The Toxicologist

Supplement to *Toxicological Sciences*

53rd Annual Meeting and ToxExpo™

March 23-27, 2014 • Phoenix, Arizona

SOT 2014 Phoenix, Arizona

An Official Journal of the Society of Toxicology

SOT | Society of Toxicology

Creating a Safer and Healthier World by Advancing the Science of Toxicology

www.toxicology.org

OXFORD UNIVERSITY PRESS

ISSN 1096-6080
Volume 138, Issue 1
March 2014

www.toxsci.oxfordjournals.org

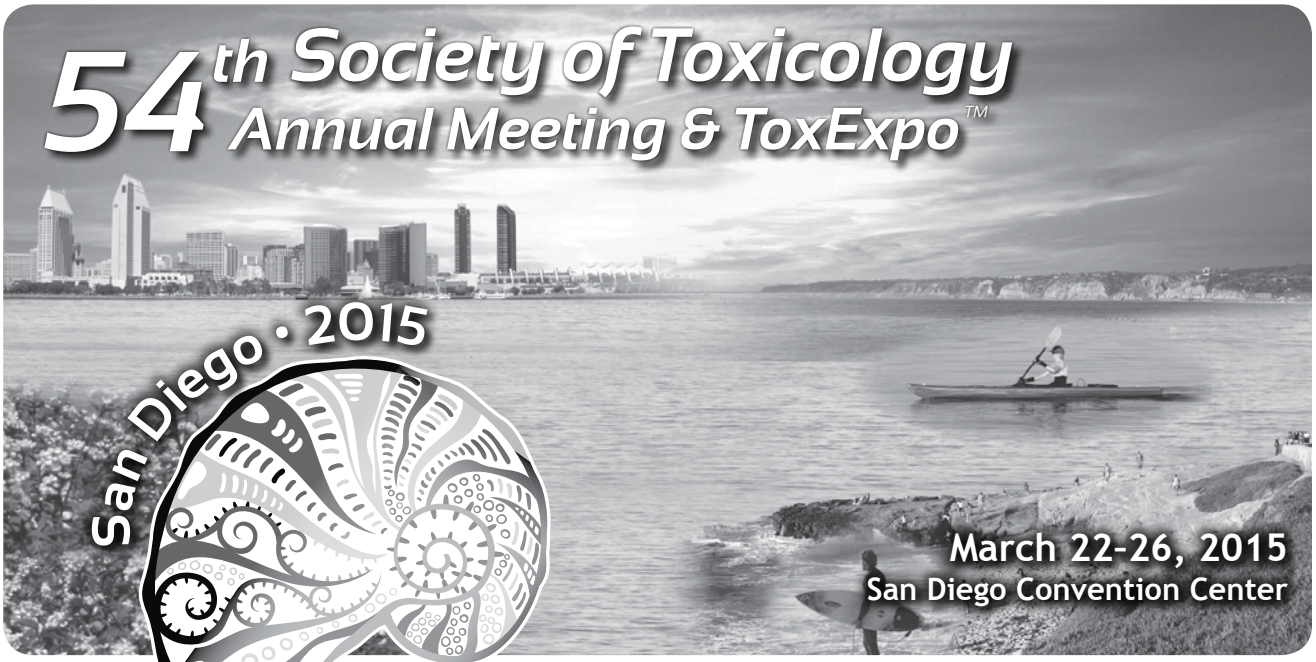

Some San Diego photos are courtesy of SanDiego.org. Some photos by Joanne DiBona.

Deadline for Proposals for SOT 2015 Annual Meeting Sessions: April 30, 2014

Why Submit a Proposal?

1. To present new developments in toxicology.
2. To provide attendees with an opportunity to learn about state-of-the-art technology and how it applies to toxicological research.
3. To provide attendees with an opportunity to learn about the emerging fields and how they apply to toxicology.

Session Types

Continuing Education—Emphasis on quality presentations of generally accepted, established knowledge in toxicology
Note: CE courses will be held on Sunday.

Symposia—Cutting-edge science; new areas, concepts, or data

Workshops—State-of-the-art knowledge in toxicology

Roundtables—Controversial subjects

Continuing Medical Education—Emphasis on state-of-the-art knowledge to assist medical doctors, health professionals, and researchers in life-long learning for providing high-quality health care
Note: Any session type may be considered for CME.

Historical Highlights—Review of a historical body of science that has impacted toxicology

Informational Sessions—Scientific planning or membership development

Education-Career Development Sessions—Sessions that provide the tools and resources to toxicologists that will enhance their professional and scientific development

Regional Interest—Central topics of relevance that describe public health and/or ecological problems of a particular region

Submit your proposal online at www.toxicology.org

The Toxicologist

Supplement to *Toxicological Sciences*

53rd Annual Meeting and ToxExpo™

March 23-27, 2014 • Phoenix, Arizona

An Official Journal of the Society of Toxicology

SOT | Society of Toxicology

Creating a Safer and Healthier World by Advancing the Science of Toxicology

www.toxicology.org

OXFORD UNIVERSITY PRESS

ISSN 1096-6080
Volume 138, Issue 1
March 2014

www.toxsci.oxfordjournals.org

Preface

This issue is devoted to the abstracts of the presentations for the Continuing Education courses and scientific sessions of the 53rd Annual Meeting of the Society of Toxicology, held at the Phoenix Convention Center, March 23–27, 2014.

An alphabetical Author Index, cross referencing the corresponding abstract number(s), begins on page 627.

The issue also contains a Keyword Index (by subject or chemical) of all the presentations, beginning on page 655.

The abstracts are reproduced as accepted by the Scientific Program Committee of the Society of Toxicology and appear in numerical sequence.

NOTE: Abstract numbers including a lower-case letter were programmed during second submission phase.

Scientific Session Types:

- **EC** Education-Career Development Sessions
- **HH** Historical Highlights Session
- **IS** Informational Sessions
- **PL** Platform Sessions
- **PS** Poster Sessions
- **RI** Regional Interest Session
- **R** Roundtable Sessions
- **S** Symposium Sessions
- **W** Workshop Sessions

Scan Me!

The 2014 SOT Mobile Event App and Event Website

Use the enhanced planning and networking tools to access the latest meeting information, connect with fellow attendees, build your own schedule, view presentation details, abstracts, and ePosters, request meetings with attendees and exhibitors, and navigate ToxExpo with an interactive floor plan. In addition to these networking and meeting planning tools, use the mobile event app and website to access a complete Phoenix city guide including hotels, restaurants, attractions, nightlife, and shopping. One-on-one technology training and support is available during the meeting; visit the @SOT Center—Internet Access and App Training located outside the ToxExpo on the Lower Level or the SOT Pavilion in ToxExpo.

Copies of *The Toxicologist* are available at $50 each plus $5 postage and handling (US funds) from:

Society of Toxicology
1821 Michael Faraday Drive, Suite 300 • Reston, VA 20190

www.toxicology.org

© 2014 Society of Toxicology

All text and graphics are © 2014 by the Society of Toxicology unless noted. For promotional use only. No advertising use is permitted.

This abstract book has been produced electronically by ScholarOne, Inc. Every effort has been made to faithfully reproduce the abstracts as submitted. The author(s) of each abstract appearing in this publication is/are solely responsible for the content thereof; the publication of an article shall not constitute or be deemed to constitute any representation by the Society of Toxicology or its boards that the data presented therein are correct or are sufficient to support the conclusions reached or that the experiment design or methodology is adequate. Because of the rapid advances in the medical sciences, we recommend that independent verification of diagnoses and drug dosage be made.

CE 1 Combination Products: Toxicology and Regulatory Challenges

J. N. Cammack[1], C. Ghosh[2] and T. Nguyen[2]. [1]*AstraZeneca Biologics, Gaithersburg, MD and* [2]*US FDA, Silver Spring, MD.*

Therapeutic and diagnostic products that combine drugs, devices, and/or biological elements are termed and regulated by US FDA as combination products. Technological advances continue to merge product types and blur the historical lines of separation among traditional drugs, biologics, and medical devices. Concomitantly, FDA's medical product centers, the Center for Biologics Evaluation and Research (CBER), the Center for Drug Evaluation and Research (CDER), and the Center for Devices and Radiological Health (CDRH), are employing ever-evolving collaborative efforts to address the regulatory complexities of combination products. Because combination products involve components that would normally be developed and regulated under different types of processes and policies (and frequently submitted to different FDA Centers), these products raise challenging development, regulatory, and review management questions. Differences in these pathways for each combination product type can impact the processes for all aspects of product development and management (especially preclinical testing), but also clinical investigation, marketing applications, manufacturing and quality control, adverse event reporting, promotion and advertising, and post-approval modifications. Trends and strategies for addressing the impact of overlapping technologies and evolving regulatory processes in developing a successful preclinical evaluation program will be highlighted. A regulatory overview of definitions and combination product examples, as well as a high-level review of FDA's final rule (effective July 22, 2013), will be included. A primary focus of the course is discussion of approaches in optimizing a pre-clinical program for a hypothetical drug-device combination product (e.g., a monoclonal antibody packaged in a pre-filled syringe). Additionally, regulatory overview of the preclinical evaluation program will be provided. Future trends in combination product therapies will also be highlighted.

CE 2 Computational and Experimental Aspects of microRNAs in Toxicology

S. C. Tilton[1], K. Wang[3], I. Pogribny[2], R. J. Brennan[4] and K. Thompson[5]. [1]*Pacific Northwest National Laboratory, Richland, WA,* [2]*US FDA-NCTR, Jefferson, AR,* [3]*Institute for Systems Biology, Seattle, WA,* [4]*Sanofi, Waltham, MA and* [5]*US FDA, Silver Spring, MD.*

MicroRNAs (miRNAs) are small noncoding RNAs that function as post-transcriptional regulators of gene expression. miRNAs are increasingly recognized for their importance in regulating mechanisms of disease and exposure, including those associated with nervous system development, cardiac function, metabolism and cancer. miRNAs and their transcriptional targets are highly conserved across species. They are also stable in plasma and urine as biomarkers of tissue-specific damage or response. Furthermore, miRNAs are unique in that not only can they be experimentally measured along with their inhibitory effects on transcript and protein levels, but their post-transcriptional regulation can also be computationally predicted based on sequence specificity and conservation across species. Given the overall importance of miRNAs in toxicology, it is necessary to understand both computational and experimental aspects of miRNAs for accurate miRNA quantification and discovery of the functional consequences of their disruption by chemical or drug exposure. The goal of the course is to provide toxicologists with a better understanding of miRNA biology (biogenesis, sequence, structure, function, and species similarities), the experimental and computational resources available for identification and target prediction and how these resources can be leveraged to identify mechanisms and biomarkers of toxicity.

CE 3 Current Trends in Genetic Toxicology Testing

B. Gollapudi[1], S. Dertinger[2], R. H. Heflich[3] and M. J. LeBaron[4]. [1]*Exponent, Midland, MI,* [2]*Litron Laboratories, Rochester, NY,* [3]*US FDA-NCTR, Jefferson, AR and* [4]*The Dow Chemical Company, Midland, MI.*

The scientific discipline of genetic toxicology has played an important role in the safety assessment of existing and new chemicals during the past four decades. This field has undergone significant changes during this time, not only in its regulatory applications, but also in the tools and technologies employed to identify adverse events. While the emphasis during the early years was on protecting germ cells and future generations from the deleterious effects of mutagenic agents, the focus shifted in later years towards identifying carcinogenic chemicals through the use of short-term assays. Furthermore, genetic toxicology tended to operate as a standalone discipline, generating qualitative data and placing little importance on dose-response analysis or integration with other toxicology measurements. The field is now in the midst of a sea change. Regulatory requirements across the globe are being harmonized, with emphasis on "3 Rs". Recent changes to ICH and OECD testing guidelines promote the integration of genetic toxicology endpoints (e.g., Comet, micronucleus, and gene mutation) into repeat-dose general toxicology studies. This integrated approach benefits the interpretation of genotoxic findings by placing them in context with other toxicology data, including pharmacokinetics and pharmacodynamics. Regulatory initiatives such as REACH stress the importance of germ cell effects as part of a comprehensive assessment of genotoxicity. Guidelines for the study of mutations in germ cells of transgenic animals (OECD 488) have recently been finalized. Rapid advances in molecular biology are facilitating the integration of genomic biomarkers into standard toxicology studies to identify various classes of genotoxic agents (DNA reactive and DNA nonreactive). Genetic toxicology is moving from a qualitative science to the quantitative assessment of dose-responses including the identification of point-of-departure (PoD) metrics to extrapolate effects to realistic human exposure levels. The course is designed to provide a comprehensive overview of recent changes and newly established practices in the field with emphasis on their application in safety assessments.

CE 4 Elucidating Adverse Outcome Pathways (AOPs) for Developmental Toxicity

T. B. Knudsen[1], G. Daston[2], D. L. Villeneuve[3], N. Kleinstreuer[4] and A. Terskikh[5]. [1]*US EPA, Research Triangle Park, NC,* [2]*Procter & Gamble Company, Mason, OH,* [3]*US EPA, Duluth, MN,* [4]*NIEHS, Research Triangle Park, NC and* [5]*Sanford-Burnham Medical Research Institute, La Jolla, CA.*

An Adverse Outcome Pathway (AOP) is a theoretical construct that integrates the biological plausibility and weight of evidence supporting a linkage between a Molecular Initiating Event (MIE) to adverse response at the individual or population level. Conceptually, an AOP spans multiple levels of biological organization and organizes the stepwise propagation of chemical disruption from MIE to toxicological outcome via a series of key events. Qualitatively, the concept of an AOP is basic to establishing plausible hypotheses and weight of evidence for chemical mode of action. This has practical use in the integration of high-dimensional data with knowledge of a complex biological system and focusing research planning on critical data needs identified as gaps in the AOP, thereby enhancing current risk assessment practices. Alternatively, development of more quantitative AOP constructs requires a framework to delineate causal relationships across a temporal series of events, and will support more realistic quantitative risk assessment. As AOPs are initially governed by signaling networks and metabolic processes, SNPs in key genes relevant to the AOP could point toward susceptible populations. The course will delve into the science of AOP elucidation from a system biology perspective, focusing on developmental processes and toxicities for early life stage susceptibilities. The presenters will each focus on making extensive use of current knowledge, informatics and data-mining tools to advance predictive toxicology.

CE 5 Inhalation Studies: Challenges and Complexities

G. L. Baker[1], W. J. McKinney[2], R. F. Phalen[3], M. Oldham[2], J. R. Harkema[4] and M. A. Higuchi[5]. [1]*Battelle, West Jefferson, OH,* [2]*Altria Client Services Inc., Richmond, VA,* [3]*University of California Irvine, Irvine, CA,* [4]*Michigan State University, East Lansing, MI and* [5]*US EPA, Research Triangle Park, NC.*

The successful execution of animal inhalation studies (e.g., acute, subchronic, and chronic) present many challenges and complexities not encountered with other routes of exposure. Five inhalation study challenges will be addressed: 1) Comparison of methods of exposure and potential impact on inhalation studies; 2) Using various test materials, generating simple atmospheres (e.g., exposures to gases, nanoaerosols, bioaerosols, micron-sized aerosols) and mixtures (e.g., semi-volatile compounds and particles, tobacco smoke); 3) selection of the appropriate animal species (e.g., species specific dosimetry); 4) incorporating standard and novel toxicological endpoints; 5) deciding which regulatory guidance document or specifications (e.g., US EPA, US FDA, OECD and NTP) to follow. The diversity of presenters' backgrounds (government, contract research organization, industry, and academic), and depth of experience, will provide a broad and rich resource for the participants.

CE 6 Methodologies in Human Health Risk Assessment

Q. J. Zhao[1], B. Meek[2], H. A. Barton[3] and J. C. Lipscomb[1]. [1]*US EPA, Cincinnati, OH,* [2]*University of Ottawa, Ottawa, ON, Canada and* [3]*Pfizer Inc., Groton, CT.*

This course provides an overview of more advanced aspects of chemical risk assessment, following up from a successful CE course on basic principles offered at the Annual Meeting in 2013. This new course will focus on methodologies, which incorporate increased use of biological and chemical specific data as a basis to provide more accurate estimates of risk. In addition, it will address evolving areas such as problem formulation as a basis to better target toxicity testing and tailor assessments to the needs of risk management. The course will feature presentations and discussions focusing on the value of mode of action analysis for characterization of hazard, the fundamental tenets of physiologically based pharmacokinetic (PBPK) model development and implementation, use of benchmark dose (BMD) models to identify points of departure, and use of chemical specific adjustment factors to address inter- and intraspecies uncertainty and variability. The principles and key components of these methodologies will be illustrated with applied case examples from the regulatory risk assessment arena.

CE 7 Nonclinical Animal Models Enabling Biopharmaceutical Advances in Translational Medicine

T. M. Monticello[1], R. Dixit[2], S. Morgan[3], N. Ganerup[4], V. J. Kadambi[5] and J. T. Sullivan[1]. [1]*Amgen Inc., Thousand Oaks, CA,* [2]*MedImmune, Gaithersburg, MD,* [3]*Abbvie, Abbott Park, IL,* [4]*Ellegaard Göttingen Minipigs A/S, Dalmose, Denmark and* [5]*Millennium, Cambridge, MA.*

A fundamental theme in drug discovery and nonclinical development is the utilization of appropriate animal models that are predictive for efficacy or adverse events in humans administered a novel biopharmaceutical. The accurate prediction of human adverse effects using nonclinical animal toxicology studies remains a major goal in drug development and relies on appropriate animal models. Essential attributes for an appropriate animal model include similar target distribution, target pharmacology, systemic pharmacokinetics, metabolism, and distribution to those of humans. Utilization of the most appropriate animal model aligns with the 2011 US FDA Strategic Plan to advance regulatory science and modernize toxicology in order to enhance product safety and develop better models of human adverse responses. The Preclinical Safety Leadership Group (PSLG) of the International Consortium for Innovation and Quality in Pharmaceutical Development (IQ) is creating a contemporary industry-wide database to determine accuracy with which the interpretation of nonclinical safety assessments in animal models correctly predicts human risk. The course will present considerations for the selection of an appropriate animal model for nonclinical safety, the use of animal models of disease in safety testing, emerging use of the minipig in safety testing, data from an industry-wide nonclinical to clinical translational database, and the use of animal safety data in the design and conduct of clinical trials. Output from the course will help identify advances and remaining gaps in the utilization of animal models in biopharmaceutical development.

CE 8 Nanotoxicology: Past Achievements, Future Challenges, and Potential Solutions

S. M. Hussain[1], D. B. Warheit[2], L. K. Braydich-Stolle[1], C. Grabinski[1], K. K. Comfort[3] and C. Geraci[4]. [1]*US Air Force, Wright-Patterson AFB, OH,* [2]*DuPont Haskell Laboratories, Newark, DE,* [3]*University of Dayton, Dayton, OH and* [4]*CDC-NIOSH, Cincinnati, OH.*

Nanomaterials (NM) possess tremendous promise to advance consumer, military, and medical applications due to their unique physicochemical properties, such as enhanced surface area, tunable size, modifiable surface chemistry, and particle reactivity. However, these same properties have made NMs a potential health hazard, thus giving rise to the field of nanotoxicology (NT), which has become a prominent player in toxicological advancement and research over the past decade. Initial NT studies were limited by a lack of both available materials and characterization tools. Through advances in material science, enhanced capabilities have been developed that allow for the synthesis of distinctive NMs and the ability to accurately evaluate their characteristics. Taking advantage of these developments, NT has made remarkable progress in evaluating the hazards of NMs and correlating specific properties, such as size, shape, coating, and composition, to observe cytotoxicity. However, even with these numerous advances, there are still a number of constraints plaguing the field of NT. One principal area of concern is the development of procedures that account for new NT facets; including NM behavior in a physiological environment, varied aggregate structure, role of ionic dissolution, and realistic modes of exposure. Another limitation is the need for new and more powerful characterization tools. Recently, the question of dosimetry has become a forefront topic and whether a universal, conceptual standard should be adopted, such as mass, surface area, or particle number. Arriving at a consensus on this issue is critical for the establishment of NM exposure limits and risk assessment metrics, which are significantly lacking. To accomplish accurate risk assessment and regulatory evaluations, NT will have to develop a means to improve the correlation of *in vitro* data to *in vivo* predictions, via enhanced cell models, relevant dosages (low vs. high), and realistic exposure scenarios. This CE course will evaluate where NT stands, by highlighting key research successes, identifying challenges facing the field today, and exploring solutions to overcome current limitations.

CE 9 Epidemiology for Toxicologists: What the Numbers Really Mean

N. B. Beck[1], M. Goodman[2], S. Eftim[3], J. E. Goodman[4] and J. Bus[5]. [1]*American Chemistry Council, Washington, DC,* [2]*Emory University, Atlanta, GA,* [3]*George Washington University School of Public Health, Fairfax, VA,* [4]*Harvard School of Public Health and Gradient, Cambridge, MA and* [5]*Exponent, Midland, MI.*

21st Century risk assessment relies on data from multiple lines of evidence. High quality human epidemiology data are generally preferred for regulatory decision-making, but the body of evidence often includes animal toxicity, *in vitro, in silico,* animal dosimetry, and human exposure data. The quality of individual epidemiology studies can be highly variable and dependent on study design as well as other critical factors that sometimes cannot be controlled for. For risk assessors to fully understand the implications of epidemiology evidence, they must understand how the overall integration of toxicity and mechanistic data with human epidemiology findings facilitates science-informed decision-making. A sufficient understanding of the epidemiology data is a necessary starting point for appropriately integrating all the available information. The course is geared towards the toxicologist who is trying to determine how to appropriately evaluate, use, and integrate epidemiology data in a weight-of-evidence evaluation or risk assessment. Attendees first will be given a basic overview of epidemiology, with a focus on different epidemiology study designs and their strengths and weaknesses. Attendees will also gain an understanding of exposure assessment and biomonitoring, and how this information is used and evaluated in epidemiology studies. Additional learning objectives of the course: How to determine when an association may be supportive of a causal relationship and what confidence intervals mean; how to use trend information; how to evaluate and understand adjustments that are made for potential confounding factors; and how to evaluate several epidemiology studies on the same topic, particularly in light of available toxicity and mechanistic data. Finally, attendees will learn to integrate all types of data streams with a real example. Attendees will leave the course with a stronger understanding of how to interpret and use epidemiology data in their weight-of-evidence analyses and risk assessments, and how epidemiology can help inform regulatory decision-making.

CE 10 Innovations in Methodologies for Inhalation Exposure and Interpretations of *In Vivo* Toxicity

J. Pauluhn[2], J. D. McDonald[3], B. T. Chen[4], T. E. Kleindienst[1] and M. A. Higuchi[1]. [1]*US EPA, Research Triangle Park, NC,* [2]*Bayer HealthCare, Wuppertal, Germany,* [3]*Lovelace Respiratory Research Institute, Albuquerque, NM and* [4]*NIOSH, Morgantown, WV.*

The respiratory system presents most diverse structural and cellular heterogeneity suited to handle complicated aspects of air liquid interface such as the direct exposure of the delicate cellular and capillary surfaces to the atmosphere and the encounter of lung epithelial cells to complex mixtures of particles and gases. Not only the respiratory depositions of inhaled substances vary regionally but also the regional responses generated by the respiratory tract. Recently the field of inhalation technology and respiratory toxicology has seen revolutionary growth because of the emergence of the use of nanomaterials and renewable energy sources creating new environmental challenges. Moreover, the paradigm shift of toxicology testing to high throughput screening has led to the development of novel inhalational approaches for cells. Speakers will cover the recent advances in inhalation methodologies for various types of emerging inhalants and focus on generation of atmospheres for *in vivo* and *in vitro* toxicity assessment. These aerosols will include gas and particulate emissions from vehicles using old and new energy sources, forest fires, coal combustion, manufactured nanomaterials and mixtures formed from atmospheric aging. The dynamic of physicochemical composition of such mixed aerosols will be discussed to allow for identification of causative constituents and lung site-specific injuries. Structural differences in the respiratory tract of rodents and large mammals, including humans, impacting dosimetry will be discussed. Respiratory system heterogeneity between humans and animals, and their differential neurohumoral mechanisms will be discussed to aid in interpretation of inhalational hazard for

humans. This course will be useful for those involved in air pollution toxicology, nanotoxicology, novel drug delivery systems, pulmonary toxicology, and risk assessment.

CE 11 Nonclinical Pediatric Drug Development: Considerations, Study Designs, and Strategies

K. E. Thompson[1], E. M. Lewis[2], K. Davis-Bruno[3], J. Carleer[4], S. B. Laffan[5] and G. J. Chellman[6]. *[1]Bristol-Myers Squibb Company, New Brunswick, NJ, [2]Charles River Laboratories, Horsham, PA, [3]US FDA, Silver Spring, MD, [4]Belgian Federal Agency for Medicines and Health Products, Brussels, Belgium, [5]GlaxoSmithKline, King of Prussia, PA and [6]Charles River Laboratories, Reno, NV.*

Although nonclinical and clinical testing needs for drugs for pediatric populations have been discussed for more than 40 years, there is no default approach to evaluating safety in this age group. Over the last decade there has been a heightened awareness of the differences between the pediatric and adult patient, and these differences are being addressed by the pharmaceutical and healthcare industries, as well as the governmental and regulatory bodies that sanction the development and testing of drugs for children. As regulatory demands evolve for nonclinical safety assessments in juvenile animals, industry leaders are developing innovative ways to meet the regulatory expectations and to overcome the challenges associated with pediatric drug development. Many practical issues regarding nonclinical testing in immature animals have been surmounted, using novel and/or adapted approaches. There are considerations related to the differences in regional guidelines (US FDA, EU, and Japan), therefore development of appropriate information for submission to worldwide agencies is critical. History and experience provide the best scientific arguments as to why juvenile animals can be useful. There are numerous examples of drugs that have identified findings in various species, including information regarding kinetic and toxicity differences that highlight considerations regarding nonclinical testing models. Additionally, there are unique challenges associated with nonclinical juvenile toxicity testing for biopharmaceuticals, including selection of appropriate animal models, immunogenicity, dose selection (toxicity vs. pharmacology), and relevant endpoints. Developing a juvenile animal program requires an appreciation of the complexity of the nonclinical strategies to enable pediatric trials and an overview of the historical perspective and the current approaches to evaluating safety during this unique period of life.

CE 12 Stem Cells in Toxicology

E. J. Tokar[1], M. P. Waalkes[1], R. Deans[2] and K. L. Kolaja[3]. *[1]NIEHS, Research Triangle Park, NC, [2]Athersys Inc., Cleveland, OH and [3]Cellular Dynamics International, Montclair, NJ.*

Stem cells are revolutionizing toxicological research and remain an area with tremendous potential. Recently, research on stem cells has generated tremendous public and professional interest. However, some areas of toxicological research have lagged behind in the integration of stem cells as a concept in toxicant-induced disease etiology. We will describe the utility and suitability of the assorted types of stem cell models (i.e. embryonic, fetal, progenitor, induced pluripotent, immortalized stem cell lines, etc.) for various research purposes, including disease modeling, drug discovery and toxicity testing in order to describe the potential applications of stem cells in toxicological research. This important overview of stem cells will highlight their nomenclature, properties, and their roles in the genesis of various diseases.

CE 13 Translational Biomarkers in the Assessment of Health and Disease

V. S. Vaidya[1], M. Moses[4], D. L. Mendrick[2], J. Aubrecht[3] and C. Leptak[5]. *[1]Harvard Medical School, Boston, MA, [2]US FDA-NCTR, Jefferson, AR, [3]Pfizer Inc., Groton, CT, [4]Children's Hospital Boston, Boston, MA and [5]US FDA, Silver Spring, MD.*

Biomarkers serve as quantitative measures of chemical exposures and biologically effective doses, early warning signals of biologic effect, predict outcome in a patient with disease, and identify who will respond to an intervention and whether the intervention is working. The current era of scientific discovery has brought seemingly limitless opportunities for improvements in medical care. Translational biomarkers that can be measured in blood or urine in both experimental animals and man are of particular interest. Given the importance to the clinical, pharmaceutical, and regulatory communities motivated by more specific and timely diagnoses, early intervention and safer therapies, clinically useful biomarkers have evolved over time, reflecting the scientific and technologic progress made over the centuries. An increasing number of clinically relevant tests and procedures are available to estimate organ injury and guide treatment. The use of molecular signals in the assessment of health and disease is not new; however, the concept of what constitutes a useful biomarker has evolved considerably in the past two to three decades given the advanced enabling technologies, deeper molecular understanding of disease, and the advent of a regulatory framework for biomarker qualification. Our panel experts will highlight the potential of these biomarkers over a wide variety of applications spanning preclinical-clinical safety in liver and kidney, to disease monitoring in cancer. The panel will also demonstrate the application of translational biomarkers in clinical trial design. Coordinated efforts at biomarker discovery and validation as well as technologies for biomarker measurement will help ensure that the ultimate goal of safer drugs, a cleaner environment, and improved patient outcomes are realized.

S 14 Air Pollution and Cardiovascular Effects: Mechanisms and Role of Lipid Peroxidation

D. J. Conklin. *Cardiovascular Medicine, University of Louisville, Louisville, KY.*

The mechanisms by which air pollution, including particulate matter ($PM_{2.5}$) and volatile gases, affect human cardiovascular health are incompletely known. Yet many animal studies performed to probe these mechanisms have observed changes in the levels of lipids and/or lipid peroxidation products regardless of the specific form of air pollution, e.g., diesel engine exhaust, concentrated ambient particulate matter, or volatile gases, used in the exposure that associates with severity of injury. These studies suggest a potential common pathway of injury that is dependent on oxidative stress and an increased production of lipid mediators. The role of lipids and lipid peroxidation as final common mediators of air pollution-induced injury in the cardiovascular system is the focus of this symposium. Speakers will address how exposures to diverse types of air pollutants, including complex mixtures, traffic emissions, volatile acrolein, and concentrated ambient particulate matter, result in alterations in circulating lipid levels, lipids structure and function, and lipid peroxidation products in target organs including lungs, blood, and the vasculature. Collectively, these presentations will shed light on the specific role of lipids and lipid peroxidation in air pollution-induced cardiovascular injury.

S 15 Air Pollution, Lipid Oxidation, and Cardiovascular Effects in Humans and Animals Models

A. Bhatnagar. *Cardiovascular Medicine, University of Louisville, Louisville, KY.*
Sponsor: D. Conklin.

Epidemiological studies indicate that ambient air pollution enhances the incidence and progression of cardiovascular disease and increases the risk of cardiovascular mortality primarily by promoting acute coronary syndromes and ischemic heart disease. Exposure to air pollutants associates with systemic lipid peroxidation, which has been shown to be an important marker and pathogenic mediator of atherosclerosis, acute plaque rupture and myocardial infarction. This symposium will address the relationship between air pollutants and lipid peroxidation that often accompanies exposures resulting in altered tissue and blood lipids. Moreover, this symposium will address the question whether and how these changes contribute to subsequent cardiovascular dysfunction and potentially increase the risk of cardiovascular disease.

S 16 Vascular Lipid Peroxidation Induced by Complex Emissions Indicates Gas-Particle Interactions in Driving Systemic Toxicity

M. Campen. *Pharmaceutical Sciences, University of New Mexico, Albuquerque, NM.*

Air pollution is associated with adverse cardiovascular events in epidemiological studies. Several recent studies have indicated a role for oxidative changes to phospholipids following inhalation of various pollutants, which leads to altered biological activity of those modified lipids. To better understand the important causal components of the ambient pollution mixtures, we have investigated the relative lipid peroxidation induced in the murine aortic wall by diverse exposure conditions involving fresh emissions of gasoline and/or diesel engines, resuspended road dust, and secondary particulates of sulfate or nitrate composition. We noted that emissions containing mixtures of particulate and gas phase components typically induced greater vascular lipid peroxidation than did individual components. Moreover, our data suggest that gases may deposit on particulates, thereby driving toxicity in a surface area-dependent manner. Further studies highlight a role for modified lipids and metabolites in the circulation after exposures, in human and rodent studies, that may drive the accumulation of vascular lipid peroxides.

S 17 Effects of Acrolein or Concentrated Ambient Particulate Matter Exposure on Plasma Lipids and Vascular Targets

D. J. Conklin. *Cardiovascular Medicine, University of Louisville, Louisville, KY.*

Acute exposure to the inhaled carbonyl, acrolein, or to fine (concentrated) ambient particulate matter (CAP) leads to alterations in plasma lipids, oxidized lipids, circulating progenitor cells and vascular insulin resistance but how these divergent endpoints are related to each other is not clear. Because vascular dysfunction and vascular insulin resistance are two early events associated with metabolic syndrome and the progression to diabetes (and in order to interrogate mechanistic relationships between disparate endpoints), we studied whether changes induced in lipids and the vasculature were shared across different pollutant exposures (gas or CAP) and to similar degrees dependent on exposure level to reveal potential common mechanisms of action.

S 18 Vehicle Emissions-Exposure Results in Increased Cerebrovascular Lipid Peroxidation Associated with Altered Blood Brain Barrier Permeability

A. K. Lund. *Biological Sciences, University of North Texas, Arlington, TX.*

Traffic-generated air pollution-exposure has recently been associated with adverse effects in the central nervous system (CNS) including neuroinflammation and neurodegeneration. While alterations in the blood brain barrier (BBB) have been implicated as a potential mechanism of air pollution-induced CNS pathologies, there is currently little known about the pathways involved. Lipid peroxidation and oxidative stress are known to regulate air pollution-mediated effects in the systemic vasculature resulting in progression of vascular disease states; therefore, we investigated their role in altered signaling, transport, and permeability in the cerebral vasculature after inhalation exposure to vehicle emissions. We observed significant increases in lipid peroxidation in the cerebral vasculature of mice, resulting from exposure to vehicle emissions, which was associated with increased BBB permeability. Additionally, we measured increased matrix metalloproteinase-9 activity and decreased tight junction expression in the cerebral vessels from exposed animals. Further studies using plasma from exposed vs. control mice in an in vitro BBB co-culture model suggest that a circulating "reactive factor" may mediate the observed alterations in BBB permeability and transport. Collectively, these data suggest that lipid peroxidation may mediate alterations in signaling and structural proteins responsible for maintaining BBB integrity.

S 19 Air Pollution, Lipid Peroxidation, and Alterations in HDL Functionality

J. Araujo. *Medicine, University of California Los Angeles, Los Angeles, CA.* Sponsor: D. Conklin.

Exposure to ambient particulate matter (PM) lead to enhanced atherosclerosis in experimental animal models. Particle size and composition play a role in the extent how atherosclerosis is promoted. We have reported that inhalation of concentrated fine and ultrafine ambient particles led to alteration of plasma HDL anti-inflammatory capacity in ApoE null mice that correlated with their ability to enhance atherosclerotic lesion formation. In addition, we have also shown that exposures to diesel exhausts result in alteration of HDL anti-oxidant capacity. This presentation will focus on our studies that have evaluated whether HDL functional changes, induced by air pollutants, are related to effects on lipid peroxidation in the lungs, circulating blood and systemic tissues.

S 20 Carbon Nanotubes Are Toxic in Experimental Models: What's Next, Who's Being Exposed, and Should We Be Concerned?

A. Erdely and J. M. Antonini. *CDC-NIOSH, Morgantown, WV.*

Engineered nanomaterials have vast potential with applications in medicine, electronics, and composites. Carbon nanotubes (CNT) represent one such material with broad applications, but this material also has the propensity for significant toxicity. Toxicities include pulmonary and systemic inflammation, fibrosis, immunosuppression, and cardiovascular dysfunction, and evidence is growing that CNT may have properties that influence carcinogenicity. Over the past decade there has been a significant investment in research to examine the *in vivo* and *in vitro* toxicity of CNT. Conversely, very little is known about the exposure level and chemical and physical properties of airborne CNT that humans are exposed to, especially in the workplace. These deficiencies make the interpretation of the vast number of experimental studies to human relevance difficult. Initial findings from epidemiological studies of workers handling engineered nanomaterials, recent advancements in detailed facility exposure assessment, pertinent *in vivo* toxicology studies with dosimetry-based human health implications, regulatory aspects, and risk assessment based on results from animal inhalation studies will be included. The outcome of this session is to provide the most recent human exposure assessment and epidemiological findings and to gather perspective on *in vivo* toxicology studies involving risk estimates and potential carcinogenicity. This data should have direct influence on the course of newly designed studies and add perspective on previous studies of CNT-induced toxicity.

S 21 Epidemiological Study of Workers Handling Carbon Nanotube and Engineered Nanomaterials

S. Liou[1], H. Liao[1], W. Wu[1], Y. Chung[1] and M. Lin[2]. [1]*Division of Environmental Health & Occupational Medicine, National Health Research Institutes, Miaoli County, Taiwan and* [2]*Institute of Occupational Safety and Health, Council of Labor Affairs, Taipei, Taiwan.* Sponsor: J. Antonini.

The aim of this study was to investigate the health hazards of workers handling nanomaterials. Study population was 206 nanomaterial-handling workers and 108 unexposed workers recruited from 14 manufacturing factories in Taiwan and were followed up for no less than 2 times. For each participant, a self-administered questionnaire was used to collect personal habits, work history, potential confounding exposure, and detailed information of work conditions and nanomaterials handled after informed consent. Since there was still a lack of personal sampling methodology and summary index for heterogeneous exposure, we adopted the control banding nanotool risk level matrix proposed by Dr. Paik to categorize the risk level for each participant as a surrogate of exposure. There were 108 workers in risk level 1, 91 workers in risk level 2, and 7 in risk level 3. The markers of health outcomes include pulmonary and cardiovascular disease markers, inflammation markers, oxidative stress markers, antioxidant enzymes activity, and genotoxicity markers in blood, urine and exhaled breath condensate (EBC). Generalized Estimating Equation (GEE) model was applied to analyze no less than 2 repeated measurements in 4-year follow-up. Increase and a risk level gradient of antioxidant enzymes, superoxide dismutase (SOD), were found in nanomaterials and carbon nanotube handling workers with compare to controls. But cardiovascular dysfunction, lung inflammation and lung function, oxidative stress, and genotoxic markers were not associated with nanomaterials handling in this four-year follow-up study. Pilot environmental study indicates that the exposure level of nanoparticles in the workplace was low. Nanomaterials handling in current negligible emission scenario may not have health impact on the workers, except for increase of antioxidant enzyme.

S 22 Carbon Nanotube Exposure Assessment: An Evaluation of Workplace Exposures in the US

M. Dahm[1], M. Schubauer-Berigan[1] and A. Erdely[2]. [1]*CDC-NIOSH, Cincinnati, OH and* [2]*CDC-NIOSH, Morgantown, WV.*

Just as there has been much advancement in the field of toxicology over the past decade relative to health outcomes from carbon nanotube (CNT) exposures, similar strides are being made in the field of exposure assessment. Recent developments in sampling methodologies have led to more accurate estimates for worker exposure levels as compared to preliminary studies, which may have overestimated exposures. As part of an ongoing NIOSH exposure assessment and epidemiologic study, worker exposure to CNT has been examined by sampling 14 different worksites across the US over a three year period. Personal breathing zone exposure levels were measured using a chemical specific marker for the mass concentration of elemental carbon (EC) at both the inhalable and respirable size fractions. The sampling methodologies are in accordance with the NIOSH Current Intelligence Bulletin on CNTs and carbon nanofibers which set a mass based Recommended Exposure Limit at 1 μg/m^3 of EC at the respirable size fraction. Overall, personal workplace exposures at the respirable size fraction to EC ranged from 0.02 – 1.47 μg/m^3 with an 8 hr time weighted geometric mean of 0.16 μg/m3. Inhalable personal breathing zone exposures ranged from 0.003 – 22.40 μg/m^3 with a geometric mean of 0.38 μg/m^3. Concurrent personal breathing zone samples were also collected and analyzed by electron microscopy using methods similar to the asbestos counting convention. CNT structure agglomerate sizes averaged > 4 μm while few single CNT fibers were found. This study also focused on how exposure level and type change within the various industries in which CNTs are being applied (composites, electronics, production), between types of materials (multi-walled vs. single-walled), and under varying work conditions. The detailed information from these exposure assessment findings bring awareness to industries with higher

exposure potentials and provide valuable data on job specific tasks where exposures are likely to occur. In addition, the findings from this study can provide valuable insight for designing and interpreting *in vivo* exposures.

S 23 Relationship between *In Vivo* Carcinogenicity and Human Risk to Carbon Nanotubes

L. M. Sargent[1], D. W. Porter[1], L. Staska[2], A. F. Hubbs[1], M. L. Kashon[1], D. T. Lowry[1], L. A. Battelli[1], B. T. Chen[1], D. G. Frazer[1], V. Castranova[1] and S. H. Reynolds[1]. *[1]CDC-NIOSH, Morgantown, WV and [2]Integrated Laboratory Systems, Inc., Morrisville, NC.*

In vitro genotoxicity investigations have shown that high aspect ratio carbon nanotubes induce cell cycle disruption and errors in chromosome number. A subsequent *in vivo* multiwalled carbon nanotube (MWCNT) whole body inhalation exposure study further demonstrated that MWCNTs promoted the growth of DNA damaged (initiated) lung cells to form lung adenomas and adenocarcinomas. Twenty-three percent of the filtered air controls, 27% of the MWCNT-exposed, and 52% of the methylcholanthrene (MCA) followed by air-exposed mice, had a mean of 1.3, 1.3 and 1.4 lung tumors per mouse, respectively. By contrast, 91% of the mice exposed to MCA followed by inhaled MWCNTs (MCA/MWCNT) had an average of 3.24 tumors per mouse. A total of 61 adenocarcinomas and 3 metastatic adenocarcinomas were observed in 55 MCA/MWCNT-treated mice. Furthermore, MWCNT inhalation increased the incidence of serosal tumors consistent with the diagnosis of sarcomatous mesothelioma from 2% in the MCA-exposed mice to 9% in the MCA/MWCNT, a 4.5 fold increase. These data demonstrate that inhaled MWCNTs are strong promoters of pulmonary adenomas and adenocarcinomas in B6C3F1 mice. The presence of metastatic disease in 15% of the MCA/MWCNT-exposed mice compared to 1.6% in the MCA-exposed group suggests that carbon nanotubes also induce cancer progression. The mouse MWCNT lung burden in this study approximated feasible human occupational exposures at the NIOSH Recommended Exposure Limit (REL). Given that recent measurements of carbon nanotubes in the workplace indicate levels of nanotubes that can be higher than the NIOSH REL, adverse outcomes in occupationally exposed humans is a possibility. The presentation will include a discussion of the mechanism of MWCNT-induced tumor promotion and progression as well as work in progress to examine the dose response of MWCNT-induced tumor promotion.

S 24 Review of CNT Health and Environmental Risks under TSCA, and Areas Where More Data Are Needed

P. Sayre. *US EPA, Washington, DC.*

EPA, under the Toxic Substances Control Act, reviews numerous types of nanomaterials prior to their entry into the market, including a substantial number of carbon-based materials. For each one a risk assessment and a risk management plan are developed that address human and environmental risks, including occupational risks. Approaches for addressing the risks of CNTs will be discussed, based on available hazard and exposure data available. More information is needed that would allow predictive determinations of hazards and exposures. Predictive frameworks could be based on hazard and exposure categories, streamlined testing strategies, and/or control banding. Additional data are needed to underpin such frameworks.

S 25 Evaluation of Human Risks on Animal Models

J. Pauluhn. *Bayer Pharma AG, Wuppertal, Germany.*

Current inhalation testing approaches are designed to evaluate and assess systemic and portal-of-entry related toxicities of soluble and bioavailable chemical substances. Insoluble chemical structures may cause toxicity by two major mechanisms: The first depends on the site and acute dose of initial deposition and the cause of localized toxicity may depend mainly on physical factors, such as solubility, particle surface activity including size, and shape. The second depends more on its durability and total dose accumulated with exposure time with time. It seems that the accumulated particle volume of inhaled low-density nanostructures delay clearance with associated faster manifestation of lung overload and toxicity. Each mechanism can dose-dependently destabilize the pulmonary barrier function, giving the structure access to the systemic circulation, depending on the degree of local inflammation. Toxicologists need to disentangle which of these etiopathologies is causing the critical toxic response under exposure conditions relevant to humans. Multiple chemical-, particle-, and experimental design-specific factors may affect the outcome of experimental studies with multi-walled Carbon Nanotubes (CNT). This adds another dimension of complexity as nanostructured particle morphologies change with their degree of agglomeration and purpose-driven modified surface characteristics. All may affect their compartmentalized retention within the lung and associated localized toxicity. Humans exposed chronically to CNTs may accumulate these structures over time and the mere exhaustion of the existing, physiological capacity of the lung may cause lung toxicity. Experimental models that do not observe these model-specific constraints may generate findings difficult to extrapolate to any real-life scenario of humans. This paper addresses as to how CNT-specific human risks can be evaluated and assessed in controlled experimental models and how kinetic modeling can be used to estimate safe Occupational Exposure Levels with a minimum number of animals.

S 26 Computational Approaches to Predict Repeat-Dose Toxicity: Lessons Learned from Cosmetic Ingredients

M. T. Cronin[1] and C. Yang[2]. *[1]Liverpool John Moores University, Liverpool, United Kingdom and [2]Altamira LLC, Columbus, OH.*

Assessing the toxicity of cosmetic ingredients presents numerous challenges, the solution of which will contribute to the general understanding of chemically-induced toxicity. The goal is to predict the effects to humans of long-term repeated low-dose exposure to chemicals used in cosmetics. For risk assessment, the results of *in vivo* assays are often distilled in terms of NOAELs and LOAELs. However, alternatives are required for cases where animal test data are lacking or cannot be obtained due to cost, time, or legislation. The past decade has seen an immense growth in attempts to predict toxicity computationally, but even with these advances traditional approaches (e.g., quantitative structure-activity relationships (QSARs)) are limited due to the lack of understanding of xenobiotic targets and small molecular interactions associated with observed phenotypic effects. QSAR is also not appropriate for making reliable estimates of NOAELs; thus, a new paradigm is being sought. Despite these drawbacks, the key premise is that structure-based computational analysis of a chemical of interest and close structural analogues for which experimental data are available will lead to improved predictivity due to greater association with mechanisms of toxicity. Exposure is often dermal, but inhalation or oral routes are also possible. Penetration and metabolism within the dermis, possibly followed by target organ toxicity, must all be considered and accounted for when necessary. The combined factors of relatively low-dose, dermal ADME properties and toxicity to specific organs are amongst the greatest challenges facing computational toxicology for the prediction of the effects of exposure to cosmetics. This session will address these issues and review the current state of the art of computational modeling at the organ level to support risk assessment as it is being developed in a unique European Union Project called COSMOS. The funding of the COSMOS Project is from the European Commission and Cosmetics Europe.

S 27 Databases, Tools, and TTC Approach Applied to Chemicals in Cosmetics Products

C. Yang[1], M. Ambrosio[2], K. Arvidson[3], M. T. Cronin[4], E. Fioravanzo[5], K. Muldoon-Jacobs[3], D. Keller[6], J. Rathman[1], A. N. Richarz[4], L. Terfloth[7], I. Tsakovska[8], V. Vitcheva[8] and A. P. Worth[9]. *[1]Altamira LLC, Columbus, OH, [2]ILSI Europe, Brussels, Belgium, [3]CFSAN, US FDA, College Park, MD, [4]Liverpool John Moores University, Liverpool, United Kingdom, [5]S-IN, Vicenza, Italy, [6]Henkel AG & Co. KGaA, Dusseldorf, Germany, [7]Molecular Networks, Erlangen, Germany, [8]BAS, Sofia, Bulgaria and [9]EC JRC, Ispra, Italy.*

The COSMOS consortium developed new databases and tools central to its mission of assisting in the ultimate replacement of animal testing of cosmetic products. COSMOS Database includes a new Cosmetics Inventory of more than 19,000 substances reported by EU CosIng and the US Personal Care Products Council. The chemical in-use functions include antioxidants, hair dyes/colorants, emollients, emulsifiers/surfactants, perfumes, preservatives, skin/hair conditioners, and UV absorbers/filters. A new toxicity database enriched with oral repeat dose studies for cosmetics ingredients was developed by compiling data from public sources including US FDA, EPA, EU SCCS, ECHA, and literature. A new non-cancer TTC database for cosmetics-related chemicals has been compiled by augmenting the COSMOS DB with relevant Munro data. The resulting TTC database contains over 500 chemical structures with reported NOAEL. The inclusion and selection criteria of the NOAEL decisions were established. ILSI Europe experts reviewed toxicity data for the high impact portion of the database, the lowest 10th percentile plus compounds for which there is a large variation across different sources. The chemical space of the new TTC database was compared with other TTC databases to demonstrate the coverage suitable for the assessment of cosmetics. A decision tree workflow incorporating structural and usage exposure categories specific to cosmetics to address the oral-to-dermal extrapolation of repeat dose toxicity data was also devised. Thus this talk addresses overall COSMOS efforts on the TTC

approach to chemicals used in cosmetics products, building from the databases to implementation of tools. Abstract does not reflect US FDA or EC JRC policies. Authors acknowledge ILSI Experts.

S 28 Role of Bioavailability in Risk Assessment of Cosmetic Ingredients: Kinetics, Permeation, and Metabolism

E. Fioravanzo[1], M. T. Cronin[2], A. R. Pery[3], L. Terfloth[4], I. Tsakovska[5], C. Yang[6] and A. P. Worth[7]. *[1]S-IN Soluzioni Informatiche, Vicenza, Italy, [2]Liverpool John Moores University, Liverpool, United Kingdom, [3]INERIS, Verneuil en Halatte, France, [4]Molecular Networks GmbH, Erlangen, Germany, [5]Institute of Biophysics and Biomedical Engineering, Sofia, Bulgaria, [6]Altamira LLC, Columbus, OH and [7]EC JRC, Ispra, Italy.*

When assessing the impact of cosmetics ingredients on human health risk assessment, the chemical's toxicity is influenced by the degree to which it is absorbed into the body (i.e. its bioavailability). When developing Threshold of Toxicological Concern (TTC) categories for chemicals used in cosmetics products the comparison of exposure from the oral and dermal routes is mandatory as existing TTC approaches for an assessment of repeated dose toxicity are based on the oral route of administration. This presentation demonstrates the role of the prediction of permeability from the dermal and the oral routes and their role in toxicity prediction. This includes the use of relevant QSARs (e.g. the Potts and Guy equation for skin permeability) and more recent models. These models have been evaluated using two new databases: a database of skin permeability values (over 2,000 entries for more than 350 compounds) and a database of PAMPA permeability values. Prediction of skin metabolism is also considered in the context of identifying chemicals that may be activated or detoxified more significantly than from the oral route. A scheme for implementing predictions of dermal and oral absorption to identify possible compounds where consideration of an oral NO(A)EL may not be protective of the dermal route has been developed. This scheme is based on a "tiered box" approach for chemicals' bioavailability which identifies four general scenarios according to the degree of oral and dermal absorption with each being subsequently considered for differences in metabolism.

S 29 Adverse Outcome Pathways (AOPs) for Target Organ Effects: The Role of Structural Alerts and Chemotypes for Liver Toxicity to Group Compounds and Apply Read-Across

M. T. Cronin[1], E. Fioravanzo[2], A. R. Pery[3], L. Terfloth[4], I. Tsakovska[5], A. P. Worth[6] and C. Yang[7]. *[1]Liverpool John Moores University, Liverpool, United Kingdom, [2]S-IN Soluzioni Informatiche srl, Vicenza, Italy, [3]INERIS, Verneuil en Halatte, France, [4]Molecular Networks GmbH, Erlangen, Germany, [5]Institute of Biophysics and Biomedical Engineering, Sofia, Bulgaria, [6]EC JRC, Ispra, Italy and [7]Altamira LLC, Columbus, OH.*

AOPs provide a framework to organise information at the mechanistic and pathway level, providing evidence that a molecular initiating event (MIE) is linked, through a pathway, to an (adverse) effect. This allows for a direct linkage of chemistry to adverse effects. Capturing the chemistry related to organ level mechanisms of action has provided the capability to profile, and hence group, compounds together. Over 100 structural alerts, which form the basis of chemotypes, have been developed for liver toxicity. These alerts are for effects such as reactive hepatotoxicity, phosopholipidosis and other liver toxicities. They were developed from grouping of known liver toxicants and are supported by mechanistic information within the AOP framework. The alerts, in the form of chemotypes, have been developed to extend the traditional structural fragment approach by incorporating not only structural information but also physico-chemical properties. They show great potential for group grouping chemicals together to perform read-across predictions for complex endpoints. The alerts are freely available as a stand-alone toxicity profiler or as part of KNIME Workflows. KNIME is a flexible computational workflow technology that allows the user and developer to build flexible, adaptable and transparent models for toxicity prediction. Together with AOP-based profilers for other organs and adverse effects they create computational approaches to predict systemic toxicity and assist in risk assessment.

S 30 Applying Databases and Tools from COSMOS to the Scientific Needs of US FDA's CERES Project

K. Arvidson[1], A. McCarthy[1], D. Hristozov[1], C. Yang[2] and M. T. Cronin[3]. *[1]CFSAN OFAS, US FDA, College Park, MD, [2]Altamira LLC, Columbus, OH and [3]Liverpool John Moores University, Liverpool, United Kingdom.*

The Chemical Evaluation and Risk Estimation System (CERES) project aims to establish a single, unified data repository that compiles available information on a food substance, including: chemical structures and properties, regulatory records, summarized toxicity data, and other biological screening assays for the Office of Food Additive Safety's (OFAS) pre- and post- market safety evaluations. In cases where no information is available for a particular substance, CERES provides tools to identify potential safety concerns by applying mode of action-driven QSAR prediction models as well as to identify and analyze data on structural and biological analogs. As such, CERES was designed with a robust foundation for handling chemical and toxicity data as well as knowledge derived from these data. In order to expand the diversity of CERES' chemical space and incorporate additional high-quality toxicity data from oral repeated dose studies, CERES is exchanging knowledge with the COSMOS DB project. Although OFAS does not regulate cosmetics ingredients, the chemical space within OFAS has significant overlap with many cosmetic ingredients, including colorants, flavors, antimicrobials, anti-oxidants, emulsifiers and surfactants. Thus, scientifically, the setting of study inclusion criteria for the COSMOS TTC DB and data and tools developed by COSMOS are relevant to the CERES project. The chemical space of the COSMOS DB and CERES has been profiled using appropriate chemotypes. Chemotypes representing both the COSMOS DB and CERES are correlated with various phenotypic effects in the oral repeated-dose toxicity studies available within COSMOS and CERES. Results from both the COSMOS DB and TTC databases are used in this analysis. This analysis is able to identify gaps in the chemical domain of the databases so that we may better understand the applicability domain of the systems as well as identify where additional biological data are needed. Abstract does not reflect US FDA policy.

S 31 US EPA's ToxCast, Tox21, and COSMOS Projects: Cheminformatics Approaches to Creating Data Linkages and Synergies

A. M. Richard[1], C. Yang[2], J. Rathman[2], R. Bienstock[3], M. T. Martin[1], L. Truong[1], M. T. Cronin[4], A. Tarkhov[5] and C. Schwab[5]. *[1]NCCT, US EPA, Research Triangle Park, NC, [2]Altamira LLC, Columbus, OH, [3]Lockheed Martin, Contractor to the US EPA, Research Triangle Park, NC, [4]Liverpool John Moores University, Liverpool, United Kingdom and [5]Molecular Networks, Erlangen, Germany.*

The ToxCast and Tox21 projects are generating high-throughput screening (HTS) data for thousands of structurally diverse chemicals, spanning multiple use categories and chemical functionalities, and probing a wide diversity of biological targets, pathways and mechanisms related to toxicity. The ToxCast and Tox21 chemical libraries include substances of environmental, agrochemical, and industrial relevance, including drugs, food contact substances and cosmetics. Whilst there are a number of common chemicals within the ToxCast, Tox21 and the COSMOS databases, there are even greater overlaps in "chemotype" space in these libraries. Chemotypes are fundamental units of chemical structure (structural features and associated atom/bond properties) that have been distilled from existing knowledge of metabolic transformations and structure-based mechanisms of toxicity. Using the concept of chemotypes as a holistic guiding principle, cheminformatics approaches were applied to highlight overlapping areas of chemical space in the ToxCast, Tox21 and COSMOS inventories, to focus mechanistic investigations, and to establish data linkages and synergies across the different project data landscapes. In particular, we illustrate how ToxCast Phase II HTS assays that are significantly linked to chemotypes enriched within the chemical space of the COSMOS RepeatDose toxicity database provide a conduit for leveraging ToxCast data across Tox21 and COSMOS. Similarly, chemotype analysis of the COSMOS RepeatDose toxicity data has been projected back onto the ToxCast and Tox21 inventories to both focus (mechanistically) and broaden (chemically) investigations to cover a wider range of environmentally relevant chemicals beyond cosmetics. Abstract does not represent EPA policy.

S 32 Induced Human Pluripotent Stem Cells and Their Differentiated Progeny Cells: Implementation in Toxicity Testing

B. D. Anson. *Cellular Dynamics International, Madison, WI.* Sponsor: K. Kolaja.

Over the past two decades stem cell technology has progressed from isolating murine and nonhuman primate embryonic stem cells (ESCs) to reprogramming fully differentiated human samples into induced pluripotent stem cells (iPSCs). Concurrent advances have been made in the differentiation of stem cells into progeny tissue cells and the ability of those cells to increasingly recapitulate native behavior. Together, these advances have driven the translation of this technology from small-scale basic biological investigations into large-scale use within the pharmaceutical industry and potential clinical applications. This symposium will focus on several examples of iPSC-derived tissue cell use in understanding and translating preclinical cardiotoxicity to the clinic; hepatocyte function, toxicity, and idiosyncratic drug-induced liver injury; and developmental neuronal toxicity. Particular emphasis will be placed on practical implementations in toxicity testing as well as the ever-expanding functional incorporation of samples from clinic populations.

S 33 Engineering the Microscale Environment around iPSC-Derived Human Hepatocytes *In Vitro*

S. R. Khetani. *Colorado State University, Fort Collins, CO.* Sponsor: K. Kolaja.

Engineered in vitro models of the human liver have proven utility in assessing liver metabolism and toxicity in preclinical drug development. Isolated primary human hepatocytes (PHHs) are ideal for constructing such models, but there is a shortage of donor livers, and PHH quality can vary widely. Induced pluripotent stem cells (iPSCs) derived from somatic cells can address the limitations of PHHs and have future potential for personalized drug screening and therapy, however, current methods yield more fetal-like hepatocytes that display only a fraction (<10%) PHHs functions. We utilized microfabrication to investigate the effects of controlled homotypic and heterotypic cell interactions and extracellular matrix (ECM) cues on long-term iPSC-HH liver functions in vitro. We found that 3T3-J2 murine embryonic fibroblasts, previously shown to positively affect PHH functions, also induced liver functions (albumin secretion, urea synthesis, CYP3A4 activity) in iPSC-HHs when micropatterned onto collagencoated domains. Further, the addition of a Matrigel overlay enhanced both albumin production and CYP3A4 activity. We also assessed the utility of the iMPCC model for assessing drug toxicity and showed that prototypical liver toxins (i.e. diclofenac, acetaminophen) caused dose-dependent down-regulation of liver functions, while non-toxins (i.e. aspirin, propranolol) had little to no effects. Our current focus is on expanding these studies to include growth factors as well as more systematic presentations of ECM mixtures towards designing differentiation protocols that will be useful for the field at large while exploring the role of liver-derived stromal cells on iPSC-HH differentiation in vitro.

S 34 iPSC-Derived Liver Cultures to Study Mechanisms Underlying Idiosyncratic Hepatotoxicity

P. B. Watkins[1, 2]. [1]*The Hamner Institutes For Health Sciences, Research Triangle Park, NC and* [2]*Institute for Drug Safety Sciences, University of North Carolina at Chapel Hill, Chapel Hill, NC.*

There are no accepted animal models of idiosyncratic drug-induced liver injury (IDILI); indeed, the vast majority of humans are not good models for IDILI since they are not susceptible to it. Because it is generally not possible to obtain liver biopsies for research purposes from patients who have experienced DILI, induced pluripotent stem cell (iPSC) technology is an alternative approach to develop liver culture systems capable of testing the components of the prevailing causal hypothesis. We have demonstrated that IPSC derived hepatocytes (iH) exposed to isoniazid (INH) create protein adducts qualitatively similar to those of primary human hepatocytes and that IPSC derived macrophages (IMØ) secrete major cytokines in response to stimulation with lipopolysaccharide; two primary components thought to contribute to IDILI. We are now proceeding with preparation of iH and iMØ co-cultures from INH-DILI subjects as well as from INH-tolerant (control) subjects to identify susceptibility factors for these and other contributing factors. These studies have already yielded novel information and hold the potential to further advance our understanding of mechanisms underlying IDILI due to INH and establish an experimental template that can be used to define mechanisms underlying IDILI due to other drugs implicated in the DILIN registry.

S 35 Induced Pluripotent Stem Cell-Derived Neurons As a Human Model for Testing Environmentally-Induced Developmental Neurotoxicity

I. L. Druwe[1], T. J. Shafer[2], K. A. Wallace[2], P. A. Valdivia[3] and W. Mundy[2]. [1]*Curriculum in Toxicology, University of North Carolina at Chapel Hill, Chapel Hill, NC,* [2]*Integrated Systems Toxicology Division, NHEERL, US EPA, Research Triangle Park, NC and* [3]*Axion Biosystems, Atlanta, GA.*

Exposure to environmental toxicants during development and early childhood can result in adverse effects in the developing nervous system. Because of the cost and time required, most chemicals currently in commerce have not been evaluated for developmental neurotoxicity (DNT). To date, methods to screen for chemical effects on the critical events of DNT (e.g., proliferation, migration, neurite outgrowth, synaptogenesis) have utilized both human and rodent cell lines or primary rodent neural cultures. Unfortunately, chemical effects in rodent models do not always extrapolate to humans due to species-specific mechanisms and pathways. This talk will center around two cell-based assays that utilize human induced pluripotent stem cell (iPSC)-derived neurons to assess the impact of environmental chemicals on DNT. High content analysis of neurite outgrowth and synaptogenesis were examined in both rodent neurons and human iPSC using a "training set" of chemicals with known effects *in vitro*. Multi-electrode array technology monitors the functional development of neuronal electrical and network activity. Together these techniques and technologies offer a viable high-throughput screening option for testing both existing and newly created environmental chemicals. *This abstract does not necessarily reflect US EPA policy.*

S 36 Improved Translation from Preclinical to Clinical Outcomes Using Human IPSC-Derived Cardiomyocytes

H. Shi. *Cardiovascular Safety Pharmacology, Discovery Toxicology, Bristol-Myers Squibb Company, Hopewell, NJ.* Sponsor: K. Kolaja.

In vitro cardiovascular safety pharmacology and toxicity studies have traditionally been carried out on nonprimate tissues and cell models. While these models have demonstrated utility and have been the mainstay of many programs, they are less than perfect and results from the *in vitro* work can have difficulty predicting the *in vivo* effect in large animals and humans. To improve the translational power of preclinical assays, we have been coupling multielectrode array (MEA) technology with organotypic cultures of embryonic rat cardiomyocytes (rE CMs) or human induced pluripotent stem cell-derived cardiomyocytes (hiPSC CMs). Compounds from different discovery programs for which standard CV safety assays did not predict adverse preclinical or clinical HR, QRS and QT findings were evaluated. In several cases, MEA assays utilizing human iPSC-derived cardiomyocytes better predicted cardiovascular outcomes than standard assays. These results highlight the value and potential utility for human multicellular model use earlier in drug discovery and toxicity testing.

S 37 Methylmercury's Modes of Action: New Approaches to Understanding an Old Problem

N. V. Ralston. *University of North Dakota, Grand Forks, ND.*

Recent advances in understanding of methylmercury (MeHg) chemistry and ecogenetics provide important insights into its molecular mechanisms of toxicity and modes of action in cells of various tissues. These new perspectives clarify MeHg's pathophysiological effects at the organism level and indicate that the findings of epidemiological studies that were thought to be in conflict are actually highly consistent with expectations. Biochemical associations between MeHg and various biomolecules influence its bioavailability, tissue distributions, dose-effect relationships, and its characteristic signs and symptoms of toxicity. Sensitivity to MeHg exposure is also notably dependent upon other physiological factors, some which have been recognized for decades, but are only now becoming well understood, as well as emerging concepts such as epigenetics and gene-environment interactions. Like other soft electrophiles, MeHg's notable toxicity occurs as a direct result of binding with biological ligands from the chalcogen series (group 16 in the periodic table), which include sulfur (S), and selenium (Se). Speakers will provide the latest information and evidence regarding the molecular targets, genetic/epigenetic underpinnings, and physiological pathways that are modulated by MeHg and how these aspects correlate with disease outcomes. Participation in this symposium acquaints the audience with the latest developments and scientific breakthroughs regarding molecular targets of Hg, its modes of action, neurodevelopmental effects, and outcomes of epidemiology studies. This will inform toxicologists, neurobiologists, and biochemists, and will be of interest to anyone who wants to understand MeHg's roles in human and environmental health.

S 38 What Can Be Learned from the Nematode (*C. elegans*) about Molecular Targets Associated with MeHg Toxicity?

M. Aschner and K. J. Helmcke. *Department of Pediatrics, Vanderbilt University Medical Center, Nashville, TN.*

Methylmercury (MeHg) has been linked to neurodevelopmental and neurodegenerative disease states. Due to its widespread existence in the environment, understanding the mechanisms of its cellular detoxification is of utmost importance. Organisms have evolved cellular detoxification systems including glutathione, metallothioneins (mtl), pumps and transporters, and heat shock proteins (hsp) to regulate intracellular metal levels, including MeHg. The model organism, *Caenorhabditis elegans* (*C. elegans*) contains these systems and provides several advantages for deciphering the mechanisms of MeHg detoxification. We hypothesized MeHg would induce expression of gst, hsp or mtl *in vivo* since glutathione (GSH), heat shock proteins (HSPs), and metallothioneins (MTs) have shown involvement in MeHg toxicity. Our studies demonstrated a modest, but significant increase in fluorescence in gst-4::GFP and mtl-1::GFP strains at an acute, low L1 MeHg exposure, whereas chronic L4 MeHg exposure induced expression of gst-4::GFP and hsp-4::GFP. Knockout gst-4 animals showed no alterations in lethality sensitivity compared to wildtype animals whereas mtl knockouts displayed increased sensitivity to MeHg exposure. GSH levels were increased by acute MeHg treatment and depleted with chronic exposure. We also demonstrate that MeHg induces hormesis, a phenotype whereby a sublethal exposure to MeHg rendered *C. elegans* resistant to subsequent exposure to the organometal. In addition, we show that pdr-1 (the human parkin homolog) knockout worms are more sensitive to MeHg than wildtype worms. Combined, these results implicate GSH, HSPs, and MTs in protecting *C. elegans* from MeHg toxicity and show a potential role of gst-4 in MeHg-induced hormesis (Supported by the National Institute for Environmental Health Sciences R01ES07331 and R01ES020852).

S 39 Inhibition of the Human Thioredoxin System As a Mechanism of Mercury Toxicity

C. M. Carvalho. *Faculdade de Farmácia, Universidade de Lisboa, Lisbon, Portugal.* Sponsor: N. Ralston.

Mercury toxicity mediated by different forms of mercury is a major health problem; however, the molecular mechanisms underlying toxicity remain elusive. We analyzed the effects of mercuric chloride (HgCl2) and monomethylmercury (MeHg) on the proteins of the human thioredoxin system, the selenoenzyme thioredoxin reductase (TrxR) and thioredoxin (Trx), and the glutaredoxin system: GSH, glutathione reductase (GR) and glutaredoxin (Grx). HgCl2 and MeHg inhibited recombinant rat TrxR with IC50 values of 7.2 and 19.7 nM, respectively. Fully reduced human Trx1 bound mercury and lost all five free thiols and activity after incubation with HgCl2 or MeHg, but only HgCl2 generated dimers. Mass spectra analysis demonstrated binding of 2.5 mol of Hg and 5 mol of MeHg/mol of Trx1 with the very strong Hg complexes involving active site and structural disulfides. Inhibition of both TrxR and Trx activity was observed in HeLa and HEK 293 cells treated with HgCl2 or MeHg. GR was inhibited by HgCl2 and MeHg in vitro, but no decrease in GR activity was detected in cell extracts treated with mercurials. Human Grx1 showed similar reactivity as Trx1 with both mercurial compounds, with the loss of all free thiols and Grx dimerization in the presence of HgCl2, but no inhibition of Grx activity was observed in lysates of HeLa cells exposed to mercury. Overall, mercury inhibition was selective toward the thioredoxin system. In particular, the remarkable potency of the mercury compounds to bind to the selenol-thiol in the active site of TrxR should be a major molecular mechanism of mercury toxicity.

S 40 Inherited Effects of Low Levels of Methylmercury in Neural Stem Cells

S. Ceccatelli, R. Bose, K. Edoff, M. Moors and N. Onishchenko. *Department of Neuroscience, Karolinska Institutet, Stockholm, Sweden.*

Epidemiological studies have shown that chronic prenatal exposure to low levels of methylmercury (MeHg) can cause long-term neuropsychiatric alterations even in subjects who did not present signs of toxicity at birth. The mechanisms underlying the long-lasting consequences of MeHg exposure in early life are still unclear. The present study was designed to investigate short-term direct and long-term inherited effects of low levels of MeHg using primary cultures of rat embryonic neural stem cells (NSCs). We found that exposure to MeHg at nM concentrations decreased NSC proliferation and altered the expression of cell cycle regulators, such as p16 and p21, senescence-associated markers, including Bmi1 and Hmga1, and genes encoding mitochondrial respiratory chain proteins. MeHg induced a decrease in global DNA methylation, which pointed to the occurrence of epigenetic modifications. Interestingly, all changes occurring in NSCs directly exposed to MeHg (parent cells) were also present in their daughter cells kept in MeHg-free culture conditions. Data from adult mice exposed to low doses of MeHg in the perinatal period showed that the exposed mice, in addition to long-lasting behavioral alterations, exhibited a decreased proliferation of the neural stem/progenitor cells in the subgranular zone of the hippocampus, as well as long-lasting epigenetic modifications. The programming effects induced by MeHg in NSCs provide an explanation for the long-term consequences of developmental exposure to low levels of MeHg, which can predispose to neurodevelopmental disorders and/or neurodegeneration.

S 41 Can Genetic Polymorphisms and Epigenetics Advance Mercury Risk Assessment? Evidence from Humans and Animals

N. Basu[1, 2]. [1]*University of Michigan School of Public Health, Ann Arbor, MI and* [2]*McGill University, Montreal, QC, Canada.*

The risk assessment of mercury is complicated due to innate inter-individual variation in exposure, biomarker values, and adverse outcomes. Recent findings by us and others suggest that epigenetic mechanisms and gene-environment interactions may help explain some of this variation. For epigenetics, studies on laboratory models (mink, chicken, perch) and wild animals (polar bears) reveals mercury-associated global DNA hypomethylation and impaired DNMT activity in some, but not all, organisms. Candidate gene studies in a cohort of dental professionals reveals that methylation of SEPP1 is associated with significant changes in hair mercury levels in males only. In terms of gene-environment interaction studies, work by us and others show that some genes that influence the absorption, distribution, metabolism and elimination (ADME) of mercury have polymorphic variants that can affect biomarker levels. For example, epidemiological research by our group has shown that polymorphisms in MT1A, MT1M, GSTP1, and SEPP1 can be associated with altered levels of urine and hair mercury. For both epigenetics and gene-environment interactions, high-throughput approaches are commercially available which we are now exploring in a range of studies. This presentation will provide a rationale by which ecogenetic and molecular understanding, in both human and animal models, can be used to improve our ability to assess the risks (both exposure and adverse outcomes) of mercury and help identify vulnerable groups.

S 42 The "SOS" Molecular Mechanisms of Mercury Toxicity

N. V. Ralston. *University of North Dakota, Grand Forks, ND.*

Selenium (Se) physiology is particularly vulnerable to high mercury (Hg) exposures and the loss of Se-dependent enzyme activities appear to coincide with the effects of Hg toxicity. Among other functions, Se is the functional moiety of the reactive side groups of selenocysteine (Sec). The Se of Sec is the most potent intracellular nucleophile, enabling genetically unique Se-dependent enzymes (Se-enzymes) to catalyze redox biochemistry reactions. Unfortunately, this same unique biochemistry makes Se-enzymes vulnerable to reactions with soft electrophiles such as Hg in its various forms. No other environmental insult has been shown to be capable of diminishing Se-enzyme activities in brain and endocrine tissues, but methylmercury (MeHg) is effective in this regard. Although MeHg is initially associated with the cysteine thiols (MeHg-Cys), it transfers to Se as the system approaches equilibrium. Since MeHg-Cys substrates enter the active site of selenoenzymes in the proper orientation to expedite exchange of MeHg from the substrate Cys to the active site Sec, MeHg-Cys acts as a "suicide substrate" that selectively and irreversibly inhibits selenoenzyme activities. As quantities of MeHg approach or exceed equimolar stoichiometries with tissue Se concentrations, Se-enzyme activities are irreversibly inhibited and tissue Se reserves progressively diminish. Results of in-silico, cell culture, animal, and human epidemiological studies coincide in confirming that MeHg exposure risk assessments require concurrent consideration of dietary Se intakes. Since Se-enzymes perform vital functions in prevention and reversal of oxidative damage to lipids and proteins in brain and endocrine tissues, and have regulatory roles in thyroid hormone and calcium metabolism, the effects of MeHg toxicity that have been observed correspond well with those predicted by the selenoenzyme inhibition hypothesis of MeHg toxicity. (Supported by the U.S. Environmental Protection Agency; EPA-G2009-STAR-B1 RD834792-01).

S 43 To Bug or Not to Bug the Immune System: Benefits and Consequences of Altering the Microbiome

V. J. Johnson[1] and B. Yucesoy[2]. [1]*BRT-Burleson Research Technologies, Morrisville, NC and* [2]*CDC/NIOSH, Morgantown, WV.*

The Human Microbiome Project, a NIH initiative to understand the complexity, constitution, and diversity of microbes living on and in the human body, was recently completed in 2012. The term "Super-Organism" was coined to describe humans as a result of characterization of the breadth and diversity of microbes that live on the external surface as well as in the blood, tissues, and cells of the human body. What role do commensal organisms play in health and disease? What role do pathogenic microbes play in health and disease? For decades, a major emphasis in the field of immunotoxicology has been to understand the impact of environmental/occupational/therapeutic exposures on host defense against invading and opportunistic pathogens. Mounting evidence suggests that equal effort should be provided to understanding the relationship between the human microbiome and how alterations thereof can have profound implications for the development of complex immune and inflammatory diseases. Individuality of the microbiome contributes to immune-diversity, "metagenetic" diversity, and interindividual differences in susceptibility to many complex diseases, including allergic disease, autoimmune diseases, cancer, and others. Evidence suggests that development of an individual's microbiome begins before birth, and the nature of this colonization can influence susceptibility to disease later in life. In addition, homeostasis of the microbiome is under continual attack due to exposures encountered in daily life. Recent research shows that exposure to toxic chemicals can shift the dominant characteristics of the microbiome, thereby providing a strong contribution to disease susceptibility. Therefore, it is important to consider this research in the context of human health risk assessment. The purpose of this symposium is to provide evidence of beneficial and detrimental contributions of the microbiome to the development of immune and inflammatory diseases and provide insight into how microbiome research integrates into human health risk assessment.

S 44 Living with a Microbiome: The Role of Exposures and Toxicity in Shaping "The Completed Self"

R. R. Dietert. *Department of Microbiology and Immunology, Cornell University, Ithaca, NY.*

"The Completed Self" model for formation of the human-microbial superorganism in early life posits that: 1) symbiotic self completion is a critical step in the developmental programming of later-life health vs. disease, 2) the immune definition of self includes our internal microbial ecosystem, and 3) commensal-driven host metabolism and immune maturation are critical factors in subsequent tissue homeostasis. A consideration of humans as beyond-mammalian could shift our prevailing view of toxicity, health hazards, and preventive measures as well as the tools we employ for effective safety assessment. Prenatal, postnatal and even transgenerational epigenetic factors have the capacity to either support or interfere with the establishment of the microbiome and/or immune-microbiome interactions. Lack of self completion appears to be an important route to metabolic disorders, immune dysfunction, misregulated inflammation, tissue pathologies and chronic disease. Environmental risk factors (e.g., environmental chemicals, drugs, diet, physical and lifestyle factors) during development are considered in light of the goals of self completion in the child and a fully-developed immune system to support the newly-formed human-microbial symbiont.

S 45 Toxic Exposures and the Microbiome: Their Input Counts, Too

E. Silbergeld. *Environmental Health Sciences, Johns Hopkins Bloomberg School of Public Health, Baltimore, MD.*

Humans are colonized, on external and internal surfaces of the body, with a wide range of microorganisms known collectively as a microbiome defined by niche. Several studies have demonstrated that differences in the diversity or composition of the microbiome can be associated with disease states, including environmentally relevant diseases such as obesity and autism. The microbiome is exquisitely sensitive to external factors, such as birth route, diet, and antibiotic use, and recent data has indicated that it may also be affected by exposure to environmental chemicals. In addition, the microbiome itself influences our responses to exposures from environmental or occupational chemicals, pharmaceuticals, and foods, among other things. In fact, the gut microbiome has been proposed as an additional "portal" for understanding ADME in toxicology and epidemiology. This talk will focus on the role of the gut microbiome as a "gate keeper" between external exposures and internal dose, and the implications of these events for a more holistic understanding of metabolism prior to absorption and distribution. This talk will review state of the art information on this topic along with a discussion of the implications for understanding the contribution of the gut microbiome to host response and susceptibility.

S 46 The Human Microbiome and Autoimmunity

A. Proal. *Autoimmunity Research Foundation, Thousand Oaks, CA.* Sponsor: V. Johnson.

The current concept of autoimmunity, in which the body creates autoantibodies against "self" was developed at a time when the human body was believed to be largely sterile. However, the discovery of the human microbiome calls for a re-evaluation of this model. The microbiome, which persists in tissue and blood, influences almost every human metabolic process. Numerous studies demonstrate dysbiosis of the microbiome in patients with autoimmune and inflammatory conditions, suggesting that autoantibodies are actually generated in response to persistent infectious agents. Intracellular pathogens associated with autoimmune disease often slow activity of the innate immune response by disabling expression by the VDR nuclear receptor. This causes a cascade of dysregulation that progressively moves the body away from a state of homeostasis. Such pathogens are able to directly interfere with transcription, translation, and DNA repair processes. Molecular mimicry between pathogen and host multiplies the scale and dysfunction of the interactome. The combined effects of different microbes on the interactome likely contribute to any single autoimmune diagnosis, the specifics of which result from the unique microbiome of each individual. This is reflected in the high levels of comorbidity observed among patients with inflammatory disease. The state of the microbiome and subsequently the innate immune response play a significant role in determining how individuals responds to toxic threats. We have retargeted an approved pharmaceutical in an effort to reactivate the VDR nuclear receptor in patients in inflammatory disease. This appears to strengthen the immune response and gradually correct microbial dysbiosis. Although the treatment generates significant immunopathology, patients are demonstrating both improved objective and subjective markers and some even exhibit recovery. We have anecdotal reports that levels of heavy metals, including mercury have decreased in patients over the course of therapy. This suggests that strengthening the innate immune response may allow the body to better manage toxic insult as it brings inflammatory disease under control.

S 47 The Microbiome in Human Health Risk Assessment: Where Do We Go from Here?

K. L. Dearfield. *Food Safety and Inspection Service, US Department of Agriculture, Washington, DC.*

It is recognized that the complex collection of microbes in our gut, the microbiome, plays a critical role in our health and well-being. It influences our responses, e.g., immunological, and reacts to environmental exposures, such as from food, drugs, and environmental contaminants. Regulatory agencies are putting a great deal of effort into understanding the sequence of mechanistic events that lead to disease. However, they haven't generally incorporated the importance of the microbiome to a great extent and how it can provide insight into human health risk assessment. We will likely need to rethink some of the risk assessments to take into account the contribution of the microbiome. Research will greatly help assessments by addressing the lack of understanding of how xenobiotic exposures can affect the composition and function of the microbiome as well as how the microbiome can affect bioavailability of contaminants and susceptibility to pathogens. Also, the interplay between chemical exposures and pathogens with commensal gut flora and with each other need to be examined as potential risk factors. While the microbiome raises the complexity of the research in disease etiology, it will help human health risk assessors to rethink how chemicals and pathogens interact with exposed people.

W 48 Developmental Programming of Hepatic Metabolism: Assessing the Impact of Perinatal Exposure to Xenobiotics

L. M. Aleksunes[1], A. L. Slitt[4], J. Richardson[1], X. Zhong[2] and W. Huang[3]. [1]*Rutgers, The State University of New Jersey, Piscataway, NJ,* [2]*University of Connecticut, Storrs, CT,* [3]*City of Hope National Medical Center, Duarte, CA and* [4]*University of Rhode Island, Kingston, RI.*

It is becoming increasingly evident that epigenetics is important in the ontogeny of hepatic metabolism and transport pathways. This workshop highlights the most recent knowledge of the developmental regulation of hepatic metabolism through transcriptional and epigenetic mechanisms in rodents and humans. Interestingly,

emerging research from a number of laboratories demonstrates that maternal exposure to environmental chemicals during the perinatal period alters the expression and function of metabolic and transport proteins in progeny later in life. Up- or down-regulation of key hepatic metabolic processes, including cytochrome (Cyp) P450 and carboxylesterase (Ces) enzymes, as well as excretory transporters, may have a significant impact on the pharmacological and toxicological responses to xenobiotics during puberty and adulthood and, additionally, impact systemic hormone levels. The purpose of this workshop is to bring together experts in the field of toxicology to highlight the regulatory mechanisms underlying the developmental programming of hepatic metabolism and transport, and to discuss the potential impact of early exposure to xenobiotics on the ability of the liver to metabolize and excrete chemicals later in life. Experimental design and cutting-edge technologies will also be discussed. The workshop contains presentations and a roundtable discussion that will address four questions: What is the role of nuclear receptors and transcription factors in the ontogenic regulation of hepatic metabolism? What epigenetic mechanisms are involved in the hepatic programming of the liver? Do environmentally-relevant concentrations of chemicals alter the developmental programming of xenobiotic metabolism pathways? What are the potential long-term consequences resulting from altered hepatic programming of metabolic enzymes, including the toxicity of pollutants and the efficacy of pharmaceuticals?

W 49 Hepatic Ontogeny of Drug Processing Genes in Mouse Liver

X. Zhong[1], L. Peng[1], J. Cui[2], H. J. Renaud[2], B. Yoo[3], S. Gunewardena[3], H. Lu[4] and C. D. Klaassen[2]. *[1]University of Connecticut, Storrs, CT, [2]University of Kansas Medical Center, Kansas City, KS, [3]Kansas Intellectual and Developmental Disabilities Research Center, Kansas City, KS and [4]State University of New York, Syracuse, NY.*

Drug processing gene encoded proteins are involved in the absorption, distribution, metabolism, and excretion (ADME) of drugs and play an important role in determining the pharmacokinetics of drugs in the body. Liver is the major organ that processes ADME reactions; however, the functions of most drug processing proteins are not mature at birth, which markedly affects ADME processes in newborns. Therefore, characterization of the gene expression profiles of drug processing genes and their regulatory mechanisms during liver maturation is needed for improving drug therapy in pediatric patients. Mouse is frequently used as an experimental model to determine how developmental expression of drug processing genes in postnatal liver is regulated. Hence, we applied RNA sequencing (RNA-Seq) to provide a "true quantification" of mRNA expression of drug processing genes, including Phase-I/Phase-II enzymes and transporters as well as nuclear receptors and epigenetic modifiers in mouse liver during development. Liver samples from male C57BL/6J mice were collected at 12 different ages from prenatal to adulthood (n=3 per age) for RNA-Seq. Several distinct ontogenic patterns were identified among the drug processing genes, which reflect a functional transition of liver from a hematopoietic organ in prenatal stage to a metabolic organ in postnatal stages during maturation. A correlation of the gene expression patterns among the Phase-I/Phase-II enzymes, transporters, and nuclear receptors was recognized, which provides a valuable foundation for mechanistic studies in the future.
This study was supported by the National Institute for Environmental Health Science [R01ES-019487] (to Xiao-bo Zhong, Curtis D. Klaassen, and Hong Lu); the National Institute of General Medical Sciences [R01GM-087376] (to Xiao-bo Zhong); the National Institute for Environmental Health Science [R01ES-009649] (to Curtis D. Klaassen).

W 50 Xenobiotic Receptor CAR and Epigenetic Misprogramming

W. Huang. *Beckman Research Institute, City of Hope National Medical Center, Duarte, CA.* Sponsor: L. Aleksunes.

Constitutive androstane receptor (CAR; NR1I3) is a central regulator of drug/xenobiotic and endobiotic metabolism. CAR also regulates other metabolism, such as glucose and lipid metabolism. Interestingly, a transient activation of CAR during animal development induces epigenetic changes, which results in epigenetic memory and permanent changes of liver drug metabolism and detoxification. CAR activation by neonatal exposure to its ligand, 1,4-bis[2-(3,5-dichloropyridyloxy)] benzene (TCPOBOP), persistently induces the expression of CAR target genes Cyp2B10 and Cyp2C37 throughout the life course. These mice also show a permanently reduced sensitivity to zoxazolamine treatment. The induced expression of CAR target genes in hepatocytes isolated from these mice is more sensitive to low concentrations of CAR agonist TCPOBOP in vitro. There are significant changes of histone modifications at the gene promoters of Cyp2B10 as analyzed by chromatin immunoprecipitation assays. These results demonstrate that epigenetic misprogramming mediated by CAR may result in a long-term epigenetic memory and permanent effect on the health of subjects.

W 51 Pharmacokinetic and Pharmacodynamic Consequences of Long-Term Increases in Carboxylesterase Expression following Developmental Pesticide Exposure

J. Richardson[1, 2]. *[1]Department of Environmental and Occupational Medicine, Rutgers Robert Wood Johnson Medical School, Piscataway, NJ and [2]Environmental and Occupational Health Sciences Institute, Rutgers, The State University of New Jersey, Piscataway, NJ.*

Carboxylesterases (Ces) play important roles in mediating the metabolism of therapeutic drugs and environmental chemicals. As such, developmental exposures that cause changes in Ces expression and activity have the potential to exert significant influence on the metabolism of drugs and chemicals. We have identified that developmental pyrethroid exposure causes persistent increases in Ces mRNA expression, protein levels and activity that appear to be mediated through the constitutive androstane receptor. These increases have functional consequences, decreased peak plasma and brain levels of methylphenidate, a drug commonly used to treat ADHD, are observed after oral dosing. These decreased levels of methylphenidate also result in decreased efficacy of methylphenidate in raising brain neurotransmitter levels. Data will also be presented regarding potential mechanisms responsible for persistent Ces up-regulation, including alterations in DNA methylation and histone modifications. Supported by NIEHS R01ES015991, T32ES007148, and P30ES005022.

W 52 Developmental Bisphenol A Exposure Alters Hepatic Phase II Metabolism and Transport via Histone Deacetylase

A. L. Slitt. *Department of Biomedical and Pharmaceutical Sciences, University of Rhode Island, Kingston, RI.*

Developmental exposure to Bisphenol A (BPA), a component of plastics manufacturing, is associated with adverse effects in rodents through epigenetic mechanisms. Multiple mechanisms and etiologies for BPA effects have been examined, with few examining BPA effects on hepatic metabolism and excretion, despite its importance in maintaining metabolic and endocrine balance for the body. We hypothesized that maternal BPA exposure could affect liver metabolism and disposition in resulting progeny. Virgin females (C57BL/6, a/a) were fed one of the following diets containing corn oil, BPA, BPA in combination with genistein, or ethinyl estradiol (EE) through gestation and lactation. Exposure ceased at weaning and livers were collected from male progeny at 135 days of age or older. Developmental BPA and EE exposure decreased UDP-glucuronosyl transferase (Ugt) and Multidrug Resistance-Associated Protein 2 (MRP2/ABCC2) expression and function, which was associated with significant alteration in nuclear receptor expression and binding. Developmental BPA and EE exposure decreased BPA glucuronidation and hepatic dibromosulfothalein (DBSP) clearance. Lastly, down regulation of mouse MRP2/ABCC2 expression was associated with increased Histone Deacetylase 2 (HDAC2) and decreased acetylated Histone 3 recruitment to functional antioxidant response elements for the Nrf2 transcription factor in the mouse MRP2/ABCC2 promoter. These observations were not observed in progeny from dams that were fed diet containing BPA and genistein. Together, these data illustrate that BPA exposure early in life can reprogram liver function, which is associated with altered Nrf2 receptor binding and histone recruitment.

W 53 New Concerns and New Science Addressing Environmental Asbestos Exposures

D. J. Carlin[1] and R. N. Hines[2]. *[1]NIEHS, Research Triangle Park, NC and [2]USEPA, Research Triangle Park, NC.*

Although extensive research has been conducted on asbestos health effects for specific fiber types, there are still many unresolved issues and controversies, particularly related to environmental asbestos exposures. Further, the health effects of mixtures of elongate mineral fibers have not previously been studied in detail. Approximately 120,000 asbestos-related deaths occur in the US and worldwide every year, and it has been well known for the past 30–40 years that occupational exposure to asbestos causes mesothelioma, asbestosis, and lung cancer. Moreover, environmental asbestos exposures have led to a declared public health emergency in Libby, Montana, an area known to have a higher incidence of asbestos-related diseases than the rest of the US. Other areas, such as El Dorado Hills, California, and Nooksack and Sumas, Washington, are also currently being evaluated for asbestos-contaminated soils and potential exposure to populations living in these areas. Although occupational asbestos exposures have been limited, there is increased concern related to exposures to environmental asbestos. For both environmental and occupational exposures, there are a number of critical issues, including: (1) How can complex mixtures of different forms of asbestos and nonasbestos contaminants be evaluated?; (2) What are the cellular and systemic mechanisms resulting

in fibrosis and/or tumor development?; (3) What is the relative toxicity of different forms of asbestos?; (4) What is the proper dose-metric to consider (e.g., mass, fiber number, or surface area of fibers) when interpreting asbestos toxicity?; (5) What are the effects of asbestos exposure on susceptible populations (e.g., children and adolescents)?; and (6) How do we implement toxicological findings into risk assessment and clean-up efforts? This workshop has been designed to present the latest epidemiological and basic research findings in an attempt to address some of these questions, and to highlight the efforts of all stakeholders in determining the role of asbestos in various disease endpoints.

W 54 Human Health and Environmental Exposure to Libby Amphibole Asbestos

T. Larson. *ATSDR, Atlanta, GA.* Sponsor: D. Carlin.

The public health situation in Libby, Montana has afforded a body of new research on the impacts of asbestos exposure on human health. While the focus of much of the preexisting asbestos literature has been on occupational cohorts comprising mostly men, the spectrum of exposures in Libby includes low levels among residents without occupational exposure. Consequently, ATSDR and EPA have funded a program of community-based epidemiologic research in Libby. Research topics include pulmonary disease progression using computed tomography, pulmonary health of child residents of Libby who subsequently moved away, and study of the relationship between residential exposure, system autoimmunity, and asbestos-related pulmonary disease. In addition to this in-process research program, several papers have been published examining health outcomes in sensitive subpopulations, health effects not classically associated with asbestos exposure, and health outcomes in residents. Self-reported pulmonary symptoms have been associated with frequency of handling vermiculite in Libby residents who were minors while the Libby vermiculite mine was operational and pleural plaque has been detected on the chest radiographs of Libby children. Residents of Libby who reported frequent contact with vermiculite also demonstrated elevated risk for systemic lupus erythematosus, scleroderma, or rheumatoid arthritis. Also among residents, radiographic pleural plaque was associated with restrictive spirometry.

W 55 Autoimmune Responses following Asbestos Exposure

J. C. Pfau. *Idaho State University, Pocatello, ID.*

Immune dysfunction is well established as part of the response following asbestos exposures, ranging from the inflammatory component of fibrotic disease to increased autoantibody production. However, epidemiological data clearly linking asbestos exposure to autoimmune disease is lacking, with only one study showing an increased risk of systemic autoimmune diseases in an amphibole exposed population. Because that study population was Libby, MT, where both occupational and environmental exposures occurred, hypotheses regarding the autoimmune component focus on differences either in exposure levels or exposure type – environmental versus occupational and/or chrysotile versus amphibole. Recent work is beginning to tease apart these issues using both human cohort comparisons and mouse models, revealing that the immune dysfunction following fiber exposure is highly complex and fiber specific. While amphibole asbestos clearly affects autoantibody production in both mice and humans, the human health outcomes do not seem to fit into current diagnostic criteria for specific rheumatic disease, but may dramatically impact pulmonary outcomes for environmental amphibole exposures. A key objective for research, therefore, is to identify specific immune changes that may be predictive of severity or progression of disease.

W 56 Determinants of Toxicity of Environmental Asbestos Fibers

S. H. Gavett. *US EPA, Research Triangle Park, NC.*

Recent EPA-led studies have addressed the comparative toxicity and pathological mechanisms of environmental asbestos samples from Libby, Montana and other communities in the United States. Longer amosite fibers induce a 4-10 fold greater induction of pro-inflammatory mediators COX-2 and HO-1 than Libby fibers in human airway epithelial cells, as well as a number of other genes involved in cellular stress and toxicity. Similarly, equal mass doses of longer amosite fibers administered intratracheally to F344 rats cause greater pathological effects than Libby fibers, from 1 day to 2 years post-exposure. However, both intratracheal and inhalation studies show comparable effects of Libby fibers and shorter UICC amosite fibers. Dosimetry modeling and potency analysis studies are using these data to predict effects in humans. Libby fibers induce an acute phase response and systemic increases in selected markers of inflammation, and induce components of the NALP-3 inflammasome in the lung, while surface complexed iron inhibits these responses. Libby fibers alter genes involved in inflammation, immune regulation, and cell-cycle control, and also induce autoimmune responses in a rat model. Comparative toxicity studies showed that chrysotile fibers from Sumas Mountain, Washington caused greater lung interstitial fibrosis than Libby fibers, which were significantly more potent than tremolite fibers from El Dorado, California and actinolite "cleavage fragments" from Ontario, Canada. These data are improving the scientific basis for the risk assessment of asbestos-contaminated communities, defining key determinants of internal dose, and providing critical insight on additional key health or pathologic endpoints.

W 57 Role of Inflammasomes in Malignant Mesotheliomas

A. Shukla. *University of Vermont, Burlington, VT.* Sponsor: D. Carlin.

Asbestos fibers cause a number of respiratory diseases including pleural fibrosis and malignant mesothelioma (MM), however, the mechanisms initiating these diseases are not well understood. We are the first to demonstrate that asbestos-induced MM development involves activation of the NOD like receptor protein 3 (NLRP3) inflammasome, caspase-1 activation and mature IL-1β release from human mesothelial cells (HMC). This priming and activation of NLRP3 in HMC by asbestos does not require exogenous TNFα or lipopolysaccharide to initiate the response. In addition, using an IL-1 receptor antagonist, Anakinra, we document that there exists an autocrine feedback loop for activation of the inflammasome and production of cytokines perpetuating inflammation in mesothelial cells. Other studies in human MM tumors and MM cells have shown significantly decreased levels of NLRP3 and caspase-1, in contrast to normal mesothelial cells, which may in part be responsible for increased drug resistance observed in these tumors. Based on our findings, the use of chemotherapeutic drugs including Bcl-2 inhibitors in combination with an IL-1 receptor antagonist could be projected as better treatment strategies for MMs. The data generated by our research will help in understanding the mechanism(s) by which asbestos can cause MM and eventually may lead to development of beneficial therapeutic strategies for asbestos-associated diseases.

W 58 Challenges and Recommendations for Future Asbestos Research

A. Miller. *NIEHS, Bethesda, MD.*

In an effort to address a host of new challenges associated with environmental asbestos exposures the NIEHS, USEPA, ATSDR, NIOSH, and academic institutions have closely collaborated over the past several years. Multidisciplinary research teams comprised of epidemiologists, toxicologists, mineralogists, clinicians, and statisticians have worked through array of complex issues elucidated by the Libby, Montana site, as well as other sites around the United States containing hazardous mineral fibers. Such issues include exposures to non-work populations including children, development of more robust sampling and analytical approaches to better characterize environmental exposures, and new epidemiologic and medical studies to understand resultant health effects including autoimmune and inflammatory health endpoints. Utilizing collaborative research platforms, Interagency Working Groups, and workshops such as an NIEHS-sponsored Mechanisms of Action Workshop that occurred in December 2009 (Chapel Hill, NC) experts from these organizations have identified data gaps and mechanistic, epidemiologic, and exposure assessment research needs. Recent collaborative research efforts also include investigations of exposures and risks among communities in North Dakota and Turkey exposed to erionite, an unregulated but very hazardous mineral fiber. Recently, the NIEHS National Toxicology Program has been designing projects (e.g. 2 year bioassays) to better assess the toxicity of Libby amphibole material in conjunction with a comprehensive program to study naturally occurring asbestos and related mineral fibers. These studies will consist of collecting toxicity data, complete detailed physical and chemical characterizations, dose-response characterization for the fibers, and the influence of mineralogy and morphology on toxicity. It is anticipated that these collective efforts will lead to an improved understanding of fiber induced illnesses and new risk assessment strategies to help protect impacted communities.

PL 59 Analysis of EPA FQPA Safety Factors for 363 Pesticides

A. A. Li[1] and B. M. Polakoff[2]. [1]*Health Sciences, Exponent, Inc., San Francisco, CA and* [2]*Health Sciences, Exponent, Inc., Washington, DC.*

The Food Quality Protection Act (FQPA) of 1996 requires a default 10x safety factor (SF) be added to the traditional interspecies and intraspecies uncertainty factors (UF) for all food-use pesticides, resulting in an initial 1000-fold UF in the derivation of all acute and chronic reference doses (RfD). The FQPA SF is required

by law to account for potential pre- and post-natal toxicity and completeness of the data with respect to exposure and toxicity to infants and children. Understanding EPA's rationale for retaining the FQPA SF is essential for determining how data impacts the risk assessment. Towards this purpose, the FQPA SF decisions for pesticides listed in the EPA's Human Health Benchmarks for Pesticides (HHBP) were analyzed. The HHBP tabulates FQPA SF for 363 pesticides and provides the URL link to the EPA's risk assessment document for each pesticide. Between 1998 and 2012, an FQPA SF of 10x or 3x was retained for 30 out of the 363 pesticides. Neurotoxicity data gaps were the most frequently cited reasons for retaining some or all of the FQPA SF (23 of 30 pesticides). Case studies for imazalil, bifenthrin, phosmet and asulam illustrate the following trends for application of FQPA SF: (1) increased susceptibility in offspring or endocrine concerns are no longer an automatic reason to retain FQPA as long as data sufficient to characterize the endpoint of concern for the appropriate populations of concern are provided; (2) scientific literature or studies submitted to EPA on the pesticide or similar class of chemistry can result in the retention of FQPA factors; (3) more recently, the 10x FQPA SF has been divided into separate pharmacokinetic and pharmacodynamic factors (3x each). EPA's decisions for retaining the FQPA factor have evolved over the past 15 years and are customized for the route and duration of exposure and population of concern depending on the scientific literature and database available for the pesticide and similar classes of chemistry.

PL 60 Predicting Children's Internal Exposure to Pyrethroids Using a Physiologically-Based Pharmacokinetic Model with Age-Appropriate *In Vitro* Metabolism Data

H. J. Clewell[1], H. Wu[1], B. G. Lake[2], T. G. Osimitz[3], N. Assaf[4] and M. Yoon[1]. [1]*The Hamner Institutes for Health Sciences, RTP, NC,* [2]*LFR Molecular Sciences, Surrey, United Kingdom,* [3]*Science Strategies, LLC, Charlottesville, VA and* [4]*Valent BioSciences, Libertyville, IL.*

Due to species differences in physiological and biochemical maturation as well as differences in major metabolic pathways, predicting early age sensitivity to a chemical exposure based on animal data requires caution. In our previous modeling with deltamethrin (DLM), while lower metabolic clearance of DLM resulted in increased sensitivity in neonatal rats, no age related sensitivity was predicted for humans. In this study, the DLM model was tested as a general platform to predict age-dependent pharmacokinetic sensitivity to other pyrethroids using compound specific kinetic parameters for trans-permethirn (TPM). In addition to maturation physiology, developmental changes in pyrethroid hydrolysis by carboxylesterases (CESs), the major metabolic pathway for both DLM and TPM in humans, were incorporated in the model. Age-appropriate hydrolysis estimates were obtained based on adult data measured in hepatic microsomes and cytosol, and ontogeny of CESs. No substantial age-differences in brain exposure to pyrethroids were predicted for TPM at a constant daily exposure (0.1 mg/kg/d) as shown by less than a 2-fold difference in average daily brain AUCs across ages. This study demonstrates that taking into consideration species-specific enzyme ontogeny and the resulting age-dependent changes in metabolic clearance of a given pyrethroid is critical in estimating early age sensitivity. The difference between environmentally relevant exposure levels and dose levels used in animal toxicity studies also needs to be considered. This modeling platform can serve as a tool to properly evaluate children's sensitivity to pyrethroids when combined with age-appropriate metabolism data and environmentally relevant exposure estimates for children (supported by the Council for Advancement of Pyrethroid Human Risk Assessment, LLC [CAPHRA]).

PL 61 Using a Two-Dimension Monte Carlo Model to Develop Chemical Specific Adjustment Factors (CSAFs) for Chlorpyrifos and Chlorpyrifos Oxon

P. S. Price[1], T. S. Poet[3], M. J. Bartels[1] and D. R. Juberg[2]. [1]*Toxicology & Environmental Research & Consulting, Dow Chemical Company, Midland, MI,* [2]*Dow AgroSciences, Indianapolis, IN and* [3]*Summit Toxicology, Richland, WA.*

The traditional values of 10 for inter- and intra-individual uncertainty factors have been recognized as resulting in overly conservative health-based standards for most chemicals (Baird et al. 1996; Gaylor and Kodell, 2000). This paper presents chemical specific adjustment factors (CSAFs) for setting the acute oral Population Adjusted Doses (aPADs) for chlorpyrifos and chlorpyrifos oxon consistent with recent WHO and USEPA guidance. The CSAFs are developed using data generated by a Biologically Based Dose Response Model (BBDR). The BBDR is based on a PBPK/PD model (Smith et al. 2013) that simulates the inhibition of red blood cell acetylcholinesterase (RBC AChEI). This model is placed in the framework of a two-dimensional Monte Carlo model of uncertainty and variation in the response. RBC AChEI is the critical effect used by USEPA in setting the aPADs for chlorpyrifos. Using the predicted average response in humans and the 99th percentile of variation in sensitivity, the inter- and intra-individual CSAFs for chlorpyrifos are 1.3 and 2.7, respectively. The corresponding values for chlorpyrifos oxon are 0.9 and 2.4. The relatively small CSAFs (as compared to traditional values) for the compounds are due to the use of RBC AChEI as the critical effect. RBC AChEI is a marker for a key event (AChEI in brain and other tissues) that occurs early in the compounds' adverse outcome pathways (AOPs). The slightly larger values for chlorpyrifos CSAFs are due to the additional activation step (conversion of chlorpyrifos to oxon) in the chlorpyrifos AOP. Variation in activation increases the intra- and inter-species differences in response for chlorpyrifos and thus the CSAF values. The approach used for the design of the BBDR and its use in setting CSAFs can be applied to other chemicals where chemical reactions are events, or markers of events, that occur early in a chemical's AOP.

PL 62 Predicting Inhalation Toxicity of Bifenthrin Using a Pharmacokinetic Rationale

Z. Liu, A. Chandrasekaran and D. W. Gammon. *FMC Corporation, Ewing, NJ.*

Numerous studies with the pyrethroid bifenthrin have demonstrated relatively low acute inhalation toxicity in rats. However, due to increased toxicity following inhalation exposure for some pyrethroids, such as flumethrin and cyfluthrin, there was hesitation to assign an inhalation BMDL for bifenthrin. The objective of this work was to use a pharmacokinetic (PK) basis for setting an inhalation BMDL for bifenthrin. To obtain internal exposure data and disposition characteristics, two PK studies were conducted in rats. These studies used far fewer rats than a Guideline 28-day or acute inhalation neurotoxicity study. In the first study, bifenthrin concentrations were measured in brain and plasma after a single oral gavage (3.1 mg/kg) or inhalation exposure (0.018 mg/L for 4 hours, equivalent to the same delivered oral dose), relative to time. The maximum concentrations (Cmax) and area under the concentration curves (AUCs) in both plasma and brain were slightly lower following inhalation than those after oral dosing. These new PK data for oral exposure were comparable to previous literature data. After intravenous administration to rats (1 mg/kg) in the second study, bifenthrin elimination was relatively rapid with a plasma half-life of 13.4 hours, i.e. limited tendency to bioaccumulate. Since bifenthrin peak neurotoxicity is proportional to Cmax in brain and/or plasma, an inhalation BMDL of 3.5 mg/kg/day was calculated based on the oral BMDL of 3.1 mg/kg/day and a ratio of 1.14 (brain oral Cmax/brain inhalation Cmax). These PK data demonstrate that there is an acceptable margin of safety even for the worst case worker exposure scenario, having an inhalation MOE=946 using the inhalation BMDL (3.5 mg/kg/day). Furthermore, the PK properties shown here for bifenthrin after multiple exposure routes, enable a complete picture of internal exposure levels to emerge for this pyrethroid, having predictive value for risk assessment without conducting additional animal toxicity studies.

PL 63 Refinement of an Acute Inhalation Reference Concentration for 1, 3-Dichloropropene

A. Maier[1], A. Parker[2], L. T. Haber[2] and S. C. Gehen[3]. [1]*University of Cincinnati, Cincinnati, OH,* [2]*Toxicology Excellence for Risk Assessment, Cincinnati, OH and* [3]*Dow AgroSciences, LLC, Indianapolis, IN.*

The acute inhalation reference concentration (aRfC) is an important component of fumigant health risk assessment. For the soil fumigant 1,3-dichloropropene (1,3-D) there have been two aRfC values derived which differ significantly. We conducted a critical analysis of the basis for the differences between these values and provide an updated aRfC incorporating additional data. Key elements of the aRfC derivation process include point of departure (POD) selection, dosimetric adjustments, and uncertainty factor use. For POD selection, the acute studies have insufficient information to characterize the dose-response for the pertinent effects. Well conducted repeat-exposure studies are available, but comparison of dose and temporal concordance patterns indicated that these studies were inappropriate in terms of temporal relevance for the aRfC. For the updated assessment a LOAEL of 357 ppm, based on decreased body weight and clinical signs, was selected as the POD from a 4-hour inhalation study in albino Wistar rats. The two assessments also differ in terms of dosimetry methods used to estimate a human equivalent concentration (HEC). One based the HEC on partition coefficient ratios, while the other used respiratory rates for this conversion. The choice of methods depends on toxicokinetic behavior following acute exposure and on whether the critical effect is related to systemic or portal of entry toxicity. Additional analysis of the rate at which steady-state toxicokinetics would be reached for 1,3-D suggested that the approach based on partition coefficient ratios is most appropriate. Thus, the LOAEL of 357 ppm was adjusted for exposure duration (4 h/24 h) and a factor of 1 was applied to reflect species differences in steady-state blood concentrations, resulting in a HEC value of 60 ppm. An updated aRfC of 0.6 ppm was derived by applying a composite uncertainty factor of 100 to this POD. Overall, the analysis highlights the importance of a systematic analysis of each step in the aRfC derivation process.

PL 64 Integrating Toxicokinetics into the Human Health Risk Assessment Process for Agrochemicals: Halauxifen-methyl

C. Terry[1], L. A. Murphy[2], K. Saffour[1], A. T. McCoy[2], M. Aggarwal[1], L. G. McFadden[2], R. J. Rasoulpour[2], D. Rick[2], M. J. Bartels[2] and R. Billington[1]. [1]*Human Health, Dow AgroSciences, Oxon, United Kingdom and* [2]*TERC, The Dow Chemical Company, Midland, MI.*

Toxicokinetic (TK) data can provide valuable information for human health risk assessment. The following describes the advantages of integrated TK (no additional animal usage) to the process of risk assessment, using halauxifen-methyl, a new herbicide, as a case-study to show integrated TK allows:
Hazard Identification: Available TK data, including target tissue concentrations, provided insight as to why acid- and methyl-forms of halauxifen had different primary target organs, kidney and liver, respectively. Halauxifen-methyl is rapidly hydrolyzed in liver to the primary metabolite, halauxifen-acid, such that post-hepatic systemic exposure is exclusively to the acid. However, unlike the acid, its methyl ester was subsequently shown to selectively activate the hepatic AhR, and be responsible for its hepatotoxicity.
Dose-Response Assessment: Halauxifen-methyl has a rapid half-life of elimination (<6 hrs in rats); metabolism data in primary hepatocytes were used and AhR activation as measured by Cyp1a1 transcript levels was assessed. Subsequent primary hepatocyte studies in rats, mice and humans, using rat TK-based target tissue concentrations, provided data on AhR activation across species at relevant concentrations.
Exposure Assessment: PBPK models for rats and humans predicted similar systemic exposures, primarily to halauxifen-acid. Dietary exposures at the NOAEL of 10 mg/kg/day from the rat 90-day study were modeled. Similar results were obtained at relevant human exposure levels (i.e., proposed chronic RfD).
Risk Characterisation: In vitro, cross-species comparative hydrolysis data and integrated TK analyses supported quantitative non-human relevance of the halauxifen-methyl AhR-mediated hepatotoxicity in rodents by establishing: 1) a clear threshold for rat liver effects, 2) that systemic exposure is to acid, and 3) a chronic RfD significantly higher than any potential human exposure.

PL 65 Mode of Action Profiles for Pesticide Compounds with Rodent Liver Tumor Outcomes

A. D. Lake[1], S. D. Hester[1], J. Liu[2], J. Rowland[3] and C. E. Wood[1]. [1]*National Health and Environmental Effects Research Laboratory; Integrated Systems Toxicology Division, U.S. Environmental Protection Agency, Research Triangle Park, NC,* [2]*National Center for Computational Toxicology, U.S. Environmental Protection Agency, Research Triangle Park, NC and* [3]*Health Effects Division, Office of Pesticide Programs, U.S. Environmental Protection Agency, Washington, DC.*

Mode of action (MOA) provides a central framework for assessing human relevance of adverse health outcomes observed in nonclinical safety studies. The goal of this study was to characterize MOA profiles for known rodent liver tumorigens identified from a database of pesticides assessed by the U.S. Environmental Protection Agency (EPA) Office of Pesticide Programs. Among 464 compounds with mouse and rat carcinogenicity study data, liver tumor effects were observed for 23% of compounds (108/464; 95/464 for mouse and 32/464 for rat). Of these, 74% (80/108) were classified by the EPA as possible (43%) or probable/likely (31%) human carcinogens. Twenty-one compounds had a MOA proposed by the registrant for liver tumor outcomes used in quantitative risk assessment. Of these, 16 MOAs were accepted by the EPA Cancer Assessment Review Committee. Molecular initiating events for these MOAs included constitutive androstane receptor (CAR) activation (10/16), peroxisome proliferator-activated receptor (PPAR)α activation (4/16), and sustained hepatic cytotoxicity (2/16), followed by increased liver cell proliferation as measured by BrdU, Ki67, or PCNA labeling index (LI). A significant increase in proliferation was observed at ≤7 days for 13/14 compounds with accepted mitogenic (CAR- and PPARα-mediated) but not cytotoxic (0/2) MOAs, while short-term effects on proliferation LI were not provided (4/5) or were inconclusive (1/5). None of the compounds included decreased liver cell apoptosis as a key event. These findings highlight the central role of quantitative proliferation data in MOA evaluation and support current efforts to prioritize potential hepatotoxicants based on early key biological effects.

PS 66 Dose Assessment of Inhaled Cigarette Smoke Particles in the Oral Cavity and Lungs

O. Price[1], B. Asgharian[1], J. McAughey[2] and Y. Caner[2]. [1]*Arlington Division, Applied Research Associates, Raleigh, NC and* [2]*British American Tobacco, Southampton, United Kingdom.*

Many chemicals present in cigarette smoke are in particulate form upon generation. The delivered and deposited doses of inhaled cigarette smoke particles are needed to link with biological response for assessing the health impact from smoking. Cigarette smoke particles contain various components such as nicotine, water, and tar, which undergo phase change between vapor and particulate form when inhaled into the lung. The assessment of the fate of these components in the respiratory tract allows for development of refined, compound-specific risk models. A model for cigarette smoke particle size change was developed based on phase change and solubility for each of its constituents. In addition, when generated, cigarette smoke particles have a high number concentration and, thus, underwent rapid coagulation leading to an increase in size. A deposition model specific to cigarette smoke particles was developed based on cloud behavior of the smoke puff through lung airways. Particle size characteristics were used in the deposition model for cigarette smoke particles to predict regional deposition fractions in the oral cavity and lung following a typical puff/breathing scenario. Evaporation of cigarette smoke components by phase change occurred rapidly, but particles continued to grow in size by coagulation. The final diameter of cigarette particles reached twice their initial diameter. Particle deposition in the lung concentrated around two regions: the first few upper airways of the lung and the deep lung. Pulmonary deposition of particles was found to be greater than deposition in the tracheobronchial region. Model predictions agreed with reported measurements of smoke particle deposition in the lung. The dosimetry model developed in this study can be used to inform deposition levels of various components of cigarette smoke to help risk analysis. This study was funded by British American Tobacco.

PS 67 Inhalation Dosimetry and Dose-Response Analysis of the Flavoring Agents Diacetyl, 2, 3- Pentanedione, and Acetoin in the Rodent Respiratory Tract

J. D. Schroeter[1], J. Kimbell[2], B. Asgharian[1], O. Price[1], J. Randazzo[3], D. T. Kirkpatrick[3], D. Vitale[4] and M. Singal[4]. [1]*Applied Research Associates, Raleigh, NC,* [2]*Otolaryngology/HNS, University of North Carolina, Chapel Hill, NC,* [3]*WIL Research, Ashland, OH and* [4]*Research Institute for Fragrance Materials, Woodcliff Lake, NJ.*

Diacetyl, 2, 3-pentanedione, and acetoin are flavoring agents used to impart a buttery flavor and aroma. During certain food manufacturing processes, there is potential for vapor inhalation and subsequent absorption in the respiratory tract. An anatomically accurate computational fluid dynamics (CFD) model of the upper respiratory tract of the rat was used to simulate airflow and vapor uptake of these three compounds. The Multiple-Path Particle Dosimetry (MPPD) model for inhaled vapors was used to simulate uptake in each airway generation of the rat lung. Absorption rates were calculated from air:tissue partitioning, diffusivity, and saturable metabolism using parameters from the literature. At an exposure concentration of 1 ppm, nasal uptake of diacetyl, 2, 3-pentanedione, and acetoin was 37, 30, and 74%, respectively; total respiratory tract uptake was 61, 56, and 85%, respectively. At higher exposure concentrations, uptake was predicted to decrease slightly due to the effects of saturable metabolism. Diacetyl and 2, 3-pentanedione displayed similar uptake behavior with limited penetration to the pulmonary region. Acetoin, being more soluble, did not reach the terminal bronchioles. Dosimetry results from the CFD and MPPD models were used in conjunction with pathology data from nose-only inhalation exposure studies (animals were exposed 6 hours/day, 5 days/week for two weeks at target concentrations of 8.8, 17.5, and 35 ppm) to develop dose-response relationships for each compound. Internal dose predictions from respiratory dosimetry models can be used to extrapolate pathologic observations to humans based on dosimetric relationships to derive exposure limits for these compounds.
This study was funded by the Research Institute for Fragrance Materials.

PS 68 Evaluation and Comparison of Inhalation Dosimetric Models for Applicability to Diesel Exhaust Particle (DEP)-Retention Modeling

A. Willis[1], L. T. Haber[1], L. M. Sweeney[1] and C. J. Matz[2]. *[1]Toxicology Excellence for Risk Assessment (TERA), Cincinnati, OH and [2]Air Health Effects Assessment Division, Ottawa, ON, Canada.*

To aid in completing the human health risk assessment (HHRA) for diesel exhaust (DE), inhalation dosimetry models (addressing deposition and clearance) were compared, with particular attention to applicability to DE particle (DEP) retention modeling. The literature was reviewed, and the six models of greatest relevance were identified. The model evaluation included: model compartments, clearance and deposition approach, species extrapolation approach, model assumptions and validation, usability and applicability to DEP. The model comparison highlighted model aspects that reflected state of the science/best practice, as well as issues that could decrease the reliability or validity of the results. For example, the Yu and Yoon (1992) model uses chemical-specific clearance information, including separate accounting for clearance of particles and of organics adsorbed to particles, but the human model has not been verified. Conversely, MPPD reflects the state of the science for deposition modeling, and the current version (2.2) includes alveolar clearance. We found that predicted or optimized deposition efficiencies were generally similar across the models; to a large degree, the observed differences reflect differences in the assumed ventilation rate, rather than inherent model differences. This observation is consistent with the finding by U.S. EPA (2002) that the alveolar deposition was very similar among the Yu and Yoon, ICRP, and MPPD (ver. 1.1) models. However, under conditions of continuous exposure, the net cumulative dose to the lung reflects the balance between delivery and clearance, and model differences in clearance appeared to be larger than for deposited dose. Based on these results, the MPPD model was deemed most appropriate for re-evaluation of the dosimetry and inclusion in a human health risk assessment of DE, to reflect the understanding of the science.

PS 69 Cross-Species Dosimetry for Upper Respiratory Tract Naphthalene Exposure with a Hybrid CFD-PBPK Model

J. Campbell, M. E. Andersen and H. J. Clewell. *The Hamner Institutes, Research Triangle Park, NC.*

A hybrid CFD-PBPK model for naphthalene in the rat and human was developed to support cross-species dosimetry comparisons of naphthalene concentrations in the nasal respiratory and olfactory epithelium. The model reproduces time courses of naphthalene blood concentrations from intravenous and inhalation exposures in rats, and upper respiratory tract extraction data in both naïve rats and rats pretreated to inhibit nasal metabolism. Metabolic rates in the nasal tissue compartments were based on in vitro to in vivo extrapolation from published studies employing nasal tissue microsomes in rats and monkeys. The model was applied to estimate human equivalent inhalation concentrations (HECs) in dorsal olfactory and ventral respiratory tissues (i.e., nasal regions where tumors were observed in the NTP animal studies) corresponding to several endpoints for cancer and non-cancer effects of naphthalene in rats, as well as benchmark doses for genomic responses observed in rat studies conducted at The Hamner Institutes. Two approaches for cross-species extrapolation were compared: (1) equivalence based on tissue naphthalene concentration, and (2) equivalence based on amount metabolized per minute (normalized to tissue volume). At the NOAEL of 0.1 ppm (based on absence of hyperplasia in nasal tissue in a 90 day exposure study), the RGDR based on naphthalene concentration was 0.2 for the dorsal olfactory; however, the ratio rises to 5.3 when based on the normalized amount metabolized due to the lower of expression of CYP2F2 isozymes in the nasal epithelium of primates and humans. HECs based on amount of naphthalene metabolized per minute could be not estimated at TWA concentrations above 0.54 ppm in the dorsal olfactory region or 0.018 ppm in the ventral respiratory region due to saturation of metabolic activity in the human nasal epithelium.

PS 70 A Regional Model of Lung Metabolism for Improving Species-Dependent Descriptions of 1, 3-Butadiene and Its Metabolites

C. Van Landingham[1], S. Crowell[2], R. Gentry[1], D. Kaden[3], S. A. Fiebelkorn[4] and A. Loccisano[5]. *[1]ENVIRON International Corporation, Monroe, LA, [2]Pacific Northwest National Laboratory, Richland, WA, [3]ENVIRON International Corporation, Boston, MA, [4]British American Tobacco, Group Research and Development, Southampton, United Kingdom and [5]R. J. Reynolds Tobacco Company, Winston-Salem, NC.*

1,3-Butadiene (BD), a volatile organic chemical used in synthetic rubber production and other industrial processes, is detectable at low levels in outdoor air and in tobacco smoke. Exposures to high concentrations of BD have been associated with cancer in humans and animals, although there are species differences in sensitivity. Following inhalation, respiratory tissues are a primary site of BD metabolism as well as targets for epoxide-induced damage and carcinogenicity. Pulmonary Type I epithelial cells, Type II epithelial cells and Clara Cells are metabolically active cells and thus potential targets of BD metabolite-induced toxicity. Metabolic capacities of these cells, their regional densities, and distributions vary throughout the respiratory tract as well as between species and cell types. Despite these differences in lung physiology/metabolic capacity, physiologically based pharmacokinetic (PBPK) models for BD to date have relied on metabolic parameters derived from whole-lung studies, and treat the lung as a homogenous organ. Here we present a novel regional model of lung metabolism for improving species dependent descriptions of BD metabolism for PBPK modeling. The overall structure of the model was also expanded by adding a kidney compartment and descriptions of higher order metabolism to allow consideration of available urinary and blood biomarker data in animals and humans to enable better model calibration between exposure and internal levels. Simulation results of inhalation exposures to BD indicate that incorporation of differential lung metabolism is important in describing species differences in pulmonary response and that these differences may have implications in cross-species extrapolation for risk assessment of BD.

PS 71 Development of an Inhalation PBPK Model for Benzo[a] pyrene in Rats and Humans

M. H. Lumpkin[1], S. Crowell[2], A. Franzen[3], R. Gentry[3], D. Kaden[4], C. Meredith[5] and R. J. Potts[6]. *[1]ENVIRON International Corporation, Atlanta, GA, [2]Pacific Northwest National Laboratory, Richland, WA, [3]ENVIRON International Corporation, Monroe, LA, [4]ENVIRON International Corporation, Boston, MA, [5]British American Tobacco, Group Research and Development, Southampton, United Kingdom and [6]R. J. Reynolds Tobacco Company, Winston-Salem, NC.*

Benzo[a]pyrene (BaP) is a by-product of incomplete combustion of fossil fuels and plant/wood products, including tobacco. Since human inhalation exposure to BaP is most commonly associated with particles, the bioavailability of inhaled BaP in humans is uncertain; however, PBPK models may assist in estimating internal dosimetry. The existing PBPK model of Crowell et al. (2011) for BaP in rats was extended to simulate inhalation exposures to BaP in rats and humans. An important step identified in modeling inhaled BaP was the impact of BaP-carrier particle dissociation on lung dosimetry. A kidney compartment was also added to allow preliminary reverse dosimetry using human urinary biomarker data to determine if carrier particle-specific BaP dissociation rates in the lung significantly impact long-term BaP dosimetry. Existing data for inhalation of BaP coated on various particle types suggested that lung clearance is bi-phasic. However, this behavior may be driven by rapid and slow particle desorption phases, the effect of mucociliary clearance, or a combination of these processes. Thus, parameter values for BaP-particle dissociation were estimated, tested in the extended inhalation model for rats, and optimized to the available rat data. Simulations of acute inhalation exposures suggest that diffusion-limited transfer of BaP from lung tissue to blood, ciliated clearance, swallowing of BaP particles, or all of these processes, may be critical for modeling lung dosimetry over time. Modeling of long-term human urinary biomarker data informed the relative significance of accounting for particle dissociation rates on chronic human dosimetry.

PS 72 Predicting Blood Lead Following Short-Term Exposures Using the All Ages Lead Model (AALM)

R. DeWoskin[1], J. S. Brown[1], G. L. Diamond[2], M. H. Follansbee[2], C. R. Partridge[3] and K. Keteles[3]. *[1]ORD/NCEA, US EPA, Research Triangle Park, NC, [2]SRC, Inc., Syracuse, NY and [3]Region 8, US EPA, Denver, CO.*

Models currently used by EPA to predict blood lead concentration following exposure to lead (Pb) in environmental media are limited with respect to the exposure pathways and durations that can be simulated (e.g., the Integrated Exposure Uptake

Biokinetic [IEUBK] model for Pb in children, and the Adult Lead Methodology [ALM]). In some cases, inputs into these models must necessarily approximate actual exposures, adding to uncertainty in model results and strategies to meet remediation goals. To improve estimates of Pb internal dosimetry following a wide range of exposure conditions and populations, EPA developed (and is testing) a PBPK model called the All Ages Lead Model (AALM). The AALM predicts blood and tissue Pb concentrations following Pb intake from contaminated air, drinking water, surface dust, food, or miscellaneous ingestion pathways. The AALM exposure module (an Excel™ interface) allows users to simulate multi-pathway exposures that are constant or that vary in time increments as small as one day, and that occur at any age from birth to 90 years. Values for gastrointestinal absorption fractions for any age as well as values for relative bioavailability of Pb from all ingestion pathways are set by the user. The AALM model is implemented in acslX™ using either a Leggett et al. (AALM-LG) or O'Flaherty et al. (AALM-OF) based biokinetic submodel. The deposition and absorption parameter values (for either submodel) are those used in ICRP's Human Respiratory Tract Model. Two case studies for short-term exposures (exposures<30 days) demonstrate the expanded capability of the AALM model: 1) exposures to construction workers, and 2) exposures to children following a home renovation. Additional AALM capabilities are listed, and next steps in the AALM model development and testing are discussed. [The views expressed are those of the authors, and do not necessarily reflect the views or policies of the U.S. EPA. Mention of any products does not constitute endorsement or recommendation for use.]

PS 73 Sensitivity Analysis of Internal Dose-Metrics for Hexavalent Chromium Toxicity Using Physiologically-Based Pharmacokinetic Modeling

A. F. Sasso[1] and P. M. Schlosser[2]. *[1]NCEA, US EPA, Washington, DC and [2]NCEA, US EPA, Research Triangle Park, NC.*

Hexavalent chromium (Cr(VI)) is an environmental and occupational contaminant, and is present in both soil and drinking water in the United States. In 2-year drinking water bioassays, the National Toxicology Program observed effects including carcinogenicity of the gastrointestinal (GI) tract in mice and oral cavity in rats. Physiologically-based pharmacokinetic (PBPK) models have been developed to estimate interspecies differences in toxicity and assess human health risk from oral exposure to Cr(VI). However, there are significant uncertainties and inter-individual variabilities to consider when modeling chromium in the gastrointestinal tract. Hexavalent chromium is rapidly reduced to trivalent chromium (Cr(III)) in the GI lumen, and only total chromium can be analytically measured *in vivo*. The reduction and absorption of hexavalent chromium will vary with intestinal pH, dietary intake, and gastric contents and physiology. These factors vary over time and between individuals. In addition, multiple PBPK models have been developed for hexavalent chromium, and a variety of different internal dose-metrics may be applied to link external exposure and toxic effects. Toxicity may be correlated to 1) concentration of Cr(VI) in the GI tract lumen; 2) absorption of Cr(VI) into specific GI tract tissue sites; 3) total absorption of Cr(VI) in the full GI tract. This work quantifies the impact of different modeling assumptions on the interpretation of toxicological data in rodents, and extrapolation to humans. It was found that the choice of dose-metric has a significant impact on the evaluation of potential human health effects from oral exposure to hexavalent chromium.
The views expressed are those of the authors, and do not necessarily represent the views or policies of the US EPA.

PS 74 Improved Toxicokinetic Model for Cadmium Using Urine, Blood, and Kidney Cortex Concentrations from Living Kidney Donors

M. N. Fransson[1], L. Barregard[2], G. Sallsten[2], M. Akerstrom[2] and G. Johanson[1]. *[1]Institute of Environmental Medicine, Karolinska Institutet, Stockholm, Sweden and [2]Department of Occupational and Environmental Medicine, Sahlgrenska University Hospital, University of Gothenburg, Gothenburg, Sweden.*

Several toxicokinetic models have been developed to describe the relation between external exposure, tissue levels and urinary excretion of cadmium. The aim of the present work was to analyse and validate one of the most common models (K&N, Kjellström & Nordberg. Environ Res, 1978) by using new data on cadmium concentrations in kidney cortex, blood and urine (Barregård et al., Environ Res, 2010). Measured data from 30 living kidney donors (14 males, 16 females) were selected from a total of 109 based on completeness of information on cadmium levels in urine, whole blood, plasma and kidney cortex, and donor status as never smokers. Markov-chain Monte Carlo simulations and flat priors were used to estimate posterior parameter distributions for the three most sensitive of the independent parameters in the model, including the systemic uptake (not to be confused with oral intake). Two additional parameters accounting for the covariate effects of gender and serum ferritin on uptake were also tested. For the gender effect, the uptake was 48% (posterior median) higher in women. For gender and serum ferritin combined, the uptake was 44% (posterior median) higher in women and 20% higher in individuals who had a serum ferritin level <30 μg/L. However, the uncertainty in the effect of serum ferritin included the null value, indicating that the parameter may not be significant. In conclusion, the K&N model described the new data well; however these new data suggest that the uptake is higher in females than in males and that this can be accounted for by a gender-specific uptake parameter.

PS 75 Pharmacokinetic Modeling of Inhaled Cadmium Oxide (CdO) Nanoparticles in Pregnant Mice to Interpret Observed Developmental Effects

Y. Zhao[1], M. Yoon[1], J. L. Blum[2], J. T. Zelikoff[2], T. Fennell[3] and H. J. Clewell[1]. *[1]The Hamner Institutes for Health Sciences, Research Triangle Park, NC, [2]New York University School of Medicine, Tuxedo, NY and [3]RTI International, Research Triangle Park, NC.*

Fetal and neonatal periods may represent vulnerable life stages for exposure to nanoparticles (NP). In this study, we used a physiologically based pharmacokinetic (PBPK) model to simulate Cd disposition in pregnant mice from two different inhalation exposures to CdO NPs: every other day inhalation at 100 μg CdO/m3 and daily inhalation at 230 μg/m3 between gestation day (GD) 4.5 and 16.5. Although there was no difference in Cd levels in the maternal placenta or uterus between the two exposures, developmental effects were observed only with daily inhalation of 230 μg CdO NP/m3. The respiratory tract deposition of inhaled CdO NPs was simulated using the Multiple-Path Particle Dosimetry model and was linked to the PBPK model. The saturable accumulation of CdO in the placenta was based on the reported involvement of active transporters such as DMT-1 and ZIP14 for uptake of Cd and subsequent induction of metallothionein (MT) that retains Cd in the placenta. The simulated total Cd contents in the lung, blood, liver, placenta, uterus, and kidney in the dam on GD 17.5 were in good agreement with the observed values. The model predicted a rapid build-up of Cd in the placenta and uterus with daily inhalation exposure to CdO NPs compared to a relatively slower increase resulting from every other day exposure. Although the Cd levels were similar on GD 17.5, the AUC values in the placenta and uterus from the daily exposure were 1.4 and 1.8 fold higher, respectively, compared to those from every other day exposure indicating that the observed effects on fetal and neonatal development and growth may be attributable to the difference in time profiles of Cd exposure in the placenta and uterus. The current modeling approach to estimate the internal exposure to CdO NPs in the placenta and the fetus can also be applied to other NPs (This work was supported by NIEHS Award #U19ES019525)

PS 76 Updating Physiologically-Based Pharmacokinetic Models for Manganese to Include Rates of Cellular Uptake and Efflux

C. Peeples[1], M. Yoon[1], A. M. Keene[2], M. Taylor[3], H. J. Clewell[1] and M. E. Andersen[1]. *[1]The Hamner Institutes for Health Sciences, Cary, NC, [2]Afton Chemical Corporation, Richmond, VA and [3]NiPERA, Research Triangle Park, NC.*

Previously, we developed a series of physiologically based pharmacokinetic (PBPK) models for manganese (Mn) in which saturable tissue binding and dose-dependent biliary induction were key determinants of Mn homeostasis. These models effectively reproduced the non-linear behavior of Mn kinetics in different tissues, accounting for dose-dependent changes in Mn kinetics with relatively slow association and dissociation rate constants for Mn binding in tissues. However, metal homeostasis depends on regulation of uptake into and efflux out of tissues. In our updated model, the binding is more reflective of general cellular requirements for Mn. To this end, a common dissociation constant (KD = 0.5 μM) was used across tissues. Variability in the presumed binding capacities accounted for different background levels of Mn in particular tissues. In this model, the rates of entry of Mn in the tissue and interactions with binding pools within tissues are rapid. This alternative structure successfully described Mn kinetics in tissues in adult rats exposed to Mn both in their diet and by inhalation, indicating that the two model structures – our earlier binding-oriented model and this second-generation transporter-based model – both capture the dose-dependent and tissue-specific kinetic behavior of Mn in adult rats. Although published models that emphasize the role of tissue binding rate constants in non-linear behaviors capture all relevant dose-dependent kinetic behaviors of this metal, more biologically relevant models will provide greater confidence in using the Mn PBPK models for risk assessment.

PS 77 A Refined Co Biokinetic Model Based on Human Data

K. Unice[1], B. D. Kerger[2], D. J. Paustenbach[3], B. L. Finley[3] and B. E. Tvermoes[4]. [1]*ChemRisk, Pittsburgh, PA,* [2]*ChemRisk, Aliso Viejo, CA,* [3]*ChemRisk, San Francisco, CA and* [4]*ChemRisk, Boulder, CO.*

Cobalt (Co) supplements are available for sale, and concerns about metals released in patients with Co-containing hip implants have been raised. However, simultaneously collected whole blood, serum, urinary excretion and serum protein binding data have not been available to evaluate Co biokinetic models. Blood and urine data from ten healthy volunteers who ingested ~1.0 mg Co/day of a Co supplement for three months were used to refine previously published Co-biokinetic models. The model was modified to account for three key experimental observations: 1) an increase in serum protein bound Co from 95% during dosing to 99% after dosing, 2) a linear decrease in Co red blood cell concentration post-dosing period, and 3) Co renal clearance consistent with estimated glomerular filtration rates. New model compartments included: 1) albumin bound Co in intravascular fluid (serum), 2) albumin bound Co in extravascular fluid exchanging with intravascular albumin, and 3) a series of compartments representing red blood cell ages between 1 and 120 days. Renal excretion was estimated by glomerular filtration rates and free Co2+ concentration. Agreement between the modeled and measured urine, serum, and whole blood concentrations were observed (r>0.8) with oral absorption rates between 10% and 65%, a RBC Co transfer coefficient equal to 10% of the rate suggested in vitro studies, and albumin binding rate constants adjusted to reflect the measured fraction of large molecular serum protein bound Co before and after dosing. Distribution of Co to systemic tissues over three months of dosing was approximately 1/10th of the amount suggested by historical single-dose radiological tracer studies, and the increase in albumin-bound Co after dosing is consistent with exchange of albumin-bound Co from extravascular fluid to intravascular fluid after source elimination. Our revised model provides useful insight on human Co kinetics, and should be helpful in the evaluation of elevated blood Co concentrations in MoM hip implant patients.

PS 78 A Physiologically-Based Pharmacokinetic Model of Alpha-Tocopherol in Squalene-Containing Emulsion Vaccine Adjuvants

M. Tegenge and R. J. Mitkus. *Center for Biologics Evaluation and Research, USFDA, Rockville, MD.*

In recent years, oil-in-water (O/W) emulsion adjuvants have emerged as a novel class of vaccine adjuvant systems. For example, ASO3® is an O/W emulsion adjuvant that contains both squalene and α-tocopherol in the oil phase and is used in certain influenza vaccines in Europe. In the absence of relevant experimental data in humans, we constructed a PBPK model for emulsified α-tocopherol in sheep based on limited blood time course data, and, after optimization, used it to inform an independent PBPK model we constructed for man. Both models incorporated the physicochemical properties of α-tocopherol; estimates of cracking of an O/W emulsion; anatomical and physiological parameters; assumptions of preferential local lymphatic transport, and flow-limited and well-stirred distribution. For adipose tissue a diffusion-limited dual compartment (deep and shallow) was employed. Receptor-mediated uptake of α-tocopherol into tissues was modeled based on the binding of I-125-labeled low-density lipoprotein to its receptor. In vitro studies using rat microsomes and mRNA expression of CYP4F2 taken from human tissues were used to estimate the rate of metabolism of α-tocopherol. Our modeling results indicate that following IM injection of intact AS03®, α-tocopherol will rapidly transfer into draining lymph nodes. The concentration of α-tocopherol was shown to peak in plasma within 8 hrs post-dose. Preliminary predictions of the distribution to other tissues, including liver, brain, and spleen indicated that α-tocopherol reached maximal levels of 4.7%, 3.6%, and 0.15% of the injected dose, respectively, within 8 hrs. With a log P >10, α-tocopherol was estimated to accumulate in deep adipose tissue (50% of injected dose within five days). This study extends a previous estimate of the potential in vivo fate of squalene-containing emulsion adjuvants and provides quantitative estimates of the human tissue distribution of a second oil-phase component, α-tocopherol. Our results also contribute to an enhanced understanding of the immunodynamics of this class of vaccine adjuvants.

PS 79 Improvements of Structure-Based Guidance Tools in Early Drug Discovery: Evaluation of the Relative Influence of Active and Passive Transport Processes in Drug Absorption

M. Kansy[1], L. Fenu[3], P. Matsson[2] and P. Artursson[2]. [1]*Non Clinical Safety / Translational Technologies & Bioinformatics, F. Hoffmann-La Roche, Basel, Switzerland,* [2]*Department of Pharmacy, Uppsala University, Sweden, Uppsala, Sweden and* [3]*CADD Group, Eli Lilly & Co, Erl Wood Manor, Windlesham, United Kingdom.*

We assembled a comprehensive collection of reported Km and Vmax data for drug transport via the major intestinal drug uptake (PepT1, MCT-1, OATP2B1) and efflux (MDR1, BCRP, MRP2) transport proteins, based on public data sources and the peer-reviewed literature. The collected data were used to assess differences and similarities in Vmax and Km distributions among the transporters. A mechanistic model was developed in house to determine the relative importance of passive and active transport on the intestinal absorption of transporter substrates.

Results

For substrates of high capacity uptake transporters (e.g. PepT1), the maximum active transport capacity Vmax is the main determinant of the concentration/time profile, followed by the passive membrane permeability and the intestinal solubility of the compound. Compounds that are substrates of low-capacity uptake transporters (–e.g. OATP2B1) will almost invariably be transported predominantly through passive diffusion, at the relevant concentrations observed in the intestine after oral dosing. For efflux transporter substrates the compound's solubility and passive membrane permeability play a major role in determining whether the active transport has an appreciable impact on its overall absorption profile. For simulated intestinal perfusions in rodents, the passive component of transport was well explained. Physiologically reasonable values of capacity could satisfactorily explain the active component.

PS 80 Physiologically-Based Pharmacokinetic Modeling for Telmisartan and Its Glucuronide and Their Liver Transporter Activity in Humans

H. A. Barton[1], R. Li[2], A. Ghosh[2], E. Kimoto[1] and T. S. Maurer[2]. [1]*Pharmacokinetics, Pharmacodynamics, and Metabolism, Pfizer, Inc., Groton, CT and* [2]*Pharmacokinetics, Dynamics, and Metabolism, Pfizer, Inc., Cambridge, MA.*

Predicting human pharmacokinetics for acid liver transporter substrates is needed due to the increasing frequency of novel acid substrates in drug discovery and development. Initially, a previously developed prediction method using sandwich cultured human hepatocytes (SCHH) and human liver microsomes (HLM) was applied to telmisartan. The human data show experimental and pharmacogenomic variability; the predictions were moderately successful using empirically determined *in vitro* to *in vivo* extrapolation scaling factors. Several improvements for the modeling were considered. Partition coefficients (Kp) were estimated from positron emission tomography (PET) data for tissues other than liver considered to have limited transporter activity. These Kp values were largely within the 3-fold error associated with Kp prediction methods, but improved the plasma profile predictions. Telmisartan is largely metabolized to a glucuronide conjugate, so a minimal model for the glucuronide was incorporated to predict PET data for the liver. Parameters were estimated from HLM, with cofactor added, and SCHH in which parent and glucuronide distribution in cells and media was measured. The longer times (>2.5 hr) for the plasma telmisartan profiles were substantially underpredicted suggesting that enterohepatic recirculation played an important role. An empirical recirculation description was added incorporating meal induced gall bladder emptying, biliary efflux transport of the glucuronide, and instantaneous cleavage to parent in the gut. This provided reasonable simulation of the plasma profile. Overall, this modeling demonstrated that while prediction of liver transporter activity is necessary for transporter substrates, simulation of additional pharmacokinetic processes can be essential including better estimates of partition coefficients and enterohepatic recirculation.

PS 81 A Physiologically-Based Pharmacokinetic and Pharmacodynamic (PBPK/PD) Model of Daily Chlorpyrifos Exposure in Egyptian Agricultural Workers

S. T. Singleton[1], J. B. Knaak[1], C. A. Ellison[1], R. McDougall[2], D. Rohlman[3], W. K. Anger[4], T. Taghreed Farahat[5], F. Farahat[5] and J. R. Olson[1]. [1]*University at Buffalo, Buffalo, NY,* [2]*The AEgis Technologies Group, Huntsville, AL,* [3]*University of Iowa, Iowa City, IA,* [4]*OHSU, Portland, OR and* [5]*Menoufia University, Shebin El-Kom, Egypt.*

Chlorpyrifos (CPF), an organophosphorus pesticide (OP), is metabolized by CYPs to the detoxified metabolite trichloro-2-pyridinol (TCPy), or to the active metabolite, chlorpyrifos-oxon (CPF-O), which is a potent esterase inhibitor. For CPF, urinary TCPy concentrations are a reliable biomarker of CPF exposure while RBC acetylcholinesterase (AChE) and plasma butyrylcholinesterase (BuChE) are biomarkers of effect. A PBPK/PD model was developed to predict exposure to CPF, dermal absorption, distribution, metabolism, elimination and adverse health effects in Egyptian agricultural workers based on urinary TCPy, blood AChE and BuChE data collected in the field over a period of 33 consecutive days. Regression analysis of 24 hr urinary TCPy values was used to establish an array of 33 daily linear transfer coefficients of CPF to clothing and skin of 35 workers (14 backpack applicators, 9 technicians and 12 engineers). The array based model predicted skin exposure (dose) for the workers, ranging from 0.07 to 9.05 mg/kg/day, dermal absorption (1.88% of skin dose), daily wash-off (95.5% of dose), evaporation (2.14% of dose), and total overall recovery (99.6% of dermal dose). Model simulations estimate CPF and CPF-O blood levels as high as 124000 and 1275 pmol/L, respectively, with model Ki values for blood AChE and BuChE varying between 1.03 x 10-4 and 1.03 x 10-3 pM-1hr-1 for applicators and between 1.03 x 10-4 and 6.0 x 10-3 for technicians and engineers. PBPK/PD modeling is generally consistent with human biomarker data, however, there is some variability between model estimates and observed ChE inhibition, suggesting that there may be genetic susceptibility components that can alter an individual's sensitivity to CPF. (US EPA STAR, grant R-83068301 and NIEHS grants ES016308, ES022163).

PS 82 Multiroute PBPK/PD Model for Predictions of Chlorpyrifos Exposure and Effects in Humans and Rat

M. J. Bartels[1], T. S. Poet[3], P. S. Price[1], J. A. Hotchkiss[2], D. R. Juberg[2] and S. Marty[1]. [1]*Toxicology, Dow Chemical, Midland, MI,* [2]*Regulatory Laboratories, Dow AgroSciences LLC, Indianapolis, IN and* [3]*Summit Toxicology, LLC, Richland, WA.*

Chlorpyrifos (CPF) is an important pesticide used to control crop insects. Biological effects occur following metabolic activation to chlorpyrifos oxon, and these effects are monitored using RBC cholinesterase inhibition. Non-occupational exposures to CPF will occur primarily through residues on foods, with occupational exposure also from dermal contact or low-level inhalation exposures to the non-volatile CPF. A physiologically based pharmacokinetic/pharmacodynamic (PBPK/PD) model has been developed that describes the relationship between oral, dermal, and inhalation doses of chlorpyrifos and key associated events in the pathway for cholinergic effects. Pharmacokinetic data is available for controlled human exposures via the oral and dermal routes and from multiple oral or inhalation studies in rats. The multi-route model was developed in these two species to validate all modeled scenarios in a parallelogram design. Since bioactivation is key to CPF effects, small amounts of metabolism in tissues potentially have a great affect on PK and PD. Metabolism was therefore added in diaphragm, brain, lung, and skin, based on published data. For most tissues, metabolism that represented 2% of the measured hepatic metabolism resulted in fits to available cholinesterase inhibition and dosimetry. Due to the lipophilic nature of CPF most of the inhaled dose will either be delivered via superficial nasal deposition into the stomach or associated with the metabolically active pulmonary tissue, thus metabolism in the lung is comparable to liver. The resultant model fits to human and rat multi-route data, and shows that CPF Cmax will be higher through non-oral routes while cholinesterase inhibition in non-portal of entry tissues will be less following exposure via these non-oral routes. This resulting model will be highly useful in risk assessments for CPF from one or more routes of exposure.

PS 83 Comparison of the Toxicokinetic Modeling of Permethrin and Cypermethrin Biomarkers of Exposure

J. Côté and M. Bouchard. *Department of Environmental and Occupational Health, University of Montreal, Montreal, QC, Canada.*

The measurement of pyrethroid metabolites in urine has been proposed for the biomonitoring of exposure in workers, but this requires a thorough knowledge of their kinetics. A human toxicokinetic model was elaborated to describe the kinetics of key biomarkers of exposure common to permethrin and cypermethrin, based initially on published urinary time courses in volunteers exposed orally and dermally to 3.3 and 31 mg of cypermethrin (≈0.05 and 0.5 mg/kg), respectively. The model parameter values were refined in this work from best-fits to novel data gathered on the time courses of metabolites in blood and urine of volunteers orally exposed to 0.1 mg/kg of permethrin and cypermethrin. The mean elimination half-life of *trans*-DCCA, *cis*-DCCA and 3-PBA metabolites from the body (through faeces, urine or metabolism) was found to be 6.9, 6.6 and 8.9 h, respectively following permethrin treatment and 6.1, 5.2 and 7.8 h after cypermethrin dosing. The average final fractions of administered dose recovered in urine as *trans*-DCCA, *cis*-DCCA and 3-PBA were 28, 11 and 50%, for permethrin dosing and 27, 11 and 31% for cypermethrin administration, respectively. The average blood clearance rate of these metabolites calculated from the permethrin and cypermethrin data was 998 ml/h and 1328 ml/h while the predicted volume of distribution was 9.6 l and 15.8 l, respectively. Our mathematical model is in complete accordance with both independent measurements of metabolites in blood (R^2=0.90-0.97 depending on the metabolite) and urine (R^2=0.97-0.99) as well as previous experimental data published in the literature.

PS 84 A Population PBPK Model for Acetaminophen and Its Key Metabolites

T. Zurlinden[1] and B. Reisfeld[1, 2]. [1]*Department of Chemical and Biological Engineering, Colorado State University, Fort Collins, CO and* [2]*School of Biomedical Engineering, Colorado State University, Fort Collins, CO.*

Acetaminophen (paracetamol, APAP) is one of the most widely used analgesic and antipyretics in the world. It is a well-known hepatotoxicant and, owing to its ubiquitous usage, is the principal cause of acute liver failure in both the United States and the United Kingdom. APAP is metabolized primarily by sulfation and glucuronidation. However, it can also be oxidized by CYP isozymes to form the reactive metabolite, and putative mediator of toxicity, N-acetyl-p-benzoquinonimine (NAPQI). Characterizing and quantifying the role of these pathways and the formation and clearance of key metabolites can be facilitated through predictive models that incorporate salient biochemical and physiological phenomena in a tissue-specific manner. To this end, we present a PBPK model for APAP that incorporates detailed metabolism and drug absorption sub-models and show comparisons to data from multiple studies in the literature for parent chemical and metabolite concentrations. Through the use of a hierarchical Bayesian approach, parameter distributions were found that accurately describe the pharmacokinetic variability among different ethnic populations and account for the uncertainty among and between different studies. Model predictions generally showed good agreement to experimental data across multiple datasets and dosages and should allow the model to be used to better understand and quantify how administered dose can lead to hepatotoxicity for this important drug.

PS 85 A Multiscale *In Silico* Modeling Framework of Xenobiotics

J. P. Sluka, X. Fu, J. Belmonte, A. Cosmanescu, M. Swat and J. A. Glazier. *Physics, Indiana University, Bloomington, IN.* Sponsor: J. Klaunig.

Recent efforts to reduce the use of experimental animals in toxicology research has led to interest in developing *in silico* models of toxicity. *In silico* models can be used to help map data from experimental animals to humans and can potentially be used to map *in vitro* data to animals. A long term goal is the development of reliable *in silico* models that would reduce or eliminate the need for animal studies. Since toxicological and pharmacological processes occur across a wide range of spatial and temporal scales and include multiple organ systems, a comprehensive *in silico* toxicological model must include sub-models that cover multiple spatiotemporal scales, tissues and absorption, metabolism and clearance pathways in a flexible way. We have developed a liver-centric multiscale *in silico* simulation framework for xenobiotic toxicity and metabolism that incorporates the common *in silico* biological modeling scales. In particular, we link a 1) PBPK whole body representation for adsorption, distribution and excretions, 2) a tissue level (multicell) model of a liver lobule that includes blood flow (arterial and venous), cellular uptake and cell migration and death, and 3) a subcellular model that can describe subcellular signaling, gene expression and metabolic pathways. The models at each of these three scales communicate with the models at higher and/or lower scales. To create our *in silico* framework, we link existing open source tools into an aggregate model and avoided building a single monolithic program. This approach allows us to leverage both existing model building tools as well as existing *in silico* models at the individual scales. The individual models the three scales can be run as standalone (single scale) models. This facilitates validation at the individual scales and simplifies incorporating single scale models developed by others. As an example of linking these disparate *in silico* models, from the whole body to the subcellular, we present a model of Acetaminophen ADME and liver toxicity.

PS 86 A General PBPK Model for IV-Injected Nanoparticles

U. Carlander and G. Johanson. *IMM, Unit of Work Environmental Toxicology, Karolinska Institutet, Stockholm, Sweden.*

In order to link NP exposure to toxicity, information about absorption, distribution, degradation and excretion (ADME) is essential. Experience from pharmaceutical drugs and industrial chemicals shows that the ADME can successfully be simulated, described and predicted by physiologically based pharmacokinetic (PBPK) modeling. The few PBPK models for NPs published to date have been developed and evaluated for a single type of NP. The aim of this study was to develop a general NP-PBPK model for intravenously injected NPs in rats. The model was based on a recently developed PBPK model for pegylated polyacrylamide (PAApeg) NPs (Dingsheng et al., submitted manuscript), which in turn was developed using detailed experimental data (time courses of NP mass in different tissues) after single intravenous administration (Wenger et al., *Toxicol. Appl. Pharmacol.* 2011). In addition to PAApeg, we retrieved intravenous rat data for nonpegylated PAA, gold and polymethylidene malonate NPs (Lescure et al., *Pharm. Res.* 1994; Wang et al., *Anal. Bioanal. Chem.* 2010). NP-dependent parameters were adjusted by best fit to each data set, whereas NP-independent physiological and anatomical parameters were kept constant. The general model was able to adequately describe the ADME behavior of all four NP types. The fitted parameters that varied most were the clearance to urine and feces, the blood:tissue permeability coefficients and the uptake rate and capacity of phagocytic cells. Additional data on NP properties such as corona formation and physiological parameters, such as number of phagocytic cells in different tissues and their capacity and turnover, are required to further improve the model. The study was supported by the Swedish Research Council for Health, Working Life and Welfare (Forte).

PS 87 A PBPK Model of Hypobaric and Hyperbaric Toluene Exposure

C. Hack[1], T. R. Covington[1], P. J. Robinson[1], P. Shiyanov[1], D. A. Mahle[2] and J. M. Gearhart[1]. [1]*HJF, AFRL, Wright-Patterson AFB, OH and* [2]*RHDJ, AFRL, Wright-Patterson AFB, OH.*

Modern high-performance jets achieve extreme altitudes and operate in hypobaric pressure environments. Conversely, divers operate at hyperbaric depths. Inhalation exposure to toxins in these extreme pressure environments may result in altered kinetics, and therefore, altered response and exposure safety guidelines. Such pressure-dependent differences in kinetics have been observed for some compounds, while absent for others. To test whether toluene kinetics are sensitive to pressure, we developed a physiologically-based pharmacokinetic (PBPK) model as a tool for examining potential physiological contributors to such differences. Our approach was to compare model predictions to hypobaric and hyperbaric toluene kinetics data in Sprague-Dawley (SD) rats, and then adjust model parameters and/or processes to fit the data, thereby identifying potential effectors of observed differences. The model was based on a typical Ramsey-Andersen model of isopropanol, with tissue compartments for the brain, liver, fat, skin, and lumped rapidly perfused and slowly perfused tissues. Toluene parameters were obtained from literature sources. The model was verified for normal pressure through comparison with previously published data and models in the literature, and produced good agreement with the data. For hyper/hypobaric simulations, the model was first adjusted with explicit implementation of the ideal gas law for conversion of ppm to mass at different pressures. Male and female SD rats were exposed to toluene via inhalation, and the data were compared with model predictions. Initial model predictions underestimated the experimental data. However, the model predicted decreased toluene in tissues with decreasing pressure, which was consistent with the experimental data. Predictions of published hyperbaric exposures slightly overestimated those data by about 30%. Future work will focus on comparison of predictions with additional hypobaric and hyperbaric, and examination of other potential physiological contributors to pressure-dependent kinetic differences.

PS 88 Understanding the Differences in the Toxicity of Tolcapone and Entacapone: A Comparative Study Using the Virtual Liver Platform—Heptox

R. Kumar, S. Das, A. Khanna, D. Srivastava, S. Louha, K. Rajendran, B. Thota, D. Raman, N. Mandyam, N. Rajeswara, S. Raghavan and K. Subramanian. *Strand Life Sciences, Bangalore, India.*

The effect of two catechol-O-methyltransferase (COMT) inhibitors, entacapone and tolcapone are compared using our toxicity prediction platform, a combination of an in silico model of liver metabolism with a set of in vitro biochemical measurements. Although both tolcapone and entacapone show similar on-target inhibitory potencies (Ki for COMT ~10nM), their off-target effects in the liver and their pharmacokinetic and pharmacodynamic properties are different.
We measured the dose- and time-dependent impact of both drugs on key liver metabolic pathways using a HepG2 cell system. HepG2 cells were treated for different time periods up to 72 hours, and we estimated both the direct action of the drug on enzyme activity as well as compensatory mechanisms that are invoked with time in response to the drug treatment. This information is used to simulate a virtual clinical trial for both the drugs using their respective pharmacokinetic data as input. Tolcopone with a three fold higher Cmax than entacapone, as well as higher plasma half-life (2.9 vs 0.9 hrs) has a far greater impact on the off-targets leading to more toxicity when compared to entacapone. In this study we show a relationship between drug-exposure and the toxic impact of these two drugs on different off-targets, and derive an explanation as to why tolcopone is more hepatotoxic than entacapone. Our simulations indicate the onset of tolcapone induced toxicity starts in after 6 weeks of treatment and predicts that over a period of 3 months, tolcapone induces mitochondrial damage, inhibits transport of ATP across the mitochondrial membrane and leads to a lowering of cytosolic ATP and eventual necrotic damage.

PS 89 The Association between Prenatal Exposure to Perfluoroalkyl Substances (PFAS) and Reduced Birth Weight: Is Glomerular Filtration Rate the Underlying Cause?

M. Verner[1, 2], A. Loccisano[3], M. Yoon[3], H. Wu[3], R. McDougall[4], M. Maisonet[5], M. Marcus[5], R. Kishi[6], C. Miyashita[6], M. Chen[7], W. Hsieh[7], M. E. Andersen[3], H. J. Clewell[3] and M. P. Longnecker[8]. [1]*Harvard Medical School, Boston, MA,* [2]*Karolinska Institutet, Stockholm, Sweden,* [3]*The Hamner Institutes for Health Sciences, Research Triangle Park, NC,* [4]*Aegis Technologies, Huntsville, AL,* [5]*Emory University, Atlanta, GA,* [6]*Hokkaido University, Sapporo, Japan,* [7]*National Taiwan University College of Medicine, Taipei, Taiwan and* [8]*National Institute of Environmental Health Sciences, Research Triangle Park, NC.*

Prenatal exposure to PFAS has been associated with lower birth weight in epidemiologic studies. Because glomerular filtration rate (GFR) during pregnancy is associated with PFAS excretion and birth weight, the observed association between PFAS levels and reduced birth weight could be driven by GFR. We used an existing physiologically-based pharmacokinetic (PBPK) model of human pregnancy to simulate PFAS in maternal and cord blood and to subsequently assess how much of the PFAS-birth weight association observed in epidemiologic studies might be attributable to GFR. We modified the model to reflect the association of birth weight with GFR. Data from 100,000 Monte Carlo simulations was analyzed using linear regression to evaluate the association between simulated PFAS levels and birth weight. Based on the simulations, we estimated reductions of 2.61 g and 6.23 g in birth weight for each 1 ng/ml increase in cord PFOS and PFOA, respectively. Each 1 ng/ml increase in simulated maternal blood PFOS and PFOA levels at delivery was associated with reductions of 1.84 g and 6.99 g in birth weight. In comparison, a meta-analysis of published epidemiologic studies suggested that each 1 ng/ml increase in prenatal PFOS and PFOA levels is associated with 5.00 g and 14.72 g reductions in birth weight. Our results revealed that a substantial portion of the reported association between prenatal PFAS and birth weight might be attributable to GFR. This study shows that PBPK models can be used to assess how much of an epidemiologic association can be explained on the basis of pharmacokinetics.

PS 90 PBPK Modeling of Human PFOA Exposure Predicts Measured Serum Concentrations from Consumption of Contaminated Drinking Water

R. R. Worley[1, 2], D. A. Fowler[1], C. Welsh[1] and J. Fisher[3, 2]. [1]*Division of Community Health Investigations, Centers for Disease Control/Agency for Toxic Substances and Disease Registry, Atlanta, GA,* [2]*Interdisciplinary Toxicology Program, University of Georgia, Athens, GA and* [3]*National Center for Toxicological Research, Food and Drug Administration, Jefferson, AR.*

Human exposure to perfluorooctanoic acid (PFOA) is common and widespread - PFOA is regularly found in human blood samples as reported by the National Health and Nutrition Examination Survey (NHANES). A physiologically-based pharmacokinetic (PBPK) model was developed that predicts the behavior of PFOA in humans and computational research is underway to evaluate human biomonitoring data collected in a community with known exposures to PFOA as a result of contaminated drinking water. Exposure scenarios that may approximate those occurring in the community are simulated and the resulting PFOA-serum concentrations are compared to those measured in the field study. The water supply for this community was known to be contaminated with PFOA for at least 12 years and biomonitoring samples were collected in 2009. Thus, model simulations are run to simulate exposure to PFOA in drinking water at background concentrations (0.01 ppb) for 38 years, followed by 12 years of exposure to PFOA in drinking water at

either 0.4 ppb (EPA's Provisional Health Advisory Level) or 2.2 ppb (a concentration measured in a private well in the community and considered to be at the high end of plausible drinking water concentrations from private wells). A simple description of PFOA elimination kinetics using a urinary clearance coefficient of 4.0 x 10-5 L/hr/kg body weight and drinking water intake rate of 2 liters per day resulted in predictions that were similar to the measured PFOA-serum concentrations for both public and private water consumption. This computational modeling research is important because it adds a valuable site-specific perspective to the assessment of PFOA and will enable exposure scientists and public health officials to better understand biomonitoring data for regulatory science applications.

PS 91 Can the Association between Serum Perfluorooctanoic Acid (PFOA) and Delayed Menarche Be Explained on the Basis of Physiology and Pharmacokinetics?

H. Wu[1], M. Yoon[1], M. P. Longnecker[2] and H. J. Clewell[1]. [1]*The Hamner Institutes for Health Sciences, RTP, NC and* [2]*National Institutes of Environmental Health Sciences, RTP, NC.*

An association between serum PFOA and delayed age at menarche was reported in a cross-sectional study of adolescents with a relatively high exposure via contaminated drinking water. Since PFOA has a half-life of about 3 years, it is expected that growth dilution and the development of a new route of excretion through menstrual cycling can affect PFOA kinetics. Therefore, the role of physiological changes during puberty in the reported association needs to be investigated prior to causal inference. A Monte Carlo (MC) Physiologically-based Pharmacokinetic (PBPK) model of PFOA was used to simulate distributions of serum PFOA levels from 2 to 20 years old. PFOA levels were simulated in a hypothetical population with similar physiological characteristics (Mean [SD] BMI: 22.1 [5.8]) to those in the epidemiologic study (Mean [SD] BMI: 22.3 [5.5]). Correlations among physiological parameters of maturation and timing of pubertal milestones such as growth spurts and menarche were also incorporated in the model. The prevalence of menarche and distributions of age-dependent physiological parameters in the simulated subjects were comparable to those reported in the epidemiologic study. The serum PFOA concentration quartiles (Q1: 11.0, Q2: 24.8, Q3: 58.2 ng/ml) in the simulated adolescent girls were comparable to the observed data (Q1: 11.4, Q2: 23, Q3: 58 ng/ml). Association between PFOA level and menarche age was estimated by logistic regression. Our results suggest that variations in PFOA kinetics due to growth dilution and an additional excretion route associated with menstruation may underlie the reported relationship between serum PFOA levels and age at menarche. Our study showed that MC PBPK modeling can be used to assess whether and how much of the apparent epidemiological association can be explained on the basis of pharmacokinetic variability rather than the chemical itself (supported by 3M and DuPont).

PS 92 Evaluation of the Observed Association between the Early-Age Exposure to Polybrominated Diphenyl Ethers (PBDEs) and Altered Age at Menarche on the Basis of Kinetics

M. Yoon[1], H. Wu[1], M. Luo[1], M. P. Longnecker[2] and H. J. Clewell[1]. [1]*The Hamner Institutes for Health Sciences, RTP, NC and* [2]*National Institutes of Environmental Health Sciences, RTP, NC.*

Epidemiological associations between blood PBDEs and earlier menarche in the general population have raised concerns for possible reproductive health effects. However, rapidly changing physiology during puberty that can affect the kinetics of a chemical may underlie the observed associations. To assess the role of pharmacokinetic variability during puberty on the reported PBDE epidemiological associations, blood concentrations of BDE-47, one of the most abundant PBDE congeners, were simulated in a hypothetical population with similar physiological characteristics to those in the epidemiologic study. To simulate a realistic time-course of blood BDE-47 during puberty it was necessary to incorporate correlations in the model among physiology and timing of pubertal events such as growth spurts and menarche in addition to distributions of physiological parameters across ages. The distributions of simulated physiological parameters from birth to adulthood, as well as timing of growth spurts and menarche, were comparable to those reported in population studies. The average blood concentrations of BDE-47 and its distribution in simulated females were comparable to those in NHANES. Preliminary results showed that each natural log unit of BDE-47 is related to a change of -0.034 (95% CI: -0.09, 0.03) years of menarche age in the simulated girls, which was close to the reported change of -0.10 (95% CI: -0.33, 0.13) years of menarche age in an epidemiologic study that analyzed NHANES data. This suggests that the reported relationship between blood PBDE and earlier menarche may be explained by inter-individual variability in PBDEs kinetics resulting from individual differences in physiological changes. The current approach can be applied to evaluate similar associations that have been reported for other chemicals on the basis of pharmacokinetics instead of chemical effect itself (supported by the ACC-LRI).

PS 93 Assessing the Dosimetry of Polybrominated Diphenyl Ethers Using a Harmonized Physiologically-Based Pharmacokinetic Model

A. Nong[1], C. M. Tremblay[1, 2] and P. Brochu[2]. [1]*Environmental Health Sciences and Research Bureau, Health Canada, Ottawa, ON, Canada and* [2]*Département de Santé Environnementale et Santé au Travail, Université de Montréal, Montreal, QC, Canada.*

Environmental persistent chemicals are of concern due to their ability to accumulate in different media and in high level organisms such as animals and human. This environmental persistency can be due to prolonged exposure of a stable chemical or bioaccumulation in body stores from highly lipophilic compounds. However, the pharmacokinetics of highly lipophilic compounds can be affected by binding to blood lipoproteins and rapid clearance from the body. Polybrominated diphenyl ethers (PBDE) are highly lipophilic compounds that undergo extensive oxidative mediated metabolism. The aim of this work is to describe the dosimetry for different congeners of PBDEs using a harmonized physiologically-based pharmacokinetic (PBPK) model. A PBPK model was developed based on single pharmacokinetic structure that can predict tissue and blood concentrations for BDE 47, 99, 100, and 153 in rodents. The model structure was derived using adipose tissues divided into blood lipoproteins, typical fatty tissues, and deep storing fatty tissues, as was demonstrated for siloxanes. Metabolism of the congeners were based on in vitro measurements and then fitted with available rodent pharmacokinetic data. Blood and tissues estimations were consistent for all congeners using the same model structure. Each congener had small changes for a few model parameters (exchange rates between blood lipoproteins, liver tissues and fatty tissues). The model simulations suggest a more rapid uptake in blood lipoproteins compared to fatty tissues for the lesser brominated congener. From this pharmacokinetic evidence, accumulation of PBDEs can be contributed by both a slow uptake of these compounds into adipose tissues and prolonged exposure from the environment. This work presents the application of PBPK modeling with chemical exposure data to support dosimetry estimation for the risk assessment of PBDEs and flame retardants.

PS 94 A Multiscale Mechanistic Model of TCDD-Induced Toxicity for Assessing Expected Dose-Responses for Adverse Outcome Pathways in Liver

S. Bhattacharya, P. D. McMullen, S. Pendse and M. E. Andersen. *Institute for Chemical Safety Sciences, The Hamner Institutes for Health Sciences, Research Triangle Park, NC.*

Ongoing efforts to describe and apply adverse outcome pathways (AOPs) for risk assessment require linkage of early molecular interactions to phenotypic responses. New advances in multiscale "virtual tissue" models provide a quantitative framework to link together: (a) tissue disposition of a chemical; (b) molecular initiating events such as receptor binding; (c) explicit models of intracellular and organism level AOPs; and, (iv) phenotypic endpoints like cell proliferation. Here we describe our development of a virtual tissue model of the rodent liver lobule for activation of the aryl hydrocarbon receptor (AhR) toxicity pathway in hepatocytes exposed to 2,3,7,8-tetrachlorodibenzo-p-dioxin (TCDD). This case study shows the process of data integration and multiscale model development for mechanistic dose-response prediction and application of the AOP framework to risk assessment. First, a modified cluster aggregation algorithm provided a two-dimensional computational representation of the rodent liver lobule. This multicellular lobular model was linked to the CompuCell3D modeling environment that incorporated a network representation of intra-hepatocyte activation of the AhR signaling pathway. A PBPK description of TCDD uptake in the liver through hepatic sinusoids estimated differential cellular dosimetry as an input to the spatial model. Zonal heterogeneity in TCDD-induced cytochrome induction arises from for descriptions of spatial gradients in basal AhR expression across the lobule. Simultaneously, a combination of published gene expression and chromatin immunoprecipitation data served to refine a detailed transcriptional network of the AhR pathway with differential sensitivity ascribed for different liver regions. Overall, the multiscale model accurately simulated the observed dose-responses for various endpoints. Virtual tissue models promise more quantitative linkage to AOPs than possible through simple narrative descriptions of these processes.

PS 95 Dosimetric Analysis of VITROCELL VC10® Smoke Exposure System with Photometer and Quartz Crystal Microbalance

W. Fields[1], K. Fowler[1], V. Hargreaves[2], L. Walker[2] and B. Bombick[1]. [1]*Research & Development, R. J. Reynolds Tobacco Co., Winston-Salem, NC and* [2]*Genetic & Molecular Toxicology, Covance Laboratories Ltd., Harrogate, United Kingdom.*
Sponsor: P. Harp.

Air liquid interface whole smoke exposure technologies such as the VITROCELL VC10® smoke exposure system (VC10) are applied to assess the effect of cigarette smoke on biological endpoints (e.g. cytotoxicity, mutagenicity and DNA modifications). Presently, dose response evaluations have been primarily determined on an airflow dilution basis following smoke generation under ISO or intense smoking regimes. Correlation of the biological response to dose is important for comparative analyses of products and data from other smoke exposure systems and may be facilitated by dosimetry tools such as photometers, quartz crystal microbalances (QCMs) and carbon monoxide monitors. The goals of this study were to 1) assess the consistency of particle detection via deposition or mass with QCMs and photometers, respectively, across all dilution bars and at airflows spanning the operating range of the VC10, 2) assess consistency of particle detection in multiple exposure modules and 3) correlate photometer readings at set airflows to deposited mass such that estimates of mass can be derived from the VC10 Photometer Monitor Software.
Consistency in particle deposition and mass was generally observed across all dilution bars and between modules at a range of airflows that spanned the operating range of the VC10. Consistency was also observed across all chamber positions within modules from 12 to 1L/min while some variability was observed at 0.5L/min. Linear correlations between particulate deposition and measured particulate mass were observed, and statistical and power curve analyses confirmed the accuracy of the predicted QCM data generated with the VC10 Photometer Monitor Software.
Collectively, we report the capacity to assess deposited mass with reproducibility with QCMs and to accurately estimate mass based on area under the curve data from photometer readings. These data will be helpful in correlating biological responses to dose related exposures with the VC10.

PS 96 Predicting Tissue:Plasma Partition Coefficients: Interindividual and Interspecies Variability

C. D. Ruark[1], C. Hack[1], P. J. Robinson[1], D. A. Mahle[2] and J. M. Gearhart[1]. [1]*HJF, Molecular Bioeffects Branch, Bioeffects Division, 711 Human Performance Wing, Human Effectiveness Directorate, Air Force Research Laboratory, Wright-Patterson AFB, OH and* [2]*Molecular Bioeffects Branch, Bioeffects Division, 711 Human Performance Wing, Human Effectiveness Directorate, Air Force Research Laboratory, Wright-Patterson AFB, OH.*

A tissue composition based mechanistic model for the prediction of steady state tissue: plasma partition coefficients ($K_{t:p}$) of organic chemicals in mammalian species was used to assess interindividual and interspecies variability. The approach predicts $K_{t:p}$ using available chemical properties (lipophilicity, binding to phospholipid membranes, and pK_a), together with biological properties of the tissue itself (fraction of water, neutral lipids, neutral and acidic phospholipids, proteins and pH). Biological properties were identified from the biomedical literature for rat, pig, human, guinea pig, monkey, mouse, beagle dog and rabbit species. Property means and coefficients of variation were used in a Monte carlo simulation to assess variability within and between species. The results show that interindividual and interspecies variability becomes more pronounced as $LogP_{O:W}$ increases and the difference is insignificant for compounds with $LogP_{O:W}<2.0$. Interspecies variation for ionizable compounds is shown to be driven by differences in the acidic phospholipid composition. The Monte carlo composition based mechanistic model can be used to predict $K_{t:p}$ for organic chemicals across 8 different species and can be an important component in population physiologically based pharmacokinetic (PBPK) modeling, safety evaluation, chemical risk assessment and screening.

PS 96a Integrating Biological Variability with QSARs in PBPK Models to Simulate Distributions of Internal Dose in Humans

K. Krishnan and T. Peyret. *Universite de Montreal, Montreal, QC, Canada.*

Existing mechanistic algorithms use point estimates for blood and tissue composition to predict the blood:air and tissue:air partition coefficients (PCs) required for PBPK modeling. The objectives of this study were: i) to develop a framework to predict the probability of distributions of PCs; and ii) to incorporate them, along with published information on the variability of cytochrome P450 CYP2E1 content and physiological parameters, within a human PBPK model to simulate the variability of toxicokinetics of inhaled VOCs. Previously published human and rat data on matrix:air PCs of toluene and acetone (in blood, fat, liver, and muscle tissue:air PCs), along with data on oil:air and water:air PCs were used in a Markov chain Monte Carlo (MCMC) approach to characterize the distributions of human blood and rat tissue composition parameters in the mechanistic algorithm for PCs (i.e., neutral lipid, water and protein contents). The posterior distributions resulting from the MCMC analysis were used along with physicochemical properties predicted with QSARs to compute distributions of chemical-specific tissue:blood and blood:air PCs. Monte Carlo simulations were then carried out with the PBPK model to predict the blood kinetics of VOCs (benzene (25 ppm, 2 h), styrene (80 ppm, 6 h) and trichloroethylene (100 ppm, 4h)) following inhalation exposures. For these VOCs, the predictions of the PBPK model compared well with the available human volunteer data. Overall, this study demonstrated the feasibility of using PBPK models to simulate the combined impact of the variability of biological and chemical properties on the internal dose of chemicals. (Supported by Natural Sciences and Engineering Research Council of Canada)

PS 96b PBPK Models for Gasoline-Ethanol Biofuels in Adult and Pregnant Rats

S. A. Martin[1], W. M. Oshiro[1], P. Evansky[2], J. Ford[3], L. L. Degn[1], H. A. El-Masri[4], E. D. McLanahan[5], D. MacMillan[3], W. K. Boyes[1] and P. J. Bushnell[1]. [1]*TAD, Durham, NC,* [2]*EPHD, Durham, NC,* [3]*RCU, Durham, NC,* [4]*ISTD, NHEERL, ORD, US EPA, Durham, NC and* [5]*NCEA, ORD, US EPA, Durham, NC.*

As utilization of biofuels (BF) in the commercial marketplace has increased in recent years, so has the need for evaluation of exposure-related health effects, such as developmental neurotoxicity. This research describes the development of inhalation life-stage physiologically-based pharmacokinetic (PBPK) models for vapors of gasoline (E0) and two BF blends, E15 (15% EtOH) and E85 (85% EtOH). Time-course blood hydrocarbon concentration (BHC) data were collected from non-pregnant female rats exposed to E0, E15, and E85, at total hydrocarbon concentrations (THC) of 3K, 6K, and 9Kppm (≤6h exposure, 4-6 time points per dose). Peak (end-of-exposure) BHC data were also collected from pregnant dams exposed to 9Kppm (6.33h, GD9, 16, 20) of E0 or E15. These datasets were used to evaluate and refine PBPK models for each mixture and to compare estimates of BHCs across BF types at comparable THCs. PBPK models were constructed using a series of sub-models for prominent aromatic and aliphatic HCs representing ~45-66% of total vapor (depending on BF), while the remaining fractions were lumped. The overall modeling framework allowed for flexibility across blend compositions. The sub-models were parameterized with literature and structure-activity-based estimates; estimated physiochemical and metabolic parameters were used for the lumps. The models adequately simulated BHCs for most aromatic and aliphatic HCs across the various exposure scenarios. Specifically, HCs with robust calibration literature were usually well simulated, while clearance rates for the other aliphatics often did not adequately match model BHC predictions. Simulations for aromatics at high vapor concentrations were improved by including metabolic interactions; HCs at low concentrations were often better simulated without these interactions. The final models may be relevant for simulations of other blend ratios. Abstract does not reflect EPA policy.

PS 96c Evaluation of Semi-Generic PBTK Modelling for Emergency Risk Assessment after Acute Inhalation Exposure to Volatile Hazardous Chemicals

J. Olie[1, 2], C. C. Hunault[1], J. Bessems[3], H. J. Clewell[4] and J. Meulenbelt[1, 5, 6]. [1]*National Poison Information Center, University Medical Center Utrecht, Utrecht, Netherlands,* [2]*University of Nijmegen, Nijmegen, Netherlands,* [3]*EC JRC, Institute for Health and Consumer Protection, Ispra, Italy,* [4]*The Hamner Institutes, Research Triangle Park, NC,* [5]*IRAS, Utrecht University, Utrecht, Netherlands and* [6]*Department of Intensive Care Medicine, UMC Utrecht, Utrecht, Netherlands.*

Rationale: Physiologically Based Toxicokinetic Models (PBTK) may facilitate emergency risk assessment after chemical incidents, but are rarely used due to their relative complexity and skill requirements. We aimed to evaluating a semi-generic PBTK model built in MS Excel for nine chemicals that are widely-used and often released in a chemical incident.
Methods: The semi-generic PBTK model was used to predict blood concentration-time curves using exposure scenarios from human volunteer studies (low exposure doses), case reports (medium to high exposure doses) and hypothetical exposures at ERPG-3levels (high exposure doses). Semi-generic means the model uses built-in QSARs to set some parameter values. Predictions were compared to measured blood concentrations from volunteer studies or case reports as well as to

blood concentrations predicted by chemical-specific models. The performances of the semi-generic model were evaluated on biological rationale, accuracy and shape of predicted concentration-time profiles, ease of use and range of application.
Results: Our results indicate that the semi-generic PBTK model can be readily used to predict blood levels for 6 out of 9 parent chemicals (benzene, xylene, toluene, styrene, trichloroethylene and tetrachloroethylene), with the exception of methanol, 2-propanol and dichloromethane. The semi-generic model could not cope with the endogenous production of methanol and acetone (metabolite of 2-propanol). The model could not simulate the formation of HbCO, which is one of the toxic end-points of dichloromethane.
Conclusion: For some hazardous chemicals, a semi-generic PBTK modelling approach to can be just as accurate as a more chemical-specific PBTK modelling approach.

PS 96d Interpreting NHANES Biomonitoring Data: Dioxins

P. Ruiz[1], T. Simon[2] and M. Mumtaz[1]. [1]*Computational Toxicology Lab, ATSDR/CDC, Atlanta, GA and* [2]*Ted Simon LLC, Winston, GA.*

Polychlorinated dibenzo-p-dioxins (PCDDs), polychlorinated dibenzofurans (PCDFs), mono-ortho and non-ortho polychlorinated biphenyls (dioxin-like PCBs) are identified as a family of organic compounds known as "dioxins". Dioxins are persistent endocrine-disrupting chemicals that bioaccumulate following environmental exposure or dietary intake. Additional adverse health effects of dioxin exposure in humans include the development of serious diseases such as diabetes, cancer, deleterious effects such as an altered immunological response and changes in the expression of receptors and metabolic enzymes. As part of translational research to make computerized models accessible to health risk assessors we recoded the Concentration-and-Age-Dependent Model (CADM) for pharmacokinetics of dioxins in Berkeley Madonna simulation language. The recoded model was evaluated by comparing simulations to other published model simulations and to human data sets. Overall, there was good agreement between the estimated and measured values. Our recoded model allows the estimation of dioxin concentrations in breastfed infants. Also presented is an application of the recoded model to interpret biomonitoring data from the National Health and Nutritional Examination Survey (NHANES). The model simulated the NHANES-measured data very well from ages 6 to 60+ years. The model describes TCDD cumulative nature in humans and accommodates the observed variation in exposure/uptake over the course of a lifetime. Hence, this model may be useful as a screening tool that can provide information on interpreting biomonitoring data and risk assessment.

PS 96e Physiologically-Based Pharmacokinetic (PBPK) Models Application to Screen Environmental Hazards Related to Adverse Outcome Pathways (AOPs)

L. Adams[1], S. A. Marchitti[2], T. L. Tal[1], N. C. Baker[3], J. F. Wambaugh[3], C. Mazur[1], J. F. Kenneke[2] and H. A. El-Masri[1]. [1]*NHEERL, USEPA, Research Triangle Park, NC,* [2]*NERL, USEPA, Athens, GA and* [3]*NCCT, USEPA, Durham, NC.*

PBPK models are useful in estimating exposure levels based on in vitro to in vivo extrapolation (IVIVE) calculations. Linkage of large sets of chemically screened vitro signature effects to in vivo adverse outcomes using IVIVE is central to the concepts of the National Academy of Sciences' Toxicology in 21st century vision. Except for metabolic clearance, most parameters used to develop PBPK models are readily available in literature, or calculated using chemical structure activity relationships. Lack of computational methods to determine clearance inhibits the application of PBPK models to large set of chemicals without conducting costly and time-consuming experiments. This problem, however, should not exclude the use of PBPK models to screen a large set of chemicals for possible environmental exposure levels that can lead to adverse outcome effects. This can be accomplished by developing "generic" PBPK models. Metabolic clearance capacity in the generic model is set to zero to estimate maximal exposure level (EXPmax) that will yield parent chemical tissue levels equivalent to in vitro levels identified for the signature effects along an identified adverse outcome pathway (AOP). EXPmax levels are then screened against environmental exposure levels (EXPenv). If EXPenv is less than EXPmax, then parent target tissue levels of the chemical under the environmental exposure scenarios will be less than toxicologically-effective in vitro levels (EC50s or LELs), indicating that the assumption of zero clearance is health hazard conservative. For chemicals where EXPenv is larger than EXPmax, metabolic clearance of these chemical may be a critical factor in determining their health risks. This abstract does not necessarily reflect EPA policy.

PS 96f Evaluation of the Pharmacokinetics of Methylphenidate in Juvenile and Adult Humans and Nonhuman Primates Using a Physiological Model

X. Yang[1], S. Morris[1], J. M. Gearhart[2], C. D. Ruark[2], M. G. Paule[1], W. Slikker[1], D. R. Mattison[3], N. C. Twaddle[1], D. R. Doerge[1], J. F. Young[1] and J. Fisher[1]. [1]*U.S. Food and Drug Administration, National Center for Toxicological Research, Jefferson, AR,* [2]*The Henry M. Jackson Foundation for Military Medicine, Wright-Patterson Air Force Base, OH and* [3]*Risk Sciences International, Ottawa, ON, Canada.*

Methylphenidate (MPH) is a psychostimulant drug marketed for treatment of attention deficit hyperactivity disorder in children and adults. A physiologically-based pharmacokinetic (PBPK) model was developed to characterize the age- and species-dependent pharmacokinetics of MPH in juvenile and adult humans and rhesus monkeys. The model was first calibrated in adult humans for MPH enantiomers and then extrapolated to children and monkeys. The calibrated MPH PBPK model was then utilized to extrapolate to children the pharmacokinetic MPH serum profiles associated with toxicity observed in juvenile monkeys. MPH is extensively and rapidly metabolized in the liver and gastrointestinal tract, primarily by carboxylesterase 1, with minor contributions from oxidative enzymes. Juvenile monkeys and children appear to metabolize MPH more rapidly than adults, with more rapid metabolism in juvenile monkeys than in children. Juvenile monkeys chronically exposed to oral MPH doses of 2.5 and 12.5 mg/kg (twice per day) showed a temporary delay in puberty (Mattison et al. 2011). Pharmacokinetically equivalent MPH doses for a 15-year-old boy were estimated to be 0.3 and 0.1 mg/kg using Cmax and AUC dose metrics from juvenile monkeys given 2.5 mg/kg of MPH. Therapeutic MPH doses in children ranging from 0.3-0.8 mg/kg, given twice a day, produce MPH kinetic profiles similar to those in juvenile monkeys that experienced delays in puberty. This computational analysis suggests that continued pharmacovigilance is prudent.

PS 96g Intra- and Interspecies Extrapolation of Dose during the Developmental Period Using PBPK Models

J. W. Fisher, D. R. Doerge, A. Lumen, A. Fu and X. Yang. *Biochemical Toxicology, FDA/NCTR, Jefferson, AR.*

PBPK models are increasingly used to extrapolate the pharmacokinetics of a chemical or drug within a species from adult to young (intraspecies extrapolation) and between species, young animals to children (interspecies extrapolation). We developed adult and neonatal monkey and adult human and newborn PBPK models for bisphenol A (BPA) and for methylphenidate (MPH, Ritalin), adult and juvenile monkey and adult human and children PBPK models. Both the BPA and the MPH models relied on intra- and interspecies extrapolation. PBPK models were constructed using pharmacokinetic studies in infant (PND 5 to77) and adult monkeys and adult humans for BPA and for MPH, juvenile (4-5 years) and adult monkeys and children (boys, 6 to 15 years old) and adult humans. These PBPK models were constructed using literature on the physiology of young and adult monkeys and humans and body weight scaling of chemical- or drug-specific model parameters (intra- and interspecies extrapolation). The acceptance or recalibration of the scaled parameters was determined by comparing predicted serum time courses data with observed data. Scaling of hepatic metabolism (iv dosing of adult monkey and infant monkey) and systemic (urinary) clearance of BPA metabolites (oral dosing of adult monkey and adult human) was not adequate to describe the kinetics of BPA and its metabolites, thus these model parameters were recalibrated. Lack of data precluded the evaluation of the human infant. For MPH, scaling of hepatic metabolism (hydrolysis) was successful for the oral administration of MPH in the child, adult human and adult monkey, but not in the juvenile monkey. Systemic clearance of the ritilinic acid metabolite of MPH could be described by scaling for the adult and juvenile monkey and the adult human and child. The successful use of adult scaled parameters in PBPK models to predict pharmacokinetics during the developmental period is a useful method to evaluate age dependencies for both intra- and interspecies extrapolation.

PS 96h Assessing Biomonitoring of Bisphenol A in Infants and Pregnant Women Using a Lifestage Physiologically-Based Pharmacokinetic Model

D. Lefebvre, C. Lang, M. Fisher, T. E. Arbuckle and A. Nong. *Environmental Health Sciences and Research Bureau, Health Canada, Ottawa, ON, Canada.*

Growing concerns about exposure to various contaminants in the environment has led to major efforts at gathering a database of chemicals measured in blood and/or urine. These biomonitoring surveys provide a wealth of information on the levels of chemicals or metabolites detected in the general population and only give an

indication on the possible dose exposure leading to these observed internal levels. A study led by Health Canada scientists, the Plastics and Personal-care Product use in Pregnancy (P4) is a great example of where urine levels of chemicals are being measured in pregnant woman-infant pairs. The objective of this work is to explore biomonitoring and exposure data of Bisphenol-A (BPA) in pregnant women and levels found in their infants using biological models. At various life stages from infancy to adulthood, physiologically-based pharmacokinetic (PBPK) models can be used to describe age-dependant changing biological processes that can affect the fate of a chemical in the body. A lifestage PBPK model was developed to estimate the changing levels of BPA internally in women and infants. Datasets collected from human and animal studies were used to define these biological processes in the models. Parameters for human pregnancy kinetics, such as mother placental transfer to the foetus, cord blood distribution or neonatal metabolism of BPA, were extrapolated from published pregnancy studies in monkeys. Model simulations of adult women urine levels were compared against data from the P4 study to evaluate species differences of the biological processes. The PBPK model was also simulated and examined against meconium levels from the P4 study during foetal stages. Model simulations of urine levels were generally consistent, within a two-fold difference, with the pregnancy data. As a tool to support risk assessments of chemicals, the present PBPK lifestage model will help in the evaluation of exposure in pregnant women as measured in BPA biomonitoring which can affect body burdens in their infants.

PS 96i Investigation of Bias in Epidemiologic Associations Using a PK Model for DEHP

M. B. Phillips[1], K. Christensen[2], T. Blessinger[2], M. Lorber[2], J. Sobus[3] and Y. Tan[3]. *[1]NERL ORD, US EPA, Duluth, MN, [2]NCEA ORD, US EPA, Washington, DC and [3]NERL ORD, US EPA, RTP, NC.*

Previous studies have reported that body mass index (BMI) is associated with urinary concentrations of di-2-ethylhexyl phthalate (DEHP) metabolites. These studies assume that biomarker concentrations are good proxies for human DEHP exposure. However, some metrics of exposure may be biased because of confounders with BMI, leading to spurious associations.
A computational approach was used to investigate bias introduced into the estimation of associations between DEHP intake and BMI. First, a simulated population based on the 2009-2010 NHANES was assigned intake doses based on published distributions, but independent of other factors, so that all associations between intake doses and BMIs should be null. A pharmacokinetic model predicted urinary DEHP metabolites based on intakes for 2749 subjects (age 18+ with DEHP metabolite measurements). The molar excretions were summed and five exposure metrics were calculated for each individual: molarity (nM), molar amount (nmol), molar excretion rate (nmol/min), creatinine corrected concentration (nmol/g creatinine), and body weight corrected daily intake dose (nmol/kg/day). The first three exposure metrics showed no significant associations with BMI. In contrast, creatinine corrected concentration showed a significant negative correlation, and daily intake dose showed a significant positive correlation, indicating the introduction of bias away from the true null association. Our findings suggest that the choice of exposure metric can introduce significant bias of varying magnitude and direction into estimated associations.

PS 97 MiR-216a & miR-217 As Potential Biomarkers of Acute Exocrine Pancreatic Toxicity

J. Wang, R. L. Yafawi, W. Huang, W. Hu, S. Thibault, W. Scott, E. Kindt, H. Gukasyan, R. Ashoor, A. Vitsky and A. John-Baptiste. *DSRD, Pfizer Inc, San Diego, CA.*

The ability to monitor pancreatic injury both in drug development and in the clinic is often challenging because of the absence of reliable predictive markers. Both classical biomarkers, amylase and lipase, are neither sensitive nor specific for monitoring exocrine pancreatic injury. Novel biomarkers for drug-induced pancreatic injury are needed to improve safety assessment during drug development, i.e. stop programs earlier, improve patient selection and reduce late-stage attrition rates. Serum miR-216a & miR-217 have been reported as potential biomarkers of acute pancreatic injury. In this pilot study, we evaluated miR-216a & miR-217 as potential biomarkers for acute exocrine pancreatic injury in rat models induced by Caerulein or Cyanohydroxybutene (CHB) and monitored amylase and lipase as comparators. Caerulein is a synthetic cholecystokinin analog, while CHB is a natural toxin found in Brassica species, and both compounds cause excessive secretion of pancreatic enzymes.
Two pancreatic injury models were tested in male Wistar Han rats. (1) Caerulein: animals were dosed by IP injection on day 1 at 0, 15 or 50 μg/kg x3, one hour apart; (2) CHB: animals were dosed by SQ injection on day 1 at 0, 50 or 150 mg/kg. Serum samples were collected at 1, 6, 24, and 48 hr post last dose. Fasted animals were sacrificed 48 hr post treatment on Day 3.
Pancreatic injury was observed in rats treated with Caerulein at 15 or 50 μg/kg and CHB at 150 mg/kg. Both miR-216a and miR-217 correlated with acinar cell injury in each rat model however miR-217 was more sensitive with a larger magnitude of response. While lipase and microRNAs correlated well in the Caerulein treated animals, miRNAs remained elevated longer than lipase. In conclusion, our data show that in rats, miR-216a & miR-217 are sensitive indicators of acute exocrine pancreatic toxicity that are equal to, or better than, amylase and lipase. Further validation of these miRNAs as exocrine pancreatic injury biomarkers in rats and other nonclinical species with other pancreatic toxicants is needed.

PS 98 Circulating miRNAs As Potential Biomarkers of Pancreatitis

C. M. Karbowski[1], R. Hu[1], D. Andrews-Cleavenger[1], J. R. Turk[2], C. Afshari[1], H. Hamadeh[1] and P. Nioi[1]. *[1]Discovery Toxicology, Amgen, Thousand Oaks, CA and [2]Pathology, Amgen, Thousand Oaks, CA.*

MicroRNAs (miRNAs) are small, single stranded, non-coding RNAs that function as post-transcriptional regulators. Upon binding, target mRNA transcripts undergo degradation or translational repression. Dysregulation of miRNAs has been implicated in the pathogenesis of many disease states. Extracellular miRNAs have been detected in the blood and body fluids of animal models and patients. These, circulating miRNAs (cmiRNAs) have high potential utility in preclinical toxicology as biomarkers of organ toxicity because they are minimally-invasive, stable in biofluids, and likely translatable to humans due to their high cross-species conservation. We hypothesized that a rat model of pancreatic injury would have circulating miRNA biomarkers of injury. Sprague-Dawley rats were treated with intraperitoneal injection of 0.05 mg/kg caerulein once per hour for three consecutive hours to induce pancreatitis. Microscopic examination of pancreatic slices along with increased lipase and amylase levels confirmed pancreatic injury. 742 miRNA were assayed in plasma by quantitative PCR analysis. There were 17 miRNA which showed greater than a 3-fold difference between treated and control rats. 4 of these miRNAs were increased in rats treated with caerulein when compared with vehicle treated controls. In particular, miR-375-3p was increased 32-fold in treated rats. miR-375 is a relatively well studied miRNA reported to be expressed in pancreatic islets and brain. It is documented to play a role in pancreatic cell development and has been reported as a biomarker of beta cell death and diabetes in mice. The large increase in circulating miR-375-3p and clear link with pancreatic biology suggests that miR-375-3p is a potential candidate biomarker for pancreatic injury. Confirmation and characterization of sensitivity and specificity is underway with a larger study size and other treatment conditions.

PS 99 Characterization of Urinary microRNAs As Biomarkers of Acetaminophen Toxicity in Children

X. Yang[1], W. F. Salminen[2], Q. Shi[1], J. Greenhaw[1], P. S. Gill[3, 4], S. Bhattacharyya[3, 4], R. D. Beger[1], D. L. Mendrick[1] and L. P. James[3, 4]. *[1]FDA/NCTR, Jefferson, AR, [2]PAREXEL International, Sarasota, FL, [3]Department of Pediatrics, University of Arkansas for Medical Sciences, Little Rock, AR and [4]Arkansas Children's Hospital Research Institute, Little Rock, AR.*

Acetaminophen (APAP) is the most common drug used for the treatment of pain and fever in children. While generally considered to be safe, APAP is also responsible for 14% of acute liver failure cases in children. Recently, several studies have reported human circulating microRNAs (miRNAs) as novel biomarkers of APAP hepatotoxicity. Elevations of urinary miRNAs have been detected in rats administered toxic doses of APAP. This study examined urinary miRNA as a potential biomarker of APAP toxicity in children. Real-time quantitative polymerase chain reaction (qRT-PCR) arrays were used to detect global expression of miRNAs from three pediatric subgroups: i) healthy children (n=10, ALT median 18, range 10-37 IU/L), ii) hospitalized children receiving therapeutic doses of APAP (n=10, ALT median 26, range 6-177 IU/L) and iii) children hospitalized for APAP overdose (n=9, ALT median 2314, range 25-9909 IU/L). Urinary miR-375 was significantly increased in children with APAP overdose, compared to control subjects and therapeutic exposure subjects ($p<0.05$). The elevation of urinary miR-375 was further confirmed by qRT-PCR single reaction. Urine levels of miR-375 correlated with serum APAP protein adducts, an indicator of the oxidative metabolism of APAP ($r=0.61$). In conclusion, this study suggests that urinary miR-375 could represent a non-invasive clinical biomarker of APAP toxicity in children.
This study was funded in part by a grant (R01 DK75936 to LPJ) from the National Institutes of Diabetes, Digestive and Kidney Diseases.

PS 100 MicroRNA Profiling for Discovery of Early Biomarker(s) of Doxorubicin-Induced Cardiac Tissue Injury in B6C3F1 Mice

V. Desai[1], J. C. Kwekel[1], V. Vijay[1], C. Moland[1], T. Han[1], T. Lee[2], E. Herman[3], S. Lewis[4] and J. C. Fuscoe[1]. [1]*Division of Systems Biology, NCTR/FDA, Jefferson, AR,* [2]*Department of Mathematics, Korea University, Sejong, Republic of Korea,* [3]*Division of Drug Safety Research, CDER/FDA, Silver Spring, MD and* [4]*Office of Scientific Coordination, NCTR/FDA, Jefferson, AR.*

MicroRNAs (miRNAs) are increasingly emerging as promising biomarkers of cardiovascular pathologies and therapeutic response. While cardiac troponins are used as clinical biomarkers of cardiac tissue injury, there is a lack of biomarkers of early events of cardiac cell damage. Using a newly developed chronic cardiotoxicity mouse model, expression profiling of 1179 unique miRNAs was performed to identify early predictive biomarkers of cardiac tissue damage. Male B6C3F1 mice were given a weekly dose of 3 mg/kg doxorubicin (DOX; an anti-cancer drug), or an equivalent volume of saline via tail vein for 2, 3, 4, 6, and 8 weeks, resulting in cumulative DOX doses of 6, 9, 12, 18, and 24 mg/kg, respectively. Mice were euthanized a week after the last dose. Plasma levels of cardiac troponin T indicated cardiac cell injury following exposures to 18 mg/kg DOX and higher, whereas microscopic examination of heart tissues revealed the presence of cardiac lesions at 24 mg/kg. Thirty-three heart miRNAs showed significant (FDR<0.1) perturbation in expression, with the expression of 1, 1, 2, 8, and 24 miRNAs being affected at cumulative doses of 6, 9, 12, 18, and 24 mg/kg DOX, respectively. miRNA-34a was the only miRNA that showed increased expression at all DOX doses and exhibited a significant dose response. Considering the pro-apoptotic effects of miR-34a during myocardial infarction and cardiac aging, up-regulation of miR-34a at 6 mg/kg cumulative DOX dose may indicate apoptosis as an early event in hearts of DOX-treated mice. Increased transcription of apoptotic genes in the heart further support this notion. These data suggest the utility of miRNAs as predictive biomarkers of early stages of cardiac cell injury that may serve as a potential tool in therapeutic risk assessment.

PS 101 The Rat miRNA Body Atlas: Species Translatable Biomarkers

A. T. Smith[1], J. Calley[1], S. X. Mathur[1], H. Qian[1], M. Farmen[1], S. K. Engle[1], F. Caiment[2], P. R. Bushel[3], J. Li[3], C. D. Fisher[4], P. Kirby[4], E. Koenig[5] and D. E. Watson[1]. [1]*Investigative Toxicology, Eli Lilly and Company, Indianapolis, IN,* [2]*Department of Toxicogenomics, Maastricht University, Universiteitsingel, Netherlands,* [3]*Biostatistics Branch, National Institute of Environmental Health Sciences, Durham County, NC,* [4]*Drug Safety Evaluation, Takeda Pharmaceuticals, Cambridge, MA and* [5]*Molecular Pathology, Takeda Pharmaceuticals, Cambridge, MA.*

MicroRNAs (miRs) are expressed in an organ specific manner and are easily detectable in serum or plasma. In contrast to protein biomarkers, many miR sequences are conserved across species and assays are readily available for quantitation. This has elicited interest in miRs as sensitive, specific and species translatable biomarkers for organ toxicity. In fact, liver (miR-122), skeletal muscle (miR-133a) and brain (miR-124) have been shown to be increased in the serum of rats with the respective organ toxicity. Interpretation of serum miR changes with respect to organ toxicity necessitates an understanding of the tissue(s) of origin of each miR and its isomiR(s). In order to confirm existing miRs and discover novel miRs we have utilized Illumina deep sequencing to construct a rat miR body atlas which consists of ~20 tissues of toxicologic interest. The data has confirmed many of the known tissue enriched miRs and revealed novel tissue enriched miRs such as liver miR-802-5p, brain 125a-5p, pancreas 148a-3p, adrenal 351-5p and stomach 205-5p. Serum miR profiling in rat and dog with histopathologic evidence of caerulein induced pancreatic injury revealed that miRs-375 and 216a increased in the serum, suggesting they may be translatable biomarkers of pancreatic injury. Takeda Pharmaceuticals created a dog miR body atlas utilizing deep sequencing and, in conjunction with HESI (Health and Environmental Sciences Institute), we have compared the rat and dog atlases for conserved tissue enriched miRs. We believe the combined data sets will be a valuable miR biomarker resource for application in pre-clinical toxicology studies.

PS 102 Building the Beagle Dog microRNA Atlas: Potential Translatable Biomarkers of Organ Toxicity

C. D. Fisher[1], E. Koenig[2], J. Senn[1], M. Gallacher[1], S. Tirrell[2], M. Carsillo[1], V. J. Kadambi[1], A. T. Smith[3], D. E. Watson[3] and P. Kirby[1]. [1]*Drug Safety Evaluation, Takeda Pharmaceuticals International Co., Cambridge, MA,* [2]*Molecular Pathology, Takeda Pharmaceuticals International Co., Cambridge, MA and* [3]*Investigative Toxicology and Translational Sciences, Lilly Research Laboratories, Indianapolis, IN.*

MicroRNAs (miRs) are stable RNA which are detectable in tissues and biofluids and thus have potential as biomarkers of tissue injury. An ideal miR biomarker would be tissue specific with sequence homology across different species. Identification of such candidates requires generation of a miR tissue atlas and subsequent expression profile comparison across tissues. Here we report results from a beagle dog miR tissue atlas and the identification of tissue specific/enriched miRs with sequence homology across relevant nonclinical species and human. Tissues from 5 male Marshall Beagle dogs were acquired from Bioreclamation, LLC (Hicksville, NY). RNA from 20 individual tissues was analyzed by microRNA-SEQ using the Illumina platform. miR sequences were aligned to the canine genome. MiR counts were quantified, normalized, and analyzed for statistical significance (*p*value < 0.005). Specific miRs indentified in pancreas (miR-216a, miR-216b, miR-802, miR-200), testes (mir-34a) and sciatic nerve (mir-432) have potential as new biomarkers for tissues which currently have limited or no validated biomarkers of injury. In a dog proof of concept study, plasma levels of two liver injury candidate miRs, miR-122 and miR-885, were demonstrated to be elevated following 7-days treatment with Compound X, and correlated with ALT and liver pathology. In collaboration with Eli Lilly and Co., via HESI Genomics Group, we are in the process of comparing rat and dog tissue atlases to pinpoint miRs with sequence homology and tissue specificity in both species. Preliminary results of the atlas comparison suggest good correlation between tissue specific miRs (miR-122, liver) and non-specific miRs (miR-192). Results of this comparison suggest that certain miRs have the potential to be translatable biomarkers of target organ injury.

PS 103 Potential Utility of microRNAs As Circulating Biomarkers in Asthma

H. Lin[1], C. Carmichael[1], M. Kasaian[2], A. Brennan[2], K. Hammerman[1] and S. K. Ramaiah[1]. [1]*DSRD, Pfizer Inc., Cambridge, MA and* [2]*ImmunoScience, Pfizer Inc., Cambridge, MA.*

MicroRNAs (miRNAs) are single-stranded, non-coding RNAs that mediate post-translational inhibition or promote degradation of mRNA targets. miRNA profiles have been shown to be detectable in cell-free body fluids including serum and plasma samples. Moreover, circulating miRNAs have been proposed as attractive blood biomarkers of human diseases and toxicities because of their disease/toxicity-specific dysregulation and their relative stability compared with mRNAs. Asthma is a chronic disorder of the airways characterized by complex interaction of airflow obstruction, bronchial hyperresponsivity, inflammation, and tissue remodeling. An essential role for Th2-mediated immune response has been demonstrated in animal models of allergic asthma. We hypothesized that miRNAs may be involved in the homeostatic regulation of asthmatic inflammatory responses, and their disease-associated dysregulation could be detected in circulating miRNA signatures. Specific miRNAs with important roles in regulating key pathogenic mechanisms in asthmatic inflammation were selected to assemble a Taqman assay panel for screening of plasma from asthmatic patients (FEV_1, 51~69%) and healthy volunteers. We found that the profile of circulating miRNAs is capable of distinguishing healthy volunteers from severe asthmatic patients. In particular, circulating 34/449 family, let-7 family, and smooth muscle-specific miR-133 levels were upregulated in the asthmatic subjects. Interestingly, 34/449 family has been previously demonstrated to be transcriptionally regulated by IL-13[a], a Th-2 centric cytokine, as well as a direct target of let-7 family members[b]. And miR-133 has been found to be regulated in airway smooth muscle cells after IL-13 stimulation[c]. The results described here have implications for the use of circulating miRNA profiles as non-invasive biomarkers for asthma.

Refs:
a.Ostrin EJ et al. Am J Respir Crit Care Med. 2013;187:A3443, ATS International Conference
b.Kumar M et al. J Allergy Clin Immunol. 2011;128:1077
c.Chiba Y et al. Am J Respir Crit Care Med. 2009;180:713

PS 104 Characterization of microRNA Expression Profiles in a Rat Model of IL-2-Mediated Vascular Injury

C. Bertinetti-Lapatki[1], N. Keirstead[2], S. Fischer[1], D. M. Knapp[2], M. Albassam[2], A. B. Roth[1], F. Schuler[1], T. Singer[1] and I. Mikaelian[2]. [1]*Non-Clinical Safety, Hoffmann-La Roche, Inc., Basel, Switzerland and* [2]*Non-Clinical Safety, Hoffmann-La Roche, Inc., Nutley, NJ.*

The use of IL2 is limited in the clinic because of its unmonitorable vascular toxicity. Here, we assessed tissue and circulating microRNAs as candidate biomarkers of vascular injury in male Wistar-Han rats administered IL2 for up to 5 days. Vascular changes consisted of endothelial hypertrophy/hyperplasia and/or medial vascular hyalinization and perivascular inflammation, most notably in the liver, kidneys, pampinform plexus and areas of injection, with perivascular mixed cell infiltrates. These changes were accompanied with increased expression of CD31 as assessed by immunohistochemistry, decreased expression of miR-126 as assessed by in situ hybridization, and increases in circulating miR-145 and miR-155. These changes and the histomorphologic findings were partially reversible after a 7 day recovery period. These observations identify increases in circulating miR-145, a marker of smooth muscle cells, prior to the onset of necrosis of the vascular wall, and support the further evaluation of miR-145 as a marker of acute vascular injury.

PS 105 Urinary Expression of microRNA-21 in Response to Toxic Kidney Injury

O. Nicoara[1], D. Antoine[3], J. Koyner[4] and V. S. Vaidya[2]. [1]*Nephrology, Boston Children's Hospital, Boston, MA,* [2]*Nephrology, Brigham and Women's Hospital, Boston, MA,* [3]*Molecular and Clinical Pharmacology, University of Liverpool, Liverpool, United Kingdom and* [4]*Nephrology, University of Chicago, Chicago, IL.*

Background: The kidney is an important site of organ damage caused by drug toxicity due to its high filtration capacity. Nephrotoxicity is one of the major dose-limiting side effects of most drugs that are eliminated by the kidney. The most efficient way to prevent drug-induced nephrotoxicity (DIN), is to have sensitive and specific biomarkers. MicroRNAs (miRNAs) are a family of non-coding RNAs that stably exist in various body fluids and have emerged as potential biomarkers. The aims of our current study was to investigate if urinary miR-21 could differentiate patients with acetaminophen (APAP)-overdose kidney injury from those without acute kidney injury (AKI), and between ICU patients who required Renal Replacement Therapy (RRT) from those that developed AKI but did not require RRT.
Methods: Urine samples were obtained from APAP-overdose patients and from ICU patients with AKI. The experiment was done using a 384-well custom plate from Qiagen that had specific probes for miR-21 and miR-489 (previously identified as an invariant miRNA). A real time PCR analysis was performed using ABI-7900HT instrument.
Results: MiR-21 were able to successfully distinguish the APAP overdose patients (n=70) from healthy controls (n=65). It was also found that miR-21 levels was significantly different between patients with APAP-induced kidney injury (n=43) and patients with APAP-overdose but no kidney injury (n=27): miR-21 (p=0.01). Urinary levels of miR-21 are significantly higher in patients admitted to the ICU who develop AKI which progresses to RRT or death (n=10) as compared to those who do develop AKI but do not require RRT (n=15) as well as those who do not develop AKI (n=9).
Conclusions: We report urinary miR-21 as potential novel translational urinary biomarker of drug-induced nephrotoxicity (DIN).

PS 106 Doxorubicin-Induced Glomerular Injury Is Associated with Urinary microRNA Alterations in the Rat

R. J. Church[1], J. E. McDuffie[2], M. Sonee[3], M. Otieno[3], P. B. Watkins[1] and A. H. Harrill[4]. [1]*Institute for Drug Safety Sciences, The Hamner Institutes for Health Sciences, Research Triangle Park, NC,* [2]*Drug Safety Sciences, Janssen Research and Development LLC, San Diego, CA,* [3]*Drug Safety Sciences, Janssen Research and Development LLC, Springhouse, PA and* [4]*The University of Arkansas Medical Sciences, Little Rock, AR.*

There is a critical need to identify sensitive and specific biomarkers of renal injury in order to detect toxicity potential during drug development. Advances in biomarker qualification have yielded biomarkers specific to discrete areas of the nephron; however, there are no biomarkers specific to the glomerulus. MicroRNAs (miRNAs) show considerable promise as biomarkers because they are relatively stable compared to proteins and because they are largely conserved across species. In this study, release of miRNAs by doxorubicin (DOX)-induced glomerular injury into the urine was quantified over a two week time course in rats. Male Sprague-Dawley rats (n=6/treatment/time point) were dosed once, weekly, with DOX (5 mg/kg, i.v.) or Vehicle (saline) and necropsy occurred on study day (D) 7 and D14. While no histological renal injury was evident on D7, significant urinary albumin elevations measured for DOX treated animals, compared to vehicle-treated controls, suggested ongoing glomerular injury at this time point. By D14, following a second drug injection given on D7, rats developed overt glomerular and tubular injury accompanied by further urinary elevation of albumin, along with urinary elevations in tubular injury markers lipocalin-2, kidney injury molecule-1, cystatin c, and β-2 microglobulin, compared to vehicle-treated controls. Microarray profiling identified eight miRNA species significantly elevated in urine during time points at which albumin was significantly elevated and six of these species make attractive biomarker candidates based on proposed function. Additionally, three of these miRNAs show suggestive elevations in urine prior to observable changes in albumin concentrations, which may indicate that these miRNA biomarkers may be sensitive for the detection of glomerular injury.

PS 107 IL-22 mRNA Expression in Blood Samples Is a Useful Biomarker for Assessing the Adverse Health Effects of PCBs in Allergic Children

M. Tsuji[1, 2], T. Kawamoto[2], C. F. Vogel[1] and F. Matsumura[1]. [1]*Environmental Toxicology, UC Davis, Davis, CA and* [2]*Environmental Health, University of Occupational and Environmental Health, Kitakyusyu, Japan.*

While it is widely accepted that persistent environmental pollutants such as PCBs pose a health hazard to people, particularly on vulnerable populations such as young children and the elderly, it has been very difficult to obtain any epidemiological proof of direct associations between exposure to low levels of air pollution and definite adverse health effects. To facilitate the assessment of adverse effects of very low concentrations of air pollutants on general populations, we planned to establish a reliable biomarker that is also useful in identifying vulnerable populations. For this purpose we monitored several inflammation markers in blood samples from 2 year old Japanese children (N = 30), and found that those children living close to major highways (<50m) show higher levels of IL-22 mRNA expression in their blood samples than those living further away (+50m). This tendency was more pronounced among subjects showing positive IgE against egg and milk. We further examined associations between IL-22 mRNA expression and PCB residues and found a number of significant positive correlations between each individual PCB congener and IL-22 expression. To identify the most vulnerable population among those children we selected asthma as a typical allergy-related disease, and found that there are significant differences in the levels of IL-22 mRNA expression between IgE negative non-asthmatic subject and asthmatic children showing positive IgE reaction toward egg or milk. These observations support our main conclusion that IL-22 expression is a sensitive biomarker which is useful in identifying sub-populations of children who are especially vulnerable to pollution.

PS 108 Urinary Mitochondrial DNA As a Novel Biomarker of Mitochondrial Dysfunction in Human Acute Kidney Injury

L. J. Stallons[1], J. Arthur[2, 3], C. Beeson[1] and R. Schnellmann[1, 3]. [1]*Dept of Drug Discovery and Biomedical Sciences, Medical University of South Carolina, Charleston, SC,* [2]*Dept of Medicine, Division of Nephrology, Medical University of South Carolina, Charleston, SC and* [3]*Ralph H. Johnson Veterans Administration Medical Center, Charleston, SC.*

Acute kidney injury (AKI) is defined by the abrupt reduction in kidney function and can be caused by numerous insults including surgery, drugs, toxicants, trauma, and ischemia/reperfusion (I/R). Animal models of AKI have demonstrated an important role for mitochondrial dysfunction as a pathological mediator of AKI. While there are numerous biomarkers of renal injury, there are no biomarkers of mitochondrial injury. The purpose of this study was to determine if urinary mitochondrial DNA (mtDNA) is a biomarker of renal mitochondrial dysfunction in human AKI. mtDNA was quantified in the urine of human patients with AKI after cardiac surgery, patients with no AKI after cardiac surgery, and control humans with normal renal function (N=170 total). Urine was concentrated using centrifugal filters, total DNA was isolated, and qPCR was performed for the mitochondrial gene ND1. The nuclear gene β-actin was used as a control. Urinary ND1 increased 10-fold in AKI patients versus healthy controls and 3-fold versus post-operative patients without AKI. Urinary β-actin did not change in any group. When normalized to β-actin, ND1 increased 10-fold in AKI patients versus surgery patients without AKI ($p<0.05$). In a mouse model of I/R-induced AKI with established mitochondrial dysfunction, urinary ND1 increased 8-fold 24 h post-reperfusion, coincident with maximal kidney injury. These results show that urinary nuclear DNA did not increase in human AKI while mtDNA is selectively released from the kidney during AKI and may be a novel, noninvasive biomarker of mitochondrial dysfunction in AKI.

PS 109 Isoproterenol-Induced Cardiotoxicity and Increases in Serum microRNAs in Rats

J. Calvano, L. T. Rosini-Marthaler, M. Tirmenstein, R. Mangipudy and W. E. Achanzar. *Drug Safety Evaluation, Bristol-Myers Squibb Company, New Brunswick, NJ.*

Cardiac troponin I (cTnI) is an established biomarker of cardiotoxicity, but its utility is limited by its short half-life. The present study was conducted to identify potential circulating cardiotoxicity miRNA biomarkers as an alternative to cTnI using a rat isoproterenol myocardial-injury model. In an initial screen, 9 heart or heart/skeletal muscle specific mRNA's were identified out of 768 miRNA's across a panel of tissues from untreated male Sprague-Dawley rats. The same panel of miRNA's was assessed in the serum following cardiac injury. In a subsequent experiment, male Sprague-Dawley rats received a single subcutaneous injection of isoproterenol (0.05 mg/kg) or vehicle. All surviving rats were sacrificed 24 hours post-injection, and cardiotoxicity was confirmed by histopathology. Serum was collected just prior to sacrifice from treated and control rats for analysis of circulating miRNAs. Plasma samples were collected predose and 24 hrs post dose for cTnI measurements. Consistent with its short half-life, plasma cTnI levels at 24 hrs post dose were comparable to baseline despite histologic evidence of cardiac injury. Several miRNA's were only present in the serum from isoproterenol-treated rats relative to controls. However, of the 9 heart- or heart/skeletal muscle-specific miRNAs identified in the tissue screen, only miR-208, a potential biomarker of cardiac toxicity was detected in the serum following isoproterenol treatment 24 hrs post dose. To our knowledge, this represents the first report of tissue expression profiling to identify heart-specific miRNAs. Ongoing work is examining the serum half-life of miR-208 after cardiac injury following isoproterenol treatment.

PS 110 Potential Biomarkers Detected by Metabolomics Analysis for Isoproterenol-Induced Cardiotoxicity in Rats

K. Hashimoto[1], N. Maeda[2], K. Watanabe[1], K. Ito[1], K. Takasuna[1], T. Yamoto[1] and W. Takasaki[1]. [1]*Medicinal Safety Research Laboratories, Daiichi Sankyo Co., Ltd., Tokyo, Japan and* [2]*Translational Medicine & Clinical Pharmacology Department, Daiichi Sankyo Co., Ltd., Tokyo, Japan.*

Cardiotoxicity is one of the critical toxicities and it is important to appropriately detect cardiotoxicity. However, there are few helpful biomarkers for cardiotoxicity. This study was conducted to obtain possible biomarkers for estimating cardiotoxicity. Isoproterenol (ISO, 5 mg/kg), an adrenergic β agonist which can induce cardiotoxicity, was intraperitoneally administered to male F344 rats at 7 weeks old (3 or 4 animals/group). The heart for the histopathological analysis and the plasma for the metabolomics analysis were obtained from the rats 2, 6, 24 and 48 hours after the administration. Metabolites were measured using an UPLC/TOF-MS, and a principal component analysis (PCA) was used for screening of potential biomarkers. In the histopathological analysis, focal vacuolar degeneration and coagulation necrosis at 2 hours, sporadic coagulation necrosis at 6 hours, inflammatory cell infiltration in coagulation necrosis at 24 hours, and fibrotic changes along with the infiltration at 48 hours were observed in the ISO-treated groups. The most severe changes in histopathology were observed at 24 hours during the progress of the heart damage. In the metabolomics analysis, PCA indicated the clear differentiation of the control and ISO-treated groups at 2 and 6 hours, and 9 metabolites including arachidonic acid contributed to the differentiation. These metabolites in the ISO-treated groups were increased more than those in the corresponding control groups at 2 and 6 hours, and the metabolites in the ISO-treated groups were equivalent to the corresponding control groups at 24 and 48 hours. These results showed that the identified metabolites were increased along with the histopathological changes in the heart and these metabolites achieved the peak levels earlier than the histopathological changes. Additionally the identified metabolites can be the possible biomarkers for ISO-induced cardiotoxicity.

PS 111 ATP Synthase Subunit Beta Is a Novel Urinary Biomarker of Renal Mitochondrial Dysfunction

M. Korrapati[1], R. M. Whitaker[1], L. J. Stallons[1], J. Arthur[2] and R. Schnellmann[1, 2]. [1]*Drug Discovery and Biomedical Sciences, Medical University of South Carolina, Charleston, SC and* [2]*Ralph H. Johnson Veterans Administration Medical Center, Charleston, SC.*

Diverse acute insults from surgery, ischemia/reperfusion (I/R), trauma, drug and environmental chemical toxicity lead to mitochondrial dysfunction, and renal cell injury/death. Consequently, there is a great need for non-invasive biomarkers of renal mitochondrial dysfunction. We hypothesized that urinary mitochondrial ATP synthase subunit beta (ATPSβ) protein is a sensitive and specific marker of mitochondrial dysfunction in acute kidney injury (AKI). We used two nonlethal rodent AKI models to test our hypothesis. Myoglobinuric AKI was induced by glycerol injection into rats, and mice were subjected to I/R AKI. Animals in both models had elevated serum creatinine, indicative of renal dysfunction, 24 h after injury which partially recovered over 144 h post-injury. LC-MS/MS studies of 24 h urine samples revealed increased urinary ATPSβ protein in mice subjected to I/R-induced AKI and rats subjected to glycerol-induced AKI when mitochondrial function was decreased. Consistent with LC/MS-MS data, Western blotting of 24 h urine samples revealed increased ATPSβ protein in mice subjected to a range of I/R times and degrees of kidney injury. Also, preliminary LC-MS/MS findings revealed that urinary ATPSβ in human subjects with post-cardiac bypass surgery-induced AKI increased when compared to controls. These studies provide evidence that ATPSβ is a urinary marker of mitochondrial dysfunction and will permit better understanding of the timing and mechanisms of renal injury and the state of mitochondrial homeostasis during AKI.

PS 112 Clinical Performance of Translatable Biomarkers for Drug-Induced Vascular Injury

K. Bendjama[2] and M. Lawton[1]. [1]*Pfizer, Groton, CT and* [2]*Firalis, Huningue, France.*

Drug-induced vascular Injury (DIVI) is a preclinical toxicity usually characterized by hemorrhage, vascular endothelial and smooth muscle damage and inflammation. Preclinical DIVI findings cause delays or termination of drug candidates due to low safety margins, the absence of non-invasive biomarkers for monitoring vascular injury and the uncertain relevance to humans. Under the framework of the EU-funded IMI SAFE-T consortium, we are qualifying a set of translatable biomarkers associated with the onset of histopathologic damage in various vascular beds in humans. Patients with conditions involving inflammatory infiltrates, activation and injury to the vascular endothelium and fibrinoid necrosis of the media were included, along with age- and sex-matched healthy volunteers. Twenty soluble proteins were measured in serum samples collected in healthy subjects and in patients during the acute and the resolution phases of disease. The panel of markers included inflammatory factors as well as endothelial proteins: CRP, E-Selectin, GROa, IL-6, IL-8, IP-10, I-TAC, NGAL, MCP-1, MIG, MIP-1, P-Selectin, SAA, sICAM-1, sICAM-3, sVCAM-1, thrombomodulin, TIMP-1, TNFRSF1A and VEGF. Univariate analysis showed that no single marker measurement provided a sufficient predictive power with an area under ROC curve (AUROC) above 0.8. In contrast, multivariate analysis allowed a robust separation of healthy volunteers from patients with vascular injury, and further separated the latter group into those in the acute and quiescent stages of disease. Of the several machine learning approaches used to calculate the performance of combinations of markers, a naive Bayes classifier based on 10 parameters (MIP-1, SAA, TNFRSF1A, TIMP-1, P-Selectin, sVCAM-1, sICAM-1, thrombomodulin, age and sex) achieved the best diagnostic performance (AUROC = 0.88). Studies to further validate these biomarkers are currently on-going. The panel of biomarkers established in this study shows promise as a clinical monitoring tool for compounds that cause DIVI in preclinical studies.

PS 113 Evaluation of Urinary L-FABP As a Nephrotoxicity Biomarker in Rats

T. Kadota[1], Y. Suzuki[1], H. Komatsu[1], K. Taguchi[2] and T. Sugaya[2]. [1]*CMIC Bioresearch Center Co., Ltd., Yamanashi, Japan and* [2]*CMIC Holdings Co., Ltd., Tokyo, Japan.*

L-type Fatty Acid Binding Protein(L-FABP), which is located in the cytoplasm of renal proximal tubular cells, responses to ischemia and oxidative stress and is excreted in urine. KDIGO (Kidney Disease Improving Global Outcomes) selected L-FABP as one of the major 5 biomarkers (L-FABP, cystatin C, NGAL, Interleukins, Kim-1) for detecting the acute kidney injury. The L-FABP ELISA kit has already been approved as a clinical diagnostic agent for renal injury in Japan and EU. However, the usefulness of L-FABP has not been established in experimental animals widely used in non-clinical toxicity studies.

The purpose of this research was to evaluate L-FABP as a nephrotoxicity biomarker in gentamicin-induced (GM) renal injury model in Sprague-Dawley and Wistar male rats. Gentamicin was injected subcutaneously at 200 mg/kg/day for 4 days. Urinary L-FABP by ELISA and urinary enzymes such as LDH, γ-GTP and NAG were determined in urine collected periodically. In addition, conventional serum and urinary clinical parameters were measured.

Urinary L-FABP elevated remarkably within 6 hours on Day 1 in both strains of rats. The peak levels of urinary L-FABP in Sprague-Dawley and Wistar rats were more than 200-fold and 75-fold of pre values, respectively. The sensitivity of the L-FABP was superior to traditional biomarkers such as BUN and serum creatinine and urinary enzymes. Urinary γ-GTP and NAG were significantly increased from Day 2, urinary LDH was not changed. There was no apparent difference between

both strains in urinary L-FABP excretion. Histological observation revealed that foamy eosinophilic globules slightly existed in proximal tubule on Day 4 and those urinary L-FABP excretion elevated on Day 1 in correspondent rats.
These results suggest that the urinary L-FABP may be a very useful sensitive biomarker of nephrotoxicity not only in humans but also in experiment animals.

PS 114 Preclinical Nephrotoxicity Biomarker Analysis Using Toxicoproteomics Approaches

L. Yu[1], Z. Li[2], Z. Cao[1], Y. Gao[1] and T. Chen[2]. [1]*Biomarkers and Alternative Models Branch, Division of Systems Biology, National Center for Toxicological Research, FDA, Jefferson, AR and* [2]*Division of Genetic and Molecular Toxicology, National Center for Toxicological Research, FDA, Jefferson, AR.*

Increased application of proteomics approaches to toxicological studies has led to the development of a new discipline that is being called "toxicoproteomics". Major research areas of toxicoproteomics include development of biomarkers of toxicity, identification of molecular targets of toxicants, and elucidation of toxicity mechanisms. To understand the molecular mechanisms of nephrotoxicity and identify kidney injury biomarkers, quantitative proteomic analyses were conducted on kidneys from aristolochic acid (AA)-treated rats. Animal treatment was conducted according to the protocol approved by the NCTR Institutional Animal Care and Use Committee. Big Blue rats were treated with 0.9% sodium chloride as the control or AA at 10 mg/kg body weight, five times/week, for 12 weeks. Kidneys were collected one day after the last treatment. Kidney tissues from the control and the AA-treated rats were processed for proteomic analysis using stable isotope labeling and two-dimensional liquid chromatography coupled online with tandem mass spectrometry (LC-MS/MS). More than 100 proteins changed their abundance as a result of AA treatment, which may be related to the toxicity and carcinogenicity of AA. Intriguingly, several FDA-qualified preclinical kidney injury biomarkers were identified in this study, and their abundance showed significant changes. A mass spectrometry-based multiplex kidney injury biomarker assay was developed for targeted quantitative measurement of the biomarker candidates discovered in this study, and many of the expression-changed proteins were confirmed. The combined open discovery and targeted proteomics approaches facilitated the identification of kidney injury biomarkers. Additional studies need to be performed in animals and humans to investigate their translational nature.
The views presented do not necessarily reflect those of the U. S. Food and Drug Administration.

PS 115 Detailing the Human Exposome: Mass Spectrometry-Based Chemical Profiling of Human Mitochondria

D. I. Walker[1, 2], K. D. Pennell[1] and D. P. Jones[2]. [1]*Civil and Environmental Eng, Tufts University, Medford, MA and* [2]*Clinical Biomarkers Laboratory, Emory School of Medicine, Atlanta, GA.*

While most studies have utilized easily accessible bio-fluids to monitor environmental agents and associated metabolic response, few have measured exogenous compounds within sub-cellular compartments. The purpose of this study was to profile the endogenous and exogenous mitochondrial metabolome of human organ tissue, with an emphasis on identifying the presence of environmental agents. Viable mitochondria were obtained from human adrenal glands (n=5) within 36 hours of removal using a differential centrifugation isolation procedure. Isolates were normalized on a per protein basis (250 ug), and analyzed in tandem with blood plasma using liquid chromatography followed by dual polarity electrospray ionization and high resolution mass spectrometric detection. Mitochondria specific metabolites and environmental agents were tentatively identified by matching (mass error ≤ 10 ppm) the mass-to-charge (m/z) ratio to the Kyoto Encyclopedia of Genes and Genome (KEGG) and EPA ToxCast database. Following data extraction and threshold filtering, 5773 unique features were obtained. Pathway mapping indicated that the adrenal mitochondria metabolome was well covered, with metabolites corresponding to mitochondrial specific pathways such as cysteine and methionine metabolism (n=27), drug metabolism by cytochrome P450 (n=60), and steroid hormone biosynthesis (n=54). Ions corresponding to exogenous chemicals were also present, which matched m/z's corresponding to fungicides, carbamate insecticides and herbicides. Compounds with known endocrine disrupting tendencies where similarly matched (n=6), including di-n-propylpthalate, di-n-hexylphthalate and styrene. Future work will include confirmation of chemical identities and absolute quantification. These results indicate that high-resolution chemical profiling of cellular organelles can be utilized to both identify exogenous agents within mitochondria and their associated metabolic response, providing relevant, in vivo toxicological information.

PS 116 Proteomic Analysis of Dried Blood Spots for Biomonitoring Organophosphorus Exposures

J. Marsillach Lopez[1, 2], E. J. Hsieh[2], R. J. Richter[1, 2], M. J. MacCoss[2], A. N. Hoofnagle[3] and C. E. Furlong[1, 2]. [1]*Medicine (Division of Medical Genetics), University of Washington, Seattle, WA,* [2]*Genome Sciences, University of Washington, Seattle, WA and* [3]*Laboratory Medicine, University of Washington, Seattle, WA.*

Organophosphorus (OP) compounds are involved in most of the occupational and environmental intoxications reported worldwide. They inhibit cholinesterases and other serine hydrolases, leading to neurological damage and serious health effects. The standard methods used for biomonitoring OP exposures are the Ellman assays, which measure the enzymatic activity of either red blood cell (RBC) acetylcholinesterase or plasma butyrylcholinesterase (BChE). Despite being fast and inexpensive, these assays suffer from several drawbacks.
We have developed a rapid immunomagnetic bead (IMB) purification for biomarkers of OP exposure, followed by OP-adduct identification on active site serines by high-resolution mass spectrometry (MS). The IMB-MS methods have been adapted to identify OP insecticide adducts on both plasma BChE and RBC acylpeptide hydrolase (APH), two known biomarkers of OP exposure. Plasma, RBCs or dried blood spots (DBS) are used for our IMB-MS methods. The methods have been designed for adaptation to high-throughput protocols to facilitate their transfer to clinical laboratories.
These methods will be validated using a cohort of Washington State agricultural workers with characterized OP exposures to chlorpyrifos or azinphos-methyl. The IMB protocols purify BChE and APH from as low as 25 μL of plasma or RBCs, respectively, or from DBS.
The use of DBS will facilitate sample collection, shipping, and archiving as well as the analysis of already archived samples. The IMB-MS protocols have significant advantages: they do not require a pre-exposure measurement, they can detect low levels of exposure, they can be automated, and they provide information on both the OP and percentage modification of the active site serines.
Supported by NIH (P42ES04696, R01ES009883, ES09601/EPA-R826886, P41GM103533); the PNASH Center (U50OH07544-10); and by financial support from the CDC (Atlanta, GA).

PS 117 Toxicometabolomics Approach to Prediction of Hepatotoxicity by Troglitazone/LPS in Rats

K. Kim[1], J. Kim[2, 1], S. Ryu[1], D. Nam[1], S. Kim[3] and S. Kim[3]. [1]*Pharmacy, Dankook University, Cheonan, Chungnam, Republic of Korea,* [2]*Pharmacology, CKD Research Institute, Yongin, Gyeonggi, Republic of Korea and* [3]*Chemistry and Chemistry Institute for Functional Materials, Pusan National University, Busan, Busan, Republic of Korea.*

Troglitazone (TGZ) is a thiazolidinedione antidabetic agent which is the synthetic ligands for the peroxisome proliferator-activated receptor γ (PPAR γ). However, it was withdrawn from the market in 2000 due to liver injury in humans. In this study, we endeavored to discover surrogate biomarkers which are correlated with hepatotoxicity induced by TGZ using urinary proton nuclear magnetic resonance (1H NMR) spectral data. A procedure of 1H NMR urinary and serum analysis using pattern recognition was proposed for early screening of the hepatotoxicity of TGZ with lipopolysaccharide (LPS) in rats. Alanine aminotransferase (ALT) and aspartate aminotransferase (AST) were the highest in 6 hours and hepatic inflammation, in histopathology, was observed in 2 hours. All treated animals were divided into two groups of responder and non-responder based on the ALT and AST levels because the levels of ALT and AST were not changed dose-dependently after treatment of TGZ (2 g/kg, p.o). In urinary analysis, 1H NMR spectroscopy did not show different clustering between responder and non-responder in global metabolic profiling through principal component analysis (PCA). However, it was significantly separated in orthogonal projections to latent structures-squares discriminant analysis (OPLS-DA). In targeted profiling, endogenous metabolites of phenylacetylglycine, glucose, acetate, 2-oxoglutarate, formate, creatine, citrate, 3-indoxysulfate, hippurate, acetone, phenylalanine, glycine, betaine, cis-aconitate, and tyrosine were selected as putative biomarkers for hepatotoxicity by TGZ. In serum analysis, pattern recognition was similar to the results of the urinary analysis, and then we could select putative 6 endogenous metabolites such as ethanol, glucose, alanine, glutamine, lactate, and 3-hydroxybutyrate. According to these results, toxicometabolomics can be used to predict or screen hepatotoxicity caused by TGZ in urine and serum of rats.

PS 118 Quantification of CD11b Levels on Cynomologus Macaque Eosinophils by Flow Cytometry Provides PK/PD Support for the Development of an Anti-Cytokine Receptor Antibody (ACRA)

D. L. Clark[1], M. Retter[2], D. E. Wilkins[3], A. Ellingwood[3] and P. Narayanan[1]. *[1]Discovery Toxicology, Amgen, Seattle, WA, [2]Pharmacokinetics & Drug Metabolism, Amgen, Thousand Oaks, CA and [3]Laboratory Sciences, Preclinical Services, Charles River Laboratories, Reno, NV.*

Pro-inflammatory signals upregulate expression of cell surface αM integrin CD11b on eosinophils, favoring cell adhesion to airway epithelium in chronic disorders such as asthma. Absence of CD16B (CD16-) is used to differentiate eosinophils from other granulocytes (CD16B+), in humans. However, in cynomolgus macaques (CM), alternative methods must be used to identify eosinophils due to the absence CD16B expression on granulocytes in this species. To resolve this, we used the inherent autofluorescence of CM eosinophils to differentiate them from other granulocytes, and monitored CD11b up-regulation *ex vivo*, following I.V. administration of either 1 or 10 mg/kg ACRA. Blood samples were collected on day-1, pre-dose, 2, 8, 15, 28, and 43 days and exposed, *ex vivo*, to increasing concentrations of a pro-inflammatory cytokine for 30 min at 37°C. Samples were acquired on a flow cytometer following red blood cell lysis and staining with anti-CDllb alllophycocyanin-conjugated antibody. CDllb median fluorescence intensity on eosinophils, identified by their granularity and autofluorescence, was reported for each sample. Animals given 10 mg/kg of ACRA had complete suppression of eosinophil activation over 43 days (plasma levels > 10,000 ng/ml). Suppression of eosinophil activation returned to baseline in animals dosed with 1 mg/kg of ACRA after 28 days, when drug plasma levels were ≤ 240 ng/ml, the EC50 derived from *in vitro* eosinophil CDllb activation assays. Thus, although some understanding of target coverage was known from *in vitro* studies, the eosinophil PD assay applied in this PK study provided valuable information about target coverage *in vivo*. The PD data from this PK study was subsequently used to model dosing for subsequent toxicology studies and clinical studies to support development of this ACRA program.

PS 119 Performance of the Gyrolab® xP for Custom Development of Biomarker Assays for Safety Testing in Preclinical Drug Development

D. M. Hamlin, V. S. Hughes and H. W. Smith. *Investigative Toxicology, Eli Lilly and Company, Indianapolis, IN.*

The drive to reduce drug development cycle time & increase the number of cycles to select promising drug candidates has included the use of biomarkers as tools for early identification of efficacy & toxicity. This strategy requires expedited fit-for-purpose biomarker assay development & validation. Although commercial immunoassay kits are available for many biomarkers, many more novel biomarker assays are custom, "in-house" developed, using commercial or internally-produced antibodies and proteins. The development & validation of custom methods on conventional 96-well immunoassay platforms is time-consuming and the assays can be problematic to transfer to external labs. Utilization of an alternative platform, the Gyrolab® xP, resulted in the rapid development, optimization & validation of urinary renal injury biomarker assays for canine KIM1 & Cynomolgus NGAL. In comparison to conventional 96-well immunoassays, the Gyros® assays were developed & validated 3-times faster, were more accurate & precise methods which had broader quantitation ranges and reduced sample analysis time by 60%. The Gyros® NGAL assay was determined to be robust across different reagent preparations (<15% CV), for multiple CD lots (<10% CV) and was readily & successfully transferred to an external lab. As with other immunoassay platforms that have "wash" steps, lower affinity antibody reagents are not optimal in a 3-step Gyros® method, causing a loss of assay sensitivity and/or precision. For a custom rat IL1b inflammation biomarker assay, this limitation was overcome by modifying the standard Gyros® method to incorporate a preincubation step; resulting in a 7-fold increase in assay sensitivity and the modified rat IL1b Gyros® assay was successfully transferred & validated at an external lab. The Gyrolab® system is a valuable immunoassay platform for the rapid development & validation of accurate, precise, robust & transferrable custom-developed assays for novel biomarkers to support early safety & efficacy assessment in preclinical drug development.

PS 120 Predictive Performance of a Rat-Based *In Vivo* Metabolomics Database (MetaMap®Tox) As Compared to Classical Toxicological Assessments

G. Montoya-Parra[1], E. Fabian[1], M. Herold[2], G. Krennrich[1], L. Ralf[2], W. Mellert[1], N. Moeller[3], E. Peter[2], V. Strauss[1], T. Walk[2], B. van Ravenzwaay[1] and H. Kamp[1]. *[1]Toxicology, BASF SE, Ludwigshafen/Rhein, Germany, [2]metanomics, Berlin, Germany and [3]metanomics health, Berlin, Germany.*

The identification of potential hazards is a key outcome of toxicity studies. With the introduction of omics-technologies into toxicological research, questions have been raised concerning the sensitivity of these methods. We have developed the MetaMap® Tox database with toxicity and metabolome data of 500 reference compounds obtained from rat studies. Plasma metabolome analysis was performed after 7, 14 and 28 days. We have evaluated the predictive performance of MetaMap®Tox using 78 substances for which the predicted mode of action based on metabolomics was compared to the actual outcome of the guideline studies. Overall, 85% of the effects observed with classical parameters have also been predicted by the metabolome data. Out of 43 compounds that did show effects in classical parameters in male animals, 36 compounds (84%) do show these effects also in the metabolome analyses and can be considered as correctly positively predicted. 7 out of these 43 compounds (16%) were found to be false negative. Out of 35 not showing any effect in the classical parameters, 30 substances (86%) did also not show an effect on the metabolome (correctly negatively predicted), whereas 5 compounds (14%) did show effects in the metabolome (false positive predictions). The numbers for female animals are 36 out of 42 correct positive predictions (86%, based on 42 compounds showing toxicity in classical parameters) and 6 out of 42 false negative predictions (14%), 30 out of 36 correct negative predictions (83%, based on 36 compounds showing no effects in classical parameters) and 6 out of 36 false positive predictions (17%). In conclusion our analysis indicates that metabolome data can be used to predict toxicological effects in rats. Since metabolome data often provides a deeper mechanistic insight into the effects observed, metabolome analysis gives an added value for systemic toxicity testing.

PS 121 Comparison of Analytical Methods (ELISPOT, RT-QPCR and Luminex®) for the Detection of IL-17 following *In Vitro* Stimulation of Human PBMCs

C. Dumont[1], O. N. Diallo[1], E. Moisan[1], E. Marcotte[1], A. Keightley[1], J. L. Maisonneuve[2] and M. S. Christin-Piche[1]. *[1]Charles River, Montreal, QC, Canada and [2]PATH, Seattle, WA.* Sponsor: M. Vézina.

Purpose: Detection of *in vitro* cytokine secretion is a useful tool in safety, efficacy or pharmacology assessments of new drugs. Depending on the selected cytokines, the sensitivity of the detection method can be challenging. The goal of this study was to identify the optimal method for the detection of IL-17 following *in vitro* stimulation with *S. pneumoniae* inactivated whole cell vaccine (SPWCV), in order to define the T cell response. IL-17 is thought to be important for anti-pneumococcal immunity and its *in vitro* monitoring could be a useful tool in the development of candidate pneumoccocal vaccines.
Methods: Given that most adults have previously been exposed to *S. pneumoniae*, peripheral blood mononuclear cells (PBMC) from 2 normal human volunteers were used for method development. PBMCs were incubated *in vitro* in the absence or presence of SPWCV (3 concentrations) and analyzed for IL-17 mRNA expression by RT-QPCR and for IL-17 secretion by Luminex® and ELISPOT.
Results: Expression of IL-17 mRNA was detected in both donors following SPWCV stimulation for 48 hours at all concentrations. After 5 days, SPWCV stimulation induced detectable levels of IL-17 by Luminex® at the mid and high concentrations while the IL-17 ELISPOT results showed a dose-dependent response at all concentrations. For all methods used, one donor gave a consistently higher response to SPWCV stimulation.
Conclusion: The ELISPOT method was shown to be more sensitive for the detection of IL-17 following *in vitro* stimulation compared to the Luminex®. Further comparison of the RT-QPCR and ELISPOT methods using samples from vaccinated donors is planned in order to determine which method is more sensitive for detecting increases in cellular responses, which, ultimately could be used in clinical trials to select optimal vaccine candidates. In summary, monitoring of enhanced *ex vivo* cytokine responses using optimal methods can be useful to evaluate T cell functions in vaccine studies.

PS 122 Subchronic Aflatoxin B1 Exposure Produces Expression of Novel Liver Transcripts

J. S. Chang[1], D. P. Phadke[2], R. Shah[2], S. S. Auerbach[1], R. R. Tice[1] and B. A. Merrick[1]. [1]*Biomolecular Screening Branch, NIEHS, Research Triangle Park, NC and* [2]*Bioinformatics, Social & Scientific Systems, Durham, NC.*

Global gene expression studies of liver from carcinogen-exposed animals using RNA-Seq can provide insights into regulatory genes and critical pathways that might lead to hepatocellular carcinoma. We recently conducted RNA-Seq analysis on liver RNA from male F344 rats exposed to 1 ppm aflatoxin B1 (AFB1) in feed for 90 days, prior to the appearance of tumors. Among the more than 1,000 differentially expressed genes, we found a total of 49 potentially novel Cufflinks-assembled transcripts of which 21 transcripts had Ensembl annotation and 28 transcripts did not. Ten of these novel AFB1 altered transcripts were validated by PCR and specific regions were sequenced for eventual assembly into expression systems. Data showed a 5-fold increase in the stem cell marker, Sox-9, and the increased reads revealed a longer transcript than predicted for the rat Ensembl transcript or mouse and human orthologs. Similarly, AFB1 produced a 50-fold increase in the p53-regulated transcript, Eda2R (ectodysplasin A2 receptor), for which an extensive, unannotated 3'-region became evident. The set of 28 unannotated, novel transcripts showed AFB1 altered expression ranging from a 5 fold decrease to 659 fold increase. We previously reported two unannotated transcripts from this dataset, termed HAfT1 and HAfT2 (hepatic aflatoxin altered transcripts 1 and 2). Here, we selected 8 other unannotated novel Cufflinks transcripts from RNA-Seq data for PCR amplification and cloning for which partial sequence was obtained that correctly mapped back to each chromosomal location. One of these included a low copy transcript increased 281 fold by AFB1 that contained at least 4 exons in an unannotated region of Chr16 flanked by Fgfr1 and Tacc1 genes. Rapid amplification of cDNA ends (RACE) procedures was used to determine complete cDNA sequence for cloning, expression and cellular function. Complete sequencing of such transcripts could pave the way for a new set of biomarkers for chemical hepatocarcinogenesis prior to tumor formation.

PS 122a Metalloproteinase-Disintegrin Adam8: A Potential Biomarker for 2-Aminoanthracene Toxicity in the Liver of Fisher-344 Rats

J. A. Rasdall[1], R. D. Ford[1], E. Rasmussen[1], S. Jiang[2] and W. E. Gato[1]. [1]*Chemistry, Georgia Southern University, Statesboro, GA and* [2]*Department of Biomedical Science, Mercer University School of Medicine, Savannah Campus, Savannah, GA.*

Adam8 belongs to a disintegrin and metalloprotease family of genes. This protein has been implicated in a various cellular processes including cell-cell adhesions, muscle development, neurogenesis and asthma. Recently a hepatic global gene expression analysis of the liver was undertaken to identify specific genes that mediate 2-aminoanthracene (2AA) toxicity in the liver. Findings from this study showed Adam8 to be highly expressed in liver tissues of Fisher-344 (F344) rats that consumed dietary 2AA. The goal of the present study was to examine the hepatic expression of Adam8 in F344 rats that ingested 0 mg/kg- (control), 50 mg/kg- (low dose), 75 mg/kg-(medium dose) and 100 mg/kg-diet (high dose) of 2AA for 2 and 4 weeks. The arylamine 2-aminoanthracene (2AA) is an aromatic hydrocarbon employed in manufacturing of chemicals, dyes, inks, and as curing agents in epoxy resins and polyurethanes. 2AA is also present in tobacco smoke as well as over-cooked food. The gene expression of Adam8 was analyzed by quantitative real-time polymerase chain reaction (qRT-PCR). Adam8 expression in the livers was dose-dependent. This transcript was highly expressed in the high-dose animals of the 2 weeks group. Similar pattern of gene expression was observed in the four weeks group. Relative quantification of Adam8 mRNA was greater in the 2 weeks group than the four weeks set. Specific immunostaining for Adam8 in various tissues has been undertaken with results being analyzed. This will be followed by western blot assay to detect Adam8 protein expression.

PS 122b CD1X on Dendrtic Cells: A Biomarker of Metallic Allergens and Metallic Nonallergens *In Vitro*

Y. Mu[1], A. M. Keene[2], H. Degheidy[3], Z. Zhang[4], C. Li[5], C. Ghosh[6] and J. L. Weaver[7]. [1]*US FDA, Silver Spring, MD,* [2]*Afton Chemical, Richmond, VA,* [3]*US FDA, Silver Spring, MD,* [4]*US FDA, Silver Spring, MD,* [5]*US FDA, Silver Spring, MD,* [6]*US FDA, Silver Spring, MD and* [7]*US FDA, Silver Spring, MD.*

The FDA has seen an increase in the incidence of allergy/immunotoxicity related post market adverse events associated with medical devices. Biomarkers are commonly used in toxicology for risk assessment and clinically as diagnostic and monitoring tests. We developed a new in vitro model where human dendritic cells (DC) were used as a biomodulator to predict allergic responses to medical device materials. The cells were exposed for 24 hr to the following metal allergens and non-allergens for biomarker identification and development by employing flow cytometry. Interestingly, of 16 selected cell surface markers (CD1a, CD1X, CD44, CD54, CD56, CD80, CD83, CD86, CD141, CD154, CD184, CD197, CD206, CD208, HLA-DR, TLR-9), we found a new functionality for the protein CD1X on DC. The expression was down-regulated significantly following exposure to 8 metallic allergens (ammonium hexachloroplatinate(IV), cobalt(II) chloride, nickel(II) sulfate, nickel(II) chloride, mercury(II) chloride, beryllium(II) sulfate, gold(I) chloride, potassium dichromate(VI)) while the expression was similar to controls (no metal treatment) when exposed to 10 metallic nonallergens (aluminum(III) chloride, potassium(I) hydroxide, sodium(I) lauryl sulfate, zinc(II) sulfate, lead(IV) acetate, manganese(II) chloride, barium(II) chloride, iron(III) chloride, copper(II) chloride, magnesium(II) chloride). The statistical evaluation on CD1X alone yielded a p value < 0.0001, 88% sensitivity, 90% specificity and 89% accuracy based on receiver operating characteristic (ROC) analysis. We also confirmed that the protein CD86 alone consistently acts as a predictive biomarker for allergenicity of metal and/or alloy containing device materials. Thus, the data indicate that CDX1 shows promise for use as a pre-clinical biomarker for screening potential allergenic responses to metal containing devices.

PS 122c Serum microRNAs As Potential Biomarkers of Nephrotoxicity in Male Fischer 344 Rats Orally Challenged with Melamine and Cyanuric Acid

D. Williams, K. Kelly, G. Gamboa da Costa and L. Camacho. *NCTR, FDA, Jefferson, AR.*

MicroRNAs are small noncoding RNA molecules that play a key role in regulating numerous biological processes. Data suggest that modulations in the systemic circulation of microRNAs can be indicative of tissue injury or disease. The objective of this study was to assess if serum microRNAs could be used as biomarkers of melamine and cyanuric acid-induced kidney toxicity. Male Fischer 344 rats were a fed diet fortified with equal amounts of melamine and cyanuric acid (0, 180, or 240 ppm each) for 28 consecutive days. Nephrotoxicity, as assessed by increased blood urea nitrogen (BUN) and serum creatinine versus control, was observed in the 240 but not 180 or 0 ppm dose group. Serum samples from the three dose groups were prepared from terminal blood and checked for hemolysis prior to evaluating microRNA expression. Equal volumes of nonhemolytic sera were pooled from a minimum of 3 animals per dose group. Using a PCR array, the relative expression of 373 microRNAs was measured. Based on the screening data, 30 microRNAs were modulated by approximately 4-fold compared to the control. To validate these data, the expression of the 30 microRNAs was measured by quantitative real-time PCR in each of the three individual samples per dose group. Circulating levels of rno-miR-144-3p were down-regulated in sera of rats dosed with 240 ppm melamine and cyanuric acid in comparison to the control group. The down-regulation of rno-miR-144-3p was further confirmed using a larger sample size (n = 12 per dose group; P < 0.025). These data suggest that rno-miR-144-3p may be a minimally-invasive biomarker of kidney injury induced by melamine and cyanuric acid, and is at least as sensitive as the currently used biomarkers BUN and serum creatinine. Future studies will evaluate the expression of rno-miR-144-3p following exposures to additional nephrotoxicants. IAG FDA 224-12-0003/NIH ES12013.

PS 122d MiRNA Profiles in Liver and Kidney during the Rat Life Cycle Show Age, Sex, and Tissue Differences

J. C. Kwekel, V. G. Desai, V. Vijay, T. Han, C. Moland and J. C. Fuscoe. *Systems Biology/Personalized Medicine Branch, FDA/National Center for Toxicological Research, Jefferson, AR.*

The liver and kidney are fundamentally important tissues for drug metabolism, disposition, and excretion. Growing evidence suggests epigenetic mechanisms of gene regulation may play a role in susceptibility to certain toxicities and adverse drug reactions. miRNAs continue to show promise as biomarkers. While relatively immature compared to other genomic resources, growing knowledge of individual miRNAs and their putative gene targets allows for large scale inquiry into genome-wide miRNA expression. miRNA expression in liver and kidney tissues was examined in F344 rats during their life cycle. Animals were evaluated at 2, 5, 6, 8, 15, 21, 52, 78, and 104 weeks of age in both sexes (n=5) using Agilent 8x15k rat miRNA microarrays. 263 and 275 miRNAs were found to be expressed in the liver and kidney, respectively, in at least one age and sex. 221 miRNAs were commonly expressed in both liver and kidney. Filtering criteria of 1.5 fold change and ANCOVA (FDR 5%) revealed 249 (94%) differentially expressed miRNAs (DEMs) in the liver, while 210 (76%) were differentially expressed in the kidney. Of the 305 total DEMs, 154 miRNAs were differentially expressed in both tissues. A notable age difference in expression consisted of 28 miRNAs showing 2

week-specific expression in the liver but not in the kidney. The genes encoding 26 of these 28 miRNAs are located on rat chromosome 6. Nine miRNAs showed sex differences in both tissues and only 1 miRNA (miR-22) showed a similar expression pattern in both tissues; male-specific up-regulation at 21 weeks of age. miR-22 has been shown to post-transcriptionally inhibit PGC-1α, PPARα and Sirt1, key regulators in metabolism pathways. These results comprise one of the first large-scale comparisons of global miRNAs in the liver and kidney over the rat life cycle that may impact susceptibility to adverse drug reactions.

PS 122e Next-Generation Sequencing of Plasma, Urine, and Tissue microRNA from Sprague-Dawley Rats Treated with Acetaminophen or Cisplatin

F. Wolenski, P. Shah, S. Wyllie, M. Gallacher, C. D. Fisher, T. Sano, V. J. Kadambi, E. Koenig and P. Kirby. *Drug Safety Research and Evaluation, Takeda Pharmaceuticals International Co., Cambridge, MA.*

MicroRNAs (miRNA) are short single-stranded RNA sequences comprised of approximately 22 nucleotides that have a role in the post-transcriptional regulation of genes. The identification of tissue specific or enriched miRNAs may be useful as novel safety biomarkers. Recent work has demonstrated that both the presence and magnitude of miRNA in biofluids (e.g., plasma and urine) can be associated with tissue-specific damage. This study is the first to use next generation sequencing to analyze changes in miRNA profiles of plasma, urine and tissue samples of rats treated with either a hepatotoxicant (Acetaminophen [APAP]) or a nephrotoxicant (Cisplatin). To verify tissue-specific damage, an analysis of histopathology and serum chemistry was performed. In animals treated with APAP, eight miRNAs were significantly ($p<0.05$) altered in the liver, 45 in plasma and none in urine. Consistent with the literature, levels of miR-122 (193-fold) and miR-192 (63-fold) were significantly ($p<0.001$) upregulated in plasma from these animals. Histopathology and increases in liver enzymes demonstrated liver necrosis for APAP-dosed rats without a concomitant kidney injury. In Cisplatin-treated animals, 20 miRNAs were significantly ($p<0.05$) altered in the kidney, nine in plasma and six in urine. Also consistent with the literature, levels of miR-34a were significantly ($p<0.004$) upregulated in the kidney (6.1-fold) and plasma (7.2-fold); a significant ($p<0.002$) 10.0-fold increase in the expression of miR-378 in the urine has not been previously reported. Histopathology and changes in serum markers for kidney injury confirmed kidney but not liver damage in Cisplatin-treated rats. We next plan to use qPCR to validate the next generation sequencing of urine miRNA. Taken together, comparative analysis of urine, plasma, and tissue miRNA demonstrated the utility of miRNA as biomarkers of organ injury and identified miR-378 as a potential novel urine marker for Cisplatin-induced injury.

PS 122f Circulating microRNAs As Potential Non-Invasive Biomarkers in Patients with Crohn's Disease

A. Kalbasi[2], H. Lin[1], N. Alsahwi[2], S. K. Ramaiah[1], C. Lepsy[3], S. C. Robson[2] and D. Solar[4]. [1]*DSRD, Pfizer Inc., Cambridge, MA,* [2]*BIDMC, Boston, MA,* [3]*PDM, Pfizer Inc., Boston, MA and* [4]*CTI, Pfizer Inc., Boston, MA.*

MicroRNAs (miRNAs) are a class of small, non-coding RNAs that negatively regulate gene expression, thereby affecting crucial processes in pathogenesis of human diseases and toxicities. Circulating miRNAs offer great potential as biomarkers for disease detection because of their remarkable stability in blood and their characteristic expression in different diseases and toxicities. Differential expression of miRNAs has been described in multiple autoimmune-associated diseases. Recently, unique miRNA expression profiles have been described in the intestinal epithelial cells and in the peripheral blood of patients with Crohn's disease (CD). We hypothesized that miRNAs may be involved in the homeostatic regulation of CD-associated inflammatory responses, and their disease-associated dysregulation could be detected in circulating miRNA signatures. Specific miRNAs with important roles in regulating key pathogenic mechanisms in CD inflammation were selected to assemble a Taqman assay panel for screening of plasma from CD patients (Montreal classification, B1~B3) and healthy volunteers. We found that the profile of a number of circulating miRNAs is capable of distinguishing healthy volunteers (HV) from CD patients. In particular, miR-182 levels were upregulated in the CD subjects (B3 vs HV, $p=0.006$). Interestingly, tumor necrosis factor (TNF)-like ligand 1A (TL1A) is a direct regulated target of miR-182. Numerous genome wide association studies have linked several polymorphisms of the TL1A gene to CD, and inflamed intestinal tissue from patients with inflammatory bowel disease show high expression levels of TL1A. Additionally, an intestinal enriched miRNA, circulating miR-194, was upregulated in the CD subjects (B3 vs HV, $p<0.001$). The results described here have implications for the use of circulating miRNA profiles as potential non-invasive biomarkers for CD detection.

PS 122g Novel Kidney Injury Biomarker Panels to Detect Nephrotoxicity in Mouse Models

W. Zheng[1], R. Maheshwari[1] and V. Sabbisetti[2, 3]. [1]*EMD Millipore, St. Charles, MO,* [2]*Brigham and Women's Hospital, Boston, MA and* [3]*Harvard Medical School, Boston, MA.* Sponsor: P. Hewitt.

Kidney is the primary organ for drug toxicity. The application of kidney injury biomarkers has greatly improved the detection of nephrotoxicity during drug development and will accelerate the speed to bring more effective and safe drugs to market. Over the past decade, a panel of novel urinary kidney biomarkers has been approved by the FDA, EMA and PMDA to detect acute nephrotoxicity in preclinical rat studies. Even though mouse models are widely used in drug development process, lack of reliable assays to quantitatively assess multiple protein markers in small volumes of mouse urine has limited the application of these markers in mouse models.

In the present study, we developed multiplexed immunoassays for two panels of mouse kidney urinary biomarkers. Furthermore, we validated the sensitivity and specificity of these assays in two different mouse kidney injury models.

To induce kidney injury, BALB/C mice were subjected to either bilateral ischemic reperfusion (I/R) for 30 minutes or one dose of cisplatin treatment. Urine specimens were collected and analyzed for urinary protein markers with MILLIPLEX® MAP Mouse Kidney Injury Magnetic Bead Panels. There was a significant increase in many of the novel markers in both I/R and cisplatin treated mice models reflecting tubular damage. In conclusion, we have developed novel multiplexed assays for mouse urinary kidney biomarkers and validated them in both ischemia and drug induced kidney injury models in mice. The simultaneous measurement of these proteins with multiplex technology offered a robust and convenient method to study these biomarkers in small volume of mouse urine samples.

PS 122h Validation of an Immunoassay for Analysis of Oxytocin in Sheep Plasma to Support Progress towards a Novel Drug Delivery Strategy for the Treatment of Postpartum Hemorrhage

E. Weber[1], T. Nett[1], V. Oliver[2], P. Lambert[2] and M. McIntosh[2]. [1]*Bioanalytics Group, Endolytics, LLC, Fort Collins, CO and* [2]*Drug Delivery Disposition and Dynamics, Monash University, Parkville, VIC, Australia.* Sponsor: W. Hanneman.

Postpartum hemorrhage is the single largest contributing factor to global maternal mortality, with the burden occurring overwhelmingly in low income countries (WHO & UNICEF 2012). Monash University is working to develop a heat stable and non-injectable oxytocin (OXT) product that can be simply administered by all levels of healthcare personnel.

In support of Monash University's pre-clinical program, we have validated a radioimmunoassay for the detection of OXT (oxRIA) in sheep plasma, and generated preliminary data on the dose pharmacokinetics (PK) of OXT in sheep, after intravenous (IV) delivery. Validation of the oxRIA, and subsequent studies were carried out using OXT Radioimmunoassay Kits (Phoenix Pharmaceuticals, Inc.). The mean lower limit of quantification for the oxRIA, over three assays, was 760fg. Recovery of OXT in biological matrix was determined by adding standard OXT at three concentrations to sheep serum, with six replicates at each concentration. After correction for extraction efficiency (69.1%, 0.70% CV), the amounts of OXT recovered from serum was >99%. Slope of the regression line was 1.0986 and r-value was 0.9986. Mean intra- and inter-assay coefficients of variations were 4.6% and 7.5% respectively, over six assays.

To assess the PK of IV-dosed OXT, six sheep were administered 10 IU (~16μg) OXT directly into the jugular vein. Following injection, blood was sampled at ten time points, and plasma concentrations of OXT were determined. Half-life (t1/2) of OXT was determined to be ~5 min.

In conclusion, we have shown the oxRIA is reliable for analysis of OXT in sheep serum. The assay was used to assess the t1/2 of OXT delivered to sheep IV, and this value agreed favorably with the t1/2 of OXT reported for other species. On-going pre-clinical studies include the evaluation of both the PK and pharmacodynamics of OXT formulations administered by intramuscular (IM) injection, pulmonary and nasal delivery.

PS 122i Urinary Marker Expression May Be Gender Specific Predictor of Oxidative Stress and Inflammatory Conditions from Drug Use

M. M. Bourgeois and I. Richards. *EOH, USF COPH, Tampa, FL.*

Males and females exhibit different morbidity and mortality across a wide range of conditions which suggests basic pathophysiology may control the incidence of multiple disease processes. Women suffer disproportionately higher rates of many of these diseases, particularly autoimmune and inflammatory diseases. Inflammatory processes induce oxidative stress and reduce cellular antioxidant capacity. This investigation examined the relationship between oxidative stress and inflammatory marker expression and gender in addition to determining the effect of confounders such as drug use, lifestyle and medical history. These conditions are linked to physiological changes that may alter the expression of certain biomarkers of inflammation and oxidative stress. Urine specimens (n=62) were assayed for Myoglobin, C Reactive Protein, Myeloperoxidase, Estradiol, Testosterone, Malondialdehyde, 8OHdG, and Interleukins 1α and 6 using ELISA. Laboratory reference ranges for urine, serum and plasma do not typically differentiate between genders. More importantly, gender-based ranges of urinary concentrations have not been determined for many oxidative stress (OS) and inflammatory cytokines linked to common chronic diseases. Multivariate regression analysis suggest predictors of oxidative marker expression may include gender, preexisting disease and drug use. The results suggest significant gender-based differences may exist in the expression of inflammatory and oxidative biomarkers in the urine of drug users.
This work has been supported in part by the Agency for Community Treatment and Services of Tampa and the Laboratory of Occupational and Public Health Toxicology.

PS 123 Characterization of Reactive Species Produced by the Human THP-1 Cell Line in Response to Contact Sensitizers

M. Azoury[1], M. Pallardy[1], S. Karaki[1], C. Migdal[1], E. Gimenez-Arnaud[2], J. Lepoittevin[2] and S. Kerdine-Römer[1]. *[1]UniverSud, INSERM UMR 996, Faculté de Pharmacie, Châtenay-Malabry, France and [2]Université de Strasbourg, CNRS UMR 7177, Laboratoire de Dermatochimie, Châtenay-Malabry, France.*

Allergic contact dermatitis (ACD) is generally induced by low molecular weight electrophilic chemicals. Chemical contact sensitizers trigger reactive species (RS) production. It is also known that RS participate to the maturation and activation of dendritic cells (DC) thus participating in the adaptive immune response. However the mechanisms underlying RS production in DC by chemical sensitizers has not been elucidated.
In this study we quantified RS production, analyzed the type of RS produced and identified the potential sites of RS production in THP-1 cells.
Treatment of THP-1 cells with 2,4-dinitrochlorobenzene (DNCB) and cinnamaldehyde (CIN) increased RS levels in a time-dependent manner and peaked at 2 hours. RS were measured using the H2DCFDA probe and flow cytometry. Our data also showed that reactive oxygen species (ROS) were induced by both DNCB and CIN and only DNCB induced reactive nitrogen species (RNS) production in THP-1 cells. Potential sources of RS production were evaluated using antimycine A, an inhibitor of the mitochondrial electron transport chain complex III; allopurinol, a xanthine oxydase inhibitor; L-NIL (N6 (1-iminoethyl)-L-lysine dihydrochloride), an inhibitor of the inducible nitric oxide synthase (iNOS) or carbonyl cyanide m-chlorophenylhydrazone (CCCP), an efflux pump inhibitor. Our results showed that DNCB-induced RS was related to the mitochondrial electron transport chain complex with the participation of the xanthine oxydase system and iNOS catalysis. Conversely, CIN-induced RS was only related to the mitochondrial electron transport chain complex and to the xanthine oxydase system.
In conclusion, these results suggested that the mechanisms underlying RS generation in THP-1 cells might differ depending on the chemical sensitizer with different types of RS emerging from different sources of RS in THP-1 cells.
Azoury M. & Karaki S. Contributed equally to this work.

PS 124 Factors Influencing Adverse Skin Responses in Rats Receiving Repeated Subcutaneous Injections and Impact on Behavior

S. N. Levoe[1], L. Brignolo[2], D. M. Imai[3], D. Bruun[1] and P. Lein[1]. *[1]Molecular Biosciences, University of California, Davis, Davis, CA, [2]Campus Veterinary Services, University of California, Davis, Davis, CA and [3]Comparative Pathology Laboratory of Veterinary Medicine, University of California, Davis, Davis, CA.*

A common route of exposure for chronic toxicity studiesis repeated subcutaneous (s.c.)injection. In a pilot study of chronic organophosphate (OP) neurotoxicity, we noted a significant incidence of skin abnormalities in young adult male Long Evans rats receiving s.c injections in the subscapular region of Planter's® peanut oil at 1.0ml/kg daily for 21 d. Both OP-treated and vehicle control groups were affected and lesions were not restricted to the site of injection, suggesting skin responses were not due to the toxicant or to repeated needle sticks. Histopathological analysis was consistent with a foreign body reaction to the injected peanut oil. We next determined whether these unanticipated skin abnormalities were related to the vehicle type, the type of bedding, or the vendor from which the animals were obtained, and further, whether these adverse reactions influenced neurobehavioral outcome. Rats injected daily with Planter's® peanut oil had an earlier onset and greater incidence of skin abnormalities than rats receiving an equal volume of either Sigma® peanut oil or Neobee-5. Daily s.c. injections of Planter's peanut oil elicited skin abnormalities in a significantly greater percentage of animals housed on corn cob versus CareFresh® bedding. Comparison of animals from different vendors exposed to the same injection paradigm (Sigma® peanut oil, 1.0 ml/kg daily, s.c.) revealed significant differences in the severity of skin abnormalities. However, animals from different vendors did not perform differently in a Pavlovian fear conditioning task. Collectively, these data suggest that environmental factors can influence the incidence and severity of skin abnormalities to repeated s.c. injections, but these adverse responses do not significantly influence performance in at least one test of learning and memory. Supported by NIH grant ES016308.

PS 125 Identification of MHC Haplotypes Associated with Drug-Induced Hypersensitivity Reactions in Cynomolgus Macaques

H. Wu, K. Adkins, C. Houle, L. Nelms, K. R. Tartaro, A. Hudson, T. T. Kawabata and J. Whritenour. *Drug Safety Research and Development, Pfizer Inc, Groton, CT.*

The occurrence of immune-mediated drug hypersensitivity reactions (IDHRs) can have a significant impact on therapeutic drug use and development. While the mechanism(s) and risk factors are not fully understood, an association between specific human leukocyte antigen (HLA) alleles and IDHR has been described for some drugs (e.g. abacavir and HLA B*57:01). However, whether such an association exists between IDHR and major histocompatibility complex (MHC) alleles from other species has not been described. In this study, genomic DNA samples were obtained from 62 cynomolgus macaques from several preclinical toxicology studies (with and without IDHR) and genotyped using microsatellite analysis to determine the MHC haplotype for each animal. Of the 62 macaques, 9 animals had clinical evidence of IDHR (manifested as skin lesions). The M1, M2, M3, M4, M5, M6, and M7 haplotype frequencies in the MHC regions were identified to be 17%, 8%, 15%, 19%, 2.4%, 7.3%, and 2.4%, respectively in these monkeys. Recombinant MHC haplotypes and undetermined MHC alleles were represented at frequencies of 23% and 6.5%, respectively. Genetic association analysis identified alleles from the M3 haplotype of the MHC B region containing B*011:01, B*075:01, B*079:01, B*070:02, B*098:05, and B*165:01 alleles were significantly associated (χ2-test for trend, $P < 0.05$) with the occurrence of IDHR (skin lesions) in this population. These data suggest that cynomolgus macaques may be a good preclinical model for studying mechanisms underlying IDHR. However, additional genetic haplotype analysis is warranted to determine the potential polymorphism(s) that may be functionally important in IDHR in cynomolgus macaques.

PS 126 Defective TGFβ Signaling in Dermal Dendritic Cells Leads to Their Reduced Lymph Node Migration and Contact Hypersensitivity Responses with Ultraviolet B Irradiation

A. Ravindran[1], K. Breech[1], J. Mohammed[2, 1] and A. Glick[1]. *[1]Veterinary and Biomedical Sciences, The Pennsylvania State University, State College, PA and [2]Dermatology, University of Minnesota, Minneapolis, MN.*

Transforming Growth Factor-β1 (TGFβ1) is an important immunoregulatory cytokine in the skin critical for the development of epidermal dendritic cell (DC) subset-Langerhans cells (LCs). However, the role of TGFβ signaling for the immunostimulatory function of LCs or other skin-resident DC subsets- CD207- dermal DCs (dDCs) and CD103+ CD207+ dDCs in response to Ultraviolet B (UVB) irradiation is not clear. Mice expressing a dominant negative TGFβ Type II receptor (DNR) specifically in CD11c+ DCs displayed reduced steady-state migration of all three DC subsets compared to WT C57BL/6 mice. Acute UVB-induced migration of dermal DC subsets, CD207- and CD207+ dDCs in DNR to skin-draining lymph nodes (SDLNs) was reduced in DNR compared to WT mice, which correlated with a reduced percentage of p-Smad2+ and CD86high dermal DCs in DNR mice with UVB. There was no significant difference in UVB-induced migration of LC subset between DNR and WT mice. In addition, the UVB-induced migration of CD207- and CD207+ dDCs subsets in a chronic UVB model as well as migration of CD207- subset in an ear explant assay was suppressed in DNR when compared to WT mice with no difference in LCs. Consistent with reduced

steady state and UVB-induced migration of dermal DC subsets, ear thickness response measured in a contact hypersensitivity model (CHS) with and without UVB, was reduced in DNR mice compared to WT with an associated reduction in memory effector differentiation and IFNγ, IL17 and IL2 cytokine profile of CD4+ and CD8+ T cells. Together, these results suggest that TGFβ signaling in DCs is important for UVB-induced skin inflammation and optimal response to hapten sensitization in a CHS model, both mediated through the DC-T cell arm of the immune response.

PS 127 Alteration of Cytoskeletal Molecules in a Human T Cell Line Caused by Continuous Exposure to Chrysotile Asbestos

T. Otsuki[1], M. Maeda[2], H. Matsuzaki[1], S. Lee[1], N. Kumagai-Takei[1] and Y. Nishimura[1]. [1]*Hygiene, Kawasaki Medical School, Kurashiki, Japan and* [2]*Agricultural and Life Science, Okayama University, Okayama, Japan.*

We have been investigating the immunological effects of asbestos, since the silicosis patients who had exposed silica, the core chemical of asbestos, SiO2, often complicate the autoimmune diseases such as Rheumatoid arthritis, SSc, and ANCA-related vasculitis. Therefore, we are considering asbestos may possess the immunological effects, although the physical fibrous form is differed from particulated silica. We considered the target of asbestos may be the anti-tumor immunity, since the major complications of asbestos-exposed patients are the cancers. In this report, we investigated alteration of protein expression among MT-2 original cells that had no contact with asbestos, and six chrysotile-continuously exposed independent sublines using ProteinChip and two-dimensional gel electrophoresis (2DGE) assays. Further confirmation of the changes in protein expression due to asbestos exposure was obtained after the 2DGE method indicated protein modification of β-actin. β-actin was upregulated in mRNA, as were the levels of protein expression and phosphorylation. Moreover, a binding assay between cells and chrysotile showed that various molecules related to the cytoskeleton such as vimentin, myosin-9 and tubulin-β2, as well as β-actin, exhibited enhanced bindings in asbestos-exposed cells. The overall findings indicate that the cell surface cytoskeleton may play an important role in inducing the cellular changes caused by asbestos in immune cells, since fibers are not incorporated to the cells and how the alterations of cytoskeleton determined cell destiny to cause the reduction of tumor immunity is important to consider the biological effects of asbestos. Further studies to target several cytoskeleton-related molecules associated with the effects of asbestos will result in a better understanding of the immunological effects of asbestos and support the development of chemo-prevention to recover anti-tumor immunity in asbestos-exposed patients.

PS 128 Analysis of Blood DcR3 Concentration and Its Correlation to Clinical Parameter of Autoimmune Diseases in Silicosis Patients

S. Lee[1], Y. Nishimura[1], S. Yamamoto[1], T. Hatayama[1], H. Matsuzaki[1], N. Kumagai-Takei[1], H. Hayashi[2], M. Kusaka[3], W. Fujimoto[2] and T. Otsuki[1]. [1]*Hygiene, Kawasaki Medical School, Kurashiki, Okayama, Japan,* [2]*Dermatology, Kawasaki Medical School, Kurashiki, Okayama, Japan and* [3]*Kusaka Hospital, Bizen, Okayama, Japan.*

Silicosis patients frequently complicate with autoimmune diseases. Dysregulation of apoptosis, particularly in the Fas/Fas ligand (FasL) pathway, has been considered to play a role in the pathogenesis of autoimmune diseases. DcR3 is known as an intrinsic decoy receptor that binds FasL and inhibits FasL-induced apoptosis. Initial studies showed that DcR3 expression is elevated in cancer cells, however, later work showed that DcR3 expression is also increased in inflammatory diseases, where serum DcR3 levels correlate with disease progression (Linn WW & Hsieh SL 2011). Our previous report showed DcR3 mRNA expression increased in PBMC of silicosis patients (Otsuki T et. al., 2000). In this study, we analyzed blood DcR3 concentration and correlation to clinical parameter of autoimmune diseases.
Plasma samples that included 19 of healthy volunteers (age 42.94±7.95, men 8: female 11), 20 of silicosis patients (age 74.85±5.35, men 19: female 1), 25 of systemic sclerosis patients (age 62.32±12.06, men 3 : female 1) were provided from Kawasaki Medical School hospital and Kusaka hospital (Bizen, Okayama). All factors were analyzed with ELISA. Statistic analysis was performed using SPSS. DcR3 blood level was remarkably increased in silicosis patients compare to healthy volunteers. This result suggested that blood DcR3 increment may cause complication of autoimmune diseases through impair Fas/FasL pathway in silicosis patients. Furthermore this study showed there are no correlation between plasma DcR3 and any other clinical parameter of autoimmune diseases in silicosis patients. This result indicated plasma DcR3 elevation means impairment of immune system rather than directing particular autoimmune disease.

PS 129 FoxO1 Regulates Apoptosis Induced by Asbestos in the Human T Cell Line MT-2

H. Matsuzaki[1], S. Lee[1], M. Maeda[2], N. Kumagai-Takei[1], Y. Nishimura[1] and T. Otsuki[1]. [1]*Kawasaki Medical School, Kurashiki, Okayama, Japan and* [2]*Okayama University, Okayama, Okayama, Japan.*

Asbestos is known to cause malignant mesothelioma and lung cancer. Recent studies indicate the implication of tumor immunity in development of various tumors including malignant mesothelioma. Thus, human T cell line MT-2 cells were cultured to asbestos for longer than 8 months and resultant cells were designated MT-2Rst. Gene expression analysis revealed that the amount of forkhead transcription factor FoxO1 mRNA decreased after long term exposure to asbestos in MT-2 cells. According to the reduction of FoxO1, pro-apoptotic Foxo1 target genes, Puma, Fas ligand, and Bim, were down-regulated in MT-2Rst cells. Furthermore, shRNA-mediated knock-down of FoxO1 reduced number of apoptotic cells after treatment with asbestos in parental MT-2 cells. On the other hand, over expression of FoxO1 does not affect on asbestos-induced apoptosis in MT-2Rst cells. These results suggest that FoxO1 play an important role in regulating of asbestos-induced apoptosis, and the presence of multiple pathways regulating resistance to asbestos in MT-2Rst cells.

PS 130 Contribution of Autoantibodies to Fiber-Induced Fibrosis

K. Serve, C. N. Zebedeo, C. Davis, K. Ng and J. C. Pfau. *Biological Sciences, Idaho State University, Pocatello, ID.*

Non-malignant pleural abnormalities arising from asbestos exposure may manifest as pleural plaques, diffuse pleural thickening, or pleural effusions. Clinical observations suggest amphibole, but not chrysotile, exposures are linked to diffuse pleural thickening and progressive loss of lung function. Recent research suggests that factors such as pathogenic autoantibodies and fiber-induced tissue damage contribute to these different clinical outcomes. In order to study the contribution of these factors to pleural disease, we used microscopy to quantify collagen deposition within the pleura and peritoneal cavities of mice exposed to amphibole or chrysotile asbestos or to the carcinogenic fiber erionite. Multiphoton microscopy was used to analyze collagen density of the lung visceral pleura or of peritoneal tissue (i.e. diffuse collagen deposition) and the dissection microscope was used to assess localized collagen plaques. Mouse sera were examined for anti-nuclear antibodies (ANAs) to determine potential correlations with collagen density. Intra-tracheal exposure to fibers resulted in an overall increase of ANAs compared with saline control exposures, with the highest ANA level associated with erionite exposure. Erionite exposure was also associated with the highest collagen density within the peritoneal cavity while amphibole was associated with the highest collagen density within the pleural cavity. Collagen density was slightly increased in amphibole-exposed, ANA-positive mice compared to ANA-negative mice; however, no there was no significant correlation between ANA presence and pleural plaques. Further study is needed regarding the possible contribution of anti-fibroblast and anti-mesothelial cell autoantibodies to collagen deposition, since these antibodies are shown to directly increase collagen production by pleural and peritoneal cells. Overall, these data suggest that fiber exposure increases diffuse collagen deposition within the pleural and peritoneal cavities, with autoantibodies potentially contributing to diffuse, but not localized, collagen deposition.

PS 131 Antinuclear Autoantibodies and IL-17 Are Induced in C57BL/6 Mice following Amphibole, but Not Chrysotile, Exposure

J. C. Pfau[1], A. Ferro[2], C. N. Zebedeo[1], C. Davis[1] and K. Ng[1]. [1]*Biological Sciences, Idaho State University, Pocatello, ID and* [2]*College of Osteopathic Medicine, Pacific Northwest University of Health Sciences, Yakima, WA.*

Exposure to amphibole asbestos has been shown to increase production of autoantibodies in mice and humans and to increase the risk of systemic autoimmune disease. However, epidemiological studies of chrysotile exposure have not indicated an increased risk for autoimmunity. To explore these apparently different responses to asbestos exposures in mice, and to suggest possible mechanistic explanations for the difference, C57BL/6 mice were exposed intratracheally to amphibole or chrysotile asbestos, or to saline only. Serum antinuclear antibodies (ANA), antibodies to extractable nuclear antigens (ENA), serum cytokines, and immunoglobulin isotypes were evaluated 8 mo after the final treatment. The percentages of lymphocyte subsets were analyzed in the spleen and lungs. The results demonstrate that amphibole, but not chrysotile, asbestos increases the frequency of ANA/ENA in mice. Both fiber types increased multiple serum cytokines, but only amphibole increased IL-17. Changes to immunoglobulin isotypes were minimal except for a decrease in IgG1 with both fiber types. Although there were no gross changes in

overall percentages of T and B-cells in the spleen or lungs of exposed mice, chrysotile induced a significant increase in the normally rare populations of suppressor B-cells (CD19+, CD5+, CD1d+) in both the spleen and lungs. Overall, the results suggest that while there may be an inflammatory response to both forms of asbestos, there is an autoimmune response in only the amphibole-exposed, but not the chrysotile-exposed mice. These data have critical implications in terms of screening and health outcomes of asbestos-exposed populations.

PS 132 Effect of Perinatal BPA Exposure on Spleen and Serum Pro-Inflammatory Cytokines in Weaned Rats

A. Kelly[1], D. R. Mierke[1], R. N. Sadowski[2], L. M. Wise[2] and S. N. Lavergne[1]. *[1]Comparative Biosciences, University of Illinois, Urbana, IL and [2]Psychology, University of Illinois, Urbana, IL.*

Bisphenol A (BPA) is an environmental endocrine disruptor, well known for its repro-and neurotoxicity, but it can also interact with immunity and inflammation. We have shown that perinatal exposure to BPA and gender affect MHC II levels in spleens of weaned rat. We here report the effect of perinatal BPA exposure (400ug/kg/day) on spleen and serum levels of 3 key pro-inflammatory cytokines (IL-1b, IL-6, TNFa) in both female and male rats. Oral exposure lasted throughout pregnancy and until PND9; rats were then humanely euthanized at weaning. Spleens and sera were collected, snap frozen, and stored at -80'C. Cytokines levels were measured using a multiplex approach. Spleen IL-1b was similar between females and males in both vehicle and BPA groups, but was lower in BPA-treated animals for both genders. Spleen IL-6 was similar between females and males in the vehicle group, but was higher in BPA males compared to vehicle males. Spleen TNFa was low and not affected by BPA. Serum IL-1b was lower in males compared to females in the vehicle group, but lower in BPA females compared to vehicle females. We did not detect any IL-6 or TNFa in these rat sera. Finally, there was no correlation between serum and spleen levels for each cytokine, but spleen cytokine levels correlated with each other. In conclusion, it appears that perinatal exposure to BPA affects peripheral pro-inflammatory cytokines, with some gender-specific effects. In addition, serum did not appear to be an adequate spleen surrogate tissue for IL-1b, IL-6, or TNFa.

PS 133 Perinatal Exposure to Bisphenol A Alters Immune Cell Differentiation at Systemic and Intestinal Level in Young Offspring Rats

L. Guzylack, S. Ménard, C. Cartier, C. Lencina, M. Gillet, E. Gaultier and E. Houdeau. *Toxalim, Research Centre in Food Toxicology, NeuroGastroenterology & Nutrition, INRA, Toulouse, France.* Sponsor: B. Salles.

Aims: Previous data in rats showed that perinatal exposure to bisphenol A (BPA) altered intestinal immune homeostasis in young offsprings, weakening host defenses to intestinal infection. We aimed to investigate whether developmental immunotoxicity during BPA perinatal exposure resulted from early alteration in immune cell differentiation. Methods: Dams were treated with BPA [5 μg/kg/d] or vehicle (corn oil) from day 15 of gestation until weaning (postnatal day (PND) 21). Immune cells from spleen, mesenteric lymph node (MLN) or jejunal lamina propria were harvested from female offspring at PND25. Analysis of immune cell frequency for T regulatory (Treg) and T helper (Th) cells, or dendritic cell (DC) was performed by flow cytometry using specific cell markers. Total and *E. coli*-specific IgA responses in PND25 offspring were also measured. Results: Perinatal BPA treatment decreased frequency of Treg cells (0.33+/-0.04 vs 0.39+/-0.02% of total splenocytes in controls, $p<0.02$) and of Th cells in spleen ($p<0.01$) and MLN ($p<0.04$). These data were associated with a decline in migratory DC frequency at systemic level (0.09+/-0.01 vs 0.16+/-0.04% of total splenocytes in controls, $p<0.04$), as well as in the gut and associated MLN ($p=0.04$). Moreover, the decline in DC and Th cells questioned the ability of BPA-exposed rats to induce B cell response. As expected, a decrease in *E. coli*-specific IgA response ($p<0.0001$) was observed in serum of BPA-exposed rats, while total IgA were not impacted. Conclusion: This study shows that perinatal exposure to BPA at a dose close to the estimated dietary exposure in human (0.3-0.9 μg/kg/day, 95th percentile, European Food Safety Agency 2013) impacted the frequency of antigen presenting cells in young offspring with consequences on T helper differentiation. This led to a decline of T regulatory cells concomitant to altered IgA response toward microbiota, two important actors for systemic and local immune homeostasis.

PS 134 Transmaternal Exposure to Bisphenol A, but Not Phthalates, Accelerates Diabetes Type 1 Development in NOD Mice

J. Bodin[1], A. K. Bølling[2], A. Wendt[3], L. Eliasen[3], F. Kuper[5], R. Becher[2], M. S. Lovik[1, 4] and U. C. Nygaard[1]. *[1]Food, Water and Cosmetics, Norwegian Institute of Public Health, Oslo, Norway, [2]Air Pollution and Noise, Norwegian Institute of Public Health, Oslo, Norway, [3]Islet Cell Exocytosis, Clinical Sciences Malmö, Malmö, Sweden, [4]Cancer Research and Molecular Medicine, Norwegian University for Science and Technology, Trondheim, Norway and [5]Nutrition and Food Research, TNO, Zeist, Netherlands.*

Type 1 diabetes (T1DM) is an autoimmune destruction of insulin producing beta cells in the pancreas with a genetic predisposition that can be triggered by environmental factors. We have previously shown that bisphenol A (BPA) accelerates the spontaneous diabetes development in the diabetes-prone NOD mice. Here, we hypothesized that oral exposure to a combination of the rapidly metabolized endocrine disruptors BPA and phthalates, which is relevant for human mixed exposures, might give a further effect on diabetes development in NOD mice. A possible link between the development of T1DM and exposure through drinking water from before birth and throughout life to BPA (1mg/l), a mixture of phthalates (DEHP 1mg/l, DBP 0.2mg/l, BBP 10mg/l and DiBP 20mg/l) and a combination of BPA and the phthalate mixture was investigated in NOD mice. Presently, BPA exposure resulted in increased prevalence of diabetes and decreased number of tissue resident macrophages. Interestingly, BPA exposure also impaired the phagocytic activity of peritoneal macrophages. None of these effects were observed after phthalate exposure alone or together with BPA. Exposure to BPA alone or in combination with phthalates resulted in decreased cytokine release (TNFa, IL-6, IL-10, IFNg, IL-4) from in vitro stimulated splenocytes, indicating a systemic change in immune function. We conclude that BPA, but not phthalates or the combination of BPA and phthalates, accelerates the diabetes development in NOD mice, possibly via decreased number and function of macrophages in pancreatic islets.

PS 135 Total Blood Mercury, Fish Consumption, Proximity to Alluvial Arsenic Deposits, and Serum Autoantibodies among the Cheyenne River Sioux Tribe Members

E. Erdei[1], J. Ong[1], R. L. Rubin[2], C. Ducheneaux[3], M. O'Leary[4], B. Pacheco[1], K. M. Pollard[5], C. Miller[1] and J. L. Lewis[1]. *[1]Community Environmental Health Program, University of New Mexico, Albuquerque, NM, [2]Molecular Genetics and Microbiology, University of New Mexico, Albuquerque, NM, [3]Environment and Natural Resources, Cheyenne River Sioux Tribe, Eagle Butte, SD, [4]Research Nurses Group, Missouri Breaks Industrial Research, Eagle Butte, SD and [5]The Scripps Research Institute, La Jolla, CA.*

Mercury (Hg), known to induce autoimmunity in rodents, is a ubiquitous toxicant on the Cheyenne River Sioux Tribal (CRST) lands. Mercury exposure happens through fish consumption (FC), a part of Native culture that supports subsistence. Our goals were to ascertain whether total blood Hg levels (THg) reflect Hg exposure via FC, smoking, and determine if THg is associated with the production of anti-nuclear antibody (ANA) and specific auto-antibodies (sAuAb).
We recruited 75 people who consume fish from CRST waters. Hg exposure via FC and smoking were assessed using questionnaires. Blood samples were collected and THg was assessed by mass spectrometry (ICP-MS). Immunofluorescence was used for serum ANA. Native, denatured DNA, chromatin and histone AuAbs and other diseases sAuAbs were measured by ELISAs. We modeled these immune measures using demographic (age, gender) and exposure predictors.
Female gender, age and FC were significant predictors of THg; self-reported smoking was not. 31% of participants tested positive for ANA stained stronger than ≥2+. Even ANA was not significantly associated with THg, the interactions of gender with THg and close proximity to As deposits were statistically significant. Also, female gender, age and FC were significantly associated with elevated sAuAb. Although FC resulted in detectable body burden of Hg, THg alone did not explain ANA or sAuAb in this population. We are working with CRST communities to investigate the relationships among FC, complex metal exposures and the community's immune responses.

PS 136 Altered Lyn Phosphorylation May Be a Key Mediator of Autoimmunity Associated with Mercury Intoxication of B Cells

A. J. Rosenspire[1], J. Caruso[2], R. Gill[1], P. M. Stemmer[2], N. Caruthers[2] and M. J. McCabe[3]. [1]*Immunology and Microbiology, Wayne State Univ, Detroit, MI,* [2]*Institute of Environmental Health Science Research, Wayne State University, Detroit, MI and* [3]*Environmental Medicine, University of Rochester Medical Center, Rochester, NY.*

Inorganic mercury (Hg2+) is a potent immunomodulator that has been implicated as a factor contributing to autoimmune disease in animal models as well as in humans. At this time a mechanistic understanding of how Hg2+ disrupts immune function remains elusive. Furthermore, while studies clearly demonstrate an association between Hg2+ exposures and increased risk of autoimmume disease on a population level, there are currently no biomarkers that can be utilized to identify Hg-induced autoimmunity. Recently there has been increased appreciation of the involvement of B cells in autoimmune disease. We have employed advanced proteomic and multicolor phosphoflow cytometric approaches to investigate the interaction of Hg2+ with immature (T1 and T2) and mature mouse B cells. Defects in the B Cell Receptor (BCR) signaling pathway of T1 and T2 B cells is known to be associated with autoimmune disease. Lyn is a Src family protein tyrosine kinase known to be intimately involved in the initiation and regulation the BCR signaling pathway in all B cells. Lyn kinase activity is both positively and negatively regulated by phosphorylation of several strategic tyrosine residues. Results from both the proteomic and phosphoflow approaches have converged on supporting the hypothesis that altered Lyn phosphorylation and functionality consequent to mercury exposure may be key interrelated phenomena mediating immuntoxicity of mercury intoxicated B cells and the emergence of an autoimmune B cell repertoire in mercury intoxicated individuals. This being the case, expression of specific Lyn phosphorylation profiles in B cells may be useful biomarkers of Hg-induced autoimmunity in Hg2+ exposed individuals. Supported by NIH grant ES019228.

PS 137 Modeling Mechanism by Which Trichloroethylene Inhibits Liver Repair in Mouse Model of Autoimmunity

S. Erickson[1], K. Gilbert[1], B. Reisfeld[2], T. Zurlinden[2], M. Kreps[1] and S. J. Blossom[1]. [1]*University of Arkansas for Medical Sciences/Arkansas Children's Hospital Research Institute, Little Rock, AR and* [2]*Colorado State University, Fort Collins, CO.*

Chronic exposure to industrial solvent and water pollutant trichloroethylene (TCE) in female MRL+/+ mice generates disease commensurate with human autoimmune hepatitis. The current study was initiated to investigate why TCE-induced autoimmunity targeted the liver. The time- and dose-dependent effects of TCE on pro-inflammatory events in liver and macrophages from female MRL+/+ mice were examined. Compared to other tissues the liver has an unusually robust capacity for repair and regeneration that protects against pathology. Consequently, the impact of TCE on these hepatoprotective events were also examined. The addition of TCE to drinking water for 12 weeks induced a dose-dependent decrease in macrophage production of IL-6 at both the transcriptional and protein level. Although often regarded as a pro-inflammatory cytokine, IL-6 is primarily protective in the liver. TCE had little effect on liver expression of pro-inflammatory genes (Tnfa, Saa2 or Cscl1) until the end of a 40-week exposure. Instead, TCE suppressed hepatic expression of genes involved in IL-6 signaling (Il6r, gp130, and Egr1). Linear regression analysis confirmed liver histopathology in the TCE-treated mice correlated with decreased expression of Il6r. A toxicodynamic model was developed to define the effects of TCE on IL-6 signaling and liver pathology under different levels of exposure and rates of repair. This study underlined the importance of longitudinal studies in mechanistic evaluations of immuntoxicants. It showed that later-occurring liver pathology caused by TCE was associated with early suppression of hepatoprotection rather than an increase in conventional pro-inflammatory events. This information was used to create a novel toxicodynamic model of TCE-induced liver inflammation.

PS 138 Activation of Poly(ADP-Ribose)Polymerase-1 in Trichloroethene-Treated MRL+/+ Mice: Potential Role in Autoimmunity

H. Ma, G. Wang and M. Khan. *Pathology, University of Texas Medical Branch, Galveston, TX.*

The mechanisms by which trichloroethene (TCE) induces/exacerbates an autoimmune response are not well understood. Previously, we have shown that TCE exposure leads to oxidative stress which contributes to TCE-mediated autoimmunity. This study was aimed to further assess the role of oxidative stress in TCE-induced autoimmunity by assessing the role of poly(ADP-ribose)polymerase-1 (PARP-1, which is mainly involved in DNA repair, and apoptosis by depleting NAD+ and ATP). To achieve this, groups of female MRL +/+ mice were given TCE, N-acetylcysteine (NAC) or TCE + NAC for 6 weeks (TCE, 10 mmol/kg, i.p., every 4th day; NAC, 250 mg/kg/day through drinking water). TCE exposure led to significant increases in serum levels of anti-nuclear (ANA) and anti-dsDNA antibodies. TCE treatment also led to significant increases in the levels of 8-hydroxy-2'-deoxyguanosine (8-OHdG) in kidney (1.7 fold) and liver (1.6 fold) compared to controls, suggesting increased oxidative DNA damage. TCE-induced DNA damage was also associated with significant increases in PARP-1 levels which were 2.8- and 2.9-fold higher in kidney and liver, respectively. Remarkably, NAC supplementation not only attenuated DNA damage and its repair (reduced 8-OHdG and PARP-1 levels), but also the TCE-mediated autoimmunity as evident from significantly reduced serum ANA and anti-dsDNA. These results suggest that TCE-induced oxidative DNA damage along with increased PARP-1 levels may play a role in TCE-mediated autoimmunity, and excessive activation of PARP-1 presents a potential mechanism of TCE-mediated autoimmunity via increased apoptosis of the cells. Supported by NIH ES016302.

PS 139 Evaluation of Nitrosative Stress in the Pathogenesis and Prevention of Autoimmunity Mediated by Trichloroethene

G. Wang, J. Wang and M. Khan. *Pathology, University of Texas Medical Branch, Galveston, TX.*

Exposure to trichloroethene (TCE), a ubiquitous environmental contaminant, has been linked to a variety of autoimmune diseases (ADs) including SLE, scleroderma and hepatitis. Mechanisms involved in the pathogenesis of such ADs are largely unknown. Earlier studies from our laboratory in MRL+/+ mice suggested the contribution of oxidative/nitrosative stress in TCE-induced autoimmunity, and N-acetylcysteine (NAC) supplementation provided protection against autoimmunity by attenuating oxidative stress. This study was undertaken to evaluate the role of nitrosative stress in TCE-mediated autoimmunity. Groups of female MRL +/+ mice were given TCE, NAC or TCE + NAC for 6 weeks (TCE, 10 mmol/kg, i.p., every 4th day; NAC, 250 mg/kg/day through drinking water). TCE exposure led to significant increases in serum levels of anti-nuclear (ANA) and anti-histone antibodies. TCE exposure also led to significant induction of iNOS and increased formation of nitrotyrosine in the sera and livers. Proteomic analysis (2D gel followed by mass spectrometry) identified several nitrated proteins in the livers of TCE-treated mice, also suggesting an overall increase in nitrosative stress. Furthermore, TCE exposure led to decreased GSH levels and increased NF-κB p65 expression. Remarkably, NAC supplementation not only ameliorated the TCE-induced nitrosative stress, reduced GSH levels and NF-κB p65 activation, but also the markers of autoimmunity, as evident from decreased levels of autoantibodies in the sera. These findings provide further support the role of nitrosative stress in TCE-induced autoimmune response. Attenuation of TCE-induced autoimmunity in mice by NAC provides an approach for designing preventive and/or therapeutic strategies. Supported by NIH ES016302.

PS 140 Docosahexaenoic Acid Consumption Suppresses Silica-Induced Pneumonitis and Glomerulonephritis in Lupus-Prone NZBWF1 Mice

M. Bates[1], C. Brandenberger[1], I. Langohr[1], L. Bramble[1], A. Holian[2], J. R. Harkema[1] and J. J. Pestka[1]. [1]*Michigan State University, East Lansing, MI and* [2]*University of Montana, Missoula, MT.*

Exposure to environmental agents such as silica is suspected to contribute to initiation and exacerbation of autoimmunity in genetically predisposed individuals. In prior work, we observed in lupus-prone mice that intranasal exposure to crystalline silica induced a marked inflammatory response in the lungs characterized by elevated pro-inflammatory cytokines, perivascular lymphoplasmacytic infiltration, and secretion of IgG, as well as comparable systemic effects that resulted in early onset of glomerulonephritis. Consumption of the n-3 polyunsaturated fatty acid (PUFA) docosahexaenoic acid (DHA) has been demonstrated to prevent inflammation and progression of autoimmunity in both animal and human studies, suggesting that diet is an important factor in autoimmune disease-prone individuals. The purpose of this study was to test the hypothesis that DHA consumption can prevent silica exacerbated lupus nephritis. Lupus-prone NZBWF1 mice were fed a modified AIN-93G diet supplemented with 0, 1, 3 or 6% DHA-enriched algal oil for 2 wk prior to intranasal silica exposure (1 mg weekly for 4 wk) and maintained on experimental diets until sacrifice. Diets supplemented with 3% and 6% DHA markedly repressed perivascular lymphoplasmacytic infiltration in lungs of silica-treated mice. Repressed pneumonitis was temporally related to reduced pro-inflammatory cytokines, IgG secretion, and autoantibodies to dsDNA in both bronchoalveolar lavage fluid and plasma. The anti-inflammatory effects of DHA were

further reflected in the kidneys of lupus-prone mice by delayed onset of proteinuria and reduction of glomerulonephritis. The percent energy intake from 3% and 6% DHA-enriched AIN-93G diet were comparable to 2.7% and 5.5% respectively, of dietary intake or pharmacological supplementation in humans. Taken together, these results suggest that consumption of the n-3 PUFA, DHA, might be effective in preventing silica-induced acceleration and exacerbation of autoimmunity.

PS 141 Early Immunomodulatory Effects of Dermal Triclosan Exposure in Mice

N. B. Marshall, S. E. Anderson, K. L. Anderson, C. M. Long, E. Lukomska and B. J. Meade. *CDC/NIOSH, Morgantown, WV.*

It has recently been shown that dermal application of the commonly used antimicrobial compound triclosan, enhanced allergic responses in a mouse asthma model. To help elucidate the mechanisms of this augmented allergic response, we investigated the early immune-related effects of dermal triclosan exposure in mice. Triclosan was applied daily to the dorsal surface of the ears of BALB/c mice at concentrations ranging from 0%-3%, and leukocytes were examined in different organs over time using flow cytometry. Examination of the draining lymph nodes revealed a dose-dependent increase in cell numbers and enhanced GATA-3, IL-4, IL-21 and IL-17 expression suggesting enhanced Th2- and Th17-like effector T cell polarization. Effects on antigen presenting cells were also observed including increased expression of MHC class II, CD80 and CD86. In mice sensitized to ovalbumin (OVA) and subsequently challenged with OVA through pharyngeal aspiration on day 7, mice exposed to triclosan had increased cell numbers in the bronchoalveolar lavage and mediastinal LN by 24 hours compared to vehicle-treated mice. Interestingly, the introduction of OVA into the airway of triclosan-exposed mice was associated with increased swelling of the ear tissue along with an influx of CD11b+ cells and dramatic increase in TSLP and TNF-alpha expression. Taken together, the early immunomodulatory effects of triclosan suggest an adjuvancy-type effect that involves CD4 T cells and antigen presenting cells which may contribute to the augmentation of allergic responses.

PS 142 An Immunologic Role of microRNA 210 in a Murine Model of Dermal Toluene-2, 4-Diisocyanate Sensitization

C. M. Long[1, 2], N. B. Marshall[1], P. D. Siegel[1], B. J. Meade[1], E. Lukomska[1], K. L. Anderson[1], D. Beezhold[1] and S. E. Anderson[1]. [1]*Centers for Disease Control and Prevention-National Institute for Occupational Safety and Health (CDC-NIOSH), Morgantown, WV and* [2]*Immunology and Microbial Pathogenesis Graduate Program, West Virginia University, Morgantown, WV.*

Diisocyanates, such as toluene 2, 4-diisocyanate (TDI) are the principal cause of occupational asthma induced by low molecular weight chemicals. Recently, the study of immune regulation by microRNAs has revealed the importance of these regulatory molecules in allergic disease. Our laboratory has shown that miRNA 210 (miR-210) expression increases in the draining lymph nodes (DLN) following dermal exposure to TDI in a murine model, however, the role of miR-210 in allergic disease is unknown. These studies were conducted to elucidate the functional role of miR-210 during sensitization to TDI. Female BALB/c mice were dermally exposed to TDI (4%) or vehicle. RNA was isolated from specific cellular subsets (T-cells and B-cells) at four days post exposure and analyzed for miR-210 expression using real-time quantitative polymerase chain reaction analysis. A statistically significant increase in miR-210 expression occurred in the DLN CD4+ cell population of TDI-exposed mice. Confirmed (foxp3) and predicted (runx1t1, runx3, smad4, and stat6) miR-210 transcription factor targets were identified using computational algorithms. Augmentations in foxp3 protein expression and decreases in runx1 and foxp3 mRNA occurred concurrently with expression of miR-210 following dermal TDI exposure. Understanding the immunologic mechanisms of allergic disease is critical for the development of preventative and therapeutic strategies and these studies suggest a functional role for miR-210 in the regulatory T cell pathway and ultimately in the pathogenesis of TDI sensitization.
Funding: This work was supported by internal funds from the Health Effects Laboratory Division of the National Institute for Occupational Safety and Health

PS 143 Differential Susceptibility to Suppression of Human Peripheral Blood T Cells by Sodium Arsenite and Monomethylarsonous Acid

F. T. Lauer[1], D. MacKenzie[1], E. Beswick[2], A. J. Gandolfi[3], L. G. Hudson[1], K. Liu[1] and S. W. Burchiel[1]. [1]*Pharmaceutical Sciences, University of New Mexico College of Pharmacy, Albuquerque, NM,* [2]*Molecular Genetics and Microbiology, University of New Mexico School of Medicine, Albuquerque, NM and* [3]*Pharmacology and Toxicology, University of Arizona College of Pharmacy, Albuquerque, AZ.*

Human exposure to arsenic in drinking water is known to contribute to many different health outcomes such as cancer, diabetes, and heart disease. Several epidemiological studies suggest that T cell function is also altered by drinking water arsenic exposure. However, it is unclear how individual responses differ to various levels of exposure to arsenic. Our laboratory has recently identified differential responses of human peripheral blood mononuclear cell (HPMBC) T cells as measured by polyclonal T cell activation following sodium arsenite exposure. Certain healthy individuals exposed to low concentrations (0.1- 100 nM) of arsenic in vitro showed a dose-dependent suppression at low concentrations of arsenite, whereas other individuals were not suppressed at low concentrations. In a series of 30 normal donors, we found that three individuals were sensitive to low dose sodium arsenite-induced inhibition of T cell proliferation produced by phytohemagglutinin (PHA) and anti-CD3/anti-CD28. There also appeared to be a correlation with the amount of IL-2 produced by these cells in culture. Current studies suggest that donors who are sensitive to As+3 may be even more sensitive to monomethylarsonous acid (MMA+3) at concentrations of 0.1-100 nM. Our studies demonstrate for the first time that low doses of As+3 and MMA+3 are immunosuppressive to HPBMC T cells in some individuals.
This work is supported by 1R01ES019968

PS 144 Association of Pro-Inflammatory and Apoptotic-Related Genes Expression with Lymphocyte DNA Telomere Length (LTL) in a Mexican Population Exposed to Arsenic

C. Escudero-Lourdes[1], A. S. Perez-Martinez[1], L. M. Del Razo[2], J. Alegria-Torres[3] and P. Mandeville[1]. [1]*Laboratorio de Inmunotoxicologia, Universidad Autonoma de San Luis Potosi, San Luis Potosi, Mexico,* [2]*Toxicologia, Centro de Investigación y Estudios Avanzados, México, D.F., Mexico and* [3]*Laboratorio de Investigación en Nutrición, Universidad del Centro de México, San Luis Potosi, Mexico.*

Long term exposure to inorganic arsenic (iAs) leads to a sustained inflammatory response. Chronic inflammation is frequently associated with oxidative stress which may cause telomere dysfunction, leading to apoptosis or, on the opposite side, to cells malignant transformation. It has been reported that during acute inflammation telomeres length increase temporarily, maybe as a strategy to assure cell expansion and insult elimination. However, telomere length shortening has been reported in peripheral blood lymphocytes as a marker of accumulated effect of oxidative stress and inflammation. In this work we evaluated the expression of inflammation and apoptotic related genes and its association with leucocyte telomere length (LTL) in a Mexican population chronically exposed to iAs (n=128) in drinking water. Results showed a positive association between iAs exposure and granulocyte and macrophage colony stimulating factor (GM-CSF) gene expression (p=0.00305) and LTL was positively associated with urinary concentration of DMA III+V (p= 0.044), but only when variables corresponding to Apaf-1, TGF-β e IL-8 gene expression were included in the multivariate model. These preliminary results suggest that inflammatory responses may contribute to lymphocyte telomere dysfunction and it could represent a mechanism associated with an increased risk for iAs-related diseases development in exposed populations.

PS 145 Inhibition of Early T Cell Cytokine Production by Arsenic Occurs Independently of Nrf2

K. R. VanDenBerg[1] and C. E. Rockwell[1, 2]. [1]*Pharmacology and Toxicology, Michigan State University, East Lansing, MI and* [2]*Center for Integrative Toxicology, Michigan State University, East Lansing, MI.*

Nuclear factor erythroid 2-related factor 2 (Nrf2) is a stress-activated transcription factor that induces the expression of a variety of cytoprotective genes. Nrf2 has also been shown to mediate immunosuppressive effects in multiple inflammatory models. Upon activation, Nrf2 dissociates from its repressor protein, Keap1, and translocates to the nucleus to induce the expression of Nrf2 target genes. This Nrf2-Keap1 interaction can be disrupted by the environmental toxicant and chemotherapeutic agent arsenic trioxide (ATO). The purpose of this study was to determine the effects of ATO on early events of T cell activation and the role of Nrf2 in those effects. The Nrf2 target genes Hmox-1, Nqo-1, and Gclc were all

found to be upregulated by ATO treatments (1-2 μM) in splenocytes derived from wild-type, but not Nrf2-/-, mice, suggesting that Nrf2 is activated by ATO in splenocytes. ATO was also found to inhibit IFNγ and IL-2 production in wild-type splenocytes activated with the T cell activator, anti-CD3/anti-CD28. However, ATO also inhibited IFNγ and IL-2 production from Nrf2-null mice, suggesting the inhibition is independent of Nrf2. In contrast, ATO had little effect on either protein or mRNA expression of the cell surface receptors CD25 and CD69. Collectively, this study suggests that although ATO activates Nrf2 in splenocytes, inhibition of early T cell cytokine production by ATO occurs independently of Nrf2. (This work is supported by NIH grant: ES018885)

PS 145a Cross-Reactivity of Halogenated Platinum Salts

D. M. Lehmann[1], E. H. Boykin[1], C. Copelnd[1], L. B. Copeland[1], S. J. Quell[2] and W. Williams[1]. [1]*NHEERL, U.S. EPA, Research Triangle Park, NC and* [2]*Student Contractor, Youngsville, NC.*

Halogenated platinum (Pt) salts are well-known respiratory sensitizers associated with the development of asthma. People may be exposed to a variety of platinum compounds in different contexts (e.g. occupationally, automobile exhaust). Published reports suggest that sensitization to one Pt compound may result in hypersensitivity reactions to other Pt compounds. We investigated the potential for this type of cross-reactivity using a mouse model of Pt hypersensitivity. Mice were sensitized through application of 100 μL 1% ammonium hexachloroplatinate (AHCP) in DMSO to the shaved back on days 0, 5 and 19, and 25 μl to each ear on days 10, 11 and 12. Unsensitized mice received vehicle. On day 24, mice were challenged by intratracheal aspiration (IA) with saline or 100 μg AHCP or 100 ug ammonium tetrachloroplatinate (ATCP) in saline. Before and immediately after dosing, airway responses were assessed using whole body plethysmography (WBP). On day 26, changes in ventilatory responses to methacholine (Mch) aerosol were assessed by WBP. All mice dosed with AHCP demonstrated significant increases in total serum IgE, suggesting the animals were sensitized. An immediate airway response (IAR) was observed in mice sensitized and challenged with AHCP. Dose-dependent increases in Mch responsiveness occurred in mice sensitized and challenged with AHCP. Bronchoalveolar lavage fluid (BALF) harvested from mice sensitized and challenged with AHCP contained an average of 5% eosinophils compared to less than 0.5% in control mice ($p < 0.05$). When challenged with 100 ug ATCP, AHCP sensitized mice also exhibited an IAR. Compared to control mice, BALF harvested from the lungs of ATCP challenged mice also contained elevated numbers of eosinophils and were responsive to Mch aerosol. Our data demonstrate that ATCP can trigger allergic lung responses in AHCP sensitized mice. This abstract does not represent EPA policy.

PS 145b Contact Sensitizing Potential of 2-Ethylhexyl p-methoxycinnamate in Female BALB/c Mice

R. P. Frawley[1], D. R. Germolec[1], B. McIntyre[1], M. J. Smith[2], K. L. White[2] and T. L. Guo[2]. [1]*National Toxicology Program, NIEHS, Research Triangle Park, NC and* [2]*Virginia Commonwealth University, Richmond, VA.*

2-Ethylhexyl p-methoxycinnamate (EHMC) is a common, active ingredient in sunscreens that absorbs in the ultraviolet B range. EHMC has been detected in both the plasma and urine of humans 3-4 hours after topical application. Published reports suggest that EHMC may be a contact sensitizer or irritant in humans, and may modulate immune responses related to hypersensitivity. The objective of this study was to evaluate the direct hypersensitivity potential of EHMC in female BALB/c mice following dermal exposure using the ICCVAM-validated local lymph node assay (LLNA) in combination with a measurement of irritancy (IRR), and the mouse ear swelling test (MEST). EHMC was applied to the dorsa of both ears daily for three days. Statistically significant ear swelling, relative to the vehicle control (acetone:olive oil, 4:1), was observed 24 hours following the third application of EHMC at concentrations ranging from 1% to 50% (v/v), however, there was no increase in cervical (auricular) lymph node cell proliferation at 0.25%-50% EHMC. In the MEST, at 48 hours post-challenge only, mice sensitized and challenged with 5% EHMC exhibited increased ear swelling, compared to the vehicle control. Because this dose had induced an irritancy reaction in the LLNA/IRR, and because there was no significant difference between the 0.15% 2,4-dinitrobluorobenzene positive control and the positive control-challenge only groups, a second MEST was conducted at non-irritating concentrations. At 0.25%-1.0% EHMC sensitization/0.5% EHMC challenge, there was no increase in ear swelling at either 24 or 48 hours post-challenge. In summary, based on the irritancy response in the absence of lymph node cell proliferation in the LLNA/IRR, and the lack of edema at non-irritating concentrations in the MEST, EHMC can be characterized as an irritant, but not a sensitizer, under the conditions of this study. This research was supported by the Intramural Research program of the NIH, NIEHS.

PS 146 Identification of Chemical-Specific Toxicity Transcript Profiles *In Vitro* Using a Comprehensive or a Custom-Made Microarray

J. M. Naciff[1], Y. Shan[1], X. Wang[1], K. N. De Abrew[1], R. Adams[1], J. P. Tiesman[1], R. S. Settivari[3], E. W. Carney[3], B. A. Wetmore[2], R. S. Thomas[2] and G. Daston[1]. [1]*Procter and Gamble, Cincinnati, OH,* [2]*The Hamner Institutes for Health Sciences, Research Triangle Park, NC and* [3]*The Dow Chemical Company, Midland, MI.*

We have demonstrated that it is possible to define chemical mode of action (MOA) by assessing chemical-specific changes in gene expression in a small number of cell types enriched in relevant pathways for such MOA. Looking for more cost effective approaches to gain information to define MOA for chemicals of interest, we have evaluated the transcriptional profile elicited by 34 chemicals in Ishikawa (uterine) and MCF7 (breast cancer) cells, using two platforms: a conventional microarray-based method (U219, Affymetrix) and a custom approach which measures the expression levels of approximately 1000 landmark genes, and uses a computational model trained to infer the response of the other genes (L1000; Genometry). Each of the 34 chemicals was tested at 3 doses and at 3 different time points. In order to compare the two platforms, Affymetrix U219 chip ID was converted to U133A chip ID, since the latter array was used to derive the probes for the L1000 array, using Affymetrix best match list. The same number of up or down regulated genes from each platform were used to query the cMap database (Broad Institute). Of the 34 chemicals evaluated, 23 are represented in the database. For those chemicals, data from either platform was specific enough to identify matches in the database for the same chemical or comparable agents acting via the same mechanism or mode of action. For chemicals not in the database, the highest ranking connections are with agents that act via the same MOA. For example, the transcriptional signature of bisphenol A, a weak estrogen, matched the one elicited by other estrogens in the database, most prominently with estradiol and genistein. These results support a conclusion that the L1000 array may be useful as a low-cost alternative source of cMAP data. We are comparing data obtained with the same 34 chemicals tested in two additional cell types to further test this idea.

PS 147 Toxicological Effects of Toluene and Thinner in *Tribolium castaneum* Herbst

N. Pajaro-Castro, K. Caballero-Gallardo and J. Olivero-Verbel. *Environmental and Computational Chemistry Group, University of Cartagena, Cartagena, Colombia.*

Thinner is a solvent widely used in many industries. It contains mainly toluene (60-70%), although in general, xylene, ethylbenzene and other substances are also present in the mixture. Toluene is a compound possessing strong neurotoxic properties. The aim of this study was to examine the toxicological effects of thinner and toluene inhalation in *Tribolium castaneum*, a beetle toxicologically sensitive to volatile aromatic compounds. Adult insects were exposed to toluene and thinner at 0, 40, 80, 120, 160 and 240 μL/L air in glass vials. LC50 values were calculated by Probit analysis for 24 h and 48 h exposure, and RT-PCR was carried out to evaluate mRNA expression for selected genes. Thinner and toluene induced lethargy in exposed insects at concentrations equal or greater than 80 and 120 μL/L, respectively. The LC50 values for toluene and thinner at 24 h exposure were 129.66 μL/L and 107.35 μL/L, respectively, whereas at 48 h those were 126.45 μL/L and 99.82 μL/L, respectively. RT-PCR analysis performed on insects exposed to thinner revealed the activation of glutathione-S-transferase, an oxidative stress marker. Toluene alone, in addition to glutathione peroxidase, also overexpressed other genes such as hypoxia-inducible factor 1 α, DNA Ligase IV and delta-9 desaturase. These results suggest *T. castaneum* is a suitable alternative animal model for the study of toxicological effects of volatile aromatic compounds. This insect may help predicting the toxicity of volatile chemicals, as it reproduces some of the effects observed in mammalian model systems. Grant from University of Cartagena. Program to Support Research Groups (2013–2014). K.C. is sponsored by the National Program for Doctoral Formation (Colciencias, 567-2012).

PS 148 Screening of Compounds That Alter Sleep-Wake State Alteration in Zebrafish

A. Alzualde and A. Muriana. *BBD BioPhenix S.L., San Sebastian, Spain.*

The zebrafish is emerging as alternative to mammalian animal models. Although it is more phylogenetically distant from humans than mammals, zebrafish are vertebrate that display other advantageous characteristics including embryo transparency, which allows direct visualization and evaluation of internal organs; or small size, which allows to manipulate them easily and to use 96- and 384-well plates to

array embryos. The model is ideal to be used as a predictive tool in Drug Discovery, being able in a high extent to compare the results with those obtained in mammals. Increasing knowledge in zebrafish gives more support to this alternative model.
Physiological, biochemical and behavioral daily rhythms are regulated by circadian clock. The sleep-wake cycle is a well-studied output of the circadian clock. Apart from having many biological advantages, zebrafish are diurnal and present highly conserved circadian and sleep regulation systems, so they have been postulated also as a good model for circadian rhythm studies. Behavioral profiling in zebrafish reveals a conserved vertebrate neuropharmacology and identifies regulators of rest/wake states. For screening purposes, working with zebrafish larvae has many advantages in terms of rapidity and throughput.
The main objective of this study was to validate a protocol to detect compounds with potential to alter rest/wake states in zebrafish. For this purpose, zebrafish larvae were exposed to melatonin and other reference drugs as barbiturates and benzodiazepines directly in 96 well plates. After treatment larvae movement was tracked during 24 hours automatically. Diurnal and nocturnal locomotor activity and responsiveness of larvae are the main endpoints related to sleep states. This study supports the use of zebrafish in order to detect compounds that alter the sleep-wake states.

PS 149 Studying Obesogens Using Zebrafish

C. W. McCollum[1], A. Riu[1], C. L. Pinto[1], M. Grimaldi[2], A. Hillenweck[3], E. Perdu[3], D. Zalko[3], L. Bernard[4], V. Laudet[4], P. Balaguer[2], M. Bondesson[1] and J. Gustafsson[1]. *[1]CNRCS - Biology & Biochemistry, University of Houston, Houston, TX, [2]Universite de Montpellier 1, INSERM U896, IRCM, Montpellier, France, [3]Research Center in Food Toxicology, INRA, UMR 1331, Toxalim, Toulouse, France and [4]Molecular Zoology Team, Institut de Genomique Fonctionnelle de Lyon, ENS de Lyon, Lyon, France.*

There is a growing prevalence in adult and childhood obesity, which leads to medical complications such as heart diseases, diabetes and other metabolic abnormalities. More than 35% of adults and roughly 17% of children in the U.S. are obese, with a projected increase in obesity prevalence in 2030 estimated at 33%. Recently, the American Medical Association officially classified obesity as a disease. Human health has been shown to be affected by the increasing presence of environmental pollutants in forms of industrial products (pesticides, drugs, plasticizers, etc.), some of which have been reported to lead to obesogenic effects in animal models. Indeed, exposure *in utero* to tributyltin (TBT) has been shown to predispose obesity in mice. Previously, we reported tetrabromobisphenol A (TBBPA) and tetrochlorobisphenol A (TCBPA), both commonly used as flame retardants, activate human and zebrafish peroxisome proliferator-activated receptor gamma (PPARγ) *in vitro* and induce adipogenesis in 3T3-L1 preadipocytes. PPARγ, highly expressed in adipose tissues, promotes adipogenesis and regulates lipid metabolism. To further investigate the link between environmental pollutants and obesity, we have utilized zebrafish as an obesogen model. We describe the metabolic fate of TBBPA and TCBPA to better assess the use of zebrafish as a vertebrate model for mammalian endocrine disruption. Additionally, we explore *in vitro* and *in vivo* activation of both human and zebrafish PPARγ by pharmaceutical human PPARγ ligands, TBBPA, TCBPA and TBT. We also show that TBBPA, TCBPA and TBT act as obesogens and promote lipid accumulation in zebrafish larvae, as well as induce late-onset obesity.

PS 150 Effects of LXR Activation on Lipid Metabolism and Visual Function in Zebrafish

C. L. Pinto, A. Riu, J. Gustafsson, M. Bondesson and P. Jonsson. *Center for Nuclear Receptors & Cell Signaling, University of Houston, Houston, TX.* Sponsor: D. Zalko.

Liver X receptor (LXR), a ligand-activated transcription factor, is a key regulator of multiple pathways involved in lipid, cholesterol and carbohydrate metabolism. While there are two LXR isoforms in mammals, LXRα (NR1H3) and LXRβ (NR1H2), only one LXR gene with higher sequence similarity to mammalian LXRα has been reported in zebrafish (zf). LXR has been shown to be expressed at early developmental stages in zf, suggesting a primordial role of LXR. To assess the effects of LXR activation during zf development, zf larvae were exposed to the LXR agonists T0901317 (2μM) and GW3965 (1μM) from 4 to 6 days post-fertilization (dpf), and RNA was extracted for microarray and qRT-PCR analyses. Microarray data demonstrated several conserved effects of the LXR ligands with mammalian models, including upregulation of known mammalian LXR target genes, and several genes involved in fatty acid and cholesterol biosynthetic pathways. These genes could potentially be used to assess the effects of environmental compounds targeting LXR in zebrafish. Our data shows that LXR plays an important role in lipid metabolic pathways during zf development and supports zebrafish as an alternative model for LXR-related studies involving lipid metabolism. Moreover, zf exposure to the LXR ligands resulted in regulation of genes associated with eye development and visual perception, including photoreceptor and lens-specific genes, suggesting that LXR may also play a role in eye development and visual function in zebrafish.

PS 151 Comparing the Effects of Bisphenol A and Its Substitute BPS on Reproduction Using *C. elegans*

Y. Chen and P. Allard. *Department of Molecular Toxicology, UCLA School of Public Health, Los Angeles, CA.*

While the toxic effects of Bisphenol A (BPA) have come under heavy scrutiny, Bisphenol S (BPS), one substitute of BPA, is increasingly used in the "BPA-free" plastic manufacturing industry. Sharing a similar structure and bioactivity with BPA, BPS also poses a potential threat to human health. However, information regarding the toxicity of BPS is still limited. In this study, the reproductive toxicity of BPS is investigated by using the nematode *Caenohabditits elegans* (*C. elegans*). Worms were grown in media containing 125, 250 and 500μM BPS or BPA. The number of apoptotic germ cells in the gonad was performed by using acridine orange staining and DAPI staining was utilized to examine the gonad structure and chromosomal abnormalities in oocytes. The effect on brood size and larvae lethality were also evaluated. Our preliminary results show that 125μM and above concentration of both BPS (7.6+3.6) and BPA (8.1+2.2) can significantly increase the apoptotic cell number in each side of the gonad, when compared to the control group (5.5+1.9). The brood size in all of the BPS and BPA groups were significantly increased except the 500μM BPA group, in which this number was dramatically reduced. These findings were consistent with the changes observed in DAPI staining, which included increased number of gaps in germline. Interestingly, both chromosomal abnormalities in oocytes and larvae lethality were only increased by BPA but not BPS. Our results reveal that BPS, like BPA, elicits detectable reproductive toxicity and has the potential to affect reproductive function in human. Future works will concentrate on examining the distinct effects on larvae lethality between BPA and BPS as well as investigating the effect of combination of BPA and BPS.

PS 152 High-Content Screening in Zebrafish Embryos Identifies Butafenacil As a Potent Inducer of Anemia

J. K. Leet, C. Lindberg, L. Bassett, G. Isales, K. Yozzo, T. Raftery and D. Volz. *Department of Environmental Health Sciences, University of South Carolina, Columbia, SC.*

Targeted high-throughput assays are needed to better predict morphologic and functional effects of chemicals on cardiovascular development. Using transgenic zebrafish (*fli1:egfp*) that stably express eGFP within vascular endothelial cells, we recently developed and optimized a 384-well high-content screening (HCS) assay that enables us to screen and identify chemicals affecting cardiovascular function at non-teratogenic concentrations. Within this assay, automated image acquisition procedures and custom image analysis protocols are used to quantify body length, heart rate, arterial circulation, pericardial area, and intersegmental vessel area within individual live embryos exposed from 5-72 hours post-fertilization (hpf). After ranking acute toxicity data generated from the U.S. Environmental Protection Agency's (EPA's) zebrafish teratogenesis assay, we screened ~10% of the most potent chemicals within EPA's ToxCast™ Phase-I library in concentration-response format (0.05-50 μM) using this HCS assay. Based on this screen, we identified butafenacil as a potent inducer of anemia, as exposure to 0.39-3.125 μM butafenacil completely abolished arterial circulation of blood cells in the absence of effects on all other endpoints evaluated. Although the cause of anemia is currently unclear, butafenacil is a herbicide that inhibits protoporphyrinogen oxidase (PPO) – an enzyme necessary for heme production in vertebrates – suggesting that severe butafenacil-induced anemia in zebrafish may be due to a loss of hemoglobin and red blood cell production during segmentation (10-24 hpf). Therefore, we are currently screening other PPO inhibitors within the ToxCast™ Phase-I library to determine whether anemia represents a common adverse outcome for these herbicides. Overall, this study highlights the ability of this assay to (1) screen chemicals for targeted effects on cardiovascular function and (2) prioritize chemicals for future hypothesis-driven and mechanism-focused investigations within zebrafish and mammalian models.

PS 153 Effects of Methylmercury on Dopaminergic Neuron Development in Zebrafish Larvae

S. S. Huang, R. Godoy, M. Ekker and L. Chan. *Biology, University of Ottawa, Ottawa, ON, Canada.*

Methylmercury (MeHg) is a well known neurotoxin capable of altering the structure and function of the central nervous system. Many signs of MeHg toxicity, including hypoesthesia and tremors, are similar to that of many neurodegenerative diseases, most notably Parkinson's disease (PD). The disease is pathologically characterized by the progressive loss of dopaminergic (DA) neurons in the midbrain, resulting in the reduction of dopamine secretion and the development of movement disorders. Wild type zebrafish (ZF; *Danio rerio*) and the transgenic strain (Tg(dat:EGFP)), expressing green fluorescence protein (GFP) in DA neurons of the ventral diencephalon, were used to evaluate the effects of environmentally relevant concentrations of MeHg on the progression of PD-like phenotypes. Three day old ZF larvae were exposed to either 0.06 or 0.3 μM MeHg for 48h. Preliminary data from whole-mount immunostaining for thryosine hydroxylase and live fluorescence imaging of dopamine transporters suggested disruption of the typical horseshoe pattern of DA neurons in MeHg exposed wild type and Tg(dat:EGFP) larvae. The effects of MeHg on DA neurons appeared to be dose correlated. Preliminarily locomotor assessments also showed a decreased mobility in MeHg exposed fish. There appeared to be a trend of reduced swimming activities in the 0.06 μM MeHg treated larvae, similar to those treated with 250 μM of 6-hydroxydopamine hydrochloride, a positive control for PD-like phenotype. Morphological changes such as endema, curvature of the spine, and hemorrhages confirmed MeHg toxicity in the exposed fish. mRNA expressions of parkin, PINK1, and LRRK2, genes associated with the recessive familial PD, were also determined. The preliminary results suggest that exposure to MeHg may increase the predisposition to neurodegenerative diseases, particularly PD, in a zebrafish model.

PS 154 The Challenge of Studying Exposure in Zebrafish Embryos

A. Wolterbeek[1], V. van der Weijden[1], T. Maarschalkerweerd[1], C. Snel[1], A. Beker[1], E. Hansen[2], F. Van Goethem[2], A. Menke[1] and N. Mesens[2]. *[1]TNO, Zeist, Netherlands and [2]Janssen, Pharmaceutical Companies of Johnson & Johnson, Beerse, Belgium.* Sponsor: R. Woutersen.

The embryonic and/or larval zebrafish model is rapidly gaining popularity to study toxicity of new compounds. Various characteristics warrant the zebrafish as an ideal non-mammalian whole organism model that could bridge gaps between in vitro cell systems and complex higher animal models.
A draw-back of the zebrafish model is that the chorion, a shell that protects the embryo in its earliest days, can act as a barrier for test compounds which might results in false negative test outcomes. However, using whole-organism homogenates to analyse total body burden might not give a realistic picture of the internal exposure of the embryo since compounds might stick to the outside of the chorion. Furthermore, in larvae, this approach will not give any information about the biodistribution of compounds.
In the present project we studied the uptake and biodistribution of a series of test compounds with different physical and chemical properties. Hereto, zebrafish embryos and larvae were treated with radioactive labeled test compounds for various time periods at different time points of development. By using autoradiography of serial microscopic sections, it was shown that both molecular weight and logP influenced the passage through the chorion, the uptake into the embryo and the biodistribution of the compounds. In general, total body burden of hydrophilic compounds is higher than that of hydrophobic compounds. Most hydrophilic compounds however stick to the chorion. In addition, it was shown that although total body burden analysis of compounds with a high molecular weight suggested considerable uptake by larvae, these compounds did not pass the epithelial cells of the gastrointestinal tract and stayed in the lumen. Consequently, internal exposure to these compounds was limited.
By testing the biodistribution of more compounds and taken into account the physical chemical properties of a compound, the predictability of the zebrafish model will be improved.

PS 155 High-Content Screening Assay for Identification of Chemicals Impacting Spontaneous Activity in Zebrafish Embryos

T. Raftery, G. Isales, K. Yozzo and D. Volz. *Environmental Health Sciences, Arnold School of Public Health, University of South Carolina, Columbia, SC.*

Although cell-based assays exist, there is a lack of rapid and cost-efficient high-content screening (HCS) assays within intact organisms to support prioritization for developmental neurotoxicity (DNT) testing in rodents. During zebrafish embryogenesis, spontaneous tail contractions represent the first sign of locomotion and result from innervations of primary motoneuron axons to target axial muscles. This behavior occurs from late-segmentation (~19 hours post-fertilization, hpf) through early-pharyngula (~29 hpf), and is an endpoint amenable for rapid detection of DNT. Moreover, as a single zebrafish embryo develops normally in 50 μl of water, potential chemical effects on this behavior can be evaluated in 384-well format. Thus, we have developed and optimized a 384-well-based HCS assay that quantifies spontaneous activity within single zebrafish embryos after exposure to test chemicals in concentration-response format. For this assay, we rely on transgenic zebrafish (fli1:egfp) that stably express eGFP beginning at ~14 hpf, allowing us to track locomotion in the absence of shading effects under transmitted light. After manual loading and exposure from 5-24 hpf at 28°C, live embryos (one per well) are acclimated at 25°C for 1 h and imaged for 6 s each under fluorescence using a 2X objective and automated stream acquisition procedure. After converting streams to AVI files, spontaneous activity within each embryo is quantified using an automated procedure in our behavioral analysis software. Control embryo survival under these conditions is consistently >85%. We screened 16 chemicals within EPA's ToxCast™ Phase-I library, and found that exposure to abamectin and emamectin benzoate – both potent avermectins – abolished spontaneous activity in the absence of gross malformations. Overall, compared to existing locomotion-based zebrafish assays conducted later in development, this method provides a simpler discovery platform for identifying potential developmental neurotoxicants.

PS 156 High-Content Screening Assay for Identification of Chemicals Impacting Cardiovascular Function in Zebrafish Embryos

D. Volz, K. Yozzo, G. Isales and T. Raftery. *Environmental Health Sciences, University of South Carolina, Columbia, SC.*

Targeted assays are needed to better evaluate effects of chemicals on organogenesis and begin classification of chemicals by toxicologically relevant modes-of-action. Using transgenic zebrafish (fli1:egfp) that stably express enhanced green fluorescent protein (eGFP) within vascular endothelial cells, we have developed and optimized a 384-well-based high-content screening (HCS) assay that enables us to screen and identify chemicals affecting cardiovascular function at sub-lethal, non-teratogenic concentrations. Following static exposure of one embryo per well from 5-72 hours post-fertilization (hpf), automated image acquisition procedures and custom image analysis protocols are used to quantify body length, circulation, heart rate, pericardial area (a biomarker for cardiac looping defects), and intersegmental vessel area within freshly hatched live embryos. After optimizing 72-hpf anesthetization procedures, we evaluated each endpoint across four independent control plates containing 384 initial embryos per plate. Survival and imaging success rates across these plates ranged from 93-99% and 42-74%, respectively. Criteria were then defined for assay success and analysis of treatments, and 10 chemicals were screened for targeted effects on cardiovascular function. Compared to existing zebrafish-based assays, this method provides a comprehensive discovery platform with 1) increased sample sizes; 2) broad concentration-response format; and 3) the ability to identify chemicals that target cardiovascular function at non-teratogenic concentrations.

PS 157 A Novel Transgenic Zebrafish Model to Predict Organ Toxicities in Mammals

C. McGinnis[1], X. Wang[2], H. Wang[2], Z. Zhao[2], N. Kaur[2], S. Mathavan[3], S. Fowler[1], T. Weiser[1], S. Cohen[2] and P. Ingham[2]. *[1]Roche, Basel, Switzerland, [2]Institute for Molecular and Cell Biology, Singapore, Singapore and [3]Genomics Institute, Singapore, Singapore.*

Zebrafish have many attractions for toxicity testing: they are cheap and easy to breed under laboratory conditions, can readily be exposed to chemical and pharmaceutical compounds and are susceptible to genetic manipulation. Reference compounds with known or no in vivo liver toxicity were tested on larval and adult zebrafish as well as isolated liver microsomes and the effects compared to available in vitro (hepatocyte) and in vivo (clinical/preclinical) data. Uptake and metabolism of compounds was analysed by LC/MS. To maximize test compound throughput, transgenic reporter lines have been generated based on our analysis of the transcriptional response of zebrafish larvae to a set of reference compounds. One potential limitation of the zebrafish is the functional divergence of its bioactivation and detoxification systems compared to those of preclinical mammalian models used in drug development: testing with human CYP3A4 specific substrates revealed differences in their metabolism between zebrafish and human. To circumvent this limitation we have generated "humanized" transgenic zebrafish using either a human Bacterial Artificial Chromosome (BAC) containing the human CYP3A4 locus or the human CYP3A4 cDNA cloned downstream of a liver specific promoter. Enzyme activity studies with the human CYP3A4 substrate, midazolam,

showed a significant increase in 1-hdyroxy-midazolam metabolite generation in these transgenic lines compared to wild-type. The metabolic and transcriptional response of the "humanized" fish to a set of test compounds has been compared to that of wild-type fish. The results will be presented and discussed in the context of the utility of the humanized line for pre-clinical safety testing.

PS 158 Novel System for Express Screening of Organ/Tissue-Specific Toxicity in Live Juvenile and Adult Zebrafish

S. Revskoy. *Pharmacology, Toxicology Research Laboratory, UIC, Chicago, IL.*
Sponsor: A. Lyubimov.

We propose a cost-effective high throughput-screening model for in vivo testing of organ/tissue-specific toxicity and efficacy in real time in adult zebrafish whose internal organs/tissues are selectively labeled with an endogenously expressed fluorescent protein, which is released into circulation upon toxic destruction of the organ/tissue. Thus, the fluorescence can be detected in off-site tissues as a result of the fluorescent protein molecules release from damaged cells followed by the fluorescent protein diffusion and distribution via circulation from the targeted organ to neighbor and distant tissues. This ectopic fluorescence can be detected and quantitatively assessed in vivo by a comparison of fluorescence in the non-targeted tissue in untreated/non-transgenic fish vs. treated fish, wherein the change is indicative of the toxic/pharmacological activity. The accuracy of detection of ectopic fluorescence has further been enhanced by using optically transparent zebrafish strains (sheer or casper) expressing fluorescent proteins in targeted organs, e.g. liver, pancreas, heart, brain etc. With multiple reporter fluorescent proteins the measurements are carried out in different spectral conditions specific for each reporter. This technology has been tested using DEN toxicity towards liver and pancreas in transgenic zebrafish harboring DsRed2- and GFP-tags in liver and pancreas, respectively. Transgenic zebrafish (i.e., an optically transparent strain) with high levels of a fluorescent reporter in hepatocytes has responded to hepatotoxic compound DEN by releasing DsRed2 fluorescent protein into circulation. As a result fluorescence has been accumulated in areas distant from the liver, such as tail, fin and others. In contrast, DEN had no effect of GFP release from pancreas. This assay is non-invasive and can be carried out on the same fish multiple times for monitoring time-course toxicity. The same strategy will be applied to an assessment of pharmacological effects of antitumor drugs on syngeneic and allogeneic tumors, growing in fish.

PS 159 Cytotoxicity of Natural Toxins Mediated by the Organic Anion Transporting Polypeptide (OATP1B3)

V. Charoensuk, D. Huang, L. Xie and D. W. Kinniburgh. *Physiology & Pharmacology, Alberta Centre for Toxicology University of Calgary, Calgary, AB, Canada.*

Microcystins (MCYSTs) are natural toxins that inhibit serine-threonine protein phosphatase. The protein phosphatase inhibition assay (PPIA) has been used in our laboratory as a screening method to detect MCYSTs in lake water since 2007. We recently developed a novel assay using the real-time cell analyzer (RTCA, Roche xCELLigence) for detecting MCYST cytotoxicity. The assay is based on the fact that MCYSTs toxicity requires the active uptake of MCYSTs into the cytoplasma membrane which is mediated by the organic anion transporting polypeptides (OATPs). The aims of this study were (1) to investigate differential cytotoxicities of other natural toxins that possibly presented in water including nodularin, tautomycin, and MCYST analogues and (2) to observe the role of transporters in the toxicities of these natural toxins.
The wild type Chinese hamster ovarian cells (CHO/WT) and CHO with OATP1B3 expression (CHO/OATP1B3) were exposed to the toxins using the RTCA method. After 48h of incubation, no toxic effect was observed in CHO/WT, while growth inhibition was demonstrated in CHO/OATP1B3. Co-incubation of toxins with the known substrates of OATPs, taurocholate (TC) and bromosulfophthalein (BSP), inhibited the uptake of toxins through the OATP1B3 transporter and decreased the cytotoxic effects. The in vitro analysis of inhibition on purified protein phosphatase, PP1, was also performed to compare the differential potencies of the toxins. Inhibition concentrations at 50% (IC50) from both cytotoxicity and PPIA were compared.
In conclusion, we demonstrated that some natural toxins, such as nodularin, tautomycin and MCYSTs, require the active uptake by the OATP1B3 to induce cytotoxicity. The cytoxicity potencies are not necessarily related to the PP1 inhibition potencies.

PS 160 Development of an *In Vitro* Assay Measuring Estrogenic Responses for Use in Chemical Safety Assessment

R. Alyea, C. Le Sommer, P. Balbuena, S. Ross, P. D. McMullen, M. E. Andersen and R. A. Clewell. *The Hamner Institutes for Health Sciences, Research Triangle Park, NC.*

To support the vision outlined in the 2007 report "Toxicity Testing in the 21st Century: A Vision and A Strategy", our laboratory is evaluating key cell response networks to develop proof of concept safety assessments for a series of prototype compounds and networks, including the estrogen receptor (ER)-mediated uterine proliferation pathway. We evaluated the ability of a human uterine epithelial adenocarcinoma cell line (Ishikawa) to recapitulate in vitro phenotypic responses to ethinyl estradiol (EE), including proliferation, epithelial-to-mesenchymal transition (EMT), and transcriptional activation of key ER-mediated genes (PGR, ALPP, GREB1). Cells were treated with vehicle (ethanol; EtOH) or EE (18 doses, 10-14 to 10-6M) for 1-6 days and cell viability was measured. This phenotypic anchor, an approximate 1.2 fold increase in cell viability, helped inform the dose range selection of EE that caused no effect, minimal effect, or maximal effect, which were then used to further examine transcriptional responses encompassing several earlier time points (6, 12, 24, 72 hours) as an indicator of transcriptionally mediated precursor events. The lowest concentration at which we observed gene expression changes was 1pM at 12, 24, and 72 hours, the same dose at which we observed a phenotypic effect. Interestingly, DEPTOR, a negative regulator of mTOR, is upregulated at these low doses. EMT, an additional in vivo and in vitro phenotypic outcome associated with estrogen signaling, occurred at doses and times similar to those inducing proliferation (day 3; 10pM). Our results suggest that EE induced increased cell viability, EMT, and transcriptional activation occur at similar doses and are consistent with in vivo responses providing evidence that Ishikawa cells are an adequate platform for evaluating estrogen mediated cellular response networks.

PS 161 A Robotic MCF-7:WS8 Cell Proliferation Assay to Detect Agonist and Antagonist Estrogenic Activity

W. Casey[1], C. Z. Yang[2], M. Stoner[2], G. J. Kollessery[2], A. Wong[2] and G. D. Bittner[2, 3]. [1]*NICEATM, National Institute of Health, Research Triangle Park, NC,* [2]*CertiChem, Inc., Austin, TX and* [3]*Neurobiology Section, School of Biology, University of Texas in Austin, Austin, TX.*

Endocrine disrupting chemicals with estrogenic (EA) or anti-estrogenic (AEA) activity have been extensively reported to possibly have many adverse health effects. We have developed robotized assays using MCF-7:WS8 cell proliferation (or suppression) to detect EA (or AEA) of 78 test substances supplied by the Interagency Coordinating Committee on the Validation of Alternative Methods (ICCVAM) and the National Toxicology Program's Interagency Center for the Evaluation of Alternative Toxicological Methods (NICEATM) for validation studies. We also assayed ICI 182,780, a strong estrogen antagonist. Chemicals to be assayed were initially examined for solubility and volatility to determine optimal assay conditions. For both EA and AEA determinations, a range-finder assay was conducted to determine the concentration range for testing, followed by a comprehensive assay. Test substances with potentially positive results from an EA comprehensive assay were subjected to an EA confirmation assay that evaluated the ability of ICI 182,780 to reverse chemically-induced MCF-7 cell proliferation. The AEA assays examined the ability of chemicals to decrease MCF-7 cell proliferation induced by non-saturating concentrations of 17β-estradiol (E2), relative to ICI or raloxifene (RAL), also a strong estrogen antagonist. To be classified as having AEA, a saturating concentration of E2 had to significantly reverse the decrease in cell proliferation produced by the test substance in non-saturating E2. We conclude that our robotized MCF-7 EA and AEA Assays have accuracy, sensitivity, and specificity values at least equivalent to validated test methods accepted by the US EPA and the Organisation for Economic Co-operation and Development (OECD).

PS 162 Evaluation of the p53-Mediated DNA Damage Response Toxicity Pathway Using Chemicals with Distinct Mechanisms of DNA Damage

R. A. Clewell[1], B. Sun[1], Y. Adeleye[2], P. L. Carmichael[2], P. D. McMullen[1], S. Pendse[1] and M. E. Andersen[1]. [1]*Institute for Chemical Safety Science, The Hamner Institutes for Health Sciences, Research Triangle Park, NC and* [2]*SEAC, Unilever, PLC, Colworth Science Park, Sharnbrook, Bedfordshire, United Kingdom.*

As part of a larger effort to provide proof of concept *in vitro* only risk assessments, we have developed a suite of high throughput assays for key readouts in the p53 DNA damage response toxicity pathway: double strand breaks (p-H2AX), fixed chromosomal damage (micronuclei; MN), p53 activation (p53, p-p53), p53 tran-

scriptional regulation (MDM2, WIP1, p21) and cell fate (cell cycle, apoptosis). 18 point dose-response curves were generated for protein and cell fate endpoints in a p53 competent cell line (HT1080) for 3 mechanistically-distinct chemicals: etoposide, methylmethane sulfonate, and quercetin. Gene array analysis was also performed for each chemical at 7 doses ranging from those with no effect, minimal effect, or maximal effect on MN response. Evaluation of cellular response across chemicals and doses revealed two important observations. 1) The p53 transcriptional program is chemical dependent. At similar levels of DNA damage, the three chemicals cause very different protein and cellular responses (apoptosis vs. arrest). Together with published ChIP-seq studies, our transcriptomic data indicate that these different responses are determined very early (*i.e.*, prior to transcriptional activation) and are likely a result of differential kinase activation and augmentation of the general p53 transcriptional response by co-regulators. 2) The p53 transcriptional response does not prevent permanent DNA damage induction at low doses. MN induction occurs at doses equal to, or lower than, doses required to activate p53-mediated gene transcription. This observation is important because it indicates that any protective effect of p53 is likely due to p53's activity as a recruitment factor for repair proteins at the site of DNA damage. We are currently evaluating the role of post-translational p53 activities (repair center formation) in the prevention of permanent DNA damage at low chemical doses.

PS 163 Embryonic Stem Cells Carrying a Transgenic BMP-Reporter Construct: A Useful Tool for the Identification and Analysis of Teratogenic Compounds *In Vitro*

J. Kugler[1], J. Tharmann[1], S. M. Chuva de Sousa Lopes[2], C. L. Mummery[2], R. Kemler[3], A. Luch[1] and M. Oelgeschlaeger[1]. [1]*Federal Institute for Risk Assessment, Berlin, Germany,* [2]*Dept. of Anatomy & Embryology, Leiden University Medical Center, Leiden, Belgium and* [3]*Department of Molecular Embryology, Max Planck Institute of Immunobiology and Epigenetic, Freiburg, Germany.* Sponsor: A. Haase.

Embryonic stem cells (ESC) are used as a tool for the identification of teratogenic modes of action in the analysis of chemicals or pharmaceuticals. In particular, the embryonic stem cell test (EST) has been scientifically validated previously and is now used for screening purposes. The differentiation of ESC into various tissues is regulated by a set of essential signaling pathways, including the TGFβ, Wnt, and Shh pathway as well as tyrosine kinase receptors mediating FGF or EGF signaling. For some of these essential signaling pathways, transgenic reporter mice have been developed that allow the *in vivo* analysis of pathway activity during embryonic development.
We have isolated and characterized embryonic stem cells from transgenic mice carrying a EGFP transgene under the control of a BMP responsive element that has been shown to nicely recapitulate *in vivo* BMP activity (Monteiro *et al*, 2008). During the differentiation of ESC into cardiomyocytes, we analyzed the differentiation process using quantitative RT-PCR, FACS, quantitative EGFP measurements, and the functional analysis of contracting cardiomyocytes. Our results show that the activity of the reporter gene can be used for the detection of teratogenic activities of valproic acid, retinoic acid, and 6-aminonicotinamide *in vitro*. In addition these cells provide a useful tool to characterize the molecular mechanism underlying the activity of chemicals or pharmaceuticals on the differentiation process during early embryonic development.
Monteiro, R.M., S.M.de Sousa Lopes, M.Bialecka, B.S.de, A.Zwijsen, and C.L.Mummery. 2008. Real time monitoring of BMP Smads transcriptional activity during mouse development. *Genesis*. 46:335-346

PS 164 Cyclosporin A Pharmacokinetics in *In Vitro* Systems

P. Bellwon[1], T. Schmidt[1], G. Truisi[2], C. Savary[3], C. Parmentier[4] and W. Dekant[1]. [1]*Department of Toxicology, University of Wuerzburg, Wuerzburg, Germany,* [2]*Non-Clinical Safety, Merck Serono, Merck KGaA, Darmstadt, Germany,* [3]*Inserm, University of Rennes, Rennes, France and* [4]*KaLy Cell, Plobsheim, France.*

The immunosuppressant Cyclosporin A (CsA) is administered to reduce graft rejections after transplantation in patients, but it is also nephro-, hepato- and neurotoxic. Hepatotoxicity is related to elevated CsA blood levels and CYP3A4/5 activity in patients. Nephro- and hepatotoxicity can be diminished by drug monitoring and adjusted CsA administration. In this work, Cyclosporin A was used as a model compound to assess the kinetic profiles in three liver models (primary human hepatocytes [PHH], primary rat hepatocytes [PRH] and HepaRG cells) after repeated dosing. Cells were treated for up to 14 days with a high (TC10) and a non-toxic concentration (1/10th of TC10) specifically determined for each model. CsA concentrations were measured by LC-MS/MS in the treatment solutions, cell culture media, cell lysates and plastic binding samples at 5 specific time points on the first and the last treatment day. Comparisons across the models revealed three different kinetic profiles. Both PHH and HepaRG cells significantly metabolized CsA and no bioaccumulation was observed after repeated dosing. Instead, CsA accumulated in PRH. Comparison of kinetics in HepaRG cells and PHH indicated the difference between a cell line and a primary cell culture, with the latter showing biological variability between different human donors. These results underline the interspecies difference for the CYP3A metabolism route between human and rat hepatocytes, which can also be observed in vivo.

PS 165 Utilizing Human Population-Based *In Vitro* Model to Investigate Pesticide Mixtures and Drug/Metabolite Pairs

N. Abdo[1], P. Marlot[2], P. Munir[2], D. Shea[3], F. A. Wright[3, 1] and I. Rusyn[1]. [1]*UNC at Chapel Hill, Raleigh, NC,* [2]*University of Liverpool, Liverpool, United Kingdom and* [3]*North Carolina State University, Raleigh, NC.*

A population-based human *in vitro* model offers exceptional opportunities for evaluating the potential hazard, mode of action, and population variability in response to chemicals. Challenges remain that require further assessment to increase the utility of the information obtained from this model. This study was designed to address two of these challenges: limited metabolic capacity of lymphoblasts and the potential to screen complex mixtures. We selected lymphoblast cell lines from 4 racially and geographically diverse populations based on availability of genome sequence and basal RNA-seq. For the mixtures experiment, 146 cell lines were exposed to pesticide mixtures (organochlorine pesticide environmental mixture extracted from a passive surface water sampling device, or a mixture of 36 currently used pesticides). For the drug/metabolite experiment, we exposed 331 cell lines to Carbamazepine, Sulfamethoxazole, or two major metabolites of each drug. Concentration-response cell viability data was used to derive a 10% effect (or no-effect) level for each compound/cell line. We found that a mixture of pesticides currently in-use was less toxic but more variable than a mixture of organochlorine pesticides. A significant correlation between pesticide mixtures indicates that cells that were sensitive to one pesticide mixture were likely sensitive to the other. Significant population differences were found for the currently used pesticide mixture. For drug/metabolite pairs, we observed a wide range of inter-individual variability in cytotoxicity. Significant pairwise correlations of EC10 were found for each drug and its two metabolites. We found statistically significant and/or suggestive associations between genetic variants and cytotoxicity of each drug/metabolite. These data provide the opportunity to establish population-based confidence intervals in cytotoxicity, as well as probe candidate susceptibility pathways.

PS 166 Toll-Like Receptor 4 Signaling Heterogeneity in Different Cell Models Can Impact Data Interpretation and Toxicity Testing

B. Franz[1], M. Davidson[2], N. Hibbard[1] and J. M. McKim[1]. [1]*CeeTox, Inc, Kalamazoo, MI and* [2]*Kalamazoo College, Kalamazoo, MI.*

Toll-like receptor (TLR) mediated pro-inflammatory signaling in response to pathogen-associated molecular patterns (PAMPs) and endogenous ligands has been implicated in a diverse array of destructive immunopathological consequences. Divergence and heterogeneity in TLR4 surface expression and signaling in immortalized cell models may present advantages or limitations in experimental applications. The aim of the present study was to evaluate TLR4 functionality in *in vitro* models of diverse human tissue origin: THP-1 acute monocytic leukemia, HepG2 hepatocellular carcinoma, Caco2 colorectal adenocarcinoma, and H295R adrenocortical carcinoma. LPS-mediated induction of the TLR4 pathway was assessed by seeding cells into 96-well plates at 10,000 cells/well followed by 24 hr equilibration at 37°C, 5% CO_2. Cells were exposed to LPS (0.1, 1, 10, 100, 1000, and 10,000 ng/mL), an antagonist naloxone (1, 10, 100, and 1000 μM), or LPS + naloxone for a period of 24 hr. Media was collected for IL8 ELISA quantitation. The THP-1 cell line exhibited a clear concentration-response to LPS, reaching a maximum of 375 pg/mL IL8 at 10,000 ng/mL LPS. HepG2 cells showed a small increase at the highest LPS exposure (150 pg/mL IL8 at 10,000 ng/mL LPS). Caco2 (≈50 pg/mL IL8 at 10,000 ng/mL LPS) and H295R (<5 pg/mL IL8 at 10,000 ng/mL LPS) cells also showed minimal effects. These data indicate concentration-responsiveness of THP-1 to LPS and attenuation of LPS-mediated activity by simultaneous naloxone exposure (e.g., 60 pg/mL IL8 at 10,000 ng/mL LPS + 1000 μM naloxone). IL8 expression exhibited by the other *in vitro* models indicates low background production of the cytokine and an apparent lack of LPS concentration-dependent upregulation. Interestingly, naloxone appears to inhibit the expression of IL8 in the absence of LPS stimulation in all cell lines tested, with the exception of the monocytic THP-1. In conclusion, selection of a cell line can greatly influence the data obtained and subsequent interpretations regarding the role of TLR4 in any observed effects.

PS 167 Assessing Cellular Stress via Hif-1α and Nrf2 Signaling Using Protein Stability and Transcriptional Reporters

A. Landreman, M. Robers, M. Bratz, J. Wilkinson, C. A. Zimprich, J. Hartnett, B. Binkowski and M. Cong. *Promega Corporation, Madison, WI.*

The signaling pathways involved in the cellular stress response have been identified as useful screening targets for assessing potential compound toxicity that can be studied in a variety of *in vitro* cell model systems. We have used reporter gene assays to study two specific pathways involved in cellular stress response: hypoxia and antioxidant response as mediated by Hif1-α and Nrf2 transcription factors respectively. For both pathways we tested the hypothesis that monitoring stability of the transcription factor protein directly using novel protein fusion reporters would accurately reflect changes in transcriptional activity as measured by the expression of a reporter being driven by response element containing promoters. Assessment was performed in transiently transfected human induced pluripotent stem cell (iPSC)-derived cardiomyocytes (iCell® Cardiomyocytes) followed by treatment with cobalt chloride or 1,10-phenanthroline (Hif1-α) and D,L-sulforaphane or tert-butylhydroquinone (tBHQ) (Nrf2). Results demonstrate that changes in the signal from the protein reporter consistently reflect the observed changes in transcriptional activity at similar exposure concentrations. In addition, treating HEK293 cells stably transfected with Hif1-α or Nrf2 response element reporter constructs with the chemical inducers described above demonstrates that transcriptional induction can be multiplexed with a cell viability assay allowing for direct measurement of both reporter gene and cell viability from the same assay well. As toxicity assessment efforts continue to move towards utilizing more physiologically relevant *in vitro* model systems, the ability to monitor cellular stress using endpoints closer to the primary signaling event, such as the stability of the transcription factor protein directly, may be a useful compliment to more traditional transcriptional reporter assays. In addition, the ability to multiplex reporter and viability assays may be valuable, particular when utilizing limiting cell types such as iPSC or primary cells.

PS 168 Characterization of a 3D Scaffold-Free Culture of Human Breast Carcinoma Cells to Understand Estrogenic Endocrine Disruption

M. M. Vantangoli, S. Petren and K. Boekelheide. *Pathology and Laboratory Medicine, Brown University, Providence, RI.*

The use of scaffold-free agarose hydrogels provides a system in which cells form spheroids, initiating contact with other cells and the matrix. We have demonstrated the use of this system to culture MCF-7 human breast carcinoma cells. MCF-7 cells within this model self-aggregate and develop into differentiated spheroids, possessing a defined luminal space. As shown by transmission electron microscopy, cells in MCF-7 spheroids display tight junctions, desmosomes and apical/basal polarity. MCF-7 cells grown in 3D display increased expression of breast-differentiation markers including cytokeratin 18 (KRT18). When compared to 2D cultures, 3D cultures show a reduced fold induction of mRNA of estrogen responsive genes (GREB, PGR and CTSD) following estradiol exposure in concentration response and time course studies. The expression of e-cadherin (CDH1) was downregulated in 2D cultures following estradiol exposure. Interestingly, CDH1 mRNA was increased in 3D cultures as soon as 2 hours post-exposure as demonstrated by RT-PCR and Western blotting. We propose to use this system to assess the molecular and phenotypic changes associated with exposure to endocrine disrupting compounds (EDCs), including diethylstilbestrol, bisphenol A and genistein. The use of a differentiated scaffold-free 3D culture system offers a unique opportunity to study the phenotypic and molecular changes associated with exposure to EDCs. 3D cell culture models are intriguing due to their ability to bridge the gap between animal models and traditional 2D cell culture. 3D models allow for the growth of human cells in an environment that is closer to the in vivo environment compared to tissue culture plastic. While many 3D models rely on scaffolded matrices for the growth of cells at low densities, scaffold-free models allow cells to aggregate and maximize cell-cell contact, free of the influence of surrounding matrix.

PS 169 Effects of Phenylethylamines on Huh-7 Human Hepatoma Cells Studied with Untargeted Global Metabolomics

T. J. Flynn[1], Y. Liu[1] and S. Pugh Bishop[1, 2]. [1]*Division of Toxicology, US Food and Drug Administration, Laurel, MD and* [2]*Oak Ridge Institute for Science and Education, Oak Ridge, TN.*

Phenylethylamines such as β-phenylethylamine (PEA) and N,N-dimethylphenylethylamine (DMPEA) are found in products marketed as dietary supplements. While the major safety concern with this class of compounds is cardiovascular toxicity, the hepatotoxicity of some phenylethylamines such as methamphetamine and MDMA is well established. PEA and DMPEA were initially screened in Huh-7 cells at concentrations from 5 to 1000 μg/mL for 48 hours. Significant cytolethality was observed at 500 μg/mL and above for both compounds. PEA but not DMPEA showed a significant dose-related increase in reactive oxygen species at concentrations as low as 10 μg/mL. LC/MS-based metabolomics studies were conducted on cells treated with PEA or DMPEA at 100 μg/mL for 48 hours. Examination of the supernatant culture medium identified several putative metabolites of both PEA and DMPEA. The most prominent metabolite for both compounds was N-phenylacetyl glutamine suggesting that the major pathway for metabolism for both compounds was through oxidative de-ammoniation by monoamine oxidase to phenylacetaldehyde. Significant ($p<0.05$, fold change>1.5) metabolomic changes in the supernatant medium from PEA treatment included increased release of mevalonic acid from the cells, suggesting increased activity of the cholesterol synthesis pathway. Significant metabolomic changes in the supernatant medium from DMPEA treatment included: increased utilization by cells of amino acids from the medium, suggesting increased cellular flux through protein synthesis pathways; and, decreased release of creatine and 1-methylnicotinamide from cells, suggesting decreased flux through intracellular bioenergetic pathways. These findings suggest that PEA and DMPEA are extensively metabolized by Huh-7 cells and that these compounds and/or their metabolites can alter liver metabolism in ways that could lead to liver toxicity.

PS 170 An Integrative Approach for the Prediction of Acute Oral Toxicity: Past and Future

R. R. Note[1], H. Noçairi[1], D. Blanchet[2], J. M. McKim[3], V. Michaut[1], G. Ouédraogo[1], S. Martinozzi Teissier[1], F. Leroy[1] and J. Cotovio[1]. [1]*Dept for The Development of Predictive Models and Methods, L'Oréal, Aulnay sous Bois, France,* [2]*Worldwide Safety Evaluation, L'Oréal, Asnières sur Seine, France and* [3]*Ceetox, Kalamazoo, MI.* Sponsor: D. Bury.

The model presented assesses results of mechanism-based in vitro assays and relevant physical-chemical properties to predict an LD50 value, the standard measurement of acute oral toxicity. The uniqueness of such a model is that it can serve multiple purposes, at a multidisciplinary level (Chemistry, Biology and Safety Evaluation): to rank-order compounds and guide the design or identification of hits for further testing, to identify potential subcellular targets and hypothetical mechanisms of acute oral toxicity, and to provide an estimate of acute oral toxicity for labeling purposes. Such a model was constructed and validated in the frame of a long-range research program with CeeTox, Inc. (SOT 2010, 2011, 2012 and 2013). The predictive performance of our model was assessed using a set of 100 public domain compounds. Chemicals were defined as toxic (T) or non-toxic (NT) on the basis of an in vivo LD50 threshold of 500 mg/kg, a value that could be acceptable for early efficacy testing. We showed that the overall concordance was above 85%, the sensitivity and the specificity being 87% and 89% respectively. To expand the applicability domain of the model and anticipate the complexity and diversity of cosmetic products, a set of reactive and non-reactive proprietary compounds was evaluated. The model remained highly predictive of the 39 chemicals categorized as non reactive (sensitivity = 83%, specificity = 94%) while for the 43 reactive compounds, the model could not be applied. This study is a clear demonstration that one way to address acute oral toxicity is to combine multiple, mechanism-based parameters and key chemical properties. However, further efforts are needed to fully handle the complexity of cosmetic ingredients. Incorporating SAR and metabolism for example, could be a way to expand the applicability domain of this model.

PS 171 DNA Damage and Adduct Formation by Prototype Metabolic Activation-Dependent DNA-Reactive Carcinogens in Chicken Embryo-Fetal Liver

G. M. Williams[1], A. M. Jeffrey[1], J. Duan[1], K. D. Brunnemann[1], M. J. Iatropoulos[1], E. H. Vock[2] and U. Deschl[2]. [1]*Chemical Safety Laboratory, Dept of Pathology, New York Medical College, Valhalla, NY and* [2]*Boehringer Ingelheim Pharma GmbH & Co., Biberach an der Riss, Germany.*

Prototype metabolic activation-dependent DNA-reactive carcinogens and structurally related, mutagenic, but less potent carcinogens or noncarcinogens were evaluated in the chicken egg genotoxicity (CEGA) assay, which provides a non-animal intact and aseptic test organism. In the assay, 3 daily doses, 48, 24 and 3 hr prior to termination, were administered to 9 to 11 day old embryo-fetuses and livers were harvested for measurement of two endpoints, DNA breaks using the alkaline single cell gel electrophoresis (comet) assay and DNA adducts using the ^{32}P-nucleotide postlabeling (NPL) assay. The effects of four carcinogens of different structures requiring distinct pathways of bioactivation, 2-acetylaminofluorene (AAF), aflatoxin B_1, benzo[a]pyrene (BaP), and diethylnitrosamine, were compared to their structurally related noncarcinogens fluorene (FLU) and benzo[e]pyrene (BeP) or

weak carcinogens, aflatoxin B_2 and nitrosodiethanolamine. The four prototype carcinogens produced DNA breaks, whereas less potent carcinogens and noncarcinogens yielded borderline or negative results, respectively. AAF and BaP also produced DNA adducts, whereas none was found with FLU or BeP, consistent with comet results. Thus, the CEGA, using comet and NPL, is capable of detecting the genotoxicity of diverse carcinogens while not yielding false positives for non-carcinogens.

PS 172 Genetic Deletions in Mitochondrial Cholesterol Transporters Result in Germline Defects in *C. elegans*

D. W. Ferreira and P. Allard. *Institute for Society and Genetics, University of California, Los Angeles, Los Angeles, CA.*

Basic DNA replication and mitochondrial machinery are conserved in the nematode *C. elegans*. Because of this, it is a prime organism to investigate the contributions of individual mitochondrial cholesterol transporters to normal cholesterol homeostasis within the developing germline. Previous studies performed by our laboratory and others indicate that Bisphenol A (BPA) causes defects in the developing germline of both *C. elegans* and rodent models. In *C. elegans*, defects are prevented by the addition of cholesterol to the treatment medium. To investigate whether inhibiting cholesterol uptake affects germline development, we have characterized several strains of *C. elegans* with null deletions in one or more mitochondrial cholesterol transporters. Preliminary experiments in adult *C. elegans* lacking either functional Steroid Acute Regulator Protein (StAR) or 18kDa translocator protein (TSPO) orthologs show an increase in the incidence of apoptosis in germ cell nuclei relative to control worms as determined by acridine orange staining. Furthermore, DAPI staining of mutant worms uncovered the presence of gaps in the pachytene region of the gonad, where germ cell nuclei are normally present. Closer examination of StAR mutant worms revealed a reduction in Syp-1 (a synaptonemal complex protein) immunofluorescence, indicating incomplete synapsis of chromosomes during germ cell meiosis. Overall fertility was also affected in these worms as measured by a decrease in total brood size. Together, the data collected in cholesterol transport mutants show similar defects in the germline as BPA treated worms. Future studies will investigate the relationship between cholesterol and BPA uptake within the germline of *C. elegans*.

PS 173 Validation of the Yeast Androgen Screen for Identification of Endocrine Active Substances That Interact with the Androgen Receptor

B. van Ravenzwaay[1], T. Ramirez[1], C. Woitkowiak[1], H. Hüner[1], C. Schönlau[2], H. Hollert[2], S. Broschk[3], O. Zierau[3], G. Vollmer[3], M. Jäger[4], A. H. Poth[4], E. Higley[5], M. Hecker[5] and R. Landsiedel[1]. *[1]Toxicology, BASF SE, Ludwigshafen/Rhein, Germany, [2]RWTH University, Aachen, Germany, [3]Technical University, Dresden, Germany, [4]Harlan CCR, Rossdorf, Germany and [5]University of Saskatchewan, Saskatoon, SK, Canada.*

Endocrine disruptor compounds (EDCs) are a group of natural or synthetic compounds that have the capacity to interact with the endocrine system of living organisms and consequently causes adverse health effects in an intact organism, its progeny, or (sub)populations. Due to the potential impact on human health, there is increasing interest in assessing the risk of the exposure to EDCs. Currently, several in vitro and in vivo assays have been developed and few of them validated and regulatory accepted. Herein, we report on the inter-laboratory validation of a yeast androgen screen assay (YAS), which is a non-animal alternative that identifies potential EDCs that interact with the androgen receptor (AR). The validation exercise was performed in 5 laboratories from Canada and Germany. It demonstrates that the method can be performed with a high intralaboratory reproducibility (>90%) and also among the laboratories (between reproducibility >85%). The analysis of the predictivity was performed using 15 reference blinded compounds, the data demonstrates a very low rate of false predictions, resulting in a specificity above 95% and a sensitivity >85%. Remarkably, the accuracy to identify agonistic compounds was >90% and >87% for the antagonistic effects. In conclusion, the validation exercise demonstrates that the method is suitable to be used as a robust in vitro alternative to identify EDCs that interact with the AR.

PS 173a Development of an Electrical Impedance-Based Device for Real-Time Assessment of Pulmonary Toxicity

C. M. Randall[1, 2, 3], S. D. Cole[1, 2, 3], D. J. Angelini[1, 2], T. B. Datta-Chaudhuri[4], R. M. Dorsey[1], E. Smela[4] and H. Salem[1, 5]. *[1]Edgewood Chemical and Biological Center, Edgewood, MD, [2]National Research Council, Washington, DC, [3]Defense Threat Reduction Agency, Fort Belvoir, MD, [4]Department of Mechanical Engineering, University of Maryland, College Park, MD and [5]Department of Homeland Security, Chemical Security Analysis Center, Edgewood, MD.*

Many of the chemical/biological warfare agents (CBWAs) have been shown to induce severe pulmonary toxicity and thus present a serious risk. Additionally, there is a paucity of human toxicological data for emerging threat agents. Advances in pulmonary biology have made it possible to study human pulmonary toxicity in vitro. One of the premier systems to evaluate human pulmonary toxicity is the Air-Liquid Interface (ALI) culture of Normal Human Bronchial Epithelial Cells (NHBECs). These cultures exhibit many hallmarks of normal human lung tissue. Measuring Trans-Epithelial Electrical Resistance (TEER) has long been the preferred mode of assessing epithelial tissue integrity in culture. Traditional TEER measurements assess resistance orthogonally through the epithelial cell layer requiring the cultured cells be submerged in media. To date, there is no method that allows TEER measurements to be taken in ALI cultures. Here we describe a novel method for assessing TEER of NHBECs grown at the ALI. To this end, gold electrodes were deposited onto the top surface of Boyden cell culture chambers to allow for resistance to be measured laterally across the chamber membrane in the ALI system. Unfortunately, no significant TEER values were detectable using this detection method. However, TEERs were readily detected in these chambers using the traditional method. Future efforts will focus on developing modified devices to increase the sensitivity and consistency of the TEER measurements. Such a device would allow for assessment of pulmonary toxicity in real-time.

PS 173b Profiling of the Tox21 10K Compound Library for Agonists and Antagonists of the Estrogen Receptor Alpha Signaling Pathway

R. Huang[1], S. Sakamura[1], M. T. Martin[2], D. Reif[3], R. Judson[2], K. Houck[2], W. Casey[3], J. Hsieh[3], K. Shockley[3], P. Ceger[3], J. Fostel[3], K. L. Witt[3], W. Tong[4], D. Rotroff[2], A. Simeonov[1], D. J. Dix[2], C. P. Austin[1], R. Kavlock[2], R. R. Tice[3] and M. Xia[1]. *[1]NCATS, NIH, Rockville, MD, [2]NCCT, EPA, RTP, NC, [3]NTP, NIH, RTP, NC and [4]NCTR, FDA, Little Rock, AR.*

Humans are occupationally and environmentally exposed to large numbers of chemicals that have never been adequately tested for toxicological effects, including endocrine disrupting potential. The quantitative high-throughput screening (qHTS) paradigm has provided a more efficient and cost-effective alternative to traditional toxicity tests for profiling environmental chemicals for toxicity. The U.S. Tox21 program has screened a library of approximately 10K chemicals in three independent runs for estrogen receptor alpha (ERα) agonist and antagonist activity using two types of ER reporter gene cell lines, one with an endogenous full length ERα (ER-luc; BG1 cell line) and the other with a transfected partial receptor consisting of the ligand binding domain (ER-bla; ERα β-lactamase cell line), in a qHTS format. Concentration-response data were analyzed by three Tox21 partners (NCGC, EPA, and NTP) using different analysis approaches to determine activity. The ability of the two assays to correctly identify ERα agonists and antagonists was evaluated using a set of 39 reference compounds with known ERα activity. Although both assays demonstrated adequate (i.e. >85%) predictivity, the ER-luc assay was more sensitive and the ER-bla assay more specific. The qHTS assay results were compared with results from previously published ERα binding assay data and showed >80% consistency. Actives identified from both the ER-bla and ER-luc assays were analyzed for structure-activity relationships (SARs) revealing known and potentially novel ERα active structure classes, e.g. steroid hormones and flavonoids. The results demonstrate the feasibility of qHTS to identify environmental chemicals with the potential to interact with the ERα signaling pathway and the two different assay formats improve the confidence in correctly identifying these chemicals.

PS 173c Developing Osteoblasts As an Endpoint for the Mouse Embryonic Stem Cell Test

X. Chen[1], G. Nolen[1], D. K. Hansen[1], J. Fisher[2], W. A. Harrouk[2], M. Tassinari[2] and A. Inselman[1]. *[1]Division of System Biology, NCTR/FDA, Jefferson, AR and [2]CDER/FDA, Silver Spring, MD.*

The mouse Embryonic Stem cell Test (mEST) is a promising in vitro assay for detecting potential embryotoxicity; however, the addition of another endpoint may improve the predictive value of the test. Differentiation of mouse embryonic

stem cells (mESCs) to osteoblasts was examined as such an endpoint. A number of variables such as culture conditions, starting cell number and genetic background of the cell lines were investigated. Direct plating of D3 ESCs in the presence of ascorbic acid, β-glycerophosphate and dexamethasone resulted in the most consistent and robust differentiation to osteoblasts which was detectable by alizarin red staining as early as culture day 7. Differentiation continued to increase to at least culture day 14 as indicated by levels of osteocalcin mRNA and other osteoblast lineage specific markers. The 14 day D3 culture system was then used to test the predictivity of osteoblast differentiation as an endpoint in the mEST; determination of cytotoxicity was performed as in the validated mEST using both the D3 and 3T3 cell lines; osteocalcin mRNA was used as the differentiation endpoint in the osteoblast EST. We have tested seven compounds used in the mEST validation experiments using the prediction model developed in the validation study. These compounds include 5-fluorouracil (CAS NO. 51-21-8), diphenhydramine hydrochloride (CAS NO. 147-24-0), methotrexate hydrate (CAS NO. 133073-73-1), lithium chloride (CAS NO. 7447-41-8), acrylamide (CAS NO. 79-06-1), valproic acid (CAS NO. 1069-66-5), and penicillin G (CAS NO. 69-57-8). Our results show that this osteoblast EST can correctly classify the embryotoxicity for all of the tested compounds. These results suggest that differentiation to osteoblasts may be used as an additional endpoint for the mEST. Future work will focus on compounds that were misclassified by the validated mEST and compounds which produce limb defects.

PS 173d Analysis of High-Throughput, High-Content Data in a *C. elegans*-Based Toxicity Assay

R. B. Goldsmith[1], J. Pirone[2], W. A. Boyd[1] and J. H. Freedman[1]. *[1]DNTP, NIEHS/NIH, Research Triangle Park, NC and [2]Social & Scientific Systems, Inc., Durham, NC.*

To quantitatively assess the effects of chemical exposures on transcription, an automated high-throughput *in vivo* toxicity assay was developed. This assay measures changes in the levels and cell-specificity of expression of individual genes in *C. elegans.* Transcriptional responses of archetypical stress-inducible target genes were measured by qRT-PCR in response to: juglone, an oxidative stressor; N-methyl-N'-nitro-N-nitrosoguanidine, a DNA damaging agent; cadmium, a heavy metal; chlorpyrifos, an organophosphate neurotoxin; and tunicamycin, an endoplasmic reticulum stressor. Genes were selected that were significantly upregulated in response to at least one toxicant, had large dynamic ranges (i.e., low constitutive levels of expression), and demonstrated a mechanistically relevant response. Individual strains of transgenic *C. elegans* that express fluorescent proteins under the control of cyp-35A2, gst-4, hsp-16.2, hsp-16.41, hsp-4 and mtl-2 were exposed to six concentrations of each toxicant. Florescence data were measured from images (N=12 per replicate) acquired using a high content imager and subsequently analyzed using CellProfiler's WormToolbox; high-throughput imaging analysis software designed for use with nematodes. Image analysis yielded a large number of highly variable nematodes at each concentration. A robust Bayesian method was used to compare the fluorescent intensity in control animals to the highest concentration of toxicant for each gene/toxicant combination. Parameters describing the distributions of nematode intensities were estimated using Markov chain Monte Carlo methods, and the difference in the means of the control and treated distributions were compared. A threshold for significance was set based on the 95% highest density interval for the difference in means and visual confirmation of fluorescence. The results obtained using this novel image-based assay were consistent with the cognate steady-state mRNA levels. These results show that this assay can be used to assess the effect of toxicants on gene expression *in vivo.*

PS 173e Quantitative Model of Systemic Toxicity Using ToxCast and ToxRefDB

L. Truong[1], G. Ouédraogo[2], S. Loisel-Joubert[2] and M. T. Martin[1]. *[1]EPA - NCCT, Durham, NC and [2]L'Oreal, Paris, France.*

EPA's ToxCast program profiles the bioactivity of chemicals in a diverse set of ~700 high throughput screening (HTS) assays. In collaboration with L'Oreal, a quantitative model of systemic toxicity was developed using no effect levels (NEL) from ToxRefDB for 633 chemicals with HTS data, chemical fingerprints, and a subset with reverse toxicokinetic (RtK) data. Floor and ceiling performance baselines (95% Confidence Intervals) were estimated to be 5 and 3 orders of magnitude uncertainty (OMU), respectively based on historical NEL distributions and reproducibility across study type and species. An initial read-across model was developed using chemical fingerprints to identify structurally similar neighbor NEL values resulting in 4.6 OMU, a 1/5th reduction in model uncertainty based on our performance baselines. HTS data was then incorporated into the model using 74 groups of assays based on biology (ie: response data, gene families), technology annotation (assay mechanisms, signal directions), and assay confounders (oxidative stress, cytotoxicity). For each assay grouping, a mean activity value was computed and adjusted for confounders. Incorporating HTS data with read-across resulted in a 4.2 OMU, a total reduction in model uncertainty of 2/5th. RtK steady-state concentrations were then incorporated to adjust in vitro concentration (uM) to in vivo dose (mg/kg/day). Although RtK values were only available for a subset of the total chemical set (211), including RtK further lowered the overall model uncertainty to 3.7 OMU, roughly 3/5th of the total model uncertainty we expect to be able to reduce. Herein, we have identified a model that incorporates HTS (dynamics), read-across (chemistry) and RtK (kinetics) to predict systemic NEL harnessing and incorporating the power of both new and existing data. This abstract does not necessarily represent EPA policy.

PS 173f A High-Throughput Microscopy Pathway in Toxicity Reporter Platform for Chemical Safety Assessment

S. Wink, B. van de Water and S. Hiemstra. *Division of Toxicology, LACDR, Leiden University, Leiden, Netherlands.*

Chemicals react or interact with cellular components leading to a perturbation of signal transduction networks as the cell tries to reestablish homeostasis. In case these perturbations are detrimental to cells adaptive stress responses are activated. However, if cellular stress is too severe these adaptive stress responses are unable to reestablish homeostasis and a threshold will be reached where the cell activates cell death responses to avoid cell community-level detrimental effects. We anticipate that high content imaging of critical cellular stress response hallmarks in the development of specific toxicities will be instrumental to assess toxicological hazard. To this end we have developed a set of endogenously regulated BAC-based GFP reporter HepG2 cell lines that enable the live cell visualization of dynamic responses of cellular adaptive stress response programs, including reporters for oxidative stress (Keap1, Nrf2 and Srxn1), DNA damage response (P53BP1, p53, p21 and Mdm2) and the unfolded protein response (ATF4, XBP1, BiP and CHOP). We have carefully characterized these reporters with respect to induction of GFP fusion products and dependence on the anticipated transcriptional control by RNAi mediated knockdown. Moreover, each adaptive stress response reporter is preferentially activated by their respective model compounds (oxidative stress: iodoacetamide, diethylmaleate; DNA damage: cisplatin and etoposide; UPR: thapsigargine and tunicamycin). As a next step we applied these HepG2 reporter cell lines to assess the activation of cellular stress responses by 150 compounds that are associated with drug-induced liver injury. All compounds were evaluated at 1, 5, 10, 50 and 100 Cmax and evaluated for the induction of Srxn1-GFP (Nrf2 activation) or CHOP-GFP (UPR activation). We identified specific sets of DILI compounds that strongly activate both, one or none of the stress response reporters. We anticipate that our cellular stress response reporters in combination with HCI may play a key role in future safety assessment of chemicals.

PS 173g Transcriptomic Characterization of Mouse Embryonic Stem Cell Differentiation and Its Modulation by Thalidomide

X. Gao, J. Yourick, V. Topping, K. Belgrave and R. Sprando. *Division of Toxicology, Office of Applied Research and Safety Assessment, U.S. Food and Drug Administration, Laurel, MD.*

The Tox21 program calls for transforming toxicology testing from traditional in vivo tests to less expensive and higher throughput in vitro methods. In developmental toxicology, a spectrum of alternative methods has been developed including cell line based tests. In particular, embryonic stem cells (ESCs) have received widespread attention as a promising alternative model for developmental toxicity assessment. Here, we characterized gene expression changes during mouse ESC differentiation and their modulation by thalidomide. C57/BL6 ESCs were allowed to differentiate spontaneously and RNA of solvent controls was collected at 0, 24, 48, 72, 96, 120 and 168 h after embryoid body (EB) formation; RNA of thalidomide-exposed EBs were collected at 24, 48 and 72 h. Samples were hybridized to Affymetrix Mouse Gene 2.0 ST Array; using a stringent cut-off criteria of Bonferroni-adjusted $p < 0.05$ and fold change > 2.0, a total of 1501 probesets were found differentially expressed among the solvent controls at different time points. Out of these probesets 1032 were mapped on the DAVID database as annotated genes, and gene ontology (GO) analysis showed these regulated genes were mostly involved in differentiation-related processes such as development, metabolism, morphogenesis, cell differentiation, cell organization and biogenesis, embryonic development, and reproduction. Principal component analysis (PCA) based on these genes showed that the unexposed solvent controls appeared in chronological order in the PCA plot, which when connected by the regression curve formed a differentiation track. The thalidomide-exposed cultures appeared to deviate from this differentiation track, suggesting its modulating effects on the differentiation process.

The differentiation track defined in this study may be further exploited as a baseline for developmental toxicity testing, with compounds causing significant deviation from the differentiation track being predicted as potential developmental toxicants.

PS 173h Performance of the BG1Luc and ER β-Lactamase Estrogen Receptor Transactivation Assays in Tox21

L. Rinckel[2], W. Casey[1], R. Huang[3], J. Hsieh[1], K. Shockley[1], M. Xia[3], R. R. Tice[1] and P. Ceger[2]. [1]*NIEHS, Durham, NC,* [2]*ILS Inc, Durham, NC and* [3]*NCGC, Rockville, MD.*

Two estrogen receptor (ER) transactivation (TA) assays, the BG1Luc and HEK293 ER β lactamase (ER-bla) methods, were adapted for use in the U.S. Tox21 high-throughput screening program. Both in vitro assays detect substances with ER agonist or antagonist activity. BG1Luc endogenously expresses full-length ER (α and β) and is stably transfected with a plasmid containing four estrogen responsive elements (ERE) upstream of a luciferase reporter gene. ER-bla is a mammalian one-hybrid system stably expressing a β-lactamase reporter gene under the control of the GAL4 DNA-binding site and a fusion protein consisting of the human ERα ligand-binding domain and the GAL4 DNA-binding domain. Approximately 10,000 chemicals were tested three times in both assays in agonist and antagonist modes. To differentiate true ER antagonists from cytotoxic substances, cell viability was determined. Concentration-response data (N=15) were analyzed to evaluate the performance of the two assays. The assay data quality was high in both agonist and antagonist modes as indicated by acceptable signal to background ratio (2.5 to 8), CV (<10.5%), reproducibility (outcome matches across triplicate runs, ≥87%), and Z' factor (≥0.4). Sensitivity and specificity of the assays were compared to ER TA performance standards that were developed with the OECD for the BG1 manual method. Sensitivity was 100% for BG1 agonist, 85% for ER-Bla agonist, and 100% for both antagonist assays. Agonist and antagonist specificity were 100% for BG1 and ER-Bla. Reference standard values were: estradiol EC50 30 pM for BG1 and 275 pM for ER-Bla, and hydroxytamoxifen IC50 71 nM for BG1 and 6 nM for ER-Bla. Understanding the differences behind the performance of these assays is critical to their acceptance and utilization by both regulators and industry. This project was funded in whole or in part with Federal funds from the NIEHS, NIH under Contract No. N01-ES-35504.

PS 173i Functional Assays and Alternative Species: Using Larval Zebrafish in Developmental Neurotoxicity Screening

S. Padilla[1], M. Culbreth[1, 2], R. C. MacPhail[3, 4], D. L. Hunter[1], K. A. Jarema[3], K. F. Jensen[3], J. Olin[1] and A. Tennant[1]. [1]*ISTD, U.S. EPA, Research Triangle Park, NC,* [2]*Albert Einstein College of Medicine, Bronx, NY,* [3]*TAD, U.S. EPA, RTP, NC and* [4]*VA Tech, Blacksburg, VA.*

The U.S. Environmental Protection Agency is evaluating methods to screen and prioritize large numbers of chemicals for developmental toxicity. As such, we are exploring a behavioral testing paradigm, which can assess the effects of sublethal and subteratogenic concentrations of developmental neurotoxicants on 6 day larval zebrafish (*Danio rerio*). This assay simultaneously tests individual zebrafish under both light and dark conditions in a 96-well plate using a video tracking system. By controlling the duration and intensity of light, we are able to detect changes in locomotion during light-dark transitions, and adaptation to both light and dark during the approximate 1.5 hour testing period. Multiple chemicals at several concentrations (≤ 120 μM nominal concentration) can be tested in large numbers of larvae using this method. We have evaluated a training set of chemicals (n=22) that are generally considered positive (n=16) or negative (n=6) controls for developmental neurotoxicity in mammals. Many of the developmentally neurotoxic compounds perturbed behavior at subteratogenic doses (e.g, lead, heptachlor, chlorpyrifos, chlorpyrifos oxon), while many non-neurotoxic compounds did not (e.g., acetaminophen, saccharin, glyphosate). Exposure to developmental neurotoxicants altered the overall activity level in light and dark conditions, and/or the activity pattern. The zebrafish neurodevelopmental assay using this training set of chemicals had a sensitivity of 0.875 and a specificity of 0.833. The training set results, therefore, indicate that careful evaluation of zebrafish larvae behavior is capable of identifying mammalian developmental neurotoxicants. *This abstract may not necessarily reflect official Agency policy.*

PS 173j Effects of ToxCast Phase I Chemicals on Steroidogenesis in H295R Human Adrenocortical Carcinoma Cells

M. T. Martin[1], A. L. Forgacs[1], D. L. Filer[1] and C. Toole[2]. [1]*ORD/NCCT, USEPA, Research Triangle Park, NC and* [2]*CeeTox, Inc., Kalamazoo, MI.*

A delicate balance of steroid hormones is essential for proper development and reproduction. Disruption of steroidogenesis by environmental toxicants results in altered hormone levels causing adverse reproductive and developmental effects. H295R human adrenocortical carcinoma cells were used to evaluate the effect of chemicals on steroidogenesis. Using a 96-well format, cells were pre-stimulated with 10μM forskolin for 48 hr to induce steroidogenesis followed by chemical exposure for 48 hr. Media were removed and 13 hormone analytes were quantified by HPLC-MS/MS including progestagens (e.g., pregnenolone [PREG], progesterone [PROG]), glucocorticoids, androgens, and estrogens. Initially, 311 unique ToxCast Phase I chemicals (primarily pesticides) were tested at a single non-cytotoxic concentration. 220 chemicals were found to alter the levels of at least one hormone analyte. Based on the single concentration analysis, 96 chemicals disrupting 4≤ hormones were selected for six-point concentration-response evaluation (0.003 – 100 μM). Concentration-dependent disruption of at least one hormone was observed with 68 of the selected chemicals. By evaluating the effects of chemicals on 13 hormones this assay provides valuable mechanistic insight into the possible targets for chemical perturbance in the steroidogenic pathway. For example, <10 chemicals altered PREG or 17αOH-PREG while 27 and 35 chemicals had an effect on PROG and 17αOH-PROG levels, respectively. These results demonstrate that the chemicals evaluated likely do not target CYP17a hydroxylase activity. However, 33 chemicals altered testosterone levels and 38 chemicals concentration-dependently altered estradiol levels revealing significant disruption of subsequent dehydrogenation and aromatization steps. Cumulatively, these results suggest CYP17a lyase and hydroxysteroid dehydrogenase activity are the most likely targets for the disruption of steroidogenesis by the subset of ToxCast Phase I chemicals evaluated. This abstract does not necessarily reflect US EPA policy.

PS 173k *In Vitro* Safety Profile of Personal Care Products—Use of an *In Vitro* Testing Platform Based on a Reconstructed Vaginal Tissue Model

C. Moudgal[1], L. Strazdas[1], D. Sheehan[2], D. Wolfinger[2], N. Wilt[2], G. Costin[2], S. Ayehunie[3] and A. Armento[3]. [1]*The Clorox Company, Pleasanton, CA,* [2]*Institute for In Vitro Sciences, Inc. (IIVS), Gaithersburg, MD and* [3]*MatTek Corporation, Ashland, MA.*

One of the common goals of industry is to confirm the safety of their products. Ethical concerns have led to the use of alternative testing methods in lieu of traditional testing methods. Several studies have shown good correlation between alternative test methods, traditional testing methods and human exposure. In the current study, the safety profile of three products with potential for vaginal exposure was assessed using the reconstructed human vaginal EpiVaginal™ model (MatTek Corporation, USA); the assay negative control (sterile, deionized water) and positive control (1% Triton®-X-100) were tested alongside. To increase the confidence in the test outcome, histopathology evaluation was conducted to assess the extent of cellular damage. Two liquid products were directly applied to the EpiVaginal™ tissues, while the wet wipe product was placed in direct contact with the tissue. Vaginal irritation expressed as ET_{50} values (3.32 and 12.71 hours) showed a higher irritation potential for the liquid formulations compared to the wipes (>24 hours). The lower irritation potential of the wipe product may be related to the availability of a rather limited amount of the liquid formulation in the wipes compared to the liquid formulations. Histology evaluations showed good correlation between the ET_{50} and change in tissue structure. The results of this *in vitro* test methodology confirmed the safety profile of the products, should vaginal exposure occur during use. This two-endpoint testing platform (viability and histology) provided not only a correlative interpretation of the data, but also indication of the structural changes of the tissues exposed to the test article that are relevant to human exposure. Future plans include further exploring the capability of this *in vitro* testing platform for screening products before entering clinical trials.

PS 173l Chemotherapeutic Class-Specific Neurotoxic Effects on Rat DRG Cells Using High-Content Analysis

H. Behrsing[1], F. Cutuli[1], J. Hamre[1], M. A. Davis[2] and L. Guo[1]. [1]*Leidos Biomedical Research, Inc., Frederick, MD and* [2]*Division of Cancer Treatment and Diagnosis, National Cancer Institute, Bethesda, MD.*

We exposed primary rat dorsal root ganglion (DRG) to peripheral neuropathy (PN)-causing drugs and evaluated cell-based changes using high content analysis (HCA). Neuron-specific BIII tubulin was stained along with other cell markers

to evaluate subcellular changes following DRG culture exposure to PN-causing drugs. Cultures consist of mostly non-neuronal cells (e.g. Schwann and satellite cells), but neuronal and support cell growth is highly interlaced. Nuclear, neurite/process (N/P), and Nissl changes were evaluated at 0, 24 or 72hr following drug exposure (0.003-30 μM, 24hr). Drug inter- and intra-class-specific changes were identified for anti-tubulin drugs (hyperstabilizers and destabilizers), alkylating agents, a proteasome inhibitor, and other anti-cancer drugs (doxorubicin, lapatinib, birinipant, and thalidomide). Destabilizers all caused varying loss of N/P and Nissl area staining, but drug-specific variations on other marker responses were found. Hyperstabilizers caused mild N/P loss, increased acetyl alpha tubulin intensity, decreased Nissl area, but had no effect on Nissl intensity. At 10 and 30 μM, cisplatin and oxaliplatin (but not carboplatin) caused Nissl marker changes, but N/P and cell loss was delayed. At different concentrations doxorubicin and lapatinib caused similar nuclear, Nissl, N/P, and cell loss. Thalidomide and birinipant caused no significant changes at any concentration tested. Interestingly, different classes of drugs showed effects on non-neuronal cells. The use of HCA in combination with specific markers has allowed us to class-rank the drugs tested. Moreover, this complex culture model demonstrates concordance with reported morphological changes induced by these classes of agents in vivo. Funded by NCI Contract No. HHSN261200800001E.

PS 173m Effect of Nicotine on Zebrafish Embryos: High-Content Analysis to Assess Developmental Toxicity

S. F. Ali, S. Lantz-McPeak, E. Cuevas, M. G. Paule and J. Kanungo. *Division of Neurotoxicology, NCTR, Jefferson, AR.*

Zebrafish embryos represent one of the only vertebrate model systems amenable to high throughput toxicity screening. Nicotine, a drug of abuse, has been reported to have many adverse effects on the developing nervous system. Several studies have shown that zebrafish adults and embryos are ideal for monitoring nicotine effects. Previously, we reported that nicotine alters the expression of biomarkers of endocrine function in zebrafish embryos. This observation is concordant with mammalian and human data depicting nicotine as an agent that can modulate hormone levels. Additionally, nicotine exposure has been shown to affect the nervous system of zebrafish larvae and juveniles generating abnormal arborization of axons, suggesting a defective path-finding signaling process. Here, we report automated fluorescent image acquisition of hb9-GFP transgenic embryos that express green fluorescent protein as a reporter in their motoneurons and axons, to detect nicotine's effects. The experiment is performed in vivo using embryos arrayed in 384-well plates. Post-acquisition image analysis provides average motoneuron axon lengths for control and experimental groups. The data show no significant difference in the ventral axon length between the control and the nicotine-treated groups when the embryos were treated at 28 hours post-fertilization for 24 hours. However, nicotine–treated embryos were slightly and significantly smaller than the controls. These observations are in agreement with previous studies reporting that nicotine promotes arborization (axon pathfinding) but does not have any drastic effect on axonogenesis. Protocol # E0735901.1

PS 173n 4-Vinylcyclohexene-Induced Changes in Gene Expression and Antioxidant Status Is Mediated via Oxidative Stress in *Drosophila melanogaster*

A. O. Abolaji[1, 2], J. P. Kamdem[2], T. H. Lugokenskia[2], T. K. Nascimento[2], E. P. Waczuk[2], E. O. Farombi[1] and J. B. Rocha[2]. [1]*Biochemistry, University of Ibadan, Ibadan, Nigeria and* [2]*Departamento de Quimica, Bioquímica Toxicológica, Universidade Federal de Santa Maria, Santa Maria, Rio Grande do Sul, Brazil.*

4-Vinylcyclohexene (VCH) is a by-product of pesticides, plastic, rubber, flame-retardants and tyre productions. The ovotoxicity of VCH has been reported in animal models. However, there is the dearth of information on the possible involvement of oxidative stress in the toxicity of this occupational chemical. Thus, this study was designed to investigate the effect of VCH on selected genes expressions, antioxidant status and oxidative stress markers in *Drosophila melanogaster* model. Flies (both genders) of 1-to 3- days old were orally treated with different concentrations of VCH (10 μM-1mM) in the diet for 5 days. Subsequently, the survival and negative geotaxis assays in the flies were determined, as well as the quantification of reactive oxygen species (ROS) generation. In addition, the real time RT-PCR expressions of selected oxidative stress and antioxidant mRNA genes of HSP27, 70 and 83, SOD, Nrf2, MAPK and catalase were determined. Furthermore, we evaluated selected enzyme concentrations such as catalase, GST, δ-ALA-D and acetylcholinesterase (Ache). Our data showed that VCH oral exposure is accompanied by the reduction in negative geotaxis. Also, VCH caused significant inductions of the mRNA of SOD, Nrf2 and MAPK genes expressions, which was associated with increased ROS production, altered activities of antioxidant enzymes (GST and catalase), and inhibition of δ-ALA-D and Ache concentrations ($p < 0.05$). These data imply that, VCH mechanism of toxicity is mediated by oxidative damage, as evidenced by the alteration in the oxidative stress-antioxidant balance. Thus, *D. melanogaster* has provided further insights into the mechanism of VCH-induced toxicity.

PS 173o Similar Toxicity of Three Fluoridation Compounds to the Nematode *Caenorhabditis elegans*

W. A. Boyd[1], J. R. Rice[1], D. Chandra[2], M. Smith[3], P. K. Den Besten[2] and J. H. Freedman[1]. [1]*NIEHS, Research Triangle Park, NC,* [2]*UCSF, San Francisco, CA and* [3]*Social & Scientific Systems, Inc., Durham, NC.*

Fluorides are commonly added to drinking water in the United States to decrease the incidence of dental caries. However, the use of fluorides in drinking water has been controversial, primarily due to unresolved toxicological questions. Silicofluorides, such as sodium hexafluorosilicate (Na_2SiF_6) and fluorosilicic acid (H_2SiF_6), are the compounds most often used for fluoridation, although fluoride salts such as sodium fluoride (NaF) are also used. Interestingly, only the toxicity of sodium fluoride has been examined and not that of the more often-used silicofluorides. In the present study, the toxicities of sodium fluoride, sodium hexafluorosilicate, and fluorosilicic acid were compared in the alternative toxicological testing organism *Caenorhabditis elegans* using three quantitative, high-throughput toxicological assays: growth, reproduction, and feeding. Within each assay, the toxicities of the three fluoride compounds varied considerably when expressed as millimoles of compound, seemingly indicating that sodium fluoride was less toxic than the silicofluorides. However, both silicofluorides contain 6 fluoride ions per molecule. Thus, when toxicity was expressed in parts per million (ppm) fluoride, all three fluoride compounds produced concentration–response toxicity profiles with almost identical EC50s and LECs, suggesting that silicofluorides have toxicities similar to sodium fluoride.

PS 173p Using Acute Toxicity, Transcriptomics, Metabolomics and Lipidomics to Understand Effects of Chemical Flame-Retardants on Eco-Indicator *Daphnia magna*

L. D. Scanlan[1], A. Loguinov[1], P. Antczak[2], Q. Teng[4], H. Stapleton[3], F. Falciani[2] and C. Vulpe[1]. [1]*U.C. Berkeley, Berkeley, CA,* [2]*University of Liverpool, Liverpool, United Kingdom,* [3]*Duke University, Durham, NC and* [4]*United States EPA, Athens, GA.*

The effects of legacy flame-retardant (FR) chemicals octa and penta brominated diphenyl ether (PBDE) and pentaBDE replacement formulation Firemaster550® (FM550) were analyzed on freshwater crustacean *Daphnia magna*, an ecological keystone species used in fresh water quality assessment. Acute 48-hour LC50 values were determined for penta and octaBDE and for five FM550 formulations and related compounds: FM550, bis (2-ethylhexyl) tetrabromophthalate (BEH-TEBP), triphenyl phosphate (TPHP), Firemaster® BZ-54 (BZ54) and the non-brominated BEH-TEBP analog bis (2-ethylhexyl) phthalate (BEHP). Microarray transcriptomics, HNMR-based metabolomics, and lipidomics were utilized to investigate mode of toxicity. Nominal LC50 values ranged from 58 μg/L (pentaBDE) to 3.96 mg/L (octaBDE) and were not correlated to LogKow. Microarray gene expression analyses performed at 1/10 LC50 found that BEH-TEBP and BZ54 caused similar gene expression patterns while the responses to other FRs were distinct. OctaBDE, BZ54 and BEH-TEBP caused changes in the expression of signal transduction genes located in the cellular membrane, but affected different signal systems and therefore caused different biological effects. PentaBDE affected protein synthesis and turn-over and FM550 appeared to cause nutritional dysregulation. Results indicate that hydrophobic FR compounds affect *Daphnia* in unique ways, not via a general narcotic mechanism.

PS 174 Exposure to 2, 3, 7, 8-Tetrachlorodibenzo-*p*-Dioxin (TCDD) Induces Expression of Prostaglandin E2 Receptor 4 (EP4) Gene in the Developing Anteroventral Periventricular Nucleus (AVPV)

J. Del Pino Sans[1, 2] and S. Petersen[1]. [1]*Veterinary and Animal Sciences, University of Massachusetts, Amherst, MA and* [2]*Toxicology and Pharmacology, Universidad Complutense de Madrid, Madrid, Spain.*

Developmental exposure to 2,3,7,8-tetrachlorodibenzo-*p*-dioxin (TCDD) interferes with masculinization of gonadotropin release patterns, most likely by blocking estradiol (E2)-dependent sexual differentiation of the anteroventral periventricular nucleus (AVPV). The process of sexual differentiation involves both cell death and alterations in neurite outgrowth, but the underlying molecular mechanisms are unclear. It has been reported that dendritic spine number and shape is modified

by TCDD. PGE2 induces formation of dendritic spines on preoptic area (POA) neurons through its EP receptor interaction. EP receptors have been implicated in sexual differentiation of dendritic outgrowth and synaptogenesis in other brain regions, and neonatal activation of EP2 and EP4 receptors are both necessary and sufficient for the organization of male sexual behavior in the preoptic area (POA). To date, no work has examined whether similar processes specifically regulate differentiation of the AVPV, a nucleus in the rostral POA. To determine whether these EP receptors are altered by TCDD in the AVPV, we administered vehicle or TCDD 600 ng orally to rat dams on the first post-partum day. Pups were euthanized the following day (PND2) and AVPV regions microdissected from frozen sections. Using QPCR, we found that only the EP2 and EP4 receptors were differently expressed in both sexes and only EP4 receptor was significantly upregulated by TCDD in males. These findings suggest that TCDD may interfere with masculinization of the AVPV by increasing EP4 receptor.

PS 175 Neonatal Exposure to Pesticides in Mice Alters Neuroprotein Levels Important for the Developing Brain

I. Lee, H. Viberg and A. M. Al-Refai. *Uppsala University, Uppsala, Sweden.*

Pesticides are used for plant protection and are divided into different chemical classes. In this study we investigate developmental neurotoxic effects of three different classes of pesticides; organophosphate (chlorpyrifos), carbamate (carbaryl) and organochlorine (endosulfan). It has been recognized that the developing mammalian brain have critical periods when the brain is more sensitive to toxic insults. When these insults occur during a period of rapid brain growth they can cause developmental neurotoxic effects and may alter adult susceptibility to other toxicants. Therefore, timing of exposure is of significance.
We have recently seen that these pesticides can induce behavioral neurotoxic effects. Therefore the aim of the present study was to explore if neonatal exposure to these pesticides can affect neuroprotein levels e.g. calcium/calmodulin-dependent kinase II (CaMKII), growth-associated protein-43 (GAP-43), glutamate receptor-1 (GluR1), postsynaptic density protein 95 (PSD95), synaptophysin and tau, which are important for normal development, of the mouse brain. Male NMRI-mice were exposed, on postnatal day 10, to a single oral dose of 5 mg chlorpyrifos/kg bw, 0.5-20 mg carbamate/kg bw or 0.1-0.5 mg endosulfan/kg bw and control animals received a 20% fat-emulsion vehicle. The animals were euthanized 24h after exposure and the neuroprotein levels in hippocampus and cerebral cortex were analyzed. Significant increased levels of GAP-43, GluR1 and tau, and significant decreased levels of CaMKII and synaptophysin compared to control was seen. The neurotoxic effects differed between the brain regions.
The results from the present study show that a single oral exposure to pesticides, during a critical period of brain development, can cause developmental neurotoxic effects, shown as changed neuroprotein levels. The neurotoxic effects are in line with previous behavioral studies. Further investigations on the developmental neurotoxic effects of pesticides are needed to understand the mode of action and assess the effects of low dose interaction of mixtures.

PS 176 Arsenic Inhibits Hedgehog Signaling during P19 Cell Differentiation

J. Liu[2] and L. J. Bain[1, 2]. [1]*Biological Sciences, Clemson University, Clemson, SC and* [2]*Environmental Toxicology, Clemson University, Clemson, SC.*

Arsenic is a toxicant found in ground water the world, and human exposure mainly comes from drinking water or from crops which are irrigated by contaminated ground water. Epidemiology studies have shown that arsenic exposure during development decreased intellectual function, reduced birth weight, and altered locomotor activity, while *in vitro* studies have shown that arsenite decreased muscle and neuronal cell differentiation. The sonic hedgehog (Shh) signaling pathway plays an important role during the differentiation of both neurons and skeletal muscle. Therefore, the purpose of this study was to investigate whether arsenic can disrupt Shh signaling in P19 mouse embryonic stem cells, leading to changes muscle and neuronal cell differentiation. P19 embryonic stem cells were exposed to 0, 0.25, or 0.5 μM of sodium arsenite for up to 9 days during cell differentiation. Arsenic exposure decreased the numbers of skeletal myotubes and neurons formed, based on morphology. Arsenite exposure also significantly reduced transcript levels of genes in the Shh pathway in both a time and dose-dependent manner. This included the Shh ligand, which was decreased 2- to 3-fold, the Gli2 transcription factor, which was decreased 2- to 3-fold, and its downstream target gene Ascl1, which was decreased 5-fold. Immunofluorescence data also showed reduced Gli2 protein expression. Taken together, we conclude that arsenic exposure affected Shh signaling, ultimately decreasing the expression of the Gli2 transcription factor. Further studies are needed for elucidating the exact mechanism by which arsenic affects Shh signaling during cell differentiation.

PS 177 Contribution of DEHP in Malformation of Fetal Brain Development

C. Tseng[1, 2, 3], Y. Chuang[1], Y. Yang[2], S. Tong[2], Y. Chen[1], Y. Chang[1], C. Lin[1] and M. Chao[1, 3]. [1]*Bioscience Technology, Chung Yuan Christian University, Chung-Li, Taiwan,* [2]*Biomedical Engineering, Chung Yuan Christian University, Chung-Li, Taiwan and* [3]*Center of Nanotechnology, Chung Yuan Christian University, Chung-Li, Taiwan.*

DEHP, Di-(2-ethylhexyl) phthalate, a phthalate plasticizer used most often in the world. It can be leached into a liquid that comes in contact with plastics, suggesting concerns about the health risk of human exposure. Previous animal studies have suggested that maternal exposure to phthalates during fetal and/or neonatal periods may cause reproductive and developmental toxicities in offspring due to their actions as endocrine disrupting chemicals (EDCs). DEHP is converted to the presumed toxic metabolite, MEHP, by lipase enzymes in the gastrointestinal tract. Upon ingestion, DEHP is rapidly metabolized to MEHP by pancreatic lipases in the lumen of the gut in both rodents and humans, before being further converted into oxidative metabolites and glucuronidated for excretion in the urine and faeces. Since DEHP is converted to MEHP in the gastrointestinal tract, it remains unclear whether DEHP is harmful to fetal brain development by parenteral routes of exposure. We therefore gave DEHP to pregnant Sprague-Dawley rats by gavage and to assess whether DEHP have direct impact on the neural cells viability and patterning of dendrites in fetal rat. DEHP treatment results in induction of oxidative stress leading to disrupt the developmental processes of the central nervous system. MTS was used to examine DEHP reduce dose dependent cell viability. With using immunofluorescence microscopy, malformation of neural morphology in fetal brain was detected. Therefore, our data summarized that DEHP is cytotoxic to the fetal neural cells and requires induction of ROS to exert their developmental alternation effects.

PS 178 Developmental Vulnerability of Rat Hippocampal Neural Stem Cells to the Neurotoxicant Methylmercury (MeHg)

M. Obiorah[1], K. B. Sokolowski[2] and E. DiCicco-Bloom[1, 2]. [1]*Neuroscience and Cell Biology, Rutgers RWJMS, Piscataway, NJ and* [2]*Toxicology, Rutgers University, Piscataway, NJ.* Sponsor: J. Richardson.

The developing brain is sensitive to environmental neurotoxicants such as methylmercury (MeHg), to which humans are exposed via tainted seafood. Studies implicate association of perinatal exposure with learning, memory and IQ deficits in children, suggesting hippocampal dysfunction. Using single-cell analysis, we showed that after 24 hours, a single, low exposure (0.6μg/g) adversely affects neurogenesis in postnatal day 7 (P7) rat hippocampus (akin to 3rd trimester in humans), a period of major neural stem cell (NSC) proliferation. NSC proliferation continues but wanes during prepubescence (P14) and adolescence (P21). Yet, the period of developmental vulnerability and lasting consequences of exposure on future neurogenesis remain undefined.
To define developmental vulnerability, we injected s.c P14 and P21 rats once with a low or high (5μg/g) MeHg dose and sacrificed 24h later, pulsing with S-phase marker EdU 2h before sacrifice. S-phase cells at P14 were not vulnerable to the low dose, but the high dose reduced mitotic cells in the dentate gyrus hilus by 29% without inducing cell death (cleaved caspase-3) or altering the size of the intermediate neural progenitor pool (Tbr2+ cells). These results indicate that P14 rats retain some vulnerability to MeHg. In contrast, P21 exposure (24 or 48 h) had no effect on S-phase cells nor apoptosis at either time point. To determine long-term effects of early exposure, P7 rats were injected once with MeHg and assessed with BrdU immunolabeling at P21. Both low and high exposures reduced S-phase cells by 24% and 33% (respectively) at P21, suggesting a lasting deficit in the NSC pool. Consistent with reduced mitosis, preliminary studies suggest immature Dcx+ neurons are reduced by 20%, suggesting reduced neurogenesis. These studies will provide insights into vulnerable periods in hippocampal neurogenesis that may inform guidelines for seafood consumption in humans. Supported by the CounterACT Program, NIH OD, and NIEHS, Grant Number [ES019762]. NS082015, NSF DGE 0801620

PS 179 Human Embryonic Stem Cells and Their Neuronal Descendants Exhibit Differential Sensitivity to PBDEs

J. F. Robinson, N. Larocque, M. McMaster and S. J. Fisher. *Department of Obstetrics, Gynecology, & Reproductive Sciences, University of California, San Francisco (UCSF), San Francisco, CA.*

Polybrominated diphenyl ethers (PBDEs) are ubiquitous environmental pollutants of major concern due to their possible effects on human neurodevelopment. At a cellular level, the potential mechanisms include disrupting proliferation and dif-

ferentiation, perturbing thyroid hormone signaling, and/or generating oxidative stress. Additional studies are needed to understand the molecular bases of PBDE-induced neurotoxicity and the potential developmental risks associated with these exposures. Knowledge gaps include: 1) PBDE effects in human model systems; and 2) windows of vulnerability to PBDE exposures during neurogenesis. In this study, we used human embryonic stem cells (hESCs; UCSF4) and their progeny, neuronal progenitors (NPGs), to investigate the dose-dependent effects of two commonly used PBDE congeners (BDE-47 and -99). The approaches included a combination of assays for assessing cell viability, death, proliferation, differentiation and thyroid hormone receptor (THRA, THRB) expression. PBDEs had dose-dependent toxic effects on both cell types with NPGs exhibiting greater sensitivity than hESCs. NPG responses included reduced expression of PAX6, a transcriptional regulator of neural development. In line with previous studies using rodent cell models, BDE47 or -99 significantly reduced THRA and increased THRB expression in NPGs. For example, 25μM BDE47 or -99 exposure for 24h upregulated expression of THRB mRNA levels by 22- and 38-fold, respectively. In summary, our results imply that human exposures to PBDEs during the early embryonic period may alter neurogenesis and that sensitivity varies during development. Follow-up studies are focusing on the mechanisms underlying differences in sensitivity of hESCs vs. NPGs and the relevance of our results to human in vivo brain development.

PS 180 Alterations of Postnatal Development of Feedback Inhibition and Basic Excitability in the Hippocampus of Rats Prenatally Exposed to Valproic Acid

Y. Fueta[1], Y. Sekino[2] and S. Ueno[3]. [1]*Department of Environmental Management and Control, University of Occupational and Environmental Health, Kitakyushu, Japan,* [2]*Division of Pharmacology, National Institute of Health Sciences, Tokyo, Japan and* [3]*Department of Occupational Toxicology, University of Occupational and Environmental Health, Kitakyushu, Japan.*

There is a concern about the impact of exogenous chemical substances on the neuronal development of children. Current developmental neurotoxicity guideline (TG426) is mainly based on *in vivo* animal studies such as behavior and pathological examinations, without any electrophysiological testing. Valproic acid (VPA), used as an antiepileptic drug and a mood stabilizer, is known to produce animal models of autism spectrum disorder. We aimed to clarify whether prenatal VPA affects early postnatal development of neuronal circuitry with our electrophysiological approach. VPA was orally administered to the pregnant day15 Wistar rats with the concentrations of 0 (control, saline only), 150, 300 or 600 mg/kg. On the days of PND 13, 14 and 15, field potentials were recorded from the CA1 area of hippocampal slices obtained from the control and VPA groups to test development of the local circuits. Stimulation/response curves of field excitatory postsynaptic potential and those of population spike (PS) enhanced at PND14 and 15 in the VPA-300 group, indicating an enhancement of spike generation or glutamatergic synaptic transmission. The ratios of paired-pulse responses of PS were almost equal to 1 in the control group, showing a lack of feedback inhibition, but decreased in the VPA-300 group from PND13 to 15, suggesting a developed feedback inhibition. Our results provide the evidence that prenatal VPA exposure enhances inhibitory circuits and then potentiates basic excitability in the hippocampal CA1 area. The present results were similar to those obtained from prenatal exposure to an industrial chemical 1-bromopropane, suggesting our electrophysiological evaluation may be useful for developmental neurotoxicity to predict producing a neuropathology after growth.

PS 181 Neurobehavioral Effects of Developmental Exposure to 2, 2', 4, 4'-Tetrabromodiphenyl Ether (BDE-47) and Mechanistic Exploration Using Whole-Genome Transcriptional Profiling

D. E. Haggard, M. T. Simonich, L. Truong, S. M. Bugel, B. C. Goodale and R. L. Tanguay. *Department of Environmental and Molecular Toxicology, Oregon State University, Corvallis, OR.*

Polybrominated diphenyl ethers (PBDEs) are a class of high production volume flame retardants used in a variety of consumer products that are considered ubiquitous environmental pollutants. 2,2',4,4'-tetrabromodiphenyl ether (BDE-47) is one of the predominant PBDE congeners found in environmental and biological samples. Developmental exposure to PBDEs, including BDE-47, is associated with neuronal and developmental effects in humans and wildlife; however, the exact mechanism is unknown. We utilized the embryonic zebrafish to assess the developmental and neurobehavioral responses induced by developmental BDE-47 exposures. Zebrafish were exposed at 6 hours post fertilization (hpf) and general mortality and malformations were assessed at 24 and 120 hpf. We examined the effects of BDE-47 exposure on photo-motor response in 24 hpf embryos using our lab-derived Photo-motor Response Assessment Tool (PRAT), and we investigated effects on 120 hpf photo-induced larval locomotion using the VeiwPoint Zebrabox system. We also ascertained the consequences of developmental BDE-47 exposure on adult zebrafish cognitive development using an active avoidance learning assay. Developmental exposure to BDE-47 up to 20μM resulted in no overt toxicity. BDE-47 exposure led to a dose-dependent increase in activity in the locomotor assay. Adult zebrafish cognition was negatively affected by developmental BDE-47 exposure, as measured by a decrease in the learning rate in the active avoidance task. To explore the mechanism by which early life-stage BDE-47 exposure initiates the observed behavioral effects, whole transcriptome RNA sequencing was performed on embryonic zebrafish exposed from 6-48 hpf. We observed distinct gene expression changes induced by BDE-47 compared to control animals, and functional analyses revealed possible mechanisms important in the behavioral effects of BDE-47.

PS 182 An Automated High-Content Screen for Migration of Neural Crest Precursor Cells

A. Essex, B. Cai, E. Batchelder, S. Feng, P. McDonough and J. Evans. *Vala Sciences, San Diego, CA.*

Cell motility is fundamental to development of neural-crest-derived structures in the embryo. Using neural crest stem cells (NCSCs) derived from induced pluripotent stem (iPS) cells, we developed a scalable high content screening (HCS) assay to measure the effect of chemicals on NCSC migration. The assay format involves "scratching" a confluent cell monolayer with a Teflon-coated pin tool (V&P Scientific, CA). In order for the assay to be routinely performed on hundreds of test chemicals, the pin tool incorporates 384 elements so that each well is scratched in parallel and reproducibly. The pin tool creates a cell-free region in each well that is 600 microns in diameter. Importantly, "scratching" did not appear to damage the culture surface, which might prevent cell migration due to removal of serum proteins or introduction of grooves running perpendicular to the cell borders. We showed that removal of the cells with the pin tool was spatially consistent well-to-well enabling automated image analysis to assess cell migration into the cell-free region. In order to control for false positives (e.g. pro-proliferative chemicals that lead to an increase in cell count within the cell-free region and cytotoxic chemicals (i.e. chemicals that lead to overall cell loss), cell density outside of the "scratched" region was measured and compared to neutral controls. The scalability of this assay enabled us to rapidly screen the NCC2 library of FDA-approved drugs as well as several reference compounds such as Cytochalasin D and paclitaxel. Not only did the imaging-based format of this assay enabled large-scale screening via fixed-endpoint screening, but it also allowed follow-up screens that incorporated staining for markers such as Sox10, and in some cases live-cell imaging to measure alterations in directional persistence for individual cells.

PS 183 Molecular Analysis of Rat Palatal Development

J. Wright[2], L. Vicario-Rodriguez[1], J. Dixon[1], M. Rattray[1], E. Barnes[2] and M. J. Dixon[1]. [1]*Faculty of Life Sciences, University of Manchester, Manchester, United Kingdom and* [2]*Jealott's Hill International Research Centre, Syngenta, Bracknell, United Kingdom.*

Development of the secondary palate involves cell growth, adhesion, differentiation and apoptosis. Cleft palate, which results from failure of these processes, involves interplay between teratogenic and genetic factors. A diverse range of molecules increases the incidence of cleft palate in the rat, data derived from this species are used in human risk assessment during development of New Chemical Entities. A deeper understanding of the molecular perturbations that lead to cleft palate would refine the utility of the rat in assessing risks to human health.

Rat palatal shelves initiate from the maxillary processes on embryonic day (E)13 and grow lateral to the tongue during E14 and E15. During E16 the palatal shelves re-orientate to a horizontal position above the tongue and fuse via their medial edge epithelia by E17. While it is believed that the molecules driving palatogenesis in the rat are identical to those underlying mouse palatal development, this assumption has not been verified.

To profile the genes expressed during palate development, we performed RNA-seq analysis of palatal shelves dissected from rat embryos at eight developmental stages between E14.5 and E17 and recovered ~10 μg of RNA from each pair of palatal shelves. Sequence analysis generated an average of 54 million reads from each sample, ~85% of which mapped to unique positions in the rat genome. To calculate gene expression levels we mapped reads to the transcriptome and used a Bayesian deconvolution algorithm to infer transcript expression levels. Transcript levels for each gene were combined to obtain gene expression levels which showed a dynamic range of five orders of magnitude. Strong, temporally-coherent signals were observed for thousands of genes. Comparison of the expression profiles of a subset of genes that play an essential role in mouse palatal development with their rat orthologues indicated similar expression patterns suggesting that the principal underlying pathways are conserved between mouse and rat.

PS 184 The Role of the Epicardium in Cardiogenesis: Insights from the *EHC* Mouse

E. Barnes[1], J. Wright[1], L. Ridge[2], G. Tenin[2] and K. Hentges[2]. [1]*Syngenta, Jealott's Hill International Research Centre, Bracknell, United Kingdom and* [2]*Faculty of Life Sciences, University of Manchester, Manchester, United Kingdom.*

Congenital heart defects and cardiovascular disease cause significant morbidity and mortality. Researching heart formation will increase our understanding of the processes that underpin these conditions. Our research has focused on the epicardium, the epithelial layer that covers the heart. Epicardial derived cells (EPDCs) migrate into the myocardium where they differentiate into fibroblasts and smooth muscle cells essential for the development of the coronary vasculature. EPDCs also provide signals required for myocardial proliferation and functionality. However, the precise mechanisms that regulate epicardial cell biology remain unclear.
The *EHC* mouse has a recessive embryonic lethal mutation in *Myh10*, and as a consequence develops multiple cardiac defects, including abnormal epicardial cell morphology and no functional coronary network. The localization of Wilms Tumour 1 (WT1), a marker of both epicardial cells and EPDCs, was explored using immunohistochemistry (IHC). Embryonic day 14.5 *EHC* embryos were genotyped by DNA sequencing; hearts were frozen and sectioned using a cryostat. Sections were stained using an anti-WT1 rabbit polyclonal antibody and fluorescence labeled anti-rabbit secondary antibody. Abnormal clusters of WT1 positive cells were observed at the interface between the epicardium and myocardium, suggesting *EHC* epicardial cells have a reduced ability to migrate into the subepicardial space. We are currently investigating the cell specific requirement for *Myh10* by generating myocardial *Myh10* knock out embryos (MHCαCreflox/flox). Initial IHC results show NMIIB protein localisation is reduced in the embryonic myocardium, indicating *Myh10* ablation in cardiomyocytes. Preliminary data indicates that *Myh10* expression in cardiomyocytes is not required for coronary vessel development.
The findings in the *EHC* mutant will improve our understanding of the complexities of embryonic coronary vessel development and the potential for abnormalities to arise.

PS 185 Intravenous Infusion in the Juvenile Rat

L. Allais, N. Truchot, P. Vignand, S. David, D. Ravelo and J. Briffaux. *WIL Research Europe-Lyon, St Germain-Nuelles, France.*

Toxicology studies in juvenile animals are part of non-clinical development of pediatric therapeutics and could be conducted in various species, the rat still being the most commonly used species. Most of the administration routes are technically feasible in the juvenile rat but more complex methods of administration, such as intravenous infusion, require challenging design adaptations. A feasibility study was first performed in close collaboration with our animal welfare group to develop continuous intravenous infusion in the juvenile rat surgically implanted with a catheter on postnatal day (PND) 21. Following anaesthesia with isoflurane, a catheter was implanted into the posterior vena cava via the femoral vein. The pups were continuously infused (24 h/day) with sterile physiological saline for 4 weeks. The technical challenges, such as the length of the catheter and the implantation site, associated with infusing a juvenile rat during a phase of rapid growth were investigated. The feasibility study was then followed by a complete juvenile study using a higher number of animals (20 males and 20 females). Half of the rats was necropsied at 7 weeks of age after the end of the 4-week infusion period and the other half was retained without further infusion for up to 11 weeks of age. Standard toxicology and developmental endpoints such as clinical observations, growth, food intake, clinical pathology, sexual maturation, auditory and pupillary reflexes were evaluated throughout the study. Two behavioral tests (open field and water maze) were also conducted during the observation period. The in-life results were compared with background data from non catheterized animals at a similar age and histology results at 7-week and 11-week sacrifice time-points were compared with those from catheterized rats used in general toxicology studies.
The present evaluation demonstrated that a 4-week continuous intravenous infusion period is feasible using equipment, procedures and welfare practices adapted to the juvenile rat and did not interfere with the growth or development from PND 21 to 11 weeks of age.

PS 186 Social Housing of Mature Males in a Nonhuman Primate Breeding Program

S. M. Henwood, J. Edwards and F. Gruenig. *Toxicology, Covance Laboratories Inc., Madison, WI.*

The cynomolgus monkey (*Macaca fasicularis*) is the preferred species for nonhuman primate (NHP) developmental toxicity studies for biopharmaceuticals. Social housing of NHPs has become mandatory in many countries. The revised USDA regulations require social housing of all social species, which includes NHPs. Although social housing of females and juvenile male NHPs is easily achieved, pair-housing of sexually mature adult males is considered challenging and even more so for male breeder animals. We have implemented a Three Pillar Concept for conducting developmental toxicity studies in NHPs, which addresses pen housing, training, and behavioral assessment of animals for selection of compatible cage mates. This Concept has been applied to our male breeder program. The assessment of social ranking by observance of aggressive and submissive behaviors allows the development of a hierarchical structure with ranking of animals as alpha, submissive, or subordinate. Assessments must be done by a trained animal behaviorist with an understanding of social structure of primate societies. Following establishment of ranking on the dominant-subordinate spectrum, a three-phase approach is used to ensure sustainable commingling pairs. An appropriate familiarization period is key to establishing successful pairs. Effects following initial pairing of males, such as delayed body weight gain, are transient. During active mating, the male pair is separated and housed individually. The female is placed in the male cage for up to 48 hours. Following completion of the mating period, the female is removed and the male commingling pair is reunited. Careful monitoring and management is critical to ensure successful commingling pairs and to minimize aggression. Challenges are mainly related to appropriate training, experience, and timing. To date, we have established 16 male breeder pairs with mature males with body weights up to 15 kg. This demonstrates that sexually mature breeding males can be socially housed successfully even during an ongoing mating program.

PS 187 The Non-Obese Diabetic (NOD) Mouse As a Model for Diabetic Pregnancy

C. Kappen[1] and J. Salbaum[2]. [1]*Developmental Biology, Pennington Biomedical Research Center, Baton Rouge, LA and* [2]*Regulation of Gene Expression, Pennington Biomedical Research Center, Baton Rouge, LA.*

Diabetes in pregnancy is a well-known risk factor for neural tube defects (NTDs). In previous work, we used Streptozotocin induction of diabetes in the mouse as a model of type I diabetes during pregnancy. We reported that embryonic gene expression is altered under diabetic conditions, and we also observed a general increase in variability of expression levels. To determine whether this is a general feature in diabetic pregnancies, we employed a model of spontaneous Type I diabetes occurrence, the non-obese diabetic (NOD) strain of mice. In this strain, litters in diabetic dams exhibit NTDs at a rate of ~40%, with no malformations found in normoglycemic pregnancies. Gene expression profiling by microarrays and next-generation sequencing, at two different developmental time points, also indicated greater variation of gene expression levels within the group of diabetes-exposed embryos. On the basis of these finding, we propose a variation-based theoretical model to explain the incomplete penetrance of the NTD phenotype in diabetic pregnancies of inbred strains in mice. We also illustrate the discovery-advancing power of this paradigm. Beyond genetic models, our concept has broad impact for incomplete penetrance of outcomes from teratogen/toxin exposures in general, and for prevention strategies.

PS 188 Fetal Myocardial Reduction in Hyperglycemic Mouse Pregnancy Is Associated with Dysregulated Expression of the Antiapoptotic Gene BCL-2 in the Developing Heart: Preliminary Results

S. D. Holladay[1], J. C. Gutierrez[2], M. R. Prater[2], P. Navarrette[2] and R. M. Gogal[1]. [1]*Vet Biosciences & Diagnostic Imaging, University of Georgia, Athens, GA and* [2]*Biomedical Sciences & Pathobiology, Virginia Tech, Blacksburg, VA.*

A growing number of environmental contaminants may adversely affect fetal development through disruption of glucose homeostasis. We previously detected significant late-gestation ventricular myocardial reduction in fetal mouse hearts collected from pregnant mice dosed with streptozotocin, which is toxic to insulin-producing beta cells of the pancreas and induces hyperglycemia. Flow cytometric analysis of the myocardial cells showed an enhanced rate of apoptosis, suggesting dysregulated cell death as a mechanism associated with the myocardial defect. The present study therefore examined expression of the anti-apoptotic gene Bcl-2 in fetal myocardium from hyperglycemic mouse dams on days 14 and 17 of gestation. The hyperglycemia was induced in female Rockefeller (inbred CD1) mice, 6 to 8 weeks old, by pre-breeding streptozotocin (STZ) injection. Expression of Bcl-2 in the fetal myocardium from the diabetic dams was decreased by 53% and 51% at GD14 and 17, respectively. These results suggest maternal hyperglycemia may damage the developing myocardium by altering expression of gene pathways that regulate cell death.

PS 189 Human Hepatic CES1 and CES2 Ontogeny

D. McCarver, J. He, P. Simpson and R. N. Hines. *Pediatrics, Medical College of Wisconsin, Milwaukee, WI.*

Human CES1 and CES2 are critical in pyrethroid insecticide disposition and toxicity. In spite of concern for increased pyrethroid juvenile susceptibility, CES1 and CES2 ontogeny has not been well characterized. To define human hepatic microsomal and cytosolic CES1 and CES2 developmental expression patterns, microsomal and cytosolic fractions were made from subjects without liver disease [N=165, 1d-18 yrs]. Proteins were fractionated and quantitated by western blotting. CES1 expression was universally measurable by 3 weeks of age, whereas CES2 onset was slightly later. Over the entire population, microsomal and cytosolic CES1 varied about 30- and 70-fold, respectively; microsomal and cytosolic CES2 varied about 11- and 8-fold, respectively. Median microsomal CES1 was lower among samples from subjects < 3 weeks of age (N=36) compared to older subjects (N=126; 6.27 vs 17.5 pmoles/mg microsomal protein, respectively; p<0.001; Kruskal Wallis test). Cytosolic CES1 increased sequentially with expression being lowest among samples from individuals between birth and 3 weeks of age (N=36), markedly greater among those from ages 3 weeks to 6 years (N=90), and then modestly greater still among those over 6 years (N=36; median values=4.7, 15.8, and 16.6 pmoles/mg cytosolic protein, respectively; p values <0.001 and 0.05, respectively, Kruskal Wallis test). Microsomal CES2 also increased sequentially across the same 3 age groups with median values of 1.8, 2.9, and 4.2 pmoles/mg microsomal protein, respectively (p<0.001, both), whereas for cytosolic CES2, only the youngest age group differed from the two older groups (p<0.001; median values=1.29, 1.93, 2.0, respectively). When age category, gender and race were considered simultaneously, only age category remained associated with CES1 or CES2 expression in both the microsomal and cytosolic compartments (p<0.001, each model; ANOVA). These data suggest that infants < 3 weeks of age would have significantly lower metabolic clearance for CES1 and CES2 substrates compared to older individuals. Funded by the Council for for the Advancement of Pyrethroid Human Risk Assessment (CAPHRA).

PS 190 Impact of Fatty Acids on Human UDP-Glucuronosyltransferase 1A1 Activity and Its Expression in Neonatal Hyperbilirubinemia

R. Fujiwara, A. Shibuya and T. Itoh. *School of Pharmacy, Kitasato University, Tokyo, Japan.*

While breast milk has been known as a cause of neonatal hyperbilirubinemia, the underlying mechanism of breast milk-induced jaundice has not been clarified. Here, the impact of fatty acids on human UDP-glucuronosyltransferase (UGT) 1A1 – the sole enzyme that can metabolize bilirubin – were examined. Oleic acid, linoleic acid, and docosahexaenoic acid (DHA) strongly inhibited UGT1A1 activity. Forty-eight hours after a treatment with a lower concentration of DHA (10 mg/kg), total bilirubin significantly increased in neonatal hUGT1 mice, which are human neonatal jaundice models. In contrast, treatments with higher concentrations of fatty acids (0.1–10 g/kg) resulted in a decrease in serum bilirubin in hUGT1 mice. It was further demonstrated that the treatment with higher concentrations of fatty acids induced UGT1A1, possibly by activation of peroxisome proliferator-activated receptors. Our data indicates that activation of peroxisome proliferator-activated receptors would increase UGT1A1 expression, resulting in reduction of serum bilirubin levels in human infants.

PS 191 Genistein Reduces Human Placental BCRP/ABCG2 Transporter Expression and Function *In Vitro*: Potential Risk for Fetal Drug Exposure

K. M. Bircsak[1, 2], Q. Wang[1], Y. Lin[1] and L. M. Aleksunes[1]. [1]*Department of Pharmacology and Toxicology, Rutgers University, Piscataway, NJ and* [2]*Joint Graduate Program in Toxicology, Rutgers University, Piscataway, NJ.*

Pregnant women with gestational diabetes are often treated with the hypoglycemic drug glyburide because of its minimal accumulation in the fetus. Low levels of glyburide result from its transport away from the fetus and back to the maternal circulation by the breast cancer resistance protein (BCRP/*ABCG2*) expressed on placental syncytiotrophoblasts. The purpose of this project was to determine the effect of the soy isoflavone, genistein, on the 1.) regulation (protein and function) of BCRP in the placenta and 2.) direct inhibition of glyburide transport by BCRP in cell-based systems. Human choriocarcinoma BeWo cells were incubated with genistein (0-10 μM) for 48 h and collected for western blot and functional analysis. For the functional inhibition studies, BeWo cells and cells overexpressing the wild-type (WT) or functionally-reduced variant (C421A) of BCRP were incubated with increasing concentrations of genistein (0-100 μM) for 1 h. Retention of BCRP substrates Hoechst 33342 or BODIPY-glyburide was quantified with an automated fluorescent cell counter. Genistein reduced the protein expression of BCRP and increased the cellular retention of Hoechst up to 40% in BeWo cells at 48 h. In the direct inhibition studies, genistein enhanced the accumulation of Hoechst in placental BeWo cells (50%) and both BCRP-overexpressing cells (WT and C421A, 300%), with a trend for the C421A-BCRP cells to accumulate even more Hoechst in the presence of genistein. Interestingly, genistein increased the accumulation of BODIPY-glyburide up to 70% only in the C421A-BCRP cells. In conclusion, genistein decreases the placental expression and direct transport of glyburide by BCRP. Pregnant women that express the common C421A-BCRP variant and/or consume soy may be at an elevated risk for drug-induced neonatal hypoglycemia. Support: ES020522, ES005022, ES007148, and an AFPE Predoctoral Fellowship.

PS 192 Human Hepatic UGT2B15 Developmental Expression

K. Divakaran, R. N. Hines and D. McCarver. *Pediatrics, Medical College of Wisconsin, Milwaukee, WI.*

Human hepatic UGT2B15 expression changes during development may alter metabolic capacity for important drugs and toxicants such as bisphenol A (BPA). UGT2B15 ontogeny knowledge to date is limited to transcript data, a dubious surrogate for protein expression. Our objective was to elucidate the UGT2B15 protein expression pattern among 236 liver samples (8 weeks gestation to 18 years). We also probed the impact of a common, functional SNP (g.253G>T), present in both *UGT2B15*2* and **5* haplotypes, on UGT2B15 expression. Quantitative western blot analysis and PCR-based single base extension genotyping were performed on liver microsomal fractions. Classification regression tree analysis was used to stratify the data into age groups. UGT2B15 expression onset occurred during late fetal life (after 24 weeks) at ~20% of mature values (median values=48 & 267 pmoles/mg of microsomal protein, respectively; p < 0.001; Kruskal Wallis test). UGT2B15 neonatal (infants < 3 wks, n=39) and late fetal (GA 28 weeks to term, n=10) expression levels were similar to each other, but strikingly lower than that of infants between 3 and 15 weeks postnatal age (n=46; median values =38, 48 & 404 pmoles/mg microsomal protein, respectively; p < 0.001; Kruskal Wallis testing). UGT2B15 content was higher and more variable in the older infant group compared to the next age group (n=82; 15 weeks to 18 years) (p < 0.001; Kruskal Wallis test). UGT2B15 expression variation was 31-fold across the entire sample set and was demonstrable within all age groups, ranging from 4- to 27-fold. Considered together, age group, the presence of g.253T and male gender were significantly associated with greater UGT2B15 expression (p < 0.001, < 0.01 and < 0.05, respectively; stepwise linear regression). In summary, hepatic UGT2B15 protein onset begins in late gestation; however, the greatest rate of change occurs during the first few weeks after birth. From these data, we speculate that the fetus and neonate may have lower clearance of some UGT2B15 substrates, such as BPA, compared to that of older individuals.

PS 193 *In Utero* Exposure of C57BL/6J Mice to 2, 3, 7, 8-Tetrachlorodibenzo-*p*-Dioxin (TCDD) Disrupts Epidermal Tight Junctions

C. S. Muenyi, S. Leon Carrion, L. A. Jones, C. H. Sutter and T. R. Sutter. *Biological Sciences, University of Memphis, Memphis, TN.*

The incidence of atopic diseases is high, affecting as many as 20 percent of children in the United States. Defects in tight junction (TJ) component of the epidermal permeability barrier (EPB) are linked to atopic dermatitis, a disease that may be predisposing to both food allergies and asthma. Here, we report on developmental effects of exposure to TCDD on EPB function. Timed pregnant C57BL/6J mice were gavage with TCDD (10 μg/kg body weight) or corn oil control vehicle on gestation day 12. Embryos were collected on embryonic days 15 (E15), E16, E17 and postnatal day 1 (PND1). Skin permeability assay showed that TCDD accelerated the timing of EPB formation, beginning at E15. This was accompanied by significant decrease in transepidermal water loss (TEWL), and enhanced epidermal stratification and formation of the stratum corneum (SC). Levels of several ceramide classes were significantly increased at E15 and E16. By PND1, histology revealed that TCDD caused acanthosis and epidermal hyperkeratosis, both of which are observed in people with TCDD-induced chloracne. Moreover, TJ functional assay revealed that TCDD significant increased the percentage of terminal TJs with biotin leakage in the PND1 pups. As these animals did not have enhanced rates of TEWL, a commonly observed phenotype in animals with TJ defects, we performed six sequential tape-strippings of epidermis to remove the SC. Complete removal of the SC resulted in significant increase in TEWL in TCDD-exposed PND1 pups compared with their control group. These data support the idea that TCDD-induced hyperkeratosis is a compensatory response in these mice with disrupted TJ barrier, and along with elevated levels of ceramides, may mitigate transepidermal water loss. Together, these findings demonstrate that the effects of TCDD to ac-

celerate EPB formation result in an abnormally functioning barrier. Furthermore, defects in TJ component of EPB that result from in utero exposure to TCDD may contribute to atopic disease.

PS 194 Ethanol (EtOH) Alters the Redox Environment, Histiotrophic Nutrition Pathways (HNP), and the Thiol Proteome during Rat Organogenesis

J. L. Jilek[1], K. E. Sant[1], K. H. Cho[1], M. S. Reed[2], J. Pohl[2], J. M. Hansen[3] and C. Harris[1]. *[1]Environmental Health Sciences, University of Michigan, Ann Arbor, MI, [2]Biotechnology Core Facility Branch, Centers for Disease Control, Atlanta, GA and [3]Division of Pulmonary, Allergy/Immunology, Cystic Fibrosis and Sleep, Department of Pediatrics, Emory Medical School, Atlanta, GA.*

Ethanol is a known teratogen involved in the etiology of structural and functional defects by mechanisms that include redox regulation and related disruption of the actin cytoskeleton, although, modes of action are not well defined. This study uses the rat whole embryo culture (rWEC) model to further elucidate the relationships between embryonic nutrition, redox environment and observed changes in the thiol proteome following EtOH exposures (1.5–6.0 mg/ml). Soluble thiol concentrations (GSH and Cys) and their respective intracellular redox potentials (Eh) were determined using HPLC. EtOH reduced GSH and Cys concentrations in embryo (EMB) and visceral yolk sac (VYS) tissues, and also in yolk sac fluid (YSF) and amniotic fluid (AF). These changes were accompanied by greater oxidation as indicated by increasingly positive Eh values. Disruption of nutrient transport and cytoskeletal dynamics has been previously shown following EtOH exposure. EtOH reduced HNP activity in rWEC as measured by the clearance of FITC-albumin from the culture media. A significant decline in total FITC clearance was observed at all doses, showing an optimal >50% change at the high dose. EtOH-induced changes in protein concentrations within the thiol proteome were measured in EMBs and VYSs using isotope-coded affinity tags (ICAT). Decreases for specific proteins involved in cytoskeletal dynamics and endocytosis (α-actin, α-tubilin, cubilin, and actin-related protein) and in proteins involved in nuclear trafficking (Ran and RanGAP) were observed. This study suggests that EtOH can alter redox environments, HNP activities, and concentrations of the thiol-reactive proteins involved with cellular transport systems, which all may collectively contribute to EtOH-induced developmental toxicity during early organogenesis.

PS 195 Two Alleles of Med31 Provide a Model to Study Defects in Cellular Proliferation and Endochondral Ossification

K. Wolton[1], J. Wright[2] and K. Hentges[1]. *[1]University of Manchester, Manchester, United Kingdom and [2]Syngenta, Berkshire, United Kingdom.*

Over 400 different skeletal dysplasias have been characterised and represent a significant global health concern., with incidence rates estimated around 1 in every 4000-5000 live births. Understanding the mechanisms which govern early skeletal development in the embryo is key to developing potential therapeutics.
We have isolated two separate mouse lines with mutations in the Mediator complex gene Med31 derived from an ENU mutagenesis screen. The first mouse is null for the Med31 protein during development, and displays delays in the development of the limbs. Using a combination of wholemount staining for the mitotic marker phospho-histone H3 on E10.5 embryos and immunohistochemistry on E16.5 paraformaldehyde fixed sections using the Ki-67 antibody, we have confirmed that the mutants have cell proliferation defects which contribute to delays in bone ossification. The second mouse line has a Med31 missense mutation (Y57C), confirmed by genomic sequencing, which we predict affects the ability of the Med31 protein to interact with Med7N within the Mediator complex. Individual null or Y57C heterozygous mice are phenotypically normal, whilst double mutants, of the genotype 'Med31 null/ Med31 Y57C' show delays in limb development similar to Med31 null mice, when stained with Alcian blue and Alizarin red in skeletal preperations.
To further understand the function of Med31 in the context of cellular proliferation in the developing limb, we have developed a cell culture knock out model, in which we reduce Med31 expression using shRNA transfection into the mesenchymal cell line C3H10T1/2. We will use a combination of cell culture and whole embryo models to further elucidate the function of Med31 in limb development.

PS 196 The Effects of Thalidomide on Fgf8, Bmp4 and Hoxa11 Expression in the Limb Bud in Rabbit Embryos

Y. Kawamura, T. Yamashita, T. Yamauchi, K. Matsumoto and K. Sato. *Drug Safety Research Laboratories, Takeda Pharmaceutical Company Limited, Fujisawa, Kanagawa, Japan.* Sponsor: K. Takami.

Thalidomide (TM) induces limb defects in humans and some animal species including rabbits. Although the mechanism of TM-induced limb defects has been investigated for a long period, the limb development-related genes expressions have not been vigorously characterized in rabbits. In this study, we investigated the Fgf8, Bmp4 and Hoxa11 expressions in the limb buds in TM-treated Kbl:JW rabbit embryos on gestation day (GD) 10, 11 and 12 by whole mount in situ hybridization.
It has been reported that Fgf8 and Bmp4 expressions were changed in the limb bud in TM-treated rabbit and chick embryos, respectively. Hoxa11 was selected because Hoxa11-knockout mice show morphological changes at the ulna and radius and the radius malformation was observed in TM-induced rabbit fetuses.
On GD 10 and 11, growth retardation of the whole body was induced by TM treatment. The expression lengths of Fgf8 on GD 10 and 11 in the forelimb bud were significantly or tended to be decreased in the TM-treated embryos, which was correlated to the growth retardation and was not considered to be directly relevant to the teratogenic effect of TM on the forelimb. Hoxa11 is not expressed on GD 10. The TM-induced characteristic changes in the expression pattern of Hoxa11 on GD 11 and Bmp4 on GD 10 and 11 were not noted.
On GD 12, there was no effect of TM on growth retardation. The expressions of Fgf8 and Bmp4 were not changed by TM on GD 12, while Hoxa11 expression was narrowed by TM at the anterior region and was not changed at the middle and posterior regions in the forelimb bud and in all regions in the hindlimb bud. The anterior region was located on the radial side and the radius malformation was observed in the TM-treated rabbit fetuses. Therefore, the decrease in the Hoxa11 expression on GD 12 was related to the limb defects induced by TM and can be a good marker for early prediction of the teratogenic effect of TM on the forelimb.

PS 197 Humoral Immunity and Lymphocyte Immunophenotyping Control Background Data in Mainland and Indonesian Cynomolgus Monkey Infants

S. Oneda[1], N. Yee[1], N. Lalayeva[1], R. E. Watson[1], N. Makori[1], S. Graza[1], P. Franklin[1], T. Beck[1], K. Fukuzaki[1] and R. Nagata[2]. *[1]Safety Assessment, SNBL USA, Ltd., Everett, WA and [2]Shin Nippon Biomedical laboratories, Ltd., Tokyo, Japan.*

Background: Lymphocyte immunophenotyping (LIP) and T-cell dependent antibody response (TDAR) are the most common tests in assessing potential developmental immunotoxicology in pre- and postnatal developmental (PPND) studies. Background data from Mainland (ML, China and Cambodia) and Indonesian Island (IL) Cynomolgus monkeys were compared in order to accurately assess the presence or absence of test article-related changes in treated monkeys from different sources.
Methods: Control data were analyzed retrospectively from a total of 14 and 10 PPND studies for LIP and TDAR data, respectively. Blood samples for LIP by flow cytometry in infants were collected throughout the postnatal period and analyzed for total CD3+ T cells, CD3+CD4+ Helper T cells, CD3+CD8+ Cytotoxic T cells, CD3-CD20+ B cells, and CD3-CD16+ or CD3-CD159a+ Natural Killer (NK) cells. To evaluate TDAR, keyhole limpet hemocyanin (KLH) was injected twice, and primary and secondary IgM and IgG levels in serum were measured by ELISA.
Results: IL monkeys generally had higher absolute counts and relative percentages of NK cell populations, and lower circulating B cell numbers when compared to ML monkeys. IgM levels elevated rapidly after the 1st and 2nd doses, with peak IgM concentrations in IL 24-27% lower than that observed in ML. IgG levels elevated gradually after the 1st dose and increased rapidly after secondary challenge. The highest IgG levels after primary KLH challenge in IL was 24% lower than ML. After the 2nd dose, the highest IgG in IL was 39% higher than ML. The trends of IgM and IgG were similar between IL and ML.
Conclusions: There were distinct differences in NK and B-cell populations and IgM/IgG responses between infants of ML and IL origin, suggesting origin-specific differences in lymphocyte development and function. These reference background data are useful to assure that accurate assessments of test article-related effects on these parameters.

PS 198 Development and Validation of an Analytical Method for Monobutylphthalate, a Metabolite of Di-n-Butylphthalate, in Harlan Sprague-Dawley Rat Pup and Fetus by Ultra-Performance Liquid Chromatography-Tandem Mass Spectrometry (UPLC-MS/MS)

R. A. Fernando[1], M. A. Silinski[1], T. A. Freed[1], F. K. Thomas[1], V. G. Robinson[2] and S. Waidyanatha[2]. [1]*RTI International, Research Triangle Park, NC and* [2]*Division of National Toxicology Program, NIEHS, Research Triangle Park, NC.* Sponsor: K. Levine.

Di-n-butyl phthalate (DBP) is a common plasticizer used in a variety of consumer products. Exposure to DBP is widespread, and its potential toxicity has been, and continues to be, investigated. The objective of this work was to develop and validate a method to quantitate mono-n-butyl phthalate (MBP), the major metabolite of DBP, in rat pup and fetus. Samples were prepared by spiking 0.5 g of pup or fetus homogenate with 25 µL of water, 25 µL of internal standard solution (MBP-d4 in water), and 300 µL of 0.1% formic acid in water. Analyte extraction was achieved by the addition of 1 mL of acetonitrile, vortex mixing, and centrifugation. The supernatant was filtered, submerged into liquid nitrogen, and centrifuged to facilitate lipid separation. The method was successfully validated over the range 50-5000 ng/g in pup, with cross-validation for fetus. Validation parameters included linearity ($r \geq 0.99$), recovery (mean recovery = 109%), sensitivity (limit of detection = 9.4 ng/g; experimental limit of quantitation (ELOQ = 50 ng/g), precision (relative standard deviation ≤10%), and accuracy (relative error ≤ 10%). Background phthalate interference was detected in both pup and fetus, but MBP peak area ratios for the blanks were ≤ 40% of those for the ELOQ standards, demonstrating acceptable selectivity. Stability was established for frozen matrix samples stored at -20°C for 60 days, matrix samples subjected to freeze-thaw (3 cycles over 3 days), and also ambient and refrigerated extracts for 3 days. It was also demonstrated that pup samples as high as 7,500 ng/g and fetus samples as high as 25,200 ng/g could be accurately quantitated by diluting into the calibration range.The method is being applied for quantitation of MBP in pup and fetus samples from rats administered 0, 300, 1000, 3000, or 10,000 ppm DBP in feed.

PS 199 Developmental Toxicity Assessment of Multiwall Carbon Nanotubes in Pregnant Mice after Intratracheal Instillation

N. Kobayashi[1], T. Numano[2, 3], R. Kubota[1], Y. Ikarashi[1] and A. Hirose[1]. [1]*National Institute of Health Sciences, Tokyo, Japan,* [2]*DIMS Institute of Medical Science Inc., Ichinomiya, Aichi, Japan and* [3]*Department of Molecular Toxicology, Nagoya City University Graduate School of Medical Sciences, Nagoya, Aichi, Japan.*

In order to evaluate the developmental toxicity of multi-wall carbon nanotubes (MWCNTs) via inhalation exposure, we conducted an intratracheal instillation study of MWCNTs in pregnant mice. MWCNTs (MWNT-7) dispersions were prepared by ultrasonication using an ultrasonic bath for 30 min. In order to compare the biological effect of dispersion media, we used two different media, mouse serum and 2% (w/v) of sodium carboxymethyl cellose (CMC-Na) solution. The MWCNT dispersions in serum were administered to pregnant Crlj:CD1(ICR) mice on gestation day 9 at dosage of 0, 3.0, 5.0 and 7.0 mg/kg bw (mouse serum). The MWCNT dispersions in 2% CMC-Na solution was administered at dosage of 5.0 mg/kg bw. Ten pregnant mice per group were evaluated and dissected on gestation day 17. Decreased body weights in all MWCNT exposed pregnant mice were observed, although there were no clear dose-dependent changes. No statistically significant difference was observed between the control group and MWCNT exposed groups in the numbers of corpora lutea, dead fetuses (early or late resorption), and live fetuses, or sex ratio. Body weight of fetuses and placental weights were significantly decreased in the most MWCNT exposed groups, although no clear dose-dependency was observed. Furthermore, external malformations (i.e., oligodactyly, extensive contracture, kinked tail, cleft lip, and cleft palate) were observed in all MWCNT exposed groups. The fetuses with external malformations were derived from the same litters. The equivocal dose-dependent effects may be due to a litter dependent toxic mechanism. These results suggested the intratracheal exposure of MWCNT caused teratogenic effects in mice in spite of different dispersion media. Further examinations are needed to clarify the mechanism of the developmental toxicity by MWCNTs.

PS 200 Elucidation of a Novel Molecular Mechanism of Dioxin Toxicity

N. Fujisawa, W. Yoshioka and C. Tohyama. *Graduate School of Medicine, The University of Tokyo, Tokyo, Japan.*

Exposure to 2,3,7,8-tetrachlorodibenzo-*p*-dioxin (TCDD) exerts a variety of toxicity. Beside the essential role of aryl hydrocarbon receptor (AhR), the molecular basis of TCDD toxicity has been elusive. Recent *in vitro* experiments showed that TCDD activates $cPLA_2\alpha$ via a different pathway from transactivation of AhR target genes. Thus, there is a research need to elucidate the possible involvement of this alternate pathway in the manifestation of TCDD toxicity *in vivo*. First, we administered TCDD to fetuses, lactational pups, and adults of wild-type or $cPLA_2\alpha$ KO mice to find out the manifestation of toxicity. Next, among a variety of dioxin toxicity, we studied the molecular mechanism of toxicity by focusing on the neonatal hydronephrosis. Finally, using AhR^{nls} mice, we investigated the role of AhR localization into nucleus with regard to the alternate pathway.
Fetal toxicity: $cPLA_2\alpha$ (+/-) pregnant mice were administered TCDD on gestational day (GD) 12.5, and onset of hydronephrosis and cleft palate and changes in fetal survival rate were examined on GD18.5. $cPLA_2\alpha$ was found to take an important part in the manifestation of neonatal and fetal hydronephrosis, and at the same time in the reduction of TCDD-induced fetal lethality. Neonatal toxicity: $cPLA_2\alpha$ (+/-) dams and AhR^{nls} dams were orally administered TCDD on postnatal day (PND) 1. Pups were sacrificed on PNDs 7 and 14 to examine the development of hydronephrosis. Hydronephrosis was not developed in either $cPLA_2\alpha$ KO or AhR^{nls} mice. Adult toxicity: $cPLA_2\alpha$ (+/+) and $cPLA_2\alpha$ (-/-) mice aged 12 week old were injected i.p. with TCDD. Hepatotoxicity and thymic atrophy were examined on day 8. In adult mice, $cPLA_2\alpha$ was found not to be associated with the manifestation of these kinds of TCDD toxicity.
In conclusion, using different stages of mice, neonatal hydronephrosis was found to be a good model to study the molecular basis of a novel pathway in the induction of TCDD toxicity. The nuclear localization of AhR was suggested to play an essential role in the activation of the novel pathway.

PS 201 Evaluation of the Sodium Valproate-Induced Developmental Abnormalities and Its Mechanisms in Zebrafish

A. Yamashita[1], H. Inada[1], K. Chihara[1], T. Yamada[1], T. Yabe[2], S. Takada[2], J. Deguchi[1] and H. Funabashi[1]. [1]*Preclinical Research Laboratories, Dainippon Sumitomo Pharma Co., Ltd., Osaka, Japan and* [2]*Division of Molecular and Development Biology, National Institute for Basic Biology, Aichi, Japan.*

Sodium valproate (VPA) is known to induce developmental abnormalities such as spina bifida, craniofacial anomalies and developmental neurotoxicity (DNT) in mammals. In the present studies, we evaluated the VPA-induced developmental abnormalities in zebrafish and analyzed the mechanisms of the abnormalities focusing on the craniofacial anomaly and DNT. [Study 1] Zebrafish (*Tupfel Longfin*) were exposed to VPA at 75 µM from 5 to 144 hours post fertilization (hpf), and morphological evaluation was conducted at 144 hpf. Additionally, gene expression analysis of *dlx2*, a marker for neural crest cells, was performed by *in situ* hybridization on staged embryos. VPA-treated larvae showed abnormal findings in the notochord and lower jaw, corresponding to the phenotypes observed in VPA-exposed mammals, and the lower jaw anomaly was accompanied with a decrease in *dlx2* expression in the hyoid arch. These results imply that the VPA-induced morphological anomaly in the lower jaw is related to morphogenesis failure of the neural crest-derived structures in zebrafish. [Study 2] Zebrafish were exposed to VPA at 40 µM from 5 to 144 hpf. After VPA-free period for 24 hours from 144 hpf, locomotor activity was evaluated under 10 minutes light and dark cycles, and gene expression analysis of *tyrosine hydroxylase* (*th*), a marker for dopaminergic neuron, was performed on staged embryos. VPA-treated larvae showed an increase in locomotor activity during the dark period and a decrease in *th* expression in the hypothalamus. These results imply that the VPA-induced DNT is related to inhibition of the dopaminergic neuron development in zebrafish. In conclusion, our studies revealed that VPA induces some developmental abnormalities in zebrafsh and suggested that inhibition of the neural crest-derived craniofacial and dopaminergic neuron development is related to these developmental abnormalities.

PS 202 Evaluation of Teratogenicity of IMiD® Compounds Using the Zebrafish Developmental Toxicity Assay

J. Y. Hui[1], P. J. Sherratt[1], B. D. Jeffy[1], K. Tang[1] and D. J. Fort[2]. [1]*Celgene Corporation, Summit, NJ and* [2]*Fort Environmental Laboratories, Stillwater, OK.*

IMiD immunomodulatory agents are analogues of thalidomide that represent a promising class of drugs for the treatment of inflammatory, autoimmune, and cancerous diseases. To investigate the usefulness of the zebrafish development toxicity

assay (ZFDA) as a screen for the teratogenicity potential of the IMiD compounds, thalidomide, lenalidomide, pomalidomide and CC-10015 were evaluated in this assay. All of these compounds have in vivo embryo-fetal developmental (EFD) toxicity data in at least one species; therefore, data from the ZFDA can be compared to those obtained from standard species used in EFD evaluation.
Treatment of zebrafish embryos started at 2 hours post-fertilization (hpf), and evaluation was performed after 96 hours of exposure. Evaluation included development of head, tail and trunk; further examination of head, eye and brain size was conducted by photo-digitization. Results showed that thalidomide and CC-10015 produced malformations at concentrations below those that resulted in general toxicity to zebrafish. Visceral defects were observed with thalidomide and CC-10015, and pectoral fin defects were observed with thalidomide only. Pomalidomide resulted in an increase in brain size at concentrations that produced growth retardation or lethality. A few malformations were observed with lenalidomide at lethal concentrations. Studies were also conducted to determine the critical time window when thalidomide produces teratogenicity. Data showed that exposure during the first 12 hours (2-14 hpf) was critical in producing pectoral fin defects.
Development of the pectoral fin shares a similar molecular pathway as those of tetrapod limbs; however pectoral fin defect was only observed with thalidomide in the ZFDA. These data with the IMiD compounds show a lack of concordance of developmental defects between zebrafish and other species commonly used for EFD evaluation because limb malformations have been reported with thalidomide and pomalidomide in rabbits, and with lenalidomide in non-human primates.

PS 203 Expression of Glyoxylase 1 (glo1) throughout Zebrafish Embryonic Development and Alterations following Atrazine Exposure

G. A. Ryan[1], G. J. Weber[1], S. M. Peterson[1], M. M. Sepulveda[2] and J. L. Freeman[1]. [1]*Health Sciences, Purdue University, West Lafayette, IN and* [2]*Department of Forestry and Natural Resources, Purdue University, West Lafayette, IN.*

Atrazine, a commonly used herbicide in the Midwest, is an endocrine disruptor and a suspected carcinogen. Although atrazine was recently banned by the European Union for widespread contamination risks in potable water supplies, this herbicide is still commonly used in the United States with a current maximum contaminant level (MCL) of 3 ppb in drinking water. The health risks associated with this MCL are currently being reviewed by the Environmental Protection Agency; however, the mechanisms of atrazine toxicity are not well defined. In this study transcriptomics was first used to identify genes with altered expression following exposure to 0, 0.3, 3, or 30 ppb atrazine during embryogenesis with the zebrafish model system. This analysis showed that expression alterations were enriched with genes associated with neuroendocrine development and function, cell cycle regulation, and carcinogenesis. From this list of genes, glyoxylase 1 (glo1) was targeted for further study. glo1 is part of the glyoxylase system which converts methylglyoxal to S-D-lactoylglutathione. Upregulation of glo1 is linked to cell proliferation and is associated with various cancers in humans. To further our understanding of this genetic target, expression was analyzed at five developmental time points (24, 36, 48, 60, and 72 hpf). in situ hybridization was used to characterize spatial gene expression of glo1 throughout development under normal conditions and after exposure to 0, 0.3, 3, or 30 ppb atrazine. glo1 was found to be ubiquitously expressed at each time point with most of the staining concentrated in the brain. A high level of expression was also observed in the liver. Quantitative PCR (qPCR) is also being applied to determine gene expression levels of glo1 throughout development. This data is furthering our understanding of glo1 expression during development and alterations induced by embryonic atrazine exposure.

PS 204 Deregulation of miRNA-126 Expression in Developing Zebrafish Exposed to the Herbicide Atrazine

K. Schlotman, S. Wirbisky, G. J. Weber and J. L. Freeman. *Health Sciences, Purdue University, West Lafayette, IN.*

Atrazine is a commonly used herbicide in the United States that is reported to frequently contaminate drinking water sources. Studies have indicated atrazine to adversely impact the neuroendocrine and reproductive systems and to be a potential carcinogen. The current maximum contaminant level for atrazine in drinking water set by the US Environmental Protection Agency is 3 parts per billion (ppb); however, levels higher than 3 ppb are often reported. Ongoing studies in our laboratory are investigating the immediate and latent adverse health outcomes associated with a developmental atrazine exposure and identifying the genetic and epigenetic mechanisms of atrazine toxicity using the zebrafish model system. MicroRNAs (miRNAs) are epigenetic regulators that post-transcriptionally control the translation of mRNA. To identify if an embryonic atrazine exposure would alter miRNA expression, a unique microarray platform containing all known zebrafish and human miRNAs was designed. Zebrafish embryos were exposed to 0, 0.3, 3, or 30 ppb atrazine through 72 hours post fertilization (hpf), and miRNA expression was analyzed using the microarray platform. Expression of 18 zebrafish and 9 human miRNAs were significantly altered in response to atrazine exposure. One of the more robustly changed miRNAs was miR-126, a miRNA associated with angiogenesis and tumorigenesis. To further investigate the developmental expression of miR-126 and its deregulation by atrazine exposure, quantitative PCR (qPCR) was first used to profile expression throughout embryogenesis in control conditions at 12, 24, 36, 48, 60, and 72 hpf. Expression of miR-126 was developmental time point specific with an increase in expression after 12 hpf and a peak in expression at 36 hpf. Following a decrease in expression at 48 hpf, expression levels were significantly higher at 60 and 72 hpf. Deregulation of miR-126 following exposure to 0, 0.3, 3, or 30 ppb atrazine at all six developmental time points was also analyzed to further our understanding on the impacts of atrazine exposure on miR-126 expression.

PS 205 Exposure to Chemicals Found in Umbilical Cord Blood Alters Kisspeptin/GPR54-GnRH Pathway Expression and Development in the Zebrafish Embryonic Development Model

J. P. Crago and D. Schlenk. *Environmental Sciences, University-California, Riverside, Riverside, CA.*

There are numerous positive and negative inputs that affect the development of the hypothalamus–pituitary–gonadal axis during fetal and early-life stages. Therefore, alterations in reproductive function that manifest later in life, such as the earlier onset of puberty could be a result from perturbations or exposures during critical neural developmental time-points. Recent work has identified Kisspeptin (KISS), expressed in the arcuate nuclei (ARC) region of the brain, that are vital for the central regulation of gonadotrophin releasing hormone (GnRH) neurosecretory activity and timing of puberty. At present, there is little research examining the effect of chemicals found in the umbilical cord blood on KISS mRNA levels or on the development of KISS positive gonadotropes in any developmental vertebrate model. The goal of this study is to use the developing zebrafish embryo model to determine the impact of individual chemicals and low-level mixtures of compounds that are present in the umbilical cord blood on KISS-NK-DYN-GnRH signaling system. Embryos were exposed to several compounds at concentrations reported in umbilical cord blood. KISS 1 and 2, GPCR54-1 and 2, and GNRH3 mRNA expression was measured at 2 hour intervals for the first 24 hours. We first identified mRNA expression of two orthologs of KISS 1 and 2 and GPCR54-1 & 2 during initial stages of development. This is subsequently followed by GnRH expression at 23 hpf. Initial exposures to either estradiol or the anti-diabetic drug metformin increased mRNA expression of KISS 1 and 2 as well as shifted the timing of expression. Our results indicate that there is a shift in timing and mRNA expression that may impact GnRH neuronal signaling and development.

PS 206 Induction of Vitellogenin in *Trachemys scripta* Exposed to Atrazine

E. R. Thomas[1] and R. Valverde[2]. [1]*Biological Sciences, Southeastern Louisiana University, Hammond, LA and* [2]*Biological Sciences, Southeastern Louisiana University, Hammond, LA.* Sponsor: A. Hoberman.

Due to their ubiquitous presence, persistence, and tendency to bioaccumulate, endocrine disrupting chemicals (EDCs) may cause significant impacts on the health of wildlife. Atrazine, a commonly used pesticide in the United States, is a type of EDC that is causing much concern due to the recent finding that it may cause adverse effects at low doses. This study focuses on the estrogenic effects of atrazine (2-Chloro-4-ethylamino-6-isopropylamino-s-triazine). Since it has been shown that atrazine caused two male American leopard frogs (*Rana pipens*) to have oocytes that were vitellogenic, we hypothesized that exposure to atrazine may result in the induction of vitellogenin in hatchling red eared slider turtles (*Trachemys scripta*). Vitellogenin is the egg yolk precursor protein that is typically found when female oviparous vertebrates are reproductively active. Because males also carry the gene that codes for vitellogenin, this protein is a reliable biomarker in oviparous vertebrates for exposure to estrogenic compounds. Hatchling female and male *T. scripta* received intraperitoneal injections of one of four different concentrations of atrazine (0.0001, 0.01, 0.1, or 1 ng/g bm), estradiol-17β in two doses (1 or 1000ng/g bm), or vehicle (saline) only. Plasma vitellogenin concentration was measured using an ELISA developed specifically for *T. scripta* vitellogenin. Significant production of vitellogenin occurred in turtles in both the estradiol groups as well as the atrazine groups in a dose response manner. Our data shows that exposure to low doses of atrazine causes induction of vitellogenin in the turtle and demonstrates the potential for this compound to act as an EDC.

PS 207 Developmental Exposure to Benzo[a]pyrene Affects Behavior and Energetics in Larval and Adult Zebrafish

A. Knecht, R. L. Tanguay and L. Truong. *Dept of Environmental and Molecular Toxicology, Oregon State University, Corvallis, OR.*

Polycyclic aromatic hydrocarbons (PAHs) are ubiquitous environmental contaminants present in urban air, dust, and soil resulting from incomplete combustion of organic materials or fossil fuels. It is widely recognized that PAHs pose risks to human health, especially for the developing fetus and infant, where PAH exposures have been linked to in-utero mortality, lower intelligence, and cardiovascular effects. Using the zebrafish model, we evaluated the developmental toxicity of PAH exposures. Zebrafish embryos were exposed from 6-120 hours post fertilization (hpf) to B[a]P, Ba[A]Q, BEZO, and 9,10-PHEQ concentrations that caused no observable morphological toxicity. Using the Seahorse Extracellular Flux Analyzer, we measured *in vivo* respiration in 26hpf embryos exposed to PAHs. Exposure to B[a]P, Ba[A[Q, BEZO, and 9,10-PHEQ caused decreased oxygen consumption rates, indicative of mitochondrial damage. Developmental B[a]P and Ba[A] Q exposure also resulted in hyperactive swimming at 120hpf. To determine if behavioral and physiological effects persisted, a subset of exposed animals were raised to adulthood in chemical-free water and assessed for learning and energetic deficits. Preliminary results indicate B[a]P-dependent deficiencies in learning and performance in an active avoidance conditioning test. To determine if adult physiological function is altered by developmental PAH exposure, a swim tunnel respirometer was used to measure total oxygen consumption. Animals developmentally exposed to B[a]P demonstrate a significant increase in oxygen consumption rates. Finally, to explore what transcriptional events are occurring prior to the onset of developmental toxicity, mRNA expression changes in B[a]P-exposed embryos were examined with whole-genome RNA-seq at 48hpf. Collectively, these data demonstrates that developmental PAH exposure results in a number of non-cancer endpoints and we are now positioned to identify the mechanisms underlying these complex responses. This research was supported by NIEHS grants P42ES016465 and P30ES000210.

PS 208 Effects of Benzo[a]pyrene and *Cyp19b* Knockdown on Early Zebrafish Development

K. M. Alharthy[1], F. T. Booc[1], J. Corrales[1], C. Thornton[1], W. Dong[2] and K. L. Willett[1]. [1]*Department of Pharmacology and ETRP, University of Mississippi, University, MS and* [2]*Nicholas School of the Environment, Duke University, Durham, NC.*

Benzo[a]pyrene (BaP) is a ubiquitous environmental contaminant that is an endocrine disrupting and carcinogenic PAH. Previously we found that BaP significantly decreased fish brain aromatase (CYP19b) expression, a key enzyme in steroidogenesis. We hypothesized that BaP deregulates the steroid hormone hypothalamus-pituitary-gonad feedback loop adversely affecting development and physiology. Here, we consider whether the toxicities observed following BaP exposure are comparable to those following transient CYP19b knockdown during early development. One-cell zebrafish embryos were injected with a CYP19b morpholino or the Genetools control-MO. Other non-injected embryos were exposed to nominal waterborne concentrations of BaP (0, 10 & 50 µg/L) for 96 hours post-fertilization (hpf). BaP and CYP19b knockdown resulted in a number of similar phenotypic endpoints. Cumulative mortality of zebrafish larvae was significantly increased by 5, 6, and 20% for low BaP, high BaP, and CYP19b knockdown, respectively, compared to controls. Hatching efficiency was significantly decreased by all treatments at 48 hpf. In a treatment-blinded morphological assessment of larvae at 96 hpf, the body length, optic vesicle, and swim bladder inflation of larvae were significantly decreased while pericardial and abdominal edema were increased by high BaP and CYP19b knockdown. The incidence of normal larval body, tail and pectoral fin shape was significantly decreased in both treatments. To identify the effects of BaP and CYP19b knockdown on primordial germ cell (PGC) migration, in-situ hybridization was done on embryos at the 25 somite stage; preliminary results suggest that BaP may affect PGC migration. Zebrafish were collected at 28, 32, 35 & 52 days post-fertilization to determine if gonad maturation was delayed. Results suggest BaP effects in zebrafish embryos are similar to the effects observed by aromatase knockdown. Supported by NIEHS R03 ES018962.

PS 209 Chemical-Specific Oxidative Stress Response in Zebrafish Embryos

M. E. Hahn[1], S. I. Karchner[1], D. G. Franks[1], A. R. Timme-Laragy[1, 2] and A. G. McArthur[3]. [1]*Biology, Woods Hole Oceanographic Inst, Woods Hole, MA,* [2]*Public Health, Univ of Massachusetts, Amherst, MA and* [3]*AGM Consulting, Hamilton, ON, Canada.*

Exposure to natural and anthropogenic stressors often leads to oxidative stress—a disruption in the regulation of intracellular redox conditions. Animals have evolved protective responses to mitigate damage caused by oxidative stress, but the mechanisms by which the oxidative stress response is regulated during development are poorly understood. Oxidants, electrophiles, and some phenolic anti-oxidants initiate this response by activating NF-E2-related factor 2 (NRF2) and related cap'n'collar-basic-leucine zipper family proteins, which bind to anti-oxidant response elements and activate transcription of genes such as glutathione S-transferases, NAD(P)H-quinone oxidoreductase, glutamate-cysteine ligase, and superoxide dismutase. To identify the genes that are induced or repressed in response to oxidative stress during development, and determine whether there is a "core" set of oxidant responsive genes that is induced by structurally distinct activators of NRF2, zebrafish (*Danio rerio*) larvae (96 hours post-fertilization) were exposed to model oxidants (tert-butylhydroquinone (tBHQ), tert-butylhydroperoxide (tBOOH), diquat (DQ) or sulforaphane (SFN)) and gene expression was measured 6 hr later by microarray and Q-RT-PCR. There was a robust response to oxidative stress by all chemicals, with a total of 1281 probes significantly altered in expression. The compounds caused overlapping but distinct patterns of altered gene expression. A core set of genes responded to all oxidants. However, other genes exhibited oxidant-specific changes in expression. Principal components analysis revealed that the changes in gene expression caused by SFN, a sulfhydryl-reactive agent, were distinct from those produced by the other oxidants. The results demonstrate that the oxidative stress response in developing animals is dependent upon the nature of the oxidative stress. [NIH R01ES016366 and F32ES017585]

PS 210 Knockdown of the TCDD-Regulated Transcription Factor, Foxq1a, Alters Pathways Involved in Neurological, Skeletal, and Muscular Development

C. J. Mattingly, D. Reif and A. Planchart. *Biology, NC State University, Raleigh, NC.*

Developmental exposure to 2,3,7,8-tetrachlorodibenzo-p-dioxin (TCDD), a potent activator of the aryl hydrocarbon receptor (AHR), is associated with adverse phenotypes including craniofacial, cardiovascular and skeletal defects. Despite much progress, the molecular mechanisms by which activated AHR leads to these phenotypes remain unclear. Work previously conducted in our laboratory identified foxq1a (previously foxq1b) as a target of TCDD-mediated upregulation in the jaw primordium. To gain insight into the developmental pathways and functions regulated by foxq1a, we knocked down its expression by morpholino injection and sequenced the transcriptome from control and morphant zebrafish embryos at 24 hours post-fertilization. Triplicate control and morphant RNA samples were depleted of rRNA and barcoded libraries were prepared using the Ion Total RNA-Seq Kit (v2) for whole transcriptome libraries (Life Technologies). Sequencing was performed using the Ion Torrent Personal Genome Machine (Life Technologies). After data processing, we obtained 3.6 million high-quality reads with a mean length of 130 base pairs. Differentially expressed genes were identified using Cuffdiff with a q-value cutoff of 0.05, yielding 117 significant genes. We used Ingenuity Pathway Analysis (Ingenuity Systems) to identify enriched molecular networks and biological functions. Top-scoring networks were associated with neurological, immune, skeletal and muscular disorders. Our data set was significantly associated with the canonical pathway for AHR signaling, consistent with out original identification of foxq1a as a target of the activated AHR pathway. These results provide new insights into the function of foxq1a and by inference, mechanisms by which TCDD mediates specific developmental phenotypes.

PS 211 Estrogen Receptor-Dependent and Independent Developmental Effects of Phytoestrogens in Zebrafish (*Danio rerio*)

S. M. Bugel and R. L. Tanguay. *Dept of Environmental & Molecular Toxicology, Oregon State University, Corvallis, OR.*

Flavonoids are a group of structurally diverse phytochemicals that humans are exposed to through dietary means (supplementation and natural sources). These chemicals are found in baby formulas and other foods, and due to their ubiquity they are detected in human urine, plasma, and breast milk. The biological activity of flavonoids are varied and include modulation of endocrine, neuroendocrine and

anti-oxidant pathways. Therefore, we explored the potential for these compounds to produce adverse developmental effects using zebrafish (*Danio rerio*) as a model vertebrate. We specifically tested the hypothesis that flavonoids exhibit effects on development through ER-dependent and –independent mechanisms. Embryos were exposed to 5 representative flavonoids (apigenin, biochanin A, S-equol, galangin and kaempferol), 1-50 μM, from 6 hours post fertilization (hpf) to 120 hpf. Effects included yolk-sac and pericardial edemas, axial defects, fin dysmorphogenesis and craniofacial abnormalities. Two compounds (S-equol and biochanin A) induced estrogen-responsive genes (vitellogenin, cyp19a1b, lhb) indicative of nuclear ER activation. Co-exposure with the ER antagonist tamoxifen significantly inhibited induction of these genes, but did not rescue against developmental toxicity. We also observed spastic pectoral fin and caudal tail movements for all compounds, which is suggestive of neurotoxicity, and not phenotypic of estrogen action. We therefore assessed acute effects on neurobehavior in naïve 120 hpf larvae challenged with a battery of 24 flavonoids. All induced hyperactive swimming behavior suggesting that flavonoids have stimulant properties at these concentrations. These results taken together indicate that although the estrogen receptor mediates some effects on gene expression, developmental toxicity and neurobiohavioral effects are likely not a result of nuclear ER action. This research is supported by NIEHS grants P30 ES00210, RC4 ES019764 and T32 ES07060.

PS 212 Monosubstituted Isopropylated Triaryl Phosphate, a Major Component of Flame Retardant Mixture Firemaster 550, Is an AhR Agonist That Exhibits AhR-Independent Cardiac Toxicity

C. V. Gerlach[1], S. R. Das[1], D. Volz[2] and R. L. Tanguay[1]. [1]*Department of Environmental and Molecular Toxicology, Oregon State University, Corvallis, OR and* [2]*Department of Environmental Health Sciences, University of South Carolina, Columbia, SC.*

Firemaster 550 (FM550) is an additive flame retardant mixture used within polyurethane foam and is increasingly found in house dust and the environment due to leaching. Despite the widespread use of FM550, very few studies have investigated the potential toxicity of its ingredients during early vertebrate development. In the current study, we sought to specifically investigate mono-substituted isopropylated triaryl phosphate (mITP), a component comprising about 32% of FM550, which has been shown to cause cardiac toxicity during zebrafish embryogenesis. Previous research showed that developmental defects are rescued using an aryl hydrocarbon receptor (AHR) antagonist (CH223191) and thus suggested that mITP-induced toxicity was completely AHR dependent. As zebrafish have three known AHR isoforms, we used a functional AHR2 knockout line along with AHR1A- and AHR1B-specific morpholinos to determine which AHR, if any, mediates mITP-induced cardiac toxicity. Measuring CYP1A mRNA and protein expression as biomarkers for AHR activation, we determined that mITP principally interacts with AHR2 but may also bind with AHR1A and AHR1B to induce CYP1A expression. However, triple knockdown of all AHR isoforms failed to prevent mITP-induced cardiac toxicity even though there was no detectable CYP1A expression. These results suggest that mITP causes AHR-independent toxicity through a pathway that is also antagonized by CH223191.

PS 213 Combined Effects of Selenomethionine and Osmotic Stress on the Unfolded Protein Response and Apoptosis during Embryonic Development

A. J. Kupsco[1] and D. Schlenk[2]. [1]*Environmental Toxicology, University of California-Riverside, Riverside, CA and* [2]*Environmental Sciences, University of California-Riverside, Riverside, CA.*

Pregnancy-Induced Hypertension (PIH) can lead to increased risk of adverse fetal and maternal outcomes by generating hyperosmotic conditions for the mother and developing fetus. Although osmotic stress may not have direct lethal effects, it may alter the toxicities of xenobiotics during development. Organic forms of selenium, such as selenomethionine (SeMet), are often taken as dietary supplements, yet SeMet's pro-apoptotic tendencies may harm the developing fetus. Japanese medaka (*Oryzias latipes*) are a euryhaline fish and a good model organism for studying fetal responses to SeMet and osmotic stress. SeMet has demonstrated embryo toxicity to fish at high concentrations. It has been previously shown to cause oxidative stress in Japanese medaka embryos and when combined with hypersalinity decreased embryo hatch. The objective of this study was to examine the role of the unfolded protein response (UPR) and apoptosis following exposure to SeMet and osmotic stress. Japanese medaka eggs were treated with 50μM selenomethionine alone and with 16ppth salinity, then sampled at 2, 4, 8 and 12 hours for measurements of CASP3A and BAX transcripts. In SeMet only treatments, the apoptotic effector, BAX, was upregulated after 12 hours of selenomethionine treatment. Additionally, transcripts for genes regulating UPR, BiP, IRE1, ATF6 and ATF4 were measured. ATF4, IRE1 and BiP were up-regulated in a time-dependent manner after 4 and 8 hours and BiP continued to increase at 12 hours. Osmotic stress without SeMet induced IRE1 and ATF6 after 24 hours. These results indicate embryo lethality may occur through apoptosis and the unfolded protein response and that osmotic stress may compound these effects.

PS 214 Ethanol Exposure during Medaka (*Oryzias latipes*) Embryogenesis: Impact on Cannabinoid Receptors

A. K. Dasmahapatra[1, 2] and I. A. Khan[1, 3]. [1]*National Center for Natural Product Research, University of Mississippi, University, MS,* [2]*Department of Pharmacology, University of Mississippi, University, MS and* [3]*Department of Pharmcognosy, University of Mississippi, University, MS.*

Developmental ethanol exposure is able to induce Fetal Alcohol Spectrum Disorder (FASD) phenotypes in medaka (*Oryzias latipes*). This study investigated possible expression of cannabinoid receptor (*cnr*) mRNAs during medaka embryogenesis and variability to ethanol-induced FASD phenotypes. Data base searching (GenBank, Ensembl) indicates that medaka genome includes three human orthologs *CNR* (*cnr1a, cnr1b* and *cnr2*). A quantitative real-time PCR (qPCR) technique was used to analyze the expression of these three *cnr* during medaka embryogenesis and their response to ethanol. Embryos at different stages of development and hatchlings were utilized for RNA extraction followed by qPCR analysis of *cnr1a, cnr1b* and *cnr2* genes at the message level. Moreover, fertilized medaka eggs (Iwamatsu stage 10) were exposed to ethanol (300 mM) either for 2 days or for 6 days followed by *cnr1a, cnr1b* and *cnr2* mRNA analysis. qPCR analyses indicate that the expression of all three, *cnr*s is developmentally regulated and only *cnr2* mRNA showed maternal expression. The mRNA concentrations of all *cnr*s were found to be enhanced after 3 dpf and attained maximal level either prior to or after hatching. Embryos exposed to ethanol (300 mM) two days are unable to produce any significant effect in *cnr* gene expression immediately after ethanol removal; however, if these embryos were maintained in clean hatching solution without ethanol for another four days (6 dpf), only *cnr1a* mRNA was reduced significantly. Expression of other two *cnr* mRNAs (*cnr1b* and *cnr2*) either in 2 dpf or in 6 dpf remained at the same level as in controls. Six dpf exposure of the embryos to ethanol (300 mM) is also showed significant reduction in *cnr1a* mRNA content; however, *cnr1b* and *cnr2* mRNAs maintained the same status as in the controls. Among the three, ethanol disrupts the expression of only *cnr1a* that may probably lead the development of FASD phenotypes in medaka.

PS 215 PAH Exposure in Early Xenopus Embryos Alters Cardiac Function and Aryl Hydrocarbon Receptor (AhR) Signaling

J. Pinette, B. Pyram, L. Hebert and S. L. Whittemore. *Biology, Keene State College, Keene, NH.* Sponsor: A. Andrew.

The incomplete combustion of fossil fuels results in deposition of the polyaromatic hydrocarbons (PAHs), pyrene (PYR) and phenanthrene (PHE), into air, soil, and water. These common and persistent contaminants are also present in tobacco smoke, coal tar sealant, and weathered crude oil and have been detected at significant levels in human milk and cord blood. Surprisingly little is known about their toxicity to humans, particularly during development. To gain a better understanding of potential risks to humans, we characterized the effects of PHE and PYR exposure on cardiac function and AHR signaling using embryos of *X. laevis*, an important model of vertebrate development. We exposed albino embryos, at the onset of gastrulation, to 0.25, 2.5, or 25 μM PHE or PYR for 120 hr and recorded the cardiac activity at various stages of heart development using an inverted dissecting microscope, Leica™ video camcorder, and recording and editing software (Camtasia™ and ImageJ™) to determine heart rate, interbeat variability, and contractility. The mRNA levels for the two CYP1A genes, CYP1A6 and CYP1A7, and for the AHRR gene (AHR repressor) were quantified for whole embryos exposed for 96 hr to PYR at 0.5 and 25 μM. At stage 42 (72 hr, during heart valve formation), PHE treatment (2.5 and 25 μM) was associated with decreased heart rate and increased interbeat variability ($P< 0.01$), a measure of arrhythmia, while exposure to PYR at these same doses led to increases in both heart rate and contractility ($P<0.01$). These two PAHs have distinct impacts on cardiac signaling, suggesting the Xenopus heart may serve as an excellent developmental system for investigating PAH-induced alterations in signaling. In addition, exposure to 0.5 μM, but not 25 μM, PYR for 96 hr was associated with 2-3 fold increases in CYP1A6 and AHRR mRNA levels ($P<0.01$), indicating activation of AHR signaling, a pathway essential to normal development, and a possible low-dose effect for PYR.

PS 216 An Integrative *D. discoideum*, *C. elegans*, and *D. rerio* Strategy to Assess Potential Hazardous Compounds

M. Wildwater[1] and R. Pieters[2]. [1]*University of Applied Sciences Arnhem and Nijmegen, Nijmegen, Netherlands and* [2]*Institute for Risk Assessment Sciences, Utrecht, Utrecht, Netherlands.*

Innovative toxicity test systems that are translational to effects in humans and that allow reduction, refinement and replacement (3Rs) of vertebrates to assess chemical safety are urgently needed for ethical, scientific and economic reasons. Whereas cell culture systems may have predictive value, they lack the multicellular or multi organ complexity of whole organisms. In addition, in view of developmental and reproductive toxicology (DART), they lack a complete life cycle. Therefore, we have compared *D. discoideum* (slime mold), *C. elegans* (nematode) and embryos of *D. rerio* (zebrafish) as possible systems to test for DART. These systems have gained attention as highly promising 3R alternatives since they have highly conserved genotypes, tissue types and molecular responses. We have performed a combinatorial knowledge and experimental based comparison to align *D. discoideum, C. elegans* and *D. rerio* in order to identify common denominators as translational biomarkers for DART. We exposed the three systems to 4 compounds, the kinase inhibitor H89, antimicrobial agent moxifloxacine, boric acid and valproate. Interestingly, although individual species showed species specific phenotypic effects upon compound application, these phenotypes were indicative of alterations in conserved and expected core molecular pathways, like PKA and inositol signaling. Individual test systems further showed differences in sensitivity to compounds. In all test systems, RNA-sequencing revealed that alterations in gene expression profiles are additive between test species and that they represent genes that have orthologs in humans. We concluded from these findings that the combinatorial use of surrogate systems may be a valuable tool for predictive DART testing. Further validation includes benchmarking of well known DART toxicants and building of a Weight of Evidence platform.

PS 217 Disruption of Collagen Biosynthetic Pathway Is a Key Mechanism in Zearalenone-Induced Reproductive and Developmental Toxic Effects in *Caenorhabditis elegans*

Z. Yang[2], L. Tang[1], X. Sun[2] and J. Wang[1]. [1]*University of Georgia, Athens, GA and* [2]*Jiangnan University, Wuxi, China.*

Zearalenone (ZEA), a mycotoxin produced mainly by *Fusarium graminearum*, is a very common contaminant in cereal grains. ZEA was a potent environmental endocrine disruptor and caused reproductive and developmental toxic effects in many biological models, including *C. elegans*. In this study, we investigate the molecular mechanism of ZEA-induced toxic effects. The worms were treated with ZEA (10, 40, 80mg/L) for 48 h and total RNA from each treated group was made. Microarray analysis identified over 3,148 gene expressions were down- or up- regulated (> 2 fold) in the high dosing group. Real-time PCR analyses reconfirmed a dramatic increase in the expression of the dpy-31 gene (20.6 fold up-regulated), sqt-3 gene (20.9 fold up-regulated), and a decrease of dpy-17 gene (4.5 fold down regulated) followed exposure to ZEA (80 mg/L), which indicated the importance of these genes in ZEA-induced toxicity. Further pathway specific mapping showed that all dpy-31, sqt-3, and dpy-17 genes regulate collagen synthetic pathways, for example, dpy-31 gene encodes a procollagen C-terminal processing enzyme, which is required for proper cuticle formation in collagen biosynthetic pathway. The exoskeleton or cuticle performs many key roles in the development and reproduction of *C. elegans*. Furthermore, confocal microscopy and fluorescence spectrophotometer analyses found that the ZEA treated *C. elegans* significantly expressed much higher R151.5::GFP (DPY-31) in germline than non-treated controls. However, much less R151.5::GFP appeared in the treated worms embryo's exoskeleton, indicating that ZEA treatment blocks the normal collagen processing and cuticle formation. These results are consistent with what we found in ZEA treated *C. elegans*: delayed embryo hatching time and germline development, lower embryo numbers in ovarian and abnormal egg laying muscles. Taken together, our studies demonstrate that disruption of collagen biosynthetic pathway is a key mechanism in ZEA-induced reproductive and developmental toxic effects in *C. elegans*.

PS 218 Knockdown of *Drosophila* MRP (dMRP) Expression in Target Organs Increases Developmental Susceptibility to Methylmercury Toxicity

L. Prince[1], M. Korbas[2] and M. D. Rand[1]. [1]*Environmental Medicine, University of Rochester, Rochester, NY and* [2]*Canadian Light Source, Saskatoon, SK, Canada.*

The developing nervous system is particularly sensitive to MeHg toxicity. Exposure to the developing brain is largely dependent on transport mechanisms that regulate MeHg toxicokinetics. MeHg conjugation to GSH is a first step in preventing MeHg toxicity, resulting in a complex that is a substrate for transport and excretion via the the multidrug resistance-associated proteins (MRP). We therefore hypothesize that variant MRP activity may influence susceptibility to MeHg toxicity. We also sought to identify target organs where MRP activity has the most impact on MeHg toxicity during development. We first identified sites of MeHg accumulation in the developing tissues of *Drosophila* by analyzing MeHg exposed larvae with X-ray synchrotron fluorescence (XRSF). We find high levels of Hg in the gut epithelium, the Malpighian tubules (the renal organ), the brain and thoracic ganglion. We therefore hypothesized that knocking down dMRP, specifically in these organs, would increase susceptibility to MeHg. Using GAL4>UAS targeted expression of RNAi, knockdown of dMRP was achieved in four organs: brain (glia and neurons), fat body (the liver structure), gut, and Malpighian tubules. Our results show that knockdown of dMRP in either the gut or the Malpighian tubules greatly increased susceptibility to MeHg, as determined by a decrease in successful development on MeHg food in an established eclosion assay. Knockdown in neurons had a significant but less robust impact. Together, these data demonstrate that 1) gut, renal and brain tissues are predominant sites of MeHg accumulation during *Drosophila* development and 2) reduced expression of dMRP in these developing organs can compromise overall development of the MeHg exposed organism. dMRP and human MRP1, MRP2 and MRP3 sequences are highly conserved, indicating a similar role for MRPs in MeHg toxicity during mammalian development. (Funded by NIEHS R01 ES01219, ViCTER sub-award to M.D.R.).

PS 219 Exposure to Pyrene and Phenanthrene Alters Normal Pigmentation in *Xenopus laevis* Embryos

E. Masure, K. Rosato, D. Snoke and S. L. Whittemore. *Biology, Keene State College, Keene, NH.* Sponsor: A. Andrew.

Pyrene (PYR) and phenanthrene (PHE) are among the most abundant of the polyaromatic hydrocarbons (PAHs) deposited into the environment. Despite the observation that both are present in human milk and cord blood, little is known about their developmental toxicity. Our lab uses a well-established amphibian model of vertebrate development, the African clawed frog *Xenopus laevis*, to assess the developmental impacts of PYR or PHE exposure. Melanophores are the amphibian cellular equivalent of human melanocytes that produce the brown-black pigment melanin. Embryos, at the onset of gastrulation, were exposed to 0, 0.25, 2.5, or 25 μM PHE or PYR for 96 hr and melanophore number and dendricity (branched or Dalmatian spot appearance) were observed. By 96 hr, melanophore dendricity was drastically reduced in embryos exposed to 25 μM of either PHE or PYR ($P<0.001$), effects that were not reversed after return to control conditions for 24 hr. In addition, while there was no effect at 96 hr on melanophore number (or density), the distance migrated by the melanophores was reduced in embryos exposed to either PHE or PYR at 25 μM ($P< 0.01$). Loss of dendricity can disturb the dispersal and transfer of melanin to surrounding keratinocytes, thus interfering with UV protection in the skin. Melanophores could serve as an accessible indicator cell system for potential PAH-induced negative impacts on developing tissues, particularly for other neural crest-derived cells including neurons, where dendricity is also critical to function. To study these effects of PAHs on pigmentation *in vitro*, we are currently culturing isolated melanophores from *Xenopus* neural crest explants.

PS 220 Prediction of Developmental Toxicity—Validation Results of an Integrated *In Silico*/*In Vitro* Testing Strategy

A. Amberg[1], H. Spirkl[1], M. Stolte[1], F. Schmidt[1], D. Mulliner[1], E. Krupp[1], S. Barbellion[2], B. Beyer[3], A. Rogissart[4], N. Roome[2] and A. Czich[1]. [1]*Preclinical Safety, Sanofi, Frankfurt, Germany,* [2]*Preclinical Safety, Sanofi, Paris, France,* [3]*Preclinical Safety, Sanofi, Bridgewater, NJ and* [4]*Preclinical Safety, Sanofi, Montpellier, France.* Sponsor: M. Bonnefoi.

The prediction of developmental and reproductive toxicity (DART) was investigated by an integrated *in silico*/*in vitro* testing strategy using 100 drug candidates with known *in vivo* DART-inducing potential in rat, rabbit and mouse (71 positives, 29 negatives).

For the *in silico* prediction of DART, several public and commercial models were investigated, including DEREK, Leadscope, Caesar, ToxTree, OECD QSAR toolbox, etc. These rule- and structure-fragment-based *in silico* systems were able to identify ~50% of the DART positive compounds with acceptable specificities (~80%). Additionally, several in-house *in silico* models were investigated for prediction of DART related off-targets, like estrogen-, dihydrofolate reductase-, many neural- and vascular-relevant receptors, etc. Interestingly, many off-targets which play a role in genotoxicity showed correlations to DART effects. These are many off-targets involved in cell cycle and spindle apparatus formation, like histone deacetylase, microtubules formation, etc. With these additional models it was possible to significantly improve the ratio of identified DART positive compounds.

Secondary, non-mammalian *in vitro* assays were used for the prediction of DART, mainly results from the FETAX (Frog Embryo Teratogenesis Assay Xenopus) and ZETA (Zebrafish) assays. The predictivity of these *in vitro* assays when used as single results were similar to the *in silico* models. But a combined *in silico*/*in vitro* approach was able to identify and evaluate compounds inducing DART effects with sensitivities up to 75% and specificities around 70%, depending on the *in silico* models used and available *in vitro* results.
These validation results showed that an integrated testing strategy of *in silico* models and *in vitro* assays is able to predict the *in vivo* DART inducing potential of drug candidates effectively and early in development.

PS 221 Transgenerational Effects of the Endocrine-Disrupting Herbicide Atrazine in Zebrafish

J. L. Freeman[1], G. J. Weber[1], S. Wirbisky[1] and M. M. Sepulveda[2]. [1]*Health Sciences, Purdue University, West Lafayette, IN and* [2]*Forestry and Natural Resources, Purdue University, West Lafayette, IN.*

Atrazine, an agricultural herbicide that is a common contaminant of potable water supplies, is implicated as an endocrine disruptor and potential carcinogen. Ongoing studies are defining the genetic and epigenetic mechanisms of an embryonic exposure to atrazine, assessing the later in life adverse health outcomes in the exposed generation, and transgenerational effects using the zebrafish model system. Embryos were exposed to environmentally relevant concentrations of atrazine shortly after fertilization through the end of embryogenesis. Transcriptomic profiles immediately following the exposure identified expression alterations in genes associated with neuroendocrine function, cell cycle regulation, and carcinogenesis. Adults developmentally exposed to atrazine had a significant difference in the number of pairs that successfully bred and was coupled to a distinct altered reproductive phenotype in the exposed females. To determine if adverse effects were passed onto progeny, an unexposed generation was created from adults developmentally exposed to atrazine to assess paternal and/or maternal inheritance (F2). RNA-sequencing of the F2 at the end of embryogenesis revealed enrichment of expression alterations in genes associated with embryonic and tissue development and with neurological and ophthalmic diseases. Furthermore, the beta-estradiol pathway was predicted to be inhibited. The F2 were raised to maturity and significant differences in reproductive function outcomes were observed with the greatest impacts in the cross of the males developmentally exposed to atrazine with control females. No significant differences were observed in the F3 larvae in regards to survivorship, hatching or morphological analysis of whole larvae, head, or eye length. Overall these results indicate that transgenerational effects on the female reproductive system are most pronounced in progeny from the males developmentally exposed to atrazine with control females suggesting transmission through the male germ line.

PS 222 Evaluation of Teratogenic Effect of BMP2-Inducible Kinase Inhibition in Zebrafish by Using Morpholino Antisense Oligonucleotides

C. Zhang, J. Panzica-Kelly, R. R. Denton and K. Augustine. *Bristol-Myers Squibb, Pennington, NJ.*

Bone morphogenic protein 2 (BMP2) has regulatory role in attenuating the program of osteoblast differentiation. BMP2 inducible kinase (BIKE2) is a serine/threonine protein kinase upregulated during BMP2 activation. Since there are no published reports related to BIKE2 inhibition inducing embryo malformation, we evaluated roles of BIKE2 in embryo development in zebrafish using morpholino antisense oligonucleotides (oligos) targeting BIKE2 and p53. (Anti-p53 mitigates morpholino-associated apoptosis/toxicity in embryos). Zebrafish embryos (2 -32 cell stage) were micoro-injected with BIKE2 antisense, or non-sense control oligonucleotides and subsequently evaluated for developmental malformations 5 days post fertilization/post-injection. Craniofacial, heart, and profound axial malformations, including caudal dysgenesis and ectopic tails were observed in groups injected with BIKE2 morpholino antisense oligos. The spectrum of malformations was similar to the "super-dorsalization" phenotype previously reported with BMP2 inhibition. Compared with control non-sense oligos, malformations were significantly higher in embryos containing antisense BIKE2 oligos (5 % in control vs 20% using a single BIKE2 antisense oligo, and 37% using a combination of two BIKE2 antisense oligos, respectively). Compounds that bind with high affinity and specificity to BIKE2 also caused teratogenic effects including skeletal abnormalities consistent with gene targets downstream of BMP2 and/or involved in dorsalization using RT-PCR. Reductions of the gene products osterix (regulating osteocyte precursors for bone cell differentiation), pax2a (required for midbrain–hindbrain boundary formation, which affects dorsal expansion), eve1, (a ventral signal required for normal mesodermal progenitor cells development), and krox-20 (required for hindbrain formation and specification) were observed. Together the studies indicate that inhibition of BIKE2 has teratogenic effect on zebrafish embryo development.

PS 223 Tributyltin (TBT) Exposure Promotes Zebrafish Sexual Differentiation

C. L. McGinnis, K. Kosior, J. Kowalski and T. Lombardi. *Quinnipiac University, Hamden, CT.*

Tributyltin (TBT), an antifouling agent, has been implicated in the masculinization of fish species worldwide, however the molecular mechanism is still not completely understood. Our lab has previously examined the actions of TBT as an endocrine disruptor in zebrafish (*Danio rerio*) and determined, *in vitro*, that TBT inhibits zfER specific activity in a dose dependent manner and may potentially act through the RXR portion of the PPAR-RXR (peroxisome proliferator-activated receptor gamma - retinoid X receptor alpha) heterodimer. Additionally, zebrafish were exposed to increasing concentrations of TBT and sexual differentiation genes were analyzed via qPCR. Results from qPCR focused our experimental efforts on the candidate gene, SRY-box containing gene 9a (Sox9a). Sox9a is a key regulator in mammalian testis differentiation, where it is shuttled to the nucleus upon differentiation; this appears to be a conserved mechanism across fish, marsupials and placental mammals. Developing zebrafish were exposed to 1pM and 2.5pM TBT from 10 days post hatch (dph) to 90 dph and sampling was done at 25, 40, 60 and 90 dph. Fish were treated three times per week with TBT, estrogen, testosterone, or vehicle. Following treatments, tissues were fixed in 4% PFA, processed, paraffin imbedded, and then immunohistochemical (IHC) analysis was performed to assess Sox9a nuclear or cytoplasmic localization.

PS 223a Mitochondrial Uncoupling Disrupts Neurodevelopment in Zebrafish Embryos

S. Chan, J. Bestman, J. J. Rahn and K. D. Stackley. *Drug Discovery and Biomedical Sciences, Medical University of South Carolina, Charleston, SC.* Sponsor: R. Di Giulio.

Caloric restriction is a proven method for weight loss and possible lifespan extension. However, caloric restriction is detrimental in early development as malnourished mothers produce offspring with low birth weights, developmental delay and neurodevelopmental defects, which have been linked with diseases in later life. Inhibiting mitochondrial energetics, such as through exposures to uncouplers like 2,4-dinitrophenol (DNP), mimics caloric restriction. DNP disrupts the proton gradient needed for ATP synthesis by oxidative phosphorylation, and is a common environmental toxicant in automobile exhaust, industrial waste and pesticides. DNP is also seeing resurgence as an illicit weight-loss drug, particularly with women of childbearing age due to its ready availability online. Thus it is important to analyze the effects of exposures to mitochondrial toxicants such as DNP on the developing embryo, as a potential cause of some birth defects and neurological disorders. We use zebrafish embryos to study the effects of mitochondrial uncoupling on embryonic development, as breeding pairs produce hundreds of transparent embryos that develop rapidly outside of the mother and hatch within 3 days post-fertilization (dpf). Here we show that mitochondrial uncoupling by DNP disrupts embryonic development, causing developmental delay and neurodevelopmental defects. The development of the primary motor neurons and retinal layers were particularly impacted, which may explain the locomotor defects observed in DNP exposed embryos. Biochemically, we observed that mitochondrial ATP turnover was decreased throughout embryonic development. Likewise, protein oxidation and other markers of oxidative stress response were decreased. As reactive oxygen species (ROS) are required for nervous system development, we propose that the neurodevelopmental defects we observe are likely due to decreased ROS signaling in embryos.

PS 223b Relative Developmental Toxicity of Pentachlorophenol and Pentachloroanisole in Zebrafish (*Danio rerio*)

Y. Cheng and L. Chan. *University of Ottawa, Ottawa, ON, Canada.*

Pentachlorophenol (PCP) and pentachloroanisole (PCA) are widely distributed chlorinated aromatic compounds and have been found in the environment and human populations. The objective of this study is to characterize and compare the effects of PCP and PCA on development using a fish model. Zebrafish embryos were exposed to 0.1, 1, 10, 100, 500, 1000 μg/L PCP and PCA respectively for 96 h. The sub-lethal and lethal effects were studied through malformation observation, LC50 testing for survival rate at 96 hpf and EC50 testing for hatching rate at 72 hpf. The mRNA gene expression changes related to brain growth and thyroid

hormone regulating pathways were investigated. LC50 at 96 hpf was 3.04 μg/L for PCP << 336.0 μg/L for PCA, and EC50 for hatching at 72 hpf was 2.74 μg/L for PCP << 339.1 μg/L for PCA, indicating that the developmental toxicity of PCP was at least 100 times higher than that of PCA. Other sub-lethal effects, such as yolk deformation, malformation of tail, scoliosis, hemorrhage and pericardial edema, were observed. Both PCP and PCA showed hyperthyroid effects similar to that of triiodothyronine (T3) resulting in increased mRNA expressions of Synapsin I (SYN), Iodothyronine Deiodinase type II (Dio2), Iodothyronine Deiodinase type III (Dio3), Thyroid hormone receptor alpha a (THRαa) and Thyroid hormone receptor beta (THRβ). Our results on the relative developmental toxicity of PCP and PCA and the possible underlying mechanisms will be useful to support further research in human populations.

PS 223c Transcriptional Regulation of the Nuclear Factor Erythroid-2 Related Factor (NRF) Family by the Aryl Hydrocarbon Receptor (AhR)

L. Williams, Y. Chen and J. Meyo. *Biology, Bates College, Lewiston, ME.*

The interaction between regulatory pathways is an important mechanism by which organisms can adapt to their environment and respond to endogenous stress. One interaction that recently has been identified in adult mammals, cell culture, and fish embryos is that occurring between the aryl hydrocarbon receptor (Ahr) and members of the nuclear factor erythroid-2 related factor (nrf) family. Each transcription factor regulates numerous downstream genes involved in the cellular response to toxicants and oxidative stress; they each also play a role in normal development. In zebrafish embryos, where there are six nrf genes, developmental gene expression of all nrfs has been shown to be altered in the absence of Ahr1B protein using morpholino knockdown. The mechanism of this altered transcriptional response by Ahr1B has been explored using Chromatin Immunoprecipitation (ChIP) in zebrafish embryos to test the hypothesis that Ahr1B is binding directly to cis-promoter elements to regulate the developmental transcription of nrf genes. Using ChIP coupled with PCR, Ahr1B has been shown to directly bind to XREs on the promoter of each nrf gene in the presence of TCDD, confirming its role as a transcriptional regulator of the entire nrf gene family. This research highlights the importance of the TCDD-Ahr-Nrf gene battery during the most sensitive life stage, the embryo, and provides a better understanding of how combinatorial molecular signaling can protect embryos from potentially embryotoxic events following toxicant exposure.

PS 223d Toxicity Screening of the ToxCast Phase II Chemical Library Using a Zebrafish Developmental Assay

S. Mosher[1], K. Houck[1], S. L. Frady[1], R. Judson[1], J. F. Wambaugh[1], D. Reif[2] and S. Padilla[1]. *[1]US EPA, Durham, NC and [2]Department of Biological Sciences, NCSU, Raleigh, NC.*

As part of the chemical screening and prioritization research program of the US EPA, the ToxCast Phase II chemicals were assessed using a vertebrate screen for developmental toxicity. Zebrafish embryos (*Danio rerio*) were exposed in 96-well plates from late-blastula stage (6hr post fertilization, pf) through day 5pf (1-2 days post-hatch). All exposures were by immersion and renewed daily. The 700 chemicals included food additives, consumer use product ingredients, pesticides, failed pharmaceuticals, and "green" plasticizers (http://epa.gov/ncct/toxcast/chemicals.html). Intra- and inter-plate replicates were included for quality control. Developmental toxicity was initially assessed using a single nominal concentration of 80 μM: positives and a selection of negatives were confirmed by concentration-response determinations. On day 5pf, larvae were moved from exposure solution to a control solution without chemical, and on day 6pf were assessed for overt toxicity (i.e., death, non-hatching and dysmorphology; n=4 embryos per chemical). Dysmorphology was a combined score using both in-life observation and brightfield, high-content image analysis. Overt toxicity was noted with 46% of the chemicals tested, compared to 62% positive chemicals when the ToxCast Phase I library, consisting of mostly pesticide active ingredients, was previously tested. As with the Phase I library, the octanol-water partition coefficient (logkow) of the Phase II library chemicals was positively correlated with overt toxicity: there were 18% positive chemicals with logkow <0; 41% positive chemicals with logkow of 0 to 4; and 67% positive chemicals with a logkow >4. All chemicals positive at the single concentration were further assessed for potency using a Dose-Response Study (8-point, semi-log concentration curve: n=3 embryos per concentration). These data demonstrate the utility of zebrafish in medium-throughput chemical testing programs for detection of adverse developmental outcomes. This abstract may not necessarily reflect official Agency policy.

PS 223e AhR-Dependent and AhR-Independent Genes Involved in the Synergistic Cardiac Developmental Toxicity of PAHs

R. Di Giulio[1], N. Jayasundara[1], L. Garner[2], K. Erwin[3] and J. N. Meyer[1]. *[1]Nicholas School of the Environment, Duke University, Durham, NC, [2]Cardno ENTRIX, Portland, OR and [3]Duke University Medical Center, Durham, NC.*

Polycyclic aromatic hydrocarbons (PAHs) are known to induce developmental defects in vertebrates, and exposures of fish embryos to PAHs have been shown to cause cardiac deformities. However, the mechanisms underlying this toxicity remain unclear. The aryl hydrocarbon receptor (AHR), a transcription factor, is activated by and mediates toxicity of some PAHs. Exposure to a simple PAH mixture consisting of an AHR agonist (benzo(a)pyrene-BaP) and fluoranthene (FL), an inhibitor of cytochrome p450 1(CYP1) - a gene induced by activation of the AHR - results in pericardial effusion and an elongated heart. Knockdown of AHR2 prevents this toxicity. In this study, we used a microarray analysis to identify genes involved in this toxicity. To determine the role of AHR2 by knocking down this gene, we used zebrafish embryos injected with a control morpholino and AHR2 morpholino. Embryos at 36hpf were then exposed to DMSO, 100 μg/L BaP, 500 μg/L FL, or 100 μg/L BaP + 500 μg/L FL. We extracted heart tissues at various time points (2h, 6h, 12h, and 18h) for RNA. Overall data showed that gene expression differences between the AHR knockdown and control embryos decreased over time, suggesting that the AHR mediated gene expression due to PAHs decrease within 18 h of exposure. Furthermore, despite BaP+FL resulting in a deformed heart, this mixture resulted in smaller effect on overall gene expression compared to BaP or FL alone. Differentially expressed genes by BaP+FL in AHR knockdown and control embryos were primarily involved in Ca2+ cycling, cardiac muscle contraction, suggesting that PAH affects on cardiac muscle function may underlie the structural deformities. Furthermore, several genes such as Pdlim - a gene involved in cardiac looping – that were identified may play a direct role in underlying cardiac deformity in fish. Ingenuity pathway analysis on transcriptomic data suggested that FOS signaling pathway might be playing a key role in mediating AHR- dependent cardiac toxicity.

PS 223f Serum Gamma Glutamyl Transferase Is Associated with Higher Blood Pressure and Lead-Induced High Blood Pressure: A Model Pathway Using NHANES 2007-2010

F. Scinicariello, M. C. Buser, H. Pohl, H. G. Abadin and H. Murray. *DTHHS, ATSDR/CDC, Atlanta, GA.* Sponsor: P. Ruiz.

Background: Lead exposure has been associated with high blood pressure. Oxidative stress and inflammation have also been independently associated with high blood pressure.
Objective: We examined the association of blood lead levels, serum gamma-glutamyl transferase (GGT), and serum C-Reactive Protein (CRP) levels with systolic blood pressure (SBP), diastolic blood pressure (DBP), and hypertension in adult participants in the National Health and Nutrition Examination Survey (NHANES) 2007-2010.
Methods: The outcomes of interest were SBP and DBP, hypertension, blood lead levels, serum GGT, and serum CRP. Serum CRP, serum GGT, and blood lead were log normal transformed. Blood lead was also analyzed using weighted quartiles. Linear regression, logistic regression and multilog procedures were used with a priori covariates age, race/ethnicity, gender, education, smoker status, alcohol use, diabetes, body mass index, and serum creatinine.
Results: Higher SBP statistically correlated with blood lead and serum GGT in all adults and in male and female subgroups. Blood lead and serum GGT were associated with hypertension when all individuals were entered in the model and in the female subgroup after stratification. Elevated serum CRP was associated with serum GGT and with DBP, but not with blood lead, SBP, or hypertension.
Conclusions: This study demonstrates a possible biological pathway through which lead induces hypertension and increases SBP. Our results indicate that lead may work through a direct mechanism as well as through the indirect mechanism of oxidative stress in order to affect these outcomes.

PS 223g Association of Urinary Dichlorophenols with Increased Body Weight Measures and Obesity in Children and Adults: Analyses of NHANES 2007-2010

S. Z. Ingber, M. C. Buser and F. Scinicariello. *DTHHS, ATSDR/CDC, Atlanta, GA.* Sponsor: P. Ruiz.

Background: Exposure to environmental chemicals may play a role in the development of obesity. There is evidence that dichlorophenol exposure may be associated with obesity in children and adults.

Objective: To examine the association of urinary levels of the environmental pesticides 2,5-dichlorophenol (2,5-DCP) and 2,4-dichlorophenol (2,4-DCP) and the environmental phenol triclosan with body weight outcomes in children, adolescents and adults participants in the National Health and Nutrition Examination Survey (NHANES) 2007-2010 .
Methods: We performed multivariate linear and logistic regression to analyze the association of BMI z-score, waist circumference, and obesity with urinary pesticide concentration in children and adolescents. We conducted the same analyses in adults with the outcomes of BMI, waist circumference and obesity.
Results: We found a statistically significant positive association ($p<0.05$) between both 2,5-DCP and 2,4-DCP and BMI z-score and obesity in children and adolescents. In adults, there was a statistically significant positive association ($p<0.05$) between 2,5-DCP and BMI, waist circumference, and a non-monotonic association with obesity. However, a statistically significant relationship between 2,4-DCP and body weight outcomes was not found in adults. No associations were found between triclosan and any of the body weight outcomes for either children or adults.
Conclusions: We found an association between dichlorophenols and increased body weight measures in both children/adolescents and adults. Additionally, we found an association between dichlorophenols and obesity in children/adolescents and a non-monotonic response in adults.

PS 223h Airway Inflammation Markers in Exhaled Breath from Children Are Linked with Exposure to Black Carbon

S. De Prins[1, 2], E. Dons[1], M. Van Poppel[1], L. Int Panis[1, 3], E. Van de Mieroop[4], V. Nelen[4], B. Cox[3], T. Nawrot[3], G. Schoeters[1, 2] and G. Koppen[1]. *[1]VITO, Mol, Belgium, [2]University of Antwerp, Antwerp, Belgium, [3]Hasselt University, Diepenbeek, Belgium and [4]Provincial Institute of Hygiene, Antwerp, Belgium.*
Sponsor: P. Hoet.

The current study assessed the associations between airway oxidative stress and inflammation markers and BC exposure in primary school children in a Western European urban area.
In 130 children 6-12 years old, the fraction of exhaled nitric oxide (FeNO), exhaled breath condensate (EBC) pH, 8-isoprostane and IL-1β were measured in two seasons. Acute BC exposure on the sampling day was assessed using BC measurements at a central monitoring site. Land use regression (LUR) models were applied to estimate weekly and seasonal average BC exposure. Associations between biomarkers and exposure were tested using linear mixed effects regression models. Next to single exposure models, models combining multiple exposures were analyzed.
Oxidative stress and inflammation markers were associated with BC levels, independent of gender, age, allergy status, parental education level and meteorological conditions on the sampling day. Depending on the considered single or multiple exposure model, IQR increases in acute BC exposure (3100 ng/m3) were linked with higher 8-isoprostane ranging from 5.9 (95% CI 0.1-12.0) to 9.4% (95% CI 2.1-17.2). Increased FeNO levels ranging from 12.1 (95% CI 2.5-22.8) to 15.2% (95% CI 4.4-27.0) were associated with IQR increases in weekly BC (1730 ng/m3). IQR increases in acute and weekly BC were linked with increases in IL-1β between 19.3 (95% CI 1.3-40.5) and 42.8% (95% CI 11.2-83.2).
Acute BC exposure was associated with airway oxidative stress while weekly and acute exposure was linked with airway inflammation. The association between BC exposure and IL-1β in EBC reflects activation of cells involved in first line defense mechanisms of the airways such as airway epithelial cells and macrophages, as was previously suggested by in vitro studies.

PS 223i Arsenic Level in Drinking Water and Lung Cancer Mortality among 127 United States Counties from 1950 to 1979

S. H. Lamm[1, 2], E. K. Dissen[1], M. Feinleib[2], J. Li[1, 2] and E. Hatef[1, 2]. *[1]Center for Epidemiology and Global Health (CEOH), Washington, DC and [2]JHU Bloomberg School of Public Health, Baltimore, MD.* Sponsor: J. Tsuji.

Background: Studies from Asia and Latin America found arsenic to be a risk factor for bladder and lung cancers in areas with high levels of arsenic (> 100-200 ug/L) in drinking water. Evidence for cancer risk at the < 100 ug/L arsenic levels found in the US is scant. We previously examined the role of drinking water arsenic as a risk factor for bladder cancer mortality using NCI/EPA data for 1950-1979 for US counties where groundwater was the exclusive known source of drinking water supply (Lamm, 2004). We now use the same method and sources to assess the relationship between drinking water arsenic levels and lung cancer mortality.
Materials and Methods: County-specific, decade-specific lung cancer counts and rates were extracted from the NCI/EPA US Cancer Mortality Rates and Trends, 1950-1979. County-specific groundwater arsenic levels and their distributions (including median) were obtained from the US Geological Survey (USGS). State health or environment departments identified counties where ground water was the unique source of public drinking water. We used the merged dataset to evaluate the relationship between drinking water arsenic level and lung cancer mortality. County-specific tobacco use data did not exist for the time-period of this study.
Results: No arsenic-related increase in lung cancer mortality was found over the exposure range of 3 to 60 ug/L using graphic, stratified, and regression analyses. The slope of the county-specific lung cancer risk on the median groundwater arsenic level was negative but not different from zero. The median groundwater arsenic levels provided no (< 0.5 %) explanatory power for the distribution of the county-specific lung cancer mortality rates.
Conclusion: This study adds to the accumulated literature on ingestion of low-levels of arsenic in groundwater and lung cancer mortality. This study showed no evidence of arsenic-related lung cancer mortality risk in the range of drinking water arsenic levels generally experienced by the US population.

PS 224 Urinary Concentrations of 2, 5-Dichlorophenol and Increased Waist Circumference in US Adults

Y. Wei[1] and J. Zhu[2]. *[1]Department of Community Medicine, Mercer University School of Medicine, Macon, GA and [2]Department of Mathematics and Computer Science, Fort Valley State University, Fort Valley, GA.*

Exposure to para-dichlorobenzene (p-DCB) from indoor environments has become a particular concern because p-DCB products, such as mothballs, air fresheners, and toilet deodorizer blocks, are widely used in the home and in buildings in the United States and other countries. Recent studies have suggested that exposure to p-DCB could be associated with obesity, earlier age of menarche, and related metabolic effect. In this study, we examined associations between urinary concentrations of 2,5-dichlorophenol (2,5-DCP), the major metabolite of p-DCB, and increased waist circumference (WC), a metabolic risk factor for type 2 diabetes and cardiovascular disease, by analyzing the 2005-2008 U.S. National Health and Nutrition Examination Survey data. Adult participants, aged 20-79 years, were selected and categorized as having increased WC (i.e. abdominal obesity) if their WC was ≥ 102 cm for men or ≥ 88 cm for women. A significantly higher geometric mean of urinary 2,5-DCP was seen in participants with increased WC, as compared with the reference group. A dose-dependent increase in the prevalence of abdominal obesity was observed in the study participants across increasing levels of urinary 2,5-DCP (p-trend = 0.0011). Multivariate logistic regression analyses revealed that urinary concentrations of 2,5-DCP were significantly associated with increased WC, after adjustment for age, gender, race, education, total fat intake, physical activity, and urine creatinine. This study demonstrated the association between exposure to p-DCB, measured as urinary 2,5-DCP, and increased WC in U.S. adults, and provided further evidence on potential roles of p-DCB in obesity, type 2 diabetes, and associated metabolic syndrome. Further prospective studies measuring exposure during etiologically relevant periods and metabolic outcomes are warranted.

PS 225 Age-Related Trends in US Pleural Mesothelioma and Soft Tissue Sarcoma Rates: Evidence for a Longevity Effect

B. D. Kerger[1], C. J. Ronk[2], M. Glynn[3], B. L. Finley[2] and D. J. Paustenbach[2]. *[1]Cardno ChemRisk, Aliso Viejo, CA, [2]Cardno ChemRisk, San Francisco, CA and [3]Cardno ChemRisk, Chicago, IL.*

We hypothesized that greater longevity may influence age-adjusted incidence of two selected mesenchymal cancer types since enhanced robustness in older age groups may more accurately reflect age-related cancer trends. Using SEER 9 registry data we examined age-adjusted pleural mesothelioma (PM) and soft tissue sarcoma (STS) incidence rates for 1973 through 2010 in conjunction with concurrent changes in age distribution of the US population. The overall age-adjusted rate per 100,000 person-years for PM significantly (* $p<0.05$) increased by 185%* from 1973 to its peak value in 1992, then decreased by 18%* from 1992 to 2010. The 75+ yr age group dominated the early PM trends, increasing by >600%* for 1973-1992, and again by 19%* for 1992-2010. In contrast, the 0-74 yr age group showed a 96%* increase in age-adjusted PM for 1973-1992, and then declined by 47%* for 1992-2010. By comparison, overall age-adjusted STS rates were increased by 17%* for 1973-1992 and again by 29%* for 1992-2010. The 75+ yr age group dominated the STS trends in both intervals, increasing by 43%* for 1973-1992, and again by 41%* for 1992-2010, while the 0-74 yr age group showed only 11% (n.s.) and 25%* increases in these respective intervals. The SEER 9 registry exhibits significant increases in the 75+ yr population at risk from 1973 (3.7%) to 1992 (7.4%*) and again for 2010 (10.1%*). We conclude that the continuing shift toward greater longevity since 1992 may help to explain the greater elevation in age-adjusted PM and STS rates among the increasingly robust 75+ yr age group. Regulatory controls on asbestos may explain the 47% decline in PM for the 0-74 yr age group from 1992 to 2010, while the 19% increase in the 75+ yr age group may represent a longevity effect that is apparent for both PM and STS. Enhanced diag-

nostic methods and changes in disease classification since 1992 also may contribute to these trends, and the issue of longer latency for asbestos-related PM should be examined further.

PS 226 Aflatoxin Exposure Associates with Abnormal Liver Function and Infections with HIV and TB in Uganda

M. Kang[1], L. Tang[1], P. M. Nkurunziza[2], R. Muwanika[3], A. Nkwata[1], J. Seeley[2], C. C. Whalen[1] and J. Wang[1]. *[1]University of Georgia, Athens, GA, [2]MRC Uganda Unit, Entebbe, Uganda and [3]Rakai Health Program, Rakai, Uganda.*

Aflatoxins (AF) exposure is a serious global health threat. The epidemic of liver disease and infections with HIV and TB was associated with AF exposure in Ghana; however, the correlation between AF exposure and the progression of these epidemic diseases has not been firmly established in other African populations. In this study we assessed AFB-lysine adduct level in serum samples collected from a normal human group (n=267), a group with abnormal liver function (n=132), a group with HIV infection (n=536), and a group with HIV/tuberculosis co-infection (n=62) in Uganda. AFB-lysine adduct was measured via high-performance liquid chromatography (HPLC)-fluorescence detection with a limit of detection of 0.4 pg/mg albumin. Median serum AFB-lysine adduct level was 1.54 pg/mg albumin (range=0.45-253.11) among normal human group; median serum AFB-lysine adduct level was 2.88 pg/mg albumin (range=0.54-153.06) among the group with abnormal liver function; median serum AFB-lysine adduct level was 3.19 pg/mg albumin (range=0.41-167.04) among the group with HIV infection; and the median serum AFB-lysine adduct level was 8.90 pg/mg albumin (range=0.54-70.41) among the group with HIV and tuberculosis co-infection. Groups with abnormal liver function ($p<0.01$), HIV infection ($p< 0.01$), and HIV/tuberculosis co-infection ($p<0.001$) had significantly higher AFB-lysine adduct levels than that in the normal human group. Patients with severe HIV progression, dependent on CD4+T cell counts, had a significant higher adduct level than those with minor progression (Ptrend=0.0062). In addition, the adduct level was synergistically increased in HIV patients infected with tuberculosis compared to the HIV patients without tuberculosis and non-infected normal group (Ptrend<0.0001). This study confirms previous finding and implies that mitigation of AF exposure not only can reduce liver diseases, but also an innovative strategy to reduce the spreading of HIV and tuberculosis in epidemic sub-Saharan African countries.

PS 227 A Systematic Review of the Epidemiologic Evidence on Low-Level Arsenic Exposure and Cognitive Function in Children: Applicability for Risk Assessment

V. Perez[1], J. S. Tsuji[2], M. R. Garry[3] and D. D. Alexander[4]. *[1]Exponent, Inc., Chicago, IL, [2]Exponent, Inc., Bellevue, WA, [3]Exponent, Inc., Bellevue, WA and [4]Exponent, Inc., Boulder, CO.*

The U.S. Environmental Protection Agency is currently revising their 1988 non-cancer and cancer risk assessments for inorganic arsenic. Cognitive function in children is an endpoint for which several recent studies bear consideration in deriving a non-cancer reference dose (RfD). We conducted a systematic review of the epidemiologic literature for scientific evidence on possible neurobehavioral effects at lower exposure levels in children. Eleven cross-sectional, case-control, and cohort studies were identified that report on the association between low-level arsenic exposure (e.g., including <100 μg/L of arsenic in drinking water) or exposure in utero and cognitive function in children. Although none of the identified studies presented a clear dose-response relationship in the region of a lowest- or no-observed-adverse-effect-level, a possible association between arsenic exposure, predominantly concurrent exposure, and cognitive function in older children (e.g., aged >5 years) was observed overall. A population-based randomized trial from Matlab, Bangladesh (Hamadani et al. 2011), provided the best evidence for informing a quantitative risk assessment (results reported separately), with supporting evidence from another region of Bangladesh. In this study, verbal and, to a lesser extent, full-scale IQ scores were inversely associated with log urinary arsenic levels in girls, but not boys, at age 5 years. It remains unclear whether the findings in the available literature are applicable to similar child populations in the United States. Standard cognitive test measures have not been developed for Bangladesh, and issues such as differences in cultural practices, poor nutrition, adequate correction for maternal IQ, presence of other neurotoxicants in some studies, and dietary deficiencies in Bangladesh greatly limit generalizability to U.S. populations.

PS 228 Clinical and Molecular Features of Myelodysplastic Syndrome following Benzene Exposure

P. Kerzic[1] and D. Pyatt[2, 3]. *[1]Pacific Coast Toxicology, Reseda, CA, [2]Summit Toxicology, Superior, CO and [3]School of Public Health, University of Colorado, Aurora, CO.*

Chronic exposure to benzene is associated with several possibly related and overlapping hematopoietic diseases such as aplastic anemia (AA), myelodysplastic syndrome (MDS), and acute myeloid leukemia (AML). Recent reports indicate that MDS developing subsequent to benzene exposure may represent the main risk of hematologic disease associated with benzene, and that MDS may develop following exposures to benzene at lower concentrations than previously reported. In addition, cytogenetic abnormalities long assumed to be induced by benzene such as aneuploidy or loss of all or part of chromosomes 5 or 7, which are associated with some forms of therapy related MDS/AML, may not be associated with benzene exposure after all. We have compiled MDS cases from the peer-reviewed literature with documented benzene exposure and describe the clinical and molecular features of benzene-associated MDS (BZ-MDS). We believe such analysis will help to clarify the etiology and pathogenesis of the disease. We report that BZ-MDS cases frequently feature hypoplastic bone marrow, clear indications of an autoimmune mechanism, marked eosinophilia, relatively young age at diagnosis, and increased survival relative to de novo MDS. In addition, cytogenetic features frequently seen in therapy-related MDS (tMDS) do not appear to be prominent features of BZ-MDS. These results highlight a need for additional study of BZ-MDS and suggest a picture of BZ-MDS that is distinct from both tMDS and de novo disease.

PS 229 The Biomarkers of Exposure to ARsenic (BEAR) Pregnancy Cohort in Mexico: Arsenic Methylation Linked to Poorer Birth Outcomes

J. E. Laine[2], K. Bailey[1], M. Rubio-Andrade[3], A. F. Olshan[2], L. Smeester[1], Z. Drobna[4], A. H. Herring[5], M. Styblo[4], G. G. Garcia-Vargas[3] and R. Fry[1]. *[1]Department of Environmental Sciences and Engineering, UNC, Chapel Hill, NC, [2]Department of Epidemiology, UNC, Chapel Hill, NC, [3]Facultad de Medicina, Universidad Juarez del Estado de Durango, Gómez Palacio, Mexico, [4]Department of Nutrition, UNC, Chapel Hill, NC and [5]Department of Biostatistics, Gillings School of Global Public Health, UNC, Chapel Hill, NC.*

Exposure to inorganic arsenic (iAs) from drinking water is a global public health problem yet much remains unknown about the extent of exposure in susceptible populations, including pregnant women and children. Higher prenatal iAs exposure has previously been associated with a greater risk of adverse pregnancy outcomes and later life health effects. Our objective for this study was to establish the Biomarkers of Exposure to ARsenic (BEAR) prospective pregnancy cohort in order to better to understand the effects of iAs exposure and iAs metabolism during pregnancy on maternal-fetal health, with the ultimate aim of increasing awareness and reducing potential exposures to iAs. Concentrations of iAs in drinking water (DW-iAs) and maternal urinary concentrations of iAs and its metabolites (U-tAs) were determined. Birth outcomes were recorded and analyzed for their relationship to DW-iAs, U-tAs, and concentrations and proportions of individual urinary arsenicals. DW-iAs for the study subjects ranged from <0.5 to 236 μg As/L. More than half of the women (53%) had DW-iAs that exceeded the World Health Organization's recommended guideline of 10 μg As/L. DW-iAs was significantly associated with U-tAs. Overall, neither DW-iAs nor U-tAs were associated with any birth outcomes. However a significant inverse relationship was observed between urinary concentrations and proportions of MMAs and birth weight with an average decrease of 25 g. Biomonitoring results demonstrate that pregnant women in Gómez Palacio are exposed to potentially harmful levels of DW-iAs. A relationship between iAs metabolism and adverse birth outcomes were established.

PS 230 A Cross-Sectional Study of Blood Level Lead and Attention-Deficit/Hyperactivity Disorder by Parental Socioeconomic Status amongst Korea Children

H. Kwon[2], O. Yi[1] and D. Kim[3]. *[1]National Health Insurance Services, Health Insurance Policy Research, Seoul, Republic of Korea, [2]Department of Preventive Medicine, Dankook University College of Medicine, Cheonan, Republic of Korea and [3]Health Promotion Research Division, Korea Institute for Health and Social Affairs, Seoul, Republic of Korea.* Sponsor: J. Park.

Background: It has been reported that blood lead level increases the risk of ADHD of children.
Objectives: We estimated the effect of blood lead level on ADHD controlling for parents' socioeconomic status (SES).

Methods: Whether or not blood lead level was associated with ADHD by parental SES was evaluated using information on 3,666 school aged children in Korea. Associations between parental SES and the blood lead level were examined by estimating fixed effects model.
Result: After adjustments for potential confounding variables, children with mother in the lowest education (Odds Ratio (OR): 2.38, 95% CI=1.40-4.03) and those living in the most deprived area (OR=1.29, 95% CI =1.01-1.66) were significantly more likely to be associated with ADHD.
Conclusion: Our findings suggest that the association between blood lead level and ADHD vary by characteristics of parents' SES.
Keywords: ADHD, blood lead level, SES

PS 231 Cumulative Risk Assessment of Urban Air Toxics: A Pilot Study in San Antonio, Texas

D. Proctor[1], M. Suh[1], J. A. Tachovsky[2], L. Abraham[3], G. Hixon[2], G. Brorby[4] and S. Campleman[5]. [1]*ToxStrategies, Mission Viejo, CA,* [2]*ToxStrategies, Austin, TX,* [3]*ToxStrategies, Houston, TX,* [4]*ToxStrategies, Richmond, CA and* [5]*Electric Power Research Institute, Palo Alto, CA.*

A pilot cumulative risk assessment project was conducted to test a modeling strategy for estimating the community health burden potentially associated with air toxics while simultaneously accounting for background air toxics, criteria air pollutants, and non-chemical stressors in an urban population of San Antonio, TX. Generalized additive models (GAMs) were used to quantitatively evaluate the potential association between airborne exposure to certain air toxics (lead, arsenic, antimony and chloromethane) generated by two coal-fired electricity generating units (EGUs), background levels of these air toxics, PM2.5, ozone, and social stressors on all cancer and heart disease mortality for 34 census tracts within the 10-mile radius of the EGUs. Four demographic and socioeconomic indicators (i.e., percent African American, percent female, age, and poverty) were significantly associated with all cancer and heart disease mortality, accounting for 70.6% and 79.1% of the variance, respectively. Accounting for these four demographic and socioeconomic indicators in the GAMs, concentrations of the four EGU-specific air toxics were not significantly associated with either all cancer or heart disease mortality in the study area. However, arsenic from non-EGU related on-road and non-road sources was significantly associated with all cancer mortality (88.8% of the residualized variance). PM2.5, lead from non-point sources, and ozone were significantly associated with heart disease mortality (88.1% of the residualized variance). With 17.9 and 21.27 degrees of freedom for cancer and heart disease, respectively, the GAMs were highly complex and non-linear. Although this pilot study has several limitations, it utilizes an innovative approach to quantitatively assess cumulative risk from non-chemical and chemical stressors and may serve as a preliminary model for future analysis.

PS 232 Weight-of-Evidence Evaluation of the Respiratory Effects Associated with Diacetyl

B. L. Finley[1], J. S. Pierce[2], K. Neier[2] and L. J. Roberts[2]. [1]*Cardno ChemRisk, Brooklyn, NY and* [2]*Cardno ChemRisk, Chicago, IL.*

Recent case reports and epidemiologic investigations have concluded that diacetyl inhalation in the workplace may be associated with serious adverse respiratory effects, including the relatively rare and lethal disease bronchiolitis obliterans (BO). The concern stems from a series of cases of fixed obstructive lung disease consistent with BO that were reported in eight former employees from the Gilster-Mary Lee microwave popcorn plant in Jasper, Missouri. However, over 100 volatile organic compounds were identified in air samples collected in the workplace, and the majority of the cohort was non-occupationally exposed to respiratory irritants, including known inducers of BO. A weight of evidence analysis was conducted to determine if the suggested associations between diacetyl and BO and pulmonary function decrements (e.g., fixed obstruction, decline in FEV1 and FVC) satisfy the Bradford Hill criteria of causation. Based on our analysis, none of the criteria were satisfied. Specifically, no risk estimates for BO have been reported in the literature and inconsistent associations have been reported between diacetyl exposure and various pulmonary function deficits (across studies and within a single cohort). Furthermore, temporality cannot be established because baseline medical evaluations were not performed on any of the worker cohorts, and none of the epidemiology investigations demonstrate the presence of an exposure-response relationship that can be attributed to diacetyl. In addition, the lack of deep lung effects observed in experimental animals exposed to concentrations of diacetyl that are orders of magnitude higher than the occupational setting contradicts the hypothesis that diacetyl is the probable cause for lung disease in these workers. Thus the weight of evidence does not support the hypothesis that exposure to diacetyl causes BO and/or pulmonary function decline.

PS 233 Applying the Bradford Hill Criteria in the 21st Century: How Advances in Molecular Epidemiology Have Changed Causal Inference

K. Fedak, S. A. Gross, A. Bernal and Z. Capshaw. *Cardno ChemRisk, Boulder, CO.*

The Bradford Hill Criteria is a set of concepts used to evaluate evidence of causality in epidemiological studies. Since they were written in 1965, the criteria have come to serve as a framework for establishing existence of a causal relationship between an agent and a disease. However, when Hill published his list of nine criteria, epidemiological research was more simplistic and disease causation was understood on a more elementary level. Advancements in genetics, molecular biology, toxicology, exposure science, and statistics have increased analytical capabilities for exploring potential cause-and-effect relationships, and resulted in greater understandings of the complexity behind human disease onset and progression. Modern molecular epidemiology has provided additional tools to advance beyond the human-subjects research designs of classic epidemiology, making it necessary to re-evaluate how one interprets and applies each Bradford Hill criterion. Herein, we explore how each criterion is affected by modern analytical tools and advances, and the implications of applying the criteria to data from modern study designs in order to support causal inferences. For example, advanced abilities to monitor molecular-level perturbations paired with understandings of hormesis and other complex dose-response relationships alter interpretations of the biological gradient criterion. The consistency criterion is impacted by the ability to pull supporting information from alternative designs, such as in vitro cellular assays. Epigenetics is continuing to change our understandings of temporality, and challenge our ability to correctly observe and identify the biological initiation of health impacts. Using examples of recently-characterized causal relationships in human disease, we discuss how 21st century tools in molecular epidemiology, which incorporates the concepts of epigenetics, biomarkers, mechanistic toxicology, genotoxicology, toxicokinetics, meta-analysis, and predictive modeling, combine with classic epidemiology to bring the Bradford Hill Criteria into the 21st Century.

PS 234 Polychlorinated Biphenyls and Thyroid Antibodies in the Anniston Community Health Survey

N. Dutton[1, 2] and M. Pavuk[2]. [1]*Oak Ridge Institute for Science and Education (ORISE fellow at ATSDR), Atlanta, GA and* [2]*Agency for Toxic Substances and Disease Registry, Atlanta, GA.* Sponsor: M. Cave.

The present study examined associations between serum PCB concentrations, presence of thyroid autoantibodies, and other thyroid disease indicators in adult residents of Anniston, Alabama.
Thirty-five ortho-substituted PCB congeners were measured in participants of the Anniston Community Health Survey using high-resolution gas chromatography/isotope-dilution high-resolution mass spectrometry. Serum total T4 (TT4), thyroid-stimulating hormone (TSH), thyroglobulin antibodies (TgAb) and thyroid peroxidase antibodies (TPOAb) were analyzed in 743 participants. Multivariable logistic regression was used to estimate odds ratios of TgAb or TPOAb presence, as well as of combined indicators of thyroid disease (TgAb or TPOAb, TT4 or TSH concentration outside normal range, and/or thyroid medication use). Models were adjusted for serum total lipids, age, sex, current smoking, body mass index (BMI) and family history of thyroid disease.
The geometric mean serum concentration for the sum of 35 PCBs was 2.8 times higher among African-Americans as among Whites (5.39 vs. 1.93 ng/g wet weight; adjusted). TgAb or TPOAb presence was more prevalent among Whites than African-Americans (22.4% vs. 13.0%), as was the presence of thyroid disease indicators (45.0% vs. 29.0%). In adjusted analyses, odds of antibody presence was significantly lower among those with higher PCB levels in the total sample (OR = 0.75, 95% CI 0.60-0.94), while odds decreased in African-Americans (OR = 0.71, 95% CI 0.48-1.07) but were elevated in Whites (OR = 1.09, 95% CI 0.75-1.60). Similar divergent patterns were seen in adjusted analyses for odds of having any thyroid disease indicator. In the total sample and African-Americans, we found lower odds of having any indicator in higher quartiles of serum PCB concentrations, but elevated odds were seen among Whites.
In a community with high environmental PCB exposures, we observed inverse associations between serum PCBs and thyroid disease indicators, with a divergence in results by race.

PS 235 Measuring Personal Exposure to Heat and Volatile Organic Compounds in Groundskeepers

M. C. Bernhard, J. M. Gohlke, S. T. Kent, M. E. Sloan, M. B. Evans and L. A. McClure. *Environmental Health Sciences, University of Alabama at Birmingham (UAB), Birmingham, AL.*

Identification of heat-related health risks is of critical importance for outdoor workers, particularly in the Deep South, where heat indexes often reach high stress levels in the summertime. We hypothesize that significant differences in vulnerability to heat-related health risks exist in urban groundskeeper populations due to the urban heat island effect and that volatile organic compound (VOC) exposure will be heightened for groundskeepers at urban sites in close proximity to roads with high traffic volumes or major point source industries, particularly when temperatures are high. We set out to determine whether a small, inexpensive temperature/sunlight monitor attached to the shoe could be used to estimate heat exposure. We recruited 21 groundskeepers to wear temperature/sunlight and passive VOC monitors for 7 consecutive days during the summer. Urban and rural non-occupationally exposed participants were also recruited (N=60). In response to an exit survey, most participants (86%) found wearing the monitor on their shoe was very comfortable and reported the monitor was not hard to remember to wear (81%). When data from the individual monitors were compared to data from the closest weather station, weather stations overestimated average heat exposure. In contrast, daily maximum temperatures from a nearby weather station underestimated maximum temperatures experienced by urban participants. A small proportion of the samplers analyzed suggest elevated time-weighted average toluene and benzene exposure for non-smoking participants when compared to ambient levels measured in the recent Birmingham Air Toxics study and estimated benzene levels for at least two participants are over the EPA chronic inhalation reference concentration for cancer risk. The investigation contributes to exposure research by determining the effect of microclimates within urban settings on assessing the heat and VOC related health risks associated with outdoor work in the summertime.

PS 235a Urinary Polycyclic Aromatic Hydrocarbons Are Associated with Childhood Obesity

M. C. Buser and F. Scinicariello. *DTHHS, ATSDR/CDC, Atlanta, GA.* Sponsor: P. Ruiz.

Background: Polycyclic aromatic hydrocarbons (PAHs) are known carcinogens and suspected endocrine disruptors. Prenatal exposure to PAHs results in increased rates of obesity in early childhood.
Objective: We examined the association of urinary PAH metabolites with adiposity outcomes (BMI z-score, waist circumference, and rate of obesity) in children and adolescents.
Methods: We performed whole-sample analyses of 3,189 individuals 6-19 years of age who participated in the 2001-2006 National Health and Nutrition Examination Survey. We performed multivariate linear and logistic regression to analyze the association of BMI z-score, waist circumference (WC) and obesity with concentrations of single urinary PAH compounds and the sum of PAHs. Furthermore, the analyses were stratified by developmental stage [i.e. children (6-11) and adolescents (12-19)].
Results: An association was found between BMI z-score, WC, and obesity and the molecular mass sum of the PAHs (∑molPAHs). Similarly, an association was found between the total sum of naphthalene metabolites (∑NAPHT) and BMI z-score, WC, and obesity.
Conclusions: We found that the total molar sum of the PAHs is associated with higher body mass index, waist circumference and obesity in children, ages 6-11. However, this association was not found amongst adolescents in the same survey. We found that urinary naphthalene is associated with higher BMI z-score, WC and obesity in both children and adolescents. It is interesting to note that the main source of naphthalene exposure is through inhalation of polluted air while the main source of exposure for other phthalates is through diet.

PS 236 Mechanisms for the Development of Rat Lung Tumors following Inhalation Exposures to MDI

A. Poole[2], A. H. Chappelle[1] and M. A. Collins[1]. [1]*International Isocyanate Institute, Manchester, United Kingdom and* [2]*Toxicology Advice & Solutions, Wollerau, Switzerland.*

Although the endpoint of greatest concern after inhalation exposure to methylene diphenyldiisocyanate (MDI) (101-68-8) is occupational asthma, it has been suggested that evidence from cancer incidence and mortality studies of workers is insufficient to determine if exposure to MDI is causally associated with cancer. Chronic administration (17 h/d) of MDI aerosol results in proliferative and fibrotic responses and low incidence of bronchoalveolar (BA) adenomas in rats. This poster reviews, evaluates and characterizes studies investigating early events of MDI pulmonary toxicity. Evidence indicates compensatory homeostatic mechanisms leading to pulmonary tumors. Key events include continued exposures to respirable MDI aerosols, localized particle deposition at concentrations depleting protective biomolecules in fluid lining the lung surface, and exposure duration. Once deposited in the BA region, MDI particles interact chemically with biological macromolecules, including surfactant and other proteins, reducing their concentrations in the lung lining. To maintain normal homeostasis increased synthesis of secretory proteins by Type II pneumocytes is induced. As the increased synthesis becomes maximized but demand for protective proteins is maintained there is a secondary, compensatory response characterized by an increase in cell replication resulting in BA hyperplasia in the terminal bronchioles and ultimately, after prolonged exposure/cellular stress, to the development of adenomas. The observation that MDI particulates do not accumulate in the lung at doses producing lung tumors, together with the lack of chronic inflammation/cytotoxicity at lower exposures, supports a non-genotoxic, compensatory response of the lung to maintain homeostasis. In conclusion, while the intrinsic properties of respirable MDI might pose a similar hazard for disease in both rat and humans, for humans the risk situation is entirely different. Rat lung tumors after chronic exposure to MDI are not predictive of the potential for human carcinogenicity.

PS 237 Is There Evidence of an Increased Risk to Human Health from Low-Level Exposure to Benzene?

S. A. Fiebelkorn and C. Meredith. *Group R&D, British American Tobacco, Southampton, United Kingdom.*

Benzene is a volatile chemical used in industry and present in petrol, exhaust fumes and tobacco smoke. Several epidemiological studies have demonstrated an association between occupational benzene exposure and increased leukaemia risk, in particular acute myeloid leukaemia (AML). However, there is still some uncertainty as to the risk to the general population from low-dose benzene exposure. The main route of human exposure is via inhalation of benzene present in the environment or tobacco smoke. Smoking can contribute up to 90% of an individual's exposure. In order to investigate the risk associated with low-dose exposure, potency estimates for benzene have been generated from individual occupational studies and meta-analysis data, and an exposure assessment for three population sub-groups, non-smokers, light smokers and heavy smokers carried out. Subsequently, various techniques including life table analysis have been used to evaluate risk of leukaemia and AML. The use of epidemiological data to generate a margin of exposure (MOE) was investigated and suggested benzene may be a high priority for risk management actions based on lifetime exposure estimates and its potency as a leukaemogen. Further assessment using meta-analyses data resulted in estimates of the excess lifetime risk of leukaemia at up to 0.006% for non-smokers and up to 0.06% for heavy smokers. For AML this was 0.003% for non-smokers and 0.03% for heavy smokers. The contribution of benzene to smoking induced leukaemia was estimated at between 8 and 26% (UCL 12-33%). For AML this contribution was estimated as 15 to 31% (UCL 28-60%). The estimates for AML are subject to some uncertainty due to limitations of the available data and further work would be required to confirm these findings. Future work may also include the use of alternative modelling techniques for epidemiological data, the use of biomarker data and further investigation of benzene metabolites and target tissue dose. It may also be possible to apply these methods to additional tobacco smoke toxicants and other smoking related disease endpoints.

PS 238 Mode of Action and Lack of Human Relevance of Benzovindiflupyr (Solatenol™)-Induced Thyroid Follicular Cell Adenomas in Male Han Wistar Rats

R. Green[2], P. P. Parsons[2], R. C. Peffer[1], J. Wright[2] and R. Currie[2]. [1]*Product Safety, Syngenta Crop Protection, LLC, Greensboro, NC and* [2]*Jeallott, Syngenta Ltd., Bracknell, Berkshire, United Kingdom.*

Benzovindiflupyr (Solatenol™) is a novel succinate dehydrogenase inhibitor fungicide (FRAC class C2). In a 2-year dietary administration study with Han Wistar rats (0, 25, 100 and 600[♂]/400[♀] ppm), an increased incidence of benign thyroid follicular cell adenomas was observed in males in the 600 ppm group only (17% vs. 2% in controls). There were no treatment-related increases in the incidence of any other tumour type in the rat or mouse.
Specific mode of action (MOA) studies were conducted and, in conjunction with the regulatory toxicology studies, demonstrate a MOA for induction of thyroid follicular cell adenoma in male rats comprising the following key events: 1) Induction of hepatic UDPglucuronosyltransferase. 2) A decrease in circulating T3/T4 levels. 3) A compensatory increase in circulating thyroid stimulating hormone (TSH) via the hypothalamus-pituitary-thyroid (HPT) axis. 4) Increased proliferation in thy-

roid follicular cells. 5) Under the sustained proliferative stimulus of TSH, thyroid follicular cells progress to form follicular cell adenomas. Furthermore, benzovindiflupyr is not genetically toxic; causes no thyroid histopathology in the mouse, dog or female rat; nor does it inhibit rat thyroid peroxidase *in vitro*. Therefore alternative MOAs can be excluded.
There are well-documented physiological differences in the HPT axis between rats and humans. Enhanced hepatic clearance of T3/T4 in humans does not result in an increase in plasma TSH levels and does not cause tumours (Dellarco *et al.*, 2006). Therefore, the established MOA for the benzovindiflupyr-induced thyroid follicular adenomas is rat specific and not relevant for human hazard/risk assessment purposes. In summary, the data support the conclusion that benzovindiflupyr does not pose a carcinogenic hazard to humans.
Reference:
Dellarco *et al.*, 2006. Crit. Rev. Toxicol. 36: 793-801.

PS 239 Integrated Analysis of Mechanistic Considerations Informative to Cancer Mode of Action in the Upper Respiratory Tract following Formaldehyde Inhalation

J. M. Fritz, L. L. Adams, A. D. Kraft, B. S. Glenn, D. DeVoney, S. V. Vulimiri and R. P. Subramaniam. *U.S. EPA, Washington, DC.*

Formaldehyde (FA) is used in both industrial applications and consumer goods, and exposure is associated with irritation of the nasal epithelium as well as pathologies such as hyperplasia, metaplasia and squamous cell carcinoma. This work presents a mode of action (MOA) analysis, conducted to examine the interdependence and collective contribution of these and other effects to upper respiratory tract (URT) carcinogenesis. Data were sorted by species and endpoint and evaluated for consistency, magnitude, specificity, plausibility and coherence across multiple data-streams. DNA damage in the nasal passages is evident within days of exposure in animals, consistent with the clastogenicity observed in the nasal/buccal epithelium of humans after months to years of exposure. In conjunction with genotoxicity, FA elicits other effects in the respiratory epithelium, such as changes in cell proliferation rates, and cytotoxicity following ciliastasis and mucous flow interruption, which progresses to regenerative proliferation at higher concentrations. As related events, genotoxicity, cytotoxicity and proliferation likely interact in a feed-forward manner, with each contributing to the amplification of initiated clones as a function of increasing FA exposure. For example, at low exposure levels both genotoxicity (DNA-protein crosslinks) and irritation may occur at the cellular level, triggering metaplastic transition and transient proliferation at the tissue level. This proliferative burst may indirectly augment direct FA genotoxicity and trigger an outgrowth of nascent clones. Sustained regenerative proliferation may further enhance cellular genotoxicity and promote the expansion of mutant cells. By evaluating the potential for complementarity, this integrated analysis highlights the relationships and relative contributions of cytotoxicity, proliferation and genotoxicity to URT carcinogenesis. The views expressed are those of the authors and do not necessarily reflect the views or policies of the U.S. EPA.

PS 240 Arsenite and Methyl Methanesulfonate Co-Exposures Induce Synergistic Cellular Responses Associated with Carcinogenic Pathways

P. Balbuena[1], B. Sun[1], S. Ross[1], L. Recio[2], J. Winters[2], H. J. Clewell[1] and R. A. Clewell[1]. [1]*The Hamner Institutes for Health Sciences, Research Triangle Park, NC and* [2]*Integrated Laboratory Systems, Research Triangle Park, NC.*

Arsenite (AsO2-) inhibits DNA repair, exacerbating effects of genotoxic chemicals. MMS induces DNA strand breaks. In this study we determined how concurrent exposure to AsO2- alters the cellular response to DNA damage from a direct mutagenic compound in vitro. We assessed whole genome transcriptomics together with markers of genotoxicity (micronucleus formation), DNA damage (Comet assay, pH2AX protein), apoptosis (Bcl2), antioxidant response (NQO1), and DNA damage response (p53) following 24 hr treatment with AsO2- (3 nM and 300 nM) and MMS (1, 3, 10, 30, and 100 μM) alone or in combination in a human fibrosarcoma cell line (HT1080) expressing wild-type p53. Previously, HT1080s showed similar NQO1 and p53 responses to AsO2- compared with primary cultures of human uroepithelial cells (target for arsenic-induced bladder cancer), indicating that this is a reasonable in vitro model for AsO2- response. Transcriptomic analysis indicated that AsO2- co-exposures were associated with increased anti-apoptotic signaling and a reduced nuclear excision repair response, with a concomitant increase in non-homologous end-joining of double-strand-breaks. 3nM AsO2-/MMS mixtures induced significant increases in protein expression for Bcl2 and NQO1 when compared to MMS alone. Co-exposure to 300 nM AsO2- increased the expression of these proteins at least two fold compared to MMS alone. In contrast, co-exposure to AsO2- did not significantly change the p53 response. Mutagenic effects were not detected by micronucleus analysis, even at the highest concentrations; however, increased DNA damage was detected by the comet assay and pH2AX expression in the AsO2-/MMS mixtures compared to MMS. Both DNA damage and apoptosis markers showed increases that were consistent with a synergistic response (more than additive). These results suggest that the co-mutagenicity of AsO2- involves increased survival signaling, together with inhibition p53 DNA damage response.

PS 241 Maternal Arsenic Exposure of C3H Mice Increases Hepatic Tumor with an Activating Mutation in the Oncogene Ha-ras in the F2 Generation

K. Nohara[1, 2], K. Okamura[1, 2], T. Suzuki[1], H. Murai[1], T. Ito[3], K. Shinjo[4] and Y. Kondo[4]. [1]*Center for Environmental Health Sciences, National Institute for Environmental Studies, Tsukuba, Japan,* [2]*Grad. Sch. of Life & Environ. Sci., University of Tsukuba, Tsukuba, Japan,* [3]*Kumamoto Univ. Grad. Sch. Med. Sci., Kumamoto, Japan and* [4]*Aichi Cancer Ctr. Res. Inst., Nagoya, Japan.*

Maternal arsenite exposure of C3H mice has been reported to increase hepatic tumors in male offspring (F1) at 74 weeks-old. Using this experiment model, we previously showed that maternal arsenite exposure particularly increased hepatic tumors with a C61A activating mutation in the oncogene Ha-ras. Since C to A mutation can be attributed to oxidative-stress-induced G:C to T:A transversion, the results suggested the involvement of oxidative stress in the hepatic tumorigenesis. We also found that two genes (Creld2, Slc25a30) were up-regulated and two genes (Fabp4, Ell3) were down-regulated more than twofold in the normal livers of F1 mice maternally-exposed to arsenite compared to the control mice at 74 weeks-old. In this study, we further investigated whether maternal arsenite exposure induces tumor-promoting changes in the F2 mice. The present study revealed that maternal arsenic exposure surprisingly increased hepatic tumors with a C61A Ha-ras mutation even in the F2 mice. No Ha-ras mutation was detected in the normal liver tissues, indicating that the mutation was somatically acquired. In the tumors with Ha-ras mutation, ERK was hyperphosphorylated, showing activation of oncogenic ERK pathway. On the other hand, the expression of Creld2 and Slc25a30 were lower and the expression of Ell3 was higher in the normal liver of F2 mice in the arsenic-treated group compared to the control group, contrary to the changes in the F1 mice. The F1 mice directly underwent arsenite exposure on the liver and the F2 mice underwent exposure as germ cells. The exposures at different time resulted in different outcomes in the gene expression and both increased hepatic tumors harboring Ha-ras mutation. The mechanism should be clarified by further studies.

PS 242 Identification of DNA Methylation Changes in the Liver Tumors Induced by Gestational Arsenic Exposure Using Genome-Wide Analysis

T. Suzuki[1], S. Yamashita[2], T. Ushijima[2], S. Takumi[1, 3], T. Sano[1], T. Michikawa[1] and K. Nohara[1]. [1]*National Institute for Environmental Studies, Tsukuba, Japan,* [2]*National Cancer Center Research Institute, Tokyo, Japan and* [3]*The Jikei University School of Medicine, Tokyo, Japan.*

Inorganic arsenic is classified as a human carcinogen. Since DNA methylation changes have been shown to be associated with tumors induced by arsenic, DNA methylation changes specific for tumors induced by arsenic will be useful in distinguishing tumors caused by arsenic from those induced by other factors. Previous studies have shown that gestational arsenic exposure of C3H mice increases the incident of tumors in male offspring. In this study, we used the same experimental model and performed genome-wide analysis by methylated DNA immunoprecipitation (MeDIP)-CpG island microarray to identify the region where DNA methylation was specifically changed in the liver tumors of arsenic-exposed offspring. Methylation specific PCR (MSP) was used to validate the data of MeDIP analysis. We selected 16 DNA regions where DNA methylation greatly changed in the liver tumor of arsenic-exposed mice compared to the normal liver of control mice from the data of MeDIP analysis. We found that DNA methylation was mostly changed in the gene body. The MSP analysis revealed that the DNA methylation changes in 11 DNA regions were well corresponded to the data of MeDIP analysis. Interestingly, among such regions, DNA methylation level of the *Fosb* was significantly higher in the liver tumors of arsenic-exposed mice than in those of control mice. Furthermore the expression of *Fosb* gene was increased in the liver tumors of arsenic-exposed mice. This finding is consistent with the previous reports that the increase of DNA methylation in gene body corresponds to the increase of gene expression. The results of this study suggested that DNA methylation change can be used to identify the liver tumors induced by gestational arsenic exposure.

PS 243 Significant Nonlinearity of Lung Cancer Risk in Relation to Arsenic in Drinking Water in Northeastern Taiwan

K. T. Bogen[1], C. Chen[3] and J. S. Tsuji[2]. [1]*Health & Environmental, Exponent, Oakland, CA,* [2]*Health & Environmental, Exponent, Seattle, WA and* [3]*Graduate Institute of Clinical Medicine, College of Medicine, National Taiwan University, Taipei, Taiwan.*

Carcinogenic effects of ingested inorganic arsenic (InAs) have been addressed by ecological studies of increases in skin, lung, and bladder cancer in impoverished villages in southwest Taiwan and elsewhere. More recently, increased lung cancer incidence (LCI) was shown in a cohort of 6,888 residents of 3,901 households located in 18 villages in northeast Taiwan who were followed for 11 years [Chen et al. Environ Res 2010; 110(5):455–462]. That study estimated InAs exposure from thousands of household-well-specific measurements classified into five categories (range: undetectable [≤0.15] to >3,000 μg/L), and adjusted by age, gender, education, and consumption of cigarettes and of alcohol. A parallel cohort study by Chen et al. (2010) showed similar effects for bladder cancer. To refine dose-response analysis, the combined LCI and exposure data were re-binned into six exposure categories using residents who did not drink well water as the reference group (~16% of all residents and of all person-years of exposure). Log adjusted relative risk (RRadj) was modeled as log(RRadj) = b log(1+X) + c log(1+X)2, with exposure (X) defined as InAs concentration or as cumulative InAs exposure. Good fits to the re-binned data ($p > 0.7$, chi-square test) were obtained using each dose metric, but the estimated initial-slope parameter b is significantly negative in each case (2-tail $p = 0.043$ and 0.029, respectively), consistent with estimates of RRadj ≤ 1 at InAs levels <55 μg/L and <1,720 μg y/L, respectively. This appears to be the first reported observation of a statistically significant hormetic dose-response relationship (i.e., one with a significantly negative initial slope) for a single chemical carcinogen based on epidemiology data. Further analysis of potential confounding factors affecting non-drinkers of well water in this study is needed to better assess the nature and magnitude of any low-dose nonlinearity of LCI that occurred in this cohort.

PS 244 Arsenic and Cadmium-Transformed UROtsa Bladder Cells Stably Expressing SPARC Will Reduce SPARC Expression during the Formation of a Tumor Heterotransplant

J. R. Dunlevy[1], A. Slusser[2], A. R. Klinger[1], J. L. Larson[1], X. Zhou[2], S. H. Garrett[2], S. Somji[2] and D. A. Sens[2]. [1]*Basic Sciences, University of North Dakota, Grand Forks, ND and* [2]*Pathology, University of North Dakota, Grand Forks, ND.*

SPARC, secreted protein acidic and rich in cysteine, is an extracellular matrix protein that can bind to structural molecules such as type I collagen yet SPARC's role in the matrix is a non-structural one. SPARC functions to regulate cell signaling, migration, angiogenesis, and cell proliferation acting more like a cytokine than a matrix molecule. SPARC clearly has a strong role in cancer however, in some types of cancers SPARC is elevated and in others reduced. Our previous studies showed that in an environmental model of bladder cancer utilizing the UROtsa cell line SPARC was drastically reduced in cells transformed with arsenic or cadmium and that this reduction occurred early in the transformation process upon exposure to low doses of either metal. In this study, SPARC was stably transfected into 2 arsenic and 2 cadmium UROtsa cell lines thereby re-establishing SPARC mRNA and protein levels comparable to those in the UROtsa parent cell line. These SPARC-expressing cells were then injected into nude mice and the resulting tumor heterotransplants were characterized. Results showed there were again non-detectable levels of SPARC protein by immunohistochemistry. In Western analyses SPARC levels were barely detectable if at all in the heterotransplants generated with SPARC-expressing cells. Real time PCR analyses showed that SPARC mRNA was being expressed in the tumors but when compared to the expression of the vector blasticidin transcript (BSD), the ratio of SPARC to BSD was reduced in the heterotransplant tumors compared to the cell lines. The possibility of down regulation of SPARC mRNA via miRNAs is being determined. In conclusion, the results of this study show that despite being stably transfected, SPARC expression is greatly reduced in heterotransplants. Therefore, shutting down SPARC protein expression appears to be strongly advantageous to tumor formation.

PS 245 Peroxisome Proliferator-Activated Receptor-β/D (PPARβ/D) Inhibits Cell Proliferation and MMP-2-Mediated Tumorigenesis in Human Testicular Embryonal Carcinoma Cells

P. Yao[1], L. Chen[1], B. Zhu[1], F. Gonzalez[2] and J. M. Peters[1]. [1]*Department of Veterinary and Biomedical Sciences and The Center of Molecular Toxicology and Carcinogenesis, the Pennsylvania State University, University Park, PA and* [2]*Laboratory of Metabolism, National Cancer Institute, Bethesda, MD.*

Testicular germ cell tumors are most prevalent in young adult men ages 15-40 years, and arise as a result of abnormal testicular development. Peroxisome proliferator-activated receptors β/δ, (PPARβ/δ) regulates a variety of biological processes but the function of PPARβ/δ in carcinogenesis remains controversial. Stable human testicular cancer cell lines (NT2/D1 and Tera2) that constitutively over-express PPARβ/δ were produced to effectively examine the role of this receptor in human cancer models. Over-expression and/or ligand activation of PPARβ/δ increased expression of angiopoietin-like protein 4 (*ANGPTL4*) mRNA, a known PPARβ/δ target gene. Over-expression of PPARβ/δ inhibited cell proliferation in both NT2/D1 and Tera2 cells compared to controls. Ligand activation of PPARβ/δ both in NT2/D1 and Tera2 cells over-expressing PPARβ/δ caused a significant decrease in clonogenicity compared to controls. Over-expression and/or ligand activation of PPARβ/δ had no effect on either staurosporine-induced or UVB-induced poly(ADP-ribose) polymerases (PARP) cleavage; however, an increase in annexinV-positive NT2/D1 and Tera2 cells over-expressing PPARβ/δ, indicative of increased apoptosis, was found using flow cytometric analysis. Over-expression and/or ligand activation of PPARβ/δ inhibited MMP2 and MMP9 activities, presumably associated with the decreased invasion and migration in NT2/D1 and Tera2 cells. The MMP2/9 inhibitor SB-3CT suppressed the PPARβ/δ antagonist GSK3787-enhanced gelatinolytic activities, invasion, and migration in NT2/D1 control and/or over-expressing PPARβ/δ cells. This finding confirms a definitive requirement of PPARβ/δ in MMP2/9-mediated metastasis in vitro. Combined, these novel observations demonstrate the inhibitory effect of activating or over-expressing PPARβ/δ on tumorigenesis in human testicular cancer cells.

PS 246 Ligand Activation of Peroxisome Proliferator-Activated Receptor-B/D (PPARB/D) Attenuates Liver Tumorigenesis in HBV Transgenic Mice

G. Balandaram[1], L. R. Kramer[1], B. Kang[2], F. Gonzalez[3] and J. M. Peters[1]. [1]*Pennsylvania State University, University Park, PA,* [2]*Non-clinical Research Institute, Chemon Co., South Korea, Democratic People's Republic of Korea and* [3]*Laboratory of Metabolism, NCI, Bethesda, MD.*

PPARβ/δ can inhibit pro-inflammatory activities in the liver. Since chronic inflammation often precedes liver carcinogenesis, the role of PPARβ/δ in modulating liver cancer was examined. Male hepatitis B virus (HBV) transgenic mice, which develop hepatocellular injury around 2-3 months of age, followed by hyperplasia and neoplasia by 9-12 months of age, eventually developing hepatocellular carcinoma by 18 months, were used for this study. Whole liver was isolated from 7-month-old mice treated with PPARβ/δ ligand for three weeks (short term study). Ligand activation of hepatic PPARβ/δ in these mice attenuated pro-inflammatory genes, tumor necrosis factor-alpha (Tnfα) and inducible nitric oxide synthase (iNos) mRNA. In addition, serum levels of alanine amino transaminase (ALT) were also attenuated in ligand treated HBV mice. These effects were not observed in the control mice. Prolonged PPARβ/δ ligand treatment (8 months long term study) of HBV mice of the same age showed attenuation of tumor multiplicity and average number of liver foci as compared with the control group. Ligand activation of PPARβ/δ in liver of HBV mice increased expression of the PPARβ/δ target gene, angiopoietin-like 4 (Angptl4) mRNA. Western blot analysis of whole liver from these HBV mice showed reduced NF-κB activation indicated by attenuated expression of phosphorylated p65 and phosphorylated IκBα protein levels in ligand activated liver tissues. In addition, protein levels of the cell proliferation marker CYCLIN D1 and the oncogene c-MYC were significantly attenuated in livers of ligand treated HBV mice as compared to controls. Combined, results from these studies suggest that PPARβ/δ inhibits hepatic inflammation, and has the potential to attenuate hepatic tumorigenesis.

PS 247 Ligand Activation of Peroxisome Proliferator-Activated Receptor-β/δ (PPARβ/δ) Inhibits TGFβ1-Induced Epithelial-Mesenchymal Transition (EMT) in a Human Lung Cancer Cell Line

K. C. Pramanik[1], A. Pidathala[1], B. Zhu[1], F. Gonzalez[2] and J. M. Peters[1]. [1]*Department of Veterinary and Biomedical Science, Penn State University, State College, PA and* [2]*Laboratory of Metabolism, National Cancer Institute, Bethesda, MD.*

PPARβ/δ regulates fatty acid catabolism, glucose homeostasis, cellular differentiation and numerous anti-inflammatory activities, but the role of PPARβ/δ in carcinogenesis remains controversial. Surprisingly, the role of PPARβ/δ in metastasis has not been extensively investigated to date in any cancer model. Thus, the present study examined the role of PPARβ/δ in tumor growth factor-β-1 (TGFβ1) stimulated lung cancer cells in stable cell lines over-expressing PPARβ/δ in the presence or absence of a potent PPARβ/δ ligand. Ligand activation of PPARβ/δ in A549 cells over-expressing PPARβ/δ resulted in a significant increase of epithelial markers, (e.g; E-CADHERIN and OCCLUDIN) with a concomitant decrease in mesenchymal markers, including N-CADHERIN and VIMENTIN without affecting the parent and A549-Migr1 vector control cells. Further, ligand activation of PPARβ/δ increased E-CADHERIN and suppressed VIMENTIN mRNA levels in A549 cells over-expressing PPARβ/δ. Migration and invasion is a known phenotype associated with cells undergoing metastasis. Ligand activation of PPARβ/δ inhibited TGFβ1-induced migration and invasion in A549 cells over-expressing PPARβ/δ, indicating an anti-metastatic effect of PPARβ/δ. Furthermore, MMP-2 and MMP-9 mRNA levels were decreased by ligand treatment in cells over-expressing PPARβ/δ. Ligand activation of PPARβ/δ in A549 cells over-expressing PPARβ/δ not only inhibited TGFβ1-induced morphology but also reversed TGFβ1-induced expression of E-CADHERIN and VIMENTIN protein. Interestingly, the PPARβ/δ antagonist GSK3787 treatment in A549 cells over-expressing PPARβ/δ prevented ligand-induced inhibition of EMT, indicating that PPARβ/δ is required for the inhibition of EMT. Collectively, these results suggest that ligand activation of PPARβ/δ could be potential therapeutic target for lung cancer metastasis.

PS 248 Evidence the PPAR Beta/Delta and BCL6 Pathway Is Involved in Pancreatic Cancer Development and Progression

R. W. Smith[1], J. D. Coleman[1], J. T. Thompson[1], B. Prokopczyk[2] and J. Vanden Heuvel[1]. [1]*Veterinary and Biomedical Sciences, Penn State University, State College, PA and* [2]*Pharmacology, Penn State University, Hershey, PA.*

The nuclear receptor Peroxisome Proliferator-Activated Receptor β/δ (PPARβ/δ) regulates expression of genes involved in inflammation, metabolism, and cancer directly or in concert with the transcriptional repressor B-Cell Lymphoma 6 (BCL6) in the pancreas. Ligand-dependent activation of PPARβ/δ causes the dissociation of BCL6 from the complex, which in turn suppress genes involved in inflammation and invasion. In this study we have examined the mRNA expression of several cancer biomarkers as well as PPARβ/δ and BCL6 target genes in human pancreatic tissue of matched normal and tumor biopsies as well as the LSL-Kras(G12D); Pdx-1-Cre mouse model of pancreatic cancer. This mouse strain contains a latent point mutant allele of Kras2 in which expression leads to pancreatic tumors in heterozygous mice. Pancreatic PPARβ/δ expression was higher in tumors than in surrounding tissue in humans and was augmented in Kras(G12D) expressing mice compared to non-recombinant counterparts. There was no change in BCL6 expression. BCL6 target genes, MCP1 and NFκB1 involved in inflammation, and VCAM1 in cell adhesion showed significant increases in both human tumors and in pancreas from Kras(G12D) expressing mice. MMP9, another BCL6 target responsible for regulation of cell migration and metastasis, also showed elevated expression from normal tissue in humans. Increased expression of PPARβ/δ, in tumors and in pre-neoplastic lesions may sequester the transcriptional repressor BCL6 and hence play an important role in cancer development and progression and suggests means for treating pancreatic cancer.

PS 249 Ligand Activation of PPARB/Δ Inhibits Invasion and Formation of Three-Dimensional Spheroids of the LNCaP Prostate Cancer Cell Line

P. Krishnan and J. M. Peters. *Penn State University, University Park, PA.*

Prostate cancer is second to lung cancer in causing death from cancer in American men. The American Cancer Society estimates that about 240,000 new cases of prostate cancer will be diagnosed and about 30,000 men will die of prostate cancer in 2013. Our previous studies have shown that ligand activation of PPARβ/δ plays a role in inhibiting skin cancer and colon cancer. The hypothesis that ligand activation of PPARβ/δ will inhibit prostate cancer progression was examined in these experiments. To study the role of PPARβ/δ, human PPARβ/δ was over expressed in LNCaP cells using the Migr1 retroviral system. Western blot analysis showed about 3 times the expression of the PPARβ/δ compared to the parent LNCaP cell line and the control Migr1 infected LNCaP cells. The LNCaP cells were treated with the highly specific PPARβ/δ agonist GW0742 (0.01 to 10 μM) and the invasion was measured using the xCELLigence system. Invasion was dose-dependently decreased following ligand activation of PPARβ/δ in LNCaP cells over-expressing PPARβ/δ compared to the parent LNCaP cells and LNCaP-Migr1 control cells. To mimic in vivo tumor growth, the LNCaP cells were plated as three dimensional (3D) hanging drops and then plated in poly(2-hydroxyyethyl methacrylate) (Poly- HEMA) coated wells and treated with transforming growth factor-β1 (2 ng/mL) and tumor necrosis factor-α (10 ng/mL) for 96 h. Morphological analysis showed that LNCaP cells and LNCaP-Migr1 control cells formed microspheres while the LNCaP cells over-expressing PPARβ/δ were more or less flat. The initial clonogenic assay results showed a dose dependent decrease in the number of clones formed in the LNCaP cells. Combined, these results suggest that activation of PPARβ/δ may play a role in preventing and/or treating prostate cancer. Analysis of the role of PPARβ/δ activation in inhibiting epithelial to mesenchymal transition by studying the changes in the marker proteins like E-CADHERIN, VIMENTIN and N-CADHERIN in this 3D spheroid model are underway.

PS 250 Uncoupling-Induced Metabolic Reprogramming Provides Insights into Skin Cancer Resistance

A. Solmonson[1, 2], S. M. Nowinski[2], M. Keaton[3], E. Morin-Kensicki[3], J. E. Rundhaug[4] and E. M. Mills[1, 2]. [1]*Institute for Cell and Molecular Biology, University of Texas at Austin, Austin, TX,* [2]*College of Pharmacology and Toxicology, University of Texas at Austin, Austin, TX,* [3]*Metabolon Inc., Research Triangle, NC and* [4]*The University of Texas MD Anderson Cancer Center Science Park Research Division, Smithville, TX.*

Metabolic reprogramming is a hallmark of tumorigenesis and malignancy across a variety of cancer types. Reduced oxidative phosphorylation and increased ATP synthesis by glycolytic upregulation is thought to provide both the energy and metabolic precursors necessary to meet the increased biosynthetic and energetic demands associated with malignancy. We hypothesized that since uncoupling protein 3 (UCP3) dissipates the mitochondrial electrochemical proton gradient, it may lead to the consumption or depletion of biosynthetic substrates necessary for carcinogenesis. In support, previous studies from our lab have shown that mice expressing a keratin 5-UCP3 transgene are completely resistant to chemically- and Ras-induced skin carcinogenesis; however the metabolic consequences of UCP3 overexpression in relation to cancer resistance are unclear. To examine the metabolic changes associated with UCP3 expression and this profound skin cancer resistance, we performed metabolomic analysis of more than 350 metabolites in epidermis from K5-UCP3 and wild type FVB/N littermate mice. Results of this analysis show significant UCP3-dependent changes in metabolites indicative of increased energy harvesting via glycolysis, breakdown of phospholipids and increased beta oxidation. Consistent with decreased energy reserve, K5-UCP3 epidermis exhibits increased uncoupled respiration, decreased ATP and increased AMP levels, which correspond to increased AMP Kinase (AMPK) activation (Thr172 phosphorylation). Taken together, these data suggest that uncoupling proteins might function to oppose the metabolic demands of tumorigenesis and suggest that targeting mitochondrial uncoupling may be a novel and effective strategy in cancer prevention and treatment.

PS 251 Does PCE Cause Non-Hodgkin's Lymphoma?

D. G. Dodge[1] and B. D. Beck[2]. [1]*Gradient, Bend, OR and* [2]*Gradient, Cambridge, MA.*

Tetrachloroethylene (PCE) is a volatile, chlorinated hydrocarbon used as a solvent in the dry cleaning and textile-processing industries and as an agent for degreasing metal parts. It is also a widespread environmental contaminant. In 2012, US EPA classified PCE as "likely to be carcinogenic in humans by all routes of exposure" based, in part, on epidemiologic evidence associating PCE exposure and Non-Hodgkin's Lymphoma (NHL). We critically analyzed human, animal, and mechanistic evidence, including epidemiologic studies published subsequent to US EPA's analysis, to address the question of whether PCE causes NHL in humans. A number of epidemiologic studies in populations exposed to PCE have been conducted, principally in laundry and dry cleaning workers and populations exposed to chlorinated solvents in drinking water. Most of the studies addressing a potential association between PCE exposure (or imperfect surrogates such as occupation) and NHL do not report statistically significant results, including those with higher quality exposure-assessment methodologies. Limitations (e.g., lack of an exposure-response

gradient, small numbers of cases, internal inconsistencies, and potential exposure misclassification) in many of the positive studies weaken the evidence of a causal relationship. In experimental animals, high doses of PCE have been associated with a number of cancers. Potentially the most relevant of these to NHL is mononuclear cell leukemia (MNCL) in aging F344 rats in more than one study. Though the etiology and mode of action of MNCL in F344 rats is not established, some factors suggest that it should not be considered a reliable indicator that PCE poses a carcinogenic hazard to humans. For example, while MNCL is extremely common in F344 rats, it is rare in other rat strains and not seen in mice. Although F344 rats are genetically predisposed to develop MNCL, there is no such predisposition in humans toward the development of the human leukemia that most resembles MNCL in F344 rats. We conclude that weak epidemiologic data and lack of human-relevant animal data indicate PCE is not likely to cause NHL in humans.

PS 252 Bisphenol A Induces Prostate Cancer Progression and Differential Gene Expression

E. Ricke[1], A. B. Theberge[1], M. A. Moses[2] and W. A. Ricke[1]. [1]*Urology, University of Wisconsin, Madison, WI and* [2]*Environmental Medicine, University of Rochester, Rochester, NY.* Sponsor: R. Peterson.

Introduction and objectives: Estrogen in combination with androgen has been shown to induce prostate diseases including prostate cancer. Bisphenol A (BPA), a small molecule used to manufacture polycarbonate plastics, is one of the most prominent EDCs and has been identified as a xenoestrogen. Humans are exposed to BPA as it leaches from food and beverage containers made of polycarbonate. Our goal was to determine if BPA could substitute for estrogen at inducing prostate cancer progression in a tissue recombination model. Furthermore, we wanted to determine if cells isolated from cancers would have different gene expression signatures indicative of hormonal regiment used.
Methods: Tissue recombinants composed of BPH1 + rUGM were surgically grafted to the renal capsule of adult male athymic mice that were subcutaneously implanted with either 25 mg of testosterone (T)+ 2.5 mg estradiol-17 beta (E2) or T+BPA (25 mg) and grown for 4 months. Grafts were excised at necropsy and BPH1 cells were isolated. RNA was collected from BPH1-BPA and BPH1-E2 as well as parental BPH1 cells. Gene expression profiles were created using quantitative PCR.
Results: BPA induced tissue recombinants composed of BPH1 + rUGM to develop into cancer similar to that of E2. Changes for INHBA expression increased in BPH1-BPA over BPH1 and BPH1-E2 cells (BPH1: 100%, BPH1-E2: 52%, BPH1-BPA: 190%). Conversely, BPH1-BPA showed lower expression than BPH-1 and BPH1-E2 for PPARγ (BPH1: 100%, BPH1-E2: 901%, BPH1-BPA: 83%). Whereas, CTNNB1 expression was higher in BPH1-E2 and BPH1-BPA compared to BPH1 cells (BPH1: 100%, BPH1-E2: 201%, BPH1-BPA: 182%). Lastly, there was minimal change in expression between cell lines for CDH1 (BPH1: 100%, BPH1-E2: 90%, BPH1-BPA: 105%).
Conclusions: These data support the concept that BPA acts as an estrogen to promote prostate cancer progression. Although, BPA induced cancers share some similarities with E2 induced cancer, BPA may have a distinct tumor gene expression profile that may distinguish it from other cancers.

PS 253 hTERT-Immortalized Renal Proximal Tubule Epithelial Cells: Characterizing a Model System for Testing the Role of Cadmium and Benzo[a]pyrene in the Development of Renal Cancer

B. R. Simon[2, 1], M. J. Wilson[1] and J. K. Wickliffe[1]. [1]*Global Environmental Health Sciences, Tulane University School of Public Health and Tropical Medicine, New Orleans, LA and* [2]*Biomedical Sciences, Tulane University School of Medicine, New Orleans, LA.*

In order to elucidate the mechanisms by which the heavy metal cadmium (Cd) acts as a co-carcinogen, we aim to characterize a newly developed cell line derived from renal proximal tubule epithelial cells (RPTEC) of a healthy human male donor. The RPTEC/TERT1 cell line has been immortalized with the human telomerase reverse transcriptase (hTERT) subunit only and does not exhibit chromosomal abnormalities. We have conducted controlled exposure experiments designed to demonstrate toxicological responses, DNA repair capacity, and mutagenicity in these cells, which will serve as a model for renal cell carcinogenesis. We are conducting exposure experiments to mixtures of the common environmental contaminants, Cd and benzo[a]pyrene (B[a]P). Our studies are the first to provide information regarding toxicological responses in this novel RPTEC/TERT1 cell line. A significant increase in the expression of genes coding for B[a]P metabolizing enzymes (CYP1A1, CYP1B1) occurred in a dose- and time-dependent manner at 3, 6, and 24 hours post exposure. Likewise, a significant increase in the heavy metal responsive gene MT2A was observed following exposure to Cd. The presence of BPDE-DNA adducts confirms that the RPTEC/TERT1 cell line responds to B[a]P consistent with what is known regarding these cell types in a normal, health kidney. Future studies will be conducted to test mutagenesis under conditions of co-exposure to Cd and B[a]P. We hypothesize that Cd inhibits DNA repair processes, therefore, causing BPDE-DNA mutations to become fixed in the genome which may lead to carcinogenesis.

PS 254 Chronic Alcohol Intake Promotes Tumor Growth in a Diethylnitrosamine-Induced Hepatocarcinogenesis Mouse Model through Increased Wnt/β-catenin Signaling

K. E. Mercer[1, 3], L. Hennings[2], N. Sharma[3], C. Chandler[3], R. Wynne[3], M. J. Ronis[1, 3] and T. M. Badger[1, 3]. [1]*Pediatrics, UAMS, Little Rock, AR,* [2]*Pathology, UAMS, Little Rock, AR and* [3]*Arkansas Children's Nutrition Center, Little Rock, AR.*

Ethanol (EtOH) metabolism is involved in both initiating and promoting mechanisms in hepatocellular carcinoma progression in chronic alcoholics. In this study, we developed a mouse model to test the hypothesis that chronic EtOH consumption promotes tumor growth irrespective of EtOH-related initiating mechanisms. Male mice received a single dose of diethylnitrosamine (DEN) on postnatal day 13, and were assigned to either an EtOH-liquid diet, a control liquid diet pair-fed (PF) to the EtOH group, or a standard chow diet 47 days post-DEN injection. After 16 wks of EtOH feeding (5.0% v/v) we observed a 2-4 fold increase tumor multiplicity, but not tumor incidence in EtOH+DEN treated livers compared to PF+DEN and chow+DEN groups, $p<0.05$, which corresponded to a 4-fold increase in hepatocyte proliferation in EtOH+DEN non tumor liver tissues, $p<0.05$. In the EtOH+DEN non tumor liver tissues, we also observed a significant increase in β-catenin expression and changes in β-catenin localization when compared to DEN treated PF and chow controls. More important, in a separate rodent model of alcoholic liver disease, prolonged feeding of EtOH alone significantly reduced hepatic retinol and retinoic acid concentrations, increased cytosolic β-catenin expression, phosphorylated (Ser 21/9) GSK3b expression, and increased nuclear accumulation of β-catenin in rat hepatocytes, $p<0.05$. In addition, RNA analysis using a targeted Wnt PCR array revealed a significant up-regulation of soluble Wnts, transcription factors associated with a proliferative phenotype, and β-catenin targets associated with disease progression, $p<0.05$. These findings suggest a link between alcohol-related retinoid depletion, up-regulation of Wnt/β-catenin signaling, and tumor growth and progression in our mouse model of HCC. Supported by NIH AA018282.

PS 255 Orally Administered Nicotine Induces Urothelial Hyperplasia in Rats and Mice

P. R. Dodmane, L. L. Arnold, K. L. Pennington and S. M. Cohen. *Pathology and Microbiology, University of Nebraska Medical Center, Omaha, NE.*

Tobacco smoking is a major risk factor for multiple human cancers including urinary bladder carcinoma. Tobacco smoke is a complex mixture containing chemicals that are known carcinogens in humans and/or animals. Aromatic amines a major class of DNA-reactive carcinogens in cigarette smoke, are not present at sufficiently high levels to fully explain the incidence of bladder cancer in cigarette smokers. Other agents in tobacco smoke could be excreted in urine and enhance the carcinogenic process by increasing urothelial cell proliferation. Nicotine is one such major component, as it has been shown to induce cell proliferation in multiple cell types in vitro. However, in vivo evidence specifically for the urothelium is lacking. We previously showed that cigarette smoke induces increased urothelial cell proliferation in mice. In the present study, urothelial proliferative and cytotoxic effects were examined after nicotine treatment in mice and rats. Nicotine hydrogen tartrate was administered in drinking water to rats (52 ppm nicotine) and mice (514 ppm nicotine) for 4 weeks and urothelial changes were evaluated. Histopathologically, 7/10 rats and 4/10 mice showed simple hyperplasia following nicotine treatment compared to none in the controls. Rats had an increased mean BrdU labeling index compared to controls, although it was not statistically significantly elevated in either species. Scanning electron microscopic visualization of the urothelium did not reveal significant cytotoxicity. These findings suggest that oral nicotine administration induced urothelial hyperplasia (increased cell proliferation), possibly due to a mitogenic effect of nicotine and /or its metabolites.

PS 256 IL6 Can Induce Epigenetic Change in Colonic Cells Grown As 2D and 3D Cultures Resulting in Increased Activation of Dietary Carcinogens and DNA Damage

S. Patel, R. David and N. J. Gooderham. *Surgery and Cancer, Imperial College London, London, United Kingdom.*

Colorectal cancer (CRC) occurs more prevalently in developed countries where it is the second highest cause of cancer-related mortality. Only 15-20% of CRC cases have a genetic pre-disposition, while the remaining 80-85% are caused by environment and lifestyle. Epidemiological studies have suggested a strong link between diet and CRC. Western-style diets can induce local colonic inflammation, which is also strongly associated with CRC development. Benzo[a]pyrene (BaP) and 2-amino-1-methyl-6-phenylimidazo[4,5-b]pyridine (PhIP) are dietary pro-carcinogens found in meats cooked at high temperatures common in Western-style diets and require metabolic activation to their genotoxic agents by cytochrome P450 (CYP) 1A and 1B1 enzymes. We previously observed overexpression of CYP1B1 and pro- inflammatory cytokine interleukin-6 (IL6) in malignant tissue resected from CRC patients, indicating that inflammation and changes in metabolic competency occur in CRC tissue. To further understand the link between diet, inflammation and CRC, we investigated the effect of IL6, BaP and PhIP on human colon epithelial cell lines HCT116 and SW480 grown as 2D and 3D cultures. We measured DNA damage using the micronucleus (MN) assay and determined CYP1A1 and CYP1B1 expression along with associated micro-RNA (miRNA) changes. In both cell lines, MN frequency was increased dose-dependently with BaP and PhIP treatment while pre-treatment with IL6 further enhanced DNA damage. Induction of CYP1B1 gene expression was shown following IL6 treatment while CYP1A1 expression was not changed. Additionally, treatment with IL6 decreased expression of miR-27b, a miRNA known to target CYP1B1 mRNA. Taken together, these data demonstrate that exposure of colonic cells to IL6 alters metabolic competency of the cells through epigenetic changes. Similar events occurring in colorectal epithelial cells could lead to increased dietary pro-carcinogen-induced DNA damage, thereby contributing to colorectal carcinogenesis.

PS 257 Extracellular Signal-Regulated Kinases 1/2-Dependent Stimulation of Mouse Epidermal JB6 Cl 41-5a Cell Proliferation by Triclosan

Y. Wu, F. A. Beland and J. Fang. *Division of Biochemical Toxicology, National Center for Toxicological Research, Food and Drug Administration, Jefferson, AR.*

Triclosan is a broad spectrum anti-bacterial agent widely used in many personal care products, household items, medical devices, and clinical settings. Human exposure to triclosan is mainly through oral and dermal routes. Although it has been reported that long-term oral exposure of mice to triclosan induces liver tumors, the dermal carcinogenicity of triclosan in either animals or humans is unknown. In this study, using mouse epidermal JB6 Cl 41-5a cells, triclosan within a narrow range of concentrations (3 - 6 μM), stimulated anchorage-dependent cell growth in a concentration- and time-dependent manner. Higher concentrations of triclosan (8 μM) inhibited cell growth, which was due to necrotic cell death. Although triclosan failed to promote anchorage-independent cell transformation in a soft agar colony formation assay, enhanced cell proliferation was demonstrated by a substantial increase in the percentage of BrdU positive cells and an elevation in the protein levels of cyclin A, even at a concentration that triggered necrosis. Western-blotting analysis revealed that triclosan transiently induced the activation of extracellular signal-regulated kinases 1/2 (ERK1/2), c-Jun N-terminal kinases (JNK), and p38 MAP kinase (p38). Pre-treatment with the MEK1/2 inhibitor PD184352 blocked triclosan-mediated the phosphorylation of ERK1/2 and substantially suppressed triclosan-stimulated cell proliferation, whereas the JNK inhibitor SP600125 or p38 inhibitor SB203580 had little or no effect on triclosan-stimulated cell proliferation. These data suggest that triclosan stimulated mouse epidermal cell proliferation in an ERK1/2-dependent manner and raises concerns about potential dermal carcinogenicity of triclosan.

PS 258 Metformin Blocks Lipogenesis in Pancreatic Cancer Cells by Downregulating Specificity Protein Transcription Factors

V. Nair[1] and S. H. Safe[1, 2]. [1]*VTPP, Texas A&M University, College Station, TX and* [2]*IBT, TAMUHSC, Houston, TX.*

There are increasing epidemiological and experimental studies supporting the activity of metformin, the most commonly used antidiabetic drug, as an antitumor agent. However the mechanisms associated with the anti-neoplastic activity of metformin remain unclear. De novo lipogenesis is considered as one of the hallmarks of cancer and fatty acid synthase (FAS), which plays a major role in lipogenesis is a negative prognostic factor for patient survival in pancreatic cancer. A key transcriptional regulator of FAS is SREBP (Sterol Regulatory Binding Protein) which is one of the downstream effectors of mTOR signaling. Treatment of Panc28 and L3.6pL pancreatic cells with 5-15 mM metformin decreased phospho- mTOR (p-mTOR) but not mTOR protein and this was accompanied by decreased expression of SREBP and FAS. Previous reports have linked IGFR to activation of mTOR in pancreatic cancer cells and knockdown of IGFR by RNA interference decreased mTOR signaling; moreover, metformin also decreased IGFR expression suggesting the mTOR inhibition by metformin is due to IGFR downregulation. Previous reports suggest that IGFR expression is regulated by specificity protein (Sp) transcription factors (TFs) and we have shown that metformin decreases expression of Sp1, Sp3 and Sp4 transcription factors in pancreatic cancer cells. The role of Sp transcription factor in regulating IGFR and mTOR was further investigated by knockdown of Sp1 (iSp1), Sp3 (iSp3), Sp4 (iSp4) or their combination (iSp1/3/4) by RNAi and this resulted in decreased expression of IGFR and inhibited mTOR signaling and its downstream effectors in pancreatic cancer cell lines. These data indicate that metformin blocks lipogenesis in pancreatic cancer cells through downregulation of Sp transcription factors and Sp regulated IGFR, resulting in inhibition of mTOR signaling.

PS 259 EGCG Elicits Stage-Specific Sensitivity and Affects Hsp90 in a Novel Human Prostate Cancer Progression Model

M. A. Moses[1], D. P. Rotella[2], W. A. Ricke[3] and T. A. Gasiewicz[1]. [1]*Environmental Medicine, University of Rochester, Rochester, NY,* [2]*Chemistry, Montclair State University, Montclair, NJ and* [3]*Urology, University of Wisconsin-Madison, Madison, WI.*

Epigallocatechin gallate (EGCG), a major tea catechin, has been shown to have anti-cancer effects, however, the mechanism of action is less understood. We made the novel discovery that EGCG is a heat shock protein 90 (hsp90) inhibitor. Utilizing non-tumorigenic (NT), tumorigenic, and metastatic prostate cancer (PRCA) cells from a human PRCA progression model, we tested the hypothesis that malignant cells are more sensitive to EGCG in a stage-specific manner and that sensitivity is related to hsp90 inhibition. Treatment of cells with EGCG (25-50μM) in vitro decreased the viability and proliferation, and induced apoptosis selectively in PRCA cells compared to NT cells. Moreover, when tumorigenic or metastatic cells were grown in vivo, mice supplemented with 0.06% EGCG in drinking water had significantly smaller tumors than those of the untreated group. To elucidate the mechanism of EGCG sensitivity, we performed affinity chromatography with EGCG-Sepharose. Binding assays revealed that hsp90 from metastatic cells had a higher affinity for EGCG than NT cells. Furthermore, EGCG disrupted hsp90 complex formation, as analyzed by NativePAGE, leading to an accumulation of dimeric hsp90, and promoted the degradation of hsp90-client proteins such as HER2, Akt, and Raf1 in metastatic cells at concentrations that affected viability. These data suggest that EGCG may be an efficacious small molecule for the treatment of PRCA because it selectively targets PRCA cells and inhibits a molecular chaperone involved in many pro-cancer signaling cascades. However, EGCG also has low bioavailability, which may limit its therapeutic efficacy. Using an hsp90-dependent luciferase-refolding assay, several EGCG analogs were found to be stronger inhibitors of luciferase refolding relative to EGCG. Use of these analogs may lead to enhanced bioavailability/stability and more potent anti-cancer activity. Funded by NIH Grants AT006366 & ES01247.

PS 260 Modulation of Human Malignant Melanoma Cell Line Proliferation by PPARβ/δ and PPARγ

M. G. Borland[1, 2], E. Ola[1], A. M. Pritzlaff[1], P. P. Albrecht[2], T. S. Lahoti[2], F. Gonzalez[3] and J. M. Peters[2]. [1]*Chemistry & Biochemistry, Bloomsburg Univesity of PA, Bloomsburg, PA,* [2]*Veterinary and Biomedical Sciences, Penn State University, University Park, PA and* [3]*Laboratory of Metabolism, NCI, Bethesda, MD.*

The incidence of melanoma continues to rise at an alarming rate, and the five-year survival for malignant melanoma remains near 10%. Thus, there remains a need for new melanoma therapeutic approaches to be investigated, including the potential targeting of the peroxisome proliferator-activated receptor (PPAR) class of nuclear hormone receptors. Of the three PPAR isoforms (PPARα, PPARβ/δ, and PPARγ), both PPARβ/δ and PPARγ are known to modulate cell proliferation in non-melanoma skin tumorigenesis models. To investigate the functional role of PPARβ/δ and PPARγ in melanoma with greater detail, the Migr1 retroviral system was used to generate stable PPAR over-expression in the UACC903 human malignant melanoma cell line. Elevated expression of PPARβ/δ and PPARγ in the respective stable cell lines caused enhanced expression of known a PPAR target gene following ligand activation of either PPARβ/δ or PPARγ. Over-expression of either PPARβ/δ or PPARγ decreased the percentage of G1 and S phase cells and increased the percentage of cells in G2/M based on flow cytometric analysis. While ligand activation of PPARγ augmented these cell cycle changes, PPARβ/δ ligand

administration did not further modulate the observed receptor-dependent effects. Ligand activation of PPARβ/δ or PPARγ also reduced cell growth in stable cell lines over-expressing these receptors. An analysis of clonal expansion also revealed that elevated expression of PPARβ/δ reduced plating efficiency; furthermore, ligand activation of either PPARβ/δ or PPARγ reduced the surviving fraction in a dose-dependent manner. Collectively, these observations demonstrate that both PPARβ/δ and PPARγ decrease human malignant melanoma cell line proliferation. These results also demonstrate the utility of the Migr1 model to dissect the functions of PPARβ/δ and PPARγ, including the targeting of these receptors for potential malignant melanoma therapies.

PS 261 The Trichloroethylene-Associated P81S VHL Hotspot Mutation Alters Tumor Microenvironment: Metabolic Reprogramming, DNA Damage Response, and Radiation Resistance

M. C. DeSimone[1], W. Rathmell[2] and D. W. Threadgill[1, 2]. [1]*Biological Sciences, NCSU, Raleigh, NC and* [2]*Lineberger Comprehensive Cancer Center, UNC, Chapel Hill, NC.*

Occupational exposure to trichloroethylene (TCE), a solvent found in contaminated groundwater, has been associated with the P81S hotspot mutation in the von Hippel-Lindau (*VHL*) tumor suppressor gene in cases of clear cell renal cell carcinoma. There remain considerable mechanistic gaps in the kidney cancer risk assessment of TCE due to lack of appropriate model systems. We purport that specific mutations in *VHL* that uniquely alter its protein function may provide a selective growth advantage to somatic cells harboring these mutants, leading to clonal expansion. For this study, we developed a stem cell model system to study the unique biology of the P81S mutation. VHL deficient (*Vhl -/-*) mouse embryonic stem cells were generated that stably express either wild-type, P81S, or R167Q human VHL protein and were examined *in vitro* under hypoxic conditions for hypoxia-inducible transcription factor family stabilization and E3-ubiquitin ligase complex interactions. To examine the microenvironmental stress response, cell lines grown as teratomas were examined for size, proliferation, and apoptosis, were subjected to whole genome microarray analysis, and were exposed to 5Gy ionizing radiation to quantify apoptotic response. The P81S mutation disrupts VHL-E3 complex formation *in vitro*, and *in vivo*, teratomas gained a growth advantage resulting from apoptotic resistance, not enhanced proliferation. Transcriptomic analysis suggests that a key component of this survival advantage is metabolic reprogramming and disabling of the DNA damage response, conferring radiation resistance. This work demonstrates a novel interaction between VHL and the ATM-mediated DNA damage response network, and highlights the potential of the TCE-associated P81S *VHL* mutation to initiate an adaptive response required for selective tumor growth through effects on metabolic diversification, apoptosis suppression, and alteration of the DNA damage response.

PS 262 Hydrolysis of DNA-Protein Crosslinks Forms Formaldehyde-DNA Adducts

Y. Lai and J. A. Swenberg. *Department of Environmental Sciences and Engineering, University of North Carolina at Chapel Hill, Chapel Hill, NC.*

Formaldehyde causes squamous cell carcinomas in the nasal passages of rats and has been classified as a known human carcinogen by IARC. The primary genotoxic effects of formaldehyde include the formation of DNA-protein crosslinks (DPCs) and hydroxymethyl DNA adducts. Formaldehyde induced DPCs showed a rapid loss in lymphocyte cultures and no accumulation was observed in rats after repeated exposures. Previous research indicated that formaldehyde induced DPCs were lost through spontaneous hydrolysis rather than DNA repair. In this study, we investigated hydrolytic degradation of formaldehyde induced DPCs with deoxyguanosine linked to cysteine (dG-CH2-Cys), glutathione (dG-CH2-GSH) and N-terminal acetylated 12-mer human O6-alkylguanine DNA methyltransferase peptide (dG-CH2-AGT). Under physiological pH and temperature conditions, the determined half-life for dG-CH2-Cys and dG-CH2-GSH was 11.6 min (R2=0.9807) and 87.8 min (R2=0.9935), respectively. The degradation kinetics of dG-CH2-AGT consisted of an initial rapid degradation rate with half-life of 7.4 min followed by a much slower degradation rate with half-life of 90.7 min (R2= 0.9987). During the hydrolysis of DPCs, dG could be directly formed if bond cleavage occurs between dG and methylene (N2-dG-CH2 bond). However, no dG was detected in the first 3 min, 20 min and 10 min incubation for dG-CH2-Cys, dG-CH2-GSH and dG-CH2-AGT, respectively. On the other hand, N2-hydroxymethyl-dG (HO-CH2-dG) was readily formed and increased rapidly after initiating reaction for all tested crosslinks, suggesting cleavage of the CH2-Cys bond, but not the N2-dG-CH2 bond. HO-CH2-dG can be degraded to dG following incubation for longer time periods. Thus, the mechanism of DPCs hydrolysis involved the production of HO-CH2-dG before forming end product of dG. These results suggest that DPCs are likely to be an important source of formaldehyde DNA monoadducts and that monoadducts represent a biomarker of both direct attack of DNA and a breakdown product of DPC.

PS 263 Differential Gene Expression Analysis of TPA/UVC Co-Treated TK6 Cells Reveals a Novel Gene Signature Important in Carcinogenesis by Combining DNA Damage and Tumor Promoting Pathways

K. P. Glover[1], Z. Chen[2], L. K. Markell[1] and X. Han[1]. [1]*Haskell, DuPont, Newark, DE and* [2]*I&CT, DuPont, Wilmington, DE.*

Environmental and chemical carcinogens have been shown to act as both initiators and promoters of cancer. In the present study, we attempted to reveal critical pathways in chemical carcinogenesis that were triggered from converging processes of initiation (via UVC irradiation) and promotion (via 12-O-tetradecanolyphorbol acetate (TPA) treatment) in cultured TK6 cells. We have previously shown that TPA-pretreated TK6 cells undergo a synergistic increase in apoptosis and delayed γH2AX clearance following DNA damage induced by UVC-irradiation. To elucidate the cellular pathways responsible for the synergistic interaction between TPA-pretreatment and UVC-irradiation we analyzed the global transcriptional profile with RNA-sequencing. Differential expression analysis revealed significantly deregulated genes associated with the combination of TPA-pretreatment and UVC-irradiation (TPA+/UVC+) compared to either stress alone (TPA+/UVC- or TPA-/UVC+). To focus our analysis on genes specific to the combined exposure, we filter the gene list for those that occurred in a TPA-dependent dose responsive trend and significantly up- or down- regulated in the TPA+/UVC+ cells compared to TPA+/UVC- and TPA-/UVC+ ($p<0.05$, FC 2). We found a set of 84 genes (46 up, 38 down) specific to the combined exposure that are significantly deregulated and likely responsible for the increased sensitivity to UVC-induced DNA damage. Major up-regulated genes include TNFSF4, GDF15, ATF3, SERPINE1, IL29, LIF, FOS, IFNG, SNAI1, NOXA and GADD34a. Major down-regulated genes include POU2AF1, PAX5, GBP1, SPIB, ASK1, GBP6, LYN, TRAF5 and CLIC4. Overall, most genes were connected to pathways important in inflammatory driven carcinogenesis including TNFα, Interferon-γ, TGFβ, AP1, and p53. Here we show that TPA-pretreatment causes an increased sensitivity to UVC-induced DNA damage which is accompanied by an exacerbation of immune/inflammatory pathways that may be important for tumor promotion.

PS 264 The Aryl Hydrocarbon Receptor Controls Breast Cancer Stem-Like Cell Development and Function

E. A. Stanford[2, 1], A. J. Parks[2], O. Novikov[2, 1] and D. H. Sherr[1]. [1]*Environmental Health, Boston University, Brookline, MA and* [2]*Molecular and Translational Medicine, Boston University School of Medicine, Boston, MA.*

In 1940, an American woman's risk of getting breast cancer was 1 in 14. Since then, the age-adjusted incidence of breast cancer has increased such that 1 in 8 women born this year will be diagnosed with breast cancer in her lifetime. Analyses of known risk factors such as diet, exercise, and hormone replacement therapy do not completely explain the increase in breast cancer incidences or the genesis of breast cancers not associated with inheritance of susceptibility genes. A meta-analysis of over 150 published studies on breast cancer and the environment implicates a number of environmental chemicals, including aryl hydrocarbon receptor (AhR) ligands, in breast cancer risk. Tumor invasion and metastasis following relapse is the cause of death in nearly all breast cancer patients. The cancer stem cell (CSC) theory hypothesizes that cancers and their metastases are driven, to a disproportionate extent, by breast cancer stem-like cells (BCSLCs). BCSLCs are defined by their activity and expression of aldehyde dehydrogenase (ALDH), expression of a set of genes associated with "stem-ness", ability to self-renew, expression of genes consistent with epithelial-to-mesenchymal transition (EMT), and resistance to chemotherapeutics. Recent studies have implicated the AhR, a transcription factor involved in tumorigenesis, in the development and/or function of stem cells, which share properties with CSCs. From these studies, we postulated that the AhR may play a role in the development or function of BCSLCs. Here, we present data demonstrating high levels of constitutively active AhR in BCSLC from aggressive human ER-, PR-, Her2- and inflammatory breast cancers. The results indicate that AhR hyper-activation with exogenous ligands increases and AHR inhibition with pharmacological or molecular agents decreases expression of BCSLC characteristics. Our findings further implicate environmental chemicals in breast cancer risk through increasing breast cancer progression and survival after chemotherapy.

PS 265 Vacuum Tower Distillation Temperature for Controlling Carcinogenicity of Residual Aromatic Extracts

M. H. Kung[1], K. Goyak[1], C. Sircar[2], K. Aldous[3] and J. J. Freeman[1]. *[1]ExxonMobil Biomedical Sciences, Inc., Annandale, NJ, [2]ExxonMobil Fuels, Lubricants & Specialties Marketing Company, Fairfax, VA and [3]ExxonMobil Research and Engineering, Fairfax, VA.*

Residual aromatic extracts (RAE) are petroleum streams derived as by-products during solvent extraction of vacuum tower bottoms (VTB) often used in tire extender oils and specialty petroleum products. Due to process conditions, RAEs may have high levels of polycyclic aromatic compounds (PACs), which are thought to drive carcinogenicity in animal bioassays. To maximize the use of these substances while protecting human health, a more efficient method for separating potentially harmful PACs during vacuum distillation was investigated. This work identifies a correlation between carcinogenicity and boiling point which can identify optimal conditions for vacuum distillation to minimize the toxicity of RAEs. Using the modified Ames assay, samples of VTB, raffinate, and RAE were obtained from five refineries to evaluate relationships between mutagenicity index (MI), PAC ring content and boiling point by GC distillation (GCD). As expected, a positive linear relationship between MI and PAC content occurred for 3-6 ring PAC (R2=0.68), regarded as the carcinogenic PACs. A negative correlation between MI and boiling point (5% vaporization by GCD, R2=0.72) indicated that lower boiling samples (<~470C) were more likely to be mutagenic. This inverse relationship was further demonstrated by distillation of select samples (MI=0.50+0.07 (n=5)) into low and high boiling range fractions. Mutagenicity and 3-6 ring PAC content were markedly higher in low boiling fractions (MI=2.36+0.55 vs.0.17+0.11, PAC=5.2+0.7 vs. 0.97+0.35%, respectively). These results support the hypothesis that PACs are key contributors to the mutagenic potential of petroleum substances that can be separated by boiling point. Because vacuum distillation can be continuously measured and manipulated at refineries, these findings provides a means to readily monitor and minimize the carcinogenic potential of RAEs in situ to ensure continued product safety.

PS 265a Quantification of Somatic Hotspot Oncogene Mutations in Normal Human Breast and Ductal Carcinoma

M. Banda, M. B. Myers, K. L. McKim, Y. Wang and B. L. Parsons. *National Center for Toxicological Research, Jefferson, AR.*

The COSMIC database indicates a number of hotspot oncogene mutations occur at lower frequency in breast tumors than in other tumor types (e.g., colon and lung). We hypothesized that greater sensitivity is required to detect somatic mutations in breast tumors, due to their clonal complexity. Therefore, the sensitive and quantitative Allele-specific Competitive Blocker PCR (ACB-PCR) method was used to quantify hotspot point mutations in KRAS, HRAS, BRAF, EGFR, and PIK3CA, in DNA isolated from normal human breast and ductal carcinoma (DC) samples (n=10). The following geometric mean mutant fraction (MF) measurements were obtained from normal breast: KRAS codon 12 GGT→GAT and GGT→GTT, 1.74 x 10-5 and 6.81 x 10-6, respectively; BRAF codon 600 GTG→GAG, 2.02 x 10-6; and HRAS codon 12 GGC→GAC, 2.12 x 10 5. Geometric mean MF measurements from DCs were: KRAS codon 12 GGT→GAT and GGT→GTT, 1.36 x 10-5 and 7.51 x 10-6, respectively; BRAF codon 600 GTG→GAG, 5.22 x 10-6; and HRAS codon 12 GGC→GAC, 3.35 x 10-4. This analysis showed that 80% of DCs carry HRAS codon 12 GGC→GAC mutation at a level greater than the upper 95% confidence interval of the HRAS MF present in normal breast. Importantly, no breast tumor had a HRAS codon 12 GGC→GAC MF ≥10-1 (i.e., that detectable by DNA sequencing). We previously demonstrated that significantly higher levels of KRAS mutation are present in colon and lung tumors relative to the cognate normal tissue; however, the frequency of KRAS codon 12 GGT→GAT and GGT→GTT MF in normal breast and in DCs were quite similar. Therefore, somatic mutations in HRAS may play a greater role in the development of breast cancers than those in KRAS. Also, this work demonstrates it is possible to empirically define "pathological" levels of specific tumor-associated oncomutations. Ongoing analyses of additional tumors of different breast cancer subtypes will provide a better understanding of the role of somatic mutations in breast cancer.

PS 265b Dysregulation of Cellular Iron Metabolism during Hepatocarcinogenesis Is Associated with Alterations in Iron Uptake/Export

I. Kindrat[1], T. Kobets[1], A. Erstenyuk[2], F. A. Beland[1] and I. Pogribny[1]. *[1]NCTR, Jefferson, AR and [2]Ivano Frankivsk National Medical University, Ivano Frankivsk, United Arab Emirates.*

Hepatocellular carcinoma (HCC) is one of the most prevalent life-threatening human cancers, with a rapidly increasing incidence worldwide. The pathogenesis of HCC is complex and consists of multiple interconnected molecular alterations. Current evidence indicates that altered iron metabolism plays an important role in the development and progression of HCC; however, there is a lack of conclusive information regarding the mechanisms of this dysregulation. In the present study, using in vitro and in vivo models of liver carcinogenesis, we investigated the underlying mechanisms of iron metabolism disturbances in the hepatocarcinogenic process. The results of our study demonstrate a prominent dysregulation of cellular iron homeostasis in rat and human HCC cell lines, characterized by a significant increase in the levels of transferrin receptor 1 (TRFC) mRNA and protein, a major protein controlling cellular iron uptake. In contrast, the level of ferroportin (FPN), the only known exporter of intracellular non-heme associated iron in mammalian cells, did not differ in the HCC cell lines compared to non-malignant liver cells. This resulted in a substantial increase in TRFC/FPN ratio, favoring an accumulation of iron in the HCC cells. This suggestion was supported further by a marked up-regulation of the main iron-storage proteins ferritin heavy chain (FTH) and ferritin light chain (FTL) in the HCC cells. Similar trends in TRFC and FPN ratios were found in preneoplastic livers of Sprague-Dawley rats that had been treated with the model genotoxic liver carcinogen 2-acetylaminofluorene for 24 weeks, and in livers of Fisher 344 rats subjected to a classic "resistant hepatocyte" model of liver carcinogenesis. These findings indicate that dysregulation of cellular iron metabolism during liver carcinogenesis is driven by an up-regulation of TRFC, which occurs at early stages of the hepatocarcinogenic process.

PS 265c Human Hepatocytes Support the Hypertrophic but Not the Hyperplastic Response to the Murine Nongenotoxic Hepatocarcinogen Sodium Phenobarbital in *In Vivo* Study Using Chimeric Mouse with Humanized Liver

Y. Okuda[1], T. Yamada[1], M. Kushida[1], H. Takeuchi[1], H. Nagahori[1], B. G. Lake[2], S. M. Cohen[3] and S. Kawamura[1]. *[1]Sumitomo Chemical Co., Ltd., Osaka, Japan, [2]Univ. of Surrey, Surrey, United Kingdom and [3]Univ. of Nebraska Medical Center, Omaha, NE.*

In a rodent tumor bioassay, high doses of sodium phenobarbital (NaPB), a constitutive androstane receptor (CAR) activator, produced hepatocellular tumors. Previous mode of action (MOA) studies have demonstrated that NaPB induces hepatic microsomal cytochrome P450 (CYP) 2B enzymes and hepatocyte replicative DNA synthesis in rodents, suggesting that the MOA for rodent liver tumor formation is a mitogenic activity via CAR activation. In this study the effects of NaPB on liver weight and histopathology, hepatic CYP2B activity, hepaocyte replicative DNA synthesis, and mRNA expressions of CYP2B/3A and selected genes related to cell proliferation, were examined after 1-week treatment with NaPB at 500, 1000, 1500, and 2500 ppm in males of CD-1 mice, Wistar Hannover (WH) rats, and humanized mice (chimeric mice with human hepatocytes). The treatment of humanized mice with 1000-1500 ppm NaPB resulted in plasma levels around 3-5 fold higher than those observed in human subjects given therapeutic dose of NaPB. NaPB produced dose-dependent increases in liver weight, CYP2B activity, and CYP2B/3A mRNA in CD-1 mice and WH rats and also produced effects on these parameters in humanized mice. While NaPB produced a dose-dependent increase in hepatocyte replicative DNA synthesis in CD-1 mice and WH rats, no increase in replicative DNA synthesis was observed in humanized mice. In addition, NaPB produced no increases in Ki-67, PCNA, GADD45β, and MDM2 mRNA expression in humanized mice but significantly increased those in CD-1 mice and/or WH rats. Thus, while NaPB could activate CAR/PXR, as demonstrated by increased CYP2B/3A mRNA levels, NaPB did not increase cell proliferation in human hepatocytes of humanized mice. As human hepatocytes are refractory to the mitogenic effects of NaPB, the data demonstrate that the MOA for NaPB-induced rodent liver tumor formation is not relevant for humans.

PS 265d Integrated microRNA, mRNA, and Protein Expression Profiling Reveals Dysregulated Expression of microRNAs and Their Targets in Rat Kidney Treated with a Carcinogenic Dose of Aristolochic Acid

T. Qin, Z. Li, M. Hackenberg, J. Yan, K. Wang, Y. Gao, L. Yu, L. Shi, Z. Su and T. Chen. *National Center for Toxicological Research, Jefferson, AR.*

Aristolochic Acid (AA), is classified as a group 1 carcinogen by the International Agency for Research on Cancer. MicroRNA (miRNA) alterations are involved in the initiation and progression of human cancer, but their roles in AA-induced carcinogenesis remain unknown. In order to search for miRNA regulation and identify their functional targets, we have employed a novel approach integrating miRNA, transcriptome and proteome profiling and a computational target predicting algorithm. We treated rats with 10 mg/kg AA and vehicle control for 12 weeks and eight kidney samples (4 for the treatment and 4 for the control) were used for examining miRNA and mRNA expression by deep sequencing, and protein expression by proteomics. AA treatment resulted in significant differential expression of miRNAs, mRNAs and proteins as measured by both principal component analysis (PCA) and hierarchical clustering analysis (HCA). Specially, 63 miRNAs (adjusted p value < 0.05 and fold change > 1.5), 6,794 mRNAs (adjusted p value < 0.05 and fold change > 2.0), and 800 proteins (fold change > 2.0) were significantly altered by AA treatment. To investigate the influence of miRNA on these processes, we combined proteomic and transcriptomic data into three groups containing responses indicating translational repression (163), translational activation (236), and transcriptional destabilization (460). Our predicted miRNA targets were further compared and validated from experimentally validated targets in miRTarBase (P = 4.96e-06). Cancer is identified as the top function by ingenuity pathway analysis (IPA) for identified 399 targets. Our findings suggest that dysregulated miRNAs and their targets are involved in kidney carcinogenesis in the AA-treated rats.

PS 265e The Role of Cancer Stem-Like Cells in Cr(VI)-Induced Malignant Cell Transformation and Tumorigenicity

J. Dai and Z. Zhang. *University of Kentucky, Lexington, KY.*

Hexavalent chromium (Cr(VI)) compounds are well-known human carcinogens. Epidemiological studies have shown that occupational and environmental exposure to Cr(VI) is associated with a high rate of lung cancer. Cancer is a disease driven by cancer stem cells (CSCs). In the present study, we hypothesize that stem-like cells (SCs) play a key role in the Cr(VI)-induced malignant cell transformation, contributing Cr(VI)-induced lung cancer. Our results show that chronically exposure to low dose of Cr(VI) up to six months caused the malignant transformation of human bronchial epithelial BEAS-2B cells. To examine the existence and nature of SCs in those Cr(VI)-transformed cells, SCs were isolated by collecting floating cells and were enriched by forming spheres under anchorage-independent growth in serum-free medium. The results show that cancer epithelial stem cell biomarkers such as Notch1 and ALDH were highly expressed in SCs as compared to normal BEAS-2B cells and Cr(VI)-transformed BEAS-2B cells. The results from hetero-transplanted animal study show that SCs were able to cause tumor growth in immune-deficient nude mice at 100 cells, while Cr(VI)-transformed cells failed to grow tumor, indicating potent self-renewal and essential for tumorigenicity of those SCs. Further investigation indicates that those CSCs exhibited apoptosis resistance and reduced capacity of generating reactive oxygen species (ROS), indicating of potent cell proliferation/growth and capacity against exotic oxidative stress. Notably, oxygen consumption rate (OCR) was significantly decreased in SCs compared to normal BEAS-2B cells or Cr(VI)-transformed cells, indicating a metabolic alteration in SCs associated with augmented tumorigenicity and potent survival characteristics. The decrease in OCR in SCs might be due to the loss of fructose-1,6-biophosphatase (FBP1) which is a rate-limiting enzyme in gluconeogenesis. In summary, the present study suggests that CSCs are critical in Cr(VI)-induced malignant cells transformation and tumorigenicity.

PS 266 Refining the Caco-2 Model to Evaluate the Impact of Intestinal Hydrolysis on Parabens Absorption in the Gut

X. Sun, Y. Zhao, J. Dong, H. J. Clewell and M. Yoon. *The Hamner Institutes for Health Sciences, RTP, NC.*

The oral bioavailability of environmental esters such as parabens can be greatly affected by intestinal hydrolysis, but little is known about this metabolic pathway largely due to lack of relevant experimental systems. The conventional Caco-2 model which overexpresses carboxylesterase-1 (CES-1) is not appropriate to this end, because the CES-2 isoform is predominantly expressed over CES-1 in human enterocytes. In this study, we stably expressed CES-2 in Caco-2 cells, while knocking down CES-1, to appropriately evaluate the impact of hydrolysis on the absorption of parabens. Western blot analysis showed that the expression of CES-2 in the Caco-2/CES-2 cells was comparable to that in human enterocytes. Studies on transport and metabolism of methyl- and buthylparabens were performed with the Caco-2/CES-2 cells. The results showed that parabens are rapidly hydrolyzed while they are being absorbed across the Caco-2 monolayer. When buthylparaben (10 μM) was applied to the apical side, all of the parent compound was converted to p-hydroxybenzoic acid (pHBA) within 30 min, most of which was found in the apical side indicating the location of hydrolysis being at or closer to the apical membrane and the efficient efflux of pHBA into the apical side (i.e., luminal side in the gut). Additional experiments with a general CES inhibitor, bis-para-nitrophenylphosphate, further supported these findings. An in vitro kinetic model was developed to describe the kinetic behaviors of parabens and pHBA in the Caco-2/CES-2 cells and extrapolate to humans in vivo. The refined Caco-2/CES-2 system, together with pharmacokinetic modeling can provide accurate estimates of oral bioavailability of parent parabens and their metabolites under different exposure conditions, which will contribute to reducing uncertainties in assessing safe human exposure to parabens and other environmental esters (supported by the ACC-LRI).

PS 267 Toxicological Effects of Antibody-Mediated TGF-beta Antagonism in Cynomolgus Monkeys

C. Horvath[1], C. Hendricks[1], P. Finn[2] and L. Andrews[1]. [1]*DSAR, Sanofi, Waltham, MA and* [2]*Genzyme Biologics, Genzyme, a Sanofi Company, Framingham, MA.*

Transforming growth factor beta (TGF-beta) is a multifunctional cytokine that has an important role in various processes, including cell proliferation and differentiation, angiogenesis, and wound healing. Overexpression of TGF-beta can lead to fibrosis and it has been proposed that pan-neutralization of TGF-beta by the antibody GC1008 may modify this pathologic process. The toxicological impact of chronic TGF-beta neutralization was evaluated in juvenile cynomolgus monkeys. Repeat dose toxicity studies (28 days, 3 months and 6 months) were conducted with GC1008 at dose levels ranging from 0.1 to 50 mg/kg (dosed every other week or every third day). In all studies, the toxicokinetics of GC1008 were highly variable, but adequate exposure was obtained to allow for interpretation of the toxicological findings. When dosed every third day, diminished systemic exposure was observed following 7 doses in a single animal; this animal tested positive for anti-drug antibodies. Across all studies, consistent findings related to treatment with GC1008 were observed. Clinical observations included bleeding, often associated with erupting teeth, and hematomas. Alterations in hematology parameters included dose dependent, reversible, decreases in red blood cell counts, hemoglobin, and hematocrit values. In the 3 and 6 month studies, epithelial cell hyperplasia was noted at varying locations. The epithelial hyperplasia observed in these studies may have been associated with exacerbation of pre-existing background lesions (i.e. periodontitis, rhinitis, cystitis). Overall, these studies have characterized the potential risks associated with chronic neutralization of TGF-beta and suggest that the majority of homeostatic roles of TGF-beta in these normal juvenile primates were not significantly disrupted by antibody-mediated antagonism of this biologically important growth factor.

PS 268 Safety Assessment of Flt3 Ligand: 28-Day Toxicity Studies in Rats and Monkeys

L. J. Thomas[1], E. M. Forsberg[1], L. E. Gergel[1], L. A. Vitale[2], B. J. Karalius[1], K. M. Borrelli[1], H. C. Marsh[1] and T. Keler[2]. [1]*Celldex Therapeutics, Needham, MA and* [2]*Celldex Therapeutics, Phillipsburg, NJ.*

Flt3 Ligand (also referred to as Flt3L, fms-like tyrosine kinase 3 ligand, or CDX-301) is a hematopoietic cytokine which stimulates the proliferation and differentiation of various blood cell progenitors. Nonclinical safety was assessed in two GLP-compliant toxicology studies where Flt3L was administered subcutaneously for 28 days to Cynomolgus monkeys and rats (5, 25, 200 and 1600 ug kg-1 d-1). For all animals, mortality, clinical signs, body temperature, body weights, and clinical pathology were recorded throughout the study. Detailed necropsies were performed in a subgroup of animals 48 hours after the last administration of CDX-301 and on the remaining animals after a 2-week recovery period. Selected tissues were collected for histopathology evaluation and bone marrow smears were evaluated. Blood samples were collected periodically for the determination of pharmacokinetics, anti-drug antibodies and, in the monkeys, for immune cell analysis. No gender differences were observed in the pharmacokinetics of Flt3L. Many animals developed anti-Flt3L antibodies, which were neutralizing in some rats. An increase in dendritic cells and monocytes, but not regulatory T cells, was seen in the monkeys following Flt3L exposure. Flt3L was well tolerated in both monkeys and rats. The most significant test article-related findings were bone marrow hyperplasia (considered a pharmacological effect of Flt3L), an increased severity of chronic inflammation at the injection site, increased severity of mononuclear cell infiltration

in various tissues, and thymic atrophy. Adverse findings were observed only in the 200 and 1600 ug kg-1 d-1 dose groups in either species. Based on these results, 25 ug kg-1 d-1 was determined to be a no observed adverse effect level (NOAEL) for both species.

PS 269 Immune-Mediated Hepatotoxicity in Monkeys following Administration of a Highly Conserved Biotherapeutic Protein

C. de Zafra[1], A. Ashkenazi[2], W. Darbonne[3], M. Cheu[4], B. Mounho-Zamora[5], K. Totpal[2], S. A. Ortega[1], B. Lum[6], B. Kabakoff[7], H. Flores[7], J. L. Bussiere[8] and N. Dybdal[1]. *[1]Safety Assessment, Genentech, Inc, So SF, CA, [2]Molecular Oncology, Genentech, Inc, So SF, CA, [3]Oncology Biomarker Development, Genentech, Inc, So SF, CA, [4]BioSample Analysis & Technology, Genentech, Inc, So SF, CA, [5]ToxStrategies, Inc, Bend, OR, [6]Clinical Pharmacology, Genentech, Inc, So SF, CA, [7]Pharmaceutical Development, Genentech, Inc, So SF, CA and [8]Amgen, Inc, Thousand Oaks, CA.*

Drug-induced liver injury (DILI) is a frequent adverse event leading to the attrition of drug candidates during development and to the withdrawal of approved therapeutics from the market. There are several causes of DILI, including immune-mediated. We report an atypical, but clearly immune-mediated drug-related hepatotoxicity in monkeys associated with a recombinant human protein (rhApo2L/TRAIL; dulanermin) formerly in development for the treatment of cancer. The cynomolgus monkey was chosen as the pharmacologically relevant species for the safety assessment of rhApo2L/TRAIL because the sequence identity between the human and cynomolgus monkey proteins was approximately 98%; additionally, rhApo2L/TRAIL bound to human and monkey cognate receptors with comparable affinities. During the course of the toxicology program, hepatotoxicity was observed in repeat-dose monkey toxicology studies. There was a strong correlation between hepatotoxicity and the presence of anti-drug antibodies (ADAs). The human and monkey proteins differ only by 4 amino acids, and the X-ray crystal structure of the human protein indicated that 3 of the 4 distinct side-chains were surface-exposed. We hypothesized that these 3 amino acids could serve as epitopes for the development of cross-species ADAs, resulting in ADA-mediated hepatotoxicity in monkeys. In vitro and in vivo investigative toxicity studies supported the ADA-mediated hepatotoxicity hypothesis and demonstrated that the equivalent autologous monkey protein was well-tolerated. The thorough characterization of the ADA-mediated toxicity in monkeys enabled the successful transition of rhApo2L/TRAIL into human clinical trials.

PS 270 Comparison of Three Methods for the Evaluation of Cytokine Storm Risk in Early- and Clinical-Stage Biopharmaceutical Development

G. dos Santos and E. Clarke. *ReachBio LLC, Seattle, WA.*

Cytokine Release Syndrome (CRS) and Cytokine Storms (CS) are common and potentially dangerous side effects of anti-T cell antibodies and other immunomodulatory therapies. Therapy-induced CRS occurs quickly following infusion and results in the activation of T cells and the release of a wide range inflammatory cytokines, including IL2, IL4, IL6, IL8, IL17, TNFα and/or IFNγ.
We compared three methods to identify a robust assay that allows for the assessment of potential CRS and CS risk. In Method 1 (Romer, 2011), human PBMCs were pre-incubated for 48 hrs at 1 x 10^7 cells per mL, followed by culture on tissue-culture plastic in the presence of test (anti-CD3 clone OKT3 or anti-CD28 superagonist clone ANC28.1) or control (humanized anti-CD20 or humanized anti-TNFα) antibodies. In Method 2 (Findlay, 2011), human PBMCs were cultured on a HUVEC monolayer in the presence of test or control antibodies. In Method 3, a combination of the first two, human PBMCs were pre-incubated at 1 x 10^7 cells per mL, followed by culture at 1 x 10^6 cells per mL on a HUVEC monolayer in the presence of test or control antibodies. In all studies, supernatants were harvested after 24 hours and evaluated for TNFα and/or IFNγ by ELISA. Using Method 1, no measureable IFNγ production in the presence of any concentration of anti-CD3 or anti-CD28 was detected. Method 2 resulted in the production of ng per mL quantities of IFNγ in the presence of at least 100 ng/mL anti-CD3, but not with anti-CD28 up to 10 μg/mL. Method 3 resulted in the production of ng per mL quantities of IFNγ and high-pg/mL quantities of TNFα when > 1 ng/mL anti-CD3 or >1 μg/mL anti-CD28 was present.
Method 2 appears to be the most suitable protocol to assess new antibodies and biologics for stimulation of inflammatory cytokine release and therefore as a potential model for CRS and CS induction. It could be extended to compare cytokine profiles with either human or non-human primate PBMCs and may be amenable to further refinement through lymphocyte subset analysis by flow cytometry.

PS 271 Aerosol and Ocular Toxicity of AERAS-402 in Nonhuman Primates

C. S. Godin[1], D. A. Hokey[2], R. Wachholder[2], P. Darrah[3], D. Bolton[4], M. Douoguih[5], R. Seder[3], M. Roederer[3] and D. Sizemore[6]. *[1]Smithers Avanza, Gaithersburg, MD, [2]Aeras, Rockville, MD, [3]Vaccine Research Center, NIAID, Bethesda, MD, [4]US Military HIV Research Program, Silver Spring, MD, [5]Crucell Holland BV, Leiden, Netherlands and [6]Ke`aki Technologies, Frederick, MD.*

AERAS-402 is a novel tuberculosis vaccine comprised of a recombinant, replication-deficient adenovirus, serotype 35 (Ad35), expressing a fusion protein of three mycobacterial antigens. This study assessed the toxicity of aerosol vaccination with AERAS-402 following three doses of 10^{11} viral particles (vp) to Rhesus monkeys and evaluated toxicity following a single ocular topical administration. Twelve monkeys received test article via aerosol inhalation on Study Day (SD) 1, 8, and 15, and subjected to a full gross necropsy on SD 18 or 43. Two monkeys were administered test article via ocular topical application on SD 1, and subjected to a full gross necropsy on SD 43. Four monkeys were administered control article via aerosol inhalation and ocular topical administration on SD 1, 8, and 15, and subjected to a full gross necropsy on SD 18 or 43. Test article-related organ weight alterations on SD 18 were limited to apparent increased absolute and relative lung weights that correlated with microscopic findings in the lung, mediastinal lymph nodes, bronchus-associated lymphatic tissue, and the naso-oropharynx. All effects were expected with vaccination via the aerosol route, considered non-adverse, and completely resolved by SD 43. There were no test article-related organ weight or microscopic pathology findings following ocular delivery. All animals receiving aerosolized vaccine generated neutralizing antibodies to Ad35 and elicited strong, multifunctional CD4+ and CD8+ T cells by SD 43 in the lungs (obtained from BAL fluid). In addition, low-level, peripheral blood T cell responses were shown in 9/12 vaccinated animals on SD 18 which diminished by SD 43. Based on these findings the no-observed-adverse-effect level (NOAEL) is at least 10^{11} vp when administered via aerosol inhalation or ocular topical application.

PS 272 Evaluation of Paracetamol Toxicity in the Cynomolgus Monkey

H. Yu[1], N. C. Barrass[1, 2], S. Gales[1, 2], E. Lenz[2], D. Weston[2], I. Wilson[2], T. Parry[2], H. Powell[2], D. Thurman[1, 3], J. Qiao[1], Q. Qin[1] and J. Ren[1]. *[1]Center for Drug Safety and Evaluation, Shanghai Institute of Materia Medica, Shanghai, China, [2]AstraZeneca Safety Assessment, Alderley Park, United Kingdom and [3]AstraZeneca R&D, Boston, MA.*

Paracetamol (Acetominophen, APAP) was administered orally in a rising dose protocol to 2 male and 2 female Cynomolgus monkeys to determine the Maximum Tolerated dose (MTD) for subsequent toxicology investigations. In the subsequent repeat dose study involving 6 monkeys, no dose-limiting toxicity was seen at up to 900 mg/kg/day APAP for 14 days. Toxicokinetic analysis showed that plasma exposure rose, albeit less than proportionally, with increasing dose. There were some fluctuations in clinical chemistry and haematology parameters, but these were not dose-related, and there were no compound-related findings observed microscopically. Both monkeys at 900 mg/kg/day had a 5 cm, gas filled segment in their large intestine that was considered compound-related. Metabolite profiling of the urine showed parent and glucuronidated APAP, but the cysteinyl conjugate which would be anticipated if the monkey has similar metabolism to rats and man was notably absent. This opens the possibility that metabolism in the cynomolgus monkey differs from that in the other species, and shows that the cynomolgus monkey is a poor model for investigating paracetamol-mediated toxicity in humans.

PS 273 Development of a Novel Model of Pseudophakia in Nonhuman Primates to Assess Ocular Particle Movement Risk following Intravitreal Administration of Suspension Formulations

E. A. Thackaberry[1], V. Bantseev[1], C. Schuetz[1], F. Zhong[1], E. Budzynski[2], M. C. Struck[3], C. Trost[2], C. Farman[1] and E. Bentley[4]. *[1]Safety Assessment, Genentech, Inc., South San Francisco, CA, [2]Covance Laboratories, Inc., Madison, WI, [3]Department of Ophthalmology and Vision Sciences, University of Wisconsin-Madison, Madison, WI and [4]School of Veterinary Medicine, University of Wisconsin-Madison, Madison, WI.*

The development of suspensions for intravitreal (ITV) injection carries a risk for particle movement within the eye, leading to visual disturbances or blockage of Schlem's canal and increasing intraocular pressure (IOP). The risk of such particle movement may be increased in patients who have undergone cataract surgery, specifically patients with artificial intraocular lenses (IOLs), termed pseudophakic patients, and pseudophakic patients who have undergone posterior capsulotomies.

To directly evaluate particle movement in a nonclinical setting, a pseudophakic non-human primate (NHP) monkey model was created to mimic clinical procedures for surgical intervention for cataracts. This model was then validated using Triesence®, an approved ITV suspension with a history of successful use in pseudophakic patients. The lenses of the right eye of 11 cynomolgus monkeys were removed by aspiration and replaced with FDA-approved acrylate/methacrylate IOLs in the capsular bag. 5/11 animals then underwent a posterior mechanical capsulotomy in the same eye. Following 4-6 weeks of post-surgical recovery, animals were dosed bilaterally with ITV Triesence®. Following ITV Triesence® dosing, no significant particle movement was observed in the control (non-surgery) eyes or the pseudophakic eyes. A small amount of test article moved into the anterior chamber of 2/5 pseudophakic + capsulotomy eyes only. Movement of Triesence® did not result in increased IOP or any other clinical complications. These results are in line with the clinical performance of Triesence® in these patient populations, and suggest that this pseudophakic NHP model may be appropriate for the assessment of particle movement with novel ITV suspensions.

PS 274 Polysomnography Using Video Electroencephalogram, Electro-Oculogram, and Electromyogram Monitored Continuously by Telemetry in Cynomolgus Monkeys

R. Mikaelian[1], S. Authier[1, 2], M. Pouliot[1], E. Troncy[2], R. Forster[1] and D. Paquette[1]. *[1]CiToxLAB North America, Laval, QC, Canada and [2]Faculty of Veterinary Medicine, University of Montreal, St-Hyacinthe, QC, Canada.*

Medication-induced sleep disturbances are a major concern in drug development as a multitude of prescription drugs cause abnormalities at polysomnography. Rodent sleep architecture (nocturnal) differs from larger mammals (diurnal) which present higher translational value. Polysomnography is used in clinical diagnostic but is also applicable to cynomolgus monkeys when using telemetry with continuous electroencephalogram (EEG), electro-oculogram (EOG) and electromyogram (EMG) monitoring with video. Sleep stages in cynomolgus monkeys include wake, N1 (somnolence), N2 (sleep characterized by the presence of sleep spindles and K complexes), N3 (deep sleep with slow waves) and rapid eye movements (REM) and are quantified with automated or manual scoring. Optimal cynomolgus data filters included EOG low pass <25 Hz, EEG band pass 0.7-50Hz and EMG high pass >5Hz. As observed in humans, cynomolgus monkeys present a progressive increased in REM sleep duration with a parallel progressive decrease in N3 sleep during the night. REM sleep was characterized by muscle atonia, high frequency (mostly theta) low amplitude EEG in all animals and EOG activity in most but not all epochs. Total sleep time was 70.3±2.2% of the 12 hour dark cycle. Sleep stages N1, N2, N3 and REM were typically observed in sequence and represented 1.1±0.3%, 65.2±5.3%, 16.0±5.6% and 17.7±2.4% of total sleep time, respectively. Amphetamine (1 mg/kg, PO) significantly reduced total sleep time and all stages. Spectral analysis revealed a significant increase in higher frequency bands after amphetamine. As expected for benzodiazepine, Diazepam (2 mg/kg, PO) significantly reduced N3 sleep compared to control (-340%) but with no effect on total sleep time. Video- EEG, EOG and EMG by telemetry is a useful non-clinical model to investigate drug induced sleep disturbances.

PS 275 Video-Electroencephalography in Conscious Rats, Dogs, and Nonhuman Primates Using Telemetry and Computer Analysis: The Gold Standard to Assess Seizure Liability

R. Kubaszky[1], D. Paquette[1], R. Forster[1], M. Pouliot[1], E. Troncy[2] and S. Authier[1, 2]. *[1]CiToxLAB, Laval, QC, Canada and [2]Faculty of Veterinary Medicine, University of Montreal, St-Hycinthe, QC, Canada.*

EEG investigations are required to characterize drug induced adverse neurological effects. Seizure liability studies generally aim to: 1) confirm drug-induced seizures are self-limiting, 2) determine plasma level at seizure onset 3) identify prodromal clinical signs which can be monitored in clinical trials 4) confirm that conventional drugs (e.g. diazepam 6 mg/kg, IP for rats and 1 mg/kg, IV for large animals) can treat drug-induced seizure and 5) confirm the NOAEL by absence of paroxysmal activity at lower dose level of the test article. Cynomolgus monkeys, Beagle dogs and Sprague-Dawley rats were instrumented with telemetry implants with EEG electrode placement based on the 10-20 system combined with EMG. After 24 h of continuous video-EEG monitoring, animals received an IV infusion of pentylenetetrazole (PTZ) until convulsions followed by diazepam. A seizure detection protocol with a dynamic spike train threshold was used for the EEG monitoring period (total of 44 h). Spectral analysis quantified absolute and relative amplitudes of EEG frequency bands (delta, theta, alpha, sigma, beta and individual frequencies). The PTZ dose required to induce convulsion was 31.2, 35.6, 48.3 mg/kg, in Sprague-Dawley rats, Beagle dogs and cynomolgus monkeys, respectively. Most common prodromal signs included tremors, salivation, emesis, ataxia and nystagmus. Spike trains were detected by computerized analysis in all animals. Seizure peak frequency was 3-6 Hz. Spectral analysis revealed an increase power from higher frequency bands (i.e. theta, alpha, sigma and beta) starting on average at 6 min 9 sec prior to ictus. EEG-video was useful to characterize neurological adverse effects and identify prodromal signs. Computerized EEG analysis was a valuable tool to investigate proconvulsant risks.

PS 276 Comparative Nonclinical Assessments of the Potential Biosimilar PF-06410293 and Adalimumab

M. Derzi[1], S. L. Ripp[2], C. Ng[3], A. M. Shoieb[2], G. Finch[2], L. G. Lorello[2] and M. W. Leach[3]. *[1]Pfizer Inc, Cambridge, MA, [2]Pfizer Inc, Groton, CT and [3]Pfizer Inc, Andover, MA.*

Rationale: Adalimumab (Humira®) is a recombinant fully human immunoglobulin (IgG1) monoclonal antibody targeting tumor necrosis factor-α (TNFα). Adalimumab is approved for the treatment of rheumatoid arthritis, juvenile idiopathic arthritis, psoriatic arthritis, ankylosing spondylitis, Crohn's disease, ulcerative colitis and plaque psoriasis. To support clinical development, nonclinical studies evaluated the structural, functional and in vivo toxicologic, toxicokinetic (TK) and pharmacodynamic (PD) similarity of PF-06410293 and adalimumab.
Methods: Structural similarity was determined by peptide mapping. Cynomolgus monkeys were administered PF-06410293 or adalimumab-EU by subcutaneous (SC) injection at weekly dose levels 0 or 157 mg/kg (total 5 doses) for 1-month. Assessments included mortality, clinical parameters, clinical pathology, TK, anti-drug antibodies (ADA), histopathology and pharmacodynamics.
Results: Peptide mapping showed similar chromatographic profiles and consistent measured masses for PF 06410293, the US-licensed (adalimumab-US) and EU-approved (adalimumab-EU) products. The results of comparative functional and binding assessments (TNF-induced inhibition of apoptosis in U937 cells and Fc-based functionality) were also similar. PF-06410293 and adalimumab-EU were well tolerated in cynomolgus monkeys. PF-06410293 and adalimumab-EU-related effects were limited to microscopic observations of decreased cellularity of lymphoid follicles and germinal centers in the spleen. There were no biologically or toxicologically relevant differences in the incidence or severity of these microscopic findings between PF-06410293 and adalimumab-EU groups. Systemic exposure appeared similar, with systemic exposure (Cmax and AUC168) ratios of PF 06410293 relative to adalimumab-EU ranging from 1.0 to 1.2. These studies supported entry of PF 06410293 into clinical development.

PS 277 A Repeat IV Dose Toxicity Study of Gemcitabine Formulations in Male and Female CD-1 Mice

J. Risvanis[1], C. S. Godin[2], A. Knill[1], B. Currow[1] and E. Koo[1]. *[1]Hospira Inc., Lake Forest, IL and [2]Smithers Avanza, Gaithersburg, MD.*

This study compared the toxicity of Hospira's Gemcitabine Injection (Test Article) with Gemzar® (Reference Article), when administered to CD-1 mice. Test and Reference Articles were composed of the same cytotoxic active ingredient but Test Article contained additional impurities formed after accelerated degradation.
One hundred and sixty mice were assigned to one of eight groups (10 mice/sex/group) and dosed with Vehicle, Test or Reference Article at doses of 0, 100, 500, or 600 mg/kg. Mice were dosed by IV administration via the lateral tail vein on Study Day (SD) 1 and 8. Surviving animals were euthanized on SD 15. Mortality, clinical and post dose observations, body weights, food consumption, ophthalmologic examinations, clinical pathology, gross pathology, organ weights, and histopathology were assessed.
There were no consistent premonitory adverse clinical signs, and no visible lesions at necropsy. There were no adverse effects of the Test or Reference Articles on clinical, cage side, or post dose observations, body weight, food consumption or gross pathology. Treatment with Test and Reference Articles both led to reduced red blood cell count, hemoglobin, hematocrit and absolute lymphocyte counts, increased absolute reticulocyte counts and red cell distribution width, increased absolute and relative spleen weights, decreased absolute and relative thymus and testis weights, increased splenic hematopoiesis and testicular germ cell depletion at doses ≥100 mg/kg. Lymphocytolysis and/or lymphoid depletion of spleen, thymus and lymph nodes were also observed and thymic atrophy was noted at 600 mg/kg. Most observations were of no toxicological significance; however testicular germ cell depletion is adverse due to potential effects on reproductive function. Lymphoid organs and testes are the primary target organs for both articles.
In conclusion, the toxicological profile of Hospira's Gemcitabine Injection containing additional impurities was no different to that of the Reference Article, Gemzar®.

PS 278 Placental Transfer of Fc-Containing Biopharmaceuticals across Species, an Industry Survey Analysis

C. J. Bowman[1], W. Breslin[2], A. Connor[3], P. L. Martin[4], G. J. Moffat[5], L. Sivaraman[6], M. Tornesi[7] and S. Chivers[8]. *[1], Pfizer Inc, Groton, CT, [2]Lilly Research Laboratories, Indianapolis, IN, [3]Nonclinical Consulting Services, San Francisco, CA, [4]Janssen Research and Development, Spring House, PA, [5]Amgen Inc., Seattle, WA, [6]Bristol-Myers Squibb Company Research and Development, New Brunswick, NJ, [7]AbbVie, North Chicago, IL and [8]Novartis Institute for Biomedical Research, Basel, CH, Switzerland.*

Understanding species differences in placental transfer of Fc-containing biopharmaceuticals (particularly monoclonal antibodies) will improve human risk extrapolation from nonclinical embryo-fetal development toxicity data. Maternal and fetal concentration data from 10, 15, 8 and 34 Fc-containing biopharmaceuticals in the rabbit, rat, mouse and cynomolgus monkey, respectively from an industry survey were analyzed for trends in placental transfer. Embryonic (prior to the end of organogenesis) exposure was assessed in 1 molecule each in rabbit, rat and mouse but detectable levels were present only in rodents. Rodent fetal blood levels were relatively constant through gestation while maternal serum concentrations increased or remained constant in rat and decreased in mice. In rabbits, following the cessation of dosing on Gestation Day (GD) 19, fetal levels increased markedly (up to 600-fold) in late gestation while maternal levels decreased. In the cynomolgus monkey, fetal levels increased substantially from GD 50 to 100 and were maintained relatively constant through parturition (~GD 165). In both the monkey and rabbit, IgG1 molecules appeared to transfer more readily than other isotypes in late gestation. Across all species, there was no differential transfer based on pharmacological target being soluble or membrane bound. Within each species there was a correlation between maternal and fetal exposure suggesting it may be possible to predict fetal exposures from maternal exposure data. These nonclinical data (both temporal and quantitative aspects) are discussed in a comparative context relative to our understanding of IgG placental transfer in humans.

PS 279 Diversity Outbred Mice As a Model for Pharmaceutical Toxicity Testing

D. M. Gatti[1], N. C. Goodwin[2] and G. A. Churchill[1]. *[1]Systems Genetics, The Jackson Laboratory, Bar Harbor, ME and [2]Cancer In Vivo Pharmacology Services, The Jackson Laboratory, Sacramento, CA.* Sponsor: A. Harrill.

Chemotherapeutic agents carry a significant risk of off-target toxicities, one of which is neutropenia. The severity of neutropenia varies across individuals and these differences may be due to genetic polymorphisms. Due to their rarity, these polymorphisms are difficult to detect in human genome wide association studies. We hypothesized that genetically diverse mouse models may mimic human toxicity responses to chemotherapeutics and accelerate the discovery of toxicity related genes. Diversity Outbred (DO) mice are a next-generation mouse population that contains over 40 million polymorphisms and structural variants, comprising a genetic diversity that surpasses the human population, but in which the frequency of rare alleles is much higher (12.5%). We investigated the utility of the DO to model human-relevant chemotherapy induced neutropenia by administering a single dose of either doxorubicin (20 mg/kg, n = 388) or cyclophosphamide (200 mg/kg, n = 192). Both doxorubicin and cyclophosphamide administration resulted neutropenia after 5 days, with an average decrease in neutrophil counts of 67% and 72%, respectively (t-test $p < 2x10-16$). We performed genetic mapping to identify genes related to doxorubicin and cyclophosphamide induced neutropenia. For doxorubicin, we identified a region on Chr 5 (5–9 Mb, $p < 0.0001$) containing Abcb1a & b, efflux transporters that are associated with doxorubicin resistance. For cyclophosphamide, we identified a region on Chr 11 (68.5–71.5 Mb, $p < 0.001$) containing Trp53, a DNA checkpoint gene that has been implicated as a risk marker for this toxicity. The identified genes comprise validated risk factors for chemotherapy-induced neutropenia, highlighting the power of the DO approach to efficiently identify clinically relevant pharmacogenetic risk factors. This study serves as a proof of principle that DO mice may be a powerful model for modeling adverse drug responses and for accelerating discovery of genes responsible for drug toxicity.

PS 280 Tolerability of Multicomponent Intravenous Vehicles Delivered As Bolus Injection or Infusion to Rats

K. D. Williams, B. A. Starch and G. Hoffman. *Nonclinical Safety Assessment, Covance Laboratories, Inc., Madison, WI.*

Vehicles A, B, and C, composed of N-methylpyrrolidine (NMP), polyethylene glycol 400 (PEG400), Kolliphor® HS15 (KP), and Lutrol® F68 (LF68) in sterile water, were assessed for tolerance in rats after intravenous injections or infusions of various durations. Vehicle A contained 5% NMP, 20% PEG400, 15% KP, 0.6% LF68; Vehicle B contained 5% NMP, 30% PEG400, 15% KP, 2.5% LF68; and Vehicle C contained 0% NMP, 30% PEG400, 15% KP, 2.75% LF68. Vehicle A given as a 45s bolus at 8 mL/kg to 2 rats caused tremors and irregular respiration followed by rapid death; the lungs had multiple 10mm2 areas. Vehicle A infusions at 4 mL/kg over 4m were rapidly lethal, whereas extension to 8m with either Vehicle A or B produced no adverse clinical signs, but did cause reddened areas to appear in lungs. Infusions of 30m and 60m of Vehicle A, B, or C at 4 and 8 mL/kg were then tested. No animals developed respiratory difficulties and plasma samples collected after the infusion did not appear hemolyzed. Near the end of the infusions, red colored urine was noted in both rats given Vehicle C at 8 mL/kg, and a rat given 8 mL/kg Vehicle C over 30m had reddened areas in the lungs. The macroscopic appearance of kidneys of all 12 rats tested in the Vehicle A, B, C comparison were normal. Thus, with 8 mL/kg infusions, Vehicles A and B were better tolerated than Vehicle C. In a repeat dose intermittent infusion study with 5 male and 5 female rats, Vehicle B (7 ml/kg) infused 1 hour per day for 5 days (phosphate buffered saline infused at all other times) resulted in no adverse clinical signs or clinical pathology changes, although some anatomical abnormalities typical of continuous infusion studies were noted in injection and catheter sites, and in lungs. Vehicles A or B appear adequate for use in intermittent infusion studies in rats with appropriate limitations imposed on infusion rate and duration. An independent vehicle group with no organic components should be included in future such studies to allow possible novel effects of the organic vehicle components to be assessed.

PS 281 Body Composition in Preclinical Studies: DXA and pQCT Precision for Fat and Muscle Analysis

A. Varela and S. Y. Smith. *Bone Research, Charles River, Montreal, QC, Canada.* Sponsor: M. Vézina.

Assessment of potential test article–related body composition effects is increasingly important for various indications and critical for diabetes, obesity, metabolic disorders, cachexia and muscle disease indications. New techniques are available to evaluate fat and lean mass in preclinical studies. The purpose of this study was to evaluate the precision of fat and muscle parameters by bone densitometry: Dual X-ray Absorptiometry (DXA) and peripheral Quantitative Computed Tomography (pQCT) in rats and in non-human primates (NHP).

DXA whole body scans (WB) were done on four rats and 4 NHPs, 4 times each with repositioning between scans using 2 separate scanners. Legs and arms scans were also performed in NHPs. pQCT scans were performed at the proximal tibia diaphysis for the calf muscle or at the femur diaphysis for the thigh muscle, in vivo and ex vivo in rats. Scanners were operated with software validated for the conduct of GLP studies. The coefficients of variation (%CV) were calculated from each series of 4 scans performed on the same animal.

The %CVs obtained for rat WB fat and muscle were below 4% and 1% respectively. The %CVs obtained for NHP WB fat and muscle were 35% and below 2% respectively. Fat mass in NHPs were very low at around 200g explaining the larger variability observed. Similar results were obtained for the two DXA machines. For the right arm, the % CV was below 10% for lean mass (7.3%) and below 11% for fat parameters (g and %). For the right leg, the % CV was below 3% for lean mass (2.4%) and below 25% for fat parameters (g and %). Additionally, body mass estimated by DXA differed by 4 % relative to the actual NHP body weight. With pQCT, the % CV was below 4% for lean mass and below 20% for fat parameters. DXA and pQCT provide reproducible non-invasive measurements of fat and muscle mass in rats and NHP which can also be combined with bone mass assessments. These data support the use DXA and pQCT densitometry in preclinical studies, to provide comprehensive measures of the body composition in nonclinical drug development programs.

PS 282 Fetal Blood Collection via the Axillary Artery—A Novel Method Which Does Not Compromise Visceral or Skeletal Examinations

M. O'Hara, C. Grace, J. Hardy and L. Schroeder. *Covance Laboratories, Greenfield, IN.*

Embryo-Fetal Development (EFD) study designs for risk assessment often include satellite groups for the assessment of toxicokinetics, increasing animal utilization and the associated labor. Additionally, if homogenized tissue is analyzed for exposure data, this prohibits a direct comparison of drug levels in the maternal and fetal circulation. Therefore, we have investigated an alternative blood sampling method which allows for collection of fetal blood yet does not hinder visceral or skeletal evaluations for the same fetuses. By collecting from the axillary artery and pooling by litter, sufficient blood volumes have been obtained from gestation day 21 (GD21) Sprague-Dawley rat fetuses to conduct either toxicokinetic or antibody titer analyses on fetal blood. Clinical pathology and hematology samples of approximately 1mL were gathered across 24 litters and directly compared. Standard

clinical chemistry (GLU, UN, CREA, AST, ALT, etc.) and hematology (RBC, etc) parameters indicated that samples collected via the axillary artery were equivalent to blood collected via cardiac puncture. However, cardiac puncture often produces structural damage to at least the thoracic cavity which would negate the possibility of further fetal evaluations. It can therefore be concluded that this bleeding procedure offers a way to meaningfully reduce satellite animal requirements without a negative impact on the visceral and skeletal evaluations required of the study design.

PS 283 A Novel Approach for Assessing the Safety of Pharmaceuticals

S. Gaukler, J. Ruff, L. Morrison and W. Potts. *University of Utah, Salt Lake City, UT.* Sponsor: G. Lamb.

Too often, prescription medications once thought safe for human use cause adverse health consequences and fail during clinical testing or are recalled after public release. One major problem is the inability of current toxicity assessment methods to detect many toxicities caused by pharmaceuticals during preclinical trials. We have developed a novel toxicity discovery method known as the organismal performance assay (OPA), that is capable of revealing mammalian health consequences. OPAs utilize genetically diverse wild mice (*Mus musculus*) that compete amongst each other for limited resources in semi-natural enclosures. This assay is sensitive, broad and functional because it demands high performance of most physiological systems in order for individuals to be successful. OPAs have proven powerful in detecting adverse health affects from inbreeding, genetic manipulations and dietary fructose. We tested the safety of Paxil (paroxetine) and Baycol (cerivastatin). Performance of pharmaceutical-exposed mice was analyzed when competing directly against control mice in OPAs. Performance was measured by territoriality, survivorship and reproductive success. We hypothesized that pharmaceutical-exposed individuals will suffer significant fitness declines compared to control individuals. Paxil-exposed breeding pairs took significantly longer to produce their first litter ($p=0.05$) and these litters were significantly biased towards female offspring ($p=0.0021$; 39:61 M:F). Paxil-exposed offspring also weighed significantly less than controls ($p<0.0001$). We detected a significant decline in reproductive success in both sexes and treatments (Paxil F: $p<0.001$; M: $p<0.01$, Baycol F: $p<0.001$; M: $p<0.001$). Pharmaceutical-exposed males were significantly less dominant than controls (Paxil $p<0.0001$; Baycol $p<0.0001$). Baycol-exposed individuals suffered higher mortality ($p=0.0116$). These pharmaceutical-caused health declines were missed by previous animal testing, indicating that OPAs provide superior sensitivity compared to conventional approaches. The data indicate OPAs could be a useful tool in safety testing during pharmaceutical development.

PS 284 Recovery Assessment in Preclinical Drug Safety Testing—A Retrospective Analysis of Value and Timing

R. Roberts, S. Robinson, R. Callander, D. Lees and S. Horner. *Drug Safety & Metabolism, AstraZeneca, Macclesfield, United Kingdom.*

We have previously reported the profile of target organ toxicities in first time in man (FTiM) toxicity studies conducted in rodents and non-rodents for 77 AstraZeneca candidate drugs (CDs) across a range of therapy areas (Horner et al., 2013, Reg Tox Pharm, 65, 334-343). Here, we present a further analysis of which target organ toxicities subsequently recovered after a dose free period and whether that profile differed for CDs that progressed into man and those that did not. We also report which additional target organ toxicities (defined as toxicities in a target organ not previously noted) were observed in chronic (≥ 3 month) studies conducted to support later stage clinical programmes across the different intended therapy areas (Cardiovascular/Gastrointestinal: CVGI; CNS/Pain: CNSP; Respiratory and Inflammation: RITA; Oncology/Infection: O/I). Target organ toxicity was primarily defined as compound-related histopathological changes. Overall, the analyses showed that >85% of findings were either fully or partially resolved at the end of the recovery period; lack of recovery in the dog male reproductive tract was the most frequent finding. Interestingly, profiles of recovery were largely similar for those CDs that progressed into man and those that did not and were also similar across therapy areas with the exception of oncology, where more findings persisted at the end of the recovery phase. Compared to observations in chronic studies, >60% of toxicities were identified in the FTIM studies with varying detection rates across the target organs. Overall, these data support inclusion of recovery on the FTiM studies and also demonstrate that chronic toxicology studies provide additional information of great value in risk assessment for longer term dosing in humans.

PS 285 Validation of a CYP1A2 and a CYP3A4 Induction Assay Using Puracyp's 1A2-DRE™, and DPX2™ Cell Lines: Comparison between the Gene-Reporter Assay and Human Hepatocytes Data

A. Watanyar, J. Enoru, K. Draper and W. DeMaio. *Ricerca Biosciences, Concord, OH.*

Induction of Cytochrome P_{450} drug metabolizing enzymes (DME) can lead to rapid elimination of APIs resulting in reduced efficacy and increased metabolism which can potentially lead to formation of toxic metabolites. The FDA routinely requests data on induction of human CYP450 enzymes CYP1A2 and CYP3A4 by new chemical entities in early development. CYP1A2 expression is regulated via the aryl hydrocarbon receptor (AhR), while CYP3A4 is predominantly regulated via the pregnane X receptor (PXR). Human primary hepatocytes are the preferred *in vitro* model for studying induction of DME, but their use is limited by unpredictable supply of tissues and interindividual donor variability. In this study, two gene reporter assays for evaluating induction of CYP1A2 and CYP3A4 were validated, using Puracyp's 1A2-DRE™ (a HepG2 derived cell line stably transfected with human AhR gene and a luciferase reporter gene linked to CYP1A2 promoter and the dioxin response element enhancer), and DPX2™ (a HepG2 derived cell line stably transfected with human PXR gene and a luciferase reporter gene linked to the CYP3A4 promoter and enhancer). CYP1A2 inducers naphthoflavone, omeprazole, 3-methylcholanthrene (3-MC), and lansoprazole increased CYP1A2 luciferase activity in a concentration dependent manner, resulting in EC50 and Emax values of 0.56 μM and 30-fold, 9.7 μM and 24.5-fold, 1.9 μM and 27.4-fold, and 3.3 μM and 37.8-fold, respectively. Similarly, CYP3A4 inducers rifampicin, phenobarbital, clotrimazole, erythromycin, and phenytoin increased CYP3A4 luciferase activity resulting in EC50 and Emax values of 0.85 μM and 7.8-fold, 119.8 μM and 5.0-fold, 0.5 μM and 5.0-fold, 10 μM and 4.2-fold and 17.5 μM and 4.0-fold, respectively. Our reporter gene assay data showed good correlation with data generated using human hepatocytes. Therefore, these validated assays can be used in early development for evaluating induction of CYP1A2 and CYP3A4, providing guidance on compound selection and potential for clinical drug-drug interactions.

PS 286 Acute Kidney Injury Biomarkers following Low-Dose Gentamicin Treatment of Rats

G. Marceau[1], L. Kolodzieyski[1], G. Diagne[1], J. Tremblay[1], S. Thébaud[1], M. Toneva[1], K. Scribner Doering[2], C. Kostrub[3] and A. Nelson[1]. [1]*ITR Laboratories Canada, Inc, Baie d'Urfe, QC, Canada,* [2]*ALPCO Diagnostics, Salem, NH and* [3]*CK Scientific, Belmont, CA.* Sponsor: W. Lee.

Rationale
The use of biomarkers as part of the preclinical assessment of kidney injury is now a well established goal. Published analysis of multiple datasets from the toxicology industry has convincingly identified a panel of urine and serum biomarkers which correlate with drug induced kidney injury. Several biomarkers have been shown to be superior to blood urea nitrogen (BUN) and serum creatinine at detecting renal injury. The present study correlates histopathologic evidence of kidney damage with urinary and serum biomarkers after very low dose regimens of Gentamicin.
Experimental procedures
Male Sprague-Dawley rats received daily subcutaneous injections of Gentamicin sulfate for 15 days at dose levels of 5, 15, and 50 mg/kg/day. Urine samples were collected over 16 hours for biomarker assessment at multiple timepoints (Pre-Tx, Days 4, 10, and 16). Blood was also collected at the end of a fasting period and serum preserved. A panel of biomarkers was tested in urine (Albumin, B2M, clusterin, cystatin C, KIM-1, NAG, NGAL, OPN, RBP) and serum (BUN, creatinine, and cystatin C). Kidney histology was assessed on days 4 and 16.
Results
Increased excretion of urinary biomarkers was observed on Days 10 and 16 of gentamicin treatment, and was associated with histologic changes on Day 16. Serum and urine creatinine and BUN remained unchanged over the treatment period.
Conclusions
As previously reported, creatinine and BUN levels were insensitive to low levels of acute kidney injury. Increased urine excretion of a group of biomarkers was associated with histopathological findings despite the normal values of creatinine and blood urea nitrogen. These biomarkers are candidate diagnostics and potential surrogates to histological evaluation of acute kidney injury.

PS 287 Comparison of Routine Clinical Pathology Parameters in Young Adult SD Rats from Different Geographical Regions

S. McPherson, S. Mason and Q. He. *WuXi AppTec, Suzhou, China.*

Clinical Pathology parameters are routinely assessed during the conduct of toxicology studies. This study was conducted to see if there were any differences in hematology, coagulation and clinical chemistry parameters among Sprague Dawley rats sourced from Charles River sites based in the USA, China and Taiwan. Control group data from completed and ongoing toxicology studies were used to see if there were any differences between the three sources of animals. The results from the three data sets were analyzed using the Charles River USA-supplied rat as reference control point. Analysis of the hematology data showed for males slightly lower white blood cell count (WBC), red blood cell count(RBC), hemoglobin (HGB), mean corpuscular hemoglobin concentration (MCHC) and neutrophils and increased mean corpuscular hemoglobin (MCH) for animals from both China and Taiwan when compared to the USA. In addition, decreased group mean lymphocytes and monocytes were observed for animals from China only. For the female rats decreased WBC, RBC, HGB, HCT, MCV lymphocytes, monocytes and eosinophils and mean platelet volume (MPV) were observed for animals from China only. For both males and females from both China and Taiwan, decreased Prothombin time were observed when compared to the USA-sourced rat. Differences in clinical chemistry were observed for rats from both China and Taiwan and included a reduced total protein due to a reduced albumin, reduced potassium and increased globulin when compared to the USA rat. The results of the analysis indicated that those rats sourced from Taiwan were closer to those sourced from China in terms of clinical pathology profile. These observed differences between the three sources of animals enforce the need to be consistent in the source of animals for a toxicology development program and also the need for maintaining separate back ground data bases.

PS 288 Lower Susceptibility to Histaminergic Reactions in Rodents Using Continuous Infusion: Advantages for Safety Assessment of Parenteral Peptide/Protein Drugs

H. van Wijk[1], P. Baldrick[1] and U. Wirnitzer[2]. [1]*Covance Laboratories Ltd, Harrogate, United Kingdom and* [2]*Bayer Pharma AG, Wuppertal, Germany.* Sponsor: A. Jackson.

Some drugs elicit histaminergic responses in vitro and in vivo, with the rat shown to be particularly sensitive in toxicology testing. As more parenteral therapeutic peptides/proteins are developed a model less prone to histamingeric reactions would offer improved safety testing. Such a model could be continuous vascular infusion via surgically implanted indwelling catheter in rodents and would allow comparison of histamine release response compared to bolus administration. In this study, the sensitivity of mouse and rat to histamine release after bovine pancreatic trypsin inhibitor drug Aprotinin (Trasylol®) given as a bolus or 6hrs intravenous infusion was investigated.
Rodents with implanted indwelling femoral vein catheter were bolus injected with 120.000, 240.000 or 300.000 U/kg or infused over 6hrs with 240.000 or 300.000 U/kg. After bolus injection, mice developed mild clinical signs, while rats developed clear histaminergic symptoms (cyanosis, swellings, reddening). Reddening was also seen in 1 rat after 300.000 U/kg infusion over 6hrs. Predose histamine levels in mice were markedly (~15-fold) lower than in rats. Induced histamine release after bolus administration was above the upper calibration limit in all rats and most mice. One mouse treated at 120.000 U/kg, had a histamine level in the predose range, 2 mice treated at 300.000 U/kg had clearly increased histamine levels within the calibration range. After 6hr infusion, mice at both dose levels had histamine levels in the predose range. Plasma histamine levels after 6hr infusion in rats were distinctly lower than after bolus injection and also within the predose range.
Although preliminary data, the results suggest that adverse histaminergic responses seen in toxicology testing following bolus injection could be avoided by use of continuous/repeated infusion. Furthermore, these data confirm the feasibility of dosing freely moving rodents by continuous infusion via indwelling vein catheter, allowing blood sampling during or after treatment.

PS 289 Induction of NADPH Oxidase and Apoptosis by CoCr-Alloy Implant Debris: Implications for Metal-on-Metal Hips

P. A. Potnis[1], D. K. Dutta[1], J. Schumacher[2] and S. C. Wood[1]. [1]*Division of Biology, Center for Devices and Radiological Health, Food and Drug Administration, Silver Spring, MD and* [2]*University of Rochester, Rochester, NY.* Sponsor: P. Goering.

Metal orthopedic implant-derived wear particles and released metal ions have been recognized to be a major concern in patients with prosthetic hips. Although the pathogenic effects of wear debris in peri-implant cells such as macrophages have been well studied, their effects on cellular oxidative stress and related events remain unknown. In this study, we investigated the ability of Cobalt Chromium-alloy (CoCr ASTM F-75, 1-5 μm) particles to produce reactive oxygen species and induce apoptosis in human monocytes. Human peripheral blood mononuclear cells (PBMC) or human monocytic cell line THP-1 were cultured with CoCr particles for up to 48 h. Exposure of cells to particles elicited a robust increase in dihydroethidium (DHE) fluorescence, compared with untreated controls, indicating enhanced production of particle-induced intracellular superoxide anion radicals. Real time RT-PCR and Western blot analysis of expression of NADPH oxidases (NOX) revealed enhanced expression of NOX subunits such as gp91 Phox, p67 Phox, p47 Phox and p22 Phox, at both the gene and protein levels, in response to CoCr-alloy particles. Flow cytometric analysis showed early apoptotic changes as revealed by increase in active caspase-3 activity. Additionally, particle-exposure resulted in enhanced staining for cleaved poly (ADP-ribose) polymerase-1 (PARP-1), a protein fragment produced by caspase cleavage. These results demonstrate that orthopedic implant-derived CoCr-alloy particles are associated with NADPH oxidase-induced generation of reactive oxygen species and excessive apoptosis. Data suggest that wear debris derived from orthopedic implants induce the generation of pro-oxidative and pro-apoptotic environment in the periprosthetic tissue surrounding these metallic implants.

PS 290 Methylmercury (MeHg) Induces Caspase-Dependent Apoptosis and Autophagy in Human Neural Stem Cells (NSCs), HB1.F3

S. Chang[1], K. Lee[1] and M. Cho[1, 2, 3]. [1]*Laboratory of Toxicology, College of Veterinary Medicine, Seoul National University, Seoul, Republic of Korea,* [2]*Graduate Group of Tumor Biology, Seoul National University, Seoul, Republic of Korea and* [3]*Graduate School of Convergence Science and Technology, Seoul National University, Seoul, Republic of Korea.*

Methylmercury (MeHg) is well known as human neurotoxic agent whose exposure sources are mainly environmental and aquatic-derived food. MeHg is reported to induce central nervous system (CNS) disability. However, the exact mechanism of MeHg-induced neurotoxic effects is still unknown. In this study, to investigate which cell death signaling pathway is related with MeHg-induced cytotoxicity, the effects of MeHg on apoptosis and autophagy were evaluated in human neural stem cells (NSCs), HB1.F3. Human NSCs were treated with 1 μM of MeHg for 48 hr and the effect of MeHg on cell signaling pathway was elucidated. MeHg inhibited Akt1/mTOR signaling that led to induction of caspase-dependent apoptosis and autophagy in the NSCs. Furthermore, retinoic acid (RA)-induced neuronal differentiation was inhibited by MeHg. Taken together, these results suggest that MeHg inhibits the differentiation of human NSCs by induction of caspase-dependent apoptosis and autophagy.

PS 291 Verifying Performance of Cell Viability and Apoptosis Assays Applied to 3D Microtissues

T. L. Riss[1], M. P. Valley[2], K. R. Kupcho[2], D. F. Lazar[2] and C. A. Zimprich[2]. [1]*Cell Health, Promega Corporation, Madison, WI and* [2]*Research, Promega Corporation, Madison, WI.*

Multicellular 3D culture systems containing more than one cell type and exhibiting formation of a complex extracellular matrix represent a more physiologically relevant environment for performing in vitro cytotoxicity testing, yet provide a challenge for assay chemistries originally designed for measuring events from 2D monolayers of cells. The approach of this research was to investigate whether increasing detergent concentrations to increase lytic capacity or providing physical disruption of samples would improve the results of cell viability and apoptosis assays applied to microtissues grown using 3D culture models. Results demonstrate that increasing detergent concentration in assay reagents has limits that depend on the source and stability of the luciferase enzyme. Introducing a physical disruption step in the protocol (shaking multi-well plates for 5 minutes at 450 rpm) improves the generation of signal from the luminescent ATP assay applied to microtissues grown in 3D models. Physical disruption also improved signal intensity from measurement of caspase-3/7 activity as a marker of apoptosis. Validation of assays designed for 2D monolayers is necessary prior to application to 3D culture models.

PS 292 Activation of the Aryl Hydrocarbon Receptor by Endogenous Agonist Cinnabarinic Acid Induces Stanniocalcin-2 to Elicit Cytoprotection against ER and Oxidative Stress

D. Carter, A. Joshi, T. Harper and C. J. Elferink. *Pharmacology and Toxicology, University of Texas Medical Branch, Galveston, TX.*

The Aryl Hydrocarbon Receptor (AhR) is a cytosolic ligand activated transcription factor historically known for its role in xenobiotic metabolism. However, endogenous tryptophan catabolites such as cinnabarinic acid possess the capacity to activate the AhR. Our lab has recently identified stanniocalcin 2 (STC2) as a novel AhR target gene that was induced in an AhR dependent manner after adenoviral infection of mouse primary hepatocytes. We hypothesized that AhR induction of STC2 plays a cytoprotective role in the mouse liver. Here we demonstrate for the first time that cinnabarinic acid activation of the AhR induces STC2 to elicit protection against ER stress and oxidative stress-induced apoptosis in mouse primary hepatocytes. We confirmed AhR activation and AhR targeting of the STC2 gene after cinnabarinic acid treatment by conducting immuno-cytochemistry and chromatin immuno-precipitation experiments, respectively. Our preliminary data demonstrates that cinnabarinic acid treament of primary hepatocytes causes significant enrichment of the STC2 protein while decreasing caspase 3 activities in a dose dependent manner. We also show that primary hepatocytes pre-treated with cinnabarinic acid for 24 hours exhibited reduced caspase 3 activities and reduced percentages of TUNEL positive cells after treatments with thapsigargin, hydrogen peroxide or ethanol when compared to non cinnabarinic acid pre-treated cells. Using AhR conditional knockout primary hepatocytes as well as STC2 knockdown using siRNA, we were able to confirm the direct involvement of STC2 in the cytoprotection of mouse primary hepatocytes against ER stress and oxidative stress-induced apoptosis. Our data conclusively demonstrates that AhR induction of STC2 in the liver plays a crucial cytoprotective role against ER stress and oxidative stress-induced apoptosis. Therefore, our goal is to elucidate the cytoprotective mechanism of STC2 in mouse primary hepatocytes.

PS 293 CYP1B1 Inhibits TRAIL-Mediated Apoptotic Pathway followed by Sp1 Induction

Y. Chun, Y. Kwon, N. Park, S. Shin, D. Ye and M. Hong. *College of Pharmacy, Chung-Ang University, Seoul, Republic of Korea.*

Cytochrome P450 1B1 (CYP1B1) belongs to the CYP1 family and shares the feature as an enzyme for drug metabolisms. It has been reported that CYP1B1 expression is higher in the tumor tissues than the normal ones, especially in hormone-related cancers such as breast, ovarian and prostate cancer cells. To explore the role of CYP1B1 on cancer cell proliferation, we investigated whether CYP1B1 blocks apoptotic pathways. Using Western blot and RT-PCR, the expression of anti-apoptotic factors such as Bcl-2, Bcl-xL, XIAP, survivin and Mcl-1 were examined and showed to be promoted followed by CYP1B1 overexpression or treatment with CYP1B1 inducer, 7, 12-dimethylbenz[α]anthracene (DMBA). These promoting results were reversed when cells were transfected with siRNA for CYP1B1 or treated with a CYP1B1 inhibitor, tetramethoxystilbene (TMS). Moreover, AIF, a widely known pro-apoptotic factor, showed to be translocated to cytosol from mitochondria after treatment with TMS. The expression of TRAIL, a member of tumor necrosis factor superfamily, was also examined followed by alteration of CYP1B1 expression and it showed similar changes in expression level to pro-apoptotic factors. Sp1, a transcription factor, has been reported to suppress TRAIL expression by binding TRAIL promoter. To identify whether Sp1 mediates the suppression of TRAIL, we examined Sp1 expression after changes of CYP1B1 expression level and it showed that Sp1 is promoted by CYP1B1. Moreover, Sp1 knockdown with specific siRNA showed promotion of TRAIL-related apoptotic factors and these results were reversed by Sp1 overexpression. Moreover, attenuation of Sp1 DNA binding activity using mithramycin A, a well known Sp1 binding inhibitor, resulted in recovery of TRAIL expression formerly suppressed by treatment with DMBA. Taken together, these data suggest that CYP1B1 blocks apoptosis via TRAIL suppression and this is mediated by Sp1 induction.

PS 294 Intact 20kDa Extracellular Domain of APO2L/TRAIL Bioanalysis by HRMS: A Potential Cancer Therapeutic Protein

F. Garofolo. *Bioanalytical Services, Algorithme Pharma Inc., Laval, QC, Canada.*

Recombinant APO2L/TRAIL (Apo2 ligand/tumor necrosis factor-related apoptosis-inducing ligand), typically analyzed by LBA, was successfully quantified as intact protein by High Resolution Mass Spectrometry (HRMS). The chromatographic separation of intact APO2L/TRAIL for mass spectrometric analyses was found to be challenging with silica columns. Whereas, polymer column greatly improved peak shape and reproducibility. Moreover, the column temperature had an important impact on the amount of APO2L/TRAIL recovered from column upon injection: Increasing the column temperature from 22°C to 70°C increased the recovery by at least 4-time and improved peak shape. Data processing method was optimized to avoid interferences, it was possible to quantitate only the most abundant charge state and isotopomer or the sum of each charge state and isotopomers. APO2L/TRAIL signal was found to have charge state distributions from +12 to +27 with the 6 most intense charge states being from +18 to +23. Monitoring only one charge state (+20), with an XIC of 10mDa, led to variability and unacceptable peak shape. After summing the 6 most abundant multiple charge states with an XIC window of 10mDa around the most abundant isotopomer, a S/N=8 was observed at the LLOQ. The method showed very good results: dynamic range was linear (weighted to 1/x2) with a correlation of r=0.9960. The assay precision was below 5% and with accuracy between 101-108% for the LLOQ QCs and 3 additional QC levels. This data successfully confirmed the possibility to use HRMS for intact protein quantification without tryptic digestion.

PS 295 Preventive Effect of Nonmitogenic Acidic Fibroblast Growth Factor on Diabetes-Induced Testicular Cell Death and Atrophy

M. Skibba[1], C. Zhang[2], X. Jiang[2] and L. Cai[1, 2]. [1]*Pharmacology and Toxicology, University of Louisville, Louisville, KY and* [2]*KCHRI and Department of Pediatrics, University of Louisville, Louisville, KY.*

Fibroblast growth factor (FGF) family members in previous studies were shown to prevent various oxidative stress-induced cardiac, neuronal and retinal inquires. Particularly, FGF-1 was found to protect the heart from ischemia-, doxorubicin- and diabetes-induced damage, suggesting the potential clinical application. However, long-term use of FGF-1 was restricted for its potential risk of carcinogenesis due to its non-specific proliferating activity. Thus a cluster of amino acids responsible for proliferation were deleted in the native FGF-1 to create a modified non-mitogenic FGF-1 (nmFGF-1). The present study tested if the nmFGF-1 protects male germ cells from diabetes-induced apoptotic cell death and testicular atrophy. Mice were treated with multiple low-doses of streptozotocin (STZ) to induce type-1 diabetes and then treated with nmFGF-1 for 6 months. Diabetic mice showed a decrease in testicular weight and an increase in apoptotic cell death (detected by TUNEL staining). Treatment with nmFGF-1 alleviated diabetic effects on testicular weight and apoptotic cell death. Mechanistically, the diabetes induces, the mitochondrial apoptotic pathway due to a significant increase in BAX/Bcl-2 ratio, determined with Western blotting assay. Diabetes also induced mild increases in endoplasmic reticulum stress and associated cell death, reflected by increases in cleaved-caspase 12, CHOP, and GRP-78 expression, and a significant increase in TNF-alpha expression as an index of inflammation. All these effects induced by diabetes were attenuated by treatment with nmFGF-1. Therefore, these results suggest that nmFGF-1 is able to prevent the apoptotic-effect of diabetes on the testes via the mitochondrial pathway predominantly, resulting in prevention of diabetes-induced testicular atrophy.

PS 296 *Nelumbo nucifera* Leaf Extract-Induced Pancreatic Cancer Apoptosis via JNK/ERK Activation-Regulated Mitochondria-Dependent and ER Stress-Triggered Signaling Pathways

Y. Chen[1], C. Su[2], T. Lu[1], C. Yen[5], Y. Chung[5], K. Chen[6], C. Wu[3], S. Liu[7] and C. Huang[4]. [1]*Department of Physiology and Graduate Institute of Basic Medical Science, China Medical University, Taichung, Taiwan,* [2]*Department of Otorhinolaryngology, Changhua Christian Hospital, Changhua, Taiwan,* [3]*Department of Public Health, China Medical University, Taichung, Taiwan,* [4]*School of Chinese Medicine, China Medical University, Taichung, Taiwan,* [5]*Department of Occupational Safety and Health, Chung Shan Medical University, Taichung, Taiwan,* [6]*Department of Urology, China Medical University Hospital, Taichung, Taiwan and* [7]*Institute of Toxicology, National Taiwan University, Taipei, Taiwan.*

In this study, we investigated the pharmacological effects of *N. nucifera* leaf in anti-pancreatic cancer and elucidate its molecular mechanisms. The results found that *Nelumbo nucifera* leaf extract (NNE) significantly caused cytotoxicity in PANC-1 cells with a dose-dependent manner and induced several features of apoptosis signals in PANC-1 cells. NNE was also capable of increasing the protein phosphorylations of JNK and ERK-1/2, but not that p38-MAPK. Transfection of PANC-1 cells with JNK1- and ERK2-specific si-RNA could inhibit JNK-1 and ERK-2 activation and attenuate caspase-3/-7 activity induced by NNE, respectively. Furthermore, exposure of PANC-1 cells to NNE could trigger endoplasmic reticulum (ER) stress indicating by the increase in ER stress-related molecules. Transfection of PANC-1 cells with GRP78- and GRP94-specific si-RNA could effectively prevented the NNE-induced caspase-3/-7 activity, respectively. More

importantly, quercetin, not that catechin, was the mainly active component of NNE in NNE-induced cytotoxicity and apoptosis in PANC-1 cells. In conclusion, these results demonstrate that NNE induces pancreatic cancer cell apoptosis via the JNK/ERK activation-regulated mitochondria-dependent and ER-stress-triggered signaling pathways. And quercetin is the mainly active component of NNE.

PS 297 Most Bioactivation-Dependent Nephrotoxins Induce Apoptotic Death along with Unique Patho-Morphological Characteristics in Mouse Kidneys

J. J. Earhart and S. D. Ray. *Dept of Pharma. Scs, Manchester Univ. College Pharmacy, Fort Wayne, IN.*

Critical issues in the pathophysiology of toxic renal injury includes drug metabolism within target cells, changes in gene expression, oxidative stress, inflammation and various types of cell deaths. Drug-induced nephrotoxicity is often viewed as an endpoint in animal toxicity studies, and the diagnosis of various forms of kidney injury based on clinical data remains very challenging because of the difficulty in interpreting histopathology. Our earlier studies showed most bioactivation-dependent nephrotoxins cause oxidative stress and apoptotic death. Therefore, this study analyzed the histopathological changes induced by several different bioactivation-dependent nephrotoxins [chloroform (CHCl3), diclofenac (DCLF), salicylic acid (SA) and furosemide (FUR)] to profile common and uncommon pathological features to hypothesize whether a subset of changes can be used to categorize nephrotoxins. Mice were administered CHCl3 (1ml/kg orally), DCLF (300 mg/kg, ip), SA (300 mg/kg, ip) and FUR (500 mg/kg, ip) and sacrificed 24 hours later. PAS or H&E stained kidney sections were examined under a brightfield microscope to assess changes in proximal (PT) and distal tubules (DT), Bowman's capsule, ureter, brush borders, Bowman's space, glycogen depletion trend and inflammation. Results indicated that all the toxins induced nephrotoxicity as judged by elevated serum BUN (5 fold or higher by all toxins), increased BUN/creatinine ratios and tissue MDA levels (6 fold or higher). Pathomorphologically, the most common features were distorted PTs and DTs along with brush border injury, scattered apoptotic nuclei and abundant inflammatory cells. DCLF showed hypertrophied tubular cells with massive induction of apoptotic nuclei, SA showed degeneration of brush borders with tubular dye accumulation, whereas FUR showed global injury throughout the tissue. Thus, this study may have discerned a novel way of profiling xenobiotic-induced nephrotoxicity [Suppo. by Dept. of PScs of Manch. Univ. Coll of Pharm. & AMS Coll of Pharm & HScs, NY]

PS 298 Anthracenyl Isoxazole Amides (AIMs) As Mitochondrial Modulators of Apoptosis

A. K. Kearns, M. J. Weaver, P. K. Shaw, N. R. Natale and H. D. Beall. *Biomedical and Pharmaceutical Sciences, Univ Montana, Missoula, MT.*

Development of G-quadruplex ligands for the treatment of solid tumors is an emerging field of research. G-quadruplex structures within the nucleus of cells are the target for these ligands with the goal of inhibiting telomerase and causing replicative senescence or selective apoptosis of tumor cells. We have previously shown that novel anthracenyl isoxazole amides (AIMs), such as NSC 748994 (AIM1), bind telomeric G-quadruplex DNA and exhibit single digit micromolar IC50 values in SNB-19 glioblastoma cells, suggesting their potential as G-quadruplex-directed antitumor agents. However, confocal microscopy with MitoTracker Red showed that AIM1 was primarily localized within the mitochondria of cells, with less distribution to the nucleus. As a result, the present study was conducted to determine if the AIMs modulate mitochondrial function in SNB-19 glioblastoma cells. Our hypothesis was that the AIMs produce cell death via mitochondrial-mediated apoptosis. AIM1 significantly increased both early and late apoptosis at 5 μM compared to control after 24 hours as measured by Annexin V/flow cytometry. JC-1 staining indicated that mitochondrial membrane potential was significantly reduced by 5 μM AIM1 while reactive oxygen species generation was increased at the 1 μM level using MitoSox Red, a mitochondrial indicator of superoxide anion. In addition, exposure to 5 μM AIM1 resulted in caspase-9 activation, an indication of intrinsic, mitochondrial-mediated apoptosis. Although these findings suggest that the mitochondria is one possible target of AIM-associated toxicity, these effects could also be triggered by AIM binding to G-quadruplex in nuclear DNA (via human telomerase catalytic subunit hTERT shuttling) or directly to G-quadruplex in mitochondrial DNA. Further studies on the mechanisms of AIM toxicity are ongoing. Supported by NIH Grant P20RR017670 (HDB).

PS 299 Assessment of an *In Vitro* Model for Evaluating the Role of PARP in Ethanol-Mediated Hepatotoxicity

J. Coyle[1], G. T. Johnson[1], M. M. Bourgeois[1], A. Mayo-Perez[1], S. Morris[2] and R. D. Harbison[1]. [1]*Environmental and Occupational Health, University of South Florida, Tampa, FL and* [2]*College of Nursing, University of South Florida, Tampa, FL.*

This investigation assesses the role of poly(ADP-ribose) polymerase in ethanol-mediated hepatotoxicity using the untransfected HepG2 hepatocellular carcinoma line, an established, well-characterized toxicological model. HepG2 cells were treated with ethanol at concentrations between 100 mM and 800 mM, and assessed for markers of cytotoxicity. PARP-1 activity in total cell protein lysates was quantified as a proxy of apoptotic induction at six hours. Our results demonstrated a 1.43-fold AST activity increase in culture medium isolates of cells exposed to 800 mM without significant effect on cellular viability. PARP-1 activity varied greatly and results for enzyme activity remained inconclusive. The results suggest a high degree of insensitivity to ethanol toxicity and nuclear enzyme activity, demonstrating the metabolic irrelevance of untransfected HepG2 in ethanol toxicosis. There is a need to characterize phase 1 metabolic enzyme expression profiles relevant to ethanol for CYP2E1 and ADH pathways to facilitate comparisons across toxicological models using transfected, as well as the untransfected HepG2 model.

PS 300 Genotoxicity of DEHP and Its Metabolite

Y. Chang[1], C. Tseng[1, 2, 3], Y. Chen[1], Y. Chuang[1] and M. Chao[1, 3]. [1]*Bioscience Technology, Chung Yuan Christian University, Chung-Li, Taiwan,* [2]*Biomedical Engineering, Chung Yuan Christian University, Chung-Li, Taiwan and* [3]*Center of Nanotechnology, Chung Yuan Christian University, Chung-Li, Taiwan.*

DEHP, Di-(2-ethylhexyl) phthalate, the most common phthalate plasticizer used in manufactures. It can be leached into a liquid that comes in contact with plastics, suggesting concerns about the health risk of human exposure. Several in vivo studies have shown that DEHP can be metabolized in the intestine and converted to MEHP, mono-ethylhexyl phthalate. The metabolite can be absorbed through the villi and travel in the circulation system then causes series damages in endocrine and reproductive system. In addition, investigations also demonstrated an association with elevated induction of rat hepatic cancer, testicular cancer, and developmental toxicity in reproductive system under MEHP exposure. However, the mechanism regarding to carcinogenicity induced by DEHP or its metabolite MEHP remains unclear up to date. We therefore are investigating the cell viability and mutagenicity of DEHP and MEHP in Chinese hamster ovary (CHO) cells. Cytotoxicity and DNA damages induced by these chemicals in nucleotide repair-proficient AA8 and repair-deficient UV5, and base excision repair-deficient EM9 cell lines. Results show that the parental chemical, DEHP, as well as MEHP derivatives caused dose-dependent decreases in cell survival, but with very different potencies: MEHP has the high potency; and DEHP lower. Exposure to these compounds induced dose-dependent production of ROS, as determined by Cm-H2DCF-DA fluorescence. Comet assay shows the DNA damages in the trend as same as cytotoxicity, but no difference observed between NER and BER deficient cells exposed to these treatments, even at highly toxic doses. It was noted however that simultaneous treatment of ROS scavenger N-acetylcysteine (NAC) shows the protection against DEHP and MEHP induced DNA damages. In summary, DEHP and MEHP are cytotoxic to the cells and require induction of ROS to exert their genotoxicity effects.

PS 301 Exposure of V79 Hamster Cells to Cadmium Chloride Results in the Production of Double-Strand Breaks and Cell Cycle Changes

J. Comotto, C. Donald and M. Reynolds-Walsh. *Washington College, Chestertown, MD.*

Cadmium is a ubiquitous metal used in many industrial applications, resulting in widespread environmental pollution. Exposure to this metal occurs through inhalation and can result in numerous respiratory disorders, as well as cancer. Non-occupational exposure occurs through inhalation and the ingestion of cadmium from polluted food and water. This study investigates the effects of cadmium exposure on cytotoxicity, genotoxicity and cell cycle progression in V79 hamster cells. Western-blot analysis of caspase and PARP cleavage were used to determine cytotoxicity while genotoxicity and cell cycle changes were analyzed using H2AX, cyclins A and B, and cyclin dependant kinases 1 and 2. To determine if cadmium damage was cell cycle specific propidium iodide analysis was performed on cells synchronized in G2/M, G0, and S phases, using nocodazole, serum starvation, and aphidicolin treatments, respectively. Genotoxicity was measured following analysis of mutations at the HPRT gene. Results determined that cadmium expo-

sure resulted in a dose-dependent increase in apoptosis and double strand break formation which correlated with a greater uptake of cadmium as measured by ICP/MS. Downregulation of cyclins A and B and cdks 1 and 2 occurred indicating there was a cell cycle arrest following cadmium exposure. Cells arrested in G2/M by nocodazole prior to exposure demonstrated increased G0/G1 arrest which was p53-dependent. Collectively, this study indicates that cadmium induces genotoxic lesions and causes alterations in normal cell cycle progression.

PS 302 Induction of Apoptosis by PQ1, a Gap Junction Enhancer That Upregulates Cx43 and Activates the p38-MAPK Signaling Pathway in Mammary Carcinoma Cells

T. A. Nguyen and S. N. Shishido. *Diagnostic Medicine/Pathobiology, Kansas State University, Manhattan, KS.*

Cell death induced by the gap junction enhancer, PQ1, was studied in mammary carcinoma cells (FMC2u) derived from a malignant neoplasm of a female PyVT transgenic mouse. PQ1 was determined to have an IC50 of 6.5 μM in FMC2u cells, while inducing an upregulation in Cx43 expression. The mechanism behind PQ1 induced cytotoxicity in mammary carcinoma cells is thought to be attributed to the change in Cx43 expression; therefore, the effects of Cx43 modulation in FMC2u cell survival was determined through transfection experiments with Cx43 cDNA, which induced an elevated level of protein expression similar to that seen with PQ1 exposure, or siRNA to silence Cx43 protein expression. Overexpression of Cx43 led to a reduction in cellular viability, while an increase in viability was observed after silencing of Cx43 in FMC2u cells. The mitogen-activated protein kinase (MAPK) family has been implicated in the regulation of cell survival and cell death; therefore, the GJIC-independent function of PQ1 and Cx43 in the MAPK-dependent pathway of apoptosis was explored in mammary carcinoma cells. Both the overexpression of Cx43 and PQ1 treatment stimulated an increase in the phosphorylated form of p38-MAPK, reduced levels of the anti-apoptotic protein Bcl-2, and increased the cleavage of pro-caspase-3. Silencing of Cx43 protein expression led to a reduction in the phosphorylation of p38-MAPK and an increase in bcl-2 expression. These results suggest that PQ1 affects not only GJIC, but also cellular survival via a MAPK-dependent pathway. Cx43 may be the key element in the mechanism of PQ1 induced apoptosis.

PS 303 Zebrafish Assay Format for Determining Compound-Induced Apoptosis Inhibition and Activation

P. McGrath. *Phylonix, Cambridge, MA.*

During development, naturally occurring apoptosis plays an important role in tissue modeling. However, uncontrolled apoptosis is associated with numerous diseases as well as compound toxicity. Here we describe an assay format used to assess compound induced apoptosis inhibition or activation that relies on the presence of developmentally regulated cell death in live 2 day post fertilization (dpf) zebrafish. At 2 dpf, developmental apoptosis present in the hatching gland and nasal placode can be assessed by acridine orange (AO) live dye fluorescence staining. In contrast, at this stage only a few dispersed apoptotic cells are present in the zebrafish tail. By 3 dpf, essentially no apoptosis is visible at any site.
Using these inherent assay parameters, in this study, we assessed 4 characterized inhibitors: Ac-DNLD-CHO, Ac-DEVD-CHO, Z-VAD-fmk, and Q-VD-Oph and 3 activators: Staurosporine, Borrelidin, Gambogic acid, and 1 negative control compound, Buthionine sulfoximine, shown not to affect apoptosis in mammals. Zebrafish (N = 10) were exposed to the MNLC of each compound for 24 hrs, incubated with AO (1 mg/ml), washed and anesthetized. Effects were initially assessed visually followed by quantitative morphometric image analysis. Compared to the DMSO control, significant inhibition ($P < 0.05$) of developmentally regulated apoptosis in the hatching gland and nasal placode was observed for Ac-DNLD-CHO (73.7 + 22.6%), Ac-DEVD-CHO (99.60 + 0.4%), Z-VAD-fmk (70.9 + 27.7), and Q-VD-Oph (68.40 + 23.5%), and significant activation ($P < 0.05$) of apoptosis in the tail was observed for Staurosporine (933 + 701%), Gambogic acid (2692 + 1205%), and Borrelidin (9227 + 6017%). Buthionine sulfoximine, the negative control, did not significantly affect AO staining. Student's t-test was used to determine significance ($P < 0.05$). Effects in zebrafish were then compared with results in mammals. The overall correct prediction rate was 100%, considered excellent by ECVAM. These data support use of zebrafish as a predictive model for assessing cell death for safety, toxicity and efficacy studies.

PS 304 Non-Tubulin Mitotic Disruptors Induce Apoptosis in Cancer Cells

J. C. States, D. J. Saforo, N. A. Klimchak and J. O. Trent. *University of Louisville, Louisville, KY.*

Disrupting mitosis is a validated approach for cancer chemotherapy. Mitotic disruptors (e.g. taxanes) are common components of combination chemotherapy used to treat cancers of lung and other organs. These agents induce mitotic arrest and apoptosis in cancer cells. Chemotherapeutic success is limited by development of resistance and dose-limiting toxicity. Mitotic disruptors currently in use, and most of the new agents in development, target tubulin. An alternative approach is to target the regulators of mitosis. The anaphase promoting complex/cyclosome (APC/C) is the master regulator of mitosis and cell cycle, and is a novel anti-cancer target. Using an in silico approach, candidate compounds were identified to disrupt APC/C assembly. Compounds were tested for ability to induce cytotoxicity in colony forming and AlamarBlue assays and to induce increases in mitotic index in a variety of human cancer, SV40-transformed and diploid cell lines. Compounds containing a 1-aminopropan-2-ol core were found to induce mitotic arrest and cell death as predicted in lung and ovarian cancer cells, malignant melanoma and HeLa cells and SV40-transformed fibroblasts and bronchial epithelia, while sparing normal diploid cells. These results indicate that targeting the disruption of the APC/C is a viable approach for developing a new class of mitotic disruptors useful for cancer chemotherapy.

PS 305 Salubrinal Differentially Modulates Mitochondrial Dysfunction-Induced by Halogenated Analogs of 3, 3'-diindolylmethane (DIM) in Prostate Cancer Cells

T. Sanderson[1], D. Montes-Grajales[2], J. Olivero-Verbel[2], S. H. Safe[3] and A. Goldberg[1]. [1]*INRS-Institut Armand-Frappier, Laval, QC, Canada,* [2]*Environmental and Computational Chemistry Group, University of Cartagena, Cartagena, Colombia and* [3]*Veterinary Physiology and Pharmacology, Texas A&M University, College Station, TX.*

We have previously shown that halogenated analogs of 3,3'-diindolylmethane (DIM), termed ring-DIMs, induce apoptosis and necrosis in human prostate cancer cells. We now show that ring-DIMs at toxic concentrations induce endoplasmic reticulum (ER) stress in human prostate cancer cells, and that cell death induced only by 4,4'-dihaloDIMs is abrogated by pre-treatment with the ER stress inhibitor, salubrinal. Salubrinal reduced phosphorylation of eIF2alpha in cells treated with 4,4'-dibromoDIM and did not increase phosphorylation of eIF2alpha in cells treated with 7,7'-dichloroDIM or DIM. We also found that neither CHOP nor ATF4 levels, both indicators of ER stress, were decreased after pre-treatment with salubrinal. The effect of salubrinal appeared to be linked to mitochondrial stability as pre-treatment with salubrinal negated the decrease in mitochondrial membrane potential (MMP) and mitochondrial abundance in cells treated with 4,4'-dibromoDIM. In contrast, salubrinal exacerbated the cytotoxic effects of 7,7'-dibromoDIM, 7,7'-dichloroDIM and DIM by further increasing the loss of MMP and mitochondrial abundance induced by these compounds. We found that an inhibitor of the mitochondrial permeability transition pore, cyclosporine A, prevented the loss of cell viability, MPP and mitochondrial abundance caused by co-treatments of 7,7'-dihaloDIMs with salubrinal. An in silico 3D docking analysis to find binding partners for salubrinal and the ring-DIMs point to targets other than ER stress and eIF2alpha as mediators of salubrinal's apparently contradictory modulation of cell death induced by the ring-DIMs.

PS 306 Targeting CamKII in Prostate Cancer Cells: Induction of Mitochondrial Dysfunction and ER Stress by Halogenated Analogs of 3, 3'-Diindolylmethane

A. Goldberg[1], A. Beach[3], D. Montes-Grajales[2], V. Titorenko[3], J. Olivero-Verbel[2], S. H. Safe[4] and J. Sanderson[1]. [1]*Toxicology, INRS, Laval, QC, Canada,* [2]*University of Cartagena, Cartagena, Colombia,* [3]*Concordia University, Montreal, QC, Canada and* [4]*Texas A&M, College Station, TX.*

We have previously shown that a series of halogenated analogs of 3,3'-diindolylmethane (DIM), termed ring-DIMs, induce apoptosis and necrosis in androgen-dependent and androgen-independent prostate cancer cells, with 4,4'-dibromoDIM having the greatest anti-cancer activity. To understand the upstream events leading to the activation of caspases in response to treatment with dihalo-DIMs in androgen-dependent LNCaP and androgen-independent LNCaP C4-2B cells, we monitored the onset of endoplasmic reticulum (ER) stress and the dysregulation of mitochondrial respiration. We found that 4,4'-dibromo- and 7,7'-dichloroDIM and DIM itself caused ER stress-dependent upregulation of CHOP and ATF4, while only 4,4'-dibromo- and 7,7'-dichloroDIM increased phosphorylation of eIF2alpha

and JNK. The 4,4'-dihaloDIMs and DIM, but not 7,7'-dihaloDIMs, caused loss of mitochondrial membrane potential (MMP) within 1 hour of exposure, before the appearance of later stage apoptotic events such as chromatin condensation. In silico binding affinity studies showed that the dihalo-DIMs could potentially interact with several subunits of calmodulin-dependent kinase II (CamKII). The selective CAMKII inhibitor KN93, but not inactive KN92, inhibited cell death induced by 4,4'-dibromoDIM only. KN93 also inhibited the mitochondrial dysfunction and ER stress associated with 4,4'-dibromoDIM toxicity. We observed phosphorylation of CamKII after 1 hour of exposure to 4,4'-dibromoDIM, suggesting that 4,4'-dibromoDIM interacts with CamKII directly, thereby causing prostate cancer cell death.

PS 307 Validation of a Novel Cell Culture System to Perform 3D *In Vitro* Cytotoxicity Analyses Using Primary Hepatocytes

T. Moeller[1], B. Larson[2], G. Cameron[3] and P. Banks[2]. [1]*BioreclamationIVT, Halethorpe, MD,* [2]*BioTek, Winooski, VT and* [3]*TAP Biosystems, Royston, Hertfordshire, United Kingdom.*

Hepatocytes are the primary cell type of the liver providing the majority of the detoxification which increases the potential for cellular dysfunction and death. Though the source of the insult may be caused by several factors, exposure to drugs represents a significant concern warranting FDA guidance on drug-induced liver injury (DILI). *In vivo* studies are still the gold standard; however, *in vitro* screening has gained importance for reducing animal exposure, amendable to high-throughput platforms and better equipped to study cellular mechanisms of action.
Typically *in vitro* screening has incorporated primary hepatocytes cultured in a two dimensional (2D) format where the cells form a monolayer across the bottom of a well. However, when cultured and studied in this fashion they rapidly lose their key functions and de-differentiate over the course of only a few days. The ability to culture, characterize and challenge primary cells in a biomimetic 3D environment enables the performance of longer term studies.
Here we present data demonstrating the differences in response between human primary cells cultured in 2D and in the RAFT 3D cell culture system which has the benefits of a collagen hydrogel with tissue-like properties. Camptothecin and pyocyanin were tested for their ability to cause short-term oxidative stress, as well as long-term induction of apoptosis and necrosis. Kinetic live cell imaging was performed using multiple fluorescent non-perturbing probes to monitor the various effects in real time with incubations up to 48 hours which enabled a thorough assessment of the toxin profile. Image overlay allowed for discrete cellular analysis. Variations in cytotoxicity levels were observed after a 24 hour 800 nM camptothecin treatment (75%:2D; 28%:3D). ROS induction was less in 3D than 2D system. Overall, cells exhibited greater viability using the RAFT system, and were less sensitive to toxins than observed in traditional 2D culture for the endpoints which may indicate a more robust cell culture system.

PS 308 Heat Shock Response Antagonism: From Toxicological Liability to Cancer Chemotherapeutic Opportunity

A. L. Davis, C. M. Cabello, S. Qiao, S. Azimian and G. T. Wondrak. *Pharmacology and Toxicology, College of Pharmacy and Arizona Cancer Center, University of Arizona, Tucson, AZ.*

The cellular heat shock response plays an essential role in cytoprotection that involves maintenance of proteostasis and suppression of apoptosis. Based on an increased vulnerability of cancer cells to proteotoxic stress, small molecule heat shock response inhibitors are now an emerging class of cancer-directed experimental therapeutics. Guided by a phenotypic screen, we have interrogated a focused compound library for functional heat shock response antagonism targeting a panel of malignant melanoma cell lines (G361, LOX-IMVI, A375). From a collection of pro-oxidant 3,7-diamino-phenothiazinium derivatives [methylene blue (MB), azure A, azure B] we have identified the redox-drug MB, used clinically for the infusional treatment of methemoglobinemia, as a negative modulator of heat shock response gene expression in human A375 melanoma cells. Stress and toxicity response gene array analysis using the RT2 Profiler™ technology (SuperArray, Frederick, MD; MB: 10 μM, 24 h) revealed that MB-treatment selectively suppressed expression of Hsp70 family members (*HSPA1A, HSPA8*) and Hsp27 (*HSPB1*), a finding confirmed at the protein level. Importantly, MB sensitized melanoma cells to the apoptogenic activity of geldanamycin, an Hsp90 antagonist that induces the counter-regulatory upregulation of Hsp70 expression underlying cancer cell resistance to geldanamycin chemotherapy. Similarly, MB-cotreatment sensitized melanoma cells to other apoptogenic chemotherapeutics. Taken together, these data suggest feasibility of repurposing the non-oncological redox drug MB as a proteotoxic heat shock response antagonist for chemotherapeutic intervention. Supported in part by grants from the National Institutes of Health [R01CA122484, R03CA167580, R21CA166926, ES007091, ES06694].

PS 309 Apoptosis Modulates Hepatotoxic Effects of 2-Aminoanthracene in Fisher 344 Rat

W. E. Gato[1], D. B. Hales[2], S. McGee[2] and J. C. Means[3]. [1]*Department of Chemistry, Georgia Southern University, Statesboro, GA,* [2]*Department of Physiology, Southern Illinois University, Carbondale, IL and* [3]*Environmental Science & Management, University of California Santa Barbara, Santa Barbara, CA.*

The arylamine 2-amino-anthracene (2-AA) is an aromatic hydrocarbon employed in manufacturing of chemicals, dyes, inks, and as curing agents in epoxy resins and polyurethanes. 2-AA has been detected tobacco smoke and cooked foods. The modulation of the toxic effects of 2-AA on the liver by apoptosis was investigated on twenty four post-weaning 3-4 week old F-344 male rats exposed to 0 mg/kg-diet (control), 50 mg/kg-diet (LD), 75 mg/kg-diet (MD) and 100 mg/kg-diet (HD) 2-AA for 14 [2WK] and 28 days [4WK]. Analysis of total mRNA extracts from liver for apoptosis-related gene expression changes in AEN, BAX, CASP3, JUN, MDM2, P53, and GAPDH genes by qRT-PCR was coupled with liver tissue histology (H&E staining), TUNEL (Terminal deoxynucleotidyl transferase dUTP nick end-labeling) assay and Caspase (Caspase Glo assay) activity. Dose-related histological changes in liver cell architecture were observed at the highest doses in both 2WK and 4WK exposures. Dose-related increases in TUNEL-positive staining were also observed. Caspase3 assays showed dose-dependent increases (2WK) but suppression in LD and MD [4WK] rat livers and an increase in HD rats. Dose-related increases in expression were observed in all genes measured.

PS 310 Glutathione Levels and Susceptibility to Chemically-Induced Injury in Human Prostate Cancer Cell Lines

L. H. Lash, D. A. Putt and A. Jankovich. *Pharmacology, Wayne State University School of Medicine, Detroit, MI.*

More aggressive or invasive prostate cancer cells (PCCs) are often resistant to chemotherapy and have poor prognosis. Differences exist in redox status and mitochondrial metabolism that may help explain this phenomenon. We compared two immortalized human PCC lines, PC-3 cells (more aggressive) and LNCaP cells (less aggressive), with regard to cellular glutathione (GSH) levels and susceptibility to either oxidants (tert-butyl hydroperoxide [tBH] or methyl vinyl ketone [MVK]) or GSH depletors (diethyl maleate [DEM] or diamide). We tested the hypothesis that compared to less aggressive PCCs, more aggressive PCCs exhibit higher GSH concentrations and are relatively resistant to cytotoxicity from exposure to various oxidants. PC-3 cells exhibited 4.2-fold higher GSH concentration than LNCaP cells. PC-3 cells only exhibited lower lactate dehydrogenase (LDH) release after toxicant exposures than LNCaP cells at some time points but only LNCaP cells underwent diamide-induced apoptosis. Expression of several proteins involved in stress response and regulation of cell growth and proliferation were measured to determine the possible role of altered levels of certain signaling molecules with differential redox state and susceptibility to toxicants. PC-3 cells exhibited higher levels of Bax and caspase-8 cleavage product and lower levels of Bcl-2 than LNCaP cells. Consistent with higher susceptibility to Fas-induced apoptosis, LNCaP cells exhibited higher expression of FasR than PC-3 cells. Consistent with a compensatory response to lower GSH concentrations and generally greater susceptibility to oxidative stress, LNCaP cells exhibited higher levels of GADD153, p53, Hsp27, Cyclin A, SOD2, Trx2, and mitochondrial GSH transporters than PC-3 cells. Thus, significant differences in redox status and expression of proteins involved in apoptosis and stress response may contribute to PCC aggressiveness.

PS 311 Coupling of PARP-1 and Store-Operated Calcium Entry Is Independent of PARG Activity in TGHQ-Induced Cell Death

F. M. Ramirez[1, 2], S. S. Lau[1, 2] and T. J. Monks[1, 2]. [1]*Pharm/Tox College of Pharmacy, U of Arizona, Tucson, AZ and* [2]*SWEHSC, U of Arizona, Tucson, AZ.*

Many pathological conditions, including renal disease, are associated with oxidative stress. 2,3,5-tris(Glutathion-*S*-yl)hydroquinone (TGHQ), a potent nephrotoxic metabolite of benzene and HQ, generates reactive oxygen species (ROS). ROS generation results in damage to cells, including DNA strand breaks, which activate DNA repair enzymes such as poly(ADP-ribose) polymerase (PARP)-1. Under robust oxidative damage, PARP-1 is hyper-activated, leading to increases in intracellular calcium concentrations (iCa^{2+}) as well as NAD^+ and ATP depletion, and ultimately cell death. We are determining the relationship between Ca^{2+} and PARP-1 during cell death of human renal proximal tubule epithelial cells (HK-2). We have shown that extracellular Ca^{2+} is responsible for coupling PARP-1 activation to increases in iCa^{2+} during TGHQ-induced cell death. PARP-1 inhibition attenuates iCa^{2+} increases induced by TGHQ, and treatment with 2-APB, a store-operated Ca^{2+} channel (SOC) inhibitor, restored levels of NAD^+, with simultaneous de-

creases in PAR protein-ribosylation. Since SOC activation has a direct effect on PARP-1 activity, and PARP-1 inhibition attenuates increases in iCa^{2+}, the results show that PARP-1 and SOCs are coupled in TGHQ-induced cell death. We further elucidated the relationship between SOC activation and PARP-1 downstream of PARP-1 activity. Poly(ADP-ribose)glycohydrolase (PARG), which catalyzes the degradation of PARs to yield free ADP-ribose (ADPR), is known to activate SOCs. siRNA knockdown of PARG partially increases PAR ribosylation, but does not restore cell viability in the presence of TGHQ, indicating that free ADPR is not responsible for SOC activation in HK-2 cells. Overall, we show that PARP-1 and Ca^{2+} are coupled through SOC entry, and that the relationship may involve alternative PAR metabolic pathways. We are further investigating the connection between SOCs and PAR metabolism, and other potential mechanism(s) by which PARP-1 and Ca^{2+} interact to contribute to cell death.

PS 312 Flavonoids Kaempferol but Not Morin Showed Toxic Effects to HepG2 Cell Line

M. J. Tasso[1], A. O. Souza[1], L. C. Pereira[2], M. F. Bernardes[2] and D. J. Dorta[1]. *[1]Faculdade de Filosofia, Ciências e Letras de Ribeirão Preto – FFCLRP/USP, Ribeirão Preto, Brazil and [2]Faculdade de Ciências Farmacêuticas de Ribeirão Preto – FCFRP/USP, Ribeirão Preto, Brazil.*

INTRODUCTION: Kaempferol and Morin are polyphenolic compounds belonging to a class of chemicals called flavonoids. Both substances have very similar structures, which differ only in the presence of an extra hydroxyl substituent in Morin. Although flavonoids are widely known due to their anti-oxidant and anti-inflammatory properties, toxic effects were already shown in literature. Therefore, this study was aimed to assess the effects of Morin and Kaempferol in HepG2 cells to check for induction of cell death evidences and to verify if the structural difference influences on toxic effects. METHODS: HepG2 cells were incubated at 37°C, in an atmosphere containing 5% CO2 and 96% relative humidity for 24 hours before treatment and the flavonoids were tested in concentrations ranging from 1μM to 100μM for 24, 48 and 72 hours. Induction of cell death was evaluated by phosphatidylseryne exposure at the outer cell membrane using Anexin V and propidium iodide (PI), followed by the assessment of nuclear fragmentation using Hoechst 33342 fluorescent dye. RESULTS: Kaempferol caused toxic effects in HepG2, since at the highest concentration and all times it increased significantly the phosphatidylseryne exposure. Moreover, it showed significant increase in nuclear fragmentation at 50 and 100μM in 24, 48 and 72h. On the other hand, Morin did not show any toxic effects in both experiments at same conditions. CONCLUSIONS: Kaempferol showed a potencial cytotoxic effect in HepG2 cells at the highest concentrations tested. The cell death observed may occur by apoptotic pathway, since the increase in nuclear fragmentation and in phosphatidylseryne exposure are evidences of this mechanism. However, Morin did not present any cytotoxic effects at same conditions. These results show the importance to do a structure-activity analysis when performing the risk assessment for flavonoids uptake.
Acknowledgments: CNPq - Brazil

PS 312a Diesel Exhaust Particle Exposure Causes Endothelial Cells Apoptosis via Autophagy Pathway

J. Wang[1], C. Tseng[2, 3], J. Chang[1], M. K. Gordon[4] and M. Chao[1, 3]. *[1]Bioscience Technology, Chung Yuan Christian University, Chung-Li, Taiwan, [2]Biomedical Engineering, Chung Yuan Christian University, Chung-Li, Taiwan, [3]Center for Nanotechnology, Chung Yuan Christian University, Chung-Li, Taiwan and [4]Joint Program of Toxicology, Rutgers University, Piscataway, NJ.*

It is well known that inhaled diesel exhaust particles (DEP) injure human endothelial cells. To elucidate the mechanism, we used an in vitro monolayer HUVEC culture model system. 25000 HUVECs were plated in the well of 24-well dishes overnight. Automobile DEP collected from Japan (courtesy of Dr. Sagai, Tokyo) were sonicated in 0.05% Tween80 with PBS for 1 min, then added immediately at 25 μg/mL and 50 μg/mL medium-diluted DEP solution to the dishes. The Cell Titer 96 Aqueous One Solution Assay (Promega) was applied to detect viable cells after at 1, 2, 4, 8, 16, and 24 h after the treatments. We found the cell viability decreased in both time and dose dependent manner, and only 40% and 20% cell survive respectively at 24 h of 25 and 50 μg/mL DEP. For more detail in sample of 50 μg/mL DEP, TUNEL method was used and demonstrated that those 80% dead cells were killed with apoptosis induction. In order to determine by what mechanism that DEP exposure results in apoptosis, the treated cells were harvested for immunofluorescence microscopy and immunoblotting. Interestingly, autophagy markers LC3-II and Atg12 appeared at 2 h and disappeared at 8 h after exposure to DEP. Their expression both reached the maximal level at 4 h. Furthermore, the upregulated expression of caspase3, caspase7, caspase9 were confirmed at various time point as well to indicate DEP induce apoptosis in HUVECs. And, ELISA analysis suggested that caspase 3 and caspase 7 expressions increased in a time dependent manner from 8 h to 24 h, while caspase 9 was initiated to be up-regulated from 16 h. In summary, the upregulation of LC3-II and Atg12 unveiled that DEP might induce HUVEC apoptosis via autophagy pathway.

PS 312b Presence of EndoG in Apoptotic Nuclei during Cisplatin Kidney Injury: A Sign of What?

A. G. Basnakian[1, 2], D. D. Zhdanov[1], T. Fahmi[1], T. Fite[1], K. Topiwala[1] and S. V. Shah[1, 2]. *[1]University of Arkansas for Medical Sciences, Little Rock, AR and [2]Central Arkansas Veterans Healthcare System, Little Rock, AR.*

Endonuclease G (EndoG, EG) is a mitochondrial endonuclease that translocates to nucleus during apoptosis. However, it is unknown whether EG directly causes apoptotic DNA fragmentation and cell death or it is anti-apoptotic. Unlike other apoptotic endonucleases, EG is the only endonuclease found in nucleus during apoptosis, has RNase activity, and induces inactive truncated isoform of another endonuclease, DNase I (DI). We hypothesized that the role of EG in apoptosis depends on the presence of DI in the cell, and used cisplatin kidney injury in vitro and in vivo models to test this. Our pilot observations were that although EG sometimes was present in TUNEL-positive nuclei of cisplatin-treated kidneys, overall it did not coincide with TUNEL. Unlike other endonucleases including DI, EG did not colocalize with DNase activity measured by DNase activity probe in pyknotic nuclei in the cultured kidney tubular epithelial NRK-52E cells. EG overexpression in DI-positive NRK-52E cells showed EG was not cytotoxic but instead protective against cisplatin injury (60 μM) as determined by flow cytometry. EG overexpression induced alternative splicing and inactivation of DI. DI overexpression was also not cytotoxic by itself but it promoted cisplatin injury to the cells. When the same experiment was repeated using DI-negative HCC1954 cells, EG was shown to be cytotoxic and promoting cisplatin-induced cell death. Further study showed that EG was induced but was not cytotoxic in cisplatin kidney injury in vivo. After injection of cisplatin (20 mg/kg), no protection in EG null mice versus wild-type mice was observed by BUN, SCr or histology. EG induction by cisplatin in WT mice was associated with the decrease of native DI expression and appearance of inactive truncated DI. In conclusion, this study showed that EG acts as a proapoptotic enzyme in the absence of DI and it is anti-apoptotic in the presence of DI in kidney cells and the kidney during cisplatin injury.

PS 312c Neuroprotective Effects of Natural Compounds against Dopamine Toxicity

S. Potdar and J. Cavanaugh. *Pharmaceutical Sciences, Pharmacology, Duquesne University, Pittsburgh, PA.* Sponsor: P. Pradeep.

Natural dietary supplements are being hailed as age defying and may, in some cases, present a sustainable medical solution for people around the world. Within the next few decades the aged population in the U.S. will be greater than ever before, increasing the demand for cost-effective medicine for the elderly. One of the major health problems in the elderly are motor deficits, caused, in part, by a loss of dopaminergic neurons. Oxidative stress is known to play a part in this neuronal loss. Resveratrol, a natural compound found in grapes and wild blueberries, has antioxidant, anticancer, and anti-inflammatory properties. Our lab has shown that resveratrol protects dopaminergic-like cells (SH-SY5Y) against oxidative stress induced by high dopamine concentrations. However, resveratrol has low bioavailability, making it important to find alternative compounds with similar properties. Piceid (RV8), an analog of resveratrol, has greater bioavailability than resveratrol. Similar to resveratrol, RV8 protects SH-SY5Y cells against oxidative stress produced by exposure to dopamine, as seen by cell viability assays (CellTiter-Glo® and Dead protease fluorescence assay). Interestingly, RV8 activates the MAP kinases ERK1/2 and ERK5; as seen using western blot analysis. Following inhibition of the ERK1/2 or ERK5 pathways, the neuroprotection afforded by RV8 is lost. In order to test if apoptotic pathways are also involved in RV8 mediated neuroprotection, we examined the expression of Bcl-2, an anti-apoptotic protein, following dopamine +/- RV8 exposure using western blot. Cells exposed to dopamine alone showed reduced Bcl-2 levels. RV8 pretreatment inhibited this dopamine-induced loss of Bcl-2. Overall, these findings suggest that the neuroprotective effects of RV8 are mediated via the activation of ERK1/2, ERK5, and anti-apoptotic proteins.

PS 312d Tert-Butylhydroquinone Antagonizes Arsenic-Induced Oxidative Injury and Apoptosis by Activation of Both NF-E2-Related Factor 2 and B Cell CLL/Lymphoma 2 in Cultured Human Keratinocytes

B. Li, X. Duan, D. Liu and G. Sun. *Department of Occupational and Environmental Health, Key Laboratory of Arsenic-Related Biological Effects and Prevention and Treatment in Liaoning Province, School of Public Health, China Medical University, Shenyang, China.* Sponsor: J. Pi.

Oxidative stress plays crucial roles in exerting a variety of damages upon arsenic exposure, and NF-E2-ralated factor 2 (Nrf2) is a crucial transcriptional regulator protecting cells and tissues from oxidative injury. Here, we tested the antagonistic effects of tert-butylhydroquinone (tBHQ), a well-known synthetic Nrf2 inducer, on arsenic-induced oxidative injuries and apoptosis using cultured human HaCaT cell line. Cells were exposed to sodium arsenite (25 μM) with or without tBHQ (50μM, 12 h) pretreatment for 24 h, and cell proliferation activity, oxidative injury, apoptosis, as well as expression of relevant genes and proteins were examined. Arsenic-induced cytotoxicity, the enhancement of reactive oxygen species generation and lipid peroxidation, and the impairment of anti-oxidative enzymes activity, were all suppressed by tBHQ administration. Arsenic was also found to induce phosphatidylserine externalization, disrupt the mitochondrial membrane potential ($\Delta\Psi m$), release cytochrome c into the cytosol, and trigger the cleavage of caspase-3, typical characteristics of mitochondria-dependent apoptosis. tBHQ co-treatment effectively rescued the cells from arsenic induced apoptosis and related alteration of mitochondria. tBHQ pretreatment resulted in a significant accummulation of nuclear fraction of Nrf2 proteins (155% of control), and Nrf2-regulated downstream genes, heme oxygenase-1 (HO-1) and NADPH:quinine oxidoreductase 1 (NQO1) mRNA expressions were overexpressed. In addition, tBHQ released anti-apoptotic Bcl-2 protein (130% of control), increased Bcl-2:Bax heterodimers and reduced cellular apoptosis. Thus arsenic induces cell apoptosis through the mitochondrial pathway, and the protection of tBHQ appears to include both Nrf2 anti-oxidation and Bcl-2 anti-apoptosis in human keratinocytes.

PS 312e Compound-Induced Bioenergetic Alterations and Cell Loss in Excitable and Nonexcitable Tissues: Relevance to Pathophysiology

W. A. Irwin[1], D. A. Fox[2] and J. Liccione[1]. [1]*HED, US EPA, Crystal City, VA and* [2]*College of Optometry, University of Houston, Houston, TX.*

Cellular processes require consistent and large amounts of energy (high energy phosphates) and ion gradients provided by glycolysis and/or mitochondria. Toxicant-induced energy deficits can result in cellular dysfunction and cell death. Some pathophysiology attributed to direct toxicant effects may partially be explained by decreased energy charge ([ATP]+0.5[ADP]/[ATP+[ADP]+[AMP]) since energy deficits decrease muscle strength and retinal function. Also, dysfunction of the liver, a mitochondrial rich tissue, is a major limitation in drug development. Our goal was to determine the relationship between cellular bioenergetics, function and viability data using a broad range of compounds. Isolated liver and muscle cells and whole retina were acutely exposed to different concentrations of several different compounds (e.g., antimycin A, bupivacaine, cerivastatin, cyclosporin, fructose, D- vs L-glyceraldehyde, lead or oligomycin). The following bioenergetic toxicity metrics were obtained: mitochondrial membrane potential (MMP), energy charge ([ATP] + 0.5[ADP] / [ATP] + [ADP] + [AMP]), [NADH], [lactate], muscle force, and/or oxygen consumption (QO2). Reliable viability data (LDH release, nuclear staining and cell counts, TUNEL) were obtained and compared to the bioenergetic metrics. For most of the above compounds, ATP levels alone did not correlate well with inhibition of cellular metabolism, cell viability or cell number. Energy charge and MMP were superior indicators of overall cellular/tissue metabolism, health and viability. Moreover, [lactate] and [NADH] were good indicators of QO2 inhibition and mitochondrial toxicity. The data for each compound was compared and modeled in these contexts. These findings have relevance for other excitable and non-excitable tissues and suggest that altered bioenergetics contributes to toxicant-induced pathophysiology.
Disclaimer: The opinions listed are those of the authors alone and not necessarily those of the US EPA

PS 312f Frankincense and Myrrh: A Sticky Combination for the Treatment of Lung Cancer

E. R. Esposito[1], M. V. Bystrek[2], S. Boyle[2], J. Borders[2], L. Willinger[2] and K. R. Adair[2]. [1]*Pharmaceutical Sciences, Sullivan University College of Pharmacy, Louisville, KY and* [2]*Pharm D. Candidate, Sullivan University College of Pharmacy, Louisville, KY.*

Purpose: Frankincense (*Boswellias*) and myrrh (*Commiphora*) are two essential oils used as sources of natural medicine for many health conditions. Historically, these oils possess antibacterial, antifungal, anti-inflammatory, and potentially anti-neoplastic properties. Limited studies have been conducted characterizing the effects of these oils specifically on lung cancer cell growth. Using an in vitro model, we aim to characterize the apoptotic effects of these oils in human alveolar adenocarcinomic (A549) cells compared to MRC-5 control cells.
Methods: Cell viability and early/late stages of apoptosis were measured using trypan blue and annexin-V assays. A549 and MRC-5 cells were treated with frankincense and myrrh using 1:500-1:4000 dilutions for 24 hrs and assessed in triplicate. Additionally, experiments using Beta-cyclodextrin and ethanol extractions were used to increase solubility of the myrrh essential oil.
Results: Data suggests that frankincense killed both cell lines at high doses, however cancerous cells did not undergo apoptosis until a higher dose was used (>1:2000 dilutions). Control and cancer cells treated with myrrh alone were non-adherent and suggested apoptosis. Further evaluation of cell permeability suggested that approximately 50% of the non-adherent cells remained viable. Literature suggests that viable, non-adherent cells could be a model of metastizing cancer cells. This suggests that myrrh would not be an advisable treatment option for lung cancer. Future studies are needed to determine if these effects are of significance. Data are the average of three independent experiments +/- standard error of the mean (S.E.M.) Statistical significance is determined $p < 0.05$.

PS 313 A Survey of AflatoxinM1 Levels in White Cheese

R. Ortiz-Martinez, C. De Luna -Lopez, A. G. Valdivia and T. Quezada-Tristan. *Disciplinas Pecuarias, Universidad Autonoma de Aguascalientes, Aguascalientes, Mexico.* Sponsor: G. Pallas-Guzman.

AFM1 is a metabolite of aflatoxin B1 which remains intact even after boiling or pasteurization processes. According to numerous reports, AFM1 is the most frequently detected aflatoxin in dairy products. The International Agency for Research on Cancer (IARC) classified AFB1 and AFM1 as class 1(carcinogenic to humans) and 2B (potentially carcinogenic to humans) respectively. The aim of our study was to assess AFM1 contamination in white cheese, in Aguascalientes, Mexico.
Cheese samples were obtained from convenience stores in eight main localities.
The samples were transported and maintained in a refrigerated insulated container, and stored at 4oC for further analysis. Sample's natural characteristics, lot and brand were identified and recorded. The analyzed cheese was the most affordable presentation of the most popular brands. All samples were analyzed for AFM1, via commercial ELISA kit. Detection range was 5 to 80 ppt.
The results showed that 87% of cheese samples (87/100) had detectable levels of AFM1 which ranged from 5 to 80 ng/kg (mean= 12.85 ± 5.4 ng/kg). In all localities, cheese with AFM1 was found. In addition, all cheese brands exposed contaminated samples too. In our study, AFM1 detected levels were lower than recorded in other countries which have studied AFM1 contamination in dairy products. Levels in some cases exceeded international limits allowed.
Despite Mexico not having tolerance limits for AFM1 in cheese, the results obtained confirm that cheese contamination in the Aguascalientes influence area is a real problem. It is necessary to establish remedial strategies to ensure healthy dairy products.

PS 314 *In Vivo* Metabolism of Fumonisin B_1 to *N*-Acylated Cermaide-Like Compounds

K. A. Voss[1], H. Harrer[2], R. T. Riley[1] and H. Humpf[2]. [1]*Toxicology & Mycotoxin Research Unit, USDA, ARS, Athens, GA and* [2]*Institute of Food Chemistry, University of Münster, Münster, Germany.*

Fumonisins are toxic and carcinogenic mycotoxins found in corn-based foods. Fumonisin B_1 (FB_1) metabolism to ceramide-like cytotoxic *N*-acylated FB_1 ($NAFB_1$) compounds has been shown *in vitro*, but *in vivo* metabolism has not been reported. Therefore, male Sprague-Dawley rats (2/group) were given 5 daily ip doses of 0 (vehicle), 0.5, 1.0 or 2.0 mg/kg body weight (BW) FB_1 (= 0.69, 1.38 and 2.77 μmol/kg BW, respectively). A positive control group was similarly treated with 1.0 mg/kg BW (2.47 μmol/kg BW) hydrolyzed FB_1 (HFB_1), an FB_1 derivative that is metabolized by rats. After the animals were euthanized, FB_1, HFB_1 and their *N*-acyl metabolites were quantified in liver and kidney by HPLC-MS/MS

analysis. Unmetabolized FB_1 accumulated in kidney in a dose-related manner at concentrations of up to 10 nmol/g tissue. Its concentrations in liver were 12 to 20-fold lower. In contrast, more HFB_1 (1.8 nmol/g) was found in liver than in kidneys (0.3 nmol/g). Low levels of $NAFB_1$ and *N*-acylated HFB_1 species ($NAHFB_1$) were found in both tissues. Metabolites having longer fatty acyl chains predominated in liver whereas those with shorter chains were prevalent in kidney: the different chain lengths likely reflecting differences in tissue-specific ceramide synthase isoforms. Metabolite concentrations decreased in the order: $NAHFB_1$ in liver > $NAHFB_1$ in liver > $NAFB_1$ in liver ≥ $NAFB_1$ in kidney. Recoveries (% of dose) of total FB_1 species from the tissues were < 1%. Recovery of HFB_1 species was more variable ranging from about 0.1 % in kidney to about 2% in liver. Except for FB_1 in kidney, where unmetabolized FB_1 was predominant, recoveries (μmolar basis) of parent and metabolites from the tissues were similar. The results show that FB_1 is metabolized by ceramide synthases in vivo to *N*-acylated ceramide-like compounds. Additional studies are needed to determine the toxicological significance of the $NAFB_1$ and $NAHFB_1$ metabolites.

PS 315 Presence of Aflatoxins and Fumonisins in Nixtamalized Masa from Mills in the Metropolitan Area of Monterrey, México

J. M. Villarreal-Guerra[1], P. Gonzalez-Barranco[2], F. Picon-Rubio[3], H. Bernal-Barragan[4] and A. G. Marroquin-Cardona[1]. *[1]Department of Physiology, Pharmacology and Toxicology, Faculty of Veterinary Medicine, Universidad Autonoma de Nuevo Leon, Escobedo, Nuevo Leon, Mexico, [2]Department of Biopharmacy, Faculty of Chemistry Sciences, Universidad Autonoma de Nuevo Leon, San Nicolas de los Garza, Nuevo Leon, Mexico, [3]Department of Nutrition and Metabolism, Faculty of Veterinary Medicine, Universidad Autonoma de Nuevo Leon, Escobedo, Nuevo Leon, Mexico and [4]Department of Nutrition, Faculty of Agronomy, Universidad Autonoma de Nuevo Leon, Escobedo, Nuevo Leon, Mexico.*

Aflatoxins (AFs) and fumonisins (FBs) are toxic metabolites produced by *Aspergillus* and *Fusarium* species that frequently contaminate maize, generating a public health risk due to their hepatotoxic and carcinogenic effects. Traditional nixtamalization (treatment of maize with calcium hydroxide) is partially effective in reducing these toxins but under certain circumstances the toxins can prevail in the masa. The aim of this study was to determine the concentration of AFs and FBs in samples obtained from corn mills in the metropolitan area of Monterrey, México. In total 62 samples of masa were dried, ground and sieved before methanolic extraction of mycotoxins. Samples were analyzed by competitive ELISA (AgraQuant®) for detection of total AFs and FBs. In the results, AFs values ranged from 0 to 22.6 μg/kg, while FBs values ranged from 0 to 16.68 mg/kg. Results showed that some samples had AFs values above the permissible limit (12 μg/kg) according to the official regulation in México (NOM-247-SSA1-2008), while other samples had FBs values exceeding the permissible international limits (4 mg/kg), since México does not have specific limits for FBs. Therefore, we concluded that consumption of nixtamalized masa from some of the mills included in this study may represent a risk for human health.

PS 316 The Effect of Aflatoxin-B1 on Red Drum (*Sciaenops ocellatus*) and Assessment of Dietary Supplementation of NovaSil for the Prevention of Aflatoxicosis

K. Zychowski[1], A. Rodrigues Hoffmann[1], H. J. Ly[1], C. Pohlenz[1], A. Buentello[1, 2], A. A. Romoser[1], D. Gatlin[1] and T. D. Phillips[1]. *[1]Veterinary Integrative Biosciences, Texas A&M University, College Station, TX and [2]Schillinger Genetics, West Des Moines, IA.*

Aflatoxin B1 (AFB1) is a potent carcinogen that causes growth stunting, immunosuppression and liver cancer in multiple species. The recent trend of replacing fishmeal with plant-based proteins in fish feed has amplified the AFB1 exposure risk in farm-raised fish. NovaSil (NS), a calcium montmorillonite clay, has previously been shown to reduce AFB1 bioavailability safely and efficaciously in several mammalian species. This study was designed to: (1) evaluate AFB1 impact on cultured red drum, *Sciaenops ocellatus*, over the course of seven weeks; and (2) assess NS supplementation as a strategy to prevent aflatoxicosis. Fish were fed diets containing 0, 0.1, 0.25, 0.5, 1, 2, 3, or 5 ppm AFB1. Two additional treatment groups were fed either 5 ppm AFB1 + 1% NS or 5 ppm AFB1 + 2% NS. Aflatoxin B1 negatively impacted red drum weight gain, survival, feed efficiency, serum lysozyme concentration, hepatosomatic index (HSI), whole-body lipid levels, liver histopathological scoring, as well as trypsin inhibition. NovaSil inclusion in AFB1-contaminated diets improved weight gain, feed efficiency, serum lysozyme concentration, muscle somatic index, and intraperitoneal fat ratios compared to AFB1-treated fish. Although not significant, NS reduced AFB1-induced histopathological changes in the liver and decreased Proliferating Cell Nuclear Antigen (PCNA) staining. Importantly, NS supplementation improved overall health of AFB1-exposed red drum.

Reprinted from the journal Toxins:
Zychowski, K.E.; Hoffmann, A.R.; Ly, H.J.; Pohlenz, C.; Buentello, A.; Romoser, A; Gatlin, D.M.; Phillips, T.D. The Effect of Aflatoxin-B1 on Red Drum (*Sciaenops ocellatus*) and Assessment of Dietary Supplementation of NovaSil for the Prevention of Aflatoxicosis, Toxins 2013, 5, 1555-1573.

PS 317 Increased Aflatoxin Exposure in Human Populations Residing in West and East Texas, USA

L. Tang[1], M. Kang[1], G. Qian[1], K. S. Xue[1], A. A. Romoser[2], M. F. Carden[4], H. G. Hayes[4], B. H. Pollock[4], F. A. Guerra[3], T. D. Phillips[2] and J. Wang[1]. *[1]University of Georgia, Athens, GA, [2]Texas A&M University, College Station, TX, [3]San Antonio Metropolitan Health District, San Antonio, TX and [4]University of Texas Health Science Center, San Antonio, TX.*

Recently, high levels of aflatoxin (AF) contamination were reported in animal feeds and human foods in US and EU markets. In this study we assessed levels of AFB-lysine adduct, a reliable biomarker of AF exposure, in archived human serum samples collected from previously conducted or current on-going studies in West and East Texas. AFB-lysine adduct was measured via HPLC-fluorescence detection with a limit of detection of 0.4 pg/mg albumin. In West Texas, AFB-lysine adduct was detectable in 9.3% (5/54) of serum samples collected in 2004 with a median level of 0.63 pg/mg albumin (range=0.53-0.91). The detection rate of AFB-lysine adduct was 33.75% (54/160) in serum samples collected in 2006-2007 with a median level of 2.72 pg/mg albumin (range=0.66–62.74). The detection rate of AFB-lysine adduct was 100% (140/140) in serum samples collected in 2008–2009 with a median level of 3.98 pg/mg albumin (range=0.52–11.23). The increase in AFB-lysine adduct detection rate and level among three different collection periods is highly significant (Ptrend<0.001). In East Texas, the AFB-lysine adduct was detectable in 26.7% (46/172) of serum samples collected in 2007–2008 with a median level of 2.35 pg/mg albumin (range=0.41–16.57). The detection rate of AFB-lysine adduct was 87.6% (204/233) in serum samples collected in 2012–2013 with a median level of 3.94 pg/mg albumin (range= 0.41–19.65). The detection rate and levels of AFB-lysine adduct are significantly different between these two collection times (p< 0.001) in East Texas. Results of this study support the hypothesis that AF exposure in US human populations is increasing due to widespread AF contamination in corn and grains. These data suggest that adverse health effects arising from AF exposure should be assessed and that strategies to reduce AF exposure in these human populations need to be developed and implemented.

PS 318 Elderly Male Mice Display Impaired Clearance of Deoxynivalenol

E. S. Clark[1, 2], M. Bates[1, 2], C. J. Doan[1] and J. J. Pestka[1, 2]. *[1]Food Science and Human Nutrition, Michigan State University, East Lansing, MI and [2]Center for Integrative Toxicology, Michigan State University, East Lansing, MI.*

Deoxynivalenol (DON), a trichothecene mycotoxin, is a common cereal grain contaminant that is resistant to processing, leading to contamination of human and animal food. The aim of this study was to test the hypothesis that increased susceptibility to DON-induced anorexia observed in elderly male mice is, in part, due to impaired organ clearance of this mycotoxin. We employed a mouse anorexia bioassay previously described by our lab (Food Chem. Toxicol. 49:1863-1869) to compare the effects of DON exposure in young adult and elderly male mice. Briefly, mice were acutely exposed to 0 and 1 mg/kg bw via IP injection and animals were euthanized at 1, 2, 4, and 12 h post exposure to DON. Organ and plasma DON concentrations were measured using a Veratox High Sensitivity (HS) ELISA with modifications (Food Chem. Toxicol. 46:2826-2831). The rank order of DON concentration measured in organs and plasma was observed to be: kidney > liver > plasma > spleen > heart > brain. Overall, DON concentrations were higher in elderly males versus young adults. The gut satiety hormones, peptide YY (PYY) and cholecystokinin (CCK), were also elevated in elderly mice. These results suggest that impaired metabolism of DON contributes to prolonged feed refusal in elderly male mice. Future research exploring population susceptibility to DON induced-anorexia should consider metabolic differences as contributing factors to susceptibility.

PS 319 *In Vitro* Mechanism Study of *Ginkgo biloba* Leaf Extract-Induced Genotoxicity

N. Mei, H. Lin, X. Guo, S. L. Dial, L. Guo, M. G. Manjanatha and M. M. Moore. *NCTR/FDA, Jefferson, AR.*

Ginkgo biloba has been used for many thousand years as a traditional herbal remedy and its extract has been consumed for many decades as a dietary supplement. *Ginkgo biloba* leaf extract is a complex mixture with many constituents, including flavonol glycosides and terpene lactones. The National Toxicology Program 2-year bioassays found that *Ginkgo biloba* leaf extract targets liver, thyroid gland, and nose of rodents. However, the mechanism of *Ginkgo biloba* leaf extract-associated carcinogenicity remains unclear. In the current study, the *in vitro* genotoxicity of *Ginkgo biloba* leaf extract and its eight constituents were evaluated using the mouse lymphoma assay and the Comet assay, and the underlying mechanisms of *Ginkgo biloba* leaf extract-associated genotoxicity were explored. *Ginkgo biloba* leaf extract, quercetin, and kaempferol resulted in a dose-dependent increase in the mutant frequency and DNA double-strand breaks (DSBs). Western blot analysis confirmed that both quercetin and kaempferol activated DNA damage signaling pathway with increased expressions of γ-H2AX and phosphorylated Chk2 and Chk1. In addition, *Ginkgo biloba* leaf extract produced reactive oxygen species and decreased glutathione levels in L5178Y cells. Loss of heterozygosity analysis indicated that *Ginkgo biloba* leaf extract, quercetin, and kaempferol treatments resulted in extensive chromosomal damage. These results suggest that *Ginkgo biloba* leaf extract and its two constituents, quercetin and kaempferol, are mutagenic to the mouse L5178Y cells with induction of DSBs. Quercetin and kaempferol may be responsible for *Ginkgo biloba* leaf extract-induced genotoxicity. More studies on the mechanism of genotoxicity and carcinogenicity of *Ginkgo biloba* leaf extract warrant for its risk assessment.

PS 320 *In Vitro* Safety Assessment of Pet Food Ingredients on Canine Renal Proximal Tubule Cells

J. Koci[1], B. Jeffery[2], J. E. Riviere[1] and N. A. Monteiro-Riviere[1]. [1]*Department of Anatomy and Physiology, College of Veterinary Medicine, Kansas State University, Manhattan, KS and* [2]*Global Quality and Food Safety, Mars, Inc., McLean, VA.*

In vitro models are useful tools to assess the safety of pet food ingredients. Clove leaf oil (CLO), eugenol (EUG), and lemongrass oil (LGO) are used in flavorings but their toxicity is unknown. These additives and positive control nephrotoxicants ochratoxin A (OTA) and neomycin (NEO) were assessed in canine primary renal proximal tubule cells (RPTC) from dogs (n=5) euthanized for clinical reasons with owner consent, using collagenase digestion, Percoll separation and cell-specific gene-based characterization. AlamarBlue, renal biomarkers (KIM-1, cystatin C and clusterin), and transmission electron microscopy (TEM) were assessed in RPTC after exposure to ingredients ranging from 0.1% (CLO and EUG) and 0.5% (LGO) to 0.0078% (CLO and EUG) and 0.0000064% (LGO) for 24 h. OTA at 25 μM to 25 nM and NEO at 55 mM to 66 μM were exposed to RPTC for 24, 48 and 72h. OTA was toxic to RPTC with comparable LC_{50} values over time of 2.7±1.5 μM (24h), 2.3±0.8 μM (48h) and 2.1±0.6 μM (72h). NEO reduced viability at high concentrations of 40.1±16.8 mM (24h), 17.1±3.4 mM (48h), and 11.9±1.9 mM (72h). LGO was 40-fold more toxic than CLO and EUG with mean LC_{50} values of 0.001±0.001% vs. 0.04±0.01% and 0.04±0.01%, respectively. Despite the fact that LC_{50} and LC_{80} concentrations of CLO, EUG and LGO induced TEM changes in RPTC, renal markers were not significantly different from controls. This study shows that OTA was significantly more potent than NEO in RPTC. LGO was more toxic to RPTC than CLO and EUG, of which the LC_{50} was similar, since EUG constitutes ~80% of CLO. LGO and CLO have not been reported to have adverse effects in dogs, while EUG causes acute oral toxicity with an LD_{50} of 500mg/kg. These findings support the use of in vitro RPTC as a suitable prescreening tool for the safety of pet food ingredients. Future studies using additional and chemically diverse additives will expand the chemical space to which such tools may be applicable.

PS 321 Levels of Benzoic Acid, Sulphur (IV) Oxide, and Sorbic Acid in Commonly Consumed Fruit Drinks and Juices Sold in Lagos Metropolis, Nigeria

C. T. Onwordi[1], A. I. Olanrewaju[1], A. D. Wusu[2], B. Oguntade[3] and O. Ademuyiwa[4]. [1]*Chemistry, Lagos State University, Lagos, Lagos, Nigeria,* [2]*Biochemistry, Lagos State University, Lagos, Lagos, Nigeria,* [3]*Science Laboratory Technology, Federal Polytechnic Ilaro, Ilaro, Ogun, Nigeria and* [4]*Biochemistry, Federal University of Agriculture, Abeokuta, Ogun, Nigeria.*

Residual sulphite as sulphur dioxide causes severe systemic reaction characterised by difficulty in breathing and cardiovascular collapse. Few studies have described exposure of humans to excessive preservatives from food and beverage products in Nigeria. Little is also known about the levels of preservatives such as benzoate, sorbates, sulphur dioxide and ascorbic acid in fruit juices and drinks. Commonly consumed fruit drinks (45) and fruit juices (22) purchased in various markets in Lagos metropolis were analysed for the preservative contents using standard methods. Residual sulphite levels expressed as sulphur dioxide in fruit drinks ranged from 2.0 - 18.4 mg/L, while in fruit juice it ranged from 3.2 - 22.0 mg/L. Ascorbic acid, citric and benzoic acids contents ranged from 6.61-92.50 mg/L, 0.09-0.89 % m/v and 127-799 mg/L respectively. The pH of the drinks ranged from 2.46-5.58. 55% of the samples analysed have benzoic acid content below the regulatory limit. Values of pH, ascorbic acid and sulphur dioxide for all samples were in conformity with standards. 30% of the samples have the citric acid values above required limit of 0.5%m/v (max). 45 % of the total samples analysed have preservative combination of benzoic acid, citric acid and sulphur dioxide levels above the national permitted level of 250ppm mg/L. Benzoic acid concentration was higher in fruit drinks than fruit juice while levels of sulphur dioxide, ascorbic acid content and citric acid were more in fruit juice than drinks. The study showed that more of the fruit drinks analysed did not satisfy the Nigeria Industrial Standard on preservative contents.

PS 322 Association between Advanced Glycation End Products (AGE) and the Receptor for AGE in Colon Carcinogenesis of Azoxymethane-Injected Fischer 344 Rats Fed with a High-Linoleic Acid and High-Glucose Diet

T. Shimomoto and H. Kuniyasu. *Department of Molecular Pathology, Nara Medical University, Kashihara, Nara, Japan.* Sponsor: Y. Satomi.

Advanced glycation end products (AGE) generated by nonenzymatic reactions under hyperglycemic and oxidative condition and the receptor for advanced glycation end products (RAGE) are closely associated with colon cancer progression. And western influence on diet, which typically means increased fat and glucose intake, has increased the incidence of colon cancer. We used an azoxymethane-injected Fischer 344 rat model as one of the animal models for colon carcinogenesis, and examined the association between AGE and RAGE in colon carcinogenesis of the rats fed with the high-linoleic acid and high-glucose diet that represented the feature of western diet. The rats fed with 15% linoleic acid diet and 10% glucose drink showed the pronounced multiplicity of aberrant crypt foci (ACF) and colon carcinomas, 16 weeks and 50 weeks since the feeding respectively, with increased mucosal AGE and RAGE compared with ones fed with normal diet. IEC6 rat intestinal epithelial cells treated with AGE showed increased RAGE expression, which was inhibited by treatment with metformin, a hypoglycemic drug or losartan, an angiotensin receptor antagonist. Treatment for the initially-used rat model with metformin or losartan suppressed the levels of AGE and RAGE and the multiplicity of ACF and colon carcinomas. These results suggest that AGE-RAGE signaling induced by high-linoleic acid and high-glucose diets substantially enhances colon cancer development; thus, suppression of AGE-RAGE signaling could be a potential target for colon cancer chemoprevention.

PS 323 Xenoestrogens in Your Diet?

I. M. Omoruyi, G. Kabiersch and R. Pohjanvirta. *Food Hygiene and Environmental Health, University of Helsinki, Helsinki, Finland.* Sponsor: M. Viluksela.

Processed and packaged food items as well as ready-to-eat snacks are neglected and poorly characterized sources of human exposure to EDCs. In this study, we investigated the presence of xenoestrogens in commercially processed and packaged foods, arising from substances deliberately added to or inadvertently contaminating the food, substances formed as a result of food processing, or substances leaching from food packaging materials. Samples were obtained in 3 separate batches of equivalent products and extracted by solid-phase extraction method. Their endocrine disrupting potential was determined by yeast bioluminescent assay, using two recombinant yeast strains *Saccharomyces cerevisiae* BMAEREluc/ERα and BMA64/

luc. The majority of samples (both foodstuffs and wrappers) analysed proved negative. However, all batches of industrially prepared hamburgers (but not those obtained from a hamburger restaurant) as well as pepper salami significantly induced luciferase activity in the test system, indicating the presence of xenoestrogens, with estradiol equivalents of these products ranging from 0.2 to 443pg/g. All three products contained soy-based ingredients which apparently accounted for, or at least contributed to, their high estrogenic activity, since no signal was observed with extracts of the packaging material, while two different soy sauces tested yielded an intense signal (28 and 54pg/ml estradiol equivalent). These findings imply that by and large, chemicals arising in the processing or packaging of foodstuffs in Finland constitute an insignificant source of xenoestrogens to consumers. However, soy-derived ingredients in certain food items might render the entire products highly estrogenic. The estrogenic activity of soy is attributed to isoflavones whose health effects – though widely considered beneficial – are controversial. As hamburgers are a popular type of food among children, our findings are noteworthy and possibly of concern.

PS 324 Genotoxicity Testing of Genipin, a Precursor in the Derivation of the Natural Food Colorant Gardenia Blue

C. A. Hobbs[1], C. Swartz[1], J. Davis[2], R. R. Maronpot[3], K. Shepard[1], J. Winters[1], A. Green[1], P. Garibaldi[1], P. Allen[4], E. Phillips[2], M. Nixon[2], L. Recio[1] and S. Hayashi[5]. *[1]Genetic and Molecular Toxicology Division, ILS, Inc., Research Triangle Park, NC, [2]Investigative Toxicology Division, ILS, Inc., Research Triangle Park, NC, [3]Maronpot Consulting LLC, Raleigh, NC, [4]Consultant, Cary, NC and [5]San-Ei Gen F.F.I., Inc., Osaka, Japan.*

Gardenia blue is widely used in Eastern Asia as a natural colorant in foods. To evaluate the genotoxic potential of genipin, the natural starting material from which gardenia blue is produced, we conducted a GLP-compliant test battery in accordance with OECD guidelines. No evidence of mutagenicity was measured in a bacterial reverse mutation assay up to a non-cytotoxic dose of 640 mg/plate in *Salmonella* strains TA98, TA100, and TA1535 and in *E. coli* WP2 *uvrA* pKM101, with or without metabolic activation; an equivocal response occurred in *Salmonella* TA97a without metabolic activation. Genipin was also tested for induction of chromosome structural damage in micronucleus (MN) and chromosome aberration assays using human TK6 and Chinese hamster ovary cells, respectively, with and without metabolic activation. The results of both of these *in vitro* tests were positive under some test conditions. To assess the ability to induce DNA damage in a rodent model, we conducted a combined MN/Comet assay in male B6C3F1 mice. Genipin was administered by gavage once daily for 3 consecutive days. Samples were collected 3 hours after the final dosing for measurement of micronucleated reticulocyte (MN-RET) frequencies in blood by flow cytometry and assessment of DNA damage in liver using the Comet assay. No effect of genipin occurred at doses reaching maximal toxicity (8, 25, and 74 mg/kg) on blood MN-RET frequency or DNA damage in the liver of exposed mice. Thus, although our studies showed some *in vitro* evidence of genotoxic potential of genipin, there was no *in vivo* evidence of DNA or chromosome structural damage under the conditions tested. Our results indicate that, with respect to genotoxicity, consumption of genipin in food does not pose a significant concern for humans.

PS 325 Predicting Public Health Consequences of Toxic Chemical Contamination of Food

J. Moser[1, 2] and R. Jablonski[1]. *[1]Chemical Security Analysis Center, Department of Homeland Security, Gunpowder (APG-EA), MD and [2]Battelle Memorial Institute, Columbus, OH.*

To assess the risks (likelihood x consequence) associated with chemical contamination within the U.S. food supply system, it is essential to evaluate potential public health consequences resulting from the dissemination of toxic chemicals through food. The Chemical Security Analysis Center (CSAC), a knowledge analysis and management center under the Department of Homeland Security, developed several hazard and risk assessments related to chemical contamination of food. For the hazard assessments, 12 different food scenarios were evaluated. In each scenario, food was contaminated at a particular point in the manufacturing process; a total of 10 chemicals were analyzed. The CARVER plus Shock method was used as the primary tool to assess the hazard within a specific food processing system. For the risk assessments, 103 chemicals were individually evaluated as threats to human health through contamination and ingestion of 11 different foods. The Chemical Terrorism Risk Assessment (CTRA) Desktop Consequence Calculator, a tool developed by CSAC that incorporates existing models and data inputs from the 2012 CTRA into an easy-to-use platform, was used to determine consequences. This presentation compares the hazard assessment (CARVER plus Shock) and risk assessment (CTRA desktop tool) methodologies used to examine food process systems and provides examples of potential public health consequences that could result from chemical food contamination. The assessments demonstrate the wide range of hazards posed by varying the chemical, varying the contaminated food product, and, in some cases, varying the point of contamination in a food processing system.

PS 326 Inactivation of Pathogens on the Surfaces of Sterile Swabs, Fruits, and Vegetables Using Sanitizing Substances Produced by Radiant Catalytic Ionization

W. J. Mackay[1], C. H. Sommers[2], D. Fulford[1], C. Steele[1], J. T. Mannozzi[1], J. Wallace[1] and V. Filbert[1]. *[1]Biology & Health Services, Edinboro University of PA, Edinboro, PA and [2]Food Safety Group, USDA, Wyndmoor, PA.*

Foodborne illness outbreaks linked to fresh products are becoming more frequent and widespread. The United States Department of Agriculture has estimated the costs associated with foodborne illnesses to be between $2.3 billion and $4.6 billion a year. The areas impacted include fruits and vegetables, meats, seafood, poultry, baking, canning, and dairy industries. Reducing pathogens and additional microbial contamination on food contact surfaces will improve the quality and shelf life of many food products. New sanitizing technologies have emerged in recent years and are being widely used in a multitude of places to better decontaminate contact surfaces. Historically, both ozone-and peroxide-based technologies have been used as disinfectants in numerous applications. Radiant Catalytic Ionization (RCI) technology, particularly ozone, is thought to be safe to humans and the use of ozone is now considered to be an organic form of treatment to disinfect food contact surfaces. RCI technology has been widely accepted within the food processing industry during recent years. Ozone and hydrogen peroxide, generated by RCI, has countless applications for reducing the number of bacteria. This study has focused on the potential use of oxidative gases, including ozone and peroxide, generated by an RCI photocell for the inactivation of *Escherichia coli*, *Listeria inocula*, *Pseudomonas aeruginosa*, *Salmonella typhimurium*, and *Staphylococcus aureus*, introduced on the tips of sterile cotton swabs, and a number of fruits and vegetables which include apples, bananas, spinach, strawberries, oranges, and lettuce. Our results indicate a 99.9% killing of bacteria with a 90 minute exposure to RCI, demonstrating that the low level of oxidative gases produced by RCI has the potential to be an effective surface disinfectant tool for use in food processing.

PS 327 Toxicological Evaluation of Oleic-Rich Algal Oil

M. R. Bauter[1], S. McQuaid[2], T. Chan[2], P. Licari[2], S. Franklin[2], J. Carney[2], R. Green[2], H. Hofman-Hüther[3], N. J. Szabo[4], R. A. Matulka[4] and P. Marone[1]. *[1]Toxicology, Product Safety Labs, Dayton, NJ, [2]Solazyme, South San Francisco, CA, [3]BioService Scientific Laboratories, Behringstrasse, Planegg, Germany and [4]Burdock Group, Orlando, FL.*

The advancement of algae-based food ingredients is ideal for enriching the nutritional profile and functionality of food products. As a prospective new food ingredient, oleic-rich algal oil has been investigated for its potential to induce gene mutations as well as its toxicological potential in a subchronic study in rats. According to a plate incorporation and pre-incubation test by *Salmonella typhimurium* strains and an *E. coli* tester strain at concentrations of 31.6, 100, 316, 1000, 2500 and 5000 μg/plate, no toxic effects, precipitation, or biologically relevant increases in revertant colony numbers of the test item were noted in any of the tester strains used up to the highest dose group evaluated. Therefore, oleic-rich algal oil did not cause gene mutations by base pair changes or frameshifts in the genome of the strains used and was considered to be non-mutagenic in the bacterial reverse mutation assay. In a subchronic study in rats, CD IGS Sprague-Dawley rats consumed 2.5, 5, and 10% test substance in the diet for 90 days and were evaluated. There were no test substance-related changes in viability, behavior, clinical signs, body weight, organ weight, and relative organ weight values between control and treated animals. Decreases in high dose male food consumption throughout the study were not accompanied by decreases in body weight, body weight gain, and food efficiency, and were therefore considered non-adverse and toxicologically insignificant. There were no hematology, clinical chemistry, urinalysis, as well as macroscopic or microscopic observations, post-mortem that were attributed to the administration of oleic-rich algal oil. Based upon these toxicological endpoints, it was concluded that the no-observed-adverse-effect-level (NOAEL) for oleic-rich algal oil is 10% in the diet with no toxicity observed, a level calculated to provide a dietary intake of 5200 and 6419 mg/kg/day in males and females, respectively.

PS 328 Safety Evaluation of TCT Catalase from *T. reesei* for Use in Dietary Supplements

S. MacKenzie[1], E. M. Donner[1], D. Hoban[1], J. Caverly Rae[1], L. A. Belcher[2] and Q. Bui[3]. [1]*DuPont Haskell Global Centers for Health and Environmental Sciences, Newark, DE,* [2]*DuPont Industrial Biosciences, Wilmington, DE and* [3]*DuPont Industrial Biosciences, Palo Alto, CA.*

TCT Catalase is an enzyme used for the production of gluconates, which are used as dietary supplements. The enzyme is produced from a recombinant strain of *Trichoderma reesei*. A battery of toxicology studies was conducted to investigate its potential to cause adverse effects in humans. All studies were conducted according to OECD Principles of Good Laboratory Practice and in compliance with OECD test guidelines. Catalase (from a different microbial host) was not an eye irritant and not toxic by oral gavage, with an oral LD50 in rats greater than 5000 mg/kg body weight (bw). In an *in vitro* cytogenetic test using human peripheral blood lymphocytes, TCT Catalase did not induce structural or numerical chromosomal aberrations in the presence or absence of metabolic activation (S-9 mix) up to the highest concentration tested (5000 μg total protein (TP)/ml). No mutagenic activity was noted in the bacterial reverse mutation (Ames) assay in the presence or absence of S-9 mix, when tested up to 5000 μg TP/plate. In a subchronic 90-day oral gavage study in Crl:CD(SD) rats, no biological or statistically significant differences were observed on in-life, neurobehavioral, clinical pathology (hematology, coagulation, clinical chemistry, urinalysis), or anatomic pathology (organ weights, macroscopic or microscopic pathology) endpoints. The NOAEL was established at 700 mg total organic solids (TOS)/kg bw/day (544 mg total protein/kg bw/day). Under the worst-case scenario that 100% of the catalase is present in the supplement, the maximum daily ingestion under intended usage is 0.1 mg/day or 0.02 mg/kg bw/day, yielding an estimated margin of safety (MOS) of greater than 27,000. Based on this high MOS, the use of TCT Catalase in dietary supplement production is not of toxicological concern.

PS 329 Toxicological Safety Assessment of a *Sceletium tortuosum* Extract

T. Murbach, A. Clewell and J. R. Endres. *AIBMR Life Sciences, Inc., Puyallup, WA.*

A standardized hydroethanolic extract of *Sceletium tortuosum*, a South African plant with a long history of traditional use, is marketed under the trade name Zembrin® as an ingredient for use in functional foods and dietary supplements. It is standardized to contain 0.35–0.45% total alkaloids (mesembrenone and mesembrenol ≥60%, and mesembrine <20%). A 14-day repeated oral toxicity study was conducted at 0, 250, 750, 2500, and 5000 mg/kg bw/d. A 90-day subchronic repeated oral toxicity study was conducted at 0, 100, 300, 450, and 600 mg/kg bw/d. Because *Sceletium tortuosum* has a long history of human use for relaxation, a functional observation battery (FOB), including spontaneous locomotor activity measured using LabMaster ActiMot light-beam frames system was employed. Several parameters such as: locomotion (time resting, moving, and hyperactive in seconds); rearing behavior (time in rearing, number of rearings); spatial parameters; and turning behavior were investigated in the final week of the study. No deaths or treatment-related adverse effects were observed in male or female Crl:(WI)BR Wistar rats in the 14- or 90-day studies. In the 14-day study, the MTD and the NOAEL were concluded as 5000 mg/kg bw/d. The NOAEL from the 90-day study was determined to be 600 mg/kg bw/d, the highest dose tested.

PS 330 Oral Toxicity Assessment of siRNAs and Long Double-Stranded RNAs

J. S. Petrick, J. H. Sherman, W. F. Heydens and S. L. Lemke. *Toxicology, Monsanto Company, Saint Louis, MO.*

New crop traits harnessing RNA interference are being developed using agricultural biotechnology. For example, when expressed in corn plants, double stranded RNA (dsRNA) targeting corn rootworm vacuolar ATPase (vATPase) provides protection against corn rootworm. Although ingested RNA is not known to be toxic, we conducted oral proof of concept toxicity studies in CD-1 mice with dsRNA targeting the mouse ortholog of vATPase. Mice were gavaged with a 218 bp dsRNA or a pool of four 21-mer small interfering RNAs (siRNAs) in an acute oral toxicity study at 2000 mg/kg and in a 28 day oral toxicity study at 1, 10, and 100 mg/kg. Test substances did not affect in-life or necropsy endpoints in either study (e.g. body weight, food consumption, clinical observations, or gross pathology). There were no treatment-related effects on clinical chemistry, hematology, histopathology, or vATPase gene expression in selected tissues (qPCR) in the 28 day study. The NOAELs for both test materials in the acute and 28-day studies were 2000 mg/kg and 100 mg/kg, respectively, the highest doses tested. The proof of concept toxicity assessment for dietary double stranded RNAs presented herein support the conclusions that ingested RNA is not toxic to mammals at large multiples of anticipated human exposure and that toxicological studies with dietary RNAs will contribute little, if anything, to mammalian/human risk assessment.

PS 331 A 3-Week Dietary Toxicity Study of Octenyl Succnic Anhydride (OSA)—Modified Starch in Preweaning Farm Piglets

B. Mahadevan[1], B. A. Thorsrud[2] and H. Ferguson[3]. [1]*Regulatory Affairs, Abbott Nutrition, Abbott Laboratories, Columbus, OH,* [2]*MPI Research, Inc., Mattawan, MI and* [3]*Abbott Nutrition, Abbott Laboratories, Columbus, OH.*

Octenyl Succinic Anhydride (OSA) is a chemically modified starch produced by treating starch with succinic acid and octanol. In infant formula OSA functions as both emulsifier and an emulsion stabilizer. A study in preweaning farm piglets was conducted with OSA to evaluate the safety and impact on growth after 3 weeks of dietary administration starting two days after birth. Three treatment groups of six animals/sex domestic farm piglets were offered OSA in infant formula at respective dose levels of 2, 4 and 20g/L/day. The control article, Amioca Powder, was supplemented in the low- and mid-dose levels of OSA to balance the nutritional profile of the formulations. One additional group of six animals/sex served as the control and received only the Amioca Powder, in infant formula. The control or test article was offered to all groups orally, six times per day for 20 consecutive days and both clinical and general observations for morbidity, mortality, injury, and the availability of food/food consumption were conducted for all animals. Body weight measurements, blood samples for clinical pathology evaluations were also collected from all animals at designated time points. Results from the study indicated that dietary administration of OSA at concentrations of 2, 4, and 20 g/L/day to neonatal piglets over a 3-week period after birth was well tolerated and did not produce any definitive test article-related effects on growth. All animals survived to scheduled necropsy. In addition, the clinical pathology parameters, evaluated, were all within the expected range of variability for this age of animals and species. Also, macroscopic and microscopic observations of the gastrointestinal tract did not reveal any treatment related cellular or tissue effects. Taken together, this study demonstrates the safe use of OSA – modified starch in infant formula using a neonatal piglet model.

PS 332 Nanostructured Synthetic Amorphous Silica—Absence of Disintegration in Intestinal Environment

M. Maier[1], P. Albers[2], R. Retamal Marin[3], F. Babick[3] and M. Stintz[3]. [1]*Inorganic Materials, Evonik Industries AG, Hanau, Germany,* [2]*Aqura GmbH, Hanau, Germany and* [3]*Technical University, Dresden, Germany.* Sponsor: D. Warheit.

Synthetic amorphous silica (SAS) is a nanostructured material formed by flame hydrolysis or precipitation. In commercial SAS products, basic structural elements (fused nanosized primary particles) are submicron aggregates that themselves form micrometer (or even larger) agglomerates. As SAS is employed in processed food, e.g. as free-flow agent, we aimed to investigate potential structural changes following oral uptake.

In a previous study no significant changes in the structure and size distribution of SAS during heating in water (e.g. food processing) and in acid environment (pH of gastric juice) were observed. We now investigated potential structural changes of SAS during the intestinal passage. Intestinal milieu is quite different from gastric conditions with respect to pH as well as the presence of natural solubilizers and residence time is significantly higher.

Food grade precipitated and pyrogenic SAS were studied in an in vitro model. FeSSIF is a fed-state simulated intestinal fluid (acetate buffer, pH 5.0) containing the natural solubilizers sodium taurocholate (bile salt) and phosphatidylcholine (lecithine) in physiological amounts. Following suspension in FeSSIF, SAS was slightly agitated for up to 48 hours (37 °C). To check for the presence or absence of changes in particle size distribution and potential surface degradation samples were analysed by laser diffraction (volume weighted size distribution) and transmission electron microscopy.

Simulated intestinal conditions did not lead to an increase of fine, nanosized SAS particle fractions. There was no indication of chemical reactions or dissolution processes at the surface of SAS particles. In contrast, partial agglomeration of dispersed SAS aggregates was observed shifting the size distribution to its coarse end with large flocculates of several hundreds of micrometers. In conclusion, SAS was shown not to experience additional dispersion or any other type of degradation during the simulated intestinal passage.

PS 333 Toxicological Evaluation of High Purity Genistein from an Alternative Synthetic Route

J. A. Edwards, P. Beilstein and M. Hugentobler. *Product Safety, DSM Nutritional Products, Kaiseraugst, Switzerland.* Sponsor: A. Davidovich.

Genistein is a naturally-occurring isoflavone found in soy. geniVida (≥ 98.5% genistein, manufactured by DSM) has been assessed previously for safety based on a range of toxicity studies (McClain *et al*, three publications in 2005, one in 2007) and obtained self-GRAS status in 2010. An alternative manufacturing process has been developed for genistein. It has the same high purity of ≥ 98.5% but with different trace components to those in the original manufacturing process. A safety assessment of the new process geniVida and its by-products was undertaken. The assessment process comprised:
- Analytical identification of the new by-products
- Literature review for information on new by-products
- *In silico* analysis (DEREK) for toxic alerts of new by-products
- *In vitro* evaluation of estrogenic potential of two potential impurities
- Ames tests (Salmonella Typhimurium Reverse Mutation Assays) and a 13-week rat bridging toxicity study with the new process material
- Comparison of data from the bridging studies and previous studies
- Definition of a new upper limit specification for newly identified by-products

Information presented from this assessment process includes summarized data from the Ames test, which showed no mutagenic potential, with or without S9, and also from the 13-week bridging toxicity study.
From the assessment of all this information it was concluded that ≥ 98.5% geniVida produced from the alternative route is safe and suitable for use as a component of specified foods for consumption by post-menopausal women and mature men, as defined in the GRAS evaluation of the original process material.
McClain RM *et al*, Food and Chemical Toxicology, safety studies with genistein, three publications in 2005, one in 2007.

PS 334 USDA Survey of Dioxins and Dioxin-Like Compounds in the US Domestic Meat and Poultry Supply

P. Basu[1], S. Lupton[2] and M. O'Keefe[1]. [1]*US Department of Agriculture, Food Safety & Inspection Service, Washington, DC and* [2]*US Department of Agriculture, Agricultural Research Service, Fargo, ND.* Sponsor: K. Dearfield.

The USDA Food Safety and Inspection Service (FSIS) and the Agricultural Research Service, conducts periodic, statistically based survey of dioxins and dioxin-like compounds (DLC) in domestic meat and poultry, to estimate the levels of DLCs in FSIS-regulated meat and poultry products, to compare levels found in the various products to past years' results and collaborate with other Agencies to investigate causes of any detected spikes in dioxin levels. These surveys have been held every 5 years since the mid-1990. From the data, background levels of dioxins in domestic beef, pork and poultry are determined.
Since mid-1990s, DLC levels in beef, pork and poultry have either declined or remained static. In the last 2007-08 dioxin survey, 17 toxic PCDD and PCDFs and 4 PCBs were measured in 510 beef, market hog, young turkey and young chicken samples. In the Fiscal Year (FY) 2013 dioxin survey, FSIS plans to duplicate the previous survey. The FY-13 survey data will also be compared to past results to determine temporal trends. Along with consumption data for beef, pork, and poultry, the survey data are used to calculate consumer exposure estimates to dioxins.
EPA released their chronic oral reference dose (RfD) for 2,3,7,8-TCDD of 0.7pg/kg-day for human exposure in 2002. For the FY-13 survey, calculations based on the EPA RfD were used to determine dioxin trigger levels (2pg TEQ/g fat for beef and 4pg TEQ/g fat for poultry and pork) that would initiate on-farm investigations for samples above the trigger level. Thus far 6 beef samples were found to be above the trigger level and are under FDA investigation. Current beef, pork, chicken and turkey dioxin levels are 0.088-6.46 pg TEQ/g fat, 0.051-0.36 pg TEQ/g fat, 0.046-0.39 pg TEQ/g fat, and 0.052-1.32 pg TEQ/g fat, respectively. Comparing the median of these data to previous surveys, there are decreases in the overall levels of dioxins over the past 5 years.

PS 335 The Supplement Quercetin Synergistically Augments Tamsulosin-Induced Vasorelaxation

M. Vrolijk, G. Haenen, A. Opperhuizen and A. Bast. *Department of Toxicology, Maastricht University, Maastricht, Netherlands.*

Tamsulosin (Tams) belongs to the drugs of first choice in the pharmacotherapy of prostate disorders. A major side effect is orthostatic hypotension, which is caused by vasorelaxation resulting from α1-adrenergic blockade. Orthostatic hypotension drastically increases the risk of falling. Fall related injuries are the fifth leading cause of death in elderly. The supplement quercetin (Q) is often used as self-medication in the treatment of prostate disorders. Q, similarly to Tams, induces vasorelaxation, thereby increasing the risk for orthostatic hypotension. This overlapping profile prompted us to investigate the interaction of Q with Tams. Since Q is extensively metabolized, the effects of the metabolites Q-3-glucuronide and 4'O-methyl-Q on Tams effects are also included.
We have determined the potentiating effects Q and Q metabolites on Tams-induced vasorelaxation. This was tested on rat mesenteric arteries constricted by the α1-adrenergic agonist phenylephrine.
Tams (0.1 nM) decreased phenylephrine-induced vasoconstriction 16-fold. Q (5, 10 and 20 μM) caused a substantial concentration-dependent (of 5, 7 and 9-fold respectively) decrease of phenylephrine-induced vasoconstriction, while Q-3-glucuronide (10 μM) and 4'O-methyl-Q (10 μM) only slightly decreased this activity (3 and 2-fold).The combination of Tams with Q or Q metabolites proved to be very potent. Q, Q-3-glucuronide and 4'O-methyl-Q synergistically increased the Tams effects to 275, 57 and 169-fold respectively.
Our results show that there is a drastic pharmacodynamic interaction between the drug Tams and the supplement Q. Tams effects are synergistically amplified by Q, 4'O-methyl-Q or Q-3-glucuronide. The interaction of Q and Tams with potentially serious consequences draws attention to drug-supplement interactions that have been neglected thus far.

PS 336 Physiological Effects of Endophyte-Infected Perennial Ryegrass Straw on Female Camels in the Middle East

J. M. Duringer[1], L. L. Blythe[2], K. Alabdouli[3], A. Elkhouly[3], A. Al Juboori[3] and A. M. Craig[2]. [1]*Environmental and Molecular Toxicology, Oregon State University, Corvallis, OR,* [2]*College of Veterinary Medicine, Oregon State University, Corvallis, OR and* [3]*Al Ain Veterinary Laboratory, Abu Dhabi Food Control Authority, Al Ain, United Arab Emirates.*

The Unites Arab Emirates is currently evaluating external sources of forage, including perennial ryegrass (*Lolium perenne*) straw, for its rapidly growing livestock industry. Unfortunately, perennial ryegrass may be infected with the endophyte *Neotyphodium lolii* which produces lolitrem B, a toxic alkaloid responsible for the neurological syndrome ryegrass staggers. Thus, a range-finding study was conducted in 24 female camels fed four doses (0, 1111, 1478 and 2273 ppb) of lolitrem B-containing perennial ryegrass straw over 56 days to establish a threshold of toxicity in camels so that perennial ryegrass straw can be safely fed as part of their dietary ration. Morphometric and blood chemistry values were evaluated. Body weight was adversely affected by consumption of lolitrem B-camels fed a diet free of lolitrem B gained more (7.4%) than the other three groups (-2.5%, 0.5% and -8.8% for 1111 ppb, 1478 ppb and 2273 ppb, respectively ($p < 0.001$)). Blood urea nitrogen increased significantly in the three treatment groups ($p < 0.001$), which is indicative of kidney damage. Brain edema, degenerative renal and hepatic lesions as well as Purkinje cell vacuolar degeneration were observed in two necropsied camels receiving the highest dose of lolitrem B. Neurological deficits were assessed by videotape and scored using an established scale for ryegrass staggers. Mean date of onset of ataxia was 35.8, 43.7 and 19.8 days (1111, 1478 and 2273 ppb, respectively). A "lip droop" was also seen in affected camels in which the lower lip was amyotonic and fell ninety degrees perpendicular to the lower jaw, similar to a partial facial nerve paralysis; this has not been reported in other ryegrass toxicosis studies. Based on these observations, we recommend that endophyte-infected perennial ryegrass straw be fed at 500 ppb or lower lolitrem B to avoid clinical disease in camels.

PS 337 Do Highly Purified Steviol Glycoside Sweeteners Cause Food Allergies?

J. D. Urban[1], C. L. Doepker[2], N. Cuellar-Kingston[3], J. van de Ligt[3] and M. Carakostas[4]. [1]*ToxStrategies, Austin, TX,* [2]*ToxStrategies, Fort Thomas, KY,* [3]*Cargill Incorporated, Wayzata, MN and* [4]*ToxStrategies, St. Helena Island, SC.*

Steviol glycoside sweeteners were permitted for use in the United States by the FDA beginning in late 2008. Prior to that, they were only allowed as dietary supplements, and most stevia products before 2008 were not highly purified (≥ 95% steviol glycosides). Steviol glycoside sweeteners are extracted from the plant *Stevia rebaudiana* (Bertoni), a member of the *Asteraceae* (Compositae) family. A number of member plants from this family can induce hypersensitivity reactions via multiple routes of exposure: dermal, inhalation, and ingestion. Well-known members of this plant family include the common herbs, widely consumed foods, and the allergens ragweed, goldenrod, and Chrysanthemum. Based on this common taxonomy, food allergy warnings for stevia are given in some popular food information sources. Not surprisingly, many non-scientific media reports and resources allege the potential for stevia allergy. To determine if such allergy warnings are warranted on stevia products, a comprehensive literature search was conducted to identify all available data related to consumption of stevia extracts or highly purified steviol

glycoside products and allergic responses. Based on the peer-reviewed literature, hypersensitivity to stevia is rare, and the few cases documented in the literature were reported prior to the introduction of high-purity products to the market, which was considered when global regulatory authorities affirmed the safety of steviol glycosides. Additionally, neither stevia manufacturers nor food allergy networks have reported significant numbers of any adverse events related to ingestion of this sweetener. Diligently maintained manufacturer post market surveillance data indicate a normalized (to sales) incidence rate of <1.1 incident/10 million servings. There have been no reports in the scientific literature since 2008 of stevia-related allergy. Therefore, there is little evidence to support warning statements to consumers about allergy to highly purified stevia extracts.

PS 338 A 28-Day Gavage Toxicity Study in Fischer 344 Rats with 3-Methylfuran

S. S. Gill[1], M. Kavanagh[1], W. Cherry[1], M. Barker[1], M. Weld[2] and G. Cooke[1]. [1]*Toxicology Research Division, Health Canada, Ottawa, ON, Canada and* [2]*Chemical Health Hazard Assessment Division, Health Canada, Ottawa, ON, Canada.*
Sponsor: R. Mehta.

3-Methylfuran is produced in foods during food processing and preservation techniques that involve heat treatment such as cooking, jarring, canning and pasteurization. Currently there are no studies available on the toxicity of 3-methylfuran. We conducted a 28-day gavage toxicity study (7 days per week) using doses of 0.0, 0.1, 0.3, 1.5, 3.0, 6.0, 12.0 and 25.0 mg/kg bw/day to in order to determine the dose range needed to establish a No Observed Adverse Effect Level (NOAEL) and to better characterize non-neoplastic effects including those affecting hematology, clinical biochemistry, gross morphology and histopathology. Histological changes of the liver were noted in all treated animals and gross changes were noted beginning at 3.0 mg/kg bw/kg. Alterations in the activity of serum enzymes indicative of effects on the liver were observed, including increases in levels of ALT and ALP at the highest dose. There was a significant increase in serum thyroxine (T4) and triiodothyronine (T3) which was not accompanied by histological changes in the thyroid. For the most part, statistically significant changes were seen only at the highest dose for hematology and at the two highest doses for clinical chemistry parameters. In contrast, mild histological lesions in the liver were observed even at the lowest dose of 0.1 mg/kg bw/day.

PS 339 Safety, Efficacy, and Toxicological Evaluation of a Novel, Patented Antidiabetic Extract of *Trigonella foenum-graecum* Seed Extract (CR0010810)

M. Bagchi[1], A. Swaroop[2], D. Bagchi[2] and P. Kumar[2]. [1]*Dr. Herbs LLC, Concord, CA and* [2]*R&D, Cepham Inc, Piscataway, NJ.*

This study was conducted to examine the safety and efficacy of a novel, patented *Trigonella foenum-graecum* seed extract (Fenfuro, CR0010810). This study evaluated the safety of CR0010810 in a variety of toxicological assays including acute oral toxicity studies in male and female Sprague-Dawley rats and Swiss albino mice, as well as repeated dose 28-days oral toxicity study in rats. Four groups of male and female rats and mice (n=5) were orally administered a single dose of either 0, 500, 1000 or 2,000 mg/kg body weight. Rats and mice were euthanized and gross necropsy examinations were carried out on the 15th day. No observable toxic effects were observed in rats or mice. In another set of experiment, Sprague-Dawley rats were orally administered either 0, 250, 500 or 1,000 mg/kg/day over a period of 28 consecutive days. No toxicological or clinical abnormalities were observed. The anti-diabetic potential of CR0010810 (150 and 450 mg/kg p.o.) was chronically evaluated for 30 days, once daily orally for first 20 days and later administered twice for the last 10 days, in type 2 diabetic rat model (streptozotocin 55 mg/kg i.p.). CR0010810 (450 mg/kg) treatment in streptozotocin-induced diabetic rats exhibited significant hypoglycemic activity (approximately 31.5%) as compared to insulin (48.2% with 1 U/kg i.p.). Further studies in animals and humans are in progress to unveil the broad spectrum safety and anti-diabetic potential of this novel fenugreek extract CR0010810.

PS 340 Effect of Omega-3 Fatty Acid Oxidation Products on the Cellular and Mitochondrial Toxicity of BDE 47

A. Yeh[1], S. E. Kruse[2], D. J. Marcinek[2] and E. P. Gallagher[1]. [1]*Department of Environmental and Occupational Health Sciences, University of Washington, Seattle, WA and* [2]*Department of Radiology, University of Washington, Seattle, WA.*

High levels of the toxic PBDE flame retardant 2,2',4,4'-tetrabromodiphenyl ether (BDE 47) detected in fish species such as salmon have raised concern over the safety of salmon consumption. However, salmon are also rich in omega-3 polyunsaturated fatty acids, specifically, eicosapentaenoic acid (EPA) and docosahexaenoic acid (DHA), which are potent antioxidants. In particular, recent reports implicate the oxidation products of omega-3 fatty acids as critical mediators of the beneficial cellular antioxidant responses associated with dietary intake of omega-3s. In the current study, we used an in vitro approach to test the hypothesis that oxidized omega-3s can ameliorate the cellular and mitochondrial toxicity of BDE 47. HepG2 cells were treated with a mixture of oxidized EPA and DHA (oxEPA/oxDHA) to induce a maximal cellular antioxidant response as evidenced by glutathione (GSH) biosynthesis, followed by exposure to BDE 47. Significant induction of GSH by the oxEPA/oxDHA mixture was associated with a small but significant protective effect against BDE 47-induced loss of cell viability, and with significant protection against loss of mitochondrial membrane potential. Examination of mitochondrial respiration in permeabilized cells revealed that oxEPA/oxDHA pretreatment partially but significantly protected against loss in both State 3 mitochondrial respiration and maximum respiratory capacity (uncoupled respiration). Pretreatment with oxEPA/oxDHA also tended to protect against loss of proton leak respiration (State 4), and of flux capacity through complexes II and IV. Our results support a chemoprotective effect of dietary antioxidants against co-consumed persistent contaminants. This study also provides some biochemical insight into assessing the safety of, and risks associated with, seafood consumption.

PS 341 Safety of Carrageenan in Infant Formula: A 4-Week Toxicity Study in Preweaning Piglets

M. L. Weiner[1], H. Ferguson[4], B. A. Thorsrud[2], K. G. Nelson[3], W. Blakemore[5] and B. Frantz[2]. [1]*TOXpertise, LLC, Princeton, NJ,* [2]*Developmental & Reproductive Toxicology, MPI Research, Mattawan, MI,* [3]*Pathology, MPI Research, Mattawan, MI,* [4]*Abbott Nutrition, Columbus, OH and* [5]*Celtic Colloids, Topsham, ME.*

Carrageenan (CGN) is a sulfated galactose polymer extracted from seaweed widely used in the food industry. The potential effects of κ/λ-CGN (Mw 700 kDa, viscosity 80cps) fed to preweaning Yorkshire crossbred piglets (6/sex/group) 2 days after birth for 28 days were evaluated at concentrations of 0, 300, 1000 & 2250 ppm in infant formula, offered 6x/day, at a volume of 500 mL/kg/day. Clinical observations, body weight & food consumption were recorded daily on each animal. Food efficiency & compound consumption were calculated. Blood was collected for hematology, clinical chemistry & coagulation parameters. Urinalysis was performed via cystocentesis. At scheduled necropsy, piglets were evaluated macroscopically and a complete list of tissues was examined microscopically. There were no deaths from CGN. The CGN formulations were well tolerated by the piglets with clinical findings, body weight & food consumption comparable among all groups. No effects seen on hematology, clinical chemistry & coagulation due to CGN, compared to control animals. Glucosuria was noted in 1 male & 3 female piglets at 2250 ppm on day 29, but blood glucose & renal histopathology were normal. Thus, glucosuria was not considered toxicologically meaningful. No adverse tissue histopathology was noted related to CGN treatment. Toluidine blue staining of gastrointestinal tissues for mast cell assessment showed no differences due to CGN. Assessment of Periodic Acid-Schiff staining of the jejunum goblet cell showed no differences due to CGN. In conclusion, the results of this study verified that dietary exposure to CGN at concentrations of 2250 ppm in infant formula (430-448 mg/kg/day) produced no adverse or treatment-related changes in the growth & development of preweaning piglets or any adverse changes to the parameters evaluated. Funded by FMC Corporation & the International Formula Council.

PS 342 Safety of Carrageenan in Infant Formula: A 4-Week Study of the Potential Immune System Effects in Preweaning Piglets

B. Zeigler[2], M. J. Cameron[2], K. G. Nelson[3], B. A. Thorsrud[4], M. L. Weiner[1], H. Ferguson[5], B. Frantz[4] and W. Blakemore[6]. [1]*TOXpertise, LLC, Princeton, NJ,* [2]*Immunology, MPI Research, Mattawan, MI,* [3]*Pathology, MPI Research, Mattawan, MI,* [4]*Developmental & Reproductive Toxicology, MPI Research, Mattawan, MI,* [5]*Abbott Nutrition, Columbus, OH and* [6]*Celtic Colloids, Topsham, ME.*

Exposure to κ/λ-carrageenan (Mw 700 kDa, η 80cps) at concentrations of 0, 100, 300 & 2250 ppm in infant formula was evaluated for potential effects on the immune system in preweaning Yorkshire crossbred piglets, using validated methods

for immunophenotyping, circulating cytokines & immunohistochemistry (ICH) of the stomach, duodenum, jejunum, ileum proximal & distal colon, cecum, rectum. Piglets (6/sex/group) were offered infant formula 6 times/day at a volume of 500 mL/kg/day from 2 days of age for 28 days. Whole blood was collected from animals on days 14 & 19 & evaluated for peripheral blood leukocytes by flow cytometry. All cells types analyzed (lymphocytes, monocytes, B cells, helper T cells, cytotoxic T cells, mature T cells) did not show a biologically significant effect in relative cell percentage or absolute cell counts after carrageenan administration at 2250 ppm. No significant effects across gender or time interval (Day 14 or 19) were observed. Sandwich immunoassays were used for cytokine evaluation. Serum samples were evaluated for IL-6 & IL-8, and plasma samples were evaluated for IL-1β & TNF-α, using commercial, validated ELISA kits. There were no test article effects on levels of any of the cytokines. A validated ICH method was used to evaluate gastrointestinal tissue samples for IL-8 & TNF-α. H&E staining was used to complement the ICH. The results of the ICH evaluation were negative for all treated groups; less than the positive control (Dextran Sodium Sulfate) between study controls (0 ppm carrageenan) & carrageenan-treated animals. In conclusion, carrageenan at concentrations of 2250 ppm in infant formula did not cause any treatment-related immunotoxicity or immunomodulation in preweaning piglets using three validated methods. Funded by FMC Corporation & the International Formula Council.

PS 343 Safety of Carrageenan in Infant Formula: A 4-Week Toxicokinetic Evaluation in Preweaning Piglets

W. Blakemore[4], A. Brant[2], L. Cochrane[2], M. Pellerin[2], B. A. Thorsrud[3], M. L. Weiner[1], H. Ferguson[5] and B. Frantz[3]. *[1]TOXpertise, LLC, Princeton, NJ, [2]BioAnalytical, MPI, Mattawan, MI, [3]Developmental & Reproductive Toxicology, MPI, Mattawan, MI, [4]Celtic Colloids, Topsham, ME and [5]Abbott Nutrition, Columbus, OH.*

A toxicokinetic evaluation was performed in Yorkshire crossbred preweaning piglets fed κ/λ-carrageenan (Mw 700 kDa, η 80cps) at concentrations of 0,100, 300 & 2250 ppm in infant formula. Piglets (3/sex/group) were fed formula 6x/day at a volume of 500 mL/kg/day from 2 days old for 28 days. Blood was collected on days 3 & 28 via the vena cava for analyses of poligeenan (PGN) plasma concentrations. Due to the strong binding of carrageenan to plasma proteins, analysis of carrageenan was not feasible. Thus, the lower molecular weight sulfated polygalactan, PGN, was a reasonable surrogate for carrageenan. A method was developed using LC-MS/MS for the determination of plasma PGN concentrations with a Limit of Quantitation of <10 μg/mL. The results showed a positive signal on days 3 & 28, similar to PGN, in some plasma samples at relatively low concentrations (~20-30 μg/mL) in control & treated animals, without a dose relationship, mostly in male piglets. This pattern is not consistent with exposure, based on the compound consumption of carrageenan because (1) a positive signal was seen in all male control animals; (2) similar values were observed in all males at 300 & 1000 ppm; (3) the signal did not produce a dose-response in treated groups, only 1 male & 1 female had positive signals at 2250 ppm & (4) a positive signal was almost exclusively limited to males. It is highly unlikely that the signal is PGN, as control animals were not exposed to carrageenan & all the treated animals were exposed to increasing amounts based on the dose group, as confirmed by formulation analysis. In summary, the pattern of signal using this method is more consistent with a signal produced by an endogenous moiety in plasma with a higher incidence in males. It is concluded that carrageenan is not absorbed by preweaning piglets. Funded by FMC Corporation and the International Formula Council.

PS 343a Evaluation of Concentrations of Nickel, Lead, Cadmium, and Vanadium in Marine Species of the Market "La Nueva Viga," Using ICP-MS

L. V. Saldívar, L. G. Hernández, G. B. Torres, T. Rodríguez Salazar and M. Espejel. *Analytical Chemistry, UNAM, Mexico City, Mexico.* Sponsor: D. Acosta.

Toxic metals adversely affect people's health. In very small quantities, many of these metals are necessary to keep good health. However, in larger amounts, they become toxic. The toxicological and environmental studies have focused interest in the determination of toxic metals in foods, particularly fish in the marine environment. In this work cadmium, vanadium, lead, and nickel were analyzed in fish: "mojarra tilapia" and "sierra" sampled in the largest seafood market of Latin America "La Nueva Viga" located in Mexico City. The best sold fish species are the "mojarra tilapia", "sierra", shrimp, octopus, crab, sea bass and red snapper. Inductively Coupled Plasma Mass Spectrometry (ICP-MS) was used, because it presents wide spectral range, good accuracy and precision, high sensitivity and selectivity. This technique permits the simultaneous detection of elements at low concentration and very small samples. The sample of "mojarra tilapia" and "sierra" was collected in 6 sectors of the market. Samples were dried, grinded and homogenized. The chemical treatment was performed using a Microwave Digestion System prior to the quantification. Analytical parameters were obtained with certified reference material (Dogfish Muscle DORM-2 and Lobster Hepatopancreas TORT-2 (limit of detection, limit of quantification, linear and working range, accuracy and precision). Important for the method development was the selection of the analyte isotope and the internal standards. The mentioned elements were determined finding the following concentrations:
"mojarra tilapia" muscle: Ni (0.2-1.2) mg/kg; Pb (0.03-0.12) mg/kg; Cd (0.19-0.22) mg/kg and V (0.043-0.048) mg/kg
"sierra" muscle: Ni (0.2-0.3) mg/kg; Pb (0.03-0.16) mg/kg; Cd (0.20-0.22) mg/kg and V (0.010-0.012) mg/kg
The results were compared with national and international norms and all the values were below the maximum allowable limit.

PS 343b Evidence for Fumonisin Inhibition of Ceramide Synthase in Humans: Validation in Follow-Up Studies in Guatemala

R. T. Riley[1], J. L. Showker[1], K. A. Voss[1], J. B. Gelineau-van Waes[2], J. R. Maddox[2], A. E. Ashley-Koch[3], S. G. Gregory[3], J. Matute[4] and O. Torres[4]. *[1]Toxicology and Mycotoxin Research Unit, USDA-ARS, Athens, GA, [2]Pharmacology, Creighton University School of Medicine, Omaha, NE, [3]Medicine, Duke University Medical Center, Durham, NC and [4]Centro de Investigaciones en Nutrición y Salud, Guatemala City, Guatemala.*

Fumonisins (FB) are mycotoxins found in corn. FB1 is the most common FB. It is the cause of farm animal diseases and is carcinogenic in rodents. The mode of action is the inhibition of ceramide synthase (CerS). Inhibition of CerS in mice causes a dose-dependent accumulation of sphinganine 1-phosphate (Sa1P) in blood and an increase in the ratio of Sa1P/sphingosine 1-phosphate (So1P). The purpose of this IRB approved study was to validate recent findings in Guatemala showing a significant direct correlation between urinary FB1 and the Sa1P/So1P ratio in blood spots collected from 1240 women in 2011 and 2012 from three separate departments, Chimaltenango (low FB intake), Escuintla (low FB intake) and Jutiapa (high FB intake). Based on a survey of FB in corn conducted in May to October 2012, three different departments were selected for the validation study: Sacatepéquez, Chiquimula and Santa Rosa. The average total FB in the corn from the three departments, respectively, was 1.0 mg/kg (n=48), 4.6 mg/kg (n=33), and 3.8 mg/kg (n=42). Approximately 300 urine and blood spot samples were collected in March and April 2013 from the three departments. Corn samples (n=30) from the same locations and times were collected and analyzed for FB to confirm low and high contamination. The level of FB in corn collected from local markets was significantly higher in Chiquimula and Santa Rosa compared to Sacatepéquez. The urinary FB1, the Sa1P/So1P ratio, and Sa1P/mg protein in blood spots were also significantly higher in Chiquimula and Santa Rosa compared to Sacatepéquez. This study confirms the findings of the earlier study. The results are consistent with the hypothesis that FB1 disrupts sphingolipid metabolism in humans consuming large amounts of FB contaminated corn. Supported by NIH grant # 1 RC4 HD067971-01.

PS 343c Evaluation of Food-Relevant Chemicals in ToxCast Phase II

A. L. Forgacs[1, 3], J. Hsieh[2] and K. Houck[3]. *[1]Technical Committee on Food and Chemical Safety Summer Fellow, ILSI North America, Washington, DC, [2]NTP, NIEHS, RTP, NC and [3]NCCT, EPA, RTP, NC.*

Phase II of the ToxCast screening program evaluated 1892 chemicals across hundreds of in vitro assays aiming to help prioritize chemicals that may need more extensive toxicological evaluation and to identify targets for potential toxicity pathways. To evaluate the possible impact on food safety, the ToxCast chemical inventory was mined for food-relevant chemicals including direct food ingredients classified as Generally Recognized As Safe (GRAS) and Food Contact Substances (FCS) and indirect food additives. Publicly available FDA sources including the Everything Added to Food in the US (EAFUS), GRAS and FCS databases identified 5,322 food-relevant chemicals. The 1892 ToxCast phase II chemicals included 828 food-relevant chemicals, of which 507 are FCS and 321 are either GRAS or direct food ingredients. The median AC50 values for food-relevant chemicals across assays were largely 10-100 uM, consistent with the entire ToxCast chemical library. Leadscope chemoinformatics identified 191 chemical clusters using physical/structural properties, with 105 chemicals as singletons not included in the clusters. "Enrichment" between clusters and assays using a modified Fisher's test revealed all assays had at least one chemical cluster enriched. Most assays had <10 enriched clusters. Identification of 8 chemical clusters enriched in more than 100 assays and 78 chemical clusters not enriched in any assay suggests that this clustering approach successfully identified properties associated with biochemical activity in the in vitro assays. In conclusion, using Leadscope chemical clustering to evaluate food-relevant chemicals in the ToxCast screening data successfully identified assays in which

specific food-relevant chemical clusters are enriched. These assays may be candidates for initial screening of chemicals for food safety. This work was sponsored by the ILSI NA Food and Chemical Safety Committee 2012 Summer Fellowship Program. This abstract does not necessarily reflect US EPA policy.

PS 343d β-Alanine: Absorption, Distribution, and Elimination following Single or Repeated Administration to Rats

A. Augustine[1], R. Slauter[1], C. Rosenfeld[1], J. Mielke[1], B. Frantz[1], A. Miedema[1], B. Fuller[1], J. Librizzi[1], B. Molitor[1], S. Smith[1], T. Dubnicka[1] and H. Ferguson[2]. [1]*Drug Metabolism and Pharmacokinetics, MPI Research, Inc., Mattawan, MI and* [2]*Abbott Nutrition, Inc., Columbus, OH.*

β-alanine (BA) is a nutritional supplement used to enhance workout capacity and delay fatigue. To ensure the safety of BA when used as a dietary supplement, a complete understanding of the absorption, distribution and elimination (ADE) of BA and it's metabolites is necessary. These studies assess the ADE of [14C]BA and its radiolabeled metabolites following single or daily oral administration of BA.
A single, oral dose of 2-[14C]BA was given to groups of adult, male, Sprague-Dawley rats once, or following 28 days of daily oral gavage administration at 1,000 or 2,000 mg BA/kg body weight. No adverse effects of either single or daily administration of BA for 28 days occurred. There were no quantitative or qualitative differences in the ADE profiles between animals receiving [14C]BA once and animals that received 28 days of BA prior to receiving a single dose of [14C]BA. BA was absorbed into and disappeared rapidly (T1/2 < 4hr) from the plasma. Total radioactivity in the plasma persisted, however (T1/2 >24 hours). Excretion in urine predominated (~40% of dose), followed by exhalation of [14C]O2 (26.7% of dose); 5.8% of the dose was excreted in the feces. The results of Quantitative Whole Body Autoradiography (QWBA) showed that BA and its radiolabeled metabolites were widely distributed. On average, only 6% of the administered dose remained in the body168 hours following [14C]BA, uniformly distributed in skeletal muscle.
In summary, there were no adverse effects caused by repeated, high-dose administration of BA. Excretion was predominantly in the urine, followed by exhaled [14C]O2, and feces, during the 168 hours following [14C]BA. Daily administration of BA for 28 days had no effect on the ADE of BA and its metabolites. Approximately 6% of the administered dose remained in the residual carcass, on average, 168 hours following administration of the radiolabeled dose.

PS 343e Oral Repeated 28-Day Study of Moniliformin in Sprague-Dawley According to OECD 407 Rats

K. Peltonen[1], M. Jonsson[1], M. Jestoi[1], A. Nathanail[1], J. Atosuo[2], U. Kokkonen[1], M. Anttila[1], P. Koivisto[1] and E. Lilius[2]. [1]*Finnish Food Safety Authority, Helsinki, Finland and* [2]*Biochemistry and Food Chemistry, University of Turku, Turku, Finland.*

Moniliformin, a Fusarium mycotoxin commonly present in grains in Northern Europa was tested in an oral repeated 28 days study conducted according to OECD 407 guideline. We have shown earlier that a LD50 cut off value of monilifirmin is 25 mf/kg bw in Sprague-Dawley rats. In this study five exposed (3, 6, 9, 12 and 15 mg/kg bw day) and two satellite groups (12 and 15 mg/kg bw day) were exposed daily to moniliformin by gavage (male Sprague-Dawley rats, 9 to 10 weeks, weight from 217 to 307 g, five animals in each group). 36 animals survived without a clear sign of toxicity. Two out of 40 rats showed decreased activity and acute heart failure. No treatment related differences between control and exposed groups were recorded (body weight, feed and water consumption, organ weights). We observed degreased phagocyte activity in exposed animals and neutrophil activity even in low dose group (3mg/bw day) was less than 59%. The activity did not recover during the two weeks period in the satellite group in which the activity even further decreased beeing only 72% after two weeks of exposure. Clearance of moniliformin to urine was only 20 to 31% of administered dose and no significant differencies were seen between dose groups. Moniliformin excretion to feces was less than 1%.
Academy of Finland is acknowledged for financial support.

PS 343f Carrageenan Is Not a Ligand for Toll-Like Receptor 4 (TLR4) in a Human Embryonic Kidney (HEK) Cell Model

J. M. McKim[1], P. C. Wilga[1], J. Pregenzer[1] and W. Blakemore[2]. [1]*CeeTox, Inc., Kalamazoo, MI and* [2]*Celtic Colloids, Inc., Topsham, ME.*

Carrageenan (CGN) belongs to a group of viscosifying polysaccharides that are extracted from certain species of red seaweeds in the family *Rhodophyceae*. CGN is composed of a linear backbone of galactose sugars linked together by alternating alpha 1-3 and beta 1-4 glycosidic linkages. CGN sugar units are both sulfated and non-sulfated. There are three major commercial forms of CGN (lambda-, kappa-, and iota-) which differ by the number and position of the sulfate moieties. CGN is used by the food industry as a thickening and stabilizing agent. Several recent studies using a human colonic cell line (NCM460) have reported that CGN is a ligand for TLR4 and that binding of CGN to TLR4 leads to inflammation. To date, direct binding to TLR4 by CGN has not been shown. Therefore, the aim of this study was to characterize the possible binding of CGN to TLR4 and subsequent activation of downstream signaling events. To accomplish this, a stably co-transfected HEK293 cell line that expresses full-length TLR4 and the secreted alkaline phosphatase (SEAP) under the control of NF-kB response element (Imgenix) was used. Cells were treated with the positive control, lipopolysaccharide (LPS), and to food grade CGN, commercially available lambda-, kappa- and iota-CGN, and to clarified locust bean gum (CLBG), a negative control. All test agents were administered to the cells at concentrations ranging from 0.1-5000 ng/mL and incubated for 24 hr at 37°C in the presence of 10% fetal bovine serum. Each treatment group was prepared in triplicate wells and the experiment repeated on two separate days. Following the exposure period, activation of TLR4 signaling was assessed by measuring SEAP in the culture medium. LPS increased SEAP in a concentration-dependent manner with a maximum response at 50 ng/mL. In contrast, there was no detectable increase in SEAP following exposure to CLBG, or to any form of CGN. These data indicate that under standard cell culture conditions, CGN is not a ligand/agonist for TLR4 in this HEK cell model.

PS 343g Maximum Concentration of Oils Tested in 13-Week Dietary Studies in Rats: Is Five Percent Optimal?

L. Dolan[1], R. Green[2] and G. A. Burdock[1]. [1]*Burdock Group, Orlando, FL and* [2]*Solazyme, Inc., San Francisco, CA.*

An increasing number of "healthy" fats or oils are being developed to replace "unhealthy" fats. Producers of "healthy" fats often propose high human usage levels (typically on the order of 10 - 40 g/day), necessitating demonstration of safety in laboratory animals at high doses. The time-tested convention of using 5% as the upper concentration in subchronic, dietary toxicity studies of macroingredients in rats is being revisited by regulatory agencies based on the fact that the margin of safety between a no observable adverse effect level (NOAEL) of 5% in the rat and estimated consumption of the ingredient in humans is substantially lower than the classical value of 100 fold. Therefore, unless properties of the oil (e.g. laxative, taste) necessitate use of lower doses, it may be prudent to use concentrations higher than 5% in 13-week dietary studies in rats. A comprehensive search of the literature on oils was conducted to determine the optimum high dose of oils for use in 13-week rat studies. The maximum concentrations of oils used in the studies ranged from 1.5 - 25%. The highest dose used in most of the studies was 10% or 15%. NOAELs for most oils were 1.5 - 10% (if tested). For some oils, adverse effects were observed at the highest doses. In general, lipidosis and toxicity to the liver were observed at concentrations ranging from 12.5 - 25%. Toxicological effects that were oil-specific were identified using concentrations ≤ 5%. The results support use of 5 -10% as the highest concentration, unless particular oil characteristics prompt concerns that use of such a dose would be expected to cause harm to the animal. Use of higher concentrations may cause nonspecific or secondary effects due to administration of large amounts of oil, which may confound interpretation and have no relevance for humans consuming oils at the levels used in food. The lack of reports of toxicity in humans of oils used in food supports the hypothesis that the maximum doses of oils that have been used historically in 13-week dietary studies in rats are sufficient for risk assessment purposes.

PS 343h Safety Evaluation Methods for Supplemental Nutrients

A. W. Wong[1] and J. N. Hathcock[2]. [1]*Council for Responsible Nutrition, Washington, DC and* [2]*John Hathcock Consulting, Alexandria, VA.*

With increasing use of dietary supplements, including those containing nutrients, it is important to determine levels that may be safely consumed. Several regulatory and authoritative bodies have employed the Tolerable Upper Intake Level (UL) method for assessing their safety. For most nutrients, the UL applies to total intake from all sources rather than to supplemental sources. The Council for Responsible Nutrition (CRN) has developed safety evaluation methods to identify an Upper Level for Supplements (ULS). Using these methods, an UL is set if evaluation of the data shows risk. If no risk is identified, a Highest Observed Intake (HOI) can be established as the highest intake as reported within (a) study(ies) of acceptable quality. When appropriate data on supplemental intakes are available, the ULS may be determined by risk assessment directly (direct safety method). If such data are not available, an indirect/difference method may be used by determining the UL or HOI of a nutrient from all sources, identifying usual intakes from foods, and calculating the ULS as a difference. Both methods rely almost exclusively on human data because extrapolation from animals, regardless of how robust and

extensive the dataset, carries a large uncertainty. Application of the CRN methods allows for the derivation of an ULS based on a HOI value for nutrients with no established adverse effects (e.g. vitamin B12), whereas the decision by some authoritative bodies not to set an UL for these nutrients may not adequately communicate the abundance of data available, leading to a perception that there is insufficient evidence to evaluate safety. Additionally, the CRN methods only consider effects that represent a true hazard rather than nuisance effects (e.g. skin flushing associated with niacin). Moreover, these methods conservatively select human No-Observed-Adverse-Effect Levels that do not require adjustment by an uncertainty factor (e.g. vitamin D). The CRN methods are a valuable tool for consumers and their health care providers to make informed decisions about safe and appropriate supplementation levels.

PS 343i Assessing Potential Interactions of "Active" Ingredients in Food

B. S. Lynch and A. Roberts. *Cantox Health Sciences International, Mississauga, ON, Canada.*

Over the past few decades, many foods have come to contain "active ingredients", often marketed to perform a functional role in maintenance of health or improvement in athletic and/or cognitive performance. Safety concerns about potential interactions of these active ingredients have been raised, a case in point being that of "energy" or "sport" drinks. Currently there is no consensus on methodology by which biological interactions of ingredients can be assessed. Also, there are generally few studies available specifically designed to assess interactions. We describe a paradigm, using "first principles" of pharmacokinetics, physiology, pharmacology, and toxicology, for assessing interactions of biologically active food ingredients. The method involves assessment of pharmacokinetics and physiological activity, and of the toxicological outcomes, of the ingredients individually, then using this information to predict potential for additive, synergistic, or antagonistic effects at doses encountered in food. As a case study, the potential for adverse effects from the interaction of common "active" ingredients in energy drinks was evaluated. Caffeine is ubiquitously present in energy drinks. Other ingredients commonly found in these products include: guarana seed extract, d-glucuronolactone, taurine, L-carnitine, inositol, quercetin, and ginseng extract. Typically, caffeine and taurine are present at about 200 and 1000-2000 mg/container, respectively, while the concentrations of the other ingredients generally ranges from 25 to 200 mg/container. Following compilation of the available data for each ingredient, and application of the "first principles" analysis, we found little to no potential for interaction for all but caffeine and taurine. In fact, it is likely that taurine may ameliorate some of the cardiovascular and neurological stimulant properties of caffeine. The results of our analysis are consistent with previously published opinions with respect to the effects of caffeine, taurine and other ingredients present in energy drinks.

PS 343j Assessment of Human Exposures to Fumonisin B1 in Ghana Using LC MS/MS

K. Rychlik[1], N. J. Mitchell[1], S. Elmore[1], A. A. Romoser[1], P. Jolly[2] and T. D. Phillips[1]. [1]*Veterinary Integrative Biosciences, College of Veterinary Medicine and Biomedical Sciences, Texas A&M University, College Station, TX and* [2]*School of Public Health, University of Alabama at Birmingham, Birmingham, AL.*

Humans can be exposed to fumonisin B1 (FB1) through ingestion of contaminated grain products. FB1 has been shown to co-occur with other mycotoxins including aflatoxin, and may act as a pro-carcinogen. Evaluating toxin exposures through the use of biological markers in vulnerable populations is essential for risk determination and the development of food safety strategies. An ultra-performance liquid chromatography/electrospray ionization tandem mass spectrometry method (UPLC/ESI-MS/MS) has been developed to detect FB1 in human urine following purification and concentration with a fumonitest immunoaffinity column. Cleanup conditions were optimized to obtain maximum analyte recovery and sensitivity. Validation was performed in the range of 2-200 μg/L based on expected urinary concentrations. LOD for the method was equal to 0.01 μg/L with an LOQ of 0.1 μg/L. A mean apparent recovery of 71.5% with an inter-day precision of 24.69% relative standard deviation (RSD) was achieved. In this study, 40 urine samples were collected from three Regions in Ghana (i.e., Central, Ashanti, and Greater Accra), and evaluated for the presence of FB1. Our results indicated that 16 out of 40 (40%) of the samples were positive for FB1 (37.5% in the Central, 46% in the Ashanti, and 36% in the Greater Accra Regions). These samples were previously shown to be positive for aflatoxin M1, indicating that Ghanaians exposed to aflatoxins may be co-exposed to fumonisins and that mitigation strategies for multiple mycotoxins are needed in high-risk populations (Research supported by NIH1R01MD005819-01).

PS 344 Chronic Intrathecal Infusion/Sampling via a Surgically Implanted Access Port with Functional Observation Battery Evaluation in Cynomolgus Monkeys

R. Tavcar[1], S. Authier[1], M. Meghazzi[1], S. Groom[1] and R. Forster[2]. [1]*CiToxLAB North America, Laval, QC, Canada and* [2]*CiToxLAB France, Evreux, France.*

Intrathecal administration (IT) and sampling continues to be critical in non-clinical pharmaceutical development for drugs that must be delivered across the blood-brain barrier or to allow sampling of cerebral spinal fluid (CSF) to investigate pharmacokinetics. In alignment with the 3Rs (reduction, replacement, refinement) we have refined a method to allow long term intrathecal administration of candidate drugs and/or sampling of CSF. In addition, a modified function observation battery (FOB) often conducted as part of the ICH S7A safety pharmacology core battery, was developed for the evaluation of neurological changes in non-human primates. A cerebrospinal fluid catheter was inserted into the intrathecal space in the vertebral lamina (L3) and connected to a vascular access port. Implanted animals were first used for the evaluation of the cerebrospinal pharmacokinetics of a pharmaceutical, with CSF sampling of 10 timepoints over a period of 36 hours. Following the end of the first phase the animals were fitted with a jacket and tether system to evaluate the feasibility of continuous infusion for 28 days with PBS. Following the 28 day period, the animals were assessed using a FOB evaluation and euthanized for histopathological evaluation. No neurological abnormalities were observed and minimum to mild catheter-associated chronic granulomatous inflammation was associated with the catheter in the subarachnoid space at the injection/sampling site, next to the spinal cord and spinal nerve roots. Similar moderate catheter-associated chronic granulomatous inflammation was also noted along the catheter track beside the vertebral body and dorsal spinal process below the lumbar muscles. In conclusion, the port/catheters were patent for the duration of the experiments (over 100 days in total), greater than the duration of a chronic study. Therefore the improved method was deemed to be appropriate for long term toxicological, neurological and pharmacokinetic evaluations in Cynomolgus monkeys.

PS 345 Successful Conduct of Continuous Intravenous Infusion Combined with Intrathecal Implantation and Administration in the Juvenile Monkey

J. Douville, T. Robillard and L. Bernier. *Charles River, Monteal, QC, Canada.* Sponsor: M. Vezina.

Early childhood onset of neurological diseases present several challenges and often these diseases represent rare, unmet medical needs. Potential drug candidates may need to cross the blood-brain barrier to reach their target, which may or may not be feasible via systemic administration depending on the nature of the compound. To mimic the clinical scenario as closely as possible, intravenous (IV) infusion and/or cerebrospinal administration in juvenile animals would be indicated. Undertaking such surgical procedures and achieving a viable model in juvenile animals also presents significant challenges. Herein, we show that concomitant surgical implantation of a femoral IV catheter and an intrathecal (IT) catheter at the lumbar level (comparable to clinical site of injection) in juvenile cynomolgus monkeys (18-23 months old) can be successfully achieved. The IT catheter was implanted via a microlaminectomy procedure of the L5 vertebra followed by a durotomy and catheter insertion in the IT space. A subcutaneous pocket was created in the lumbar region, cranial to the catheter site, and the access port was secured to the muscle and the catheter connected to the port. For the IV cannulation, the femoral vein was isolated and the catheter was inserted; the tip of the catheter was placed in the vena cava. The catheter was secured in place with appropriate suture material and brought subcutaneously to an exteriorization point on the animal's back. Post surgical recovery was completed over a 7-day period. Animals were administered saline by continuous IV infusion and by IT injection every other day over 14 days. Endpoints evaluated included body weights, clinical observations, hematology, coagulation, clinical biochemistry, neurological examinations, gross observations at necropsy as well as histopathology. The results obtained are comparable to historical data obtained in animals of 2 to 5 years undergoing similar experimental procedures and as such feasibility of continuous IV infusion combined with IT implantation at the lumbar level for injection was confirmed.

PS 346 A Validation Safety Pharmacology Study of the Central Nervous System, Employing a Functional Observational Battery (FOB) in Female Cynomolgus Monkey

L. Hu[1], W. Zheng[1], B. Platzack[1, 2], R. A. Bialecki[1, 2], Y. Chen[1, 3], H. Yu[1] and J. Ren[1]. [1]*Center for Drug Safety and Evaluation Research of the Shanghai Institute of Material Medica, Shanghai, China,* [2]*Global Safety Assessment, AstraZeneca, Alderley park, United Kingdom and* [3]*AstraZeneca R&D, Boston, MA.*

The objective of this study was to establish and validate a functional observational battery (FOB) at the Center for Drug Safety Evaluation & Research (CDSER) that provides a basic neurological and behavioral assessment in group housed Cynomolgus Monkey.
Four female cynomolgus monkeys were assigned to this study and were given vehicle, chlorpromazine, (+)MK-801 or caffeine in 4 separated days. A FOB was performed and recorded by two independent observers for each animal at designated time points in order to minimize the subjective biases.
The administration of 5 mg/kg chlorpromazine resulted in sedative effect between 0.5 and 3 hrs and decreased body temperature at 1 hr post dose. The dose of (+)MK-801 (0.1, 0.5, 1.25 and 2.5 mg/kg) resulted in suppressed behavior (low arousal, infrequent vocalization, hypoactive), autonomic responses (salivation, decreased respiration and rectal temperature) and sensorimotor/neuromuscular alternations (un-coordinated, lack of auditory response, tremor/convulsion) at all doses, and unconscious/pupil dilation at high doses (1.25 and 2.5 mg/kg). Caffeine resulted in stimulant behavioral (high arousal, hyperactivity and intermittent circling behavior) at dose of 30 mg/kg and one of two monkeys at dose of 45 mg/kg (between 0.5 and 4.5 hr post dose). At higher doses (one at 45 mg/kg and one at 60 mg/kg), caffeine resulted in decreased arousal and hypoactive between 0.5 and 3 hrs post dose. Autonomic alteration was evidenced by vomiting/retching seen in 45 and 60 mg/kg monkeys between 0.5 and 3 hrs post dose.
In conclusion, the observations recorded in this study were consistent with expected pharmacological effects of the neurosedative or neurostimulant reference substances. A FOB in group housed cynomolgus monkeys has been successfully established at CDSER for safety pharmacology and/or toxicology studies to support regulatory submission.

PS 347 Comparative Neurotoxicity and Sex Sensitivity of Neurotoxicants in Wistar Rats

S. Jadhav[1], D. Gohel[1], M. V. Patel[1], V. J. Piccirillo[2], P. Mehta[1], K. Shah[1] and M. Pandya[1]. [1]*Toxicology, Jai Research Foundation, Valvada, Gujarat, India and* [2]*VJP Consulting, Inc, Ashburn, VA.*

Various toxicity data of selected chemicals are prevailing in published literatures which are contradictory at many places. Hence, the aim of the study was to compare effects of model neurotoxicants in 10 male and 10 female Wistar rats per chemical and avail the data on ideal dose levels and dosing frequency. Single dose of Carbaryl (CBR) and Triademafon (TDF) were administered at 100 and 150 mg/kg b. wt. via oral gavage. Trimethyltin (TMT) was administered at 5 mg/kg b. wt./day through intraperitoneal route for 3 days. ALM was administered at 30 mg/kg b. wt./day via oral gavage for 16 days. Dose levels and frequency of dosing were decided based on dose range finding study and published data. Vehicle control groups were dosed with either corn oil or 0.5 % CMC. A Functional Observational Battery (FOB) was performed at 0.5-1 hour (CBR), 1-2 hours (TDF), on day 3 (TMT) and on day 15 (ALM) to evaluate differences in the neurotoxicity and behavioural effect and sex sensitivity considering the time of peak effect. At termination, all the animals were sacrificed and subjected to gross and neuropathological examination. Animals dosed with CBR developed signs of neurotoxicity; impaired mobility, motor activity and rearing counts, lacrimation, salivation and low grip strength. TDF dosing caused hyperactivity with increased rearing counts and motor activity in rats. In TMT dosed rats, low rearing count and motor activity, affected approach and touch response, abnormal righting reflex and piloerection, neuronal degeneration and karyorrhexis in brain were noted. ALM induced impaired mobility, rearing count and motor activity and low grip strength. These results supports that the dose levels and dosing frequency selected were ideal to evaluate different signs of neurotoxicity. However, inspite of pronounce effect, no sex related differences revealed with any of the chemicals tested.

PS 348 Side Effects of MK-801 As a Positive Control for a Rat Neurotoxicity Study

W. F. Roosen, E. J. De Waal, D. Abbott, A. Vynckier, Y. Van Bekkum, A. Lampo and W. Coussement. *Drug Safety Sciences, Janssen Research & Development, a Division of Janssen Pharmaceutica N.V., Beerse, Antwerp, Belgium.*

N-methyl-D-aspartate (NMDA) receptor antagonists have been shown to produce neuronal vacuolation and degeneration in the posterior cingulate and retrosplenial cortex of the rat brain after a single dose. The NMDA receptor antagonist MK-801 (dizocilpine) is well known to produce these so-called Olney lesions in rats after a single subcutaneous dose of 0.5 to 10 mg/kg. In the literature these dose levels have been administered to rats generally without apparent side effects. However, occasionally recumbency of dose-related duration was reported at 1 to 5 mg/kg. Females were particularly prone to this effect. Female rats are also known to more vulnerable to the induction of Olney lesions than males.
In preparation of a full single dose neurotoxicity study with an investigative NMDA receptor antagonist in rats to investigate its potential to induce Olney lesions, first a small scale single dose neurotoxicity study in female rats was conducted to investigate the tolerability of the positive control MK-801 at 0.5, 1, 2 or 5 mg/kg. On the 4th day after dosing, the rats were killed and the brains were sampled and perfused with 3% glutaraldehyde.
At 0.5, 1 and 2 mg/kg pronounced clinical signs were noted showing a dose-related increased in severity and duration. The main observations were hypotonia, decreased general activity, decubitus (at 2 mg/kg), salivation and body weight loss during the first 24 hours. Thereafter ataxia and a general poor condition (chromodacryorrhea, piloerection, hunched back) occurred at 0.5 and 1 mg/kg up to 48 hours post-dose, and at 2 mg/kg till necropsy. A partial or full recovery was observed at 0.5 and 1 mg/kg on the 4th day after dosing, but not at 2 mg/kg. The intended dose of 5 mg/kg was not given due to severe symptoms noted at lower doses. Olney lesions were observed histologically at 0.5, 1 and 2 mg/kg.
It can be concluded that a single dose of 1 mg/kg is the maximum tolerated dose level of MK-801 in females, based on the prolonged clinical signs and body weight loss.

PS 349 Potential Mechanisms Leading to Neurotoxicity following N-Butanol Exposure

A. S. Bale. *National Center for Environmental Assessment, US EPA, Washington, DC.*

There is growing interest with respect to potential widespread human exposure of n-butanol toxicity due to consideration of usage as a fuel additive. However, limited evidence of toxicities, including neurotoxicity, following exposure to n-butanol is available. Neurotoxicity effects resulting from either an acute or subchronic exposure to n-butanol primarily consist of disruption in motor movement and coordination in experimental animal studies conducted to date. In humans, one study reported that exposure to n-butanol exacerbated hearing impairment in workers chronically exposed to high noise conditions. Studies with n-butyl acetate, a metabolic precursor to n-butanol, have reported no neurobehavioral changes with repeated exposure in rodent studies. However, significant decreases in absolute brain weight in male rats have been observed following n-butyl acetate exposure. The purpose of the current investigation is to examine available mechanistic data with n-butanol and explore potential mechanisms that might lead to the observed neurotoxic effects. Acute mechanistic studies with n-butanol have suggested a linkage between the observed neurological effects and alterations in neuronal receptors (e.g. ion channels, g-protein coupled receptors), transport systems, and direct interaction with phospholipases and cellular adhesion molecules. These findings from the mechanistic data suggest that there may be some similarities with n-butanol to other known neurotoxicants such ethanol. (Disclaimer: The views expressed are those of the authors and do not necessarily represent the views or policies of the US EPA.)

PS 350 1, 3-Dinitrobenzene Induces Age-, Region-, and Pathway-Specific Oxidative Modification of Mitochondria-Related Proteins

L. Kubik[1], R. W. Landis[1], H. A. Remmer[2], M. Ford[3] and M. A. Philbert[1]. [1]*Toxicology Program, University of Michigan, Ann Arbor, MI,* [2]*Department of Biological Chemistry, Medical School, University of Michigan, Ann Arbor, MI and* [3]*MS BioWorks, LLC, Ann Arbor, MI.*

The mechanistic basis of the selective vulnerability of brain regions to xenobiotics and increased sensitivity as a function of age is poorly understood. 1,3-Dinitrobenzene (DNB) causes spongiform changes in the energy-demanding regions of the brainstem in rats. Male Fisher 344 rats (1mo, 3mo and 18mo)

were exposed to 10mg/kg DNB, i.p., and mitochondria (mt) isolated from cortex and brainstem by differential centrifugation. Mitochondrial proteins were separated by SDS-PAGE and analyzed by LC-MS/MS to identify protein modifications. Database searches were performed using the Mascot search engine and NCBI & UniProt databases. Results were displayed in ScaffoldTM software and the Normalized Spectral Abundance Factor (NSAF) and %Oxidation were calculated. Proteins were selected for pathway analysis in the Database for Annotation, Visualization and Integrated Discovery (DAVID) based on <0.25 or >4.0-fold changed by NSAF or %Oxidation. Brains from 1mo control rats had significantly higher levels of native proteins in several key metabolic pathways, whereas brains from older control animals showed lower levels of native protein. While cortical %Oxidation was not affected by age, specific brainstem mt-proteins were more prone to oxidation, i.e, the number of oxidized brainstem mt-proteins increased with age. Pathway analysis revealed that DNB caused age-related oxidation specific for protein and nucleotide binding [cation transmembrane transporters, nucleoside-triphosphatases, pyrophosphatases, and hydrolases, ($p<0.05$)]. These data suggest that oxidation of the brain mitochondrial proteome is region, age and pathway specific and that brainstem mitochondria are more susceptible to oxidative xenobiotic injury as a function of age than their cortical counterparts. This work was supported by NIH 2R01 ES08846 (MAP) and NIH 2T32 ES007062 (LLK).

PS 351 Dioxin-Like and Non-Dioxin-Like Polychlorinated Biphenyls (PCBs) Modulate Basal and Activity-Dependent Dendritic Arborization in Primary Neuronal Cell Cultures

C. Barnhart, W. Feng, Y. Dong, I. N. Pessah and P. Lein. *Molecular Biosciences, University of California, Davis, Davis, CA.*

PCBs are ubiquitous environmental contaminants that have been linked to cognitive and behavioral deficits in children and experimental animals. We previously demonstrated that exposure to the non-dioxin-like (NDL) PCB congener 95 increases dendritic arborization of primary hippocampal neurons in vitro via activation of the ryanodine receptor (RyR) calcium channel. However, whether other PCBs similarly trigger dendritic growth via RyR-dependent mechanisms is unknown. To address this question, we measured the effects of NDL PCB congeners 95 and 52 and dioxin-like (DL) PCB congener 77 on RyR activation and on dendritic arbor complexity. Radioligand-receptor binding analysis with tritiated ryanodine (3H-Ry) showed that PCBs 95 and 52 increased specific receptor occupancy, indicating RyR sensitization; however, the concentration-effect relationships differed. In contrast, PCB 77 did not affect 3H-Ry binding. To determine whether RyR sensitization predicted effects on dendritic growth patterns, primary cultures of perinatal rat hippocampal neurons were exposed to varying concentrations of each congener for 48 h, and the number of dendritic termini was quantified as a measure of dendritic arbor complexity. Each congener enhanced dendritic growth, but exhibited a unique concentration-effect relationship that did not correlate with potency of RyR activation. PCB exposure reduced arbor complexity in neurons treated with bicuculline, a GABA receptor antagonist that stimulates dendritic arborization, indicating an antagonistic interaction between PCBs and activity on dendritic growth. These data demonstrate that dendritic arborization may be a convergent cellular outcome in PCB developmental neurotoxicity, but that NDL and DL PCBs may stimulate dendritic growth via RyR-dependent and/or –independent pathways. This work was supported by NIH (grants R01 ES014901, R01 ES017425, T32 ES007059), the ARCS Foundation, and the Superfund Research Program (P42 ES04699).

PS 352 Perfluorobutyrate (PFBA) Produces Dose-, Time-, and Sex-Dependent Pupillary Light Reflex (PLR) Deficits and Retinal Degeneration

D. A. Fox[1], J. A. Hart[2], T. N. John[3], D. J. Ehresman[2], S. Chaney[1], R. Hamilton[1], S. Chang[2] and J. L. Butenhoff[2]. *[1]Univ Houston, Houston, TX, [2]3M, St. Paul, MN and [3]Pace Analytical, Minneapolis, MN.*

During toxicological evaluation of PFBA, we saw a delayed direct PLR in Sprague-Dawley male, but not female, rats exposed to 30 mg/kg PFBA by oral gavage for 90 days. No other signs of neurotoxicity were seen (Reprod Toxicol 2012). To characterize this unusual deficit, retinas from males and females were stained and examined. To determine time course and dose-dependence, the PLR was assessed prior to and weekly during a 28 day exposure of male rats to 0, 30 and 150 mg/kg PFBA (n=18-40/group) followed by retinal histology and immunocytochemistry (n=6-10/group). Staining of the 90 day PFBA retinas with the fluorescent nuclear dye DAPI revealed significant decreases in outer (ONL), inner (INL), ganglion cell layer (GCL) and total retinal (TR) thickness in males, but not females, relative to controls. PLR studies in dark-adapted 0, 30 and 150 PFBA groups showed significant dose- and time-dependent delays beginning 1 week after exposure. DAPI staining revealed significant dose-dependent decreases in ONL, INL, GCL and TR thickness. In the 150 PFBA group compared to controls, single- and double label confocal studies demonstrated a loss of bipolar cells and retinal ganglion cells (RGCs), with no increase in GFAP immunoreactivity (no reactive gliosis). Consistent with the loss of photoreceptors and inner retinal cells, mitochondrial cytochrome oxidase IV immunoreactivity was decreased in photoreceptor inner segments and their synapses (outer plexiform layer), bipolar/GCL synapses (inner plexiform layer) and GCL. Western blots confirmed the confocal results. Together, these novel findings establish that PFBA produces dose-dependent functional and structural retinotoxic effects in male, but not female, rats: consistent with the shorter PFBA half-life in the latter. Although the molecular mechanism is unknown, we suggest that the synaptic connections and somas of the intrinsically photosensitive RGCs mediating the PLR were lost. Supported by 3M and NIH grants EY07024 and EY07551.

PS 353 The Toxicity of Low Doses of Ultrafine Diesel Exhaust Particles on Bovine Brain Microvessel Endothelial Cells

Y. Kim[1], Y. Choi[1], S. Eom[1], S. F. Ali[2], S. Lantz[2], W. Trickler[2], M. T. Kleinman[3] and H. Kim[1]. *[1]Dept. of Preventive Medicine, College of Medicine, Chungbuk National University, Cheongju, Republic of Korea, [2]Neurochemistry Laboratory, National Center of Toxicological Research/Food and Drug Administration, Jefferson, AR and [3]Department of Medicine, University of California at Irvine, Irvine, CA.*

Diesel exhaust particles (DEPs), originated from combustion of diesel fuel, are one of major pollutant in urban area. DEPs are consisted of various sized of particles, the most of them are ultrafine particles, chemicals, and gases. DEPs are known as an important risk factor for various health problems including brain diseases. However, we have limited evidence for the toxicity of low doses of ultrafine DEPs on brain. This study was performed to evaluate the neurotoxicity of low doses of ultrafine DEPs with bovine brain microvessel endothelial cells (bBMEC) as a blood-brain barrier (BBB) model. Various concentrations of DEPs (from 1.28 ng/mL to 20 μg/mL) were exposed to bBMEC for 24 h in vitro. After exposure, we evaluated cytotoxicity with lactate dehydrogenase (LDH) activity, reactive oxygen species (ROS) generation with DCFH-DA method, total antioxidant capacity (TAC) with bathocuproinedisulfonic acid disodium salt, and permeability by measuring the flux of fluorescein. As results, low doses of DEPs decreased cell viability and induced oxidative stress by increasing ROS generation and decreasing TAC with dose-dependent manner. Additionally, BBB permeability was showed to increase by DEPs exposure. This study showed that exposure to low doses of ultrafine DEPs might disrupt BBB function accompanied with oxidative stress generation. This suggests a possibility that exposure of DEPs, even if the dose is extremely low, may induce adverse effects on CNS by altering the integrity of BBB.

PS 354 Role of Oxidative Potential versus Nicotine in Tobacco Smoke-Induced BBB Toxicity: Genomic and Proteomic Assessment of BBB Endothelial Dysfunction

P. Naik[1], N. M. Fofaria[2] and L. Cucullo[1]. *[1]Pharmaceutical Sciences, Texas Tech University Health Sciences Center, Amarillo, TX and [2]Biomedical Sciences, Texas Tech University Health Sciences Center, Amarillo, TX.*

Until recently toxicological studies on tobacco smoke (TS) have preferentially focused on lung and cardiovascular physiology leaving out the blood-brain barrier (BBB) and the cerebrovascular system. Previous studies from our group have shown that BBB impairment by TS is mediated through induction of vascular adhesion molecules, pro-inflammatory cytokines and matrix metalloproteinases from activated leukocyte and endothelial cells (EC). These TS-dependent inflammatory stimuli are suppressed by antioxidants. Thus, we hypothesized that TS-induced oxidative stress (including nitric oxide release) is a major determinant for BBB toxicity of cigarette products. For this purpose, we assessed the impact of soluble cigarette smoke extract (CSE) on gene and protein expression levels in BBB EC. Herein we report the specific impact of nicotine (100ng/ml) versus CSE from full flavor (FF) and ultralow nicotine (ULN) cigarettes. Initial profiling showed that levels of reactive oxygen (ROS) and nitrogen species (RNS) were significantly higher in ULN product compared to the FF and nicotine alone thus indicating a higher oxidative potential. Down regulation of BBB endothelial tight junction (TJ) proteins such as ZO-1 was observed in both ULN and FF cigarettes but not in nicotine-exposed EC. In addition, the membrane expression of VE-cadherin was up-regulated; perhaps a failsafe (compensatory) mechanism to inhibit leukocytes transmigration across the BBB. Nrf-2- a transcription factor involved in anti-oxidant response signaling was also increased in CSE-exposed endothelial cells substantiating the role of the ROS generation in BBB toxicity. In summary, our results suggest that BBB toxicity of tobacco products correlates to their relative oxidative capacity which also implies that labeling low-nicotine product as light or less harmful in misleading.

This work was supported by NIH/NIDA R01-DA029121-01A1 & A.R.D.F. to Dr. Luca Cucullo.

PS 355 Neurotoxic Effects of the Global Smokeless Tobacco Product, Gutkha

D. E. Lauterstein[1], C. Hoffman[1], A. Hawkins[1], C. Klein[1], M. Rice[2] and J. T. Zelikoff[1]. *[1]Environmental Medicine, NYU, Tuxedo, NY and [2]Neurosurgery, NYU, New York City, NY.*

Gutkha, a smokeless tobacco (ST) product manufactured in India and readily available in the U.S. (used extensively by South Asian immigrant communities), is composed of powdered tobaccos, areca nut, and a variety of spices. To assess the neuropharmacological effects of subacute gutkha usage, adult male mice were exposed via daily "painting" of the oral mucosa with either water (control), gutkha, or nicotine for 7 d. Serum cotinine levels for all groups were analyzed upon sacrifice within 1 hr post-exposure; gutkha and nicotine alone had comparable cotinine levels ranging between 18-50 ng/mL and 20-60 ng/mL, respectively. Evaluation of methylation status of genes in the frontal cortex demonstrated that gutkha treatment increased methylation state of genes known to be associated with specific mental disorders (e.g. Bdnf, Avp, and Comt1). In follow-up experiments, gutkha's effects on local dopamine (DA) regulation in the striatum, important for executive function and reward-related events, were evaluated using ex vivo voltammetry. Brain slices were exposed ex vivo to varying concentrations of nicotine or gutkha and the lowest concentration causing nicotinic acetylcholine receptor (nAChR) desensitization. These studies demonstrated that a >10-fold higher concentration of gutkha (concentration determined by nicotine content in gutkha mixture) than nicotine was needed to cause nAChR desensitization ($p<0.05$). The results suggest that: (1) effects of gutkha on certain brain parameters may be due to gutkha-associated toxicants other than nicotine; (2) gutkha causes changes in the epigenome that could be associated with development of certain mental disorders; and, (3) higher doses of gutkha may need to be consumed in order to desensitize nAChRs associated with nicotine dependence. Thus, gutkha, and possibly other ST products, poses a public health threat that requires further investigation and ultimately enhanced regulation. Supported by Memorial Sloan Kettering Cancer Center and NYU NIEHS Center of Excellence Grant No. ES000260.

PS 356 Assessment of the Neurotoxic Potential of 50 Hz Extremely Low-Frequency Electromagnetic Fields in Naïve and Chemically-Stressed PC12 Cells

M. de Groot, M. Kock and R. H. Westerink. *Toxicology Division, Institute for Risk Assessment Sciences, Utrecht, Utrecht, Netherlands.*

The increasing exposure to extremely low frequency electromagnetic fields (ELF-EMFs, 50 Hz), generated by power lines and electric appliances, is associated with childhood leukemia. This raised public and scientific concern about (other) potential adverse health effects of ELF-EMFs. The central nervous system is expected to be particularly vulnerable to ELF-EMFs as its function strongly depends on electrical excitability and ion channel activity. Moreover, potential neurotoxic effects more likely occur in developing or aged/stressed neuronal cells.
We therefore investigated effects of ELF-EMFs on stressed/aging neuronal cells as these have higher levels of iron and reactive oxygen species (ROS) and are thus more sensitive to environmental insults. We exposed naïve and chemically-pre-treated pheochromocytoma (PC12) cells acutely (30 min) and chronically (48 h) to 50 Hz ELF-EMFs (0.1 – 1000 μT) and measured changes in Ca^{2+}-homeostasis using Fura-2 single cell fluorescent microscopy. Additionally, effects on ROS production and cell viability were assessed using H_2-DCFDA and a combined Alamar Blue/CFDA/Neutral Red assay respectively.
Our data demonstrate that PC12 cells pre-treated with iron or L-DOPA have a stressed phenotype compared to naïve PC12 cells, including increased ROS production and α-synuclein expression. However, both acute and chronic exposure of the different PC12 models to 50 Hz ELF-EMFs up to 1000 μT, i.e. 10,000 times above background exposure, failed to affect basal or K^+-evoked $[Ca^{2+}]_i$, cell viability and ROS production. This suggests that 50 Hz ELF-EMFs do not induce neurotoxic effects *in vitro*. Moreover, stressed neuronal cells do not appear more vulnerable to ELF-EMFs. Our future experiments in *in vitro* models for developmental neurotoxicity aim to elucidate the toxic potential of ELF-EMFs to developing neuronal cells.
Funding: ZonMw NL (85300003).

PS 357 Bisphenol A and 4-Methyl-2, 4-bis(4-hydroxyphenyl)pent-1-ene Induces Neuronal Cell Apoptosis via Akt/Endoplasmic Reticulum Stress-Regulated Signaling Pathway

C. Huang[1], C. Su[2], T. Lu[3], Y. Chung[4], C. Wu[5], C. Yen[4], S. Liu[6] and Y. Chen[3]. *[1]School of Chinese Medicine, China Medical University, Taichung, Taiwan, [2]Department of Otorhinolaryngology, Changhua Christian Hospital, Changhua City, Taiwan, [3]Department of Physiology and Graduate Institute of Basic Medical Science, China Medical University, Taichung, Taiwan, [4]Department of Occupational Safety and Health, Chung Shan Medical University, Taichung, Taiwan, [5]Department of Public Health, China Medical University, Taichung, Taiwan and [6]Institute of Toxicology, National Taiwan University, Taipei, Taiwan.*

Objectives: Bisphenol A (BPA) and 4-methyl-2,4-bis(4-hydroxyphenyl)pent-1-ene (MBP), an active metabolite of BPA, are an endocrine disrupting chemicals (EDCs) or environmental estrogenic property which can disrupt the hormones produced or secreted in mammalian. Several studies have been reported BPA and MBP can cause severely toxicological effects, including neurological dysfunction. However, effects and action mechanisms of BPA and MBP-induced neurotoxicity remained unclear.
Results: BPA significantly decreased cell viability (the LD50 was determined to be approximately 75 μM) and induced the increase in sub-G1 hypodiploid population, annexin V-FITC binding, and the protein expressions of caspase-3/-7 in Neuro-2a cells, indicating that BPA could induce neuronal cell apoptosis. Exposure of Neuro-2a cells to 75 μM BPA also could trigger ER-stress as indicated by several key markers (GRP-78, GRP-94, CHOP, and XBP-1) and caspase-12 cleavage. Moreover, treatment of Neuro-2a cells with MBP more markedly reduced the number of viable cells (the LD50 was determined to be approximately 10 μM), which was associated with inducing apoptotic events and the expression of ER stress-related key molecules and decreased the phosphorylation of Akt. Transfection with specific si-RNA (GRP-94, CHOP, and XBP-1) and over-expression of constitutive activation of Akt (c.a. Akt), respectively, effectively attenuated MBP-induced neuronal cells apoptosis.
Conclusions: These results indicate that Akt/endoplasmic reticulum (ER) stress-regulated apoptotic pathway plays the crucial role in BPA and MBP-induced neuronal cell death.

PS 358 Quinone-Induced Protein Handling Changes: Implications for Major Protein Handling Systems in Quinone-Mediated Toxicity

R. Xiong, D. Siegel and D. Ross. *Department of Pharmaceutical Sciences, Skaggs School of Pharmacy and Pharmaceutical Sciences, Anschutz Medical Campus, University of Colorado, Aurora, CO.*

Para-quinones such as 1,4-benzoquinone (BQ) and menadione (MD) and ortho-quinones including the oxidation products of catecholamines, are derived from the metabolism of xenobiotics as well as endogenous molecules. Both BQ and MD have been shown to perturb protein-handling systems and we have demonstrated that the dopamine-derived quinone aminochrome (AC) could inhibit proteasomal activity. Since the potential hazardous effects of quinones on protein handling systems, including the 20/26S proteasome, the ER stress/unfolded protein response (UPR), autophagy, heat shock proteins (Hsps) and aggresome formation have not been investigated in detail, we conducted this study to systematically examine quinone-induced protein handling changes. In addition, the potential importance of NAD(P)H: quinone oxidoreductase 1 (NQO1) in modulating protein handling changes and toxicity was investigated using stable transfection to generate an isogenic NQO1-overexpressing neural cell line. Our data showed that both BQ and AC could inhibit proteasomal activity and activate the ER stress response in rat dopaminergic N27 cells as indicated by increased phosphorylation of eIF2α. While menadione had no significant effect on any protein handling systems, AC was able to stimulate autophagic flux and induce formation of aggresomes as determined by increased LC3 I/II turnover and the formation of ubiquitin positive inclusion bodies. By modulating quinone-induced ER stress responses, NQO1 protected against BQ toxicity but potentiated AC and MD toxicity. This suggests that NQO1 mediated reduction to unstable hydroquinones and subsequent redox cycling was important for the activation of the ER stress response and toxicity of AC and MD in N27 cells. In summary, our data demonstrates that quinone-specific changes in protein handling are evident in N27 cells and the induction of the ER stress response is associated with quinone-mediated toxicity (supported by R01ES018943).

PS 359 Scavenging Seizure-Induced Reactive Oxygen Species with a Catalytic Antioxidant Attenuates Oxidative Stress and Neuroinflammation in the Pilocarpine Model of Nerve Agent Toxicity

P. Bhuyan[1], L. Liang[1], S. D. Rowley[2], J. N. Pearson[2], A. White[3], B. J. Day[4, 1] and M. N. Patel[1, 2]. [1]*Department of Pharmaceutical Sciences, University of Colorado Denver, Aurora, CO,* [2]*Neuroscience Training Program, University of Colorado Denver, Aurora, CO,* [3]*Department of Pediatrics, University of Colorado Denver, Aurora, CO and* [4]*Department of Medicine, National Jewish Health, Denver, CO.*

Seizure activity is a critical injury response following exposure to nerve agents. Reactive oxygen species (ROS) have been identified as key mediators of seizure-induced neuronal damage, along with aberrant inflammation. One potential avenue of controlling pro-inflammatory responses is by scavenging seizure-induced ROS and thereby improving the redox balance. Adult male rats were subjected to pilocarpine induced status epilepticus (SE) and proinflammatory cytokine production was assessed in the hippocampus and piriform cortex which revealed acute increases in their levels. To determine the role of ROS in SE-induced cytokine production, a separate cohort of rats were treated with AEOL10150 [Mn(III) tetrakis (N,N′-diethylimidizolium-2-yl) porphyrin], a catalytic antioxidant with high superoxide dismutase and catalase activities and sacrificed after 24h. Pilocarpine-induced SE significantly increased 3-Nitrotyrosine/Tyrosine (3NT/Tyr) ratio, decreased glutathione redox status (GSH/GSSG), decreased mitochondrial respiration and increased proinflammatory cytokine production, which were significantly attenuated by AEOL10150. Treatment with AEOL10150 also decreased microgliosis and neuronal death, without altering pilocarpine-induced SE. These results demonstrate that scavenging ROS can decrease indices of seizure-induced neuroinflammation and oxidative stress and highlight the importance of redox mechanisms in controlling inflammation in nerve agent-induced toxicity.
Supported by the CounterACT Program, NIH OD and NINDS Grants R21 NS072099 and UO1NS083422 (M.P.) and NINDS Grant RO1 NS039587 (MP).

PS 360 Combined Therapy with Allopregnanolone and Diazepam Mitigates TETS-Triggered Hyperexcitability of Neuronal Networks *In Vitro* and Rescues Mice from TETS-Induced Seizures and Death

D. Bruun[1], Z. Cao[1], S. Hulsizer[1], B. Inceoglu[2], S. Vito[2], I. N. Pessah[1] and P. Lein[1]. [1]*VM Molecular Bioscience, UC-Davis, Davis, CA and* [2]*Entomology, UC-Davis, Davis, CA.*

Tetramethylenedisulfotetramine (TETS) is a potent convulsant $GABA_A$ receptor antagonist considered to be a chemical threat agent. Mice that receive a lethal dose of TETS (0.15 mg/kg, i.p.) can be rescued by the $GABA_A$ receptor positive allosteric modifier diazepam (DZP) when administered at a high dose (5 mg/kg, i.p.) immediately after the second clonic seizure (~20 min after TETS injection). However, at this dose, DZP significantly reduces blood pressure and mobility but does not suppress TETS-induced neuroinflammation in the brain. To identify alternative medical countermeasures, we used a primary culture cell model to screen $GABA_A$ receptor agonists, singly or in combination. Acute exposure of cultured mouse hippocampal neurons to TETS reversibly alters the pattern of spontaneous Ca^{2+}oscillations and increases discharge frequency and synchronicity as determined by Fluo-4 fluorescence and extracellular microelectrode array recording. Low concentrations (0.1 μM) of DZP and allopregnanolone (AlloP) that are minimally effective when added singly to cultures, show synergism in suppressing TETS-induced alterations of Ca^{2+} dynamics and electrical discharges when added in combination 20 min after cultures are exposed to TETS. As predicted by the in vitro experiments, doses of DZP (0.03 mg/kg) and AlloP (0.03 mg/kg) that are minimally effective when administered singly, increase survival to nearly 100% and reduce the total number of seizures when given in combination immediately after the second clonic seizure. In contrast to high dose DZP, this combinatorial therapy has no effect on blood pressure or mobility, and mitigates TETS-induced activation of microglia but not astrocytes. These studies indicate that in vitro studies can be used to predict effective drug combinations for post-exposure prevention of TETS-induced death. This work is supported by NINDS CounterACT Program grant U54 NSS079202.

PS 361 Effect of Q-VD-OPh on Neurodegeneration and Neuroinflammation of Sarin-Exposed Mice

E. J. Shah, W. Grunwald, T. L. Garrett, J. B. Lucot, T. L. Brown and D. R. Cool. *Wright State University, Boonshoft School of Medicine, Dayton, OH.*

Organophosphates (OP) cause CNS hyperstimulation resulting in seizures, convulsions and brain damage. Sarin is a toxic OP nerve agent that was used in Syria, the Gulf War and in terrorist attacks in Japan. Exposure to sarin has been associated with presence of dead neurons, activation of astrocytes and microglia and neuroinflammation. Since, cell death and neuroinflammation are prevalent in sarin exposed animals, we were interested in seeing the efficacy of Q-VD-OPh, a broad spectrum caspase inhibitor that prevents cell death and has anti-inflammatory properties. Current treatments available for such exposures are effective only if administered within first 30-40 minutes of exposure. In this study, adult female C57BL/6 mice were subjected to a dosing sequence that mimics chronic OP toxicity in humans via the injection of 1.5 mg/kg CBDP before a 0.04mg/kg injection of sarin followed by 20 mg/kg injection of Q-VD-OPh 30 minutes after sarin injections. Mice were sacrificed at two and fourteen day time points followed by BioPlex (Bio-Rad) cytokine analysis of amygdala, hippocampus and piriform cortex. The mice were divided into six different groups; CBDP+Sarin, CBDP+Sarin+Q-VD, CBDP+Sarin+Q-VE, CBDP+Sarin+Diazepam, CBDP+Sarin+Diazepam+Q-VD and CBDP+Sarin+Diazepam+Q-VE. At the two day time point, there was a significant decrease ($p<0.05$) in IL-1b, IL-2, IL-3, IL-10, IL-12(p40), IL-13, MIP-1b and TNF-a in the CBDP+Sarin+Q-VD group in comparison to CBDP+Sarin. Also, CBDP+Sarin+Diazepam group showed a significant decrease ($p<0.05$) in IL-1b, IL-3, IL-10 and IL-12(p40) when compared to the group CBDP+Sarin. Q-VE-OPh did not appear to have an effect. The data strongly suggests that Q-VD-OPh provides neuroprotective and anti-inflammatory properties in mice exposed to sarin. This project was supported by a grant from the NIH R21NS072103-03. Dr. Cool and Dr. Brown have an equity interest in Apoptrol, LLC (Vice President and President, respectively) which supplied the Q-VD-OPh and Q-VE-OPh for the study.

PS 362 Investigations on Neurotoxicity of Carbonyl Sulfide in Mice

P. V. Anantharam[1], E. Whitley[3], V. Anantharam[2], A. G. Kanthasamy[2], A. Kanthasamy[2], P. Imerman[1], S. Ensley[1], J. Koziel[4] and W. K. Rumbeiha[1]. [1]*VDPAM, Iowa State University, Ames, IA,* [2]*BMS, Iowa State University, Ames, IA,* [3]*VPTH, Iowa State University, Ames, IA and* [4]*AgBio, Iowa State University, Ames, IA.*

Carbonyl sulfide (COS) is a toxic gas whose molecular structure is similar to that of carbon disulfide and hydrogen sulfide. It is both an environmental and occupational hazard. Over 16 million pounds of COS are released in the environment every year. It is very persistent in the environment with a half-life of 1-2 years in air. The Department of Homeland Security has designated COS as a potential terror weapon. Even so, there is very minimal research on this chemical which has shown COS to be a potential neurotoxin. The underlying neurotoxic mechanisms are unknown. The EPA designated COS as a priority clean air chemical. Our long-term objective is to characterize the neurotoxicity of COS in the mouse model. We recently conducted acute dose-response studies. C57BL/6J mice were exposed to 0, 250 and 476 ppm of COS for 4h/day on day 0 and day 1 in whole body inhalation chambers. Mice were tested for behavioral endpoints in open field testing and the Rotorod test and for neurochemicals including dopamine, srotonin and their metabolites, and histopathological analysis of the brain tissue. Behavioral testing showed a significant increase in activity for the 250 ppm treatment group, while showing a decrease in activity for both the 476 ppm treatment groups. No significant differences were found in striatal dopamine, DOPAC, and HVA concentrations in any of the treatment groups as compared to the controls. Histopathological investigation of the 476 ppm group, showed that all mice developed lesions in the inferior colliculus, and all but one had lesions in the ventral cochlear nucleus and paraolivary region. Some of these mice also developed lesions in the thalamus, retrosplenial cortex, and pretectal area. The inferior colliculus appeared to be the most sensitive region affected by COS. These results indicate that COS is neurotoxic in mice.

PS 363 *Toxoplasma gondii* Impairs Memory in Infected Seniors

P. D. Gajewski, M. Falkenstein, J. G. Hengstler and K. Golka. *Leibniz Research Centre for Working Environment and Human Factors, Dortmund, Germany.*

Almost 30% of humans present a Toxoplasma gondii positive antibody status. The central nervous system is the main target. However, little is known about the influence of asymptomatic toxoplasmosis on cognitive functions. We performed a blinded study classifying individuals from a basis sample (N=131) of healthy par-

ticipants with an age of 65 years and older into T-pos (IgG≥50 IU/ml) and non-infected individuals (T-neg; IgG=0 IU/ml). Their cognitive status was evaluated by standardized quantitative tests of memory-based and non-memory-based cognitive functions. The depressive state and the quality of life were assessed by questionnaires. Infected individuals showed an impairment of different aspects of memory. In contrast, executive functions were not affected. In particular, lower performance in T-pos seniors was found in a short-term verbal memory test, both regarding immediate recall (P=0.022) and delayed recognition (P=0.037) and in recall from long-term memory assessed by the word fluency tests (P=0.029). Moreover, the rate of correctly detected target symbols in a 2-back task was decreased (P=0.048), indicating a reduced working memory capacity. Decreased memory functions in T-pos seniors were accompanied by a decreased self-reported quality of life. The observed association is relevant for public health considering the high prevalence of toxoplasmosis. The relatively large effects on some of the here reported memory functions correspond to the mean decrease usually observed between year 60 and 70.

PS 364 Microcystins Alter Behavior by Uniquely Targeting the AWA Sensory Neuron in *Caenorhabditis elegans*

C. Moore and B. Puschner. *Molecular Biosciences, UC Davis, Davis, CA.*

Climate change and eutrophication trigger harmful algal blooms, exposing humans and animals to microcystins (MCs) through contaminated water. While acute hepatotoxic exposure to these ubiquitous toxins has been well documented, toxicity due to sub-lethal exposure to MCs is less well-understood. During blooms the most commonly tested variant, MC-LR, has been found at concentrations from 2.5 to above 500 μg/L. Studies suggest other MC variants may be more harmful to the central nervous system. MCs are known to inhibit protein phosphatases (PP) 1 and 2A, which are critical for neuron function. The alternative model *Caenorhabditis elegans* (*C. elegans*) was used to study whether MCs target neurons. Two strains of adult *C. elegans*, N2 (wildtype) and bah-1 (weakened cuticle around the head), were exposed to 0, 1, 10, 40, 80, 160, 320, 500 μg/L MC-LR, and 0, 1, 10, 100, 500 μg/L MC-LF, okadaic acid (OA) and tautomycin (TA) for 24 hours with food. OA and TA inhibit only PP2A and PP1, respectively, and were used to discern inhibition of PP1 and PP2A. The chemotaxis behavior assay was conducted with two odors, benzaldehyde and diacetyl. The *C. elegans* AWC sensory neuron detects benzaldehyde while the AWA sensory neuron detects diacetyl. The proportion of worms that detect an odor after toxin exposure was evaluated using a binomial regression with quasibinomial error. MC-LR did not significantly impact N2 AWC function, but did impair AWA function up to 320 μg/L. At 500 μg/L MC-LR did not impair either AWC or AWA function. MC-LR did not impact bah-1 AWC function, but may increase AWA function up to 500 μg/L. At low doses, MC-LR impaired AWA function while at high doses it may cause stimulation. MC-LF did not alter N2 AWC neuron function but may impair AWA function more potently than MC-LR. OA decreased N2 AWC and AWA neuron function, while TA only decreased N2 AWA neuron function, similar to MC exposure. The similar pattern in toxicity between MC and TA exposure suggests that MCs alter neuron function through inhibition of PP1.

PS 365 Effects of Microcystin Exposure on the Phosphorylation State of GSK-3 Beta in Human Neuronal Cells

D. R. Dietrich, M. Helmer, J. Behr and F. Polzer. *Human & Environmental Toxicology, University of Konstanz, Konstanz, Germany.*

Microcystins (MCs) are a group of heptapeptide toxins with more than 100 congeners known produced by several strains of cyanobacteria. Due to their widespread abundance in surface waters and algae food supplements, MCs can be a serious human health hazard. MCs are often described as hepatotoxins, although nephrotoxic and neurotoxic effects have also been demonstrated. MCs are known to inhibit protein phosphatases (PP) 1 and 2A. In the study presented the focus was set on the neurotoxic effects of microcystins. Therefore the downstream effects of an inhibition of PP1 and PP2A were studied in the human neuroblastoma cell line SH-SY5Y subsequent to neuronal differentiation using repeated exposure to retinoic acid. As a downstream target PP inhibition, GSK-3β was chosen due to its role as a key regulator of neuronal cell phosphorylation homeostasis. Furthermore GSK-3β, as a Tau kinase, regulates tau binding to microtubules and hence is involved in microtubular stability. Cells were exposed to 3 different non-cytotoxic concentrations of microcystin (MC) congeners –LR, -RR, -LF and –LW and harvested after 24 h of treatment. SDS-PAGE and Western Blot were performed followed by immunocytochemistry with antibodies recognizing whole GSK-3β molecule and phosphorylation sites S9, Y216 and T390. Whereas phosphorylation at Y216 and T390 was not changed, phosphorylation at the GSK-3β-activity regulating site S9 was increased significantly following exposure to the MC-LF and -LW. These results suggest that exposure to MCs may affect the phosphorylation/dephosphorylation homeostasis in human neuronal cells and thereby lead to progressive neuronal damage or loss.

PS 366 Transcriptional Regulation of Brain ABC Transporters during Acute Acetaminophen (APAP) Intoxication in Mice and the Possible Role of the Nuclear Factor-Erythroid 2-Related Factor 2 (Nrf2)

C. I. Ghanem[1], S. Rudraiah[2] and J. E. Manautou[2]. [1]*Pharmacological Research Institute, Pharmacy School, CONICET-University of Buenos Aires, Buenos Aires, Argentina and* [2]*Department of Pharmaceutical Sciences, University of Connecticut, Storrs, CT.*

Changes in gene and protein expression of liver ABC transporters have been previously described during acute APAP intoxication. However, the effect of hepatotoxic doses of APAP on brain ABC transporters has never been studied. The aim of this study was to evaluate the effect of APAP on brain ABC transporter expression and the role of the transcription factor and the oxidative stress sensor Nrf2 thereon. For this purpose, male C57BL6 mice received APAP (400mg/kg) or vehicle. 24 h later, brains were removed and protein expression of Mrp1-Mrp5, Bcrp and P-gp was determined by Western blotting from total brain homogenates. mRNA expression for these ABC transporters was also assayed by q-RT PCR between 6 and 24 hr after APAP. The results show that APAP treatment significantly increases the expression of brain P-gp (195%), Mrp2 (293%) and Mrp4 (38%) proteins relative to controls, with no changes in Bcrp, Mrp1 and Mrp5 detected. Mrp3 protein was not detectable in either group. The increased protein expression for P-gp, Mrp2 and Mrp4 correlated with changes in mRNA expression. In agreement with protein content, mRNA expression for Bcrp, Mrp1, Mrp3, and Mrp5 did not change with APAP treatment. Indicative of Nrf2 activation, mRNA and protein expression of NAD(P)H:quinone oxidoreductase 1 increased significantly in brain tissue with APAP treatment. Furthermore, nuclear content of Nrf2 protein was found to increase by 50% at 12 hr after APAP. In conclusion, acute APAP intoxication induces protein expression of several brain ABC transporters through a transcriptional mechanism. This study also suggests that these changes may be due to in situ Nrf2 activation by APAP. The functional consequences of these changes in brain ABC transporters by APAP deserve further attention.

PS 367 Effect of Different Durations of Morphine Exposure on Mesencephalic Dopaminergic Neurons in Morphine-Dependent Rats

Y. Li[1], W. Shi[1], F. Liu[2], Q. Qi[1], J. Wang[1], J. Liu[1] and B. Cong[1]. [1]*Hebei Medical University, Shi Jiazhuang, He Bei, China and* [2]*National Center for Toxicological Research, Jefferson, AR.*

Mesencephalic dopaminergic neurons are heavily involved in the development and maintenance of drug dependence. Therefore, the morphological changes in dopaminergic neurons of the substantia nigra (SN) and ventral tegmental area (VTA) in morphine dependent rats were investigated. Models of morphine dependence were established in rats, and paraffin-embedded sections, immunohistochemistry and immunofluorescence were used to observe the changes in expression of tyrosine hydroxylase (TH) protein, a specific marker of dopaminergic nerve cells. Fluoro-Jade B staining was used to detect degeneration and necrosis, and terminal deoxynucleotidyl transferase-mediated dUTP nick-end-labeling (TUNEL) detected apoptosis of mesencephalic dopaminergic nerve cells. The number of TH positive cells significantly decreased in rats that were morphine dependent for a longer period of time. With prolonged morphine exposure, SN and VTA dopaminergic nerve cells showed degeneration and necrosis, while apoptotic cells were not observed. The number of SN and VTA dopaminergic nerve cells decreased with increasing periods of morphine dependence, which was most likely due to degeneration and necrosis of nerve cells induced by morphine toxicity.

PS 368 Morphine Sulfate Concomitantly Alters Mouse Stem Cell Differentiation and Opioid Receptor Gene Expression

S. L. Dholakiya and F. A. Barile. *Pharmaceutical Sciences, St. John's University College of Pharmacy, Queens, NY.*

In order to advance treatments for narcotic addiction, we need to better understand the influence of opioids on neuronal differentiation, receptor expression, withdrawal and tolerance in the central nervous system. In this study, mouse embryonic stem (mES) cells were used as an in vitro model for neural development to determine the relationship between opioid receptor expression and mES cell

differentiation. We manipulated mES cells in culture to differentiate in 3 stages: cell transformation to embryoid bodies (EBs); EB differentiation to neural progenitor cells (NPC); and, mES cell differentiation to neural/glial cells. Cell types are confirmed by monitoring expression of Oct4, nestin, mtap-2, and GFAP, as cell-specific markers for stem cells, NPC, neurons, and astrocytes, respectively, using RT-PCR and flow cytometry analysis. Similarly, opioid receptor gene expression for mu (μ), kappa (κ) and delta (δ) receptors, was confirmed in each cell type. Our results demonstrate that 100 μM morphine sulfate (MS) for 24-hrs does not alter cell viability or cell cycle kinetics in mES cells. In addition, MS does not alter μ-opioid receptor gene expression nor receptor protein expression after 24-hrs exposure. However, MS causes internalization of μ-receptors in a concentration-dependent manner, and down regulation of κ-receptor gene expression in stem cells. Chronic exposure of stem cells during transformation to EBs and NPC results in down regulation of both μ-receptor gene expression and NPC-specific marker expression of nestin, respectively. Overall, these results indicate that acute MS exposure does not alter self-renewal of mES cells; however, chronic treatment inhibits differentiation to NP cells. Consequently, the project focuses on the significance of the relationship between MS administration in early and late stage differentiation, and opioid receptor expression and receptor activity. Understanding this mechanism has particular clinical applications for the prevention or treatment of fetal and childhood narcotic addictions.

PS 369 Effect of Prenatal Methadone on Reinstated Behavioral Sensitization Induced by Methamphetamine in Adolescent Rats

L. Tien[1], C. Wong[1, 2], Y. Lee[1], Y. Chiang[3, 4], L. Fan[5] and I. Ho[3, 4, 6]. *[1]School of Medicine, Fu Jen Catholic University, New Taipei City, Taiwan, [2]Department of Anesthesiology, Cathay General Hospital, Taipei, Taiwan, [3]Center for Drug Abuse and Addiction, China Medical University Hospital, Taichung, Taiwan, [4]Graduate Institute of Clinical Medical Science, China Medical University Hospital, Taichung, Taiwan, [5]Pediatrics Newborn Medicine, University of Mississippi, Jackson, MS and [6]Neuropsychiatric Research Center, National Health Research Institutes, Zhunan, Taiwan.*

The present study was to investigate the effect of prenatal exposure to methadone on methamphetamine (METH)-induced behavioral sensitization as an indicator of drug addiction in later life. Pregnant rats received saline or methadone (7 mg/kg, s.c.) twice daily from E3 to E20. To induce behavioral sensitization, offspring (5 weeks old) were treated with METH (1 mg/kg, i.p.) or saline once daily for 5 consecutive days. Ninety-six hours (day 9) after the 5th treatment with METH or saline, animals received a single dose of METH (1 mg/kg, i.p.) or saline to induce the reinstated behavioral sensitization. Prenatal methadone treatment enhanced the level of development of locomotor behavioral sensitization to METH administration in adolescent rats. Prenatal methadone treatment also enhanced the reinstated locomotor behavioral sensitization in adolescent rats after the administration had ceased for 96 hours. These results indicate that prenatal methadone exposure produces a persistent lesion in the dopaminergic system, as indicated by enhanced METH-induced locomotor behavioral sensitization (before drug abstinence) and reinstated locomotor behavioral sensitization (after short term drug abstinence) in adolescent rats. These findings show that prenatal methadone exposure may enhance susceptibility to the development of drug addiction in later life. This could provide a reference for drug usage such as METH in their offspring of pregnant woman who are treating with methadone.

PS 370 Inhibition of the Vesicular Monoamine Transporter 2 Alters the Acute and Long-Term Effects of 3, 4-(±)-Methylenedioxymethamphetamine

L. E. Lizarraga, A. M. Phan, S. S. Lau and T. J. Monks. *Pharmacology/Toxicology, University of Arizona-College of Pharmacy, Tucson, AZ.*

3,4-(±)-Methylenedioxymethamphetamine (MDMA, Ecstacy) exerts a biphasic pharmacological response on the brain resulting in contrasting acute and long-term effects. During the acute phase, MDMA causes major monoamine release into the synapse, primarily of serotonin (5-HT), inducing hyperthermia and hyperactivity (5-HT syndrome). Conversely, long-term serotonergic neurotoxicity manifests as a prolonged depletion in 5-HT, and structural damage to 5-HT nerve terminals. The vesicular monoamine transporter 2 (VMAT2) is involved in the transport of monoamine neurotransmitters, in particular dopamine (DA) and 5-HT, into intra-neuronal storage vesicles. As such, VMAT2 is critical for maintaining neuronal health by preventing neurotransmitter oxidation within the cytosol. Previously, we showed that pretreatment with VMAT2 inhibitor, Ro 4-1284 (10mg/kg, ip), one hour prior to MDMA exposure (20mg/kg, sc), attenuates MDMA-mediated hyperthermia, locomotor activity and long-term 5-HT depletion in Sprague-Dawley (SD) rats. In the present study, microdialysis was used to measure MDMA-mediated monoamine release in the striatum of SD rats. As expected, MDMA significantly increased DA and 5-HT release in the caudate putamen. Ro 4-1284 pretreatment had little effect on MDMA-mediated increases in dialysate monoamine concentrations. However, increases in dialysate concentrations of DA and 5-HT metabolites (DOPAC and 5-HIAA, respectively) were indicative of increased monoamine turnover. Immunohistochemistry revealed that Ro 4-1284 prevents striatal depletion of the 5-HT reuptake transporter in MDMA-treated rats, consistent with findings that inhibition of VMAT2 protects against long-term MDMA serotonergic neurotoxicity. In conclusion, we have demonstrated that VMAT2 inhibition by Ro 4-1284 has significant effects on the acute and long-term effects of MDMA. Further studies are required to decipher the mechanisms by which Ro 4-1284 protects against MDMA neurotoxicity. (DA023525, P30ES006694, & T32ES007091).

PS 371 Enhanced Vesicular Function and Reduced Neurotoxicity in Mice Overexpressing the Vesicular Monoamine Transporter

G. W. Miller, K. Lohr, A. I. Bernstein, K. Stout, A. R. Dunn and A. Salahpour. *Environmental Health, Emory University, Atlanta, GA.*

The vesicular monoamine transporter 2 (VMAT2) packages monoamine neurotransmitters into vesicles for rapid release at the synapse. In addition to its role in neurotransmission, VMAT2 also sequesters toxicants away from their sites of action in the cell. Our laboratory has previously characterized mice with reduced vesicular capacity, which results in progressive degeneration of dopamine and norepinephrine neurons and motor and non-motor deficits (J. Neurosci., 2007; J. Neurosci., 2009; Neuropharmacology, 2013). However, it was unknown if an increase in VMAT2 level would result in increased vesicular function in an animal model. We created a BAC transgenic VMAT2 overexpressing (VMAT2-HI) mouse line to determine the effects of increased vesicular monoamine filling on associated neurochemical, behavioral, and toxicological outcomes. The increased vesicular filling in the VMAT2-HI mice results in an enhanced vesicular storage capacity for dopamine as shown by increased vesicular uptake and increased vesicle size. This corresponds to a 21% increase in striatal dopamine content, suggesting a sustained enhancement of the dopaminergic system in the VMAT2-HI mice. This increased dopamine storage also results in an 80% increase in synaptic dopamine release as measured by fast-scan cyclic voltammetry. Further, VMAT2-HI mice show behavioral changes, including increased locomotor activity and an enhanced response to amphetamine. VMAT2-HI mice also show improved outcomes on measures of anxiety and depressive-like behaviors, including a 42% reduction in marble burying and a 22% decrease in immobility time on the forced swim test. Finally, since VMAT2 level is a neuroprotective mechanism in monoaminergic systems, we tested the vulnerability to the parkinsonism-inducing neurotoxin MPTP and found that the VMAT2-HI mice had reduced dopaminergic toxicity. These data suggest that monoamine vesicular capacity can be increased and this increased capacity corresponds to reduced toxicity.

PS 372 Diverse Models of Neurotoxicity Link Induction of Astrogliosis to Activation of STAT3

K. A. Kelly, D. B. Miller and J. P. O'Callaghan. *CDC-NIOSH, Morgantown, WV.*

Dr. Paul Greengard received the 2000 Nobel Prize in Physiology or Medicine for identifying the dopamine- and cAMP-regulated neuronal phosphoprotein (DARPP-32) signaling pathways in medium spiny striatal neurons. Identification of multiple phospho-sites on DARPP-32 revealed upstream effectors regulating the activation of this specific neuronal cell type. We adopted the same approach to map signaling pathways upstream of the key astrocyte damage marker, glial fibrillary acidic protein (GFAP). In a 1-methyl-4-phenyl-1,2,3,6-tetrahydropyridine (MPTP) model of dopaminergic neurotoxicity, we demonstrated the development of neuroinflammation (upregulation of proinflammatory cytokines/chemokines) and activation of the janus kinase and signal transducer and activator of transcription (JAK2-STAT3) pathway preceding the up-regulation of GFAP in astrocytes in the brain. Here, we show that multiple mechanistically distinct models of neurotoxicity (MPTP, amphetamine (AMP), methamphetamine (METH), 3,4-methylenedioxyamphetamine (MDA), 3,4-methylenedioxymethamphetamine (MDMA), kainic acid (KA) and trimethyltin (TMT)) engender the same neuroinflammatory response and STAT3 activation in target brain regions of the respective neurotoxicants. Pharmacological antagonism of neurotoxic effects of MPTP, METH and KA with nomifensine, ethanol and diazepam, respectively, blocked the neuroinflammation, phosphorylation of STAT3 and GFAP induction, indicating neuronal damage as a component of the initiation of astrogliosis. Deletion of astrocytic STAT3 in conditional knockout mice prevented the induction of GFAP in MPTP-treated mice. Double immunostaining of GFAP and STAT3 showed

enhanced nuclear staining localized to astrocytes in association with the induction of astrogliosis. These findings strongly implicate the STAT3 pathway in astrocytes as a key signaling pathway for astrogliosis.

PS 373 BAC-TRAP Technology in Neurotoxicology: The ALDH1L1 BAC-TRAP Mouse As a Tool to Assess Astrocyte Specific Responses to Neural Injury

J. P. O'Callaghan, K. A. Kelly and D. B. Miller. *CDC-NIOSH, Morgantown, WV.*

A central problem in neurotoxicology is detecting the selective and unpredictable damage to specific cells produced by toxic agents and mixtures. Evaluating astrogliosis overcomes this problem because reactive astrocytes show the location of toxicant-induced damage occurring anywhere in the CNS. Enhanced expression of GFAP is a hallmark of reactive astrocytes; however, few other astrogliosis biomarkers are known. Thus, determining the specific in vivo transcriptomic profile of astrocytes under control and reactive conditions will allow for the identification of additional astrogliosis biomarkers. Heintz and Greengard (2008) introduced BAC-TRAP (translating ribosome affinity purification) technology as an approach for identification of cell-type-specific responses in vivo. Here, we implemented this approach for the assessment of mRNA translation specific to astrocytes responding to damage caused by known neurotoxicants. ALDH1L1 is an enzyme thought to serve a housekeeping function in astrocytes. Using hippocampal and striatal damage due to TMT and MPTP, respectively, we evaluated the localization and response of ALDH1L1 compared to astrogliosis seen by GFAP immunohistochemistry and ELISA. Staining of ALDH1L1 revealed localization to astrocytes after TMT and MPTP, while immunoblots of ALDH1L1 revealed basal expression of this protein but little enhanced expression after MPTP and TMT, confirming it to be an astrocytic "housekeeping" gene/protein. We then used the ALDH1L1 BAC-TRAP mouse to evaluate astrocytic-specific mRNA with expression analyses by gene array in control conditions. Tissue was subjected to TRAP utilizing an eGFP antibody that only binds to actively translating RNA in astrocytes. This revealed numerous genes in "resting" astrocytes, including genes previously localized to astrocytes (e.g., GFAP), as well as novel genes to this cell type (e.g. PHOX2A). MPTP expression data are reported in accompanying poster. The ALDH1L1 BAC-TRAP mouse represents a promising tool to investigate astrocytic responses to neural injury.

PS 374 BAC-TRAP Technology in Neurotoxicology: Assessing the Astrocyte Response to MPTP-Induced Damage in the ALDH1L1 BAC-TRAP Mouse

D. B. Miller, K. A. Kelly and J. P. O'Callaghan. *CDC-NIOSH, Morgantown, WV.*

A central problem in neurotoxicology is detecting the selective and unpredictable damage to specific cells produced by toxic agents and mixtures. Evaluating astrogliosis overcomes this problem because reactive astrocytes show the location of toxicant-induced damage occurring anywhere in the CNS. Enhanced expression of GFAP is a hallmark of reactive astrocytes; however, few other astrogliosis biomarkers are known. Heintz & Greengard (2008) introduced BAC-TRAP (translating ribosome affinity purification) technology that allows the characterization of the actively translating transcriptome of a particular cell type. For example, ALDH1L1 is an astrocyte specific enzyme thought to be a housekeeping gene. Thus, ALDH1L1 BAC-TRAP mice can be used to characterize the transcriptome of astrocytes under various conditions. To begin to characterize additional biomarkers of astrogliosis occurring in response to neurotoxic damage ALDH1L1 BAC-TRAP mice were given a single 12.5 mg/kg s.c. dose of MPTP, a well characterized dopaminergic neurotoxicant that induces significant astrogliosis, Striatal tissue was obtained at 12, 24, and 48 hrs following a single s.c. dosage of saline or 12.5 mg/kg MPTP. Striatal tissue was subjected to TRAP utilizing an eGFP antibody that only binds to actively translating RNA in astrocytes. Changes in the actively translating RNA induced by MPTP damage were determined by microarray (Illumina MouseWG-8 v2 Expression BeadChip) and the dataset interrogated using Ingenuity Pathway Analysis (IPA). MPTP induced robust transcriptome changes in genes previously identified as astrocyte specific (e.g., 403, 399, 804 fold increases in TIMP1 at 12, 24, 48 hrs, respectively) as well as others not previously considered astrocyte-specific (e.g., 219, 203, 3.69 fold increases in PHOX2A at 12, 24, 48 hrs). Our data indicate the BAC-TRAP technology can be used to identify additional biomarkers of astrogliosis and will aid in characterizing various astrocyte phenotypes.

PS 375 Human iPSC Neurons: *In Vitro* Models to Predict Clinical CNS Toxicity

C. A. Snyder, K. Staflin and D. L. Misner. *Safety Assessment, Genentech, South San Francisco, CA.*

A major cause of drug attrition from clinical trials is neurotoxicity, a problem stemming from the lack of a relevant model to predict human CNS safety. Current neurotoxicity assessment depends on in vivo animal models, which are time-consuming and expensive. In vitro models consist of immortalized cell lines and primary rodent cultures, which are often a poor representation of human physiology. There is need for high throughput, human-based assays that can narrow down drug candidate panels for in vivo animal studies, and augment those studies with human data before initiation of clinical trials. We chose to establish such assays with human induced pluripotent stem cells (iPSCs) that have been differentiated into mature neurons. These iPSC neurons offer a renewable source of mature cells, relevant to human drug safety, and free from ethical concerns. CNS toxicity results from disruption of complex neural networks, which is why our test panel addresses neuronal activity, in addition to neurite outgrowth, cytotoxicity and mitochondrial stress. Few studies tackle neuronal activity in a high throughput system, and fewer still integrate changes in activity with other functional toxicity endpoints. Our novel platform will combine a semi-high throughput multi-electrode array (MEA) with high throughput neurotoxicity assays for potential screening of drug candidates. By using a panel of test compounds known to cause CNS toxicity in vivo we put forward a panel of in vitro human physiological-based assays to evaluate the translatability of drug safety.

PS 376 Live Cell-Based Assay Using GFP+ Human Stem Cell-Derived Neurons

J. N. Le. *ArunA Biomedical Inc, Athens, GA.* Sponsor: S. Stice.

Adverse outcome pathways (AOP) are conceptual frameworks that portray existing knowledge concerning the linkage between a molecular initiating event and an adverse outcome. High throughput screening (HTS) and high content screening (HCS) approaches seek to gain a greater perspective of the AOP, leading to more efficient and reliable identification of adverse outcomes of compounds and chemicals. However, HCS assays often utilize primary or stem cell sources which are not amenable to large scale screening and can require extensive cell culture, fixation and permeation, and immunocyotochemistry prior to imaging. Thus, major costs are associated with 96-well based high content neurotoxin screening. In addition, preserving or fixative steps can alter cell architecture and a new plate of cells is required for each time point, thus introducing variability to data. This new human cell-based assay provides a scalable solution to the previously labor intensive, single-end-point, and hence limited nature of neurotox assays, while preserving the breadth and quality of data. The assay utilizes clonal, embryonic stem cell derived, human neural cells that have been genetically modified with a non-viral vector encoding a Green Fluorescent Protein (GFP) reporter gene driven by a ubiquitous promoter. Previously, hN2™ human neuronal cells faithfully reproduced early brain development, providing a cell model > 95% positive for neuronal markers while demonstrating higher sensitivity to neural toxins than mouse cortical neurons, and our new GFP+ neurons are equally sensitive. Additionally, previous studies using rodent primary cells examined mixed and unknown ratios of neural cells, often at various stages of proliferation and differentiation. These new GFP+ neurons are differentiated from a clonal GFP+ neural progenitor population, thus removing variability from cultures while maintaining an adherent monolayer amenable to high content imaging. By eliminating the need for fixing and staining cells, these GFP+ human neurons provide a scalable means to analyze neurite outgrowth in live cells spanning the course of hours to days following exposure to test compounds.

PS 377 A Functional Phenotypic Screen for Synapse Formation in Human iPS-Derived Neurons

B. Cai, A. Essex, E. Batchelder, S. Feng, P. McDonough and J. Evans. *Vala Sciences, San Diego, CA.*

Exposure to low levels of neuronal toxicants may affect neuronal structure subtly, leading to developmental and cognitive impairment. Synaptic transmission is the fundamental unit of communication between healthy neurons. We used human induced pluripotent stem (iPS) neurons grown in low volume 384 well dishes for 1-3 weeks to measure synapse formation. Work done in other laboratories has demonstrated that these cells are capable of electrical transmission. Therefore, we used antibodies to measure expression levels of the pre- and post-synaptic proteins, Synapsin I and post-synaptic protein 95 (PSD95), respectively. Furthermore, using advanced image analysis algorithms we masked neurite regions demarked by

expression of Tuj1 (beta-III tubulin) and measured colocalized signals for the pre- and post-synaptic markers only in these functionally-relevant regions. Additional information that may be related to the mechanism of action for chemicals that showed an effect in the assay included the amount of neurite outgrowth (Tuj1) and alterations in nuclear texture (Hoechst 33342). Our high content screening (HCS) approach enabled us to screen a library of FDA-approved drugs (the NCC2 library) as well as other agents such as forskolin, estrogen, and tamoxifen known to modulate neuronal function. Using this approach we have developed a robust platform for large-scale screening of chemicals that affect synapse formation, the basic unit of neuronal function in humans.

PS 378 eCiphrNeuro: A High-Throughput Assay to Detect Neurotoxic Compounds in Early Drug Discovery

J. Bradley, C. Strock, H. Luithardt and J. Gilbert. *Cyprotex, Watertown, MA.*

Seizurogenic neurotoxicity produces significant drug attrition during drug discovery. Currently available in vitro assays cannot predict this toxicity due to the failure of general cytotoxicity assays to predict sublethal target specific electrophysiological liabilities. Ion channel and receptor activity assays can be used to predict some seizure potential, but these only focus on specifically measured targets for prediction and may miss a response which relies on a combination of endpoints. Most evaluation of seizure inducing compounds occurs later in preclinical development in in vivo studies which have much higher costs. Therefore, the development of a high-throughput in vitro assay to screen compounds for seizurogenic potential would lead to evaluating compounds earlier at lower cost and greater reliability. Here we demonstrate the use of a 48-well microelectrode array (MEA) to screen for seizurogenic compounds using rat cortical neurons. Spikes were measured and the results were computed for mean firing rate, synchrony, and spike train organization (inter-spike and burst statistics) using custom Matlab scripts and NeuroExplorer. All of the seizurogenic compounds, including GABA -A antagonists, showed significant changes in MFR, synchronization, and spike train and burst organization, while all of the negative controls were ineffective. Glutamate, the excitatory neurotransmitter, showed a robust increase in activity. Neuroinhibitory molecules such as Domoic Acid, a neurotoxin, GABA (GABA agonist), Tetrodotoxin (sodium channel blocker) and TEA (potassium channel blocker) were also tested and found to block activity. These results illustrate the power of a high-throughput rat cortical neuron MEA assay for predicting compound induced neural toxicity.

PS 378a Low Frequency Activity of Cortical Networks Is Differentially Altered by Bicuculline and Carbaryl

D. Hall[1], C. M. Mack[2], D. W. Herr[2] and T. J. Shafer[1]. [1]*ISTD, US EPA, RTP, NC and* [2]*TAD, US EPA, RTP, NC.*

Thousands of chemicals need to be characterized for their neurotoxicity potential. Neurons grown on microelectrode arrays (MEAs) are an in vitro model used to screen chemicals for functional effects on neuronal networks. Typically, after removal of low frequency components, effects on high frequency events (neuronal action potentials, or "spikes") are used to differentiate chemical effects. However, such approaches discard information and low frequency activity has yet to be examined for its utility in screening chemicals. In this pilot study, spontaneous network activity in primary cultures of rat cortex was collected in MEAs and differential effects of bicuculline (BIC 25 μM, n=4) and carbaryl (CAR 30μM, n=2) as compared to controls were examined. Activity was sampled at 25 kHz and subsequently separated into low (1-100 Hz) and high (>200 Hz; spikes) frequencies for separate analysis. Low frequency activity was extracted in Matlab in 1 sec segments for 300 seconds/electrode/well using a Kaiser window with no overlap. Spectral amplitudes (FFT transformation; μV) were grouped into 5 frequency bands of interest: δ (1-4Hz), θ (4-8Hz), α (8-14Hz), β (14-30Hz), and γ (30-50Hz). Amplitudes in a given band were averaged across pre- and post-treatment for every electrode and the difference calculated. The resulting electrode amplitude differences were averaged across a well to obtain an average power difference. BIC had significantly higher amplitude vs control in the δ, θ, α, β, and γ ($p<0.01$) bands. By contrast, CAR showed an increased amplitude difference in the θ and α bands ($p<0.05$). For high frequency activity, BIC increased spike rates to an average of 225% of control, while CAR decreased spike rates to 20% control. This study demonstrates that low frequency activity is differentially altered by chemical treatment, and may be useful in distinguishing chemical influence on neuronal networks. (This abstract does not represent Agency Policy)

PS 378b Evaluation of the Neuroactivity of ToxCast Compounds Using Multiwell Microelectrode Array Recordings in Primary Cortical Neurons

P. A. Valdivia[1], M. T. Martin[2], W. LeFew[3], D. Hall[3], J. Ross[1], K. Houck[2] and T. J. Shafer[3]. [1]*Axion Biosystems, Atlanta, GA,* [2]*NCCT, US EPA, RTP, NC and* [3]*ISTD, US EPA, RTP, NC.*

Assessment of spontaneous activity in neuronal cultures using multi-well microelectrode arrays (MEA) systems is a rapid, efficient and sensitive method to detect neuroactivity of drugs, chemicals, and particles. Effects of 68 ToxCast compounds (biased for neuroactive compounds) on neuronal activity using 48 well MEA plates were examined previously. In this experiment, effects of 20 additional ToxCast compounds, with a bias towards those inactive in ToxCast ion channel assays, were examined. Five additional compounds, known to be without effect on neuronal function in MEAs (negatives) were included. Further, these experiments refined data analysis approaches by considering recording stability post-hoc and establishing criteria for data inclusion. On day in vitro 14, 1 hr of baseline activity was recorded prior to exposing the cortical networks to 40 μM of each compound for 1 hr; the percent change in mean firing rate (MFR) was determined in the absence and presence of each chemical. Post-hoc analysis determined that the first 20 min of baseline recording was a period of activity stabilization and thus were omitted from analysis. A hit detection threshold of a 39.1% change in weighted (wMFR) was determined based on 2 standard deviations beyond the mean response to DMSO treatment; none of the 5 known negatives altered wMFR beyond this threshold. However, of the 20 ToxCast chemicals, 12 altered wMFR beyond the hit threshold. Hits included tetramethrin and fenthion, 4/5 conazoles, piperonyl butoxide, vinclozolin, lactofen, prochloraz, butyl benzyl phthalate and genistein. None of the 25 chemicals were cytotoxic. Concentration-response assessments were concordant with the single point screen result for 7/8 chemicals. These results indicate that spontaneous activity of cortical neurons measured with MEAs may be sensitive to chemicals with actions on endpoints other than ion channels. (This abstract was supported by CRADA #644-11 with Axion Biosystems and does not reflect EPA Policy)

PS 378c Effects of Organophosphorus Flame Retardants on Spontaneous Activity in Neuronal Networks Grown on Microelectrode Arrays

T. J. Shafer[1], K. A. Wallace[1], W. Mundy[1] and M. Behl[2]. [1]*Integrated Systems Toxicology, U.S. Environmental Protection Agency, Research Triangle Park, NC and* [2]*NIEHS, Research Triangle Park, NC.*

Organophosphorus compounds are increasingly used as alternatives to brominated flame retardants (BFRs) and thus are commonly found in house air and dust. However, there is limited information on their potential health effects. Assessment of spontaneous neural network activity using microelectrode arrays has been shown to be a sensitive method to screen chemicals for potential neuroactivity/toxicity. Therefore, this study compared the effects of nine organophosphorus flame retardants (OPFs) with the BFR tetrabromobisphenol A to determine their ability to alter network function in primary cultures of rat cortical neurons grown on 48 well microelectrode array (MEAs) plates. On day 13 or 14 in vitro, 1 hr of baseline activity was recorded prior to exposure to flame retardants (0.1 to 30 μM). Changes in spontaneous mean firing rate (MFR) relative to the vehicle control were assessed 1hr after exposure. The BFR tetrabromobisphenol A and the OPF tris (2-chloroethyl) phosphate did not alter the spontaneous activity at any concentration tested. The remaining 8 OPFs decreased spontaneous activity in a concentration-dependent manner, with EC_{50} values ranging from 6.6 to 18.6 μM in the following order: t-butylphenyl diphenyl phosphate ≥ tricresyl phosphate ≥ 2-ethylhexyl diphenyl phosphate ≥ isopropylated phenyl phosphate ≥ isodecyl diphenyl phosphate ≥ ortho-tricresyl phosphate ≥ triphenyl phosphate ≥ tris (1,3-dichloroisopropyl) phosphate. None of the flame retardants decreased the viability of cortical cells at any concentration tested. This data indicates that some OPFs have the ability to alter the spontaneous activity in neuronal networks in vitro at micromolar concentrations. *This abstract does not necessarily reflect U.S. EPA policy.*

PS 378d Neurotoxic Effects of Tri-Ortho-Cresyl Phosphate *In Vitro*

V. Hausherr[1], N. Schöbel[1, 2] and C. van Thriel[1]. [1]*Neurotoxicology and Chemosensation, IfADo - Leibniz Research Centre for Working Environment and Human Factors, Dortmund, NRW, Germany and* [2]*Animal Physiology, Ruhr-University Bochum, Bochum, NRW, Germany.*

Tri-ortho-cresylphosphate (TOCP) provokes organophosphate-induced delayed neuropathy (OPIDN) in the peripheral nervous systems of humans and sensitive animals. On the cellular level axon swelling and disturbance of axonal transport

are the initial events of OPIDN. Low-dose effects of TOCP on central nervous system (CNS) functions on a cellular level have only been rarely studied yet. In the present study, we investigated neurotoxic effects of TOCP on neurons of mice cerebral cortices in vitro. We evaluated cell viability, neurite outgrowth, and the functionality of neurochemical processes. A 24 h exposure of mouse primary cortical neurons (pCNs) to TOCP yielded dose-dependent cytotoxic effects. 89 μM TOCP were associated with significant reduction of about 50 % in cell viability. In addition, TOCP impaired neurite outgrowth and caused degeneration of neurite networks with a lowest effective dose of 1 μM. Using fluorescence-based life-cell Calcium imaging, we investigated TOCP effects on signals evoked by the main excitatory neurotransmitter glutamate. Glutamate-evoked signals in pCNs were significantly decreased after 24 h exposure to TOCP 100 nM. Both, the percentage of glutamate-responsive neurons and the mean response amplitudes were decreased. In addition to these results, we observed a direct inhibition of glutamate receptor-mediated responses by TOCP. In detail, the simultaneous application of TOCP (100 μM) together with the glutamate stimulation resulted in a block of glutamate-induced responses by 70 %. In summary, we showed here low and lowest-dose effects of TOCP on functional parameters of CNS neurons. Further research aims at investigating the mode of action of TOCP on glutamate receptors and the identification of receptor subtypes that might be affected. Possibly, the effects described here are associated with some neurobehavioral symptoms related to the aerotoxic syndrome.

PS 378e Rat Brain Neurolemma Microtransplanted into Xenopus Oocytes Is a Useful Tool to Examine the Effects of Environmental Toxicants on Endogenous Voltage-Sensitive Ion Channels

S. B. Symington[1], E. Murenzi[2], T. G. Osimitz[3], L. P. Sheets[4], D. Minnema[5], M. Brooks[6], D. W. Gammon[7] and J. M. Clark[8, 3]. *[1]Biology and Biomedical Science, Salve Regina University, Newport, RI, [2]Molecular and Cellular Biology, University of Massachusetts, Amherst, MA, [3]Science Strategies LLC, Charlottesville, VA, [4]Bayer CropScience, Research Triangle Park, NC, [5]Syngenta Crop Protection, Greensboro, NC, [6]Ag-chem Consulting, Clifton, VA, [7]FMC, Ewing, NJ and [8]Vet and Animal Science, University of Massachusetts, Amherst, MA.*

Microtransplantation of mammalian neurolemma is a tool to study the structure and function of transmitter receptors and ion channels associated with the central nervous system. Microtransplanted neurolemma can originate from a variety of sources, posses ion channels and receptors in their native configuration and lipid matrix, and are applicable to examine diseases associated with different channelpathies. This functional system makes neurolemma-injected Xenopus oocytes a viable method for detailed investigations of toxicants on ion channel function. Our preliminary results indicate that Xenopus oocytes, injected with rat brain neurolemma are capable of reconstituting native ion currents into their plasma membrane. Expressed ion currents were sensitive to tetrodotoxin, ω-conotoxin MVIIC, and TEA; indicating the presence multiple voltage-gated ion channels (voltage-gated sodium channel, calcium channel and potassium channel, respectively). Furthermore, neurolemma-injected oocytes, exposed to increasing concentrations of permethrin, exhibited a concentration-dependent increase TTX-sensitive current. Once completely characterized, this procedure will also be amenable to the study of the developmental and reproductive toxicity of various drugs and other environmental contaminants and for the study of additional agents causing acute, chronic and developmental neurotoxicity in mammalian neuronal tissues, including those from knockout mice models and humans.

PS 378f Noninvasive Magnetic Resonance Imaging Marker of White Matter Neurotoxicity Caused by Hexachlorophene in the Rat Brain

S. Liachenko[1], J. Ramu[1], S. Sarkar[1], M. G. Paule[1], L. Schmued[1] and J. P. Hanig[2]. *[1]Division of Neurotoxicology, NCTR/FDA, Jefferson, AR and [2]Office of Testing and Research, CDER/FDA, White Oak, MD.*

Neurotoxicity assessment in drug development is accomplished using microscopic analysis, which may require different types of histological staining depending upon the type of damage to be assessed. Histopathology studies can be time consuming and easily miss lesions if the wrong stain or locus for tissue sampling is selected. In this study we used magnetic resonance imaging (MRI) to detect presumably neurotoxic changes in the rat brain caused by hexachlorophene (HC). Adult male Sprague-Dawley rats (N = 7, 347 ± 20 g) were given either HC (30 mg/kg, N = 5) or pure vehicle (corn oil, 1 ml/kg, N = 2) orally once a day for 5 consecutive days. Animals were imaged using MRI T_2 mapping before the treatment and at 4 and 6 days after the start of the treatment. At the time of imaging, animals were anesthetized with isoflurane and positioned inside a 7 tesla MRI scanner. T_2 relaxation mapping of the whole brain was performed at a resolution of 0.2 × 0.2 × 1.0 mm per pixel. All rats were perfusion-fixed at the end of the observation and their brains underwent histopathological assessment using aminocupric silver (classic neurotoxicity) and black gold (white matter damage) stains. MRI revealed significant increases in T_2 values in all HC-treated animals in areas which correspond closely to white matter. Histological sections stained with aminocupric silver did not show any damage in HC-treated rats and were classified as 'normal' by a neuropathologist. However, black gold-stained sections revealed the vast damage to white matter, which was seen in the non-invasive MRI scans. Controls treated with corn oil did not exhibit any changes in MRI scans or histology. These data suggest that MRI has significant utility in detecting neurotoxic changes in different structures of the brain and could be used to guide not only the loci for histopathology sectioning but also the type of stain used for histopathological studies. (Supported by NCTR and CDER, FDA, #E0741801).

PS 378g Mitochondrial Bioenergetics in Young, Adult, Middle-Age, and Senescent Brown Norway Rats

J. D. Pandya[2], A. Sebastian[2], J. E. Royland[3], R. C. MacPhail[1], P. G. Sullivan[2] and P. S. Kodavanti[1]. *[1]Neurotoxicology Branch, US EPA, Research Triangle Park, NC, [2]Dept of Anatomy and Neurobiology, University of Kentucky, Lexington, KY and [3]Genetic and Cellular Toxicology Branch, US EPA, Research Triangle Park, NC.*

Mitochondria are central regulators of energy homeostasis and may play a pivotal role in mechanisms of cellular senescence and age-related neurodegenerative and metabolic disorders. However, mitochondrial bioenergetic parameters have not been systematically evaluated under identical physiological conditions within multiple organ samples in diverse age-groups. In the present study, we used the Seahorse Extracellular Flux Analyzer (Seahorse Bioscience XF-24) to compare four different life-stages [i.e. 1 Month- Young (Y), 4 Month- Adult (A), 12 Month- Middle-Aged (M) and 24 Month- Old-Aged (O)] of Brown Norway rats (n=5 animals/group). Mitochondrial (15-40 μg/well) bioenergetic parameters were evaluated together from five brain regions [brain stem (BS), frontal cortex (FC), cerebellum (CER), striatum (STR), hippocampus (HIP)] and three peripheral organs [heart (HRT), liver (LVR), lung (LNG)]. In general, all the regions of the brain followed identical patterns where the maximal respiratory capacities (State V and State VSucc) were reduced with age (Y>A>M=O). The State III respiration in BS, CER and HIP demonstrated a similar pattern like State V (Y>A>M=O); whereas the FC and STR displayed highest State III rates in adult group (A>Y≥O≥M). The proton leak (State IV) remained unaffected. In peripheral organs, the State V and State III rates were highest in younger animals followed by gradual decline with aging as evident in both HRT (Y>A=O>M) and LNG (Y>A=O=M). In LVR, the NADH-linked bioenergetics remained unchanged whereas the FADH-linked maximal respiratory (State VSucc) rates increased gradually as a function of age (Y<A<M=O). In summary, the comparative data analysis of this study gives valuable insight into the metabolic status of various organs that could potentially lead to age-associated changes in neurodegenerative or metabolic disorders. Additionally, the observed changes in mitochondrial bioenergetics will serve as a basic platform to elucidate chemically-induced life-stage susceptibility mechanisms important in community health-related research. (This abstract does not necessarily reflect USEPA policy).

PS 378h Optineurin Expression in Dopaminergic Neurons and Response to Parkinson's Disease Relevant Insults

J. Wise[1], Z. S. Agim[1], M. A. Tambe[2], J. Rochet[2] and J. R. Cannon[1]. *[1]Health Sciences, Purdue University, Lafayette, IN and [2]Medicinal Chemistry and Molecular Pharmacology, Purdue University, Lafayette, IN.*

Optineurin (OPTN) is a protein that was first identified in 1998 as a genetic factor in normal tension glaucoma. Since then, multiple functional roles have been identified for OPTN, including roles in vesicle trafficking, Golgi organization, induction of macroautophagy and cell cycle. Recent data has also shown that OPTN aggregates in sensitive neurons in several neurodegenerative diseases, including Parkinson's disease (PD). The characteristic pathology of PD includes the aggregation of α-synuclein into Lewy bodies and the progressive loss of DA neurons in the substantia nigra. Macroautophagy is a primary route for degradation of α-synuclein but is dysregulated in PD. Currently, data on potential roles for OPTN in the pathogenesis of PD is very limited. Given OPTN's roles in many cellular pathways implicated in PD pathogenesis, we wished to characterize basal brain expression and response to dopaminergic (DA) neurotoxicants. Here, for the first time, we show immunohistochemical evidence that OPTN is enriched in the pars compacta region of the substantia nigra of untreated rats, in cells with a morphology characteristic of dopaminergic neurons. In primary rat mesencephalic cultures containing dopaminergic and nondopaminergic neurons, OPTN was primarily localized in DA neurons. We also demonstrate increased OPTN expression in DA neurons after methamphetamine exposure, compared to control, assessed by quantitative immunofluorescence. These data demonstrate that OPTN has high expression in

dopaminergic neurons, and its expression is increased after neurotoxicant insult, perhaps via a mechanism related to induction of macroautophagy. Our next steps are to investigate the interaction between OPTN and proteins involved in macroautophagy after PD-relevant toxicant insults.
Acknowledgments: We thank Vartika R. Mishra for technical assistance.
Funding: NIEHS/NIH ES019879 (J.R.C.).

PS 378i Methamphetamine Induces Neurotoxicity in Blood-Brain Barrier Endothelial Cells: Protective Role of Prolactin

H. Rosas-Hernandez[1, 2], E. Cuevas[1], S. Lantz-McPeak[1], M. G. Paule[1], Q. Gu[1], S. Z. Imam[1], J. Kanungo[1], S. F. Ali[1] and C. Gonzalez[2]. *[1]Division of Neurotoxicology, NCTR, Jefferson, AR and [2]Laboratorio de Fisiologia Celular, Universidad Autonoma de San Luis Potosi, San Luis Potosi, SLP, Mexico.*

Methamphetamine (METH) is a highly addictive psychoestimulant drug, which exerts its toxic effects by affecting the dopaminergic system. Recent reports suggest that METH disrupts the blood-brain barrier (BBB) by increasing apoptosis, permeability and decreasing tight junction proteins. On the other hand, the hormone prolactin (PRL) exerts protective vascular effects associated with the stimulation of endothelial cell proliferation. Because of that, the aim of this study was to evaluate the possible protective effect of PRL in the METH-induced neurotoxicity in bovine brain microvessel endothelial cells (bBMVEC) as an in vitro model of BBB. Confluent bBMVEC monolayers (cultured 10-14 days) were treated with increasing concentrations of METH (100 μM – 2.5 mM), and co-treated with METH and 100 nM PRL for 24 hours. METH increased the permeability of the BBB in vitro model associated with a decrease in the transendothelial electrical resistance (TEER), in a dose-dependent manner (250 μM-2.5 mM). The changes in permeability were related with a reduction in the expression of the tight junction (TJs) proteins claudin-5 and occludin The effects of METH on TEER and TJs proteins were prevented by co-administration with 100 nM PRL at all concentrations of METH except 2.5 mM. METH also decreased bBMVEC proliferation and increased apoptosis just at concentrations of 1 and 2.5 mM. 100 nM PRL protected against the effects in cellular proliferation and apoptosis induced by METH at 1 mM, but not at 2.5 mM. These data suggest that PRL may be useful to prevent the METH-induced neurotoxicity in bBMVEC by restoring the permeability of the BBB.

R 379 Environmental Factors in Dysregulation of Puberty Timing and Progression

X. Ye[4], E. Eugster[2], T. M. Plant[3] and W. D. Kempinas[1]. *[1]Morphology, Institute of Biosciences, State University of São Paulo, Botucatu, São Paulo, Brazil, [2]Pediatrics, Riley Hospital for Children, Indiana University School of Medicine, Indianapolis, IN, [3]Obstetrics, University of Pittsburgh School of Medicine, Pittsburgh, PA and [4]Physiology and Pharmacology, College of Veterinary Medicine, University of Georgia, Athens, GA.*

Puberty is a time of dramatic developmental changes, characterized by the transition from childhood to adulthood. The initiation of puberty is triggered by re-activation of a pulsatile pattern of hypothalamic gonadotropin-releasing hormone (GnRH) secretion, which in turn drives the pituitary-gonadal axis. Pubertal timing greatly varies among individuals, and recent studies have demonstrated a progressive decrease in age of onset of puberty in children around the world. This is generally accepted to be due to a complex interaction between genetic, neuroendocrine, and environmental factors, acting in concert with one another in each individual, determining pubertal timing. It has been demonstrated in animal and human studies that a highly heterogeneous group of exogenous substances interfering with the endocrine and neuroendocrine systems, imitating or antagonizing the action of endogenous hormones, have effects on the onset of puberty. Moreover, links between dietary factors, obesity, and dysregulation in puberty onset have been reported. The aim of this roundtable is to present the state of this important issue and discuss future directions of research, prioritizing a multidisciplinary approach.

IS 380 Nonrodents Can Be Monitored, Too…Characterization of Novel Biomarkers of Drug-Induced Kidney Injury (DIKI) in Rats, Canines, Nonhuman Primates, and Humans

J. E. McDuffie[1], S. Adler[2], J. A. Phillips[3], M. Sonee[4], K. Lynch[6], J. Gautier[5] and D. Burt[7]. *[1]Janssen Research & Development, LLC, San Diego, CA, [2]AstraZeneca, Wilmington, DE, [3]Boehringer Ingelheim Pharmaceuticals, Inc., Ridgefield, CT, [4]Janssen Research & Development, LLC, Spring House, PA, [5]Sanofi, Paris, France, [6]GlaxsoSmithKline, King of Prussia, PA and [7]Pfizer, Inc., Groton, CT.*

The purpose of this informational session is to broaden the dialog around the necessities for translatable DIKI biomarkers for use in drug discovery and development, as well as highlight ongoing research relative to the discovery and qualification of DIKI biomarkers across species. Traditional parameters used to detect DIKI include serum creatinine (sCr) and blood urea nitrogen (BUN). In all species, sCr and BUN lack sensitivity and/or specificity in detecting early stages of renal tissue injury identified by routine histopathology. The Critical Path Institute's Predictive Safety Testing Consortium, the Foundation for the National Institutes of Health, the International Life Sciences Institute-Health and Environmental Sciences Institute (ILSI-HESI), and the European Union Innovative Medicines Initiative (IMI) Safer and Faster Evidence-Based Translation program are in the process of identifying and qualifying novel biomarkers of kidney injury and dysfunction. Eight novel urinary protein kidney biomarkers have already been qualified for specific "context of use" in rat preclinical safety studies. Ongoing qualification of additional biomarkers in rats will be discussed. The potential utilities for the qualified rat renal biomarkers in canine and nonhuman primate preclinical toxicology studies will be reviewed. Paramount is the need for qualified renal biomarkers that allow for the monitoring of DIKI in the clinical setting. Efforts have been focused on bridging the gap between biomarkers being qualified in rats to nonrodent species and humans. During this informational session, selected data and other relevant information will be presented that underpins our overall translational strategy for the validation of biomarkers in rodents leading to the qualification of safety biomarkers for use in the clinical trials.

EC 381 The Role of Consultants in the Science and Practice of Safety Assessment

M. S. Miller. *Cancer Biology, Wake Forest School of Medicine, Winston-Salem, NC.*

During the past decade, a significant number of industrial and academic scientists have pursued full or part-time careers in toxicology consulting. Resources describing the nuts and bolts of how to set up a consulting business are often very general and do not address specific issues related to toxicology. The best safety assessment and product development efforts take a village, namely a team with a wide variety of detailed scientific knowledge, regulatory skills, and practical experience in product development, occupational toxicology, genetic toxicology and carcinogenesis, public health, etc. In many cases such knowledge, skill, and experience lie outside the internal resources of a firm. Toxicology consultants are a diverse external resource with varied specialties who can quickly and effectively address serious issues in safety assessment and/or product development. They can also perform more standard tasks when firms are constrained by the availability of internal toxicologists. In addition, toxicology consultants play a critical role in the interface between the scientific and lay communities when legal issues arise. This career development session will provide practical advice for those considering entering the field of toxicology consulting on a part-time or full-time basis, provide a comprehensive discussion of how toxicology consultants can satisfy critical needs of various types of clients, and provide guidance on leveraging their expertise in advancing the science and practice of toxicology. The talks will cover the full spectrum of consulting environments, including independent consultants, consulting in an academic environment, and consulting as part of a large firm, as well as examples of the client-consultant relationship.

PS 382 Mechanisms of Triclosan Effects on Mast Cell Function

L. Weatherly[1, 2], J. Shim[2], R. Kennedy[1, 2], L. Hutchinson[2], H. Hashmi[2], K. Blais[2], J. Pelletier[2], B. Burpee[2], B. Evans[2], Z. Kormendy[2], S. McGillicudy[2], E. Rice[2], Z. Tranchemontagne[2] and J. A. Gosse[1, 2]. *[1]Graduate School of Biomedical Science and Engineering, University of Maine, Orono, ME and [2]Department of Molecular and Biomedical Sciences, University of Maine, Orono, ME.*

Triclosan (TCS) is an antimicrobial that is used widely in hospitals, consumer goods, and personal care products such as hand soaps at concentrations ~10 mM. TCS has been found in clinical studies to be a therapeutic aid in human atopic skin disease, the mechanism of which is unknown. Using a well-characterized mast cell model, rat basophil leukemia (RBL-2H3) cells, we previously showed that non-cytotoxic concentrations of TCS inhibits antigen-mediated degranulation,

which is the release of histamine and other mediators. Mast cells are key players in allergy, infectious disease, carcinogenesis, and even a host of neurological functions and diseases such as autism. We have now also demonstrated TCS dampening of degranulation in a human mast cell line (HMC-1.2). In order to avoid use of an organic solvent, which could have cellular side effects, we have developed a method of TCS dissolution, along with UV-Vis spectrophotometry concentration determination for these studies. We have found that TCS strongly inhibits F-actin polymerization and membrane ruffling, suggesting that TCS's target is common to both the ruffling and degranulation pathways. Using Ca^{2+} ionophore stimulation to bypass early signaling events, we have found that TCS's suppressive effects are actually enhanced. When Ca^{2+} levels in the cell are directly measured with fluo-4 fluorescence, following antigen stimulation, TCS has no effect on Ca^{2+} influx into the cell. Taken together, these data suggest that TCS's target is likely downstream of the calcium machinery.

PS 383 Effects of Nitrated Fatty Acids on Phthalate-Induced Inflammation in Neonatal Neutrophils

M. Mohammed[1], F. E. Archer[1], S. Gowda[1], J. Abukharmah[1], I. Malik[1], D. L. Laskin[2], B. Weinberger[1] and A. M. Vetrano[1]. *[1]Pediatrics, Rutgers University-Robert Wood Johnson Medical School, New Brunswick, NJ and [2]Pharmacology and Toxicology, Rutgers University, Piscataway, NJ.*

Rationale: Hospitalized infants are exposed to numerous devices that contain the plasticizer di-(2-ethylhexyl)phthalate (DEHP). Metabolites of DEHP, including mono-(2-ethylhexyl) phthalate (MEHP), are markedly elevated in the urine of premature infants and have the ability to alter neutrophil function. MEHP binds PPAR-γ, a nuclear transcription factor that mediates the resolution of inflammation, a process that is developmentally impaired in neonatal neutrophils. Nitroalkene derivatives of fatty acids (NO-FA), such as linoleic acid (LA, LNO_2) and oleic acid (OA, OA-NO_2), are formed naturally in the body and are potent PPAR-γ ligands. We hypothesized that NO-FA would suppress the effects of MEHP by competitively binding to PPAR-γ. Methods: Neutrophils from umbilical cord and adult peripheral blood were isolated by density centrifugation and treated with LA, OA, LNO_2, OA-NO_2 (1μM) or medium control, in the presence or absence of MEHP (100 - 500 μM). H_2O_2 production was measured by Amplex Red assay. Cytokines were measured by cytometric bead array analysis, and gene expression was measured by qPCR.
Results: MEHP induces dose dependent increases in H_2O_2 production and Cox-2 expression in neonatal neutrophils. Both OA-NO_2 and LNO_2 inhibit MEHP-induced hydrogen peroxide production and cyclooxygenase-2 (Cox-2) expression in neonatal neutrophils. While OA and LA did not inhibit hydrogen peroxide production, they were effective inhibitors of Cox-2 expression. $OANO_2$ inhibited both basal and MEHP-stimulated IL-1β production.
Conclusions: These data demonstrate that nitrated lipids are capable of down-regulating MEHP-induced effects on neonatal neutrophil activity. Nitrated fatty acids are generated physiologically from dietary lipids. Our findings suggest that specific dietary alterations may help reduce the burden of inflammatory diseases in hospitalized neonates.
Supported by: NIEHS R21ES021170, ES ES005022, The Gerber Foundation

PS 384 Lipidomic Changes in the Pancreas and Plasma of Hepatic Alcohol Dehydrogenase-Deficient Deer Mice after Long-Term Ethanol Feeding

H. Fernando, K. K. Bhopale, G. A. Ansari and B. S. Kaphalia. *Pathology, The University of Texas Medical Branch, Galveston, TX.*

Alcoholic pancreatitis (AP) is a major disease causing significant morbidity and mortality among chronic alcohol abusers. Dysregulation of lipid metabolism is one factor that is involved in the early stage of AP can lead to inflammation and fibrosis and may be pancreatic cancer in some cases. However, the mechanism of AP is not well understood due to the lack of a suitable animal model. Earlier, we reported pancreatic injury and a significant endogenous formation of fatty acid ethyl esters (FAEEs) in the pancreas in hepatic alcohol dehydrogenase (ADH)-deficient (ADH-) deer mice fed 3.5 % ethanol daily for 2 months. Therefore, we evaluated the lipidomic changes and FAEE levels in the lipids extracted from the pancreas and plasma of ADH- deer mice fed ethanol for 3 or 6 months using 800 MHz proton (1H)-NMR spectroscopy and GC-MS. NMR data was analyzed by hierarchical clustering and principal component analysis. Pancreatic and plasma total lipids increased in mice fed ethanol daily for 3 months, but decreased for those fed daily for 6 months. Decreases were found for phospatidylcholine (PC) related protons in plasma of mice fed ethanol for 3 or 6 months while this change was significant only at 3 months in the pancreas. However, peaks corresponding to the protons of the diallylic group were increased in the pancreatic lipids as compared to a decrease at 3 months and an increase at 6 months in the plasma. The increased signals of FAEEs in the pancreas were confirmed by GC-MS analysis. Our findings suggest that metabolism of ethanol under hepatic ADH deficiency (a metabolic condition found during chronic alcohol abuse) generates FAEEs and decreases PC resulting in mild fatty deposition in the pancreas and its progression to pancreatitis with increasing the duration of ethanol feeding.

PS 385 3, 3-Diindolylmethane (DIM) Ameliorates SEB-Induced Acute Lung Injury: A Role for microRNA

D. M. Elliott, P. S. Nagarkatti and M. Nagarkatti. *Pathology, Microbiology and Immunology, University of South Carolina School of Medicine, Columbia, SC.*

Acute lung injury (ALI) and acute respiratory distress syndrome (ARDS) are characterized by pulmonary infiltration, hypoxemia, and edema. Among other etiologies, inhalation of toxic substances can lead to this serious condition. Staphylococcal enterotoxin B (SEB), a CDC select agent and public health threat during nosocomial infections, can be used to model ALI. Current clinical therapies for ALI and ARDS remain unreliable and mortality rates are still high. 3,3-diindolylmethane (DIM), a dietary compound found in cruciferous vegetables, has been recently shown to have anti-inflammatory properties and provides a potential therapeutic for ALI. We studied the mechanism underlying the ameliorative effects of DIM on SEB-induced ALI. Mice were exposed to SEB [50 mg; intranasal] and administered DIM [100 mg/kg] via oral gavage. Forty-eight hours after SEB exposure, serum, lung tissue and lung infiltrating mononuclear cells were collected. DIM treatment led to a decrease in lymphocytic infiltration, specifically CD4+, CD8+ and Vβ8+ T cells. DIM also led to a reduction of vascular leakage in lungs. Isolated mononuclear cells were subjected to high throughput microarray analysis to ascertain global microRNA expression levels. SEB led to dramatic miRNA dysregulation; in particular, modulating miRNAs such as miR-34a, -15a [decreased] and miR-221, -222 [increased], which were reversed in DIM treated mice. These microRNA have various gene targets dispersed throughout the apoptotic and cell cycle pathways, including SIRT1 and Bcl-2, as well as p27kip1, PUMA, CCND1, and CDK6, respectively. Moreover, DIM [10, 25, 50 μM] induced apoptosis in splenocytes and CD3+ T cells treated in vitro with SEB in a dose-dependent manner. Together, these studies demonstrate that DIM treatment may suppress SEB-mediated ALI by induction of apoptosis in T cells via alteration in expression of miRNA.
(Supported in part by NIH grants P01AT003961, R01AT006888, R01ES019313, R01MH094755 and VA Merit Award 1I01BX001357)

PS 386 Regulation of Nod2-Linked Proinflammatory Signals by Epithelial Ribosomal Insults

S. Park[1], D. Kim[2] and Y. Moon[1]. *[1]Department of Biomedical Sciences, Pusan National University School of Medicine and Immunoregulatory Therapeutics Group in Brain Busan 21 Project, Yangsan, Republic of Korea and [2]National Institute of Animal Science, RDA, Suwon, Republic of Korea.*

In response to excessive nucleotide-binding oligomerization domain–containing protein 2 (Nod2) stimulation caused by mucosal bacterial components, gut epithelia need to activate regulatory machinery to maintain epithelial homeostasis. Activating transcription factor 3 (ATF3) is a representative regulator in the negative feedback loop that modulates TLR-associated inflammatory responses. In the current study, the regulatory effects of ribosomal stress-induced ATF3 on Nod2-stimulated pro-inflammatory signals were assessed. Ribosomal inactivation caused persistent ATF3 expression that in turn suppressed pro-inflammatory chemokine production facilitated by Nod2. Decreased chemokine production was due to attenuation of Nod2-activated NF-kB and early growth response protein 1 (EGR-1) signals by ATF3. However, the underlying molecular mechanisms involve two convergent regulatory pathways. Although ATF3 induced by ribosomal inactivation regulated Nod2-induced EGR-1 expression epigenetically through the recruitment of histone deacetylase 1, NF-kB regulation was associated with posttranscriptional regulation by ATF3 rather than epigenetic modification. ATF3 induced by ribosomal inactivation led to the destabilization of p65 mRNA caused by nuclear entrapment of transcript-stabilizing human Ag R protein via direct interaction with ATF3. These findings demonstrate that ribosomal stress-induced ATF3 is a critical regulator in the convergent pathways between EGR-1 and NF-kB, which contributes to the suppression of Nod2-activated pro-inflammatory gene expression.
(This work was carried out with the support of "Cooperative Research Program for Agriculture Science & Technology Development (Project No. PJ008405032012)" Rural Development Administration, Republic of Korea).

PS 387 Role of TRIF and MAP Kinases in TLR3 & 4-Mediated Regulation of Drug Metabolizing Enzymes and Transporters

P. Shah, R. Ghose, T. Guo and O. Omoluabi. *Pharmaceutical and Pharmacological Sciences, University of Houston, Houston, TX.*

Purpose: The expression and activity of hepatic drug metabolizing enzymes and transporters (DMET) is altered on activation of an inflammatory response by bacterial or viral components. Inflammation in the liver is mediated primarily by the Toll-like receptors (TLRs). TLR3 and TLR4 mediate responses by viral and gram -ve bacterial components respectively, through adaptor molecules Toll/interleukin (IL)-1 receptor (TIR) domain containing adaptor protein and TIR domain containing adaptor inducing interferon (IFN)-β (TRIF). We have shown TLRs regulate gene expression of DMET however, the mechanism by which TLR signaling regulates these genes is not known. We hypothesize that TRIF and MAP kinases (MAPK) play a role in down-regulation of DMET through TLR3 & TLR4.
Methods: Male, TRIF+/+ and TRIF-/- mice (6-8 weeks) were treated with saline, Poly I:C (5mg/kg) or LPS (2mg/kg) for 8 and 16 h respectively. Liver tissues were harvested and stored at -80°. To assess the roles of MAPK, primary hepatocytes were isolated from C57BL/6 mice and treated with and without the following inhibitors: JNK (SP00125, 10μM), ERK (PD98059, 20μM) and p38 (SB203580, 25μM) for 30 min followed by treatment with Poly I:C (50μg/ml) or LPS (1μg/ml). RNA was extracted from livers/cells and gene expression was analyzed by qPCR analysis.
Results: In TRIF+/+ mice, Poly I:C treatment led to down-regulation of Cyp3a11,Cyp2a4, Cyp1a2, Cyp2e1, Ugt1a1, Mrp2 genes where as LPS treatment led to down-regulation of Cyp3a11, Cyp2a4, Ugt1a1 and Mrp2 genes. Surprisingly, this down-regulation was not attenuated in TRIF-/- mice. In hepatocytes, Poly I:C and LPS down-regulated the gene expression of DMET in the absence of inhibitors. While JNK inhibitor completely attenuated the down-regulation, p38 and ERK inhibitors did not affect down-regulation of DMET through TLR3 or TLR4.
Conclusion: These results show that down-regulation of DMET through TLR3 & 4 is dependent on JNK where as it is independent of the adaptor protein TRIF.

PS 388 Coculture of Hepatocytes and Kupffer Cells As an *In Vitro* Model of Inflammation and Liver Hepatotoxicity

K. Rose, N. S. Holman, M. E. Anderson and E. LeCluyse. *The Hamner Institutes for Health Sciences, Research Triangle Park, NC.*

Immune-mediated chemical-induced hepatotoxicity, i.e. indirect hepatocellular toxicity resulting from immune cells activating liver inflammatory responses, is often overlooked as a potential mode of action due to unavailability of appropriate in vitro models. We have established an in vitro rat co-culture model using Kupffer cells (KCs) and hepatocytes (HC) to study how inflammation impacts chemical-induced effects on liver. Optimal cell culture conditions have been identified for the maintenance of co-cultured KC and HC including cell ratios of KCs and hepatocytes. Hepatocytes and KCs were cultured for 48 hours with varying doses of several chemicals with hepatotoxic potential, with or without 1 μg/ml lipopolysaccharide (LPS) to mimic normal and inflammatory conditions. Trovafloxacin (TVX) was used as a benchmark for comparison to other chemicals. IL-6 and TNFα levels were assessed by ELISA and CYP3A was measured using Luciferin-IPA as a probe substrate to monitor endotoxin-induced functional changes in metabolic capacity. Cocultures showed varied cytokine responses depending on the compound tested, with corresponding differences in CYP3A activity levels. LPS-treated co-cultures exhibited marked down-regulation of CYP3A activity, which correlated with up-regulation of IL-6 production. This response was blunted in co-cultures treated with LPS and TVX, showing no changes to CYP3A activity and significantly lower production of IL-6. However, TNFα production was unaffected in TVX/LPS-treated co-cultures. Acetaminophen (APAP) showed a similar trend to TVX, although not all compounds tested had this modulating effect on LPS-induced IL-6. In most cases, treated co-cultures exhibited increased hepatocellular injury at higher doses of chemicals +/-LPS, represented by decreased ATP content, compared to hepatocyte monocultures alone. Results showed diverse effects on cytokine profiles that may be reflective of compound-specific mode of action in vivo.

PS 389 Adoptive Transfer to Study Cell Populations in Bleomycin-Mediated Lung Injury

T. Golden, M. Mandal, D. L. Laskin and A. Gow. *Pharmacolgy and Toxicology, Rutgers University, Piscataway, NJ.*

Intratracheal Bleomycin (ITB) induces pulmonary injury, inflammation, resolution and subsequent fibrosis. We hypothesize that recruited cells are critical for the inflammatory process, while resolution is dependent upon resident cells. To study the cell populations involved in ITB we used green fluorescent protein (GFP) chimeric mice. Recipient bone marrow was ablated with X-ray radiation and subsequently replaced with GFP+ bone marrow cells. Following 6 weeks of recovery, mice were either intratracheally instilled with saline or 3units/kg bleomycin. Mice were sacrificed at 8 (inflammation) or 15 (resolution) days post ITB. Bone marrow cells and BAL cells were collected and analyzed by flow cytometry. The mean bone marrow replacement was 85% ± 5 GFP+; while resident alveolar macrophages were GFP-. 8 days post injury, GFP- populations were similar between groups in number and appear as mature macrophages (F4/80+ CD11c+). The recruited populations, GFP+, are also primarily F4/80+ CD11c+. In saline treated mice the GFP+ cells are unactivated (CD11b(low)Ly6C-). In ITB treated mice these cells are activated (CD11b(high)Ly6C+). At 15 days there is minimal change in either resident or recruited cell populations with respect to 8 days for saline treated mice. However, in ITB treated mice GFP-F4/80+CD11c+ cells are reduced in number, while GFP+F4/80+CD11c+CD11b(high)Ly6C+ are increased in relative quantity. In addition, a novel population of F4/80+ CD11c- is seen in both recruited and resident cells. Recruited but not resident F4/80+ CD11c- cells are activated as they are Ly6C+. We propose that the GFP-F4/80+CD11c- cells are resident macrophages that are mediating the resolution process. These studies show that only recruited cells display an acute activation profile in response to ITB at either 8 or 15 days. However, resident cells do differentiate their phenotype by 15 days post ITB, possibly as a mechanism to mediate resolution. Supported by NIH grants F31GM108463, HL086621, TES005022

PS 390 Inhalation Exposure to the Tobacco Smoke Component Acrolein Enhances Allergic Responses to Ovalbumin

E. O'Brien[1], P. Spiess[1], A. Habibovic[1], M. Hristova[1], R. A. Bauer[1], M. J. Randall[1], M. E. Poynter[2] and A. van der Vliet[1]. [1]*Pathology, University of Vermont, Burlington, VT and* [2]*Medicine, University of Vermont, Burlington, VT.*

Acrolein, an α-β-unsaturated aldehyde generated in part through cooking oils and smoking tobacco, is a highly reactive electrophilic respiratory irritant implicated in asthma pathogenesis. However, few studies have directly investigated the influence of acrolein exposure on allergen sensitization and pulmonary inflammation. This study uses a murine inhalation model to examine whether inhaled acrolein alone or in combination with inhaled ovalbumin (OVA) enhances allergic sensitization to subsequent OVA challenge. Adult male C57BL/6 mice were sensitized to inhaled OVA (1%, 30 min/day, 4 days/week) and/or inhaled acrolein (5 ppm, 4 h/day, 4 days/week) over 2 weeks before challenge with aerosolized OVA (1%, 30 min/day) over three days. Sera, bronchoalveolar lavage (BAL) fluids, and lung tissues were collected after OVA challenge to assess pulmonary inflammation and allergic sensitization. Serum anti-OVA IgG1 levels were increased 4-fold in animals sensitized to both OVA and acrolein, compared to animals sensitized to OVA alone or acrolein alone. In addition, differential cell counts revealed an increase in BAL neutrophils among animals sensitized to OVA and acrolein. Acrolein sensitization was also observed to increase lung mRNA levels of Il13 and Il1a. Interestingly, exposure to both OVA and acrolein did not influence Il13 and Il1a mRNA levels, though it did significantly increase Ccl20 mRNA levels. This study suggests that acrolein inhalation can enhance allergen sensitization and lead to worsened airway inflammation.

PS 391 Effects of Current Tobacco Exposure on T Cell Immune Responses

U. C. Nygaard[1, 2], K. M. Hew[1], S. Mackey[3], L. Jack[4], G. E. Swan[4], R. Krasnow[4], S. Runyon[1], H. T. Maecker[3], C. L. Dekker[3] and K. Nadeau[1]. [1]*Dept of Pediatric Allergy and Immunology, Stanford University, Stanford, CA,* [2]*Div. of Environmental Medicine, Norwegian Institute of Public Health, Oslo, Norway,* [3]*Stanford University, Stanford, CA and* [4]*Center for Health Sciences, SRI International, Menlo Park, CA.*

Epidemiological studies have shown that smokers suffer from more frequent infections and infectious complications. The scope of the present study was to test the hypothesis that tobacco smoke exposure (TSE) modulates T cell function, thereby leading to impairment of cellular and humoral responses to the influenza vaccine. Monozygotic twins (MZT) ages 5 to 55 yrs were studied. Each participant's PBMC immune profile was determined 7 days after flu immunization by measuring expression of 37 different cell surface markers using CyTOF analyses and 51 different serum proteins using Luminex technology. Influenza vaccine responses were quantified by hemagglutination inhibition (HAI) 28 days after immunization. Associations between TSE and a selection of T cell subsets, some related serum cytokines and vaccine responses were investigated by comparing twins discordant for TSE (i.e. ever smoked vs. never smoked) and concordant for TSE (i.e. both ever smoked or both never smoked).

The percentage of T cells, CD4+, CD8+ and regulatory T cells ($p<0.001$), as well as serum levels of IFNγ, IL-5 and TNFα ($p<0.05$), were significantly lower in ever smoking individuals compared to their non-smoking twins (n=16 pairs). If restricted to only current smokers (n=12), stronger significances were seen ($p\leq0.0002$). No differences were seen between TSE concordant twins. Preliminary results indicate no significant differences (p=0.94, n=4 pairs) in vaccine responses between smoking and non-smoking twins, but a larger number of current smokers is needed to draw conclusions.
Overall, our preliminary data suggest that current tobacco smoke exposure may affect T cell immune responses and related cytokines, which may have implications for the development of immune diseases and infection resistance.

PS 392 Exposure to Sidestream Tobacco Smoke Induces Airway Hyperresponsiveness and Inflammation in Early Postnatal Mice

Z. Wu, D. D. Hunter, T. P. Batchelor and R. D. Dey. *Neurobiology and Anatomy, West Virginia University, Morgantown, WV.* Sponsor: T. Nurkiewicz.

There are abundant epidemiological studies linking early environmental tobacco smoke (ETS) exposure with childhood asthma. The present study was designed to determine changes on airway responsiveness and innervation after ETS exposure during early postnatal period. The postnatal day (PD) 2 mice were exposed to either ETS or filtered air (FA) for 10 consecutive days. Lung function, substance P (SP) airway innervation, and nerve growth factor (NGF) and cytokines in bronchoalveolar lavage (BAL) fluid were measured 1, 3 and 7 days after last ETS exposure. 1 day after the last ETS exposure, airway responsiveness and SP innervation in airway smooth muscle were significantly increased, as well as altered airway inflammation, which include significant elevated levels of IL-1β, IL-4, IL-6, IL-10, TNFα and INFγ in BAL compared with FA exposure. Interestingly, 3 days after ETS exposure, airway hyperresponsiveness and SP innervation in airway smooth muscle remained elevated, parallel with high levels of IL-1and NGF. These results indicated that the change in SP airway innervation play an important roles in airway inflammation and hyperresponsiveness induced by ETS exposure during early in life.

PS 393 Comparison of Proinflammatory Cytokine (IL-6 and IL-8) Release from Two Types of Cells Exposed to Mainstream Cigarette Smoke Total Particulate Matter

X. Li, P. Shang, F. Xie, H. Liu and J. Xie. *Key Laboratory of Tobacco Chemistry, Zhengzhou Tobacco Research Institute of CNTC, Zhengzhou, Henan, China.* Sponsor: R. Meng.

Mainstream cigarette smoke is a complex aerosol consisting of thousands of chemical compounds and oxidants, which can cause cellular oxidative injury and inflammation involved in the development and progression of human respiratory diseases such as chronic obstructive pulmonary disease (COPD). Many cell lines are available to be used as the *in vitro* models for investigating the mechanisms of cigarette smoke-induced diseases. Different types of cells can respond to cigarette smoke-induced toxicity differently. A549 cells (human adenocarcinoma cells) and BEAS-2B cells (human bronchial epithelial cells) widely used in many laboratories are representative two types of cells. The purpose of this study was to compare the difference in proinflammatory cytokine release from two types of cells in response to cigarette smoke total particulate matter (TPM). Cells were exposed to TPM for 24 h. The neutral red uptake (NRU) assay was employed to assess the cytotoxicity of cigarette smoke, and the levels of proinflammatory cytokine (IL-6 and IL-8) were measured by ELISA. The results showed that BEAS-2B cells were more sensitive to smoke-induced cytotoxicity than A549 cells. TPM of mainstream cigarette smoke caused dose-dependently increase of cytokine IL-6 and IL-8 release from BEAS-2B cells. While the induction of IL-6 and IL-8 release from A549 cells was not impacted after TPM exposure, and in contrary, the release of IL-6 and IL-8 decreased with the concentration of TPM solutions increased, compared to control cells. These results indicate that the inflammatory response to cigarette smoke can be different depending on the characteristic of cells, and non-tumor cells might be an appropriate model for investigating the smoke-induced inflammatory mechanisms.
This work was supported by the National Natural Science Foundation of China (No. 21007094).

PS 394 The Effects of Ozone Exposure on Inflammasome Activation and Heart Failure during CVB3 Myocarditis

M. M. Aladdin, A. Bucek and D. Fairweather. *Environmental Health Science, Johns Hopkins University Bloomberg School of Public Health, Baltimore, MD.*

Ozone (O3) is a common secondary air pollutant that contributes to increased morbidity and mortality. Studies have shown a positive correlation between O3 exposure and emergency department visits for the exacerbation of pulmonary conditions. Ozone is also linked to cardiovascular conditions such as cardiac ischemia and heart attacks. In this study, we explored the effects of O3 on heart failure (HF) during coxsackievirus B3 (CVB3) myocarditis. Myocarditis is an autoimmune disease that is characterized by inflammation of the myocardium with or without cardiomyocyte damage. Viral infections, such as CVB3, are the most common cause of myocarditis in the US. Myocarditis is a very important public health issue as it goes largely undiagnosed, and can progress to other conditions like HF and dilated cardiomyopathy (DCM). The Fairweather lab found marked sex differences in the incidence and severity of disease; and has established that testosterone increases myocarditis and DCM in mice with CVB3 myocarditis by increasing IL-1β and the inflammasome. Air pollution can exacerbate the underlying inflammation in myocardium and drive HF. O3 has been shown to increase this pathway in the lung.
We hypothesized that O3 exposure during CVB3 myocarditis activates the inflammasome via TLR4 and increases IL-1β, which may drive HF in males. We explored this hypothesis by injecting 8-10 week old BALB/c mice with CVB3 or PBS intraperitoneally at day 0, and then exposing them to either room air (RA) or ozone (O3) at 0.3 ppm, continuously for 48 hours at days 8 and 9. Mice were subsequently sacrificed at day 10. The interaction of CVB3 and O3 increased protein expression of IL-1β. Furthermore, pressure-volume loop data showed that simultaneous exposures to O3 and CVB3 increased the risk for HF in mice. To our knowledge, this is the first study to explore the interaction between CVB3 infection and O3 exposure in HF. Through this study we can provide a mechanistic explanation for how air pollution increases the risk for cardiovascular events.

PS 395 Role of Spleen Monocytes (Mo) in Ozone-Induced Lung Inflammation and Injury

M. Francis, M. Mandal, H. Choi, J. D. Laskin and D. L. Laskin. *Rutgers University, Piscataway, NJ.*

Ozone is a ubiquitous air pollutant known to damage the lung. Activated macrophages (MP) have been implicated in ozone toxicity; however, the origin and phenotype of these cells is unknown. Evidence suggests that the spleen functions as an extramedullary source of inflammatory monocytes (Mo). In these studies we used splenectomized (SPX) mice to assess the contribution of spleen Mo to the pulmonary inflammatory response to inhaled ozone. Lung, spleen, and bone marrow were collected 24-72 h after exposure of mice to ozone (0.8 ppm, 3 h) or air and analyzed by flow cytometry. Ozone caused increases in bronchoalveolar lavage (BAL) protein and MP, markers of lung injury and inflammation. Resident alveolar MP from control animals expressed F4/80 and Cd11c+, but not CD11b. Following ozone exposure, increases in immature Cd11b+F4/80- and mature Cd11b+F4/80+ MP were observed in the lung. Subpopulations of these cells were identified that expressed high and low levels of the proinflammatory Mo/MP marker, Ly6C. Both immature Cd11b+F4/80-Ly6Chi and mature Cd11b+F4/80+Ly6Chi proinflammatory MP increased in the lung after ozone, reaching a maximum at 48 h. This correlated with a decrease in Cd11b+Ly6chi Mo in the spleen. Conversely, Cd11b+F4/80-Ly6Chi proinflammatory Mo increased in the bone marrow. Splenectomy resulted in a decrease in the total number of inflammatory cells in the lung after ozone, and reduced tissue injury. Flow cytometric analyses revealed a reduction in immature (Cd11b+F4/80-Ly6Chi) and mature (Cd11b+F4/80+Ly6Chi) proinflammatory MP in lungs of SPX mice, but increases in mature Cd11b+F4/80+Ly6Clo anti-inflammatory MP. Cd11b+F4/80-Ly6chi immature proinflammatory Mo in bone marrow of ozone-treated SPX mice were also decreased relative to sham control. These data suggest that the spleen is a source of proinflammatory/cytotoxic MP that contributes to ozone-induced lung injury. Moreover, in the absence of this splenic reservoir, there is a compensatory increase in inflammatory cells generated in the bone marrow. Supported by NIH ES004738, CA132624, AR055073, ES007148and ES005022.

PS 396 Subsequent Ozone Exposures *In Vitro* Result in Attenuation of Inflammatory Response

E. C. Bowers[1, 2], S. D. McCullough[2], L. A. Dailey[2] and D. Diaz-Sanchez[2]. [1]*UNC Chapel Hill, Chapel Hill, NC and* [2]*United States Environmental Protection Agency, Clinical Research Branch, Chapel Hill, NC.*

Approximately 133 million residents of the United States live in areas where ozone levels exceed the National Ambient Air Quality Standards. Some of these regions may experience such exceedances on a daily basis. While the health effects of acute ozone exposure are well documented, the effects of chronic exposures are less understood. Given that many people are exposed to harmful levels of ozone on a chronic basis, it is important to characterize the physiological effects of subsequent, daily exposures. Controlled human exposure studies have shown that response to ozone varies between acute and chronic exposure conditions. If only exposed to ozone for one to two days, subjects present with increased airway inflammation and decreased lung function. However, additional exposures up to six days result in the attenuation of these effects. We were interested in investigating the mechanism underlying this phenomenon using an *in vitro* model. To accomplish this we used primary human bronchial epithelial cells from healthy volunteers grown in air–liquid interface culture and exposed them to 0.3 ppm ozone or clean air for two hours per day for seven consecutive days. Because inflammatory state varied between chronic and acute exposures, we chose to measure the expression of IL-8, IL-6, and IL1-α, as these are key mediators of inflammation. The expression of these genes peaked following a single day of ozone exposure. During subsequent days of exposure the ozone-mediated induction of pro-inflammatory mediators declined and eventually approached baseline levels. Thus daily ozone exposure *in vitro* produces a similar suppression of the pro-inflammatory response as observed in clinical studies. Using this model, we plan on identifying the central mechanisms responsible for this effect, which may include altered signaling pathways and epigenetic modifications. Understanding the health consequences of this effect may help identify and treat vulnerable populations.

PS 397 Development of an *In Vitro* Functional Assay for Human Macrophages

A. Hudson, C. Bono, J. Whritenour and S. Casinghino. *Pfizer, Inc., Groton, CT.*

Macrophages play a critical role in the defense against pathogens. Drugs being developed to treat inflammatory diseases often target macrophages, which are potent producers of cytokines and other inflammatory mediators. These drugs have the potential to compromise host resistance by inhibiting other macrophage functions (e.g. oxidative burst and phagocytosis) besides cytokine production. The objective of these studies was to develop an in vitro method to measure oxidative burst and phagocytosis in human monocyte-derived macrophages. CD14 positive monocytes were isolated from whole blood using magnetic beads and then stimulated with granulocyte macrophage colony stimulating factor to generate macrophages, and cultured for various incubation periods (from 2-9 days). The macrophage phenotype was verified using anti-CD206 antibody and intracellular reactive oxygen species (ROS) generation and phagocytosis were measured using FcOxyburst and pHrodo® Bioparticles, respectively. Assay conditions (4 days of culture and 50,000 cells per assay tube) and length of pre-incubation time with inhibitors were optimized for maximal viability and function of the macrophages. Typical assay results show that more than 50% of the CD206-expressing macrophages are phagocytic and more than 90% produce ROS. Cytochalasin D and N-acetyl cysteine were used to inhibit phagocytosis and ROS generation, respectively. Results showed that macrophage immune functions could be measured and inhibited in this assay. These data suggest that the macrophage function assay can be used as a tool for determining the potential of drug candidates to inhibit phagocytosis and oxidative burst.

PS 398 Evaluation of Sex Sensitivity in Local Lymph Node Assay Using Butachlor and α-Hexylcinnamaldehyde

M. V. Patel[2], V. R. Dalal[2], V. J. Piccirillo[1], R. Chhimwal[2], N. Patel[2], S. Jaiswal[2], B. Prajapati[2], D. R. Boverhof[3] and M. R. Woolhiser[3]. [1]*VJP Consulting, Inc., Ashburn, VA,* [2]*Toxicology, Jai Research Foundation, Valvada, Gujarat, India and* [3]*TERC, The Dow Chemical Company, Midland, MI.*

The current OECD Test Guideline for the conduct of the Local Lymph Node Assay (LLNA) recommends the use of only female mice for the assessment of skin sensitization potential for a given chemical. The NIH publication no. 99-4494 recommends that only female CBA mice be used, as they reportedly develop a stronger contact dermatitis response when compared to males however if male to be used, systematic studies evaluating potential sex differences should be conducted. Males were also reported to display a larger variation in response due to a greater tendency to fight and to be involved in 'social ranking' behavior when group housed. However, there are several advantages to consider with the inclusion of male mice in LLNA testing including a more refined and responsible use of animals. Therefore, to begin to systematically assess the appropriateness of using male mice in the LLNA a comparative guideline study was conducted with individual housing of mice using the sensitizer, Butachlor 50% EW (BU50) and α-hexylcinnamaldehyde (HCA) respectively. The study compared 5 male and 5 female CBA/J mice/group, at three BU50 concentrations [10%, 25%, 50% (v/v)] and a single HCA concentration [25%] using 1% L92 as the vehicle. Stimulation indices for the three BU50 treatment groups were 2.07, 3.85, and 5.25 for male and 1.45, 3.65 and 6.79 for females, respectively and stimulation index for the HCA treated group were 5.92 for male and 4.16 for females. The results revealed no significant difference between samples means or variability between the sexes and the SI values observed for both male and female mice of positive control were within the range of historical control data for female mice. These data provide initial support for the use of male mice in the LLNA and will be followed by further experimentation.

PS 399 Evaluation of Sex Sensitivity in Local Lymph Node Assay Using Acephate and α-Hexylcinnamaldehyde

V. R. Dalal[2], V. J. Piccirillo[1], M. V. Patel[2], R. Chhimwal[2], N. Patel[2], S. Jaiswal[2], B. Prajapati[2], D. R. Boverhof[3], M. R. Woolhiser[3] and S. Balakrishnan[4]. [1]*VJP Consulting, Inc, Ashburn, VA,* [2]*Toxicology, Jai Research Foundation, Valvada, Gujarat, India,* [3]*TERC, The Dow Chemical Company, Midland, MI and* [4]*Department of Zoology, Faculty of Science, The M.S. University of Baroda, Vadodara, Gujarat, India.*

The current OECD Test Guideline for the conduct of the Local Lymph Node Assay (LLNA) recommends the use of only female mice for the assessment of skin sensitization potential for a given chemical. The NIH publication N° 99-4494 recommends that only female CBA mice be used, as they reportedly develop a stronger contact dermatitis response when compared to males however if male to be used, systematic studies evaluating potential sex differences should be conducted. Moreover, males were reported to display a larger variation in response due to a greater tendency to fight and to be involved in 'social ranking' behavior when group housed. However, there are several advantages to consider with the inclusion of male mice in LLNA testing including a more refined and responsible use of animals. Therefore, to begin to systematically assess the appropriateness of using male mice in the LLNA a comparative guideline study was conducted with individual housing of mice using a non-sensitizer and a sensitizer viz., Acephate 97 DF (AC97) and α-hexylcinnamaldehyde (HCA) respectively. The study compared 5 male and 5 female CBA/J mice/group, at three AC97 concentrations [10%, 25%, 50% (w/v)] and a single HCA concentration [25%] using dimethylformamide as the vehicle. Stimulation indices (SI) for the three BU50 treatment groups were 1.16, 1.58 and 1.59 for male and .39, 1.55 and 1.56 for females, respectively and SI for the HCA treated group were 4.31 for male and 5.44 for females. The results revealed no significant difference between samples means or variability between the sexes and the SI values observed for both male and female mice of positive control were within the range of historical control data for female mice. These data provide initial support for the use of male mice in the LLNA and will be followed by further experimentation.

PS 400 Impact of Collection Site and Method on Blood Lymphocyte Subsets in Sprague-Dawley Rats

G. Burleson, F. G. Burleson and R. Mikkelsen. *BRT-Burleson Research Technologies, Inc., Morrisville, NC.*

Immunotoxicology studies in rats often include peripheral blood collection from multiple anatomical sites, and can vary due to non-terminal or terminal collection. Differences in lymphocyte subset counts based on collection site in humans and mice have been recently reported. In order to better control for potential cell count differences between multiple anatomic blood sampling sites in rat research studies, lymphocyte cell counts were performed for samples from the lateral tail or saphenous veins (non-terminal) or inferior vena cava (terminal) of Sprague Dawley rats. Non-terminal samples were collected without anesthesia, and terminal samples were collected after CO2 overdose. Additional lateral tail vein samples were drawn after animals were heated to dilate the vein, for comparison to samples from non-heated animals. T, B, and natural killer (NK) cell subsets were evaluated using a flow cytometer.

In two separate studies, it was found that NK cell percentage and counts were increased, while total T cell percentage and counts were decreased in inferior vena cava terminal samples compared to non-terminal samples. Cytotoxic and helper T cell counts were concomitantly lower in inferior vena cava samples relative to

non-terminal samples. B cell and total CD45+ lymphocyte counts were not impacted by collection site. Pre-heating animals to dilate the lateral tail vein did not impact lymphocyte subset counts.
These results highlight the importance of understanding the possible impact of non-terminal and terminal blood collection, or collection from peripheral and central anatomic sites, on study design and data interpretation.

PS 401 The Guinea Pig Systemic Anaphylaxis Model Revisited

J. Descotes[1], M. Duclos[2], V. Haag[2] and R. Forster[2]. [1]*Poison Center, Lyon, France and* [2]*CiToxLab, Evreux, France.*

The guinea pig systemic anaphylaxis model was introduced decades ago to evaluate the sensitizing potential of pharmaceuticals and chemicals. After years of use, it was nearly abandoned, but is attracting renewed interest for the evaluation of pharmaceutical macromolecules or medical devices. As standardization of this model has been meager, the aim of this study was to analyze data obtained with the positive reference compound ovalbumin (OVA) using various experimental modalities. A total of 14 studies including 285 male Dunkin-Hartley guinea pigs were selected. Groups of 5 animals received 1, 2, 3 or 6 sensitizing injections of 0.2, 2 or 20 μg OVA by the intraperitoneal (0.5 ml), subcutaneous (0.1 ml) or intradermal route (0.1 ml). Few animals received aluminum hydroxide with the first sensitizing injection. The delay between the injections was 7 days, except in some animals (2 injections, 14 days apart). After a rest period of 7 or 14 days, the animals were challenged with 0.2 or 20 μg OVA (0.1 ml) via the penile vein (or the ear vein in rare animals). Controls received injections of saline using the same route, volume and injection schedule. Sensitization was evaluated from signs of anaphylaxis observed during a one-hour follow-up. The retrospective analysis of the results shows that the optimal sensitizing dose of OVA was 2 μg. Inconsistent results were obtained with 0.2 μg. Results were similar with the subcutaneous and the intradermal route, but were more variable with the intraperitoneal route. Similar clinical signs were observed after 2, 3 or 6 sensitizing doses with the same challenging dose, but were less consistent after 1 sensitizing dose. The optimal challenging dose of OVA was 20 μg and no overt differences were seen in animals given aluminum hydroxide. The conclusion of this retrospective analysis is that an optimal study plan consists of 2 sensitizing subcutaneous injections of 2 μg OVA with a 7-day interval followed by a challenging intravenous injection of 20 μg OVA after a 14-day rest period.

PS 402 Transferability and Reproducibility of the Myeloid U937 Skin Sensitization (MUSST) Test for Skin Sensitization Testing

C. Piroird, L. Nardelli, J. Cotovio and N. Alépée. *L'Oréal, Aulnay sous Bois, France.* Sponsor: D. Bury.

Skin sensitization is a disturbed immunological process in which a sensitizer is a substance that triggers an immunological cellular response. Initially, the substance penetrates the epidermis prior to the formation of a stable conjugate with skin proteins. This stable conjugate is then processed by the epidermal dendritic cells, which subsequently mature and migrate out of the skin to the local lymph nodes.
The MUSST test method is modelling the dendritic cell activation upon exposure to sensitizers by means of measuring phenotypical changes in the U937 human myeloid cells. Like the dendritic cells, upon contact with sensitizers, U937 cells induce CD86 expression as they are activated. Cell viability is assessed using propidium iodide exclusion. Both parameters are measured by flow cytometry. The prediction model is defined by a stimulation index above 150 with a dose response relationship and at least 2 concordant experiments, for identifying a substance as Sensitizer S /Non-Sensitizer NS.
The aim of this study is to demonstrate the transferability and reproducibility of the MUSST in 4 laboratories and define its predictivity.
The main determinant of the test method reliability assessment was the concordance of classification, S/NS. The intra-laboratory reproducibility (WLR) study was assessed with 21 chemicals tested in 3 independent experiments within L'Oreal. Similar prediction was obtained resulting in a WLR of 95%. Eleven out of the 14 substances were consistently classified (S/NS) by the 4 laboratories resulting in an inter-lab reproducibility (BLR) of 79%. The BLR for the pair-wise comparisons was comprised between 86-93%.
To determine the predictive capacity of the MUSST, a set of 123 substances has been evaluated. The predictive capacity of the MUSST is 86.2% with a sensitivity of 86.1% and a specificity of 86.4%.
The MUSST is an efficient transferable and reproducible assay for the skin sensitization hazard characterization, promising as a tool to be integrated within a battery of assays to perform a skin sensitization risk assessment.

PS 403 Time Course Difference in Severity and Sensitivity of Immunotoxicity of Cyclophosphamide in Female Swiss Albino Mice

P. Mehta[1], D. Gohel[1], V. J. Piccirillo[2], M. V. Patel[1], S. Jadhav[1], K. Shah[1] and M. Pandya[1]. [1]*Toxicology, Jai Research Foundation, Valvada, Gujarat, India and* [2]*VJP Consulting, Inc, Ashburn, VA.*

The study was conducted to evaluate the time course difference in severity and sensitivity of in-house bred female Swiss Albino mice to the immunosuppressive effect of Cyclophosphamide Monohydrate (CPM). The mice were treated with CPM by intraperitoneal administration for 4 consecutive days at dose levels of 5, 25 and 50 mg/kg body weight/day, dissolved in Phosphate Buffer Saline (PBS). Concurrent control group animals were dosed with vehicle (PBS) alone. On the first day of treatment, all animals were treated with SRBCs (Innovative Research, USA) in normal saline (8 x 107 RBCs) at fixed dose volume of 0.2 mL/animal intravenously. Eight animals from each group were sacrificed on day 5 and four animals per group were sacrificed on day 15. Significant reductions in anti-SRBCs IgM antibody level, WBC count, neutrophil count and absolute and relative weight of spleen and thymus were observed in animals sacrificed on day 5 from groups treated with 25 and 50 mg of CPM/kg body weight whereas significant changes were not observed in animals treated with 5 mg/kg b. wt. dose. Animals sacrificed on day 15 showed no significant immunotoxic changes when compared to control group suggesting recovery. The effects observed in the 25 and 50 mg/kg dosed animals sacrificed on day 5 were consistent with immunotoxic effect of CPM seen in previous immunotoxicity studies in mice. Based on these results, it can be concluded that the time course for treatment and sacrifice of Swiss albino mice in immunotoxicity studies is critical and also demonstrates that in house Swiss Albino mice give responses similar to other recommended strains (e.g. B6C3F1 hybrid mouse).

PS 404 Quantitation of Leukocyte Subsets and Leukocyte Activation in Canine Blood Using a 7-Colour Flow Cytometry Assay

A. J. Beavis, M. S. Perpetua, S. Harvey and G. Bannish. *Biomarkers, Bioanalysis, and Clinical Sciences, Huntingdon Life Sciences, East Millstone, NJ.*

We developed and validated a 7-color flow cytometry assay to identify lymphocytes, monocytes, granulocytes, T cells, T cell subsets, B cells and HLADR expression in canine whole blood. Six commercial antibody conjugates recognizing canine leukocyte antigens were used; CD3FITC, CD21PE, HLADRPECy5, CD4PECy7, CD8AF647 and CD14AF647, in combination with the DNA-binding dye DAPI and the LiveDead viability dye. Whole blood (EDTA, 100 μL) was incubated with lysing buffer, washed and labeled with the viability dye. Cells were stained with CD3/CD21/CD4/CD8,CD14 and HLADR or control, washed, fixed and incubated in DAPI. Counting beads were added and samples analysed on the flow cytometer. Data for frequency (%), absolute number (cells/μL) and HLADR mean fluorescence intensity (MFI) were reported. Viable leukocytes were identified with DAPI and LiveDead stain. Monocytes were gated as the CD3-/AF647+ cluster from a plot of CD8/CD14 versus CD3. Lymphocytes were identified by light scatter and Boolean Logic to exclude monocytes. The T and B cells were identified by expression of CD3 and CD21 respectively and T cell subsets by expression of CD4 and CD8 antigens. Granulocytes were identified from a plot of side scatter (SSC) and CD4 with the granulocyte cluster expressing the CD4+ phenotype and a granulocyte subpopulation with CD4- phenotype. In naïve animals, differential MHC class II expression was observed on T cells, B cells and monocytes but not on granulocytes. Intra-assay precision of ≤ 20 % CV was demonstrated for all major cell types for frequency, absolute values and MFI. Whole blood was stable up to 24H post-collection and stained samples stable up to 24 H when stored refrigerated. This assay was validated with acceptable precision, stability and robustness and is applicable for assessing the impact of test articles on leukocytes and leukocyte activation in canine peripheral blood.

PS 405 Comparison of the Lymphocyte Subpopulations from Peripheral Blood of CD1, CBA/J and Swiss Albino Female Mice following Administration of Cyclophosphamide Monohydrate

D. Ujawane[1], M. V. Patel[1], V. J. Piccirillo[2], K. Hadiya[1], M. Shinde[1], M. Poshiya[1], D. Gohel[1] and J. Mistry[1]. [1]*Department of Toxicology, Jai Research Foundation, Valvada, Gujarat, India and* [2]*VJP Consulting, Inc., Ashburn, VA.*

The prevalent guidelines (OCSPP: 870.7800) for determination of immunotoxic potential recommend use of CD1 mice. Considering the diversity of strains existent with different toxicology labs, a comparative study or immunosuppressive activity induced by cyclophosphamide monohydrate (CPM) was evaluated in CD1,

CBA/J, and Swiss Albino Mice (SAM). The study included evaluation of peripheral blood lymphocyte (WBC) and subpopulations of the cluster of differentiation (CD) cell. Each mouse strain was dosed with 25-mg/kg CPM for four consecutive days via intraperitoneal injection. The vehicle (reverse osmosis water) was injected in the concurrent control groups. Peripheral whole blood was collected on day 5 and subjected to estimation of WBC count using automated haematology analyzer (ADVIA 120), while the subpopulation of CD cells was determined using flow cytometer FACSVerse (BD). All the strains displayed, comparable WBC counts. No change in WBC counts was seen in any of the strain specific control. Consistent decreases in percent population of CD19+, CD16/32+, CD3-, CD16/32+ and CD3-CD19+ were seen in all three strains, as compared to strain matched controls. Further, CPM treatment resulted in an increase in percent population of CD4+ cells in all the strains as well as decreases in NK cell marker (CD3-, CD16/32+) and B lymphocyte (CD19+). The results of this preliminary study support the use of either of the CD1, CBA/J or SAM mouse strains for use in immunotoxicity testing.

PS 406 A Comparison of Mauritius and Chinese Cynomolgus Monkeys in the Natural Killer Cell Cytotoxicity Assay

J. E. Arrington[1], G. Ferency[3], A. Guerrero[2], M. Fort[2] and P. Narayanan[2]. *[1]Toxicology Study Direction, Covance, Madison, WI, [2]Amgen, Inc., Seattle, WA and [3]Clinical Pathology Services, Covance, Inc., Madison, WI.*

The purpose of this study was to compare the natural killer cell (NK) cytotoxicity assay results from Mauritius origin and Chinese (mainland) origin cynomolgus monkey peripheral blood. Known differences in peripheral blood cell numbers of Mauritius monkeys in comparison to Chinese origin cynomolgus monkeys are described in the literature, but no data regarding differences in NK cell function was included. Evaluation of the innate immune response is important for certain immunomodulatory compounds and the NK cell cytotoxicity assay has been established to assess functional changes in the NK cell response. The study results showed that different methodologies for isolating peripheral blood mononuclear cells (PBMC) were required for Mauritius origin monkeys than for Chinese origin monkeys and that the methodology also affected the NK cell cytotoxicity assay activity. Comparison of lytic units (LU) for Mauritius and Chinese origin monkeys showed that the NK cell cytotoxicity data was comparable, however, LU values for Mauritius animals tended to be lower and more variable [Mauritius-origin mean LU of 35.9% with coefficient of variation (CV) of 86.7%, while Chinese-origin had LU of 72.8% and CV of 60.4%]. In summary, assessment of innate immune function via the NK cell cytotoxicity assay can be done effectively in Mauritius origin monkeys, but the study results highlight the need to assess differences in animal origin for any assay being used to make decisions on compound development or safety assessment.

PS 407 Validation of a Functional Assay to Detect Nonhuman Primate Natural Killer Cell Activity

V. J. Johnson[1], R. Mikkelsen[1], N. Makori[2], F. G. Burleson[1] and G. Burleson[1]. *[1]BRT-Burleson Research Technologies, Morrisville, NC and [2]SNBL USA, Everett, WA.*

The immunotoxicity of a compound is ideally determined by assessing all three arms of the immune response: humoral, cell-mediated, and innate immunity. Although humoral immunity is now routinely assessed in non-human primates by evaluation of the T-dependent antibody response (TDAR), assessments of innate and cell-mediated immunity are more difficult to integrate into non-human primate studies.

The purpose of this study was to validate a functional killing assay to detect NK cell activity in PBMCs obtained from male and female cynomolgus monkeys. The human erythroleukemia K562 cell line was labeled with ^{51}Cr and used as the target cell population. This assay detected NK cell-mediated lysis and killing of K562 targets by quantifying the release of ^{51}Cr into the cell culture media.

Target cell killing showed a strong positive correlation with the effector:target (E:T) ratio (6.25:1 to 50:1). At the lowest E:T ratio of 6.25:1, NK cell activity was clearly discernible from the spontaneous target cell death background. Spontaneous target cell death was consistently low with an average of 8%. Intra- and inter-assay precision were below 6% and 24% CV, respectively. Intra- and inter-animal variability were both below 35% CV for all animals. Treatment of NK cells with R(+)-Verapamil, a known inhibitor of NK function, caused robust concentration-dependent (8.3-225 μm) inhibition of target killing. The assay detected at statistically significant 12% reduction in NK cell activity following treatment with 8.3 μm R(+)-Verapamil.

An assay was developed and validated to determine the ability of monkey NK cells to kill target cells, a critical innate immune function. This assay can be used to assess the impact of drugs and chemicals on NK cell activity in monkeys, as a key component of an immunotoxicity evaluation. Future studies will include development of an assay to measure CTL function by direct assessment of antigen-specific target cell killing by non-human primate CD8+ T cells.

PS 408 Quantitative Immunophenotypic Analysis of Rat Thymocytes

H. Hu, J. Puchalski, F. Cheung, J. Olsen, G. Ferency, T. Klein, P. Brewer and J. E. Arrington. *Covance Laboratories Inc., Madison, WI.*

Quantitative immunophenotypic analysis of rat thymocytes is often required for the evaluation of test article effects; changes of thymocyte subsets reveal the test article effects and the severity of the effects. In this study, two methods for assessment of absolute thymocyte numbers were evaluated. Thymuses were harvested and weighed from 15 male and 15 female rats at 12 to 13 weeks of age. Single cell suspension was prepared and thymocytes enumerated for FACS analyses. Thereafter, two ways of absolute cell number evaluation were compared: cell number per thymus and cell number normalized by thymus weight. Cell number per thymus was positively correlated to thymus weight; heavier thymuses yielded more cells, thus male rats had more thymocytes per thymus compared to female rats (Mean±SD: 1136.7±296.4 million cells/thymus and 990.3±218.1 million cells/thymus for male and female rats, respectively). These variations (CV=25%) indicate that cell number per thymus is not a valid basis for calculation of absolute numbers for thymocyte subsets. However, when thymocyte numbers were normalized by thymus weight, results were more comparable among all rats (CV=14%) and between sexes (Mean±SD: 2714.1±359.8 million cells/g and 2712.0±421.5 million cells/g for male and female rats, respectively). Based on the weight normalized thymocyte number, absolute number can be calculated for thymocyte subsets: CD3- cells, CD3-CD4+CD8- cells, CD3-CD4-CD8+ cells, CD3-CD4+CD8+ cell, CD3+ cells, CD3+CD4+CD8+ cell, CD3+CD4+CD8- cells, and CD3+CD4-CD8+ cells. In conclusion, weight normalized thymocyte numbers are a valid basis for calculation of absolute numbers of thymocyte subsets. These absolute numbers can be used for statistical analyses to assess the effects of test articles on the thymus. Furthermore, because the variation of weight normalized thymocyte numbers is small between male and female rats, the two sexes can be combined for statistical analyses when animal numbers/sex/ group are inadequate.

PS 408a Application of the KeratinoSens™ Assay for Assessing the Skin Sensitization Potential of Crop Protection Active Ingredients and Formulations

R. S. Settivari[1], S. C. Gehen[2], R. Acosta Amado[2], N. Visconti[1], A. Natsch[3], E. W. Carney[1] and D. R. Boverhof[1]. *[1]The Dow Chemical Company, Midland, MI, [2]Dow AgroSciences LLC, Indianapolis, IN and [3]Givaudan Schweiz AG, Dübendorf, Switzerland.*

Recent regulations have advocated for the development of non-animal approaches that can reliably predict the skin sensitization potential of low molecular weight chemicals. The KeratinoSensTM assay has emerged as one of the most promising in vitro assays for predicting skin sensitization of single chemicals, however its performance with formulations and mixtures has not been previously addressed and is a significant need. To assess this potential application, the KeratinoSensTM assay was conducted for 8 crop protection active ingredients including 3 sensitizers (acetochlor, meptyldinocap, triclopyr butoxyethyl ester), 5 non-sensitizers (aminopyralid, clopyralid, florasulam, methoxyfenozide, oxyfluorfen) and 10 corresponding agrochemical formulations for which the in vivo sensitization data were already available. The assay correctly predicted the sensitization potential of all the active ingredients when tested individually. The assay approach was then modified to allow for the testing of agrochemical formulations, which can be considered complex mixtures of crop protection active ingredients and co-formulants. The assay correctly predicted the sensitization potential for 3 of 4 sensitizing formulations and all six non-sensitizing formulations relative to available in vivo data. The assay misclassified the sensitization potential of the Meptyldinocap-containing formulation due to the cytotoxicity of its co-formulants. Overall, the KeratinoSensTM assay demonstrated good performance for the formulations with sensitivity, specificity and accuracy of 75, 100 and 90%, respectively, relative to available in vivo data. Taken together, these results provide evidence to support the potential application of the KeratinoSensTM assay for the evaluation of the skin sensitization potential of crop protection active ingredients and their corresponding agrochemical formulations.

PS 408b Assessment of the Usefulness of the Murine Thymoma Cell Line EL-4 for Immunotoxicity Screening by Transcriptomics

P. Hendriksen[1], P. C. Schmeits[1], H. Van Loveren[2] and A. Peijnenburg[1]. [1]*Toxicology, RIKILT Institute of Food Safety, WUR, Wageningen, Netherlands and* [2]*National Institute for Public Health and the Environment (RIVM), Bilthoven, Netherlands.*

For immunotoxicity testing, there is a big demand to replace animal testing by in vitro experiments. Whole genome mRNA expression analysis on cells exposed to test chemicals in vitro promises to be a valuable option for this aim. The immunological response involves many different cell types. It is therefore likely that multiple immune cell types have to be included to enable adequate evaluation of immunotoxic hazard.
In this study, the value of the mouse thymoma EL-4 cell line as an in vitro screening model for immunotoxicity was assessed using two immunotoxic model compounds, the mycotoxin deoxynivalenol (DON) and the organotin compound tributyltin oxide (TBTO). EL-4 cells were exposed to 0.25, 0.5 and 1 μM DON for 3, 6 or 11 h or to 0.5 and 1 μM TBTO for 3 or 6 h. Biological interpretation of the microarray data revealed that part of the previously detected modes of action of TBTO and DON in the Jurkat T cell line were not observed in the EL-4 cell line. TBTO induced genes involved in calcium signalling and ER stress but did not induce genes involved in T cell activation and apoptosis. DON induced RNA related processes and ribosome biogenesis. Furthermore, DON downregulated ER stress, T cell activation and apoptosis which is opposite to the mechanism of DON observed in the mouse thymus in vivo and in Jurkat T cells in vitro. Apparently, EL-4 cells lack factors that are important to link ribotoxic stress to ER stress and cannot elicit a T cell activation response. Based on the results obtained for TBTO and DON, it can be concluded that the EL-4 cell line has no added value for immunotoxicogenomics based screening.

PS 409 Dynamic Changes in Ribosome-Associated Proteome and Phosphoproteome during Deoxynivalenol-Induced Translation Inhibition and Ribotoxic Stress

X. Pan[1, 2], D. A. Whitten[1], C. G. Wilkerson[1] and J. J. Pestka[2]. [1]*Biochemistry and Molecular Biology, Michigan State University, East Lansing, MI and* [2]*Food Science and Human Nutrition, Michigan State University, East Lansing, MI.*

Deoxynivalenol (DON), a trichothecene mycotoxin produced by Fusarium that commonly contaminates cereal-based food, interacts with the ribosome to cause translation inhibition and activate stress kinases in mononuclear phagocytes via the ribotoxic stress response (RSR). The goal of this study was to test the hypothesis that the ribosome functions as a platform for spatiotemporal regulation of translation inhibition and RSR. Specifically, we employed stable isotope labeling of amino acids in cell culture (SILAC)-based proteomics to quantify the early (≤ 30 min) DON-induced changes in ribosome-associated proteins in RAW 264.7 murine macrophage. Changes in the proteome and phosphoproteome were determined using off-gel isoelectric focusing and titanium dioxide chromatography, respectively, in conjunction with LC-MS/MS. Following exposure of RAW 264.7 to a toxicologically relevant concentration of DON (250 ng/mL), we observed an overall decrease in translation-related proteins interacting with the ribosome, concurrently with a compensatory increase in proteins that mediate protein folding, biosynthesis, and cellular organization. Alterations in the ribosome-associated phosphoproteome reflected proteins that modulate translational and transcriptional regulation, and others that converged with signaling pathways known to overlap with phosphorylation changes characterized previously in intact RAW 264.7 cells. These results suggest that the ribosome plays a central role as a hub for association and phosphorylation of proteins involved in the coordination of early translation inhibition as well as recruitment and maintenance of stress-related proteins - both of which enable cells to adapt and respond to ribotoxin exposure. This study provides a template for elucidating the molecular mechanisms of DON and other ribosome-targeting agents.

PS 410 System-Biological Screening of Polybrominated Diphenyl Ethers (PBDEs)

E. Demchuk[1], J. J. Irwin[2], C. V. Smith[1] and H. G. Abadin[1]. [1]*Dept.Tox.Hum. Health Sci, ATSDR, Atlanta, GA and* [2]*Dept.Pharm.Chem., UCSF, San Francisco, CA.* Sponsor: M. Mumtaz.

Toxicological profiles (TPs) are comprehensive peer-reviewed public documents developed by ATSDR per mandate from the Congress. ATSDR is implementing a systematic review process in TP development with focus at multifaceted health effects caused by hazardous chemicals. A systematic review begins with framing scientific questions and searching for relevant studies that address these questions. The search and further analysis rests on stipulation of the questions. In the present work, we investigate if a system-biologic screening of the chemicals, conducted before the search, is capable of expanding prior knowledge available for framing the questions. Isocyanates, DEET, tribufos, toluene, and PBDEs were screened using the Similarity Ensemble Approach (SEA) against ChEMBL ver.12, WOMBAT, and KEGG enzyme databases using ECFP-4 fingerprints. With the exception of PBDEs, no significant molecular target was identified for the listed compounds at selected false-positive/negative rates. It suggests that these parent compounds (metabolites were not considered) are unlikely interfering with known *in vivo* molecular pathways as represented by drugs and research compounds available in current databases. For PBDEs, however, several candidate targets for the mechanism of action were identified. They were leukotriene A4 hydrolase (LH), arachidonate 12-lipoxygenase (AL), and aldose reductase (AR). The likelihood of interactions with these receptors was dependent on the level of BDE halogenation. For DE, mono- and di-BDEs, LH came up as a likely molecular target. For tetra- to hepta-BDEs (peaked at hexa-BDEs) it was AL, and for octa- and nona-BDEs it was AR. AL and LH are involved in omega-6 fatty acid metabolism. Medium-brominated PBDEs are known to inhibit AL in micromolar concentrations and cause death of cerebellum granule cells, while AR is implicated in the etiology of diabetes-induced blindness. These findings suggest that SEA did not generate false-positive outcomes. Therefore, the new methodology may successfully complement the traditional approach to TP development.

PS 411 The Comparative Toxicogenomics Database

A. P. Davis[1], C. J. Mattingly[1], C. G. Murphy[1], J. M. Lay[1], K. Lennon-Hopkins[1], D. Sciaky[1], C. Saraceni-Richards[1], B. L. King[2], M. C. Rosenstein[2] and T. C. Wiegers[1]. [1]*Biological Sciences, NC State University, Raleigh, NC and* [2]*MDIBL, Salisbury Cove, ME.*

The Comparative Toxicogenomics Database (CTD; http://ctdbase.org) is a free resource that informs hypothesis development about environmental effects on human health. CTD content consists of manually curated chemical-gene-disease interactions, which are integrated with functional information, canonical pathways, and novel tools to infer relationships between chemical exposures and biological events. Here, we highlight new analysis and data visualization features of CTD, including the ability to generate novel pathways associated with chemicals and diseases. We also report results from a pilot project in which we expanded our curation to include relationships between chemicals and non-disease phenotypes (e.g., cell proliferation, adipogenesis). The goal of this project was to determine if including chemical-phenotype data in CTD could advance: a) understanding of environmental disease progression, b) identification of exposure biomarkers, and c) the capacity to conduct and interpret studies across species and experimental systems. We integrated chemical-phenotype and disease data from this pilot project and performed a two-dimensional hierarchical clustering that revealed 18 disease clusters with distinct phenotype profiles. Our results suggest the potential for this strategy to generate meaningful links between chemicals, early cellular phenotypes and diseases. We continue to expand the depth and functionality of CTD to meet the evolving needs of the environmental health research community.

PS 412 DILIsym® Provides a Potential Insight into the Mechanism of Hepatotoxicity for Carbon Tetrachloride

L. Shoda, S. Q. Siler, P. B. Watkins and B. A. Howell. *Hamner Institutes for Health Sciences, Research Triangle Park, NC.*

Drug-induced liver injury (DILI) is one of the leading causes of drug development failures and drug withdrawals. DILIsym® is being developed to identify and mitigate DILI risk through in silico analysis of compounds. The DILIsym® representation of the innate immune response was initially based on acetaminophen (APAP) data. Carbon tetrachloride (CCl4), a compound with hepatotoxic similarities to APAP, was simulated for further evaluation of the innate immune response to liver injury. DILIsym® simulation results for CCl4 pharmacokinetics were consistent with published PK data. CCl4 is generally thought to induce hepatotoxicity via a free radical metabolite which drives lipid peroxidation. However, when CCl4 was simulated via DILIsym®, free radical generation and lipid peroxidation to levels consistent with the public literature were insufficient to drive hepatotoxicity. Analysis demonstrated that saturation of the metabolic pathway generating the free radical limited the extent of lipid peroxidation and thus the extent of cell death. In comparison, the APAP metabolic pathway had a greater dynamic range, resulting in higher levels of lipid peroxidation and cell death. Papers were identified in which lipid peroxidation independent mechanisms of cell death were suggested, including lipid peroxidation independent mitochondrial toxicity. The CCl4 representation was modified to induce mitochondrial electron transport chain (ETC) inhibition. Concurrent induction of lipid peroxidation and ETC inhibition mechanisms permitted reconciliation of simulated hepatotoxicity with published data. For exam-

ple, >3x ALT elevations were simulated at doses <50 mg/kg, with the highest ALT elevations (>1000 U/L) at doses >100 mg/kg in mice. Simulated CCl4 was then used to evaluate and further refine the innate immune response. In summary, quantitative analysis of CCl4 in DILIsym® not only permitted evaluation of the innate immune response, but also suggested a limitation in the putative primary mechanism of hepatotoxicity.

PS 413 Organotypic Tissue Cultures As Models to Study the Impact of Cigarette Smoke on Human Upper and Lower Respiratory Tract

M. Talikka[1], R. M. Kostadinova-Angelova[1], Y. Xiang[1], D. Kuehn[1], S. Majeed[1], C. Mathis[1], S. Frentzel[1], N. Ivanov[1], F. Martin[1], A. Hayes[2], J. Hoeng[1] and M. Peitsch[1]. [1]*Biological Systems Research, PMI, Neuchatel, Switzerland and* [2]*Spherix Consulting, Rockville, MD.*

Cigarette smoke (CS) is etiologically linked to fatal respiratory diseases. To enable the development of modified risk tobacco products (MRTPs) to reduce the risk of smoking related diseases, there is a need to understand the mechanisms whereby CS causes damage. As an alternative to animal experimentation, the principles of 3 R's, necessitate the establishment of reliable in vitro models, which may also provide a better predictability of exposure response, when derived from human cells. Among the in vitro models, the three-dimensional organotypic pseudo-stratified culture systems better mimic the morphological, physiological, and molecular attributes of human respiratory tract than primary or immortalized cells cultured as a submerged monolayer.
The bronchus and lung parenchyma are the primary sites that manifest smoking related respiratory diseases, however, nasal epithelium has been proposed as a surrogate tissue to study smoking effects on the respiratory tract. We are evaluating the utility of organotypic culture systems derived from upper and lower respiratory tract in the assessment of exposure response to CS and prototypic MRTPs. Repeated whole CS exposure showed that both bronchial and nasal organotypic cultures tolerated in a similar manner the two CS concentrations (10% and 16%), measured by tissue integrity (trans epithelial electric resistance) and cellular toxicity (lactate dehydrogenase) assays. By combining the transcriptomic data with computable biological network models, we further showed that several biological processes, including those related to cellular stress response and proliferation, were perturbed in both nasal and bronchial tissues in response to smoke exposure. In summary, the study gives valuable insight into the effect of repeated whole CS exposure on organotypic models derived from both the upper and lower respiratory tract.

PS 414 Integration of the Hepatic and Urinary Metabolome with Hepatic Differential Gene Expression in C57BL/6 Mice following Repeated TCDD Dosing

T. R. Zacharewski[1], S. Y. Lunt[2], L. Newhouse[2] and R. Nault[1]. [1]*Biochemistry & Molecular Biology, Center for Integrative Toxicology, Michigan State University, East Lansing, MI and* [2]*Department of Physiology, Michigan State University, East Lansing, MI.*

2,3,7,8-Tetrachlorodibenzo-*p*-dioxin (TCDD) is a potent aryl hydrocarbon receptor agonist that elicits hepatic lipid accumulation in mice. To further investigate TCDD-induced metabolic disruption, intact female C57BL/6 mice were orally gavaged every 4 days for 28 days with sesame oil vehicle or 8 doses of TCDD (0.01-30 μg/kg). Hepatic gene expression was examined using Agilent 4x44K microarrays identifying 1,434 unique differentially expressed genes (|fold-change|≥1.5, P1(t)≥0.9999) while the hepatic and day 26 urinary metabolomes (vehicle, 3, 10, and 30 μg/kg only) were determined by targeted LC-MS/MS that detected 159 metabolites. Mapping differential gene expression to metabolite changes indicated alterations in lipid transport, processing and metabolism, the TCA cycle, and the pentose phosphate pathway (PPP). For example, TCDD increased PPP metabolites ribose- and ribulose-5-phosphate levels ~2-fold with a 2- to 5-fold decrease in 6-phosphogluconic acid, erythrose-4-phosphate, fructose-6-phosphate and glucose-6-phosphate. Concomitant alterations in glucokinase/hexokinase and hexose-6-phosphate dehydrogenase expression suggests glucose-6-phosphate routed towards the PPP to produce reducing equivalents in support of TCDD-induced NADPH-dependent reactions such as those catalyzed by cytochrome P450s. Decreases in acyl-CoA lipid precursors levels, and acetyl-CoA acyl transferase (thiolase) and acyl-CoA synthetase (acetyl-CoA carboxylase) mRNA levels are also consistent with inhibition of β-oxidation. Limited acetyl-CoA availability may also compromise the TCA cycle resulting in the 11-fold increase in oxaloacetate. Collectively, TCDD-elicited hepatic lipid accumulation involves disruption of multiple metabolic pathways by altering gene expression with corresponding changes in hepatic metabolite levels. Funded by SRP P42ES04911.

PS 415 Cigarette Smoke-Induced Perturbations of Molecular Pathways in Human Organotypic Cultures of Buccal and Gingival Mucosa

M. Cabanski[1], C. Mathis[1], R. M. Kostadinova-Angelova[1], S. Wagner[1], S. Frentzel[1], D. Kuehn[1], S. Majeed[1], M. Geertz[1], F. Talamo[1], E. Guedj[1], Y. Xiang[1], F. Martin[1], W. K. Schlage[1], A. Hayes[2], M. Peitsch[1] and J. Hoeng[1]. [1]*Philip Morris International, Neuchatel, Switzerland and* [2]*Spherix Consulting, Rockville, MD.*

Smoker's oral mucosa is subject to cigarette smoke (CS)-induced cytological, genomic, and transcriptional changes that could potentially lead to the development of mouth disease. To characterize CS effects, we used two human organotypic *in vitro* models of the buccal and gingival epithelia (MatTek®). Both *in vitro* models were exposed at the air-liquid interface to fresh, diluted CS (one reference cigarette 3R4F at a time, with Health Canada smoking regimen and nicotine doses of 0.279mg/L or 0.557mg/L) on 4 occasions with 1h intervals between exposures where the tissues were kept in the incubator under appropriate culture conditions. Systems biology endpoints (gene and miRNA expression) were determined at time 0 following the 4th exposure and 4h, 24h, 48h after exposure to investigate time- and dose-dependent CS effect on both tissues. Other endpoints (e.g. cytotoxicity, pro-inflammatory marker release, cytochrome P450 (CYP) activity, histology) were also measured for some time points.
The release of pro-inflammatory markers such as VEGF and MMP-1 was up-regulated in both CS-exposed buccal and gingival tissues 24h after exposure. However, only gingival tissues showed a significant up-regulation of CYP1A1/CYP1B1 activity 48h after exposure. By using computational approaches and by capturing systems biology endpoints, various perturbations of biological processes (e.g. inflammation, proliferation, cellular stress) triggered by repeated CS exposure were observed in both buccal and gingival *in vitro* models.
We describe here for the first time the impact of CS exposure on human buccal and gingival organotypic models using various approaches combining systems biology, biological network models, computational methods and standard endpoints.

PS 416 Tobacco-Specific Gene Profiles in Korean Male Smokers

H. Na and M. Yang. *Research Center for Cell Fate Control, College of Pharmacy, Sookmyung Women's University, Seoul, Republic of Korea.*

Tobacco smoking-related cancers can be protectable with well controlled cancer prevention strategies. Particularly, the prevalence of male smoking in Korea belongs to the world's highest levels. Therefore, we performed microarray to find out Korean-specific genetic factors associated with tobacco smoking among age- and sex-matched healthy male smokers and nonsmokers (age=38.9±3.7, N=12) with Illumina human HT-12 platform with 47,231 transcript probes. Subjects were evenly divided into tobacco-high and low exposed groups, according to levels of urinary cotinine, a major metabolite of nicotine, which was measured with HPLC-UVD. We also performed qRT-PCR to confirm microarray results, and further compared the expression patterns of blood to those of buccal cells. Finally, we performed gene network analyses using DAVID Bioinformatics and KEGG pathways to integrate tobacco smoking-responses. As results, smoking-upregulated genes were 16 genes including ARPC3, CXCR4, ACTG1, and CYP1B1 ($p<0.01$ and >1.5-fold change). On the other hand, smoking-downregulated genes were 22 genes including DEFA4, VAV3, and FCGR3A. The expression levels of FCGR3A in blood were correlated with those in buccal cells ($r2=0.85$, $p<0.01$). After network analyses, we found that Korean male smokers differentially expressed immune responsive pathways such as Fcγ-receptor mediated phagocytosis and leukocyte transendothelial migration, compared to non-smokers. In conclusion, our findings provide new insights in understanding of ethnical specific toxic mechanisms and health end points of tobacco smoking.

PS 417 Systems Biology to Identify Stage-Specific Biomarkers of Acute Liver Injury

K. C. Wu, R. Degonkar, A. Sarma, S. Phat, E. Grund, L. Rodrigues, V. Vishnudas, N. Narain and R. Sarangarajan. *Berg, LLC, Framingham, MA.*

Acetaminophen (APAP) is a leading cause of acute liver injury; early intervention is essential for mitigation of permanent liver damage. The fact that treatment in the ER settings is still based on normograms established in 80's, indicates need for biomarkers to detect early signs of APAP induced liver toxicity. The present study describes a novel process, in which an in-depth interrogation of the biological sequela of APAP toxicity using in vitro liver models was undertaken by generating a pan-omic biomolecular multi-matrix subjected to artificial intelligence modeling using Bayesian Network Inference (BNI). Toxicity in liver cells at 4h, 8h, and 24h was benchmarked against APAP concentration dependent decrease in mitochon-

drial ATP, cytosolic GSH depletion, LDH release, and oxidative stress at 1-10mM. APAP induced toxicity was minimal at 4h, moderate at 8h, and substantial after 24h of exposure, suggestive of early, middle, and late stage of injury. A LC/MS/MS based proteomic analysis was performed to investigate alterations of molecular signature in the liver model. Differential expression proteomic signatures were identified by linear model with Empirical Bayes Method (FDR-adjusted $p < 0.05$). Total of 306, 323, and 485 proteins were found to be differentially expressed at 4h, 8h, and 24h, respectively. Pathway analysis demonstrated that the proteome of the APAP liver toxicity model was enriched in ribosomal proteins, mitochondria content, and stress response proteins. Among the proteins that differentially expressed, 26, 21, and 26 proteins were exclusively altered at 4h, 8h, or 24h by lethal dose acetaminophen (10mM), with potential utility as stage specific markers of APAP toxicity. In addition, two specific proteins were dose-dependently induced or suppressed at 24h, suggesting their potential utility as biomarkers to assess the severity of liver injury. Efforts are underway to validate these proteins in rodent and human serum samples. Validation of these biomarkers will aid in shaping clinical intervention in APAP overdose.

PS 418 Use of Mummichog to Map the Exposome: Associating Environmental Chemicals with Perturbed Metabolic Pathways

S. Li[1], J. Roede[2], K. Uppal[1] and D. P. Jones[1]. [1]*Dept Medicine, Emory University, Atlanta, GA and* [2]*Skaggs School of Pharmacy and Pharmaceutical Sciences, University of Colorado, Aurora, CO.*

High-resolution metabolomics (HRM) using liquid chromatography and high-resolution mass spectrometry now routinely capture >20,000 chemicals in biologic samples. Among these, about 2000 appear to be endogenous intermediary metabolites and the majority appears to represent low-abundance metabolites and environmental chemicals, which have not been fully characterized. How to interpret such data in the appropriate biological context remains a great challenge, and the identification of chemicals is often the rate-limiting step. This is especially problematic for the >10,000 chemicals used in commerce, where systematic analytic methods for biomonitoring are not available and potential biologic impacts of environmental products have not been fully explored. We have recently described a set of computational algorithms that directly predict pathway and network activities from high-resolution metabolomics, by leveraging the collective power in genome scale metabolic models (Li et al. PLoS Comp Biol 9: e1003123). This approach greatly speeds up the analysis of metabolomics data, since metabolite identification can be deferred to a posterior confirmation step. In a case study using in vitro models of Parkinson disease, we extended these algorithms to integrate metabolomics and transcriptomics. Our results revealed that a metabolic network of oxidative phosphorylation and carnitine shuttle is dysregulated by the herbicide paraquat. The results establish a research paradigm using high-resolution metabolomics to investigate dose-response associations of environmental agents with biologic responses in human populations.

PS 418a Computational Embryology and Predictive Toxicology of Hypospadias

M. C. Leung[1], N. S. Sipes[1], N. C. Baker[2], B. Ahir[1], C. J. Wolf[3], A. W. Seifert[4], M. Hutson[5], S. P. Darney[3], R. M. Spencer[2] and T. B. Knudsen[1]. [1]*National Center for Computational Toxicology, U.S. Environmental Protection Agency, Research Triangle Park, NC,* [2]*Lockheed Martin, Research Triangle Park, NC,* [3]*National Health and Environmental Effects Research Laboratory, U.S. Environmental Protection Agency, Research Triangle Park, NC,* [4]*Department of Biology, University of Kentucky, Lexington, KY and* [5]*Departments of Physics and Biological Sciences, Vanderbilt University, Nashville, TN.*

Hypospadias, one of the most common birth defects in human male infants, is a condition in which the urethral opening is misplaced along ventral aspect of the penis. We developed an Adverse Outcome Pathway (AOP) framework and computer simulation that describes the pathogenesis of hypospadias. We first utilized semi-automated literature mining to identify 511 PubMed hypospadias articles based on MeSH annotations with 'chemicals' and 'proteins'. This information was used to develop an AOP framework linking potential molecular initiating events, altered cellular behaviors, tissue morphogenesis, and abnormal organogenesis. We selected vinclozolin (hypospadias in rats at 96 mg/kg/day in ToxRefDB, AC50 = 0.307 μM for inhibition of the human androgen receptor binding in ToxCast) as a reference for proof-of-concept. A multicellular computer simulation model capable of rendering key events in GT development was built in CellDesigner for simulation using a cellular agent-based model (CompuCell3D.org) by incorporating key signals (e.g., SHH, FGF10, EphB2, and androgen) and cellular behaviors (e.g., selective adhesion, motility) to control urethral tubulogenesis. Overall, the AOP approach and computer simulation: 1) provide a platform for integrating available biological information to predictively model the complex pathogenesis of hypospadias; 2) enable the generation of new research hypotheses; and, 3) contribute to better mechanistic understanding of this adverse developmental outcome. [This work is approved by EPA but does not necessarily reflect official Agency policy].

PS 418b Using High-Content Screening Data from ToxCast to Analyze Cell State Dynamics

I. Shah[1], W. Setzer[1], J. John[2], K. Houck[1], T. B. Knudsen[1], M. T. Martin[1], D. M. Reif[2], A. M. Richard[1], D. J. Dix[1] and R. J. Kavlock[1]. [1]*National Center for Computational Toxicology, US EPA, Durham, NC and* [2]*NCSU, Raleigh, NC.*

We developed a novel approach for analyzing chemical-induced dynamic cell 'state' changes using in vitro data. The ToxCast project conducted a high content screening study in which HepG2 cells were treated with 10 concentrations (ranging from 0.4 to 200 μM) of 976 diverse chemicals, and 10 cellular end points were measured after 1, 24 and 72 h of exposure. After analyzing the concentration response data we found 669 chemicals significantly changed one or more end points including: mitochondrial functions (435), cell cycle (412), cytoskeletal stability (332), JNK (253), p53 (253), and cell number (510). In order to capture the overall response to each chemical at a single time point, we constructed a bioactivity vector based on the magnitude and the direction of the change in each end point. The bioactivity vectors for all chemicals were analyzed using the Euclidean distance metric, K-means and cluster quality analysis to identify 15 clusters. We assumed that these clusters capture a range phenotypic 'states' of the HepG2 system as it responds to different perturbations ranging from normality to adversity (defined by significant cell loss). By translating bioactivity vectors to cellular states, the temporal effects of each chemical can be described as a sequence of states, called a trajectory. A trajectory describes the dynamic sequence of changes in the HepG2 system as it adapts to chemical exposure. Chemicals with similar mechanisms such as, mitochondrial disruptors, cytoskeletal disruptors and stress kinase activators, produced similar trajectories. On the other hand, structurally similar chemicals, such as thiazoladinediones, produced different trajectories that were consistent with their known toxicity. By analyzing trajectories, it is possible to characterize chemicals that cause adaptive changes that lead to recovery, or those that lead to adversity. Further work is necessary to evaluate the relevance of this work to *in vivo* outcomes.
This abstract does not reflect EPA Policy.

PS 418c Using Targeted Proteomics and Next-Generation Sequencing Approaches to Identify New Plasma Biomarkers and Assess Systematic Drug-Induced Adverse Effects

K. Wang, S. Qin, Y. Zhou and L. Hood. *Institute for Systems Biology, Seattle, WA.* Sponsor: S. Tilton.

Adverse effects caused by therapeutic drugs are a serious and costly health concern. Despite the body's systemic responses to therapeutics, the liver is often the focus of damage and is usually the focus of studies of toxic effects due to its active roles in the metabolism of xenobiotics. Applying sensitive and high throughput proteomics and transcriptomics technologies including Selected Reaction Monitoring (SRM) and next generation sequencing (NGS) on body fluid samples open a window to identify new biomarkers and assess adverse effects at systems level. To explore this, we utilized SRM and NGS technologies to quantify and profile circulating protein and cell-free RNA in plasma using a well-characterized acetaminophen (APAP) overdose mouse model.
As a proof principle study, we initially focused on the levels of 85 liver-enriched proteins. Among them, 52 showed concentration changes in plasma after APAP overdose. Some of the proteins showed better performance than the existing blood markers for detecting and monitoring acute drug-induced injury. From NGS profiling of circulating RNA, the levels of a number of transcripts, both protein-coding and noncoding RNAs, showed changes in plasma. The results are in agreement with our previous report on the association of blood miR-122 levels with liver injury. Detailed analysis revealed the changes of circulating RNA reflected not only the liver injury induced by APAP overdose, but also damage in tissues other than the liver. Besides endogenous RNAs, we also identified a significant amount of exogenous RNAs (exRNAs). The changes in exRNAs also reflect alteration of dieting behavior after APAP overdose.
Besides the identification of new blood biomarker candidates, this study illustrates the possibility of using SRM and NGS to assess global effects of therapeutics. This could lead to a new approach for a more comprehensive assessment of the efficacy and safety of therapeutics.

PS 418d Functional Profiling to Reveal Adverse Outcome Pathways

C. Vulpe[1], W. Varsally[2], B. Gaytan[1], V. De La Rosa[1], D. Faulkner[1], P. Antczak[2] and F. Falciani[2]. [1]*Nutritional Science and Toxicology, University of California, Berkeley, Berkeley, CA and* [2]*Institute of Integrative Biology, University of Liverpool, Liverpool, United Kingdom.*

Converging scientific opinion from both the regulatory and scientific community recognize the importance of developing a new mechanism driven toxicity assessment paradigm. We use functional profiling in yeast, *Saccharomyces cerevisiae*, to identify the fundamental adverse outcome pathways involved in cellular toxicity. The ~4500 viable deletion barcoded strains are pooled, grown for multiple generations in the presence of a toxicant, and sensitivity/resistance of each strain to the toxicant is individually quantified. We screened a diverse variety of industrial chemicals at multiple doses and determined the functional importance of each gene for optimal growth in the presence of each toxicant. We used our functional profiling dataset for diverse toxicants and the network inference ARACNE algorithm to infer a network representing toxicity related functional linkages between non-essential genes in *S. cerevisiae*. We identified key network modules enriched in different functional properties impaired upon toxicant exposure which we hypothesize represent common cellular response and adverse outcome hubs. We subsequently identified adverse outcome hubs associated with each individual toxicant. Additional dose response analysis enabled us to identify candidate adverse outcome pathways linking early cellular response through to adverse outcomes for each toxicant. We suggest that this functional approach in yeast and development of functional networks provides a unique insight into both the shared and unique molecular responses to toxicant exposure.

PS 418e Potential Use of ToxCast Assays for Assessing Drug-Induced Liver Injury in Humans

M. Lee[1], J. Zhang[1], Y. An[2], C. Chang[1] and W. Tong[1]. [1]*National Center for Toxicological Research, Jefferson, AR and* [2]*Hanyang University, Gyeonggi-Do, Republic of Korea.*

Predicting a drug's potential to cause drug-induced liver injury (DILI) is still a major challenge with the animal models. A paradigm shift from *in vivo* animal testing to *in vitro* system has been proposed, but met with challenges. The EPA has assayed many chemicals with an array of mechanism-based *in vitro* systems, providing an opportunity to develop *in vitro* prediction system for DILI. We developed a robust quantification of dose response for the ToxCast assay data coupling with the DILI annotation by the FDA's Liver Toxicity Knowledge Base (LTKB) to investigate the potential use of the ToxCast data to predict DILI in humans. Specifically, the LTKB developed 287 benchmark drugs and some of which were assayed by ToxCast, which was used in this study. Area under the dose-response curve, with the median value from each concentration, was calculated for each drug/assay combination and the assay potential for predicting DILI was evaluated by area under Receiver Operating characteristic (AUROC). With the criteria of AUROC > 0.6 and p-value < 0.05, 42 endpoints out of 451 assayed by ToxCast were identified with the prediction potential. Some of these endpoints associated with key mode of actions underlying DILI mechanisms including mitochondria damage, oxidative stress, PPARγ and NURR pathways. The findings are encouraging and indicate the potential utility of the ToxCast system for DILI assessment in humans. The future study will be focused on applying the identified assays to rank and prioritize the ToxCast chemicals accordance to the DILI potential and improving mechanistic understanding on DILI.

PS 419 Development of a Novel Method for Deriving Thresholds of Toxicological Concern (TTCs) for Vaccine Constituents

J. White[1, 2], C. Wrzesinski[1], M. Green[1], G. T. Johnson[2], J. D. McCluskey[2] and R. D. Harbison[2]. [1]*Division of Vaccine and Related Products Applications, Food and Drug Administration, Rockville, MD and* [2]*Environmental and Occupational Health, University of South Florida, Tampa, FL.*

Safety assessment of impurities, residual materials and contaminants in vaccines is an important risk assessment process for evaluating public health risks associated with new and existing vaccines. Defining thresholds of toxicological concern (TTCs) is a concept that can be applied for screening vaccine constituents and evaluating the toxicity of specific vaccine constituents with little or no toxicity data. TTCs are mathematically modeled and extrapolated levels, below which adverse human health effects are not expected to occur. Probit and lowest-toxic-dose (TDLo) data were obtained from INCHEM, RepDose, RTECS and TOXNET. ToxTree software using three different algorithms (The Cramer Extended, the In Vivo Rodent Micronucleus Assay algorithm, and the Benigni-Bossa rule base for carcinogenicity by ISS) was applied to assign the chemical test set (n= 197) into structural families based on structural alerts (SAs). This resulted in six potential methods for elucidating TTCs: In Vivo Rodent Micronucleus Assay/ probit, Benigni-Bossa/ probit, Cramer Extended/ probit, In Vivo Rodent Micronucleus Assay / TDLo, Benigni-Bossa/ TDLo, and the Cramer Extended/ TDLo. These were subjected to a preliminary analysis in JMP statistical software v9, resulting in two TTC methods for further consideration: Benigni-Bossa/ probit and the Cramer Extended/ probit. The Benigni-Bossa/ probit method outperformed the Cramer Extended/ probit method in terms of specificity (87.2 vs. 48.1%), accuracy (65.2 vs. 52.94%), positive predictivity (66.6 vs. 50%), negative predictivity (64.8 vs. 56.5%), receiver operating characteristics (ROC)+ (2 vs. 1) and ROC- (1.84 vs. 1.3). Our results indicated that the Benigni-Bossa/ probit was the most appropriate method. These comments are an informal communication and represent our own best judgment. These comments do not bind or obligate FDA.

PS 420 Comparison of Cramer Class Prediction between Toxtree, OECD QSAR Toolbox, and Expert Judgment—Strategies for Refinement

S. Bhatia[1], J. Shen[1], L. Kromidas[1], T. W. Schultz[2], R. Ford[1], D. Roberts[3] and A. Api[1]. [1]*RIFM, Woodcliff Lake, NJ,* [2]*University of Tennessee, Knoxville, TN and* [3]*Liverpool John Moores, Liverpool, United Kingdom.*

The Threshold of Toxicological Concern (TTC) approach is used to predict the toxicity of compounds with low oral exposure. The Cramer classification decision tree is used extensively for TTC estimation. Assigning an accurate Cramer class to a material is a crucial step to preserve the integrity of the risk assessment. The Cramer class of over 1000 fragrance materials across diverse chemical classes were determined by using the OECD QSAR Toolbox (TB), Toxtree and expert judgment. Concordance between Cramer class predictions by Toxtree, OECD Toolbox and expert judgment are presented. The overall concordance between expert judgment and Toxtree was 76%, Toxtree (with extensions) 72%, TB (with extensions) 65%, TB 72%. The concordances between predictions and expert judgment for different chemical classes were also analyzed. The concordance between Toxtree (with extensions) and expert judgment for esters, alcohol, ketones and aldehyde chemical classes was 77%, 76%, 72 and 82% respectively. The concordance between TB and expert judgment for esters, alcohol, ketones and aldehyde classes was 79%, 58%, 54% and 81% respectively. The concordance between TB (with extensions) and expert judgment for esters, alcohol, ketones and aldehyde classes was 70%, 61%, 51%, and 61% respectively. The concordance between Toxtree (with extensions) and expert judgment for esters, alcohol, ketones and aldehyde classes was 82%, 50%, 54%, and 91% respectively. More detailed evaluation of chemical categories (subgroups) suggested that the lowest concordance between expert judgment and in silico tools (Toxtree and TB) to be among Heterocycles/Oxygen Containing/ Furan/Monocyclic/Saturated (<30%), Alcohol/Aryl alkyl (<55%) and Ketone/ Cyclic/Monocyclic/Saturated (<55%). Strategies and guidance on determining the Cramer class for various chemical classes are discussed. The suitability of software for specific chemical classes and possible re-coding of rules are presented.

PS 421 xMSanalyzer and xMSannotator: R Packages for Systematic Study of the Exposome

K. Uppal[1, 2] and D. P. Jones[1]. [1]*Emory University, Atlanta, GA and* [2]*Georgia Institute of Technology, Atlanta, GA.*

Improved analytical technologies and better data extraction algorithms for high-resolution mass spectrometry have enhanced the coverage of chemical detection for metabolic profiling and environmental biomonitoring, including detection of low abundance environmental chemicals and their metabolites. Our recently published software, xMSanalyzer (Uppal et. al, 2013), includes utilities that allow quantitatively reliable measurement of metabolites detected in individual biological samples. A number of databases and online tools are available to perform mass spectrum searches, but most of the web-based tools allow query of only few hundred mass-to-charge values in a single search. No convenient interface exists to query and bridge information concerning environmental chemicals across multiple chemical, disease, environmental, and pathway databases. Here we introduce xMSannotator, an R package that uses the KEGG REST, METLIN REST, and ChemSpider SOAP APIs to allow metabolome-wide querying of high-resolution mass spectrometry data against several compound, disease, drug, reaction, and pathway databases, including toxic substance databases such as ACToR, Comparative Toxicogenomics Database, and ToxCast. The package allows users to define search parameters including data sources to be searched within ChemSpider and can be used in combination with existing R packages for processing environmental metabolomics data. Our results demonstrate that together, xMSanalyzer and xMSannotator allow reliable detection of environmental chemicals in individual biological samples and facilitate the ability to gauge the physiological relevance of the environmental chemicals and their metabolites.

PS 422 Standard Operating Procedures for Cumulative Exposome Research with Liquid Chromatography High-Resolution Mass Spectrometry

V. Tran[1], K. Uppal[1], D. I. Walker[3], T. Yu[2] and D. P. Jones[1]. [1]*Pulmonary, Emory University, Atlanta, GA,* [2]*Biostatistics & Bioinformatics, Emory University, Rollins School of Public Health, Atlanta, GA and* [3]*Department of Civil and Engineering, Tufts University, Medford, MA.*

The exposome is the array of environmental influences and cumulative biological responses throughout an individual's lifespan, including exposures from the environment, diet, behavior, and endogenous processes. To operationalize exposome research, an "open" database structure is needed in which data from newly acquired samples can be added to existing data in a sufficiently rigorous manner to allow time-dependent studies of an individual over years to decades. Liquid chromatography high-resolution mass spectrometry with triplicate analysis, improved data extraction and automated 24/7 operation now provides capability to measure >100,000 ions, representing >20,000 chemicals, in a few microliters of biological samples. The number of ions and presence of many unidentified low-abundance chemicals (m/z range 85-2000) makes commonly used analytic procedures, such as MS/MS with calibration against authentic standards, impractical for routine measurement. Consequently, we have devised and begun to test standard operating procedures for exposome research. Analysis of samples in triplicate facilitated detection of chemicals present at low abundance and present in only a small percentage of individuals. Inclusion of a mixture of stable isotopic standards in each sample provided authentication of instrument calibration and consistency of response; single internal standards were insufficient for this goal. The standards also allowed direct determination of consistency of elution characteristics. With daily Quality Control (QC) using apLCMS with xMSanalyzer (Uppal et al BMC Bioinformatics 2013) and routine replacement of columns and instrument cleaning after 25 days of continuous operation, the results are sufficiently robust to warrant evaluation as a routine pipeline for combination of data in a cumulative exposome research database.

PS 423 Exposure Data and the Comparative Toxicogenomics Database (CTD)

C. J. Grondin, A. P. Davis and C. J. Mattingly. *Biology, North Carolina State University, Raleigh, NC.*

Exposure science studies and characterizes the interactions between environmental stressors and human or ecological receptors. This research plays a critical role in the translation of toxicity data to prioritize research, assess human health risks, and inform public health decisions. To facilitate the characterization of stressor-receptor interactions (including identification of connections between real-world exposures, chemicals, genes and proteins, diseases, and molecular pathways), we initiated a project to curate and integrate chemical exposure data into the publicly available Comparative Toxicogenomics Database (CTD; http://ctdbase.org). CTD is a manually curated database containing over 21 million toxicogenomic relationships for chemical-gene-disease interactions, Gene Ontology (GO) annotations, and molecular pathways that are integrated with analysis tools to promote understanding of the molecular mechanisms underlying environmental diseases. In our exposure curation paradigm, the peer-reviewed literature is manually curated using several controlled vocabularies and free text to capture details in more than 50 data fields characterizing the four major exposure concepts defined by the Exposure Ontology (ExO): Stressor, Receptor, Event, and Outcome. To date, over 600 articles have been curated, resulting in more than 21,000 exposure statements for 550 unique chemicals, 95 distinct receptor populations from 70 countries,154 diseases, and 70 phenotypic outcomes. Integrating this information with core CTD data will allow exposure science data to be queried, retrieved, and contextualized within CTD's broader biological framework. This integrated platform will help promote mechanistic understanding of environmental influences on human health.

PS 424 LocaTox: An Interactive Tool Linking Known Environmental Contaminants, Associated Chemical-Human Gene Interactions, and Birth Defect Statistics in Specific Locales

K. Aquino, K. Hald, M. Reyna, M. Zamora and D. Johnson. *Nutritional Sciences & Toxicology, UC Berkeley, Berkeley, CA.*

Several areas in the US have higher incidences of birth defects than the national average, yet do not display clusters of a single type of congenital abnormality where an association with a specific chemical contamination can be made. To aid in current research on environmental chemicals and birth defects, we hope to develop an interactive tool, LocaTox, where an extensive array of data can be integrated on specific locales including topography, local infrastructure, specific industries and levels of air, water, and ground pollution. These environmental factors are then associated with specific birth defect statistics and are paired with chemical-gene and gene-birth defect interactions. A user can actively explore potential connections as an opening to developing research questions. As a prototype, we selected Fresno County California where statistics show a higher rate of birth defect-related infant deaths compared to the cumulative rate in California and where the causes of many birth defects remain unknown. In this study we identified some of the most prominent environmental pollutants in Fresno and their associations, if any, with a wide array of birth defects. Resources used included DART, CTD, ChemIDPlus, t3db, Scorecard and websites such as Pesticide Action Network (PAN) and several US EPA resources. Chemicals prominent in Fresno County previously associated with birth defects were identified and specific chemical-disease-gene relationships were identified. One valuable result from the searching capability is the possibility of linking several exposures rather than individual chemicals to various birth defects which possibly expands the overall environmental risk assessment. The content-design of the tool can be adapted for any specific locale of interest.

PS 425 iLINCS—A Web-Based Portal for Integrative Analysis of Multidimensional Data

J. F. Reichard[1], M. Medvedovic[2], S. Sivagas[2], J. Chen[2], M. Phatak[2] and W. Niu[2]. [1]*Toxicology Excellence for Risk Assessment, Cincinnati, OH and* [2]*Environmental Health, University of Cincinnati, Cincinnati, OH.*

New technologies and systems approaches are being applied to identify biological signatures that are common across chemicals sharing similar modes of action or predictive of disease outcomes. However application of systems data for risk assessment requires integration of multidimensional endpoints (readouts) acquired from multiple "omic", network and biochemical platforms. The effective application of these distinct readouts to risk assessment requires advances in biostatistics, bioinformatics, and computational methods. The NIH Library of Integrated Network-based Cellular Signatures (LINCS) program aims to create a network-based understanding of biology by cataloging changes in gene expression and other cellular processes (http://www.lincsproject.org/). Previously, we demonstrated that integration of transcriptomic and transcription factor DNA-binding profiles significantly improves detection of otherwise obscured chemical signatures. Here, we introduce the web-based iLINCS (Integrative LINCS) Genomics Data Portal; a computational biology tool integrating various types of systems biology readouts (http://eh3.uc.edu/GenomicsPortals/viewiLincs.jsp). Currently, these readouts include publicly accessible data from Broad Institute (LINK signatures, Connectivity Map signatures), ENCODE transcription factor binding signatures, and disease-related signatures (NCBI GEO GDS collection). The objective is to leverage publicly available libraries of the signatures, meta-signatures and regulatory network signatures to evaluate and identify chemical-related network signatures shared or common to diseases, chemical exposures and transcription factor pathways. The iLINCs web-based portal enables the identification of functional connections between chemicals, genes and diseases. Integrative analysis based on multidimensional data will vastly improve in vitro prediction of apical toxicological outcomes for chemicals lacking in vivo toxicological data. Supported by: U01HL111638.

PS 426 Harnessing the Wealth of Pharmaceutical Preclinical Toxicity Data—The eTOX Database (eTOX Part I)

T. Steger-Hartmann[1], F. Pognan[2] and K. Briggs[3]. [1]*Investigational Toxicology, Bayer HealthCare, Berlin, Germany,* [2]*Discovery Investigative Safety, Novartis, Basel, Switzerland and* [3]*Lhasa Ltd., Leeds, United Kingdom.*

Most preclinical data acquired during drug development are not available in the public domain due to attrition of projects or IP issues. Lack of data accessibility was identified by the European Federation of Pharmaceutical Industries and Associations (EFPIA) as an obstacle to read-across approaches, development of new in silico tools and data mining for biomarkers.

In the framework of the European Innovative Medicines Initiative, 13 pharmaceutical companies and 12 public partners initiated the eTOX project to collect unpublished preclinical safety data and build a database covering multiple endpoints. The participating EFPIA companies identified archived reports on systemic tox studies (paper or pdf) and manually extracted them. In parallel a trusted organisation ("honest broker" - Lhasa Ltd., Leeds) set up the database. The data sets were sent to the honest broker and incorporated into the database after quality check. Due to data heterogeneity a major effort was undertaken for data harmonization and ontology work (see abstract eTOX Part II).

The steadily growing database currently contains 2127 reports (status: Aug 2013) of systemic toxicity studies with more than 800 different chemical structures. The database was populated with virtually all endpoints investigated in systemic toxicity

studies according to guidelines, i.e. clinical observations, clinical chemistry, hematology, macroscopic findings and histopathology. The majority of datasets pertain to rats (72%), followed by dogs, primates and mice. Reported findings are strictly attributed to treatment-related or non-treatment based on the original report. Liver was the most frequently (30 % of the findings) affected organ, followed by spleen (19 %), kidney (17 %) and thymus (16 %).
The eTOX database should become one of the largest and most granular preclinical databases for pharmaceuticals. It will facilitate comparison of early candidates ("read-across") and pave the way for the development of new in silico tools (see abstract eTOX Part III).

PS 427 eTOX Ontologies: Enhancing Standards for Better Knowledge Management of Animal Study Data (eTOX–Part II)

P. Marc[1], P. J. Clements[2], A. Piaia[1], A. M. Ryan[3], M. Stolte[4], C. Ravagli[1], F. Sanz[5], T. Steger-Hartmann[6] and F. Pognan[1]. *[1]Preclinical Safety, Novartis, Basel, Switzerland, [2]GlaxoSmithKline, Ware, United Kingdom, [3]Pfizer, Groton, CT, [4]Sanofi, Frankfurt, Germany, [5]GRIB (IMIM-UPF), Barcelona, Spain and [6]Bayer Schering Pharma, Berlin, Germany.*

Multiple data types are collected during preclinical animal studies and alignment of terms used in study reports is a real endeavor started many years ago by the toxicologist community. The work done is now rewarded with the materialization of data exchange mechanisms driven by the CDISC-SEND consortium. Use of common code lists to describe studies and findings is a key enabler for increasing interoperability, empowering knowledge management, data mining and predictive modeling. The IMI eTOX consortium has collected data from more than 5000 toxicology reports from 13 companies in order to enable data mining and structure-based prediction. Data from these reports were manually extracted and verbatim findings were stored "as is". In order to make that collection of diverse data and terminologies useful, relevant code lists had to be identified and the 1.5 million extracted finding verbatim terms mapped to the appropriate locations.
Developments delivered by eTOX include the OntoBrowser, an open source tool dedicated to the mapping of verbatim term to preferred terms and maintenance of created ontologies. On top of existing code lists from SEND, a complete ontology was also developed, which included dependencies of terms in order to facilitate endpoint definition and database queries. The most challenging ontology was derived from standard pathology texts, includes the evolving INHAND terms and describes the microscopic anatomic pathology findings. All these ontologies will be shared in the public domain in order to increase inter operability of data in the preclinical safety world.

PS 428 New Frontiers in the *In Silico* Prediction of *In Vivo* Drug Toxicity: The IMI eTOX Project (eTOX Part III)

M. Pastor and F. Sanz. *Research Programme on Biomedical Informatics (GRIB), IMIM - Universitat Pompeu Fabra, Barcelona, Spain.* Sponsor: F. Pognan.

The IMI eTOX project [1] is a European-wide R&D initiative that, for the first time, is collecting and integrating information from *in vivo* preclinical toxicity reports buried in the archives of the pharmaceutical companies. The resulting repository, complemented with information obtained from public sources, is being exploited using methods as read-across and a fully integrated *in silico* prediction system.
The project, started in 2010, begins to yield valuable outcomes. So far the 13 participating pharmaceutical companies have already donated more than 5,000 toxicology reports (see eTOX Part I), the consortium has developed ad hoc ontologies to facilitate data integration (see eTox Part II) and nearly a hundred models have been developed and implemented. With respect to methodological outcomes, the project has developed an integrated prediction system using an original architecture based on independent virtual machines developed by academic partners and interconnected using web services. This solution allows efficient academic-industry collaboration and a safe deployment of the software within the pharmaceutical companies. Predictive models are being developed using a new integrated modeling framework that facilitates their development and maintenance and incorporates functionalities such as structure normalization or assessment of the predictions applicability domain. The predictive models already developed address most of the endpoints classically studied in toxicology. Moreover, since the project is specifically aimed to the prediction of *in vivo* and organ level toxicological endpoints, some of these models implementing multilevel and multiscale approaches [2].

1. Integrating bioinformatics and chemoinformatics approaches for the development of expert systems allowing the *in silico* prediction of toxicities (eTOX). IMI-JU project 115002. http://www.etoxproject.eu
2. Obiol-Pardo C, Gomis-Tena J, Sanz F, Saiz J, Pastor M. A Multiscale Simulation System for the Prediction of Drug-Induced Cardiotoxicity. J Chem Inf Model 2011; 51(2): 483-92

PS 429 An Ensemble Model of *In Silico* Tools to Improve Toxicity Prediction

P. Pradeep[1], R. J. Povinelli[1], R. Brown[2], S. White[2], A. Korolev[2] and S. J. Merrill[1, 2]. *[1]Department of Math, Statistics and Computer Science, Marquette University, Milwaukee, WI and [2]Center for Devices and Radiological Health, US FDA, Silver Spring, MD.*

Quantitative structure activity relationship(QSAR) are theoretical models that relate a quantitative measure of chemical structure to a physical property, or a biological effect. Such models are of particular interest in regulatory settings for toxicity (adverse affect) profiling of drugs or compounds that may be released from medical devices. Free/proprietary in silico tools are gaining wider acceptance as a faster alternative to otherwise time-consuming clinical and animal testing methods. However, different in silico tools often make contrasting predictions for a given chemical and also vary in the accuracy of prediction across different chemical datasets. The objective of this study is to apply the ensemble learning approach in machine learning paradigm for combining predictions from different models, based on the understanding that consensus predictions are better than an individual prediction.
We have developed a novel hybrid QSAR model based on a decision tree framework using Bayesian classification. We compare the predictive performance of in-silico tools (Toxtree, Lazar, OECD Toolbox and Danish QSAR) and the ensemble model for carcinogenicity prediction for a dataset of air toxins (332 compounds), medical device leachables (84 compounds) and the gold carcinogenic potency database (480 compounds). The results show that the ensemble model has improved overall performance (Accuracy: 83.81%, 88.10% and 81.04%) and highest inter-rater agreement, (kappa (κ): 0.6322, .759 and 0.6164). The study suggests that the ensemble model significantly improves the quality of predictions from a regulatory standpoint.

PS 430 DIAMONDS: Data Infrastructure for Applying Models ON Design and Safety

E. Kroese, E. van Someren, J. Venhorst, H. E. Buist, S. Bosgra, J. T. Vogels, M. M. van Lipzig and R. H. Stierum. *TNO, Zeist, Netherlands.* Sponsor: R. Woutersen.

Innovations in many industrial sectors involve the development of new chemical entities with improved properties. Regulatory frameworks in place may differ per industrial sector, but all have the avoidance of harmful effects to exposed humans as major objective. Safe limit values are often driven by complex endpoints like repeated dose toxicity, carcinogenicity, or reproductive toxicity. Until recently, these limits could only be established by animal studies on a compound by compound basis. Today, developments in toxicological sciences, systems biology and computational chemistry, provide opportunities to predict toxicological profiles of chemicals with highly reduced in vivo testing. At TNO, we are developing 'DIAMONDS', a data infrastructure with statistical and computational tools that achieves and visualizes exactly this goal: the efficient prediction of complex toxicological hazards of new molecules. The applied methodology, detailed in this poster, relies on the combined knowledge of known toxicologically characterized toxicants. By extracting the determinants of a specific toxicological outcome, the toxicological profile of a novel compound can be predicted and its probability specified. In addition, DIAMONDS encompasses the use of (in vitro) screening models for 'biological verification', as structural similarity does not guarantee similar toxicological profiles, and to use that screening model outcome for prediction of the potential toxicity of novel molecules. Our visualization tool allows a rapid interpretation of toxicity prediction probability on the basis of all available data. We have applied this tool on TG GATEs, and ToxCast/ToxRef databases and found associations between structural properties, Omics pathway signatures and toxicity/pathology profiles. We found a strong diversity in predictive performance depending on the chosen endpoint. ToxCast assay data did not provide additional predictive value compared to structural fingerprint-based data (Grants NGI-NTC, Cefic-LRI-AIMT-2&3, ZonMW-ASAT).

PS 431 Collaborative Interoperability between Public Projects to Support Replacement of *In Vivo* Repeated Dose Toxicity Testing

D. Hristozov[1], N. Jeliazkova[2], T. Kleinoeder[3], S. Miller[4], D. Neagu[5], Y. Lan[5], A. N. Richarz[6], B. Hardy[7], M. T. Cronin[6] and C. Yang[1]. [1]*Altamira LLC, Columbus, OH,* [2]*Ideaconsult, Sofia, Bulgaria,* [3]*Molecular Networks, Elrangen, Germany,* [4]*Leadscope, Columbus, OH,* [5]*University of Bradford, Bradford, United Kingdom,* [6]*Liverpool John Moores University, Liverpool, United Kingdom and* [7]*Douglas Connect, Zeiningen, Switzerland.*

SEURAT-1 (Safety Evaluation Ultimately Replacing Animal Testing) is a cluster jointly funded by the European Union and Cosmetics Europe with the aim to develop knowledge and technology for the replacement of repeated dose systemic toxicity testing *in vivo* used for the assessment of human safety. The COSMOS and ToxBank projects are part of the SEURAT-1 cluster. The management and sharing of chemical and biological data play a central role. COSMOS developed a web-based database with searching capabilities for both structures and toxicity data. The chemistry content includes a cosmetics inventory compiled from EU COSING database and US PCPC list for cosmetics-related chemicals. COSMOS DB also supports repeated dose toxicity, metabolism information and dermal absorption. It also houses the COSMOS oRepeatDoseDB and TTC database. A web-based data entry system which allows both data entry and quality control has been also developed. Version 1.0 will be publicly available by the end of 2013. ToxBank is the SEURAT-1 cross-cluster infrastructure project aimed at the development of a data warehouse which provides a shared repository for protocols and experimental results across the cluster. In addition, ToxBank supports the mode-of-action framework across the cluster by the selection of reference compounds. A pilot case study was designed to retrieve relevant information from either COSMOS DB or ToxBank to promote analysis across different data domains, for example, *in vivo* toxicity and *in vitro* testing results. The integration between both systems is presented based on open standards, which allows seamless exploration of the data available across public projects including SEURAT-1 cluster. *Supported from the EU FP7 COSMOS and ToxBank Projects.*

PS 432 Hazard Evaluation Support System Database (HESS DB) for Repeated-Dose Toxicity of Chemical Substances: A Multifunctional Tool for Hazard Assessment and Predictive Toxicology

T. Yamada[1], T. Abe[1], R. Hasegawa[1], Y. Sakuratani[1], J. Yamada[1], T. Yamashita[2], K. Yoshinari[3], Y. Yamazoe[3], A. Hirose[4] and M. Hayashi[5]. [1]*National Institute of Technology and Evaluation, Tokyo, Japan,* [2]*Fujitsu Limited, Chiba, Japan,* [3]*Tohoku University, Sendai, Japan,* [4]*National Institute of Health Sciences, Tokyo, Japan and* [5]*BioSafety Research Center, Iwata, Japan.*

Repeated-dose toxicity (RDT) is one of the key regulatory endpoints in the hazard assessment of chemical substances. We have recently released Hazard Evaluation Support System (HESS) and the attached database (HESS DB). HESS is compatible with OECD QSAR Toolbox and has a supportive function to group structural analogs with toxicity data. HESS DB contains test data of RDT studies for currently about 600 industrial chemicals, most of which were conducted in accordance with GLP principles. The DB also includes reference information on ADME and toxicity mechanism for some of those chemicals. Here we demonstrate that HESS DB is very useful for hazard assessment and predictive toxicology. HESS DB has full data set at all tested doses. That allows us to calculate bench mark dose1) and find a parameter useful for hazard assessment2). Moreover, chemicals causing similar toxicity can be efficiently searched with the DB, facilitating to find marketed toxic chemicals and new structural alerts whose mechanistic information is limited. These are new targets of toxicological research. Finally, HESS DB provides information on predictable or measurable key events identified on adverse outcome pathways. The combination use with HESS supports to perform category approach or integrated testing strategy to predicting the primary toxicity of untested chemicals in a transparent and interpretable manner3). Both HESS DB and HESS are donwloadable from the website of NITE at no charge (http://www.safe.nite.go.jp/english/kasinn/qsar/hess-e.html).

1) Yamada et al., J. Toxicol. Sci., 37, 503-512, 2012. 2) Yamada et al., J. Toxicol. Sci., 38, 291-299, 2013. 3) Yamada et al., Regul. Toxicol. Pharmacol., 65, 189-195, 2013.

PS 433 A Web Application for Estimating Provisional Health Guidance Values of Diverse Environmental Chemicals Using Reliable QSAR Models

A. Prussia, N. M. Khalil and E. Demchuk. *Division of Toxicology and Human Health Sciences, Agency for Toxic Substances and Disease Registry, Chamblee, GA.* Sponsor: A. Prussia.

ATSDR is congressionally mandated to develop health guidance values, defined as minimal risk levels (MRLs), to be used for assessing the risk of exposure to hazardous environmental chemicals. Epidemiological data and/or toxicity data from animal studies are the preferred sources of information for developing MRLs. However, such in vivo data exist for only a few hundred chemicals compared to the many thousands present in the environment. Though quantitative structure-activity relationship (QSAR) models for predicting these properties exist in the literature, the models generally lack defined measures of reliability and are difficult to apply to the current chemical of interest. To address these issues, a web application was developed for prediction of rat chronic oral toxicity endpoints known as lowest-observed-adverse-effect-levels (LOAELs). The user need only supply a CAS number for an organic compound of interest, which is interpreted and applied to QSAR models developed from 159 environmental chemicals with experimental LOAELs. The general reliability of these models is confirmed through application of an external test set (Q2 = 0.53); the specific reliability for the chemical of interest is determined through a distance metric to the models' descriptor space. In the future, web-based use of further validated QSAR models may provide quick and reliable toxicity predictions to guide Agency decisions on risk assessment, provisional exposure levels and investigational priorities.

PS 434 Toxicophores: Identification, Validation, and Application

B. M. Paisley, C. M. Zwickl and T. K. Baker. *Investigative Toxicology, Eli Lilly, Indianapolis, IN.*

Growing pressure to move away from animal testing, forge a need for more predictive *in vitro* and computational tools. Cheminformatics is an attractive approach as it is inexpensive and enables early safety assessment. Our goal was to identify toxicophores, substructures with an increased potential for specific toxicological outcomes within a defined chemical and/or biological context. Over 1000 internal compounds with 4 to 14 day rat and dog histopathology data from toxicology studies were included. The compounds comprise diverse pharmacological (NHRs, kinases, GPCRs, ion channels), physicochemical and toxicological properties. Leadscope® was utilized to identify substructures of compounds within the dataset with statistical significance at any of 50 toxicological end points we considered. These "substructure correlates" were evaluated, prioritized and validated against an external test (Pharmapendium®) and an internal test set. *In vivo* and *in vitro* ADMET data paired with structural, pharmacological and other data were used to determine the context in which each toxicophore has an increased likelihood of an adverse event in rat or dog 4 to 14 day tox studies. Eight toxicophores for 3 target organ toxicities have been identified to date. Current chemistry containing these substructures are evaluated visually and screened through the relevant *in vitro* surrogate assays to assess relevance and to determine potential for preclinical toxicity risks. Despite the high predictive power of QSAR models, complex molecular descriptors typically do not provide information on what to modify to mitigate risk. The toxicophore approach is a combined knowledge- and judgment-based method with lower applicability compared to QSAR; however, for compounds containing these toxicophores, it can provide strong chemically and biologically relevant hypotheses to interrogate risk. Our data demonstrate an inexpensive, ethical and informative approach to identify molecules with potential preclinical *in vivo* toxicology risks.

PS 435 Mechanistic Modeling of Acute Oral Toxicity for Rat

S. Ringeissen[1], A. Detroyer[1], R. R. Note[1], D. Nedelcheva[2], N. Dimitrova[2], S. Dimitrov[2] and O. Mekenyan[2]. [1]*Advanced Research, L'Oreal R&I, Aulnay-sous-Bois, France and* [2]*LMC-OASIS, Bourgas, Bulgaria.* Sponsor: D. Bury.

Our aim is to develop a structure-activity model for acute oral toxicity (AOT) of chemicals to rats. The presented AOT model is based upon a category approach: chemicals are grouped in the same category based on their common interaction mechanism and toxicological mode of action. The formed categories include two types of toxicity: basic and excess. Basic toxicity results from the chemical affecting the most basic function of the cells. Most of the chemicals in this category are non-reactive chemicals acting by narcosis mechanism, which alter reversibly the physiological properties of cell membranes. Chemicals having reactive groups could also reveal basic toxicity because of their limited bioavailability. Excess toxicity is a result of destroying some critical processes for the cells or the whole organism.

Chemicals of this category have highly reactive groups acting by specific interaction mechanisms, which result in an enhanced toxicity as compared to the basic toxicity. Two types of excess toxicity were defined: bioavailability dependent and invariable excess toxicity. Bioavailability dependent excess toxicity of chemicals is conditioned by two factors: bioavailability and reactivity. The solubility or partitioning parameters are considered to be adequate descriptors for bioavailability of toxicants. After reaching a certain threshold of water solubility the reactivity factor is starting to play role increasing acute toxicity. The toxic potency of chemicals revealing invariable excess toxicity does not depend on their bioavailability and they possess a constant toxicity within the studied range of solubility or partitioning parameters. The current version of TIMES-AOT model contains 2500 training chemicals. Some data were provided with thanks to the Dow Chemical Company. Based on the structure analysis, mechanisms of interaction and toxicological modes of action, 64 AOT categories were already determined. For each of them, local models for predicting AOT were derived.

PS 436 Computational Analysis of the Combined Therapeutic Effects of Traditional Chinese Medicines and Western Therapeutics in Breast Cancer

A. Chu, M. Lin, D. Loomba, J. Ma and D. Johnson. *Nutritional Sciences & Toxicology, UC Berkeley, Berkeley, CA.*

Alleviating the side effects of chemotherapy drugs with herbal remedies is increasing in popularity. In this research, we used a computational systems pharmacology/toxicology approach to study Taxol and Traditional Chinese Medicine (TCM) recipes used in conjunction to treat and alleviate side effects in breast cancer treatment regimens. Phytochemicals from TCM recipes were determined from the TCM Database@Taiwan and the mechanism of action, potential molecular targets, metabolic pathways, herb-herb and herb-drug interactions, and potential toxicity of individual phytochemicals were elucidated using several resources including the Comparative Toxicogenomics Database (CTD), DrugBank, ToxNet, Toxin and Toxin Target Database (t3db), Side Effect Resource (SIDER), Search Tool for Interactions of Chemicals (STITCH), and Pathwaycommons. Phytochemical findings were integrated into Taxol/breast cancer pathways to elucidate potential synergistic and inhibitory effects. This study provides insight on the potential benefits – and some potential negative effects – of commonly used TCMs and Taxol in the treatment of breast cancer. Relevant findings include the induction of ghrelin by atractydolin, inhibition of VEGF and cMyc by baicalin and baicalein, and inhibition of cyclin D by tashinones. This research supports the continued search for isolated phytochemicals (and structural analogues) from TCM recipes for use in breast cancer treatments.

PS 437 Computational Analysis of Potential Interactions from the Combined Use of Western Therapeutics and Traditional Chinese Medicines in Postmenopausal Osteoporosis

R. Chang and D. Johnson. *Nutritional Sciences & Toxicology, UC Berkeley, Berkeley, CA.*

Osteoporosis is a disease that significantly decreases bone mineral density and increases the risk for fractures. Boniva® and BoneVigor® are two medications used to treat osteoporosis in postmenopausal women. Boniva® contains ibandronate sodium (IS), while BoneVigor® is a Traditional Chinese Medicine (TCM) that contains the herb *Psoralea corylifolia*. Bakuchiol (Bk) is one of the 35 active phytochemicals found in the herb. Many osteoporotic patients choose to use a combination of both Western and TCM treatments for osteoporosis, but their possible interactions are unknown. By using the Comparative Toxicogenomics Database (CTD), KEGG, PharmGKB, Meteor Nexus, and SMARTcyp, we examined a possible overlap between the major Bk metabolite and IS pathways involved in osteoporosis. CTD, KEGG, and PharmGKB were used to provide detailed biological information involved in the mevalonate and osteoporotic pathways. IS inhibits farnesyldiphosphate synthase in the mevalonate pathway and is not metabolized by CYP450 enzymes, while Bk is an ER-α agonist and subject to CYP450 metabolism. From Meteor Nexus and SMARTcyp, Bk was predicted to undergo allylic hydroxylation and then oxidation in mammals to yield a metabolite susceptible to further Phase I biotransformation. This metabolite contains a trisubstituted alkene that is susceptible to epoxidation by CYP2C19 and the opening of its hydrolytic ring by epoxide hydrolase. This Bk metabolite resembles mevalonic acid and presumably can enter the mevalonate pathway which may account for its biological effects. Accordingly, polymorphisms in CYP2C19 and CYP19 may affect Bk metabolism in osteoporotic patients, thereby affecting the way Bk would interact with IS. This study provides a better understanding of how Bk may be metabolized and interact with IS to help develop more personalized medicine regimens for osteoporotic patients with different CYP2C19 and/or CYP19 polymorphisms.

PS 438 Network Motif Basis of Threshold Responses

Q. Zhang[1], S. Bhattacharya[1], R. B. Conolly[2], H. J. Clewell[1], N. E. Kaminski[3] and M. E. Andersen[1]. [1]*Institute for Chemical Safety Sciences, The Hamner Institutes for Health Sciences, Durham, NC,* [2]*Integrated Systems Toxicology Division, NHEERL, USEPA, Durham, NC and* [3]*Department of Pharmacology & Toxicology, Michigan State University, East Lansing, MI.*

There has been a long-running debate over whether or not environmental toxicants exhibit thresholds for adverse health effects. The difficulty in answering the question stems from two fundamental challenges: (i) statistical analysis by itself cannot prove the existence of a threshold; and (ii) there has been little progress in developing a more mechanistic understanding of how threshold phenomena might arise in biological systems. We believe that mechanistic evidence for the existence of thresholds has to come from studying the underlying biological networks as nonlinear dynamical systems. We computationally analyzed the abilities of several intracellular biochemical network motifs to generate threshold responses. These motifs include proportional and integral feedback control, incoherent feedforward control, saddle-node, pitchfork, and transcritical bifurcations, and ultrasensitivity. For each motif, we present mathematical models to illustrate the kinetic basis for threshold responses. We conclude that integral feedback, feedforward and transcritical bifurcations can generate well-defined thresholds below which the response does not deviate from non-stressed control. Other motifs, such as proportional feedback and ultrasensitivity, can give rise to "threshold-like" responses where the low-dose region rises slowly staying close to the baseline. Feedforward control can also produce nonmonotonic/hormetic responses. In conclusion, threshold behaviors may be understood at the level of network motifs, the study of which is necessary for the emerging, toxicity pathway-based approach for chemical safety assessment. This is an abstract or a proposed presentation and does not necessarily reflect USEPA policy. Mention of trade names or commercial products does not constitute endorsement or recommendation for use.

PS 439 Post-Translational Control of Adaptive Cellular Stress Responses and Its Implications in Toxicity Testing and Risk Assessment

M. E. Andersen, Q. Zhang, S. Bhattacharya and J. Pi. *Institute for Chemical Safety Sciences, The Hamner Institutes for Health Sciences, Durham, NC.*

Transcriptional induction of stress genes constitutes a major cellular defense program against a variety of stresses arising from exposures to environmental toxicants. Besides these transcriptional programs, which are slow to activate, fast-acting, post-translational control mechanisms are also at work in the face of cellular stresses. Through computational systems biology pathway models, we are examining processes that would lead to a dose-dependent transition from posttranslational control to transcriptional control with increasing stress levels. These models indicate that posttranslational control serves at least two functional purposes: (1) it handles small and/or transient stress in a timely manner and alleviates the initial impact of persistent stress; and (2) it stabilizes the transcriptional network, which by itself is prone to oscillation due to its delayed negative feedback nature. Posttranslational control, in a feedback or feedforward manner, can underpin perfect adaptation and thus produce thresholds in the responses against external perturbations. Subthreshold stresses are unable to activate the transcriptional program, whereas supra-threshold stresses can transcriptionally induce stress genes, with concomitant alterations of expression of genes regulating cell metabolism, proliferation and apoptosis. These transcriptional alterations may be associated with adverse cellular outcomes. Posttranslational and transcriptional control pathways, acting in concert, may constitute a stratified cellular defense program, allowing cells to handle stresses of wide-ranging intensity coherently. As cell-based in vitro assays become a more significant focus for chemical toxicity testing, examination of protein activity changes in the absence of transcriptional changes deserves more attention. Biomarker monitoring for safety assessment at low stress levels may also need a shift in focus to posttranslational pathways.

PS 440 Computational High-Throughput Quantitative Analysis of Dose-Dependent Histological Features

R. Nault[1, 3], D. Colbry[4], J. R. Harkema[2, 3] and T. R. Zacharewski[1, 3]. [1]*Department of Biochemistry & Molecular Biology, Michigan State University, East Lansing, MI,* [2]*Department of Pathobiology & Diagnostic Investigation, MSU, East Lansing, MI,* [3]*Center for Integrative Toxicology, MSU, East Lansing, MI and* [4]*Institute for Cyber-Enabled Research, MSU, East Lansing, MI.*

Manual quantitation of stained features can be onerous and subjective, yet valuable when integrated with complementary molecular responses. Alternatively, computational approaches such as image segmentation can be used to quantify features.

We have developed a high throughput Matlab®-based tool that runs within the MSU High Performance Computing Center to quantify the level of vacuolization (Oil Red O), immune cell infiltration (H&E or F4/80), and fibrosis (picrosirius red). To test the tool, volume density (V_v) was manually estimated by point counting using STEPanizer©, and computationally estimated for 2,723 Oil Red O stained hepatic sections from mice orally gavaged with 9 doses (0 to 30 μg/kg) of 2,3,7,8-tetrachlorodibenzo-*p*-dioxin (TCDD) every 4 days for 28 days. Significant correlations were calculated between the manual and computational V_v estimates demonstrating the reliability and accuracy of the tool to identify and quantify histological features. Furthermore, unlike manual approaches, the tool was also used to simultaneously quantify vacuole number and size revealing both an increase in number of vacuoles at 30 μg/kg TCDD as well as a dose-dependent increase in size, consistent with a change from micro- to macro-vesicular steatosis noted following visual assessment. Dose-response modeling of Oil Red O stained features estimated ED_{50}, BMD, and BMDL values of 10, 0.26, and 0.12 μg/kg TCDD, respectively, using manual counting and 27, 1.40, and 1.01 μg/kg TCDD, respectively, using our computational tool. In summary, high throughput image segmentation dramatically reduced analysis time to ~1h, facilitated large-scale assessment of histopathological features, and is a viable alternative that is consistent with results from the ≥ 60h manual assessment. Funded by SRP P42ES04911.

PS 440a Deriving Points of Departure and Performance Baselines for Predictive Modeling of Systemic Toxicity Using ToxRefDB

K. W. McLaurin[1], L. Truong[1], G. Ouédraogo[2], S. Loisel-Joubert[2] and M. T. Martin[1]. [1]*NCCT/ORD, US EPA, Raleigh, NC and* [2]*L'Oréal, Paris, France.*

A primary goal of computational toxicology is to generate predictive models of toxicity. An elusive target of alternative test methods and models has been the accurate prediction of systemic toxicity points of departure (PoD). We aim not only to provide a large and valuable resource of PoD, but to also scope the problem by generating floor and ceiling baseline uncertainty bounds for which to judge future models. EPA's ToxRefDB, originally populated with pesticide registration data, has grown to incorporate guideline-like studies from the pharmaceutical industry, National Toxicology Program, and publicly available research literature. Over 6000 high quality animal studies on 1071 chemicals were captured using standardized study design, treatment and effect vocabulary. Systemic lowest and no effect levels (LEL/NEL) were obtained from each study across a diverse set of study types including systemic sub-acute (SAC), subchronic (SUB), chronic (CHR) studies as well as systemic adult effects observed in developmental (DEV) and reproductive (MGR) studies. Species and study type adjusted chemical-level NEL were derived demonstrating a floor baseline of roughly 5 orders of magnitude uncertainty (OMU; 95% CI) based on the default distribution of NEL. Using SUB to predict CHR rat and mouse to predict rat CHR NEL, ceiling baselines were established of 3 and 3.5 OMU, respectively. Further classification of study types based on exposure duration (short = SAC, DEV; medium = SUB; long = CHR), established a ceiling baseline for short vs medium, and long vs medium to be 3.3 and 3.9 OMU, respectively. Thusly, the goal of any predictive model of systemic toxicity is to improve upon the 5 OMU and approach 3-3.5 OMU, but cannot be expected to exceed the inherent uncertainty in toxicological testing and evaluation. This abstract does not necessarily reflect US EPA policy.

PS 440b Dynamic Interaction between Human Serum Albumin and PFOS: A Theoretical Study

A. Zhang, H. Cao and J. Fu. *Research Center for Eco-Environmental Sciences, CAS, Beijing, China.* Sponsor: B. Zhao.

Numerous studies have focused on whether or not PFOS may displace fatty acids bound to human serum albumin (HSA) since the famous persistent organic pollutant exhibited a long half-life of elimination in human serum, approximately 5.4 years. However, there is insufficient information on both PFOS binding sites with HSA and the potential biological function induced by the PFOS-HSA interaction. Recent study of PFOS-HSA complex structure at extremely high PFOS concentration revealed two PFOS binding sites in HSA which overlapped with fatty acid binding sites FA3/4 and FA6, respectively. Unfortunately, such still can not elucidate which site acts as the preferable binding cavity at rational human exposure concentration. Therefore, molecular simulation was adopted to answer the question in the present study. The allosteric modulation associated with PFOS-PFOS effect between 2 binding sites of HSA, FA3/4 and FA6, was analyzed using molecular dynamics simulations and binding free energy calculations. FA6 site was firstly recognized by PFOS binding to HSA although PFOS exhibit higher binding affinity with FA3/4 site. Single binding PFOS at FA6 site can generate allosteric modulation of subdomain 3A through increasing cavity volume of FA3/4 site. Key residues R410 and Y411 locating at entrance of FA3/4 site controlled the allosteric effect and the binding procedure of second PFOS molecule in FA3/4 site subsequent to the first PFOS in FA6. Besides, FA6 may act as only binding site for PFOS at environmental exposure dose, while both crystallographic structures of ligands-HSA complex and binding free energies analysis excluded the possibility that PFOS binding HSA at FA6 site would significantly affect blood delivery of fatty acids in normal physiological conditions. Nevertheless, PFOS binding at FA6 site can still lead to the potential disturbance in natural transport function of HSA due to conformation alterations induced in other subdomains.

PS 440c Utilization of Gene Expression Marker Data to Computationally Generate Nested Networks Underlying Embryonic Stem Cell Differentiation

W. LeFew, J. Crooks, S. Hunter, M. B. Rosen and K. J. Chandler. *US EPA, Durham, NC.*

Predictive tools which model the differentiation of stem cells under a variety of stresses are an area of current research interest. The biological stem cell differentiation network delineates which cell differentiates into which cell. However, the underlying rules which determine when cells differentiate are not fully understood. We suggest there exists a nested regulatory network that governs, controls, and modifies the probabilities of lineage specification.
Pluripotent J1 mouse embryonic stem cells (mESCs) were maintained on a mouse embryonic feeder (MEF) cell layer supplemented with LIF. mESC differentiation was initiated on culture day zero using an adherent cell model. MEF-depleted pluripotent mESCs were seeded onto 96-well gelatin-coated plates in the presence of fetal bovine serum without LIF. Cultures were maintained through day nine (cardiomyocyte formation). On days zero through nine, RNA was isolated from the cell population and analyzed using the MouseRef-8 v2.0 Expression BeadChip (Illumina).
To detect the regulatory network, genes were selected as biomarkers of specific cell types (pluripotent, ectoderm, primitive streak, mesoderm, and endoderm cells). A novel model formulation was used to calculate plausible daily cell counts for each cell type using biomarker expression data, supplemented with cell number counts on each culture day. Computationally generated daily counts for each cell type were used to generate possible nested regulatory networks. Networks were generated using a Bayesian optimization approach over a stochastic model describing differentiation and proliferation. We will demonstrate the model in control and perturbed systems of differentiation. The methodology is scalable to larger systems and modular so that improvements to any feature may be applied independently. This abstract does not necessarily reflect EPA policy.

PS 440d Development of Quantitative Adverse Outcome Pathways Using Health-Protective Assumptions to Fill Data Gaps

R. B. Conolly[1], W. Cheng[1], D. L. Villeneuve[2] and G. T. Ankley[2]. [1]*US EPA, Research Triangle Park, NC and* [2]*US EPA, Duluth, MN.*

In an adverse outcome pathway (AOP), the target site dose participates in a molecular initiating event (MIE), which in turn triggers a sequence of key events leading to an adverse outcome (AO). Quantitative AOPs (QAOP) are needed if AOP characterization is to address risk as well as hazard. A QAOP is based on data from and, in its mature form, has the ability to predict the dose response and time course (DRTC) behaviors linking toxicant dosimetry, the MIE, and the key events with each other and with the AO. Identification of data gaps during QAOP development is common and, typically, some of the gaps cannot be filled given constraints of time and resources. In such situations, alternative assumptions can be identified about how the missing data would affect DRTC behaviors and the more risk-conservative assumptions incorporated until the missing data become available. We are developing a QAOP for fathead minnows. The MIA is inhibition of CYP19A, which converts testosterone to estradiol (E2). Depression of plasma E2, upregulation of CYP19A mRNA, and reduced levels of the glycolipoprotein egg yolk precursor vitellogenin (VTG) are key events. Depression of VTG is associated with decreased fecundity, the AO. Available data include time-course studies with 3 doses of the CYP19A inhibitor fadroloze, plasma E2 and VTG levels, ovarian CYP19A mRNA levels, and fecundity. In this presentation we show how quantitative dose-response relationships between key events, such as expression of CYP19A mRNA as a function of decreased plasma E2 levels, while constrained by data, can be described by alternative functions with different low dose behaviors. These alternative assumptions provide different DRTC behaviors for the overall relationship between the MIA and the AO and can be selected to bias the QAOP to provide risk conservative predictions. This is an abstract or a proposed presentation and does not necessarily reflect EPA policy. Mention of trade names or commercial products does not constitute endorsement or recommendation for use.

PS 440e Evaluation of Alternative Hypotheses for the Linkage of Aromatase Inhibition with Vitellogenin Levels in Fathead Minnows

W. Cheng[1], A. Schroeder[2], D. L. Villeneuve[2], G. T. Ankley[2] and R. B. Conolly[1]. [1]*US EPA, Research Triangle Park, NC and* [2]*US EPA, Duluth, MN.*

The aromatase inhibitor fadrozole inhibits CYP19A, a key enzyme that converts testosterone to estradiol (E2). In fish, E2 levels control synthesis of the glycolipoprotein vitellogenin (VTG), an egg yolk precursor protein essential to oocyte development and larval survival. Fathead minnows were exposed to various concentrations of fadrozole continuously for 8 days and then held in control water for an additional 20 days. Plasma E2 and plasma VTG concentrations were reduced during exposure. While E2 concentrations recovered to control levels post-exposure, VTG concentrations did not fully recover, even after 20 days of depuration. We developed alternative hypotheses to explain the effect of fadrozole on VTG levels. First, it is possible that hepatic production of VTG returned to normal as the E2 concentration recovered. However, plasma VTG could remain depressed for an extended period while oocyte VTG is being replenished. A second hypothesis is that the plasma VTG concentration is not simply proportional to the level of E2 but rather, involves a more complicated biological circuit with alternative setpoints, or attractors, to which it would move after the initial perturbation by fadrozole (i.e., allostasis). Computational modeling cannot by itself identify the actual biological structure of this circuit but it can identify candidate structures that could be investigated in the laboratory. We modeled a candidate circuit that reproduces the VTG data. Our approach is intended to identify the underlying biological explanation for the dynamics of VTG perturbations by fadrozole. This work illustrates the application of computational modeling to evaluate alternative hypotheses and to thereby identify the most appropriate hypothesis for follow-up experimental work. *This is an abstract or a proposed presentation and does not necessarily reflect EPA policy. Mention of trade names or commercial products does not constitute endorsement or recommendation for use.*

PS 440f Development of Population-Based BBDR-HPT Axis Model for Near-Term Pregnancy

A. Lumen[1], C. Hack[2], N. George[3], K. McNally[4], G. D. Loizou[4], D. R. Mattie[5] and J. Fisher[1]. [1]*Biochemical Toxicology, FDA/NCTR, Jefferson, AR,* [2]*Henry M. Jackson Foundation for the Advancement of Military Medicine, WPAFB, OH,* [3]*Bioinformatics and Biostatistics, FDA/NCTR, Jefferson, AR,* [4]*Health & Safety Laboratory, Buxton, United Kingdom and* [5]*Bioeffects Division, 711 Human Performance Wing, Human Effectiveness Directorate, Air Force Research Laboratory, WPAFB, OH.*

A deterministic biologically based dose response (BBDR) model was developed for the hypothalamic-pituitary-thyroid (HPT) axis to evaluate the effects of iodide intake and perchlorate exposure in the near-term pregnant woman and fetus. The goal of the current study is to extend the model to a probabilistic framework evaluating the response of pregnant population to thyroid disturbances. Maternal thyroid hormones play a crucial role in the fetal neurodevelopment. Perturbation of serum levels of maternal free thyroxine (fT4) following inhibition of thyroidal uptake of iodide by perchlorate was chosen as the relevant endpoint. Global sensitivity analysis was carried out to identify input parameters that significantly impact model output and quantify their individual and interaction effects. Monte Carlo (MC) methods are used to evaluate the effect of parameter variabilities and uncertainties on maternal fT4 levels. Physiological and thyroid function variances reported in the literature were obtained, as available, and used as initial estimates of input parameter distributions and bounds. A computational framework for probabilistic evaluation was developed and the preliminary results include identification of the subset of influential parameters and MC analysis of maternal fT4 levels for varying iodide intake. Model predictions provide a good representation of the maternal fT4 levels and urinary iodide levels observed in the pregnant population. The population-based model also addresses correlations between input parameters and captures the nonlinearities associated with predicted levels of maternal thyroidal iodide stores. Efforts are underway to account for variability in perchlorate exposure and its subsequent influence on maternal fT4 levels.

PS 440g A Preliminary Model for the Protective Role of the Endocannabinoid 2-Arachydonylglycerol in Neuroinflammation

E. A. Merrill[1], R. R. Chapleau[1], J. Schlager[2], J. M. Gearhart[1] and P. J. Robinson[1]. [1]*Henry M. Jackson Foundation, 711 HPW/RHDJ, AFRL, Wright-Patterson AFB, OH and* [2]*Molecular Bioeffects Branch, 711 HPW/RHDJ, AFRL, Wright Patterson AFB, OH.*

Activation of cannabinoid receptors, CB1 and CB2, via their endogenous ligands, anandamide (AEA) and 2-arachidonylglycerol (2-AG), yield both anti-inflammatory and anti-excitatory properties. Specifically, basal levels of 2-AG in the nM range are tightly maintained by monoacylglycerol lipase (MAGL), which converts 2-AG into arachidonic acid (AA). Therefore, selective MAGL inhibitors are attracting significant attention as a treatment modalities for conditions that are exacerbated by inflammation. For example, while AA is typically considered the main precursor of inflammatory prostaglandins via oxidative conversion by COX-2, 2-AG has also been found to be a direct substrate for COX-2 metabolism. However, compensatory responses of elevated 2-AG results in reduced expression of COX-2 through activation of the CB1 receptor. To account for the complexities of the system, we have developed a preliminary model for the effect of 2-AG and its metabolites on neuroinflammation in which 2-AG modulates the behavior of the immune response (PGE2 production) to a stressor by altering the magnitude of self-recruitment (via the CB2 receptors on immune cells), while at the same time being metabolized by MAGL to AA, and added with inhibition of COX-2 mediated metabolism of AA and 2-AG (via neuronal CB1 activation). Our model comparisons aligned with observed changes in 2-AG, AA and PGE2 levels induced by JZL 184 found by Nomura et al. (2011) and predicted 75- 95% MAGL inhibition by JZL 184. The modeling also was able to predict reduced 2-AG levels observed by Pope et al. (2013) following exposure of rats to the OPs chlorpyrifos and parathion give model-based predictions of 53% and 20% MAGL inhibition, respectively.

PS 440h Use of the Zebrafish Developmental Screen and Estimation of Internal Concentration to Assess Toxicity

J. T. Hamm[1], N. Kleinstreuer[1], S. Padilla[2] and W. Casey[3]. [1]*ILS, Inc., Research Triangle Park, NC,* [2]*NHEERL/ORD, EPA, Research Triangle Park, NC and* [3]*DHHS/NIH, NIEHS/NTP/NICEATM, Research Triangle Park, NC.*

Traditional toxicology tests required by US regulatory agencies are expensive and time consuming especially in light of the many chemicals that require such testing. An alternative vertebrate model for developmental toxicity is the zebrafish embryo (*Danio rerio*). In this study, 309 environmental chemicals were screened, mainly pesticides and antimicrobials from the ToxCastTM Phase I chemical library. Embryos were immersed in media containing chemical concentrations from 0.001 to 80 μM and the half-maximal activity concentration (AC50) for toxicity (lethality, non hatching, or dysmorphology) determined. To extrapolate to mammalian toxicity, the demonstrated relationship between lipophilicity (LogP) and bioconcentration was used to estimate a body burden associated with developmental toxicity (EC50). Toxicity potency rankings derived from AC50 and EC50 calculations were compared. Some chemicals (for example, thiram, rotenone, butafenacil) were highly toxic regardless of how toxicity was expressed. In contrast, assessing potency by EC50 substantially affected the ranking for a number of chemicals. Daminozide had a high AC50 (66.5 μM) but due to its low LogP, limited uptake was predicted with a very low EC50 (0.04 μM). In contrast, the pyrethroids (n=12) were among the most toxic chemicals with a mean AC50 of 4.01 μM. Due to their high LogP (mean = 5.78), however, the mean EC50 for the class was estimated at 843.25 μM. To further assess extrapolation to mammalian systems, oral equivalent doses from reverse toxicokinetic studies were used to correlate *in vitro* concentrations with potential *in vivo* effects. The ability of the zebrafish developmental screen to predict mammalian toxicity was then assessed by examining the correlation between chemical potencies based on EC50, chemical class, and known *in vivo* effects. This abstract does not necessarily reflect EPA or NIEHS policy.
This project was funded in whole or in part with Federal funds from the NIEHS, NIH under Contract No. N01-ES-35504.

PS 440i Developing QSAR Models of Major Human Membrane Transporters for the Application in Drug Design and Drug Safety Evaluations

A. Sedykh, S. Chakravarti and R. D. Saiakhov. *MultiCASE Inc, Beachwood, OH.*

Membrane transporters are present in all tissues, where they modulate permeability and biological effects of small molecules. Knowledge of transporter interactions is crucial for drug pharmacokinetics and adverse effects, but requires a large-scale

research effort which is the goal of International transporter consortium (ITC). In this study, based on public sources, we have developed a panel of CASE Ultra modules for 14 human drug transporters expressed in intestine, liver, kidney and brain (MDR1, MRP1-5, BCRP, ASBT, NTCP, BSEP, OATP2B1, OCT1, MCT1, PEPT1). The modules provide evidence of active transport or its inhibition and are based on datasets that range in size from 34 molecules (BCRP substrates) to 1,585 chemicals (MDR1 inhibitors). Performance of the modules was evaluated by 10% bootstrapping and 10-fold external cross-validation. All modules achieve good sensitivity (60-100%), specificity (60-100%), balanced accuracy (70-100%), as well as positive (60-100%) and negative (60-100%) prediction rates. The panel of transporter modules was then applied to 1,543 FDA approved drugs. Only 20% of the drugs were predicted to have no active transport, while over half were predicted as substrates of two or more transporters. The developed panel of modules can be used for assessing transporter interactions at early stages of drug development or chemical hazard evaluation.

PS 440j Computational Modeling of OATP1B1 Inhibitors

M. Lawless, R. D. Clark, M. Bolger and W. Woltosz. *Simulations Plus, Lancaster, CA.* Sponsor: S. Ferguson.

OATP1B1 (organic anion transporting polypeptide 1B1) is a member of the solute carrier family of transporters. It is expressed predominantly in the liver where it occupies the basolateral side of hepatocyte cell membranes and transfers molecules from the blood stream into the liver. OATP1B1 substrates include natural products such as bile salts as well as pharmaceuticals such as statins and sartans. OATP1B1 is inhibited by several compounds including cyclosporine A and rifampicin. Drug-drug interactions can occur when an inhibitor of the transporter is coadministered with a substrate drug. For example, when orally administered pravastatin is taken with cyclosporine A, the area under the curve of pravastatin increases almost 900%, potentially leading to toxicological effects. The first International Transporter Consortium report identified OATP1B1 as one of the seven most important transporters in drug disposition.
A data set of 336 compounds was compiled from recent publications. The data consisted of single-concentration, percent inhibition data with either estradiol-β17-glucuronide or estrone-3-sulfate as the substrate. These values were first converted to IC50 values and then to inhibition constants (Ki) using the Cheng-Prusoff equation. Compounds with Ki values less than 20 μM were classified as inhibitors. The overall data set contained 74% noninhibitors and 26% inhibitors, so the population was skewed towards noninhibitors. An artificial neural network classification ensemble (ANNCE) model was trained on 80% of the compounds with the remaining 20% set aside as an external test set. The best model consisted of seven descriptors and six hidden neurons. The model includes lipophilic, atomic charge, and sigma Fukui index descriptors. It has high specificity (90%), sensitivity (89%), and overall concordance (90%) when applied to the external test set. The model was used to predict OATP1B1 inhibition of a subset of about 2,300 compounds from the World Drug Index (WDI). The model predicted 26.5% of the compounds to be OATP1B1 inhibitors with less than 1.5% of the molecules outside the model's applicability domain.

PS 440k Interpretable QSAR of Skin Sensitization for Screening Cosmetics and Environmental Chemicals

R. D. Saiakhov, S. Chakravarti and A. Sedykh. *MultiCASE Inc, Beachwood, OH.*

Computational models of skin sensitization provide important alternative to animal testing of chemicals. However, many of reported models have limited applicability due to small training sets, insufficient validation, and unclear interpretation of results. To address this, we have compiled from scientific literature a harmonized dataset of 374 small molecules with categorical data from local lymph node assay (LLNA). We used CASE Ultra expert system (v.1.4.7.0) to derive two types of models. Model 1 defined strong and extreme sensitizers as active group (73 cmpds), moderate sensitizers as marginally active (103 cmpds), and treated weak and non-sensitizers as inactive (198 cmpds). Model 2 defined strong, extreme, and moderate sensitizers as active (173 cmpds), weak sensitizers as marginal (108 cmpds), and non-sensitizers as inactive (93 cmpds). External cross-validation (10-fold) for Model 1 yielded sensitivity of 50% and specificity of 90%, while for Model 2 - sensitivity of 80%, and specificity of 52%. The developed models have distinct advantages (lower false positives vs. lower false negatives) and can be used jointly for early prioritization of skin care products, topical drugs and environmental chemicals. Major chemical features found by these models to be associated with sensitization were various aromatic, phenolic and ketone groups.
Exemplary screening with these models 298 skin application drugs from DrugBank and Drugs@FDA databases suggested that 15 to 30% of them may have some skin sensitizing effect.

PS 440l Global Phosphoproteome Dynamics of Zebrafish (*Danio rerio*) Embryos

O. Kwon[1], S. Kim[1], J. Sim[1], M. Song[1], K. Yun[2], J. Kim[2], T. Jeong[3] and S. Lee[1]. [1]*College of Pharmacy, Kyungpook National University, Daegu, Republic of Korea,* [2]*Mass Spectrometry Research Center, Korea Basic Science Institute, Ochang, Republic of Korea and* [3]*College of Pharmacy, Yeungnam University, Gyeongsan, Republic of Korea.*

The zebrafish (*D. rerio*) is a popular animal model in studies of vertebrate development and organogenesis. Recent research has shown a similarity of about 70% between the human and zebrafish genomes and of 84% of human disease-causing gene. In particular, zebrafish embryos show a number of desirable features, such as, transparency, a large size, and rapid embryogenesis. Protein phosphorylation is a well-known post-translational modification (PTM), and performs various biological functions. Recent mass spectrometry (MS) developments have been used to study global phosphorylation using MS-based proteomics coupled TiO2 phosphopeptide enrichment. In the present study, we identified 3,500 non-redundant phosphorylation sites on 2,166 phosphoproteins and 1,564 quantified phosphoproteins in zebrafish embryos. The distribution of Ser/Thr/Tyr phosphorylation sites in zebrafish embryos was found to be 88.9%, 10.2%, and 0.9%, respectively. Using Motif-X analysis, a potential kinase motif was predicted for 80% of the identified phosphorylation sites, motif related to MAPK has been found the most frequently appearing. In particular, we found that the pSF motif of 35 phosphorylation sites has not been previously reported in vertebrates. In addition, we created 6 of phosphoproteins cluster pattern during developmental stages in zebrafish embryos. Throughout these results, we reported the largest data set for phosphoprotein in zebrafish embryos and the pSF motif at the first time in vertebrate found. Finally, our zebrafish results can be used the further studies of phosphorylation site or dynamic phosphoproteins in zebrafish embryos.

PS 441 Genotoxic Compound Profiling Using MILLIPLEX® MAP DNA Damage/Genotoxicity 7 Plex Panel

J. Hwang[1], N. Scott[1, 2], T. Warmke[1], R. Maheshwari[1] and R. Wiese[1]. [1]*R&D Immunoassays, EMD Millipore Corp., St. Charles, MO and* [2]*Biomedical Engineering, Washington University, St. Louis, MO.*

A cell's response to DNA damage involves many complex pathways and mechanisms, collectively called the DNA damage response. Once initiated, these pathways ultimately lead to the repair of the damage or the initiation of apoptosis. The DNA damage response plays a crucial role in maintaining the function, genomic stability, and viability of the cell and organism at large. Dysfunctions in the response are implicated in many disease states including cancer, premature aging, and neurodegenerative disease. We have developed a Luminex® bead based multiplex immunoassay that allows for the simultaneous detection of multiple DNA damage proteins in a single well, including phosphorylated Chk1, Chk2, H2A.X, and p53, and total protein levels of ATR, MDM2, and p21. Using the DNA Damage/Genotoxicity 7 Plex panel, we analyzed the levels of phosphorylated and total proteins in HEPG2 and HEK293 cells treated with genotoxic compounds (ethylnitrosourea, methyl methansulfonate, cisplatin, p-chloroaniline, etoposide, hydroquinone, sodium arsenite, paclitaxel and chloramphenicol) and non-genotoxic carcinogens (D-limonene and diethanolamine). Genotoxic compounds, but not non-genotoxic carcinogens, resulted in changes in DNA damage response in a dose and time dependent manner. However, the profile of the genotoxic compounds showed differential regulation of the seven analytes in the DNA Damage/Genotoxicity panel, which implies different modes of action. Cell toxicity was also confirmed using the Human Kidney Toxicity Panel 2 on HEK293 cells. These studies demonstrate the validity of using the DNA Damage/Genotoxicity 7 Pplex panel in screening genotoxic compounds.

PS 442 Ochratoxin A Induces DNA Double-Strand Breaks and Large Deletion Mutations in the Carcinogenic Target Site of *Gpt* Delta Rats

K. Kuroda[1], D. Hibi[1], Y. Ishii[1], S. Takasu[1], A. Kijima[1], K. Matsushita[1], K. Masumura[2], M. Watanabe[3], Y. Sugita-Konishi[4], T. Nohmi[5], K. Ogawa[1], A. Nishikawa[5] and T. Umemura[1]. [1]*Division of Pathology, National Institute of Health Sciences, Tokyo, Japan,* [2]*Division of Genetics and Mutagenesis, National Institute of Health Sciences, Tokyo, Japan,* [3]*Division of Microbiology, National Institute of Health Sciences, Tokyo, Japan,* [4]*Department of Food Life Science, Azabu University, Kanagawa, Japan and* [5]*Biological Safety Research Center, National Institute of Health Sciences, Tokyo, Japan.*

Ochratoxin A (OTA) is a carcinogen targeting proximal tubules at the renal outer medulla (ROM) in rodents. We previously reported that OTA increased mutant frequencies of the *red/gam* gene (Spi^-), suggesting deletion mutations. In the present study, Spi^- assays and mutation spectrum analyses of the Spi^- mutants were performed using additional samples collected in our previous study. Spi^- assay results were similar to those in our previous study, revealing large (over 1 kb) deletion mutations in the *red/gam* gene. To clarify the molecular progression from DNA damage to gene mutations, *in vivo* comet assays and analysis of DNA damage/repair-related mRNA and/or protein expression was performed using the ROM of *gpt* delta rats treated with OTA at 70, 210, or 630 μg/kg/day by gavage for 4 weeks. Western blotting and immunohistochemical staining demonstrated that OTA increased γ-H2AX expression specifically at the carcinogenic target site. In view of the results of comet assays, we suspected that OTA was capable of inducing double-strand breaks (DSBs) at the target sites. mRNA and/or protein expression levels of homologous recombination repair (HR)-related genes (*Rad51*, *Rad18*, and *Brip1*), but not nonhomologous end joining-related genes, were increased in response to OTA in a dose-dependent manner. Moreover, dramatic increases in the expression of genes involved in G_2/M arrest (*Chek1* and *Wee1*) and S/G_2 phase (*Ccna2* and *Cdk1*) were observed, suggesting that DSBs induced by OTA were repaired predominantly by HR, possibly due to OTA-specific cell cycle regulation, consequently producing large deletion mutations at the carcinogenic target site.

PS 443 A 6-Week Inhalation Protocol to Measure Cigarette Smoke-Induced Damage in the Rat Lung by *Ex Vivo* Comet and Histopathological Analysis

A. Dalrymple[1], D. Thorne[1], P. Ordoñez[2], D. Walker[1], O. Camacho[1], D. Dillon[1] and C. Meredith[1]. [1]*Group R&D, British American Tobacco, Southampton, United Kingdom and* [2]*Parque Científico de Madrid, VIVOTECNIA Research S.L, Tres Cantos, Madrid, Spain.*

Guidelines for the provision of genotoxicity data in mammalian cells have been re-defined such that an *ex vivo* study is preferable to a second *in vitro* mammalian study. We have explored the potential of the Comet assay to monitor DNA damage in rat lung alveolar type II epithelial cells (AECII) isolated from rats exposed to cigarette smoke (CS) via inhalation for 6 weeks. Concurrent histopathology was undertaken to monitor characteristic lesion formation following CS exposure.
Female and male rats were exposed to sham air or 0.6 mg/L 3R4F reference CS for 1h or 2h a day for 6 weeks. Lungs were collected, the left lobe processed for histopathology and AECII isolated from the right lobe. Histopathological evaluation demonstrated that goblet cells in the main bronchus, plus unpigmented macrophages and pigmented macrophages in the alveolar lumina were statistically significantly increased in CS exposed rats when compared to sham air. Values obtained (mean severity scores ± SEM) were 0.44±0.16, 1.47±0.30 and 1.38±0.26 for goblet cells, 0.45±0.15, 1.85±0.18 and 2.42±0.19 for unpigmented macrophages and 0.00, 0.45±0.14 and 1.11±0.17 for pigmented macrophages following exposure to sham air, 1h 3R4F CS or 2h 3R4F CS respectively. The level of DNA damage in isolated AECII was statistically significantly increased in CS exposed rats when compared to sham air. Values obtained (mean % tail DNA ± SD) were 3.19%±7.29, 13.43%±14.54 and 13.83%±16.20 for the Alkaline Comet assay and 18.58%±15.52, 37.75%±16.17 and 39.84%±17.56 for Modified Alkaline Comet following exposure to sham air, 1h 3R4F CS or 2h 3R4F CS respectively.
In conclusion, we have developed a 6 week inhalation protocol with an *ex vivo* endpoint. This protocol may have potential use to monitor characteristic lesion formation alongside DNA damage induced by CS.

PS 444 Identification of Genotoxic Compounds Using Isogenic DNA Repair Deficient DT40 Cell Lines in a Quantitative High-Throughput Screening (qHTS) Platform

K. Nishihara[1], J. Zhao[2], R. Huang[2], K. L. Witt[3], R. R. Tice[3], S. Takeda[1] and M. Xia[2]. [1]*Radiation Genetics, Graduate School of Medicine, Kyoto University, Kyoto, Japan,* [2]*National Center for Advancing Translational Sciences, Bethesda, MD and* [3]*National Institute of Environmental Health Sciences, Research Triangle Park, NC.*

DNA repair pathways play a critical role in cellular homeostasis by repairing DNA damage induced by endogenous processes and xenobiotics. Isogenic chicken DT40 cell lines deficient in different DNA repair pathways can be used to identify genotoxic compounds and aid in characterizing the nature of the induced DNA damage. As part of the U.S. Tox21 program, we previously optimized several DT40 isogenic clones for qHTS in a 1536-well format and confirmed the utility of this screening system, which is based on measuring differential cytotoxicity in wild-type and DNA repair deficient clones following exposure to chemicals. In this study, we screened the Tox21 10K compound library against two isogenic DNA repair deficient DT40 cell lines (ku70/rad54 and rev3) and one wild-type cell line using a cell viability assay based on measuring ATP levels. Ku70 and rad54 are associated with DNA double-strand break repair, and rev3 is associated with translesion DNA synthesis pathways. From the primary screening, we identified several well-known genotoxic compounds (e.g., melphalan, alachlor) that induced significantly greater cytotoxicity in the rev3 deficient cell line compared to the wild type cell line. Moreover, several previously unknown compounds were identified as potential direct-acting genotoxic chemicals in our assay. Our results demonstrate the utility of this approach for evaluating the genotoxic activity of chemical compounds using 1536-well based qHTS and for acquiring detailed information on the type(s) of DNA damage induced by these compounds. Supported by NIEHS Interagency Agreement Y3-ES-7020-01.

PS 445 Integration of Pig-a Mutation and Micronucleated Reticulocyte Frequencies in a 28-Day Repeat Dose Study

R. Naravaneni, S. Sharma and R. D. Mehta. *Genetic Toxicology, PBR Laboratories Inc., Edmonton, AB, Canada.*

Genotoxicity of N-ethyl-N-nitrosourea (ENU) was evaluated for Pig-a gene mutation and micronucleated reticulocyte (MN-RET) endpoints in rat peripheral blood using high throughput flow cytometry-based methods. Male Sprague Dawley rats (7-8 weeks age, 6 animals/group/dose) were treated via oral gavage for 28-consecutive days with several doses of ENU (0.625, 2.5, or 10mg/kg/day) or the vehicle (Phosphate Buffered Saline, pH 6.0). Blood samples were collected from the tail vein on days 0, 15, 29 and 46 for measuring Pig-a gene mutation frequencies in total red blood cells (RBCs) and reticulocytes (RETs) using MutaFlow-PLUS kit reagents. On day 4 and day 29 of the study, blood samples were processed for measurement of MN-RET frequencies with MicroFlow-PLUS kit reagents. Mutant RBCs and RETs exhibited significant dose and time-dependent increases on days 15, 29 and 46 at all the dose levels tested except at the lowest dose (0.625mg/kg) on day 15. This 0.625mg/kg dose induced a small but significant increase only in mutant RETs frequencies at this early time point, whereas both mutant RBCs and mutant RETs were elevated on days 29 and 46. With regard to MN-RET frequencies, a significant increase was found on day 4 and day 29 at the highest dose level (10mg/kg). The mid dose (2.5mg/kg) was significantly elevated on day 29. In conclusion, the lowest dose of ENU tested in this study (0.625mg/kg) was observed to cause marked increases in Pig-a mutation despite the fact that it is lower than the threshold dose of 0.88 mg/kg estimated by Dobo and colleagues who also studied the Pig-a endpoint (Mutat. Res., 725:13-21). This increased sensitivity may be attributable to our use of immunomagnetic column separation step that allowed scoring of many times more cells per sample. In addition, the results validated the simultaneous scoring of two genotoxicity endpoints as well as provided a statistical robustness to the data collected. This approach of analyzing more than one endpoint in a single study results in reducing the number of animals used and proves highly cost-effective.

PS 446 *In Vivo* Genotoxicity of 1, 4-Dioxane in Rats

C. Hattori, M. Nagata, S. Itoh and W. Takasaki. *Medicinal Safety Research Laboratories, Daiichi Sankyo Co., Ltd., Tokyo, Japan.*

1,4-Dioxane is used widely as a solvent in the manufacture of chemicals, and as a laboratory reagent. 1,4-Dioxane induces liver adenomas and carcinomas in mice and rats, and is categorized into IARC Group 2B chemicals. 1,4-Dioxane has been reported to be non-genotoxic in *in vitro* studies, e.g. Ames, mouse lymphoma TK, chromosomal aberration, *in vitro* micronucleus and sister-chromatid exchange assays. In the *in vivo* studies, positive results were obtained in bone marrow micronu-

cleus assay in C57BL6 and CD-1 mice, and liver micronucleus assay with or without partial hepatectomy (PH) in CD-1 mice. However, negative results were also observed in many *in vivo* genotoxicity studies; e.g. drosophila sex-linked recessive lethal, rat liver DNA alkaline elution, rat liver DNA repair, bone marrow (BALB/c mice) and peripheral blood (CD-1 mice) micronucleus assays. Therefore, there is no clear conclusion for its *in vivo* genotoxicity in rodents. In the present study, we investigated the ability of 1,4-dioxane to induce micronuclei in rat bone marrow and liver. In the liver micronucleus assay, we performed the juvenile animal method and two PH methods (dosing before PH or after PH). We also evaluated the mutagenicity of 1,4-dioxane by Pig-a gene mutation assay using rat peripheral blood. As a result, all methods of liver micronucleus assay detected micronucleus induction by 1,4-dioxane. In the sensitivity to liver micronucleus induction by 1,4-dioxane, the dosing before the PH method, a suitable method for structural chromosome aberration inducer, is the highest among the three methods. This finding is consistent with a report that 1,4-dioxane induces chromosome breakage in the liver. Negative results were observed in the bone marrow micronucleus and Pig-a gene mutation assays. These results suggested that 1,4-dioxane is genotoxic in the liver but not in the bone marrow of rats. The fact that genotoxicity of 1,4-dioxane in the liver was detected in rats as well as mice supports the usefulness of the rat liver micronucleus assay because the rat is more common species in toxicology research and requires easier operation in PH.

PS 447 Combination of Multitissue Micronucleus Assay and Gene Mutation Assay: Simultaneous Detection of Multitissue Micronucleus Inducibility and Gene Mutation in Gpt Delta Transgenic Rats

J. Tanaka, M. Natsume, S. Kasamoto, K. Suzuki, M. Nagai, F. Uno, M. Fukumuro, S. Masumori and M. Hayashi. *Biosafety Research Center (BSRC), Iwata, Shizuoka, Japan.*

Recently, the combination or integration assay attracts attention because the reduction in the number of experimental animals is required from the viewpoint of the animal welfare. If the evaluation of multi-tissue gene mutation assay using transgenic rat is combined to the results of micronucleus assay which shows different genotoxicity endpoints, it is expected that more information will be obtained from the same animals.
The gpt delta male rats were orally administered with 1, 2-dimethylhydrazine dihydrochloride (DMH) at day 1 and N-nitroso-N-methylurea (MNU) at day 3 and 4. DMH and MNU are known to induce micronuclei in the glandular stomach and colon, respectively. The colon, glandular stomach, peripheral blood and liver were removed from the animals euthanized on one day after the final administration. The gpt assay and Spi- assay were conducted using these tissues. The micronucleus assay was conducted using the colon, glandular stomach and peripheral blood.
In the results, statistically significant increases in the frequency of micronucleated cells in the colon, glandular stomach and peripheral blood were observed in the DMH and MNU-treated groups compared with the negative control. In the gpt assay, mutant frequencies in all assayed organs were also significantly increased. In the Spi- assay, mutant frequency in the liver only was significantly increased.
These results suggest that the multi-tissue gene mutation assay using transgenic rat can be combined to the micronucleus assay in gastrointestinal tract.

PS 448 Toxicity of Chemical Dispersants, Oil, and Chemically Dispersed Oil in Sperm Whale Skin Cells

C. Wise[1, 2], J. Wise[1, 2], S. Wise[1, 2, 3] and J. P. Wise[1, 2, 3]. [1]*Wise Laboratory of Environmental and Genetic Toxicology, Portland, ME,* [2]*Maine Center for Toxicology and Environmental Health, Portland, ME and* [3]*Department of Applied Medical Science, University of Southern Maine, Portland, ME.*

Two major oil crises in United States history, the 1989 Exxon-Valdez oil spill in Alaska and the 2010 Deepwater Horizon Oil Rig explosion in the Gulf of Mexico, drew attention to the need for toxicological experiments on oil, chemical dispersants, and chemically dispersed oil. We are still learning the effects these spills had on wildlife. However, little data is known about the toxicity of these substances in marine mammals. The objective of this study is to determine the toxicity of the two dispersants (Corexit 9500 and 9527), Alaskan and Gulf oil, as well as chemically dispersed oil. Corexit 9500 and 9527 are both cytotoxic to sperm whale skin fibroblasts. Corexit 9527 is less cytotoxic than 9500. S9 mediated metabolism did not alter cytotoxicity of either dispersant. Both dispersants are genotoxic to sperm whale skin fibroblasts; S9 mediated metabolism increased Corexit 9527 genotoxicity. Oil experiments were performed using the water accommodated fraction of oil (WAF). The Alaskan WAF is not cytotoxic to sperm whale skin cells. Chemically dispersed Alaskan oil (CEWAF) is more cytotoxic and genotoxic than the WAF. S9 mediated metabolism increased genotoxicity caused by CEWAF and WAF.

PS 449 *In Vitro* Cytotoxicity and Genotoxicity Testing Using upcyte® Hepatocytes

A. Nörenberg. *Medicyte GmbH, Heidelberg, Germany.* Sponsor: P. Hewitt.

We have developed a novel technique which causes primary human hepatocytes to proliferate whilst retaining an adult phenotype including functional phase 1 and 2 metabolism. In this study we evaluated the resulting "upcyte® hepatocytes" for their potential use in cyto- and genotoxicity testing.
For the establishment of an upcyte® hepatocytes based genotoxicity test we adapted the conditions of the frequently used micronucleus test. Conditions for upcyte® hepatocytes from a single donor (Donor 740) showed that a treatment duration of 96 h, without a recovery period was optimal for detecting both directly acting and metabolically activated genotoxins, whilst true negative and "misleading" positive compounds were correctly identified as negative. The micronucleus rate (%MN) in upcyte® hepatocytes treated with DMSO, cyclophosphamide and MMC was essentially unaffected by the growth stage (between a population doubling of 18 and 59). In conclusion, these data support the use of upcyte® hepatocytes in the MN test, since they were able to correctly identify known direct and metabolically activated genotoxicants, while misleading positives and true negative compounds resulted in negative outcomes.
The cytotoxicity of 31 compounds was measured using upcyte® hepatocytes derived from four donors to include effects due to donor variation. The compounds were classified as either severely, moderately or non-hepatotoxic. There was a very good intra- and inter-experimental reproducibility of the measurements. The cytotoxicity of the majority of compounds was donor-dependent. The predictive capacity of the assay was generally good such that known non-hepatotoxicants were clearly negative and compounds that were associated with hepatotoxicity caused damage to the upcyte® hepatocytes.
In conclusion, these studies show that use of upcyte® hepatocytes which combine proliferation with long-term stable expression of adult hepatic phenotype enables the development of new in vitro liver cell models for metabolic drug and toxicity analysis.

PS 450 The Liver Micronucleus Test Integrated into 5-Day Repeated-Dose Toxicity Study in Mice Would Be Useful to Detect the Genotoxicity of Hepatocarcinogens

A. Maeda, K. Takahashi, H. Tsuchiyama, Y. Asaoka, M. Mutsuga, K. Oshida and Y. Miyamoto. *Pharmaceutical Research Laboratories, Toray Industries, Inc., Kamakura, Kanagawa, Japan.*

The liver micronucleus test has the potential to detect liver carcinogens due to the accumulation of micronuclei by repeated dosing and could be expected to be integrated into repeated-dose toxicity study. In this study, to assess the possibility of its integration into 5-day repeated-dose toxicity study in mice, genotoxic hepatocarcinogens; diethylnitrosamine (DEN), 2,4-diaminotoluene (2,4-DAT), 2,4-dinitrotoluene (2,4-DNT) and 2-acetylaminofluorene (2-AAF), non-genotoxic hepatocarcinogen; clofibrate, and non-carcinogen; 2,6-diaminotoluene (2,6-DAT), were administered orally to male ICR mice once daily for 5 consecutive days. Hepatocytes were collected 24 h after the final administration, and the frequencies of micronucleated hepatocytes (MNHEPs) were examined. Significant increases in MNHEPs were observed in DEN- and 2,4-DAT-treatment groups, but not in 2,4-DNT-, 2-AAF-, 2,6-DAT- and clofibrate-treatment groups. 2-AAF might not induce MNHEPs because of its mitosis inhibitory effect on parenchymal hepatocytes. The result of 2,4-DNT is reasonable because it is a hepatocarcinogen in rats, but not in mice. In conclusion, the liver micronucleus test integrated into 5-day repeated-dose toxicity study in mice would be useful to detect the genotoxicity of hepatocarcinogens with consideration on results of general toxicity studies.

PS 451 Evaluation of Reactive Textile Dyes with Organs-Specific Genotoxicity Using *In Vitro* Flow Cytometry-Based Micronucleus Assay

D. M. Leme[1], A. Sehr[2], T. Grummt[2] and D. P. Oliveira[1]. [1]*FCFRP-USP, Ribeirão Preto, São Paulo, Brazil and* [2]*Umweltbundesamt, Bad Elster, Germany.*

Introduction: The textile industry extensively uses synthetic chemicals as dyes. There are several studies reporting the deleterious effects (e.g. DNA damage) of dyes to humans. Humans can be exposed to toxic dyes either through ingestion of contaminated waters or dermal contact with colored garments. Thus, genotoxicity assessments of these chemicals using organ-specific cell lines can be relevant to estimate their hazard. Objective: Cyto- and Genotoxicity of the textile dyes Reactive Green 19 (RG19), Reactive Blue 2 (RB2), Reactive Blue 19 (RB19), Reactive Black 5 (RB5), Reactive Red 120 (RR120) and Reactive Orange 16 (RO16) were assessed using in vitro MicroFlow® kit (Litron Laboratories Ltd.)

with immortalized human keratinocytes (HaCaT) and human hepatoma cells (HepaRG TM, Biopredic International, Rennes, France, purchased at Fisher Scientific). Methodology: HaCaT and HepaRG TM at 1x105 and 2x105 cells/mL, respectively, were exposed in a 96-well format to six concentrations of the test dyes (at 31.25 to 1000 μg/mL), PBS 20%-v/v (solvent control), Mitomycin at 2.5 to 10μg/mL and Vinblastine at 12.5 -50 ng/mL (positive controls) for 48 and 24 h, respectively. 2-fold over concurrent solvent control mean (EMA-fold: cytotoxicity, MN-fold: genotoxicity) were used to define the positive results. Results and Discussion: A dose-dependent cytotoxicity was observed using HaCaT cells for all tested dyes, unlike in the experiments carried out with HepaRG TM, which cytotoxic effects were detected only for RB19 and RO16 at the highest concentration (1000 μg/mL). Genotoxicity was not observed for any of the tested dye under both experimental conditions (HaCaT and HepaRG TM). Conclusion: Based on our findings, HaCaT cells showed to be more sensitive to detect the cytotoxic effects of textile dyes than HepaRG TM. The reactive dyes studied herein can be considered not hazard to human health in respect to the capacity of induce genotoxicity in these target tissue (epidermis and liver). Financial Support: FAPESP (Process No. 2010/14941-3)

PS 452 Kinetics and Dose-Response Assessments of Cisplatin-Induced Genotoxicity in Sprague-Dawley Rats

S. Dertinger[1], S. Phonethespwath[1], S. Avlasevich[1], D. K. Torous[1], C. Labash[1], J. Cottom[1], J. Mereness[1], S. Bryce[1], J. Bemis[1] and J. T. MacGregor[2]. [1]*Litron Laboratories, Rochester, NY and* [2]*Toxicology Consulting Services, Arnold, MD.*

Cisplatin and other platinum-type drugs exhibit tremendous efficacy in treating some types of malignancies, for example testicular cancer. However, secondary malignant neoplasms are common, with some estimates suggesting rates as high as one in three. We set out to determine whether a rat model and two blood-based endpoints could be used to effectively study the genotoxicity of cisplatin at low, tumorigenic dose levels. Male Sprague Dawley rats, age 7 weeks, were administered cisplatin *via* ip injection at 0, 0.05, 0.1, 0.2 and 0.4 mg/kg/day for 28 consecutive days. Allometric scaling suggests that the highest dose level corresponds to a human equivalent of 2.4 mg/m^2—well below typical therapeutic levels of 20 mg/m^2 iv (once/day for 5 days/cycle). Two endpoints of genotoxicity were studied: micronucleated reticulocytes served as an indicator of chromosomal damage and were measured on days 4 and 29, and *Pig-a* mutant phenotype cells were scored in blood samples collected on days 15, 29, 56 and 84. Even the earliest time points evaluated showed dose-related increases for both endpoints, long before tumors or pre-neoplastic lesions would be expected. The lowest significant dose level was 0.4 mg/kg/day for micronuclei, and 0.05 mg/kg/day for *Pig-a*. These data illustrate the potential of these sensitive blood-based endpoints to provide dose-response and temporality information for assessing whether suspected leukemogenic agents such as cisplatin contribute to the risk of secondary malignancies through a genotoxic mode of action. Furthermore, given the pharmaceutical industry's desire to combine platinum drugs with novel anti-neoplastic agents, we speculate that this rodent model may prove useful for studying adjuvants' effects on platinum drug-induced DNA damage, and by extension the tumorigenicity of combination therapies.

PS 453 Development of a Flow Cytometric Assay for Measuring *In Vivo* Mutation in an Autosomal Gene

J. A. Bhalli[1, 2], V. N. Dobrovolsky[1] and R. H. Heflich[1]. [1]*Division of Genetic and Molecular Toxicology, National Center for Toxicological Research, Jefferson, AR and* [2]*Genetic Toxicology, Covance Laboratories Inc, Greenfield, IN.*

The product of the X-linked Pig-a gene is essential for the synthesis of glycosyl phosphatidyl inositol (GPI) anchors that link specific proteins to the cell surface. Although an assay that detects in vivo mutation in the Pig-a gene (the Pig-a assay) has generated considerable interest in the regulatory community, the Pig-a assay is not expected to detect an important class of mutation, i..e., loss of heterozygosity (LOH). LOH mutations can most readily be detected using a heterozygous autosomal reporter gene, as is the case with the heterozygous Tk gene employed in the mouse lymphoma assay. In this study, we investigated the feasibility of a flow cytometric Pig-a-like assay using an autosomal gene that codes for a GPI-anchored surface marker protein, CD24. CD24+/- mice were generated by breeding CD24 knockout (KO) males to wild-type females. A labeling strategy was devised to differentiate between Pig-a and CD24 mutant RBCs. Leukodepleted blood was labeled with a PE-conjugated anti-mouse CD24 antibody and FLAER (AlexaFluor®488-conjugated nontoxic variant of proaerolysin), which binds to GPI anchors. A pilot study was performed by treating groups of five 6-8-week-old male CD24+/- mice with single doses of 0 or 140 mg/kg ENU by oral gavage; blood was collected on Days -1, 15 and 29, labeled, and processed by flow cytometry to quantify fluorescently labeled and unlabeled erythrocytes. Significant increases in the frequency of FLAER-negative (presumably Pig-a mutant) and CD24-negative (presumably Pig-a and CD24 mutant) erythrocytes were observed in ENU-treated animals, with CD24-negative erythrocyte frequencies being somewhat higher. Additional studies using agents that induce high frequencies of LOH-type mutations (e.g., ionizing radiation) should be conducted in order to confirm that the CD24-negative phenotype is detecting a greater number of mutations than Pig-a-negative phenotype.

PS 454 Evaluation of Thioacetamide Genotoxicity in Rat Liver and Stomach As Measured by the *In Vivo* Alkaline Comet Assay

R. Neft[2] and C. Beevers[1]. [1]*Covance Laboratories Ltd, Harrogate, North Yorkshire, United Kingdom and* [2]*Covance Laboratories Inc, Greenfield, IN.* Sponsor: J. Bhalli.

Thioacetamide is a known hepatotoxic agent and dietary administration caused hepatocellular carcinoma in mice and rats and tumors of the bile duct in rats. It is negative in Ames and in vitro chromosome aberration tests, however, there are conflicting reports regarding its genotoxicity in vivo. It induced micronuclei in the bone marrow of two strains of mice, albeit mostly at lethal dose levels, but similar effects were not seen in rats. No micronuclei were induced in the liver or peripheral blood of thioacetamide treated rats. In the Comet assay, thioacetamide was positive in stomach, colon and urinary bladder, but not in bone marrow or liver of mice treated by intraperitoneal injection. We examined thioacetamide activity (up to a maximum tolerated dose) in a rat alkaline comet assay and measured DNA migration in liver and stomach after 3 exposures (21-24 hours apart), sampling 3 hours after the final administration. Thioacetamide caused an increase in DNA migration in the stomach of rats treated at 38 and 75 mg/kg/day as well as an increase in hedgehogs, a Comet morphology indicative of highly fragmented DNA that is excluded from Comet analysis. Thioacetamide did not cause any increase in DNA migration in the liver, despite evidence of marked hepatotoxicity. These findings confirm that toxicity does not always confound assessment of genotoxicity-related DNA migration in the Comet assay.

PS 455 Evaluation of the DNA Adductome Approach to Assess the DNA Reactivity of Chemicals in Rat Liver

S. Muto, K. Yamada, K. Kato, E. Yamamura, Y. Iwase and Y. Uno. *Safety Research Laboratories, Mitsubishi Tanabe Pharma Corporation, Kisarazu, Japan.* Sponsor: J. Shinouka.

The usefulness of DNA adductome approach, a complehensive measurement of DNA adducts using highperformance liquid chromatography equipped with tandem mass spectrometry (LC–MS/MS), was evaluated to assess the DNA-damaging capability of chemicals *in vivo*.
Male Sprague-Dawley rats were treated with compounds from three categories: (1) genotoxic carcinogens causing DNA alkylation, dimethylnitrosamine (DMN) and methylnitrosourea (MNU); (2) genotoxic carcinogens producing DNA bulky adducts, 2-acetylaminofluorene (2-AAF), 2,4-Diaminotoluene (2,4-DAT), 7,12-dimethylbenz[a]anthracene (DMBA) and 4-Nitroquinoline 1-oxide (4NQO), and (3) non-genotoxic carcinogen, Di(2-ethylhexyl)phthalate (DEHP). DNA extracted from liver samples were enzymatically hydrolyzed to deoxyribonucleoside by micrococcal nuclease/bovine spleen phosphodiesterase or P1 nuclease method, and subsequently applied to the LC/ESI-MS/MS analysis. The methods was designated to detect the neutral loss of deoxiribose from positively ionized deoxynucleoside adducts by monitoring the DNA samples transmitting their [M+H]+>[M+H-116]+ transitions. The transitions were monitored over the m/z range of 250-702.
All genotoxic carcinogens produced various DNA adduct peaks in the liver. Some of DNA adduct peaks had the m/z values corresponded to compound-derived adducts (methyl-dG for DMN and MNU, aminofluorene-dG for 2-AAF, DMBA-diol-epoxide-dG for DMBA, 4-aminoquinoline 1-oxide-dG for 4NQO). On the contrary, no DNA adduct peak was detected in liver of DEHP treated rats.
These results indicate that this DNA adductome approach would be useful to identify the DNA reactivity of compounds, and to support the understanding of their mechanism of action.

PS 456 Detection of Germ Cell Mutagens in the MutaMouse Transgenic Mutation Assay

C. Beevers. *Covance Laboratories Ltd, Harrogate, North Yorkshire, United Kingdom.* Sponsor: J. Bhalli.

OECD test guideline 488 describes optimum study designs for determination of mutagenicity in a variety of rodent tissues. For male germ cells sampling times should be carefully selected to ensure the range of exposed cell types throughout germ cell development is sampled and that each stage targeted has had sufficient exposure. The guideline recommends one of two approaches for germ cell muta-

tion assessment: 1) to dose for 28 days plus 3 days expression period and sample both developing germ cells from the seminiferous tubules and mature sperm from the cauda epididymis/vas deferens or 2) to dose for 28 days and sample only mature sperm a minimum of 7 weeks (mice) or 10 weeks (rat) after last treatment. Option 1 has significant advantages in terms of logistics, duration and cost of the study. Even more importantly where somatic tissues are investigated alongside germ cells, Option 1 is more ethically justified as it would use up to half the number of animals as Option 2. However, it has been questioned whether all stages of germ cell development are adequately covered by the 28 plus 3 day study design to ensure accurate detection of germ cell mutagens. We treated male MutaMice with saline or the potent mutagen ethylnitrosurea (ENU). Animals were treated orally by gavage for 28 consecutive days at 10 mg/kg/day. On Day 31, animals were necropsied and developing germ cells from the seminiferous tubules and mature sperm from the cauda epididymis/vas deferens were isolated. Both cell types were examined for mutation in the neutral lacZ transgene using positive selection methods. Clear increases in mutant frequency were detected in developing germ cells, however, weaker, equivocal increases were detected in the mature sperm, supporting the idea that a 28 plus 3 day study design is not optimal for robust detection of germ cell mutagens.

PS 457 Genotoxic Effects on HepG2 Cells Induced by Brominated Flame Retardant (BDE-47)

A. O. Souza[1], M. J. Tasso[1], L. C. Pereira[2], D. P. Oliveira[2] and D. J. Dorta[1,2]. [1]*Química, FFCLRP-USP, Ribeirão Preto, SP, Brazil and* [2]*Análises Clínicas, Toxicológicas e Bromatológicas, FCFRP, Ribeirao Preto, SP, Brazil.*

INTRODUCTION: BDE-47, a brominated flame retardant, shows evidences of potential toxicity to the organisms and the environment. The levels of BDE-47 on biotics and abiotics systems are increasing and its high bioaccumulation has leading to growing concerns about its presence in the environment and the consequences to the human helath, such as its genotoxic potential. BDEs genotoxic potentials had been shown for some cell lines, but there is no information to the liver cells, which are one of the main targets of BDEs. Therefore, the full evaluation about the risks of BDE use are still necessary to better understand their toxicity to the human health. OBJETIVE: The aim of the work was to investigate the genotoxic effects of the BDE-47 on human hepatoma cells (HepG2). METHODOLOGY: Briefly, cells were incubated at 37°C, in an atmosphere containing 5% CO2 and 96% relative humidity and treated with concentrations ranging from 0.1 to 25μM for 4 hours. After the exposure period, the HepG2 cell were mixed with agarose and transferred to slides. The cell on the slides were lysed for 2 hours and submitted to electrophoresis (300 mA and 25 V for 20 min). Then, the cells were stained with propidium iodide solution (10 μg/ml) and examined using fluorescence microscopy. RESULTS: Our results showed the capacity of BDE-47 to cause DNA damage at doses starting at 10 μM ($p < 0.05$) while at lower concentration there isn't difference between treatments and negative control (without BDE-47). CONCLUSIONS: According to these results, BDE-47 showed the ability to cause DNA damage of HepG2 cells after the high concentration exposure. These conclusions contribute with evidences to the genotoxic potential of BDE-47, which high bioaccumulation potential can easily lead to a high concentration into the organism.

PS 458 BDE-153 is Genotoxic to HepG2 Cells and Lead to Apoptotic Cell Death

L. C. Pereira[1], A. O. Souza[2], M. F. Bernardes[1], M. J. Tasso[2], D. P. Oliveira[1] and D. J. Dorta[2]. [1]*FCFRP, Universidade de São Paulo, Ribeirão Preto, Brazil and* [2]*Química, FFCLRP, Ribeirão Preto, São Paulo, Brazil.*

INTRODUCTION: Polybrominated diphenyl ethers have been used in diverse products and are ubiquitous contaminants in sediments and biota. They are also found in human tissues, food and wildlife. There is a lot of information about the presence of brominated flame retardants in the environment, however little is known about their mechanisms of inducing toxicity. The use of different assays as well as monitor different endpoints is important to evaluate the hazard potential of chemicals OBJECTIVE: The aim of this work was to investigate the mechanisms by which BDE-153 (penta-BDE) can induce toxicity to HepG2 cells in concentrations ranging from 0.1 to 25 μM. METHODS: Briefly, the effects of BDE-153 in HepG2 cells were evaluated by different endpoints. First, we assessed the exposure of phosphatidylserine on the outer cell membrane after 24 and 48 hours of exposure to BDE-153. After that, we assessed nuclear fragmentation using the fluorescent dye Hoechst 33342, and finally, we evaluated the genotoxic potential of the compound through the comet assay. RESULTS: We observed that in concentrations of 5 μM and higher BDE-153 was able to induce apoptotic cell death since it was observed exposure of phosphatidylserine in the outer cell membrane and nuclear fragmentation of HepG2 cells after 24 h of exposure to the compound. In addition BDE-153 is able to induce primary DNA damage observed by comet assay at the same concentrations but much earlier, with only 4 hours of cell exposure to the compound. CONCLUSIONS: The results reinforce the importance of using different assays for toxicological analyzes and suggest that BDE-153 induces genotoxic effects that can lead the cell to death by apoptosis.
Supported by: FAPESP - Proc. 2012/13123-0
"The opinions, assumptions, and conclusions or recommendations expressed in this material are those of the authors and do not necessarily reflect the views of FAPESP"

PS 459 Validation of an Expert Rule-Based System to Support the ICH M7 Guideline on Drug Impurities

G. J. Myatt, K. P. Cross and D. Bower. *R&D, Leadscope, Columbus, OH.*
Sponsor: R. Benz.

The ICH M7 guideline on drug impurities states that two distinct in silico methodologies can be used to qualify certain drug impurities as not mutagenic. This poster outlines a new expert rule-based system to predict the results of a bacterial mutagenesis assay. In the development of this system, an initial library of mutagenicity structural alerts was identified from the literature. This process included consolidating the same or similar alerts cited in multiple publications. Information on plausible mechanisms was collected alongside the structural definitions. Factors that deactivate the alerts were also identified from the literature and through an analysis of the corresponding data using the Leadscope data mining software. Over 200 distinct alerts were identified and these alerts were further validated against a database of over 7,000 chemicals with known bacterial mutagenesis results. Only validated alerts with a sufficiently strong association with positive expert-reviewed calls from *Salmonella* and *E. coli* strains were included. A prediction of the bacterial mutagenesis assay can be made using these validated alerts; however, this is only possible where the compound is within the applicability domain of the alert system. In addition, a confidence score based on information collected for each alert is provided alongside the positive or negative call. This poster outlines the expert system along with the results of validating the system, both as a standalone system as well as in combination with a statistical-based approach. The system was tested using a set of 3,734 compounds with concordance of 79.4% and coverage of 99.8%.

PS 460 An *In Vivo* Mutagenicity Test of Hydroquinone Using the *lacZ* Transgenic Mice

A. Ono[1], M. Honma[2], S. Masumori[3], M. Matsumoto[1], M. Hirata-Koizumi[1] and A. Hirose[1]. [1]*Division of Risk Assessment, National Institute of Health Sciences, Tokyo, Japan,* [2]*Division of Genetics and Mutagenesis, National Institute of Health Sciences, Tokyo, Japan and* [3]*Genotoxicology Laboratory, Biosafety Research Center, Shizuoka, Japan.*

Hydroquinone (HQ) is used as an antioxidant in rubber industry and as a developing agent in photography. HQ is also used as a skin-lightening agent, and some cosmetics with an excess of content over 10% are marketed in Japan. Health risks in general population may be of concern due to highly absorbed HQ via dermal exposure. Carcinogenicity of HQ was suggested from previous studies in which HQ induced hepatocellular ademonomas and forestomach hyperplasias in mice and renal tubular cell adenomas in male rats. In genotoxicity tests, positive results in chromosomal aberration tests and micronuclei tests both *in vivo* and *in vitro* were reported, whereas most reported results in Ames tests were negative except in a few studies.
In this study, the *lacZ* transgenic mouse (Muta™ Mouse) model was used to clarify whether mutagenic mechanisms are involved in HQ-induced carcinogenesis in according to the OECD guideline 488. Male Muta™ mice were subjected to repeated oral administration of HQ at dosages of 0, 50, 100, or 200 mg/kg/day for 28 days. High dose was set based on the result of the NTP fourteen day gavage study using B6C3F1 mice in which HQ related death was observed in males receiving 250 mg/kg/day. Body weight was not affected by HQ administration up to 200 mg/kg/day. Mutant frequency in the liver and stomach of HQ treated mice were not significantly different from the negative control. *N*-Ethyl-*N*-nitrosourea, used as a positive control, induced mutation at a frequency 2-fold higher in the liver and 11-fold higher in the stomach than in their respective negative control organs. These results suggest that the mutagenic mechanism is not responsible for carcinogenesis of HQ.

PS 461 Oligoquat M Does Not Induce Mutagenesis and Chromosome Aberration in the V79 and CHL Cell Lines

Z. Lu[1, 2], J. Liang[1] and M. Wang[1]. [1]*The Institute of Toxicological and Functional Evaluation, Jiangsu Provincial Center for Disease Control and Prevention, Nanjing, China and* [2]*Basic Medical Sciences, University of Arizona Medical College-Phoenix, Phoenix, AZ.* Sponsor: S. Qiu.

Oligoquat M is a novel cationic moisturizing polymer derived from sugar cane with the active ingredient being stearyl dihydroxypropyldimonium oligosaccharides. Oligoquat M is used as a personal hygiene product and therefore warrants a detailed assessment of its safety, including mutagenesis potential. In this study, the toxicity of the Oligoquat M to the Chinese hamster lung cells (V79 and CHL) was tested in the presence and absence of the metabolic system (S9), and the V79 HGPRT gene mutation and the CHL chromosome aberration induced by Oligoquat M were tested. We found that the half of the growth inhibitory concentration (IC50) was 209μg/mL to the CHL cell. The number of resulting mutant clones from V79 cells treated by the dose levels of 75, 150 and 300μg/mL were similar to those of the negative control (P>0.05); in contrast, the cell mutation frequency (MF) of positive control was 49.4/10E6 and 63.0/10E6 for EMS and MCA, respectively, which was greater than 3 times of the negative control group (4.4/10E6 and 3.5/10E6 with or without S9, respectively). In the dose level of 50, 100 and 200μg/mL, the incidence of the chromosome aberration of CHL cells were less than 4% in the presence and absence of S9, and showed no clear dose-response relationships. We can conclude that Oligoquat M has no significant mutagenic and chromosome aberration effects in V79 and CHL cells under this laboratory conditions.
KEYWORDS: Oligoquat M; HGPRT locus; Gene mutation; Chromosome aberration

PS 462 Assessment of Genotoxicity and Antigenotoxicity of Ethanolic Extract of *Spondias mombin* L. (Anacardiaceae) Leaves in *In Vitro* and *In Vivo* Models

O. E. Ola-Davies[1], J. E. Mata[2], A. O. Adeogun[3] and O. S. Olawuwo[1]. [1]*Department of Veterinary Physiology, Biochemistry and Pharmacology, University of Ibadan, Ibadan, Oyo, Nigeria,* [2]*Department of Basic Medical Sciences, College of Osteopathic Medicine of the Pacific, Western University of Health Science, Lebanon, OR and* [3]*Department of Zoology, University of Ibadan, Ibadan, Oyo, Nigeria.*

Spondias mombin, a medicinal plant found in Nigeria contains high amounts of phenolic compounds with antioxidant activity. The ethanolic extract of the leaves was evaluated for its safety and beneficial effects using genotoxicity and toxicity tests. None of the plant fractions had detectable mutagenic activity. The *S. mombin* fractions were not only non-mutagenic in *Salmonella typhimurium* strains TA98 in the presence and absence of metabolic activation, but also exhibited antimutagenic activities against 2 – amino – 3 methyl – 3H – Imidazo(4, 5 - F) quinoline (IQ) - induced mutagenesis.
Phytochemical screening of *S. mombin* extract revealed the presence of alkaloids, tannins, saponins, phlobatanins, flavonoids and anthraquinones. The administration of *S. mombin* at concentration of up to 8,000 mg/kg body weight did not induce acute toxicity in rats. A bone marrow micronucleus test was performed to detect clastogenicity and anticlastogenicity. The extract in the dose of 2,000 mg/kg did not cause micronucleus formation in the bone marrow of rats. Furthermore, in rats administered 50–100 mg/kg of the extract, no anticlastogenicity effect against sodium arsenite induced micronucleus formation was observed. These studies provide data concerning the safety and antimutagenic potency of an ethanolic extract of *Spondias mombin* leaves.

PS 463 Detection of Sulfur Mustard-Induced DNA Adducts in Human Skin Cells with Laser Scanning Microscopy

K. Kehe[1], S. Müller[2], D. Steinritz[2] and H. Thiermann[2]. [1]*E - Research and Development, Bundeswehr Medical Academy, München, Germany and* [2]*Bundeswehr Institute of Pharmacology and Toxicology, Munich, Germany.*

Introduction: Sulfur mustard (SM) and 2-chloroethyl ethylsulfide (CEES) are bi- and monofunctional DNA alkylating agents, respectively. SM is an old chemical warfare agent causing blisters (vesicant). Both chemicals react with N7 guanine. SM will form 7-Hydroxyethylthioethylguanine for SM. A specific monoclonal antibody (2F8) exists which detects SM at N7 position.
Aim: The 2F8 antibody was used to develop a microscopique technique for detection of SM exposure in human keratinocytes (HaCaT cells).
Methods: HaCaT cells were cultured on cover slips and exposed with different concentrations of SM (30 min). After exposure, cells were fixed and treated with Proteinase K. Subsequently, the preparation was treated with the monoclonal 2F8-antibody against the N7- guanine monoadduct. Next, the antibody molecules attached to the DNA damage were made visualized by binding to a goat-anti-mouse antibody that contains covalently a fluorescent group emitting red light to bind to them. The preparation was also treated with DAPI to counterstain cell nuclei. By means of laser scanning microscopy, red fluorescence was quantified. Results: DNA adducts were concentration dependent detected after SM exposure below 30 μM which is the vesicant threshold.
Conclusion: The presented technique is potentially able to detect and quantify SM exposure in HaCaT cells in vitro. The technique may be useful to confirm SM exposure in blister roofs of intoxicated patients.

PS 464 Response of Human Peripheral Blood Lymphocytes to Model Clastogens and Aneugens in an *In Vitro* Micronucleus Test

N. N. Patel[1], R. M. Nagane[1], J. R. Rana[1], K. R. Nikam[1], S. S. Gaikwad[1] and V. J. Piccirillo[2]. [1]*Toxicology, Jai Research Foundation, Vapi, Gujrat, India and* [2]*VJP Consulting, Inc., Ashburn, VA.*

The *in vitro* micronucleus assay has been gaining considerable popularity in recent years as a preferred assay for evaluating cytogenetic effects. This study was undertaken to evaluate the response of human peripheral blood lymphocytes after exposure to reference chemicals, in the absence and presence of S9 using the cytochalasin-B cytokinesis block method. Forty-four hours after phytohaemagglutinin stimulation, the cells were exposed for 3.5h to NaCl, pyrene, nalidixic acid, di(2-ethylhexyl)phthalate, mitomycin-C, cyclophosphamide, benzo(a)pyrene, vinblastine, colchicine and cytosine arabinoside. The cells were harvested following a 24h recovery period. Vinblastine and mitomycin-C were additionally tested with 28h continuous treatment. MN frequencies were determined in 2000 binuclear lymphocytes/concentration and cytotoxicity was estimated based on replicative index. Results showed that these clastogens and aneugens caused dose dependent, biologically relevant and statistically significant increases in micronuclei with frequencies ranging from 1.9-7.1% (cytostasis ≤55%). On the other hand, the negative control chemicals had MN frequencies ranging from 0.1-0.7% which were not significantly different from solvent controls. In order to obtain optimal contrast between nuclei and cytoplasm, a staining time of 30 min. using Giemsa stain was found to be appropriate versus recommendations of 5-15 minutes in publications. Some authors have recommended air drying the slides but precipitation was observed after air drying, which also caused alteration in cellular and nuclear morphology and made it difficult to analyze the cells. Use of a slide warmer to dry the slides at 50±5 °C resolved this problem. Careful titration of concentrations spacing was found to be necessary in order to elicit a positive response with colchicine. In summary, the reference chemicals examined elicited the expected responses in primary cultures of human peripheral blood lymphocytes demonstrating the portability of the assay.

PS 465 Strategies and Endpoints in the Detection of Weak Genotoxins: Opportunities and Challenges

G. Jena. *Department of Pharmacology & Toxicology, National Institute of Pharmaceutical Education and Research (NIPER), Mohali, Punjab, India.*

Chemical mutagens which induce weak/equivocal responses are difficult to reproduce and assess the biological relevance. The lists of such chemicals are increasing and the recommendations from the latest OECD guidelines and reports from the International Workshops on Genotoxicity Testing (IWGT) have been considered. Improvement in the detection limit and the sensitivity of genotoxicity assays are required, as the standard test battery concept fails to detect some non-genotoxic carcinogens and marginal genotoxins. Previously, we have reported that prior bleeding increases the sensitivity of micronucleus (MN) assay in juvenile rats. Further, more work is carried out to improve the sensitivity of genotoxicity assays, which includes erythropoietin in combination with prior bleeding and inhibiting the histone deacetylases (HDAC) with sodium valproate in rodent models. One of the mechanisms involved in the detection of weak genotoxins depends on the DNA repair efficiency of the cell under investigation. Further, an attempt has been made to enhances the detection limit, to facilitate the screening of weak genotoxins in the presence of 3-aminobenzamide (3-AB), a Poly (ADP-ribose) polymerase inhibitor in mice. Results demonstrate that 3-AB increases the genotoxicity of several chemicals, but its effect was more pertinent on weak genotoxins, however, 3-AB per se did not show any genotoxicity. This approach may be applied to the evaluation of genotoxicity of marginal/weak clastogens as well as chemical producing short- lived reactive metabolites. Collectively, each model has to be carefully validated and the results should be critically evaluated to avoid any false positives and false negatives in the risk assessment process.

PS 466 Investigation of the Genotoxic and Cytotoxic Activities of the LLL-3, a STAT3 Inhibitor, Using Micronucleus and WST Assays

E. A. Ferraz, A. S. Fernandes, I. Felzenszwalb and A. Mencalha. *Department of Biophysics and Biometry, State University of Rio de Janeiro, Rio de Janeiro, Brazil.*
Sponsor: D. Oliveira.

Introduction: LLL-3, an anthracene derived compound, has been shown to be a promising therapeutic agent in the treatment of some kinds of cancer such as chronic myeloid leukemia. This compound is derived from the commercial product STA21 and acts by inhibiting the STAT3, which has been associated with the induction of proliferation and survival of cancer cells. Although LLL-3 has presented good properties to be a potential therapeutic agent in the treatment of some types of cancer, there is no data in the literature about the toxic properties of this compound.
Objective: To investigate the genotoxic and cytotoxic activities of the LLL3 by Micronucleus (MN) and WST assays, using mouse macrophage cell line RAW 264.7.
Material and Methods: MN assay was performed according to Hori et al. (2006) with some modifications. Briefly, 2 x 105 of RAW 264.7 cells were exposed to LLL-3 for 3 hours, fixed in petri dishes and stained with DAPI. To determine the mitotic index and the number of cells with micronuclei, 3000 cells/concentration were analyzed under a fluorescence microscope. In WST assay, the cells were exposed to LLL-3 for 3 hours, it was added WST dye and the absorbance was measured in 450 nm.
Results and Discussion: LLL-3 did not induce genotoxicity in RAW 264.7 cells, moreover, it was no observed apoptosis or necrosis cell death in these cells, although the mitotic index decreased after exposure in the same tested conditions, which may suggest some cytostatic effect, since this compound acts by inhibiting the STAT3. Besides, the cell viability evaluated by WST assay was not affected by LLL-3. Once LLL-3 did not show mutagenic activity as most of other drugs used in cancer treatment, our results increase the chance of using this drug in cancer therapy.
Conclusion: LLL-3 should be of interest to further explore the possibility of using it as a potential agent for human cancer treatment.
Acknowledgements: FAPERJ and CNPq.

PS 467 Genotoxicity Assessment of Sandalwood (*Santalum album*) Essential Oil on Human Breast Adenocarcinoma Cells (MCF-7)

C. M. Ortiz-Sanchez[1], L. Morales[1], M. Sastre[2], A. Castro[3] and J. L. Matta[1]. [1]*Physiology, Pharmacology and Toxicology, Ponce School of Medicine and Health Sciences, Guayama, Puerto Rico,* [2]*Biology, University of Puerto Rico, Humacao, Puerto Rico and* [3]*Microbiology, University of Puerto Rico, Humacao, Puerto Rico.*

Sandalwood essential oil (SEO) is extracted from *Santalum album* trees that grow in Malaysia, Australia, and India. Its main constituents are (Z)-α-santalol and (Z)-β-santalol which are responsible of its woody odor. SEO is used in food industry as a flavoring ingredient with a daily consumption of 0.0074 mg/kg. It is also used in perfumery and other cosmetic products. Recently, there has been an increased interest regarding the pharmacological properties of EOs. SEO has antiviral and antimicrobial properties. However, its genotoxic effect on human cells is largely unknown. The main objective of this study was to assess the genotoxic effects of SEO on human adenocarcinoma and mammary epithelial cell lines (MCF-7 and MCF-10A). Cells were exposed to SEO in a concentration range from 8 – 160 μg/mL for 24 hours. Cell proliferation was determined by the tetrazolium salt (MTT) assay while genotoxicity assessment was performed using the alkaline comet assay. Cells were visually scored according to tail length into four classes: (1) class 1: undamaged, no tail, (2) class 2: tail shorter than diameter of the head (nucleus), (3) class 3: tail as long as 1–2x the diameter of the head, and (4) class 4: tail longer than 2x the diameter of the head. Our results show that as concentration of SEO is increased, there is a reduction in class 1 comets; therefore, increasing the appearance of class 2 and 3 comets in MCF-7 cells. These results lead us to conclude that SEO is capable of inducing DNA double strand breaks on this cell type. However, this genotoxic effect was not seen in the normal human breast cell line, MCF-10A. These results provide the first evidence that SEO may be genotoxic to MCF-7 breast cancer cells.
Research supported by: RISE grant R25GM082406 from the National Institutes of Health, 1CSA157250, 9SC1CA182846-04, and the Molecular Biology Core Lab (Grant RR003050/MD007579).

PS 467a *In Vivo* Genotoxicity Study of Estragole and Safrole

W. Ding[1], D. D. Levy[2], M. E. Bishop[1], M. G. Pearce[1], K. J. Davis[3], A. M. Jeffrey[4], J. Duan[4], G. M. Williams[4], G. A. White[3], L. E. Lyn-Cook[1] and M. G. Manjanatha[1]. [1]*Division of Genetic and Molecular Toxicology, FDA/NCTR, Jefferson, AR,* [2]*FDA/CFSAN, College Park, MD,* [3]*Toxicologic Pathology Associates, FDA/NCTR, Jefferson, AR and* [4]*New York Medical College, Valhalla, NY.*

Estragole and safrole, naturally-occurring constituents of various herbs and spices, are rodent liver carcinogens. To further understand the mechanisms underlying their carcinogenicity, genotoxicity was measured in rats using Comet, 32P-postlabeling DNA adduct and micronucleus assays, combined with histopathological analysis. Oxidative damage was measured using human 8-oxoguanine-DNA-N-glycosylase (hOGG1) and Endonuclease III (EndoIII)-modified Comet assays. Groups of 5 seven-week old male F344 rats were administered corn oil or with various doses of estragole or safrole in corn oil by oral gavage at 0, 24, and 45 hr and were sacrificed at 48 hr. Estragole induced a dose-dependent increases in DNA strand breaks, DNA adducts, and oxidative DNA damage in the liver, the cancer target organ. DNA strand breaks were not detected in kidney, stomach or bone marrow, non-target tissues for cancer. Peripheral blood micronuclei were observed at the highest dose in estragole treated animals. Safrole also induced dose-dependent increases in DNA strand breaks and oxidative DNA damage in the liver. No DNA damage was detected in kidney, stomach or bone marrow nor was micronuclei elevated in peripheral blood in safrole treated animals. Evidence of inflammation, single-cell necrosis, and cell proliferation were found in estragole but not safrole-treated rat livers. Taken together, these results imply mixed genotoxic mechanisms. The direct genotoxic effects, indicated by DNA strand breaks and DNA adducts, are associated with the generation of initiated cells; while an indirect genotoxic effect, involving oxidative stress, accompanied by inflammation and cell proliferation, could be associated with tumor development.

PS 467b Evaluation of Mutagenicity of Vinyl Acetate and Acetaldehyde in *Gpt* Delta Mouse Lung Fibroblast Cell Line, GDL-1

M. G. Manjanatha[1], S. D. Shelton[1], Y. Chen[1], R. A. Mittelstaedt[1], R. Budinsky[2], R. J. Fensterheim[3], B. Gollapudi[4], L. T. Haber[5], R. Valentine[7], M. S. Stavanja[6], E. Rushton[8], J. Piper[6], T. S. Lardie[2], R. J. Albertini[9] and M. M. Moore[10]. [1]*Genetic and Molecular Toxicology, FDA/NCTR, Jefferson, AR,* [2]*The Dow Chemical Co, Midland, MI,* [3]*RegNet Environmental Services, Washington, DC,* [4]*Center of Toxicology and Mechanistic Biology, Exponent, Midland, MI,* [5]*Toxicology Excellence for Risk Assessment, Cincinnati, OH,* [6]*Celanese International Corporation, Dallas, TX,* [7]*Health and Environmental Sciences, DuPont Haskell Global Centers, Newark, DE,* [8]*LyondellBasell Co, Houston, TX,* [9]*The University of Vermont, Burlington, VT and* [10]*ENVIRON International Corporation, Little Rock, AR.*

Vinyl acetate monomer (VAM) induces nasal tumors in rats and oropharyngeal tumors in rats and mice. VAM is weakly genotoxic in vitro and non genotoxic in vivo. A critical key event in VAM's rodent carcinogenicity is its carboxylesterase-dependent hydrolysis to acetaldehyde (AA), a genotoxic metabolite. The mutagenicity of VAM and AA was evaluated in a newly established *gpt* delta mouse lung fibroblast cell line (GDL1) harboring two reporter genes, *gpt* and *red/gam* (Spi^-) employing either horse serum (HS) or fetal bovine serum (FBS) since HS was shown to rapidly metabolize VAM to AA. GDL1cells were exposed to VAM and AA at concentrations ranging from 0.5 mM to 10 mM for 24 hr. Cells were washed and further cultured for 6 days for mutation fixation. Cytotoxicity was measured by relative cell count and ethylnitrosourea and mitomycin C were used as positive controls. VAM was also tested for micronuclei (MN) induction in GDL cells. VAM and AA were not mutagenic at the Spi^- locus which detects large deletion mutations in GDL cells. In contrast, VAM induced a dose-dependent increase in the MN frequency which was higher in the HS than in FBS. Apparent increases in the MFs at the *gpt* locus were observed with doses up to 5 mM of VAM and AA with cytotoxicity ranging up to 70% whereas the higher doses induced severe cytotoxicity reaching 95%. These results suggest that the Spi^- assay may not be as sensitive as the MN assay for detecting VAM-induced genotoxicity.

PS 467c Effects of Ethyl Methanesulfonate on DNA Damage of Uterine Mucosa in Rats

R. Tanaka, S. Masumori, M. Ueda, M. Fukumuro, S. Tanaka, A. Shiga, F. Mizuhashi and M. Hayashi. *Biosafety Research Center (BSRC), Iwata, Shizuoka, Japan.*

It is known that the DNA damage in the multiple organs can be detected by the in vivo comet assay. However, this assay that uses the uterus as a target organ is hardly known. The in vivo comet assay was examined by using ethyl methanesulfonate (EMS) whether there was a difference in DNA damage in the uterine mucosa when dosed in each stage of the estrous cycle. EMS was administered orally to female rats at a single daily dose of 200 or 300 mg/kg for 2 days. The 10 weeks old female rat when the estrous cycle was steady was used. At 3 hours after the final dosing, the uterus was removed, and specimens were prepared. The % tail DNA, an indicator of DNA damage, was determined. As a result, DNA damage was observed dose-relatedly in the EMS dosing group compared with the negative control (distilled water) group. The influence by the difference at the estrous cycle was not admitted in the negative control group and EMS dosing group.

PS 467d *In Vitro* Toxicity Testing of 2, 4, 6-Trinitrotoluene (TNT) Contaminated Soil

L. K. Markell[1], M. P. Mawn[2], C. E. Pooler[3], A. Myhre[1], P. Bloxham[2], A. Faranda[1], E. M. Donner[1], X. Han[1] and T. S. Bingman[4]. *[1]DuPont Haskell Laboratories, Newark, DE, [2]DuPont Corporate Center for Analytical Sciences, Newark, DE, [3]URS Corporation, Louisville, KY and [4]DuPont Corporate Remediation Group, Wilmington, DE.*

Remediation of 2,4,6-trinitrotoluene (TNT) contaminated soil at explosive manufacturing sites may use approaches for monitoring the remediation progress. Previous studies have identified TNT as a mutagen and extracts from TNT contaminated soil show mutagenicity in a number of in vitro assays. The purpose of this study was to demonstrate proof-of-concept for in vitro mutagenicity testing of contaminated soil, which may be used to validate the effect of future remediation processes. Here, we use an extraction procedure based on the EPA 8330B method, which includes the use of a ring and puck mill to homogenize the soil, incremental sampling and subsampling and LC/UV analysis. Acetonitrile extracts from soil contaminated with TNT and soil determined to be free of TNT, as well as a TNT standard were tested in a Reverse Bacterial Mutation (Ames) assay. *Salmonella typhimurium* strains TA98, TA100, TA1535, and TA1537 and the *Escherichia coli* WP2uvrA strain with and without Aroclor 1254 induced rat liver S9 metabolic activation were used. Results from soil extracts absent of TNT yielded no mutagenicity. As expected, treatment with the TNT standard yielded a positive response with 4 strains (TA98, TA100, TA1537, WP2uvrA) and a dose response trend with TA1535. A similar mutagenicity profile was observed with extracts from soil contaminated with TNT, indicating that the extraction procedure and Ames assay are appropriate methods. The addition of the S9 fraction reduced the number of bacterial revertants, demonstrating that metabolism reduces mutagenic potential of TNT. Yet, it is possible that other unidentified contaminants in the soil may be contributing to the Ames results. This study verifies the methodology used for in vitro mutagenicity testing of soil contaminated with TNT and demonstrates a simple and inexpensive technique by which effective hazard reduction may be demonstrated following remediation.

PS 467e Evaluation of Genotoxicity of 6-Diazo-5-Oxo-L-Norleucine (DON)

R. Kulkarni[1], E. W. Dakoulas[1], K. E. Miller[2] and P. S. Terse[3]. *[1]BioReliance, Rockville, MD, [2]Kemmx Corporation, Sapulpa, OK and [3]National Center for Advancing Translational Sciences, NIH, Bethesda, MD.*

6-Diazo-5-oxo-L-norleucine (DON), a glutamine antagonist, was isolated originally from Streptomyces in a sample of Peruvian soil and was demonstrated to exhibit analgesic and anticancer properties. The current study was performed to characterize its in vitro and in vivo genotoxic potential. DON was tested in the Bacterial Reverse Mutation Assay (Ames test) for its mutagenic potential using *Salmonella typhimurium* tester strains TA98, TA100, TA1535 and TA1537 and *Escherichia coli* tester strain WP2 uvrA with and without S9 and also with reductive S9. DON was tested for the chromosome aberrations in Chinese Hamster Ovary (CHO) cells with or without S9 to evaluate the clastogenic potential of the test article. DON was also evaluated for its clastogenic activity and/or disruption of the mitotic apparatus by detecting micronuclei in polychromatic erythrocyte (PCE) cells in mouse bone marrow. In the mutagenicity assay using the plate incorporation method with and without S9 and using the preincubation method with uninduced hamster liver S9, no positive mutagenic responses were observed. In the in vitro chromosome aberration assay, dose dependent statistically positive increase in structural aberrations was observed at 4 and 20 hour exposure without S9 and also at 4 hour exposure with S9. In the in vivo micronucleus assay, bone marrow was collected from the male mice dosed intravenous with 100, 10, 1 and 0.1 mg/kg at 24 and 48 hour post dose. Three animals dosed with 500 mg/kg were also analyzed 24 hours post injection for micronucleus induction. A statistically positive response for micronucleus formation was observed at 500, 100 and 10 mg/kg at 24 and 48 hour post exposure. Thus, DON appears to be negative in the Ames test but positive in the in vitro chromosome aberration assay and in the in vivo micronucleus assay. In conclusion, the results indicate DON is a potential genotoxic compound with a plausible epigenetic mechanism of action. (Supported by NCI-SAIC Contract No. HHSN261200800001E and NIAMS under BrIDGs Program).

PS 467f Ames Bacterial Mutation Test—Comparative Sensitivity of Standard and Micro Formats

R. Proudlock, K. Evans and J. Rundell. *Moltox, (Molecular Toxicology Inc.), Boone, NC.*

The Ames test is the most widely used genotoxicity assay and is a regulatory requirement for almost all new chemicals that enter the environment. Because of its importance as an early predictor of carcinogenicity, a screening version using modifications to reduce compound requirement is often employed at an early stage of compound development. The 24-well plate micro screen (μAmes) employs virtually the same methods as the standard test but uses 95% less compound while reducing labor costs significantly. Since the methodology is so similar to the standard Ames test it should, theoretically, be highly predictive of the eventual full-scale GLP assay and allow extrapolation from one version to the other. One important question that remains largely unanswered for this and other screening versions of the test is 'How do the two methods compare in terms of sensitivity?' We have determined the lower limit of sensitivity of the two formats using a wide range of 40 mutagens with different physical and chemical characteristics to provide an objective and quantitative answer to this question. The 40 compounds include those recommended as standard positive controls by OECD, compounds in the NTP database and diagnostic mutagens recommended by Ames and others.
The reduced culture volume in the μAmes theoretically reduces the sensitivity of the method; this is compensated for by increasing the number of replicate control cultures, resulting in improved reliability and reduced variability of the estimate of the background mutation rate. The μAmes test gives almost identical results to the standard assay while using 5 to 10 times less test material. In summary, the μAmes appears highly predictive of the standard Ames, at least for potent mutagens, while being less labor-intensive and using much less material. We are extending this validation of the μAmes using compounds which are only weakly active in the Ames test to elucidate possible limitations of the screening method.

PS 467g Development of a High-Throughput Homogenous Assay to Detect DNA Double-Strand Breaks

B. Goodwin[1], T. Khuc[1], R. Huang[1], K. L. Witt[2], R. R. Tice[2] and M. Xia[1]. *[1]Division of Preclinical Innovation, NCATS, Rockville, MD and [2]Division of the National Toxicology Program, NIEHS, Research Triangle Park, NC.*

Identification of compounds with the potential to induce DNA damage is an important component of the chemical safety evaluation process. The most deleterious DNA lesions are DNA double strand breaks (DSBs), which, if unrepaired, can lead to cell death or mutations leading to cancer. Following DSBs, the histone H2A variant, H2AX, is rapidly phosphorylated at serine-139 by ataxia telangiectasia mutated (ATM) kinases and accumulates in foci at the sites of damage in the nucleus. A homogenous assay was developed in a high throughput screening format for detecting phosphorylated H2AX (γH2AX) using homogenous time resolved FRET (HTRF) technology. To optimize the assay condition, the best pair of antibodies for detecting γH2AX-responsive DNA damage was identified after testing multiple antibodies labeled with donor and acceptor fluors. Following treatment with compounds for one hour, the cells are lysed, and an anti-γH2AX antibody labeled with the donor fluor, Europium cryptate, and an anti-H2AX antibody labeled with the acceptor fluor, d2, are combined and added to the cell lysate. In the presence of phosphorylated H2AX, the donor fluor transfers energy to the acceptor fluor, which emits at 665 nm. Signal is detected as the ratio of 665 nm:615 nm on an Envision plate reader. Using camptothecin, this assay was optimized in CHO-K1 and HepG2 cells, with good performance (e.g., signal to background of 3.5 fold, coefficients of variation of <5%, Z' factor of 0.7). This assay was further validated by screening the 1280 compounds in the Library of Pharmacologically Active Compounds in both cell lines; the resulting hit rate was 2.0% for CHO-K1

and 0.6% for HepG2. All known genotoxicants including etoposide, mitomycin C, and gemcitabine the library were active in CHO-K1 cells. Therefore, this assay has been selected for screening the Tox21 10K compound library using CHO-K1 cells as part of Tox21 screening program.

PS 467h Cytotoxicity and Genotoxicity Assays for Assessing the Toxicity of the Reactive Black 5 Dye

G. A. Oliveira[1], E. S. Paula[2], D. M. Leme[2], A. Sehr[3], T. Grummt[3] and D. P. Oliveira[2]. *[1]Faculdade de Farmácia, Universidade Federal de Goiás - FF/UFG, Goiânia, Goiás, Brazil, [2]Departamento de Análises Clínicas, Toxicológicas e Bromatolóicas, Universidade de São Paulo - FCFRP/USP, Ribeirão Preto, São Paulo, Brazil and [3]Umweltbundesamt, Bad Elster, Germany.*

Introduction: The textile industry plays a key role among the main economic activities of Brazil. However, during textile processing, inefficiencies in dyeing result in large amounts of dyes that are directly discharged into water bodies, contaminating the environment and endangering human health. The amount of dye that is lost during the dyeing processes depends on the class of dye used, which may vary from 2% to 50% for basic and reactive dyes, respectively. Reactive Black 5 (RB5) is an azo compound, commonly used in textile industry. Cytotoxicity and genotoxicity assays are crucial tools for predicting both human and environmental health risks. Objective: Evaluate the cytotoxicity and genotoxicity of the RB5 dye. Methodology: Cultures of HepG2 cells were exposed to RB5 dye at concentrations ranging from 1.5 to 500 μg/mL and cytotoxicity was evaluated after 4, 24 and 48 hours using the MTT test. Analysis of micronucleus (MN) in HepG2 cells was performed by flow cytometry-based in vitro MN assay (In Vitro MicroFlow® Kit) and 2-fold over concurrent solvent control mean were used to define the positive results. Results: RB5 dye showed cytotoxic effect in a dose- and time-dependent manner ($p<0.05$) and a significant increase of MN frequencies was produced by the dye at 50 and 100 μg/mL. Discussion: Overall, our data indicate that RB5 dye is cytotoxic and genotoxic to human hepatocarcinoma cell line. Conclusion: The use of these bioassays showed to be an efficient approach for the initial screening of different dyes and dye containing effluents, in order to establish toxicological information about textile dyes, avoiding damages on humans and to the aquatic environment.
Acknowledgments: FCFRP/USP

PS 468 Continuous, Telemetric Blood Pressure Measurement in Conscious, Freely Moving Cynomolgus Monkeys following Oral Etilefrine Administration Using Different Technologies (JET-BP and Physiotel Digital)

M. Niehoff[1], D. Staub[1], B. Niggemann[1], M. Foley[2], J. Saul[3] and M. Holbrook[3]. *[1]Covance Laboratories GmbH, Muenster, Germany, [2]Covance Laboratories Inc., Madison, WI and [3]Covance Laboratories Ltd., Harrogate, United Kingdom.* Sponsor: G. Weinbauer.

The determination of adverse cardiovascular events in non-clinical studies is a pivotal requirement in drug development. Compound attrition due to adverse cardiovascular side effects occurs rarely in phase I clinical trials, but the frequency increases in phase II and III, suggesting that measurement of cardiovascular endpoints and decision making in non-clinical studies requires improvement. In this project, we compared different technologies (Physiotel digital and JET-BP) and dosing regimens (Latin square cross-over and parallel design) for cardiovascular assessment using a positive control, etilefrine (a sympathomimetic that directly stimulates adrenergic receptors to induce hypertension). In the first model, etilefrine was administered orally (0, 2, 5 and 10 mg/kg) in a Latin square design to 4 male animals pre-implanted with an L21 full implant and systemic blood pressure measured using Physiotel™ digital system. A slight (2 mg/kg) to marked (5 and 10 mg/kg) increase in mean, systolic, diastolic blood pressure and pulse pressure for up to 2 hours (2 mg/kg) or 5 (5 and 10 mg/kg) hours post dose was measured. In our second model, etilefrine was administered at 0, 1, or 10 mg/kg on 3 occasions [days 1, 8, and 15] to 12 female animals (4/group) and blood pressure measured using JET-BP technology. Systolic blood pressure was slightly increased at 1 mg/kg and markedly increased at 10 mg/kg. The magnitude of change for systolic pressure was higher using Physiotel digital and the Latin square design with a maximal increase of 10 (2 mg/kg), 20 (5 mg/kg), and 40 (10 mg/kg) mmHg and 10 (1 mg/kg) and 25 (10 mg/kg) mmHg using JET-BP and a parallel design. These data indicate that these technologies and study deigns allow good sensitivity for the detection of CV effects.

PS 469 Tethered Subcutaneous Infusion in Telemetry-Instrumented Nonhuman Primates for Cardiovascular Assessment of Short-Half-Life Compounds

K. Rasmussen, N. West, C. Douglas, H. Drey, R. Haas, J. Nelson and A. N. Alexander. *Nonclinical Safety Assessment, Covance Laboratories Inc, Madison, WI.*

Assessing potential cardiovascular (CV) effects of a compound in experimental pharmacology and toxicology studies is critical to understanding the compounds safety profile in humans. Frequently, the half-life of a compound is such that T max occurs shortly after administration; therefore, potential test article related CV findings can be masked by "background noise" associated with animal response to human presence in the animal room for dose administration. For this study we developed a novel approach to subcutaneous infusion in which the telemetry-instrumented cynomolgus monkeys were surgically implanted with subcutaneous catheters in the dorsal region to facilitate remote dose administration. Animals were fitted with an infusion jacket and tether system post surgery and connected to an external syringe infusion pump. Catheter patency was maintained through continuous infusion of 0.9% sodium chloride at a rate of 0.3 mL/hr. During dose administration, two infusion pumps were used per animal. Both pumps were programmed for delayed start, with one pump programmed to deliver the control or test article (known to cause immediate CV effects) over approximately 1 minute and the second pump programmed to deliver a flush to clear the remaining control or test article from the infusion apparatus post-dose administration. Animals exhibited minimal signs of discomfort during dose administration. Statistical analysis of cardiovascular data (hemodynamics) indicated a significant, dose dependent response to compound administration within 5 minutes of the start of infusion. Given the impact of human presence during and after room entry (background noise), using standard subcutaneous dosing procedures would have masked CV responses, and made it difficult to accurately describe the profile and time course of action of the test article. This novel approach to dose administration appears to be a viable option when short half-life and/or human presence–related artifact are considerations for study design.

PS 470 Utilisation of JET-BP (Jacketed External Telemetry with Blood Pressure) for Collection of Cardiovascular Data in the Minipig: Administration of a Positive Control

P. J. Priestley and B. Marshall. *Pharmacology, Covance Laboratories Ltd., Harrogate, North Yorkshire, United Kingdom.* Sponsor: A. Jackson.

JET-BP (DSI) enables continuous collection of cardiovascular data from toxicology study animals for extended periods of time without the need for animal restraint, therefore resulting in the capability to acquire not only an increased quantity of data, but increased quality. The mini-pig, whilst commonly utilised in dermatalogical-related evaluations, is an increasingly popular laboratory species due to anatomical and physiological similarities to humans. Male mini-pigs (purpose bred Gottingen ApS mini-pigs obtained from Ellegaard Gottingen, Denmark) surgically implanted with calibrated sensors (DSI C10 series) for arterial blood pressure (ABP) in conjunction with electrocardiographic (ECG) measurements using jacketed external telemetry (JET) were orally administered Moxifloxacin (fluoroquinolone antibiotic). Data were acquired pre-dose and for up to 24 hours post-dose. Administration of Moxifloxacin at 30, 100 and 300 mg/kg elicited a dose related increase in QTcF of up to 10-20% (300 mg/kg), compared to control (0.5% methylcellulose) treated animals. The increase was evident within the first 2 hours following dose administration and was maintained throughout the majority of the post-dose data collection period. Whilst the intended cardiovascular effect was evident following Moxifloxacin administration, the data highlighted the challenges that are associated with the twice daily feeding required for mini-pigs. Significant changes in cardiovascular parameters are evident around the time of day of the second daily feed (approximately 6 hours post-dose) and although consistent with the effects in the control treated group could potentially be an issue depending on the profile of the compound.
In conclusion, JET-BP is an acceptable method of cardiovascular data collection in mini-pigs. Special considerations, unique to the general care of mini-pigs must be taken into consideration during study design, in relation to the profile of the compound to be administered, in order to avoid mis-interpretation of the data-set.

PS 471 Noninvasive (Jacketed) ECG Monitoring with Telemetry in Beagle Dogs, Göttingen Minipigs, and Cynomolgus Monkeys: Benefits from Multiple Derivations

F. Duguay[1], R. Forster[1], A. Ascah[1], M. Pouliot[1], E. Troncy[2] and S. Authier[1, 2]. [1]*CiToxLAB, Laval, QC, Canada and* [2]*Faculty of Veterinary Medicine, University of Montreal, St-Hyacinthe, QC, Canada.*

Non-invasive telemetry monitoring is widely used to investigate potential ECG effects in toxicology studies. Data quality is one of the most critical success factors when using non-invasive ECG monitoring technologies. Beagle dogs (n=4), Göttingen minipigs (n=4) and cynomolgus monkeys (n=4) were fitted with jackets and undershirts and leads from a telemetry transmitter with 3 bipolar channels were applied using cutaneous adhesive patches. All animals were instrumented to record 3 Einthoven standard ECG derivations (Lead II, V4 and Lead III) throughout the acclimation period and for 24 hours prior to and after dosing with sotalol (PO, 15 mg/kg). Lead II was used for ECG interval analysis while all derivations were used for interpretation when suspected arrhythmias were present. The period of ECG monitoring prior to dosing was used to establish parameters for individual QTc calculations as previously described (Spence et al., Toxicol Sci, 1998, 45(2), 247-58). Evaluation of ECG data revealed that acclimation to experimental procedures varied between animals from 12hrs to 2 days as evidenced by the presence of normal stable circadian cycle for heart rate and values in the normal range from implanted telemetry. As expected, the methodology identified a decrease in heart rate with peak effects at 137 min post sotalol administration. Sotalol also induced a significant increase in QTc in all species (+83 msec, $p<0.01$). The use of 3 derivations was useful for qualitative evaluation ECG tracings in presence of arrhythmia and/or artifacts. Specifically, review of the same ECG complex in various derivations enabled differentiation between true abnormal complexes and electromyographic artifacts. This methodology was useful to investigate potential ECG liabilities in toxicology studies using Beagle dogs, Göttingen minipigs or cynomolgus monkeys for QTc effects but also during critical ECG tracing review for potential arrhythmias.

PS 472 Evaluations for Variance in Jacketed External Telemetry Electrocardiography (JET ECG) Data in Conscious Beagle Dogs and Cynomolgus Monkeys and for Predicting QT Interval Prolongation Using Individual Reference Intervals

T. Yoshikawa, D. Matsushita, T. Hirayama, N. Terashita, K. Hashiguchi, T. Koga, Y. Deguchi, T. Yamamoto, H. Sameshima and R. Nagata. *Shin Nippon Biomedical Laboratories (SNBL), Ltd., Kagoshima, Japan.*

JET is widely used for the evaluation of effects of biologics and anticancer drugs on ECG parameters in general toxicology (TOX) studies under ICH S6 and S9 guidelines, as an alternative to cardiovascular safety pharmacology studies. The purpose of this study was to determine the physiological variance in control ECG data acquired via a JET system from conscious cynomolgus monkeys and beagle dogs and to evaluate drug induced QT interval prolongation using these reference intervals.
JET ECG data from conscious, unrestricted cynomolgus monkeys (272 males and 270 females) and beagle dogs (81 males and 81 females) in TOX studies were used. ECG parameters (PR and QT intervals, QRS duration) and heart rate (HR) were recorded and analyzed by a JET system (Ponemah Physiological Platform, Data Science, Inc.). The overall and individual reference intervals (IRI) were calculated. The ECGs showed wide individual and time variability and clear circadian rhythms of HR and QT in both species. These results suggest that IRI at the point can be used for evaluation of drug effects on ECG parameters in small-scale-design studies, especially preliminary TOX studies. To evaluate the validity of IRI, data on sotalol-induced QT interval prolongation (at 3 and 10 mg/kg, po) in monkeys was analyzed using the IRI. Sotalol at 10 mg/kg statistically significantly prolonged QT interval when compared with the control. Sotalol at 3 mg/kg prolonged QT interval beyond the IRI at some time points after dosing, where there was no statistically significant difference from the control.
IRI analysis is considered helpful for detecting possible adverse effects on cardiovascular systems in TOX studies, especially preliminary study. A combination of statistical comparison between groups (standard method) and IRI analysis enhances the ability to predict toxicity of drug in TOX studies.

PS 473 A Comparison of Cardiovascular Parameters in Beagle Dogs Sourced from Two Different Geographic Regions

L. Qu, S. Mason, S. McPherson and Q. He. *Wuxi AppTec, Suzhou, China.*

Electrocardiography is now one of the standard investigations performed in preclinical toxicology studies. One of the key parameters is the QT interval, as certain types of drugs have the capacity to delay cardiac repolarization, an effect seen in the electrocardiogram traces as a prolongation of the QT interval. Even when this effect is part of the therapeutic mechanism of an anti-arrhythmic drug, excessive QT interval prolongation is also undesirable as this can provoke new arrhythmias (torsades de pointes) and sudden death. The detection of drug induced QT interval changes is sometimes masked by concurrent heart rate changes and therefore it is normalized by means of various formulae (such as Bazetts, Frederica,Van der Waters and Linear regression analysis) into a heart rate independent corrected value known as the QTc interval. The purpose of this publication is to compare the hemodynamic and electrocardiographic parameters from naive telementry-instrumented beagle dogs (*Canis familiaris*) from two suppliers one in the USA and the other in China. The control cardiovascular data for the USA animal were obtained from published data (Soloviev MV, et. al.. 2006). The mean systolic and diastolic pressures for Chinese dogs were 125/69 mmHg and 134/72 mmHg for male and female animals respectively, compared with 142.5 and 84.7 mmHg. The mean heart rate were slightly higher in the Chinese Beagle (126 bpm and 112 bpm for males and females respectively) when compared to the published data for the USA animal of 95.6 bpm. The QT and QTC intervals for the Chinese beagle were, 198 ms and 241 ms for males and, 209 ms and 246 ms for females respectively, compared with the published values of 217 ms and 245 ms. respectively In conclusion the the cardiovascular parameters collected from beagles sourced in China were essentially similar to those reported for USA sourced animals.

PS 474 Assessment of ECG and Hemodynamic Changes in Nonhuman Primates Given Four Reference Compounds in Pen or Individual Housing

L. Kreckler, J. Grosh, J. Schneider and M. Foley. *Nonclinical Safety Assessment, Covance Inc, Madison, WI.*

An evaluation of the effect of a compound on the cardiovascular (CV) system is a critical part of safety assessment and can be achieved in general toxicology studies using jacketed external telemetry (JET) with an implanted telemetry blood pressure (BP) transmitter. We assessed CV changes using JET-BP in nonhuman primates (NHPs) in response to administration of four different reference compounds under two different housing conditions, pen and individual housing. Thirty-six male NHPs group-housed in pen-style caging (three animals/pen) were dosed with etilefrine (sympathomimetic; 1 or 10 mg/kg), hydralazine (vasodilator; 1 or 10 mg/kg), sotalol (nonspecific β-blocker; 3 or 30 mg/kg), or moxifloxacin (antibiotic known to prolong QT; 10, 50, or 175 mg/kg). Following the last dose, animals were transferred to individual housing, allowed to acclimate, and the same dosing regimen was repeated except that hydralazine was given at 10 or 30 mg/kg. Continuous JET-BP measurements were recorded for at least 90 minutes prior to dosing through 20 hours postdose. Electrocardiographic (ECG) parameters of PR, QT, and rate-corrected QT interval and hemodynamic parameters of systolic, diastolic, and mean arterial pressure; heart rate; and arterial pulse pressure were determined. Etilefrine at 10 mg/kg increased systolic and pulse pressure at a similar magnitude in both housing conditions. Hydralazine did not decrease BP at 10 mg/kg (pen and individual housing) or 30 mg/kg (individual only). Sotalol and moxifloxacin significantly prolonged QT with no change in BP, and changes were of similar magnitude under both housing conditions. Finally, hemodynamic parameters of control animals when housed in pen or individual housing were compared. Systolic, diastolic, and mean arterial pressure and heart rate were slightly lower when animals were housed in pens than when housed individually. In summary, ECG and BP changes caused by four different reference compounds were detectable using JET-BP technology in NHPs under two different housing conditions.

PS 475 Potential Advantages for Combining Gender for the Assessment of Cardiovascular Effects: A Case Study with Three Positive Control Articles

J. J. Kremer[1], H. Chen[2], A. J. Bills[1], N. Hanke[1], M. Foley[1] and M. Osinski[1]. [1]*Covance Laboratories Inc., Madison, WI and* [2]*Covance Laboratories Inc., Chantilly, VA.*

Nonclinical safety studies are increasingly incorporating cardiac safety endpoints into toxicology studies, either as a supplement or replacement for traditional standalone safety pharmacology studies. One liability to this approach is the reduction in sensitivity to detect test article-related changes due to the study design (e.g. cross-

over versus parallel), room environment, telemetry technology, etc. One potential strategy to boost statistical power is to increase group size by combining CV data across gender.
Methods: Thirty-six male and female beagle dogs (n=6/sex/group) were outfitted with jacketed external telemetry and an implanted miniature blood pressure transmitter (JET-BP) and administered control (RO water, all days) or etilefrine (1,10 mg/kg, day 1), sotalol (3,30 mg/kg, day 8), and hydralazine (1,10 mg/kg, day 15). Telemetry data were collected pre-dose and up to 20 hours post-dose. Test article exposure for each positive control article was confirmed at 7 hours post-dose.
Results: Prior to combining the CV data across sex, it was confirmed that the test article exposure and pharmacodynamic responses (e.g. changes in ECG or hemodynamic data) were consistent across males and females. Exposure levels were dose-dependent and were within 41% (etilefrine), 6% (sotalol), or 14% (hydralazine) when comparing males and females. When genders were combined, additional statistically-significant changes were noted as compared to when genders were analyzed separately. Increased sensitivity was confirmed by retrospective power analysis of genders separately or combined, respectively, that had minimum detectable differences of 16 or 12 msec (QTci interval), 11 or 9 mmHg (systolic pressure), 10 or 7 mmHg (diastolic pressure), and 11 or 8 bpm (heart rate).
Discussion: This case study demonstrates the potential advantages of combining CV data across gender when the test article exposure and pharmacodynamics were consistent.

PS 476 Safety Pharmacology Time Interval Considerations in Repeated Measures Statistical Analysis

W. Miner, R. Collins, T. Vidmar and L. L. Freshwater. *BioSTAT Consultants, Portage, MI.*

The ability to collect continuous measurement (heart rate, blood pressure, etc) on animals during a safety pharmacology study has become increasingly common. Repeated measures statistical analysis relies on the underlying assumption that responses measured repeatedly over time are correlated. This correlation is then used to test for treatment effects. It is not uncommon for a safety pharmacology study to include 24 hours of continuous data. This data is then 'binned' into time intervals by the study scientist for summary and analysis. It is important that the scientist consults with a statistician regarding the analysis in terms of analysis blocks (subphases of the 24 hour collection) as well as the number of binned time points within individual analysis blocks. Environmental conditions and drug characteristics are essential considerations in analysis block selection. An example is demonstrated where the inclusion of too many time points masks the beginning and the end of a significant drug effect. If smaller block sizes are used, that drug effect is apparent. Further, there are statistical results that suggest that the use of too many time points may impact the power in the statistical analysis. It is recommended to limit the number of time points in an analysis block to no more than 12. At the other extreme, a "super interval" is when only one response (average) per animal per analysis block is included in the statistical analysis. The super interval may be a procedure where the binning process has been taken too far resulting in meaningful peak effects diluted by the volume of data included in the single, average response. A procedure between these two extremes is recommended. Repeated measures statistical analysis is appropriate when a response is measured multiple times on a subject. The results of a repeated measures analysis can vary depending on the defined analysis blocks and therefore it is important to understand the objective of the analysis and consult a statistician.

PS 477 An Improved ECG Processing Algorithm for Interval Measurement and Arrhythmia Detection

M. Brockway[1, 2], M. Miyamoto[3], B. Brockway[2] and R. Hamlin[4, 5]. [1]*University of Minnesota, St Paul, MN,* [2]*VivaQuant, St Paul, MN,* [3]*Huntingdon Life Sciences, E. Millstone, NJ,* [4]*QTest Labs, LLC, Columbus, OH and* [5]*The Ohio State University, Columbus, OH.*

Most existing commercialized ECG analysis algorithms employ template matching techniques that originated in the 1980's. Originally developed for ECG recordings from a hospital environment or other situations where the ECGs are relatively noise free, they have since been widely adopted for ambulatory ECGs. Template matching algorithms require considerable computing resources and, in the presence of noise, have difficulty achieving a template match and can exhibit unpredictable template switching that results in high interval measurement variability. A new technology, referred to as Multi-Domain Signal Processing (MDSP) addresses these shortcomings. In this study, we evaluated MDSP performance for interval measurement and arrhythmia detection in preclinical surface ECG recordings. Results show that MDSP provides equivalent interval measurements for noise-free recording segments but substantially reduces measurement variability when noise is present. For nine 24-hour NHP JET recordings, the average Standard Deviation (SD) for 60-second mean QT intervals was 3 msec (range for all subjects 1.9 to 4.5). SD for all intervals for individual series was 2-5 lower than Ponemah and published values, depending on the level of noise in the recording. A 24-hour recording is processed in about 5 minutes on an ordinary PC. On average MDSP provided accurate interval measurements for about 80% of available beats in these nine recordings. MDSP provides high Sensitivity and Positive Predictive Value for detection of arrhythmias of interest in safety pharmacology and toxicology. The ability of MDSP to deal effectively with noise results in a significant reduction in false positive events and "blind spots" that require manual review and hence is highly efficient for assessing arrhythmia burden. The reduction in measurement variability and high data density provided by MDSP should result in greater sensitivity to drug-induced changes in ECG, lower cost, and reduce animal use.

PS 478 Multielectrode Array and xCELLigence: Synergistic Platforms for Cardiovascular Risk Assessment

G. C. Luerman, J. A. Denker, C. A. Obejero-Paz, J. W. Kramer, A. M. Brown and A. Bruening-Wright. *Chantest Corporation, Cleveland, OH.*

Emerging plate-based technologies allow electrical recording from human induced pluripotent stem cell-derived cardiomyocytes (hiPSC-CMs) in medium-throughput formats. hiPSC-CMs demonstrate consistent intrinsic beating/contraction patterns that are readily monitored. Although drug-induced block of the hERG ion channel is the main culprit responsible for the delayed repolarization of the cardiac action potential and may lead to lethal cardiac arrhythmias, recent evidence suggests that a model that incorporates multiple ion channel effects (MICE, Kramer et al., Sci Rep. 2013) may provide improved prediction of proarrhythmic potential. Multi-electrode array (MEA) technology measures the extracellular potential of beating cardiomyocyte monolayers which produce electrocardiogram (ECG)-like waveforms. All ion channels that contribute to the cardiac action potential are therefore incorporated into this ECG-like recording. Importantly, the xCELLigence RTCA Cardio system can indirectly monitor cardiomyocyte contraction and cellular viability in real-time using impedance-based measurements. As a corollary, while not detected on MEA, compounds that affect long-term cell viability (such as doxorubicin), or contractility (such as blebbistatin) in the absence of electrophysiological effects, can be accurately detected. The combination of these two synergistic platforms provides for a thorough and cost-effective pre-clinical assessment of cardiac risk. Our data compare the effects of multiple compounds from different drug classes across both platforms, and highlight the utility of each platform.

PS 479 Use of Bayesian Tolerance Intervals to Interpret Absolute and Relative Heart Weights

A. Stokes[1], P. Torres-Saavedra[2] and C. Kimbrough[3]. [1]*Safety Assessment, GlaxoSmithKline, Research Triangle Park, NC,* [2]*Mathematical Sciences, University of Puerto Rico at Mayaguez, Mayaguez, Puerto Rico and* [3]*Statistical Sciences, GlaxoSmithKline, Research Triangle Park, NC.*

Changes in absolute and relative heart weights are important indicators of cardiovascular function and can predict structural and functional alterations in the cardiovascular system. Detecting these changes, especially in shorter term studies (e.g., 7-Days) with limited animal numbers, can be challenging. The work described here presents a graphical representation using Bayesian tolerance limits set at 80% content level and 95% confidence level based on heart weight data collected on control rats of the same gender and of similar age and weight. Included in the analysis were absolute and relative (to brain and body weight) heart weight data used to generate Bayesian tolerance limits to aid in the interpretation of the data. This analysis also demonstrates the relationship between absolute and relative heart weight data by using color and spatial relationship to plot individual heart weight values in two dimensions. Animals with absolute heart weight values that fall outside of the tolerance intervals for absolute heart weight values are graphed in a different color (red) to quickly identify these values. Individual relative heart weight values and tolerance limits relative to body and relative to brain weight are plotted on the x and y-axes, respectively. Using this tool, scientists are easily and quickly able to identify test article-related dose responses in absolute and relative heart weight data to aid in the interpretation of biologically significant effects in Groups with sizes that may not be powered appropriately for traditional comparative statistical methods (e.g., t-test).

PS 480 Metallothionein As a Compensatory Component Prevents Intermittent Hypoxia-Induced Cardiomyopathy in Mice

S. Zhou, X. Yin, Y. Tan, W. Feng, P. Epstein, J. Cai and L. Cai. *University of Louisville, Louisville, KY.*

Obstructive sleep apnea (OSA) causes chronic intermittent hypoxia (IH) to induce cardiovascular disease, which may be related to oxidative damage. Metallothionein (MT) is a potent and highly inducible antioxidant protein that is expressed in the heart. The present study was to test the hypotheses that MT as a potent antioxidant protects the heart from OSA derived IH-induced cardiomyopathy. Mice were exposed to IH for 3 days to 8 weeks, which is consisted of alternating cycles of 20.9% O2 /8% O2 FIO2 (30 episodes per h) with 20 seconds at the nadir FIO2 for 12 h a day during daylight. IH significantly increased the ratio of heart weight to tibia length at 4 weeks with a decrease in cardiac function from 4 to 8 weeks, shown by decreased left ventricular ejection fraction (EF) and fractional shortening (FS). Cardiac oxidative damage and fibrosis were observed after 4 and 8 weeks of IH exposures. Endogenous MT expression was up-regulated in response to 3-day IH, but significantly decreased at 4 and 8 weeks of IH. In support of MT as a major compensatory component, mice with cardiac overexpression of MT gene and mice with global MT gene deletion were completely resistant and highly sensitive, respectively, to chronic IH-induced cardiac effects. These findings show that chronic IH induces cardiomyopathy characterized by oxidative stress and cardiac damage. The antioxidant MT protects the heart from such pathological changes.

PS 481 Lack of Recovery from Lead-Acetate-Induced Cardiotoxicity in Wistar Rats

T. O. Omobowale[1], A. S. Akinrinde[2], A. A. Oyagbemi[2], A. B. Saba[2], B. S. Ogunpolu[1] and O. T. Daramola[1]. *[1]Department of Veterinary Medicine, University of Ibadan, Ibadan, Oyo State, Nigeria and [2]Departments of Veterinary Physiology, Biochemistry and Pharmacology, University of Ibadan, Ibadan, Oyo State, Nigeria.*

Lead poisoning continues to be a serious health problem and more significantly so in developing countries with ineffective waste disposal systems. Recent efforts at solving lead poisoning issues have seen entire towns being re-settled from lead-contaminated areas. This study was designed to investigate whether withdrawal of lead exposure results in a resolution of toxic effects of lead to cardiac tissues. Adult male Wistar rats were exposed orally to lead acetate at doses of 0.25, 0.5 and 1.0mg/ml for 6-week duration, after which one-half was sacrificed and the remaining left for a further 6 weeks without lead treatment. Exposure of rats to lead acetate produced significant decline ($p<0.05$) in the activities of antioxidant parameters, including Glutathione peroxidase (GPx), Glutathione S-transferase (GST), Catalase (CAT), Superoxide dismutase (SOD) and Reduced glutathione (GSH), while Malondialdehyde (MDA) concentration was significantly elevated. Animals from the withdrawal period exhibited similar pattern of alterations, with significant ($p<0.05$) reduction in GSH, GPx and SOD and significant elevation in MDA and H2O2 concentrations. However, GST activity was elevated, while CAT activity remained unaltered in the recovery period. The results of this study showed that cardiotoxicity indicated by induction of oxidative stress and reduction in antioxidant parameters in this study failed to resolve upon withdrawal of lead exposure in male rats during the period of study.
Keywords: Cardiotoxicity, oxidative stress, Lead acetate, antioxidants, rats
indicated by induction of oxidative stress and reduction in antioxidant parameters in this study failed to resolve upon withdrawal of lead exposure in male rats during the period of study.

PS 482 Methyl Honokiol Prevention of High-Fat Diet-Induced Cardiac Hypertrophy and Dysfunction Is Associated with Attenuating Lipid Accumulation and Insulin Resistance

Z. Zhang[1, 2], S. Zhou[1, 2], X. Yan[1], Y. Tan[1], K. Kim[3], K. Kim[3], Y. Zheng[2], L. Cai[1] and Y. Kim[3]. *[1]KCHRI at the Department of Pediatrics, University of Louisville, louisville, KY, [2]The First Hospital of Jilin University, Changchun, Jilin, China and [3]Bioland Nature, Science & Life, Shanghai, China.*

Obesity is associated with inflammation, oxidative stress, apoptotic cell death, cardiac hypertrophy and cardiac dysfunction. Magnolia as an herbal material obtained from Magnolia officinalis has been found to play an important role in anti–inflammation, anti-oxidative stress and anti-apoptosis. This study was designed to investigate the effect of methyl honokiol (MH, an activity standard of Magnolia) on obesity-associated insulin resistance, lipid accumulation and inflammation in the heart. C57BL/6 mice were fed with a low-(10 Kcal% fat) or high-(60 Kcal% fat) fat diet (LFD and HFD, respectively) for 24 weeks to induce obesity and insulin resistance. HFD-fed mice were given a gavage of vehicle, 0.5 or 1 mg/kg body weight of MH daily. Treatment with 0.5 mg/kg MH significantly ameliorated insulin resistance and slightly decreased HFD-caused body weight gain. Both 0.5 and 1 mg/kg MH treatments significantly attenuated HFD-induced cardiac hypertrophy and dysfunction, cardiac lipid accumulation (reflected by increasing Oil Red O and down-regulating fatty acid translocase), and cardiac inflammation (evidenced by down-regulating TNF-α and PAI-1 expression). Treatment with 0.5 and 1 mg/kg of MH also ameliorated HFD-induced cardiac insulin resistance, shown by up-regulating Akt and Akt2 phosphorylation and hexokinase II expression. This study demonstrates that MH treatment can attenuate HFD-associated cardiac damage through the prevention of HFD-induced cardiac lipid accumulation, inflammation and insulin resistance.

PS 483 Metallothionein Preservation of Cardiac Akt2 Function and Insulin Signaling by Down-Regulating TRB3 Prevents Diabetic Cardiomyopathy

Y. Tan[1, 2], X. Yan[1, 2], S. Zhou[1, 2], C. Zhang[1, 2], Y. Li[1], Y. Li[1] and L. Cai[1, 2]. *[1]KCHRI, Departments of Pediatrics, Biochemistry and Surgery Oncology, University of Louisville, Louisville, KY and [2]Chinese-American Research Institute for Diabetic Complications, Wenzhou Medical University, Wenzhou, Zhejiang, China.*

Cardiac insulin resistance is a key pathogenic factor for diabetic cardiomyopathy, but its mechanism remains largely unclear. Here we demonstrated that diabetes significantly inhibited cardiac Akt phosphorylation from 2 weeks to 2 months in wide-type (WT) mice, but not in cardiac-specific metallothionein-transgenic (MT-TG) mice. Cardiac Akt2 expression and phosphorylation was decreased and insulin-induced cardiac Akt2 and GSK-3β phosphorylation and GS dephosphorylation were also significantly attenuated in WT, but not MT-TG diabetic mice. Deletion of Akt2 gene either in vitro H9c2 cells or in vivo significantly impaired glucose metabolic signaling. In addition, diabetes significantly increased cardiac Akt negative regulator tribbles (TRB)3 expression only in WT mice, suggesting the possible contribution of MT inhibition of diabetic up-regulation of TRB3 to Akt2 function preservation. Cardiac H9c2 cells with and without forced MT-overexpression (MT-H9c2) were treated with tert-butyl hydroperoxide (tBHP), which significantly reduced Akt2 phosphorylation in both basal and insulin-stimulating conditions only in H9c2 cells. Silencing TRB3 expression with SiRNA completely prevented tBHP's inhibition of insulin-stimulated Akt2 phosphorylation in H9c2 cells, while overexpression of TRB3 in MT-H9c2 cells completely abolished MT preservation of insulin-stimulated Akt2 phosphorylation. Forced-overexpression of TRB3 by adenovirus-mediated gene delivery in MT-TG hearts also abolished MT's preservation of cardiac insulin signaling and prevention of diabetic cardiomyopathy. These results suggest that diabetes-attenuated cardiac Akt2 function via up-regulating TRB3 plays a critical role in diabetic inhibition of insulin signaling in the heart. MT preservation of cardiac Akt2-mediated insulin signaling by inhibition of TRB3 prevents diabetic cardiomyopathy.

PS 484 Intratracheal Exposure to PVP-Coated Nanosilver Expands Cardiac I/R Injury in Male Sprague-Dawley Rats Seven Days after Exposure

N. A. Holland[1], D. P. Becak[1], R. M. Lust[1], S. C. Sumner[2], T. Fennell[2] and C. J. Wingard[1]. *[1]Physiology, East Carolina University, Greenville, NC and [2]RTI International, Research Triangle Park, NC.*

The potential uses of engineered nanomaterials have expanded in biomedical technology and consumer manufacturing. Our lab has demonstrated expansion of myocardial infarction in male Sprague-Dawley (SD) rats 24 hours after intratracheal (IT) instillation of nanosilver (AgNP). We hypothesized that pulmonary exposure to AgNP induces a persistent increase in circulating proinflammitory cytokines which results in expansion of cardiac ischemia-reperfusion (IR) injury. To test this hypothesis, we exposed male SD rats to an instillation of 200 μg of 20 nm or 110 nm PVP coated AgNP, or a respective small and large PVP vehicle. Serum samples were collected prior to instillation and 1, 3, 6, 24, 48, 72, and 168 hours following instillation. Serum samples were analyzed by multiplex assay for concentrations of: G-CSF, IL -1β, IL-2, IL-6, IL-18, MCP-1, and TNF-α. 168 hours after exposure, cardiac ischemia was induced by left anterior descending coronary artery ligation for 20 minutes followed by 2 hours of reperfusion. IT exposure to 20 nm (37.8 ± 2.7) and 110 nm (42.1 ± 4.7) AgNP resulted in expansion of IR injury (% infarcted area/area at risk) compared to small PVP (23.6 ± 1.2), large PVP (27.2 ± 2.2) and naïve (17.0 ± 0.6). Exposure to 20 nm AgNP resulted in higher aggregate serum concentrations of: G-CSF (287.3 ± 17.4 pg/mL), IL-2 (606.7 ± 29.74 pg/mL), IL-6 (1799 ± 195.7 pg/mL), IL-18 (479.6 ± 28.7 pg/mL), and MCP-1(2465 ± 86.0 pg/mL) compared to small PVP vehicle: (181.2 ± 23.1 pg/mL), (250.1 ± 25.9 pg/mL), (468.2 ± 103.9 pg/mL), (250.1 ± 103.9 pg/mL), (207.4 ± 22.2 pg/mL), and (1767 ± 107.9 pg/mL) respectively. No statistical differences were demonstrated between 110 nm AgNP and large PVP. Based on these

data, IT AgNP exposure increases circulating levels of several proinflammitory cytokines which may contribute to the expansion of IR injury. Supported in part by NIEHS U19 ES019525 and ECU.

PS 485 Intratracheal Instillation of Multiwalled Carbon Nanotubes Increases Vasoconstrictor Responses in Pregnant Sprague-Dawley Rats

C. J. Wingard[1], A. K. Vidanapathirana[1], L. C. Thompson[1], J. Dawkins[1], N. A. Holland[1], S. C. Sumner[3], T. Fennell[3] and J. M. Brown[2]. [1]*Physiology, East Carolina University, Greenville, NC,* [2]*Pharmaceutical Sciences, University of Colorado Denver, Aurora, CO and* [3]*Discovery Sciences, RTI International, Research Triangle Park, NC.*

Multiwalled carbon nanotubes (MWCNTs) are being increasingly designed for industrial/biomedical applications raising concerns on their safety, especially during unique life-stages such as pregnancy. We hypothesized; pulmonary MWCNT exposure during pregnancy will increase vasoconstrictor responses in uterine and placenta derived blood vessels by increasing rho-kinase (ROCK) signaling. We exposed gestational day 17-19 pregnant and non-pregnant female Sprague Dawley rats to 100μg/kg of MWCNTs suspended in 10% Infrasurf surfactant by intratracheal instillation. Vasoactive responses of uterine, mesenteric, aortic and umbilical vessels were studied 24h post-exposure by wire myography. Maximum stress generation in the uterine artery following MWCNT exposure was increased during pregnancy in response to phenylephrine by 2.6 mN/mm2 (+37%) and to angiotensin II by 4.9 mN/mm2 (+118%), as compared to naïve response. Following MWCNT exposure serotonin induced ~4 mN/mm2 increase in stress generation of the mesenteric artery from both pregnant and non-pregnant rats as compared to vehicle response. Wire myographic studies in the presence of a ROCK inhibitor did not reveal significant changes. RhoA and ROCK mRNA/protein expression in rat aortic endothelial cells were unaltered with in vitro exposure to MWCNTs, suggesting absent/minimal contribution of ROCK to the enhanced contractions following MWCNT exposure. The reactivity of the umbilical vein was not changed; however, mean fetal weight gain was reduced by 7% with MWCNT exposure. These results suggest a higher susceptibility of the uterine vasculature to MWCNT induced vasoconstriction predisposing reduced fetal blood supply/growth during pregnancy. This work is supported in part by NIEHS U19ES019525, RO1ES5016246, AHA Mid-Atlantic Affiliate Predoctoral Fellowship and East Carolina University.

PS 486 Spatially-Distinct Cardiac Mitochondrial Dysfunction following Pulmonary Exposure to Various Carbon-Based Nanomaterials

C. E. Nichols[1], A. Erdely[2], D. L. Shepherd[1], D. Thapa[1], R. Salmen[2], C. E. McLoughlin[2], T. M. Sager[2], J. R. Roberts[2] and J. M. Hollander[1]. [1]*Exercise Physiology, West Virginia University, Morgantown, WV and* [2]*NIOSH, Morgantown, WV.*

While carbon-based nanomaterial use continues to grow, the health effects are not fully realized. Nanomaterial inhalation affects lung mitochondria, but cardiac mitochondrial effects are not well defined. Within the heart, analyses are complicated by the presence of two mitochondrial subpopulations: the subsarcolemmal (SSM), beneath the sarcolemma, and interfibrillar (IFM), between the myofibrils. The current study investigated the impact of pulmonary exposure to various carbon-based nanomaterials on the function of cardiac mitochondrial subpopulations. Male C57BL/6 mice were exposed using pharyngeal aspiration to either 40 μg of <2 μm x <2 μm x 1-2 nm graphene (GP-1), 5 μm x 5 μm x 7 nm (GP-5), multi-walled carbon nanotubes (MWCNT), or carbon black; 10 μg of MWCNT; or sham, dispersion media. Four or 24 h after exposure, cardiac mitochondrial subpopulations were isolated and run through polarographic assessments for mitochondrial oxygen consumption. Mitochondrial hydrogen peroxide (H2O2) production was measured using the fluorescent dye Amplex red. The IFM of mice exposed to GP-1 had decreased active respiration 24 h after exposure compared to shams ($P<0.05$). Exposure to GP-1, GP-5, and carbon black increased IFM H2O2 production compared to shams 4 h post-exposure ($P<0.05$). Both doses of MWCNT decreased active respiration rates in the IFM at 4 h compared to controls ($P<0.05$), but no difference at 24 h. Increased production of IFM H2O2 were seen 24 h after exposure to 40 μg MWCNT as compared to shams ($P<0.05$). No effects were observed in any SSM population. In conclusion, cardiac mitochondrial dysfunction was observed solely in the IFM following pulmonary exposure to carbon-based nanomaterials. Decreased function and increased H2O2 production in the mitochondria between the myofibrils can promote cardiovascular dysfunction.
AHA 13PRE16850066;NIH DP2DK083095;NSF DGE1144676;NIH T32HL090610;NIOSH NTRC

PS 487 Radical-Containing Ultrafine Particulate Matter Exacerbates Cardiac Functional Decline Induced by Ischemia-Reperfusion Injury

B. R. Burn and K. J. Varner. *Dept. of Pharmacology, Louisiana State University Health Sciences Center, New Orleans, LA.*

Epidemiological studies continue to link increases in particulate air pollution to adverse cardiovascular events, including the incidence and severity of myocardial infarction. Within environmental air samples, our colleagues have identified environmentally persistent free radicals (EPFRs), capable of the continuous generation of free radicals. We have shown that inhalational exposure to a model EPFR (1,2-dichlorobenzene chemisorbed to 200nm Si-CuO particles at 230°C - DCB230) decreases left ventricular (LV) cardiac function in rats, in part due to increased pulmonary resistance and decreased ventricular filling. DCB230 also produces oxidative stress in the serum and LV. Given the cardiac effects of exposure to EPFRs, the aim of this study was to investigate whether inhalational exposure to DCB230 could increase the severity of ischemia-reperfusion (I-R) injury. Male rats (DCB230 n=9, vehicle n=8) were exposed via nose-only inhalation to either DCB230 (~ 110μg/m3) or vehicle for 20 min/d for 7 days. I-R injury was induced 24 hr after the final exposure by ligation of the left anterior descending artery for 45 min followed by 24 hr of reperfusion, after which LV function was assessed using a pressure-volume catheter. Sham I-R rats (n=8) were also studied. I-R injury in vehicle-treated rats significantly decreased end systolic pressure (ESP) when compared to sham I-R (82.6 vs. 98.6mmHg respectively). Vehicle exposed I-R rats compensated for the decrease in ESP and maintained a cardiac output (CO) similar to shams (41.3 vs. 40.3mL/min). In contrast, rats exposed to DCB230 before I-R had significantly smaller end diastolic volume (154.9 vs. 184.0μL), stroke volume (86.1 vs. 106.4μL), and CO (33.3 vs. 41.3mL/min) compared to vehicle exposed I-R rats. These data indicate that prior exposure to EPFRs exacerbates the decline in function induced by I-R injury and could help explain the link between air pollution and increased cardiac morbidity and mortality from ischemic events. Supported by NIEH P42ES013648 and NIH/NCRR P20RR018766.

PS 488 Nano-Cerium Dioxide Exposure and Arteriolar Dysfunction: What Is the Mechanism?

V. C. Minarchick[1], P. G. Stapleton[1], N. R. Fix[3], S. S. Leonard[3], E. M. Sabolsky[2] and T. R. Nurkiewicz[1]. [1]*Center for Cardiovascular and Respiratory Sciences, West Virginia University, Morgantown, WV,* [2]*Department of Mechanical Engineering, WVU, Morgantown, WV and* [3]*NIOSH, Morgantown, WV.*

Applications of nano-cerium dioxide (CeO_2) are potentially endless, but its biologic interactions must first be understood. We have reported that pulmonary CeO_2 exposure results in endothelium-dependent and -independent arteriolar dysfunction. Based on these observations, we predict that this dysfunction is mechanistically linked to impaired nitric oxide (NO) signaling. Rats were intratracheally instilled (65 μg) or intravenously injected (IV,100 μg) with CeO_2 suspended in saline (5% serum). Mesenteric arterioles were examined post 24 hrs via intravital microscopy or isolated vessels. Arteriolar reactivity was evaluated by using acetylcholine (ACh, 10^{-9}-10^{-4} M), and spermine NONOate (10^{-9}-10^{-4} M). The role of NO synthase and cyclooxygenase reactivity was tested in the presence of Nω-Nitro-L-arginine methyl ester hydrochloride (L-NMMA) and/or indomethacin (INDO) (respectively). Soluble guanyl cyclase activator (YC-1) and cyclic guanosine monophosphate mimetic (8-Bromo-cGMP) assessed smooth muscle activation. Electron spin resonance and a free radical analyzer assessed the ability of NO to react with CeO_2 and the level of tissue free radicals. At the time of writing, results were similar in both models and exposure routes. Control animals responded normally to increasing concentrations of ACh (80±4%) and this dilation was impaired in the presence of L-NMMA (34±9%) or INDO (45±11%). Pulmonary CeO_2 exposure significantly impaired this dilation (30±4%). INDO treatment did not alter this impairment (44±10%) but there was a partial restoration in function during L-NMMA treatment (51±11%). Smooth muscle activation was intact following both exposure routes. CeO_2 is capable of reacting with NO and there appears to be minimal changes in free radicals. These results are consistent with the notion that CeO_2 exposure impairs endothelial function at least in part via a NO dependent mechanism. RO1-ES015022(TRN), NSF IGERT(VCM), F32-ES023435(PAS)

PS 489 Effects of Estrogenic Compounds on Cardiac Development in Zebrafish

G. Diamante and D. Schlenk. *University of California, Riverside, Riverside, CA.*

Several studies have shown that exposure to estrogenic compounds like 17β-estradiol (E2) can cause cardiac edema in developing vertebrates including zebrafish. Exposure to endocrine disruptors could lead to a disruption in the of signal trans-

duction events required for normal heart development via activation of G protein-coupled estrogen receptor 1 (GPER). Potential targets include, GATA4, ERK, PKA and NFAT. GATA4 regulates the expression of Hand2 and Lrrc10, which are involved in heart cell differentiation and development. This transcription factor can be activated by several kinases, such as ERK and PKA, both of which are downstream targets of the estrogen signaling pathway. GATA4 has also been proposed to interact with NFAT, whose activation is regulated by calcium influx. We hypothesize that exposure to E2 would alter the expression of important heart determinant genes such as Hand2 and Lrrc10, as well as calcium homeostasis in zebrafish. To explore potential molecular mechanisms of cardiac dysfunction, expression of genes involved in signal transduction and calcium homeostasis were examined in zebrafish embryos following exposure to E2. Embryos were exposed to 2μM and 5 μM of E2 at 2 hpf and RNA was extracted at 28hpf. Preliminary qPCR results suggest that E2 exposure during early embryogenesis causes a decrease in the expression of Lrrc10 and Hand2. Additional studies will not only measure the expression of other genes related to GPER activation by estrogen, but also measure intracellular calcium to better understand how endocrine disruptors alters cardiac development.

PS 490 Investigating Proepicardial, Epicardial, and Myocardial Cells As Targets of TCDD Cardiotoxicity in Zebrafish Embryos

M. S. Yue[1], J. S. Plavicki[2], M. Kim[2], P. J. Hofsteen[2], R. E. Peterson[1, 2] and W. Heideman[1, 2]. [1]*Molecular and Environmental Toxicology, University of Wisconsin Madison, Madison, WI and* [2]*School of Pharmacy, University of Wisconsin Madison, Madison, WI.*

Exposure to the ubiquitous environmental contaminant 2,3,7,8-tetrachlorodibenzo-p-dioxin (TCDD) causes severe cardiovascular toxicity via activation of the AHR pathway. These effects are likely due to failure of the epicardium to form. The epicardium is the outer layer of the heart, and is important for heart development and regeneration. In the zebrafish heart the epicardium is derived from the proepicardium (PE), which forms adjacent to the heart and begins to migrate to the myocardium at 70 hours post fertilization (hpf). Recent work has shown that exposure to TCDD inhibits PE formation, epicardial progenitor cell migration, and the spread of epicardial cells across the myocardium. We hypothesize that the myocardium is a target site of TCDD that contributes to inhibition of PE migration and epicardial spread in TCDD-exposed hearts. To investigate this, we have activated AHR2 expression exclusively in myocardial cells using constitutively activated AHR2 (caAHR2) linked to the cardiac myosin light chain 2 (cmlc2) promoter. Here we show that caAHR2 in myocardial cells does not inhibit development of the PE, however, the PE or PE cells fail to migrate onto the myocardium. This may explain the lack of epicardium formation in these caAHR2 embryos. Additionally, using scanning electron micrography (SEM), we show that TCDD-exposed hearts have a smooth myocardial surface topography, which contrasts significantly from the rough and pockmarked surface of controls. To further examine the role of the myocardial cells on epicardium formation, we are developing an epicardial migration assay to assess the ability of untreated epicardial cells to spread onto the myocardium of TCDD-treated hearts in vitro, and to test whether caAHR2 myocardial cells are receptive to migrating epicardial cells. (Supported by NIH ES012716 and 5T32ES007015-35)

PS 491 Comparison of Exposure Route on Cardiorespiratory Effects following Acute Benzo[a]pyrene in Adult Zebrafish (*Danio rerio*)

L. P. Weber[1, 2] and C. J. Gerger[2]. [1]*Veterinary Biomedical Sciences, University of Saskatchewan, Saskatoon, SK, Canada and* [2]*Toxicology Graduate Program, University of Saskatchewan, Saskatoon, SK, Canada.*

Polycyclic aromatic hydrocarbons (PAHs) are ubiquitous environmental contaminants. PAH exposure causes developmental toxicity in multiple fish species, but acute adult fish toxicity is thought to be minimal. However, there is some indication of sublethal PAH effects. We hypothesize that acute PAH exposure in adult fish will cause cardiorespiratory impairment that will not differ with exposure route. In order to investigate this hypothesis, adult zebrafish (*Danio rerio*) were injected (i.p.) twice with increasing concentrations of the prototypical PAH, benzo[a] pyrene (BaP; 0.1, 10, and 1000 μg/kg) or exposed aqueously (static, renewal at 24 hr; 16.2 and 162 μg/L) for 48 hr and compared to corresponding dimethylsulfoxide controls. No mortalities or significant effects on weight of the fish were noted at any exposure concentration or route. At 48 hr, fish were subjected to swimming tests with concurrent oxygen consumption measurement (n=10 fish/treatment) or echocardiography (n=12 fish/treatment). Oxygen consumption (MO2) was increasingly higher as swimming speed increased in all injected BaP groups compared to control ($p<0.01$ in Fisher's LSD tests after two-way ANOVA). In contrast, aqueously BaP-exposed fish showed increased MO2 under basal conditions. Despite increased oxygen demand, cardiac output and ventricular rate were significantly decreased in BaP-exposed fish, both injected and aqueously-exposed. The primary mechanism for the reduced cardiac output appeared to differ between exposure routes. BaP-injected fish suffered from significant atrio-ventricular conduction blockade, while aqueous BaP exposure caused significant suppression of ventricular function (reduced end-systolic and end-diastolic volumes). In conclusion, acute BaP exposure in adult zebrafish had negative effects on cardiorespiratory function sufficient to impair fitness of the fish, but the primary mechanism behind these effects differed slightly with exposure route.

PS 492 Diesel Exhaust Causes Stress-Induced Cardiac Conduction Instability in Hypertensive Rats As Demonstrated by a Novel Measure of Refractoriness

M. S. Hazari[1], J. Lancaster[2], J. Starobin[2], A. K. Farraj[1] and W. Cascio[1]. [1]*Environmental Public Health Division, Environmental Protection Agency, Research Triangle Park, NC and* [2]*University of North Carolina at Greensboro, Greensboro, NC.*

Loss of cardiac refractoriness, which prevents early stimulation in the heart, increases the risk of arrhythmogenesis. Although the heart has a large reserve of refractoriness (RoR), disease can cause impairment, particularly when under stress or toxic insult, and thus conduction instability and mechanical dysfunction. RoR is an assessment of the heart's minimum level of refractoriness as compared with the critical level associated with conduction instability. We previously showed that diesel exhaust (DE) causes cardiac electrical disturbances in rats during exercise-like stress. To further assess the subtle impacts of DE on the intrinsic conduction properties of the heart, we used the Chernyak-Starobin-Cohen (CSC) model to calculate RoR and thereby analytically determine conduction stability during dobutamine (DOB) challenge, which mimics exercise by increasing heart rate and contractility (i.e. pacing). We hypothesized that spontaneously hypertensive (SH) rats would have a greater decrease in RoR than Wistar-Kyoto (WKY) rats during pacing, and that DE would exacerbate the response. WKY and SH rats exposed to 150μg/m3 of DE were challenged with increasing doses of DOB. The CSC model was customized for each rat; QT and RR intervals taken from the electrocardiogram after a given dose of DOB were used to determine action potential duration and diastolic interval. These values were then analyzed to calculate model conductance parameters and determine RoR. Air-exposed WKY and SH rats did not have any decrease in RoR during pacing; however, DE caused a significant decrease during pacing in both strains. SH rats had an eight times steeper decrease in RoR when compared with WKY suggesting greater risk. These data indicate that after exposure to DE, risk of cardiac instability increases with increasing stress, particularly with underlying cardiovascular disease. (This abstract does not reflect EPA policy)

PS 493 Prevention of Angiotensin II-Induced Cardiomyopathy by Sulforaphane-Activated Nrf2 Partially via AKT/GSK-3β/Fyn Pathway

Y. Xin[1], X. Jiang[2], Y. Bai[2] and L. Cai[1]. [1]*University of Louisville, Louisville, KY and* [2]*The First Hospital of Jilin Unviersity, Changchun, Jilin Province, China.*

Angiotensin II (Ang II) is an important causative of diabetic cardiomyopathy. Sulforaphane (SFN) is anti-oxidative supplement through activation of Nrf2 pathway. The present study examined whether SFN could protect from Ang II-induced cardiomyopathy and the underlying mechanism. FVB mice were given subcutaneous injection of Ang II (0.5 mg/kg) for 2 months with or without SFN treatment (0.5 mg/kg) for 3 months and then kept until 6 months. At 3 and 6 months, blood pressure and cardiac function were assessed. SFN significantly prevented Ang II-induced high blood pressure at 6 months and cardiac dysfunction at both 3 and 6 months. Ang II caused remarkable pathological changes, including myocardial hypertrophy and collagen accumulation, along with increases in cardiac oxidative damage (3-NT and 4-HNE), inflammation (TNF-α and PAI-1), and fibrotic response (TGF-β1 and CTGF). Those damages were almost completely prevented by 3-month SFN treatment that up-regulated Nrf2 function, reflected by increased Nrf2 phosphorylation and downstream antioxidants. To define the direct role of SFN-activated Nrf2 in preventing Ang II-induced cardiomyopathy, in vitro H9c2 cells were treated with Ang II in the absence or presence of Nrf2 siRNA to silence Nrf2 expression. SFN significantly up-regulated Nrf2 and also prevented Ang II-induced CTGF and PAI-1expression, which were completely abolished by Nrf2 silence. Furthermore, cardiac-overexpressing Nrf2 gene (Nrf2-TG) and wild-type (WT) mice were treated with Ang II (0.5 mg/kg) for 2 months. Ang II-induced cardiomyopathy was seen in WT mice, but not in Nrf2-TG mice. To dissect the mechanism for SFN activation of Nrf2, H9c2 cells were given SFN (10 μM) simultaneously with and without Akt inhibitor (LY294002, 10 μM). SFN's activation of Nrf2 was partially inhibited by Akt inhibition that also induced GSK-3β activation

and Fyn nuclear accumulation. These results suggest that Ang II-induced cardiomyopathy can be prevented by SFN via Akt/GSK-3β/Fyn-mediated activation of Nrf2 antioxidant pathway.

PS 494 (+)-Usnic Acid-Induced Myocardial Toxicity in Rats

Y. Yokouchi, M. Imaoka, N. Niino, N. Kiyosawa, A. Sayama, T. Jindo and W. Takasaki. *Medicinal Safety Research Laboratories, Daiichi Sankyo Co., Ltd., Tokyo, Japan.*

(+)-Usnic acid (UA) has been known to be a strong uncoupler, and mitochondrial and endoplasmic reticulum (ER)-related stresses are suggested to be involved in the mechanism of hepatotoxicity. However, it has not been clarified whether UA causes toxicity in other mitochondria-rich organs. We confirmed whether UA induced cardiotoxicity and its mechanism. In the preliminary study of oral administration at 100 mg/kg/day of UA for 14 days in rats, cytoplasmic rarefaction of myocardium and swollen mitochondria were observed. Immunohistochemically, increased intensity of prohibitin, a marker for mitochondrial imbalance, were demonstrated. Toxicogenomic analysis indicated oxidative stress, ER stress, and amino acid limitation as a possible cardiotoxicity mechanism of UA. In the present study, rats were orally given 100 mg/kg/day of UA for 1, 4, 7 and 14 days, and were sacrificed on the next day of final dosing. The day of first dosing was defined Day 1. The gene expression analysis of the heart by real-time RT-PCR for representative oxidative stress (*Nqo1* and *Txnrd1*), ER stress (*Casp4*, *Trib3* and *Ddit3*), and amino acid limitation-related genes (*Mthfd2*, *Asns* and *Atf5*) were performed in combined with histopathological examination. No changes were detected on Day 2, while up-regulation or up-regulating tendency were shown in *Nqo1* and *Mthfd2* on Day 5, and in *Nqo1*, *Txnrd1*, *Trib3*, *Mthfd2*, *Asns* and *Atf5* on Day 8. Up-regulation of *Mthfd2*, *Asns* and *Atf5* were sustained on Day 15. Ultrastructurally, swollen mitochondria were seen only on Day 15. In conclusion, it was manifested that amino-acid limitation and oxidative stress preceded the morphological change of mitochondria, and were initial phenomena implying their key role in UA-induced mitochondrial toxicity.

PS 495 Water Fluoridation at WHO-Recommended Concentration Accelerates Medial Vascular Calcification in Uremic Rats

V. Sorribas[1], A. Martín-Pardillos[1], C. Sosa[1] and A. Millan[2]. [1]*Laboratory of Molecular Toxicology, University of Zaragoza, Zaragoza, Spain and* [2]*Institute of Materials Science of Aragon, CSIC-University of Zaragoza, Zaragoza, Zaragoza, Spain.* Sponsor: A. Anadon.

Public water fluoridation is a common policy for improving dental health. Fluoride replaces the hydroxyls of hydroxyapatite, thereby improving the strength of tooth enamel, but this process can also occur in other active calcifications. This work studies the effects of water fluoridation during the course of vascular calcification in renal disease.

The effect of fluoride was studied in vitro and in vivo. Rat aortic smooth muscle cells were calcified with 2 mM Pi for 5 days. Fluoride concentrations of 5-10 μM –similar to those found in people who drink fluoridated water– partially prevented calcification, death, and osteogene expression in vitro. The anticalcifying mechanism was independent of cell activity and exhibited an IC50 of 8.7μM fluoride. Most likely this effect is based on an action on the nucleating sites of proteins. In vivo, however, fluoridation of drinking water at 1.5 mg/L (concentration recommended by the World Health Organization) and 15 mg/L dramatically increased the incipient aortic calcification observed in rats with experimental chronic kidney disease, CKD (5/6-nephrectomy), fed a Pi-rich fodder (1.2% Pi, a western-like diet). Fluoride further declined the remaining renal function of the CKD animals, an effect that most likely overwhelmed the positive effect of fluoride on calcification in vitro. Ultrastructural analysis revealed that fluoride did not modify the Ca/P atomic ratio of deposits, but it was incorporated into the lattice of in vivo mineralization. Fluoride also converted the crystallization pattern from plate to rode-like structures.

In conclusion, while fluoride prevents calcification in vitro, the WHO's recommended concentrations in drinking water become nephrotoxic to CKD rats, thereby aggravating renal disease and making media vascular calcification significant.

PS 496 Mechanisms of How Arsenicals Impact TGF-beta2 Signaling in Cardiac EMT

T. Huang[1] and T. D. Camenisch[1, 2, 3]. [1]*Pharmacology & Toxicology, The University of Arizona, Tucson, AZ,* [2]*Southwest Environmental Health Sciences Center, The University of Arizona, Tucson, AZ and* [3]*Bio5 Institute, The University of Arizona, Tucson, AZ.* Sponsor: N. Cherrington.

Chronic exposure to environmental arsenic contributes to cardiovascular ailments including heart disease and aneurysms. Monomethylarsonous acid [MMA(III)] is the most potent metabolite of inorganic arsenic and has been shown to partly account for arsenic induced toxicity. However the impact of arsenicals on blood vessel formation and function during coronary artery development has not been studied. The TGFbeta family of ligands and receptors are essential for developmental cardiac epithelial to mesenchymal transition (EMT) and differentiation into coronary smooth muscle cells during embryogenesis. In this study, we use a primary mouse cardiac epithelial cell line to study the effects of arsenicals exposure on developmental EMT. 24 hour exposure to 1.34 uM arsenite and 0.13uM MMA(III) disrupt developmental EMT programming in murine epicardial cells causing a deficit in cardiac mesenchyme. The expression of EMT programmed genes are also decreased in a dose-dependent manner following exposure to arsenite and MMA(III). Smad-dependent TGFbeta2 canonical signaling and the non-canonical Erk signaling pathways are abrogated as detected by decreases in phosphorylated Smad2/3 and Erk5. There is also loss of nuclear accumulation of pSmad and pErk due to arsenicals exposure. These observations coincide with a decrease in vimentin positive mesenchymal cells invading three-dimensional collagen gels. However, arsenicals do not block TGFbeta2 stimulated p38 activation. Additionally, smooth muscle cell differentiation which is proven to be governed by p38 signaling in epicardial cells also remains intact with arsenicals exposure. Overall these results show that MMA(III) is 10 times more potent than arsenite. Arsenicals exposure blocks developmental EMT gene programming in murine coronary progenitor cells by disrupting the activation of Smad2/3 and Erk5 and that smooth muscle cell differentiation and p38 signaling are refractory to this arsenicals toxicity.

PS 497 Arsenite Exposure Decreases eNOS Protein Levels and Activity

T. D. Camenisch, P. Sanchez Soria, P. Allison, D. Espiritu and D. Broka. *Pharmacology and Toxicology, University of Arizona, Tucson, AZ.*

Previous work has shown that mice exposed to environmentally relevant dose of arsenic through the drinking water (100ppb As(III)) results in increased blood pressure and concentric left ventricular hypertrophy. In order to understand the underlying mechanism or arsenic related hypertensive pathology, a human placental endothelial cell line, EA.hy 926 was used to explore the effects of arsenic exposure on endothelial nitric oxide synthase (eNOS) function and stability. Preliminary results indicate that several phosphorylation sites are altered by arsenic exposure. EA.hy 926 cells were exposed to 500 μM sodium arsenite for 30 minutes to evaluate phosphorylation changes, and to 100 μM sodium arsenite for 6 hours to evaluate protein stability. Phosphorylation of eNOS was dysregulated by arsenic exposure, including phosphorylation of Ser632, which increased significantly. Moreover, arsenic exposure substantially increased eNOS ubiquitination levels and reduced total eNOS protein levels after a 6 hr exposure. To test whether arsenic can directly reduce nitric oxide (NO) production, we used an inducible cell system for iNOS expression and NO synthesis. We detect inhibition of NO production by arsenic in this doxycycline inducible iNOS cell line (HTRiNOS). This suggests that arsenic exposure affects NOS function by increasing its degradation rate and altering phosphorylation of key residues necessary for adequate nitric oxide production and vasomotor regulation. (NIH ES 04940; ES06694; SWEHSC P30ES006694)

PS 498 1, 1-Difluoroethane Abuse and Possible Routes for Mechanistic Studies

K. P. Joshi, J. Wurpel and M. Barletta. *Pharmaceutical Sciences, St. John's University, Queens, NY.* Sponsor: D. Hardej.

Inhalant abuse is the intentional inhalation of chemical vapors to attain euphoric effect. Many common household products are abused by inhalation and one of them is 1, 1-Difluoroethane (DFE). DFE (Freon 152A) is a halogenated hydrocarbon used as a propellant in dust-off spray and airbrush painting. The electrocardiogram monitored effects of multiple inhaled doses of DFE on cardiovascular system. In addition, enzyme and electrolyte levels after DFE inhalation were also measured. Electrolyte and enzyme levels served as primary experiments for mechanistic studies. In this study an animal model was used to simulate the conditions of

inhalation abuse that result in sudden death due to DFE. Many human DFE abuse cases have been studied but the exact cause and the mechanism behind their death is still unknown.
To investigate arrhythmogenic effect Sprague dawley rats (n=8) were exposed to 30 sec of 20 L/min DFE. Arrhythmogenic effects were evaluated by electrocardiographic monitoring (ECG test). These effects were quantified after multiple DFE doses. In addition, severity of those arrhythmias was evaluated. Furthermore, using the same procedure for DFE administration, electrolyte and some enzyme levels were evaluated. Following DFE administration blood was collected by cardiac puncture. Sodium, potassium, calcium and magnesium levels were measured, and Lactate dehydrogenase (LDH) and Creatine Kinase (CK) levels represented cardiac markers.
Electrocardiographic monitoring showed that DFE resulted in graded severity of arrhythmias from minor skipped beat to serious ventricular fibrillation. Electrolyte levels showed a change in plasma potassium and magnesium level while sodium and calcium levels did not change. In addition, LDH and CK levels in DFE administered rats were higher as compared to control rats. Further organ bath experiments will be performed to determine the possible mechanism.
These results suggest DFE show cardiotoxic effects in form of arrhythmias and in addition, there were altered plasma potassium and magnesium levels followed by higher LDH and CK levels.

PS 499 Effects of Methanolic Extract of *Clerodendrum violaceum* Leaf on Selected Indices of Cardiovascular Diseases in Rat

E. A. Balogun, H. I. Zailani and J. O. Adebayo. *Biochemistry, University of Ilorin, Ilorin, Kwara, Nigeria.*

Clerodendrum violaceum is a medicinal plant used indigenously in Nigeria for the treatment of various diseases, especially malaria. However, the toxicity of the indigenously used leaf extract of this plant has not been extensively studied. Therefore, the possible toxic effects of the methanolic extract of *C. violaceum* leaf was evaluated in this study using selected indices of cardiovascular indices. Thirty mice were randomly divided into six groups (A, B, C, D, E and F) of five mice each. Distilled water was administered orally to mice in group A (control) while mice in groups B, C, D, E and F were administered orally 31.25, 62.5, 125, 250 and 500 mg/Kg body weight of methanolic extract of *C. violaceum* leaf for 28 days. Then alkaline phosphatase (ALP), creatine kinase (CK) and aspartate aminotransferase (AST) activities in the heart and serum of the mice were determined. Also, the serum lipid profiles of the mice were determined. The results revealed that the methanolic extract of *C. violaceum* leaf did not cause any significant change ($P>0.05$) in heart ALP activity at all doses administered but significantly increased ($P<0.05$) serum ALP in a dose-dependent manner compared to controls. The methanolic extract of *C. violaceum* leaf caused no significant change ($P>0.05$) in creatine kinase activities in the heart and serum at all doses administered compared to controls. However, the extract significantly reduced ($P<0.05$) AST activities in the heart and serum at the highest dose administered compared to controls. The extract did not cause any significant alteration ($P>0.05$) to serum lipoprotein (a) concentration at all doses administered but significantly reduced ($P<0.05$) serum total cholesterol, LDL-cholesterol and atherogenic index in a dose dependent manner compared to controls. The results of this study suggest that the methanolic extract of *Clerodendrum violaceum* leaf may not predispose subjects to cardiovascular diseases, especially at lower doses.

PS 500 Species Difference in Isoproterenol-Induced Cardiotoxicity between Sprague-Dawley Rats and Duncan Hartley Guinea Pigs

M. Pannirselvam, J. Wan, J. Ooi, S. Bolts, M. Sanders and D. W. Brewster. *Drug Safety Evaluation, Vertex Pharmaceuticals, Cambridge, MA.*

In the clinical setting, serum levels of cardiac troponin I and cardiac troponin T are widely used in the detection of acute myocardial infarction and other cardiac conditions. These along with other cardiac specific biomarkers such as fatty acid-binding proteins have been previously measured in several experimental models utilizing rats, mice, dogs and non-human primates. The objective of the present study was to compare isoproterenol-induced cardiotoxicity in rats and guinea pigs using the meso scale discovery (MSD) rat muscle injury panel along with histopathology. Male guinea pigs and rats were injected subcutaneously either with saline at 1 ml/kg or single dose of isoproterenol at 4 mg/kg. Four and 24 hours post injection, blood samples were collected for troponin levels and at 24 h heart and skeletal muscle were harvested for histopathological examination. Isoproterenol injection in rats induced a significant increase in the cardiac troponin I levels, fatty acid binding protein and myosin light chain at 4 h and correlated to ventricular damage on histopathology. Surprisingly, there was a significant increase in the skeletal muscle troponin levels at four hours. Selectivity of cardiac vs. skeletal troponin detection was confirmed using heart and skeletal muscle homogenate as well as with purified proteins. However, the same dose of isoproterenol did not induce any change in cardiac troponin level or histopathological lesions in guinea pigs. In summary, our data suggests a species difference in the cardiac injury to isoproterenol.

PS 501 DAPM-Induced Alterations in Serotonergic Signaling May Be Aryl Hydrocarbon Receptor-Mediated in a Novel Model for Female-Specific Pulmonary Arterial Hypertension

M. A. Carroll Turpin, V. Y. Hebert, T. Chotibut and T. R. Dugas. *Pharmacology, Toxicology and Neuroscience, LSUHSC-Shreveport, Shreveport, LA.*

Pulmonary Arterial Hypertension (PAH) is a cardiovascular disorder characterized by elevated pulmonary artery pressure as a result of arterial wall thickening. Though relatively rare, it is inevitably fatal. The few available therapies only slow progression – there is no cure. Patients are 3-4 times more likely to be women than men. Our purpose was to develop a relevant animal model of PAH in order to identify sex differences that contribute to disease progression, and in doing so, identify potential new treatment strategies. 4,4'-Methylenedianiline (DAPM) is an aromatic amine used industrially in the synthesis of polyurethanes. Chronic, intermittent treatment of rats with DAPM results in medial hyperplasia of pulmonary arterioles, exclusively in females, coupled with increases in pulmonary arterial pressures. After 12 wk, significant increases in plasma levels of serotonin (5-HT) were observed in females but not males treated with DAPM. This elevated 5-HT was also significantly correlated with peak pressure gradient, an indirect measure of pulmonary arterial pressure. DAPM-treated females also exhibited increased levels of the serotonin transport protein 5-HTT, or SERT, in their pulmonary arteries. 5-HT is known to induce HPVSMC proliferation and its role in PAH has been established.
In culture, DAPM stimulated female human pulmonary artery endothelial cells (HPAEC) to release 5-HT. No such response was seen in male cell isolates. Additionally, human pulmonary artery smooth muscle cells (HPAVSMC) were stimulated to take up 5-HT, and to proliferate, when treated with DAPM. In our attempts to determine the mechanism(s) by which DAPM elicits these effects, we have observed DAPM-induced activation of the DNA binding target of the aryl hydrocarbon receptor (AhR) - the xenobiotic response element (XRE). Ongoing studies are seeking to address the extent at which the AhR mediates the observed DAPM-induced effects *in vitro* and *in vivo*.

PS 502 Fenofibrate Reduces Cardiac Fibrosis Due to the Reduction of the DNA Binding Activity of the Hypoxia-Inducible Factor-1/Aryl Hydrocarbon Receptor Nuclear Translocator Complex

S. Ichihara[1], Y. Suzuki[1], S. Tada-Oikawa[1] and G. Ichihara[2]. [1]*Mie University, Tsu, Japan and* [2]*Nagoya University Graduate School of Medicine, Nagoya, Japan.*

Background: The aryl hydrocarbon receptor (AHR) is a transcription factor that binds to DNA as a heterodimer with the AHR nuclear translocator (ARNT) after interaction with ligands such as polycyclic and halogenated aromatic hydrocarbons found in tobacco smoke and the environment. We investigated the roles of AHR-ARNT signaling on the development of left ventricular hypertrophy and cardiac fibrosis by angiotensin II (Ang II) infusion in mice lacking the AHR gene (AHR-/-). Moreover, we accessed the hypothesis that peroxisome proliferator-activated receptor-α activator, fenofibrate reduces cardiac fibrosis through the ARNT signaling.
Methods and Results: Male AHR-/- and age-matched wild type (WT) mice (n = 8 for each group) were treated with Ang II, infused at a rate of 100 ng/kg/min for 2 weeks. Ang II elevated systolic blood pressure to comparable levels in AHR-/- and WT mice. AHR-/- mice developed prominent concentric cardiac hypertrophy and prominent fibrosis after Ang II infusion compared with WT mice. The expression of ARNT and hypoxia-inducible factor-1α (HIF-1α) as well as genes inducible by HIF-1α, vascular endothelial growth factor (VEGF) were significantly enhanced in the left ventricles of AHR-/- mice after Ang II infusion compared with those of wild-type mice. Moreover, fenofibrate (100 mg/kg/day for 2 weeks, n = 8) reduced the cardiac fibrosis. Fenofibrate inhibited the HIF-1α activity of binding to the VEGF gene promoter and the inhibition was associated with the reduction of the DNA binding activities of the HIF-1α/ARNT complexes.
Conclusions: Ablation of the AHR resulted in enhancement of Ang II-induced cardiac fibrosis. This effect was likely attributable to the associated enhancement of VEGF expression. Fenofibrate reduced cardiac fibrosis and enhanced VEGF expression due to the reduction of the DNA binding activity of the HIF-1α/ARNT complexes.

PS 503 Acute Oral Cardiopulmonary Safety Pharmacology Study of CBL0137 in Cynomolgus Monkeys

K. Kearney[1], P. Atterson[1], A. Purmal[2] and C. Chow[2]. [1]*WIL Research, Ashland, OH and* [2]*Cleveland BioLabs, Buffalo, NY.*

According to the ICHS7A guidelines, new chemical entities (NCE) must be evaluated for potentially undesired effects on the cardiovascular (CV), respiratory, and central nervous systems. Additionally, the ICHS7B guidelines were established to assess the potential of NCE to affect the ventricular repolarization and proarrhythmic risk. Advancements in telemetry technology allow for the concomitant capture of CV, ECG, and respiratory endpoints in conscious, freely moving animals. Such collection paradigms allow researchers to evaluate the relationship between the CV and respiratory systems concurrently, thus providing a more robust risk assessment in a single study, whilst using fewer animals and less test compound.
The objective of the presented investigation was to evaluate the potential acute effects of CBL0137 on respiratory, CV, and ECG following nasogastric administration in telemetry-implanted cynomolgus monkeys. Cardiovascular and ECG data were acquired from implanted telemetry devices, while concurrent respiratory data was acquired via a jacketed system in conjunction with respiratory inductance plethysmography (RIP).
Acute nasogastric administration of CBL0137 to radiotelemetry-implanted male cynomolgus monkeys at 10 and 30 mg/kg resulted in lower arterial blood pressure (systolic, diastolic, and mean arterial pressure) and lower body temperature; and at 30 mg/kg resulted in test article-related prolongation of the heart rate corrected QT (Bazett) intervals. CBL0137 administration at all dose levels had no affect on heart rate, pulse pressure, PR, QRS, and RR interval, ECG waveforms, or respiratory function (respiratory frequency, tidal volume, or minute volume). It is concluded that preclinical safety pharmacology results do not preclude the FIH (First-in-Human) study of CBL0137.

PS 504 Inhibition of Gene Expression of Carnitine Palmitoyltransferase I and Heart Fatty Acid Binding Protein in Cyclophosphamide and Ifosfamide-Induced Acute Cardiomyopathic Rat Models

M. Sayed-Ahmed, M. L. Aldelemy, O. A. Al-Shabanah and M. M. Hafez. *Pharmacology and Toxicology, King Saud University, Riyadh, Saudi Arabia.* Sponsor: S. Albakheet.

It is well documented that high therapeutic doses of cyclophosphamide (CP) and ifosfamide (IFO) are associated with acute and lethal cardiotoxicity. Therefore, this study has been initiated to investigate whether CP and IFO therapy alters the expression of the key genes engaged in long-chain fatty acid (LCFA) oxidation outside rat heart mitochondria, and if so, whether these alterations should be viewed as a mechanism during CP and IFO-induced cardiotoxicity. To achieve the ultimate goals of this study, a total of 60 adult male Wistar albino rats were assigned to one of six treatment groups namely, control, L-carnitine, CP, IFO, CP plus L-carnitine and IFO plus L-carnitine. Treatment with CP and IFO significantly decreased expression of hear fatty acid binding protein (H-FABP) and CPT I genes in cardiac tissues. Moreover, CP but not IFO significantly increased Acetyl-CoA Carboxylase (ACC) mRNA expression. Conversely, IFO but not CP significantly decreased mRNA expression of Malonyl-CoA Decarboxylase (MCD). Both CP and IFO significantly increased serum lactate dehydrogenase (LDH), creatine kinase isoenzyme MB (CK-MB), and malonyl-CoA content in cardiac tissues. Interestingly, carnitine supplementation completely reversed all the biochemical and gene expression changes-induced by CP and IFO to the control values, except CPT I mRNA and protein expression remained inhibited by IFO. Data from the current study suggest that: (1) CP and IFO therapy are associated with the inhibition of the expression of H-FABP and CPT I genes in cardiac tissues with the consequent inhibition of mitochondrial transport and oxidation of LCFA. (2) The progressive increase in cardiotoxicity enzymatic indices and the decrease in H-FABP and CPT I expression may point to the possible contribution of these genes in CP and IFO-induced cardiotoxicity.(3) L-carnitine prevents CP and IFO-induced cardiotoxicity by modulating the expression of genes involved in LCFA oxidation.

PS 504a Effects of Isoproterenol HCl and Moxifloxacin HCl on Cardiovascular, ECG, and Blood Pressure Parameters Assessed via Jacketed External Telemetry (JET) in the Freely Moving Minipig

L. Diehl[1], W. Nungester[1] and D. Regalia[2]. [1]*Charles River, Spencerville, OH and* [2]*Charles River, Reno, NV.*

Telemetric cardiovascular and blood pressure monitoring of minipigs in repeat-dose toxicology studies is beneficial as the minipig is a viable alternative to other socially-conscious species and contributes to the 3Rs of animal testing. Three male and 3 female Gottingen minipigs 4 to 6 months of age were implanted with TA11PAC10-TOX-LA (DSI, St. Paul, MN) devices in the femoral artery. Jacket acclimation was performed for at least 7 consecutive days with at least a 3 day rest period prior to dosing. The animals were treated in a cross-over study design that consisted of subcutaneous administration of isoproterenol HCl on Study Days 1, 7, and 14 at doses of 10 and 30 μg/kg to demonstrate arterial blood pressure decreases and oral administration of moxifloxacin HCl on Days 17, 23, and 30 at doses of 30 and 100 mg/kg to elicit prolongation of the QT interval. Cardiovascular and blood pressure parameters were collected at least 3 hours pre dose to at least 21 hours post dose to encompass both light and dark photoperiods. As minipigs are known to exhibit cardiovascular changes as an anticipatory response to food, feedings were scheduled with other room activities. Decreases in arterial blood pressure from approximately 90-105 to 58-70 mmHg were observed 80 minutes post dose and persisted for 2-5 hrs post dose. Increases in QT interval up to approximately 15 msecs and 35 msecs were observed compared to baseline and control, respectively. The QT prolongation effects manifested approximately 90 minutes post-dose and were still evident at 24 hrs, consistent with established moxifloxacin exposure data in minipigs. This study successfully demonstrated that the laboratory minipig, a commonly used and scientifically and socially-justified species in regulatory toxicity testing can be safely implanted, sufficiently acclimated, and dosed appropriately to collect quality cardiovascular and blood pressure data via external and minimally-invasive telemetric methods.

PS 504b Cardiac Myocyte-Specific AhR Activation Phenocopies Embryonic Dioxin Exposure in Zebrafish

K. A. Lanham, J. S. Plavicki, R. E. Peterson and W. Heideman. *School of Pharmacy, UW Madison, Madison, WI.*

Exposure of zebrafish embryos to 2,3,7,8-tetrachlorordibenzo-p-dioxin (TCDD) activates the zebrafish aryl hydrocarbon receptor 2 (Ahr2) to produce developmental and cardiovascular toxicity. It has been hypothesized that cardiovascular collapse following exposure to TCDD is the cause of early life stage mortality in fish and other species; however, since TCDD acts systemically it is difficult to determine its influence on any one tissue or system. We have constructed a constitutively active AHR (caAHR) that is functional in zebrafish and expressed it tissue specifically to test whether AHR activation in the myocardium reproduces cardiovascular endpoints of TCDD toxicity. We show that AHR activation within the myocardium reproduces most, if not all, of the cardiovascular defects seen following TCDD exposure, in addition to other endpoints outside of the cardiovascular system. This work identifies a single cellular site of TCDD action, the myocardial cell, that can sufficiently account for the cardiovascular collapse and mortality observed following early life stage exposure to TCDD.

PS 504c Cardiovascular Effects of Diesel Exhaust Exposure

M. Berg[1], J. Harrill[2], D. R. Cawthon[2], K. C. Scribner[2], P. T. Goad[2] and T. Hesterberg[3]. [1]*Toxicology, Center for Toxicology and Environmental Health, LLC, Kemah, TX,* [2]*Toxicology, Center for Toxicology and Environmental Health, LLC, Little Rock, TX and* [3]*Toxicology, Center for Toxicology and Environmental Health, LLC, Denver, CO.*

Emissions from diesel engines are a highly variable and complex mixture of particulate and gas-phase compounds derived from the incomplete combustion of fuels, fuel-additives, and lubricating components. While recent scientific evaluations of Traditional Diesel Exhaust (Pre-1988; TDE) continue to show adverse cardiovascular effects at elevated exposures, it is hypothesized that New Technology Diesel Exhaust (Post-2007; NTDE) will not produce such impacts. To evaluate potential cardiovascular endpoints, we reviewed the recent scientific literature, restricting our analyses to publications with well-defined exposures, limited confounders, and occurring through the inhalational route. While controlled human-exposure studies using TDE or TDE-like exhaust examined a variety hemodynamic, inflammatory, thromobogenic, and atherogenic responses; the most consistently observed effect was a marginal, albeit transient, alteration in cardiovascular vasomotor response (e.g. attenuation of vasodilation) in acute, elevated (≥300 μg/m3 DPM) exposures.

These effects appeared reduced or absent in the limited number of studies which evaluated exposure to NTDE or NTDE-like exhausts. Recent animal studies provide mechanistic insight into these cardiovascular endpoints via knockout (ApoE-/-) or spontaneously-hypersensitive animals – models representing sensitive human receptors. The use of these findings to predict potential TDE health effects in most occupationally-exposed individuals is problematic because the DE concentrations used in the animal and human studies were 1-2 orders of magnitude higher than above-ground occupational exposures. While further research on NTDE is needed, an individualistic evaluation of both forms of diesel exhaust is of significant regulatory importance because it provides additional data from which to evaluate whether or not current emission standards are effective in preventing human disease.

PS 505 Identification of Inhibitors of Cytochrome P450 (CYP) 1B1

L. H. Kennedy[1], M. P. Connor[1], J. E. Powers[1], D. Tran[2], A. Parrill-Baker[2], C. H. Sutter[3] and T. R. Sutter[3, 2]. *[1]Chemistry, United States Naval Academy, Annapolis, MD, [2]Chemistry, The University of Memphis, Memphis, TN and [3]Biological Sciences and the W. Harry Feinstone Center for Genomic Research, The University of Memphis, Memphis, TN.*

Cytochrome P450 (CYP) 1B1 is known to be overexpressed in several types of human malignancies, including breast, endometrial and prostate cancers. The role of CYP1B1 in estradiol metabolism to catalyze the hydroxylation at the C-4 position is of specific importance in estrogen-related tumorigenesis. Finding a potent and safe inhibitor to this critical step could lead to chemoprevention of several forms of human cancer. We used the Chembridge online database (www.hit2lead.com) to perform similarity searches, using 2,3',4,5'-tetramethoxystilbene (TMS), a compound known to inhibit CYP1B1 activity, as the search target. A 50% similarity threshold was used, reporting all compounds with a similarity of ≥50% as hits. The database determines the similarity of a compound with respect to the lead compound using the Tanimoto coefficient. Ultimately, 64 compounds were tested at a single concentration for inhibition of CYP1B1 catalyzed ethoxyresorufin-o-deethylase (EROD) activity. Five compounds inhibited EROD activity to an extent equal to or greater than TMS, and were considered positive hits. CYP1-selectivity was determined using the EROD assay, several concentrations of the five compounds, and CYP1A1, CYP1A2, and CYP1B1. The five compounds varied in selectivity, but all were more selective for CYP1B1 than either CYP1A1 or CYP1A2. Kinetic studies were used to determine the K_i and the mechanism of enzyme inhibition for these compounds. Spectral binding analysis using recombinant CYP1B1 was used to determine the observed binding spectrum; type I, reverse type I, or type II. Several of these lead compounds are more potent and selective than TMS for inhibition of CYP1B1 and could potentially lead to new discovery in the treatment and prevention of cancer.

PS 506 CYP1B1 Expression Is Induced by Leptin through Ligand-Independent Activation of ERα Pathway in MCF-7 Cells

T. Khanal, H. Kim, J. Choi and H. Jeong. *Pharmacy, Chungnam National University, Daejeon, Republic of Korea.*

Leptin, a hormone with multiple biological actions, is produced predominantly by adipose tissue. Among its functions, leptin is able to stimulate tumor cell growth. Estrogen receptor-alpha (ER-alpha), which plays an essential role in breast cancer development, can be transcriptionally activated in a ligand-independent manner. This study investigated the effect of leptin on CYP1B1 expression and its mechanism in breast cancer cells. Leptin induced CYP1B1 protein, messenger RNA expression and promoter activity in ER-alpha-positive MCF-7 cells but not in ER-alpha-negative MDA-MB-231 cells. Transient transfection with CYP1B1 deletion promoter constructs revealed that the estrogen response element (ERE) plays important role in the up-regulation of CYP1B1 by leptin. Furthermore, leptin stimulated phosphorylation of ER-alpha at serine residues 118, 167, and 305 and increased the ERE-luciferase activity, indicating that leptin induced CYP1B1 expression by ER-alpha activation. Finally, leptin activated ERK, Akt, and PKA signaling pathways which are upstream kinases related to ER-alpha phosphorylation induced by leptin. These results indicate that leptin-induced CYP1B1 expression is mediated by ligand-independent activation of the ER-alpha pathway as a result of the activation of ERK, Akt, and PKA in MCF-7 cells.

PS 507 Metformin Inhibits Aryl Hydrocarbon Receptor-Mediated Induction of CYP1A1 and CYP1B1 in Breast Cancer Cells

M. Do, T. Tran, H. Kim and H. Jeong. *Pharmacy, Chungnam National University, Daejeon, Republic of Korea.*

Induction Cytochrome P450 (CYP) 1A1 and CYP1B1 by endogenous ligands or xenobiotic compounds through the activation of the aryl hydrocarbon receptor (AhR) has been implicated in a variety of cellular processes relate to cancer such as transformation and tumorigenesis. Here, we study the effects of anti-diabetes drug metformin on the expression of CYP1A1 and CYP1B1 in breast cancer cells under basal and inducible conditions. Results showed that metformin markedly reduced the expression of CYP1A1 and CYP1B1 mRNAs and proteins in breast cancer cells under basal and TCDD-induced conditions. The inhibition of AhR expression is required for the reduction of CYP1A1 and CYP1B1 transcriptional expression by metformin. The down-regulation CYP1A1 and CYP1B1 expression by metformin was independent of ERα. Additionally, metformin significantly down-regulated Sp1 protein expression in breast cancer cells, and the use of genetic and pharmacological means demonstrated that the down-regulation of AhR expression by metformin mediated through the reduction of Sp1 protein. Our findings indicate that metformin suppresses CYP1A1 and CYP1B1 expression in breast cancer cells by down-regulating AhR signaling pathway. These results provide evidences for the use of metformin as a drug for cancer prevention and treatment.

PS 508 Suppression of NADPH-Cytochrome P450 Reductase Causes Vacuolization in Renal Proximal Tubules in Mice

S. Liu[1, 2], K. Dickman[3], S. Sell[1], X. Ding[1], C. Mei[2] and J. Gu[1]. *[1]Wadsworth Center, Albany, NY, [2]Changzheng Hospital, Shanghai, China and [3]Stony Brook University, Stony Brook, NY.*

Cytochrome P450 reductase (CPR or POR) is an obligatory redox partner for all microsomal P450 enzymes, which play crucial roles in the metabolism of numerous drugs, environmental chemicals, and endogenous regulatory molecules. Germline deletion of mouse Por is known to disrupt embryonic development, and POR functional deficiency resulting from genetic polymorphisms in people leads to disordered steroidogenesis and Antley-Bixler syndrome. Large interindividual variations in levels of POR expression are found in human liver and extrahepatic tissues; but the impact of such variations on physiology or disease risk is unknown. A substantial decrease in POR expression, in a mouse model with global suppression of POR expression (named Cpr-low mouse), was previously found to lead to altered sex steroid hormone homeostasis and female infertility, as well as decreased capacity for xenobiotic metabolism. The aim of this study was to further characterize the Cpr-low mouse model, in order to identify additional phenotypes that may reveal vulnerability in people with low POR expression. Here we report age-dependent appearance of marked vacuolization in the proximal tubules of 4-9 month old male (but not female) Cpr-low mice. The vacuoles, which were negative for fat (Oil-red O) and glycogen (PAS) staining, were localized in S1/S2, but not S3, segment of the proximal tubules. Further analysis with electron microscopy revealed that the vacuoles ranged from small, clear structures to large osmophillic bodies consistent with lysosomes. Given the known association of proximal tubule vacuolization with renal diseases and chemical-induced renal injuries, our results suggest that chronic suppression of POR expression may lead to increased susceptibility to renal injuries/diseases. Further studies are under way to delineate the mechanisms of the renal vacuolization and characterize any associated deficits in renal function.

PS 509 First Report of Possible Biotransformation of Tetracycline to Doxycycline in *Brassica chinensis* L

H. Chen[1], P. Chen[1], R. Lee[2], C. Wei[1] and C. Chou[1]. *[1]Veterinary Medicine, National Chung-Hsing University, Taichung, Taiwan and [2]Chemistry, National Chung-Hsing University, Taichung, Taiwan.*

Metabolic biotransformation referred to the process by which a drug is structurally modified in a living entity, presumably to reduce associated toxicity (detoxification) of the drug and to accelerate elimination. However, bioactivation can also occur, complicating the prediction of the metabolic outcome. Cytochrome P450 are enzymes responsible for drug biotransformation in both animals and plants but the metabolites may differ significantly. For instance, the biotransformation of tetracycline (TC) to epimer-tetracycline and hydroxytetracycline has been reported in animals but not in plants. In a pharmacokinetic study of TC in *Brassica chinensis* L. grown hydroponically, we found initial evidence that TC was uptaken and possibly biotransformed to doxycycline (DC) in the leaves after 5 days of cultivation. The suspected DC compound was first identified by HPLC-UV chromatogram and further confirmed by liquid chromatography–electrospray ionization-mass spectrometry (LC–ESI/MS) in positive mode. The protonated molecule, [M+H]+ of

m/z 445 was used to confirm the presence of TC and DC. It is interesting to note that DC was not found in the petioles or roots and not detectable in the leaves until day 5 (prior sampling was on day 2), suggesting likely a tissue specific and relatively slow biotransformation process. Since biotransformation has great potential to generate novel products or to produce known products more efficiently, further studies to establish the time-dependency of DC production from TC and to delineate possible involving enzymes are warranted.

PS 510 Disposition of 2, 2', 3, 3', 6, 6'-Hexachlorobiphenyl (PCB 136) in Mice with Liver-Specific Deletion of the Cytochrome P450 Reductase Gene

X. Wu, A. Kammerer and H. Lehmler. *Univ. of Iowa, Coralville, IA.*

PCB 136 is oxidized by hepatic cytochrome P450 enzymes to neurotoxic hydroxylated PCB metabolites (OH-PCBs) in mice. We hypothesized that mice with a liver-specific depletion of the cytochrome P450 reductase (cpr) gene oxidize PCB 136 more slowly compared to wild type, thus resulting in overall higher PCB 136 tissue levels compared to wild type mice. To test this hypothesis, eight week old female mice with a liver-specific deletion of the cpr gene (KO; n=7) and their wild type littermates (WT; n=4) were dosed orally with PCB 136 on a cookie (30 mg/kg b.w.). KO (n=5) and WT (n=5) control animals received the vehicle (cookie) only. Animals were euthanized 3 days after PCB administration and PCB 136 and OH-PCB levels were determined in adipose, blood, brain and liver tissues. PCB 136 levels decreased in the order adipose > liver > brain > blood in both KO and WT mice. OH-PCBs were detected in the blood and liver, but not the adipose and brain from KO and WT mice. PCB 136 levels in all tissues investigated were higher in KO compared to WT mice. In contrast, OH-PCB levels were either not significantly different between both mouse strains or significantly higher in KO mice. Feces was the major route of elimination of PCB 136 and OH-PCBs in both mouse strains; however, the time course of elimination differed between KO and WT mice. Significantly more PCB 136 and OH-PCBs were eliminated with the feces on day 1 in WT compared to KO mice (24% vs. 17% of the total dose, respectively). The opposite was true in day 3 feces samples, with 6.6% and 3.5% of the total dose being eliminated from KO and WT animals, respectively. These findings suggest considerable differences in the toxicokinetic of PCB 136 in KO versus WT mice due to an altered metabolism of PCB 136. KO mice may be a good genetic model to study the role of metabolism in the developmental neurotoxicity of PCBs.

PS 511 Influence of Human Cytochrome P450 2A13 in Tobacco-Specific Nitrosamine-Induced Carcinogenesis with a Transgenic Zebrafish Model

H. Chiang[1], T. Liu[1], M. You[2, 3], Y. Shen[4], J. Wu[5] and T. Tsou[1]. [1]*Division of Environmental Health and Occupational Medicine, National Health Research Insititutes, Zhunan, Taiwan,* [2]*Institute of Molecular and Genomic Medicine, National Health Research Institutes, Zhunan, Taiwan,* [3]*Taiwan Zebrafish Core Facility at ZeTH, National Health Research Institutes, Zhunan, Taiwan,* [4]*Pathology Core Laboratory, National Health Research Institutes, Zhunan, Taiwan and* [5]*Institute of Cellular and Organismic Biology, Academia Sinica, Taipei, Taiwan.* Sponsor: P. Lin.

The carcinogenicity of tobacco-specific nitrosamines (TSNAs) mainly depends on metabolic activation of TSNAs by cytochrome P450 enzymes (CYPs). CYP2A13 expression potentiates the TSNAs-induced mutagenesis *in vitro*, suggesting the important role of CYP2A13 in the TSNAs-induced carcinogenesis. Because zebrafish, with no CYP2A orthologous gene, have extremely low CYP2A enzyme activity, establishment of a CYP2A13-transgenic zebrafish model is a promising strategy to minimize the interference of endogenous CYP2As and to highlight the impact of CYP2A13 on the CYP2A13-mediated biological consequences, such as tumor formation. The present study aimed to determine the *in vivo* effect of human CYP2A13 on the TSNAs-induced carcinogenesis by using zebrafish models. A transgenic zebrafish model with a CYP2A13-mCherry fusion protein specifically expressed in liver was established. CYP2As enzyme activity in the CYP2A13-transgenic zebrafish was significantly higher than that in the wild-type control. Following TSNAs treatments, the TSNAs-induced DNA adducts and metabolites were significantly increased in the CYP2A13-transgenic zebrafish. Furthermore, we found marked changes in liver histology in the CYP2A13-transgenic zebrafish with chronic TSNAs treatments, including severe liver steatosis, bile duct proliferation, hepatoma and bile duct carcinoma. The present study reveals the metabolic effects of CYP2A13 on the TSNAs-induced genotoxicity *in vivo*. It is noted that CYP2A13 expression potentiates the TSNAs-induced carcinoma formation in zebrafish, supporting the important role of CYP2A13 in the TSNAs-induced carcinogenesis in humans.

PS 512 Cytochrome P450 Monooxygenases Expression in Human Bronchial Epithelial Calu-3 Cells under Different Culture Conditions

T. Hansen, M. Niehof and J. Knebel. *In vitro and Mechanistic Toxicology, Fraunhofer Institute of Toxicology and Experimental Medicine, Hannover, Germany.* Sponsor: C. Dasenbrock.

The pulmonary epithelium is the first barrier for airborne xenobiotics and inhaled drugs and the cell line Calu-3 is a well characterized model for *in vitro* tracheobronchial epithelial permeability. To serve as a model for toxicity testing of airborne substances (gases, aerosols, particles), Calu-3 cells can be cultured under air interfaced culture (AIC) conditions. However, there is little information regarding the metabolic properties of Calu-3 cells under AIC conditions compared to conventional liquid covered culture (LCC) conditions. It was thus the goal of this study to characterize the basal and inducible cytochrome P450 (CYP) isoform expression in Calu-3 cells under AIC and LCC conditions. Calu-3 cells were cultured under AIC and LCC conditions and induction experiments were started on day 11 after passage. The transepithelial electrical resistance (TEER) was measured to monitor the barrier properties of the cell monolayers. CYP expression was determined using real-time reverse transcription quantitative polymerase chain reaction (RTqPCR). Comparable basal expression of CYP1B1, CYP2B6/7, CYP2J2, CYP2C, CYP2E1, CYP2D6, CYP1A1, CYP3A4, CYP3A5 and CYP3A7 was detected under both conditions, which is consistent with expression in the human lung. Omeprazole, a well-known activator of the aryl hydrocarbon receptor (AhR) induced CYP1A1 and CYP1B1 in Calu-3 cells under both conditions, with stronger induction being observed in AIC cultures. Dexamethasone acts via glucocorticoid receptors and we found slight but significant induction of CYP3A4 and CYP3A5 in LCC cultures only. In summary, Calu-3 cells express a broad range of CYPs under both culture conditions with preserved inducibility for the main lung CYPs 1A1 and 1B1 and are thus a valuable model of the airway epithelial barrier for *in vitro* toxicity testing of airborne substances.

PS 513 Analysis of DNA-Adducts in Lymphatic Tissues of Mice Treated with the Polycyclic Aromatic Hydrocarbon Dibenzo[def, p]chrysene

T. Harper[1, 2], F. T. Lauer[3], L. K. Siddens[2], J. Morre[4], S. W. Burchiel[3] and D. E. Williams[1, 2, 4]. [1]*Linus Pauling Institute, Oregon State University, Corvallis, OR,* [2]*Superfund Research Program, Oregon State University, Corvallis, OR,* [3]*Pharmaceutical Sciences, University of New Mexico College of Pharmacy, Albuquerque, NM and* [4]*Environmental Health Sciences Center, Oregon State University, Corvallis, OR.*

The polycyclic aromatic hydrocarbon (PAH) dibenzo[def,p]chrysene (DBC, also known as dibenzo[a,l]pyrene) is a ubiquitous environmental contaminant. In the laboratory DBC is a potent carcinogen reported to cause skin, lung, and ovarian tumors in mice. The U.S.-EPA considers DBC approximately 30-times more potent as a carcinogen than benzo[a]pyrene. The International Agency for Research on Cancer (IARC) recently increased DBC's classification to a probable human carcinogen (class 2A). Metabolism of DBC to the ultimate genotoxic metabolite, 11,12-dihydrodiol-13,14 epoxide (DBCDE), by CYP1B1 is reported to form DNA adducts in oral tissues and ovaries of DBC-exposed mice. Furthermore, our laboratories have demonstrated that DBC is an immunotoxicant resulting in suppression of T cell-dependent antibody response (TDAR) in splenic cells of mice exposed orally, and an inducer of T-cell lymphoma in offspring exposed transplacentally. We therefore hypothesize that DBC-mediated immunotoxicity in orally exposed mice is a result of DNA-adduct formation leading to genotoxicity targeting the immune system and lymphatic organs. To test this hypothesis we treated 8-week old male C57Bl/6J mice with 10 mg/kg DBC in pill form for 5 consecutive days. The mice were euthanized 3 days after the last exposure. Liver, lung, lymphatic organs, and bone marrow cells were snap frozen and stored at -80°C. Preliminary analysis, using stable isotope dilution UPLC-MS/MS, successfully separated and detected 15N labeled DBCDE-dA internal standards establishing the required parameters for adduct detection in a more complex matrix such as mouse lymphatic tissues. This research was supported by PHS NIH grants ES019968 and ES016465.

PS 514 Evaluating the FAD-Reduction and Transfer Reaction in a Engineered Styrene Monooxygenase System

N. Okonkwo, B. Aseffa, J. Brionies and G. Gassner. *Chemistry and Biochemistry, San Francisco State University, San Francisco, CA.* Sponsor: F. Bayliss.

More than 20-million tons of styrene are produced annually in the United States for use in the synthesis of commercial plastics and rubbers. Styrene and its metabolites act as biological membrane disrupters and intracellularly where they are trans-

formed by cytochrome p450 isoforms to form styrene oxides and vinylphenols, which have biological activity as pulmonary and hepatic poisons. This toxic vinyl benzene is a danger to living systems and for this reason we have focused our research on the styrene detoxification pathway in *Pseudomonas putida* (S12) bacteria. The first enzyme, styrene monooxygenase (SMO), a two-component flavoenzyme with an NADH specific reductase, SMOB, and a FAD specific epoxidase, SMOA, which catalyzes the epoxidation of styrene to yield styrene oxide. Here, SMOB binds NADH and oxidized FAD as substrates and catalyzes the reduction of FAD by a hydride-transfer mechanism. The recently reported crystallographic and mechanistic investigation of SMOB suggests that disorder in the N-terminal region of the reductase may play an important role in the SMOB-SMOA interaction and subsequent FAD transfer. Studies of naturally occurring and engineered SMO fusion proteins further support this idea.
Our present research evaluates the catalytic mechanism of an N-terminally histidine-tagged version of styrene monooxygenase reductase (N-SMOB). We found that the impact of this N-terminal tag is manifested in an increase FAD-binding affinity (Kd ~ 50 nM), which is nearly an order of magnitude greater than that of the wild type reductase, SMOB. The change in FAD-binding affinity impacts the steady-state kinetic mechanism, which changes from sequential in the wild-type enzyme to double displacement in the case of N-SMOB. Non-linear least squares curve fitting gives estimates of the Km values of NADH, and FAD and Vmax of N-SMOB to be 5.0 μM, 3.7 μM, and 38.0 μMs-1, respectively. These findings will be presented together with their implications in the single turnover hydride- and flavin-transfer reactions of the two-component SMO system.

PS 515 Elimination Kinetics of 4-Chlorobiphenyl (PCB3) after Acute Inhalation Exposure

K. Dhakal[1, 2], A. Adamcakova-Dodd[2], H. Lehmler[1, 2], P. S. Thorne[1, 2] and L. W. Robertson[1, 2]. [1]*Interdisciplinary Graduate Program in Human Toxicology, The University of Iowa, Iowa City, IA and* [2]*Occupational and Environmental Health, The University of Iowa, Iowa City, IA.*

PCB3 is a semi-volatile, lower chlorinated congener of Polychlorinated Biphenyls (PCBs). Semi-volatile PCBs are found in the buildings built before 1970s. Previously, we reported that PCB3 undergoes rapid metabolism by hydroxylation, sulfation, and glutathione conjugation following i.p and inhalation exposures. Here we investigated tissue disposition, elimination, and general toxicity after inhalation exposure to PCB3 in rats after acute inhalation exposure for 2h. The experiment was carried out in two shifts in a setting that generated air concentrations of PCB3 of 2.1 and 1.4 mg/m3. Rats in the first shift (n=3) received an estimated dose of 35 μg/rat, and were immediately transferred to metabolism cages for the collection of urine and feces, and killed at 24 h. In the second shift (n=12), they received 21 μg/rat, and killed at 0, 1, and 4 h. At 0 h after exposure, the concentration of hydroxylated (OH-PCB3) and sulfated metabolites were 7±1 and 560± 60 ng/mL serum, 213±123 and 842± 80 ng/g liver, 110 and 87 ng/g lung, and 40 and 6 ng/g brain, respectively. They followed first-order kinetics with elimination half-lives of 5.2 and 9.9, 3.5 and 8.3, 3.8 and 8.7, 4.2 and 8.0 h for OH-PCB3, 4'PCB3 sulfate, 3'PCB3 sulfate, and 3PCB3 sulfate from serum and liver, respectively. Approximately 1/3 of the dose was recovered from urine within 24 h, which consisted of OH-PCB3 and sulfates in the ratio of 1:6. While OH-PCB3 and PCB3 were also recovered from feces, the fecal route was minor. Although PCB3 metabolites penetrated the brain, and have been reported to displace thyroxine (T4) from transthyretin in vitro, serum T4 levels were normal. There was no difference in 8-oxo-dG levels in urine, a marker of oxidative stress due to electrophilic bioactivation of PCB3, between control and PCB3 exposed rats.Our findings will be useful for future PBPK modelling of inhalation exposure to airborne PCBs. (P42 ES 013661)

PS 516 2-DE and MALDI-TOF/TOF As a Tool to Monitor CYP2 Family Isoforms in the Phenobarbital-Treated Mouse Liver Microsomes

M. Lauan[1], K. Suzuki[2], T. Agusa[1] and H. Iwata[1]. [1]*Center for Marine Environmental Studies(CMES), Ehime University, Matsuyama, Japan and* [2]*Graduate School of Science, Hiroshima University, Hiroshima, Japan.*

Cytochrome P450s (CYPs) constitute a superfamily of membrane-bound proteins that participate in metabolism of environmental contaminants and drugs. Advances in mass spectrometry (MS)-based proteomics have provided a potential for the identification of CYPs. However, the application of MS-based proteomics is still limited due to the high sequence homology and insolubility of CYP proteins. A comprehensive analysis of CYP isoform-specific expression is essential for a better understanding of the molecular basis of xenobiotic metabolisms and their toxic mechanisms. The goal of the present study was to identify a variety of CYP proteins, and to characterize their protein expression levels by two-dimension electrophoresis (2-DE) and matrix-assisted laser desorption/ionization time-of-flight tandem mass spectrometry (MALDI-TOF/TOF). Liver microsomes were prepared from female MRL/lpr mice treated with phenobarbital (PB). Following isoelectric focusing with three immobilized pH gradient strips (pH 6-11, 3-10 and 3-11) and staining the 2-D gels with Coomassie blue, protein spots detected in the range of 45-60 kDa and pH 5.5-11 were picked up and digested with trypsin. Extracted peptides were subjected to MALDI–TOF/TOF for the identification of proteins by peptide mass fingerprinting (PMF) and MS/MS analysis. The CYP isoforms identified were 2B10, 2F2, 2C29, 2C37, 2C50, 2C54, and 2C55. Higher protein expression levels of some CYP2s were found in the hepatic microsomes of PB-treated mice, compared with control mice. Multiple spots were identified as CYP2C29 in the PB-treated mice, suggesting PB-induced post-translational modifications of this CYP isoform. Induction of CYP2B and CYP2Cs was further confirmed by pentoxy- and benzyloxyresorufin O-dealkylase assay and Western blot analyses. These results suggest that the combination of 2-DE and MALDI-TOF/TOF would be a useful tool to comprehensively monitor the "Omics" of CYP proteins.

PS 517 Biotransformation of Organohalogen Compounds in the Liver Microsomes of Cats and Dogs

H. Mizukawa[1], K. Nomiyama[2], S. Nakatsu[3], A. Kubota[4], H. Iwata[2], Y. Ikenaka[1], S. Tanabe[2] and M. Ishizuka[1]. [1]*Hokkaido University, Sapporo, Japan,* [2]*Ehime University, Matsuyama, Ehime, Japan,* [3]*Nakatsu Veterinary Surgery, Sakai, Osaka, Japan and* [4]*Woods Hole Oceanographic Institution, Woods Hole, MA.*

The present study was conducted to identify and quantify metabolites of polychlorinated biphenyls (PCBs) in liver microsomes of cats and dogs. Following the treatment of the microsomes with a mixture of 64 PCB congeners, the microsomes were incubated, and derived hydroxylated PCBs were analyzed by gas chromatography-mass spectrometer. The chemical analysis showed higher levels of 3-4Cl OH-PCBs in the cat liver microsomes. These OH-PCBs may be products of PCBs with hydrogens at adjacent ortho- and meta- positions of biphenyl rings, suggesting the catalytic reaction CYP1A enzymes for the PCB metabolisms. In fact, an immunoblot analysis revealed higher levels of CYP1A expression in cats than in dogs. Biotransformation rates from anticipated precursor PCBs to identified OH-PCB metabolites were estimated to be a few percentages (0.23-1.2 %). However, decrease rates of precursor PCBs (0.80-54 %) were higher than biotransformation rates as identified above. This suggests that PCBs are degraded not only to identified OH-PCBs but also to other unexpected products such as di-hydroxylated and/or dechlorinated congeners. Tri- to hepta-chlorinated OH-PCBs were detected in the hepatic microsomes of dogs. This result was in contrast with our previous findings showing that these OH-PCBs were not found in the dog blood, suggesting that lower chlorinated OH-PCBs were easily eliminated through the phase II conjugation reaction. Decrease rates of precursor PCBs were 0.50-100 % in the dog microsomes, whereas identified OH-PCB metabolites accounted only for 0.77-7.9 % to the parent PCBs. Especially, 4OH-CB187 which was a dominant congener in the dog blood was not detected in the hepatic microsomes. This implies that 4OH-CB187 is less produced in the liver of dogs but it may be retained in the blood of dogs by binding to transthyretin. The toxicological risk posed by hydroxylated metabolites should be assessed in future studies.

PS 518 Polymorphic Human Flavin-Containing Monooxygenase 3 (FMO3)-Mediated Drug Interactions

M. Shimizu and H. Yamazaki. *Showa Pharmaceutical University, Machida, Tokyo, Japan.*

Human flavin-containing monooxygenase 3 (FMO3) in the liver catalyzes a variety of oxygenations of nitrogen- and sulfur-containing medicines and xenobiotic substances. Loss-of-function mutations of the FMO3 gene, the enzyme responsible for trimethylamine N-oxygenation, cause the inherited disorder trimethylaminuria. From viewpoint of expanding interests for drug interactions mediated by polymorphic FMO3, sulindac sulfide S-oxygenation by human liver microsomal FMO3 was investigated as a model reaction in the present study. Competitive inhibition by methimazole (0–50 μM) on sulindac sulfide S-oxygenation was observed in six individual human liver microsomes (1.0 mg protein/mL) or recombinatly expressed FMO3 proteins (0.025 mM equivalent) in bacterial membrane after co-incubation for 15 min at 37°C. Kinetic analysis showed that activity was inhibited by methimazole in a dose-dependent manner, presumably because of competitive interaction in this study. Sulindac sulfide S-oxygenation activities in human liver microsomes genotyped as homozygous for p.[Glu158Lys; Glu308Gly] FMO3 gene were likely to be suppressed more by methimazole than liver microsomes genotyped as wild type or heterozygotes and had an apparently half inhibition constant (Ki) value. These tendencies were confirmed with recombinantly expressed wild-type and [Glu158Lys; Glu308Gly] variant FMO3 proteins. These results suggest that genetic polymorphism in the human FMO3 gene might lead to some

changes of catalytic efficiency and drug interactions for N- or S-oxygenations of xenobiotics and endogenous substances. In conclusion, since even the most common [Glu158Lys; Glu308Gly] variant FMO3 protein could result in stronger inhibition potential, genetic polymorphism of human FMO3 gene might lead to unexpected drug interactions via modulation of FMO3 catalytic efficiency.

PS 519 Assessment of Metabolic Potential of PCB Congeners in the Baikal Seal (*Pusa sibirica*) Using the Liver Microsome

J. Yoo[1], H. Mizukawa[1, 2], K. Nomiyama[1], C. Kanbara[1], A. Kubota[3], T. Agusa[1], E. Kim[4], S. Tanabe[1] and H. Iwata[1]. [1]*Center for Marine Environmental Studies, Ehime University, Matsuyama, Japan,* [2]*Graduate School of Veterinary Medicine, Hokkaido University, Sapporo, Japan,* [3]*Woods Hole Oceanographic Institution, Woods Hole, MA and* [4]*Department of Life and Nanopharmaceutical Science and Department of Biology, Kyung Hee University, Seoul, Republic of Korea.*

Polychlorinated biphenyls (PCBs), consisting of 209 congeners are biomagnified in the food web and exhibit a broad range of adverse effects. Biotransformation of PCBs is initiated with the insertion of an oxygen atom into the biphenyl ring by cytochrome P450s (CYPs). Toxicokinetics of PCBs occurs in a congener- and species-specific manner. Baikal seals (*Pusa sibirica*) accumulate high levels of some PCB congeners. However, there still remains unknown how CYPs can metabolize PCB congeners in the Baikal seal. We thus assessed the metabolic potential of PCB congeners by CYPs using Baikal seal liver microsomes. The microsomal reaction solution containing a mixture of 62 PCB congeners was incubated with NADPH for 180 min, and the parent PCBs and their hydroxylated metabolites (OH-PCBs) were analyzed by a gas chromatography-mass spectrometry. The factors that potentially affect the metabolism of PCBs were further explored by principal component analysis (PCA). The microsome incubation showed that over 50% of CB19 and CB37 and 20-50% of CB22, CB54, CB77 and CB105 were metabolized by CYP. The PCA analysis suggested that highly chlorinated PCB congeners are less susceptible to metabolism, while congeners with more hydrogen atoms at *meta*- and/or *para*-position(s) of the biphenyl ring are more metabolized. 3Cl- and 4Cl-substituted OH-PCBs were the major metabolites. 4OH-CB79 that may be formed from CB77 was detected at the highest level among the identified OH-PCBs, followed by 4'OH-CB26 and 4OH-CB29, whereas more than 50% of the amount of detected OH-PCBs was unidentified. Only 11.5% of added amount of parent PCBs was recovered as OH-PCBs. These results indicate that there are large unknown CYP-dependent metabolic pathways of PCBs in the Baikal seal.

PS 520 Selective Effects of a Therapeutic Protein-Targeting Tumor Necrosis Factor-Alpha on Cytochrome P450 Regulation during Infectious Colitis: Implications for Disease-Dependent Drug-Drug Interactions

M. D. Merrell[1], B. A. Nyagode[1], R. Jahangardi[1], M. G. Tansey[2] and E. T. Morgan[1]. [1]*Pharmacology, Emory University, Atlanta, GA and* [2]*Physiology, Emory University, Atlanta, GA.*

We studied the impact of administering XPro1595, a novel antagonist of soluble tumor necrosis factor-α (TNFα), on the regulation of hepatic cytochrome P450 enzymes in the *C. rodentium* model of infectious colitis. XPro1595 was administered subcutaneously every three days throughout the infection, or as a single injection near the peak of infection. When given throughout the infection, XPro1595 selectively blocked the down-regulation of Cyp3a11 and 3a25 mRNAs and Cyp3a protein, as well as the induction of Cyp2a4/5, without affecting the down-regulation of Cyp4a10, Cyp4a14, Cyp2b10 or flavin-mooxygenase-3. Induction of Cyp3a11, Cyp3a25, Cyp2c29 and Cyp3a13 mRNAs were observed only in XPro1595-treated mice. Administration of a single dose of XPro1595 was relatively ineffective. These results a) confirm the role of soluble TNFα in hepatic Cyp3a regulation during infectious colitis deduced from studies in TNFR1-null mice; b) indicate the potential for soluble TNFα-specific antagonists to cause disease-dependent drug-drug interactions; and, c) suggest a novel mechanism by which an anti-inflammatory therapeutic protein can produce an opposite effect to that of the disease by selectively neutralizing one of multiple signals regulating drug-metabolizing enzyme expression. More research is needed to determine whether or not this is applicable to other diseases or disease models.

PS 521 Identification of Interspecies Differences in Phase II Reaction in Nonexperimental Mammalian Species

Y. Ikenaka, A. Saengtienchai and M. Ishizuka. *Hokkaido University, Sapporo, Japan.*

Chemical sensitivities have wide degree of variation among species, that why it is important to estimate it in each species. An interspecies difference of xenobiotic metabolism is one of the keys to determine sensitivity. However, especially in non-experimental animals as wildlife and domesticated animals, there is still insufficient information. In the present study, we aimed to evaluate the interspecies differences of phase-II conjugation reaction by using environmentally exposed pyrene (PY) as the indicator. We collected urine from 16 mammalian species and analyzed the PY metabolites from each urine sample. From our results, we found that the glucuronide conjugates were the dominant metabolites in the urine of many species, including deer, humans, cattle, pigs, and horses, etc. However, glucuronide conjugates could not be detected in ferret urine even though ferret UDP-glucuronosyltransferase 1A6 (UGT1A6) was not a pseudogene. Sulfate conjugates were mainly detected in the urine of cats, ferrets, and rabbits. Interestingly, sulfate conjugates had detected in pig urine, although pig is well known species that have limited aryl-sulfotransferase (SULT) activity. However, we couldn't detected the sulfate conjugates from hedgehog's urine. It's indicated that the limited in SULT activity in hedgehogs. We found clear interspecies differences of PY metabolite *in vivo* with nonexperimentally exposed condition, which can reflect the difference in phase-II conjugation reactions.

PS 522 Metabolism of Unsaturated Fatty Acids by CYP2B6

W. S. Baldwin, E. J. Litoff and R. Kumar. *Biological Sciences, Clemson University, Clemson, SC.*

Cyp2bs are crucial in the metabolism of drugs, environmental toxicants, and endobiotics. We produced a Cyp2b-knockdown (KD) mouse for subsequent study of Cyp2b function using lentiviral-promoted shRNA homologous to all five murine Cyp2b subfamily members (Cyp2b10, 2b9, 2b13, 2b19, and 2b23). Wild-type (WT) and Cyp2b-KD mice were treated ip with the Cyp2b-inducer, TCPOBOP dissolved in corn oil, corn oil as a control, or left untreated. Interestingly, the corn oil treated Cyp2b-KD mice retained lipids in their livers as discerned from Oil Red O staining. Corn oil treated WT did not show retention of lipids in the liver and neither did the TCPOBOP-treated Cyp2b-KD mice suggesting that murine Cyp2bs are involved in the metabolism of the lipids in the corn oil (primarily linoleic acid). Serum cholesterol and triglycerides are also higher in the corn oil treated Cyp2b-KD mice relative to their WT counterparts. To discern whether CYP2B's are potentially metabolizing fatty acids and may compete with toxicant metabolism, we examined whether fatty acids, toxicants, and known CYP2B substrates inhibit human CYP2B6. Endosulfan, parathion, atrazine, and triclosan, as well as fatty acids such as linoleic acid, DHA, and arachidonic acid inhibited CYP2B6. Subsequent results were compared to CYP3A4 and atrazine, parathion, and arachidonic acid are significantly more potent CYP2B6 inhibitors than CYP3A4. Linoleic acid, DHA, endosulfan, and triclosan were slightly more potent at inhibiting CYP2B6 than CYP3A4. We are currently investigating the ability of CYP2B6 to metabolize 13Clinoleic acid via GC-MS. In summary, in vivo and in vitro evidence indicates that CYP2B isoforms have an endogenous function in dietary fat metabolism in addition to their role in xenobiotic metabolism. Lipids may compete with toxicants for Cyp2b metabolism and this could lead to hepatotoxicity and fatty liver, especially during consumption of high fat diets such as the current western diet.

PS 523 Contribution of Six Human CYP Enzymes to the Metabolism of the Food Constituents Methyleugenol, Methylisoeugenol, Alpha-, Beta-, and Gamma-Asarone

A. T. Cartus and D. Schrenk. *Food Chemistry and Toxicology, University of Kaiserslautern, Kaiserslautern, Rhineland-Palatinate, Germany.*

Previously we investigated the phase I metabolism of different phenylpropenes (PP) present in food, including the allylic methyleugenol (ME) and gamma-asarone (gA), as well as the propenylic methylisoeugenol (MIE), alpha- (aA), and beta-asarone (bA). ME, aA, and bA are carcinogenic to rodents, whereas MIE is not, and gA has not been investigated so far. Activation of ME occurs via a genotoxic mechanism by forming a sidechain alcohol (1'-OH-ME) which is afterwards sulfonated. After loss of sulfate, it forms a reactive carbocation, which can react with DNA. The molecular mechanism responsible for the carcinogenicity of aA and bA is still not understood.

Here, we performed *in vitro* studies to elucidate the contribution of six prominent human cytochrome P450 enzymes (CYP) to the metabolism of the PP mentioned above. Therefore we incubated Supersomes™ (expressing human CYP1A2, 2A6, 2C19, 2D6, 2E1 or 3A4) with the test compounds at different start concentrations (50–800 μM) over different time spans (20 and 60 min). Main reactions were side chain hydroxylation at the 1'- and 3'-position, oxidation of those alcohols, formation of side chain epoxides and hydrolysis to the corresponding diols, demethylation, and hydroxylation of the benzene ring.
CYP1A2 was by far the most potent enzyme in all incubations with respect to turnover rates, pattern of metabolites, and catalytic efficiencies. In contrast, CYP2A6 was nearly inactive for all substrates.
In case of ME, the formation of the proximate carcinogen 1'-OH-ME, was catalyzed effectively by CYP1A2, moderately by 2C19, 2D6 and 3A4, and very weakly by 2A6 and 2E1. In contrast, CYP2E1 was most active in formation of the ME-epoxide, and the corresponding ME-diol.
CYP3A4 was the most active enzyme in formation of the side chain diols of the propenylic PP MIE, aA and bA.
Taken the different CYP activities of the used Supersomes™ and of human liver microsomes into account, CYP1A2 and 3A4 are the predominant enzymes involved in the biotransformation of the investigated PP.

PS 524 Toxicity Profiling of Breast Cancer-Associated Compounds and ToxCast Chemicals in "Humanized" Budding Yeast Expressing P450 Genes

B. Gaytan[2], D. Faulkner[2], M. Proctor[2], R. Rudel[3], C. Vulpe[2] and M. Fasullo[1]. *[1]Nanobiosciences, College of Nanoscale Sciences and Engineering, Albany, NY, [2]Toxicology, University of California Berkeley, Berkeley, CA and [3]Silent Spring Institute, Newton, MA.*

Many environmental toxicants require bioactivation to become potent genotoxicants. We introduced the P450 genes, CYP1A1, CYP1A2, and CYP3A4 into yeast strains that are deficient in either poly-drug resistance or both recombinational and nucleotide excision DNA repair. We screened over 50 agents and classified the compounds whose toxicity 1) not influenced by P450 expression, 2) enhanced by P450 expression, and 3) reduced by P450 expression. Compounds not influenced by P450 expression include those that directly interact with DNA, such as 4-nitroquinilone oxide, and 12-dibromo-24-dicyanobutane. Compounds whose toxicity is enhanced by P450 expression include testosterone and 2-methoxy-3-aminodbenzofuran. Compounds whose toxicity is decreased by P450 expression include zearalenone. These studies demonstrate that expressing P450 genes can modulate toxicity and genotoxicity of select compounds.

PS 525 A Cocrystal of m-Chlorobenzoic Acid with Furosemide: Prospective Applications

B. London[1], M. O. Claville[2], F. R. Fronczek[3] and R. M. Uppu[1]. *[1]Environmental Toxicology, Southern University and A&M College, Baton Rouge, LA, [2]School of Science, Hampton University, Hampton, VA and [3]Department of Chemistry, Louisiana State University, Baton Rouge, LA.*

Furosemide is a highly used diuretic for the treatment of hypertension and edema and, to a lesser extent, hypercalcemia. This furan containing compound is of interest; however, the toxicity elicited by these core compounds is not well understood. The free furan itself is a known hepato-carcinogen and toxicant as studied in rats and mice. The epoxide metabolite of furans, formed in CYP450-mediated oxidations, can isomerize to highly reactive electrophilic intermediates such as cis-2-butene-1,4-dial. We have performed the oxidation of furosemide with m-chloroperbenzoic acid (m-CPBA), and isolated various epoxide and isomerized products in support of our efforts to understand this type of toxicity mechanism, and to also identify potential biomarkers for furosemide in humans. During the separation and drying of the products of the furosemide-m-CPBA reaction, we observed the formation of crystals in the mother liquor (the organic layer). Analysis of these crystals by X-ray crystallography revealed a nonahydrate cocrystal of furosemide (starting material) with that of m-chlorobenzoic acid (an inadvertent contaminant or the reduced product of m-CPBA). Analogous to the known properties of cocrystals of furosemide with nicotinamide and their pharmaceutical importance, we believe that the cocrystals of furosemide with m-chlorobenzoic acid could have useful applications in drug development and may lead to formulations with improved potency, solubility, and stability. Therefore, this serendipitous finding may have important applications for improving furosemide bioavailability [Support from NSF ACE Implementation grant (HRD-1043316) and the US Department of Education (PO31B040030) is acknowledged; corresponding author's email: rao_uppu@subr.edu].

PS 526 Genome Profiling of Saccharomyces Cerevisiae Resistance to Aflatoxin B1 (AFB1), a Potent Liver Carcinogen

M. Fasullo[1, 2], J. Bard[3], C. Cera[2], P. Egner[4] and T. J. Begley[1, 2]. *[1]Nanobiosciences, College of Nanoscale Sciences and Engineering, Albany, NY, [2]Biomedical Sciences, State University of New York at Albany, Albany, NY, [3]Center of Excellence in Bioinformatics, State University of New York at Buffalo, Buffalo, NY and [4]Bloomberg School of Public Health, John Hopkins University, Baltimore, MD.*

The mycotoxin aflatoxin B1 (AFB1) is a potent liver carcinogen. A signature p53 mutation is found in tumors from liver cancer patients who inhabit AFB1-contaminated areas, suggesting that AFB1 is a potent genotoxin. P450 enzymes convert AFB1 into a highly reactive epoxide that forms N7-guanine DNA adducts, which are unstable and convert into AFB1-formamidopyrimidine (FAPY)-derivatives. These AFB1-associated adducts are either mutagenic or block DNA replication in vitro. In CYP1A2-expressing budding yeast, AFB1 is a weak mutagen but a potent recombinagen, and triggers the formation of recombinational repair foci. A DNA damage-checkpoint response correlates with a delay in cell cycle progression. Microarray analysis reveals that that both DNA repair and stress response genes are up regulated. To elucidate the functional significance of transcriptional induction, we are profiling the yeast genome for AFB1 resistance, using state-of-the-art next generation sequencing to identify molecular barcodes. We introduced the human CYP1A2 into ~90% of the deletion library, and pooled samples have been exposed to 50 μM and 100 μM AFB1 for 20 hrs. We identified genes that confer resistance to AFB1 by barcode sequencing, and additional genes by growth curves. DNA metabolism genes include RAD55, RAD17, REV1, and REV3, emphasizing the potency of the mycotoxin to trigger replication stress. Additional genes include those that function to elevate deoxynucleotides, maintain mitochondria, promote cellular growth and rearrange the cytoskeletal architecture. The ultimate aim will be to identify corresponding mammalian genes. The yeast libraries will be valuable for additional high-throughput studies using other metabolically-activated drugs and carcinogens. Grant support: NIH : R21ES1954, F33ES021133

PS 527 Development of a Selective CYP2B6 and Cell Viability Duplex Assay

M. Curtin, J. J. Cali, D. Ma, H. Wang and P. Meisenheimer. *Promega Corporation, Madison, WI.* Sponsor: T. Riss.

CYP2B6 induction affects drug clearance and potentially contributes to adverse drug interactions in humans. To predict CYP induction in vitro cultured hepatocytes are exposed to a probe CYP substrate and compounds that accelerate probe conversion are scored as CYP inducers. However, induction may be underestimated when cytotoxic compounds reduce CYP activity indirectly by cell killing. To selectively measure effects on CYP2B6 activity while controlling for cytotoxicity we developed a novel CYP2B6/cell viability multiplex assay. For CYP2B6 we synthesized 6-((4,4-dimethoxybutan-2-yl)oxy)benzo[d]thiazole-2-carbonitrile as a probe substrate. This probe is a luciferase pro-substrate that is activated by CYP2B6 then detected as light from a luciferase reaction. A screen of 21 recombinant human CYPs showed strong CYP2B6 selectivity. Selective inhibition of liver microsome probe reactions by known CYP2B6 inhibitors provided further evidence for selectivity. With adherent hepatocytes initial test compound or vehicle treatments were followed by incubation with the probe. The product of the CYP probe reaction is found in the medium so samples were removed and mixed with a luciferase formulation to give luminescence that reflects CYP activity. Hepatocyte viability was then measured by a lytic ATP-based luminescent assay and values from CYP measurements were normalized to respective viability values. Cell based data was consistent with CYP2B6 selectivity in that CYP2B6 inducers and inhibitors respectively elevated or reduced activity (e.g. CITGO vs. Clopidogrel). Fold inductions and IC50s correlated well with reported values from LCMS-based CYP2B6 assays. This approach provides convenience and selectivity for CYP2B6 studies and enhanced biological relevance by normalization to cell viability.

PS 528 Role of CYP2ABFGS in NNK Bioactivation and Lung Tumorigenesis: Insights from a Novel *Cyp2abfgs*-null Mouse

L. Li, V. Megaraj, Y. Wei and X. Ding. *Health Research Inc., Albany, NY.*

Enzymes encoded by the mouse Cyp2abfgs gene cluster are preferentially expressed in the respiratory tract, and a number of these are active toward xenobiotic compounds, including many drugs and a tobacco-specific lung procarcinogen 4-(methylnitrosamino)-1-(3-pyridyl)-1-butanone (NNK). CYP2A5 is already known to mediate a significant fraction, but not all, of NNK bioactivation in the lung. This study was aimed to test the hypothesis that, besides CYP2A5, other CYP2ABFGS enzymes also play significant roles in NNK-induced lung tumorigenesis, with use of a novel Cyp2abfgs-null mouse. Deletion of the constitutive genes in the

Cyp2abfgs cluster was confirmed by RNA-PCR analysis in tissues known to express each gene. The Cyp2abfgs-null mouse was viable, fertile and without any obvious developmental deficits, and they appeared to have no compensatory increase in the expression of other P450s. NNK bioactivation in vitro and NNK-induced DNA adduction and lung tumorigenesis in vivo were studied in wild-type, Cyp2a5-null, and Cyp2abfgs-null mice. The Cyp2abfgs-null mice exhibited significantly lower rates of NNK bioactivation in lung and liver microsomes, compared to either wild-type mice or Cyp2a5-null mice. Consistent with the in vitro data, the levels of lung O6-methyl guanine (O6-mG, the DNA adduct highly correlated with lung tumorigenesis) were substantially reduced in the Cyp2abfgs-null mice, compared to either wild-type mice or Cyp2a5-null mice. Moreover, the Cyp2abfgs-null mice were largely resistant to NNK-induced lung tumorigenesis at a high NNK dose (200 mg/kg), in contrast to the wild-type mice or Cyp2a5-null mice. These results indicate that, collectively, the CYP2ABFGS enzymes play essential roles in mediating NNK-induced lung tumorigenesis.

PS 529 Identification of P450 Activity As a Risk Factor for Metabolism-Dependent Drug-Induced Hepatotoxicity

U. Doshi and A. P. Li. *In Vitro Toxicology, In Vitro ADMET Laboratories LLC, Columbia, MD.*

A possible risk factor for drug-induced hepatotoxicity is drug metabolizing enzyme activity which may vary among individuals due to genetic (genetic polymorphism) and environment factors (environmental pollutants, foods and medications that are inhibitors or inducers of drug metabolizing enzymes). We hypothesize that P450 activity represents one of the key risk factors for hepatotoxicity for drugs that are metabolically activated to cytotoxic/reactive metabolites. After evaluation of >20 lots of human hepatocytes, each from a different donor, we identified one lot, HH1020 (from a 21 year old Caucasian female) to have uniquely P450 high activities for several major human P450 isoforms, with CYP2B6 (bupropion hydroxylation), CYP2D6 (dextromethorphan O-demethylation), and CYP3A4 (midazolam 1-hydroxylation) activities to be 700%, 200% and 800%, respectively, of the average values for the other donors. We evaluated the in vitro cytotoxicity of three metabolism-dependent hepatotoxicants acetaminophen (APAP), cyclophosphamide (CPA), and aflatoxin B1 (AFB1) as well as a direct-acting cytotoxicant, tamoxifen (TMF), in HH1020 versus hepatocytes from two other donors. The hepatocytes were cultured in collagen-coated plates and treated after 4 hours of plating for 24 hrs, following by viability determination using cellular ATP as endpoint. The EC50 values were as follows: APAP: 2.3 mM (HH1020), 9.4 and 10 mM (others), CPA:1.8 mM (HH1020), >5 mM (others), AFB1: 2.8 uM (HH1020), 10 and 22 uM (others), and TMF: 26 uM (HH1020), 29 and 30 uM (others). In a separate experiment, HH1020 was treatment with CPA and AFB1 in the presence of the non-selective P450 inhibitor aminobenzotriazole (ABT). Dose-dependent reversal of cytotoxicity by ABT was observed, confirming the role of P450 metabolism on CPA and AFB1 hepatotoxicity. Our results showed convincingly that HH1020 hepatocytes were significantly more sensitive to metabolism-dependent drug-induced hepatotoxicity, and therefore support the hypothesis that P450 activity is a probable risk factor towards drug-induced hepatotoxicity.

PS 530 Effect of Vinclozolin on Liver Cytochrome P450 Expression and Testosterone and Estradiol Serum Levels During Pregnancy

F. G. Garcia-Montes de Oca[1], M. L. Lopez-Gonzalez[1], R. Chavira-Ramirez[2] and A. Sierra-Santoyo[1]. *[1]Toxicology, CINVESTAV-IPN, Mexico City, Mexico and [2]Instituto Nacional de Ciencias Medicas Y Nutricion "Salvador Zubiran", Mexico City, Mexico.*

Vinclozolin (V) is a fungicide used for agricultural settings. V and its metabolites M1 and M2 bind to the androgen receptor (RA) and act as RA antagonists. They inhibit the androgen-dependent gene expression. V is able to regulate adult rat liver cytochrome P450 (CYP) expression in a complex manner. The information about effects of V on rat liver is limited and there is no information about the effect on testosterone and estradiol serum levels during pregnancy. The aim of this study was determine the effect of V on regulation of rat liver CYP during pregnancy and how affect testosterone and estradiol bioavailability. Pregnant Wistar rats were administered at the dose of 150 mg V/kg/d suspended in corn oil by gavage during gestational days 14-21. Mothers were sacrificed by asphyxia with CO_2. Liver was removed and processed to obtain the microsomal fraction. V exposure increased about 8-fold the content of liver microsomal immunoprotein of CYP2A and 3A2, while CYP1A1, 2B1/2 and 3A1 were induced about 26.7-, 25.6- and 43.7-fold, respectively. On the contrary, the content of CYP1A2 decreased 60% in comparison to non-treated pregnant rats. Likewise, enzyme activities of MROD and PROD increased 21.7- and 817-fold, respectively, and 7α- and 6β-testosterone hydroxylase increased 1.7- and 4.4-fold, respectively. In V-treated pregnant rats testosterone serum levels decreased 56.6% and interestingly estradiol serum levels increased 1.6-fold. These effects produced an increase of 3.5-fold on the estradiol/testosterone ratio. These results indicate that V regulates hepatic CYP expression and alters estradiol and testosterone homeostasis during pregnancy. In addition, they could help to explain the antiandrogenic effects on reproductive system in male offsprings during uterine exposure. (Supported by CONACYT-Mexico No. 168384).

PS 531 Role of P450 Enzymes in Cigarette Smoke-Induced Acute Lung Injury

M. A. Hartog[1, 2] and X. Ding[1, 2]. *[1]Wadsworth Center, New York State Department of Health, Albany, NY and [2]School of Public Health, State University of New York at Albany, Albany, NY.*

The aim of this study is to test the notion that microsomal P450 enzymes can influence the risks of cigarette smoke (CS) induced lung inflammation and tissue damage, an idea supported by the fact that multiple, toxicologically relevant, compounds found in CS are P450 substrates. Based on the protease-antiprotease hypothesis of emphysema development and when considering the inflammatory events observed in COPD, it is thought that pulmonary recruitment of neutrophils and macrophages may play a key role in CS-induced lung diseases. Thus, we examined the cellular profiles in the lungs of wild type (WT) mice and mice with selective abolition of P450 activity; the animals (adult female, all on B6 genetic background) were pre-exposed to either filtered air (FA) or environmental tobacco smoke (ETS) via nose-only inhalation for 5.5 h at a dose of 250 mg/m3 total particulate matter. We found that, the numbers of total cells and of macrophages in bronchoalveolar lavage (BAL) were not significantly different between WT and LCN mice (liver-specific P450 reductase null mice, with little P450 activity in hepatocytes) that were pre-exposed to FA; however, the numbers were 1.5-1.6 fold greater in LCN than in WT mice that were pre-exposed to ETS. ETS-exposed WT and LCN mice both had significant increases in the number of neutrophils in BAL, compared to FA-exposed mice; but the numbers were not different between the two strains. Furthermore, ETS exposure failed to induce a significant increase in the number of BAL neutrophils in Cyp2abfgs-null mice, where all Cyp genes of the Cyp2a, 2b, 2f, 2g, and 2s subfamilies have been deleted throughout the body. An enhanced pulmonary inflammation in ETS-exposed LCN mice, compared to ETS-exposed Cyp2abfgs-null mice, was further confirmed by histological analysis of H&E-stained lung tissue sections. Taken together, these results support the hypothesis that hepatic P450s protect against, whereas lung CYP2ABFGS mediate, the development of ETS-induced acute lung toxicity.

PS 532 Role of Human CYP2A13 and CYP2F1 in Naphthalene Bioactivation and Toxicity in the Lung and Nasal Mucosa of a CYP2A13/2F1-Humanized Mouse

X. Ding[1], L. Li[1], K. Jia[1], M. A. Hartog[1], Y. Wang[1] and L. S. Van Winkle[2]. *[1]Health Research Inc., Albany, NY and [2]UC Davis, Davis, CA.*

The aim of this study is to characterize the expression and activity of CYP2A13 and CYP2F1, two human P450 enzymes expressed preferentially in the respiratory tract. CYP2A and CYP2F enzymes have been reported to metabolize many lung toxicants, including naphthalene (NA). The function of human CYP2A13 and CYP2F1 in NA bioactivation and respiratory tract toxicity was examined in this study, using CYP2A13/2F1-humanized mice and CYP2A13(only)-humanized mice (on Cyp2abfgs-null background). In vitro studies indicated that, while the activity in the nasal olfactory mucosa (OM) of the CYP2A13/2F1-humanized mice was primarily contributed by CYP2A13, the activity in the lung was mainly contributed by CYP2F1. Further in vivo studies were conducted, in order to assess the capabilities of CYP2A13 and CYP2F1 to mediate acute inhalation toxicity of NA, at an NA dose relevant to occupational exposure (10 ppm for 4 h). CYP2A13/2F1-humanized mice showed greater sensitivity than Cyp2abfgs-null mice did, to NA-induced depletion of non-protein sulfhydryl and occurrence of cytotoxicity (observable by routine histology) in the OM (but not lung), when examined at 2 or 24 h after termination of NA exposure. However, preliminary results showed that the lungs of NA-treated CYP2A13/2F1-humanized mice had greater numbers of dye-permeable (injured) cells than that of NA-treated Cyp2abfgs-null mice, in both proximal and distal bronchioles, when examined using an ethidium homodimer incorporation assay, which is more sensitive than routine histology examination. These results demonstrate that both CYP2A13 and CYP2F1 are active toward NA in the lung and OM of the CYP2A13/2F1-humanized mice, and they play a significant role in NA-induced toxicity.

PS 533 Essential Role of the Cytochrome P450 Enzyme CYP2A5 in Olfactory Mucosal Toxicity of Naphthalene

J. Hu[2], L. Sheng[2], L. Li[1], X. Zhou[1], F. Xie[1], J. D'Agostino[1], Y. Li[2] and X. Ding[1]. [1]*Health Research Inc., Albany, NY and* [2]*Institute of Materia Medica, Chinese Academy of Medical Sciences & Perking Union Medical College, Beijing, China.*

Naphthalene (NA), a ubiquitous environmental pollutant that can cause pulmonary and nasal toxicity in laboratory animals, requires cytochrome P450 (P450)-mediated metabolic activation in order to cause toxicity. Our recent study using a Cyp2f2-null mouse showed that CYP2F2 plays an essential role in NA-induced lung toxicity, but not in NA-induced nasal toxicity. The aim of this study was to determine whether mouse CYP2A5, abundantly expressed in nasal olfactory mucosa (OM) and liver, but less in lung, plays the major role in the bioactivation and toxicity of NA in the OM. We found, by comparing Cyp2a5-null and wild-type (WT) mice, that the loss of CYP2A5 expression led to substantial decreases in rates of NA metabolic activation by OM microsomes. The loss of CYP2A5 did not cause changes in systemic clearance of NA (at 200 mg/kg, i.p.). However, the Cyp2a5-null mice were much more resistant than were WT mice to NA-induced nasal toxicity (though not lung toxicity), when examined at 24 h after NA dosing (at 200 mg/kg i.p.), or to NA-induced depletion of total nonprotein sulfhydryl in the OM (though not in the lung), examined at 2 h after dosing. Thus, mouse CYP2A5 plays an essential role in the bioactivation and toxicity of NA in the OM, but not in the lung. Our findings further illustrate the tissue-specific nature of the role of individual P450 enzymes in xenobiotic toxicity, and provide the basis for a more reliable assessment of the potential risks of NA nasal toxicity in humans.

PS 534 High-Throughput Screening to Identify Substrates of Zebrafish Cytochrome P450 1A

J. Y. Wilson and D. H. Alsop. *Biology, McMaster University, Hamilton, ON, Canada.*

Cytochrome P450 (CYP) 1 isoforms catalyze the metabolism of steroids, pharmaceuticals and environmental contaminants in vertebrates. In the world of fish aquatic toxicology, CYP1A is perhaps the best known of the family due to its induction and role as a biomarker with contaminant exposure (often examined with the EROD assay). However, only a handful of substrates for CYP1A have been identified in fish. Presently, we have used heterologously expressed zebrafish CYP1A in a high-throughput screen (HTS) with thousands of bioactive compounds, with the aim of identifying the substrate specificities of this enzyme. Catalytic activity was determined in 50 µl reactions in 384 well plates, testing for NADPH consumption. We screened a 6,400 bioactive compound library consisting of off-patent, natural or pharmacologically active compounds with an average molecular weight of 350 g/mol. NADPH consumption rates were compared to negative (DMSO) and positive (7-methoxyresorufin) controls. A total of 87 and 33 compounds activated NADPH consumption at rates greater than 50% and 100% of the positive control, respectively. However, 13 of the top 40 hits induced significant NADPH loss in the absence of CYP1A enzyme, indicating a small but significant degree of false positives. The top 160 hits were screened for ROS formation, where rates greater than 25% of our positive control (pentoxyresorufin) were observed in 31 compounds (19%), indicating some hits may induce uncoupled reactions. The confirmed top hits included a number of drugs (such as antibiotics and NSAIDs). In addition, there were also a number of endogenous compounds (such as neurotransmitters, peptides and bile acids) and plant compounds (garlicin, chalconoids, flavonoids, alkaloids and monoterpenoids). Although CYP1A is a key enzyme in the context of present day polluted aquatic ecosystems, perhaps the endogenous and plant (dietary) compounds identified here may provide a clue as to substrates that shaped the evolution of this enzyme. Present HTS studies are examining the remaining zebrafish CYP1 isoforms (CYP1B, 1C1, 1C2, 1D) and CYP3A65.

PS 535 Mechanistic Role of Cytochrome P450 (CYP)1A2 in the Persistent Induction of CYP1A1 by the Polycyclic Aromatic Hydrocarbon 3-Methylcholanthrene (MC) in Mouse Heptoma Cells (hepa-1)

S. R. Kondraganti, C. Chu, W. Jiang, L. Wang and B. Moorthy. *Pediatrics, Baylor College of Medicine, Houston, TX.*

Humans are constantly exposed to environmental carcinogenic polycyclic aromatic hydrocarbons (PAHs) through cigarette smoke, diesel exhausts, charcoal-broiled meats, etc. Cytochrome P4501A (CYP1A) enzymes play important roles in the activation of PAHs such as 3-methylcholanthrene (MC) to carcinogenic DNA-binding metabolites. We reported earlier that MC causes persistent induction of hepatic and pulmonary CYP1A1 in mice for several weeks after MC withdrawal, and that the phenomenon of sustained hepatic CYP1A1 induction is lost in Cyp1a2-null mice. In this study, we tested the hypothesis that MC elicits persistent CYP1A1 induction in hepa-1 cells, and that CYP1A2 contributes mechanistically to this phenomenon. Hepa-1 cells were treated with the MC (2.5 µM), or dimethylsulfoxide (DMSO) as control, and at selected time points, CYP1A1 promoter activity, CYP1A1 enzyme activities, contents, and CYP1A1 mRNA levels were studied. We found that MC markedly and persistently induced CYP1A1 promoter activity, transcription, apoprotein expression, and the CYP1A1 associated ethoxyresorufin O-deethylase (EROD) activities for up to 5 days. Transfection of cells with CYP1A2 siRNA resulted in knockdown of CYP1A2 mRNA by 70%, but a statistically significant increase of basal CYP1A1 mRNA by 35-40%. The induction of CYP1A1 promoter activity, CYP1A1 mRNA, CYP1A1 protein, and EROD activity by MC were not affected by CYP1A2 siRNA at the 24 h time point, but was significantly attenuated by Cyp1a2 siRNA on day 5. These results suggest that CYP1A2, possibly via a metabolite, contributes to the sustained induction of CYP1A1 by MC in hepa-I cells. Further investigations into the mechanisms of persistent induction of CYP1A1 by MC could lead to novel preventative/therapeutic strategies against PAH-mediated carcinogenesis in humans.

PS 536 Role of Intestinal Cytochrome P450 Enzymes in Protection against Colon Inflammation in a Mouse Model of Dextran Sulfate Sodium-Induced Colitis

Q. Zhang[1, 2], Y. Zhu[2], F. Xie[1] and X. Fan[2]. [1]*Wadsworth Center, NYSDOH, Albany, NY and* [2]*School of Public Health, SUNY at Albany, Albany, NY.*

The aim of this study was to determine the roles of intestinal microsomal cytochrome P450 (P450) enzymes in protection against colon inflammation, by studying dextran sulfate sodium (DSS)-induced colitis in an intestinal epithelium (IE)-specific P450 reductase knockout (IE-Cpr-null) mouse model, which has little microsomal P450 activity in the epithelial cells. DSS treatment (2.5% in drinking water for 6 days) caused more severe colon inflammation in IE-Cpr-null than in wild-type (WT) mice, as evidenced by the presence of higher levels of myeloperoxidase, an indicator of neutrophil infiltration, and proinflammatory cytokines (TNF-α, IL-6 and IL-1β), accompanied by greater weight loss, colonic tissue damage, and colon shortening. A deficiency in colonic corticosterone (CC) synthesis was identified in the IE-Cpr-null mice, as indicated by decreases, compared with WT mice, in rates of CC production in ex vivo cultured colon tissues from both vehicle-treated (by ~30%) and DSS-treated mice (by ~70%). Co-treatment of DSS-exposed mice with deoxycorticosterone, a precursor of CC biosynthesis via mitochondrial CYP11B1, abolished the hypersensitivity of IE-Cpr-null mice to DSS-induced colon inflammation. Taken together, our results strongly support the notion that microsomal P450 enzymes in the intestine play an important role in protecting colon epithelium from DSS-induced inflammation, possibly through increased local CC synthesis in response to DSS challenge.

PS 537 Identification of a P450-Mediated Hepatotoxicity-Associated Glutathione-Conjugate of Phenytoin in Phenytoin-Induced Liver Injury in Mice

T. Yokoi[1, 2], E. Sasaki[1], A. Iwamura[3], T. Fukami[1], M. Nakajima[1] and T. Kume[3]. [1]*Graduate School of Medical Science, Kanazawa University, Kanazawa, Ishikawa, Japan,* [2]*Department of Drug Safety Sciences, Nagoya University Graduate School of Medicine, Nagoya, Aichi, Japan and* [3]*DMPK Research Laboratory, Mitsubishi Tanabe Pharma Corporation, Toda, Saitama, Japan.*

Phenytoin (DPH) is widely used as an anticonvulsant agent. Hepatic necrosis was rarely observed in patients who received DPH. The formation of reactive metabolites are believed to involve the developing of DPH-induced live injury, however, evidence for reactive metabolites formation, their thiol conjugates, such as glutathione (GSH), formation and their effects on developing of DPH-induced liver injury are largely unknown. We previously demonstrated that DPH treatment decreased the hepatic GSH contents, and GSH depletion exacerbated the liver injury in mice. In this study, we first identified the GSH-DPH adduct, conjugate of putative electrophilic arene oxide metabolite with GSH, in the bile of the liver-injured mice, administered with DPH for 5 days with GSH biosynthesis inhibitor, L-buthionine-S,R-sulfoximine (BSO), in female C57BL/6 mice. In the plasma, N-acethylcysteine- and S-cysteine-DPH conjugates were detected. In addition, the peak time of the concentration of conjugates were corresponded to that of plasma alanine aminotransferase (ALT) levels. The plasma conjugates concentrations were significantly reduced by the cytochrome P450s inhibitor, 1-aminobenzotriazole (ABT), treatment. Furthermore, elevation of plasma ALT levels and hepatic GSH depletion were significantly suppressed by ABT, fluconazole, and ketoconazole treatment. Although single administration of DPH could not elevate plasma ALT levels, induction of Cyp2c caused significant elevation for plasma ALT levels. In

conclusion, we firstly identified hepatotoxicity-associated GSH conjugate of DPH, and suggested that Cyp2c-mediated metabolism could contribute to the development of the liver injury via arene oxide formation.

PS 538 Increased Susceptibility to Hyperoxic Lung Injury and Alveolar Simplification in Newborn Rats by Prenatal Administration of Benzo[a]pyrene

X. Couroucli, V. S. Thakur, Y. W. Liang, W. Jiang, L. Wang and B. Moorthy. *Pediatrics, Baylor College of Medicine, Houston, TX.*

Maternal smoking is one of the risk factors for pre-term birth and for the development of bronchopulmonary dysplasia (BPD). In this study, we tested the hypothesis that prenatal exposure of rats to benzo[a]pyrene (BP) will result in increased susceptibility of newborns to oxygen-mediated lung injury and alveolar simplification, and that cytochrome P450 (CYP)1A and 1B1 enzymes and oxidative stress mechanistically contribute to this phenomenon. Timed pregnant Fisher 344 rats were administered BP (25 mg/Kg) or the vehicle corn oil (CO) on gestational days 18, 19 and 20, and newborn rats delivered from the mothers of both these groups were either maintained in room air or exposed to hyperoxia (85% O2) for 7 or 14 days. Hyperoxic newborn rats prenatally exposed to the vehicle CO showed lung injury and alveolar simplification, and inflammation, and these effects were potentiated in rats that were prenatally exposed to BP. Prenatal exposure of BP also resulted in significant modulation of hepatic and pulmonary cytochrome P450 (CYP)1A and 1B1 enzymes at PND 7-14. These rats also displayed significant oxidative stress in lungs at postnatal day (PND) 14, as evidenced by increased levels of the F2-isoprostane 8-iso-PGF2α. In conclusion, our results show increased susceptibility of newborns to oxygen-mediated lung injury and alveolar simplification following maternal exposure to BP, and oxidative stress as well as modulation of CYP1A and 1B1 enzymes contribute to this phenomenon.

PS 539 Increased Susceptibility of Mice Lacking the Gene for Cytochrome P450 (CYP)1A1 to Hyperoxic Lung Injury *In Vivo*

B. Moorthy, K. Lingappan, L. Wang, X. Couroucli and W. Jiang. *Pediatrics, Baylor College of Medicine, Houston, TX.*

Supplemental oxygen therapy is often required for treatment of preterm infants with pulmonary insufficiency, as well as adults suffering from acute lung injury (ALI)/ acute respiratory distress syndrome (ARDS). However, hyperoxia contributes to the development of bronchopulmonary dysplasia (BPD) in premature infants and may exacerbate lung injury in ALI/ARDS patients. In this investigation, we tested the hypotheses that mice lacking the gene for the cytochrome P450 (CYP)1A1 would be more susceptible to hyperoxic lung injury than wild type (WT) mice, and that the protective role of CYP1A1 in the WT mice is in part due to mechanisms involving CYP1A1-mediated detoxification of lipid hydroperoxides such as F2-isoprostanes and isofurans. Twelve week-old male wild type (WT) (C57BL/6J) or Cyp1a1-null mice were exposed to hyperoxia (greater than 95% O2) or room air for 24-72 h. Lung injury was evaluated by measuring lung weight/ body weight (LW/BW) ratios, and by histology. The Cyp1a1-null mice were more susceptible to oxygen-mediated lung damage and inflammation than WT mice, as evidenced by increased LW/BW ratios, enhanced airway and endothelial injury, and neutrophil recruitment. Hyperoxia for 24-48 h elicited significant induction of CYP1A1 expression at the catalytic, apoprotein, and mRNA levels in liver and lung in the WT mice. The increase in lung injury in the Cyp1a1-null was accompanied by augmented expression of IL-6 and TNF-α in the lungs of these mice, compared to WT mice at the 72 h time point. Levels of pulmonary F2-isoprostanes and isofurans were significantly elevated in the lungs of hyperoxic WT as well as Cyp1a1-null mice, with Cyp1a1-null mice showing higher levels after 48-72 h after hyperoxia. Our results support the hypothesis that CYP1A1 protects against hyperoxic lung injury by detoxifying lipid hydroperoxides such as F2-isoprostanes and isofurans in vivo. Future research could lead to the development of novel strategies for the prevention and/or treatment of BPD in premature infants and ALI/ ARDS in adults.

PS 539a Biochemical Characterization of Cytochromes P450 2B from the Desert Woodrat

R. Wilderman[1], H. Jang[1], J. R. Malenke[2], M. Salib[1], E. Angermeier[1], S. Lamime[1], D. Dearing[2] and J. R. Halpert[1]. [1]*SSPPS, University of California, San Diego, La Jolla, CA and* [2]*Department of Biology, University of Utah, Salt Lake City, UT.* Sponsor: R. Tukey.

RATIONALE: Mammalian detoxification processes have been the focus of intense research, but little is known about how wild herbivores process plant secondary compounds, many of which have medicinal value or are drugs.
PROCEDURES: cDNA sequences that code for three enzymes of the cytochrome P450 (CYP) 2B subfamily, here termed 2B35, 2B36, and 2B37, have been recently identified from a wild rodent, the desert woodrat (*Neotoma lepida*). Two variants of each enzyme were engineered to increase protein solubility and to facilitate purification. Protein-ligand interactions were investigated using the model substrates 7-ethoxy-4-(trifluoromethyl)coumarin (7-EFC) and 7-benzyloxyresorufin (7-BR) and the monoterpene (+)-α-pinene.
RESULTS: When expressed in *E. coli* each of the woodrat proteins gave the characteristic maximum at 450 nm in a reduced carbon monoxide difference spectrum but generally expressed at lower levels than rat CYP2B1. 2B36 and 2B37 showed dealkylation activity with 7-EFC and 7-BR, whereas 2B35 was inactive. Binding of (+)-α-pinene produced a Type I shift in the absorbance spectrum of each enzyme. Mutation of 2B37 at residues 114, 262, or 480, key residues governing ligand interactions with other CYP2B enzymes, did not significantly change expression levels or produce the expected functional changes. Stoichiometry measurements of coupling of reducing equivalents to product formation were unique for each enzyme.
CONCLUSIONS: In summary, two catalytic and one ligand-binding assay are sufficient to distinguish among 2B35, 2B36, and 2B37. Differences in functional profiles between 2B36 and 2B37 are partially explained by changes in substrate recognition site residue 114, but not 480. The results advance our understanding of the mechanisms of detoxification in wild mammalian herbivores and highlight the complexity of this system. Reported CYP2B gene sequences from *N. lepida* allow for larger scale analyses of the structure-function relationships among these enzymes.

PS 539b Estimation of Bisphenol A Toxicity with the Datachip/ Metachip Technology

S. Park[1], S. Yi[2] and M. Yang[1]. [1]*Research Center for Cell Fate Control, Sookmyung Women, Seoul, Republic of Korea and* [2]*Central R & D Institute, Samsung Electro-Mechanics Co, Suwon, Republic of Korea.*

Bisphenol A (BPA) is a well known endocrine disrupting chemical, however, its toxic mechanisms and health end points are not clearly understood, yet. Particularly, most metabolic studies of BPA were performed in animal studies. Therefore, new technologies to estimate BPA toxicity in human have been required. For this purpose, we used the DataChip/MetaChip platform, an alternative to animal testing by supplying more in vivo-like environment with high throughput screening manner, for estimating metabolism-based hepatotoxicity of BPA with 28 individual metabolic enzymes. DataChip consisted of 532 micro-pillars with 3D cultured Hep3B cells encapsulated in alginate, indicating cytotoxicity of BPA and it's metabolites. The complementary MetaChip consisted of micro-wells with individual metabolic enzymes, generating metabolites of BPA on the chip. Metabolism-induced toxicity assays were performed by stamping the DataChip onto the MetaChip. After incubation for 1 day with BPA and for 2 days without BPA, viability of Hep3B on the DataChip was measured by calcein AM staining and IC50 values were calculated. As results, we found that cytotoxicity of BPA was increased by CYP2E1 (IC50: control vs. CYP2E1, 260 +/- 20 uM vs. 129 +/- 29 uM), however, decreased by SULT1E1(IC50 : 403 +/- 49 uM).. These results are quite different from those obtained by animal studies, which emphasized roles of UGTs. Therefore, we estimate BPA is mainly bioactivated by CYP2E1 and detoxified by SULT1E1 in human with the new alternative to animal tests.

PS 539c Comparative Characterization of Feline Cytochrome P450 3A by Fluorescent Inhibition Assay

H. Teraoka, G. Okamatsu, T. Komatsu and T. Kitazawa. *School of Veterinary Medicine, Rakuno Gakuen University, Ebetsu, Hokkaido, Japan.*

Cytochrome P450 3A (CYP3A) is the major subfamily of CYP, most important metabolizing enzymes for pharmaceutical drugs and toxicants in humans and other mammals, including first-pass effects. Although domestic cats (*Felis catus*) are the most common companion animal, the properties of their CYPs are obscure. Many drugs developed for humans are used for cats as well as dogs at the discretion of

the veterinarians, as insufficient numbers of drugs are approved for veterinary use. Therefore, doses of these drugs are empirically determined with reference to human information. In this study, we developed heterologously expressed feline CYP3A and the orthologues of dogs and humans for comparison, individually with human P450 oxidoreductase to generate functional monooxygenase systems in *Escherichia coli*. We found two novel CYP3A genes, CYP3A131 and CYP3A132 in cats. Both feline CYP3As show high identity with canine CYP3A homologues and those of some artiodactyls. CYP3A131 transcripts were expressed predominantly in liver and small intestine, while CYP3A132 was only detected in liver with much lesser amount. Feline CYP3A131 extensively metabolized a fluorescent substrate, 7-benzyloxy-4-trifluoromethylcoumarin (BFC) to 7-hydroxy-4-trifluoromethylcoumarin (HFC) with Km value similar to human CYP3A4 and canine CYP3A12 (Km 271-413 μM), except human CYP3A5 (63 μM). As indicated by Ki values, there were general similarities between human, canine and feline CYP3As in binding affinities of some CYP3A inhibitors, such as miconazole, erythromycin, cimetidine, dexamethasone and medetomidine except human CYP3A5, which was very resistant to these inhibitors. The present study provides a high-throughput system to assess possible drug interactions in feline CYP3A metabolism in comparison with canine and human CYP3As.

PS 539d PAH Dibenzo[def, p] Chrysene-Induced Adult On-Set Lung Tumors and T Cell Acute Lymphoblastic Leukemia Utilizing a CYP1B1 Humanized Mouse Model: A Transplacental Model

H. You, E. Madeen, T. Harper, D. E. Williams, W. M. Baird and C. V. Löhr. *Environmental & Molecular Toxicology, Oregon State University, Lake Oswego, OR.*

Polycyclic aromatic hydrocarbons (PAHs) ubiquitously contaminate food crops through atmospheric deposition. Dibenzo[def,p]chrysene (DBC, an IARC class 2A probable human carcinogen), is carcinogenic in animal models and is a human health concern. We induce adult onset T-cell acute lymphoblastic lymphoma (T-ALL) and lung tumors in mice by transplacental fetal exposure via a single gavage dose of DBC to pregnant B6/129SF1 dams on gestation day 17. The maternal doses tested were 6.5 or 12 mg DBC/Kg. Cytochrome P450 (Cyp) 1b1 is required for DBC-dependent T-ALL (at 4-6 months of age) Lung tumor development (hyperplasia, adenoma, adenoma with progression, and carcinoma) at 10 months of age is due to both Cyp 1a1 and 1b1 bioactivation of DBC. We utilized 129S males, null for mouse cyp 1b1, to cross with B6/129SF1 dams null for mouse cyp1b1 and expressing one allele of human CYP 1B1. There was no significant mortality in the null and humanized hemizygous 1B1 groups, however the T-ALL dependent mortality rate for wild type groups were 42% in the low dose (6.5mg/kg) and 66% in the high dose (12 mg/kg) groups, n~35 per group. At 10 months of age, lung tumor multiplicity was assessed. Corn oil treated groups did not develop lung tumors. Low dose treated groups developed similar numbers of tumors; null = 9±7 tumors, n=26 with 96% incidence; hemizygous 1B1 = 7±5 tumors, n=25 with 96% incidence; and wild type = 8±6 tumors, n=18 with 100% incidence. Similar numbers of tumors were found among high dose treated groups. Null = 12±7 tumors, n=49 with 98% incidence; hemizygous 1B1 = 12±9 tumors, n=23 with 97% incidence; and wild type = 13±5 tumors, n=10 with 100% incidence. The "humanized" hemizygous 1B1 transgenic mouse did not contribute to increased susceptibility to T-ALL or lung tumor compared to 1b1 null mouse. Current work is focused on tissue specific expression of the humanized transgenic 1B1 in mice. Supported by NIH grant P42 ES016465.

PS 539e Metabolism of 4-Methylimidazole in the Rat and Mouse

T. Fennell, R. Snyder, S. Watson and S. Dhungana. *RTI International, Research Triangle Park, NC.*

4-Methylimidazole (4-MeI) is found in numerous heated foods and in some caramel colors used in foods and beverages. In long-term cancer bioassays 4-MeI induced alveolar/bronchiolar tumors in mice, but not in rats. This study was conducted to investigate the metabolism of 4-MeI in vitro in rat, mouse, and human lung and liver microsomes and S-9 fractions, and in vivo in rats and mice. No metabolites were detected by HPLC analysis in rat, mouse, and human lung and liver microsomes, or S-9 fractions. Male and female F-344 rats and B6C3F1 mice administered [^{14}C] 4-MeI at doses of 50 and 150 mg/kg by gavage to track the disposition and metabolism of 4-MeI in vivo. Animals were placed in metabolism cages for collection of excreta and exhaled CO_2 and volatiles for 48 h. In rats administered [^{14}C] 4-MeI, the major route of elimination was via urine, with 79-89% of the radioactivity in urine, 3-9% in cage rinse, 2-4% in feces, 1-2% exhaled as CO_2, 1-2% in carcass, and 0.1 % or less as exhaled volatiles. In mice, 41-70% of the administered dose was recovered in urine, 4-12% in feces, 18-34% in cage rinse, 2-4 % exhaled as CO_2, and 1-3% in carcass, and 0.1 % or less as exhaled volatiles. In rats and mice, the majority of the radioactivity (71-88%) in urine was present as unchanged 4-MeI, characterized by HPLC with detection of radioactivity, and by LC-MS. Additional radioactive peaks were detected (with the largest metabolite ranging from 8 - 18 % of the activity), and characterized by LC-MS/MS as 4-hydroxymethylimidazole, two other oxidized products, possibly hydroxylated on the 2- and 5-positions, and a glucuronide of 4-hydroxymethylimidazole. This study demonstrated that 4-MeI is largely excreted unchanged in male and female rats and mice. However, limited oxidative metabolism and conjugation was observed in rats and mice. 4-MeI is not oxidized in microsomes or S-9 from rat, mouse and human lung and liver. Overall, there was no indication of metabolism of 4-MeI to reactive species. This work was funded by the American Beverage Association.

PS 540 PON 1 Enzyme Activities in a Mississippi Population Vary with Substrate, Genotype, and Race

M. Dail[1], C. McDaniel[1], R. Wills[1], H. W. Chambers[2] and J. E. Chambers[1]. *[1]Center for Environmental Health Sciences, Mississippi State University, MS State, MS and [2]Biochem., Mol. Biol., Entom., Plant Path., Mississippi State University, MS State, MS.*

Paraoxonase (PON1) hydrolyzes paraoxon (PO) and diazoxon (DZO), the active metabolites of the insecticides parathion and diazinon, respectively. The human PON1 gene has several single nucleotide polymorphisms (SNPs). The SNP involving arginine (R) to glutamine (Q) substitution at codon 192 is associated with catalytic efficiency while that involving methionine (M) to leucine (L) substitution at codon 55 is associated with serum concentration. PON1 polymorphisms and activities have been linked to cardiovascular and other diseases. Since Mississippians have high disease rates, 186 cardiology clinic patients were evaluated. Hydrolysis rates of PO (POase), DZO (DZOase), dihydrocoumarin (lactonase) and phenyl acetate (arylesterase) were evaluated for associations with race, gender, age, and PON1 55/192 SNP genotypes. The variables were analyzed both individually and in combination. African Americans had higher levels ($p<0.02$) of POase and arylesterase than Caucasians but Caucasians had higher DZOase and lactonase values ($p<0.05$). Since lactonase activity may be the most critical PON1 enzyme activity for LDL oxidation prevention, this might partially explain the health disparity paradox of why African Americans have higher POase and arylesterase activities than Caucasians yet still have higher rates of coronary disease. Significant ($p<0.0001$) differences in arylesterase activities were seen amongst the genotypes with QQMM having the lowest and RRLL the highest activities. This opposes the prevailing belief that arylesterase is unaffected by genotype and suggests that this activity cannot be used to quantify PON1 protein. The differences in PON1 activities indicate the need to specify substrate and demographic data for enzyme assays. (Support NIH ES015170)

PS 541 Contribution of CYP2B6 Alleles in Sudden Death of Methadone Users: A CYP2B6 Genetic Polymorphism Study

T. Ahmad[1], L. Richards-Waugh[2], S. Sabet[1] and G. O. Rankin[1]. *[1]Pharmacology, Physiology & Toxicology, Marshall University, Huntington, WV and [2]Forensic Science Graduate Program, Marshall University, Huntington, WV.*

West Virginia (WV) and Kentucky (KY) ranked in the top ten states for increases in fatal methadone overdoses in 1999-2004. Cytochrome P450 2B6 (CYP2B6) plays a significant role in stereoselective metabolism of (S)-methadone to 2-ethyl-1,5-dimethyl-3,3-diphenylpyrolidine (EDDP). Elevated (S)-methadone can cause cardiotoxicity by prolonging the QT interval. Large interindividual variability in the pharmacokinetics of methadone causes ambiguity in the relationship between dose, plasma concentration levels, and side effects. The purpose of this study was to determine if single nucleotide polymorphisms (SNPs) in the CYP2B6 gene can lead to decreased metabolism of methadone leading to fatal concentrations. Genomic DNA was isolated from blood stain cards prepared during autopsies at the WV and KY Offices of the Chief Medical Examiner. DNA samples underwent real time polymerase chain reaction utilizing TaqMan Allelic Discrimination Analysis to determine the genotypic frequencies of four CYP2B6 gene SNPs (rs8192709, rs4803149, rs3745274, and rs3211371) in the methadone only fatality (136) and control (269) cases. All four of the SNPs studied were within Hardy-Weinberg equilibrium. The observed genotypic frequencies were significantly different than the frequencies for the general population ($p<0.05$) for three of the four (rs4803149, rs3745274, and rs3211371) SNPs. With the Kruskal Wallis test, the rs3745274 SNP showed a significant difference between [methadone]/[EDDP] ratio for the methadone only overdoses ($p = 0.019$). Although, the rs4803149 and rs3211371 SNPs were not found to be significantly associated with an increase in [methadone]/[EDDP] ratio, there is an apparent enrichment of the minor allele in the methadone fatality group. Based on these results, SNP rs3745274 is likely linked with a slow-metabolizer phenotype for methadone. Supported in part by NIH grant P20RR016477.

PS 542 Proteomic Insight of Isoniazid Immunomodulatory Activity: Considerations for Tuberculosis Therapy

S. R. Khan[1], A. Baghdasarian[2], R. Fahlman[3] and A. G. Siraki[4]. [1]*Pharmacy and Pharmaceutical Sciences, University of Alberta, Edmonton, AB, Canada,* [2]*Pharmacy and Pharmaceutical Sciences, University of Alberta, Edmonton, AB, Canada,* [3]*Department of Biochemistry, University of Alberta, Edmonton, AB, Canada and* [4]*Pharmacy and Pharmaceutical Sciences, University of Alberta, Edmonton, AB, Canada.*

Immunotherapy is thought of as an emerging strategy for tuberculosis (TB) management. The most effective immunotherapy is the immunomodulatory methods that target the Th1/Th2 imbalance and focus on enhancing Th1 responses to release interferon gamma to activate bactericidal macrophages/monocytes. Because monocytes/macrophages are the first line of defense for TB, infection mainly depends on the number of functional monocytes/macrophages. We investigated isoniazid (INH), which is one of the main drugs used against TB, for its potential immunomodulatory action using human promyelocytic leukemia cells (HL-60) as a model for immune cell precursors. We hypothesized that in addition to its well-known bactericidal actions, INH has immunomodulatory effects which reinforce its therapeutic importance in TB therapy. We employed assays including the NBT reduction assay, superoxide release assay, and flow cytometry to identify the differentiation of HL-60 cells treated with INH. Additionally, we applied quantitative proteomics which revealed certain cellular pathways related to HL-60 cell differentiation, particularly towards monocytic differentiation. Proteomic data also revealed cellular mechanisms involved in INH detoxification. In conclusion, our study revealed that INH induced monocytic differentiation in HL-60 cells. These findings emphasize that INH may yet play important therapeutic roles in multidrug resistant and extremely drug resistant TB and therefore should be continued in these cases.

PS 543 Prdm2 Is Identified As a Potential Risk Factor for Zileuton-Induced Liver Injury Using a Mouse Genetic Diversity Panel

M. Mosedale[1], K. Adkins[2], H. Wu[2] and A. H. Harrill[1, 3]. [1]*The Hamner Institutes for Health Sciences, Research Triangle Park, NC,* [2]*Pfizer Inc., Groton, CT and* [3]*UAMS, Little Rock, AR.*

Zileuton, an orally active inhibitor of 5-lipoxygenase, is used clinically for the maintenance treatment of asthma. Zileuton is also a candidate for the treatment of other inflammatory diseases that involve leukotrienes, but this application is hampered by serious, idiosyncratic drug-induced liver injury associated with its use. Previous studies have demonstrated the utility of a mouse diversity panel (MDP), comprised of 34 genetically diverse inbred strains, for the identification of genetic risk factors associated with drug-induced injury. In this study, serum and liver tissue were collected from 34 mouse strains treated with zileuton (300 mg/kg, *i.g.*) or vehicle once daily for 7 days. Significant elevations in serum alanine aminotransferase (ALT) levels in zileuton-treated animals relative to vehicle-treated controls were observed in 9 of the 34 strains ($p<0.05$). ALT fold change was significantly correlated with serum aspartate aminotransferase and glutamate dehydrogenase levels (Pearson correlations, ($p=0.0002$ and $p=0.0033$, respectively) and associated with microscopic findings of hepatocellular hypertrophy and parenchymal inflammation and necrosis. Zileuton-induced ALT changes, however, were not correlated with drug exposure. Genome wide association mapping conducted using ALT fold change identified a significantly associated SNP ($-\log(p)=5.85$) in PR domain zinc finger protein 2 (*Prdm2*), a transcriptional regulator of the cytoprotective enzyme heme oxygenase 1. Basal *Prdm2* levels were found to be significantly decreased in strains with the minor allele of the polymorphism ($p=0.0018$). In summary, the MDP approach defined a possible risk factor that can be evaluated in humans and has the potential to identify patients with genetic susceptibility to zileuton-induced liver injury.

PS 544 Next-Generation Sequencing Reveals Baseline Gender and Species Differences in Renal Transcript Expression in the CD1 Mouse and Wistar Han Rat

P. Pande[1], J. Yuan[1], J. Hill[2] and W. W. Ku[1]. [1]*Integrative Toxicology, Nonclinical Drug Safety, Boehringer Ingelheim Pharmaceuticals, Inc., Ridgefield, CT and* [2]*Computational Biology, Scientific Knowledge Discovery, Boehringer Ingelheim Pharmaceuticals, Inc., Ridgefield, CT.*

Mammals exhibit major gender differences in kidney function under various physiological, pharmacological, and toxicological conditions. To gain better understanding of the molecular differences in kidney between mammalian sexes and between rodent species, we have utilized next generation sequencing to evaluate potential species and gender differences in the transcriptomes in the CD-1 mouse and the Wistar Han rat strains. Enriched renal cortex tissue was collected from 7 weeks CD-1 mice and 9-10 weeks Wistar Han rats. The whole transcriptome in kidney was profiled using Illumina HiSeq 2000. Baseline gene expression was compared between male and female in CD-1 mouse and Wistar Han rat. Our data showed the major gender biased gene expression in kidney cortex of rodent species. Male and female CD-1 mice kidney exhibit gender specific expression in drug metabolism enzyme and transporter and female CD-1 mice have higher expression in genes related to osmotic regulation and glutathione detoxification in kidney. In contrast, Wistar Han rats showed a different profile of gender biased expression in drug metabolism and transport functions. The gender differential expression is less detected in Wistar Han rat kidney comparing with CD-1 mice. The elucidation of baseline molecular differences in kidney function between genders and rodent species would enable us to better evaluate the occurrence and development of drug-related gender and species specific changes that may be relevant to understanding mechanisms of drug-induced nephrotoxic effects.

PS 545 Refinement of N-Acetyltransferase 2 Phenotype Prediction for Activity and Urinary Bladder Cancer Risk Prediction

K. Golka[1], M. Blaszkewicz[1], K. Ickstadt[2], J. G. Hengstler[1] and S. Selinski[1]. [1]*Leibniz Research Centre for Working Environment and Human Factors, Dortmund, Germany and* [2]*Faculty of Statistics, TU Dortmund University, Dortmund, Germany.*

Polymorphisms of N-acetyltransferase 2 (NAT2) are well-known to modify urinary bladder cancer risk as well as efficacy and toxicity of pharmaceuticals via reduction of the enzyme's acetylation capacity. Nevertheless, the discussion about optimal NAT2 phenotype prediction, particularly differentiation between different degrees of slow acetylation is still controversial. Therefore, we investigated the impact of single nucleotide polymorphisms (SNPs) and their haplotypes on slow acetylation in vivo and on bladder cancer risk. For this purpose we used a study cohort of 1,712 bladder cancer cases and 2,020 controls genotyped for NAT2 and the tagSNP rs1495741 of whom 344 individuals were phenotyped by the caffeine test in vivo. We identified an 'ultra-slow' acetylator phenotype based on combined *6A/*6A, *6A/*7B and *7B/*7B genotypes containing the homozygous minor alleles of C282T (rs1041983, *6A, *7B) and G590A (rs1799930, *6A). 'Ultra-slow' acetylators have significantly about 32% and 46% lower activities of caffeine metabolism compared to other slow acetylators and to the *5B/*5B genotypes, respectively ($P < 0.01$, both). The 'ultra-slow' genotype showed an association with bladder cancer risk in the univariate analysis (OR = 1.31, P = 0.012) and a trend adjusted for age, gender and smoking habits (OR = 1.22, P = 0.082). In contrast, slow acetylators in general were not associated with bladder cancer risk, neither in the univariate (OR = 1.02, P = 0.78) nor in the adjusted (OR = 0.98, P = 0.77) analysis. In conclusion, this study suggests that NAT2 phenotype prediction should be refined by consideration of an 'ultra-slow' acetylation genotype

PS 546 Potential Role of Carbonyl Reductase 3 in Doxorubicin-Induced Cardiotoxicity

C. M. Schaupp[1], C. White[1], G. F. Merrill[2] and T. Kavanagh[1]. [1]*Department of Environmental and Occupational Health Sciences, University of Washington, Seattle, WA and* [2]*Department of Biochemistry and Biophysics, Oregon State University, Corvallis, OR.*

Doxorubicin is highly effective at inducing DNA double-strand breaks in rapidly dividing cells, which has led to it being a widely used cancer chemotherapeutic. However, clinical administration of doxorubicin is limited by off-target cardiotoxicity, thought to be mediated by the primary alcohol metabolite of doxorubicin, doxorubicinol. Carbonyl reductase 1 (CBR1), a well-characterized monomeric enzyme present at high basal levels in the liver, is known to exhibit activity toward doxorubicin. Little is known about a closely related enzyme, carbonyl reductase 3 (CBR3), which is present in the liver at low basal levels but is highly inducible by the transcription factor Nrf2. Polymorphisms in *CBR3*, but not *CBR1*, are associated with differential cardiac outcomes in doxorubicin treated patients. *Cbr3* mRNA and CBR3 protein are highly expressed in the livers of *Gclm -/-* mice (a mouse model of glutathione deficiency) relative to wildtype mice. In the present study, we first investigated the ability of CBR3 to metabolize doxorubicin. Incubations of doxorubicin and purified recombinant murine CBR3 (mCBR3) were analyzed for doxorubicinol formation using HPLC, revealing for the first time that doxorubicin is a substrate of mCBR3. Moreover, hepatocytes from *Gclm -/-* mice produced more doxorubicinol than *Gclm +/+* hepatocytes. In addition, differentiated rat myoblasts (C2C12 cells) co-cultured with primary *Gclm -/-* murine hepatocytes were more sensitive to doxorubicin-induced cell death than incubations with *Gclm +/+* hepatocytes. Our results indicate an important mechanistic role for CBR3 in doxorubicin-induced cardiotoxicity. Because there is likely to be variability in hepatic CBR3 activity in humans (due to either genetic or epigenetic

influences on expression), these data also suggest that inhibition of CBR3 may provide protection from doxorubicinol cardiotoxicity. Supported by NIH grant P30ES007033 and UW DEOHS.

PS 547 Synergistic Interaction between Genetics and Disease on Pravastatin Disposition

J. Clarke[1], R. N. Hardwick[1], A. D. Lake[1], A. J. Lickteig[2], C. D. Klaassen[2] and N. J. Cherrington[1]. [1]*Pharm/Tox, University of Arizona, Tucson, AZ and* [2]*University of Kansas Medical Center, Kansas City, KS.*

Genome wide association studies have implicated the hepatic uptake transporter organic anion transporting polypeptide-1B1 (OATP1B1) in the pharmacokinetics and musculoskeletal toxicity of statin drugs, such as pravastatin. Along with OATP1B1, other OATP uptake transporters can participate in the transport of pravastatin, partially compensating for the loss of OATP1B1 in polymorphic patients. Nonalcoholic steatohepatitis (NASH) in humans and in a diet-induced rodent model alters the expression of multiple OATP and multidrug resistance-associated protein (MRP) transporters. Genetic loss of Oatp1b2, the rodent ortholog of human OATP1B transporters, caused a modest increase in pravastatin plasma concentrations in mice with healthy livers. Although a diet-induced model of NASH did not alter the disposition of intravenously administered pravastatin compared to WT control mice, the combination of NASH and Oatp1b2 genetic loss caused a synergistic increase in plasma area under the curve (AUC) and tissue concentrations in kidney and muscle. These data reveal a potential mechanism for this synergistic increase in pravastatin exposure that involves NASH-induced alterations in the expression of multiple hepatic uptake transporters which, due to overlapping substrate specificity among the OATP transporters, may combine with the pharmacogenetic loss of OATP1B1 to increase the risk of statin-induced adverse drug reactions.

PS 548 The Role of the Folate Pathway in Pancreatic Cancer Risk

S. Chittiboyina, L. M. Kamendulis and B. A. Hocevar. *Environmental Health, Indiana University School of Public Health, Bloomington, IN.*

Pancreatic cancer is a devastating disease, with poor prognosis for survival. Most cancers, including pancreatic cancer, develop through interactions between genes and environmental/lifestyle factors. Risk factors for pancreatic cancer development include a low dietary intake of folate. In conjunction with diet and lifestyle determinants, an individual's folate pathway status is determined by their genetic makeup. Expression of single nucleotide polymorphisms (SNPs) of genes in the folate pathways have been shown to modulate susceptibility to pancreatic cancer. In particular, homozygous expression of the TT allele of methylene tetrahydro-folate reductase (MTHFR) at nucleotide position 677, which causes decreased enzymatic activity, has been associated with an increased risk for development of pancreatic cancer and low folate levels. In the present study, we measured serum and red blood cell folate levels and determined SNP expression in selected genes in the folate metabolic pathway in a cohort of pancreatic cancer patients and healthy related and unrelated control groups. While serum folate levels did not differ between patients and controls, red blood cell folate levels were significantly lower in pancreatic cancer patients compared to controls ($p<0.05$). As expected, we find that the TT allele of MTHFR C677T is associated with low serum folate levels and significantly associated with low red blood cell folate levels compared to the CC or CT genotype. We also performed analysis for gene-gene interactions among SNPs in the folate pathway in relation to pancreatic cancer risk. We find that individuals expressing the SHMT1 L474F/MTHFR C677T diplotypes LF+FF/CC and CT+T/LF+FF exhibit an increased risk for pancreatic cancer (OR -2.234 95%CI 1.08-2.51 ; OR 2.11 95%CI 1.06-4.62 respectively). Collectively our results suggest that both environmental factors (diet) and genetics contribute to the risk for the development of pancreatic cancer.

PS 549 Functional Effect of Polymorphic Variations of Human Cytochrome P450 2D6 (P34S, E418K, S486T, and R296C)

D. Kim, J. Kim, Y. Lim, S. Han and H. Park. *Konkuk University, Seoul, Republic of Korea.* Sponsor: T. Jeong.

Cytochrome P450 2D6 is responsible for the metabolism of various clinical drugs and its genetic polymorphisms can significantly influence the metabolic activity. In this study, we analyzed the functional activities of four nonsynonymous single nucleotide polymorphisms from P450 2D6*52 allele, which were recently found, and one found frequently in P450 2D6 alleles. Recombinant variant enzymes of E418K, S486T, and R296C were successfully expressed in Escherichia coli and purified. However, a P450 holoenzyme spectrum of P34S variant was not detected in E. coli whole cell level. Structural analysis indicated that P34S mutation seemed to perturb a highly conserved proline-rich N-terminus of P450 2D6. Steady state kinetic analyses showed the significant reductions of enzymatic activities in E418K and R296C variants. In the case of bufuralol 1'-hydroxylation, a novel mutant, E418K, showed 32 % decrease in catalytic efficiency (kcat/Km) mainly due to the decrease of kcat value. R296C showed much greater reduction in the catalytic efficiency (9 % of wild-type) due to both of a decrease of kcat value and an increase of Km value. In the case of dextromethorphan O-demethylation, E418K showed both of a decrease of kcat value and an increase Km value to result in ~43 % reduction of catalytic efficiency. A highly decreased catalytic efficiency (~6 % of wild-type) in the mutant of R296C also was observed mainly due to the dramatic change of kcat value of dextromethorphan O-demethylation. These results suggested that individuals carrying these allelic variants are likely to have the altered metabolic abilities of many clinical drugs therefore, these polymorphisms of P450 2D6 should be much concerned for reliable drug treatment.

PS 550 Polymorphism of RGS9: Association with Obesity

M. Sharma[1], C. Shen[2], D. Reid[3], J. Celver[5], J. Chen[5], N. Seman[6, 7], S. K. Vasan[6], H. Wang[2], T. Gu[6], Y. Liu[4], W. W. Mohamud[7], K. Brismar[6], W. G. Fairbrother[3], A. Kovoor[5] and G. Harvest[6]. [1]*Dr BR Ambedkar Center for Biomedical Research, University of Delhi, Delhi, India,* [2]*Epidemiology and Biostatistics, Nanjing Medical University, Nanjing, China,* [3]*Molecular Biology, Cell Biology and Biochemistry, Brown, Providence, RI,* [4]*National Laboratory of Medical Molecular Biology, Basic Medical Sciences, Beijing, China,* [5]*Biomedical and Pharmaceutical Sciences, University of Rhode Island, Kingston, RI,* [6]*Research Center for Diabetes and Endocrinology, Karolinska, Stockholm, Sweden and* [7]*Cardiovascular Diabetes and Nutrition Research Centre, Medical Research, Kuala Lumpur, Malaysia.*

RGS9-2 is a member of Gα GTPase accelerating proteins that regulates G protein signaling (RGS). It has been shown recently that RGS9 knockout mice have increased adiposity. In the present study we evaluate the genetic effect of RGS9 gene on obesity and genotyped 9312 obese, type 2 diabetes and healthy Chinese and Malaysian subjects for insertion/deletion (TTTCT I/D) polymorphism (rs3215227) in the gene. The deletion polymorphism of RGS9 was associated with decreased prevalence of obesity in woman ($P=0.003$) and girls ($P=0.002$), moderate in boys ($P=0.039$) and non-significant in men. We did not find any significant association of RGS9 polymorphism with type 2 diabetes. Since the deltaTTTCT deletion was close to the branch point for RNA splicing and corresponded to a binding motif for polypyrimidine tract binding protein (PTB), we attempted to determine RGS9 binding affinity with the region. We found that deletion variant showed 10 fold reductions in PTB binding in vitro. We also demonstrated the differential effect of overexpression of PTB on the splicing of the two polymorphic forms of RGS9 minigene. We observed that overexpression of PTBP1 and PTBP2(Brain specific) significantly decreased the splicing in wild type construct of RGS9 minigene. Thus, our data suggest that RGS9 has genetic effect on obesity but not on type 2 diabetes. The altered post-transcriptional processing of the RGS9 I/D polymorphic alleles through an altered affinity for the splicing factor PTB could be causal for the inverse association between the polymorphism and obesity.

PS 551 Gene Environment Interaction in Urinary Bladder Cancer

B. D. Banerjee[1], T. Sharma[1], A. Verma[2] and S. Gupta[2]. [1]*Biochemistry, University College of Medical Sciences and GTB Hospital, Delhi, India and* [2]*Surgery, University College of Medical Sciences and GTB Hospital, Delhi, India.* Sponsor: S. Goel.

Urinary bladder cancer (UBC) is a common disease worldwide with a high incidence. The etiology of UBC includes both environmental and endogenous factors. Environmental risk factors include exposure to heavy metals, aromatic amines and environmental pollutants including pesticides mainly organochlorine pesticides (OCPs). OCPs are potent endocrine disrupters, are found to be associated with several cancers. Glutathione S-transferase(GST) involved in the detoxification of numerous environmental toxins including OCPs. The present study was carried out in UBC and healthy control subjects with an aim to determine the role of GSTM1 and GSTT1 polymorphism and its implication on the OCP detoxification or bioaccumulation which may increase the risk of UBC in humans. This study was also designed to identify the "gene-environment interaction" specifically between gene polymorphism in xenobiotic metabolizing genetic enzyme(s) and OCP residue levels in blood. GSTM1/GSTT1 gene polymorphism was analysed by using multiplex PCR. OCPs levels in whole blood were estimated by gas chromatography. The results demonstrated a significant ($p<0.05$) increase in frequency of GSTM1-/GSTT1- (null) genotype in UBC cases without interfering the distribution of other GSTT1/GSTM1 genotypes. The blood levels of α,β,γ,total–HCH and p,p'-DDT were found to be significantly ($p<0.05$) high in UBC cases as compared to controls. Multiple regression analysis revealed a significant interaction

between β-HCH and GSTM1-genotype (p<0.05) as well as between β-HCH and GSTT1- genotype (p<0.05) respectively. These findings indicate that "gene-environment interaction" may play a key role in increasing the risk for UBC in individuals among North Indian population who are genetically more susceptible due to presence of GSTM1/GSTT1 null deletion during their routine encounter with exposure to OCPs.

PS 552 Human ALDH1B1 Polymorphisms May Affect the Metabolism of Acetaldehyde and All-Trans Retinaldehyde—*In Vitro* Studies and Computational Modeling

B. C. Jackson[1], P. Reigan[1], D. Thompson[2] and V. Vasiliou[1]. [1]*Department of Pharmacetuical Sciences, University of Colorado Anschutz Medical Campus, Aurora, CO and* [2]*Department of Clinical Pharmacy, University of Colorado Anschutz Medical Campus, Aurora, CO.*

Purpose: To test the metabolism of novel substrates by ALDH1B1 and to predict the effect that human ALDH1B1 polymorphisms will have on these and previously described substrates.
Methods: Purified human recombinant ALDH1B1 was used to determine the capacity of ALDH1B1 to metabolize nitroglycerin and all-trans retinaldehyde. Computational-based molecular modeling was used to predict the binding affinities of the substrates acetaldehyde, 4-hydroxynonenal, nitroglycerin, and all-trans retinaldehyde to ALDH1B1 and three human polymorphisms ALDH1B1*2 (A86V), ALDH1B1*3 (L107R), and ALDH1B1*5 (M253V). The binding of the cofactor NAD+ to ALDH1B1 and its polymorphisms was also modeled computationally.
Results: ALDH1B1 metabolizes and appears to be inhibited by nitroglycerin and has favorable kinetics for metabolism of all-trans retinaldehyde. Differences in calculated docking poses and weak interactions between ligands/cofactor and ALDH enzymes from modeling studies provided a basis for predicting the capacity of each of the variants to metabolize acetaldehyde, nitroglycerin, and all-trans retinaldehyde. Modeling indicated that ALDH1B1*2 and ALDH1B1*5 likely bind NAD+ poorly compared to ALDH1B1 and ALDH2, and all ALDH1B1 mutants had poor binding affinities for nitroglycerin.
Conclusions: ALDH1B1 metabolizes the novel substrates nitroglycerin and all-trans-retinaldehyde, and two human polymorphisms (ALDH1B1*2 and ALDH1B1*5) are likely to metabolize substrates poorly, which may affect the roles of ALDH1B1 in stem cells and ethanol metabolism.

PS 552a SLC19A1, SLC46A1 and SLCO1B1 Polymorphisms Are Associated with Methotrexate-Related Overall Toxicity in Portuguese Rheumatoid Arthritis Patients

A. Lima[1, 2, 3], R. Azevedo[2], H. Sousa[2], M. Bernardes[4], R. Medeiros[2, 3] and V. M. Seabra[1]. [1]*IINFACTS/CESPU, ISCS-Norte, Gandra, PRD, Portugal,* [2]*Molecular Oncology Group, IPO, Porto, Portugal,* [3]*ICBAS, University of Porto, Porto, Portugal and* [4]*Rheumatology Department, São João Hospital Center, Porto, Portugal.*

Methotrexate (MTX) is used for rheumatoid arthritis (RA) treatment with a wide variety of clinical responses, especially of concern is the development of MTX-related toxicity (MTX-Tox). Studies have described a possible role of genetic polymorphisms that alter MTX transporters influx (solute carriers, SLC) and/or efflux (ATP-binding cassette, ABC) in MTX-Tox development. The aim of this work was to evaluate the influence of several single nucleotide polymorphisms (SNP) in genes codifying MTX transporters with the occurrence of MTX-Tox in Portuguese RA patients. A total of 233 RA patients were included in the study and genotyped by Sequenom MassARRAY® for 20 SNPs (SLC16A7, SLC19A1, SLC22A6, SLC22A11, SLC46A1, SLCO1B1, ABCB1, ABCC1, ABCC2 and ABCG2). Binary logistic regression analysis were performed and adjusted to possible confounder variables (related to patient, disease and treatment). Haplotype analysis was used to test SNPs revealing statistical significance and a risk index for MTX-Tox was created. In this study, SLC19A1 rs7499 G carriers (P=0.013;OR=4.07), SLC19A1 rs2838956 A carriers (P=0.045;OR=2.81), SLC46A1 rs2239907 G homozygotes (P=0.031;OR=2.31) and SLCO1B1 rs4149056 T carriers (P=0.037;OR=2.82) were associated with increased risk for MTX-Tox. SLC19A1 rs7499 and rs2838956 revealed to be in linkage disequilibrium (P<0.001, D=0.90), nevertheless the estimated haplotypes were not associated with MTX-Tox. In addition, the risk index revealed that patients with the 4 risk variants (SLC19A1 rs7499 GG, SLC19A1 rs2838956 AA, SLC46A1 rs2239907 GG and SLCO1B1 rs4149056 TT) had a 14-fold increased risk for MTX-Tox (P=0.011;OR=14.1). This study revealed that SNPs in ABC transporter genes do not seem to be associated with the development of MTX-Tox, whereas SLC19A1, SLC46A1 and SLCO1B1 genotypes may help clinicians to identify patients with increased risk for MTX-related overall toxicity.

PS 552b Role of CYP3A5 in the Metabolic Activation of Lapatinib

K. D. Hardy[1, 2], M. Wahlin[2] and A. E. Rettie[2]. [1]*Department of Pharmaceutical Sciences, Lipscomb University College of Pharmacy, Nashville, TN and* [2]*Department of Medicinal Chemistry, University of Washington School of Pharmacy, Seattle, WA.* Sponsor: R. Totah.

Idiosyncratic hepatotoxicity has been associated with the oral tyrosine kinase inhibitor lapatinib, which is used in the treatment of metastatic breast cancer. However, the mechanism(s) of this toxicity are unknown. Lapatinib is extensively metabolized via *O*-debenzylation by CYP3A4/5 to form a phenolic metabolite. Further oxidation yields a reactive quinone imine, which can potentially lead to liver injury. While CYP3A4 is abundantly expressed in human liver, CYP3A5 expression is highly polymorphic. Individuals with the *CYP3A5*1* allele express high levels of the functional protein, whereas the *CYP3A5*3* variant allele results in low to undetectable levels of CYP3A5. We hypothesized that polymorphic expression of CYP3A5 may contribute to inter-individual differences in the generation of reactive metabolites of lapatinib. To address this hypothesis, we first examined the kinetic parameters of lapatinib *O*-debenzylation by CYP3A4 and CYP3A5 Supersomes™ utilizing LC-MS/MS analysis. Both recombinant enzymes turned over lapatinib rapidly (15-18 min^{-1}) and with high affinity (1.0-2.2 μM), albeit CYP3A4 exhibited an overall 2.5-fold higher catalytic efficiency than CYP3A5. In individual genotyped human liver microsomal preparations, the rates of debenzylation of lapatinib (5 μM) were comparable between carriers of the *CYP3A5*1* wild-type allele and CYP3A5 non-expressers (*CYP3A5*3/*3*). Next, glutathione (GSH) trapping experiments were conducted with debenzylated lapatinib as substrate (5 μM) to assess the formation of GSH adducts of the quinone imine reactive metabolite (RM-SG). Kinetic analysis revealed that CYP3A5 Supersomes were seven times more efficient than CYP3A4 for generation of RM-SG adducts. Finally, the levels of RM-SG formed were significantly higher (P= 0.03) in human liver microsomes from *CYP3A5*1* expressers compared to *CYP3A5*3/*3* livers. These data show that CYP3A5 is a quantitatively important contributor to hepatic lapatinib bioactivation *in vitro*.

PS 552c A Genetic Variant Associated with Clopidogrel Responses: Exome Sequencing and Validation

B. Ning[1], L. M. Yerges[2], C. Chang[1], D. Yu[1], A. Fisch[2], D. Thierry-Mieg[3], J. Thierry-Mieg[3], B. Green[1], Z. Su[1], J. R. O'Connell[2], M. A. Pacanowski[4], W. Tong[1], L. Shi[1] and A. R. Shuldiner[2]. [1]*National Center for Toxicological Research, FDA, Jefferson, AR,* [2]*University of Maryland School of Medicine, Baltimore, MD,* [3]*National Center for Biotechnology Information, Bethesda, MD and* [4]*Center for Drug Evaluation and Research, FDA, Silver Spring, MD.*

Clopidogrel is an anti-platelet drug used for prevention of thrombotic events in patients with coronary artery disease. Residual ADP-stimulated platelet aggregation in clopidogrel-treated patients is highly heritable; however, with the exception of loss of function variants in CYP2C19, the underlying genetic contributions have not been identified. The elucidation of these genetic variants could enable more efficacious approaches to anti-platelet therapy. To identify novel genetic variants associated with clopidogrel response, we performed exome sequencing of DNA samples from extreme clopidogrel responders and non-responders from the Amish Pharmacogenomics of Anti-platelet Intervention (PAPI) Study. We identified 15 variants in candidate genes whose frequencies were enriched in one of the extremes (p<0.0001). These variants were genotyped in the full PAPI cohort (n=668). One SNP, rs41291122 in PLCE1, was associated with post-clopidogrel ADP-stimulated platelet aggregation in the full cohort (p=0.001). Luciferase reporter studies in HEL cells revealed that the G allele of the SNP had an increased promoter activity compared to the reporter constructs containing the T allele of the SNP. These results suggest for the first time that variants in PLCE1 influence clopidogrel response. If this SNP is found to be associated with clinical outcomes in clopidogrel-treated coronary artery disease (CAD) patients, it may be useful as a prognostic marker in CAD patients. Furthermore, these findings unveil novel platelet biology and potential new drug targets.

PS 552d Genistein Nanoparticles Protect Against Radiation-Induced Injury by Multiple Mechanisms

M. R. Landauer. *Armed Forces Radiobiology Research Institute, Bethesda, MD.*

Medical radiation countermeasures have applications in clinical oncology, space travel, radiation site cleanup and radiological terrorism. We demonstrated previously that the soy isoflavone genistein protects against acute hematopoietic radiation injuries by increasing hematopoietic stem cell survival and decreasing proinflammatory cytokines. Genistein is a phytoestrogen that has been established to have weak estrogenic activity. In the present study, we evaluated the radiation pro-

tective effects of a nanoparticle formulation of genistein after the administration of an estrogen receptor antagonist. Male CD2F1 mice received an intramuscular (IM) injection of the estrogen receptor antagonist, ICI 182,780 (ICI), or corn oil vehicle daily for 4 days. On the fourth day, mice received a second IM injection of either vehicle or genistein nanosuspension (150 mg/kg). All mice then received a single dose (9.25 Gy) of total body gamma irradiation (cobalt-60), 24 h after the second injection. Results showed that 30-day survival for both the vehicle and ICI groups was 25%, whereas 90% of genistein-treated mice survived. Mice that received ICI followed by genistein exhibited a significant decrease in survival rate (45%). These results demonstrate that the radiation protective effects of genistein are mediated in part through an estrogen receptor pathway.

PS 552e Arsenicals, Lewisite- and Phenylarsine Oxide-Induced Cutaneous Inflammation Response and Cell Death Are Regulated by UPR Signaling Pathway

R. K. Srivastava, C. Li, S. C. Chaudhary, Z. Weng, F. Afaq and M. Athar. *Dermatology, University of Alabama at Birmingham, Birmingham, AL.* Sponsor: S. Beedanagari.

Vesicants are a group of chemical agents that cause skin blistering and inflammation following their cutaneous exposure. These agents were synthesized as chemical weapons to be used during warfare. Lewisite, an arsenicals is an important war threat agent. It is known to manifest severe cutaneous inflammation and blistering. However, the exact molecular mechanisms underlying there effects remain undefined. We develop a novel mouse murine model which is highly sensitive to inflammatory inducing agents and manifests similar responsces as observed in humans. Here, we show that topical exposure to lewisite and its analog phenylarsine oxide (PAO) on the skin of Ptch+/-/SKH-1 hairless mice induced erythema, edema and microvesication associated with the enhanced production of pro-inflammatory cytokines and reactive oxygen species (ROS). A huge cell death was also observed particularly at the site of lewisite exposure. These effects were found to be regulated via unfolded protein response (UPR) signaling pathway activation. UPR inhibitor, 4-phenylbutyric acid (PBA), an antioxidant N-acetyl-cysteine (NAC) or their combination were highly effective in diminishing PAO-induced erythema, edema and microvesication. Similarly, a dose- and time-dependent up-regulation of inflammatory and UPR pathways by arsenicals were observed in human skin keratinocytes. PERK-regulated UPR proteins GRP78, p-PERK, p-eIF2α, ATF4 and CHOP were particularly induced in these cells. PBA and NAC significantly attenuated these effects in keratinocytes. Employing siRNA approaches, CHOP was found to be the key apoptosis and pro-inflammatory responses inducing protein. These data provide evidence that lewisite and its analog PAO which is also a degradation product of other arsenicals have potent inflammation, vesication and cell death inducing properties in the skin and may have long term environmental and human health consequences.

PS 552f Arg-1 Is Associated with the Development of Late Pulmonary Fibrosis following Irradiation

C. J. Johnston, A. M. Groves, J. P. Williams, T. Beach and J. N. Finkelstein. *Pediatrics, University of Rochester, Rochester, NY.*

Macrophages are found in close proximity with collagen-producing myofibroblasts and indisputably play a key role in fibrosis. With their potential to act in both a pro- and antifibrotic capacity, as well as regulate the activation of resident and recruited myofibroblasts, macrophages and the factors they express are integrated into all stages of the fibrotic process. Classical activation by microbial agents and/or T helper cell type 1 (Th1) cytokines, interferon-γ (IFN-γ), in particular, is associated with the production of nitric oxide (NO) and proinflammatory cytokines involved in cytotoxicity, microbial killing, and regulation of cell proliferation (M1 or type-1 polarization). More recently, it was shown that macrophages could also follow a different activation pathway after stimulation with the Th2 cytokines interleukin (IL)-4 or IL-13 (M2 or type-2 polarization). Our hypothesis is that the induction of Arg-1 in these "alternatively activated" cells leads to development of radiation-induced fibrosis. 8 week old female C57BL/6J or C3H/HEJ mice were irradiated with 5 Gy total body irradiation followed by a dose of 10 Gy to lung only. Mice were examined at 24 or 72 hours or 1,4,12,18 or 26 weeks post irradiation. Our findings demonstrate a dramatic increase in Arg-1 and MCP-1 expressing macrophages associated with the progression of fibrosis. These results correlate with later time points where C57BL/6J mice are exhibiting a robust fibrotic response but C3H/HeJ demonstrate little pathology. Injuries which generated robust inflammatory responses but did not develop fibrosis demonstrated induction of iNOS but not Arg-1. These data suggest a role for Arg-1 expressing macrophages in the development of inflammation and demonstrate that differential activation of Arg-1/NOS-2 is a potential determinant in the pathogenesis of pulmonary fibrosis development. This information may provide an important target for potential mitigation agents that could be effective in reducing the development of fibrosis following irradiation.

PS 552g Soman-Induced Convulsions Change the Phosphorylation State of the Potassium-Chloride Cotransporter (KCC2)

C. Smith[1], S. M. Miller[1], T. Z. Deeb[2], L. Silayeva[2], S. J. Moss[2] and J. H. McDonough[1]. [1]*US Army Medical Research Institute of Chemical Defense, Aberdeen Proving Ground, MD and* [2]*Tufts Medical School, Boston, MA.*

Exposure to nerve agents induces numerous symptoms, including seizures that become resistant to benzodiazepines within 40 minutes of onset. This resistance may result from the internalization of GABAA receptors; however, this process is likely too slow to account for this rapid benzodiazepine resistance. An alternate hypothesis is that dysfunction of KCC2, a protein that permits GABA's inhibitory tone by maintaining the Cl- gradient, may decrease the efficacy of benzodiazepines following prolonged seizures. As little as 15 minutes of seizure-like activity decreases KCC2, which may in turn increase concentrations of intracellular Cl- and reduce GABA-mediated inhibition. The current experiment examined the concentrations of KCC2 and phosphorylation at two key regulatory residues, S940 and T906, in C57BL/6 mice following the onset of soman-induced convulsions. Importantly, the phosphorylation of S940 (pS940) increases KCC2 activity, whereas the phosphorylation of T906 (pT906) decreases KCC2 activity. Mice were exposed to soman, and brain tissue was collected at 0, 15, 30, or 60 minutes following the onset of convulsions. In the hippocampus, soman increased pT906 within 15 minutes of convulsion onset and continued to increase over time up to 60 minutes. In contrast, soman-induced convulsions did not significantly alter pS940 or total KCC2. In the cortex, soman-induced convulsions increased both pT906 and pS940 at 15 minutes; however, concentrations of pS940 decreased to levels equivalent to saline-exposed mice by 60 minutes. Congruent with results from the hippocampus, total KCC2 levels did not change in the cortex. These results suggest that soman-induced convulsions are associated with time-dependent changes in the phosphorylation state of KCC2. Reactivating KCC2 may thus serve as a potential therapeutic strategy for terminating benzodiazepine-resistant seizures.

PS 553 Flavanone Silibinin As Potential Therapeutic against Skin Injuries by Vesicating Agents

N. Tewari-Singh[1], A. K. Jain[1], S. Inturi[1], D. Kumar[1], D. Orlicky[2], C. Agarwal[1] and C. White[3]. [1]*Department of Pharmaceutical Sciences, University of Colorado Denver, Aurora, CO,* [2]*Department of Pathology, University of Colorado Denver, Aurora, CO and* [3]*Department of Pediatrics, University of Colorado Denver, Aurora, CO.*

Chemical warfare agent sulfur mustard (SM) and its analog nitrogen mustard (NM) inflict delayed blistering and incapacitating injuries on skin tissue. Our previous findings have demonstrated therapeutic efficacy of silibinin in reversing monofunctional alkylating SM analog 2-chloroethyl ethyl sulfide (CEES)-induced skin injuries. To translate this effect using a bifunctional alkylating vesicant, efficacy studies were carried out with NM-induced injury biomarkers established in SKH-1 hairless mice. Topical application of silibinin 30 min after NM exposure decreased NM-induced 60% mortality (120 h exposure) and NM-induced toxic skin injury attributes in SKH-1 mice. Following 1 or 2 mg silibinin treatment, a dose-dependent reduction of NM-induced increases in epidermal thickness, microvesication, dead and denuded epidermis, parakeratosis and scab formation was observed. All NM-induced lesions were assessed at 24, 72 or 120 h time point depending on their optimum injury. Silibinin (2 mg dose) caused complete prevention of NM-induced H2A.X phosphorylation indicating reversal of DNA damage, large incidences of microvesication (>500μm2) and parakeratosis. Silibinin (2 mg) application also caused 52% and 77% ($p<0.05$) reversals in NM-induced increase in COX-2 and myeloperoxidase levels, respectively. These findings indicate that attenuation of NM-induced skin injuries by silibinin is due to its multiple effects targeting pathways associated with DNA damage, inflammation and vesication. Together, these studies suggest therapeutic potential of silibinin against skin injuries by NM and support its further optimization as an effective treatment for skin injuries by SM and other vesicating agents.

PS 554 Topical Nitrogen Mustard Exposure Causes Systemic Toxic Effects in Mice

R. Agarwal[1], D. Kumar[1], D. G. Goswami[1], N. Tewari-Singh[1], S. Inturi[1], D. Orlicky[2], A. K. Jain[1], R. C. Rancourt[3], C. White[2] and C. Agarwal[1]. [1]*Department of Pharmaceutical Sciences, University of Colorado Denver, Aurora, CO,* [2]*Department of Pathology, University of Colorado Denver, Aurora, CO and* [3]*Department of Pediatrics, University of Colorado Denver, Aurora, CO.*

Vesicating agents sulfur mustard (SM) and nitrogen mustard (NM) are easily absorbed by skin causing cutaneous injuries and blistering. To study clinical, histopathological, and molecular features of cutaneous lesions from topical vesicant exposure, we used NM. Our studies showed that topical NM (3.2 mg) exposure in SKH-I hairless mice not only caused skin injuries but also lead to significant body weight loss and 40-60% mortality (120 h exposure), suggesting systemic effects of its topical exposure. Studies in these mice showed that, though a decrease in heart and breath rate was only observed at 120 h following exposure, NM exposure initiated an increase in blood leucocyte count by 24 h and thereafter leucopenia 72 h post-exposure. Examination of the blood revealed an increase in neutrophils and decrease in lymphocytes 24 h post exposure. H&E staining of the small intestine revealed NM-related toxic effects including loss of membrane integrity of surface epithelium and abnormal structure of glands as well as degeneration of villi starting by 24 h and observed mainly 72-120 h after exposure. NM exposure also resulted in a reduction in T-cells from the splenic peri-arterial lymphatic sheath as well as macrophages and RBCs from the red pulp. At later time points (72 and 120 h), NM exposure resulted in dilation of glomerular capillaries and loss of cells from the renal corpuscles. It has been reported that exposure to higher SM levels (total body exposure) can cause damage to the bone marrow and hematopoietic system, liver and kidney failure, and toxicity to the spleen and GI tract. Our results with NM indicate that these organs are also affected from only topical vesicant exposure and can lead to mortality. These outcomes could help identify useful countermeasures against skin injuries and toxic systemic effects after topical vesicant exposure.

PS 555 Nitrogen Mustard-Induced Corneal Injury Involves DNA Damage and Induction of Pathways Related to Inflammation, Vesication, and Neovascularization

D. G. Goswami[1], N. Tewari-Singh[1], D. Dhar[1], D. Kumar[1], C. Agarwal[1], D. A. Ammar[2], R. Kant[1], J. Petrash[2] and R. Agarwal[1]. [1]*Department of Pharmaceutical Sciences, University of Colorado Denver, Aurora, CO and* [2]*Department of Ophthalmology, University of Colorado Denver, Aurora, CO.*

To develop effective therapies against ocular injuries by vesicating agents, investigation of mechanistic aspects of vesicant-induced ocular injuries is important. Accordingly, toxic effects and associated mechanisms were examined in maximal affected corneal tissue with nitrogen mustard (NM), an analog of sulfur mustard (SM). Analysis of 100 nmol NM-exposed rabbit corneas for 2 h (washed and cultured for 24 h), evidenced increases in epithelial thickness, apoptotic cell death, epithelial-stromal separation, increase in the levels of angiogenic regulator VEGF, and induction of COX-2 and MMP-9. Since vesicating agents mainly target the corneal epithelial cells, we also employed human corneal epithelial cells (HCEC) to study and compare the mechanism/s of action of NM-induced injury in these cells with rabbit cornea. Exposure (48 h) to NM (50 and 100 μM) caused a dose-dependent decrease in HCEC viability and DNA proliferation.. These toxic effects could be related to NM-induced DNA damage (p53 phospho ser15, total p53 and H2A.X phospho ser139) in HCEC. In addition to p53 phosphorylation, NM also induced caspase-3 and PARP cleavage, suggesting their role in NM-related HCEC death and apoptotic cell death in rabbit cornea. Similar to studies in rabbit cornea, NM exposure also caused an increase in COX-2, MMP-9 and VEGF levels in HCEC, indicating a role of these molecules and related pathways in NM-induced corneal inflammation, epithelial-stromal separation and neovascularization. NM exposure in HCEC also instigated an increase in phosphorylation of MAPKs and activation of AP-1 family proteins. Increase in lipid peroxidation and protein oxidation in HCEC by NM suggests the role of oxidative stress in the activation of signaling pathways by NM. These molecular targets could be supportive in development of therapeutics against vesicant-induced corneal injuries.

PS 556 Neural Protection Demonstrated in the Central Nervous System by Novel Pyridinium Oxime Reactivators of Organophosphate-Inhibited Acetylcholinesterase

R. Pringle[1], E. C. Meek[1], H. W. Chambers[2], J. M. Gearhart[3] and J. E. Chambers[1]. [1]*CEHS, Mississippi State Univ., Mississippi State, MS,* [2]*Biochem., Mol. Bio., Ent. and Plant Path., Mississippi State Univ., Mississippi State, MS and* [3]*AFRL, WPAFB, OH.*

Exposure to toxic levels of organophosphates (OPs), such as nerve agents and some insecticides, compromises the cholinergic system by inhibiting acetylcholinesterase (AChE), resulting in neural damage and potential detrimental long-term cognitive effects. The efficacy of novel phenoxyalkyl pyridinium oxime reactivators, created with moieties to increase blood-brain barrier penetration, was tested *in vitro* using highly relevant surrogates for sarin (phthalimidyl isopropyl methylphosphonate; PIMP), cyclosarin (nitrophenyl cyclohexyl methylphosphonate; NCMP), and VX (nitrophenyl ethyl methylphosphonate; NEMP), as well as with paraoxon, the active metabolite of the insecticide parathion. Rat brain homogenate was incubated with OP concentrations yielding about 80% AChE inhibition, followed by a novel oxime (0.1mM) and AChE activity measured. Oximes resulting in good reactivation potential were also tested *in vivo* against surrogates for sarin (nitrophenyl isopropyl methylphosphonate; NIMP) and VX (NEMP). Glial fibrillary acidic protein (GFAP) and brain monoamines were evaluated as markers of neural damage and brain activity, respectively. *In vitro* AChE reactivation by oximes was similar for PIMP (14-79%) and NEMP (23-76%). Fewer oximes were efficacious with NCMP, with lower reactivation (0-25%). Reactivation varied by individual oximes for paraoxon (16-93%) compared to nerve agent surrogates, but the overall range was similar. *In vivo* several oximes reactivated AChE inhibited by NIMP and NEMP (up to 35% by 2 hours). The most efficacious oxime exhibited neural protection (less GFAP accumulation in key brain regions following oxime treatment), accompanied by protection from OP-induced seizures. These results suggest the innovative oxime chemistry may be therapeutic after OP exposure and could protect from neural damage. Support: Defense Threat Reduction Agency: 1.E0056_08_AHB_C

PS 557 Behavioral Assessments in NIH Swiss Mice Acutely Intoxicated with Tetramethylenedisulfotetramine (TETS)

B. Flannery[1], J. L. Silverman[2], D. Bruun[1], J. N. Crawley[2] and P. Lein[1]. [1]*Molecular Biosciences, University of California Davis School of Veterinary Medicine, Davis, CA and* [2]*MIND Institute and Psychiatry and Behavioral Sciences, University of California Davis School of Medicine, Sacramento, CA.*

TETS, a GABAA receptor antagonist, is a potent rodenticide with no known antidote. Acute TETS intoxication can cause seizures, convulsions, status epilepticus and death. Little is known about the long-term neurobehavioral consequences in individuals who survive acute TETS intoxication. Here, we address hypothesized consequences using the NIH Swiss mouse. Mice received TETS (0.15 mg/kg, i.p.) or saline vehicle followed by diazepam (5 mg/kg, i.p.) after 2 clonic seizures (≈ 20 min post TETS-exposure). Behavioral endpoints were assessed at 1 week and 1 month post-TETS injection in two separate cohorts of mice. Mice were evaluated for anxiety-like behaviors using the elevated plus-maze and light↔dark transition test, and for depression-relevant behaviors using tail suspension and forced swim tests. Learning and memory were evaluated using Pavlovian fear conditioning. There were no significant effects of TETS treatment on anxiety and depression tests. Fear conditioning results were inconclusive because NIH Swiss mice were insufficiently responsive to footshock training. A follow up study revealed this insensitivity is likely due to increased pain threshold and that novel object recognition is a more suitable test of learning and memory in this mouse strain. Collectively, acute TETS intoxication did not cause long-term behavioral deficits in our mouse model. Support provided by the NIH NINDS CounterAct Program (U54 NS079202).

PS 558 Atropine Therapy Alone in Guinea Pigs Does Not Improve Survivability against Most G Agents, VX, Paraoxon, and Chlorpyrifos Oxon

T. H. Snider[1], C. Wilhelm[2], M. C. Babin[1], D. Jett[3], G. Platoff[2] and D. T. Yeung[1]. [1]*Biomedical Research Center, Battelle, Columbus, OH,* [2]*National Institute of Neurological Disorders and Stroke, National Institutes of Health, Bethesda, MD and* [3]*National Institute of Allergy and Infectious Diseases, National Institutes of Health, Bethesda, MD.*

Dose-lethality response curves were characterized in non-sedated, atropinized Dunkin-Hartley male guinea pigs for the nerve agents tabun (GA), sarin (GB), soman (GD), cyclosarin (GF), VX, the pesticides parathion and phorate, and the oxon metabolites paraoxon, phorate oxon (PHO), and chlorpyrifos oxon (CPO)

administered either by subcutaneous (SC) injection in, or percutaneously on, guinea pigs that subsequently received atropine free base at 0.4 mg/kg. The human-equivalent dose in guinea pigs for three DuoDote® autoinjectors was estimated to be 0.4 mg/kg. Lethality rates were obtained at 24 hr after challenge for all but parathion by percutaneous challenge, which required 48 hr to allow for bioactivation to the oxon form. Probit analysis was used to calculate the median lethal dose (LD50). Protective ratios (PR) for atropine were calculated as the LD50 for a challenge material (CM) in atropinized guinea pigs divided by the LD50 for the same CM in no-therapy guinea pigs using data from either the literature or concurrent experiments. Phorate, paraoxon, and CPO did not present significant percutaneous threats, and attempts to obtain an LD50 were abandoned. Statistically significant ($p < 0.05$) therapy in terms of survival was attributed to atropine therapy against a SC challenge of GA alone. Atropine alone did not improve survivability against any other CM exposure by either SC injection or topical application on clipped skin.

PS 559 Identification of Glutaredoxin As a Molecular Target for the Sulfur Mustard Analog Bis(2-chloroethyl)methylamine

Y. Jan[1], D. E. Heck[2], R. P. Casillas[3], D. L. Laskin[4] and J. D. Laskin[1]. *[1]Environmental & Occupational Medicine, Rutgers University-Robert Wood Johnson Medical School, Piscataway, NJ, [2]Environmental Health Science, New York Medical College, Valhalla, NY, [3]MRI-Global, Kansas City, MO and [4]Pharmacology & Toxicology, Rutgers University, Piscataway, NJ.*

The glutaredoxin system, which consists of glutaredoxin (Grx), glutathione, and glutathione reductase (GR), plays a key role in antioxidant defense and cell growth control. Due to their high structural similarity, glutaredoxin and thioredoxin often display overlapping functions. Bis(2-chloroethyl)methylamine (HN2), a bifunctional alkylating agent commonly used as a model compound to study sulfur mustard-induced injury, is known to cause oxidative lung injury. Previously, we reported that HN2 selectively targets the thioredoxin system in lung A549 epithelial cells resulting in enzyme inactivation, a process contributing to oxidative stress and toxicity. In this study, we examined the effects of HN2 on the glutaredoxin system. HN2 treatment was found to cause a concentration- and time-dependent inhibition of Grx, but not GR, in A549 cells. Immunoblot analysis revealed a band corresponding to tetramers of Grx in HN2-treated cells, but not in control cells, indicating that HN2 caused inter-molecular Grx crosslinks. Using recombinant human Grx1 and mass spectrometry, HN2 was found to selectively alkylate cysteine and lysine residues on the enzyme, including cysteine-23 and cysteine-26 in the redox center of the enzyme. Several inter-peptide crosslinks were also identified in HN2-treated Grx1, providing a mechanism for the formation of Grx tetramers in A549 cells. These data demonstrate that glutaredoxin is a molecular target of HN2. Inhibition of the glutaredoxin system may be an important mechanism by which vesicants, including sulfur mustard, induce oxidative tissue injury. Support: NIH grants AR055073, ES004738, CA132624, and ES005022.

PS 560 Functional Properties of Bispyridinium Non-Oxime Compounds on Muscle-Type Nicotinic Acetylcholine Receptors Using a Bilayer-Based Method

H. Thiermann, T. Seeger, L. Florian, F. Worek and K. V. Niessen. *Bundeswehr Institute of Pharmacology and Toxicology, Munich, Germany.*

Objective: In poisoning with some nerve agents, e.g. soman, therapeutic efficacy is limited. A direct intervention at nicotinic acetylcholine receptors (nAChR) might be an option. Studies with bispyridinium non-oxime compounds demonstrated therapeutic effects against soman in vitro and in vivo. Consequently, these results arouse increasing interest in functional properties on nAChRs, especially the muscle-type. The Torpedo electric organ is regarded as a suitable surrogate. For functional characterization, cell-free electrophysiological methods based on solid supported membranes (SSM) can be useful in cases where conventional electrophysiology cannot be applied. In this bilayer based sensor technique, charge translocation is measured via capacitive coupling of the supporting membrane. Functional interactions of bispyridinium compounds were investigated.
Experimental procedures: Purified plasma membrane vesicles from Torpedo californica electric tissue were adsorbed to SSM under varying conditions. Voltage dependent sodium channels were blocked by ambroxol. Rapid exchange to a buffer containing the agonist carbamoylcholine initiated Na+ influx in the membrane vesicles. Various concentrations of agonist and bispyridinium compounds were tested.
Results: Depending on particle size, zeta potential and adsorption procedures, stable and reproducible cholinergic signals were recorded (> 1 nA). Ambroxol prevented a premature collapse of the sodium gradient. High carbamoylcholine concentrations (1-10 mM) seemed to induce desensitization. Small size bispyridinium compounds affected receptor desensitization. However, in absence of an agonist, no intrinsic effect was generated.
Conclusion: The results demonstrated here show that functional measurements can be performed with this technique by using membranes of Torpedo californica electric tissue. Bispyridinium compounds seemed to interact as positive allosteric modulators, thereby affecting desensitisation. Further research is necessary to verify this hypothesis.

PS 561 Attenuation of Nitrogen Mustard (NM)-Induced Pulmonary Injury and Inflammation by Antitumor Necrosis Factor (TNF)alpha Antibody and the Inducible Nitric Oxide Synthase (iNOS) Inhibitor, N-(3-(Aminomethyl)benzyl) acetamidine (1400W)

R. Malaviya[1], V. Sunil[1], A. Venosa[1], K. Vayas[1], P. J. Sinko[1], J. Shen[1], L. Hall[2], D. Shealy[2], N. Heindel[3], C. J. Lacey[3], J. D. Laskin[1] and D. L. Laskin[1]. *[1]Pharmacology and Toxicology, Rutgers University, Piscataway, NJ, [2]Johnson & Johnson, Raritan, NJ and [3]Lehigh University, Bethlehem, PA.*

NM (mechlorethamine) is a vesicant which causes severe damage to the lung leading to pulmonary fibrosis; this is associated with oxidative stress and inflammation. Using transgenic knockout mice, we previously demonstrated that the proinflammatory cytokine, TNFα and nitric oxide generating enzyme, iNOS, play key roles in the pathogenic response to NM. In these studies we analyzed the ability of anti-TNFα antibody and 1400W, alone and in combination, to mitigate NM-induced lung injury. Treatment of male Wistar rats (250 g) with NM (0.125 mg/kg, i.t.) resulted in histopathologic changes in the lung 3-7 d post exposure, and induced expression of cleaved caspase-3 (Casp-3), a marker of apoptosis. This was correlated with increases in bronchoalveolar lavage (BAL) cell and protein content, indicating damage to the alveolar-epithelial barrier. NM also caused increased expression of cyclooxygenase (COX)-2 and heme oxygenase (HO)-1 in lung macrophages, as well as YM-1, a marker of oxidative stress and alternatively activated macrophages. Treatment of rats with anti-TNFα antibody (15 mg/kg, i.v., 1x), 1400W (50 mg/kg, i.p., 1x/d), or a combination of anti-TNFα + 1400W 30 min after NM reduced lung injury and inflammation, as measured by BAL cells, protein and histology. NM-induced expression of COX-2, HO-1, YM-1 and Casp-3 were also reduced. Although the combination of anti-TNFα + 1400W was more effective in down regulating expression of Casp-3, COX-2, HO-1 and YM-1 at 3 d than either agent alone, fibrotic changes at 7 d were only inhibited by anti-TNFα antibody. These data demonstrate that inhibiting TNFα and/or iNOS represents an important approach to mitigating acute and long-term lung injury induced by vesicants. Supported by NIH Grants HL096426, AR055073, ES004738, CA132624, and ES005022.

PS 562 Inhibition of Multidrug Resistance-Associated Protein (MRP) Efflux Transporters Increases the Sensitivity to Vesicant-Induced Growth Inhibition in Lung Epithelial Cells

R. G. Udasin[1, 2], K. M. Bircsak[1, 2], V. Mishin[2], D. E. Heck[3], L. M. Aleksunes[1, 2], D. L. Laskin[1, 2] and J. D. Laskin[1, 4]. *[1]Joint Graduate Program in Toxicology, Rutgers University, Piscataway, NJ, [2]Pharmacology & Toxicology, Rutgers University, Piscataway, NJ, [3]Environmental Health Science, New York Medical College, Valhalla, NY and [4]Environmental & Occupational Medicine, Robert Wood Johnson Medical School, Rutgers University, Piscataway, NJ.*

Sulfur mustard and the related vesicant nitrogen mustard (mechlorethamine, HN2) are bifunctional alkylating agents that cause oxidative stress and persistent lung damage. In the present studies, we examined the role of MRP in modulating the sensitivity of lung cells to HN2. MRP transporters 1, 2, and 3 remove glutathione (GSH)-modified electrophiles from cells. HN2 causes tissue injury by reacting with cellular components such as DNA, proteins, and lipids. By reacting with GSH, monofunctional adducts form, and these adducts contribute to cytotoxicity. MRPs export these adducts, limiting toxicity. Western blot analysis revealed that MRP 1, 2, and 3 are expressed in A549 human lung epithelial cells. To assess the role of these transporters in the cytotoxic actions of HN2, we used MK-571, an inhibitor of MRP1, 2 and 3. Pretreatment of cells with 25 μM MK-571 for 1 h caused a marked inhibition of MRP activity. This was associated with increased sensitivity of the cells to HN2-induced growth inhibition (IC50 = 27 nM with MK-571 vs IC50 = 114 nM with control at 72 h). In contrast, growth inhibition induced by the monofunctional half mustard, chloroethyl ethyl sulfide, which is detoxified by GSH, was not altered by treatment with MK-571 (IC50 = 385 μM with MK-571 vs 325 μM with control). Taken together, these data demonstrate that MRP-mediated efflux transport is key in regulating HN2-induced growth inhibition in lung epithelial cells. Enhancing the activity of these transporters may represent a promising route to mitigate vesicant-induced cytotoxicity. Support: NIH grants AR055073, ES004738, ES007148, CA132624, and ES005022.

PS 563 Sulfur Mustard Alters Sebocyte Differentiation in Hairless Mouse Skin

D. E. Heck[1], L. B. Joseph[2], J. A. Cervelli[2], G. M. Composto[2], R. P. Casillas[3], D. R. Gerecke[2], P. J. Sinko[2], D. L. Laskin[2] and J. D. Laskin[4]. [1]*New York Medical College, Valhalla, NY,* [2]*Rutgers University, Piscataway, NJ,* [3]*MRIGlobal, Kansas City, MO and* [4]*Rutgers University-Robert Wood Johnson Medical School, Piscatway, NJ.*

Sebaceous glands secrete sebum, a lipid containing mixture important in lubricating and waterproofing the hair and skin. Sulfur mustard (SM) is a vesicant known to damage the skin and suppress the production of epidermal lipids. Using a vapor cup model, we examined the effects of SM on sebocyte differentiation in male SKH1-Hr hairless mice. The dorsal skin of mice was analyzed 1, 3, 7, and 14 days after exposure to saturated SM vapor for 6 min. In control mice, prominent sebocytes are evident in the sebaceous glands. These glands, which are composed of immature flattened peripheral sebocytes with differentiated lipid (sebum) laden cells in the central core, expressed fatty acid synthase (FAS), a marker of de novo fatty acid synthesis, inducible nitric oxide synthase (iNOS), and proliferating cell nuclear antigen (PCNA). FAS and PCNA were more prominent in cells near the distal end of the sebaceous gland and in nucleated sebocytes. As sebocytes ascend the sebaceous glands, there is a loss of foamy cytoplasm, an increase in cells containing pyknotic nuclei, and decreased expression of FAS and PCNA. One day post SM, distortions in the sebaceous glands and loss of sebocytes were observed. Sebocytes within both unilobate and multilobate sebaceous glands were swollen, with disintegrated nuclei and poorly defined cell margins. Three days post SM exposure, FAS, iNOS and PCNA expression was down regulated. At 7 days post SM, only sebaceous gland remnants were evident with scattered sebocytes expressing iNOS and PCNA. At 14 days post SM-exposure, no sebaceous glands were present in the skin. Taken together, these data indicate that SM alters sebocyte differentiation, a process which may contribute to epidermal injury. Support: NIH AR055073, ES004738, CA132624, and ES005022.

PS 564 Comparative Efficacy Assessments of Oxime Therapies against Subcutaneous Organophosphate Challenges in the Hartley Guinea Pig

C. Wilhelm[1], T. H. Snider[1], M. C. Babin[1], G. Platoff[2], D. Jett[3] and D. T. Yeung[3]. [1]*Battelle, Columbus, OH,* [2]*National Institutes of Health/National Institute of Allergy and Infectious Diseases, Bethesda, MD and* [3]*National Institutes of Health/National Institute of Neurological Disorders and Stroke, Bethesda, MD.*

Organophosphorus (OP) compounds, including pesticides and chemical warfare nerve agents (CWNAs) represent a threat to the general population not only as possible weapons of terrorism, but also as chemicals that could be released from transportation and storage facilities during industrial accidents. Given the rapid onset of symptoms and toxicity of OP agents, a quick-acting therapeutic regimen that is efficacious over the broad spectrum of OPs is urgently needed. The current regimen includes the administration of atropine in combination with an acetylcholinesterase (AChE) reactivator (oxime; 2-PAM C1). An anticonvulsant (diazepam) is administered if convulsive symptoms are observed. Although this treatment approach is effective against OP intoxication, more effective treatments are being investigated to improve the nation's medical response capabilities. The objective of the current study was to perform a head-to-head comparison of the leading oxime therapies (2-PAM Cl, HI-6 DMS, obidoxime Cl2, TMB4, MMB4-DMS, HLö7 DMS, MINA and RS194B) under standardized conditions against the CWNAs tabun, sarin, soman, cyclosarin, VX, and the pesticides paraoxon, chlorpyrifos oxon and phorate oxon administered by the subcutaneous (SC) route in atropinized guinea pigs. The various oxime reactivators were dosed at a level that was the molar equivalent (145 μmol/kg) of the currently fielded oxime 2-PAM Cl. In another study the dose was based on the therapeutic index of 2-PAM Cl. OP challenges were performed with the 85th percentile lethality dose (LD85) of each agent. The preponderance of evidence from clinical observations, lethality, quality of life scores and cholinesterase reactivation rates across the challenge materials indicates that MMB4 DMS and HLö7 DMS were the two most consistently efficacious oximes.

PS 565 The Sulfur Mustard Analog Bis(2-chloroethyl) Methylamine Induces Oxidative Damage in Mouse Skin

L. B. Joseph[1], G. M. Composto[1], J. A. Cervelli[1], D. R. Gerecke[1], R. P. Casillas[2], D. L. Laskin[1], J. D. Laskin[3] and D. E. Heck[4]. [1]*Rutgers University, Piscataway, NJ,* [2]*MRIGlobal, Kansas City, MO,* [3]*Rutgers University-Robert Wood Johnson Medical School, Piscatway, NJ and* [4]*New York Medical College, Valhalla, NY.*

The sulfur mustard analog (bis(2-chloroethyl) methylamine, HN2) is a potent skin vesicant. As a bifunctional alkylating agent, HN2 can directly modify DNA, a process that can result in strand breaks. Recent evidence suggests that HN2 is also a potent inducer of epidermal oxidative stress. In the present studies we determined if HN2-induced epidermal DNA strand breaks were associated with expression of markers of oxidative stress. CD-1 female mice (6-8 weeks of age) were treated on the dorsal skin with HN2 (20 μmoles). After 1, 3 and 5 days, expression of markers of oxidative stress including 4-hydroxynonenal (4-HNE)-modified proteins and 8-oxo-2'-deoxyguanosine (8-OHdG), and histone phospho-H2A.X, a marker of DNA double strand breaks, was analyzed in the skin using techniques in immunohistochemistry. We found that 8-OHdG and phospho-H2A.X were coordinately upregulated in the nuclei of interfollicular and follicular epidermal cells throughout the wound one day post-treatment. In contrast, 4-HNE modified proteins were identified only in the stratum granulosum and the follicular epidermis. By day 3, phospho-H2A.X and 8-OHdG were upregulated in a thick eschar above the wound and within the interfollicular epidermis and the sebocytes, while 4-HNE was expressed in the hypertrophic epidermis underlying the eschar and interfollicular epidermis. At 5 days post exposure, phospho-H2A.X was confined to the stratum basale with scattered expression in the dermis, while 8-OHdG was expressed in the dermis and the hypodermis. 4-HNE was down regulated and restricted to the hyperplastic stratum granulosum and stratum spinosum. These data indicate that HN2 induces lipid peroxidation and oxidative DNA damage in mouse skin, a process which likely contributes to tissue injury following exposure to vesicating agents. Support: NIH AR055073, ES004738, CA132624, and ES005022.

PS 566 New Approach for Neuroprotection: Novel Peptides Ameliorate Neuroinflammation

U. Wormser[1], B. Brodsky[1], M. Aschner[2], Y. Finkelstein[3] and E. Proscura[1]. [1]*Institute of Drug Research, The Hebrew University, Jerusalem, Israel,* [2]*Department of Molecular Pharmacology, Albert Einstein College of Medicine, New York, NY and* [3]*Neurology and Toxicology Service and Unit, Shaare Zedek Medical Center, Jerusalem, Israel.*

Nerve agents cause neuroinflammatory response that may potentially be treated by novel anti-inflammatory peptides. The way of their discovery is described.
Previous studies demonstrated the potent effect of topical iodine against skin toxicity induced by sulfur mustard and other chemical and thermal stimuli. While exploring the mechanism of iodine we discovered that it induces the production of a nonapeptide, a fragment of H2A histone termed IIIM1. This peptide showed counterirritating and antiinflammatory activities in the ear swelling test and carrageenan-induced hind paw edema assay.
Being an antiinflammatory peptide, IIIM1 was evaluated as a potential drug candidate for pathologies-associated with neuronal damage such as experimental autoimmune encephalitis (EAE), an animal model of multiple sclerosis (MS). The peptide dramatically ameliorated the neurological symptoms in the diseased mice, reduced proinflammatory cytokines, elevated Th2 cytokines and caused proliferation of T-regulatory cells. In addition to its immunomodulatory/antiinflammatory properties, IIIM1 significantly reduced cytotoxicity and oxidative stress in astrocytes exposed to methyl mercury. The neuroprotective effects of IIIM1 strongly support the notion that this peptide may be used as a neuroprotectant in organophosphate exposure.
Further mechanistic studies revealed that IIIM1 induced a 16 amino acid peptide termed RA1 that surprisingly, is present in Japanese rice. RA1 ameliorated neurological symptoms in EAE mice, reduced proinflammatory cytokines and elevated Th2 cytokines. This peptide may be associated with the low incidence of MS in Japan.
In view of their antiinflammatory characteristics both IIIM1 and RA1 are potential candidates for treatment of neuroinflammation caused by exposure to nerve agents.

PS 567 Are Current Antidotes for Organophosphorus Nerve Agent Effective against the Toxic Effects of Carbamate Poisoning in the Hartley Guinea Pig?

M. K. Brittain[1], J. A. Harvilchuck[1], M. C. Babin[1], D. Jett[2], G. Platoff[3] and D. T. Yeung[2]. [1]*Biomedical Research Center, Battelle Memorial Institute, Columbus, OH,* [2]*National Institute of Neurological Disorders and Stroke, NIH, Bethesda, MD and* [3]*National Institute of Allergy and Infectious Diseases, NIH, Bethesda, MD.*

Aldicarb and methomyl are highly toxic carbamate insecticides and known groundwater contaminants. Both carbamates have been implicated in animal and human poisonings. Consequently, they pose a threat to the general population not only as possible weapons of terrorism, but also from environmental and occupational exposures. Like the more common organophosphorus pesticides (OPs) and nerve agents, the mechanism of toxicity is cholinesterase (ChE) inhibition which can result in cholinergic crisis. Inhibition of ChE reverses fairly rapidly when compared to inhibition from OPs. Based on its primary mechanism of toxicity as an anticholinesterase, the administration of atropine and the oxime 2-PAM C1 is the proposed therapeutic approach after carbamate poisoning. This study evaluated the dose-lethality response curves characterized in non-sedated, Hartley male guinea pigs exposed to either aldicarb or methomyl, administrated via a single subcutaneous (SC) injection. The median lethal dose (MLD) for aldicarb was determined to be 0.86 mg/kg while methomyl was approximately 10-fold less toxic at 8.06 mg/kg. Atropine (Atr) free base was administered at human equivalent dose (HED) levels for the guinea pig, 0.4 mg/kg, via the intramuscular route. Due to toxicity in the guinea pig, 2-PAM Cl was administered at the human-relevant dose of 25.7 mg/kg and was via the same administration route. Atropine alone and in combination with 2-PAM Cl demonstrated significant protection against lethality. However, the addition of 2-PAM Cl had no statistical effect on the efficacy of atropine alone. The observation that 2-PAM Cl did not reduce the overall efficacy of this treatment regimen is encouraging given previous concerns regarding the potential problematic interactions between carbamates and oximes.

PS 568 Paraoxonase 1 (PON1) Enhancers Accelerate the Detoxication of Organophosphates (OP) Including Nerve Agent Surrogates

J. E. Chambers, E. C. Meek, R. Pringle and H. W. Chambers. *Coll Vet Medicine, Mississippi State Univ, Mississippi State, MS.*

PON1, a calcium dependent hydrolase, is associated with the high density lipoproteins in human serum. PON1, named for its ability to hydrolyze paraoxon, the active metabolite of the OP insecticide parathion, can hydrolyze some OPs, but most with low efficiency. PON1 uses a hydroxide ion from water as the nucleophile to accomplish the degradation of the OP. Novel substituted phenoxyalkyl pyridinium oximes have been developed as more potent nucleophiles with the expectation that they might enhance the efficacy of PON1 in degrading OPs. The substrates tested were surrogates for sarin and VX, nitrophenyl isopropyl methylphosphonate (NIMP) and nitrophenyl ethyl methylphosphonate (NEMP), respectively, and paraoxon. Commercially available human serum was used as the source of PON1. The length of the alkyl chain varied from 6-10 carbons, and the molecules contained various substitutions on the phenoxy moiety. A direct assay was employed using 0.3mM NIMP or NEMP or 1.2mM paraoxon and 0.1mM nucleophile, monitoring the released 4-nitrophenol spectrophotometrically following a 15 min incubation with serum. About 20 novel nucleophiles were tested. Enhancement of degradation of over 10% occurred with 10 of the nucleophiles with NIMP, with 8 of these yielding over 20% enhancement. Enhancement of degradation of over 10% occurred with 9 of the nucleophiles with NEMP, with 3 of these yielding over 20% enhancement. Only 1 of these nucleophiles enhanced the degradation of paraoxon. An indirect assay used 120 nM NIMP or 30 nM NEMP (i.e., more realistic concentrations), and monitored residual anticholinesterase activity of undegraded surrogate as an index of PON1 activity. This indirect assay showed 11 nucleophiles able to enhance NIMP degradation by up to 50% and 7 nucleophiles able to enhance NEMP degradation by up to 35%. These nucleophiles show potential to be developed as drugs with a novel mechanism of antidotal activity. (Supported by Defense Threat Reduction Agency HDTRA1-12-1-0043)

PS 569 Δ^9 Tetrahydrocannabinol Prevents Mice from Staphylococcal Enterotoxin B-Induced Toxic Death by the Modulation of the miR-17-92 Cluster and *De Novo* Induction of T-Regulatory Cells

R. Rao, P. S. Nagarkatti and M. Nagarkatti. *University of South Carolina, Columbia, SC.*

The superantigen Staphylococcal enterotoxin B (SEB) is a potent activator of Vβ8+T-cells which results in the clonal expansion of ~30% of the T-cell pool. Consequently, this leads to the substantial release of inflammatory cytokines, induction of toxic shock, and eventually death. In the current study, we sought to investigate if Δ^9 Tetrahydrocannabinol (THC), a marijuana cannabinoid known for its anti-inflammatory properties, could prevent SEB-induced mortality and alleviate symptoms of toxic shock. Intranasal followed by intraperitoneal dual administration of SEB resulted in acute mortality, while THC treatment led to 100% survival. Additionally, THC treatment significantly decreased numerous SEB-mediated clinical parameters, such as production of inflammatory cytokines, immune cell infiltration into the lung, vascular leak, and improved airway resistance. Microarray analysis revealed that a prominent miRNA signature upon SEB exposure was the induction of the miR-17-92 cluster. Mechanistically, we found the miR-17-92 cluster targets Pten (phosphatase and tensin homolog), an inhibitor the PI3K/Akt signaling pathway, thereby promoting cellular proliferation and the suppression of T-regulatory cells. THC treatment, however, inhibited the individual miRNAs in the cluster. Moreover, in its ability to act as a PI3K/Akt inhibitor, THC treatment led to the induction of CD4+Foxp3+ T-regulatory cells and suppressed cellular proliferation. We report, for the first time, a miRNA expression profile in response to SEB. Furthermore, our results suggest that THC is a potent anti-inflammatory compound that acts by modulating critical miRNA involved in SEB-induced toxicity and death. (Supported in part by NIH grants P01AT003961, R01AT006888, R01ES019313, R01MH094755, P20RR032684 and VA Merit Award BX001357)

PS 570 Store-Operated Calcium Entry As a Mechanism of Phosgene Toxicity

D. K. Andres[1], B. Keyser[1], B. J. Benton[1], A. Appell[1], D. Olivera[2], W. Holmes[2], D. Paradiso[2], D. Anderson[2] and R. Ray[1]. [1]*Research Division, US Army Medical Research Institute of Chemical Defense, Aberdeen Proving Ground, MD and* [2]*Analytical Toxicology Division, US Army Medical Research Institute of Chemical Defense, Aberdeen Proving Ground, MD.* Sponsor: J. Yourick.

Phosgene (CG, COCl2) is a chemical used in the manufacturing of pharmaceuticals, dyes, and polyfoam rubber products; however, it is highly toxic. The risk of human exposure is via industrial accidents, natural disasters, or acts of terrorism. CG causes bronchoconstriction, vasoconstriction and associated pathological effects that could be life threatening. Currently, there is no effective medical countermeasure for complications resulting from CG exposure. We hypothesize that the broncho- and vasoconstriction effects of CG are due to disturbed intracellular free Ca2+ concentration ([Ca2+]i) regulation in bronchial smooth muscle cells and vascular endothelial cells. We studied [Ca2+]i changes in 80-90% confluent monolayer cultures of human bronchial smooth muscle cells (BSMC) and human pulmonary microvascular endothelial cells (HPMEC) exposed to CG (16 ppm, 8 min) using an air/liquid interface exposure system. Intracellular free Ca2+ was measured using Fluo-4 fluorescence. CG increased [Ca2+]i ($p<0.05$) in both BSMC and HPMEC. This [Ca2+]i increase was blocked ($p<0.05$) by two types of store operated calcium entry (SOCE) channel blockers, SKF-96365 and Compound A. These effects correlate with the in vivo efficacies of these compounds to protect against 24 hr lethality from CG inhalation in mice (data not shown). Thus the SOCE mechanism appears to be one of the targets for intervention in CG toxicity. Disclaimer: The views expressed in this abstract are those of the authors and do not reflect the official policy of the Department of Army, Department of Defense, or the U.S. Government. This research was supported by an interagency agreement between NIH/NIAID (Y1-A1-6179-04) and the USAMRICD (A120-B.P2009-03).

PS 571 Accumulation of Distinct Macrophage (MP) Subpopulations in the Lung following Nitrogen Mustard (NM) Exposure; Contribution of Splenic Monocytes

A. Venosa, R. Malaviya, J. D. Laskin and D. L. Laskin. *Joint Graduate Program in Toxicology, Rutgers University/Robert Wood Johnson Medical School, Piscataway, NJ, Piscataway, NJ.*

NM (mechlorethamine) causes lung injury and fibrosis. This is associated with MP accumulation in the tissue and the release of mediators implicated in toxicity. Herein, we assessed the phenotype and origin of MP accumulating in the lung after NM. Cells were collected by bronchoalveolar lavage (BAL) 1-28 d after i.t. saline or NM (0.125 mg/kg) administration to Wistar rats and stained with antibodies to Mac-1 (inflammatory cells) and CD43 (monocyte-derived MP). The majority (>97%) of cells from control animals were Mac-1-/CD43-, consistent with a resident alveolar MP phenotype. NM caused an increase in Mac-1+/CD43+ and Mac-1+/CD43- cells in the lung, which peaked at 3 and 7 d, respectively. By 28 d post NM, cells more closely resembled resident alveolar MP. To characterize these subpopulations, cells were analyzed for expression of pro- (CCR2, iNOS) and anti-inflammatory (IL-10) genes. NM caused a persistent increase (4-6 fold) in CCR2 expression by resident alveolar MP (Mac-1-/CD43-), with no change in iNOS or IL-10. Increased CCR2 was also observed in infiltrating Mac-1+/CD43- and Mac-1+/CD43+ cells after NM; at 3 d, expression was 2-3 greater than resident alveolar MP. CCR2 remained elevated for at least 7 d in Mac-1+/CD43+ cells. These cells also expressed increased iNOS, and to a lesser extent, IL-10, suggesting that within this population there are phenotypically distinct subsets. Splenectomized (SPX) rats were used to assess the role of the spleen as an extramedullary source of lung MP. Increased tissue damage was noted in histologic sections of SPX rats 3 d post NM; this correlated with increased Mac-1+/CD43+ cells in the lung. These studies show that NM treatment leads to infiltration of multiple inflammatory subpopulations into the lung some of which originate in the spleen. Moreover, it appears that spleen derived cells contribute to down regulating inflammation and initiating wound repair. (NIH AR055073, ES004738, CA132624, and ES005022)

PS 572 Mechlorethamine Dermatotoxicity Is Potentiated by the Absence of Nrf2 in the Mouse Ear Vesicant Model

O. Sparavalo, H. Tumu, K. Giusto, S. Nicholson, M. Guralnik, L. Nogueira, S. E. Reznik, L. D. Trombetta and B. Billack. *Department of Pharmaceutical Sciences, St. John's University, College of Pharmacy and Health Sciences, Jamaica, NY.*

Vesicants are chemicals with a blistering activity which pose a threat to the public. The prototype vesicant is sulfur mustard (SM), which is highly toxic and which requires specialized laboratory facilities for handling. The related vesicant mechlorethamine (HN2) has been used as a chemical surrogate for SM in numerous studies aimed at identifying countermeasures to chemical threats. HN2 increases oxidative stress in the skin and also possesses an alkylating property, leading to adduct formation of cellular macromolecules. Nrf2 is a transcription factor involved in cellular detoxification of free radicals and oxidants. Based on the propensity of HN2 to induce oxidative stress and the role of Nrf2 in detoxifying oxidative stress, a pilot study was conducted to determine if Nrf2 deficiency would result in an exaggerated toxic response of skin to HN2 exposure. To this end, the mouse ear vesicant model (MEVM) was utilized in wildtype and Nrf2(-/-) C57BL/6J female mice and the effects of HN2 upon ear tissue histology and thickness were measured 24 h after vesicant exposure using a qualitative histological scoring scale and quantitative morphometric analysis. Test doses of HN2 were applied topically and DMSO served as the vehicle in all studies. As the dose of HN2 applied to the ear was increased, an increase in edema, epithelial hyperplasia, vesication and inflammatory cell infiltrates were observed in both strains. Nrf2 knockout animals exhibited a higher incidence of vesication than wildtype mice after a single exposure to HN2 (at test doses ≥ 1 μmol/ear); however, statistically significant differences between wildtype and Nrf2 deficient animals in the areas of edema and epithelial hyperplasia were not observed. The data here suggest that Nrf2 status in the skin may specifically impact the oxidative stress and cellular injury that account for the vesicant activity of HN2.

PS 573 Quantitative Proteomic Analysis of the Guinea Pig Brainstem following Exposure to Sarin

M. L. Meade[1], M. K. Makley[1], J. J. Schlager[2], T. H. Snider[3] and J. M. Gearhart[1]. [1]*Henry M Jackson Foundation, Wright Patterson AFB, OH,* [2]*Air Force Research Lab 711 HPW/RHDJ, Wright Patterson AFB, OH and* [3]*Battelle Biomaedical Research Center, West Jefferson, OH.*

Sarin (O-isopropyl methylphosphonofluoridate; GB) is a toxic organophosphorus (OP) nerve agent developed during WWII. It has been used in both military and civilian attacks, and reports suggest its use in the ongoing Syrian civil war. It is a potent inhibitor of acetylcholinesterase (AChE). The brainstem controls breathing and circulation, among other processes, and asphyxiation is typically the cause of death from GB poisoning. The purpose of this study is to perform quantitative protein profiling using tandem mass spectrometry (MS/MS) to determine mechanisms of toxicity from a GB exposure.

Four male and four female guinea pigs were exposed to 2xLD50 of sarin subcutaneously. Clinical observations were taken following the exposure and brains excised and flash frozen following death. Brainstems were homogenized in a lysis buffer and proteins digested with trypsin and labeled with iTRAQ reagents. Samples were separated on a Waters NanoUPLC prior to on-line injection to the Thermo LTQ Orbitrap Velos for data-dependent MS/MS analysis. Western blotting was performed as a confirmation of the MS data.

The MS analysis quantitated approximately 300 proteins in the brain stem. Relative to controls, 76 proteins increased in concentration and 36 decreased. The increased proteins include: DNA-repair, apoptotic, and glutamatergic proteins, among others. Two of the most increased proteins identified were GLAST-1, a protein that actively transports and removes released glutamate, and MYCBP2, a protein involved in respiratory distress. Decreased proteins include astrocyte related, glycolytic, and cytoskeletal proteins. Proteins that have been found to be modulated following exposure, including alpha tubulin and myelin basic proteins, were also confirmed through this method. The quantitative profiling data gives further understanding to the mechanisms of toxicity of GB and may aid in identification of targets for therapeutic intervention.

PS 574 Solubility and Efficacy Studies with Three Poorly Water Soluble Sulfur Donors As Potential Cyanide Antidotes

I. Petrikovics, A. Duke, S. A. Lee, S. Racheed, J. Olvera, S. Angalakurthi, S. De Jesus, J. Aleman, E. Miller, C. Chou and K. Kovacs. *Chemistry, SHSU, Huntsville, TX.*

Poor water solubility is one of the main reasons why many potent drug molecules cannot be used efficiently in combating illnesses, diseases or intoxications. The purpose of these studies was to establish optimal solubilizing systems that could be used as in vivo solvents for three tested sulfur donors (SD) in cyanide (CN) antidotal studies: tetramethylthiuram disulfide (TMTDS), methyl propyl trisulfide (MPTS) and bis(p-tolylsulfonyl) trisulfide (BPTSTS). Earlier in vitro efficacy studies indicated that all the three tested SDs are highly superior to sodium thiosulfate (TS), the SD component of one the present CN therapies of NithiodoteTM: TMTDS=3x, MPTS=5x, and BPTSTS showed 153x more in vitro activity than TS. For the solubility studies the surfactants Cremophor EL, Cremophor RH40, Polysorbate 80, sodium cholate and sodium deoxycholate at concentrations of 1, 5, 10, 15 and 20%, the co-solvents ethanol, PEG200, PEG300, PEG400 at concentrations of 10, 25, 50 and 75%, and the combinations of these surfactants and co-solvents were employed. The solubilities of the SDs were determined by HPLC-UV methods. For MPTS the surfactant Cremophor EL in 20% concentration provided the maximum solubility of 45 mg/ml, and it was enhanced to 430 mg/ml by adding 75% ethanol. For TMTDS the solubility the maximum solubility of 12.1 mg/ml was achieved with the solubilizing system containing 75% PEG400. While the in vitro efficacy with BPTSTS was the highest, the regular surfactant and co-solvents systems in various concentrations and their combinations did not provide enough solubility for in vivo studies, due to the required high injection volume. The in vivo efficacy was determined on CD-1 mice model, and expressed as antidotal potency ratio (APR = LD50 of CN with antidote/LD50 of CN without antidote). APR with MPTS (200 mg/kg, intramuscular administration) was over 3, that is a 2x higher antidotal protection than by TS at the same dose.

PS 575 Targeting Connexin 43: Cutaneous Wound Repair Using the Sulfur Mustard Analog, Nitrogen Mustard, Hairless Mouse Skin Model

Y. Chang[1], J. D. Wang[1], R. A. Hahn[1], H. Chang[1], R. P. Casillas[2], M. K. Gordon[1] and D. R. Gerecke[1]. [1]*Dept of Pharm and Tox, Ernest Mario School of Pharmacy, Rutgers University, Pisacataway, NJ and* [2]*MRI Global, Kansas City, MO.*

Sulfur mustard [SM, Bis (2-chloroethyl) sulfide], a potent vesicant agent, induces dermal toxicity which includes edema, inflammation, fluid-filled blistering, dermal-epidermal junction (DEJ) disruption, delayed wound repair, and scarring. Studies have shown that down regulation of the gap junction protein, connexin 43 (Cx43) accelerates wound closure and improves wound reepithelialization. We performed a time course study using nitrogen mustard [NM, Bis (2-chloroethyl) methylamine] to establish an alternative to the SM skin injury model. We also evaluated the wound repair response using a Cx43 antisense oligodeoxynucleotide (asODN) topical treatment on NM exposed hairless (SKH-1) mouse skin. NM exposure alone caused most of the dermal toxicity produce by SM exposure. In addition we examined several skin markers: keratin 5 (K5, basal keratinocyte marker); keratin 10 (K10, keratinocyte differentiation marker); Ki67 (proliferation marker); laminin 332 (LM332, basement membrane marker). Immunofluorescent (IF) studies showed reduced K5 expression, loss of K10 and Ki67, and an interrupted LM332 pattern of expression 1 day after NM exposure. By day 3, K10 reappeared in a diffuse pattern. By day 7, the LM332 appearance was thick and continuous. By day 10, there was intense expression of Ki67, accompanied by extreme hyperplasia. Animals treated with Cx43AsODN after NM exposure had an accelerated wound rate and improved reepithelialization so that the skin marker patterns above appeared at earlier timepoints. RT-PCR and Western blot analysis showed significant reduction of Cx43 at days 3 and 7. Cx26 and Cx30 were significantly reduced at days 1 and 3 by RT-PCR analysis. IF studies showed that Cx43 asODN treatment successfully reduced Cx43 expression and modulated higher Cx26 expression in the wound margin by day 3. The data suggest that the use of Cx43asODN may improve vesicant wound repair. Supported by ES005022, ES004738, EY09056, and NIAMS U54AR055073

PS 576 Inhibitors of Poly (ADP-Ribose) Polymerase 1 (PARP-1) As Protective Agents against HN2 Toxicity in a Skin Cell Model

M. A. Pino[1, 2], M. Patel[1], T. Talele[1] and B. Billack[1]. [1]*College of Pharmacy and Health Sciences, St John's University, Jamaica, NY and* [2]*Department of Basic Biomedical Science, Touro College of Osteopathic Medicine, New York, NY.*

Mechlorethamine (HN2) is an alkylating agent and sulfur mustard mimetic. Mustard cytotoxicity involves oxidative stress and DNA damage. Numerous strand breaks lead to supraphysiological PARP-1 activation, resulting in NAD and ATP depletion, and subsequent necrosis. In the present work, four selected inhibitors of PARP-1, including 3-aminobenzamide (3-AB), 3-indazolinone (TT-1), indazole-3-carboxamide (TT-2), and 1-(3-(isatin-1-yl)propyl)-1H-indazole-3-carboxamide (TT-3) were tested for the ability to reduce HN2 toxicity in A-431 skin cells. A cell-free system was also utilized to determine the extent to which these compounds exhibited PARP-1 inhibitory activity. All compounds tested were observed to reduce the activity of this enzyme. The MTT (3-(4,5-dimethylthiazol-2-yl)-2,5-diphenyltetrazolium bromide) assay was performed after 24 h to determine the effect of each test compound upon cellular viability in the presence or absence of HN2 (40 μM). It was observed that TT-1 interfered with the MTT reagent; therefore viability studies performed with this PARP-1 inhibitor were evaluated using the trypan blue dye exclusion method. In the absence of HN2, all the tested PARP-1 inhibitors, except TT-1, were found to be free of toxicity at concentrations of 75, 150 or 300 μM. When cells were co-incubated with HN2 and test compound, no protection was observed for TT-1or TT-3. However, the compounds 3-AB and TT-2 were observed to reduce cell death. Among them, 3-AB was able to improve cell viability at all three tested concentrations, while TT-2 only showed protection at the highest concentration. Light microscopy confirmed these findings for the two effective compounds. These data indicate that selected inhibitors of PARP-1 may protect A-431 skin cells from HN2 toxicity by a mechanism that prevents energy depletion in mustard treated cells.

PS 577 AEOL 10150 Improves Morbidity and Mortality after Lethal Lung-Sulfur Mustard Exposures

C. McElroy[1, 2], E. Min[2], J. Huang[2], J. Loader[1], T. Hendry-Hofer[1], R. Garlick[1], J. Rioux[1], L. Veress[1], R. Smith[1], C. Osborne[1], D. Anderson[3], W. Holmes[3], D. Paradiso[3], C. White[1] and B. J. Day[2, 1]. [1]*University of Colorado, Aurora, CO,* [2]*National Jewish Health, Denver, CO and* [3]*USAMRICD, Aberdeen, MD.*

Sulfur mustard (bis 2-chloroethyl ethyl sulfide, SM) is a powerful bi-functional vesicating and potent alkylating chemical warfare agent. SM causes blistering of exposed epithelial surfaces, leading to inflammation and necrosis. The respiratory tract is highly susceptible to SM-mediated injury. Although the exact mechanism of SM toxicity has not been elucidated, it is believed that it causes tissue injury through excessive production of reactive oxygen species resulting in DNA damage, and depletion of glutathione. The manganese porphyrin, AEOL10150, is a catalytic antioxidant with a broad spectrum of activities including superoxide and hydrogen peroxide dismutation, and is also capable of scavenging peroxynitrite and lipid peroxides. To evaluate the effectiveness of AEOL10150 in suppressing oxidative stress leading to toxicity in vivo, we delivered 1.4mg/kg sulfur mustard (approximate LD50 at 48 hours) from a water jacketed vapor generator directly into anesthetized rats via intratracheal intubation, followed 1 hour later by administration of either AEOL10150 (5 mg/kg, sc) or saline (sc) and comparing several AEOL10150 dosing regimens. Our results show that AEOL10150, when used as a rescue agent, was able to effectively improve survival from sulfur mustard inhalation from 33% (controls) to 89% (AEOL 10150, Q4H). We have demonstrated an improvement in clinical markers with AEOL10150 administration (Q4H), including pulse oximetry (23% increase), heart rate (21% increase), and clinical scoring (decrease of 4.3 on a scale of 0-10, where 0 is no outward distress) at euthanasia, when compared to saline controls. There was also a 56.3% reduction in the lung occlusive casts that result from sulfur mustard exposures in the major airways of animals that received AEOL10150 (Q4H). Support provided by NIH-CounterACT grant U54ESO15678.

PS 578 Assessment of Corneal Wound Healing Seven Days after Mustard Exposure

A. DeSantis Rodrigues[1], I. Po[1], R. A. Hahn[1], D. R. Gerecke[1], K. K. Svoboda[2] and M. K. Gordon[1]. [1]*Ernest Mario School of Pharmacy, Rutgers Univ, Piscataway, NJ and* [2]*Biomedical Sciences, Baylor College of Dentistry, Texas A & M, Dallas, TX.*

Our overall goal is to understand ocular mustard injury. We have exposed corneas in organ culture to levels of UVB and NM that resulted in 60% epithelial-stromal separation at 24 hr post exposure. UVB-exposed corneas reestablished their epithelial-stromal junction by 7 days after the exposure. However, corneas exposed to the dose of nitrogen mustard causing equivalent injury only partially healed in 7 days. One characteristic of these corneas was a reduction in the number of fibroblasts in the anterior stroma. Even in areas where the epithelial-stromal junction was reestablished, the number of fibroblasts in the anterior stroma showed little improvement in 7 days. Two types of mustard exposure were used to assess proteins that could potentially play a role in delaying healing: rabbit eyes exposed to sulfur mustard in vivo, and rabbit corneas in organ culture exposed to NM. Both the in vivo corneas and the organ cultured corneas showed imperfect healing by histology at 7 days post exposure. In addition to the lack of fibroblasts in the anterior stroma, local areas where the epithelial-stromal junction was imperfectly reformed were always observed. Immunofluorescence of organ cultured corneas demonstrated that the expression of the enzymes MMP9 and furin were still elevated 7 days after exposure. SPARC, a component of the provisional wound bed matrix, further confirmed incomplete remodeling towards the healed phenotype. The activity of MMP9 and furin, plus the persistence of provisional matrix in the wound bed may contribute to perpetuating injury after mustard exposure.

PS 579 High-Resolution 7T Magnetic Resonance Imaging (MRI) of Brain Damage in a Rat Model of Acute Organophosphate Intoxication

B. A. Hobson[1], S. Siso[2], D. Rowland[3], D. Bruun[1], J. Garbow[4] and P. Lein[1]. [1]*Molecular Biosciences, University of California Davis, Davis, CA,* [2]*Pathology, Microbiology & Immunology, University of California Davis, Davis, CA,* [3]*Center for Molecular and Genomic Imaging, University of California Davis, Davis, CA and* [4]*Department of Radiology, Washington University, St. Louis, MO.*

Organophosphates (OPs) pose a threat to human health due to accidental, suicidal, and terrorism-related exposures. Current standard treatments for acute OP exposure reduce mortality, but are ineffective in preventing delayed neurodegeneration. We recently demonstrated that acute intoxication by the OP diisopropylfluorophosphate (DFP) produces region-specific delayed neuronal cell death and

neuroinflammation in the rat brain, as determined by histological assessment. The goal of the current study was to test high-field MRI as a tool for monitoring the progression of neurologic damage following acute DFP intoxication. Adult male Sprague-Dawley rats were given pyridostigmine (0.026 mg/kg, i.m.) prior to successive administration of DFP (4 mg/kg s.c.), atropine sulfate (2mg/kg, i.p.), and 2-PAM (25 mg/kg, i.m.). This treatment paradigm resulted in moderate-to-severe seizure activity as determined using a modified Racine scale. Animals were imaged on a Bruker 7T MRI at baseline, and then at two of five time points post-intoxication (3, 7, 14, 21, or 28 days). At each time point, animals were euthanized and brains collected for histological evaluation. DFP exposure produced significant abnormalities in T2-weighted and diffusion tensor imaging out to 28 days post intoxication. Regions such as the dorsolateral thalamus, amygdala, hippocampus, and piriform cortex showed changes in MR endpoints (e.g., intensity, ADC, and anisotropy). These same brain regions exhibited severe neuronal necrosis. These results demonstrate that MRI is a powerful tool for longitudinal assessments of neuropathology following acute OP poisoning that may prove useful for screening candidate neuroprotective therapies. Supported by the NIH CounterACT program (grant #U54 NS079202) and by an NIH training grant (T32 GM099608).

PS 580 A New Purpose for Ebselen As a Prophylactic to Chemical Threats?

A. Lulla, S. E. Reznik, L. D. Trombetta and B. Billack. *Department of Pharmaceutical Sciences, College of Pharmacy and Allied Health Professions St. John's University, Jamaica, NY.*

Sulfur mustard (SM) is a chemical warfare agent that can cause severe acute and chronic injury to the eyes, skin and respiratory tract. The nitrogen mustard mechlorethamine (HN2) has a toxicity profile similar to that of SM and is recognized as a SM mimetic. Whereas previous studies in this and other laboratories have demonstrated that ebselen (EB-1) is effective at protecting cells from HN2 toxicity *in vitro*, the present study investigated whether or not EB-1 can reduce the dermal toxicity of HN2 *in vivo*. The mouse ear vesicant model was utilized, with mouse ears topically exposed to HN2 and biopsied 24 h after exposure. Ear punches were then fixed, sectioned and stained with H&E for inspection by light microscopy. HN2 produced a dose-dependent inflammatory response, characterized by edema, epithelial hyperplasia, increased neutrophil infiltrates and vesication. A histopathological scoring scale analysis of ear tissue sections was developed and used to qualitatively assess HN2-mediated injury. In addition, the morphometric index (MI) of exposed tissues was calculated using the formula, MI = (thickness of treated tissue/average thickness of vehicle exposed ears) * 100%. Both histopathological score analysis and morphometric analysis revealed statistically significant injury at doses of HN2 ≥ 0.250 μmol/ear. To test the efficacy of EB-1 as a prophylactic to HN2, three topical treatments with EB-1 (1 mg/ear or 2 mg/ear) were performed at 8 h, 4 h and 15 min prior to HN2 exposure. Quantitative morphometric analysis of tissue samples collected 24 h post HN2 demonstrated that EB-1 significantly reduced HN2-induced tissue swelling at both doses. Similar results were obtained using histopathological score analysis, where a trend toward EB-1 mediated protection was also observed. Taken together, the data presented here suggest that repositioning EB-1 from a drug previously thought to be useful for stroke treatment to one with a new purpose as a prophylactic to chemical threats may be warranted.

PS 581 Exposure-Response Modeling and Simulation to Support Human Dosing for Botulism Antitoxin Heptavalent (A, B, C, D, E, F, G)–(Equine) or H-BAT

A. L. Menard[1], D. Douglas[2], K. Atnikov[2], J. F. Marier[1] and M. Beliveau[1]. [1]*Pharsight Consulting Services, Certara, Montreal, QC, Canada and* [2]*Cangene Corporation, Winnipeg, MB, Canada.*

Exposure-response modeling and simulation was performed to support Cangene's human dosing recommendations for BAT™, Botulism Antitoxin Heptavalent (A,B,C,D,E,F,G) – (Equine). A compartmental model was constructed to assess the pharmacokinetics (PK) of H-BAT in humans, guinea pigs and Rhesus macaques. A traditional allometric power model was used to scale compartmental PK parameters in humans according to the corresponding body weight of each species. This relationship was used to simulate exposure to H-BAT in any species and according to any dosing scenarios. Subsequently, an exposure-response model was constructed to provide a mechanistic understanding of the relationship between exposure to H-BAT and response to BoNT intoxication (survival) based on the available post-exposure prophylaxis study information (guinea pig and Rhesus macaque). Exposure to H-BAT was simulated using the PK model and survival probability in humans was predicted based on the above exposure-response model. H-BAT exposure (AUC) in humans was compared to a minimum efficacious exposure (MEE) to identify the margin of efficacy (MOE = $AUC_{Human\ Dose}$ /AUC_{MEE}). The MOE ratio provides an estimate of the "safety" margin for the product. The survival probability derived using specification potency was 99.9, 95.6, 97.5, 93.1, 99.0, 99.5 and 97.4% for serotypes A to G respectively. Based on the exposure-response models, the MOE for all antitoxin serotypes were above 1 and the predicted probability of survival in humans following exposure to all serotypes of BoNT was more than 93.1% following administration of the one vial of H-BAT.

PS 581a Corneal Endothelial Toxicity following Corneal Exposure to Sulfur Mustard Vapor: Is Endothelial Loss the Pathophysiology Responsible for Long-Term Ocular Injury?

K. M. Tuznik, P. McNutt, M. R. Nelson, A. L. Adkins, M. E. Lyman and T. Hamilton. *USAMRICD, Aberdeen Proving Ground, MD.*

Sulfur mustard (SM) is a highly reactive vesicant that causes severe ocular injuries. Following exposure to moderate or high doses, a subset of victims develop a chronic injury known as mustard gas keratopathy (MGK), involving a keratitis of unknown etiopathogenesis with secondary keratopathies such as persistent epithelial lesions, corneal neovascularization and progressive corneal degeneration. The etiology of these recurrent keratopathies is unknown. Diverse therapeutic approaches have failed to mitigate the delayed injury, suggesting that researchers need an improved understanding of the mechanisms underlying injury progression. We have developed a novel rabbit corneal vapor exposure model that exhibits acute and long-term sequelae commensurate with human clinical reports and have characterized consistent and reproducible metrics of injury progression. In preliminary ultrastructural analyses a chronic pathology was observed in the corneal endothelium of MGK corneas. To determine whether (a) SM exposure evokes acute endothelial toxicity and (b) endothelial pathologies were specifically observed in MGK corneas as opposed to healed corneas, we evaluated the corneal endothelium at 1 d and 8 wk after exposure using scanning electron microscopy (SEM), transmission electron microscopy (TEM), in vivo confocal microscopy (IVM), fluorescent microscopy and functional measures of endothelial barrier function. All methods revealed the appearance of a centripetal endothelial lesion at 1 d after exposure, and longitudinal analysis using IVM revealed additional cytotoxicity between 1-13 d. In contrast to healed corneas at 8 wk, which appeared similar to sham-exposed naïve eyes, MGK corneas exhibited significant evidence of continued pathological changes in the endothelium. These data indicate that endothelial toxicity occurs at the right time and with the appropriate pathophysiology to contribute to MGK and explicates many of the previously confusing aspects of clinical progression.

PS 581b Deterministic Models of Inhalational Anthrax in New Zealand White Rabbits

B. Gutting. *NSWCDD, Dahlgren, VA.*

Computational models describing bacterial kinetics were developed for inhalational anthrax in New Zealand white (NZW) rabbits following inhalation of Ames strain *B. anthracis*. The data used to parameterize the models included bacterial numbers in the airways, lung tissue, draining lymph nodes and blood. Initial bacterial numbers were deposited spore dose. The first model was a single exponential ordinary differential equation (ODE) with three rate parameters that described mucociliated (physical) clearance, immune clearance (bacterial killing) and bacterial growth. At 36 hours post-exposure, the ODE model predicted 1.7 x 10^7 bacteria in the rabbit, which agreed well with data from actual experiments (4.0 x 10^7 bacteria at 36 hours). Next, building on the single ODE model, a physiological-based biokinetic (PBBK) compartmentalized model was developed where one physiological compartment was the lumen of the airways and the other was the rabbit body (lung tissue, lymph nodes, blood). The two compartments were connected with a parameter describing transport of bacteria from the airways into the body. The PBBK model predicted 4.9 x 10^7 bacteria in the body at 36 hours and by 45 hours the model showed all clearance mechanisms were saturated, suggesting the rabbit would quickly succumb to the infection. As with the ODE model, the PBBK model results agreed well with laboratory observations. These data are discussed along with the need and potential application of the models in risk assessment, drug development and as a general aid to the experimentalist studying inhalational anthrax.

PS 581c Evaluation of the Antihistamine Promethazine against Acute Soman Intoxication

R. K. Kan, J. A. Leuschner, S. W. Kaski, A. N. Sbarra, L. J. Shumway, C. R. Braue and T. L. Dao. *Pharmacology, USAMRICD, Aberdeen Proving Ground, MD.* Sponsor: T. Shih.

The present study was designed to evaluate the effectiveness of the antihistamine promethazine in rats following exposure to the chemical warfare nerve agent soman. Acute soman intoxication was induced using a soman model that produces convulsive seizures in 100% of the intoxicated animals. Rats pretreated with the oxime reactivator HI-6 (125 mg/kg, ip) 30 min prior to soman challenge (2.0 LD50 or 225 ug/kg, sc) were treated with atropine methylnitrate (AMN, 2.0 mg/kg, im). Promethazine (32 or 40 mg/kg, ip) was given at 1 min after soman injection or at the onset of soman-induced seizures. Controls received an equivalent of sterile water instead of promethazine. When given at 1 min after soman exposure, promethazine at the dose of 32 or 40 mg/kg decreased the incidence of seizures from 100% to 0% or 40%, respectively. Interestingly, the 40% of the animals that developed seizures after promethazine treatment at 1 min after soman exposure had their seizures spontaneously terminated. Promethazine given at 1 min after soman exposure at the dose of 32 or 40 mg/kg also increased the survival rate from 0% to 75% or 100%, respectively. When promethazine at the dose of 32 or 40 mg/kg was administered at the onset of seizures, seizures were terminated in 100% of animals, and the survival rate was increased from 0% to 100%. At 24 hr, promethazine-treated animals behaved like non-exposed animals. Brains from promethazine-treated animals were evaluated for brain injury. None of the animals treated with promethazine, either at 1 min after soman administration or at the onset of seizures, exhibited neuronal damage in any of the brain regions examined. These observations indicate that promethazine treatment can effectively control seizures, improve survival and prevent brain injury following exposure to 2.0 LD50 of soman.

PS 581d Pharmacokinetics of Nitrocobinamide (NCbi), a Novel Cyanide Antidote

K. O'Loughlin[1], R. Swezey[1], W. Shinn[1], G. R. Boss[2] and C. E. Green[1]. [1]*Toxicology & Pharmacokinetics, SRI International, Menlo Park, CA and* [2]*University of California, San Diego, CA.*

The cobalamin analog cobinamide (Cbi) has a high affinity for cyanide and is a potent cyanide antidote after im injection. Pigs are rescued from a lethal cyanide dose by 12.5 mg/kg of Cbi. The objective of the current study was to determine the pharmacokinetics of NCbi, a formulation developed to optimize drug absorption. Male Sprague Dawley rats received either 30 mg/kg iv, 65, 95, or 130 mg/kg as single im injection or 65 mg/kg split into two im injections. Plasma drug levels were determined at 5, 10, 20, 30, 60 min and 2, 4, 6, 8, 24 and 48 h post dose. After an iv dose, Cbi was rapidly distributed and eliminated with $t_{1/2}$ of 11.6 ± 3.6 h and clearance of 45.5 ± 7.3 ml/h/kg. The plasma concentration extrapolated to time 0 was 378 ± 62 μg/ml and the AUC was 670 ± 101 μg•h/ml. The volume of distribution was 0.74 ± 0.13 l/kg, consistent with distribution to extracellular water. After an im dose, the plasma Cbi concentration increased rapidly with mean T_{max} values ranging from 0.8 ± 0.3 h (high dose) to 1.7 ± 0.6 h (mid dose). The C_{max} and AUC values were dose dependent, although the increase in exposure was not linear from the mid to the high dose. The mean $t_{1/2}$ was about15 h for the single injection im groups. When the low dose was given as two injections of 100 mM, Cbi was absorbed faster (T_{max} of 0.6 ± 0.3 h vs 1.3 ± 0.6 h) and the C_{max} was ~ 40% higher than after a single injection of 100 mM. At a concentration of 50 μg/ml N-Cbi, 83.0 ± 2.89% of Cbi was bound to rat plasma proteins. In summary, NCbi absorption after im injection reached maximum plasma levels at 0.5 to 2 h. Exposure, based on C_{max} and AUC, increased with dose but tended to plateau, suggesting that Cbi absorption becomes saturated at higher formulation concentrations. The administration of the low dose, split and injected at two sites, yielded faster absorption and higher C_{max} values than a single injection. The average bioavailability of Cbi after im administration of N-Cbi was excellent, >75%. This research was supported by NIH Contract HHSN271200623691C.

PS 581e Zebrafish As a Novel Animal Model for Chemical Warfare Nerve Agent (CWNA) Biomedical Research

T. Dao, T. A. Shih, R. Kim, C. R. Braue, J. Koenig, J. A. Leuschner and R. K. Kan. *USAMRICD, Aberdeen Proving Ground, MD.*

Zebrafish only express the acetylcholine hydrolyzing enzyme acetylcholinesterase (AChE). This unique genotype makes the zebrafish an ideal animal model to study the toxicological effects of organophosphorus nerve agent (NA) AChE inhibitors and the effectiveness of oximes to reactivate NA-inhibited AChE. The present study determined the LC50 of sarin and evaluated the efficacy of 2-PAM in reactivating sarin-inhibited AChE. Larval zebrafish at 6 days postfertilization (dpf) were exposed to various concentrations of sarin for 1 hr to determine the LC50 of sarin. Following sarin exposure, zebrafish larvae were screened under a dissecting microscope to observe the overt signs of toxicity. Death was determined by the cessation of heart beats. The mortality rate was 0, 20, 45, 35, 43, 75, 75, 90 or 100% after exposure to 0, 12.5, 25, 50, 75, 100, 150, 250 or 500 uM of sarin, respectively. By regression analysis, the LC50 of sarin for 1 hr exposure at 24 hr was estimated to be 80 uM. Twenty-four-hour survivors exhibited behavioral changes, including an inability to maintain buoyancy, hanging vertically in water and laying on the side. To evaluate the effectiveness of 2-PAM to reactivate sarin-inhibited AChE, 6 dpf larvae were exposed to 25 uM of sarin, and their AChE activity was measured by the Ellman assay. When the larvae were completely immobile after 5 mins of exposure, they were treated with 0 or 50 uM of 2-PAM. The percentage of AChE inhibition was 98% when the larvae lacked locomotion. With 2-PAM treatment, the AChE percentage inhibition was decreased from 98% to 18%. The results suggest that 1) zebrafish larvae are sensitive to the toxic effects of sarin in a concentration-dependent manner and 2) zebrafish larvae AChE inhibited by sarin can be reactivated by 2-PAM, an oxime reactivator currently used as standard treatment for CWNAs in the military. These observations provide evidence that the zebrafish is a suitable animal model system for in vivo evaluation of NA toxicity and novel oxime reactivators.

PS 581f Melatonin Treatment Reduces Corneal Injury after Nitrogen Mustard Exposure

A. L. Miller[1], H. Yaren[2], H. Yaman[3], R. A. Hahn[1], P. Zhou[1] and M. K. Gordon[1]. [1]*Pharmacology and Toxicology, EMSOP, Rutgers University, Piscataway, NJ,* [2]*Department of CBRN Defense, Gulhane Military Medical Academy, Ankara, Turkey and* [3]*Biochemistry, Gulhane Military Medical Academy, Ankara, Turkey.*

Mustards are vesicants that induce separations between the corneal epithelial and stromal layers, impairing vision. To identify therapies for ocular mustard injury, we have tested whether topical delivery of the immunomodulatory component, melatonin, might decrease corneal injury after mustard exposure. Rabbit corneal organ cultures were exposed to 100 nmol nitrogen mustard (NM) for 2 hr, after which medium was changed. The corneas then received either topical melatonin, or topical N-hydroxy-octylhomovanillamide, aka NDH4417 (an ADAM17 inhibitor) as therapies. Control cultures were unexposed or NM-exposed, followed by applications of culture medium at the same volume as the therapies. All post exposure treatments were applied 3 times over the course of 22 hr following the 2 hr exposures. The extent of corneal injury was then assessed by histology. When only medium was applied after NM exposure, ~60% of the epithelial layer was separated from the stroma. When melatonin was applied 2 hr post exposure, epithelial-stromal separation was reduced to ~45%. However, when NDH4417 was applied post NM exposure, epithelial-stromal separation was 17%. Future work will assess whether topical melatonin treatment reduces inflammatory cytokines expression in NM-exposed corneas and whether a combination therapy of melatonin and NDH4417 would reduces epithelial stromal-separation even further.

PS 581g Government Toxicologist: A Veteran's View of Professionalism and Ethical Expectations in the Context of Veterans' Exposure Claims and the Society of Toxicology Code of Ethics

W. T. Carter. *C-123 Veterans Association, Fort Collins, CO.* Sponsor: L. Birnbaum.

Different professions, different ethics, different loyalties, and different expectations of the professional can be a function of profession and employer. Public expectations of a scientist's loyalties and ethics are different than those demanded of other professionals. Science is truth. What truth comes from the toxicologist–the truth of science, or the "truth" of the scientist's employer? Government toxicologists are faced with agency agendas that they are challenged to respect yet still deliver clean science. Too often, the government-employed toxicologist might falter, yielding through loyalty or career concerns, fielding work products fitting the agency's agenda, disserving science and the public. I discuss the 2012 Society of Toxicology poster "AGENT ORANGE: THE 50 YEAR HISTORY" from the Department of Veterans Affairs (DVA) in which exposure was explicitly redefined: "Exposure=concentration present+bioavailability." This blocked dioxin (TCDD) exposure claims from 1560 veterans who flew C-123 transports after the Vietnam War. The C-123s remained contaminated after spraying Agent Orange. DVA's redefinition is unscientific and an example of an agency-driven work product. The redefinition was advanced in light of professional challenge by other toxicologists and National Institute of Environmental Health Sciences and the Agency for Toxic Substances and Disease Registry, but without noting any controversy. Veterans'

laws do not mention bioavailability. SOT's Code of Ethics should have compelled more science, not policy-driven results. The reader's attention is drawn to the Code: "Abstain from professional judgments influenced by undisclosed conflict of interest, disclose any material conflicts of interest, and avoid situations that imply a conflict of interest." The poster's authors were responsible to DVA for creation of negative responses to concerns raised by exposed veterans. No disclosure was offered or mention made of challenges raised by other toxicologists not employed by the DVA, which was not in keeping with the Code.

PS 581h Blood Pressure, Heart Rate, Temperature, and Central Nervous System Evaluation of Cyanide Intoxication in Juvenile and Adult Mice

M. Hawk, G. Ritchie, T. Vinci, K. A. Henderson, S. Behringer, K. Knostman, B. Roche, C. L. Sabourin and P. Sabourin. *Battelle, Columbus, OH.*

Cyanide (CN) affects organ systems with the highest demand for energy such as the central nervous, cardiovascular (CV), and pulmonary systems. A mouse model of oral KCN intoxication is needed for screening and testing of CN countermeasures. Adult and juvenile CD-1 mice were dosed orally with a single dose of water or 8 mg/kg KCN, a toxic but generally non-lethal dose. Sensory, motor, cognitive, and behavioral changes were measured using a functional observation battery (FOB) and Tier II CNS testing up to 42 days post-dosing. Histopathology was conducted on select tissues and telemetry was used for CV evaluations and body temperature. KCN reduced sensorimotor responsivity or spontaneous locomotor activity (FOB and Tier II testing) in juvenile and adult mice at 30 min post-dose. Core body temperature decreased at 30 min post-challenge consistent with the general malaise observed. No FOB differences were observed on Day 2 (24 hr post-dose), but decreases in spontaneous locomotor activity and/or rectal temperature were observed on Days 7, 14, 28, and 42. Tier II tests demonstrated no significant differences between KCN-treated and control groups on Days 2, 7, 14, 28, or 42. KCN caused immediate effects related to bradycardia, hypotension, and hypothermia with recovery 1 to 3 hours post-dosing. Twenty percent of mice in the KCN group experienced ECG events within the first 5 min post-dosing that ranged from bradycardia, to left ventricular premature contractions (VPCs), and a large Ta wave. At 30-min post-dosing, ECG included PR prolongation, alternans, and Ta prolongation. The bradycardia and VPCs as well as the PR and Ta prolongation appear to be effects of KCN in a small percentage of mice, most likely due to effects on the SA node. There were no KCN related histological findings through Study Day 42. The effect of treatments on KCN-induced changes in CV and CNS parameters can be used in subsequent studies to determine the efficacy of countermeasures.

PS 581i Younger Rats Are More Susceptible to the Lethal Effects of Sarin Than Adult Rats: 24 h LC50 for Whole-Body (60 Min) Exposure

L. K. Wright[1], D. B. Miller[2], W. T. Muse[2], E. J. Emm[2], R. B. Lee[1], C. E. Whalley[2] and L. A. Lumley[1]. [1]*US Army Medical Research Institute of Chemical Defense, Aberdeen Proving Ground, MD and* [2]*Edgewood Chemical Biological Center, Aberdeen Proving Ground, MD.*

Chemical warfare nerve agents (CWNA) are among the most lethal chemicals known to man, and children are a particularly vulnerable subpopulation because of their smaller body masses, smaller airway diameters, higher respiratory rates and immature central nervous systems. While there have been a handful of studies on the effects of CWNA in younger animals, exposure routes relevant to battlefield or terrorist situations (inhalation for G-agents and dermal for V-agents) were not used. Thus, we determined the 24 h LC50 for whole-body (60 min) exposure to sarin using a stagewise, adaptive dose design. Briefly, both male and female Sprague-Dawley rats were exposed to a range of sarin concentrations at five different time points during their development (postnatal day [PND] 7, 14, 21, 42 and 70). For both male and female rats, the lowest LC50 value was observed on PND 14 and the highest LC50 value on PND 42. Females had slightly smaller LC50 values than males at all five time points, and the LC50 values were significantly smaller on PND 21 and 70. Thus, younger rats are more susceptible to the lethal effects of whole-body exposure to sarin than older rats, and females are more susceptible than males. The views expressed in this abstract are those of the authors and do not reflect the official policy of the Department of Army, Department of Defense, or the U.S. Government. The experimental protocol was approved by the Animal Care and Use Committees at USAMRICD and ECBC, and all procedures were conducted in accordance with the principles stated in the Guide for the Care and Use of Laboratory Animals and the Animal Welfare Act of 1966 (P.L. 89-544), as amended. This research was supported by interagency agreement between the Biomedical Advanced Research and Development Authority and USAMRICD.

PS 581j Natural History Study of Cyanide Intoxication in Adult and Juvenile Mice

P. Sabourin[1], C. Kobs[1], B. Horne[2], E. Psurny[1], C. Matthews[1], K. M. Patton[1], S. Gibbs[1] and C. L. Sabourin[1]. [1]*Battelle, Columbus, OH and* [2]*Best Center, Battelle, Aberdeen, MD.*

Cyanide (CN) is an inhibitor of cytochrome C oxidase causing rapid death due to hypoxia. CN is of concern due to its use as a warfare agent, industrially, exposure from burning plastics, and possible terrorist use. A well-characterized model of oral KCN intoxication is needed to test new therapeutics for KCN intoxication under the FDA Animal Rule. The objective was to describe CN intoxication after a single lethal and sub-lethal acute oral KCN administration to juvenile and adult mice. The oral LD50 of KCN was 11.5 ± 0.4 mg/kg KCN in adult mice and 10.4 ± 0.3 mg/kg KCN in juveniles. The oral KCN LD50 value for male mice was about 0.9 mg/kg greater than female mice, for either age. Death following KCN challenge occurred within 30 min post-dose in adult and juvenile mice at doses above 10 mg/kg. Juveniles tended to have a shorter time to death with a rapid seizure response. CN and its major metabolite, thiocyanate, were quickly metabolized (Tmax of 0.5 hr and 2-4 hrs, respectively) and excreted. A survey of biomarkers indicated that blood pH and lactate were rapid and quantitative, although non-specific, markers of CN intoxication. Serum FABP3 increased with KCN dose in adult, but not juvenile, mice. No microscopic pathological findings were observed 1 day post-dose. The model description indicates that the effects of KCN are rapid and, at doses up to a least the LD50, completely reversible in surviving mice. The toxicokinetics of CN in mice is consistent with the rapid clinical signs and recovery. Based on the rapid toxicity observed, treatment would have to be initiated quickly following exposures for optimal results. Rapid analysis of blood pH and/or lactate using a point of care device, such as the I-Stat, could be used as a trigger for treatment in efficacy studies. The results provide a well characterized model of acute oral KCN intoxication of adult and juvenile mice that may be used to screen or conduct pre-clinical efficacy studies of potential countermeasures.

PS 581k Treatment of Lung Injury from Phosgene Chemical Inhalation with NOS-2 Inhibition

P. Filipczak[1, 2], J. D. McDonald[1], L. Fredenburgh[1, 2] and R. Baron[1, 2]. [1]*Lovelace Respiratory Research Institute, Albuquerque, NM and* [2]*Division of Pulmonary and Critical Care Medicine, Brigham and Women's Hospital, Harvard Medical School, Boston, MA.*

Acute lung injury (ALI) induced by the chemical agent phosgene (CCl2O) is characterized by increased lung expression of inducible nitric oxide synthase (iNOS, NOS2) and production of reactive nitrogen species including peroxynitrite, which triggers epithelial and endothelial cell injury, surfactant dysfunction, and loss of alveolar epithelial barrier integrity. Our research demonstrates that phosgene-induced lung injury also leads to significant reduction in the tight junction protein zonula occludens (ZO)-1, resulting in exaggerated alveolar epithelial permeability in response to acute phosgene exposure. We have previously demonstrated that NOS2 expression in lung epithelial cells plays a key role in surfactant dysfunction and is critical for the development of endotoxin-induced ALI. Furthermore, we have identified that NOS2-derived NO from lung epithelial cells downregulates surfactant protein B (SP-B) expression at the transcriptional level. We therefore hypothesized that NOS2-generated NO contributes to phosgene-induced ALI and that selective inhibition of NOS2 in the lung epithelium will attenuate surfactant dysfunction, disruption of tight junction proteins, and vascular leak induced by phosgene. Our research demonstrates that administration of a NOS2-specific inhibitor 1400W delivered via inhalation, but not systemically, dramatically attenuates phosgene-induced lung injury. Aerosol delivery of 1400W augmented SP-B expression and restored ZO-1 expression in the lung leading to attenuation of histologic lung injury and physiologic dysfunction in a murine phosgene ALI model. Consistent with our previous studies and work by other investigators, these findings support a role for inhibition of localized NOS2 production within the lung in attenuating chemical agent-induced lung injury. We will present on this research, and consider the current proposed standard of care for phosgene induced ALI against this potential therapy in terms of feasibility and efficacy.

PS 582 Modulation of Inflammasome Activation by Carbon Nanotubes in Asthma

K. A. Shipkowski, A. Taylor, E. Thompson and J. C. Bonner. *North Carolina State University, Raleigh, NC.*

Introduction: Multi-walled carbon nanotubes (MWCNT) represent a potential health hazard for human lung disease based on studies in mice which show lung inflammation after exposure. A possible mechanism of MWCNT-induced inflam-

mation is inflammasome activation in lung macrophages and secretion of IL-1β. Allergen-challenged mice are susceptible to MWCNT-induced airway inflammation and have elevated levels of the Th2 cytokines IL-13 and IL-4. We postulate that Th2 cytokines modulate MWCNT-induced inflammasome activation and IL-1β release by human monocytes (THP-1 cells) in vitro and in the lungs of mice in vivo following house dust mite (HDM) allergen challenge. Methods: THP-1 cells were differentiated with vitamin D3 and TPA, primed with LPS, and dosed with MWCNT alone or with IL-13 or IL-4. IL-1β in cell supernatants was measured by ELISA. C57Bl/6 mice were exposed to HDM allergen intranasally for two weeks, dosed with MWCNT (2mg/kg via oropharyngeal aspiration), and necropsied 1 day post-MWCNT exposure. Bronchoalveolar lavage fluid (BALF) and serum were analyzed for IL-1β and IgE, respectively, via ELISA. BALF was also used to determine inflammatory cell differential counts. The left lung was formalin-fixed for histopathology. Results: THP-1 cells treated with MWCNT showed a dose-dependent increase in IL-1β, while IL-13 or IL-4 significantly decreased MWCNT-induced IL-1β. HDM sensitization significantly decreased MWCNT-induced IL-1β levels in BALF from the lungs of mice. MWCNT suppressed HDM-induced serum IgE, but enhanced HDM-induced eosinophil counts in BALF. Conclusions: The allergen-inducible cytokines IL-13 and IL-4 negatively regulate MWCNT-induced production of IL-1β by macrophages in vitro. HDM allergen also decreases MWCNT-induced IL-1β production in the lungs of mice in vivo. However, MWCNT enhance HDM-induced eosinophilic lung inflammation. Further study will address the mechanism through which Th2 cytokines modulate MWCNT-induced inflammasome activation and how MWCNT exacerbate allergic airway inflammation in asthma.
Funding: Supported by NIEHS grants RO1-ESO20897 and RC2- ESO18772.

PS 583 Atomic Layer Deposition Coating of Multiwalled Carbon Nanotubes with Aluminum Oxide Alters Innate Immune Responses *In Vitro* and *In Vivo*

A. Taylor[1], K. A. Shipkowski[1], E. Thompson[1], C. Devine[2], G. Parsons[2], S. Garantziotis[3], S. Hussain[3] and J. C. Bonner[1]. [1]*Biological Sciences: Toxicology Program, North Carolina State University, Raleigh, NC,* [2]*Chemical & Biomolecular Engineering, North Carolina State University, Raleigh, NC and* [3]*Laboratory of Respiratory Biology, National Institute of Environmental Health Sciences, Research Triangle Park, NC.*

Multi-walled carbon nanotubes (MWCNTs) pose a possible human health risk for lung disease as a result of occupational or environmental exposure. Macrophages are the first line of defense that engulf and remove inhaled MWCNTs from the lungs. MWCNTs stimulate macrophage inflammasome activation and interleukin (IL)-1β release, key cellular components of the innate immune response that mediate the initiation and resolution of acute inflammation. Alternatively, macrophages are a source of secreted osteopontin (OPN), which promotes tissue matrix remodeling and fibrosis. Atomic layer deposition (ALD) is a novel process used to enhance surface and functional properties of MWCNTs. The purpose of this study was to determine whether ALD coating with Al2O3 would alter toxicity, phagocytosis, or the production of soluble mediators (IL-1β or OPN) in human macrophages or monocytes exposed to MWCNTs as well as in mice in vivo. IL-1β and OPN protein secretion was measured via ELISA at 24hr post nanotube exposure. ALD surface coating of MWCNTs with Al2O3 enhanced IL-1β secretion, yet inhibited OPN production by THP-1 cells. Experiments conducted with primary peripheral blood monocytes obtained from normal human donors also showed that the Al2O3-coating on MWCNTs enhanced IL-1β secretion and yet suppressed OPN production. C57BL6 mice exposed to uncoated MWCNTs for 1 day had increased levels of IL-1β and OPN in the bronchoalveolar lavage fluid. ALD coated MWCNTs increased IL-1β in the BAL fluid as well, yet had a suppressive effect on OPN levels. These findings indicate that thin film surface coating of MWCNTs with Al2O3 by ALD enhances the innate immune response of mononuclear phagocytes but decreases pro-fibrogenic activity in vitro and in vivo.

PS 584 Activation and Interplay of the Tumor Suppressor Genes p53 and STAT-1 in Response to Multiwalled Carbon Nanotubes

E. Thompson, K. A. Shipkowski, A. Taylor and J. C. Bonner. *Department of Biological Sciences, Environmental and Molecular Toxicology Program, North Carolina State University, Raleigh, NC.*

Multi-walled carbon nanotubes (MWCNTs) are engineered nanomaterials that possess unique physical properties, making them ideal candidates for use in electronics, engineering and medicine. As they are used in increasing quantities, the potential for occupational and/or environmental exposures is inevitable. There is increasing evidence that MWCNTs may produce toxic effects both in cultured cells and in the lungs of rodents. Studies in human epithelial cells and rats *in vivo* have shown MWCNTs to cause DNA damage. The tumor suppressor gene p53 is a DNA damage inducible transcription factor involved in cell cycle arrest and apoptosis. Likewise, the transcription factor, STAT-1 serves many of the same functions as p53 and STAT-1 has been found to interact with p53 in mouse embryonic fibroblasts and human fibrosarcoma cells *in vitro*. We explored a possible relationship between p53 and STAT-1 in human mesothelial cells, the target cells of mesothelioma, as well as in the mouse lung *in vivo*, following exposure to MWCNTs. Human mesothelial cells (Met5A cells) were dosed with 10 μg/cm^2 MWCNTs, and using western blot analysis, we observed that the phosphorylated or "active" forms of both p53 and STAT-1 were increased 4 hours post-exposure. To determine whether the induction in p-p53 was affected by the presence of STAT-1, we utilized both STAT-1 siRNA to knockdown STAT-1 message in the Met5A cells, as well as a STAT-1 knockout mouse model. In both models, decreased or absent STAT-1 protein, resulted in decreased p53 protein levels. Our results suggest that both p-p53 and p-STAT-1 can be induced as a result of MWCNT exposure and that the induction in p-p53 is dependent on the presence of STAT-1. The findings are relevant to our understanding of the potential for carbon nanotubes to cause pleural disease after inhalation exposure.
Funding: Supported by NIEHS grant RO1-ESO20897.

PS 585 Different Functionalizations of MWCNT Influence Transformation Potential in Primary Human Lung Epithelial Cells

T. A. Stueckle[1], R. Derk[1], M. Chen[2], V. Castranova[1, 2], Y. Rojanasakul[2] and L. Wang[1, 2]. [1]*NIOSH, Morgantown, WV and* [2]*West Virginia University, Morgantown, WV.*

MWCNT have received increased scrutiny for potential human health impacts based on their fibrogenicity and promotion of pulmonary carcinogenesis. Functionalized CNT (fCNT) development has intensified to improve surface activity in technological applications, and potentially reduce toxicity. Subchronic *in vitro* CNT exposure causes neoplastic-like transformation; however, tumorigenic risk associated with fMWCNT exposure in human lung epithelium is presently unknown. To identify early steps in fMWCNT-induced cell transformation, this study hypothesized that different functional groups of MWCNT determine their neoplastic transformation potential in primary human small airway epithelial cells (SAECs). Cells were continuously exposed (0.06μg/cm^2) to dispersed pure (pMWCNT), carboxylated (cMWCNT), and aminated MWCNT (nMWCNT) for 8 and 12 weeks. Dispersed ultrafine carbon black (UFCB) and crocidolite asbestos served as controls. Exposed cells were assessed for several established cancer hallmarks and morphological transformation. UFCB and pMWCNT cells at 48h and all MWCNT cells at 6d post-treatment exhibited significant increased proliferation compared to controls. UFCB exposure stimulated significant invasion and migration behavior while pMWCNT and cMWCNT showed moderate significant increases; however, these trends disappeared at 6d post-exposure. Conversely, nMWCNT displayed the largest significant increase in colony formation potential while UFCB showed a moderate significant increase. All other treatments did not differ from controls. UFCB and nMWCNT cells exhibited increased foci frequency, indicative of neoplastic transformation, compared to all other treatments. In summary, surface charge characteristics of carbon nanoparticles can impact transient, early neoplastic transformation events *in vitro* following occupationally relevant exposures.
Disclaimer: Present findings and conclusions are the authors and do not necessarily represent the views of the National Institute for Occupational Safety and Health.

PS 586 Lactoperoxidase-Mediated Degradation of Oxidized Single-Walled Carbon Nanotubes and Its Modulatory Effects on Airway Antibacterial Activity

K. Bhattacharya[1], R. El-Sayed[1], F. T. Andón[1], A. Fornara[2], H. Li[3], J. Gregory[1], K. Leifer[3], S. Dahlén[1], A. Star[4] and B. Fadeel[1]. [1]*Institute of Environmental Medicine, Karolinska Institutet, Stockholm, Sweden,* [2]*Unit for Chemistry, Materials and Surfaces, SP Technical Research Institute of Sweden, Royal Institute of Technology, Stockholm, Sweden,* [3]*Department of Engineering Sciences, Ångström Laboratory, Uppsala, Sweden and* [4]*Department of Chemistry, University of Pittsburgh, Pittsburgh, PA.*

Studies in recent years have shown that carbon nanotubes (CNTs) may elicit inflammatory responses. On the other hand, enzymatic biodegradation of CNTs by inflammatory cells has also been reported thus illustrating the reciprocal interactions between CNTs and the immune system. Here we analyzed the biodegradation of oxidized SWCNTs by recombinant lactoperoxidase (LPO), in the presence or absence of lung surfactant (Curosurf®). UV/Vis-NIR and Raman spectroscopy techniques were employed to monitor the biodegradation. There was effective degradation of SWCNTs by LPO and no interference by Curosurf®. AFM and

SEM analyses suggested the attachment of LPO on the carboxylated side-walls of the bundles of SWCNTs. We also confirmed the ex vivo biodegradation of SWCNTs in murine bronchoalveolar lavage (mBALF) shown to express peroxidase activity. Lastly, we addressed whether the pre-occupancy of LPO with SWCNTs would interfere with its antibacterial properties. To this end, experiments with Pseudomonas aeruginosa, an opportunistic human pathogen, were conducted and we noted that the pre-occupancy of LPO with SWCNTs severely impaired the antibacterial activity of LPO. Our study provides evidence for the degradation of carboxylated SWCNTs by LPO, a secreted peroxidase that is present in the airways. However, the antibacterial activity of LPO is impaired as a result of the pre-occupancy of LPO with SWCNTs. This latter finding implies that airway defenses may be compromised in individuals exposed to SWCNTs, possibly leading to more persistent infections.

PS 587 Effects of MWCNT and Nitrogen-Doped MWCNT in Lung Epithelial Cells

A. Mihalchik[1, 2], D. W. Porter[2], V. Castranova[2], S. Tsuruoka[3], M. Endo[3] and Y. Qian[2]. *[1]Pharmaceutical and Pharmacological Sciences, West Virginia University, Morgantown, WV, [2]Health Effects Laboratory Division, National Institute for Occupational Safety and Health, Morgantown, WV and [3]Research Center for Exotic Nanocarbons, Shinshu University, Nagano, Japan.*

The growing use of multi-walled carbon nanotubes (MWCNT) and their derivatives in academic and industrial settings has raised the need to efficiently and accurately determine their potential toxicity in the workplace. Nitrogen-doped multi-walled carbon nanotubes (ND-MWCNT) are modified MWCNT that have enhanced electrical conductivity and are increasingly used in a variety of aerospace and fuel cell applications. Although similar in structure to MWCNT, limited toxicological data is available, and the biocompatibility and mechanism of action of ND-MWCNT have yet to be elucidated. Recent in vivo data showed that ND-MWCNT induced inflammation and fibrosis in mouse lungs. In this study, we assess uptake of ND-MWCNT into small airway epithelial cells (SAEC), which may induce molecular toxicological effects. We showed that ND-MWCNT induced higher levels of reactive oxygen species (ROS) in SAEC when compared to their parent MWCNT in short-term in vitro exposure. Treatment of SAEC with low doses (1.2μg/mL) of ND-MWCNT and MWCNT indicated that both induced a significant increase in cell proliferation in a time-dependent manner. Furthermore, significant alterations to the cell cycle were observed in cells treated with both ND-MWCNT and MWCNT in a time- and dose-dependent manner, as shown by an increased percentage of cells in the S and G2 phases of the cell cycle. Confocal images showed alterations in acetylated and total tubulin levels in both ND-MWCNT and MWCNT treated cells as well. Since increases in ROS production and cellular proliferation are associated with multiple pathological conditions, ND-MWCNT exposure may play a role in the initiation of these diseases.

PS 588 Autophagy and Extracellular HMGB1 Are Mediators of Inflammasome Activity in Response to MWCNT Exposure

F. Jessop, R. Biswas and A. Holian. *Center for Environmental Health Sciences, University of Montana, Missoula, MT.*

RATIONALE: Pulmonary exposure to Multi-walled Carbon Nanotubes (MWCNT) has been shown to induce chronic inflammation in animal models, and therefore may pose a health risk to humans. Pathology induced by MWCNT exposure is dependent upon NLRP3 Inflammasome activity, specifically IL-1β signaling. Mechanisms regulating Inflammasome activity are not clear. In this study, we establish critical roles for High Mobility Group Box 1 (HMGB1) and autophagy in regulating Inflammasome activity. METHODS: Secretion of HMGB1 was assessed in vitro from primary Alveolar Macrophages (AM) and in vivo in C57Bl/6 mice (24 and 72 hours) after MWCNT exposure. The contribution of extracellular HMGB1 to Inflammasome activity was delineated in vitro via HMGB1 elimination by immunoprecipitation techniques and in vivo using neutralizing antibodies. To assess the contribution of autophagy in mediating inflammasome activity, primary AM exposed to MWCNT were treated with molecular inhibitors (LY294002, Bafilomycin, Imipramine) targeting different sites along the autophagic flux, and IL-1β production assessed after 24 hours. RESULTS: HMGB1 secretion and autophagic flux are increased following MWCNT exposure. HMGB1 removal by immunoprecipitation techniques or neutralization reduces IL-1β production in primary AM in vitro and in vivo, respectively. Additionally, targeting autophagy by stabilizing the lysosome also decreases IL-1β production after MWCNT exposure. However, inhibition of PI3 kinase activity, responsible for autophagosome formation, enhances IL-1β secretion. CONCLUSIONS: HMGB1 signaling and autophagy play critical roles in the acute Inflammasome response to MWCNT exposure, and may be potential therapeutic targets in particle induced inflammatory diseases.

PS 589 Effects of SWCNT Fiber Length and Functionalization on ROS and Collagen Production

A. Manke[1], T. A. Stueckle[2], L. Wang[2], C. A. Dinu[3] and Y. Rojanasakul[1]. *[1]Pharmaceutical Sciences, West Virginia University, Morgantown, WV, [2]NIOSH, Morgantown, WV and [3]Chemical Engineering, West Virginia University, Morgantown, WV.*

Single-walled carbon nanotubes (SWCNTs) present a significantly higher chance of occupational and environmental exposure owing to their widespread use in technology and commercial products. Currently, there is a lack of consensus on the various CNT characteristics that induce pulmonary toxicity. Therefore, our aim was to study the effect of SWCNT length and chemical functionalization on ROS production and collagen synthesis in human lung fibroblasts. SWCNTs with varying functionalization including carboxylic acid, amine and hydroxyl, and varying lengths, i.e. long 5-30 nm and short 1-2 nm, obtained from Cheap Tubes Inc. were used. SWCNT dimension and elemental composition characterization was conducted using atomic force microscopy and energy dispersive X-ray spectroscopy respectively. SWCNT toxicity in normal human lung fibroblast were first determined using WST-1 assay and sub-toxic concentrations of SWCNTs were selected for further experiments. Cellular ROS production was determined fluorometrically using DCF-DA as fluorescent probes for peroxide measurement. Type I Collagen expression was determined by western blotting in the presence and absence of ROS inhibitors. Cellular collagen content was determined by Sircol® assay. Our results showed that: 1) Pristine > COOH > NH_2 > OH SWCNT in ROS and collagen production in a dose- and time-dependent manner; 2) longer length SWCNTs induced higher ROS generation and collagen I expression than those of short length; and 3) SWCNT-induced collagen expression was significantly blocked by various ROS inhibitors revealing a role for oxidative stress in SWCNT-induced fibrogenesis. These results suggest that SWCNT length and functionalization impact lung fibroblast ROS and collagen synthesis, which contribute to SWCNT-induced pulmonary fibrosis.
Disclaimer
Research findings and conclusions are those of the authors and do not necessarily represent the views of the National Institute for Occupational Safety and Health.

PS 590 Differential Gene Expression in SAEC and HMVEC Grown in Monoculture or Coculture and Exposed to MWCNT: Correlation with *In Vivo* Studies

B. Talkington[1], C. Dong[2], X. Zhao[2], J. Dymacek[2, 3], V. Castranova[1], Y. Qian[1] and N. L. Guo[2]. *[1]National Institute for Occupational Safety and Health, Morgantown, WV, [2]West Virginia University Mary Babb Randolph Cancer Center, Morgantown, WV and [3]West Virginia University Lane Department of Computer Science and Electrical Engineering, Morgantown, WV.*

In vitro coculture systems are at the forefront of molecular research due to their increased ability for cell-cell communication. In this study, small airway epithelial cells (SAEC) and human microvascular endothelial cells (HMVEC) were grown separately in monoculture or together in an alveolar-capillary coculture and exposed to either dispersion media control or multi-walled carbon nanotubes (MWCNT) for 6 or 24 h. Global mRNA profiling determined genes that were differentially expressed in coculture as compared to monoculture, and Ingenuity Pathway Analysis determined the biological functions and related pathways of these genes. A total of 1505 SAEC and 54 HMVEC genes, commonly involved in the cell cycle and cell proliferation, were differentially expressed in control coculture experiments as compared to monoculture (SAM 1%, FC >1.5). A total of 1601 SAEC and 2016 HMVEC genes, commonly involved in cell movement and survival, were differentially expressed in coculture as compared to monoculture following MWCNT exposure (SAM 1%, FC >1.5). A correlation study of gene expression between monoculture, coculture, and in vivo gene expression from mice lungs exposed to MWCNT determined that coculture gene expression had a better correlation with in vivo gene expression than monoculture. In this study, we determined that gene expression in cells from coculture models is different from expression in the corresponding cells in monoculture. As coculture gene expression better correlates with gene expression seen in vivo, we hypothesize that coculture may offer an enhanced in vitro model for nanoparticle risk assessment.

PS 591 Determination of Stoichiometric ROS Degeneration and Relationship between Redox Potential and Bioavailability to Design Safe CNTs

S. Tsuruoka[1], H. Matsumoto[2], K. Takeuchi[3], K. Koyama[1], N. Saito[5], Y. Usui[1], S. Kobayashi[5], E. Akiba[4], D. W. Porter[6], V. Castranova[6], F. R. Cassee[7] and M. Endo[1, 3]. *[1]Research Center for Exotic Nanocarbons, Shinshu University, Nagano, Nagano, Japan, [2]Tokyo Institute of Technology, Meguro, Tokyo, Japan, [3]Institute for Carbon Science & Technology, Shinshu University, Nagano, Nagano, Japan, [4]Kuraray Living Co., Ltd., Osaka, Osaka, Japan, [5]School of Health Science, Shinshu University, Matsumoto, Nagano, Japan, [6]NIOSH, Morgantown, WV and [7]RIVM, Bilthoven, Netherlands.*

An important goal is to design safe carbon nanotubes (CNTs) by controlling their properties. Biological evaluations have been conducted with individual CNTs, and such results have been used for risk assessment (NIOSH CIB 65, 2013). However, information is lacking to define the relationships between the chemical properties of CNTs and their bioavailability. The present work aimed to obtain a stoichiometric expression of ROS degeneration by CNTs, which predicted ROS scavenging results with CNTs. ROS degeneration rate was measured with an ESR-DMPO method. The Fenton reaction was used to generate OH radicals. To evaluate CNT surface reactions, surfactant concentration was minimized to eliminate its influence, and reactivity of CNTs was determined. Results indicate that this allows kinetic quantification of the relationship between degeneration reactions and CNT morphology. Since the degeneration of ROS is attributed to a redox reaction according to the hypothesis in reaction kinetics on CNT surface, CNT bioactivity is defined as a redox potential that can be used to elucidate the relationship between bioactivity and CNT physicochemical properties. In conclusion, redox potential will be used to predict CNT bioactivity using its surface morphology and to design safer CNTs. [This work was supported by the Exotic Nanocarbon Project, Japan Regional Innovation Strategy Program by the Excellence, JST(Japan Science and Technology Agency)(ST, KK, YU, ME)].

PS 592 Development of Determination Method of Single-Walled Carbon Nanotubes in the Lung of Intratracheal-Instilled Rat

N. Shinohara[1, 2], K. Uchino[2], K. Fujita[1, 2], S. Endoh[2], J. Maru[2] and H. Kato[1, 2]. *[1]National Institute of Advanced Industrial Science and Technology (AIST), Tsukuba, Ibaraki, Japan and [2]Technology Research Association for Single Wall Carbon Nanotubes (TASC), Tsukuba, Ibaraki, Japan.*

Novel method to determine single-walled carbon nanotubes (SWCNTs) in rat lung was developed to evaluate the pulmonary SWCNTs clearance after intratracheal instillation. First, rat lung homogenate containing SWCNTs was treated with nitric acid (HNO3) under gradual heating using microwave digestion system. After the acid treatment, SWCNT adsorbed on the PFTE tube or glass tube was desorbed with ethanol using ultrasonication. Secondly, acid-digested samples and washed ethanol were filtrated with silica wool filled in stainless tube or silica glass tube. Wool and tube had been preheated at 900 °C in a muffle furnace to reduce the contamination. The wool containing the SWCNTs was washed with pure water 5 times, and then heated gradually to 900 °C using pyrolyzer under O2 gas flow. CO2 outgas from the pyrolyzer was determined over time with IR (infrared spectroscopy) using the calibration curve created with glucose. In the IR analysis, CO2 derived from single biological carbon without SWCNTs and SWCNTs without biological carbon were separately detected under 500 °C and 500 to 900 °C, respectively. In the case acid treatment was not conducted for the biological carbon sample containing SWCNTs, however, the tailing of the IR peak of CO2 derived from biological carbon interfered the IR peak of CO2 derived from SWCNTs. After the acid treatment to the biological carbon sample containing SWCNTs, the IR peak of CO2 derived from residual biological carbon were completely separated from the IR peak of CO2 derived from SWCNTs. SWCNTs in the powder, SWCNTs in the suspension, and SWCNTs spiked to rat lung homogenate could be recovered at higher than 90% between several μg and 100 μg of SWCNTs. This developed method will be applied to determine the pulmonary SWCNTs burdens after intratracheal instillation of SWCNTs. This research was funded by NEDO, Japan (P10024).

PS 593 Acute Inhalation Toxicity of Graphene Oxide and 5-Day Repeated Inhalation Toxicity of Graphene

J. Kim[1], J. Shin[2], J. Hwang[2], J. Lee[2], T. Kim[1], J. Lee[1], Y. Kim[6], H. Lee[3], N. Song[4], K. Ahn[5] and I. Yu[1]. *[1]Institute of Nanoproduct Safety Research, Hoseo University, Asan, Republic of Korea, [2]Occupational Lung Diseases Institute, KCOMWEL, Ansan, Republic of Korea, [3]Donga University, Busan, Republic of Korea, [4]KRISS, Daejeon, Republic of Korea, [5]Hanyang University, Ansan, Republic of Korea and [6]Korea Ginseng Corporation, Daejeon, Republic of Korea.*

Hazard of graphene exposure to human health, however, has not been known well. Acute pulmonary toxic effect of graphene oxide was evaluated via nose-only inhalation for 6 hours to experimental animals. Male Sprague-Dawley rats were divided into 3 groups (4 rats in each group), the fresh air control (0 mg/m^3), low (0.46 ± 0.06 mg/m^3), and high (3.76 ± 0.24 mg/m^3) concentration group, respectively. Lactate dehydrogenase (LDH), microprotein (mP), and microalbumin (mALB) levels were evaluated from the bronchoalveolar lavage (BAL) fluid on day 1, 7, and 14 after 6 hours exposure to graphene oxide. In addition, 5-day repeated inhalation toxicity of graphene was conducted to rats by assigning 3 groups (20 rats in each group); the control (0 mg/m^3), low dose (0.68 ± 0.14 mg/m^3) and high dose (3.86 ± 0.94 mg/m^3). The rats were exposed to graphene for 6 hr/day for 5 day. The exposed rats were allowed to recover for 14 to 28 days to evaluate the biopersistent effect of graphene oxide and graphene on the lungs after the acute and 5-day repeated exposure. The ingestion of graphene oxide and graphene in the alveolar macrophages was also evaluated. There was no statistical significant difference in average concentrations of LDH, mP, and mALB in the exposed groups when comparing with the unexposed control in all post-exposure groups (1, 7, and 14 days). The ingestion of graphene oxide in the alveolar macrophages was observed in all post exposure groups of the high dose group, but it was difficult to observe the graphene oxide in the control and low concentration group. Graphene oxide did not induce acute pulmonary toxic effect in the lungs of experimental animals. Graphene also did not induce any significant body weight, organ weight and lung weight changes after 5 day exposure and during 28 days of recovery.

PS 594 Modulation of Toll-Like Receptor Activity by Pristine Single-Walled Carbon Nanotubes with Distinct Chiral Enrichment

X. Zheng[1], N. Afrooz[2], N. B. Saleh[2], J. Bisesi[1] and T. Sabo-Attwood[1]. *[1]University of Florida, Gainesville, FL and [2]University of South Carolina, Columbia, SC.*

The rapid expansion of nanomaterial use in industrial, consumer and medical sectors has raised concern regarding associated health effects from unintended exposure. There is exceptional interest in single-walled carbon nanotubes (SWNT), as they are used in many common applications. As SWNT share a resemblance to asbestos, there is concern regarding inhalation exposure and associated lung diseases. Although consequences of SWNT exposure in the lung include pulmonary injury and fibrosis, few studies have focused on the ability of these particles to modulate infections by pathogenic agents. Recognition of invading pathogens occurs through interaction with toll-like receptors (TLRs) that stimulate the immune system through activation of nuclear factor kappa beta (NF-κB). Based on this knowledge, we hypothesized that SWNT alter TLR activity and the production of pro-inflammatory cytokines through induction of NF-κB. Furthermore, SWNT of distinct chiral enrichment (SG65, SG76 and CG200) would differentially impact TLR activity. Using human embryonic kidney (HEK) cell lines which overexpress TLR2 or TLR3 and an NF-κB-driven reporter gene, we show that all of the SWNT tested failed to modulate activity of either TLR. However, SG65 SWNT significantly suppressed TLR2 activation by the agonist zymosan while significantly enhancing TLR3 activation by the agonist poly (I:C). Neither SG76 or CG200 SWNT nor the particle control carbon black (CB) had any influence on TLR2 or 3 activities. Characterization of SWNT by dynamic light scattering (DLS) reveal SG65 SWNT formed smaller aggregates and were more stable compared to the other SWNT tested. Finally, utilization of near-infrared fluorescence (NIRF) suggests that the SG65 SWNT interacted with the TLR agonists. Overall, these data suggest that chirality, aggregate size and stability of SWNTs may influence the activity of TLRs and have implications for interfering with normal pathogen defense systems.

PS 595 Carbon Nanotubes Effects on Primary Human Umbilical Vein Endothelial Cells (HUVEC) Cultures Morpholgogy and Expression of Endothelial Genes and Proteins Implicated in Fibrinolysis

Y. Rodríguez-Yáñez[1], B. Chavez-Munguia[2], B. Cisneros[3], R. López-Marure[4], S. K. González[5] and A. Albores[1]. [1]*Toxicology, Cinvestav, Mexico City, Mexico,* [2]*Infectomics, Cinvestav, Mexico City, Mexico,* [3]*Genetics, Cinvestav, Mexico City, Mexico,* [4]*Cell Biology, Instituto Nacional de Cardiología Ignacio Chávez, Mexico City, Mexico and* [5]*HG Ticomán, Mexico City, Mexico.*

Cardiovascular health effects caused by single-walled carbon nanotubes (SWCNT) pose a growing concern because of their many uses due to their physicochemical properties, i.e. biomedical equipment, including intravascular devices where endothelial cells could be affected. There is no a full description on SWCNT toxicity on the vascular endothelium and the fibrinolytic system yet. Thus, concentration- and time-dependent responses of pristine SWCNT on HUVEC's cultures were investigated by assessing SWCNT uptake and morphology changes; and their effect on the fibrinolytic system, gene expression and proteins level. HUVEC's were treated for 3, 6, 12 or 24 h with 5 or 25 μg SWCNT/ml; tumor necrosis factor-alpha (1 ng/ml) was used as positive control. Expression of tissue plasminogen-activators (*PLAT, PLAU, KLK1*) and *serpine1*, an inhibitor gene were assessed by real-time PCR, whereas ELISA was used to quantitate proteins (tPA, uPA, KLK1, PA1-1). Cell SWCNT uptake and morphological changes observed by transmission electron microscopy (TEM) included mitochondrial swelling and autophagosomes; SWCNT significantly induced serpine1 12h after treatment, while PLAT increased 3h after but decreased 6h afterwards. SWCNT caused an inverse time-dependent *PLAU* and *KLK1* induced expressions. SWCNT (5 μg /ml) induced *KLK1* but not so higher concentrations. All protein levels were assessed 24 h after exposure. In summary, SWCNT resulted in evident HUVEC's damage either by contact and/or internalization, generating endothelial dysfunction as shown by alterations on the expression or levels of genes and proteins involved in fibrinolysis, however, the capacity of SWCNT to cause circulation damage needs investigation. (Support grants: SSA/IMSS/ISSSTE/CONACYT grant 162391, ICyTDF51/2012 and CONACYT scholarship 203482 to YRY).

PS 596 Pulmonary Instillation of Multiwalled Carbon Nanotubes Increases Lung Permeability and Decreases Glycoprotein 130 Expression in the Lungs

L. C. Thompson[1], R. J. Snyder[3], B. S. Harrison[4], J. M. Brown[2] and C. J. Wingard[1]. [1]*Physiology, East Carolina University, Greenville, NC,* [2]*Pharmacology & Toxicology, East Carolina University, Greenville, NC,* [3]*NanoHealth Program, National Institute of Environmental Health Sciences, NIH, Research Triangle Park, NC and* [4]*Institute of Regenerative Medicine, Wake Forest University, Winston-Salem, NC.*

Pulmonary instillation of multi-walled carbon nanotubes (MWCNT) has demonstrated a potential to promote cardiovascular impairments, but a mechanism by which pulmonary exposure to MWCNT influences cardiovascular endpoints is unclear. We hypothesized that pulmonary exposure of MWCNT would mimic an acute lung injury-like response via increased lung permeability and decreased glycoprotein 130 (gp130) expression in the lung. We first tested the impact of 1 and 10 μg/cm2 of MWCNT on transepithelial electrical resistance (TEER) in vitro using normal - human bronchial epithelial cells. Since 10 μg/cm2 MWCNT altered the progression TEER measurements, we instilled male Sprague-Dawley rats with a corresponding concentration of 100 μg of MWCNT or Vehicle 24 hours prior to injury assessment. We measured lung water/tissue weight ratios, bronchoalveolar lavage (BAL) fluid total protein and differential cell counts from BAL. We assessed gp130 mRNA and protein expression in rat lung, heart and aortic tissue. Our findings demonstrated that pulmonary instillation of MWCNT increased lung water (6.9±1.0 vs 4.7±0.2 mg H2O/mg dry tissue), BAL protein (0.27±0.02 vs 0.21±0.01 mg/mL) and eosinophilia (7592±2457 vs 762±440 eosinophils) in rats. The MWCNT group also expressed decreased gp130 mRNA (-2.0±0.3 fold down-regulation) and protein (0.77±0.04 fold change) in the lung, but gp130 mRNA expression was elevated in aortic tissue (2.5±0.7 fold up-regulation) compared to vehicle. We conclude that pulmonary exposure to MWCNT may cause an acute lung injury-like response, which alters the circulating physiological milieu to promote cardiovascular detriments. This work is supported by NIH U19ES019525 and R01 ES016246 (CJW).

PS 597 Correlation of Toxicity and Material Properties: Oral and Inhalation Exposure of 16 Surface-Functionalized Nanomaterials

L. Ma-Hock[1], R. Büsen[1], W. Wohlleben[3], S. Gröters[1], D. Geiger[2], B. van Ravenzwaay[1] and R. Landsiedel[1]. [1]*Toxicology, BASF SE, Ludwigshafen/Rhein, Germany,* [2]*Product Safety, BASF SE, Ludwigshafen, Germany and* [3]*Material physics, BASF SE, Ludwigshafen, Germany.*

16 nanomaterials were tested by short-term inhalation studies (R. Landsiedel, et al. Advanced Materials 22.24 (2010): 2601-2627) and oral gavage (28-day OECD TG407). The results were correlated to the complete physical-chemical properties (according to the REACH R7.1 nano-specific guidance) and to the in-situ corona structures (in lung surfactant, pure lipids, serum-containing media)
The surface of suspended nanoparticles with sizes of 10 nm (ZrO2), 15nm (SiO2) and 50 nm or 200 nm (Ag) received -acid, -amino, -PEG, and -steric functionalities. The organic molecules were bound to the surface of the particles to improve properties such as processability, solubility or stability of the products. All results were benchmarked against OECD reference materials (TiO2, ZnO, BaSO4).
None of the materials elicited an adverse effect in oral testing (see separate poster). For inhalation at up to 50 mg/m3, inflammations of the lung were observed with most of the nanomaterials. In general, functionalizations reduced the acute inflammatory response, especially for negative charges and for sterically stabilized materials. The correlation of inflammatory potency (e.g. monitored by PMN) to in-situ corona parameters is vanishing. A weak correlation was found between the particle's affinity to phospholipids and the deposition rate, but not further correlated to clearance. In contrast, correlations are strong with the chemical composition of the core particle, suggesting grouping and prioritization for in-vivo testing by surface charge and by core substances.
The project NanoGEM (Nanostructured materials – Health, Exposure and Material Properties, 2010 – 2013) involved 19 research institutions and companies, supported by the Federal Ministry of Education and Research (BMBF).

PS 598 Determination of Nanomaterial Single Nanoparticle and Nanoparticle Aggregation in Complex Biological Environments

Y. Zhang[1], S. V. Jenkins[2], T. Ingle[1], R. Wang[1], J. Chen[2] and P. C. Howard[1]. [1]*NCTR/ORA Nanotechnology Core Facility, Office of Scientific Coordination, NCTR/FDA, Jefferson, AR and* [2]*Department of Chemistry and Biochemistry, University of Arkansas, Fayetteville, AR.*

The plasmonic nanomaterials are attractive for a variety of biomedical applications such as drug delivery and bio-imaging agents. Many of these nanomaterials were introduce to human or animals through intravenous injection and work most effectively following cellular uptake. However, aggregation/agglomeration of nanoparticles will affect their biological behavior, distribution and toxicity. Rapid *in situ* characterizations are urgently needed to monitor the physical nature of the nanoparticles as they were introduced into blood and intracellular compartment representing extremely complex environments. We proposed that the confocal Raman microscopy (cRM) and hyerspectral dark field microscopy (hpDFM) are able to discriminate the status of the gold nanoparticles (Au NPs) and aggregates in biological fluid blood and cultured macrophage. Citric acid coated Au nanoparticle (50 nm) and nanoparticle aggregates were characterized using transmission electron microscopy (TEM), Zetasizer, Nanoparticle Track Analysis (NTA), UV/Vis spectroscopy and induced-coupled Plasmon microscopy (ICP-MS). A series of complementary methods are used to characterize the single Au NPs and status of particle aggregates following incubation in rat blood and cultured macrophage. hpDMF was demonstrated to monitor Au NPs and aggregates in blood in situ, and the spectra were shifted from 540 nm with single particles to 600-700 nm for the nanoparticle aggregates. In contrast, Au NPs aggregates were detected in the cytosol of macrophages after exposure to Au nanoparticles. Additionally, cRM was demonstrated as complementary to detect Au NPs aggregation state. This detection method was further confirmed by single particle ICP-MS analysis. The study suggested that the hpDFM imaging system is likely robust and can be used to assess physiological status of new plasmonic nanomaterial in biological system.

PS 599 CEFIC-LRI N1 Project: Oral Toxicity of a Synthetic Amorphous Silica (SAS) in Rats

J. Buschmann, G. Lewin and O. H. Creutzenberg. *Fraunhofer ITEM, Hannover, Germany.* Sponsor: C. Dasenbrock.

The test item was a synthetic amorphous silica (SAS) coded NM-200 and available at the EU JRC nanomaterials repository. It is a nanostructured, precipitated SAS. As NM-200 is used as an ingredient in food it was the objective of this study to

evaluate oral toxicity. The toxicity of NM-200 after daily oral gavage in male rats for 28 days with an additional 14-day recovery period (OECD TG 407; in addition: Si ion and Si particle analysis in selected organs) was tested. Dose levels of 100, 300 and 1000 mg/kg bw (vehicle: 0.5% methylhydroxypropylcellulose) were used. Extra groups (control recovery; high dose recovery) were kept for additional 14 days of post-observation. Body weights, food consumption, the functional observational battery (FOB) and hematology and clinical chemistry did not reveal any treatment-related effects. Also organ weights, necropsy, and histopathological examination did not show any substance-related findings in the high dose group, as compared to controls. Chemical analysis of silicon ions in blood, kidney and liver tissues did not reveal differences between the control and the high dose group. As a result, NM-200 did not cause any substance-related effects at doses up to 1000 mg/kg b.w. after oral exposure for 28 days in male Wistar (WU) rats. Therefore, the highest dose tested (1000 mg/kg b.w.) was determined to represent the NOAEL in this study. By exemplary TEM analysis no particles of NM 200 could be detected in selected tissues.

PS 600 CEFIC-LRI N1 Project: Inhalation Toxicity of a Synthetic Amorphous Silica (SAS) in Rats

O. H. Creutzenberg, G. Pohlmann, T. Hansen, S. Schuchardt, H. Ernst, T. Tillmann and D. Schaudien. *Inhalation Toxicology, Fraunhofer Institute of Toxicology and Experimental Medicine, Hannover, Lower Saxony, Germany.* Sponsor: C. Dasenbrock.

The test item was a synthetic amorphous silica (SAS) coded NM-200 and available at the EU JRC nanomaterials repository. It is a nanostructured, precipitated SAS used in the food sector. A subacute 14-day and a subchronic 90-day inhalation toxicity test were conducted (OECD TG 412 and 413) in male Wistar rats both including an expanded endpoint pattern (i.e.toxicokinetics, genotoxicity, TEM analysis) compared to the requirements of OECD TG. In the 14-day test rats were exposed to aerosol concentrations of 1, 5 and 25 mg/m^3. No systemic but local acute effects in nose/lungs were detected, i.) mucous (goblet) cell hyperplasia and epithelial eosinophilic droplets/inflammatory cell infiltration in the nasal cavity; ii.) alveolar/ interstitial macrophage/granulocyte infiltration in the lungs of the high dose group. Statistically significant increases of polymorphonuclear neutrophils (PMN) in bronchoalveolar lavage fluid (BALF) were detected in the mid and high dose groups 1 day after exposure. These findings showed a rapid reversibility. The LOAEL was 5 mg/m^3 and the NOAEL 1 mg/m^3. In the 90-day test, conducted at aerosol concentrations of 1, 2.5 and 5 mg/m^3 the LOAEL was 1 mg/m^3, thus an experimental NOAEL could not be derived from the study. The EPA benchmark model resulted in a BMCL of 0.6 mg/m^3 based on the PMN number in BALF. Toxicokinetics followed over 90 days after end of exposure revealed a half-time of approx. 30 days (chemical Si analysis) thus indicating a high solubility. TEM analysis detected SiO_2 particles located in intraalveolar macrophages. In remote organs, however, such particles were not detectable.
Overall, NM-200 showed acute toxicity in nose and lungs after inhalation. Due to an effective clearance and solubility a full recovery of effects was found. A translocation of NM-200 particles was not observed.

PS 601 CEFIC-LRI N1 Project: Genotoxicity of a Synthetic Amorphous Silica (SAS) in Rats

J. Knebel, C. Ziemann and O. H. Creutzenberg. *Inhalation Toxicology, Fraunhofer Institute for Toxicology and Experimental Medicine, Hannover, Germany.* Sponsor: C. Dasenbrock.

There is a debate about direct genotoxic potential of nanoparticles. Due to their high specific surface area, nanostructured materials are of special interest. Thus, genotoxicity was one focus in the expanded toxicity testing of NM-200. This test item is a synthetic amorphous, precipitated silica available at the EU JRC nanomaterials repository. As part of a subacute 14-day inhalation test in Wistar rats (strain: Crl:WU) with aerosol concentrations of 1, 5 and 25 mg/m^3, a micronucleus test in vivo and a comet assay ex vivo with alveolar macrophages were conducted. Inhaled NM-200 did not significantly enhance the micronucleus frequency in polychromatic bone marrow erythrocytes of both male and female rats, i.e. was not clastogenic/aneugenic in this cell type. In the in vivo comet assay, particularly after the 14-days recovery period, a slight, concentration-dependent increase in DNA-damage was noted in BAL cells from NM-200 treated male rats, as compared to the negative controls, but there was no significant induction of oxidative DNA-damage. Nevertheless, a slight significant increase of 8-OH-dG positive nuclei was observed in lung epithelial cells by immunohistochemistry in all treatment groups at day 1 and day 14 postexposure. In a parallel in vitro comet assay with primary rat alveolar macrophages no significant clastogenic potential or potential to induce oxidative DNA-base lesions (8-OH-dG) was obvious, irrespective of cytotoxicity in the highest NM-200 concentration. In a chromosomal aberration test (OECD 473) NM-200 treated cultures demonstrated low aberration frequencies in the range of historic negative controls. Hence, the conclusion was 'unclassified' for structural chromosomal aberrations. Finally, NM-200 did not significantly increase mutant frequencies up to the limit concentration of 5000 μg/ml in a mouse lymphoma assay (OECD 476) and thus exhibited no substance-specific mutagenic potential. Overall conclusion: For NM-200 there is no evidence for systemic or local genotoxic activity if applied to lungs of animals.

PS 602 Modulation of Macrophage Phenotype and Function by Engineered Nanoparticles

V. K. Kodali[1], M. H. Littke[1], S. C. Tilton[1], H. D. Jolley[1], J. G. Teeguarden[1], C. F. Frevert[2], S. J. Skerrett[2], J. G. Pounds[1] and B. D. Thrall[1]. [1]*Systems Toxicology, Pacific Northwest National Laboratory, Richland, WA and* [2]*Department of Comparative Medicine, University of Washington, Seattle, WA.*

Epidemiological studies have established a correlation between exposure to ambient air pollution particulates and the incidence of pneumonia and lung infections. Using an in vitro assay of macrophage phagocytic function, we investigated the effects of an array of 18 different ENP types on the ability of macrophages to recognize and phagocytize *S. pneumoniae*. We identified three major groups of ENPs based on their effect on macrophage function. ENPs which most potently inhibited macrophage phagocytosis included metals and metal oxides which are expected to undergo significant dissolution and have direct cytotoxic effects. An additional group of materials, including iron oxide and MWCNTs, were found to cause dose-dependent inhibition of phagocytic function, yet had no direct cytotoxic or proinflammatory effects of their own. The third group of benign ENPs had no effect on direct cytotoxicity or phagocytic capacity. Oropharyngeal instillation of superparamagnetic iron oxide (SPIO) an ENP from group 2 in C57BL/6 mice confirmed the in vitro results, demonstrating SPIO exposure decreased *S. pneumoniae* lung clearance in vivo. Macrophage transcriptional response to two ENPs silica and SPIO from class 2 and class 3 before and after bacterial lipopolysaccharide (LPS) challenge showed that while SPIO treatment modulated nearly 500 genes, silica pretreatment regulated only 67 genes. Macrophages exposed to SPIO displayed a phenotype suggesting an impaired ability to transition from an M1 to M2-like activation state, characterized by suppressed IL-10 induction, enhanced TNFα production, and diminished expression of complement and phagocytic receptors. Our results illustrate adverse biological consequences of nanomaterials may not always be directly mediated, but may be manifested by altering susceptibility to other common environmental exposures.
Supported by NIEHS Grant U19-ES019544

PS 603 Amphiphilic Polymer-Coated CdSe/ZnS Quantum Dot-Induced Hemolysis and Glutathione Depletion Are Enhanced in Gclm Null Mouse Erythrocytes

C. Carosino[1], H. Wang[1], C. White[1], J. Shang[2], X. Gao[2] and T. Kavanagh[1]. [1]*Department of Environmental and Occupational Health Sciences, University of Washington, Seattle, WA and* [2]*Bioengineering, University of Washington, Seattle, WA.*

Quantum dot (QD) nanoparticles have unique fluorescent properties, making them ideal for biomedical imaging. However, QDs contain heavy metals such as cadmium (Cd) and selenium (Se) and have been demonstrated to generate reactive oxygen intermediates, elevate oxidative stress biomarkers such as heme oxygenase-1 (Hmox1) and to cause pulmonary inflammation in vivo. Glutamate cysteine ligase (GCL), the rate-limiting enzyme in glutathione (GSH) synthesis, is important for antioxidant defense. Absence of GCLM (GCL modifier subunit) results in greatly diminished GSH. GCLM polymorphisms exist in humans some of which have been linked to increased risk of cardiovascular disease. We tested the effects of QDs on cultured erythrocytes obtained from Gclm wild-type (+/+), heterozygous (+/-) and null (-/-) mice. Gclm+/- and Gclm-/- erythrocytes had diminished GSH as compared to Gclm+/+erythrocytes (51% and 6%, respectively). Erythrocytes from Gclm+/+ and Gclm+/- mice greatly resisted QD-induced hemolysis until 48 hours at which point a mild dose-response increase in hemolysis was observed. However, Gclm-/- erythrocytes experienced increased hemolysis as early as 12 hours with all QD treatments yielding equally high levels of hemolysis at 48 hours. Interestingly, after 24 hours of exposure to 40 nM QDs, erythrocytes from Gclm+/+ and Gclm+/- mice (but not Gclm-/- mice) had higher total GSH levels. This may be due to enhanced formation of GCL holoenzyme in these erythrocytes, thus increasing GSH synthesis. These findings suggest that QDs are capable of producing oxidative stress-mediated hemolysis and raise concerns regarding the effects of prolonged exposure to QDs or other engineered nanomaterials that cause oxidative stress, especially in individuals having genetic or epigenetic modifications to DNA resulting in low expression of GCLM. Supported by NIH Grants U19ES01945, P30ES007033, T32ES007032 and UW DEOHS.

PS 603a Assessment of the *In Vitro* Irritant Contact Dermatitis Potential of Metal-Containing Nanoparticles Using Human-Derived Epidermal Keratinocytes

M. F. Hughes[1] and V. Miyani[2]. [1]*ORD/NHEERL, US EPA, Research Triangle Park, NC and* [2]*Student Services Contractor, Morrisville, NC.*

Dermal exposure to metals may result in irritant contact dermatitis. The objective of this study was to examine the in vitro potential of metal-containing nanoparticles to elicit irritant dermatitis in human-derived epidermal keratinocytes (HDEK). These cells are cultured and form a multi-layered, highly differentiated model of human skin. Ag (14), TiO_2 (7) and CeO_2 (3) nanoparticles of various sizes (10 nm – 214 nm) were used in this study. The Ag particles were capped with either citrate or polyvinylpyrrolidone/citrate (PVP) or coated with silica. The Ag nanoparticles were suspended in saline and the TiO_2 and CeO_2 particles were suspended in cell culture media containing 10% fetal bovine serum. Stock suspensions of these particles were dispersed using a probe sonicator. The particles (1 mg/ml, 30 µl) were transferred to the epidermal surface of the HDEK in 24-well plates. Three wells of HDEK were tested per particle. The positive control was 5% sodium dodecyl sulfate (SDS) and the negative control was either saline or culture media. After 1 hr exposure at 37 °C the HDEK were washed with saline. The HDEK were then incubated for 42 hr at 37 °C with an exchange of media at 24 hr. Viability of the HDEK was assessed using the MTT assay. A test substance is considered an irritant in this assay if the HDEK viability is less than 50%. The mean viability for the SDS treated HDEK was 7.8%. The lowest viabilities (mean ± SD) for the nanoparticle treated HDEK were: Ag 75 nm PVP, 91.9 ± 3.8%; Ag 50 nm silica coated, 91.9 ± 3.6%; Ag 80 nm silica coated, 91.9 ± 5.3%; TiO_2 22 nm (anatase), 93.2 ± 22.2%; CeO_2 58 nm, 91.3 ± 3.9%. Under the in vitro conditions used in this study, the Ag, Ti and Ce nanoparticles examined were not dermal irritants to the HDEK. The formed stratum corneum of the HDEK may limit penetration of these nanoparticles to induce inflammation and cell death or their inherent dermal irritancy potential is very low. (This abstract does not necessarily represent U.S. EPA policy.)

PS 603b A Simple Approach for the Determination of Nanoparticle-Induced Cytotoxicity *In Vitro*

Q. Gu[1], S. Lantz-McPeak[1], E. Cuevas[1], H. Rosas-Hernandez[1], S. F. Ali[1], S. Sarkar[1], M. G. Paule[1] and Y. Zhang[2]. [1]*Division of Neurotoxicology, FDA/NCTR, Jefferson, AR and* [2]*Nanotechnology Core Facility, FDA/NCTR, Jefferson, AR.*

Emerging new materials utilizing nanoparticles (NPs) are being increasingly incorporated into consumer products. Thus, elucidating the potential toxicities associated with NP-exposure will lead to a better evaluation of the undesired biological impacts of NP-based materials. Here we report a simple approach for the assessment of NP-induced cytotoxicity *in vitro* using Fluoro-Jade C (FJ-C), which has been extensively utilized in *in vivo* neurotoxicity studies where they have been shown to label dead and dying neurons. In the present study, different types of cell cultures including rat brain micro-vessel endothelial cells, bovine brain micro-vessel endothelial cells, and the human cell line SH-SY5Y were examined, and potential cytotoxic effects of silver-nanoparticles (Ag-NPs) and gold-nanoparticles (Au-NPs) were tested. Whereas incubation with 20 nm diameter citrate-Ag-NPs for 24 hours induced a dose-dependent increase in the number of FJ-C labeled cells, incubation with 7 nm diameter tannate-Au-NPs for 24 hours showed few changes even at concentrations higher than those used for Ag-NP studies. The dose-dependent i*in vitro* cytotoxicity of Ag-NPs and the lack thereof for Au-NPs were further confirmed by two commonly used cytotoxicity assays, the lactate dehydrogenase (LDH) and 2,3-bis-(2-methoxy-4-nitro-5-sulfophenyl)-2H-tetrazolium-5-carboxanilide (XTT) assays. In addition to the examination of Ag-NP-induced cytotoxicity, two well known toxicants, cadmium and Thimerosal, were also employed to induce cell death *in vitro* and both elicited a significant increase in the number of FJ-C labeled cells. These results suggest that the FJ-C-based approach can provide an easily obtained assessment of NP-induced cytotoxicity and has the potential to lead to high-throughput *in vitro* screening and analyses. This simple FJ-C labeling approach may have broad application for the assessment of *in vitro* cytotoxicity following NP-exposure.

Supported by FDA/NCTR Protocols E07460 and E7524.

PS 603c Influence of Nanoparticles on Cell Death and Cell Cycle in A549 Cells

Y. Huang[1], L. M. Tolliver[1], F. S. Hou[2], R. S. Aronstam[1] and H. Lee[3]. [1]*Biological Sciences, Missouri U. of Science and Technology, Rolla, MO,* [2]*Department of Clinical Laboratory Science, Marquette University, Milwaukee, WI and* [3]*Department of Natural Resources and Environmental Studies, National Dong Hwa University, Hualien, Taiwan.*

Although frequently used in industrial and biomedical applications, fourth period metal oxide nanoparticles (NPs) display varying degrees of cytotoxicity, of which the mechanisms need further exploration. In the past, we established a trend of cytotoxicity of transition metal oxide NPs. Three distinct "tiers" of cytotoxicity was observed: low (TiO2, Cr2O3 and Fe2O3), moderate (Mn2O3 and NiO) and high (CuO and ZnO). In this report, we investigated influence of these seven NPs on cellular ROS generation, cell death and cell cycle in A549 cells. ROS generation was measured by DCFH-DA. TiO2, Cr2O3 and Fe2O3 did not elevate ROS while Mn2O3 and NiO, CuO and ZnO increased ROS by several folds. The apoptotic dyes Annexin-V conjugated fluoroisothiocyanate (FITC) and 7-Aminoactinomycin D (7-AAD) were used to characterize cell death of NP-treated cells through immunofluorescence microscopy and quantify it through flow cytometry. The flow cytometry results mimicked the same general trend of low, moderate and high toxicity. The combined populations of early apoptotic cells and late apoptotic/early necrotic cells treated with the highest concentrations of CuO (20 µg/mL) and ZnO (25 µg/mL) were 71.8%±7.6% and 59.8%±4.9%, respectively. The combined populations of early apoptotic cells and late apoptotic/early necrotic cells of the rest of five NPs range from 3.2±0.85%. The degree of apoptosis and necrosis corresponded with severity of cytotoxicity. Different NPs differentially affect different phases of cell cycle. One notable observation was that zeta potentials of NPs varied significantly in water (-7 to -34 mV), PBS solution (-22 to -30 mV), and cell medium (-6.4 to -9.2 mV). The potentials do not correlate with the trend of cytotoxicity.

PS 603d Molecular Responses to MWCNT Pulmonary Exposure at Relevant Workplace Exposure Levels

P. C. Zeidler-Erdely[1], S. Shah[2], S. Tugendreich[2], S. Bilgesu[1], T. Hulderman[1], J. Cumpston[1], D. G. Frazer[1], W. McKinney[1], B. T. Chen[1], V. Castranova[1] and A. Erdely[1]. [1]*HELD, NIOSH, Morgantown, WV and* [2]*Ingenuity Systems, Inc., Redwood City, CA.*

Pulmonary toxicity from multi-walled carbon nanotube (MWCNT) inhalation exposure is well described and includes lung epithelial hyperplasia, inflammation, and fibrosis. However, at levels relevant to workplace exposures the contributing molecular mechanisms are not well described. To address this question, a 19d inhalation exposure to MWCNT in C57BL/6J mice with daily alveolar depositions of 2340 ng (=1000 d of human exposure), 234 ng (=100 d), and 23.4 ng (=10d) was conducted. Cumulatively, these doses represent 76, 7.6, and 0.76 yr for the high, middle, and low dose, respectively, for a worker exposed to an inhalable concentration of 10 µg/m3 (average exposure from worker sampling at 8 different MWCNT sites; MMAD 5.5 µm) for 8 h/d for 250 d/yr. Mice were sacrificed at 0, 28, and 84 d post-exposure. RNA was isolated from left lung lobes and global expression analysis was performed with subsequent Ingenuity Pathway Analysis (IPA). Results indicated marked inflammation at the high dose that was sustained through 84 d post-exposure. Markers associated with pathological changes, such as fibrotic growth factors (TGFb, EGF, PDGF), were also a feature of the high dose. The middle dose was also associated with markers of inflammation (e.g. IL-6, IL-1b) but to a lesser extent and not as sustained when compared to the high dose. The middle dose showed indications of increased fibrotic markers at 0 and 28 d by BioProfiler analysis, but the response was not sustained and was absent at 84 d. The low dose showed minimal expression changes that did not form any major networks of activation. These results confirm the potential of MWCNT to induce molecular mechanisms associated with a marked inflammatory and pathological response in exposed mice. Based on exposure predictions, considerable years of exposure may be necessary at facilities operating at an inhalable concentration of 10 µg/m3 or below to elicit marked molecular changes.

PS 603e Panel Biomarker Study in Workers Exposed to Multiwalled Carbon Nanotube Aerosol

L. M. Fatkhutdinova[1], T. Khaliullin[1], E. K. Kisin[2], I. Mustafin[3], E. M. Birch[4], V. E. Kagan[5] and A. A. Shvedova[2]. *[1]Hygiene and Occupational Medicine, Kazan Medical University, Kazan, Russian Federation, [2]HELD/PPRB, National Institute for Occupational Safety and Health, Morgantown, WV, [3]Biochemistry, Kazan Medical University, Kazan, Russian Federation, [4]DART, National Institute for Occupational Safety and Health, Cincinnati, OH and [5]Department of Environmental and Occupational Health, University of Pittsburgh, Pittsburgh, PA.*

The aim of the study was to assess potential fibrogenic risk upon real occupational exposure to multi-walled carbon nanotubes (MWCNT) using biomarkers tested in preceding animal experiment. The study was conducted at 2 MWCNT-producing enterprises with the same reactor type. 11 workers who had more than 1 year contact with MWCNT aerosol composed the exposure group, the control group consisted of 14 people. Elemental carbon was evaluated in air samples and the CNT presence was confirmed by TEM-analysis. Blood and induced sputum samples were obtained from workers, TGF-β1, KL-6 and osteopontin levels evaluated. To assess the relationship between MWCNT exposure and biomarker levels (age, gender, smoking have been chosen as cofounders) generalized linear models including main effects and interactions in-pairs were created. The regression coefficients confidence intervals were refined by bootstrap analysis. TWA respirable MWCNT fraction was up to 6.11 mg/m3. TEM has shown the presence of MWCNT agglomerates sized 0,5-10 μm in all air samples. It was found that exposure to MWCNT aerosol at workplaces may alter the fibrosis biomarkers in blood serum and induced sputum. The levels of TGF-β1 in serum were dependent on exposure to MWCNTs (β=10.5, 95%BCa=1.2-51.8), the KL-6 levels in induced sputum were significantly higher in exposure group (β=235.9, 95%BCa=21.2-482). Osteopontin proved to be as an uninformative indicator. Data suggest that MWCNT exposure may lead to the changes in serum and induced sputum samples specific fibrogenic biomarkers content in workers. MWCNT-producing companies have to introduce control measures, as well as provide the adequate medical services organization.

PS 603f MWCNT Exposure Assessment in Occupational Settings

T. Khaliullin[1], R. Zalyalov[1], E. M. Birch[2], V. E. Kagan[3], A. A. Shvedova[4] and L. M. Fatkhutdinova[1]. *[1]Hygiene, Kazan State Medical University, Kazan, Russian Federation, [2]DART, National Institute for Occupational Safety and Health, Cincinnati, OH, [3]Department of Environmental and Occupational Health, University of Pittsburgh, Pittsburgh, PA and [4]HELD/PPRB, National Institute for Occupational Safety and Health, Morgantown, WV.*

The production of Multi-walled carbon nanotubes (MWCNTs) steadily increases all around the world. However, recent toxicological data raise concerns about their potential risk to human health, particularly upon occupational exposures. The aim of this study was to evaluate the occupational exposure to MWCNT at one of the manufacturing facilities in Russia. The sampling was performed at different sites during the entire technological process. Elemental carbon (EC) analysis was performed using modified NIOSH 5040 method. TEM analysis was performed using modified NMAM 7402 method. The highest MWCNT aerosol short-term concentration was registered during the reactor cleanout process, reaching 157 ug/m3. Time-weighted average (TWA) concentration was respectively 29.6 ug/m3 for the 8-hours shift. Respirable fraction TWA concentrations for EC at different workstations ranged from 0.53 to 6.11 ug/m3. TEM showed the presence of MWCNT-containing agglomerates at all technological stages, also detectable on non-working days. Agglomerates size ranged from 1 to 10 um; no individual MWCNTs were found. The highest EC values were found in samples obtained during reactor cleanout and harvesting, whereas laboratory handling produced the lowest MWCNT mass concentration values. In the absence of relevant OEL currently set in Russia we compared the maximum 8-hr TWA concentrations with the NIOSH recommended exposure level – 1 ug/m3. The 6.11 ug/m3 EC 8-hr TWA mass concentration value - determined during product harvesting - dictates the necessity of exposure control aimed at the reduction of potential adverse health effects in workers. Repeated exposure assessment is required after exposure controls installation. Direct online particle counters should be also used for mapping and identification of critical exposure points.

PS 603g Multiwalled Carbon Nanotubes Induce NLRP3 Inflammasome-Dependent Expression of Pro-Fibrotic Markers in Primary Human Bronchial Epithelial Cells

S. Hussain[1], S. Sangtian[1], R. J. Snyder[1], J. D. Marshburn[1], A. Rice[1], J. C. Bonner[2] and S. Garantziotis[1]. *[1]Clinical Research Unit, National Institute of Environmental Health Sciences (NIH), Research Triangle Park, NC and [2]Environmental and Molecular Toxicology, North Carolina State University, Raleigh, NC.*

Fibrogenic potentials of multi-walled carbon nanotubes (MWCNT) have been well documented; however mechanisms leading to lung fibrotic changes especially in primary human cells are not well understood. We aimed at deciphering the toxic effects of MWCNTs on primary human bronchial epithelial (HBE) cells and studied the effects of epithelial origin factors on human lung fibroblasts (MRC-5 cells). Well characterized MWCNTs and their suspensions were used to treat primary HBE cells (1.5-24 μg/mL). Fetal Lung fibroblasts (MRC-5 cells) were exposed to 1:4 dilated conditioned medium from MWCNT exposed BECs. MWCNT induce NLRP3 inflammasome dependent pyroptosis in HBE cells characterized by caspase-1 activation, cathepsin B release and inflammatory cell death. Cell death induction as well as inflammatory cytokine production can be significantly reduced by using siRNA to NLRP3, a caspase-1 inhibitor (z-WEHD-FMK) or a cathepsin B inhibitor (CA-074Me). Significant increase in mRNA expression of two well-known markers of fibrosis (TIMP-1 and Tenascin-C) in human lung fibroblasts was observed after treatment with conditioned media from MWCNT-treated HBE cells. Induction of these pro-fibrotic markers is significantly reduced when conditioned media from NLRP3 siRNA transfected HBE cells is used. In conclusion we demonstrate here that MWCNT induce inflammasome dependent pyroptosis in primary HBE cells which can initiate a profibrotic response. Thus we present a novel mechanism by which MWCNTs induce human airways epithelial damage.

PS 603h Mucociliary Differentiation May Protect Human Bronchial Epithelia from Multiwalled Carbon Nanotube-Induced Toxicity

R. J. Snyder[1], S. Hussain[1], S. Sangtian[1], A. Rice[1], S. Randell[2] and S. Garantziotis[1, 2]. *[1]National Institute of Environmental Health Sciences, Durham, NC and [2]University of North Carolina Chapel Hill, Chapel Hill, NC.*

Multi-walled carbon nanotubes (MWCNTs) are a form of graphitic carbon engineered for a wide variety of applications in consumer and industrial products. Their unique physiochemical properties, including high tensile strength and conduction, have made carbon nanotubes one of the most widely-used nanomaterials today. However, the increasing public use of MWCNTs elevates the risk of human exposure, both to consumers and those involved in the manufacture of MWCNT-enabled products, particularly via inhalation. Previous studies have found elevated cytotoxicity, inflammation, and fibrosis in murine lungs and human cells exposed to MWCNTs. However, the effect of these materials on the normal differentiation of human bronchial epithelial cells (BECs) is not well studied. In this study, human primary BECs derived by bronchoscopy were seeded on Millicell CM transwell inserts and allowed to reach confluence in BEGM growth medium (Lonza). Cells were then exposed to MWCNT in suspension for 24 hours at 0.06, 0.25 or 1 μg/cm2. Treatment controls included an untreated control, vehicle (BEGM with 10μg/ml DPPC, 1% BSA) control, and a 1μg/cm2 nano graphitized mesoporous carbon (NG) shape control. BECs exposed during differentiation in either air-liquid interface (ALI) or submerged culture were compared. BECs grown in ALI fully differentiated into a mucociliary pseudostratified epithelium regardless of treatment. In submerged culture, 1 μg/cm2 MWCNTs were highly cytotoxic to BECs and 0.25 μg/cm2 MWCNTs prevented the BECs from prototypical squamous differentiation. The results of this study suggest that the process of mucociliary differentiation in BECs can provide resistance to the cytotoxic effects of MWNCTs even before the cells have fully matured.

PS 603i Preparation and Antimicrobial Activity of Nanocapsules Containing Extracts of *Catharanthus roseus* and *Matricaria chamomilla*

E. G. Sanchez-Rueda[1], A. Alvarado[1], J. Soriano[1], F. Mercado[1], L. Flores[1], M. Dominguez[1], C. F. Espinoza[1], M. A. Mendez[2], L. Hernandez[2], R. E. Cachau[3], M. C. Miranda[1], Z. N. Juarez[1, 2] and T. D. Palacios-Hernandez[1, 2]. [1]*Biological Sciences, UPAEP, Puebla, Puebla, Mexico,* [2]*Chemical and Biological Sciences, UDLAP, Cholula, Puebla, Mexico and* [3]*Frederick National Laboratory for Cancer Research, Frederick, MD.*

In this project, the synthesis, characterization and antimicrobial activity of calcium alginate nanocapsules containing active ingredients of *Matricaria chamomilla* and *Catharanthus roseus*, were evaluated. Plants were collected from Puebla, Mexico, and stem, flowers, leaves and roots were employed to obtain hexane, chloroform and methanol extracts of both plants, and extracts were dissolved in glycerol and/or water. Synthesis of calcium alginate nanocapsules was developed by microemulsion method, employing the dissolved extracts during the process. The nanocapsules obtained were characterized by Low Voltage Electron Microscopy (LVEM) at 45 kV, Dynamic Light Scattering (DLS) and DRIZZLE method. Antimicrobial activity of extracts and nanocapsules was evaluated employing antibiograms containing 10 μL of suspensions containing 10, 1, 0.1 and 0.01 mg/mL of extracts, upon *Staphylococcus aureus* and *Escherichia coli* as Gram positive and Gram negative models, growth in Mueller-Hinton agar and adjusting the inoculum with the standard 0.5 McFarland. Antimicrobial activity of capsules was evaluated employing the same protocol, however their quantity was determined by DLS. Results obtained by LVEM showed that nanocapsules size range was between 35-100 nm, with morphology previously reported for soft spheres (1). DLS demonstrated a hydrodynamic ratio between 13-100 nm, and large aggregates on 1 μm. DRIZZLE analysis showed that aggregates were conformed by nanocapsules in a size range of 50-100 nm. Antimicrobial activity showed that nanocapsules containing chloroform extracts of flower and leaves in *M. chamomilla*, and nanocapsules containing hexane extracts of *C. roseus* inhibited the bacterial growth.

(1) J.P. Blitz and V.M. Gun'ko (Eds.), Surface Chemistry in Biomedical and Environmental Science, 23–34. © 2006 Springer.

PS 603j Nanoparticles from the Wear of Cobalt-Chromium Alloy Metal-on-Metal Hip Implants: Physicochemical and Dose Analysis of Patient and Toxicology Studies

M. Liong[1], M. Kovochich[3], B. L. Finley[2], D. J. Paustenbach[1] and A. Madl[3]. [1]*Cardno ChemRisk, San Francisco, CA,* [2]*Cardno ChemRisk, Brooklyn, NY and* [3]*Cardno ChemRisk, Aliso Viejo, CA.*

Wear debris analyzed in hip simulator systems and in patients with cobalt-chromium (CoCr) alloy metal-on-metal (MoM) hip implants show that the vast majority of wear particles (by number) exist in the nanometer size range. A number of studies have suggested that nanoparticles in this debris may cause local and systemic health effects. Most published papers have not evaluated toxicology studies in light of the physicochemical characteristics of wear debris in patients. The objective of this analysis was to identify the relevant physicochemical characteristics of CoCr wear nanoparticles from hip implant patients and evaluate their relevance to in vitro and in vivo toxicology studies of CoCr wear debris with respect to: 1) particle physicochemistry, 2) solubility in relation to metal ion release, 3) physicochemical variances across particle generation systems, and 4) human equivalent doses. For well-functioning MoM hip implants, the volumetric wear rate is relatively low (<1 cubic mm per million cycles or per year), and the majority of the wear debris is composed of Cr oxide nanoparticles (<100 nm) with minimal Co content. For implants with surgical malpositioning (rotational and translational), the volumetric wear rate is as high as 100 cubic mm per million cycles or per year, and the wear debris particles have larger sizes (up to 1000 nm) and contain higher Co content. The majority of in vitro and in vivo studies do not consider the clinical relevance or physicochemical characteristics of the wear debris actually found in patients or from hip simulator studies. Furthermore, many studies used doses orders of magnitude higher than implant patient experiences [when typical dose metrics (dose per gram of tissues) are applied]. We concluded that future studies need to evaluate nano and larger particles accounting for physicochemical characteristics and dose metrics relevant to those generated in patients or in properly conducted hip simulator studies.

PS 603k Metabolomic Profiles Delineate Potential Role for Glycine in Membrane and Secretion Factors Disruption Caused by Gold Nanorods in Male Germ Cells

Y. Xia, B. Xu, M. Chen, X. Ji, Z. Mao, X. Chen and X. Wang. *Institute of Toxicology, Nanjing Medical University, Nanjing, China.*

Gold nanorods (GNRs) are commonly used nanomaterials with potential harmful effects on humans. However, the mechanism by which GNRs affect reproduction remains largely undetermined. In this study, we used a metabolomics approach to comparatively analyze the metabolic changes in GNRs-treated male germ cells (GC-2 and TM-4). GC-2 and TM-4 cells were exposed to GNRs for 24h, and then the general cytotoxicity and cell health status were evaluated. MTT assay showed that neither GNRs (0.1, 1, 10 nmol/L) treatments nor control medium treatment affected cell viability. High content screening showed that GNRs could decrease membrane permeability and mitochondrial membrane potential of TM-4 cells, but GNRs had no effects on GC-2. In addition, RT-PCR indicated that the mRNA levels of secretion factors in TM-4 cells were also disrupted by GNRs. Metabolomic analysis revealed a significant GNRs-induced perturbation in metabolic pathway for Glycine, Serine and Threonine metabolism in TM-4 cells. Glycine, a non-essential amino acid involved in the body's production of phospholipids, was identified as a differential metabolite that was highly decreased during GNRs treatment. After the replenishment of glycine, the GNRs-induced harmful effects on membrane recovered. Addition of glycine also corrected the disturbance of the mRNA levels of secretion factors in TM-4 cells. Our results firstly showed that even at low doses of GNRs, there were significant toxic effects on membrane and secretion factors in TM-4 cells. Furthermore, we reveal glycine as a potentially important metabolic intermediary for the changes of membrane permeability, mitochondrial membrane potential and mRNA of secretion factors in TM-4 cells.

PS 603l 3-Dimensional Microtissues in the Assessment of Pulmonary Toxicity Induced by Engineered Nanoparticles

P. K. Kabadi and A. Kane. *Pathology and Laboratory Medicine, Brown University, Providence, RI.*

The rapid growth of nanotechnology has greatly increased the risk for environmental and human health toxicities. Current testing methods for nanoparticles (NP) largely rely on low-throughput *in vivo* studies to adequately assess toxicity and potential hazards to humans. While these methods have contributed significantly to the knowledge base on NP toxicity, they are often long term, monetarily inefficient and limited in the number of NPs that can be tested. Though alternative testing methods have utilized traditional 2-dimensional (2-D) *in vitro* assays as a more efficient means of testing large numbers of NPs, several studies have reported differential 2-D *in vitro* and *in vivo* data. To effectively evaluate NP toxicity in a pulmonary system using alternative testing methods, we used a 3-dimensional (3-D) microtissue model (Microtissues, Inc.). As most carbon-based NP exposures are pulmonary, lung macrophages and fibroblasts were grown in scaffold-free gel molds to examine the potential of carbon-based NPs in the development of granulomas and fibrotic tissue. Our data demonstrate the utility of 3-D microtissues in examining pulmonary granulomatous and fibrotic endpoints. In a preliminary study, microtissues exposed to carbon nanotubes and certain graphene NPs exhibited the development of granulomas surrounding the particles as seen by H&E staining. Further investigation of fibrotic tissue development was examined using Masson's trichrome staining and gene expression levels for collagens. The versatility of *in vitro* 3-D microtissues enables the examination of complex cell-cell interactions through the co-culture of different cell types and can be used to evaluate multiple pulmonary toxicity outcomes. Microtissues provide a unique alternative testing method, utilizing both 2-D and 3-D techniques, allowing for *in vivo*-like functionality, and moving towards a high-throughput and predictive means of NP toxicity testing. This research is supported by an NIEHS training grant (T32 ES07272) and a generous support by Donna McGraw Weiss '89 and Jason Weiss.

PS 604 Benchmark Dose Analysis of NTP Data on Tumors Induced in Rodents Chronically Exposed to Dietary Anthraquinone

A. Singhal and K. T. Bogen. *Exponent, Inc., Oakland, CA.*

Anthraquinone (AQ), a chemical present in low concentrations in food packaging products, was recently added to the California Proposition 65 list of chemical carcinogens, and also identified as a genotoxic carcinogen by the European Food Safety Authority (EFSA), based on 2005 National Toxicology Program (NTP) chronic oral bioassay data showing clearly increased B6C3F1 mouse liver and F344/N rat kidney (and other) tumors in each sex, even at dietary concentrations <1,000 ppm. To derive a point of departure (POD) for quantitative risk assessment for AQ, we performed benchmark dose (BMD) analysis to derive estimates of the 95% lower

confidence bound (BMDL) on BMD for each tumor type that NTP considered to be affected significantly by AQ. The lowest BMDL estimates obtained for increased tumor occurrence were based on tumor data for female mouse liver (7.0 mg/kg/day) and male rat kidney (14 mg/kg/day). AQ also significantly, and nearly completely, reduced mononuclear cell leukemia (MCL) in both male and female NTP rats in all exposed groups. Estimates of BMDL (and BMD) calculated for MCL suppression in male and female rats were 0.25 and 0.47 (and 0.083 and 0.16) mg/kg/day, respectively. Tumor suppression was thus clearly the most pronounced effect of chronic dietary AQ administration on tumor-incidence rates in the NTP (2005) study. A 1968 National Cancer Institute (NCI)-sponsored bioassay previously showed that 18 months of dietary exposure of male and female B6C3F1 mice to either 0 or ~1,200 ppm AQ had no significant effect on the incidence of liver or other tumors. After adjusting for study size and duration differences, the NCI liver-tumor data were found to be significantly inconsistent with those later obtained by NTP, implying that liver tumors in B6C3F1 mice are not a reliable basis for characterizing possible cancer risk posed by AQ intake. Consequently, for this endpoint, 14 mg/kg/day is an appropriate POD that conservatively ignores the possibility that human exposure to AQ may tend to reduce net cancer risk.

PS 605 Estimating an Acceptable Daily Intake of Anthraquinone (AQ) in Paper-Packaged Food

P. Sheehan, K. T. Bogen and A. Singhal. *Exponent, Oakland, CA.*

AQ is used in the pulping process in making paper and may be present in finished paper products used for food packaging. IARC recently concluded that AQ was carcinogenic based on NTP chronic dietary AQ bioassay results for B6C3F1 mice and F344/N rats, possibly with a genotoxic mode of action (MOA). This conclusion raised questions about AQ in food packaging in the European Union (EU). Exponent performed a margin of exposure (MOE) evaluation for AQ to estimate derived maximum exposure levels (DMELs) assuming that AQ is a genotoxic carcinogen, and alternatively assuming a scientifically supported nongenotoxic MOA. AQ genotoxicity is questionable because: 1) tests directly comparing purified vs. commercial sources of AQ found genotoxicity was induced only with AQ containing detectable levels of mutagenic contaminants; 2) NCI found no evidence that dietary AQ exposure of male or female B6C3F1 or B6AKF1 mice increased tumor incidence, and the NCI vs. NTP data for B6C3F1 mice are significantly inconsistent; 3) hydroxy-AQ derivatives have long been hypothesized and 1-hydroxy-AQ is known to promote tumorigenesis by PGE2-mediated target-tissue inflammation (a nonlinear MOA). In view of the contradictory NCI and NTP results for mice, a reference point of 14 mg/kg/day was identified for increased tumor risk based on benchmark dose analysis of NTP rat tumor data. Applying EU guidelines for MOE assessments, and assuming AQ is a genotoxic carcinogen with an MOE of 10,000, yields a DMEL of 98 ug/day. Assuming instead, based on the overall weight of evidence indicating that contaminant-free AQ and its in vivo metabolites are probably nongenotoxic at relevant doses, a DMEL value of 9,800 ug/day is derived using an effective MOE value of 100, the safety factor typically applied for a classical toxicity endpoint. More conservatively under this interpretation, a DMEL value of 980 ug/day was derived by applying an effective MOE value of 1,000 to address uncertainty concerning any form of genotoxicity that might dominate an otherwise predominant inflammation-mediated MOA expected for AQ and its metabolites.

PS 606 Updated Dose-Response Assessment and Derivation of Acceptable Drinking Water Levels for O-Phenylphenol

A. Gadoth, V. S. Bhat, C. J. McLellan and A. D. Phelka. *Toxicology Services Dept., NSF International, Ann Arbor, MI.*

The general population may be orally exposed to *o*-phenylphenol (OPP) or its water-soluble sodium salt (SOPP) through industrial applications that result in food and drinking water contact. Both an oral RfD and a cancer slope factor have previously been derived for OPP-induced bladder tumors in male rats, the most sensitive tested species and sex. Lacking from these analyses is a dose-response assessment for bladder hyperplasia, a precursor key event, for consideration as a point-of-departure for a threshold mode of action. In contrast to previous assessments, the key study in the present evaluation was considered the Niho et al. (2002) chronic oral study with SOPP in F344 rats, since it included additional and lower dose levels than other studies in F344 or SD rats that examined bladder lesions, thus potentially increasing confidence in quantitative dose-response modeling. Use of data for the more potent SOPP is supported by limited data suggesting SD rats may be more susceptible to bladder toxicity than F344 rats, the only strain tested chronically. The dose and temporal relationship of the necessary non-cancer precursor key events (cytotoxicity and regenerative hyperplasia) and the lack of DNA-OPP adducts in target tissue *in vivo* support the most plausible mode of action for OPP or SOPP being the ability of the reactive metabolite, phenylbenzoquinone, to react with the urothelium, possibly forming urothelial protein adducts if detoxification pathways become saturated. Benchmark dose modeling suggests only a marginal (1.5x) increased potency of SOPP compared to OPP in F344 rats when high doses associated with sodium ion-induced bladder calculi are excluded. The oral RfD for OPP of 1 mg/kg-day based on a human equivalent benchmark dose ($BMDL_{10}$) of 33 mg/kg-day for bladder hyperplasia corresponds to a total allowable concentration of 7 mg/L in drinking water. A short-term exposure level (STEL) of 20 mg/L was derived based on maternal toxicity in rats, since the weight-of-evidence does not indicate any specific effects on reproduction or development.

PS 607 Mode-of-Action Evaluation and Oral Risk Assessment of Hydroquinone

K. Cox, J. C. English, G. L. Ball and C. J. McLellan. *Toxicology Services Dept., NSF International, Ann Arbor, MI.*

The general population may be exposed to hydroquinone through dietary sources, pharmaceuticals, drinking water, cigarette smoke and metabolism of benzene and phenol. Exposure to hydroquinone may also occur by ingestion of arbutin (hydroquinone-1-*O*-β-D-glucopyranoside), a naturally-occurring conjugate of hydroquinone present in plant-derived foods. A recent oral risk level incorporating current risk assessment methodology and new data was not identified for hydroquinone and thus was the purpose of the present assessment. Due to insufficient quantitative data in humans, hazard identification relies on laboratory animal data. In chronic bioassays, hydroquinone induced atypical tubule hyperplasia and benign neoplasms in the kidneys of male F344/N rats dosed orally either by gavage or diet, and in kidneys of male B6C3F1 mice dosed via the diet. The renal lesions in male F344/N rats occurred only in areas of the kidney with severe or end-stage chronic progressive nephropathy. In female F344/N rats, a dose-related increase in mononuclear cell leukemia was observed; however, the incidences in the exposure groups were within the historical control range. Findings of hepatic adenomas in mice were not consistent between two chronic bioassays; hydroquinone exposure was associated with hepatocellular adenomas in female B6C3F1 mice in one study and in male B6C3F1 mice in another study. No increases in hepatocellular carcinomas were observed in either chronic bioassay. The combined incidence of renal tubule adenoma and atypical tubule hyperplasia observed in the male F344/N rats was selected as the critical effect with a resulting Human Equivalent $BMDL_{10}$ of 3.1 mg/kg-day. The evidence for a prooxidant, cytotoxic mode of action potentiated in male F344 rats by chronic progressive nephropathy supports a threshold. Recognizing the F344 rat as being more susceptible to hydroquinone nephrotoxicity relative to other animal models, an interspecies uncertainty factor (UF) was not applied. Using a 10x UF to account for possible human variability, an oral RfD of 0.3 mg/kg-day was determined for hydroquinone.

PS 608 Derivation of Acceptable Drinking Water Levels for *N*-Nitrosomorpholine That Accommodate Susceptibility during Early Life Stages

J. C. English, V. S. Bhat and C. J. McLellan. *Toxicology Services Dept., NSF International, Ann Arbor, MI.*

N-Nitrosomorpholine (NMOR) is a drinking water contaminant that may be present in source water and as a byproduct of disinfection. Successful methods of remediation have not been identified. The general population can also be exposed to NMOR through tobacco, air, food and consumer and industrial products. The purpose of this assessment was to establish acceptable lifetime drinking water levels for NMOR that account for potential increased susceptibility during early life stages (i.e. birth to 16 years of age). No epidemiology studies that specifically evaluated NMOR were identified, but rubber industry exposure to elevated combined NMOR/*N*-nitrosodimethylamine concentrations in the workplace was associated with increased relative risks for cancer of the esophagus, oral cavity, and pharynx. In laboratory animals NMOR is a multiple-site and species carcinogen. Target tissues following oral exposure include the liver, esophagus, nasal cavity, lung, and kidneys. Hepatocellular tumors were seen in both sexes of NMRI mice, rats of several strains, and Syrian golden hamsters. Dose-response assessment identified the liver in rats as the most sensitive target tissue and species. The weight-of-evidence for a mutagenic mode of action included mutagenicity, clastogenicity, and oxidative DNA damage *in vitro*; *in vivo* evidence for genotoxicity in the liver included the induction of micronuclei, DNA adducts, and unscheduled DNA synthesis. A 10^{-5} cancer risk level was estimated from the human equivalent benchmark dose ($BMDL_{10}$) of 250 μg/kg-day based on the incidence of hepatocellular carcinomas in female F344 rats from a chronic drinking water study in which the exposure commenced at eight weeks of age. After adjusting for potential increased susceptibility from early post-natal life-stage exposure, the drinking water unit risk was 2.9 x 10^{-4} $\mu g/L^{-1}$ corresponding to a total allowable concentration for NMOR of 40 ng/L in drinking water. Contemporary methods permit quantification of nitrosamines in water at less than part-per-trillion levels.

PS 609 Evaluation of Human Health Benchmarks of Four "Possibly" Essential Elements: Arsenic, Boron, Nickel, and Vanadium

S. Goldhaber[1] and A. Gebhart[2]. [1]*SBG Consulting, Inc., Raleigh, NC and* [2]*ToxServices, LLC, Washington, DC.*

Arsenic, boron, nickel, and vanadium are four elements for which data suggest beneficial roles in physiological processes in some species; however the data are incomplete in humans and nutritional levels such as Recommended Dietary Allowances (RDAs) have not been set for any of these elements. Key information for these elements have been evaluated, including their potential essentiality and toxicity, current areas of research, and the basis for the following human health benchmarks: Institute of Medicine's Tolerable Upper Intake Level ; EPA's Reference Dose, Maximum Contaminant Level, or lifetime Health Advisory; Agency for Toxic Substances and Disease Registry's Minimal Risk Level; California EPA's Public Health Goal; International Programme for Chemical Safety's Tolerable Daily or Weekly Intake; and other benchmarks developed by States or private organizations. An analysis of the human health benchmarks shows that the range of human health benchmarks for boron and vanadium are within a 3-fold difference between the highest and lowest benchmarks for boron and within a 6-fold difference for vanadium, while there is a large range between the human health benchmarks for arsenic and nickel (10,000-fold difference for arsenic and 254-fold for nickel). A comparison between the human health benchmarks and the average adult intake of the elements in the U.S. revealed that for boron, vanadium, and nickel, all of the benchmarks exceed the mean adult intake by 4- to 150-fold, while for arsenic, the mean adult intake exceeds two of the human health benchmarks by 100- to 1000-fold. An analysis of the reasons for the large spread between the human health benchmarks for arsenic is also presented in this work.

PS 610 24-Hour Air Monitoring Comparison Value for Hexavalent Chromium

N. K. Erraguntla and J. T. Haney. *Toxicology, Texas Commission on Environmental Quality, Austin, TX.*

The Texas Commission on Environmental Quality (TCEQ) has an extensive ambient air monitoring network that collects air toxics data, including fifteen metals (e.g., Cr) in particulate matter with an aerodynamic diameter of 10 or 2.5 microns or less (PM_{10}, $PM_{2.5}$). Metal samples are collected on 24-hour PM filters every sixth day. Historically, the TCEQ has only evaluated 24-hour data in terms of comparisons of the resulting annual averages to chemical-specific chronic Air Monitoring Comparison Values (AMCVs) to evaluate the potential for chronic health and welfare (vegetation) concerns. That is, 24-hour data were typically not evaluated from a short-term/acute perspective. However, the development of a 24-hour, health-protective AMCV for hexavalent chromium (CrVI) would allow the TCEQ to more fully utilize 24-hour data for the evaluation of potential short-term public health concerns, and is also more consistent with the intermediate exposure duration studies available in the CrVI toxicological database. Consequently, the TCEQ has developed a conservative 24-hour AMCV based on Glaser et al. (1990) study in which 8-week old male Wistar rats (30 animals/group) were exposed 22 hours/day, 7 days/week to sodium dichromate aerosol concentrations ranging from 50 to 400 μg CrVI/m^3. The increase in mean lung weight was greater than the ten percent in organ weight commonly used to define adversity in regulatory chemical assessments and was identified as the critical effect. The data on increase in mean lung weight was benchmark dose modeled since there was a clear dose-response and the increase was statistically significant in the exposure groups when compared to the controls. Additionally, animal-to-human dosimetric adjustments were also performed using the Multiple-Path Particle Dosimetry Model (MPPD v 2.11) prior to dividing the point of departure by appropriate uncertainty factors. The proposed 24-hour AMCV of 1.3 μg CrVI/m^3 will allow the TCEQ to more fully evaluate available monitoring data and is considered sufficiently health-protective of not only 24-hour exposure, but also short-term intermittent exposures.

PS 611 Health-Protective Manganese Guideline for Welding and Other Occupations

L. A. Bailey[1], L. E. Kerper[2] and B. D. Beck[2]. [1]*Gradient, Middlebury, VT and* [2]*Gradient, Cambridge, MA.*

Since manganese (Mn) particles from welding fumes are much smaller than from other Mn exposures, there is some concern that they may be absorbed more readily in the lung or travel more directly to the brain *via* the olfactory nerve. Therefore, we evaluated whether exposure guidelines considered health-protective for other Mn occupational exposures are also health-protective for welders. We critically analyzed occupational epidemiology literature associated with Mn exposures during smelting, mining, or in the production or use of Mn alloys, and from exposure to Mn in welding fumes to determine exposure-response relationships for neurological effects; welding studies were considered separately from other occupations. Given the uncertainty in Mn exposure concentrations in many of the welding studies, we also conducted a weight-of-evidence (WoE) analysis that integrated the epidemiology data with studies on Mn levels in the brains of welders (*via* pallidal index or "PI" estimated from magnetic resonance imaging or "MRI"), Mn brain concentrations and PI in monkeys, and corresponding neurological effects in monkeys at given brain concentrations, with the goal of predicting correlations between Mn exposure concentrations and neurological effects in welders. Overall, through integration of epidemiology, monkey, and toxicokinetic data, our preliminary WoE analysis suggests that predicted brain concentrations in welders at Mn exposure concentrations of 100-200 μg/m^3 are not likely to lead to more than a very small (10%) increased risk of slight to mild (subclinical) neuromotor effects; therefore, a Mn occupational exposure level of 100-200 μg/m^3 is protective for welding exposures. Our results are in contrast to the recently adopted American Conference of Industrial Hygienists (ACGIH) 8-hour time-weighted average threshold limit value (TLV-TWA) for respirable particulate Mn of 20 μg/m^3. A more statistically robust approach for derivation of the TLV (*i.e.*, benchmark dose) would be more consistent with the current standard of risk assessment practice, and would result in a TLV approximately 5- to 10-fold higher.

PS 612 Comparison of Inhalation Occupational Exposure Limits (OELs) and European Worker's Inhalation Derived No Effect Levels (DNELs) for Inorganic and Insoluble Metals

M. Jackson[1], C. J. Inhof[1], L. Fell[1] and R. Lemus[2]. [1]*ARCADIS US Inc., Brighton, MI and* [2]*ATL, Cincinnati, OH.*

The European Chemical Agency (ECHA) previously released manufacturer/importer REACH (Registration, Evaluation, Authorization and Restriction of Chemicals) chemical registration files, making available the Derived No Effect Levels (DNELs) for hundreds of substances. The DNEL is defined as "the level of exposure above which humans should not be exposed" and needs to reflect the likely route(s), duration and frequency of exposure. Specifically, worker DNELs are levels intended to protect workers during manufacture. Typically, DNELs are developed by Industry using ECHA's guidance; the registrant has the final decision on the selection of the key studies, endpoints of concern, and the assessment factors to account for sources of uncertainty. By comparison, currently accepted occupational exposure limits (OELs), such as permissible exposure limits (PELs) or threshold limit values (TLVs) developed by the Occupational Safety and Health Administration (OSHA) and the American Conference of Industrial Hygienists (ACGIH), respectively, may have been derived using different methods, some of which incorporate economic and technical feasibility concerns and/or health-based assessment. In addition, these other occupational values may have been based on different toxicological data and endpoints. Because the worker DNELs may potentially be used as guideline levels for worker exposures in Europe and have the potential to become de facto OELs in other regions due to the global extent of REACH, a comparison analysis between the long-term inhalation DNELs for the worker population and OELs developed within Europe and by OSHA and ACGIH was completed for eighteen common inorganic and insoluble metals (in powder form). This analysis showed that in most cases the long-term inhalation worker DNELs for metals that were used for comparison were equivalent to or lower than the accepted OELs.

PS 613 Principles and Practices of the Workplace Environmental Exposure Level (WEEL) Development for Chemicals: An Initiative of the Occupational Alliance for Risk Science (OARS)

T. A. Kimmel[1], T. A. Lewandowski[2], S. Barnett Bucherl[3], A. Havics[3] and A. Maier[4]. [1]*SafeBridge Consultants, Inc., New York, NY,* [2]*Gradient Corporation, Seattle, WA,* [3]*pH2, LLC, Avon, IN and* [4]*College of Medicine, University of Cincinnati, Cincinnati, OH.*

Although there are thousands of chemicals in use in the US, there are only several hundred Occupational Exposure Limits (OELs) for these chemicals. Many chemicals have sufficient toxicological data to generate OELs. However, there is still a limited pool of experts to evaluate the data and create a consensus-based OEL. One such mechanism is the approach used by the Workplace Environmental Exposure Level (WEEL) committee under the Occupational Alliance for Risk Science (OARS), a collaborative initiative managed by the not-for-profit Toxicology Excellence for Risk Assessment (TERA). The goal of this arrangement is to promote worker health through increased access to high quality OELs, enhancements in methods for establishing worker-health exposure guidelines, and education and training in occupational risk assessment methods. The OARS-WEEL Committee is

a volunteer group of toxicologists and industrial hygienists from academic, governmental, corporate, and consulting backgrounds, who create health-based guideline values for chemical agents, called WEELs. WEELs are limits that represent "safe" [or "relatively safe"] air concentrations that will protect most workers from adverse health effects related to occupational chemical exposures over a lifetime. They can be used across industries as a central tool for worker health protection. OARS promotes the development of WEELs by encouraging stakeholder engagement. This is achieved through open and transparent processes, invitation of stakeholders to attend science deliberations, free online access to WEELs and associated documentation, and active outreach, while using a scientifically-based methodological approach to evaluate the toxicological data including the application of appropriate safety & uncertainty factors. The WEEL development process will be explained using a selected WEEL as an example.

PS 614 Derivation of a Human Equivalent Concentration for Diacetyl for Hyperplasia of the Bronchiolar Epithelium

R. Adams[1], M. Glynn[1], J. S. Pierce[1] and B. L. Finley[2]. [1]*Cardno ChemRisk, Chicago, IL and* [2]*Cardno ChemRisk, Brooklyn, NY.*

Severe respiratory disorders, including bronchiolitis obliterans (BO), have been alleged in some cases in which workers and consumers were exposed to diacetyl in microwave popcorn and other products. Recently, results have become available from an unpublished study conducted by the National Toxicology Program in which rodents were exposed to diacetyl for 6 hours per day, 5 days per week for 13 to 14 weeks. Using these data, we performed a BMC analysis to estimate the diacetyl concentration associated with a 10% excess risk (BMC_{10}) of hyperplasia of the bronchiolar epithelium and a 95% lower confidence bound concentration estimate ($BMCL_{10}$). The endpoint of interest was chosen because it occurs in the deep lung and is expected to occur at concentrations below that of BO in humans. Modeling was performed using EPA guidelines, BMDS software, and the available range of dose-response models for a dichotomous outcome. The estimated $BMCL_{10}$ values were adjusted to human equivalent concentrations (HECs) using the following procedure: 1) the computed $BMCL_{10s}$ were converted to an equivalent exposure of 8 hours per day, 2) a scrubbing factor was applied using the computational fluid dynamics model developed for diacetyl for rodents and humans, and 3) a regional gas dose ratio (RGDR) was calculated and applied using EPA methods. Based on our analysis, the BMC_{10} ranged from 39.7 ppm to 92.9 ppm, and the $BMCL_{10}$ ranged from 31.9 ppm to 60.4 ppm over all models; the HECs were estimated to range from 15.9 ppm to 30.1 ppm. The results of our analysis were consistent with those reported by Maier et al. (2010), who calculated an HEC of 1.8 ppm for an endpoint of interest in the upper airways (minimal to mild peribronchial lymphocytic inflammation). Our range of HECs is based on a sensitive endpoint and newly-available data, and should be considered when evaluating the risk of developing BO and other serious respiratory diseases following diacetyl exposure.

PS 615 Critical Evaluation of EPA's Toxicological Assessment of Benzo(a)pyrene

B. Magee. *ESAP, ARCADIS, Chelmsford, MA.*

EPA's draft toxicological assessment of Benzo(a)pyrene (BaP) was released for public review with comments accepted until November 2013. The document proposed a new Oral Slope Factor of 1.0 (mg/kg-day)-1. EPA also presented four new values not currently on IRIS: Inhalation Unit Risk (0.0005 (μg/m3)-1), oral Reference Dose (0.0003 mg/kg-day), inhalation Reference Concentration (0.000002 mg/m3), and a first ever Dermal Slope Factor (DSF) (0.005 (μg/day)-1). These toxicity factors for BaP have far reaching implications because BaP is the indicator PAH and will be used to assess the risks posed by the additional 25 proposed potentially carcinogenic PAHs. The converted DSF is 350 (mg/kg-day)-1, which makes ingestion exposure moot. This talk provides a critical review of the derivation of the 5 toxicity factors. The DSF is scientifically inappropriate because it presumes that mouse skin is predictive of human skin, but ignores the large epidemiological literature on coal tar pharmaceutical users, which shows that highly exposed humans do not contract skin cancer. The DSF is also based old, poor studies in which BaP dosimetry was not carefully quantified. More importantly, several studies were ignored without cause and of the dozen studies that were considered, the two studies that were documented to have exceeded the Maximally Tolerated Dose were chosen as the basis of the DSF. The dose-response modeling was also flawed in that it (a) averaged doses over a longer period that the animals' lifespan, (b) ignored the documented depot effect for repeated skin doses of BaP, (c) used selected models, and (d) ignored EPA's own guidance on assessing model fit. The other toxicity values are similarly critiqued. Finally, the implications are discussed. For instance, if the proposals are adopted, the ingestion pathway for cancer risk assessment will be insignificant and dermal risks will dominate. The Regional Screening Level will drop to 1 part-per-billion, and it will be predicted that 30% of all skin cancer in the US will have been caused by exposure to PAHs in soil.

PS 616 Benzo(a)pyrene Cancer Toxicity Criteria Updates: Implications for Human Health Risk

T. Behrsing, K. Gettmann, E. Sciullo and M. Wade. *Dept. Toxic Substances Control, CalEPA, Sacramento, CA.*

Polycyclic aromatic hydrocarbons (PAHs) from natural and anthropogenic sources are common contaminants at CA sites. To assess risk from carcinogenic PAHs (cPAHs) other than naphthalene, cPAHs can be converted to benzo(a) pyrene-equivalents (BaP-EQ) using Potency Equivalency Factors (PEFs). The total BaP-EQ concentration is used to calculate risk and can be compared to ambient PAH levels. In recent years newer BaP cancer toxicity criteria have been developed or proposed, and early life exposure adjustments have been incorporated. In 2010, CalEPA derived an oral cancer slope factor (CSFo) of 1.7 (mg/kg-day)-1 [2.9 with Age-Sensitivity Factors], which is less than the 1993 CSFo of 12 (mg/kg-day)-1. In 2013, USEPA released a Public Comment Draft CSFo of 1 (mg/kg-day)-1, inhalation unit risk (IUR) of 5E-4 (μg/m3)-1, and dermal slope factor (SF) of 0.005 (μg/day)-1. The draft CSFo is 7-fold lower than USEPA's current criterion, and derivation of a dermal SF is unique. Use of updated criteria and early life adjustments has implications for risk as shown for Site A with 1.8 mg/kg BaP in soil. Using CalEPA's 1993 CSFo and no early life adjustments, residential risk was 4.7E-5. Using the 2010 CSFo and 2013 draft CSFo and IUR with age dependent adjustment factors (ADAFs), risks are reduced to 2.8E-5 and 1.7E-5. Industrial risk using the 1993 CSFo was 1.4E-5. Risks using the 2010 CSFo and 2013 draft CSFo and IUR are 2E-6 and 1.1E-6. Impacts of the newer criteria are greater for industrial risk because ADAFs are not used. Industrial soil risk-based levels using the 2010 CSFo and 2013 draft CSFo and IUR with standard assumptions are 0.9 and 1.5 mg/kg. These values approach or exceed upper bound ambient PAH levels often considered in remedial decisions. However, direct dermal contact risk using the draft dermal SF may impact risks conversely and methods to evaluate this exposure route are needed. Potential impacts of revised BaP criteria on PEFs must also be considered. Given the prevalence of cPAHs at CA sites, issues related to BaP toxicity criteria updates require consideration and evaluation.

PS 617 Assessment of the Developmental Effects of N-Methylpyrrolidone (NMP) in Rats Using PBPK-Derived Internal Dose Measures and Benchmark Dose Methods

R. J. Parod[1], D. E. Rodwell[2] and C. R. Kirman[3]. [1]*BASF Corporation, Wyandotte, MI,* [2]*Rodwell & Associates, El Paso, TX and* [3]*Summit Toxicology LLP, Orange, OH.*

The developmental effects of NMP are well studied in rats following oral, inhalation, and dermal routes of exposure. A hazard identification and dose-response assessment was conducted. Based on consideration of the dose-response range covered, on the inclusion of late-gestational exposures, and on consistency with current test guidelines, the oral and inhalation studies were considered to be more robust than the dermal study. Fetal body weight changes in rats are considered to be the most sensitive endpoint for NMP. However, this effect appears to be reversible, and because it reflects a cumulative response, is not expected to result from acute (1-day) exposures. Because other developmental endpoints (e.g., delayed ossification) were highly variable and occurred only at higher internal doses, these effects were considered secondary to fetal body weight changes and an inappropriate endpoint for risk assessment. Instead, two developmental endpoints were identified as suitable for human health risk assessment: (1) for acute exposures, the increased incidence of skeletal malformations, an effect noted only at doses that were toxic to the dam and fetus, was assessed using the maximum daily AUC (as estimated using a PBPK model); and (2) for repeated exposures to NMP, changes in fetal body weight were assessed using cumulative AUC. Benchmark dose methods were used to estimate a point of departure for skeletal malformations (BMDL05) and fetal body weight changes (BMDLSD). Where possible, data from multiple studies were pooled to increase the predictive power of the data set. BMDL05 values for skeletal malformations ranged from approximately 1200-1500 mg/L*hr (in terms of maximum daily AUC). Similarly, BMDLSD values for fetal body weight changes ranged from approximately 270-710 mg/L*hr (in terms of cumulative AUC). These BMD values can be used to support margin-of-exposure analyses for human health risk assessments of NMP conducted in terms of internal dose.

PS 618 Derivation of a No-Significant-Risk-Level (NSRL) for Cocamide Diethanolamine (DEA)

Z. Guerrette[1], B. Wang[2], J. Fleischer[2] and M. H. Whittaker[2]. [1]*ToxServices LLC, Ann Arbor, MI and* [2]*ToxServices LLC, Washington, DC.*

Cocamide diethanolamine (DEA) has been listed on the State of California's Proposition 65 List as a chemical known to the State to cause cancer. This listing is based on the results of a National Toxicology Program (NTP) 2-year dermal carcinogenicity study which found clear evidence of carcinogenic activity in B6C3F1 mice based on increased incidences of liver neoplasms in both sexes, and increased incidences of renal tubule neoplasms in males. Although controversy exists regarding the relevance of the NTP study to humans, industries are obligated to comply with the Proposition 65 labeling requirement and drinking water discharge prohibition, unless they are able to demonstrate that cocamide DEA levels in their products are below a specific No Significant Risk Level (NSRL). The State of California has not published a NSRL for cocamide DEA. In accordance with the guidelines of California EPA, ToxServices derived a NSRL of 13.3 μg/day for cocamide DEA based on the incidence of hepatocellular carcinoma or hepatoblastoma in female mice obtained from the NTP carcinogenicity study using benchmark dose modeling. The U.S. EPA's Benchmark Dose Software (BMDS) was used to model the cancer slope factors for the combined incidence of hepatic neoplasms. These slope factors were scaled to human equivalent doses and used to determine the lifetime average daily dose that would result in one excess cancer case in an exposed human population of 100,000. This NSRL value can be used as part of an exposure and safety assessment to evaluate compliance with Proposition 65 requirements for products sold in the State of California.

PS 619 Derivation and Application of a No-Significant-Risk-Level (NSRL) for Diethanolamine (DEA)

B. Wang, D. E. Amacher and M. H. Whittaker. *ToxServices LLC, Washington, DC.*

Diethanolamine (DEA) has been listed on the State of California's Proposition 65 List. This listing is based in part on tumors reported in a National Toxicology Program (NTP) 2-year dermal carcinogenicity study in mice which found clear evidence of carcinogenic activity in B6C3F1 mice based on increased incidences of liver neoplasms in both sexes, and increased incidences of renal tubule neoplasms in males. Although considerable controversy exists on the relevance of the NTP study to humans, industries are obligated to comply with the Proposition 65 labeling requirement and drinking water discharge prohibition, unless they are able to demonstrate that DEA levels in their products are below a specific No Significant Risk Level (NSRL). The State of California has not published an NSRL for DEA. ToxServices derived a NSRL of 5.6 μg/day and a life-stage-adjusted $NSRL_{adj}$ of 1.4 μg/day from the NTP carcinogenicity study using benchmark dose modeling based on the incidence of hepatocellular carcinoma in female mice, in accordance with the guidelines of California EPA. Subsequently, we performed exposure assessments for DEA on several personal care products and demonstrated that exposure to DEA through the intended use of most of these products does not exceed the established NSRL.

PS 620 Derivation of No Significant Risk Levels for Titanium Dioxide

J. Fleischer, B. Wang and M. H. Whittaker. *ToxServices LLC, Washington, DC.*

Titanium dioxide (TiO2) is widely used as a colorant in consumer products. Recently, TiO2 was listed by the State of California on the list of chemicals known to the state to cause cancer or reproductive toxicity (i.e., Proposition 65), due to its classification by the International Agency for Research on Cancer (IARC) as a Group 2B possible human carcinogen. Products containing Proposition 65 substances are subject to labeling requirements, unless exposure is below California's "safe harbor" level. For potential carcinogens, the safe harbor level is termed the No Significant Risk Level (NSRL). As no NSRL for TiO2 has been established by California, we derived a NSRL according to CalEPA guidelines.
We performed benchmark dose (BMD) modeling on combined lung tumor incidence data from 3 published long-term, inhalation-route rat studies. BMD modeling was based on TiO2 particle deposition in the lung, expressed as particle surface area per gram of lung tissue. The surface area metric resulted in best fit of the data and normalized strain-specific anatomic differences and differences in exposure duration across studies. This approach also accounted for the impact of different particle sizes (which have different surface areas). When extrapolating modeled animal doses to human doses, a particle dosimetry model was used to account for particle size distribution, respiration pattern, and deposition and clearance mechanisms specific to humans. Using this approach, separate NSRLs were calculated for TiO2 particles with different surface areas. For fine TiO2 particles (1-2.5 μm), the NSRLs is 27 μg/day, and for ultrafine particles (< 0.1 μm) the NSRL is 2.8 μg/day. The derivation of two NSRLs is consistent with observations in animal inhalation studies that indicate that TiO2 toxicity is particle size-dependent. Although route-specific safe harbor levels exist for other chemicals, this is the first instance of particle size-specific Proposition 65 NSRLs and thus represents a novel, toxicologically-driven approach to safe harbor determination.

PS 621 Derivation of an Intravenous Permitted Daily Exposure Value for Bisphenol A

J. W. Card, H. Fikree and L. A. Haighton. *Intertek Cantox, Mississauga, ON, Canada.*

Bisphenol A (BPA) is an industrial chemical widely used in the production of polycarbonate plastics and epoxy resins. A recent concern with BPA is its endocrine-disrupting potential, an effect attributed to free (*i.e.,* unconjugated) but not metabolized (*i.e.*, conjugated) BPA. Human exposure to BPA is primarily *via* the diet, which results in extensive gut and liver metabolism to biologically-inactive BPA. To address concerns about systemic exposure to free BPA as a leachable from implanted medical devices or intravenous (IV) drug products, work was undertaken to derive an IV permitted daily exposure (PDE) value for BPA. Oral exposure limits for BPA were adjusted for route-specific pharmacokinetics. Recently, EFSA reaffirmed an oral tolerable daily intake (TDI) for BPA of 50 μg/kg/day applicable to all age groups and sensitive populations. Data from monkeys given low oral and IV doses of deuterated BPA (100 μg/kg) suggest only 1.9 and 0.94% of an oral dose is systemically available as free BPA in neonates and adults, respectively. To be conservative, the lower value of 0.94% was assumed for all age groups. Thus, at the oral TDI, the amount of free BPA systemically available would be 0.47 μg/kg/day [calculated as: 50 μg/kg/day X (0.94/100)]. This can be considered the IV PDE value, and is equivalent to 6.5 μg/day for children ≥2 years of age (≥13.8 kg) and 23.5 μg/day for adults (≥50 kg). The IV PDE value for BPA is considered suitable because: i) it is based on an established oral exposure limit; ii) it takes into account route-to-route extrapolation based on a well-conducted study in neonatal and adult monkeys, with monkeys being the most suitable species (next to humans) with which to model BPA pharmacokinetics; and iii) there is no information to suggest that metabolism or renal excretion of BPA differs in subjects as young as 2 years of age compared with that in adults. For risk assessment comparative purposes, the reverse relationship can be used to calculate equivalent oral doses from toxicology studies that bypass the gut (*e.g.*, studies that use subcutaneously-implanted pumps).

PS 622 Development of an Oral Cancer Slope Factor and Lifetime Average Daily Dose Estimates for TBBPA

D. Wikoff[1], C. M. Thompson[2], C. S. Perry[1], M. White[1], L. M. Fitzgerald[1], S. Borghoff[3] and L. C. Haws[1]. [1]*ToxStrategies, Austin, TX,* [2]*ToxStrategies, Houston, TX and* [3]*ToxStrategies, Cary, NC.*

Tetrabromobisphenol A (TBBPA) is an important flame retardant used primarily as a reactive chemical in the synthesis of printed circuit boards. In this application, it is incorporated into the epoxy and serves a vital role in fire safety. The National Toxicology Program (NTP) recently completed a 2-year bioassay for TBBPA. The objective of this present study was to develop an oral cancer slope factor (OSF) and compare the corresponding risk specific dose (RSD) to appropriate exposure estimates. Of the two potentially treatment-related tumor types observed in the NTP study (uterine tumors in female rats-clear evidence; hepatoblastomas in male mice-some evidence), only the uterine tumors were considered for development of a cancer-based toxicity value due to a number of issues with the hepatoblastoma data (e.g., findings not significant when combined with hepatocellular adenomas and/or carcinomas; data from high dose group not considered in NTP analysis). Using benchmark dose (BMD) modeling, a 95% lower confidence limit (BMDL) was derived with a default linear multistage model with a benchmark response set to 10% extra risk. The resulting OSF was 0.0032 $(mg/kg\text{-}day)^{-1}$, which is equivalent to a RSD of 0.00031 and 0.0031 mg/kg-day at 10^{-6} and 10^{-5} risk levels, respectively. This OSF is highly conservative given that TBBPA is non-mutagenic and that tumors are likely occurring via a threshold-based response. However, additional data are required to characterize key events associated with the underlying mode of action in order to support nonlinear assessment of the cancer data. Nonetheless, the lifetime average daily dose estimates for TBBPA (based on exposures to TBBPA in breastmilk, soil/dust, water, and diet from birth through adulthood) ranged from 0.00000022 to 0.0000039 mg/kg-day for central tendency and upper-bound regulatory scenario estimates, respectively. These data indicate that there is a sufficiently large margin of safety between highly conservative cancer-based RSDs and current exposure to TBBPA.

PS 623 Development of Noncancer-Based Toxicity Factors and Daily Dose Estimates for TBBPA

L. C. Haws[1], C. M. Thompson[2], C. S. Perry[1], M. White[1], L. M. Fitzgerald[1], S. Borghoff[3] and D. Wikoff[1]. [1]*ToxStrategies, Austin, TX,* [2]*ToxStrategies, Houston, TX and* [3]*ToxStrategies, Cary, NC.*

Tetrabromobisphenol A (TBBPA) is an important flame retardant used primarily as a reactive chemical in the synthesis of printed circuit boards. In this application, it is incorporated into the epoxy and serves a vital role in fire safety. Despite its use primarily as a reactant with limited release to the environment, some concerns have been raised regarding exposure. The objective of this study was to develop non-cancer based toxicity values (reference doses, or RfDs) and to compare such to appropriate estimates of human exposure. An array of potential RfDs was developed using data reported as part of a recent 2-year bioassay conducted by the National Toxicology Program (NTP); these data indicated that chronic exposure to TBBPA induced hepatic and kidney lesions in male mice, and forestomach lesions in male and female mice. In rats, notable lesions included uterine hyperplasia and rete overii cysts at study termination, as well as decreased serum thyroxin levels after 13 weeks of exposure. These endpoints were modeled using benchmark dose (BMD) modeling; the 95% lower confidence interval values (BMDLs) were derived with a benchmark response set to 10% extra risk for dichotomous endpoints and one standard deviation for continuous endpoints. BMDL values were adjusted by allometric scaling and subsequently reduced by uncertainty factors to derive RfD values ranging from 0.03 to 3.0 mg/kg-day. In comparison, exposure estimates ranged from 0.0000003 to 0.00007 mg/kg-day based on an evaluation of exposures for infants (based on intakes due to breastmilk and soil/dust), and for children, adolescents, and adults (based on intakes due to diet, drinking water, and soil/dust ingestion). The total daily exposure estimates were generally driven by soil/dust ingestion for most receptors (and by breastmilk for infants) in reasonable maximum and upper-end regulatory default exposure scenarios. These data indicate that there is a sufficiently large margin of safety between potential RfD values and current exposure to TBBPA.

PS 624 Provisional Advisory Level (PAL) Development for Ricin

C. S. Wood[1], D. R. Mattie[2], C. Baird[3], G. M. Henningsen[4] and F. Adeshina[5]. [1]*Oak Ridge National Lab, Oak Ridge, TN,* [2]*711 HPW/RHDJ, Air Force Research Laboratory, WPAFB, OH,* [3]*USA Public Health Command, US Army, Aberdeen Proving Ground, MD,* [4]*Front Range Environmental Toxicology Services, Monument, CO and* [5]*US EPA, Washington, DC.*

PAL values developed for hazardous materials by the US EPA represent general public emergency exposure limits for oral and inhalation exposures corresponding to three different severity levels (1, 2, and 3) for 24-hr, 30-d, 90-d, and 2-yr durations. PAL 1 represents the threshold for mild effects; PAL 2 represents the threshold for serious, irreversible or escape-impairing effects; PAL 3 represents the threshold for lethal effects. PALs have not been promulgated nor have they been formally issued as regulatory guidance. They are intended to be used at the discretion of risk managers in emergency situations when site specific risk assessments are not available. PALs are developed using standard protocols based on the SOP.
Ricin is a protein found in castor beans making up 1-5% of the bean by weight. The protein is a cellular toxin which binds ribosomes inhibiting cellular protein synthesis at the portal of entry such that systemic toxicity is not a consequence of exposure by any route. Toxicity after exposure to ricin is delayed 8-24 hours due to the time required for ricin protein transport to the ribosomes. Ricin is much more toxic by inhalation exposure than by the oral route. Respiratory tract inflammation, edema and necrosis have been observed across multiple species. Following intratracheal ricin dosing of rats, effects on the respiratory tract were similar to inhalation exposure dosing studies. PAL estimates were based on adverse effects occurring in rats and mice after oral, inhalation and intratracheal ricin dosing. The oral PAL 1 value is 2.4 mg/L for 24-hr and 30-d; oral PAL 2 and 3 values are 11 and 14 mg/L, respectively, for 24 hrs. Inhalation PAL 2 and 3 values are 0.0000047 and 0.000014 mg/m3, respectively, for 24 hrs. All remaining PAL values are presently NR (not recommended) due to insufficient data. These PALs are the first guidelines proposed for ricin.

PS 625 Provisional Advisory Level (PAL) Development for 4-Aminopyridine

C. Bast[1], P. M. McGinnis[2], M. McClanahan[3] and F. Adeshina[4]. [1]*Oak Ridge National Laboratory, Oak Ridge, TN,* [2]*RG York & Associates, Syracuse, NY,* [3]*US Centers for Disease Control and Prevention, Retired, Lilburn, GA and* [4]*U.S. EPA, Washington, DC.*

PAL values developed for hazardous materials by the US EPA represent general public emergency exposure limits for oral and inhalation exposures corresponding to three different severity levels (1, 2, and 3) for 24-hr, 30-d, 90-d, and 2-yr durations. PAL 1 represents the threshold for mild effects; PAL 2 represents the threshold for serious, irreversible or escape-impairing effects; PAL 3 represents the threshold for lethal effects. PALs have not been promulgated nor have they been formally issued as regulatory guidance. They are intended to be used at the discretion of risk managers in emergency situations when site specific risk assessments are not available. Application of PAL protocols has been performed for 4-aminopyridine to estimate oral exposure limits; inhalation PAL values are not recommended (NR) due to insufficient data. 4-Aminopyridine blocks voltage-sensitive potassium channels in nerves by binding to sites within the channels. PAL values for 4-aminopyridine are based on clinical nervous system effects in humans using the SOP and QAPP requirements. The mention of trade names does not imply EPA endorsement.
4-Aminopyridine oral PAL 1 values are 0.25 mg/L for 24-hr, and 30-d, 90-d and 2-yr.
4-Aminopyridine oral PAL 2 values are 1.0 mg/L for 24-hr, and 30-d, 90-d and 2-yr.
4-Aminopyridine oral PAL 3 values are 1.5 mg/L for 24-hr, and 30-d, 90-d and 2-yr.

PS 626 Provisional Advisory Level (PAL) Development for Chlorine Gas

S. Milanez[1], L. D. Koller[2], D. C. Dorman[3], C. Baird[4] and F. Adeshina[5]. [1]*Oak Ridge National Laboratory, Oak Ridge, TN,* [2]*Environmental Health and Toxicology, Corvallis, OR,* [3]*North Carolina State University College of Veterinary Medicine, Raleigh, NC,* [4]*US Army, Aberdeen Proving Ground, MD and* [5]*US EPA, Washington, DC.*

PAL values developed for hazardous materials by the US EPA represent general public emergency exposure limits for oral and inhalation exposures corresponding to three different severity levels (1, 2, and 3) for 24-hour, 30-day, 90-day, and 2-year durations. PAL 1 represents the threshold for mild effects; PAL 2 represents the threshold for serious, irreversible or escape-impairing effects; PAL 3 represents the threshold for lethal effects. PALs have not been promulgated nor have they been formally issued as regulatory guidance, but are intended for use at the discretion of risk managers in emergency situations when site-specific risk assessments are not available. PALs are developed with appropriate human and animal data, using standard protocols based on the SOP and QAPP requirements.
Chlorine is a greenish-yellow gas with a pungent odor, a strong oxidizing agent, and very reactive. Large amounts are made worldwide, primarily for use in making PVC plastics, but also insecticides, pesticides, and bleaches. It has been used as a chemical warfare agent. Chlorine gas is a contact irritant, and in both humans and animals, the respiratory tract is the primary target for toxicity. Effects include sensory irritation, increased airway resistance, and lesions in the lungs and other organs. Death follows quickly at high concentrations. PALs were derived using controlled studies with monkeys, rats, mice, and humans. The resulting inhalation PAL 1, PAL 2, and PAL 3 values, respectively, for a 24-hour exposure are 0.096, 0.19, and 5.1 ppm; for a 30-day exposure are 0.018, 0.11, and 0.32 ppm; and for a 90-day exposure are 0.0036, 0.036, and 0.32 ppm. For a 2-year exposure, the PAL 1 and PAL 2 are 0.0036 and 0.036 ppm, respectively; a 2-year PAL 3 was not developed due to insufficient data. Oral PAL values were not developed. The PAL values were approved by the Expert Consultation Panel for PALs in April 2013.

PS 627 Development of Exposure Guidelines for Chronic Health Effects following Acute Exposures to TICs

D. Winkel[1], B. Hawkins[1], J. Jackson[1] and L. E. Roszell[2]. [1]*Battelle Memorial Institute, Columbus, OH and* [2]*US Army Public Health Command, APG, MD.*

Joint Chemical, Biological, Radiological, and Nuclear doctrine requires military commanders to minimize total risk in operational planning and execution. Incorporation of Military Exposure Guidelines (MEGs) into risk estimates can provide a mechanism to consider short- and long-term chemical exposure risks. However, current MEGs (and civilian guidelines) do not address chronic non-cancer health effects that may result from a single acute exposure. This gap is a source of concern for planners in the medical community, as these effects may have im-

plications for long-term protection of exposed military or civilian populations. Challenges in establishing this type of guideline are small sample sizes, difficulties or inconsistencies in identifying long-term effects, and uncertainty in exposure concentration and duration. Given these challenges, the current investigation describes an approach to develop such guidelines, using chlorine as an exemplar chemical. Chlorine was selected due to its use in attacks with improvised explosive devices, its significant presence in industry/transport, and the prevalence of cases reported in the literature. Reports from accidental chlorine exposures were reviewed and data on exposure concentration, duration, and long term health outcomes were compiled. These health outcomes ranged from the presence of physical symptoms (e.g., shortness of breath) to abnormal pulmonary function test results. Binomial distributions were used to address issues with a small sample population and uniform distributions were used to address incomplete exposure terms. This approach was applied to all data presently identified and a probit analysis was used to generate a probit curve capturing the dose-response of long term health effects due to acute exposure to chlorine. The curve compares favorably to existing guidelines (both military and civilian) in that only severe exposures have the potential to cause chronic health effects. This approach is believed to be novel and may be applicable to other TICs with a limited data set.

PS 628 Smoothing Regression Splines As the Basis for Dose-Response Modeling

G. Hixon[2], C. M. Thompson[1], L. Abraham[1] and A. Bichteler[2]. [1]*ToxStrategies, Katy, TX and* [2]*ToxStrategies, Austin, TX.*

In its current state, dose-response modeling employs analytical methods that include numerous candidate mathematical functions from which the analyst must choose in order to develop toxicity values such as reference doses and cancer slope factors. Smoothing regression splines offer a much simpler approach to dose-response modeling and have a number of desirable properties. They are flexible, require no pre-specification of a functional form, achieve optimal fit under a wide range of circumstances, and need little-to-no intervention by the analyst. In addition, the same smoothing regression splines can be used to unambiguously identify various types of points of departure (e.g. threshold and benchmark doses), as well as address important questions about a dose-response curve such as its overall non-linearity and non-linearity within specific regions. We compared more traditional modeling approaches with smoothing splines to illustrate how the latter provide a unified mathematical framework for estimating dose-response functions and critical quantities and often provide superior performance. For example, we compared threshold doses estimated via smoothing regression splines with other published bilinear models. Although smoothing regression splines regularly provide similar results to older approaches, when differences emerge the smoothing spline results are often clearly superior. They are more faithful to the underlying data as indexed by their solutions tracking more closely to the key visual characteristics of the plotted data, and they frequently offer narrower confidence intervals. Finally, we introduce an R package that facilitates the use of smoothing regression splines for dose-response modeling.

PS 629 Is Nonparametric Method Suitable for Benchmark Dose Analysis Using Typically Available Toxicity Study Data?

K. Shao. *NCEA, U.S. Environmental Protection Agency, Research Triangle Park, NC.*

Model uncertainty is one important problem associated with benchmark dose (BMD) analysis and has gained much attention in recent development of BMD methodology. In addition to the model averaging approach, which produces one weight-averaged BMD/BMDL estimate according to the posterior model weights, nonparametric method has been proposed as another alternative to avoid issues associated with model uncertainty. One advantage of nonparametric method for BMD estimation is that it does not assume any particular format for the dose-response model. However, it has some limitations. This study addresses two questions: (1) Is nonparametric method as reliable as parametric methods for deriving BMD/BMDL estimates from typically available dose-response data? (2) What are the general toxicity study design criteria that are suitable for nonparametric BMD analysis? These two questions are going to be answered based on results from a large simulation study using both dichotomous and continuous endpoints. The adequateness of the BMD and BMDL estimates is judged by their accuracy and coverage rate. Given a typical chronic study setting (i.e., 200 animals exposed for 2 years), the simulation study will mainly examine how dose spacing and animal distribution among dose groups can affect the nonparametric BMD analysis. Preliminary results suggest that the dose-response data from current toxicity studies may present difficult challenges for nonparametric analysis due to the limited number of dose groups used in most toxicity bioassays.

PS 630 Standardized Benchmark Dose Calculation: Opportunities to Inform Science-Based Decisions in Human Health Assessments

J. Wignall[1], A. J. Shapiro[1], F. A. Wright[1], T. J. Woodruff[2], W. A. Chiu[3], K. Z. Guyton[3] and I. Rusyn[1]. [1]*University of North Carolina, Chapel Hill, NC,* [2]*University of California, School of Medicine, San Francisco, CA and* [3]*US EPA, NCEA, ORD, Washington, DC.*

Benchmark dose (BMD) modeling computes the dose associated with a pre-specified response level. While offering advantages over traditional points of departure (POD), BMD methods have lacked consistency and transparency in application, interpretation and reporting. We aimed to apply a standardized process for conducting BMD modeling to reduce inconsistencies in model fitting and selection. Furthermore, we sought to identify study design features affecting BMD modeling fit acceptability. We evaluated dose-response data (880 datasets) for 352 environmental chemicals with existing human health assessments. We calculated benchmark doses (1 standard deviation or 10% response, BMD10/1SD) for each chemical in a standardized way with pre-specified criteria for model fit acceptance. We identified study design features associated with successful models. Our approach was successful for 255 (72%) of chemicals. Batch-calculated BMD10/1SD values were significantly and highly correlated with points of departure previously used in human health assessments, with median values similar to reported no-observed-adverse-effect-levels (NOAELs). We observed a significant trend of increasing model viability with increasing number of dose groups. At the same time, choices of dose level and spacing had little effect. BMD10/1SD values can be calculated in a standardized way for use in health assessments on a large number of chemicals/critical effects. This facilitates exploration of health effects across multiple studies of a given chemical, or when chemicals need to be compared, providing greater transparency and efficiency than current approaches. Lessons learned from successful or failed benchmark dose response modeling can inform study design and selection for future assessments. Disclaimer: The views expressed here are the authors' and not necessarily those of the US EPA.

PS 631 TTC: A New Concept for Inhalation Exposure

S. Escher[1], I. Tluczkiewicz[1], M. Batke[1], R. Kühne[2], R. Ebert[2], G. Schüürmann[2] and I. Mangelsdorf[1]. [1]*Chemical Risk Assessment, Fraunhofer Institute for Toxicology and Experimental Medicine - ITEM, Hannover, Germany and* [2]*Ecological Chemistry, The Helmholtz Centre for Environmental Research, Leipzig, Germany.* Sponsor: C. Dasenbrock.

The TTC concept derives thresholds to structural groups of compounds below which a risk for human health is not assumed for a life-time exposure. Thresholds were derived by analyzing datasets of oral in vivo studies to which the Cramer decision tree was applied. Inhalation is, however, an important route in human risk assessment e.g. for workers and consumers. The application of the Cramer decision tree to datasets of repeated-dose studies with inhalation exposure resulted in very low thresholds compared to oral TTC values. Reasons might be route specific differences e.g. an observed high sensitivity of the respiratory tract to local effects (Carthew et al. 2009, Escher et al. 2010).
We present an integrative approach to derive inhalation specific threshold values, which are based on a dataset of 296 chemicals with repeated-dose toxicity studies (www.fraunhofer-repdose.de). Systemic and local NOEC values were discriminated. Groups of compounds with specific structural features (SF) were identified based on atom centered fragments (Kühne et al. 2009). Few SF were explicit for local or systemic activity indicating that this mode of action is not a determining factor. The structural and toxicological boundaries of the initial SFs were further evaluated considering differences in absorption, published data on mechanism/metabolism and sensitive targets/effects observed in the in vivo studies. 28 SF groups resulted, 9 low (L) and 19 toxic (T) groups. About 20% of the compounds are, however, not yet grouped. Compared to the Cramer classes the T and L-groups better discriminate low toxic and toxic compounds. Two clearly distinguished TTC values are proposed.

Carthew P, Clapp C, Gutsell S 2009. Food Chem Toxicol 47, 1287-1295.
Escher SE, Tluczkiewicz I, Batke M, Bitsch A, Melber C, Kroese ED, Buist HE, Mangelsdorf I 2010. Regul Toxicol Pharmacol 58, 259-274.
Kühne R, Ebert R-U, Schüürmann G 2009. J Chem Inf Model 49, 2660-2669.

PS 632 Threshold of Toxicological Concern (TTC); A Strategy to Support Application of TTC to Dermally Applied Cosmetic Ingredients

F. M. Williams[1], M. Ambrosio[2], G. Barrett[3], M. T. Cronin[4], R. H. Guy[5], J. R. Plautz[6], N. A. Monteiro-Riviere[7], C. Roper[8], H. Rothe[9], D. Rua[10], M. Verwei[11] and C. Yang[12]. *[1]Newcastle University, Newcastle, United Kingdom, [2]ILSI Europe, Brussels, Belgium, [3]Health Canada, Ottawa, ON, Canada, [4]Liverpool John Moores University, Liverpool, United Kingdom, [5]University of Bath, Bath, United Kingdom, [6]DSM Nutritional Products, Basel, Switzerland, [7]Kansas State University, Manhattan, KS, [8]Charles River Laboratories, Edinburgh, United Kingdom, [9]Proctor & Gamble, Darmstadt, Germany, [10]US FDA, College Park, MD, [11]TNO, Zeist, Netherlands and [12]Altamira LLC, Columbus, OH.*

Threshold of Toxicological Concern (TTC) is a tool developed to provide scientific advice about possible human health risks from exposure to low levels of chemicals in the diet, when specific toxicity data are not available. It provides health protective human exposure threshold values for chemicals from a three broad ranges of structural categories (Cramer classes).
The aim of the work, as part of the EU COSMOS Project, has been to adapt the TTC concept and extend its applicability to cosmetics which are applied to the skin. A decision tree approach has been developed based on estimated usage/skin exposure, maximum possible dermal absorption derived from the J max prediction or experimental absorption data to estimate systemic dose for ranking against TTC, incorporating structural categories and Cramer class. A new dermal absorption database enriched with cosmetics-related chemicals has been established; the chemical space and domain of cosmetics-related chemicals have been also defined. Where available, experimental dermal absorption data have been ranked with predicted Jmax values.
Also assessed is the importance of local metabolism in determining differences between the oral and dermal exposure routes and its influence in decision making and use of TTC. The potential for use of TTC for cosmetics is indicated and the findings support application of TTC approaches by regulators.
Supported by the EU FP7 COSMOS Project

PS 632a By How Much Do Shapes of Toxicological Dose-Response Relationships Vary?

W. Slob[2] and W. Setzer[1]. *[1]National Center for Computational Toxicology, US EPA, Research Triangle Park, NC and [2]National Institute for Public Health and the Environment - RIVM, Bilthoven, Netherlands.* Sponsor: J. Wambaugh.

A re-analysis of a large number of historical dose-response data for continuous endpoints showed that the shapes of the dose-response relationships were surprisingly homogenous. The datasets were selected on the sole criterion that they were expected to provide relatively good information on the dose-response shape, and included a variety of endpoints and both in vivo and in vitro studies of various types. Both the four-parameter exponential and Hill model adequately described all toxicological dose-response data we considered. For a given endpoint and study type, dose-response shapes did not differ statistically significantly among chemicals in the in vitro studies considered, while a mild among-chemical variation in the steepness parameter seemed to be present in the in vivo studies. These findings have various practical consequences. For continuous endpoints, model selection in the BMD approach is not a crucial issue. The often-applied approach of using constraints on the model parameters to prevent "infinite" slope at dose zero in fitting a model is not in line with our findings, and appears to be unjustified. Instead, more realistic ranges of parameter values could be derived from re-analyses of large numbers of historical dose-response datasets in the same endpoint and study type, which would then be used as parameter constraints or informative priors in the analysis of future individual datasets. This approach would be particularly useful for weak datasets (e.g. few doses, much scatter). In addition, this approach may open the way to use fewer animals in future studies. Finally, we argue that distinctions between linear, sub/supralinear or thresholded dose-response shapes, based on visual inspection of plots, are not biologically meaningful nor useful for risk assessment. This abstract does not necessarily reflect EPA policy.

PS 632b Variation in Scaling Factors Used for *In Vitro* to *In Vivo* Extrapolation (IVIVE) and Its Impact on Internal Dose in Rats: A Case Study with Bromodichloromethane (BDCM)

E. Kenyon[1], C. R. Eklund[1], J. C. Lipscomb[2] and R. A. Pegram[1]. *[1]ORD/NHEERL/ISTD, U.S. EPA, Durham, NC and [2]ORD/NCEA, U.S. EPA, Cincinnati, OH.*

Physiologically based pharmacokinetic (PBPK) models can include values for metabolic parameters extrapolated from in vitro studies using scaling factors (SF) such as mg of microsomal or cytosolic protein per gram of liver (MPPGL and CPPGL) and liver volume (FVL). Variation in SF values impacts metabolic rate parameter estimates (Vmax) and hence estimates of internal dose used in dose response analysis. The impact of variation in MPPGL, CPPGL and FVL on toxicologically relevant dose metrics was assessed using a rat PBPK model for BDCM and Monte Carlo analysis. Values for SF were determined experimentally or obtained from the literature. Dose metrics examined include area under the curve for blood BDCM (AUCV) and amount metabolized in liver via detoxification (oxidative, AM1) and toxication (glutathione, AM2) pathways. At relatively low doses (5 mg/kg) all dose metrics evaluated were changed by less than 20%, probably because metabolism is blood flow-limited at lower doses. In contrast, at bioassay dose levels (100 mg/kg) differences of 5-, 3- and 9-fold were observed for AUC, AM1 and AM2, respectively. Sensitivity analysis for both AUC and AM1 revealed that MPPGL and FVL were highly and moderately influential parameters, respectively. The larger difference observed for AM2 is likely a consequence of higher variability in CPPGL (3 times higher coefficient of variation compared to other SF) suggesting that more precise estimates are needed for CPPGL and distribution of cytosolic enzymes in rat liver. This analysis demonstrates: 1) that variability in SF used for IVIVE of metabolic rate parameters can have a significant impact on estimates of internal dose metrics at toxicologically relevant doses, and 2) the need to evaluate both uncertainty and variability for scaling factors used for IVIVE. (This abstract does not reflect USEPA policy).

PS 632c Toluene PBPK Models to Extrapolate Neurological Effects between Rats and Humans, across Acute Durations and Severity Categories

G. M. Woodall[1], E. Kenyon[2], V. Benignus[3], C. R. Eklund[2], P. J. Bushnell[2] and W. K. Boyes[2]. *[1]NCEA, US EPA, Research Triangle Park, NC, [2]NHEERL, US EPA, Research Triangle Park, NC and [3]Retired, US EPA, Research Triangle Park, NC.*

Acute exposure to volatile organic compounds (e.g., toluene and ethanol) impairs neurological function. The degree of impairment has been quantified as a dose-response relationship using a variety of behavioral tasks, including reaction time (RT). Brain toluene concentrations (Br-TC) have been related quantitatively to blood ethanol concentrations (BEC) via changes in RT associated with each chemical (Benignus et al., 2005). A BEC of 0.08 g/dl (legal intoxication) and a Br-TC of 119 μM both produce a 13% reduction of RT. The current interim level 2 acute exposure guideline levels (AEGL-2) are based on a 70-min exposure to 2400 ppm toluene, and results in an effect level consistent with a BEC of 0.17 g/dl, as determined by our analyses. An alternate set of AEGL-2 values based on a doubling of RT in Long-Evans rats (1600 ppm for 34-mins) was determined using a rat PBPK model (Kenyon et al., 2008). The rat Br-TC at the end of exposure (535 μM; 49.2 mg/L) was reduced by a factor of 3 to derive the target concentration. AEGL-2 values (10- and 30-min, 1-, 4- and 8-hr durations) were determined from the target concentration with a human model (GPAT: Benignus et al., 2006). The same PBPK model construct was applied to determine AEGL-3 values based on a rat lethality NOAEL. The estimate of a human LC-50 was also derived for comparison to a Dutch Probit method for land-use planning. The final results were toluene exposure levels for durations from 10-mins up to 8-hrs at three levels of severity in humans: a clear decrement in RT; the threshold for lethality; and an LC-50. These analyses led to a quantitative methodology to inform revisions of AEGL values for toluene which were reviewed and approved by the National Academies of Science. The views expressed in this abstract are those of the authors and do not necessarily reflect the views or policies of the US EPA.

PS 632d Modeling of Blood Lead Levels in Astronauts Exposed to Lead from Microgravity-Accelerated Bone Loss

H. D. Garcia[1], J. S. Tsuji[2] and J. T. James[3]. *[1]Wyle Laboratories, Houston, TX, [2]Exponent Corp., Bellevue, WA and [3]NASA (Retired), Houston, TX.*

Setting Spacecraft Water Exposure Guidelines (SWEGs) for lead (Pb) in spacecraft drinking water has special challenges related to estimating blood lead levels (PbB) during the increased release of lead into systemic circulation via microgravity-in-

duced bone loss. The effects on the PbB of Pb in drinking water (PbW), Pb released from bones, and change in lead exposure before, during, and after spaceflight were evaluated using a physiologically based pharmacokinetic (PBPK) mathematical model (2013, Aviation, Space, & Environmental Medicine 84:1229-1234) that incorporates environmental lead exposure on earth and in flight and includes temporarily increased rates of osteoporosis during spaceflight. The model predicts that the average American astronaut in 2030 (the earliest anticipated launch date for a long-duration mission) would have a PbB of 1.7 μg/dL at launch and that PbB levels would decrease in microgravity at PbW values less than about 9 μg Pb/L because of reduced lead exposure during spaceflight. Currently, PbW on the International Space Station (ISS) averages <1 μg Pb/L. A SWEG of 9 μg Pb/L would protect most astronauts on long-duration spaceflights by ensuring that PbB values will not exceed pre-launch levels. At in-flight PbW concentrations <9 μg Pb/L, Pb concentrations in both bone and blood would gradually decrease below their pre-launch values. On the other hand, astronauts who have high concentrations of lead stored in bones (an unlikely possibility) could experience increased PbB levels in microgravity due to release of lead from bones. While the resultant in-flight PbBs would depend on their pre-flight bone lead levels, their PbBs will not be significantly further elevated (<1 μg/dL) by consuming water with a PbW of ≤9 μg /L. Because individuals with a history of clinical lead poisoning would likely have high concentrations of lead stored in their bones, we recommend that such individuals avoid exposure to microgravity of more than a few days' duration to prevent in-flight lead poisoning.

PS 632e Using Pharmacokinetic Modeling to Derive Infant: Mother Internal Exposure Ratios for the Prediction of Infant Exposure to POPs throughout Breastfeeding

S. Haddad[1] and M. Verner[2]. [1]*Environmental and Occupational Health, IRSPUM, Université de Montréal, Montréal, QC, Canada and* [2]*Channing Division of Network Medicine, Brigham and Women's Hospital, Harvard Medical School, Boston, MA.*

It is now well established that breastfeeding is a major source of exposure to persistent organic pollutants (POPs) in newborns and infants. These chemicals are eliminated very slowly and can rapidly accumulate in infants. Infant internal exposure may even exceed maternal levels during the breastfeeding period. Some studies suggest that high exposure to these chemicals at such a critical time in infant development can lead to certain problems later in life, hence the increasing attention in risk assessment. One of the major problems is the estimation of this exposure in children. The objective of this study was to estimate the maximal internal exposure an infant can attain compared to its mother. Using a validated pharmacokinetic model for POPs, Monte-Carlo simulations were performed to obtain distributions of infant:mother internal exposure (IMIE) ratios and these were compared to available data from a cohort where POP levels were measured in mothers at delivery and their 6-month-old infants (HCB and PCB-153). While not being overly conservative, the calculated maximal IMIE (Max IMIE) ratios were greater than all measured IMIEs of dyads that were strictly breastfed before blood measurement (n=50 per chemical). For example, the Max IMIE at 6 months of age is estimated to be 6.61 for HCB (Median=2.94) and 6.85 for PCB-153 (median=3.00) while the observed values were below the estimated 95th-ile. The peak Max IMIE is attained at 12 months and reaches 16.9 for HCB and 19.1 for PCB-153. A series of Max IMIEs were then estimated to compounds of different half-lives and for infants breastfed from birth to 24 months of age. The Max IMIE is a new exposure factor that could easily be applied in risk assessment when estimating infant exposure to breast milk with prior knowledge of maternal exposure.

PS 632f The Toxic Potency of 2, 3-Pentanedione Relative to Diacetyl

D. A. Dankovic and R. J. Smith. *Risk Evaluation Branch, CDC/NIOSH, Cincinnati, OH.*

Diacetyl is often used in the food flavoring and production industries and occupational exposure to this substance has been associated with severe respiratory responses in workers. 2,3-Pentanedione (PD) has been used as a substitute for diacetyl; it is also of concern because of its structural similarities and because toxicological studies show similar pathologic responses in the upper and lower respiratory tracts of experimental animals. An earlier analysis of the relative toxic potency of PD and diacetyl was based on pilot study data (n=5 per dose group) for diacetyl, in male mice only. This analysis presents an updated comparative potency analysis of PD relative to diacetyl, based on new data for diacetyl. A 2-week + 2 day inhalation study of rats and mice exposed to PD (n=6 per dose group) was compared to a recent 13-week NTP study of diacetyl in male and female mice and rats (n=10 per dose group), as well as the male mouse pilot study data. The results are based on multinomial regression modeling of severity-ordered pathological response data. Benchmark concentrations (BMCs) for lesion scores of 1+ (at least minimal) were estimated for those models having a significant dose-response (P<0.05) and an adequate fit (P>0.05). A more complex model was necessary for estimating mouse BMCs, in which quadratic dose terms significantly improved the fit, and adjustments for the different durations of these studies were incorporated. The relative potency estimates (diacetyl/PD) range from 0.81–7.3, depending on sex and the specific endpoint evaluated (where 1.0 would indicate equal toxic potency for the two compounds). Model-based 95% confidence limits range from 0.55–14, and the range increased to 0.44–21 when adjusted for overdispersion. These results suggest that equal or greater toxic potency for PD relative to diacetyl cannot be ruled out on the basis of currently available data.

PS 632g Dose-Response Assessment of the Nephrotoxicity of Melamine and Cyanuric Acid in Rodents—A Summary of Studies Conducted at the US FDA

G. Gamboa da Costa[1], L. Loukotková[1], L. VonTungeln[1], C. C. Jacob[2], G. Olson[3], R. Sprando[4], D. Hattan[4], C. Stine[5], R. Reimschuessel[5] and F. A. Beland[1]. [1]*US FDA National Center for Toxicological Research, Jefferson, AR,* [2]*BIOASTER, Lyon, France,* [3]*Toxicologic Pathology Associates, Jefferson, AR,* [4]*US FDA Center for Food Safety and Applied Nutrition, College Park, MD and* [5]*US FDA Center for Veterinary Medicine, Laurel, MD.*

In 2007, the intentional adulteration of pet food ingredients with melamine and cyanuric acid, caused kidney failure and death of hundreds of cats and dogs in the U.S.. Early investigation revealed that co-exposure to these compounds can elicit nephrotoxicity due to the formation of highly insoluble melamine cyanurate (MC) crystals in the nephrons. In response to these events, and later events in China in 2008 involving the contamination of infant formula with melamine, it became apparent to regulatory agencies, including the U.S. Food and Drug Administration (FDA), that further in-depth studies addressing the toxicity of melamine, cyanuric acid, and their combination were warranted. We report the design and outcome of 7- and 28-day feed, and 90-day gavage dose-response studies conducted at the FDA in male and female F344 rats on the combined nephrotoxicity of melamine and cyanuric acid. The current tolerable daily intakes (TDI) established by the FDA for dietary exposure to melamine and its derivatives are based upon a NOAEL of 63 mg/kg bw/day for dietary exposure to melamine in a 13-week rat study. The data from our current studies demonstrate that in F344 rats, oral co-exposure to melamine and cyanuric acid results in a NOAEL value 25- (based upon renal histopathological alterations such as tubule degeneration, fibrosis, dilatation and epithelium hyperplasia and elevated blood urea nitrogen and serum creatinine) to 100-fold (based upon MC crystal formation) lower than that previously considered in the risk assessments based on the NOAEL value derived from exposure to melamine alone.

PS 632h Proposed Novel Method for Assessing Risks of Inhaled Titanium Dioxide from Cosmetics

T. Jonaitis and L. A. Haighton. *Intertek Scientific & Regulatory Consultancy, Mississauga, ON, Canada.*

Titanium dioxide (airborne, unbound particles of respirable size) was added to the Proposition 65 list in 2011 as a carcinogen. Numerous notices of violation (NOV) have since been filed against cosmetic products. High dose studies show TiO2 induces lung tumors in rodents but epidemiology studies fail to show this association even with years of occupational exposure. The cancer mechanism is thought to be overloading of lung clearance due to the poorly soluble respirable particles. A Safe Harbor Level (SHL) for TiO2 has not been derived by OEHHA; however, Prop 65 regulations allow for SHL to be derived according to scientific methods. Route-appropriate (i.e., inhalation) human SHLs based on occupational data have been determined for assessing risk from cosmetics use using products with highest potential consumer exposures to TiO2: aerosol hairsprays and sunscreens. SHLs were adapted based on occupation exposure levels shown not to over burden the lungs or increase cancer risk over the course of a 40 year working career. The amortized SHLs correspond to 55, 13, and 1.6 mg/day, for TiO2 (total), fine, and ultrafine, respectively. Respirable particles (<10 μm size), may cover most of the TiO2 particles present in sunscreens; however, only about 5% of airborne particles created during spraying would be expected to be of respirable size. Thus, using data on frequency of use and use levels from survey data on cosmetics and scientifically-based exposure assessment calculations, the exposure to TiO2 would be 0.82 mg/day for hairspray and 0.32 mg/day for spray sunscreen, which are below all SHLs. TiO2 exposures from other cosmetic products such as compacts that are not aerosolized would be even lower. As such it is evident that the NOV filed against these various products are unwarranted as users would not be exposed to TiO2 levels that would cause cancer even allowing for daily lifetime applications. This work further underlines the importance of science-based decision-making in relevant risk communication in the public domain.

PS 632i Systematic Review of the Association between Lung Cancer Risk and Low Levels of Arsenic in Drinking Water

E. K. Dissen[1], M. Feinleib[2] and S. H. Lamm[1, 2]. [1]*Center for Epidemiology and Global Health, Consultants in Epidemiology and Occupational Health, Washington, DC and* [2]*JHU Bloomberg School of Public Health, Baltimore, MD.* Sponsor: J. Tsuji.

Background: Multiple studies have demonstrated the increased risk of bladder and lung cancers with exposure to drinking water containing inorganic arsenic at levels in the hundreds of micrograms/liter. The risks at lower levels are uncertain. A systematic review and meta-analysis of the risk of bladder cancers with exposure to drinking water (Mink, 2008) has found no increased risk at arsenic exposures below 200 ug/L with the exception of studies limited to tobacco smokers. No such analysis has been reported with respect to lung cancers.
Materials and Methods: Our comprehensive literature search yielded a final set of 11 papers with 17 study populations from 4 continents that reported the risks of lung cancer from lower levels of arsenic exposure in drinking water. Risk ratio and exposure metric data were extracted. Results were stratified into exposures at <10 ug/L, 10-100 ug/L, 100-200 ug/L, and >200 ug/L.
Results: The 11 studies had 3 risk estimates in the <10 ug/L range, 20 in the 10-100 ug/L range, 7 in the 100-200 ug/L range, and 9 just above 200 ug/L. The mean and median risk estimates were 0.92 and 0.94 for <10 ug/L, 1.02 and 1.02 for 10-100 ug/L, 1.51 and 1.34 for 100-200 ug/L, and 2.36 and 1.97 for >200 ug/L. Only one of 20 (5%) risk estimates at 10-100 ug/L was significantly greater than the risk at lower levels, as were 3 of 7 (43%) at 100-200 ug/L and 5 of 9 (55%) at > 200 ug/L. An arsenic-associated risk was seen among smokers only above 200 ug/L.
Conclusion: Lung cancer risk with exposure to arsenic in drinking water was not seen to rise at levels below 100 ug/L. Increased risks were observed at 100-200 ug/L and at > 200 ug/L. These results are consistent with those of bladder cancer risk with exposure to arsenic in drinking water; However, bladder cancer studies have generally separated out the risk for smokers from that of non-smokers and only two of the lung cancer studies have done so.

PS 632j Guidance for Contaminated Sites: Trichloroethylene Case Study

B. K. Gadagbui[1], M. L. Dourson[2, 1], R. Thompson[4], J. Lowe[3] and E. Pfau[5]. [1]*TERA, Cincinnati, OH,* [2]*Alliance for Risk Assessment, Cincinnati, OH,* [3]*CH2M Hill, Spokane, WA,* [4]*Alliance for Site Closure, Indianapolis, IN and* [5]*Hull and Associates, Inc, Columbus, OH.*

A methodology for interpreting a range of acceptable noncancer risks was developed, similar to the range used for cancer risks in management of waste sites, based on readily available toxicity information from U.S. EPA and elsewhere. This range enables noncancer risk to be evaluated in a way that reflects the uncertainty of the noncancer benchmark. The EPA's recently developed RfC for trichloroethylene (TCE), based on multiple endpoints, was evaluated as a case study for the noncancer risk range. For TCE, this range was judged to be 3 μg/m3 to 20 μg/m3. The results of the NTP study-based RfC were used to determine the floor and midpoint of this uncertainty range. The highly controversial results from the Johnson et al. (2003) study-based RfC, while associated with low confidence, were nevertheless used to determine the ceiling level of this uncertainty range. The proposed range was entirely within the wider individual uncertainty range from the Keil et al. (2009) study; therefore, this latter study was considered to be confirmatory. The multi-endpoint uncertainty range is composed of floor, midpoint and ceiling values derived from studies for which the appropriate averaging time corresponds to different exposure durations (i.e., developmental or chronic exposure periods). Therefore, this range can be applied to both long- and short-term exposures, with the associated differences in exposure averaging times. For shorter-term exposures, the results from the Johnson et al. study (2003) might also be used to describe the best averaging time, but if so, this averaging time should be based on the average time of cardiac development in humans during fetal growth, approximately 24 days. An assumed 24-day averaging time for cardiac development in humans is consistent with the fact that effects in the Johnson et al. study (2003), appeared to occur during the whole time of cardiac development in the rat.

PS 633 Pen Housing of Nonhuman Primates on Toxicology Studies

J. Setser, E. Lambert and G. Maginnis. *WIL Research, Ashland, OH.* Sponsor: T. O'Neill.

As part of our continuing effort to improve our animal care and use program and to exceed regulatory requirements in the housing of nonhuman primates, we have developed a pen-style housing system for use on GLP-compliant toxicology studies. The pen system was developed with three objectives 1) meet housing requirements as specified in Appendix A of the European Convention for The Protection Of Vertebrate Animals Used for Experimental and Other Scientific Purposes (Ets No. 123) 2) ability to perform all standard toxicology endpoints and 3) maintaining similar animal densities as current caging. Each pen within the housing system provides approximately 254 cubic feet of space, which is capable of housing 6 animals within the standard age range (2-4 years old) used on toxicology studies. When fully utilized, the pens provide the same animal densities as our standard pair and triad caging system. The pen system consists of panels made of colored laminate, stainless steel rods and toughened safety glass. Solid flooring, lined with natural wood chip bedding, allows for foraging opportunities and placement of novel enrichment items. Positioning of perches at various heights as well as the use of climbing aids and swings ensures utilization of all available space. To facilitate performance of various research procedures in a more controlled environment, a mobile treatment trolley was developed. The trolley is a mobile unit which allows for temporary separation of animals for research required activities. Several in-house studies were conducted to evaluate feasibility of performing and collecting standard toxicology endpoints. Study designs included various dosing routes (nasogastric, IV, IM, subcutaneous), sample collection (toxicokinetic and clinical pathology), ECGs, ocular exams, observations and body weight collections. All standard parameters were successfully performed with slight modifications to current procedures. Based on the success of our evaluation studies and meeting our initial objectives, use of the pen system is considered appropriate for use on GLP-compliant nonhuman primate studies.

PS 634 Implementing the 3R Methods and Hurdles for Their Application—A Perspective from the Chemical Industry

R. Büsen, T. Ramirez, S. S. Schneider, S. Kolle, W. Mellert, R. Landsiedel and B. van Ravenzwaay. *Toxicology, BASF SE, Ludwigshafen, Germany.*

For the safety of consumer products their toxicological potential must be determined. By law, the toxicological testing often requires animal studies. According to our commitment to animal protection we apply 3R principles whenever possible, i.e. "reduce" and "replace" animal studies by new testing strategies as well as "refine" them by humane testing conditions. Herein, we report on certain hurdles that BASF SE has faced in the recent years.
Hurdles for reduction of animal numbers used for regulatory purposes exist (i) for "reproduction toxicity studies" as the basic design of the extended one-generation reproductive toxicity study is still lacking full acceptance and (ii) for "non-rodent toxicity studies" as the redundant one-year dog study is still requested by some authorities. Hurdles for application of replacement methods exist for the endpoints (iii) "eye irritation" as technical equipment is difficult to achieve for a validated and accepted assay, and (iv) "skin sensitization" as the validation process will be completed too late for registration of many substances under the European Union legislation REACH. Hurdles for refinement were encountered when (v) the propagated use of a cytotoxicity assay for the optimal selection of the starting dose in acute oral toxicity did not prove to be as useful as anticipated.
Taken together, especially in the field of in vitro methods, many problems can be encountered during the process of development, establishment, and their application. Some of these hurdles are technical issues, some published alternatives not fulfilling inter-laboratory reproducibility requirements, and an insufficient validation procedure. Most often, in vitro methods are not validated fast enough and regulatory acceptance takes too much time. Therefore, their use for regulatory purposes is often delayed and does not match legislative and political goals (e.g. Cosmetic Directive and REACH).

PS 635 SLIM As a Smart Way to Translate 3R Innovations to Acceptance for Use in Human Risk Assessment

C. Krul[1, 2], M. Teunis[1], R. Vandebriel[3], R. A. Woutersen[2, 8], D. Kegler[4], J. Raaijmakers[5], J. Van der Valk[6] and R. Pieters[1, 7]. [1]*Department of Innovative Testing, University of Applied Sciences, Utrecht, Netherlands,* [2]*TNO, Zeist, Netherlands,* [3]*RIVM, Bilthoven, Netherlands,* [4]*Nutricia Research, Utrecht, Netherlands,* [5]*GSK, Zeist, Netherlands,* [6]*NKCA, Utrecht, Netherlands,* [7]*Institute for Risk Assessment Sciences, Utrecht University, Utrecht, Netherlands and* [8]*Wageningen University and Research Centre, Wageningen, Netherlands.*

Safety assessment of pharmaceuticals and food ingredients requires a significant number of animal experiments. Although in vitro techniques for safety assessment became available over the past years, the number of accepted methods actually implemented within industry and regulations is very low. The slow implementation process delays the innovations in product development, which is undesirable for scientific, societal and economic reasons.
The objective of the SLIM project is to obtain good practices for a faster development, (regulatory) acceptance and implementation of methods that replace, reduce or refine animal experiments. Four case studies in the field of reproductive toxicity,

food allergy, carcinogenicity and bioavailability of new products were performed. An advisory board, composed of scientists working for international regulatory agencies, has critically reviewed these case studies. Two case studies focus on retrospective analysis of the predictive value of animal experiments and aim to identify whether one animal species can be used in reproductive toxicity testing, without losing safety information or whether long-term carcinogenicity tests can be replaced with shorter tests. Other case studies focus on development of in vitro models to identify embryotoxic compounds or allergic reactions. The fourth compared different in vitro models to assess oral bioavailability. Part of all case studies include identification of barriers and drivers of (regulatory) acceptance. Case studies will be presented and show that drivers and barriers can be influenced by intensifying collaborations between stakeholders, i.e. companies, regulatory bodies and research institutes in an early phase in the assay development process.

PS 636 The Use of Weight of Evidence (WoE) for Fulfilling the 2nd Species Information Requirement for Developmental Toxicity within the REACH Framework

J. E. Foreman, M. H. Kung and G. D. Minsavage. *ExxonMobil Biomedical Sciences, Inc., Annandale, NJ.*

REACH passed into law in 2007, placing the responsibility on registrants to demonstrate that potential risks from chemical exposures are appropriately managed and communicated. The European Chemicals Agency (ECHA) has indicated that the second most frequent 'shortcoming' in REACH registration dossiers was related to the PNDT endpoint. For >100 tpa registrations, REACH mandates the information requirements for PNDT be filled by conducting OECD test guideline 414 (usually rat), with an expectation to consider further testing in a second species (usually rabbit). The necessity of conducting PNDT testing in two species has recently been evaluated in the literature. Initial conclusions indicate that a) rabbits are not inherently more sensitive detectors of human teratogenicity, b) the variability observed between species for the majority of chemicals does not exceed normal variability that occurs in multiple studies with the same species, and c) species sensitivities that do exist are driven by identifiable biological differences. A properly constructed WoE should establish whether the specific substance is expected to have a similar metabolic fate across species, and determine if there are any indicators that a unique response may be expected in different species. This evaluation can predict whether additional information for risk assessment purposes would be obtained from a second species study. Additionally, variability between NOAELs resulting from a rat and rabbit study can be estimated using existing data on substances that have been evaluated in both species. This estimate can be used in comparison with exposure scenarios to determine if the Margin of Exposure (MoE) is large enough to encompass any residual uncertainty remaining after completing a thorough substances specific evaluation. Building a WoE with perspectives from the published literature, a chemical specific evaluation, and MoE calculations should be sufficient to determine the necessity for PNDT testing in a second species within the REACH framework.

PS 637 Evaluation of a Tiered Toxicity Testing Decision Trigger for Assessing Reproductive Hazards of Commodity Chemicals

L. M. Plunkett[1], A. Kaplan[2] and R. A. Becker[3]. [1]*Integrative Biostrategies LLC, Houston, TX,* [2]*A. Michael Kaplan & Associates, Landenberg, PA and* [3]*American Chemistry Council, Washington, DC.*

A tiered toxicity testing framework for application to commodity chemical safety assessment has been developed which employs endpoint-specific decision triggers. The framework has two tiers in which hazard information can be integrated with exposure information at each tier. Decisions about testing choices for Tier 2 tests, the more complex tests, are made based on consideration of decision triggers for significant toxic effects, one of which is reproductive toxicity potential. In the current work, an initial assessment of the reliability of the proposed reproductive toxicity decision trigger was performed using reproductive toxicity data collected within the U.S. Environmental Protection Agency (EPA) Toxicity Reference database (ToxRefDB). Among the ToxRefDB chemicals which EPA previously designated as being either positive or negative for reproductive toxicity potential, 10 positive and 10 negative substances were randomly selected. Toxicity data were extracted from the ToxRefDB and entered into a database constructed for the analysis, the "Toxicity Trigger Database" (ToxTrigDB). During the evaluation, however, significant limitations were uncovered in the underlying curation of the ToxRefDB, limitations that involved interpretation of toxicity effects and designation of toxicity endpoints. As a result, not enough positive reproductive toxicants were included in the random selection, and only a limited evaluation of the proposed trigger was possible. The limited evaluation showed that the trigger's performance was dependent on the scientific evaluation criteria used, and judgments made when determining whether responses met the criteria for designating a substance as a positive or negative. Before analyses are conducted using ToxRefDB, including use in validation of prediction models, consensus criteria for designating positive and negative agents need to be developed and applied to ensure the database is adequate for this type of use.

PS 638 Association between Health Outcomes and Environmental Factors in Illinois

M. P. Chan. *Southern Illinois University Edwardsville, Edwardsville, IL.*

Research has suggested that mortality rates are positively correlated with social inequalities, race/ethnic, air pollution, elevated ambient temperature, availability of medical care, risk factors and other factors. This study develops a model that uses indicators for multiple factors to predict the mortality rates for selected diseases by county in Illinois. County-level data on 102 Illinois counties from the 2012 County Health Rankings were linked to county mortality data from the Centers for Disease Control and Prevention Compressed Mortality database. Appropriate statistical analyses were used to predict the relationship between various environmental factors and other factors to explain variations in county-specific mortality rates for the leading causes of death and lifespan in Illinois. It is anticipated that this study would suggest some adaption strategies to improve the health of residents in Illinois through working with some community organizations.

PS 639 A Novel Approach to Toxicological Hazard Assessment of CAS Number-Specific Compounds with Variable Composition

J. Zhang and A. Lewis. *Gradient Corp, Cambridge, MA.*

The rapidly changing global landscape of environmental regulations and chemical compliance presents a major challenge for chemical manufacturers and importers. Increasingly, countries are requiring hazard identification based on the Globally Harmonized System of Classification and Labeling (GHS) Guidance. The use of a GHS-based classification system is complex and calls for a level of expertise in toxicology and chemistry that was not previously needed to communicate chemical safety. As part of the hazard assessment process, Gradient has identified a recurring complication regarding hazard assignment for substances with variable compositional features but the same Chemical Abstracts Service (CAS) Registry Number. CAS numbers are unique chemical-specific identifiers; however, they are not specific to length, size, and composition. Examples include silica, petroleum distillate, alcohol ethoxylates, and glass oxide compounds. We determined that hazard conclusions can vary considerably across the publicly available literature for a specific CAS number, and information on the chemical manufacturing process is often necessary to appropriately assign hazards. For example, using just the CAS number, an evaluation of glass oxide would suggest a potential carcinogenic risk because this CAS number is classified as a class 1B carcinogen in the Registration, Evaluation, Authorisation and Restriction of Chemicals (REACH) registration dossier (without any caveats). Such a classification would trigger significant downstream regulatory requirements. Upon targeted investigation into product specifications on particle size, however, we determined that the glass oxide in question consisted of continuous filament glass fibers with aerodynamic diameters ranging between 8-26 μm, which are unlikely to deposit in the alveoli regions of the lungs and thus unlikely to pose carcinogenic risks. This poster presents several examples of complexities involved in the hazard classification of compounds with variable compositional features and the research strategy necessary to arrive at well-supported hazard conclusions.

PS 640 A Sustainable Product Risk Assessment

E. A. Choudhury, K. Enters and M. S. Stavanja. *EHS/Product Stewardship, Celanese International Corporation, Irving, TX.*

Celanese uses a global risk management process for identifying and managing product-related risk associated with raw materials, manufacturing, handling, distributing, sale and the end-use of our products. The process was developed, in support of the responsible care business approach, utilizing a framework rooted in the best practices and industry benchmarking. It involves coordination of experts to further evaluate and assess various elements, including effects on employees, customers, consumers, operating sites, the environment, and the Company. The purpose of our Product Risk Assessment process is to ensure that our products meet our corporate safety and legal targets, as well as all applicable safety, regulatory and legal requirements and possible risks in each country where the product will be marketed and used. Our internal global risk management process targets the identification and management of product related risk associated with raw materials, manufactur-

ing, handling and distribution, sale, and the end-use of our products. The system is designed to broadly review, assess, evaluate and balance risk from multiple internal and external sources. A secondary goal was to increase institutional awareness and organizational decision-making at risk relevant levels. The process includes a risk review by committees comprised of technical professionals with backgrounds in toxicology & medical technology, legal, product development, manufacturing, and others as appropriate. Success has been achieved by embedding the product risk management process into our new product commercialization systems, creating a cultural change towards proactive consideration of critical risk management elements such as product risk, increased organizational awareness, escalation of decision-making, and risk mitigation.

PS 641 A Life-Cycle Approach for Prototypical Consumer Products Containing Nanomaterials

C. M. Sayes, G. Rothrock, S. Cho, J. Child, C. Norton and P. Durham. *Center for Aerosols & Nanomaterials Engineering, RTI International, Research Triangle Park, NC.*

Nanocomposite materials (bulk materials enabled with nanoparticles) are used in the building industry. To date, a total of 250 products produced by over 100 companies incorporate nanocomposites into building or renovation plans; estimated revenues surpass $1 billion. Nanoparticles offer tailored benefits to the traditional functions of materials. Nanocomposite coatings have led to new opportunities in the world-wide market. The continued utilization of nanomaterials in the building envelope is expected to develop rapidly; however, the safety of these novel materials to humans and the surrounding environment must be studied in parallel to their incorporation into products. One way to develop safe nanomaterials is to use a product life cycle approach that integrates product development with manufacturing and worker/consumer exposure. This research approach investigates a white paint product enabled with 120 nm titanium dioxide particles as a case study. The bulk material (dry wall) is characterized with the nano-enabled product (white paint) in its intact and degraded forms. Simulated wear-and-tear scenarios are performed on the painted wall and the released airborne particles are analyzed for concentration, size, and composition. Human respiratory deposition of the airborne particles via inhalation exposure is calculated by a particle dosimetry model. The released particles are collected and exposed to normal epithelial cells from four areas of the human pulmonary airway for a toxicological evaluation. Results show that differential physicochemical properties, respiratory depositions in human airway, and toxicological responses are induced between particle-types that contain nanomaterials versus particle-types without nanomaterials. The impact of this research will help to enable sustainable opportunities of nanotechnology in the built environment and provide methodologies for understanding nanomaterial properties and potential toxicological impacts in the context of developed consumer products.

PS 642 Towards a Harmonized Evaluation of Chemical Emissions from Building Products in the EU

G. Johanson[1], C. Däumling[2] and P. Harrison[3]. [1]*Institute of Environmental Medicine, Karolinska Institute, Stockholm, Sweden,* [2]*German Federal Environment Agency, Berlin, Germany and* [3]*PTCH Consultancy, Leicester, United Kingdom.*

A prerequisite for healthy air quality indoors is the use of low emitting materials. There are three different mandatory systems in EU member states to evaluate emission properties of building products: in Germany since 2006, in France since 2012 and in Belgium beginning 2014. Besides these mandatory systems there are a number of voluntary health related quality labels in European countries. A working group with experts from nine European countries coordinated by the Joint Research Center of the European Commission has started to develop a new science-based harmonized procedure to derive health related thresholds, so called EU-LCI values (Lowest Concentration of Interest) for all substances regulated in France and Germany. EU-LCI values (usually expressed as μg/m3) are health-based reference concentrations for inhalation exposure used to assess emissions after 28 days from a single product during a laboratory test chamber procedure, as defined in the proposed standard developed by CEN TC 351. The working group generated a protocol incorporating a set of definitions, criteria for the selection of chemicals and use of read across and adjustment and assessment factors. A standardized summary fact-sheet was developed to ensure transparent derivation of LCI values. Further, a list of interim EU-LCI values for 78 compounds (including e.g. acetaldehyde, toluene, xylene, 1,2,4-trimethylbenzene, 1,4-dichlorobenzene, ethylbenzene, 2-butoxyethanol, styrene, ε-caprolactam and α-pinene) was developed. Only "regular" volatile organic compounds (VOCs), and not VVOCs, SVOCs or carcinogens, were considered at this stage. The output of the working group is under publication as European Collaborative Action (ECA) Report No. 29. It has received wide appreciation by member states and industry in the EU, and the Belgian decree already refers to a future list with EU-LCI values.

PS 643 Does Industry Take the Sensitive Subpopulation of Asthmatics into Account when Setting Derived No-Effect Levels under REACH?

M. Johansson[1], G. Johanson[1], M. Öberg[1] and L. Schenk[1, 2]. [1]*Work Environment Toxicology, Institute of Environmental Medicine, Karolinska Institutet, Stockholm, Sweden and* [2]*Department of Philosophy and History, Royal Institute of Technology, Stockholm, Sweden.*

The European Union's chemicals legislation, Registration Evaluation Authorization and Restriction of Chemicals (REACH), aims to improve the knowledge about hazardous properties of chemicals and also puts the responsibility for ensuring safe use on industry. The European Chemicals Agency (ECHA) registration database include Derived No-Effect Levels (DNELs) developed by industry. This study aims to investigate to what extent data generated from asthmatic subjects are considered in the DNEL setting process, and if this relatively common subpopulation is adequately protected by the acute/short-term inhalation DNELs. To this end, we performed an extensive literature review of published experimental data on lung function measurements during controlled exposure of healthy and asthmatic subjects to airborne chemicals. Data for 23 substances were found, 16 of these were also included in the ECHA database. However, only 8 of the 16 included studies on asthmatics as references. The acute/short-term inhalation DNELs of the 16 substances were generally close to the NOAEL/LOAEL values we identified for asthmatics, suggesting absence of or a low safety margin. Omission of asthmatics may interfere with trustful and efficient health protective actions. We suggest that the availability of data on asthmatics should be carefully examined in the development of DNELs, and that the lack of such data should be explicitly noted for respiratory irritants. Further guidance from ECHA on how to address sensitive subgroups in DNEL setting may improve the consistency of DNEL values. The study was supported by grants from the Swedish National Board of Health and Welfare (SoS), the Swedish Civil Contingencies Agency (MSB) and the Swedish Research Council for Health, Working Life and Welfare (Forte).

PS 644 A Novel Approach to Encourage Data Sharing in Chemical Registration Systems

Z. Yin. *Haskell Global Centers for Health and Environmental Sciences, DuPont, Shanghai, China.*

Data sharing is an important approach to avoid unnecessary testing in modern chemical registration schemes. In EU REACh, in order to enable test data to be shared, and thus avoid unnecessary testing and reduce costs, wherever practicable, registrations should be submitted jointly, in accordance with the rules on joint submission. In other chemical regulations, such as Chinese new chemical notification system, although joint submission is allowed in certain tonnage bands, the joint submission applicants have to share the tonnage. This was designed on purpose to preserve the environmental capability for hazardous chemical disposal. In this case, however, the registrant often is reluctant to share the tonnage, therefore joint submission becomes hard to achieve. We propose an approach which combines a chemical release information system, similar to US Toxic Release Inventory (TRI) with the current tonnage sharing rule. Thus, according to the chemical release data, if a geographic area has enough environmental capability, such as a specialized chemical manufacturing zone in mid-west, the applicant could use a prorated tonnage, whereas a manufacturing facility on the east coast where environmental capability is low will have to utilize a full tonnage. Specifically, a pro rata system is built upon Persistent Bioaccumulative and Toxic (PBT) chemicals release data. This is a novel approach to encourage data sharing by combining a chemical release information system with the tonnage sharing rule in joint submission in chemical notification systems. This would also help to encourage the chemical businesses to move their facilities to the specialized chemical manufacturing and processing zone in less populated area.

PS 645 Electronic and Conventional Cigarette Topography Differ

M. Hua, R. Z. Behar and P. Talbot. *Cell Biology and Neuroscience, University of California, Riverside, Riverside, CA.*

The topography of conventional cigarettes has been thoroughly studied. However, topography of electronic cigarettes (EC) is limited to two video studies. In this study, topography data were collected and analyzed from nine EC users (5 male; 3 female) over 2 days within a 7 day period. Individuals were prescreened to ensure they were 18 and over, experienced users, accustomed to 12-18 mg of nicotine/cartridge, and were in good health. Participants used two popular brands (A and B) and were asked to puff them as they would normally in two 10 min intervals separated by a 15 minute break on 2 different days. The brand order of use was reversed on the second day. The brands required different flow rates for activation (A = 14

ml/sec; B = 12 ml/sec). A handheld topography device (Cress Pocket, Borgwaldt KC) attached to the EC measured parameters such as puff count, puff volume, puff duration, and average airflow rate. Puff counts across both bands ranged from 21-42 puffs/10 minutes. The average puff count for individuals using brand A was 33 ± 5.9 puffs/10 min and for brand B was 27 ± 4.5 puffs/10 min for both days. The puff duration ranged from 1.24 to 3.84 seconds for brand A and from 1.59 to 3.81 seconds for brand B. Average total puff volume from the fifth puff to the last puff for brand A was 3928 ml and for brand B was 1161 ml. In addition, the average volumes/puff were 141.4 ml/puff (brand A) and 48.3 ml/puff (brand B). These values exceed the ISO standard for conventional cigarettes which is set at 35 ml/puff over 2 seconds once a minute The puff volume was larger for brand A which required the lower flow rate for activation. The average flow rates for users of brand A and B were 45.9 ml/second and 18.8 ml/second, respectively. There was no recognizable difference in the pattern of use between days. Additionally, puff interval varied among users. This study provides new data on EC topography and will be useful in future EC smoking machine protocol development and will aid researchers in designing experiments involving EC.

PS 646 A Simulation Environment for Population Dynamics Models of Tobacco Products

B. Poland[1], R. Gunawan[1] and K. Lee[2]. [1]*Consulting Services, Pharsight, A Certara Company, Sunnyvale, CA and* [2]*JT International SA, Geneva, Switzerland.*

Simulation models are being used increasingly to predict population impacts of tobacco products and tobacco control policies. Most models incorporate population- and individual-related inputs (e.g., tobacco-use behavior, product health risk, and policy changes) and simulate excess smoking prevalence and mortality over time. However, typically it is unclear how the model is built and tested and how uncertainties in input parameters affect uncertainties in outcomes. In this project, a simulation environment is developed to help standardize model development, testing, and documentation, for a population dynamic simulation model (PDSM). The model can be used to assess pre-market population impacts of new tobacco products including reduced-risk products. The environment is set up to take user inputs and their documentation, run deterministic or Monte Carlo simulations, and visualize predictions including effects of uncertainty. The model and environment are coded in Microsoft Visual Basic and Excel, with Excel as the interface. Tables and plots of population changes, for example differences between base and "what-if" scenarios, are generated automatically. A tornado plot ranks parameters from most to least sensitive with respect to key outputs, to help visualize impacts of uncertainties and focus attention on more important ones. A Scenario Manager is available to document hypothetical scenarios and facilitate reproducing them. As part of initial testing, a scenario in which no menthol cigarettes exist (from the US FDA's TPSAC 2011 menthol report) was simulated using reported parameters. The resulting excess smoking prevalence and mortality were comparable to reported predictions, which were found to be highly sensitive to a few input parameters (mortality risk; menthol/non-menthol yield experimenter to smoker; proportion of menthol users among experimenters). The simulation environment could be adapted to other types of models, thus providing a test bed for comparing alternative models with standardized outputs.

PS 647 A Chemical Risk Prioritization Scoring Process for the Oil and Gas Exploration and Production Industry

E. Freeman[1], K. Koblis[3], J. Staveley[2] and M. Kierski[2]. [1]*Center for Chemical Regulations and Food Safety, Exponent, Moon Township, PA,* [2]*EcoSciences, Exponent, Alexandria, VA and* [3]*EHS Strategic Planning, Noble Energy Inc., Houston, TX.*

The oil and gas industry has been under increased scrutiny for its use of chemicals during exploration and production. The media has raised concerns about the chemicals used for hydraulic fracturing in respect to human health and the environment, and state and federal agencies have begun issuing decisions on chemical disclosure. A chemical risk prioritization scoring process has been developed to address these issues and also demonstrate product stewardship.

Although chemical risk ranking is a recognized concept, there is no established process for its use in the oil and gas exploration and production industry. The Chemical Risk Prioritization System (CRPS) developed herein can be used to identify the chemicals which pose the highest potential risks to people and the environment. A tiered approach is taken that identifies a short list of chemicals that may need further risk characterization and risk management. The CRPS considers both chemical hazards and exposure scenarios in the determination of the relative risk to human health and/or the environment. This approach identifies the patterns of chemical use/exposure to both occupational and environmental receptors related to activities throughout the exploration and production life cycle.

A benefit of the CRPS is that it is a consistent, transparent approach tailored to company-specific activities. It streamlines the identification of chemicals where no additional concern is warranted or relative potential risk is minimal. This allows a more detailed risk assessment to occur for a smaller set of chemicals with higher potential risk. It also informs the company of chemicals where little hazard information is available, aiding industry in working with the chemical manufactures to better characterize potential risk.

PS 648 Toxicological Evaluations of Dermal Exposure to Chemicals: A Comparison of Evaluations under the European Legislations for Industrial Chemicals and Cosmetics

L. Schenk[1, 2] and E. Westerholm[2]. [1]*Institute of Environmental Medicine, Karolinska Institutet, Stockholm, Sweden and* [2]*Department of Philosophy and History, Royal Institute of Technology, Stockholm, Sweden.*

Dermal exposure to chemicals is highly relevant in relation to the use of cosmetic products, both in consumers and in individuals exposed occupationally. Regulatory frameworks exist within the EU to limit the dermal exposure of the general population and workers to chemicals in general as well as to limit the use of certain substances in cosmetic products. The objective of the study was to investigate and compare evaluations of dermal exposure performed under two regulatory frameworks. The publicly available information provided under respective regulatory framework for toxicological evaluation of the substances resorcinol, p-phenylenediamine, p-aminophenol, N-phenyl-p-phenylenediamine and diethylene glycol monoethyl ether was scrutinized. A low consistency between the existing evaluations performed under REACH and under the Cosmetics directive was observed in regards to selection of data and identification of critical effect, although no systematic differences were identified. A questionable relevance of included data was observed for some of the registrant evaluations under REACH. However, regardless of these differences the critical dose descriptors were quite similar between the evaluators (within a factor of 2.5) for these five substances. An extended comparison was performed of the critical dose descriptors for all substances evaluated under both frameworks (n=30, only including cosmetics evaluations published 2003-2013). This exercise showed that the REACH registrant's critical dose descriptor on average is 2.3 (geometric mean) higher than the SCCS critical dose descriptor, ranging from 0.5 to 57 times higher. This is partly explained by a difference in route of the critical study, as REACH registrant critical dose descriptors more often are derived from dermal exposure studies. Removing pairs of dose descriptors with different routes of exposure yields a geometric mean of 1.7, with a range of 0.5 to 40 times higher.

PS 649 The Relationship between Chemical-Induced Kidney Weight Changes and Kidney Histopathology in Rats

E. Craig and J. Zhao. *USEPA, Cincinnati, OH.*

The kidney is a major site of chemical excretion, which results in its propensity to exhibit chemically-induced toxicological effects at a higher rate than most other organs. A routine practice in the assessment of kidney toxicity in animal studies is the evaluation of kidney weight changes. However, the manner in which kidney weight is interpreted and the value of this information in predicting renal damage remains a topic of discussion. In this study we sought to determine whether a relationship exists between chemically-induced kidney weight changes and renal histopathological alterations. We also examined the relative utility of absolute and relative (kidney-to-body weight ratio) kidney weight in the prediction of renal toxicity. For this, data extracted from oral chemical exposure studies in rats performed by the National Toxicology Program (NTP) were qualitatively and quantitatively evaluated. Our analysis showed a statistically significant correlation between absolute, but not relative, kidney weight and renal histopathology in chemically-treated rats. This positive correlation between absolute kidney weight and histopathology was observed even with compounds that statistically decreased terminal body weight. Furthermore, most increases in absolute kidney weight reaching statistical significance (irrespective of the magnitude of change) were found to be relevant for the prediction of histopathological changes. Thus, compared to relative kidney weight, the evaluation of absolute kidney weight may be a preferable method for identifying potential renal toxicants.

PS 649a Assessing Drug Substances to Identify "Highly Hazardous" Compounds for Quality Risk Management Programs

R. Sussman[1], A. R. Schatz[4], T. A. Kimmel[1], A. G. Ader[2] and B. D. Naumann[3]. [1]*SafeBridge Consultants, Inc., New York, NY,* [2]*SafeBridge Consultants, Inc., Mountain View, CA,* [3]*Merck & Co., Inc., Whitehouse Station, NJ and* [4]*Ashland, Inc., Bridgewater, NJ.*

Regulatory guidance documents and audits of pharmaceutical drug product manufacturing operations are intended to preserve the quality and safety of active pharmaceutical ingredients (APIs) and drug products. Historically, regulatory authorities have assigned certain APIs to various "categories of concern," based on their toxicological properties, in the interest of protecting patients from exposure to potentially hazardous contaminants. Equipment used to manufacture multiple products has the potential of becoming cross-contaminated. In the absence of data clearly demonstrating safety, these categories were intended to provide appropriate segregation for the prevention of potential cross-contamination as outlined by current Good Manufacturing Practices. However, the use of specific categories of concern often overlooked other characteristics of the API, such as pharmacologic potency and mechanism of action, which might also trigger specific requirements for safe handling and disposal. Drug manufacturers are often asked by contract manufacturing organizations whether or not APIs are "cytotoxic", "steroids", or "hormones." As these terms were never defined, clarification is needed because the pharmacological mechanism of new APIs has dramatically changed since the time these terms were first introduced. Also, certain compounds may be inappropriately placed in one of these generic categories, giving the impression that segregation or dedication is required when in fact an acceptable daily exposure can be established and sufficient cleaning achieved. This presentation will discuss the historic use of these categories within the context of assessing their toxicological and pharmacological characteristics to help identify compounds requiring special attention within a Quality Risk Management Program.

PS 649b Cleaning Product Ingredient Safety Initiative: Development of the Hazard Database

E. Williams[1], M. Ciarlo[3], P. DeLeo[2], C. Horne[3], K. Connors[1], B. Greggs[4] and B. W. Brooks[1]. [1]*Baylor University, Waco, TX,* [2]*American Cleaning Institute, Washington, DC,* [3]*EA Engineering, Science, & Technology, Sparks, MD and* [4]*Soleil Consulting, Sanibel, FL.*

The American Cleaning Institute (ACI) is the industry trade association that represents the formulators of more than 90% of the consumer cleaning products in the United States. Under the Cleaning Product Ingredient Safety Initiative (CPISI), ACI's recent effort gathered publicly-available hazard data for each ingredient identified during the inventory phase (comprising over 900 substances in 49 chemical categories). The purpose of this project task was to acquire data to support an upcoming screening-level risk assessment. Primary data sources included EPA's HPVIS, OECD's HPV chemical archive, ECHA REACH dossiers, and the HERA project. In numerous cases, chemical ingredients were noted as safe food additives by the FDA. Acquisition of hazard data relevant to human health included standard regulatory endpoints: acute and repeated dose studies, skin and eye irritation, skin sensitization, toxicity to development and reproduction, mutagenicity, and carcinogenicity. Dose descriptors included NOAELs, LOAELs, LD50s, LC50s, and judgments on irritation and sensitization. Studies that were judged as reliable (i.e., Klimisch 1 or 2) were acquired. To date, over 5,000 hazard data points have been entered into the CPISI database. Available data on hazard for all endpoints will be presented (e.g, ranges of NOAELs, LOAELs and LD50s), using chemical groupings when available. Decision-making on hazard noted the absence of primary data for a number of ingredients, and in numerous cases read-across approaches were employed. For the majority of chemicals in the ACI Ingredient Inventory, sufficient hazard data were available in the public domain. However, for some sole-source proprietary ingredients, public hazard data were not available as these are often considered confidential between the supplier and user. A web-based clearinghouse has also been developed to provide references for publicly-available hazard data for each ingredient.

PS 649c Results of the American Board of Toxicology Standard of Knowledge Survey Instrument

J. E. Hulla[4] and D. Petersen[1, 2, 3]. [1]*American Board of Toxicology, Raleigh, NC,* [2]*University of Cincinnati, Cincinnati, OH,* [3]*EPA, Cincinnati, OH and* [4]*US Army Corps of Engineers, Sacramento, CA.*

Complexity and diversity of toxicological sciences and risk-based assessments is expanding, and there is growing need for certification of competency and command of a current professionally-based standard of knowledge (SoK). On behalf of the American Board of Toxicology (ABT) we commenced to define the breadth and depth of expertise of professional toxicologists with the intent to review and refine the ABT certification criteria. A survey instrument was designed and piloted, then distributed broadly in the second quarter of 2013. 796 respondents representing 12 professional toxicology job roles (academic, agricultural, chemical, etc.) ranked the importance of 82 knowledge elements in their current professional practice. Specific elements ranked highest (≥50%) across all roles) included: Risk and safety assessments; mechanisms of toxicity and exposure, disposition and biotransformation of toxicants; regulatory toxicology, clinical pathology; target organ systems (notably, liver, lung, kidney and reproductive) ; chemical carcinogenesis, mutagenesis, and epigenesis; study designs and in vivo methodologies. Notably, the above were ranked consistently across all 12 toxicology professions, with all differences in emphasis being those anticipated within specific professions. Knowledge elements ranked 'not needed' by ≥20% or respondents included: History of toxicology, forensics, and specially-explicit techniques. These results provide a robust basis with which to define a SoK stratifying and providing appropriate focus on knowledge elements across current professional toxicology roles, upon which specific components of a certification program can be expressly linked.

PS 649d Mercury Exposure: Risk Assessment, and Risk Management

S. G. Gilbert[1] and E. Groth[2]. [1]*INND, Seattle, WA and* [2]*Groth Consulting Services, Pelham, NY.*

There is no doubt that methylmercury (MeHg) is neurotoxic and an undesirable contaminant of fish. The potential toxicity of mercury has been known since ancient times, but more modern awareness of the tragic consequences of MeHg exposure began in the 1950s at Minamata, Japan. This and other incidents led to the realization that inorganic mercury was readily biomethylated by bacteria to MeHg, which biomagnified and bioaccumulated up the food chain. High-order fish such as shark, tuna, and swordfish accumulate MeHg in their muscle, and humans and wildlife are exposed to MeHg when they consume contaminated fish. Recent epidemiological studies including those from New Zealand, Faroe Islands, and Seychelles have reported adverse effects of methylmercury, such as lower scores for attention, language skills, memory, eye-hand coordination and other fine motor responses, at exposure levels around or even below the current mercury RfD. Epidemiology studies since 2003 have focused on lower level MeHg exposure and more subtle developmental effects such as verbal development. In 2001 the US Environmental Protection Agency set an oral RfD for MeHg at 0.1 μg/kg/day, and later established an advised MeHg fish tissue level of 0.3 ppm for human health based upon water quality standards. A summary of recent studies on the developmental effects of MeHg indicates that a new risk assessment could lower the current RfD to 0.025 μg/kg/day. There is growing recognition of health hazards to high fish consumers of all ages. What should a revised RfD be in order to protect human health? In 1969, the US Food and Drug Administration (FDA) set a 0.5 ppm action level for total mercury in fish. The FDA raised the action level for total mercury to 1 ppm in 1979, and in 1984, it switched the standard from total mercury to 1 ppm methylmercury in fish. Part of the challenge is that risk depends on dose (the product of fish Hg level, fish intake and body weight), not merely on fish Hg level, so it is conceptually not possible to define a "safe" level of Hg in fish. An additional challenge is that fish consumption has substantial nutritional benefits, not just risks.

PS 650 Industrial Effluent-Induced Chromosomal Aberration in Catfish from Ogun River, Lagos, Nigeria

O. T. Iji[1, 3] and A. A. Adeogun[2]. [1]*Department of Paraclinical Sciences, Faculty of Veterinary Sciences, University of Pretoria, Ondersteepoort, Guateng, South Africa,* [2]*Department of Zoology, University of Ibadan, Ibadan, Oyo, Nigeria and* [3]*Federal College of Animal Health & Production Technology, Ibadan, Oyo, Nigeria.*

The aim of the study is to evaluate the cytotoxic effect of effluents at inducing chromosomal aberrations, using this as a biomarker tool in wild *Clarias pachynema* for assessing and monitoring pollution of the aquatic environment. A total of 60 live fish (30 each downstream and upstream) were obtained and subjected to chromosomal analysis. Chromosomal aberration in the fish samples from the downstream sector was recorded at a rate of 30%, while there were no aberrations in the samples collected upstream the effluent discharge point. Water sample analysis revealed a high concentration of Ammonia and Nitrates above permissible standards of FEPA guidelines. Heavy metal analysis also revealed the presence of Cr (0.05), Cu (0.01), Pb (0.05), Zn (5.0) and Fe (0.3) above permissible standards from the downstream section of the river. This study shows clearly that the ever increasing discharge of effluents from the industry could increase chromosomal damage in the aquatic components.

PS 651 Enzymatic Biomarker in Blackjaw Tilapia (*Sarotherodon melanotheron*) and Bagrid Catfish (*Chrysichthys nigrodigitatus*) in the Lagos Lagoon

S. O. Ayoola and A. A. Idowu. *Marine Sciences, University of Lagos, Lagos, Lagos, Nigeria.*

The indiscriminate dumping and release of wastes and hazardous substances into rivers might lead to environmental disturbance that could be considered a potential source of stress to the biotic community. A toxicological study was carried out to ascertain the effects of aquatic pollutants in the blood of *Chrysichthys nigrodigitatus* and *Sarotherodon melanotheron* at the Lagos lagoon for a period of six weeks. Four enzymatic biomarkers which include protein, superoxide dismutase, Malondialdehyde and Reduced Glutathione and also the physiochemical parameters of the water were analyzed. The water quality parameters were Temperature which has a mean of 24.5±0.5, Dissolved oxygen 1.65±0.05; Biological oxygen demand 106±17.0 and pH 7.1±0.1. The BOD increases while DO decreases and temperature increases. The water was slightly alkaline. The lipid peroxidation and antioxidant biomarkers in the blood of *Chrysichthys nigrodigitatus* showed a significant difference ($P < 0.05$), while that of *Sarotherodon melanotheron* showed likewise except, SOD which showed that there was no significant difference ($P > 0.05$). This study indicates that there was an alteration in antioxidant enzyme and lipid peroxidase activities in both *C. nigrodigitatus* and *S. melanotheron* blood which may cause biochemical dysfunction in this specie.

PS 652 Coral Allelochemical Toxicity and the Role of Cytochrome P450 Detoxification in Butterflyfish (*Chaetodon spp.*) of Differing Feeding Strategies

A. Maldonado[1], D. Schlenk[1], R. Lavado[1], G. Ostrander[2], S. Knutson[4], M. Slattery[3] and S. Ankisetty[3]. [1]*Environmental Science, University of California, Riverside, Riverside, CA,* [2]*Florida State University, Tallahassee, FL,* [3]*University of Mississppi, University, MS and* [4]*University of Hawaii at Manoa, Honolulu, HI.*

Cytochrome P450 monooxygenase (CYP) is the primary enzyme system for detoxification of xenobiotics including dietary chemicals and pollutants. Little is known about the biotransformation and detoxification of allelochemicals derived from dietary products in marine organisms. Certain species of butterflyfish of the genus *Chaetodon* have been shown to feed on several species of chemically-defended corals including the soft corals *Sinularia spp.* 5-episinuleptolide (5ESL) is an allelochemical found at high concentrations in *Sinularia maxima*. This study examined the effects of 5ESL on the expression and catalytic activities of CYP3A and CYP2 in the butterflyfish species *Chaetodon unimaculatus, Chaetodon kleinii, Chaetodon auriga*, and *Chaetodon multicinctus*. Fish were gavaged at ecologically-relevant concentrations of 1.0 and 3.0 mg/kg of 5ESL. Testosterone hydroxylase (TOH) 16 β was 16 times higher in fish treated with 5ESL. Testosterone hydroxylase (TOH) 16 β in control animals was 6 times higher than other hard coral feeding species. These results indicate an induction of CYP2 (16-α TOH) and CYP3A (6 β, 16 β TOH) catalytic activities in detoxification of 5ESL in *C. unimaculatus*, which preferentially feed on this coral species in Guam.

PS 653 Transcriptome Analysis of Red Seabream (*Pagrus major*) Embryos Treated with 2, 3, 7, 8-Tetrachlorodibenzo-*p*-Dioxin (TCDD)

M. Iida[1], S. Fujii[1], M. Uchida[2], H. Nakamura[2], Y. Kagami[2], S. Bak[3], E. Kim[3], Y. Shima[4] and H. Iwata[5]. [1]*Computer Science and Systems Engineering, Kyushu Institute of Technology, Iizuka, Japan,* [2]*Ecogenomics, Inc., Kurume, Japan,* [3]*Department of Life and Nanopharmaceutical Science and Department of Biology, Kyung Hee University, Seoul, Republic of Korea,* [4]*Hakatajima Station, National Center for Stock Enhancement, Fisheries Research Agency, Imabari, Japan and* [5]*Center for Marine Environmental Studies (CMES), Ehime University, Matsuyama, Japan.*

TCDD induces a broad spectrum of toxic effects including craniofacial malformation and neural damage in fish embryos. These effects are mainly mediated by the aryl hydrocarbon receptor (AHR). However, there still remains a gap of mode of action between AHR activation and adverse outcomes induced by dioxins. To provide a complete picture of the AHR signaling pathway in fish embryos exposed to TCDD, red seabream (*Pagrus major*) embryos were treated with a graded concentrations of TCDD (0.3 - 36 nM) alone in seawater and with a mixture of TCDD and 500 nM of an AHR antagonist, CH223191. The transcriptome of red seabream embryos was analyzed by using our custom-made microarray with 6000 probes for this species. Jonckheere-Terpstra test was performed to detect the genes of which the mRNA expression levels were altered by TCDD exposure. Signals of total 1294 probes were significantly altered in a TCDD-dose dependent manner ($p<0.03$). These mRNA expression levels altered by TCDD exposure were recovered by co-exposure to CH223191, suggesting the mRNA expression of these genes is regulated by AHR. The microarray data further underwent Gene Set Enrichment Analysis (GSEA)-based screening of the KEGG pathway database to identify TCDD-activated pathways. The pathway analyses showed the effects of TCDD on sets of genes related to the regulation of actin cytoskeleton, endocytosis, vascular endothelial growth factor (VEGF) signaling and synaptic long-term depression (LTD) in the embryos. The results suggest that TCDD induces teratogenicity via the dysregulation of actin cytoskeleton and neurotoxicity via VEGF signaling alterations and LTD.

PS 654 Impacts of Hypersaline Acclimation on the Sublethal Toxicity of Chlorpyrifos to Salmonid Olfaction

L. A. Maryoung[1], R. Lavado[1], G. Hardiman[2], R. Sasik[2], N. Agarwal[2], K. Tierney[3] and D. Schlenk[1]. [1]*Department of Environmental Sciences, University of California, Riverside, Riverside, CA,* [2]*Department of Medicine, University of California, San Diego, San Diego, CA and* [3]*Department of Biological Sciences, University of Alberta, Edmonton, AB, Canada.*

Acclimation to hypersaline environments enhanced the acute toxicity of certain organophosphate pesticides to euryhaline fish species; however sublethal effects have been far less studied. The present study focuses on the sublethal toxicity of chlorpyrifos to salmonid olfaction after hypersaline acclimation. To determine molecular effects of combined exposure, coho salmon were acclimated to three different salinities (8, 16, and 32ppth) for one week and mRNA was collected from the olfactory rosettes. Micrroarray hybridization was used to determine differences in gene expression for the different salinity treatments. Potential target genes involved in signal transduction, which have been shown to be impacted by chlorpyrifos in zebrafish, were identified and included chloride interacellular channel 4, guanylate cyclase activator 1A (retina), G-protein (zgc:101761), calcium/calmodulin-dependent protein kinase II delta, and adrenergic alpha 2C receptor. To assess physiological effects, electroolfactograms (EOGs) were conducted on rainbow trout acclimated to freshwater and 16ppth with co-exposure to environmentally relevant concentrations of chlorpyrifos (0.5 and 5.0 μg/L). Exposure to chlorpyrifos following acclimation to hypersalinity significantly decreased the response to L-serine and decreased the response to taurocholic acid additively. Gene expression of the five target genes was examined in olfactory tissue from rainbow trout used in the EOG study. Exposure to hypersalinity and chlorpyrifos up-regulated all five target genes. The combined results from the molecular and physiological experiments show that sublethal exposure to chlorpyrifos after hypersaline acclimation negatively impacts salmonid olfaction, which may result from diminished signal transduction in olfactory neurons (NIEHS P30ES07033 and T32 ES018827).

PS 655 Subthreshold Toxic Effects of Atrazine and Three Degradates on Learning and Behavior in *Procambarus clarkii*

C. B. Starkey, A. C. Lefevre and B. L. Antonsen. *Biology, Marshall University, Huntington, WV.* Sponsor: J. Lipscomb.

Atrazine is among the most heavily applied pesticides worldwide, and recent evidence suggests that it may be unsafe at environmental levels. It has been classified as a possible human carcinogen and is an endocrine disruptor. The US EPA Maximum Contaminant Level (MCL) is 3 ug/L for human ingestion and 200 ug/L for limited human exposure. Several environmentally persistent degradates have been identified, including deethylatrazine (DEA), deisopropylatrazine (DIA) and hydroxyatrazine (HA). However, these degradates have no MCL established, although some are suggested toxins. Thus, there remains concern for the risk associated with atrazine and its metabolites in the environment. Little data exist describing sublethal effects of atrazine and its degradates. Fortunately, toxicological research has evolved past dependency on mortality measures to incorporate sophisticated behavioral studies that can elucidate the effects of sublethal exposure to toxins. The goal of this research was to use such parameters to quantify the subthreshold (below the level at which harm is immediately detected) toxic effects of atrazine, DEA, DIA and HA on learning and behavior in *Procambarus clarkii* (red swamp crayfish), a sensitive bioindicator species. Crayfish were placed in an aquatic T-maze (classic method to test cognitive ability) with a food reward in a side arm. Time needed for each animal to locate the reward over repeated trials was recorded, as was time to enter and time spent in each section of the maze. Concentrations of the chemicals tested represented an environmentally realistic range. There was an observed increase in time needed to locate reward for all treatment groups, each taking a minimum mean of 25% longer than control, and most treatment groups had a failure rate (did not find food) at least 2x greater than control. Based on these results, crayfish exposed to atrazine and its degradates at low, biologically relevant doses were lethargic, less explorative, and had impaired learning compared to untreated animals.

PS 656 Concentrations of Metals Associated with Crude Oil from the BP Macondo Spill in Fish Collected from the Northeastern Gulf of Mexico across a Four-Year Period

A. C. Nichols, D. A. Steffy, J. Morgan and S. T. Gardner. *Physical and Earth Sciences, Jacksonville State Univ, Jacksonville, AL.*

Chromium (Cr), nickel (Ni), lead (Pb) and thallium (Tl) were reported by EPA (USEPA, 2010) as components of the crude oil released into the northeastern Gulf of Mexico in the spring and summer of 2010 as a result of the Macondo spill. To investigate the uptake and duration of these metals in the marine food chain, scad mackerel (*Trachurus lathami*) collected in October and November of 2009, 2010 and 2012 were analyzed for metal concentrations. Scad were collected off of the Gulf coasts of Florida and Alabama as part of the yearly NOAA small pelagic trawl survey. Collection sites roughly followed the 200 m contour line. Freeze-dried fish tissue samples were analyzed for the four metals by ICP using USEPA Methods (1994). Tissue levels for each metal were compared among the three collection periods using one-way analysis of variance (ANOVA) and Tukey's multiple comparison test. Thallium levels were significantly higher in 2010 compared to both 2009 and 2012. Chromium and Ni levels were higher in 2010 than 2009, but the difference was not significant. However, Cr and Ni levels were both significantly higher in 2010 compared to 2012. Surprisingly, Pb tissue levels were significantly higher in 2009 compared to both 2010 and 2012. Our data indicate that during the year of the BP oil spill, levels of three of these metals increased in scad. However, this increase was transitory as two years after the oil release tissue levels had returned to pre-spill values.

PS 657 An Evaluation of Mancozeb Toxicity on Adult Zebrafish Gills

A. Shohatee and L. D. Trombetta. *Pharmaceutical Sciences, St. John's University, Queens, NY.*

Freshwater ecosystems often become susceptible to various pesticides as a result of crop dusting and/or spraying as well as run-off from agricultural plots. Exposure to these compounds can result in deleterious effects to individual species as well as upset the homeostatic nature of these ecosystems. Mancozeb, manganese-zinc ethylenebis (dithiocarbamate), is fungicide applied to a wide range of crops, vegetables, seeds and ornamental plants, which may enter such ecosystems. Previous studies have suggested that Mancozeb exerts its toxicity through mechanisms related to the induction of oxidative stress. The purpose of this study is to investigate the oxidative stress inducing potential due to Mancozeb exposure in the gills of zebrafish, *Danio rerio*. The gills of fish are permanently in contact with environmental water thus becoming a prime target for waterborne toxicants. Adult male zebrafish were exposed to 0.475, 0.95, and 1.9 mg/L (1.8, 3.6, and 7.2 μM, respectively) of Mancozeb for three hours and then immediately euthanized. Gills were extracted and processed according to each experiment's protocol. Scanning electron micrographs suggest that Mancozeb causes morphological changes to the epithelial cells comprising the surface of the gills. These changes include the appearance of rounded cells and exfoliation from the basement membrane, when compared to the flattened tightly adjoined cells found on the gills of controls. Glutathione peroxidase (GPx) activity was assessed to investigate antioxidant activity against hydrogen peroxide formation due to Mancozeb exposure. GPx activity showed a significant dose-dependent increase in activity when compared to control.

PS 658 Environmental Testing Strategy for Pharmaceuticals with Endocrine Disrupting Properties

Z. Dang[1] and C. Bodar[2]. *[1]RIVM, Bilthoven, Netherlands and [2]RIVM, Bilthoven, Netherlands.*

Environmental risk assessment (ERA) of human pharmaceuticals with endocrine disrupting properties should be performed irrespective of the quantity released into the environment. It is unknown, however, which ecotoxicity tests are needed and which should be performed first. Currently we are collecting ecotoxicity testing data on the daphnid 21-day reproduction assay, the mysid two-generation toxicity test, the harpacticoid copepod development and reproduction test, the mollusc toxicity test, the fish early-life stage toxicity test, the short term fish reproduction assay, the fish sexual development test, and fish partial/full life cycle toxicity tests. These tests have been validated, or are currently being validated within the OECD test guidelines programme. The fish short-term reproduction assay and the daphnid reproduction test were evaluated by compiling 140 studies (41 chemicals) for fish and 123 studies (85 chemicals) for crustacean. The preliminary results showed: 1) a differential sensitivity in the testing endpoints for both fish and daphnia toxicity tests: fecundity is the most sensitive endpoint, whereas sex ratio is less sensitive, and 2) biomarker responses related to endocrine-mediated effects could be observed in the fish test, but not in the daphnia test. Further analysis will include a comparison of LOECs among daphnids, mysids, copepods, molluscs and various fish tests. By analysing these ecotoxicity data, it will become clear if invertebrate toxicity tests should be performed prior to fish tests, and, if fish tests are then still considered to be needed, if both a fish development toxicity test and reproduction toxicity test have to be carried out. Based on the overall data analysis, we will propose an environmental testing strategy, which is important for minimizing vertebrate testing and costs.

PS 659 Short-Term Effects of Dechlorane Plus on Earthworm *Eisenia fetida* Determined by System Biology Approach

L. Zhang, F. Ji, M. Li, Y. Cui and B. Wu. *School of the Environment, Nanjing University, Nanjing, China.*

Dechlorane Plus (DP), a chlorinated flame retardant, has been widely detected in environmental matrices, especially in sediment and soil. DP has the characteristics similar to persistent organic pollutants. However, no toxicity data of DP on terrestrial invertebrate are available. In this study, earthworm *Eisenia fetida* were exposed to 0.1, 1, 10, and 50 mg/kg DP for 14 days. The lethality, oxidative stress and damage, neurotoxicity, and transcriptomic profiles of *E. fetida* were assessed on day 7 and day 14. Results showed that 50% lethal concentration (LC50) for DP was higher than 50 mg/kg. However, DP exposure could induce an increase of malonaldehyde (MDA) and 8-Hydroxy-2'-deoxyguanosine (8-OHdG) levels, and facilitate changes of acetylcholinesterase (AChE) activities. High throughput sequencing-based transcriptomic analysis showed that DP exposure significantly altered gene expression and pathways related to antioxidant enzyme, stress response, neurological dysfunction, calcium binding and signal transduction. The results from different toxicological endpoints indicate that DP toxicities on earthworm focus on oxidative damage and neurotoxicity. Based on these results, we deduce that the oxidative stress might be one of mechanism of DP toxicity actions. This study provides an insight into toxicological effects of DP on earthworm, and is useful for the risk assessment of DP on soil ecosystem.

PS 660 Comparison of Aquatic Toxicity between Silver Nanoparticles and Silver Nanowires

E. Sohn[1], S. Johari[2], T. Kim[1], J. Kim[1], J. Lee[1] and I. Yu[1]. *[1]Institute of Nanoproduct Safety Research, Hoseo University, Asan, Republic of Korea and [2]Aquaculture Department, University of Kurdistan, Sanandaj, Islamic Republic of Iran.*

To better understand the potential ecotoxicological impacts of silver nanoparticles (AgNPs) and silver nanowires (AgNWs) released into freshwater environments, the toxicities of these nanomaterials were assessed and compared using standard OECD guidelines including "*Daphnia* sp., Acute Immobilisation Test", "Fish, Acute Toxicity Test", and "Freshwater Alga and Cyanobacteria, Growth Inhibition Test". According to estimated median lethal/effective concentrations of AgNWs/NPs in the present study, the order of animal susceptibility was: *Daphnia magna* > *Raphidocelis subcapitata* > *Oryzias latipes*. Thus, both AgNPs and AgNWs tested in the current study should be classified according to GHS (Globally Harmonized System of Classification and Labelling of Chemicals) as "category acute 1" for *D. magna*, and "category acute 2" for *O. latipes* and *R. subcapitata*. The results showed that AgNPs were more toxic when compared with AgNWs. The change in toxicity could be because of the different degree of Ag+ dissolution due to differences in surface area between the sphere shape of AgNPs and the rod shape of AgNWs. In general, our results suggest that the release of silver nanomaterials into the freshwater aquatic environment should be carefully considered.

PS 661 Effect of Triclosan Challenges on Chlorine Tolerance in Bacteria Found in Waste Water Effluent

C. E. Woodward, C. G. Dean and J. A. Roling. *Bridgewater State University, Bridgewater, MA.*

Triclosan is a chlorinated aromatic compound that is used as an antibacterial agent in many household products such as toothpaste and antibacterial hand soaps. Triclosan from these products end up in wastewater discharge. With constant exposure to triclosan, bacterial tolerance is expected to develop in waste water effluent. Because triclosan contains chlorine within its structure, there may be a causal relationship between triclosan exposure and chlorine tolerance. Samples were collected from four rivers in Massachusetts; the Hoosic River (Adams, MA), the Nashau River (Clinton, MA), the French Stream (Rockland, MA), and the Nemasket River (Middleboro, MA). These sites were selected because the effluent

discharge was the first NPDES on each of the rivers, although no triclosan was detected in the water. River samples both upstream and downstream to the effluent discharge were collected. After plating, 288 colonies were isolated from each of the four sites. The NOAEC and LOAEC of triclosan was determined to be 0.001 mg/ml and 0.004 mg/mL, respectively. The bacteria were exposed to 0.05 and 0.001 mg/mL triclosan or to 50 mg/mL chlorine for 24 hours in an orbital shaker at 30C and 175 rpm. The bacteria that were exposed to the triclosan were then exposed to 50 mg/mL chlorine for 24 hours in the same conditions specified above. Growth was measured during the triclosan challenges and chlorine exposure using spectrophotometry absorbance at 600 nm. There is no difference in bacterial chlorine tolerance due to waste water effluent (increased tolerance in bacteria upstream and downstream were 17.2% and 12.3%, respectively). Low concentration triclosan challenges increased bacterial chlorine resistance more than high concentration triclosan challenges (9.5% and 1.7%, respectively). Incidence of increased chlorine tolerance in bacteria was independent of sample site (Hoosic: 13.9%, Nashua: 21.2%, French: 11.5%, Nemasket: 12.5%).

PS 662 Biomonitoring and Risk Assessment of Nonpoint Source Pollution in Jingchuan Wetlands of Northeast China Using Nematodes

Y. Wang[1, 3], C. He[2], L. Sheng[2], X. Wang[1] and T. Guo[3]. [1]*Northeast Institute of Geography and Agroecology, Chinese Academy of Sciences, Changchun, China,* [2]*School of Environment, Northeast Normal University, Changchun, China and* [3]*University of Georgia, Athens, GA.*

Cultivation for agricultural production often poses threats to wetlands ecosystems in fertile landscapes. Jinchuan Wetlands, located in the northeast China, is facing the risks of non-point source pollution (NPS) pollution by farmland additives from uplands draining including rainfall and snowmelt. Nematodes are frequently used as biological indicators of environmental stresses, and *Caenorhabditis elegans* could be a useful model in ecotoxicological studies. In this study, nematode ecological indexes in the wetland, the farmland, and the edge of wetland and farmland in Jingchuan Wetlands were evaluated by random sampling. In addition, we determined the main soil environmental properties that were critical for the stability of the nematode community. The 24 h mortality and changes in behavior and reproduction in *C. elegans* strains exposed to the sampled waters were also examined. Expressions of heat shock protein (Hsp) 70 and Hsp90 were measured using ELISA both in the field bacterivore nematode species related to *C. elegans*, and the standard lab strain of *C. elegans* for modeling test. Our results suggested that disturbance to wetland ecosystems by NPS pollution reduced the nematode richness (from 2.24 to 1.92), and proportions of bacterivore nematodes (from 32.0% to 19.0%). *Acrobeloides*, which was a dominant genus in the core of wetlands, had declined to less than 10% as a common genus in the edge. In summary, bacterivore nematode diversity and plant-parasitic ecological index were proven to be sensitive indicators of the ecological health of wetlands. The genus *Acrobeloides* and Hsp70 were useful biosensors to monitor and assess the levels of NPS pollution in wetlands. Furthermore, multi-level soil faunal assessments by canonical correspondence analysis showed that Jinchuan Wetlands are undergoing NPS pollution risk by nearby farmlands.

PS 663 Toxicity, Bioaccumulation, and Human Health Risk Assessment of Lead and Cadmium in *Tilapia guineensis*

O. K. Yemitan[1], O. O. Adeyemi[2] and P. F. Wright[3]. [1]*Pharmacology & Toxicology, Lagos State University College of Medicine, Ikeja, Lagos, Nigeria,* [2]*Pharmacology, College of Medicine of the University of Lagos, Lagos, Lagos, Nigeria and* [3]*Toxicology, School of Medical Sciences, RMIT-University, Bundoora Campus, Victoria, VIC, Australia.*

In Nigeria, data are sparse for the background levels, toxicity potentials as well as human health risk potentials of heavy metals in aquatic species.
This study investigated the background levels, acute (96 h) toxicity, and bioconcentration and bioaccumulation potentials of lead (Pb) and cadmium (Cd) in *Tilapia guineensis* of a Nigerian habitat in a laboratory model. A human health risk assessment was also conducted based on the measured levels of Pb and Cd in the organism and habitat waters.
Acute (96 h) exposure to graded concentrations of Pb(NO3)2 produced mortalities with LC50 values of 58 mg/L in *T. guineensis*; while CdCl2 exposure gave LC50 of 21 mg/L. The 28-day bioaccumulation studies using one-hundredth of the LC50 values of Pb or Cd produced increasing and significant ($P<0.05$, ANOVA) Pb concentrations in whole fingerlings, as well as dissected fish samples thus: fleshy muscle (1.105μg/g), liver (1.056μg/g), gills (0.702μg/g) and GIT (0.102μg/g). In the Cd study, results were liver (1.167μg/g), gills (0.518μg/g), muscle (0.372μg/g) and GIT (0.111μg/g).
In the human health-based risk assessment, the hazard quotient (HQ) for Pb or Cd did not indicate potential for adverse health effects. However, the Hazard Index (HI) for Pb in city (1.06) and riverine (1.46) children, but not adults, indicated potential for adverse health effects. In contrast, the HQs and HIs for Cd were less than 1 and as such did not indicate potential for adverse health effects. The HI for combined Pb and Cd exposure of riverine children (1.13) indicated potentials for non-cancer, but not for cancer health risks.
In conclusion, Pb and Cd are bioconcentrated in various tissues of local Nigerian fish to considerable levels, with the potential for non-carcinogenic health effects mainly from exposure to Pb in human receptor groups.

PS 664 Textile Dye Reactive Blue 15 Reduces the Reproduction in *Ceriodaphnia dubia*

D. P. Oliveira and G. Meireles. *University of São Paulo, Ribeirão Preto, Brazil.*

Introduction: Dyes are widely used in different types of industries, such as textile, pharmaceutical, food, cosmetics, photographic, among others. However, these substances can be toxic, mutagenic and resistant to many degradation processes used in wastewater treatment. It is estimated that about 15% of the dyes used in the world are lost during the dyeing process and released into the environment, affecting mainly water bodies. However, despite the large amount of commercial dyes available and high quantity released in the aquatic ecosystem, studies about the toxicity of these substances are scarce and little is known about their mutagenic and ecotoxicological effects. Objectives: The aims of this study were to evaluate the ecotoxicity and genotoxicity of the textile dye Reactive Blue 15 (RB15). Methodology: The ecotoxicological assays with *Daphnia similis, Vibrio fischeri* and *Ceriodaphnia dubia* were realized according to ABNT NBR12713:2009, ABNT NBR15411-3:2012 and ABNT NBR 13373:2010, respectively. The Comet assay was carried out according to Tice et al. (2000) and *Salmonella* mutagenicity assay was carried out according to Maron and Ames (1983) and Mortelmans and Zeiger (2000). Results: The RB15 dye was relatively non-toxic to *Daphnia similis* and reduced the *Vibrio fischeri* luminescence in high concentrations. The RB15 dye reduced fecundity of *Ceriodaphnia dubia* and was not mutagenic and genotoxic to human dermal fibroblasts. Discussion: RB15 did not induce acute toxicity but in chronic exposure the dye reduced the reproduction in *C. dubia*. This decrease can be harmful to the aquatic organisms. This dye did not induce DNA damages in the tested conditions. Conclusion: The results shows that the dye can cause adverse effects on organisms even at low concentrations in chronic exposure and that the continuous release of these substances in water bodies is worrying.

PS 665 Assessment of the Expression Levels of Genes Involved in Metal Detoxification in Killifish Inhabiting a Closed Copper Mine Superfund Site

D. Jung, A. Cravero, R. Lehman, E. Cutting, B. Jackson and B. Stanton. *Geisel School of Medicine at Dartmouth, Hanover, NH.*

The Callahan Mine Superfund site in Brooksville, ME is a closed open-pit copper mine and is currently flooded with seawater. The sediments at this site are contaminated with extremely high levels of metals such as cadmium, lead, copper, and zinc. Consequently, killifish (*Fundulus heteroclitus*) inhabiting this Superfund site are constantly exposed to these metals. A survey has shown that killifish collected from the site have significantly higher metal concentrations in tissues compared to fish collected from a nearby reference site. Therefore, we hypothesized that killifish from the Superfund site have elevated expression of genes involved in antioxidant defense induced by metals, and metallothionein (MT), a protein involved in metal detoxification. To test this hypothesis, we collected fish from three different locations within the Superfund site, as well as from a reference site nearby. Gills and livers were isolated for gene expression analysis from twelve individuals at each location. Expression levels of five oxidative stress response genes (nuclear factor erythroid-related factor-2 (Nrf2), glutathione-S-transferase-alpha (GSTα), glutamate cysteine ligase catalytic subunit (GCLc), Mn-superoxide dismutase (SOD2), and catalase) and MT were measured by Q-RT-PCR. In addition, tissues were analyzed for metal content. Tissue samples collected from the Superfund site had significantly high levels of cadmium and copper. Surprisingly, MT mRNA levels were not different in the gills and livers of fish collected from the Superfund site compared to the reference site. In addition, none of the oxidative stress response genes showed significant differences among the collection sites. Therefore, constant exposure to extremely high levels of metals does not seem to affect the expression of genes involved in metal detoxification pathways. Examination of protein expression of these genes will provide more information on whether killifish at the Callahan Mine Superfund site have adapted to high levels of metals in the environment.

PS 666 Evaluating the Relationship between Land Use and Water Quality in Non-PRASA Systems

W. Morales-Soto and J. Arce-Nazario. *Biology, University of Puerto Rico Cayey, Cayey, Puerto Rico.*

Puerto Rico currently has more than 250 non-PRASA water systems, which are water systems that are not serviced by the Puerto Rico Aqueduct and Sewer Authority (PRASA). These non-PRASA systems have limited resources for water management and are often non-compliant with the Safe Drinking Water Act. The majority of these systems are located on the rural part of the island, which are characteristically areas of increased poverty. Due to their lack of resources they are often unable to administer the proper treatments and testing for the water systems. This can be potentially hazardous to these communities since poor water quality can result in the proliferation of diseases and exposure to toxic compounds. Our goal was to use geographic analysis to determine the risks of these systems for water contamination. To evaluate how geographic factors could shape the water quality of non-PRASA systems, we (1) organized the database on water quality from the Puerto Rico Health Department for 92 non-PRASA systems, (2) defined the watershed area for each system using ArcMap, (3) evaluated the human activities within the watersheds. We found that water systems that were located near areas with high agricultural activity had the highest nitrate concentration, whereas areas that were within 500 m of a conservation area had the lowest nitrate levels. Our results also suggest that multiple variables can influence water quality, including land cover distribution, environmental factors, and socio-economic factors. Theses results have important policy implications for promoting forest conservation in non-PRASA watersheds or for connecting non-PRASA community members to PRASA systems in regions where watersheds are highly impacted.

PS 667 Metals, PAHs, and Toxicity of Sediments from Santa Marta, a Coal Port in Colombia

K. Caballero-Gallardo[1], J. De la Rosa[2], B. Johnson-Restrepo[3], A. Garcia-Cantillo[3], A. Guerrero-Castilla[1] and J. Olivero-Verbel[1]. [1]*Environmental and Computational Chemistry Group, University of Cartagena, Cartagena, Colombia,* [2]*Associate Unit CSIC-CIQSO, University of Huelva, Huelva, Spain and* [3]*Environmental Chemistry Research Group, University of Cartagena, Cartagena, Colombia.*

Extraction, transport and utilization of coal spread out coal dust. Nowadays, Colombia is one of the most important producers of this mineral in South America, being Santa Marta one of the two largest coal exporting ports in the country. The aim of this work was to assess the bioactivity, and the presence of metals and PAHs in sediments from the line coast of Santa Marta. Forty-six trace elements were analyzed by ICP/MS and 16 PAHs by GC/MS in 8 locations (S1–S8) around Santa Marta Bay, during two sampling campaigns, April (C1) and September (C2) 2011. mRNA expression was performed for selected genes in HepG2 cells treated for 12 hours with 1% sediment extracts in DMSO. PAHs levels were lower during C2 when compared to C1. The highest value for ∑PAHs was found at S9 (90 ng/g), a site located around 300 m far from the coast line at close proximity to the area where coal is loaded into cargo vessels for international shipments. At this point, the most abundant PAH was naphthalene. However, for S3, a sample taken in a beach next to the coal port in downtown Santa Marta Bay, ∑PAHs was 63 ng/g for C1 and 76 ng/g for C2, with the greatest concentration observed for fluoranthene. Pb, Zn, Zr, As and Li presented the greatest concentrations at S9, although sediments collected at S3 and S8, this last in front of the city of Cienaga, had the greater metal concentrations. Fluoranthene/Pyrene ratio revealed sources of PAHs are variable. Extract from S3 induced overexpression of CYP1A1 when compared to vehicle control, whereas those from S6-S9 overexpressed NQO1. This effect was observed during C1. These data showed the coal port of Santa Marta is a source of diverse chemicals that are toxicologically active. Colciencias-UniCartagena, 110749326186-2009. K.C. is sponsored by Colciencias, 567-2012.

PS 668 The Toxicity of Particle-Based Dispersants for Marine Oil Spills and Their Impact on Benzene Toxicity Using the Model Organism *Artemia franciscana*

A. L. Rodd[1], M. Creighton[2], R. Hurt[2] and A. Kane[1]. [1]*Pathology & Laboratory Medicine, Brown University, Providence, RI and* [2]*School of Engineering, Brown University, Providence, RI.*

Fine particles like carbon black can assemble at water-oil interfaces to stabilize oil droplets, forming what is known as a Pickering emulsion. These novel dispersants not only stabilize oil droplets like traditional surfactant-based dispersants, they can also adsorb toxic, water-soluble fractions of petroleum. Benzene was used as a model aromatic compound to determine the extent of the adsorption and retention of these fractions bound to carbon particles as a function of tunable surface hydrophilicity. Using a model marine microcrustacean, *Artemia franciscana* (brine shrimp), the toxicity of carbon dispersants, benzene, and mixtures was characterized using mortality and compared to a high-surface area powdered activated carbon adsorbent. Hsp70 protein expression was also measured as a sublethal endpoint to measure the general stress response of the larvae. At all concentrations tested (up to 50mg/L), the carbon black materials had no effect on brine shrimp viability, and no increase in Hsp70 expression up to 25mg/L. Induction of Hsp70 by the carbon black mixtures demonstrated an additive relationship between carbon black and low doses of benzene. In future work, the brine shrimp model will be further developed using additional sublethal bioassays that will provide a foundation for future studies to assess bioaccumulation in fish through trophic studies. This experimental approach will provide important information on potential adverse environmental effects of particle-based dispersants deployed in the aftermath of a marine oil spill. Research supported by BP/The Gulf of Mexico Research Initiative, US Dept. of Education GAANN Award, NIEHS Training Grant T32 ES07272, and the generous support of Donna McGraw Weiss '89 and Jason Weiss.

PS 669 Pesticide Distribution Pattern in Surface Water of a Mountainous Region River from Rio de Janeiro, Brazil

G. F. Veríssimo[1], J. Moreira[2] and A. Meyer[1]. [1]*IESC, Universidade Federal do Rio de Janeiro, Rio de Janeiro, Brazil and* [2]*CESTH, Fundação Oswaldo Cruz (FioCruz), Rio de Janeiro, Brazil.* Sponsor: G. Veríssimo.

Paraquat (PQ) is an herbicide widely used in several crops as a desiccant. Due to its moderate toxicity, the fate of PQ in the environment is of great concern. In the mountain region of Rio de Janeiro, where PQ is intensively used, the river water is used for irrigation and recreation but not directly as drinking water source. However, it's of interest to public health to evaluate the concentrations of such compound, since the local population consumes water from fountain near the river. The objective of this present study was to assess the concentrations of PQ in a river of an intensive agricultural area during all application seasons in Rio de Janeiro State, Brazil. PQ was measured in river water collected from 7 sampling sites totaling 80 samples during 12 sampling events between 2010 and 2012 in the São Lourenço River in Nova Friburgo-RJ, Brazil. PQ levels were determined by an enzyme-linked immunosorbent assay (ELISA) QuantiPlate™ Kit with a limit of quantification (LOQ) of 0,02 ppb. The pesticide was detected in measurable quantities in all samples. The last sampling site, where the volume of water is bigger, showed as most frequently contaminated with a median of 0,048 ppb (maximum 0,279 ppb). Pluviosity is an important element and the Spearman correlation showed that concentrations of PQ in river water vary with the monthly rainfall (R=0,682; p=0,015). The highest median concentrations and rainfall correlation were found in last site sampling (R=0,771; p=0,003). All others sites showed positive correlations, except for the first one that is the control site located in river springs in the mountain that showed a inverse correlation. Although the found concentrations were below of the limits established by regulatory agency (maximum 20 ppb), our results showed that the use of paraquat in this region impacts the river health, especially after a period of rain.

PS 669a Degradation of Tumor Promoter Activity of *Jatropha curcas* Phorbol Esters Derived from Jatropha Oil Cake in Soil

M. Nakao[1], Y. Shimizu[1], Y. Ishihara[1] and T. Yasuhara[2]. [1]*Public Health, Kurume University, Kurume, Japan and* [2]*Kitasato University, Tokyo, Japan.*

Background: Large amount of oil cake is generated during production of biodiesel fuel from Jatropha seeds. Although Jatropha oil cake is rich in plant nutrients, the presence of toxic phorbol esters limits the usage of oil cake as fertilizer. The objective of this study is to evaluate the contents and tumor promoting activity of phorbol esters by plants and Jatropha oil cake-supplemented soil.
Method: Contents and biological activity of Jatropha phorbol esters in soil and plants were sequentially analyzed by high-performance liquid chromatography (HPLC) and in vitro cell transformation assay, respectively.
Results: Jatropha phorbol ester-specific HPLC peaks disappeared after 5-week incubation with soil. Along with the degradation of Jatropha phorbol esters in soil, tumor promoter activity of Jatropha oil cake-supplemented soil was dramatically attenuated and finally disappeared. Jatropha phorbol esters and tumor promoter activity were not detected from mustard spinach cultured with Jatropha oil cake-supplemented soil.
Conclusions: These data showed that (1) contents and tumor promoter activity of Jatropha phorbol esters in oil cake were completely lost by 5-week incubation with soil and (2) Jatropha phorbol esters did not transfer into plants cultured with Jatropha oil cake-supplemented soil. Therefore, these results suggested that that Jatropha phorbol ester in oil cake could be degraded by indigenous bacteria and that Jatropha oil cake is useful as a safe fertilizer.

This study was supported by JICA/JST, SATREPS (Science and Technology Research Partnership for Sustainable Development), Japan.

PS 669b Degradation of the Major Toxic Component of *Jatropha curcas* Phorbol Esters by Enzymes and Sterilized Water

K. Yamauchi, M. Nakao, Y. Shimizu and Y. Ishihara. *Kurume University, Kurume, Japan.*

We found that toxic Jatropha phorbol esters are degraded in Jatropha-oil-cake-supplemented soil in 5 weeks. This study demonstrated degradation of the major toxic Jatropha phorbol esters by lipase and esterases in buffer and in sterilized water. Main toxic of Jatropha phorbol esters (DHPB) was purified and analyzed by high-performance liquid chromatography (HPLC) and its biological activity was tested in an in vitro cell transformation assay. DHPB was incubated with various concentrations of Lipase from *Aspergillus niger* (AL), esterases from *Klebsiella oxytoca* (SNSM-87) and *Acinetobacter calcoaceticus* (KM-109) in buffer and in sterilized water for 5 weeks at the optimum temperature and pH. DHPB degradation products were analyzed by HPLC and cell transformation test.
The optimum temperature, pH and the enzyme concentration were similar among AL, SNSM-87, and KM-109; 37°C, 6.5-8.5 and 50-100μg/ml, respectively. Following 4-weeks incubation of DHPB in sterilized water or phosphate buffer (pH7.0), DHPM-specific HPLC peaks decreased as much as 50% time-dependently. By addition of KM109 to these solutions, DHPB-specific HPLC peak was markedly decreased to about 65% on Day 7. The loss of DHPB reached to 95% at Day 28. However, following incubation with AL or SNSM87 and DHPB for 4-weeks showed similar decay of DHPM degradation as in the buffer or sterilized water alone. Retention times for DHPB degradation components in the HPLC analysis were different between the samples with SNSM87 in sterilized buffer or water alone at Day 7 and 28. The loss of cell transformation activity was similar to decrease of DHPB. These data showed that contents and tumor promoting activity of main Jatropha phorbol ester were decreased in the presence of water. Degradation of DHPB was promoted by esterase in water or spontaneous ester hydrolysis. Therefore, these observations suggested that Jatropha oil cake may safely be used as fertilizer as Jatropha phorbol esters in oil cake is degradated quickly by together with indigenous bacteria in water rich soil. This study was supported by JST/JICA, SATREPS, Japan.

PS 669c Preliminary Study on the Effect of Weathered Oil and Oil Dispersants on *Menidia beryllina* Embryo

O. K. Adeyemo[1], K. J. Kroll[1], G. Natalia[2] and N. D. Denslow[1]. [1]*Department of Physiological Sciences, Center for Human and Environmental Toxicology, University of Florida, Gainesville, FL and* [2]*Institute for Genomics, Biocomputing and Biotechnology, Mississippi State University, Starkville, MS.*

Environmental stress can affect an organism at any stage of life, but developing larvae are particularly susceptible. Exposure of fish embryos to relatively low concentrations of oil has been implicated in sub-lethal toxicity. However, the effect of oil and commonly used dispersants; singly and in combination should be more thoroughly evaluated to better understand and anticipate the ecological impacts. Oil (1ppm) and 0.1ppm dispersants (Corexit 9500 and 9527) were weathered singly and in combination in 25 ppt saltwater for 7 days in bottles with vortex in a hood. The aqueous part post weathering (Weathered solution, WS), was diluted at 1:5 (200 ml WS: 800 ml 25 ppt saltwater). Thereafter, 20-25 *Menidia beryllina* embryos at 30-48 hrs post-fertilization were exposed to diluted WS in quadruplicate for 72 hours as follows: Control (1 liter 25 ppt Saltwater), Oil (200 ul/L), C9500 (20 ul/L), C9527 (20 ul/L), Oil/9500 (200/20 ul/L) and Oil/9527 (200/20 ul/L). Mortality, heartbeat and embryo abnormalities were assessed. Mortality was not significantly different between treatments (p=0.68). Post-exposure, heartbeat and abnormality scores were significantly different (p=0.002 and 0.007, respectively) with the lowest heartbeats and highest abnormality scores recorded in dispersant exposed embryos. Although oil and dispersants exposed embryos developed to the hatching stage; significantly more embryos were in a state of deterioration, with arrested tissue differentiation compared with control (p=0.008). This study has shown that exposure of developing fish embryos to oil and dispersants, singly and in combination induced developmental abnormalities. Sub-lethal effects dealing with fish development could therefore be an early indicator of the long term effects of both oil spill and oil dispersants.

PS 669d Contaminant Burden Analysis in Wild Shovelnose Sturgeon (*Scaphirhynchus platorynchus*) in the Lower Mississippi River

D. R. Johnson[1, 2], C. Godard-Codding[3], T. Anderson[3], C. Ang[4], G. Cobb[5], J. Canas[3], J. Clarke[2], A. Roberts[6], K. Boysen[2], J. Killgore[2] and J. Hoover[2]. [1]*Conestoga-Rovers and Associates, Dallas, TX,* [2]*US Army Engineer Research and Development Center, Vicksburg, MS,* [3]*Texas Tech University, Lubbock, TX,* [4]*Badger Technical Services, Vicksburg, MS,* [5]*Baylor University, Waco, TX and* [6]*University of North Texas, Denton, TX.*

Long-lived benthic animals experience repeated and/or prolonged exposures to sediments and their associated anthropogenic contaminants. As a result, these animals are at risk of elevated contaminant burdens. The overall objective of this study was to determine baseline data for contaminant burdens in wild sturgeon in the lower Mississippi River watershed. A field collection on the Mississippi River near Ft. Adams, MS in January 2010 resulted in the collection of shovelnose sturgeon, a surrogate for the endangered pallid sturgeon (*Scaphirhynchus albus*). Sturgeon (n=13, 4-10 years old) were euthanized, and relevant tissues (liver, muscle) and gut content were analyzed for chlorinated pesticides, PCBs, and metals according to standard EPA methods (8081a, 8082, 6020, respectively). The Kaplan-Meier method was used to estimate the means and SD for sample sets that included observations below the detection limits (i.e., nondetects). The persistent organochlorine 1,1,1-trichloro-2,2-di(4-chlorophenyl)ethane (DDT) metabolites DDD and DDE and α- and γ-chlordanes were the most detected chemicals in the fish samples. Significant positive correlations with age ($p<0.05$) occurred with DDE, α-chlordane, and γ-chlordane in liver tissue; arsenic in gut, and copper in liver. There was no correlation between DDD or DDE concentrations in tissues (gut, liver, muscle); however, there were significant correlations between cadmium concentrations in gut and liver, chromium concentrations in liver and muscle, lead concentrations in gut and liver, and zinc concentrations in liver and muscle. These data provide a better understanding of environmental contaminant levels that are present and bioaccumulated into a long-lived benthic fish species from the nation's largest river system.

PS 669e Comparison of Cyropreserved Trout Hepatocytes and Liver S9 Fractions As *In Vitro* Models for Predicting Hepatic Clearance in Fish

K. Fay, P. N. Fitzsimmons, A. D. Hoffman and J. W. Nichols. *U.S. EPA, Duluth, MN.*

In vitro measurements of chemical clearance can be extrapolated to the whole liver and used to improve modeled predictions of bioaccumulation in fish. Fish hepatocytes and liver S9 fractions are two systems commonly used to measure in vitro intrinsic clearance (CLin vitro, int; ml/h/mg protein or 106 cells). Previously, trout S9 fractions were used to measure CLin vitro, int for six polycyclic aromatic hydrocarbons. CLin vitro, int were then extrapolated to the intact liver and compared to measurements of hepatic clearance (CLH; ml/h/g liver) by isolated perfused trout livers. In the present study, the same approach was used to evaluate CLH predictions obtained from cryopreserved trout hepatocytes. With one exception, extrapolations of CLin vitro, int to in vivo intrinsic clearance (CLin vivo,int; ml/h/g liver) using scaling factors (510 x 106 hepatocytes/g liver, 163 mg S9/g liver) resulted in similar predictions for the two in vitro systems (≤ 2 fold difference). For the test chemical benzo[a]pyrene, the CLin vivo,int predicted from hepatocyte data was nearly 10 fold lower than that obtained from the S9 system. CLin vivo,int values were then used as inputs to a well -stirred liver model, which accounts for flow limitations on clearance as well as potential binding effects. To facilitate this comparison, chemical binding in vitro and in solutions used to perfuse isolated livers were measured using solid phase microextraction. The resulting predictions of CLH were in good agreement with measured values from intact livers (< 2 fold difference for all but naphthalene), as well as earlier predictions obtained using the S9 system. This agreement can largely be attributed to the fact that CLin vitro, int rates in both in vitro systems often approached the flow rate of the isolated liver system. These findings suggest that both in vitro systems provide comparable predictions of hepatic clearance, which can be used to improve bioaccumulation assessment for fish.

PS 670 Hemp Seed Flour Impacts the Development of *Tenebrio* Larvae and Their Susceptibility to Organophosphorous Insecticides

J. Gaston, L. Edwards and S. Chao. *Fayetteville State University, Fayetteville, NC.*

Previous research studies have shown that hemp seed products can alter the development of insects. Considering hemp seed's effect on some developing insects, *Tenebrio* larvae were raised on hemp seed flour to determine any developmental dysfunction as well as possible susceptibility to insecticides such as chlorpyrifos, an organophosphorous insecticide. Three groups of larvae were tested; each group was raised on different amounts of hempseed flour (100% hemp seed flour, 0% hemp seed flour/100% wheat flour, and a mixture of hemp seed and wheat flour). Larvae from each group were exposed to chlorpyrifos using a dip technique. Larvae raised on hemp seed flour were more susceptible to chlorpyrifos based on LC50 comparisons. In addition, decreased acetylcholinesterase (AChE) activity was also demonstrated in larvae raised on hemp seed flour. Results indicate that hemp not only disrupts normal development in *Tenebrio* larvae but also increases susceptibility to organophosphates.

PS 671 Two Insecticidal Neurotoxic Mechanisms of Action of Monoterpenoids

J. R. Coats[1], A. D. Gross[1], F. Tong[1], M. J. Kimber[2] and T. A. Day[2]. [1]*Entomology, Iowa State University, Ames, IA and* [2]*Biomedical Sciences, Iowa State University, Ames, IA.* Sponsor: A. Keating.

Monoterpenoids from plant essential oils have been shown to elicit neurotoxic symptoms in insects, including rapid onset of tremors and loss of coordination, followed by death if a sufficient dose is applied. Many are "soft" insecticides that are much less potent than conventional insecticides but are very selectively toxic to insects and not to vertebrates. We have studied two specific neurotoxic mechanisms of action with respect to the actions of selected monoterpenes on insect neuroreceptors. GABA-gated chloride channel receptors from house fly were utilized for binding studies with tritiated-TBOB which binds at the picrotoxin binding site at that receptor-ionophore complex. Also microsacs were prepared from dissected cockroach ventral nerve cords; the effect of monoterpenes on GABA-gated chloride channel function was evaluated using 36Cl-uptake assays. Studies on binding at the house fly nicotinic acetylcholine receptor were conducted using a 14C-nicotine as the radioligand; when the phenolic monoterpenoid carvacrol was added to the preparation, it reduced binding of the nicotine in a concentration-dependent manner, at low micromolar concentrations.

PS 672 Evaluation of At-Home Methods to Reduce Pesticide Residue on Apples and Peaches

B. Pavilonis and C. Weisel. *Rutgers University, Piscataway, NJ.*

The diet is a significant route of pesticides exposure to the general public. Nevertheless, public health guidelines to reduce exposure by cleaning food are generally based on anecdotal reports. The objective of this study was to evaluate different methods that could be performed at home to reduce consumer pesticide exposure from apples and peaches. All treatments studied were safe to the general public, did not structurally alter the fruit, and used products that could be readily found in the home or grocery store. Fruit was obtained from the Rutgers University Extension Farm which supplied information on the pesticide applications. In this study, captan, fenpropathrin, and phosmet were quantified by gas chromatography/mass spectrometry. Mean captan and phosmet levels on peaches were 72.7±42.7 μg/fruit and 18.1±6.4 μg/fruit, respectively; while captan, fenpropathrin, and phosmet levels on apples averaged 41.9±23.5 μg/fruit, 16.7±7.6 μg/fruit, and 12.2±6.9 μg/fruit, respectively. Captan and phosmet residue were reduced by approximately 50% or more on apples and peaches by washing and wiping for 15 seconds with a homemade soap solution or a vinegar and lemon juice solution and then rinsing with water. In general, the commercially available fruit wash reduced captan and phosmet concentration better than the other treatment methods studied. On peaches an 85% and 63% reduction in captan and phosmet was observed while captan and phosmet residue was reduced 55% and 52% on apples. Compared to rinsing with water alone, the homemade and commercial fruit wash reduced pesticide levels greater, most likely due to the lipophilic nature of the pesticides. However, fenpropathrin levels present on ripened apples were not reduced by any of the washing treatments studied, possibly due to fenpropathrin's high octanol water partition coefficient. Some, but not all pesticide can be removed from fruit by washing and wiping. While washing and wiping of fruit is recommended, more effective methods are still needed to reduce dietary pesticide exposure. This work was supported by NIEHS 5T32ES019854 and P30ES005022.

PS 673 Toxicity and Safety Evaluation of Etofenprox, S-Methoprene, and Piperonyl Butoxide in Dogs Topically Exposed to Bio Spot Defense®

R. C. Gupta, S. D. Bland, M. A. Lasher and T. D. Canerdy. *Toxicology, Murray State University, Hopkinsville, KY.*

Currently, pyrethroids are more commonly used than any other class of ectoparasiticides on pets. Due to lack of safety data, pet owners have raised serious concerns for their use on dogs and cats. Concerns have also been raised about transferable residues of pesticides to the pet owners, veterinarians, veterinary technologists, and dog handlers. The present investigation was therefore undertaken with two specific objectives: (1) to determine the safety of Bio Spot Defense Flea and Tick Spot On® applied to six dogs, and (2) to determine the residue of active ingredients of the product (etofenprox, s-methoprene, and piperonyl butoxide) in blood of dogs and gloves worn to pet dogs at 24, 48, 72 h, and 1, 2, 3, 4, and 5 weeks post-application. At these time intervals, dogs were evaluated for physical examination. Residues of active ingredients were determined and confirmed using GC/MS. In the blood, etofenprox was detected as early as after 48 h (18.4±5.1 ppm) and the residue persisted until 1 week (0.8±0.4 ppm). S-methoprene and piperonyl butoxide were not detected in the blood at any time. In the gloves, the highest concentrations of etofenprox, s-methoprene, and piperonyl butoxide were determined at 24 h (9,552.0±1551.8; 2307.9±456.7; and 1286.1±0.5 ppm, respectively). Residues of all three compounds were detected in appreciable concentrations in the gloves until 1 week (294.9±27.2; 80.6±10.1; and 40.5±5.8 ppm, correspondingly). Of course, with a steep descending trend, residues of these compounds were present 5 weeks post-application. Findings of this investigation revealed: (1) none of the dogs exhibited any physical or behavioral abnormality, and (2) active ingredients of the product persisted on dog's coat for five weeks.

PS 674 Development and Validation of a QuEChERS-Based Liquid Chromatography Tandem Mass Spectrometry Method for the Determination of 143 Pesticide Residues in Tobacco

L. Chen, B. Hu, L. Pan, D. Ai and H. Liu. *Zhengzhou Tobacco Research Institute of CNTC, Zhengzhou, China.* Sponsor: R. Krieger.

In common with other crops, agrochemicals continue to be an important means of pest, disease and weed control in tobacco. To protect consumers from exposure to unacceptable levels of pesticide residues, Guidance Residue Levels (GRLs) of 120 agrochemicals in tobacco have been issued by the AgroChemical Advisory Committee (ACAC) of Cooperation Center for Scientific Research Relative to Tobacco (CORESTA). Sensitive and selective multi-residue analytical methods are needed to satisfy the demand for monitoring pesticide residues in tobacco. A reliable and rapid liquid chromatography tandem mass spectrometry (LC-MS/MS) multi-residue method for the simultaneous analysis of 143 pesticides in tobacco was developed and validated using a QuEChERS based extraction procedure. The MS was operated at electrospray ionization in both positive and negative mode. Multiple reaction monitoring mode was applied for the quantification and confirmation of those compounds. For accurate quantification, matrix matched calibration curves were applied to compensate matrix effects. Average recoveries of all of the compounds in tobacco were in the range of 60-126% with relative standard deviations of 0.5-21% at three fortification levels. The limits of quantification (LOQs) ranged from 0.008 to 0.09 μg/g. These values were within the acceptable range for trace residue analysis for demonstration of compliance with GRLs. The validated method was successfully applied to the analysis of 232 real tobacco samples, and 36 pesticides were detected. Carbendazim had the highest detected frequency (47.8%), and this was followed by propamocarb (37.9%), pendimethalin (32.3%) and triadimefon (32.3%). All the residue levels of these pesticides in 232 samples were below GRLs, excluding carbendazim (in 11 samples), propamocarb (in 8 samples), triadimefon (in 7 samples) and isoprothiolane (in 4 samples). The method greatly improved the detection performance and the range of the pesticide residues.

PS 675 Determination of Paraquat (PQ) in Urine Using Reversed-Phase HPLC/DAD

A. Meyer[1], G. F. Veríssimo[1], J. Alves[3] and J. Moreira[2]. [1]*IESC, Universidade Federal do Rio de Janeiro (UFRJ), Rio de Janeiro, Brazil,* [2]*CESTH, Fundação Oswaldo Cruz (FioCruz), Rio de Janeiro, Brazil and* [3]*Faculdade de Farmácia, Universidade Federal do Rio de Janeiro (UFRJ), Rio de Janeiro, Brazil.* Sponsor: G. Veríssimo.

Paraquat (PQ) is an extensively used herbicide in agricultural area, and is highly toxic to humans, having been implicated in many diseases among rural populations. The aim of this study was to develop and validate a method to quantify

PQ in urine. The sample preparation is simple where 1mL of sample is adjusted to a basic pH with 5mL of sodium hydroxide solution (0,1N). And the method employed a solid phase extraction using Sep-Pak C18 cartridge and a high-performance liquid chromatographic system consisting of a model 1200 binary pump with DAD detector coupled. The pretreatment is done with methanol and water passed through the SPE column. The extraction phase requires vacuum manifold, high temperature (40C) and nitrogen stream to evaporate efficiently the eluate. The separation thecnique uses an octadecyl–silica column with an eluent of 10% acetonitrile (v/v) containing 5,0 mM sodium 1-heptanesulphonic acid and 0,2 M orthophosphoric acid buffer (pH 3 with triethylamine). PQ and ethyl PQ, used as an internal standard (IS), is eluted at 40C at a flow-rate of 1,0 mL/min and monitored by UV absorption at 258 nm. The accuracy of the method was evaluated by recovery studies using spiked pull of urines. The recoveries of PQ were 74–101%. The calibration curve for PQ showed excellent linearity in the range of 1 – 10 ppm as judged by the coefficient of determination (R=0,983). The detection limit (with S/N>3) was 0,3 ppm with an injection volume of 100 ml. And the quantification limit (with S/N>10) was 1,1 ppm. The intra- and inter-day precision, expressed as the coefficient of variation, for PQ in urine samples were not greater than 13.0%. PQ was sensitively and selectively determined and quantified by HPLC/DAD from urine samples. The present method is promising for identification and quantification of PQ and can be suitable for epidemiological surveys.

PS 676 Identification of Pesticides and Other Environmental Chemicals Associated with the Development of Nonalcoholic Fatty Liver Disease in Rodents

M. Cave[1, 3], L. Al-Eryani[1], B. Wahlang[1], H. Clair[1], K. C. Falkner[1] and R. A. Prough[2]. [1]*Department of Medicine/GI, University of Louisville, Louisville, KY,* [2]*Biochemistry, University of Louisville, Louisville, KY and* [3]*Robley Rex VAMC, Louisville, KY.*

Environmental chemical exposures may contribute to the genesis and progression of non-alcoholic fatty live disease (NAFLD). However, a comprehensive list of these chemicals has not been generated. This study evaluates two large rodent exposure study databases for environmental chemicals which caused NAFLD in rodents. ToxRefDB is a database designed by the National Center for Computational Toxicology (NCCT) and Environmental Protection Agency's (EPA) Office of Pesticide Programs (OPP) containing animal toxicity testing filed during pesticide registration. 474 rat/mouse studies were queried for histologic NAFLD descriptors including fatty change, lipid deposition, steatosis and Oil red O positivity. Chemical Effects in Biological systems (CEBS) is a data repository developed by the National Toxicology Program (NTP) warehousing about 9000 rodent toxicology studies. Chemical selection was based on histopathological observations in the liver (fatty changes and the toxic hepatopathy). From TOXRefDB, 42 unique chemicals were associated with NAFLD pathologic descriptors. The 42 compounds included 22 fungicides, 13 herbicides, 6 insecticides, and 1 miticide. From CEBS, 329 studies of 83 unique chemicals reported positive NAFLD descriptors. These chemicals included 12 pesticides/intermediates; 6 dioxin-like molecules; 17 plasticizers, polymers, synthetic textiles and resins; 16 solvents and chemical intermediates; 7 paints, polishes and dyes; 10 fragrances, cosmetics and essential oils and 15 miscellaneous chemicals. 371 studies archived in federal databases linked 125 unique environmental chemicals to NAFLD in rodents. Pesticides composed 43% of these chemicals. Furthermore, nearly 10% of pesticide registration toxicity studies reported the development of NAFLD. The potential role of the identified chemicals, and in particular pesticides, in human NAFLD should be investigated.

PS 677 Trifluralin and Tebuthiuron, Two Widely Used Herbicides in Brazil, Showed Different Cytotoxic Potentials to HepG2 Cells

M. F. Bernardes[1], L. C. Pereira[1], M. J. Tasso[2] and D. J. Dorta[2]. [1]*Universidade de São Paulo (USP), Faculdade de Ciências Farmacêuticas de Ribeirão Preto (FCFRP), Ribeirão Preto, São Paulo, Brazil and* [2]*Departamento de Química, Universidade de São Paulo (USP), Faculdade de Filosofia, Ciências e Letras de Ribeirão Preto (FFCLRP), Ribeirão Preto, São Paulo, Brazil.*

INTRODUCTION: The application of pesticides, particularly herbicides, in agriculture, is a well established practice, and effective to control weeds. However, due to the length of agriculture, large amounts of herbicides have been used and they may influence non-target organisms by several mechanisms. Trifluralin (α,α,α-trifluoro-2,6- dinitro-N,N-dipropyl-p-toluidine) and Tebuthiuron (1-(5-tert-butyl-1,3,4- thiadiazol-2-yl)-1,3-dimethylurea) are herbicides widely used in crops in Brazil. OBJECTIVES: The present work aimed to analyze the the effects of this two herbicides, trifluralin and tebuthiuron, in HepG2 cell model. METHODS: Nuclear condensation and fragmentation was assessed by microscopy using the flurescent dye Hoechst 33342, and phosphatidyl serine exposure on the outer cell membrane was performed using annexin-V / propidium iodide assay. Concentrations from 1 through 100 μM of each herbicide dissolved in dimethylsulfoxide was analysed. All experiments were performed in triplicate and statistical analysis were done using ANOVA test followed by Dunnett. RESULTS: Trifluralin showed a significantly difference effect on nuclear condensation and fragmentation as well as positive marking for annexin-V at concentraton of 100uM indicating the induction of apoptotic cell death. On the other hand, Tebuthiuron did not affect these parameters at any of the tested concentrations. CONCLUSION: Our results show that trifluralin but not tebuthiuron is cytotoxic to HepG2 cells and that trifluralin induces the activation of the apoptotic pathway.
Supported by: FAPESP - Proc. 2012/15220-3
"The opinions, assumptions, and conclusions expressed in this material are those of the authors and do not necessarily reflect the views of FAPESP"

PS 678 Effect of Organochlorine Compound Exposure on Apolipoprotein B Secretion by Rat Hepatoma Cells

A. Ward, M. Dail and J. E. Chambers. *College of Veterinary Medicine, Mississippi State University, Mississippi State, MS.*

Dyslipidemia occurs in type 2 diabetes mellitus (T2D). During dyslipidemia there is increased production of lipids from the liver including apolipoprotein B (Apo B) containing very low density lipoproteins (VLDL) and low density lipoproteins (LDL). There is an increasing epidemiological association between diabetes and higher levels of serum organochlorine compounds (OC). OC exposure was found to be a predictor of dyslipidemia in diabetes and non-diabetes. The liver is a target for OC metabolism and plays a role in dyslipidemia and T2D. Therefore, the effect of a group of select OC on the dyslipidemic risk factor, Apo B, in liver cells was investigated. McArdle-RH7777 (McA) rat hepatoma liver cells were treated with 0.4 mM oleic acid (OA) for 16 hr to induce Apo B secretion. McA cells were exposed to 10 μM dichlorodiphenyldichloroethylene (DDE), dichlorodiphenyltrichloroethane (DDT), dieldrin, or chlordane simultaneously with 0.4 mM OA for 16 hr to induce Apo B secretion. McA cells were exposed to 1, 10, or 100 μM DDE simultaneously with 0.4 mM OA for 16 hr to investigate a dose-response of Apo B secretion. Immunoblotting of lipoproteins secreted into the cell media yielded significantly higher levels of secreted Apo B for exposed versus non-exposed liver cells. Immunoblotting of cell lysates revealed that intracellular Apo B levels were significantly different for OC and OA induced cells compared to non-induced cells. The OC exposed cells exhibited a trend of higher Apo B protein levels than OA induced cells. These results suggest a role of OC in lipid transport and secretion of Apo B containing lipids rather than in Apo B synthesis that is induced by lipogenic fatty acids such as OA. Based on these results, OC exposure may be associated with T2D by increasing a dyslipidemic risk factor of T2D.

PS 679 p, p'-DDE Enhances Adipogenesis in 3T3-L1 Adipocytes and Alters Cyclooxygenase-2 (COX-2) Activity in J774a.1 and THP-1 Macrophage Cells

L. Mangum, G. E. Howell, S. B. Pruett, M. K. Ross and J. E. Chambers. *College of Veterinary Medicine, Mississippi State University, Mississippi State, MS.*

Exposure to p,p'-DDE, a metabolite of p,p'-DDT, is associated with obesity, dyslipidemia, insulin resistance and incidence of metabolic syndrome. DDE has been shown to have immunomodulatory properties, affecting macrophage and T cell populations. Obesity leads to immune cell infiltration into the adipose tissue (AT) causing local inflammation. Potential mechanisms were studied by which DDE could modulate adipocyte and immune cell function and facilitate an increased risk of obesity and immune dysregulation, potentially through COX-2. Human THP-1 and murine J774a cell lines and 3T3-L1 preadipocytes were studied for the effects of DDE on prostaglandin (PG) production and adipogenesis. Macrophage cell lines were exposed to 20μM DDE or 10μM NS398, a specific COX-2 inhibitor, for 18hr before treatment with an inflammatory challenge of 0.25μg/ml lipopolysaccharide (LPS) or 200μM palmitic acid (PA). PGE2, PGD2, PGF2α, and arachidonic acid (AA) were analyzed in cell culture supernatants. The effect of DDE or NS398 on COX-2 activity was also measured indirectly in a cell-free system through addition of AA to cell lysates of LPS (1μg/ml) stimulated macrophages. In J774a and THP-1 cells, DDE or NS398 followed by immune challenge reduced cellular PG secretion and PG production in a cell free system, suggesting that DDE may interfere with COX-2 activity. 3T3-L1 cells were induced to differentiate to adipocytes using a sub-optimal differentiation cocktail with increasing concentrations of DDE (0.5-100μM). DDE increased adipogenesis in a dose-dependent manner in mature adipocytes as determined by Oil Red O staining. As PGE2 and PGF2α inhibit adipogenesis, decreased PG synthesis by resident AT macrophages may lead to increased adipogenesis and contribute to development

of obesity. These results suggest that DDE exposure may contribute to increased adipogenesis and altered PG production, potentially mediated through a COX-2 dependent mechanism.

PS 680 The Toxicity of Maneb in Human Colon Cells May Be Related to the Transchelation of the Metal Moiety and the Organic Backbone

L. M. Hoffman, L. D. Trombetta and D. Hardej. *Pharmaceutical Sciences, St. John's University, Queens, NY.*

Ethylene bisdithiocarbamate (EBDC) pesticides are used as broad range contact fungicides on a variety of crops. A subset of the metal containing EBDC pesticides includes Maneb (MB), which is complexed with the transition metal manganese (Mn). Previous testing in our laboratory has established the toxicity of this compound in transformed colon cells, HT-29 and Caco2. Significant decreases in cell viability were observed in both HT-29 (120-260μM) and Caco2 cells with MB (40-180μM). Exposure also resulted in a dose dependent increase in intracellular Mn levels within HT-29 and Caco2 cells (20-200μM). Recent scientific studies have suggested that Mn exposure may result in increases in copper (Cu) concentrations within the brain. Therefore, the purpose of the present study was to determine if MB exposure results in an increase in copper levels within HT-29 and Caco2 cells. Following exposure to MB in HT-29 (100-200μM) and Caco2 cells (20-60μM), inductively coupled plasma-optical emission spectroscopy was performed. MB exposure resulted in a significant accumulation of Cu within HT-29 and Caco2 cells (40-200μM). These data suggest that the Mn moiety of MB may transchelate with Cu and play a role in the generation of toxicity. To investigate whether Cu played a role in the cytotoxic process, cells were treated with Cu chloride ($CuCl_2$). Exposure to $CuCl_2$ produced no significant decrease in cell viability in all cell types up to 200μM. To investigate the role the EBDC backbone plays in the generation of toxicity, HT-29 and Caco2 cells were treated with Nabam (NB), an EBDC pesticide that contains the identical core organic component of MB but has sodium in place of Mn. Significant decreases in cell viability were observed with NB in HT-29 (400-3200μM) and Caco2 cells (200-3200μM). The lack of toxicity observed following treatment with NB within the same concentration range as MB suggests that the EBDC backbone and Cu moiety may be acting in conjunction to cause toxicity in human colon cells.

PS 681 Mechanism of the Toxic Effect of Carbendazim on the Pubertal Seminiferous Epithelium: An *Ex Vivo* Study

M. Perrard[1], D. Carette[2], G. Martin[3], E. Christin[3], G. Pointis[2] and P. H. Durand[3]. [1]*CNRS, Lyon, France,* [2]*U895, INSERM, Nice, France and* [3]*Kallistem, Lyon, France.* Sponsor: R. Witorsch.

Carbendazim (CBZ) is a fungicide used to prevent and eliminate fungal plant diseases. In vivo studies reported that CBZ induces severe testicular alterations in male rats. The cellular and molecular mechanisms of CBZ are not completely understood; even its status of endocrine-disruptor is still debated. We used our validated rat seminiferous tubule culture model (Bio-AlteR®) developed by Durand's team for testing concentrations of CBZ at least 60 fold lower than the serum concentrations of CBZ found in rats treated with high doses of CBZ (25 mg/kg). Cultured seminiferous tubules from 20-22 days old rats were treated with CBZ 50 nM, 500 nM or 5 μM. The integrity of the blood-testis barrier [Trans-Epithelial Electrical Resistance (TEER), immunocytochemistry of Connexine 43 (Cx43) and of Claudin11], the different cell populations (flow cytometric analyses and quantification of mRNAs specific of the different cell populations) and hormonal receptor mRNAs were studied.
The TEER was slightly increased by CBZ from day 16 onward, and the expression of Cx43 and gap junction functionality were decreased, while the expression of Claudin 11 was increased. CBZ increased somatic cells and decreased germ cells in a dose-dependent manner from day 14 onward. CBZ increased young spermatocytes only on days 7 and 14. Secondary spermatocytes were increased or decreased according to the day of culture and the concentration of CBZ. However round spermatids were always decreased by the 3 concentrations of CBZ in a dose-dependent manner indicating a blockade of the second meiotic division. These results were confirmed by measurement of mRNAs specific of the different germ cell types. CBZ induced an increase of androgen receptor mRNA on day 14, and of mRNAs of estrogen receptors 1 and 2 on days 14 and 21.
Hence, by regulating the expression of androgen and estrogen receptors, low concentrations of CBZ do possess endocrine-disruptor effects leading to alteration of spermatogenesis.

PS 682 Rynaxypyr Is Active but Significantly Less Potent toward Ryanodine Receptor Type 1 from Wild Type and Malignant Hyperthermia Susceptible Mammalian Skeletal Muscle

K. M. Truong[1], M. La Merrill[2] and I. N. Pessah[1]. [1]*Molecular Biosciences, UC Davis, Davis, CA and* [2]*Environmental Toxicology, UC Davis, Davis, CA.*

Rynaxypyr is an anthranilic diamide that represents a major emerging class of insecticide widely used to eradicate Lepidopteran agricultural pests. While Rynaxypyr is a potent activator of ryanodine receptors (RyRs) that are expressed in Leptidopterous skeletal muscle, its activity towards RyR1, which is expressed in adult mammalian skeletal muscle, has been less studied. Considering that RyRs in insect and mammalian species perform similar roles in regulating intracellular Ca2+ release from sarcoplasmic reticulum (SR) during physiological and pathophysiological processes of skeletal muscle, we explored if Rynaxypyr was devoid of activity towards adult mouse RyR1, even at high (> 1 μM) concentrations. For these initial studies we prepared skeletal muscle SR from congenic C57BL/6J wild type mice and mice that are homozygous for a human malignant hyperthermia susceptibility mutation in the C-terminal region of RyR1 (RyR1-T4826I). These SR preparations were subjected to radioligand-receptor binding analysis with [3H]ryanodine (5 nM) in the absence or presence of increasing concentrations of Rynaxypyr. As previously reported (Barrientos et al J Biol Chem 287:2863), RyR1-T4826I was found to be constitutively more active than wild type RyR1. Rynaxypyr > 10 μM significantly activated RyR1 found in both wild-type mouse muscle and in mouse muscle homozygous for the T4826I-RyR1 mutation. These results suggest Rynaxypyr is capable of altering Ca2+ dynamics mediated by RyR1 in both wild type and malignant hyperthermia susceptible mammalian muscle. There is a need to better understand how anthranilic diamides alter the function of mammalian RyR1 and RyR2 given these receptors are known to express mutations that contribute to environmentally triggered disorders of skeletal and cardiac muscle.
[Supported by P42 ES04699]

PS 683 Quantitation of the Pyrethroid Deltamethrin (DLM) in Rat Liver and Muscle Using Gas Chromatography Negative Chemical Ionization Mass Spectrometry (GC-NCI-MS)

J. V. Bruckner[1], C. White[1], D. Gullick[1], A. Popovici[1], M. Krolski[2], D. W. Gammon[3], B. S. Cummings[1] and M. Bartlett[1]. [1]*UGA, Athens, GA,* [2]*Bayer Crop Science, RTP, NC and* [3]*FMC Corp., Ewing, NJ.*

High quality trace analysis of pyrethroids in biological samples is necessary for toxicokinetic studies for risk assessments. To date highly sensitive methods to measure pyrethroids have focused on large environmental samples (water, soil, food) or urine. There are no validated methods in the literature for quantifying low concentrations of this class of compounds from small (100 uL) liver and muscle samples. DLM was extracted from homogenated liver and muscle samples by protein precipitation using acetonitrile and phosphoric acid. The samples were vortexed and centrifuged before evaporation to dryness. Samples were reconstituted and DLM extracted from the residue using toluene prior to injection into an Agilent Model 6890N gas chromatograph equipped with a Model 5973 quadrupole mass analyzer. Samples were ionized via electron capture in the negative ion mode using methane as a chemical ionization gas. Fragment ions were monitored using selected-ion monitoring for quantitation and verification of the analyte. Cis-permethrin was used as the internal standard. The method was linear from 0.3 ng/mL to 1, 000 ng/mL from both liver and muscle homogenates. The limit of quantitation was 0.3 ng/mL and the intraday precision and accuracy of the method was better than 20% at the LLOQ and better than 15% across the linear range (n=18). The method was applied to monitor tissue DLM concentrations following oral dosing of adult rats with 1 to 5 mg/kg DLM in corn oil. Liver DLM levels declined more rapidly that muscle levels. DLM in liver and muscle could be accurately measured for up to 24 hours following dosing. A novel GC-NCI-MS method for the determination of DLM from 100uL liver and muscle samples was successfully developed and validated by FDA guidelines.

PS 684 Maturation Effects on Plasma Protein Binding of Deltamethrin (DLM), Cis- (CIS), and Trans-Permethrin (TRANS) in Human and Rat Plasma

P. Sethi[1], S. Muralidhara[1], T. G. Osimitz[2], D. Minnema[3], P. M. Hinderliter[3], B. S. Cummings[1], J. V. Bruckner[1] and C. White[1]. [1]*Pharmaceutical and Biomedical Sciences, University of Georgia, Athens, GA,* [2]*Science Strategies, LLC, Charlottesville, VA and* [3]*Syngenta, Greensboro, NC.*

Plasma protein binding can influence the toxicokinetics of highly-bound chemicals by limiting the amount of compound free to reach target organs and sites of elimination. Because the influence of age on plasma protein binding of common pyrethroids is unclear, this study was undertaken to determine if binding of DLM, CIS or TRANS changes during maturation. The plasma protein binding was studied in plasma of 10-, 15-, 21- and 90-day-old rats and birth-1 wk, >1-4 wks, >4 wks-1 yr, >1-3 yrs, >3-6 yrs, >6-18 years and adult humans. A solvent extraction method was employed using radiolabled pyrethroids to quantify the binding of these highly hydrophobic compounds. Since rat plasma is known to contain esterases that metabolize pyrethroids, samples were treated with 10 ul of a 1 mM solution of NaF to inhibit carboxylesterase. Pyrethroid concentrations were determined by radioactive counting against reference counts. In all age groups, rat and human binding was linear over the concentration range of 250 to 750 nM and inversely proportional to concentrations >750 nM. Binding of all 3 compounds to rat albumin was significantly lower at PND 10 (~35%) and 15 (~40%) vs. PND 90 (~50%). Lipoprotein binding of DLM, CIS and TRANS were significantly higher at PND 10 (~35%) than at PND 90. With human plasma, the total binding of all 3 compounds in birth-1 week (~75%) and >1-4 wks (~76%) was significantly lower than in adults (~90%) at <750 nM. However, no differences in binding of any of the 3 compounds were observed in the plasma from groups of individuals older than 4 weeks. Higher free fractions of DLM, CIS and TRANS in the PND 10 and 15 rats and infants < 4 weeks may result in increased tissue deposition and effects, though this may be offset by enhanced systemic clearance.
Supported by the Council for Advancement of Pyrethroid Human Risk Assessment.

PS 685 Toxicokinetics of Deltamethrin (DLM) in Adult Male Sprague-Dawley Rats

C. Chen[1], S. Muralidhara[1], T. G. Osimitz[2], D. W. Gammon[3], S. Anand[4], B. S. Cummings[1], J. V. Bruckner[1] and C. White[1]. [1]*Pharmaceutical and Biomedical Sciences, University of Georgia, Athens, GA,* [2]*Science Strategies, LLC, Charlottesville, NC,* [3]*FMC Co, Ewing, NY and* [4]*DuPont Haskell Labs, Newark, NJ.*

Pyrethroid insecticides are used extensively in the US and Europe. Low level exposure has been observed in humans. Empirical toxicokinetic data for construction and validation of improved physiologically-based pharmacokinetic models are quite limited, particularly for very low doses close to "real life" exposure levels. This study was undertaken to determine the plasma and tissue time-courses of DLM after oral bolus doses ranging from 0.01 to 1.0 mg/kg in corn oil (5 ml/kg) in adult male Sprague-Dawley rats. Serial arterial blood samples were obtained from 4-7 cannulated rats to characterize DLM plasma kinetics. Additional groups of rats (n=5/time-point) were similarly dosed and euthanized to obtain brain, muscle, liver, and fat at selected time-points. Plasma and tissues were analyzed by GC-NCI-MS. DLM was slowly absorbed from corn oil in the GI tract, yielding peak concentrations after 5-7 hours. At DLM doses ranging from 0.01-1.0 mg/kg, the peak concentrations increased proportionately with dose. However, AUCs from 0-24h increased disproportionately with dose, while apparent oral clearance was constant. This suggests a change in bioavailability and/or tissue distribution. The effective half-life was decreased at the 0.05 mg/kg dose (254 to 118 min). This corresponded to the decrease in the apparent volume of distribution at this dose. A slow terminal elimination phase was noted at all dose levels, which was most likely primarily due to prolonged DLM release from body fat. Liver concentrations were 20-40% higher than the plasma concentrations. Brain concentrations ranged from 5- to 10-fold lower than plasma levels, which was unexpected since DLM is a highly lipophilic compound. However, extensive plasma protein and lipoprotein binding (~90%) and possibly the blood brain barrier may limit distribution of DLM to the central nervous system.
Supported by the Council for Advancement of Pyrethroid Human Risk Assessment.

PS 686 Engineering PON1 in an *E. coli* System Improves Stability and Activity

S. Suzuki[1], R. C. Stevens[4], Y. Vu[1], J. Bui[3], T. B. Cole[2], R. J. Richter[1], S. S. Park[1] and C. E. Furlong[1]. [1]*Medical Genetics and Genome Sciences, University of Washington, Seattle, WA,* [2]*Environmental and Occupational Health Sciences, University of Washington, Seattle, WA,* [3]*Biochemistry, University of Washington, Seattle, WA and* [4]*MRL Boston, Boston, MA.*

Organophosphates (OPs) are some of the most commonly-use pesticides worldwide. Paraoxonase 1 (PON1) is a calcium-dependent, HDL-associated enzyme capable of hydrolyzing OPs and is protective against specific OPs *in vivo*. Human PON1 has two common coding polymorphisms, L55M and Q192R. The Q192R polymorphism affects catalytic efficiency towards specific substrates. Rabbit PON1 is more stable than human PON1 which has been suggested as a therapeutic catalytic scavenger for OP exposures. We have developed an *E. coli* system for expressing and purifying untagged native human and rabbit PON1s and variants. The two native 192 alloforms (Q and R) were expressed and purified as well as a human PON1 variant with lysine at the 192 position (rHuPON1K192). Several variants with polymorphisms homologous to rabbit PON1 were computationally predicted to have increased stability and higher affinity calcium binding. These were also generated on the human rHuPON1K192 protein backbone. Rabbit PON1 and variant recombinant rabbit PON1Q192 (rRabPON1Q192), which is predicted to have increased activity against nerve agents, were also expressed and purified. The rHuPON1K192 variant had increased OP catalytic efficiency relative to the native human PON1s. PON1K192 was tested in a knockout mouse model and found to protect brain cholinesterase from the OP diazoxon. Mutants predicted to have increased stability were tested by heat inactivation and EDTA inhibition to determine heat stability and calcium binding affinity. The L130M and S67A variants, analogous to rabbit PON1 at these positions, had increased resistance to both heat and EDTA denaturation. rRabPON1Q192 was expressed and purified and is currently being characterized for its catalytic properties against specific OP compounds. This research was supported by NIH Grants ES09883, ES09601/EPA RD-83170901, 5P42ES04696, P30ES07033, T32ES007032.

PS 687 Chlorpyrifos Induces DNA Damage and MLL Translocations through Topoisomerase II Inhibition and Apoptosis in Human Fetal Liver Hematopoietic Stem Cells

C. Lu[1], H. Hu[2], X. Liu[1], J. Wang[1] and J. Shao[1]. [1]*School of Public Health, Dalian Medical University, Dalian, Liaoning, China and* [2]*The Second Affiliated Hospital, Dalian Medical University, Dalian, Liaoning, China.*

Chlorpyrifos (CPF) is an extensively used insecticide especially for residential indoor pest control, and therefore considered to be the main source of CPF exposure for certain population such as pregnant women, fetuses and infants. During early fetal development, liver is a hematopoietic organ with majority of cells being CD34+ hematopoietic stem cells (CD34+HSC). The in utero injury to CD34+HSC has been known to underlie the pathogenesis of several blood disorders, often involving rearrangements of the mixed-lineage leukemia (MLL) gene on 11q23. In fact, the household pesticide exposure during pregnancy has been associated with a more than two-fold increased risk in infant leukemia, and CPF is among the most frequently applied insecticides for households. In the present study, we evaluated the leukemogenic potential of CPF in human fetal liver-derived CD34+HSC. Specifically, exposure to 10 μM CPF led to a decrease in viability, an inhibition in proliferation and an induction of DNA double-strand break (DSB) by neutral Comet assay and the occurrence of MLL+ rearrangements by FISH. In particular, we observed CPF-mediated cell cycle disturbance as shown by G1 arrest, in contrast to etoposide, an anticancer drug used as a positive control and known to induce G2/M arrest. Further study on mechanisms underlying DNA DSB and MLL+ rearrangements revealed that CPF may act as topoisomerase II poison, a mechanism of action similar to etoposide. On the other hand, CPF was also shown to induce early apoptosis through active caspase-3 activation, an alternative pathway known to underlie DNA DSB and MLL+ translocations. Our data indicate that in utero injury of CD34+HSC by CPF may contribute to the increased risk of infant leukemia. Future work will elucidate the mechanism and the type of CPF-induced MLL+ translocations in HSC. All use of human tissues has been approved by the Dalian Medical University IRB.

PS 688 Inhalation of Saturated Vapor Concentrations of Chlorpyrifos or Chlorpyrifos Oxon Does Not Inhibit Cholinesterase Activity in the Lung, Brain, or Blood of Rats

J. A. Hotchkiss[1], S. M. Krieger[1], K. M. Mahoney[1], K. A. Brzak[1], D. L. Rick[1], M. J. Bartels[1], D. W. Lickfeldt[2] and D. R. Juberg[2]. [1]*The Dow Chemical Company, Midland, MI and* [2]*Dow AgroSciences, Indianapolis, IN.*

Chlorpyrifos (CPF; CAS No. 2921-88-2) is the active ingredient in DURSBAN™ and LORSBAN™ brand insecticides. Chlorpyrifos-oxon (oxon; CAS No. 5598-15-2) is an oxidative metabolite of CPF, a potent inhibitor of cholinesterase (ChE) activity and, like CPF, is hydrolyzed to 3,5,6-trichloropyridinol (TCP). Inhalation exposure to CPF and oxon vapors is an important metric for human health risk assessment. This study was designed to assess the concentration- and time-dependent effects of a single 6h, nose-only, inhalation exposure to saturated vapor atmospheres of CPF or oxon on 1) ChE activity in lung, red blood cells (RBC), plasma and brain and 2) blood concentrations of CPF, oxon and TCP in female Sprague Dawley rats. Rats (n=8/group) were exposed 6h to filtered air (control) or saturated vapor atmospheres of CPF (254 $\mu g/m^3$) or oxon (35 $\mu g/m^3$) and were sacrificed immediately or up to 24h after the end of exposure. No clinical signs of toxicity were noted in any CPF- or oxon-exposed rats. No blood oxon levels > the lower limit of quantitation (LLQ=$1.5x10^{-4}$ nmole/g blood) were measured in any control, CPF- or oxon-exposed rats at any time point. In oxon-exposed rats, blood TCP levels >LLQ (0.089 nmole/g blood) were measured through 8h post-exposure, thus confirming absorption of inhaled oxon vapors. In CPF-exposed rats, blood CPF levels were <LLQ ($1.5x10^{-4}$ nmole/g blood) by 6h post-exposure. Blood TCP levels decreased with time after exposure but were >LLQ through 12h post-exposure. No inhibition of ChE activity was measured in RBC, plasma, brain or lung at any time after exposure to CPF or oxon. Based on the absence of ChE inhibition in RBC, plasma, brain or lung (the portal-of-entry tissue), the 6h No Observed Effect Concentration (NOEC) for CPF vapors is > 254 $\mu g/m^3$ and the NOEC for oxon vapors is > 35 $\mu g/m^3$.

PS 689 Biomarkers of Chlorpyrifos and Profenofos Exposure and Effect in Adult and Adolescent Egyptian Cotton Field Workers

J. R. Olson[1], S. T. Singleton[1], O. A. Dadson[1], M. R. Bonner[1], T. Farahat[2], F. Farahat[2], G. Abdel-Rasoul[2], A. A. Ismail[2], O. Hendy[2], W. K. Anger[3] and D. Rohlman[4]. [1]*University at Buffalo, Buffalo, NY,* [2]*Menoufia University, Shebin El-Kom, Egypt,* [3]*OHSU, Portland, OR and* [4]*University of Iowa, Iowa City, IA.*

Chlorpyrifos (CPF) and profenofos (PFF) are organophosphorus (OP) pesticides that are applied seasonally in Egypt to cotton fields. Urine trichloro-2-pyridinol (TCPy), a specific CPF metabolite, and 4-bromo-2-chlorophenol (BCP), a specific PFF metabolite, are biomarkers of exposure, while inhibition of blood butyrylcholinesterase (BuChE) and acetylcholinesterases (AChE) activities are effect biomarkers which may be associated with neurotoxicity. Urine TCPy and BCP and blood BuChE and AChE activities were measured in 37 adult Egyptian Ministry of Agriculture workers during and after 9-17 consecutive days of CPF application followed by PFF (8-10 days), and a second CPF application (5 days) in 2008. In a longitudinal study, 57 adolescent applicators and 38 age-matched non-applicators were studied over 10 months in 2010. During the OP applications, mean TCPy and BCP levels were significantly higher than baseline levels and remained elevated following the application periods. Peak urinary BCP and peak TCPy levels for individuals (ranging from 13.4 to 8,052 and 16.4 to 30,107 ug/g creatinine, respectively) were also highly correlated ($r= 0.77$, $p<0.001$). In adults, a significant inverse correlation was observed between urinary TCPy and blood BuChE and AChE activities. In the adolescent study, the mean peak TCPy levels were less than the adults, but the exposure-effect relationship for BuChE inhibition was similar to adults. Both adolescent groups had elevated TCPy and depressed BuChE which persisted for 4-7 weeks after spraying ended. Biomarker data in the adolescent non-applicators, which mirrored that of the applicators, indicated that the non-applicators received environmental CPF exposures. Together, these results can serve to guide future investigations in assessing health risks of OPs and can be used in future efforts to model exposures to CPF and PFF. (NIEHS ES016308, ES022163)

PS 689a Absence of Adverse Effects on Testes or Male Reproduction in an F1 Extended Two-Generation Reproductive Toxicity Study of Carbendazim in Rats

B. Neal[1], K. Hill[2], P. Limaye[2], S. Bommegowda[2], L. Elcock[2] and D. Dandekar[2]. [1]*Toxicology and Mechanistic Biology, Exponent Inc., Alexandria, VA and* [2]*Xenometrics LLC, Stilwell, KS.*

Carbendazim is a fungicide with a mitotic spindle inhibitor mode of action. Bolus gavage dosing of carbendazim to rats in prior studies has led to testicular toxicity. Dietary studies did not confirm this effect. Many prior studies used test substance with low or unknown purity and/or failed to assess potential intergenerational effects. An F1 extended two generation reproductive toxicity study of carbendazim (> 98% pure) was conducted in Wistar rats at dietary concentrations of 0, 250, 1000 or 2000 ppm. Potential testicular effects were assessed in adult parental (P) (30/dose) and F1 generation males (two cohorts, 1a and 1b), and in juvenile F1 and F2 rats. Testosterone levels (P and F1 1b), sperm parameters, reproductive organ weights and histopathology including testicular staging were assessed in adult males. Juvenile F1 and F2 males were assessed for testes weight and F1 males for testes histopathology. Reproductive performance was assessed for the P and F1 males (both F1 cohorts). Testicular findings, considered non-adverse, were limited to slight but statistically significant decreased absolute testes weights in the adult F1 cohort 1a only at 1000 and 2000 ppm, with no effect on testes weight relative to body weight, and no effect in P or F1 cohort 1b males. Statistically significant higher testicular sperm counts were noted at 1000 ppm in F1 cohort 1a and at 2000 ppm in both F1 cohorts. There were no effects on testosterone levels, epididymal sperm count, sperm motility, progressive sperm motility, percent or type abnormal sperm, and no exposure related testicular or epididymal histopathology in adult males. Juvenile testes weights and histopathology were not affected. There was no effect on time to mating or male reproductive parameters in either generation. This study confirms a low hazard of testicular toxicity or male reproductive toxicity from carbendazim exposure in the diet.

PS 689b Metabolism of Deltamethrin (DLM), Cis-Permethrin (CPM) and Transpermethrin (TPM) by Rat and Human Liver Preparations

B. G. Lake[1], R. J. Price[1], B. R. Ing[1], M. P. Scott[1], C. Cantrill[3], J. B. Houston[3], M. Yoon[2], H. J. Clewell[2], S. Anand[4], D. W. Gammon[5] and T. G. Osimitz[6]. [1]*LFR Molecular Sciences, Leatherhead, Surrey, United Kingdom,* [2]*The Hamner Institutes for Health Sciences, RTP, NC,* [3]*University of Manchester, Manchester, United Kingdom,* [4]*DuPont Haskell, Newark, DE,* [5]*FMC, Ewing, NJ and* [6]*Science Strategies, LLC, Charlottesville, VA.*

Pyrethroids are metabolised by hepatic cytochrome P450 (CYP) and/or carboxylesterase (CES) enzymes. While CPM is mainly metabolised by CYP enzymes, DLM and TPM can be metabolised by both CYP and/or CES enzymes. The aim of this study was to determine the kinetics of pyrethroid metabolism in liver microsomes in the presence of NADPH (i.e. to determine both CYP and CES metabolism) using the substrate depletion approach. Apparent intrinsic clearance (CLint) values for DLM, CPM and TPM metabolism in both rat and human liver microsomes varied with protein concentration (0.1-1 mg protein/ml). For example, apparent CLint values for DLM metabolism in rat liver microsomes at protein concentrations of 0.1 and 1 mg/ml were 0.17 and 0.04 ml/min/mg protein, respectively. All three pyrethroids exhibited nonspecific binding to liver microsomes, with experimentally determined fraction unbound (fu) values for DLM, CPM and TPM being 0.339, 0.207 and 0.172, respectively, at a protein concentration of 0.25 mg/ml. After correction for nonspecific binding, unbound CLint values for DLM, CPM and TPM metabolism were 0.32, 1.41 and 2.46 ml/min/mg protein, respectively, in rat liver microsomes and 2.48, 0.33 and 2.44 ml/min/mg protein, respectively, in human liver microsomes. Pyrethroid metabolism in human liver microsomes was enhanced by the addition of human serum albumin (HSA), which appears to be attributable to the removal of inhibitory fatty acids by HSA. Based on these results it is crucial to take the nonspecific binding of these compounds into account in order to properly determine rates of pyrethroid metabolism in liver microsomes. The kinetic data obtained in this study will be extrapolated to in vivo to develop PBPK models for these pyrethroids. (Supported by The Council for Advancement of Pyrethroid Human Risk Assessment).

S 690 Adverse Outcome Pathways As an Integrative Framework for Predictive Toxicology: Combining Top-Down and Bottom-Up Thinking

C. Corton and I. Shah. *US EPA, Research Triangle Park, NC.*

A number of regulatory agencies have ongoing efforts to identify, describe, and categorize AOPs. Developing libraries of AOPs that can effectively address the practical needs of chemical risk assessment is a major undertaking. There is increasing consensus on the AOP concept and structure: chemical exposure triggers a molecular initiating event that leads to a series of biochemical/cellular alterations culminating in tissue effects including frank toxicity. There is recognition that a reductionist approach may not capture sufficient biological complexity of chemical-induced effects for effectively implementing the AOP framework in risk assessment. In the era of large-scale/high-throughput biology, top-down (hypothesis-driven) and bottom-up (data-driven/systems biology) thinking are both vital for building and using AOPs. This symposium will bring together cutting-edge ideas on AOPs as an integrative framework for predictive toxicology and will focus on 1) building the structure of libraries of AOPs, 2) populating the key events with chemical-induced effects from both a top-down and bottom-up (systems biology) approach, and 3) applying the AOP framework to quantitative risk assessment. The first speaker will give an overview of international efforts to build libraries of AOPs and highlight the requirements for their utility in a regulatory context. The second speaker will discuss some of the techniques and hurdles in combining top-down thinking using large-scale molecular data to characterize molecular and cellular events involved in adverse outcomes in the liver. The third speaker will present a large-scale semantic approach for linking data in relation to AOPs. The fourth speaker will present a computational framework that uses data-driven and knowledge-driven analysis to reconstruct AOPs. The last speaker will present some of the opportunities and challenges in using AOPs for qualitative and quantitative extrapolation from *in vitro* to *in vivo*. This symposium will be of wide interest to SOT members, including scientists working in the regulatory arena as well as those interested in the application of molecular and systems biology to risk assessment.

S 691 An International Program for the Development of Adverse Outcome Pathways to Support Chemical Risk Assessment

M. P. Whelan. *The Joint Research Center of the European Commission, Ispra, Italy.* Sponsor: C. Corton.

An Adverse Outcome Pathway (AOP) is a conceptual construct that is the central element of a toxicological knowledge framework built specifically to address the needs of chemical hazard and risk assessment. An AOP is reductionist at the process level, describing a sequential chain of causally linked events at different levels of biological organization that lead to an adverse health or ecotoxicological effect. AOPs can vary in resolution and expanse and can be tailored for multiple uses such as providing a blueprint for a computational prediction model or designing Integrated Approaches to Testing and Assessment (IATA). In January 2013 the Organization for Economic Cooperation and Development (OECD) officially launched the AOP Development Program. Projects being undertaken cover AOP development, AOP knowledge management tools and AOP-related guidance. At the heart of the program is the AOP Knowledge Base (AOP-KB) which is a web-accessible platform that facilitates international crowdsourcing of mechanistic knowledge through collaborative AOP development and evaluation. Emerging AOPs are being taken up within the OECD Hazard Assessment Task Force to guide the design of IATA with skin sensitization being the first case study. AOPs will also help prioritize new methods for the OECD Test Guidelines Program and the development of molecular profilers for the OECD QSAR Toolbox.

S 692 Integrating Genomics into the AOP Framework

C. Corton. *US EPA, Research Triangle Park, NC.*

Databases of gene expression information annotated for phenotypic outcomes offer opportunities for predicting key events in adverse outcome pathways (AOPs). We have developed strategies for linking gene expression changes to prediction of key events. Three comprehensive databases of gene expression changes in liver/primary hepatocytes have been annotated based on mouse, rat and human data containing ~2,000, ~10,000 and ~2,000 gene expression biosets, respectively. Signatures predictive of key events in liver AOPs were built using species-specific strategies. Mouse signatures capitalized on comparisons between chemically-treated wild-type and transcription factor (TF)-null mice. Rat signatures used known marker genes for TFs. Human signatures were developed in HepG2 cells in which gene expression was correlated to TF activation profiles examined in the same chemically-treated samples. Prediction tests of TF activation showed that balanced accuracies ranged from ~85 – 98% with signatures from mice being the most accurate. The signatures were used to predict chemically-induced key events including activation of AhR, CAR, FXR, Nrf2, PPARalpha, PXR and hormonally-induced receptors. The predictions of chemical behavior are put into the context of key events allowing predictions of AOPs in the liver. Simultaneous assessment of all known AOPs linked to liver cancer or steatosis uncovered complexities in interactions between the TFs. Because chemical-independent factors that regulate the TFs are simultaneously evaluated in the database (e.g., diet, genetic background and lifestage), the integrated predictions open the door for assessment of cumulative risk. (This abstract does not represent EPA policy.)

S 693 Opportunities in Toxicology for Large-Scale Semantic-Linked Data and Prediction

D. J. Wild. *Indiana University, Bloomington, IN.* Sponsor: C. Corton.

Technologies have recently been developed that allow large-scale, semantic integration of heterogenous biomedical and drug discovery datasets. A variety of tools and algorithms have emerged that can use this linked data for drug-target prediction and Mechanism of Action discovery, *inter alia*. Emerging opportunities will be explored for applying these in areas of toxicity and adverse event prediction, including interpretable association predictions that take into account complex inter-relations between genes, compounds, pathways and biological end-points. Examples will be given of how interpretable heterogenous data subnetworks can shed light on adverse drug events (including proposing mechanisms of action for the hepatic and cardiac events associated with the thiazolinediones Rosiglitazone and Troglitazone) and how chemical compounds can be profiled against targets and other compounds to produce interpretable predictions of biological effects.

S 694 Interactive Computational AOP Reconstruction from Data

I. Shah. *US EPA, Research Triangle Park, NC.*

While there is growing consensus on the utility of AOPs for risk assessment, developing AOPs for target organ toxicity remains a major challenge. We are a part of the OECD effort for identifying AOPs for hepatotoxicity. To streamline AOP mapping we developed computational tools to reconstruct, visualize, modify, store and share AOPs. First, we developed an ontology to standardize chemical effects on 26,419 biological endpoints including: molecular events, cellular processes, and tissue phenotypes. Second, we synthesized ~1.2M effects on 5,541 chemicals from ToxCast, ToxRefDB and the literature into a computable knowledge base. Third, we systematically mined the literature and pathway databases to calculate dependencies between all 26,419 endpoints. Finally, we developed a heuristic search algorithm to interactively and visually reconstruct putative AOPs for chemicals by inferring linkages between molecular, cellular and tissue-level events. We evaluate the utility of this framework for analyzing receptor-mediated pathways in hepatic steatosis, cholestasis, and non-genotoxic liver cancer. These results highlight the power of automated AOP reconstruction as well as important limitations. (This abstract does not represent EPA policy.)

S 695 From AOPs to Quantitative *In Vitro* to *In Vivo* Extrapolation

M. E. Andersen. *The Hamner Institutes for Health Sciences, Research Triangle Park, NC.*

There are multiple international initiatives to move toxicity testing from reliance on in-life studies to in vitro platforms that evaluate modes-of-action of chemicals using human cells. The transition from past practices requires placing the new assays in a toxicological/risk assessment context. Adverse Outcome Pathways (AOPs) link events at different levels: from cellular interaction of chemicals, through perturbations of cellular pathways, on to integrated responses at the organism level. Development of AOPs will accelerate the move to acceptance of modern methods of testing by providing convincing arguments for regulatory authorities of the utility of pathway-oriented *in vitro* assays. These assays provide output showing the concentrations at which compounds produce cellular or subcellular responses. Formal use in risk/safety assessment requires dosimetry extrapolation from *in vitro* concentrations to human exposures and low dose extrapolations based on the cellular circuitry affected by the chemicals. This talk focuses on two key methodologies required for risk/safety assessment purposes: 1) quantitative *in vitro* to *in vivo* extrapolation (qIVIVE) that relates *in vitro* concentrations to environmental exposures and 2) computational systems biology pathway (CSBP) modeling that accounts for the structure of the key signaling pathways coordinating key cellular events. The CSBP modeling tools also evaluate dose-dependent transitions and

aid in identifying responses falling within the normal range. Our pathway research with receptor-mediated signaling (PPAR and AhR) and with DNA-damage shows the application of these tools in practice.

S 696 Is Neuroimmune Crosstalk Important to Neurotoxicology? Critical Insight from Animal and Human Studies

T. A. Brown[1] and C. E. McLoughlin[2]. [1]*University of Montana, Missoula, MT and* [2]*NIOSH, Morgantown, WV.*

Convincing evidence of bidirectional communication between the immune system and the nervous system has led to a paradigm shift in our understanding of neuroimmune interactions. Emerging evidence establishes a role for immune signaling in key neurodevelopmental events. Additional evidence suggests immune system contribution to neuronal responses in the form of neuroprotection and repair of tissue injury, as well as in the pathogenesis of neurodevelopmental and neurodegenerative disease. Simultaneously, neurons may actively participate in immune responses in the nervous system by signaling to resident and infiltrating immune cells. The net result of the neuroimmune crosstalk depends on the balance between protective and destructive signaling pathways. There is increasing consensus that exposure to neurotoxicants may tip this balance towards a more disruptive outcome and augment the risk and/or severity of disease. How the immune system can act as a mediator/modulator of neurotoxicity remains elusive. Understanding gained by investigation into neuroimmune interactions will guide improvement of disease diagnosis, prevention, and treatment. This session will present evidence of neuroimmune perturbations in human studies and animal models of neurotoxicant exposure. Evidence from human studies will focus on immune alterations following developmental neurotoxicant exposure in children with documented neurological deficits and in a pediatric population with autism spectrum disorders. Supporting data from animal models will focus on peripheral immune alterations and neuroinflammation following developmental or adult nervous system insult.

S 697 Neuroimmune Interactions in CNS Development, Repair, and Damage: An Overview

M. Stamou and P. Lein. *Molecular Biosciences, School of Veterinary Medicine, University of California Davis, Davis, CA.*

It is becoming increasingly clear that the nervous system and the immune system can no longer be considered as separate entities. Evidence suggests that molecules traditionally thought to be exclusive members of either the immune or the nervous system have a dual role in both systems and can regulate CNS function and central innate immune responses, not only in disease but also during normal physiological processes (development, aging, pregnancy, chronic stress). Such molecules include complement and major histocompatibility complex proteins, cytokines, chemokines and neurotrophins. Expression patterns of these molecules are altered in Parkinson's, Alzheimer's and multiple sclerosis and mutations in some of the corresponding genes have been linked to neurodevelopmental disorders (Autism Spectrum Disorders, schizophrenia). Neurons, astrocytes and microglia express a wide variety of these molecules, which in turn function to mediate cell-cell interactions including neuronal control of microglial activation and conversely microglial regulation of neurodevelopmental events such as synaptic pruning. Depending on the timing and context of the neuroimmune interaction, such crosstalk may mediate normal neurodevelopment or, in the case of CNS insult, may result in disease or repair. The net effect depends on the balance of neuroprotective and destructive pathways activated. Exposure of the CNS to neurotoxic chemicals could tip this balance towards a detrimental outcome and evidence of immune alterations in the CNS following exposure to environmental factors such as manganese, air pollution and pesticides, provide a compelling reason for further investigation. However, our understanding of the regulatory switches that determine neuroimmune interactions, and of the implications of their perturbation is still in its infancy. This talk will provide an overview of the cell types and molecules that mediate this bidirectional communication in the CNS, assess experimental evidence of their alteration by neurotoxicants, and highlight knowledge gaps in this rapidly growing field.

S 698 Effect of Polybrominated Diphenyl Ethers (PBDEs) on Immune Function and Cellular Signaling in Children with Autism

M. Eloi Atkintunde, P. Krakowiak, R. Boyce, P. Ashwood, I. Hertz-Picciotto, I. N. Pessah and J. Van de Water. *University of California Davis, Davis, CA.*

Elucidating the impact of environmental toxicants on the pediatric population, specifically children with autism spectrum disorders (ASD), is of critical importance. Previous studies implicate gene-by-environmental interactions in the etiology of autism, a disorder characterized by abnormal neurodevelopment and immunological dysfunction. PBDEs have been shown to influence development of both the nervous and immune systems. Research in the field lacks investigation in humans, especially sensitive populations, such as children with neurodevelopmental disorders. For this study, we sought to examine the impact of a potent congener, BDE-49, on the immune function in peripheral blood mononuclear cells (PBMCs) isolated from children ages 2-5 years old with neurodevelopmental diagnoses, such as ASD, developmental delayed (DD) and aged-matched typically developing (TD) subjects. Isolated PBMCs were exposed ex vivo for 4 hours to BDE-49 (0, 50nM, 250nM) prior to challenge with bacterial lipopolysaccharide (LPS), an innate immune cell activator, or the T cell mitogen, phytohemagglutin A (PHA). Cytokine and chemokine levels from cell supernatants were analyzed via a 21-multiplex bead-based assay. Ex vivo exposure of peripheral immune cells from a pediatric population to BDE-49 had global effects on the production of certain cytokines and chemokines, regardless of diagnosis. When diagnosis was taken into account, ex vivo exposure of PBMCs to BDE-49 at 50nM resulted in a differential inflammatory immune response in children with ASD compared to TD. We found that in each population, female subjects were more immune-sensitive to BDE-49 compared to male subjects, with a down regulation of cytokine and chemokine expression. This novel human study may aid in a better understanding of the interplay between immunological and neurotoxicants and the combined role in the etiology of autism.

S 699 The Immune and Neurological Impacts of Developmental BPA Exposure

J. N. Franklin, Q. Hu, B. Rushing, M. Biller and J. DeWitt. *Brody School of Medicine, East Carolina University, Greenville, NC.*

Environmental exposure to exogenous agents during critical time points of development may be associated with the onset of deleterious effects, including autoimmune and neurological disorders. Numerous studies have shown that bisphenol A (BPA) exposure can disrupt myriad biological systems. This presentation will focus on the immune and neurological impacts of a "double hit" of developmental exposure to BPA and an acute exposure to lipopolysaccharide (LPS) in an in vivo C57BL/6 mouse model. LPS exposure given around the time of learning has been shown to "unmask" developmental deficits in learning and memory. We hypothesize that postnatal exposure to LPS will unmask BPA-induced developmental impacts to hippocampal-dependent learning and memory of C57BL/6 offspring. Behavioral changes will be correlated with markers of immune dysfunction to determine the relationship between immunological alterations and behavioral changes. C57BL/6 female mice were given 0, 0.4, or 50 mg/kg of BPA in a corn oil vehicle by gavage, beginning at pairing with males and ending at weaning of pups. Offspring were assessed on a Barnes maze at postnatal day 60 (PND60), 24 hours after challenge with LPS. Splenic lymphocyte immunophenotype, total serum immunoglobulins, and inflammatory cytokines were evaluated after behavioral testing. Our findings suggest that developmental immunotoxicity induced by BPA exposure, in the absence of a postnatal trigger, is insufficient to induce changes in learning and memory.

S 700 Exploring the Relationship between Neuroinflammation and Neurotoxicity

K. A. Kelly, D. B. Miller and J. P. O'Callaghan. *CDC-NIOSH, Morgantown, WV.*

The enhanced expression of proinflammatory cytokines and chemokines accompanies brain injury induced by neurotrauma, disease or neurotoxicity as well as systemic infection. Elevations in proinflammatory mediators may serve as modulators or mediators of astroglial and microglial activation, cellular responses associated with all types of brain injury and collectively referred to as neuroinflammation. The "acute phase" response to systemic inflammation also leads to upregulation of proinflammatory cytokines/chemokines in the brain in the absence of underling neural damage, responses thought to be mediated largely by microglia and that serve as the basis of "sickness behavior". Activated glia may have neuroprotective roles or may exacerbate neural damage. Exposure to the known dopaminergic

neurotoxicants, MPTP and methamphetamine (METH), cause nerve terminal damage followed by neuroinflammation. Genetic and pharmacological interventions have resulted in partial suppression of the neuroinflammatory responses to MPTP and METH without affecting neurotoxicity and gliosis. In an attempt to achieve a complete suppression of neuroinflammation, chronic exposure to corticosterone (CORT) was used. Surprisingly, mice treated with CORT exhibited an exaggerated neuroinflammatory response to METH coupled with potentiated neurotoxicity (loss of dopaminergic nerve terminal marker, tyrosine hydroxylase) and gliosis. As the levels of chronic CORT approached or exceeded those associated with high physiological stress, the data suggest chronic CORT therapy or sustained physiological stress sensitizes CNS neuroinflammatory and neurotoxic responses. Yet, in a model of LPS-induced systemic infection that does not induce gliosis or neural damage, chronic CORT pretreatment greatly exacerbated and prolonged neuroinflammation without evidence of neural damage or gliosis. These results show a priming of the CNS proinflammatory response to amplify future exposures to pathogens, injury or toxicity. Taken together these findings suggest that while neurotoxicity causes inflammation, neuroinflammation may potentiate, but does not necessarily cause, neurotoxicity.

S 701 Neuroautoantibodies: Biomarkers and Potential Pathogenicity

L. A. Shaiba. *Department of Pediatrics, University of British Columbia, Vancouver, BC, Canada.*

Hypoxic-ischemic events are common to neurodegeneration due to many etiologies, including neurotoxicity, with devastating neurological outcomes. There is a compelling need for reliable, translatable biomarkers. Studies of neuroimmune interactions suggest that nervous system (NS)-specific antigens provide a record of insult in the form of serum autoantibodies (NAb). Using neonatal hypoxic-ischemic encephalopathy (HIE) as a model paradigm, the humoral hypoxic response, the corresponding detection of NAb biomarkers and brain astrogliosis were delineated. Sprague-Dawley rat pups underwent left carotid ligation and 3hr of hypoxia (8% O2) on PN7. Littermates with sham surgery and normoxia were controls. Neurofilaments (NF), glial-fibrillary acidic protein (GFAP) and myelin basic protein (MBP) antigens reflect the NS's cellular heterogeneity. Serum NAb against GFAP, NF, MBP and brain GFAP, and erythropoietin (EPO), VEGF, IL-2, IL-6 and TNFα were measured post-surgery (1, 4, 7, 14, 21, 28 and 36d). All cytokines measured were elevated at 24 hours post-surgery in HIE rat pups and for the duration of the study. EPO and VEGF, elevated at 24hr, began to decline at 14d. Only HIE pups had detectable levels of IgM and IgG against NF, GFAP and MBP at 4d post-hypoxia which increased in a time-dependent manner. Significant associations between GFAP levels and serum anti-GFAP IgG were seen for thalamus and cerebellum, the two regions most affected. Presence of inflammatory cytokines is consistent with pathophysiology and the early increases in EPO and VEGF are consistent with growth and compensatory attempts. The early predominance of IgG NAb suggests isotype switching from a natural repertoire of IgM. A transient decline in NAb likely reflects release of NS antigen due to secondary insult and suggests a possible pathological role of NAb. The reactive gliosis indicated by brain GFAP, a hallmark of neurodegeneration, as indicated by serum NAb. This study of early NAb detection indicates their potential as biomarkers of brain injury in neonates and children and suggests a role of NAb in progression of injury.

S 702 Perinatal Exposures and Children's Health Outcomes

N. Holland[2] and M. C. Poirier[1]. [1]*CDI Section, LCBG, National Cancer Institute, Bethesda, MD and* [2]*School of Public Health, University of California Berkeley, Berkeley, CA.*

The developing fetus is more susceptible to xenobiotic toxicant exposures than are individuals in adulthood. This may be largely due to the rapid growth rate, the inability of the placenta to protect completely, and the undeveloped/immature fetal immune and metabolic systems. *In utero* and perinatal xenobiotic exposures may contribute to chronic diseases of adolescence and adulthood, including cancer, asthma, and obesity. Molecular epidemiology of children's environmental health, which attempts to link exposure and disease, is a fast-growing area of research, both nationally and internationally. Clinical end points examined include growth parameters, metabolism, and cognitive capacity. Biomarker studies have concentrated on revealing genotoxic and epigenetic events, as well as mitochondrial toxicity, alterations in DNA repair, estrogenic effects, prediabetic metabolic syndromes, and other changes. Epigenetic effects related to prenatal exposures, are considered to play a role in the fetal origin of adult human diseases, but the importance of this area for public health is only beginning to be understood. The relevant exposures may range from metals, polycyclic aromatic hydrocarbons associated with air pollution, and pesticides, to hormone disruptors and widely-used chemotherapeutic drugs. Fetal adverse outcome may appear early (mitochondrial toxicity, metabolic syndrome, asthma, cognitive disorder), or years later (leukemia, obesity, and diabetes). This symposium is designed to highlight the significance of adverse health outcomes induced in infants and young children by a broad range of xenobiotic exposures occurring *in utero* and/or shortly after birth. If we can elucidate underlying genetic and epigenetic mechanisms, it may be possible to devise strategies that will better protect the health of all infants and children.

S 703 Perinatal Exposures to Environmental Pollutants and Children's Health

J. J. Heindel, T. Schug and K. Gray. *NIEHS, Research Triangle Park, NC.*

There is increasing experimental and epidemiological evidence showing that development (*in utero* and the first years of life) is vulnerable to phenotypic insult due to environmental influences. This vulnerability arises at least in part because development is a highly coordinated balance between genetic and epigenetic interactions. The epigenetic system is responsible for coordinating cell differentiation, and tissue and organ formation during development based on the genetic background. The epigenome is particularly sensitive to changes in the external environment, including under- and over-nutrition, stress, drugs, infections and environmental chemicals, which cause shifts or programmatic changes in cell development. This altered "programming" is evidenced by alterations in DNA methylation and chromatin architecture, which have been linked to increased susceptibility to disease and dysfunction that show up later in life. This presentation will set the stage for the session on pollutants and children's health by focusing on the data supporting a role for environmental chemical exposures, emphasizing endocrine active chemicals, in childhood diseases including asthma, learning disabilities, susceptibility to infections, obesity, type 2 diabetes and early puberty. It will also focus on the role that the NIEHS/EPA network of Centers for Children's Environmental Health and Disease Prevention play in linking environmental exposures to these childhood diseases/dysfunctions and indicate areas of rapidly developing research and data needs such as a focus on improved exposure assessments, mixture studies, examination of multiple windows of susceptibility, examination of disease syndromes and improved interactions between animal model researchers and epidemiologists in children's environmental health research. Data, while still incomplete, support a focus on prevention of childhood diseases by reducing exposure to environmental chemicals during development.

S 704 Early-Life Metal Exposure and Epigenetics

R. O. Wright. *Mount Sinai School of Medicine, New York, NY.*

A critical issue in the toxicology of metals includes the role of early life and prenatal exposures on subsequent health outcomes, including adverse neurodevelopmental outcomes, poor growth and obesity. Metals have been associated with all of these health outcomes and epigenetics has been demonstrated to play a role in the programming of these adverse developmental phenotypes in childhood. The complexity of the interplay between metals and developmental programming is further complicated by the role of some metals as both nutrients as well as toxicants. As such, biological processes to regulate normal metabolic functions exist alongside toxicometabolic processes designed to limit their toxicity and the existence of non-monotonic dose response relationship are likely. Complexity in studying epigenetics and child development lies in the multiple epigenetic "marks" that may regulate development (DNA methylation, histone modification, microRNAs) and the role of exposure timing during critical developmental windows. The PROGRESS (Programming Research in Obesity, GRowth, Environment and Social Stressors) study is a 1000 mother-child birth cohort with longitudinal assessment of metal exposure (arsenic, lead and manganese) and assessment of later life neurodevelopment, growth and obesity up to age 7 years. In the talk new data on the relationships between metal exposure at multiple critical developmental windows and epigenomic marks in distinct target tissues (umbilical artery, vein, placenta and white blood cell DNA), using the Illumina 450K methylomic microarray, will be presented. In a pilot study, differences in methylation were seen in umbilical arteries in the glucocorticoid receptor gene and P16 promoter. In addition to methylomic data, we will present data on LINE-1 expression as they related to growth and development.

S 705 Fetal Consequences of *In Utero* Antiretroviral (ARV) Nucleoside Reverse Transcriptase Inhibitor (NRTI) Exposures in Primates

M. C. Poirier[1], O. Olivero[1], Y. Liu[1], R. L. Divi[1] and R. A. Woodward[2]. *[1]CDI Section, LCBG, National Cancer Institute, Bethesda, MD and [2]Shared Animal Facility, NICHD, NIH, Dickerson, MD.*

Maternal-fetal Human Immunodeficiency Virus-1 (HIV-1) transmission is largely preventable when ARV drugs are given to the infected mother during pregnancy. However, the NRTI zidovudine (AZT) is a transplacental carcinogen in mice, and perinatal exposure induces genotoxicity and mitochondrial toxicity in monkey and human offspring (Env. Mol. Mutagenesis, vol. 48, April 2007). Approximately 10,000 women per year in the US are HIV-1-infected and become pregnant, and essentially all will receive these highly-successful therapies. Using an Erythrocebus patas (patas) monkey model, and human tissues, we have examined the mechanistic consequences of transplacental NRTI use. The monkey dams were given human-equivalent NRTI protocols, and because they do not become infected with immunodeficiency virus, the data reflect only drug toxicity. The human infant data, however, reflect both the effects of the drug and the maternal HIV-1 infection. We have shown incorporation of the NRTIs AZT and lamivudine (3TC) into nuclear and mitochondrial (mt)DNA of newborn monkeys and humans. Subsequently, AZT/3TC-induced mutagenesis/clastogenesis was found in transplacentally-exposed human infants. Recently the patas studies revealed the persistence of chromosomal damage in cultured bone marrow taken from transplacentally-exposed offspring at birth, 1 and 3 yr of age (equivalent in maturity to a 15 yr old human). In parallel studies we found mitochondrial morphological damage and mtDNA abnormalities in heart and brain of NRTI-exposed patas at birth, 1, and 3 yrs of age. Furthermore, the brains of 1 yr old patas, exposed perinatally to combinations of 2 NRTIs, contained only half of the mtDNA found in the controls. Overall, NRTI-DNA incorporation, chromosomal aberrations, mitochondrial morphological damage and depletion of mtDNA in placenta, were similar in NRTI-exposed patas and humans suggesting that these events underlie the toxic profiles in both species, and are independent of maternal HIV-1 status.

S 706 Air Pollution and Molecular Biomarkers of Children's Health

R. J. Sram, M. Dostal, H. Libalova, A. Milcova, P. Rossner, A. Rossnerova, J. Schmuczerova and J. Topinka. *Department of Genetic Ecotoxicology, Institute of Experimental Medicine, Academy of Sciences of the Czech Republic, Prague, Czech Republic.*

The city of Ostrava has the highest level of pollution from carcinogenic polycyclic aromatic hydrocarbons (c-PAHs), like benzo[a]pyrene (B[a]P), in the Czech Republic. We studied a group of 100 asthmatic and 100 healthy children (8-15 years old) exposed to ambient air in Ostrava and 200 control children from the less polluted city of Prachatice. We measured 8-oxodG in urine and lipid peroxidation in plasma as biomarkers of oxidative damage. Gene expression profiles and DNA methylation in white blood cells were assessed by Illumina HumanHT-12 and 27K BeadChips respectively. Gene expression appears to differ between asthmatic and healthy children, and vary by the two regions. Results also indicate that higher exposure to c-PAHs may induce non-allergic asthma in children. No difference in DNA methylation was observed between children with and without asthma, but patterns in both asthmatic and healthy children varied between the cities.
We also studied the effect of prenatal exposure to B[a]P on DNA adducts, MNs and transcriptome in Prague and Ceske Budejovice. Samples were obtained from non-smoking mothers from Prague (N=35) and Ceske Budejovice (N=52), and cord blood was collected from their newborns. Mean exposures to B[a]P in subjects from these cities were 3 months prior to delivery 1.9±0.5 ng/m3 and 3.2±0.2 ng/m3 respectively. Gene expression was assessed by microarrays in peripheral blood and placentas of the mothers, and in cord blood of their newborns. Compared to subjects from Prague, pregnancies from Ceske Budejovice showed up-regulation in expression of genes related to metabolism of xenobiotics, but down-regulation of genes related to immune response. This finding corresponds with an increased level of DNA adducts and MN frequency in cord blood from Ceske Budejovice. Analysis of gene expression appears to be an important new biomarker of air pollution.
Supported by the Grant Agency of the Czech Republic (P301113-13458S).

S 707 Genetic and Epigenetic Determinants of Health Outcomes in Children with Prenatal Pesticide Exposure

N. Holland, P. D. Yousefi, K. Huen and B. Eskenazi. *CERCH, University of California Berkeley, Berkeley, CA.* Sponsor: M. Poirier.

New results from the longitudinal study conducted by the Center for the Health Assessment of Mothers and Children of Salinas (CHAMACOS) examine the effects of prenatal exposure to pesticides on the functional genomics of Paraoxonase 1 (PON1) and genome-wide DNA methylation in Mexican-American children. PON1 is a multifunctional enzyme involved in antioxidant defense and detoxification of organophosphate (OP) pesticides. The broad variability of PON1 activities within populations may confer differential susceptibility to environmental exposures. We determined PON1 genotypes and three PON1 enzyme activities in 450 mothers and their children from an agricultural cohort residing in Salinas Valley, CA. Infants and young children, particularly those with PON1 genotypes encoding for lower PON1 levels and activities, have up to 65-fold lower levels of the protective PON1 enzyme than adults and may be especially susceptible to OP exposures. Additionally, global and site-specific DNA methylation was assessed in DNA isolated from cord blood and peripheral blood of 9 year old CHAMACOS children. Measurement of global DNA methylation was performed by pyrosequencing of Alu and LINE-1 repetitive elements. Global DNA methylation was found to vary by age, sex, and was lower (hypomethylated) in relation to prenatal exposure to organochlorine pesticides and PBDE's. Site-specific DNA methylation analysis was conducted using the Illumina 450K BeadChip platform that simultaneously interrogated methylation at more than 480,000 CpG sites from over 24,000 genes. Approximately 16% of all investigated CpG sites were differentially methylated by age and more than 2% of CpG sites (in >1900 genes) showed significant differences in methylation by sex, including many CpG sites located in autosomes. We also identified CpG sites across the PON1 gene whose methylation was associated with protein expression in CHAMACOS children, suggesting that epigenetic mechanisms may also regulate PON1 activity.

S 708 The Emerging Role of Mitochondrial Turnover, Biogenesis, and Dynamics in Tissue Injury

J. Kim[1], J. J. Lemasters[2], Y. Yoon[3], R. Schnellmann[2] and H. Jaeschke[4]. *[1]Surgery, University of Florida, Gainesville, FL, [2]Drug Discovery & Biomedical Sciences, Medical University of South Carolina, Charleston, SC, [3]Physiology, Georgia Regents University, Augusta, GA and [4]Pharmacology, Toxicology and Therapeutics, University of Kansas Medical Center, Kansas City, KS.*

The mitochondria, the cell's powerhouses, provide cells with adenosine triphosphate (ATP) to drive diverse energy-requiring reactions. Besides energy generation, the mitochondria are also involved in a myriad of essential functions and signaling events in cells. Consequently, disturbances affecting mitochondrial integrity diminish the quality and function of mitochondria, ultimately leading to tissue injury and death. Indeed, mitochondrial dysfunction is a key mechanism underlying ischemia/reperfusion, aging, and drug-induced toxicity in the liver, kidney, and other organs. To maintain normal cell function and survival under the conditions of a variety of stresses, cells possess a powerful surveillance system that selectively eliminates injured or dysfunctional mitochondria in a timely manner, a process called mitophagy. Impaired or insufficient mitophagy is causatively linked to pathology of ischemia/reperfusion, aging, and alcohol- and acetaminophen-mediated hepatotoxicity. The mitochondria are newly formed, and constantly divide and fuse, and continuously change their size and morphology during times of cellular stresses or in response to environmental stimuli. The biogenesis of mitochondria is tightly regulated, and inhibition of mitochondrial biogenesis has been associated with the development of age-related degenerative diseases. Furthermore, mitochondrial dynamics not only determines mitochondrial size, but also regulates mitophagy. Growing evidence is accumulating that mitochondrial biogenesis and dynamics are neatly interconnected with mitophagy. This symposium will emphasize the emerging role of mitochondrial turnover, biogenesis, and dynamics in tissue injury.

S 709 Variants of Mitochondrial Autophagy: Types 1 and 2 Mitophagy

J. J. Lemasters. *Drug Discovery & Biomedical Sciences and Biochemistry & Molecular Biology, Medical University of South Carolina, Charleston, SC.*

Autophagy removes damaged, effete and superfluous mitochondria, a process of mitophagy. In hepatocytes during nutrient deprivation, preautophagic structures (PAS) associated with mitochondria grow into cup-shaped isolation membranes (phagophores) that sequester individual mitochondria into mitophagosomes, a process requiring phosphatidylinositol-3-kinase (PI3K). Sequestration is complete in less than 10 min and often occurs coordinately with mitochondrial fission. After

sequestration, the outer compartment between the inner and outer autophagosomal membranes acidifies likely due to fusion of mitophagosomes with lysosomes/ late endosomes. Subsequently, mitochondria depolarize and the organelles undergo lysosomal digestion. Mitochondrial damage also activates mitophagy. After photodamage to individual mitochondria of nutrient replete hepatocytes, coalescence of autophagic structures on the surfaces of depolarized mitochondria occurs after about 30 min, followed by vesicular acidification and lysosomal digestion. These examples illustrate two variants of mitophagy, Type 1 and Type 2, that differ in several respects. Type 1 mitophagy occurs after nutrient deprivation, requires PI3K activity and is associated with phagophore development and mitochondrial fission. Type 2 mitophagy occurs independently of PI3K activation and without phagophore formation or mitochondrial fission. Notably, mitochondrial depolarization occurs after autophagic sequestration in Type 1 mitophagy but prior to sequestration in Type 2 mitophagy. Nonetheless, mitophagosomes once formed by either type of mitophagy go on to acidify, fuse with lysosomes and degrade their mitochondrial contents (NIDDK).

S 710 Mitochondrial Autophagy in Ischemia-Reperfusion Injury and Age-Mediated Hepatotoxicity

J. Kim. *Surgery, University of Florida, Gainesville, FL.*

Patients with the end stage of liver disease often require transplantation and complex hepatic surgery for extirpation of a non-functional liver and are frequently hospitalized for supportive care that provides only temporary comfort. Moreover, the aged liver has significantly less reparative capacity following ischemia/ reperfusion (I/R) injury associated with these operations. Mitochondrial dysfunction plays a causative role in I/R injury. Currently, no therapeutic strategy can suppress I/R injury. Mitochondrial autophagy (mitophagy) is integral quality control machinery that timely and selectively targets and removes damaged or abnormal mitochondria. Biochemical, genetic and imaging analysis demonstrates that I/R injury to young livers and increased sensitivity of old livers to stresses are strongly associated with decreased autophagic responsiveness and subsequent mitochondrial dysfunction, due to depletion of key autophagy-related proteins. Enhanced mitophagy confers cytoprotection against I/R injury, drug-induced toxicity and aging in liver and other tissues, suggesting that mitophagy plays a pivotal role in I/R- and age-mediated hepatotoxicity, and that enhancing mitophagy has a therapeutic potential to improve hepatic function after liver surgery.

S 711 Mitochondrial Dynamics and Oxidative Tissue in Diabetes

Y. Yoon. *Department of Physiology, Georgia Regents University, Augusta, GA.*
Sponsor: J. Kim.

Mitochondria are dynamic organelles, undergoing constant shape change mainly through fission and fusion. Mitochondrial fission and fusion spend cellular energy, suggestive of their importance. However, not only functional significance of mitochondrial fission and fusion but also the mechanistic correlation between mitochondrial functionality and morphology is poorly understood. Our studies demonstrated that mitochondrial shortening by fission coincides with increases in reactive oxygen species (ROS) levels in hyperglycemic conditions. Elevated ROS level was causal for an increase of mitochondrial permeability transition (MPT) and apoptotic cell death. We were able to show that inhibiting mitochondrial fission by expression of a dominant-negative mutant, DLP1-K38A, alleviated MPT and cell injury by decreasing ROS levels. Enhanced mitochondrial ROS production arising from diabetes is pathologically linked to hyperglycemic complications in many target tissues. In an effort to evaluate the role of mitochondrial fission in diabetic tissue damage, we found that cellular ROS levels in DLP1-K38A transgenic mice made diabetic were significantly lower in both renal and hepatic tissues. While mitochondria in renal proximal tubular cells became round and 'swollen' in diabetic control mice, DLP1-K38A mice maintained normal elongated shape in diabetic conditions. Mechanistically, we discovered that fission inhibition induces an increase of respiration uncoupling to decrease ROS production from mitochondria. Importantly, DLP1-K38A expression suppressed oxidative damage and renal dysfunction in diabetic mice, indicating that mitochondrial fission can be a novel target of intervention in combating oxidative tissue damage.

S 712 Mitochondrial Biogenesis or Not Following Toxicant Exposure

R. Schnellmann. *Drug Discovery and Biomedical Sciences, Medical University of South Carolina, Charleston, SC.*

Mitochondria are direct and indirect targets of many toxicants in a number of different tissues and a large number of studies have focused on the mechanisms of mitochondrial injury and the resulting cell death. In contrast, how cells respond to mitochondrial dysfunction has received less attention. One response to toxicity is the induction of mitochondrial biogenesis (MB) to restore mitochondrial and cellular functions in sublethally injured cells and prevent cell death. In contrast, recent studies have shown that toxicants can inhibit MB. MB requires a coordinated and tightly regulated signaling system. Nuclear respiratory factors (NRF-1 and -2) bind to the promoters of the nuclear genes, leading to expression of constituent components of the oxidative metabolism enzymes and other genes regulating mitochondrial DNA (mtDNA) replication, transcription and maintenance. The transcriptional coactivator PGC-1alpha, the master regulator of MB, induces and coordinates gene expression of mitochondrial transcription A (Tfam), NRF-1 and 2, and itself. Most mitochondrial proteins are encoded by nuclear DNA but mtDNA encodes 13 proteins which are all key components of OXPHOS machinery. A number of upstream signaling pathways (e.g. p38 MAPK, SIRT1, AMPK) have been shown to be activated following injury and activate PGC-1alpha to produce MB and restore mitochondrial and cellular functions. This presentation will explore the pathways that signal MB and the functional outcomes.

S 713 Mitochondria Dynamics in Acetaminophen-Induced Liver Injury

H. Jaeschke. *Department of Pharmacology, Toxicology and Therapeutics, University of Kansas Medical Center, Kansas City, KS.*

Acetaminophen (APAP) hepatotoxicity is currently the most frequent cause of drug-induced liver failure in many countries. In addition, APAP is a widely used model to study mechanisms of drug-induced cell death. Although initiated by formation of a reactive metabolite, the mechanisms of APAP hepatotoxicity center on mitochondrial dysfunction and oxidant stress. These early events trigger activation of MAP kinase pathways, which amplify the mitochondrial oxidant stress leading to the mitochondrial membrane permeability transition pore opening and ultimately cell necrosis. Recent evidence for a role of receptor interacting kinase protein 1 (RIP1) and especially RIP3 in APAP-induced liver cell death suggests characteristics of programmed necrosis. RIP3 controls the mitochondrial translocation of dynamin related protein 1 (Drp1) implying that RIP3 promotes mitochondrial fission during APAP-induced cell death. Inhibition of Drp1 protects against cell death. However, removal of mitochondrial fragments by autophagy serves to reduce the number of dysfunctional mitochondria and limits progression of cell death signaling. This presentation will discuss the critical role of mitochondrial dynamics in cell survival and cell death during drug hepatotoxicity.

S 714 Use of Stem Cells in Toxicity Testing—From Basic Research to Personalized Toxicology

S. H. Dhalluin[1] and Y. Will[2]. [1]*New Medicines - Non-Clinical Development, UCB Pharma SA, Brussels, Belgium and* [2]*Global Research and Development, Pfizer, Groton, CT.*

Drug-induced toxicity remains a major problem for all pharmaceutical companies, and most have deployed *in silico* and *in vitro* testing paradigms throughout the drug discovery process to select safer drugs to be tested in animal models and advance to patients. Despite many advances in understanding mechanisms of toxicity, the majority of *in vitro* assays predict human risks by less than 50%, and it was shown that measuring simple mechanistic toxicity endpoints in organ-relevant cell lines does not predict organ toxicity (Lin and Will, 2012, Lu and Will, SOT 2013).This may be due to the fact that certain basic toxicity mechanisms such as apoptosis or mitochondrial dysfunction can contribute to a variety of organ toxicities and that many cell lines lack features of organ physiology, such as proper metabolism, relevant ion channel pharmacology, genetic diversity or disease background, to name a few. To build a predictive multicell model, it is necessary to begin with improved functional cell models from the relevant tissue, e.g., hepatocytes, cardiomyocytes, etc. Therefore, efforts to generate physiologically-, pharmacologically-, and toxicologically-relevant cells from ES and iPS cells are important. Progress has been made in the production of human/patient-derived pluripotent stem cells, which can be continuously expanded in the undifferentiated state and differentiated to form most cell types, potentially allowing recapitulation of genetic variation such as association with known gene variants (e.g., HLA susceptibility alleles). This symposium will contribute to our understanding of the current and future state of stem cell

usage in toxicology by: 1) providing an overview of stem cells, their characteristics in comparison to native organs, their ability to represent patient genetics and disease, 2) describing the current state of application to detect liver, heart, and kidney toxicity, 3) discussing how good patient genetic and disease background give rise to personalized toxicity assessment.

S 715 Human Pluripotent Stem Cells As Tools for Safety Toxicology

J. Thomson. *Morgridge Institute for Research, Madison, WI.* Sponsor: Y. Will.

Human ES and iPS cells offer scalable, consistent sources of normal human cell types that were previously difficult to source. Because human iPS cells offer control over genetic backgrounds, in vitro modeling of drug responses for an intended target population is practical for the first time. This talk will review the properties of iPS cells, and will discuss recent progress in the large-scale derivation of iPS cells and specific iPS cell derivatives relevant to safety toxicology and drug discovery. Specific examples of how Pharma is already using iPS cell-derived cardiomyocytes, neurons, and hepatocytes will be discussed.

S 716 The Application of Stem Cell-Derived Hepatocytes in Mechanism-Based Drug Safety Assessment

C. Goldring. *MRC Centre for Drug Safety Science, University of Liverpool, Liverpool, United Kingdom.* Sponsor: S. Dhalluin.

Recent research into idiosyncratic adverse drug reactions (ADRs) has successfully revealed novel genetic predisposing factors by utilising a candidate gene approach and through the application of genome-wide scanning techniques. However, the underlying mechanisms of ADRs such as drug-induced liver injury (DILI) are complex, multi-dimensional, and not fully amenable to testing using the currently available cell culture systems. The recent rapid advances in the ability to generate induced pluripotent stem (iPS) cells from somatic cells have provided a unique tool to derive disease-specific stem cells that may serve as a mechanistic model for the study of idiosyncratic ADRs, for the liver and other tissues. Nevertheless, work needs to be done before it is known whether this promise will be fulfilled. This talk will highlight advances in this area, and will focus on some critical hurdles in both the embryonic and the iPS fields. The prospects for personalisation in safety assessment, through the great advances in the iPS field will also be considered. Furthermore, advances in complex culture techniques, such as spheroids, bioreactors and multi-cell culture, that may enlighten the field of in vitro hepatotoxicity screening will be highlighted.

S 717 iPSCs for Cardiac Drug Testing

J. Wu[1, 2]. [1]*Stanford Cardiovascular Institute, School of Medicine, Stanford University, Stanford, CA and* [2]*Department of Medicine/Cardiology, School of Medicine, Stanford University, Stanford, CA.* Sponsor: Y. Will.

Cardiac toxicity is a side effect of many pharmaceutical compounds and is a leading cause for drug withdrawal from market because of safety concerns. Current preclinical methods to measure cardiotoxicity are inefficient and rely on genetically altered cell lines, such as human embryonic kidney cells, or Chinese hamster ovary cells, which do not accurately resemble human heart cells (cardiomyocytes). Recent technological advancement has enabled the generation of human induced pluripotent stem cells (hiPSCs) from skin, which can be used to generate patient-specific cardiomyocytes (hiPSC-CMs) in vitro. The hiPSC-CMs generated in this fashion carry all the genetic information from the individuals from whom they are derived. Here we will overview the capacity of a hiPSC-CM library to be used as a clinical trial in a dish model for accurate detection of patient-specific drug responses.

S 718 *In Vitro* Models for the Prediction of Nephrotoxicity in Humans

D. Zink. *Institute of Bioengineering and Nanotechnology, Agency for Science, Technology and Research, Singapore, Singapore.* Sponsor: S. Dhalluin.

The kidney is a major human target organ for drug-induced toxicity. Nephrotoxicity is often detected only late during drug development. Animal models have limited predictability due to interspecies variability. In vitro models are of increasing interest, but there are currently no validated or approved in vitro models for nephrotoxicology available. We developed kidney-specific two-dimensional (2D) and 3D (Zhang et al., J Cell Mol Med, 2011; Li et al., Nanotoxicology, 2012) models for in vitro toxicology and nanotoxicology. Our models are based on human primary renal proximal tubular cells (HPTC) and human renal cells derived from pluripotent stem cells (Narayanan et al., Kidney Int, 2013). Endpoint of the in vitro model with the currently highest predictability is increase in marker gene expression. This model has been validated with 41 well–characterized compounds (Li et al., Toxicology Research, 2013). The results show high sensitivity, specificity and concordance with human clinical data. All major performance metrics, including the area under the curve of the receiver operating characteristic curves are in the range of 0.8. This translates to about 80% accuracy in the predictions made with this model. An alternative model compatible with high content screening is currently under development.

W 719 Skeptically Re-Examining the Limits of Toxicology Evidence in the Courtroom

G. B. Corcoran[1], M. J. Saks[2], S. M. Bobst[3], G. E. Marchant[2], T. Simon[4] and R. T. Kennedy[5]. [1]*Pharmaceutical Sciences, Wayne State University, Detroit, MI,* [2]*Sandra Day O'Connor College of Law, Arizona State University, Tempe, AZ,* [3]*Nexeo Solutions, LLC, Houston, TX,* [4]*Ted Simon, LLC, Winston, GA and* [5]*New Mexico Court of Appeals, Albuquerque, NM.*

This session examines the legal applications and boundaries of toxicology and closes with a panel discussion and audience question and answer. Law and science exist in a time-frame dichotomy. The law needs a just jury verdict today, yet the *modus operandi* of science works over years toward more accurate theories. The adversary system and its use of experts to support a partisan position is explored. Differing models of legal and scientific interaction dictate that goals of science or of the law may suffer while the other is upheld. Toxicology stands front and center in how the law approaches scientific evidence and professional expert testimony. *Galileo's Revenge* did much to expose junk science in expert testimony. The Supreme Court selected cases rooted in toxicology to re-tool the federal approach to scientific expertise in *Daubert v. Merrill Dow* and *Joiner v. General Electric*. The courts followed with the *Federal Reference Manual on Scientific Evidence*, guiding the role of science in complex litigation. Questions about how toxic substances cause injury and how to trace and attribute responsibility remain among the most common in the courtroom. This workshop examines neurological damage and the roles of genetics and genomics. The limits of expertise to explain and predict the causes and effects are central to such cases. Experts are offered from many disciplines, some never seen before depositions. Lawyers and judges are urged by Daubert to view science as scientists do, through the scientific method. Following this skeptical evaluation of toxicology evidence in the courtroom, attendees will be better prepared to assist the higher ends of both toxicology and the law.

W 720 Trial Factfinders and Expert Evidence

M. J. Saks. *Sandra Day O'Connor College of Law, Arizona State University, Tempe, AZ.* Sponsor: G. Corcoran.

The role of the expert witness is to educate the judge and jury about facts and inferences expected to be helpful to resolving a case. The role of counsel is to advocate on behalf of a particular outcome, and to advance evidence and arguments to support that outcome. Too often, the expert becomes an assistant advocate, trying to help bring about the verdict sought by the lawyer's client. We examine the social and psychological forces that push expert witnesses beyond what they do best and beyond what the court wants of them. We consider the tensions between the law's formal expectations and the informal pressures that tend to strain the ethics of experts, distort the field's knowledge, and in the end do not serve justice or science as well as they both deserve. And we ask what professional and scientific fields might do to improve the situation.

W 721 Presentation Approach: The 5-Question Approach to Specific Causation, and Beyond

S. M. Bobst. *Nexeo Solutions, LLC, Houston, TX.*

Thomas, Bobst, and Zheng introduced the 5 Question Approach to the Society of Toxicology in 2005. Toxicity, exposure, specific case evidence, alignment or gaps with the specific tort or drug test claim, and alternative explanations are key issues for the forensic or general toxicologist to address, as an expert in the courtroom. Similar themes have been shared by other toxicology experts that address the role of the toxicologist in the courtroom, and will be referenced and presented to support

proof of concept. Case studies in chemical exposure and drug pharmacology will be explored where the 5 question approach was applied by a toxicologist for litigated tort claims, including ethyl acetate and an opoid painkiller.

W 722 Evidentiary Challenges with Genomic Data in Toxic Tort Litigation

G. E. Marchant. *Sandra Day O'Connor College of Law, Arizona State University, Tempe, AZ.*

As the genomic era continues to rapidly advance, genomic data is increasingly being introduced into toxic tort litigation by expert witnesses for both defendants and plaintiffs. This includes genetic susceptibility data that might affect the causation analysis, as well as various types of genetic biomarker evidence that may be relevant to the exposure inquiry. The attempted introduction of such data is often controversial and contested, with opposing counsel frequently arguing that such data are unreliable, inadequately validated, or irrelevant. This presentation will discuss several recent high-profile attempts to introduce genetic data into toxic tort cases involving toxicants such as benzene, lead, ionizing radiation, mercury, and PCBs, and the challenges such data presented for our evidentiary standards, expert witnesses, attorneys, judges and juries. This case study of genomic data in toxic tort litigation illustrates some of the broader issues the evidentiary and expert witness systems in our federal and state courts will encounter in the era of rapidly changing technology and knowledge. These issues include the temptation and incentives for expert witnesses to place premature or exaggerated reliance on emerging scientific knowledge, and the tension between scientific and legal standards of admission and proof.

W 723 Evidentiary Standards for Neuroactive and Neurotoxic Drug Testing

T. Simon. *Ted Simon LLC, Winston, GA.*

A number of psychoactive and potentially neurotoxic substances are often considered by courts to modify or disrupt the functioning of the brain. However, dose response is taken into account for only a single substance—ethanol. For ethanol, the societal consensus for impairment of performance has been set at 0.08% or 80 mg/dL. Because of the zero-order elimination kinetics of ethanol and the widely used Widmark pharmacokinetic model, one can determine the source of alcohol in the body based on recent consumption history and this determination can be used as legal evidence. Inorganic mercury intoxication produces a condition called "erethism" with symptoms of anxiety, mood lability, and poor anger control that may be misdiagnosed as psychosis. The "date-rape" drug gamma-hydroxybutyrate (GHB) appears to act by modulating the effects of a number of neurotransmitters, and its effects may be potentiated by nicotine. Symptoms of GHB intoxication include euphoria, relaxation, and increased sexuality. At higher doses, GHB may cause unconsciousness and even death. GHB is produced endogenously within the body. Exogenous GHB is eliminated from the body completely within 8 hours and no rapid immunological test exists—so testing for GHB in cases of drug-facilitated sexual assault is challenging. Regarding cocaine, GS-MS LC-MS and immunological assays methods are used for detection of cocaine metabolites in urine, other body fluids and even hair—with the potential for both false-positive and false-negative results from all methods. In summary, for most psychoactive substances, evidence of exposure obtained by analysis of body matrices is considered tantamount to a psychoactive effect and potential impairment by the legal system. With marijuana is now legal in 18 states, the interpretation of evidence of psychoactive drug exposure in terms of dose-response and assessment of the likelihood of impairment is becoming an important task. Currently, the question addressed by drug testing is—was the subject exposed to the drug? For marijuana especially, the question needs to be—did the subject have enough drug in his/her system to be impaired?

W 724 Challenging Toxicologists to Advance the Science of Forensics

R. T. Kennedy. *New Mexico Court of Appeals, Albuquerque, NM.* Sponsor: G. Corcoran.

Toxicological evidence in court should demonstrate the existence of a toxin, symptom, and causal relation (general/specific) between them. Lawyers ask, and judges often allow medical doctors regularly testify to causal relationships through differential diagnoses in court. This can result in the introduction of incomplete or flawed evidence. Toxicology's language confuses judges and lawyers. In criminal cases, analytical chemistry is called "toxicology." In many trials, analysts of varying skill and repute testify as "toxicologists," stating opinions linking symptoms with levels of drugs or alcohol found in body fluids or tissue. For alcohol, this is based on scant exposure to Widmark's formula. With drugs, it is common to see experts give causal testimony first ascertaining symptoms of "impairment" from a police report, then matching the test results, equating amounts found to those symptoms. The credulity of the law allows the potential for injustice. "Non-forensic" toxicology represented by SOT might provide "academic" context to apply standards of research, validation, and acceptable practice to frontier territory needing regulation, See, Strengthening Forensic Science: A Path Forward (NAS,2009). The Federal reference manual on scientific evidence applies toxicology to toxic tort and pharmaceutical litigation, but not applying guiding principles to more common appearances of "toxicology". Can forensic and legal minds grasp what "toxicology" is about? A question: "If Daubert is about applying 'science as scientists do it', why can't a qualified expert examine another researcher's data to see if it supports conclusions drawn?" Is motivation inferred from performing such an analysis for litigation any less suspect than performing research for a company desiring to move its product to market? The writer hopes for a concept and direction of how SOT and its members can advance the legal use of toxicological expertise based on objectively reasonable and established standards of scientific practice.

EC 725 Scientific Ethics in Research and Publications

W. J. Brock[1] and M. Genter[2]. [1]*Brock Scientific Consulting, Montgomery Village, MD and* [2]*University of Cincinnati, Cincinnati, OH.*

For many involved in toxicological research and publishing, it may seem strange or uncomfortable to engage in a discussion of the practicality of ethics. However, with the daily pressures of career advancements and salary increases as well as notoriety and professional recognition, engaging in this discussion will permit continued awareness of the pitfalls of poor ethical behavior that can lead to catastrophic career outcomes. The scientific community has been rocked by unfortunate media reports over the years that call into question the results of studies and fallibility of science. Although these reports may represent a small percentage of individuals, the impact is far-reaching throughout the scientific community. There have been several reports in the past few years that suggest that the number of retracted papers in scientific literature has increased 10-fold over the previous decade, and that a majority of the retracted papers was due to scientific misconduct that included fraud, plagiarism, and outright data falsification. In spite of the increase in retractions, many of those retracted papers continue to be cited in subsequent publications and grant submissions. Plagiarism by far represents the more common concern in scientific writing. Whether this occurs from the originating author or the wording is "stolen" by others to improve or even exaggerate a conclusion has led to a change in peer-review processes, development of plagiarism software, and mandatory training in certain academic circles. In addition, "ghost" and "in absentia" authors have raised significant data credibility concerns in a regulatory environment. In this session, the background of the problem is presented with real-world examples from literature and reports, and the impact of this problem on a career. Can the peer-review process reduce the likelihood of scientific misconduct? Discussion will occur on the peer-review process and how that process affects the publishing of duplicative or plagiarized data.

EC 726 Introduction to Scientific Misconduct: The Problem, the Results, and the Potential Impact of Advancing a Career Path

W. J. Brock. *Brock Scientific Consulting, Montgomery Village, MD.*

Over the last 100+ years, there have been enormous increases in scientific knowledge across all fields of science. Unfortunately, the individual desire to be a part of the technical innovations observed during this time has led to "abuse" of that innovation. In the last 15-20 years, the number of cases of scientific misconduct has been surprisingly numerous. In this presentation, the problem of misconduct will be described to include the more notable case reports that have affected our scientific understanding and ability to make judgments of human health safety. For those in the regulatory toxicology community, a description of how scientific misconduct has led to greater regulatory oversight will be presented.

EC 727 Responsible Research: What Is It and Can It Be Done?

H. Bante. *University of Cincinnati, Cincinnati, OH.* Sponsor: W. Brock.

Biomedical research continues to evolve as investigators collaborate across disciplines and institutions to solve complex health problems. These interdisciplinary interactions coupled with for-profit relationships have led to questions surrounding professional norms and ethical principles as they relate to scientific research. Recognizing these changes and in an effort to foster research integrity, the National

Science Foundation and the National Institutes of Health have mandated education of all trainees, fellows, participants, and scholars in the Responsible Conduct of Research (RCR). Despite these efforts, the incidence of scientific misconduct and questionable research practices remain problematic. This presentation will explain RCR and what it hopes to accomplish, and discuss why collapses in responsible research continue to occur.

EC 728 Authorship and Scientific Misconduct

W. B. Mattes. *PharmPoint Consulting, Poolesville, MD.*

An integral component of the practice of science is the publication of research results and analyses. Needless to say, humans conceive of, conduct, analyze, and describe the work, and participation in this endeavor is acknowledged through the author list of the resulting publication. However, professional advancement and financial rewards are often tied to the number of authored publications; in many fields, the first author is given special attention. Given this setting, authorship is often abused. "Honorary" authors are those whose names are included, yet made no real contribution to the work. "Ghost" authors are those who actually did contribute but are not listed. First authorship is often a source of conflict and is especially problematic in fields where the work requires a large number of collaborators. This presentation will review not only the well-established guidelines but also provide an analysis of the problems of authorship with proposed solutions.

EC 729 Seeking, Identifying, and Preventing Plagiarism: Manuscript Submissions and Peer Review

M. Genter. *University of Cincinnati, Cincinnati, OH.*

While plagiarism can be intentional or unintentional, and can involve an author plagiarizing himself or another author, it can have devastating effects on one's pursuit of a degree, ability to successfully compete for funding, ability to publish in the peer-reviewed literature, and success in successfully advancing up the career ladder. This presentation will focus on plagiarism from the perspective of the author, peer reviewer, and journal editor. Trainees at all levels should be mentored in the appropriate situations and ways to cite not only the work of others, but also their own work. Peer reviewers and journal editors should be aware of the high incidence of plagiarism, and should put special effort into assuring that a submitted manuscript, or parts thereof, has not been published elsewhere. Examples of self-plagiarism and plagiarism of others' works in submitted manuscripts will presented, as well as tips to identify and prevent plagiarism.

S 730 Noncoding RNAs in Human Health, Therapeutics, and Environmental Disease

N. E. Kaminski. *Michigan State University, East Lansing, MI.*

A little over a decade ago, the regulatory role of small non-protein-coding RNAs was first uncovered through experiments involving the deliberate introduction of short double-stranded RNAs (dsRNA) into plant and eukaryotic cells. These exogenous dsRNAs were found to induce post-transcriptional gene silencing, a process termed RNA interference. This seminal observation led to the discovery of novel and complex biological processes of gene regulation involving endogenous noncoding RNAs of which several varieties have been identified, including microRNA, PIWI-interacting RNA, and long noncoding RNA. During the past 10 years, significant advances have been made in gaining an understanding of the role of noncoding RNAs spanning the period from organismal development and continuing throughout all stages of life. Although the biological role of noncoding RNA has yet to be fully understood, it is important to emphasize that only a small fraction of the mammalian genome codes for mRNAs, and yet the majority of the remaining genome is transcribed into noncoding RNAs. It is tempting to speculate that a large proportion of these noncoding RNAs are transcribed for the distinct purpose of carrying out critical regulatory functions. Indeed, there is a growing literature identifying specific processes under the control of noncoding RNAs and, likewise, the pathology that can ensue when noncoding RNA regulatory processes are disrupted. Relatively little is known concerning the influence environmental factors exert on noncoding RNAs, at the level of their expression, function, or contribution to the etiology of disease processes; therefore, this represents an important frontier for toxicological investigation. In light of the importance of this relatively new area of biology and its potential impact on human health, the goal of this session is to feature eminent scientists who have made important contributions and advances to our current knowledge of noncoding RNAs. The broad areas to be addressed include: general concepts surrounding the biology of noncoding RNAs, their role in development and in specific disease processes, and their potential role in novel therapeutic approaches.

S 731 RNA at the Epicenter of Human Development

J. S. Mattick. *Garvan Institute of Medical Research, Sydney, NSW, Australia.*
Sponsor: N. Kaminski.

It appears that the genomic programming of humans and other complex organisms has been misunderstood for the past 50 years, because of the assumption that almost all genetic information is transacted by proteins. Surprisingly, the human genome contains only about 20,000 protein-coding genes, similar in number and with largely orthologous functions as those in other animals, including developmentally simple nematodes and sponges. On the other hand, the extent of non-protein-coding DNA increases with increasing developmental and cognitive complexity, reaching 98.8% in humans. Moreover, high-throughput analyses have shown that the vast majority of the human genome is dynamically transcribed to produce a previously hidden world of different classes of small and large, overlapping and interlacing intronic, intergenic and antisense non-protein-coding RNAs. The transcriptome is in fact far more complex than the genome, which is best viewed as a zip file that is unpacked in highly stage- and cell-specific patterns during development. This is illustrated by the use of targeted RNA sequencing to reveal thousands of previously unknown exons and spliced isoforms of oncogenes and tumor suppressors, as well as at least 1500 new long noncoding RNA (lncRNA) genes in intergenic GWAS regions associated with complex diseases. These RNAs fulfill a wide range of regulatory functions, with microRNAs and related species being best (although not well) understood. The functions of lncRNAs are varied and include central roles in the formation of differentiation-specific subnuclear organelles. However, recent evidence suggests that their main function is to organize chromosome territories and to guide chromatin-modifying complexes to their sites of action, to specify the architectural trajectories of development. Moreover, this system has subsequently evolved plasticity, via an as-yet-unexplored universe of retrotransposon expression and mobilization, as well as RNA editing and modification, which appears to be the molecular basis of environmental-epigenome interactions and brain function.

S 732 Role of microRNA Signaling in the Cancer Microenvironment Communication

M. Fabbri. *Departments of Pediatrics and Molecular Microbiology & Immunology, Keck School of Medicine, University of Southern California, Los Angeles, CA.*
Sponsor: N. Kaminski.

Cancer is a complex genetic disease. Recent evidence indicates that not only cancer cells but also surrounding cells, forming the so called "tumor microenvironment" play a central role in cancer biology. MicroRNAs (miRNAs), are small non-coding RNA with gene regulatory function, whose dys-regulation is observed in almost all types of human cancers (both solid and hematological malignancies). In addition to their "traditional" mechanism of action (which consists of their targeting of messenger RNAs, miRNAs affect the tumor microenvironment also through previously unknown mechanisms that will be discussed in this lecture. Particular focus will be put on their role as cancer secreted molecules within exosomes, able to trigger pro-tumoral and pro-metastatic signaling by affecting the biology of the tumor microenvironment. A better understanding of such mechanisms represents the necessary rationale for the development of new personalized treatments for cancer patients.

S 733 MicroRNAs in Hepatocellular Carcinoma

C. Lee[1, 2, 3]. [1]*Department of Biochemistry, Yong Loo Lin School of Medicine, National University of Singapore, Singapore, Singapore,* [2]*Duke-NUS Graduate Medical School, Singapore, Singapore and* [3]*National Cancer Centre, Singapore, Singapore.*
Sponsor: N. Kaminski.

Hepatocellular carcinoma (HCC) is the 3rd leading cause of cancer deaths globally with a five-year survival of ~5%. Diagnosis of HCC currently relies on routine screening of at-risk patients, including those with cirrhosis due to viral hepatitis, by screening serum alpha-fetoprotein (sAFP) levels in conjunction with hepatic ultrasonography but this combination has limitations. Although cost-effective, ultrasonography has only 60% sensitivity and 97% specificity. sAFP is only 40-60% sensitive as many tumors do not produce AFP or do so at very advanced stage. Hence, there is an urgent need to identify better, more reliable noninvasive biomarkers with higher sensitivity and specificity for early detection of HCC. Although ad-

vances have been made to our understanding of the mechanisms of HCC, it still remains incomplete as we grapple with the full spectrum of complexities of the genetic, epigenetic, molecular and cellular events in hepatocarcinogenesis. In this presentation, I will discuss the role of miRNAs in HCC and explore the potential of miRNAs as potential biomarkers and therapeutic targets for HCC.

S 734 MicroRNA Reprogramming in Cancer: Mechanisms and Therapeutic Opportunities

J. T. Mendell. *Department of Molecular Biology, University of Texas Southwestern Medical Center, Dallas, TX.* Sponsor: N. Kaminski.

MicroRNA (miRNA) gain- and loss-of-function can potently influence cellular behavior in normal physiologic states and in diseases such as cancer. The regulation of miRNA expression and activity by cellular signaling cascades can therefore result in dramatic phenotypic outputs. We previously demonstrated extensive control of miRNA expression by well-characterized oncogenic and tumor suppressor networks including the Myc, Kras, and p53 pathways. We are now employing novel mouse models with gain and loss of miRNA function to investigate the physiologic functions of the miRNAs embedded within these signaling pathways and the pathologic consequences when their functions are disrupted. Insights gained from these studies are revealing unanticipated roles for miRNAs *in vivo* and are informing our understanding of how dysregulated miRNA activity contributes to tumorigenesis. I will present our latest findings related to the regulation and function of mammalian miRNAs in normal physiology and in cancer and how these findings may be exploited for the development of novel therapeutic approaches.

S 735 Does This Chemical Make My Liver Look Fat (Environmental Exposures and Steatosis)

C. A. McQueen[1] and N. J. Cherrington[2]. [1]*US EPA, Research Triangle Park, NC and* [2]*University of Arizona, Tucson, AZ.*

Headlines have proclaimed the exponential increase in obesity, type 2 diabetes, and metabolic syndrome in the US and other developed countries. Fatty liver is associated with all of these conditions that adversely affect human health. Initially, fatty liver disease (FLD) is benign, but, unfortunately, the disease may develop into the more serious condition steatohepatitis, characterized by lipid accumulation, inflammation, and fibrosis. Further progression can result in cirrhosis and even cancer. Much research has focused on the cellular and molecular changes in order to develop better diagnostic and treatment options. In contrast, there is only limited knowledge of the causes of fatty liver disease (FLD). Upon diagnosis, FLD is classified as alcoholic fatty liver disease (AFLD), with excessive alcohol consumption identified as the cause, or the broader category of nonalcoholic fatty liver disease (NAFLD). Known causes of NAFLD include a high-fat diet and some drugs, but these only account for a fraction of the estimated 30–40 million cases in the US. A better understanding of the environmental and chemical causes of NAFLD can aid in both prevention and treatment of the disease. This symposium focuses on the role of environmental chemicals in the etiology of NAFLD. The presentations will provide a better understanding of how environmental agents, from disinfection byproducts to pesticides, result in steatosis, as well as the multigenerational persistence of the effects of these exposures. Importantly, new insights will be gained on environmental agents that may contribute to the increasing incidence of NAFLD. (This is an abstract or a proposed presentation and does not necessarily reflect US EPA policy.)

S 736 Exposure to Disinfection Byproducts of Drinking Water in Obesity: From Adipokine Imbalance to Epigenetic Alterations leading to Metabolic Syndrome, NASH, and End-Stage Liver Disease

S. Chatterjee. *University of South Carolina, Columbia, SC.*

It is hypothesized that obesity is associated with strong risks of development of chronic inflammatory liver disease and metabolic syndrome following a second hit. A series of studies in our laboratory explored the role of chronic exposure of bromodichloromethane (BDCM), a disinfection byproduct of drinking water, in causing nonalcoholic steatohepatitis (NASH), mediated by cytochrome P450 isoform CYP2E1 and adipokine leptin. Mechanisms range from free radical metabolism of bromodichloromethane, adipokine imbalance, CPG island methylation in key promoter sites of regulatory genes including tumor suppressors, regulatory roles of micro RNAs and the immune system. Diet-induced obese mice, exposed to BDCM exhibited increased hepatic leptin levels, higher proinflammatory gene expression and Kupffer cell activation. Obese mice exposed to BDCM also showed profound hepatic necrosis, Mallory body formation, collagen deposition, higher alpha smooth muscle actin expression, events that are hallmarks of NASH. BDCM-exposed obese mice had alterations in both glucose and lipid metabolism genes leading to changes in the hepatic metabolic profile. Strongly hypermethylated regions in CPG islands of tumor suppressors and regulators of lipid catabolism genes were associated with decreased mRNA and protein expression following BDCM exposure. BDCM exposure led to increased expressions of miRNA 155a, 21,105 and down regulation of miRNA 122. BDCM-administered obese mice had increased CD8+ve/CD57+ve T cell presence that was dependent both on its free radical metabolism and hyperleptinemia. These results provide novel insights into BDCM-induced NASH, hepatic metabolic reprogramming and progression of liver disease in obesity. The molecular mechanisms associated with this study in rodents both at the gene and protein levels, could lead to answers in unraveling the causes of environment-linked fatty liver disease and nonalcoholic steatohepatitis.

S 737 AhR in Fatty Liver Disease, The Expected and Unexpected

W. Xie. *Center for Pharmacogenetics, University of Pittsburgh, Pittsburgh, PA.*

AhR was initially defined as a "xenobiotic receptor." Here, we have uncovered an endobiotic role for AhR in hepatic steatosis and steatohepatitis. Activation of AhR induced spontaneous hepatic steatosis characterized by the accumulation of triglycerides. The steatotic effect of AhR is likely due to the combined up-regulation of fatty acid translocase CD36/FAT and fatty acid transport proteins (FATPs), suppression of fatty acid oxidation, inhibition of hepatic export of triglycerides, increase in the peripheral fat mobilization, and increase in hepatic oxidative stress and inflammation. Promoter analysis established CD36 as a novel transcriptional target of AhR. Moreover, the steatotic effect of an AhR agonist was inhibited in CD36 null mice. Our more recent results showed activation of AhR also sensitized mice to non-alcoholic steatohepatitis (NASH) via the deactivation of the mitochondrial sirtuin deacetylase Sirt3. Industrial or military exposures to dioxin and related xenobiotics have been linked to fatty liver and other disorders. Results from this study may help to establish AhR and its target CD36 as novel therapeutic targets for the human fatty liver diseases.

S 738 Chronic Low-Dose Perfluorooctanesulfonic Acid (PFOS) Induces Hepatic Lipid Accumulation and Dampens Caloric Restriction-Induced Lipid Loss in Mice

A. L. Slitt. *University of Rhode Island, Kingston, RI.*

A combination of caloric restriction (CR), dietary modification, and exercise is the recommended therapy to reverse nonalcoholic fatty liver disease. The ability to mount an effective response to caloric restriction required to effectively shift hepatic metabolism to fatty acid oxidation depends upon induction of sirtuins, AMP-activated kinase, and peroxisome proliferator-activated receptor-γ coactivator 1α (PGC-1α). PFOS, a fluorosurfactant previously used as a stain repellent and anti-stick material, is persistent in the environment and considered an "emerging contaminant" by the Environmental Protection Agency. PFOS (1-10 mg PFOS/kg/day) induced hepatic lipid accumulation associated with altered lipid metabolism, and gene and protein expression in mice. We hypothesized that PFOS interferes with the beneficial effects of CR on hepatic lipid utilization and glucose homeostasis. Adult male C57BL/6 mice were fed ad libitum or placed on a 25% reduced calorie diet concomitant with 100 μg PFOS/kg/day for 6 weeks. PFOS significantly increased percent body weight after 4 weeks of administration, but did not significantly alter CR-induced percent weight loss over 6 weeks. Further studies indicated that PFOS (50 nM, 1, 5, 10, and 50 uM) increased adipogenesis in 3T3-L1 cells through induction CEBPs and PPARγ. PFOS also increased hepatic triglyceride accumulation and hepatic lipid loss after CR was lower in PFOS treated mice but not associated with significant changes in lipogenic gene mRNA expression. As insulin resistance contributes to fatty liver disease, we also evaluated PFOS effects on glucose and insulin tolerance. PFOS did not markedly affect either in *ad libitum* fed mice but did interfere with CR-induced improvement of glucose tolerance. This was further associated with suppression of Glut-2 and IRS-1 mRNA expression in liver and PFOS stimulation of glucose production in isolated hepatocytes. Overall, a relatively low sub-chronic administration of PFOS had some disruptive effects for lipid and glucose homeostasis under *ad libitum* and CR conditions.

S 739 Prenatal Obesogen Exposure Causes Transgenerational Inheritance of Increased Fat Mass, Stem Cell Programming, and Hepatic Steatosis

B. Blumberg. *University of California Irvine, Irvine, CA.* Sponsor: C. McQueen.

Consumption of calorie-dense food and diminished physical activity are accepted causes of obesity. The environmental obesogen model proposes that chemical exposure during critical stages in development influences subsequent adipogenesis, lipid balance and obesity. Obesogens are chemicals that inappropriately stimulate adipogenesis and fat storage. Tributyltin (TBT) is a high-affinity agonistic ligand for RXR and PPARγ. RXR-PPARγ signaling is essential in adipogenesis and the function of adipocytes. Activation of this receptor heterodimer can elevate adipose mass in rodents and humans. Thus, inappropriate activation of RXR-PPARγ can directly alter adipose tissue homeostasis. Our previous work showed in utero exposure to TBT promoted adipocyte differentiation, modulated adipogenic genes in vivo, and increased adiposity in mice. These results are consistent with the environmental obesogen model and suggest that organotin exposure is a previously unappreciated risk factor for the development of obesity and related disorders. Prenatal and early postnatal events such as maternal nutrition, drug, and chemical exposure are received, remembered and then manifested in health consequences later in life. We hypothesized that organotin exposure during prenatal adipose tissue development favors the subsequent development of adipocytes. We found that prenatal TBT exposure altered the balance of progenitor types in the multipotent stromal stem cell (MSC) compartment predisposing them to form adipocytes at the expense of bone. Prenatal exposure to low, environmentally relevant doses of TBT in drinking water led to transgenerational effects on adipose depot weight, adipocyte size and gene expression in MSCs in F1, F2 and F3 animals. Prenatal TBT exposure also increased hepatic lipid accumulation and up-regulated hepatic expression of genes involved in lipid storage/transport, lipogenesis and lipolysis in all 3 generations. Taken together, these results illustrate how prenatal exposure to xenobiotics can have lasting, potentially permanent effects on the offspring of exposed animals.

S 740 Ocular Immunotoxicology: A Privileged View

B. Christian[1] and J. C. Schuh[2]. [1]*Nonclinical Safety Assessment, Covance Inc., Madison, WI and* [2]*JCL Schuh, PLLC, Bainbridge Island, WA.*

Vision is achieved through highly specialized ocular tissue structures and processes which refract and transmit light to the photosensitive cells of the retina. Optimal visual function depends on maintaining the integrity and transparency of cornea, aqueous, lens, and vitreous, which can be compromised by unchecked immune reactions. The eye is considered to be an "immune-privileged" organ because of its capacity to moderate intraocular inflammatory responses and protect tissues of the visual axis through anatomic barriers, as well as through local and systemic immunoregulatory mechanisms, particularly immunosuppression. Breakdown or dysregulation of ocular immune privilege can lead to inflammatory disorders such as uveitis, and progression of intraocular neoplasms, and has been implicated in age-related macular degeneration and glaucoma. In addition, ocular inflammation is a commonly encountered response to intentional breach of immune privilege via intraocular administration of therapeutics. This session will highlight the unique aspects of the immunology of the eye and the associated implications for ocular toxicology and the development of ocular therapeutics. The audience will gain current understanding of structural barriers and active mechanisms of ocular immune privilege. Examples of innate and acquired immune responses to ocular insult, including allergens, microorganisms, and ocular administration of small molecule drugs, biotherapeutics, and viral vector-based gene therapies will be presented. Routine and specialized techniques for evaluating ocular immune responses will also be described. The session will include a presentation describing a current immunomodulatory approach to treat ocular disease involving the complement pathway and possible mechanisms for toxicities in preclinical studies. The final presentation will provide clinical examples and mechanisms of drug-induced immunotoxicity.

S 741 Ocular Oversight: Immune Privilege, and Immune Regulation and Dysregulation

J. C. Schuh. *JCL Schuh, PLLC, Bainbridge Island, WA.*

Ocular immunotoxicology is an evolving field and immune modulation in the eye has implications for successful design, delivery and clinical outcomes for ocular therapeutics. Our understanding of the immunological activity of the eye, including innate, mucosal and acquired immunity has expanded greatly in the last decade. The embryology of the eye is complex and includes formation of the passive barriers of the blood:retinal and blood:aqueous partitions, which are involved in regulation of exposure to systemic immunity and in ocular pharmacokinetics. Uniquely, the eye is a prototypical site of immune privilege, which is not immunological ignorance, but a process of regulated tolerance. Local cellular and secretory activity of immunoregulatory cells in the eye provides an active barrier that minimizes destructive inflammatory outcomes through immunosuppression and anterior chamber-associated immune dysfunction. If released to systemic circulation from an injured eye, ocular antigens interacting with the systemic immune system may lead to sympathetic ophthalmia, a destructive bilateral auto-immune response. Similarly, neoplastic cells that manage to evade barriers in tissues with immune privilege are also more likely to be progressive. Intraocular uveal melanomas arising within the eye also harness the techniques of ocular immune privilege to avoid destruction upon systemic metastasis. An understanding of ocular passive and active barrier function is important to toxicologists as intraocular injection of drugs or implants, trauma, infections, chemical injuries, paracentesis, surgery, and experimental injection of antigens can result in highly destructive inflammatory responses that threaten vision. This presentation will overview ocular structures, and passive and active barriers of the eye and their relationship to immune privilege, immunological homeostasis and major dysfunctional states that distort the visual axis or result in ocular immunotoxicology.

S 742 Innate and Adaptive Immune Responses to Ocular Insult

B. Gilger. *Department of Clinical Sciences, North Carolina State University, Raleigh, NC.* Sponsor: B. Christian.

This presentation will provide an overview of the recent developments in the understanding of ocular surface and intraocular innate and adaptive immune response. Understanding the ocular immune response is essential for specific ocular and systemic general toxicology when assessing biological responses to therapies (small molecule, biologics, gene therapies) given topically, intraocularly, or systemically, their time course, and their implications for preclinical development. The innate or non-antigen specific immune response represents the first line of defense against many pathogens in the eye. The cellular effectors in the innate immune response include neutrophils, eosinophils, mast cells, macrophages, and natural killer cells. While activation of these cells is not antigen specific, innate immunity is based on the recognition of specific pathogen associated molecules through a variety of cell surface receptors. It has long been noted that certain bacterial or fungal molecules, particularly cell wall products such as lipopolysaccharides (LPS) and endotoxins, as well as certain plant-based molecules, can elicit rapid and robust inflammation and immune responses in the eye. These are common contaminates of test articles and thus they may confound ocular toxicity results. The antigen specific immune response, also termed the acquired or adaptive immune response, involves a variety of effector mechanisms involving both T cell directed cellular effectors as well as humoral or antibody driven responses to eliminate more complex pathogens. It also provides for a memory response, which is responsible for providing immunity to subsequent infections. It is also responsible for most autoimmune diseases. The antigen specific immune response is dependent on inflammation and the innate immune response for activation and direction. Routine and specialized techniques for evaluating ocular immune responses will also be described.

S 743 Complement As a Target for Ocular Disease

D. Demady. *Preclinical Science, Novartis Institute for Biomedical Research, Cambridge, MA.* Sponsor: B. Christian.

Complement pathways have been implicated in human disease for many years and more recently there has been a focus on their role in ocular diseases, including uveitis, macular degeneration and diabetic retinopathy. Complement is a component of innate and acquired immunity and its activity is tightly regulated within the eye. Control of complement activation through the use of inhibitors is an active area of ocular therapeutics. An antigen-binding fragment (Fab) was developed to intervene in the alternative complement pathway for treatment of acute macular degeneration by intravitreal administration. In a pilot safety study in cynomolgus monkeys, adverse effects, particularly in one animal, were characterized by severe inflammation, hemorrhaging, and blindness after a single dose. Investigations into the cause of the toxicities implicated the presence of high levels of anti-drug antibodies in the eye and surface bound Fab. Potential mechanisms for these adverse effects will be discussed.

S 744 Innate and Acquired Immune Responses to Ocular Viral Gene Delivery Vectors in Primate Eyes

C. R. Brandt. *Ophthalmology and Visual Sciences, University of Wisconsin School of Medicine and Public Health, Madison, WI.* Sponsor: J. Schuh.

Gene therapy for ocular diseases is an exciting prospect and recent success in treating Lehber's Congenital Amaurosis with AAV based vectors is encouraging. AAV, Lentivirus, Adenovirus, Herpes simplex virus, and Baculovirus vectors have all been used experimentally to deliver genes to ocular tissues. AAV vectors generally do not trigger ocular immunotoxicology but they have a small carrying capacity. In rodents, these viral vectors do not seem to trigger inflammation; however, a single injection of Lentivirus, Herpes simplex virus, and Adenovirus vectors into non-human primate eyes triggers a transient uveitis. This "toxic" response is an issue in determining whether to proceed with clinical development and with regulatory agencies that approve therapeutics. Vector-induced uveitis develops within a few days of injection, suggesting innate, and not adaptive immune mechanisms are involved. The uveitis does not appear to be due to endotoxin contamination of vector preparations. Cells in the retina express several Toll-like receptors and some of these are up-regulated in the presence of viral vectors. Preliminary array studies suggest that specific changes in host cell innate immunity genes are also occurring. This talk will discuss our efforts to characterize the components of innate immune responses to viruses that are present in the primate eye and how they respond to the presence of these viral gene delivery vectors in order to develop ways to inhibit the responses.

S 745 Clinical Implications of Ocular Immunotoxicology

F. W. Fraunfelder. *Casey Eye Institute, Oregon Health and Science University, Portland, OR.* Sponsor: J. Schuh.

Preclinical models may not predict manifestations of ocular immunotoxicity and this may result in unexpected ocular disease in clinical trials and marketed therapeutics. This presentation will report on clinically relevant immunotoxicity associated with ocular therapeutics. Case reports from spontaneous reporting systems and the world literature were mined for ocular immunological reactions related to medications. The reports come from the FDA spontaneous reporting database, the World Health Organization's Uppsala Monitoring Center, and the National Registry of Drug Induced Ocular Side Effects (Casey Eye Institute, Portland, Oregon). Multiple drugs were associated with immunologic related pathophysiology. Off target effects of topical ocular chloramphenicol induced aplastic anemia, bisphosphonate related ocular inflammation, and post vaccination uveitis are of particular clinical importance. A working knowledge of some the most common immunotoxicity adverse effects in ocular tissue is important for toxicologists and clinicians as rapid recognition and drug withdrawal is often curative.

W 746 Application of the Adverse Outcome Pathway (AOP) Concept to Neurotoxicology: A Challenging Approach

A. K. Price[1] and E. Fritsche[2]. [1]*Institute for Health and Consumer Protection, The Joint Research Center of the European Commission, Ispra, Italy and* [2]*IUF-Leibniz Research Institute for Environmental Medicine, Düsseldorf, Germany.*

An adverse outcome pathway (AOP) describes a sequence of key measurable events, starting by a molecular initiating event in which a chemical interacts with a biological target, followed by a sequential series of key cellular events, leading to anatomical and functional changes in biological processes and ultimately resulting in an adverse outcome relevant to the human organism and the human population. Thereby, AOP characterization could provide information on the development of structure-activity relationships, i.e., using effect information from one chemical to predict effects for other structurally similar chemicals. Finally, AOPs provide evidence important for qualitative and quantitative predictive models of the adverse outcome that result from triggering molecular initiating or other key events for which high-throughput testing methods can be developed. There are a large number of cellular and molecular processes known to be critical to proper function of the central (CNS) and peripheral nervous systems (PNS). However, comprehensive understanding of pathways leading from chemical exposure to an adverse outcome in the CNS or PNS is sparse. In this session, five AOPs with relevance for human neurotoxicity will be presented, and common key events across these AOPs will be determined, increasing the possibility to identify potential neurotoxicants, even if toxicity is mediated by various pathways. Moreover, vulnerable windows of susceptibility to chemical exposure during brain development and aging will be discussed.

W 747 Introduction to the Session: Application of the Adverse Outcome Pathway (AOP) Concept to Neurotoxicology: A Challenging Approach

A. K. Price. *Institute for Health and Consumer Protection, The Joint Research Center of the European Commission, Ispra, Italy.* Sponsor: E. Fritsche.

The lack of knowledge on Adverse Outcome Pathways (AOPs) hampers the development of alternative testing methods for neurotoxicity evaluation, especially for regulatory purposes. The majority of alternative methods used for neurotoxicity testing are not able to clearly explain how the prediction is derived and why it is relevant for the decision-making process. In this context,the concept of AOPs is proposed as a tool to link molecular/cellular toxicology data to in vivo adverse outcomes in humans. The main goal of the session is to present the selected AOPs relevant to various human neuropathologies as a tool for mechanism-based neurotoxicity testing. The common key events for various pathways of neurotoxicity across different AOPs will be determined as they could serve as the basis for assays development. A short introduction to the AOP concept and to the selected AOPs presented during the session will be briefly discussed.

W 748 Organophosphate-Induced Neurotoxicity

A. Hargreaves. *School of Science and Technology, Nottingham Trent University, Nottingham, United Kingdom.* Sponsor: E. Fritsche.

Organophosphorus compounds (OPs) are still very widely used in agriculture, capitalizing on their ability to bind covalently to and irreversibly inhibit acetylcholinesterase activity in target organisms. However, OPs are also able to interact with a variety of other proteins in non-target organisms, including other serine hydrolases and cytoskeletal proteins. A small number of OPs have been found to be able to induce a condition known as organophosphate induced delayed neuropathy (OPIDN) the clinical signs of which can occur several weeks after exposure. Early molecular lesions preceding clinical signs of the conditions include inhibition and aging of the serine hydrolase neuropathy target esterase (NTE) and cytoskeletal disruption possibly as a consequence of disrupted calcium homeostasis and / or increased oxidative stress. Features that OPIDN has in common with other chemically induced neuropathies include cytoskeletal disruption, impaired nerve regeneration and inhibition of axonal transport. Exposure to some OPs have also been linked to effects on cognitive function as well as developmental and neurobehavioral deficits in mammalian studies. Such OPs are also able to inhibit the outgrowth of neurites in differentiating neuronal cell lines, the latter also being associated with cytoskeletal disruption. An AOP is proposed to involve multiple initiating OP binding events that trigger key events such as disruption of Ca2+ homeostasis, cell signaling and the cytoskeleton, leading ultimately to impaired neurite outgrowth or Wallerian degeneration, depending on the developmental stage at which exposure occurs.

W 749 N-Methyl-D-Aspartate Receptor (NMDA-R) Overactivation As a Pathway for Neurotoxicity

C. Suñol. *IIBB-CSIC-IDIBAPS, Barcelona, Spain.* Sponsor: E. Fritsche.

Glutamate is the major excitatory neurotransmitter in the central nervous system (CNS). It mediates key aspects of normal brain function such as sensory information, motor coordination, emotions and cognition. However, it has neurotoxic effects when it is present in excess causing neuronal dysfunction and degeneration (excitotoxicity hypothesis). Most neurons have the ionotropic glutamatergic N-methyl-D-aspartate, α-amino-3-hydroxy-5-methyl-4-isoxazolepropionic acid and kainic acid receptors (NMDAR, AMPAR, KAR), and glutamate-induced neurotoxicity occurs due to their over activation, mainly the NMDAR, which allows the influx of cations, most notably calcium. The activation of NMDAR requires not only binding of various ligands but also cellular depolarization that can be triggered by the activation of AMPAR and KAR. NMDAR are predominantly distributed in the hippocampus, cortex and basal ganglia, where they play a major role in the processes of learning and memory that occur in the hippocampus.
The Adverse Outcome Pathway (AOP) methodology is designed to provide a causative link between a Molecular Initiating Event (MIE) and an adverse health effect due to exposure to toxicants. An AOP is proposed that links domoic acid (DA) neurotoxicity (manifested by seizures and loss of memory and histopathological hallmarks like cell death in the hippocampus and other brain areas) with the activation of KAR as the Molecular Initiating Event. Key events in this process are the high affinity of DA to bind KAR, the influx of Na+ and Ca2+ leading to cell depolarization, the release of glutamate from hippocampal neurons, which in turns over activates NMDAR that leads to hippocampal cell death. Data gathered from the bibliography related to the effects of domoic acid-contaminated mussels on human

health, as well as the effects of domoic acid on animal status, on glutamate receptors in in vitro preparations and on cultured neuronal cells allow to get a picture of this pathway of neurotoxicity.
Supported by the Spanish Grant FIS PI10/0453 cofinanced with European Social Funds

W 750 SH-Group Binding-Induced (Developmental) Neurotoxicity

C. van Thriel. *IfADo-Leibniz Research Center for Working Environment and Human Factors, Dortmund, Germany.*

The adverse effects of methylmercury (MeHg) on the nervous system have been observed in humans, experimentally studied in animals, and MeHg serves as a test compound in many alternative in vitro NT and DNT methods. Like other electrophilic neurotoxins MeHg binds to sulfhydryl groups on macromolecules in cells and body fluids. Such interactions might be the molecular initial event (MIE) in the AOP of several neurotoxins sharing the feature of electrophilicity. In case of MeHg the formation of a methylmercury cysteine complex (MeHg(Csy)2), mimicking methionine, enables the compound to cross membranes (e.g. blood brain barrier) via specific amino acid transporters. Due to this event, and in contrast to inorganic mercury, MeHg becomes a potent neurotoxin that causes disturbances of glutamate uptake by astrocytes or induces ROS by affecting the mitochondrial electron transfer chain. Like other electrophilic neurotoxins MeHg might bind to glutathione (GSH) reducing the antioxidant capacity of neurons. Thus, in case of MeHg one key event of the AOP is reinforced by another. Such multiple and sometimes interactive molecular and cellular events might cause disturbance in brain physiology (e.g. reduce activity-dependent neuronal plasticity) resulting in the neurobehavioral phenotype of MeHg poisoning.

W 751 Adverse Outcome Pathway (AOP) for Neuroinflammation

F. Tschudi-Monnet[1] and A. K. Price[2]. *[1]Department of Physiology, University of Lausanne and Swiss Center for Applied Human Toxicology (SCAHT), Lausanne, Switzerland and [2]Joint Research Centre, European Commission, Institute for Health and Consumer Protection, Ispra, Italy.* Sponsor: E. Fritsche.

Neuroinflammation implies the reactivity of microglial cells and astrocytes. It can be triggered following neuronal stress, injury, or death, following demyelination, or direct activation of microglia and astrocytes.
Several classes of toxicants acting via diverse molecular initiating events leading to oxidative stress, calcium overload, cytoskeleton instability, synapse impairment, or apoptosis, can trigger a neuroinflammatory response. Therefore, neuroinflammation is a common key event.
Depending on the pathogenic context and/or on the duration of neuroinflammation, glial cells can acquire a neurodegenerative phenotype, which will cause neurodegeneration. Neurodegeneration, the adverse outcome, will exacerbate the neuroinflammatory response and lead to a self-sustained neurodegenerative loop.
It is generally accepted that neuroinflammation is involved in several neurodegenerative diseases, playing an important and early role in the disease process. Therefore the detection of neurotoxicant-induced increased expression of the markers of the microglial neurodegenerative phenotype (Itgam, CD86), of some pro-inflammatory cytokines (TNF-alpha, IL-1beta ; IL-6), of the reactive oxygen species production (i-NOS, hsp32) and of the astrocyte reactivity (GFAP) associated to a decrease of the markers of the microglial reparative phenotype (Arg1, MRC1) and of some anti-inflammatory cytokines (IL-4, IL-13), completed with morphological observations of an increased number of microglial cells and of markers of their macrophagic state (ED1) will provide early alert for neurotoxicants that may be considered as risk factors for the development of neurodegenerative diseases. The use of in vitro models for screening strategies is possible providing that cultures contain all types of brain cells, since cell-cell interactions are crucial for the neuroinflammatory process.

W 752 Oxidative Attack of the Neural Progenitor Cell Niche As an AOP for Neurotoxicity of the Elderly

E. Fritsche. *IUF-Leibniz Research Institute for Environmental Medicine, Düsseldorf, Germany.*

Hippocampal neurogenesis accompanied by neural progenitor cell (NPC) proliferation and differentiation takes place in the adult human and rodent brain. Thereby, loss in regenerative (functional) capacities of NPC, i.e. decline in NPC proliferation and neuronal differentiation, causes the steady process of 'Normal Brain Aging' with increasing cognitive decline over time. Loss of antioxidative response is one cause for brain aging and decreasing amounts of the major antioxidative transcription factor Nrf2 are found in brains/NPCs of aged rodents in vivo. Just as in vivo, in vitro aged NPCs also loose Nrf2 function. Applying a lenti-viral shRNA approach, we identified Nrf2 as a critical pathway contributing to decline in hNPC proliferation and neuronal differentiation thus proving its causal role in declined hNPC function during aging. Shifting the cellular redox balance towards the oxidative side produces accumulation of intracellular NAD+ (molecular initiating event). NAD+ serves as a co-factor for the HDAC Sirt1, which is involved in inhibition of pro-neuronal gene transcription like Mash1 by association with Hes1. On the contrary, reducing conditions favor transcription of Mash1 leading to neuronal differentiation. Thus, oxidative stress supported by decline in Nrf2 leads to decreased neuronal differentiation in adult brains by activation of the HDAC Sirt1 (Key event). This diminished neuronal regeneration causes cognitive decline on the individual and therefore also on the population level (adverse outcome).

W 753 Idiosyncrasies of Cells in Culture: Lessons from Genetic Toxicology

M. M. Moore[1], J. Clements[2], M. J. LeBaron[3], P. White[4] and S. Pfuhler[5]. *[1]ENVIRON International Corporation, Little Rock, AR, [2]Covance Laboratories, Harrogate, North Yorkshire, United Kingdom, [3]The Dow Chemical Company, Midland, MI, [4]Health Canada, Ottawa, ON, Canada and [5]Proctor & Gamble, Mason, OH.*

Because of a desire to reduce laboratory animal use and a goal to provide information using human cells in culture, rather than rodents, there is an international focus on developing *in vitro* predictive toxicology assays for chemical hazard assessment. These factors, coupled with the new molecular 'omics technologies, have provided the major impetus behind the Tox21, ToxCast, and other efforts to move toward an all *in vitro* hazard test battery. The genetic toxicology community began developing *in vitro* assays to predict both cancer and human heritable genetic disease in the early 1970s. Ultimately, a regulatory test battery was established and is used by the majority of international regulatory agencies. Over the decades there has been substantial knowledge gained concerning the strengths and weaknesses as well as the important issues involved in using *in vitro* assays for hazard assessment. In addition, major improvements to the genetic toxicology assays and the interpretation of data have been accomplished over this time period. Currently, there is a multi-sector international effort with a focus on better understanding the issues around cell stewardship, cell line characteristics, and the appropriate strategies for providing/assuring the required metabolic activation for *in vitro* systems. This effort, coupled with other genetic toxicology community experience, including the use of 2D vs. 3D cell cultures, and the selection of endpoints and correlations with apical health outcomes, provide extensive information that should inform the current efforts to establish all *in vitro* approaches for chemical hazard assessment.

W 754 Overview and Perspective Based on Lessons Learned from the Evolution of *In Vitro* Genetic Toxicology

M. M. Moore. *ENVIRON International Corporation, Little Rock, AR.*

The discipline of genetic toxicology began more than four decades ago with the development of a large number of assays in a large number of different organisms and *in vitro* cell types. Early on, the possibility that an *in vitro* assay using reverse mutations in bacteria (generally known as the Ames Test) would be a good predictor of chemicals that cause cancer was proposed and demonstrated with a limited set of test data. This prompted the hope that genetic toxicology tests would prove to be inexpensive and reliable predictors of chemical carcinogens and the subsequent utilization of data from genetic toxicology tests in various regulatory decisions. Unfortunately, over time, with the testing of more chemicals and the addition of more *in vitro* assays, it became clear that the Ames Test and other assays were not completely satisfactory for reliable and accurate carcinogen prediction. The fact that the apical health outcome (the induction of tumors) is not the result of a single biological effect (mutation) that leads, in every case, to a tumor, adds complexity to the situation. Generally, when regulatory agencies selected their preferred genetic toxicology test battery, assays were chosen based on the type of genetic damage that they detect rather than correlation with rodent cancer bioassays. There are currently many parallels between the emerging field of all *in vitro* toxicology testing and the evolution of *in vitro* genetic toxicology tests. Many major issues were identified and tackled for *in vitro* genetic toxicology assays that are just now being recognized as important for the new 21st century *in vitro* assays. The experiences and lessons learned from the evolution of genetic toxicology will be put into a perspective to provide insight into optimal development, validation and ultimate utilization of new *in vitro* systems to predict toxicological outcomes.

W 755 Know Your Cells: Importance of Cell Line Stewardship in Toxicity Testing

M. J. LeBaron. *Toxicology & Environmental Research & Consulting, The Dow Chemical Company, Midland, MI.*

Good cell culture practices are of critical importance for the reliability and reproducibility of results obtained from *in vitro* cell systems. In addition to quality standards applied to any cell system, cell cultures used for toxicity testing should demonstrate their ability to accurately detect the endpoint of interest. Experience with genetic toxicology testing emphasizes the importance of avoiding "genetic drift" and minimizing selective pressure that could potentially interfere with the system used to detect the event of interest. Although cell culture based genetic toxicology tests have been in use for several decades, it is only recently that experts in the field have embarked on a mission to provide well characterized, documented, and continuously available stocks of the most common cell lines used in genotoxicity testing. One of the first tasks was to identify the cell line isolate as close as possible to those described in the original publications and characterize these cells on their performance and, where possible, spectral karyotype analysis. These well characterized cells were deposited at multiple locations globally (European Collection of Cell Cultures – U.K., Sigma – U.S., and Japanese Collection of Research Bioresources - Japan) to ensure the continuous availability of certified cells for use in genotoxicity testing. This experience from genetic toxicology should be extended to other toxicity test systems in view of the growing interest in the application of in vitro test systems for high throughput (*e.g.*, ToxCast/Tox21) and other regulatory-mandated safety assessment studies (*e.g.*, Endocrine Disruptor Screening Program of the U.S. EPA). It is imperative that consistent performance and reliability of all aspects of these *in vitro* test systems are critical elements of realizing the U.S. National Academy of Sciences vision of "Toxicity Testing in the 21st Century."

W 756 Impact of Cell Type on Toxicity Testing—Implications for Assay Interpretation

J. Clements, J. Whitwell and R. Smith. *Genetic Toxicology, Covance Laboratories, Harrogate, North Yorkshire, United Kingdom.* Sponsor: M. Moore.

In vitro genetic toxicology assays have been reported to have a high rate of positive results that are not confirmed in *in vivo* and/or carcinogenicity studies raising the question of relevance to human risk assessment. This observation led to several studies in which initial observations appeared to indicate that there might be a difference between cells with normal and impaired p53 function, altered DNA repair capacity and/or human versus rodent origin. As part of an on-going collaborative programme of work looking to improve existing *in vitro* assays (reducing the rate of so called "false positive" results) commonly used mammalian cell types of different species origin, with differing p53 status have been investigated. This present study compared human versus mouse and p53 competent versus p53 mutated function. Nine reproducibly 'false positive' chemicals were tested in a micronucleus study using mouse lymphoma L5178Y-3.7.2C (mutated p53), human TK6 (functional p53) and WIL2-NS (TK6 related with mutated p53). Although p53 functionality does not seem be the overriding factor impacting the generation of positive responses, rodent versus human origin and apoptosis (measured via Caspase-3/7 activity) may have a role to play. This experience emphasizes that differences in qualitative and quantitative responses among cell lines is generally not based on one or perhaps a small number of cell line specific characteristics. Rather, it indicates the importance of understanding the individual cell lines used in toxicological evaluations and accepting the fact that there will be differences in the responses and that proper test interpretation requires that cell line characteristics be factored into test interpretation.

W 757 *In Vitro* Simulation of Endogenous Mammalian Metabolism: Lessons From Genetic Toxicology

P. White[1], J. Cox[2] and M. Fellows[3]. [1]*Environmental Health Science & Research, Health Canada, Ottawa, ON, Canada,* [2]*Environmental Health Science & Research, Health Canada, Ottawa, ON, Canada and* [3]*R&D Alderley Park, AstraZeneca, Macclesfield, Cheshire, United Kingdom.* Sponsor: M. Moore.

Seminal research published in the 50's and 60's carefully elucidated the metabolism of N-alkyl-nitroso compounds, and *in vivo* generation of potent alkylating agents. Metabolites rapidly react with DNA, contributing to formation of genetic mutations and the initiation of chemical carcinogenesis. Later works noted that dimethylnitrosamine (DMN) can induce mutations in *Drosophila*, but not in bacteria or yeast exposed *in vitro*. In 1971, Malling published a landmark work that used murine hepatic microsomes for *in vitro* simulation of mammalian DMN metabolism, and the results showed effective reversion of *Salmonella histidine* auxotrophs. Ames and colleagues later established a standard *in vitro* metabolic activation mixture containing hepatic microsomes from male rats exposed to AhR agonists (e.g., PCBs). Indeed, rat liver microsomal preparations (i.e., S9) have become the standard for *in vitro* assessment of chemical mutagenicity. The system is not without its problems however, and researchers have investigated the utility of S9 preparations from a wide range of tissues and animals, as well as a host of alternative approaches for simulating mammalian metabolism *in vitro*. Fast forward to 2007, and the launch of the ToxCast program for rapid, high-throughput *in vitro* assessment of chemical toxicity. The ToxCast and Tox21 programs are employing a wide range of *in vitro* assessment tools, capable of monitoring a vast array of endpoints, to screen over 10,000 substances. However, incorporation of mammalian xenobiotic metabolism into the quantitative high-throughput screening (qHTS) paradigm has proved difficult. Several options are being explored (e.g., metabolically competent cells, coculture, etc), some of which were initially developed for *in vitro* assessment of genetic toxicity. The presentation will provide an overview of the technical challenges underscoring effective *in vitro* simulation of mammalian xenobiotic metabolism, and highlight promising avenues for effective qHTS.

W 758 Utility of Three-Dimensional Tissue Constructs for Toxicity Testing

S. Pfuhler. *Global Product Stewardship, Human Safety, Procter & Gamble, Mason, OH.* Sponsor: M. Moore.

In vitro toxicity assays are based on mammalian cell culture systems using 'immortal' cells with compromised cell functions that are limited in their ability to deal with stress. Such 2-dimensional static cell culture systems are artificial and far removed from the *in vivo* state, while 3D tissue constructs allow for more natural cell-cell and cell-matrix interactions and show '*in vivo*-like' behavior for key parameters like cell viability, proliferation, differentiation, morphology, gene and protein expression, and function. Because of these advantages, 3D tissue constructs, usually based on primary cells of human origin, are being increasingly utilized in the field of toxicology. Examples include the use of 3D ocular models for eye irritation testing, 3D lung models for respiratory irritation and nanoparticle toxicity/uptake, and 3D liver models for metabolism studies. Moreover, for the evaluation of a chemical's potential to cause skin irritation or corrosion, 3D skin models have become the standard tool that has replaced animal studies in a regulatory context. Such skin tissues have now also been successfully established for genotoxicity testing and are available in a format that allows for low-medium throughput. The results obtained thus far demonstrate good inter- and intra-laboratory reproducibility, as well as a higher predictive capacity than 2-dimensional static cell culture systems. This indicates that these models behave more '*in vivo*-like' and are less prone to react to non-physiological stress than 2D cell cultures and they therefore hold promise for use in 21st century toxicity testing strategies.

W 759 Photosafety Evaluation of Pharmaceuticals without Testing in Animals

L. B. Kinter[1] and A. Jacobs[2]. [1]*Global Safety Assessment, AstraZeneca, Wilmington, DE and* [2]*US Food & Drug Administration, White Oak, MD.*

Advances in understanding of photochemistry, photoreactivity, and phototoxicity of pharmaceuticals offer for the first time the opportunity to appropriately evaluate the potential for photosafety risk in humans while minimizing or eliminating testing in animals. Generally, compounds that absorb light in the visible and UV ranges and generate reactive oxygen species (ROS) pose a potential risk for phototoxicity. Photoreactivity tests to detect generation of ROS and *in vitro* bioassays to detect phototoxicity (3T3-NRU and 3D-skin assays) offer high sensitivity (e.g., few false negatives) but lower selectivity (higher numbers of false positives) with which to predict phototoxicity potential in humans. To support an integrated assessment strategy, it is most important these assays show high sensitivity, because negative assay results are usually conclusive and do not warrant further photosafety evaluation. Thus, it is not essential that positive assay results always predict a clinically relevant phototoxic response, and the fact that these assays measure entirely different endpoints lowers the probability of multiple false-positive findings, such that one negative finding with other positives is generally sufficient to indicate negligible photosafety risk. Finally, compounds that absorb in the relevant spectrum and test positive in chemical and/or *in vitro* assays can be evaluated for photosafety in clinical trials with proper precautions, without intermediate *in vitro* or animal testing if the sponsor chooses (ICH M3(R2) 2010). The session will be of broad interest to academic, industry, regulatory, and consultant toxicologists concerned about the current status of photosafety testing and/or advances in nonclinical safety assessment that reduce or replace animal testing (e.g., 3Rs).

W 760 Chemical Methods for Detection of Photoreactive Pharmaceuticals

S. Onoue. *School of Pharmaceutical Sciences, University of Shizuoka, Shizuoka, Japan.* Sponsor: L. Kinter.

For a chemical to demonstrate phototoxicity and/or photoallergy, the following characteristics are critical: Absorbs light within the range of natural sunlight (290-700 nm); generates a reactive species following absorption of UV/visible light (UV/VIS); and distributes sufficiently to light-exposed tissues. UV/VIS absorption by chemicals alone may not always directly correlate with phototoxic potential and may provide false photoreactivity predictions; however, when UV/VIS absorption is associated with a molar extinction coefficient (MEC) of less than 1,000 $M^{-1}cm^{-1}$, there is little phototoxic risk since this low level of light absorption is unlikely to be harmful. Reactive oxygen species (ROS) are generated via energy transfer mechanisms following UV/VIS excitation, including superoxide and singlet oxygen. The ROS assay has been designed to assess photoreactivity of pharmaceuticals, of which the principle is to monitor types I and II photochemical reactions of the test chemicals when exposed to simulated sunlight. This simple analytical test could be used to screen potential chemical scaffolds, leads, and candidate drugs to identify and/or select away from those having phototoxic potential. The validation study for the ROS assay has been being carried out by the Japan Pharmaceutical Manufacturers Association (JPMA), supervised by the Japanese Center for the Validation of Alternative Methods (JaCVAM). Although several false positives appeared, the ROS assay on 42 coded chemicals has provided no false negative predictions. The validation study tentatively indicates satisfactory outcomes in terms of transferability, intra- and inter-laboratory variability, and predictive capacity. Thus, a negative result in this ROS assay would indicate a very low probability of phototoxicity, whereas a positive result would be a flag for follow-up assessment. In conclusion, UV/VIS analysis, MEC, and the ROS assay are non-biological assessments useful for the prediction of the photochemical reactivity, and their strategic use can minimize animal use in phototoxicity testing of pharmaceuticals.

W 761 How *In Vitro* Phototoxicity Data May Inform Selection and Later Risk Assessment of Investigational Drugs

D. Bauer. *Preclinical Safety, Novartis Institutes for Biomedical Research, Basel, Switzerland.* Sponsor: L. Kinter.

Evaluation of active pharmaceutical ingredients in the presence or absence of simulated sun light using *in vitro* cell culture assays is often part of a step-wise photosafety testing strategy. The *in vitro* 3T3 Neutral Red Uptake Phototoxicity Test (3T3-NRU-PT, OECD TG 432) is a widely recognized, sensitive and accepted assay for this purpose. Based on the quantitative Photo-Irritation Factor (PIF) it supports threshold-based conclusions. This test can also be modified to tolerate significant amounts of (inherently cytotoxic) UVB irradiation by using appropriate light source/filter combinations. Especially for compounds to be used in topical formulations such improved conditions would extend the current applicability domain. However, for systemic drugs UVB is considered less important than UVA due to very limited penetration into skin and standard irradiation conditions may suffice. The demonstrated high sensitivity justifies, that negative test results do not warrant further testing for systemic drugs (neither in animals nor in human) and are sufficient to support a definitive human photosafety risk assessment. Conversely, due to lower specificity positive results do not necessarily predict clinical outcomes, mainly because this *in vitro* assay cannot account for pharmacokinetic properties, e.g., distribution into light exposed tissues.

If used as a highly standardized screening assay the 3T3-NRU-PT is a valuable tool guiding further testing and finally selection of drug candidates: clearly negative compounds may progress without any concern, while highly positive compounds may need supporting *in vivo* data in order to estimate human photosafety risk and to justify further investments (e.g. conducting GLP toxicity studies or clinical trials). Ultimately, it depends on the therapeutic context (indication, duration, systemic exposure, etc.) and remains the decision of the drug developer whether additional *in vivo* data for weakly positive *in vitro* result are crucial and immediately decision-relevant. Otherwise, photosafety assessment within human clinical trials may be an option.

W 762 *In Vitro* 3-Dimensional Skin Models for Testing Phototoxic Potential of Dermal Formulations

H. Kandarova. *MatTek* In Vitro *Life Science Laboratories, Bratislava, Slovakia.*

Reconstructed human skin models, with the presence of a stratum corneum and lipid barrier, permit testing of various types of topically applied materials ranging from neat chemicals to final clinical formulations. To date, the methods developed have been based on measuring cell viability in the tissue with and without irradiation. The release of cytokines/chemokines into the medium can be informative as well. In the 1990's, an ECVAM pre-validation phototoxicity study on the EpiDerm™ model (Liebsch et al., 1999) showed that reconstructed human epidermis (RhE) models are capable of correct detection of the acute human phototoxins and non-photo toxins. Several studies with other commercially available reconstructed tissue models (EPISKIN®, SkinEthic™) confirmed these findings. The sensitivity and specificity of assays developed with RhE models for prediction of acute skin phototoxicity are close to 100%. Use of RhE-based phototoxicity assays for prediction of the topical phototoxicity testing was recently implemented into the draft ICH Guidance Document on Photosafety Testing (S10) .As shown in a feasibility study with EpiDerm sponsored by ECVAM between 2002-2005 (contract No. 19868-2002-09 F1ED ISP DE), these models can also be used to assess photo-potency, i.e. to assess the phototoxic strength of a topical phototoxin and to estimate the non-phototoxic concentrations that can be safely used in human (e.g. for therapeutic use). Based on comparison between in vitro and in vivo human studies, a safety factor of 10 fold can be recommended when extrapolating the in vitro results to man. This presentation will focus on current 3-D skin models for the assessment of the phototoxicity potential of dermal formulations. The presentation will provide an overview of RhE-based phototoxicity assays and discuss their strengths and weaknesses for photo-safety assessment in toxicology and pharmacology.

W 763 Evaluation of Phototoxicity of Pharmaceuticals in Clinical Trials

D. R. Bickers[1] and H. Ko[2]. [1]*Columbia University Medical Center, New York City, NY and* [2]*US FDA, Silver Spring, MD.* Sponsor: L. Kinter.

Clinical development of therapeutic products may encounter issues related to photosafety. This can be due to photoirritation or to a photoallergic reaction, both broadly covered under the indiscriminate term "photosensitivity". Over 300 therapeutic products are reported to have given photosensitivity reactions, including a variety of pharmacologic classes and biologic agents. Lack of an accurately defined population base makes it difficult to estimate the real incidence of photosensitivity associated with pharmaceutical use. Of the implicated medications, only a minor proportion is of sufficient frequency to be studied in greater detail.

Clinical manifestations of adverse drug reactions upon light exposure depend on the interaction between the host, the agent, and the radiation. They range from an acute inflammatory skin reaction, unusual clinical patterns, to photocarcinogenicity. Thus, prediction of the potential for photo-reactions in humans is challenging, both for frequency and severity, and standardized conditions for studies intended to compare pharmaceuticals for photosafety are important.

Current approaches to the evaluation of photosafety in clinical trials are primarily based on adverse event reporting or active solicitation of anticipated events, as well as search for possible findings when there is suspicion from nonclinical studies. Issues concerning this strategy include bias introduction, limitation of sample size in premarket trials, and variability in usage in postmarket studies. For topical products, drug development necessitates predictive testing under standard conditions when the to-be-marketed formulation contains ingredient(s) absorbing visible or ultraviolet light. Such testing for photoirritation and photocontact allergy is informative for the design of precautions and safety monitoring in later-phase clinical trials as well as for product labeling.

As there are advances in in vitro studies for photo-reactions and the development of human biomarkers for adverse experiences, it is likely that these will impact future approaches to the clinical evaluation of photosafety.

W 764 Stem Cell-Derived Cardiomyocytes: An Alternative Cardiac Toxicity Model for Assessing Drug Safety and Chemical Health Risk

K. Dreher[1] and S. D. Pettit[2]. [1]*US EPA, Research Triangle Park, NC and* [2]*ILSI, Health and Environmental Sciences Institute, Washington, DC.*

Cardiac safety is a major cause of attrition, withdrawal, and adverse reactions in drug development. It is estimated that adverse cardiac and/or vascular reactions account for greater than 20% of drug attrition over the preclinical, clinical trials, and post-market phases. Effective chemical safety evaluations are also critical for protecting public health. Significant adverse cardiac effects following exposure to a variety of chemicals present in the environment have been reported by the World Health Organization and other researchers. Cardiac safety associated with pharmaceutical drugs and chemical exposures are a mutual focus of keen interest for clinical and public health researchers, academic scientists, government regulators, and industrial scientists worldwide. The development of alternative testing methods predictive of drug and/or chemical toxicity could impact drug discovery and safety evaluations as well as chemical health risk assessment. This workshop brings together a trans-sector and multidisciplinary group of experts to present and discuss

the use of stem cell-derived cardiomyocytes as an alternative model to determine alterations in cardiac electrophysiology, contractility, and structural and developmental toxicity following drug or chemical exposure. Presenters and discussions will address the sensitivity, reproducibility, and biological relevance or "fit for purpose" of stem cell-derived cardiomyocytes and how these factors relate to the use of such data in a screening, risk, or safety evaluation for drugs and chemicals.

W 765 Transitioning Cardiac Stem Cells from Research Platforms to Predictive Tools

S. D. Pettit. *ILSI, Health and Environmental Sciences Institute, Washington, DC.*

The availability and use of induced, stem-cell derived cardiac myocytes has grown exponentially in the last 10 years. With this growth has come a concurrent diversification of the potential applications for these assays – for structural, functional, and toxicity based assessments as well as direct clinical translation. This presentation will highlight key areas that could benefit from greater consensus and weight of evidence. These include the sensitivity, reproducibility, and biological relevance of these cell lines and how these factors relate to the use of such data in a screening, risk, or safety evaluation context.

W 766 Stem Cell-Derived "Cardiomyocytes" and Their Application to Cardiac Safety Assessment: Ready for Primetime?

H. M. Vargas. *Toxicology Sciences, Amgen Inc., Thousand Oaks, CA.* Sponsor: K. Dreher.

Human stem cell-derived cardiomyocytes (SC-CM) are an emerging model for the study of drug safety, in particular drug-induced changes in cardiac electrophysiology and contractility. The potential for SC-CM to be used for proarrhythmia assessment is also being considered. An advantage of this test system is that safety pharmacology studies can be performed in human embryonic progenitor cells or adult fibroblasts transformed to resemble mature cardiac myocytes, which could assist translation of nonclinical to clinical findings, and risk assessment. The utilization of an *in vitro* human SC-CM system to de-risk candidates during preclinical drug development could improve our ability to bring forward novel and safe drug candidates for clinical evaluation. However, the application of SC-CM for drug safety requires robust validation of these cells, to understand how closely they resemble authentic mature ventricular myocytes, and their performance relative to conventional assays used in cardiovascular safety testing. What are the limitations of the human SC-CM model? This presentation will explore the electrophysiological evaluation of SC-CM, their response to a variety of ion channel blockers known to alter cardiac conduction and repolarization, and discuss some of the challenges that need to be overcome to validate the use of SC-CM for cardiovascular safety assessment.

W 767 Stem Cell-Derived Cardiac Cells in High-Throughput Screens for Modulators of Contractility

M. Mercola. *Department of Bioengineering, University of California San Diego, San Diego, CA.* Sponsor: S. Pettit.

Human stem cell-derived cardiac myocytes (SCC) are an emerging model for the study of drug safety, in particular drug-induced changes in cardiac function. The application of SCC in drug safety evaluation requires robust validation of these cells, to understand their performance relative to other pharmacological assays used in cardiovascular safety testing. To facilitate high throughput analyses of cardiomyocyte physiology, we developed kinetic imaging cytometry, a new high content screening technology capable of measuring cardiomyocyte contractile calcium transients and voltage action potential kinetics and morphology. The instrument and dedicated software are now commercially available, and function by optically recording and analyzing the fluorescence changes of small molecule calcium and voltage sensing probes in response to electrical field stimulation and exposure to ion channel blockers known to alter cardiac conduction and repolarization. We have begun to evaluate the technology using a panel of safe and arrhythmogenic drugs, revealing EC50 values similar to the reported EC50 and/or IC50 values obtained by biochemical and traditional electrophysiological studies. The presentation will discuss current progress and limitations in the optical, high throughput measurements of electrophysiological parameters to assess arrhythmogenic risk. Furthermore, we have used kinetic imaging cytometry in screening campaigns to identify molecules and targets to sustain cardiomyocyte contractility in heart failure, leading to the development of a potential RNA therapeutic that shows efficacy in halting the progression of established heart failure in a mouse pressure overload model.

W 768 High-Content Screening of Bioenergetic Modulation of Kinase Inhibitor Mitochondrial Toxicity in Human Stem Cell-Derived Cardiomyocytes

N. Thomas. *GE Healthcare, Whitchurch, Cardiff, United Kingdom.* Sponsor: S. Hunter.

Cardiotoxicity is a significant issue in the development of new drugs targeting key cellular kinases. Human embryonic stem cell (hESC) derived cardiomyocytes cultured in glucose and galactose media were used to examine the cardiotoxicity of twenty six kinase inhibitors and other drugs using high content screening (HCS) to examine a number of key mitochondrial and cellular parameters indicative of toxicity. Analysis of HCS data revealed a number of compounds with increased toxicity under conditions of mitochondrial oxidative phosphorylation. The tyrosine kinase inhibitor Mubritinib, was non-toxic in cells cultured in glucose but exhibited very significant mitochondrial toxicity in galactose media which correlated with the direct impact of the compound on mitochondria measured by respirometry. HCS is a sensitive and efficient approach to surveillance of drug cardiotoxicity in hESC derived cardiomyocytes with multi-parameter analysis providing insight into toxicity mechanisms and that cellular bioenergetics can significantly influence drug cardiotoxicity.

W 769 Evaluating Chemical Safety, Molecular Targets, and Toxicity Pathways in Mouse Embryonic Stem Cell Differentiation to Cardiomyocytes

E. S. Hunter. *US EPA, Research Triangle Park, NC.*

As one of the earliest systems to develop and function, evaluation of the cardiovascular system is a critical target for chemical safety and risk assessment. Cardiogenic anlagen are established with formation of cardiac plate mesoderm, cardiomyocyte differentiation and establishment of a beating heart tube. The embryonic stem cell test examines compound effects on differentiation of pluripotent mouse ESC to beating cardiomyocytes. Our modified Adherent Cell Differentiation and Cytotoxicity assay evaluates differentiation to cardiomyocytes using myosin heavy chain (MHC) or gastrulation using goosecoid (GSC) as biomarker proteins (In-Cell Western analysis). Additionally, differentiation to multiple cell lineages is assessed using mRNA biomarkers (quantitative nuclease protection assay). Cell number was determined to account for induction of excess cell death or altered proliferation. We evaluated 276 chemicals of the ToxCast phase I library for effects on MHC and GSC. Twenty six chemicals produced a >50% change in the cardiomyocyte differentiation biomarker and 80 chemicals s produced more than a 20% change. Two predominant "targets" were identified for chemicals that decreased cardiomyocyte formation, BMP signaling and altered redox potential. Cardiomyocyte differentiation requires normal development and function of the lineages that precede its specification. A comparison of chemical effects indicated that 45% of chemicals that perturb cardiomyocyte differentiation also affect gastrulation, raising questions of selectivity and specificity of targets and pathways. Thus, ESC can be used to evaluate compound effects on cardiomyocyte formation. Studies that characterize the cell lineage ontology are needed to determine the target cell population and define molecular targets for an assessment of the specificity of effects on cardiomyocyte differentiation. This abstract does not represent EPA policy.

W 770 The Doorway between Exposure and Response: How Biologically-Based Inhalation Dosimetry Models Enhance Human Health Risk Assessment

J. A. Hotchkiss[1] and J. B. Morris[2]. [1]*The Dow Chemical Company, Midland, MI and* [2]*University of Connecticut, Storrs, CT.*

The respiratory tract is the portal of entry for inhaled gasses, vapors, and particles, providing a route of entry for systemic exposure and a potential target for toxic agents. The inhaled dose is dependent on the physical state, solubility, reactivity and concentration of the material, the structural and functional characteristics of the respiratory tract, and the types and metabolic capability of the surface epithelial cells. It is also contextual and dependent on the dose metric used, whether it is the systemic blood or tissue concentration or the regional dose to specific anatomic sites or target cell populations in the respiratory tract. Human risk assessments are often based on inhalation toxicity studies in rodents, yet a number of vapors, including hydrogen fluoride and diacetyl, have been shown to produce nasal and large airway injury in rodents but small bronchiolar airway injury in humans. Computational modeling has confirmed significant differences in regional vapor absorption patterns between rats and humans that provide a rational framework to explain the observed differences in site-specific injury between species. Multiscale

computational models of the respiratory system that incorporate species-specific anatomic details and data derived from *in vivo* measurement of particle deposition/clearance and vapor absorption have been developed to improve estimates of material transport and regional dosimetry. Model accuracy is greatly improved by incorporating regional morphologic characteristics of the mucosa and exposure-response data to validate model predictions of site- and species-specific dosimetry. The goal of this workshop is to provide participants with a working knowledge of the state-of-the-art computational tools available to predict regional deposition, absorption and dose of inhaled materials in laboratory rodents, the essential data needed to validate these predictions, and the use of biologically-based computational modeling in human health risk assessment applications and related research.

W 771 Site-Specific Airway Pathology and Dosimetry of Inhaled Toxicants

J. R. Harkema. *Department of Pathobiology and Diagnostic Investigation, Michigan State University, East Lansing, MI.*

Injury caused by acute and chronic inhalation exposures to airborne toxicants (gases and particles) is site specific in the respiratory tract, and dependent on airway dosimetry and cell/tissue sensitivity. Airway dosimetry and injury of inhaled toxicants are further determined by many additional factors such as the physicochemical character of the inhaled toxicant, exposure regimen, host species/strain, age, gender, diet and overall health. In this talk, the speaker will briefly review comparative anatomy and physiology of the respiratory tract in laboratory animals (rodents and nonhuman primates) and humans. He will further provide examples of site-specific nasal and pulmonary pathology caused by exposures to various gaseous and particulate toxicants (e.g., aldehydes, chlorine, ozone, nanoparticles). In addition, examples of state-of-the-art, yet practical, approaches to unbiased determination of exposure-related morphometric, molecular, and biochemical alterations (i.e., computational toxicologic pathology) will be discussed. The talk will conclude with a description of methods to correlate site-specific pathology with estimated 3D-airway dosimetry and modeling of both the upper and lower respiratory tract in laboratory animals that can be used in predictive toxicology to estimate human risk to toxicant exposure.

W 772 *In Vivo* Measurements of Dosimetry: What Do the Data Say?

J. B. Morris. *Pharmaceutical Sciences Toxicology Program, University of Connecticut, Storrs, CT.*

This presentation will discuss *in vivo* measurements of regional vapor absorption and integration of that data into computational models of inhaled dose of absorbed vapors for purposes of human health risk assessment. In rodents a large dataset exists on vapor uptake in the isolated upper respiratory tract (URT). Data are also available on whole respiratory tract uptake. Data on URT uptake reveal the critical importance of solubility (as measured by tissue:air partition coefficient), local metabolism, and direct reactivity in influencing vapor absorption in that site. Physiologically based pharmacokinetic (PBPK) model structures accurately predict the importance of these parameters in controlling uptake, thus providing validation of the PBPK-based approach. Extension of this modeling approach to the whole respiratory tract also provides accurate prediction of total vapor uptake in the rodent. A rich data set from mouth-breathing experiments is available on lower respiratory tract (LRT) vapor uptake in humans. As for the rodent, vapor solubility, local metabolism and direct reactivity are important factors influencing vapor uptake and PBPK-based model structures accurately predict the data that has been obtained. Diacetyl is a vapor that causes nasal and large airway injury in rodents but is associated with bronchiolar injury in man. Application of the PBPK-based modeling approach to diacetyl vapor predicts that the delivery of diacetyl to the lower airways in the human is much greater than in the rat particularly in mouth breathing humans undergoing light exercise. This difference is greatest at lower exposure concentrations at which local airway metabolic pathways are not saturated. The rodent-human difference in airway delivered dose likely reflects a general pattern rather than one specific to diacetyl. Thus, modern validated modeling approaches provide key insights that can be incorporated in quantitative inhalation risk assessments.

W 773 Interspecies Differences in Respiratory Dosimetry of Volatile and Aerosol Materials Using Multiscale Computational Models

R. A. Corley. *Exposure Science & Systems Toxicology, Pacific Northwest National Laboratory, Richland, WA.*

Computational models are often used to link exposures to target tissue doses and responses to inhaled gases, vapors and aerosols. Models have ranged from empirical to compartmental, or mechanistic approaches, depending upon the application and available data. For materials that target specific sites or cell types within the respiratory tract, computational fluid dynamics (CFD) airflow-based models that explicitly incorporate 3D anatomy and physiology have emerged as a leading choice for predicting species- and site-specific exposure-dose-response relationships. In the past, development of such models was expensive, time-consuming, and limited to highly specialized applications. Using modern 3D and 4D imaging and computational methods, CFD models have become more widely available for use in chemical, pharmaceutical, and biological exposure assessments in multiple species including mice, rats, rabbits, monkeys, and humans. These models can extend from the nose/mouth to the bronchiolar airways of the lung. Lower dimensional models can be added to 3D models to address tissue mechanics and the impact of disease on airflows and tissue dosimetry in the deep lung. Likewise, physiologically based pharmacokinetic (PBPK) models have been utilized as airway boundary conditions in CFD models for material transport, uptake, metabolism, and clearance by respiratory tissues along conducting airways. This talk will emphasize the experimental foundation for the development, evaluation, and refinement of these multiscale models, including 3D and 4D CT imaging of normal and diseased animals and humans; MR imaging of hyperpolarized 3He gas flows; airway extraction studies with volatile chemicals; and particle deposition using breath analysis, SPECT/CT imaging; and post-mortem tissue analysis. The potential impacts these multiscale computational models have on relating exposures to site-specific "doses" that are critical for toxic responses and potential risk assessments will be demonstrated for several volatiles and aerosolized materials.

W 774 Material Transport, Deposition, and Clearance in the Respiratory Tracts of Humans and Animals

B. Asgharian. *Health Effects and Medical Response, Applied Research Associates, Inc., Raleigh, NC.*

Assessment of the dose and site of deposition of inhaled materials in the lung aids in the interpretation of biological response. The deposited dose provides the link between external exposure and potential adverse effects. While high fidelity computations of the dose are only feasible for the proximal regions of the lung which fall within the resolution of scanned images, anatomically accurate and physiologically relevant mathematical models of material transport and deposition in the entire respiratory tract are developed for humans and a few selected animals to predict site-specific dose and tissue uptake, and allow interspecies extrapolation based on various dose metrics. Mathematical models have been formulated for insoluble, hygroscopic, nonspherical (fibers and nanotubes) particles as well as for vapors and mixtures. Modeling approach and application to a few specific scenarios will be discussed and a few examples will be presented.

W 775 The Role of Inhalation Dosimetry Models in Multiscale Support to a Range of Risk Assessment Applications

A. M. Jarabek. *National Center for Environmental Assessment, US EPA, Research Triangle Park, NC.*

Inhalation dosimetry models afford the flexibility and versatility to support a range of potential applications in human health risk assessment that spans aiding *in vitro* experimental design, through translation of dose across various test species, to facilitating inferences regarding pathogenesis processes typically represented by endpoints that may also span a scale from genomic profiling in specific target tissues to population biomonitoring. Understanding how the various model structures discussed in the previous presentations can aid these various applications in risk assessment is critical to advancing the accuracy of it as a science-based discipline. This presentation addresses how to best marry available model structure to risk assessment application with examples for both particles and gases. Impact of model applications illustrated include *in vitro* dosimetry for the design of nanoparticle experiments, translation of fiber dose across species, inferring exposure from biomonitoring of solvents, and using models to inform the plausible mode of action for reactive gases. Opportunities for refining current default inhalation dosimetry algorithms used in dose-response analysis, originally already based on fuller model forms, will be highlighted to show how risk assessment applications continue to evolve as more sophisticated computational structures emerge. Ultimately such

computational models of inhalation dosimetry will serve as the bridge to virtual tissues and systems biology descriptions of the cardiopulmonary system, and link models of multi-pollutant exposures in a given airshed to a multi-dimensional description of mode of action and resultant disease. (The views expressed in this abstract are those of the author and do not necessarily represent the views or policies of the U.S. Environmental Protection Agency.)

PL 776 Adverse Outcome Pathways As a Method to Characterize Potential Sources of Increased Risk of Health Effects Attributed to Inorganic Arsenic

J. Lee[1], J. Sacks[2], R. Jones[2], L. Joca[2] and J. Cowden[2]. *[1]NCEA-IRIS, US EPA, Research Triangle Park, NC and [2]NCEA-RTP, US EPA, Research Triangle Park, NC.*

Inorganic arsenic is associated with a number of human health effects including the development of tumors and other diseases. These health effects can be organized into collections of biological responses, i.e., key events that represent adverse outcome pathways (AOPs). An analysis of AOPs may be useful in characterizing the potential impact of sources of variability for health effects, such as the increased risk for particular key events or adverse outcomes. A literature review was conducted to identify the factors that may increase risk for an arsenic-induced adverse outcome, transitional cell tumors of the urinary bladder. Using an AOP framework, we characterized potential impacts of individual-level factors (e.g., sex, genetic polymorphisms, nutritional status, and cigarette smoking status) and life stages (e.g., childhood and *in utero*) on the risk of bladder cancer. Preliminary results support the hypothesis that factors associated with reduced secondary methylation [i.e., the conversion of monomethylarsonic acid (MMA) to dimethylarsinic acid (DMA)] may also correlate with increased risk of bladder cancer, including sex, genetic polymorphisms, nutrition, and smoking. Our results demonstrate the utility of an AOP analysis in identifying events to which certain human populations may be at increased risk to arsenic-induced bladder cancer.
Disclaimer: The views expressed are those of the authors and do not necessarily represent the views or policies of the US EPA.

PL 777 Evaluation of an Arsenic Reference Dose for Potential Neurobehavioral Effects in Children

M. R. Garry[1], J. S. Tsuji[1], V. Perez[2] and D. D. Alexander[3]. *[1]Exponent, Bellevue, WA, [2]Exponent, Chicago, IL and [3]Exponent, Boulder, CO.*

Health effects associated with low-dose exposures typically occur only after long-term, repeated exposures. However, a health-protective dose based on neurobehavioral effects in children has the potential to be lower than a lifetime-average dose that is protective of chronic health effects. Since an earlier review finding skin lesions as the most sensitive endpoint for populations of arsenic-exposed children, more recent studies have examined cognitive effects in populations exposed to lower arsenic levels in drinking water (<100–200 μg/L). Based on a systematic review of the epidemiological literature (reported separately), we identified critical studies to assess a point of departure (POD) for evaluation of a reference dose (RfD) for neurobehavioral effects. Data from a population-based longitudinal cohort study in Bangladesh provided the strongest evidence for quantifying an association between low-level arsenic exposure and neurobehavioral effects in children. Based on the specific test, gender, and age with the highest positive association between cognitive results (verbal IQ in girls at age 5) and speciated urinary arsenic level, a 38 μg/L speciated urinary arsenic level is a POD, assuming a decrease of 1 IQ point. This urinary arsenic level is well above the distribution in U.S. children. Using an age-specific urinary excretion rate and population-specific body weight, the POD was converted to an absorbed dose of 0.001 mg/kg-day. Uncertainty factor selection considered study population sensitivity and potential bias toward overestimation (highest dose-response used, malnutrition, incomplete correction for maternal IQ and other socioeconomic factors). Application of an uncertainty factor of 1 to 3 would result in RfDs in the range of 0.001 to 0.0003 mg/kg-day. The existing RfD for chronic exposure in adults (0.0003 mg/kg-day) is thus also protective of potential neurobehavioral effects in children.

PL 778 Characterization of Blood Lead Levels for Children in a Community Affected by Historical Mining Activities

R. Schoof[1], D. L. Johnson[1], A. Feldpausch[1], E. R. McConnell[1], C. Van Landingham[2], L. Dell[3], M. Das[1] and A. Gallagher[3]. *[1]ENVIRON, Seattle, WA, [2]ENVIRON, Monroe, LA and [3]ENVIRON, Amherst, MA.*

Numerous studies of child blood lead levels (BLLs) were conducted during the 1980s and 1990s in former mining communities in the western U.S.; however, data characterizing contemporary BLLs in such communities are not readily available. For the past decade, blood lead samples have been analyzed for children ages 1-5 in Butte, MT where mining and mineral processing activities have occurred for more than a century within the community. Additional samples were also collected for some children outside the area most affected by mining, and for infants and pregnant women. An electronic database has been compiled from the Silver Bow County Health Department paper records that includes over 6600 records for infants, children and pregnant women. Our study focusses on over 3,500 records for Butte children 12 to 60 months old for the period from 2002 through 2011. Each record includes gender, birthdate, sample date, and a blood lead result. House age data were obtained from the Montana Cadastral online land survey repository. Consistent with nationwide trends, average Butte BLLs have declined by more than 50% from 2002 through 2011. BLLs are higher in 1-2 year olds compared with 3-5 year olds. Strong seasonal variation in BLLs is evident with peak levels in late summer. More than 55% of the children resided in homes built before 1950 and BLLs correlated with house age. A reference population was created by considering the comparability of prominent risk factors between the Butte dataset and the NHANES blood lead database. Weighting factors are applied to adjust for differences in gender balance, child age distribution, and house age distribution. Additional adjustments considered differences in distributions for race/gender and poverty level. Comparisons with the reference population and assessment of variations in BLLs across neighborhoods will guide assessment of ongoing remediation and lead abatement activities.

PL 779 Variation Analysis of PBPK Model Parameters for Describing the Delivery of Cr(VI) to the Small Intestines of Humans

C. R. Kirman[1], D. Proctor[2], M. Suh[2], C. M. Thompson[3], M. A. Harris[3], L. C. Haws[4] and S. M. Hays[5]. *[1]Summit Toxicology LLP, Orange, OH, [2]ToxStrategies, Rancho Santa Margarita, CA, [3]ToxStrategies, Katy, TX, [4]ToxStrategies, Austin, TX and [5]Summit Toxicology, Lyons, CO.*

Sensitivity analyses were used to identify PBPK model parameters that are important for predicting the delivered dose of Cr(VI) to the small intestines in humans. These include physiological parameters (GI lumen pH, transit rates, reduction capacities, and volumes), chemical-specific parameters (pH-dependent reduction rate, absorption rates), and exposure parameters (number of drinking events, event duration). Monte Carlo methods were used to characterize the impact of parameter variation on PBPK model predictions for Cr(VI) internal dose. Coefficients of variation for the key model parameters ranged from approximately 25% to 120%. The impact of correlations between model parameters was assessed. Monte Carlo simulations were conducted for neonates, infants/children, youths, adults, and elderly, using two exposure levels, and two measures of internal dose to the small intestines. Model parameters contributing to greater than 10% of the variance in the predictions for both dose measures include the reduction rate constant and gastric transit rate. Stomach lumen volume was an important contributor to gastric flux, and the absorption rate constant was an important contributor to SI flux. At high doses, the number of drinking water events per day and exposure event time (during fed or fasted states) also become an important variables. The results of the initial analyses were used to calculate data-derived extrapolation factors to account for inter-individual variation. The ratios of the predicted 95th percentile to predicted mean lifetime average dose of CrVI delivered to the small intestines, ranged from approximately 2 to 4. These results indicates the default value of 3 (USEPA) or 4 (IPCS) for intraspecies variation in toxicokinetic processes sufficiently characterizes variability in Cr(VI) SI tissue dose.

PL 780 Development of a Unit Risk Factor for Hexavalent Chromium and Compounds Based on an Updated Carcinogenic Toxicity Assessment

J. T. Haney[1], N. K. Erraguntla[1], R. L. Sielken[2] and C. Valdez-Flores[2].
[1]*Toxicology Division, Texas Commission on Environmental Quality, Austin, TX and* [2]*Sielken & Associates Consulting, Bryan, TX.*

It is important for the Texas Commission on Environmental Quality (TCEQ) to conduct up-to-date assessments of all carcinogens (e.g., hexavalent chromium) emitted in Texas based on the latest scientific data and analyses. Consequently, TCEQ has developed an inhalation unit risk factor (URF) for hexavalent chromium (CrVI) based on excess lung cancer mortality in two key epidemiological studies of chromate production plant workers. One of the studies (Crump et al. 2003) concerns the Painesville, OH worker cohort and is an update to an earlier study (Mancuso 1975) used by USEPA (1984) to derive a URF, while the other (Gibb et al. 2000) regards a Baltimore, MD worker cohort used previously to calculate occupational URFs. A cohort of workers from four low-dose chromate plants (Corpus Christi, TX, Castle Hayne, NC, two in Germany) was used for a supporting quantitative dose-response assessment (URFs for other studies also calculated). For the Painesville cohort (Crump et al. 2003), grouped observed and expected number of lung cancer mortalities along with the cumulative exposures to CrVI were used to obtain the maximum likelihood estimate and asymptotic variance of the slope (β) for the linear multiplicative relative risk model using Poisson regression modeling. For the Baltimore cohort (Gibb et al. 2000), Cox proportional hazards modeling was performed with optimal exposure lag and adjusting for the effect of covariates (e.g., smoking) to estimate β values as more detailed, individual, data were available. Life-table analyses were used to develop URFs for each of the two key studies, which were then combined using weighting factors relevant to confidence to derive the final URF for CrVI of 2.3E-03 per $\mu g/m^3$. The de minimis air concentration corresponding to a 1 in 100,000 extra lung cancer risk level is 0.0043 $\mu g/m^3$. The TCEQ will use this value to protect the general public in Texas against the potential carcinogenic effects from chronic exposure to CrVI in ambient air.

PL 781 Chronic Beryllium Disease Risk Assessment for Occupational Beryllium Exposure

K. S. Crump[2], M. Suh[1], G. Brorby[4], A. Bichteler[3], G. Hixon[3] and D. Proctor[1].
[1]*ToxStrategies, Inc., Mission Viejo, CA,* [2]*Kenny S. Crump, Ruston, LA,* [3]*ToxStrategies, Inc., Austin, TX and* [4]*ToxStrategies, Inc., Richmond, CA.*

Quantifying the risk of chronic beryllium disease (CBD) from occupational beryllium (Be) exposure is challenging because of limitations in the exposure characterization and interindividual variability in sensitivity. Using worker-specific average exposures and prevalence data for beryllium sensitization (BeS) and CBD for 264 workers at a primary manufacturing facility investigated by NIOSH, the risk of CBD was quantified using logistic, log-logistic and log-logistic transformed regression models. Several modeling approaches and assumptions regarding background risk were explored to estimate the added risk of CBD using models of CBD and bifurcated models of BeS and CBD. Bifurcated models assume two populations with different sensitivities. For both approaches, the average Be concentration associated with a 1/1000 added risk of CBD (RSACs) ranged from 0.02 to 0.22 μg/m3, with median values of 0.05-0.13 μg/m3. Bifurcated models estimate that approximately 16% of the cohort was more sensitive, with the remaining members being highly insensitive. These data may be used to inform an Occupational Exposure Limit (OEL) protective of CBD; however, OELs are limits that are not to be exceeded on a day-to-day basis, whereas the RSACs are measures of average exposure. To determine an OEL consistent with these data, 4,016 total Be lapel samples from the same facility that were used in the exposure reconstruction were further analyzed. Cluster analysis and homogeneity testing was conducted to group the data by job codes with airborne concentrations fitting the same distribution. Of eight statistically distinct groups found, two had mean concentrations of 0.05 and 0.12 μg/m3, consistent with the estimated range of median RSACs. For these groups, 0.2 μg/m3 occurs at the 99th and 84th percentiles, respectively. Thus, setting an upper limit of exposure at 0.2 μg/m3 is associated with average exposures consistent with a 1/1000-increased risk of CBD.

PL 782 Antiperspirants Contribute Considerably to the Total Systemic Exposure to Aluminum in Humans

B. Granum, I. L. Lillegaard, I. Steffensen, A. Ruus and H. Amlund. *Norwegian Institute of Public Health, Oslo, Norway.*

Important exposure routes for aluminum (Al) are diet and use of cosmetics. Reproductive toxicity and neurotoxicity have been observed in animal experiments. In 2012 the Joint FAO/WHO Expert Committee on Food Additives established a provisional tolerable weekly intake (PTWI) of 2 mg Al/kg body weight (bw).
The total Al exposure in the Norwegian population from the diet and use of cosmetics (antiperspirant, lipstick/lip gloss) was estimated based on analyses of the Al content in selected products. National food consumption surveys were used to estimate oral exposure to Al. Nine-year old children, adolescents and adults were assumed to be exposed to Al through the use of cosmetics. Systemic exposure to cosmetics was estimated using default values from the Scientific Committee of Consumer Safety's Notes of Guidance for the Testing of Cosmetic Ingredients and Their Safety Evaluation. To sum up the two exposure routes, the dietary exposure was converted to a systemic exposure dose taking into account the low bioavailability (0.1%) of Al after oral intake. Thus the PTWI was converted to a systemic PTWI of 2 μg Al/kg bw/week.
The mean dietary exposure to Al varied from 0.22 to 0.89 mg/kg bw/week depending on age group, corresponding to estimated systemic exposure doses of 0.22 to 0.89 μg/kg bw/week. By adding lipstick/lip gloss, none of the estimated total systemic exposures exceeded the systemic PTWI. However, by adding the use of antiperspirant, the estimated total exposures were 50 and 30 μg Al/kg bw/week for adolescents and adults, respectively. In a worst case scenario (cosmetic product applied on damaged skin), the estimated total exposure were 940 and 600 μg Al/kg bw/week, for adolescents and adults, respectively.
This risk assessment showed that none of the estimated mean dietary exposures to Al exceed the PTWI in any age groups. Antiperspirants, however, contributed considerably to the total systemic exposure to Al in Norwegian adolescents and adults, leading to a large exceedance of the PTWI.

PS 783 Virtual Screening for the Discovery of Bioactive Natural Compounds against DNA Methyltransferases, Protein Targets in Skin Cancer

W. Maldonado-Rojas and J. Olivero-Verbel. *Environmental and Computational Chemistry Group, University of Cartagena, Cartagena, Colombia.*

The thinning of the ozone layer and the lack of natural protection again UV radiation are main factors in the increase of skin cancer incidence. As this disease has been growing at an alarming rate and becoming resistant to conventional chemotherapy, it requires the search for new sources of more effective drugs. Natural product structures have had a vast influence in approved drug therapies, especially for several types of cancers. However, the precise molecular mechanisms of these compounds remain unexplored. In this work, virtual screening methodologies were employed for the search of natural molecules with the ability to inhibit the activity of DNA methyltransferases (DMTs), referenced as pivotal protein targets in the development of skin cancer. In total, 800 structures were downloaded from The NatProd Collection (www.msdiscovery.com/natprod.html), and evaluated in silico on fourteen 3D DMT structures (64% Homo sapiens, 36% Mus musculus) from Protein Data Bank (PDB), using molecular docking protocols with AutoDock Vina program. The results showed that digitoxin (glycoside extracted from Digitalis purpurea L.) had the best AutoDock Vina affinity value (-13.1 kcal/mol). However, other molecules such as gitoxin, chrysantellin A and huperzine, also presented significant affinity values (−12.1 kcal/mol, for each one). These results are promising, in particular when calculating the theoretical affinity for known DMTs inhibitors, such as zebularine, decitabine, fazarabine and azacitidine (-6.7, -7.0, -7.1, -6.9 kcal/mol, respectively). Computational approaches suggest natural compounds reported here should be evaluated as possible DMTs inhibitors, and also provide a platform for structure-based design of new compounds for treatment/prevention of skin cancers. W. Maldonado is sponsored by the National Program for Doctoral Studies in Colombia, Colciencias, 528-2011.

PS 784 Investigation of the Mutagenic, Genotoxic, and Cytotoxic Acivities of *Sanionia uncinata* Extracts

A. D. Campos[1], J. Mazzei[2], H. Evangelista[1] and I. Felzenszwalb[1]. [1]*Department of Biophysics and Biometry, State University of Rio de Janeiro, Rio de Janeiro, Rio de Janeiro, Brazil and* [2]*Center for Chromatography, Platform of Analytical Instruments, Oswaldo Cruz Foundation, Rio de Janeiro, Rio de Janeiro, Brazil.* Sponsor: D. Oliveira.

Introduction:The Antarctic moss *Sanionia uncinata* has presented high contents of chromophores after exposition to high levels of natural ultraviolet B radiation and can be an important source of antioxidants. The photoprotective activity of this moss has been observed. However, there is no data in the literature about toxicological research.
Objective:To investigate the mutagenic, genotoxic and cytotoxic activities of the *S. uncinata*.
Material and Methods: The *Salmonella* microssome assay was performed using the pre-incubation protocol. The mixture of 100 μL of the stationary culture of *Salmonella enterica* serovar Typhimurium strains TA97, TA98, TA100, TA102 and TA104 and 500 μL of the S9 mix was incubated for 20 min with 100 μL of different concentrations of the hydroethanolic (HE) and ethanol (EE) extracts. Top-agar was added and poured into a Petri dish containing minimal agar medium. After 72h the number of revertants was counted. In MN assay HepG2 cells were exposed to HE and EE for 3 hours, fixed and stained with DAPI. To determine the mitotic index and the number of cells with micronuclei, 6000 cells/ concentration were analyzed under fluorescence microscope. In WST assay, the cells were exposed to HE and EE for 3, 24 and 72 hours, it was added WST dye and the absorbance was measured in 440nm.
Results and Discussion: The extracts did not show mutagenic activity in the *Salmonella* strains and did not induce genotoxicity in HepG2 cells, moreover, it was no observed apoptosis or necrosis cell death in these cells. Besides, the cell viability evaluated by WST assay was not affected by HE and EE. Our results showed that in metabolically competent cells, the HE and EE did not induce mutagenic, genotoxic and cytotoxic effects.
Conclusion: The HE and EE should be of interest to further explore the possibility of using it as potential photoprotective.

PS 785 Cytotoxicity of Extracts of Three Medicinal Plant Species Used to Treat Inflammation-Related Conditions in South Africa

S. A. Adebayo[1, 2], J. L. Shai[1] and K. A. Eloff[2]. [1]*Biomedical Sciences, Tshwane University of Technology, Pretoria, South Africa and* [2]*Phytomedicine Programme, Department of Paraclinical Sciences, University of Pretoria, Pretoria, South Africa.*

Extracts of medicinal plants are widely used in developing countries for the treatment and management of many diseases. The safety or hazards presented by the consumption of these substances is scarce in literature. There are many cases of fatal intoxication from plants in hospitals. The aim of this study was to assess the safety of oral consumption of extracts derived from the selected medicinal plant species using *in vitro* cytotoxicity tests.
Dried leaves portion of *Acacia sieberiana*, *Erythrophleum lasianthum* and *Tecomaria capensis* were ground into a fine powder. The ground materials were extracted with cold and hot distilled water, as well as ethanol, representing traditional methods of extraction. The dried extracts were re-constituted in dimethylsulphoxide at a concentration of 20 mg/ml. These extracts were tested against isolated mononuclear leucocytes, U937 macrophage, vero kidney and liver cell lines maintained in Dubelco's Minimum Essential Medium (DMEM) for 72 hours. The assessment of cytotoxic effects were done using both the reduction of yellow tetrazolium salt (3-(4, 5-dimethylthiazolyl-2)-2, 5-diphenyltetrazolium bromide (MTT) and Excelligence RTCA assay systems.
Overall, the results indicated that all the extracts tested were not cytotoxic to the cell lines used when compared with hydrogen peroxide (1 mM) and Doxorubicin hydrochloride (2 mg/ml) positive controls. The vero kidney cell lines grew at optimal rate when cultured in the presence of ethanolic extracts of *A. sieberiana*, while the least growth was observed when the same cell lines were cultured in the presence of cold water extracts of *E. lasianthum*. The cold water extracts of *E. lasianthum* had the least effects on mononuclear leucocytes using the MTT assay among the extracts tested. This indicated that the choice of evaluation method is critical for results interpretation. However, there is a need for *in vivo* study using a model animal to validate these results.

PS 786 The Effect of Eukaryotic Initiation Factors on the Activity of Pokeweed Antiviral Protein

S. Cheng, A. Domashevskiy and L. Kobilinsky. *Sciences, John Jay College of Criminal Justice, New York, NY.*

Ribosome-inactivating proteins (RIPs) are found in numerous plant, fungi and bacterial species, and are recognized to have a broad spectrum of anti-viral activity. RIP function is characterized by depurination, the N-glycosidase activity, of the conserved sarcin/ricin loop of the large ribosomal subunit. PAP is also able to depurinate mRNA at specific nucleotide locations, by binding to the m7G cap at the 5'-end of the mRNA, and interaction with eukaryotic initiation factors (eIFs). These biological functions suggest that the mechanism of PAP action is complex, yet information about the molecular mechanism of how this toxin causes apoptosis or the basis for its selection of RNA for depurination scares. In order to determine the role of multiple protein-protein interactions (PAP, eIFiso4E, and eIFiso4G) in PAP function, the pull-down assay and the fluorescent-resonate energy transfer assay (FRET) have been investigated here. Our results indicate that eIFiso4E binds to m7GpppG cap analog. PAP competes with eIFiso4E for binding to the m7GpppG cap analog. eIFiso4G does not bind to the m7GpppG cap analog. However, eIFiso4E and eIFiso4G bound together as the eIFiso4F complex to m7GpppG cap analog and this binding cannot be overcompeted by PAP. eIFiso4G repressed the competition of PAP with eIFiso4E for m7GpppG cap analog binding. FRET energy transfer study revealed that eIFiso4E and eIFiso4G bind in close proximity as PAP and eIFiso4G bind close enough to cause FRET energy transfer. PAP and eIFiso4E interact with each other; this interaction produces only low level of FRET energy transfer. PAP, eIFiso4E and eIFiso4G bound closely to each other to increase FRET energy transfer dramatically. This triplex protein interaction demonstrated eIFiso4G plays a key role in regulation of PAP binding.

PS 787 Effect of Sesamin on Endothelial Nitric Oxide Synthase Activation via Multiple Pathways

S. Jin, H. Kim, J. Choi, S. Won, S. Oh and H. Jeong. *Pharmacy, Chungnam National University, Daejeon, Republic of Korea.*

Endothelial nitric oxide synthase (eNOS) is the key regulator of vascular functions in the vascular endothelium. While many pathways are involved in the regulation of eNOS activity, phosphorylation at the most thoroughly studied site at Ser1177 is generally found to be a critical requirement for eNOS activation. Sesamin, one of the major lignans in sesame seeds and oil, has been reported to have many benefits and medicinal properties including anti-hypertensive effect, but its influence on intracellular pathways underlying eNOS remains unclear. Sesamin increased the phosphorylation of eNOS in a concentration-dependent manner in human endothelial cells. In addition, sesamin increased the phosphorylation of Akt, ERK1/2, JNK1/2, and p38 MAPK in cells. Furthermore, sesamin increased the phosphorylation of AMP-activated protein kinase (AMPK) and calmodulin-dependent protein kinase II (CaMKII). eNOS phosphorylation was inhibited by specific upstream inhibitor of ERK1/2 (PD98059), p38 (SB203580), AMPK (compound C), and CaMKII (BAPTA, W7). These results indicate that sesamin stimulates eNOS phosphorylation via the activation of ERK1/2, p38, AMPK, and CaMKII.

PS 788 Amelioration of Sodium Arsenite and Potassium Chromate Toxicities by Methanolic Extract of *Rauvolfia vomitoria*

K. A. Akinwumi[1, 2], O. A. Odunola[1], A. N. Dosunmu[2], O. B. Owolabi[2], A. Songonuga[2], O. A. Aboyewa[2], O. A. Olatunji[2] and O. O. Osifeso[3]. [1]*Dept. of Biochemistry, University of Ibadan, Ibadan, Oyo, Nigeria,* [2]*Dept. of Chemical Sciences, Bells University of Technology, Ota, Ogun, Nigeria and* [3]*Dept. of Science Laboratory, Moshood Abiola Polythenic, Abeokuta, Ogun, Nigeria.* Sponsor: J. Landolph.

Exposure to arsenic and hexavalent chromium is a major public health concern especially in the developing part of the world and there is still no reliable treatment. This study therefore evaluates the effect of methanolic leaf extracts of *Rauvolfia vomitoria* (MRV) on mice exposed to sodium arsenite (NaAsO2) and/ potassium heptaoxochromate VI (K2Cr2O7). Test and control mice were pre-treated with 275mg/kg body weight MRV before being challenged with either NaAsO2 and/ K2Cr2O7 on the seventh day. The negative control animals were exposed to distilled water, while the positive control mice were exposed to a single dose of either 2.5 mg/kg body weight NaAsO2 and/ 12mg/kg of K2Cr2O7 a day before the animals were sacrificed. The frequency of micronucleated polychromatic erythrocytes (mPCEs) was monitored in bone marrow cells, while aspartate aminotransferase (AST) and alanine aminotransferase (ALT) activities were assessed in the plasma. Hepatic glutathione (GSH) and malondialdehyde (MDA) levels as well as catalase (CAT) and glutathione-S-transferase (GST) activities were also monitored.

NaAsO2 and K2Cr2O7 significantly (P<0.05) increased the frequency of mPCE formation, AST, ALT, CAT and GST activities when compared with the control. Simultaneous exposure to NaAsO2 and K2Cr2O7 further increased (p<0.05) the levels of the markers. In addition, GSH and GST were significantly (p<0.05) reduced in mice exposed to NaAsO2 or K2Cr2O7 or their combination. However, pre-treatment with MRV restored the markers towards that of the control. Our study therefore suggests that MRV ameliorates NaAsO2 and K2Cr2O7 induced toxicities via reduction of oxidative stress and fortification of anti-oxidant system.

PS 789 Cytotoxic and Genotoxic Assessments of the Natural Dye Erythrostominone

F. R. Abe and D. P. Oliveira. *University of São Paulo, Ribeirão Preto, São Paulo, Brazil.*

Introduction: Synthetic dyes are used extensively for pharmaceutical, cosmetic or food industries. These industrial sectors are attracted by the low cost, easy availability and high diversity of colors and shades of synthetic dyes, however, several of these compounds present inherent toxicity, and can be precursors of toxic intermediates and/or mutagens produced during metabolism. Thus, natural dyes obtained by the fermentation processes of micro-organisms are alternatives for the substitution of synthetic dyes in some applications. Additionally, they have low cost, and require little space for the large-scale production, increasing the economic viability for industrial use. Objectives: The present work aimed to evaluate the cytotoxicity and genotoxicity of the natural dye erythrostominone extracted from micro-organism. Methodology: Cultures of HepG2 cells were exposed to erythrostominone at concentrations of 35, 87, 174, 261, 348, 522, 696 and 870 mg/l and to negative (NC-DMSO) and positive controls (PC-CCCP) and cytotoxicity was evaluated after 24 hours using MTT assay. After exposure, cell viability was analyzed by spectrophotometry. The comet assay verified the genotoxicity of the dye at concentrations of 35, 87, 174, 261, 348, 435 and 522 mg/l, NC (DMSO) and PC (MMS). The DNA tail formation was analyzed with fluorescence optic microscopy. The values of cell viability and tail moment were analyzed statistically by the software GraphPad Prism 5.01. Results: Erythrostominone dye at 522, 696 and 870 mg/l presented statistically significant difference in cell viability, when compared to the NC. No statistically significant difference was observed in tail moment. Discussion: Erythrostominone dye is cytotoxic at higher concentrations, however it does not induce genotoxicity in tested concentrations. Conclusion: According to our data, erythrostominone dye can be used in industrial sectors as a substituent of synthetic dyes, since it has no citotoxicity and genotoxicity at concentrations lower than 522 mg/l. Others toxicological studies are necessary to investigate possible damage to human and environmental health.

PS 790 Comparison of the Estrogenic Modulating Activities of Dong Quai with Hops and Red Clover

B. M. Dietz, T. Gödecke, T. S. Tewolde, A. Hajirahimkhan, H. Dong, Y. Choi, S. Chen, D. Nikolic, R. B. van Breemen, G. F. Pauli and J. L. Bolton. *Medicinal Chemistry and Pharmacognosy, University of Illinois at Chicago, Chicago, IL.*

Many women use dong quai (*Angelica sinensis*, (Oliv.)) dietary supplements as over-the-counter medication to relief menstrual irregularities and menopausal symptoms in a natural and safe way. However, despite the widespread use of dong quai in the US, its efficacy and safety has not been demonstrated. Data in the literature about dong quai's estrogenic/antiestrogenic activities are contradictory. To analyze this controversy, a lipophilic (CO2) and hydrophilic (EtOH 75%) dong quai extract was systematically analyzed for its estrogen receptor (ER) modulating activities in estrogenic bioassays in endometrial and breast cancer cells. Our preliminary data suggest that the 75% EtOH and CO2 supercritical fluid extracts show opposing estrogenic and antiestrogenic activities in endometrial cells. Partitioning of an EtOH extract leads to at least three fractions with distinct estrogenic/antiestrogenic activities in breast and uterine cells. The fractions that showed partial agonistic activities in an ERE-luciferase assay contained ligustilide as major constituent. Ligustilide itself displayed weak antiestrogenic activities in the endometrial cancer cell line, Ishikawa, and in the breast cancer cell line, MCF-7, and significant estrogenic activities in the ERE-luciferase assays in both cells. In comparison to other estrogenic botanical dietary supplements, such as hops and red clover, dong quai extracts show both, antiestrogenic as well as estrogenic properties. While hops and red clover contain phytoestrogens that bind to the ER and elicit estrogenic activities, ligustilide appears not to be an ER ligand. The present data suggest that distinct dong quai extracts may have diverse estrogen modulating activities in reproductive tissue and highlight the importance of standardization for dong quai botanical dietary supplements.
Support for this work was provided by P50 AT00155

PS 791 Extracts of *Protea cynaroides* Are Cytotoxic toward Hormone-Resistant Breast and Prostate Cancer Cells

P. Gwavava, F. Imhoff-White, B. Cridge, S. Taurin and R. J. Rosengren. *Pharmacology & Toxicology, University of Otago, Dunedin, New Zealand.*

This study was designed to determine the optimal extraction method for extracting phenolic compounds from the plant *Protea cynaroides*. In all extraction methods, 1 g of leaves were thoroughly washed and submerged in 0.1 N HCl prior to extract preparation. Immediate freezing and grinding in LN2 followed by freeze drying produced the freeze dried extract. Leaves that were oven dried were subjected to water, alcohol and alcohol/water extraction methods. All stock solutions were sterilised using a 0.22 μm filter. Cytotoxicity was determined using the sulforhodamine B assay. Phenolic content of the extracts was determined using the Folin-Ciocalteu method. The results showed that the alcohol/water extraction method produced a 2-fold greater amount of phenolic compounds compared to water extraction (100 vs 50 μg/ml, respectively). This correlated with more potent cytotoxicity of the alcohol/water extract toward both cell lines. Specifically, 92, 94 and 97% of MDA-MB-231 cells were killed by the alcohol/water extract compared to 47, 55 and 55% for the water extract at concentrations of 0.9, 1.8 and 9 mg/ml, respectively. A similar trend was seen in PC3 cells as 83, 93 and 99% of cells were killed following treatment with the alcohol/water extract compared to 55, 76 and 86% for identical concentrations of the water extract. However, freeze-dried extracts were equally cytotoxic at 9 mg/ml concentrations, as > 94% of PC3 and MDA-MB-231 cells were killed at this concentration by both freeze-dried and alcohol/water extracts. However, alcohol/water extracts were more potent than freeze-dried extracts at the lower concentrations of 0.9 and 1.8 mg/ml. The results of this study show that water, alcohol/water and freeze drying are all viable methods of extracting phenolic compounds from *Protea cynaroides*. However, alcohol/water extraction is the preferred method as it produces a more potent extract that is cytotoxic toward ~90% of MDA-MB-231 and PC3 cells at concentrations of 0.9 mg/ml.

PS 792 Differential Effects of Biz-2 in Cancer Cells

O. S. Phillip[1], K. Harris[2] and W. G. Gray[2, 1]. [1]*Environmental Toxicology, Southern University and A&M College, Baton Rouge, LA and* [2]*Department of Chemistry, Southern University and A&M College, Baton Rouge, LA.*

Prostate cancer (PCa) is the leading cause of cancer death in men in the USA, making it a major problem with a socio-economic burden in the millions of dollars. Despite rapid advancements in the early detection and treatment of PCa over the past fifty years, there are no effective cures for this disease. It is of paramount importance to develop new, effective ways of addressing PCa. Our laboratory has been studying the mechanism of the bioactive chemicals present in the *Kola acuminate*, a "cure-all" herbal medicine known to the Ettu people of Jamaica as bizzy nut. Based on the ethnobotanical and anecdotal data available on this natural product, we hypothesized that bizzy nut contains one or more bioactive compounds that can modulate prostate biology. Using cell cytotoxicity, androgen receptor (AR) binding and AR gene expression as indices of androgenicity, we found that the ether extract of bizzy (Biz-2) contains compounds with potent anti-androgenic potential in both AR+ and AR- prostate cells. Biz-2 was able to inhibit the proliferation of prostate cells (DU145 and LNCaP) in a concentration-dependent manner. We observed that the Biz-2 extract displays cell-specific cytotoxicity toward PCa cells, with no toxicity towards breast (MCF-7), lymphocyte (THP-1) or neuronal (GT1-7) cancer cells. Furthermore, our current data show that low doses of Biz-2 kill PCa cells, but show no apparent effect on normal, transformed prostate cells, or display any in vivo toxicity in mice. Next, we examined the mechanism of action of Biz-2-induced cytotoxicity by examining LNCaP and DU145 cells exposed to Biz-2 for morphological signs of apoptosis, along with the expression of several apoptotic markers. In those experiments, we found that Biz-2 was able to induce apoptotic cell death in PCa cells. Biz-2 was twice as potent in inducing apoptosis in AR- DU145 cells as in the AR+ LNCaP cells. This study has demonstrated that Biz-2 can modulate prostate cancer cell function. (Work was supported by a NIH grant, Grant No. 3P20RR016456-08S1)

PS 793 Antioxidant Activity of Extracts of Stem Bark of *Enantia chlorantha* (Oliv)

O. E. Adebiyi and O. M. Abatan. *Department of Veterinary Physiology, Biochemistry and Pharmacology, University of Ibadan, Nigeria, Ibadan, Oyo, Nigeria.*

Enantia chlorantha is an ornamental tree that has been reported to posses haemostatic antimalarial, antibacterial, antiviral and hepatoprotective properties. The hexane, chloroform, ethyl acetate and methanol extracts of stem bark from *Enantia chlorantha* stem bark were assessed for *in vitro* antioxidant activity using Ferric

reducing antioxidant power (FRAP) and 1,1-diphenyl-2-picrylhydrazyl (DPPH) scavenging assay at 0.04, 0.06, 0.08 and 0.10 mg/ml. The results were compared with that of ascorbic acid.
Antioxidant activity of the different solvents extract with the DPPH radical scavenging and iron (III) to iron (II) reducing activity were in the order of methanol extract > chloroform methanol > ethyl acetate > hexane. In the DPPH scavenging assay the potency of methanol extract of *E. chlorantha* stem bark (85.8% inhibition) was of the same magnitude as that of reference ascorbic acid. Further phytochemical screening of the methanol extract of *E. chlorantha* stem bark revealed the presence of phenolics, flavonoids, alkaloids, glycosides, saponins and resin.
The results suggest that extracts from the stem bark of *Enantia chlorantha* have strong antioxidant activity. The antioxidant activities of *E. chlorantha* may be responsible for its pharmacological properties.

PS 794 Synthesis and Biological Evaluations of Amino Acid Conjugates As Potential Prodrugs of Curcumin

D. You[1], L. Chen[1], S. Tu[2], C. S. Yang[2, 3] and L. Hu[1, 3]. [1]*Medicinal Chemistry, Ernest Mario School of Pharmacy, Rutgers University, Piscataway, NJ,* [2]*Chemical Biology, Ernest Mario School of Pharmacy, Rutgers University, Piscataway, NJ and* [3]*Cancer Institute of New Jersey, New Brunswick, NJ.* Sponsor: L. Aleksunes.

Curcumin, a phytochemical found in Tumeric, has been widely studied for its potential in the prevention of different types of cancer. However, it only has limited clinical applicability because of its low oral bioavailability. One of the approaches to improve curcumin's bioavailability is to develop curcumin prodrugs. Ester prodrugs are the most common type that can be easily converted back to the active agent by esterases found in the body. A series of aminoacyloxymethyl prodrugs of curcumin was designed and synthesized incorporating amino acids such as leucine, isoleucine, and valine. Mono-conjugated (only one phenol group in curcumin was conjugated with an amino acid moiety) and di-conjugated (both phenols were modified) products were observed. The conjugates were then evaluated in cytotoxicity assays using different prostate cell lines and in cancer prevention screening assay using sphere formation in gastric cancer cells. Overall, valine conjugates were less cytotoxic than curcumin while mono-isoleucine conjugates had comparable cytotoxicity to curcumin. Two mono-conjugates were screened for their cancer preventive effects. The results showed that curcumin and both amino acid conjugates significantly reduced sphere formation. This indicates that curcumin analogs, which are expected to have better aqueous solubility and improved oral bioavailability, have similar chemopreventive effects to curcumin, possibly at reduced cytotoxicity.

PS 795 Suppression of PMA-Induced Tumor Cell Invasion by Kahweol via the Inhibition of Akt/ERK/NF-kB and AP-1-Dependent MMP-9 Expression

H. Kim, J. Choi and H. Jeong. *Pharmacy, Chungnam National University, Daejeon, Republic of Korea.*

Kahweol, the coffee-specific diterpene, has been reported to have anti-carcinogenic properties. Animal data support such a chemopreventive effect of coffee. However, the precise underlying protective mechanisms are poorly understood. This study examined the inhibitory effect of kahweol on phorbol myristate acetate (PMA)-induced MMP-9 expression in HT-1080 human fibrosarcoma cells. Kahweol reduced PMA-induced activation of MMP-9 and further inhibited cell invasion and migration. Kahweol suppressed PMA-enhanced expression of MMP-9 protein, mRNA and transcription activity levels through suppression of NF-kB and AP-1 activation without changing the tissue inhibitor of metalloproteinase (TIMP)-1 level. In addition, kahweol suppressed PMA-induced phosphorylation of Akt and ERK1/2, upstream factors involved in NF-kB and AP-1 pathways. Therefore, the inhibition of MMP-9 expression by kahweol might have therapeutic potential for controlling the growth and invasiveness of cancer cells.

PS 796 Bioactive Compounds in Hops (*Humulus lupulus L.*) Differentially Modulate Oxidative Estrogen Metabolism: Isoxanthohumol Correlates with Chemopreventive Activity

S. Wang, C. Snelten, R. F. Ramos, S. Chen, G. F. Pauli, B. M. Dietz and J. L. Bolton. *Medicinal Chemistry and Pharmacognosy, University of Illinois at Chicago, Chicago, IL.*

Long term exposure to estrogens, particularly through hormone therapy, has been listed as a major risk factor for breast cancer development. Accordingly, many women have turned to botanical dietary supplements (BDS) for the alleviation of post-menopausal symptoms. Hops (*Humulus lupulus L.*) is one of the widely used BDS for which safety and efficacy claims remain to be demonstrated. It has been shown previously that a standardized hops extract reduces the formation of key oxidative estrogen metabolites, which further form DNA-damaging estrogen quinones contributing to estrogen carcinogenicity. However, what hops constituents contribute to this chemopreventive activity is not known. Analyzing the influence of three bioactive hops constituents, 8-prenylnarigenin (8-PN), xanthohumol (XH), and isoxanthohumol (IX) on oxidative estrogen metabolites formation using an LC-MS/MS method, we demonstrated that 8-PN enhanced and IX reduced the carcinogenic 4-hydroxylation pathway, while the amount of 4-hydroxylated products remains unaffected by XH. Cytochrome P450 1A1 (CYP1A1) and 1B1 (CYP1B1) catalyze 2- and 4-hydroxylation of estrogen into precursors of carcinogenic quinones. Modulation of mRNA levels and activity of CYP1A1 and CYP1B1 were measured to assess possible mechanisms of actions. The results correlated with the 4-hydroxylation metabolism data; 8-PN significantly induced CYP1B1 mRNA expression and IX preferentially inhibited CYP1B1 activity. Evaluation of the influence of an IX-rich (57.6% w/w) hops extract on 2- and 4-hydroxylation of estradiol by LC-MS/MS revealed that the extract reduced the carcinogenic 4-hydroxylation pathway similar to pure IX. These data suggest that hops constituents differentially modulate estrogen carcinogenesis and underscore that standardization of hops extracts is essential for the reproducibility of biological outcome.
Support for this work was provided by P50 AT00155.

PS 797 Evaluation of Cell Viability and Mitochondrial Protective Effects of Quercetin in Rat L6 Cells

V. Kale and J. Radhakrishnan. *College of Pharmacy, Roseman University of Health Sciences, South Jordan, UT.*

Mitochondrial biogenesis plays an important role in the etiology of many diseases, including neurodegenerative disorders, diabetes, and cardiovascular myopathies, as well as the aging process and poor exercise tolerance. Quercetin is one of a broad group of natural polyphenolic flavonoids that is being investigated for its widespread health benefits. These benefits have generally been ascribed to its combination of antioxidant and anti-inflammatory activity. The present study sought to investigate whether quercetin could protect mitochondria against oxidative damage and to elucidate its mechanism for mitochondrial protection in rat L6 cells. Rat L6 cells were grown in DMEM media with glutamate supplemented with 10% FBS and antibiotics (PenStrep). For cytotoxicity and ATP measurements, cells were treated with various concentrations of quercetin (0, 50, 100, 250 and 500μM) dissolved in DMSO and incubated for 24 and 48h ($3x10^4$ cells/well in 96 well plates, 5% CO_2, 37°C and 95% relative humidity). For all experiments final DMSO concentration was 0.1% v/v. The % LDH released (Mean±SE) from L6 cells treated with quercetin was significantly different from vehicle treated group for 100, 250 and 500μm at 24h (3.5±1.0, 6.3±1.1, 8.0±1.0, 12.0±0.9, 17.1±0.9) and for all concentrations at 48h time point (8.7±1.8, 18.0±2.5, 27.7±3.7, 35.7±5.8, 31.8±5.9). The % ATP levels (Mean±SE) were also correlated with decrease in cell viability. ATP levels were significantly lower from vehicle control for concentrations 250 (65.5±4.5) and 500 μM (62.4±8.4) at 48h and no significant differences were seen at 24h time point for all concentrations tested. These results suggest that the quercetin causes limited cytotoxicity and concentration and time-related decrease in ATP levels in L6 cells. Currently, we are identifying the protective effects of quercetin on Antimycin A-induced mitochondrial damage, cellular & mitochondrial processes modulated by quercetin and its possible mechanism of mitochondrial protection in myocytes. (Support: Roseman University of Health Sciences).

PS 797a Effect of Caffeic and Phenethyl Ester on Endothelial Nitric-Oxide Synthase Activation

B. Park, H. Kim, J. Choi, S. Jin and H. Jeong. *Pharmacy, Chungnam National University, Daejeon, Republic of Korea.*

NO production is used as a marker of endothelial function, which is mediated by endothelial nitric-oxide synthase (eNOS) activation in the vasculature. Caffeic acid phenethyl ester (CAPE) is an active component of honeybee propolis extracts which has anti-inflammatory, immunomodulatory, anti-proliferative, and anti-oxidant properties. Nonetheless, the effects of CAPE on endothelial nitric oxide synthase (eNOS) activation have not been characterized. This study investigated molecular mechanisms by which CAPE stimulated eNOS activation in human endothelial cells. Results showed that CAPE increased eNOS phosphorylation in a concentration- and time-dependent manner. CAPE activated eNOS phosphorylation via Akt, ERK1/2, and AMP-activated protein kinase (AMPK) signaling. In addition, CAPE stimulated AMPK phosphorylation through ca2+/calmodulin-dependent protein kinase II (CaMK II). Moreover, inhibitors of Akt (LY294002), ERK1/2 (PD98059), AMPK (compound C), and CaMKII (W7) suppress CAPE-induced eNOS phosphorylation. These results indicate that CAPE

stimulates eNOS phosphorylation via the activation of Akt, ERK1/2, AMPK, and CaMKII. These results demonstrate that CAPE might be useful for the treatment or prevention of endothelial dysfunction associated with atherosclerosis and cardiovascular disease.

PS 797b Kahweol Induces Apoptosis in HER2-Overexpressing Breast Cancer Cells through a Down-Regulation of HER2/SREBP-1/FAS Pathway

S. Oh, M. Do and H. Jeong. *Pharmacy, Chungnam National University, Daejeon, Republic of Korea.*

Breast cancer is the leading cause of cancer-related death among women worldwide. Kahweol, natural diterpenes from coffee, has been reported to exhibit anti-cancer activities. This study investigated molecular mechanisms by which kahweol induced apoptosis in HER2-overexpressing breast cancer cells. Results showed that kahweol strongly inhibited cell growth and induced apoptosis in SKBR3 breast cancer cells through caspase-3 activation and induction of PARP cleavage. Kahweol markedly reduced HER2 protein levels in a concentration-dependent manner. Kahweol significantly suppressed fatty acid synthase (FAS) mRNA and protein levels in SKBR3 cells. Kahweol inhibited Akt activation, leading reduction of mature sterol regulatory element-binding protein (SREBP)-1 protein levels. Furthermore, using specific PI3K inhibitor LY294002 confirmed that the blockade of Akt/SREBP-1 signaling pathway caused FAS reduction in SKBR3 cells. These results demonstrate that kahweol down-regulates HER2/SREBP-1/FAS pathway and induces apoptosis in breast cancer cells, suggesting a potential role in prevention and treatment of human breast cancer.

PS 797c Antiproliferative and Apoptotic Effect of *Rhus trilobata* Extracts on SKOV-3 Ovarian Cancer Cells

B. E. Sánchez Ramírez[1], E. SaénzPardo-Reyes[1], C. González-Horta[1], R. Infante-Ramírez[1] and P. Talamás-Rohana[2]. [1]*Graduate Program in Biotechnology, Universidad Autonoma de Chihuahua, Chihuahua, Chihahua, Mexico and* [2]*Infectómica y Patogénesis Molecular, Centro de Investigación y Estudios Avanzados del IPN, México, DF, Mexico.* Sponsor: L. Del Razo.

Rhus trilobata, known as Skunk brush, is a plant from northern Mexico frequently used in traditional medicine for different types of cancer. The aim of this work was to analyze the effect of extracts of *Rhus trilobata* on proliferation and apoptosis of SKOV-3 ovarian cancer cells. Extracts were prepared by ebullition in distilled water (AE) or with 70% methanol (ME) using stems of the plant recollected in November 2012. Sub-fractions of both extracts were obtained using Sep-Pak C18 cartridges and different solvents. Crude extracts and sub-fractions were tested on SKOV-3 ovarian cancer cells; viability and cytotoxicity or apoptosis were determined in cultures using the ApoToxGlo kit, and mitotic index was calculated for all treatments. Cultures without treatment or incubated with Vincristine or Curcumine, were used as controls. Results showed that both extracts, AE and ME, significantly decreased proliferation (mitotic index < 1) and cell viability at concentrations < 20 μg/mL at 24 and 72 h, compared with untreated cultures ($p < 0.05$); no significant differences were found with cultures treated with 20 μg/mL of Vincristine. Fractionation of crude extracts produced seven fractions that were evaporated to dryness previous to their use. The fractions that showed greater antiproliferative effect were 3, 4, and 7 from the AE, and 2, 5, and 7 from ME at a concentration of 5 μg/mL ($p < 0.05$). Apoptosis assays showed that antiproliferative effect was associated with an increase in caspase activity in cells treated with 5 μg/mL of AE, ME, or active sub-fractions. No cytotoxic effect was detected at any of the concentrations tested. Results presented here demonstrate that *Rhus trilobata* stems contain active compounds with an important antiproliferative effect on SKOV-3 ovarian cancer cells, may be related to the induction of apoptosis rather than a cytotoxic effect. Supported by FOMIX CHIH-2010-C01-147532.

PS 798 Comparison of Myelostimulation by *Echinacea purpurea* Extracts with Analytical Fingerprints to Identify Active Constituents

S. A. Meyer[1], H. F. Hussin[1] and K. A. El Sayed[2]. [1]*Toxicology, Univ LA-Monroe, Monroe, LA and* [2]*Basic Pharmaceutical Science, Univ LA-Monroe, Monroe, LA.*

We have previously described a myelostimulatory activity of *Echinacea* herbal supplement (Spring Valley Natural Whole Herb, Idea Sphere Inc., American Fork, UT) (Ramasahayam et al. 2011. Planta Med. 77:1883-9). Product label described the encapsulated material as *Echinacea purpurea* (aerial part) with gelatin and medium-chain triglycerides. A 75% ethanol extract administered orally for 7d at 50-100 mg dried extract/kg/d, as recommended for human intake, to female Sprague-Dawley rats yielded a 70% increase in femur myeloid progenitors, i.e., CFU-GMs, from nucleated bone marrow cells upon culture in methylcellulose with csf2, IL-3 and SCF (HALO assay, Hemogenix, Colorado Springs, CO). To determine that bioactivity was due to plant-derived material, we obtained plant source material (CP) of the supplement (Ray Jaglowski, Twinlab Corp., Grand Rapids, MI), extracted with ethanol (EtCP) and tested for CFU-GMs. Since Echinacea aerial part contains lipophilic N-alkylamides as a primary constituent class, we also determined myelostimulatory activity of n-hexane-washed EtCP (HxEtCP). Analytical fingerprints of EtCP and HxEtCP constituents were acquired with HPTLC and ^{1}HNMR (400 MHz, 20 mg/700 ul MeOH-d4). Increase in CFU-GMs of EtCP was comparable to that previously determined for herbal supplement and HxEtCP activity, normalized to source EtCP (~95% yield), was 2 times more potent than EtCP. Hexane wash fraction of CP did not affect CFU-GMs. Proton NMR spectra of hexane wash contained prominent peaks from β-sitosterol, as verified from spectra of pure standard (ChromDex,Irvine, CA). Similarly, ^{1}HNMR spectral peaks with shifts equivalent to those of dodeca-2,4,8,10-tetraenoic acid isobutylamide (PhytoLab, Vestenbergsgreuth, Germany) were evident in hexane wash. HPTLC confirmed that these lipophilic constituents were removed from EtCP by washing with n-hexane. In conclusion, these studies demonstrated that myelostimulation of supplement Echinacea was due to phytomaterial other than lipophilic constituents.

PS 799 Inhibitory Effects of *Platycodon grandiflorum* Root-Derived Saponins on DNCB-Induced Atopic Dermatitis-Like Skin Lesions in Mice and the Possible Mechanisms in Cells

J. Choi[1], S. Jin[1], B. Park[1], H. Kim[1], Y. Chung[2] and H. Jeong[1]. [1]*Pharmacy, Chungnam National University, Daejeon, Republic of Korea and* [2]*Department of Food and Medicine, International University of Korea, Jinju, Republic of Korea.*

Platycodon grandiflorum root-derived saponins (Changkil saponins, CKS) have many biological and pharmacological effects, including anti-inflammatory, anti-oxidative, and ant-obesity effects, but its influence on contacted allergens-induced atopic dermatitis (AD) remains unclear. The consequences of precipitously rising allergic skin inflammation rates worldwide have accelerated the risk of AD. AD is a major health problem all age in globally. This study investigated the inhibitory effect of CKS on AD-like skin lesions in mice and the possible mechanisms in cells. DNCB treatment for 9 weeks led to marked AD-like skin lesions as assessed by AD severity, ear thickness, serum level, and histopathological examination in mice. DNCB-induced AD severity, serum level of IgE and TARC, and mRNA expression of TARC, TNF-alpha, IFN-gamma, IL-4, IL-5, and IL-13 attenuated by CKS treatment in NC/Nga mice. Histopathological examination showed that DNCB-induced thickness of the epidermis/dermis and dermal infiltration of inflammatory cells and mast cells reduced by CKS treatment in the ear lesions. Also, CKS suppressed TNF-alpha/IFN-gamma-induced TARC expression in HaCaT cells. CKS inhibited TNF-alpha/IFN-gamma-induced NF-kB activation as well as STAT1 activation. Furthermore, CKS increased Nrf2/ARE-mediated HO-1 expression. These results indicate that CKS suppressed DNCB-induced AD-like skin lesions by regulating cytokine mediators in NC/Nga mice and TNF-alpha/IFN-gamma-induced TARC expression through the suppression of NF-kB and STAT1 and induction of Nrf2/ARE-mediated HO-1 expression in HaCaT cells, which may be an effective alternative therapy for AD-like skin symptoms.

PS 800 Inhibitory Effects of *Platycodon grandiflorum* Root-Derived Saponins on High-Fat Diet-Induced Nonalcoholic Steatohepatitis in Rat

Y. Chung[2], S. Jin[1] and H. Jeong[1]. [1]*Pharmacy, Chungnam National University, Daejeon, Republic of Korea and* [2]*Department of Food and Medicine, International University of Korea, Jinju, Republic of Korea.*

Platycodon grandiflorum root-derived saponins (Changkil saponins, CKS) have many biological and pharmacological effects, including anti-inflammatory, anti-oxidative, and ant-obesity effects, but its influence on obesity-induced nonalcoholic steatohepatitis (NASH) unclear. NASH is regarded as the hepatic manifestation of the metabolic syndrome, which correlates with the existence of an inflammatory response, also known as metabolic-triggered inflammation secondary to high intake of fats and carbohydrates. This study investigated the inhibitory effects of CKS on high fat diet (HFD)-induced NASH in rat. HFD fed with 8 weeks led to mark NASH as assessed by serum biochemistry, histopathological examination, lipid peroxidation, and collagen content. CKS suppressed HFD-increased body and liver weights. CKS attenuated HFD-induced serum alanine aminotransferase (ALT) and aspartate aminotransferase (AST) activities and hepatic malondialdehyde (MDA) level. Histopathological examination showed that CKS attenuated severe hepatic damage and collagen deposition. Also, HFD-induced hepatic collagen content attenuated by CKS treatment. HFD-induced fibrosis-related expression of matrix

metalloproteinase-13 (MMP-13), tissue inhibitor of metalloproteinase-1 (TIMP-1), tumor necrosis factor-alpha (TNF-a), alpha-smooth muscle actin (SMA), and collagen type I inhibited by CKS treatment. Moreover, CKS inhibited HFD-induced cyclooxygenase-2 (COX-2) protein expression, NF-kB p65 nuclear translocation, and IkBalpha degradation. These results indicated that CKS manifests hepatocellular protective action and ameliorative effects against chronic liver injury and developing NASH induced by HFD treatment.

PS 801 Inhibitory Effects of *Platycodon grandiflorum* Root-Derived Saponins on Ovalbumin-Induced Airway Hyper-Responsiveness in Mice

Y. Lee[2], J. Choi[1], S. Jin[1], H. Kim[1], Y. Chung[3] and H. Jeong[1]. [1]*Pharmacy, Chungnam National University, Daejeon, Republic of Korea,* [2]*Jangsaeng Doraji Research Institute of Biotechnology, Jangsaeng Doraji Co., Ltd., Jinju, Republic of Korea and* [3]*Department of Food and Medicine, International University of Korea, Jinju, Republic of Korea.*

Platycodon grandiflorum root-derived saponins (Changkil saponins, CKS) have many biological and pharmacological effects, including anti-inflammatory, anti-oxidative, and ant-obesity effects, but its influence on inhaled allergens-induced airway hyperresponsiveness remains unclear. Allergic asthma is a chronic respiratory disease caused by inappropriate responses to inhaled allergens and is characterized by reversible obstruction of airway hyperresponsiveness, infiltration of inflammatory cells, mucus overproduction, and the overexpression of inflammatory cytokines and chemokines. This study investigated the inhibitory effects of CKS on ovalbumin (OVA)-induced airway inflammation in mice and PMA-induced MUC5AC expression in A549 cells. Mice were sensitized and challenged with OVA developed inflammation and remodeling in airway. The inhibitory effect of CKS on OVA-induced airway inflammation was evaluated by number of total and differential leukocytes, level of IgE, MCP-1 chemokine, and cytokines, and histopathological study. CKS attenuated OVA-induced number of total cells, eosinophils, basophils, lymphocytes, and macrophages, level of TNF-alpha, IFN-gamma, IL-4, IL-5, IL-13, MCP-1, and IgE in bronchoalveolar lavage (BAL) fluid. CKS suppressed OVA-increased mRNA expression of MMP-2/9 and MUC5AC in mice. Additionally, CKS attenuated airway hyperresponsiveness, inflammatory cells and goblet cells hyperplasia in lung tissue. CKS blocked NF-kB p65 nuclear translocation from lung tissues of OVA-sensitized/challenged mice. Furthermore, CKS suppressed PMA-induced MUC5AC mRNA expression and luciferase activity in cells. These results indicate that CKS suppressed the development of the airway inflammation-like symptoms and MUC5AC expression by suppressing of NF-kB activation in mice, and so may be a useful tool in the therapy of airway inflammation-like symptoms.

PS 802 Inhibitory Effects of *Platycodon grandiflorum* Root-Derived Saponins on Estrogen Deficiency-Induced Osteoporosis in Mice

H. Jeong[1], J. Choi[1], B. Park[1], K. Lee[2] and Y. Chung[3]. [1]*Pharmacy, Chungnam National University, Daejeon, Republic of Korea,* [2]*College of Pharmacy, Chonnam National University, Gwangju, Republic of Korea and* [3]*Department of Food and Medicine, International University of Korea, Jinju, Republic of Korea.*

Platycodon grandiflorum root-derived saponins (Changkil saponins, CKS) have many biological and pharmacological effects, including anti-inflammatory, anti-oxidative, and ant-obesity effects, but its influence on estrogen deficiency-induced osteoporosis remains unclear. Osteoporosis is a reduction in bone mass and the micro-architectural weakening of bone tissue, with a resultant increase in bone fragility and vulnerability to fractures. Osteoporosis is a major health problem in postmenopausal and aged women in the world. This study investigated the inhibitory effect of CKS on osteoporosis induced by ovariectomy (OVX) in mice. OVX animal model has been widely used to evaluation for postmenopausal osteoporosis with estrogen insufficiency. The inhibitory effect of CKS on OVX-induced osteoporosis was evaluated by body weight, plasma parameters, and micro-computed tomography for bone turnover in mice. After 4 weeks of recovery from surgery, the OVX mice were randomly divided into three groups and orally treated with saline or CKS for 3 weeks. CKS attenuated OVX-induced body weight. CKS improved OVX-reduced plasma levels of alkaline phosphatase, phosphorus, and calcium. Also, CKS restored the bone deterioration of trabecular microarchitecture. These results indicate that CKS attenuate OVX-induced bone turnover and lower the risk of osteoporosis.

PS 803 Toxicological Evaluation of Methanol Leaf Extract of *Alchornea cordifolia*

T. O. Ajibade and F. O. Olayemi. *Department of Veterinary Physiology, Biochemistry and Pharmacology, University of Ibadan, Nigeria, University of Ibadan, Nigeria, Ibadan, Oyo, Nigeria.*

Alchornea cordifolia is commonly used as a medicinal plant and widely distributed throughout Africa including Nigeria and Democratic Republic of Congo (DRC). The leaves are traditionally used for the treatment of venereal diseases. Thirty six male Wistar albino rats were randomly divided into six groups of six rats each. The toxic effects of the methanol extract of *Alchornea cordifolia* leaves were investigated on reproductive and hematological parameters of male rats at 0, 100, 200, 400, 800 and 1600 mgkg-1. The Red Blood Cell (RBC) count, packed cell volume (PCV), hemoglobin concentration (Hb) and hematmetric indices except mean corpuscular volume decreased ($p<0.05$) significantly at the 1600 mgkg-1 dose compared to the control. Markers of hepatic damage alanine and aspartate aminotransferases (ALT and AST) and renal damage (Urea and Creatinine) were significantly elevated ($p<0.05$) at 800 and 1600 mgkg-1. Similarly, significant increases were observed in testicular weight, spermatozoa count and motility with concomitant increase in serum testosterone levels in all treatment groups. Severe deleterious effects were not recorded at doses below 400 mgkg-1. However, the leave extract of *Alchornea cordifolia* at 800 and 1600 mgkg-1 has hematotoxic, hepatotoxic and nephrotoxic effects. In conclusion, caution is therefore required for the medicinal usage of this plant because of its potential toxic effects on the liver, kidney and blood cells

PS 804 Elucidation of the Mechanisms of Teratogenicity of Some Commonly Used Medicinal Plants

G. O. Afolayan[1], M. J. Carvan[1], O. Awodele[2] and E. O. Agbaje[2]. [1]*School of Freshwater Sciences, University of Wisconsin-Milwaukee, Milwaukee, WI and* [2]*Department of Pharmacology, University of Lagos, Lagos, Nigeria.*

An array of studies has proven the efficacy of numerous medicinal plants against ailments ranging from pain to microbial infection. However, their teratogenic potentials have not been well elucidated. One such ethnobotanical survey was used to determine the types of medicinal plants used by pregnant women in Lagos, Nigeria. The aim of this study is to determine the possible teratogenic effects on the cardiovascular and nervous systems and the mechanism of teratogenicity of these commonly used medicinal plants.

The aqueous extracts of some of the most commonly used plants (*Enantia chlorantha, Morinda lucida* and *Moringer olifera*) were prepared. Pregnant Wistar rats were treated with several doses (150-600 mg/kg) of these extracts at gestational day six and the litters were examined for any defects at gestational day 20. There was no significant change in the number of litters and their gross morphology. However, there was a significant increase in fetal resorptions, and the overall body weight and crown to rump length of the litters was affected in a dose dependent manner of which the direction is dependent on the plant species. Zebrafish embryos were also exposed to several concentrations (0-1.28 mg/ml) of the extracts between 4-144 hours post-fertilization. A dose dependent effect was observed in the developmental processes of the zebrafish resulting in embryo lethality, skeletal dysmorphogenesis and pericardial edema leading to the formation of a tubular heart. However, there was no significant change in locomotor activity of the eleutheroembryo at six days post-fertilization when there was no overt teratogenicity.

These research findings offer a basis for further investigation of the cellular and molecular mechanisms by which these extracts cause developmental defects in both zebrafish and rat whole embryo culture. These approaches remove the influence of maternal metabolism and other influences, and will provide valuable endpoints for exploration in pregnant mammals and newborns.

PS 805 Effect of α7 Nicotinic Acetylcholine Receptor Agonists and Antagonists on Motor Function in Mice

K. Welch[1], J. A. Pfister[1], F. Lima[2], K. E. Panter[1], B. T. Green[1] and D. R. Gardner[1]. [1]*Poisonous Plant Research Laboratory, USDA-ARS, Logan, UT and* [2]*Federal University of Goias, School of Veterinary Medicine, Goiania, Goias, Brazil.*

Nicotinic acetylcholine receptors (nAChR) are ligand-gated cation channels found throughout the body, and serve to mediate diverse physiological functions. Muscle-type nAChR located in the motor endplate region of muscle fibers play an integral role in muscle contraction and thus motor function. The toxicity and teratogenicity of many plants are due to various toxins that bind to nAChRs including deltaline and methyllycaconitine (MLA) from larkspur (*Delphinium*) species, and nicotine and anabasine from tobacco (*Nicotiana*) species. The primary result of the actions of these alkaloids at nAChRs is neuromuscular paralysis and respiratory failure. The objective of this study was to further characterize the motor coordination deficien-

cies that occur upon exposure to a non-lethal dose of nAChR antagonists MLA and deltaline as well as nAChR agonists nicotine and anabasine. We evaluated the effect of nAChR agonists and antagonists on the motor function and coordination in mice using a balance beam, grip strength meter, rotarod, open field analysis and tremor monitor. These analyses demonstrated that within seconds after treatment the mice had significant loss of motor function and coordination that lasted up to one min, followed by a short period of quiescence. Recovery to normal muscle coordination was rapid, typically within approximately 10 min post-dosing. Additional studies were conducted to determine if the α7 nAChR subunit plays a role in these motor coordination deficiencies by comparing the motor function and coordination in wild-type mice to mice lacking the α7 subunit of the nAChR, after treating them with a non-lethal dose of MLA or anabasine. The results from this study suggest that the α7 nAChR subunit does not play an integral role in the acute effects of MLA or anabasine on motor function/coordination.

PS 806 Toxic Effects of Root Extract of *Cnestis ferruginea* (de Candolle) on the Blood Profiles of Male Rats

F. O. Olayemi. *Veterinary Physiology, Biochemistry and Pharmacology, University of Ibadan, Ibadan, Nigeria.* Sponsor: A. Adedapo.

Cnestis ferruginea belongs to the family *Connaraceae* and it possesses antibiotic activities. It has alkaloid as its main bioactive constituent and our preliminary investigation revealed that it has antifertility property. The toxic effects of methanolic root extract of *Cnestis ferruginea* on the blood profiles were studied in male albino rats. The rats were treated with daily oral administration of 500mg kg-1bw of *Cnestis ferruginea* for 5, 30 and 60 days. The erythrocyte values (red blood cell (RBC), packed cell volume (PCV), haemoglobin (Hb), mean corpuscular haemoglobin (MCH), mean corpuscular haemoglobin concentration (MCHC) and mean corpuscular volume (MCV) and leucocyte values (total white blood cell (WBC), lymphocyte, eosinophil and monocyte counts) and plasma concentrations of aspartate aminotranferase (AST) and alanine aminotranferase (ALT) were not affected by the extract after the 5days treatment period. However, there were significant reductions in the values of RBC ($P<0.001$) and PCV ($P<0.02$) on the 60th day of treatment. The values of Hb and MCV were not affected while those of MCH and MCHC were increased ($P<0.001$) after 60 days of treatment. Furthermore, the total WBC, neutrophil, eosinophil and monocyte counts were not affected by prolonged treatment. The plasma level of AST was not affected by prolonged treatment, but the plasma levels of ALT increased ($P<0.01$) on the 60th day of treatment. In the recovery experiment, the values of PCV, MCH, MCHC and plasma ALT were also restored to the pre-treatment values. This study revealed that prolonged administration of the crude root extract of *Cnestis ferruginea* may induce anaemia.

PS 807 Acute and Subchronic Oral Toxicity Studies of Stem Bark Extract of *Syzygium guineense* (Myrtaceae) in Rats

O. A. Salawu[1], M. Hafeez[2] and A. Y. Tijani[1]. [1]*Pharmacology and Toxicology, National Institute for Pharmaceutical Research and Development (NIPRD), Abuja, Nigeria and* [2]*Pharmacology and Therapeutics, Ahmadu Bello University, Zaria, Nigeria.*

Introduction/Objective: *Syzygium guineense*, widely used in African Traditional Medicine, has been evaluated for its effect on diabetes mellitus, Herpes zoster in combination with other medicinal plants, malaria, bacterial infections, diarrhoea and hypertension. To confirm its safe use, the present study evaluated the potential toxicity of a methanol extract of *S. guineense* stem bark after acute and subchronic administration in Wistar rats.
Materials and Methods: The oral acute toxicity of the extract was studied using the modified Lorke's method, and the rats were then monitored for 14 days. In the subchronic toxicity study, the extract was administered orally to groups of rats (6 rats/dose/sex) at doses of 250, 500 and 1000 mg/kg/day for 90 consecutive days. Measurements included clinical observations, water and food consumption, body weight, haematology, blood chemistry, urinalysis, gross necropsy, organ weight and histopathology.
Results: There was no mortality or signs of acute or subchronic toxicity. There was no significant difference in body weight, relative organ weight or haematological, liver function monitoring parameters, urea, creatinin and electrolytes at 42 and 90 days respectively in the subchronic toxicity study. No abnormality of internal organs was observed in both gross and histopathological examinations between treatment and control groups.
Conclusion: These results suggest that the lethal oral dose of the stem bark extract of *Syzygium guineense* is more than 5000 mg/kg in both male and female rats and the no-observed-adverse-effect level (NOAEL) of the extract for both male and female rats is considered to be 1000 mg/kg per day for 90 days.

PS 808 Enzymic and Nonenzymic Antioxidant Status in Wistar Rats Administered Aqueous Leaf Extract of *Morinda morindoides*

D. I. Akinloye[1], E. A. Balogun[4, 1], T. O. Sunmonu[2] and S. O. Omotainse[3]. [1]*Biochem., Fed. Univ. of Agric., Abeokuta, Ogun, Nigeria,* [2]*Biolog. Sci., Al-Hikman Univ., Ilorin, Kwara, Nigeria,* [3]*Vet. Patholgy, Fed. Univ. of Agric., Abeokuta, Ogun, Nigeria and* [4]*Biochem., Univ. of Ilorin, Ilorin, Kwara, Nigeria.*

Morinda morindoides is a medicinal plant in some African countries where its leaves are used for treating malaria. Information on biochemical changes induced following oral administration of this plant is scarce in the literature. Hence, this study was designed to investigate the enzymic and non-enzymic antioxidant status in Wistar rats administered aqueous leaf extract of *M. morindoides* using activities of catalase (CAT), glutathione peroxidase (GPX), glutathione reductase (GSH.RD), superoxide dismutase (SOD), glutathione-S-transferase (GST), gamma glutamyl transferase (GGT) and levels of reduced glutathione (GSH), total-thiol (T.SH), vitamin C and E as indices. *In vitro* antioxidant activity of the extract and its *in vivo* effects on malondialdehyde (MDA) concentration and histology of liver and kidney were also investigated. Thirty rats grouped into five (A, B, C, D, and E) were used for the study. Group A served as control and was administered distilled water while groups B, C, D and E were given 100, 200, 400 and 800 mg/Kg body wt of the extract for 28 days. Phytochemical analysis revealed that the plant is rich in phenolic and flavonoid compounds. Plasma vitamins C and E, T.SH and GSH were significantly ($P<0.05$) increased while a significant ($p<0.05$) reduction in plasma concentration of MDA and activities of erythrocytes GPX, GSH.RD as well as liver activities of SOD and CAT occured when compared with control. These are indications of antioxidant property of *M. morindoides*. The extract showed significant scavenging effects on hydrogen peroxide, nitric oxide, ABTS radical cation and DPPH radical. Histological investigations revealed mild vacuolar degeneration of hepatocytes and moderate tubular degeneration of the kidney. These findings indicate that *M. morindoides* possesses *in vivo* and *in vitro* antioxidant activities but may be slightly injurious to the tissues studied.

PS 809 The Antioxidant, Anti-Inflammatory, and Antinociceptive Activities of the Ethanol Leaf Extract of *Andrographis paniculata Nees* (Family *Acanthaceae*)

A. A. Adedapo[1], B. O. Adeoye[1], A. A. Oyagbemi[1] and M. O. Sofidiya[2, 1]. [1]*Veterinary Physiology, Biochemistry and Pharmacology, University of Ibadan, Ibadan, Oyo, Nigeria and* [2]*Pharmacognosy, University of Lagos, Lagos, Lagos, Nigeria.*

Introduction
Andrographis paniculata Nees commonly known as king of bitters is well-known medicinal properties (Sandberg 1994, Samir & Amrit 2002, Adedapo et al 2009). This study is to evaluate the medicinal property of this plant obtained in the wild in Nigeria.
Materials and Methods
Ethanol extract (EE) was prepared by dried ground leaf material (200g) in absolute 1 L ethanol for 48 h, filtered, dried and then used for the pharmacological investigations. Standard phytochemical methods were used to test for the presence of phytoactive compounds in the plant. Acute toxicity was carried out in mice to determine safe doses for this plant extract. Anti-oxidant activities of the plant were assessed using ABTS, DPPH, FRAP and total phenolics test. The anti-inflammatory activities were conducted using carrageenan and histamine-induced tests while antinociceptive activities were carried out using writhes and formalin licking tests.
Results
Acute toxicity test showed that no animals died at the doses even at 1600mg/kg dose. The extract at 50, 100 and 200mg/kg body weight caused a significant reduction in the anti-inflammatory and analgesic activities though not in the same magnitude as indomethacin, the reference drug used in this study. In the case of anti-oxidant activities, the extract caused 82.7% ABTS inhibitory activity i.e. 6.21±0.003 gallic acid equivalent; 76.61% DPPH inhibitory activity (12.91±0.007 ascorbic acid equivalent); 50.37±0.23 (42%) ascorbic acid equivalent for FRAP and 78.56±0.04 (58.43%) gallic acid equivalent for total phenolics.
Conclusion
The results from this study may have validated the traditional basis for the use of *Andrographis paniculata* as medicinal agent. The pharmacological activities noted in this study may be attributed to the presence of flavonoids and other phenolics contained in this plant.

PS 810 Identification of Methylated and Microbial Metabolites of Green Tea Polyphenols in Humans

Y. Wang, L. Tang, K. S. Xue, M. Kang and J. Wang. *University of Georgia, Athens, GA.*

Green tea polyphenols (GTP) are found to protect against many chronic diseases in animal models and human studies. There are four major GTP: EC, ECG, EGC, and EGCG in green tea. They mainly undergo phase 2 metabolism, including glucuronidation, sulfation, and methylation. In addition, there was significant metabolism by gut microflora in the colon. The lack of sufficient information on the biotransformation of GTP has limited our understanding of its possible beneficial health effects. In this study we determined the metabolic fate of GTP in humans with particular emphasis on their methylated forms and microbial metabolites. After feeding 600 mL of green tea (5 g tea leaves), human urine samples were collected for analysis by HPLC with a multi-channel coulometric electrochemical detector (HPLC-ECD) and liquid chromatography-mass spectrometry (LC-MS). The major methylated metabolites appeared in human urine were identified as 4'-O-methyl-(-)-epigallocatechin (4'-Me-EGC), 4''-O-methyl-(-)- epigallocatechin-3-gallate (4''-Me-EGCG) and 4',4''-di-O-methyl-(-)-epigallocatechin-3-gallate (4',4''-DiMe-EGCG). Only trace amounts of 4'-O-methyl-(-)-epigallocatechin-3-gallate (4'-Me-EGCG) were found. These methylated metabolites were mostly in glucuronidated form (50-75%) in human subjects and the renal excretion peaked 4.5-5.5 h after the dose. The cumulative excretion of 4'-Me-EGC, 4''-Me-EGCG, and 4',4''-DiMe-EGCG during a 8 h period ranged from 4 to 100 μg, 15 to 18 ug, and 5.9 to 300 μg, respectively. The amount of 4'-Me-EGC excreted in urine was about 20% of total excreted EGC, and accounted for about 1% of EGC ingested, whereas excreted 4',4''-DiMe-EGCG accounted for about 0.1% of ingested EGCG. Microbial metabolites such as (-)-5-(3',4',5'-trihydroxyphenyl)-γ-valerolactone (M4), (-)-5-(3',4'-dihydroxy- phenyl)-γ-valerolactone (M6), and (-)-5-(3',5'-dihydroxyphenyl)-γ-valerolactone (M6') were also detectable and predominantly in glucuronidated and sulfated forms in the urine. These results will enhance our understanding of protective characteristics of green tea constituents against human diseases.

PS 811 Subchronic Oral Gavage Safety of Beta-Alanine in Rats

D. W. Poage[1], B. Frantz[1], P. Hanlon[2] and H. Ferguson[2]. [1]*MPI Research, Mattawan, MI and* [2]*Abbott Nutrition, Columbus, OH.*

A common amino acid, β-alanine (BA) is frequently used as a nutritional supplement to enhance workout capacity in athletes and delay fatigue; effects potentially attributable to enhanced buffering in muscle resulting from increased carnosine content. The present study in rats was designed to assess the safety of BA exposure over a prolonged period of time.
BA was administered to 8-month old Sprague-Dawley rats at concentrations of 0, 100 and 250 mg/mL via oral gavage twice per day for total daily doses of 0, 2000 and 5000 mg/kg. Deionized water served as the vehicle for BA administration. Ten animals per sex were administered each dose for a total of 13 weeks. Treatment with BA did not reduce body weight or food consumption in either treatment group, and clinical observations were also not indicative of an effect of BA. Safety of BA administration was also evaluated through clinical pathology, gross pathology, organ weights, and tissue histopathology. Preliminary results from this study indicated that twice daily, oral administration of BA at doses of 2000 and 5000 mg/kg/day to rats over a 13-week period did not produce any definitive adverse test article-related effects.

PS 812 Acute and Subacute Toxicity Study of *Zanthoxylum armatum* Leaves in Mice

N. Verma[1] and R. Khosa[2]. [1]*School of Pharmacy & Emerging Sciences, Baddi University of Emerging Sciences & Technology, Baddi, Himachal Pradesh, India and* [2]*School of Pharmacy, Bharat Institute of Technology, Meerut, Uttar Pradesh, India.*
Sponsor: D. Mishra.

The present study was carried to evaluate acute and sub-acute toxicity of ethanolic extract of *Zanthoxylum armatum* (EEZA) in Swiss mice. Taxonomically identified and authenticated leaves of *Z. armatum* (voucher specimen NHCP/NBPGR/2007/99/2225) were extracted with ethyl alcohol (95%). For acute toxicity studies the animals were divided in to one control group and five treated groups. The control group received saline and each treated group received the EEZA in dose of 100, 500, 1000, 2000 and 4000 mg/kg through gastric intubation. The animals were monitored continuously for 3 h and thereafter were kept on observation each hour during a 24 h period to see observe change (if any) in their general behavior or other physiological activities. For subacute toxicity studies the animals were divided in to one control group and four treated groups. The control group received saline and each treated group received the EEZA in dose of 500, 1000, 2000 and 4000 mg/kg through gastric intubation for 15 days (once a day in the morning). At the end of the experiment, blood was collected from the orbital sinus under ether anesthesia for biochemical and hematological analysis. The animals were sacrificed by cervical displacement and selected organs (liver, heart, spleen, left kidney and left lung) were removed for macroscopic analysis. Oral administration of the alcoholic extract of *Z. armatum* in a dose from 100 to 4000 mg/kg did not produce any significant changes in behavior, breathing, cutaneous effects, sensory nervous system responses and gastrointestinal tract effect in mice. In conclusion these results showed that in single dose, there is no adverse effect of *Z. armatum* indicating that the medium lethal dose (LD50) is higher than 4000 mg/kg for both male and female mice. The macroscopic analysis of the target organs of the treated animals (liver, lungs, heart, spleen and left kidney) did not shows any significant changes in colour and texture when compared with control group.

PS 813 Investigation on the Toxicity of *Aconitum brachypodum* Diels *In Vitro* and *In Vivo*

X. Huang, H. Zhou, Y. Jiang and M. Zheng. *South-Central University for Nationalities, Wuhan, China.*

To investigate the toxities of four active extracts from *Aconitum brachypodum* Diels *in vitro* and *in vivo*. LD50 was detected to estimate the toxicity of the extracts after intragastric administration to Kunming mice. The results showed that the extracts from *Aconitum brachypodum* Diels have different degrees of toxic effects on mice. The toxic symptom included reduced activity amount, retching, abdominal breathing, diaphoresis, exorbitism and convulsion. The chloroform extract even lead to fatality of some mice at doses above 25 mg/kg. LD50 of chloroform extract, petroleun benzin extract and n-butanol extract were 38.0 mg/kg, 6766.9 mg/kg and 5492.3 mg/kg respectively. The rank of their toxicity was: chloroform extract > n-butanol extract > petroleun benzin extract. MTT assay was used for Vero cells *in vitro* and different cytotoxicities were also obtained from the four extracts, respectively. The 24 h inhibition rate of chloroform extract, petroleum ether extract, n-butanol extract and ethyl acetate extract at dose of 400 μg/ml on Vero cells were 69.7%, 63.9%, 32.9% and 18.2% respectively. The rank of the cytotoxicity was: chloroform extract > petroleun benzin extract > acetic ether > n-butanol extract. The present study compared the toxic fractions of *Aconitum brachypodum* Diels *in vivo* and *in vitro*.
Acknowledgements: Supported financially by National Natural Science Foundation of China (No: 81102897, 81374064) and Chinese National Project of "Twelfth Five-Year" Plan for Science & Technology Support (2012BAI27B06-2).

PS 813a Toxicity in Mice and Rats Associated with Inhalation of the Flavor and Fragrance Ingredient Alpha-Pinene

C. V. Rider, M. D. Stout and R. A. Herbert. *NTP/NIEHS, Research Triangle Park, NC.*

α-Pinene is the main component in turpentine and is used as a fragrance and flavoring ingredient. Due to widespread exposure potential and a lack of available toxicity data, the National Toxicology Program conducted 2-week and 3-month inhalation studies in male and female F344/N rats and B6C3F1/N mice. In the 2 week studies, groups of 5 male and 5 female rats and mice were exposed to α-pinene by whole body inhalation at concentrations of 0, 100, 200, 400, 800, or 1,600 ppm, 6 hours plus T90 (12 minutes) per day, 5 days per week for 16 (rats) or 17 (mice) days. There was significantly decreased survival in the 800 and 1,600 ppm male and female rats and mice, clinical signs of toxicity in rats (400 ppm and greater) and mice (800 and 1600 ppm), and increased liver weights in both species. In the 3-month studies, groups of 10 male and 10 female rats and mice were exposed to α-pinene at concentrations of 0, 25, 50, 100, 200, or 400 ppm, 6 hours plus T90 (10 minutes) per day, 5 days per week for 14 weeks. All exposed male rats and male and female mice survived to the end of the studies, while six 400 ppm female rats died before the end of the study. The major targets for α-pinene toxicity were the urinary system and the male reproductive system. Increased kidney weights in male (100 ppm and greater) and female (50 and 200 ppm) rats were accompanied by histopathological lesions (i.e., granular casts and hyaline droplet accumulation) in all dosed groups of male rats only. A dose-dependent increase in the incidence of transitional epithelium hyperplasia in the urinary bladders was observed in male (70%, 100%, and 100%) and female (60%, 100%, and 100%) mice exposed to 100, 200, and 400 ppm α-pinene, respectively. Finally, there were significantly decreased numbers of cauda sperm in 200 ppm and above male rats and 100 ppm and above male mice, reaching a maximum 53% decrease in 400 ppm male mice. Based on these toxicity findings, chronic inhalation studies with α-pinene are warranted. This research was supported by the NIH, National Institute of Environmental Health Sciences.

PS 813b Protective Effect of *Andrographis paniculata* against Sodium Arsenite-Induced Clastogenicity and Hepatotoxicity in Wistar Rats

A. M. Adegboyega[1, 2], M. A. Gbadegesin[1] and O. A. Odunola[1]. [1]*Biochemistry, University of Ibadan, Ibadan, Oyo, Nigeria and* [2]*Department of Chemistry, The Polythenic of Ibadan, Ibadan, Oyo, Nigeria.*

Arsenic toxicity has been associated with diverse ailments including cancer in both experimental animals and humans. Hence, the search for agents that can protect/reduce arsenic-induced toxicities. In the present study, the anticlastogenic and hepatoprotective abilities of aqueous leaf extract of *Andrographis paniculata* (Ap) against sodium arsenite (NaAsO2)-induced toxicities were examined in male albino rats. The *in vitro* antioxidant activity of the extract was also determined as compared with standard antioxidants. Test and control rats were exposed to 200, 500 and 1000 mg/Kg body weight of Ap for 28 days. Simultaneously, the animals were treated with 5mg/kg body wt of NaAsO2 on the 7th, 14th, 21st and 28th day of the experiment before they were sacrificed. The frequency of micronucleated polychromatic erythrocytes (mPCEs) as monitored in bone marrow cells while aspartate aminotransferase (AST), alanine aminotransferase (ALT), alkaline phosphatase (ALP) and gamma glutamyl transferase activities were assessed in the serum. NaAsO2 induced significantly ($p<0.05$) mPCEs formation and the activities of all the hepatic enzyme markers. Pre-treatment with Ap significantly ($P<0.05$) reduced levels of serum enzymes and mPCEs close to the levels observed for the negative control. The phytochemical constituents of the extract include alkaloids, flavonoids, tannins and phenols. The aqueous extract of Ap also possess strong antioxidant and reducing capacity, which may be responsible for the anticlastogenic and hepatoprotective effect observed. Our study suggests that aqueous leaf extract of Ap may be useful in the management of arsenic toxicity.

PS 813c Naringenin Attenuates DMH-Induced NF-κB and COX-2 Expression in Rat Colon: Abrogation of Oxidative Stress, Inflammatory Responses and Proinflammatory Cytokine Production

M. U. Rehman[1, 2], A. Farooq[1], A. Arif[2], S. A. Bhat[2], R. Razzaq[2], B. Ahmad[2], M. R. Mir[2] and M. Y. Shah[1]. [1]*Department of Pharmaceutical Sciences, University of Kashmir, Srinagar, J&K, India and* [2]*Veterinary Biochemistry, Faculty of Veterinary Science & Animal Husbandry, SKUAST-Kashmir, Srinagar, J&K, India.* Sponsor: S. Beedanagari.

Purpose: Colon carcinogenesis is a multistep process and it emanates from a series of molecular and histopathological alterations. Naringenin is a natural occurring flavonoid abundantly found in grapes. It has several pharmacological and biological properties such as anti-inflammatory, immunomodulatory and anti-cancer. In the present study, we investigated the chemopreventive potential of Naringenin against 1,2-dimethyhydrazine (DMH)-induced colon toxicity and its role in regulating the inflammation in the colon of Wistar rats.
Methods: Animals were divided into 5 groups. In group III, IV and V, Narigenin was administered once daily for 14 consecutive days at the doses of 40, 80 and 80 mg/kg b.wt. respectively. On day 7, a single injection of DMH was given subcutaneously in the groin at the dose of 40 mg/kg body weight. Animals were euthanized on day 15
Results: Naringenin supplementation suppressed the oxidative insult and inflammatory burst and suppressed the immunostaining of, NF-kB-p65, COX-2, and iNOS. Narigenin treatment significantly attenuated the level of TNF-α and IL-6. Pretreatment with Naringenin significantly reduced the severity of submucosal edema, regional destruction of the mucosal layer and intense infiltration of the inflammatory cells in mucosal and submucosal layers of the colon.
Conclusion: The data of the present study suggest that Naringenin effectively suppress DMH induced colonic mucosal damage by ameliorating oxidative stress and inflammatory. Further studies are warranted to elucidate the precise mechanism of action of Naringenin.

PS 813d Green Tea Epigallocatechin Gallate Binds to and Inhibits Respiratory Complexes in Swelling but Not Normal Rat Hepatic Mitochondria

Z. Weng[1], P. Zhou[1], W. F. Salminen[1, 2], X. Yang[1], A. H. Harrill[3], D. L. Mendrick[1], W. B. Mattes[4] and Q. Shi[1]. [1]*Division of Systems Biology, US FDA, NCTR, Jefferson, AR,* [2]*PAREXEL International, Sarasota, FL,* [3]*Department of Occupational and Environmental Health, University of Arkansas for Medical Sciences, Little Rock, AR and* [4]*PharmPoint Consulting, Poolesville, MD.*

Epigallocatechin gallate (EGCG), the major flavonoid in green tea, has been associated with cases of hepatotoxicity in humans and animals. Here the EGCG effect on rat liver mitochondria was examined as a useful model of xenobiotic hepatotoxicity. Though EGCG showed negligible effects on oxidative phosphorylation at 7.5-100 μM in normal mitochondria, respiratory chain complexes (RCCs) were profoundly inhibited in mitochondria undergoing calcium overload-induced mitochondrial permeability transition (MPT). As RCCs are located in mitochondrial inner membranes (IM) and matrix, it was reasoned that EGCG could not readily pass through IM to affect RCCs in normal mitochondria but may do so when IM integrity is compromised. This speculation was substantiated in three ways. (1) Purified EGCG-bound proteins were barely detectable in normal mitochondria and contained no RCCs as determined by Western blotting, but swelling mitochondria contained about 1.5-fold more EGCG-bound proteins which included four RCC subunits together with cyclophilin D that locates in mitochondrial matrix. (2) Swelling mitochondria consumed more EGCG than normal ones as determined by HPLC. (3) MPT blocker cyclosporine A diminished the above-mentioned difference. Among four subunits of RCC II, only SDHA and SDHB that locate in mitochondrial matrix, but not SDHC or SDHD which insert into the IM, were found to be EGCG targets. Interestingly, EGCG promoted calcium overload-induced MPT only when moderate MPT already commenced. The data suggest EGCG could be detrimental in MPT-associated diseases and toxicities by causing synergistic or additional mitochondrial damages.

PS 814 Computational and Experimental Deconvolution of the Role of Silver Nanoparticles and Ions on Macrophage Cellular Toxicity *In Vitro*

J. G. Teeguarden[1, 2], P. Munusamy[1], D. Thomas[1], J. N. Smith[1], V. K. Kodali[1], H. Shankaran[1], H. D. Jolley[1], P. Demokritou[3], J. Cohen[3], D. R. Baer[1] and B. D. Thrall[1]. [1]*Systems Toxicology and Exposure Science, Pacific Northwest National Laboratory, Richland, WA,* [2]*Environmental and Molecular Toxicology, Oregon State University, Corvallis, OR and* [3]*Center for Nanotechnology and Nanotoxicology, Harvard School of Public Health, Cambridge, MA.*

Nanoscale silver is a member of a broader class of soluble metal nanoparticles that cause co-exposure to both solubilized ions and nanoparticles in cell culture and in vivo test systems. The presence of two forms of silver, the changing nature of particles and ion/particle concentration dynamics in solution due to dissolution are significant obstacles assessing the role of particle characteristics on toxicity. We have developed a conceptual model and from it, a computational model of the processes influencing silver nanoparticle dissolution, and the uptake of both ions and nanoparticles by cells in common in vitro systems (ISDD-D). The dissolution of 20 nm and 110 nm silver nanoparticles at 1-50 μg/ml was monitored over time in RPMI media with 10% FBS by ICPMS. The asymptotic silver ion concentration (~2.7 μg/ml) was well described by equations relating the kinetics of silver dissolution to particle concentration, surface area and a solubility product (ksp). Dissolution of silver nanoparticles reduced the primary particle size (agglomerate), affecting particle delivery rates. The kinetics of ion and nanoparticle cellular uptake in murine macrophages were characterized independently, and used to calibrate the ISDD-D kinetic model. ISDD-D was applied toxicity studies to deconvolute the role of silver ions and silver nanoparticles on toxicity during exposure to dissolving 20 and 110 nm particles. Silver ions alone were more toxic EC50 (2 μg/ml) than silver nanoparticles (EC50 40 μg/ml). Using ISDD-D to devonvolute the role of ions and particles, we found that silver content in cells was dominated by material in nanoparticle form, strongly suggesting that ionic silver drives the toxicity of silver nanoparticles in vitro.

PS 815 Physiologically Based Pharmacokinetic Modeling of Cerium Oxide Nanoparticles by Pulmonary Exposure in Rats

D. Li[1], J. Barres[1], U. Carlander[2], E. Eagle[3], C. Emond[4], G. Johanson[2], M. Morishita[1], J. G. Wagner[5], M. Wooldridge[3] and O. Jolliet[1]. *[1]Environmental Health Science, University of Michigan, Ann Arbor, MI, [2]Environmental Medicine, Karolinska Institutet, Stockholm, Stockholm, Sweden, [3]Mechanical Engineering, University of Michigan, Ann Arbor, MI, [4]BioSimulation Consulting Inc, Newark, DE and [5]Center for Integrative Toxicology, Michigan State University, East Lansing, MI.*

In vitro studies have reported toxic effects of cerium oxide nanoparticles (CeO_2 NPs) which can be used as a diesel fuel additive, thus it is important to understand the biodistribution of CeO_2 NPs in the body via plumonary exposure. The aim of this study was to measure this biodistribution and to develop a physiologically based pharmacokinetic model of CeO_2 NPs in rats. Our model has 10 compartments (blood, lungs, gastrointestinal tract, liver, kidney, lungs, heart, brain, spleen, and rest of the body) interconnected via the blood circulation. Each compartment includes phagocytizing cells which may take up NPs in a saturable manner. We therefore exposed Sprague-Dawley rats by nose-only exposure to 3.5mg/m^3 CeO_2 NPs (~80nm) for 5 hours and measured concentrations in different organs over 14 days. These results were then compared to the organs concentrations after intratracheal delivery of 200µg CeO_2 NPs (~6.6nm) over 28 days measured by He et al. (2010). High concentrations of CeO_2 NPs were found in the lungs and feces: about 2mg/g and 12mg/g of NPs were found respectively in the lungs and feces 1 day post inhalation exposure. Concentrations in other organs were 3-4 orders of magnitude lower at this time. By comparison, the intratracheal instillation study had similar tendencies in the concentrations among organs but captured a higher fraction of the total administrated NPs in the lungs compared to the nasal exposure study (78% versus 4%). The simulated time courses of NPs biodistribution agreed well with experimental data, yielding R^2 of 0.73 for the inhalation exposure study and 0.95 for the intratracheal instillation study. Further investigations are ongoing to study the sensitivity of the model parameters and to support the most critical parameters.

PS 816 Comparative Analysis of Predictive Models Used to Identify Drivers of Nanomaterial Toxicity

B. Harper[1], R. Liu[2], Y. Cohen[2] and S. L. Harper[1, 3]. *[1]Environmental and Molecular Toxicology, Oregon State University, Corvallis, OR, [2]Center for Environmental Implications of Nanotechnology, University of California, Los Angeles, Los Angeles, CA and [3]School of Chemical, Biological and Environmental Engineering, Oregon State University, Corvallis, OR.*

Understanding the inherent and conditional factors associated with nanomaterial toxicity is critical to the development nanotechnologies that pose minimal threats to humans and the environment over the life cycle of the nanomaterial. We compared the results of several different models built to predict toxicity from the open-source data on nanomaterial toxicity to embryonic zebrafish (*Danio rerio*) found in the Nanomaterial-Biological Interactions (NBI) knowledgebase at Oregon State University. Model comparisons included the ABMiner predictive models, MATLAB clustering analysis and the use of Self-Organizing Map (SOM) based consensus clustering conducted on the data in the NBI knowledgebase (nbi.oregonstate.edu). Overall results suggest that exposure concentration and outermost surface chemistry (and thus surface charge) both should be considered in conjunction with the core composition of nanomaterials when trying to develop predictive models for developing zebrafish. Core composition was found to be a significant contributor to the ABMinor predictive model. MATLAB clustering grouped materials into two clusters with outermost surface chemistry being the primary determinant. The SOM modeling identified five significant clusters (clustering index = 0.89); while no core materials occurred in all 5 clusters, 4 material types (based on core composition) occurred in 4/5 clusters and 15 material types occurred in 3/5 clusters. In addition, over half of the materials appeared in multiple clusters depending on the dose applied. Thus, classification of nanomaterials by simple descriptors such as core composition may not be sufficient for predicting nanomaterial toxicity or managing nanomaterial risks.

PS 817 Development and Validation of a Dosimetric Platform for *In Vitro* Nanotoxicology

J. Cohen and P. Demokritou. *Harvard School of Public Health, Boston, MA.* Sponsor: J. Brain.

There is a great need for developing screening tools capable of rapidly and accurately assessing engineered nanomaterial (ENM) toxicity. One impediment to the development of reliable in vitro screening methods is the need for accurate dosimetry. In a typical in vitro cytotoxicity study ENM powders are suspended in liquid media for application to cells. ENMs in liquid suspension can form large fractal agglomerates thereby altering (1) the total number of free particles, (2) the total surface area available for biointeractions, and (3) the effective size and density of the particles, two properties that influence their fate and transport and determine the effective dose actually delivered to cells in culture over the duration of exposure. We present here a methodology for in vitro nanotoxicology that takes into consideration particokinetics and enables accurate determination and reporting of effective dosimetry. This multi-step methodology includes: (1) standardization of ENM liquid suspension preparation; (2) careful characterization of critical ENM transformations in exposure media; and (3) numeric calculation of the delivered to cell dose as a function of exposure time.
The described methodology was then used to derive simple mathematical equations called Relevant In Vitro Dose (RID)f functions for an extensive panel of nano metal and metal oxide ENMs. The RID functions can be used by nanotoxicologists to accurately calculate the particle mass (RIDM), particle surface area (RIDSA), or particle number (RIDN) delivered to cells dose as a function of exposure time, or to perform meta analyses on previously reported toxicity datasets taking dosimetry into consideration.

PS 818 A Pharmacokinetic Modeling Framework for Interspecies Extrapolations of Nanoparticle Biodistribution Taking into Account Biocorona Dynamics Independent of Species-Specific Disposition Processes

J. E. Riviere[1, 2], F. D. Sahneh[1], C. Scoglio[1, 2] and N. A. Monteiro-Riviere[2]. *[1]Institute of Computational Comparative Medicine, Kansas State University, Manhattan, KS and [2]Nanotechnology Innovation Center of Kansas State, Kansas State University, Manhattan, KS.*

Formation of a corona complex around engineered nanoparticles (NP) dramatically alters their biodistribution. A common practice in nanotoxicology and nanomedicine is to extrapolate results from in vitro cell culture or in vivo rodent models to humans. There are concerns about the reliability of these approaches: one being whether the fate of NP in rodent models with high basal metabolic rates (BMR) and short blood circulation times can predict the fate of the NP in large mammals that have a lower metabolic rate and a greater circulation time? The interaction of two major processes determines the NP biodistribution: delivery to target cells with an allometrically scalable rate across species and an independent process of NP corona formation. Long circulation times in humans allows for the formation of a mature hard corona complex potentially masking the NP originally engineered purpose with specific surfaces for target cell receptors. A simple and descriptive compartmental model is proposed to compare the potential fate of NP in rodent models versus humans by allometrically scaling those components dependent upon BMR and separately describing the dynamic of protein corona formation using normal time scales. Our model shows while engineered NP can successfully reach the target cells in rodent models the results may be different for humans due to the available time for further biocorona evolution. We propose a framework model for proper development of interspecies extrapolation of NP biodistribution incorporating mixed effects of interspecies allometric scaling coupled to the dynamics of corona formation. This model also serves as a tool to allow NP protein corona dynamic data generated in vitro to be extrapolated to different animal species and humans in vivo.

PS 819 Understanding the Dynamic Behavior of the Protein Corona and Its Influence on the Physicochemical Composition of Silver Nanoparticles

A. Sasidharan[1], R. Chen[1, 2], S. Oldenburg[3], J. E. Riviere[1, 2] and N. A. Monteiro-Riviere[1]. *[1]Nanotechnology Innovation Center of Kansas State, Kansas State University, Manhattan, KS, [2]Institute of Computational Comparative Medicine, Kansas State University, Manhattan, KS and [3]nanoComposix, Inc, San Diego, CA.*

The health effects and safety of nanoparticles (NP) are of a great concern due to their increasing availability and use in consumer products and biomedical applications. It has been established that NP tend to interact with proteins to form a protein corona upon entering biological fluids. The dynamic interactions of the protein corona with NP may significantly influence the bio-identity of NP, leading to diverse biological outcomes, especially at the cellular level. Since NP-protein interactions are poorly understood, a fundamental understanding of the complexity and dynamic interactions of the protein corona with NP is crucial. A systematic investigation on time dependent adsorption kinetics of the protein corona formation was conducted with citrate or lipoic acid coated silver NP (AgNP) of 40nm. AgNP were exposed to human serum albumin (HSA) and fibrinogen at their in vivo physiological concentrations. Dynamic light scattering, zeta potential, NP tracking analysis and transmission electron microscopy were used to monitor kinetics of the

AgNP protein corona formation. Data on time evolution revealed that irrespective of the surface chemistry, rapid and prominent binding of HSA at 40mg/ml formed coronas with both citrate and lipoic acid coated AgNP and caused an increase in size to 60nm which was stable. In contrast, AgNP in fibrinogen at 2mg/mL showed a time dependent decrease in stability with aggregation within 1 to 4h with a significant reduction in NP concentration and size (24.8nm) over 12h at 37°C. These results showed that the corona proteins at their physiological concentrations interacted rather differently with AgNP; whereby HSA prevented NP dissolution and aggregation, while fibrinogen caused a significant size reduction and aggregation.

PS 820 Toxicity Assessment of Six Titanium Dioxide Nanoparticles in Human Epidermal Keratinocytes

N. A. Monteiro-Riviere[1], L. W. Zhang[1] and B. Veronesi[2]. [1]*Nanotechnology Innovation Center of Kansas State, Kansas State University, Manhattan, KS and* [2]*United States Environmental Protection Agency, Research Triangle Park, NC.*

Nanoparticle uptake in cells may be an important determinant of their potential cytotoxic and inflammatory effects. Six TiO_2 NP (A=Alfa Aesar, 10nm, A*= Alfa Aesar, 32nm, B=P25, 27.5nm, C=Acros, 200nm, C*= NanoAmor, 30-40nm, and D*=Mkano 200-400nm) and controls were assessed for their size, effect on cell viability, agglomeration, cytokine release, and cellular uptake in human epidermal keratinocytes (HEK). TiO_2 NP were suspended in water or in culture medium, and characterized by transmission electron microcopy (TEM) and dynamic light scattering (DLS). TiO_2 NP did not change shape with any NP type in medium by TEM but DLS showed an increase in size and in agglomerations. TiO_2 NP were assessed for viability with CellTiter 96® AQueous One (96AQ), MTT and alamar Blue (aB) assays. All NP interfered with 96AQ and MTT but aB was minimal. Therefore, aB assay was selected to assess all NP in serial dilutions ranging from 0.0125 to 0.4mg/ml for 24h. Only TiO_2 sample B had a statistically significant decrease in aB viability at 0.4mg/ml. Also, interleukin (IL)-1β, IL-6, IL-8, IL-10, and TNF-α were evaluated and slight increases were noted in samples A, A*, C, D* at medium or high concentrations, while A* and B showed an increase in IL-6. IL-10 and IL-1β release was noted for all NP but was at or below the detection limit. A significant decrease in IL-8 was noted for all NP at the highest concentrations which demonstrates assay interference except for sample C. All NP were localized within the intracellular cytoplasmic vacuoles of HEK and the element titanium (Ti) was detected and confirmed by energy-dispersive x-ray spectroscopy (EDX). In conclusion, based on cell viability only sample B was slightly cytotoxic to HEK and samples B and A* have the potential to cause inflammation indicated by an increase in IL-6. (Supported by USEPA)

PS 821 Characterization of a Complex Protein Corona on Silver Nanoparticles and Its Influence on Cellular Interactions

J. Shannahan[1], F. A. Witzmann[2] and J. M. Brown[1]. [1]*University of Colorado, Aurora, CO and* [2]*Indiana University, Indianapolis, IN.*

Silver nanoparticles (AgNP) have been incorporated in biomedical and consumer products as antimicrobial agents. Upon introduction into physiological environments NPs associate proteins forming a protein corona (PC). The PC alters the NP-cell interface resulting in modified uptake, activity, clearance, and toxicity. Here we characterized the formation of a complex PC (consisting of multiple proteins) on AgNPs and examined its alterations in cellular interactions. To characterize the formation of the PC, PVP- or citrate-suspended AgNPs of 20 or 110 nm were incubated in DMEM containing 10% FBS. PC formation was indicated by alterations in the hyperspectal image of AgNPs such as a broadening of peaks and a red shift in the spectra. Spectral profiles were altered due to the size and surface coating of the AgNPs suggesting dissimilar PC formation. Individual PC components were identified and quantified via label-free mass spectroscopy. All AgNPs associated unique complex PCs that included different amounts of a common subset of 11 proteins including albumin and certain apolipoproteins. 110 nm AgNPs were found to associate the greatest number of proteins compared to 20 nm AgNPs, suggesting differences in PC formation based on surface curvature, whereas the PC on 20 nm AgNPs consisted of more hydrophobic proteins. These findings demonstrate the significance of electrostatic and hydrophobic interactions in the formation of the PC. To assess how the PC influences cellular interactions, macrophages were exposed to AgNPs (25 μg/ml) coated with a complex PC and differences in uptake were analyzed by hyperspectral dark field microscopy and flow cytometry. Addition of the PC was observed to increase uptake for all AgNPs (110 nm > 20 nm) by flow cytometry. By using spectral libraries we were able to intracellularly observe AgNPs and qualitatively determine differences in uptake by image analysis. These findings demonstrate the influence of variations in NP size and surface coatings, on the formation of the PC and modifications of cellular interactions.

PS 822 Metabolic Behavior and Effects of Ion and Nanoparticle Forms of Silver in the Mouse Lung and Macrophages

T. Miyayama[1, 2], Y. Arai[3] and S. Hirano[2, 3]. [1]*Hygiene and Public Health I, School of Medicine, Tokyo Women's Medical University, Shinjyuku-ku, Tokyo, Japan,* [2]*Environmental Nanotoxicology Project, National Institute for Environmental Studies, Tsukuba, Ibaraki, Japan and* [3]*Graduate School of Pharmaceutical Sciences, Chiba University, Chiba, Japan.*

Health effects of silver nanoparticles (AgNPs) have not been well investigated, although AgNPs are now widely used in consumer products. We have investigated metabolic behavior and inflammatory responses of intratracheally instilled AgNPs and silver nitrate ($AgNO_3$) in the mouse lungs. Male ICR mice were administered with AgNPs or $AgNO_3$ at a dose of 10μg Ag per animal. Contents of Ag in lungs of the AgNPs-treated mice were significantly and 4.27 and 4.47 times higher than those of the $AgNO_3$-treated mice at 4 and 24 h post administration, respectively. In the $AgNO_3$-treated mice, Ag concentration in the lungs was not changed between 4 and 24 h. To evaluate neutrophil and pro-inflammatory cytokines after AgNPs or $AgNO_3$ instillation, we performed bronchoalveolar lavage (BAL) to mice. $AgNO_3$ significantly increased numbers of neutrophils at 24 h after instillation. On the other hand, AgNPs slightly increased neutrophil numbers at 24 h. In the BAL fluid (BALF), the concentrations of IL-1β significantly increased 24 h after $AgNO_3$ and AgNPs instillation. We also investigated uptake and intracellular distribution of Ag in vitro exposing mouse macrophage cell cells (J774.1) to either $AgNO_3$ or AgNPs. Ag was located to the insoluble fraction of the cells after exposure to AgNPs in a time dependent manner. Ag bound metallothionein (MT), which was measured by HPLC-ICP-MS, increased up to 3 h in J774.1 cells following exposure to AgNO3. On the other hand, Ag was not distributed to MTs and localized in lysosomes following exposure to AgNPs. These results suggest that AgNPs were first incorporated in lysosomes of macrophages and induced inflammatory stimuli to the cells or tissues. In contrast $AgNO_3$ probably induced inflammatory stimuli first and increased Ag-bound MT levels in the cytosol.

PS 823 Acute and Subchronic Exposure to Inhaled Silver Nanoparticles Results in Alterations in Gene Expression, Gene-Specific Promoter Methylation, and Mitochondrial Integrity

M. A. Popovech, E. L. Saunders, K. Galdanes, J. M. Vaughan, L. Chen and T. Gordon. *Environmental Medicine, New York University School of Medicine, Tuxedo, NY.*

The use of silver nanoparticles (AgNPs) is ubiquitous. Legitimate toxicology concerns exist, and a number of recent studies suggest that AgNPs pose a threat to human health. This study was conducted to examine the effects of acute and subchronic exposure to inhaled AgNPs. Male FVB/NJ mice were exposed to AgNPs generated using a Palas spark generator, via nose only inhalation, at either a single 4 hr exposure of 1 mg/m3, or at an exposure of 0.25 mg/m3 for 30 days. At 24hr, 48hr, and 7d post-exposure, animals were euthanized and blood, lavage and tissue were collected, and fresh mitochondria was isolated within one hour of sacrifice. Lavage was analyzed for total cell counts, differential cell analysis, and protein levels. Fifty-four samples, isolated from lung and liver tissue, were used in Affymetrix Mouse Gene 2.0 ST Array Analysis. Microarrays were analyzed using Agilent GeneSpring and results verified by real-time qPCR. DNA isolated from lung and liver tissue was used in the analysis of gene-specific promoter methylation using Epitect Methyl II arrays. Inner mitochondrial membrane integrity was quantified using JC-1 staining and fluorescence microscopy. Outer mitochondrial membrane integrity was examined by measuring cytochrome c oxidase activity in the presence and absence of n-dodecyl beta-D-maltoside. Highly significant alterations in gene expression were observed in response to both acute and subchronic AgNP exposure, in both lung and liver tissues, in a time dependent manner. In addition, AgNP exposure resulted in significant decreases in both inner and outer mitochondrial membrane integrity. These experiments suggest that exposure to inhaled AgNPs results in gene expression alterations, which may be regulated by alterations in promoter methylation, in a time dependent manner. Further, cellular uptake of inhaled AgNPs, in lung and extra-pulmonary organs results in detrimental effects on mitochondrial membrane integrity.

PS 824 Gene Expression Alterations in the Brain Elicited by Inhalation of Silver Nanoparticles

P. B. Tijerina, M. A. Popovech, K. Galdanes, E. L. Saunders, L. Chen and T. Gordon. *Environmental Medicine, NYUMC, Tuxedo, NY.*

The use of silver nanoparticles (AgNPs) in consumer products has vastly increased due to their antimicrobial activity. However, recent reports suggest the inhalation of AgNPs can lead to neurodegeneration due to translocation via olfactory nerves. Previous studies fail to evaluate biologically relevant exposure routes and concentrations. Therefore, this study evaluated the effects of inhaled AgNPs on gene expression within distinct subregions of the brain under diverse exposure terms. Adult-male FVB/NJ mice were exposed via nasal inhalation to AgNPs produced by a Palas spark generator. Animals were assigned to 3 exposure groups: 1) single exposure (1mg/m3), 2) subacute repeated dose (30d, 0.25mg/m3), or 3) subchronic repeated dose (90d, 0.25mg/m3). Tissue samples were taken at 24hr, 48hr, and 7d post-exposure for the single exposure group, and repeated group animals at 24 hr. Animals were euthanized and brains removed and dissected into three portions: olfactory bulb (OB), cerebellum (CB), and midbrain (MB). Isolated total RNA was analyzed by real-time RT-PCR using various oxidative stress-associated gene primers. Overall a variety of gene expression alterations were found for each neural subregion. Most interesting, the single exposure resulted in gene expression alterations for amyloid beta (A4) precursor protein (APP), which is associated with Alzheimer's, a detrimental neurodegenerative disease. APP upregulation was segregated to the OB, where it remained high 7d post-exposure suggesting possible long-term neurological effects from a single exposure to AgNPs. Conversely, Amyothropic Lateral Sclerosis (ALS) associated gene was only mildly changed in all sub-regions, suggesting a specific mechanism of toxicity. Additionally, oxidative stress related genes were upregulated within the MB and CB at 48 and 72 hr and returned to control levels by 7d post-exposure. Together these results demonstrate that inhalation of AgNPs can result in oxidative stress and gene expression alterations which could contribute to neurotoxicity and potentially neurodegeneration.

PS 825 A Comparative Pulmonary Response: Inflammation, Injury, and Clearance of Silver Nanoparticles in Two Mouse Strains

E. L. Saunders[1], M. A. Popovech[1], T. Gordon[1], L. Chen[1], K. Galdanes[1], S. Chillrud[2] and J. Ross[2]. [1]*Environmental Medicine, New York University, Brooklyn, NY and* [2]*Earth Sciences, Columbia University, Palisades, NY.*

The research presented here shows the difference in pulmonary inflammation, injury, and clearance of two common strains of mice exposed via nose only inhalation to Silver (Ag) nanoparticles (NPs). This study was conducted as part of ongoing research to establish the pulmonary and systemic differences in sensitive and resistant mouse strains. Our study used FVBN/J and C57BL/6J mice and has established baseline parameters for mechanistic and kinetic studies. Animals were exposed for 4 hours to Ag NPs produced via spark generation from rods of 99.99% purity to an average concentration of 0.5 mg/m3 ± 10%, and lung inflammation measured 24 hrs post exposure. The FVBN/J mice displayed an 8% influx of polymorphonuclear leukocytes (PMNs) in bronchoalveolar lavage fluid (BALF) as well as significant pulmonary protein leakage versus control animals. The C57BL/6J mice displayed no increases in protein and a < 1% PMN response. To further explore the pulmonary response difference between the strains, repeated exposures were conducted at 0.25 mg/m3 for 4 and 30 days and euthanized at 24 hrs post final exposure. The FVB/NJ's showed a marked inflammatory response with a 28% influx of PMNs at 4 days, increasing to 44% at 30 days. The C57BL/6J's, however, demonstrated a clear response and recovery to Ag NPs with a 31% PMNs at 4 days, recovering to ~9% at 30 days. To better understand these strain-dependent response differences, and potential systemic clearance, pulmonary and secondary tissues were digested and analyzed for Ag at 0, 24, 72, and 168 hrs after a single exposure. This comparison of whole body elimination between the two strains is important to better understand the amount of Ag available to elicit the pulmonary inflammatory response in the two strains.

PS 826 Role of Scavenger Receptor B1 in Macrophage Uptake and Activation by Silver Nanoparticles

A. Aldossari, J. Shannahan and J. M. Brown. *University of Colorado, Aurora, CO.*

Silver nanoparticles (AgNPs) are currently being incorporated into a variety of consumer products such as sunscreens, cosmetics, and water filters due to their antimicrobial activity. Due to these extensive applications, concerns have been raised regarding their potential adverse health effects. Macrophages are likely to interact with AgNPs as they form the first line of immune defense against invading pathogens and foreign particles. Macrophages express multiple types of receptors that facilitate their phagocytic response. Scavenger receptor B1 (SR-B1) is expressed by macrophages and has been reported to play a role in recognition of negatively charged particles. We therefore hypothesized that SR-B1 contributes to macrophage uptake of AgNPs and subsequent cellular activation. To test this hypothesis, we exposed a mouse macrophage cell line (RAW 264.7) and bone marrow-derived macrophages (BMDM) to 20 nm citrate-suspended AgNPs. To verify the role of the SR-B1 receptor, we utilized Blt-2, an SR-B1 pharmacological inhibitor. Flow cytometry was used to evaluate cellular uptake following exposure to AgNPs (50 μg/ml). Exposure to AgNPs led to increases in the side scatter of macrophages indicating cellular uptake. Inhibition of SR-B1 with Blt-2 reduced RAW and BMDM uptake of AgNPs. To further examine the role of SR-B1 in macrophage uptake of AgNPs, BMDMs were derived from SR-B1$^{-/-}$ mice. Following AgNP exposure, SR-B1$^{-/-}$ BMDMs demonstrated decreased uptake by flow cytometry. To confirm flow cytometry findings, cells were imaged following AgNP exposure with hyperspectral dark field microscopy and quantitatively assessed by ICP-MS. *In vivo* studies confirmed the role of SR-B1 in AgNP-induced toxicity. C57BL/6 mice receiving a pulmonary instillation of AgNPs demonstrated increases in lung inflammatory cells, and lung tissue IL-6 and IL-1β gene expression. In comparison, SR-B1$^{-/-}$ mice showed a significant decrease in AgNP-induced inflammatory cell recruitment and gene expression. In conclusion, macrophage SR-B1 activation contributes to the inflammatory response induced by AgNPs.

PS 827 Effects of Repeated Intranasal Administration of Silver Nanoparticles on Learning and Memory in Mice

L. L. Davenport[1], H. Hsieh[1], M. T. Williams[2, 3], C. V. Vorhees[2, 3] and M. Genter[1]. [1]*Department of Environmental Health, University of Cincinnati, Cincinnati, OH,* [2]*Department of Pediatrics, University of Cincinnati, Cincinnati, OH and* [3]*Division of Neurology, Cincinnati Children's Research Foundation, Cincinnati, OH.*

Silver nanoparticles (AgNPs) have been increasingly used in manufactured goods for their bactericidal properties. Previous work has shown these particles to be toxic to the nervous and immune systems under various dosing regimens. A previous study from our lab demonstrated localization of AgNPs in the brain following a one-time intranasal (IN) administration of 50 mg/kg AgNPs. We also found increased *Hmox1* gene expression, a marker of oxidative stress, in the hippocampus of the silver-treated mice. To examine possible functional consequences of AgNP accumulation and increased *Hmox1* gene expression, behavioral experiments were performed to characterize changes in learning and memory following IN AgNP exposure. Adult male C57BL/6 mice were dosed for 7 consecutive days with uncoated AgNPs (0 or 50 mg/kg; average diameter 35.7 nm) to mimic repeated workplace exposure in adult humans. One week after the end of AgNP administration, the behavior of the mice was assessed via novel object recognition and Morris Water Maze. AgNP-treated mice exhibited no significant difference in exploration of the novel object during testing. No significant difference was observed between the control and treated groups during the acquisition, reversal, or cued phases of Morris Water Maze testing. Blood cell counts were similarly unaffected between the control and AgNP-treated mice, with the exception of a significant increase in the number of eosinophils. No differences were found in spleen and thymus weights between groups. Further studies into the localization of silver following repeated doses and exposure of animals at different life stages will lead to a greater understanding of the effects of repeated exposure to these toxic particles. This work was funded in part by NIEHS T32ES016646 and NIEHS P30ES006096.

PS 828 Deposition and Retention of Inhaled Silver Nanoparticles in the Rat Lung

D. S. Anderson[1], E. S. Patshin[1], R. Silva[1], D. Uyeminami[1], T. Gordon[2], L. Chen[2], K. E. Pinkerton[1] and L. S. Van Winkle[1]. [1]*Center for Health and the Environment, University of California, Davis, Davis, CA and* [2]*Department of Environmental Medicine, NYU, Tuxedo, NY.*

Silver nanoparticles (AgNPs) have antimicrobial activity and unique electrical properties, resulting in increasing use. While biological effects of AgNPs have been studied, there has not been a comparison of particle size on aerosol-delivered AgNPs persistence. We investigated lung deposition and retention of 20 and 110nm citrate-coated spherical AgNPs. Aerosol of AgNPs was generated using a nebulizer. Adult male rats were exposed nose-only for 6 h to either 20nm or 110nm AgNPs (8mg/m3 and 6.2mg/m3) or 2mM citrate buffer vehicle control. Tissues were collected immediately following exposure (T0) and 1, 7 and 21 days post-exposure (DPE). Ag was quantified using inductively-coupled plasma mass spectrometry and tissue distribution was defined using autometallography (AMG). Each lung lobe and the trachea were measured to determine differences between lobes at T0. At T0 the mean Ag concentration of 110nm AgNPs ranged from 11.89 -18.95μg/g tissue with no significant difference between lobes. 20nm AgNPs T0 lobes were significantly different from each other and ranged from 2.05-9.28μg/g

tissue. The concentration rank by lobe was: left>caudal>cranial>accessory>middle. At 1 DPE, both AgNPs had a diffuse pattern of silver AMG tissue staining, with heavy localization in macrophages. At 7 DPE, Ag localized to the epithelium in the bronchoalveolar duct junction (BADJ), in addition to macrophages. At 21 DPE, the Ag was found in the subepithelium of the bronchoalveolar duct junction with fewer stained macrophages observed. At 21 DPE similar amounts of Ag remained in the lung for 110nm and 20nm AgNPs (4.25μg/g and 3.64μg/g, respectively). We conclude that 1) the 110nm AgNPs dispersed more uniformly than the 20nm AgNPs between lung lobes, 2) the pattern of silver distribution indicates prolonged localization to the BADJ and 3) the lung retains approximately 25% of delivered dose at 21 DPE. Support:U01ES02027 and P42ES004699. AgNPs supplied by NIH NCNHIR consortium.

PS 829 Inhaled Nano-TiO2 Size Distribution along with Mass Concentration Define Lung Responses

A. Noel[1, 4], Y. Cloutier[2], M. Charbonneau[3], K. Maghni[1], R. Tardif[1] and G. Truchon[2]. [1]*School of Public Health, University of Montreal, Montréal, QC, Canada,* [2]*Institut de Recherche en Santé et en Sécurité du Travail, Montréal, QC, Canada,* [3]*INRS-Université du Québec, Laval, QC, Canada and* [4]*SVM, Louisiana State University, Baton Rouge, LA.*

Currently, there is no consensus regarding the exposure metric that best expresses the nanoparticle (NP) dose. Although the surface area was extensively studied for the inflammatory reaction, it has not been validated for cytotoxicity or oxidative stress. Since inhaled NP deposit and interact with lung cells according to their agglomerates size, we hypothesized that the mass concentration combined to the aerosol's size distribution is suitable for NP risk assessment. The objective of this study was to evaluate different exposure metrics for inhaled 5 nm TiO2 aerosols composed of small (SA) (<100 nm) or large (LA) (>100 nm) agglomerates at 2, 7 and 20 mg/m3 on rat lungs inflammatory, cytotoxicity and oxidative stress responses. Six groups of male F344 rats (n=6) were nose-only exposed for 6 hr to the different 5 nm TiO2 aerosols. The control group was exposed to air. Exposures were characterized by weight measurement for mass concentration and with an electrical low pressure impactor for number concentration and size distribution. Bronchoalveolar lavages (BAL) were analyzed 16 hr after exposure. Our results showed that the 7 mg/m3 LA and the 20 mg/m3, both LA and SA aerosols, increased the number of neutrophils compared to controls. The 20 mg/m3 SA significantly ($p<0.05$) increased LDH activity and 8-isoprostane concentration compared to controls. When the size distribution of NP was considered with the mass as an exposure metric, we found a strong correlation ($r>0.97$) with the number of neutrophils for SA and LA. For LDH and 8-isoprostane, we observed a high correlation ($r>0.89$) only with SA. These data show that the mass concentration alone is not sufficient to adequately predict oxidant and cytotoxic pulmonary effects. Overall, our study indicates that considering the NP size distribution along with the mass concentration contribute to a more mechanistic discrimination of respiratory effects.

PS 830 Cell Transformation Potential of Nano-Cerium Oxide ($nCeO_2$), Nano-Ferric Oxide (nFe_2O_3) Compared to Multiwalled Carbon Nanotubes (MWCNT)

L. Wang[1], T. A. Stueckle[1], P. Demokritou[2], M. Chen[3], R. Derk[1], S. Luanpitpong[3], J. Y. Ma[1], V. Castranova[1] and Y. Rojanasakul[3]. [1]*NIOSH, Morgantown, WV,* [2]*Harvard University, Boston, MA and* [3]*West Virginia University, Morgantown, WV.*

Unique physicochemical properties of engineered nanomaterials (ENMs), including CNTs and metal oxides, are distinct from their micron-sized counterparts evidenced by their unique biological effects. Previous studies have suggested potential lung disorders induced by these EMNs. Recent animal study indicated cancer promotion by MWCNT. Our previous *in vitro* work showed subchronic single walled CNT or MWCNT exposure can cause human lung epithelial cell transformation which formed tumors when subcutaneously injected into mice. These findings raise ENM-induced carcinogenesis concerns due to rapid growth in ENM applications, including widely used $nCeO_2$, nFe_2O_3 and MWCNT. The present work tested cell transformation potential of $nCeO_2$ and nFe_2O_3 compared to MWCNT as a positive tumorigenic control. Primary human small airway epithelial cells were treated with a sub-toxic, low dose of ENMs (62.5 ng/cm^2 of $nCeO_2$ and nFe_2O_3, or 60 ng/cm^2 of MWCNT), with albumin and saline as dispersant and no treatment controls, respectively. Cells were continuously exposed to ENM containing medium for 6 weeks. Following exposure, cells were assayed for cell transformation and cancer hallmark analysis. Increased cell proliferation suggested significant cell stimulation by $nCeO_2$ and MWCNT. Next, nFe_2O_3 and MWCNT-treated cells formed soft agar colonies and significantly enhanced cell invasion which suggests their potential cell transformative effect. These results will guide future *in vivo* studies to confirm the observation and to assess the relevancy of our subchronic *in vitro* exposure model. Such an *in vitro* model may serve as a simple/fast/high throughput tool to screen countless ENM to predict cell transformation/carcinogenic potential and addresses a critical need in ENM risk assessment.
Disclaimer: Presented findings and conclusions are the authors and do not necessarily represent those of the National Institute for Occupational Safety and Health.

PS 831 Evaluation of Pulmonary Response to Tungsten Oxide (WO_3) Nanoparticles in Golden Syrian Hamsters

M. V. Prajapati and J. M. Cerreta. *PHS, St. Johns University, Queens, NY.*

Tungsten oxide (WO_3) nanoparticles possess excellent photochromic, electrochromic, thermochromic and catalytic properties. Extensive industrial and military uses have raised the possibilities of human occupational and environmental exposure with concomitant health concerns. To evaluate the effects of such particles in the lung, Golden Syrian Hamsters were exposed by inhalation to aerosols of WO_3 nanoparticles (Nanostructured and Amorphous Materials, Inc., TX). Hamsters were divided into four groups – a control group that was exposed to distilled water and 3 treatment groups that were exposed to 5, 10 or 20 mg/m^3 WO_3 nanoparticles (4 hrs/day, for 4 days). Animals were euthanized 24 hours post-exposure and bronchoalveolar lavage fluid (BALF) was collected. Lungs were then fixed by insufflations of 10% formalin. Tissue sections were analyzed using bright and dark field microscopy. The average size of WO_3 nanoparticles, 71 ±34 nm, was confirmed using TEM. There was a significant increase ($p<0.05$) in total cell counts 22.3 ±0.1, 21.6 ±2.5, and 29.3 ±0.1 (x10^4 cells/ml) of BALF from treated groups (5, 10 or 20 mg/m^3 respectively), as compared to controls (15.6 ±1.4 x 10^4 cells/ml). BALF protein levels increased in treated groups (106.1, 110.7 and 124.1 μg/ml) as compared to controls (98.9 μg/ml). The number of macrophages increased in the BALF treated group (76.8, 65.6 and 145.5 cells/field at X400) as compared to controls (29.2 cells/field at X400) without increase in the number of PMN's. Dark field micrographs of tissue sections revealed WO_3 nanoparticles present in alveolar macrophages that were dispersed in large numbers throughout the lung. Nanoparticles were also identified on airway epithelium, within airway epithelial cells and in interstitial areas of alveolar structures. Results from these experiments indicate that WO_3 nanoparticles can reach alveolar space, enter epithelial layers and penetrate to interstitial structures.

PS 832 Evaluating Metallic NP-Induced Stress Using a Neuronal Coculture Model

M. Grogg, L. K. Braydich-Stolle and S. M. Hussain. *Molecular Bioeffects Branch, Bioeffects Division, 711HPW/AFRL, Wright Patteson AFB, OH.*

To date nanotoxicity studies on the central nervous system are limited and conflicting with discrepancies between animal models and humans adding to the complexity. A previous study focused on establishing a neuronal co-culture model which included neurons and their microglia, to evaluate the phagocytic response effects of nanoparticles (NPs). As a continuation, the present study examined the toxicity of different nanometals which included silver (Ag) and gold (Au) as well as known neurotoxicants manganese (Mn), aluminum (Al), and copper (Cu); and while all of the metallic NPs had an initial size of 80 nm, dispersion resulted in varying degrees of aggregation. The cells were dosed with realistic exposure levels of the different metallic NPs to represent a daily or weekly exposure based on the current limits reported for the bulk metals by OSHA. In addition to viability and reactive oxygen species (ROS) production, key stress genes (NF-κB, TNFα, IL-6) were selected to examine changes following varying times of exposure (4, 8, and 24 h) to metallic NP. The Mn-NPs induced significant toxicity at daily and weekly exposure levels, while Cu-NP showed toxicity only at the weekly exposure level. Furthermore, the Mn-NP treatment demonstrated concentration dependent increases in ROS production and TNFα and IL-6 expression over time while NFκB remained unchanged. Surprisingly, while the Cu-NP treatment induced toxicity, and increased ROS production, the stress response profiles showed no changes at 4 h, and d decreased expression for IL-6 and TNF-α following 8 and 24 h. In comparison, the Ag-, Au-, and Al-NP treatments did not induce toxicity or significant increases in ROS and showed no changes in gene expression at either treatment concentration or time point. Taken together, the results demonstrated that the co-culture model provides enhanced sensitivity for studying NP induced stress responses and the nanometals displayed differential toxicity with Mn>Cu>Al/Ag/Au.

PS 833 Unique Mode of Toxicity of Cu Nanoparticles Compared to Their Micron and Ionic Analogs in *E. coli* and *L. brevis*

C. Kaweeteerawat[1, 2], A. Ivask[2], C. Chang[2], P. Holden[2, 3] and H. Godwin[1, 2]. [1]*Molecular Toxicology, UCLA, Los Angeles, CA,* [2]*UC Center for Environmental Implication of Nanotechnology, UCLA, Los Angeles, CA and* [3]*Donald Bren School of Environmental Science and Management, UCSB, Santa Barbara, CA.*

Nanotechnology has grown rapidly over the past decade, promising benefits in diverse areas of society. However, the rate of toxicological analysis of nanoparticles (NPs) has not kept pace with the rate of development, leading to concerns over the potential biological toxicity and environmental contamination of NPs. Here, we report toxicity ranking as well as mechanisms of toxicity for a series of Cu particles, including nano Cu, nano CuO, nano Cu(OH)2, micro Cu and micro CuO as well as ionic Cu (CuCl2 and CuSO4) in bacteria (*Escherichia coli* and *Lactobacillus brevis*). Fluorescent assays such as PI/SYTO, XTT, DiBAC, and H2DCFDA were used to measure viability, respiration rate, membrane potential, and ROS production, respectively. IC50 values were calculated from growth inhibition curves, revealing that Cu and CuO NPs are more toxic than their micro-sized counterparts, with toxicities approaching that of ionic Cu. Strikingly, the NPs showed distinct differences in their mode of toxicity when compared to the Cu ions, highlighting the unique toxicological properties of materials at the nanoscale. Moreover, cells treated with nano Cu showed higher levels of bioavailable Cu++ than cells treated with ionic Cu. 3D tomography from electron microscopy of cells exposed to the NPs revealed the presence of intact NPs inside the cells.

PS 834 Physicochemical Characterization and Ecotoxicological Evaluation of TiO_2 Nanoparticles in Earthworm *Eisenia foetida*

B. Siva Prasad, S. Ashwini and P. Sankar Ganesh. *Biological Sciences, Birla Institute of Technology and Science Pilani, Hyderabad Campus, Hyderabad, India.*

Wide spread application and use of nanoparticles such as TiO_2 confers their release into various compartments of environment thereby raising concerns about their health impacts. It is essential to assess the ecotoxicity and implications of TiO_2 on the flora, fauna and ecosystem as a whole. Although there are studies reporting toxicity of TiO_2, but specific findings on its effect and underlining toxicity mechanisms in terrestrial organisms such as earthworms remain poorly understood and documented. Hence in this study, ecotoxicological evaluation of the rutile form (10-100nm) of TiO_2 nanoparticles on earthworm, *Eisenia foetida* was conducted as per the modified filter paper test of OECD-207 guidelines. Physicochemical characterization of TiO_2 nanoparticles was carried out using zeta sizer and scanning electron microscope. Earthworms were exposed to a series of concentrations (0.05, 0.1, 0.15, 0.2 and 0.25 mg/cm^2) of TiO_2 nanoparticles. Mortality of earthworms was determined after 48h exposure to TiO_2. Activity of the enzymes, catalase, super oxide dismutase and glutathione reductase was assessed in whole body homogenate of the worms surviving after exposure. Lipid peroxidation was measured to define the levels of oxidative stress during toxicity assessment. Perturbations caused by TiO_2 nanoparticles resulted in the oozing of coelomic fluid and pale coloration of earthworm body. Mortality rate, activity of antioxidant enzymes and lipid peroxidation were influenced by size and charge of TiO_2 nano particles rather than concentration. Results of the study showed that agglomeration of TiO_2 nanoparticles is responsible for the variation in their size and charge. The finding is first of its kind to establish ecotoxicity of rutile form of TiO_2 nanoparticles on earthworms. Similar studies will eventually help in developing strategies to predict ecotoxicity of TiO_2 in the soil environment.

PS 835 Gene Expression Changes in Secondary Organs of Rats Intratracheally Exposed to Silver Nanoparticles

T. Coccini[1], R. Gornati[3], I. Vanetti[3], E. Signoretto[3], F. Rossi[3], G. Bernardini[3] and L. Manzo[1, 2]. [1]*Toxicology Division, Maugeri Foundation IRCCS, Institute of Pavia, Pavia, Italy,* [2]*University of Pavia, Pavia, Italy and* [3]*Department of Biotechnology and Life Sciences, University of Insubria, Varese, Italy.*

Studies in rats have demonstrated the ability of silver nanoparticles (AgNP) to translocate to secondary target organs (e.g. liver or kidney) after administration by respiratory route (Takenaka et al, Environ Health Perspect, 2001). In this study, the expression profile of genes involved in oxidative stress (Gpx1, SOD, Gss, FMO2, Gsr, Txnrd1), metal toxicity (mt1), apoptosis/cell cycle (Casp3, p53), and protein folding (Hsp70) was investigated in liver and testis of rats at different time intervals after i.t. instillation of AgNP. AgNO3 was used as a positive control. Groups of adult male Sprague-Dawley rats received 50 μg/rat of AgNP (20 nm), 7 μg/rat of AgNO3 or 100 μL aqueous solution/rat (control). At days 7 and 28 post-administration, the transcriptional profile of selected genes was examined in tissues by cDNA microarray analysis coupled with bioinformatics and functional gene annotation studies. Semiquantitative followed by Real Time PCR was performed to quantify gene expression changes.
At day 7, changes in gene expression that selectively involved antioxidant enzymes were observed in both liver and testes. In particular, Gpx1, FMO2 and SOD genes were upregulated. No changes were seen for the other genes. At day 28 the AgNP-treated animals exhibited a tissue gene expression profile similar to control. None of the investigated genes was shown to be affected by treatment with AgNO3 at both time points considered. The results suggest the potential of AgNPs to cause, at low doses, subtle molecular changes in secondary target organs, in contrast with Ag ions, possibly reflecting the strong tendency of Ag ions to form inert complexes with cellular or blood components or be neutralized by defense mechanisms. (Grants: Italian Ministries of Health, Research & Education; & CARIPLO foundation-Rif. 2011-2096).

PS 836 The Influence of UV Light on the Genotoxicity of Engineered Nanoparticles

D. Cupi and A. Baun. *Environmental Engineering, DTU (Technical University of Denmark), Kongens Lyngby, Denmark.*

TiO2 nanoparticles (NPs) are one of the most commonly used engineered nanomaterials due to their use in a large variety of applications as photocatalytic agent. The inherent properties of TiO2 might however, lead to photo-induced toxicity in human and animal tissue. Under UV irradiation, TiO2 NPs can produce ROS which is damaging to DNA and other biomolecules.
In this study we used a chemical test for quantifying ROS generation in combination with the umu-test which is a short-term genotoxicity assay providing high throughput screening (96-well plates). Various nanoparticles (SiO2, CeO2, ZnO, and TiO2) were screened using concentrations of 0.0125-0.1 mg/mL with a 2 hour incubation/exposure time and no metabolic activation. No genotoxicity was induced for any of the NPs in the absence of UV light in the concentration range tested.
The next set of experiments involved the use of full spectrum UV light. Methylene blue dye decomposition was used for assessing the photocatalytic activity of TiO2 for an exposure period of 5-80 minutes. Maximal degradation of methylene blue occurred after 60 minutes. In order to investigate the effect of UV on Salmonella typhimurium bacteria, growth rate was investigated at 10, 20, 30, 40, 50, 70 min of exposure. Less than 15% decrease was observed for all the exposed bacteria compared to control. Therefore, an exposure period of 60 minutes was chosen to observe the ability of OECD reference hydrophilic (NM-104) and hydrophobic (NM-105) TiO2 NPs to induce genotoxic effects in the presence of UV light compared to absence of UV light. Concentrations of 0.25, 0.5, 1 mg/mL (45, 90, 180 μg/well) increased the β-galactosidase activity indicating a possible genotoxic effect in the presence of UV light.

PS 837 Monocyte Activation by Particulate Matter and Reactive Oxygen Species Formation

K. I. Tran[1], P. Pakbin[2], A. Kim[1], C. Sioutas[2] and A. Campbell[1]. [1]*Department of Pharmaceutical Sciences, Western University of Health Sciences, Montclair, CA and* [2]*Sonny Astani Department of Civil and Environmental Engineering, University of Southern California, Los Angeles, CA.*

Acute as well as chronic exposure to ambient air particulate matter (PM) has been implicated in playing a part in adverse health outcomes. Formation of reactive oxygen species (ROS) is one pathway by which PM exposure may disrupt normal physiological balance leading to disease pathogenesis. This study used human monocytic (THP-1) cells to assess potential activation and subsequent production of reactive oxygen species. THP-1 cells were seeded in 96-well plates and then exposed for 24 hrs to particulate matter collected from a site in Los Angeles. The particles were smaller than 100 nm in aerodynamic diameter and were collected in an urban site of downtown Los Angeles. Two different doses 2 or 20 μg/m3 were used. Levels of ROS were measured by a fluorescent method. After exposure, there was a dose-dependent increase in the amount of ROS formation. Mitochondrial activity, measured by the MTS assay, was increased at both doses. This increase was not due to changes in cell number. Indeed at the highest dose, we noted a decrease in cell number which may reflect decreased cell proliferation or viability. The data shows that THP-1 cells may be activated by PM leading to ROS formation. Further co-culture studies are needed to determine how activation of monocytes may affect normal human cells. This is the current focus of our laboratory.

PS 838 Semi-Quantitative Analysis for the Uptake of Fluorescently Labeled Carboxylated Nanocrystalline Cellulose in Zebrafish Embryos (*Danio rerio*)

A. N. Clendaniel[1], J. A. Bonventre[1], B. Harper[1] and S. L. Harper[1, 2]. [1]*Environmental and Molecular Toxicology, Oregon State, Corvallis, OR and* [2]*Chem, Bio and Envl Engineerin, Oregon State, Corvallis, OR.*

Uptake and biodistribution of nanomaterials in an in vivo model system are important considerations for nanotoxicology. The use of fluorophore labeling can help with identifying particle location within a specimen and enable particle tracking. This study aimed to quantify the uptake of rhodamine labeled carboxylated nanocrystalline cellulose (NCC) throughout development in the model vertebrate, Danio rerio. NCC was selected for initial investigation because it elicits low toxicity in zebrafish embryos and is increasingly important in commerce. Similar to unlabeled NCC, no significant mortality or developmental abnormalities were observed at the highest dose tested. Fluorescent microscopy images of control embryos and embryos exposed to 500ppm rhodamine labeled NCC were taken on days 1- 5. Integrated density (ID) was used as a surrogate measure for uptake. The experiment was repeated using embryos with and without intact chorions. On day 1, embryos exposed without a chorion had an ID value 3 times higher than those with the chorion intact. On day 2, the chorion off embryos had an ID value 1.43 times that of the chorion on embryos. After hatching, the ID values were not significantly different. There was a linear increase in uptake over the first 4 days, and then an exponential increase on day 5, possibly due to the onset of mouth gaping. From this data, dermal and oral uptake rates were calculated. Confocal microscopy was used to identify heavily concentrated locations within the embryos that seem to be associated with the integumentary system. Our data demonstrates that carboxylated NCC was taken up both dermally and orally by the embryos depending on the stage of development. In addition, the chorion does pose a barrier for these particles prior to hatching which is important when assessing toxicity within the first 72 hours of development.

PS 839 Biodisposition Kinetics of Titanium Dioxide Nanoparticles and Induced Oxidative Stress after Intravenous Administration in Rats

D. Dieme, I. Pujalté, S. Haddad and M. Bouchard. *Environmental and Occupational Health, University of Montreal, Montreal, QC, Canada.*

The wide production and use of titanium dioxide (TiO2) nanoparticles (NPs) is of concern due to insufficient knowledge of potential health effects in workers particularly. Published NP disposition studies have focussed to date mostly on the respiratory tract, the main route-of-entry in workers. To understand pathophysiological mechanisms of NPs, intravenous (iv) exposure studies are important to ensure 100% bioavailability. The biodisposition kinetics of TiO2 NPs and associated oxidative stress were studied in iv exposed rats. Adult male Sprague-Dawley were injected with 1 mg/kg bw of commercial anatase TiO2 NPs (~20 nm core size). Blood samples were collected at 0, 2, 4, 8, 12, 24 and 72 h post-dosing (n = 5 rats) and rats were sacrificed at 1, 3, 7 and 14 days (n = 5 per group) after exposure. Ti levels were quantified by ICP-MS in blood, tissues (lungs, liver, kidneys, spleen), and excreta (urine, feces). Oxidative stress was measured 72 h post-dosing, by following increases of malondialdehyde (MDA) and 8-isoprostane (8-isop) in blood and tissues. NPs were found to accumulate mainly in liver, with peak values observed 72 h post-exposure (on average 3 μg Ti/g liver) followed by a progressive decrease until 336 h (on average 0.330 and 0.011 μg Ti/g liver at t=336 h post-dosing and in controls, respectively). This shows a removal of NPs by the hepatobiliary route. At 72 h, levels in other organs followed the order: spleen>lungs>kidneys. Blood Ti levels remained low beyond 24 h post-dosing. Induced oxidative stress was observed, as indicated by increased MDA concentrations in blood and kidneys, with values of 68.1 and 350.3 μM/mg of protein 72-h post-dosing compared to 30.9 and 238.7 μM/mg of protein in controls ($p<0.05$); increased 8-isop levels were also found in kidneys with values of 70.3 μg/mg of protein 72-h post-treatment compared to 47.7 μg/mg of protein in controls ($p<0.05$). This study further documented the fate of TiO2 NPs in the body and early biological alterations, for risk assessment.

PS 840 Synthesis and Effects of Functional Gold Nanoparticles As Potential Transfection System for Mammalian Cells

A. M. Mendez[1, 2], M. E. Martinez-Leija[1], G. Palestino[2] and M. Salgado[1]. [1]*Facultad de Medicina-Departamento de Bioquimica, Universidad Autónoma de San Luis Potosi, San Luis Potosi, San Luis Potosi, Mexico and* [2]*Facultad de Ciencias Quimicas, Universidad Autonoma de San Luis Potosí, San Luis Potosí, San Luis Potosi, Mexico.*

Gold nanoparticles (AuNPs) have unique properties for been considered as transfection vectors for gene delivery. Using gold nanoparticles for gene therapy brings a new opportunity for enhance the level of transfection and protect the genetic sequence to be delivered. However, the AuNPs application for biomedical topics could be limited for cytotoxicity. In order to decrease the cytotoxicity and enhance the gene delivery efficiency we synthetized AuNPs using polyethilenimine (PEI)as reducing agent, a 25 kDa polycationic branched polymer, which is actually used in DNA transfection protocols. The nucleotide si-miR-148a sequence were grafted to the AuNPs and labeled with carboxyfluorisceine (CFSE). Optical feature, shape and size distribution of AuNPs were examined using UV-Vis spectroscopy, transmission electron microscopy (TEM) and dynamic light scattering (DLS). The results showed the absorbance plasmon centered at 420 ± 5 nm usually attributed to AuNPs spheres, the size of particle-size was at t 5 nm with narrow distribution. Zeta potential measurements indicate that PEI produced more stable NPs (-35 mV) compared with those synthetized by using other reducing agents (citric acid) (-10 mV). We evaluated the cell viability (HeLa cells) through the resazurin assay and follow the nanoparticles distribution into cells using fluorescence microcopy and flow citometry. We found that the HeLa cells viability was up to 95%, and the interaction between AuNPs vector and HeLa cells was evident through positive fluorescence of CFSE by microscopy and flow citometry as cells complexity augmented due to AuNPs intake. These results suggest that AuNPs transfection system brings stability and is biocompatible for be used in mammalian cells.

PS 841 *In Vivo* Study of the Role of Endocytosis and Lysosome Function in Silver Nanoparticle Uptake and Toxicity in *Caenorhabditis elegans*

X. Yang, A. Schindler, R. Taggart, H. Hsu-Kim, D. Sherwood, D. E. Hinton and J. N. Meyer. *Duke University, Durham, NC.*

We used the nematode *Caenorhabditis elegans* to study the roles of endocytosis and lysosomal function in uptake and subsequent toxicity of silver nanoparticles (Ag NPs). Because we wanted to focus on Ag NP uptake and effects, we used citrate-coated Ag NPs (CIT), which dissolved the least of all the Ag NPs we have tested. We found that the clathrin-mediated endocytosis inhibitor chlorpromazine reduced the toxicity of CIT, but not AgNO3. We also tested the sensitivity of three endocytosis-deficient mutants (rme-1, rme-6 and rme-8), two lysosomal function deficient mutants (cup-5 and glo-1), and one coelomocyte fluid endocytosis mutant (cup-4), as compared to wild-type (N2 strain) *C. elegans*. One of the endocytosis-deficient mutants (rme-6) took up less silver and was resistant to the acute toxicity of CIT as compared to N2s, and none of those mutants showed altered sensitivity to AgNO3. Interestingly, the lysosomal mutants were not more resistant to the growth-inhibiting effects of CIT, and were in fact more sensitive to CIT-mediated inhibition of reproduction. Most intriguingly, the glo-1 mutants were much more sensitive than wild type to inhibition of reproduction after exposure to CIT, but not AgNO3, constituting a clear nanoparticle-specific toxic effect. Microscopic examination of the reproduction-impaired glo-1 mutants revealed a phenotype of bagging (retention of developing eggs in the adult), resulting from blockage of embryo transport to the vulval opening by excess yolk accumulation.

PS 841a Silver Nanoparticle-Induced Toxicity to Terrestrial Invertebrates in Different Soil Orders

R. Boyd[1], D. R. Johnson[2, 1] and J. A. Steevens[1]. [1]*Environmental Laboratory, U.S. Army Engineer Research & Development Center, Vicksburg, MS and* [2]*Conestoga-Rovers and Associates, Dallas, TX.*

Silver nanoparticles (AgNPs) are incorporated into a wide variety of products, yet the environmental effects of these novel particles once released into the environment are just beginning to be understood. While preliminary ecotoxicity data exist for AgNPs, additional soil studies are needed to fully understand the effects of these novel nanoparticles in true soil environments. Thus, this study examines the acute toxicity of polyvinylpyrrolidine (PVP)-coated AgNPs to terrestrial invertebrates in multiple soils spanning several soil orders. Briefly, earthworms (*Eisenia fetida*, n=10, 3 replicates per soil) were exposed to increasing concentrations of PVP-AgNP in Memphis Silt (alfisol order), Sunev (mollisol order), Camp Shelby (ultisol order), and Big Black (entisol order) soils. Earthworms were also exposed

silver nitrate (AgNO3) as a positive control in the same soils. Soil exposures lasted for 14 days, after which surviving earthworms were counted and the median lethal concentration for 50% of the population (LC50) was calculated according to the trimmed Spearman-Karber method. PVP- AgNP LC50 in the Memphis Silt soil was 2828.43 mg/kg; in contrast, AgNO3 was much more toxic than PVP-AgNP in the same soil (LC50=223.31 mg/kg). The PVP coating did not contribute to PVP-AgNP soil toxicity (PVP LC50 > 40,000 mg/kg). PVP-AgNP LC50 in Sunev, Camp Shelby, and Big Black soil were all >1000 mg/kg. These data demonstrate that PVP-AgNP is less toxic in a soil environment than the ionic form (AgNO3). Furthermore, by utilizing four soils that cover over 50% of the soil in the contiguous U.S., these data provide quantitative soil toxicity values to better evaluate the effects of PVP-AgNP in soil environments.

PS 841b Transmission Electron Microscopic (TEM) Evaluation of Silver Nanoparticles (AgNP) or Silver Acetate (AgOAc) Deposition in Selected Tissues of Sprague-Dawley (SD) Rats

M. S. Imam[1], M. D. Boudreau[1], G. Olson[2] and A. Paredes[1]. [1]*National Center for Toxicological Research, Jefferson, AR and* [2]*Toxicologic Pathology Associates, Jefferson, AR.*

This study investigated the deposition of silver (Ag) in selected tissues (ileum, jejunum, colon, kidney, liver, spleen and mesenteric lymph nodes) of SD rats administered AgNP (10, 75, and 110 nm) at 36 mg/kg/day or AgOAc at 56 mg/kg/day by daily oral gavages for 13 weeks. The levels of Ag detected by TEM were highest in the small and large intestine of both male and female rats administered either AgNP or AgOAc. A subtle surface difference between AgNP and AgOAc deposition were observed in the colons and kidneys of rats. Rats treated with AgNP showed fine, spherical, and measurable Ag granules, whereas AgOAc showed irregular, flower-shaped surface depositions. The majority of Ag granules were located within the lamina propria and basement membrane of the intestinal epithelial cells. The localization and distribution of Ag varied in the other tissues, including the kidneys, livers, and mesenteric lymph nodes. Ag granules were entrapped by the macrophages in the mesenteric lymph nodes, whereas in the kidneys, the Ag deposition was observed in the basal lamina of the glomeruli involving podocytes and endothelia cells. In particular, the 10 nm AgNP had greater deposition in mesenteric lymph nodes, kidneys, and colons of both male and female rats suggesting size-dependent bio-distribution. Furthermore, the energy-dispersive X-ray spectral analysis revealed that Ag deposition in the kidneys, colons, and mesenteric lymph nodes consisted of silver and often coexisted with selenium, silicon and sulfur containing granules. A gender-related difference in Ag deposition was noted in the kidneys and colons, with greater Ag deposition in females compared to males. This study provides new insights into the bio-distribution patterns of AgNP or AgOAc in the major tissues and proposes a need for further research. This study is supported, by interagency agreements 224-12-0003 and AES12013 between the NCTR/FDA and NIEHS/NTP

PS 841c Toxicity and Allergy Responses in the Lung following Pulmonary Exposure to Nanoparticle Silver in Mice

C. E. McLoughlin, S. Anderson, K. L. Anderson, D. Schwegler-Berry, B. T. Chen and J. R. Roberts. *NIOSH, Morgantown, WV.*

Silver nanoparticles (AgNP), due to antimicrobial properties, are widely used in medical applications and consumer products. Expansive use of AgNP in manufacturing raises the concern of effects following respiratory exposure in workers. Previous work in the laboratory has shown dose-dependent lung toxicity with inflammation and alterations in lung immune parameters in rodents. The goal of the current study is to characterize effects of AgNP for potential exacerbation/attenuation of respiratory allergy in an ovalbumin (OVA)-induced allergy model in BALB/c mice. For range-finding (RF) studies, mice were exposed to physiological dispersion medium (DM), 6.1µg (LO), 18.2µg (ME), or 73µg (HI) AgNP. AgNP were 20 nm diameter with 0.3% wt polyvinylpovidone coating (NanoAmor, Inc.), were suspended and sonicated before exposures by pharyngeal aspiration (PA) on day 0. For RF studies assays were conducted on days 1, 10, and 29 post exposure—time points chosen to correspond with the allergy paradigm time course. Airway hyperreactivity was measured as PenH, bronchalveolar lavage (BAL) was performed on the whole lung, cells and fluid were retained for analysis of lung-associated injury and inflammation and phenotyping by flow cytometry, lymph nodes (LN) were harvested for enumeration and phenotyping. Changes in PenH did not occur with AgNP alone at any time point. Results indicated a dose-dependent injury and inflammation by day 10 which began to resolve by day 29. For the allergy model, DM and OVA served as controls and ME and HI were chosen for study. Animals received i.p. injections of OVA + aluminum hydroxide gel (alum) during the sensitization phase on days 1 and 10. To elicit an OVA-specific response, 2 PA challenges of OVA were given on days 19 and 29. Dose dependent increases in PenH, BAL and LN cell number were observed in mice exposed to AgNP over OVA controls. Results indicate potential for AgNP to exacerbate allergic response in the lung.

PS 841d Differential Genomic Effects on Signaling Pathways by Two Different CeO2 Nanoparticles in HepG2 Cells

K. T. Kitchin, K. A. Wallace, C. P. Jones, H. Ren, B. T. Castellon, J. Crooks and S. Thai. *US EPA, Durham, NC.*

Nanoparticles composed of CeO2 are of particular interest in toxicological studies due to their growing use in pharmaceutics, biomedical products, cosmetics, polishing materials and as automotive fuel additives. Human liver HepG2 cells were exposed for three days to two different forms of nanoparticles both composed of CeO2 (0.3, 3 and 30 ug/mL) and a genomic study performed. The two CeO2 nanoparticles have dry primary particle sizes of 8 nanometers {(M) made by NanoAmor}and 58 nanometers {(L) made by Alfa Aesar}and differ in various other physical-chemical properties as well. This systems biological genomic study showed that the major altered pathways were protein synthesis, stress response, proliferation/cell cycle, cytoskeleton remodeling/actin polymerization and cellular metabolism. Some of the canonical pathways affected were mTOR signaling, EIF2 signaling, fatty acid activation, G2/M DNA damage checkpoint regulation, glycolysis and ubiquitination. Nanoparticle M showed a normal dose-response pattern with 363, 633 and 1273 differentially expressed genes (DEGs) at 0.3, 3 and 30 ug/mL, respectively. M is more active than L in respect to altering the pathways of mitochondrial dysfunction, acute phase response, apoptosis, 14-3-3 mediated signaling, remodeling of epithelial adherens junction signaling, actin nucleation by ARP-WASP complex, and altered TCA cycle. However, L is more active than M in respect to the pathways of NRF2-mediated stress response and hepatic fibrosis/hepatic stellate cell activation. In summary, these two CeO2 nanoparticles effected both many shared and some differing toxicity pathways. Disclaimer: [This is an abstract or a proposed presentation and does not necessarily reflect EPA policy. Mention of trade names or commercial products does not constitute endorsement or recommendation for use.]

PS 841e Aggregation of Gold Nanoparticles with Thioether-Containing Amino Acids

S. Babu[1], F. Jaetae Seo[1], R. M. Uppu[2] and M. O. Claville[1]. [1]*School of Science, Hampton University, Hampton, VA and* [2]*Department of Environmental Toxicology and the Health Research Center, Southern University and A&M College, Baton Rouge, LA.*

Gold nanoparticles (Au NPs) have vast applications in drug therapy because of their unique optical, electronic and molecular properties. The toxicity of the Au NPs varies in cellular environment, depending on the physiochemical properties such as size, shape, surface chemistry, and the molecules with which they interact. When blue mussels, *Mytilus edulis*, are exposed to Au NPs of particle size < 5 nm, they exhibit an increase in oxidative stress and decrease in thiol-containing proteins. These organisms also contain methionyl peptides that are hypothetically subject to oxidation due to Au NP exposure. In this present study, we present preliminary findings regarding the interaction of Au NPs with methionyl compounds, L-Methionine(Met), D/L-Met, N-Acetyl-L-Met, L-Met Ethyl Ester, and Met-Glycine. The average sizes of the eight Au NPs used in the study are ~5, ~10, ~15, ~20, ~30, ~32, ~35, and ~40 nm diameters. The UV-Vis spectral studies showed that Au NPs exhibit a strong plasmon at ~530 nm while the methionyl compounds displayed an additional plasmon band at ~785 nm, indicating the formation of Au NPs aggregates. Methionine was found to aggregate Au NPs (conc. $3.487E^{-10}$ M) with size ~35 nm at higher concentration (final 0.125 M) with the color change from red to blue. While lower concentration of L-Met and D/L-Met did not aggregate immediately, N-terminal (N-Acetyl-L-Met) and C-terminal protected Met (Met Ethyl Ester) readily formed Au NPs aggregates. Methionine-Glycine dipeptide was only slightly better than D/L-Met at inducing aggregation of Au NPs. The results provide insight into the impact of NP size, peptide sequence, and concentration of NPs, on aggregation. We strongly believe aggregation size and kinetics may have a role in the etiology of cellular response which needs to be systematically evaluated. [This research is supported by grants from NSF-1230357 (formerly 0847742), NSF HRD–1238838, NSF HRD–1137747, and ARO W911NF-11-1-0177.]

PS 842 Toxicogenomic Analysis of Low-Dose CT Exposure in Neonatal Mouse Lungs

H. Wang, J. E. Moore, M. C. Walb, J. Winslow, M. T. Munley, L. D. Miller, X. Zhou and M. S. Miller. *Wake Forest School of Medicine, Winston-Salem, NC.*

Young children are exposed to substantial amounts of low dose radiation (LDR) during diagnostic imaging. The long term carcinogenic effects of LDR are not known, especially when prior exposure to environmental chemicals could sensitize to LDR. We previously reported in adult mouse models, in which lung cancer was induced by either transgene expression or chemical carcinogen treatment, that whole-body CT doses approximating clinical screening doses significantly increased tumor multiplicity by 40 to 100%. Pregnant C57BL6-BALB/c mice were treated *in utero* with vehicle or a single 45 mg/kg dose of 3-methylcholanthrene (MC). Half of the male and female offspring in each group were exposed to a single dose of 50 mGy of LDR from a clinical CT scanner 4½ weeks after birth. RNA was isolated 10 min post-exposure. Affymetrix gene chip expression profiling followed by gene ontology analysis identified 32 differentially expressed genes that were altered by *in utero* exposure to MC but were not altered in response to neonatal LDR. Using DAVID, we identified clusters of genes under the categories response to stimulus and immune system process that were significantly altered following neonatal exposure to LDR, with network centers in the p38 MAPK pathway. When male and female responses to LDR were determined, significant gender related differences were identified. For females, the top network was related to cardiovascular disease, cardiovascular system development and function, and cell morphology. In males, differentially expressed genes were enriched in two networks. The first was related to connective tissue development and function, tissue morphology, and lymphoid tissue structure & development, and the second to functions in cancer, involving cell-cell signaling & interaction and cellular growth & proliferation. Our data demonstrate gender related differences in LDR-induced differential gene expression following neonatal exposure in gene pathways related to disease pathogenesis that may be responsible for the long term toxic responses to radiation.
(NIH grant CA136910)

PS 843 Lead Pollution in Soil, Domestic Animals, and Children from Townships near a Lead-Zinc Mine in Kabwe, Zambia

S. M. Nakayama[1], J. Yabe[2], Y. Ikenaka[1], Y. B. Yohannes[1], B. Oroszlany[1], N. Bortey-Sam[1], K. Muzandu[2], K. Choongo[2], A. N. Kabalo[3], J. Ntapisha[3], A. Mweene[2], T. Umemura[1] and M. Ishizuka[1]. [1]*Hokkaido Univ, Sapporo, Japan,* [2]*University of Zambia, Lusaka, Zambia and* [3]*District Health Office, Kabwe, Zambia.*

In Africa, major sources of childhood Pb poisoning include Pb mining and smelting. In Kabwe, the capital of Zambia's Central Province, extensive Pb contamination of township soils in the vicinity of a Pb-Zn mine has been reported and poses a serious health risk to children in these townships. Therefore, this study investigated Pb levels in soil, edible tissues of cattle and chickens as well as blood lead levels (BLLs) in children exposed to Pb pollution. The concentrations of Pb (9-51188 mg/kg) in Kabwe soil (n=101) were much higher than benchmark values. Pb levels in tissues of Kabwe cattle were higher than those in other Zambian towns. Moreover, mean concentrations of Pb exceeded maximum levels for human consumption in some organs including muscle in free-range chickens, in contrast to low levels in broiler chickens. Given these results of Pb pollution in soil and domestic animals, we investigated BLLs in children (n = 246), under the age of 7 years, in townships around the Pb-Zn mine in Kabwe and to identify children with BLLs that require medical intervention. Almost all of the sampled children had BLLs exceeding 10 μg/dL. Children in these areas could be at serious risk of Pb toxicity as 18% of the sampled children in Chowa, 57% (Kasanda) and 25% (Makululu) had BLLs exceeding 65 μg/dL; the threshold widely considered to result in Pb toxicity. A total of 8 children had BLLs exceeding 150 μg/dL. These levels were markedly high, especially that concentrations of up to 427 μg/dL were recorded. Therefore, it is recommended that medical intervention be commenced in the children with BLLs exceeding 45 μg/dL and other interventions to reduce Pb exposure in the affected townships.

PS 844 Gene Expression Profiles in Asthmatic Children Living in Localities with Different Extent of the Air Pollution

H. Libalova, J. Topinka, M. Dostal and R. J. Sram. *Department of Genetic Ecotoxicology, Institute of Experimental Medicine AS, Prague, Czech Republic.*

This study is a part of the broader molecular epidemiology study dealing with health effects of the air pollution in children living in the heavily polluted industrial area of the Czech Republic, Ostrava region, where the incidence of asthma bronchiale in children is extremely high (30-40 %). We hypothesized that high level of the air pollution by polycyclic aromatic hydrocarbons (mostly bound on PM10) is associated with increased asthma morbidity in children from Ostrava region. We compared gene expression profiles in leukocytes of asthmatic children (aged 6 - 16 years) with profiles of healthy children without asthma using Illumina HumanHT-12 BeadChip in a group of 200 children living in Ostrava-Radvanice and Ostrava-Bartovice (100 asthmatic and 100 healthy children) and a control group of 200 children living in rural district of Prachatice (100 asthmatic and 100 healthy children). Our results indicated completely different gene expression profiles among localities. We identified significantly deregulated genes specific for Ostrava or Prachatice, however, no gene was found to be commonly deregulated in both localities. Gene expression data of asthmatic children from Prachatice showed increased expression of SIGLEC8, CLC, CCL23 and CACNG6, genes related to the presence of bronchial eosinophilic inflammation suggesting allergic phenotype of asthma. Skin tests also confirmed the diagnosis of allergy in most cases. In contrast, children living in industrial Ostrava region exhibited upregulation of gene associated with neutrophilic inflammation and non-atopic asthma phenotype (DEFA4) which could be triggered by air pollutants. Moreover, upregulation of HBG2 and AHSP genes may imply the role of hypoxia in asthma development. Taken together, our results demonstrated the existence of distinct phenotype of asthma in children living in polluted Ostrava region compared to children living in rural district of Prachatice.

PS 845 The Development and Validation of Methods for Evaluating the Immune System in Preweaning Pigs

B. A. Thorsrud[7], M. J. Cameron[6], B. Zeigler[6], K. G. Nelson[2], J. M. McKim[3], M. L. Weiner[1], H. Ferguson[4], B. Frantz[7] and W. Blakemore[5]. [1]*TOXpertise, LLC, Princeton, NJ,* [2]*Pathology, MPI, Mattawan, MI,* [3]*CeeTox, Kalamazoo, MI,* [4]*Abbott Nutrition, Columbus, OH,* [5]*Celtic Colloids, Topsham, ME,* [6]*Immunology, MPI, Mattawan, MI and* [7]*Developmental & Reproductive Toxicology, MPI, Mattawan, MI.*

Methods were developed to evaluate immunotoxicity effects of chemicals in preweaning piglets using immunophenotyping (IP), circulating cytokine evaluation & immunohistochemistry (IHC) of the gastrointestinal tract (GIT). Yorkshire crossbred piglets were offered ProNurse® formula 6x/day at 500 mL/kg/day for 4 weeks. Groups were Formula Control; Phosphate Buffered Saline (PBS) Control (im injection); Lipopolysaccaride (LPS) Positive Control (im injection); PBS Control by percutaneous endoscopic gastrostomy (PEG) tube & Dextran Sodium Sulfate (DSS) (as positive control). Piglet tissue & blood were used for evaluations. The IP method used whole blood from control animals on Days 13, 14, 28, and 29 to evaluate peripheral blood leukocytes by flow cytometry. The cytokine method used blood from PBS control & LPS groups collected to evaluate IL-1β, IL-6, IL-8, and TNF-α. ELISA kits were used to detect cytokines. The ICH method used tissues obtained from the stomach, duodenum, jejunum, ileum, proximal & distal colon & cecum on for IL-6, IL-8 and TNF-α staining. These tissues were collected from PBS controls & DSS animals. H&E staining was used to confirm tissue ICH changes. Results of the IP evaluation confirmed that it was a precise assay for evaluating lymphocytes, mature T-cells, helper T-cells, cytotoxic T-cells, B-cells & monocytes in preweaning piglet blood. Cytokine evaluations confirmed an increase in cytokine levels in LPS-treated animals. Immunohistochemistry evaluation confirmed increased IL-8 & TNF-α staining in the proximal &/or distal colon in DSS animals. H&E staining was associated with colonic inflammation/edema in tissues of DSS animals. In conclusion, these three methods were confirmed to be robust assays to evaluate the immune system of preweaning piglets. Funded by FMC Corp. & the International Formula Council.

PS 846 Increased Prevalence of Asthma in Children Exposed to Pyrethroids in Housedust

S. L. Shalat[2], M. Ramagopal[1], B. Buckley[2], K. Black[2] and G. Mainelis[2]. [1]*Pediatrics, Rutgers-RWJMS, New Brunswick, NJ and* [2]*E.O.H.S.I., Piscataway, NJ.*
Sponsor: J. Richardson.

The household environment is recognized as a potentially important factor in the early childhood development and exacerbation of asthma and allergies. In recent years pyrethoid pesticides have become widely used for control of household insect pests, based upon the widespread acceptance of their safety for use in and around children. A study was conducted in households in New Jersey to examine the nature of the relationship between housedust and its common constituents and the prevalence of asthma and allergies in young children (ages 6 months to 5 years). A total of 75 children and households were enrolled in the study. Health endpoints were assessed by a technician-administered questionnaire. The parents of the study subject were asked a questionnaire based upon that employed in the International Study of Asthma and Allergies in Children (ISAAC). Environmental sampling was carried out with vacuum sampling for dust, and aerosol (inhalable) sampling for particulate matter. Housedust was analyzed for the presence of a panel of 10 pyre-

throid pesticides by GC/MS. A multivariate logistic regression analysis was carried out for total pyrethroids in housedust. All non-detects (N=9) were included at half the limit of quantitation and log transformations of the data carried out. Additional variables in the final model included age (years), gender, and family history of asthma (yes/no first degree relative). The model for parental reporting of the child having had a physician diagnosis of asthma was statistically significant at the 0.003 level with log total pyrethroids OR = 1.25 (95% 1.03-1.51). When pyrethroid exposure was examined as quartiles the results for the top three quartiles with the bottom quartile as reference was OR = 1.05, 2.55, and 5.77 respectively, with the top quartile statistically significant (P = 0.027). The presence of a dose response increase in reporting of asthma in young children is suggestive that pyrethroid pesticides may play a role in early childhood asthma.

PS 847 Femoral Growth Plate Dysplasia in Juvenile Rabbits Dosed with a Spleen-Like Kinase (Syk) Inhibitor

P. Duffy[1], T. Mitchard[1], G. R. Clemens[2] and P. A. Hall[1]. [1]*Drug Safety and Metabolism, Astrazeneca, Macclesfield, United Kingdom and* [2]*Rigel Pharmaceuticals Inc, South San Francisco, CA.*

Tyrosine Kinase inhibitors with inhibitory activity at the VEGF receptor have been associated with effects on the epiphyseal growth plates in rodents. This has potential impact for clinical trials and therapy in paediatric patients. This study was designed to investigate the potential for off target effects of a syk inhibitor in juvenile rabbits. Three groups of juvenile New Zealand White rabbits, each consisting of 10 males and 10 females, were given the test syk inhibitor orally, twice daily, for 1 month. The control group consisted of 11 males and 9 females and was similarly treated with vehicle. The dose levels were 0, 5, 15 or 30 mg/kg bid. The animals were 9 weeks old at the start of dosing. After dosing with 15 or 30 mg/kg bid, histopathological changes were evident in the proximal femur (growth plate dysplasia; reduced bone marrow cellularity), femoro-tibial joint (growth plate dysplasia; reduced bone marrow cellularity) and sternum (reduced bone marrow cellularity). The treatment-related dysplasia noted in the growth plate of the proximal femur was characterised by the thickening, fissuring and in some animals, fracturing of the growth plate due to the accumulation of hypertrophic chondrocytes. In conclusion, the syk inhibitor produced growth plate dysplasia in the proximal femur and femoro-tibial joint and reduced bone marrow cellularity in the femur and sternum at 30 and 60 mg/kg/day. These findings were consistent with those seen in toxicity studies in rodents. The chondrodystrophy/growth plate dysplasia in rat and rabbit is considered to be related to off target inhibition of VEGF and subsequent reduced angiogenesis and is limited to actively growing bones (before growth plate closure).

PS 848 Persistent Mitochondrial Damage in Offspring of Patas Monkeys Exposed *In Utero* to Antiretroviral Nucleoside Reverse Transcriptase Inhibitors (NRTIs)

Y. Liu[1], A. T. Gibbons[1], E. Shim[1], P. Nguyen[1], R. L. Divi[2], R. A. Woodward[3], M. J. Sowers[3] and M. C. Poirier[1]. [1]*Carcinogen and DNA Interactions Section, LCBG, CCR, National Cancer Institute, NIH, Bethesda, MD,* [2]*DCPC, National Cancer Institute, NIH, Bethesda, MD and* [3]*Animal Center, NIH, Dickerson, MD.*

Combinational antiretroviral therapy containing NRTIs is highly successful in controlling HIV-1 infection, and reducing mother-to-child HIV-1 transmission. However, NRTI exposure may cause mitochondrial dysfunction in infants born to mothers receiving NRTIs during pregnancy. To model NRTI use in human pregnancy, patas dams received human-equivalent protocols of antiretroviral drug combinations, and the offspring were examined for mitochondrial integrity. Dams were given combinations of 3 NRTIs, zidovudine (AZT)/ lamivudine (3TC)/abacavir (ABC), or 2 NRTIs, AZT/3TC, plus a non-NRTI, Nevirapine (NVP), for the last 10 wk (50%) of gestation. Heart and brain tissues, collected from offspring at birth, 1 and 3 yrs of age, were examined by electron microscopy (EM) to evaluate mitochondrial morphology. The EM photomicrographs of heart and brain from drug-exposed offspring revealed damaged mitochondrial membranes with mitochondrial swelling, loss of cristae, and increased lucency. Scoring of coded EM photomicrographs, by 3 independent investigators, revealed significantly higher damage in 1 yr old patas exposed to both drug combinations in utero, compared to 1 yr old unexposed patas ($P<0.05$). In addition, the 3 yr old drug-exposed patas had levels of heart and brain mitochondrial damage similar in magnitude to the 1 yr old drug-exposed animals, and significantly higher than the unexposed 1 yr old patas. Additional evaluations, including mtDNA levels, and mitochondrial oxidative phosphorylation assays are in progress. Because the drug-induced damage was persistent in 3 yr old patas, an age equivalent to 14 years in human life, this study provides powerful evidence for the persistence of NRTI-induced mitochondrial damage, and helps to explain the mitochondrial dysfunction observed in NRTI-exposed children.

PS 848a Isotopic Analyses of Lead in Blood of Children to Identify Sources and Routes of Pollution in a Mexican Mining Site

P. R. Rebeca Yasmin[1], C. L. Javier[1], G. T. Arturo[2] and P. A. Ofelia[2]. [1]*Universidad Autonoma de San Luis Potosí, San Luis Potosí, Mexico and* [2]*Universidad Autónoma de México, Querétaro, Mexico.* Sponsor: M. Gonsebatt.

Lead (Pb) is a highly toxic element to the human body and even at low concentrations (<10 μgdL−1) it will have severe physiological or neurological effects particularly for children; it is well known that can be provided by different sources such as paint, ceramic, mining residues, etc.
In semiarid Mexican mining and metallurgical centers such Cedral San Luis Potosí, Mexico, the residues of these activities containing high concentrations of heavy metals (Pb, As, Cd, Hg) are generally deposited in uncovered piles, which constitute a source of contamination due to the wind dispersion. Human population can be exposed to these particles by different routes through inhalation or ingestion, and this source of pollution could be the cause of adverse effects associated to Pb. Some health affections in this community have been reported, but it has not been identified the source or sources of Pb to which the children are exposed.
The aim of this study is to trace the origin of Pb pollution and identify the principal source of environmental and human Pb contamination, using isotopic methods.
Pb concentrations and isotopic compositions in blood samples of children (4–8 years old) were determined by MC-ICPMS and compared to those of associated environmental samples (soil, residues, outdoor and indoor dust). Pb concentrations of soil, residues and dust ranged between 73-2640, 1736-6700, 144-3550 mgKg−1 respectively. Blood Pb concentrations levels (11.0 ± 5.3 μgdl−1) in children ranged between 2.7-36 μgdl−1, which is 3–14 times higher than the current average (1.9 μgdl−1) of children in the US. We find that blood Pb isotopic ratios (206Pb/204Pb 18.7872±0.0003) strongly correlates with those values determined in atmospheric particles (206Pb/204Pb 18.7754±0.0003) and the latter correlates with the isotopic value of samples coming from residues (206Pb/204Pb 18.7749±0.0003). The results indicate that the main source of Pb in this site is mining residues, which are dispersed through wind

PS 848b Impulsivity and Attention in Fluoxetine-Treated Juvenile Monkeys

M. Golub[1], C. Hogrefe[2] and E. Hackett[2]. [1]*Environmental Toxicology, University of California Davis, Davis, CA and* [2]*California National Primate Research Center, University of California Davis, Davis, CA.*

The psychopharmacological agent fluoxetine is approved by FDA for use in children and is widely prescribed for a variety of developmental disorders. Possible adverse consequences of chronic fluoxetine treatment during brain development are being investigated in a rhesus monkey model. PK/PD studies were first conducted to select a dose with serum concentrations of active agent comparable to therapeutic use in children. Fluoxetine (2.2 mg/kg/d) or vehicle control was then administered orally to male rhesus monkeys (N=15,16 per group) daily between 1 and 2 years of age (equivalent to 4-8 years of age in humans). A reward delay (impulsivity) test and an automated Continuous Performance Test (CPT) were administered. Fluoxetine-treated monkeys demonstrated shorter average response latencies during the reward delay test and more immediate responses to presentation of the test. During 15 CPT sessions conducted in the home cage room, fluoxetine-treated monkeys showed more omission errors taking into account cage location, which also influenced this measure. The study suggests that response inhibition and attention, two executive functions important to daily life in children, can be influenced by fluoxetine at therapeutic dose levels. Supported by HD065826.

PS 848c Perinatal Bisphenol A Exposure Changes Expression of Airway Secretory Products in the Developing Mouse Lung

P. Edwards, L. S. Van Winkle, K. Lee and S. Carratt. *Center for Health & Environment, UC Davis, Davis, CA.*

Bisphenol A (BPA) is a component of plastics. Recent work has shown that BPA exposure alters mucous cell development in fetal rhesus monkeys. While perinatal BPA exposure has been shown in a mouse model to increase airways hyperresponsiveness and alter immunity, the ability of BPA to change normal growth and development of secretory cells, including mucous cells, in the airways of mice, has not been studied. To address this, we exposed timed pregnant NIH Swiss mice to 10ug/ml BPA in drinking water beginning on gestational day 14 (GD14) and continuing for the length of the study. We examined the proximal (extrapulmonary trachea/bronchi) and distal (intrapulmonary bronchioles) conducting airways of both male and female offspring using histopathology and gene expression approaches at 1d, 3 weeks and 8 weeks of age to span birth, weaning and young adulthood. Mucous cell abundance was defined using AB/PAS histologic staining

and muc5B/muc2 gene expression. Club (Clara) cell abundance was defined using immunohistochemistry and gene expression of secretaglobin 1A1 (sgb1A1). We found that continual BPA exposure beginning in the third trimester and extending to 3 wks postnatal resulted in site-specific changes in Muc5B expression. Proximal extrapulmonary airways had a 2 fold decrease in Muc5B gene expression in males and females, which achieved statistical significance in males. In contrast, the more distal, intrapulmonary airways of both males and females had a greater than 2 fold increase in muc5B expression. This was mimicked by Muc2 gene expression but only in male mice and an increase insgb1A1 gene expression only in female mice. When the abundance of sgb1A1 protein was assessed, the amount per cell was diminished in the distal airways of BPA treated mice suggesting a mismatch between mRNA expression and protein expression which might be explained by accelerated secretion. We conclude that BPA exposure during lung development changes secretory product expression, even in species with limited mucous cells such as mice.
Supported by NIEHS R21 ES021600

PS 849 BMS-986094: Nonclinical Investigative Studies on a Nucleoside Analog Intended for Treatment of Hepatitis C Virus Infection

M. Davies, M. J. Graziano and T. Sanderson. *Drug Safety Evaluation, Bristol-Myers Squibb Company, Princeton, NJ.*

BMS-986094 (formerly INX-08189), a 2'-C-methylguanosine prodrug with pivalate and 1-naphthol moieties, was withdrawn from clinical trials because of a serious safety issue. Events included decreased left ventricular ejection fraction, electrocardiogram changes, and acute kidney injury.
In prior animal studies, tolerated doses associated with minimal and reversible skeletal muscle degeneration were established. Since skeletal muscle degeneration correlated with increases in standard serum analytes (e.g., transaminases), it was expected that clinical dosing could proceed safely with careful monitoring prior to onset of more severe events.
Because the onset and severity of clinical adverse events (heart and kidney) were unexpected, Bristol-Myers Squibb Company conducted a robust series of in vitro and in vivo investigative studies including innovative, and in some cases newly developed, mechanistic and diagnostic methodologies, to further characterize BMS 986094 toxicity. These studies focused on several potential mechanisms including: 1) reactive metabolites and cytotoxicity of BMS-986094 and its prodrug moieties, 2) mitochondrial toxicity, 3) pivalate involvement in tissue energy status, 4) plasma and tissue metabolomic changes, 5) tissue transcriptional changes, and 6) levels of BMS 986094 and its metabolites in plasma and tissues.
Although these studies extended the understanding of the nonclinical toxicities of BMS 986094, they did not identify a specific underlying mechanism. Observations included possible novel kidney injury biomarkers; an apparent correlation of tissue nucleoside triphosphate levels to toxicity; that predominate BMS 986094 metabolism was not associated with reactive metabolites or oxidative stress; and preliminary evidence that, although some potential secondary energy utilization changes were observed, BMS 986094 does not appear to be a direct mitochondrial toxicant.
A series of eight abstracts herein (searchable by "BMS-986094") describe these investigations in greater detail.

PS 850 BMS-986094: Investigation of Potential Biomarkers and Mechanisms of Toxicity in Cynomolgus Monkeys

K. Horn[1], T. Sanderson[1], R. White[1], E. Renshaw[1], D. Nelson[1], S. Clark[1], T. R. Van Vleet[1], D. Simic[1], B. Baumgart[1], B. Wang[3], J. Lute[5], E. Janovitz[4], M. J. Graziano[2] and M. Davies[2]. *[1]Drug Safety Evaluation (DSE), Bristol-Myers Squibb (BMS), Mt. Vernon, IN, [2]DSE, BMS, Lawrenceville, NJ, [3]DSE, BMS, New Brunswick, NJ, [4]Discovery Toxicology, BMS, Hopewell, NJ and [5]Bioanalytical Sciences, BMS, Lawrenceville, NJ.*

BMS-986094 (formerly INX-08189), a 2'-C-methylguanosine prodrug, was withdrawn from clinical trials due to a serious safety issue. Events included decreased left ventricular ejection fraction, electrocardiogram changes, and acute kidney injury. This study evaluated non-routine potential biomarkers and mechanisms of myocardial and renal toxicities associated with BMS-986094 and reversibility of any changes.
BMS-986094 was given orally at 0, 15, or 30 mg/kg/day for ≤ 1 month + a 6-week dose-free period. The major plasma BMS-986094-related analyte was INX-08032 (initial nucleoside), followed by INX-08144 (O-methyl nucleoside), INX-09054 (prodrug less naphthol), and BMS-986094. BMS-986094 was clinically tolerated at 15 mg/kg/day (INX-08032 AUC 668 ng•h/mL), but 3 monkeys at 30 mg/kg/day (INX-08032 AUC 1110 ng•h/mL) were euthanized after ~3 weeks. The magnitude of changes were generally dose- and time-related with observations at both doses including prolonged QT interval and flattened and inverted T-waves; urine myoglobin output, and kidney injury biomarkers (serum calbindin, β2 microglobulin, and clusterin); and cardiomyocyte degeneration. However, there were no consistent serum markers of cardiac injury. At 30 mg/kg/day, further changes were macroscopic and ultrastructural changes indicative of acute renal proximal tubular degeneration and skeletal myocyte degeneration/regeneration. There were no changes in heart or kidney mitochondrial respiration or DNA copy number, and mitochondrial morphology appeared normal by electron microscopy. Except for QT prolongation, all changes appeared to recover.
While a mechanism of toxicity was not established, the changes associated with BMS-986094 were inconsistent with a direct effect on mitochondria. Additionally, potential novel biomarkers for kidney injury were identified.

PS 851 BMS-986094: Repeat-Dose Oral Cardiovascular (CV) Safety Pharmacology Study in Monkeys

M. W. Gill[1], J. K. Hennan[1], L. V. Buchanan[1], W. A. Warner[1], L. M. Dillon[1], P. C. Levesque[1], M. Davies[2], T. Sanderson[2] and M. J. Graziano[2]. *[1]Discovery Toxicology, Bristol-Myers Squibb, Princeton, NJ and [2]Drug Safety Evaluation, Bristol-Myers Squibb, Princeton, NJ.*

BMS-986094 (formerly INX-08189), a 2'-C-methylguanosine prodrug, was withdrawn from clinical trials because of a serious safety issue. Events included decreased left ventricular ejection fraction, electrocardiogram changes, and acute kidney injury.
To characterize any CV changes, BMS-986094 was given to 5 telemetered monkeys/group at 0 or 15 mg/kg/day (45 days) or 30 mg/kg/day (30 days) with recovery for ≤91 days. Key criteria included toxicokinetics, serum cardiac troponin (cTnI) and N-terminal brain naturetic peptide (BNP), echocardiography, arterial and left ventricular (LV) pressures, LV dP/dt, and electrocardiography (ECG). The predominant plasma analyte (74-89% total AUC) was INX 08032 (initial nucleoside, 534 and 3400 ng•h/mL at 15 and 30 mg/kg/day, respectively). There were no LV ejection fraction [EF], % fractional shortening [%FS], or stroke volume [SV] changes at 15 mg/kg/day. Beginning Day 32, ventricular dilatation occurred at 15 (2.1× pretest) and 30 mg/kg/day (4.0×). Day 32 changes (vs. pretest) at 30 mg/kg/day were decreased mean LV EF (0.43×), % FS (0.35×), and SV (0.62×), with recovery by Day 39. Absolute LV EF ranged from 12 to 43%. Dose-related LV dP/dt decreases at 15 (0.78×) and 30 mg/kg/day (0.45×) occurred with nadirs on Days 33-47 at 15 and Days 26-53 at 30 mg/kg/day. Potential cardiac biomarkers (cTnI, BNP) did not correlate in individual monkeys. ECG changes were prolonged QT interval at both doses, and flat and inverted T waves and ST-segment depression at 30 mg/kg/day. Two 30 mg/kg/day monkeys were euthanized on Day 32; with their hemodynamic and anatomic pathology changes suggesting heart involvement. CV changes in survivors exhibited partial to complete recovery.
In summary, BMS-986094 was not tolerated at 30 mg/kg/day, and partial-to-complete reversible, dose- and time-related ventricular dilatation, decreased ventricular function, and ECG interval and morphology changes were observed at both doses.

PS 852 BMS-986094 and Its Metabolites in Target and Nontarget Monkey Tissues

K. J. Trouba[1], J. Wang[2], A. Liu[2], B. Wang[3], M. J. Graziano[2], T. Sanderson[1] and M. Davies[2]. *[1]Drug Safety Evaluation, Bristol-Myers Squibb (BMS), Mt Vernon, IN, [2]BMS, Lawrenceville, NJ and [3]BMS, New Brunswick, NJ.*

BMS-986094 (formerly INX-08189), a 2'-C-methylguanosine prodrug, was withdrawn from clinical trials because of a serious safety issue. Events included decreased left ventricular ejection fraction, electrocardiogram changes, and acute kidney injury. BMS-986094 and selected BMS-986094 metabolites were measured in target (heart, kidney, diaphragm, and liver) and non-target (lung) tissues under optimal stabilization to determine any associations between analyte levels and toxicity. Consistent with companion studies, BMS-986094 was dosed orally at 0, 15, or 30 mg/kg/day to cynomolgus monkeys for 3 weeks + a 3-week treatment-free period. BMS-986094, INX-09054 (prodrug less naphthol), INX-08032 (initial nucleoside), INX-08144 (O-methyl nucleoside), and INX-09114 (triphosphorylated nucleoside) were measured by LC/MS in plasma and peripheral blood mononuclear cells (PBMC) in Weeks 1, 3, and 6; and in tissues in Weeks 3 and 6. INX-08032 was the major circulating analyte (66-68% of total AUC) followed by INX-08144 (<16%). BMS-986094, INX-09054, and INX-09114 levels (<22%) in plasma were low and INX-09114 levels in PBMCs could not be quantified. In Week 3, INX-09114 (≤ 4280 ng/mL) was high in heart and kidney, and males had higher (3.3×) heart levels than females at 30 mg/kg/day. Other analytes increased dose dependently in target and non-target tissues with BMS-986094 highest in diaphragm (≤ 4400 ng/mL) followed by INX-08032 in liver and kidney (≤ 1360 ng/mL) and low INX-08144 and INX-09054 levels (≤ 124 ng/mL) in other tissues. After the treatment-free period (Week 6), heart and kidney INX-09114 remained high (≤ 1870 ng/mL). Tissues and plasma had low INX-08032 levels (≤ 37 ng/mL), and other analytes were not detected. Persistent INX-09114 in heart and

kidney appeared to correlate with toxicities in these tissues in companion studies; however, higher tissue INX-09114 in males did not translate to increased toxicity in this sex. There were no other correlations between analytes and target organ toxicity.

PS 853 BMS-986094: Metabolomic Assessment of Cardiotoxicity in Monkeys and Mice

D. Robertson[1], P. Shipkova[1], N. Aranibar[1], P. Virdi[1], M. Reily[1], T. R. Van Vleet[2], K. Horn[2] and K. J. Trouba[2]. [1]*Applied and Investigative Metabolomics, Bristol-Myers Squibb Co., Princeton, NJ and* [2]*Drug Safety Evaluation, Bristol-Myers Squibb Co., Mt. Vernon, IN.*

BMS-986094 (formerly INX-08189), a 2'-C-methylguanosine prodrug, was withdrawn from clinical trials because of a serious safety issue. Events included decreased left ventricular ejection fraction, electrocardiogram changes, and acute kidney injury.
Pivalate prodrugs, as is BMS-986094, can be metabolized to pivaloylcarnitine (PVC) which is not further metabolized, and is eliminated in urine potentially leading to systemic carnitine depletion and, after prolonged high doses, secondary cardiomyopathy. Some monkeys and mice given BMS-986094 develop cardiomyocyte degeneration and to a lesser extent skeletal muscle degeneration. During mechanistic evaluation of potential BMS 986094 cardiotoxicity, metabolomics in monkey plasma and tissue (0, 15, or 30 mg/kg/day, 3-4 weeks) and in mouse heart (0 or 150 mg/kg/day, 2 weeks) were conducted. In monkey plasma, a dose-proportional, novel MS peak, isobaric with valeryl and isovaleryl carnitine, was identified as PVC. PVC was not evident in control or recovery monkeys. In monkey heart, acetylcarnitine was markedly depleted (0.15× control) and free carnitine (0.7×) and mid-chain acylcarnitines (0.4-0.6×) were both moderately depleted after 3 or 4 weeks of treatment. For comparison, heart PVC was the third most abundant acylcarnitine (C3-C18), but much less than free carnitine and acetylcarnitine. However, plasma carnitine was only modestly depleted suggesting that its depletion was not relevant to potential cardiotoxicity. No change was noted on any measured acylcarnitine in diaphragm despite having PVC levels similar to heart, suggesting tissue specificity. In mouse heart, there were no decreases in free carnitine or acetylcarnitine on Day 2, with only modest reduction (0.7× control) subsequently.
Tissue acetylcarnitine changes, a reflection of acetyl CoA status, were disparate across species suggesting acylcarnitine changes are likely secondary, and not indicative of a cardiac toxicity mechanism.

PS 854 BMS-986094: Transcriptional Profiling in Monkeys and Mice

T. R. Van Vleet, D. Simic, K. Horn, R. White, R. Bunch, M. Davies, T. Sanderson and M. J. Graziano. *Drug Safety Evaluation, Bristol-Myers Squibb, Mt. Vernon, IN.*

BMS-986094 (formerly INX-08189), a 2'-C-methylguanosine prodrug, was withdrawn from clinical trials because of a serious safety issue. Events included decreased left ventricular ejection fraction, electrocardiogram changes, and acute kidney injury.
Transcriptional changes (TC) associated with potential BMS-986094 toxicities were evaluated in monkeys dosed (0, 15, or 30 mg/kg/d) for 1 month and mice dosed (0, 25, or 150 mg/kg/d) for 2 weeks. For gene expression analysis, tissues were collected after the last dose (monkey) or on Days 1 (6 and 24 h), 3, 8, and 15 (mouse, time-course study). In both species, the primary target tissues were heart, kidney, and skeletal muscle, and in these tissues TC generally separated from control in PCA space. No consistent pattern of TC (up- or down-regulated) was apparent.
In monkeys, heart TC was greatest (≤ 16% total genes) with much fewer kidney TC and still fewer in skeletal muscle. Heart TC suggested cytoskeleton/myofibers/sarcomeres, GTPase (Rho, Rab, Rac, and Ras), Ca2+ and redox signaling, mitochondria, and purine synthesis involvement. Kidney TC suggested altered transport/endocytosis. Skeletal muscle TC was similar to heart, but at lower magnitude. In mice, kidney TC was greatest (≤ 13% total genes) with fewer skeletal muscle and heart TC. Early gene expression changes in kidney were associated with GTPase signaling (Rho and Rab), the cytoskeleton, Ca2+-related genes, and endocytosis-related genes. Early TC in heart was associated with cytoskeleton/myofibers/sarcomeres and GTPase and Ca2+ signaling. Most mitochondrial gene expression changes were in kidney (mostly tRNA and ribosomal genes). Gene expression changes in skeletal muscle were similar to those in heart, but lower in magnitude and delayed in onset.
Overall, TC timing and magnitudes were generally associated with the level of toxicity in target tissues. The earliest TC appeared related to cytoskeleton/myofiber/sarcomere, and GTPase and Ca2+ signaling with other TC (e.g., mitochondrial changes) likely secondary.

PS 855 BMS-986094: Investigations of *In Vitro* Metabolism, Reactive Metabolite Formation, and Oxidative Stress in Human Liver Microsomes, Hepatocytes, and Cardiomyocytes

W. Li[1], L. Ma[1], W. Zhao[1], J. Kwagh[2], C. Storck[2], Y. Zhu[1], A. Liu[1], O. Flint[2] and W. G. Humphreys[1]. [1]*Bristol-Myers Squibb, Lawrenceville, NJ and* [2]*Bristol-Myers Squibb, Pennington, NJ.*

BMS-986094 (formerly INX-08189), a 2'-C-methylguanosine prodrug, was withdrawn from clinical trials because of a serious safety issue. Events included decreased left ventricular ejection fraction, electrocardiogram changes, and acute kidney injury.
These experiments evaluated in vitro metabolism and reactive metabolite formation of BMS-986094 (non-labeled) or single BMS-986094 diastereomers (14C- or 3H-labeled BMS-986095 and BMS-986096) in human liver microsomes (HLM), hepatocytes (HH) and cardiomyocytes (HCM). Incubates were analyzed by LC-MS/radioactive detection or targeted LC-MS/MS assays. Protein covalent binding (PCB) in HLM, and intracellular glutathione (GSH), adenosine triphosphate (ATP), and reactive oxygen species (ROS) in HH or HCM were measured.
BMS-986095 and BMS-986096 were extensively metabolized in HLM, but via different oxidative pathways. Substantial PCB was detected in HLM with both diastereomers, with higher levels of PCB being produced by BMS-986095 than BMS-986096. PCB derived from the 14C-labeled naphthyl moiety was higher than that from the 14C-labeled guanine moiety for both diastereomers. GSH conjugates derived from the naphthyl moiety were detected. In human hepatocytes and cardiomyocytes, hydrolysis was the predominant metabolism pathway for both diastereomers, which led to the formation of the pharmacologically active triphosphate metabolite. Oxidative metabolisms were minor in these cells. BMS-986094 was not associated with reduced intracellular GSH in either HH or HCM, or with ROS induction in HH.
These data suggest that reactive metabolite formation by BMS-986094 in HLM was mainly associated with oxidative metabolism at the naphthyl moiety, but the predominate metabolism pathway (hydrolysis) of BMS-986094 in HH and HCM was not associated with the formation of reactive metabolites or oxidative stress.

PS 856 BMS-986094: Potential Cytotoxicity in Differentiated Human Cardiomyocytes

J. Kwagh, C. Storck, H. Shi, M. Huang, P. C. Levesque and O. Flint. *Discovery Toxicology, Bristol-Myers Squibb, Princeton, NJ.*

BMS-986094 (formerly INX-08189), a 2'-C-methylguanosine (2CMG) prodrug with pivalate and 1-naphthol moieties, was withdrawn from clinical trials because of a serious safety issue. Events included decreased left ventricular ejection fraction, electrocardiogram changes, and acute kidney injury.
2CMG-triphosphate (2CMG-TP), pivalate and 1-naphthol are formed by cellular metabolism of BMS-986094. The objective of these studies was to assess potential cytotoxicity of these 3 metabolites in cultures of differentiated human cardiomyocytes (hCM).
hCM, derived from induced pluripotent stem cells, were cultured up to 10 days. Cell viability and function endpoints included total ATP, caspase 3/7 activity, beat rate, and contractility by impedance (eXCELLigence). Glucose- and fatty acid-driven mitochondrial respirations were assessed using the Seahorse XF®96 analyzer and acylcarnitine formation was measured by HPLC.
Based upon ATP depletion, BMS-986094 IC50 values on Days 1, 3, 6 and 10 were >50, 17.3, 2.1 and 0.6 μM, respectively. Caspase 3/7 activity, a measure of apoptosis activation, was increased on Days 3, 6 and 10. Decreased hCM contractility (amplitude) was associated with reduced cell viability. Other changes associated with BMS-986094 (10 μM) included: (1) inhibition of mitochondrial respiration as early as Day 1 (IC50 7.7 μM); (2) inhibition of palmitate-fueled oxygen consumption after 4 days; and (3) reduced glucose-driven basal cell oxygen consumption on Days 6 and 10. In contrast, 1-naphthol (100 μM) and pivalate (10 μM), when added directly to cultures, were not associated with reduce cell viability when tested up to 10 days.
BMS-986094 was associated with concentration- and time-related cytotoxicity and altered energy utilization in hCM cells. However, the relevance of these observations to in vivo findings remains unclear. Pivalate and 1-naphthol, principal BMS-986094 prodrug metabolites, were not cytotoxic.

PS 857 BMS-986094: *In Vitro* Mitochondrial DNA Replication, Transcription, and Translation

O. Flint[1], F. Wang[1], J. Kwagh[1], C. Storck[1], T. Sanderson[1], J. Arnold[2], C. Cameron[2] and S. Sharma[2]. [1]*Discovery Toxicology and Drug Safety Evaluation, Bristol-Myers Squibb, Princeton, NJ and* [2]*Biochemistry and Molecular Biology, The Pennsylvania State University, University Park, PA.*

BMS-986094 (formerly INX-08189), a 2'-C-methylguanosine prodrug, was withdrawn from clinical trials because of a serious safety issue. Events included decreased left ventricular ejection fraction, electrocardiogram changes, and acute kidney injury.
The objective was to assess any changes on mitochondrial DNA (mtDNA) replication, transcription, or mRNA translation in HepG2 cells and in differentiated human cardiomyocytes (hCM), derived from induced pluripotent stem cells, exposed to BMS 986094. HepG2 and hCM were exposed to BMS-986094 (0.2-2 μM) for ≤19 days. The mitochondrial genes ATP8 and COXII, total cell number, protein, ATP, and lactate were assayed by qPCR. In separate experiments (0.1, 1, and 10 μM; 24 hours), transcripts of the mitochondrial genes ND1 and ND5 were assayed by Northern blot in Huh7 cells and the respiratory chain proteins ND1 and COXII were assayed in hCM by in-cell Western.
BMS-986094 at >1 μM was associated with concentration- and time-related cytotoxicity after 3 days. At non-cytotoxic concentrations (<1 μM), BMS 986094 was not associated with HepG2 or hCM mtDNA reductions after 19 or 10 days, respectively. BMS 986094 at high concentrations (9-10 μM) was associated with reduced ND1 and ND5 transcription in Huh7 cells and ND1 and COXII proteins in hCM within 24 h. Other observations at 10 μM were inhibition of mtRNA polymerase-driven mRNA transcription (POLRMT) and reduced expression (translation) of respiratory chain proteins. These latter observations are consistent with a recent report [Arnold et al, PLoS Pathog 8(11): 2012] that 2'-C-methylguanosine is a terminator of POLRMT-driven mRNA strand elongation.
In summary, BMS-986094 was not associated with mtDNA replication inhibition, but was associated with POLRMT inhibition and reduced respiratory chain protein expression. However, the relevance of these in vitro observations to in vivo findings remains unclear.

PS 858 Altered Vascular Nitric Oxide Production in Diabetics and Control Subjects following Acute Traffic Pollution Exposure

A. Pettit[1], H. Kipen[2, 3], R. Laumbach[2, 3], Z. Fan[3], P. Ohman-Strickland[4], C. Cepeda[3] and A. Gow[3, 5]. [1]*Graduate School of Biomedical Sciences, Rutgers University, Piscataway, NJ,* [2]*Robert Wood Johnson Medical School, Rutgers University, Piscataway, NJ,* [3]*Environmental and Occupational Health Sciences Institute, Rutgers University, Piscataway, NJ,* [4]*School of Public Health, Rutgers University, Piscataway, NJ and* [5]*Ernest Mario School of Pharmacy, Rutgers University, Piscataway, NJ.*

The vascular endothelium modulates arterial tone through production of endothelial-derived nitric oxide (EDNO). Loss of EDNO has been implicated in the pathogenesis of vascular conditions including diabetes(T2DM). Exposure to traffic-related air pollution (TRAP) has been found to negatively impact clinical vascular outcomes,possibly through loss of endothelial function. Reactive hyperemia (RH), a potent inducer of EDNO, is reduced in T2DM and following exposure to TRAP. In this study we examined impact of an acute 2 hour highway TRAP exposure on NO metabolism in 20 type II diabetic and 20 control subjects. Plasma nitrite (NO2-), a proximal measure of EDNO, and nitrate (NO3-), a further oxidized metabolite, were measured prior to and following RH, before and after pollution exposure. Diabetics displayed a higher resting NO2- level than controls at baseline (230 vs. 182.6nM, $p<0.06$). Resting NO2- in diabetics decreased by 18.3% following the car ride ($p<0.06$), while controls decreased by 2.9%($p<0.08$). Controls responded with a significant increase in NO2- following RH (15.9%, $p<0.02$) that was blunted by TRAP exposure (5.0%, ns). Diabetics showed no change in NO2- due to RH (1.8%, $p<0.8$) that was unaffected by TRAP. The ratio of NO2- to NO3- showed no change in controls due to TRAP. This ratio shifted toward NO3- in diabetics. Therefore, TRAP appears to lower the RH response in EDNO production, a property that is already lost in T2DM. Meanwhile TRAP strongly impacts the handling of NO within T2DM,favoring oxidation. Oxidative metabolism of NO in T2DM, leading to loss of endothelial function, appears to be further increased following TRAP exposures, implying this population may be more susceptible to adverse clinical events from traffic.

PS 859 Anterior Chamber Model to Evaluate Drug Effects on Corneal Wound Repair

A. Vickers[1], J. Herrmann[1] and R. Fisher[2]. [1]*Allergan Inc, Irvine, CA and* [2]*Vitron Inc, Tucson, AZ.*

Human and rabbit response to drug effects on corneal wound healing was evaluated in an anterior chamber model. New Zealand white rabbit eye globes were obtained and placed in Optisol. Human eyes were procured with donor consent through Midwest Eye-Banks (Ann Arbor, MI) and The Lions Eye Institute for Transplant and Research (Tampa, FL). Wounding, anterior keratectomy (AK), was induced by scoring the cornea (rabbit 2.5 mm, human 8 mm), and removing the epithelium using a gill knife. The anterior segment of the eye was dissected and cultured in complete medium on a rotating platform to maintain tissue differentiation for several days. The initial wound and progression of wound closure was visualized with fluorescein (0.015%), and the area recorded with a digital photo and quantified with Image J. Wound closure in untreated AK cornea occurred at different rates, rabbit (75% at 72 h) compared to human (24 h). Diclofenac (DCF) a nonsteroidal anti-inflammatory agent often used post-surgery and dosed topically (0.1%), impaired wound healing in both species. Rabbit AK cornea treated with DCF exhibited more gene changes in immune/inflammation, cell adhesion/chemotaxis, apoptosis, hypoxia/oxidative stress and angiogenesis than AK only. DCF also suppressed cell cycle/proliferation and protein folding genes altered by AK alone. Human gene expression changes altered by DCF included immune/inflammation, cell adhesion, remodeling and angiogenesis responses; apoptosis related genes were not altered. DCF has been shown to decrease early epithelialization in rabbits in vivo and corneal changes in humans. This anterior chamber model allows for the evaluation of human response to drugs and formulations on untreated eyes as well as the effects on wound repair.

PS 860 Establishment and Characterization of a New Rat Bronchial Organotypic Model Resembling the *In Vivo* Situation

C. Mathis[1], S. Huang[2], S. Frentzel[1], D. Kuehn[1], F. Talamo[1], M. Guertz[1], E. Guedj[1], Y. Xiang[1], A. Hayes[3], S. Constant[2], M. Peitsch[1] and J. Hoeng[1]. [1]*Philip Morris International, Neuchâtel, Switzerland,* [2]*Epithelix Sarl, Plan-les-Ouates, Switzerland and* [3]*Spherix Consulting, Rockville, MD.*

Organotypic *in vitro* culture of primary human airway epithelial cells grown at the air/liquid interface have been shown to be a powerful model to investigate normal biological processes, disease mechanisms, and responses to toxic exposures of the respiratory system. Up to now, a rodent derived counterpart of such *in vitro* model was unavailable, which could help to elucidate species translatability and minimize the use of animals in research.
This present work describes the development of a rat organotypic bronchial model from a joint effort among Epithelix, Philip Morris International R&D, and the Nickel Producers Environmental Research Association (NiPERA). After various experimental optimizations, a fully differentiated rat organotypic bronchial model (MucilAir™) has been successfully developed. Time-course trans-epithelial electrical resistance measurements indicate stable tissue integrity after 17 days and up to 26 days in culture. A morphological characterization of the rat MucilAir™ model demonstrates the presence of functional ciliated cells, mucus secreting cells, and basal cells. A similar tissue organization as seen *in vivo* was also observed. Additionally, this rat model possesses active ion transport (as demonstrated by isoproteronol or a specific inhibitor of cystic fibrosis transmembrane conductance regulator), good metabolic activity, and active secretion of inflammatory cytokines upon challenges. The data suggest that the rat Mucilair™ model is a relevant *in vitro* rat model that can be used for translational toxicology studies from rodent to human and for toxicological assessment of a variety of products including novel Modified Risk Tobacco Products.
[Supported by Philip Morris International, R&D and NiPERA]

PS 861 Application of Reduced Blood Volumes in Rodent Toxicology Designs; Enhancing Translation of Data and Reduce Number of Animals

A. Prefontaine, L. Bernier and C. Copeman. *Toxicology, Charles River, Montreal, QC, Canada.* Sponsor: M. Vézina.

Blood volume limitations are often a challenge in preclinical rodent studies, especially for studies with biologics where immunogenic and pharmacodynamic parameters are key endpoints. Additional animals and terminal blood collection are often required on these studies resulting in composite data sets from multiple satellite groups. This can be limiting as correlations and extrapolations are required between animals. To decrease the amount of data fragmentation and increase the types and amount of data from individual animals, we investigated various study designs

using micro-bioanalysis and/or reduced blood volume techniques for clinical pathology (CP) assessments. These study designs were created using recommended guidelines for weekly blood volume collections (7.5% of total blood volume/week). Study designs included a 4 week dosing period with a 4 week recovery period using a large molecule test article and included toxicokinetic (TK) and anti-drug antibody (ADA) endpoints, one pharmacodynamic marker (PD) and clinical pathology (CP) assessments. In rat studies, we were able to reduce the total blood volume that was collected on a weekly basis by up to 15 fold using micro-bioanalysis. This resulted in a 1 to 2 fold decrease in number of animals for the study. Additionally, we demonstrated that by combining micro-bioanalysis with reduced blood volumes for CP assessments it would be possible to perform a rat study with no satellite groups and collect all required samples from the same animals (TK, ADA, PD and CP). In mouse study designs, the difference was greater, by incorporating micro-bioanalysis and reduced CP volume, we could not only reduce the number of animals by 4 fold, but also perform some study endpoints using the same animal; increasing greatly the value of the data from each animal. Toxicology rodent studies can be greatly improved by incorporating reduce blood volume assays into their designs, allowing reduction in animal and improving data interpretation. These practices all support and incorporate the principles of the 3Rs.

PS 862 Exploration for Mitochondrial Toxic Oxidative Stress in Pregnant Women on Iron Supplements in a Population with High Maternal Mortality Rate

J. I. Anetor[1], E. I. Diala[1], A. Arowojolu[1], L. B. Amoo[1] and G. O. Anetor[2]. [1]*Departments of Chemical Pathology & Obstetrics/Gynaecology, University of Ibadan, Ibadan, Oyo, Nigeria and* [2]*Health Education, University of Ibadan, Ibadan, Oyo, Nigeria.*

Although Iron (Fe) is a common supplement in pregnancy, it generates toxic oxygen species (TOS). Manganese(Mn) is vital for mitochondrial function; key component of the mitochondrial antioxidant, MnSOD which scavenges TOS. Fe competes with Mn for a common transporter, transferrin (Tf). The contribution of this interaction to mitochondrial toxic oxidative stress in at risk populations has received little attention. Sixty-three pregnant women on Fe supplements (FeSO4) covering the 3 trimesters, and 63 non-pregnant women, were investigated. Fe and indices of Fe homeostasis, Mn and key components of the antioxidant system were evaluated in serum in all groups and sub-groups. The levels of Mn, SOD, and Tf were raised in pregnant subjects vs control ($p < 0.05$). In contrast, levels of Fe, ferritin, Cu, uric acid, TIBC, % saturation, and Zn were significantly reduced in the same group ($p<0.05$). The first trimester demonstrated significant elevations in Mn and Tf compared to control ($p <0.05$), while Fe, Cu, Zn, Hct, ferritin were decreased. The second trimester exhibited significant elevations in the levels of Mn, Tf and SOD. In contrast, Fe, Cu, Zn, ferritin & TIBC were significantly reduced; as for the first trimester ($p < 0.05$). In the third trimester, Mn and Tf were again significantly elevated like the previous trimesters. The levels of other bioindicators were identical with those of earlier trimesters. The consistent increase in Mn and Tf levels in the pregnant compared to non-pregnant states, and the 3 trimesters, with inverse patterns in Fe level and key components of the antioxidant system may in addition to increased demand for Fe, reflect antioxidant dynamics consistent with oxidative stress, including toxic mitochondrial oxidative perturbation. Mild to moderate mitochondrial impairment contributes to many pathologies. Understanding these interactions may improve strategies for addressing the refractory high maternal mortality rate in this high risk population.

PS 863 ELISA Detection of Zilpaterol in Retinal Tissue

C. Wilson[1, 2], M. Mengel[1] and J. Butz[1]. [1]*Indiana Animal Disease Diagnostic Laboratory, Purdue University, West Lafayette, IN and* [2]*Comparative Pathobiology, Purdue University, West Lafayette, IN.*

Zilpaterol is a β-adrenergic agonist feed ingredient intended for livestock animals in order to enhance lean muscle mass and increase feed efficiency. Unfortunately, due to zilpaterol's anabolic properties, it can be abused as a performance enhancing drug in livestock show and racing animals. Illicit abuse of the drug also extends into use of the product in animals for which the drug is not approved. Drug testing in animals commonly involves screening urine or serum samples; however, zilpaterol has a rapid rate of elimination and a short half-life. β-Adrenergic agonists, such as zilpaterol, have been shown to accumulate and persist longer in melanin-containing biological matrices, such as retinal tissue. Therefore, development of a method to detect zilpaterol in retinal tissue would be beneficial in monitoring abuse of the drug. This study highlights the use of a method that extracts zilpaterol from retinal tissue. The extract generated can then be applied to an ELISA specific for zilpaterol detection. Briefly, this method involves the following: 1) homogenizing approximately 0.40 g retinal tissue with acetonitrile:isopropanol (4:1) and 0.24 g NaCl, 2) drying the extract with 0.10 g MgSO4 and 0.80 g Na2SO4, 3) N2 evaporating the extract to dryness, reconstituting with 0.4 mL PBS, and 4) analyzing 50 μL of the reconstituted sample by ELISA. Sample optical densities less than or equal to the optical density of the 10 ppb positive control were considered positive. Using this protocol, zilpaterol was detected in the retinal tissue of 2 steers fed 96 mg zilpaterol/head/day for 26 days. The average optical density in the 2 samples was 0.050, while the 10 ppb positive control average optical density was 0.280. This study shows that zilpaterol can be detected in retinal tissue from animals being fed the drug and provides a means by which the presence of zilpaterol can be monitored in animals for which the drug is being abused or being used off-label.

PS 864 Monitoring GI Liability of EGFR Inhibitors with a Scratch Wound Assay in Intestinal Epithelial Cells

J. Harney[1], M. Hemkens[2] and G. Yanochko[2]. [1]*Drug Safety Research and Development, Pfizer, Inc., Groton, CT and* [2]*Pfizer, La Jolla, CA.*

Clinically, the use of epidermal growth factor receptor (EGFR) inhibitors for oncology includes gastrointestinal (GI) toxicity and is dose limiting. EGFR is a member of the ErbB receptor tyrosine kinase family. In normal cells, EGFR signaling is important for migration, survival, and proliferation and promotes epithelial restitution after normal GI mucosal damage. In cancer cells, activating EGFR mutations drive the development of a specific subset of non-small-cell lung cancers and in 50% of these patients the use of wild type (WT) EGFR inhibitors such as erlotinib and gefitinib is limited by the development of a T790M secondary mutation. To target patients who harbor both primary and secondary mutations, selective EGFR double mutant (DM) inhibitors are in development. We sought to determine if DM compounds would have a better GI safety profile over WT inhibitors. We used a rat intestinal epithelial cell line (IEC-6) in a scratch-wound assay (SWA) as a model for restitution of the GI epithelium. The ability of WT or DM compounds to prevent TGF-α-induced repair of wounded IEC-6 cell monolayers was measured using the IncuCyte to monitor real time wound closure (WC) (Essen BioScience). Seven WT and five DM targeted compounds were tested. WT inhibitors prevented TGF-α-induced WC. The IC50 range for the rate of WC from 0-6 hours was 0.009±0.001 to 1.15±1.38 μM with a mean of 0.19±0.56 μM and was not due to cytotoxicity as IC50 values for cytotoxicity were ≥30 μM (Promega). Inhibition of WC was associated with the WT inhibitor potency at EGFR; R2 = 0.60. In contrast to WT inhibitors, the IC50 range for the rate of WC from 0-6 hours for five DM compounds was 1.16±1.16 to 34.32±12.92 μM with a mean of 11.41±15.52 μM and was significantly greater than that for WT inhibitors ($p<0.0001$). There was some overlap between inhibition of WC and cytotoxicity in this group of compounds: IC50 values for cytotoxicity ranged from 20-100 μM. Collectively, these data suggest that the DM EGFR inhibitors should have reduced GI liability in vivo compared to WT inhibitors.

PS 865 The Protective Effects of Short-Term Fasting against 60Co-γ Ray Radiation

J. Li[1, 2]. [1]*soochow University, Suzhou, China and* [2]*RIRBM, Hiroshima University, Hiroshima, Japan.*

To investigate the antagonistic effects and mechanism of short-term fasting against 60Co-γ ray radiation *in vivo* and *in vitro*.
ICR mice were randomly divided into control, 12h, 48h, and 72h fasting group and were irradiated 7.5Gy. General symptoms, organ ratio, WBC, ROS, SOD, MDA, T-AOC and eNOS were detected. To observe the differential effects and mechanism on glucose restriction against 60Co-γ ray radiation to normal and tumor cell. V79 and A549 cells were irradiated 12Gy. V79 and A549 cells were divided into 9 groups, including high glucose of 3.0g/l with 10% serum group (3.0g/l+10% group), normal glucose of 1.0g/l with 10% normal serum group(1.0g/l+10%), 0.5g/l+10%, 3.0g/l+5%, 1.0g/l+5%, 0.5g/l+5%, 3.0g/l+1%, 1.0g/l+1% and 0.5g/l+1% group.
In vivo, the survival rates of ICR mice were 0 for the control and 12h group, 12.5% for the 48h group and 50% for the 72h group respectively. Compared with 0h group, ROS content and eNOS activity of 72h group were reduced and increased respectively. SOD, T-AOC activity of 72h group was less than 0h group. The viability of V79 and A549 cell was related to the dose level of γ ray, when the dose was 12Gy. Toxic effects and differential stress resistance (DSR) could be observed. As a result of interaction between serum restriction and radiation, the concentration of glucose in the media was reduced to mimic STS. After 60Co-γ ray radiation, V79 cell viability of the high, normal, low glucose group was reduced to 46%, 23% and 1% respectively, and A549 cell was reduced to 37%, 50% and 48%; The apoptosis rate of V79 cell of low glucose contents was reduced significantly, but A549 cell had no significant difference among groups. ROS production of V79 cell with low glucose was reduced, SOD activity was increased significantly, in contrast, ROS production of A549 cell was increased and SOD reduced significantly.

So, short-term fasting may attenuate injuries induced by radiation, as evidenced by a significant increase in mice survival rate. Glucose restriction based on differential stress resistance (DSR) protect normal cell V79 but not tumor cell A549 against 60Co-γ ray radiation.

PS 866 Effect of GDC-0941 Treatment in Combination with T-DM1 on Formation of Megakaryocytes

H. Uppal, D. L. Misner, A. H. Kim and P. Dhawan. *Safety Assessment, Genentech Inc., South San Francisco, CA.*

PI3 kinase inhibitors are being developed for several clinical indications including metastatic breast cancer in women overexpressing HER2. GDC-0941 is a potent pan PI3K inhibitor, which when given in combination with trastuzumab emtansine (T-DM1) showed >Grade 3 thrombocytopenia. The purpose of the present study was to examine the potential of GDC-0941 alone and in combination with T-DM1 to effect megakaryocyte production and proliferation *in vitro*. We utilized human *in vitro* model for the study which consisted of deriving the human hematopoietic stem cells (CD34+) (HSCs) from healthy donor bone marrow and differentiating them into megakaryocytes, during which cells were collected for cytotoxicity, cell number and CD41/CD61 expression. We evaluated the cytotoxic effect of GDC-0941 treatment on human megakaryocyte formation from CD34+ HSCs. We further co-treated GDC-0941 with T-DM1 to evaluate whether effects on human megakaryocyte formation were additive/synergistic. The data showed that GDC-0941 treatment caused a decrease in megakaryocyte production from hematopoietic stem cells and cell proliferation over a period of 14 days. Further, the treatment of GDC-0941 in combination with T-DM1 showed an enhanced cytotoxicity leading to a decrease in production of megakaryocytes over a period of 14 days when compared to GDC-0941 alone. The results show consistency when tested in additional donors. Thus, the human *in vitro* bone marrow model is very useful to evaluate the potential of a drug candidate to cause thrombocytopenia or bone marrow toxicity.

PS 867 Serum Biomarkers of Mitochondrial Damage in Survivors and Nonsurvivors of Acetaminophen-Induced Acute Liver Failure: Implications for the Mechanism of Hepatotoxicity in Humans

M. R. McGill[1], W. M. Lee[2, 3] and H. Jaeschke[1]. [1]*Pharmacology, Toxicology, and Therapeutics, University of Kansas Medical Center, Kansas City, KS,* [2]*Digestive and Liver Diseases, University of Texas Southwestern Medical Center, Dallas, TX and* [3]*Acute Liver Failure Study Group, Dallas, TX.*

Acetaminophen (APAP) overdose is a major problem. Although most patients survive, the volume of cases makes it the most common cause of acute liver failure (ALF) and ALF-related deaths in the US. We are only beginning to translate the mechanisms of hepatotoxicity from rodents to humans. Our group recently reported evidence of mitochondrial dysfunction in APAP overdose patients using biomarkers of mitochondrial damage (mitochondrial DNA [mtDNA], glutamate dehydrogenase [GDH], and nuclear DNA [nDNA] fragments). In this study, we wanted to determine if these markers correlate with death or survival. We measured mtDNA by qPCR, GDH activity by kinetic assay, and nDNA fragments by ELISA in serum from APAP-induced ALF patients who did (n = 35) and did not (n = 34) survive. All three parameters were elevated at or near the time of peak ALT in patients with APAP-induced liver injury. Unlike ALT, peak levels of both GDH and nDNA fragments were higher in serum from non-survivors than survivors (1,083±177 vs. 513±74 U/L and 259±2 vs. 209±4 % of control, respectively). GDH and nDNA fragments also exhibited weak but significant correlations with ALT, prothrombin time, and with each other. Importantly, receiver operating characteristic (ROC) curve analysis revealed that higher peak levels of both GDH and nDNA fragments better associated with non-survival (AUC=0.68 and 0.65 for GDH and nDNA, respectively; $p<0.03$) than ALT (AUC=0.60, $p=0.11$). Limited data suggest similar results for mtDNA. Conclusions: Biomarkers of mitochondrial damage are higher in non-survivors with APAP-induced ALF. This indicates that patients with more mitochondrial damage are less likely to survive. Mitochondrial biomarkers could be useful as part of a panel for patient prognosis. (NIDDK U-01 DK58369 to the Acute Liver Failure Study Group)

PS 868 A Labor of HERCULES: Curation of the Environmental Metabolome for Exposome Research

D. P. Jones[1], K. Uppal[1], D. I. Walker[2], V. Tran[1], Y. Liang[1], Y. Go[1], E. Voit[3], D. B. Barr[1], P. Tolbert[1], K. D. Pennell[2] and G. W. Miller[1]. [1]*Dept of Medicine, Emory University, Atlanta, GA,* [2]*Civil and Environmental Engineering, Tufts University, Medford, MA and* [3]*Georgia Technology Institute, Atlanta, GA.*

Liquid-chromatography high-resolution mass spectrometry with advanced algorithms for data extraction, termed "high-resolution metabolomics" (HRM), now enables routine measurement of >20,000 chemicals in biologic samples. As part of the new NIEHS-funded P30 Center at Emory University and Georgia Tech called the Health and Exposome Research Center: Understanding Lifetime Exposures (HERCULES), we have initiated systematic curation of the environmental metabolome through cross-platform statistical tests of results from validated, targeted analyses of environmental chemicals and HRM analyses of the same samples. The principles of the approach were validated using quantitative results obtained commercially (Metabolon) and compared to HRM using "targeted MWAS" (Metabolome-Wide Association Study). In this validation, the values for specific chemical targets in a series of 50 samples were regressed against the intensities for all ions [mass/charge (m/z) features] detected by HRM. The cross-platform targeted MWAS for >100 metabolites were performed, with each displayed as Manhattan plots of –log p (p value for t-test) as a function of m/z, along with false discovery rate correction. Co-elution of authentic standards and MS^n confirm metabolite identity from HRM. Results with internal standards and calibration against pooled reference samples demonstrate that HRM can be used for absolute quantification, with initial curation results also verifying the detection of environmental agents (e.g., dibutylphthalate, triphenylphosphate, pirimicarb, atrazine metabolites) and associated physiological metabolites. As part of the NIEHS Center program, HERCULES provides a robust foundation for exposome research, applying this methodology to develop a knowledgebase of environmental chemicals and their distribution among human populations and ecologic systems.

PS 869 Pathogenic Mechanisms in Highly Active Antiretroviral Therapy (HAART)-Induced Hepatotoxicity: Role Phosphodieaterase 4 (PDE4) and ER-Stress

H. Donde[1], P. Barve[1], D. Barker[1], S. Joshi-Barve[1], L. Gobejishvili[1], C. McClain[1, 2] and S. Barve[1]. [1]*Department of Medicine/GI, University of Louisville, Louisville, KY and* [2]*Robley Rex VAMC, Louisville, KY.*

HIV protease inhibitors (HIV-PIs) are the major components of the highly active anti-retroviral therapy (HAART) and have been successfully used in the treatment of HIV-1 infection in the past two decades. However, it has been shown that HIV-PIs induce endoplasmic reticulum (ER) stress response and subsequent activation of unfolded protein response (UPR) leading to dys-regulation of hepatic lipid metabolism and hepatotoxicity. Our recent work shows that PDE4/cAMP metabolism plays a significant role in alcohol-induced hepatic steatosis and injury. Hence in the present study, we examined the potential mechanisms underlying HIV-PI induced hepatic ER stress and toxicity with a particular emphasis on the pathogenic role of PDE4 family of enzymes.
The effects of clinically used HIV-PIs [ritonavir (RIT) and lopinavir (LOP)] were examined both in a rat hepatoma cell line (H4IIE) as well as rat primary hepatocytes. The data obtained from these studies demonstrated that RIT+LOP led to a significant loss of hepatocyte survival. Notably, inhibition of PDE4 by a specific PDE4-inhibitor, rolipram, markedly attenuated hepatotoxicity induced by PI treatments. Examination of the mechanistic role of PDE4 showed that PDE4 inhibition significantly decreases the expression of the ER stress related proteins CHOP, ATF-4 and -3 induced by PIs. Furthermore, examination of the PDE4/cAMP-regulated downstream signaling demonstrated the involvement of Exchange proteins activated by cAMP (EPAC). Specifically, similar to rolipram, EPAC cAMP analogue (8-pCPT-2'-O-Me-cAMP) downregulated the expression of the PI-induced ER-stress genes. These data strongly support and identify a pathogenic/mechanistic role for PDE4 regulated cAMP-EPAC in the development of HIV-PI induced ER-stress leading to hepatic steatosis and injury.

PS 870 Dual Regulation of Calcineurin Activity following Lymphocyte Activation: Contribution to Cyclosporine-Induced Toxicity?

S. Sanquer[1], C. Lena[1], L. Herry[1], M. Stern[2] and R. Barouki[1]. [1]*INSERM UMR-S 747, Paris Descartes University, Paris, France and* [2]*Hôpital Foch, Suresnes, France.*

Introduction: The standard for rejection prevention in transplantation includes a calcineurin (CN) inhibitor, such as cyclosporine (CsA). It was thought that high CN activity (CN-a) reflected inadequate immunosuppression (IS) with insufficient

therapy that may lead to rejection, whereas low CN activity reflected excessive IS that would facilitate the development of adverse events. We have recently found that in several transplanted patients, both rejection and CsA-related adverse events were paradoxically accompanied by a decreased CN-a. The aim of this study was to provide a molecular explanation for such discrepancies.
Methods: We measured CN-a in human lymphocytes up to 48 h following stimulation by PMA/ionomycin. The induction of lymphocyte activation was verified by assessing the gene expression of IL6, IL2RA and IL17 by qPCR. The effect of CsA was measured in both resting and activated lymphocytes. CN-a was quantified by using tandem mass spectrometry.
Results: In resting lymphocytes, CsA led to a dose-dependent decrease in CN-a. In stimulated lymphocytes, CN-a was increased at short time-points after stimulation but was gradually decreased at later time-points. In addition, this down-regulation was even more dramatic in the presence of CsA. The transient activation of CN-a was accompanied by a lasting effect on other markers of lymphocyte activation.
Conclusion: Our results demonstrate that lymphocyte activation in vitro triggers a dual regulation of CN-a. The fact that the addition of CsA led to a more potent inhibition of CN-a when cells were activated suggests that two distinct mechanisms might concomitantly decrease CN-a: one mediated by CsA itself and another one mediated by an endogeneous down-regulation of the CN/NFAT signalling pathway. We anticipate that the activation of such mechanisms following lymphocyte activation could contribute to the toxicity induced by CNIs, especially as the CNI dosage is generally increased when rejection is suspected.

PS 871 Derivation of Induced Pluripotent Stem Cells and Their Potential Application for Cardiac Regeneration in a Porcine Model

B. Kumar[1, 2], T. Kim[1], W. Lee[1], Y. Lee[1], R. Jeon[1], S. Jang[1], S. Lee[1], S. J. Peng[3], H. Kim[3], S. L. Park[3] and G. Rho[1]. [1]*Department of Theriogenology and Biotechnology, College of Veterinary Medicine, Gyeongsang National University, Jinju, Republic of Korea,* [2]*Centre for Stem Cell Research & Regenerative Medicine, K.S. Hegde Medical Academy, Nitte University, Deralakatte, Mangalore, India and* [3]*PWG Genetics, Singapore, Singapore.* Sponsor: W. Koh.

Porcine induced pluripotent stem cells (iPSCs) offer a great promise to advance the strategies for cardiac therapy using a large animal model. Therefore, the present study investigated the derivation of iPSCs and their potential application for the treatment of myocardial infarction in a porcine model. Porcine bone marrow derived mesenchymal stem cells (BMSCs) were reprogrammed to iPSCs by the lentiviral transduction of transcription factors Oct4, Klf4, Sox2 and c-Myc. Generated iPSCs exhibited alkaline phosphatase activity and expressed pluripotent markers. Porcine iPSCs differentiated well into three germ layer-derived cells in vitro. Further, they efficiently formed teratomas in immunodeficient mice and the tumor tissues revealed the tissues of three germ layers. The efficiency of iPSCs to differentiate in vitro into cardiomyocytes was greatly enhanced in the presence of 5-azacytidine. To demonstrate the therapeutic potential, porcine iPSCs labeled with a membrane dye PKH26 were transplanted into miniature pigs with myocardial infarction generated by coronary artery ligation and reperfusion. Four weeks after transplantation, compared with control, animals injected with porcine iPSCs showed significant functional improvement measured by echocardiography. PKH26 labeled cells were detected in iPSCs transplanted groups, and showed the expression of cardiac specific markers in ischemic microenvironment. No inflammation or teratoma formation was observed in pigs that received iPSCs. The findings revealed the potential of porcine iPSCs as ideal cellular models for cardiac cell therapy and preclinical assessments.

PS 872 Engineered Nanomaterial Exposure and the Metabolic Syndrome

P. G. Stapleton, V. C. Minarchick, J. Yi, J. Frisbee and T. R. Nurkiewicz. *Physiology and Pharmacology, WVU, Morgantown, WV.*

Metabolic syndrome (MS) is a diagnosable condition, affecting the microcirculation, represented by a set of cardiovascular risk factors. Engineered nanomaterial exposure (ENM) has been shown to lead to a variety of cardiovascular effects. In this study, we evaluated coronary microvascular reactivity within the Zucker rat model of MS after ENM exposure, to determine if exposure would exacerbate microvascular dysfunction. Nine and 17-week (w) old lean control (LZR) and obese MS (OZR) male Zucker rats were exposed to filtered air or a single inhalation exposure (count median aerodynamic diameter of 152±2nm, 11±0.2mg/m3, 5hrs/day) to nano-titanium dioxide aerosols 24h before sacrifice producing calculated pulmonary depositions of 36.6-38μg, respectively. Coronary arterioles (<150μm) were evaluated within an isolated microvessel preparation. Vascular reactivity analysis was performed based on responses to endothelium-dependent (acetylcholine, ACh, 10-9-10-4 M and adenosine, ADO, 10-4 M) and –independent stimuli (spermine-NONOate, SPR, 10-9-10-4 M and seratonin, 5-HT, 10-9-10-4 M). Within the control, the LZR exhibits reduced dilator reactivity (ACh and SPR) after ENM exposure at 17w. With respect to ADO, a profound vasodilator, ENM exposure led to a 28.6% reduction in dilation at 9w, limiting reactivity to aged levels. This response was echoed, although not significant, at 17w. Additionally, reactivity to the vasoconstrictor 5-HT, is abolished at 17w, after ENM exposure. Within the MS, ENM exposure further reduced (to significance) impaired endothelium-dependent vasodilation at 9w (ACh [>10%] and ADO [21.7%]). ENM exposure within the aged group also significantly reduced ADO stimulated dilation. SER reactivity was significantly impaired with aging; however there were no additive differences associated with ENM exposure. While microvascular dysfunction was evident after ENM exposure in both age groups, there was a greater decline associated with metabolic syndrome progression than an additive effect stemming from ENM exposure.
NIH-F32-ES023435 (PAS)
NIH-RO1-ES015022 (TRN)
NSF-1003907 (VCM)

PS 873 Cyclophilin Inhibitor Alisporivir (DEB025) Is Not Toxic to Mitochondria: A Comprehensive *In Vitro* and *In Vivo* Assessment

F. Pognan[1], K. Balavenkatraman[1], P. Couttet[1], R. Kreutzer[1], S. B. Helliwell[1], D. Brees[1], A. Cordier[1], S. Chibout[1], N. Naoumov[2], A. Wolf[1] and M. Uteng[1]. [1]*NIBR, Novartis, Basel, Switzerland and* [2]*Pharma, Novartis, Basel, Switzerland.*

Some pancreatitis cases were reported in clinical studies with alisporivir (ALV) in combination with peg-interferon/ribavirin treatment of hepatitis C patients. The potential of ALV to affect mitochondrial function or morphology was assessed both *in vitro* and *in vivo*.
In vitro, a dose range of ALV and Zalcitabine (ddC - mitochondrial toxin) were tested in proliferating cell lines HepG2, Panc-1 and Capan-1 after 7 and 14 days of continuous treatment. Viability, ATP content, mitochondrial mass, mitochondrial DNA (mtDNA) and oxygen consumption rates (OCR) were measured as endpoints. With ALV, OCR paralleled cytotoxicity, reflecting cell death; however with ddC, OCR decreased even at non-cytotoxic concentrations, demonstrating mitochondrial specific impairments. At cytotoxic concentrations of either agent only ddC provoked a decrease of mtDNA content. To further assess potential mitotoxicity, similar readouts were assessed in galactose-adapted HepG2 and Molt4 cells (T-cell line sensitive to mitochondrial toxins). Galactose forces metabolism via OxPhos and thus reveals mitochondrial toxin effects not detectable in glucose. Galactose grown HepG2 and Molt4 cells were more susceptible to ddC after 14 and 25 days treatment compared to glucose, but no differential cytotoxicity or mitotoxicity was observed with ALV compared to glucose grown cells. Hence, ALV was shown to be devoid of mitotoxicity in these *in vitro* assays.
In vivo, the morphology of mitochondria in pancreas, heart and skeletal muscle from mice treated daily with DEB025 at an oral dose of 300mg/kg for 26 weeks and rats treated daily for 2-weeks at an oral dose of 100 mg/kg were examined by electron microscopy. No differences in the ultrastructure of mitochondria were observed between samples from control and DEB025 treated animals in any of the tissues examined in either species. In conclusion, the results demonstrate that alisporivir is not a mitochondrial toxin.

PS 874 Sulforaphane Protects against Influenza Virus Infection in the Nasal Mucosa of Smokers

E. Glista-Baker[1], L. Müller[2], R. N. Bauer[3], M. Meyer[4], S. Z. Jones[1], H. Zhang[5], H. Zhou[1, 5], T. Noah[1, 6] and I. Jaspers[1, 3, 6]. [1]*Center for Environmental Medicine, Asthma and Lung Biology, University of North Carolina, Chapel Hill, NC,* [2]*University Children's Hospital Basel, Basel, Switzerland,* [3]*Curriculum in Toxicology, University of North Carolina, Chapel Hill, NC,* [4]*Department of Microbiology and Immunology, University of North Carolina, Chapel Hill, NC,* [5]*Department of Biostatistics, University of North Carolina, Chapel Hill, NC and* [6]*Department of Pediatrics, University of North Carolina, Chapel Hill, NC.*

Influenza continues to affect approximately 5-20% of people in the United States. Moreover, studies show that exposure to cigarette smoke increases the susceptibility to and severity of respiratory virus infections. Researchers have explored nutritional antioxidants as a preventative therapy for viral infection. In the current study, we evaluated whether the antioxidant sulforaphane (SFN), an isothiocyanate found in cruciferous vegetables, could modify viral replication in the nasal mucosa of smokers and non-smokers *in vivo*. Separate cohorts of smokers and non-smokers were randomized to consume either a SFN-rich broccoli sprout homogenate or placebo (alfalfa sprout homogenate) once daily for four consecutive days. On day two, all subjects were inoculated with a standard dose of live attenuated influenza virus (LAIV) vaccine. Markers of viral replication, heme oxygenase-1 (HO-1), and

NAD(P)H dehydrogenase (NQO1), were analyzed in nasal lavage fluid (NLF) cell pellets and nasal epithelial biopsies (NB) using qRT-PCR. Endpoints were analyzed for baseline responses to SFN supplementation prior to inoculation with LAIV, as well as effects of SFN on LAIV-induced mucosal immune responses. Results suggest that supplementation with SFN increases levels of NLF HO-1 and NQO1 in both smokers and non-smokers. However, in response to LAIV, only smokers supplemented with SFN saw a decrease in markers of viral replication. Our data suggest that supplementation with SFN could be utilized as a novel therapeutic strategy to improve respiratory defense, particularly in susceptible populations, such as smokers.

PS 875 Trauma and Drugs of Abuse in Puerto Rico: A Retrospective Study

H. Jirau[1,5], F. Colón[2,5], M. Figueroa[4], G. Rodríguez[3], P. Rodríguez[3,4] and B. D. Jimenez-Velez[2,5]. [1]*Biology, University of Puerto Rico Rio Piedras Campus, San Juan, Puerto Rico,* [2]*Biochemistry, University of Puerto Rico School of Medicine Medical Science Campus, San Juan, Puerto Rico,* [3]*Surgery, University of Puerto Rico School of Medicine Medical Science Campus, San Juan, Puerto Rico,* [4]*Trauma Center, San Juan, Puerto Rico and* [5]*Center for Environmental and Toxicological Research, San Juan, Puerto Rico.*

It is well established that young drivers are at high risk for accident involvement and for alcohol-related fatal crashes. Alcohol-related motor vehicle crashes are the number one cause of death for American youth. This study evaluates the use of drugs and alcohol with trauma in Puerto Rico during the last 20 years. The rate of traffic accidents, violent crimes, and patients admitted to trauma units in Puerto Rico is rapidly increasing. Few studies have evaluated the use of alcohol and drugs of abuse simultaneously with other drugs. Blood and urines were collected during this period and analyzed for seven types of drugs. In 1992, 58.2% of trauma patients recruited were involved in traffic accidents, 36.7% were associated with violent crimes and 5.1% were related to accidental falls. The percent of trauma patients between 18-25 years of age has declined since 1992 from 41% to 25 % until present. The use of abused substances in trauma has declined in the last 20 years. However, alcohol still prevails as number one trauma drug declining from 26.6% to 20.5% since 1992, closely followed by cocaine (22.4% to 17.4%) and cannabinoids (13.3% to 13.1%). At least one drug was detected in 56.1% of the patients recruited of which 30.6% tested positive to one drug, while 26.0% were positive to two or more drugs (p=0.03). At least one drug remained constant across age groups (p=0.001). Most of cocaine users fell in the category of gunshot wound (p=0.002) ranging between 21-35 years old (p=0.04). Benzodiazepines had the highest prevalence as prescription drugs, especially in those related to violent crimes (p=0.04). Our results support the hypothesis that alcohol and drugs are major etiologic factors in both accidental and violent crime-related trauma in Puerto Rico.

PS 876 Production of Recombinant Antibody Fragments Targeting Soluble Epoxide Hydrolase

Z. Majkova, H. Kim, C. Morisseau, S. Lee, S. J. Gee and B. D. Hammock. *University of California, Davis, CA.*

Recombinant antibody technology allows for generation of reagents that are economical to produce and easily replenishable. Camelid heavy chain antibodies are uniquely amenable to truncation and expression in bacteria as soluble single domain antibodies (sdAbs). In this study, we created sdAbs targeting human soluble epoxide hydrolase (sEH). The enzyme sEH catalyzes conversion of epoxides to dihydrodiols. Its affinity for endogenous substrates, particularly epoxides of polyunsaturated fatty acids, makes sEH a key regulator in many physiological processes and pathologies. Inhibition of sEH can improve inflammation, hypertension, pain, and other conditions. With a goal to use the sdAb in Western blots, an alpaca was immunized with denatured purified human sEH. Lymphocyte RNA was isolated and upon reverse transcription to cDNA, genes corresponding to variable domains of heavy chain antibodies (IgG2 and IgG3) were cloned into phagemid vector pComb3X. sdAbs were displayed on surface of filamentous bacteriophage M13. This sdAb library was used for selection of antibodies binding sEH by biopanning. The total of six sdAbs with different sequences were isolated and expressed as soluble proteins of ~17 kDa. These sdAbs recognize denatured sEH with high affinity and bind weakly native sEH. sdAb that exhibited the highest sensitivity was further tested by Western blotting. The antibody cross-reacts with human and mouse sEH at ~1 ng. Binding specificity was confirmed by the use of purified sEH standards, as well as tissues from sEH knockout mice; and the antibody exhibited negligible background binding. In order to improve utility of the sdAb for Western Blot and immunohistochemistry applications, fusion proteins with AviTag (biotin conjugation), alkaline phosphatase (AP), and enhanced green fluorescent protein (EGFP) were cloned and expressed. These reagents provide valuable tools to explore factors involved in regulation of sEH and its role in health and disease. (This work was supported by the NIEHS Superfund Basic Research P42 ES04699.)

PS 876a Mobile Augmented Reality Displays for Personalized Exposure Informatics

A. J. Larkin[1,2], D. E. Williams[1,2,3] and W. M. Baird[1,2]. [1]*Environmental and Molecular Toxicology, Oregon State University, Corvallis, OR,* [2]*Superfund Research Center, Oregon State University, Corvallis, OR and* [3]*Linus Pauling Institute, Oregon State University, Corvallis, OR.*

Smartphones, tablets, and similar mobile technologies are widely utilized by the general public. Current estimates place the number of smartphone users at more than 1 billion. These devices are deeply integrated within modern communication networks and have vast potential for providing personalized health care-related information in real time. We have previously linked smartphones with atmospheric pollution models for providing predicted pollutant concentrations at smartphone locations. Public concern regarding personal air quality conditions, however, are focused on minimizing future risk rather than evaluating air quality in the recent past. We extended our smartphone technology software to inform users of predicted future atmospheric pollution levels in addition to past and present levels. Spatial extents of model predictions were enlarged to include the 20 km2 area surrounding the smartphone location. Users are informed of predicted air quality conditions in the surrounding area via an augmented reality heads-up display (HUD). The orientation of the smartphone device and cardinal direction the smartphone user is facing (N,S,E,W) is determined, and predicted exposure level at the current smartphone location, as well as the direction the user is facing, displayed on the HUD as 95% confidence intervals, color coded according to EPA air quality index categories. Arrows on the HUD inform users which direction in the surrounding location has the best predicted air quality, as well as which directions have predicted air quality that exceed warning levels. Future directions include incorporating the smartphone program into smartglass hardware such as Google glass and expanding the prediction algorithm for providing directions to destinations. We conclude that mobile technologies coupled with accurate, high-resolution environmental models can inform users of predicted near future air quality conditions. Funded by NIH P42ES016465.

PS 876b Clinical Toxicology and Community Health Education: National Poison Prevention Week in the United States

M. Broderick Pritty[1] and T. Dodd-Butera[2]. [1]*San Diego Division, California Poison Control System, San Diego, CA and* [2]*Nursing, CSU San Bernardino, College of Natural Sciences, San Bernardino, CA.*

Unintentional poisoning deaths increased by 160% from 1999 to 2009 in the United States (CDC, 2012). Approximately 4 million calls were reported by regional centers in 2010, to the American Association of Poison Control Centers. Unintentional poisonings occur primarily in the home, in children under six years of age. However, poisonings are also one of the leading causes of death among adults. Thus, educational outreach in communities, across the lifespan, fulfills a significant need for mitigating acute toxicological exposures. In 1961, the U.S. Congress established National Poison Prevention Week - held annually in the third week of March and organized by the Poison Prevention Week Council. The focus is on raising awareness and providing education and prevention efforts to the public and public health community. In addition, resources are provided to assist in prevention and treatment of intentional and unintentional poisonings throughout the year. Examples include offering the toll-free number to the PoisonHelp Line from the American Association of Poison Control Centers (AAPCC); and websites, such as PoisonPrevention.org (http://www.poisonprevention.org/index.htm); and resources about poisoning from the Centers for Disease Control (http://www.cdc.gov/features/poisonprevention/), along with educational materials developed by the AAPCC in multiple languages. Annual data from the National Poison Data System (NPDS) is reported to identify numbers and severity of exposures in human poisonings, and it is used to assess the risk to public health. Select topics of concern are chosen as the focus of National Poison Prevention Week. National Poison Prevention Week continues to be a source of community health education after more than 50 years, and supports the efforts of AAPCC to inform, advocate, and educate about acute toxicology incidents.

PS 876c Dermatoxicologic Clinical Solutions: Textile Dye Dermatitis Patch Testing

N. Blickenstaff, G. Coman and H. I. Maibach. *Dermatology, University of California San Francisco, San Francisco, CA.*

Textile contact dermatitis results when a patient develops skin manifestations due to clothing or other fabrics that contact the skin, commonly from the chemical additives used in processing the fabric, such as textile dyes, tanning agents, and finishing resins. In this study the authors provide a framework for working up and counseling a patient with suspected textile dermatitis, focusing on identifying which textile materials are most likely to be the cause of the eczematous lesions, the current clinical guidelines, the utility and appropriateness of patch testing, the limitations of these guidelines, and our pro tempore recommendations. Although there are many challenges to correctly identifying and counseling patients on how to avoid the offending textile products in a patient with suspected textile dye dermatitis, there is value in following the guidelines set forth to help identify the textile dermatitis source.

Clinicians should instruct patients to categorize and list all colored-fabric textile products that contacted the affected skin areas. The fiber composition, corresponding colorant class, and dye fastness of each suspected garment should then be noted. Lastly, fabrics should be prioritized based on color darkness. While patch tests can be useful, dermatologists should understand the limitations of standardized patch testing for patients with suspected textile dye induced dermatitis. These guidelines are expected to increase the likelihood of identifying the causative textile(s) so that patch testing can be supplemented with swatch testing and chemical dye extraction to help discover the allergenic dye.

PS 876d Cardiovascular Effects of Diesel Exhaust and Ozone in a Multipollutant Context

T. Stevens[1], M. Case[2], A. Rappold[2], J. Pleil[3], D. Diaz-Sanchez[2], W. Cascio[2] and M. C. Madden[2]. [1]*ORISE/EMAG/NCEA/ORD, EPA, RTP, NC,* [2]*CRB/EPHD/ORD, EPA, Chapel Hill, NC and* [3]*HEASD/NERL/ORD, EPA, RTP, NC.*

The cardiovascular effects of two common pollutants, diesel exhaust (DE) and ozone (O3), were examined alone and in combination in an IRB approved clinical study. Consenting healthy subjects (n=15) were exposed for 2 hrs with intermittent, moderate exercise on Day 1 to 0.3 ppm O3, 300 µg/m3 DE, both O3 and DE, or filtered air (FA). On Day 2, subjects were exposed to 0.3 ppm O3. Cardiac electrophysiology and venipuncture were performed pre and post exposure. In addition, blood pressure (BP) was measured pre, post, and every hour up through 4 hrs post on days 1 and 2. Relative to air exposure values, maximum heart rate decreased ~12% immediately post DE exposure, and the cardiac QTc interval (QTcDYN) increased ~2% immediately post O3 and DE+O3 exposure. Systolic BP was significantly decreased immediately post DE+O3 exposure compared to air. Plasma lipid profiles were altered significantly immediately after day 1 exposure. Specifically, after DE+O3 exposure triglycerides were decreased (vs O3), and VLDL decreased compared to O3 and DE. LDL and HDL levels increased compared to O3 and air, respectively. Evidence was found for independent effects of acute O3 and DE exposures alone and in combination on some outcomes. These data suggest that either interactions of ambient air pollutants or individual pollutants themselves may play a role in inducing adverse health outcomes. [Disclaimer: The views expressed are those of the authors and do not necessarily reflect the official views or policies of the US EPA.]

PS 877 Development and Validation of an Analytical Method to Quantitate 2-Ethylhexyl p-Methoxycinnamate in Rat Plasma: Application to a Preliminary Toxicokinetic Study

C. R. Croutch[1], C. Dillon[1], A. Gutierrez[1], F. Hubbard[1], R. Mathias[1], D. Logan[1], B. Sitzmann[1], J. Cobb[1], K. Dunn[1], J. Roseman[1], S. Kerns[1], D. Slade[1], K. Aillon[1], J. Algaier[1], R. Harris[1], B. Collins[2] and S. Waidyanatha[2]. [1]*MRIGlobal, Kansas City, MO and* [2]*NIH/NIEHS/DNTP, Research Triangle Park, NC.*

2-Ethylhexyl p-methoxycinnamate (EHMC) is a UVB filter ingredient found in many sunscreen formulations sold in the United States. As a result of increased public awareness of the dangers of UV radiation, sunscreen use has increased, leading to possible chronic exposure to sunscreen ingredients. EHMC is currently under study by the National Toxicology Program (NTP). We have developed an analytical method to measure EHMC in plasma in order to support planned NTP toxicity and toxicokinetic (TK) studies. Development of the method proved challenging due to the labile nature of EHMC in rat plasma. The validated method used addition of ~100mM sodium fluoride (NaF) to the plasma, processing of samples on ice, followed by protein precipitation with acetonitrile and analysis by LC-MS/MS.

The method was validated over the range of 6-110 ng/mL in plasma, resulting in acceptable linearity ($r \geq 0.99$), accuracy (% relative error ≤ 24.8%), and precision (% relative standard deviation (%RSD) ≤ 9.1%). EHMC was stable (loss ≤ 15.9%) in plasma for 6 days at ≤ –70C; acetonitrile extracts were stable (loss ≤ 6.8%) for 5 days under ambient or refrigerated conditions. The method was applied to plasma samples from a preliminary toxicokinetic study where male and female Harlan Sprague Dawley rats were intravenously administered 8 mg/kg EHMC. Blood samples were collected using a NaF stabilizing procedure, in which the dead space of the syringe was filled with a ~ 1100 mM solution of NaF. The plasma concentration vs. time course followed first order kinetics for both genders with estimated half-lives of < 35 minutes. The validated method will be used to analyze plasma from NTP reproductive and definitive TK studies.

PS 878 Validation of an ELISA for Quantitation of the Lysosomal Protein Saposin C following Protein-Lipid Nanovesicle BXQ350 Delivery to Nonhuman Primates

M. Shelton[1], R. Takigiku[2], R. Wimalasena[3], C. Cruze[2], J. Davis[1] and K. Draper[1]. [1]*Ricerca Biosciences, Concord, OH,* [2]*Bexion Pharmaceuticals, Covington, KY and* [3]*The Proctor & Gamble Company, Cincinnati, OH.*

BXQ-350 is a nanovesicle formulation of the lysosomal protein Saposin C and phospholipid dioleoylphosphatidylserine (DOPS) (SapC-DOPS) that selectively induces apoptosis in tumor cells, using a novel mechanism of action. A sandwich ELISA method for determination of SapC concentrations in K2EDTA-containing cynomolgus monkey plasma was developed and validated to support bioanalytical work on GLP-compliant toxicology studies. The calibration standard curve ranged from 0.43 to 12.4 ng/mL. Monkey plasma spiked with BXQ350 at the concentration of the lower limit of quantitation (LLOQ), low, mid and high assay ranges, and upper limit of quantitation (ULOQ) was used as quality control (QC) samples to evaluate overall performance of the assay including intra-day and inter-day accuracy and precision. Dilutional linearity was established for spiked QC samples diluted from 1:1,000 (minimal required dilution) to 1:50,000. No differences were observed between standard curve samples prepared in 0.1% monkey plasma and those prepared in buffer, suggesting that plasma was a suitable matrix for the assay. Although the assay was vulnerable to artifacts in spiked QC samples, selectivity was demonstrated using both spiked and unspiked samples at the ULOQ and LLOQ for the assay. Stability of SapC within stock solutions of BXQ350 was established for 193 days of storage at -20 °C. Stability of SapC in QC plasma samples was determined for 2 hours of short-term storage at room temperature and in incurred study samples for 229 days of long-term storage at -20 °C. In conclusion, a suitable validated ELISA method for quantitation of SapC in monkey plasma was developed.

PS 879 Intact versus Signature Peptide Approach to Reach Optimal Sensitivity in Large Molecule Quantification by LC-MS: Exenatide Case Study

D. Leroux-Petersen and F. Garofolo. *Bioanalytical Services, Algorithme Pharma Inc., Laval, QC, Canada.*

Direct comparison of two different quantification approaches; intact versus signature peptide, for the quantification of Exenatide in human plasma. The exenatide amino acids sequence analysis revealed 3 theoretical trypsin cleavage sites which would result in the generation of 4 tryptic peptides. However, experimental digestion data performed in solution showed the presence of only 3 tryptic peptides, which only one showed to be more suitable for quantification. This peptide almost exclusively ionized to the +2 charge state (m/z 474.8) and clearly fragmented to one singly charged product ion (m/z 688.4). It was observed that the detection of exenatide tryptic peptide was 5 times more sensitive than the intact exenatide. The SPE extraction efficiency of exenatide was 61% and the digestion efficiency was 80%. Overall, the entire extraction process (SPE+digestion) efficiency was calculated to be 49%. The lower limit of quantification (LLOQ) achievable using the tryptic digestion approach was 10pg/mL, which is significantly lower than the reachable LLOQ for the intact exenatide. The calibration curve was linear (weighted 1/x2) with a coefficient of correlation of 0.9951. Accuracy for 3 levels of quality control samples (QCs) ranged between 102-103% and precision between 4-7%. The method was also tested for specificity, matrix effect, preliminary human plasma stabilities, which met acceptance criteria. This study demonstrates that the tryptic digestion approach is suitable for the quantification of exenatide in human plasma. On-going work is performed on the novel QTRAP6500 to further decrease the LLOQ to low pg/mL.

PS 880 Glucagon Bioanalysis by LC-MS: Unprecedented Level of Sensitivity (10pg/mL) for a Novel Formulation

M. Raigneau and F. Garofolo. *Bioanalytical Services, Algorithme Pharma Inc., Laval, QC, Canada.*

Development of LC-MS method more sensitive than LBA for challenging quantification of Glucagon at low pg/mL level in new formulation which is easier to administer than the currently available formulations. A bioanalytical method for glucagon in human plasma was validated on API5000. However, the LLOQ (100pg/mL) was not adequate to cover the pharmacokinetic profile of a novel formulation. Therefore, the method was re-developed on two different instruments to reach higher level of selectivity and sensitivity. TripleTOF5600 was tested in full scan TOFMS (30K resolution). The 3 most abundant isotopomers of +5 charge state of glucagon were summed. Moreover, MRMHS (15K resolution targeted approach), was also evaluated and the 3 most abundant isotopomers of the +5 charge state product ion (neutral loss of NH3) were summed. This experiment revealed that using a targeted quantification approach (MRMHS) led to a 10-fold increase in sensitivity over TOFMS. Hence, it was possible to have on a TripleTOF5600 the same sensitivity of a API5000. QTRAP6500 was able to reach the LLOQ of 10pg/ml (10-time lower than validated LLOQ on API5000). The calibration curve was linear (weighted 1/x2) for the concentration range 10-10000pg/mL with a coefficient of correlation of 0.9990. The accuracy for the LLOQ was 88% with 16% precision. The accuracy for quality control samples ranged between 91-101% while the precision between 3-9%. The outcome of this research showed that it possible the development an LC-MS method more sensitive than LBA for the challenging quantification of Glucagon at low pg/mL level for a novel formulation.

PS 881 Advanced Use of High-Resolution Mass Spectrometry (HRMS) to Overcome Triple Quadrupole Limitations in Large Molecules Quantification

R. Sabelli and F. Garofolo. *Bioanalytical Services, Algorithme Pharma Inc., Laval, QC, Canada.*

The use of HRMS (QTOF) to overcome limitation of triple quadrupole for development of Large Molecule bioanalytical assays. To achieve the lowest LLOQ possible during the method development of somatostatin and enfurvirtide, the use of HRMS was preferred over triple quadrupole. For somatostatin, a large cyclic peptide known for ineffective fragmentation, a parent-to-parent approach was selected to limit loss of sensitivity during the fragmentation process. This approach is practically impossible with a triple quadrupole due to high chemical noise generated. The LLOQ achieved on HRMS with the summation of the two most intense isopotomers was 12pg/mL (S/N 22 vs. 9 on triple quadrupole). For enfurvirtide, the product ion used was 1343, which is outside the normal mass range of the quadrupole (m/z 1200). When compared to the most sensitive fragment obtained with the triple quadrupole (465.1m/z) the LLOQ was easily decreased from 100 to 50pg/mL with S/N=15. Calibration curves were found linear (weighted 1/x2) and coefficients of correlation were 0.9995 for somatostatin and 0.9987 for enfurvitide. The CV% calculated from five replicate injections of QCLLOQ was 6% for somatostatin and 9% for enfurvirtide. For both compounds, the precision of the QC samples were all within 15% and accuracy between 96-102%. This study demonstrated that HRMS instrument is more adapted and suitable than the regular triple quadrupole for overcoming of complex analytical challenges as in the case of Large Molecule quantitation. The HRMS was able in both case studies to allow more flexibility in the quantification to increase selectivity and sensitivity of the assays.

PS 882 Human Metabolism Studies of High-Molecular Weight Polycyclic Aromatic Hydrocarbons Utilizing UPLC-Moving Wire Solid Sample Feed-Accelerator Mass Spectrometry

E. Madeen[1], R. A. Corley[2], M. A. Malfatti[3], T. Ognibene[3], K. W. Turteltaub[3], T. McQuistan[1] and D. E. Williams[1]. [1]*OSU, Corvallis, OR,* [2]*Pacific Northwest National Laboratories, Richland, WA and* [3]*Lawrence Livermore National Laboratory, Livermore, CA.*

High molecular weight polycyclic aromatic hydrocarbon (PAH) exposure occurs from atmospheric deposition of incomplete combustion products to food crops and from flavoring/preserving food smoking processes. High molecular weight PAHs are carcinogenic to laboratory animals and are probable human carcinogens. Human PAH studies was previously not possible due to exposure occurring as mixtures and ethical concerns of administering the PAHs in detectable quantites to human volunteers. The application of the traditional carbon dating instrument, the accelerator mass spectrometer, to biological sample analysis is now possible with de miniumus health risk due to the improved sensitivity (one 14C molecule per 1024 molecules of 12C) and efficiency (100% transfer from UPLC eluent to AMS). We were able to detect parent and metabolites of our model PAH, dibenzo(def,p)chrysene (DBC), in the urine and plasma of human volunteers from an oral microdose of 29ng/5nCi. Volunteers, n=9, were selected to be non-homogenous of age, sex, BMI, and ethnicity to represent the variability of human metabolism. Total 14C-eq of DBC resulted in pharmacokinetic parameters of plasma Cmax=61.5 ± 42.9 fg DBC eq, Tmax= 2.25 ± 0.95 hr, α-phase T½= 5.3 ± 3.28 hr, while α-Kel= 0.19 ± 0.01 fg*h-1, followed by a prolonged β-phase parameters. Current work is focused on UPLC separation of urine and plasma metabolites and detection using the moving wire solid sample interface as well as upcoming studies of human metabolism with PAHs phenanthrene and benzo(a,l)pyrene microdosing. This data is used to validate physiologically based pharmacokinetic models of human PAH metabolism with the goal of future mixture modeling.

PS 883 Development and Characterization of a LC-MS/MS Method for Antifolate Compounds for the Treatment of *Bacillus anthracis* Infections

P. J. Kuehl[1], C. Bourne[2], K. Berlin[3], R. A. Bunce[3], J. Lucak[1], J. Marsters[1], B. C. Moeller[1], M. Valderas[1] and W. Barrow[2]. [1]*Lovelace Respiratory Research Institute, Albuquerque, NM,* [2]*Department of Veterinary Pathobiology, Oklahoma State University, Stillwater, OK and* [3]*Department of Chemistry, Oklahoma State University, Stillwater, OK.*

Bacillus anthracis is a category A priority pathogen as classified by the National Institute of Allergy and Infectious Disease division of the National Institutes of Health. Exposure to *Bacillus anthracis* is currently treated by antibiotics (ciprofloxacin, doxycycline, penicillin, etc.), however antibiotic resistance has been produced in the laboratory. Therefore a medicinal chemistry program has been created to synthesize compounds that overcome the trimethoprim resistance observed in *B. anthracis*. This program has selected two early lead compounds, RAB1 and #53. In order to support preclinical development programs, a liquid chromatography-tandem mass spectrometry method was developed for quantification of these leads in mouse biological matrices (plasma, urine and GI content). The bioanalytical assay achieves separation via a reversed phase method and by detection multiple reaction monitoring. The extraction procedure uses a two-step protein precipitation method (MeOH and ACN) to prepare samples for analysis. This extraction procedure was selected as it provides sample sterilization prior to analysis, which is required for sample analysis from *B. anthracis* challenged animals. The assay was found to be specific and selective for both lead compounds with an LLOQ of 1 ng/mL in mouse plasma. The linear range was shown to be 1.0 to 200 ng/mL with dilutional linearity up to 6,000 ng/mL. Additionally, the mass spectrometer was selectively tuned to screen for phase I metabolites (mono- and di-hydroxylation; and mono- and di-demethylation). Application of the assay to plasma protein binding studies (using rapid equilibrium dialysis) indicated that both compounds are highly protein bound (99%) in mouse plasma. This method allows for quantification of both lead compounds in preclinical pharmacokinetic and efficacy studies.

PS 884 Differential Pharmacokinetics of Tetracycline and Sulfamethoxazole in *Brassica chinensis* L. Grown Hydroponically

C. Chou, Y. Wu, P. Chen and H. Chen. *Veterinary Medicine, National Chung-Hsing University, Taichung, Taiwan.*

Veterinary antibiotics in edible vegetables have quietly become an increasing food safety concern as these antibiotic-containing vegetables may find their way back to the human food chain. Although much has been studied on the deposit levels of antibiotics in plants, relatively little is known regarding the fate of antibiotics with time once they got entry to the plant. The pharmacokinetics (uptake, distribution, metabolism and elimination) of two most commonly detected antibiotics in soil and river, tetracycline (TC) and sulfamethoxazole (SMX) in edible vegetable *Brassica chinensis* L. were investigated. The vegetable was exposed to 100 μg/mL of drugs in cultivation fluid for 24 hrs, drug concentrations in roots, petioles and leaves at 0.5, 3, 6, 12 and 24 hrs were quantified by HPLC-UV method and the bioaccumulation factors (BAF) were calculated. The results suggested significant differential uptake and distribution of the two antibiotics evidenced by a BAF of 21/0.4 in the roots and 1.3/0.2 in the leaves for TC/SMX, respectively and by a concentration ranking of roots>leaves>petioles for TC versus roots>petioles≧leaves for SMX. The Cmax and Tmax in the roots are 948±132 μg/mL at 6 hrs for TC and 33±4 μg/mL at 24 hrs for SMX, whereas in the leaves they are 92±4 μg/mL at 12 hrs (TC) versus 7±1 μg/mL at 24 hrs (SMX). The percentage uptake of drugs by the vegetable were similar at 3 concentration levels (100, 10 and 1 μg/mL) indicating the appropriateness of the current model and the ability of *Brassica chinensis* L. to uptake high amount of TC. Possible biotransformation of TC (but not SMX) was detected only in the leaves. Elimination of drugs from the vegetable was most noted in the roots mainly in the first 0.5 hr (30% reduction for TC and

15% for SMX); refreshing the cultivation fluids maximized the reduction to 50%. In conclusion, it appeared that the pharmacokinetic behaviors of TC in *Brassica chinensis* L. acted in a controlled manner while SMX followed the passive water transport in xylem.

PS 885 Comparative Metabolism and Pharmacokinetics of Diisobuyl Ketone and Diisobutyl Carbinol in Male SD Rats

F. Zhang, M. J. Bartels, A. J. Clark, J. J. Staley, T. S. Lardie, D. A. Markham, B. J. Hughes and N. N. Ball. *TERC, The Dow Chemical Company, Midland, MI.*

Diisobutyl ketone (DIBK) and diisobutyl carbinol (DIBC) are important organic solvents widely used as industrial intermediates. It was hypothesized that DIBC and DIBK have common metabolic pathways and metabolites and as such toxicological data on DIBK could be used to characterize the hazards of DIBC. To confirm or refute this hypothesis a comparative metabolism and pharmacokinetics assessment of DIBK and DIBC was conducted via single oral gavage dosing in male SD rats, followed by blood collection, metabolite identification, major biomarker quantitation, and pharmacokinetics analysis. Overall, the major metabolites of both DIBC and DIBK in blood were their corresponding monohydroxylated metabolites (DIBC alcohol and DIBK alcohol) with the site of hydroxylation at the σ and σ-1 positions, respectively. Quantitative analysis of DIBC, DIBK, DIBC-alcohol, and DIBK-alcohol in blood samples collected from 5 min to 120 hr after single dosing indicated the following: 1) DIBC and DIBK are both well absorbed following oral gavage with substantial evidence of enterohepatic recycling of DIBK, DIBC, DIBK-alcohol, and DIBC-alcohol; 2) DIBK and DIBC are also interconverted in rats; 3) DIBC and DIBK have similar bioavailability (AUC) after oral administration; 4) higher bioavailability (AUC) was found for DIBK-alcohol than DIBC-alcohol, implying that DIBC-alcohol may be more easily conjugated and eliminated in bile, thus leading to lower systemic exposure than from DIBK-alcohol. In summary, the metabolic similarities and the metabolite bioavailability difference between these substances observed in the current study support the hypothesis that DIBC will have a low potential toxicity similar to that of DIBK.

PS 886 Short-Acting and Long-Acting Buprenorphine Therapeutic Drug Levels following Single Subcutaneous Administration in Diabetic Yucatan Miniswine

B. C. Hanks[1], S. Schlink[1], L. Brown[1], M. Luna[2], Y. Liu[2], J. Liu[1], A. Stricker-Krongrad[1] and G. Bouchard[1]. *[1]Sinclair Research, Auxvasse, MO and [2]KCAS, LLC, Shawnee, KS.*

Sustained and controlled analgesia for animals involved in potentially painful procedures is required for animal welfare and ethical considerations. We designed a study to assess the PK for buprenorphine (BUP) analgesics in diabetic Yucatan miniswine. Four castrated male alloxan diabetic animals weighing approximately 30 kg were used in a complete cross-over design. For BUP, animals were dosed subcutaneously (left flank fold) with either 0.01 mg/kg (low-dose) or 0.02 mg/kg (high-dose), while for BUP SR(sustained release) the dose was either 0.12 mg/kg (low-dose) or 0.24 mg/kg (high-dose) s.c. in left flank-fold. Washout was set at 9d before animals were redosed with another formulation. For the BUP, blood samples were collected at pre-dose, 0, 15, 30, 60, 120, 240 and 480 minutes (8 timepoints targeted). For the BUP SR, samples were collected at pre-dose, 0, 30, 60, 90, 240 and 480 minutes, and 12h, 24h, 48h, 72h, and 96h (12 timepoints targeted). Buprenorphine was analyzed in K2EDTA plasma samples by liquid-liquid extraction and LC-MS/MS (quantitation range is 50 to 5000 pg/mL). Results were reported in picograms/mL of plasma. All data were quality controlled and outliers removed before summary statistics were calculated and plotted. Results for buprenorphine high- & low-dose plasma drug profile curves showed that BUP peaked at 2192 pg/ml for the high-dose and 842 pg/mL for the low dose. Following single s.c. administration, shorter-acting BUP drug was in plasma for 240-480 min (above 0.1 ng/mL efficacious threshold for 480 min or 8 hrs). Results for BUP SR plasma drug profile curves showed peaks at 1795.5 pg/ml at 240 min (high-dose) and at 1531.8 pg/mL (low dose) at 30 min. Sustained release drug was present in plasma for 96 hrs for both high- & low-dose (above 0.1 ng/mL). In conclusion, these data show that these dose levels provide sufficient plasma levels of drug for analgesia (>0.1 ng/mL) for at least 8 hr (short-acting BUP) or 96 hr (long-acting BUP SR).

PS 887 Oxycyte®, a Perfluorocarbon Emulsion Drug Candidate for the Treatment of Ischemic Brain Injury, Has Similar Pharmacokinetic Characteristics across Rodent and Nonrodent Species, Including Humans

T. B. Grizzle[2], T. Bradshaw[1] and S. Anderson[1]. *[1]Oxygen Biotherapeutics Inc, Morrisville, NC and [2]Toxicology Services Inc, Chapel Hill, NC.*

Oxycyte is a 60% w/v perfluoro(t-butylcyclohexane) intravenous emulsion being developed as a novel treatment for a variety of ischemic conditions, including traumatic brain injury. The pharmacokinetics (PK) of Oxycyte's perfluorocarbon, FtBu, across two rodent species, two nonhuman primate species, and humans were compared with the objective of using exposure ratios to assist in the selection of clinically relevant doses for future nonclinical studies. Following intravenous administration of Oxycyte in BALB/c mice and Sprague Dawley rats (3, 6, 12 mL/kg), cynomolgus monkeys (4 and 10 mL/kg), olive baboons (3 and 12 mL/kg) and humans (0.5, 1.5 and 3 mL/kg), concentrations of FtBu in whole blood generally decreased over time in a monoexponential manner. In all species, while peak exposures (C_{max}) were roughly dose proportional, overall exposure (AUC) more than doubled with each doubling of Oxycyte dose (e.g., 3 to 6 mL/kg; 6 to 12 mL/kg). In addition, FtBu half-life ($T_{1/2}$) increased with increasing Oxycyte dose, whereas values for systemic clearance (Cl) decreased. Oxycyte emulsion particles are removed from circulation via phagocytic cells of the reticuloendothelial system with the metabolically inert perfluorocarbon eventually exhaled during respiration. The nonlinearity between the systemic exposure and elimination data reflect, at least partially, saturation of this clearance mechanism with increasing dose levels. By comparing FtBu systemic exposures (AUC ratio), it was determined that in previous animal safety studies Oxycyte dose levels provided systemic exposures up to 25-fold higher than those expected at the highest clinical Oxycyte dose (3 mL/kg). Based on the comparison of PK parameters, the pharmacokinetics of FtBu are similar across species, including humans. Therefore, exposure estimates can be used to determine appropriate, clinically relevant, Oxycyte doses for use in future animal safety and pharmacology studies.

PS 888 Iron Sucrose Nanoparticles: Effects on Tissue Iron Levels and Hepatic Gene Expression in the Rat

N. J. Pearson[1], R. Forster[1], J. Bouchard[1], L. Jaillet[1], A. Rogue[1] and P. Elford[2]. *[1]CiToxLAB, Evreux, France and [2]Azad Pharma AG, Toffen, Switzerland.*

The generic Iron Sucrose Azad (ISA) or reference iron sucrose drug Venofer® were administered intravenously to (non-anemic) male rats at 15 mg/kg, a supratherapeutic dose level. Tissue iron levels in plasma and selected tissues were determined over 28 days using an ICP-MS method. Hepatic gene expression was evaluated by microarray analysis of mRNA from samples taken 24 hours after drug administration. Iron concentration/time profiles for plasma and tissues were quantitatively similar; circulating iron levels briefly exceeded transferring binding capacity and there was a transient increase in hepatic iron. Iron levels remained elevated in the bone marrow. No increases in tissue iron were observed in the heart, stomach or lungs of treated rats and small transient increases were recorded in the kidney. Spleen iron levels increased over the 28 day period in treated and control rats. The effects of ISA and Venofer® on hepatic gene transcription were similar. There was no systematic effect of either treatment on transcriptional profiles. Only a small number of genes showed significant modulation of expression. No transcriptional pattern matches with toxicity pathways were found in the ToxFX database for either treatment. No modulation of key genes in apoptosis, inflammation or oxidative stress pathways was detected. The biodistribution of administered iron is essentially similar for Iron Sucrose Azad and Venofer® and iron sucrose partitions predominantly into the liver, spleen and bone marrow. Hepatic gene expression studies did not provide any evidence of hepatic toxicity.

PS 889 Comparative Metabolism and Pharmacokinetics of Pterostilbene in Rhesus Macaques, Cynomolgus Macaques, and Common Marmosets

M. Muzzio, T. G. Ooms, W. D. Johnson and D. L. McCormick. *Life Sciences, IIT Research Institute, Chicago, IL.*

Resveratrol (3,5,4'-trihydroxy-trans-stilbene) is a natural polyphenol that demonstrates cancer chemopreventive, antiinflammatory, and cardioprotective activities in animal models. Although resveratrol has a number of desirable biological effects, its activity may be limited by poor oral bioavailability and rapid metabolism. Pterostilbene [3,5-dimethoxy-4'-hydroxy-trans-stilbene] is the dimethyl ether analog of resveratrol. Like resveratrol, pterostilbene is found in grapes and other foods, and has antiinflammatory and cancer chemopreventive activities. In a comparative

PK and metabolism study in rats, we found that total absorption (AUC) and peak plasma levels (Cmax) of pterostilbene (parent) are 10 to 40-fold higher than those of resveratrol (parent) after oral dosing. Plasma levels of resveratrol glucuronide and resveratrol sulfate are comparable after a single oral dose, whereas metabolism of pterostilbene is overwhelmingly by sulfation. The present study was performed to compare the PK and metabolism of pterostilbene in three species of non-human primates. Although common marmosets (*Callithrix jacchus*) are used much less often in preclinical development studies than are cynomolgus macaques (*Macaca fascicularis*) or rhesus macaques (*Macaca mulatta*), their smaller body size may offer important benefits, particularly when drug supply is limited or synthesis costs are high. Groups of 3 to 4 animals per species received a single gavage dose of pterostilbene (50 or 100 mg/kg); the 100 mg/kg dose is an interspecies extrapolation of the rat NOAEL for resveratrol. Timed blood collections were performed over 24 hours after dosing. No evidence of pterostilbene toxicity was seen in any animal. Plasma levels of pterostilbene (parent) were generally comparable in common marmosets and in the two species of macaques over the 24 hour collection period. These data suggest that common marmosets may provide a useful model for preclinical drug development, particularly in situations when test article availability is limited.

PS 890 Toxicokinetics of Combined Treatment with Melamine and Cyanuric Acid in Male Sprague-Dawley Rats

T. Jeong[1], G. Kim[1], Y. Um[1], C. Seo[1], K. Noh[1], W. Kang[1], H. Kim[2] and M. Kang[1]. *[1]College of Pharmacy, Yeungnam University, Gyeongsan, Republic of Korea and [2]College of Pharmacy, Sungkyunkwan University, Suwon, Republic of Korea.*

When melamine is combined with cyanuric acid, melamine-cyanuric acid crystals can easily be formed, by which nephrotoxicity of melamine would be aggravated. In the present study, toxicokinetics of melamine and cyanuric acid was studied in male SD rats orally received either melamine or cyanuric acid alone and combination of melamine and cyanuric acid for 7 consecutive days. Melamine and cyanuric acid in serum, urine and kidney were determined by liquid chromatography-mass spectroscopy. In the groups of both melamine and cyanuric acid alone, they reached the maximal serum concentration at 1 hr after dosing. Melamine and cyanuric acid were eliminated almost completely within 24 hr without a sign of accumulation. On the other hand, they were not rapidly eliminated when combined. In sera, they were increased in dose- and time-dependent manners with the sign of accumulation. The sign was also seen in kidney. In addition, the combined treatment could induce severe nephrotoxicity when compared to the group of either melamine or cyanuric acid alone. Taken together, the toxicokinetic characteristics suggested that the combination of melamine and cyanuric acid might be responsible for the severe nephrotoxicity which was not seen in either melamine or cyanuric acid alone. Supported by the grant from KFDA (09162KFDA542).

PS 891 An Updated PBPK Model for RDX (Hexahydro-1, 3, 5-Trinitro-1, 3, 5-Triazine) and Its Metabolites in Mice

C. J. Brinkerhoff[1, 2] and L. J. D'Amico[1]. *[1]ORD/NCEA-IRIS, US EPA, Washington, DC and [2]Oak Ridge Institute for Science & Education, Oak Ridge, TN.*

RDX is a military explosive that has been detected at or near military bases and munitions plants and storage facilities in air, soil, and ground water. Mice, but not rats, exposed to RDX in the diet for 2 years show an increasing trend in the combined incidence of hepatocellular adenomas and carcinomas (Lish et al. 1984). Physiologically-based pharmacokinetic (PBPK) models can aid in interpreting toxicological data and extrapolations across dose, species and exposure routes, and a PBPK model for RDX has previously been developed for mice based on oral absorption of RDX from single gavage doses (Sweeney et al. 2012 Regul. Toxicol. Pharmacol., 2012 v. 64, p. 205-224). Recently the absorption, distribution, and biotransformation of RDX administered to mice in feed for 28 days has been measured by Pan et al. (Environ. Toxicol. Chem., 2013 v. 32, p. 1295-1303). These new toxicokinetic data were used to evaluate the PBPK model of RDX in mice. The PBPK model was modified to account for absorption of RDX from feed and the metabolism of RDX to N-nitroso compounds in the GI tract. The resulting model simulations are consistent with experimental measurements of RDX concentrations in plasma, liver and brain tissues, reported by Pan et al. (2013). The model is used to evaluate correlations between the internal dose metrics of RDX and its metabolites with tumor incidence in mice.
The views expressed in this abstract are those of the authors and do not necessarily reflect the views or policies of the U.S. Environmental Protection Agency or other affiliations.

PS 892 Scoping the Need for PBPK Modeling of Child-Adult Metabolism Differences: Case Studies Applying an Enzyme Ontogeny Database

S. V. Vulimiri[1], Y. Lin[1], J. Kancherla[1], G. L. Ginsberg[2], B. P. Foos[3] and B. R. Sonawane[1]. *[1]U.S.EPA, ORD/NCEA-W, Washington, DC, [2]Connecticut Dept. of Public Health, Hartford, CT and [3]U.S.EPA, OCHP, Washington, DC.*

Knowledge of the ontogeny of Phase I and Phase II metabolizing enzymes could be essential in determining internal dose and risk of xenobiotic exposure to children in comparison to adults. Early life ontogeny of metabolizing systems has been considered in therapeutic drug monitoring, animal toxicology, gene expression studies, and physiologically-based pharmacokinetic (PBPK) modeling; however, this body of literature has not previously been organized into a single database. We created an Enzyme Ontogeny Database (EOD) for selected Phase I and Phase II enzymes commonly encountered in xenobiotic metabolism. This EOD can be used to screen child-adult metabolism differences and whether such differences should be the focus of PBPK modeling. This scoping function was exemplified with case studies of 5 chemicals, 3 of them (acetaminophen, toluene, and chlorpyrifos) were proof of concept examples because they have sufficient data to know whether enzyme ontogeny affects risk and two (trichloroethylene and aromatic amines) demonstrate how to prioritize with limited data. This analysis demonstrated that early life stages are likely to be more vulnerable to toluene and chlorpyrifos, but not to acetaminophen. Scoping for both trichloroethylene and aromatic amines indicates immaturities in cytochrome P450 enzymes (2E1 & 1A2) and conjugation systems (glutathione and N-acetylation) that may tend to offset one another. However, these predictions need to be further explored with PBPK modeling. The EOD combined with knowledge of chemical metabolism and mechanism of action may provide the basis for scoping as well as any PBPK analyses needed to determine whether children are at heightened risk due to metabolic factors.
Disclaimer: The views expressed in this presentation are those of the authors and do not necessarily reflect the views or policies of the US EPA.

PS 893 Distribution of Capecitabine and Its Metabolites 5'-Deoxy-5-Fluorocytidine, 5'-Deoxy-5-Fluorouridine, and 5-Fluorouracil in a Preclinical Mouse Model of Brain Metastases of Breast Cancer

R. Balyan, H. R. Thorsheim, R. Samala and Q. R. Smith. *Department of Pharmaceutical Sciences, Texas Tech University Health Sciences Center, Amarillo, TX.* Sponsor: S. Srivastava.

Capecitabine is an oral triple prodrug of 5-fluorouracil (5-FU), which is successful against many types of systemic tumors. Capecitabine itself is approved for treatment of breast and colorectal cancer. However, there is no information on the distribution or uptake of capecitabine and its metabolites in brain metastases of breast cancer (BMBC). We investigated conversion and extent of exposure of capecitabine and its metabolites in brain metastasis and peripheral tumors in a mouse preclinical model. Dose levels that produce plasma levels matching those in humans were selected. Xeloda (capecitabine, 150 mg/kg) was administered orally to athymic NuNu mice bearing intracranial MDA-MB-231BR human breast cancer tumors. Tissue and plasma samples were collected from 0.5-8 h and compound levels were measured by LC-MS/MS. Enzymatic biotransformation of capecitabine and its metabolites in brain and tumor was also assessed in vitro. Improved uptake and conversion of capecitabine and its prodrug metabolites was observed in brain metastases compared to healthy brain. Integrated exposure of capecitabine and its nucleoside prodrugs in brain metastases were 12-39% of plasma level and 3.5-fold higher than healthy brain ($P<0.05$). The 5-FU levels in brain metastases were 6.7 times higher than in brain ($P<0.05$) with Cmax approaching values associated with antitumor activity in vitro. Cytidine deaminase and thymidine phosphorylase enzyme activities were higher in intra-cranial tumor than healthy brain. The results demonstrate that capecitabine and each of its prodrug metabolites exhibit improved uptake and distribution in BMBC relative to normal brain.

PS 894 Disposition of the Actinide Chelating Agent 3, 4, 3-LI(1, 2-HOPO) in Swiss-Webster Mice Using C-14 As a Radio-Tracer

T. A. Choi, D. An, J. A. Morales-Rivera, J. A. Villalobos and R. J. Abergel. *Chemical Sciences Division, Lawrence Berkeley National Laboratory, Berkeley, CA.* Sponsor: R. Abergel.

In a continuing effort to remediate the harmful effects of internally deposited radioactive actinides, our research group is investigating a linear octadentate spermine based ligand, 3,4,3-LI(1,2-HOPO), for clinical application. In order to

comprehensively evaluate the disposition and tissue pharmacokinetics of this compound, 3,4,3-LI(1,2-HOPO) labeled with C-14 was administered to healthy, male and female Swiss-Webster mice by oral, intraperitoneal or intravenous route (dose level = 100 μmol/kg; C-14 activity = 100 μCi/kg). Plasma, kidney, liver, urine, and feces were collected over a course of 24 hours post single administration and analyzed using liquid scintillation counting (LSC). The study demonstrated that the ligand was rapidly distributed and cleared from tissues and was predominantly excreted through the biliary route. In order to improve the oral bioavailability of the ligand, the compound was formulated with a permeability enhancer and was administered by oral route. The maximum concentration (Cmax) of the ligand in plasma improved by 3-fold when administered with a permeability enhancer. Additional toxicity studies were performed; no toxic effects were observed in mice at the highest administered oral dose (1800 μmol/kg). The results clearly show that 3,4,3-LI(1,2-HOPO) exhibits promising activity and merits further investigation.

PS 895 Effect of Altitude on Tissue Distribution of Toluene in S-D Rats

D. A. Mahle[1], P. R. Eden[1], P. Shiyanov[1, 2], E. Hack[1, 2], L. Qi[1, 2], B. A. Wong[2, 4], W. R. Howard[4] and A. James[3, 4]. *[1]711 HPW/RHDJ, USAF, Wright Patterson AFB, OH, [2]Henry Jackson Foundation, WPAFB, OH, [3]Camris International, WPAFB, OH and [4]NAMRU-D, WPAFB, OH.*

Extreme altitude is one of the unique stressors experienced by pilots of high performance jets such as the F-22. In-line sampling from an OBOGS (On Board Oxygen Generating System) product line has identified a number of volatile organic compounds (VOCs), such as toluene, that have the potential to affect a pilot's air quality. A typical dose-response to an inhaled compound at standard conditions would likely be altered under the stress of altitude. A potential outcome of this shift in dose-response is unpredictable effects on performance and cognitive function. Adult male and female S-D rats were exposed to 200 ppm toluene for 1 hr using a single pass, nose only exposure system at simulated altitudes of 940 (ambient), 10,000 or 20,000 feet above sea level. At the end of the exposure, blood, liver, brain, lung and muscle were collected into headspace vials and analyzed for toluene. Development of a physiologically-based pharmacokinetic model of toluene with adjustments based on the ideal gas law was initiated to elucidate the mechanisms of pressure dependent changes in toluene distribution. Model simulations predicted decreasing toluene uptake as altitude increases. At ambient pressure, blood toluene from males was 30.5 ± 12.4 mg/L, while lung was the lowest at 15.6 ± 5.6 mg/L and liver the highest at 78.5 ± 43.3 mg/L. At ambient pressure, females had no significant differences from males in tissue toluene concentration with the exception of blood, which was 35% lower than male blood toluene concentration. Levels of toluene decreased significantly in blood, liver, brain, lung and muscle from male rats at 20,000 ft as compared to male rats at ambient pressure. All tissues from female rats at 10,000 or 20,000 ft had significantly lower levels of toluene than ambient with the exception of lung at 10,000 ft. The potential payoff of this research is the establishment of exposure limits of selected VOCs under extreme conditions associated with the operation of high performance combat aircraft.

PS 896 Airborne PCB11 Does Not Bioaccumulate: The Fate of ^{14}C-Labelled PCB11 and Its Metabolites *In Vivo*

X. Hu, A. Adamcakova-Dodd and P. S. Thorne. *Occupational and Environmental Health, University of Iowa, Iowa City, IA.*

Background: The production ban of polychlorinated biphenyl (PCB) technical mixtures has left the erroneous impression that PCBs exist only as legacy pollutants. Some lower-chlorinated PCBs are still being produced and contaminate both indoor and ambient air.
Objectives: To inform PCB risk assessment, we characterized lung uptake, distribution, metabolism and excretion of 3,3'-dichlorobiphenyl (PCB11) as a signature compound for these airborne non-legacy PCBs.
Methods: After delivering [^{14}C]PCB11 to the lungs of male rats, radioactivity in 34 major tissues and 5 digestive matter compartments was measured at 12, 25, 50, 100, 200 and 720 min postexposure, during which time the excreta and exhaled air were also collected. [^{14}C]PCB11 and metabolites in liver, blood, digestive matter, urine, feces and adipose tissues were extracted separately to establish the metabolic profile of the disposition.
Results: [^{14}C]PCB11 was distributed rapidly to all tissues after 99.8% pulmonary uptake and quickly underwent extensive metabolism. The major tissue deposition of [^{14}C]PCB11 and metabolites translocated from liver, blood and muscle to skin and adipose tissue 200 min postexposure, while over 50% of administered dose was discharged via urine and feces within 12 h. Elimination of the [^{14}C]PCB11 and metabolites consisted of an initial fast phase ($t_{½}$ = 10-30 min) and a slower clearance phase to low concentrations. Phase II metabolites dominated in liver, blood and excreta within 25 min after exposure.
Conclusions: This study shows that PCB11 is completely absorbed after inhalation exposure and is rapidly eliminated from most tissues. Phase II metabolites were eliminated more slowly than the PCB11 or phase I metabolites and thus can better serve as urine biomarkers of exposure.

PS 897 Tissue to Blood Partition Coefficients for Deltamethrin (DLM), Cis-Permethrin (CIS), and Trans-Permethrin in Adult Male Sprague-Dawley Rats and 21-Day Old Pups

M. Amaraneni[1], S. Muralidhara[1], T. G. Osimitz[2], S. Anand[3], D. W. Gammon[4], C. White[1], B. S. Cummings[1] and J. V. Bruckner[1]. *[1]PBS, University of Georgia, Athens, GA, [2]Science Strategies, LLC, Charlottesville, VA, [3]DuPont Haskell, Newark, DE and [4]FMC, Ewing, NJ.*

Pyrethroids are used to control a wide variety of pests in homes and in agriculture. Children ages 1 to 3 years generally have greatest exposure to pyrethroids due to their higher hand-to-mouth behavior. Differences in the pharmacokinetics between children and adults may influence their relative sensivitiy to pyrethroids. The tissue to blood partition coefficients (Kt:b) for pyrethroids in adults rats have been reported, there are no studies reporting Kt:b in pups. Thus, we determined the Kt:b of the commonly used pyrethroids, DLM,CIS and TRANS in adults and 21-day old pups. Kt:b values for DLM in 21-day old pups at 72 hr ranged from 0.4 to 0.7 for brain, liver and muscle, and were 4.6 for skin. The Kt:b values for adults were similar to those in pups, with the exception that the Kt:b for adult skin was 29.0, and that a Kt:b for fat was determined, which was 102.3. Kt:b values for CIS in 21-day old pups were 2.8 for brain, 1.4 for liver, 2.8 for muscle and 8.2 for skin. This was in contrast to 1.8 for brain, 0.8 for liver, 8.9 for muscle, 140.0 for fat and 47.3 for skin in adults. The Kt:b values for TRANS in brains of 21-day old pups were lower than adults (0.4 Vs. 2.9), as were the Kt:b values for the liver (0.4 Vs. 6.5). In contrast, the Kt:b for TRANS for muscle (7.6) and skin (43.5) in 21-day old pups were higher than adults (1.8 for muscle and 11.7 for skin). The fat Kt:b in adults for TRANS was 67.0. Kt:b values for fat in 21-day old pups were not able to be calculated for any pyrethroid due to the small amount of this tissue in this age group. These data show the novel finding that the Kt:b for several common pyrethroids differ between adults rats and 21-day old pups. It is unknown if such differences contribute to age-depenent differences in the toxicokinetics of these pesticides.

PS 898 Rapid Clearance of Murine IgG1 and IgG2 Monoclonal Antibodies in Pregnant Mice

K. Ishida[1], A. H. Nguyen[1], S. L. Wild[1], W. Sohn[1], N. Chirmule[1], M. B. Hock[1], M. J. Horner[1], E. M. Lewis[2], G. J. Moffat[3] and J. L. Bussiere[1]. *[1]Amgen, Thousand Oaks, CA, [2]Charles River Laboratories, Horsham, PA and [3]Amgen, Seattle, WA.*

Background: Three embryofetal development studies in mice with Fc-containing biotherapeutics revealed lower drug exposure in pregnant mice than nonpregnant mice, lower maternal exposure in late gestation than early gestation and higher fetal exposure than maternal exposure at gestation day [GD]18. Methods: Pregnant mice received subcutaneous injections of one of two murine surrogate monoclonal antibodies (mAb A [IgG2] 30 or 300 mg/kg or mAb B [IgG1] 300 mg/kg) on GD6 and 13. The PK profile for mAb A was compared to nonpregnant mice. PK profiles were also compared between GD6 and GD13 doses. At GD18, fetal and maternal (F/M) exposure ratio was assessed. Results: mAb A exposure (AUC) after GD6 dose was 48-54% lower in pregnant mice compared to nonpregnant mice, which was primarily attributed to more rapid clearance. For both mAb A and mAb B, clearance was also enhanced in late gestation compared to early pregnancy (AUC[GD13-18] for mAb A and mAb B was 39-65% and 52% lower than AUC[GD6-12], respectively). Anti-drug antibody development did not impact exposure. At GD18, fetal exposure was higher than maternal exposure (F/M ratio was 8.2-29 for mAb A and 29 for mAb B). Fetal plasma concentrations on GD18 for mAb A and mAb B were 51.5-258 and 111 ug/mL, respectively, which were within the pharmacologically relevant range for both mAbs. Conclusion: Clearance of murine IgG1 and IgG2 mAbs was more rapid in pregnant mice than nonpregnant mice. The rapid clearance is further enhanced in late gestation compared to early stage, leading to high F/M exposure ratios in late gestation. However, for conclusions related to placental transfer of mAbs in mice and pharmacological relevance to the fetus, it is more important to consider the absolute fetal plasma concentration.

PS 899 An Evaluation of the Feasibility and Toxicokinetics of Administering Ultra Low Doses of a Fully Humanized Monoclonal Antibody to Rats for Up to 26 Weeks

T. A. Henriques[1], D. Seemann[2], K. Marsh[1], B. Stine[3], R. Caldwell[1] and R. Yeager[1]. *[1]AbbVie Inc., North Chicago, IL, [2]AbbVie Deutschland GmbH & Co. KG, Ludwigshafen, Germany and [3]AbbVie Bioresearch Center, Worcester, MA.*

A key objective for a preclinical toxicology program with a fully humanized monoclonal antibody was to determine a dose level that maintained serum exposures in rat over time without the test-item related, rat-specific dose limiting toxicity (DLT). To this end, extensive feasibility and compatibility work was conducted to evaluate whether an ultra low dose could be formulated consistently (within 15% of target concentration) and administered by i.v. bolus without dosing apparatus interference. Upon confirmation of the feasibility of formulating and administering ultra low doses, a definitive single-dose pharmacokinetic study was conducted in male rats at i.v. bolus doses of 0.01, 0.1, 1.0, and 3.0 mg/kg. At doses of 1.0 and 3.0 mg/kg, one of five animals per group had early evidence of the rat specific DLT. Evaluation of the single-dose rat study pharmacokinetic (PK) parameters revealed a dose exposure profile that was predicted by a two-compartmental PK model with parallel linear and nonlinear (Michaelis-Menten) elimination. The rat exposure profiles may be explained by the formation of anti-drug antibodies or target mediated disposition. For the 26-week rat study, the dose of 0.01 mg/kg/week produced variable serum exposure levels that were not maintained beyond 96 hours after the initial dose in the majority of animals. Serum test item levels were also inconsistent among individual animals administered 0.1 mg/kg/week and the rat-specific DLT was observed at the beginning of Week 3. At 1.0 mg/kg/week, serum test item concentrations were high; however, this group was terminated during Week 8 of the study based on the occurrence of the rat-specific DLT. The early feasibility and single dose PK studies enabled ultra low dose administration on the 26-week rat toxicology study, which demonstrated that consistent serum exposures could not be maintained at a dose below the level that caused the rat-specific DLT.

PS 900 Oatp Subtypes Expressed in Zebrafish Liver and Kidney Transport Various Microcystin-Congeners

K. Steiner[1], D. R. Dietrich[1], L. Zimmermann[1], T. Karner[1] and B. Hagenbuch[2]. *[1]Human & Environmental Toxicology, University of Konstanz, Konstanz, Germany and [2]University of Kansas Medical Center, Kansas City, KS.*

Microcystins (MCs) are cyanobacterial toxins produced by several cyanobacteria genera. More than 100 variants of the cyclic-heptapeptide MCs, which primarily differ in their variable L-amino acid composition, have been identified so far. MC toxicity is mediated via the specific inhibition of protein phosphatases (primarily PP 1 and 2A), concomitant with protein hyperphosphorylation and subsequent collapse of the cytoskeleton and loss of cellular function and integrity. However, in order to exert cytotoxicity, MCs needs to be transported into the cell via organic anion transporting polypeptides (Oatp).
Nine Oatp subtypes from zebrafish were cloned in the vector ptracer-CMV/Bsd and transfected in HEK293 cells to test their capability to transport MCs. In order to analyze the functional expression of the transfected transporters uptake experiments were performed using the typical Oatp substrates Estrone-3-sulfate, Methotrexate and Taurocholate. Transport of Microcystin was demonstrated by exposing transfected cells to MC-LR, -RR, -LF and –LW for 24h and subsequent immunoblotting using an anti-adda antibody. Organ distribution was determined for two subtypes (Oatp1f and 1d1) using real time PCR.
Oatp1d1 is mainly expressed in the liver and transports all tested MC congeners. The kidney specific Oatp1f2 and 1f4 only transport the congeners -LW and -LF. All other Oatp subtypes do not seem to transport the MC congeners tested.

PS 901 Biliary Drug Excretion in Sandwich-Cultured Human Hepatocytes: Predicted from Inverted Membrane Vesicles and Targeted Proteomics

J. M. Pedersen[1, 2], E. Svedberg[2], Y. Lai[3], A. Noren[2], J. Palm[4], J. Hoogstraate[5] and P. Artursson[2]. *[1]The Hamner Institutes of Health Sciences, Durham, NC, [2]Uppsala University, Uppsala, Sweden, [3]Bristol-Myers Squibb, Princeton, NJ, [4]AstraZeneca R&D, Mölndal, Sweden and [5]Acturum Life Science AB, Södertälje, Sweden.* Sponsor: M. Kansy.

ABC multidrug-resistance proteins in the canalicular membrane are important contributors to the pharmacokinetic properties of drugs and endogenous compounds. In this study, a new approach for determining the individual contributions from three ABC transporters to biliary clearance was implemented. First, the inhibition of P-glycoprotein (Pgp/ABCB1), Breast Cancer Resistance Protein (BCRP/ABCG2) and Multidrug-Resistance Associated Protein 2 (MRP2/ABCC2) was investigated in inverted membrane vesicles from HEK293 cells overexpressing each of the ABC proteins. Inhibition profiles of prototypic substrate transport were obtained for 24 compounds and compared with results obtained in alternative expression systems. A good correlation between the HEK-MRP2 and Sf9-MRP2 vesicle data was observed. However, up to 40-fold lower IC50-values were obtained for Pgp and BCRP in the HEK vesicles compared to those in cellular expression systems. Next, estradiol 17β-glucuronide (E17G) was found to be a substrate for all three transporters. The contribution of each transporter to the E17G biliary efflux was investigated in HEK vesicles and in sandwich-cultured human hepatocytes (SCHH), using nine inhibitors with different specificities for the three ABC-proteins. The SCHH identified ABC inhibitors from the HEK vesicles that lost their inhibition in this physiologically more relevant model. Finally, the maximal transport activity (MTA) of each transporter was calculated and their contribution to the biliary clearance of E17G was predicted, using transport kinetics and protein expression. The canalicular efflux of E17G in SCHH was predicted with an accuracy of 90%.

PS 901a Toxicokinetics: Role in Improving Guideline Toxicological Studies for Agrochemicals

S. A. Saghir. *Intrinsik Environmental Sciences Inc., Mississauga, ON, Canada.*

Dose is central to our understanding of biological responses and used in developing toxicity criteria and ADI. In guideline toxicity studies, top dose is selected based on MTD to provide an adequate margin of safety for human exposure. Responses at such high doses likely overwhelm physiological parameters (e.g., ADME) which, for agrochemicals, are not relevant to humans due to a very large MOE (animal = mg/kg vs. human = μg or ng/kg). Ideally, the top dose in animal studies would be selected based on the POD from linear kinetics of biomarker(s) in blood to obtain a kinetically-derived maximum dose (KMD). KMD ensures the use of appropriate doses, eliminates the generation of data at irrelevantly high doses and additional MOA studies, reduces animal use, and avoids unnecessary classification (e.g., carcinogen or developmental toxicant). Sulfoxaflor (an insecticide) doses for a 13-week dietary mice study were based on the MTD of a 4-week study that showed nonlinear TK responses. Systemic dose (plasma AUC_{24h}) became supra-linear in males and remained sublinear in females between the mid and the high doses without reaching the MTD. The KMD was used to select the top dose (which was 1.1×10^6 fold higher than expected human exposure) for the chronic mice study resulting in TK linearity across doses, avoiding possible nonspecific toxicity. The plasma AUC_{24h} of 2,4-D (a herbicide) became nonlinear at doses ≥25 mg/kg/day in F0 female rats after 28 days of dietary exposure with higher nonlinearity during pregnancy and lactation due to increased dietary intake. In pups of both genders, TK became nonlinear at maternal doses of ≥40 mg/kg/day. Based on these data, the top dose was selected slightly above the KMD (~50 mg/kg/day; 8×10^5 fold higher than expected human exposure) for the subsequent extended one-generation reproductive toxicity study. This dose was ½ of the MTD and accepted by EPA and PMRA. Use of KMD-derived top dose avoided kidney and neurotoxicity, which would have resulted from the saturation of OAT1-dependent elimination at MTD-derived doses. Additionally, this procedure allowed the removal of 3X safety factor.

PS 901b Fates of Two Emerging Brominated Flame Retardants, 2-Ethylhexyl Tetrabromobenzoate and Bis(2-ethylhexyl) Tetrabromophthalate, in Female Sprague-Dawley Rats

G. A. Knudsen, J. M. Sanders, A. M. Sadik and L. S. Birnbaum. *Toxicology and Toxicokinetics, NCI at NIEHS, Research Triangle Park, NC.*

2-ethylhexyl tetrabromobenzoate (TBB; MW 550 g/mol) and bis(2-ethylhexyl) tetrabromophthalate (TBPH; MW 706 g/mol) comprise the brominated components used in several 'alternative' flame retardant mixtures (Firemaster 550, BZ-54, DP-45) introduced after the phase-out of lower-brominated polybrominated diphenyl ether (PBDE) mixtures. As replacements for 'Penta' PBDE flame retardants, TBB & TBPH are used in a wide variety of consumer products, most notably in polyurethane foams. TBPH & TBB have been detected in household dust, surface waters, adsorbed to sediment, and air samples. [14C]-labeled TBB was administered to female Sprague Dawley rats by gavage at 0.1, 1, 10, or 100 μmol/kg (6 or 25 μCi/kg). [14C]-TBPH was administered at 0.1 or 10 μmol/kg. TBB is extensively absorbed, readily metabolized, and eliminated by both urinary and fecal routes. More than 80% of administered radioactivity was recovered after 24 h at doses up to 10 μmol/kg, with fecal recoveries increasing with dose (24 h: 33→45→50%; 72h: 39→51→60%). Urinary recovery peaked between 8 and 24 h at these doses. Administration of 100 μmol/kg TBB resulted in a clear delay in both urinary and fecal recoveries, indicating saturation of elimination pathways. [14C]-radioactivity recovery exceeded 93% by 72 h after all doses and

retention of [14C]-radioactivity in tissues was minimal. HPLC analyses of urinary [14C]-radioactivity detected up to 6 metabolite peaks. The number and relative proportion of each metabolite present in urine were time and dose-dependent. The principal moieties present in fecal extracts corresponded to parent TBB and tetrabromobenzoic acid. TBPH was poorly absorbed and was primarily eliminated as parent compound in the feces at both doses tested. These findings indicate that while TBB & TBPH are structurally similar, they have very different disposition. This work was supported by the Intramural Research Program of the National Cancer Institute at the National Institutes of Health [Project ZIA BC 011476].

PS 901c Durable Pharmacological Responses from the Peptide ShK-186, a Specific Kv1.3 Channel Inhibitor That Suppresses T Cell Mediators of Autoimmune Diseases

E. J. Tarcha[2], E. J. Munoz-Elias[2], D. Bailey[1], G. W. Ruppert[1], S. E. Boley[1], R. Slauter[1], B. Knapp[1], D. Kentala[1], M. W. Pennington[3], C. Beeton[4], K. Chandy[5], S. P. Iadonato[2] and S. W. Frantz[1]. *[1]Gen. Toxicology & DMPK, MPI Research Inc., Mattawan, MI, [2]R&D, Kineta Inc., Seattle, WA, [3]R&D, Peptides International, Louisville, KY, [4]Molecular Physiology and Biophysics, Baylor College of Medicine, Houston, TX and [5]Physiology & Biophysics and Surgery, University of California, Irvine, Irvine, CA.*

The Kv1.3 channel is a recognized target for drug development to treat autoimmune diseases and organ rejection. ShK-186, a specific peptide inhibitor of Kv1.3, has shown promise in animal models of both multiple sclerosis and rheumatoid arthritis. Here, we describe the pharmacokinetic/pharmacodynamic (PK/PD) relationship for ShK-186 in rats and monkeys. The PK profile was evaluated with a validated high-performance liquid chromatography-tandem mass spectrometry method to measure the peptide's concentration in plasma. These PK results were compared with the single-photon emission computed tomography/computed tomography data for ShK-186 that were collected with an 111In-1,4,7,10-tetraazacyclododecane-1,4,7,10- tetraacetic acid-conjugate of ShK-186 to assess whole-blood PK parameters as well as the peptide's absorption, distribution, and excretion profiles. Analysis of these data support a model wherein ShK-186 is absorbed slowly from the injection site, resulting in blood concentrations above the Kv1.3 channel blocking IC50 value for up to 7 days in monkeys. PD studies on human peripheral blood mononuclear cells showed that brief exposure to ShK-186 resulted in sustained suppression of cytokine responses and may contribute to prolonged drug effects. Delayed-type hypersensitivity, chronic relapsing-remitting experimental autoimmune encephalomyelitis, and pristane-induced arthritis rat models all show that single doses of ShK-186 every 2 to 5 days are as effective as a daily administration. ShK-186's slow distribution from injection sites and its long Kv1.3 channel residence time contribute to the prolonged therapeutic effects of ShK-186 in animal models of autoimmune disease.

PS 901d Comparison of the Disposition and Pharmacokinetics of 14C-Octamethylcyclotetrasiloxane (D4) following a Single Low Dose in Rodent Liquid Diet or a High Dose in Corn Oil via Oral Gavage to Fischer 344 Rats

J. Domoradzki[1], C. Sushynski[1], C. Van Landingham[2] and K. P. Plotzke[1]. *[1]Dow Corning Corporation, Auburn, MI and [2]ENVIRON International Corp., Monroe, LA.*

The absorption, distribution, metabolism and excretion of D4 in Fischer 344 rats following a single oral gavage administration of a low dose, 30 mg 14C-D4/kg, in a rodent liquid diet or a high dose, 300 mg 14C-D4/kg, in corn oil were evaluated. Parent D4 and total radioactivity were measured in blood through 168 h post-dosing and in various tissues. Animals were housed in metabolism cages for collection of urine, feces, expired volatiles (EV) and CO2. Blood AUCs were not proportional to dose. About 25% more of the dose was absorbed following the low dose administration with a greater % of radioactivity compared to parent than in the high dose study. Parent D4 and radioactivity were measurable in all tissues with the highest concentration found in fat and majority of the recovered radioactivity being eliminated by 24 h post-dosing following either dose. Following a high dose in corn oil (females), 41% of the recovered dose was found in feces, 26% in urine, 14% in EV, 4% in CO2 and 8% in carcass. Following a low dose in rodent liquid diet (females), 23% of the dose was found in feces, 32% in urine, 30% in EV, 3% in CO2 and 11% in carcass. An increase in the % of dose in EV and a decrease in the % of dose in feces was noted in the low dose study with metabolites being present in both feces and EV. Urinary elimination consisted entirely of polar metabolites for either dose. Metabolism appeared to be increased following low dose administration driving a greater absorption. Since an earlier PBPK model based on the high dose study did not adequately describe oral uptake, low dose data will be used to refine the model. Considering the effective removal of D4 through metabolism and exhalation, accumulation in the body after repeated low oral exposures is unlikely despite its high lipophilicity. This study was supported in part by the Global Silicone Industry.

PS 901e Mass Spectrometry Imaging in Toxicology Study: Biodistribution of Unlabeled Bleomycin in Induced Interstitial Pulmonary Fibrosis (IPF) Model

D. Bonnel[1], M. McElroy[2], S. Madden[2] and J. Stauber[1]. *[1]Imaging Department, ImaBiotech, Loos, France and [2]Charles River Discovery Research Services, Edinburgh, United Kingdom.* Sponsor: D. Bonnel.

One of the main difficulties in toxicology study is to identify the potential causes of the histopathologic/functional tissue changes. Mass spectrometry imaging (MSI) technology has been used to address these crucial issues. The main advantage of this label free imaging technique is the detection of all molecules of interest directly on-tissues with high specificity. Indeed the molecular distribution of some unlabeled targeted molecules could be directly correlated with some histopathologic and functional tissue changes. MSI was used to identify the cause and to improve the understanding of the Bleomycin interstitial pulmonary fibrosis rat model.
Experimental procedures: Rats were administered seven doses of bleomycin delivered to lung by the oropharangeal aspiration route and followed for 7 days. Control animals received seven doses of saline. Three control and three treated animals were sacrificed and lungs were collected. Several fresh sections were prepared and then the distribution of the Bleomycin was determined by high resolution mass spectrometry imaging with a MALDI-FTICR. The images were generated by Quantinetix software.
Results: This work illustrates a technique for identifying the causes of some histopathologic and functional tissue changes correlated with a drug administration in toxicology study. We describe a process which combines MSI and classical staining approach directly on tissue to follow the distribution of targeted molecules implicated in a fibrosis model generation, and allows a better understanding of the toxicity model.
Conclusions: We have demonstrated the use of Mass Spectrometry Imaging to follow the distribution of a non-labeled drug and to understand its application in interstitial pulmonary fibrosis model generation. Mass Spectrometry Imaging could also allow the detection of other important endogenous molecules in the same or adjacent tissue section, such as specific disease or toxicity markers, thus allowing further understanding of PK-Tox relationships.

PS 901f A Simplified and Reliable Capillary Microsampling Procedure to Support Preclinical Regulatory Studies in Rodents

R. Mader[1], S. Iqbal[2], J. Bravo[1], J. Burnett[2], P. Kilford[2] and M. Fraschini[1]. *[1]Debiopharm International SA, Lausanne, Switzerland and [2]Covance Laboratories Ltd, Harrogate, United Kingdom.* Sponsor: A. Jackson.

Until recently, blood sampling in rodents for toxicokinetic (TK) assessment required separate satellite groups in order to obtain complete TK profiles. Due to blood volume limitations, especially so in mice, these profiles, composed of samples taken from different animals at each time point, resulted in an apparent average systemic exposure not reflecting individual exposure. Serial sampling from toxicity animals is preferable over the use of separate satellite groups, not only to correlate individual animal exposure to observed toxicity but also to reduce the overall number of animals. The recent introduction of highly sensitive mass spectrometry into routine sample analysis has enabled drug concentrations to be measured from a significantly reduced plasma volume allowing the move towards low volume blood sampling (<100 μL).
The new technique proposed involved, at the initial blood sample processing stage, that the plasma remaining within the original sampling capillary after centrifugation is placed directly into a labeled holding tube for storage and transportation. At the bioanalytical laboratory, the sample is thawed and a measured volume (currently 10 μL) removed by pipette and subsequently diluted as part of the pre-analysis procedure. This removes the need for the error-prone original capillary to volumetric micro-capillary plasma transfer, thereby reducing the sample processing time and allowing all the plasma harvested to be available for analysis.
The data presented demonstrate the feasibility of this approach in the frame of a 4 week GLP toxicity study in mice from which good TK profiles were obtained by taking serial samples (5 time points, blood volume <60 μL) from 4 mice/group/sex only. Moreover, the addition of a single blood sample from the toxicity animals at Cmax allowed observed toxicity in individual animals to be correlated directly with exposure. In addition to producing good quality data, the method also follows the principles of 3Rs by importantly reducing the number of mice required for TK.

PS 902 Crosstalk between Aryl Hydrocarbon Receptor and the Inflammatory Response: A Role for NF-κB

C. F. Vogel[1], E. Kahn[1], P. Leung[2], M. Gershwin[2], T. Haarmann-Stemmann[4], A. Hoffmann[3] and M. Denison[1]. [1]*Environmental Toxicology, University of California, Davis, CA,* [2]*Division of Rheumatology, Allergy and Clinical Immunology, University of California, Davis, CA,* [3]*Department of Microbiology, Immunology and Molecular Genetics, University of California, Los Angeles, CA and* [4]*Leibniz Research Institute for Environmental Medicine, Institute for Environmental Research, Düsseldorf, Germany.*

The Aryl hydrocarbon receptor (AhR) is involved in the regulation of immune responses, T-cell differentiation and immunity. Here we show that inflammatory stimuli such as lipopolysaccharide (LPS) induce the expression of AhR in human dendritic cells (DC) associated with an AhR-dependent increase of Cytochrome P4501A1 (CYP1A1). In vivo data confirmed the elevated expression of AhR by LPS and the LPS-enhanced 2,3,7,8-tetrachlorodibenzo-p-dioxin (TCDD)-mediated induction of CYP1A1 in thymus of B6 mice. Inhibition of nuclear factor-kappa B (NF-κB) repressed both normal and LPS-enhanced, TCDD-inducible, AhR-dependent gene expression and canonical pathway control of RelA regulated AhR-responsive gene expression. LPS-mediated induction of AhR was NF-κB-dependent as shown in mouse embryonic fibroblasts (MEFs) derived from Rel null mice. AhR expression and TCDD-mediated induction of CYP1A1 was significantly reduced in RelA deficient MEF compared to wildtype MEF cells and ectopic expression of RelA restored the expression of AhR and induction of CYP1A1 in MEF RelA null cells. Promoter analysis of the human AhR gene identified three putative NF-κB-binding elements upstream of the transcription start site. Mutation analysis of the AhR promoter identified one NF-κB site as responsible for mediating the induction of AhR expression by LPS and electrophoretic shift assays demonstrated that this NF-κB motif is recognized by RelA/p50 heterodimer. Our results show for the first time that NF-κB RelA is a critical component regulating the expression of AhR and the induction of AhR-dependent gene expression in immune cells illustrating the interaction of AhR and NF-κB signaling.

PS 903 Toxicogenomic Evaluation of Dose-Dependent TCDD-Elicited Effects in the Jejunal Epithelium of C57BL/6 Mice

K. A. Fader[1], R. Nault[2, 3] and T. R. Zacharewski[2, 3]. [1]*BioMolecular Sciences, Michigan State University, East Lansing, MI,* [2]*Department of Biochemistry & Molecular Biology, Michigan State University, East Lansing, MI and* [3]*Center for Integrative Toxicology, Michigan State University, East Lansing, MI.*

2,3,7,8-Tetrachlorodibenzo-*p*-dioxin (TCDD) exerts its effects primarily through activation of the aryl hydrocarbon receptor (AhR). We have previously demonstrated that dietary fat rather than *de novo* synthesis is the primary lipid source in TCDD-elicited hepatic steatosis in C57BL/6 mice. This study examined the dose-dependent effects of TCDD (0.01, 0.03, 0.1, 0.3, 1, 3, 10 or 30 μg/kg body weight (bw)) on gene expression in the jejunum of mice orally gavaged every 4 days for 28 days. Agilent 4 x 44K microarray analysis of jejunal epithelium identified 439 genes differentially expressed (|fold change| ≥ 1.5, P1(*t*) ≥ 0.999) across one or more doses. Dose-response modeling (ToxResponse Modeler) identified 264 sigmoidal, 28 Gaussian and 47 exponential responses from differentially expressed genes, with ED_{50} values for sigmoidal responses ranging between 0.019 to 29.0 μg/kg. Functional analysis associated differential gene expression with lipid/cholesterol transport and metabolism, lipoprotein receptor activity, and immune response. Dioxin response elements (DREs) were identified in the promoter/genomic regions of 9 of 16 lipid-related regulated genes, suggesting DRE-dependent and -independent mechanisms are involved. The induction of *Pnlip*, *Cd36*, and *Scarb1* at 10 and/or 30 μg/kg TCDD suggests enhanced dietary fat hydrolysis and uptake which coincides with mild to moderate hepatic lipid accumulation. There was also suppression of several major histocompatibility complex (MHC) class II genes at 10 and/or 30 μg/kg TCDD. Hematoxylin and eosin staining of the jejunum did not reveal any histologic differences between TCDD-treated and control mice. These results suggest dietary lipid transport and processing in the jejunum is dysregulated by TCDD. Funded by SRP P42ES04911.

PS 904 Modulation of TCDD-Mediated Induction of Cytochrome P450 1A1 by Cadmium Ion (Cd^{2+}) in a Zebrafish Liver Cell Line

Y. Chen and K. M. Chan. *Biochemistry, School of Life Science, The Chinese University of Hong Kong, Hong Kong, China.*

Trace metal ions, such as cadmium (Cd^{2+}), and trace organics typified by 2,3,7,8-Tetrachlorodibenzo-p-Dioxin (TCDD), are common co-contaminants in the environment that pose serious health risks. However, the knowledge of their joint toxic effects is largely unknown. In this study, we evaluated the effects of Cd^{2+} on the transcriptional and post-transcriptional regulation of the cytochrome P450 1A1 (CYP1A1) gene induced by TCDD, To determine the effects, Zebrafish liver cells were treated with TCDD (3 nm or 30 nm) with or without increasing concentrations of Cd^{2+} (0–30 μm), Alamer-Blue, Ethoxyresorufin-O-deethylase (EROD), real-time PCR and luciferase assay were employed to determine the cytotoxicity, enzyme activity, gene expression levels and transcriptional regulation of CYP1A1. Our results showed that TCDD, at both concentrations, can inhibit Cd^{2+}-induced cell viability and the inhibition effect is especially stronger at higher concentration of TCDD (30 nm). Cd^{2+}, at all concentrations used significantly inhibit TCDD mediated induction of CYP1A1 activity and aryl hydrocarbon receptor (AHR2), aryl hydrocarbon receptor nuclear translocator 2b (ARNT2B) as well as CYP1A1 mRNA expression levels. Luciferase assay of different deletion mutants of the CYP1A1 gene promoters also showed that co-treatment with Cd^{2+} (0–15μM) and TCDD (3 nm) produced inhibition in the activity of gene construct harboring distal promoter region (P -2626/-2009) of CYP1A1 and 3XRE reporter gene compared to TCDD (3 nm) treatment alone. In contrast, co-treatment with Cd^{2+} (30μM) and TCDD (3nm) result in a increase induction in proximal promoter (P-2626/+36) region of CYP1A1 induction compared to TCDD (3 nm) treatment alone, indicating the different contributions of CYP1A1 promoter regions on the inhibition effects induced by Cd^{2+},These data showed the ability of Cd^{2+} to alter the capacity of AhR ligands to induce the bioactivating phase I enzymes (CYP1A1), which would have effects on the carcinogenicity and mutagenicity of the AhR ligands.

PS 905 Dioxin Blocks Initiation of β-Catenin Signaling in Developing Mouse Prostate

A. J. Schneider[1], R. W. Moore[1], A. Branam[1], V. Mehta[2], L. L. Abler[2], K. P. Keil[2], C. M. Vezina[2] and R. E. Peterson[1]. [1]*School of Pharmacy, University of Wisconsin, Madison, WI and* [2]*School of Veterinary Medicine, University of Wisconsin, Madison, WI.*

In utero exposure to 2,3,7,8-tetrachlorodibenzo-p-dioxin (TCDD) impairs prostate development in mice by blocking prostatic bud specification and initiation in the ventral urogenital sinus (UGS). The result is complete ventral prostate agenesis. β-catenin (CTNNB1) is a key regulator of prostate development with multiple functions that include cell adhesion and transcriptional activation. Genetic knockout of Ctnnb1 in the UGS prevents budding initiation and causes complete agenesis of the entire prostate. Prior results from *in vitro* culture of UGSs have suggested that TCDD can downregulate CTNNB1 signaling. Therefore we sought to determine if *in utero* exposure to TCDD likewise downregulates CTNNB1 signaling in the ventral UGS. Pregnant C57BL/6J dams were exposed to either vehicle or TCDD (5 μg/kg) at embryonic day 15.5 (E15.5), and UGSs from the embryos were harvested at different developmental times thereafter. Nuclear localization of CTNNB1 and expression of CTNNB1 target genes like lymphoid enhancer factor 1 (LEF1) are hallmarks of activated CTNNB1 signaling. Using immunohistochemical staining, we found that between E16.0 and E17.0 there is a pronounced increase in the nuclear localization of CTNNB1 and expression of LEF1 in the ventral UGS epithelium (UGE) in vehicle-exposed embryos. In contrast, we did not observe an increase in CTNNB1 nuclear localization or LEF1 expression in the ventral UGE of age-matched, TCDD-exposed embryos. Furthermore, we identified Wnt inhibitory factor 1 (Wif1) and receptor tyrosine kinase-like orphan receptor 2 (Ror2) as putative target genes of CTNNB1 signaling in the UGS, and show by *in situ* hybridization that TCDD downregulates the transcription of both genes. Thus, exposure of the C57BL/6J mouse fetus to TCDD negatively regulates CTNNB1 signaling in the UGE, which could cause ventral prostate agenesis. (Supported by NIH grant ES01332.)

PS 906 Aryl Hydrocarbon Receptor Regulation of miR-196a Controls Lung Fibroblast Proliferation via the Cell Cycle Inhibitor p27kip1

M. Zago[1], E. Hecht[1], J. Sheridan[1], P. Nair[2], J. B. Matthews[3], A. Gomez[3], Q. Hamid[1], D. H. Eidelman[1] and C. J. Baglole[1]. [1]*Medecine, McGill University, Montreal, QC, Canada,* [2]*McMaster University, Hamilton, ON, Canada and* [3]*University of Toronto, Toronto, ON, Canada.*

Rationale: The Aryl hydrocarbon receptor (AhR) is a ligand-activated transcription factor that regulates cell proliferation. Cells from chronic obstructive pulmonary disease (COPD) subjects have reduced proliferation, but the association with the AhR is unknown. Activation of the AhR by benzo[a]pyrene (B[a]P) inhibits the cell cycle by controlling the levels of p27kip1, a cyclin-dependent kinase inhibitor. The mechanism by which the AhR regulates proliferation may be in part due to miR-

196a which has been shown to control proliferation associated with the expression of p27kip1. Hence, we propose that AhR-dependent regulation of miR-196a promotes proliferation by inhibiting the p27kip1 expression.
Methods: AhR+/+ and AhR-/- mouse lung fibroblasts were treated with B[a]P (1uM) with or without the AhR antagonist CH-223191 (10 uM) and miR-196a assessed by qRT-PCR. miR-196a was also assessed in A549 cells where AhR expression was knocked-out using zinc finger nuclease technology. p27kip1 and AhR protein levels were assessed by western blot. Proliferation was evaluated by thymidine incorporation. Human lung fibroblasts (HLFs) derived from smoker or COPD individuals were used for AhR protein and miR-196a analysis.
Results: AhR-/- cells (lung fibroblast and A549 cells) have a significant decrease in basal miR-196a expression compared to control cells. Both B[a]P and CH-223191 decreased miR-196a and AhR protein expression. AhR expression promoted proliferation concurrent with a reduction in p27kip1 protein. Finally, AhR protein levels in HLFs were significantly less in COPD cells as was miR-196a.
Conclusions: We report miR-196a regulation as a potential novel endogenous role for the AhR. The regulation of p27kip1 could also be how the AhR controls cell proliferation. Elucidating the role of the AhR in cell cycle progression may provide novel therapeutic options for lung diseases which have significant alterations in proliferation, such as COPD.

PS 907 Ligand Promiscuity of Aryl Hydrocarbon Receptor Agonists and Antagonists Revealed by Site-Directed Mutagenesis

A. Soshilov and M. Denison. *Environmental Toxicology, University of California Davis, Davis, CA.*

The aryl hydrocarbon receptor (AhR) is a ligand-dependent transcription factor that can be activated by structurally diverse chemicals. Although AhR ligand-binding promiscuity appears to be determined by distinct binding mechanisms within the ligand-binding pocket, direct experimental evidence is lacking. To examine the mechanisms responsible for the promiscuity in AhR ligand binding, we determined the effects of mutations within the mouse AhR ligand-binding domain (LBD) on the activity of diverse AhR ligands. AhR point mutations were generated using site-directed mutagenesis. Mutant AhR proteins were expressed in vitro and their ligand-dependent DNA binding was analyzed by gel retardation assay and functional activity confirmed by analysis of reporter gene expression in transfected cells. Site-directed mutagenesis identified Ile319, and to a lesser extent Phe318, as residues involved in ligand-selective modulation of AhR transformation and DNA binding using a panel of twelve AhR ligands. These ligands could be categorized into four distinct structurally related groups based on their ability to activate AhR mutants at position 319 in vitro. The AhR containing I319K was selectively activated in vitro and in cell culture by FICZ but not by other examined ligands. F318L and F318A mutations resulted in conversion of the AhR agonists β-naphthoflavone and 3-methylcholanthrene, respectively, into partial agonists/antagonists. Additionally, Hsp90 binding to the AhR was decreased with several mutations and was inversely correlated with AhR ligand-binding promiscuity. Together, these data identify overlapping amino acid residues within the AhR LBD that are involved in the selectivity and promiscuity of ligand binding, agonist or antagonist mode of ligand binding and hsp90 binding and provide further insights into molecular determinants of ligand activation of the AhR. Supported by the NIEHS (R01ES007685).

PS 908 The Ah Receptor Recruits IKK-alpha to Phosphorylate Ser10 in Histone H3 of the *Cyp1a1* Promoter Chromatin

H. Kurita and A. Puga. *Environmental Health, University of Cincinnati, Cincinnati, OH.*

Halogenated aromatic hydrocarbons such as 2,3,7,8-tetrachlorodibenzo-*p*-dioxin (TCDD) cause many types of toxicity via the aryl hydrocarbon receptor (AHR). One of the best known proteins induced by TCDD is the cytochrome P450 CYP1A1. Induction of this enzyme requires AHR ligand-dependent activation followed by binding of the activated AHR to AHR responsive elements (AhRE) in the promoter region of the *Cyp1a1* gene. Histone modifications are well-known epigenetic markers modulating the activity of transcription factors by alteration of chromatin states. Among histone modifications, phosphorylation of serine-10 in histone H3 (H3S10ph) by various kinases has been reported to play a role in mitosis. Prior work from this lab has shown that the level of H3S10ph in the AhRE enhancer region of the *Cyp1a1* promoter was elevated by AHR activation, which led us to search for responsible kinases that would be recruited by the ligand-activated AHR. To search for candidate kinases that phosphorylate H3S10 in an AHR dependent manner, we performed chromatin immunoprecipitation (ChIP) assays for the enhancer region of *Cyp1a1* in TCDD-treated Hepa-1 cells and C35 (AHR mutant) cells by using antibodies for AHR, H3S10ph and various kinases previously reported to phosphorylate this site. We found that binding of a subset of kinases, including IKKα, MSK1 and MSK2, to the *Cyp1a1* enhancer region was absent in control cells and significantly increased by TCDD treatment in an AHR dependent manner. In addition, Cyp1a1, Aldh3a1 and Nqo1 mRNA induction, and the level of H3S10ph in the *Cyp1a1* enhancer region of in TCDD-treated cells transfected with IKKα-shRNA was significantly decreased in comparison to TCDD-treated cells transfected with a scrambled-shRNA. We conclude that IKKα is recruited by AHR to the *Cyp1a1* enhancer region and that phosphorylation of H3S10 is a main requirement for Cyp1a1 induction. *Supported by NIH grant R01 ES 06273*

PS 909 RNA-Seq Analysis Reveals Roles for Aryl Hydrocarbon Receptor in Endogenous Lipid Synthesis and TNF Signaling

T. B. Salisbury[1], J. K. Tomblin[1], D. Primerano[2], G. Boskovic[2], J. Fan[2], A. R. Chaudhry[1], G. Morris[3] and J. Denvir[2]. *[1]Pharmacology, Physiology and Toxicology, Joan C Edwards School of Medicine, Marshall University, Huntington, WV, [2]Biochemistry and Microbiology, Joan C Edwards School of Medicine, Marshall University, Huntington, WV and [3]Department of Science and Mathematics, Glenville Sate College, Glenville, WV.*

Aryl hydrocarbon receptor is a major xenobiotic sensing transcription factor involved in the metabolism of toxicants. This study uses RNA-seq analysis to further characterize endogenous AHR roles in the absence of xenobiotics in human MCF-7 breast cancer cells. Reducing AHR with short interfering RNA significantly reduced AHR levels compared to control cells. AHR knockdown induced statistically (false discovery rate < 10%) significant changes in the expression of 634 genes compared to controls. Ingenuity pathway analysis identified that differentially expressed genes in AHR knockdown cells were significantly associated with several process that are important for endogenous lipid processing including: conjugation of lipid, conjugation of 12-hydroxyeicosatetraenoic acid, glucuronidation of leukotriene B4, synthesis of lipid, fatty acid metabolism, metabolism of eicosanoid, metabolism of prostaglandins, synthesis of fatty acid, synthesis of prostaglandins and synthesis of eicosanoids. Based on the patterns of expression of differentially expressed genes, the activity of tumor necrosis factor (TNF) was predicted to be inhibited in AHR knockdown cells. TNF responsiveness was further investigated by treating cells with TNF and measuring the induction of TNF targets p53, p21 and the antioxidant manganous superoxide dismutase (MNSOD). AHR knockdown significantly compromised TNF induction of MNSOD protein. Collectively, these results suggest that AHR (1) is active in the absence of exogenous AHR ligands (2) could play a role in signaling by controlling the expression of genes that generate bioactive intracellular lipids and (3) modulate cellular responses to intracellular reactive oxygen species (ROS).

PS 910 Dexamethasone Induces Fibroblast Growth Factor (FGF) 21 in Humans and Mice

S. Vispute and X. Cheng. *Department of Pharmaceutical Sciences, St. John's University, Queens, NY.*

Fibroblast growth factor (Fgf) 21, a recently identified master metabolic regulator, plays an important role in glucose and lipid metabolism. Fgf21 is recognized as a potential therapeutic candidate for the treatment of metabolic syndrome. Fgf21 can be induced in the mouse and human liver by activation of PPARα, triggered by fasting and ketogenic diets. Nuclear receptors, such as PPARα, PXR, and CAR, play an important role in mediating the mode of action and disposition of endogenous and exogenous compounds. We investigated whether activation of PXR and CAR also regulates Fgf21 in mouse liver. Amongst PXR ligands (spironolactone, pregnenolone 16α-carbonitrile, and dexamethasone [DEX]) and CAR ligands (TCPOBOP, Phenobarbital, and diallylsulfide), only DEX, a therapeutic drug for treatment of inflammatory and autoimmune disorders, up-regulated Fgf21 mRNA expression in mouse liver in a time- and dose-dependent manner. In addition, 72 hours treatment of 10μM DEX induced Fgf21 mRNA expression in cultured mouse (Hepa1c1c7) and human (Hep3B) hepatocytes. DEX can activate both glucocorticoid receptor (GR) and/or pregnane-X-receptor (PXR). Our data also demonstrated that DEX induced Fgf21 mRNA expression in both wild-type and PXR-null mouse liver, indicating that the induction of Fgf21 by DEX is PXR-independent. *In silico* DNA analysis of mouse and human Fgf21/FGF21 gene promoter sequences revealed the presence of several putative GR response elements (GREs) in the promoter region of both mouse and human Fgf21/FGF21 gene. Taken together, DEX significantly induced Fgf21 expression in both mouse and human hepatocytes. DEX induced Fgf21 mRNA expression in mouse liver in a PXR-independent manner.

PS 911 Transcriptiome Analysis of PXR-Regulated Gene Expression in HepG2 Cells

G. Wang[1], E. Yang[1], S. Ke[2], J. Cai[1] and Y. Tian[2]. [1]*Department of Veterinary Integrative Biosciences, College of Veterinary Medicine, Texas A&M University, College Station, TX and* [2]*Department of Physiology and Pharmacology, College of Veterinary Medicine, Texas A&M University, College Station, TX.*

Pregnane X receptor (PXR, NR1I2) is a ligand-dependent nuclear receptor (NR) that functions as a xenobiotic sensor and effector in coordinately regulating expression of genes of the xenobiotic detoxification network. PXR exerts its transcriptional regulatory functions by dimerization with retinoic X receptor (RXR), and PXR-RXR complex binds to specific DNA sequences for regulating gene expression. Whole-genome transcriptome analysis based on next generation sequencing technology (RNA-Seq) provides unprecedented opportunity to study the PXR-regulated gene expression. PXR-HepG2 cells were generated by stable transfection of PXR gene in human liver cell line HepG2 and treated with PXR ligand rifampicin (10 μM, 48 hr). PolyA RNA was isolated and the samples were subjected to RNA-Seq analysis. We have found around 2000 genes were significantly up-regulated by ligand treatment in PXR in a PXR-dependent manner, including classic PXR-regulated phase I enzymes such as CYP3A family, phase II enzymes UGT1A family and GST1As. Interestingly, we have identified PXR-regulated novel intergenic noncoding RNAs that were significantly regulated by ligand-activated PXR. In addition, we have identified alternative RNA splicing process in certain genes appears to be regulated by PXR. Our results suggest that RNA-seq through next-generation sequencing is an important tool in anaylzing the transcriptome and using this technology would enable us to gain in depth understanding of alteration of gene expression induced by xenobiotics.

PS 912 Using Three-Dimensional Cell Culture to Understand Ethanol Toxicity in Mammary Cells

R. David and N. J. Gooderham. *Imperial College London, London, United Kingdom.*

Mechanistic studies are best performed in highly controlled experimental models such as cell culture. Yet cell monolayers (2D) are generally only useful for acute exposure to toxicants and are not representative of the cellular environment found within an organism as most physiological parameters are lost. Three dimensional (3D) cell culture is reported to better represent the *in vivo* structure of tissues and tumours regarding cell shape and their environment, thus culturing in 3D is suggested to decrease the gap between cell culture and physiological tissue.
The current study aimed to determine whether 3D cell culture provides a more *in vivo*-like model of ethanol-induced toxicity to mammary cells. MCF-7 cells in 2D or 3D (spheroid) culture were exposed to a dose range (1-100mM) of ethanol for an acute (24-72h) or chronic repeat dose (10 cycles of 72h treatment, 3D only) study following which proliferation, migration, spheroid size, signal transduction and gene expression were measured.
Acute exposure of 2D MCF-7 cells to ethanol increased proliferation dose and time-dependently over 72 h. Cell migration was also increased at 100mM compared to control. Acute exposure of 3D MCF-7 spheroids to ethanol (up to 100mM) showed a trend for increased signal transduction (p-ERK ratio) consistent with increased proliferation.
Chronic repeated exposure of spheroids to ethanol dose-dependently decreased spheroid size by cycle 5. With continued exposure to low doses of ethanol (1-10mM) the decrease in size was reversed. Total cell number, however, was unaffected by treatment. At cycle 10 signal transduction (p-ERK ratio) was reduced for all treatments in line with rat *in vivo* data, where continuous/intermittent alcohol exposure (Sanna et al. Brain Res 948 P186 2002) and chronic ethanol exposure (45 days) (Sampey et al. J Biol Chem 282 P1925 2010) decreased levels of p-ERK. In contrast there was a trend for induction of the oncogenic microRNA miR-21 (anti-apoptotic) at cycle 10.
These data indicate that chronic ethanol exposure induces phenotypic change in 3D cultured mammary cells that has similarities to ethanol exposure *in vivo*.

PS 913 Low-Dose Transplacental Arsenic Exposure Alters Expression of Cell Cycle Genes in Lung Tissues of C57BL/6 Mice

D. J. Udawatte[1], X. Li[2], P. Carlson[3] and R. J. Van Beneden[1, 3, 4]. [1]*Molecular and Biomedical Sciences, University of Maine, Orono, ME,* [2]*Center for Molecular Medicine, Central South University, Changsha, Hunan, China,* [3]*Graduate School of Biomedical Sciences and Engineering, University of Maine, Orono, ME and* [4]*School of Marine Sciences, University of Maine, Orono, ME.* Sponsor: J. Gosse.

Arsenic is an environmental toxicant associated with several human diseases including cancer. The current EPA and WHO maximum allowable level for arsenic in drinking water is 10 ppb. This level is often exceeded in private wells in the state of Maine and many places world-wide, and poses a potential health concern. Molecular mechanisms of arsenic-induced carcinogenesis are still not well defined. In this study, we hypothesized that transplacental arsenic exposure alters cell cycle regulatory gene expression which may lead to a predisposition to carcinogenesis in the lung. F0 female C57BL/6 mice (Mus musculus) were exposed to 0, 10, 50 or 500 ppb sodium arsenite in their drinking water throughout mating, gestation and nursing. F1 generation mice were exposed to arsenic only during gestation and nursing. F2 mice were not directly exposed to arsenic. The expression of three cell cycle regulatory genes, Foxm1, Cdc25a and Cdc6, from the lung tissue of F1 and F2 mice was evaluated using quantitative real time PCR (qRT-PCR). Preliminary findings showed a significant change in expression of FoxM1 and Cdc6 at doses as low as 10 ppb. Histological findings suggest arsenic exposure induce inflammation in lung tissues. These results suggest low-dose transplacental arsenic exposure alters the transcription levels of several genes involved in cell cycle regulation. Our findings contribute an important insight toward the identification of a mechanism for cell cycle deregulation, following exposure to low doses of arsenic.

PS 914 Hormonal Changes and Gene Signaling Pathways in Female Rat Thyroids Exposed to Acrylamide

R. C. Colli-Dula[1], N. D. Denslow[1] and M. A. Friedman[2]. [1]*CEHT, Universy of Florida, Gainesville, FL and* [2]*Kennesaw State University, Kennesaw, GA.*

In this study, we used biological endpoints and transcriptomics to identify molecular events associated with acrylamide (AA) exposure. Pregnant female RccHan Wistar rats were treated with 3 mg AA/kg in drinking water from gestational day 6 to post natal day 30. Thyroid glands were collected from female pups at 10 AM and at 10 PM. While control animals showed no statistical difference in serum levels of TSH, T3 and T4 between AM and PM, animals exposed to AA and collected in the AM showed significant increase in serum levels of TSH and PM animals showed significant increases in levels of T4 and T3, compared to controls. In terms of gene expression changes, there were fewer changes in the AM animals compared to PM animals, consistent with their increased activity and dietary patterns at night. PM animals treated with AA showed decreases in transcripts involved in metabolic activity such as insulin-like growth factor 2, transforming growth factor beta, and glucose-6-phosphate transporter compared to controls, while these same transcripts were not altered in AM animals. In addition, the PM animals showed up-regulation of transcripts involved in detoxification, oxidative stress, apoptosis, neurotoxicity, tumorigenesis, among others. But, there were also changes seen in morning animals that were specific to that time point such as up regulation of branched chain amino acid metabolism and aspartate metabolism. There were commonalities among both morning and night animals which included up-regulation of transcripts related to the checkpoint pathways, DNA replication and sister chromatid cohesion, among others. This analysis indicates that the time of collection of animals is important in assessing how acrylamide affects gene expression in the thyroids of treated animals.

PS 915 Development of a Nanoparticle Platform for the Targeted Delivery of siRNA to HER2-Positive Breast Cancers

D. Castro[1, 2], W. Ngamcherdtrakul[2], J. Morry[2], T. Sangvanich[2], S. Gu[2], S. Goodyear[2] and W. Yantasee[1, 2]. [1]*PDX Pharmaceuticals, Portland, OR and* [2]*Biomedical Engineering, Oregon Health and Science University, Portland, OR.*

Successful siRNA based therapy has the potential to revolutionize cancer therapy by mediating the silencing of any gene deemed important for disease progression. We are developing an effective siRNA based nanoparticle platform that would overcome traditional shortcomings of siRNA based therapies such as poor bioavailability and off-target effects. The platform utilizes a mesoporous silica nanoparticle electrostatically loaded with siRNA and conjugated with an antibody for target homing. The human epidermal growth receptor type 2 (HER2) is a highly validated therapeutic target in breast cancer due to its prognostic role in cancer aggressiveness and drug resistance when overexpressed in tumors. Suppression of HER2

with siRNA based therapy (siHER2) offers a new treatment modality and provides a testable system for the development of our nanoparticle platform. Incorporation of Herceptin, a monoclonal antibody which binds to HER2, will serve to selectively target HER2-positive cancer cells. We first evaluated our nanoconstruct loaded with a highly optimized siHER2 sequence against a panel of HER2-positive (HCC1954, JIMT-1, BT474) and HER2-negative (MCF-7, MCF-10A, HDFa) cell lines to assess HER2 silencing efficacy and specificity of the nanoconstructs. We proceeded to establish knockdown of our target gene (77% reduction of HER2 mRNA) and a concomitant decrease in cell viability that was specific to HER2-positive cell lines. More importantly, siHER2-nanoconstruct treatment effectively inhibited growth in HER2-positive cell lines resistant to Herceptin and Lapatinib. The in vitro success translated well to tumor growth inhibition in a HCC1954 mouse tumor model following i.v. injection of our siHER2-nanocontruct. Current efforts are directed toward immune cell function and hematology assays to generate an immunological safety profile of the nanoconstruct.

PS 916 Pentoxifylline Induces GSK-3β-Independent Proteasomal Degradation of Cyclin D1 and Arrests Renal Cancer Cells in the G1 Phase

W. Cai, N. Mastrandrea, K. Y. Tham, S. S. Lau and T. J. Monks. *Pharmacology and Toxicology, University of Arizona, Tucson, AZ.*

Cyclin D1 is required for progression from the G1 phase into the S phase of the cell cycle. Over-expression of cyclin D1 causes an increase in cell cycle progression and proliferation, implicating it in a variety of tumors. Canonical cyclin D1 degradation is initiated by phosphorylation of Thr286 by GSK-3β. Quinol Thioether Rat Renal Epithelial (QTRRE) cells are a rodent cell model for renal cell carcinoma (RCC) and are derived from the Eker rat, which carries a germline mutation in the tuberous sclerosis-2 tumor-suppressor locus (TSC-2Ek/+). Through exposure to a toxic metabolite of benzene, 2,3,5-Tris-(glutathion-S-yl)HQ, the TSC-2 locus in QTRRE underwent loss of heterozygosity, rearing no functional TSC-2 protein. ACHN cells, also null for TSC-2, are a human RCC cell line. Both cell lines exhibit elevated levels of cyclin D1. Pentoxifylline (PTX), a non-specific phosphodiesterase inhibitor, is used as an adjunct in chemotherapy to treat cachexia. We report that PTX causes a time- and dose-dependent decrease in cyclin D1 protein levels and G1 cell cycle arrest in QTRRE and ACHN cells. RT-PCR analysis showed no significant changes in cyclin D1 mRNA. However, PTX's ability to decrease cyclin D1 protein was prevented in the presence of a proteasome inhibitor, MG-132. Inhibition of GSK-3β with LiCl in the presence of PTX failed to rescue cyclin D1 levels. PTX increases the phosphorylation of Ser9 on GSK-3β, indicative of an inhibition of GSK-3β activity. Following siRNA knockdown of GSK-3β, PTX retains the ability to decrease cyclin D1 levels. Moreover, PTX treatment in the presence of MG-132 revealed no increase in phospho-Thr286 compared to control. Our data indicate that PTX initiates GSK-3β- and phospho-Thr286-independent proteasomal degradation of cyclin D1 and arrests the RCC cell models in the G1 phase. Because our findings demonstrate a novel anti-cancer property of PTX, its use as an adjuvant therapy in RCC treatment should be further explored.

PS 917 Regulation of Intestinal Drug-Processing Genes in Germ-Free Mice

J. Cui, F. Selwyn and C. D. Klaassen. *Department of Internal Medicine, University of Kansas Medical Center, Kansas City, KS.*

Little is known regarding how the gut microbiome regulates the drug-processing genes (DPGs) in various sections of the intestine, which is an important metabolic organ for orally administered drugs. The goal of this study was to determine the regulation of DPGs in intestine of germ free (GF) mice. Total RNAs from duodenum, jejunum, ileum, and colon of adult male GF and Conventional mice (n=3 per group) were isolated, and the transcriptome was quantified using RNA-Seq (50 cycles paired end). Over 35 million reads were generated per sample, of which >96% were mapped to the mouse mm10 genome (Tophat). Among 23,846 genes in mice, jejunum had the largest number of differentially regulated genes (2514, FDR-BH<0.05), followed by colon (835), duodenum (435), and ileum (368). In duodenum, drug metabolism was among the top most differentially regulated networks in GF mice. In all 3 sections of the small intestine, Cyp1a1 was among the top most down-regulated genes within the transcriptome, suggesting that the aryl hydrocarbon receptor signaling is attenuated in the small intestine of GF mice. In duodenum and ileum, many of the Cyp2b, 2c and 3a mRNAs were down-regulated in GF mice, suggesting attenuated signaling of the pregnane X receptor and constitutive androstane receptor. In duodenum, there was a decrease in the mRNAs of glutathione-S-transferases, which are responsible for detoxifying electrophiles and oxidative stress. In jejunum, many alcohol dehydrogenases, aldo-keto reductases (Akrs), aldehyde dehydrogenases, and the Cyp4 family members, were up-regulated. In ileum, the apical sodium-dependent bile acid transporter (Asbt) and Akr1c19 were among the top most up-regulated genes in the transcriptome. In colon, most differentially regulated DPGs were up-regulated, exemplified by increased mRNAs of Asbt and organic solute transporter α. In conclusion, our study was the first to quantitatively determine the regulation of all DPGs in GF mice, and identified that distinct sections of intestine respond differently to the absence of the gut microbiome.

PS 918 Caudal-Related Homeodomain Protein 2 (Cdx2) and the Hepatocyte Nuclear Factor 4α(HNF4α) Synergize to Regulate UDP-Glucuronosyltransferase (UGT) 1A8 Gene Expression

S. N. Mubarokah[1, 2], P. A. Gregory[3], P. I. MacKenzie[1] and R. Meech[1]. [1]*Clinical Pharmacology, Flinders University, Adelaide, SA, Australia,* [2]*University of Islam Malang, Malang, East Java, Indonesia and* [3]*Centre for Cancer Biology, Adelaide, SA, Australia.* Sponsor: C. Reilly.

UGT1A8 gene has been reported to possess important DNA sequence motifs on its proximal promoter which significantly contribute to its intestinal-specific transcriptional regulation. Cdx2 and HNF4α are identified within 1kb of the transcription start site and have been found to play an important role in the regulation of the UGT1A8-1A10 gene cluster. HNF4a is reported to be mainly involved in hepatic regulation of UGTs, while Cdx2 is reported to be involved in the intestinal expression. The role of HNF4α and its interaction with Cdx2 in the intestinal expression of UGT1A8 has not been investigated. The present study aims to determine the role of HNF4α in the regulation of UGT1A8 by Cdx2. We carried out an In Vitro study in transiently transfected Caco-2 cells using promoter-luciferase constructs and mutational analysis. RT-qPCR analysis was used to examine expression of endogenous UGT mRNA. Our results define a novel functional HNF4α site in the proximal promoters of the UGT1A8 genes. We also show for the first time that HNF4α and Cdx2 synergistically activate this UGT1A8 promoters in Caco-2 cells. Mutational analysis of the UGT1A8 promoter shows that the novel HNF4α site located at -31 to -44 is essential for the synergy between HNF4α and Cdx2, but does not mediate regulation by HNF4α alone. Further analysis shows that the synergy does not involve a previously defined HNF4α motif located at -808 to -821. Consistent with the UGT1A8 promoter analysis result, the endogenous UGT1A8 mRNA is induced by Cdx2 and synergistically by Cdx2 and HNF4α. These findings provide a novel function for Cdx2 and HNF4α in cooperatively controlling intestinal UGT regulation. They also show that HNF4α has a profoundly different function in regulation of intestinal Vs hepatic UGT expression. The synergistic mechanism described here may be critical for differentiation-dependent UGT expression in intestine.

PS 919 CYP2S1 Depletion Promotes Cell Growth in Human Lung Cells

T. Madanayake and A. M. Rowland. *New Mexico State University, Las Cruces, NM.*

Cytochrome P450 2S1 (CYP2S1) expression is elevated in several epithelial derived cancers including squamous cell carcinoma. Although the expression pattern of CYP2S1 suggests an important physiological function, it is still considered as an orphan enzyme with unknown endogenous substrate. We reasoned that changes in CYP2S1 expression would initiate metabolic shifts in pathways linked to CYP2S1-mediated metabolism of endogenous substrates, and that these pathways can be identified through transcriptional alterations. CYP2S1 expression was depleted in human BEAS-2B cells, using RNA-interference targeting the 3'UTR (759) and exon 3 (984) of the CYP2S1 gene, and compared with a non-targeting shRNA control (SCRAM). Transcriptome analysis was performed on CYP2S1 depleted (759) and scrambled control (SCRAM) BEAS-2B cells using RNA-sequencing (RNA-seq). Pathway analysis of differentially expressed genes, using the Database for Annotation, Visualization, and Integrated Discovery (DAVID) analysis, revealed pathways consistent with previously published endogenous substrates and phenotypes. Additionally, analysis also revealed significant changes within mTOR signaling in response to CYP2S1 depletion. mTOR signaling is involved in regulating cell growth. Consistent with changes in cell growth, both CYP2S1 depleted cell lines, 759 & 984, exhibited an approximate 10% increase in cell diameter and 50% increase in cell volume. Western analysis reveals post-translational modifications within the mTOR signaling cascade consistent with increased cell size in CYP2S1 depleted cells (759 & 984) compared with control (SCRAM). CYP2S1 depleted cells specifically exhibit increased phosphorylation of mTOR, and its downstream target S6 kinase. These data suggest that alterations in CYP2S1 expression, and presumably CYP2S1-mediated endogenous metabolism, influence cell size through regulation of mTOR signaling. We are currently pursuing the mechanistic link between CYP2S1-mediated metabolism of endogenous substrates and mTOR signaling.

PS 920 Functional Genetic Screen in Human Haploid Cells to Identify Genes Involved in Susceptibility to Chemical Exposure

H. Shen, M. T. Smith and L. Zhang. *Environmental Health Sciences, University of California Berkeley, Berkeley, CA.*

Functional genetic screening systems have been successfully applied to study susceptibility to chemical toxicity. However, some approaches have certain limitations, such as lack of relevance to humans of yeast mutant screen findings and incomplete gene knock-out and off-target effects of RNA interference. Human haploid cell models are advantageous as an induced gene mutation can result in a clear phenotype due to the absence of a second gene copy. We recently developed a more efficient semi-solid medium based screening platform that employs a human haploid cell mutant library (KBM7-Mu) to identify genes that modulate sensitivity to chemical exposures. Compared to the liquid medium-based approach, our method allows for simultaneously screening and generating mutant colonies from cells resistant to the chemical of interest. This shortens the entire screening process by approximately 3 weeks and decreases the rate of false positives. Using this new approach, we identified eleven human genes that confer the resistance to formaldehyde (FA), a known human leukemogen. Among these genes, LPR5 (Low-density lipoprotein receptor-related protein 5), GOT1 (Glutamic-oxaloacetic transaminase 1) and M1AP (Meiosis 1 Associated Protein) were confirmed in two independent screening experiments. LRP5, GOT1 and M1AP mutant KBM7 cells showed significant resistance to FA-induced toxicity compared to wild type cells (KBM7-Wt). Further studies on LPR5 mutant KBM7 cells using quantitative RT-PCR and western blotting confirmed the knockdown of transcription and knockout translation of the LRP5 gene. These findings suggest that LPR5, GOT, M1AP and other genes are involved in susceptibility to FA toxicity. They further demonstrate the broad applicability of this optimized approach to screen genetic susceptibility to toxic chemicals, identify novel susceptibility genes, and gain insight into potential mechanisms of toxicity of chemical exposures.
(Supported by NIEHS P42ES004705 to MTS and R01ES017452 to LZ)

PS 921 Carbon Monoxide Modulation of mRNA in Human Airway Smooth Muscle Cells

B. A. Rolls[1], L. Aguilera-Aguirre[1], L. M. Hallberg[1], I. Boldogh[1], A. J. Halayko[2] and B. T. Ameredes[1]. [1]*University of Texas Medical Branch, Galveston, TX and* [2]*University of Manitoba, Winnipeg, MB, Canada.*

Rationale: Asthma is a chronic inflammatory airway disease involving disregulation of human airway smooth muscle cell (HASMC) function; subsequently, asthmatics may be more susceptible to the adverse affects of inhaled pollutants, such as carbon monoxide (CO). CO is toxic at high concentrations due to asphyxia resulting from carboxyhemoglobin formation, but may also have non-hemoglobin related effects. Thus, we investigated the effect of CO exposure in HASMC, to determine its effect on intracellular message regulation.
Methods: Cultures of primary HASMC at passage 6 were serum-starved for 24hr, refed, and stimulated with 1ng/mL IL-1β for 2-10hr, or exposed to 500ppm CO for 8hr, following the 2hr stimulation period. Inflammatory cytokine and receptor mRNA levels were assayed by q-PCR; the significant modulation threshold was taken as (+ or -) changes >5-fold.
Results: mRNAs were upregulated from 24- to over 2300-fold. Of the 84 messages we assayed in controls (IL-1β only), TNF was the main upregulated early message (2hr), while IL-1β receptor antagonist (IL1RN) was the primary upregulated late message (10 hr). IL-8, CXCL1, CXCL2, CXCL3 and CCL20 were upregulated at 2 hr, and maintained at 10hr, while CXCL5 and CXCL6 were further upregulated by 10 hr. At 10hrs, exposure to 500ppm CO upregulated SPP1, TNFβ, IL-10, TNF, and IL-13 (7- to 32-fold), while downregulating CXCL5, IL-1β, CXCL2, CXCL6 and IL1RN (5- to 24-fold).
Conclusions: We conclude that CO exposure can upregulate specific messages in HASM to a greater extent than IL-1β alone. Conversely, CO exposure can also downregulate specific messages, at least two of which are involved in the IL-1β pathway, namely, IL-1β and IL1RN. These results show that CO exposure can have direct effects on the intracellular mRNA levels in HASMC, an airway cell relevant to environmentally-associated asthma.
Supported by: NIEHS T32ES007254, NIEHS 5P30ES006676, The Sealy Center for Environmental Health and Medicine, and the Brown Foundation.

PS 922 Role of microRNA in the Induction of Immunosuppressive MDSC by Δ^9-THC *In Vivo*: Regulation of Transcription Factor C/EBPα by miR-690

V. L. Hegde, S. Tomar, A. R. Jackson, R. Rao, X. Yang, U. Singh, N. P. Singh, P. S. Nagarkatti and M. Nagarkatti. *Pathology, Microbiology & Immunology, University of South Carolina, Columbia, SC.*

Δ^9-tetrahydrocannabinol (THC), the major psychotropic component of marijuana has been shown to induce potent myeloid-derived suppressor cells *in vivo*. We investigated the role of miRNA in this process. $CD11b^+Gr\text{-}1^+$ MDSCs were purified from peritoneal cavities of BL/6 mice injected with THC. Genome-wide profiling of 690 mouse miRNA by microarray analysis showed significantly altered expression in THC-MDSCs vs control BM precursors, with 13 miRNA identified as differentially expressed (>2 fold). We used a robust combination of TargetScan, RNAhybrid and miRanda algorithms (Poisson $P \leq 0.05$, predicted by at least 2) to identify the targets. Ingenuity pathway analysis revealed that cell growth, proliferation, and myeloid differentiation were the top significantly enriched canonical pathways. Several specific, potentially important miRNA-target interactions were identified. MiR-690 was the highly overexpressed miRNA in THC-MDSC (~16 fold). Transcription factor C/EBPα involved in myeloid differentiation was identified as the potential functional target of miR-690 with a good seed-sequence binding site within its mRNA 3'UTR. C/EBPα expression was found to be higher in BM precursors with a significant decrease in THC-MDSC, while showing inverse correlation with miR-690 expression. Knock-down of miR-690 in THC-MDSC following transfection with stable, peptide nucleic acid (PNA) antagomiR resulted in unblocking, and significant increase in C/EBPα levels. Further, FACS sorted, THC-induced $CD11b^+Ly6G^+Ly6C^+$ granulocytic and $CD11b^+Ly6G^-Ly6C^+$ monocytic MDSC subtypes showed similar levels of miR-690 and attenuated C/EBPα suggesting that mir-690 is a pan MDSC marker, and miR-690-C/EBPα is a common pathway in MDSCs. Select miRNA and their targets play a key role in the induction of immunosuppressive MDSC following cannabinoid exposure, and hence, in cannabinoid-induced immune suppression. *Supp.by NIH P01AT003961,P20RR032684,R01AT006888,R01ES019313, R01MH094755 & VA 1\01BX001357.*

PS 922a Profile of Six Hepatic Insulin Signaling Pathway Genes in Response to 2-Aminoanthracene Dietary Ingestion

J. W. Jay[1], G. W. Barnett[1], J. C. Means[2] and W. E. Gato[1]. [1]*Chemistry, Georgia Southern University, Statesboro, GA and* [2]*Bren School of Environmental Science & Management, UC Santa Barbara, Santa Barbara, CA.*

Six genes that regulate various processes in the insulin signaling pathway were profiled. These transcripts were reported to regulate other genes that are essential for glucose metabolism, fatty acid and lipid biosynthesis. In a previous hepatic global gene expression analysis followed by DAVID bioinformatics analytics showed ampk, g6pc, gck, pp1, srebp-1C and socs2 to be likely modulated by 2-aminoanthracene (2AA) dietary consumption. The goal of the current study is to evaluate the responses of these proteins in the liver of Fisher-344 (F344) rats exposed to 2AA. 2AA belongs to a class of compounds referred to as polycyclic aromatic hydrocarbons (PAHs). This compound has been detected in broiled food and tobacco smoke. F344 rats were fed 2AA adulterated diets of 0 mg/kg, 50 mg/kg, 75 mg/kg and 100 mg/kg for 14- and 28-days. Differential gene expression of ampk (Prkab1), g6pc, gck, pp1, srebp-1C, socs2 and gapdh were be carried out by qRT-PCR. Results seem to suggest 2AA modulates different genes related to energy metabolism in the liver. Relative quantification of these products indicated an up-regulation of the ampk and socs in animals treated to 100 mg/kg-diet and 50 mg/kg-diet respectively during 14 days of feeding. The rest of the mRNA transcripts were down-regulated in the treated rats relative to the control group. G6pc gene was highly up-regulated in all animals that ingested 2AA for 28 days. Pp1 protein was also up-regulated in the 75 mg/kg-diet rats. The rest of the genes tested were not differentially altered. This result will be followed by a protein immunoblot assay to examine the expression of g6pc and ampk.

PS 922b Effects 2-Aminoanthracene Exposure on Insr, Irs, Akt and Glut4 Expression

N. D. Mattis[1], J. J. Rosaldo[1], J. C. Means[2] and W. E. Gato[1]. [1]*Chemistry, Georgia Southern University, Statesboro, GA and* [2]*Bren School of Environmental Science & Management, UC Santa Barbara, Santa Barbara, CA.*

The modulation of the toxic effects of 2-aminoanthracene (2AA) on the expression of insulin receptor (Insr), insulin receptor substrate (Irs1), v-akt murine thymoma viral oncogene homolog 1 (Akt1) and solute carrier family2, facilitated glucose transporter member 4 (Glut4) liver is being investigated. These genes play vital

roles including regulatory activity in insulin signaling and glucose metabolism (Akt1), important glucose transporter essential for the development of type 2 diabetes (Glut4) and activation and processing of insulin signaling transduction (Insr, Irs). In a previous study to assess the toxic effects of 2AA using global gene expression coupled with DAVID bioinformatics tool, it was found that several genes that regulate the insulin signaling pathway may be altered by 2AA toxicity. The objective of the current investigation is to examine the mRNA expression of four specific genes that mediate insulin signaling due to 2AA toxicity. Polynuclear aromatic amine, 2AA is a by-product of cigarrete smoke and broiled meat. Twenty four post-weaning 3-4 week old F-344 male rats were exposed to 0 mg/kg-diet (control), 50 mg/kg-diet (Low Dose - LD), 75 mg/kg-diet (medium dose - MD) and 100 mg/kg-diet (high dose - HD) 2-AA for 2wks and 4wks. The mRNA expression of Insr, Irs1, Akt1 and Glut4 was determined by quantitative real-time PCR followed by the quantification of Akt1 via enzyme-linked immunosorbent assay (ELISA) assay. Transcripts Glut4 and Insr were not expressed at all in all treatment groups. Akt1 gene was up-regulated in animals treated to 2AA for both two and four weeks. Similarly, Irs1 mRNA was only up-regulated in rats that ingested 2AA for four weeks. It appears Akt1 and Irs1 proteins were targets of 2AA intoxication. This study is still ongoing to quantify the level of protein expression of Akt1 in the livers of rats exposed to 2AA.

PS 922c Functional Analysis of the Dioxin Response Elements (DREs) of the Murine *Cyp1a1* Gene Promoter: Beyond the Core DRE Sequence

S. Li, X. Pei, H. Xie and B. Zhao. *Research Center for Eco-Environmental Sciences, Chinese Academy of Sciences, Beijing, China.*

Aryl hydrocarbon receptor (AhR) is a ligand-dependent transcription factor that mediates biological and toxicological effects of halogenated aromatic hydrocarbons such as 2,3,7,8-tetrachlorodibenzo-p-dioxin (TCDD). DREs are located upstream of cytochrome P4501A1 (CYP1A1) and other AHR-responsive genes and binding of the AHR complex, stimulates their transcription. Although CYP1A1 expression has been used as the model system to define the biochemical and molecular mechanism of AhR action, there is still limited knowledge about the roles of each of the seven DREs located in the CYP1A1 promoter. These seven DREs are conserved in mouse, human and rat. Deletion analysis showed that a single DRE at -488 was enough to activate the transcription. Truncation and mutation analysis demonstrated that the DRE at site -981 has the highest transcriptional efficiency in response to TCDD, suggesting that the conserved DRE at site -981 could represent a significant and universal AHR regulatory element for CYP1A1. And reversed 5 bp core sequences of seven DREs did reduce the transcriptional efficiency, which illustrated that the adjacent sequences of DRE played a vital role in activating transcription. The reversed 25bp sequences including DREs showed that the core DRE sequence (5'-TNGCGTG-3') tends to show higher transcriptional level than that of the core DRE sequence (5'-CACGCNA-3') triggered by TCDD. Furthermore, in the core DRE (5'-TNGCGTG-3') sequence, when 'N' is Thymine or Cytidine (T, C), the transcription efficiency was stronger compared with that of the other nucleotides. This study reported systematically the effects of DRE orientation, DRE adjacent sequences, and the nucleotide "N' in the core DRE (5'-TNGCGTG-3') sequence on the AhR-regulated CYP1A1 transcription in response to TCDD and laid a good foundation for further investigation into the AhR-dependent transcriptional regulation triggered by dioxin and dioxin-like compounds.

PS 922d The Effects of Five Days of Tetrabromobisphenol A (TBBPA) Treatment in Female Rats

J. M. Sanders[1], G. A. Knudsen[1], S. J. Coulter[1], J. K. Dunnick[2] and L. S. Birnbaum[1]. *[1]NCI, RTP, NC and [2]NIEHS, RTP, NC.*

TBBPA, a widely used brominated flame retardant, is an endocrine disruptor in rodents. In a recent chronic toxicity study, the National Toxicology Program observed increased incidence of uterine epithelial tumors in TBBPA-treated female Wistar Han rats and hepatoblastoma in male B6C3F1 mice. The mechanisms of TBBPA-induced toxicity in rodents may include disruption of thyroid homeostasis, oxidative stress, and perturbations of lipid and endogenous estrogen metabolism. The present work investigated modes-of-action of TBBPA-mediated toxicity in female Wistar Han rats. Each rat received five consecutive daily doses of either 250 mg/kg TBBPA (n = 10) or corn oil (n = 10) by gavage. Twenty-four hours following the final dose, the rats were euthanized and biological changes were assessed in blood, liver, and uterus. TBBPA treatment resulted in a statistically significant decrease in the serum concentration of T4. No significant changes in serum concentration of T3 or TSH were observed in the animals. An increase in mRNA for thyroid receptor alpha (TRα) was observed in liver and uterus following TBBPA treatment. TRβ mRNA was unchanged in the uterus and decreased in liver. The concentration of serum estradiol was statistically similar in the two treatment groups. However, mRNA for estrogen receptor alpha (ERα) increased in uterine tissue of TBBPA–treated rats. ERβ mRNA increased in the distal, but not proximal segment of the uterine horn. Genes associated with metabolism were differentially expressed between treatment groups and tissue types. *Ppara* expression decreased in liver, but increased in the uterus of TBBPA-treated rats. *Ugt1a1* expression increased in the uterus. *Sult2a1* expression increased in the proximal, but not distal segment of the uterine horn. The expression of *Ugt1a1* was unchanged, *Sult2a1* was decreased, and *Cyp2b2* was increased in liver. In conclusion, the biological changes observed in the present study may correlate to specific toxicities observed in TBBPA-treated female rats. (Supported by the Intramural Research Programs of NIH/NCI and NIEHS.)

PS 923 2-Amino-1-Methyl-6-Phenylimidazo(4, 5-b)Pyridine (PhIP) Neurotoxicity in Primary Midbrain Cultures

Z. S. Agim[1], A. M. Griggs[1, 2], V. Mishra[2], K. W. Turteltaub[3], A. E. Director-Myska[4], J. Rochet[2] and J. R. Cannon[1]. *[1]School of Health Sciences, Purdue University, West Lafayette, IN, [2]Department of Medicinal Chemistry and Molecular Pharmacology, Purdue University, West Lafayette, IN, [3]Biosciences & Biotechnology Division, Lawrence Livermore National Laboratory, Livermore, CA and [4]Science and Technology, Defense Threat Reduction Agency, Fort Belvoir, VA.*

Parkinson's disease (PD) is characterized behaviorally by cardinal motor features that arise due to dopamine (DA) neuron loss in the substantia nigra. Much epidemiological research suggests that environmental factors have a role in etiology. Dietary factors may be encountered frequently and in high doses. 2-amino-1-methyl-6-phenylimidazo[4,5-b]pyridine (PhIP) is a heterocyclic amine produced during high-temperature cooking of meat products. PhIP bears structural resemblance to dopamine and known dopaminergic toxicants. PhIP is a suspect carcinogen, but effects on the nervous system are not known. Here, we tested the hypothesis that PhIP is toxic to dopaminergic neurons. Primary midbrain neuronal cultures containing DA and non-DA neurons and glial cells were treated with PhIP or select Phase I metabolites for 24 hours. DA neurons and total neurons were quantified using immunofluorescence staining and fluorescence microscopy. Our data demonstrates that PhIP or N-OH-PhIP is selectively toxic to DA neurons. We also tested whether a blueberry extract with antioxidant activity and the antioxidant molecule N-acetyl-cysteine (NAC) are protective. Treatments with either antioxidant prevented PhIP- and N-OH-PhIP-induced toxicity to DA neurons. Further studies quantified 4-hydroxynonenal (4-HNE) and nitrotyrosine (NT) as measures of oxidative damage. We observed a significant increase in 4-HNE and NT in PhIP-treated primary midbrain cultures, suggesting that PhIP-mediated toxicity to DA neurons is mediated by oxidative stress. Our future studies will assess PhIP neurotoxicity in vivo.
Acknowledgments: We thank Mitali A. Tambe for technical assistance.
Funding: Showalter Trust (J.R.C. and J.-C.R.), NIEHS/NIH ES019879 (J.R.C.).

PS 924 Dopamine-Induced Post-Translational Modifications of α-Synuclein

A. B. Cholanians, S. S. Lau and T. J. Monks. *College of Pharmacy, University of Arizona, Tucson, AZ.*

α-Synuclein (SYN) plays a central role in synucleinopathies. SYN comprises the major component of aggregates present in Lewy Bodies, a hallmark of Parkinson's disease (PD). Moreover, dopamine (DA) mediated SYN post-translational modifications (PTM) play an important role in the etiology of the disease. At physiological pH, DA readily oxidizes to the corresponding reactive ortho-quinone species, which interacts with SYN causing crosslinking of the protein, SYN-aggregation, and subsequently cytotoxicity. However, since there is a paucity of information on DA-induced SYN PTMs, and of the consequences of such modification, we examined the effects of DA and of some of its thioether conjugates on SYN aggregation. MALDI-TOF and Western blot analysis of DA-modified SYN, revealed an addition of 4.5 kDa to the SYN monomer, and up to 9 kDa to the SYN dimer, suggesting poly-DA interaction with SYN, crosslinking of protein, and aggregation of SYN. Acetylation of SYN at lysine (K) residues by acetylsalicylic acid or acetic anhydride ameliorates DA-induced SYN aggregation, indicating an interaction between K and DA. To overcome the complexity of protein crosslinking and poly-DA formation, N-acetylcysteine (NAC) and glutathione (GSH) were utilized for synthesis of DA conjugates. NAC and/or GSH occupy one of the reactive sites on the aromatic ring of DA, leading to oxidized conjugates with only one reactive electrophilic sites. Mono-DA-NAC and mono-DA-GSH conjugates oxidize and generate SYN adducts in a pH-dependent manner similar to DA, but fail to crosslink and/or cause SYN aggregation. MALDI-TOF and Western blot analysis of DA conjugates with SYN reveal addition of up to 5 kDa to SYN monomer, with very low levels of SYN dimer formation. The findings reveal that scavenging of DA quinone by cysteine and/or GSH has profound effects on the interaction of DA

with SYN, and on subsequent aggregation reactions. Redox modulation of SYN PTMs and of SYN aggregation suggests potential interventions to alleviate SYN-dependent cytotoxicity. (P30ES006694 & T32-ES016652)

PS 925 Linking Nicotinamide Nucleotide Transhydrogenase (Nnt) Activity and Respiration-Dependent H2O2 Consumption through the Mitochondrial Thioredoxin/Peroxiredoxin System in Cell-Based Model of Parkinson's Disease

P. Lopert[1], L. Liang[2] and M. N. Patel[2]. [1]*Neuroscience, University of Colorado Anchutz Medical Campus, Aurora, CO and* [2]*Pharmaceutical Sciences, University of Colorado Anchutz Medical Campus, Aurora, CO.*

Mitochondrial reactive oxygen species (ROS), such as hydrogen peroxide (H2O2) are implicated in neurodegenerative diseases such as Parkinson's disease (PD). Epidemiological studies have shown pesticide exposure can increase the risk of developing PD and many pesticides/herbicides, such as Paraquat (PQ) work through redox cycling or inhibiting the electron transport chain. Mitochondria are thought to be net producers of ROS but recently it was shown brain mitochondria can consume H2O2 in a respiration-dependent manner by the thioredoxin/peroxiredoxin (Trx/Prx) system (Drechsel, 2010). This study wanted to determine the mechanism linking mitochondrial respiration with H2O2 consumption in a cellular model of PD. We examined the role of Nicotinamide Nucleotide Transhydrogenase (Nnt), which uses the proton gradient to generate NADPH from NADH and NADP+, to detoxify H2O2 by the Trx/Prx system. Pharmacological inhibition of Nnt in isolated brain mitochondria significantly decreased their ability to consume H2O2 in the presence, but not absence, of respiration substrates. Nnt inhibition in liver mitochondria, which do not need substrates to detoxify H2O2, had no effect. Pharmacological inhibition or shRNA knockdown of Nnt in N27 cells a) decreased H2O2 consumption b) decreased TrxR activity c) decreased NADPH and increased NADP+ levels and d) decreased basal, spare and maximal mitochondrial oxygen consumption rates. Nnt deficient cells where more susceptible to ROS production and cell death following exposure to subtoxic levels of PQ. This data implicates Nnt as a critical link between the metabolic and antioxidant functions in brain mitochondria and suggest Nnt as a potential therapeutic target to improve the redox balance in conditions of oxidative stress associated with neurodegenerative diseases. Funding: RO1NS45748

PS 926 Environmental/Mitochondrial Toxicity Induced by Paraquat and MPP+ Is Associated with a Decrease in Ubiquitination- and p62/Autophagy-Mediated Clearance of Oxidized Proteins

J. Navarro-Yepes[1, 2], A. Anandhan[1], B. Quintanilla-Vega[2] and R. Franco[1]. [1]*School of Veterinary Medicine and Biomedical Sciences, University of Nebraska-Lincoln, Lincoln, NE and* [2]*Toxicology, CINVESTAV, IPN, Mexico City, D.F., Mexico.*

A hallmark of neurodegenerative diseases is the accumulation/aggregation of misfolded or damaged proteins, which has been associated with increased oxidative stress and dysfunction in protein degradation pathways (ubiquitin-proteasome system and autophagy). α-Synuclein, ubiquitin and p62 are major components of Lewy body inclusions in Parkinson's disease. In this work, we aimed to study the effect of environmental/mitochondrial toxins in the ubiquitin-proteasome- and autophagy-mediated degradation pathways in human neuroblastoma and dopaminergic mesencephalic cell cultures. Using the ubiquitin-proteasome and the proteasome-only reporters, GFPμ and GFP-ODC, and western blot analysis of ubiquitin-bound proteins and changes in the autophagy flux, we observed that paraquat- and 1-methyl-4-phenyl-1,2,3,6-tetrahydropyridine (MPP+)-induced cell death was associated with a decrease in protein ubiquitination. Decreased protein ubiquitination induced by paraquat or MPP+ was paralleled by a decrease in the autophagic flux (LC3-II accumulation in the presence of chloroquine) and an increase in p62 accumulation. Paraquat-induced oxidative stress was paralleled by the accumulation of oxidized (sulfenylated) proteins. Neither paraquat nor MPP+ toxicity was increased by the presence of the proteasomal inhibitor MG132. However, overexpression of a dominant-negative form of the autophagy protein 5 (dnAtg5) increased both paraquat and MPP+ toxicity. We hypothesize that impairment of protein ubiquitination by paraquat or MPP+ is compensated by autophagic clearance of p62-bound oxidized protein aggregates, and that inhibition of autophagy potentiates the toxicity of these environmental/mitochondrial toxicants.

PS 927 Evidence for the Involvement of Protein Kinase C Delta (PKCδ)-Mediated Epigenetic Deregulation in the Histone Deacetylase Inhibitor Trichostatin-A-Mediated Neurotoxicity in N27 Dopaminergic Neuronal Cells

V. J. Lawana, N. Singh, V. Anantharam, H. Jin, A. Kanthasamy and A. Kanthasamy. *Interdepartmental Toxicology, Iowa State University, Ames, IA.*

Acetylation and deacetylation of histones has been shown to be a critical regulator of gene transcription and chromatin remodeling. We have previously demonstrated that NF-κB activation is critically linked to trichostatin A (TSA)-induced apoptotic cell death in N27 dopaminergic cells. However, the influence of protein kinase c delta (PKCδ), a redox sensitive kinase, on histone hyperacetylation and its impact on dopaminergic neuronal survival remains to be established. Therefore in the present study we sought to investigate the link between PKCδ dependent oxidative stress and histone hyperacetylation. Herein we show that exposure of N27 cells to TSA for various time periods (3-12h) induced a time dependent increase in Bax activation, dissipation of MMP, caspase activation, NADPH oxidase activation, and GSH depletion. These changes preceded the drug induced apoptotic cell death. Intriguingly, a concomitant activation of PKC delta that paralleled histone hyperacetylation was evidenced in TSA treated cells. Moreover, TSA- induced increase in the expression of transcriptional regulators, such as p53, STAT1, and NF-κB, positively correlated with increased expression of pro-apoptotic factors. Notably, down regulation of PKCδ levels via ectopic overexpression of a caspase cleavage mutant of PKCδ (D327A) or small interference RNA-mediated gene silencing attenuated mitochondria mediated oxidative cell signaling events, transcription factor activation, histone hyperacetylation, and apoptotic cell death. Collectively, these findings identify PKCδ as a key regulator of TSA-induced hyperacetylation of histones and suggest that oxidative stress mediated proteolytic activation of PKCδ contributes to dopaminergic neuronal demise at least in part via deregulation of cellular epigenetic mechanisms (ES10586 and NS065167).

PS 928 Loss of NF-κB p50 Amplifies Microglia Priming in the Aged Brain

T. Taetzsch, S. Brookins, S. Levesque, C. McGraw and M. L. Block. *Virginia Commonwealth University, Richmond, VA.*

Excessive and chronic microglial activation has been implicated in degeneration of dopaminergic (DA) neurons in the substantia nigra (SN) during Parkinson's disease (PD). Aging, a key risk factor for PD, is associated with enhanced sensitivity of microglia to pro-inflammatory stimuli, but the mechanisms are poorly understood. NF-κB p50 is a regulator of inflammation and NF-κB p50 expression is reduced in post mortem SN tissue of Lewy Body Dementia patients, supporting a role for loss of NF-κB p50 function in neurodegeneration. To examine the consequences of loss of NF-κB p50 function in microglial activation, 1.5-2.0 month old NF-κB $p50^{+/+}$ and NF-κB $p50^{-/-}$ mice were injected with LPS (5mg/kg, IP). Expression of the pro-inflammatory genes TNFα and IL-1β in the midbrain as well as serum TNFα levels were higher in LPS treated NF-κB $p50^{-/-}$ mice at 3h post-injection. Kinetics studies demonstrated that TNFα and iNOS expression is increased at 6h and 12h, but not 3h post-LPS treatment in NF-κB $p50^{-/-}$ mixed glia cultures, implicating NF-κB p50 in resolution of the glial pro-inflammatory response. Consistent with this premise, NF-κB $p50^{-/-}$ cultures expressed lower levels of the M2 marker arginase-1 in response to LPS, indicating impairment of the resolution of iNOS activation. To examine how loss of NF-κB p50 function affects microglial activation in the aged brain, 1.5-3.0 and 16-18 month old male mice (NF-κB $p50^{+/+}$ & NF-κB $p50^{-/-}$) were injected with LPS IP. Aged LPS treated NF-κB $p50^{-/-}$ mice had the highest levels of serum TNFα as well as midbrain TNFα and IL-1β expression at 3h. Furthermore, higher numbers of microglia with activated morphology were observed in the SN of aged LPS treated NF-κB $p50^{-/-}$ mice. These results support that loss of NF-κB p50 function increases neuroinflammation and microglial activation, impairs pro-inflammatory resolution and that these effects are further magnified by aging.

PS 929 Exploring Gene-Environment Interactions Implicated in Parkinson's Disease Using a Paraquat and Maneb Model in *Drosophila*

V. Nunez[1], C. A. Martin[3] and D. Krantz[2]. [1]*Society and Genetics, University of California, Los Angeles, Los Angeles, CA,* [2]*Neuroscience, University of California, Los Angeles, Los Angeles, CA and* [3]*Molecular Toxicology, University of California, Los Angeles, Los Angeles, CA.*

Parkinson's disease (PD) is a neurodegenerative disease characterized by the loss of dopaminergic neurons and a loss in both motor and non-motor functions. Overexpression and mutations of the alpha-synuclein gene in humans has been linked to familial forms of Parkinson's disease. However, inheritable forms of PD are rare. The vast majority of PD cases are sporadic, thus, disease progression likely relies on an individual's genetic background and/or environmental exposures. Exposure to environmental toxins, such as pesticides or heavy metals, has been shown to increase the risk of developing PD in humans. In particular, prolonged exposure to the pesticides paraquat and maneb has also been shown to increase the risk of PD up almost two fold. Interestingly, individuals with variants in the alpha-synuclein gene were shown to be at increased risk of PD, compared to control, when they were exposed to pesticides. The complex nature of gene-environment interactions in sporadic PD has made it difficult to understand disease etiology using traditional rodent models. Thus, our lab has developed a paraquat and maneb model of PD in *Drosophila melanogaster*, which is amenable to multiple genetic modifications which can be easily combined with various environmental toxin exposures. In our model, survival and motor ability significantly decreased when exposed to paraquat alone or with paraquat and maneb combined. Dopaminergic cell counts decreased only when exposed to both paraquat and maneb. Additionally, we assessed the dopaminergic cell counts, survival curves and climbing assay of our model in the presence of over-expression of human mutant alpha-synuclein. Thus our work confirms epidemiological data in addition to further exploring implicated gene-environment interactions.

PS 930 The Parkinson's Disease-Linked Pesticide Ziram Causes Deregulation of the Synapse

C. A. Martin[1] and D. Krantz[2]. [1]*Molecular Toxicology, University of California, Los Angeles, Los Angeles, CA and* [2]*Neuroscience, University of California, Los Angeles, Los Angeles, CA.*

Exposures to environmental toxins, such as pesticides, have long been implicated in neurodegenerative diseases such as Parkinson's disease (PD). Recent epidemiological studies demonstrate that chronic exposure to the pesticide ziram results in over a two-fold increase in the risk of contracting PD. PD is a devastating disease that affects millions of people worldwide. PD patients suffer from an irreversible and progressive loss of dopaminergic neurons that results in motor deficits as well as impairment of other non-motor functions regulated by dopamine such as mood, sleep, smell and digestion. The molecular and physiological changes in dopaminergic neurons that precede cell death and disease are unclear, particularly in the case of sporadic disease onset, which accounts for the vast majority of PD cases. Our aim was to investigate how exposure to the PD-linked pesticide ziram may alter neuron physiology and behavior. By using the well-characterized *Drosophila* neuromuscular junction (NMJ) preparation, we were able to assess for the first time ziram's affect in an intact synapse. The large array of live-imaging genetic reagents available in the fly allowed for us to quantify ziram's affect on the essential neuronal processes of synaptic vesicle release, reuptake and action potential dependent calcium influx. We report that ziram alters synaptic behavior at both excitatory, glutamatergic terminals and modulatory, aminergic terminals at the *Drosophila* NMJ. Interestingly, aminergic terminals are particularly sensitive to disruption by ziram exposure, resulting in a robust decrease in the rate of endocytosis. Additionally, we observe spontaneous depolarization of aminergic, but not glutamatergic, nerve terminals in the presence of ziram. We hypothesize that chronic exposure to ziram results in preferential deregulation of aminergic terminals and may be responsible for its link to PD in the human population.

PS 931 Mitochondrial DNA Damage and Dysfunction and Their Effects on Dopaminergic Neurodegeneration after Chemical Insult in *Caenorhabditis elegans*

C. P. Gonzalez, I. T. Ryde and J. N. Meyer. *Nicholas School of the Environment, Duke University, Durham, NC.*

Mitochondrial dysfunction has been linked to neurodegenerative diseases including Parkinson's Disease (PD). Neurons are cells with a high energy demand, and as a result are hypothesized to be particularly vulnerable to mitochondrial dyshomeostasis. We investigated dopaminergic neuron viability after chemical insult in *Caenorhabditis elegans* strains with gene knockouts of *pink-1* and *pdr-1*, which are involved in mitochondrial dynamics. These genes are the nematode homologs of the human genes PINK1 and PARK2 which when mutated cause familial PD. The four cephalic dopaminergic neurons were visualized with fluorescent microscopy, and assigned a score based on the level of damage observed. Each neuron was scored from 0 to 2, with zero representing an intact dendrite and 2 representing the highest level of neurodegeneration observed .The strain BY200 (*dat-1*::GFP) was used as wild type for the strains UA226 (*dat-1*::GFP; *pink-1*) and UA227 (*dat-1*::GFP; *pdr-1*), all generously provided by Guy Caldwell (University of Alabama). After 6-hydroxydopamine (6-OHDA) exposure, both mutant strains showed different levels of neurodegeneration compared to wild type, with the *pink-1* mutant exhibiting less neuronal damage than wild type. We also performed quantitative polymerase chain reaction (QPCR) after 6-OHDA exposure and observed significant levels of DNA damage to both nuclear and mitochondrial genomes. This genotoxic effect of 6-OHDA could be in part responsible for the degeneration observed in dopaminergic neurons after exposure to this chemical. Previous results obtained in the laboratory indicate that knockdown of *pink-1* inhibits removal of mitochondrial DNA (mtDNA) damage, presumably inducing mitochondrial fusion and functional complementation and potentially explaining the resistance to neurodegeneration observed in the *pink-1* mutant. Further studies are being performed to fully characterize the fate of mtDNA damage induced by environmental toxicants and its effect on neuronal viability and mitochondrial health.

PS 932 Identification of Novel Genes and Epigenetic Mechanisms in *C. elegans* Models of Idiopathic Parkinson's Disease

W. Li[1], N. M. VanDuyn[1], J. Trinidad[2] and R. M. Nass[1]. [1]*Pharmacology and Toxicology, Indiana University School of Medicine, Indianapolis, IN and* [2]*Chemistry, Indiana University, Bloomington, IN.*

Background: Idiopathic Parkinson's disease (PD) is an oxidative stress-related disorder that result in abnormal dopamine (DA) signaling and cell death. Although the origin of the pathogenesis in PD remains unclear, corollary evidence suggests both genetic and environmental contributions. Recently we have shown that the PD-associated transcription factor SKN-1/Nrf2 is expressed in *C. elegans* DA neurons and inhibits PD-associated DA neurodegeneration. Aims/Objectives: In this study we asked what are the genes, molecular pathways, and mechanism involved in DA neuron vulnerability to PD-associated toxicants. Methods: We utilized reverse genetics, biochemical assays, immunofluorescence, transgenic *C. elegans*, RT-PCR, Western analysis, mass spectrometry, and behavioral and neuronal morphology analysis to characterize expression, localization and the role that SKN-1, IDN-1, and post-translational modifications play in 6-OHDA-, rotenone-induced neuronal death. Results: In this study we demonstrate that IDN-1 mutants render DA neuron up to over 10-fold more resistant to the neurotoxicants relative to WT. We show that IDN-1 is expressed in DA neurons, and IDN-1 overexpression results in a 2-fold increase DA neuron vulnerability. We also show that DA neuron vulnerability is affected by transcriptional and post-translational modifications of involving these and other proteins identified using RNAi affects DA neuron vulnerability. Conclusions: This study identifies novel genes and molecular pathways involved in DA neuron vulnerability in PD, and shows that common epigenetic mechanism modulate DA neuron vulnerability to PD-associated neurotoxicants. Support: NIEHS ES014459 and ES003299 to RN, and EPA STAR Graduate Fellowship to NVD.

PS 933 LRRK2 Transgenic Rats Exhibit Heightened Sensitivity in a Colitis Model

J. Lee[1], J. Park[2], C. H. Kim[2] and J. R. Cannon[1]. [1]*School of Health Sciences, Purdue University, West Lafayette, IN and* [2]*Comparative Pathobiology, Purdue University, West Lafayette, IN.*

Accumulating evidence suggests that chronic systemic inflammation is associated with the pathophysiology of Parkinson's disease (PD). Leucine-rich repeat kinase 2 (LRRK2) has been identified as the gene most frequently mutated in autosomal dominant familial PD. LRRK2 is also a major susceptibility gene for inflammatory bowel disease (IBD) and has an immunoregulatory function. Pathological functions of LRRK2 in both IBD and PD are not well understood. The goal of this project was to examine how potential interactions between IBD and PD models might be mediated by LRRK2. In a preliminary study, BAC transgenic (TG) rats expressing human G2019S mutated LRRK2 or wild-type (WT), littermate controls were exposed to daily dextran sodium sulfate (DSS, 2.5-5% W/V in drinking water) over 21 days to induce experimental colitis. During the trial, daily disease activity index (DAI), including body weight loss, stool score and fecal occult blood test, was quantified. At day 21, after euthanasia the brains were removed and processed for neurotransmitter analysis and histology. Also, the blood and gastrointestinal tract were collected for immunological determination. DSS-treated LRRK2

G2019S transgenic rats (DSS-TG) showed significantly increased DAI compared to DSS-treated wild type (DSS-WT) or untreated rats (control). Surprisingly, neurotransmitter analysis showed that WT animals exhibited decreased striatal dopamine and DOPAC in response to DSS, with TG animals showing no such response. Serotonergic neurotransmission was not affected. Further, immunohistochemistry data suggest that DSS-WT animals also exhibit decreases in striatal tyrosine hydroxylase levels, in the absence of overt dopaminergic terminal loss. Here again, TG animals did not exhibit such a response. In summary, rats expressing G2019S LRRK2 exhibited heightened clinical sensitivity in a colitis model and did not exhibit adaptive changes in nigrostriatal dopamine transmission observed in WT animals treated with DSS. More studies are needed to confirm these initial observations.

PS 934 Neuroproective Effect of Tauroursodeoxycholic Acid (TUDCA) in Parkinson's Disease Mouse Model

S. Chigurupati, J. Reymick, L. Schmued, M. G. Paule, J. F. Bowyer and S. Sarkar. *Neurotoxicology, NCTR/FDA, Jefferson, AR.*

Parkinson's disease (PD) is a progressive motor disease of unknown etiology. The motor impairments of PD arise from selective degeneration of dopaminergic (DA) neurons in the substantia nigra pars compacta (SNc). These DA neurons project to the striatum (CPu) to release dopamine. Clinical symptoms of Parkinsonism emerge when more than half of the dopaminergic nerve terminals are damaged in the striatum. In the current therapeutic in vivo mouse model study, we used TUDCA as a neuroprotectant and 1-methyl-4-phenyl-1,2,3,6-tetrahydropyridine (MPTP) as neurotoxicant. TUDCA is a molecular chaperone which modulates cell death by interrupting classic pathways of apoptosis, modifying the expression of certain Bcl-2 family members, as well as NF-kB activity. In the present study mice were divided into three groups (Saline/Probenecid [250mg/kg, control], MPTPp [25mg/kg-10 doses+Probenecid, positive control] and TUDCA+MPTPp [200mg/kg+25mg/kg, treatment group]). Using immunohistochemical and analytical chemistry techniques, we showed that the SNc and CPu are significantly protected from MPTP induced damage after TUDCA treatment compared to MPTP+Probenicid group. Tyrosine hydroxylase and dopamine transporter immunoreactivity in the ventral midbrain SNc and striatum are more protected from MPTP damage in TUDCA treated mice compared to its positive controls. Microglial activation, depletion of striatal fibers and dopamine and the development of motor deficits are significantly less in TUDCA treated group. Together, our results suggest that new mechanisms may be involved in the pathogenesis of PD and that might be exploited in the development of novel therapeutics aimed at slowing or halting neurodegeneration in patients with PD

PS 935 Ceftriaxone Ameliorates L-DOPA-Induced Dyskinesia, a Side Effect of Parkinson's Disease Treatment

T. Chotibut, V. Fields and M. F. Salvatore. *Pharm., Tox. & Neuroscience, LSUHSC, Shreveport, LA.*

Parkinson's disease (PD) is a neurodegenerative disease characterized by motor impairment arising from the loss of dopaminergic neurons. Currently, pharmacological dopamine (DA) replacement with L-DOPA is the gold standard treatment for PD. Unfortunately, chronic L-DOPA therapy induces abnormal involuntary movements termed L-DOPA-Induced-Dyskinesia (LID) in over 90% of PD patients over time. Furthermore, once dyskinesia manifests, it occurs with every subsequent exposure to L-DOPA. The prevalence and permanence of LID makes L-DOPA's side effect profile a highly relevant clinical obstacle especially given the primary role L-DOPA plays in PD treatment. Glutamate mediates excitatory signal transduction and in excess (excitotoxicity), can contribute to loss of DA neurons in PD. Thus, suppression of glutamate-mediated excitotoxicity could prolong the longevity of nigrostriatal neurons in PD progression. The beta-lactam antibiotic, ceftriaxone (cef), increases the expression of GLT-1, a glutamate transporter responsible for glutamate clearance in the CNS. We examined whether Cef could ameliorate dyskinesia when given 7 days post lesion in a 6-OHDA LID model. Chronic Cef (200mg/kg i.p) significantly delayed and attenuated dyskinesia in 6-8 month male Sprague Dawley rats compared to saline. Striatal GLT-1 expression was also increased in both Cef and Cef + L-DOPA treated rats compared to L-DOPA suggesting a cef-induced increase in synaptic glutamate clearance. Tyrosine hydroxylase (TH), a marker for DA, was measured in the lesioned striatum. Compared to its contralateral control, Cef treated rats had the highest remaining striatal TH with 81%, L-DOPA + Cef had 55%, and L-DOPA had 18%. Our data suggest that chronic Cef + L-DOPA may not only halt TH destruction, but also potentially reverse striatal TH loss in a 6-OHDA LID model. Given that Cef is already FDA-approved, these data support the repositioning of the antibiotic based on its ability to not only mitigate dyskinesia severity, but also protect against further DA loss in a Parkinson's disease rodent model.

PS 936 Quercetin Treatment Protects Progressive Nigral Dopaminergic Neuronal Degeneration in Cell Culture and MitoPark Animal Models of Parkinson's Disease by Activating PKD1 Signaling

M. Ay, J. Luo, A. Kanthasamy, V. Anantharam, M. R. Langley, H. Jin and A. Kanthasamy. *Biomedical Sciences, Iowa State University, Ames, IA.*

Oxidative stress has been associated with many neurological diseases including Parkinson's disease (PD). Therefore, identifying cell signaling mechanisms associated with oxidative stress is critically important to the development of new treatment strategies for PD. We have recently identified a novel oxidative stress-associated signaling pathway in which protein kinase D1 (PKD1) plays a major compensatory survival role in dopaminergic neurons. Therefore, we adopted a rationale based pharmacological screening approach to identify activators of PKD1 using dopaminergic neuronal cell model. Herein, we identified quercetin, a natural flavonoid widely found in vegetables and fruits can effectively activate PKD1 protective signaling. Western blotting analysis revealed that quercetin treatment significantly induced the phosphorylation and activation of PKD1 as well as CREB and Akt phosphorylations in MN9D dopaminergic neuronal cells. Activation of Akt, however, was inhibited by siRNA knockdown of PKD1, suggesting that Akt acts as a downstream target of PKD1 signaling during quercetin treatment. Results from qRT-PCR, Western blot analysis, mtDNA content analysis, and Mitotracker assay experiments revealed that quercetin can induce mitochondrial biogenesis in MN9D cells. Importantly, quercetin treatment protected against 6-OHDA-induced neurotoxicity in MN9D cells. Next, we evaluated the neuroprotective efficacy of quercetin against the progressive neurodegenerative process by using MitoPark mouse model of PD. Administering quercetin (25 mg/kg) once daily to 12-week-old Mitopark mice via oral gavage for 6 weeks significantly reversed behavioral deficits, striatal dopamine depletion, and TH neuronal cell loss in MitoPark mice. Our findings suggest that quercetin, by virtue of its ability to activate the PKD1-mediated neuroprotective signaling, is a promising neuroprotective drug candidate for the treatment of PD (NIH NS74443).

PS 937 Nonmotor Symptoms in MitoPark Mouse Model of Parkinson's Disease

M. R. Langley, M. Ay, S. Ghaisas, H. Jin, V. Anantharam, A. Kanthasamy and A. Kanthasamy. *Biomedical Sciences, Iowa State University, Ames, IA.*

Mitochondrial dysfunction has been implicated as a key player in the pathogenesis of Parkinson's disease (PD). The MitoPark mouse, a transgenic mitochondrial impairment model recently developed by specific inactivation of Tfam in dopaminergic neurons, spontaneously exhibits progressive behavioral deficits and neurodegeneration, recapitulating several features of PD. Since non-motor symptoms are now recognized as key features of the pre-symptomatic stage of PD, we monitored the clinically relevant motor and non-motor symptoms of PD from 8-24 wks of age in MitoPark and C57 wild type mice. As expected for MitoPark mice, motor deficits begin around 12 weeks and become severe by 18-24 wks. Interestingly, male MitoPark mice showed memory deficits before female mice, beginning at 8 wks and becoming most severe between 20-24 wks, as determined by Morris Water Maze. When compared to age-matched naive C57 black mice, MitoPark mice exhibited olfactory deficits in novel and social scent tests as early as 12 wks. MitoPark mice between 16-24 wks spent more time immobile in forced swim and tail suspension tests, and made fewer entries into open arms of the Elevated Plus Maze, indicating a depressive- and anxiety-related phenotype, respectively. Preliminary analyses revealed that sleep disturbances and gastrointestinal problems may also be present in MitoPark mice. Collectively, our results indicate that MitoPark mice progressively exhibit deficits in cognitive learning and memory, olfactory discrimination, sleep latency, and anxiety- and depressive-like behaviors. Thus, MitoPark mice can serve as an invaluable model for studying motor and non-motor symptoms in addition to studying pathology in PD (supported by NIH grants ES10586 and NS074443 and NS039958).

PS 938 Prevalence and Titers of Neuroantibodies (NAb) in Hemodialysis Patients (HD): Associations with Vitamin D Receptor (VDR) Polymorphisms (SNP) and Blood Lead (BPb)

H. A. El-Fawal[1], A. Johnson[1, 2], P. Storrs[2], J. Bishop[3], K. Elnagar[4] and D. Mason[2]. *[1]Neurotoxicology Laboratory, Albany College of Pharmacy and Health Sciences, Albany, NY, [2]ANephRx Core Laboratory, Albany College of Pharmacy and Health Sciences, Albany, NY, [3]Pharmacogenomics Laboratory, College of Pharmacy, University of Illinois, Chicago, IL and [4]Neuropsychiatry Services, Albany Medical Center, Albany, NY.*

There is evidence of neurological deficits (ND) and heavy metal accumulation in HD. VDR SNPs are risk factors for both. 229 (23% African-Americans) HD patients were recruited and VDR SNPs: rs1544410 (Bsm1), rs2228570 (Fok1), rs731236 (Taq1) and rs7975232 (Apa1) determined by PCR for association with NAb, IgG, against neurofilaments (NF-L, NF-M and NF-H), GFAP and myelin basic protein (MBP) and BPb. Except for Folk1, SNPs were in Hardy-Weinberg equilibrium. Stratification by SNP alleles indicated a tendency towards higher BPb levels for Taq1_T and Apa1_C (p=0.06), whereas Bsm1_C allele in Caucasians (p=0.009) was associated with higher BPb. NAb had a high prevalence in HD (>50%), anti-NF-H, GFAP and MBP the most prevalent. Based on genotype stratifications, Bsm1 (C) and Taq1 (C) [homozygotes and heterozygotes] had higher levels of anti-NF-L, NF-H and GFAP (p<0.01-0.05). Bsm1_CT genotype, only, was associated with a nearly two-fold increase in the odds of anti-NF-M presence (p=0.02), the NAb best correlated (r=0.24, p=0.008) with BPb, although BPb did increase the odds of anti-MBP detection (OR: 1.13, C.I. 1.034-1.232, p=0.003). Overall, multivariate regression revealed that BPb was a significant determinant of anti-NF-M, GFAP and MBP titers (p=0.04, 0.03, 0.005, respectively). Although vitamin D is neuroprotective, VDR SNPs have been associated with ND. In addition, VDR SNP, particularly the major Bsm1_C allele, as well as Taq1_T, alleles have been shown to promote Pb accumulation, an observation confirmed here. Taken together, this study indicates that NAb, may be useful for detection of ND in environmentally and genomically vulnerable populations and suggests that heavy metals, like Pb, may contribute to ND in HD patients.

PS 939 Pb Exposure, Histone Methylation, and the S-Adenosylmethionine (SAM) Pathway: Implications for Alzheimer's Disease

A. Eid[1], H. Huang[3, 2], S. W. Bihaqi[2] and N. Zawia[1, 2]. *[1]Interdisciplinary Neurosciences Program, University of Rhode Island, Kingston, RI, [2]Biomedical and Pharmaceutical Sciences, University of Rhode Island, Kingston, RI and [3]School of Public Health, Zhengzhou University, Zhengzhou, Henan, China.*

Alzheimer's disease (AD) is a neurodegenerative disorder and is the most common type of dementia, and is the sixth leading cause of death in the United States. It presents as two forms, either early onset Alzheimer's disease (EOAD) that is primarily genetic in nature, or late onset Alzheimer's disease (LOAD) which is sporadic and afflicts 90% of those diagnosed with AD. Epidemiological data seem to suggest that both LOAD and late-onset dementia have early origins. Previous work in our lab has shown that early life exposure to lead (Pb) results in epigenetic reprogramming, partially through DNA methylation (Alashwal et al., 2012, Dosunmu et al., 2012). Our lab has shown that epigenetic marks have been correlated with alterations in the expression of genes associated with Alzheimer's disease (Wu et al., 2008; Hui et al, 2012; Syed and Zawia, 2013). It is also known that epigenetic reprogramming may occur via histone modifications. This in vitro study focuses on changes in histone methylation, and on the methyl donor S-adenosylmethionine (SAM) and its role in epigenetic reprogramming. We compare changes in histone methylation as a result of Pb exposure with levels of SAM and the enzymes involved in its biosynthesis.

PS 940 Inhibitory Effect of Curcumin on HMGB1 Release in LPS-Stimulated Microglia Cell

M. Entezari[1], M. Javdan[2] and N. Hussain[1]. *[1]Natural Science, LaGuardia Community College, Long Island City, NY and [2]Biological Sciences and Geology, Queensborough Community College, Bayside, NY.*

Alzheimer Disease (AD) is one of the most common neurodegenerative disorders. Accumulation of Aβ-containing amyloid plaque is a neuropathological hallmark of Alzheimer's disease (AD) but inflammatory process triggered by Aβ deposition and microglia activation is significantly related to the pathogenesis of AD. Studies on brain tissues of the patients with AD show the elevated levels of pro-inflammatory cytokines such as IL-1β, and IL-6. Several research studies have shown the therapeutic potential of curcumin in neurodegenerative diseases including AD through its antioxidant, anti-inflammatory and anti- Aβ protein aggregation effects. However, the effect of curcumin on microglia functions and its underlying mechanism is not elucidated yet. The aim of this study was to investigate the anti-inflammatory properties of curcumin on LPS-stimulated microglia cells and its effect on microglia's functions. We previously demonstrated inhibition of a High Mobility Group Box 1(HMGB1) in LPS- stimulated microglia BV2 cells improves the phagocytosis ability in these cells. Our current study demonstrated that pre-treatment with 5μM curcumin suppresses LPS-induced proliferation and HMGB1 overexpression in BV2 cells that corresponds with markedly decreased the expressions of Toll like receptor 4(TLR4). Moreover, administration of curcumin significantly improved the LPS-induced phagocytic impairment in BV2 cells. The present results propose curcumin, which inhibits HMGB1/TLR4 in microglia cells may offer a novel and probable benefit against AD-associated neuro-inflammation.

PS 941 Cellular Transport of the Nonprotein Amino Acid BMAA in Three Cell Lines: A Comparison of the L- and D-Enantiomer

L. Ersson[1], M. Andersson[2], U. Bergström[2], O. Karlsson[1] and E. B. Brittebo[1]. *[1]Pharmaceutical Biosciences, Uppsala University, Uppsala, Sweden and [2]Environmental Toxicology, Uppsala University, Uppsala, Sweden.* Sponsor: M. Stigson.

The cyanobacterial neurotoxin β-N-methylamino-L-alanine (L-BMAA) has been implicated in the etiology of amyotrophic lateral sclerosis/parkinsonism dementia complex in humans. Previous studies demonstrate that neonatal exposure to BMAA induces cognitive impairments as well as altered protein expression and degenerative changes in the adult hippocampus in rodents. Furthermore, autoradiographic imaging studies show that BMAA is rapidly transported into the mammary gland and breast milk of lactating dams, and that the subsequent transfer to the suckling pup results in a high exposure of the neonatal brain. The present study aimed to characterize and compare the uptake of D- and L-enantiomers of 14C-BMAA in the murine mammary gland epithelial cell line HC11, the human glioblastoma cell line U343 and the human neuroblastoma cell line SH-SY5Y differentiated by trans-retinoic acid. Uptake of radioactive 14C-BMAA was determined via liquid scintillation counting. The results revealed a more rapid influx and efflux of L-BMAA than of D-BMAA in HC11 cells suggesting enantiomer-selective transport. Competition experiments with other amino acids and a low sodium dependency of the transport of L-BMAA in HC11 cells suggested that the amino acid transporters LAT 1 and LAT 2 were involved the transport of L-BMAA into milk. Furthermore, the results revealed a more rapid uptake of BMAA in the human U343 cells and SH-SY5Y cells than in the murine HC11 cells. Competition experiments with other amino acids indicated that BMAA may be taken up also by other transporters, and that there may be a differential expression of these amino acid transporters in the three cell lines.

PS 942 Gene-Microarray Analysis of Brain Tissues in a Multiple Sclerosis Mice Model: 6-Weeks vs. 15-Months Mice

J. Seo[1, 2], M. Hasan[1, 2], M. Kang[2, 3], B. Jung[2, 3], S. Nam[4], W. Park[4], H. Kim[4] and O. Kwon[1, 2]. *[1]Toxicology Lab, Doping Control Center, Korea Institute of Science and Technology, Seoul, Republic of Korea, [2]Biological Chemistry, University of Science and Technology, Daejeon, Republic of Korea, [3]Molecular Recognition Research Center, Korea Institute of Science and Technology, Seoul, Republic of Korea and [4]The Catholic University of Korea, Seoul, Republic of Korea.*

Identified have many genes been that contribute to course of multiple sclerosis (MS) and its animal model, experimental autoimmune encephalomyelitis (EAE). Genes related MS or EAE with aging remains to be studied. To identify highly associated genes between EAE and aging, the gene was analyzed by cDNA microarrays in mice brain tissues of different ages (6 weeks, Y; 15 months, O). In our results, 4 up- and 19 down-regulated genes were overlapped in old-control (O-CON) vs. Y-CON (up, 136; down, 74) and O-EAE vs. Y-EAE (up, 40; down, 126) which were related to aging effects with EAE disease. The up-regulated pathways of cell adhesion molecules and adherens junction were involved in aging with EAE effects. Also 44 up- and 4 down-regulated genes were expressed together in Y-EAE vs. Y-CON (up, 162; down, 34) and O-EAE vs. O-CON (up, 106; down, 81) which affected to EAE induction or pathogenesis regardless of age, relating to activation of pathways for antigen processing and presentation, cell adhesion molecules, and chemokine signaling. Overlapping genes (up, 13; down, 24) in O-EAE vs. O-CON and O-EAE vs. Y-EAE may be aggravate EAE disease because O-EAE showed more severe symptom than Y-EAE. In addition, tripartite motif (23 and 35) and septin 7 genes were verified by qRT-PCR to be increased, showing the consistent result with their microarray data. These genes reportedly have functions of apoptosis, protein

ubiquitination, nucleotide- and metal ion-binding. A profile of gene expression related to EAE and aging was exhibited, suggesting that monitoring of these genes may be a main subject of possible targets for treatment of the disease.

PS 942a Toxicology of Targeted Drug Delivery to the Midbrain for Parkinson's Disease Treatment

R. Grondin[1], Y. Ai[1], P. A. Hardy[1], M. T. Butt[2], G. A. Gerhardt[1], D. M. Gash[1], D. A. Bumcrot[3] and Z. Zhang[1]. [1]*Anatomy & Neurobiology, University of Kentucky, Lexington, KY,* [2]*Tox Path Specialists, LLC, Frederick, MD and* [3]*David H. Koch Institute, Cambridge, MA.* Sponsor: M. Vore.

Direct drug administration into the brain parenchyma offers a high degree of targeting, while reducing the risks of unwanted side-effects by limiting systemic exposure. Drug delivery to the midbrain region remains a challenge. Here, we used an investigational catheter and cranial anchor system coupled to implanted programmable pumps to continuously infuse 5mM gadopentetate dimeglumine (Magnevist®) into the substantia nigra (SN) of female rhesus monkeys to lay the foundation for delivering drug therapies to the midbrain region. Flow rate tolerability of either 0.1 μL/min to the right SN for 14 days or 0.2 μL/min to the left SN for 14 days was assessed by monitoring clinical observations, body weights and histopathological examinations of the striatum and midbrain regions. Evaluation of post-surgical MRI indicated that the placement of each intranigral catheter was within a 2-mm radius from the intended surgical target and that all catheters were patent, as evidenced by the presence of Magnevist® at the catheter tip. The volume of distribution achieved in the midbrain region with Magnevist® infused at a rate of 0.2 μL/min was greater than that achieved at 0.1 μL/min by nearly 2-fold. There were no indications of toxicity as noted in clinical observations and body weight values. Histopathological evaluations indicated that the catheter tip was placed in or near the SN pars compacta region in all animals. There was no evidence of infection at any of the catheter sites and no difference between the two infusion rates with respect to changes indicating inflammation. There was no discernible difference regarding the microglial reaction at the two different infusion rate sites. There was no detectable decrease of tyrosine hydroxylase staining in the striatum in any of the sections and no detectable necrosis of neurons in the SN pars compacta region. Our data support that direct drug delivery to the midbrain maybe used for the treatment of Parkinson's disease.

PS 942b Studying Aspects of Parkinson's Disease in a Zebrafish Model of Ziram Toxicity

A. Lulla[1, 2], L. Barnhill[1, 2], M. Stahl[2], A. G. Fitzmaurice[1, 2], S. Li[2] and J. Bronstein[2, 1]. [1]*Molecular Toxicology, UCLA, Los Angeles, CA and* [2]*Neurology, UCLA, Los Angeles, CA.*

Parkinson's disease (PD) is the second most common neurodegenerative disease. Genetic causes of PD account for 5% of cases suggesting that the environment has a role in disease etiology. Epidemiological studies indicate that exposure to pesticides increases the risk for PD. We previously found that exposure to ziram increases the risk of developing PD in humans and causes selective dopaminergic cell toxicity, inhibition of the ubiquitin prosteasome system (UPS), and increased α-syn levels in primary neuronal cultures. Here we utilize zebrafish embryos (ZF, *Danio rerio*) to investigate the mechanisms of ziram's toxicity.
ZF embryos were exposed to ziram at an environmentally relevant concentration (50nM), A transgenic ZF line expressing green fluorescent protein driven by vesicular monoamine transporter protein 2 (VMAT2) promoter was used to study the effects of ziram on aminergic neurons. Embryos treated with 50nM ziram were found to have a reduction of VMAT-GFP expressing neurons by approximately 30%. Ziram was not toxic to non-DA sensory neurons. Additionally, exposure to ziram resulted in a 138% increase in expression of TH.
The closest ZF homologue to human α is ZF γ1-syn (zsyn), which was found to aggregate when overexpressed in ZF. Treatment with 50nM ziram resulted in an increase in zsyn expression as measured by western blot. Knockdown of zsyn via antisense was found to protect against ziram's dopaminergic cell toxicity, resulting in approximately 75% attenuation of VMAT-GFP expressing neuronal death. The mechanism by which ziram increases ZF γ1-syn appears to involve inhibition of protein degradation pathways, as concentrations as low as 1nM ziram inhibited the UPS. In a preliminary experiment a 6 fold increase in fluorescence of LC3, a marker of autophagy was observed for embryos treated with ziram. These studies demonstrate that ziram toxicity is at least partially mediated by synuclein and add to the understanding the etiology PD.

PS 942c In-Depth Toxicogenomic Analysis of a Dopamine Transporter Knockout Animal: Transporter-Associated Behavioral and Signaling Changes in a *C. elegans* Parkinson's Disease Model

R. M. Nass[1], N. VanDuyn[1], J. Duerr[4], J. Trinidad[2], W. Li[1] and G. Wong[3]. [1]*Pharmacology and Toxicology, Indiana University School of Medicine, Indianapolis, IN,* [2]*Chemistry, Indiana University, Bloomington, IN,* [3]*Biosciences, Kuopio University, Kuopio, Finland and* [4]*Biological Sciences, Ohio University, Athens, OH.*

Background: The loss of DA from basal ganglia results in the devastating neurological disorder Parkinson's disease (PD). DA transporters (DATs) regulate synaptic DA availability and play a role in neuronal vulnerability, yet the molecular modulators associated with DAT are poorly defined. Aims/Objectives: In this study we determined which genes are involved in DAT-associated gene expression and neuron vulnerability. Methods: We utilized RNA-seq, microarrays, behavioral and biochemical assays, immunofluorescence, transgenic *C. elegans*, RT-PCR, LC-MS, HPLC, Western analysis, and neuronal morphology analysis to characterize DAT-associated gene and protein expression, post-translational modifications, and toxicant-associated DA neuron vulnerability. Results: Approximately 20,000 genes were analyzed. Over 54 genes were overexpressed in the DAT knockout strain and 33 genes were under expressed. These genes were strongly biased to water homeostasis, cation transport, and G-protein mediated signalling. Specifically, tyrosine hydroxylase (TH), the rate limiting step for DA synthesis, as well as DA is significantly reduced (approximately 50%) as determined by RNAseq, immunofluorescence, Western analysis, and HPLC. DAT knockout animals also displayed mechanosensory-associated movement defects. Furthermore, 6-OHDA treated DAT knockout animals showed a dramatic change in gene expression (44 genes enriched in oxidative phosphorylation, exocytosis, and GTPase function) relative to WT suggesting novel pathways involved in 6-OHDA mediated toxicity independent of DAT. Conclusion: This study describes a novel whole genome analysis of the role that the DAT and associated genes and signalling pathways play in DA neuron vulnerability that may provide useful therapeutic targets to inhibit PD-associated cellular pathologies.

PS 942d Alterated Expression of Amyloid Beta (Aβ) Deposit-Related Molecules in the Aging Brain

D. Kim, J. Park and B. Choi. *Preventive Medicine, Chung-Ang University, Seoul, Republic of Korea.*

Alzheimer's disease (AD) is most common form of dementia characterized by the presence of Aβ plaque and neurofibrillary tangles. Aging is the main risk factor for AD. However, the underlying mechanisms are not completely understood. We focused the alteration of the expression related to Aβ production, degradation and transport in the different age rats.
We used Sprague-Dawley male rats at ages 7, 26, 52, 96 weeks. We analyzed the protein expression of amyloid precursor protein (APP), beta-site APP-cleaving enzyme 1 (BACE1), neprilysin (NEP), and insulin degrading enzyme (IDE) in the hippocampus and low-density lipoprotein receptor-related protein 1 (LRP1) and receptor for advanced glycation end products (RAGE) in the brain capillary endothelium (BCE) using Western blot.
The LRP1 expression in BCE of 96-week rats were lower than 26- and 52-week rats, however higher than 7-week rats. The RAGE exspression in BCE was positively associated with age. However, other molecules, such as APP, BACE1, NEP and IDE in HC did not change according to aging.
These results imply that age is related with reduction of Aβ transportation. It might lead to accumulation of Aβ in brain extracellular space.

PS 942e Changes of Tight Junctions in the Blood-Brain Barrier Are Mediated by Aβ25-35-RAGE Interaction

E. Cuevas[1], H. Rosas-Hernandez[1, 2], S. Lantz-McPeak[1], M. G. Paule[1], Q. Gu[1], C. Gonzalez[2], S. Z. Imam[1], J. Kanungo[1] and S. F. Ali[1]. [1]*Division of Neurotoxicology, NCTR, Jefferson, AR and* [2]*Laboratorio de Fisiologia Celular, Universidad Autonoma de San Luis Potosi, San Luis Potosi, SLP, Mexico.*

Recently, we demonstrated that microinjection of Aβ25-35 into the rat hippocampus produces neurotoxicity mediated by advanced glycation end products (RAGE). It has been demonstrated that RAGE interact with amyloid β-peptide (Aβ) and mediate Aβ transport across the blood-brain barrier (BBB), contributing to the deposition of Aβ in the brain. However, molecular mechanisms underlying Aβ-RAGE interaction-induced alterations in the BBB are poorly understood. In order to determine whether the toxicity induced by Aβ25-35-RAGE interaction is involved in tight junction disruption at the blood-brain barrier (BBB), a primary culture of rat brain microvessel endothelial cells (rBMVEC) was created by enzy-

matic digestion and differential centrifugation as an in vitro model of the BBB. Confluent rMVEC monolayers (cultured 10-14 days) were treated with Aβ25-35 or Aβ35-25 (as control) at 20 μM for 24 hours. RAGE, occludin, and claudin-5 expression were measured by Western blotting. Cytotoxicity was evaluated using a lactate dehydrogenase (LDH) assay for cell death, an XTT (2,3-bis(2-methoxy-4-nitro-5-sulfophenyl)-2H-tetrazolium-5-carboxanilide) assay for mitochondrial function, and detection of 2', 7'- dichlorofluorescin diacetate (DCFH-DA) to measure ROS production. Aβ25-35 produced an increase in RAGE and occludin; and a decrease in claudin-5 expression. Significantly decreased mitochondrial function and increased oxidative stress (ROS production) with no effect on LDH leakage were also observed. These data suggest that Aβ25-35-RAGE interaction induced toxicity involved increased occludin and decreased claudin-5 expression. Further studies are underway to determine if these events are associated with disruption in the permeability of the BBB.

PS 943 *In Vitro* Skin Irritation Testing: Characterization of Mid-Range Tissue Viability

B. Lundell[1], C. Dingee[1], Y. Huang[2], J. Li[2] and D. M. Colleluori[2]. [1]*WuXi AppTec, St. Paul, MN and* [2]*WuXi AppTec, Philadelphia, PA.* Sponsor: R. White.

Introduction
In vitro skin irritation testing is gaining acceptance to replace animal testing. Poor intra-assay reproducibility for chemicals with viabilities in the mid-range can potentially hamper classification near the prediction threshold of 50%. This in vitro study characterized a test article having poor-intra-assay reproducibility in the 30-70% range.
Materials and Methods
Based on testing of medical device extracts, triplicate wells of EpiDerm™ were exposed to 100 μl of test material for 24 hours. After washing, wells were processed for histology or tissue viability. Test materials were Dulbecco's phosphate buffered saline (DPBS, negative control), 0.125% sodium lauryl sulfate (SLS) in DPBS (positive control), 3.25% lactic acid (LA) in DPBS and 5.0% LA in DPBS. After exposure, culture medium was harvested for analyses of human Interleukin 1 alpha (IL-1α), Interleukin 1 Receptor Antagonist (IL-1RA), Interleukin 8 (IL-8) and Leukemia Inhibitory Factor (LIF) using Quantikine® ELISA kits. Data were shown as mean ± SD. Values were compared to the negative control using student's t test. A (p) value of less than 0.05 was considered statistically significant.
Results
The controls gave expected viabilities, 100 ± 4.9% and 18.3 ± 2.3%. Exposure to 3.25% LA decreased viability to the mid-range and demonstrated poor reproducibility (mean 47.7 ± 30.7%). Exposure to 5.0% LA consistently decreased viability to the low range (mean 8.2 ± 0.9%).
The levels of IL-8, IL-1RA and IL-1α were significantly increased and LIF levels were below the limit of detection for all treatments. Poor intra-assay reproducibility with 3.25% LA was confirmed for viability, IL-1RA, and histology. Of the biomarkers evaluated, IL-1α was more sensitive to the treatment of SLS than LA.
Conclusions
Poor-intra assay variability associated with in vitro skin irritation testing is a true chemical response, not technical artifact. Establishing threshold levels for proinflammatory biomarkers may aid in classification of chemicals with viabilities near the prediction threshold of 50%.

PS 944 Evaluation of an *In Vitro* Assay for the Detection of Skin Irritants in Medical Devices

C. Nycz and A. Y. Sawyer. *Corporate Preclinical Development and Toxicology, BD, Research Triangle Park, NC.*

The objective of this work is to identify alternative in-vitro methods to screen medical device materials for the presence of skin irritants. Current testing for the presence of skin irritants is done exclusively using a rabbit animal model. Medical device extracts or materials are exposed to the skin of the animal. The material is removed and the affected skin area is observed daily for 3 days and evaluated for erythema and edema. Efforts seeking to improve upon this model by eliminating or reducing the number of animals used in such testing while maintaining or improving sensitivity in identifying such irritants is a focus of ISO TC/194 a standards organization for the Biological Evaluation of Medical Devices. A cultured human skin tissue model, EpiDerm, (Mattek Corporation) allows the direct exposure of test materials to the cultured skin. This model recently demonstrated acceptable performance as a part of the ECVAM international validation study for the in vitro identification of chemical irritants. This cultured human skin model is now being evaluated for its ability to identify irritants present in extracts of medical materials and devices. Medical device and device materials present unique problems as the irritants exist within a solid material and are generally present in low levels. We adapted the model protocol and evaluated multiple materials for their irritancy potential. Essentially, the cultured skin tissue was exposed to solvent material extracts for 24 hours. The extract was removed and the skin tissue was allowed to recover for 24 hours. MTT uptake was used to determine irritancy potential (cell cytotoxicity), 50% of control. In addition, IL-1α production was determined via ELISA, to detect increased expression as compared to controls. We have identified 2 materials, when extracted in non-polar solvents, Buna O-rings and Vicryl, that demonstrate an irritancy potential with elevated (≥ 1.5 fold) IL-1α production. This is the first successful demonstration of the use of this in vitro methodology for the identification of irritants in device materials.

PS 945 Does Leaching of Bisphenol A (BPA) from Dental Composites Contribute to Neuropsychological Deficits in Children? An Evaluation of Plausibility

J. E. Reynolds[1], L. H. Moilanen[1], E. Hope[1] and J. K. Dahms[2]. [1]*Medical Department, 3M Company, St. Paul, MN and* [2]*3M ESPE, 3M Company, St. Paul, MN.*

Composite dental restorations are placed in more than 10 million U.S. children each year with significant benefits for oral health. Two recent publications have suggested that BPA leached from dental composites contributes to neuropsychological deficits including decreased executive and memory functioning in children, based on results from standardized tests for assessment of psychosocial function. Both publications were based on secondary analyses of data collected for the New England Children's Amalgam Study, a randomized clinical trial comparing the health of children whose caries were restored using either dental amalgam or mercury-free composite materials. We evaluated the plausibility of the hypothesis that BPA leached from dental composites contributes to neuropsychological deficits based on a review of the methodology used in the studies, as well as review of published literature describing dental composite composition, evidence for BPA release from dental composites, and known toxicokinetic and toxicological properties of BPA. Possible misclassification of subjects, confounding, and lack of statistical robustness weaken the strength of the study conclusions. Published data indicate that BPA exposure from dental materials occurs primarily from trace amounts of residual BPA in composite monomers synthesized from BPA. Exposure might also occur by enzymatic degradation of certain dental monomers by esterases. Measured dental-related BPA exposures are small (ng/kg-day) and of acute duration. Bioavailable BPA from dental composites is likely rapidly metabolized and excreted, minimizing exposure. At present, a specific mechanism to explain the putative neuropsychological effects of trace levels of BPA has not been articulated. Based on the weight of the examined evidence, the plausibility of neuropsychological deficits in children caused by BPA released from dental composites is low.

PS 946 Potential Confounders of Bisphenol A Analysis in Dental/Orthodontic Materials

E. Hope[1], D. R. Reed[2] and L. H. Moilanen[1]. [1]*Medical Department, 3M, Saint Paul, MN and* [2]*Corporate Research and Development Analytical Laboratories, 3M, Saint Paul, MN.*

Bisphenol-A (BPA)-based dental/orthodontic ingredients such as Bisphenol-A diglycidyl ether dimethacrylate (Bis-GMA) may contain trace amounts of BPA as a chemical synthesis residue. Accurate determination of BPA in final product formulations is essential for reliable health risk assessments. A cured Bis-GMA-based material representative of commercial dental products was extracted according to international guidelines for medical devices. The extraction solvent was spiked with d16BPA as an internal standard. Sample processing followed expert recommendations for minimizing BPA sample contamination. Extracts were analyzed for BPA using high performance liquid chromatography (HPLC) with either ultraviolet (UV) or Multiple Reaction Monitoring (MRM) detection. The BPA concentrations appeared about 30-fold higher using HPLC-UV vs. HPLC-MRM. Full scan liquid chromatography/mass spectrometry (HPLC/MS) was used to elucidate the different results, and showed a compound co-eluting with BPA which interfered with LC/UV analysis. The co-eluting compound derived from ethyl-4-dimethyl aminobenzoate, a co-initiator used by many dental product manufacturers. These results highlight the potential difficulties in accurate analysis of BPA in complex mixtures such as dental product extracts. Both good separation methodology and a detection method with high specificity and sensitivity are important to avoid incorrect assignment of extractables, and consequent inaccurate quantification of BPA.

PS 947 Biocompatibility Assessment of Multipurpose Contact Lens Solution: Points to Consider for *In Vitro* Cytotoxicity Testing

M. Salvador-Silva and L. Huang. *Biological Sciences, R&D, Abbott Medical Optics, Santa Ana, CA.*

New Multipurpose Contact Lens Solution (MPS) formulations are required to demonstrate disinfection efficacy, stability, biocompatibility, preclinical and clinical safety in accordance with recognized national and international standards. Specific *in vitro* tests include medium elution, agar overlay, neutral red uptake for cytotoxicity, colony formation for proliferation, and MTT/XTT assays for metabolic activity. Different parameters used in testing, such as cell line sensibility detection response to toxic agents, exposure time, and MPS dilution, can lead to contradictory results between various *in vitro* studies and suggest a lack of correlation to clinical results. This study evaluates the correlation among *in vitro* models for assessing cytotoxicity and biocompatibility of MPS containing disinfectant polyhexamethylene biguanide (PHMB). The biological effects of MPS were evaluated following USP Direct Contact test and Colony Formation Assay (ISO 10993-5) in mouse (L-929) and hamster (V79) fibroblast, respectively, and Cell Viability Assay by alamarBlue in human corneal epithelial cells (HCEC). The dose-dependent effects and uptake-release kinetics of PHMB by contact lens materials were evaluated. Results of the USP Direct Contact test indicated that MPS-induced cytotoxicity are dependent upon the lens PHMB uptake and release profiles. MPS cytotoxicity effects on V79 fibroblasts demonstrated a concentration-dependent response, where cytotoxicity increased with MPS concentrations (1.25%, 2.5%, 5%, and 10%) after long-term exposure (7 days) while MPS concentrations at 100%, 75% and 50% in HCEC showed a shorter time exposure dependency (15-60 minute) when evaluated by alamarBlue Cell Viability Assay. These results indicate that correlations between preservative concentration-response curves and lens uptake-release profiles should be considered as part of the battery of tests to demonstrate MPS biocompatibility.

PS 948 Safety Assessment of Colorants Used in Cardiac Lead Implant Devices—Applying the Threshold of Toxicological Concern Approach

F. K. Hsia[1], M. P. Beauchane[1], B. J. Swackhamer[2] and E. E. Reverdy[1]. [1]*Global Toxicology and Biocompatibility Services, Boston Scientific Corporation, Maple Grove, MN and* [2]*CRT Leads Development, Boston Scientific Corporation, St. Paul, MN.*

The use of printing inks in cardiac leads was evaluated following the 2013 FDA draft guidance on the *"Use of International Standard ISO 10993,"Biological Evaluation of Medical Devices - Part 1: Evaluation and Testing"*. Cardiac leads are used for defibrillation and resynchronization therapies in heart failure patients. Printing ink will be used on silicone lead connector boots as a visual indicator facilitating the connection of the leads to the correct pulse generator connector cavities. To demonstrate the potential bioavailability of pigments present in the printing inks, an exhaustive extraction study was completed using test samples with exaggerated printing. The challenges and successes in demonstrating the safety of the pigments used in this application are presented here. Test samples were extracted at 50ºC for 7 days in water, 9% ethanol and hexane. These aggressive extraction conditions maximized the potential to extract colorant and were not intended to represent clinical use. Different analytical techniques (LCMS and ICP-MS) were used based on the types of pigments present in the inks (organic vs. inorganic). All results were blank subtracted and adjusted relative to spike sample recovery levels. The worst-case exposure estimates were calculated by normalizing the adjusted amounts proportionally to the maximum printed surface area on the device. The normalized amounts ranged from < 0.01 – 1.5 µg/device. The safety assessment was conducted following *ISO 10993-17: Establishment of Allowable Limits for Leachable Substances*. The threshold of toxicological concern (TTC) approach was applied for pigments with insufficient toxicological data. It was concluded that the printing ink pigments used in the cardiac lead permanent implant devices are eluted from the device at toxicologically insignificant amounts when extrapolated to the clinical exposure.

PS 949 Chemical Safety Risk of Blue Colorant Present in a Limited Contact Device by Exaggerated Extraction Testing and TTC

E. E. Reverdy, A. Hood and M. P. Beauchane. *Boston Scientific Corporation, Natick, MA.*

Patient safety of colorants used in medical devices is an essential part of evaluating device biocompatibility. C.I. Pigment Blue 28 (CAS# 1345-16-0) was proposed for use in two polyether ether ketone (PEEK) resin (2% C.I. Pigment Blue 28) patient contacting components of an imaging catheter (limited, externally communicating, contact with blood). Safety concern over C.I. Pigment Blue 28 was due to the presence of cobalt. The total surface area (mass) of the two colored patient contacting parts (i.e., tubes) were 70.39cm2 (12.8mg) and 20.06 cm2 (8.4mg) respectively. The extractable amounts of colorant C.I. Pigment Blue 28 present in this device were determined by exaggerated extraction, followed by digestion of the non-volatile residue (NVR) portion, and analysis by Inductively Coupled Plasma-Mass Spectroscopy (ICP-MS) to quantify the cobalt (Co) metal ion present in the C.I. Pigment Blue 28 molecule. The amount of C.I. Pigment Blue 28 extracted from OptiCross was determined using percent composition (metal-to-colorant mass ratio). None of the extracts contained a detectable amount of cobalt above the method detection limit (MDL) of 0.8µg/L (ppb) for colbalt, which corresponds to a MDL of 0.3µg C.I. Pigment Blue 28. From this analytical data, the worst-case total exposure was calculated to be less than 0.8µg of C.I. Pigment Blue 28 per device, which was at least 112 times less than the threshold of toxicological concern (TTC) value of 90µg/day. Therefore, chemical safety risk of the extractable amount of C.I. Pigment Blue 28 from OptiCross under exaggerated conditions is assessed to be acceptable.

PS 950 Safety Evaluation of an Intravascular Catheter Securement Device

N. V. Soucy[1] and D. Conrad-Vlasak[2]. [1]*Medical Department, 3M Company, St Paul, MN and* [2]*C3SD, 3M, St. Paul, MN.*

3M™ Tegaderm™ IV Advanced Securement Dressing is an intravascular catheter securement device designed to be placed over a catheter to keep it securely anchored to the skin. In the US it is classified as a Class I device (FDA 21 CFR880.5210) and subject to ISO 10993 Biological Evaluation of Medical Devices - Part 1: Evaluation and Testing within a Risk Management Process, which requires that a risk management framework be used when implementing a biological evaluation program. The dressing is constructed from a polyurethane film, polyester soft cloth material and two different acrylate adhesives. As such, it was necessary to evaluate both the film/adhesive and the backing/adhesive combinations. The nature, degree, frequency and cumulative duration of exposure are important considerations in this evaluation and the following biological effects should be considered for a device classified as a surface device with permanent contact (>30d) to intact skin: cytotoxicity, irritation and sensitization; additionally, genotoxicity and subchronic toxicity should be considered for >30 d contact to breached skin. Potential cytotoxicity of leachable materials present in the dressing was evaluated in both the MEM elution assay and the Agar overlay assay in L-929 mouse fibroblast cells (ISO 10993-5). Potential irritation was evaluated following 24 hr dermal exposure in the New Zealand White rabbit and the dermal sensitization potential was evaluated in the guinea pig maximization test (ISO 10993-10). Under the conditions of these studies, no appreciable cytotoxicity, irritation, or sensitization was observed for the film/adhesive or the backing/adhesive combinations that comprise the device. Genotoxicity and subchronic toxicity data were bridged from a predicate product on the basis of toxicological equivalence. Based on the overall assessment (chemical composition, available literature and biological test data), it can be concluded that the 3M™ Tegaderm™ IV Advanced Securement Dressing is safe for its intended use as an IV catheter securement device.

PS 951 Evaluation of Extract Particulates on Biocompatibility Test Results

A. Hood, M. P. Beauchane, P. Edelman, A. Larson and E. E. Reverdy. *Boston Scientific Corporation, Natick, MA.*

Particulates in biocompatibility test extracts may raise questions during a regulatory submission if the source of the particulates and impact on the test result are not understood. The purpose of this study was to confirm the source of sodium chloride (SC) extract particulates (50°C for 72 hours with agitation), and assess their impact on the Guinea Pig Maximization Test (GPMT) and Intracutaneous Irritancy test results (negative) that were performed at two independent laboratories. No visible evidence of device degradation was observed post-extraction. Particulate source was evaluated by filtering the SC extracts followed by automated counting and sizing software, which showed the extract contained ~900 particles ≥50µm (~17,700 particles/device), and FTIR analysis that showed the particles as predominately cellulosic. Presence of cellulosic material in the SC extract indicated the source to be environmental foreign material (FM) that may have been introduced during device manufacturing. Review of manufacturing processes confirmed the devices came in contact with a cellulosic type material. Impact of SC extract particulates on the two biocompatibility test results was assessed by the Liquid Laser Particulate Test. The Liquid Laser Particulate Test is a validated particulates test method based on USP <788> that determines particulate count and size. An average of 5,019 particles ≥10µm, with a maximum of 8,350 particles ≥10µm, was observed. The worst-case particles observed were 9-times below the historical level of allowable particulates

for limited-duration, blood-contacting devices (75,000 particles ≥10μm). Because the device category is limited duration and breached or compromised surface contact per ISO 10993-1, the size and number particles present on the device are acceptable and did not adversely impact the test results of the sensitization and intracutaneous reactivity biocompatibility tests.

PS 952 High-Density Polyethylene Controls in Toxicological Implant Studies

I. Trausch and R. D. White. *WuXi Apptec, St. Paul, MN.*

Implant toxicity studies for medical devices require controls that are similar in size, shape, and configuration to the test article. USP High Density Polyethylene (HDPE) is commonly used as a reference material (negative control) for implant studies when a predicate device control is not available, or not feasible for the study design. HDPE controls are matched as closely as possible to test articles by size, shape, and surface area. However, limitations in commercially available USP HDPE often preclude a close geometrical match to a test article, leading to concerns regarding the use of controls and test articles of unmatched dimensions and surface areas in medical device implant toxicity studies. A recent 13 week implantation toxicity study in rabbits compared the clinical pathology and histopathology of animals implanted with a test article to animals implanted with HDPE of two different dimensions and surface areas.
Bilateral intramuscular implants were made in 24 animals. Eight test group animals were implanted with bar-shaped stainless steel /nitinol implants approximately 1 x 0.1 x 0.1 cm in size and a surface area of 0.4 cm2. One group of eight control animals were implanted with USP HDPE of the same dimensions and surface area as the test article, and a second group of eight control animals were implanted with USP HDPE of a flat rectangular shape, 1 x 1.25 x 0.1 cm in size with a surface area of 3.0 cm2. All animals were terminated after thirteen weeks. Gross necropsy, hematology, clinical chemistry, and histopathology of local and systemic tissues were evaluated and compared for each of the three groups.
No significant differences were seen in clinical pathology parameters or local and systemic tissue reactions between the two control groups, or between the test group and either control group. Based on these results, using HDPE negative controls unmatched in size, shape and surface area to the test article does not significantly affect the clinical pathology or histopathology evaluation of subchronic intramuscular implantation toxicity studies in rabbits.

PS 953 Infusion Pump Accuracy Assessment: Weighing Syringes and IV Bags Not Necessary As Secondary Accuracy Check on Infusion Studies

L. Hudgens, J. K. Herman, K. Rasmussen, N. West and A. N. Alexander. *Nonclinical Safety Assessment, Covance Laboratories Inc, Madison, WI.*

It is common in some academic and preclinical safety assessment labs to weigh syringes and intravenous (IV) dosing bags pre and post dose administration to confirm dose delivery on infusion studies as a secondary accuracy check. This practice is very laborious, especially for preclinical studies using hundreds of animals, and difficult to document to GLP standards. We chose to assess the accuracy of several commercially available syringe and peristaltic infusion pumps to determine if weighing syringes and IV bags was necessary to confirm dose delivery.
Surgically catheterized dogs and rats were infused using a tethered infusion apparatus and external peristaltic or syringe infusion pumps for three dosing cycles at various dose rates to mimic typical preclinical intermittent safety assessment infusion studies. Syringes and IV bags were weighed pre- and post-dose administration and dose volume delivered computed by subtracting the two values and employing a density correction for saline. The calculated dose volume was compared to the dose delivery volume listed on the infusion pump display screen. Percent of theoretical volume delivered was calculated for each animal on each dosing day.
A total of 226 rats and 30 dogs were infused for three dosing cycles over 17 days. A total of 2096 syringe doses and 338 IV bag doses using peristaltic pumps were administered over the course of the study. At a threshold of +/-10% of theoretical, 98.7% of the doses listed on the infusion pump met acceptance criteria compared to the calculated dose volume for syringe pumps (99.4% for peristaltic pumps). At a threshold of +/- 5% of theoretical, the correlation was 90% and 77.8%, respectively.
The accuracy of the syringe and peristaltic infusion pumps exceeded expectations and were comparable with acceptance criteria of other laboratory equipment used on GLP studies. Therefore, there is no scientific rationale for recording syringe weights pre- and post-dose delivery as a secondary infusion pump accuracy check.

PS 954 Comparison of Optical Coherence Tomographic and Histopathological Retinal Images and Investigation of Age-Related Change in Retinal Thickness in Cynomolgus Monkeys

K. Nishi, T. Araki, T. Okazaki, K. Kabayama, Y. Motomura, H. Sameshima and R. Nagata. *Shin Nippon Biomedical Laboratories (SNBL), Ltd., Kagoshima, Japan.*

Purpose: Optical coherence tomography (OCT) captures images of ocular fundi non-invasively in real time, based on light reflected from surfaces of interest. In this study, retinal thickness was measured in cynomolgus monkeys using OCT and histopathological (HP) images, and the results were compared to investigate the utility of OCT. Age-related changes in retinal thickness were also investigated with OCT.
Methods: For comparison of OCT and HP (eyeballs were fixed in a mixture of 3% glutaraldehyde/2.5% formalin), 10 male monkeys (age: 3–5 years) with no history of retinal disease were used. Retinal thickness was measured using OCT and HP images at the mid point between the optic papilla and macula, in total and for the following 10 layers: internal limiting membrane (ILM), nerve fiber layer (NFL), ganglion cell layer (GCL), inner plexiform layer (IPL), inner nuclear layer (INL), outer plexiform layer (OPL), outer nuclear layer (ONL), external limiting membrane (ELM), photoreceptor cell (PR), and retinal pigment epithelial layer (RPE). For investigation of age-related change, retinal thickness was measured using OCT for each of the 10 layers in 40 female monkeys (10 animals/age at 1, 5, 10 and 13 years). These data were analyzed statistically.
Results: No difference was noted in total retinal thickness (approx. 340 μm) between OCT and HP images. GCL, INL and OPL were thinner (approx. 30-40%), and IPL and ONL were thicker (approx 50%), in OCT images than HP images. With increase in age, NFL thickness decreased by 23% (1 vs. 13 years) and ONL and INL showed a tendency toward decrease in thickness. IPL, OPL, GCL and RPE showed a tendency toward increase in thickness from 5 years; PR, ILM and ELM showed no age-related change in thickness.
Conclusion: Ocular examinations and evaluations in cynomolgus monkeys with OCT should be carried out taking differences between OCT and HP measurements and age-related change in retinal thickness into consideration.

PS 954a Creating a Holistic Extractables and Leachables (E&L) Program for Biotechnology Products

K. L. Li[1], A. Mire-Sluis[1, 2] and B. Cherney[1, 2]. [1]*Corporate Environment, Health and Safety, Amgen Inc., Thousand Oaks, CA and* [2]*Corporate Quality, Amgen Inc., Thousand Oaks, CA.*

The risk mitigation of extractables and leachables (E&L) presents significant challenges to regulators and drug manufacturers with respect to the development, as well as the lifecycle management of drug products. A holistic program is proposed, using a science- and risk-based strategy for testing E&L for primary containers, drug delivery devices and single-use systems for the manufacture of biotechnology products. The strategy is phase-appropriate, progressing from extractables testing for material screening/selection/qualification through leachables testing of final products. The strategy is designed primarily to ensure patient safety and product quality of biotechnology products.
The holistic program requires robust extraction studies using model solvents, with careful consideration of solvation effect, pH, ionic strength, temperature, product contact surface and duration. From a wide variety of process- and product-contact materials, these extraction studies have identified and quantified over 200 organic extractable compounds. The commonly observed compounds are siloxanes, fatty acid amides and methacrylates. The extractables profiles often show degradation products of the chemical additives. Toxicology assessments have been conducted on these compounds using risk-based decision analysis. Safety thresholds have been derived, as appropriate, for the majority of these compounds. Analysis of safety thresholds has helped to establish action thresholds to target and monitor high risk compounds in drug products on stability until expiry. Action thresholds serve to trigger quality investigations to determine potential product impact.
The holistic program also has in place processes to assess the impact of E&L compounds to product quality attributes and risk for immunogenicity. This science- and risk-based approach for primary drug containers and drug delivery devices is also suitable for single-use systems when justified with a historical knowledge base and understanding of the manufacturing processes of biotechnology products.

PS 954b Medical Device Thrombogenicity Testing Using Molecular Indicators of Thrombin Generation: An *In Vitro* Alternative to the NAVI Model

M. F. Wolf[1], S. Hoffmann[2], C. E. DeRusha[3, 1], A. A. Anderson[4, 1], J. Rodriguez[1] and A. Y. Sawyer[5]. [1]*Core Technologies, Medtronic Inc., Minneapolis, MN,* [2]*SEH Consulting + Services, Paderborn, Germany,* [3]*Biochemistry, University of Wisconsin, Stevens Point, WI,* [4]*Chemistry, University of Minnesota, Minneapolis, MN and* [5]*Biological Sciences, Becton Dickinson & Company, Research Triangle Park, NC.*

The ISO 10993-4 standard describes pre-clinical biological tests for the evaluation of blood-contacting cardiovascular medical devices. FDA's interpretation of this standard often calls for an in vivo non-anticoagulated venous implant (NAVI) test in large animals to estimate potential thrombosis risk. This work explores an in vitro alternative to the NAVI test that details necessary in vitro experimental conditions and measures key coagulation proteins TAT and F1.2 which are reflective of thrombin generation upon blood contact with the device. Medical device materials of known low, intermediate, and high NAVI scores (0-5 scale) were tested in simple static-tube and dynamic-pulsatile-loop in vitro blood contact models. Study variables were: model, material, anticoagulation (0.6 to 2.0 IU heparin/mL blood), exposure time (30 to 90 minutes), and donor. Statistical analyses were performed on ELISA measurements of plasma TAT and F1.2 following exposure of six different materials to fresh human blood. Significant ($P < 0.05$) TAT and F1.2 thrombin generation responses were attributable to each study variable and were reflective of observed in vivo NAVI scores. Significant two-factor interactions were also observed. In summary, modern molecular tools for in vitro measurement of human blood coagulation proteins showed that levels of such proteins from controlled material exposure to blood correlate with in vivo thrombus scores achieved in the NAVI model. With carefully defined in vitro blood-contact models and test conditions, these tools provide a simple, accurate, and reproducible estimation of risk for medical device-associated thrombotic responses. Therefore, this approach may be an acceptable replacement for the NAVI animal model, which is costly and known to be a poor predictor of human safety.

PS 954c Comparable Results from 2 *In Vitro* Cytotoxicity Tests Used in the Evaluation of Medical Devices

R. T. Przygoda[1] and D. E. Malek[2]. [1]*Life Cycle Materials, Johnson & Johnson, Cincinnati, OH and* [2]*Malek Toxicology Delaware LLC, Greenville, DE.*

ISO 10993-1 includes an *in vitro* cytotoxicity test as part of a biological evaluation of medical devices. Two cytotoxicity tests commonly used in this evaluation are the MEM elution (ME) and Colony Formation (CF). Previous data from the ME and CF tests for 43 test samples showed 86% agreement. In this current study, results from five commonly used positive controls from both the ME and CF tests were evaluated. The tests for each positive control were performed at two separate laboratories. The ME test was performed according to ISO 10993-5, Section 8.2 with the addition of serial dilutions of the extract with doses ranging from 0.391% to 100%. The CF test was performed according to ISO 10993-5, Annex B with doses ranging from 0.098% to 100%. In the MEM elution tests, results for powder free latex (PFL) and the black rubber stopper (BRS) were inconsistent. BRS at laboratory A was completely toxic (scores of 4) at 25, 50 and 100% but the same doses were scored as non-toxic (scores of 2) in laboratory B. PFL at laboratory A was completely toxic (scores of 4) at 6.25, 12.5, 25, 50 and 100% and the doses between 3.25 to 100% were scored as non-toxic (scores of 2) in laboratory B except for 6.25% which was toxic (scores 4). Results for the PFL were reproducible in laboratory B. The difference in results may be contributed to the difference in the sterilization states of the test samples. In the CF tests, the IC_{50} values for PFL, cadmium chloride and the BRS showed significant variation between laboratories. However, for polyurethane containing 0.1% ZDBC and polyurethane containing 0.25% ZDEC the IC_{50} values from each laboratory were nearly identical. If the two non-sterile samples are eliminated, the cytotoxicity categorizations using MHLW notification 0301 No.20, 2012 were identical for both ME and CF tests. Therefore, either test may be used potentially to predict the same category of cytotoxicity (strong, moderate, weak or none).

PS 954d *In Vitro* Genotoxicity Assays with Co and Cr(III) Ions and Alloy Particles: Implications for Cancer Risks to Hip Implant Patients

W. V. Christian[1], L. D. Oliver[2], M. Kreider[1] and B. L. Finley[2]. [1]*Cardno ChemRisk, Pittsburgh, PA and* [2]*Cardno ChemRisk, Brooklyn, NY.*

Cobalt-chromium (CoCr) alloys have long been used in metal-containing hip implants because of their biocompatibility. Like all implant materials, CoCr alloys undergo some degree of wear and corrosion *in vivo*, and as a result implant patients typically have blood and tissue Co and Cr(III) concentrations that are a few-fold higher than background levels associated with dietary intake. Although to date epidemiology studies do not indicate an increased incidence of cancer in patients with hip implants, questions continue to be raised about the potential cancer risk posed by CoCr-containing implants. This analysis was conducted to determine whether the existing toxicology data support epidemiological findings. We evaluated the results of over 60 *in vitro* genotoxicity assays in human cell lines treated with Co and Cr(III) ions and particulate; endpoints included chromosomal aberrations, micronuclei formation, DNA breakage, and oxidative DNA damage. The *in vitro* concentrations at which genotoxic effects occurred (and did not occur) in these studies were compared to tissue concentrations of Co and Cr(III) that we conservatively estimated would exist in patients with normal functioning CoCr metal-on-metal (MoM) hip implants (wear rates of 1 mm^3/year). For metal particulates, we found that in general, the minimum concentrations required to cause genotoxic effects *in vitro* ($10^4 – 10^8$ μg/g) were more than 1,000-fold higher than those likely present in tissues of implant patients; similar results were obtained for studies on Co and Cr(III) ionic solutions. Thus, exposures to CoCr wear debris from MoM prostheses would not likely be genotoxic *in vivo*, and this is consistent with cancer epidemiology studies conducted to date.

PS 954e CYP2C9 Regulation by Epigenetic Modification of Histone H3—Involvement of Med25 As the Key Regulator

N. Englert, G. Luo, S. Surapureddi and J. A. Goldstein. *Laboratory of Toxicology and Pharmacology, National Institute of Environmental Health Sciences, Research Triangle Park, NC.*

Cytochrome P450 (CYP450) enzymes are important for the hepatic metabolism of exogenous chemicals including common pharmaceutical drugs such as Warfarin and Ibuprofen, as well as the metabolism of endogenous substrates. The CYP2C9 gene is regulated by nuclear receptor HNF4α, which has been shown to recruit Med25, a subunit of the Mediator complex. The Mediator complex is involved in the transcriptional regulation of most genes by recruiting Polymerase II, thus revealing its importance in controlling cellular function. Here, we examined whether Med25 is involved with epigenetically regulating the expression of CYP2C9, through modifying histone markers in the chromatin of the CYP2C9 promoter. We hypothesize that Med25 is important not only for Polymerase II recruitment, but for controlling the chromatin architecture, and thus the expression, of target genes. Chromatin immunoprecipitation in HepG2 cells indicated that altering Med25 expression modified H3K27 status; in the presence of Med25, the HNF4α binding site was enriched for activating markers H3K27ac and H3K27me1, with progressive demethylation. When Med25 expression was silenced, H3K27 was highly methylated (H3K27me3), which is a prototypical gene-silencing marker; PRC2 proteins were recruited to the site in the absence of Med25. CYP2C9 transcript levels were reduced after silencing Med25 expression. Coimmunoprecipitation revealed a reduced association of PRC2 proteins with HNF4α when Med25 was expressed. These data indicate that Med25 induces a permissive chromatin state at the CYP2C9 proximal promoter. Additionally, confocal microscopy revealed that Med25 colocalized with activating histone markers (H3K27ac) in the nucleus of HepG2 cells while it did not colocalize with repressive markers (H3K27me2, H3K27me3). Our data indicate that Med25 is important for changing the epigenetic landscape to allow for increased levels of transcriptional activation of highly inducible genes such as the hepatic cytochrome P450s.

PS 954f Regulation of Chromatin Assembly by Environmental Toxicant

C. Jin[1], D. Chen[1], L. Fang[1], H. Li[1] and L. Huang[2]. [1]*Environmental Medicine, NYU School of Medicine, Tuxedo, NY and* [2]*Physiology & Biophysics, UC Irvine, Irvine, CA.* Sponsor: M. Costa.

Appropriate chromatin assembly ensures the maintenance of proper chromatin structure, genome integrity, and gene expression. Abnormal chromatin assembly could be a cause or significant contributor to pathogenesis. In the presented study, we investigated how environmental toxicant modulates chromatin assembly pathway. Acrolein is abundant in the environment, especially in tobacco smoke. It has

been implicated in neurodegenerative diseases and cancer, yet the mechanisms by which it act have remained largely unknown. As an α,β-unsaturated aldehyde, acrolein could react nucleophilic amino acid residues such as lysine in susceptible proteins. The fact that histone proteins are rich in lysines raised the possibility that acrolein targets lysine residues in histone tails, affecting their physiological posttranslational modifications. Because appropriate histone lysine modifications are crucial for genome function, the formation of acrolein-histone adducts should have significant impact on cellular processes. Biochemical and Mass Spectrometry analyses show that acrolein forms adducts with some but not all lysines on histone proteins in vitro and in vivo and preferentially reacts with free histones rather than with nucleosomal histones. Cellular fractionation analyses reveal that acrolein exposure specifically inhibits acetylations of N-terminal tails of cytosolic histones H3 and H4, modifications that are important for nuclear import and chromatin assembly. Notably, acrolein exposure compromises the delivery of histone H3 into chromatin and increases chromatin accessibility as measured by Chromatin Immunoprecipitation and Micrococcal Nuclease Digestion analyses. Moreover, changes in nucleosome occupancy at several genomic loci are correlated with transcriptional responses to acrolein exposure. We propose that reacting with newly synthesized not yet modified histones thereby affecting histone modification and chromatin assembly pathway represents a novel mechanism whereby certain environmental factors interact with the genome and influence genome function

PS 954g Multifocal Defects in the Hematopoietic and Lymphoid Compartments in Mice Dosed with a Broad BET Inhibitor

D. U. Lee, P. Katavolos, C. Sioson, A. Katewa, J. Pang, E. Choo, N. Ghilardi, D. Diaz and D. M. Danilenko. *Genentech, South San Francisco, CA.*

Bromo and extra terminal (BET) proteins (BRD2, BRD3, BRD4 and BRDT) are epigenetic transcriptional regulators required for efficient expression of growth promoting, cell cycle progression and antiapoptotic genes. Through their bromodomain, these proteins bind to acetylated lysine residues of histones and are recruited to transcriptionally active chromatin. Inhibition of the BET-histone interaction provides a tractable therapeutic strategy to treat diseases that may have epigenetic dysregulation. JQ1 is a small molecule that blocks BET interaction with histones. It has been shown to decrease proliferation of patient-derived multiple myeloma in vitro and decrease tumor burden in vivo in xenograft mouse models. While targeting BET appears to be a viable and efficacious approach, the safety profile of BET inhibition is largely unknown. In this study, we used JQ1 as a tool molecule to explore the potential safety issues related to BET inhibition, and provide early de-risking of the target. Mice dosed with JQ1 at efficacious exposures develop multifocal defects in the lymphoid and immune cell compartments. At higher doses, JQ1 was not tolerated and resulted in significant body weight loss in mice, which were subsequently euthanized early in the study. Flow cytometry analysis of lymphoid tissues showed a decrease in both B and T lymphocytes and a concomitant decrease in peripheral white blood cells were confirmed by hematology & histopathology. Further investigation is required to determine if these toxic effects are associated with BET inhibition or more specifically related to the chemical structure of JQ1.

PS 954h Sex-Dependent Effects of Lead and Prenatal Stress on Histone Modifications in Frontal Cortex and Hippocampus of the Developing Brain

J. Schneider[1], D. W. Anderson[1], S. Kidd[1], M. Sobolewski[2] and D. A. Cory-Slechta[2]. [1]*Thomas Jefferson University, Philadelphia, PA and* [2]*University of Rochester, Rochester, NY.*

Sex-dependent differences characterize the response of the brain to lead (Pb) and prenatal stress (PS), but the molecular mechanisms are unknown. This study examined the potential epigenetic basis of Pb ± PS effects on expression of sexually dimorphic histone modifications, H3K9/14Ac (associated with gene activation) and H3K9Me3 (associated with gene silencing), in frontal cortex (FC) and hippocampus (HIPP) in males and females at 2 developmental periods (PN0, PN6). C57/Bl6 mouse dams received 0 or 100 ppm Pb in drinking water 2 mos prior to breeding and through PN6. Half of the dams in each Pb group were exposed to restraint stress (PS) 3x/day for 30 min from gestational day 11-19 or no stress (NS). Treatment groups/sex were: 0-NS, 0-PS, 100-NS and 100-PS. FC and HIPP from PN0 and PN6 brains were processed for immunoblotting for H3K9/14Ac and H3K9Me3. At PN0, FC H3K9/14Ac levels were decreased by Pb alone in females, but were increased synergistically by Pb + PS in males. FC H3K9Me3 levels were increased by PS and Pb + PS in females, but not by Pb alone, while effects of Pb + PS, but neither alone were seen in males. There were no sex differences or Pb ± PS effects on FC H3K9/14Ac or H3K9Me3 levels at PN6. HIPP H3K9Me3 and H3K9/14Ac changes were seen only in females and only at PN0; these included increases in the H3K9/14Ac response to PS and Pb + PS and to PS only for H3K9Me3 levels. These results suggest that Pb ± PS alters H3 acetylation/trimethylation early during development in a sex-dependent manner, leading to potential errors in transcriptional regulation. FC appeared more vulnerable than HIPP. Enhanced effects of combined Pb + PS were seen only in males; effects were prominent at P0 but not P6. Histone modifications are involved in many aspects of brain development including neurogenesis, synapse formation, and cell differentiation/migration. Sex differences in histone modification may underlie different functional outcomes from Pb ± PS in males and females. ES021534-01

PS 955 Global DNA Methylation Profiling of Hepatocellular Carcinomas from *Ginkgo biloba* Extract-Treated and Vehicle Control B6C3F1 Mice

S. Bhusari[1], A. R. Pandiri[1, 3], D. Mav[2], R. Shah[2], H. Hong[1], T. Ton[1], D. Malarkey[1], R. Sills[1] and M. Hoenerhoff[1]. [1]*CMPB, NTP, NIEHS, RTP, NC,* [2]*SRA, INTL., RTP, NC and* [3]*EPL, Inc., RTP, NC.*

Epigenetic modifications, such as DNA methylation, play an important role in the development of hepatocellular carcinoma (HCC). In a recent NTP 2-year carcinogenicity bioassay, chronic exposure of B6C3F1 mice to *Ginkgo biloba* extract (GBE) resulted in a high incidence of HCC. To better understand the gene-specific methylation alterations in HCC due to GBE exposure, we performed global methylation profiling on HCC from GBE exposed mice (GBE-HCC; n = 5), spontaneous HCC from vehicle control mice (spont-HCC; n = 5), and age-matched normal liver from vehicle control mice (VN; n = 5), in order to identify differentially methylated regions (DMRs) in HCC from GBE exposed animals. The global methylation profiling included 20,404 promoter regions and 15,988 annotated CpG islands, and methylation changes were correlated to corresponding transcriptomic changes. Compared to VN liver, 1400 CpG sites in GBE-HCC and 849 CpG sites in spont-HCC were differentially methylated (DM; $P < 0.01$). Compared to spont-HCC, 138 CpG sites were DM in GBE-HCC ($P < 0.01$). Using pyrosequencing, we confirmed promoter-specific hypomethylation of the *cMyc* oncogene in GBE-HCC compared to spont-HCC ($P<0.001$), with a corresponding increase in gene expression showing significant negative correlation with methylation changes ($r = - 0.93$; $P = 0.01$). In addition, we also confirmed hypermethylation of tumor suppressors (*Spry2, Cdkn2a, Dusp5*) in GBE-HCC compared to spont-HCC ($P < 0.001$) with a corresponding decrease in gene expression. In conclusion, we have identified DMRs in promoter CpG islands of relevant cancer genes altered in GBE-HCC compared to spont-HCC, suggesting that such promoter CpG island DMRs could be used to differentiate treatment-related tumors from background, spontaneous tumors in cancer bioassays. Furthermore, these data provide additional understanding of the underlying epigenetic mechanisms of chemical carcinogenesis in animals and their relevance to human health and hazard identification.

PS 956 Hepatic Epigenome Controls the Severity of Liver Injury in Mice Induced by a Choline- and Folate-Deficient Diet

V. Tryndyak[1], T. Han[2], J. C. Fuscoe[2], F. A. Beland[1] and I. Pogribny[1]. [1]*Division of Biochemical Toxicology, FDA-NCTR, Jefferson, AR and* [2]*Division of Systems Biology, FDA-NCTR, Jefferson, AR.*

The importance of epigenetic changes in etiology and pathogenesis of disease has been increasingly recognized. However, the role of epigenetic alterations in the genesis of nonalcoholic fatty liver disease (NAFLD) and cause of variations in individual susceptibilities to this disease are largely unknown. In the present study we investigated whether or not the epigenetic profile of normal liver affects the severity of NAFLD-associated liver injury. Male WSB/EiJ and A/J inbred mice were maintained on either control or choline- and folate-deficient (CFD) diets for 12 weeks and the status of DNA methylation and histone H3 lysine 4 trimethylation (H3K4me3) was determined using whole genome methylated DNA immunoprecipitation (MeDIP) and H3K4me3-chromatin immunoprecipitation (ChIP)-on-chip techniques. Feeding the CFD diet for 12 weeks caused significantly greater liver injury in WSB/EiJ mice as compared to A/J mice. MeDIP analysis shows that the greater vulnerability of WSB/EiJ mice was associated with a hypomethylated liver phenotype. This was evidenced by a greater number of hypomethylated CpG domains than hypermethylated CpG regions, 3429 and 471, respectively, and consequently a high hypomethylated/hypermethylated CpG domain ratio in DNA isolated from normal livers of WSB/EiJ mice. In contrast, DNA isolated from normal livers of A/J mice contained approximately an equal number of hypomethylated and hypermethylated CpG regions, 2044 and 1856, respectively. ChIP-on-chip analysis showed differential histone H3K4me3 enrichment throughout the genome in the normal livers in WSB/EiJ and A/J mice, but it was not associated with the extent of the CFD diet-induced liver injury. Interestingly, feeding a CFD diet caused opposite effects on DNA methylation: increased methylation in the livers of

WSB/EiJ mice and decreased in A/J mice. Our findings indicate that the status of hepatic epigenome is the important factor determining the individual vulnerability to NAFLD.

PS 957 Epigenetic Alterations in the Livers of Fisher 344 Rats Exposed to Furan

T. Kobets, A. de Conti, C. Escudero-Lourdes, B. Montgomery, V. Tryndyak, F. A. Beland, D. R. Doerge and I. Pogribny. *Division of Biochemical Toxicology, National Center for Toxicological Research, Jefferson, AR.*

Furan is a volatile heterocyclic compound widely used in the chemical manufacturing industry. It is also found in a variety of common cooked foods consumed by adults and infants. Lifetime exposure to furan causes liver tumors in rats and mice (NTP, 1993); however, the mechanisms of the furan hepatocarcinogenicity are still unclear. The goal of the present study was to investigate whether or not the exposure to furan causes epigenetic alterations in rat liver. Male Fisher 344 rats were treated by gavage with different doses of furan [0, 0.92, 2.0, or 4.4 mg/kg/body weight(bw)/day] dissolved in corn oil. The exposure of Fisher 344 rats to furan produced dose- and time-dependent epigenetic changes in the livers consisting of alterations in the global pattern of histone lysine methylation and acetylation, gene-specific methylation, and altered expression of chromatin modifying genes. Specifically, there was a sustained decrease in the levels of histone H3 lysine 9 and H4 lysine 20 trimethylation in the livers after 180 and 360 days of furan exposure, and a marked reduction of histone H3 lysine 9 and H3 lysine 56 acetylation after 360 days of treatment at 4.4 mg/kg/bw/day. These histone modification changes were accompanied by a reduced expression of related Suv39h1, Prdm2, and Suv4-20h2 histone methyltransferases, Ep300 histone acetyltransferase, and an up-regulation of Sirt6 histone deacetylase. The exposure to furan at doses 0.92, 2.0, and 4.4 mg/kg/bw/day caused global demethylation of hepatic DNA after 360 days of treatment. Additionally, furan at 2.0, and 4.4 mg/kg/bw/day doses induced hypermethylation-dependent down-regulation of the Rassf1a tumor suppressor gene in the livers after 180 and 360 days of treatment. In summary, these findings indicate possible involvement of dose- and time-dependent epigenetic modifications in the hepatotoxicity and carcinogenicity of furan.

PS 958 Genome-Wide DNA Methylation Changes Influence Gene Expression in Arsenic-Transformed Human Prostate Cells

B. A. Merrick[1], E. J. Tokar[1], D. P. Phadke[2], R. Shah[2], X. Wang[3], M. A. Bostrom[3], O. Gordon[3], G. M. Wright[3], M. Burke[3], K. E. Pelch[1], S. S. Auerbach[1], R. R. Tice[1] and M. P. Waalkes[1]. *[1]DNTP, NIEHS, NIH, Research Triangle Park, NC, [2]Social & Scientific Systems, Durham, NC and [3]DHMRI, Kannapolis, NC.*

NextGen sequencing provides genome-wide coverage at base-pair resolution of DNA alterations for environmentally-related diseases, like cancer. In this study, methylated DNA was affinity-enriched, bisulfite treated and sequenced for high-resolution detection of differential methylation in arsenic-transformed, CAsE-PE cells derived from normal, RWPE-1 human prostate cells. We hypothesized that changes in methylation status might change gene expression in CAsE-PE cells and contribute to malignancy. A total of 74-84 million bisulfite-treated DNA sequenced reads (100bp, paired end) were produced. Analysis focused on the most differentially methylated bases (cytosines), termed DMBs, and showed a >50% change in methylation state. We organized DMB's into structural units of 'differentially methylated clusters' (DMC), as short regions with 4 or more DMBs. More than 7,000 DMCs were found in the two cell lines. There were >500 genes with at least one DMC in the promoter region for which >40 hypermethylated cytosines and 10 hypomethylated sites have been independently validated by 454 pyrosequencing. However, only 25% of all DMBs were found within CpG islands or shores while the majority of DMBs were not. Data suggest that CpG-based platforms (e.g. CpG bead arrays) may underrepresent the methylome and not be fully capable of measuring differential methylation. Additionally, RNA-Seq showed a large increase in KRAS mRNA in CAsE-PE cells compared to RWPE-1. KRAS is a well-known oncogene whose enhanced activity (mutated forms) or increased mRNA levels can be upregulated in many types of tumors. While no mutations were seen in KRAS mRNA in either cell line, other oncogenic mechanisms may have occurred that play a major role in malignant conversion to form CAsE-PE cells. We believe these data will offer insights into epigenetic effects of arsenic carcinogenesis and a technical approach to studying epigenetic mechanisms.

PS 959 Environmental Health Disparities in the Age of Epigenetics

K. Olden, Y. Lin and B. R. Sonawane. *ORD, EPA, Washington, DC.*

Over the past decades, genome-wide association studies have identified certain genetic loci for numerous diseases and traits. However, genetic variations identified to date account for only a small proportion of disease phenotypes. Growing evidence suggests that environmental exposures can influence human disease risk through the accumulation of epigenetic modifications. This general hypothesis provides a broad umbrella to examine how the environment "gets under skin" among selected racial, ethnic and/or socioeconomic groups. We systematically reviewed published literature and propose the "neighborhood-specific" epigenome analysis as a promising approach to study environmental health disparities. In this treatise, environment is characterized in the broad sense of "non-genetic" factors including social, biological, chemical and physical stressors. The hypothesis suggests that understanding the complex interactions between genes, the environment and chronic disease requires the examination of the role of epigenetics in regulating genetic susceptibility to environmental stressors. The slow progress in understanding disparities in disease susceptibility may be in part related to the fact that studies have not considered the cumulative effect of environmental exposure to both chemical and non-chemical stressors on genetic substrates. "Geographical neighborhood-specific" epigenetic markings can potentially be used as a tool to investigate proposed mechanisms to account for well documented racial and ethnic disparities in health. Also, by comparing neighborhood-specific epigenetic profiling, one could then identify novel targets for population-based prevention efforts. This proposed neighborhood-specific epigenome approach promises to provide considerable insight into the causes of health disparities and their potential prevention and intervention strategies.

PS 960 Cadmium Alters Histone Modifications in Mouse Embryonic Stem Cells

S. R. Gadhia and F. A. Barile. *Pharmaceutical Sciences, St. John's University College of Pharmacy, Queens, NY.*

Epigenetic changes in histone modifications due to cadmium exposure early in life results in pathologies observed during adulthood. We tested the effects of low dose acute Cd exposure on cell viability, total histone protein (THP) production, H3K27 mono-methylation (H3K27me1) levels and cell cycle progression in mouse embryonic stem (mES) cells. Exposure to 10 μM Cd altered cell cycle progression at 1-h and 24-h (± recovery) but differentiation patterns were affected only during 72-h exposures. In addition, flow cytometry data demonstrated that Cd IC25 concentration decreased the number of cells appearing in the S-phase and reduced newly synthesized DNA during acute exposures, where as cell differentiation is inhibited during chronic exposures in mES cells. Also, we previously showed that Cd alters THP production and H3K27me1 levels (Gadhia et al, 2012), suggesting chromatin damage and transcriptional changes. Whereas H3K27me1 is a precursor to H3K27me2/me3 states, and since the reaction is catalyzed by a methyltransferase enzyme, EZH2, a member of the PRC2 complex, we monitored EZH2 expression. However, 10 μM Cd exposures up to 72-h did not demonstrate any change in EZH2 expression. Consequently, the results are accounted for by a change in EZH2 activity. The results also confirm the conversion of transcriptionally active H3K27me1 to repressive H3K27me2/me3 modifications. We also studied the heritable effects of acute Cd exposure in stem cells. The data shows that Cd toxicity is transferred from parental mES cells to subsequent generations, without the continued presence of Cd. Interestingly, epigenetically controlled H3K27me1 changes may not be expressed in all subsequent generations. Thus we report that toxic consequences of low dose acute Cd exposure in mES cells are not only cumulative but also inherited.

PS 961 Comprehensive DNA Methylation and Gene Expression Study on Livers Using 2-Stage Hepatocarcinogenesis Model in Rats

K. Omura[1, 2], T. Uehara[2, 3], Y. Morikawa[2, 3], H. Hayashi[4, 5], K. Mitsumori[4], K. Minami[2, 6], M. Kanki[1, 2], H. Yamada[2], A. Ono[2, 7], Y. Ohno[7] and T. Urushidani[2, 8]. *[1]Astellas Pharma Inc., Osaka, Japan, [2]Toxicogenomics Informatics Project, Osaka, Japan, [3]Shionogi & Co., Ltd., Osaka, Japan, [4]Tokyo University of Agriculture and Technology, Tokyo, Japan, [5]Gifu University, Gifu, Japan, [6]Ono Pharmaceutical Co., Ltd., Ibaraki, Japan, [7]National Institute of Health Sciences, Tokyo, Japan and [8]Doshisha Women's College of Liberal Arts, Kyoto, Japan.* Sponsor: Y. Miyamae.

Recent studies have revealed that epigenetic alteration correlates to carcinogenesis in various tissues. Identification of epigenetic alterations in the early stage of carcinogenesis promises a great contribution for mechanism analysis and marker

exploration for the drug development. For this purpose, we conducted comprehensive analyses for DNA methylation and gene expression in livers obtained from a rat 2-stage carcinogenesis study using nitrosodiethylamine (DEN), thioacetamide, methapyrilene and acetaminophen as an initiator and phenobarbital as a promoter. DEN induced glutathione S-transferase-placental form (GST-P) positive foci dose dependently. Pathway analysis revealed that genes changed in expression and DNA methylation were related to PTEN signaling and immune responses in DEN-treated livers. Interestingly, these genes showed similar expression profiles in livers treated with various hepatotoxicants especially genotoxic and/or oxidative stress-type non-genotoxic carcinogens. These results suggested that altered methylation state could trigger the initiation of the future carcinogenic pathway. It was noteworthy that MHC class Ib gene, *RT1-CE5* was persistently hypomethylated proximal to exon 1 in DEN-treated livers. Moreover, this gene was specifically up-regulated in livers treated with various types of carcinogens. These results suggested that early induction of the gene reflects one side of carcinogenesis like tumor immunity. In conclusion, we identified the specific profile of DNA methylation and gene expression in livers with preneoplastic foci and the results suggested that early epigenetic perturbation relates to the early events of carcinogenesis.

PS 962 Effect of THC on Genome-Wide Histone Methylation in Immune Cells

X. Yang, V. L. Hegde, J. Zhang, P. S. Nagarkatti and M. Nagarkatti. *PMI-SOM, University of South Carolina, Columbia, SC.*

Despite the fact that marijuana may have beneficial medical effects in patients with certain diseases, increasing evidence indicates that marijuana suppresses immune function. Therefore marijuana use may increase susceptibility to infection and some types of cancer. To further investigate the effect of marijuana on immune function, we used an animal model to determine the role of Δ9-tetrahydrocannabinol (THC), the major effective component in marijuana, in epigenetic modification of genes in immune cells. Since epigenetic modification plays a critical role in immune cell differentiation and linage commitment, we sought to investigate whether THC alters global histone methylation. Using ChIP-Seq technology, we compared genome-wide histone H3K4, H3K27, H3K9 and H3K36 trimethylation patterns between THC and vehicle treated activated popliteal lymph node cells. Our results show that THC treatment leads to the association of active modification signals with Th2 cytokine genes and suppressive modification signals with Th1 cytokine genes. These results suggest that THC inhibits Th1 cells while promoting Th2 cells through histone modification. At the genomic level, a significant amount of histone methylated regions are altered by THC. Functional classification of these histone methylation associated genes shows that these differentially associated genes are involved in various cellular functions, from cell cycle to metabolism, suggesting that THC regulates global gene expression in immune cells through histone modification. (Supported in part by NIH grants P01AT003961, R01AT006888, R01ES019313, R01MH094755, P20RR032684 and VA Merit Award BX001357)

PS 963 Prenatal Exposure to TCDD Triggers Epigenetic Modifications Including DNA Methylation and microRNA Induction That Target Genes Which Regulate Immune Functions

N. P. Singh[1], X. Yang[1], U. Singh[1], J. Zhang[2], I. K. Abbas[1], M. Nagarkatti[1] and P. S. Nagarkatti[1]. [1]*Pathology, Microbiology, and Immunology, University of South Carolina School of Medicine, Columbia, SC and* [2]*Epidemiology and Biostatistics, University of South Carolina, Columbia, SC.*

TCDD (2,3,7,8-tetrachlorodibenzo-p-dioxin) is a potent aryl hydrocarbon receptor (AhR) ligand and an environmental contaminant. Prenatal exposure to TCDD is well known to cause thymic atrophy as well as alterations in T cell differentiation, the precise mechanisms of which are unclear. In the current study, therefore, we investigated the role played by epigenetic mechanisms in regulating the immunotoxic effects of TCDD following prenatal exposure. To this end, pregnant mice on gestational day 14, were injected with TCDD (5 μg/kg) and on postnatal day 4, the thymi were harvested and high-throughput microRNA (miR) and genome-wide MeDIP methylation arrays were performed. We observed more than 69 miRs to be up- or down-regulated greater than 2 fold in fetal thymocytes post TCDD exposure when compared to controls. We validated the expression of several miRs by performing Real-Time PCR. The data obtained from miR arrays of fetal thymi post-TCDD exposure demonstrated changes in miR profile that affected expression of important genes such as, AhR, CYP1A1, Foxp3, IL-17, Fas and FasL, which are known to regulate signaling, toxicity, apoptosis, thymic atrophy, and immunosuppression caused by TCDD. The data obtained from methylation arrays, upon further analysis, showed significant differences in methylation status of specific genes such as AhR, CYP1A1, IFN-γ, IL-4, FoxP3, and IL-17 in thymus following prenatal exposure to TCDD. We also noted induction of regulatory T cells and suppression of Th17 cells. Together, our studies suggest that prenatal exposure to TCDD triggers significant alterations in miRs as well as methylation status of a wide range of genes that regulate the immune functions (Supported in part by NIH grants P01AT003961, R01ES019313, R01MH094755, P20RR032684 and VA Merit Award BX001357).

PS 964 Physiological Effects of Developmental Lead (Pb) Exposure on Weight, Food Intake, Body Fat, and Insulin in Mice

C. Faulk, A. K. Barks, B. N. Sánchez, Z. Zhang, O. S. Anderson, K. E. Peterson and D. Dolinoy. *Environmental Health Sciences, University of Michigan, Ann Arbor, MI.*

Developmental exposure to lead (Pb) can have persistent effects on physiology and has been associated with lower body weight in human infants and late onset obesity in mice. Epigenetic reprogramming of transposons and imprinted genes during development is a plausible mechanism linking early exposures and physiological changes later-in-life. Mouse dams (n=49) were randomized to one of four groups where drinking water was supplemented 2 weeks prior to mating, through weaning, with 0 (control), 2.1 (low), 16 (medium), or 32 (high) ppm Pb. We measured 18 outcomes in offspring (n=30 control, n=28 low, n=33 medium, and n=29 high): physiological measures at 3, 6, and 9 mos of age, and epigenetic drift in tail DNA from weaning to 10 mos. We estimated average, sex-specific changes in physiological outcomes over time and their differences across exposure using repeated measures models adjusted for within-litter and within-mice correlations. Overall both sexes exhibited increased energy expenditure ($p<0.0001$) as well as increased food intake ($p<0.0001$) compared to controls. Similarly, body weight increases were found in males at medium ($p=0.004$) and high ($p<0.029$) exposure, whereas overall, total body fat increased in males and decreased in females (both $p<0.0001$). However, relative to controls, insulin was increased only in males at the medium level ($p<0.05$). We measured linear trends in relative methylation shift over time vs. exposure level using a linear mixed model. Epigenetic drift measured at the transposon linked metastable epiallele, CabpIAP had significant, exposure-dependent increases over time ($p<0.02$). In general, imprinted genes increased in methylation over time but had locus-specific responses to Pb. For example, Igf2 showed no association with Pb, while Igf2r exhibited increased methylation with Pb ($p=0.045$), and H19 displayed moderately increased methylation with Pb ($p=0.085$). Perinatal Pb exposure has both physiological and epigenetic effects over life course in mice that vary by sex and locus.

PS 965 Effect of 2, 3, 7, 8-Tetrachlorodibenzo-*p*-Dioxin (TCDD) Exposure on the Expression of DNMT Genes during Development in Zebrafish (*Danio rerio*)

E. Kuo[1, 2], Z. Yu[3], S. I. Karchner[1] and N. Aluru[1]. [1]*Biology, Woods Hole Oceanographic Institution, Woods Hole, MA,* [2]*Stanford University, Stanford, CA and* [3]*New England Biolabs, Ipswich, MA.*

DNA methylation is one of the most important epigenetic modifications involved in the regulation of gene expression. Recent studies have demonstrated that environmental toxicants can affect normal development by altering DNA methylation patterns. However, the mechanisms of action of these chemicals are poorly understood. Hence, we tested the hypothesis that developmental exposure to TCDD affects DNA methyltransferase (DNMT) gene expression patterns. To address this hypothesis, zebrafish embryos were exposed to 5 nM TCDD for one hour from 4 to 5 hours post-fertilization (hpf) and sampled at 12, 24, 48, 72 and 96 hpf to determine DNMT gene expression patterns and global methylation patterns. Results demonstrate that TCDD upregulates DNMT1 gene expression, whereas DNMT3 genes (DNMT3a1, 3b1, 3b4) are downregulated following exposure. These results suggest that TCDD exposure may impact both maintenance and de novo methylation. To characterize the TCDD effects, we screened the 2 kilobase region of the DNMT gene promoters for xenobiotic response elements (XRE). We identified at least one XRE in each DNMT promoter. We are characterizing the function of these XREs in *in vitro* luciferase reporter assays. Furthermore, we are quantifying global DNA methylation levels using liquid chromatography to correlate changes in gene expression with methylation patterns. Funding for this project was provided by WHOI Ocean Life Institute and NIH grant P01ES021923 and National Science Foundation Grant OCE-1314642 through the Woods Hole Center for Oceans and Human Health.

PS 966 Time-Dependent, CpG Specific Changes in DNA Methylation Found in CD4+ T Cells from Trichloroethylene-Treated Mice

K. Gilbert[1], S. Erickson[1], S. J. Blossom[1], B. Broadfoot[1], K. West[1], G. Chandler[1] and C. Cooney[2]. *[1]University of Arkansas for Medical Sciences/ Arkansas Children's Hospital Research Institute, Little Rock, AR and [2]Central Arkansas Veterans Healthcare System, Little Rock, AR.*

Adult exposure to water pollutant trichloroethylene (TCE) in drinking water has been shown to induce autoimmune hepatitis in female MRL+/+ mice. This was accompanied by expansion of activated/memory CD4+T cells that secreted increased levels of IFN-γ. Several aspects of normal and autoreactive CD4+T cell function, including differentiation and cytokine production, are regulated by gene-specific alterations in DNA methylation. In the current mechanistic study transcriptomics and toxicogenomics were used to define time-dependent alterations in gene expression and related DNA methylation in CD4+ T cells from MRL+/+ mice exposed to TCE for up to 40 weeks. Naive and memory/activated subsets of CD4+T cells were examined separately. We observed differential DNA methylation in CD4+ cells from TCE and control mice. These TCE-induced alterations in DNA methylation were CpG-, time-, and subset-specific. The alterations encompassed genes important in CD4+ T cell differentiation, cell cycle proliferation and cytokine production. This study is the first to document that low level adult exposure to TCE induces temporal, specific, and potentially functionally important, epigenetic alterations in CD4+ T cells.

PS 967 Nickel Exposure Causes Epigenetic Dysregulation on a Genome-Wide Scale

C. C. Jose[1], B. Xu[2], R. K. Mallela[1], D. E. Schones[2] and S. Cuddapah[1]. *[1]Department of Environmental Medicine, New York University School of Medicine, Tuxedo, NY and [2]Department of Cancer Biology, Beckman Research Institute, City of Hope, Duarte, CA.* Sponsor: M. Costa.

Nickel, an environmental carcinogen, is a widely used metal and release of nickel compounds into atmosphere occurs during various stages of industrial processes. Nickel compounds have been conclusively shown to induce lung and nasal cancers in humans. In spite of its proven carcinogenicity, the mutagenic potential of nickel is very low. Therefore, nickel-induced carcinogenesis appears to be initiated predominantly by non-genotoxic mechanisms. It has been shown earlier that exposure to nickel alters the levels of various epigenetic modifications and growing evidence points to epigenetic dysregulation as a major outcome of nickel exposure. However, the mechanistic basis of nickel-induced epigenetic alterations is not fully understood. In this study, using ChIP-Seq, we comprehensively analyzed NiCl2-induced alterations to several activating and repressive histone modification marks on a genome-wide scale in the immortalized non-cancerous human lung epithelial, BEAS-2B cells. Using RNA-Seq, we detected hundreds of genes with altered expression due to nickel exposure. A large majority of these genes had altered epigenetic profiles in their promoters and gene body regions indicating the extent of epigenetic alterations induced by nickel. Interestingly, the nickel-induced alterations to histone modification marks were not only limited to promoters and regulatory regions of the genome, but also extended to large genomic regions. Taken together, our results indicate disruption of chromatin structure as an important mechanism in nickel-induced gene expression alterations, which could potentially lead to carcinogenesis. We believe that our findings will serve not only as a model to understand the mechanism involved in epigenetic alterations induced by an environmental carcinogen, but also help comprehend how epigenetic aberrations contribute to carcinogenesis. Supported by National Institutes of Health grants R01ES023174 and P30ES000260.

PS 968 Differences in Methylation of Immune Response Genes in Germ-Free and Control Mice

Z. I. Cordero Badillo[1], D. Shubitowski[2] and S. Ewart[2]. *[1]University of Puerto Rico, Rio Piedras, San Juan, Puerto Rico and [2]Michigan State University, East Lansing, MI.* Sponsor: W. Atchison.

RATIONALE: Asthma is a chronic inflammatory disease of the airways that has both environmental and genetic causes. The hygiene hypothesis links asthma to lack of exposure to microorganisms, like bacteria, early in childhood shifting the T helper (Th) 1/Th2 balance towards the Th2 response, which has been associated with immunological disorders. Our lab has shown in a mouse model a relationship between the microbiota of an organism and its epigenome through changes in methylation in *Gata3*,*Il13ra1* and *Pax1* genes that relate to expression of asthma. To further understand this relationship genes previously associated with allergic diseases, *Gata3*, *Il13ra1* and *Pax1* were studied more in depth. We hypothesized that the difference in microbiota in germ-free (GF) and control mice will produce differential methylation in these immune response genes.
METHODS: DNA methylation in *Gata3*, *Il13ra1* and *Pax1* was compared between GF and control mice. We identified CpG islands and assessed methylation percentages in these genes as follows. DNA from spleens was bisulfite converted, gene-specific CpG islands were amplified by PCR and products pyrosequenced.
RESULTS: Methylation of CpG sites in the *Il13ra1* CpG island was increased in GF mice as compared to controls ($p<0.05$). Differential methylation was not found in *Gata3* or *Pax1*.
CONCLUSIONS: The microbiome, or its absence, has a significant impact on methylation of select immune response genes.
FUNDING: NIH grant R25HL103156

PS 969 DNA Hypermethylation of Tumor Suppressor Genes in Chromate Workers

H. Sun, T. Kluz, Q. Qu and M. Costa. *Environmental Medicine, NYU School of Medicine, Tuxedo, NY.*

Hexavalent chromium [Cr(VI)] is a potent human carcinogen. Occupational exposures haves been associated with increased risk of respiratory cancer. Increasing evidences suggests that multiple mechanisms might contribute to Cr(VI) induced carcinogenesis, including DNA damage, genomic instability, and epigenetic modulation. As an important epigenetic regulator of gene expression, DNA methylation in the promoter region of genes is inversely correlated to gene transcription. Aberrant DNA methylation in the gene promoter region has been found in many human tumors, which is responsible for their silencing. Previous studies on chromate-induced human cancer revealed a decreased expression of MLH1 and p16 that was accompanied by an increased DNA methylation in their promoter region, indicating that chromium was able to silence tumor suppressor genes by modulating DNA methylation status. To further investigate the effect of chromate on DNA methylation of other tumor suppressor genes, we analyzed the promoter methylation of 22 tumor suppressor genes in workers from a chromate factory and referent subjects using EpiTect Methyl II PCR array. Among 22 tumor suppressor gene promoters whose hypermethylation was frequently observed in many human cancers, three genes (WIF1, APC and MLH1) exhibited elevated promoter DNA methylation in chromate workers compared to referent subjects. Multiple linear regression analysis indicated a positive correlation between promoter DNA methylation of these three tumor suppressor genes and the levels of Cr(VI) in air and in the red blood cells. Our studies have identified new target tumor suppressor genes that were silenced in human by chromate through epigenetic regulation.

PS 970 Epigenetic Promoter Histone Modifications Play a Key Role in Regulating FasL Gene Expression and Alcohol-Induced Immunotoxicity in CD4+ T Lymphocytes

S. Ghare[1], S. Joshi-Barve[1], A. Moghe[1], M. Patil[1], D. Barker[1], L. Gobejishvili[1], M. Cave[1, 2], C. McClain[1, 2] and S. Barve[1]. *[1]Department of Medicine/GI, University of Louisville, Louisville, KY and [2]Robley Rex VAMC, Louisville, KY.*

Mechanisms underlying alcohol induced immunotoxicity are poorly understood. FasL plays a critical role in regulating physiologic as well as pathologic apoptotic death of CD4+ T cell and the immune response. Although transcriptional regulation of FasL has been extensively studied, the role of epigenetic mechanisms is only poorly understood. Accordingly, immunotoxic effects of alcohol on promoter histone modifications regulating FasL gene expression in human primary CD4+ T cells were examined.
Effect of stimulation and alcohol exposure on FasL promoter-histone modifications was examined in chromatin samples prepared from CD4+ T cells obtained from non-alcoholic and alcohol abusing study subjects by quantitative chromatin immunoprecipitation (ChIP) analysis. In comparison to normal CD4+ T cells, alcohol exposure significantly increased transcriptionally permissive trimethylation at histone H3 lysine 4 (H3K4me3), with a coordinate decrease in transcriptionally repressive trimethylation at H3 lysine 9 (H3K9me3). Commensurate with the decrease in H3K9me3, the acetylation of H3K9 (H3K9ac) which is an essential modification for transcriptional activation and is mutually exclusive to methylation, was further increased upon alcohol exposure. Notably, increase in H3K9ac was determined to be critically regulated by the p300 histone acetyltransferase (p300-HAT). Further, in correspondence with transcriptionally germane histone modifications, alcohol enhanced the recruitment of relevant transcription factors and RNA polymerase II to the FasL promoter, which correlated with increased FasL expression and apoptotic death. Overall, these data identify the dynamic interplay between promoter H3K4 and H3K9 methylation and acetylation as a significant mechanism regulating FasL gene expression in alcohol-induced immunotoxicity.

PS 971 Chemical Allergen-Induced Perturbation of the Mouse Lymph Node DNA Methylome

V. Chapman[1, 2], T. Zollinger[2], R. Terranova[2], J. Moggs[2], I. Kimber[1] and R. J. Dearman[1]. [1]*Manchester University, Manchester, United Kingdom and* [2]*Discovery and Investigative Safety, Novartis Institutes for Biomedical Research, Basle, Switzerland.*

Epigenetic regulation of gene expression plays a pivotal role in the orchestration of immune responses and may impact their vigor, quality or longevity. Chemical allergens can be broadly divided into two categories; contact allergens (e.g. dinitrochlorobenzene; DNCB) and respiratory allergens (e.g. trimellitic anhydride; TMA) that induce polarized type 1/type 17 or type 2 responses, respectively. To explore the molecular regulation of such responses, the genome wide pattern of DNA methylation following treatment with allergen was examined. Mice (n=5 per group) were exposed to DNCB, TMA or vehicle control for 13 days, and draining auricular lymph nodes excised. DNA was extracted and processed for methylated DNA immunoprecipitation then hybridization to a high resolution DNA promoter array covering promoter regions and known CpG islands. Changes in DNA methylation profiles for allergen-activated tissues were compared with vehicle-treated samples ($p<0.01$ cut off). Selected differently methylated regions (DMR) were technically validated by qPCR and were 90% concordant with the array data. More DMR (~3-fold) were recorded for DNCB than TMA, with approximately half of the TMA DMR common to DNCB. For promoter region DMR, 781 and 140 genes were uniquely associated with DNCB or TMA treatment, respectively. Such DMR were generally hypomethylated whereas DMR common to both allergens were equally hypo- and hypermethylated. Pathway analysis of these DMR failed to show immunological pathway enrichment whereas the tight junction pathway was enriched by hypomethylated genes for both allergens and the olfactory transduction pathway was associated with hypo- and hypermethylated genes after DNCB and TMA treatment, respectively. These data demonstrate characteristic DNA methylation patterns indicative of epigenetic regulation of the allergic response, with both DNCB and TMA associated with unique activating epigenetic marks.

PS 972 Assessment of Dose-Response Relationship between Epigenetic and Apical Endpoints following Short-Term Exposure to Nongenotoxic Rodent Hepatocarcinogens

M. R. Schisler[1], L. A. Murphy[1], I. Racine Miousse[2], M. J. LeBaron[1], I. Koturbash[2] and R. J. Rasoulpour[1]. [1]*The Dow Chemical Company, Midland, MI and* [2]*University of Arkansas for Medical Sciences, Little Rock, AR.*

The current product safety assessment paradigm identifies adverse apical effects to establish a no-observed-adverse-effect level (NOAEL) which is utilized for human risk assessment. Some hepatocellular carcinogens induce apical liver effects (i.e. hepatomegaly, hypertrophy, and hyperplasia) which could be mediated in part by epigenetic mechanisms. However, it is currently unknown whether these epigenetic mechanisms: 1) occur within the dose response range for apical effects, 2) are key events in the mode of action (MoA) for apical liver effects or 3) represent unrelated events that simply occur in parallel. In order to determine the dose response for epigenetic mechanisms and relationship to the MoA for apical liver effects, we evaluated both apical and epigenetic changes in the livers of male F344/DuCrl rats following seven day exposures to the rodent hepatocarcinogens, phenobarbital (PB) and clofibrate (CF). Exposure to PB (0; 5, 25, and 100 mg/kg/day) or CF (10, 50, 250 mg/kg/day) resulted in dose-dependent increases in relative liver weights and transcript levels of Cyp2b1(PB) and Cyp4a1(CF) along with hepatocellular hypertrophy and hepatocellular proliferation. Pyrosequencing-based analysis of LINE1 repetitive element revealed a significant decrease in liver DNA methylation after treatment with 100 mg/kg/day PB while the expression of LINE1 was unchanged. There were no changes in methylation status observed in kidney which supports that the changes in liver DNA methylation are compound- and MoA-specific. Although epigenetic mechanisms, such as methylation of LINE1, could be key events in the MoA for apical liver effects, our findings support that these changes occur within the same dose response as apical liver effects. Funded in part by the UAMS CTCA UL1TR000039 and KL2TR000063 (IK), ABI (IK), and Dow (RR).

PS 973 Epigenetic Regulation of Dopamine Transporter Expression

A. L. Green[1, 3], L. Zhan[2], H. Zarbl[2], G. L. Guo[2] and J. Richardson[1]. [1]*Department of Environmental and Occupational Medicine, Robert Wood Johnson Medical School, Rutgers University, Piscataway, NJ,* [2]*Department of Pharmacology and Toxicology, Ernest Mario School of Pharmacy, Rutgers University, Piscataway, NJ and* [3]*Joint Graduate Program in Toxicology, Rutgers University, Piscataway, NJ.*

The dopamine transporter (DAT) is the key regulator of dopaminergic transmission and is a target of several xenobiotics, including pesticides and pharmacological agents. Therefore, determination of the mechanisms by which DAT expression is regulated may provide insight into the actions of these compounds on the nervous system. Using in silico analyses, we identified regions within the DAT promoter which may contribute to its regulation at the mRNA level. The DAT promoter is CpG rich, indicating potential regulation by DNA methylation. Additionally, the lack of a conserved TATA box suggests regulation by histone acetylation. To determine the relative roles of DNA methylation and histone acetylation, we utilized a rat dopaminergic cell line (N27) to probe the responsiveness of the DAT to manipulations by inhibitors of DNA methyltransferases (DNMT) and histone deacetylases (HDAC). Inhibition of DNMTs using 5-aza-2-deoxycytidine led to a 1.25-fold increase in DAT mRNA expression. This was confirmed by siRNA experiments. However, valproate exposure increased DAT mRNA expression by up to 10-fold. To confirm the mechanism of HDAC inhibitor-mediated increase in DAT mRNA, chromatin immunoprecipitation assays were used to determine proteins recruited to the DAT promoter following valproate treatment. Data demonstrate a 4-fold increase in acetylation of histone 3 on lysines 9 and 14 (H3K9/K14ac) in the DAT promoter. Together, these results indicate that histone acetylation appears to be a plausible mechanism for DAT regulation by valproate and perhaps, by other xenobiotics. Support provided by NIEHS grants P30ES005022, R01ES015991, T32ES007148.

PS 974 Epigenetic Changes TNF-α Related in Human Mononuclear Cells Due to Polycyclic Aromatic Hydrocarbons Expose *In Vitro*

J. A. Varela Silva and M. Salgado. *Bioquímica, Universidad Autonom de San Luis Potosí, San Luis Potosí, San Luis Potosí, Mexico.*

Introduction: Polycyclic aromatic hydrocarbons (PAHs) are a group of over 100 different compounds which belong of biomass incomplete combustion. The public health agencies had been concern about worldwide distribution and the reports that health effects in human due expose to PAHs had been augmented since last decade. Several health effects related to exposure of different PAHs, including benzo[a]pyrene (BaP), were reported as asthma, genotoxicity, altered neurodevelopment and interestingly highlight the proinflammatory effects. Recently, it has been reported the increased expression of TNFα, IL-1β and IL-8 in mononuclear cells in culture exposed to BaP. However, only in human population has been observed an TNFα expression increased due to HAPs exposure. So far, the effects on the proinflammatory cytokines induction are attributed to the activation of the aryl hydrocarbon receptor (AhR). However, the molecular mechanisms involved in proinflammatory effects due benzo(a)pyrene are not absolutely elucidated. Interestingly, the main epigenetic mechanisms such as DNA methylation, histone modification and microRNAs are be able to respond to external factors as pollutants. In this work we explored if BaP be able to modify two epigenetics mechanisms. We found that miRNAs expression are altered due BaP exposure in human MNC *in vitro.*

PS 975 Epigenetic Regulation Is a Crucial Factor for the Tissue-Specific Expression of Human UGT1A10

S. Oda[1, 2], T. Fukami[2], T. Yokoi[1, 2] and M. Nakajima[2]. [1]*Graduate School of Medicine, Nagoya University, Nagoya, Aichi Prefecture, Japan and* [2]*Faculty of Pharmaceutical Sciences, Kanazawa University, Kanazawa, Ishikawa Prefecture, Japan.*

UDP-glucuronosyltransferases (UGTs) are a family of phase II drug-metabolizing enzymes that catalyze the glucuronidaton of compounds to facilitate their excretion. Among 19 members of the UGT1 and UGT2 families identified in human, UGT1A10 is not expressed in the liver; however, UGT1A10 is exclusively expressed in the intestine, contributing to presystemic first-pass metabolism of a variety of drugs and xenobiotics. Earlier studies revealed that hepatocyte nuclear factor (HNF) 1α and Sp1, as well as an intestine-specific transcription factor, caudal type homeobox (Cdx) 2, are involved in the constitutive expression of UGT1A10. However, why UGT1A10 is not expressed in the liver, where HNF1α and Sp1 are abundantly expressed, is unknown. In this study, we sought to elucidate the mechanism, focusing on epigenetic regulation. Bisulfite sequence analysis revealed that the CpG-rich region (-264 to +117) around the UGT1A10

promoter was hypomethylated (11%) in the epithelium of the small intestine, whereas the UGT1A10 promoter was hypermethylated (89%) in hepatocytes. A luciferase assay revealed that the methylation of the UGT1A10 promoter by SssI methylase abrogated transactivity even with overexpressed Cdx2 and HNF1α. The UGT1A10 promoter was highly methylated (86%) in liver-derived HuH-7 cells, where UGT1A10 is not expressed. In contrast, the UGT1A10 promoter was hardly methylated (19%) in colon-derived LS180 cells, where UGT1A10 is expressed. Treatment with 5-aza-2'-deoxycitidine (5-Aza-dC), an inhibitor of DNA methylation, resulted in an increase in UGT1A10 mRNA expression only in HuH-7 cells. Moreover, the overexpression of HNF1α and Cdx2 further increased UGT1A10 mRNA only in the presence of 5-Aza-dC. Collectively, we found that DNA hypermethylation would interfere with the binding of HNF1α and Cdx2, resulting in the defective expression of UGT1A10 in human liver. Thus, epigenetic regulation is a crucial determinant of the tissue-specific expression of UGT1A10.

PS 976 Circulating microRNA Profiles Altered in Mice after 28 Days Exposure to Perfluorooctanoic Acid

J. Dai, Y. Shengmin, W. Jianshe and W. Zhang. *Institute of Zoology, Beijing, China.*

Perfluorooctanoic acid (PFOA) is a stable man-made compound with many industrial and commercial uses. Recently, however, concern has been raised that it may induce various toxicological effects such as hepatotoxicity, immunotoxicity, and developmental toxicity. Because levels of circulating microRNAs (miRNAs) can be altered in several clinical diseases, they may serve as potential novel biomarkers. Here, we explored differences in the profiles of circulating miRNAs in mice after PFOA exposure. Using TaqMan miRNA arrays, we determined that the levels of 24 circulating miRNAs were altered in mice dosed with PFOA at 1.25 mg/kg/d and 73 were altered in mice dosed with 5 mg/kg/d. Eight miRNAs, namely miR-28-5p, miR-32-5p, miR-34a-5p, miR-122-5p, miR-192-5p, miR-200c-3p, miR-26b-5p and miR-199a-3p, were further validated using TaqMan Real-Time PCR assays. Results were consistent with those obtained from the TaqMan miRNA arrays, except for miR-199a-3p. The most remarkable of the circulating miRNAs (miR-26b-5p and miR-199a-3p) were also up-regulated in the serum of occupational workers in our previous epidemiological study. We also found similar patterns in mice exposed to PFOS and the observed increase of circulating miRNAs may not only be specific for PFOA but also for PFOS and even other PFASs. These results demonstrated that circulating miRNA profiles were altered after exposure to high concentrations of PFOA and miR-28-5p, miR-32-5p, miR-122-5p, miR-192-5p, and miR-26b-5p in serum may be potential biomarkers of PFOA induced toxicological effects, especially in occupational exposed people.

PS 977 Correlation between Whole Genome DNA Methylation and Biomarkers of Arsenic Toxicity in Arsenic-Exposed Populations of West Bengal, India

M. Majumder[1], U. B. Dasgupta[2], D. N. GuhaMazumder[3] and N. Das[1]. *[1]Dept. of Molecular Biology, Surendranath College, Kolkata, West Bengal, India, [2]Dept. of Life Science and Biotechnology, Jadavpur University, Kolkata, West Bengal, India and [3]DNGM Foundation, Kolkata, West Bengal, India.*

Background: Arsenic is a potent environmental toxicant. Number of individuals in West Bengal, India are endemically exposed to inorganic arsenic, far above the acceptable limit (10μg/L). Though Pigmentation, keratosis are the specific skin lesions characteristic of chronic arsenic toxicity, various systemic manifestations are there over and above skin lesions, like chronic lung diseases, skin, lung urinary bladder cancer. Despite being recommended as a Group 1 carcinogen, arsenic is a poor *in-vitro* mutagen in both bacterial and mammalian systems. Thus, epigenetic mechanisms of carcinogenesis (hyper/hypo methylation of DNA) has been invoked. Arsenic exposure may result in global DNA hyper methylation in human; still the association between DNA methylation and the known biomarkers of arsenic toxicity remains to be determined.
Objective: The objective of the study presented here is to find if there is any correlation between biomarkers of arsenic toxicity like skin manifestation score, arsenic intake, hair and urinary arsenic deposition, smoking and tobacco chewing habit, gender with whole genome DNA methylation in exposed individuals of West Bengal.
Method: PBL DNA quantification and methylation, plasma and urinary arsenic concentrations, smoking habit and skin manifestation were assessed in a study population, in the district of Nadia,West Bengal. Genomic DNA methylation was measured by using ELISA-based assay. An Institutional Ethical committee (IRB) meeting was held to review the project in depth and approved.
Result: Our data indicated positive correlation between whole genome DNA methylation and skin score (p=0.004).
Conclusion: Skin manifestation showed positive association with whole genome DNA methylation in a dose-dependent manner while other biomarkers did not indicate any. The underlying mechanisms and physiologic implications of the increased skin manifestation need further study.
[PBL: Peripheral Blood Leukocyte]

PS 978 Genotoxic and Epigenotoxic Effects of 1, 3-Butadiene: Putative Mechanisms of Tissue Specificity in Adverse Health Outcomes

G. Chappell[1], B. O'Brien[1], T. Kobets[2], N. Tretyakova[3], D. Sangaraju[3], O. Kosyk[1], K. G. Sexton[1], W. Bodnar[1], I. Rusyn[1] and I. Pogribny[2]. *[1]Environmental Sciences and Engineering, UNC Chapel Hill, Chapel Hill, NC, [2]National Center for Toxicological Research, US Food and Drug Administration, Jefferson, AR and [3]Department of Medicinal Chemistry, University of Minnesota, Minneapolis, MN.*

1,3-Butadiene (BD) is a widely used industrial chemical and a ubiquitous environmental pollutant that is a known human carcinogen. Although genotoxicity is an established mechanism of the carcinogenicity of BD, epigenotoxicity has also been observed in livers of mice exposed to the chemical. To better understand the molecular mechanisms associated with BD effects in other tissues, we evaluated BD genotoxicity and epigenotoxicity in both target (lung and liver) and non-target (kidney) tissues of butadiene-induced carcinogenesis. We hypothesized that epigenotoxic effects may explain, at least in part, the tissue-specific differences in BD carcinogenicity in mice. Male C57BL/6 mice were exposed to 0 or 425 ppm of BD by inhalation (6 hr/day, 5 days/week) for 2 weeks. For assessment of genotoxic and epigenetic alterations, we evaluated THB-Gua adducts and bis-N7G-BD crosslinks, and levels of histone and DNA methylation, respectively. Liver and lung tissues of BD-exposed mice exhibited DNA damage as well as epigenetic alterations indicative of genomic instability. Marked genotoxic effects of BD were also observed in the kidneys, but epigenetic alterations clearly differed in this non-target tissue as compared to liver and lung. Specifically, trimethylation of histones H3K9, H3K27, and H4K20, all marks of condensed heterochromatin and transcriptional silencing, was increased in the kidneys of treated mice as compared to controls. These modifications may represent a post-repair chromatin restoration response at sites of DNA damage and present a potential mechanistic explanation for the lack of tumor susceptibility of this non-target tissue. These results indicate that tissue-specific epigenetic alterations are associated with tissue specificity in carcinogenesis, even in cases of known genotoxic carcinogens.

PS 978a DNA Methylation Profiling in the Liver during the Life Cycle of Rats

T. Han, C. Moland, V. Vijay, K. Wang, J. C. Kwekel, V. G. Desai and J. C. Fuscoe. *Personalized Medicine Branch, Division of Systems Biology, National Center for Toxicological Research/FDA, Jefferson, AR.*

Epigenetic modifications of DNA, such as methylation of cytosine, play a critical role in regulating mRNA expression, miRNA levels, and cellular development, and have been linked to human diseases such as cancer. The role of epigenetics in liver development and diseases has been recently reviewed; however, there is a lack of a comprehensive study to understand the epigenetic effects on liver disease susceptibility and response to xenobiotics at different life stages. Furthermore, these epigenetic changes may serve as biomarkers for disease progression. Recent advances in high throughput technologies make it possible to monitor the methylation aberrations at the whole genome level. In this study, liver tissues from both sexes of Fischer 344 rats at 2, 5, 6, 8, 15, 21, 52, 78, and 104 weeks of age were examined for sex- and age-specific alterations in DNA methylation using Roche 385k rat promoter methylation microarrays. The raw image data were extracted and analyzed by DEVA software (v1.2.1) to determine the methylation changes in these samples. Tukey's biweight mean centering normalization was applied before downstream analysis. One-way ANOVA was used to identify differences between groups. Principal component analysis indicated that there are greater sex differences than age difference in terms of methylation patterns. Within each sex, the results also showed methylation changes occurring from early age through old age. In contrast, the differences between 52wk, 78wk, and 104wk animals were much smaller in male animals compared to female animals, in which there were greater differences between 52wk and older animals. The number of methylated sites was very similar between different groups although there was variability in the chromosomal sites. These age- and sex-related differences in DNA methylation may provide insights in susceptibility to liver disease, adverse drug events and their progression.

PS 978b Establishment of a Unique Profiling Method for DNA Methylation Frequency and Its Application to Toxicology

T. Aiba[1], T. Saito[2], A. Hayashi[2], S. Sato[3], H. Yunokawa[3], H. Kurita[1], T. Maruyama[4], W. Fujibuchi[4], C. Tohyama[1] and S. Ohsako[1]. [1]*Grad. Sch. Med., The Univ. of Tokyo, Tokyo, Japan,* [2]*Nat'l Inst. Radiol. Sci., Chiba, Japan,* [3]*Maze Inc., Tokyo, Japan and* [4]*Ctr. iPS Cell Res. Appl., Kyoto Univ., Kyoto, Japan.*

Epigenomic changes induced by environmental factors are important for the acquired phenotype. It is thought that degree of its variability is small and that its deviation is large among individuals. Since no appropriate method has been available to quantify CpG-methylation frequency (MF) in a genome-wide manner in terms of accuracy, precision, and cost, we developed a novel method (methylated site display (MSD)-AFLP) and then applied this method to examine influence of bisphenol-A (BPA) exposure on DNA methylation in mouse tissues. MSD-libraries prepared by HpaII digestion and adaptor-ligation were used to obtain AFLP-chart data of the DNA methylation of C57BL/6J mouse tissues (liver, kidney and hippocampus). Many CpG-sites suspected to be the tissue-specific differentially methylated regions (tDMRs) were detected by 16-selective primer sets. Nucleotide sequences adjacent to these methyl-CpG sites were determined and the MF was analyzed by MSRE-PCR to confirm the precision of the AFLP analysis. The differences of the MF among tissues were almost identical in the both methods. Additionally, AFLP data from SssI-treated genomic DNA was used to calculate MF from MSD-AFLP. Many CpGs showing less than 5% of statistically significant tissue-specific difference and less than 10% of degree of variability were detected, suggesting that MSD-AFLP is a highly precise analytical method. Finally, hippocampus DNAs from male pups exposed to 200 μg/kg BPA (n=6) in utero and from control pups (n=6) were analyzed by MSD-AFLP. No statistically significant change of MF by BPA exposure was detected in 43,840-CpGs, despite using the full 256-selective primer sets. Our newly developed method will provide accurate values in MF and be useful to screen unknown subtle differences of methyl-CpGs in a genome-wide manner. In addition, nearly no influence of in utero BPA exposure on DNA methylation was observed in mouse hippocampus.

PS 978c Epigenetic Study of Dioxin Response Elements in Tregs and Th17 Cells

M. E. Martinez-Leija and M. Salgado. *Bioquímica, Universidad Autonoma de San Luis Potosí, San Luis Potosí, San Luis Potosí, Mexico.*

Actually, it is known that aryl hydrocarbon receptor (AhR) plays an important role as modulator of the adaptive immune responses. Furthermore, AhR activation behind linked with the different ligands promote different responses. When lymphocites T cells naïve are exposed to 2,3,7,8 -Tetrachlorodibenzo-p-dioxin (TCDD) in vitro induce Tr1 differentiation but, when Tcells cultures are stimulated with 6-Formylindolo (3,2-b) carbazole (FICZ) promotes Th17 cell induction via AhR activation. However, if epigenetic mechanisms are implicated are still unknown. Hence, to study whether the AhR may cause changes in the methylation patterns by interacting directly, or indirectly due changes in the expression patterns of miRNA modulators of DNMTs is relevant. To observe the effects of two differents AhR ligands, in this study we isolated CD4+ T cells and cultivated with 10 nM of TCDD or 300 nM FICZ by 24 h then, several gene expression and miRNAs that associated with DNA methylation were evaluated by real time PCR. We found that no change in the AhR expression to 24 hours under the different conditions of cultures. Interestingly, a increased expression of CYP1A1 gene were founding, whereas gene expression of DNMT1 when AhR are activated. In addition, we found that miR-21 and miR-126a expression are augmented in cultures exposed to TCDD and FICZ. The results suggests that aryl receptor ligands may be affecting the activity of DNA methylation by DNMT1 and that ligand could be altere miRNAs associated with methylation expression levels. As a preliminary conclusion is that AhR activated due to FICZ by TCDD ligands also be able to induce epigenetics changes as DNA methylation to the modulate the expression of DNMT1 and miR -21 as miR -126.

PS 978d Protective Effect of CAPE against ROS-Induced Proapoptotic miRNA Expression and Apoptosis Pathway Activation

C. E. Cross[1], M. F. Tolba[2], C. M. Rondelli[1], M. Xu[1] and S. Abdel-Rahman[1]. [1]*Obstetrics & Gynecology, UTMB, Galveston, TX and* [2]*Pharmacology and Toxicology, Ain Shams University, Cairo, Egypt.*

In early pregnancy, the conceptus is highly sensitive to reactive oxygen species (ROS). During implantation, maternal spiral artery remodeling and trophoblast invasion serves as the beginning of placental development and results in increased protection of the fetus to ROS signaling. However, improper invasion and remodeling can result in disease development. Although debated, the current proposed model for preeclampsia development is aberrant maternal spinal artery remodeling, subsequent altered angiogenesis and localized ischemia/reperfusion due to continued muscularization of the spinal arteries leading to an increase in trophoblast apoptosis and premature placental failure. Preeclampsia is associated with low birth weight, preterm labor, small gestational age, and intrauterine growth restriction as well as altered gene expression in the placenta as a result of increased ROS production. We previously demonstrated an increase in apoptosis, modulated by the natural product CAPE, and alteration of the normal miRNA profile in first trimester cytotrophoblasts exposed to ROS. Thus we hypothesized that CAPE would modulate ROS-induced apoptotic miRNA changes and protein changes as a protective mechanism. Villous 3A cells were mock exposed, exposed to 25μM H2O2 or 10μM CAPE, and co-exposed to 25μM H2O2 and 10μM CAPE for 4 hours. Data indicates a protective effect of CAPE by decreasing caspase-3 activation. In addition, CAPE ameliorated the H2O2-induced miRNA changes for 3 apoptotic miRNAs. CAPE alone and co-exposure of CAPE with H2O2 induced expression of 5 anti-apoptotic miRNAs. Further research will be conducted to determine the protein targets of these miRNAs. (Supported by T32-07454; P30-006676 and JSME bridging grants).

PS 978e Evaluation of Epigenetic Properties of Dioscin and Diosgenin Isolated from Wild Yam (*Dioscorea villosa*) Root Extract

P. Aumsuwan[1, 2], S. I. Khan[1, 3], I. A. Khan[1, 3], L. A. Walker[1, 2], Z. Ali[1] and A. K. Dasmahapatra[1, 2]. [1]*National Center for Natural Product Research, University of Mississippi, University, MS,* [2]*Department of Pharmacology, University of Mississippi, University, MS and* [3]*Department of Pharmacognosy, University of Mississippi, University, MS.*

Previously, we have observed that wild yam root extract (WYRE) is able to enhance DNA methyltransferase (*DNMT*) mRNA expression in human breast cancer cells, MCF-7(GATA3-positive, non-invasive, epithelial) and MDA-MB-231(GATA3-negative, invasive, mesenchymal) followed by demethylation and activation of gata binding protein-3 (GATA-3). We hypothesize that WYRE was able to demethylate GATA-3 promoter and activate *GATA-3*. The present study was aimed to evaluate the epigenetic effects of two bioactive constituents of WYRE (dioscin and diosgenin) in MCF-7 and MBA-MB-231 cells. The anti-cell proliferative activity of dioscin (DC) and diosgenin (DG) was determined by treating the cells either with DC or DG for 72h. The IC50 is 3.85 μM for MCF-7 and 2.07 μM for MDA-MB-231 by DC and 29.35 μM for MCF-7 and 20.15 μM for MDA-MB-231 by DG. qPCR analysis of *DNMT1, 3A, 3B, GATA3,ZFPM2, CDH1, MMP9* and *VIM* indicate that in response to DC (5.76 μM) *DNMT1* mRNA remained unaltered in both cell lines whereas *DNMT3A* increased in MDA-MB-231. *DNMT 3B* mRNA showed significant increase in both cell lines. Upon DG treatment (24.17μM), *DNMT1* remained unaltered in MCF-7 but increased (24.17μM) in MDA-MB-231, while *DNMT3A* and *3B* remained unaltered in both cells. Although in these cells, *GATA3* mRNA expression remained unaltered by both compounds, *ZFPM2*, an upstream *GATA-3* gene, was significantly increased only by DC. *E-cadherin*, a downstream gene of *GATA-3* and a cellular transition marker, is also increased in both cell lines by DS (5.76 μM) but decreased by DG (24.17μM). Other cell transition markers such as *MMP9* remained unaltered in both, while *VIM* showed cell-specific response with an increase in MCF-7 and a decrease in MDA-MB-231. These data indicate that DS is more epigenetically effective than DG in breast cancer cells.

PS 979 Weathered Marine Crude Oil Exposure Induces Skin Inflammation in Mice

J. M. Kemp, L. R. Luckett-Chastain, W. M. McShan and R. Gallucci. *Pharmaceutical Sciences, OU Health Sciences Center, Oklahoma City, OK.*

The Deepwater Horizon oil spill in the Gulf of Mexico (2010) is undoubtedly the worst marine oil spill in US history. Spill remediation workers are exposed to weathered oil and tend to suffer a myriad of health effects, including contact dermatitis. Since little is known concerning the effects of exposure to weathered crude oil, a mouse model was used to investigate this pathology. Denuded skin of C57BL/6 and BALB/c mice was exposed to weathered oil or acetone (control) for 7 days. Histopathology revealed inflammation in the oil exposed skin, primarily characterized by epidermal thickening and neutrophil infiltration which was most pronounced in BALB/c mice. CD86 (macrophage/APC) mRNA expression was increased in oil exposed skin, but not the M2 marker CD206. Multiplex analysis of skin inflammatory cytokine expression showed that oil exposure increased IL-6, CXCL10, and CCL2 protein levels, the extent of which varied relative to mouse strain. Cytokine mRNA expression was altered as well; however, it did not necessarily correspond with protein expression. Thus, it appears that weathered oil is

indeed a skin irritant, as evidenced by PMN and inflammatory macrophage infiltration and activity. Furthermore, characteristic inflammation may be dependent on genetic background.

PS 980 Comparative *In Vivo* and *Ex Vivo* Toxicity Studies of Wildfire Particulate Matter

Y. Kim[1], M. Daniels[2], E. H. Boykin[2], T. Krantz[2], J. McGee[2], M. Hays[3], J. A. Dye[2] and I. Gilmour[2]. [1]*Curriculum in Toxicology, University of North Carolina, Chapel Hill, NC,* [2]*NHEERL, U.S. Environmental Protection Agency, Research Triangle Park, NC and* [3]*NRMRL, U.S. Environmental Protection Agency, Research Triangle Park, NC.*

Inhalation of particulate matter (PM) generated from biomass burning is of concern particularly as the frequency and severity of wildfires have been increasing. Size-fractionated PM samples (ultrafine, <0.2 μm; fine, 0.2-2.5 μm; coarse, 2.5-10 μm) were collected downwind from a peat-bog wildfire in Eastern North Carolina from 6/26/2008 – 7/11/2008 when the fire was smoldering (ENCF-1), or at a later time from 8/8/2008 – 8/19/2008 after the fire had been controlled but not fully extinguished (ENCF-4). Wildfire PM samples were extracted in methanol for toxicity studies and chemical analysis, and then given by oropharyngeal aspiration to mice at 100 μg/50 μl saline or cultured with lung tissue slices at 11 μg per lung slice (8 mm diameter). At 4 h and 24 h post-exposure, biomarkers of lung injury and inflammation were assessed in lung lavage fluid from mice, and in conditioned medium from the lung slices. In addition, lung slices were also exposed to wildfire PM pre-treated with the endotoxin inhibitor (polymyxin B). The results showed that both ENCF-1 and -4 coarse PM had 4-8 times greater endotoxin content than the fine and ultrafine PM. Moreover, only the coarse PM significantly increased neutrophils and biomarkers of inflammation (e.g., interleukin-6) in the lung lavage fluid at any time point, and similar patterns of pro-inflammatory effects were observed in the lung tissue slice model. Finally, the inflammatory effects in the lung slices were significantly diminished after exposure to the PM pre-treated with polymyxin B. We conclude that exposure to wildfire coarse PM caused substantial acute toxicity in the mouse lung in association with endotoxin content, and that the lung slice *ex vivo* model provides a good alternative for *in vivo* lung toxicity testing. (This abstract does not represent U.S. EPA policy).

PS 981 The Impact of Endotoxins in African Dust: Cause for Inflammatory Response

M. G. Ortiz-Martínez and B. D. Jimenez-Velez. *Biochemistry and Center for Environmental and Toxicological Research, University of Puerto Rico-Medical Sciences Campus, San Juan, Puerto Rico.*

African Dust Events (ADE) are believed to be associated with respiratory diseases such as asthma in Puerto Rico. Particle pollution in the form of PM_{10} contained in windblown dust is known to possess bacterial molecules such as endotoxins (ENX) as part of its biological components. ENX are able to signal the activation of pro-inflammatory genes through the Toll-like receptors (TLR2, 4) signaling pathway. We had demonstrated that ENX in PM_{10} from an urban and rural site were in part responsible for the release of IL-6 and IL-8 from human bronchial epithelial cells (BEAS-2B). The use of a specific ENX inhibitor (polymyxin B) indicates ENX are responsible for increase in TLR4 mRNA expression and transcription factor, nuclear factor kappa (NF-κB) activation (preliminarily). Taqman® Real-Time PCR, antibody based and transcription factor assays were employed for these outcomes. We report here that urban extracts are more proficient in the induction of pro-inflammatory responses than rural extracts. Results highlight ENX as important constituents of PM_{10} ADE-induced cellular effects in vitro with particular contribution at the urban site. Also, these findings suggest the influence of local PM_{10} sources on dust reaching a Puerto Rican urban site and how it is capable of stimulating the molecular mechanism of Toll-like receptors in BEAS-2B. Support provided by MBRS-RISE Grant R25GMO61838.

PS 982 Addition of a Methoxymethyl Side Chain into p-Phenylenediamine Yields 2-Methoxy-Methyl-*p*-Phenylenediamine, a Hair Dye with Reduced Skin Sensitizing Properties

C. Goebel[1], J. Troutman[2], J. Hennen[3], H. Rothe[1], H. Schlatter[1], G. Gerberick[2] and B. M. Blomeke[3]. [1]*Central Product Safety, Procter & Gamble, Darmstadt, Germany,* [2]*Central Product Safety, Procter & Gamble, Cincinnati, OH and* [3]*Environmental Toxicology, Trier University, Trier, Germany.*

p-Phenylenediame (PPD) and p-toluylenediamine (PTD) are the most important hair dye primary intermediates for oxidative hair coloring and are regarded as the key drivers of hair dye allergy. Adding a methoxymethyl side chain to the PPD molecule yields the derivative 2-methoxy-methyl-p-phenylenediamine (ME-PPD) with reduced sensitizing properties compared to PPD and PTD. ME-PPD showed an attenuated innate immune response when analyzed for its protein reactivity and dendritic cell activation potential. In the local lymph node assay (LLNA) in mice, the concentration of ME-PPD needed to induce lymphocyte proliferation 3-fold above background (EC3 value) was 4.3%, indicating a moderate skin sensitizing potency, whereas EC3 values of 0.1 and 0.17% correspond with an extreme to strong potency for PPD and PTD. Quantitative risk assessment (QRA) of the skin sensitizing potency of ME-PPD under hair dye usage conditions indicated an allergy induction risk negligible compared to PPD or PTD.

PS 983 Comparison of Different Sampling Methods for Assessment of Biological Activity of Dust from Moisture Damaged Buildings

J. Tirkkonen[1], K. Huttunen[1], M. Täubel[1, 2], H. Leppänen[1, 2], A. Hyvärinen[2] and M. Hirvonen[1]. [1]*Department of Environmental Sciences, University of Eastern Finland, Kuopio, Finland and* [2]*Department of Environmental Health, National Institute for Health and Welfare, Kuopio, Finland.* Sponsor: M. Viluksela.

The poor quality of indoor air in the moisture damaged buildings leads to several kinds of symptoms and diseases. There is an evident need for better tools to measure the severity of the damage. In this study, the aim was to compare sampling methods for analysis of biological activity of dust in moisture damaged and reference school buildings. Two kinds of samples were collected in one moisture damaged and one reference school: three active air samples (Button sampling, 4L/min) for five days during working hours, and six settled dust box samples during a two week period. All dust samples were weighed and then extracted directly into cell culture medium. The toxicity testing was done by exposing RAW 264.7 mouse macrophages to three dilutions of dust samples for 24 hours. After the exposure, the viability of the cells and production of inflammatory mediators nitric oxide (NO) and cytokine tumor necrosis factor (TNF) α were measured. The amount of dust was smaller in the damaged school compared to the reference school. The biological activity of the actively collected dust was slightly higher in the sample collected from the moisture damaged school, but the small amount of material in the sample limited the assay. A similar, clearer trend could be seen in the settled dust samples, and the difference was even more pronounced when the sampling sites within the schools were compared according to the damage observations. The results indicate that the biological activity of the dust collected with these sampling methods seems to be higher in the water damaged school compared to reference school, but the method may not differentiate the buildings reliably enough for the needs of risk assessment. Further testing of different sampling approaches should be done to improve the method.

PS 984 Role of ROS and HMGB1 in Chemical Allergen-Induced IL-18 Production in Human Keratinocytes

E. Corsini, V. Galbiati, C. L. Galli and M. Marinovich. *DiSFeB, Università degli Studi di Milano, Milan, Italy.*

We have recently identified the possibility to use interleukin-18 (IL-18) production for the *in vitro* identification of contact allergens. Previously, we demonstrated a role for oxidative stress, NF-κB and p38 MAPK activation in p-phenylenediamine (PPD)-induced IL-18 production. The purpose of this study was to characterize the molecular mechanisms underlying allergen-induced IL-18 production, in order to identify the cellular source of reactive oxygen species (ROS) and the danger signals involved.

Selective inhibitors were used to characterize the source of ROS and to identify the damage-associated molecular pattern molecules (DAMPs) triggered by contact allergens. The human keratinocyte cell line NCTC2544 was exposed to three contact allergens, namley PPD, 2,4-dinitrochlorobenzene and citral in the presence or absence of diphenylene iodonium (DPI), allopurinol and rotenone to identify

the source of ROS, and to antiTLR4 antibody and glycirrizic acid to characterize the DAMPs. In the case of PPD, the induction of IL-18 can be modulated by rotenone, allopurinol and DPI, indicating the involvement of different sources of ROS. In the case of DNCB, rotenone completely prevents the induction of IL-18, suggesting a central role of mitochondria-derived ROS, while for citral DPI completely prevents the induction of IL-18, indicating the central of NADPH oxidase. Allergen-induced IL-18 involves the activation of the inflammasome and TLR4, as it can be modulated by the caspase inhibitor Z-VAD FMK and anti-TLR4 antibody. As DAMPs, we demonstrated the ability of all allergens tested to induced the release of HMGB1 (high mobility group box-1) and its sequester by glycirrizic acid significantly modulate PPD-induced IL-18 production and completely prevents DNCB and citral-induced IL-18, confirming the role of HMGB1.
Overall, we found that different intracellular source of ROS are triggered by contact allergens and an important role for HMGB1 in chemical allergen-induced IL-18 production was demonstrated.

PS 985 Human Skin Explants: An Alternative Method to Assess Allergenic Potential of Chemicals

L. Mathieu[2], P. Grascha[1], F. Burgher[2], E. Lati[3], J. Blomet[2] and H. I. Maibach[4]. *[1]DEB Group, Denby, United Kingdom, [2]PREVOR Laboratory, Valmondois, France, [3]Bio-Ec Laboratory, Longjumeau, France and [4]Department of Dermatology, UCSF Medical School, San Francisco, CA.*

Aims of the study
This study is aimed to assess predictive allergenic potential of chemicals through a histological expertise of the general morphology of the skin after staining according to Masson's trichrome and by the counting of Langerhans cell as after immunostaining of CD1a.
The study is also an opportunity to develop a model for evaluation of protective creams against professional chemical allergens.
Method
84 human skin explants from abdominoplasty. 8 allergens frequently used at workplaced were evaluated: Tetramethylthiuram disulfide, 2-Mercaptobenzothiazole, Benzyl carbamate, Bisphenol, Ethyl acrylate Kosher, Araldite 506 epoxy Resin, Hevein (latex) and Formaldehyde 30 %. The allergens stayed in contact with the skin for 24 hours. 3 series were compared: the 8 allergens as positive control, cream excipient, creams with different potential protective agents. Epidermic Langerhans cells were stained with a monoclonal anti-CD1a antibody (IM1590, clone O10, Beckman Coulter) for one hour, then enhanced with a streptavidin/biotin system (Vector, PK-7200) and at the end revealed using VIP (Vector, SK-4600). The mean number per centimetre of epidermic Langerhans cells was calculated to objective their migration as a proof of skin sensitization.
Results
In our operating conditions, allergenic tested molecules in contact with the skin for 24 hours induce Langerhans cells migration. When the skin was pre-treated with excipient or skin protective cream, less significant migration of the Langerhans cells was induced by the allergens ($p < 0.05$).
Conclusion
This method is efficient to show the hypersensitivity potential of known chemical allergen. It could be useful "for alternative to animal testing" for skin sensitization. It also could be a model for testing skin protective creams.

PS 986 Comparing Lymphocyte Subsets in the Mouse Allergy Model and Local Lymph Node Assay by Multiparameter Flow Cytometry

X. Zhu, S. H. Cole, T. T. Kawabata and J. Whritenour. *Immunotoxicology CoE, Drug Safety Research and Development, Pfizer Inc., Groton, CT.*

A validated animal model is needed to predict the potential of drugs administered by oral or parenteral routes to produce hypersensitivity reactions (HR). Recently, the mouse allergy model (MAM) was developed as a predictive model where subcutaneous injection of drugs associated with HR in the clinic produce a marked increase in the cellularity of the draining lymph nodes (LN). The murine local lymph node assay (LLNA) has been used extensively as a tool to predict for contact HR but does not appear to predict for systemically administered drugs. In the LLNA, topical application of contact sensitizers to the ears of mice causes an increase in cell counts in draining LN. The objective of this study was to compare the responses in the MAM and LLNA to determine if similar mechanisms may be involved in driving these responses. The MAM and LLNA assays were performed and the draining LN lymphocyte subsets and surface marker expression of CD62L/ L-selectin and CCR7 were evaluated by flow cytometry. In the MAM, amoxicillin (100 mg/kg) treatment resulted in a proportional increase in absolute counts of CD4 and CD8 T cells and B cells, whereas a significant (2-fold) increase in the percentage of B cells was observed in the LLNA with 0.25% Dinitrofluorobenzene (DNFB) treatment. Increased expression of the chemokine receptor CCR7 (key molecule governing lymphocyte entry into the LN) and down-regulation of CD62L was observed in draining LN cells in animals treated with amoxicillin (MAM) while no changes on these endpoints were observed following DNFB administration (LLNA). These data suggest that the mechanisms for the increased LN cellularity may differ between the MAM and LLNA. The MAM response may be partially due to increased lymphocyte entry and migration into the LN under the regulation of CCR7 accompanying the loss of CD62L, whereas an increase in B cells by other mechanisms may have a greater role in increasing LN cellularity with contact sensitizers in the LLNA.

PS 987 Identification and Frequency of Naïve T Lymphocytes Specific for Penicillin: Implication in Drug-Allergy

M. Pallardy[1], M. Azoury[1], N. Scornet[2], C. Nhim[1], D. Joseph[2], S. Delarue-Cochin[2], S. Delluc[3], B. Maillere[4], R. Weaver[5] and N. D. Claude[5]. *[1]UMR996, UniverSud, Châtenay-Malabry, France, [2]UMR CNRS8076, UniverSud, Châtenay-Malabry, France, [3]Platine Pharma Service, Lyon, France, [4]SIMOPRO, IbiTec, CEA, Saclay, France and [5]Intitut de Recherches Internationales Servier, Suresnes, France.*

Allergic reactions to drugs are unpredictable and have many side effects. According to the hapten theory, these compounds are capable to bind to proteins and form immunogenic complexes. Antigen presenting cells, such as dendritic cells (DC), internalize haptenized complexes, digest them into peptides and present them on HLA molecules to drug-specific T cells inducing an immune response. Knowing that drugs provoke IgE mediated hypersensitivity reactions in treated patients, the CD4+ T-cell response to benzyl-penicillin (BP) was investigated. The aim of the study was to determine the size of the BP-specific naïve CD4+ T-cell repertoire, and to identify peptide epitopes haptenized with BP and presented to T cells via HLA-II molecules.
Since BP is known to bind covalently to proteins, human serum albumin (HSA)-BP bio-conjugates were synthesized at basic pH and BP binding-sites on HSA were identified using mass-spectrometry. 12 peptides of 15 mer long including the identified BP binding sites were synthetized. Naïve CD4+ T cells from non-allergic donors were stimulated once a week with autologous DC loaded with HSA-BP or with peptide-BP to amplify respectively HSA-BP- or peptide-BP-specific T cells. Activation of specific CD4+ T cells was detected using interferon-γ EliSpot and their frequency was calculated.
Results of the CD4+ T-cell response to BP were as follow:
- Detection of BP-specific CD4+ T cells in 12/13 tested donors with a mean frequency of 0.26 cells/million of CD4+ T cells
- Identification of 17 binding sites of BP on HSA
- Specific naïve CD4+ T cells recognized 3 specific peptides, from HSA, haptenized by BP.

This study showed the capacity of HSA-BP to be recognized by naïve T-cells from multiple donors and the possibility to identify epitopes involved in the allergic reaction to BP.
Azoury M. & Scornet N.: Contributed equally to this work.

PS 988 Molecular Profile Analysis of Allergenic Acid Hydrolyzed Wheat Protein

S. Sakai[1], R. Adachi[1], R. Nakamaura[1], Y. Kimura[1], R. Nakamura[1], K. Sasaki[2], K. Nishijima[2], H. Ataku[2], Y. Fukutomi[3], T. Nishimaki-Mogami[1] and R. Teshima[1]. *[1]National Institute of Health Sciences, Tokyo, Japan, [2]National Institute of Technology and Evaluation, Tokyo, Japan and [3]Sagamihara National Hospital, Sagamihara, Japan.*

Hydrolyzed wheat protein (HWP; hydrolyzed gluten) is used in various products worldwide. Several cases of systemic wheat allergy caused by HWP have been reported, including wheat-dependent exercise-induced anaphylaxis following sensitization to HWP in cosmetics in Japan. Moreover, an increasing number of studies have shown that HWP can induce IgE-mediated hypersensitivity by skin contact and/or food ingestion. It is considered that these allergic manifestations result from deamidated glutens in HWP. However, the relationship between the essential molecular properties of HWP and its allergenicity remains unknown.
In this study, we prepared several HWPs with different degrees of acid hydrolysis (0.1 N hydrochloric acid treatment at 100°C for 0.5, 1, 3, 6, 9, 12, and 24 h). In profiling analysis of these HWPs, size exclusion chromatography showed that the average molecular weight of HWP decreased depending on the extent of acid hydrolysis. In contrast, proteomics analysis showed that the deamidation level increased depending on the extent of acid hydrolysis, and this level reached a plateau after 6 h of hydrolysis. The allergenicity of gluten and two HWPs (0.5- and 9-h hydrolysis sample) was compared by transdermal administration to BALB/c mice. Among these HWPs, the 0.5-h hydrolysis sample showed significantly increased

antigen-specific serum IgE titer. After skin sensitization for 4 weeks, intraperitoneal injection of this HWP caused active systemic anaphylaxis, resulting in marked decrease in rectal temperatures, increase in anaphylaxis scores, and increase in plasma histamine levels. The effect of skin sensitization with gluten and 9-h hydrolysis samples was significantly weaker than that with the 0.5-h hydrolysis sample.
In conclusion, we demonstrated that allergenic HWP has specific molecular properties and the results showed that it may be possible to reduce the risk of skin sensitization to HWP by extensive acid hydrolysis.

PS 989 Impact of Aggregation on Immunogenicity: Relevance for Biopharmaceuticals

K. Ratjani[1], J. Derrick[1], R. Thorpe[2], M. Wadhwa[2], I. Kimber[1] and R. J. Dearman[1]. [1]*Faculty of Life Sciences, Manchester University, Manchester, Greater Manchester, United Kingdom and* [2]*Institute for Biological Standards and Control, Potter Bar, United Kingdom.*

The clinical use of protein therapeutics has increased dramatically over the last decade. One important safety issue with such molecules is the development of anti-drug antibodies in patients that may cause adverse events or may reduce efficacy of the protein therapeutic. Protein aggregation can be associated with the induction of vigorous immune responses, for example with certain preparations of interferon-β. As a result, regulatory guidelines recommend screening for and minimising protein aggregation during bioprocessing, despite a lack of understanding regarding the mechanisms and the size/nature of problem aggregates that can trigger such responses. In the current experiments a humanized single chain Fv (scFv) antibody fragment expressed by *Escherichia coli* was purified using Protein A affinity chromatography (monomeric fraction; mean diameter 7nm). Reproducible aggregates within the subvisible particle size range (mean diameter 1900nm) were formed by incubation at 40oC for 20 min at pH 7.0. Antibody responses induced in BALB/c strain mice by intraperitoneal exposure to the monomeric fraction or the aggregated scFv (1 mg/ml) were characterised. Sera were analysed for protein specific total IgG and IgG1 and IgG2a subclasses by enzyme-linked immunosorbant assay. Immunisation with both forms of scFv induced relatively vigorous IgG and IgG1 antibody responses of equivalent magnitude. However, the aggregated fraction stimulated significantly higher titers of IgG2a antibody than did the monomeric fraction. Titers were independent of whether aggregated or monomeric protein was used a substrate in the analysis. Thus, aggregated protein induces a preferential Th1 type response (IgG2a>IgG1) whereas the monomer elicits a selective Th2 response (IgG1>IgG2a). Th1 responses are typically mounted against intracellular bacteria and viruses, suggesting that the aggregated protein may stimulate polarized Th1 responses by mimicking the repetitive structures found in viruses.

PS 990 Allergen-Induced Langerhans' Cell (LC) Migration: Role of Interleukin (IL)-1β

L. Eaton[1], O. Metryka[1], R. Roberts[2], I. Kimber[1] and R. J. Dearman[1]. [1]*Manchester University, Manchester, United Kingdom and* [2]*Safety Assessment, AstraZeneca, Alderley Park, United Kingdom.*

Epidermal LC play key roles in the initiation and regulation of immune and allergic responses. LC migration induced in mice by topical exposure to the contact allergen oxazolone (Ox) requires two independent cytokine signals delivered by tumor necrosis factor (TNF)-α and IL-1β. However, another potent skin allergen, 2,4-dinitrochlorobenzene (DNCB), provokes TNF-α-independent migration. Here we have investigated whether DNCB-induced LC migration is a function of local IL-1β availability. BALB/c mice were treated topically on the dorsum of the ear with lactoferrin (LF; an iron-binding glycoprotein that inhibits skin TNF-α production) or vehicle alone. After 2h, mice were injected intradermally with 50ng or 300ng IL-1β at the same site. Mice were terminated 4h later, ears were removed, the epidermis isolated and LC frequency determined by fluorescence microscopy. In parallel investigations, skin IL-1β mRNA expression profiles induced by 6h exposure to either 0.5% Ox or 1% DNCB were examined by quantitative real time PCR. Both doses of IL-1β induced significant LC migration in vehicle-treated mice compared with resting LC frequencies in naïve control mice. As observed previously, the 20-30% of LC available for rapid mobilization were stimulated to migrate. However, LF pre-treatment inhibited LC mobilization provoked by low dose IL-1β. In contrast, 300ng IL-1β was able to induce LC migration regardless of LF pre-treatment. Topical treatment with 1% DNCB provoked more vigorous IL-1β expression than that stimulated by 0.5% Ox; concentrations that in each case induce maximal LC migration. Taken together these data demonstrate that if local IL-1β concentrations are very high, LC migration is independent of TNF-α. This contrasts with the prevailing view that all LC migratory stimuli (allergens, irritants, UVB, trauma) are dependent upon the local availability of TNF-α. These data also highlight that skin sensitizing chemicals may act through subtly different mechanisms to provoke optimal LC migration.

PS 991 Cytokine Fingerprinting for Chemical Respiratory Allergens: Use of a Nonstandard Vehicle

R. J. Dearman and I. Kimber. *Manchester University, Manchester, United Kingdom.*

We have demonstrated previously that prolonged (13 day) topical exposure of BALB/c mice to the reference contact allergen 2,4-dinitrochlorobenzene (DNCB), or to the reference respiratory allergen trimellitic anhydride (TMA) induces selective type 1 or type 2 cytokine secretion profiles, respectively. Similar divergent cytokine expression patterns have been shown for a number of other contact allergens (such as formaldehyde, isoeugenol) and respiratory allergens (including diisocyanates). In these experiments, compounds have been formulated exclusively in the standard local lymph node assay acetone:olive oil (AOO) vehicle for topical exposure. In the current experiments, responses provoked by respiratory sensitizers formulated in dimethyl formamide (DMF) have been examined. Mice were exposed topically to allergen over a 13 day period, 13 days after the initiation of exposure, draining auricular lymph node cells (LNC) were isolated. Single cell suspensions were prepared and cultured; cytokine secretion profiles were measured. Initial experiments with DNCB and TMA formulated in either AOO or DMF revealed that, with the exception of interleukin (IL)-4 which was recorded at low levels in TMA/DMF treated animals, TMA treatment induced a type 2 phenotype with high levels of IL-5, 10 and 13 and relatively low levels of interferon-gamma when formulated in either vehicle. The converse type 1 pattern was provoked by DNCB exposure independent of vehicle, however, cytokine levels were more variable and patterns less divergent when DMF was used. Cytokine fingerprinting experiments conducted with additional respiratory sensitizers (chloramine T; reactive dyes) formulated in DMF revealed the expected type 2 phenotype. These data suggest that the measurement of induced cytokine secretion profiles in the BALB/c strain mouse provides a robust method for hazard identification and characterization of respiratory chemical allergens. Furthermore, DMF is an appropriate alternative vehicle although AOO is still the vehicle of choice.

PS 992 Interleukin (IL)-1 Expression by Dendritic Cells (DC): Evidence for Intracellular Degradation

I. Kimber[1], J. Ainscough[1], G. Gerberick[2] and R. J. Dearman[1]. [1]*Manchester University, Manchester, United Kingdom and* [2]*Procter & Gamble, Cincinnati, OH.*

DC play pivotal roles in the development of immune and allergic reactions, including skin sensitization, the commonest form of immunotoxicity. A key event in contact allergy is the production of the proinflammatory cytokine IL-1β. This cytokine is not secreted via the classical pathway, instead, 2 independent signals are required. The first induces up-regulation of pro-IL-1β, and the second drives cleavage and secretion of the bioactive molecule. The intracellular regulation of expression of this cytokine in immature (day 8) mouse bone marrow (BM) DC has now been characterized. Cells were stimulated with lipopolysaccharide (LPS; 0.1μg/ml) and the IL-1α and β content of supernatants (secreted cytokine) and cell lysates (intracellular cytokine) was analyzed by ELISA. The impact of cyclohexamide (CHX), the proteasome inhibitor MG132, and the autophagy inhibitor 3-methyladeninde (3-MA) on IL-1 production was examined. The role of ubiquitination was examined by IL-1β immunoprecipitation and Western blotting. LPS treatment stimulated a marked increase in intracellular IL-1, peaking at ~8hr and declining rapidly thereafter. There was no concomitant detection of secreted product, indicating that in the absence of a second signal, LPS-induced IL-1α and β were rapidly degraded. Using a 1hr CHX (10μg/ml) pulse to inhibit de novo translation revealed a 4-hr lag before IL-1 degradation was detected. Treatment with MG132 (10μM), but not with 3-MA (10mM), inhibited significantly IL-1 degradation without impacting upon cell viability. Furthermore, following MG132 inhibition of degradation, Western blotting with anti-ubiquitin antibodies revealed an accumulation of ubiquitinated IL-1β. Thus, IL-1α and β conform to the ubiquitin-proteasome paradigm of protein degradation and this process is initiated following DC activation in the absence of secretion. Therefore, the regulation of IL-1 proteasomal degradation may control the vigor of IL-1 secretion, and ultimately may influence the potency of pro-inflammatory responses.

PS 993 Enteropathogenic *Escherichia coli* As a Mucosa-Associated Exposome Extends Epithelial NF-κB Activation via Macrophage Inhibitory Cytokine 1

H. Choi and Y. Moon. *Department of Biomedical Sciences, Pusan National University School of Medicine and Immunoregulatory Therapeutics Group in Brain Busan 21 Project, Yangsan, Republic of Korea.*

Commensal bacterial community shifts in the pathogenic colonic environment and chronic colonization of mucosa-associated *Escherichia coli* (MAEC) has been linked to chronic colonic inflammatory diseases. Enteropathogenic *Escherichia coli*

(EPEC) is one of commonly identified MAEC in inflammatory bowel disease patients. The aim of this study is to address the contribution of MAEC colonization to human inflammatory signals such as nuclear factor kappa B (NF-κB). The present study was conducted to investigate the prolonged epithelial responses to persistent EPEC infection via NF-κB activation. EPEC infection led to sustained activation of NF-κB signal in mouse intestinal epithelial cells *in vivo* and *in vitro*, which was positively associated with a type III secretion system, whereas early NF-κB is regulated. Moreover, prolonged NF-κB activation was found to be a part of macrophage inhibitory cytokine 1 (MIC-1)-mediated signaling activation, a novel link between NF-κB signaling and infection-associated epithelial stress. Functionally, both EPEC-induced MIC-1 and NF-κB signaling mediated epithelial survival by enhancing the expression of cyclin D1, a target of NF-κB. In summary, the results of the present study suggest that MIC-1 serves as a mediator of prolonged NF-κB activation, which is critical in maintaining gut epithelial integrity in response to EPEC-induced injuries (This work was supported by the Basic Science Research Program through the National Research Foundation of Korea, funded by Ministry of Education, Science and Technology Grant 2012R1A1A2005837, and a grant from the Korean Health Technology Research and Development Project, Ministry of Health and Welfare, Republic of Korea (HI13C0259).).

PS 994 The Role of Endothelin-1 in Endotoxin-Triggered Release of Placental Proinflammatory Cytokines

P. R. Mahajan[1], R. Donepudi[3], F. Einstein[3] and S. E. Reznik[1, 2, 3]. [1]*Pharmaceutical Sciences, St. John's University, Jamaica, NY,* [2]*Pathology, Albert Einstein College of Medicine, Bronx, NY and* [3]*Obstetrics and Gynecology and Women's Health, Albert Einstein College of Medicine, Bronx, NY.* Sponsor: L. Trombetta.

Background: Premature delivery occurs in 12% of all births and accounts for 60 to 80% of perinatal mortality in non-anomalous infants. Despite advances in obstetrics and neonatology, there is no FDA approved therapy for preterm labor. We have shown that the ECE-1 inhibitor, phosphoramidon, the selective endothelin receptor A antagonist, BQ-123 and a novel synthetic ET A receptor antagonist synthesized by our group rescue mice from LPS-induced PTB. Finally, we have been able to prevent PTB in LPS-stimulated animals, using RNA silencing, by hydrodynamic transfection of E15 mice with ECE-1 RNAi.
Objective: Our aim was to test the hypothesis that ET-1 contributes to the cause of preterm birth by up-regulating pro-inflammatory cytokines.
Methods: Chorionic villous explants from full term human placentae obtained by Cesarean delivery were cultured under aseptic conditions and were divided into four groups: sham, endotoxin-treated, endotoxin plus low concentration BQ-123-treated, and endotoxin plus high concentration BQ-123-treated. Explant supernatants from all groups were collected 24 hours after the addition of LPS and evaluated for changes in levels of interleukin 1 β (IL-1 β) and tumor necrosis factor α (TNF α) by Western blot analysis.
Results: Villous explants treated with LPS released significantly higher amounts of both IL-1 β and TNF α into culture media than sham explants. This pro-inflammatory response was reversed, in a concentration-dependent fashion, with the ET A receptor antagonist, BQ-123.
Conclusion: IL-1 β and TNF α, pro-inflammatory cytokines closely linked to infection-associated PTB, are ET-1 dependent. The mechanism of action of ET-1 blocking agents in tocolysis involves decreased ET-1-dependent release of these mediators. Further evaluation of inflammatory mediators affected by ET-1 action may lead to the identification of novel targets for preventive therapy for PTB.

PS 995 Classical and Alternative Activation of Cyanobacterium *Anabaena* sp. Lipopolysaccharide (LPS)-Treated Rat Brain Microglia

C. Osterbauer[1], D. MacAdam[1], M. L. Hall[1], D. Feher[2], P. Williams[2] and A. M. Mayer[1]. [1]*Pharmacology, Midwestern University, Downers Grove, IL and* [2]*Chemistry and Biochemistry, University of Hawaii at Manoa, Honolulu, HI.*

Cosmopolitan Gram-negative cyanobacteria may contaminate freshwater by releasing toxins, such as lipopolysaccharide (LPS), thus affecting human health. We reported that cyanobacterium *Anabaena* sp. LPS (AnaLPS) elicited classical activation of rat microglia (BMG) and MIP-1α (CCL3) and IL-6 release *in vitro* (The Toxicologist CD 132 (S-1), 2013). We hypothesized that AnaLPS activates classical and alternative activation of BMG *in vitro* and concomitant release of cytokines and chemokines. AnaLPS was prepared by hot phenol/water extraction. *E. coli* LPS (EcLPS) 026:B6 from Difco Lab, Detroit, MI was used as a positive control. BMG were isolated from neonatal rats, and treated *in vitro* in a concentration-dependent manner with either AnaLPS or EcLPS for 18 hours at 35.9 °C. Cytokines and chemokines were determined by Milliplex® MAP rat cytokine/chemokine multiplex immunoassays. Results were the following: EcLPS and AnaLPS stimulated concentration-dependent and statistically significant release of (a) Pro-inflammatory cytokines: IL-6>IL-1β>TNF-α; (b) Pro-inflammatory chemokines: MIP-2(CXCL2)>CINC(CXCL1)>MIP-1α (CCL3)>MCP-1(CCL2)>IP-10(CXCL10)>RANTES(CCL5); and the (c) Anti-inflammatory cytokine: IL-10, at > than 1ng/mL EcLPS and 10^4ng/mL AnaLPS. We thus conclude that an 18 hour *in vitro* treatment with AnaLPS stimulated both classical and alternative activation of rat brain microglia, but was considerably less potent than EcLPS. Continued investigation of the mechanism responsible for the differential response observed between EcLPS and AnaLPS on BMG is ongoing in our laboratory. Financial support by Midwestern University and the University of Hawaii at Manoa is gratefully acknowledged.

PS 996 Behavioral and Neurochemical Alterations in Adult Mice with Low-Grade Chronic Inflammation Caused by Repeated Peripheral Lipopolysaccharide Exposure

S. Krishna[1], C. A. Dodd[1, 2] and N. M. Filipov[1]. [1]*Physiology and Pharmacology, Univ. of Georgia, Athens, GA and* [2]*Biology, Fort Valley State University, Fort Valley, GA.*

Sickness behavior following acute inflammation, modeled by acute peripheral lipopolysaccharide (LPS) administration, can later transition into depressive behavior. In light of the limited information on the impact of chronic peripheral inflammation on the induction of depressive behavior and other behavioral alterations and on their persistence after inflammatory stimuli exposure termination, this study assessed behavioral and neurochemical effects of chronic (25 weeks), low dose (0.25 mg/kg body weight; twice weekly) peripheral (intraperitoneal) LPS exposure in adult male C57BL/6 mice. Behavioral tests were performed 6 and 12 weeks post LPS/saline treatment as well as in mice exposed to 13-week LPS/saline treatment followed by an 11-week period without any treatment. Following sacrifice (at 13 and 25 weeks), striatal concentrations of dopamine, serotonin and their metabolites were analyzed. LPS-exposed mice were hypoactive in the open field after 6 weeks, whereas significant hyperactivity was observed in the 12 week LPS and 13 week LPS on+11 week off groups. Similar biphasic responses were observed in the time in the center of the open field arena between the 6 week LPS (decreased) and 13 week LPS on+11 week off groups (increased), suggestive of increased and decreased anxiety, respectively. In forced swim test, mice exhibited significant increase in the immobility time (depressive behavior) at all three time points. Neurochemistry data are still being analyzed. Above findings demonstrate that chronic peripheral inflammation initially causes decreased locomotion and increased anxiety, followed by persistent hyperactivity and decreased anxiety. Notably, chronic low-dose LPS-induced depressive behavior appears early and persists long after termination of LPS exposure. Collectively, these data emphasize the need to pay more attention on the lasting behavioral alterations induced by chronic peripheral inflammation. Supported by: R01ES016965 (NIEHS).

PS 997 Sex Differences in Gene Expression Profiles in Individuals with Idiopathic Pulmonary Fibrosis; Potential Targets of Xenoestrogens?

L. C. Smith[1], S. P. McGee[2], W. Karmaus[3], H. Zhang[3] and T. Sabo-Attwood[4]. [1]*Physiological Sciences, University of Florida, Gainesville, FL,* [2]*Bayer CropScience LP, Research Triangle Park, NC,* [3]*Epidemiology, Biostatistics, and Environmental Health, University of Memphis, Memphis, TN and* [4]*Environmental and Global Health, University of Florida, Gainesville, FL.*

Epidemiological studies suggest sex-specific trends in the prevalence and mortality of idiopathic pulmonary fibrosis (IPF) and chronic obstructive pulmonary disease (COPD). While the expression of several immune and extracellular matrix (ECM) genes in the lung have been well characterized in these diseases, investigations aimed at elucidating their sex-specific expression by disease type and severity, and the evaluation of hormone-related genes, has not been well studied. To begin to examine sex-specific expression profiles we performed targeted analysis of 48 genes, those involved in inflammation, ECM remodeling and hormonal processes, in lung tissues from males and females with mild or medium severity IPF or COPD. Results revealed a subset of genes that are differentially expressed among sex, disease type and severity. The most significant observations were the increased expression primarily of ECM genes in medium severity IPF (CATHK, COL1A1, COL3, MMP1, MMP7, IL1RN) compared to mild IPF and COPD. Interestingly, two genes, CH3L1 and MMP7 showed a significant interaction of sex and disease in individuals with IPF. While there were no significant differences in any of the hormonal genes between the IPF groups, ESR1 and AR expression levels were higher and lower, respectively, compared to COPD samples. Based on these data we are investigating a role for (xeno)estrogens in the transcriptional control of these select genes in lung epithelial cells through modulation of the nuclear and membrane

estrogen receptor. Overall, these results highlight molecular targets that could play a role in differential trends in lung disease incidence and severity between men and women and their influence by contaminants with hormonal activity.

PS 998 S-Nitrosoglutathione Reductase (GSNOR) Activity Is Differentially Regulated within Macrophage Phenotypes

C. Guo, J. Gow, M. Govindraj and A. Gow. *Rutgers University, Piscataway, NJ.*

Macrophages (MΦ) play a crucial role in innate immunity. Upon stimulation, MΦ are divided by two main phenotypes, classic (M1) and alternative (M2) activation, distinguished by their functional patterns. M1 MΦ produce large amount of NO, which reacts with glutathione (GSH) to form S-nitrosoglutathione (GSNO). GSNO can transnitrosate the thiol residues of proteins to form S-nitrosothiols (SNO), with functional consequences. GSNO reductase (GSNOR) reduces the SNO moiety in the presence of NADH to regenerate GSH and produce hydroxylamine. It is a major regulator of intracellular SNO levels. We hypothesized that GSNOR activity is regulated within MΦ activation in order to regulate SNO accumulation within phenotypic differentiation. We have utilized LPS or IL-4 to stimulate a M1 or M2 phenotype respectively in a range of MΦ cultures including Raw264.7, Raw Blue, bone marrow derived MΦ (BMDM) and alveolar MΦ. Incubation of all MΦ with LPS dramatically increased iNOS expression and NO production in all cell systems. IL-4 induced arginase but not iNOS expression. LPS induced M1 MΦ had increased SNO content and SNO-proteins as determined by Cu-Cys reduction assay and biotin-switch. IL-4 reduced total intracellular SNO content and SNO-proteins. LPS treatment decreased MΦ GSNOR expression within 1-6 hours, while IL-4 treatment stimulated expression of GSNOR. These changes were matched by reduced GSNOR activity within cellular lysates. LPS mediated increased in iNOS expression were associated with NF-κB activity in Raw blue cells, and the NF-κB inhibitor CAPE reduced iNOS expression in Raw264.7 cells. However, CAPE had no effect on GSNOR expression, suggesting that GSNOR expression is NF-κB independent. These changes were not specific to cell lines as they were also observed in BMDM and alveolar MΦ. SNO regulation in MΦ in the different phenotypes suggests that SNO plays an important role in MΦ activation. Regulation of GSNOR activity may provide novel therapeutic avenues within inflammatory disease. Supported by NIH HL086621.

PS 999 *Salvia plebeia* Extract Alleviates Inflammatory Response in Murine Arthritis Model and Human Rheumatoid Synovial Fibroblasts

J. Choi, M. Jin, I. Je and S. Kim. *Pharmacology, School of Medicine, Kyungpook National University, Daegu, Republic of Korea.*

Salvia plebeia R. Br (*S. plebeia*) has been used for the treatment of a variety of inflammatory diseases and anti-oxidant as an oriental folk medicine. In this study, we investigated the effects of *S. plebeia* extract (SPE) on inflammatory arthritis and underlying mechanisms of action. We used a collagen-induced arthritis (CIA) model in BALB/c mice by immunized with type II collagen. SPE was orally administrated during 5 weeks of arthritis induction. Oral administration of SPE decreased arthritis symptoms such as, physiologic arthritis score, footpad thickness, histopathological changes, in addition to serum IgG1 and IgG2a levels. SPE inhibited Th1/Th2/Th17 phenotype CD4+ T lymphocytes expansion in draining lymph node, expression of inflammatory mediator cytokines, matrix metalloproteinase (MMP)-1 and MMP-3 in the ankle joint tissue. To define the underlying mechanisms of action, tumor necrosis factor-α stimulated rheumatoid arthritis synovial fibroblasts were used. SPE significantly suppressed the expression of inflammatory cytokines and MMP-1 by the down-regulation of nuclear factor-κB and mitogen-activated protein kinases. Taken together, the results indicate that SPE has therapeutic efficacy for chronic inflammatory arthritis, suggesting that SPE might be a candidate for the treatment of RA.

PS 1000 Optimization and Evaluation of Metabolite Extraction Methods for Untargeted Metabolomic Study by LC-QTOF/MS for the Evaluation of Effects of 12-Diindolymethane on RAW 264.7 Murine Macrophages

J. Berkbigler. *Center For Environmental Medicine, Colorado State University, Fort Collins, CO.*

Advances in accurate mass spectrometry, better data analysis software and availability of biological pathway databases have allowed for more accurate untargeted metabolomic investigations. The purpose of this study was to optimize the harvesting, extraction and LC-QTOF/MS parameters for the metabolic evaluation of the effects of 12-diindolylmethane (12-DIM) on RAW264.7 murine macrophages. 12-DIM is part of a family of potential anti-inflammatory compounds isolated from Brassica vegetables, such as broccoli, kale and brussel sprouts, and a metabolomics study will evaluate the potential for anti-inflammatory properties of 12-DIM. The optimal harvesting and extraction procedure was quenching with cold methanol and cell scraping, compared to the standard trypsin/ethylenediaminetetraacetic acid (EDTA) treatment. Four different extraction methods were compared to elucidate the highest efficiency for intracellular and extracellular metabolite extraction, including: methanol/chloroform/water, methanol/chloroform/0.1% formic acid, methanol/chloroform and methanol/water. Extraction with cold methanol/chloroform was found to extract the most definable molecular features. The ideal mobile phases were found to be water/0.1% formic acid and methanol, which gave a better chromatographic baseline as compared to acetonitrile. The source parameters including: nebulizer, sheath gas temperature, gas flow, gas temperature and the fragmentor for the LC-QTOF/MS were also optimized. These refined parameters provide a sensitive and reproducible sample preparation and extraction of cellular metabolites from RAW264.7 macrophage cells for a global metabolomics study of the effects of 12-DIM.

PS 1001 Nebulized Thiocyanate Attenuates Inflammation and Oxidative Stress in the Airway and Liver of ENaC Mice

J. D. Chandler[1, 2], E. Min[1], J. Huang[1], D. P. Nichols[1] and B. J. Day[1, 2]. *[1]DEOHS, National Jewish Health, Denver, CO and [2]Pharmaceutical Sciences, University of Colorado, Denver, CO.*

The pseudohalide thiocyanate (SCN-) has been implicated in innate immune function in mammals but less is known about its impact on inflammation and oxidative stress. SCN- is dysregulated in cystic fibrosis (CF), a disease marked by chronic airway inflammation. Previously, we have shown that nebulized SCN- decreases inflammatory and bacterial burden in B6 mice infected with P. aeruginosa while sparing the antioxidant glutathione (GSH). To investigate the role of SCN- in pathogen-independent inflammation, we administered nebulized SCN- or normal saline vehicle to ENaC mice, a phenotypic model of CF, and wild type littermate controls. Nebulized SCN- significantly decreased airway neutrophil infiltrate concurrent with rescue of the ratio of GSH to oxidized glutathione (GSSG) in airway leukocytes and epithelial lining fluid (ELF) of ENaC mice compared to control. Similarly, nebulized SCN- rescued the GSH:GSSG ratio in lung and liver tissue of ENaC mice to levels comparable to littermate controls. These results demonstrate that SCN- directly impacts pathogen-free airway inflammation and attenuates oxidative stress with both local and systemic protective effects. These results are supported mechanistically by the ability of SCN- to scavenge hypohalous acids, strong oxidants produced by neutrophils, forming a less reactive oxidant (hypothiocyanous acid) that we have previously demonstrated is safely metabolized by mammalian cells. Our findings support nebulized SCN- as a potential pharmacologic agent in diseases of chronic inflammation such as CF. Continuing studies will investigate the effect of nebulized SCN- during chronic infection of ENaC mice and littermates and changes in cytokine characteristics that may affect neutrophil trafficking. This work was supported by NIH grant RO1 HL084469 and a Cystic Fibrosis Foundation Research Grant.

PS 1002 Redox Cross-Talk between Myeloid-Derived Suppressor Cells and Dendritic Cells in Cancer: Accumulation of Oxygenated Lipid Droplets and Suppression of Antigen Cross-Presentation

V. A. Tyurin[1, 2], W. Cao[3], A. Amoscato[1, 2], J. Loomen[3], D. Gabrilovich[3] and V. E. Kagan[1, 2]. *[1]EOH, University of Pittsburgh, Pittsburgh, PA, [2]Center for Free Radic Antioxidant Health, University of Pittsburgh, Pittsburgh, PA and [3]The Wistar Institute Cancer Center, Philadelphia, PA.*

Accumulation of myeloid-derived suppressor cells (MDSCs), and expansion of immature dendritic cells (DCs) with aberrant cross-presentation – are important immunological abnormalities in cancer. While interactions between these cells are recognized as contributors to the failed anti-tumor immunity, their molecular mechanisms remain elusive. Excessive formation of lipid droplets (LDs) affects DC's immune functions. We show that DCs from tumor-bearing mice or treated with tumor explant supernatants (EL4, MC38) contained oxygenated neutral lipids: triglycerides (oxTAGs), free fatty acids (oxFFAs) and cholesterol esters (oxCE). LC-ESI-MS/MS revealed that oxTAGs were represented by a spectrum of truncated molecular species 39:1; 39:0; 41:1; 41:0; 43:2; 43:1; 43:0 and 45:2 with 9-oxo-nonanoic and 7-oxo-heptanoic acids. We hypothesized that MDSC – with their high ROS and myeloperoxidase activity - might be a source of oxygenated lipids. To test this, DCs were co-cultured with MDSC (Gr-1+,C57BL6 BM, pre-cultured with GM-CSF and deuterated linoleic acid, LA-d4) followed by purification of DCs from the mixture of cells. We found that LA-d4 was incorporated into

TAGs and several classes of phospholipids in MDSC and DC. Further, we demonstrated the transfer of LA-d4 from pre-loaded MDSC to DCs whereby increased amounts of oxFFAs and oxTAGs, including truncated TAGs, were identified. In contrast, no oxidized phospholipids were observed in either MDSC or DCs. By using a lipid-soluble radical azo-initiator, AMVN, we bolstered oxidation of LDs of LA-supplemented DCs and showed that accumulation of oxidized neutral lipids inhibited antigen cross-presentation. This suggests a novel role for oxidized lipids in immune responses – as regulators of antigen cross-presentation. Supported by NIH grants CA165065, U19 AI068021, and NIOSH OH008282.

PS 1003 Signaling Role of Cardiolipin Externalization in Elimination of Damaged Mitochondria in Lung Epithelial Cells

V. E. Kagan[1], J. Jiang[1], Z. Huang[1], V. A. Tyurin[1], Y. Tyurina[1], D. Stolz[3], S. Watkins[3] and R. Mallampalli[2]. *[1]EOH, University of Pittsburgh, Pittsburgh, PA, [2]Medicine, University of Pittsburgh, Pittsburgh, PA and [3]Cell Biology, University of Pittsburgh, Pittsburgh, PA.*

Bacterial pneumonia triggers an exuberant host response characterized by excessive inflammation, oxidative stress, and epithelial cell damage culminating in the acute respiratory distress syndrome (ARDS). In ARDS, virulent bacterial pathogens directly damage host cells, activate innate immune responses, and trigger a burst in reactive oxygen species resulting in epithelial cell death. However, specific pathways involved in the evolution of epithelial injury with attendant release of novel damage signals remain elusive. We suggested that one critical damage signal is mitochondrial cardiolipin (CL). We found that mitophagy and reduced levels of distal mitochondrial protein markers were detectable in murine models of bacterial pneumonia. In addition, we demonstrated that early on after bacterial infection of murine lung epithelial cells (MLE15), CL transmigrates from the IMM to OMM; the unmasked externalized CL serves as a novel signal for mitophagy. A typical inducer of mitophagy, carbonyl cyanide m-chlorophenylhydrazone (CCCP) – acting as a protonophoric uncoupler - induced CL externalization to the OMM in MLE15 cells. This was evidenced by a robust decrease of the ratio of CL in the IMM and OMM from 18.6±0.3 in control MLE15 cells to 3.7±1.4 after treatment with CCCP. The externalization of CL was accompanied by activation of autophagy (LC3-I/II conversion) and decreased levels of mitochondrial marker proteins (TOM40, TIM23 and MnSOD) - consistent with mitophagy activation. CCCP-induced mitophagy in MLE was also confirmed by co-localization of mitochondria and lysosomes. Manipulations of CL levels or proteins involved in CL externalization (PLSR3) affected sensitivity of MLE to pro-mitophageal stimulation. These data are compatible with a hypothesis that externalized CL acts as an "eat-me" signal in depolarized mitochondria. Supported by NIH ES021069, U19 AI068021, NIOSH OH008282.

PS 1004 Resveratrol Protects against a Mouse Model of Multiple Sclerosis via Regulation of T Cell miRNA Expression

K. Orr Gandy, P. S. Nagarkatti and M. Nagarkatti. *Pathology, Microbiology and Immunology, University South Carolina School of Medicine, Columbia, SC.*

Resveratrol is a plant-derived phytoestrogen with antioxidant, anti-carcinogenic and anti-inflammatory actions. Resveratrol has been extensively studied in cancer and in cardiovascular disease and has recently emerged as a potential therapeutic for the treatment of various inflammatory diseases. In this study, we evaluated the mechanistic effects of resveratrol on the pathogenesis of a mouse model of multiple sclerosis, experimental autoimmune encephalitis (EAE). We hypothesized that resveratrol protects against myelin oligodendrocyte peptide (MOG35-55)-induced neuroinflammation via regulation of T cell microRNA (miRNA) expression. Analysis of miRNA expression in CD4+ T cells from brains of EAE mice revealed significant up-regulation of miR-124,-128,-132,-138 and -155 with resveratrol treatment. Predicted and validated target genes were chosen for further examination based on gene ontology and functional analysis. miRNAs and target gene expression were validated by qRT-PCR. We found that resveratrol treatment leads to miRNA-mediated down regulation of genes essential for cell cycle progression (Rb1 and Cyclin D1) and growth and proliferation (p38 and Sphingosine Kinase 1) in CD4+ T cells. We also found that resveratrol decreases immune cell infiltration into the brain and impairs activation. While studies evaluating the effect of resveratrol on immune cells in the periphery exist, few studies have examined its effect on T cells in the target organ, the brain. Given the established neuroprotective effects and the rapidly growing anti-inflammatory properties, resveratrol is emerging as an ideal candidate for the treatment of multiple sclerosis and other neuroinflammatory diseases. (Supported in part by NIH grants P01AT003961, R01AT006888, R01ES019313, R01MH094755, P20RR032684 and VA Merit Award BX001357)

PS 1005 CCR2 Regulates Proinflammatory Macrophage Migration into the Liver during Acetaminophen (APAP)-Induced Hepatotoxicity

M. Mandal[1], R. Sun[1], S. Lad[1], H. Choi[1], J. D. Laskin[2] and D. L. Laskin[1]. *[1]Pharmacology & Toxicology, Rutgers University, Piscataway, NJ and [2]Robert Wood Johnson Medical School, Rutgers University, Piscataway, NJ.*

Inflammatory macrophages (MP) have been shown to play an important role in APAP-induced hepatotoxicity. Mechanisms mediating their accumulation in the liver have not been established. The C-C chemokine receptor, CCR2 has been shown to regulate inflammatory cell trafficking into injured tissues. In the present studies, we analyzed the phenotype of MP migrating into the liver following APAP intoxication and the role of CCR2 in this response. Mice were fasted overnight prior to administration of APAP (300 mg/kg, i.p.) or PBS. Liver, spleen and bone marrow (BM) were collected 24-96 h later and analyzed by flow cytometry. APAP caused a time-dependent increase in CD11b+Ly6Chi pro-inflammatory MP in the liver, but a transient decrease in CD11b+Ly6Clo anti-inflammatory/wound repair MP. Loss of CCR2 significantly reduced CD11b+Ly6Chi cells accumulating in the liver in response to APAP. We previously showed that the spleen is a source of hepatic inflammatory MP. Following APAP administration, increases in CD11b+Ly6Chi monocytes were observed in the spleen, with no effect on CD11b+Ly6Clo monocytes. Loss of CCR2 reduced numbers of pro-inflammatory monocytes in the spleen. In contrast, no differences were observed in monocyte subsets in the BM between wild type (WT) and CCR2-/- mice. We also identified a subpopulation of CD11b+Ly6G+Ly6C+ myeloid derived suppressor cells (MDSC) in the liver and spleen of WT mice, which decreased 72 and 96 h after APAP. In contrast, in CCR2-/- mice, MDSC increased within 24 h of APAP, remaining elevated for 72-96 h. Taken together, these results indicate that CCR2 plays a role in the emigration of CD11b+Ly6Chi pro-inflammatory MP into the liver from BM and spleen following APAP hepatotoxicity. Moreover, loss of CCR2 results in increased MDSC in the liver which may contribute to tissue repair. Supported by NIH ES007148, ES004738, CA132624, AR055073, and ES005022.

PS 1006 Collagen Synthesis and Degradation Are Enhanced in Chronic Bacterial-Induced Prostatic Inflammation

L. Wong, P. Hutson and W. Bushman. *University of Wisconsin-Madison, Madison, WI.*

Benign prostatic hyperplasia (BPH) is a common disorder in aging men. Prostatic inflammation-induced fibrosis is suggested to be a major contributor of BPH etiology. Collagen deposition was increased in our previously described mouse model of bacterial prostatic inflammation. The goal of this study is to investigate the synthesis and degradation of newly synthesized collagen in bacterial-induced prostatic inflammation.

Adult C3H/HeOuJ male mice were transurethrally instilled 200ul of 2x106/ml of uropathogenic *E. coli* 1677 or saline to induce prostatic inflammation. Prostates were harvested to perform immunohistology at selected timepoint following infection. To measure collagen synthesis, mice were injected with 15μCi of 3H-proline on day 0, 5, 12, 19, 26 post-instillation. Prostates were harvested 2 days after 3H-proline injection. To measure collagen degradation, mice were injected with 15μCi of 3H-proline every 2 days for 28 days. Prostates were harvested on day 0, 4, 8, 15, 22, 29, 36, 57, 78, 113 after the last injection of 3H-proline. The incorporation of 3H-hydroxyproline was determined by measuring 3H radioactivity using a liquid scintillation counter.

Collagen synthesis was significantly increased in the infected prostates between 5 and 7 days, and 12 and 14 days post-instillation. Immunostaining to determine collagen-producing cell revealed that there were abundant CD45+Vimentin+ fibrocytes coexpressing with the collagen synthesizing enzyme prolyl hydroxylase in the infected prostates on day 7 after infection. The newly synthesized collagen in prostatic inflammation was less stable than that in the saline-instilled prostates. The half-life of collagen in the saline prostates was 18.6 days while collagen in the infected prostates had a half-life of 13.7 days.

Our study showed that increased collagen turnover and the presence of fibrocytes characterize prostatic fibrosis in bacterial-induced inflammation. This finding provides a basis for future study to elucidate the cellular and molecular mechanisms of collagen deposition in inflammation-associated prostatic diseases.

PS 1006a Screening for Allergic Antibody Responses to 2nd Generation Biofuel Sources

M. D. Ward[1], L. B. Copeland[1], M. A. Bollman[2], L. Watrud[2] and D. Olszyk[2]. *[1]NHEERL/EPHD, US EPA, Research Triangle Park, NC and [2]NHEERL/WED, US EPA, Corvallis, OR.*

The use of cellulosic biofuels crops can potentially reduce our carbon footprint. However, they may have unintended ecological and health effects such as increased competitiveness and allergenicity. Climate change may impact the quality or quantity of allergens produced in elevated temperatures. The goal of these studies was to 1) develop a method to assess the potential allergenicity of the various grass components to which workers will be exposed and 2) determine if there are differences based on grass growth temperature (gt).
The biofuel grass components (leaves, flowers/stems, anthers, pollen) of *Sorghum bicolor* and *Panicum virgatum* were extracted in an excess of 0.2 mM Tris pH 8. Following centrifugation the supernatant was concentrated and protein content assayed. Female BALB/c mice were dosed 4X over a 4 week period by intratracheal aspiration to a pool of equal protein amounts from each of the component extracts/species/gt to induce an IgE antibody response. Three days after the final exposure the mice were exsanguinated and the blood pooled by species and gt.
Western blots of the component extracts were probed with species/gt specific serum for IgE reactivity. IgE reactive proteins were identified only in pollen extracts. Blots of *S. bicolor* pollen extract identified 2 IgE reactive protein bands. Grass gt had no apparent effect on IgE reactivity (densitometry). Blots of *P. virgatum* pollen identified 4 IgE reactive protein bands in the control gt extract and 5 additional protein bands in the high gt extract. There was a reduced intensity in the 4 common *P. virgatum* protein bands in the control gt extract compared to the high gt extract.
This limited dataset suggests that pollen is the most relevant source of allergenic proteins and that elevated growth temperatures may alter the IgE reactive profile for some but not all species.
(This abstract does not reflect EPA policy.)

PS 1006b Oxidized Lipid Macromolecules by Lipopolysaccharide (LPS) May Identify a Biomarker of Inflammatory Oxidative Insult

M. B. Kadiiska. *National Institutes of Health/National Institute of Environmental Health Sciences, Research Triangle Park, NC.*

Many techniques exist that potentially allow the measurement of inflammatory oxidative stress in animal models and humans. The goal of our multi-laboratory international study is to validate the best markers of inflammatory oxidative stress which are applicable to different oxidative insults and measurable in stored specimens. Also, to determine which of the available methods for measurement of oxidative products of lipids, proteins and DNA in biological fluids are highly specific, sensitive and selective indicators of inflammatory oxidative stress. In the present study, various oxidative products of lipids, proteins DNA were measured in plasma and urine of experimental mini-pigs using LPS treatment as an oxidative insult. The time (2h, 16h, 48h and 72h) and dose (2.5 μg/kg iv., and 5 μg/kg iv.)-dependent effects of LPS on plasma and urine lipid hydroperoxides, TBARS, malondialdehyde (MDA), isoprostanes, tyrosine oxidation products, protein carbonyls, methionine sulfoxides, DNA strand breaks were investigated with different techniques. Comparisons about the sensitivity of a given assay were carried out as well.
It was found that plasma F2-isoprostanes (by GC/MS) were increased by LPS only at the early time point (2h) and were not changed at later time points. However, urinary concentrations of F2-isoprostanes (by ELISA) were raised at all time points by both LPS doses. Urinary MDA concentration was significantly increased by both LPS doses at only later times (48h and 72 h). Generally, LPS did not cause significant differences in all other products of lipid-, protein-, or DNA oxidation. It is concluded that measurement of urinary MDA and F2-isoprostanes fulfilled the oxidative biomarker criterion of significant effects measured in biological fluid and seen at both doses at more than one time point. Measurements of MDA and F2-isoprostanes in the urine are sensitive biomarkers for oxidative damage induced by the LPS and may be the tool of choice for the assessment of inflammatory oxidative damage by LPS in vivo.

PS 1007 Concentration-Dependent Changes of Anti-BPDE-DNA-Adduct Rates in Human Lung Cells in Binary PAH Mixtures

S. Plöttner, B. Marczynski, P. Welge, H. U. Käfferlein and T. Brüning. *Institute for Prevention and Occupational Medicine of the German Social Accident Insurance - Institute of the Ruhr-Universität Bochum (IPA), Bochum, Germany.*

Polycyclic aromatic hydrocarbons (PAHs) comprise several hundred compounds with different carcinogenic potentials and are invariably found in mixtures. Due to a lack of data, risk estimations for PAH mixtures are usually based on those for benzo[a]pyrene (B[a]P). Individual substances within PAH mixtures, however, may influence genotoxic properties and act synergistically or antagonistically. In the present study we examined influences on the formation of B[a]P-specific anti-B[a]P-7,8-diol-9,10-epoxide (anti-BPDE) DNA-adducts by pyrene. Human A549 lung cancer cells were exposed to B[a]P (0.01-10 μM), pyrene (0.01-10 μM) or binary mixtures of 1 μM B[a]P + pyrene (0.01-10 μM) for 24 h. Specific anti-BPDE-DNA-adducts were determined in terms of the B[a]P-tetrol I-1 by HPLC with fluorescence detection. Additionally, changes in cytochrome P450 1A1/1B1 (CYP1A1/1B1) activities were measured in intact cells utilizing a luminescence-based assay. B[a]P alone led to a concentration-dependent formation of anti-BPDE-DNA-adducts after 24 h, with maximum adduct rates at 1 μM. After co-incubation with 1 μM B[a]P + 0.01 μM pyrene, adduct rates were enhanced compared to 1 μM B[a]P alone. But, with further increasing pyrene-concentrations in the binary mixtures, anti-BPDE-DNA-adduct rates constantly decreased compared to 1 μM B[a]P alone. All changes in DNA-adduct formation were accompanied by similar changes in CYP1A1/1B1 activities. Incubation with pyrene only resulted in concentration-dependent decreases of CYP1A1/1B1 enzyme activities. Our results show that genotoxicity of B[a]P was systematically modulated by pyrene, but, not unidirectional in terms of increasing or decreasing genotoxicity. The observed effects were closely related to the bioactivation of B[a]P. These findings are important especially with respect to the fact that PAH mixtures to which humans are exposed vary in their compositions.

PS 1008 Toxicological Evaluation and Risk Assessment for Effects of Fusarium Toxin Mixtures on Intestinal Immunity Using a Fractional Factorial Design

L. Wan[1], P. Turner[2], K. Allen[3] and H. El-Nezami[1]. *[1]The University of Hong Kong, Hong Kong, Hong Kong, [2]University of Maryland, College Park, MD and [3]University of British Columbia, Vancouver, BC, Canada.*

Toxicological evaluation and risk assessment of chemical mixtures using a factorial design allows us to estimate not only main effects but also toxin interactions. This study evaluated individual and combined effects of four common Fusarium mycotoxins, DON (2μM), NIV (2μM), ZEA (40μM) and FB1 (40μM) on immunological defense mechanisms of intestinal epithelial cells (IECs) using pro-inflammatory cytokine synthesis (IL1α, IL1β, IL6, IL8, TNFα and MCP-1), antimicrobial peptide (pBD-1 and pBD-2) synthesis and secretion on porcine intestinal epithelial IPEC-J2 cells, as well as secretory mucin (MUC5AC and MUC5B) synthesis and secretion on human intestinal epithelial cells (Caco-2) and mucin-producing cells (HT29-MTX) co-cultures as end-point measures. These Fusarium mycotoxins differentially modulated the synthesis and secretion of IL1α (up to 6-fold), IL1β (up to 22-fold), IL6 (up to 2.6-fold), IL8 (up to 20.5-fold), TNFα (up to 21-fold) and MCP-1 (up to 24.5-fold), pBD-1 (up to 15-fold) and pBD-2 (up to 39-fold), as well as MUC5AC (up to 18.5-fold) and MUC5B (up to 40-fold). Statistical analyses showed significant interactions between treatments would indicate that the addition of more than one mycotoxin has a non-additive effect (i.e. antagonism or synergy), whereas an observed lack of interaction would indicate additive effects. Results showed that additive effects were noted in most of the toxin mixtures. Therefore, these results provide evidence demonstrating that Fusarium toxins, individually and in mixtures, expressed different responses on intestinal immunological defense mechanism. Moreover, the data on toxin mixtures will contribute to improved understanding and risk assessment for common mycotoxin combinations observed in contaminated food and feed.

PS 1009 Multiple Exposures to Indoor Pollutants: Derivation of Benchmark Doses Based on Reprotoxic Effects

K. Fournier[1, 2], P. Glorennec[1, 2], D. Zmirou-Navier[1, 2, 3] and N. Bonvallot[1, 2]. *[1]EHESP School of Public Health, Sorbonne Paris Cité, Rennes, France, [2]INSERM UMR 1085 IRSET, Rennes, France and [3]Lorraine University Medical School, Nancy, France.* Sponsor: C. Emond.

Many semi-volatile organic compounds (SVOCs) are commonly present in dwellings (plasticizers, flame retardants, etc) and are suspected to have reprotoxic effects mediated by endocrine disruption mode of action. In view to carry out a cumu-

lative risk assessment for children, this work is to derive comparable benchmark doses (BMD) for SVOCs acting on the reproductive system through the same mode of action.
The choice of chemicals was based on: detection frequency (>10%) in French dwellings, availability of data on the mechanism / mode of action for reproductive toxicity, and availability of comparable dose-response relationships (in terms of species, route and window of exposure). Lower bound of 95% confidence interval of BMDs corresponding to a decrease in 10% and 50% of serum testosterone were derived using BMDS software (US EPA, 2013).
Among 51 SVOCs previously selected, 12 (6 phthalates, 1 polybromodiphenyl-ether, 3 pesticides, benzo[a]pyrene and bisphenol A) have been described to act on the Leydig cells by inhibition of an enzyme activity responsible of testosterone production, resulting in a decrease in serum testosterone levels. Only 7 have sufficient and comparable data to derive BMDs. Considering the decrease of serum testosterone levels, benzo[a]pyrene has the most potent toxicity (BMDs' lower bounds: 0.0023-0.015mg/kg BW/d) and benzylbutylphthalate has the less potent toxicity (BMDs' lower bounds: 52.73 - 346.89mg/kg BW/d). Relative potencies ranked as: benzo[a]pyrene > bisphenol A > 2,2',4,4',5-pentabromodiphenyl-ether > permethrine > diethylphthalate > cypermethrine > benzylbutylphthalate.
The main limitation for a cumulative risk assessment remains the lack of comparable toxicological data but this approach allows taking into account pollutants from diverse chemical families, with similar mode of action. These BMDs make possible a cumulative risk assessment for children exposed in indoor, in view to protect them from reproductive effects in adulthood.

PS 1010 Human Health Hazard Assessment of Hydroprocessed Esters and Fatty Acids (HEFA) Bio-Based Jet Fuels

D. R. Mattie[1], L. M. Sweeney[2, 3], K. L. Mumy[2], B. A. Wong[2, 3] and T. R. Sterner[1, 3]. *[1], 711 HPW/RHDJ, WPAFB, OH, [2]NAMRU-D, WPAFB, OH and [3]HJF, WPAFB, OH.*

The 2007 Office of the Secretary of Defense Assured Fuels Initiative directs the pursuit of domestically produced alternative fuels for military use to decrease dependence on foreign oil sources. Although bio-based jet fuels are similar to petroleum-derived JP-8, the traditional military fuel, the overall chemical composition is different. Therefore, potential health effects must be studied during development of alternative jet fuels. The body of toxicological data for Hydroprocessed Esters and Fatty Acids (HEFA) fuels from feedstocks including Camelina seed (HEFA-C), tallow (HEFA-T) and mixed animal fats and oils (HEFA-F) were examined in order to develop an occupational exposure limit (OEL) for HEFA fuels. Dermal irritation studies showed that HEFA fuels are less irritating or equivalent to JP-8. Mutagenicity and genotoxicity assays were negative. Acute and short-term inhalation studies resulted in transient effects at low levels that were not seen in the 90-day inhalation study; additional reproductive endpoints were negative and no significant neurobehavioral effects were observed based on functional observational battery and motor activity tests. Sensory irritation assays never reached 50% respiratory depression at saturation doses. HEFA toxicity data were compared with toxicity data from synthetic paraffinic kerosene (SPK) alternative jet fuel and petroleum derived JP-8. A comparative OEL for HEFA fuels was developed that concurs with the current JP-8 OEL (200 mg/m^3).

PS 1011 Xenobiotic Mixtures Decrease Human Hepatic Gluconeogenesis and Glucose Oxidation

A. Leblanc[1], E. Blanc[1], A. Ambolet-Camoit[2], C. Benelli[1], S. Bortoli[1], R. Barouki[1] and M. Aggerbeck[1]. *[1]UMR-S 747, INSERM, Paris, France and [2]845, INSERM, Paris, France.*

Epidemiological studies have shown that exposure to certain xenobiotics is associated with an increased prevalence of metabolic diseases. Since humans are exposed to mixtures of xenobiotics detoxified by the liver, we used two xenobiotics, both endocrine disruptors and persistent organic pollutants, which use different signaling pathways, to study hepatic energy metabolism: 2,3,7,8 tetrachlorodibenzo-p-dioxin (TCDD), which uses the AhR, and α-endosulfan, an organochlorine pesticide, which acts via the PXR and/or the estrogen receptor.
Differentiated HepaRG cells, which resemble human hepatocytes, were exposed for 30h to 25nM TCDD, 10 μM α-endosulfan, or the mixture. Gene expression was measured by transcriptomics and RT-qPCR. Oxidation of glucose to CO2 (radioactive incorporation) and production of lactate and glucose (colorimetry) were measured.
The expression of two genes of hepatic gluconeogenesis critical for hepatic energy metabolism, glucose transporter 2 (GLUT2) and glucose-6-phosphatase (G6Pc), were reduced 80% by the mixture (more than either xenobiotic alone). The expression of other glucose metabolism genes (pyruvate kinase, glycogen synthase, glycogen phosphorylase, pyruvate dehydrogenase 2) also was decreased suggesting that the mixture may markedly impact carbohydrate metabolism. Glucose production decreased 40% with the mixture under gluconeogenic conditions. Under glycolytic conditions, although the oxidation of glucose into CO2 decreased 30% after 72h exposure to the mixture, lactate production was not affected. Long-term treatment (8 days) with lower doses (0.2 to 5 nM TCDD, 3 μM α-endosulfan) similarly decreased G6Pc and Glut2 expression.
Thus, the mixture of TCDD and α-endosulfan decreases, in vitro, the expression of hepatic glucose metabolism genes even at low doses and decreases hepatic gluconeogenesis and glucose oxidation. Chronic exposure of individuals to low doses of xenobiotics might significantly affect hepatic carbohydrate metabolism and be a contributing factor in the development of the metabolic syndrome.

PS 1012 Studying the Impact of Volatile Organic Chemical Coexposures on the Urinary Excretion of Their Metabolites in Human Volunteers

A. Marchand[1], R. Aranda-Rodriguez[2], A. Nong[2] and S. Haddad[1]. *[1]Environmental and Occupational Health, IRSPUM, Université de Montreal, Montréal, QC, Canada and [2]Environmental Health Sciences and Research Bureau, Health Canada, Ottawa, ON, Canada.*

It is common practice to assess volatile organic compounds (VOCs) exposure by monitoring their corresponding urinary metabolite, assuming no interactions between co-exposed chemicals. There is a dearth of information concerning the impact of VOC co-exposure on the excretion of metabolites used for biomonitoring. The objective of this study was to collect metabolite excretion data and parent compound kinetics from inhalation exposures in human of four common VOCs (i.e. chloroform [CHL], toluene [TOL], ethylbenzene[EBZ] and m-xylene [XYL]). Five human volunteers were exposed by inhalation to 18 different combinations of chemicals (single, in binary combination with chloroform, or all 4 VOCs) at ¼ or 1/8 TLV for 6 hours each with a week of interval between each exposure. Parent compounds were measured in exhaled air and blood samples taken during and following exposures. Metabolites, such as o-cresol (TOL), mandelic acid (EBZ), m-methylhippuric acid (XYL) and 2,4-dimethylphenol (XYL), were quantified in urine (collected during and after exposure) after derivatization. No interactions were observed in exhaled air between exposures. No statistically significant interactions were observed on metabolites except for 2,4-dimethylphenol, which showed a decrease of 25% to 36% in total excreted amount in the presence of CHL alone or in the presence of all VOCs in air. Although average total amount of o-cresol excreted is increased by 50-72% when co-exposed to EBZ and XYL in air, and CHL in drinking water, this was not shown to be statistically significant. More effort will be place to understand the contradictory mixture interaction (i.e., decreased xylene blood levels but decreased metabolite excretion). These data will help to develop and validate an interactions-based physiologically-based pharmacokinetic modeling approach to assess VOCs exposure from urinary biomonitoring data.

PS 1013 Pharmaceutical, Metal, and Ammonia Mixtures: Widespread Additive Toxicity in Zebrafish Larvae

D. H. Alsop and J. Y. Wilson. *Biology, McMaster University, Hamilton, ON, Canada.*

Urban and industrial effluents (e.g. wastewater, agricultural and mining effluents) can introduce many contaminants into our aquatic ecosystems. Indeed, multiple contaminants in a single polluted site is the norm. Aquatic life has little say in the matter and are susceptible to contaminant exposure, given their constant contact with the aqueous environment. The acute toxicities of a variety of environmental contaminants were examined using the larval stage of a model organism, the zebrafish (Danio rerio; 4–8 days post fertilization). Toxic interactions were observed between metals such as nickel, cadmium and copper. For example, sublethal copper exposure (6% of the copper LC50 or 13% of LC01) decreased the cadmium 96 h LC50 by 47%. In addition, pharmaceuticals in the environment are a growing concern, and selective serotonin reuptake inhibitors (SSRIs) are particularly toxic to fish. Fluoxetine (ProzacTM) and sertraline (ZoloftTM, LustralTM) mixtures displayed additive toxicity; sublethal fluoxetine (one-third of the LC50, 40% of the LC01) decreased the sertraline LC50 by 46%. Most surprising, however, were the observations that mixtures of acutely toxic environmental contaminants from different chemical classes also displayed additive toxicity. For example, ethinyl estradiol (EE2; bioactive estrogen in the female oral contraceptive pill) displayed additive toxicity with copper and sertraline. Similarly, sublethal ammonia (a component of fertilizer) increased the toxicities of sertraline and fluoxetine. Mixtures were typically additive or greater than additive. In the search for a common toxic mechanism, it was discovered that larvae exposed to metals, SSRIs or ammonia (around their respective LC50s) all experienced whole body ion loss. Decreases were greatest for Na+, as high as 39% in 48 h. Water quality criteria should ultimately recognize additive toxicity in order to protect our aquatic ecosystems.

PS 1014 Assessing Neurological Risks from Oral Exposure to Mixtures of Organophosphorus (OP), Carbamate, and Pyrethroid Insecticides

P. McClure[1] and H. Pohl[2]. [1]*SRC, Inc., East Syracuse, NY and* [2]*US Public Health Service ATSDR, Atlanta, GA.*

Data on interactions were evaluated to develop approaches to screening level assessments of human neurological hazard from oral exposure to mixtures of OP, carbamate, and pyrethroid insecticides. PubMed and Toxline were searched for data on interactions among 34 OPs, 16 pyrethroids, and 14 carbamates. Using ATSDR's 2004 binary weight-of-evidence framework, the following determinations were made: 1) There are inadequate data to assess the direction of possible interactions between pyrethroids and carbamates; 2) There is some evidence for >dose -additive action between pyrethroids and OPs, but only at near lethal levels in rodents; and 3) There is evidence for dose-additive action for carbamates and OPs on neurological endpoints in rats [brain cholinesterase and associated thermoregulatory endpoints]. Additionally, pirimicarb-elimination kinetics was unchanged in humans exposed to low doses of pirimicarb and chlorpyrifos-methyl. Overall, the evidence is not compelling to move from a dose-additive approach. Dose-additivity most closely describes the joint toxic action of adverse neurological effects from oral exposures to mixtures of OPs, carbamates, or pyrethroids. A relative potency factor (RPF) Hazard Index approach would be an appropriate approach using RPFs and index chemicals determined by the USEPA Office of Pesticide Programs (EPA 2006, 2007, 2011) and provisional oral Minimal Risk Levels for index chemicals of each class.

PS 1015 Potential Toxicity of Electronic Cigarette Liquids and Aerosols As Measured by Four *In Vitro* Assays

R. Leverette, M. Misra, B. T. Cooper and M. B. Bennett. *Technology Development/Life Sciences, Lorillard Tobacco Company, Greensboro, NC.*

The popularity of electronic cigarettes (E-cig) continues to increase worldwide, with several major tobacco companies entering the E-cig market. A typical E-cig delivers a flavored propylene glycol or glycerol based aerosol, with or without nicotine, via vaporization by a battery-powered heating element. Currently, data regarding the potential toxicity of E-cigs is limited. To further our understanding, an in vitro battery of established assays was used to examine the mutagenicity (Ames), cytotoxicity (Neutral Red Uptake; NRU), genotoxicity (Micronucleus; MN) and inflammatory (IL-8 release) response of a set of glycerol-based commercial E-cigs, specifically the neat E-cig liquids, pad-collected aerosol extracts and freshly generated whole aerosols. Pad-collected smoke condensates and whole smoke from traditional tobacco burning cigarettes (3R4F, 1R5F and one commercial cigarette) were included for comparison. All E-cigs and traditional cigarettes were smoked under Canadian Intense parameters (55 mL puff volume, 2 second puff duration, 30 second puff interval, 100% blocked air dilution). At the levels tested, exposures with neat E-cig liquids and pad-collected aerosol extracts showed no-to-extremely low activity in the Ames, NRU, MN and IL-8 assays when compared to responses from the traditional tobacco burning cigarettes. Results with E-cig samples without nicotine were very similar in all assays, indicating that the presence of nicotine, at the levels tested, did not significantly contribute to any cytotoxic and genotoxic effects observed at high doses. Whole aerosol exposures are ongoing, but preliminary results (Ames) show no activity. Overall, results from this study indicate, under the experimental conditions utilized, E-cigs do not produce any meaningful toxic effects when compared to traditional cigarettes, as measured by the four in vitro endpoints used in this study.

PS 1016 Concentration Addition and Toxic Equivalent Factors: When Do They Apply?

T. Webster. *Dept Environmental Health, Boston University School of Public Health, Boston, MA.*

Dose addition/concentration addition (CA) is the principle criterion used in toxicology for judging interaction of compounds that act via similar mechanisms. Deviations from CA are then said to display synergy (more properly, greater than CA) or antagonism (less than CA). Following Berenbaum and others, by CA we mean that one compound can substitute for another at a constant ratio at any constant effect level. This is equivalent to having linear isoboles: the contours of the joint dose-response surface are straight lines. It is not widely understood that Toxic Equivalence Factors (TEFs) is a special case in which the dose ratio is the same at all effect levels (Isoboles are then parallel which they need not be in the more general case). Confusion has crept into the literature as a result. Indeed, some alternative definitions of concentration addition lead to strange results. First, suppose that fa(A) describes the dose-response curve for compound A and fb(B) for compound B. Let the mathematical inverses of these functions be ga(E) and gb(E), respectively: they tell us the dose of A alone or B alone needed to achieve any given effect level E. One alternative definition of CA calculates the combined effect of A and B under no interaction as fa(A+ga(fb(B)) or fb(gb(fa(A)+B). We show that these two expressions are equal only under the TEF case; in other situations they can lead to different isoboles. Second, it has been claimed that joint dose-response surfaces with linear isoboles are rare. It is widely known that TEFs apply when the joint response of A and B is fa(A+r*B) where r is the relative potency of B compared to the reference compound A. While it can be shown that this is the only situation where TEFs apply, it places little restriction on the types of dose-functions fa(.). Finally, we might ask what kinds of joint dose-response functions obey CA. It can be shown that applying another function h(E) to a response function changes the height of the response function but not the shape of its isoboles. Hence the kinds of dose-response-functions which can obey CA is enormous.

PS 1017 Toxicology and Risk Assessment of Chemical Mixtures

M. Krishan and A. Kretser. *ILSI, North America, Washington, DC.*

Evaluation of potential health risk from simultaneous exposure to multiple chemicals has been one of the major challenges for toxicology research and risk assessment (RA). Terminology and problem formulation is complex and the framework for mixture RA varies greatly among different agencies. As part of the International Life Sciences Institute North America Technical Committee on Food and Chemical Safety, 2013 Summer Fellowship Program, we analyzed current methods to achieve the following: 1) Describe the landscape of RA for chemical mixtures; 2) Characterize differences in RA frameworks; and 3) Assess regulatory acceptance of these frameworks with a focus on food mixtures. Reviews were completed for mixture RA paradigms used by US federal agencies, non-profit organizations (WHO, IPCS) and international agencies (EU). There are significant overlaps and differences between paradigms and there appears to be no single unified method, is apparent from our research. US EPA's original framework forms the basis of most of the globally accepted methods for mixtures RA. Whole mixture, sufficiently similar mixture or component-based approaches are used for mixture RA depending on data availability. Differences in hazard assessment approaches were found among agencies, including differences in criteria (e.g., mode of action, health outcome) for grouping chemicals in assessment groups. WHO, IPCS and EU recommend the use of a tiered approach and dose additivity as the default approach. We developed a framework based on a food mixture scenario to select the set of parameters to guide use of appropriate RA methods. These parameters include target population, exposure routes, availability of data on the exposure levels and toxicology interactions for the whole mixture or individual components. Future methods could incorporate high throughput screening data (e.g., toxicogenomics and biomonitoring) to improve risk characterization of food mixtures. Considering the current challenges in food mixtures such as heavy metals, pesticides and migrants from packaging, a case study was done to compare different methods and test their applicability to food safety assessments.

PS 1018 The Modulation of Antioxidant Enzyme Activities and Glutathione Levels in the Livers of Mice after Subchronic Exposure to Mixtures of Dichloroacetate and Trichloroacetate

E. Hassoun and J. M. Cearfoss. *Pharmacology, University of Toledo, Toledo, OH.*

Dichloroacetate (DCA) and trichloroacetate (TCA) are drinking water chlorination byproducts that were found to be hepatotoxic/ hepatocarcinogenic in rodents. Mixture of the compounds were previously found to induce additive or greater than additive effects on various biomarkers of oxidative stress (OS) in the hepatic tissues of B6C3F1 male mice after subchronic exposures, and that was suggested to modulate the hepatotoxic/ hepatocarcinogenic outcomes of the compounds. In order to determine the role of antioxidant enzymes and glutathione (GSH) on the effects of the mixtures, groups of male B6C3F1 mice were treated daily, by gavage, with 3 different doses of DCA (7.5, 15 and 30 mg/kg/day), 3 different doses of TCA (12.5, 25, and 50 mg/kg/day) and 3 different mixtures (Mix I, Mix II and Mix III) of the compounds for 13 weeks. The concentrations of the compounds in Mix I, II and III, respectively corresponded to those producing approximately 15%, 25% and 35% of maximal induction of OS by the individual compounds in the subchronic studies. The mice were euthanized at the end of the treatment period and livers were assayed for the activities of superoxide dismutase. catalase, glutathione peroxidase and glutathione level. While the individual compounds effects on the enzyme activities and glutathione were demonstrated as either suppression or stimulation, the mixture effects were demonstrated as the net effects of the two compounds in the mixtures. The results indicate significant contribution of the antioxidants to the outcome of OS in the livers of B6C3F1 mice after long term exposure, and that the effects of mixtures of the compounds are different from

those produced by the individual compounds. Hence, mixtures of DCA and TCA may result in modulation of the hepatotoxic/hepatocarcinogenic outcomes of the individual compounds. (Supported by NIH/NIEHS grant # R15ES013706-01A2)

PS 1018a Cumulative Toxicity of an Environmentally Relevant Mixture of Nine Regulated Disinfection By-Products in a Multigenerational Rat Reproductive Bioassay

J. Simmons, M. G. Narotsky, G. Klinefelter, J. M. Goldman, A. B. DeAngelo, D. S. Best, A. McDonald, L. F. Strader, A. S. Murr, J. S. Suarez, M. H. George and S. Hunter. *NHEERL/ORD, U.S. EPA, RTP, NC.*

Disinfection of water has advanced public health by decreasing waterborne disease. Dsinfectants react with organic materials in the water to form complex mixtures of disinfection by-products (DBPs). While a large unknown fraction remains, >600 DBPs have been identified. Most prevalent in chlorinated water are trihalomethanes (THMs) and haloacetic acids (HAAs); 4 THMs (chloroform, bromodichloromethane, chlorodibromomethane, bromoform) and 5 HAAs (chloroacetic, dichloroacetic, trichloroacetic, bromoacetic, dibromoacetic acid) are regulated by EPA as a group at 80 μg/L and 60 μg/L, respectively. This is the first multigenerational reproductive toxicity bioassay in animals with a drinking water mixture of the regulated THMs and HAAs. At realistic proportions, a mixture was prepared at 0, 500×, 1000×, and 2000× of EPA's maximum contaminant levels (MCLs). Timed-pregnant Sprague-Dawley rats (P0 generation) were exposed from gestation day 0 until weaning of the F1 offspring. Weanlings continued in their treatment groups, were examined for reproductive endpoints and bred to produce F2 litters. Pre- and postnatal survival was unaffected. F1 pup weights were unaffected at birth but reduced at 2000× on postnatal day (PND) 6 and at ≥1000× on PND 21. Males at 2000× had a small but significantly increased incidence of retained nipples and effects on sperm motility. Onset of puberty showed dose-related delays at 1000× and 2000×. F1 estrous cycles, breeding, and fertility were unaffected and F2 litters showed no effects on pup weight, or prenatal or neonatal survival. Histologically, P0 dams had nephropathy and adrenal cortical pathology at 2000×. In sum, while puberty was delayed at DBP concentrations ≥1000× and males at 2000× had retained nipples and altered sperm motility, exposure at these concentrations to an environmentally realistic mixture of 9 regulated DBPs did not affect F1 animals' ability to reproduce. (This abstract does not reflect EPA policy.)

PS 1018b Toxicity Testing of Water, Air, and Soil near Mountaintop Removal Mining Sites in the Southern Coalfields of West Virginia Using *In Vitro* Methods—What the Data Can Tell Us

L. M. Crosby[1], W. Orem[1], C. DeVera[1], K. Charles[3], M. Varonka[1], A. Bates[1], T. Westphal[1], A. Kolker[1], C. Tatu[2, 1] and N. Geboy[1]. *[1]Eastern Energy Resources Science Ctr, US Geological Survey, Reston, VA, [2]University of Medicine and Pharmacy, Timisoara, Romania and [3]J. Craig Venter Institute, Rockville, MD.*

As a result of published epidemiological studies indicating health impacts in mountaintop removal coal mining (MTR) areas of southern West Virginia (WV), the USGS conducted a survey of air, water and soil in the impacted area and at WV State Parks which served as control sites with no MTR. The analytes measured were organics, metals, and in vitro toxicity, collected over 2 years. Toxicity testing included three assays which measured 24 hr toxicity, 1 week clonal outgrowth and anchorage-independent growth effects of water and soil sample extracts on human cells. A case study was then conducted on samples collected from Artie, WV in close proximity to active mountaintop removal mining. Private wells, surface waters, soil, fruit/vegetable matter were sampled. Grab sampling was conducted during one week periods over the first year of the survey over all seasons at locations in several counties and at two State Parks outside the active mining area. Year two sampling concentrated on Artie, WV during spring and summer. From the sampling in year one, 2 of 22 samples (March), 3 of 21 (May), 4 of 18 (December) showed significant toxicity to human cells, while from the Artie, WV sampling in year two toxicity was seen in 16 of 19 (August) but 0 of 23 (December) samples. Ground whole apples from a site sampled in August also showed significant toxicity. This variation could be due to episodes of mining activity, seasonal differences in temperature, or water abundance and movement through the aquifer. The air, water and soil organics, metals, and fine particulates showed important differences between mined and non-mined locations. We will discuss how the latter relate to the toxicity results, potential overall importance and context within recent literature findings regarding the possible health effects of mountaintop mining removal.

PS 1018c Assessment of *In Vivo* Toxicological Interactions from Criteria Air Pollutant Mixtures

L. Datko-Williams[1], B. Young[1], A. Wilkie[1], M. Madden[1], J. Dubois[1], L. W. Stanek[2], D. Johns[3] and E. Oesterling Owens[1]. *[1]NCEA, US EPA, RTP, NC, [2]NERL, US EPA, RTP, NC and [3]NIOSH, US CDC, Morgantown, WV.*

The US EPA sets National Ambient Air Quality Standards for criteria air pollutants, recognizing that air pollution in the environment exists as a complex mixture. Potential interactions between mixture components within biological systems are not well characterized. We reviewed past literature investigating the effects of mixtures of criteria air pollutants, starting with mixtures containing NO_X (nitrogen oxides), and evaluated the presence of *in vivo* toxicological interactions. All endpoints and NO_X-containing mixtures were considered, however, most studies evaluated respiratory effects of NO_X+O_3 (ozone). Studies were classified into two categories: complete or incomplete response data. Complete data included the number of observations, mean response, and variance for each treatment group in the study. Studies lacking single pollutant exposures or complete response data were reviewed qualitatively. Of the 13 animal studies and 7 human studies in the qualitative analysis, 6 animal studies and 0 human studies suggested there may be interactions, though no pattern of response among the endpoints or exposures was apparent. Studies with complete data were analyzed quantitatively, and the response to the mixture was compared statistically to the sum of the responses to individual pollutants; the absence of a difference was defined as additive (H_0: combined effects = sum of individual effects, p=0.05). Of the studies in the quantitative analysis, all animal studies (n=17) had at least one non-additive endpoint, while the majority of endpoints evaluated in human studies (n=9) were additive. Among the studies that deviated from additivity, no pattern of response emerged in endpoints or exposure conditions. Thus, this analysis suggests that deviations from additivity exist in criteria air pollutant mixtures; however, many of the studies did not demonstrate interactions other than additivity.
The views expressed in this abstract are those of the authors and do not necessarily represent the views or policies of the U.S. EPA.

PS 1018d Mixture Effects at Human Relevant Exposure Levels?

A. Vinggaard[1], N. Hadrup[1], M. Pedersen[2], K. Skov[2], L. O. Bertelsen[1], H. Frandsen[2], K. G. Kongsbak[1], J. Boberg[1] and U. Hass[1]. *[1]Div. Toxicology & Risk Assessment, Technical University of Denmark, Søborg, Denmark and [2]Division of Food Chemistry, Technical University of Denmark, Søborg, Denmark.*

Mixtures of endocrine active chemicals usually act additively irrespective of the applied model system and the complexity of the endpoint measured. Most studies performed so far have tested doses ≥ NOAEL for individual chemicals. But what happens when we test mixtures of EDC's at doses close to human relevant exposure levels? We had the hypothesis that a low dose mixture of environmental chemicals and active food ingredients would not affect toxicity induced by perfluornonanoic acid (PFNA). PFNA was given at 13, 250 or 5000 μg/kg/day to male rats with or without a cocktail containing 14 chemicals including phthalates, bisphenol A, parabens, UV filters, pesticides, and the CYP3A4 inhibitors bergamottin (from grape fruit) and glabridin (from liquorice) at human relevant exposure levels (totally 2.5 mg/kg/day'). The lowest PFNA dose corresponded to an internal dose of ~6-fold total human PFC exposure. We did histology, hormone analysis, metabolomics in plasma and gene expression analysis in liver, testis and fat tissue. PFNA induced steatosis at the highest dose. At the low dose PFNA+Cocktail pronounced increases of androgen levels (dehydroepiandrosterone, androstenedione & testosterone) were evident. Gene expression analysis in low dose PFNA+Cocktail treated animals showed that CYP19 mRNA was affected in testis and fatty tissues. At higher PFNA doses several steroidogenic enzymes were down-regulated. Overall, we suggest that low dose PFNA+Cocktail affect the kinetics of androgens causing increased androgen levels. In addition the Cocktail protected against PFNA-induced increases in corticosterone levels via an effect on11β-HSD. The observations are effects at the molecular level that may be considered as biomarkers of direct adverse effects. This is to our knowledge a first indication that mixture effects appear in rats at doses close to human relevant exposure levels.

PS 1018e Chemical and Toxicological Assessment of Vapor from a Novel Tobacco-Heating Device

J. C. Miller Holt[1], M. Meger[1], T. Bonk[1], J. Pani[2], E. Weber[2] and I. W. Jones[1]. [1]*JT International SA, Geneva, Switzerland and* [2]*Ökolab Gesellschaft für Umweltanalytik Ges.m.b.H, Vienna, Austria.*

Devices which heat, rather than combust, tobacco are delivering an aerosol which is chemically less complex and biologically less active than smoke from a conventional cigarette. This study examines the emissions chemistry and in vitro toxicological activity of a new battery-powered device which heats tobacco to 170 ± 10oC to produce a vapor for users to inhale.
Constituent analysis of the vapor reveals it to be chemically distinct to the smoke from a standard reference cigarette, with most constituents measured, being reduced by at least 90%. These results are consistent with the fact that the product heats rather than burns tobacco.
In vitro toxicological assessment of the vapor was conducted using the Ames Salmonella mutagenicity assay, the Neutral Red Uptake assay and the micronucleus assay. In the Ames assay, vapor extract did not show a significant increase in activity above the negative control in any of the Ames tester strains evaluated (TA98, TA100, TA102, TA1535, TA1537), with or without metabolic activation (S9). Similarly, no significant increase above the negative control is observed in the micronucleus assay in any of the testing regimes (Short-term treatment in the presence and absence of S9 and long-term continuous treatment in the absence of S9). In the neutral red uptake assay, no dose-response curve could be established for particulate or gas vapor phases.
These data are broadly in agreement with observations made by previous authors investigating the biological activity of emissions generated when tobacco is heated rather than burnt.

PS 1018f Respiratory Dose Analysis for Components of Ambient Particulate Matter

C. S. Kim[1, 2]. [1]*USEPA, Research Triangle Park, NC and* [2]*North Carolina State University, Raleigh, NC.* Sponsor: M. Madden.

Particulate matter (PM) in the atmosphere is a complex mixture of particles with different sizes and chemical compositions. Although PM is known to cause health hazard, specific attributes of PM that may cause health effects are somewhat ambiguous. Dose of each specific component of PM together with relevant dose metrics may shed insights into understanding of PM related health effects. We have attempted to analyze lung deposition dose of typical bimodal ambient aerosols composed of two distinct aerosols with mass median diameter of 0.3 um (A1) and 5.0 um (A2) with geometric standard deviation of 1.8 – 2.0. Mass fractions, MF = A1/(A1+A2), were varied in order to reflect aerosol characteristics of different regions. Lung deposition including tracheobronchial (TB) and alveolar (AL) regions was calculated by using a mathematical model built upon Weibel's lung morphology for mass, surface area and number of each of three size fractions, ultrafine (UF, PM0.1), fine (F, PM0.1-2.5) and coarse (C, PM2.5-10) at inhalation patterns mimicking resting and mild to moderate exercise. Overall, mass deposition of C decreases whereas deposition of F increases in both TB and AL as MF increases during normal breathing at rest. Combined deposition of C and F shows a decrease in TB but an increase in AL resulting in a slight increase in TB+AL. Surface area deposition is resulted mainly by F with a minor contribution from UF at MF>0.2 whereas number deposition comes from both UF and F at a ratio of 1.5:1. During exercise, mass deposition increases greatly (~140%) in TB but decreases (15%) in AL resulting in a moderate increase of 40% in TB+AL in C whereas F decreases by 15% ~ 40%. This results in variable changes (+/-20%) of F+C as compared with resting condition. Surface area and number deposition shows a decrease of ~20% in a wide range of MF. In conclusion, PM size fractions of ambient aerosols contribute differently to lung deposition dose in terms of mass, surface area and number. Significance of roles of each size fraction and their combined effects need to be considered in toxicological and health risk assessment.

PS 1019 Application of the Neutral Red Release and EpiOcularTM Assays in a Tiered Approach for Evaluating the Eye Irritation Potential of Agrochemical Formulations

E. W. Carney[1], R. S. Settivari[1], S. C. Gehen[2], R. Acosta Amado[2], M. Corvaro[2], L. Kan[1], D. Wilson[1] and D. R. Boverhof[1]. [1]*TERC, The Dow Chemical Company, Midland, MI and* [2]*Dow AgroSciences LLC, Indianapolis, IN.*

Evaluation of chemicals for eye irritation potential is an important aspect of safety assessment. Although the rabbit Draize test has served as the conventional approach, recent global regulations and responsible stewardship programs are driving the development of non-animal approaches. Cytotoxic potential is one of the primary modes of action that can result in eye irritation. Herein, we describe our evaluation of two cytotoxicity-based in vitro approaches, the neutral red release (NRR) and EpiOcularTM (EO) assays, for the evaluation of the eye irritation potential of prospective crop protection products. The NRR has been shown to have good performance for identification of strong irritants but may exhibit reduced performance for moderate and mild irritants. In contrast, EO performs well with moderate and mild irritants but may fail to correctly identify strong irritants. Therefore, the assays were implemented in a tiered approach starting with the higher-throughput 2D culture NRR assay and implementing the 3D culture EO assay if further refinement was needed. In the first tier assessment, the NRR assay was conducted on 51 agrochemical formulations and co-formulants and the results were compared to Draize data. The assay exhibited good performance in correctly predicting all the tested 15 strong irritants; however, the assay tended to over-predict the irritation potential of moderate, mild and non-irritants. To address this limitation, the EO assay was used as the second tier test for 14 of the NRR-over-predicted formulations. The EO assay demonstrated good performance with 86% concordance for correctly classifying the NRR-over predicted irritants. Overall, this evaluation highlights the strengths and limitations of the assays as well as presents a potential tier-based approach for assessing the eye irritation potential of crop protection products.

PS 1020 Testing Framework for Prediction of Ocular Irritation Using the Bovine Corneal Opacity and Permeability (BCOP) Assay and Chorioallantoic Membrane Vascular Assay (CAMVA)

A. Carrao[1], K. Norman[2], D. Cameron[1], G. Mun[2], N. Wilt[2], A. Hilberer[2], J. Avalos[1] and F. Simion[1]. [1]*Kao USA Inc., Cincinnati, OH and* [2]*Institute for In Vitro Sciences Inc., Gaithersburg, MD.*

In vitro ocular irritation assays, such as the Chorioallantoic Membrane Vascular Assay (CAMVA) and Bovine Corneal Opacity and Permeability (BCOP) test, are routinely used by personal care products companies because they are rapid and economical to conduct, do not require the use of live animals, and provide reliable predictive data. Previous research using an extensive CAMVA and BCOP database at Kao USA Inc. has shown that ocular irritation potential for new hair shampoos, ethanol-based hair stylers, skin cleansers, and skin lotions can be reliably predicted using a decision tree that systematically compares the ingredient composition, particularly ethanol and surfactant content, of the new formulation to previously tested formulations. Because the studies comprising this original database were conducted at a single contract laboratory, a follow-up study using a second contract laboratory was conducted to demonstrate inter-laboratory reliability of the CAMVA/BCOP data-derived decision tree for prediction of ocular irritation potential. Thirty-five personal care products were tested using the CAMVA and/or BCOP assays. The ethanol and surfactant content of each test material was evaluated, and the results of the assays were compared to the decision tree-based predictions of ocular irritation potential. Our data confirmed the ocular irritation predictions made using the decision tree model for 33 of 37 test samples (89% correlation rate) and verified the inter-laboratory reliability of the CAMVA and BCOP assays when conducted using appropriate controls. Our results also strengthened the ocular irritation decision tree model by confirming that deodorants are consistently predicted not to be ocular irritants based on composition.

PS 1021 Investigations on Reducing Ocular Irritation Associated with Harsh Ingredients by Altering Physicochemical Properties of the Formulation

K. N. Boyd[1], E. A. Sly[2] and K. Norman[2]. [1]*SC Johnson and Son Inc., Racine, WI and* [2]*Institute for In Vitro Sciences, Inc., Gaithersburg, MD.* Sponsor: H. Raabe.

With the upcoming implementation of the Globally Harmonized System of Classification and Labeling of Chemicals (GHS) in various forms throughout the world and a global movement towards a reduction in animal testing, more emphasis is placed on utilizing the inherent hazards of chemicals for classification and labeling; however, the assessment of the toxicity of chemical mixtures, particularly ocular irritation, can be complex. The ability to formulate mixtures to be less irritating with minor modifications to the physical form would be very beneficial. The present study used the Bovine Cornea Opacity and Permeability (BCOP) assay, which is an OECD-approved *in vitro* method to assess ocular irritation, to investigate how physical properties (e.g., viscosity) affect ocular irritation. We found that the BCOP *in vitro* scores of irritating chemicals from several classes, including strong bases, were diminished by altering the viscosity of the aqueous medium or by dosing the solution as a foam. Our data show that a 1% NaOH solution in water produced an *in vitro* score of 165; however, when the medium was thickened with 1% Carbopol®, the *in vitro* score dropped to 67.6. A change of this nature is significant, and if this were an EPA-registered antimicrobial cleaner, for example, this reduction in the *in vitro* score would lower the hazard category.

Product form and usage can clearly impact exposure, and the present results suggest that modifications to the physical properties of chemical mixtures can alter their ocular irritation potential; perhaps by affecting exposure to the eye. Although no formal comparisons were performed in animals, the BCOP assay is an OECD-validated method to assess ocular irritation, and studies have shown that the BCOP assay does not under-predict the results of traditional animal tests; thus, there are no obvious reasons to suggest that the present results would not correlate to animals or humans.

PS 1022 Assessing Default GHS Classifications for Eye Toxicity with Alternative Ocular Assays

N. Pechacek[1], J. Caudill[2] and T. O'Brien[1]. [1]*Ecolab, St. Paul, MN and* [2]*Ecolab, Naperville, IL.*

The Globally Harmonized System of Classification and Labeling of Chemicals (GHS) represents an international approach to standardize the classification and hazard communication for chemicals in the work place. Institutional cleaning products, due to their surface-active chemistries, commonly carry a classification of serious eye damage or irritation. For appropriate product stewardship, such products must be correctly classified for eye effects. Ocular testing is a common approach for attaining a proper GHS classification. Current GHS criteria for classifying this endpoint are based primarily on interpreting in vivo data. However, due to animal welfare concerns, there is a shift in testing emphasis to alternative assays. Two such assays are the Bovine Corneal Opacity Permeability Assay (BCOP) and Chorioallantoic Membrane Vascular Assay (CAMVA). The BCOP uses excised bovine corneas to evaluate ocular irritation. The CAMVA uses the vascular network of fertilized chicken eggs as a conjunctival model to assess ocular irritation. For this study, institutional cleaning products were assigned default GHS classifications for eye effects based on an algorithm prescribed by GHS. Twenty-six products had joint BCOP/CAMVA tests conducted to assess such classifications. Based on the test results from the joint BCOP/CAMVA studies conducted for each product, GHS classification were re-assigned and compared to the default classifications. Of the 26 products evaluated, 17 had test-based classifications aligning with default classifications, 6 had test-based classifications lower than the default classifications and 3 products had test-based classifications higher than the default classifications. Based on this particular dataset of 26 products, the results suggest the GHS algorithm assigns appropriate (~65%) or conservative (~23%) eye classifications with a relatively small (~11%), but not insignificant, minority of under classifications. A larger dataset is needed to make a definitive conclusion for this observation.

PS 1023 Exploration of New Transcriptomic Biomarkers for Eye Irritation Test Using a New 3D Reconstructed Human Corneal Epithelial Model, MCTT HCE™

K. Lim[1], S. Choi[1, 2], M. Lee[1] and Y. Chun[2]. [1]*College of Pharmacy, Ewha Womans University, Seoul, Republic of Korea and* [2]*College of Pharmacy, Chung-Ang University, Seoul, Republic of Korea.*

Evaluation of the eye irritation is essential in the development of new cosmetic products since they are to be used directly on face. Since 1960s, the draize rabbit eye irritation test has been widely used in which chemicals are directly applied to rabbit eye, and the symptoms and signs of eyes are scored. However, due to the invasive test procedure, this test causes a substantial level of pains and discomfort to animals. So, it has been a primary target of animal welfare activities. To resolve this ethical issue, it is essential to develop a verified and credible animal alternative testing methods. Recently, 3D reconstructed human cornea models like EpiOcularTM, SkinEthics HCETM receives enormous interests owing to the similarity in structural and functional characteristics to real human cornea. Previously, we also reported an eye irritation test method using a new human corneal epithelial model (MCTT HCE™) which is reconstructed from remaining human tissues after a corneal transplantation. This model exhibited an excellent predictive capacity (sensitivity 100%, specificity 77% and accuracy 88% vs GHS for 25 chemicals). To improve the test accuracy for this model, we explored new biomarkers for the eye irritation using toxicogenomics approach. We selected 3 surfactants among the known eye irritants that include sodium lauryl sulfate, benzalkonium and triton X-100. After the test chemicals were treated at various concentrations, we investigated the differentially expressed genes in negative control (PBS) and test chemicals through a whole gene microarray (Affymetrix GeneChip® Human Gene 2.0 ST Array). As a result, we identified that cornifelin, a constituent of the insoluble cornified cell envelope (CE) of stratified squamous epithelia and early growth response 1 gene, a nuclear transcriptional regulator that are important for cornea epithelial differentiation and proliferation are significantly changed in three eye irritants.
This work is supported by MFDS CAMSEC grant (13172MFDS98)

PS 1024 Development of an *In Vitro* Microelectric Cell Sensing Technique to Assess Cytotoxicity of Ocular Irritants

K. Berezowski[1], D. Y. Huang[1], S. Gabos[2] and D. W. Kinniburgh[1]. [1]*Physiology & Pharmacology, Alberta Centre For Toxicology, University of Calgary, Calgary, AB, Canada and* [2]*Department of Laboratory Medicine & Pathology, University of Alberta, Edmonton, AB, Canada.*

The Draize rabbit eye test is currently the most widely accepted method for assessing ocular irritancy of chemicals. However, due to a variety of limitations and concerns with the test, along with changes to legislation, such as the European Union Cosmetics directive regarding the use of experimental animals, alternative methods are being developed at a rapid pace. The result has been the introduction of a broad spectrum of assays, none of which can singularly replace the Draize rabbit eye test. The pursuit of a toxicological tool box of tests, that when taken together, could eventually replace the Draize test, continues to drive the need for new technologies and methods of assessment of ocular irritation.
With this study, our objective was to develop and optimize a novel high throughput cell based *in vitro* method to measure the potential of chemicals, mixtures and commercial products to cause eye irritation. This was undertaken by evaluating the cytotoxicity of compounds exposed to a cell panel using a micro electric cell sensing technology, the Real Time Cell Analyzer (RTCA™) from ACEA Biosciences Inc. Three cell lines were used in this study: SIRC, ARPE-19, and BJ. These three cell lines were exposed to 6 known ocular irritants and 3 known ocular non-irritants in quadruplicate. The 50% cell growth inhibitory concentration values (IC_{50}) at 0, 6, 12, 48, 60, and 72 hours were calculated for each compound and each cell line using RTCA™ technology in tandem with the MTT assay for validation of the results. Comparative analysis of results from the two assays shows reasonable correlation. Results generated by RTCA™ and MTT were subjected to comparison to historical Draize data, again with good correlation. In conclusion, RTCA™ technology in general appears to be a strong candidate as an alternative ocular irritation test.

PS 1025 Cultured Porcine Cornea Assay Using Confocal Microscopy for High Resolution Detection and Quantification of Sub-Mild Ocular Irritation

M. Piehl, M. R. Carathers, E. Ryan, W. R. Hahn, D. R. Cerven and G. L. DeGeorge. *MB Research Laboratories, Spinnerstown, PA.*

A critical need exists for a non-animal ocular irritation assay that is sensitive to sub-mild ocular irritation. We have developed a novel assay, PorFocal, which can quantify individual dead corneal epithelial cells in porcine corneas using confocal microscopy. PorFocal uses phosphate buffered saline (PBS) as a negative control and 0.01% benzalkonium chloride (BAK) as a positive control. In 17 experiments, 0.01% BAK always caused more cell death than PBS, and statistically ($p<0.05$) more in 15 of 17 replicates. The PorFocal assay detected a significant dose-response with BAK dilution series treatment. Treatment with 0.01% BAK-preserved lubricant eye drops showed a statistically significant ($p<0.05$) greater than 3-fold increase in cell death when compared to the preservative-free version. To examine the potential of the PorFocal to detect human eye sting of a known stinging chemical (avobenzone), we compared a low avobenzone (LA) to a high avobenzone (HA) content sunscreen. The HA caused significantly more cell damage (7-fold increase) than the LA. We then compared PorFocal to an industry standard 3D reconstructed human tissue (RhT) ocular irritation assay. The RhT detected four of nine materials while the PorFocal assay detected eight of nine materials tested as statistically greater than PBS values. Overall, this indicates a great degree of sensitivity with PorFocal assay, previously not attainable by existing methods.

PS 1026 Using Benzalkonium Chloride and POLYQUAD® to Test the *In Vitro* Reconstituted Human Corneal Epithelium Model As a Replacement for *In Vivo* Ocular Screening

F. Zhang[1], L. Walker[1], R. Rice[2] and D. P. Rodeheaver[1]. [1]*Preclinical Safety, Alcon, Fort Worth, TX and* [2]*Preclinical Development, Alcon, Fort Worth, TX.*

The aim of this investigation was to evaluate whether the reconstituted human corneal epithelium (RHCE) in vitro model (SkinEthic Laboratory, Nice, France) is a reliable indicator of in vivo acute topical ocular irritation. Two preservatives commonly found in topical ocular formulations, benzalkonium chloride (BAC) and POLYQUAD® (PQ, polyquaternium-1) solutions, were utilized as model compounds in the test system.
Both BAC and PQ solutions were evaluated in the in vitro RHCE model at concentrations of 0.01, 0.02, 0.1 or 0.5%. Test solutions were applied on the surface of each RHCE tissue for 10 min, 1 hr or 24 hrs, respectively. Cell viability, histopathology, interleukin-1α, -6 and -8 were evaluated. Test solutions, except 0.5%

BAC, were also evaluated in a one-day in vivo topical ocular dosing study in NZW rabbits. The in vitro results classified PQ as a non-irritant at all concentrations and at all time points by cell viability. BAC was classified as an irritant in the in vitro study after both 1 hr and 24 hrs exposures at ≥0.1% by cell viability. Histological and interleukin analyses did not correlate as well and appeared to be more sensitive. Results from the in vitro RHCE model using cell viability assay appear to correlate with results from in vivo study with rabbits. These results suggest the RHCE using cell viability assay may have utility in screening topical ocular formulations for potential acute ocular irritation. Also, interleukins and histopathology could provide valuable data but require further investigation.

PS 1027 The Importance of Understanding Drivers of Irritation *In Vivo* for Selection of Chemicals Used in the Development and Evaluation of *In Vitro* Eye Irritation Assays: Cosmetics Europe Analysis

J. Barroso[1], N. Alépée[2], A. De Smedt[3], B. De Wever[4, 10], J. Hibatallah[5], P. McNamee[6], K. Mewes[4], M. Millet[7], U. Pfannenbecker[8], M. Tailhardat[9] and M. Templier[7]. *[1]Cosmetics Europe, Brussels, Belgium, [2]L'Oréal, Aulnay, France, [3]Janssen Research & Development, Beerse, Belgium, [4]Henkel AG & Co. KGAelopment, Düsseldorf, Germany, [5]Chanel Parfums Beauté, Neuilly sur Seine, France, [6]The Procter & Gamble Company, Egham, United Kingdom, [7]Pierre Fabre, Castres, France, [8]Beiersdorf AG, Hamburg, Germany, [9]LVMH Recherche, St. Jean de Braye, France and [10]ALTEXA Development, Monte Carlo, Monaco.*

Cosmetics Europe's Task Force Eye Irritation is actively involved in the development and evaluation of in vitro methods to assess the eye irritation potential of cosmetic ingredients. Selecting adequate chemicals based on a proper understanding of what drives irritation in classification of ocular effects of chemicals in the in vivo Draize eye test is a critical element that enables identification and evaluation of predictive capacity and applicability domain at an early stage of in vitro methods development. As such, an in depth analysis of the data available from external databases containing in vivo eye irritation data for chemicals tested in the Draize eye test (from more than 500 independent studies) has been undertaken. This analysis is based on having good quality in vivo data that has allowed a clear understanding of the different ocular tissues effects that drive classification. These include the degree of severity and/or the persistence of corneal opacity, iritis, conjunctiva redness and/or conjunctiva chemosis. In addition, all chemicals were screened for their commercial availability, assurance that they cover the whole range of irritation potential and represent relevant chemical classes and physical states. The approach used to define the drivers of irritation and the importance of each of them for the classification and labeling of chemicals is described. This work demonstrates e.g., the high involvement of corneal effects and the low prevalence of iritis driving classification, and the importance of conjunctiva effects in classification of GHS Cat 2A versus 2B.

PS 1028 Tiered Testing Strategy Using Validated *In Vitro* Assays for the Assessment of Skin and Eye Corrosion/Irritation of Pharmaceutical Intermediates

S. Calufetti[1], C. Callis[1], K. Nelson[1], M. Krcha[2], N. Wilt[2] and G. Costin[2]. *[1]Eli Lilly and Company, Indianapolis, IN and [2]Institute for In Vitro Sciences, Inc. (IIVS), Gaithersburg, MD.*

The safety of workers handling solid pharmaceutical intermediates was assessed using a tiered testing strategy based on regulatory validated *in vitro* assays. The Top-Down approach was initiated with the *in vitro* skin corrosion assay (OECD TG 431) followed by the *in vitro* skin irritation assay (OECD TG 439) using the reconstructed human epidermis model from MatTek Corporation. Of the ten pharmaceutical intermediates tested, nine were predicted to be non-corrosive to skin and were subsequently confirmed as non-irritants. The only intermediate predicted corrosive to skin was further tested using the Corrositex assay (OECD TG 435) and was assigned a corrosive packing group II classification. Furthermore, three intermediates predicted non-corrosive/non-irritant to skin were tested as 20% dilutions in water in the *in vitro* Bovine Corneal Opacity and Permeability (BCOP) assay (OECD TG 437) and they were predicted as non-irritant to the eye. Our tiered skin and eye corrosion/irritation testing strategy proved to be a very useful platform for the assessment of the potential safety risk posed to workers during manufacturing operations used for pharmaceutical intermediates.

PS 1029 Study of Cosmetics Europe for Skin Sensitization Hazard Characterization and Risk Assessment without Animal Testing

A. G. Schepky[1], K. Reisinger[2], N. Alépée[3], S. Martinozzi Teissier[3], G. Maxwell[4], P. Kern[5], H. Sakaguchi[6], J. Barroso[7], T. Ashikaga[8] and M. Tailhardat[9]. *[1]Beiersdorf AG, Hamburg, Germany, [2]Henkel AG & Co. KGaA, Duesseldorf, Germany, [3]L'Oréal, Paris, France, [4]Unilever, Colworth, United Kingdom, [5]The Procter and Gamble Company, Cincinnati, OH, [6]Kao Corporation, Tokyo, Japan, [7]Cosmetics Europe, Brussels, Belgium, [8]Shiseido Corporation, Tokyo, Japan and [9]LVMH, Paris, France.*

Cosmetics Europe (CE) intends to develop a testing strategy for sensitizer potency prediction without animal testing. In this regard, potency is defined as the entire spectrum of skin sensitisation, ranging from non-sensitiser to extreme sensitisers.
To reach this aim a method evaluation study was initiated to identify appropriate in vitro methods. In a joint effort CE and 15 test developers systematically evaluated 16 in vitro methods. 10 chemicals were blind tested by each test method developer: 4-Nitrobenzylbromide, Methyldibromoglutaronitrile, 2-Mercaptobenzothiazole, Cinnamal, Tetramethyl thiuram disulphide, Salicylic acid, Lactic acid, Sodium lauryl sulphate, Phenyl benzoate, Lauryl gallate. Additional information was shared on the protocol, prediction model and existing data for previously tested chemicals: Of the 16 test methods evaluated for hazard prediction (sensitiser vs non-sensitiser) 14 misclassified a maximum of 2 substances, 3 correctly predicted all 10 substances. 7 methods provided useful potency information for the assessment of skin sensitisation, subcategorise in 5 classes as defined for the LLNA. 5 methods misclassified a maximum of 3 substances, usually being only one category off. One test method misclassified more substances, while the 7th method was not evaluated in detail as only for 4 substance results were available.
Phase II of the method evaluation study started in 2013 with ten prioritized methods to build a data base used for the data integration approach staring Q1 2014.

PS 1030 Predictability of *In Vitro* Dermal Assays When Evaluating Fatty Amine Derivatives

P. J. Rugen, S. Grundén, D. Hart and E. Houthoff. *Product Safety & Regulatory Affairs, AkzoNobel, Chicago, IL.*

It is widely accepted in the world of *in vitro* toxicology that skin assays can be used in place of *in vivo* testing to accurately predict corrosivity and/or irritancy of commodity chemicals. Due to REACh legislation, various categories of fatty amines have been evaluated. Historical worker occupational experience has exhibited that various fatty acid amines are corrosive to the skin. Coco-Amidopropyldiethanolamine (Coco-APDEA) contains both secondary and tertiary amines and is used as a surfactant in numerous industries. In the EpiDerm (EPI-200) Skin Model, skin corrosion is expressed as the remaining cell viability after exposure to the test substance. The relative mean tissue viability obtained after the 3 minute and 1 hour treatments with Coco-APDEA was 80% and 70% respectively. Since the mean relative tissue viability was not below 50% after the 3 minute treatment and not below 15% after the 1 hour treatment, Coco-APDEA is not considered to be corrosive in this assay. In the EpiSkin-SMTM irritation assay, a positive result is determined when viability is below 50% following a 15 minute exposure. Coco-APDEA exhibited 1% viability at the 15 minute exposure period which would be considered an irritant in this assay. Because the results from the *in vitro* assays with the human three dimensional epidermal models did not align with historical data, a limited *in vivo* rabbit study was employed. This test involved one animal and had to be terminated on day 2 because of severe reactions following the 3 minute exposure. Histopathology performed showed marked necrosis of the epidermis of the treated skin, with a marked heterophylic cell infiltrate in the underlying dermis. Based on the results of the histopathology (full thickness destruction) findings, the substance was considered to be corrosive. The results obtained for Coco-APDEA shows that these assays do not always predict corrosivity correctly. Modifications to protocols should be considered when testing amines.

PS 1031 Prediction of Systemic Bioavailability Using *In Vitro* Skin Absorption and Epidermal and Hepatic Metabolism of Aromatic Amine Hair Dyes

J. Manwaring[1], H. Rothe[3], C. Obringer[1], D. Foltz[2], T. Baker[2] and C. Goebel[3]. *[1]Global Product Safety, Procter & Gamble, Mason, OH, [2]Global Analytical, Procter & Gamble, Mason, OH and [3]Global Product Safety, Procter & Gamble, Darmstadt, Germany.* Sponsor: G. Daston.

Approaches to assess the role of absorption, metabolism and excretion (AME) of cosmetic ingredients that are based on the integration of different in vitro data are important for their safety assessment specifically due to the ban on animal testing

in the European Union. In order to estimate systemic exposure (AUC) to each of 5 aromatic amine hair dyes (A027 (4-amino-2-hydroxytoluene), A074 (4-amino-m-cresol), A158 (2-amino-5-ethylphenol HCl), A005 (toluene 2,5-diamine) and A154 (1-hydroxyethyl 4,5-diamino pyrazole sulphate)) following typical product application conditions, the bioavailable fraction was first determined using *in vitro* skin penetration experiments and human keratinocyte (HaCaT) metabolism. This was followed by an estimation of the systemic AUC by additionally utilizing hepatic clearance values. The fraction of the dermally applied dose that reaches the systemic circulation was estimated using measured Michaelis-Menten descriptors of epidermal metabolism, skin penetration rates, viable epidermis measurements, mean residence time and skin permeability coefficients. Predictions of the nonmetabolized fraction were equal to or less than 0.25% of the applied dose. Separate *ex vivo* studies using viable human skin explants produced values that were within the same order of magnitude as those predicted from the above *in vitro* AME approach. In the final step, *in vitro* hepatocyte Km and Vmax values and whole liver mass and cell density were used to calculate the scaled hepatic clearance to predict systemic exposure in the general circulation (AUC) based upon the estimated dermally absorbed dose. The overall approach provides a quantitative prediction of the internal exposure using appropriate toxicokinetic information that can be generated based solely on *in vitro* data and showed that none of the applied dose avoided effects of metabolism either by the skin upon entry into the body or by the liver systemically.

PS 1032 The Use of Human Skin Equivalents for Identification of Contact Sensitizers

A. H. Poth, C. Behle-Wagner and L. Theis. *Alternative and Genetic Toxicology, Harlan Cytotest Cell Research GmbH, Rossdorf, Germany.*

Dermal sensitizers are currently identified using animal based tests such as the mouse local lymph node assay, the guinea pig maximisation test and the Buehler test. Minimizing the use of animals for chemical testing has been increased the development of new in vitro testing strategies. Gibbs et al., 2013 developed a protocol using different 3D- epidermal models to explore the possibility of assessing the release of Interleukin-18 (IL-18) for identification and classification of skin sensitising chemicals including a putative prediction model. In our study we have investigated two sensitizers (Cinnamaldehyde and 2,4-Dinitrochlorobenzene) and two irritants (SDS and salicylic acid). The aim of our study was to determine on whether the three prediction models proposed for this test system are able to distinguish clearly between sensitizers and irritants. The two sensitizers were clearly identified by the three prediction models proposed. However, for the irritant compounds it turned out that at higher cytotoxicity ranges IL-18 was also significantly and dose-dependently released and by using the three prediction models the compounds were wrongly classified as sensitizers. Lowering the cytotoxicity ranges, both the sensitising compounds as well as the irritants were correctly classified which may indicate a modification of the prediction models proposed.

PS 1033 A Highly Differentiated 3D Epidermal Skin Model to Characterize Skin Sensitizers in Mixtures

L. F. Pratt, M. Troese and G. L. DeGeorge. *MB Research Laboratories, Spinnerstown, PA.*

Strong support exists in the consumer products, pharmaceutical and cosmetics industries to develop in vitro assays to identify and characterize skin sensitizers. We have adapted the keratinocyte interleukin-18 (IL-18) response assay developed by Corsini and colleagues in 2009 for use with epiCS®, a highly differentiated epidermal model. epiCS® comprises primary human keratinocytes, grown into a 3D skin model at the air-liquid interface. The IL-18 response assay measures release of this cytokine into the culture medium of test substance-treated tissues over 24 hours, by ELISA. Results are expressed as a Stimulation Index (SI) when compared to vehicle control treatment and an SI value of >1.5 was considered indicative of a positive sensitizer response. Four vehicles – Ethanol, AOO 4:1, Ethanol:DMSO 4:1, and Petrolatum – were compared for their effects on three sensitizers (dinitrochlorobenzene, eugenol and citral). Ethanol:DMSO 4:1 yielded the highest SI values for the three sensitizers. The basal amount of IL-18 release for all vehicles ranged from 1.1 pg/ml to 17 pg/ml. DNCB at 0.15% consistently produced the highest SI values with the vehicles, and a clear dose-response at concentrations of 0.018%-0.3% was seen. In addition, a dose-response was caused by nitrobenzylbromide (0.025%-0.2%) and p-phenylenediamine (PPD, 0.1%-2.0%) in ethanol vehicle, while cinnamic alcohol and resorcinol were negative. However, resorcinol was clearly positive (SI = 2.7) in AOO 4:1 vehicle. The irritant/nonsensitizers 2% phenol and glycerol were both negative (SI < 1.5). Lastly, consumer product mixtures, specifically hair dyes containing PPD to yield light brown, dark brown and black colors were tested neat on the epiCS® tissues. A clear increase in IL-18 over sham-treated controls (13 pg/ml) was observed in hair dyes ranging from 71 pg/ml to 76 pg/ml to 85 pg/ml, respectively (SI values 5.7, 6.0 and 6.8). Further work is necessary to investigate different categories of chemicals and mixtures and their mechanisms of toxicity, to adapt and improve the prediction model accordingly.

PS 1034 A Dermal Sensitization Assay Using SkinEthic™ RHE

M. Troese and G. L. DeGeorge. *MB Research Laboratories, Spinnerstown, PA.*

International regulatory agencies, as well as animal welfare groups, are seeking in vitro assays for assessing the toxicity of chemicals and products. One of the most difficult challenges has been to develop non-animal tests for skin sensitization. As an outcome of the Sens-it-iv project in Europe, Corsini and colleagues developed an Interleukin-18 (IL-18) response assay in monolayer keratinocytes as an indicator of sensitization in 2009. Here we report release of IL-18 into the culture medium of SkinEthic RHE™ treated with sensitizers, but not with irritants or non-sensitizers. Sensitizer-induced IL-18 release by RHE tissues was observed to occur in a concentration-dependent manner. RHE tissues were exposed to test substances for 24 hours. Data were expressed as a Stimulation Index (SI) calculation. An SI ratio of >2.0 was considered a positive result for a dermal sensitizer. A range of slight to severe sensitizers, as well as nonsensitizers and irritants were tested. A commercially available ELISA measured IL-18 and tissue viability was determined by the MTT assay. Of the twelve known positive sensitizers tested (4-Nitrobenzyl bromide, p-Phenylenediamine, 2,4-Dinitrochlorobenzene, Eugenol, Citral, Resorcinol, Glyoxal, α-Hexyl cinnamaldehyde, Cinnamaldehyde, Cinnamic Alcohol, IsoEugenol and 2-Mercaptobenzothiazole), ten were correctly predicted. In addition, six of seven irritants (Chlorobenzene, Lactic Acid, Phenol, Methyl Salicylate, Salicylic Acid and Tween-20) and nonsensitizer (Glycerol) were correctly predicted. Overall accuracy of the assay was calculated to be 84%. In conclusion, an in vitro assay for characterization of dermal sensitizers was developed in SkinEthic™ RHE. This assay is promising for identification of sensitizers with high accuracy and predictivity, and for further research into the mechanism of dermal sensitization mediated by Interleukin-18.

PS 1035 Coculture Assay for the Identification and Investigation of Dermal Sensitizers (Epi-DC)

G. L. DeGeorge[1], M. Troese[1], L. F. Pratt[1], M. Piehl[1], P. J. Hayden[2] and S. Ayehunie[2]. *[1]MB Research Laboratories, Spinnerstown, PA and [2]MatTek Corporation, Ashland, MA.*

In order to investigate the mechanism of dermal sensitization, a co-culture model of human keratinocytes and dendritic cells was developed and optimized. This model (Epi-DC) consists of a 3D epidermal organotypic tissue, EpiDerm™, grown atop a suspension culture of plasmacytoid dendritic cells (DCP-100), in a medium that allows both cellular components to express normal viability, expression of IL-18, and the activation of surface markers CD86 and CD54 on DC. In this model, test chemicals were dosed topically on the EpiDerm™ tissue for 24 hours. The criteria for change in biomarkers to indicate a positive sensitizer included: (1) an increase of IL-18 release into the culture medium of >1.6-fold over vehicle, or (2) an increase in percentage of DCP-bearing activation surface markers CD86+ or CD54+ of >1.5-fold over vehicle controls, as measured by flow cytometry. Dinitrochlorobenzene (DNCB; 0.003% to 0.1%) and cinnamaldehyde (CA; 0.0003% to 0.006%) were tested diluted in the ethanol vehicle.
Results: Basal secretion in vehicle control co-cultures was 23.8 pg/ml of IL-18. Treatment of Epi-DC with DNCB yielded IL-18 concentrations that peaked at 0.1% DNCB, resulting in a release of 44.5 pg/ml (1.9-fold increase). Vehicle control cultures had 9.1% CD86+ DC, and a dose-dependent increase of CD86+ DC was shown with treatment of DNCB ranging from 0.003% to 0.1% DNCB, peaking at 18.7% positive CD86+ DC (2.1 fold increase). No significant increases in CD54 expression were observed. At 0.006% CA, increases of 1.6-fold over control were observed in CD86 expression. No increases in CD54+ DC were seen at any of the test substance treatments. Thus, in this initial evaluation, the Epi-DC co-culture model has shown to be a useful and predictive tool for identifying dermal sensitizers without the use of animals.

PS 1036 Human Skin Assays (SkimuneTM) for the Detection of Adverse Reactions, Potency, and Efficacy

M. Matevia[1], C. Willett[1], S. Ahmed[2], A. M. Dickinson[2], X. Nong Wang[3] and R. Stebbings[4]. *[1]Regulatory Toxicology, The Humane Society of the United States, Washington DC, WA, [2]Alcyomics Ltd, Newcastle University, Newcastle upon Tyne, Tyne and Wear, United Kingdom, [3]Haematological Sciences, Newcastle University, Newcastle upon Tyne, Tyne and Wear, United Kingdom and [4]Biotherapeutics Group, National Institute for Biological Standards and Control, London, Hertfordshire, United Kingdom.*

We describe a human-based *in vitro* skin explant test (Skimune™) that improves predictivity relative to the use of animal models for adverse immune reactions. The test involves exposing dendritic cells from a healthy volunteer to a test compound followed by incubation with autologous T cells.The T cells are then tested for immune reactivity *in vitro* on a skin biopsy from the same volunteer. If the compound is a sensitizer, coculture of activated T cells with the skin gives rise to an adverse immune reaction, graded histopathologically from I-IV. The test was evaluated using a range of chemical sensitizers and nonsensitizers, with 95% concordance with the mouse local lymph node assay (LLNA)(P<0.001,sensitivity 95%, specificity 95%). The test correctly identified chemicals negative in the LLNA but positive in man (e.g.nickel sulphate) and correlated with T cell proliferation and interferon gamma secretion assays. The test also predicts adverse immune reactions to biologics such as the Tegenero antibody (TGN1412) and overcomes interspecies barriers which often prevent detection of adverse effects during safety testing. Compounds tested included: maleic anhydride, glutaraldehyde, trimellitic anhydride, paraphenylendiamine, cinnamic alcohol, isoeugenol, eugenol, 2,4,dinitrochlorobenzene, mercaptobenzothiazole, cinnamaldehyde, oxazolone, glyoxal, resorcinol, 4-nitrobenzylbromide, potassium dichromate, ethylendiamine, hexylcinnamicaldehyde, and 2-hydroxyethylacrylate, and the nonsensitizers sodium dodecyl sulfate, glutamic acid, triton-X-100, zinc sulphate, dimethylsulfoxide, potassium permanganate, isopropanol, dimethylformamide, glycerol, tween80, phenol, ethylvanillin, octanoic acid, propyleneglycol,4-aminobenzoicacid, methylsalicylate, chlorobenzene, diethylphthalate,p-hydroxybenzoic acid, and benzaldehyde.

PS 1037 Inter-Laboratory Validation of an *In Vitro* Method to Classify Skin Sensitizers

A. J. Clippinger[1], J. M. McKim[2], D. Keller[2], P. C. Wilga[2], A. R. Van Rompay[3] and H. Witters[3]. *[1]PETA, Norfolk, VA, [2]CeeTox Inc., Kalamazoo, MI and [3]Flemish Institute for Technological Research, Mol, Belgium.*

This study builds upon previous studies showing that CeeTox's *in vitro* SenCeeTox® assay can correctly identify and categorize chemical sensitizers when used in-house. The aim of this project was to further validate the SenCeeTox® assay by conducting an inter-laboratory validation at the Flemish Institute for Technological Research (VITO). In this study, MatTek's three-dimensional human skin model, EpiDerm (EPI-296, EpiDerm 96-well reconstituted human epidermis), was treated in triplicate with six concentrations of each test article. Test articles were run in a blinded manner. The test articles evaluated were: metol, isoeugenol, 2,3-butanedione, 2-mercaptobenzothiozol, eugenole, 1-chloro-2,4-dinitrobenzene, glycerol, 2-hydroxyethylmethacrylate, 2-hydroxyethylacrylate, and lactic acid. Following 24 hr exposure to the test articles, the following endpoints were measured: 1) cytotoxicity, 2) the ability of each chemical to directly react with glutathione, and 3) expression of key genes. The gene expression levels of seven target genes controlled by the Nrf2/Keap1/ARE signaling pathway were examined: NADPH-quinone oxidoreductase 1, aldoketoreductase 1C2, interleukin 8, cytochrome P450 1A1, aldehyde dehydrogenase 3A1, heme-oxygenase 1, and glutamate cysteine ligase catalytic subunit C. The data were then analyzed in a blinded manner using a proprietary algorithm to predict each chemical's likelihood of causing a human sensitization reaction. The results confirm the inter-laboratory reproducibility of SenCeeTox® which accurately predicted the ability to elicit a sensitization reaction for all 10 blinded compounds tested at VITO. Furthermore, it correctly predicted the sensitization potency category for 9 out of the 10 compounds, missing the 10th compound by only one potency category. In conclusion, SenCeeTox® can predict the sensitization potency of chemicals ranging from nonsensitizers to strong-extreme sensitizers.

PS 1038 New Sloughing and Oral Irritation Assays Using Organotypic Human Tissue Models

B. Breyfogle, P. J. Hayden, M. A. Bachelor and M. Klausner. *MatTek Corporation, Ashland, MA.*

Oral irritation can result from exposure of soft tissue to dentifrice and oral rinse formulations. *In vitro* tissue models (MatTek Corporation) produced from normal human oral keratinocytes were exposed to common oral care excipients, dentifrice supernatants, and mouth rinses to determine the potential irritation of oral care excipients/formulations, including SLS, poloxamer, NaF dentifrice, and pyrophosphate (PPi)/NaF dentifrices.
As a measure of mucosal irritation, cell viability was monitored for up to 24 hours using the MTT assay. The expression of pro-inflammatory cytokines, IL-1β and IL-1α, were also monitored via ELISA. In addition, a novel oral sloughing assay was developed to quantitate the level of physical damage to the oral tissue when exposed to mouth rinses containing various levels of surfactant. Tissues treated with SLS solutions (0.2%-0.6%) provided a clear dose response with ET-50 values ranging from 10.5 to < 2 hrs. A dose response was also observed for IL-1α and IL-1β expression in SLS-treated tissues. The addition of poloxamer to SLS solutions increased tissue viability and decreased levels of pro-inflammatory cytokines. Treatment of tissues with NaF and PPi/NaF dentifrices (10% supernatants) exhibited differences in both ET-50 values and cytokine expression levels. In addition, the cell viability results strongly correleated to cytokine expression levels. Differences in the level of sloughed protein were observed following application of various oral rinse formulations to the organotypic oral epithelium. Findings from the oral sloughing assay strongly correlated to changes in tissue thickness (Pearson's r-value > 0.8). The oral tissue models represent highly reproducible, non-animal means to screen newly developed oral care products for oral irritation and should be useful to study the innate immunity, biology, and pathology of the oral mucosa.

PS 1039 Identifying Interspecies Variations in Uro-Epithelial Cell Culture Models

E. Bowen[1], S. Baker[1], P. Rawlinson[2], P. Mistry[2], J. Wright[2] and J. Southgate[1]. *[1]Jack Birch Unit for Molecular Carcinogenesis, University of York, York, United Kingdom and [2]Syngenta, Bracknell, United Kingdom.*

Toxicity testing of novel chemicals is a necessary process to safeguard human health. The current system, which relies heavily on rat *in vivo* models, has high ethical and financial costs and can produce results that do not accurately translate to humans. Use of human *in vitro* models have the potential to bridge the gap between rats *in vivo* and man, reducing animal usage and increasing the relevance of toxicity tests to humans. The aim of this project was to use a basic cell culture system to identify any fundamental differences in the cellular physiology of human and rat epithelial cells as a basis for understanding species variations in xenobiotic toxicity. To achieve this, pathways regulating proliferation were studied in an established human *in vitro* system of the bladder epithelium (urothelium) and compared to a system developed using normal rat urothelial (NRU) cells. Our results indicate differences in the pathways regulating proliferation between normal human and rat urothelial cells under standard (low calcium) culture conditions. Normal human urothelial (NHU) cell proliferation is known to be driven via the epithelial growth factor receptor involving Erk and β catenin activation. In NRU cells, phospho-Erk was minimally expressed under standard conditions and pharmacological activation of the β-catenin pathway did not affect cell proliferation. Activation of the Akt pathway by insulin growth factor 1 produced a significant increase in the expression of the proliferation marker Ki67 in NRU cells but not in NHU cells. In addition, cellular phenotype varied with markers of differentiation being lost by NHU cells but maintained by NRU cells. Our results reveal physiological differences in the pathways regulating proliferation and the phenotype of human and rat urothelial cells *in vitro*. It is not yet known whether these differences underlie altered responses to xenobiotics and so future work will proceed to further investigate whether these differences contribute to species variations in xenobiotic toxicity.

PS 1040 A Novel Organotypic 3-D Human Small Intestinal Tissue to Assess Drug Safety and Inflammation

S. Ayehunie[1], Z. Stevens[1], T. Landry[1], M. Taimi[2], A. Armento[1], M. Klausner[1] and P. J. Hayden[1]. *[1]MatTek Corporation, Ashland, MA and [2]Apredica, Watertown, MA.*

The intestinal epithelium plays a key role in defining the bioavailability of orally administered drugs. The colon cell line, Caco-2, is commonly used to study intestinal drug safety and inflammation but it does not recapitulate the structure or physiology of small intestine (SI) tissue. This study evaluates the functionality of a novel in vitro tissue model reconstructed from normal human primary SI epithelial

cells and fibroblasts. Primary cells were expanded in monolayer culture and seeded onto microporous membrane inserts to reconstruct 3D organotypic SI tissues. Tissue morphology, surface marker expression, ultrastructural features, and barrier integrity of the tissues were characterized. In addition, efflux drug transporter expression was analyzed by RT-PCR and drug permeation was examined using LC-MS/MS with 3 model drugs previously tested with Caco-2 cells. Inflammatory responses were examined by exposing the tissue to TNF-α for 24 hr. Analysis of the SI tissue model revealed: 1) wall-to-wall tissue growth, 2) columnar epithelial cell morphology similar to human SI, 3) a physiological TEER value of 60-180 Ω*cm2 mimicking the SI microenvironment, 4) expression of MUC-2, CK19, and villin, and 5) formation of brush borders and tight junctions. RT-PCR also showed expression of the prominent efflux drug transporters P-gp (MDR-1), MRP-1, MRP-2, BCRP and the main metabolic enzyme, CYP3A4 similar to human SI explants. Initial permeation studies using 2 P-gp substrates, ranitidine and talinolol, demonstrated active transport while warfarin, a non-PgP substrate, did not. Treatment of the SI tissue with TNF-α induced a proinflammatory response by inducing the release of chemokines including IL-8 and GRO-α. We anticipate that this new human cell-based SI tissue will be useful for pre-clinical assessment of drug safety and mucosal inflammation and at the same time will reduce the use of animals for experimentation.

PS 1041 Comparison of Three Different *In Vitro* Intestinal Barrier Models for Assessing the Oral Fraction Absorbed of Pharmaceutical and Nutritional Products

H. Wortelboer[3], J. Westerhout[3], S. Vaessen[2], M. Bol-Schoenmakers[1], B. J. Blaauboer[1], J. Schrickx[1], M. Verwei[3] and R. Pieters[1, 2]. [1]*Institute for Risk Assessment Sciences, Utrecht University, Utrecht, Netherlands,* [2]*Dept Innovative Testing, University of Applied Sciences, Utrecht, Netherlands and* [3]*TNO, Zeist, Netherlands.*

In development of pharmaceutical and nutritional products an accurate prediction of the oral fraction absorbed in humans is essential, as the bioavailability of a compound at the target site co-determines the efficacy of the active compound. Currently, animal models, *in vitro* (mainly cell lines) and *in silico* tools are applied preclinically, but their predictive value to assess oral bioavailability in humans is often insufficient.
Here, we aim to design a decision tree based on several *in vitro* intestinal barrier models, but to increase acceptance and implementation, data obtained with intestinal barrier models should be translatable to human *in vivo* data. Apparent permeability (Papp) values of 15 model compounds with different physicochemical properties were tested in the Caco-2 model and the InTESTine™ model using porcine jejunal tissue and compared with published human Papp values. In addition, cells and porcine and human intestinal segments were analyzed for abundance of transporter proteins and metabolic enzymes.
Papp values of compounds determined using the InTESTine™ system were in the same range as the human Papp values (based on Ussing data), whereas data obtained with Caco-2 cells showed major differences probably due to differences in effective surface area. As expected, major differences were found in the levels of active transport systems and metabolic enzymes in both Caco-2 cells and porcine jejunal tissue in comparison with human intestinal tissue. Results provide important characteristics of different *in vitro* permeability models and will help to design a predictive decision tree feeding into human PBPK modelling.

PS 1042 Evaluation of the Toxicity Profiles of Selected Bioactivated Compounds in Primary Rat Hepatocytes Cultured in Micropatterned Cocultures

O. Ukairo[1], M. McVay[1], S. Krzyzewski[1], K. Rose[2], M. E. Anderson[2], S. Khetani[1] and E. LeCluyse[2]. [1]*Hepregen Corporation, Medford, MA and* [2]*The Hamner Institutes for Health Sciences, Research Triangle Park, NC.*

Drug-induced liver injury is often caused by cytochrome P450-dependent activation of drugs into reactive metabolites. *In vitro* models, which can mimic *in vivo* responses and allow the evaluation of initial and adaptive responses to bioactivated compounds over prolonged periods, offer potentially valuable tools for toxicological assessment. We have previously developed a model in which primary hepatocytes (rat, human) are seeded onto ECM-coated domains of optimized dimensions and subsequently cocultivated with murine embryonic fibroblasts [i.e. micropatterned cocultures (MPCC)]. This model retains key biochemical functions of *in vivo* liver with long term stability. Here, we assess the bioactivation and cytotoxicity of acetaminophen (APAP) and other compounds in the 96-well rat MPCC. APAP is a well-known hepatotoxin and exerts its toxic effects through bioactivation associated, in part, with cytochrome P450 3A (CYP3A). Rat MPCCs were exposed to increasing concentrations of APAP (over 5 days) and assessed for changes in hepatic ATP content, glutathione (GSH) levels, albumin secretion and urea synthesis. Similar concentration-dependent cytotoxicity profiles (AC50=8.4 ± 2.4mM for GSH depletion and 14.17 ± 3.5mM for urea synthesis inhibition) were obtained over the course of the 4-week study. Addition of 200μM L-buthionine (S, R)-sulfoximine (BSO), an inhibitor of GSH synthesis, or 10μM dexamethasone (DEX), an inducer of rat CYP3A1/2, to rat MPCCs potentiated APAP-induced hepatotoxicity in these cultures irrespective of culture age (over 4 weeks). These findings are consistent with the known *in vivo* mechanisms of APAP toxicity in rats. In conclusion, rat MPCCs provided reproducible APAP-induced cell cytotoxicity profiles over a 4 week period and can be used to assess the effects of chronic exposure to bioactivated compounds. The toxicity profiles of selected bioactivated compounds are also reported here.

PS 1043 Upregulation of CYP3A4 and CYP1A1/2 Activities in Huh-7 Human Hepatoma Cells with DMSO and Use of These Induced Cells to Evaluate CYP Inhibition by Botanical Extracts and Their Components

Y. Liu[1], S. Pugh Bishop[1, 2] and T. J. Flynn[1]. [1]*Food and Drug Administration, Laurel, MD and* [2]*Oak Ridge Institute for Science and Education, Oak Ridge, TN.*

Liver metabolic enzyme inhibition and induction are the leading causes for severe drug-drug and drug-dietary supplement interactions which may result in increased toxicity or loss of treatment efficacy. *In vitro* cell line-based models are needed as an alternative to the "gold standard" primary hepatocytes, which are expensive and may exhibit problematic batch-to-batch variability. In the current study, human hepatoma Huh7 cells were treated with 1% dimethyl sulfoxide (DMSO) for two weeks after reaching confluence. Basal gene expression and enzyme activity levels of cytochrome P450 1A1/2 and 3A4 were compared between DMSO-treated and non-treated Huh7 cells cultured in parallel. Real-time PCR analysis revealed that DMSO treatment up-regulated gene expression for CYP1A1, CYP1A2, and CYP3A4 by 2.3 to 3.0 fold. Additionally, CYP1A2 and 3A4 activity (measured by specific luminescence assays) was 4.5 to 5.0 times higher in DMSO-treated Huh7 cells versus non-treated cells. Finally, the cell-based system was used to investigate the CYP3A4 inhibition by both whole *Psoralea corylifolia* extract and its major characteristic phytochemical components psoralen and isopsoralen. Psoralen and isopsoralen (1 μM to 50 μM), as well as *Psoralea corylifolia* extract (5 μg/mL to 20 μg/mL), inhibited CYP3A4 activity in a dose-dependent manner. No cytotoxicity was observed at these concentrations. In conclusion, Huh7 cells treated with 1% DMSO differentiate into a metabolically competent cell line, especially with regards to basal CYP1A1/2 and CYP3A4, which can be useful in studying the effects of botanicals and related pharmacological compounds on CYP1A1/2 and CYP3A4 function.

PS 1044 Evaluation of Hepatotoxic Effects of Acetaminophen and Arsanilic Acid on the Human Adipose Tissue-Derived Hepatocytes

H. Yi, M. Kwon, Y. Park, B. So and H. Kang. *Veterinary Drugs and Biologics Division, Animal and Plant Quarantine Agency, Anyang City, Gyeonggi-do, Republic of Korea.*

Hepatocyte-like cells (HLCs) derived from human adipose-derived stem cells (hADSC) could provide availability as *in vitro* hepatotoxicity model. In this study, we improved the differentiation strategy of hADSCs into HLCs by shortening the period of differentiation and evaluated the effect of acetaminophen (AAP) and arsanilic Acid (Ars), on the differentiation of hADSCs to HLCs. hADSC was used for hepatogenic differentiation. At final differentiation day (day 13), enzyme activities (LDH, ALT, AST), expression of hepatocyte specific genes (ALB, AFP, CYP3A4, CK18, C/EBP) and CYP450 activity (CYP1A2, CYP3A4) were determined. 1 and 2.5mM of Ars and 5mM of AAP showed cytotoxicity. Enzymatic activity was not changed by Ars treatment. In AAP treated groups, LDH activity was increased dose-dependently, and AST activity was also increased by the treatment of 2.5mM and 5mM, and ALT activity was increased by 5mM AAP. In the Ars-treated groups, the expression of ALB was decreased by 0.25, 0.5 and 2.5mM treatment without showing dose-dependent manner. In the AAP-treated groups, the expressions of ALB and AFP were significantly decreased by all dose of AAP. The expression of CYP3A4 was decreased only by 5mM AAP compared to non-treated group. Interestingly, the expression of CK18 was increased by 5mM AAP. C/EBP expression was not different in all concentration of AAP. The activity of CYP1A2 in AAP increased in dose-dependent manner and CYP3A4 was decreased by 0.625mM of AAP. In the Ars treated groups, CYP1A2 activity was decreased and CYP3A4 activity was not significantly different from non-treated group. Conclusively, Ars decreased the expression of ALB and CYP1A2 activity whereas AAP increased activity of ALT, AST, LDH and decreased the expression of

ALB, AFP and CYP3A4. We suggest that HLCs differentiated from hADSCs can be used as *in vitro* hepatotoxicity test model in drug development in that this model recapitulates the hepatic differentiation process *in vivo*.

PS 1045 Human Induced Pluripotent Stem Cell-Derived Hepatocytes As a Model to Investigate Mechanisms of Isoniazid IDILI

J. Lu[1], I. G. Metushi[2], J. Uetrecht[2], S. Einhorn[3], D. A. Mann[3], R. P. Hanzlik[4], P. B. Watkins[1] and E. LeCluyse[1]. [1]*The Hamner Institutes for Health Sciences, Durham, NC,* [2]*Department of Pharmacology and Toxicology, University of Toronto, Toronto, ON, Canada,* [3]*Cellular Dynamics International, Madison, WI and* [4]*Department of Medicinal Chemistry, The University of Kansas, Lawrence, KS.*

Isoniazid (INH), prescribed for tuberculosis, has been associated with idiosyncratic drug-induced liver injury (IDILI). It is speculated that genetic factors contribute to susceptibility towards INH hepatotoxicity. In the current study, induced pluripotent stem cell derived hepatocytes (iHC), which carry the donor's genetic information, were characterized for studying INH hepatotoxicity. Specific probe substrates demonstrated that Vmax/mg protein of CYP1A2, CYP2B6, CYP2C8, CYP2C9, CYP2C19, CYP2D6, CYP2E1, CYP3A4 in iHC were comparable to those reported in primary human hepatocytes (pHH). Both iHC and pHH demonstrated dose- and time-dependent INH-protein adduct formation and reduction in binding was observed after treating the cells with pan P450 inhibitors. Major bands of INH-adducted proteins in both cell types were qualitatively, but not quantitatively, similar. Proteomic analysis identified prohibitin-2 and macrophage navigation inhibitory factor as major proteins adducted by INH in iHC. INH, up to 10 mM, which is 100 fold higher than the Cmax in patients serum, does not cause ATP loss, lactate dehydrogenase (LDH) release or morphological changes in iHC. However, at non-cytotoxic concentrations, INH reduced the oxygen consumption rate as well as mitochondrial membrane potential and there was an increase in iHC release of microparticles (~0.1 micron) into the medium which may represent a mechanism for neoantigen and "danger signal" release. In summary, the iHC exhibited many CYP activities comparable to pHH. At non-cytotoxic concentrations, INH formed protein adducts, altered mitochondrial function and released microparticles in iHC cultures. We conclude that iHC are appropriate for study of INH DILI and preparation of cultures from INH DILI subjects is now underway.

PS 1046 Hepatotoxicants-Induced Cytokine Imbalance between Pro- and Anti-Inflammatory Cytokines: A Possible Role in Innate-Immune Mediated Drug-Induced Liver Injury

S. Goto, J. Deguchi, N. Nishio, T. Yamada, N. Nomura and H. Funabashi. *Dainippon Sumitomo Pharma Co., Ltd., Osaka, Japan.*

In recent years, innate-immune mediated drug-induced liver injury (DILI) has been focused as one of the mechanisms of idiosyncratic DILI. Kupffer cell (KC), a hepatic resident macrophage, is known to have a central role in innate-immune induction, and activation of KCs appears to modulate DILI through the release of pro- and anti-inflammatory mediators, such as cytokines and chemokines. In this study, we examined the fluctuations of cytokine levels by hepatotoxic compounds in isolated KCs and discussed the relation between the fluctuations and the potential of innate-immune mediated DILI. KCs, isolated from a Sprague-Dawley rat by density-gradient centrifugation and pre-cultured for 24 hours, were treated with hepatotoxic (acetaminophen, troglitazone, trovafloxacin) or non-hepatotoxic (pioglitazone, levofloxacin) compounds with or without LPS. After 24 hour treatment, cell culture supernatants and total RNA were collected and examined the release and mRNA expression of inflammatory mediators (TNF-alpha, IL-1beta, IL-6, IL-10). Cytokines released by cultured KCs were not affected by the hepatotoxicants without LPS. LPS alone induced the releases of above cytokines into culture supernatants and elevated their mRNA. Hepatotoxic compounds concentration-dependently suppressed the LPS-induced increases of IL-6 and IL-10 levels without the effects on TNF-alpha or IL-1beta. Hepatotoxic compounds also down-regulated the LPS-induced increase of IL-10 mRNA expression at which concentration there were no effects on the expression levels of TNF-alpha and IL-1beta. Neither release nor mRNA levels of IL-6 or IL-10 were affected in non-hepatotoxic compound treatment. Based on these results, it is suggested that the levels of some cytokines are affected by DILI related drugs with LPS stimulation, and imbalance between pro- and anti-inflammatory cytokines, induced by down-regulation of IL-6 or IL-10, is one of the key role for innate-immune mediated DILI.

PS 1047 Long-Term *In Vitro* Three-Dimensional Cocultured Human Liver Microtissues: Characterization and Implication for Drug-Induced Hepatotoxicity Studies

P. Gunness[1], S. Messner[1], L. Fredriksson[2], J. M. Kelm[1], W. Moritz[1] and M. Ingelman-Sundberg[2]. [1]*InSphero AG, Schlieren, ZH, Switzerland and* [2]*Department of Physiology and Pharmacology, Karolinska Institutet, Stockholm, Sweden.*

Drug-induced liver injury (DILI) remains the main cause of acute liver failure and post-market drug withdrawals. The well-documented limitations of pre-clinical in vivo animal studies and in vitro two-dimensional (2D) human hepatic models hinder the accurate prediction of DILI in humans. The objective of this study was to characterize long-term three-dimensional (3D) co-cultured human liver microtissues (MTs) to assess its suitability for use in drug-induced hepatotoxicity studies. 2D monolayer and 3D co-cultures of cryopreserved primary human hepatocytes and Kupffer cells were maintained for 2 (2D cultures) or 5 (MTs) weeks and systematically assessed for viability, liver-specific morphology, functionality and mRNA expression over the culture period. Results illustrated that the MTs had a longer (5 times) life span than the conventional 2D cultures and maintained a consistent diameter (250 – 300 μM) in the absence of a necrotic core over the culture period. CYP3A4, CD68, cytokeratin 7 and bile salt export pump proteins were expressed in the MTs. Albumin secretion was significantly higher in the MTs. Lipopolysaccharide stimulation induced interleukin-6 secretion in the MTs over the culture period. Transcriptomic analyses revealed differential regulation of 145 genes in the MTs versus the 2D cultures on culture day 7, including those involved in immune reactions, liver-specific functions and the processes of absorption, distribution, metabolism and excretion. The activities of CYPs 3A4, 1A2, 2B6, 2D6, 2A6 were higher (≥ 2-fold) in the MTs versus the 2D cultures on culture day 7, and was maintained only in the MTs thereafter. Taken all together, the results illustrate that the MTs maintain a differentiated liver-specific phenotype for at least 4 weeks and are a valuable in vitro model to study chronic and immune-mediated DILI in humans.

PS 1048 Studying the Anti-Inflammatory Role of Alkaline Phosphatase in the Liver *In Vitro*

B. J. Blaauboer[1], A. F. Pike[1], N. Kramer[1], W. Seinen[1, 2] and R. Brands[1, 2]. [1]*Institute for Risk Assessment Sciences, Utrecht University, Utrecht, Netherlands and* [2]*Alloksys Life Sciences BV, Bunnik, Netherlands.*

Alkaline phosphatase (AP) is a hydrolase enzyme regulating inflammatory immune responses by dephosphorylating lipopolysaccharides (LPS). AP is present in all tissues, but it is particularly concentrated in the liver. Upon a pro-inflammatory stimulus, AP is released from liver into the circulation, but is quickly used up. Clinically, it has been shown that open-heart surgery patients injected with a bolus and subsequent infusion of bovine AP during surgery produced more endogenous AP than patients who did not receive the bolus, thus reducing the risk of systemic inflammatory response syndrome (SIRS). The aim of this study is to investigate the effect of pro-inflammatory stimulants on alkaline phosphatase production by hepatocytes in vitro. Co-cultures of HepaRG (a human liver carcinoma cell line) and THP-1 (a monocytic cell line) were exposed to pro-inflammatory stimulants including lipopolysaccharides, nucleotides and hypoxia inducing agents. Results indicate that AP gene expression and release into the culture medium is induced upon high concentrations of LPS stimulation. We hypothesize that AP induction after LPS stimulation is an indirect effect and that the release of necrotic factors including ATP, ADP, and adenosine, through CD39 and 73 membrane receptors are responsible. An insight into the mechanism of AP induction should improve the search for drugs and techniques to prolong the residence time of AP in the bloodstream of patients with, for example, rheumatitis and SIRS.

PS 1050 Improvements of the ALI *In Vitro* testing Method for Inhalable Compounds

D. Ritter[1], J. Knebel[1] and C. Brodbeck[2]. [1]*Fraunhofer ITEM, Hannover, Germany and* [2]*Fraunhofer SCAI, Sankt Augustin, Germany.* Sponsor: C. Dasenbrock.

In the course of legislation (REACH) and ethical standards the testing of inhalable substances by appropriate in vitro methods is required. In this context, the air-liquid interphase (ALI-) method has emerged as the standard technique for exposure of cell lines, primary cells or co-cultures of the respiratory tract. A currently finished round-robin pre-validation study with model gases revealed the sensitivity and relevance of this method in principle. At the same time, several weak points in the concept concerning robustness, practicability, applicability and efficacy of the method regarding aerosol applications were discovered, which presently prevent an acceptance of this promising method for routine testing. This study aimed on

a fundamental improvement of the technology by focusing on two main aspects: (i) to re-design the workflow of the procedure for reduction of cellular stress and experimental complexity and (ii) to clearly improve the deposition of airborne particulate matter on the cellular surface during aerosol testing.
As a result, an advanced procedure including a novel type of exposure device was developed. It permits a uniform and smooth processing of cells leading to higher robustness, practicability and ease of use. Repeated dose exposures and less time and material consuming routine use are enabled. To increase the applicability of the ALI-method in aerosol testing, numerical CFD simulations were applied for the optimization of the stagnation flow setup. A combination of different particle deposition mechanisms such as sedimentation, diffusion and thermophoresis was balanced. First results of simulation and laboratory experiments showed a clearly increased deposition efficiency of particles from aerosols in the test system without observation of adverse effects on the exposed cells. Therefore, the improvements of the procedure so far seem promising to further enhance the applicability and acceptance of alternative methods in the study of inhaled substances significantly.

PS 1051 Use of Rat Precision-Cut Lung Slices for Long-Term Functional Evaluation

V. Neuhaus[1, 2], A. Braun[1, 2] and K. Sewald[1, 2]. [1]*Fraunhofer ITEM, Hannover, Germany and* [2]*Biomedical Research in Endstage and Obstructive Lung Disease Hannover (BREATH), Member of the German Centre for Lung Research (DZL), Hannover, Germany.* Sponsor: C. Dasenbrock.

The need of alternative methods for animal studies to investigate basic inflammatory mechanism and to test toxicological potential of new substances has been increased during the last decades. Precision-cut lung slices (PCLS) have been proven to be a valuable alternative for mammalian *in vivo* studies reflecting relevant factors of the respiratory tract in accordance with the three R principles. However PCLS have been used mostly for short-term cultivation (≤ 72h) only, which limits their use to certain questions. When it comes to analyses of slowly metabolized chemicals and to repeated application of compounds, the long-term cultivation of PCLS might be utterly important. In this study viability and maintenance of structure and functionality of long-term cultured (≥ 14 days) rat PCLS was investigated.
Rat PCLS were cultured for 15 days. Readout parameters for vitality (WST-1 assay) and functionality were assessed at different time periods. Ability to secret the pro-inflammatory cytokine Tumor necrosis factor alpha (TNF-α) upon lipopolysaccharide stimulation was used as marker for functionality. Additionally, methacholine-induced bronchoconstriction was measured at different time points. WST-1 assay showed more or less constant mitochondrial activity over time, though a slight decrease towards the end. The ability to secret TNF-α upon stimulation decreased significantly from day 1 till day 15. Bronchoconstriction was inducible at all times, though the sensitivity decreased ($EC50_{1d}$=8x10^{-8} M vs. $EC50_{15d}$=5x10^{-7} M). Also the maximum reduction of the initial airway area altered (1d=28.5% vs. 15d=56.5%).
Overall these results show that a general long-term cultivation of rat PCLS with a good preservation of the viability is feasible. However, the decreased functionality indicates that some cellular alterations have been taken place. This implies that the long-term cultivation of rat PCLS is feasible for bronchoconstriction studies and toxicity assays, but unusable yet for induced cytokine secretion.

PS 1052 Characterization of Aerosolized Zinc Oxide Exposures to Lung Epithelial-Macrophage Cocultures at the Air-Liquid Interface (ALI) Using the NACIVT System

S. P. Ng and D. B. Warheit. *DuPont Haskell Global Centers for Health and Environmental Sciences, Newark, DE.*

The successful implementation of animal-alternative, *in vitro* lung toxicity screening assays to replace *in vivo* inhalation animal testing is critical for product development. To optimize *in vitro* aerosol methodologies using the Nano-Aerosol Chamber for In Vitro Toxicology (NACIVT) system, rat lung epithelial L2 cells and NR8383 macrophages were co-cultured on an ALI system and exposed to fine-sized ZnO particles or room air at 25 mL/min in a temperature- and humidity-controlled deposition chamber. Exposure of the co-cultures (n=6/group) to generated air for 10, 30, or 60 minutes resulted in 8-16% decrease in viability (determined by XTT assays performed within 15 min post-exposure) compared to unexposed controls maintained in an incubator; LDH assay results revealed a 6.3% reduction in viability after 60-min air exposure. Aerosolized test atmospheres of ZnO particles were then generated in a glass cylindrical chamber using a jetmill device and entered the deposition chamber inlet through a connection tube. Source particle concentration and chamber deposition were monitored and analyzed gravimetrically. Multiple ZnO exposures were conducted with source particle concentrations ranging from 34-88 mg/m^3 (MMAD=0.85μm, GSD=2.5) and results indicated that deposition efficiencies (at 25-47%) were inversely proportional to the source particle concentrations. Co-cultures exposed to 27 ug/cm^2 ZnO particles for an hour resulted in 55 ± 4.4 % reduction in viability at 24-hr post-exposure (vs. air-exposed controls). In conclusion, these ongoing studies were developed to characterize the performance of the NACIVT system, i.e., to expose epithelial-macrophage co-cultures to airborne particulates. This system is designed to simulate aerosol particulate exposures to physiologically relevant lung cell-types *in vitro*, cultured at the ALI (relative to submerged cell culture systems) and represents an important step in facilitating the development of a reliable, high-throughput toxicity screening system.

PS 1053 A Coculture Model of the Air-Blood Barrier Reconstructed from Primary Human Cells

P. J. Hayden, G. Jackson, C. Mankus, J. Oldach, M. Child, M. Spratt and S. Ayehunie. *MatTek Corp., Ashland, MA.*

Reliable *in vitro* human models for investigating airway toxicity are needed to advance Tox21 efforts to replace animal testing with human-based model systems. *In vitro* airway models based on primary human cells have been described. However, models based on animal cells or human cell lines are still most commonly employed. In the present work, we describe development of an *in vitro* air-blood barrier model derived from primary human alveolar epithelial cells, pulmonary endothelial cells and monocyte-derived macrophages. The model was constructed by seeding endothelial cells on the underside of a microporous membrane. Alveolar epithelial cells were then cultured on the top surface of the membrane. The epithelial /endothelial co-culture was continued until barrier development occurred. Finally, monocyte derived macrophages were seeded onto the apical surface of the model. The triple cell co-culture model was characterized by histological and immunohistochemical methods and transmission electron microscopy. Barrier formation was assessed by measurement of transepithelial electrical resistance (TEER). Expression of drug transporter genes including ABC family efflux transporters BCRP, MRP1 and MRP2, and organic cation uptake transporters OCTN1, OCTN2 and OCT3 was demonstrated by RT-PCR. Macrophage purity was > 95% (CD14+) as assessed by flow cytometry. Confocal imaging demonstrated epithelial staining for cytokeratin 19 and carboxypeptidase M (alveolar type 1 cell markers), as well as tight junction proteins ZO-1 and occludin, while the endothelial cell layer stained positive for von Willebrand factor and e-cadherin. Celltracker dye was used to visualize macrophages on the luminal side of the alveolar cultures. The model developed peak TEER of > 1,000 Ω x cm2 within 9-12 days, and maintained TEER > 400 Ω x cm2 for up to 30 days. This new human model system shows promise as a useful tool for *in vitro* airway toxicity and drug-drug interaction investigations.

PS 1054 Systems Toxicology Approach for the Biological Impact Assessment of Conventional Cigarette Smoke Fractions and Aerosol Fractions from a Prototypic Modified Risk Tobacco Product on Normal Human Bronchial Epithelial Cells

U. Kogel[1], Y. Xiang[1], E. Dossin[1], P. Guy[1], C. Mathis[1], I. Gonzalez Suarez[1], G. Vuillaume[1], A. Hayes[2], J. Hoeng[1] and M. Peitsch[1]. [1]*Philip Morris International R&D, Neuchatel, Switzerland and* [2]*Spherix Consulting, Rockville, MD.*

Smoking causes serious fatal diseases such as lung cancer and chronic obstructive pulmonary disease. Bronchial epithelial cells as the first barrier against invading organisms and exposure to chemicals play a major role in the pathogenesis of these diseases.
In order to demonstrate the applicability of a systems toxicology approach to evaluate the risk associated with prototypic modified risk tobacco products (pMRTPs), normal human bronchial epithelial (NHBE) cells were exposed to an aqueous cigarette smoke fraction (smoke bubbled into phosphate-buffered saline/sbPBS) from the 3R4F reference cigarette at three non-toxic doses based on cell viability for either 4 or 24 hours. The pMRTP aerosol doses in sbPBS were matched to the highest concentrations of 3R4F in terms of puff/ml.
A static headspace GC/MS method focusing on volatile and semi-volatile constituents revealed that most of the levels of the 85 monitored constituents were lower in sbPBS of the pMRTP as compared to the 3R4F.
Whole genome transcriptomics analysis of NHBE cells demonstrated a dose-dependent increase in the number of differentially expressed genes for the 3R4F sbPBS exposure. Fewer genes were differentially expressed after exposure to sbPBS from the pMRTP. Analysis using computable biological network models showed the perturbation of biological processes related to cell stress and senescence after 4 hours of exposure to sbPBS from 3R4F, whereas after 24 hours of exposure the cell proliferation network was most perturbed. Exposure to the pMRTP resulted in much attenuated perturbation of biological networks.
In summary, we provide mechanistic insight of the biological impact on key cellular processes in NHBE cells upon sbPBS exposure, suggesting reduced biological network perturbation from exposure to pMRTP compared to 3R4F.

PS 1055 Multiplexed High-Content Screening Analysis Reveals Reduced Toxicity of a Prototypic Modified Risk Tobacco Product (pMRTP) As Compared to a Conventional Cigarette

I. Gonzalez Suarez[1], D. Marescotti[1], S. Acali[1], D. Goerdetier[1], S. Frentzel[1], C. Mathis[1], A. Hayes[2], J. Hoeng[1] and M. Peitsch[1]. [1]*Philip Morris International R&D, Philip Morris Products S.A., Neuchatel, Switzerland and* [2]*Spherix Consulting, Rockville, MD.*

Exposure to cigarette smoke (CS) causes lung toxicity and increases the risk of developing chronic obstructive pulmonary disease and cancer. Gaining insight into the cellular processes impacted upon exposure would be very useful to understand CS toxicity and aid the development of Modified Risk Tobacco Products (MRTP) products. The aim of the study was to investigate the biological impact of a smoke condensate from a prototype (p)-MRTP product, compared to the reference cigarette 3R4F. For this purpose, we performed a High Content Screening analysis on normal human bronchial epithelial cells. Thriteen multi-parametric indicators of cellular toxicity were measured over a range of condensate concentrations and at different time points.
Exposure to 3R4F resulted in increased cytotoxicity after 24h. Moreover, compared to vehicle control, 3R4F induced a dose-dependent increase in DNA damage at 4h and 24h. Genotoxicity was accompanied by cell growth arrest, consistent with activation of DNA repair, as well as dose-dependent responses on markers of cellular stress (ROS production, c-Jun activation and glutathione depletion), mitochondrial health (mitochondrial membrane potential and mitochondrial mass) and cellular integrity (cellular membrane permeability). Compared to 3R4F, exposure to a pMRTP product resulted in significant decreases in all tested endpoints at 4h and 24h and more than 90% decrease in cytotoxicity after 24h.
In summary, we provide mechanistic insight into the mode of action of CS on lung cells, and how, by lessening the biological impact on key cellular processes, exposure to a pMRTP reduces overall toxicity when compared to CS. Moreover, the ability to detect biological perturbations at sublethal doses strongly supports the use of HCS-based approaches for toxicological assessment.

PS 1056 Identification of Cytotoxic Chemicals in Thirdhand Smoke

V. Bahl[1], S. Schick[2], M. Sleiman[3] and P. Talbot[1]. [1]*Cell Biology and Neuroscience, University of California Riverside, Riverside, CA,* [2]*Department of Medicine, University of California San Fransisco, San Fransisco, CA and* [3]*Indoor Environment Group, Lawrence Berkeley National Laboratory, Berkeley, CA.*

Little information is available on the health effects of thirdhand smoke (THS). Our work evaluates the effect of THS on mouse neural stem cells, an *in vitro* model for neonatal brain. Cytotoxicity was studied using the MTT assay which evaluates conversion of a tetrazolium salt to a colored formazan by mitochondrial reductases. Terry cloth exposed to cigarette smoke for 110 hours over 1 year was stored at room temperature to allow aging of THS, and extracts were prepared after different times of aging. THS aged for 11 months caused complete cell death in the MTT assay at the highest dose and 50% cell death at the 30% dose. Cytotoxicity was lost when THS was aged for an additional 5 months. Another sample of terry cloth was exposed to cigarette smoke for 19.5 hours over 1 month. The THS extract obtained immediately after the smoking period caused 50% cell death at the highest dose, but lost its activity when aged for an additional 45 days. This shows that cytotoxicity of THS is lost with aging. The decrease in cytotoxicity could be due to loss of volatile organic chemicals (VOC) in cigarette smoke or degradation of chemicals. VOC in THS were identified using Thermal Desorption Gas Chromatography-Mass Spectrometry and authentic standards were tested to identify the cytotoxic VOC. Of the 20 chemicals tested, only 2,5-dimethylfuran (2',5'-DMF) and acrolein were cytotoxic causing complete cell death at a 10-3M dose. Combinations of VOC were not cytotoxic. Due to their high volatility, an additional trial was performed with each VOC being replaced at 4 hour intervals for 48 hours. Results were not affected except for 2,5'-DMF which had increased potency in this experiment causing 50% cell death at 10-4M dose. Results show that 2',5'-DMF and acrolein contributed to the cytotoxicity THS extracted from terry cloth.

PS 1057 Prevalidation of the *Ex Vivo* Model PCLS for the Prediction of Acute Inhalation Toxicity

K. Sewald[1], A. Hess[2], L. Lauenstein[1], X. Schneider[3], S. Vogel[2], M. Steinfath[4], R. Pirow[4], M. Liebsch[4], S. Kolle[2], L. Ma-Hock[2], R. Landsiedel[2], C. Martin[3] and A. Braun[1]. [1]*Fraunhofer ITEM, Hannover, Germany,* [2]*BASF SE, Ludwigshafen, Germany,* [3]*RWTH Aachen, Aachen, Germany and* [4]*BfR ZEBET, Berlin, Germany.*

In acute inhalation toxicity studies, animals inhale substances at given concentrations. Without additional information, it is difficult to estimate the appropriate starting concentration for *in vivo* inhalation studies. The goal of this BMBF-funded project was the standardization and pre-validation of precision cut lung slices (PCLS) as a suitable *ex vivo* alternative approach to reduce animal numbers used in inhalation toxicology. The project was conducted in three independent laboratories (Fraunhofer ITEM, BASF SE, RWTH Aachen). BfR provided support in biostatistics.
In all participating laboratories, rat PCLS were prepared and exposed to 20 substances under standard submerged culture conditions for 1 hour. Toxicity was assessed by measurement of released lactate dehydrogenase (LDH assay) and mitochondrial activity (WST-1 assay) after 23 hours post-incubation. In addition, protein content and IL-1α were measured. For all endpoints a sigmoid dose-response model was fitted to the data and IC50 values were calculated.
This study shows the final results for all 20 chemicals. More than 900 dose-response curves were fitted and analysed. Log10[IC50 (μM)] obtained for all assay endpoints showed best intra-laboratory consistency for the data obtained by WST-1 and BCA assays. While WST-1 and LDH indicated toxic effects for majority of the substances, only few of the substances induced increase in IL-1α. The reproducibility within the participating laboratories appeared to have acceptably low between-laboratory variations for WST-1 and BCA assay. The results show (i) that the test protocol used in this study is adequately transferable for practical use and (ii) that the tissue model using the WST-1 endpoint is reliable. Binary prediction model showed promising results.

PS 1058 Quantification of Neuron Maturation and Neurite Outgrowth *In Vitro* Using Human Neural Progenitor Cells

X. Wu[1, 2], E. Jordan[2], J. Donnell[4], J. Chilton[3] and S. Stice[2, 1, 3]. [1]*UGA ITP, Athens, GA,* [2]*Animal and Dairy Science, The University of Georgia, Athens, GA,* [3]*ArunA Biomedical, Inc, Athens, GA and* [4]*Infectious Disease, The University of Georgia, Athens, GA.*

Human embryonic stem cells based developmental neural toxicity (DNT) assays mimic neuron development in vitro and have become an alternative to expensive and time consuming animal DNT models. Previously using human embryonic stem cell derived neuronal cells, an in vitro human neural culture system assay for neurite extension/recovery has been employed as a DNT assay. Our objective was to mimic in vivo neural tube development starting with proliferative neural progenitor (NP) cells for high content image screening in 96-well plates and to characterize the time point for neurite extension and NP cell transition to post mitotic neurons. In our lab we have generated differentiated neurons from NP cells without basic fibroblast growth factor (bFGF) but with leukemia inhibitory factor (LIF) in 2 weeks. During differentiation, Bis 1 dose solutions were applied to the cells 6 h after plating for 2 weeks and then immunostained cell cultures in 96 well plates were loaded into a Cellomics ArrayScan VTI HCS reader high-content imaging system for automated image acquisition and morphometric analyses. Here our results show that expression of post mitotic neuronal cell marker HuC/D increased from 3.4 % at day 0 to 63.5 % by 2 weeks but did not significantly increase at later times. Thus we used this period of time in a multiplex assay to determine the effects of Bis1, a known neural toxicant on neurite outgrowth and maturation to HuC/D positive neural cells. Bis1 inhibited neurite extension in a dose dependent manner starting at 0.1mm without significantly affecting neuron maturation over the 2 weeks. We have developed a multiplex high content assay to determine the effects of toxicant in cells representative of the developing human neural tube and for the first time demonstrated that Bis1 specifically affects neurite outgrowth at lower concentrations than acute neurite recovery assays.

PS 1059 An Analysis of the Toxicity of Ximelagatran Using a Combination of *In Vitro* and *In Silico* Methods

A. Khanna, S. Das, R. Kumar, D. Srivastava, S. Louha, K. Rajendran, B. Thota, D. Raman, N. Mandyam, N. Rajeswara, S. Raghavan and K. Subramanian. *Strand Life Sciences, Bangalore, India.*

Hepatotoxicity associated with increase in liver enzymes has been observed on long term (>35 days) treatment with Ximelagatran, an oral thrombin inhibitor causing the drug to be withdrawn from the market. We used a combination of in vitro and in silico methods to understand the mechanisms underlying its toxic behaviour.
We first tested Ximelagatran in a series of in vitro assays designed to understand its dose-dependent impact upon key pathways in HepG2 cells and derived a dose-relationship for each of them. The in vitro treatment was performed for 72 hours allowing us to build a robust relationship between drug exposure and inhibitory effects on key liver enzymes and transporters. We then simulated a virtual clinical trial using the pharmacokinetic data as input into our in silico model of liver metabolism assuming the tissue drug concentration of the drug to be higher than the plasma concentration, since the volume of distribution is high.

Our simulations indicate that the drug has an impact on mitochondrial function by affecting multiple targets that eventually lead to depletion of cellular energy and production of reactive oxygen species. We hypothesize that this is due inhibition of mitochondrial energy transport. Furthermore, these effects are exposure-dependent leading eventually to depletion of cellular GSH and hepatocellular necrosis. Our simulations predict that these effects will manifest after 30 days of exposure in vivo and hence not be detectable in acute exposure models.
This study proves the utility of combining in vitro and in silico methods to predict and understand mechanisms of in vivo toxicity that can manifest over longer periods of exposure.

PS 1060 Evaluation of *In Vitro* Cardiac Electrophysiological Assessments on the ACEA xCELLigence and Axion Maestro Platforms

M. A. Kauss, H. Uppal and D. L. Misner. *Safety Assessment, Genentech, South San Francisco, CA.*

Introduction: Cardiotoxicity liabilities persist as a major cause of pre-clinical and clinical drug attrition today. Recent advancements in both biological models and electrophysiological technologies allow for faster and longer-term in vitro methodologies to assess beat rate and functional alterations. We sought out to utilize label-free, electrode-based, high throughput platforms to detect cardiomyocyte beating and functionality.
Methods: Both the xCELLigence from ACEA and the Axion Maestro systems are label-free, electrode-based, high throughput platforms used to detect in vitro cardiomyocyte beating and functionality through detection of impedance and voltage, respectively. To evaluate each system, we used a set of four potent anti-cancer molecules that had previously shown significant effects on cell viability (IC50s under 10nM), along with one structurally similar but biologically inactive molecule as a negative control, and then determined the effects on human stem-cell derived cardiomyocytes, both functionally and electrophysiologically.
Results: Both platforms were able to accommodate the multiple-day experiments required to detect significant changes in beating over time. In these time course studies, both systems showed that the most toxic doses had dramatic effects on cardiomyocyte functionality, ultimately stopping beat rate entirely, and doses closer to the IC50s had more intermediate effects of reduced beat rate and amplitude. In contrast, inactive molecules were benign, demonstrating specificity of the compounds' effect.
Conclusions: Measurements from both systems were sensitive enough to detect on-target, time dependent and mechanism-specific responses. Additionally, the Maestro detected spike slope, as well as T wave position, which allowed for assessment of repolarization periods ("QT intervals"), which helped to further discriminate the mechanisms of functional toxicity versus viability effects across molecules.

PS 1061 Preclinical Profiling and Comparison to a Human Response Database of an *In Vitro* Cynomolgus Macaque Vascular System As a Nonhuman Primate Surrogate

M. Simmers[1], R. Feaver[1], B. Cole[1], A. W. Pryor[1], J. R. Turk[2], D. Manka[1], B. R. Wamhoff[1], C. W. Qualls[2] and B. Blackman[1]. [1]*HemoShear LLC, Charlottesville, VA and* [2]*Amgen Inc., Thousand Oaks, CA.* Sponsor: A. Dash.

The cynomolgus macaque (CYNO) can be critical for de-risking and validating preclinical candidates for on- or off-target vascular responses. However, it is often difficult to translate mechanism of action studies from CYNO to humans. Previously we established a human primary vascular endothelial (EC) and smooth muscle cell (SMC) co-culture system, which recapitulates hemodynamic forces and restores cell biology and responsiveness to drugs at physiologically relevant levels. From this, we generated a predictive human response database (HRDB) comprising responses to >120 clinically relevant drugs, including atorvastatin (AS), simvastatin (SS), cerivastatin (CS) and rosuvastatin (RS). In the current study, we established a co-culture system with primary ECs and SMCs from CYNO arteries and exposed them to hemodynamics captured directly from CYNO arteries, inflammatory stimuli, and four different statins. Using RNAseq transcriptomics we profiled responses observed in the CYNO co-culture system and compared this to the HRDB. As in the HRDB, the expression of CYNO vascular genes (KLF-2, KLF-4, eNOS) that serve an atheroprotective function was significantly increased by healthy regional hemodynamics compared to atheroprone hemodynamics. The addition of advanced inflammatory conditions dramatically increased the expression of genes associated with oxidative damage (SOD2) and inflammation (MCP-1, IL-8) in both the CYNO system and the HRDB. Treatment with 3 out of 4 statins (AT, SS, CS) restored KLF-2 and KLF-4 under advanced inflammatory conditions; the exception was RS, which failed to restore these protective genes. A transcriptomic analysis will be presented comparing and contrasting the responses to statins of the human and CYNO systems. In summary, the CYNO vascular system described here mirrors many well-known responses of the human vascular system, and should provide a valuable preclinical tool for understanding mechanisms of action.

PS 1062 The Use of the SHE Cell Transformation Assay for the Safety and Risk Assessment of Compounds under the EU REACH Regulation

A. Heppenheimer and A. H. Poth. *Alternative and Genetic Toxicology, Harlan Cytotest Cell Research GmbH, Rossdorf, Germany.*

The 2-year bioassay is the standard method for carcinogen detection which is time and resource intensive. Many short-term tests, especially genotoxicity tests have been developed to aid in identification of potential carcinogens. The SHE cell transformation assay is simulating the process of animal two-stage carcinogenesis and is suited to detect a carcinogenic potential of test compounds vitro including genotoxic and non-genotoxic mechanisms. For mechanistic investigations of Berrylium (first phase of REACH), three different genotoxicity tests (Ames-, Mammalian Gene Mutation- and Chromosomal aberration test) together with the SHE cell transformation assay were carried out. Due to the insolubility of the metal powder and the metal alloy, these studies were conducted on extracts. No genotoxic effects where obtained with both extracts in the genotoxicity assays performed. However, in the SHE cell transformation assay dose-dependent increases in morphologically transformed colonies were obtained both with the metal alloy as well as with the metal powder, which indicates a non genotoxic mechanism of the metal powder and the alloy.
The SHE cell transformation was also carried out on a compound (first phase of REACH) with a structural alert for carcinogenicity (pararosaniline derivative). A significant dose-dependent increase in morphologically transformed colonies was obtained with the pararosaniline derivative indicating the usage of in vitro data to demonstrate similarities across a chemical category (read-across).
Our data indicate that the SHE cell transformation assay in combination with other information such as genotoxicity data, structure activity analysis, in vivo toxicity data and pharmaco-/toxicokinetic information can facilitate a relatively comprehensive assessment of a carcinogenic potential of a chemical.

PS 1062a Adverse Outcome Pathway for Embryonic Vascular Disruption and Alternative Methods to Identify Chemical Vascular Disruptors during Development

T. L. Tal[1], N. Kleinstreuer[2], P. Harris[3], J. Olin[1], A. Palekar[1], T. Toimela[4], R. Sarkanen[4], T. Heinonen[4], T. B. Knudsen[5] and S. Padilla[1]. [1]*ISTD, U.S. EPA, RTP, NC,* [2]*ILS, Inc./NICETUM, RTP, NC,* [3]*GED, U.S. EPA, Gulf Breeze, FL,* [4]*FICAM, University of Tampere, Tampere, Finland and* [5]*NCCT, U.S. EPA, RTP, NC.*

Chemically induced vascular toxicity during embryonic development can result in a wide range of adverse prenatal outcomes. We constructed an embryonic vascular disruption adverse outcome pathway (AOP) based on molecular initiating events corresponding to genetic models with phenotypic evidence of abnormal embryonic vascular development in the Mouse Genome Informatics Database. ToxCast high throughput screening data for 25 assays mapping to targets in the AOP were used to prioritize >1000 chemicals for their potential to disrupt vascular development. A subset of 38 predicted vascular disrupting chemicals (pVDCs) or non-pVDCs were selected for targeted testing in zebrafish (*D. rerio*). To test computational predictions, TG(flk1:GFP) zebrafish embryos were used to visualize and quantify blood vessel formation during development. Manual and automated methods of vessel quantification were developed, and the assay was evaluated with anti-angiogenic reference compounds PTK787 and AG1478, small molecule inhibitors of VEGFR2 and EGFR, respectively. The functional consequence of developmental vascular toxicity was assessed in larval and juvenile zebrafish. The assay was used to test the effects of 38 pVDCs and non-pVDCs including pesticides, flame retardants, and endocrine active compounds. The test chemicals were also evaluated in a functional angiogenesis assay comprised of a human endothelial cell and fibroblast co-culture system. Chemical rankings were well correlated among the predictive signature and zebrafish and *in vitro* tubulogenesis assays. Taken together, the zebrafish assay meets a critical need for an *in vivo* platform that can assess predictions generated by computational models of developmental vascular toxicity. This abstract does not necessarily reflect EPA policy.

PS 1062b Mechanism of Cadmium-Induced Tight Junction Disruption in an *In Vitro* Human Airway Air-Liquid Interface Tissue Model

X. Cao[1], H. Lin[1], L. Muskhelishvili[2], J. R. Latendresse[2], P. Richter[3] and R. H. Heflich[1]. [1]*DGMT, FDA/NCTR, Jefferson, AR,* [2]*TPA, Jefferson, AR and* [3]*FDA/CTP, Silver Spring, MD.*

Prolonged exposure to cadmium (Cd) in cigarette smoke has been associated with adverse health effects involving damage to pulmonary and cardiovascular tissue. Cd is known to induce oxidative stress, inhibit DNA repair, and interfere with essential metals. A recent study with Calu-3 cells also described its ability to disrupt tight junctions (TJs), possibly by a direct effect on adherens junction proteins. Herein, we report a novel mechanism of Cd-mediated TJ disruption in an in vitro human air-liquid-interface (ALI) airway tissue model derived from normal primary human bronchial epithelial cells. Cultures were exposed basolaterally to 10-100 μM CdCl2 for 16 h, which, while considerably higher than the ~15 nM Cd found in smokers' blood, was non-cytotoxic to ALI cultures based on the MTS assay. Treatment with 100 μM CdCl2 resulted in the collapse of barrier function as demonstrated by Trans-Epithelial Electrical Resistance (TEER), immunofluorescence staining with TJ markers, ZO-1 and occludin, and histopathology staining. PCR array analysis of human TJ genes indicated that CdCl2 exposure altered the expression of several groups of genes encoding proteins associated with TJ assembly. Immunoblotting of select junction interacting proteins demonstrated down-regulation of their expression, suggesting that disruption of junctional complexes essential for maintaining TJ integrity is a possible mechanism for Cd toxicity. Furthermore, inhibition of kinase signaling using specific inhibitors prevented the down-regulation of junction interacting proteins, inhibited the up-regulation of tyrosine phosphorylated occludin, and preserved the integrity of TJs. Our findings indicate that acute doses of Cd likely disrupt TJ integrity through kinase activation and occludin hyperphosphorylation. Whether or not Cd causes similar toxicity with chronic, low level exposures experienced by smokers remains to be determined.

PS 1062c Predicting Skin Sensitization Using 21st-Century Toxicology

N. Kleinstreuer[1], J. A. Strickland[1] and W. Casey[2]. [1]*ILS, Inc., Research Triangle Park, NC and* [2]*NIEHS/DNTP, DHHS/NIH, Research Triangle Park, NC.*

Allergic contact dermatitis (ACD) is an adverse health effect that develops following repeated exposure to skin sensitizing chemicals and products. To minimize the occurrence of ACD, regulatory authorities require testing, such as with the mouse local lymph node assay (LLNA), to identify potential skin sensitizers. The Organization for Economic Cooperation and Development (OECD) established an Adverse Outcome Pathway (AOP) for skin sensitization. In an effort to reduce or replace animal use, OECD is also pursuing the development of integrated testing strategies using novel in vitro and in silico approaches. The U.S. Tox21 and ToxCast projects include high-throughput screening (HTS) assays that map to key events in the skin sensitization AOP (e.g., oxidative stress, cytokine expression) and from which data on hundreds of potential skin sensitizers have been generated. We built a cross-validated random forest model using ToxCast Phase II data and a balanced training set of 60 chemicals. The model predicted LLNA results with 80% accuracy. The assays with highest variable importance in the random forest model included known AOP targets (e.g., Nrf2, T-cell proliferation) as well as targets outside of the current AOP (e.g., Coll III, PPAR, PXR, ER). Well-characterized AOPs like skin sensitization provide opportunities to use HTS data to develop efficient testing strategies that minimize the use of animals in regulatory testing.
This project was funded in whole or in part with Federal funds from the NIEHS, NIH under Contract No. N01-ES-35504.

PS 1062d A Cellular Impedance-Based Human iPSC-Cardiomyocyte Model to Screen for Cardiotoxicity

L. Guo[1], M. Furniss[1], J. Mussio[1], S. Eldridge[2], R. Parchment[1] and M. A. Davis[2]. [1]*Laboratory of Investigative Toxicology, Applied/Developmental Directorate, Leidos Biomedical Research, Inc. Frederick National Laboratory for Cancer Research, Frederick, MD and* [2]*DCTD, National Cancer Institute, Bethesda, MD.*

Cardiotoxicity is frequently a dose-limiting factor of chemotherapeutics. Human induced pluripotent stem-cell derived cardiomyocytes (hiPSC-CMs) may be useful for early detection of such liabilities in new therapy development. We applied cellular impedance (CI) technology that detects beating cardiomyocytes to measure cardiotoxicity endpoints in vitro. For model qualification, 40 drugs (including 26 anticancer agents) with well-defined clinical cardiotoxicity profiles were tested for effects on CI, ATP content and spontaneous contraction patterns. Chemotherapeutics known to induce ventricular dysfunction or congestive heart failure reduced CI and ATP dose-dependently. The receiver-operating characteristic (ROC) analysis revealed that a threshold of CI IC50 ≤ 30 μM for class determination resulted in an optimal in vitro-in vivo concordance of 85% that identified 16 of 17 positive and 18 of 23 negative cardiotoxicants, namely, 94% sensitivity and 78% specificity for prediction of structural cardiotoxicity. Incorporation of clinical exposure (Cmax) improved model performance; a cutoff of IC50/Cmax ratio ≤10 resulted in 90% concordance with 88% sensitivity and 91% specificity. Using ATP IC50 either alone or with Cmax was less predictive. Chemotherapeutics associated with clinical QT prolongation or arrhythmic liabilities reduced spontaneous beating rate and induced irregular beats frequently at the concentration relevant to clinical exposure. Signature irregular beats that are coupled to delayed repolarization were induced by nilotinib, sunitinib, dasatinib and lapatinib, which have black-box warnings for clinical QT prolongation, torsade de pointes or sudden cardiac death. Collectively, these results demonstrated the ability of a hiPSC-CM impedance model to identify structural and functional cardiac liabilities of chemotherapeutics.
Funded by NCI Contract # HHSN261200800001E.

PS 1062e Data Integration of Nonanimal Tests for the Development of a Test Battery to Predict Human Skin Sensitizing Potential

M. Miyazawa, O. Takenouchi, T. Nishijou, K. Saito, Y. Nukada and H. Sakaguchi. *Kao Corporation, Tochigi, Japan.* Sponsor: J. Avalos.

Recent changes in regulatory restrictions and social views against animal testing have accelerated development of reliable alternative tests for predicting skin sensitizing potential and potency of many chemicals. Lately, the approach of using a battery of in vitro tests instead of a single in vitro test has been suggested as a replacement for animal tests. In this study, we created a dataset of 66 test chemicals with human sensitizing potential data, human cell line activation test (h-CLAT), direct peptide reactivity assay (DPRA), and the in silico prediction system DEREK Nexus. DPRA, based on the covalent binding between proteins and haptens, and h-CLAT, emulating dendritic cell activation in the skin during sensitization, have been successfully pre-validated under ECVAM. For DEREK, 21 out of 66 chemicals have been used as the training dataset.
The results of these tests were converted into a score from 0 to 2, taking into account the integrated testing strategy concept. For the 66 test chemicals, the total battery score between 0 and 5 was calculated by the sum of individual scores. When we set the positive criteria as more than a score of 2, the score-based battery system provided an accuracy of 94%, sensitivity of 96%, and specificity of 85% for the human sensitizing potential. We next developed a tiered approach, weighing the predictive performance of the h-CLAT and DPRA. The h-CLAT indicated a higher sensitivity than the DPRA. Thus, we determined the h-CLAT was a good first step for a tiered approach. The tiered system provided an accuracy of 89%, sensitivity of 98%, and specificity of 60%. Both battery systems showed a higher sensitivity compared with the h-CLAT or DPRA alone. In summary, our data not only demonstrates that the h-CLAT could be part of a non-animal test battery together with the DPRA and other methods for the assessment of skin sensitization but also supports the practical utility of a tiered system where h-CLAT and DPRA are the first screening methods for skin sensitization.

PS 1062f Using the *Drosophila melanogaster* Genetics Reference Panel (DGRP) to Identify Toxicity Pathways for Airborne Chemicals

K. R. Tatum-Gibbs[1], P. Bushnell[2], J. M. McKee[2], P. Evansky[2], M. A. Higuchi[2], S. D. Hester[2], R. Judson[3], W. K. Boyes[2] and D. Reif[4]. [1]*ORISE, Research Triangle Park, NC,* [2]*NHEERL, US EPA, Research Triangle Park, NC,* [3]*NCCT, US EPA, Research Triangle Park, NC and* [4]*NC State University, Raleigh, NC.*

High-throughput screening assays are generating information regarding the toxicity of thousands of untested environmental chemicals. However, current methods are unable test volatile organic compounds (VOCs). In addition, mechanistic information is needed to link effects at molecular targets to adverse outcomes in whole organisms. This study is designed to address these issues using the *Drosophila* Genetic Reference Panel (DGRP), a set of genetically well-characterized strains of fruit flies. The goals of the project are to determine whether fruit flies can be used to screen VOCs for toxicity, and to identify adverse outcome pathways associated with acute exposure. The first phase of this study was to determine dose-effect functions using behavior endpoints for 3 VOCs that differ in their mode of action. In a second phase, behavioral response profiles across strains of DGRP flies will be determined at the EC20 of each VOC and mapped to genetic markers of effect. We used a hybrid line of flies derived from ~ 40 DGRP lines to identify an EC20 for each chemical. Individual flies were placed in 5mm dia. glass tubes and exposed for 4 hours at various concentrations of toluene vapor (n= 16/sex/dose); controls received air. Real-time locomotor activity was observed at 10-minute intervals for both sexes. Males were overall more active than females. Toluene decreased activity in both

sexes in a dose-dependent fashion, particularly in the second 2 hr of exposure. The sexes did not differ in their sensitivity to toluene: mean (95% CI) EC20 values were 764.9 (672.4 – 870.2) for males and 823.1 (578.5 – 1171.0) ppm for females. These results suggest that *Drosophila* can be used as viable organism to screen VOCs using motor activity; their utility for characterizing toxicity pathways remains to be determined. This abstract does not necessarily reflect U.S. EPA policy.

PS 1062g In-House Validation and Technology Transfer of the GARD Assay for Prediction of Sensitizing Compounds

E. L. Roggen[1], A. Forreryd[2], H. Johansson[2], F. Rydnert[2], A. Albrekt[2], C. A. Borrebaeck[2] and M. Lindstedt[2]. [1]*3Rs Management and Consulting, Lyngby, Denmark and* [2]*Immunotechnology, University of Lund, Lund, Sweden.*

Background: Allergic contact dermatitis is caused by an adverse immune response towards chemical haptens. The disease affects a significant proportion of the population, with increasing incidences, which leads to a substantial economic burden for society. New legislations on the registration and use of chemicals within chemical and cosmetic industries require development of alternative, high-throughput, in vitro assays for the prediction of sensitization, to replace current animal-based experiments.
Results: We have developed a human cell-based assay for the prediction of sensitizing chemicals, called Genomic Allergen Rapid Detection, GARD. By analyzing the transcriptome of the MUTZ-3 cell line after 24 h stimulation with well characterized skin sensitizing chemicals (N=20) and controls (N=20), we have identified a genomic biomarker signature with potent discriminatory ability. The prediction accuracy of the assay has been assessed in three separate in-house, blinded, validation studies (N=37), and is thus far 89% (sensitivity: 92%, specificity: 83%). In order to further adapt the assay to a high-throughput screening mode, we evaluated the performance of three non-array based platforms using a restricted set of probes from the biomarker signature. Results from the evaluation mimicked previous data from genome wide transcriptome analysis in terms of reproducibility and robustness while alternative platforms proved to be superior in terms of cost efficiency, increased sample throughput and simplified protocols.
Conclusions: The GARD assay was demonstrated to have potent ability to predict sensitization. By changing the technical platform for gene expression analysis, we could retain the robustness and discriminatory power of GARD and at the same time simplify assay procedures, reduce assay cost and increase sample throughput providing a first step towards formal validation and adaption of the assay for industrial screening of potential sensitizers.

PS 1062h Risk Assessment of Paracetamol-Induced Liver Toxicity Based on Human *In Vitro* Data

G. M. Groothuis[1], N. Mafirakureva[1], J. Proost[1], M. Jetten[2], J. Kleinjans[2], A. Lommen[3], A. Peijnenburg[3], G. Vredenburg[4], N. Vermeulen[4] and F. Russel[5]. [1]*Pharmacy, Division Pharmacokinetics, Toxicology & Targeting, University of Groningen, Groningen, Netherlands,* [2]*Toxicogenomics, Maastricht University, Maastricht, Netherlands,* [3]*Institute of Food Safety, Toxicology and Effect Analysis, Wageningen University, Wageningen, Netherlands,* [4]*Chemistry & Pharmaceutical Science, Free University Amsterdam, Amsterdam, Netherlands and* [5]*Pharmacology and Toxicology, Radboud University Medical Center, Nijmegen, Netherlands.*

Currently risk assessment is based on animal experiments with limited success. The aim of this study was to explore the feasibility to replace the use of animals in risk assessment for drug-induced liver injury, by hazard identification and kinetic modeling based on human in vitro data for metabolism and toxicity. Paracetamol was used as model compound. Human hepatocytes were used to elucidate the toxic mechanisms by transcriptomics and metabolite formation. Time- and dose-dependent toxicant exposure of the human liver was modeled with a mechanism-based physiology-based toxicokinetic (PBTK) model (Simcyp®) and time and concentration-dependent metabolite production and exposure of the hepatocytes to the toxic reactive metabolite was modeled with an in vitro biokinetic model using experimentally derived and literature data on metabolism. Plasma concentration profiles were adequately modeled and the effect of individual variability in metabolism was assessed. Phase 2 metabolism as observed in human hepatocytes was well predicted by the biokinetic model. However the rate of phase 1 metabolism was over predicted in both models. Pathway analysis learned that oxidative phosphorylation, drug metabolism and immune response were consistently regulated, suggesting that adverse effects of paracetamol are related to oxidative stress and immune dysfunction. The results indicate the feasibility of in vitro-based risk assessment of xenobiotics for the human population without the use of animals taking into account the individual variation in drug metabolism. For future refinement more data on metabolizing enzyme and transporter protein abundance is required.

PS 1062i Human Brain Endothelial Cells Exposed to PCB Congener 126 Show Increased Angiogenic Response in the 3D Cell Model

J. K. Das and Q. H. Felty. *Environmental & Occupational Health, Florida International University, Miami, FL.*

Cerebral microvascular endothelial cells have been reported to serve as a vascular niche for the recruitment of neural stem cells, regulation of breast tumor metastasis to the brain, and promote the self-renewal of cancer stem like cells in gliobastoma multiforme (GBM). We previously reported the effect of the noncoplanar PCB153 on human brain endothelial cell line hCMEC/D3. PCB153 exposed hCMEC showed a significant increase in stem cell markers CD34, CD133, and VEGFR-3. Exposure to PCBs may severely compromise normal function and lead to increased level of stem cell markers that participate in the development and promotion of brain tumors. We tested our hypothesis using in vitro 3D endothelial spheroid cell model that may serve as a rapid and cost-effective alternative to animal testing. The goal of the current study was to develop a 3D in vitro model to evaluate the effects of another PCB congener 126. PCB126 belongs to the coplanar dioxin-like group of PCBs that act through an aryl hydrocarbon receptor (AhR) mechanism. We show that PCB126 [100ng/ml] significantly increased the size of 3D endothelial spheroids over a 48h time period in the ID3 endothelial cell clone. MTT assays confirmed spheroid cell viability and flow assisted cell sorting (FACS) showed significantly less apoptosis in spheroids exposed to PCB126. Both stem markers VEGFR3 and CD133 were significantly increased from PCB126 exposure as shown in FACS studies and Western blot. Our results indicate that PCB126 may contribute to brain tumor angiogenesis by enhancing VEGFR3 signaling. For instance, elevated tissue levels of the isoforms VEGFC and VEGFD have been shown in human brain and tumor derived endothelial cells receiving anti-VEGF therapy. Since these isoforms are known to contribute their effects via VEGFR3 signaling, our findings support the hypothesis that environmental pollutants may angiogenically activate the brain microvasculature and exacerbate brain cancer or other brain disorders through their effects on the neurovascular niche.

PS 1063 Profiling of Compound-Induced Modulation of ERalpha-Coregulator Interaction As a Means to Compare Bisphenol A Analogs

R. Houtman[1], R. van Beuningen[1], N. Bastiaensen[1], T. Khuc[2], B. Goodwin[2], C. T. Teng[3] and R. R. Tice[3]. [1]*PamGene International BV, Den Bosch, Netherlands,* [2]*NCAT, NIH, Rockville, MD and* [3]*DNTP, NIEHS, Research Triangle Park, NC.*

Bisphenol A (BPA) and its analogs (BPAF, BPS) are well-known endocrine disruptor compounds (EDCs). We have previously shown that BPA induces estrogen receptor (ERα) but not androgen receptor (AR) activation in luciferase reporter assays. BPA also represses androgen-induced reporter activity in transiently transfected CV-1 cells. Nuclear receptor (NR) target gene transcription levels are dictated by ligand-binding, altered receptor conformation and subsequently modulation of recruitment of coregulator proteins, which modify chromatin accessibility for RNA polymerase. The best-characterized NR-interaction surfaces of coregulators contain highly conserved helical LxxLL (NR-box, coactivators) or LXXXIXXXL (CoRNR-box, corepressors) motifs. To understand the co-regulator interaction with the BPA-bound ERα or AR, we applied MARCoNI which mimics NR-coregulator interaction in vitro. Crude lysate of U2OS cells transfected with EGFP-tagged full-length NR were incubated with a peptide array of 154 CoR- and NR-boxes. The latter serves as a sensor for NR conformation, and hence activity status as a function of ligand. To investigate and compare the mechanisms of action by which compounds modulate ERα activity we quantified the ERα binding profile of BPA, BPAF, BPS, 17-β-estradiol (E2, the natural ligand) or solvent (2% DMSO) only. Compound response profiles, i.e. compound-induced log-fold change of ERα binding, were subjected to hierarchical clustering and demonstrated clear differences between compounds and their ability to modify ERα conformation. All four compounds induce repulsion of a similar set of coregulators. ERα interaction with a second set of coregulators is enhanced by E2 and BPS (with partial efficacy), largely unaffected by BPA, and moderately decreased by BPAF.

PS 1064 Nonestrogenic Bisphenols: Black Swans or Pink Unicorns?

M. S. Maier and E. Weaver. *The Valspar Corporation, Pittsburgh, PA.*

Bisphenol A (BPA) is used to make resilient epoxy coatings for food cans. These coatings are required to protect food quality. Although science-based regulatory bodies, including the U.S. FDA and the European Food Safety Authority, conclude that BPA is safe for use in making food-contact coatings, the market has begun to de-select materials containing BPA because it is has very weak agonist

activity toward the estrogen receptor. After years of research, no polymers other than epoxies have been identified that are able to fulfill all integrity demands of light metal food packaging.
Alternate bisphenols that technically could be used to replace BPA in epoxy coatings include bisphenol F, S, M, B, AP and AF. Unfortunately, these and most other common bisphenols, like BPA, are weakly estrogenic. This fact has led some policy makers to believe that all potential BPA replacement bisphenols are estrogenic. Using drug-discovery techniques such as QSAR, followed by rigorous in vitro testing, it was possible to identify and verify that some bisphenols exhibit no estrogenicity whatsoever, and a subset of these non-estrogenic bisphenols can be used to make robust epoxy food can coatings.
Valspar identified 4,4'-methylenebis(2,6-di-tert-butylphenol), CASN 118-82-1, and 2,2'-methylenediphenol, CASN 2467-02-9, as likely to have no estrogenicity using a simple QSAR technique in ChemDraw® that measures the immutability of the methylene bridge angle at low temperature. Molecules selected in this way were negative in the yeast estrogen screen (YES) assay. Bisphenols that were negative in the YES assay, and from which epoxy coatings could be made, were further tested and found to be uniformly negative in the U2OS ER green fluorescent protein redistribution assay, the ER Calux® assay, and even in the low-specificity MCF-7 cell proliferation assay (EScreen).
It can be concluded that not all bisphenols are estrogenic. Furthermore, some of these non-estrogenic bisphenols can be used to make robust food-contact epoxy coatings with performance that is comparable to BPA-based polymers.

PS 1065 Interpreting Estrogen Screening Assays in the Context of Potency and Human Exposure Relative to Natural Exposures to Phytoestrogens

K. Wise[1], L. Aylward[2], S. M. Hays[3], C. R. Kirman[4] and R. A. Becker[5].
[1]American Chemistry Council, Washington, DC, [2]Summit Toxicology LLP, Falls Church, VA, [3]Summit Toxicology LLP, Lyons, CO, [4]Summit Toxicology LLP, Orange Village, OH and [5]American Chemistry Council, Washington, DC.

Indication of exposure to potentially endocrine active substances can be detected in urinary biomonitoring studies. While EPA and OECD have validated in vitro & in vivo screening assays to measure interaction of substances with estrogen, androgen & thyroid pathway components, to date, methods to contextualize such results in terms of potencies & actual human exposures are lacking. Although urinary concentrations of substances can be compared on a mass per volume basis, such comparisons are not biologically meaningful because a receptor response is dependent upon potency and the concentration of the active moiety at the receptor. To understand endocrine screening results in terms of potency & human exposure, we propose a method that entails 1) calculating a benchmark dose (BMD) for a response measured in an endocrine screen; 2) estimating the human urinary concentration (Biomonitoring Equivalent, BE) expected to correspond to this dose (BE_{BMD}); 3) deriving the Exposure:Activity Ratio (EAR) by comparing actual urinary values from human biomonitoring studies (e.g. NHANES) to the BE_{BMD} ; and 4) comparing the EAR for a substance to one for a reference chemical. Using OECD uterotrophic assay validation studies and NHANES results, we calculated EARs for genistein (EAR_{GEN}=6.6E-4), and bisphenol A (EAR_{BPA}=8.8E-7). GEN, a dietary phytoestrogen, is recommended as a reference to interpret the significance of an EAR for estrogenic response, and to calculate the Relative Endocrine Exposure Activity Quotient (REEAQ; defined as $EAR_{CMPND} \div EAR_{GEN}$). The $REEAQ_{BPA/GEN}$=1.34E-3, indicates the EAR (uterotrophic) for geometric mean GEN exposure is more than 700-fold greater than the EAR_{BPA} for typical BPA exposures in the US. Such methods may be applied to additional compounds & endocrine assays; substances with low EARs and low REEAQs may not warrant additional testing.

PS 1066 Adaptation of T47D-KBluc and MDA-kb2 to Screening and Comparison to Other Receptor Reporter Platforms

K. B. Paul[1, 2], D. L. Filer[1, 4], R. Judson[4], V. S. Wilson[3], K. Crofton[4], S. O. Simmons[2] and M. T. Martin[4]. *[1]Oak Ridge Institute for Science Education, Oak Ridge, TN, [2]Integrated Systems Toxicology Division, US EPA, Durham, NC, [3]Toxicity Assessment Division, US EPA, Durham, NC and [4]National Center for Computational Toxicology, US Environmental Protection Agency, Durham, NC.*

A concern in the use of high-throughput screening assays is a potential inability to detect low potency chemicals with assays that demonstrate less sensitive, or right-shifted, response profiles. This work tested the hypothesis that use of T47D-Kbluc estrogen receptor (ER) and MDA-kb2 (AR) androgen receptor transactivation assays, well-characterized and responsive to hormones at physiologically-relevant concentrations, will increase detection of low potency AR- and ER-active chemicals. First, we tested whether the T47D-KBluc and MDA-kb2 assays could be miniaturized to a 384-well format, and used quality metrics (controls, dynamic range, variability, Z') to evaluate this effort. The MDA-kb2 assay was miniaturized without shifts in quality metrics, but the T47D-KBluc assay was automated in 96-well plates to maintain dynamic range. Comparative data were generated for a 90-chemical training set with the T47D-KBluc and MDA-kb2 assays, in agonist and antagonist modes, to discern if they might yield different activity predictions compared to the ER BG1 Luc, ERα β-lactamase, and the AR β-lactamase assays. The ER reporter assays and AR reporter assays predicted similar positives in the agonist and antagonist modes, but using all three assays for ER increased predictive power. Further, the data suggest that though 17β-estradiol and dihydrotestosterone were more potent in the T47D-KBluc and MDA-kb2 assays, as expected, the potencies for chemicals active at micromolar concentrations were not uniformly left-shifted when compared to the other receptor reporter assays. Automated adaptation of the T47D-KBluc and MDA-kb2 assays provides an additional endocrine screening tool, and supports development of predictive models for estrogen and androgen activity using multiple assays. This abstract does not necessarily reflect U.S. EPA policy.

PS 1067 Estrogenic Activity of Aromatic Substances from Mineral Oil Used in Printing Inks

P. Tarnow[1], C. Hutzler[1], K. Schoen[1], T. Bovee[2], T. Tralau[1] and A. Luch[1].
[1]Product Safety, German Federal Institute for Risk Assessment, Berlin, Germany and [2]RIKILT, Wageningen, Netherlands. Sponsor: A. Haase.

Mineral oils (MO) used as ingredients for many printing inks are complex mixtures of hydrocarbons. Although migration of MO from paperboard food packaging made of recycled paper into food has been shown, the toxicological relevance of these findings is elusive. Therefore we investigated the estrogenic potential of mineral oil using different *in vitro* assays. Proliferative effects of MO in the estrogen responsive human breast cancer cell line MCF7 were assessed in the E-screen, and endogenous estrogen responsive gene expression was quantified by real-time PCR. Transactivation assays were performed in HeLa9903 containing the human estrogen receptor α (ERα) and an estrogen responsive element (ERE)-driven luciferase as well as in yeast containing ERα and an ERE-dependent green fluorescent protein. MO primarily consist of mineral oil saturated hydrocarbons (MOSH) and mineral oil aromatic hydrocarbons (MOAH). These two fractions were separated by preparative HPLC and also assessed in the bioassays. MO in a thousand fold dilution stimulated MCF7 proliferation but did not induce reporter gene expression neither in yeast nor in HeLa9903 cells. Furthermore, expression of the estrogen responsive genes PGR and TFF1 in MCF7 cells was induced after 24 h exposure to total MO. The estrogenic effects were derived from the MOAH fraction, as exposure of MCF7 cells to this fraction induced gene expression and increased proliferation. In conclusion estrogenic action of aromatic substances derived from MO could be shown *in vitro*.

PS 1068 Estrogenicity and Androgenicity Screening of 8 Individual PCB Sulfate Monoesters in Human Breast Cancer MCF-7 Cells

S. Flor, H. Lehmler and G. Ludewig. *Univ of Iowa, Iowa City, IA.*

Lower chlorinated PCBs undergo oxidative metabolism to hydroxylated PCBs which are important contributors to PCB toxicity. These metabolites are substrates of cytosolic phase II enzymes which produce PCB sulfates as a new class of metabolites. Because very little is known about the biological and metabolic disposition of this class of metabolites, 8 sulfate monoesters which are either derived from PCB3, a congener shown to be biotransformed to sulfate monoesters, or are derivatives of a paint-specific congener or from OH-congeners shown to interact with sulfotransferases (i.e. 2, 3, 2', 3' and 4'PCB3 sulfate, 4PCB11, 4PCB39, and 4PCB53 sulfate) and 4'-OH-PCB3 as positive control. These compounds were tested for estrogenic and anti-estrogenic, androgenic and anti-androgenic potential at concentrations from 100 μM to 1 pM in the E-and A-screen as well as evaluated for cytotoxicity. These screens are quantitative assays which identifies potential xeno-estrogens. Only 4'OH-PCB3 is highly cytotoxic, while the 4PCB53 and 3PCB3 sulfates are weakly cytotoxic. Regarding endocrine disruption, our data suggest that there is a structure-activity relationship, with the 4'OH-PCB3 (1 uM) and its sulfate ester (100 μM) as most active estrogenic compounds followed by 2'PCB3 sulfate, 4PCB39 and 4PCB53 sulfates (100 μM). The same compounds and 3PCB3 sulfate with lower concentrations also exhibited anti-estrogenic activity. 4'PCB3 sulfate is the most potent androgenic compound, visible at the highest concentration tested, followed by 3'PCB3 sulfate and 4PCB53 sulfate. Also weakly androgenic are 4PCB11 sulfate, 4PCB39 sulfate and 4'OH-PCB3. Anti-androgenicity was observed with 2'PCB3 and 3'PCB3 sulfates at very low concentrations. Endocrine-disrupting chemicals often display U-shaped or inverted U-shaped nonmonotonic dose-response curves. Similarly no classical dose-response

curves were seen in our experiments. These preliminary data suggest that these PCB sulfate monoester have very low cytotoxic potential in human breast cancer cells as well as very low potential to act as endocrine disrupting agent.

PS 1069 Pharmacophore Model of Natural Phytoestrogens Which Induce Estrogen Receptor Alpha/Beta Heterodimerization

C. Coriano[1,2], C. Sievers[3], J. Kolesar[4], J. Shull[1,2] and W. Xu[1,2]. [1]*Oncology, University of Wisconsin, Madison, WI,* [2]*Molecular & Environmental Toxicology, University of Wisconsin, Madison, WI,* [3]*Cellular & Molecular Pathology, University of Wisconsin, Madison, WI and* [4]*Pharmacy, University of Wisconsin, Madison, WI.*

Estrogen plays an important role in the normal development and growth of the mammary gland. The binding of 17β-estradiol (E2) and other estrogenic compounds to the estrogen receptor (ER) leads to its dimerization and consequent genomic transcription and cascade of biological activities. ERα and ERβ have been shown to exhibit a "Ying and Yang" relationship in regulating breast cancer cell growth: ERα promotes cell growth while ERβ inhibits it. At the receptor level, ERβ appears to negatively regulate the proliferative role of ERα through the formation of ERα/β heterodimers. The objective of this study is to identify natural estrogenic compounds which promote the formation of ERα/β heterodimers, thereby activating ERβ while dampening ERα activity, which might have a protective effect in breast cancer. We initially screened 37 phytoestrogenic compounds from four flavonoid subclasses in a two-step screening process that include activation of ER gene transcription using an ER-dependent reporter assay and dimerization using the Bioluminescent Resonance Energy Transfer (BRET) assay where 6 slightly selective ERα/β heterodimer inducing compounds were identified. In silico studies were then performed to identify the pharmacophore that confers ERα/β heterodimer specificity in order to design high affinity ligands. We have proposed to test the cancer preventive effects of compounds that induce the ERα/ERβ heterodimer in the E2-induced breast cancer model of ACI rats.

PS 1070 Disruption in the Hypothalamus Neonatally Exposed to P-Tert Octylphenol Is Essential for Induction of Early Occurrence of Persistent Estrus, a Feature of Delayed Effect in Rats

M. Yoshida[1], R. Ichimura[1,2], K. Inoue[1], G. Watanabe[2] and M. Takahashi[1]. [1]*Department of Pathology, National Institute of Health Sciences, Tokyo, Japan and* [2]*Veterinary Physiology, Tokyo University of Agriculture and Technology, Tokyo, Japan.*

Neonatal exposure to estrogenic compounds induces delayed effect characterized as early occurrence of persistent estrus (Takahashi et al., 2012), but its mechanism has not been undetermined. The delayed effect is a big concern for offspring toxicity because reproductive toxicity studies couldn't detect it. We investigated which organ, the hypothalamus or the ovary, is essential for the delayed effect of estrogenic compound. Female Donryu rats were treated with 100 mg/kg p-tert-octylphenol (OP) sc 3 times during 5 days after birth (PND5), which treatment is inducible delayed effect, and 8 times of the same manner as PND5 during 15 days (PND15) to induce typical androgenization. The bilateral ovaries in the PND5 or PND15 OP treated or the control groups were dissected at the 4-week of age, and transplanted into the subcutis of ovariectomized rats at the same age in each group. Estrous cyclicity were checked up to 17 weeks of age and compared to rats with intact ovaries in the corresponding groups. The transplanted ovaries were morphologically examined. In the control group, most of rats received the donated ovaries from control and all treated groups showed normal cycle within 4 weeks after the transplantation, and corpora lutea (CL) were observed in all donors' ovaries. In the PND5 group, normal cyclicity changed to persistent estrus 1.5 months after the transplantation in the rats donated the ovaries from control and PND5 groups, the status being similar to corresponding ovary-intact animals. In the PND15 group, all rats with and without the transplantation showed persistent estrus up to 8 weeks of age. Microscopically, few CL were observed. These results indicate that any disruption in the hypothalamus exposed to OP neonatally at delayed effect inducible dose plays an essential role for early occurrence of persistent estrus.

PS 1071 Pituitary Proliferation Is Affected by Bisphenol A Exposure, but Recovers upon Its Removal

K. Eckstrum[1], K. Brannick[1], W. Wang[2], J. A. Flaws[2] and L. Raetzman[1]. [1]*Molecular and Integrative Physiology, University of Illinois Urbana Champaign, Urbana, IL and* [2]*Comparative Biosciences, University of Illinois Urbana Champaign, Urbana, IL.*

Bisphenol A (BPA) impacts the hypothalamic-pituitary-gonadal (HPG) axis, affecting neuroendocrine differentiation, reproductive capacity, and puberty. Although the pituitary gland is a central component, little is known about its response to BPA exposure. We previously demonstrated that environmentally relevant BPA treatment during the embryonic period leads to increased pituitary proliferation and gonadotrope cell numbers in female mice. It is unknown whether the effects of prenatal exposure to BPA would cause persistent increases in progenitor proliferation or if the critical window of postnatal pituitary expansion is directly impacted by BPA treatment. Therefore, we formed two hypotheses. First, that embryonic treatment of BPA would have lasting effects into the early postnatal period. To test this, mice were dosed with 0.5 or 50μg/kg/day BPA from embryonic day 10.5 to postnatal day (PND)0 and collected at PND4. No differences were seen in proliferation or gonadotrope number between groups, indicating removal of BPA restored the pituitary to normal conditions. Second, we hypothesized that BPA would have a direct effect on the postnatal pituitary. To test this, we cultured intact PND0 pituitaries with 0.05 or 50 μg/ml of BPA, 10 nM 17β estradiol, or ethanol for 48 hours. QRT-PCR revealed that mki67 (a proliferation marker) decreased with both doses of BPA, however estradiol raised mki67 levels. Progesterone receptor (Pgr) mRNA, a known target of estrogen signaling, was raised in the presence of estradiol, but unchanged by BPA. Interestingly, levels of Esr1 were decreased with BPA treatment, but unaltered by estradiol. From these data, we conclude that BPA affects proliferation and gene expression in the postnatal pituitary directly in a manner dissimilar to estradiol. These studies also highlight that Influence of the HPG axis or time of dosing may be contributing to pituitary effects of BPA. Supported by P01 ES022848, R01 DK076647, T32 ES007326.

PS 1072 New Sites for Old Suspects: Endocrine Disrupting Chemicals Targeting Human Estrogen Receptor Nonligand Binding Sites

C. G. Katche[2], B. Asare[1] and R. V. Rajnarayanan[1]. [1]*Pharmacology and Toxicology, SUNY University at Buffalo, Buffalo, NY and* [2]*Phamaceutical Sciences, SUNY University at Buffalo, Buffalo, NY.* Sponsor: R. Rajnarayanan.

Estrogen receptors (ER) play a critical role in development of breast carcinoma. Estrogen activates ER by directly binding to its ligand binding domain and mediates a cascade of cellular signaling events that promote cell growth and proliferation. Upon activation, ER recruits co-activators which enable the transcriptional activity of ER at the target genes. Endocrine disrupting chemicals (EDC) including alkylphenols, bisphenols, diethylstibesterol (DES) binds directly to ER LBD and enable ER dimerization and estrogen response element (ERE) mediated transcription of target genes. While these EDCs have the required pharmacophore to induce agonist conformation of ER, many EDCs that are currently classified as weak estrogens produce considerable endocrine damage even at low exposure. Plasticizers, alkoxybisphenols and phthalate esters, do not share estrogen pharmacophore but are misclassified as compounds binding to ER-LBD. Here we report our integrated in silico and in vitro structure-activity analyses of phthalate esters and their ability to module ER-ERE based transactivtion by activing on a non-ligand binding site. Compounds were assessed for their ability to compete with fluorescent-labeled estradiol and FITC-tagged peptides binding to non-ligand binding sites using a fluorescence polarization based high throughput screen. Computational screening of library of 87,000 EDCs against pseudoreceptor-shape-based pharmacophores yielded a focused library of ER binding compounds. We identified 1870 chemicals bound to ER-LBD and 276 bound to a specific non-ligand binding site near the co-regulator binding site. Phthalate esters diethylhexylphthalate, monoethylhexylphthalate, dimethylphthalate, butylbenzylphthalate, dibutylphthalate and dioctylphthalate bound to this site with higher affinity than alkoxybisphenols.

PS 1073 Vitellogenin Gene Expression and Gonadal Alterations in Cichlids from a Man-Made Lake in Nigeria

A. O. Adeogun[1], S. D. Adeduntan[1], O. E. Ola-Davies[2] and O. A. Fagbohun[3].
[1]Department of Zoology, University of Ibadan, Ibadan, Nigeria, [2]Department of Veterinary Physiology, Biochemistry and Pharmacology, University of Ibadan, Ibadan, Nigeria and [3]Department of Veterinary Microbiology and Parasitology, University of Ibadan, Ibadan, Nigeria.

There is growing concern worldwide on the effect of endocrine disrupting chemicals (EDCs) on aquatic organisms and wildlife. Aquatic organisms are particularly vulnerable to exposure because their ecosystems act as sinks for a wide variety of pollutants. Vitellogenin expression, gonad histological alterations are amongst specific biomarkers for monitoring the effects of EDC's in fish. Vitellogenin expression in male, female and juvenile fish and gonad histopathological alterations were evaluated in Cichlids: *Tilapia zillii, T. guineensis, Sarotherodon melanotheron, S. galilaeus, Oreochromis niloticus, Hemichromis fasciatus* and *Chromidotilapia guentheri* from Eleiyele reservoir to assess endocrine disruption in fish.Vitellogenin-B2a (VTG-B2a) gene expression in the liver of fish was detected using RT-PCR. Intersex was observed in 33.3% of sampled fish of which 29.0% were adult and 71.0 % juvenile male fish. The highest occurrence of intersex was in *T. zillii* and histological appearance of intersex included the development of primary oocytes alongside maturing spermatocytes (juveniles)/matured spermatocytes within testicular tissue. A significant expression of Vtg-B2a gene was observed in all adult male and some juvenile male fish suggesting exposure to EDCs. VTG gene expression correlated with pathological presentation of intersex observed in adult/juvenile male fish. Further studies to quantify the level of VTG expression by RT-qPCR is on-going but available data indicate that Cichlids could be sentinel species for evaluating the presence of EDCs in lotic waters because of their commercial importance to the population structure of lakes. This is a first report of responsiveness to EDCs in a man-made lake in Nigeria.

PS 1074 Vitellogenin Expression and Steroid Hormone Levels As Biomarkers of Endocrine Disruption in Tilapias from Ogun River, Nigeria

O. R. Ibor[1], A. O. Adeogun[1], A. V. Chukwuka[1] and O. A. Fagbohun[2].
[1]Department of Zoology, University of Ibadan, Ibadan, Nigeria and [2]Department of Veterinary Microbiology and Parasitology, University of Ibadan, Ibadan, Nigeria.

The presence of vitellogenin (a female specific egg yolk precursor protein) in the liver and blood of male/juvenile oviparous vertebrates is widely used as an indicator of endocrine disruption. 426 Tilapias (*Oreochromis niloticus, Tilapia zillii, Tilapia guineensis, Sarotherodon melanotheron* and *Sarotherodon galileaus*) were collected from three sampling points reflecting different degrees of anthropogenic contamination and control along the length of Ogun River with the aim of investigating the existence of endocrine disruption in fish. Vitellogenin B2a gene (Vtg-B2a) expression was detected from the liver using Reverse Transcriptase Polymerase Chain Reaction (RT-PCR). The levels of some reproductive hormones (Luteinizing hormone (LH), Follicle stimulating hormones (FSH), Testosterone, Cholesterol and Oestrogen) were measured by Enzyme linked immunosorbent assay (ELISA). Significant expression of Vtg-B2a gene was detected in male and juvenile fish from polluted points of the river compared with the control where Vtg-B2a gene was not detected. Control fish showed the normal sex distinct six stages of gonad development for male and female fish respectively which reflected the gonochoristic nature of these species, while fish from polluted points along the river displayed occurrence of testis and ovaries existing in one fish. Significant decreases ($p<0.05$) in levels of Luteinizing hormone (LH), Follicle stimulating hormones (FSH), Testosterone and Cholesterol were also recorded in fish from polluted points of the river compared with the control. Significantly increases ($p<0.05$) in oestrogen levels were recorded in fish from polluted points compared with the control and this increase was 2 times higher in males (10.00±0.23 lU/L) compared with females (5.00±0.11 1U/L) indicating a disruption in the steroidal hormones signaling pathway. Our results represent the first indication of endocrine disruption in Tilapias from Ogun River.

PS 1075 Naringenin and 8-Prenylnaringenin Arrest Oocyte Maturation and *In Vitro* Embryo Development by Affecting the Cumulus-Oocyte Complex

K. Solak[1], R. R. Santos[1], B. A. Roelen[2], B. J. Blaauboer[1], M. Van den Berg[1] and M. B. van Duursen[1]. *[1]IRAS, Utrecht University, Utrecht, Netherlands and [2]Department of Farm Animal Health, Utrecht University, Utrecht, Netherlands.*

Granulosa cells in immediate contact with the oocyte are called the cumulus cells (CC). During oocyte maturation, cumulus cells change from a compact cell mass into a dispersed structure of cells, a process called cumulus expansion, and influence oocyte development in a paracrine fashion. In this study, potential effects of two flavanones naringenin (NAR) and 8-prenylnaringenin (8PN) were determined on porcine oocyte maturation and its intrinsic capacity to produce embryos after parthenogenic activation. Additionally, effects of NAR and 8PN on aromatase (CYP19) were determined in human KGN granulosa cells. Estradiol (E2; 3.12 μM) did not affect CC expansion, whereas naringenin (0.3, 1 and 3 μM) and 8-PN (1 and 3 μM) significantly decreased CC expansion up to 30%. Meiotic spindle formation was affected in oocytes e\xposed to E2, NAR and especially 8PN, indicating an effect on oocyte maturation. Upon parthenogenic stimulation, oocyte cleavage and blastocyst formation was decreased by NAR and, to a lesser extent, 8PN. Because granulosa cells are responsible for local estrogen formation during the preovulatory period, effects of NAR and 8PN on CYP19 gene expression and activity were investigated. In both primary pig CCs and human KGN cells, 8PN but not NAR caused a significant upregulation of CYP19 gene expression. However, 8PN completely inhibited CYP19 activity (IC50 value of 10 nM), while NAR induced CYP19 activity by 53% at 3 μM in KGN cells. KGN cell migration was reduced by 30% by 8PN but not NAR at 3 μM. Taken together, these data indicate that NAR and 8PN can cause an arrest in oocyte maturation and decrease of in vitro embryo production and/or development by affecting the cumulus-oocyte complex. Considering that oocyte maturation arrest is considered a cause of infertility, precautions are in place and high intake of these phytochemicals should better be avoided by women who are trying to conceive.

PS 1076 Effects of Resveratrol and Resveratrol Analogs on Steroidogenesis in Human Adrenocortical H295R Cells

A. Oskarsson[1], Å. Ohlsson Andersson[1], C. Spatafora[2] and C. Tringali[2].
[1]Department of Biomedical Sciences and Veterinary Public Health, Swedish University of Agricultural Sciences, Uppsala, Sweden and [2]Dipartimento di Scienze Chimiche, University of Catania, Catania, Italy.

Resveratrol (RSV, trans-3,5,4'-trihydroxystilbene) and piceatannol (PIC, 3,5,3',4'-tetrahydroxystilbene) are phytoalexins, present in grapes and wine and considered to have antiproliferative, antioxidative and antiinflammatory activity. Furthermore, RSV has been demonstrated to modulate androgen and estrogen receptors and exert an inhibitory effect on steroidogenesis in different cell types, which may be of potential therapeutic relevance to conditions associated with excessive androgen production, such as prostate cancer. However, oral bioavailability is low and resveratrol analogs have been synthetized in an attempt to improve beneficial effects. We have investigated the effects of RSV and PIC and the synthetic analogs 3,5,4'-triacetylresveratrol (RSVTA), 3,5-diacetylresveratrol (RSVTM) and 3,5,4'-trimethylresveratrol (RSTVM) on steroid hormone synthesis in the human adrenocortical cell line H295R, which expresses all enzymes required for secretion of adrenocortical and sex hormones. Cells were treated with 1-50 μM of test compounds for 24 hours and levels of progesterone, aldosterone, cortisol and sex steroids were determined by ELISA or RIA. Strong inhibitory effects were demonstrated on secretion of dehydroepiandrosterone (DHEA), testosterone and cortisol, while secretion of progesterone and aldosterone increased. Inhibition of CYP17A1 enzyme activity was demonstrated and could explain this steroid secretion pattern. Increased levels of estradiol were found after treatment of cells with RSV, PIC, RSVTA and RSVTM, but not RSVTM. Estradiol accumulation was found to result from inhibition of estrogen sulfate conjugation, catalyzed by SULT1E1. The effects on steroidogenesis were demonstrated at concentrations of resveratrol compounds well below those causing effects on cell proliferation. The reduced testosterone production may be of relevance in prostate cancer chemoprevention.

PS 1077 Orally Subchronic Exposure to Benzo[a]pyrene Alters Reproductive Hormone Profile

A. Jeng[1] and Y. Chen[2]. [1]*Old Dominion University, Norfolk, VA and* [2]*Department of Nuclear Medicine, Kaohsiung Medical University Chung-Ho Memorial Hospital, Kaohsiung, Taiwan.*

The objective of this study was to assess whether benzo(a)pyrene (B[a]P) alters reproductive hormones, which in turn leads to decreased spermatozoa quality and spermatogenic cell levels. Hsd: ICR (CD1) 10-week old males were orally exposed to B[a]P at 1, 10, 50, and 100 mg/kg/day of body weight for 30 and 60 days. At the end of the experiment, mice were anesthetized and reproductive tissues, i.e. testes, seminal vesicles, and epididymis, were collected. Spermatogenic cells and mature spermatozoa were recovered from the testes and cauda epididymis, respectively. Spermatozoa quality, including concentration, morphology, motility and viability, was examined. Testosterone, estradiol, follicle stimulating hormone (FSH), and luteinizing hormone (LH) levels in serum were determined using the Enzyme Immunoassay/Enzyme Linked Immunosorbent Assay (EIA/ELISA). Mice exposed to B[a]P at 50 mg/kg/day and 100 mg/kg/day for 30 days and 60 days exhibited a significantly decrease in serum testosterone and estradiol levels as compared with the control, while FSH and LH remained stable. The levels of testosterone and estradiol were positively correlated with decreased spermatozoa motility (p=0.025 and 0.014, respectively), viability (p=0.002 and 0.018, respectively), and morphology (p=0.007 and 0.018, respectively), but the hormone levels did not correlate with spermatozoa levels. The testosterone and estradiol levels did not correlate with the levels of spermatogonia, pachytene spermatocytes, round spermatids, and elongated spermatids. Subchronic exposure to B[a]P could modulate the production of testosterone and estradiol, which subsequently influence spermatozoa quality.

PS 1078 Testing Mixtures of Antiandrogens *In Vivo* at Human-Relevant Exposure Levels

K. Fussell[1], S. S. Schneider[1], S. Melching-Kollmuss[1], S. Gröters[1], V. Strauss[1], B. Siddeek[2], M. Benahmed[2], M. Frericks[1] and B. van Ravenzwaay[1]. [1]*Toxicology, BASF SE, Ludwigshafen/Rhein, Germany and* [2]*INSERM, Nice, France.*

Endocrine disruption has become an important topic of public concern. Despite an increasing amount of public attention, little is understood about whether human-relevant doses of endocrine disrupting chemicals (EDCs) affect homeostasis. To address these concerns we performed pre-/post-natal reproductive toxicity studies to measure the developmental toxicity of low single- and mixture-doses of three substances with an anti-androgenic mode of action: vinclozolin, flutamide and prochloraz. Doses were selected to mimic a LOAEL, a NOAEL for endocrine effects, and the acceptable daily intake (ADI) for each compound, which were then combined together into three mixtures of the LOAELs, NOAELs, and ADIs. In addition to standard regulatory parameters, a number of molecular endpoints were also incorporated within the same study design. Thus, single- and mixed-exposures can be compared from molecular to pathological levels in one and the same animals.

While female offspring developed normally, the male offspring demonstrated anti-androgenic effects at the single and mixed LOAEL doses only. A significant decrease in ano-genital distance on PND 1 and an increase in the number of nipples/areolas on PND 12 were noted in these animals. In the mixture LOAEL dose group a number of animals still had nipple/areolas at PND 20. The male offspring in these LOAEL dose groups which were reared to young adulthood displayed additional anti-androgenic effects including delayed sexual maturation and reduced sex organ sizes and weights. No adverse effects were noted at either the NOAEL or ADI dose levels. Assessment of the nature of the combined effects and the molecular endpoints including the transcriptome, miRNome and metabolome (with hormone levels) is ongoing.

PS 1079 Conazole Fungicides Inhibit Leydig Cell Testosterone Secretion and Androgen Receptor Activation *In Vitro*

M. Roelofs[1], R. Temming[1], A. H. Piersma[2, 1], M. Van den Berg[1] and M. B. van Duursen[1]. [1]*IRAS, Utrecht University, Utrecht, Netherlands and* [2]*Center for Health Protection, National Institute for Public Health and the Environment (RIVM), Bilthoven, Netherlands.*

Conazole fungicides are widely used in the cultivation of crops, hence frequent exposure is common. Several studies suggest that these fungicides can cause endocrine disrupting effects including effects on male fertility. In this study, the potential effects of cyproconazole (CYP), fluconazole (FLUC), flusilazole (FLUS), hexaconazole (HEXA), myconazole (MYC), penconazole (PEN), prochloraz (PRO), tebuconazole (TEBU), triadimefon (TRIA), and triticonazole (TRIT) were assessed on androgen receptor (AR) activation and testosterone (T) secretion, two important factors in male fertility. Seven of the tested conazoles caused a decrease in T secretion by murine Leydig MA-10 cells with CYP, FLUS, HEXA, PRO, TEBU, and TRIT showing >50% inhibition at 10 μM. Yet, expression of steroidogenic (3β-HSD1, 17β-HSD3, Cyp11A1, Cyp17, and StAR) and cholesterol biosynthesis (Cyp51, HMG-CoA reductase, and Por) genes was not changed by conazole exposure. None of the tested conazoles induced AR activation in human T47D cells stably transfected with an androgen responsive element with a firefly luciferase reporter gene. However, nine of the selected conazoles decreased T-induced AR activation with FLUS being the most potent antagonist (IC50 of 11.9 μM) and MYC being the least potent conazole (IC50 of 71.5 μM). Our results show clear in vitro anti-androgenic effects of several conazole fungicides that have been linked to male reprotoxic effects. Nevertheless, better biomonitoring and exposure data are needed in order to perform proper human and environmental risk assessment for human male reprotoxic effects of conazole fungicides.

PS 1080 Mechanistic Investigation of Testicular Tumor Formation in Rats Treated with the SGLT2 Inhibitor Canagliflozin

P. Vinken[1], S. De Jonghe[1], T. Nett[3], L. Lammens[1], M. Srinivas[2] and M. D. Johnson[2]. [1]*Janssen Research & Development, a division of Janssen Pharmaceutica NV, Beerse, Belgium,* [2]*Janssen Research & Development LLC, Raritan, NJ and* [3]*Colorado State University, Fort Collins, CO.*

Canagliflozin, a sodium glucose cotransporter 2 (SGLT2) inhibitor induced Leydig cell tumors (LCTs) in a 24-month rat carcinogenicity study in male rats at dose levels ranging from 10 to 100 mg/kg/day. There were no corresponding preneoplastic lesions in the 3-month or 6-month repeated dose toxicity studies. No tumor development was present in the mouse carcinogenicity study with this compound. A 7-month repeated dose toxicity study was conducted in two groups of 30 male Sprague-Dawley rats receiving vehicle or 100 mg/kg/day canagliflozin by oral gavage to investigate the potential mechanism of LCT formation. Blood samples were collected monthly for measurement of luteinizing hormone (LH) and testosterone (T) and pathology of testis and secondary sex organs was assessed at the end of the study.

Compared to vehicle, serum LH concentrations were increased after 1 month of dosing and generally remained elevated throughout the dosing period. Circulating testosterone levels were unchanged at all time points in comparison to the vehicle. There was a decrease in the weight of the secondary sex organs in the canagliflozin treated group with no change in testis weights. Histopathological examination showed a slight increase in interstitial cell hyperplasia in the canagliflozin treated rats and this was correlated with the increased LH levels.

Disruption of the hypothalamic-pituitary-gonadal axis, resulting in sustained increases in LH levels is an established mechanism of toxicity described for a number of non-genotoxic compounds causing LCT's in male rats. Clinically, no increases in LH were seen in male subjects treated with canagliflozin for 12 weeks. Therefore the formation of LCT's in male rats treated with canagliflozin is not relevant to humans.

PS 1081 The Fungicide Prochloraz Induces Transporter Breast Cancer Resistance Protein BCRP (ABCG2) in Human Mammary and Adrenocortical Cells

J. Lundqvist, Å. Ohlsson Andersson, J. Tallkvist and A. Oskarsson. *Dept of Biomedical Sciences and Veterinary Public Health, Uppsala, Sweden.*

The imidazole fungicide prochloraz is widely used in horticulture and agriculture, e.g. as a post-harvest anti-mold treatment of fruits and vegetables. Prochloraz is a known endocrine disruptor causing developmental toxicity with multiple mechanisms of action. In this abstract, we report a new mechanism by which prochloraz may exert toxicity on a wide range of cells. BCRP is an efflux transporter, with a broad substrate specificity ranging from xenobiotics such as chemotherapeutics, antibiotics, and the dietary carcinogen PhiP (2-amino-1-methyl-6-phenylimidazo-pyridine) to endogenous substances such as estrone-3-sulfate and DHEA-sulfate. BRCP is widely expressed, e.g. in the intestine, liver, kidney, testis and brain, where it can restrict the cellular uptake of xenobiotics and facilitate the excretion of endogenous substances. BCRP is also present in the mammary gland, where it may cause secretion of xenobiotics into breast milk and dairy milk. The aim of the present study was to investigate the effects of prochloraz on BCRP gene expression in two human cell models, representing mammary tissue (MCF-7) and adrenocortical tissue (H295R). Cells were treated with 0.1-10 μM prochloraz for 24 h. RNA was isolated and relative BCRP gene expression measured by real-time RT-PCR. All experiments were conducted using non-toxic levels of prochloraz as determined by MTS assay. We found that prochloraz is able to induce BCRP in both cell lines in a dose dependent manner. The gene expression of BCRP was increased 1.5 to 3 fold. In addition to the previously reported mechanisms for prochloraz-induced toxicity, our results show a novel mode of action for prochloraz, which might be

important in a wide range of tissues. A prochloraz-induced stimulation of BCRP could alter both the milk excretion of BCRP substrates, and the steroid availability via increased efflux of estrone-3-sulfate and DHEA-sulfate from endocrine tissues.

PS 1082 Polybrominated Diphenyl Ether Congener 47 Increases Aldosterone Secretion in a Human Adrenocortical Cell Line

P. G. Kopf and B. Dungar. *Department of Pharmacology, Midwestern University, Downers Grove, IL.*

Elevated circulating aldosterone levels are associated with hypertension, thrombosis formation, cardiac hypertrophy, and congestive heart failure. Polybrominated diphenyl ethers (PBDEs) and their metabolites have been previously shown to alter various endocrine biosynthetic pathways including thyroid hormone, estrogens, and androgens. Additionally, PBDEs have been shown to accumulate in the adrenal gland. Therefore, we characterized the effect of PBDE-47 on aldosterone secretion in a human adrenocortical cell line. HAC15 cells were exposed to vehicle or various concentrations of PBDE-47 (10 nM-100 μM). After 72 h, cell viability, aldosterone secretion, and gene expression of enzymes and cofactors involved in aldosterone synthesis was examined. The only concentration of PBDE-47 that affected cell viability was 100 μM. PBDE-47 induced basal aldosterone secretion at 10 and 100 μM (in ng/mL: vehicle, 9.0±1.7; 10 μM PBDE-47, 70.2±9.8; 100 μM PBDE-47, 78.5±19.8; n=4, $p<0.05$). PBDE-47 also increased Ang II-stimulated aldosterone secretion at 10 μM, but decreased Ang II-stimulated aldosterone secretion at 100 μM (in ng/mL: vehicle, 137.9±6.7; 10 μM PBDE-47, 200.4±9.3; 100 μM PBDE-47, 80.1±20.6; n=4, $p<0.05$). Gene expression of several enzymes and cofactors involved in aldosterone synthesis were increased by 10 μM PBDE-47. These data indicate that PBDE-47 disrupts the regulation of aldosterone secretion and provides further evidence that PBDEs are potential endocrine disruptors.

PS 1083 NQO1, a Component of the Plasma Membrane Electron Transport System, Regulates Redox Status in Clonal Pancreatic Beta Cells and Primary Islets

E. A. Heart[1], C. E. McCue[2], N. E. Corbett[2], A. K. Jaiswal[3] and J. P. Gray[2,1]. [1]*Cellular Dynamics, Marine Biological Laboratory, Woods Hole, MA,* [2]*Science, United States Coast Guard Academy, New London, CT and* [3]*Pharmacology, University of Maryland School of Medicine, Baltimore, MD.*

Plasma membrane electron transport (PMET) is a ubiquitous system which transports electrons out of cells while re-oxidizing intracellular reduced equivalents NADH and NADPH. Recently, NQO1, NAD(P)H-dependent quinone reductase 1, well known for its role in 2-electron reduction of quinones, was shown to be a mediator of PMET in pancreatic beta cells, where it helps to support glucose metabolism and subsequent insulin secretion following exposure of these cells to elevated glucose levels. Our previous work showed that NQO1 positively regulates glucose-stimulated insulin secretion (GSIS), suggesting a role for NQO1 in glucose metabolism and homeostasis. In the current work, we characterized the role of NQO1 in the PMET pathway of pancreatic beta cells and its role in the alteration of intracellular oxidative state in the presence of the redox cycling pro-oxidant menadione. Adenoviral-mediated over-expression of NQO1 resulted in the increase of the NQO1 protein and NQO1 enzymatic activity, and reduced the level of menadione-dependent ROI production in both clonal INS-1 832/13 cells and isolated islets. In islets isolated from global NQO1 knockout mice, menadione-dependent ROI production was elevated. This is consistent with NQO1's role in detoxification of menadioen in other tissues via two-electron reduction. In the absence of menadione, NQO1 over-expression or knock-out decreased or increased, respectively, the $NAD(P)H/NAD(P)^+$ ratio consistent with its role in the Plasma Membrane electron transport (PMET), particularly at elevated glucose levels. Together, these data show that NQO1, as a member of the PMET pathway, is an important regulator of the intracellular redox state of the beta cell and is important for insulin secretion at elevated glucose levels.

PS 1084 *In Utero* Exposure to Perfluorooctanoic Acid (PFOA) or Perfluorooctane Sulfonate (PFOS) Did Not Increase Body Weight, Blood Glucose, or Small Intestinal Tumorigenesis in Min Mice

I. Steffensen, H. Ngo and R. B. Hetland. *Department of Food, Water and Cosmetics, Norwegian Institute of Public Health, Oslo, Norway.* Sponsor: B. Granum.

According to the environmental obesogen hypothesis, exposure to some environmental contaminants may initiate or exacerbate the development of obesity and its associated health consequences. Obesity is now regarded as a risk factor for colon cancer. Perfluorinated compounds (PFCs) are used in applications such as clothing, carpets, food packaging, fire extinguishers etc. We examined effects of exposure to the PFC chemicals PFOA and PFOS during critical periods of development (*in utero*) in the intestinal cancer mouse model C57BL/6J-*Min*/+ (multiple intestinal neoplasia). The dams were exposed to PFOA or PFOS (0.01, 0.1 and 3.0 mg/kg bw/day) by oral gavage on gestational days 1-17. Body weight of the pups was recorded from birth until termination at 11 weeks and presented as area under the curve (AUC). The small intestine was fixed, stained with 0.2% methylene blue, and tumors scored by an inverse light microscope. Plasma glucose levels (non-fasted) were measured by glucometer at age 6 and 11 weeks, to study the hypothesis of disrupted glucose regulation as a link between obesity and intestinal tumor development.

After 3.0 mg/kg bw/day PFOA very few live pups were obtained, whereas this dose of PFOS and the other two doses of both chemicals gave enough mice for statistical analysis. No obesogenic effect of PFOA or PFOS was observed up to 11 weeks of age. Compared with mice exposed to water, mice treated with 0.1 mg/kg bw PFOA had significantly lower AUC on days 3-18 and weeks 3-11, and also compared with mice treated with 0.01 mg/kg bw PFOA on weeks 3-11, indicating a toxic effect of PFOA. None of the doses of PFOA or PFOS increased the plasma glucose levels at either time point or increased the number of small intestinal tumors compared with mice given the vehicle distilled water.

Conclusion: Exposure to PFOA or PFOS *in utero* did not have obesogenic effect, at least not up to 11 weeks of age, and did not increase blood glucose levels or intestinal tumorigenesis in Min mice.

PS 1085 Emerging Toxicants Induce Adipogenesis and Suppress Osteogenesis in Mouse Mesenchymal Stromal Cells

J. Watt, T. Webster and J. J. Schlezinger. *Boston University School of Public Health, Boston, MA.*

Environmental obesogens are a newly recognized category of endocrine-disrupting chemicals that are thought to be contributing to rising rates of obesity in the United States. While obesity is typically regarded as an increase in visceral fat, adipocyte accumulation in the bone has been linked to lower bone density, osteoporosis and increased fracture risk Exposure to environmental toxicants that activate PPARγ, a critical regulator of the balance between adipogenesis and osteogenesis, may generate adverse effects in bone, which have increased in prevalence over the last several decades. Using a primary mouse bone marrow culture model, we tested the hypothesis that obesogens acting as PPARγ agonists divert the differentiation pathway of multipotent mesenchymal stromal cells towards adipogenesis and away from osteogenesis. The toxicants tested included organotins (tributyltin and triphenyltin), a phthalate metabolite (mono-(2-ethylhexyl)phthalate, MEHP), and brominated flame retardants (tetrabromobisphenol-a, TBBPA, and mono-(2-ethylhexyl)tetrabromophthalate, METBP). All of the compounds increased adipogenesis (e.g. lipid accumulation, FABP4 expression) and suppressed osteogenesis (e.g. alkaline phosphatase activity, Osterix expression) with different potencies and efficacies. Despite structural dissimilarities, there was a strong correlation between induction of adipogenesis and suppression of osteogenesis. Only the organotins were distinct in their exceptional ability to suppress osteogenesis. Additionally, we have investigated combinatorial effects of full and partial PPARγ-agonists, both synthetic and endogenous, using reporter assays and generalized concentration addition modeling.

PS 1086 Influence of Halogenated Phenolic Compounds on Thyroid Hormone System via Inhibition of Iodotyrosine Deiodinase Activity

R. Shimizu[1], M. Yamaguchi[1], N. Uramaru[2], H. Kuroki[3], S. Ohta[4], S. Kitamura[2] and K. Sugihara[1]. [1]*Faculty of Pharmaceutical Sciences, Hiroshima International University, Hiroshima, Japan,* [2]*Nihon Pharmaceutical University, Saitama, Japan,* [3]*Daiichi University of Pharmacy, Fukuoka, Japan and* [4]*Graduate School of Biomedical and Health Sciences, Hiroshima University, Hiroshima, Japan.* Sponsor: M. Takiguchi.

Hydroxylated polychlorinated biphenyls (PCBs) and polybrominated diphenyl ethers (PBDEs) are detected in human plasma as the metabolites of PCBs and PBDEs, their configuration are similar to that of thyroid hormone, and their effect on thyroid hormone system are concerned. Iodotyrosine deiodinase (IYD) has an ability to salvage iodide from iodotyrosine that are generated as byproducts of thyroid hormone biosynthesis. This enzyme has also been discovered to act as a dehalogenase of bromo- and chlorotyrosine. The aim of this study was to investigate the possible influence of halogenated compounds on thyroid hormone metabolism, IYD-inhibitory activity by 44 halogenated compounds, PCBs, PBDEs, agrichemicals, antiparasitics, pharmaceuticals and food colorants, were examined in vitro using microsomes of HEK-293T cells expressing recombinant human IYD. Among them, 22 halogenated phenolic compounds inhibited IYD activity. Rose bengal was the most potent inhibitor, followed by erythrosine B, phloxine B, benzbromarone, 4'-hydroxy-2,2',4-tribromodiphenyl ether, 4-hydroxy-2,3',3,4'-tetrabromodiphenyl ether, 4-hydroxy-2',3,4',5,6'-pentachlorobiphenyl, 4'-hydroxy-2,2',4,5'-tetrabromodiphenyl ether, triclosan, and 4-hydroxy-2,2',3,4',5-pentabromodiphenyl ether. However, among PCBs and PBDEs without a hydroxyl group, including their methoxylated metabolites, none inhibited IYD activity. These results suggest that halogenated compounds may disturb thyroid hormone homeostasis via inhibition of IYD, and that the structural requirements for IYD-inhibitory activity include halogen atom and hydroxyl group substitution on a phenyl ring.

PS 1087 Effects of Exposure to 1-Bromopropane on the Level of Thyroid Hormone in Cerebrospinal Fluid of Rats

L. Zhang[1], C. Zong[1], N. Koibuchi[2], S. Ichihara[3], H. Fujita[4], J. Chang[1], J. Huang[1], H. Naito[1], M. Kato[1] and G. Ichihara[1]. [1]*Occupational and Environmental Health, Nagoya University Graduate School of Medicine, Nagoya, Japan,* [2]*Gunma University Graduate School of Medicine, Mebashi, Japan,* [3]*Mie University Graduate School of Rennovation Studies, Tsu, Japan and* [4]*Hoddaido University School of Medicine, Sapporo, Japan.*

Purpose: A previous epidemiological study showed dose-dependent increase in TSH level in the serum of the workers exposed to 1-bromopropane (1-BP). Hyperthyroidism-like signs were observed in rats exposed to 1-BP, such as irritating behavior as well as decreased cholesterol and increased protein levels in plasma. The present study investigated effects of exposure to 1-BP on transthyretin (TTR), which is a carrier of thyroid hormone from blood to cerebrospinal fluid (CSF), as well as the level of thyroid hormone in the CSF and blood to understand the possible involvement of thyroid hormone in the toxicity of 1- BP to the central nervous system.
Methods: Forty-eight male F344 rats were divided into four equal groups and exposed to 1-BP at 0, 200, 400 and 800 ppm 8 h/d for four weeks. Distribution of TTR protein in the brain was examined by immunhistochemistry. The levels of TTR mRNA in the choroid plexus and liver were measured by quantitative real time PCR. Free triiodothyronine (Free-T3) in the CSF and plasma was measured using ELISA kit. Total triiodothyronine was also measured in the plasma.
Results: Four-week exposure to 1-BP at 200 and 400 ppm significantly increased mRNA of TTR in the chroid plexus of the lateral ventriculi and fourth ventriculus, but reduced that at 800ppm. The level of TTR mRNA didn't show any change in hippocampus. Free-T3 increased significantly at 400 and 800 ppm in the CSF after four-week exposure to 1-BP but didn't change in the plasma. Free thyroxine (T4) in the plasma significantly decreased in all the 1-BP exposure groups.
Conclusion: The study showed increase in free T3 in the CSF of the rats exposed to 1-BP, which may explain the irritating behavior as well as low cholesterol and high protein in serum of rat exposed to 1-BP.

PS 1087a Enhancement of the Endocrine Disruptor Knowledge Base for Assessing Endocrine Activity of Untested Chemicals

H. Hong[1], H. Ng[1], H. Fang[2], R. Perkins[1] and W. Tong[1]. [1]*Division of Bioinformatics and Biostatistics, National Center for Toxicological Research, Jefferson, AR and* [2]*Office of Scientific Coordination, National Center for Toxicological Research, Jefferson, AR.*

Endocrine disruptors (EDs) are exogenous chemicals with potential to disrupt the endocrine system. EDs came under international scientific discussion and debate some two decades ago, sparking regulatory attention. Accordingly, FDA developed the Endocrine Disruptor Knowledge Base (EDKB) and made it publically available. Since then, the EDKB has been widely used by the scientific community. It was recently updated with more comprehensive data and corresponding predictive models. Effects mediated by the estrogen receptor homodimer complex are a primary ED concern. Since many EDs exhibit estrogenic activities, affecting normal estrogen signaling pathways, we first updated the estrogenic data and augmented the EDKB with a comprehensive database of chemicals assayed for estrogenic activity. The database contains over 21,000 estrogenic activity data points across more than 8,000 compounds assayed among 11 species. It also contains protein subtypes and domains used in the assays. Original data were converted into the same units, such as logRBA for competitive receptor binding. Quality control was performed to ensure data quality. It was built using Instant JChem and subsequently instantiated in a web-based software system for users to browse, search and export data. It enables search across multiple fields such as chemical structure, substructure, chemical name, CAS, assay type, species, activity range, and references using logical operators. Additionally, data for binding affinity to α-Fetoprotein (AFP) for 125 chemicals are included. The AFP 3D structure was modeled using homology and molecular dynamics (MD) simulations, and AFP-ligand binding modes elucidated for 13 binders. With the recent enhancements, the EDKB provides the scientific and regulatory communities a free source to search endocrine activity data and to develop predictive models for predicting endocrine activity of chemicals for which no data are available.

PS 1087b Effects of Triclosan on Iodide Uptake and the Expression of Genes Related to Thyroid Hormone Synthesis in Rat and Human Thyroid Follicular Cells

J. Fang, Y. Wu and F. A. Beland. *Division of Biochemical Toxicology, National Center for Toxicological Research, Food and Drug Administration, Jefferson, AR.*

Triclosan, an anti-bacterial agent widely used in many personal care and household products, has been reported to decrease serum thyroid hormone (TH) levels in rats following oral exposure and in mice following dermal exposure. Disruption of TH homeostasis may occur via several pathways, including alteration of TH synthesis, transport, and/or metabolism. Iodide uptake, mediated by the sodium/iodide symporter (NIS, encoded by the gene SLC5A5) in thyroid follicular cells, is a key step during TH synthesis. In this study, we examined the effects of triclosan on iodide uptake and the expression of genes related to TH synthesis, including SLC5A5, thyroperoxidase (TPO), and thyroglobulin (TG), in rat thyroid follicular FRTL-5 cells and human thyroid follicular Nthy-ori 3-1 cells. In FRTL-5 cells incubated with 10 μM sodium iodide and various concentrations of triclosan (0 – 40 μM) for 60 min, triclosan inhibited NIS-mediated iodide uptake in a concentration-dependent manner, with an IC50 of 6.6 μM. In further kinetic studies, the initial velocity of iodide uptake was determined in FRTL-5 cells incubated with various concentrations of triclosan (0 – 40 μM) and sodium iodide (10 – 320 μM) simultaneously for 5 min; the data showed that triclosan acted as a non-competitive inhibitor of NIS, with a Ki of 37.3 μM. There were no significant changes in the transcriptional expression levels of SLC5A5, TPO and TG in either FRTL-5 or Nthy-ori 3-1 cells upon treatment with non-cytotoxic concentrations (2.5 – 10 μM) of triclosan for 24 or 48 h, while a cytotoxic concentration of triclosan (20 μM) induced a slight increase in the expression levels of SLC5A5 (1.9-fold), TPO (1.4-fold), and TG (2.2-fold) in FRTL-5 cells, but not in Nthy-ori 3-1 cells, following a 48 h exposure. These data suggest that triclosan inhibited NIS-mediated iodide uptake in a non-competitive manner, but had little effect on the expression of SLC5A5, TPO and TG in either rat or human thyroid follicular cells.

PS 1087c International Validation of Two Human Recombinant Estrogen Receptor (ER alpha) Binding Assays

V. S. Wilson[1], S. C. Laws[1], A. Freyberger[3], Y. Akahori[4], M. Takeyoshi[4], M. Jacobs[5], D. R. Dietrich[6], K. L. Hamernik[2] and M. K. Manibusan[2]. [1]*ORD, NHEERL, USEPA, RTP, NC,* [2]*OSCP, USEPA, Washington, DC,* [3]*Bayer HealthCare, Elberfeld, Germany,* [4]*CERI, Saitama, Japan,* [5]*Public Health England, Chilton, United Kingdom and* [6]*U. Konstanz, Konstanz, Germany.*

An international validation study has been successfully completed for 2 competitive binding assays using human recombinant ERα. Assays evaluated included the Freyberger-Wilson (FW) assay using a full length human ER, and the Chemical Evaluation and Research Institute (CERI) assay using a ligand-binding domain of the human ER. Twenty three compounds were tested in 6 laboratories for the FW assay and 5 for the CERI assay, which included three controls (used with every run), 9 uncoded, and 14 coded chemicals across 3 subtasks. The overall goal of this validation study was to demonstrate the ability of each of the two assays to reliably classify the test chemicals as binders or non-binders. Laboratories had little trouble with the ER binders that produced a full binding curve when using either the CERI or FW assays. As is typical with all ER competitive binding assays, the weak binders proved to be more challenging. However, overall results from both the FW and CERI assays were consistent and in agreement with expected classifications regardless of the form of the hrER (i.e., full length ER versus an ER ligand binding domain) or the subtle differences in the protocols for conducting each assay. The reproducibility and accuracy for classification of chemicals as potential ER binders and non-binders using the FW and CERI hrER binding assays were comparable to that of the U.S.EPA's existing ER binding test guideline OPPTS 890.1250, while providing an improved, higher throughput method that does not require animal tissue as the source of receptor. An OECD test guideline is currently being drafted. This abstract does not reflect US EPA policy. Parts of this work were supported through the EU sponsored project ReProTect ((LSHB-CT-2004-503257), ECVAM, and USEPA.

PS 1087d Comparison of *In Vitro* and *Ex Vivo* Thyroid Hormone Synthesis Inhibition Results and *In Vivo* Outcomes for a Series of Benzothiazoles

M. W. Hornung, J. T. Haselman, J. Korte, P. Kosian, K. Challis, S. Hall and S. Degitz. *ORD, NHEERL, Mid-Continent Ecology Division, US EPA, Duluth, MN.*

Assessing how *in vitro* data may be used to predict adverse effects *in vivo* is critical as efforts are advanced to incorporate *in vitro* assays into a risk assessment framework. Within the context of a thyroid hormone (TH) synthesis inhibition adverse outcome pathway (AOP), *in vitro*, *ex vivo* and *in vivo* assays were used to study the TH disrupting potential for a series of benzothiazoles: benzothiazole (BTZ), 2-mercaptobenzothiazole (MBT), 5-chloro-2-mercaptobenzothiazole (CMBT), 2-aminobenzothiazole (ABT), 2-hydroxybenzothiazole (HBT), and 2-(methylthio) benzothiazole (MTBT). A thyroid peroxidase (TPO) inhibition assay was used to determine the activity of these chemicals *in vitro*. The rank order potency for TPO inhibition was MBT=CMBT>ABT>BTZ>HBT. MTBT did not inhibit TPO activity. The benzothiazoles were tested further in *Xenopus laevis* thyroid gland explant culture with inhibition of TH release as the endpoint. Toxicity was assessed as decreased glandular ATP. MBT inhibited TH release at non-cytotoxic concentrations and with similar potency to methimazole. The benzothiazoles with greatest potency for T4 release inhibition were MBT, CMBT, and HBT, with IC50s of 3, 30, and 133 μM, respectively, but all benzothiazoles showed some inhibitory activity. Benzothiazoles were further assessed *in vivo* in a 7-d *X. laevis* tadpole assay. MBT and CMBT were the most potent for affecting endpoints of thyroid hormone synthesis inhibition, whereas others showed little or no effect. Both MBT and CMBT significantly increased sodium iodide symporter (NIS) mRNA indicative of compensatory TSH stimulation in response to decreased circulating TH. Taken as a whole, these results indicate the utility of *in vitro* assays for queuing chemicals for further testing, but illustrate the need for caution in interpreting results of *in vitro* or *ex vivo* inhibition assays especially where toxicity may be a confounding factor. *This abstract does not necessarily reflect U.S. EPA policy.*

PS 1087e Triclosan-Induced Cell Growth Was Reversed by a Phytoestrogen, Kaempferol, via Regulating Cell-Cycle Related and Apoptosis-Related Genes in MCF-7 Breast Cancer Cells

S. Kim and K. Choi. *Laboratory of Biochemistry and Immunology, College of Veterinary Medicine, Chungbuk National University, Cheongju, Republic of Korea.*

Triclosan is one of endocrine disrupting chemicals (EDCs) which are scattered with environment agents, such as toothpastes, deodorant and cleaning supplies. As a phytoestrogen, kaempferol is one of bioflavonoids, which has been found at variety of vegetables including broccoli, tea and tomato. Although kaempferol may have anti-cancer activity, its exact mechanism is under investigation in the induction of apoptosis and inhibition of cell proliferation or angiogenesis. In this study, we examined the anti-proliferative effects of kaempferol in triclosan-induced cell growth in MCF-7 breast cancer cells. A proper concentration of kaempferol or triclosan was determined in MCF-7 cells measured by MTT assay. In this study, kaempferol significantly reduced the viability of MCF-7 cells compared to a negative control treated with DMSO, and that kaempferol reversed triclosan-induced MCF-7 cell growth at 50 uM. To confirm that kaempferol inhibited triclosan-induced cell growth, we examined the transactional levels of cell growth and apoptosis-related markers, i.e., cyclin D, p21, cyclin E, p27 and bcl-2, and bax genes, using reverse transcription (RT)-PCR. The expression levels of cyclin D, cyclin E and bax/bcl-2 ratio were increased, while that of p21 and p27 mRNAs was decreased by triclosan in MCF-7 cells. In addition, kaempferol reversed triclosan-induced gene expressions in an opposite manner. Taken together, these results indicated that kaempferol may inhibit the growth MCF-7 cells via regulating of cell cycle and apoptosis-related genes. In addition, EDCs-induced progression of breast cancer may be suppressed by a phytoestrigen, i.e., kaempferol, in a specific manner. [This work was supported by National Research Foundation of Korea (NRF) grant funded by the Ministry of Education, Science and Technology (MEST) of the government of Republic of Korea (2013R1A1A2059092).]

PS 1087f *In Vitro* Metabolism of Tamoxifen in Human, Rat, and Fish Microsomes

S. C. Laws[1], W. M. Henderson[2], M. G. Hotchkiss[1] and L. J. Mills[3]. [1]*TAD, NHEERL, ORD, U.S. EPA, Research Triangle Park, NC,* [2]*ERD, NERL, ORD, U.S. EPA, Athens, GA and* [3]*AED, NHEERL, ORD, U.S. EPA, Narragansett, RI.*

Results from an *in vivo* study comparing biologically-active metabolites in the plasma of Wistar rats and cunner fish (*Tautogolabrus adspersus*) treated with tamoxifen indicate notable differences in circulating metabolite concentrations between these two species. After a single oral dose of tamoxifen (25 mg/kg), the predominant metabolite observed from 1 to 72 hrs in rats was N-desmethyltamoxifen while in cunner it was 4-hydroxytamoxifen. The predominant metabolite in humans has been reported to be N-desmethyltamoxifen. To investigate if these species differences could be predicted using an *in vitro* assay, hepatic microsomes from cunner fish, Wistar rats, and humans were used. The experiment was designed to measure metabolic activity in all 3 species at 37° and 18°C, but in preliminary experiments, fish microsomes were shown to be inactive at 37°C. Thus, metabolism among all 3 species was compared at 18°C (1,2,3, 4 hrs), and rat and human microsomes were also compared at 37°C (0.5, 1, 1.5, 2 hrs). Final assay concentrations of microsomes (0.4 mg/mL), tamoxifen (10μM), and NADPH (30μM) were prepared in KPO_4 (pH 7.4, 100mM). Metabolic activity was quenched by adding 0.5 mL of ice cold acetone. Samples were stored at -80°C until analyzed for tamoxifen and metabolites using LC-MS/MS. The highest concentrations of N-desmethyltamoxifen and 4-hydroxytamoxifen at all time points were observed in rat microsomes. In rat and human microsomes, N-desmethyltamoxifen was the predominant metabolite at both 18°C and 37°C. While formation of 4-hydroxytamoxifen was minimal with human microsomes, this metabolite doubled from 1 to 2 hrs in fish and rat microsomes (18°C). Unlike *in vivo* results, fish microsomes produced about twice as much N-desmethyltamoxifen as 4-hydroxytamoxifen during 4 hrs in the *in vitro* assays. Thus, though these *in vitro* results are similar to *in vivo* studies reported for human and rats, they do not reflect *in vivo* results observed for cunner fish. This abstract does not necessarily reflect U.S.EPA policy.

PS 1087g Fenhexamid Regulated the Transcripts of Aryl Hydrocarbon Receptor, Aryl Hydrocarbon Receptor Nuclear Translocator and Cell Cycle Related Genes in Human BG-1 Ovarian Cancer Cells Expressing Estrogen Receptors

R. Go and K. Choi. *Laboratory of Biochemistry and Immunology, College of Veterinary Medicine, Chungbuk National University, Cheongju, Republic of Korea.* Sponsor: M. Cho.

Fenhexamid is antifungal agents used in agricultural applications, which are present at measurable amounts in fruits and vegetables. Fenhexamid has been reported to act as an anti-androgen in an androgen receptor reporter assay in engineered human breast cancer cells. Aryl hydrocarbon receptor (AhR) is a ligand-activated transcription factor, which translocates into nucleus and dimerizes with aryl hydrocarbon receptor nuclear translocator (ARNT). In this study, we examined the effects of fenhexamid, a pesticide, on the expressions of AhR, CYP1A1, CYP1B1, ARNT, and p21 by RT-PCR analysis. To evaluate the ability of cell viability, BG-1 cells were cultured with a negative control (0.1% DMSO), 17b-estradiol (E2; 1x10-9 M), 2,3,7,8- tetrachlorodibenzo-ρ-dioxin (TCDD; 1x10-8 M), or fenhexamid (1x10-5 - 1x10-8 M). E2 as a positive control markedly increased BG-1 cell proliferation compared to DMSO. In addition TCDD and fenhexamid increased BG-1 cell proliferation at the concentration of 1x10-8 M and 1x10-5 M, respectively. The transcriptional level of p21 was reduced at 6 h by E2, TCDD, or fenhexamid, while its level was reversed at 24 h following their treatments. The mRNA expression of AhR was reduced by E2, TCDD, or fenhexamid in a time-dependent manner, while its level was reversed in the presence of alpha-naphthoflavone, an AhR inhibitor. In contrast, the transcriptional level of ARNT appeared to be increased by E2, TCDD, or fenhexamid. Taken together, these results indicate that fenhexamid may regulate AhR, ARNT and p21 to induce cell growth in BG-1 ovarian cancer cells expressing estrogen receptors. A further study will continue to examine disruptive effects of pesticides in estrogen receptor expressing cells or tissues. [This work was supported by National Research Foundation of Korea (NRF) grant funded by the Ministry of Education, Science and Technology (MEST) of the government of Republic of Korea (2013R1A1A2059092).]

PS 1087h Effects of *In Vivo* Exposure to Tamoxifen on a Nontarget Species, the Marine Fish Cunner (*Tautogolabrus adspersus*)

L. J. Mills[1], S. Jayaraman[1], R. Gutjahr-Gobell[1], D. Borsay Horowitz[1], G. Zaroogian[1] and S. C. Laws[2]. [1]*ORD, NHEERL, AED, U.S. Environmental Protection Agency, Narragansett, RI and* [2]*ORD, NHEERL, TAD, U.S. Environmental Protection Agency, Research Triangle Park, NC.*

Tamoxifen is an endocrine-active pharmaceutical that is used world-wide to treat certain breast cancers. Because tamoxifen has been detected in aquatic environments, a study was undertaken to investigate its biological effects in a non-target species, the marine fish cunner (*Tautogolabrus adspersus*). Effects of a 17-day exposure to two different oral doses of tamoxifen (0.5 and 5 mg/kg fish weight) on reproduction in spawning cunner were examined relative to controls. Results show mean egg production in tamoxifen-treated cunner was significantly less than controls. No significant effects were observed in fertile or viable eggs relative to controls, although a downward trend for both endpoints was noted. After the 17-day exposure, activity of the steroidogenic enzyme aromatase in brains and ovaries from these fish was also evaluated. Ovarian aromatase activity was significantly increased in cunner treated with 5 mg/kg of tamoxifen. There were no significant differences in brain aromatase activity or gonadosomatic index in either sex compared to controls. In a separate experiment, formation of biologically active metabolites over time (from 1 to 72 hours) after a single oral dose of tamoxifen (25 mg/mg) was compared in Wistar rats versus cunner. The predominant metabolite in plasma from rats was N-desmethyltamoxifen, while in plasma from cunner it was 4-hydroxytamoxifen. This difference suggests that the effects of exposure to tamoxifen could be magnified in cunner, since 4-hydroxytamoxifen is considered to be about 100 times more efficacious than tamoxifen or N-desmethyltamoxifen. Overall, differences in circulating metabolites between species and a significant reduction in egg production in spawning cunner treated with tamoxifen both suggest that exposure to tamoxifen could present a tangible ecotoxicological risk to fish such as cunner. *This abstract does not necessarily reflect US EPA policy.*

PS 1087i Subchronic Toxicology of Tetrabromobisphenol A (TBBPA) in CD® Rats

T. G. Osimitz[1], W. Droege[1] and A. Hayes[2]. [1]*Science Strategies, Charlottesville, VA and* [2]*Vision and Strategy, Harvard University, Boston, MA.*

This study was conducted to evaluate the subchronic toxicity of the flame retardant tetrabromobisphenol A (TBBPA) in CD® rats. Three treatment groups, ten rats/sex/group, were gavaged daily at 100, 300, or 1000 mg/kg/day for 90 days. Recovery animals (five rats/sex) were included in the control and high-dose groups and evaluated 6-weeks post-treatment. In addition to routine observations, organ weights, hematology, and clinical chemistry, a Functional Observational Battery (FOB) was conducted pretest and at Week 12. Motor activity was also evaluated during Week 12. Moreover, thyroid hormone levels (TSH), T3, and T4, were evaluated at 33 days, termination, and recovery. T4 levels were statistically significantly lower in males in all dose groups relative to controls at Day 33 (-26.2%, -31.0%, -31,7% at 100, 300, 1000 mg/kg, respectively) and at Day 90 (-35.8%, -33.4%, -39.3% at 100, 300, 1000 mg/kg, respectively). T4 levels were comparable to controls in the 1000 mg/kg recovery animals. T4 levels were statistically significantly lower in females in all dose groups relative to controls only at Day 33 (-22.5%, -24.1%, -22.0% at 100, 300, 1000 mg/kg, respectively). No changes were noted at Day 90. No changes in TSH or T3 levels relative to controls were noted in either sex at any time point. No toxicologically significant changes were observed in any of the other parameters. The reduction in serum T4 levels was not accompanied by evidence of toxicity or adverse effects, and the animals were clinically normal. Moreover, because the decrease in T4 levels was not of sufficient magnitude to alter mean serum TSH or T3 levels, thyroid histopathology, thyroid weight, or other parameters indicative of thyroid pathology (e.g., body weight), the decrease in serum T4 levels was not considered adverse. Thus, in this rat 90-day oral toxicity study with TBBPA, the No Observed Adverse Effect Level (NOAEL) was at least 1000 mg/kg/day, the highest dose tested. Supported by the NAFRA Panel of the American Chemistry Council.

PS 1087j Adverse Human Reproductive Outcomes and Body Burdens of Endocrine Disrupting Compound—Polychlorinated Biphenyls

D. Roy, M. Morgan and C. Yoo. *Florida International University, Miami, FL.*

Inconsistent evidence exists for an association between polychlorinated biphenyls and adverse human reproductive outcomes. Therefore, the goal of our study was to determine if risk of reproductive and endocrine dysfunction in humans is increased due to exposure to endocrine disrupting compound - polychlorinated biphenyls. The CDC's NHANES data was used to examine exposure levels of PCBs and the association between blood levels of PCBs and self-reported reproductive health outcomes among U.S. women. The study population ranged from 3109 to 3192 female participants (12 years of age and older) of the National Health and Nutrition Examination Survey who provided blood samples between 1999 and 2004. Individual levels of 7 PCB congeners (PCB 074, 099, 118, 138, 153, 170, and 180), the sum of dioxin-like PCB congeners (PCB 074, 118), and the sum of non-dioxin-like PCB congeners (PCB 099, 138, 153, 170, and 180) were used in conjunction with data obtained from the medical and reproductive health questionnaires. Self-reported reproductive health outcomes were obtained from the interviews of female participants 12 years of age and older. The following outcomes were evaluated using categorical data: age at first live birth, age at menarche, age at menopause, having undergone a medical procedure, uterine fibroids, endometriosis, parity, having a baby with low birth weight, and menstrual cycle regularity for the past 12 months. Separate analyses showed that body burdens of PCBs in blood were significantly higher among women with breast cancer, women with a history of uterine fibroids, and women who had undergone surgical removal of their uterus and/or ovaries when compared to the rest of the study population. While these results do not provide any evidence of causal associations, it is noteworthy that women with these reproductive outcomes have significantly higher body burdens of PCBs than women without them.

PS 1087k Developmental Exposure of Zebrafish to Dieldrin Alters Gene Expression Associated with Energy Homeostasis

M. H. O'Brien and I. P. Callard. *Department of Biology, Boston University, Boston, MA.*

Environmental exposure to xenobiotics has been suggested to modify energy balance and increase the risk for obesity, metabolic syndrome, and diabetes incidence. The importance of developmental exposure to pollutants and the associated risk for disease later in life is not clear. Reproductive development and energy homeostasis are tightly linked. Our previous studies have shown reproductive abnormalities in

freshwater turtles near the Massachusetts Military Reservation (MMR) Superfund Site where pesticides and other persistent pollutants have been detected in egg yolk. To explore the mechanisms of developmental toxicity of these pollutants we used a zebrafish (*Danio rerio*) whole embryo model. Quantitative RT-PCR analysis showed that exposure of zebrafish to pond water contaminated by the MMR, relative to water from a control pond, induced vitellogenin and aromatase B but did not alter estrogen receptor alpha, cytochrome P4501a, or metallothionein gene expression. Upon individual examination of pollutants from pond water we found the pesticide dieldrin, but not p,p'-DDE, had a significant effect on global gene transcription patterns. Gene Set Enrichment Analysis (GSEA) of microarray results indicated that exposure to dieldrin disrupted many pathways including insulin secretion, glucose secretion and metabolism, and adipocytokine signaling. Using Quantitative RT-PCR we further investigated a panel of dieldrin-responsive genes (neuronal PAS domain protein 4, pyruvate dehydrogenase kinase 2, phosphoenolpyruvate carboxykinase 1, hydroxysteroid 11-beta dehydrogenase 2, pre-proopiomelanocortin, and insulin-induced gene 1). For all genes examined we found an inverted U-shaped dose response curve with dieldrin exposure. The normal developmental pattern of these dieldrin-responsive genes was also characterized. We found that neither MMR-contaminated pond water nor p,p'-DDE exposure had a significant effect on genes regulating energy homeostasis. In addition to other pollutants at the MMR, dieldrin is a concern and is shown here to alter energy balance signaling.

PS 1087l The Role of Mn in Skeletal Development

C. J. Richardson[1], D. Smith[1], S. Fendorf[2], J. Lezama Pacheco[2], R. Ritchie[3] and N. Dave[3]. [1]*Microbiology and Environmental Toxicology, University of California Santa Cruz, Santa Cruz, CA,* [2]*Environmental Earth System Science, Stanford University, Stanford, CA and* [3]*Materials Sciences Division, Lawrence Berkeley National Laboratory, Berkeley, CA.*

Objective:
To determine the affects of early postnatal manganese(Mn) exposure on skeletal Mn accumulation and development in pre and post weaned rats.
Rationale:
Mn is essential for proper bone development and growth however overexposure to Mn can impair proper bone formation. Mn is incorporated in bone mineral as a biological analog to calcium, although the extent of accumulation in bone is not well known.
Approach:
Male Long Evans rats were orally exposed to 0,25 or 50 mg Mn/kg/d over the pre-weaning period only (PND 1-21) or lifelong, and sacrificed at age PND 24,66,400 for collection of femur, tibia and fibula tissue. Bone tissues were analyzed for Mn using ICPMS and calcium using OES. Tibia samples were pulverized and analyzed for molecular coordination and speciation using X-Ray diffraction (XRD) and X-Ray absorption(XAS) techniques. Femurs were tested for fracture resistance using an instron at PND 66.
Results:
1) Results indicate that within an age group of lifelong exposure, PND 24,66,or 400 continuously exposed to Mn had an increased Mn accumulation relative to exposure.
2) Bone Mn levels in young PND 24 animals were substantially higher than levels in PND 66 and 400 animals.
3) Bone Mn levels in PND 66 and 400 animals that were exposed to Mn only over the pre-weaning period (PND 1-21) still showed evidence of slightly elevated bone Mn levels compared to controls never exposed .
4) Bone Ca levels were significantly lowered in the PND 66 group.
5) Preliminary Instron analyses of bone strength suggests that Mn exposure may reduce bone strength,while preliminary XRD results do not suggest any gross alteration in the macroscopic mineral composition.
Conclusions: Collectively these results suggest that elevated early life and lifelong Mn exposure may lead to increased bone Mn accumulation into adulthood, and reduce overall bone strength, with implications of osteoporosis and compromised bone integrity.

PS 1087m Interaction of Manganese, Iron, and Stress on Spatial Learning and Memory after Developmental Exposure

R. M. Amos-Kroohs[1], L. L. Davenport[2], N. Atanasova[3], C. V. Vorhees[1] and M. T. Williams[1]. [1]*Neurology, Cincinnati Children's Hospital, Cincinnati, OH,* [2]*Environmental Health, University of Cincinnati, Cincinnati, OH and* [3]*Philsophy, University of Cincinnati, Cincinnati, OH.*

Manganese (Mn) is neurotoxic at higher concentrations. Mn toxicity occurs in children from sources such as soy-based infant formulas, well-water, and air pollution near heavy manufacturing. Children's gastrointestinal systems allow Mn to more readily enter circulation and accumulate in brain. Subclinical iron (Fe) deficiency (FeD), which affects up to 15% of US children, exacerbates Mn toxicity due to increased Mn bioavailability during FeD. FeD is prevalent in impoverished and low socioeconomic environments that are considered stressors. To model developmental stress (DS), pregnant rats and their litters were housed in cages with a wire grid floor or standard bedding from embryonic day (E)7 to postnatal day (P)28. Dams were fed a 90% Fe deficient or standard NIH-07 diet from E15 through P28. Within each litter, different offspring were treated with 100 mg/kg Mn (100Mn) by oral gavage or vehicle from P4 to P28. As adults, offspring were tested in the Morris Water Maze (MWM). Progeny in the 100Mn group, regardless of FeD or DS, showed increased latency on acquisition trials and decreased platform crossings on the probe trial. The interaction of FeD and DS also impaired MWM performance. A potential mechanism underlying these deficits in 100Mn animals is decreased long-term potentiation that we observed in slice preparations in the hippocampus. DMT1 and ZIP8, metal transporters in the CNS, showed increased protein in the hippocampus via Western blot in treated groups; ZIP8 was decreased only in the FeD/100Mn compared with controls. Together these data suggest that multifactorial models may reveal effects not observed when only one factor is studied at a time. (Supported by NIH T32 ES07051 and P30 ES006096)

PS 1087n Characterization of the Neuropathological Consequences of Plac1 Ablation in the Developing Mouse Embryo

J. Bourgeois[1], X. Kong[2], J. Fuentes[2], R. D. Harbison[1], G. T. Johnson[1, 2] and M. Fant[2]. [1]*Environmental and Occupational Health, College of Public Health, University of South Florida, Tampa, FL and* [2]*Pediatrics, College of Medicine, University of South Florida, Tampa, FL.*

Placenta-specific 1 (Plac1) is an X-linked gene that is essential for normal placental development. Plac1 is also expressed in the fetal brain and paternally imprinted. Expression is markedly downregulated immediately after birth. Plac1 ablation predisposes Plac1-null males and Xm-X Hets (inactive maternal allele) to an increased risk of developing lethal postnatal hydrocephalus suggesting a functional role for Plac1. The objective of this study was to characterize the effect of Plac1 on brain development. A mutant Plac1 mouse model, established on the C57BL/6J background, was studied. Embryo and brain sections were obtained at various stages of development. Plac1 expression was assessed by qRT-PCR, immunohistochemistry (IHC), and in situ hybridization (ISH). Brain structure was assessed by histopathological and magnetic resonance imaging. Results revealed Plac1 expression throughout the embryonic brain when assessed by qRT-PCR, IHC, and ISH at E14.5-E18.5. MRI analysis of an adult Plac1 knockout (KO) brain revealed microcephaly (10%), a dysmorphic cerebellum, and increased heterogeneity of the medulla. Consistent with these findings, H&E staining of the KO brain revealed a smaller cortical mantle, a dysmorphic hippocampus, and a dysmorphic cerebellum with reduced folia and major disruptions in development and significantly reduced neuronal cell numbers. Similarly, anti-NeuN staining of an Xm-X Het revealed decreased neuronal cell numbers. In conclusion, Plac1 is a paternally imprinted, X-linked gene that is essential for normal brain development. Plac1 ablation is associated with the disruption of axonal development and decreased neuronal cell number. The Plac1 promoters are under the control of RxR in combination with other transcriptional regulators. It is therefore likely that Plac1-mediated signaling pathways are relevant to neuropathies associated with disruptions in retinoic acid signaling.

PS 1087o Evaluation of Environmental Chemicals Computationally Predicted to Disrupt Angiogenesis

T. Heinonen[1], T. Toimela[1], T. B. Knudsen[2], N. Kleinstreuer[3] and R. Sarkanen[1]. [1]*FICAM, University of Tampere, Tampere, Finland,* [2]*National Center for Computational Toxicology, US EPA, RTP, NC and* [3]*ILSI, Inc./ NICEATM/NIEHS, RTP, NC.*

The aim of this study was to investigate the effect of 10 chemicals, predicted by ToxCast and a virtual tissue model to impact angiogenesis at varying degrees, in an in vitro human cell-based angiogenesis assay. Angiogenesis is critical for embryonic development and reproduction in general, and contributes to the pathogenesis of numerous disorders. This human cell based angiogenesis assay may serve as a test to detect potential antiangiogenic substances including teratogens. The test chemicals were selected from the ToxCast project based on predicted antiangiogenesis activities (strong, weak, negative). The co-culture of human fibroblasts and human endothelial cells (HUVEC) was exposed to test chemicals at a concentration range of 10 pM to 10 mM (limited by the solubility). After 24 h, the neutral uptake assay (NRU) was performed for EC80 cytotoxicity value for each test chemical. Extent of tubule formation was microscopically assessed after 6 days in culture. The concentrations of each test chemical that produced less than 20% cytotoxicity in the NRU test were selected for tubule formation analysis. Potency order for in

vitro inhibition of tubule formation (IC50) was: Octyl gallate 1 μM > Triclosan 1.7μM > 1-hydroxypyrene 11 μM> Disulfiram 23 μM> Sodium dodecylbenzene sulfonate 44 μM > Diethanolamine 1788 μM. With Sodium dodecylbenzene sulfonate the inhibition of tubule formation was considered to be cytotoxicity-related. Tert-butylhydroquinone did not inhibit tubule formation at non-cytotoxic concentrations. Tris- (2-chloroethyl) phosphate, Mannitol and Decane were neither cytotoxic at the concentration range tested nor markedly inhibited tubule formation. Decane showed only minor inhibition of tubule formation. The in vitro results were generally consistent with prospective predictions from the in silico models with respect to antiangiogenic potential. This abstract does not necessarily reflect US EPA policy.

PS 1087p Computational Modeling of Limb Development Using ToxCast High-Throughput Screening Data for Predictive Toxicology

B. K. Ahir[1], N. S. Sipes[1], N. C. Baker[2], R. M. Spencer[2], M. C. Leung[1], R. DeWoskin[3], R. Judson[1], M. T. Martin[1] and T. B. Knudsen[1]. *[1]U.S. EPA-ORD, NCCT, RTP, NC, [2]U.S. EPA-ORD, NCCT-Lockheed Martin, RTP, NC and [3]U.S. EPA-ORD, NCEA, RTP, NC.*

Skeletal defects are one of the major adverse outcomes observed across many prenatal developmental toxicity studies. We mined the ToxCast database (ToxCastDB) for in vitro chemical-bioactivity profiles that significantly correlated with skeletal defects in the Toxicity Reference Database (ToxRefDB). Using high-throughput screening (HTS) data from >1060 chemicals tested in 860 assays, 734 chemicals had in vivo developmental toxicity data in ToxRefDB and 44 (4-5%) produced fetal limb defects. In addition, we identified 112 ToxCast chemicals not in ToxRefDB that according to published articles produced limb defects. Significant univariate associations (e.g., assay-endpoint) were used to filter HTS assays based on statistical correlation ($p<0.05$) with distinct in vivo developmental limb defects. Retinoic acid receptors (RARs) assays emerged as the top target and were activated by 17 ToxCast chemicals. Retinoic acid (RA) signaling plays an essential role in limb patterning as a ligand for nuclear RA receptors. We incorporated RA signaling into a multicellular agent-based model (ABM) of early limb development in CompuCell 3D. The ABM stimulates complex cellular interactions (adhesion, apoptosis, chemotaxis, migration, mitosis, secretion) through formation of apical epidermal ridge, zone of polarizing activity, and expansion of mesenchyme driven by morphogenetic signals (BMPs, FGFs, SHH, RA). To evaluate the model we selected two known prototypes: Dieldrin (AC50 = 4.8 μM on RARγ, and 0.974 μM on RARα) and Aldrin (AC50 = 45.5 μM on RARγ, and inactive on RARα) based on ToxCast data. Simulating the impact of RAR disruption by these compounds on other pathways (e.g. SHH, FGFs) in the limb model can provide insight into the spatial-temporal dynamics of altered limb development as a tool for predictive toxicology. [This abstract does not necessarily reflect EPA policy.]

PS 1087q Evaluation of the Mechanism of Misoprostol-Induced Limb Defects Using a Late Organogenesis Rat Embryo Culture

M. Cavieres[1, 2] and O. Madrid[1]. *[1]Facultad de Farmacia, Universidad de Valparaíso, Valparaíso, Chile and [2]Centro Regional de Estudios de Alimentos Saludables, Valparaíso, Chile.* Sponsor: E. Faustman.

Prostaglandins of the E-series play an important role on bone metabolism and limb development. Misoprostol is a prostaglandin E1 analog and is registered in Chile for the prevention and treatment of non-steroidal anti-inflammatory peptic ulcers. It is also used to induce abortions. In utero exposure to misoprostol, after failed abortion attempts, has been associated to joint and skeletal defects, although the mechanism of action which mediates this teratogenicity is unknown. Since misoprostol can act on prostanoid receptors expressed during limb development, we hypothesized that this interaction could explain the induction of limb defects. In order to test this hypothesis, we established a late organogenesis embryo culture to model the effect of misoprostol on limb development in which to evaluate functionality, growth and morphology. GD13.5-collected rat fetuses were cultured for 24 hours at 37 °C, in rat serum diluted in Hank's solution which also contained either 200, 2.000 or 20.000 pg/mL misoprostol, PGE2 or the EP1 and EP2 antagonist, AH6809. 1000 mg/L sodium penicillin G and 50 μg/ml ketoconazole were used as negative and positive control, respectively. All concentrations of misoprostol, PGE2 and the antagonist induced similar toxicity, inducing abnormal clefts and decrease of bone development in anterior limb digital rays. However, they did not alter growth and functionality parameters. In conclusion, misoprostol induces overt manifestations of alterations of limb development, which may not be mediated by prostanoid receptors EP1 or EP2.

PS 1087r Peripheral Blood Changes in Rats Developmentally Exposed to Volatile Organic Compounds: Shifts in Leukocyte Distribution

E. Quist[1, 2], A. J. Filgo[1, 3], D. H. King[1], G. Travlos[1], C. D. Bortner[1], M. I. Sifre[1], G. Kissling[1] and S. E. Fenton[1]. *[1]NIEHS, Research Triangle Park, NC, [2]Comparative Biomedical Sciences, North Carolina State University, Raleigh, NC and [3]Curriculum in Toxicology, University of North Carolina, Chapel Hill, NC.*

Volatile organic compounds (VOCs) such as benzene, trichloroethylene (TCE), 1,2-dichloroethylene (1,2-DCE), perchloroethylene (PERC) and vinyl chloride (VC) are important industrial solvents used in dry cleaning agents, dyes, and varnishes, among others. Since the mid-1970s, environmental or occupational exposures to these VOCs have been associated with increased incidences of cancer, particularly leukemia and lymphoma. Epidemiological studies indicate that ingestion of contaminated drinking water or inhalation of volatile gases in the air, are the most likely routes of environmental VOC exposure. Developmental exposures to VOCs (e.g. during pregnancy or in infancy) can be especially detrimental and often result in malformations, congenital abnormalities and later life disease. In this study, Harlan Sprague-Dawley rats were pre-natally and peri-natally exposed to drinking water containing a VOC-mixture of 5, 10 and 50-fold well water concentrations (5X, 10X, 50X) of benzene, TCE, DCE, PERC and VC from gestation day 12 (GD 12) through post-natal day 48 (PND 48). While all dosed animals exhibited elevated leukocyte counts compared to age-matched controls, 5-7-fold elevations were observed within the two higher dose groups (10X and 50X). In addition, examination of peripheral blood smears of the 10X and 50X animals revealed increased numbers of circulating large granular lymphocytes, particularly within the 10X group. These changes possibly suggest a bone marrow response in leukocyte production or, more likely, a shift in leukocyte distribution from the tissue reservoir to the circulatory pool as a result of developmental exposure to VOCs.

PS 1087s DNA Methylation Is Required for Mouse Prostate Development

K. P. Keil[1], L. L. Abler[1], V. Mehta[1], H. M. Altmann[1], J. Laporta[2], L. L. Hernandez[2] and C. M. Vezina[1]. *[1]Comparative Biosciences, University of Wisconsin Madison, Madison, WI and [2]Dairy Science, University of Wisconsin Madison, Madison, WI.*

A number of dietary and environmental chemicals including but not limited to bisphenol-A (BPA), bis(2-ethylhexyl)phthalate (DEHP), and 2,3,7,8 tetrachlorodibenzo-p-dioxin (TCDD) are capable of altering ductal development and disrupting DNA methylation patterns in developing mouse prostate. Whether these actions are mechanistically linked is not known in part because the role of DNA methylation in neonatal mouse prostate development is not known. The purpose of this study was to determine whether DNA methylation participates in mouse prostate development. 14 days post coitus (dpc) mouse urogenital sinuses were cultured for 2 days in the presence or absence of a DNA methylation inhibitor and then 1, 3 or 5 days in media containing dihydrotestosterone (androgen) without DNA methylation inhibitor. At the end of the culture period, *in situ* hybridization was used to visualize and count prostatic buds, immunohistochemistry was used to determine the index of androgen receptor (AR) positive cells, and methylated DNA immunoprecipitation was used to assess *Ar* DNA methylation. The DNA methylation inhibitor reduced *Ar* promoter methylation, increased AR protein abundance, increased the number and rate of prostatic buds formed, and caused prostatic buds to form in response to a lower concentration of androgen. Thus, we conclude that DNA methylation creates a permissive environment for mouse prostatic outgrowth, and primes the prostate primordium to respond to developmental cues mediating prostate ductal development. These results raise the possibility that endocrine disrupting chemicals could alter prostate development by perturbing DNA methylation. Supported by NIH grant DK096074 and ES001332 and NSF grant DGE-0718123.

PS 1087t Pregestational Ethinylestradiol Exposure Postpones Pubertal Onset and Decreases Body Weight in Both Male and Female Offspring in Rats

D. Wu, W. Zhang, K. Xu, D. Chen and X. Wang. *Department of Toxicology, Nanjing Medical University, Nanjing, Jiangsu, China.*

Ethinylestradiol (EE) is used for medical treatment and as contraceptives in females and its exposure during gestational period has been proved to elicit reproductive abnormalities in both male and female offspring. To test whether pre-gestational EE exposure also affects reproductive development, especially pubertal timing in the offspring, female Sprague-Dawley rats were treated orally with EE (0, 50, 200, 800 μg/kg/d) for 15d. Another 30d later, they mated with normal males and gave

birth to the offspring. Litter size and litter sex ratio were recorded. Anogenital distance (AGD) and body weight were measured every 5d since postnatal day 1(P1). Age at vagina opening in females and penis stripping in males were recorded to mark pubertal onset. Rats were sacrificed on P51. Ovarian/testis mass, serum estrodial (E2)(females), testosterone (T)(males) levels were detected. Results showed no significant difference in litter size and litter sex ratio. However, mothers with pre-gestational 50, 200, 800 μg/kg/d EE treatment had offspring with significantly lower body weight and higher AGD/body weight ratio than the control group since P1. Maternal pre-gestational EE exposure significantly postponed the puberty onset in male and female offspring in 200 and 800 μg/kg/d groups. Body weight at pubertal onset was significantly lower in 50 μg/kg/d group in males and females. Hormone assay data indicated T in males was higher in 200 and 800 μg/kg/d groups than control and no difference was found in E2 in females. Ovarian/body weight ratio in females and testis/body weight ratio in males were not different among groups. These data indicated that maternal pre-gestational EE exposure might cause alteration in the neuroendocrine system to give rise to pubertal developmental disruption but might not lead to adverse effects in gonads. Since no significant sex-specific difference was observed and all treated groups had lower body weight, alteration of metabolic signals activating the reproductive axis may underlie the induced pubertal development disruption.

PS 1087u Characterization of Developmental Aryl Hydrocarbon Receptor Signaling in the Mouse

B. P. Johnson, E. Stevens and C. A. Bradfield. *Oncology, UW-Madison, Madison, WI.*

The aryl hydrocarbon receptor (AHR) is a ligand binding transcription factor known for its role in the adaptive metabolism of xenobiotics. Phenotypic observations of untreated AHR mutant mice suggest that the AHR is also involved in natural developmental processes. Mutants at Ahr display vascular aberrations such as a patent ductus venosus (DV), poor hepatic perfusion and late embryonic stage hepatic necrosis in developing pups, although the nature and function of AHR signaling in this context is still uncharacterized. We set out to narrow down the timing and cellular location of these natural AHR signaling events and to characterize the transcriptional targets and pathways mediated by "natural" AHR activation. We employed mice carrying Cre-recombinase transgenes driven by various promoters crossed with mice carrying a conditional Ahr allele and identified TEK+ and CDH5+ "endothelial" cells as those cells where intact AHR signaling is required for normal DV closure and to prevent hepatic necrosis. We then isolated this cell population using CDH5+ dependent cell sorting and transcriptionally profiled these cells from wild-type (WT) and Ahr-/- mice at E15.5 and E18.5. We found that loss of AHR in this cell population resulted in the dysregulation of transcripts activated by the hypoxia signaling pathway and biomarkers of renal toxicity, but not of known AHR target genes. Next, we applied an inducible Cre-recombinase model and identified the critical window of "natural" AHR signaling, just after birth, and found that this signaling is sensitive to xenobiotic ligand. Given that AHR signaling is required for normal vascular development and that the phenotypes studied herein were initially identified as subtle differences found in adult mice, it is plausible that exposure to xenobiotic AHR ligands at birth could interfere with normal signaling processes and have subtle deleterious effects on vascular development.

PS 1087v Influence of Maternal Stress on Gestational Parameters and Prenatal Development in Himalayan Rabbits

S. S. Schneider[1], I. Fegert[2], C. Werner[2] and B. van Ravenzwaay[1]. [1]*Toxicology, BASF SE, Ludwigshafen/Rhein, Germany and* [2]*Regulatory Toxicology Crop Protection, BASF SE, Ludwigshafen, Germany.*

Gestational stress is hypothesized to enhance the developmental toxicity of chemicals. Single stress factors like food restriction have been reported to be associated with resorptions, abortions, reduced fetal weight, and alterations in ossification in rabbits. But, little is known about how maternal stress from handling alters fetal development, confounding the data interpretation of regulatory prenatal toxicity studies. In the present experiment we exposed 25 pregnant Himalayan rabbits per group to two daily handling protocols aimed to increase maternal stress: restraint (15 min per day) and restraint plus dressing the animals with stretchable bandages for 6 hours per day. These groups were compared with an unexposed control group. Investigations and data assessment were made in accordance with standard regulatory guidance, i.e. OECD TG 414 and OPPTS 870.3700. Neither stress protocol affected any of the parameters routinely used to characterize maternal toxicity. No adverse clinical signs were noted; nor was food consumption or (net) body weight gain in the pregnant rabbits influenced. Restraint stress alone had no influence on prenatal development; however, the combination of restraint plus dressing stress produced 4 abortions and an early resorption rate of almost 50%. Prenatal development of the surviving offspring was not impaired. Thus, a combination of two handling stressors which do not evoke obvious pathological findings in pregnant rabbits is able to produce severe prenatal developmental toxicity. When taken together with other investigations, these data suggest that the nature of these findings, in this case intrauterine death, is likely specific to the stressor and hypothetically even the species or the strain being tested. Furthermore, we speculate that when combined with handling, the stress due to chemical exposure may cause developmental findings in the absence of frank maternal toxicity, simulating a test substance-specific effect.

PS 1087w An Oral Prenatal Developmental Toxicity Study with Tetrabromobisphenol A (TBBPA) in CD Rats

M. L. Dourson[1], R. Cope[1] and S. Kacew[2]. [1]*Toxicology Excellence in Risk Assessment, Cincinnati, OH and* [2]*Cellular and Molecular Medicine, Faculty of Medicine, University of Ottawa, Ottawa, ON, Canada.*

The objective of this GLP OECD TG 414/US EPA OPPTS GL No. 870.3700 study was to discern the effects of oral TBBPA (0, 100, 300 or 1000 mg/kg bw/d; gavage) on embryonic/fetal development from gestation days (GDs) 0 to 19.No test article-related mortality was observed in any of the dams. Sporadic ptyalism in dams was associated with the administration of TBPPA at doses of ≥ 300-mg/kg bw/d. Because of the sporadic nature of this effect, and lack of a clear dose response, the effect was regarded as being non-adverse and related to the normal taste response following exposure to residual amounts of the test article on the dosing catheters. No other test article-related effects including clinical examinations, gestational parameters, body weight, body weight gain, food consumption, uterine implantation, gravid uterine weight, number of uterine implantations, number of corpora lutea, number of early/late resorptions, number of viable/non-viable fetuses, fetal sex distribution, individual fetal weights, liver weights of dams, fetal external examinations, fetal visceral examinations, fetal skeletal examinations and macroscopic pathology examinations of the dams were observed.The NOEL for maternal and developmental toxicity was 1000 mg/kg bw/d, the highest dose evaluated.

PS 1087x An Oral Two Generation Reproductive, Fertility and Developmental Neurobehavioral Study of Tetrabromobisphenol A (TBBPA) in CD Sprague-Dawley Rats

R. Cope[1], M. L. Dourson[1] and S. Kacew[2]. [1]*Toxicology Excellence in Risk Assessment, Cincinnati, OH and* [2]*Institute of Population Health, University of Ottawa, Ottawa, ON, Canada.*

The objective of this GLP US EPA OPPTS 870.3800 study was to discern the effects of TBBPA (10, 100 or 1000 mg/kg bw/d; gavage) over the course of 2 generations (P and F1) on growth and development of offspring (F1 and F2). A developmental neurotoxicity/neuropathology assessment was also conducted on a F2 generation cohort.

Exposure to ≥ 100-mg/kg bw/d TBBPA was associated with changes in the peripheral thyroid levels in rats that were explainable on the basis of induction of liver catabolism, a phenomenon that is known to be not relevant to humans. TBBPA at up to 1000 mg/kg bw/d was not associated with any significant non-neurological effects on reproduction, growth and development. A subtle reduction, of unknown biological relevance, in the thickness of the parietal cortexes of 11-day-old F2 pups from the 1000 mg/kg bw/d group was noted. However, this change was not accompanied by evidence of micro-anatomic change. The functional relevance of this finding at present remains obscure and needs to be interpreted with caution given the limitations of the morphometric analysis. No other test article-related effects on developmental neurotoxicity/neuropathology were present including no test article-related effects on detailed clinical observations, developmental maturation landmarks, neurobehavioral evaluations and Day 60 brain weights.

PS 1088 Effect of a Nutrient Mixture on Matrix Metalloproteinase-9 Dimers in Various Cancer Cell Lines

M. Roomi, M. Rath and A. Niedzwiecki. *Dr. Rath Research Institute, Santa Clara, CA.*

Strong clinical and experimental evidence demonstrates association of elevated levels of matrix metalloproteinase (MMP)-9 with cancer progression, metastasis and shortened patient survival, as it plays a key role in tumor cell invasion and metastasis by digesting the basement membrane and ECM components. MMP-9 is secreted in both monomer and dimer forms. Though there is little research on MMP-9 dimers, some studies have shown the dimer to be associated with more

aggressive tumor progression. Our objective was to study the relative secretion patterns of MMP-9 dimer in various carcinomas, sarcomas, adenocarcinomas and leukemias and the effect of a nutrient mixture (NM) containing lysine, proline, ascorbic acid and green tea extract on dimer secretion.
The cancer cell lines were grown in their respective media, supplemented with 10% FBS, penicillin (100 units/ml), and streptomycin (100 μg/ml) in 24-well tissue culture plates. At near confluence, the cells were treated with NM at 0,10, 50, 100, 500 and 1000 μg/ml. Parallel sets of cultures were treated with phorbol 12-myristate 13-acetate (PMA) 100 ng/ml for induction of MMP-9. Cell MMP-9 secretion was assayed by gelatinase zymography.
No MMP-9 dimer secretion was observed in prostate, pancreatic, colon, bladder, head and neck, glioblastoma and leukemia cell lines. MMP-9 dimer secretion only with PMA induction was seen in sarcomas, melanoma and breast, lung and tongue cancer cell lines. Cervical, renal and hepatic carcinomas exhibited MMP-9 dimer without PMA treatment and increased secretion with PMA treatment. Sarcomas demonstrated the highest combined levels of MMP-9 monomer and dimer with and without PMA among these cancer cell lines. NM showed dose-dependent inhibition of MMP-9 monomer and dimer in all cell lines tested.
In conclusion, high MMP-9 secretion levels correlated with more aggressive cancer cell lines. NM was effective in inhibiting MMP-9 monomer and dimer secretion in all cell lines tested, suggesting its therapeutic potential as an antimetastatic agent.

PS 1089 Increased Susceptibility of Rats versus Mice to N-Butyl-N-(4-hydroxybutyl) Nitrosamine (BBN)-Induced Urinary Bladder Tumors

M. Tirmenstein[1], E. Janovitz[2], Y. Song[3], S. Chen[3], K. Phillips[3], T. Dorr[1], M. J. Graziano[3] and T. P. Reilly[3]. [1]*Bristol-Myers Squibb, New Brunswick, NJ,* [2]*Bristol-Myers Squibb, Hopewell, NJ and* [3]*Bristol-Myers Squibb, Princeton, NJ.*

BBN is a potent and specific urinary bladder carcinogen that has been utilized in experimental models of 2-stage tumor promotion. However, the dose-response of BBN on key tumorigenic events are not well understood since they have not been systematically evaluated and BBN is usually administered in drinking water as a single concentration. The current study was conducted to better understand the dose-response relationship between BBN administration and the incidence of urinary bladder tumors in mice and rats. BBN was administered by oral gavage twice weekly for 6 weeks to either male C57Bl/6J mice (0, 125, 250, 500 mg/kg; N= 45) or male Sprague-Dawley rats (0, 100, 200, 400, 800 mg/kg; N = 20). Necropsies were conducted at 10 (mice only), 14 and 24 weeks following the initiation of BBN administration. In mice (10 weeks) and rats (14 weeks), BBN caused a dose-dependent increase in oxidative DNA damage (8-hydroxguanosine staining) and cell proliferation (Ki-67 staining) in urinary bladder transitional cells. Despite the urinary bladder transitional cell hyperplasia, BBN was associated with a very low incidence of urinary bladder tumors (≈1% incidence) in mice over the full 24-week period. In contrast, BBN-treated rats exhibited a dose-dependent increase in atypical hyperplasia and transitional cell papillomas and carcinomas in the urinary bladder, with a 20, 47, 57, and 93% incidence of urinary bladder tumors across doses after 24 weeks. Thus, BBN induced urinary bladder tumors in male Sprague-Dawley rats with a steep dose response relationship, but was not effective in producing bladder tumors in male C57Bl/6J mice at comparable doses despite underlying evidence of DNA damage and hyperplasia. The steep dose response observed with BBN and relative species susceptibility highlight important considerations in designing urinary bladder tumorigenesis studies with BBN.

PS 1090 Reduced Body Weight Gain Prolongs Early-Life Levels of Tyrosine Hydroxylase Expression in Hypothalamic Tuberoinfundibular (TIDA) Neurons in Wistar Rats

S. Plummer[1], M. Beltran[1], N. Kuan[1], M. Millar[2], R. Weigand[3], R. Currie[4], R. Green[4] and J. Wright[4]. [1]*MicroMatrices Associates Ltd, Dundee, United Kingdom,* [2]*MRC Centre for Reproductive Health, Edinburgh, United Kingdom,* [3]*MRC Centre for Inflammation Research, Edinburgh, United Kingdom and* [4]*Syngenta Ltd, Bracknell, United Kingdom.*

Calorific restriction in Wistar rats leads to a decreased incidence of mammary and pituitary tumours and an increase in uterine tumours (1, 2, 3) relative to concurrent controls. Previously we found (4) that lean female Wistar rats (>30% body weight gain reduction cf. controls) from a 2 year bioassay showed increased expression of tyrosine hydroxylase (TH) mRNA and protein in hypothalamic TIDA neurons. We have postulated that alterations to leptin signalling, resulting from reduced body fat, could maintain dopaminergic inhibition of prolactin secretion and prolong pro-oestrogenic stimulation of the uterine epithelium. The present study explored (i) the time–dependency of the effects on TIDA neuron TH expression, using immunostaining (IHC), in situ hybridisation (ISH) and image analysis on FFPE tissue from 90 day, 12 month and 2 year studies; and (ii) pathways involved in prolactin and oestrogen signalling, regulated by the hypothalmo-pituitary axis, that might promote uterine carcinogenesis.
TH RNA and protein expression decreased with time in controls, whilst lean rats maintained their TH levels. Laser dissection targeted microarray analysis of hypothalamus, pituitary and uterus revealed down-regulation of pituitary prolactin, hypothalamic GABA B receptors, and leptin receptor (LEPR) signalling molecules STAT3 and PDE3B, and up regulation of uterine oestrogen receptor alpha (ESR1). Immunostaining for ESR1 showed increased expression in uterus. These results support previous observations that chronic reduction in bodyweight gain alters regulation of hypothalamic dopamine, with downstream consequences on hormonal control of prolactin, oestrus cycle prolongation, and potential to increase the incidence of uterine tumours.

1. Roe et al. 1995;
2. Keenan, et al. 1995;
3. Harlemann et al. 2012.
4. Plummer et al 2013

PS 1091 The Effects of Testosterone on NNK-Induced Lung Tumorigenesis in Female and Male A/J Mice

Y. Nakano[1], M. Yokohira[1], F. Ninomiya[1], S. Kishi[1], K. Yamakawa[1], S. Kanie[1], K. Saoo[1, 2] and K. Imaida[1]. [1]*Onco-Pathology, Kagawa University, Faculty of Medicine, Kita-gun, Kagawa, Japan and* [2]*Tomakomai City Hospital, Tomakomai, Hokkaido, Japan.*

It is well known that there is sex difference of the sensitivity of the lung carcinogenesis. In human, lung adenocarcinomas of female are higher incidence than those of male. In experimental animals, A/J mice shows similar pattern with humans. So, the lung carcinogenesis might be associated with sexual hormones. The present study is conducted to investigate the effects of testosterone on the lung carcinogenesis in A/J mice.
In experiment 1, female A/J mice were separated into 4 groups. Groups 1 and 2 were treated with interperitoneal injections (i.p.) of 4-(methylnitrosamino)-1-(3-pyridyl)-1-butanone (NNK) (2mg/0.1ml saline/mouse) at weeks 0 and 1. At week 3, testosterone pellets (90-day release, 25mg/pellet/mouse, Innovative Research of America) were implanted under the shoulder skin in groups 1 and 3, and control pellets (placebo) were implanted in groups 2 and 4. All mice were sacrificed at week 15.
In experiment 2, male A/J mice at 6 week-old were separated into 6 groups. Group 1, 2, 5 and 6 were castrated two weeks ago before groups 1, 2, 3 and 4 were treated with i.p. of NNK at weeks 0 and 1. At weeks 3 and 9, testosterone pellets were implanted in groups 1, 3 and 5. Groups 2, 4 and 6 were implanted placebo pellets at week 3 and treated sham operation at week 9. All mice were sacrificed at week 15.
In experiment 1, the female mice showed significant decreasing of multiplicity of lung tumors with higher testosterone level in their blood. However, in male mice (experiment 2), there were no significant differences of the multiplicity or area of lung tumors with no different concentrations of testosterone in the serum. Therefore, testosterone has possibilities to inhibit NNK-induced lung carcinogenesis in female A/J mice, but not in male mice.
In conclusion, the testosterone is suggested to have tumor-suppressing effecton lung tumorigenesis, but there could be sex difference or other factors.

PS 1092 Activation of ERK1/2 on NNK-Induced Lung Carcinogenesis in A/J Mice

K. Yamakawa[1], S. Kishi[1], M. Yokohira[1], Y. Nakano[1], F. Ninomiya[1], S. Kanie[1], K. Saoo[2] and K. Imaida[1]. [1]*Onco-Pathology, Kagawa University, Faculty of Medicine, Kita-gun, Kagawa, Japan and* [2]*Tomakomai City Hospital, Tomakomai, Hokkaido, Japan.*

The extracellular signal-regulated kinase 1/2 (Erk1/2) signaling pathway is activated by several growth factors and mitogens, and up-regulation has been noted in many human cancers, including lung cancers. In this study, we examined immunohistochemical expression of phosphorylated forms of Erk1/2 (pErk1/2) and correlation between Erk activation and mutation of *Kras* encoding an upstream activator of Erk1/2, in a mouse lung carcinogenesis model. Female 7-week old A/J mice were administered a single dose of 4-(methylnitrosamino)-1-(3-pyridyl)-1-butanone (NNK), then maintained without additional treatment until sacrifice at week 52. We analyzed immunohistochemical expression of pErk1/2 in 26 hyperplasias, 50 adenomas, and 17 adenocarcinomas. The pErk1/2-positive cells were relatively rare expression levels in adenocarcinomas being markedly higher than in hyperplasias and adenomas (~5-fold, ~4-fold; $p<0.01$). In adenocarcinomas, the pErk1/2 positive cells were scattered at the periphery of the tumor. In many areas of pErk1/2 positive cells in adenocarcinoma, level of PCNA expression was higher than in pErk1/2 negative portions. Activating mutations of *Kras* gene at codons 12

or 13 were detected in 19 of 25 adenomas (76%), and 10 of 14 adenocarcinomas (71%). The vast majority of adenomas harboring *Kras* mutation, were negative or had only faint expression of pErk1/2, and level of pErk1/2 expression did not correlate with the *Kras* mutation status in either adenomas or adenocarcinomas. These results suggest that activating Erk1/2 plays a key role in malignant transformation during mouse NNK-induced lung carcinogenesis, apparently independent of *Kras* mutation.

PS 1093 Effects of Gonadectomy on Lung Carcinogenesis Induced by 4-(methylnitrosamino)-1-(3-pyridyl)-1-butanone (NNK) in Both Sexes of A/J Mice

F. Ninomiya, M. Yokohira, S. Kishi, Y. Nakano, K. Yamakawa, T. Inoue, T. Kuno and K. Imaida. *Onco-Pathology, Kagawa University, Faculty of Medicine, Kita-gun, Kagawa, Japan.*

It is well known that female mice are more sensitive to chemical lung carcinogenesis than males. In order to investigate our hypothesis that the lung carcinogenesis may be affected by sex hormone levels, both sexes of A/J mice were gonadectomized and were examined about their lung carcinogenesis induced by 4-(methylnitrosamino)-1-(3-pyridyl)-1-butanone (NNK). NNK is a tobacco-specific N-nitrosamine which is considered to play important roles in cigarette-related lung cancer, and also induces lung adenocarcinoma in rodents.
In the present experiment, 18- and 56-week studies were conducted. Male and female A/J mice were separated into gonadectomized and unoperated groups. All animals were treated intraperitoneal injection of NNK at the dose of 2 mg/mouse, with 2 injections at weekly interval in the 18-week study and 1 injection in the 56-week study. All of surviving mice were sacrificed at the ends of an experiment period.
Lung proliferative lesions were detected in all mice of all groups. In the control groups of 18- and 56-week studies, the multiplicities of lung nodules were significantly greater in females than in males. In the 56-week study, the males showed the multiplicity of macroscopical lung nodules, histopathological bronchiolo-alveolar hyperplasias, adenomas and tumors were increased significantly by castration. In the 18-week study, females showed the multiplicity of adenomas were decreased significantly by ovariectomy.
From these results, female A/J mice are more susceptible for lung carcinogenesis induced by NNK than males and gonads play important roles in determining sex differences in the lung carcinogenesis in A/J mice. It is suggested that the progression of lung tumor could be inhibited by testosterone and promoted by estradiol.

PS 1094 7-GSH-Pyrrole Adducts Is a Potential Active Metabolite Leading to Pyrrolizidine Alkaloid-Induced Cytotoxicity and Tumorigenicity

Q. Xia[1], L. Ma[1], L. Cai[2] and P. Fu[1]. *[1]NCTR, FDA, Jefferson, AR and [2]Biotranex LLC, Monmouth Junction, NJ.* Sponsor: L. Guo.

Pyrrolizidine alkaloid (PA)-containing plants are the most common poisonous plants affecting livestock, wildlife, and humans. PAs require metabolic activation to form pyrrolic metabolites, including (±)-6,7-Dihydro-7-hydroxy-1-hydroxymethyl-5H-pyrrolizine (DHP), to exert cytotoxicity and tumorigenicity. We previously determined that four DNA adducts were formed in rats dosed with tumorigenic PAs. The structures of the four DNA adducts were elucidated as (i) a pair of epimers of 7-hydroxy-9-(deoxyguanosin-N2-yl)dehydrosupinidine adducts (termed as DHP-dG-3 and DHP-dG-4) as the predominant adducts; and (ii) a pair of epimers of 7-hydroxy-9-(deoxyadenosin-N6-yl)dehydrosupinidine adducts (termed as DHP-dA-3 and DHP-dA-4 adducts). 7-GSH-DHP is a metabolite of PAs formed in vivo and 7,9-di-GSH-DHP is a metabolite found in vitro. Glutathione (GSH)-pyrrolic conjugates were considered as detoxified metabolites. In this study, we determined that reaction of 7-GSH-DHP and dexoyguanosine (dG) in water formed both DHP-dG-3 and DHP-dG-4 adducts in a concentration and time dependent manner. Besides, DHP-dG-1 and DHP-dG-2 adducts, of which dG binds to the C7 position of DHP, were formed as predominant products. Similarly, reaction of 7-GSH-DHP with deoxyadenosine (dA) generated DHP-dA-1 and DHP-dA-2 as predominant adducts and DHP-dA-3 and DHP-dA-4 as minor adducts. The structures of all these adducts were determined by comparison of their HPLC retention times, UV-visible absorption spectra, and LC/MS data with those of previously synthesized standards. In contrast, no DHP-dG or DHP-dA adducts were formed from reaction of 7,9-di-GSH-DHP with dG or dA. This study represents the first report that a GSH-pyrrole adduct can be a potential active metabolite leading to PA-induced cytotoxicity and tomorigenicity. (This article is not an official guidance or policy statement of the U.S. FDA. No official support or endorsement by the U.S. FDA is intended or should be inferred.)

PS 1095 ALDH1B1 Is Required for Colon Tumorigenesis by Modulating WNT-Signaling and Metabolizing Retinaldehyde

S. Singh[1], J. Arcaroli[3], Y. Chen[1], B. C. Jackson[1], W. Messersmith[3], D. Orlicky[4], D. Thompson[2] and V. Vasiliou[1]. *[1]Department of Pharmaceutical Sciences, University of Colorado Anschutz Medical Campus, Aurora, CO, [2]Department of Clinical Pharmacy, University of Colorado Anschutz Medical Campus, Aurora, CO, [3]Division of Medical Oncology, University of Colorado School of Medicine, Aurora, CO and [4]Department of Pathology, University of Colorado School of Medicine, Aurora, CO.*

Aldehyde dehydrogenase 1B1 (ALDH1B1) is a mitochondrial enzyme that shows 65% and 72% amino acid homology with ALDH1A1 and ALDH2, respectively. In human normal colon, ALDH1B1 is expressed only at the crypt base, along with stem cells. It is highly expressed in all cancerous cells of human colonic adenocarcinomas. This pattern of expression corresponds closely to that observed for Wnt signaling activity in normal and cancerous colon. In the present study, we show that shRNA mediated knockdown of ALDH1B1reduced the number and size of spheroids formed by human colon cancer cells in a three-dimensional matrigel culture. In addition, ALDH1B1 knockdown depletes the putative highly carcinogenic ALDHbright colon cancer cells and significantly decreased xenograft tumor formation in athymic (nu+/nu+) mice. Gene expression studies on the Wnt-signaling pathway revealed upregulation of Axin2 (a negative regulator of the Wnt pathway) and downregulation of beta-catenin (a critical protein in the canonical Wnt-signaling pathway) and Wnt dependent transcription of cMyc in ALDH1B1-depleted colon cancer cells. We have also found that ALDH1B1 metabolizes all trans-retinaldehyde efficiently with Km of 25 μM to generate retinoic acid which has been reported to increase expression of pro-survival genes and tumor growth by activating PPARβ/δ in colon cancer. In summary, our data demonstrate that ALDH1B1 plays a functional role in colon cancer tumorigenesis by modulating the Wnt signaling pathway and participating in retinoic acid formation.

PS 1096 Increased Growth and Tumorigenicity of MCF-7 Breast Cancer Cells by Chronic Exposure to Oxidative Stress

P. S. Mahalingaiah, K. P. Singh and L. Ponnusamy. *Environmental Toxicology, The Institute of Environmental and Human Health (TIEHH), Texas Tech University, Lubbock, TX.*

Breast cancer is the second leading cause of cancer related death in women. Exposure to environmental estrogenic chemicals has been shown to be associated with breast cancer development and progression through various mechanisms. Though, the increased oxidative stress by xenoestrogens-generated reactive oxygen species (ROS) has been hypothesized as a potential mechanism for breast cancer growth and progression, there is no direct evidence for the ROS-induced growth and tumorigenicity of breast cancer cells. Therefore the objective of this study was to evaluate the chronic effect of hydrogen peroxide (H2O2) generated ROS on the growth and tumorigenicity of MCF-7 breast cancer cells. MCF-7 cells were exposed to H202 for both acute (48 hrs) and chronic (3 months) period. Cell growth and viability were evaluated by cell count and MTT assay and were confirmed by cell cycle analysis. Expression of genes related to cell cycle, cell survival, and metastasis were measured by quantitative real-time PCR. Soft agar assay was also performed to determine the effect of H202 on anchorage independent growth of MCF-7 cells. Results of cell count, MTT and cell cycle analysis revealed increased growth, and survival of MCF-7 cells chronically treated with H2O2. This was further confirmed at molecular level by increased expression of Cyclin D1, Survivin and Bcl2 in H2O2 treated cells. Significant increase in number of soft agar colonies in H202 treated cells further suggest that chronic oxidative stress causes increase in tumorigenic phenotype of MCF-7 cells. Up regulation of pro-metastatic genes like VEGF, WNT1 & CD44 and down regulation of anti-apoptotic gene E-cadherin indicates that persistent oxidative stress may enhances metastatic potential of MCF-7 cells. In summary, this study for the first time provided direct evidence for the increase growth, tumorigenicity, and metastatic potential of breast cancer cells by chronic exposure to oxidative stress.

PS 1097 Effect of Melatonin on Colitis-Associated Colon Carcinogenesis in Mice: Role of Autophagy and Nrf2 Signaling Pathways

P. P. Trivedi and G. Jena. *Pharmacology and Toxicology, National Institute of Pharmaceutical Education and Research, Mohali, Punjab, India.*

Ulcerative colitis, a chronic gastrointestinal disorder, gradually leads to colon carcinogenesis. Various pre-clinical and clinical studies have shown that melatonin has beneficial effects in cancer. However, elucidation of the detailed molecular

mechanisms involved in melatonin-mediated protection against colon carcinogenesis deserves further investigation. The present study was aimed at deciphering the effect of melatonin on autophagy and Nrf2 signaling pathways in a mouse model of colitis-associated colon carcinogenesis (CACC). For the induction of CACC, male Swiss Albino mice were administered a single i.p injection of 20mg 1, 2-dimethylhydrazine dihydrochloride (DMH)/kg bw, followed by 3 cycles of 3% w/v dextran sulfate sodium (DSS) (one cycle consisted of 7 days of DSS-treated water followed by 14 days of normal drinking water) 1 week after DMH injection. One week after the initiation of DSS administration, melatonin was administered at the dose of 1mg/kg bw for 8 and 18 weeks, and mice were sacrificed at 10 and 20 weeks after DMH treatment respectively. Melatonin treatment decreased the progression of colon carcinogenesis, inflammation, oxidative stress and DNA damage in the colon of mice with CACC. Further, CACC in mice led to an increased autophagy in the colon as revealed by the expression of various autophagy markers such as Beclin-1, LC3B-II/LC3B-I and p62. Decreased p62 expression in the colon of mice with CACC was associated with decreased nuclear factor-erythroid 2 (NF-E2)-related factor 2 (Nrf2) expression. Melatonin treatment reduced autophagy and increased the expression of Nrf2 and the associated antioxidant enzymes, NAD(P)H:quinone oxidoreductase (NQO-1) and heme oxygenase-1 (HO-1) in the colon of mice with CACC. The results of the present study demonstrated that melatonin attenuated the progression of CACC in mice by modulating autophagy and Nrf2 signaling pathways.

PS 1098 Novel Role of STAT3 in Anoikis Resistance and Tumor Cell Metastasis

N. M. Fofaria and S. K. Srivastava. *Biomedical Sciences and Cancer Biology Center, Texas Tech University Health Sciences Center, Amarillo, TX.*

Anoikis is an anchorage independent cell death. Resistance to anoikis is one of the key features of metastatic cells. The role of STAT-3 in anoikis resistance in various melanoma, pancreatic, breast, ovarian, lung and colon cancer cells was analyzed in the current study. Marked anoikis was induced in cells that were grown under anchorage-independent conditions. Cells that resisted anoikis were observed to a have higher rate of migration and invasion as compared to the cells grown under anchorage dependent conditions, as observed by cell migration and invasion assays. The anoikis resistant cells also had significantly higher expression and phosphorylation of STAT-3 at Tyr 705 than the cells that were attached to the basement membrane. Treatment of these cells with IL-6, a cytokine which phosphorylates STAT-3, prevented the induction of anoikis. STAT-3 inhibitors AG490 and piplartine induced anoikis in a concentration-dependent manner in anoikis resistant cells, whereas IL-6 blocked anoikis. Over-expression of STAT-3 by transfection, not only increased the anoikis resistance, but also protected the cancer cells from piplartine-induced anoikis, confirming the role of STAT-3 in anoikis resistance. On the other hand, silencing STAT-3 decreased the potential of cancer cells to resist anoikis. Furthermore, STAT-3 (-/-) cancer cells were more sensitive to anoikis, as compared to cells overexpressing STAT-3 (+/+) cells. The STAT-3 (+/+) cells also had enhanced migration potential, as compared to STAT-3 (-/-) cells. STAT-3 -/- cells and piplartine treated cells completely failed to form tumors in SCID-NSG mice, as compared to untreated anchorage independent cells. Similarly, piplartine treated or STAT-3 -/- cells failed to metastasize to lungs and liver, as compared to untreated anchorage independent cells which extensively metastasized. The metastasis was confirmed by H & E staining as well as bioluminescence. In summary, our results establish STAT-3 as a critical player that renders anoikis resistance to the cancer cells and enhance their metastasis potential.

PS 1099 Toxicokinetic Mode-of-Action (MOA) Investigation of Liver Tumors Induced by Chronic Oral Exposure to Biphenyl in Female BDF1 Mice

J. Klapacz, F. Zhang, A. J. Clark, K. A. Brzak and M. J. Bartels. *TERC, The Dow Chemical Company, Midland, MI.*

Biphenyl (BP) is a high production volume chemical used in USA and EU in closed system applications as a synthesis intermediate and component of heat transfer fluids. The rich toxicological dataset, with a number of cancer bioassays, notes two cases of neoplastic effects from high-dose BP exposures that are species, sex and strain specific. MOA investigations have demonstrated that urinary bladder tumors seen in male F344 rats occur from calculi development at specific pH and potassium concentrations, conditions that are not relevant for humans. Recently, Umeda et al. (2005) demonstrated increased tumor incidence from high-dose dietary BP exposures in female BDF1 mice, while in males, decreased tumor incidence occurred with increasing doses. Different explanations have been proposed, but there is no clear understanding of the underlying MOA for these liver tumors or their relevance to humans. In order to better understand this cancer MOA, absorption, metabolism and elimination of 14C-BP in BDF1 mice following 900 mg/kg gavage dosing was evaluated. Absorption, metabolism and BP metabolite profiles were comparable between sexes. BP is rapidly absorbed and excreted primarily via urine. The majority of radioactivity was eliminated within 24 hrs post-dosing. No bioaccumulation was observed after 168 hrs post-dosing in either sex. BP was mainly metabolized by hydroxylation, followed by methylation, and conjugation with sulfate and glucuronide, resulting in 26 identified metabolites. However, systemic exposure to BP and metabolites was substantially higher in females, as evidenced by slower terminal blood elimination half-life of 671 hrs vs. 99 hrs for males, and 2-fold higher blood AUC in females than in males. Thus in females, slower clearance results in higher systemic exposure. These results are consistent with Umeda et al. (2005) findings and point to differences in sex-specific systemic exposures at high BP doses underlying sex-specific liver tumor findings in BDF1 mice. Sponsored by the Biphenyl Work Group of SOCMA.

PS 1100 Mice with a Heterozygous Deletion of S-Nitrosoglutathione Reductase (GSNOR/ADH5) Display Normal O6-alkylguanine-DNA Alkyltransferase Levels and Are Protected from DEN-Induced Hepatocarcinogenesis

D. B. Colagiovanni, S. Mutka, L. Green, W. Schauer and G. J. Rosenthal. *Life Sciences, N30 Pharma, Boulder, CO.*

Recently, studies have demonstrated that total genetic deletion of S-nitrosoglutathione reductase (GSNOR) in mice (GSNOR-/-) leads to a higher incidence of hepatocellular carcinoma (HCC), possibly through uncontrolled iNOS-induced nitrosation and subsequent proteosomal degradation of O6-alkylguanine-DNA alkyltransferase (AGT). Mice deficient in AGT show increased susceptibility to hepatocarcinogenesis induced by DEN as compared to WT mice. The objectives of these studies were to investigate whether mice with a heterozygous deletion of GSNOR/ADH5 (GSNOR+/-) were protected from nitrosative inactivation of AGT and subsequent hepatocarcinogenesis following treatment with diethylnitrosamine (DEN) as compared to mice containing a complete genetic deletion of GSNOR (GSNOR-/-) or wild type (WT) control mice. Additionally, we investigated iNOS expression in embryonic fibroblasts of WT and GSNOR-/- mice and liver cancer cDNA arrays for ADH expression. GSNOR+/- mice were given a single IP injection of DEN and later sacrificed to study AGT protein expression and tumor development in the liver. In the DEN-treated GSNOR+/- mice, AGT levels were equivalent to levels seen in WT control animals and with no increased incidence of hepatocellular tumors. Mechanistically, iNOS expression appeared to be critical to the development of HCC, rather than GSNOR expression. We also observed that multiple ADH genes, which reside at the same chromosomal locus as GSNOR (4q23), were depleted in HCC patients, and the reduction in expression level correlated with more advanced tumors. The findings indicate that, in contrast to complete genetic deletion of GSNOR, GSNOR+/- mice express normal AGT activity and DEN treatment did not increase the incidence of HCC. Lastly, ADH profiling of the liver cancer cDNA arrays demonstrated broad effects on the ADH genes, rather than a GSNOR-specific effect, correlating with the advancement of the tumors.

PS 1101 Histone Acetylation Alterations and Monomethylarsonous Acid (MMAIII)-Induced Cell Malignant Transformation

X. Ren[1, 2], Y. Ge[1], Z. Gong[1], H. Zhang[1] and J. R. Olson[2, 1]. *[1]University at Buffalo, Buffalo, NY and [2]Pharmacology and Toxicology, University at Buffalo, Buffalo, NY.*

Chronic arsenic exposure is known to be associated with increased morbidity and mortality from both cancerous and non-cancerous effects. Inorganic arsenic (iAs) and its high toxic metabolite, monomethylarsonous acid (MMAIII), is capable of inducing malignant transformation in human cells, and population-based studies have shown that an increase in the percentage of urinary and blood arsenic present as MMAIII, is linked to increased susceptibility to skin lesions and several types of cancer. The mechanism through which MMAIII induces cell transformation and carcinogenicity has not yet been elucidated but studies suggest the involvement of epigenetic mechanisms. We recently demonstrated a global and lysine specific decrease in histone acetylation upon acute MMAIII exposure in human urothelial cells (UROtsa cells), the target for arsenic-induced carcinogenesis. To investigate the effects of prolonged exposure to an environmentally relevant level of MMAIII on histone acetylation modification and its association with MMAIII-induced neoplastic transformation, we utilized UROtsa cells and examined the mechanisms and tumorigenic outcomes of histone acetylation changes upon MMAIII exposure. We demonstrated that prolonged exposure to low-level MMAIII in human urothelial cells significantly increased the expression and activity of histone deacetylases (HDACs) with an associated reduction of histone acetylation levels both globally and lysine specifically. Administration of the HDAC inhibitor, suberoylanilide hydroxamic acid (SAHA), at 4 weeks after the initial MMAIII treatment inhibited

the MMAIII-mediated up-regulation of the expression and activities of HDACs, leading to increase histone acetylation and prevention of MMAIII-induced malignant transformation. These new findings suggest that histone acetylation dysregulation may be a key mechanism in MMAIII-induced malignant transformation and carcinogenesis, and that HDAC inhibitors could be targeted to prevent or treat arsenic-related cancers.

PS 1102 The Biology of Srx-Prx1 Interaction: Structure to Molecular Insights

M. Mishra, H. Chawsheen, L. Wu, H. Jiang and Q. Wei. *Graduate Center for Toxicology, University of Kentucky, Lexington, KY.*

Sulfiredoxin(Srx) is the exclusive enzyme that reduces overoxidized Peroxiredoxins(Prx). The Srx-Prx axis is one of the critical components of antioxidant system in eukaryotes. Among them, the Srx-Prx1 interaction is involved in the pathogenesis of various oxidative stress induced conditions including cancer, inflammation, and cardiovascular and neurological diseases. The purpose of this study is to understand the biology of the Srx-Prx1 axis by studying their interaction at the structural and molecular levels, which may be of significance for the identification of molecular targets for the development of novel therapeutics. Firstly, homology modeling and protein-protein docking approaches were applied to examine the Srx-Prx1 interaction using in-silico methods including ITASSER, Phyre2, Swissmodel, MZDOCK and ZDOCK. By in-silico studies, we identified a 26-amino acid motif at the C-terminus of Prx1 that may be a steric hindrance for the kinetics of Srx-Prx1 interaction. Then we tested these findings in-vitro using purified recombinant proteins including Srx, Prx1 and Prx1Mut (deleted C-terminal motif). Surface Plasmon Resonance was used to examine the real-time kinetics of the interaction. We found that deletion of the C-terminal motif of Prx1 significantly enhanced its association with Srx, a >1000 fold increase in the ka, but has marginal effect on dissociation (kd). These results were further validated by immunoprecipitation to examine the stable interaction. With the same amounts of Srx input, significant increased levels of Prx1Mut were co-precipitated by Srx compared with those of Prx1. Finally, we expressed Srx into HEK293 cells and exposed them to oxidative stress. With an antibody specifically recognizing the overoxidized Prxs, we examined and interpreted the substrate specificity of Srx for different isoforms of Prxs. Taken together, our data add novel molecular and structural insights critical for the understanding of the biology of Srx-Prx interaction, and may facilitate future development of targeted therapeutics for the prevention and treatment of human diseases.

PS 1103 Differential Tumor Promoting Properties of Low-Molecular-Weight Polycyclic Aromatic Hydrocarbons

R. S. Osgood[1], K. Velmurugan[2], C. Alexander[2], K. Xiong[2], P. Babica[4], B. L. Upham[3] and A. K. Bauer[2]. [1]*Pharmaceutical Sciences, University of Colorado Denver, Aurora, CO,* [2]*Environmental and Occupational Health, University of Colorado Denver, Aurora, CO,* [3]*Pediatrics and Human Development, Michigan State University, East Lansing, MI and* [4]*RECETOX, Masaryk University, Brno, Czech Republic.*

Polycyclic aromatic hydrocarbons (PAHs) are ubiquitous environmental contaminants, major components of secondhand smoke, and have been associated with carcinogenesis. Most research has focused on the ability of high molecular weight PAHs to act as complete carcinogens or initiators, however, recent evidence suggests that the low molecular weight (LMW) PAHs may act through distinct mechanisms to promote, rather than initiate, neoplasia. We evaluated four secondhand smoke PAHs in single treatment and in mixtures (1- and 2-methylanthracene ((1- and 2-MeA), fluoranthene (Flthn) and pyrene (Py) isomers) for their ability to dysregulate gap junction intercellular communication (GJIC), decrease connexin 43 (Cx43; a gap junction protein) expression, activate mitogen activated protein kinases (MAPK), induce several key inflammatory markers, as well as other indicators of promotion, such as proliferation. C10 cells (a mouse, non-tumorigenic type II cell line and progenitor cell for lung adenocarcinoma) were used for these studies with scrape-load/dye transfer assays, immunoblotting, qRT-PCR, and proliferation assays to determine the effects of these LMW PAHs. 1-MeA and Flthn dysregulate GJIC, as well as their mixtures, and decreased Cx43 expression, however, no changes were observed from their respective isomers (2-MeA, Py), likely due to structural differences. 1-MeA activated ERK1/2 and p38 MAPK, induced several inflammation pathways, and increased proliferation, however only p38 inhibition reversed GJIC-dysregulation and inflammation pathways. The differences observed between isomers (1- and 2-MeA and Flthn and Py) suggest that the ability of LMW PAHs to act as tumor promoters is likely dependent on chemical structure. Future work will address whether these differences are indicative of discrete toxicological mechanisms.

PS 1104 Transcriptomics to Elucidate Oxidative Stress Mechanisms Involved in Genotoxic and Nongenotoxic Liver Carcinogenesis

L. Deferme, J. Wolters, J. Kleinjans and J. Briede. *Toxicogenomics, Maastricht University, Maastricht, Limburg, Netherlands.* Sponsor: H. van Loveren.

Genotoxic (GTX) and non-genotoxic (NGTX) carcinogens are known to induce multiple molecular changes and cellular damage in causing liver toxicity and/or carcinogenesis. Currently, the specific mechanisms for these different classes of compounds that induce hepatocarcinogenesis are still unknown but oxidative stress seems to be important. Therefore, a better understanding of cellular changes induced by compounds from these different classes in relation to oxidative stress is needed.
We selected 3 oxidative stress-inducing compounds (Azathioprine (AZA), Tetradecanoyl phorbol acetate (TPA), Diazinon (DZN)) and 3 non-oxidative stress related compounds (Furan (Fu), Tetrachloroethylene (TCE) and D-mannitol (Dman)). In a human hepatoma cell line (HepG2), Whole genome gene expression was measured, analyzed and correlated to (oxidative) DNA damage and cell cycle changes at 5 different time points (4, 8, 24, 48 and 72h) after exposure to these compounds.
ROS formation and (oxidative) DNA damage and cell cycle arrest was confirmed after AZA, TPA and DZN treatment and appeared to be related to a 10-fold higher number of gene expression changes over time compared to Fu, TCE or Dman treatment, indicating that this is due to cellular oxidative stress. Different genes and pathways were found over time between the different classes, however, a higher number of gene expression changes overlapped between AZA, TPA and DZN being especially involved in oxidative stress, DNA damage and immune responses Genes such as NRF2, GCLC, HMOX1 and GSR were significantly upregulated. This was not observed after Fu, TCE or Dman treatment, thus indicating that carcinogenic processes are not solely caused by oxidative stress. However, cellular oxidative stress has a high impact on cellular changes such as DNA damage gene expression and cell cycle distribution, and for certain compounds, may represent the underlying cause for increasing the risk of liver toxicity and even carcinogenesis.

PS 1105 Functional Role of Long-Noncoding RNAs in Rhabdomyosarcoma Cells and Tumors

G. Chadalapaka[1], I. D. Jutooru[1] and S. H. Safe[1, 2]. [1]*VTPP, Texas A&M University, College Station, TX and* [2]*Institute of Biosciences and Technology, Texas A&M Health Science Centre, Houston, TX.*

Long noncoding RNAs (lncRNAs) >200 bp in length are now emerging as critical factors in tumor biology. Reports suggest that dysregulated lncRNA expression in cancer correlates with disease progression and may serve as an independent predictor for patient outcomes. Little is known about the lncRNA regulation in rhabdomyosarcoma (RMS), a disease which is prevalent in children is the most common soft-tissue sarcoma and accounts for approximately 50% of soft-tissue sarcomas. Regulation of lncRNAs is not well defined and development of drugs that target oncogenic lncRNAs has not been reported. 'HOXA transcript at the distal tip' (HOTTIP) is a 3,764 bp lincRNA located ~330 bases upstream of HOXA13 and Metastasis-associated lung adenocarcinoma transcript 1(MALAT1) are two lncRNAs highly expressed in RH30 and RD RMS cell lines and the function of the lncRNAs was investigated by RNA interference (RNAi). Knockdown of MALAT-1 in RH30 and RD cells resulted in a 57% and 60% decrease in cell proliferation respectively and we also observed a > 60% decrease in cell migration in a Boyden chamber assay. We also observed that MALAT-1 silencing increased markers of apoptosis (PARP cleavage) in RMS cells and these were consistent with a pro-oncogenic function for MALAT-1 in RMS and similar results were reported in other solid tumors. In contrast, the function of HOTTIP has not previously been reported in cancer cells and our results show that like MALAT-1, knockdown of HOTTIP by RNAi also decreases cell proliferation and migration and induces apoptosis. Current studies are focused on the overlapping and independent regulation of genes by MALAT-1 and HOTTIP and development of agents that target these pro-oncogenic lncRNAs.

PS 1106 HOXA Transcript at the Distal Tip (HOTTIP) is a Pro-Oncogenic Long-Noncoding RNA in Pancreatic Cancer

Y. Cheng[1], I. D. Jutooru[2], G. Chadalapaka[2] and S. H. Safe[1, 2]. [1]*Institute of Biosciences and Technology, Texas A&M Health Science Centre, Houston, TX and* [2]*VTPP, Texas A&M University, College Station, TX.*

Recent studies demonstrate that non-coding RNAs (ncRNAs) are differentially expressed and play an important role in gene regulation and influence normal and cancer cell phenotypes, and this is due, in part, to association with chromatin-mod-

ifying complexes. HOXA transcript at the distal tip (HOTTIP) is a 3,764 bp lncRNA transcribed from 5'tip of HOXA gene cluster and is expressed in anatomically distal cells. Previous studies in our laboratory showed that HOTTAIR is a negative prognostic marker in pancreatic cancer and HOTAIR cooperatively represses gene expression with complexes such as Polycomb Repressive Complex 2 (PRC2). It has been reported that HOTTIP interacts with MLL-1 complexes by specifically binding the WDR5 adapter protein leading to a loss of H3K4me3 across the HOXA locus. In this study, we investigated the functional role of HOTTIP in Panc1 and L3.6pL pancreatic cancer cell lines. Knockdown of HOTTIP by RNA interference studies (siHOTTIP) resulted in ~50% reduction in cell survival within 72 hr after transfection and siHOTTIP also decreased pancreatic cancer cell migration. In addition, overexpression of HOTTIP also induced proliferation of Panc28 cells. An in vivo study was performed using L3.6pL cells transfected with siHOTTIP in a mouse xenograft model and after 15 days of knockdown there was a significant reduction in tumor volumes and weights (≥70%). Knockdown of HOTTIP induced & decreased expression of 514 & 757 genes respectively in Panc1 cells. RT-PCR confirmed that HOTTIP regulated expression of several pro-oncogenic factors including Aurora kinase A (AURKA), AHNAK, CD44. Knockdown of MLL-1 also decrease AURKA expression, however regulation of AURKA by HOTTIP/MLL-1 was WDR5-independent. Further analysis of array data suggests a less prominent role for HOTITP, MLL1/WDR5 interactions in pancreatic cancer cells compared to non-tumor cells (fibroblasts). Functional interactions of HOTTIP with other chromatin-modifying complexes are currently being investigated.

PS 1107 Determination of Artifacts, the Steady State, and Half-Life of N2-Hydroxymethyl-dG Adducts *In Vitro*, and in a 28-Day 13CD2-Formaldehyde Inhalation Exposure Study

R. Yu[1], B. C. Moeller[2], M. Doyle-Eisele[2], D. Kracko[2], W. Bodnar[1], T. B. Starr[3] and J. A. Swenberg[1]. [1]*ESE, University of North Carolina at Chapel Hill, Chapel Hill, NC,* [2]*LRRI, Albuquerque, NM and* [3]*TBS Associates, Raleigh, NC.*

Rationale: N2-HOMe-dG is the main formaldehyde-induced DNA mono-adduct, which plays important roles in mutagenesis and carcinogenesis. The purpose of this study is to provide the distribution pattern of exogenous DNA adducts, and further tell whether or not inhaled formaldehyde can reach tissues distant to sites of initial contact. We have also undertaken studies related to artifact formation during DNA isolation and processing.
Methodology: DNA was isolated, reduced, digested, and injected onto an Agilent HPLC-UV for adduct fractionation. DNA adducts were quantitated using nano-LC-MS-MS (with a limit of detection of 1.25 attomolar).
Results: Artifacts formation was less than 0.56% and 0.46% of the average amounts of endogenous adducts in all tissues (n=205) from sodium phosphate buffer and NucleoBond DNA isolation kit, respectively. Exogenous adducts were only detected in rat nasal respiratory epithelium, the amounts of which were 3- to 8-fold lower than the average amounts of endogenous adducts. Additionally, inhaled exogenous adducts were found to accumulate, with the time to steady-state concentrations being 28 days. The unstable exogenous adducts were found to follow a biphasic decay model in vivo, and the half-life was determined to be 5.2 days. The unstable exogenous adducts were also found to follow a biphasic decay model in isolated calf thymus DNA in vitro.
Conclusions: Our study showed that inhaled formaldehyde only reached rat nasal respiratory epithelium. For the first time, this study has elucidated accumulation of exogenous adducts, the time to reach steady state, and the half-life for the repair/loss of exogenous adducts in vivo. Overall, the data generated in this study provide pivotal information to understand the toxicity and carcinogenicity of formaldehyde, as well as the biological plausibility of leukemia induction following inhalation exposure of formaldehyde.

PS 1108 Ablation of the bZIP Transcription Factor, CCAAT Enhancer Binding Protein-β (C/EBPβ), in Skin Protects Mice from Skin Cancer Induced by Ultraviolet B Radiation

H. W. Tam, S. Zhu and R. C. Smart. *Department of Biological Sciences, Toxicology Program, NC State University, Raleigh, NC.*

Nonmelanoma skin cancer (NMSC) is the most common cancer in the United States. Each year there are more cases of NMSC than all cases of breast, prostate, lung and colon cancers combined. The majority of NMSCs is caused by solar UVB radiation which causes DNA damage. Sunlight is a ubiquitous environmental carcinogen and p53 plays a key role in the response of skin keratinocytes to UVB-induced DNA damage by causing cell cycle arrest and apoptosis. We observed that C/EBPβ is abundantly expressed in epidermis and that C/EBPβ protein levels are induced by UVB radiation in mouse and human keratinocytes in culture as well as in mouse epidermis in vivo. Activation of C/EBPβ often involves phosphorylation at threonine 188 (T188) and UVB treatment increased the phosphorylation of C/EBPβ at T188. In order to understand the function of C/EBPβ in UVB-induced responses in epidermis and in skin cancer, we developed a C/EBPβ deficient (C/EBPβ$^{-/-}$) SKH-1 hairless mouse model. SKH-1 hairless mice are an established experimental model relevant to UVB-induced human skin cancer. Treatment of C/EBPβ$^{-/-}$ mice with UVB, resulted in increased apoptotic cell death in epidermal keratinocytes when compared to similarly treated control mice. C/EBPβ$^{-/-}$ mice were highly resistant to UVB-induced skin cancer. In order to determine whether the resistance of C/EBPβ$^{-/-}$ mice to UVB-induced skin cancer is due to an intrinsic keratinocyte effect, we developed an epidermal specific C/EBPβ conditional knockout (CKOβ) SKH-1 mouse. In this model, the keratin 5 promoter directs Cre recombinase expression to the epidermis to delete floxed C/EBPβ alleles. CKOβ mice were highly resistant to UVB-induced skin cancer and displayed increased levels of UVB-induced apoptosis. These studies indicate that C/EBPβ is induced and activated by UVB and has critical role in the development of UVB-induced skin cancer where it suppresses UVB-induced apoptosis and in doing so may allow the survival of keratinocytes with DNA damage and mutations.

PS 1109 Western Diet Accelerates Benzo(a)pyrene [B(a)P]-Induced Colon Tumorigenesis in the PIRC Rat Model

K. Harris[1], S. R. Pulliam[1], M. S. Niaz[1], M. K. Washington[2], S. E. Adunyah[1] and A. Ramesh[1]. [1]*Biochemistry & Cancer Biology, Meharry Medical College, Nashville, TN and* [2]*Pathology, Vanderbilt University Medical Center, Nashville, TN.*

Colorectal cancer ranks third in terms of mortalities in the United States. Consumption of Western Diet (WD; rich in red meat and fats), contaminated with polycyclic aromatic hydrocarbons (PAHs) has been implicated as one of the causative agents for sporadic colon cancer. Therefore, the aim of this study was to investigate whether the colon polyp burden was potentiated by WD when exposed to benzo(a)pyrene [B(a)P], a PAH compound. To test this concept, we have used an adult male transgenic rat model, the Polyposis In the Rat Colon (PIRC) kindred type. Treatment consisted of 25, 50 and 100 μg B(a)P/kg bw dissolved in tricaprylin, administered to rats daily via oral gavage for 60 days. One group of B(a)P-treated rats were fed with AIN-76A regular diet (RD) and the other group with WD throughout the study. Rats that received the diets alone, but no B(a)P served as controls. Food consumption and body weights were periodically monitored. Subsequent to exposure, rats were sacrificed; colons, and other tissues were retrieved and preserved in 10% formalin for observation of gross pathological changes. Blood samples were collected and concentrations of cholesterol, triglycerides, and adiponectin were measured. There was no change in food consumption, but body weight loss of WD group compared to RD group and controls ($p < 0.005$) was noticed. An increased incidence of adenomas and high grade dysplasia were encountered in rats that were fed with WD compared to RD and controls ($p < 0.05$). The colon tumor numbers showed a B(a)P dose-response relationship. Rats that received B(a)P + WD showed increased levels of cholesterol and triglycerides in comparison to rats that received B(a)P + RD and also controls. Levels of adiponectin did not vary much between B(a)P + WD, and B(a)P + RD groups. Our results showed that WD accelerates the development of colon tumors induced by B(a)P through proinflammatory action, characterized by gain in tumor number and sizes, and body weight loss.

PS 1110 Nuclear Receptor-Mediated Effects of the Mammary Carcinogens Benzo[a]pyrene and PhIP in MCF-7 and MDA-MB-231 Cancer Cell Lines

D. S. Malik, R. David and N. J. Gooderham. *Imperial College, London, United Kingdom.*

Breast cancer is the most commonly diagnosed malignancy in females. Its aetiology is multifactorial, and the role of environmental exposure to DNA damaging chemicals has been widely investigated. Benzo(a)pyrene (BaP) and 2-Amino-1-methyl-6-phenylimidazo [4,5-b]pyridine (PhIP) are mammary carcinogens in rodents. Both compounds require cytochrome P450 (CYP) mediated metabolic activation to DNA damaging species, and both induce transcriptional responses through the nuclear receptors Aryl hydrocarbon receptor (AhR) and estrogen receptor α (ERα). The objective of this research was to investigate the molecular toxicology of BaP and PhIP in ERα positive (MCF-7) and ER-negative (MDA-MB-231) cancer cell lines. MCF-7 and MDA-MB-231 cells were incubated with various concentrations of BaP and PhIP for up to 96 hrs. Genotoxicity, drug metabolism activity, CYP expression, proliferation and cell migration were examined. BaP showed a dose-dependent increase in micronuclei (MN) formation in both cell lines, while PhIP was positive only in MCF-7 cells. Ethoxyresorufin-O-deethylase (EROD; CYP1A) activity and CYP1A1 and 1A2 expression was induced in both cell lines by BaP, but PhIP only induced CYP1A2 mRNA in MCF-7 cells. Cell proliferation and migration was induced in both cell lines by BaP, but only in MCF-7 cells by PhIP.

These data demonstrate the ability of BaP and PhIP to induce DNA damage and receptor-mediated effects in mammary cells. Furthermore, the differential effect of PhIP in the two cell lines supports the role of ERα in the toxicity of PhIP.

PS 1110a Estrogen Receptor Alpha Modulation and Differential Cytotoxicity of Caffeic Acid Phenethyl Ester in Prostate Cancer Cells

M. F. Tolba[1, 2], S. S. Azab[1], A. E. Khalifa[1], S. Abdel-Rahman[2] and A. B. Abdel-Naim[1]. *[1]Department of Pharmacology and Toxicology, Faculty of Pharmacy, Ain Shams University, Cairo, Egypt and [2]University of Texas Medical Branch, Galveston, TX.*

Caffeic acid phenethyl ester (CAPE) is a promising natural component of propolis that possesses selective estrogen receptor modulatory (SERM) activity. The class of compounds known as SERMs are promising therapeutic agents for patients with castration-resistant prostate cancer (PC). However, the potential SERM activity of CAPE in PC has not been evaluated before. In this investigation we test the hypothesis that, in PC cells (PC-3, DU-145, LNCaP), the differential cytotoxicity of CAPE is dependent on the cells' estrogen receptor (ER) status. To test our hypothesis, we assessed CAPE cytotoxicity in the androgen dependent cell line LNCaP and the androgen-independent cell lines PC-3 and DU-145 using sulforhodamine B (SRB) assay. CAPE exhibited greater cytotoxicity in PC-3>>DU-145>LNCaP and was least potent in nontransformed prostate epithelial cell line BPH1. Western blot analysis for ER-α in the 3 cell lines confirmed that only PC-3 expresses this ER subtype. Furthermore, we evaluated the impact of CAPE on AKT1/2/3 (Ser473) as well as ERK1/2 (Thr202/Tyr204, Thr185/Tyr187) activation in the tested PC cells since Akt and ERK pathways are crucial for PC tumor aggressiveness and progression and due to their known cross-talk with ER-α. Our data indicate that CAPE significantly reduced both Akt and ERK activation in PC-3 cells while it only reduced the activation of Akt in LNCaP and ERK in DU-145 cells. Our study shows, for the first time, that CAPE-induced inhibition of Akt activation is more pronounced (1.7 folds higher) in cells expressing ER-α such as PC-3 cells compared to LNCaP. CAPE treatment reduced ER-α phosphorylation at Ser-167, which is known to be related to Akt activation, further supporting the evidenced reduction in Akt activation by CAPE in this specific cell line. These data indicate that the cytotoxic effects of CAPE in prostate cancer are partly mediated by ER-α modulation.

PS 1110b Cholorogenic Acid Rich Plum Juice Inhibited AOM Treated Colorectal Aberrant Crypt Foci (Acf): Potential Role of miR143/MTOR Pathway

N. Banerjee[1, 2], H. Kim[1, 2], M. Nemec[1] and S. Talcott[1, 2]. *[1]Toxicology, Texas A&M University, College Station, TX and [2]Nutrition and Food Science, Texas A&M University, College Station, TX.*

The antitumorigenic and cytotoxic,activities of polyphenols, chlorogenic acid and neo-chlorogenic acid in plum juice (PL) have been previously studied in various cancer models. Our preliminary result exhibited anti-inflammatory property of PL which decreased the expression of VCAM-1and the activation of PI3K/AKT, in AOM treated in vivo study. The objective of this study was to investigate the underlying cytotoxicity mechanisms involving miR143/PI3K/AKT/mTOR in PL-mediated anti-inflammatory and anti-carcinogenic effects in vivo and in vitro.
Sprague Dawley rats (n=10/group) received PL juice (1345.68ppm GAE) or a polyphenol-free control beverage ad libitum for 10 weeks and were injected with azoxymethane (AOM) subcutaneously (15 mg/kg) at weeks 2 and 3.
Consumption of PL juice suppressed the number of high multiplicity aberrant crypts foci (HMACF>4 ACF) by 47.98% ($P<0.05$) and significantly lowered proliferation of mucosa cells. The results were accompanied by a downregulation of nuclear factor kappa B (NF-κB), inducible nitric oxide synthase (iNOS), cyclooxygenase-2 (COX-2), vascular adhesion molecule-1 (VCAM-1) and mRNA and protein. PL also inhibited phosphorylation of PI3K/AKT, and mTOR/HIF-1α pathways. PL increased the expression of miR143 expression.
In summary, PL suppressed number of HMACF formation, colon tumorgenesis where microRNA-143-regulated pathways significantly contributed in the underlying cytotoxicity mechanisms.

PS 1110c ARNT Isoforms Differentially Regulate Cancer Cell Growth through a p53-Dependent Mechanism

K. Gardella[1, 2, 3], I. Muro[2, 3], G. Fang[2, 3], K. Sarkar[1, 2, 3] and C. Wright[1, 2, 3]. *[1]The Institute for Cellular and Molecular Biology, The University of Texas at Austin, Austin, TX, [2]Division of Pharmacology and Toxicology, College of Pharmacy, The University of Texas at Austin, Austin, TX and [3]Center for Molecular and Cellular Toxicology, The University of Texas at Austin, Austin, TX.*

In addition to its roles in xenobiotic and hypoxic responses, we have shown that the arylhydrocarbon receptor nuclear translocator (ARNT) is an integral cofactor of NF-kappaB signaling. However, these initial observations of ARNT-mediated NF-kappaB modulation were based on simultaneous suppression of the two ARNT isoforms, isoform 1 and 3, and therefore precluded the isolated examination of each isoform's function. We show here that lymphoid malignancies exhibit a shift to higher levels of ARNT isoform 1, compared to normal lymphocytes that harbor equal levels of isoform 1 and 3. The increase in ARNT isoform 1 is necessary for the growth of these cancer cells as suppression of isoform 1 resulted in S-phase cell cycle arrest. Interestingly, NF-kappaB signaling was unaffected by suppression of isoform 1. However, co-suppression of p53 with ARNT isoform 1 rescued the arrest phenotype, suggesting that the observed cell cycle arrest was dependent on p53 activity in the absence of isoform 1. Furthermore, suppression of isoform 1 sensitized cells to low levels of doxorubicin, an effect that was also rescued by suppressing p53. These findings reveal that ARNT isoform 1 potentiates cell growth by antagonizing a p53 cell cycle inhibitory mechanism and suggests that ARNT targeted therapies would benefit chemotherapy regimens.

PS 1110d Ligand-Dependent Activation of EGFR Mediates Malignant Cell Transformation Induced by Chronic Exposure to Hexavalent Chromium

D. Kim. *University of Kentucky, Lexington, KY.* Sponsor: Y. Son.

Hexavalent chromium (Cr (VI)) compounds are well-established lung carcinogens. The carcinogenic mechanisms of Cr (VI) are currently under investigation. Epidermal growth factor receptor (EGFR) is a tyrosine kinase transmembrane receptor that regulates cell survival, cell cycle progression, tumor invasion, and angiogenesis. The present study investigates the role of EGFR in Cr(VI)-induced cell transformation and tumorigenesis. Our results show that chronic exposure of human bronchial epithelial (BEAS-2B) cells to Cr (VI) caused malignant cell transformation. The Cr (VI)-transformed cells exhibited apoptosis resistance with reduced expressions of cleaved Poly ADP ribose polymerase (C-PARP) and Bax and enhanced expressions of Bcl-2 and Bcl-xL. Reduced capacity of generating reactive oxygen species (ROS) along with elevated expression of antioxidant manganese superoxide dismutase (SOD2) was also found in Cr (VI)-transformed cells. Phosphorylation of EGFR was dramatically increased in both Cr (VI)-transformed BEAS-2B cells and lung tissue of animals exposed to Cr(VI) particles. Expression of amphiregulin (AR), a EGFR ligand, was elevated in Cr (VI)-transformed cells. Knockdown of EGFR or AR increased ROS generation, resulting in elevated expressions of C-PARP and Bax and reduced expression of Bcl-2, leading to reduced apoptosis resistance in Cr (VI)-transformed cells. PI3K and AKT, downstream targets of EGFR, were also activated in Cr (VI)-transformed cells. Treatment the Cr (VI)-transformed cells with LY492002 and wortmannin, inhibitors of PI3K, caused ROS generation, resulting in increased Bax expression and reduced Bcl-2 expression, leading to increase of apoptosis. Most importantly, the results from xenograft mouse tumor study showed that knockdown of EGFR reduced both the size and frequency of tumor compared to Cr (VI)-transformed cells. In summary, the present study indicates that ligand-dependent activation of EGFR plays an important role in Cr (VI)-induced malignant cell transformation and tumorigenesis.

PS 1110e The Effects of Quercetin on the Placental Transport of the Dietary Carcinogen 2-Amino-1-methyl-6-phenylimidazo(4, 5-b)pyridine

M. McNerney, M. A. Malfatti, K. W. Turteltaub, G. Bench and K. Kulp. *BBTD, Lawrence Livermore National Labs, Livermore, CA.*

The heterocyclic amine 2-amino-1-methyl-6-phenylimidazo(4,5-b) pyridine (PhIP) is a dietary carcinogen formed from cooking meats at high temperatures. PhIP readily passes through the intestinal barrier, as well as, the placental barrier, increasing bioavailability and potentially exposing a developing fetus to harmful substances. Recent evidence has shown that certain flavonoids increase PhIP intestinal barrier crossing in vitro, and increases bioavailability in vivo, although it is unclear if this is also the case with the placental barrier. The current study aimed to determine the extent at which PhIP crosses the placental barrier using BeWo cells as a model, and determine if flavonoids can influence the rate of transport across

the barrier. BeWo cells were first cultured in transwell plates and dosed with 0, 1, 5, 10, or 100uM PhIP, and the barrier penetration was quantified at 0, 30, 60, 120 and 240min after dosing. The amount of PhIP crossing over time was concentration-dependent, which is similar to Caco2 cells. However, when the BeWo cells were incubated with 2 or 20uM quercetin prior to a dose of 10uM PhIP, there were no observable changes in the rate or amount of PhIP penetration. This is in contrast with the Caco2 cell culture models, suggesting a different transport mechanism between the cell types.

This work was performed under the auspices of the U.S. Department of Energy by Lawrence Livermore National Laboratory under Contract DE-AC52-07NA27344.

PS 1110f Evaluation of a Potential Mechanism for Formaldehyde-Induced Leukemia in C3B6.129F1-Trp53tm1Brd Mice

D. L. Morgan[1], D. Dixon[1], M. P. Jokinen[2], D. H. King[1], H. Price[3], G. Travlos[1], R. A. Herbert[1], J. E. French[1] and M. P. Waalkes[1]. *[1]NTP, Research Triangle Park, NC, [2]ILS, Research Triangle Park, NC and [3]Alion Sci Tech, Research Triangle Park, NC.*

Formaldehyde (FA) inhalation is linked to nasopharyngeal and sino-nasal cancer and myeloid leukemia in humans. While there is a strong mechanistic basis behind FA inhalation and causation of nasal cancer in humans, the mechanism linking FA and leukemia is unclear. Cell proliferation and DNA adducts in the nasal cavity are recognized as key mechanistic events in the induction of nasal cancer. Inhaled FA does not induce formation of detectable levels of DNA adducts at sites other than the nasal cavity; however, FA may cause leukemia by another mechanism. It was hypothesized that inhaled FA could cause significant genetic damage to stem cells in the nasal epithelium or circulating in local blood vessels. These damaged stem cells could reach the general circulation, seek out tissue sites that support the hematopoietic niche, undergo lodgment and become leukemic stem cells. We tested this hypothesis by exposing groups of 25 male C3B6.129F1-Trp53tm1Brd mice to 0, 7.5 or 15 ppm FA 6h/d, 5d/w for 8w and then holding mice without further exposure until 50 weeks old. At necropsy, blood was collected for hematology, and tissues were collected for histopathology. There were mice in all groups (10/75), including control, that died early or were euthanized in moribund condition. Moribund mice had reduced body weights and most had visible tissue masses. There was no evidence of leukemia in FA exposed mice based on hematology. Nose, larynx, lung, liver, spleen, thymus, lymph nodes, kidney, and gross lesions were evaluated microscopically. The primary exposure-related finding was minimal to mild squamous metaplasia of the respiratory epithelium of the nose. The incidence of this lesion increased with exposure concentration: 0/21, control, 14/21, 7.5 ppm, 21/22, 15 ppm. No cases of leukemia or lymphohematopoietic neoplasia were seen. Under the conditions of this study, FA inhalation did not cause leukemia in these genetically predisposed mice.

PS 1110g Detection of Endogenous and Exogenous DNA Adducts of Acetaldehyde

E. Mutlu[1], W. Bodnar[1], L. Collins[1], L. Recio[2], A. Green[2] and J. A. Swenberg[1]. *[1]Environmental Sciences and Engineering, University of North Carolina, Chapel Hill, NC and [2]Integrated Laboratory Systems, Research Triangle Park, NC.*

Acetaldehyde (AA) is a possible human carcinogen that is widely used in industry. It is also present in tobacco, automotive exhaust and several consumer products, as well as a metabolite of ethanol. AA is also formed endogenously by metabolic oxidation of ethanol and reacts with 2'-deoxyguanosine to form two DNA adducts, N^2-ethylidene-2'-deoxyguanosine, and 1,N^2-propano-2'-deoxyguanosine. Unlike 1,N^2etheno-2'-deoxyguanosine which arises from endogenously formed aldehydes such as crotonaldehyde, 1,N^2-propano-2'-deoxyguanosine arises from both exogenous AA and endogenously formed aldehydes due to lipid peroxidation. In our laboratory we have developed a method to measure endogenous and exogenous formation of 1,N^2-propano-2'-deoxyguanosine along with endogenous formation of 1,N^2etheno-2'-deoxyguanosine. In this method DNA was enriched by HPLC following enzyme hydrolysis and analyzed by nano LC-MS/MS on an AB Sciex 6500 triple quadrupole mass spectrometer. Limit of quantitation was 0.1 fmol for both 1,N^2etheno-2'-deoxyguanosine and 1,N^2-propano-2'-deoxyguanosine. Endogenous 1,N^2etheno-2'-deoaxyguanosine and 1,N^2-propano-2'-deoxyguanosine were detected at ~ 0.15 and ~ 3.4 fmol respectively in 1.25 μg calf thymus DNA. TK 6 cells were exposed to [$^{13}C_2$]-acetaldehyde in 0, 0.25, 0.5, 1, and 2 mM concentrations to analyze endogenous and exogenous formation of AA DNA adducts. The data obtained from these cells will enable us to determine both endogenous DNA adducts and the adducts from acetaldehyde exposure.

PS 1111 Human Stem Cell-Derived Cardiomyocyte—Bringing Cardiovascular Toxicity Screening to the Front Line

M. Peters, S. D. Lamore, J. Sasaki and C. W. Scott. *AstraZeneca, Waltham, MA.*

Cardiovascular (CV) toxicity is a prominent cause of drug attrition and withdrawal. Introducing new in vitro assays with higher throughput should permit earlier hazard identification and enable medicinal chemists to design-out CV liabilities. A central hurdle to developing in vitro CV assays has been the dual challenge of replicating integrated cardiovascular physiology while achieving a format with the throughput and consistency required for screening. The emergence of human stem-cell derived cardiomyocytes (CM) which beat spontaneously appears to address the first of these technical challenges and provides a foundation for developing screens. One screening platform, cellular impedance assays, has been validated for CM screening showing excellent predictivity for arrhythmia (Guo et al Tox Sci 2013) and contractility (Scott et al, in preparation). To complement validation data, in this poster we provide data to illustrate 3 points. (1) Changes in beat rate and amplitude are typically related. Across a wide range of stimuli the relationship is consistent with the inverse force-frequency relationship observed in force-based assays. (2) Either beat rate or amplitude can be selectively altered by compounds indicating they can be independent variables. (3) Understanding that the amplitude-frequency relationship is inverted relative to in vivo can be valuable for translating cardiomyocyte data to animal studies. In addition, we compare and contrast cellular impedance with calcium flux and MEA, two other technologies for detecting CM beating. These platforms detect different endpoints within the excitation-contraction cascade. We posit a new CV toxicity screening cascade that integrates the strengths of each platform. Key criteria include driving primary screening to achieve broad, inclusive detection followed by a choice of secondary assays to enable mechanism-appropriate follow-up.

PS 1112 Utilizing Structural and Functional Endpoints to Evaluate Drug-Induced Cardiotoxicity in Human-Induced Pluripotent Stem Cells

K. Doherty, D. Talbert, P. B. Trusk, R. Wappel, S. Shell and S. Bacus. *Quintiles, Westmont, IL.*

Safety pharmacology studies that evaluate new drug entities for potential cardiotoxicity remain a critical component of drug development. Recent studies have shown that in vitro toxicity tests utilizing human induced pluripotent-derived cardiac stem (iPS) cells reflect cardiac liabilities elucidated using the current standard testing methods(e.g., hERG, QT studies). We previously demonstrated that iPS cells could accurately predict the cardiotoxicity of 4 FDA-approved targeted oncology agents using an in vitro multi-parameter test panel assessing overall cardiac health and function. The present studies expand upon this initial report to assess whether this in vitro screen could accurately reflect known clinical cardiac risks across multiple drug classes and indications. Twenty drugs with known cardiac safety profiles were examined for their effect on iPS cell viability, reactive oxygen species (ROS) generation, lipid formation, troponin secretion, and beating activity. The results showed a unique cardiotoxic signature for these different drug classes and clinical indications. Oncology compounds induced potent structural toxicity (ROS generation, lipid formation, cell death, and troponin secretion) and subsequent disruption of beating activity. Anti-arrhythmic drugs potently disrupted cardiac cell beating in an acute time frame with minimal impact on metabolic stress or cell viability. In comparison, cardiac-safe drugs had no effect on the tested endpoints. Thus, different classes of drugs appear to show unique toxicity profiles that may reflect multiple mechanisms of cardiotoxicity. Further, this data supports previously published reports showing that the in vitro toxicity profiles of iPS cells provide an accurate and reliable model for cardiac risk assessment and appear to reflect known clinical safety outcomes. Thus, these studies show that a multi-parameter approach using iPS cardiomyocytes provides a comprehensive and robust assessment of cardiotoxic potential by evaluating several parameters important to cardiac cell health and function.

PS 1113 Real-Time Monitoring of iPSC Cardiomyocyte Contractility Assay Using a 96-Well Multielectrode Array System: A Potential Screen for Cardiotoxicity

E. Poulton, J. Morelli and Z. Jayyosi. *Predictive and Investigative Tox, DSAR, Sanofi, Framingham, MA.*

Cardiotoxicity is a leading cause of drug failure in preclinical and clinical development. An improvement in preclinical capability to predict cardiotoxicity would streamline the drug development process and reduce the likelihood of late phase drug development failures. Currently a number of in vitro electrophysiology assays are used to predict cardiotoxicity, including hERG and pukinjie fiber assays. The recent availability of well-characterized cardiomyocytes derived from induced

pluripotent stem cells (iPSCs) has made the development of assays measuring cardiomyocyte contractility possible. One such system, the xCelligence RTCA Cardio (Acea Biosciences), uses electrical impedance to measure the amount of cell to surface contact in an electrode containing tissue culture plate. We used the RTCA system to measure the effects of known cardiotoxic compounds on the contractility of iCell cardiomyocytes (Cellular Dynamics Inc.). Endpoints measured for 24 hours in cardiomyocytes included beat rate, amplitude, and beat rate irregularity. Compounds known to cause cardiotoxicity through a variety of mechanisms; including hERG channel blockers, Ca2+ channel blockers, multichannel blockers, inhibitors of myosin II, and beta blockers were used as a validation set. The validation compounds differently affected cardiomyocyte contractility following acute exposure or longer periods of treatment. For example, aconitine, which binds to sodium channels, caused an immediate increase in beating rate while pentamidine, which affects hERG trafficking to the membrane, affected beating rate only several hours following exposure. Blebbistatin, which interacts with myosin, caused a dose dependent decrease in amplitude, but did not affect beat rate until contraction was completely inhibited. hERG inhibitiors including cisapride and terfendine affected beat rate and caused irregular beats. The xCELLigence system detected the effects of diverse compounds on cardiomyocyte contractility, and may be useful for the prediction of cardiotoxicity.

PS 1114 A Novel Model for Proarrhythmia Assessment in iCell Cardiomyocyte Using a Multielectrode Extracellular Recording System

T. Taniguchi, M. Uesugi, A. Ojima, N. Miyamoto and K. Sawada. *Eisai, Tsukuba-shi, Japan.* Sponsor: A. Suganuma.

Prolongation of the cardiac action potential and the QT interval are potential causes of the ventricular tachycardia that is characteristic of torsades de pointes (TdP). However, it has been increasingly obvious that a prolongation of the QT interval does not necessarily lead to TdP. To bridge this dissociation, a lot of in vitro/vivo models for proarrthymic effects have been developed. Recently, human iPS cell derived cardiomyocytes (hiPSC-CM) have become a valuable tool for safety assessment in drug discovery. Present studies examined the effects of cell density and experimental temperature on iCell cardiomyocytes with MED64 system. Low-density cell plating lead to enlargement of hiPSC-CM. Gene expression analysis and pathway analysis reveal similarities between enlarged hiPSC-CM and cardiac hypertrophy. Low-density cell plating also caused decrease in expression of the KCNQ1 gene and affected the response to Iks blockers. The concentration-response curves for Chromanol 293B and HMR1556 shifted to the right when cell densities were decreased from 30000, 15000, 7500 and 3750 cells/well. When the experimental temperature was changed from 38.5 to 35.0 °C, the corrected field potential duration (FPDc) increased from 285 to 370 msec (24 msec/°C) almost linearly. Under the condition of both low-density cell plating and low experimental temperature, E4031 caused early afterdepolarizations (EADs) more frequent than in normal temperature. In conclusion, the plating cell density (cell size) and experimental temperature are very important as the determinants of drug sensitivity and EAD induction in field potential recoding experiments with hiPSC-CM.

PS 1115 Identification of Pro-Arrhythmic Potential with Human iPS-Derived Cardiomyocytes Using a Multiwell Microelectrode Array (MEA)

C. Strock, S. Qin, J. Gilbert and H. Luithardt. *Cyprotex, Watertown, MA.*

Cardiotoxicity is the most common reason for attrition due to toxicity. Current in vitro cytotoxicity assays identify only the most overtly toxic compounds, while assays to measure more specific liabilities such as hERG and other ion channels may fail to detect a response which relies on a combination of endpoints or a delayed response due to expression. Toxicity determination relies heavily on the later preclinical phase animal studies which have much higher costs associated and can have species specific results which may not model human responses. Therefore, an ideal assay for predicting cardiotoxicity would involve screening earlier on a platform measuring the field potential in human cardiomyocytes and which can identify the pro-arrhythmic potential of compounds.
eCiphrCardio is a multiwell MEA assay which measures the field potential of iPSC derived human cardiomyocytes. This assay provides a summation of the effects of the compounds on all channels, receptors, and pathways which affect cardiac function. This data reported is field potential duration (FPD) (QT), beat rate, Fast Na amplitude and slope. The measurement of these effects can be used to predict whether the mechanism driving a response is consistent with known responses from various reference compounds that have been evaluated in the system previously. A major liability in cardiotoxicity is associated with hERG inhibition which is linked to QT prolongation. As this MEA assay is capable of identifying a T-wave, prediction of a hERG liability can be demonstrated by a reduction in the amplitude of the T-wave as well as increase in the FPD. It is also capable of identifying Early After Depolarizations (EADs) which are common for some hERG inhibitors and can stimulate Torsades de Pointes like responses. The assay is also label free so it can also be performed over multiple time points and days to measure effects which are delayed and which patch clamp cannot detect. eCiphrCardio is a powerful, predictive assay for cardiac liabilities.

PS 1116 Advanced Cardiotoxicity Screening Using Human Stem Cell-Derived Cardiomyocytes and a Low-Impedance Microelectrode Array System for Proarrhythmic Risk Prediction

E. Navarrete[1], T. Thomas[2], B. Patlolla[4], H. Jiko[1], D. M. Bers[3] and R. Beygui[4]. [1]*AlphaMED Scientific, Ibaraki, Osaka, Japan,* [2]*Neural ID, Redwood City, CA,* [3]*UC Davis, Davis, CA and* [4]*Cardiothoracic Surgery, Stanford University, Stanford, CA.* Sponsor: M. Taylor.

Research on human heart tissue has been enabled thanks to advances in stem cell biology. In fact, the drug industry and regulatory agencies are considering human stem cell-derived cardiomyocytes (hSC-CMs) as a standard assay for preclinical cardiac safety screening. A beating cellular system integrating all the ion currents that contribute to the field potential (FP) allows in vitro testing of drug effects on the field potential duration (FPD) and thus prediction of the clinical QT interval's response. Low-impedance microelectrode arrays' (MEAs) enhanced sensitivity allows screening for early afterdepolarizations (EADs), the initiating mechanism of the drug-induced cardiac arrhythmia, Torsades de pointes. Short term variability of repolarization (STVrep), the correlate of electrical alternans, is an additional parameter whose investigation can contribute to a thorough cardiac safety assessment. hSC-CMs were plated on low-impedance MED-P5004A MEA probes and signals were acquired using a MED64 amplifier (Alpha Med Scientific Inc., Osaka, Japan) running Mobius QT software (Witwerx Inc., Tustin CA). Data were analyzed using Intelligent Waveform Service (Neural ID, Redwood City CA). A thorough panel of drugs was tested, including the torsadogenic hERG blockers sotalol and quinidine, the false positive (non-torsadogenic) hERG blocker verapamil, and the false-negative hERG blocker alfuzosin. All drugs produced the expected qualitative and quantitative effects on the FP. Most importantly, EADs and ectopic beats were found in 50% of the hiPSC preparations treated with sotalol and 40% treated with quinidine, as well as increased STVrep. We conclude the MEA/hSC-CM platform's capability to screen for EADs and STVrep is ideal for better predicting a drug's proarrhythmic risk, thus enabling a more thorough cardiotoxicity assessment, but most importantly reducing drug attrition and development costs.

PS 1117 Regulation of Superoxide and Mitochondrial Biogenesis by PGC-1α Protects against Doxorubicin-Induced Toxicity in Cardiomyocytes

S. Peng[1], H. Yuan[1], J. Guo[1], T. Zhang[1], M. Hou[1], H. Peng[1], J. Li[2] and P. L. Carmichael[2]. [1]*Academy of Military Medical Sciences, Institute of Disease Control and Prevention, Beijing, China and* [2]*Unilever Safety and Environmental Assurance Center, Sharnbrook, Bedfordshire, United Kingdom.*

Objective Doxorubicin (DOX) is an efficient and widely used anthracycline antibiotic for the treatment of tumors, but severe cardiotoxicity limits its application. Superoxide has been proposed to be mainly responsible for the cardiotoxicity of DOX, which is usually associated with mitochondrial dysfunction. PPARγ coactivator 1α (PGC-1α) is a nuclear-encoded transcriptional coactivator which plays a central role in mitochondrial biogenesis. Previous studies suggested that inhibition of mitochondrial biogenesis was responsible for the pathogenesis of DOX-induced cardiomyopathy. Nevertheless, the exact roles of PGC-1α in mitochondrial biogenesis and superoxide metabolism in DOX-induced cardiotoxicity remain unexplored. The present study was conducted to understand the exact role of PGC-1α in mitochondrial biogenesis and superoxide metabolism in DOX-induced cardiotoxicity. Methods and results A human cardiac cell line, AC16 cell, was used in the study. We treated AC16 cells with 10 different doses (0-2000 nM) of DOX for 12h. We demonstrated that low dose DOX treatment produced a low amount of superoxide in AC16 cells, which activated mechanisms of mitochondrial biogenesis (PGC-1α, NRF-1, TFAM) and the antioxidant system(SOD2,UCP2) via the PGC-1α to adapt the oxidative stress. In contrast, AC16 cells produced a large amount of superoxide following high dose DOX exposure, with down-regulated mitochondrial biogenesis, inhibited the antioxidant system and deleterious effects on mitochondrial function. Knockdown PGC-1α in AC16 cell can aggravates DOX-induced cardiotoxicity. Conclusion Taken together, these data suggest PGC-1α play a critical role in DOX-induced cardiotoxicity by regulating mitochondrial biogenesis and superoxide metabolism. Therefore, PGC-1α signaling pathway may emerge as a new potential target for future development of more effective cardioprotective strategies against DOX-induced cardiotoxicity.

PS 1118 Automated Patch Clamp and New Impedance of Stem Cell-Derived Cardiomyocytes for Safety Screening and Drug Discovery

C. Bot, G. Okeyo, J. Oestreich and R. Haedo. *Nanion Technologies Inc., North Brunswick, NJ.*

Human induced-pluripotent stem cell-derived cardiomyocytes (hiPS-CM) combine a primary cardiomyocyte-like physiology with the advantages of a cell line, e.g. large batch sizes, low batch-to-batch variation, and a convenient "ready-to-use" format. We have used hiPS cardiomyocytes from diverse cell suppliers in automated patch clamp and impedance assays and show that this approach is of great value in cardiotoxicity prediction. The label-free impedance platform, the CardioExcyte 96, allows precise impedance measurements at a time resolution of 1 ms and generates 96 recordings in parallel. The automated patch clamp device Patchliner generates up to 500 dp per day and is capable of generating pharmacological experiments, IC50 or EC50 data and action potentials recordings from hiPS-CM.
Cells from main stem cell suppliers were successfully tested and data will be compared. Dose response curves or single-point screening experiments of several drugs (e.g. hERG and Cav1.2 blockers) were collected and will be presented.The presented data show how these systems can be used efficiently to predict drug-induced arrhythmia for cardiac risk assessment.

PS 1119 Examining the Use of Human Induced Pluripotent Stem Cell-Derived Cardiomyocytes for Exploring Multiple Arrhythmogenic Endpoints in a Single High-Throughput Assay

R. Whittaker, R. Vega, F. Cerignoli and J. Price. *Vala Sciences Inc., San Diego, CA.*

Human induced pluripotent stem cell derived cardiomyocytes (HiPS-CMs) may be used as a powerful in vitro model for predictive cardiac safety assessment and could allow for better identification of compounds with poor arrhythmogenic liability profiles in the early drug discovery process. To enable HT arrhythmogenic testing in HiPS-CMs, we have developed the Kinetic Image Cytometer (KIC) for high throughput, automated cell-by-cell analysis of intracellular calcium transient dynamics. Calcium transients integrate the electrochemical signals of the action potential with the molecular signaling pathways that regulate contraction. Drug induced alterations in the shape and duration of the cardiomyocyte action potential result in changes to the shape and duration of the intracellular calcium transient. Therefore, by examining calcium transient dynamics in hiPS-CMS a single assay can be used to screen for compound effects across multiple ion channel types and is also capable of detecting multi-channel effects. In the present study, we used KIC technology to assess the predictive values of hiPS-CMs using a library of 90 compounds known to alter the activity or expression level of cardiac ion channels/receptors resulting in changes in the cardiac action potential. Our data indicate that using hiPS-CMs, KIC is able to detect known drug-induced changes in Ca2+ transients and therefore, may potentially predict drug-induced arrhythmogenic liabilities in early drug discovery.

PS 1120 Development of a Spontaneously Beating Human Cardiac Microtissue Model for the Study of Drug-Induced Cardiotoxicity

S. Ravenscroft[1, 2], A. Pointon[2], M. Cross[1] and J. Sidaway[1, 2]. [1]*MRC Centre for Drug Safety Science, Molecular & Clinical Pharmacology, Institute of Translation Medicine, University of Liverpool, Liverpool, United Kingdom and* [2]*Innovative Medicines and Early Development, Drug Safety and Metabolism, Translational Safety, AstraZeneca, Macclesfield, Cheshire, United Kingdom.*

Spontaneously beating multicellular cardiac microtissues comprising human embryonic stem cell cardiomyocytes (hESC-CM's), human cardiac microvascular endothelial cells (HCMEC's) and human cardiac fibroblasts (HCF's) have been developed using a scaffold free 96 well cell suspension method. Microtissues dramatically reduce cell culture costs, display uniform shape and size, key cellular markers and can be maintained for at least 4 weeks. The contractile properties of microtissues were assessed using a video-based edge detection method (IonOptix™, Dublin, Ireland), mounted on a heated stage (~36°C), with continued perfusion and paced at a frequency of 1Hz. After perfusion with vehicle (0.1% DMSO), microtissues were exposed to compound (8 inactive compounds; 5 positive inotropes and 12 negative inotropes) for ~ 250 seconds. Compound effects were normalized to the vehicle control for each microtissue; concentration-effect curves were constructed. Both negative and positive inotropy was detected. 88% of compound effect correlated with the known in vivo outcome, including two compounds (lapatinib, 0.86 μM; atenolol, 0.94 μM) that resulted in false negative effects in canine cardiomyocytes (Harmer et al. (2012) Toxicol. Appl. Pharmacol. 260, 162–172). These two compounds were subsequently assessed in single cell microtissues of hESC-CM's and as with the canine cardiomyocytes, false negative effects were observed. In conclusion, a spontaneously beating multicellular cardiac microtissue with video-based edge detection gives improved in vitro to in vivo correlation and this could be applied to the in vitro detection of the cardiotoxic potential of novel therapeutics.

PS 1121 Acrolein and Endothelial Cell Dysfunction: Role of the miRNA let-7a

W. T. Abplanalp[1], X. Li[2], N. Cooper[2], P. Haberzettl[1], D. J. Conklin[1], A. Bhatnagar[1] and T. O'Toole[1]. [1]*Diabetes and Obesity Center, University of Louisville, Louisville, KY and* [2]*Department of Anatomy and Neurobiology, University of Louisville, Louisville, KY.*

Several studies have linked the pervasive combustion product, acrolein, with a number of cardiovascular disorders including coronary heart disease, myocardial infarction, and atherosclerosis. These disorders typically arise from a dysfunctional endothelium, however less is understood about the mechanisms whereby acrolein affects endothelial function. To determine if acrolein does so by inducing changes in endothelial miRNAs we initially used microarray technology. We found that acrolein exposure (4hx10μM) stimulated the upregulation of 12 and the downregulation of 15 miRNAs by at least 1.5-fold in treated human umbilical vein endothelial cells (HUVECs). Selected changes were confirmed by qPCR. Among the upregulated miRNAs were 3 members of the let-7 family (let-7a, let-7d, let-7e) that have roles in cellular differentiation, growth and insulin signaling. Consistent with let-7a upregulation, acrolein-treated HUVECs had decreased expression of four of let-7a predicted protein targets: β3 integrin, Cdc34, K-Ras, and insulin receptor-β (57%, 73%, 55% and 73% of control, respectively). β3 integrin mediates endothelial migration, and exposure to acrolein reduced HUVEC migration compared with vehicle-treated cells (38% of control). These migratory defects of acrolein-treated cells were reversed by prior transfection with a let-7a antagomir (87% of control), but not with a non-specific antagomir (48% of control). In addition, we found that mice inhaling volatile acrolein (1ppm/6h/6d) developed aortic insulin resistance associated with upregulation of aortic let-7a. These studies suggest that endothelial cell miRNA, specifically members of the let-7 family, protein expression and cellular function can be acutely regulated by acrolein. This mechanism may contribute to the vascular pathologies resulting from exposure to acrolein and related environmental pollutants.

PS 1122 Dysfunction of Vascular Smooth Muscle and Vascular Remodeling by Simvastatin

K. Kim[1], S. Kang[1], H. Woo[1], K. Lim[2], M. Lee[3], O. Bae[4] and J. Chung[1]. [1]*College of Pharmacy, Seoul National University, Seoul, Republic of Korea,* [2]*College of Pharmacy, Ewha Womans University, Seoul, Republic of Korea,* [3]*College of Pharmacy, Dongguk University, Goyang, Republic of Korea and* [4]*College of Pharmacy, Hanyang University, Ansan, Republic of Korea.*

Statins, inhibitors of 3-hydroxy-3-methylglutaryl-coenzyme A reductase, are widely prescribed for hypercholesterolemia. With the increasing use of statins, numerous reports demonstrated that statin can cause damage to skeletal muscles. However, the toxicities of statins on vascular smooth muscle, which are essential to cardiovascular homeostasis, have not been elucidated. Here, we examined the effects of simvastatin on the contractile function and the integrity of vascular smooth muscle. In isolated rat thoracic aorta, simvastatin suppressed the normal agonist-induced contractile responses. The suppression was irreversible even after wash-out of simvastatin and persisted in the endothelium-denuded aortic rings, reflecting that normal function of vascular smooth muscle was altered permanently. Simvastatin abolished agonist-induced intracellular Ca2+ increase in primary cultured vascular smooth muscle cells, and suppressed the contraction induced by Bay K8644, an activator of voltage-operated Ca2+ channel (VOCC), indicating that Ca2+ influx through VOCC was disrupted. This effect was reversed by the supplementation of mevalonate and geranylgeranylpyrophosphate, suggesting that alteration of protein isoprenylation may be involved. Consistently, activation of RhoA, a representative isoprenylated protein, was disrupted by simvastatin and RhoA-mediated phosphorylation of MYPT1 and CPI-17, and tonic tension were also suppressed. Notably, prolonged treatment of simvastatin induced apoptosis in vascular smooth muscle suggesting that dysfunction may eventually lead to disruption of structural integrity. Most importantly, simvastatin treatment in vivo significantly attenuated the agonist-induced vasoconstriction in rats ex vivo and induced a decrease in luminal area of the vascular wall, demonstrating that simvastatin can impair normal vascular contractility and induce vascular remodeling.

PS 1123 Mitochondrial Dysfunction and Autophagy in Endothelial Progenitor Cells by High Glucose

K. Kim[1], Y. Shin[1], E. Kim[1], M. Akram[1], M. Noh[2] and O. Bae[1]. [1]*College of Pharmacy Institute of Pharmaceutical Science and Technology, Hanyang University, Ansan, Republic of Korea and* [2]*College of Pharmacy, Seoul National University, Seoul, Republic of Korea.*

Cardiovascular dysfunction is the most severe complication in patients with diabetes mellitus. Among several causes, it has been recently demonstrated that endothelial progenitor cells (EPCs), a circulating adult stem cell regenerating damaged vascular endothelium, are dysfunctional under diabetic condition resulting in impaired peripheral circulation. To elucidate the mechanisms underlying diabetes-associated cardiovascular impairment, we investigated the cellular alteration of EPCs under high glucose condition. Bone marrow-derived EPCs (BM-EPCs) were exposed to normal glucose-(5.5 mM) or high glucose (30 mM)-containing medium. High glucose treated-EPCs showed deceased ability to form tubule-like networks in Matrigel compared to EPCs in normal glucose. The conversion of LC3-II from LC3-I in EPCs was significantly increased, suggesting that autophagy occurs under high glucose condition. Interestingly, increased autophagy was not accompanied with phosphorylation of mTOR, reflecting that high glucose-induced autophagy was not related with mTOR signaling pathway. Increased generation of reactive oxygen species and disruption of mitochondrial function was observed in EPCs under high glucose condition. In conclusion, we demonstrated that ROS-mediated autophagy is induced in EPCs under high glucose condition, giving a new insight into the mechanism underlying dysfunction of diabetic EPCs.

PS 1124 Loss of Caveolin-1 Protects against PCB-Induced Vascular Dysfunction by Upregulating Nrf2 and the Antioxidant Response

M. C. Petriello[1, 2] and B. Hennig[2]. [1]*Toxicology, University of Kentucky, Lexington, KY and* [2]*Superfund Research Program, University of Kentucky, Lexington, KY.*

Environmental toxicants such as polychlorinated biphenyls (PCBs) have been implicated in the promotion of multiple inflammatory diseases including cardiovascular disease, but information regarding mechanisms of toxicity and cross-talk between relevant cell signaling pathways is lacking. To examine the importance of crosstalk between Cav-1 and Nrf2 in PCB-induced inflammation, we silenced Cav-1 in vascular endothelial cells and subsequently treated with PCB. Cav-1 silencing (siRNA treatment) increased levels of Nrf2-ARE transcriptional binding (EMSA) resulting in higher mRNA levels (RT-PCR) of the antioxidant genes glutathione s-transferase (GST ~ 3 fold increase) and NADPH dehydrogenase quinone 1 (NQO1 ~ 1 fold increase) in control cells. This upregulated antioxidant response was also seen in Cav-1 siRNA treated cells exposed to PCB. Mechanistically, in Cav-1 siRNA treated cells, we observed decreased protein levels of Nrf2 inhibitory proteins Keap1, Fyn kinase and Bach1. We next isolated mRNA from livers of Cav-1 -/- and C57BL/6 mice and determined that Cav-1 -/- mice display significantly decreased levels of inhibitory Keap1 compared to control. Finally, we isolated lung and aortic endothelial cells from wild-type and Cav-1 -/- mice and treated these cells with PCB 126. Cav-1 -/- endothelial cells were protected from PCB-induced cellular dysfunction as evidenced by decreased vascular cell adhesion molecule (VCAM-1) protein induction. We attributed this protection to an increased antioxidant response due to Cav-1 Nrf2 cross-talk. In this work we identified novel crosstalk between Cav-1 and Nrf2 which implicates down-regulation of Cav-1 as a protective mechanism of PCB-induced inflammation. To defend against the toxicities of Superfund chemicals we propose the use of healthful nutrients that will both downregulate pro-inflammatory Cav-1 and simultaneously upregulate the Nrf2 antioxidant response.

PS 1125 Uric Acid Induces Endothelial Dysfunction by Vascular Insulin Resistance Associated with the Impairment of Nitric Oxide Synthesis

Y. Choi[1], Y. Yoon[1], K. Lee[1], T. Hien[1], K. Kang[1], K. Kim[1], J. Lee[1], M. Lee[2], S. Lee[3], D. Kang[4] and B. Lee[1]. [1]*College of Pharmacy, Seoul National University, Seoul, Republic of Korea,* [2]*Dongguk University, Goyang, Republic of Korea,* [3]*College of Medicine, Seoul National University, Seoul, Republic of Korea and* [4]*Ewha Womans University, Seoul, Republic of Korea.*

Uric acid is the final metabolite of purine nucleotide in the species, including human, that are deficient in uricase responsible for the conversion to allantoin. Despite some evidence of the uric acid-induced cardiovascular diseases, the relationship with the insulin resistance has not been established clearly. In this study, we investigated the role of vascular insulin resistance in the uric acid-induced endothelial dysfunction. Uric acid inhibited insulin-stimulated eNOS phosphorylation and NO production in endothelial cells without any effects in the basal state. Decreased insulin response in the cells is mediated with the impairment of PI3K/Akt as well as p38 MAPK signaling pathway as verified in the p110 and CA-MKK-6 transfected cells, respectively. Uric acid also suppressed metformin- and AICAR-induced eNOS phosphorylation. The inhibitory effects of uric acid were evident between 50 and 200 μM, a concentration range found in normouricemia. We also examined the effects in mild hyperuricemic rats induced by an uricase inhibitor allantoxanamide (ATX). Treatment of rats with ATX induced mild hyperuricemia and increased mean arterial pressure significantly. While ATX treated rats did not show systemic insulin resistance, they showed impaired vasorelaxation induced by insulin or metformin but not by acetylcholine. Compromised insulin response in terms of Akt/eNOS signaling pathway was observed in aorta ring of hyperuricemic rats. Co-administration with allopurinol reduced serum uric acid and blood pressure to the level of vehicle control group and restored the action of insulin on the Akt-eNOS signaling and vasorelaxation. Taken together, uric acid induces vascular insulin resistance and endothelial dysfunction associated with the impairment of eNOS activity that can lead to the development of hypertension.

PS 1126 Cellular Impedance Assays for Deconvoluting Kinase Inhibitor-Induced Cardiotoxicity

S. D. Lamore[1], C. W. Scott[1], M. Lamb[2], C. Chuaqui[2], C. S. Boyer[1], J. Sagemark[1], L. Carlsson[1], E. Ahlberg[1] and M. Peters[1]. [1]*Drug Safety and Metabolism, AstraZeneca, Waltham, MA and* [2]*Oncology Innovative Medicines, AstraZeneca, Waltham, MA.*

Cardiovascular (CV) toxicity is a leading contributor to drug attrition and market withdrawal. There is urgent need for earlier and broader CV screening, particularly for kinase inhibitors (KI) which suffer frequent CV toxicity. Lack of kinase selectivity is a persistent hurdle to unraveling the specific kinases that contribute to CV toxicity due to the highly conserved nature of the ATP pocket. To handle KI promiscuity and discover underling kinases requires an in vitro assay with the throughput to screen kinome-spanning compound sets. Addressing CV effects requires an integrated functional assay that is downstream of the excitation-contraction cascade and capable of capturing the pleiotropic effects of kinases. The emergence of cellular impedance technology enables detection of spontaneous beating of cultured cardiomyocytes (CM) in a real-time, label-free 96-well format, and can quantify both the rate and amplitude of beating. Using this technology, we are seeking to identify specific kinase profiles that underlie functional effects on CMs. The effects on iPSC-derived CM beating were evaluated using two panels of KIs (65 and 160 compounds) whose kinome selectivity has been published. Neither KI promiscuity nor physical-chemical properties appeared to correlate with changes in CM beating. The impedance and polypharmacology results are being interrogated using machine learning methods to identify culprit kinase profiles. Initial results indicate that KI promiscuity within specific kinase families (AGC, STE, and CAMK) is associated with altered CM beating. Individual kinases that have been identified as possible contributors to functional CV toxicity by recursive partitioning or feature importance algorithms are being substantiated with siRNA-based knockdown experiments. Ultimately, this study will lead to the development of a model to predict KI CV toxicity thus enabling drug discovery programs to design-in CV safety.

PS 1127 TCDD and Omeprazole Up-Regulate Human Platelet Activation via the Aryl Hydrocarbon Receptor (AhR) Nongenomic Pathway

M. Pombo, M. Lame and F. Tablin. *VM Anatomy, Physiology and Cell Biology, University of California Davis, Davis, CA.* Sponsor: L. Van Winkle.

Platelets, anucleate cells, circulate in the peripheral blood and are essential for maintenance of hemostasis. Prior studies from our laboratory showed increased platelet activation with exposure to particulate matter containing AhR ligands. We show, using Western blot analysis and immunoprecipitation, that platelets express the AhR. Using 2,3,7,8-tetrachlorodibenzo-p-dioxin (TCDD) or omeprazole, we show that washed human platelets incubated with AhR ligand demonstrate a significant concentration dependent increase in AhR protein levels. Treatment with either AhR ligand results in statistically significant increases in phosphorylation of p38MAPK and cPLA2, two key regulatory molecules in platelet activation. To evaluate platelet function, we performed optical aggregometry studies using platelet-rich plasma incubated with either of the above AhR ligands. Aggregometry studies demonstrate that treatment with these ligands results in platelet priming, as defined by enhanced sensitivity to physiologic agonists. Incubation with either ligand significantly increased both the slope and the amplitude of the platelet-rich plasma aggregation. As further evidence of AhR function, we found that incubation of washed platelets with TCDD results in increased secretion of TXB2, an additional marker of platelet activation. Our data support a model of the platelet AhR non-genomic pathway in which incubation with ligand results in increased

expression of the AhR, phosphorylation of p38MAPK and cPLA2 and eventual secretion of TXB2 functioning in a feedback loop resulting in platelet priming. These findings suggest that ligand binding to the platelet AhR may play a key role in the vascular response to particulate matter.
All studies were conducted under IRB 299969-3. These studies were supported by a contract with the California Air Resources Board. The statements and conclusions in this study are those of the University of California Davis and are not necessarily those of the California Air Resources Board.

PS 1128 IL-33 Cardiovascular Safety Profile Redefined: Lessons Learned from Rat and NHP Cardiomyocytes, KO Mice, and Human GWAS Studies

T. Brabham[1], W. Hu[1], T. Swanson[2], L. Gauthier[1], J. Heyen[1], T. Wisialowski[1], T. LaBranche[1], M. Hemkens[1], J. Jamieson[1], K. Reibling[2], B. Hollingshead[1], L. Collis[5], N. Bing[3], L. Bloom[4], K. Nocka[5], M. Kasaian[5] and M. Vogel[1]. *[1]Drug Safety Research & Devlopment, Pfizer, Andover, MA, [2]Comparative Medicine, Pfizer, Groton, CT, [3]Biotherapeutics Clinical Research, Pfizer, Cambridge, MA, [4]Biotherapeutics Technologies, Pfizer, Cambridge, MA and [5]Immunoscience Research Unit, Pfizer, Cambridge, MA.*

IL-33 is a cytokine alarmin implicated in innate/adaptive immune responses, as well as in cardiac volume overload diseases (i.e. congestive heart failure). Some evidence suggest an IL-33-dependent decrease in cardiomyocyte hypertrophy is heart protective, rescuing the ventricles from dysfunction and fibrosis. To evaluate the role of IL-33 in normal cardiac function an IACUC approved de-risking strategy to re-define its safety profile was initiated. Methods: Cardiac structure and function were assessed in neonatal rat and adult non-human primate (NHP) cardiomyocyte hypertrophy assays, IL-33 knock out (KO) mice via echocardiography (echo) and histology; and human genome-wide association studies (GWAS) to correlate IL-33 and its receptor ST2 polymorphisms with CV disease. Results: Neonatal rat cardiomyocytes - Phenylephrine-induced cardiomyocyte hypertrophic gene expression (i.e. myosin heavy chain 7) was antagonized by rhIL-33. Adult NHP cardiomyocytes – No drug-induced cardiomyocyte hypertrophic gene expression was detected in preliminary experiments. IL-33 KO mice echo - Aged mice (~13 months): KO (n=21), heterozygote (n=15) and wild type (n=32) were assessed. Baseline values were obtained from all, with 50% re-examined after an acute dobutamine-induced cardiac inotropic challenge. No heart rate, ejection fraction, or cardiac output differences were detected across any genotypes. GWAS: No strong IL-33 or ST2 association with CV disease (p>0.01). Summary: The role of IL-33 in preventing cardiomyocyte hypertrophy (rat cardiomyocytes) was confirmed. Cardiac structure and function were not adversely affected in aged KO mice. Human GWAS analyses did not support a high probability association of CV disease and IL-33.

PS 1129 Utilization of Reverse Phase Protein Array (RPPA) Technology to Evaluate Multikinase Pathway Inhibition in Cell Lysates

D. Puppala, S. Dann and K. Leach. *Pfizer Inc., Groton, CT.*

Targeted inhibition of these kinases has been shown to be beneficial in treating certain kinds of cancers. Unfortunately, most of these inhibitors may be promiscuous as the ATP binding sites are similar amongst kinases. Although the underlying mechanisms are not clear the adverse effects (like cardiotoxicity) observed by these inhibitors are attributed to off target inhibitions. Hence understanding the off target activities associated with potential kinase inhibitors is critical for designing safer inhibitors. Towards this end, we tested the Reverse Phase Protein Array (RPPA) technology from Carna Biosciences. This technique detects the phosphorylation status of 180 proteins across 18 critical cell signaling pathways simultaneously. RPPA technology utilizes compound treated cell lysates and phospho specific antibodies for detection. We treated NCI-H1975 (adenocarcinoma) cells with four PKC pathway inhibitors from 2 different chemical series (A&B: Series 1; C&D : Series 2) for 60 min followed by treatment of phorbol esters for 30 min. Cell lysates were then subjected for RPPA evaluation and phosphorylation status of 180 proteins was obtained. 30 minute treatment with phorbol myristate acetate (PMA) alone exhibited a phosphorylation signal (>1.5 intensity) for 18 different proteins across 7/18 different pathways (PI3K-AKT-mTOR (7), Ras-Raf (3), Cytoskeleton (2), DNA damage (2), RTK (2), Angiogenesis (1) and p38 MAPK (1). PMA induced phosphorylation signal for most of the kinases was altered by compound A & B whereas compounds C & D did not alter these kinases. For example, PMA induced phosphorylation of ERK1/2 and ribosomal S6 protein was inhibited by compounds A & B (>2-9 fold) whereas C and D did not alter these signals. Overall, compounds from series 1 (A & B) clustered differently than compounds from series 2 (C & D) based on similarities in their RPPA profiles. RPPA can potentially be used to differentiate compounds based on their off- target activities. These changes in signaling pathways will be further confirmed using traditional approaches like western blotting and flow cytometry.

PS 1129a Altered Hemodynamics Play a Critical Role in Fenoldopam-Induced Mesenteric Vasculitis in the Rat

B. R. Wamhoff, M. Simmers, B. Cole, A. Mackey, D. Manka and B. Blackman. *HemoShear LLC, Charlottesville, VA.* Sponsor: A. Dash.

Mechanisms underlying drug-induced vascular injury (DIVI) are poorly understood, and although several drugs induce DIVI in preclinical species, the risk to humans is unknown. For example, fenoldopam is an anti-hypertensive agent that elicits drug-induced hemodynamic changes and DIVI in the rat mesentery but presents no known vascular injury response in humans. The purpose of this study was to determine whether the alterations in fenoldopam-induced hemodynamics were necessary for fenoldopam-induced DIVI. Rats were administered fenoldopam (100 mg/kg s.c.) to induce DIVI and changes in mesentery hemodynamic blood flow were measured by ultrasound. To replicate the observed in vivo response in vitro, we utilized a co-culture platform with rat primary endothelial and smooth muscle cells where the endothelium is exposed to in vivo-derived hemodynamic waveforms to restore in vivo-like vascular cell responsiveness. Exposure of endothelial cells to the fenoldopam-induced hemodynamic waveform enhanced permeability compared to vehicle dose waveform that was independent of the exposure to fenoldopam in the platform. Gene analysis revealed significant changes in the endothelial and smooth muscle cell response to fenoldopam or its drug-induced hemodynamic response alone. The most differentially regulated pathways were observed in ECs when fenoldopam and its drug-induced hemodynamic response were combined, suggesting synergism. Biological themes included: vascular-related biology, inflammation, oxidative stress, cell death, and cell remodeling. In conclusion, we provide evidence that supports the hypothesis that fenoldopam-induced changes in hemodynamics play a critical role in fenoldopam-induced DIVI in the rat mesentery.

PS 1129b *De Novo* Cyclin D2 Induces Cardiomyocyte Proliferation in Adult Mouse Hearts

L. Zhan, M. Soonpaa, S. Reuter and L. Field. *Riley Heart Research Center, Division of Pediatric Cardiology, Indiana University School of Medicine, Indianapolis, IN.*

Previous studies have shown that targeted expression of cyclin D2 under the regulation of the cardiomyocyte-restricted myosin heavy chain (MHC) promoter results in sustained cardiomyocyte cell cycle activity which was sufficient to promote regeneration following myocardial injury. Transgene expression in this model initiates prior to cardiomyocyte terminal differentiation. It thus remains to be demonstrated if de novo cyclin D2 expression in the adult myocardium would be sufficient to induce cardiomyocyte proliferation. In this study, we generated a model capable of conditional cyclin D2 expression in cardiac myocytes. The model utilizes an attenuated myosin heavy chain (atMHC) promoter to target expression of cyclin D2. The atMHC promoter is active only in the presence of VP16 trans-activator protein in the myocardium (MHC-tTA mice). In the absence of doxocycline (DC), the VP16 protein is active and drives transcription of the atMHC promoter. However, in the presence of DC, the VP16 protein is inactive. Thus, cyclin D2 expression in double transgenic animals can be turned off (by treating with DC) or turned on (no DC treatment). We have shown that in the absence of DC, atMHC-cycD2 / MHC-tTA double transgenic animals express cyclin D2 in cardiomyocytes and exhibit cardiomyocyte cell cycle activity as we have observed in our constitutive model. Furthermore, we demonstrated that cyclinD2 expression in the MHC-tTA/atMHC-cycD2 mice was blocked from embryo to 3 months old by low doses (10 mg/ml) of DC in the drinking water and reactivated after removing the DC for 10 days. Cardiomyocyte nuclear was identified by the introduction of β-galatosidase reporter gene under the control of cardiac myosin heavy chain promoter (MHC-nLAC). BrdU incorporation analyses revealed sustained cardiomyocyte DNA synthesis in the adult MHC-tTA/atMHC-cycD2/ MHC-nLAC mice. [supported by NIH grant R01 HL109205].

PS 1129c The Effect of Endocrine-Disrupting Chemicals on Human Stem Cell-Derived Cardiomyocytes

N. Posnack[1], H. Ding[2], G. Stybayeva[3], Z. Karabekian[1], M. Laflamme[2] and N. Sarvazyan[1]. [1]*The George Washington University, Washington, DC,* [2]*University of Washington, Seattle, WA and* [3]*University of California, Davis, CA.*

The ubiquitous nature of plastics has raised concerns pertaining to continuous exposure to plastic additives and human health risks. Of particular concern is the use of endocrine-disrupting compounds (EDCs) in plastic production, including bisphenol A (BPA) and di-2(ethylhexyl)phthalate (DEHP). We previously reported the direct effects of DEHP and BPA exposure on cardiac calcium handling and electrical conduction in rodent cardiomyocytes and heart tissue. Our goal was to investigate the applicability of our previous findings to humans by examining the direct effect of EDC exposure on human stem cell-derived cardiomyocytes (hESC-CM). hESC-CM were derived from H7 embryonic stem cells, as previously described (Laflamme 2007). After 8-10 days, hESC-CM formed a confluent network that exhibited rhythmic spontaneous contractions. Cells were treated with BPA (0.1 - 100 μM) or DEHP (1 - 50 μg/mL), loaded with 5 μM Fluo-4AM, and then calcium transients were recorded using a Zeiss confocal imaging system. BPA treatment modified calcium handling parameters, including an increase in calcium release and calcium reuptake time, and a decrease in peak fluorescence amplitude. DEHP treatment resulted in complete cessation of contractile activity, via both spontaneous cell contractions and external pacing. We observed significant changes in calcium handling in human cells at lower EDC doses than for rodent cardiac cells. These findings illustrate key differences in cardiac models and emphasize the importance of examining the effect of EDCs on human cardiac cells of different origins (atrial, pacemaker, ventricular). Supported by NIH (K99ES023477 to NGP).

PS 1129d Smoke Extracts from Tobacco Cigarettes, but Not E-Cigarettes, Delay Cardiac Maturation *In Vitro* and *In Vivo*

P. J. Hofsteen, N. Palpant, L. Pabon, H. Reineke and C. Murry. *University of Washington, Seattle, WA.* Sponsor: R. Peterson.

Maternal smoking is a risk factor for low birth weight and other developmental delays. We sought to determine the impact of extracts derived from e-cigarettes (e-cig) compared to standard tobacco cigarettes (3R4F) on heart development in vitro and in vivo. Human embryonic stem cells were used as a model for in vitro cardiac development and were differentiated using monolayer cardiac differentiation. Cells were exposed to purified nicotine or extracts from e-cig or tobacco cigarettes containing 1.7, 3.4, 6.8, and 13.7 μM nicotine, or vehicle control throughout differentiation. On day 14 control cells had an intrinsic beating rate of 39.5 ± 7.2 beats per minute (bpm), cardiomyocyte cell yield of 2.5x106 ± 4.3x105 cells, and cardiomyocyte purity of 83.6% ± 1.1% cTnT+ cells by flow cytometry. Cells exposed to purified nicotine or e-cig extracts showed no effect on intrinsic beating rate, cardiomyocyte yield, or cardiomyocyte purity under all concentrations tested. In contrast, there was no survival of cells exposed to 13.7 μM nicotine from tobacco cigarettes. Furthermore, cells exposed to 6.8 μM tobacco nicotine showed markedly reduced intrinsic beating rate (4.5 ± 0.9 bpm), but no effect on cardiomyocyte yield or purity. Cardiomyocytes exposed to 1.7, 3.4, and 6.8 μM tobacco nicotine showed significantly increased levels of α-smooth muscle actin, consistent with cardiomyocyte immaturity. To determine if these data correlate in vivo, zebrafish embryos were raised in 3.4, 6.8, and 13.7 μM e-cig, tobacco extract or control from 0-72 hours post fertilization. Tobacco-exposed fish showed significant decrease in heart rate, survival, general development and increased incidence of heart malformation in a dose dependent manner. In contrast, e-cig exposed fish closely resembled the time-matched controls. These data suggest that nicotine alone or e-cig extracts do not have a marked impact on early heart development. However, smoke extracts generated from tobacco markedly impact cardiac development by reducing cardiac beating rates and delaying cardiomyocyte maturation.

PS 1129e Engineered Heart Tissues for Cardiotoxicity Testing

T. Wakatsuki and M. Conway. *InvivoSciences, Inc., Madison, WI.* Sponsor: K. Dreher.

Nearly 45% of drugs withdrawn from the market (1975-2007) were eliminated by cardiosafety concerns. While the International Conference on Harmonization defines assays to detect inhibition of a delayed rectifier potassium current by the human hERG channel, the discovery of human induced pluripotent stem cells (iPSCs) opened up an exciting opportunity to perform cardiotoxicity testing. The drug safety community is rapidly incorporating human iPSC derived cardiomyocytes (CMs) into their safety assessment. However, iPSC-derived CMs may not predict drug-induced cardiac toxicity in adults. The iPSC-derived CMs exhibit spontaneously firing action potential profiles of immature CMs. To characterize excitation contraction coupling of human iPSC-derived CMs, human engineered heart tissues (EHTs) were developed to measure their force of contraction, Ca-transient, and their potential to develop into mature CMs in a 3D microenvironment, recapitulating post-natal cardiac development. Automatically handled viscous solutions containing fragile cardiac cells fabricated human EHTs in a 96-well plate. Cells remodeled extracellular matrix to form EHTs that maintain cardiac contractions for several months. An increasing external calcium concentrations (0-3.6mM) elevated cardiac contractility. However, positive inotropic agents including isoproterenol (100nM) had little effect on the force of contraction. Inhibitors of the sarcoplasmic reticulum Ca ATPase pump, such as thapsigargin (>30 nM), reduced peak and duration of the Ca transient, and nifedipine (>30nM)-sensitive L-type Ca channel was critical to maintain cardiac contraction and exhibited Bay-K's known dose-dependent open/close status. Antiarrhythmic agents (e.g., E4031) elongated cardiac twitch-duration at low dose (1-10 nM), but decreased twitch force at high dose (>100nM). Drug-induced changes and a slowly rising (peak in 0.5s) Ca-transient suggested a slow development of t-tubule and ryanodine receptor complex in immature CMs thickening and elongating in two week old EHTs. Gene expression data, however, holds the promise that CMs are maturing in older EHTs (3-6 mo).

PS 1129f CYP2J2 Inhibition in Cardiac Tissue Could Lead to Drug-Induced Cardiotoxicity

R. Totah[1], E. Evangelista[1] and L. Santana[2]. [1]*Medicinal Chemistry, University of Washington, Seattle, WA and* [2]*Physiology and Biophysics, University of Washington, Seattle, WA.*

Cytochrome P450 2J2 (CYP2J2) is the major human P450 isozyme expressed in cardiac tissue. CYP2J2 is unique among other cytochrome P450 enzymes in that it is a drug metabolizing enzyme with a known endogenous function. CYP2J2 is responsible for oxidizing arachidonic acid to epoxyeicosatrienoic acids (EETs), which are protective in maintaining cellular function in various organs. In the cardiomyocyte, EETs are electrophysiologically active and regulate L-type Ca2+, Na+ and ATP dependent K+ (KATP) channels, which are important in the repolarizing phase and control the QT-period during the cell's electrical cycle. Therefore any reduction in EET levels due to chemical inhibition of CYP2J2 is expected to have a toxic effect on the cardiomyocyte. In this study, the inhibition of CYP2J2 by five drugs (terfenadine, grepafloxacin, cisapride, danazol and sertindole) known to cause cardiotoxicity and especially QT-prolongation was determined in a recombinantly expressed enzyme as well as adult human cardiomyocytes. The effect of terfenadine, on the action potential duration in freshly isolated mouse cardiomyocytes was also determined using patch clamp. Data demonstrates that at physiological concentrations of 0.1-1.0 uM, the above drugs efficiently inhibit CYP2J2 (by ~80%) both in recombinant enzyme and in adult cardiomyocytes. In freshly isolated mouse cardiomyocytes, terfenadine (0.2uM) increased the action potential duration (ADP90) from 52 to 70s. This increase in ADP was completely reversed following the addition of 50nM 11,12-EET. However, 11,12-EET was not able to reverse terfenadine inhibition of hERG using CHO cells (over-expressing hERG) in an IC50 shift assay. This indicates that CYP2J2 mediated EETs, play a protective role against drug induced QT-prolongation but probably through a hERG independent pathway. Consequently, it is prudent to avoid CYP2J2 inhibition, and reduction of EETs in the cardiomyocyte, when developing new chemical entities as potential therapeutics.

PS 1130 Microbiome-Derived Tryptophan Metabolites and Their Aryl Hydrocarbon Receptor-Dependent Agonist and Antagonist Activities

U. Jin[1], S. Lee[1], G. Sridharan[2], K. Lee[2], A. Jayaraman[3,4], R. Chapkin[5], R. Alaniz[4] and S. H. Safe[1,6]. [1]*Institute of Biosciences & Technology, Texas A&M Health Science Center, Houston, TX,* [2]*Chemical & Biological Engineering, Tufts University, Medord, MA,* [3]*Chemical Engineering, Texas A&M University, College Station, TX,* [4]*Microbial & Molecular Pathogenesis, Texas A&M Health Science Center, College Station, TX,* [5]*Nutrition & Food Science, Texas A&M University, College Station, TX and* [6]*Veterinary Physiology & Pharmacology, Texas A&M University, College Station, TX.*

The tryptophan metabolites indole, indole 3-acetate and tryptamine were identified in mouse cecal extracts and fecal pellets by mass spectrometry using a triple quadruple ion trap mass spectrometer coupled to a binary pump HPLC. Levels of indole (200-400 μM), tryptamine (10-20 μM), and indole 3-acetate (10-40 μM) were variable in both extracts. The AHR agonist and antagonist activities of these microbiota-derived compounds were investigated in CaCo-2 intestinal cells as a model for understanding their potential effects on colonic tissue which is highly aryl hydrocarbon (AH)-responsive. Activation of AH-responsive genes such as CYP1A1 demonstrated that tryptamine and indole 3-acetate were AHR

agonists, whereas indole was an AHR antagonist in CaCo2 and breast cancer cells. Moreover, chromatin immunoprecipitation (ChIP) assays showed that indole inhibited TCDD-induced binding of the AHR complex to dioxin response elements on the CYP1A1 promoter. These results demonstrate that the tryptophan metabolites indole, tryptamine and indole 3-acetate modulate AHR-mediated responses in CaCo-2 cells, and concentrations of indole that exhibit AHR antagonist activity (100-250 μM) are detected in the intestinal microbiome and impacts on intestinal function are being investigated.

PS 1131 NR4A1 Antagonists Inhibit Breast Cancer Cell Growth, Survival, and Migration

E. Hedrick[1], U. Jin[2], S. H. Safe[1, 2] and S. Lee[2]. *[1]Veterinary Physiology & Pharmacology, Texas A&M University, College Station, TX and [2]Institute of Biosciences & Technology, Texas A&M Health Science Center, Houston, TX.*

The orphan nuclear receptor NR4A1 (Nur77/TR3) is overexpressed in many solid tumors, and results of RNA interference (RNAi) studies suggest that NR4A1 functions a pro-oncogenic factor. However, previous studies in breast cancer cells on the activity of NR4A1 are equivocal and we have investigated the function of this receptor in breast cancer cells by knockdown of NR4A1 (siNR4A1) or treatment with 1,1-bis(3'-indolyl)-1-(p-substituted phenyl)methanes (C-DIMs) that are NR4A1 antagonists. Transfection of breast cancer cells with siNR4A1 or treatment with a C-DIM/NR4A1 antagonist activates caspases-8 and -7 and induced cleaved PARP expression in MCF-7, MDA-MB-231 and SKBR3 breast cancer cells. Transfection of erbB2-overexprssing SKBR3 cells with siNR4A1 also decreased cell proliferation by >30% after 72 hr and cell migration in a Boyden chamber assay was decreased by >80%. NR4A regulates cell survival and mTOR pathways and maintains low levels of oxidative stress in pancreatic and lung cancer cell lines, and treatment with C-DIMs/NR4A1 antagonists or transfection with siNR4A1 decreased survival (induced apoptosis), inhibited mTOR, and induced stress in breast cancer cells. However, it was also evident that the expression of these well-characterized NR4A1-regulated pathways and the effects of NR4A1 inactivation were also highly cell context-dependent among a panel of breast cancer cell lines (MCF-7, SKBR3 and MDA-MB-231). Nevertheless, the C-DIMs/NR4A1 antagonists were effective antineoplastic agents in breast cancer cell lines and inactivated one or more NR4A1-regulated pathways.

PS 1132 AhR Knockout Rats Are Insensitive to Changes in Tissue Pathology and Serum Chemistry Markers following 4-Week Repeated-Dose Exposure to TCDD

R. Budinsky[1], R. Hukkanen[1], M. Lawson[1], A. Nyska[2], R. Manno[3], A. Grassetti[3], D. Layko[4], J. Rowlands[1], J. A. Harrill[4] and R. S. Thomas[4]. *[1]The Dow Chemical Company, Midland, NC, [2]Sackler School of Medicine, Tel Aviv University, Tel Aviv, Israel, [3]Research Toxicology Centre S.p.A., Pomezia, Rome, Italy and [4]The Hamner Institutes for Health Sciences, Research Triangle Park, NC.*

Persistent activation of the aryl hydrocarbon receptor (AhR) is believed to play a key role in the mode-of-action for TCDD-induced rat liver tumorigenesis. To evaluate the AhR-dependence of early pathological changes prior to tumor formation, we conducted a four-week TCDD repeated-dose study in adult female AhR knockout (AHR-KO) and wild type (WT) rats and investigated alterations in target tissue pathology and serum chemistry markers. Beginning at 8 weeks of age, AhR-KO and WT rats (n = 20 rats/dose/genotype) were dosed by oral gavage (4-5 doses / week, 19 total doses) with varying concentrations of TCDD in corn oil (0, 3, 22, 100, 300, 1000 ng/kg/day). Liver, lung, thymus and kidney were examined for treatment- and genotype-related gross and histopathological effects. Serum was isolated from blood samples and analyzed using a standard rat clinical chemistry panel. Treatment-related increases in the severity of hepatic and thymic pathology were observed in WT rats only. In the liver, these included hepatocytic vacuolation and hypertrophy and increased inflammation. Treatment-related increases in serum ALP, AST, cholesterol, globulin, total bile acids and total bilirubin as well as decreases in serum triglyceridses, glucose and A/G ratio were also observed in WT, but not AhR-KO rats. These data demonstrate that AhR-KO rats are insensitive to early changes in liver function and histopathology induced by repeated exposure to TCDD.

PS 1133 Epithelial Aryl Hydrocarbon Receptor Contributes to Intestinal Host-Microbe Homeostasis

I. A. Murray, K. J. Smith, A. Patterson and G. H. Perdew. *Center for Molecular Toxicology and Carcinogenesis, The Pennsylvania State University, University Park, PA.*

Recent evidence demonstrates a role of the aryl hydrocarbon receptor (AHR) within the immune compartment of the intestine in establishing tolerance to commensal microbes and suppressing pathogenic infection. However, the contribution of epithelial AHR in maintaining host-microbe symbiosis has thus far not been examined. Using C57B6/J mouse Ahrfx+/+ & epithelial Ahr knockout (IEΔAhr) models together with 16S quantitative PCR (qPCR), we have investigated the effect of epithelial Ahr ablation upon the composition of the intestinal microbiota. The data reveal a 2-fold increase in ileal bacteria of IEΔAhr mice when compared to Ahrfx/fx counterparts. ELISA data revealed that bacterial outgrowth observed with IEΔAhr mice was associated with a 50% increase in fecal IgA, suggesting a humoral response to the increased bacterial population. qPCR analysis supports the notion of a humoral response in IEΔAhr mice with increased expression of Baff together with its receptors Tnfsfr13c, Tnfsfr13a and Tnfsfr17. Furthermore, ileal expression of the acute phase proteins Saa2/3 were increased in IEΔAhr mice. Additionally, elevated hepatic Saa1 was observed, indicative of a systemic response. Coincident with the elevated bacterial population and the inflammatory response, we observed a 10-fold decrease in segmented filamentous bacteria (SFB). The association of SFB with the ileal epithelium educates the immune system with regard to commensal bacteria, prompting tolerance through the Th17/Treg system, limiting outgrowth/pathogen expansion. We therefore examined ileal Il17a mRNA expression in IEΔAhr and Ahrfx/fx mice. Data revealed that Il17a expression reflected the decrease in SFB. The deficit in Il17a expression suggests that IEΔAhr mice may exhibit a reduced capacity to respond to opportunistic pathogens. Here, we propose that ablation of epithelial Ahr restricts SFB colonization, thereby decreasing microbial tolerance, which leads to bacterial expansion, dysbiosis and an inflammatory response. Funding:NIHES004869/019964.

PS 1134 Characterisation of the Hepatic Effects of Phenobarbital in Constitutive Androstane Receptor (CAR, NR1I3) Knockout Rats

M. Chamberlain, C. Haines and C. R. Elcombe. *CXR Biosciences, Dundee, United Kingdom.*

The administration of Constitutive Androstane Receptor (CAR, NR1I3) activators to rats and mice induces hepatomegaly that is characterised by hepatocellular hypertrophy (due to the proliferation of smooth endoplasmic reticulum and concomitant induction of enzymes belonging to the CYP2B and 3A families) and hyperplasia (increased semi-conservative DNA synthesis and cell proliferation). Previous studies utilising CAR knockout (KO) mice have demonstrated that the presence of an active CAR is necessary for the induction of this hepatomegaly.This study was designed to investigate the effects of the CAR-activator phenobarbital (PB) in CAR KO rats (SAGE Labs, Boyertown, PA).

Male Wild Type (WT) and CAR KO rats (n=5 per group), which had been implanted with osmotic pumps containing BrdU to allow determination of replicative DNA synthesis (S-phase), were administered PB (500 ppm) in the diet for 7 days. Other groups of WT and CAR KO rats received control diet.

PB treatment of WT rats resulted in 1.2-fold increases in liver weight and liver/body weight ratios, centrilobular hepatocellular hypertrophy, a 5-fold increase in hepatocellular S-phase labelling index and a 3-fold increase into total microsomal P450. The microsomal CYP2B catalysed reactions pentoxyresorufin-O-depentylation (PROD) and benzyloxyresorufin-O-debenzylation (BROD) were induced 100-fold and 40-fold respectively. These changes were accompanied by increases in CYP2B1 (2600-fold) and CYP2B2 (1120-fold) mRNA. None of these PB-induced effects were observed in the CAR KO rats.

The use of Whole Genome Expression Microarrays demonstrated 343 differentially expressed genes in the PB-treated WT rats versus the WT control group (selection criteria of >1.5 fold change and a p value < 0.05). There were 200 differentially expressed genes in the PB-treated CAR KO rats compared to the untreated control CAR KO rats.

In conclusion, an active CAR is required for phenobarbital-mediated hepatomegaly in rats and only 40% of the genes regulated by PB appeared to be CAR-dependent.

PS 1135 Effects of Perfluoroalkyls on the Activations of Human CAR3, PXR, and TR Receptors *In Vitro*

D. J. Ehresman[1], P. Webb[2], S. D. Ayers[2], J. Vanden Heuvel[3, 4], G. Olsen[1], S. Chang[1] and J. L. Butenhoff[1]. [1]*3M Company, St. Paul, MN,* [2]*The Methodist Hospital Research Institute, Houston, TX,* [3]*Pennsylvania State University, State College, PA and* [4]*INDIGO Biosciences, State College, PA.*

Research studies have shown that several perfluoroalkyls substances (PFASs) have the potential to activate certain xenosensor nuclear receptors (NR) involved in regulating metabolic processes. Pleiotropic responses following activation likely are responsible for many effects observed in toxicological studies, and key differences in expressions and responses on activation are known to exist. Although many studies have investigated the potential of PFASs to activate NR1C1 (PPARα), few studies have examined potential for activation of NR1I3 (CAR3) and NR1I2 (PXR). Notably lacking are investigations into the ability of PFASs to activate the thyroid receptors, NR1A1 (TRα) and NR1A2 (TRβ). We investigated the potential of 5 PFASs (perfluorooctanesulfonate (PFOS, 2 samples), perfluorohexanesulfonate (PFHxS), perfluorobutanesulfonate (PFBS), perfluorobutyrate (PFBA), and perfluorooctanoate (PFOA)) to activate human CAR3, PXR, and TRα using chimeric systems with a luciferase reporter plasmid at PFAS concentration ranging from 0.4 to 100 μM. The same PFASs as well as perfluorononoate (PFNA) and perfluorodecanoate (PFDA) were tested for human TRα and TRβ activation in another similar system with luciferase reporter plasmid at PFAS concentrations of 10 μM. In these assays, PFOS, PFNA, and PFDA were also tested for activation at 1, 10, and 100 μM. No human TRα or TRβ activation or repression was observed with any PFAS at any concentrations tested. Weak activations that were lower in magnitudes than the respective positive controls were observed with CAR3 (PFOS, 100μM) and PXR (PFHxS, 33 and 100 μM; and PFOS, 100 μM). These PFAS concentrations (equivalent of 13,000 – 50,000 ng/mL) were several orders of magnitude higher than general population. Based on these observations and in light of known human exposure levels, the PFASs included in this study are not expected to act via direct activation of the studied NR1 sub-family receptors.

PS 1136 Activation of Aryl Hydrocarbon Receptor (AhR) Synergistically Induces Lipopolysaccharide (LPS)-Mediated Transcription of Proinflammatory Chemokine (c-c motif) Ligand 20 (Ccl20)

T. S. Lahoti, J. A. Boyer, J. M. Hughes, I. A. Murray and G. H. Perdew. *Vet. & Biomed. Sci., The Pennsylvania State University, University Park, PA.*

Chemokines, a family of chemotactic cytokines, dictate recruitment of leukocytes, and play a critical role in immune homeostasis and tumorigenesis. *Ccl20*, a pleiotropic chemokine, also known as *macrophage inflammatory protein-3α* or *Exodus-1*, was originally identified as a chemoattractant for lymphocytes and dendritic cells. *Ccl20* is highly expressed in pathological conditions such as rheumatoid arthritis, colon and pancreatic cancers and sepsis. It is the ligand for CC chemokine receptor 6 (Ccr6), which is expressed on the surface of dendritic cells, memory T cells and naïve B cells. LPS, a component of outer membrane of gram-negative bacteria, activates inflammatory signaling in macrophages, leading to enhanced secretion of pro-inflammatory cytokines and chemokines, such as *Ccl20*, via NF-κB-mediated activation. It is known that during inflammation, AhR can crosstalk with p65 subunit of NF-κB. Therefore, we examined the role of AhR in LPS-mediated activation of *Ccl20*. Primary peritoneal macrophages (1^0 Mϕ) from C57BL6/J (*Ahr*^{b}) and *Ahr* null mice (*Ahr*$^{-/-}$) were isolated and treated with AhR agonists 2,3,7,8-tetrachlorodibenzo-*p*-dioxin (TCDD) or indolo[3,2-b]carbazole (ICZ), followed by stimulation with pro-inflammatory LPS. Quantitative real time PCR revealed that the activation of AhR by TCDD and ICZ in 1^0 Mϕ from *Ahr*^{b} mice not only induces the basal levels of *Ccl20* but also synergistically promotes LPS-mediated activation of *Ccl20* mRNA. Studies performed in 1^0 Mϕ from *Ahr*$^{-/-}$ mice revealed that the basal/synergistic effects to be AhR-dependent. ELISA performed on supernatants from *Ahr*^{b} 1^0 Mϕ cells exposed to TCDD and LPS mirrored the mRNA expression, albeit without synergy. Overall, these findings suggest that activation of AHR plays an underlying role in regulating the *Ccl20* transcription in 1^0 Mϕ, and likely contribute towards AhR agonist-mediated inflammation. (Funded by: ES004869 and ES019964)

PS 1137 Aryl Hydrocarbon Receptor: Insights into Its Role in Metabolic Homeostasis

N. Girer, I. A. Murray and G. H. Perdew. *Dept. of Vet. and Biomed. Sci., Penn State University, State College, PA.*

Obesity is a multi-factorial disease governed by a complex combination of genetic, lifestyle, and environmental inputs. Obesity is often associated with hyperglycemia, hypertension, hepatic steatosis, endotoxemia, inflammation, and cancer. Numerous studies indicate these pathologies are influenced by the Aryl Hydrocarbon Receptor (AHR). Recent evidence demonstrates that AHR has the capacity to attenuate *de novo* cholesterol and fatty acid synthesis in the liver. However, AHR's role in obesity appears to be complex and requires further investigation. Here, we have examined the effect of different allelic variations and conditional knockout murine models of *Ahr* upon metabolic homeostasis and associated gene expression. We identified that male mice harboring the low-affinity *Ahr*^{d} allele are 20% more glucose tolerant than their high-affinity *Ahr*^{b} counterparts. Additionally, *Ahr*^{d} mice exhibit a 2-fold increase in liver triglyceride content, accompanied by a relevant increase in the expression of fatty acid synthesis genes (*Fasn*, *Acaca*, *Scd1*, and *Srebp1c*). Furthermore, we observed a 3-fold increase in hepatic *Fgf21* (fibroblast growth factor 21) expression among AHR-deficient mice in comparison with *Ahr*^{b} mice. Similarly, liver-specific, conditional AHR-knockout mice recapitulated the effect seen in *Ahr*-null mice, exhibiting a 2.7-fold increase in *Fgf21* expression when compared to their *Ahr*$^{Fx/Fx}$ counterparts. This suggests that AHR exerts liver-specific control over *Fgf21* gene expression. FGF21, an important regulator of the response to fasting, is known to ameliorate obesity when administered to various genetic and diet-induced murine models of the disease. Interestingly, the *Fgf21* promoter contains several putative dioxin response elements (DREs). We hypothesize that AHR is involved in the regulation of this key hormone through direct repression on the promoter. This project is supported by NIH grants ES004869 and ES019964.

PS 1138 Selective Aryl Hydrocarbon Receptor Modulator (SAhRM) SGA360 Attenuates Lipopolysaccharide (LPS)-Mediated Septic Shock

G. H. Perdew[1], T. S. Lahoti[1], J. M. Hughes[1], I. A. Murray[1], K. Gowda[2] and S. Amin[2]. [1]*Vet. and Biomed. Sci., The Pennsylvania State University, University Park, PA and* [2]*Penn State College of Medicine, Hershey, PA.*

Septic shock is a pathological condition predominantly associated with endotoxin (LPS) producing gram-negative bacteria. It requires immediate medical attention since it is the leading cause of death in patients admitted to intensive care units worldwide. LPS activates Toll-like receptor 4 leading to enhanced secretion of proinflammatory cytokines and chemokines. Overexpression of these proinflammatory mediators contributes to multi-organ dysfunction syndrome, leading to death. Aryl hydrocarbon receptor (AHR), a ligand activated transcription factor, has recently been implicated to possess immuno-modulatory effects. We have previously shown that SGA360 can be used to mitigate cytokine-mediated pro-inflammatory gene expression. Thus this study was conducted to evaluate the role of AHR in both in vivo and in vitro models of septic shock. C57BL6/J (*Ahr*^{b}), *Ahr*^{d}, and *Ahr*$^{-/-}$ mice were injected with SGA360 at -1h and +12h relative to a lethal dose of LPS. Animals from all three genotypes exposed to LPS alone showed median survival of 28h, 29h and 30h respectively. However, *Ahr*^{b} mice exposed to SGA360 followed by LPS showed a significant increase in median survival to 42h. *Ahr*^{d}, and *Ahr*$^{-/-}$ mice exposed to SGA360 followed by LPS showed poor median survival rate (27h and 20h). Macrophages have been shown to play a critical role in LPS-mediated inflammation. Thus, in order to study the ability of SGA360 to selectively modulate AHR, primary peritoneal macrophages (1^0 Mϕ) isolated from *Ahr*^{b} and *Ahr*^{d} mice were pretreated with SGA360 followed by activation with proinflammatory LPS. Quantitative real-time PCR revealed that SGA360 mitigated expression of multiple inflammatory genes induced by LPS only in *Ahr*^{b} mice. These findings suggest that selective modulation of AHR may be a viable therapeutic approach to mitigate inflammatory signaling associated with septic shock. (Funded by: ES019964)

PS 1139 Adaptation of the Human Ah Receptor to Bind Simple Indoles

T. D. Hubbard[1], D. Desai[3], W. Bisson[2], S. Amin[3] and G. H. Perdew[1]. [1]*Vet. and Biomed. Sci., Pennsylvania State University, State College, PA,* [2]*Env. & Mol. Tox., Oregon State University, Corvallis, OR and* [3]*Penn State College of Medicine, Hershey, PA.*

Recent evidence has shown that specific tryptophan catabolites are ligands for the aryl hydrocarbon receptor (AHR) and are important for the maintenance of intestinal health. The activation of AHR promotes gut immunological homeostasis

and increased epithelial barrier function. Through characterization and analysis of multiple tryptophan catabolites, we have identified a discrepancy between the ability of mouse versus human AHR to bind simple indole molecules. Computer modeling of the ligand-binding domain (LBD) of the mouse and human AHR reveal significant differences, consistent with the 10-fold decrease in affinity for TCDD observed with the human AHR, relative to the murine *Ah^b* allele. The abundant microflora tryptophan catabolite indole (20 μM) was found to increase relative luciferase activity 6-fold in a dioxin response element driven luciferase reporter human HepG2 assay, similar to results observed with 10 nM TCDD. Conversely, in a mouse hepatoma reporter line, indole induced a 10-fold induction of luciferase activity compared to a 374-fold induction by TCDD. qPCR analysis of induction of AHR target gene *CYP1A1* in Caco2 cells revealed a 307-fold increase in *CYP1A1* transcripts by indole, comparable to TCDD. Furthermore, qPCR analysis revealed tryptophan catabolite 3-methyl indole to display agonist activity specific to human AHR similar to that of indole, while isomers 1-methyl indole and 2-methyl indole failed to exhibit agonist activity. In silico molecular modeling and docking data predicts that indole binding is energetically favorable within the human AHR LBD, in contrast to mouse AHR LBD. Our optimized AHR model characterized a possible novel binding mechanism for indole in which two molecules of indole enter the ligand-binding pocket and facilitate activation of AHR. These results suggest that the human AHR has evolved to bind simple indoles produced in the gut. This project is supported by NIH grants ES004869 and ES019964.

PS 1140 Species-Specific Response to Peroxisome Proliferators in Primary Hepatocytes

P. D. McMullen, M. E. Andersen, R. A. Clewell, S. Bhattacharya, E. LeCluyse, C. G. Woods, B. Sun and S. Pendse. *The Hamner Institutes for Health Sciences, Research Triangle Park, NC.*

Exposure to environmental chemicals often leads to different outcomes in humans and rodents, calling into question the applicability of animal-based toxicity testing for human risk assessment. Peroxisome proliferators, which include several purported endogenous fatty acids and synthetic ligands, induce fatty acid metabolism in humans and have been used as therapeutic strategies for various dyslipidemias and diabetes. For rodents, in addition to regulating fatty acid metabolism, peroxisome proliferators also influence peroxisome assembly, inflammatory responses, and cell proliferation. Understanding the mechanisms for these similarities and differences is essential to translating data from animal models to human health. Here we compare genomic characterizations of human and rat primary hepatocytes exposed to the PPARα-selective agonist GW7647. We used gene expression microarray experiments to compile a highly resolved characterization—five doses (10^{-3}–10^{1}μM) across five time points (2, 6, 12, 24, and 72h)—of the PPARα-mediated response in these two species. Consistent with the qualitative differences in the response to peroxisome proliferators, we identified a substantially larger set of differentially expressed genes in rat cells (1113) compared to human (192). These additional genes include a suite of developmental processes that may account for the increased toxicity of peroxisome proliferators in rodents. We performed ChIP-seq at key time and dose points for both species to assess genomic binding of PPARα. By coupling these results with a computational motif search, we found that the canonical nuclear receptor response mechanism accounts a small fraction (31% of genes in rat; 32% in human) of the detected response, suggesting a larger role for indirect PPARα transcriptional mechanisms than was previously thought. To understand how these cell-based experiments relate to *in vivo* toxicity, we have performed a parallel study in live rats; gene expression in the liver correlates well with that in primary hepatocytes.

PS 1141 Dietary TCDF Impacts the Host-Microbiome Metabolic Axis

L. Zhang[1], J. Correll[1], R. Nichols[1], R. Hao[1, 3], P. Smith[1], E. Hatzakis[2], G. H. Perdew[1] and A. Patterson[1]. [1]*Veterinary and Biomedical Sciences, Pennsylvania State University, University Park, PA,* [2]*Department of Chemistry, Pennsylvania State University, University Park, PA and* [3]*DuPont Haskell Global Centers for Health and Environmental Sciences, Newark, DE.*

2, 3, 7, 8-tetrachlorodibenzofuran (TCDF), a potent aryl hydrocarbon receptor (AHR) ligand, is among the most environmentally toxic compounds and its impact on the gut microbiome relatively unknown. In this study, C57BL/6 mice were given TCDF for one week (24 μg/kg body weight) to assess the acute effects of TCDF on the gut microbiome. We analyzed TCDF-induced metabolic changes in multiple biological matrices (urine, plasma, feces, liver, and intestinal tissues) using a combination of mass spectrometry (MS)- and 1H nuclear magnetic resonance (1H NMR)-based metabolomics and gene expression analysis. After TCDF exposure, a significant increase in the expression of Cyp1a1 and Cyp7a1 but decreased expression of short heterodimer partner (liver) and fibroblast growth factor 15 (ileum) were observed by QPCR analyses. 1H NMR-based metabolomics results showed that TCDF exposure caused significant elevation of hepatic lipids, glycogen and nucleic acid metabolites (inosine and hypoxanthine) but reduction of hepatic glucose, lactate, choline metabolites and amino acids. We found lower fecal glucose and oligosaccharide levels together with higher succinate and short chain fatty acids (n-butyrate and propionate) levels in TCDF-treated mice. Targeted LC-MS/MS analyses showed that TCDF exposure resulted in significant reduction of primary bile acids (cholic and glycocholic acid) together with elevation of a secondary bile acid, deoxycholic acid, in liver, feces and intestinal tissues. These results indicated that TCDF exposure caused hepatic lipidosis accompanied with widespread metabolic changes in amino acid, nucleic acid and energy metabolism, fecal bacterial fermentation, and bile acid metabolism associated with gut microbiota functions. These findings provide new evidence that exposure to persistent environmental contaminants strongly impacts the gut microbiome.

PS 1142 An Aryl Hydrocarbon Receptor from the Salamander *Ambystoma mexicanum* Exhibits Low Responsiveness to 2, 3, 7, 8-Tetrachlorodibenzo-*p*-Dioxin

J. Shoots and W. H. Powell. *Biology Department, Kenyon College, Gambier, OH.*

Sequence and structural features of the aryl hydrocarbon receptor (AHR) can underlie species- and population-specific differences in its affinity for 2,3,7,8-tetrachlorodibenzo-*p*-dioxin (TCDD) and other agonists. These differences often explain the varying degrees of TCDD toxicity exhibited by distinct animal groups. Frogs, for example, are dramatically less sensitive to TCDD toxicity than many other vertebrates, and we have previously demonstrated that frog AHRs bind TCDD with low affinity. In *Xenopus laevis* AHR1β, weak TCDD binding results from the combination of three residues in the ligand binding domain: A354 and A370, along with N325. In the current study we seek to determine whether this mechanism of low TCDD responsiveness is shared by AHRs of other amphibian groups. To this end, we used RT-PCR to isolate a cDNA encoding an AHR from a salamander, the Mexican axolotl (*Ambystoma mexicanum*). It encodes a polypeptide of 95.5 KDa that shares 59% identity with *Xenopus laevis* AHR1α and AHR1β and 50% identity with mouse AHR. Phylogenetic analysis reveals that the axolotl AHR is orthologous to vertebrate AHR1s. *Ambystoma* AHR contains the same amino acid residues in the positions that confer low TCDD affinity to frog AHRs (N335, A364 and A380), suggesting that it also binds TCDD weakly. We tested this hypothesis with transactivation assays employing a luciferase reporter gene governed by the enhancer region from mouse CYP1A1 (pGudLuc6.1). For axolotl AHR, the EC50 for reporter gene induction by TCDD was 45 nM, even lower than frog AHR1β (23 nM) and dramatically less than a chimeric frog AHR containing the mouse ligand binding domain (0.2 nM). Taken together, the low TCDD responsiveness and the sequence conservation with the frog AHR ligand binding domain suggest that axolotl AHR binds TCDD with low affinity. We predict that *Ambystoma mexicanum* salamanders will exhibit resistance to the toxic effects of TCDD and other xenobiotic AHR agonists. Funded by the NIH (R15 ES011130) and the Kenyon Summer Science Scholars Program.

PS 1143 1, 1-Bis(3'-indolyl)-1-(aromatic)methanes Are NR4A1 Antagonists That Inhibit Rhabdomyosarcoma Cell Growth and Survival

A. Reeder[1], G. Chadalapaka[1], S. Lee[2] and S. H. Safe[1, 2]. [1]*Veterinary Physiology & Pharmacology, Texas A&M University, College Station, TX and* [2]*Institute of Biosciences & Technology, Texas A&M Health Sciences Center, Houston, TX.*

Rhabdomyosarcoma (RMS) is the most common tissue sarcoma that is primarily observed in children and adolescents. Cytotoxic drugs are the major chemotherapies used for RMS treatment and these are accompanied by toxic side-effects. The nuclear orphan receptor NR4A1 (Nur77/TR3) is a pro-oncogenic factor that is expressed in RMS cells, and we investigated the effects of a series of 1,1-bis(3'-indolyl)-1-(p-substituted phenyl)methane (C-DIMs) analogs that exhibit NR4A1 antagonist activity on the growth and expression of selected pro-oncogenic factors in RD and RH30 RMS cells. EC50 values for growth inhibition (2 days) by the p-hydroxyphenyl (DIM-C-pPhOH), p-cyanophenyl (DIM-C-pPhCN), and p-carboxymethyl (DIM-C-pPhCO2Me) were 14, 6.4 and 10 μM, respectively, for RH30 cells and 16, 4.4 and 11 μM, respectively, for RD cells. NR4A1 regulates multiple pro-oncogenic pathways/genes and acts as a coactivator for multiple specificity protein 1 (Sp1)-regulated genes through NR4A1-Sp1 interactions, and several Sp-regulated genes are critical for RMS cell and tumor growth. Treatment of RMS cells with 15-22.5 μM DIM-C-pPhOH significantly decreased expression of bcl-2, survivin, epidermal growth factor receptor (EGFR), cyclin D1 and c-Myc proteins, and the mechanisms of NR4A1-Sp interactions and their inactivation by C-DIMs are being investigated. Thus, NR4A1 antagonists are a novel class of relatively non-toxic agents for clinical treatment of RMS and for application of combined drug therapies.

PS 1144 Tocopherylquinone As an Activator of the Aryl Hydrocarbon Receptor

S. Olguin[1], Y. Liu[2], A. M. Fajardo[2], D. MacKenzie[2] and T. A. Thompson[2]. *[1]University of New Mexico, Albuquerque, NM and [2]Pharmaceutical Sciences, UNM Health Sciences Center, Albuquerque, NM.*

The aryl hydrocarbon receptor (AhR) is expressed in many tissues and is mainly studied in the context of environmental chemicals and toxins. For example, benzo[a]pyrene (BaP) and TCDD are well-established activators of the AhR, whereas endogenous ligands of the AhR are still uncertain. In its function as an antioxidant, vitamin E (VE as alpha-tocopherol) is oxidized to alpha-tocopherylquinone (TQ), which is widely considered to be biologically inert. Our early studies suggested that TQ may be biologically active as an activator of the AhR in prostate cancer cells (i.e. LNCaP cells). Thus, the rationale for this study was to examine TQ as an activator of the AhR. Upon completion of gene expression analyses, TQ was found to produce more than 3,800 gene expression changes (greater than 2-fold), whereas VE treatment resulted in 1,200 gene expression changes. Gene expression pathway and network analyses identified a clustering of AhR-responsive genes affected by TQ, but not VE, which was validated using qPCR for specific AhR-responsive genes (e.g., CYP1A1). Activation of AhR by TQ was further examined using an XRE/DRE-responsive luciferase reporter system where TQ, but not VE, stimulated activity. Experiments using RNAi to down-regulate AhR activity showed that the TQ-induced up-regulation of CYP1A1 expression was indeed mediated by the AhR. Finally, primary cultures of AhR knock out mouse embryonic fibroblasts (MEFs) were established. CYP1A1 expression in AhR wild-type (WT) and knock out (KO) MEF cells was determined after treatment with TQ. KO MEF cells showed little change in the expression of CYP1A1, while WT MEF cells responded to TQ treatment with increased CYP1A1 expression, establishing that the AhR is necessary for TQ-mediated up-regulation of CYP1A1. Details on the mechanism of TQ's activation of the AhR remain unclear. However, we have shown that quinone structures, as present in TQ, are effective at activating the AhR. Results from these studies provide intriguing support for TQ as an endogenous activator of the AhR.

PS 1145 Pharmacological and Electrophysiological Characterization of *Ascaris suum* Homopentameric Nicotinic Acetylcholine Receptors in *Xenopus laevis* Oocytes

M. Abongwa, S. Buxton, S. Verma, A. P. Robertson and R. J. Martin. *Department of Biomedical Sciences, Iowa State University, Ames, IA.*

Nicotinic acetylcholine receptors (nAChRs) belong to the family of ligand-gated ion channels (LGICs) and are found in both vertebrate and invertebrate species. The nAChRs in nematode parasites are pharmacologically different from mammalian host nAChRs allowing nematode selective compounds (anthelmintics) to be used for treatment and prophylaxis. Unfortunately, the widespread use of anthelmintics has given rise to the development of resistance. There is then, an urgent need to characterize the different nAChRs present in parasitic nematodes to provide a better understanding of their pharmacology for drug development and to find ways of overcoming resistance.
Using molecular cloning and the two-electrode voltage clamp electrophysiological techniques, we have cloned and expressed two nAChR subunit genes (*acr-16* and *acr-21*) from *Ascaris suum* in *Xenopus laevis* oocytes. Our results showed that ACR-16 or ACR-21 on their own can reconstitute a functional nAChR in the presence of an ancillary factor, RIC-3. Pharmacological characterization of homomeric receptors produced by ACR-16 or ACR-21 revealed that these receptors have distinct properties. The homomeric ACR-16 receptor is more sensitive acetylcholine than to nicotine and insensitive to levamisole and pyrantel. On the other hand, the homomeric ACR-21 receptor is more sensitive to nicotine than to acetylcholine but also insensitive to levamisole and pyrantel. These previously uncharacterized receptors are potential target sites for new anthelmintic compounds and are not anticipated to show cross-resistance with existing anthelmintics.

PS 1146 FICZ Is Not Responsible for the Structural Diversity of Ah Receptor Ligands/Agonists

M. Denison, D. E. DeGroot, G. He, J. Zhao and A. Soshilov. *Environmental Toxicology, University of California, Davis, CA.*

The aryl hydrocarbon receptor (AhR) is a ligand-activated transcription factor that mediates a variety of toxic and biological effects of "classical" AhR ligands (halogenated aromatic hydrocarbons and polycyclic aromatic hydrocarbons), although AhR-dependent gene expression can be stimulated by many chemicals whose structures are dramatically different from the "classical" ligands. Identification of these "nonclassical AhR ligands" has raised significant questions regarding the specificity and promiscuity of AhR ligands and the mechanisms by which these chemicals activate the AhR. Recently, Wincent and coworkers (PNAS 109, 4479 (2012)) concluded that the dramatic diversity in AhR ligand structure was an artifact of cell-based assay systems and that the AhR was not actually bound and activated by these structurally diverse chemicals, but by 6-formylindolo[3,2-b]carbazole (FICZ), a high affinity AhR agonist present in cell culture media. They proposed that activation of the AhR by these "nonclassical" ligands resulted from the ability of these chemicals to inhibit the normally rapid metabolism of FICZ, thus allowing FICZ to activate the AhR. To test this hypothesis, we tested the ability of a series of structurally diverse AhR agonists to directly activate the AhR using ligand and DNA binding assays in which FICZ can play no significant role. These results clearly demonstrate the ability of structurally diverse compounds to directly bind to the AhR and to stimulate AhR transformation and DNA binding in vitro. Since these compounds also fail to stimulate AhR-dependent reporter gene expression in cells transfected with an AhR containing a mutation in the ligand binding domain that allows it to be selectively activated by FICZ, these chemicals must not activate the AhR via FICZ. These results clearly demonstrate that the AhR can directly bind and be activated by these structurally diverse chemicals and FICZ plays little or no role in defining the structural promiscuity of AhR ligands. (NIEHS ES007685; ES004699).

PS 1147 Characterization of a Full-Length Pregnane X Receptor, *In Vivo* Expression, and Identification of PXR Alleles in Zebrafish

J. J. Stegeman[1], A. Kubota[1], J. V. Goldstone[1], B. Lemaire[1], A. Bainy[2], R. Lille-Langøy[3], S. I. Karchner[1], M. E. Hahn[1], M. Celander[4] and A. Goksøyr[3]. *[1]Woods Hole Oceanographic Institution, Woods Hole, MA, [2]Universidade Federal de Santa Catarina, Florianópolis, Brazil, [3]University of Bergen, Bergen, Norway and [4]University of Gothenburg, Göteborg, Sweden.*

The pregnane X receptor (PXR) (nuclear receptor NR1I2) is a ligand activated transcription factor, mediating responses to diverse xenobiotic and endogenous chemicals. The properties of PXR in fish are not fully understood. Here we report on characterization of full-length zebrafish PXR, *Danio rerio*, and *pxr* expression *in vivo*. Sequence variation among clones in the initial effort prompted sequencing of multiple clones from a single fish. There were two prominent variants, one sequence with S183, Y218 and H383 and the other with I183, C218 and N383, which we designate as alleles *pxr*1* (*nr1i2*1*) and *pxr*2* (*nr1i2*2*), respectively. In COS-7 cells co-transfected with a PXR-responsive reporter gene, the full-length Pxr*1 (the more common variant) was activated by known PXR agonists clotrimazole and pregnenolone 16α-carbonitrile but to a lesser extent than the full-length human PXR. Activation of full-length Pxr*1 was only 10% of that with the Pxr*1 LBD. qPCR analysis showed prominent expression of *pxr* in liver and eye, as well as brain and intestine of adult zebrafish. *pxr* was expressed in adult heart and kidney at levels similar to that in intestine. The expression of pxr in liver was weakly induced by ligands for mammalian PXR or CAR (NR1I3). *pxr* expression was also investigated in embryonic zebrafish throughout development. Ortho-PCBs do not induce *pxr* expression in 72hpf zebrafish. The results establish a foundation for PXR studies in this vertebrate model. PXR allelic variation and the differences between the full-length PXR and the LBD in reporter assays have implications for assessing the action of PXR ligands in zebrafish. Support: NIH P42ES007381, NIH R21HD073805, Norwegian Research Council MILJØ2105, 181888; Swedish Research Council Formas 216-2007-468.

PS 1148 Modes of Interaction between the Chaperone Calreticulin (CRT) and Protein Substrates

S. J. Wijeyesakere, S. M. Rizvi and M. Raghavan. *Microbiology and Immunology, University of Michigan Medical School, Ann Arbor, MI.*

CRT is a multi-domain endoplasmic reticulum chaperone with a specificity for monoglucosylated glycoproteins that plays a role in the folding of major histocompatibility complex (MHC) class I molecules that mediate immune surveillance. CRT also inhibits the aggregation of non-glycosylated proteins and contains a generic polypeptide-binding site whose location and contribution to substrate folding are unknown. Using bio-layer interferometry (BLI) and intra-molecular ensemble Förster resonance energy transfer (FRET) spectroscopy, we show that CRT binds glycosylated and non-glycosylated proteins with similar affinities but distinct kinetic profiles. Glycan-dependent interactions between CRT and immunoglobulin Y (IgY; a natively monoglucosylated protein) are characterized by rapid association (kon= 196582.5±17423.7 M-1s-1) and dissociation (koff=0.08±0.004 s-1) modes while glycan-independent interactions between CRT and enzymatically deglycosylated IgY display slower kinetics (kon=17395.7±4274.5; koff=0.01±0.002 s-1). While both interaction modes involve the glycan binding site or its vicinity, the arm-like proline-rich (P-) domain of CRT contributes to binding non-glyco-

sylated proteins. Correspondingly, ensemble FRET spectroscopy measurements indicate that glycosylated and non-glycosylated proteins induce 'open' and 'closed' P-domain conformations respectively. The co-chaperone ERp57 influences substrate-binding kinetics and induces a 'closed' P-domain conformation, even in the presence of a glycosylated substrate. Together with analysis of the interactions of CRT with cellular proteins, these findings indicate that recruitment of monoglucosylated proteins to CRT is kinetically driven, while the P-domain and co-chaperone binding contribute to stable CRT-substrate interactions. Substrate sequestration in the cleft between the glycan binding site and P-domain is a likely mechanism for CRT -assisted protein folding.

PS 1149 Quantitative Profiling of Environmental Chemicals and Drugs for Farnesoid X Receptor Activity

C. Hsu[1], J. Zhao[1], R. Huang[1], J. Hsieh[2], J. T. Hamm[2], X. Chang[2], K. Houck[3] and M. Xia[1]. *[1]NCATS/NIH, Rockville, MD, [2]DNTP/NIEHS/NIH, RTP, NC and [3]U.S. EPA, RTP, NC.*

Farnesoid X receptor (FXR), a bile acid sensor, exerts protective function in numerous diseases including cholestasis, diabetes, liver regeneration, and cancer. Despite the extensive interests in FXR ligands in drug discovery, little is known regarding potential FXR-mediated toxicity effects from xenobiotic chemicals. Here we describe the profiling of approximately 10K environmental chemicals and drugs in modifying FXR signaling and associated cytotoxicity. The FXR beta-lactamase assay was used to screen the Tox21 10K compound library, containing environmental chemicals, clinically-approved drugs and known bioactive small molecules, in a 1536-well plate format at 15 concentrations in triplicate runs. 435 potent and reproducible hits were identified and grouped into several clusters based on their chemical structure similarity and known biological function. Many environmental chemicals including synthetic hormones, pesticides, and industrial chemicals showed FXR antagonist activity. Some drugs acted as agonists, antagonists, or partial agonists of FXR. Several clusters of compounds identified from the screening were also found to be active against other functionally related nuclear receptors. These results not only provide directions for prioritizing chemicals for further testing FXR-mediated toxicity but also suggest novel signaling pathways for future mechanistic studies. Supported by EPA Interagency Agreement Y3-HG-7026-03. This work was reviewed by EPA and NTP and approved for publication but does not necessarily reflect official agency policy.

PS 1150 Thalidomide Increases Cytochrome P450 Activity and Drug Metabolism in Liver through Direct Activation of Nuclear Receptor CAR and PXR

R. van Beuningen[1], N. Murayama[2], D. Melchers[1], H. Suemizu[3], C. Guillouzo[4], N. Shibata[5], K. Yajima[2], M. Utoh[2], M. Shimizu[2], C. Chesne[4], M. Nakamura[3], R. Houtman[1] and H. Yamazaki[2]. *[1]PamGene International BV, Den Bosch, Netherlands, [2]Showa Pharmaceutical University, Machida, Japan, [3]Central Institute for Experimental Animals, Kawasaki, Japan, [4]Biopredic International, Rennes, France and [5]Nagoya Institute of Technology, Nagoya, Japan.*

We recently demonstrated heterotropic cooperativity of human cytochrome P450 (P450) 3A4/5 by the teratogen thalidomide using a model substrate midazolam in various in vitro and in vivo models. In the current study we further investigate the regulation of drug metabolizing enzymes by thalidomide in human livers. Chimeric mice with humanized liver displayed enhanced midazolam clearance upon pre-treatment with orally administered thalidomide, presumably because of human P450 3A induction. Indeed, thalidomide enhanced levels of P450 3A4/2B6 mRNA, protein expression, and/or oxidation activity in human hepatocytes indirectly suggesting activation of gene transcription factors. A key event after ligand-binding is an alteration of nuclear receptor (NR) conformation and recruitment of coregulator proteins which alter chromatin accessibility of target genes. To demonstrate direct engagement and functional alteration of pregnane X receptor (PXR) and constitutive androstane receptor (CAR) by thalidomide, we applied a peptide microarray with 154 coregulator-derived NR-interaction motifs, CoR- and NR boxes, which serves as a sensor for NR conformation and activity status as a function of ligand. Thalidomide and its human proportionate metabolite 5-hydroxythalidomide displayed significant modulation of coregulator interaction with CAR and PXR ligand-binding domains similar to established agonists for these receptors. These results collectively suggest that thalidomide could act as a ligand for PXR and CAR and cause enzyme induction. The possibilities of drug interactions during thalidomide therapy in humans should be evaluated further.

PS 1151 Novel Interaction between PXR and CAR1 in Cytochrome P450 Induction

B. C. Ho[1], L. Huang[2], J. Johnson[2], P. C. Wilga[3] and M. I. Morano[1]. *[1]Originus Inc, Ann Arbor, MI, [2]Cayman Chemical, Ann Arbor, MI and [3]CeeTox Inc, Kalamazoo, MI.*

Xenobiotics may interact with specific nuclear receptors and modulate the expression levels of cytochrome P450 (CYP) enzymes leading to drug-drug interactions. CAR and PXR are two key nuclear receptors that participate in the induction of several CYPs including CYP2B6, CYP3A4, and CYP2C9. More than 20 splice variants of CAR transcripts have been identified. CAR1 is the main isoform found in hepatocytes; however, CAR1 shows strong constitutive activity when expressed in cell lines. In contrast, two other less abundant splice variants, CAR2 and CAR3, display no constitutive activity and can transactivate CYP2B6 and CYP3A4 upon ligand binding. In order to investigate the molecular mechanism of CAR1-mediated induction in hepatocytes, we assembled secreted alkaline phosphatase (SEAP) reporter gene constructs using native promoter sequences from CYP genes. These reporters were co-transfected in HepG2 cells with combinations of CARs, PXR, and HNF4α by STEP reverse transfection. The reporter constructs were functionally verified by expressing PXR or CAR3 and stimulated with corresponding ligands. In the presence of CAR1, both the CYP2B6 and CYP3A4 reporters exhibited the expected strong constitutive activity which masked the induction effect of CAR ligand CITCO. Interestingly, the co-expression of PXR and CAR1 drastically suppressed the basal constitutive activities of CAR1 on both reporter genes. As a result, the effect of CITCO activation of CAR 1 on CYP2B6 reporter became much more prominent (>5-fold). Although CITCO binding to CAR1 or CAR3 triggered only around 2-fold induction of CYP3A4 reporter gene, the co-activation of CAR1 and PXR led to a much more robust (>11-fold) induction of CYP3A4 than by activation of either nuclear receptor alone indicating a synergistic effect. This study emphasizes the significance of nuclear receptor interactions in the regulation of gene expression and illustrates the importance of using native promoter sequences instead of short synthetic regulatory elements in reporter gene assays. (Supported by NIH grant ES019807)

PS 1152 Effects of PPAR-Alpha Activation on Liver Toxicity in Mice Exposed to Trichloroethylene

H. Yoo, V. Soldatow, O. Kosyk, W. Bodnar and I. Rusyn. *Dept. of Environmental Sciences and Engineering, University of North Carolina at Chapel Hill, Chapel Hill, NC.*

Trichloroethylene (TCE) is an environmental and occupational toxicant and is classified as 'carcinogenic to humans' by both the US EPA and IARC. It has been hypothesized that peroxisome proliferator-activated receptor alpha (PPARα) activation, mediated by oxidative metabolites of TCE, is an important mechanistic event for liver cancer in mice. Although it is known that trichloroacetic acid (TCA), a major metabolite of TCE, may activate PPARα, uncertainties remain regarding the association between the extent of oxidative TCE metabolism, PPARα activation, and toxicity pathways that may be independent of PPARα. This study investigated oxidative TCE metabolism in the context of PPARα status (wild-type, *Ppara*-null, and humanized *Ppara*) in the mouse. Male and female mice of each genotype were treated with TCE (400 mg/kg/day in 5% Alkamuls EL-620 in saline vehicle) by oral gavage for 4 weeks. Liver and serum were collected at 5 hrs after the last dose. Quantification of TCA, dichloroacetic acid (DCA), and trichloroethanol (TCOH) was performed. In addition, ALT, liver-to-body weight ratio, hepatocellular proliferation, expression of peroxisome proliferator marker genes (*Ppara*, *Acox1*, and *Cyp4a10*), inflammation, and steatosis were evaluated. We found that (1) there were significant differences in TCE metabolism between different genotypes; (2) expression of *Acox1* and *Cyp4a10* significantly increased in both wild-type and h*Ppara* mice, but not in *Ppara*-nulls; (3) spontaneous steatosis was observed in *Ppara*-null vehicle-treated, but not in mice treated with TCE; (4) mild increase in inflammation in TCE-treated group compared to vehicle was observed in h*Ppara* mice. In conclusion, these data provide additional mechanistic information for understanding the linkages between oxidative TCE metabolism, PPARα activation, and liver toxicity of TCE. This work was supported by the Superfund Basic Research Program grant P42 ES005948.

PS 1153 A Central Role of Aryl Hydrocarbon Receptor in High-Fat Diet-Induced Hepatic Steatosis

C. Xu[1], C. Wang[1], K. Bottum[2], S. Krager[2], C. Jaeger[1] and S. Tischkau[1]. [1]*Pharmacology, SIU School of Medicine, Springfield, IL and* [2]*Internal Medicine, SIU School of Medicine, Springfield, IL.*

The aryl hydrocarbon receptor (AhR) is a ligand-activated basic helix-loop-helix/period-AhR nuclear translocator-single minded transcription factor which mediates a wide range of physiological and toxicological effects upon exposure to endogenous and exogenous ligands. Recent studies have shown that activation of AhR induces hepatic steatosis through upregulation of fatty acid translocase that is responsible for fatty acid transportation into liver. The aim of this study is to determine whether AhR knockout protects against high-fat diet-induced hepatic steatosis. 6-week old wild-type (WT), AhR heterozygous (AhR+/-) and AhR knockout (AhR-/-) male mice were exposed to a normal chow diet (NCD, 10% fat diet) or a high-fat diet (HFD, 60% fat diet) for 14 weeks. AhR-/- as well as AhR+/- mice were protected from HFD-induced hepatic steatosis, impairment of the insulin signaling pathway, and inflammation, as well as systemic insulin resistance. In addition, the expression of CD36/fatty acid translocase, key lipogenic genes, fatty acid synthase (Fas) and acetyl-CoA carboxylase (Acc), peroxisome proliferator-activated receptor-α (PPARα) and fatty acid oxidation key enzymes, carnitine palmitoyl transferase-1 (CPT-1) and acyl-CoA oxidase (ACO) were lower in AhR-/- and AhR+/- mice compared to WT mice after HFD feeding. Since fatty acid oxidation was decreased as an adaptation to decreased de novo fatty acid synthesis, the gene expression profile suggests that the protective effects on HFD-induced hepatic steatosis in AhR-/- as well as AhR+/- mice resulted from upregulation of CD36/fatty acid translocase expression, thereby increasing fatty acid transportation into the liver. These findings elucidate an important role for the AhR in HFD-induced hepatic steatosis, and the AhR signaling pathway could become a potential therapeutic target for fatty liver disease.

PS 1154 Profiling of Compound-Induced Modulation of CAR-Coregulator Interactions As a Means to Differentiate between Direct and Indirect CAR Activation

J. P. Groten[1], D. Melchers[1], R. van Beuningen[1], B. Chorley[2], C. Corton[2] and R. Houtman[1]. [1]*PamGene International BV, Den Bosch, Netherlands and* [2]*EPA, Research Triangle Park, NC.*

The nuclear receptor (NR) superfamily member constitutive activated receptor (CAR) controls the expression of a large battery of genes encoding xenobiotic metabolism enzymes and transporters. CAR can be activated by at least two mechanisms: direct binding (e.g. CITCO) and subsequent recruitment of coregulator proteins which regulate target gene chromatin accessibly, or an indirect mechanism involving interference with a signaling pathway that inhibits the ability of CAR to translocate to the nucleus (e.g., phenobarbital (PB) and phenytoin (PN)). Although a large number of chemicals activate CAR, use of structure-activity relationships to predict CAR activation has been hampered due to the lack of an assay that in conjunction with classical trans-activation assays, allows chemicals to be classified as indirect or direct activators. As a potential solution for this caveat, we applied a peptide microarray with 154 coregulator-derived NR-interaction motifs, (CoR-)NR boxes, which serves as a sensor for CAR conformation and activity status as a function of ligand. Human CAR LBD-coregulator interactions were profiled in the presence of PB, PN, or CITCO, clotrimazole (antagonist) or solvent (2% DMSO). Compound response profiles, i.e. compound-induced log-fold change of CAR binding, were subjected to hierarchical clustering and demonstrated clear differences between compounds and their ability to modify CAR conformation. A large number of significant interactions between CAR and coregulators were stimulated with CITCO. Many of the same interactions were significantly decreased with clotrimazole. PB and PN exposure led to very few significant interactions indicating that they do not activate CAR directly. In summary, coregulator-NR interaction assays are promising new tools to identify chemicals that activate nuclear receptors by different mechanisms. (This abstract does not reflect EPA policy)

PS 1155 Ethanol-Induced Hepatic Expression of Cytochrome P450 (Cyp) 2b10 Is Dependent on PPARB/D

T. Koga[1], G. Balandaram[1], M. Goudarzi[2], A. Fornace[2], F. Gonzalez[3] and J. M. Peters[1]. [1]*Pennsylvania State University, University Park, PA,* [2]*Georgetown University, Washington, DC and* [3]*National Cancer Institute, Bethesda, MD.*

Because of the significant morbidity and lethality due to alcoholic liver disease (ALD), there remains a need to elucidate the mechanisms how ALD is caused. This will allow for the development of new non-invasive biomarkers of ALD that could lead to new approaches for the prevention and treatment of ALD. It was previously shown that PPARβ/δ has an important function in the ALD, and that PPARβ/δ could prevent some ethanol-induced hepatic effects as shown by differences in the urinary metabolome. Thus, the present study global gene expression patterns to begin to identify potential genes that may contribute to the differences in urinary metabolites modulated by PPARβ/δ. Chronic ethanol treatment causes increased hepatic Cyp2b10 mRNA and protein in wild-type mice, but this was not observed in Pparβ/δ-null mice. This suggests that induction of CYP2B10 by ethanol is regulated by PPARβ/δ, and this could be involved in the etiology of ALD modulated by PPARβ/δ. Interestingly, nuclear and cytosolic sub-localization of the constitutive androstane receptor (CAR), a transcription factor know to regulate Cyp2b10 expression, was not different between each wild-type or Pparβ/δ-null mice. However, peroxisome proliferator-activated receptor gamma coactivator 1-alpha (PGC1α), a transcription factor which participates in CAR transactivation of the Cyp2b10 gene, was up-regulated in wild-type mice, and this effect was not observed in Pparβ/δ-null mice. These results suggest that PPARβ/δ regulates Cyp2b10 expression indirectly by modulating PGC1α expression, not by affecting CAR translocation directly. Ongoing studies are evaluating the role of Cyp2b10 in ALD and how PPARβ/δ influences the metabolism of endogenous compounds by this drug metabolizing enzyme (Supported by AA018863 and ES016013).

PS 1156 Compromised Adaptive Upregulation of Mitochondrial Metabolism and Accumulation of Hepatic Lipids Associate with Alcoholic Liver Damage in PPARα-/- Mice

A. Fornace[1], H. Li[1], J. B. Tyburski[1], T. Mak[1] and J. M. Peters[2]. [1]*Department of Biochemistry, Georgetown University, Washington, DC and* [2]*Department of Veterinary and Biomedical Sciences, Pennsylvania State University, University Park, PA.*

Alcohol alters hepatic metabolism, and chronic alcohol consumption can result in alcohol induced liver disease (ALD). Peroxisome proliferator-activated receptor-α (PPARα), a ligand activated transcription factor modulates expression of genes that regulate fatty acid catabolism. The specific PPARα target genes that modulate ALD are unclear. There is remarkable similarity between the histopathology of ALD in Pparα–/– and in early ALD in humans. Importantly, PPARα expression and activity are thought to be lower in human liver than mouse liver. Hence, the Pparα–/– mouse is a good model to investigate ALD. In this study, Pparα–/– mice were used to elucidate whether PPARα is activated or repressed by chronic alcohol consumption. Hepatic transcriptomic and metabolomic analyses were used to examine the alterations of genes and metabolites associated with pathological changes associated with ALD. The changes triggered by chronic alcohol consumption in Pparα–/– mice were compared with those in wild-type mice. The results showed that in the presence of PPARα, energy metabolism pathways in mitochondria, namely the fatty acid β-oxidation, the TCA cycle and electron transfer chain, were induced transcriptionally in response to two-month alcohol feeding. In contrast, these responses were greatly reduced in the absence of PPARα expression. In line with the transcriptional modulations of these metabolic pathways, lipidomics profiling results showed consistent accumulation of triglycerides in Pparα–/– mice as compared to controls. A robust increase of inflammatory-response-associated metabolites, and a strong induction of fibrogenesis genes were also observed exclusively in alcohol-fed Pparα–/– mice as compared to controls. These observations indicate that PPARα plays a protective role in response to chronic alcohol consumption by adaptive transcriptional activation of this receptor.

PS 1157 A Novel Pregnane-X-Receptor (PXR) Knockout Rat Model: Characterization and Evaluation of the Role of PXR in Hepatic Lipidosis

E. Trueblood, P. Nioi, N. Everds, A. Guerrero, S. Clark, R. T. Dunn, J. Chen, J. Schroeder and M. Fielden. *Amgen, Thousand Oaks, CA.*

The PXR plays a well established role in drug metabolism and protection against toxic metabolites such as bilirubin, however its role in lipid metabolism is less well understood. Previous studies in mice have linked PXR activation to induction of hepatic lipidosis, although the consequences of PXR activation in the rat and human remain unclear. To further understand the role of PXR in lipid metabolism, we evaluated the phenotype a novel Sprague Dawley rat PXR knockout (KO) model constructed using zinc finger nuclease technology. PXR KO rats were fertile and were of similar body weight to age-matched wild type rats. There were no differences observed by light microscopy in the majority of tissues examined, however there was a consistent decrease in hematopoiesis and lymphopoiesis, which was reflected by a decrease in hematocrit and circulating red and white blood cells (all lineages), decreased bone marrow cellularity and decreased lymphocytes in the spleen. Altered basal energy metabolism in the PXR KO rats was indicated by mild decreases in serum glucose and cholesterol but no change in serum triglycerides or non-esterified fatty acids. Consistent with published studies in mice, treatment of

wildtype rats with a PXR activator (pregnenolone-16alpha-carbonitrole (PCN)) induced centrilobular hepatocellular hypertrophy consistent with enzyme induction and periportal hepatocellular microvesicular vacuolation, which stained positively for adipophilin confirming the vacuoles contain lipid. An increase in hepatic triglycerides further confirmed accumulation of hepatic lipid by PXR activation in the rat. When the PXR activator PCN was administered to PXR KO rats, no hepatocellular hypertrophy or vacuolation (and no increase in hepatic triglyceride content) was evident, thus confirming that PXR induction is associated with increased hepatocellular lipid in rats. These results are similar to those reported in mice, and further suggests PXR activation is associated with changes in hepatic lipids in rodents.

PS 1158 Aryl Hydrocarbon Receptor-Dependent Induction of Liver Fibrosis by Dioxin

X. D. Coumoul[1,2], S. Pierre[1,2], A. Chevallier[1,2], F. Texiera-Clerc[3], L. Bui[1,2], A. Bats[1,2,5], P. Fernandez-Salguero[4], M. Aggerbeck[1,2], S. Lotersztajn[3] and R. Barouki[1,2]. [1]*INSERM UMR-S 747, Paris, France,* [2]*University Paris Descartes, Paris, France,* [3]*IRMB, INSERM U955, Créteil, France,* [4]*Departamento de Bioquimica y Biologia Molecular, Facultad de Ciencias, Universidad de Extremadura, Badajoz, Spain and* [5]*AP-HP, Hôpital Européen Georges Pompidou, Service de Chirurgie Gynécologique Cancérologique, Paris, France.*

The contribution of environmental pollutants to liver fibrosis is an important and poorly explored issue. In vitro studies suggest that the environmental pollutant 2,3,7,8-tetrachlorodibenzo-p-dioxin(TCDD) and other Aryl hydrocarbon Receptor(AhR) ligands induce several genes that are known to be up-regulated during liver fibrosis. Our aim was to determine whether exposure to such pollutants can lead to liver fibrosis and to characterize the mechanisms of action. Mice were treated for 2, 14 or 42 days, once a week with 25μg/kg of TCDD. Gene and protein expression, in vitro and in vivo, as well as liver histology were investigated for each treatment. Treatment of mice with TCDD for 2-weeks modified the hepatic expression of markers of fibrosis such as collagen-1α1 and α-smooth-muscle-actin. This is not observed in AhR KO mice. Following 6-weeks of treatment, histological features of murine hepatic fibrosis became apparent. In parallel, the levels of inflammatory cytokines and of markers of activated fibroblasts were found to be up-regulated. Interestingly, we also found increased expression of genes of the TGF beta pathway and a concomitant decrease of miR-200a levels. Since the transcription factors of the Snail family were shown to be involved in liver fibrosis, we studied their regulation by TCDD. Two members of the Snail family were increased, whereas their negative targets, the epithelial marker E-cadherin and Claudin1, were decreased. Further, the expression of mesenchymal markers were increased. Finally, we confirmed that Snai2 is a direct transcriptional target of TCDD in the human hepatocarcinoma cell line, HepG2. The AhR ligand, TCDD, induces hepatic fibrosis by directly regulating pro-fibrotic pathways.

PS 1159 Identification of Environmental Chemicals Which Could Contribute to Nonalcoholic Fatty Liver Disease by Nuclear Receptor Activation

L. Al-Eryani[1], B. Wahlang[1], K. C. Falkner[1], H. Clair[1], R. A. Prough[2], J. C. States[3] and M. Cave[1,4]. [1]*Department of Medicine/GI, University of Louisville, Louisville, KY,* [2]*Biochemistry, University of Louisville, Louisville, KY,* [3]*Pharmacology & Toxicology, University of Louisville, Louisville, KY and* [4]*Robley Rex VAMC, Louisville, KY.*

Environmental chemical exposures have previously been associated with nonalcoholic fatty liver disease (NAFLD). Activation of xenobiotic receptors including pregnane-xenobiotic-receptor (PXR) and constitutive androstane receptor (CAR) by environmental chemicals may influence energy metabolism. We hypothesize that PXR activation is a mode of action for toxicants in NAFLD. The purpose of this study is to identify and validate environmental chemicals which interact with PXR or CAR and could thus contribute to NAFLD. EPA-ToxCast Phase I (320 chemicals) was screened for compounds associated with receptor activation. Human (h) and murine (m) PXR and CAR activation were examined for selected compounds from ToxCast Phase I in addition to organochlorine pesticides which were previously associated with human NAFLD. These compounds were validated in vitro for PXR/CAR activation using transient transfection assays in HepG2 cells. Nearly 2/3 of chemicals screened positive for PXR activation. 67 compounds and 102 compounds were found to activate hPXR by NGCG and Attagene assays respectively. The CellzDirect assay identified 202 compounds that were found to change CYP3A4 (PXR target gene) expression. Among chemicals selected for validation (n=9) in cell-based reporter assays, trans-nonachlor, chlordane, DDE, DDT, lindane and alachlor activated h/m PXR. Dieldrin activated mPXR only. Dieldrin, trans-nonachlor, DDT, lindane and alachlor also activated hCAR but not mCAR. Potential PXR interactions were identified for nearly 2/3 of ToxCast Phase I chemicals. However, not all chemicals identified by the ToxCast screening assays proved to be xenobiotic receptor agonists. We postulate that the environmental chemicals that activate PXR may contribute to NAFLD through the effect of this receptor on energy metabolism which may differ in humans and rodent models.

PS 1160 Involvement of Constitutive Androstane Receptor (CAR) in the Liver Hypertrophy and Hepatocarcinogenesis Induced by Three Fibrates in Mice

K. Inoue[1], D. Suzuki[1], Y. Ogawa[2], J. Maeda[1], T. Morikawa[1], R. Ichimura[1], M. Takahashi[1], Y. Kodama[3] and M. Yoshida[1]. [1]*Division of Pathology, National Institute of Health Sciences, Tokyo, Japan,* [2]*Laboratory of Comparative Toxicology, Azabu University, Sagamihara, Kanagawa, Japan and* [3]*Division of Toxicology, National Institute of Health Sciences, Tokyo, Japan.*

Fibrates are known as PPARα agonists and induce hypertrophy and tumors in mouse liver. To clarify the involvement of CAR in the mechanisms of liver hypertrophy and tumors induced by fibrates, 6-week-old male C3H (wild) and CAR knockout (KO) mice were fed a diet containing 2,000 ppm clofibrate (Clo), 2,400 ppm fenofibrate (Feno) or 5,000 ppm bezafibrate (Beza). Four-week-treatment of three fibrates induced centrilobular (Clo) or diffuse (Feno and Beza) liver hypertrophy in wild mice, while CARKO inhibited the hypertrophy of Clo only. In all treated groups of both genotypes, Cyp4a10 expression was markedly increased in the liver. All fibrates increased Cyp2b10 expression in wild mice and the expression significantly decreased by CARKO in all treated groups. However CYP2B10 protein was clearly observed in the centrilobular areas only in wild Clo group, indicating a discrepancy between mRNA and protein expression. These data suggest that CAR might involve in Clo-induced liver hypertrophy. In 27-week-feeding treatment with these three fibrates after diethylnitrosamine initiation, the numbers of basophilic altered foci and/or adenomas were significantly increased in wild mice, but not CARKO, indicating that CAR might involve in induction of basophilic foci and adenomas induced by these three fibrates. On the other hand, CARKO did not affect the increased numbers of eosinophilic altered foci and/or adenomas, which were induced by each fibrate in wild mice. In conclusion, not only PPARα but also CAR plays an important role in liver hypertrophy of Clo and in the hepatocarcinogenesis process of Clo, Feno and Beza.

PS 1161 *Ginkgo biloba* Extract Is Nongenotoxic *In Vivo* and Constitutive Androstane Receptor Is Involved in Its Hepatocarcinogenesis

J. Maeda[1], K. Inoue[1], R. Ichimura[1], T. Morikawa[1], Y. Ogawa[2], Y. Kodama[3] and M. Yoshida[1]. [1]*Division of Pathology, National Institute of Health Sciences, Tokyo, Japan,* [2]*Laboratory of Comparative Toxicology, Azabu University, Sagamihara, Kanagawa, Japan and* [3]*Division of Toxicology, National Institute of Health Sciences, Tokyo, Japan.*

Ginkgo biloba extract (GBE) is commonly used as an herbal supplement aiming to improve brain function and memory. A recent National Toxicology Program (NTP) study of GBE (TR578) reported concerns of genotoxicity and clear evidence of liver hypertrophy and hepatocarcinogenicity in mice. To understand the mode of actions of hepatocarcinogenesis of GBE, we investigated the genotoxicity of GBE *in vivo* and constitutive androstane receptor (CAR) involvement in liver hypertrophy/carcinogenesis, using wild-type and CAR knockout (CARKO) mice.
Our studies of liver comet assay and bone marrow micronucleus assay showed negative results, even at 2,000 mg/kg GBE by gavage for 3 days. This indicates that GBE is non-genotoxic *in vivo.*
In a 4-week GBE dietary treatment of doses up to 10,000 ppm, a dose-dependent hepatocellular hypertrophy accompanied by CYP2B10 expression was induced in wild-type mice. In CARKO mice, only the highest dose of GBE induced same alterations as wild-type mice, indicating that GBE-induced liver hypertrophy is mainly CAR-mediated.
In a two-stage hepatocarcinogenesis model initiated by diethylnitrosamine administration, a 27-week treatment with GBE at 10,000 ppm resulted in an increased number of liver tumors and altered foci in wild-type mice. In contrast, the lesions were far less frequent in CARKO mice.
These results demonstrate that GBE has a certain potential to induce mouse liver tumors through a non-genotoxic mechanism, and that the mode of action for hepatocarcinogenesis of GBE is CAR-mediated.

PS 1162 Activation of the Farnesoid X Receptor Restores Hepatic and Intestinal Bile Acid Synthetic Enzyme and Transporter Expression in Pregnant Mice

J. E. Moscovitz[1], B. Kong[1], G. L. Guo[1, 2] and L. M. Aleksunes[1, 2]. [1]*Department of Pharmacology and Toxicology, Rutgers University, Piscataway, NJ and* [2]*Environmental and Occupational Health Sciences Institute, Rutgers University, Piscataway, NJ.*

Bile acid (BA) homeostasis is dysregulated during pregnancy as a result of reduced signaling of the Farnesoid X Receptor (Fxr), which can lead to hypercholanemia and liver diseases such as intrahepatic cholestasis. To determine whether Fxr function could be pharmacologically rescued during pregnancy, pregnant C57BL/6 mice were treated with vehicle or 100 mg/kg GW4064 (GW), a synthetic Fxr agonist, on gestation days 13 and 14, and livers and intestines were collected for qPCR and western blot analysis. In pregnant mice, the mRNAs of hepatic transporters Ntcp, Oatp1a4, Mdr2, and Mrp3 were reduced by 50-80% as compared to virgin controls. Pregnancy also down-regulated BA metabolism genes Cyp27a1, Bal, and Baat between 35 and 40%, and enhanced Cyp7a1 mRNA by ~2-fold. Protein levels of Ntcp, Bsep and Cyp27a1 were decreased between 35 and 50%. Treatment of pregnant mice with GW increased hepatic Mrp3, Ntcp, Mdr2, Bsep and Ostb mRNAs, as well as Cyp27a1 and Bal mRNAs by 20 to 150%. Expression of Cyp7a1 mRNA was reduced in GW-treated pregnant mice to levels lower than virgin controls. In addition, GW restored expression of Ntcp, Bsep and Cyp27a1 proteins. In the ileum, treatment of pregnant mice with GW increased Fgf15 and Ostb mRNAs between 2- and 3-fold. Pregnancy also decreased the expression of the Fxr target gene and transcription factor, Shp, in liver and ileum by 65% and 98%, respectively. GW returned Shp expression to levels of virgin controls in the liver, and elevated expression by 4-fold in the ileum. These data demonstrate that pharmacological activation of Fxr during pregnancy may partially restore the down-regulation of key bile acid and xenobiotic transporters, as well as additional target genes in the Fxr pathway. Supported by R01ES020522, T32ES007148, and P30ES005022.

PS 1163 An Animal Model of Intrahepatic Cholestasis of Pregnancy

Y. Zhang[1], F. Li[2], K. Krausz[2], P. Vogel[3], F. Gonzalez[2] and J. Schuetz[1]. [1]*Pharmaceutical Sciences, St. Jude Children's Research Hospital, Memphis, TN,* [2]*Laboratory of Metabolism, NCI, National Institutes of Health, Bethesda, MD and* [3]*Pathology, St. Jude Children's Research Hospital, Memphis, TN.*

Fetal complications of Intrahepatic Cholestasis of Pregnancy (ICP) frequently include perinatal mortality. The severity is positively related to maternal serum total bile acids, but the genetic etiology remains unsolved. Respiratory Distress Syndrome (RDS) occurs in 28.6% of newborns of ICP patients. ABCB11 is a hepatic export pump for bile acids. Abcb11 KO mice show elevated serum bile acids. Therefore, we hypothesized that Abcb11 KO female mice might be a model for ICP.

Offspring from KO dams showed 100% mortality, regardless of paternal genotypes. Necropsy only revealed atelectasis in neonates from KO dams. Gene and protein expression of pulmonary cell type markers did not change. Histopathological analysis did not reveal any defect in developmental lungs of neonates from KO dams.

However, electron microscopy revealed super-coiled surfactant in the lungs of neonates from KO dams. The lipid components of pulmonary surfactant did not differ between neonates of WT and KO dams. But serum bile acids were significantly higher in KO dams during pregnancy and accordingly, higher in their neonates. However, only taurine conjugated muricholic acid (T-MCA) was elevated in the lungs of neonates from KO dams. Our data suggests that elevated T-MCA affects pulmonary surfactant, leading to poor oxygenation. This is consistent with our findings that Hif target genes are activated in the postnatal but not embryonic lungs of KO dams.

To rescue of the mice, we backcrossed Abcb11 KO into either CAR or PXR-null background. Abcb11/CAR double KO mice rendered 100% neonatal mortality rates. In contrast, maternal absence of PXR with Abcb11 produces strong neonatal rescue with about 60% of neonates.

The studies have identified Abcb11 as a major gene that accounts for neonatal RDS of cholestatic mothers. The Abcb11 KO female mice could be animal model to develop therapeutic approach.

PS 1163a Exposure to Aryl Hydrocarbon Receptor Antagonist Alpha-Napthaflavone Blocks Diet-Induced Obesity and Nonalcoholic Fatty Liver Disease

B. Moyer, I. Rojas and C. Tomlinson. *Medicine, Dartmouth College, Hanover, NH.*

Previous studies have indicated a role for the aryl hydrocarbon receptor (AHR) in mediating obesity. Mice with the Ahrd variant low-affinity allele have been shown to become less obese when fed a high-fat diet compared to mice with the high-affinity Ahrb1 allele. In the current study, we hypothesize that high doses of known AHR antagonist alpha-napthaflavone (NF) will also prevent diet-induced obesity. To test this, C57BL/6 mice were fed either a standard mouse diet, a "Western diet" containing additional cholesterol 45% of kilocalories come from fat, or these two diets containing 2% NF. Following 26 weeks of diet exposure, no adverse response to the NF was observed, and no differences in food consumption were associated with the NF diet. At 26 weeks' diet, 16 mice per group per sex were sacrificed. NF had a near-complete effect on blocking obesity. Body weights at sacrifice for females were 22.0 ±1.4 g (control), 28.7 ± 3.3 g (Western), 23.6 ± 1.8 g (control + NF), and 24.5 ± 2.2 g (Western + NF). The difference between Western diet and Western diet + NF was significant, P value < 0.05. Furthermore, histological examination of livers indicate fat accumulation indicative of non-alcoholic fatty liver disease (NAFLD) was widespread in Western diet groups, but was not widely detected in any other group. Differences in fat accumulation were also detected via MRI imaging and fat pad weights taken at sacrifice. From these data we conclude that inhibition of the AHR via dietary exposure to high levels of a known antagonist can block pathologies associated with the Western diet, including obesity and NAFLD. This further affirms a possibly major role of the AHR in regulating the body's response to diet.

PS 1163b Amphiregulin (AREG) and Transforming Growth Factor-alpha (TGF-α) Play Opposing Roles in 2, 3, 7, 8-Tetrachlorodibenzo-*p*-dioxin (TCDD)-Induced Proliferation and EGFR Signaling in Skin

C. Campion[1], C. H. Sutter[1], T. R. Sutter[1, 2] and J. A. Cole[1]. [1]*Biological Sciences, University of Memphis, Memphis, TN and* [2]*W. Harry Feinstone Center for Genomic Research, Memphis, TN.*

In the epidermis, the balance between differentiation and proliferation is modulated by epidermal growth factor receptor (EGFR) signaling. EGFR activation promotes proliferation and is dampened under differentiating conditions. Previous studies show that TCDD, calcium (Ca), and TCDD/Ca cause time- and treatment-dependent down-regulation of [^{125}I]-EGF binding, however the mechanism and implications of this down-regulation on epidermal homeostasis and EGFR signaling have not been fully addressed. In this study, we sought to identify whether secreted ligands drive EGFR down-regulation and the impact of these ligands on EGFR signaling, ligand responsiveness, and cellular proliferation in primary neonatal human epidermal keratinocytes (NHEKs). A 72 h treatment with TCDD, Ca, or TCDD/Ca reduced [^{125}I]-EGF binding to 77%, 41%, and 32% of control cells respectively without loss of EGFR protein. TCDD and TCDD/Ca-treated NHEKs showed no change in basal ERK activity but significantly enhanced responsiveness to exogenous ligand. TCDD, Ca, or TCDD/Ca caused elevated secretion of TGF-α compared to control cells while all NHEKs secreted AREG in a time-dependent manner. Using neutralizing antibodies, we showed that altering secreted ligands had no effect on total EGFR protein. TGF-α had an anti-proliferative effect and neutralization led to significantly decreased [^{125}I]-EGF binding. Conversely, neutralization of AREG led to decreased cell number in TCDD, Ca-, and TCDD/Ca-treated NHEKs. Neutralization of both ligands reversed treatment-dependent EGFR down-regulation in TCDD-, Ca-, and TCDD/Ca-treated cells, supporting that this down-regulation is modulated through the secretion of both TGF-α and AREG, which leads to an alteration, though not a loss, of EGFR signaling. TGF-α and AREG play opposing roles in downstream NHEK proliferation suggesting that TCDD pathology is in part due to imbalancing ligand-driven EGFR signaling.

PS 1164 Hepatic Overexpression of Annexin A1 in Thioacetamide-Primed Mice Protects Them from Liver Failure and Death Induced by a Lethal Dose of Acetaminophen

V. P. Dadhania[1], J. R. Latendresse[2] and H. M. Mehendale[1]. [1]*Toxicology, University of Louisiana at Monroe, Monroe, LA and* [2]*Toxicologic Pathology Associates, National Centre for Toxicological Research, Jefferson, AR.*

This study was conducted in male Swiss Webster mice to further confirm our previous findings on heteroprotection of thioacetamide (TA)-primed mice against acetaminophen (APAP)-induced lethality. The objective was to examine the role of annexin A1, an endogenous inhibitor of phospholipase A2, in heteroprotection by TA against APAP-induced liver failure and mortality. Male Swiss Webster mice were primed with a low dose of TA [40 mg/kg in 10 ml normal saline/kg, intaperitoneally (i.p.)] 36h before challenge with a lethal dose (600 mg/kg in 0.45% NaCl pH 8.2, i.p.) of APAP. Plasma alanine aminotransferase (ALT), aspartate aminotransferase (AST) were measured as biomarkers of liver injury, and plasma secretory phospholipase A2 (sPLA2) activity was measured to monitor the expansion of APAP-initiated liver injury. Hepatic glutathione (GSH) depletion following APAP treatment was measured in TA primed and non-primed mice. TA priming resulted in marginal decrease (~25%) in Cyp2e1 enzyme level, but the extent of rise in ALT and AST and decrease in hepatic GSH after APAP overdose was not affected due to TA priming. Moreover, TA priming did not affect the rise in plasma sPLA2 level at 2h following APAP treatment; however, no further rise in sPLA2 was observed at later time points in TA primed mice as compared to non-primed mice. TA priming resulted in overexpression of annexin A1 at 24 to 48h. Inhibition of annexin A1 biosynthesis using protein synthesis inhibitor cycloheximide (CHX) (40 mg/kg in 5 ml distilled water/kg, i.p.) at 1h before TA priming resulted in unabated expansion of APAP-induced liver injury and led to 100% mortality in stark contrast to 100% survival in APAP-overdosed TA primed mice that did not receive CHX intervention. In conclusion, annexin A1 overexpression in proliferating hepatocytes abolishes the expansion of liver injury after a lethal APAP overdose in mice.

PS 1165 Inhibition of Secreted Phospholipase A2 (sPLA2) Enzyme Leads to Survival of Lethally Acetaminophen-Overdosed Mice

H. M. Mehendale[1], V. P. Dadhania[1] and J. R. Latendresse[2]. [1]*Toxicology, University of Louisiana at Monroe, Monroe, LA and* [2]*Toxicologic Pathology Associates, National Centre for Toxicological Research, Jefferson, AR.*

This study was designed to test whether inhibiting secreted phospholipase A2 (sPLA2), a death protein, with a specific inhibitor, BPPA [5-(4-benzyloxy-phenyl)-4S-(7-phenylheptanoylamino) pentanoic acid], prevents the expansion of liver injury initiated by a lethal overdose of acetaminophen (APAP) in mice. Male Swiss Webster mice (25-30g) were treated with a lethal dose of APAP (600 mg/kg, ip, in warm 0.45% NaCl pH 8.2) followed by a single dose of either BPPA (20 mg/kg, ip, in DMSO 3 ml/kg) or DMSO vehicle (3 ml/kg, ip) alone injected at 2, 4 or 8h after APAP administration. Survival and mortality were recorded over the next 14 days. Plasma alanine aminotransferase (ALT) and sPLA2 activities were measured in the mice on alternate days from days 1 to 13. ALT and sPLA2 activities increased sharply in the mice treated with APAP either alone or followed by DMSO (3 ml/kg, ip) led to 80% mortality. In contrast, mice treated with BPPA at 2 and 4h after the APAP administration exhibited similar rise in sPLA2 and ALT activities on day 1 declining thereafter and suffered only 10 and 30% mortality, respectively. Covalent binding of 14C-APAP-derived reactive metabolite to liver protein, hepatic glutathione (GSH) depletion, and hepatic GSH:GSSG ratio did not change after the APAP overdose in the mice receiving the BPPA intervention. Ninety, 70, and 60 percent of the mice treated with BPPA at 2, 4, and 8h after the lethal dose of APAP, respectively, survived. We conclude that timely intervention by the administration of the sPLA2 inhibitor, BPPA, prevented the expansion of APAP-induced liver injury and death of the mice after the lethal challenge with APAP.

PS 1166 Antidiabetic and Antilipidemic Effects of *Artemisia annua* L. Extract Are Mediated by AMPK Activation

J. Lee[1], B. Lee[1], H. Yang[1], Y. Yu[1], S. Park[1], C. Choi[2], H. Kim[1], H. Jeong[3] and Y. Hwang[1]. [1]*Pharmaceutical Engineering, International University of Korea, Jinju, Republic of Korea,* [2]*Jeollanamdo Institute of Natural Resources Research, Jeollanamdo, Republic of Korea and* [3]*College of Pharmacy, Chungnam National University, Daejeon, Republic of Korea.*

Nonalcoholic fatty liver disease (NAFLD) is considered to be the most common hepatic manifestation of metabolic syndromes such as diabetes and obesity. The dysregulation of triacylglycerol metabolism may contribute to the derangement of hepatic lipid homeostasis and chronic liver damage. In this study, we evaluated body weight, liver histology, and hepatic lipid content in high-fat diet (HFD)-fed ICR mice treated with *Artemisia annua* L. extract (AAE). In addition, we characterized the underlying mechanism of AAE's effects in HepG2 hepatocytes through Western blot analysis. AAE (50 mg/kg/day) reduced weight gain, fat pad mass, and hepatic triglyceride accumulation, and improved serum lipid parameters in mice fed a HFD for 4 weeks. AAE significantly increased the phosphorylation of AMP-activated protein kinase (AMPK) and acetyl-CoA carboxylase (ACC) in the liver and HepG2 hepatocytes. In addition, AAE downregulated the levels of sterol regulatory element-binding protein-1 (SREBP-1) and its target genes including ACC and fatty acid synthase (FAS). The specific AMPK inhibitor; compound C, attenuated the effects of AAE on the expression of lipid metabolism-related proteins such as SREBP-1 and FAS in HepG2 hepatocytes. The beneficial effects of AAE on HFD-induced hepatic lipid accumulation are thus mediated through AMPK signaling pathways suggesting a potential target for the prevention of obesity.

PS 1167 *Poria cocos* Alleviates Nonalcoholic Fatty Liver by Inhibiting SREBP-1 Activity via the AMPK-SREBP Signaling Pathway

B. Lee[1], J. Lee[1], H. Yang[1], Y. Yu[1], S. Park[1], C. Choi[2], H. Kim[1], T. Sung[1], H. Jeong[3] and Y. Hwang[1]. [1]*International University of Korea, Jinju, Gyeongnam, Republic of Korea,* [2]*Jeollanamdo Institute of Natural Resources Research, Jeollanamdo, Janmheung, Republic of Korea and* [3]*College of Pharmacy, Chungnam National University, Daejeon, Republic of Korea.*

In this study, we investigated the antiobesity properties of *Poria cocos* extract (PCE) in mice in which obesity was induced with a high-fat diet (HFD). PCE administration (50 mg/kg/day) for 28 days decreased body weight gain, adipose tissue weight, and the serum triglyceride level in mice fed a HFD. PCE reduced serum levels of glutamic pyruvic transaminase and glutamic oxaloacetic transaminase as well as the accumulation of lipid droplets in the liver. PCE restored the HFD-induced decrease in phosphorylation of AMP-activated protein kinase (AMPK) and acetyl-CoA carboxylase (ACC) in liver tissue. PCE increased the phosphorylation of AMPK and ACC and decreased the expression of SREBP-1 in human HepG2 hepatocytes. The specific AMPK inhibitor; compound C, attenuated the effects of PCE on the expression of lipid metabolism-related proteins such as SREBP-1 and FAS in HepG2 hepatocytes. Taken together, these data suggest that PCE exert improving effects on HFD-induced obesity by reducing lipogenesis.

PS 1168 Translation Initiation Factor EIF4A1 Mediates TNF-Mediated Apoptosis in Drug-Induced Liver Injury through the ATF4/CHOP Pathway

B. van de Water, L. Fredriksson, B. Herpers and S. Wink. *Leiden/Amsterdam Center for Drug Research, Leiden University, Leiden, Netherlands.*

Drug-induced liver injury (DILI) is an important clinical problem. Here we used a genomics approach to establish the critical drug-induced toxicity pathways that act in synergy with the pro-inflammatory cytokine tumor necrosis factor alpha (TNF) to cause cell death of liver HepG2 cells. Transcriptomics-based analysis of the cell injury stress response pathways initiated by diclofenac (DCF) and carbamazepine (CBZ), revealed the endoplasmic reticulum (ER) stress/translational initiation signaling and Nrf2 signaling as two major pathways. ER stress was primarily related to PERK and ATF4 activation and subsequent expression of CHOP, which was all independent of TNF signaling. Identical ATF4 dependent transcriptional programs were observed in primary human hepatocytes as well as human liver slices. Subsequent targeted RNA interference studies revealed that while ER stress signaling through IRE1alpha and ATF6 acted cytoprotective against the TNF synergistic toxicity with CBZ and DCF, activation of the ER stress protein kinase PERK and subsequent expression of CHOP was pivotal for the onset of drug/TNF-induced apoptosis. While inhibition of the Nrf2-dependent adaptive oxidative stress response enhanced the drug/TNF cytotoxicity, Nrf2 signaling did not affect CHOP expression. CBZ and DCF caused an enhanced expression of the translational initiation factor EIF4A1. Importantly, depletion of EIF4A1 almost completely inhibited CHOP expression in association with protection against the drug/TNF-mediated cell killing. Our data support a model in which enhanced drug-induced translation initiates PERK-mediated CHOP signaling in an EIF4A1 dependent manner, thereby sensitizing towards caspase-8-dependent TNF-induced apoptosis.

PS 1169 Let's Talk About Sex: Is Nrf2 Responsible for Sex Differences in Susceptibility to Acetaminophen-Induced Hepatotoxicity in Mice?

P. Rohrer and J. E. Manautou. *Department of Pharmaceutical Sciences, University of Connecticut, Storrs, CT.*

Nuclear factor erythroid 2-related factor 2 (Nrf2) is a transcription factor that positively regulates the expression and activity of cytoprotective genes during periods of oxidative stress. Literature has shown that some of these genes are more highly expressed in livers of female than male mice. This may explain previous reports of greater tolerability by female mice to acetaminophen (APAP) hepatotoxicity than males. The hypothesis for this study is that resistance to APAP toxicity by female mice is due to higher basal and inducible expression of Nrf2 and Nrf2-dependent genes. Here, we examined differences in basal mRNA and protein expression for Nrf2 and Nrf2-dependent genes in naïve (fed) male and female mice and overnight-fasted mice following vehicle or APAP treatment. Alanine aminotransferase (ALT) activity was also measured as an indicator of hepatotoxicity. Hepatic mRNA and protein levels were measured by quantitative PCR and western blotting, respectively. Contrary to our hypothesis, results show that basal Nrf2 mRNA expression was significantly lower in livers of fed female than male mice. Consistent with this, basal Nrf2 protein expression was lower in livers of both fed and overnight-fasted female than male mice, with significance observed in livers of fed mice. However, greater induction of the Nrf2-dependent gene NAD(P)H quinone oxidoreductase 1 (Nqo1) and multidrug resistance-associated protein transporter 4 (Abcc4 or Mrp4) was observed in livers of overnight-fasted female than male mice. Similarly, Nqo1 protein expression was significantly higher in livers of both fed and overnight-fasted female mice. As expected, ALT activity was significantly elevated in both WT and Nrf2-null male mice following APAP treatment, but no significant increases in ALT were observed in either genotype of female mice. This unaltered tolerance by female mice lacking Nrf2 indicates that other factors, rather than Nrf2, are responsible for the lower susceptibility of female mice to APAP hepatotoxicity. Supported by NIH DK069557.

PS 1170 1, 3-Dicarbonyl Enol Compounds Modify Acetaminophen Hepatotoxicity and Liver Ischemia/Reperfusion Injury

R. LoPachin[1], T. Gavin[2], B. Kosharskyy[1], A. Vydynathan[1] and L. Zhang[1]. [1]*Anesthesiology, Albert Einstein College of Medicine, Bronx, NY and* [2]*Chemistry, Iona College, New Rochelle, NY.*

We have shown that enolates formed from 1,3-dicarbonyl compounds, such as 2-aceytylcyclopentanone (2-ACP), can provide protection in cell culture models of electrophile- or oxidative stress-induced toxicity. Here we evaluated the protective abilities of 2-ACP in a mouse model of acetaminophen (APAP) hepatotoxicity. Oral APAP overdose (500 mg/kg) was 90% lethal within 72 hrs and the resulting hepatotoxicity was associated with changes in plasma liver enzyme activities, histopathological indices and markers of hepatocyte oxidative stress. 2-ACP (i.p., 0.80 – 2.40 mmol/kg) produced dose-dependent protection against APAP lethality over a 7-day period. This effect was correlated with normalization of measured parameters. Complete protection was afforded when 2-ACP was administered 20 but not 60 minutes post-APAP. Although i.p. administration of N-acetylcysteine (NAC) was not effective (2.40-7.20 mmol/kg), temporal studies indicated that i.p. NAC was hepatoprotective when injected 60 min after APAP intoxication. Oral 2-ACP administration was associated with modest APAP protection, whereas NAC (0.80 – 2.40 mmol/kg) administered orally provided significant protection. In chemico studies and quantum mechanical calculations indicated that 2-ACP acted as a surrogate nucleophile target for the reactive electrophilic APAP metabolite N-acetyl-p-benzoquinone imine. As an in vivo model of oxidative stress, warm ischemia-reperfusion (I/R) injury of rat liver was produced by clamping the hepatic circulation for 60 mins followed by 180 mins of reperfusion. 2-ACP (i.p., 2.4 mmol/kg) administered at several times during I/R period reduced the appearance of liver enzymes (ALT, AST and LDH) in plasma by 75-85%. These data suggest that 2-ACP can prevent electrophile- or oxidative stress-induced toxicity and might therefore be useful in treating certain disease states (e.g., stroke) and/or acquired toxicities associated with electrophilic drugs, metabolites or environmental toxicants. (supported by R01 ESO3830-26)

PS 1171 Proinflammatory Oligonucleotides Do Not Potentiate Drug-Induced Hepatotoxicity in Mice

H. S. Younis, B. Adhikari, J. Hsaio, L. Shen, G. Hung and S. Henry. *Isis Pharmaceuticals, Inc., Carlsbad, CA.*

Oligonucleotide (ON)-based therapeutics are in late-stage clinical development for multiple disease indications. Several classes of ONs exist based on their mechanism of action (e.g. RNASE H, RISC, aptamer), structure (e.g., single stranded DNA, double stranded RNA) and chemical modifications. In general, ON therapeutics are associated with proinflammatory properties in animals, particularly in mice. The objective of this research was to determine if the proinflammatory effects of the phosphorothioate - 2'-methoxyethyl (PS-2'MOE) antisense class of ONs potentiates drug-induced hepatotoxicity in rodents. Mice were pretreated with proinflammatory ONs (ISIS 104838 or ISIS 421856 at 300 mg/kg/week for 2 weeks) followed by single dose administration of CCL4 (0 to 65 mg/kg) or acetaminophen (APAP, 0 to 400 mg/kg), at which point, liver function tests (ALT, AST, bili), proinflammatory markers (cytokine production, spleen weight) and liver histopathology were evaluated. The proinflammatory response as manifested by cytokine production (IL-6, IL-10, MCP-1), splenomegaly and mononuclear cell infiltration in the liver following PS-2'MOE treatment was greater for ISIS 421856 relative to ISIS 104838. CCL4 produced a dose-dependent increase in hepatotoxicity based on marked elevations of ALT, AST and bili and presence of centrilobular hepatocellular necrosis. The extent of hepatocellular toxicity following CCL4 treatment was similar in PS-2'MOE or PBS treated mice. Proinflammation following PS-2'MOE administration also had no effect on APAP-induced hepatotoxicity in mice. Thus, the low to moderate level of proinflammation produced by PS-2'MOE antisense oligonucleotides does not appear to potentiate drug-induced hepatotoxicity in mice.

PS 1172 Lower Susceptibility of Female Mice to APAP Hepatotoxicity: Role of Mitochondrial Glutathione and c-Jun-N-Terminal Kinase

K. Du, C. D. Williams, M. R. McGill and H. Jaeschke. *Pharmacology, Toxicology & Therapeuticals, University of Kansas Medical Center, Kansas City, KS.*

Acetaminophen (APAP) causes severe hepatotoxicity after an overdose in animals and humans. Despite extensive studies that have been performed to elucidate the mechanisms of APAP hepatotoxicity (Drug Metab. Rev. 44:88-106, 2012), the mechanisms underlying the gender differences have not been clarified. In our study, both female and male C57Bl/6 mice were treated with 300 mg/kg APAP after overnight fasting and liver injury was determined up to 24h after APAP administration. APAP treatment caused severe hepatotoxicity in male mice, while the liver injury was significantly lower in female animals at all time points. Equivalent cytosolic and mitochondrial APAP-protein adducts were generated between genders, indicating no gender difference in metabolic activation to initiate toxicity. Hepatic glutathione (GSH) was depleted rapidly in both genders before the initiation of liver injury, while GSH recovery was must faster in female mice in both the total liver and in mitochondria. The faster recovery of GSH, which correlated with increased glutamate-cysteine ligase expression, attenuated the mitochondrial oxidative stress in female mice, which was indicated by the lower GSSG/GSH ratio at 6h and minimal centrilobular nitrotyrosine staining. While c-jun-N-terminal kinase (JNK) activation was similar at 2 and 4h after APAP, it was much lower at 6h in female mice. However, female mice were also protected against liver injury by the JNK inhibitor SP600125. Conclusion: The lower susceptibility of female mice compared to males was not caused by a difference in metabolic activation of APAP but by the improved detoxification of reactive oxygen due to the accelerated recovery of mitochondrial GSH levels. The improved detoxification of reactive oxygen attenuated late JNK activation and liver injury. However, even the reduced injury in female mice was still dependent on JNK.

PS 1173 Dissecting the Mechanisms of Liver Regeneration after Acetaminophen Toxicity: From Incremental Dose Model to Role of Wnt/Beta-Catenin Signaling

B. Bhushan, C. Walesky, P. Borude, G. Edwards and U. Apte. *Department of Pharmacology, Toxicology, and Therapeutics, University of Kansas Medical Center, Kansas City, KS.*

Overdose of acetaminophen (APAP) is the major cause of acute liver failure (ALF) in the US with very limited treatment options. Recent studies suggest that liver regeneration is critical determinant of overall survival following APAP overdose and may have therapeutic potential. However, mechanisms of liver regeneration following APAP-induced ALF are not known. In the present study, we identified major signaling pathways involved in liver regeneration following APAP-induced

ALF using an incremental dose model. C57BL/6 mice were treated with either 300 mg/kg (APAP300, regenerative dose) or 600 mg/kg (APAP600, non-regenerative dose) APAP. Liver injury and regeneration were studied over a time-course of 0 to 96-hr. Mice treated with APAP300 developed extensive liver injury followed by significant regeneration resulting in resolution of injury by 48-hr. In contrast, APAP600 group exhibited significant progression of injury with substantial decrease in regeneration. The inhibition of regeneration in APAP600 group was associated with decreased cyclinD1 mRNA and protein expression. Further analysis of upstream signaling revealed that growth factors signaling pathways (EGFR/c-Met, downstream MAPKs) were dose-dependently activated and remain highly activated even at APAP600, where regeneration was inhibited. However, canonical Wnt/β-catenin and NF-κB signaling were activated only in APAP300 where regeneration was stimulated. Next, we investigated role of Wnt/β-catenin in further detail. ChIP analysis revealed increased binding of β-catenin to cyclinD1 promoter specifically at APAP300 correlating with higher cyclinD1 induction. Furthermore, over-expression of stable form of β-catenin (S45D) in mice resulted in induction of cyclinD1, improved liver regeneration and decreased progression of injury following APAP overdose. Overall, our study identified several potential pathways and confirmed role of Wnt signaling in regulation of liver regeneration after APAP overdose.

PS 1174 Strain Difference in Carbamazepine-Induced Hepatotoxicity

T. Fukushima, M. Nagata, K. Matsuyama, K. Masuno, S. Matsushima, M. Ueno and M. Torii. *Shionogi Co & Ltd, Toyonaka, Osaka, Japan.* Sponsor: K. Nakamura.

Carbamazepine (CBZ) is a widely used antiepileptic drug, and severe hepatotoxicity is reported in a small population of the patients who took CBZ. Recent publications suggest that the CBZ-induced hepatotoxicity is immune-mediated. The present study investigated effects of mouse strain-specific immunological back ground on CBZ hepatotoxicity. CBZ was administered to 3 mice strains, ICR (frequently used in general toxicology study), C57BL/6 (Th1 dominant) and BALB/c (Th2 dominant). These mice were given CBZ at 400 mg/kg/day for 4 days and 800 mg/kg for subsequent 1day. After 24 hr of the final dosing, all survived animals were necropsied and laboratory tests were performed. Hepatotoxicity, such as necrosis of hepatocytes along with increases in plasma AST, ALT or LDH, was observed in 0/10, 5/10 and 8/10 mice in ICR, C57BL/6 and BALB/c, respectively, among which the severity was worst in BALB/c. Blood TCR-α,β values were comparable in all 3 strains. However, RT-PCR analysis using liver revealed highly increased gene expression of pTCRα, CCL2 in C57BL/6 and BALB/c. Furthermore, there was also increased gene expression of TNF-α, IL-6 and IL-10 also increased. These responses were strongest in BALB/c. In addition, an increased gene expression of liver Hemeoxygenase-1 (HO-1) was observed in the hepatotoxicity-induced mice. Since HO-1 is reported to present in dendritic cells in the liver, HO-1 might play some role for CBZ-induced hepatotoxicity. Taken together, there were clear strain differences in incidence and severity of CBZ-induced hepatotoxicity. The different hepatotoxicity responses between the strains were correlated to different immunological responses in the liver and BALB/c was most sensitive.

PS 1175 Assessment of the Effects of Perfluorononanoic Acid on Hepatic Homeostasis

K. G. Kongsbak[1, 2], K. Skov[1], N. Hadrup[1] and A. Vinggaard[1]. [1]*National Food Institute, Technical University of Denmark, Søborg, Denmark and* [2]*Department of Systems Biology, Technical University of Denmark, Kgs. Lyngby, Denmark.*

Polyfluorinated compounds (PFC) are compounds where all or most hydrogen atoms are replaced by fluorine atoms. Due to their physical-chemical properties, PFCs are used in more than 200 industrial and consumer applications of which lubricants, fire-fighting foams, and emulsifiers for the production of fluoropolymers are a few examples. Perfluorononanoic acid (PFNA) is a nine-carbon perfluorinated compound, used as a surfactant and emulsifier.
Over the last decade (1999-2010), researchers have found a three-fold increase in PFNA concentrations in blood from the US population. Due to the long half-life of PFCs and thus the tendency to bio-accumulate, there is an increased concern about the human exposure to these compounds. PFNA is between the four most frequently detected PFC's in human serum.
To study the potential effects of PFNA on hormonal and hepatic homeostasis, we dosed adult male Wistar rats with three doses of PFNA (0.0125, 0.25, and 5 mg/kg bw/day) once daily for 14 days by gavage. After euthanization, we sampled blood and various tissues and isolated mRNA from liver samples for Agilent rat gene expression microarrays. A metabolomics analysis was performed on the blood samples using LC MS/MS. The identified perturbed targets/signaling pathways were validated using RT qPCR and immunohistochemical staining of liver slices. The highest PFNA dose caused steatosis and general toxicity. We found significant changes in plasma levels of androstenedione and testosterone at the highest dose and corticosterone at the lowest dose. Initial overrepresentation analyses of the gene expression microarray data using Gene Ontology categories suggested effects of PFNA on energy metabolism and peroxisome proliferation along with mitochondrial and endoplasmic reticulum function. This is e.g. indicated by misregulation of genes involved in mitochondrial fatty acid β-oxidation. This is in agreement with the findings from the metabolomics analysis, showing decreased levels of lipids in the plasma samples.

PS 1176 Tolerance to Acetaminophen (APAP) Hepatotoxicity in a Mouse Model of Autoprotection Is Associated with Induction of Flavin-Containing Monooxygenase-3 (Fmo3)

S. Rudraiah, P. Rohrer, I. Gurevich, T. P. Rasmussen and J. E. Manautou. *Uni. of Connecticut, Storrs, CT.*

APAP overdose is the leading cause of acute liver failure in the U.S. Rodents treated with low hepatotoxic doses of APAP become resistant to toxicity from subsequent treatment with higher doses of APAP (APAP autoprotection). Although this phenomenon is also seen in patients who repeatedly take supratherapeutic doses of APAP, the underlying mechanism(s) is not known. Previous gene microarray studies revealed a pronounced induction of liver Fmo3 mRNA expression in our mouse model of APAP autoprotection. Here, we characterized the gene regulation and protein expression of liver Fmo3 during APAP hepatotoxicity.The functional consequences of Fmo3 induction were also investigated. Plasma and livers were collected from male C57BL/6J mice over a period of 72h following a single dose of APAP (400 mg/kg) to measure Fmo3 mRNA and protein expression.Although Fmo3 mRNA levels increased significantly following APAP treatment, its protein expression marginally changed. By contrast, both Fmo3 mRNA and protein expression were significantly higher in mice pretreated with APAP (400 mg/kg) and re-exposed to a higher dose (600 mg/kg). In contrast to naïve C57BL/6J male mice, female mice have about 80-times higher basal Fmo3 mRNA and are highly resistant to APAP hepatotoxicity.Co-administration of APAP with the Fmo3 inhibitor methimazole rendered female mice susceptible to APAP hepatotoxicity, with no changes in susceptibility detected in male mice.Furthermore, a human hepatocyte cell line (HC-04)clone overexpressing human FMO3 showed enhanced resistance to APAP cytotoxicity. Taken together, these findings establish for the first time induction of Fmo3 protein expression and function by xenobiotic treatment. Our results also indicate that Fmo3 expression and function plays a role in protecting the liver from APAP-induced toxicity. Although the mechanism(s) of this protection remains to be elucidated, this work describes a novel function for this enzyme. Supported by NIH DK069557.

PS 1177 Altered Expression of Hepatic Xenobiotic Metabolism Systems in Transport Deficient (TR-) Rats

L. LeCureux, V. Bhaskaran and L. D. Lehman-McKeeman. *Discovery Toxicology, Bristol-Myers Squibb, Lawrenceville, NJ.*

TR- rats are characterized by a spontaneous mutation in the biliary transporter, multidrug resistance-associated protein-2 (Mrp2; Abcc2), and it is generally recognized that there is a compensatory increase in the expression of the basolateral transporter Mrp3 (Abcc3) in these rats. The purpose of this work was to characterize global hepatic gene expression changes in TR- rats, with emphasis on xenobiotic metabolizing systems. Liver mRNA profiles were evaluated in TR- and control Wistar rats (Affymetrix®, Rat Genome 230, 2.0 GeneChips; $p < 0.01$), and results were confirmed by RT-PCR. For Phase I metabolic enzymes, CypP450 reductase, Cyp2b1, and Cyp2a2 increased (≥ 1.5x), whereas Cyp2c40, Cyp2b2, and Cyp7a1 decreased (≥ 2.7x). For phase II conjugating enzymes, Ugt1a1 increased along with several glutathione transferases including, Gsta5, Gstm2, Gstp1, and Gstt1. Gsta5 was the most significantly increased in this family (9.4x). As expected, Abcc3 mRNA was increased, along with an increase in Abcba1 (3.9x). Hepatic expression of numerous solute carriers (Slc family) was altered, with 7 members significantly up-regulated. Of these transcripts, expression of Slc35c2, a transporter for GDP-fucose, was elevated (6x). An additional 11 Slc genes were down-regulated, including the taurine transporter Slc6a6 (4.4x) and the Na/phosphate exchanger, Slc34a2 (8.8x). These results indicate that hepatic expression of numerous genes involved in Phase I, II and III metabolism are altered in Mrp2-deficient TR- rats. The potential contribution of these changes (e.g. altered enzyme activity or transport of solutes) to the disposition of endogenous and exogenous compounds should be considered when this model is used to assess the role of Mrp2 in biliary excretion and toxicity of drugs and environmental chemicals.

PS 1178 Allopurinol Protects against Acetaminophen-Induced Liver Injury by Aldehyde Oxidase-Mediated Preconditioning

C. D. Williams, M. R. McGill and H. Jaeschke. *KUMC, Kansas City, KS.*

Acetaminophen (APAP) overdose causes severe and occasionally fatal liver injury. Numerous drugs that attenuate APAP toxicity have been described. However these compounds frequently protect by cytochrome P450 inhibition, thereby preventing the initiating step of toxicity. We have previously shown that pretreatment with allopurinol can effectively protect against APAP toxicity, but the mechanism remains unclear. In the current study, C3HeB/FeJ mice were administered allopurinol 18h or 1h prior to APAP overdose. Administration of allopurinol 18h prior to APAP overdose resulted in an 88% reduction in liver injury (serum ALT) 6h after APAP, however, 1h pretreatment offered no protection. APAP-cysteine adducts and glutathione depletion kinetics were similar with or without allopurinol pretreatment. The phosphorylation and mitochondrial translocation of c-jun-N-terminal-kinase (JNK) has been implicated in the progression of APAP toxicity. In our study we showed equivalent early JNK activation (2h) however late JNK activation (6h) was attenuated in allopurinol treated mice, which suggests that later JNK activation is more critical for the toxicity. Additional mice were administered oxypurinol (primary metabolite of allopurinol) 18h or 1h pre-APAP, but neither treatment protected. This finding implicated an aldehyde oxidase (AO)-mediated metabolism of allopurinol, so mice were treated with hydralazine to inhibit AO prior to allopurinol/APAP administration, which eliminated the protective effects of allopurinol. We evaluated potential targets of AO-mediated preconditioning and found increased hepatic metallothionein 18h post-allopurinol. These data show metabolism of allopurinol occurring independent of P450 isoenzymes preconditions the liver and renders the animal less susceptible to an APAP overdose.

PS 1179 Hepatoprotective Effects of Olive Leaves Extract (*Olea europaea*) against Acetaminophen-Induced Hepatotoxicity in Isolated Rat Hepatocytes

O. S. El-Tawil, S. M. Saleh, E. M. El-Saied, A. F. Tohamy and O. S. El-Tawil. *Toxicology Department, Faculty of Veterinary Medicine Cairo University, Giza, Cairo, Egypt.*

Olive leaf from *Olea europaea* is one of the native Mediterranean plants, and has been known for its medicinal properties since ancient times. It has diverse pharmacological properties including antioxidant and anti-inflammatory activities. The present study was planned to evaluate the potential hepatoprotective effects of olive leaves total crude extract at different concentrations against hepatotoxicity induced by acetaminophen in isolated rat hepatocytes. In addition, the mechanism of the expected protective effect of the olive leaves extract was elucidated through assessment of the exposed hepatocytes performance and cytopathological examination by light and electron microscopes. Liver cell performance and cytotoxicity were evaluated by assessing cell viability and leakage of cytosolic enzymes (LDH, ALT and AST) as well as determination of intracellular glutathione content and lipid peroxidation products. Exposure of isolated rat hepatocytes to acetaminophen (7mM) caused a significant decrease in cell viability, and a significant increase in the leakage of intracellular enzymes.As well as, acetaminophen caused progressive depletion of intracellular GSH content and significant enhancement of TBARS accumulation. The cytopathological examination revealed morphological alterations of hepatocytes. Membranous structures lost their integrity. Preincubation of hepatocytes with olive leaves extract (0.05, 0.1 and 0.2% W/V) or silymarin (0.5 mM) exerted marked protective effects against acetaminophen toxicity which was indicated by increasing cell viability and decrease the leakage of intracellular enzymes, improvement of GSH contents, and decrease lipid peroxidation products. The organelles and cytoplasm structures were widely protected against the effects of acetaminophen. The present results indicate that acetaminophen has potential cytotoxic effects in rat heptocytes; and olive leaves extract can afford a significant protection against acetaminophen–induced hepatotoxicity.

PS 1180 The Role of TLR-4 in APAP-Induced Organ Damage

M. Ellithi[1], D. Magdy[1], L. Ali[1], M. M. Salama[2, 1], M. Elgamal[2, 1], A. Abdelaziz[4], H. Sheashaa[3] and M. Sobh[3, 1]. *[1]Medical Experimental Research Center, Faculty of Medicine, Mansoura University, Mansoura, Dakahleya, Egypt, [2]Department of Toxicology, Faculty of Medicine, Mansoura University, Mansoura, Dakahleya, Egypt, [3]Department of Nephrology, Urology & Nephrology Center, Mansoura, Mansoura, Dakahleya, Egypt and [4]Pathology, Faculty of Medicine, Mansoura University, Mansoura, Dakahleya, Egypt.*

Acetaminophen (APAP) is the most common cause of acute liver failure in the United States. Beside hepatotoxicity, APAP has a nephrotoxic effect that is not related to its liver induced damage. Pro/anti-inflammatory balance plays critical role in determining the progress of APAP induced hepatotoxicity. TLR4 are major receptors for extracellular histone mediated sterile inflammation, injury and death in mouse model of APAP. The aim of this study was to elucidate the possible role of TLR-4 blockers in preventing APAP induced hepato-renal failure in comparison to conventional antidote (N-Acetyl Cysteine, NAC)
4 groups of C57BL mice were studied (n=6 in each group) vehicle treated [VEH], APAP treated (400 mg/kg ip) [APAP], NAC (204 mg/kg ip 1 h prior to APAP) pretreated plus APAP [NAC+APAP], TAK-242 (TLR-4 blocker, 1mg/kg ip 1 h prior to APAP) pretreated plus APAP [TAK+APAP]. Plasma was collected 4 h after APAP administration. ALT and creatinine levels were measured. Animals were then perfused, liver and kidney were collected and examined histologically with basic H&E staining to detect signs of necrosis and inflammation. APAP treated group showed elevated ALT and creatinine denoting hepatic and renal damage, moreover, these data were confirmed with histological evaluation denoting necrosis both in liver and kidney specimens. TAK+APAP group showed complete protection against the toxic effects of paracetamol on kidney and liver. The NAC treated group showed complete hepatoprotective effects, however, kidney specimens showed mild inflammatory infiltrates compared to the TAK+APAP group. These data provide evidence for the role of TLR-4 in APAP induced organ toxicity. Moreover, it seems that TLR4 may offer supreme protection over conventional APAP antidote [NAC] especially on the level of kidney damage.

PS 1181 Mechanisms of Acetaminophen-Induced Cell Death in Primary Human Hepatocytes

Y. Xie[1], M. R. McGill[1], K. Dorko[1], S. Kumer[2], T. Schmitt[2], J. Forster[2] and H. Jaeschke[1]. *[1]Department of Pharmacology, Toxicology & Therapeutics, University of Kansas Medical Center, Kansas City, KS and [2]Department of Surgery, University of Kansas Medical Center, Kansas City, KS.*

Acetaminophen (APAP) overdose is the most prevalent cause of drug-induced liver injury in western countries. Extensive studies have been conducted to investigate the mechanisms of injury after APAP overdose in various biological models, including mice, rats and hepatoma cell lines. However, it remains ill-defined as to how the injury progresses in humans. Primary human hepatocytes (PHH) represent the gold standard model of studying drug toxicity, and here we investigated APAP hepatotoxicity using freshly isolated PHH, isolated from either unused tissue from donor livers or material from liver resections. PHH were exposed to 5mM, 10mM and 20mM APAP over a period of 48 hours, and multiple parameters were assessed. As evidenced by the release of alanine aminotransferase (ALT), APAP dose-dependently induced significant hepatocyte necrosis starting from 24h, which correlated with the clinical onset of human liver injury after APAP overdose. Interestingly, cellular glutathione was depleted rapidly during the first 3h, which was similar to the murine model. APAP also resulted in early formation of APAP-protein adducts (measured in whole liver homogenate and in mitochondria) and mitochondrial dysfunction as shown by the loss of mitochondrial membrane potential after 12h. Furthermore, APAP time-dependently activated c-Jun N-terminal kinase (JNK). More specifically, JNK phosphorylation occurred in the cytosol within 1h after APAP exposure; phospho-JNK subsequently translocated to the mitochondria. Both pretreatment and co-treatment with JNK inhibitor SP600125 reduced JNK activation and partially attenuated cell death at 24h and 48h after APAP. Our data demonstrate for the first time detailed mechanistic events in human hepatocytes and highlight the crucial role of JNK in the progression of injury after APAP in humans. Thus, the JNK pathway may represent a therapeutic target in the clinic.

PS 1182 Acrolein, a Lipid-Derived Aldehyde Metabolite, Is a Critical Mediator of Alcohol-Induced Endoplasmic Reticulum Stress and Liver Injury

W. Chen[1], J. Zhang[1], C. McClain[1, 2], S. Barve[1] and S. Joshi-Barve[1]. *[1]Department of Medicine/GI, University of Louisville, Louisville, KY and [2]Robley Rex VAMC, Louisville, KY.*

Alcohol is the most socially accepted addictive drug, and it can cause alcoholic liver disease, which is a major cause of morbidity and mortality in the United States. Chronic alcohol consumption causes a pro-oxidant environment in the liver and increases hepatic lipid peroxidation. Acrolein is the most reactive and toxic aldehyde generated through lipid peroxidation. Acrolein is also found in fried fatty foods and is a major component of cigarette smoke, which negatively impacts chronic liver diseases. Acrolein is known to form protein adducts, and we have demonstrated that acrolein triggers endoplasmic reticulum (ER) stress leading to cytotoxicity in hepatocytes. Notably, alcohol-induced ER stress is thought to be an etiologic factor in alcoholic liver disease. This study investigates the hypothesis that acrolein is a major mediator of hepatic ER stress and injury during alcohol consumption.

Acrolein accumulation, activation of pro-apoptotic stress kinase-JNK, ER stress, and apoptotic cell death was examined in vitro in alcohol-exposed rat hepatic cells (H4IIEC), and in vivo in a mouse model of alcohol consumption. Exposure to alcohol led to substantial accumulation of acrolein adducts both in vitro and in vivo. This was accompanied by phospho-activation of JNK and upregulation of ER stress transcription factors ATF3 and ATF4, and the pro-apoptotic protein, GADD153/CHOP. Cellomics analysis revealed that accumulation of acrolein adducts correlated with (i) disruption of mitochondrial membrane potential; (ii) release of free calcium; and (iii) cell death in hepatocytes. This study demonstrates that acrolein is likely to be a major culprit in the ER stress and hepatotoxicity associated with alcohol consumption. Acrolein scavengers may have therapeutic potential in alleviating the adverse effects of alcohol consumption, and we are actively investigating this concept.

PS 1183 Mechanism of Altered Metformin Distribution in Diabetic Nonalcoholic Steatohepatitis

A. L. Dzierlenga, J. Clarke, N. Nelson, S. Werts and N. J. Cherrington. *Pharmacology & Toxicology, University of Arizona, Tucson, AZ.*

Metformin is an anti-hyperglycemic agent that is widely prescribed for type-2 diabetes and is currently being investigated for the treatment of other insulin resistance-related disorders including nonalcoholic fatty liver disease (NAFLD). NAFLD is a highly prevalent chronic liver disease with stages ranging from simple steatosis to nonalcoholic steatohepatitis (NASH). NASH, which contains various cellular stress responses including lipid accumulation, inflammation, oxidative stress and fibrosis, alters transporter expression and drug disposition. Metformin elimination is transporter-dependent, mediated by Oct2, Oct1 and Mate1 in the liver and kidney. The purpose of this study was to determine whether metformin demonstrates altered exposure and tissue distribution in diabetic and NASH mouse models. A single oral dose of [14C] metformin was administered to C57BL6 and diabetic ob/ob mice, each fed either a control diet or a methionine and choline deficient (MCD) diet to model NASH. ob/ob (diabetic) mice exhibited increased hepatic Mate1 and decreased renal Oct1 expression compared to WT, and diet-induced NASH in diabetic mice increased mRNA expression of hepatic Oct1. Both diabetes and NASH decreased Oct2 and Mate1 mRNA expression in the kidney. For metformin distribution, diabetic mice had increased plasma area under the curve (AUC) and liver and kidney metformin levels compared to WT. In both WT and ob/ob strains, the presence of NASH increased metformin exposure, with NASH mice exhibiting increased plasma AUC and muscle concentrations compared to WT, and diabetic NASH mice exhibiting increased plasma AUC, muscle and liver concentrations compared to diabetic alone. Overall, diabetes and NASH additively increased plasma AUC and retention of metformin in liver and muscle compared to WT control. These results indicate that diabetes and NASH alter transporter expression and shift the disposition profile of metformin, potentially increasing the risk of drug toxicity.

PS 1184 Altered Transcription Initiation and Exonization of the First Intron of the Human Liver *ABCC4* Gene in Tissue Specimens from Cases of Acetaminophen Overdose

X. Gu and J. E. Manautou. *University of Connecticut, Storrs, CT.*

Liver injury caused by overdose of the analgesic and antipyretic drug acetaminophen (APAP) is a serious human health problem. The precise molecular events mediating initiation, progression and recovery from APAP liver injury remain unclear. In our previous studies, mRNA and protein induction of the efflux transporter ABCC4 gene was found to be associated with APAP liver injury and recovery. In this study, we examined potential changes in transcription start site (TSS) profile and intronic exonization of the ABCC4 gene in human liver specimens from APAP overdose cases. Using 5'RLM-RACE analysis (RNA ligase mediated rapid amplification of cDNA 5′-end) and genotyping of ABCC4 mRNA intronic exons, we found multiple ABCC4 TSSs distributed in a dispersed fashion in liver samples from APAP overdose patients. Similarly, multiplicity and dispersion of ABCC4 TSSs was also observed in normal livers. However, the frequency and location of ABCC4 TSSs in APAP livers were noticeably different from those in normal livers. We also found two types of ABCC4 mRNA variants with different exonization of intron 1 in both normal and APAP livers. Lower levels of 5' uncapped mRNA variants containing a longer intronic exon, while higher levels of 5'capped mRNA variants containing a shorter intronic exon were identified in APAP livers. This indicates that during APAP toxicity, degradation of ABCC4 mRNA variants containing a longer intronic exon is enhanced while degradation of variants containing shorter intronic exon is repressed. In silico analysis showed that ABCC4 mRNA variants containing the shorter intronic exon encode for a 39-amino acid peptide that is approximately1/35th the length of the full peptide. The biological significance and function of these ABCC4 mRNA variants remains to be further investigated. Taken together, our findings provide new insights into the mechanism of ABCC4 gene regulation at the transcriptional and posttranscriptional level in association with APAP hepatotoxicity. Supported by NIH Grant DK069557.

PS 1185 Nrf2 Protects against Furosemide-Induced Hepatotoxicity

Q. Qu[1, 2], J. Liu[1], H. Zhou[2] and C. D. Klaassen[1]. [1]*Department of Internal Medicine, University of Kansas Medical Center, Kansas City, KS and* [2]*Institute of Clinical Pharmacology, Xiangya Medical School, Central South University, Changsha, Hunan, China.*

Furosemide is a diuretic drug, but its reactive intermediates lead to acute liver injury in mice. Given the essential role of Nrf2 as a cellular defense regulator, we investigated whether Nrf2 would protect against furosemide-induced liver injury using the Nrf2 "gene-dose response" mice model (Nrf2-null, wild-type, Keap1-KD and Keap1-HKO mice). Twenty-four hour after furosemide administration (250mg/kg, i.p.), serum ALT activities and histopathological analysis indicated severe hepatotoxicity in Nrf2-null and WT mice, but significantly less in the Nrf2-overexpresed Keap1-KD and Keap1-HKO mice. Furosemide increased the mRNA of genes involved in the acute phase response (Ho-1 and MT-1), ER stress (Chop10 and Gadd45), inflammatory cytokine (IL-1β), chemokines (Mip-2 and mKC), as well as apoptosis (Egr1 and Bax) in livers of Nrf2-null and wild-type mice, but increased less in mice with more Nrf2. The two genotypes of over-expressed Nrf2 mice had increased expression of the Nrf2 target genes Gclm, Gclc and Nqo1 prior to furosemide administration, and were increased further after furosemide administration. Thus, our findings provide strong evidence that over-expression of Nrf2 in Keap1-KD and Keap1-HKO mice and the increases in mRNA of a number of genes involved in anti-oxidative stress, anti-inflammation, anti-ER stress and anti-apoptosis protect against furosemide-induced hepatotoxicity.

PS 1186 Acetaminophen (APAP)-Induced Hepatic Protein Modifications in Liver and Mitochondria of C57/Bl6 Mice Are Reduced by S-Adenosylmethionine (SAMe)

A. Schnelle[2], M. S. Wright[1], H. Hedrick[1], J. Brown[1], J. G. Ball[1] and M. Valentovic[1]. [1]*Pharmacology, Physiology and Toxicology, Marshall University School of Medicine, Huntington, WV and* [2]*Wheeling Jesuit University, Wheeling, WV.*

Hepatotoxicity is associated with an overdose of the antipyretic drug, acetaminophen (APAP). APAP toxicity requires biotransformation to a toxic metabolite and increased oxidative stress. S-Adenosylmethionine (SAMe) protects mice from APAP overdose. The overall hypotheses for this study is that SAMe reduces APAP hepatic toxicity by preventing oxidative stress and post-translational modifications of proteins including the antioxidant enzyme, Manganese Superoxide Dismutase (MnSOD). Male C57Bl/6 mice were divided into 4 groups (N=5-10/group) and injected intraperitoneal (ip) as indicated: vehicle (VEH, 15 ml/kg water ip), SAMe (1.25 mmol/kg 5 ml/kg ip), APAP (250 mg/kg ip), SAMe and APAP (SAMe administered 1h after APAP). Livers were collected 4 h following APAP. Subcellular fractions were isolated from mitochondria and cytosol. Equal amounts of protein were processed for Western analysis and immunoprecipitation. SAMe administered 1 h after APAP reduced APAP hepatic toxicity when measured 4 h post APAP injection. Protein carbonylation was increased by APAP and attenuated by SAMe. 3-Nitrotyrosine (3-NT) formation was increased in mitochondria by APAP and reduced by SAMe. Mitochondrial MnSOD nitrosylation was increased by APAP and reversed in the APAP+SAMe group. In conclusion, APAP induced protein carbonylation and nitrosylation of proteins which was reversed by SAMe treatment 1 h post APAP. (Supported by NIH Grant 5P20RR016477 to the West Virginia IDeA Network for Biomedical Research Excellence).

PS 1187 Hepatic Vascular Endothelial Dysfunction in Environmental Toxin-Induced Nonalcoholic Steatohepatitis Is Regulated by TLR4-miR21-GRHL3 Axis

S. Das, R. K. Seth and S. Chatterjee. *University of South Carolina, Columbia, SC.*

The liver sinusoidal endothelium is very specialized and phenotypically differentiated. The aims of this study were to investigate the role of TLR4-linked upregulation of miR21 and its effect on the target: grainyhead-like 3 (GRHL3), in inducing the changes in liver histology and liver microvasculature. We used a murine model of environmental toxin-induced nonalcoholic steatohepatitis (NASH) where diet-induced obese (DIO) mice were exposed to disinfection byproduct bromodichloromethane (BDCM). In addition, CYP2E1 and TLR4 gene deleted mice (KOs), exposed to BDCM were used for the study; to establish the role of metabolic

oxidative stress and TLR4 in hepatic endothelial dysfunction. qRTPCR was used to detect the changes in mRNA levels for vascular endothelial dysfunction markers, GRHL3 (regulates eNOS phosphorylation and hence endothelial dysfunction), TLR4; and in levels of miR21 (targets GRHL3). Western blot, oil red O, H&E, immunofluorescence staining and microscopic techniques were also used to reach the experimental endpoints. mRNA and protein levels for vascular endothelial dysfunction markers were significantly increased in DIO+BDCM group compared to DIO, CYP2E1 KO and TLR4 KO groups. GRHL3 protein expression was significantly decreased (implying degradation of mRNA by miR21); whereas miR21 and TLR4 mRNA levels were significantly increased in DIO+BDCM group compared to DIO, CYP2E1 KO and TLR4 KO groups. The mRNA levels of inflammatory markers were significantly high in DIO+BDCM group compared to the other groups. CYP2E1 KO and TLR4 KO mice were protected from hepatic vascular endothelial dysfunction along with other NASH pathology as evidenced by decreased inflammation. In summary, our finding for the first time identifies the role of TLR4-miR21-GRHL3 axis in modulating hepatic vascular endothelial dysfunction and resultant inflammation. This forms a basis for a potential therapeutic target in the treatment of environmental toxin-induced NASH. (4R00ES019875-02 to Saurabh Chatterjee).

PS 1188 Serum and Hepatic Fibroblast Growth Factor 21 Levels Are Increased in Subjects with Alcoholic Liver Diseases and in Mice Exposed to Alcohol by Decreased Transcriptional Suppression

C. Zhao[1], Y. Liu[1], K. C. Falkner[2], M. Cave[1, 2], C. McClain[1, 2] and W. Feng[1, 2]. [1]*Hepatology and Nutrition, University of Louisville, Louisville, KY and* [2]*Pharmacology & Toxicology, University of Louisville, Louisville, KY.*

Liver-derived FGF-21 is a novel metabolic regulator of glucose and lipid metabolism. Alcohol exposure affects lipid metabolism by increasing lipogenesis and decreasing fatty acid β-oxidation. However, it is currently unknown whether alcohol exposure affects FGF-21 expression. Serum FGF-21 levels were measured in 24 consenting human subjects with severe acute alcoholic hepatitis, 20 patients with alcoholic cirrhosis, and 9 subjects with alcohol abuse, and were compared to 26 healthy, non-drinking controls by ELISA. C57BL/6 mice were fed Lieber DeCarli diet containing 5% alcohol or maltose dextrin for 4 weeks (chronic), or for 12 days and then given one dose of alcohol at 6 g/kg by gavage 6 hours before sacrificing (chronic-binge), or only one dose of alcohol by gavage (acute). Serum and hepatic FGF-21 levels and hepatic FGF-21 mRNA levels were measured. Liver triglyceride and serum FFA were also measured. Serum levels of FGF-21 were markedly increased in both human subjects with ASH and alcohol abusers without ALD, but unchanged in AC vs. non drinking controls. Serum levels of FGF-21 were also markedly increased in mice exposed to alcohol, and the hepatic expression of FGF-21 were increased by both mRNA and protein levels. The increased FGF-21 expression was positively correlated with increased hepatic levels of triglyceride and serum levels of FFA. The expression of PGC-1α and Rev-Erbα, which are important transcription suppressors of FGF-21, were decreased in mouse livers exposed to alcohol. Alcohol exposure increased hepatic and circulating FGF-21 expression likely through an inhibition of transcriptional suppression mediated by the PGC-1α-Rev-Erbα pathway. The regulation of FGF-21 expression may be associated with hepatic lipid metabolism in alcoholic steatohepatitis. The observed increase in circulating FGF-21 was conserved between animal models and human subjects with ALD.

PS 1189 FGF21 Deficiency Exacerbates Chronic Alcohol-Induced Fatty Liver Disease

Y. Liu, C. Zhao, M. Zhang, C. McClain and W. Feng. *University of Louisville, Louisville, KY.*

Alcoholic fatty liver disease (AFLD), is considered as the earliest pathological alteration in ALD. Studies demonstrated that inhibition of fat accumulation and promotion of fat clearance prevents hepatic steatosis and slows or halts the progression of ALD. Previous studies have identified extrahepatic hormones are important in alcohol-induced alteration in liver lipid metabolism, little is known whether the paracrine and endocrine signal for metabolic regulation of hepatic itself participates in alcohol exposure associated lipid accumulation. Fibroblast growth factor 21 (FGF21) is a member of the endocrine FGF subfamily and a major metabolic regulator, which plays a critical role in the glucose and lipid metabolism. Here we demonstrated that FGF21 deficiency exacerbate chronic alcohol-induced AFLD. Global FGF21 knockout mice and their controls were fed Lieber deCarli diet containing 5% alcohol or pair-fed isocaloric diet for 4 weeks. Alcohol feeding increased hepatic fatty acid and triglyceride contents and fat accumulation. There was no obvious alteration in hepatic fat accumulation in FGF21 deficiency mice under pair feeding. However, a markedly increased hepatic fat was detected in FGF21 knockout mice when fed chronic alcohol. Further studies showed that FGF21 deficiency exacerbated alcohol-induced liver injury. The FGF21 exacerbated-fat accumulation was associated with upregulation of the genes involved in fatty acid de novo synthesis, such as FAS and SCD-1, and the decrease in the gene expression responsible for fatty acid β-oxidaton, such as CPT-1. Mechanistic studies showed that FGF21 knockout decreased SIRT1 which deacetylates SREBP-1c. In addition, we showed that FGF21 deficiency also decreased LKB1 which activates AMPK. The downregulation of SIRT1 and LKB1/AMPK in FGF21 deficiency livers of mice exposed to chronic alcohol leads to SREBP-1c- and PGC-1a-mediated increased fatty acid synthesis and decreased fatty acid β-oxidation. In conclusion, FGF21 is likely required for cellular defense against hepatic lipogenesis and cellular capacity for fat clearance in subjects exposed to chronic alcohol.

PS 1190 Uric Acid Inhibits Lipid Metabolism through Suppression of Autophagy

K. Lee[1], Y. Choi[1], S. Oh[2] and B. Lee[1]. [1]*College of Pharmacy, Seoul National University, Seoul, Republic of Korea and* [2]*Research Center for Oral Disease, Regulation of the Aged, College of Dentistry, Chousn University, Gwangju, Republic of Korea.*

Fructose which is reported to be lipogenic is rapidly phosphorylated to fructose-1-phosphate by fructokinase using ATP. It results in AMP accumulation causing activation of AMP deaminase and generation of uric acid. Patients with hyperuricemia or gout usually accompany hypertriglyceridaemia and hyperuricemia is also prevalent in patients presenting nonalcoholic fatty liver disease (NAFLD) that develops hepatic steatosis in the lack of alcohol abuse. In this context, we hypothesized that uric acid which comes from the fructose metabolism promote triglyceride accumulation and development of fatty liver. Today, it is widely accepted that fatty liver mainly results from increased de novo lipogenesis, increased transport of triglyceride into the liver and decreased lipolysis. In this paper, we tried to characterize the role of uric acid in lipolysis. A newly found function of autophagy is the degradation of lipid droplets in hepatocytes. Accordingly, we hypothesized that uric acid contributes to the pathogenesis of development of fatty liver by regulation of autophagy. We found that uric acid inhibits autophagy in concentration- and time- dependent manner in HepG2 cell line. Although uric acid did not suppress the expression of autophagy related proteins but activated Akt followed by inhibitory phosphorylation of TSC2, subsequently increased phosphorylation of mTOR and decreased autophagy. It is well known that starvation-induced autophagy degrades lipid droplet and releases fatty acids for mitochondrial β-oxidation. Pretreatment of uric acid suppressed starvation-induced autophagy and decreased intracellular lipid utilization by starvation. In addition, long-term treatment of uric acid itself increased intracellular lipid content and cells incubated with oleate in the presence of uric acid deposited more lipid than those only treated with oleate. In conclusion, this study first demonstrated a novel mechanism that uric acid regulates lipid metabolism through suppression of autophagy.

PS 1191 Platelet Function Inhibits Liver Injury and Fibrosis Induced by a Bile Duct Toxicant

N. Joshi[1], A. K. Kopec[2], K. L. Towery[2], H. Cline[2], K. Williams[2], M. J. Flick[3] and J. P. Luyendyk[2]. [1]*Phm & Tox, Michigan State University, East Lansing, MI,* [2]*Pathobiology & Diag Inv, Michigan State University, East Lansing, MI and* [3]*Division of Experimental Hematology and Cancer Biology, Cincinnati Children's Hospital Medical Center, Cincinnati, OH.*

Chronic liver disease in humans and animal models is associated with hemostatic changes including platelet activation and deposition of cross-linked fibrin in the liver. Previous studies have suggested that hepatic platelet accumulation inhibits liver fibrosis and promotes liver repair. Complete fibrin(ogen) deficiency worsens liver injury in mice with chronic liver disease. However, the pathways linking coagulation to platelet activation during chronic liver disease are not known. We hypothesized that elements of platelet activation and function, including thrombin mediated protease activated receptor (PAR)-4 signaling and fibrin engagement of the αIIBβ3 integrin on platelets inhibit hepatocellular injury and fibrosis in a mouse model of xenobiotic-induced chronic liver injury and fibrosis. To test this hypothesis,mice expressing a mutant form of fibrin(ogen) incapable of binding αIIBβ3 (FibγΔ5 mice) and mice lacking PAR-4 (PAR-4-/- mice) were used. FibγΔ5 mice, PAR-4-/- mice and wild-type (WT) mice were fed a purified diet (AIN-93M) containing the bile duct toxicant alpha-naphthylisothiocyanate (ANIT) (0.025%), or control diet (AIN-93M) for four weeks. PAR-4 deficiency did not increase liver necrosis in mice fed ANIT diet. However, compared to WT mice, portal inflammation and peribiliary fibrosis increased significantly in PAR-4-/- mice fed ANIT diet. Focal hepatocellular necrosis and serum alanine aminotransferase activity were markedly increased in FibγΔ5 fed ANIT diet compared to WT mice and this corresponded with a significant induction of profibrogenic genes and increased depo-

sition of type 1 collagen protein in FibγΔ5 mice on ANIT diet. The results indicate that thrombin dependent platelet activation via PAR-4 and fibrin-αIIBβ3 integrin engagement are hepatoprotective in this model of chronic liver injury and fibrosis.

PS 1192 The RHO-Kinase Pathway Plays a Major Role in the Bile Canalicular Lumen Contraction Observed in Chlorpromazine-Induced Cholestasis

C. Guguen-Guillouzo[1, 2], A. Sharanek[2], P. Bachour El Azziz[2], R. Le Guevel[3] and A. Guillouzo[2]. [1]*Research and Development, Biopredic International, St Gregoire, Brittany, France,* [2]*INSERM 991, Rennes University, Rennes, France and* [3]*ImPACcell BIOSIT, Rennes University, Rennes, France.* Sponsor: M. Robin.

Effects of chlorpromazine (CPZ), known to induce intra-hepatic cholestasis have been analyzed using differentiated human HepaRG cells. Bile acids efflux and influx have previously been reported to be inhibited by CPZ. These changes correlated with occurrence of a strong contraction of the bile canalicular lumen (BCL). In this work we attempted to define the molecular mechanisms involved in BCL morphogenesis and reorganization in CPZ-treated HepaRG cells by imaging analyses. We observed that BCL contraction was a dose-dependent morphogenic process associated with a reduction to 2, in the number of cells clustered to form each bile canaliculus (BC), involving extensive cytoskeleton reorganization. These changes were correlated with the RHO-kinase (ROCK) pathway induction as also argued by the antagonized effects obtained with various inhibitors of this pathway. Addition of ROCK inhibitor to normal cells resulted in the development of enlarged apical lumen that shared 3 or more cells per single BC and lined with a dense F-actin network. Similar remodeling of the apical lumen of CPZ-treated cells exposed to ROCK inhibitor was observed. Using ETA, a ROCK inducer, we reversed the apical lumen remodeling to small lumen with only 2 or 3 clustered cells, thus mimicking CPZ-treated cells. In addition, inhibition of the myosin heavy chain ATPase by BDM, a down-stream ROCK target controlling contraction by actin-myosin interactions, mimicked the reorganization induced by ROCK inhibitor of the large canalicular lumen by increasing the number of cells sharing a single BC. Taken together, these results demonstrate that HepaRG hepatocytes can rapidly respond to the main factors modulating the ROCK pathway and identified as controlling the BCL morphogenesis. They highlight the critical role of this pathway in CPZ-induced cholestasis. Understanding of these control mechanisms should help development of liver-cell based therapies.

PS 1193 Mechanisms of Cholestasis Induced by Cyclosporin A in Human HepaRG® Cells

A. Guillouzo[1], A. Sharanek[1], P. Bachour El Azziz[1] and C. Guillouzo[2]. [1]*Inserm U991, University of Rennes, Rennes, France and* [2]*Research & Development, Biopredic International, Sant-Gregoire, France.* Sponsor: M. Robin.

Cyclosporin A (CsA) and tacrolimus (FK506) are powerful immunosuppressants widely used in organ transplantation. CsA is known to cause dose-dependent hepatotoxic effects characterized by an increase in bile salts levels, hyperbilirubinemia and cholestasis. By contrast, FK506 has been reported to cause only rare cases of cholestasis. Ambiguity remains regarding early and delayed effects of CsA. In this study, human HepaRG® hepatocytes were used to investigate the mechanisms involved in CsA-induced alterations of both influx and efflux of bile acids and a comparison was made with the effects caused by FK506. The earliest CsA effect was observed on efflux activity. As early as 15min after addition of 10μM CsA efflux of taurocholic acid (TA) was inhibited with a maximum after 2h and this inhibition was totally reversible after 4h. However, it became irreversible with higher CsA concentrations (≥ 50μM). The involvement of the protein kinase C-p38 pathway in the cholestatic effects was demonstrated by the use of specific inhibitors and phosphorylation of p38. At high concentrations (≥50μM) pericanalicular distribution of F-actin was altered and related to constriction of bile canaliculi. Inhibition of TA efflux by high CsA concentration was mostly prevented by N-acetyl cysteine or 4-phenyl butyric acid co-treatment, indicating a major role of oxidative and endoplasmic reticulum stresses. Compared to the efflux inhibition a delayed reduction of Na+-dependent taurocholate influx was also found with a maximum inhibition after 2h. It was completely reversible with low CsA concentrations (≤10μM) after 4h while no reversion was observed with concentrations ≥50μM. Comparatively, FK506 did not exert any cholestatic at low concentration (≤10μM) whereas a much lower inhibition of TA efflux than with CsA was detected at 50μM. In summary, our results bring new insight on the mechanisms involved in CsA-induced cholestasis and the absence of effects of FK506, at low concentrations, agrees with clinical data.

PS 1194 *Lactobacillus rhamnosus* GG Culture Supernatant Treatment Attenuates Alcohol-Induced Fat Accumulation in the Liver by Enhancing AMPK-Mediated Fatty Acid Oxidation

M. Zhang, C. Wang, C. Wang, Y. Wang, Y. Liu, C. McClain and W. Feng. *University of Louisville, Louisville, KY.*

Probiotic species produce biologically active compounds that can modulate mucosal integrity and prevent pathogen-induced intestine leakage. Our previous study showed that *Lactobacillus rhamnosus* GG culture supernatant ameliorated acute alcohol-induced intestinal permeability and liver injury. However, whether LGGs administration prevents chronic alcohol exposure-induced liver injury is unknown. The purpose of this study was to examine whether LGGs provides a protective effect and explore the underlying mechanism in chronic-induced liver injury in mice. Mice were fed Lieber DeCarli diet containing 5% alcohol for 4 weeks, and LGGs was administered at a dose of equivalent to 109 CFU/mouse with alcohol. LGGs decreased chronic alcohol-induced liver injury evaluated by measuring the activity of ALT and AST in plasma. Alcohol-induced hepatic steatosis was prevented by LGGs treatment as evaluated by triglyceride content measurement and Oil Red O staining of the liver sections. In addition, alcohol exposure also increased circulation and hepatic free fatty acid concentration, which is attenuated by LGGs treatment. Further study demonstrated that alcohol induced a significant decrease in AMPK and ACC phosphorylation, and these effects were prevented by LGGs administration in animals, which is correlated with the increase of the expression of adiponectin receptors. We also found that alcohol exposure increased hepatic SREBP-1c protein expression and LGGs treatment inhibited this increase. Further studies showed that LGGs prevented alcohol-induced hepatic apoptosis as evaluated by TUNEL assay. In vitro studies confirmed the positive effects of LGGs in promoting AMPK phosphorylation. These results suggest that LGGs is effective in preventing chronic alcohol-induced liver injury by suppression of alcohol-induced hepatic apoptosis and steatosis through AMPK phosphorylation. This finding could lead to developing new strategies for reducing chronic alcohol-induced liver injury by secreted factors of LGG culture.

PS 1195 Leflunomide Cytotoxicity in Hepatic Cells Involves Mitogen-Activated Protein Kinase Activation, Endoplasmic Reticulum Stress, and Mitochondrial Dysfunction

J. Xuan[1], T. Qing[2], S. Chen[1], A. Iyer[3], L. Couch[1], L. Shi[2, 1] and L. Guo[1]. [1]*Division of Biochemical Toxicology, National Center for Toxicological Research/U.S. Food and Drug Administration, Jefferson, AR,* [2]*School of Pharmacy, Fudan University, Shanghai, China and* [3]*University of Maryland, Baltimore, Baltimore, MD.*

Leflunomide, an anti-inflammatory drug used for the treatment of rheumatoid arthritis, has been marked with a black box warning regarding an increased risk of severe liver injury. Thus far, however, the mechanisms underlying leflunomide-associated hepatotoxicity remain unknown. Here, we performed a comprehensive study of leflunomide-induced cytotoxicity in HepG2 cells. Our data showed that leflunomide started to exhibit significant cytotoxicity at 125μM and 250 μM within 6 h, as measured by ATP content and LDH release, respectively. At toxic concentrations, leflunomide markedly upregulated the expression of TNF-alpha and activated stress signaling ERK1/2, JNK and p38 pathways. Concurrently, multiple markers of endoplasmic reticulum (ER) stress were activated, leading to cell death. Notably, the expression of eIF2α, ATF3, Gadd153/CHOP, and pro-apoptotic proteins, such as Bip, Bik, Bak and Bax, were dramatically increased. Leflunomide-induced cell death was attenuated by ER stress and ERK1/2 inhibitors. Moreover, leflunomide induced mitochondrial permeability transition, which was blocked by bongkrekic acid (BA), a specific inhibitor of adenine nucleotide translocator. Leflunomide exposure also caused ATP depletion and LDH release in HepG2 cells in a dose- and time-dependent manner, both of which were attenuated by BA. Additionally, significant differences were observed in leflunomide toxicity between cells grown in glucose- and galactose-supplemented media, suggesting an important role of mitochondria dysfunction in leflunomide-induced cytotoxicity. Our study defines fundamental mechanisms of leflunomide-associated hepatotoxicity, which may be a consequence of a cross-talk between several critical events involved in cell death.

PS 1196 Intracellular Signaling and Inflammation in the Mechanism of Furosemide Hepatotoxicity

H. Jaeschke, M. R. McGill, C. D. Williams and M. Bajt. *Pharmacology, Toxicology, and Therapeutics, University of Kansas Medical Center, Kansas City, KS.*

Furosemide (FS) is a common diuretic. Though safe when used appropriately, it is increasingly popular as a model hepatotoxicant, due in part to the fact that the histological pattern of injury resembles acetaminophen but it does not appear to involve mitochondrial dysfunction. Despite this, the mechanisms of FS-induced liver injury are unclear. It was shown that a reactive metabolite binds to proteins, and that inhibition of P450s prevents the toxicity. Beyond this, however, little is known. To explore the mechanisms of FS hepatotoxicity, we treated mice with 500 mg/kg FS and collected plasma and livers at various time points to probe for evidence of activation of cell signaling pathways. In animals with liver injury, plasma ALT increased by 6h (246±46 U/L) and was constant until at least 12h (151±15 U/L). Interestingly, ALT dramatically increased at 24h (2,241±695 U/L). Histology and TUNEL staining revealed spotty necrosis at early time points, which developed into widespread centrilobular necrosis. Immunoblotting for caspase-3 failed to provide evidence for apoptosis, and cytochrome c release into cytosol did not increase before 24h, consistent with the idea that FS toxicity does not involve mitochondrial damage. Nevertheless, JNK phosphorylation and translocation to mitochondria were observed at 6h and persisted. RIP3, which may be involved in JNK signaling, was induced by 6h. Because of the unusual time course showing an initial injury with a delayed increase, we also stained liver sections for neutrophils. Interestingly, we observed neutrophil infiltration by 6h, but the most infiltration was seen at 24h. Finally, we observed an increase in cell death (LDH release) in metabolically-competent human liver cells (HepaRG) treated with FS. Conclusions: Large doses of FS cause injury in both mice and human HepaRG cells. The mechanism of hepatotoxicity in mice may involve intracellular signaling pathways at early time points, followed by inflammation at later times.

PS 1197 Contribution of PAR-4 and Thrombin to Acetaminophen Hepatotoxicity in Mice

K. Miyakawa[1, 2], B. P. Sullivan[1], R. P. Albee[3], R. Singhal[2, 3], M. A. Scott[1], J. P. Luyendyk[1, 2], P. E. Ganey[2, 3] and R. A. Roth[2, 3]. *[1]Pathobiology and Diagnostic Investigation, Michigan State University, East Lansing, MI, [2]Center for Integrative Toxicology, Michigan State University, East Lansing, MI and [3]Pharmacology and Toxicology, Michigan State University, East Lansing, MI.*

Acetaminophen (APAP) hepatotoxicity is the main cause of acute liver failure in many countries, yet treatment options remain limited. APAP-induced liver injury in humans and in mouse models is associated with coagulation cascade activation and thrombocytopenia, both of which can be marked. We found that depleting blood platelet concentration (by antiCD41 antibody) can reduce APAP hepatotoxicity and thrombin generation. Protease-activated receptor-4 (PAR-4) is a thrombin receptor on mouse platelets, and when platelets are activated, they can contribute to thrombin generation. We hypothesized that PAR-4 and thrombin generation play important roles in APAP hepatotoxicity in mice. Wild-type and PAR-4-/- mice were treated with APAP (300 mg/kg ip). Hepatic platelet accumulation (quantified by immunolabeling) and thrombin generation (detected as increased thrombin-antithrombin complex in plasma) were significantly decreased at 2 h, and liver injury at 6 h and 24 h was markedly reduced in APAP-treated PAR-4-/- mice compared to APAP-treated wild-type mice. These findings suggest that amplification of thrombin generation is related to PAR-4-dependent platelet activation in APAP-treated mice. To determine the role of thrombin in APAP-mediated liver damage, mice were given the thrombin inhibitor lepirudin (1 mg/kg i.p. 30 min before and after APAP injection and every 2 h thereafter); lepirudin significantly reduced hepatocellular injury at 6 h in APAP treated mice. Therapeutic intervention with lepirudin beginning 1.5 h after APAP administration also reduced the liver injury. These results indicate that platelets and PAR-4 contribute to amplification of thrombin generation and to the progression of liver injury from APAP overdose and suggest that platelet-directed intervention might provide adjunctive therapy in APAP poisoning cases. (Supported by NIH grant R01DK087886.)

PS 1198 Hepatic Toxicological and Lipid Peroxidation Assessments of Pioglitazone on Albino Wistar Rats

O. O. Olubanke[1], O. E. Ogunlana[2], U. K. Stanley[1], J. A. Olagunju[3] and A. A. Akindahunsi[4]. *[1]Department of Biological Sciences, Covenant University, Ota, Ogun, Nigeria, [2]Department of Biological Sciences, Crawford University, Igbesa, Ogun, Nigeria, [3]Department of Medical Biochemistry, Lagos State University, Ikeja, Lagos, Nigeria and [4]Department of Biochemistry, Federal University of Technology, Akure, Ondo, Nigeria.*

Pioglitazone is one of the thiazolidinedione anti-diabetic drugs which have been used for the treatment of non-insulin dependent diabetes mellitus. This work aims at studying the hepatic toxicity of pioglitazone (PIO) when administered in various high concentrations in female albino Wistar rats. Four groups of seven animals each were treated with test substances for twenty eight days. Group one was given 0.5 ml distilled water, while groups 2 to 4 were given 15 mg/kg, 30 mg/kg and 45 mg/kg of body weight of PIO respectively. Using standard biochemical kits and reported chemical procedures, hepatic biochemical, histological and lipid peroxidation assessments of PIO were determined in the plasma of experimental animals. There was no significant change in aspartate aminotransaminase (AST), alanine aminotransaminase (ALT), alkaline phosphatase (ALP), total and direct bilirubin and malondialdehyde concentrations in pioglitazone-treated groups when compared to control($p<0.05$). Pioglitazone did not elicit any noticeable liver toxicity at the experimental doses used in the study in non-diabetic animal model
Email: banke.ogunlana@covenantuniversity.edu.ng
Key words: Pioglitazone; hepatic biochemical parameters; Lipid peroxidation

PS 1199 NSAIDs Synergize with Inflammatory Cytokines to Kill Hepatocytes: Implications in Idiosyncratic Reactions

A. Maiuri[1, 2], L. Gora[1], R. Parkins[3], P. E. Ganey[1, 2] and R. A. Roth[1, 2]. *[1]Pharmacology and Toxicology, Michigan State University, East Lansing, MI, [2]Center for Integrative Toxicology, Michigan State University, East Lansing, MI and [3]College of Veterinary Medicine, Michigan State University, East Lansing, MI.*

Idiosyncratic drug-induced liver injury (IDILI) occurs in a small fraction of patients taking a drug and, although rare, can result in severe liver injury or death. The mechanisms of IDILI are unknown; however, factors resulting from an activated immune system are likely to be important in the pathogenesis. The inflammatory mediators, tumor necrosis factor-alpha (TNF) and interferon-gamma (IFN) are two such factors that can activate pathways to cell death as well as proliferation. We tested the hypothesis that non-steroidal anti-inflammatory drugs (NSAIDs) associated with IDILI in humans synergize with TNF and/or IFN to cause death of hepatocytes and inhibit cell proliferation in vitro. HepG2 cells were treated with NSAIDs that have high IDILI liability (diclofenac, sulindac sulfide, bromfenac, or nimesulide) and NSAIDs with less IDILI liability (naproxen, ibuprofen, rofecoxib, and aspirin) alone and in combination with TNF and/or IFN. Treatment of cells with drugs with high IDILI liability in the presence of TNF resulted in cytotoxicity. IFN potentiated the cytotoxicity caused by diclofenac, sulindac sulfide, and bromfenac in the presence of TNF. Naproxen and ibuprofen synergized with TNF to cause cytotoxicity in HepG2 cells, but IFN did not affect the response to any of the drugs with low IDILI liability. Treatment of cells with diclofenac in the presence or absence of TNF and IFN inhibited proliferation of HepG2 cells. These data indicate that NSAID-induced hepatocellular stress interacts with TNF and IFN to cause cell death and inhibit proliferation. Given that failure of proliferative repair could magnify modest liver damage, these findings raise the possibility that some IDILI reactions result from such drug-cytokine synergy. (Supported by NIH grant DK061315 and T32 GM092715).

PS 1200 Elevation of Serum Transaminases Due to CSF1-R Inhibition

K. Ghoreishi, J. Piccotti, M. Breider, R. Magpantay, B. D. Jeffy, K. Tang and Z. Tong. *Celgene, San Diego, CA.*

Serum biomarkers such as alanine aminotransferase (ALT) and aspartate aminotransferase (AST) are well-characterized hepatotoxicity biomarkers that correlate well with liver histopathology. However, it has been reported that colony stimulating factor-1 receptor (CSF1-R) inhibition results in decreased proliferation, differentiation and function of macrophages, leading to decreased clearance of serum transaminases. In support of this observation, we previously demonstrated increases in serum AST in the absence of histopathology following treatment of rats with CC0485118, a small molecule kinase inhibitor of spleen tyrosine kinase (Syk) that also inhibits CSF1-R. In the current study, we investigated the effect of CSF1-R inhibition by CC0485118 on AST clearance in serum. Jugular vein cannulated (JVC) Sprague-Dawley rats were dosed with 400 mg/kg of CC0485118

for 4 consecutive days via oral gavage. On last day of treatment, rats were injected intravenously with 200 μl of purified rat AST. Serial blood samples were collected at baseline and up to 24 hours post-injection. In this study, clearance of AST in test article-treated animals was approximately 50% of vehicle-treated animals. Similar findings were seen in a subsequent study using radiolabeled rat AST, indicating that the increases in AST were due to deceased clearance and not increased production. This mechanism was further investigated in vitro using rat hepatocyte-Kupffer cell co-cultures treated with increasing concentrations of CC0485118 (10, 50, or 100 μM) to evaluate compound effect on the phagocytic function of Kupffer cells. Results showed that 50 μM or higher of CC0485118 attenuated the uptake of S. aureus bioparticles compared to vehicle alone. The inhibition was not due to compound toxicity as assessed by ATP assay. The evidence of in vitro inhibition of Kupffer cell function and in vivo AST clearance attenuation related to CC0485118, supports the hypothesis that the elevation of AST is caused by decreased phagocytic activity by liver macrophages.

PS 1200a Regorafenib at Clinically Relevant Concentrations Impairs Mitochondrial Functions Causing Necrosis in Primary Rat Hepatocytes

Q. Shi, Z. Weng and Y. Luo. *Division of Systems Biology, National Center for Toxicological Research, US FDA, Jefferson, AR.*

Regorafenib, a kinase inhibitor, was recently approved by regulatory agencies for cancer treatment. Based on clinical trial data, a black box warning about regorafenib-induced hepatotoxicity was included in the FDA-endorsed product label at the time of market approval. The mechanism for regorafenib associated hepatotoxicity is unknown. Isolated rat liver mitochondria or primary hepatocytes were incubated with regorafenib. Oxygen consumption was determined using a Clark electrode. Mitochondrial permeability transition (MPT) was measured by a swelling assay and the fluorescent dye calcein. Mode of cell death was determined by annexin V/propidium iodide staining supplemented with measuring lactate dehydrogenase leakage and caspase activation. In isolated mitochondria, regorafenib significantly uncoupled (but did not inhibit) oxidative phosphorylation (OXPHOS) and promoted calcium overload-induced mitochondrial swelling, with the latter being completely preventable by cyclosporin A (CsA). In primary hepatocytes, regorafenib caused strong uncoupling of OXPHOS, a rapid onset of MPT, a sharp decrease in mitochondrial inner membrane potential, a significant adenosine triphosphate (ATP) shortage, and ensuing necrosis (but not apoptosis). Pretreatment by MPT blockers CsA and trifluoperazine, or the glycolysis enhancer fructose plus the mitochondrial ATPase inhibitor oligomycin A, or their combination, significantly delayed the onset of necrosis. Remarkably, all detrimental effects were observed at clinically-relevant concentrations of 2-15 μM, which were in the range of maximal blood concentrations achieved after taking recommended daily doses. The data demonstrate that regorafenib causes necrosis in primary hepatocytes by uncoupling OXPHOS and MPT induction, indicating that mitochondrial damage possibly contributes to the pathogenesis of regorafenib-induced hepatotoxicity.

PS 1200b Targeted Serum Bile Acid Profile of Naïve Rats and Dogs over a 24h Time Course

R. Morgan[1], J. Maher[2], S. Cepa[2], C. Sensenhauser[3], D. Potter[4], L. Webster[5], K. Olson[5], M. Ameri[1], K. Stocking[1], M. Higgins[1], N. King[6] and J. Lawrence[1]. *[1]Toxicology, Amgen, Newbury Park, CA, [2]Toxicology, AbbVie, Chicago, IL, [3]DMPK, JNJ, Spring House, PA, [4]Statistics, Pfizer, Groton, CT, [5]GSK, DMPK, RTP, NC and [6]PSTC, Critical Path Institute, Tucson, AZ.*

DILI is a leading cause of attrition during drug development. Most DILI cases are rare and idiosyncratic. Inhibition of BSEP in humans is considered a susceptibility factor for DILI. Mutations in BSEP resulting in complete loss of function yield a severe form of cholestasis. In contrast, only mild evidence of cholestasis is observed in rodents with similar mutations. Further, rodents are typically insensitive to DILI with agents known to inhibit human BSEP in vitro. Although in vitro models exist to screen for BSEP inhibition, a biomarker to confirm this in vivo would be valuable. A non-invasive translatable biomarker would enable monitoring for BSEP inhibition and contribute to the development of a dataset that would clarify the role of BSEP inhibition in human DILI. Serum bile acid (BA) profiling using LCMSMS is being applied to discover such a biomarker. Baseline BA profiles were acquired for naïve rats and dogs, over a 24h time course, in four separate studies (2 rat, 2 dog). Serum was also collected for a limited clinical chemistry panel. There were no significant diurnal changes in BA or clinical chemistry parameters in naïve animals over a 24h time course. In one dog study, food was returned 6h post study initiation, and blood was collected 8h post. The 8h time point showed significant elevations in taurine-conjugated BA, ranging from 6–15 fold increase relative to fasted levels. There was appreciable inter-animal variability for both dogs (average CV across all time points 11–149%) and rats (average CV 30–80%). However, inter-animal variability was consistent across studies. In dog, glycine conjugated BA were barely present. In rat, both glycine and taurine conjugated BA were present. These data clarified the baseline BA profiles for rats and dogs and provides a foundation to design studies where known in vitro BSEP inhibitors can be administered.

PS 1200c Hepatic Effects of Aqueous Extract of *Chromolaena odorata* in Male Wistar Albino Rats

R. N. Asomugha[1], O. E. Orisakwe[2], P. N. Okafor[3], I. I. Ijeh[3] and A. L. Asomugha[4]. *[1]Pure and Indusrial Chemistry, Nnamdi Azikiwe University, Awka, Anambra State, Nigeria, [2]Clincal Pharmacy, University of Port Harcourt, Port Harcourt, Rivers State, Nigeria, [3]Biochemistry, Federal University of Agriculture, Umudike Umuahia, Abia State, Nigeria and [4]Anatomy, Nnamdi Azikiwe University, Nnewi Campus, Anambra, Nigeria.*

The hepatic effects of aqueous leaf extract of *Chromolaena odorata*, a plant commonly used for traditional medications, was evaluated using male Wistar albino rats. Acute and sub chronic toxicity was evaluated after 90 days of exposure. The LD50 was 2154mg/kg. Serum levels of glucose, lactate dehydrogenase, aspartate aminotransferase transaminase, and total bilirubin increased significantly in the 538.5 and 1077mg/kg dose groups. These two groups also had significantly reduced serum levels albumin and total serum protein when compared with the control group. Histopathological assessment showed degenerative changes in the liver. aqueous leaf extract of *Chromolaena odorata* used in traditional medical practice may be safe whereas high doses may have deleterious hepatic effects

PS 1200d CYP2A5 Contributes to Cadmium-Induced Liver Injury but Protects against Alcoholic Liver Disease

Y. Lu and A. Cederbaum. *Mount Sinai School of Medicine, New York City, NY.*

Ethanol can induce cytochrome P450 2E1 (CYP2E1), an active generator of reactive oxygen species, and CYP2E1 is considered a risk factor for alcoholic liver disease. Recently we found that ethanol can also induce CYP2A5, and ethanol induction of CYP2A5 is CYP2E1-dependent and regulated by CYP2E1-ROS-Nrf2 pathway. Cadmium can also induce CYP2A5 and cadmium induction of CYP2A5 is also regulated by Nrf2, but cadmium does not induce CYP2E1. The role of CYP2A5 in liver injury is still unclear. In this study, we examined liver injury induced by ethanol and cadmium chloride (CdCl2) in CYP2A5 knock out (cyp2a5-/-) mice and wild type (WT) mice. To examine cadmium-induced liver injury, WT and cyp2a5-/- mice (male, 8-10 weeks old) were injected CdCl2 intraperitoneally at a dose of 5 mg/kg, and then the mice were sacrificed 24 h after the CdCl2 administration. CYP2A5 was induced in WT mice but not in cyp2a5-/- mice. Serum levels of ALT and AST were increased to a greater extent in WT mice than in cyp2a5-/- mice. Cadmium-induced necrosis was more severe in WT mice than in cyp2a5-/- mice. Consistently, 3-nitrotyrosine (3-NT), a marker of oxidative stress, was induced in WT mice more than in cyp2a5-/- mice. As for alcoholic liver disease, Lieber-Decarli model was applied. After 3 weeks of feeding with Lieber-Decarli ethanol liquid diet, unlike cadmium-induced liver injury, ethanol-induced liver injury was enhanced in cyp2a5-/- mice compared with WT mice as indicated by serum ALT, hepatic fat accumulation (steatosis) and necro-inflammation observed in H&E stained liver sections. Ethanol-induced oxidative stress was also higher in cyp2a5-/- mice than WT mice. Ethanol feeding induced CYP2A5 in WT mice but not in cyp2a5-/- mice, although induction of CYP2E1 was comparable in cyp2a5-/- and WT mice. These results suggest that CYP2A5 contributes to cadmium-induced liver injury, and in contrast, CYP2A5 protects against ethanol-induced liver injury.

PS 1200e Effects of Red Ginseng Extracts on the Ethanol-Induced Hepatosteatosis *In Vivo* and *In Vitro*

S. Kim[1], J. Sim[1], O. Kwon[1], M. Song[1], H. Kim[1], S. Ki[2], T. Jeong[3] and S. Lee[1]. *[1]College of Pharmacy, Kyungpook National University, Daegu, Republic of Korea, [2]College of Pharmacy, Chosun University, Gwangju, Republic of Korea and [3]College of Pharmacy, Yeungnam University, Gyeongsan, Republic of Korea.*

l metabolism. Generally, chronic ethanol treatment causes hepatoseatosis in animal models by regulating the sterol regulatory element-binding protein 1 (SREBP1) that increase the synthesis of hepatic lipid. The effect of ethanol on SREBP-1 is mediated through mammalian sirtuin-1 (SirT1) regulation in hepatic lipid metabolism. Ginsenosides are active components mainly responsible for the therapeutic and pharmacologic properties of ginseng. We examined the effect of red ginseng extracts on regulation of SREBP-1 and SirT1 involved in lipid homeostasis in

ethanol-fed mice and hepatoma cells. Mice were randomly divided into 4 groups: control, EtOH fed group, EtOH and Korean red ginseng extracts (KRG extract) fed group (250 and 500 mg/kg) for 4 weeks. AML-12 cells were treated with EtOH and/or red ginseng extracts (0 – 1 mg/ml). Lipid droplets were determined using Oil red O staining, and expressions of SirT1 and SREBP-1 were investigated by western blotting in mouse mitochondria fraction and cells. The orally KRG extracts administrated mice showed hepatoprotective effects against EtOH-induced hepatosteatosis, and inhibited immunoreactivities, expression of nitrotyrosine as marker of iNOS related oxidative stresses and 4-HNE as marker of lipid peroxidation. Treatment of KRG extracts significantly increased SirT1 and decreased SREBP-1 in ethanol-fed mice and cells. We investigated the effect of individual ginsenoside related to regulation of SirT1 and SREBP-1 contrasted in EtOH-treated cells. This finding indicated that the treatment of KRG extracts showed hepatoprotective effects against EtOH-related hepatosteatosis *in vivo* and *in vitro*.

PS 1200f Potential Cytotoxicity of Thiazolidinedione-, Oxazolidinedione- and Succinimide-Ring Containing Compounds in HepG2 Cells

D. Almazrou, A. M. Keil, T. H. Rushmore, R. Tchao and P. J. Harvison. *Dept. of Pharmaceutical Sciences, University of the Sciences in Philadelphia, Philadelphia, PA.*

Liver damage has been reported in some patients following treatment with troglitazone (TGZ). Although the mechanism of TGZ hepatotoxicity is not known, the thiazolidinedione (TZD) ring in its molecular structure may be involved. Another TZD derivative, 3-(3,5-dichlorophenyl)-2,4-thiazolidinedione (DCPT), is hepatotoxic in rats and cytotoxic in human hepatoma HepG2 cells. Other studies have implicated the cytochrome P450 CYP3A isozyme sub-family in TGZ and DCPT toxicity. To further explore the role of TZD rings in cytotoxicity, two series of compounds were tested using HepG2 cells. DCPT analogs included N-(3,5-dichlorophenyl)succinimide (NDPS) and 3-(3,5-dichlorophenyl)-2,4-oxazolidinedione (DCPO). Structural analogs of TGZ comprised 5-(4-methoxyphenylmethyl)-2,4-thiazolidinedione (MPMT), 5-(4-methoxyphenylmethylene)-2,4-thiazolidinedione (MPMT-I), 3-(4-methoxyphenylmethyl)succinimide (MPMS), 3-(4-methoxyphenylmethylene)succinimide (MPMS-I) and 5-(4-methoxyphenylmethyl)-2,4-oxazolidinedione (MPMO). Wild-type HepG2 cells were incubated with the compounds (0-250 μM) for 24 h at 37 °C in HBSS under 95% air-5% carbon dioxide. Cell viability was assessed using the MTS assay. Compared to HBSS-treated controls, DCPT and MPMT-I were highly cytotoxic (>50% loss of viability), whereas the other compounds had little (<20%) or no effect on cell viability. To investigate a potential role for CYP-mediated metabolic activation, MPMT-I was also incubated with CYP3A4-transfected HepG2 cells. MPMT-I was more cytotoxic in the transfectants than in the wild-type cell line. Furthermore, the CYP3A inhibitor ketoconazole partially protected cells against MPMT-I-induced cytotoxicity. Our results suggest that the TZD ring can play a role in the toxicity of these compounds. Similar to TGZ and DCPT, MPMT-I cytotoxicity may involve the parent compound and a CYP-derived metabolite. Supported by PHS grant ES012499 and the USciences Department of Pharmaceutical Sciences.

PS 1200g Cellular and Genetic Liver Toxicity from Exposure to Polybrominated Diphenyl Ethers (PBDE) in Hepatic Cells *In Vitro*

J. Gomes[1], S. Ramoju[2] and D. Krewski[2]. [1]*Health Sciences, University of Ottawa, Ottawa, ON, Canada and* [2]*Toxicology, Risk Science International, Ottawa, ON, Canada.*

Polybrominated diphenyl ethers (PBDEs) are a family of synthetic chemical substances used as additive flame retardants to inhibit combustion, in a variety of consumer products (e.g., plastics, foams, electronics). The North American use of PBDE accounts for much of the world's PBDE use and in 2001about 7100 metric tons of Penta-BDE commercial mixture (namely DE-71). The continued usage of PBDE in various products amplifies the human burden of PBDEs. PBDE is bioaccumulative and persistent in the environment; and, therefore, the concentrations of PBDEs in human tissues have been increasing. BDE-47 and -99 (major components of DE-71 mixture) were predominatly detected in liver and reported to cause liver toxicity by inducing oxidative damage. Chronic liver damage can be a risk factor to liver diseases including hepatocellular carcinomas after long term exposures. In this study we investigated the mode of action of PBDE induced toxicity in human liver by exposing human hepatocarcinoma cells in a time (24-72h) and dose (0-100μM) dependent manner. The methodology includes determination of key cellular events leading to hepatotoxicity in human hepatocarcinoma cells, from exposure to DE-71 mixture and examination of molecular mechanism of stress response pathways, using Real Time-qPCR based pathway specific arrays. This study will also determine gene expression profile as biomarkers of adverse events in liver before they become histopathologically apparent. The highest test dose caused an inhibition in cell viability up to 50% after 72h, whereas lower doses (<50μM) showed slight increase in cell viability. Likewise, higher doses caused significant accumulation of intracellular ROS over time. Further, increase in caspase-3 enzyme levels and DNA fragmentation showed that, lower brominated PBDEs induce liver toxicity through accumulation of toxic metabolites and reactive oxygen species over time leading to caspase-mediated apoptotic cell death.

PS 1200h *In Vivo* Optical Imaging of Acetaminophen-Induced Liver Toxicity

J. D. Peterson, K. O. Vasquez and X. Li. *Applied Biology, PerkinElmer Inc, Hopkinton, MA.* Sponsor: D. Frazier.

Drug induced liver injury (DILI) is a major reason for late stage termination of drug discovery projects, so assessment is now routinely being integrated earlier in the drug development process. In vivo optical imaging offers non-invasive detection of biological changes in preclinical animal efficacy models, and this approach is also ideal for in vivo toxicology determination. We applied near infrared (NIR) fluorescence imaging techniques to the detection and quantification of DILI in living mice, using NIR fluorophore-labeled Annexin V (Annexin-Vivo 750 [AV750]) to detect cell surface phosphatidylserine on apoptotic and necrotic cells. AV750 was imaged 2h after injection, and could be re-injected safely every 24 h for longitudinal monitoring of the same animals. As a positive control, we used acetaminophen (APAP), a commonly used over-the-counter analgesic and antipyretic drug that is known to cause centrilobular hepatic necrosis when used at high doses. When male C57BL/6 mice were injected with a single dose (500 mg/kg) of APAP, the resulting liver necrosis peaked at 24 hours as detected by imaging with Annexin-Vivo 750 in living animals. Imaging results at 24h were statistically significant as compared to those of the PBS control group using only 3-4 mice per group. Both fluorescent tomographic imaging (FMT 4000), and higher throughput epifluorescence imaging (IVIS Spectrum CT), provided excellent detection of AV750 fluorescence in the liver. Histology and plasma ALT confirmed the kinetics of tissue necrosis, and at 48 hours more extensive liver damage was seen but with a decrease in tissue phosphatidylserine and plasma ALT, suggesting a decline in active tissue destruction. Maximal tissue damage was measured at 300 and 500 mg/kg APAP doses by AV750. Compared to conventional plasma/serum assays, in vivo imaging can offer fast, quantitative imaging results directly assessing the tissue of interest. Our results to date demonstrate the utility of optical imaging for assessing potential compound liver toxicity in early drug discovery programs.

PS 1200i Leelamine Is As a Potent Novel Inducer of Hepatic CYP2B

J. Sim[1], W. Nam[1], H. Oh[1], S. Lee[1], D. Lee[1], T. Lee[1], S. Ki[2], T. Jeong[3] and S. Lee[1]. [1]*College of Pharmacy, Kyungpook National University, Daegu, Republic of Korea,* [2]*College of Pharmacy, Chosun University, Gwangju, Republic of Korea and* [3]*College of Pharmacy, Yeungnam University, Gyeongsan, Republic of Korea.*

Cytochrome P450 (CYPs) are the important enzymes take part in a xenobiotic substance like as toxic chemicals, drugs. Many drugs may affect the activity of CYP, which is a major source of adverse drug interactions.Phenobarbital (PB), one of the antiepileptic drugs is well known to induce drug metabolizing enzymes in the liver. Especially, PB has been widely used to induce the CYP2B for investigation of the drug-drug interaction of CYP2B6 substrate drugs. Leelamine is a diterpene compound at the focus of efforts to develop a treatment for diabetes as pyruvate dehydrogenase inhibitor 4. Its potent is comparable to inductive effect of PB. In this study, we identified the selective and potent effect of leelamine on CYP2B *in vivo* and *in vitro* using a cocktail assay and LC-MS/MS system. In mice, the BROD, PROD activity was significantly increased by 2-fold and 2.5-fold at 5 mg/kg of leelamine for 1 day single treatment. Furthermore, western blot analysis showed that leelamine significantly increased the CYP2B1 protein levels by dose-dependently. We confirmed the induction effects of leelaminein *in vitro* model using mouse primary hepatocyte and mouse hepatoma cell lines (AML-12 cells). The activity of CYP2B was significantly increased by 1.7-fold and 2.2-fold at 5 μM of leelamine than PB or rifampicin as positive control of CYP2B induction, respectively. Whereas, the CYP2B activity was significantly increased by leelamine, mRNA level of *CAR* and CYP2B was no significant change after leelamine treatment. These data suggested that leelamine might be a novel inducer for CYP2B, instead of transcript activation of *Cyp2b* gene mediated *CAR* ligand receptor. Thus we suggest that leelamine is novel substitute of PB for selective induction of CYP2B *in vivo* and *in vitro*.

PS 1201 Acetaminophen Produces Oxidative Stress in the Airways and Modulates Respiratory Responses to Oxidant Challenge

G. J. Smith, J. Cichocki, J. E. Manautou and J. B. Morris. *School of Pharmacy, University of Connecticut, Storrs, CT.*

Air pollutants such as environmental tobacco smoke (ETS) and acrolein (the predominant irritant in tobacco smoke) produce oxidative stress in the respiratory tract airways. Oxidative stress plays an important role in the pathogenesis of airway diseases such as asthma. Epidemiological evidence suggests that acetaminophen (N-acetyl-para-aminophenol, APAP), a widely used analgesic, may also play a role in the pathogenesis of asthma via oxidative stress-related mechanisms, but direct data on the pro-oxidant effects of APAP in the airways is absent. To determine if APAP causes oxidative stress in the airways at near-therapeutic doses we administered APAP (ip) to female C57Bl/6J mice and measured tissue non-protein sulfhydryl (NPSH) as a marker for the antioxidant glutathione, and antioxidant response element (ARE)-dependent gene induction by qRT-PCR. Lung, trachea, and nasal NPSH levels were diminished to ~80% of control 1 hr following a 100 mg/kg dose of APAP (ip). APAP at 60 and 100 mg/kg caused significant ARE gene induction within 2hrs, and pre-treatment of mice with APAP potentiated the ARE gene response to ETS (5 mg/m3). We next determined if APAP modulated the airway responsiveness to oxidant air pollutants using sensory irritation as an index of airway response. Sensory irritation is due to stimulation of trigeminal sensory nerves and is known to be pro-inflammatory. APAP alone (100 mg/kg) did not elicit a response, but it greatly increased the sensory irritation response to both acrolein and ETS. The current results demonstrate that APAP, at near-therapeutic doses, causes oxidative stress in airway tissues and enhances the airway response to oxidant air pollutants. Children exposed to ETS are more likely to develop asthma. Modulation of airway responses to ETS provides a mechanism for the association between APAP use and the development of asthma in pediatric populations. (Supported by the University of Connecticut President's Research Award)

PS 1202 Characterization of the Blu E-Cigarette to Define the Composition of Inhaled Material

T. Holmes, J. D. McDonald, P. J. Kuehl and D. Kracko. *LRRI, Albuquerque, NM.*

In order to better define human exposure and to design experiments for toxicology systems (in vitro and in vivo) an aerosol characterization of the blu® e-cigarette was conducted. E-cig were characterized for aerosol mass, particle size, gas; particle partitioning, excipient, nicotine and formaldehyde content. We applied a modified Canadian Intensive protocol and developed a novel characterization system. The blu® e-cig heating processes resulted in generation of an aerosol mixture of particle excipients, nicotine present in both the gas and droplet phase, and small but detectable amounts of formaldehyde. There were over 1 million particles/cm3 of ~110 nm in size measured from a puff. E-cigarettes may have a decreased risk to users compared with conventional inhaled tobacco products. The aerosols were composed of excipient particles, with lesser amounts of nicotine and also other gases such as formaldehyde. This contrasts marketing for the device, which suggests that people only inhale nicotine vapor and water. The health consequence of these inhaled materials is uncertain based on available evidence, but the information provided here will assist in future risk assessments and the design of toxicology studies

PS 1203 A Mechanistic Study of Cigarette Smoke-Induced COPD in C57BL/6 Mice: The Impact of Switching to a pMRTP

E. Veljkovic[1], B. Phillips[2], M. Peck[1], A. Buettner[3], J. Hoeng[1], G. Vuillaume[1], A. Hayes[4] and M. Peitsch[1]. [1]*Philip Morris International, Neuchatel, Switzerland,* [2]*Philip Morris International, Singapore, Singapore,* [3]*Histovia, GmbH, Overath, Germany and* [4]*Spherix Consulting, Rockville, MD.*

In this study, the impact on the development of emphysema/COPD following inhalation of aerosol from two tobacco products, a reference cigarette (3R4F) and a prototypic modified risk tobacco product (pMRTP), was evaluated in C57Bl/6 mice. The mice were exposed to an aerosol from 3R4F (750 μg/l TPM, 34.4 μg/l nicotine), pMRTP (nicotine concentration-matched) or filtered air (sham) for 4 hours per day, 5 days per week, up to 7 months. After 2 months of exposure to 3R4F, switching and cessation groups were exposed to pMRTP or filtered air, respectively. To analyze the progression of emphysema, evaluations of inflammation, pulmonary function, and various histopathological and molecular changes (transcriptomics and lipidomics) were performed at months 1, 2, 3, 4, 5 and 7. Exposure to 3R4F induced molecular, cellular and physiological modifications in lungs leading to emphysematous changes. Animals exposed to pMRTP exhibited negligible changes in all parameters assessed. Both cessation and switching groups showed a reversal of the inflammatory and functional responses induced by 3R4F smoke. Histopathological evaluation revealed a slowdown in the progression of emphysematous changes in switching and cessation groups. Smoking cessation or switching resulted in the rapid recovery at the transcription level. The lipid profiles in lung, liver and plasma similarly showed a clear 3R4F effect, with minimal changes associated with pMRTP exposure, and recovery near to sham-exposed levels following either switching or cessation. These data demonstrate that exposure to pMRTP for up to 7 months resulted in a response similar to fresh air-exposed animals using a battery of physiological and molecular measures. Furthermore, following a 2 month 3R4F cigarette smoke exposure period, both cessation and switching to a pMRTP aerosol resulted in the reversal or stabilization of parameters assessed.

PS 1204 Examination of Acute Pulmonary Responses to Various Cookstove Exhaust Emissions

E. Gibbs-Flournoy[1], J. Jetter[2], T. Krantz[3], C. King[3], J. Richards[3], M. Daniels[3], E. H. Boykin[3], R. Jaskot[3], R. Harrison[3], J. Griffioen[3], I. Gilmour[3] and J. A. Dye[3]. [1]*Toxicology, UNC, Chapel Hill, NC,* [2]*NRMRL, US EPA, RTP, NC and* [3]*NHEERL, US EPA, RTP, NC.*

Air pollution is a global public heath problem, to which the emissions from rudimentary cooking devices has been estimated to contribute significantly through the burning of various types of biomass. Notably, exposure to cookstove emissions (CE) has been linked to increases in morbidity and mortality causing an estimated 4 million deaths which most frequently impact women and children. Current efforts to reduce CE have led to the development of several new cookstove (CS) designs. Although some studies have characterized improvements in the overall release of specific pollutants from modern CS, there is less information regarding the potential health benefits that may be derived from their usage. In this study, current models representing 4 different CS types, 3-Stone (3S), Forced Draft (FD), Natural Draft (ND), and Propane (PR), were used under the same cooking conditions for two consecutive cooking cycles. Exhaust emissions from each stove were characterized, and young adult female CD-1 mice were simultaneously exposed for a 3 hr period. Various endpoints examined at 0, 4, and 24 hr post-exposure (PE) included lung inflammation and changes in redox status/antioxidant capacity. Of these endpoints, CS emissions were observed to most significantly affect the pulmonary redox status of exposed animals via the oxidation of cellular glutathione. As compared to filtered air controls, lung homogenates from CE-exposed mice had consistently decreased levels of reduced glutathione (GSH), with corresponding increases in disulfide glutathione (GSSG), at 0 and 24 hr PE for all 4 CS. While no significant increases in pulmonary inflammation were observed in CE-exposed animals, macrophages from 3S and ND-exposed mice had a visible particle burden 24 hours PE, as compared to air controls. Together, these data support the need for a continued assessment of the health effects resultant from prolonged exposure to the exhaust emissions of modern CS. (Does not necessarily reflect USEPA policy)

PS 1205 Effect of Near-Road Particulate Matter on Respiratory Responses and Inflammation in Healthy and Ovalbumin-Allergic Mice

M. A. McGee[1], J. McGee[2], E. H. Boykin[2], M. Daniels[2], L. B. Copeland[2], D. Andrews[3], J. Richards[2], I. Gilmour[2] and S. H. Gavett[2]. [1]*Curriculum in Toxicology, UNC, Chapel Hill, NC,* [2]*EPHD, NHEERL, EPA, RTP, NC and* [3]*Research Cores Unit, Proteomic Research Core, EPA, RTP, NC.*

The Near-Road Exposures and Effects of Urban Air Pollutant Study (NEXUS) previously examined the association of near-roadway exposures to air pollutants and respiratory outcomes in children with asthma. This toxicological study was designed to complement NEXUS and determine which particulate matter (PM) characteristics may contribute to exacerbation of allergic asthma. Samples of coarse, fine and ultrafine PM were collected upwind and downwind from I-96 in Detroit, MI during Winter 2010/11. Healthy and ovalbumin (OVA)-sensitized female Balb/cJ mice were exposed via oropharyngeal (OP) aspiration to 20 or 100 μg coarse, fine, or ultrafine fractions of upwind or downwind PM 2 hr prior to OP challenge with 20 μg OVA. No samples caused significant changes in immediate responses to OVA challenge as determined by whole body plethysmography (WBP). Two days later, airway responsiveness to methacholine aerosol (assessed by WBP) was not significantly affected by PM exposure in either healthy or allergic mice. In OVA-allergic mice, 100 μg downwind coarse PM caused a greater increase than downwind fine or ultrafine PM in bronchoalveolar lavage (BAL) neutrophils (7x vs. control blank filter extract) and eosinophils (10x) and also caused significant increases in BAL LDH and NAG. Interestingly, 100 μg upwind fine PM produced greater increases in neutrophils (7x vs. control blank filter extract) and eosinophils (4x) than upwind coarse or ultrafine PM. Ultrafine PM did not significantly increase neutrophils or eosinophils in comparison to allergic mice given ultrafine blank filter extract. Further analyses will be conducted to investigate associations between

chemical components and phenotypic effects of allergic lung disease. We conclude that coarse PM downwind and fine PM upwind of traffic promote allergic inflammation in OVA-allergic mice. (This abstract does not represent U.S. EPA policy.)

PS 1206 Diurnal Variation in Toxicological Effects of Size-Segregated Particulate Samples Collected from High-Air Pollution Situation in China

P. I. Jalava[1], O. Uski[1], S. Kasurinen[1], K. Kuuspalo[1], J. Ruusunen[1], H. Liqing[1], O. Sippula[1], M. Happo[1], H. Koponen[1], J. Nurmela[1], Q. Wang[2], C. Gu[2], J. Jokiniemi[1] and M. Hirvonen[1]. [1]*University of Eastern Finland, Kuopio, Finland and* [2]*University of Nanjing, Nanjing, China.* Sponsor: M. Viluksela.

Air pollution is a wide recognized problem all over the world. The air pollution levels in ambient air are known cause for premature deaths, many respiratory and cardiac diseases as well as cancer. We studied the in vitro toxicological responses associated with the observed adverse health effects. Thus far, the daily variations in air pollution levels and the consequent health effects have been studied to a lesser extent. We collected the particles for toxicological and chemical analyses from University of Nanjing, Xianlin campus. The generally high air pollution situation in China allowed us to separate between the day and nighttime samplings due to sufficient collected mass. With this approach we also got information on how the atmospheric processes and changes in the emission sources alter the toxicity of the collected particulate mass. The samples were collected with high volume cascade impactor in four different size ranges (PM10-2.5; PM2.5-1; PM1-0.2; PM0.2) and then extracted from the sampling substrates. Mouse macrophage cell line was employed in detection of the toxicological responses of the particulate samples including cytotoxicity, genotoxicity and inflammatory responses. The results showed that both chemistry and toxicological responses change between day and night. Nighttime samples had much more PAHs than the daytime samples. Cytotoxicity was rather similar in the day and night samples. However, inflammatory responses and genotoxicity were significantly higher during the daytime when compared to the night. It is possible that breakdown products of the PAHs are responsible for the higher responses during the daytime. When compared to the previous results from less polluted situations in Europe, the responses were quite different. In conclusion, the toxicity of the particulate mass in polluted situation during day and nighttime showed large variation.

PS 1207 Particulate Matter from Saudi Arabia Induces Genes Involved in Cholesterol and Lipid Metabolism

J. A. Brocato[1], M. Shamy[2], M. Costa[1], M. Khoder[2], A. Mansour[2], H. Sun[1], L. Chen[1] and T. Kluz[1]. [1]*Environmental Medicine, NYU School of Medicine, Tuxedo, NY and* [2]*Faculty of Meteorology, Environment, and Arid Land Agriculture, King Abdulaziz University, Jeddah, Saudi Arabia.*

Airborne particulate matter (PM) exposure is a major environmental health concern and is linked to metabolic disorders, such as cardiovascular diseases (CVD) and diabetes, which are on the rise in the Kingdom of Saudi Arabia. This study investigated changes in mouse lung gene expression caused by administration of PM10 collected from Jeddah, Saudi Arabia. FVB/N mice were exposed to 100 ug PM10 or water by aspiration and euthanized 24 h later. The bronchoalveolar lavage fluid (BALF) was collected and analyzed for neutrophil concentration and TNF-a and IL-6 levels. IL-6 and TNF-a were significantly higher in mice exposed to PM according to an ELISA assay and neutrophil concentration was also increased in exposed mice. RNA was extracted from the lungs and whole transcript was analyzed using Affymetrix Mouse Gene 1.0 ST Array. Mice exposed to PM10 displayed an increase in neutrophil concentration and elevated TNF-a and IL-6 levels. Gene expression analysis revealed that mice exposed to PM10 displayed 202 genes that were significantly up-regulated and 40 genes that were significantly down-regulated ($p<0.05$). PM10 induced genes involved in inflammation, cholesterol and lipid metabolism. This is the first study to demonstrate that Saudi Arabia PM10 increases in vivo expression of genes located in pathways associated with diseases involving metabolic syndrome.

PS 1208 Compounds Collected from Indium-Tin Oxide Production Induce Inflammatory Responses from Cultured Macrophages and Bronchial Epithelial Cells

M. A. Badding[1], D. Schwegler-Berry[1], K. J. Cummings[2] and S. S. Leonard[1]. [1]*Health Effects Laboratory Division, NIOSH, Morgantown, WV and* [2]*Division of Respiratory Disease Studies, NIOSH, Morgantown, WV.*

Indium-tin oxide (ITO) is used to make transparent conductive coatings for touch-screen and liquid crystal display electronics. Lung disease among workers in the ITO industry is an emerging occupational health concern as the demand for consumer electronics continues to increase. Epidemiologic studies have shown indium compound-exposed workers to have pulmonary alveolar proteinosis and fibrotic interstitial lung disease. However, the molecular mechanisms behind indium compounds' toxicity remain largely unknown. Thus, we aim to uncover how compounds encountered during ITO production affect cultured cells and ultimately, contribute to the pathogenesis of indium lung disease. We hypothesize that indium compounds (8 different samples collected from various stages at an ITO facility) cause lung pathology through direct cytotoxicity and/or via inflammatory signaling from exposed cells. Preliminary studies showed that exposure of RAW 264.7 monocyte macrophages and BEAS-2B bronchial epithelial cells to indium compounds resulted in significantly reduced viability. Microscopy techniques revealed that various indium compounds interact with and are engulfed by both cell lines within 1 to 3 hours, suggesting that cellular reactions may be occurring very rapidly. Indeed, nuclear factor kappa beta (NFκB) activation occurs within 3 hours of treatment with compounds containing sintered ITO in both cell lines. Robust cytokine production (TNFα, IL-1β, IL-6, and IL-8) following cellular exposures confirmed that pro-inflammatory responses are indeed occurring. Our results suggest that inflammatory responses to indium compounds by both pulmonary macrophages and epithelial cells may initiate and propagate indium lung disease. These findings have provided a better understanding of the molecular mechanisms behind an emerging occupational health issue and will aid in the discovery of biomarkers for disease prevention.

PS 1209 Differential Diagnosis of Airways Diseases Using the Ratio of FEV1/FVC in Subjects Occupationally Exposed to Powder Particles in a Pharmaceutical Industry in Nigeria

I. O. Omotosho[1, 2]. [1]*Chemical Pathology, University of Ibadan, Ibadan, Nigeria and* [2]*University of Ibadan, Ibadan, Nigeria.*

Contribution of exposure to chemicals, fumes, dust and particles to the growing incidence of Chronic Obstructive Pulmonary Disease (COPD) has not been critically evaluated in this environment. This work was a preliminary report of the diagnostic differentials of COPD using pulmonary function indices determined in subjects occupationally exposed to chemical particles and dust in a pharmaceutical industry in Nigeria. 125 workers in the organization were screened for their pulmonary functions. Using Global Initiative for Obstructive Lung Disease (GOLD) as the mode of analysis and based on percentage FEV1/FVC ratio, 31.2% (39) had Normal Respiratory (NR) function; 24.8% (31) had Mild Restriction (MiR); 24% (30) had Moderate Restriction (MoR); 10.4% (13) had Moderately Severe Restriction(MSR); 5.6% (7) had Severe Restriction (SR); 2.4% (3) had Mild Obstruction (MO) while 0.8% (1) had Obstruction combined with Restriction (OR). Using the NR group as reference and towards stratifying the data, mean FEV1 and FVC obtained for the MiR, MoR, MSR, SR, MO and OR groups were compared with that of NR. The Mean values varied significantly in all the other groups ($P<0.005$) except with the MoR group ($P>0.005$). With this correction, 69 (55.2%) could be said to show normal pulmonary function while the remaining 53 (44.8%) had a form of respiratory abnormality or the other. The application of basic spirometry measurement and the need for enforcement of various industrial laws monitoring risk exposure towards reducing toxicity of chemicals by inhalation and the attendant airways diseases in our industries was further highlighted in this work.

PS 1210 Black Carbon Exposure Levels in New York City's Subway Stations

M. Vilcassim, G. D. Thurston and T. Gordon. *Environmental Medicine, New York University, Tuxedo, NY.*

The New York City subway is the main mode of transport for over 5 million passengers on average weekdays. Commuters are thus exposed frequently to the microenvironment in subway stations and airborne pollutants can have a significant impact on subway users if exposure levels are high. This study looked at black car-

bon (PM 2.5 size fraction) concentrations while traveling from a selected starting site and then along 4 subway lines. Exposure levels of black carbon were recorded aboveground and in selected subway stations along the commute.
Standard sampling techniques and equipment were used to measure black carbon levels and PM 2.5 levels in the subway stations. PM samples were collected on quartz filters and black carbon was measured real time using a Micro-Aethalometer and PM was measured real time with PDR 1500 Data Rams. The quartz filters were analyzed for Organic and Elemental carbon (OC/EC) (Sunset Instruments) and compared with the real time Aethalometer readings. The mean EC level was between 9 – 10 μg/m3 which agreed with the Aethalometer output, although in real time, the Aethalometers recorded BC concentrations up to 25 μg/m3. All subway black carbon readings were several times higher than roadside readings, which were generally around 1-2 μg/m3.
Therefore, this pilot study shows that black carbon levels in New York City's subways can be considerably higher than ambient urban levels and further monitoring and investigation of black carbon in other subway stations and lines is warranted. Such monitoring will be important to identify which stations have excessive air pollution and why, and also to develop plans to implement better ventilation systems for mitigation.

PS 1211 Polyhexamethyleneguanidine Phosphate-Induced Pulmonary Fibrosis Model: Comparison with Bleomycin-Induced Model

J. Song[1], D. Saputra[1], C. Song[2] and K. Lee[1]. [1]*Inhalation Center, Korea Institute of Toxicology, Jeongeup, Republic of Korea and* [2]*Toxicogenomics Center, Korea Institute of Toxicology, Daejeon, Republic of Korea.* Sponsor: S. Park.

Our prior study showed that polyhexamethyleneguanidine phosphate (PHMG-ph), one of the major constituent of biocides, caused pulmonary damage of inflammation and fibrosis in rat lungs. In this study, we examined inflammation and fibrosis in lungs induced by PHMG-ph and compared with bleomycin model, which is most often used to study the pathogenesis of pulmonary fibrosis. In a current study, we administrated 0.9 mg/kg PHMG-ph or 1.5 mg/kg bleomycin to mice intratracheally on day 1, and conducted necropsies after 1 week, 2 weeks, 4 weeks, and 10 weeks. Proinflammatory cytokines and fibrotic markers were measured from lungs tissues. We also evaluated whether PHMG-ph activates inflammasome, because a marked elevation of IL-1β was observed by 10 weeks in PHMG-ph group. As a result, PHMG-ph induced severe pulmonary inflammation with high expression of IL-1β, IL-6, MCP-1, and reduced level of IFN-γ. Increased expression of extracellular matrix proteins such as collagen and fibronectin was also observed in the lung tissues by week 10. In addition, we postulate that imbalance of metalloproteinase and tissue inhibitor of metalloproteinase accelerates the pulmonary fibrosis. On the contrary, bleomycin-induced inflammation and fibrosis sustained until week 4. Nalp3 and caspase-1 expression was elevated by 4 weeks for PHMG-P treatment group, by 2 weeks in BLM group. In addition, we observed an increased expression of Bax and caspase-3, which means that PHMG-ph induces apoptosis. This study suggested evidences that PHMG-ph-induced apoptosis continuously stimulates inflammasome, therefore impairs resolution of inflammation, which leads to pulmonary fibrosis. Also our study shows that a single dose of PHMG-P model induces acute and chronic pulmonary inflammation as well as severe fibrosis by 10 weeks, unlike BLM model.

PS 1212 Phosgene-Induced Lethal Lung Edema: Novel Mechanism-Based Biomarker of Injury and Treatment

W. Li[1], C. Hai[1], F. Liu[2] and J. Pauluhn[3]. [1]*Department of Toxicology, Fourth Military Medical University, Xi'an, Shaanxi, China,* [2]*Beijing Institute of Respiratory Medicine, Capital Medical University, Beijing, China and* [3]*Experimental Toxicology, Bayer Pharma, Wuppertal, Germany.*

Life-threatening acute pulmonary edema may occur followingl accidental exposures to phosgene. Rats exposed to phosgene at 1000 mg/m3 x min show prolonged stimulation of apnea time, bradycardia, and hemoconcentration early in onset with slow reversibility. Nitric oxide (NO) seems to be directly involved in the process of lung edema formation. Exhaled NO (eNO) was measured consecutively to phosgene exposure and served as non-invasive, instant biomarker of phosgene-induced acute lung injury in rats. It is hypothesized that NOS-inhibitors administered by inhalation mitigate cardiovascular dysfunction and lung edema accordingly. Current pharmacological interventions of phosgene-related lung edema include administration of steroidal and non-steroidal anti-inflammatory drugs. Phosgene pre-exposed rats were curatively treated with dexamethasone (DX; 100 mg/kg bw, ip) and sodium salicylate (SS; 200 mg/kg bw, ip) alone or in combination to study changes in eNO, mortality, and increased lung weights one day post¬exposure. SS showed minimal (if any) efficacy while DX, alone or in combination with SS, substantially aggravated the lung edema (lung weights) with 40% mortality and increased eNO. Non-treated phosgene-exposed and treated but non-phosgene-exposed rats survived. This experimental evidence suggested that high-dose corticoid treatments may aggravate the pulmonary toxicity of phosgene. In contrast, the NOS-inhibitor aminoguanidine reduced the magnitude of lung edema. In summary this study seems to support the view that the pro-apoptotic corticosteroids may further deteriorate the lung while the known anti-apoptotic property of SS maintains function. Inhalation therapy with an aersolized iNOS inhibitor was both efficacious to reduce eNO and lung weights. This outcome seems to suggest that cardiovascular and not irritation-related tissue destruction is the lead etiopathology of phosgene-induced lung edema.

PS 1213 The Long-Term Toxicity and Mesothelial Cell Reactions Induced by Potassium Octatitanate Fibers (TISMO) in the Left Thoracic Cavity in A/J Female Mice

M. Yokohira, S. Kishi, Y. Nakano, K. Yamakawa, F. Ninomiya, S. Kanie and K. Imaida. *Onco-pathology, Kagawa University, Faculty of Medicine, Kita-gun, Kagawa, Japan.*

The present study was performed to assess effects on mouse lung and thoracic cavity by potassium octatitanate fibers, trade name TISMO, which is often used for friction material of cars, precision filters or the others, and with the chemical formula K2O-nTiO2. Previously (SOT in 2012), we presented the 21 weeks experiment for TISMO with dimensions mostly <50μm in length and <2μm and granular-shaped micro- and nano-size order particles of titanium dioxide (TiO2). Thoracotomy was performed to infuse test particles (1.5 mg in 0.2 ml saline/mouse) directly into the left thoracic cavity of A/J mice. After 21 weeks, only the fiber-shaped TISMO, morphologically similar to asbestos, induced a severe reaction of the pleura. The results indicate that the risk of mesothelial cell reaction may depend on the shape as well as the particle size.
In the present study, 65 weeks experiment was employed to examine long-term effects and possible tumorigenesis by fiber-shaped TISMO infused into the thoracic cavity of A/J mice. The experiment was terminated for the decreasing of the effective number of animals. This experiment showed numbers of TISMO fibers in the alveoli, indicating penetration through the visceral pleura. Atypical mesothelial cells were also observed with severe pleural proliferation, but no malignant mesothelioma was detected. The additional detection of TISMO fibers in the in the liver, spleen, kidneys, ovary, heart and bone marrow histopathologically indicated their movement outside of the thoracic cavity.
In conclusion, the experiments demonstrated fiber-shaped TISMO infused into the thoracic cavity of A/J mice induced severe pleural proliferation but not malignant mesothelioma. Hazard risk should also take into account that asbestos-like fiber spread to the whole body from the thoracic cavity.

PS 1214 The Role of HIF1 alpha in Regulating Cobalt-Induced Cytokine Expression in Alveolar Type II Cells

R. Rivera-Soto[1], S. P. Proper[2, 3] and J. J. LaPres[2, 3]. [1]*Biology, University of Puerto Rico at Arecibo, Arecibo, Puerto Rico,* [2]*Biochemistry and Molecular Biology, Michigan State University, East Lansing, MI and* [3]*Center for Integrative Toxicology, Michigan State University, East Lansing, MI.*

Cobalt is a transition metal associated with allergic contact dermatitis, hard metal lung disease (HMLD) and asthma. Cobalt has been found in significant amounts in air pollution and in many industrial settings. It is also recognized as a hypoxic mimic. Similar to hypoxia, cobalt exposure triggers the stabilization of the hypoxia inducible factor (HIF), a family of proteins that regulate the cellular response to the decrease in oxygen availability. Recent studies have shown that mice deficient in the protein, HIF1α, in the alveolar type II (ATII) and club cells and exposed to cobalt exhibit an asthma-like immune response. In contrast, control mice respond to cobalt by displaying symptoms similar to HMLD. Previous research in the laboratory and literature review led us hypothesize that loss of HIF1α in ATII cells lead to a change in the cell's cytokine expression profile that promotes the observable change in cobalt-induced inflammation. To address this hypothesis, A549 cells, a human ATII-like cell line, were used. To model what happens in the transgenic mouse lung, these cells were manipulated, using siRNA, to decrease the expression of HIF1α. Following knock down, these cells, and their respective controls were exposed to cobalt for 6 and 24 hours and the expression of BCL2/adenovirus E1B 19 kDa protein-interacting protein 3 (BNIP3), vascular endothelial growth factor (VEGF) and Interleukin (IL) 5 and 10 genes was assessed by quantitative RT-PCR. The preliminary results indicate that exposure to cobalt altered the expression of cytokines in a HIF1α-dependent manner. To confirm these results, it will be important to identify clonal populations within the HIF1α-deficient cells and repeat the described experiments.

PS 1215 The Evaluation of the Biopersistence, Pathological Response, and Pleural Translocation of Chrysotile Containing Brake Dust in Comparison to Crocidolite Asbestos following Short-Term Inhalation Exposure

D. M. Bernstein[1], R. A. Rogers[2], H. Ernst[3] and J. I. Phillips[4]. [1]*Consultant in Toxicology, Geneva, Switzerland,* [2]*Rogers Imaging Corporation, Needham, MA,* [3]*Fraunhofer Institute for Toxicology and Experimental Medicine, Hannover, Germany and* [4]*Department of Biomedical Technology, Faculty of Health Sciences, University of Johannesburg, National Institute for Occupational Health, National Health Laboratory Service, Johannesburg, South Africa.*

Chrysotile asbestos has been used in the manufacturing of friction brake linings since the early 1900's. Although the use of asbestos containing products is has been reduced, chrysotile brakes continue to be manufactured and/or used in many parts of the world. This is the first inhalation study designed to provide an understanding of the biokinetics and potential toxicology of chrysotile containing brake dust following short term exposure in rats. The deposition, pathological response and translocation of brake-dust derived from brake pads manufactured with chrysotile were evaluated in comparison to the amphibole, crocidolite asbestos. This presentation presents results from the lung and in particular the quantification of measurements of fibers and pathological response in the pleural cavity. Rats were exposed by inhalation 6 h/day for 5 days to either brake-dust obtained by sanding of brake-drums manufactured with chrysotile, a mixture of chrysotile and the brake-dust or crocidolite asbestos. The crocidolite asbestos fibers initiated a rapid inflammatory response in the lung following exposure resulting in a 5-fold increase in fibrotic response within 91 days. In addition, marked increase in visceral pleural thickness and collagen deposition was observed following crocidolite asbestos inhalation. No significant pathological response was observed in the lung or the pleural cavity at any time point in either the brake-dust or chrysotile/brake-dust exposure groups. These results provide support that brake-dust derived from chrysotile containing brake drums would not initiate a pathological response in the lung following short term inhalation.

PS 1216 Klotho Overexpression in Human Lung Epithelial Cells Decrease Sensitivity to Cigarette Smoke-Induced Cell Death

D. J. Blake. *Biology, Fort Lewis College, Durango, CO.*

Chronic obstructive pulmonary disease (COPD) is currently the third leading cause of death in the United States. COPD is associated with an abnormal inflammatory response to noxious particles and gases, and is characterized by progressive airflow limitation. Cigarette smoke (CS) is the primary cause of COPD although exposure to air pollution, respiratory infections and genetic factors also contribute to the disease progression. Exposure to CS induces oxidative stress in the lung, which results in cellular senescence or aging of the lung, leading to decreased proliferation of epithelial cells and the destruction of alveolar structure resulting in pulmonary emphysema. Although aging is a natural process, in the presence of cigarette smoke cellular senescence increases dramatically. Given that cigarette smoke accelerates lung aging, therapies that significantly reduce or delay cellular senescence may be important in the overall management of this disease.
The anti-aging gene, klotho, encodes a membrane bound protein, which has been shown to be a key regulator of oxidative stress, cellular senescence and inflammation. Mice with a defect in the klotho gene have a short life span and develop a syndrome resembling emphysema. In this study the role of Klotho was investigated in human epithelial cells. Individual clones that stably overexpress Klotho were generated through retroviral transfection and geneticin selection. Klotho overexpression was confirmed through real-time PCR and Western blotting. Compared to control cells, which were stably transfected with the retroviral control vector only, constitutive Klotho overexpression resulted in decreased sensitivity to cigarette smoke induced cell death in vitro. However, compared to control cells, the generation of reactive oxygen species and the production of IL-6 and IL-8 were not altered in the presence of CS. Therefore, our results suggest that enhancing Klotho activity in pulmonary epithelial cells, particularly those exposed to CS, may be a promising strategy to alleviate apoptosis and possibly prevent the development of COPD.

PS 1217 Subchronic Inhalation Exposure of Rats to Libby Amphibole and Amosite Asbestos: Effects at 18 Months Post Exposure

D. E. Dodd[1], G. A. Willson[2], K. C. Roberts[1], H. G. Wall[2], A. M. Jarabek[3] and S. H. Gavett[3]. [1]*The Hamner Institutes for Health Sciences, RTP, NC,* [2]*Experimental Pathology Laboratories, Inc., RTP, NC and* [3]*U.S. EPA, RTP, NC.*

Increased asbestosis, lung cancer, and mesothelioma rates are evident after exposures to Libby amphibole (LA). To support dosimetry model development and compare potency, a subchronic nose-only inhalation study (6 hr/d, 5 d/wk, 13 wk) was conducted in male F344 rats. Rats were exposed to air (control), LA (LO, MED, HI; 1.01, 3.32, 10.06 mg/m^3; 159, 693, 1522 fibers/cc), or amosite (AM; 3.34 mg/m^3; 230 f/cc). Toxicity endpoints, pathology, and fiber burden evaluation were determined 18 mo post-exposure. Fiber exposure had no effect on survival. Mononuclear cell leukemia was the main cause of death prior to scheduled necropsy in all groups except the LA 3.3 group, though group incidences were below NTP historical control data. BAL cell numbers, LDH, and protein in AM and LA groups were not statistically different from the control group (n=8 rats/group), indicating resolution of earlier inflammation (Dodd, SOT 2012; Willson, SOT 2013). Histopathology of the left lung lobe, trachea, sternum, pleura, epididymis and testes, and relevant gross tissue lesions was conducted on 50 rats/group. Alveolus inflammation, pleural fibrosis, lung interstitial fibrosis, and the presence of foreign bodies were noted in all fiber-exposed groups. A greater incidence of chronic tracheal inflammation was noted in the LA groups. Alveolar bronchiolar adenoma occurred in 2 rats in each of the AM, MED LA, and HI LA groups, and 1 alveolar bronchiolar carcinoma was observed in the HI LA group; all of these findings were within historical NTP control data. No pleural mesotheliomas were observed in any treatment groups. In conclusion, both AM and LA induced dose-related lung fibrotic responses; tumor incidences were apparently increased but not beyond historical control ranges. Tissue fiber burden data are supporting dosimetry model development; comparisons of responses between fibers may change based on internal dose estimates. (This abstract does not represent US EPA policy.)

PS 1218 Sex Differences in Glutathione Levels and Cytotoxicity following Naphthalene or Acrolein Exposure in Nasal Epithelium

L. S. Van Winkle[1], J. Cichocki[2], R. Mendoza[1], P. Edwards[1] and J. B. Morris[2]. [1]*Center for Health & Environment, UC Davis, Davis, CA and* [2]*School of Pharmacy, Univ of Connecticut, Storrs, CT.*

Naphthalene causes site and dose dependent respiratory tract toxicity in rodents that is P450 mediated. The carcinogenesis bioassay found evidence for formation of olfactory neuroblastomas and respiratory adenomas in the nose of both sexes of rats. Currently, there is debate as to whether epithelial injury following naphthalene exposure occurs in humans. In this study we used nasal epithelial tissue explants obtained from rhesus monkeys culled from the colony at California National Primate Research Center for health reasons as a surrogate for human nasal epithelium. We incubated maxillo, ethmoid, and septal epithelia (N= 3 or more per group) from male and female monkeys with naphthalene (10, 50, 100 and 500 uM), acrolein (50, 150, 300 uM) or vehicle (sham) control to provide site-matched tissue pieces for 3 hrs. Samples were analyzed for amount of glutathione (GSH) depletion via HPLC and also for histology of cytotoxicity using differential incorporation of the fluorescent nuclear dye ethidium homodimer-1. We found that acrolein, a direct acting agent that does not require P450 mediated metabolism to have an effect, depleted GSH at the highest dose, in all tissues tested, except male septal epithelium. In general, females were more susceptible to GSH depletion but had higher baseline GSH levels. Naphthalene was less effective than acrolein at depleting GSH, with a trend towards depletion only seen in maxilloturbinates at the highest dose. No other nasal tissue was depleted by 500 uM NA, a high dose, likely equivalent to an inhaled concentration of >10ppm. Naphthalene cytotoxicity was rare, focal and was primarily localized to individual cells in subepithelial glands. We conclude 1) the nasal epithelium of the Rhesus monkey is resistant to glutathione depletion and that this may reflect robust resynthesis capabilities, 2) that naphthalene is poorly capable of depleting GSH in most nasal tissues tested and 3) naphthalene causes minimal cytotoxicity in this model.

PS 1219 Sex Differences in Acute Nasal Antioxidant Responses to Inhaled Naphthalene

J. Cichocki[1], L. S. Van Winkle[2], G. J. Smith[1], A. R. Buckpitt[2] and J. B. Morris[1]. [1]*Pharmaceutical Sciences, University of Connecticut, Storrs, CT and* [2]*Veterinary Medicine, University of California, Davis, CA.*

At concentrations of 10 ppm or greater, naphthalene (NA) is a nasal carcinogen inducing respiratory adenomas in male and olfactory neuroblastomas in female rats, respectively. The proposed carcinogenic mode of action includes metabolic activation via CYP450 to an electrophile with subsequent glutathione depletion, escape of electrophile, covalent binding, cell death, and regenerative cell proliferation. To fully define the effect of acute NA exposure on nasal antioxidant responses, male and female F344 rats were nose-only exposed to 0, 1, 3, 10, or 30 ppm NA vapor for 6 hours. Following exposure, nasal olfactory (OE) and respiratory/transitional (RTE) epithelia were analyzed for reduced/oxidized glutathione levels (GSH/GSSG) and for mRNA levels of selected antioxidant genes. Epithelial membrane permeability was also assessed via ethidium homodimer-1 staining as an indirect marker of cytotoxicity. Significant GSH depletion occurred at all exposure levels in

RTE and OE with maximal depletion (to ~ 25 and 40% of control levels, respectively) occurring at or above 1 ppm. Similar trends were seen in both males and females. There was significantly more induction of glutamyl cysteine ligase (gclc) and NADPH quinone oxidase 1 (nqo1) male rat OE compared to female OE. At 3 ppm in male rats, NA upregulated gclc and nqo1 12- and 16-fold, compared to 5- and 3-fold in females, respectively. Membrane permeability following NA exposure to 10 or 30 ppm NA was not dependent on sex, suggesting no sex differences in the acute cytotoxic response at these exposure levels. While no sex differences in GSH depletion were observed, sex differences in the induction of antioxidant genes suggest that induction of antioxidant protective pathways may contribute to sex differences in the carcinogenic response to NA.

PS 1220 Pulmonary Effects and Biokinetics of Nanoparticles: Whole-Body Inhalation Exposure to CeO2 in 5-Day, 28-Day, and 90-Day Rat Studies

J. Keller[1], K. Küttler[1], L. Ma-Hock[1], V. Strauss[1], S. Gröters[1], K. Wiench[2], B. van Ravenzwaay[1] and R. Landsiedel[1]. [1]*Toxicology, BASF SE, Ludwigshafen/Rhein, Germany and* [2]*Product Safety, BASF SE, Ludwigshafen/Rhein, Germany.*

CeO2 nanoparticles are widely used for biomedical, commercial and industrial applications. To assess hazard potential of air-born CeO2 nanoparticles, CeO2 (NM212), an OECD depository material, is tested in a combined chronic and carcinogenicity long-term inhalation study in rats within the framework of the EU-project NanoREG.
As a preparation work for the long-term inhalation study, 5-day and 28-day studies were performed in female rats. The rats were whole-body exposed to 0.5, 5 and 25 mg/m3 CeO2 for 6 h/d, 5 d/week for 1 and 4 weeks in the 5- and 28-day studies, respectively. A variety of biological endpoints including broncho-alveolar lavage (BAL) and histopathology were examined. The lung retention and clearance kinetics were assessed up to a post-exposure period of 129 days. Based on these results, the long-term study was started at concentrations of 0.1 mg/m3, 0.3 mg/m3, 1 mg/m3 and 3 mg/m3 CeO2. Meanwhile, the results of satellite group animals exposed for 90-days are available.
In both 5-day and 28-day studies, an increase of biochemical and cytological parameters (e.g. polymorph nuclear neutrophils, PMN) were observed in BAL fluid in a concentration-related manner. Cytokines in BAL fluid were increased significantly in both studies. These findings indicate a moderate inflammation in the lung after inhalation exposure. Consistent to BALF results, histopathology revealed substance- and concentration-related morphological changes in the lungs and lung associated lymph nodes. The effects comprised alveolar histiocytosis, granulomatous inflammation in the lung, and macrophage aggregates with particles in bronchial-associated lymphoid tissue and lung associated lymph nodes. Pulmonary effects could be correlated with high particle retention and slow clearance in the lungs and a translocation to associated lymph nodes. The no observed adverse effect levels (NOAEL) for CeO2 is 0.5 mg/m3 in both 5- and 28-day studies.

PS 1221 Inhalation Toxicity of Three Different Types of Nano-Size Organic Pigments

K. Wiench[3], P. Simmendinger[2], L. Ma-Hock[1], S. Gröters[1], B. van Ravenzwaay[1] and R. Landsiedel[1]. [1]*Toxicology, BASF SE, Ludwigshafen/Rhein, Germany,* [2]*BASF Schweiz, Basel, Switzerland and* [3]*Product Safety, BASF SE, Ludwigshafen, Germany.*

Four different organic pigments, which are nanomaterials according to the EU definition, were tested in the 5 day short term inhalation study (STIS) in rats. The STIS is a sensitive test system, which comprises a comprehensive scheme of biological effects (such as inflammatory reactions in the lung) as well as preliminary biokinetic data (such as lung burdens and potential translocation). A recovery period provides information on the persistence, progression and/or regression of effects is obtained.
The pigments represent three different chemical classes of organic pigments, the diketopyrrolopyrrol-pigments (Pigment Red 254 and DPP Orange), the arylide yellow pigments (Pigment Yellow 74) and copper phthalocyanine pigments (Pigment Blue 15). These pigments are poorly soluble particles, the average particle size distribution of these pigments are 25 – 250 nm.
The pigments were tested in the concentrations from 1 to 30 mg/m3, examination of the lung lavage as well as histopathogical examinations were performed after the exposure period as well as after a recovery period of 3 weeks.
Only mild and partly reversible morphological changes were observed in lung and lymph nodes at the highest concentrations tested with the diketopyrrolpyrrol-pigments, whereas Pigment Yellow 74 showed no changes in histopathology and lavage parameter up to the highest concentration tested.
As a first result it can be concluded these nano-size organic pigments only represent a mild inhalation hazard potential.

PS 1222 Secondary Organic Aerosols Generated from α-Pinene-Amine Mixtures: Effects on the Cardiovascular System

M. Doyle-Eisele[1], A. C. Rohr[2], E. Knipping[2], A. K. Lund[3], J. Brower[1] and J. D. McDonald[1]. [1]*LRRI, Albuquerque, NM,* [2]*EPRI, Palo Alto, CA and* [3]*University of North Texas, Denton, TX.*

The SPHERES research program was created to examine the role of inhaled secondary organic aerosol (SOA) on cardiovascular outcomes in mice. SOA was generated in a reaction chamber with alpha-pinene, and was combined with neat amines (monoethanolamine (MEA), methyl diethanolamine (MDEA), piperazine (PIP)) or carbon dioxide degraded amines (CO2-degraded MEA, CO2-degraded MDEA, CO2-degraded PIP). To examine the effects of these mixtures on vascular and lung inflammatory responses, 8 wk old male Apo E-/- mice, on a high fat diet were exposed for 7 days, and the resulting vascular expression levels of HO-1, ET-1, MMP-9, and TIMP-2 cytokines as well as the TBARS measure of lipid peroxidation were assayed in aortic tissue. Total cell counts and differentials were assayed in the bronchoalveolar lavage fluid (BALF). Exposure to some of these mixed amine/SOA atmospheres caused mild vascular and lung responses following 7 days of exposure. MEA+SOA tended to decrease expression levels of cytokines and TBARS in the vasculature, MDEA+SOA had no appreciable effect on cytokines or TBARS, and PIP+SOA led to increases in MMP-9 and TBARS expression and a decrease in TIMP-2 expression compared to control. CO2-degraded MDEA+SOA tended to decrease cytokine expression while having little effect on TBARS. The processing to determine the effects of CO2-degraded MEA+SOA and PIP+SOA are currently in progress. In the BALF, total cell and macrophage counts were non-significantly increased following exposure to MEA+SOA, MDEA+SOA, and PIP+SOA atmospheres and the CO2-degraded MDEA+SOA exposure. Neutrophil and lymphocyte counts were too low to accurately quantify. Overall, some mixed amine/SOA atmospheres caused mild responses in lung and vascular markers of inflammation.

PS 1223 Pulmonary Toxicity Screening of 1, 2-Benzisothiazol-3(2H)-One by Intratracheal Instillation

J. Kwon, H. Kim, I. Shim, P. Kim and K. Choi. *National Institute of Environmental Research, Incheon, Republic of Korea.* Sponsor: J. Kwon.

Chemicals are widely used in our daily lives for various purposes such as disinfectants, air fresheners, paints and hair sprays. In particular, chemicals used in household products (CHPs) have been shown to be a major source of inhalation exposure. However, their pulmonary toxicity has less studied compared with oral and dermal toxicity. Therefore, the purpose of this study was to determine the pulmonary inflammation responses of 1,2-benzisothiazol-3(2H)-one (BIT) used in major CHPs in Korea. Toxicity of BIT was evaluated by intratracheal instillation in SD rats exposed to 10 μg/kg B.W. (low group), 100 μg / kg B.W. (middle group) and 1000 μg / kg B.W. (high group). Animals were sacrificed at both 1 day and 1 week after installation. Toxicity was assessed by count of total and differential cells in bronchoalveolar lavage (BAL) fluid. As a result, in high exposure group, clinical abnormalities associated with the pulmonary toxicity were observed such as shortness of breath and dyspnea. Also, installation of BIT caused a decrease of body weight. The total cell count in BAL fluid increased in the middle and high exposure groups. However, middle group recovered by 1 week post-exposure. Furthermore, significant changes in the polymorphonuclear neutrophils (PMN) values as inflammation marker in the BAL fluid were observed in all exposure groups. Therefore, this study suggests that careful regulations of CHPs would be necessary in maintaining a high quality of life.

PS 1224 Acute Effects of White Spirit with Different Aromatic Content

L. Ernstgård[1], A. Iregren[2], S. A. Juran[1], B. Sjögren[1] and G. Johanson[1]. [1]*Institute of Environmental Medicine, Karolinska Institutet, Stockholm, Sweden and* [2]*Swedish Work Environment Authority, Stockholm, Sweden.*

The use of 'standard' white spirit (stdWS, 15–20% aromatics) in Europe has gradually shifted to low-aromatic or dearomatized white spirit (deWS), as the latter is considered to carry a lower risk of health effects. However, data on health risks of deWS on humans are sparse. We have performed a controlled short-term chamber exposure to compare deWS and stdWS with respect to irritation, inflammation and central nervous systems (CNS) effects. In a dose-finding study thresholds of irritation and CNS effects were identified. Eight (4 males) healthy volunteers rated symptoms related to irritation, smell and CNS effects on a 0–100 mm visual analogue scale (VAS) while exposed to increasing levels of deWS or stdWS from 0.5 to 600 mg/m3.

Based on the dose-finding study, 12 (6 males) healthy volunteers were exposed for 4 h at rest at five conditions: clean air, 100 mg/m3 deWS (0.002% aromatics), 100 mg/m3 stdWS (19% aromatics), 300 mg/m3 stdWS, and 300 mg/m3 deWS. The study was approved by the Regional Ethical Review Board in Stockholm. The following endpoints were studied: symptom ratings on VAS (irritation in the eyes, nose, throat, dyspnoea, smell, headache, fatigue, nausea, dizziness, and feeling of intoxication), neurobehavioral performance (vigilance, response inhibition, response shifting, divided attention, and working memory), pulmonary function, nasal swelling, breathing frequency, blinking frequency, plasma inflammatory markers, and biochemical variables. The only significant increase in rating (compared to clean air) except "solvent smell" was seen for eye irritation at the high stdWS exposure. Ratings during stdWS exposure tended to be higher than during deWS exposure. Weak and inconsistent impairments in working memory and response shifting were seen at high stdWS exposures, compared to clean air. No exposure-related effects on the other objective measurements were found. In conclusion, based on symptom ratings, stdWS is slightly more irritating than deWS.

PS 1225 Repeated Intratracheal Powder Aerosol Delivery in Sprague-Dawley Rats

A. Dumais[1], M. Stoute[1], S. Groom[1], R. Tavcar[1] and R. Forster[2]. *[1]CiToxLAB North America, Laval, QC, Canada and [2]CiTox LAB France, Evreux, France.*

Inhalation administration (Rx) is a highly effective delivery route allowing the bypass of first-pass metabolism and permitting local delivery to the lungs but it is expensive and requires large quantities of material. We have evaluated an alternative approach using a novel device for repeated intratracheal administration (IT Rx). Using this approach we performed single dose and 7 day repeat dose studies with administration of air, PLGA (50/50 DL-lactide/glycolide copolymer) (10 mg/day) or a pharmaceutical test item (10 mg/day) to groups of 6 female Sprague Dawley rats. Only the results of the air and PLGA control groups are presented. Repeated IT Rx resulted in procedure-related lung changes in both control groups, including perivascular/peribronchiolar infiltrate, increased alveolar macrophages, and alveolar hemorrhage. These changes were seen with higher incidence and/or severity in rats receiving PLGA. Lung changes attributable to PLGA, but not seen in the air control, included bronchioloalveolar inflammation, bronchiolar epithelium hypertrophy/hyperplasia and/or erosion, exudate/cellular debris in bronchioloalveoar lumens, foreign material, foreign body granuloma, and necrosis with or without trachea epithelium hypertrophy/hyperplasia and inflammation. Although repeated IT Rx of dry powder aerosols was feasible with this novel device, the lung mechanical damage and dose delivery variation represented significant limitations. This approach was not considered ideal for a 28-day regulatory study with the pharmaceutical test item because of these limitations. Repeated IT Rx of a dry powder aerosol in this way can be a feasible and cost effective alternative approach to inhalation exposure during early discovery allowing for preliminary toxicological and pharmacokinetic evaluation before committing to longer term inhalation studies.

PS 1226 Refinement of Acute Inhalation Toxicity Studies: The Isolated Perfused Rat Lung As a Screening Tool for Surface-Active Substances

C. Dasenbrock, M. Fischer, H. Windt and W. Koch. *Fraunhofer ITEM, Hannover, Germany.*

New surface-active agents in waterproofing sprays are often tested for acute inhalation toxicity *in vivo* on the basis of OECD Test Guideline 403. A screening test using the isolated perfused rat lung (IPRL) is proposed in order to reduce the number of acute inhalation tests and to refine these. The test comprises exposure of IPRLs to aerosolised formulations of the water proofing agents and on-line monitoring of respiratory parameters.

Substances revealing harmful effects on the IPRL, such as impaired lung compliance and atelectasis formation, did also show changes in respiratory parameters up to mortality in *in vivo* tests with rats. Thus, pre-testing in the IPRL allows the identification of surface-active substances causing acute inhalation toxicity.

To assess the potential lung toxicity of seven formulations, each tested in two male and two female IPRLs, we evaluated changes in the respiratory parameters tidal volume, compliance, and resistance, edema and atelectasis formation, taking into account the inhaled doses. These IPRL results were compared with available *in vivo* results and a good or excellent correlation in six out of seven cases was revealed.

In conclusion, the use of the IPRL is well suited for screening substances showing acute "physical" inhalation toxicity. Therefore, for future assessment of surface active substances, it is suggested to use this test prior to *in vivo* inhalation tests. Formulations with no acute harmful effects on the IPRL need to be further investigated *in vivo* for complete risk assessment. However, substances showing strong reactions in the IPRL will most likely cause lung damage *in vivo*. This is why testing in live animals is not recommended in order to avoid possible pain, suffering or distress.

PS 1227 Quantitative Evaluation of the Relationship between Vapor Characteristics and Upper Respiratory Tract Uptake Efficiencies in Rodents

K. Neier[1], M. Glynn[1], H. A. Fritz[1], J. S. Pierce[1], A. Urban[2], S. H. Gaffney[2] and B. L. Finley[3]. *[1]Cardno ChemRisk, Chicago, IL, [2]Cardno ChemRisk, San Francisco, CA and [3]Cardno ChemRisk, New York, NY.*

Characterizing the regional absorption of inhaled vapors within the respiratory tract of animals typically used in toxicology studies is essential in applying the results to human health risk assessments. It is well documented that water soluble and reactive vapors are absorbed or "scrubbed" in the upper respiratory tract (URT) of the rodent with high efficiency, thereby reducing the amount of vapor that reaches the lower airways. A literature review and analysis was performed to quantitatively evaluate the relationship between 5 vapor characteristics (pKa, Henry's Law constant (HLC), water solubility, vapor pressure, and Km) and their effects on URT uptake efficiency (UE) in rodents. Sixteen studies that examined UE of 14 vapors were identified. Linear regression modeling controlling for inhaled vapor concentration and flow rate was performed for each vapor characteristic in rats and mice to characterize their relationship with URT UE. Results indicated that pKa and HLC had significant inverse linear relationships with URT UE in rats (pKa: β= -1.18, $p < 0.0001$; R^2=0.537; HLC: β= -18780, $p < 0.0001$; R^2=0.398). Models that included both pKa and HLC yielded a slightly higher adjusted R2 than pKa and HLC alone (full model R^2=0.540; reduced models R^2=0.377-0.520). There was no significant linear relationship between URT UE and water solubility (β=0.0007, p=0.9; R^2=0.147) or vapor pressure (β= -0.0009, p=0.9; R^2=0.147) in rats, although it is possible that non-linear models may better describe these relationships. There were limited data available for mice; however, these results indicated a similar relationship between URT UE and pKa (β= -0.49, $p < 0.001$; R^2=0.333). Although limited data were available for analysis and only linear relationships were examined, these preliminary results indicated that identification of common vapor characteristics may aid in interpreting and explaining observed regional effects of vapor inhalation in rodents.

PS 1228 Comparison of the Upper Respiratory Tract Uptake Efficiencies of Vapors in Rats and Mice

H. A. Fritz[1], M. Glynn[1], K. Neier[1], J. S. Pierce[1], A. Urban[2], S. H. Gaffney[2] and B. L. Finley[3]. *[1]Cardno ChemRisk, Chicago, IL, [2]Cardno ChemRisk, San Francisco, CA and [3]Cardno ChemRisk, Brooklyn, NY.*

It has been reported that soluble and reactive vapors are readily absorbed or "scrubbed" in the upper respiratory tracts (URT) of rodents, reducing the dose that reaches the lower airways. Since the inhalation of some vapors has resulted in differences in observed regional airway effects between mice and rats, researchers have hypothesized that there is a significant difference in URT uptake efficiency (UE) between the two species. To investigate this hypothesis, a literature review was performed to identify studies that measured the URT UE of the same vapors in both mice and rats, and a quantitative comparison between the URT UEs was performed. In order for a vapor to meet the inclusion criteria, studies must have been identified that measured UEs via surgically isolated URTs for both species at comparable concentrations and flow rates. A total of eight studies that evaluated 4 vapors (naphthalene, propylene oxide, acetaldehyde, and acrolein) were included in this analysis. URT UEs were compared for each vapor individually and for all vapors together using paired t-tests. Overall, the mice had statistically significant higher mean URT UEs than rats (48.13% v. 38.15% ; $p < 0.0001$). The mean URT UEs for mice were higher than rats for naphthalene (62.26% v. 33.41%; $p < 0.0001$) and for propylene oxide, although to a lesser extent (21.75% v. 17.25%; $p = 0.008$). In contrast, there was no significant difference in URT UE of acetaldehyde between mice and rats (45.67% v. 46.52%; $p = 0.67$). A statistical comparison was not performed for acrolein due to small sample size (n = 1 for both species). Although there were a limited number of studies available, the results demonstrate that URT UE is not uniform across species, even in species as similar as mice and rats. Further, the results demonstrate the importance of taking species-specific differences into account when interpreting rodent model results and extrapolating to other species, including humans.

PS 1229 A Spray Dryer Method for the Micronization of Small Amounts of Substance in High Yield for Aerosol Generation

F. Acevedo[1] and P. Gerde[1, 2]. [1]*Inhalation Sciences Sweden AB, Novum, Sweden and* [2]*IMM, Karolinska Institutet, Stockholm, Sweden.*

Research on dry powder toxic inhalants or drug candidates for inhalation therapy typically require particulate starting materials with diameters in the range of 1- 5 μm. However, isolated toxicants or newly synthesized drug candidates are often available only in the milligram range. Yet, few systems for generation of micronized substances of these batch sizes have been available. Here we present a spray dryer method for generating micronized particles at room temperature in high yields requiring substance only in the mid-milligram range. The LaminarPace spray dryer generates micronized particles from nebulized solutions. A mesh nebulizer (Aeroneb Pro) delivers droplets to a laminar air flow in an inner column coated with a vapor-permeable membrane. A countercurrent stream of air at room temperature on the outside of the membrane removes the evaporated solvent, from which it is absorbed in a separate silica/activated carbon column in a closed loop. Dried powder product is collected on a filter at the end of the drying column. Aqueous solutions of 2% lactose and 2.5% horse radish peroxidase and an ethanol solution of 2% budesonide were micronized from batches in the range of 20 to 500 mg. Product yields were >80% and particle sizes ranged from 1 to 5 μm. The production rate varied from 0.1 to 1 mg/min. Enzymatic activity of horse radish peroxidase was fully retained after drying indicating that delicate biomolecules will retain their activity. Removal of solvent was nearly complete when nebulizer output was around 5% of its full capacity. However, using ethanol as solvent makes the transfer slightly less effective than with water. The laminar flow regime maintains particle losses in the column at less than 10%. Small portions of toxic substances or drug candidates can thus be micronized and tested via inhalation, thereby facilitating early detection of biological activity.

PS 1229a Pulmonary Responses after the Inhalation of Fumes from Resistance Spot Welding of Galvanized Zinc-Coated Steel

J. M. Antonini, A. Afshari, W. McKinney, T. G. Meighan, M. Jackson, B. T. Chen, D. Schwegler-Berry, N. B. Marshall, S. E. Anderson, A. Cumpston, J. Cumpston, H. D. Leonard, D. G. Frazer and P. C. Zeidler-Erdely. *NIOSH, Morgantown, WV.*

Spot welding (SW) of galvanized zinc (Zn)-coated steel is commonly used in the automotive industry where high speed repetitive welding of thin metal sections is needed. SW produces complex aerosols that cause bronchitis and asthma in workers. The goal was to assess the effect of SW fumes on lung responses in an animal model. Male Sprague-Dawley rats were exposed by inhalation to 25 mg/m^3 of SW aerosol for 4 h/d x 8 d. Controls were exposed to filtered air. During exposures, particle size distribution, morphology, and chemical composition of the generated aerosol were determined in the breathing zone of exposed animals. Mass median aerodynamic diameter was determined to be 0.25 μm by a MOUDI particle impactor. Particles were arranged as chain-like agglomerates composed of ultrafine primary particles. Large, more spherical particles were observed among the agglomerates. Metal analysis indicated the fumes were 90% Fe, 7% Zn, and 2% Mn. Due to the presence of Zn in the fumes and the possible development of metal fume fever, animal body temperatures were measured before and after each daily exposure. No change in body temperatures was observed throughout the exposure period when comparing the two treatment groups. At 1 and 7 d after the final exposure, bronchoalveolar lavage (BAL) was performed to assess lung toxicity. Lactate dehydrogenase (a marker of lung cell cytotoxicity), total BAL cells, and BAL neutrophils were significantly elevated ($p<0.01$) 1 d after exposure to the SW fumes compared to controls, indicating the development of acute lung injury and inflammation. However, all markers of lung toxicity returned to control values by 7 d after exposure. Acute inhalation of SW fumes from galvanized Zn-coated steel at an occupationally-relevant concentration caused significant lung toxicity, but not metal fume fever in an animal model. Importantly, the observed lung injury and inflammation subsided after a 7-d post-exposure recovery period.

PS 1229b 90-days Inhalation Toxicity Study of Manufactured Zinc Oxide Nano Particle

Y. Heo[1], Y. Kim[1], H. Yang[1], S. Bae[1], K. Lee[1], E. Jo[2], I. Eom[2] and B. Lee[2]. [1]*Inhalation Toxicology Center, Korea Institute of Toxicology, Jeongeup-Si, Republic of Korea and* [2]*Risk Assessment Division, National Institute of Environmental Research, Incheon, Republic of Korea.*

Nano-sized Zinc oxide is extremely produced for last decade, and has been used in a variety of application on the industries of food, batteries, paints, cement, cosmetics, etc. The potential risk of inhalable nano-sized ZnO is intensely raised on humans, especially workers in manufacturing company. However, the inhalation toxicology reports of ZnO nanoparticle are limited. In this study, 90-days repeated inhalation toxicology study was performed according to GLP guidelines. Nano-sized ZnO aerosol was generated using dust feeder of turntable-rotation type, and mechanically distributed with automatic aerosol dilution system. Eight-week-old SD rats divided into 4 groups (control; fresh-air, low dose; 0.5 mg/m3, middle dose; 2.0 mg/m3 and high dose; 10.0 mg/m3) were exposed to ZnO nano-aerosol for 6 hr/day, 5 day/week, and for 13 weeks. For analysis of particle characterization and size distribution, MMAD (Mass median aerodynamic diameter) and number concentration were also monitored. Clinical signs, body weight and food consumption were periodically observed during whole study duration. Total and differential cell count, total protein, LDH, and cytokines (IL-1β and IL-2) were measured from BAL fluid. As well, the distribution of inhaled ZnO particles inside lungs was observed using TEM (Transmission electrical microscopy). The male rats of high dose group showed significant changes in body weight, but female rats did not show any change for 90-day experiments. Significant differences were detected between high dose group and other dose groups on total and differential cell count values, total protein levels, LDH levels, and IL-1β and IL-2 levels. We also verified distribution of zinc oxide nanoparticle relative to different concentration on alveolar macrophage. In conclusion, it was expected sub-chronic inhalation exposure of nano-sized ZnO could have adverse effects and NOAEL (no observed adverse effect level) is considered to be above 2.0 mg/m3 under this experimental condition.

PS 1229c Use of Lung Weight As Biomarker for Assessment of Lung Toxicity in Rat Inhalation Studies

H. Zhang[1], E. Wahlström[1, 2], L. Sundius[1, 3] and A. Ollerstam[1, 4]. [1]*AstraZeneca, Mölndal, Sweden,* [2]*Karolinska Institute, Stockholm, Sweden,* [3]*Lund University, Lund, Sweden and* [4]*LEO Pharma A/S, Copenhagen, Denmark.* Sponsor: S. Platz.

Organ weight in general has been accepted as a valuable readout in toxicological studies (1). In our daily practice, we have noticed that lung weight changes were often but not always associated with lung histopathology, as observed by others (2). The variations in lung weights, together with relatively small group sizes, made it difficult to interpret the lung weight changes occurring in inhalation studies, particularly in the 1- to 2-week studies in rat. Further literature searching did not help us find sufficient information discussing the application of lung weight as a biomarker of lung toxicity and its correlation with lung histopathology.

To investigate whether the lung weight can be used as an indicator for acute lung injury, we have analyzed retrospectively the lung weight data from 30 inhalation studies in rats exposed to dry powder inhalation. The lung weight change and lung histopathology in the inhalation studies reviewed showed concordance in the majority of studies. The lung weight change in the 1- to 2-week studies was often predictable to the lung weight change in the 4-week studies with the same test compound. Under current design with 5 males and 5 females per group, the lung weight change greater than 10 to 20% of control values can be detected. The lung weight should be applied as a complementary end point to lung histopathology for assessing lung toxic effect by inhaled compounds in acute/subacute inhalation studies in rat.

1.Bailey, S. A., Zidell, R. H., and Perry, R. W. (2004). Relationships between organ weight and body/brain weight in the rat: What is the best analytical endpoint? Toxicol Pathol 32, 448–66.

2.Michael, B., Yano, B., Sellers, R. S., Perry, R., Morton, D., Roome, N., Johnson, J. K., and Schafer, K. (2007). Evaluation of organ weights for rodent and non-rodent toxicity studies: A review of regulatory guidelines and a survey of current practices. Toxicol Pathol 35, 742–50.

PS 1229d Macrophage Solubilization of Indium-Containing Particles As an *In Vitro* Correlate to Pulmonary Toxicity *In Vivo*

W. M. Gwinn[1], W. Qu[1], R. W. Bousquet[2], H. Price[2], C. Shines[2], G. Taylor[2], M. P. Waalkes[1] and D. L. Morgan[1]. [1]*NTP Laboratory, NIEHS, RTP, NC and* [2]*Alion Science and Technology Corp, RTP, NC.*

Indium-containing particles (ICPs) such as indium phosphide (InP) and indium tin oxide (ITO) are toxic to the lung. Many ICPs are insoluble and engulfed by alveolar macrophages; however, the mechanism(s) of pathogenesis is unclear. Previously, we showed in vitro that macrophage solubilization of InP and ITO via the phagolysosomal acidification pathway results in particle-induced cytotoxicity and the release of ionic indium, potentially the cytotoxic constituent of ICPs. It is undetermined whether the toxicity of ICPs relates to the total amount of indium in the compound and/or the solubility. The ICPs used in these initial studies were of different particle diameters and thus a valid comparison could not be made. In the current study, we compared the macrophage solubilization and cytotoxicity of InP and ITO with similar particle diameters (~1.5 μm) and determined if relative differences in these in vitro parameters correlated with particle-induced pulmo-

nary toxicity in vivo. RAW 264.7 macrophages were treated with InP or ITO and cytotoxicity was assayed at 24 hrs. Particle solubilization (release of ionic indium) was also measured at 24 hrs in culture supernatants by atomic absorption spectroscopy. Macrophage cytotoxicity and ionic indium release were much greater for InP compared to ITO. Next, B6C3F1 mice were treated with 1 mg/kg InP or ITO by oropharyngeal aspiration. On day 28, BAL and pleural lavage were collected and assayed for total cell numbers (and differentials), LDH activity and protein levels as markers of lung toxicity. All of these parameters were greatly increased in mice treated with InP compared to ITO. These data suggest that macrophage solubilization and cytotoxicity of ICPs in vitro may be capable of predicting pulmonary toxicity in vivo. Furthermore, these differences in toxicity were observed despite the two compounds having similar indium content suggesting that solubilization, not total indium content, may better reflect the toxic potential of ICPs.

PS 1229e Acrolein Toxicity in Endothelial Cells Involves Lipid Peroxidation, Protein Damage, and Reduced Cellular GSH and Augmented Monocyte Adhesion

R. Chitrakar[1], Z. Jia[1], H. Shah[1], A. Speen[1], J. McCormick[1], P. Nallasamy[1], P. Joubert[1], H. Zhu[2] and Y. Li[2]. *[1]University of North Carolina at Greensboro, Greensboro, NC and [2]Campbell University School of Osteopathic Medicine, Buies Creek, NC.*

Environmental pollutant exposure has been implicated in the pathogenesis of cardiovascular diseases. Acrolein is a highly reactive aldehyde pollutant mainly found in automobile exhaust and tobacco smoke. However, the action of acrolein in endothelial cells remains to be investigated. The present study examined acrolein-induced cellular injury, oxidative modifications of cellular constituents, adhesion of monocytes to endothelial cells and altered intracellular glutathione (GSH) on EAHY926 cells, a widely used endothelial cell line for study of endothelial cell dysfunction. Incubation of cells with acrolein at pathophysiological concentrations for 24 hours caused a significant decrease in cell viability measured by MTT assay and increase in release of lactate dehydrogenase (LDH), which is further confirmed by a significant change in cell morphology. Acrolein also increased the amount of thiobarbituric acid reactive substances, a marker of lipid peroxidation, and protein carbonyl levels, a marker of protein damage in the cells. Incubation of cells with acrolein also resulted in a significant depletion of cellular GSH and augmented monocyte adhesion to human endothelial cells, an important step in the development of atherosclerosis. The results of this study may contribute to our ability to assess the cardiovascular risk of human exposure to acrolein.

PS 1229f Carbon Capture and Sequestration: An Exploratory Inhalation Toxicity Assessment of Amine Trapping Solvents and Their Degradation Products

D. Kracko[1], A. C. Rohr[2], J. D. McDonald[1], M. Doyle-Eisele[1], J. Seagrave[1], E. Knipping[2] and S. Shaw[2]. *[1]LRRI, Albuquerque, NM and [2]Electric Power Research Institute, Palo Alto, CA.*

Carbon dioxide (CO2) absorption with aqueous amine solvents is a method of carbon capture and sequestration (CCS) from flue gases. One concern is possible release of amine solvents and degradation products into the atmosphere, warranting evaluation of potential pulmonary effects from inhalation. The CCS amines monoethanolamine (MEA), methyldiethanolamine (MDEA), and piperazine (PIP) underwent oxidative and CO2-mediated degradation for 75 days. C57bl/6N mice were exposed for seven days by inhalation of 25 ppm of neat amine or equivalant concentration in the degraded mixture. The aqueous solutions were nebulized to create the inhalation atmospheres. Pulmonary response was measured by changes in inflammatory cells in bronchoalveolar lavage fluid and cytokine expression in lung tissue. Ames mutagenicity and CHO-K1 micronucleus assays were applied to assess genotoxicity. Chemical analysis of the test atmosphere and liquid revealed complex mixtures including acids, aldehydes, and other compounds. Exposure to oxidatively degraded MEA increased ($p<0.05$) total cells, neutrophils, and lymphocytes compared to control mice and caused inflammatory cytokine expression (statistical increase at $p<0.05$). MEA and CO2 degraded MEA were the only atmospheres to show statistical ($p<0.05$) increased in oxidative stress. CO2 degradation resulted in a different composition, less degradation, and lower observed toxicity (less magnitude and number of effects) with no genotoxicity. Overall, oxidative degradation of the amines studied resulted in enhanced toxicity (increased magnitude and number of effects) as compared with the neat chemicals.

PS 1229g Potential Exposure Threshold of Chrysotile Asbestos

T. Hesterberg[1], P. A. Nony[2], P. Watson[4], M. Berg[3] and K. C. Scribner[2]. *[1]Center for Toxicology and Environmental Health, L.L.C., Denver, CO, [2]CTEH, L.L.C., North Little Rock, AR, [3]CTEH, L.L.C., Kemah, TX and [4]CTEH, L.L.C., Albany, NY.*

Studies have shown that various forms of asbestos (serpentine, crocidolite, and amosite) have different toxicities depending on the fiber characteristics dose, dimension, durability, and biosolubility. While some early regulations accounted for these differences, the current guidelines consider all asbestos types to have the same hazardous potential. We hypothesize that there is an exposure threshold for the health effects of a biosoluble asbestos, such as chrysotile. This has implications for whether exposures can be controlled to levels that would not be expected to cause lung disease in countries where chrysotile asbestos is still in use.

To determine the current information available regarding chrysotile asbestos, a review of available epidemiological and animal studies was performed. Epidemiology studies are difficult to use for elucidating threshold doses since asbestos type and dimension in the workplace are often not known, and worker history can be difficult to obtain. Animal research has shown that high exposure to chrysotile asbestos is associated with lung disease; however, at these high levels the disease related to a lung overload mechanism. Subchronic exposure studies have indicated a No Observed Adverse Effect Level (NOAEL) of approximately 500 f/cc, which indicates a threshold for asbestos-induced lung disease. Additional studies have shown that chrysotile has low biopersistence in the lung, does not translocate to the pleura, and does not appear to cause hyperplasias or other pleural changes.

The science indicates that low exposures to chrysotile asbestos do not present a significant risk to human health. A multi-dose, chronic inhalation study in rodents would better define the threshold for potential health effects from low exposures to chrysotile asbestos. Understanding low-dose chrysotile exposures is important to evaluating the role of past chrysotile asbestos exposures in the US and to the regulation of asbestos use in other countries.

PS 1230 Increases in the Serum Acute Phase Proteins after Ozone Exposure Are Associated with Induction of Genes in the Lung but Not Liver

A. R. Henriquez[1], D. Johnson[1], M. Schladweiler[2], J. Richards[2] and U. P. Kodavanti[2]. *[1]Curriculum in Toxicology, University of North Carolina at Chapel Hill, Chapel Hill, NC and [2]EPHD/NHEERL/ORD, US EPA, Research Triangle Park, NC.*

Acute Phase Response (APR), a systemic reaction to infection, trauma, and inflammation, is characterized by increases and decreases in plasma levels of positive and negative acute phase proteins (APP), respectively. Although the liver has been shown to contribute to APR in various pathologies, the source of circulating APP after air pollution exposure is not well characterized. We hypothesized that lungs and liver both will contribute to plasma levels APP after an acute ozone exposure. To test this hypothesis, we exposed male Wistar Kyoto rats to air or O3 (1ppm), 6hr/day for 1 or 2 consecutive days. Immediately after ozone exposure, genes encoding APP were analyzed at mRNA level in the lungs and livers and proteins were analyzed in the serum. Ozone exposure increased positive acute phase proteins in the serum, such as α-1-acid glycoprotein, AGP; α-2-macroglobulin, A2M; and decreased negative APP such as transferrin. These increases in serum proteins were associated with marked increases in mRNA expression of several APP in the lungs (A2M, AGP, α-1-antitrypsin, hepcidin, and ceruloplasmin). Ozone did not increase liver mRNA for any APP examined. However, there were remarkable tissue differences between lung and liver mRNA expression of APP in air exposed rats (liver>lung). C-reactive protein was expressed highly in the liver but minimal expression was noted in the lung (not affected by ozone in lung or liver). Thus, although liver tissue mass is ~15 times greater than lung mass, it is clear that the acute phase protein genes are induced only in the lung after ozone exposure; the role of lung should not be ignored in modulating APR and release of APP in the circulation upon the inhalation of pollutants. (This abstract does not reflect the US EPA policy).

PS 1231 Effects of Nitrogen Dioxide and Ozone on the Expression of Proinflammatory and Oxidative Stress Mediators in Primary Human Bronchial Epithelial Cells at the Air-Liquid Interface

J. E. Mirowsky[1], K. E. Duncan[1], S. D. McCullough[2], L. A. Dailey[2] and R. Devlin[2]. [1]*Center for Environmental Medicine, Asthma, and Lung Biology, University of North Carolina, Chapel Hill, Chapel Hill, NC and* [2]*National Health and Environmental Effects Laboratory, US Environmental Protection Agency, Chapel Hill, NC.*

Nitrogen dioxide (NO_2) and ozone (O_3) are environmental air pollutants capable of inducing lung injury and inflammation by causing oxidative damage to the respiratory epithelium. Mice models have suggested that these pollutants induce damage via similar mechanisms, although little work has been done to corroborate this *in vitro* – specifically in primary epithelial cells. Thus, the purpose of this study was to compare the responses between O_3 and NO_2 in a gas-phase system using primary human epithelial cells obtained via brush biopsy. These cells, obtained from 9 donors, were cultured and grown at an air-liquid interface (ALI), which closely reflects the real-life inhalation of these toxicants. After 3-4 days at ALI, the cells were exposed to NO_2 (1.0, 2.0, 3.0, or 5.0 ppm), O_3 (0.25, 0.50, 0.75, or 1.00 ppm), or clean air for 120 min. The expression of pro-inflammatory and cellular stress markers was measured using quantitative real time PCR 0, 1, 4, and 24 hours following each exposure. Expression of the pro-inflammatory cytokine IL-8 was elevated only at 24 hours post-exposure when cells were exposed to either 3.0 or 5.0 ppm NO_2; however, down-regulation of HO-1 and COX2 were observed at all time points at each dose. In contrast, the expression of IL-8, HO-1, and COX2 were up-regulated following all O_3 exposures; the greatest increases were seen 1 hour following O_3 exposures. Therefore, it is possible that NO_2 and O_3 exposures induce damage to the respiratory epithelium via differing mechanisms, in contrast to the previously tested mice models.

PS 1232 Health Effects Associated with Inhalation Exposure to Diesel Emission Generated with and without CeO2 Nano Fuel Additive

S. J. Snow[1, 2], M. Schladweiler[2], J. McGee[2], V. L. Bass[1], D. Nash[3], J. Weinstein[3], R. Willis[3], W. Linak[3], C. E. Wood[3], S. Elmore[4], R. F. Thomas[2], D. B. Miller[1], T. Krantz[2], C. King[2], C. Johnson[5], J. Morrison[5], J. Richards[2], A. Ledbetter[2], I. Gilmour[2] and U. P. Kodavanti[2]. [1]*UNC, Chapel Hill, NC,* [2]*NHEERL, EPA, RTP, NC,* [3]*NERL, EPA, RTP, NC,* [4]*NIEHS, RTP, NC and* [5]*Pathology Associates Inc., Durham, NC.*

Diesel exhaust (DE) exposure induces adverse cardiopulmonary effects. Addition of nano cerium (Ce) oxide to diesel fuel (DECe) increases fuel burning efficiency but results in altered emission characteristics and potentially altered health effects. We hypothesized that inhalation of DECe will cause greater adverse pulmonary health effects in rats compared to DE alone. Male Sprague-Dawley rats (8 wks old) were exposed to either DE or DECe (1000 μg/m3) 5 hrs/day for 2 days. We observed an increase in N-acetyl glucosaminidase in lung lavage fluid of rats exposed to DECe as compared to air group. There were also marginal but insignificant increases in several lung injury biomarkers in both exposure groups (DECe>DE). To further characterize DECe toxicity, we exposed rats to DECe (100 or 1000 μg/m3) or the gas-phase components of DECe (1000 μg/m3) 5 hrs/day for either 2 days or 4 wks (5 days/wk) with one group allowed a 14 day recovery. Ce lung burden levels indicated a time- and concentration-dependent accumulation during treatment with 35% clearance of Ce from the lung during the 14 day recovery. The high dose of DECe increased lung inflammation at the 2 day time point; this effect was reduced at 4 wks except for the sustained increases in lavage fluid activity of γ-glutamyl transferase. Increased alveolar septae thickness due to edema and increased presence of pigmented macrophages after DECe exposure was illustrated by histology and TEM. Lung effects were also evident after exposure to gas-phase of DECe, suggesting the effects of whole exhaust may be driven by gas-phase components and/or particulate effects may be modified by gas-phase components. These data indicate that exposure to DECe induces adverse pulmonary effects that on a mass basis, causes greater injury than DE alone. (Does not reflect the US EPA policy)

PS 1233 Histopathological Effects of Inhaled Diesel Exhaust from Diesel Engine in SD Rats

I. Shim, H. Kim, J. Kwon, P. Kim and K. Choi. *National Institute of Environmental Research, Incheon, Republic of Korea.*

Exposure of humans and experimental animals to Diesel Exhaust (DE) has been reported as major air pollutant to induce airway inflammation, decrease lung function and aggravate asthma because it contains hazardous materials such as particulate matters. The objective of this study is to identify the acute inhalation toxicity of DE in SD rats using wholebody exposure chamber. In this study, groups of 10 Sprague-Dawley rats were exposed to the DE from diesel engine by the route of inhalation(2h/day, 3days) at the 3 different RPM(Rotation per minute) of 0(control), Idle, 1160, 1740 rpm. As a result, there were no significant differences in body weight and organ weight gain between exposure groups and control group. Clinical examination results showed that there were no symptoms or deaths. However, the histopathological changes were found in the lungs of the male and female rats inhaled with diesel exhaust. The histiocytic inflammatory cell infiltration described as histiocytic pneumonitis was found around the terminal bronchiole and alveolar duct. The lesions were observed in the lung of Idle exposed group. These results suggest that inhalation of diesel exhaust could induce obvious histopathological changes to rats.

PS 1234 The Effects on Endothelial Cell Eicosanoid Release with Biodiesel Exhaust Soluble Fraction

L. Bhavaraju[1], R. McCormick[2] and M. C. Madden[3]. [1]*Toxicology, University of North Carolina, Chapel Hill, NC,* [2]*NREL, Golden, CO and* [3]*U.S. EPA, Chapel Hill, NC.*

Human umbilical vein endothelial cells (HUVECs) were exposed in vitro to soluble fraction of 100% soy biodiesel combustion particles (BEPE) in order to study their effect on vasodilation. Previous controlled human exposures indicate inhalation of biodiesel (BD) combustion emissions can inhibit vasodilation. We developed a study to measure a vasodilator eicosanoid, prostacyclin, in response to BEPE. Our study indicated no significant cytotoxicity, measured by LDH release, after 6h exposure with 100ug/mL BEPE. After 6h exposure the stable metabolite of prostacyclin, 6-keto PGF1α (6keto), was found significantly decreased from vehicle indicating disruption of vasodilator (6keto) release. Next we examine biochemical mechanisms involved, analyzing mRNA and protein levels of enzymes in 6-keto production. COX-1 &2 gene expression levels were significantly decreased below vehicle with BEPE at 100ug/mL after 6hrs ($p<0.05$). Western blot of COX-2 showed a decrease. Western blot of COX-1 shows no intensity changes with BEPE exposure. PGI synthase (PGIS) mRNA levels and protein levels show no change from control levels. Both COX1/2 and PGIS were challenged after extract exposure with 10uM Arachidonic acid (AA) and 1uM PGH2 respectively to verify if enzyme activity can be reversed. Post challenge, 6-keto levels ≥ vehicle with PGH2 challenge and AA challenge. The results indicate PGIS & COX-2 were not permanently affected by BEPE. Additionally PLA2 agonist challenge post exposure indicates, 6keto levels were unaltered compared to vehicle suggesting BEPE suppresses some enzymes of 6keto production. Post BEPE exposure simultaneously incubation with fresh BEPE and AA induced a decrease of 6keto. These results indicate compounds in BEPE can induce immediate impairment in 6keto release and/or detection. We postulate the saturated fatty acids from BEPE combustion disrupted the formation of complexes inhibiting 6keto temporarily and at low intracellular substrate levels. This abstract of a proposed presentation may not reflect official US EPA Policy

PS 1235 Effects of Diesel Exhaust on Markers of Genetic and Cardiovascular Toxicity in Rats: Results from the ACES Study

J. Bemis[1], L. M. Hallberg[2], D. J. Conklin[3], M. Kong[3], B. T. Ameredes[2], J. B. Ward[2], C. Hernandez[2], S. Zaas[4], C. Norton[4] and J. K. Wickliffe[4]. [1]*Litron Laboratories, Rochester, NY,* [2]*University of Texas Medical Branch, Galveston, TX,* [3]*University of Louisville, Louisville, KY and* [4]*Tulane University, New Orleans, LA.*

Exposure of humans to vehicle emissions is an unavoidable part of today's world. New engine technologies have been developed to minimize emissions and reduce potential health impact(s). The effects of exposure to 2007 model-compliant diesel engine exhaust (DE) were assessed via ancillary investigations performed under the Advanced Collaborative Emissions Study (ACES) chronic bioassay. As part of ACES performed at Lovelace Respiratory Research Institute, male and female Wistar-Han rats were exposed up to 30 months to dilutions of whole DE resulting in low, medium and high levels of exposure based on NO2 concentration. In addition to examination of lung function and general pathology (reported elsewhere), the effects on genotoxicity and vascular inflammation and aging were investigated at 1, 3, 12, and 24 months. Biomarkers of lipid peroxidation and DNA damage were examined by the Comet assay in lung, 8-OH-dG in serum, and TBARS in brain. Chromosomal damage was assessed via the flow cytometric micronucleus assay conducted in peripheral blood. Pro-inflammatory and general toxicity endpoints were measured in plasma. No statistically significant exposure-related effects were observed in the markers of genotoxicity or oxidative damage at any time point. At 24 months, exposure-related increases in plasma IL-6 and sICAM-1 were observed in female rats. Alterations in other markers of toxicity, including plasma total and non-HDL cholesterol and triglycerides were also observed in female rats

only. The ACES study represents the most comprehensive examination of the potential health effects associated with 2007 engine DE performed to date. Under the conditions described, no effects on oxidative damage or genotoxicity were observed. However, a few modest increases in markers of cardiovascular disease risk appeared dependent on age and/or exposure duration and sex.

PS 1236 ACES Phase 3: Results from the Chronic Bioassay of Rats Exposed to 2007 Compliant Diesel Emissions

J. D. McDonald, M. Doyle-Eisele, J. Seagrave, R. Miller and A. Gigliotti. *LRRI, Albuquerque, NM.*

Phase 3 of the Health Effects Institutes (HEI) ACES program was to conduct animal inhalation studies in rats for up to 24-30 months as a carcinogenicity bioassay, measuring indicators of pulmonary toxicity in rats at intervals during exposure. This presentation reports the final results of the bioassay. Atmospheres were generated from emissions of a 2007 compliant 500 hp engine and aftertreatment system operated on a variable-duty cycle. Dilutions of exhaust were maintained at average integrated concentration of 4.1, 0.8 and 0.1 ppm NO2. Exposure atmospheres were characterized in detail. Exposures were conducted for 16 hr/day, 5 days/wk. Rats were evaluated by respiratory function, hematology, serum chemistry, bronchoalveolar lavage, lung cell proliferation, and histopathological assays. Concentrations of particulate matter are generally very low and rise only during diesel filter regeneration, once or twice per 16-hr exposure period. Mild biological responses were observed, and were confined primarily to the respiratory tract and primarily at the highest exposure concentration. The primary histologic findings were minimal airway thickening in the central acinus. The severity of the lesions did not increase between 1 year and the lifetime. The observed changes were consistent with exposure to gaseous components such as NO2, and differed markedly from effects observed from traditional diesel exhaust.

PS 1237 Involvement of TLR2 and TLR4 and Th1/Th2 Shift in Lung Inflammatory Responses Induced by Fine Ambient Particulate Matter

X. R. Xia. *Peking University First Hospital, Beijing, China.*

Air quality in China is notoriously poor and recently has become an issue associated with increasing social unrest. Epidemiologic studies have reported the association between fine particles (aerodynamic diameter≤2.5μm; PM2.5) and health effects, but the immunological mechanisms are not clear. To investigate the dose and time-dependent role of toll-like receptor (TLR) and Th1/Th2 cell in local and systemic inflammation induced by PM2.5, PM2.5 was added to MH-S cells (mouse alveolar macrophage cell line) and mice were subjected to Nose and mouth exposed of 2.5, 5, or 10mg/kg PM2.5 in this study. After 24h, 72h, 7days, and 14days, mice were sacrificed to measure TLR2 and TLR4 expressions and Th1/Th2 related cytokines in bronchoalveolar lavage fluid (BALF) and peripheral blood. Histopathological changes in lung were examined. Inflammatory infiltration and macrophages with engulfed particles were found by lung histopathology after PM2.5 exposure. TLR4 positive cells decreased in BALF but increased in blood at 24h after the exposure. The low percentage of TLR4 positive cells continued to day 14 in BALF, but recovered at day 7 and decreased further to lower than the control value at day 14 in blood. TLR2 positive cell changed similar to TLR4 in BALF on the dose effects. In BALF at 24h after the exposure, the Th2 related cytokines IL-5 and IL-10 increased dose-dependently; and in blood, the Th2 related cytokines IL-4, IL-5, and IL-10 also increased. These results suggest that acute exposure of PM2.5 leads to acute inflammatory responses locally and systemically in mice. TLR2 and TLR4 are involved in this process and PM2.5 can drive a Th2-biased immune response.

PS 1238 Effect of SNPs and Glycosolyation Site Mutations on TRPA1 Activation by Particulate Material

C. Deering-Rice, D. Shapiro, E. G. Romero and C. A. Reilly. *Pharm/Tox, University of Utah, Salt Lake City, UT.*

Transient receptor potential ankyrin 1 (TRPA1) mediates nocifensive responses and inflammation caused by inhaled irritants including certain particulate air pollutants (PM). The mechanism by which insoluble components of PM activate TRPA1, as well as whether differential activation occurs as a result of single nucleotide polymorphisms (SNPs), leading to differences in individual PM sensitivity, was further explored. TRPA1 mutants were generated, transfected into HEK-293 cells, and functionality evaluated by comparing calcium flux relative to the wild-type channel. AITC, a soluble electrophilic TRPA1 agonist, was used to assess the overall functionality of each specific mutant and as a model for PM associated electrophiles.3,5-ditertbutylphenol (3,5-DTBP) is a non-electrophilic component of some PM and is a TRPA1 agonist. The insoluble PM agonist was coal fly ash (CFA). qPCR confirmed equivalent mRNA expression of all mutants and wild-type TRPA1. The N-terminal SNPs R3C and R58T exhibited increased responses to all agonists, and the pore-loop SNP, N954T exhibited a lack of response to all agonists. The ankyrin repeat SNPs E179K and K186N and the pore-loop SNP R919Q exhibited selective decreases in response to CFA, but not to AITC or 3,5-DTBP. The N-linked glycosylation site (predicted) mutants (N747A and N753A) did not effect sub-cellular localization of TRPA1 based on complete inhibition of responses by the cell-impermeable inhibitors EGTA and ruthenium red; activation by AITC and 3,5-DTBP was unaffected. However, activation by CFA was selectively decreased. These data demonstrate a role for both the N-terminal ankyrin repeat domains and cell surface N-linked glycans in mechanical activation of TRPA1 by insoluble PM, providing new insights into the structural components of TRPA1 that are involved in its mechanical sensitivity. Furthermore, the effects of SNPs on TRPA1 activation by various agonists provide rationale for studies to ascertain whether TRPA1 variants may underlie differences in individual sensitivity to PM. Support: ES017436.

PS 1239 Concentrated Ambient Fine Particulate Matter (CAP, PM2.5)-Induced Vascular Insulin Resistance: Role of Oxidative Stress

P. Haberzettl, R. Folz, I. Zelko, A. Bhatnagar and D. J. Conklin. *Medicine, University of Louisville, Louisville, KY.*

Epidemiological studies suggest that increases in fine particulate matter (PM2.5) air pollution contribute to the rapidly evolving epidemics of obesity and diabetes. Previous studies have shown that vascular insulin sensitivity is rapidly impaired by high fat feeding and long-term CAP exposures. Thus, we examined vascular insulin sensitivity and function in low- and high-fat (HFD, 60% kcal fat) fed C57BL/6J mice exposed for 9-30 consecutive days (6h/d) to air or downtown Louisville CAP. CAP exposure for 9 or 30 days impaired aortic insulin signaling measured as insulin-induced phosphorylation of Akt and endothelial-specific eNOS independent of dietary fat. Thus, aortic insulin resistance occurred rapidly in the absence of frank endothelial dysfunction (acetylcholine-induced relaxation) reflecting the high sensitivity of vascular insulin signaling to CAP. To identify the underlying mechanism of CAP-induced vascular insulin resistance, we interrogated the role of systemic or lung oxidative stress by exposing mice treated with TEMPOL (4-hydroxy-2,2,6,6-tetramethylpiperidine 1-oxyl; 1mM in drinking water, 2 days prior and throughout) and mice transgenic (Tg) for lung-specific ecSOD to air or CAP for 9 days. Both vascular insulin resistance and aortic inflammation were abolished by systemic TEMPOL. Moreover, lung-specific ecSOD-Tg mice exposed to CAP did not develop vascular insulin resistance. Collectively, these results suggest that short-term CAP induces vascular insulin resistance via local inflammation due to pulmonary oxidative stress, and thus, our model supports the idea that exposure to PM2.5 may contribute to the increased risk of developing T2D and CVD in humans.

PS 1240 PM2.5-Induced Tachycardia and Hypertension in Rats Are Linked to Elemental Carbon and Specific Temperature-Resolved Carbon Subfractions

J. G. Wagner[1], A. Kamal[2], M. Morishita[3], T. Dvonch[3], J. R. Harkema[1] and A. C. Rohr[4]. *[1]Michigan State University, East Lansing, MI, [2]USEPA, Research Triangle Park, NC, [3]University of Michigan, Ann Arbor, MI and [4]Electric Power Research Institute, Palo Alto, CA.*

Ambient fine particulate matter (PM2.5) is associated with cardiovascular morbidity and mortality. The components responsible for adverse health effects are unknown.
OBJECTIVE: We tested the hypothesis that cardiovascular responses to PM2.5 will be enhanced in hypertensive rats and associated with specific particulate components found in an urban industrial setting.
METHODS: Spontaneously hypertensive rats were exposed by inhalation to filtered air (n=8) or concentrated PM2.5 (n=8) in Dearborn, Michigan, for four consecutive summer days. Exposures were repeated in four separate groups of rats (n=32). Blood pressure (BP), heart rate (HR) and HR variability (HRV) metrics (SDNN, RMSSD) were assessed by radiotelemetry and compared to 1h- and 8h-averaged fluctuations in PM2.5 composition, with a focus on elemental carbon (EC), organic carbon (OC) and their temperature-resolved subfractions, EC1-EC5, PC (pyrrolized carbon), and OC1-OC4.
RESULTS: Exposure-related increases in mean, systolic and diastolic BP were detected as well as increased HR and decreased HRV compared to air-exposed rats. Using 1h averages, PM2.5 EC (1 μg/m3 increase) was associated with increased

HR of 11-32 bpm (4-11% increase), 22-27% decrease in HRV, 3-14 mmHg increases (1.5-8%) in systolic BP, and 4-9% increases in diastolic BP. By comparison effects of OC were negligible. Using 8h averages, EC subfractions were also associated with increased heart rate (EC1; 13bpm, EC2,EC3,PC; <5bpm) and SDNN (EC1>>EC2>EC3,EC4,PC), but with decreased RMSSD (EC2,EC5> EC3,EC4). Significant but comparatively smaller responses were associated with OC and OC1. Effects of either EC or OC subfractions on blood pressures were negligible.
CONCLUSIONS: Acute changes in cardiovascular responses associated with PM2.5 carbon species appear to be driven primarily by EC and EC1 fractions.US EPA RD83479701 & Electric Power Research Institute.

PS 1241 Differential Activation of Transient Receptor Potential Ankyrin-1 by Diesel Exhaust Particulate Materials

V. K. Mitchell, C. Deering-Rice, D. Shapiro, E. G. Romero and C. A. Reilly. *Pharmacology and Toxicology, University of Utah, Salt Lake City, UT.*

Diesel exhaust particulate matter (DEP) is a source of fine-particulate air pollution (PM). Inhaled, fine PM deposits throughout the airways inhalation of DEP can cause irritation to airways, pulmonary inflammation, exacerbation of asthma, and promote chronic pulmonary diseases. Mechanisms underlying the adverse effects of DEP and other environmental PM have been difficult to define due, in part, to the significant variation in its chemical composition arising from inconsistent combustion conditions, particle age, and other factors. PM derived from cigarette smoke, wood smoke, coal burning, and diesel combustion activate transient receptor potential ankyrin-1 (TRPA1). In the respiratory tract TRPA1 activation causes cough, bronchoconstriction, and neurogenic inflammation/edema. We hypothesized that three different DEP samples that mimic environmental DEP, would exhibit variations in potency as TRPA1 agonists due to differences in chemical composition, and that such potency differences would correlate with variations in measures of toxicity such as cell death and cytokine gene expression. NIST SRM 2975 (NIST), DEP collected from the tail-pipe of an on-road truck (JMV), and DEP recovered during diesel filter regeneration (FILTER) were used. TRPA1 activation (Ca++ flux) was determined using TRPA1-over-expressing HEK-293 cells: "JMV" DEP was most potent followed by NIST, then FILTER. The mechanism of TRPA1 activation was also investigated. TRPA1 activation by JMV and NIST were attributable to electrophiles, whereas FILTER activated via both the electrophile and menthol agonist-binding sites. Chemical analysis of DEP components (PAHs and Aldehydes/Ketones) by HPLC and LC/MS suggested a correlation between DEP potency and the abundance of perinaphthenone, benzoquinone, and 3,5-ditert-butylphenol in the DEP. Increased understanding of how different samples of DEP affect lung cells is an important step in better understanding the factors that influence the multiple reported effects of DEP in the lung. Support: ES017346.

PS 1242 Ambient PM Exposure and RAGE: Insight into an Emerging Risk for Diabetes and Cardiovascular Disease

J. M. Vaughan, B. Narayanan, A. Schmidt and L. Chen. *Environmental Health Science, New York University, Tuxedo, NY.*

Numerous epidemiological studies reveal alarming evidence that individuals with diabetes have been shown to be an especially susceptible population to the cardiopulmonary effects of particulate matter (PM) pollution. This has been thought to be due to the inherent enhanced inflammation and endothelial dysfunction seen in diabetics. Nonetheless, there is no definitive mechanism that explains the pathways responsible for these observed vulnerabilities. Recent reports have implicated activated receptors for advanced glycation end-products (RAGE) as an integral factor in the inflammatory processes of cardiovascular dysfunction and diabetes; nonetheless, it is unclear whether ambient PM alone/or in combination w/ other endogenous factors may contribute to RAGE activation and underlie these inflammatory disparities. To investigate the influence of RAGE on PM-mediated inflammation, levels of soluble RAGE (sRAGE), membranous RAGE, ligands (i.e. AGEs, S100 proteins and HMGB1) and Nf-κB were measured in human pulmonary and cardiovascular cell models (pulmonary endothelial, epithelial, macrophage and alveolar) exposed to regional PM or inert saline solution. Lastly, to validate RAGE as a mechanism of PM-induced inflammation, B6C3/F2 mice were exposed to regional PM aspirations. Results: After 24h of PM2.5 exposure, a dose dependent increase in cell proliferation and small increases in sRAGE activity at higher doses of PM was evident. Immunofluorescence detection showed an elevation in cells positive for membranous RAGE expression; accompanied w/ a 2-fold increase in mRNA for RAGE & NF-κB; as well as significant increases in measures of ligands such as AGE and HMGB-1. These findings suggest a plausible interaction between PM & RAGE resulting in the enhanced expression and activation of NF-κB and RAGE. Finally, preliminary mouse exposures have yielded supportive findings: exposed mice have shown significantly increases of RAGE expression compared to controls. Collectively, these data offer valuable insight into PM-mediated RAGE activation and its influence on diabetes.

PS 1242a Intratracheal Coexposure to Diesel Exhaust Particulate and Crystalline Silica in Rats Potentiates the Inflammatory Effects of Silica in the Lungs

B. M. Yingling[1, 2], C. E. McLoughlin[2], J. S. Fedan[2, 1], B. T. Chen[2], D. Schwegler-Berry[2], J. M. Antonini[2, 1] and J. R. Roberts[2, 1]. [1]*WVU, Morgantown, WV and* [2]*NIOSH, Morgantown, WV.*

Worker exposure to high levels of respirable dust containing crystalline silica and diesel exhaust (DE) has become a concern during hydraulic fracturing operations. The goal of the current study was to investigate the effects of acute pulmonary co-exposures to silica and DE particulate (DEP) in vivo. Doses were derived from field measures using the high point values for respirable silica, applied to a human pulmonary deposition model, and normalized to the surface area of the rat lung. The silica dose of 230 μg/rat represents 2.5 mg/m^3 for 12 hr/d for 14 d. The DEP dose of 7.9 μg represents 0.1 mg/m^3 for the same duration in a deposition model for total carbon (TC). A 50 μg dose of DEP was also used to represent ~0.6 mg/m^3 TC for the same duration. Rats were exposed by a single intratracheal instillation of sterile PBS as vehicle or one of the following doses: 7.9 μg DEP, 50 μg DEP, 230 μg silica, or silica and DEP combined for each dose of DEP. At 1 d, 1 wk, and 1 mo post-exposure, bronchoalveolar lavage (BAL) was performed on the right lungs; cells and fluid were retained to assess pulmonary injury and inflammation. Lung-associated lymph nodes (LALN) were harvested to evaluate immune responses. Silica alone caused increased inflammation and lung injury at all times post-exposure, indicated by increased neutrophil influx, oxidant production, and lactate dehydrogenase (LDH) in BAL. DEP alone caused only slight inflammation 1 d post-exposure but no effects later. At 1 wk and 1 mo after exposure, 50 μg DEP significantly increased the inflammatory effects of silica. In addition, at 1 mo, both co-exposure doses significantly enhanced the phagocyte oxidant production over silica alone. Lymphocyte counts in LALN in the co-exposures were not elevated relative to silica exposure alone. In summary, DEP alone produced relatively no pulmonary toxicity; however, DEP in a co-exposure with silica has the capability to potentiate the adverse effects of silica in the lung.

PS 1242b Inhalation of Traffic-Derived Particulates and Exposure to Social Stress Differentially Alter Cardiovascular Function in Rats

A. P. Carll[1], T. Jaeger[2, 1], D. Lamoureux[3, 1], R. Sato[2, 1], J. E. Clougherty[4, 1], V. Papapostolou[1], J. Lawrence[1], E. Diaz[1] and J. J. Godleski[1]. [1]*Environmental Health, Harvard School of Public Health, Boston, MA,* [2]*Faculdade de Medicina da Universidade de Sao Paulo, Sao Paulo, Brazil,* [3]*Laboratory of Personalized Medicine, Harvard Medical School, Boston, MA and* [4]*Environmental & Occupational Health, University of Pittsburgh Graduate School of Public Health, Pittsburgh, PA.*

Vehicular-derived air pollution includes particulate matter (PM) consisting of primary particles (P) and secondary organic aerosols (SOA) that induce adverse cardiovascular events potentially through vascular or autonomic nervous system dysfunction. Telemetered rats were exposed by whole-body inhalation to traffic-derived P+SOA denuded of combustion gases (4d/wk × 5h/d; mean $PM_{2.5}$ concentration ≈ 50 μg/m^3) for 12 d to determine effects on arterial pressure (AP) and heart rate variability (HRV, a measure of autonomic balance). P+SOA caused increased AP during exposure days 1, 4, and 6 (mean AP: +15 mmHg vs. control), sympathetic dominance during days 1 and 4 (standard deviation of interbeat intervals: −3.4 ms), supraventricular tachycardia (heart rate: +180 beats/min for up to 5 h) between days 6 and 8 in half of animals, decreased AP on day 11 (−9 mmHg mean AP), and bradycardia in half of animals during baroreflex challenge on day 12. Baroreflex sensitivity tended to increase on day 12 of exposure, indicating compensation for the hypertensive effects of P+SOA. To compare P+SOA to social stress, separate telemetered animals were introduced to a dominant rat for 20 min/d for 10 d. Social stress consistently increased heart rate (+40-100 beats/min) and mean AP (+15 mmHg) while increasing a HRV measure of vagal tone (root mean square of successive differences) potentially indicating baroreflex activation. Thus, the autonomic effects of P+SOA and social stress diverged during similar hypertensive responses. Therefore, traffic-derived PM causes hypertension, autonomic imbalance, and subsequent compensatory responses in a pattern different from acute psychological stress.

PS 1242c Potent Protection against Diesel Exhaust Particle-Caused Cytotoxicity and Vasculature Permeable through Regulation of Adherens Junction Distribution by *Ganoderma lucidum*

J. Chang[1], M. Chung[1], J. Wang[1], C. Tseng[2, 3], M. K. Gordon[4] and M. Chao[1, 3]. [1]*Bioscience Technology, Chung Yuan Christian University, Chung-Li, Taiwan,* [2]*Biomedical Engineering, Chung Yuan Christian University, Chung-Li, Taiwan,* [3]*Center for Nanotechnology, Chung Yuan Christian University, Chung-Li, Taiwan and* [4]*Joint Program of Toxicology, Rutgers University, Piscataway, NJ.*

Epidemiological studies suggest a direct correlation between exposure to diesel exhaust particles (DEP) and the onset of cardiovascular diseases presumably through the disruption of the adherens junctions. This would lead to increase of vasculature permeability and the inhaled DEP gain access into the circulation system. Although the mechanism remains unclear, our group has demonstrated the DEP-induced reactive oxygen species (ROS), which may play a key role in causing vascular permeability factor, VEGFA secretion. In order to minimize the level that DEP penetrating into the capillary lumen, 20 and 200 μg/mL *Ganoderma lucidum* (*G. lucidum*) was applied with DEP to the in vitro capillary-like HUVEC tube culture. After 24 h DEP exposure, we observed VEGFR2 dissociated from the membrane and relocalized to both cytoplasm and supernatant. It subsequently resulted in making PI3K/Akt inactivation. While with co-treatment of *G. lucidum*, Cm-H2DCFDA assay showed the ROS generation was blocked. Not only was the increased vasculature permeability reduced following by the oxidative stress inhibition, but none of secreted VEGFA was also detected. Immunoblotting further suggested the localization of VEGFR2 and PI3K/Akt activation were affected only at high dose of DEP (100 μg/mL). Additionally, immunefluorescent images revealed that VE-cadherin formed adherens junction network was destroyed in response to DEP. Once combine the treatment with *G. lucidum*, the cell-cell junctional structure was rebuilt, however, this was observed only at 1 and 10 μg/mL DEP. In summary, these results indicate that inhaled DEP may directly impact the lung vasculature, while additive *G. lucidum* may protect the endothelial tube cells and their adherens junctions from exposure to DEP.

PS 1242d Subchronic Effects of Inhaled Ambient Particulate Matter on Glucose Homeostasis and Target Organ Damage in Type 1 Diabetic Rat Model

T. Cheng[1], Y. Yan[1], C. Chou[2] and J. Wang[3]. [1]*National Taiwan University, Taipei, Taiwan,* [2]*Academia Sinica, Taipei, Taiwan and* [3]*Kaohsiung Veteran General Hospital, Kaohsiung, Taiwan.* Sponsor: L. Chen.

Epidemiological studies have reported associations between particulate matter (PM) and diabetes mellitus (DM), but the toxicological data was limited. The objective of this study is to investigate whether subchronic PM exposure alter glucose homeostasis and cause cardiovascular and renal toxicity in type 1 DM rat model. We constructed a real world PM2.5 exposure system, the Taipei Air Pollution Exposure System for Health Effects (TAPES), in order to continuously deliver non-concentrated submicron PM for subchronic exposure. Type 1 DM rat model was induced by streptozotocin (STZ) injection. Between December 22, 2009, and April 9, 2010, DM rats were exposed to PM or filtered air (FA) using TAPES in Taipei, Taiwan, 24 hours/day, 7 days/week, for a total of 16 weeks. The average concentrations of PM2.5 in the exposure and control chamber of TAPES during the study period was 13.30 and 0.13μg/m3, respectively. Glycated hemoglobin A1c (HbA1c) was significantly elevated after exposed to PM compared with exposure to FA (mean [SD], 7.4% [3.1%] vs. 5.7% [2.4%], p<.05). PM caused focal myocarditis in the myocardium and increased aortic medial thickness (mean [SD], 0.16 [0.02] vs. 0.11 [0.02] mm, p<.001). Morphometric analysis of the kidneys showed a significantly increased proportion of rats with advanced glomerulosclerosis (47.2 vs. 30.6%, p<0.05), accentuation of tubular damage (tubular damage index: 1.76 [0.77] vs. 1.15 [0.36], p<.001) and early development of kidney tumors. Our study showed that subchronic real world PM2.5 exposure altered glucose homeostasis and caused cardiovascular and renal toxicity in STZ-induced type 1 DM rat model. The results support previous epidemiological findings that PM may enhance cardiovascular diseases in DM.

PS 1242e Acute Inhalation Exposure to Mixed Vehicle Emissions Induces Serum Metabolite Changes Related to Oxidative Stress, Lipid Peroxidation, and Energy Metabolism

J. Brower[1], B. C. Moeller[1], M. Doyle-Eisele[1], S. Stirdivant[3], J. D. McDonald[1] and M. Campen[2]. [1]*Lovelace Respiratory Research Institute, Albuquerque, NM,* [2]*Pharmaceutical Sciences, University of New Mexico, Albuquerque, NM and* [3]*Metabolon Inc., Durham, NC.*

The adverse health effects of environmental exposure to gaseous and particulate components of vehicular emissions are a major concern among urban populations. A link has been established between respiratory exposure to vehicular emissions and the development of cardiovascular disease (CVD), but the mechanisms driving this interaction remain unknown. Chronic inhalation exposure to mixed vehicle emissions has been linked to CVD in animal models. This study evaluated the temporal effects of acute exposure to mixed vehicle emissions (MVE; mixed gasoline and diesel emissions) on potentially active metabolites in the serum of exposed mice. C57Bl/6 mice were exposed to a single 6 hour exposure to filtered air (FA) or MVE (100 or 300 $\mu g/m^3$) by whole body inhalation. Immediately after and 18 hours after the end of the exposure period, animals were sacrificed for serum and tissue collection. Serum was analyzed for metabolites that were differentially present between treatment groups and time points. Changes in metabolite levels representative of increased oxidative stress (oxidized glutathione, cysteine disulfide, taurine), lipid peroxidation (13-HODE, 9-HODE), energy metabolism (lactate, glycerate, branched chain amino acid catabolites, butrylcarnitine, fatty acids), and inflammation (DiHOME, palmitoyl ethanolamide) were observed immediately after the end of exposure in the serum of animals exposed to MVE relative to those exposed to FA. By 18 hours post exposure, serum metabolite differences between animals exposed to MVE versus those exposed to FA were less pronounced. Experiments are underway to investigate the potential bioactivity of these metabolites in an *ex vivo* model of vascular reactivity.

PS 1242f Electrocardiographic Changes in ApoE -/- Mice following Exposure to the Semi-Volatile Fraction of Ultrafine Concentrated Ambient Particulate Matter

A. J. Keebaugh[1], D. Herman[1], P. Pakbin[2], C. Sioutas[2] and M. T. Kleinman[1]. [1]*UC Irvine, Irvine, CA and* [2]*University of Southern California, Los Angeles, CA.*

Coronary artery disease (CAD) is the most prevalent cause of disease-related death in the US and emissions related particulate matter (PM) exposures are thought to be associated with thousands of excess deaths per year. Ultrafine particles (UF) contain a large proportion of redox-active organic compounds, exposure to which may be related to oxidative stress that is involved in the pathogenesis of heart disease, that exist in the volatile or particle phase and are considered semi-volatile organic compounds (SVOCs). We previously demonstrated an acceleration of atherosclerosis in susceptible mice associated with exposure to SVOCs from ultrafine concentrated ambient particles (CAPs). The interaction of enhanced arterial disease and CAPs derived SVOC exposure may increase the susceptibility of the heart to adverse cardiac events. We hypothesized that the SVOC exposed mice would have changes in heart rate variability (HRV), a measure of cardiac autonomic control, and in the morphology of the repolarization segment measured on an electrocardiogram. Decreased HRV is a measure in humans that has been associated with increased cardiac risk of adverse events. ApoE -/- mice, which are prone to developing atherosclerosis, were exposed to either UF CAPs or CAPs with the SVOC components removed by a thermodenuder (deCAPs) for 8 weeks in downtown Los Angeles for 5 hours/day, 4 days/week. A control group was exposed to purified, filtered air. Implanted cardiac transmitters monitored electrocardiograms from the mice. The CAPs exposed mice had diminished HRV compared to deCAPs and Air exposed mice, particularly during the latter weeks of exposure. Similarly, repolarization segment changes were observed in the CAPs exposed mice but not the Air and deCAPs exposed mice. The attenuation of cardiac effects in the deCAP group indicate that SVOCs in CAPs exposures are possibly important contributors to the toxic cardiac effects.

PS 1242g Replacing Diesel Fuel with Biodiesel: For Better or for Worse?

M. Farcas[1], N. Yanamala[1], D. Schwegler-Berry[1], J. Hummer[3], M. Shurin[5], E. M. Birch[4], D. W. Gutkin[5], E. Kisin[1], V. E. Kagan[6], A. D. Bugarski[3] and A. A. Shvedova[1, 2]. *[1]HELD/PPRB, CDC/NIOSH, Morgantown, WV, [2]Dept. of Physiology and Pharmacology, WVU, Morgantown, WV, [3]OMSHR, NIOSH/CDC, Pittsburgh, PA, [4]NIOSH/CDC, Cincinnati, OH, [5]Dept. of Pathology, UPMC, Pittsburgh, PA and [6]Dept. of Environmental and Occupational Health, University of Pittsburgh, Pittsburgh, PA.*

Employment of sustainable resources for fuel manufacture has recently gained worldwide trends to limit usage of fossil oils while providing less atmospheric greenhouse gas effects and reducing air pollution. Biodiesel (BD) fuels and biodiesel petroleum blends are used for large truck engines and small, single-cylinder basic piston operating engines. BD produced by transesterification of vegetable oil into fatty acid methyl esters is a renewable energy source. Considering BD fuel is mainly composed of unsaturated fatty acids, we hypothesize that BD exhaust particles could induce pronounced adverse outcomes, due to their ability to readily oxidize fatty acid residues interacting with biological system. We compared the effects of particulate matter (PM) generated by combustion in an engine fueled by corn-based BD to that of petroleum-based diesel (D) after pulmonary exposure of mice by pharyngeal aspiration. We demonstrated that pulmonary exposure to BD PM caused pulmonary inflammation and damage, enhanced release of inflammatory mediators found in BAL and lung tissue causing oxidative stress. Biomarkers of tissue damage, oxidative-stress and inflammation were significantly elevated in lungs of mice exposed to BD compared to those found in mice treated with D. The up-regulation of inflammatory cytokines/chemokines was also higher in lungs of mice treated with BD. Histological evaluation of mouse lungs indicated presence of lymphocytic infiltrate and impaired clearance with prolonged retention of BD PM in pigment laden macrophages. Future studies on the detailed analysis of combustion products from BD and specific mechanism of interactions of these emissions related to found inflammation, oxidative-stress and impaired clearance is underway.

PS 1242h Mutagenic Potential of Biodiesel Exhaust Particles and Effect of Engine Operating Conditions

E. K. Kisin[1], X. C. Shi[2], M. J. Keane[2], A. D. Bugarski[3] and A. A. Shvedova[1]. *[1]HELD/PPRB, CDC/NIOSH, Morgantown, WV, [2]HELD/EAB, CDC/NIOSH, Morgantown, WV and [3]OMSHR, CDC/NIOSH, Pittsburgh, PA.*

Approximately 28,000 underground miners are potentially exposed to relatively high concentrations of diesel particulate matter (PM) in the mining industry. Changing fuel supply from diesel (ULSD) to biodiesel and its blends is considered to be a viable option for controlling exposures to PM but the potential for adverse health effect has yet to be addressed. This study was conducted to investigate the mutagenic potential of diesel engine emissions from neat (B100) and blended (B50) soy-based fatty acid methyl ester (FAME) biodiesel in comparison with ULSD PM using different engine operating conditions and exhaust aftertreatment configurations. The exhaust samples were collected for engine equipped with either a standard muffler or a combination of the muffler and diesel oxidation catalytic converter (DOC) that was operated at four different steady-state modes. Bacterial gene mutation activity of exhaust PM was tested on the organic solvent extracts using the Ames Salmonella assay. The mutagenic activity was strongly affected by fuels, engine operating conditions, and exhaust aftertreatment systems. The mutagenicity was increased with the fraction of biodiesel in the fuel. While the mutagenic activity was observed in B50 and B100 samples collected from both light- and heavy-load operating conditions, the ULSD samples were only mutagenic at light-load conditions. The presence of DOC in the exhaust system resulted in decreased mutagenicity when engine was fueled with B100 and B50 and operated at light-load conditions. This was not the case with ULSD. Heavy-load operating condition in the presence of DOC resulted in a decrease of mutagenicity only when engine was fueled with B50, but not B100 or ULSD. Therefore, the results indicate that PM from neat or blended biodiesel has a higher mutagenic potency than ULSD. Further research is needed to investigate the health effects of biodiesel as well as efficiency of DOC or other exhaust aftertreatment systems.

PS 1242i Reactive Oxygen Species and Inflammatory Response of Monocytes to Ambient Particles Varies by Highway Proximity

R. E. Muller[1, 4], W. Wu[4, 2], K. Berhane[3], S. Fruin[3], F. Liu[3], I. Jaspers[1, 4], D. Diaz-Sanchez[5], D. B. Peden[4] and R. McConnell[3]. *[1]Curriculum in Toxicology, University of North Carolina at Chapel Hill, School of Medicine, Chapel Hill, NC, [2]School of Public Health, Xinxiang Medical University, Henan Province, China, [3]Preventive Medicine, USC Keck School of Medicine, Los Angeles, CA, [4]Center for Environmental Medicine, Asthma & Lung Biology, University of North Carolina at Chapel Hill, School of Medicine, Chapel Hill, NC and [5]Office of Research and Development, US Environmental Protection Agency, Durham, NC.*

Epidemiological studies have demonstrated associations of respiratory disease with near-roadway traffic related pollutant exposure, effects which are independent of those of regional air pollutants. However, there has been limited study of potential mechanisms for near-roadway effects. We examined the in vitro effects of respirable particulate matter (PM) collected adjacent to a major Los Angeles freeway and at an urban background location. PM was collected on filters during two consecutive fifteen day periods. Oxidative stress and inflammatory response (intracellular reactive oxygen species (ROS), IL-1β, IL-6, IL-8 and TNFα) to PM aqueous extract was assessed in THP-1 cells, a model for evaluating monocyte/macrophage lineage cell responses. Near-roadway PM induced statistically significantly higher levels of IL-6, IL-8 and TNFα ($P<0.01$) but not of IL-1β ($P=0.06$) or of ROS ($P=0.17$). PM stimulation enhanced activity of extracellular signal-regulated kinase (ERK) and c-Jun N-terminal kinase (JNK). Pre-treatment of THP-1 cells with kinase inhibitors or antioxidant reduced PM-induced cytokine expression. Contrast between urban background and near-roadway PM-induced inflammatory cytokines was similar in magnitude to differences between collection periods. We conclude that near-roadway PM had greater inflammatory activity than urban background PM, a finding consistent with epidemiologic findings, in pathways regulated by ROS and the MAPK pathways including ERK and JNK. THP-1 cells are a potential model for development of biologically relevant metrics of long-term spatial variation in exposure for study of disease.

PS 1243 The Role of Zinc in Altering the Detrimental Effects of World Trade Center Particulate Matter on Human Pulmonary Fibroblasts

A. DiLorenzo, S. Choi, P. Rivera, F. DaileySterling and N. Pattnaik. *Biology & Molecular Biology, Montclair State University, Montclair, NJ.*

Particulate matter from the World Trade Center (WTC) tragedy of 9-11 is linked to increased respiratory problems and emergence of World Trade Center Cough. High levels of Zinc (Zn) have been identified among the many heavy metals found in WTC dust. It has been indicated that some synergistic effects among several chemicals might be contributing to respiratory illness. The toxicity and apoptotic ability of WTC dust from the Market Street sample were carried out on MRC-5 human lung cells. The combination treatment of Zn to WTC dust mimicked the ratio of Zn identified in the total dust. Similar studies were performed to show reduction in toxicity either Lead (Pb) or Cadmium (Cd). Measurements utilizing 96 well plates were read in a Bio-Tech Synergy 2 multi plate reader . In all experiments heavy metals known to be highly damaging to human lung cells were modified by the presence of Zn. Modification of deleterious effects were noted in cells exposed to WTC dust and Zn. Without the addition of unusual high levels of Zn, both Pb, Cd, and WTC dust alone, would be more damaging to those exposed to WTC dust. These experiments suggest that the high levels of Zn found in the particulate matter at the WTC site might possibly serve as a reward in disguise to WTC victims.

PS 1244 Evaluation of Zinc and Metallothioneins in the Skin Injured after an Experimental Surgery

E. Brambila[1], T. Moreno Lopez Malo[1], N. Fernández Tamayo[2], P. Aguilar Alonso[1] and B. Leòn Chàvez[1]. *[1]Clinical Sciences, Benemérita Universidad Autónoma de Puebla, Puebla, Puebla, Mexico and [2]Pathology, ISSSTEP, Puebla, Puebla, Mexico.*

Previous studies have shown that Zn and MT are essential for tissue repair, however there are few studies that show the changes of Zn and MT in the different stages in the healing process. Therefore the aim of this study was to evaluate the changes of Zn and MTs during phases of inflammation, proliferation and maturation in the injury produced by an experimental surgery. Male NUDE rats weighing 100 to 150 g were used as a model, which underwent an abdominal incision of 3 cm. Groups of 5 animals were sacrificed at 6, 12, 24, 48 h, 7 and 28 days after surgery. Each animal skin samples were taken from the injured area, and as control skin, an

area adjacent without lesion in the same animal was used to analyzed the cellular morphology after hematoxilin-eosin stain, and to evaluate the level of Zn and MT which were determined by AAS and 109-Cd saturation method, respectively. The results showed increases of Zn at 48 hours and 7 days after surgery, whereas MTs start to increase at 6 h after surgery, maintaining this level until 48 h. Maximum increases of both metabolites occurred at 48 h, corresponded with the maximum increase of inflammatory cells (polymorphonuclear cells and macrophages). The increase of Zn in the injured area can have an important role for activation of metalloenzymes-Zn and activation of transcription factors necessary for healing, while MTs can act as a reservoir of Zn, and as antioxidant defense in the lesion site.

PS 1245 Gene Expression and Pathway Analysis of Cadmium Exposure in Human Hepatocarcinoma Cells

L. Cartularo[1], F. Laulicht[1], H. Sun[1], T. Kluz[1], J. H. Freedman[2] and M. Costa[1]. [1]*Environmental Medicine, New York University, Tuxedo, NY and* [2]*NIEHS, Research Triangle Park, NC.*

Cadmium (Cd) is a toxic and carcinogenic metal naturally occurring in the earth's crust as well as in rocks and soil. Cd can also be introduced into the environment through its many industrial uses. Cd is easily absorbed by plants from the soil, thus a common route of human exposure is via diet. Additionally, smokers are exposed to high levels of Cd from tobacco. This study examined the effects of both acute and chronic Cd exposure on gene expression in human hepatocarcinoma (HepG2) cells. HepG2 cells were treated with either 0.5 μM Cd for 24 hours or 0.1 μM Cd for three weeks and gene expression analysis was performed using Affymetrix GeneChip® Human Gene 1.0 ST Arrays. Acute and chronic exposures significantly altered the expression of 333 and 181 genes, respectively. The genes most upregulated by acute exposure include several metallothionein genes. Downregulated genes include the monooxygenase CYP3A7, which is involved in drug and lipid metabolism. CYP3A7 was upregulated by chronic Cd exposure, as was DNAJB9, which plays a role in protecting stressed cells from apoptosis. Genes downregulated due to chronic exposure include the transcriptional regulator early growth response protein 1 (EGR1). Ingenuity Pathway Analysis, IPA, revealed that the top networks altered by acute exposure are lipid metabolism, small molecule biosynthesis, and cell morphology, organization, and development; while top networks altered by chronic exposure are organ morphology, cell cycle, cell signaling, renal and urological diseases, cellular growth and proliferation, and cancer. Expression data demonstrate that exposure to Cd alters the expression levels of many different genes involved in various disease pathways. Many of the genes altered by Cd exposure may be involved in carcinogenesis, with roles in cellular growth, proliferation and apoptosis.

PS 1246 Zinc Supplementation Abates Cadmium-Induced Upregulation of Glutathione Synthesis and Oxidative Stress

S. D. Francis Stuart, R. K. Young and A. R. Villalobos. *Texas A&M University, College Station, TX.*

In primary cultures of rat choroid plexus we showed cadmium (Cd) induced oxidative stress, stimulated apical choline uptake, and up-regulated glutathione (GSH) synthesis. Zinc (Zn) supplementation prior to and during Cd exposure attenuated stimulation of choline uptake and reduced ROS accumulation. Our aim is to determine whether Zn modulates the regulation of GSH synthesis and availability in response to low dose Cd exposure. Choroid plexus primary cultures were supplemented with 25 μM Zn for 48 h then treated with 0, 250, or 500 nM CdCl2 in serum-free medium without or with 10 μM Zn for 12 h. Induction of heme-oxygenase-1 (HO-1), heat-shock protein 70 (HSP70), copper-zinc superoxide dismutase (SOD1), and metallothionein-1 (MT-1) was analyzed by immunoblot and qRT-PCR. Glutamate-cysteine ligase (GCL) is the rate-limiting enzyme in GSH synthesis; the modifier and catalytic subunits, GCLM and GCLC, were also analyzed. As compared to controls, Cd treatment induced gene expression of GCLC, MT-1, HO-1, and SOD1 by 2, 16, 12, and 3-fold. Zn supplementation, however, reduced this induction. Cd increased GSH by 2-fold and GSSG by 30-fold as compared to control, whereas in cells also supplemented with Zn, GSH and GSSG levels were decreased 25% and 44% as compared to Cd treatment alone. To determine whether effects of Zn were associated with changes in GSH availability, cells were pretreated (12 h) without or with buthionine sulfoximine (BSO, 100 μM), a GCL inhibitor, after Zn supplementation and before treatment with 0 or 250 nM CdCl2 ± Zn (10 μM) for 12 h. BSO treatment, regardless of condition (e.g., without or with Zn ± Cd), reduced GSH by 92% but increased GSSG by 15-fold above controls. BSO treatment resulted in an enhanced, compensatory induction of HO-1, HSP70, SOD1, GCLC, GCLM and MT-1 in the presence of Cd. However, this was attenuated in cells also supplemented with Zn. These data indicate Zn abates Cd-induced up-regulation of GSH synthesis and still protects when GSH synthesis is inhibited. NSF #IOS-1052654

PS 1247 Kidney Specificity in Cd-Induced Accumulation of p53 Dependent on the Inhibition of UBE2D Family Gene Expressions

M. Satoh[1], J. Lee[1], M. Tokumoto[1, 2] and Y. Fujiwara[1]. [1]*Laboratory of Pharmaceutical Health Sciences, School of Pharmacy, Aichi Gakuin University, Nagoya, Japan and* [2]*Laboratory of Chemical Toxicology and Environmental Health, Showa Pharmaceutical University, Tokyo, Japan.*

Cadmium (Cd) is an environmental metal pollutant causing renal dysfunction. However, the underlying mechanisms of Cd toxicity remain to be elucidated. Our recent study has demonstrated that overaccumulation of p53 may relate to Cd-induced apoptosis and may be due to the suppression of p53 degradation through the inhibition of gene expressions of Ube2d family in rat proximal tubular cells (NRK-52E cells). In this study, we examined whether suppression of Ube2d gene expression and p53 accumulation by Cd have kidney-specificity. In the present study, we used not only some cell lines as IEC-6 cells (rat small intestine epithelial cells), HBMECs (human brain microvascular endothelial cells), human astrocytes, and HK-2 cells (human kidney proximal tubular cells), but also kidney and liver of C57BL6/J mice. In IEC-6 cells, Cd decreased both of mRNA levels of 3 members (Ube2d1, Ub2e2d2 and Ube2d4) of Ube2d family and protein level of p53. In HBMEC, Cd increased p53 protein level without the decrease in UBE2D family gene expressions. In human astrocytes, Cd increased only the mRNA level of UBE2D3. In HK-2 cells, Cd suppressed the mRNA levels of UBE2D2 and UBE2D4, as well as increased p53 protein level. Moreover, Cd exposure for 6 months decreased mRNA levels of Ube2d family and accumulated p53 protein in kidney of mice. On the other hand, neither mRNA levels of Ube2d family nor p53 protein level are changed in liver of mice exposed to Cd for 6 months. These findings suggest that Cd accumulates of p53 protein via the suppression of Ube2d family gene expression with kidney-specificity.

PS 1248 Cadmium-Induced Apoptosis Is Mediated by p53 Accumulation through the Suppression of Gene Expression of Ube2d Family in Proximal Tubular Cells

J. Lee[1], M. Tokumoto[1, 2], Y. Fujiwara[1] and M. Satoh[1]. [1]*School of Pharmacy, Aichi Gakuin University, Nagoya, Aichi, Japan and* [2]*Showa Pharmaceutical University, Tokyo, Japan.*

Cadmium (Cd) toxicity is accompanied by disturbance of gene expressions and increases in stress-response proteins. However, the precise targets of Cd toxicity are still unknown. Our previous study demonstrated that Cd induced cellular accumulation of tumor suppressor protein p53, and inhibited the gene expressions of ubiquitin-conjugating enzyme E2 D family (Ube2d family), which involves in p53 ubiquitination for its degradation, in NRK-52E rat renal tubular epithelial cells and mouse kidney. In the present study, we examined the association of decrease of Ube2d family gene expressions with increase of p53 accumulation by Cd, and the involvement of p53 overaccumulation in Cd-induced apoptosis, using HK-2 human proximal tubular cells and kidney of C57BL/6J mice. Cd increased cellular p53 protein prior to toxic effect in HK-2 cells. Cd significantly decreased gene expressions of Ube2d2 and Ube2d4, members of Ube2d family, prior to accumulation of p53 by Cd. The double knockdown of *UBE2D2* and *UBE2D4* by siRNA caused the increase in cellular p53 protein in HK-2 cells. Moreover, Cd markedly increased nuclear phosphorylated p53 level. Not only apoptotic cell death was promoted in response to Cd, but also Cd-induced apoptosis was attenuated by knockdown of *p53* using the siRNA. In addition, 6-month exposure of mouse to Cd (300 ppm) triggered accumulation of p53 in proximal tubules, and apoptotic signals were observed on the same spots where Cd accumulated p53 in proximal tubules. The present findings suggest that cadmium excessively absorbed in proximal tubular cells may induce p53-dependent apoptosis through the suppression of Ube2d gene expression.

PS 1249 Paraoxonase Activity in Subchronic Low-Level Cadmium Exposure

O. O. Ogunrinola[1, 2], A. D. Wusu[1, 2], O. K. Afolabi[2, 4], E. A. Balogun[2, 5], E. O. Abam[2], D. O. Babayemi[2], O. A. Dosumu[2], O. B. Onunkwor[2], O. O. Odukoya[3] and O. Ademuyiwa[2]. [1]*Biochemistry, Lagos State University, Ojo, Lagos, Nigeria,* [2]*Biochemistry, Federal University of Agriculture, Abeokuta, Nigeria,* [3]*Chemistry, Federal University of Agriculture, Abeokuta, Nigeria,* [4]*Biochemistry, Ladoke Akintola University, Ogbomoso, Nigeria and* [5]*Biochemistry, University of Ilorin, Ilorin, Nigeria.*

Epidemiological studies suggest an association between cardiovascular diseases and cadmium in drinking water. While the underlying mechanism of this cadmium-mediated increase in cardiovascular risk factors remains enigmatic, studies

indicate a role for paraoxonase (PONase) in cardiovascular diseases. To investigate the association between cadmium exposure and cardiovascular diseases, male albino rats were exposed to 100, 200 and 300ppm cadmium doses for 12 weeks in their drinking water. PON activities towards paraoxon (PONase) and phenylacetate (AREase) in plasma, lipoproteins, hepatic and brain microsomal fractions were determined using standard methods. Inhibition of PONase and AREase in plasma and HDL characterised the effects of the cadmium exposure. While cadmium inhibited PONase by 64% (plasma) and 40% (HDL), AREase activity was inhibited by 30 and 45% respectively. The pattern of inhibition in plasma and HDL indicates that cadmium induced a dose-dependent inhibition of PONase and AREase. In the VLDL, cadmium inhibited PONase (39%) and AREase (59%) respectively. In the hepatic microsomal fractions, reduction in PONase and AREase activities are 58% and 33% respectively. While in the brain microsomal fraction, PONase and AREase activities was inhibited by 55% and 33% respectively. Microsomal cholesterol was decreased by exposure to cadmium resulting in increased cholesterol/phospholipid ratios. Our findings indicate that decreased PON activity observed in cadmium exposure may be an incipient biochemical step in the cardiovascular effects of cadmium. The modulation of PON activity by cadmium may also be mediated through changes in membrane fluidity brought about by changes in the concentration of cholesterol in the microsomes.

PS 1250 Cadmium-Induced Lung Emphysema and Carcinogenesis Coupled with Defect in Lysyl Oxidase in the Rat Animal Model

Y. Zhao[1], P. Toselli[1], G. Cheng[2], M. Zheng[2], J. Li[2] and W. Li[1]. *[1]Biochemistry, Boston University School of Medicine, Boston, MA and [2]Central Lab, Hebei United University Affinity Hospital, Tangshan, Hebei, China.*

Lysyl oxidase (LOX) is an extracellular matrix cross-linking enzyme and a tumor suppressor. To assess cadmium (Cd) effects on LOX expression, pathogenesis and carcinogenesis in the lung, a constant dose of $CdCl_2$ at 30 μg/rat (= 0.123 ± 0.007 mg Cd/kg body weight) in 100 μl physiological saline was intratracheally instilled into the lung of male Sprague-Dawley rats once a week for 6 weeks (total Cd dose = 110.4 μg Cd/rat). Control rats received saline only (20 rats). Rats were killed 1 or 65 weeks after the last instillation. Due to the half-life of absorbed Cd by the lung to be 9.4 year, actually, Cd exposure times in two treated groups were 7-weeks (6+1) and 71-weeks (6+65), respectively, each with 20 rats (10 rats for morphological study and 10 rats for biochemical assays) . Rats exposed to Cd for 7 weeks all exhibited extensive enlargement of airspace and multiple pulmonary bullae with or without small areas of interstitial fibrosis. EM showed the thin alveolar wall with less deposition of matrix components such as elastin and collagen. Cd exposure for 71 weeks elicited adenocarcinoma in 5 rats (25%). Some areas of lung tissues were infiltrated with cancer cells, capillaries, and hemorrhages. Biochemical assays illustrated declined levels of LOX at protein, mRNA and catalytic activities associated with downregulation of collagen synthesis in emphysematous and carcinogenic lung tissues. However, tissue thiols such as glutathione (GSH) and metallothionein as well as γ-glutamylcysteine synthetase, a key enzyme for GSH biosynthesis were constantly upregulated. Cd upregulation of cellular thiols is a critical cellular event facilitating downregulation of LOX since they trap cellular copper, a cofector of LOX. Based on LOX biological functions, Cd downregulation of LOX may play a vital role in lung emphysema pathogenesis and carcinogenesis (Supported by grant NIEHS R01-11340).

PS 1251 Acute and Chronic Cadmium Exposure Induces Transcriptional Activation of BMP-2 Signaling Cascades in a Human Renal Epithelial Cell Culture Model

A. Slusser, A. Holmquist, S. Somji, D. A. Sens and S. H. Garrett. *Pathology, University of North Dakota, Grand Forks, ND.*

Cadmium is a toxic heavy metal that is a known nephrotoxin and carcinogen. While acute exposure causes tubular necrosis (i.e. acute kidney injury), chronic exposure can result in renal fibrosis (1.e. chronic kidney disease) or cancer. Although the consequences of cadmium exposure are well characterized, the mechanisms responsible for the pathologic states remain to be fully characterized. In order to elucidate the signaling cascades elicited by cadmium, an in vitro model of exposure was developed using human renal epithelial cells derived from the proximal tubule, the main site of cadmium induced toxicity. The cells were exposed to varying concentrations of cadmium for either 24 hours (9, 27, and 45 μM) or 13 days (4.5, 9, and 27 μM). Microarray analysis revealed 387 differentially expressed genes common to both exposure time points, including bone morphogenic protein 2 (BMP-2), a member of the TGF-β superfamily of proteins. Previous studies have shown BMP-2 involvement in epithelial- mesenchymal transition (EMT), making it an interesting candidate to evaluate in the context of this study. BMP-2 acts by binding to heteromeric BMP receptor type I/II complexes at the plasma membrane, initiating a signaling cascade involving SMAD1/5/8 phosphorylation, colocalization of the phospho-SMAD1/5/8 complex with SMAD4, and nuclear translocation of the complex. Nuclear translocation of the complex activates the expression of several target genes including inhibitor of DNA binding 1 (ID1). RT-PCR results have confirmed the upregulation of BMP-2, BMPR2, and ID1 as well as FZD2 and Wnt5a indicating the possibility of cross talk between canonical Wnt signaling and cadmium induced BMP-2 signaling. Together these results indicate that exposure to cadmium either acutely or chronically may initiate EMT via synergism between BMP-2 signaling and canonical Wnt signaling pathways.

PS 1252 Diabetogenic and Obesogenic Effects of Cadmium in Rats and db/db Mice at Clinically Relevant Levels of Exposure

J. Edwards[1], J. Nguyen[1] and C. Ackerman[2]. *[1]Department of Pharmacology, Midwestern University, Downers Grove, IL and [2]Edward Via College of Osteopathic Medicine, Spartanburg, SC.*

Cadmium (Cd) is a ubiquitous environmental pollutant that has been associated with hyperglycemia or diabetes in epidemiological studies. In the current study, we show that after 12 weeks of Cd exposure in rats there was an increase in serum glucose-dependent insulinotropic polypeptide (GIP) and a decrease in the satiety hormone, leptin. Based on these observations we conducted a pilot study using rats, db/db mice (diabetic mouse model) and lean mice. All animals were given daily subcutaneous injections of Cd at a dose of 0.6 mg/kg/day for two weeks then given no Cd for another two week period. At the end of the study, all animals underwent an oral glucose tolerance test (OGTT) and body weight and fat pad weights were recorded. In the OGTT, Cd had the greatest effect on db/db mice, with all animals except one having blood glucose levels of 600 mg/dl or higher 30 min following an oral dose of glucose (2g/kg). At the same 30 min time point, the non-Cd treated db/db mice had an average blood glucose value of 507 ± 19 mg/dl. Surprisingly, at the end of the study, all Cd treated groups of animals had higher average body weight values as compared to non-Cd treated animals. This increase in body weight during the last 2 weeks of non-Cd exposure was statistically significant in rats. Epididymal and retroperitoneal fat pad weights were significantly greater in the Cd-treated lean mice as compared to non-Cd treated lean mice. Finally, Cd content of the renal cortex from Cd-treated lean mice was 45.4 ± 3.6 μg/gram tissue wet weight. This study shows that environmental substances such as Cd can have diabetogenic and obesogenic effects at low levels of exposure.

PS 1253 Analysis of Molecular Mechanisms Involved in Induction of Endoplasmic Reticulum Stress by Cadmium

G. Hwang, K. Du and A. Naganuma. *Graduate School of Pharmaceutical Sciences, Tohoku Univ, Sendai, Miyagi, Japan.*

Cadmium is a toxic heavy metal that causes renal dysfunction. However, the molecular mechanisms underlying its toxicity are not clearly understood. Recently, we employed RNA interference to identify novel factors involved in manifestation of cadmium toxicity. We found that the inhibition of the expression of endoplasmic reticulum-associated protein degradation (ERAD) system related-genes sensitized HEK293 cells to cadmium. ERAD system is a cellular response system to the ER stress, and is involved in translocation of misfolded ER proteins into the cytosol and promotion of their ubiquitination and subsequent degradation by proteasome. NHK and TCRα are well-characterized substrates for ERAD. The level of these two proteins was significantly increased by treatment of HEK293 cells, which were harboring the NHK and TCRα expression vectors, with cadmium. Cycloheximide-chase assay for determining the degradation rates showed that cadmium inhibits degradation of NHK and TCRα. The levels of these two proteins were also increased by treatment with proteasome inhibitor (MG132), but further accumulation of ERAD substrates by cadmium was hardly observed in the MG132 treated cells. These results suggest that cadmium inhibits the process leading to the proteasome-dependent degradation of ERAD substrates. VCP is involved in retrograde translocation of ubiquitinated ERAD substrate from the ER to the proteasome. When the ERAD system was inhibited by VCP knockdown, levels of ER stress markers such as BiP and CHOP were significantly increased similar to the case of cadmium treatment. This supports the possibility that cadmium induces ER stress through the accumulation of ERAD substrates in the cells. ER stress-inducing agents such as tunicamycin, thapsigargin and dithiothreitol did not affect the levels of both NHK and TCRα, suggesting that the ER stress induced through the accumulation of ERAD substrates is specifically caused by cadmium. We conclude that cadmium may induce ER stress by inhibition of the function of the ERAD system and repression of the degradation of misfolded protein.

PS 1254 Environmental Metabolome of Mouse Liver Mitochondria and Cell Nuclei

Y. Go, M. Orr, Y. Liang and D. P. Jones. *Medicine, Emory University, Atlanta, GA.*

Cd accumulates in humans from dietary, environmental including cigarette smoke, and occupational sources, and has a twenty-year biologic half-life. Our previous studies showed that environmental low dose Cd altered protein redox states resulting in stimulation of inflammatory signaling and actin cytoskeleton disruption, suggesting that Cd could impact multiple disease mechanisms. However, little is known about the relative sensitivities of cellular metabolism associated with subcellular compartmental disruption. In the current study, we investigated effects of acute Cd on mouse liver examining the metabolome of isolated mitochondria and nuclei. To identify nuclear and mitochondrial metabolites affected by Cd, liver nuclei and mitochondria isolated from Cd-exposed mice were analyzed by high-resolution metabolomics. The result showed that Cd altered levels of 1,901 and 542 metabolites in nuclei and mitochondria, respectively, compared to control group. Of these metabolites changed significantly by Cd, 1016 in nuclei and 278 in mitochondria matched to metabolites in Kyoto Encyclopedia Gene and Genome (KEGG) database. Of these, 80% of decreased features are categorized to phytochemical compounds, lipids and biologically functional compounds. On the other hand, Cd increased 262 and 88 features in nuclei and mitochondria, respectively. Of these, 24% (nuclei) and 17.1% (mitochondria) are categorized into pesticides, natural toxins and carcinogens. The results suggest that Cd -induced toxicity could be associated with substantial decrease in functionally essential biological molecules and increase in toxic chemicals in nuclei and mitochondria. Among multiple pathways analyzed by MetaCore software, metabolism associated with altered features of nuclei and mitochondria are distinct. Taken together, the results indicate that metabolomics analysis of subcellular compartments enable identifying biological molecules and toxic chemicals, and associated functional pathways, which could be applicable to determine potential markers as indication of complex mechanisms of environmental effects in disease.

PS 1255 Gastrointestinal Solubilization and Uptake of Mercury and Selenium from Wild-Harvested Inuit Foods

B. D. Laird[1], S. Palaniyandi[1], P. J. Vanié[2], M. Lemire[3], M. Kwan[4], L. Chan[2], E. Dewailly[3] and P. Ayotte[5]. [1]*School of Public Health and Health Systems, University of Waterloo, Waterloo, ON, Canada,* [2]*Department of Biology, University of Ottawa, Ottawa, ON, Canada,* [3]*CR-CHUQ, Université Laval, Québec City, QC, Canada,* [4]*Nunavik Research Centre, Makivik Corporation, Kuujjuaq, QC, Canada and* [5]*Institut National de Santé Publique du Québec, Québec City, QC, Canada.*

The Inuit of Nunavik, Canada face elevated methylmercury exposures through the consumption of traditional foods such as beluga meat. However, many of the major methylmercury sources in the Inuit diet are also rich in the essential micronutrient selenium. Although the mechanisms of interactions are largely unknown, selenium may affect the bioavailability of mercury in the gastrointestinal (GI) tract. In this work we aim to identify the bioavailability of mercury and selenium in the traditional foods of Inuit.

The traditional foods that most contribute to the dietary intake of Se and Hg by Inuit were collected in Nunavik in 2008-2012. Each of the foods was digested using an in vitro model that simulates the physiological conditions of the human GI tract to measure bioaccessibility (IVBA). Thereafter, the extracts were applied to the apical side of an intestinal epithelial model. Mercury IVBA of the traditional foods ranged between 9% (Arctic char) and 95% (Ringed seal meat). The IVBA of mercury in ringed seal liver was considerably lower (25%) than observed in ringed seal meat. Interestingly, a large variation in Hg IVBA was observed between fish species (e.g. Arctic char 9.4%; Lake trout 56%). In vitro uptake experiments using Caco-2 cells loaded in Transwell plates showed mercury bioavailability to differ between foods (ranging between 5% for ringed seal liver and 64% for arctic char). In contrast, no such differences were observed between foods for Se bioavailability. Altogether, this research indicates that constraints on dissolution and uptake may impact Inuit exposure to Hg and Se from traditional foods. Future work shall elucidate whether these differences in mercury bioaccessibility and bioavailability are associated with mercury and selenium speciation.

PS 1256 Semichronic Methylmercury Exposure Alters KCl-Induced Calcium Influx in SH-SY5Y Cells

I. Cruz-Torres, K. L. Long-Roldán, S. M. Ciotti and W. D. Atchison. *Mich State Univ, E Lansing, MI.*

Methylmercury (MeHg) causes cell-type specific damage in the cerebellum in a Ca^{2+}-dependent manner. In vitro studies have shown that acute MeHg treatment caused a biphasic increase in $[Ca^{2+}]_i$which can be delayed by voltage-gated Ca^{2+} channel (VGCC) antagonists, demonstrating their role in MeHg-induced Ca^{2+} dysregulation. We and others have shown effects of MeHg on dopamine release; numerous studies have addressed the acute effects of MeHg on cholinergic and dopaminergic cell lines and primary neurons. However, exposure to low levels of MeHg during lifetime are lacking. As such, our aim was to study effects of repeated MeHg treatment on VGCC function in differentiated SH-SY5Y cells, a dopaminergic cell line. These cells haven't been used extensively to study MeHg neurotoxicity so we first characterized acute effects of MeHg on $[Ca^{2+}]_i$ in these cells. Changes in $[Ca^{2+}]_i$ were measured using Fura-2; cells were perfused continuously with 1, 2, 5, or 10μM MeHg. MeHg caused a biphasic, concentration-dependent increase in fura-2 fluorescence; the times to onset of both phases were inversely proportional to the [MeHg]. At 1 μM Phase 1 (P1) and Phase 2 (P2) occurred at ~12 and 48min respectively, whereas at 10μM P1 occurred within 2 min and P2 within 15min. Nifedipine (Nif, 5μM) and ω-conotoxin GVIA (GVIA, 1 μM), L- and N-type antagonists respectively, delayed the onset of P2 but not P1. Effects of semichronic MeHg treatment on VGCC function were subsequently characterized. Cells were treated with 0 or 20nM MeHg for 48 or 72h. Cells were then loaded with fura-2 AM and KCl-induced (40mM) Ca^{2+} influx was monitored as an index of VGCC function. Ca^{2+} influx through L- and N-type VGCCs was isolated using GVIA and Nif respectively. The 48h treatment significantly decreased KCl-induced Ca^{2+} influx through L-type VGCCs; the 72h treatment significantly decreased KCl-induced Ca^{2+} influx through both L- and N-type VGCCs. Thus semichronic MeHg treatment affects VGCC function in a dopaminergic cell line. These may result from MeHg-induced alterations of VGCC expression, resting $[Ca^{2+}]_i$, or block of VGCCs.

PS 1257 Brain-Specific Induction of Expression of Ccl4 and Scgb3a1 by Methylmercury in Mice

M. Kim[1], T. Takahashi[1], J. Lee[1, 2], G. Hwang[1] and A. Naganuma[1]. [1]*Laboratory of Molecular and Biochemical Toxicology, Tohoku University, Sendai, Miyagi, Japan and* [2]*Laboratory of Pharmaceutical Health Sciences, School of Pharmacy, Aichi Gakuin University, Nagoya, Aichi, Japan.*

Methylmercury (MeHg) is a pollutant that causes severe central nervous system damage. However, the mechanism of MeHg toxicity remains unclear. Our previous study indicated that expression levels of 21 genes were changed in the cerebellum of mice by MeHg. In this study, we investigated effects of MeHg on the expressions of these 21 genes in various tissues (cerebrum, cerebellum, liver and kidney) of MeHg-treated mice. Scgb3a1, Ch25h, Chi3l3 Ctla2b and several chemokines (Ccl2, 4, 7, 9 and 12) mRNA expressions were significantly increased in the brain of MeHg-treated mice. Among these genes, mRNA levels of Ccl4 and Scgb3a1 were not significantly changed in the liver and the kidney. These results suggest that the MeHg-induced increases in Ccl4 and Scgb3a1 expression are brain specific in mice.

In mouse neural progenitor C17.2 cells, expression of Ccl4 or Scgb3a1 mRNA were also increased by MeHg. Involvement of mitogen-activated protein kinase (MAPK) cascades in induction of Ccl4 or Scgb3a1 expression has been known. We investigated the involvement of MAPK cascades (p38, ERK and JNK) in MeHg-induced Ccl4 or Scgb3a1 expression in C17.2 cells. Pre-treatment with a p38 inhibitor (SB203580) or a ERK inhibitor (PD98059) significantly attenuated MeHg-induced expression of Ccl4 mRNA, but not the expression of Scgb3a1 mRNA. MeHg enhanced phosphorylation of p38 and ERK in C17.2 cells. These results suggest that the activation of p38 and ERK cascade are involved at least partially in the induction of Ccl4 expression by MeHg in C17.2 cells.

PS 1258 Role of Reactive Sulfur Species in Reduction of Methylmercury Toxicity *In Vitro* and *In Vivo*

E. Yoshida[1], T. Toyama[3] and Y. Kumagai[2]. [1]*Graduate School of Comprehensive Human Sciences, University of Tsukuba, Tsukuba, Japan,* [2]*Faculty of Medicine, University of Tsukuba, Tsukuba, Japan and* [3]*JSPS Research Fellow, Tsukuba, Japan.*

Methylmercury (MeHg) is an environmental electrophile that can be covalently bound to protein sulfhydryls to form protein–MeHg complexes. These covalent modifications, referred as "S-mercuration", are associated with disruption of enzyme function and neurotoxicity. Some of MeHg unbound and/or proteins mod-

ified by MeHg undergo interaction with deprotonated glutathione (GSH) to yield its GSH adducts that are rapidly excreted into extracellular space through MRP transporters. On the other hand, hydrogen sulfide (H2S) is a gaseous, weakly acidic molecule mainly produced by cystathionine β-synthase (CBS) and cystathionine γ-lyase (CSE) in cells. Most interestingly, H2S is extensively dissociated into a nucleophile HS- because of its pKa value = 6.76 while pKa value of GSH is 9.12, implying that most of GSH exists as its protonated form at physiological conditions. However, role of H2S in chemical modification of cellular proteins and cytotoxicity during exposure to MeHg is poorly understood. We examined the contribution of H2S derived from CBS to cellular protection against MeHg. Pretreatment with NaHS or overexpression of CBS reduced MeHg cytotoxicity, whereas transfection with CBS small interfering RNA enhanced MeHg toxicity in human neuroblastoma SH-SY5Y cells. Bismethylmercury sulfide ((MeHg)2S), formed during the reaction of MeHg with H2S, was identified as a metabolite of MeHg in SH-SY5Y cells exposed to MeHg and in the livers of rats treated with MeHg. (MeHg)2S had little chemical protein modification capability and little cytotoxicity compared with MeHg in vitro and in vivo. Based on these results, we propose a novel detoxification pathway of MeHg catalyzed by cellular enzyme to generate H2S.

PS 1259 Characterization of Mercury Binding Proteins in the Liver of Northern Fur Seals (*Callorhinus ursinus*)

T. Agusa[1], S. Yasugi[1], T. Ikemoto[2], T. Kunito[3], N. Baba[4], S. Tanabe[1] and H. Iwata[1]. *[1]Ehime University, Center for Marine Environmental Studies (CMES), Matsuyama, Japan, [2]Thermo Fisher Scientific, Yokohama, Japan, [3]Shinshu University, Matsumoto, Japan and [4]National Research Institute of Fisheries Science, Yokohama, Japan.*

Marine mammals accumulate a large amount of mercury (Hg) in the liver. Our previous studies have found that most of Hg exists as an inactive form, tiemannite (HgSe) in the nuclear, lysosomal, and mitochondrial (NLM) fraction of the liver of marine mammals, whereas relatively high abundance of organic Hg was observed in the liver cytosol. This result suggests that methyl Hg is demethylated in the cytosol and Hg subsequently co-accumulates with selenium (Se) in the NLM fraction. However, it is still unknown how Hg is present in the liver cytosol fraction in marine mammals. To understand the toxicokinetics of mercury, we investigated Hg binding proteins in the hepatic cytosol of the northern fur seal (*Callorhinus ursinus*). In the cytosol, Hg concentration in the high molecular weight (HMW) fraction was higher than the metallothionein (MT) and the low molecular weight (LMW) fractions. In contrast, Se was detected in the HMW and LMW fractions, but not in the MT fraction. A significant positive correlation between Hg and Se concentrations was found in the HMW fraction of the cytosol. The molar ratio of Hg and Se reached 1:1 with an increase in Hg concentration. These results suggest that Se interacts with Hg and then bind to HMW protein(s) in the hepatic cytosol, reducing the toxicity of Hg in the liver. By the purification of proteins interacted with both of Hg and Se using an anion exchange and a gel filtration chromatography, four proteins with the molecular weight around 100 kDa and 40 kDa were obtained in the HMW fraction of the cytosol. The purified proteins may play a role in the formation of Hg-Se complex in the hepatic cytosol.

PS 1260 Effects of Single Nucleotide Polymorphisms on Blood Mercury Level of Korean Population

J. Lim[1], H. Kwon[1], H. Kim[3], Y. Kim[3], S. Eom[3], M. Hwang[4] and J. Park[2]. *[1]Dankook University, Cheonan, Republic of Korea, [2]Chung-Ang University, Seoul, Republic of Korea, [3]Chungbuk University, Chengju, Republic of Korea and [4]National Institute of Food and Drug Safety Evaluation, Cheongwon, Republic of Korea.*

Background: Recent studies have suggested that several genes that mediate mercury metabolism are polymorphic in humans.
Objectives: We hypothesized those single-nucleotide polymorphisms (SNPs) in toxicokinetics genes may influence individual difference in blood mercury levels. We studied the potential modifying effects of toxicokinetics related SNPs on blood mercury level.
Methods: We selected samples of 528 adults from "the Korean research project on the integrated exposure assessment of hazardous materials for food safety (KRIEFS)"cohort. This cohort measured blood mercury level and dietary exposure to mercury level. We analyzed SNPS of samples with a Human Exome 12 v 1.2. The blood mercury levels were compared by SNPs with linear regression model.
Results: Linear regression analysis showed that eight SNPs were statistically significant different in blood mercury level by genotype (cut off P< 10-7). When we adjusted age, sex, smoking, and dietary exposure level, TOP1MT (rs11544484) AA genotype (n=2) or AG genotype (n=57) had lower blood mercury levels than GG genotype (n=437). MBIP (rs2899849) GG genotype (n=1) GA genotype (n=24) had lower blood mercury level than AA genotype (n=471). FZD7 (rs201306518) GG genotype (n=1) or GC genotype (n=27) had lower blood mercury level than CC genotype (n=468). IL6ST (rs2228043) GG genotype (n=1) or GA genotype (n=43) had lower blood mercury level than AA genotype (n=452). Intragenic of PARP11 and CCND2 (rs11063069) AA genotype (n=1) or AT genotype (n=47) had lower blood mercury level than TT genotype (n=448). MBIP (rs3168891) AA genotype (n=1) or AC genotype (n=43) had lower blood mercury level than CC genotype (n=448).
Conclusion: Our findings suggest that some toxicokinetics related genetic polymorphism may influences blood mercury level.

PS 1261 Ras Sindoor: Ayurveda's Attempt at Detoxifying Mercury

N. Sadekar and L. D. Trombetta. *Pharmaceutical Sciences, St. John's University, Queens, NY.*

Ayurveda is a traditional medicine system or a form of alternative medicine, which is native to the Indian subcontinent. Rasa Shastra is a branch of Ayurveda that involves processes to purify metals for therapeutic use as herbo-metallic preparations. With the expanding global community, these medicinal preparations are easily available to anyone desperately seeking alternative treatment strategies. These preparations may be more likely to be toxic than therapeutic. Ras Sindoor (RS) is an inorganic compound containing mercury and sulfur, used as a form of medicine in Ayurveda. Toxicity of organic and inorganic mercury compounds has been well established, but there is a dearth of scientific investigations that study potential RS toxicity. This study utilized techniques such as SEM- X-ray Diffraction (EDAX) and the dimethyl thiazolyl diphenyl tetrazolium bromide (MTT) assay to study the effect of RS along with methyl mercury and red mercuric sulfide on rat hippocampal astrocytes. The outcome of EDAX was that both red mercuric sulfide and RS showed similar chemical composition. Rat hippocampal astrocytes (passage 12-13) seeded in 96 well plates were exposed to the three compounds at concentrations 0.5μM, 1μM, 2μM, 3.5μM and 5μM for methyl mercury and 50μM, 60μM, 70μM, 80μM, 90μM and 100μM for both red mercuric sulfide and RS for 12 hours. The MTT assay was used to assess the cytotoxicity. Red mercuric sulfide and RS showed no statistical difference from controls at the dosages tested. However, light micrographs of astrocytes exposed to red mercuric sulfide and RS, showed cell injury in the form of shortened astrocytic processes when compared to controls. RS and red mercuric sulfide demonstrated morphological changes, which apparently do not affect cell viability. These changes may indicate alterations to cytoskeletal components, which can alter cellular physiology but not viability. Further experiments are needed to elucidate the nature of such changes to determine if they result in deviation from normal cell function.

PS 1262 Involvement of Decreased Activities of Thioredoxin Reductase and Glutathione Peroxidase in the Neuronal Degeneration by Methylmercury in the Developing Rat Cerebrum

M. Yamamoto[1], M. Sakamoto[2] and K. Sakai[3]. *[1]Department of Basic Medical Science, National Institute for Minamata Disease, Minamata, Kumamoto, Japan, [2]Department of Environmental Science and Epidemiology, National Institute for Minamata Disease, Minamata, Kumamoto, Japan and [3]Japan Institute for the Control of Aging, Nikken Seil, Fukuroi, Shizuoka, Japan.*

This study was designed to investigate factors that determine susceptibility to the developmental neurotoxicity of methylmercury (MeHg). It has been previously shown that MeHg treatment decreased glutathione peroxidase (GPx) activity in the developing rat brain. In this experiment, the effects of MeHg on GPx, thioredoxin reductase (TrxR) and glutathione reductase (GR) activities were examined in postnatal developing rats. Wistar male rats of postnatal days 14 (8 rats per group) were orally administered vehicle (control) or MeHg (6.4 mg Hg/kg/day) for 10 days. The MeHg-administrated group showed a significant decrease in body weight, and half of the animals exhibited mild hind-limb crossing by day 11. Increased reactive astrocytosis was also observed in the cerebral cortex of the MeHg-administrated group. Activity of GPx and TrxR, but not GR, were significantly decreased by MeHg-treatment. MeHg inhibited TrxR activity to a greater extent than GPx activity. These results indicate that TrxR and GPx activity, Se-contained enzymes, could be significantly affected by MeHg exposure in the developing brain.

PS 1263 Interaction between Early-Life Methylmercury Exposure and Iron Deficiency in *Daphnia pulex*

S. L. Hudson, D. Doke and J. M. Gohlke. *Environmental Health Sciences, University of Alabama at Birmingham, Birmingham, AL.*

Methylmercury (MeHg) is a known neurotoxicant and bioaccumulates in fish, with exposure to humans *in utero* being of highest concern. Also, iron (Fe) deficiency, with an estimated prevalence of 49%, is particularly problematic during pregnancy and early life. Previous studies have shown that iron deficiency exacerbates manganese and cadmium toxicity. We are currently using *Daphnia pulex* as an alternative model for chronic toxicity testing due to its short lifespan, ease of culture, and transparency for physiological studies. The overall purpose of this research is to investigate the interaction between poor nutrition, particularly a low iron diet, and early life exposure to MeHg. We hypothesize when *D. pulex* are fed a low-iron diet, the toxicity associated with early exposure to MeHg will increase. We have fed *D. pulex* a standard and half Fe diet. Early life exposure to low level MeHg (1600 ng/l, 800 ng/l, 400 ng/l and 200/ng/l) was administered (for 24 hrs in first 48 hrs.). Maturation time, average brood size, total reproduction, and total lifespan were measured. In addition, the effects of Fe deficiency and MeHg exposure on lipid storage were measured using image analysis of Oil Red O staining and confirmed through biochemical analysis (triacylglyceral quantification). Also, we are investigating effects on egg size and metabolic rate. Preliminary data suggests that daphnids that are fed a standard Fe diet had a significantly longer lifespan compared to daphnids on a half-Fe diet. In addition, brood size and total reproduction on a standard Fe diet had significantly more offspring compared to those who were fed a half-Fe diet. However, the differing diets did not show a significant difference in maturation time.

PS 1264 Sex Differences in the Lipidomics of Subchronic Low-Level Inorganic Mercury Exposure in the Rat

A. D. Wusu[1], O. Ademuyiwa[2], O. O. Ogunrinola[1], O. K. Afolabi[2], E. O. Abam[2], D. O. Babayemi[2], E. A. Balogun[2] and O. O. Odukoya[3]. *[1]Biochemistry, Lagos State University, Lagos, Nigeria, [2]Biochemistry, Federal University of Agriculture, Abeokuta, Abeokuta, Nigeria and [3]Chemistry, Federal University of Agriculture, Abeokuta, Abeokuta, Nigeria.*

Inorganic mercury has been identified as a risk factor of cardiovascular diseases. The mechanisms underpinning this risk and the sex differences are not yet understood. To investigate the effects of mercury on lipid metabolism, male and female rats were exposed to mercury chloride (0.5, 1.0 and 1.5 mg/kg) for 12 weeks. Dyslipidemia caused by mercury in both sexes exhibited different patterns. At the highest dose, hypercholesterolemia characterized the effect of mercury in male as against hypocholesterolemia in female. Hypertriglyceridemia was observed in both sexes. Plasma and erythrocyte free fatty acids (FFA) increased significantly in male than in female. Reverse cholesterol transport was inhibited by mercury at 1.5mg/kg dose in male as evidenced by decreased HDL cholesterol but increased in female. Brain cholesterol and triglyceride were reduced by mercury (at 1.5mg/kg) in male as against the no effect observed in female animals. Hepatic cholesterol in male and phospholipid in both sexes were increased by mercury (1.5mg/kg). Pulmonary cholesterogenesis and phospholipidosis were observed in male whereas in female only phospholipidosis was observed. Increase in triglyceride in lung and heart of female animals and liver of both sexes were also observed. Mercury exposure caused reduction in phospholipid concentrations in brain and spleen of both sexes. Hepatic HMG-CoA reductase was up-regulated in both sexes (at 1.0 mg/kg in male but at 1.5 mg/kg in female) whereas brain HMG-CoA reductase was down-regulated in male and up-regulated in female at 1.5mg/kg. Plasma FFA and HDL cholesterol were positively associated with tissue mercury in females as against the negative associations observed in males. These findings indicate that inorganic mercury perturbs different pathways in lipid metabolism in both sexes and this may be responsible for its cardiovascular effects.

PS 1264a Cut-Off Values and Benchmark Doses (BMDs) for Cadmium Compared across Human Exposure Settings: Evidence for Protective Pathways?

M. Bhattacharyya. *Georgia Regents University, Augusta, GA.*

A benchmark dose (BMD) is the dose of a toxic compound that increases the probability of an abnormal response by a benchmark response (BMR), i.e., from P0 for a control unexposed subject to P0 +BMR for a subject at the BMD. For cadmium (Cd), dose is taken as urine Cd concentration (UCd) – a measure of internal dose. Pathways that protect against Cd toxicity, including metallothionein synthesis, are a feature of human cells. This project considers the hypothesis: 1) Cd protective pathways are effective at low levels of environmental exposure; 2) With the BMD approach, 'control' populations that differ in UCds might generate similar cut-off values for kidney dysfunction, reflective of Cd-protective pathways. To achieve uniformity of approach, 95% cut-off values for urine concentrations of beta-2 microglobulin (UB2M) and N-acetyl-beta-D-glucosaminidase (UNAG), and BMD values based on a 5% BMR, were compared across published studies. With UB2M as the marker of kidney dysfunction, Chinese and Japanese populations with similar mean UCd values (1.3-1.8 ug Cd/g cr) generated similar 95% urine cut-off values (0.415 - 0.897 mg B2M/g cr). Corresponding BMD values ranged much more widely, from 1.7 to 10.0 ug Cd/g cr. No UB2M BMD results were available for Sweden. With UNAG as the marker of kidney dysfunction, control populations with mean UCds of 0.76 (Swe), 1.3 (Jap1), and 2.4 (Jap2) ug Cd/g cr generated 95% urine cut-off values of 3.6 (Swe), 11.1 (Jap1) and 16.6 (Jap2) Units NAG/g cr. Respective BMD values were 0.64, 4.3, and 10.8 ug Cd/g cr in urine. Increases in mean UCds were directly associated with increases in cut-off values and BMD values. Results indicate that, in the mean UCd range of 0.76 to 2.4 ug Cd/g cr among control populations not impacted by known industrial sources of cadmium, no indication exists for protective pathways producing similar cut-off values independent of mean UCd values, even at very low levels of Cd exposure. Additional research is needed to investigate the extent to which differences in BMD methods among studies may have contributed to these results.

PS 1264b MTF-1 Regulates Fra-1 mRNA Expression after Cadmium Exposure

E. Braithwaite and J. H. Freedman. *National Institute of Environmental Health Sciences, Research Triangle Park, NC.*

Cadmium has been classified as a known human carcinogen based on epidemiological studies and research performed in experimental animals. One class of cadmium responsive genes includes the fos family of transcription factors. The four members of this family (c-Fos, FosB, Fra-1 and Fra-2) can heterodimerize with Jun partners to form the AP-1 transcription factor and influence cellular properties such as invasion, metastasis, proliferation, differentiation, apoptosis and angiogenesis. Aberrant expression of these proteins can ultimately promote oncogenic transformations. To better understand the mechanism by which cadmium regulates the expression of three fos family members (FosB, Fra-1 and Fra-2), we examined the role the metal regulatory transcription factor 1 (MTF-1) plays in their regulation. MTF-1 is activated upon exposure to cadmium and accumulates in the nucleus of cells. Upon binding to metal responsive elements (MREs) in genes, MTF-1 participates in a multi-protein complex to regulate transcription and influence gene expression. After exposure to cadmium, quantitative real time PCR revealed that FosB, Fra-1 and Fra-1 steady state mRNA levels increased. However, only Fra-1's mRNA expression was reduced by the presence of MTF-1. Genomic analysis revealed the presence of several MRE sequences within the Fra-1 gene and ChIP analysis localized MTF-1 to MRE sequences located within the first intron. These data suggest that MTF-1 may play a role as a tumor suppressor gene after cadmium exposure by decreasing the expression of Fra-1.

PS 1264c Immuno-Modulatory Role of N-Acetylcysteine in Cadmium Treated Human Lung Cells

C. Odewumi, M. Ruden, V. Badisa, S. Fils-Aime and L. Latinwo. *Department of Biological Sciences, Florida A&M University, Tallahassee, FL.* Sponsor: A. Becker.

DHHS, IARC and EPA have determined that cadmium (Cd) and cadmium compounds are human carcinogens. Major route of cadmium exposure to humans is via inhalation. Cd exposure has been linked to cause lung cancer which is the second leading cause of cancer related deaths in the United States and developed countries. The mortality of cancer can be prevented by reducing the Cd toxicity in the biological system by using anti-oxidants compound such as N-acetyl-cysteine (NAC). NAC contains anti-oxidant and anti-inflammatory properties. In this study, we examined the immuno-modulatory effect of NAC on the viability and cytokines expression in CdCl2-treated A549 human lung cells. Cells were treated with 0, 50, 75 and 100 μM CdCl2 alone, 2.5 mM NAC alone, and co-treated with 2.5 mM NAC and 75 μM CdCl2 for 24 h. The level of cytokines in the cells' lysate and cell culture medium was measured using Ray Biotech's Human Cytokine Array 6 in control cells, 75 μM CdCl2 alone and NAC co-treated cells. Array results were validated by ELISA kit. The viability was decreased to 44.5% in the cells treated with 75 μM CdCl2 alone in comparison to the untreated control cells (100%), while viability was increased to 84.1% in the cells treated with 2.5 mM NAC and 75 μM CdCl2. In cell lysate of CdCl2 alone treated cells, 12 cytokines were up regulated and 8 cytokines were down regulated, while in the medium 15 cytokines were up regulated and 3 cytokines were down regulated in comparison to the control cells. In the cells treated with 2.5 mM NAC and 75 μM CdCl2, the cytokines expression was modulated by the NAC treatment. All the up regulated cytokines were reduced in comparison to CdCl2 alone treated cells. The ELISA results showed the

same pattern of expression as the cytokine array. These results clearly indicate the immune-modulatory role of NAC on the viability and cytokines expression in cadmium treated human lung cells and suggests that NAC can be used as an antidote against cadmium toxicity that can reduce lung cancer mortality rate.

PS 1265 Exposure to Cobalt, Nickel, Cadmium, and Chromium Causes Changes in Gene Expression and Protein Abundance in a Human Liver-Derived Cell Line

M. Permenter[1], D. Kumsher[1], W. E. Dennis[2], J. A. Lewis[2] and J. D. Stallings[2]. [1]*Excet, Inc., Fort Detrick, MD and* [2]*USACEHR, Fort Detrick, MD.* Sponsor: D. Jackson.

In the course of military and occupational activities the Nation's Guardians routinely encounter hazardous environmental toxicants and materials which may result in adverse health effects. Cobalt, nickel, cadmium, and chromium are four such materials with wide use and distribution in industrial areas, which increases the risk of exposure. While the toxic effects of these metals have been widely studied, the exact mechanisms of toxicity remain unclear, and no biomarkers of the adverse health effects have been validated. In order to further elucidate these mechanisms in liver and identify candidate biomarkers, we exposed HepG2-C3A cells to sublethal concentrations of NiCl2, Na2Cr2O7, CdCl2, and CoCl2 for 24 hrs. We chose the treatment concentrations based on a novel qPCR assay using a panel of genes developed from previous metal toxicity studies, as opposed to traditional cytotoxicity assays, to more accurately predict gene expression endpoints. We examined changes in gene expression using DNA microarrays and changes in protein abundance using mass spectrometry.
We performed both gene-level and functional analyses of the results and observed changes in pathways consistent with the known effects of heavy metal intoxication. Comparative analysis identified both common and unique modulated transcripts and perturbed pathways among the four metals. The changes in protein abundance closely resemble and validate the conclusions we drew from the microarray analysis. This work offers key insights into the roles specific genes, proteins, and pathways play in heavy metal toxicity mechanisms, and also identifies candidate biomarkers.

The views expressed are those of the authors and do not constitute endorsement by the U.S. Army. The research described herein was sponsored by the U.S. Army Medical Research and Materiel Command, Military Operational Medicine Research Program.

PS 1266 Time Course of Lead-Induced Dyslipidemia in Male Albino Rats

O. Ademuyiwa[1], E. O. Abam[1], O. O. Ogunrinola[1], A. D. Wusu[1], O. K. Afolabi[3], O. A. Dosumu[1], O. B. Onunkwor[1], E. A. Balogun[1] and O. O. Odukoya[2]. [1]*Biochemistry, Federal University of Agriculture, Abeokuta, Ogun, Nigeria,* [2]*Chemistry, Federal University of Agriculture, Abeokuta, Ogun, Nigeria and* [3]*Biochemistry, Ladoke Akintola University of Technology, Ogbomosho, Oyo, Nigeria.*

Lead has been shown to induce dyslipidemia in rats although the attendant mechanisms have not been clearly elucidated. In order to investigate the time course of lead-induced perturbations in lipid metabolism, male albino rats were exposed to 200ppm, 300ppm and 400ppm lead as lead acetate in their drinking water for 4, 8 and 12 weeks. Control animals received distilled water for the same exposure times after which blood and vital organs were removed from the animals and analyzed for lipid dynamics. Lead accumulated in the organs in the following descending order: kidney, liver, brain, heart and lungs. At 4 weeks, plasma cholesterol increased by 5% (in the 200ppm and 400ppm groups) and 8% in 300ppm. At 8 weeks, cholesterol in the 200ppm group increased by 10%. Plasma phospholipids decreased across all study groups. Lead decreased HDL cholesterol in a time-dependent manner (17% in 4-week 400ppm, 35%, 43% and 49% in 200ppm, 300ppm and 400ppm groups respectively at eight weeks). Plasma free fatty acids (FFA) displayed a hormetic-like response at 4 weeks with the lowest dose (200ppm) resulting in a decrease of 51% while 300ppm and 400ppm displayed 2-fold and 1.5-fold increases respectively. At 12 weeks, increases in FFA were dose-dependent. While cardiac and pulmonary phospholipidosis were observed, hepatic, brain and renal cholesterogenesis and phospholipidosis were observed. Hepatic and brain HMG-CoA reductase activities were up-regulated in most of the dosage groups. A positive correlation was observed between liver lead and liver cholesterol ($r = 0.476$, $p < 0.01$) while a negative correlation was observed between blood lead and HDL cholesterol ($r = -0.523$, $p < 0.01$). These findings indicate that lead-induced dyslipidemia may be mediated through up-regulation of HMG-CoA reductase activity and enhanced phospholipidosis resulting from increased availability of FFA.

PS 1267 Failure of Recovery from Lead Acetate-Induced Erythrocyte Oxidative Stress and Alteration of Antioxidant Defense System in Wistar Rats

A. A. Oyagbemi[1], T. O. Omobowale[2, 1], A. S. Akinrinde[1], A. B. Saba[1], O. T. Daramola[2] and B. S. Ogunpolu[2, 1]. [1]*Dept of Vet. Physiology, Biochemistry and Pharmacology, University of Ibadan, Nigeria, Ibadan, Oyo, Nigeria and* [2]*Veterinary Medicine, University of Ibadan, Nigeria, Ibadan, Oyo, Nigeria.*

Environmental contamination has continued to be a global source of concern even decades to come. Lead acetate (PbA) is one of the major environmental contaminants with grave toxicological consequences both in the developing and developed countries. This study was designed to evaluate possible toxic effects of PbA following exposure and subsequent withdrawal in male Wistar rats. Control group (group I) received normal saline while groups II, III and IV received 0.25, 0.5 and 1.0mg/ml of PbA respectively for 6 weeks. One half of the population of the rats was sacrificed at 6 weeks and PbA was withdrawn from the remaining rats for another 6 weeks. The erythrocyte antioxidant status and markers of oxidative were assessed. Our results show significant ($p<0.05$) increase in erythrocyte Malondialdehyde (MDA) and Hydrogen peroxide (H2O2) generated with significant ($p<0.05$) reduction in erythrocyte Reduced glutathione (GSH), Glutathione peroxidase (GPx), Catalase (CAT) after 6 weeks of exposure. However, there was significant ($p<0.05$) increase in the activity of Superoxide dismutase (SOD). After PbA withdrawal, there was significant ($p<0.05$) reduction in erythrocyte GSH, GPx, catalase CAT and SOD. MDA and H2O2 also increased significantly. Taken together, erythrocytes antioxidant defence system failed to recover after withdrawal of the exposed PbA for the period of the study. Hence, exposure of both animals and humans to PbA could be tantamount to failure of recovery from the toxic effect.

PS 1268 Co(II) and Ni(II) Responses in Human Lung Cells: Uptake, p53 Activation, and Cytotoxic Mechanisms

A. Zhitkovich, S. Green, M. W. Luczak, J. Morse and Z. DeLoughery. *Brown University, Providence, RI.*

Cobalt(II) and nickel(II) are both hypoxia mimetics and show many similar chemical properties. However, epidemiological and animal studies have found that only soluble Co(II) but not soluble Ni(II) was carcinogenic via inhalation. To understand biological differences between these two metals, we investigated stress responses in human lung cells. We found that H460 cells accumulated several times more Co(II) than Ni(II) but upregulation of the transcriptional factor p53 measured by its protein accumulation, Ser15 phosphorylation and expression of CDKN1A and MDM2 genes was more efficient by Ni(II). A stronger activation of the p53 pathway by Ni(II) was also evident from its more than 10-fold depletion of the p53 inhibitor MDM4 (HDMX) whereas Co(II) showed no effect. Apoptosis and the overall cell death by Co(II) were delayed and weaker than by Ni(II). The role of different mechanisms of cell death was examined using shRNA and inhibitors of caspases and programmed necrosis pathways. Ni(II)-induced cell death was completely caspase-dependent and p53 was responsible for activation of the caspase-9/caspase-3 cascade. For Co(II), 55% of cell death was caused by p53-mediated apoptosis, 20% by p53-independent apoptosis and 25% was due to p53/caspase-independent mechanisms. Primary human bronchial epithelial cells also showed several times higher accumulation of Co(II) than Ni(II) and delayed and weaker caspase activation by Co(II). Our results suggest that high uptake and ineffective elimination of Co(II)-loaded cells can contribute to carcinogenicity of this metal.

PS 1269 Non-Antioxidant Role of N-Acetylcysteine in Chemoprotection against Chromate, Cadmium, and Cobalt

M. W. Luczak and A. Zhitkovich. *Pathology and Laboratory Medicine, Brown University, Providence, RI.*

N-acetylcysteine (NAC) is a clinically approved drug that has been used as antidote for acetaminophen overdose and acute heavy metal poisoning. The chemoprotective activity of NAC has been attributed to elevation of cellular levels of glutathione and its direct radical-scavenging properties. However, the antioxidant-based mode of action in NAC protection against metal toxicity is inconsistent with findings in genetic models and the absence of redox activity among some metals. In this work, we investigated a mechanism of chemoprotection of human cells by NAC against three toxic metals Cr(VI), Cd(II) and Co(II). Our results showed that NAC-mediated chemoprotection was associated with rescue of cellular metabolic activity, elimination of caspases 3/7 activation and loss of upregulation of the stress-responsive transcription factors p53, HIF-1α and HSF-1. Experiments with γ-glutamylcysteine synthetase inhibitor ruled out the participation of cellular glutathione in cytoprotective activity of NAC. Using graphite furnace atomic absorption spectros-

copy, we found that NAC dramatically decreased cellular accumulation of all three metals in both transformed and normal human cells. Suppression of chromate uptake by NAC resulted from extracellular reduction of Cr(VI) to membrane-impermeable Cr(III). Incubation of Co(II) with NAC resulted in a rapid formation of Co(II)-NAC conjugates, which were unable to cross the plasma membrane. In conclusion, we found that direct reactivity with metals is a major antioxidant-independent mechanism in chemoprotection by NAC against carcinogenic Cr(VI), Cd(II) and Co(II). Our results also suggest that the use of NAC could be beneficial for diminishing tissue accumulation of this toxic metal released during corrosion of cobalt-chromium hip implants.

PS 1270 Lack of Reversal from Lead Acetate-Induced Hepatotoxicity and Oxidative Stress in Wistar Rats

A. B. Saba[1], A. A. Oyagbemi[1], T. O. Omobowale[1, 2], A. S. Akinrinde[1], O. T. Daramola[1, 2] and B. S. Ogunpolu[1, 2]. [1]*Dept of Vet. Physiology, Biochemistry and Pharmacology, University of Ibadan, Nigeria, Ibadan, Oyo, Nigeria and* [2]*Veterinary Medicine, University of Ibadan, Nigeria, Ibadan, Oyo, Nigeria.*

Lead is a ubiquitous metal and also one of the most abundant elements present on earth. Both the developing and the developed countries have been contaminated by this element. This study was designed to evaluate possible toxic effects of lead acetate (PbA) exposure and subsequence withdrawal in male Wistar rats. Control group (group I) received normal saline while groups II, III and IV received oral administration of 0.25, 0.5 and 1.0mg/ml PbA respectively for the period of 6 weeks. One half of the population of the rats was sacrificed at 6 weeks of PbA exposure. PbA was similarly withdrawn from the remaining rats for another 6 weeks. Exposure of rats to PbA led to significant decline ($p<0.05$) in Glutathione peroxidase (GPx), Glutathione S-transferase (GST), Catalase (CAT), Superoxide dismutase (SOD), and Reduced glutathione (GSH) content. Similarly, Malondialdehyde (MDA) and H2O2 concentrations were significantly ($p<0.05$) elevated. In the same vein, Aspartate aminotransferase (AST), Alanine aminotransferase (ALT) and Alkaline phosphatase (ALP activities also increased significantly in exposed rats. Animals from the withdrawal period exhibited similar pattern of alterations, with significant ($p<0.05$) reduction in GSH, GST, GPx and SOD and significant elevation in MDA. Serum ALT, AST and ALP however remained persistently high. In conclusion, experimental animals exposed to PbA could not recover from hepatotoxicity and oxidative stress. This might be due to significant disruption of antioxidant defence system and free radical generation by PbA.

PS 1271 Long-Term Exposure of Mice to Cr(IV) in Drinking Water Disrupts the Oxidative Stress Response Induced by Benzo[a] pyrene in the Proximal Gastrointestinal Tract

F. J. Sanchez-Martin, Y. Fan, J. L. Ovesen, V. S. Carreira and A. Puga. *Department of Environmental Health, University of Cincinnati, Cincinnati, OH.*

Exposure to a single toxic compound is rare in the environment. Exposure to complex mixtures of different toxicants are more frequent, causing mixture-specific effects that cannot be attributed to a single mechanism. Complex mixtures of the heavy metal chromium IV (Cr(IV)) and the polycyclic aromatic hydrocarbon benzo[*a*]pyrene (B[*a*]P), two toxicants with unrelated modes of action, are often found in the environment. To study the biological effects of these mixtures, we exposed mice to 0, 55, 550, and, 5500 ppb Cr(IV) in drinking water for 2 months followed by 3 additional months of coexposure to Cr(VI) and B[*a*]P, the latter included in corn oil-soaked food at doses of 0, 1.25, 12.5, or 125 mg/kg/day. Gene expression changes in liver, affecting genes such as *Cdkn1a/p21* and *Mki-67*, were solely B[*a*]P-dependent and independent of whether the mice had been co-exposed to Cr(VI). The proximal (PSI) and distal (DSI) portions of the gastrointestinal (GI) tract were also collected and analyzed for gene expression changes. In the PSI section, B[*a*]P exposure up-regulated the expression of several oxidative response genes, including *Gclc*, *Gclm*, *Gpx1*, or *Gpx4*. Exposure to Cr(IV) alone caused no apparent gene expression changes, but, when administered in conjunction with B[*a*]P, it inhibited the B[*a*]P-dependent effects observed in the GI tract PSI region. We conclude that the combined effect of Cr(IV) and B[*a*]P exposure may inhibit B[*a*]P-dependent induction of the oxidative stress response in the GI tract. This effect may be particularly critical in cases of extended exposure to mixtures of these agents, as may happen in the occupational setting or in areas where drinking water contains elevated levels of Cr(VI), and may contribute to the overall mutagenicity of the mixture. *Supported by NIH grants ES010807 and R21 ES020048.*

PS 1272 Effects of Particulate Hexavalent Chromium on Centrosome Separation and the Centrosomal Kinase Nek2A

J. Martino[1, 2], A. Holmes[1, 2, 3], H. Xie[1, 2, 3], E. Nigg[4] and J. P. Wise[1, 2, 3]. [1]*Wise Laboratory of Environmental and Genetic Toxicology, University of Southern Maine, Portland, ME,* [2]*Maine Center for Toxicology and Environmental Health, University of Southern Maine, Portland, ME,* [3]*Department of Applied Medical Sciences, University of Southern Maine, Portland, ME and* [4]*Biozentrum, University of Basel, Basel, Switzerland.*

Particulate hexavalent chromium (Cr(VI)) is a human lung carcinogen. Previous studies from our laboratory show that chronic exposure to particulate Cr(VI) causes centrosome amplification, a commonly seen phenotype in solid tumors associated with aneuploidy and chromosome instability. However, the molecular mechanisms involved in particulate Cr(VI)-induced centrosome amplification are unknown. In this study, we focused on Nek2A, a kinase involved in the separation of centrosomes at the G2/M transition. Premature centrosome separation could impair spindle formation and progression through mitosis, resulting in centrosome amplification. We exposed human lung fibroblasts to zinc chromate for 24-120 hours. Immunofluorescence techniques were used to evaluate centrosome separation and centrosomal localization of Nek2A. Western blots were used to assess total protein levels of Nek2A. Our data show that chronic exposure to particulate Cr(VI) causes an increase in centrosome separation. Moreover, even though Nek2A protein levels decreased after exposure to Cr(VI), its centrosomal localization in G2 cells did not change. Current efforts are aimed at measuring Nek2A activity after Cr(VI) exposure. Our data suggest that chronic exposure to particulate Cr(VI) causes premature centrosome separation and that this may be the result of Nek2A activation. Future work aims at reversing the centrosome separation caused by particulate Cr(VI) as well as studying upstream regulators of Nek2A. This work was supported by NIEHS grant ES016893 (J.P.W.) and the Maine Center for Toxicology and Environmental Health.

PS 1273 Time Course of Lead-Induced Alterations in Paraoxonase Activity in Male Albino Rats

E. O. Abam[1, 4], O. O. Ogunrinola[1], A. D. Wusu[1], O. K. Afolabi[1], O. A. Dosumu[1], O. B. Onunkwor[1], E. A. Balogun[1, 3], O. O. Odukoya[2] and O. Ademuyiwa[1]. [1]*Department of Biochemistry, Federal University of Agriculture, Abeokuta, Ogun State, Nigeria,* [2]*Department of Chemistry, Federal University of Agriculture, Abeokuta, Ogun State, Nigeria,* [3]*Department of Biochemistry, University of Ilorin, Ilorin, Kwara State, Nigeria and* [4]*Chemical Sciences Department, Biochemistry option, Bells University of Technology, Ota, Ogun State, Nigeria.*

Studies on paraoxonase (PON) activity in lead toxicity in the past have often found lead to be associated with lower serum PON activities and lower HDL values. In order to investigate the time course of lead-induced alterations in PON activity, male albino rats were exposed to 200ppm, 300ppm and 400ppm lead as lead acetate in their drinking water for 4, 8 and 12 weeks respectively. PON activities towards paraoxon (PONase) and phenylacetate (AREase) in plasma, lipoproteins, hepatic and brain microsomal fractions were determined. Lead was also assayed in blood, liver and brain tissues. Lead inhibited plasma PONase activity at 4 weeks (35%, 53% and 24% in 200ppm, 300ppm and 400ppm groups respectively), while activating it at 8 and 12 weeks (65%, 64% and 16% at 8 weeks; and 45% and 22% at 12 weeks in 200ppm and 300ppm groups respectively). Plasma AREase was also activated in most dosage groups. On the other hand, hepatic and brain microsomal PONase and AREase were generally inhibited by all the lead doses. HDL AREase increased by 25%, 35%, and 15% in 200ppm, 300ppm and 400ppm respectively at 12 weeks. HDL PONase also increased by 35% and 42% in 300ppm and 400ppm respectively at 4 weeks and 40%, 7% and 42% respectively at 8 weeks. VLDL AREase activity also increased by as much as 72% in 200ppm group at 4 weeks. However, lead inhibited VLDL PONase in all the dosage groups at 12 weeks. Positive correlations were observed between hepatic lead and plasma AREase ($r = 0.304$, $p = 0.01$), while negative correlations were observed between blood lead and liver microsomal AREase ($r = -0.504$, $p = 0.01$) and PONase ($r = -0.506$, $p = 0.01$). The unusual activation of circulating PONase and AREase might result from damage to microsomal membrane as a result of lead exposure.

PS 1274 The Unique N and C-Terminal Domains of Metallothionein-3 Influence the Growth and Differentiation of MCF-7 Breast Cancer Cells

B. Voels, S. H. Garrett, D. A. Sens and S. Somji. *Pathology, University of North Dakota, Grand Forks, ND.*

Toxic insult from the heavy metal cadmium is known to induce the expression metallothioneins (MT) which are heavy metal binding proteins. Previous work from our laboratory has shown that over-expression of MT-3 in breast cancers is associated with poor patient outcome. Furthermore, MT-3 has shown to inhibit the growth of breast cancer and prostate cancer cell lines. The MT-3 protein contains 7 additional amino acids that are not present in any other member of the MT gene family, a 6 amino acid C-terminal sequence and a Thr inserted in the N-terminal region. The unique N-terminal sequence is responsible for the growth inhibitory activity of MT-3 in the neuronal system. The goal of this study was to characterize the function of the N- and C-terminal domains of MT-3 in the breast cancer cell line, MCF-7. For this purpose six different constructs of MTs were prepared which were as follows: wild type (WT) MT-3, MT-3 N-terminal mutation (MT-3ΔNT), MT-3 C-terminal deletion (MT-3ΔCT), WT MT-1E, and MT-1E altered to contain the N –terminal, the C-terminal of MT-3 or both the N- and the C-terminal of MT-3. Each of these constructs was stably transfected into MCF-7 cells and the growth rates and mesenchymal markers E- and N-cadherin were measured. The data obtained suggests that the N-terminal region of MT-3 is involved in growth inhibitory activity whereas the C-terminal region is involved in vectorial active transport which is indicated by the formation of domes in cell culture, and that there is no significant change in the ratio of E- to N-cadherin. In conclusion, this study further characterizes the unique properties of the N- and the C-terminal domain of MT-3 and the potential role that it may play in the differentiation of certain breast cancers.

PS 1275 Characterization of OH Radicals Induced by Particulate Matter and Associated Species with a High-Throughput Approach

Y. Son[1], V. Mishin[2], W. Welsh[3], J. D. Laskin[3] and Q. Meng[1]. [1]*School of Public Health, Rutgers University, Piscataway, NJ,* [2]*Ernest Mario School of Pharmacy, Rutgers University, Piscataway, NJ and* [3]*Robert Wood Johnson Medical School, Rutgers University, Piscataway, NJ.*

Exposure to ambient particulate matter (PM) can cause various cardiopulmonary diseases. Oxidative stress, purported to be caused by the ability of PM to induce reactive oxygen species (ROS), has been identified as one of the common mechanisms leading to the observed adverse health effects. Among the ROS, hydroxyl radical (OH) is the most destructive. However, there is no high throughput approach to measure OH generated by PM, which in turn hinders the study of the interactions between PM and our biological system.

The goals are 1) to develop a high-throughput approach to measure OH induced by PM in a cell-free system, and 2) to study the kinetics of OH formation induced by PM and its constituents (transition metals).

OH induced by PM were quantified using a fluorescence assay (microplate reader), with disodium terephthalate as the molecular probe. Employing an established approach, the kinetics of OH formation was studied by introducing PM and 9 transition metal ions into a simulated lining fluid, and the formed 2-hydroxyl terephthalate was measured at designated time points up to 2 hours.

The detection limit of OH for the devised high-throughput approach (as extrapolated from the formation of 2-hydroxyl terephthalate) was 17.6×10-3 μM. The initial rate of OH formation ranged from 1.33×10-5 μM/s for Mn (10 μM) to 1.58×10-3 μM/s for Cu (10 μM). Both statistically significant synergistic effects (e.g. Cu and Fe) and antagonistic effects (e.g. Cu and V) were observed for OH generation by a mixture of transition metal ions. Insoluble PM constituents, soluble metal ions, and other soluble constituents contributed 22%, 59% and 19%, respectively, of OH induced by PM (NIST SRM 1648).

Trace-level OH induced by PM and its constituents can be measured with the devised high-throughput approach. The initial rates of OH formation derived from the kinetic experiments will be used to evaluate PM toxicities.

PS 1276 The Cytotoxicity and Genotoxicity of Soluble and Particulate Cobalt in Human Lung Fibroblasts

A. Holmes[1], L. J. Smith[1], S. Wise[1], M. Mason[2], T. Zheng[3] and J. P. Wise[1]. [1]*Wise Laboratory of Environmental and Genetic Toxicology, University of Southern Maine, Portland, ME,* [2]*Department of Chemical and Biological Engineering, University of Maine, Orono, ME and* [3]*Department of Environmental Health Sciences, Yale School of Public Health, New Haven, CT.*

Cobalt exposure is increasing as cobalt rises in demand worldwide due to its use in enhancing rechargeable battery efficiency, super-alloys, and magnetic products. Cobalt is considered a possible human carcinogen with the lung being a primary target. However, few studies have considered cobalt-induced toxicity in human lung cells. Therefore, in this study, we sought to determine the cytotoxicity and genotoxicity of particulate and soluble cobalt in human lung cells. Cobalt oxide and cobalt chloride were used as representative particulate and soluble cobalt compounds, respectively. Exposure to both particulate and soluble cobalt induced a concentration-dependent increase in cytotoxicity, genotoxicity, and intracellular cobalt ion levels. Based on intracellular cobalt ion levels, we found that soluble cobalt was more cytotoxic than particulate cobalt; however, soluble cobalt induced less chromosome damage compared to particulate cobalt. Accordingly, we investigated the role of particle internalization in cobalt oxide-induced toxicity. We found that particle-cell contact was necessary to induce cytotoxicity and genotoxicity after cobalt exposure. These data indicate that cobalt compounds are cytotoxic and genotoxic to human lung fibroblasts, and solubility plays a key role in cobalt-induced lung toxicity. This work is supported by ARO grant # 911NF-09-1-0296 (J.P.W.) and the Maine Center for Toxicology and Environmental Health.

PS 1277 Spatial Localization and Altered Quantitative Expression of Genes Associated with Alzheimer's Disease in Zebrafish Brains during Normal Senescence and with a Developmental Lead Exposure

J. Lee, S. M. Peterson and J. L. Freeman. *School of Health Sciences, Purdue University, West Lafayette, IN.*

Developmental lead (Pb) exposure is suggested as a risk factor for neurodegenerative diseases including Alzheimer's disease (AD). To further investigate the association between early-life Pb exposure and AD pathogenesis, zebrafish embryos were exposed to a control treatment or 100 ppb Pb from 1 to 72 hours after fertilization. Larvae were then rinsed and allowed to mature under normal laboratory conditions until they reached the age of 3 months (young) or 12 months (aged) for sex- and age-specific gene expression profiling. Seven genes associated with AD including amyloid beta precursor protein (appa and appb), presenilin (psen1 and psen2), apolipoprotein E (apoea and apoeb), and sortilin-related receptor L (sorl1) were analyzed. In situ hybridization revealed spatial expression of the seven genes throughout the brain, exhibiting weak to extensive staining in the hypothalamus and/or optic tectum regions. However, location of expression was not different between sexes, ages, or in those individuals developmentally exposed to Pb. In the quantitative polymerase chain reaction analysis, a significant increase in sorl1 expression was observed in aged control brains compared to the young control brains in both sexes. In addition, a significant up-regulation of appa was also detected in the aged female brains compared to the young female brains. These results suggest that both sex-specific and non-sex-specific alterations of genes related to AD occur during normal brain senescence. Moreover, a significant down-regulation of apoeb was observed in the aged males developmentally exposed to Pb compared to the control group. No significant quantitative differences were exhibited in any other Pb treated groups analyzed. These findings along with further characterization of AD-associated genes in zebrafish will provide insight into understanding impacts of developmental Pb exposure on adult neurodegenerative disease pathogenesis.

PS 1278 Treatment of Rat Hippocampal Astrocytes with Selenium Compounds Results in Metalloid Accumulation and Release of Cytochrome C

S. Roy and D. Hardej. *Pharmaceutical Sciences, St. John's University, Jamaica, NY.*

Selenium (Se) is a metalloid and a member of group 6A in the periodic table. It is an essential trace element in mammalian systems and serves as a cofactor for some enzymes. Exposure to high levels of Se have been associated with neurotoxicity. Work in our laboratory has established the cytotoxicity of Se compounds in rat hippocampal astrocytes. The purpose of this study was to investigate the accumulation of selenium in rat hippocampal astrocytes treated with diphenyl diselenide and selenium tetrachloride and the role of cytochrome *c*, lipid peroxidation products and glutathione peroxidase in the toxicity profile. The LC_{50} of both compounds

had been previously documented to be 7.81 μM. Transmission electron microscopy was used to study morphological changes and accumulation of selenium in cells following treatments. Micrographs of controls show well defined nuclei, double layered nuclear envelopes and mitochondria with definite shape and cristae. Astrocytes treated with 7.81 μM of both compounds appear to have disrupted morphology with pyknotic nuclei. Mitochondria show distorted shapes with the presence of deposits which may be selenium compounds. An ELISA assay was used to investigate cytochrome *c* levels in cytosolic and mitochondrial fractions. There was a significant decrease in cytochrome *c* in mitochondrial fractions and a significant increase in the cytochrome *c* in cytosolic fractions of astrocytes treated with 7.81 μM and 15.62 μM of both compounds compared to controls. TBARs assay was performed to investigate lipid peroxidation products. There was a significant decrease in the products in cells treated with 15.62 μM compared to controls. There were no significant changes in the activities of GPx in any treatment group. These results suggest that the accumulation of Se in the mitochondria and release of cytochrome *c* into the cytosol result in cytotoxicity in rat hippocampal astrocytes. Oxidative stress does not appear to be involved in the process.

PS 1279 Comparative Toxicity of Hexavalent Chromium (Cr(VI)) in Human and Alligator Cells

S. Wise[1], H. Xie[1], J. P. Wise[1], C. Wise[1], L. Guillette[2] and J. P. Wise[1]. [1]*University of Southern Maine, Portland, ME and* [2]*Medical University of South Carolina, Charleston, SC.*

The American alligator (*Alligator mississippiensis*) is an established sentinel species for many aspects of human and environmental health. However, genotoxicity studies in the species are absent, limiting our understanding of the impact of environmental toxicants on alligators and the human disease aspects they can represent. Cr(VI) is a ubiquitous environmental pollutant and a known human genotoxic agent. Thus, we compared the cytotoxicity and genotoxicity of Cr(VI) in primary human skin and alligator scute cells. Cr(VI) was both cytotoxic and genotoxic to alligator cells. Concentrations of 0.1, 0.5, 1.0, 5, and 10 ug/cm2 lead chromate induced relative cell survival levels of 126, 61, 46, 26 and 9 percent, respectively; and concentrations of 0, 0.5, 1, and 5 ug/cm2 lead chromate and induced 6, 19, 39 and 53 chromosome aberrations in 100 metaphases, respectively. In human cells, the same concentrations reduced relative cell survival levels to 64, 28, 10, 0 and 0 percent, respectively, indicating the alligator cells were more resistant to Cr(VI) cytotoxicity. For genotoxicity, the concentrations used in the alligator cells induced more damage in the human cells. For example, after adjusting for background differences (by subtracting controls), 0.5, and 1 ug/cm2 lead chromate induced 13 and 33 aberrations per 100 metaphases, respectively, in alligator cells compared to 32 and 43 aberrations in human cells. Thus, alligator cells had fewer aberrations and less cell death than human cells. Together, these data show that alligators have a similar Cr(VI) response as humans although the magnitude of the effects differ, possibly reflecting differences in Cr(VI) ion uptake, or, perhaps, a novel repair response. This research was supported by NIEHS grant ES016893 (JPW).

PS 1280 Interlaboratory Validation of Bioaccessibility Test for Metals

R. Henderson[1], V. Verougstraete[2], K. Anderson[3], J. Arbildua[4], T. O. Brock[5], T. Brouwers[6], D. Cappellini[7], K. Delbeke[8], G. Herting[9], G. Hixon[1], I. Odnevall Wallinder[9], P. Rodriquez[4], F. Van Assche[10], P. Wilrich[11] and A. R. Oller[12]. [1]*ToxStrategies, Inc., Durham, NC,* [2]*Eurometaux, Brussels, Belgium,* [3]*Oregon State University, Corvallis, OR,* [4]*Adolfo Ibañez University, Santiago, Chile,* [5]*Duke University, Durham, NC,* [6]*ECTX-Consult, Hasselt, Belgium,* [7]*Kirby Memorial Health Center, Wilkes-Barre, PA,* [8]*European Copper Institute, Brussels, Belgium,* [9]*KTH Royal Institute of Technology, Stockholm, Sweden,* [10]*International Zinc Association, Brussels, Belgium,* [11]*Freie Universität Berlin, Berlin, Germany and* [12]*NiPERA, Inc., Durham, NC.*

The intra- and inter-laboratory variability of bioaccessibility tests were evaluated in synthetic fluids relevant to oral, inhalation, and dermal exposure. Using one defined protocol, five laboratories measured metal release from cobalt oxide, cobalt powder, copper concentrate, Inconel alloy, leaded brass, and nickel sulfate hexahydrate. Standard deviations of repeatability (s_r) and reproducibility (s_R) were used to evaluate the intra- and inter-laboratory variability, respectively. Examination of the s_R:s_r ratios demonstrated that, while gastric and lysosomal fluids had reasonably good reproducibility, other fluids did not show as good concordance between laboratories. Relative standard deviation (RSD) analysis showed more favorable reproducibility outcomes for some data sets, overall results varied more between than within-laboratories. RSD analysis of s_r showed good within-laboratory variability for all conditions except some metals in interstitial fluid. In general, these findings indicate that absolute bioaccessibility results in some biological fluids may vary between different laboratories. Since measures of relative bioaccessibility are typically used (e.g., in read-across approaches for hazard and risk assessment), both inter- and intra-laboratory reproducibility are relevant unless all substances are tested in the same laboratory. Deviations in protocol interpretation may provide an explanation for some of the inter-laboratory variability observed.

PS 1281 Genetic Variation of Iron Metabolism in Mice

H. Irimagawa[1], Y. He[1], D. W. Killilea[2], B. Parks[3], S. T. Hui[3], E. Eskin[4, 5], A. J. Lusis[3, 4], C. Vulpe[1] and K. E. Page[1]. [1]*Department of Nutritional Science and Toxicology, University of California, Berkeley, Berkeley, CA,* [2]*Children's Hospital Oakland Research Institute, Oakland, CA,* [3]*Department of Medicine/Division of Cardiology, University of California, Los Angeles, Los Angeles, CA,* [4]*Department of Human Genetics, University of California, Los Angeles, Los Angeles, CA and* [5]*Department of Computer Science, University of California, Los Angeles, Los Angeles, CA.*

Iron deficiency is the most common nutritional deficiency in the world, with an estimated 4-5 billion affected persons, which can lead to debilitating fatigue, altered immune function, decreased work capacity and anemia. Similarly, iron overload is a significant health concern. Iron overload targets the liver, heart, and pancreas, and can lead to multiple complications including liver disease, cardiomyopathy, and diabetes mellitus. The great diversity in genetic disorders of iron metabolism in man, rodents and other vertebrates suggest that multiple loci can contribute to the susceptibility of iron deficiency and severity of iron overload. Several individual studies have shown genetic differences in iron homeostasis between inbred strains of mice. We hypothesize that this wide genetic variation underlies the differences seen in iron metabolism between inbred mice. Here we show variation in iron metabolism in six inbred mouse strains fed low (12ppm), high (10000ppm), and sufficient (35ppm) iron diets. Variation in elemental tissue content, hematological markers of iron status, as well as body weight and obesity markers are seen in this subset of the hybrid mouse diversity panel. This study highlights the population diversity in the ability to handle iron stress (deficiency or overload), and indicates the genetic variation in this population plays an important role.

PS 1282 Cytotoxicity and Epigenetic Effects of Post-Hydraulic Fracturing Flowback Waters in the Marcellus Shale from Pennsylvania

Y. Yao[1], M. Zhong[1], L. Chen[1], J. T. Zelikoff[1], T. Chen[2], Z. Wu[2] and M. Costa[1]. [1]*New York University School of Medicine, Tuxedo, NY and* [2]*School of Material Science and Engineering, Nanjing University of Science and Technology, Nanjing, Jiangsu, China.*

The rapid development of high-volume horizontal hydraulic fracturing (HVHHF) for mining natural gas from shale has posed potentially serious impacts on human health and biodiversity. The produced flowback waters after hydraulic stimulation is known to carry high levels of saline and total dissolved solids (TDS). To understand the toxicity and epigenetic effects of these waste waters, we analyzed post-frac flowback water from 5 Marcellus wells from Pennsylvania. We characterized the composition of these samples by X-ray fluorescence (XRF) and scanning electron microscopy (SEM)/ energy dispersive X-ray spectroscopy (EDX). XRF indicated bromine (436.67±68.78 ppm), strontium (1286.08±443.49 ppm), and barium (3776.58±609.01 ppm) are most abundant in these samples. Amorphous silicon aluminum oxide (SiAlOx) nano/micro-particles ranged from 70-285nm and amorphous zirconium oxide (ZrOx) particles ranged from 40-140nm have been found by SEM/EDX analysis. A cytotoxicity assay using colony formation was carried out to decide LC50 of these samples on the human bronchial epithelial cells (Beas-2B) with 7 days repetitive treatment. The LC50 was calculated to be ~2.7 %(v/v). The 7-day-treatment also led to decreases of the levels of acetylation of H3K9 and H3K14 as well as H3K4 trimethylation. We are also studying cell transformation and epigenetic gene silencing that are induced by the flowback waters. Our study will help understand the potential health effect of post-hydraulic fracturing flowback waters in the Marcellus shale. (Supported by a supplement to NIEHS Center grant #ES 000260)

PS 1283 Tungsten Alters Bone Homeostasis by Decreasing Osteogenesis and Increasing Adipogenesis

A. M. Bolt[1, 2], M. Flores Molina[1, 2], A. D. Kelly[1, 3] and K. K. Mann[1, 2, 3]. [1]*Lady Davis Institute for Medical Research, McGill University, Montreal, QC, Canada,* [2]*Department of Oncology, McGill University, Montreal, QC, Canada and* [3]*Division of Experimental Medicine, McGill University, Montreal, QC, Canada.*

Increased use of tungsten in the manufacturing of industrial goods has led to increased contamination in the air and ground water, particularly near active mines and industrial sites. However, little data exists as to the consequences of exposure to high levels of tungsten. Tungsten rapidly accumulates in murine bone in a concentration-dependent manner, providing a source of continuous low-dose exposure to tungsten. We hypothesized that tungsten in the bone could alter bone homeostasis, a balance between bone formation by osteoblasts and bone resorption by osteoclasts. We assessed the effects of tungsten on osteoblasts using in vitro and in vivo models. Osteoblasts are derived from bone marrow-resident mesenchymal stromal cells (MSC), which can also differentiate into adipocytes. First, we tested whether tungsten changed primary murine MSC differentiation in vitro in the presence or absence of tungsten. We found that tungsten skewed MSC differentiation by decreasing osteoblast markers and increasing adipocyte markers. In vivo, tungsten increased expression of adipocyte markers in murine bone marrow after 4 weeks, but did not change expression of osteoblast markers. Tungsten also increased mouse serum sclerostin levels, a protein that inhibits bone formation and enhances apoptosis of osteoblasts. These data suggest that tungsten promotes adipogenesis potentially at the expense of osteogenesis. Next, we explored the effects of tungsten on TGF-β signaling, known to enhance osteoblast differentiation, and concomitantly inhibits osteoclast formation. In vitro, tungsten decreased TGF-β protein levels in MSC, which resulted in decreased SMAD signaling. The data presented provide evidence that tungsten is altering bone homeostasis by decreasing bone formation, potentially by decreasing TGF-β signaling. Future experiments will investigate potential effects of tungsten on osteoclasts, as well as changes to bone remodeling and integrity.

PS 1284 Lead Enhances Antibiotic Resistance in Chicken Enteric Bacterial Flora

R. M. Gogal[1], S. D. Holladay[1], M. Nisanian[1], R. P. Kerr[1], S. Williams[2], L. Stabler[1], V. McArthur[3] and C. Tuckfield[3]. [1]*Vet Biosciences & Diagnostic Imaging, University of Georgia, Athens, GA,* [2]*Poultry Diagnostic & Research Center, University of Georgia, Athens, GA and* [3]*Savannah River Ecology Laboratory, University of Georgia, Athens, GA.*

Heavy metals have been implicated for their ability to increase antibiotic resistance in bacteria collected from polluted waters, independent of antibiotic exposure. Specific Pathogen Free (SPF) Leghorn chickens were therefore given Pb acetate in the drinking water, to expose the enteric bacteria to Pb and to determine if antibiotic resistance changed in these bacteria. Concentrations of Pb used were 0.0, 0.01, or 0.1 mM. Vent culture samples were collected for bacterial cultures on day 0 before Pb exposure, day 7 and day 14, and then birds were euthanized by CO2 gas for necropsy on Day 14, at which time intestinal contents were also collected for bacterial cultures. Fecal swabs but not intestinal samples from Pb-exposed birds contained isolates that had significantly elevated antibiotic resistance, independent of antibiotic exposure having occurred. Select isolates contained bacteria that were resistant to up to 20 antibiotics. These results suggest the need for repeated studies in chickens infected with zoonotic pathogens.

PS 1285 Neurotoxic Insults Upregulate a Novel Secreted Protein to Promote Cell Survival in Dopaminergic Neuronal Cells During Early Stages of Toxicity

J. Luo, A. Kanthasamy, M. Neal, V. Anantharam, H. Jin and A. Kanthasamy. *Biomedical Sciences, Iowa State University, Ames, IA.*

Neurotoxic agents exert neuronal toxicity mainly by impairing key signaling molecules that control the balance between pro- and anti-apoptotic signaling. Although various proapoptotic signaling pathways that occur during neurotoxic stress have been elucidated, only a few studies have characterized signaling molecules that can protect neurons against toxic insults. Herein, we have identified that dopaminergic neurotoxicants MPP+ and manganese rapidly induce Prokineticin-2 (PK2), a recently discovered mammalian homolog of mamba snake venom, as determined by qPCR pathway array analysis. In order to further understand the functional role of PK2 upregulation, we created stable PK2 expressing dopaminergic cells by delivering PK2 myc-tagged cDNA into mouse dopaminergic MN9D cells. Interestingly, exposure of manganese and MPP+ to PK2 overexpressing cells showed significant protection against the neurotoxicity as compared to vector control cells, indicating that PK2 may play a neuroprotective role in dopaminergic neurons. The protective effect was both dose- and time-dependent. Furthermore, PK2 receptor blocker PC7 attenuated the PK2-induced neuroprotective effects in PK2 overexpressing cells. Measurement of apoptosis by Annexin 5 and caspase-3 activation also revealed that PK2 overexpression protects against manganese and MPP+ -induced apoptosis. We also found mitochondrial integrity was well maintained in PK2 overexpressing cells as compared to vector cells following exposure to the neurotoxic agents. Preliminary results also showed that key proteins involved in mitochondrial functions, including BCl2, PGC1-alpha and TFAM levels, were preserved in PK2 overexpressing cells during neurotoxic stress. Collectively, our results suggest that neurotoxic insults upregulate PK2 in dopaminergic neurons to protect against early stages of neurotoxicity (NS 078327 and ES 10586).

PS 1286 Acute High-Dose Manganese Inhalation Alters Systemic Iron Metabolism and Impairs Motor Coordination in Rats

J. Chang[1], D. Saputra[2, 3], K. Lee[2, 3] and J. Kim[1]. [1]*Pharmaceutical Sciences, Northeastern University, Boston, MA,* [2]*Inhalation Toxicology Center, Korea Institute of Toxicology, Jeongeup, Republic of Korea and* [3]*University of Science and Technology, Daejeon, Republic of Korea.*

Manganese (Mn) inhalation is associated with neurobehavioral problems including impaired motor coordination. In addition, a growing body of evidence from in vitro studies indicates that acute Mn exposure increases hypoxic stress and disrupts iron metabolism, resulting in inflammatory response, angiogenesis and cell death. Hence, we examined if an acute exposure to inhaled manganese at high dose would modify iron homeostasis and alter motor performance in vivo. Male Sprague-Dawley rats (10-wk-old) were exposed to manganese aerosol (1.1 μm median diameter) at a concentration of 154 mg Mn/m3 for 2 days, 4 hours/day in a nose-only inhalation chamber. Control rats were exposed to filtered air. One day after the last exposure, rats were tested for motor coordination by the rotarod device at a fixed speed of 10 rpm over 2 min. Following the test, rats were euthanized to collect blood and liver for the determination of iron levels. At 10 rpm speed, Mn-exposed rats fell off from the bar sooner than controls (59 vs 99 sec; P=0.031), although there was no statistical difference in the number of falls between Mn-inhaled and control rats (1.7 vs 0.8 times; P=0.073). During the exposure, body weight was decreased in Mn-exposed rats (from 351 to 306 g; P<0.001) but not in control rats, likely due to Mn-induced stress that could in part influence motor performance. Blood hematocrit was increased in Mn-exposed rats (51.3%) compared with controls (48.5%; P=0.024). Moreover, levels of non-heme iron in liver and serum, markers of body iron status, were also elevated by 23% and 35%, respectively (P<0.05), upon Mn exposure. Collectively, our data suggest a compensatory up-regulation of erythropoiesis in response to hypoxia mediated by Mn over-exposure even for two days, which consequently promotes neurotoxicity.

PS 1287 A Novel Associated Particle Neutron Elemental Imaging (APNEI) Technology for 3-D Noninvasive *In Vivo* Quantification of Trace Elements in Animal and Human Tissue

L. H. Nie[1] and D. Koltick[2]. [1]*School of Health Sciences, Purdue University, West Lafayette, IN and* [2]*Physics Department, Purdue University, West Lafayette, IN.*

Trace elements play a crucial role in living organisms. The distribution of trace elements in these organisms provides valuable information about their biological function. In this project, a novel APNEI technology was studied for noninvasive quantification of trace elements in vivo at high 3-D resolution required for general biological research (e.g. toxicology research). The APNEI technology uses fast neutrons produced by a compact neutron generator to extract elemental information from an animal or a human tissue. The technology has two unique features: 1) the penetration of the neutrons and γ-rays to get into the animal or human tissue and to bring the elemental information out of the tissue; and 2) the associated particles to locate the position of the element. In this project, a deuterium-deuterium (D-D) APNEI model was built using Monte Carlo (MC) simulation method. MC simulations for the interaction between a D-D neutron source and a series of elements were performed. The resulting characteristic gamma-rays of interested elements were collected by high-purity germanium (HPGe) detectors simulated in the program. Assuming a 5 mm * 5 mm * 5 mm voxel in soft tissue (about 15 cm away from the neutron source) with iron (Fe) concentration of 1300 ppm, the Fe gamma-ray signals collected by the HPGe detectors is about 120 in 10 minutes with a radiation dose of 0.3 mSv to the irradiated tissue at neutron flux of 10^8 n/s. The number for phosphorus gamma-ray is about 60 counts for a 1 cm^3 voxel in soft tissue with P concentration of 500 ppm. These results show that the technology is sensitive enough to image some trace elements in animal or human tissue with image resolution of mm order at the biologically meaningful concentrations. This

technology can be used to investigate metal toxicology or the toxicity of other toxic agents that would result in an alteration of the elemental distributions in animal or human body.

PS 1288 Early-Life Lead Exposure and Drug Abuse: A Novel Pathway to Addiction

B. Soares, K. Stansfield, J. L. McGlothan and T. R. Guilarte. *Environmental Health Sciences, Columbia University, New York City, NY.*

A recent assessment of a prospective cohort of children exposed to lead (Pb2+) in infancy has documented later effects on mental health including drug abuse (McFarlane et al., 2013). Animal studies have provided limited evidence that perinatal Pb2+ exposure enhances cocaine sensitization and Pb2+-exposed animals are more prone to relapse (Nations et al., 2000; 2003). Other animal studies have shown that Pb2+ alters dopaminergic circuitry (Cory-Slechta and Widzowski, 1991; Zuch et al., 1998) critical for drug addiction. However, there is no data on mechanisms by which Pb2+ exposure may sensitize animals to drug abuse. In the present study, we examined the effects of early life Pb2+ exposure on cocaine sensitization and dopamine receptor levels in the striatum (STR) and nucleus accumbens (NAC) in late adolescence. Rats chronically exposed to Pb2+ during early life exhibited a highly significant increase in the locomotor response to cocaine administration (15 mg/kg) relative to controls. This effect of cocaine was associated with a marked increase (20-34%) in D1-dopamine receptors (D1R) in the STR and NAC of Pb2+-exposed rats relative to controls. Activation of D1R by dopamine plays an important role in addictive and drug reinforcing properties of cocaine. We also observed a modest but significant increase in D2-dopamine receptors (D2R) in the STR and results in the NAC are forthcoming. D1R and D2R were measured using quantitative receptor autoradiography. Pharmacological studies are examining the selectivity of the sensitization to D1R and/or D2R antagonist. Together, these results show that chronic Pb2+ exposure during development alters D1R/ D2R expression and cocaine responsivity. They suggest that early life Pb2+exposure may induce a state of re-programming of the developing brain by which neuronal pathways important for drug addiction may be permanently altered, thus enhancing liability for drug use and addiction as young adults [supported by ES006189 and a pilot project from NIEHS Center ES006189].

PS 1289 Lead Inhibits Presynaptic Neurotransmitter Release in Schaffer Collateral-CA1 Synapses in the Rat Hippocampus: Understanding Mechanism(s)

P. K. Stanton[1], X. L. Zhang[1], J. L. McGlothan[2], K. Stansfield[2] and T. R. Guilarte[2]. [1]*Dept of Cell Biol & Anat, New York Medical College, New York City, NY and* [2]*Environmental Health Sciences, Columbia University, New York City, NY.*

Lead exposure during brain development inhibits neurotransmitter release and this effect is likely to contribute to impaired synapse formation, plasticity and learning deficits. However, the mechanism(s) by which lead impairs neurotransmitter release have not been fully elucidated. In primary hippocampal neurons, lead exposure inhibits vesicular release and reduces the number of fast-releasing sites, an effect mediated by NMDAR inhibition (Neal et al., 2010). Since this finding was made in primary hippocampal neurons, we wanted to determine if similar effects were also present in animals exposed to lead in vivo. In the present study, we examined the effects of chronic lead exposure on presynaptic transmitter release using two-photon laser scanning microscopy of FM1-43 vesicular release in Schaffer collateral-CA1 synapses in ex vivo hippocampal slices. We found that chronic lead exposure significantly enhanced paired-pulse facilitation (Control PPF = 1.7 versus Lead PPF = 3.0 at 30msec inter-pulse interval), an indirect measure of reduced release probability. Mean-variance analysis of evoked synaptic potentials at Schaffer collateral-CA1 synapses directly confirmed that chronic lead treatment persistently reduced transmitter release probability (Control Pr = 0.46; Pb Pr = 0.25 at 2mM [Ca2+]o). Using FM1-43 2-photon imaging of release from CA1 Schaffer collateral terminals, we found that this reduced probability was associated with reduced release of glutamate from vesicles in the rapidly-recycling vesicle pool loaded by hypertonic shock. These studies confirm and extend our previous findings in primary hippocampal neurons that lead produces profound impairments in vesicular release that are likely to contribute to deficits in synaptic plasticity and cognitive function. Current studies are examining the molecular bases of the lead inhibition of vesicular release. [Supported by grant # ES020465]

PS 1290 X-Ray Fluorescence Microspectroscopic Analysis of Duodenal Mucosae following Cr(VI) Exposure in Drinking Water

C. M. Thompson[1], D. Proctor[2], M. Suh[2], J. Wolf[3], L. C. Haws[4] and M. A. Harris[1]. [1]*ToxStrategies, Katy, TX,* [2]*ToxStrategies, Mission Viejo, CA,* [3]*Experimental Pathology Laboratories, Sterling, VA and* [4]*ToxStrategies, Austin, TX.*

Mutagenic and nonmutagenic modes of action (MOAs) have been proposed to explain duodenal tumors in B6C3F1 mice following oral exposure to hexavalent chromium [Cr(VI)]. Evidence against a mutagenic MOA includes an absence of Cr(VI)-induced crypt micronuclei or kras codon 12 mutations in the duodenum after exposure to ≤180 mg/L Cr(VI). Herein, we show that these findings can be explained, in part, by the distribution of Cr within the duodenal epithelium. Specifically, X-ray fluorescence microscopy was conducted on formalin-fixed, paraffin-embedded duodenal sections from mice exposed to 0 or 180 mg/L Cr(VI) for 90 days. Sections from treated mice indicated much higher Cr fluorescence in the duodenal villi than in adjacent crypts on the same section. Cr speciation analysis indicated that all Cr in the tissue was in the trivalent form, Cr(III). Immunostaining of phosphorylated H2AX (γ-H2AX), a marker of DNA double strand breakage, was elevated (relative to control) in the duodenal villi of mice exposed to 180 mg/L Cr(VI) for 90 days. Duodenal crypts from treated mice were visibly taller than untreated mice (190.5 vs 98.3 μm; $p \leq 0.001$) due to the increase in the number of crypt enterocytes visible in cross-sections (63.9 vs 38.4, $p \leq 0.01$). Despite the increase in crypt enterocytes due to proliferation, the overall scoring of crypt γ-H2AX staining did not differ between treated and untreated mice. The absence of treatment-related changes in γ-H2AX immunostaining, micronuclei, or kras mutations in the mouse duodenum is consistent with the low levels of Cr fluorescence in the crypt. These data support a nonmutagenic MOA whereby Cr(VI) enters anion transporters expressed on villous enterocytes, induces dose-dependent cytotoxicity and subsequent regenerative crypt hyperplasia. Such chronic compensatory crypt proliferation increases the lifetime risk of intestinal carcinogenesis.

PS 1291 A Novel Transportable Neutron Activation Analysis System to Quantify Manganese in Bone *In Vivo*: System Setup and Validation

Y. Liu, D. Koltick, W. Zheng and H. L. Nie. *Purdue University, West Lafayette, IN.*

Overexposure to manganese (Mn) can lead to "manganism", a devastating neurological disorder with symptoms closely resembling Parkinson's disease. The progressive and irreversible characteristics of manganism, even after exposure cessation, make early diagnosis of body Mn burden an urgent issue. Data in literature suggests that the amount of Mn in bone accounts for ~40% of total body burden. We hypothesize that bone Mn (MnBn) may serve as a valuable biomarker for long-term cumulative Mn exposure. To test this hypothesis, we have constructed a neutron activation analysis system and validated its usefulness for non-invasive quantification of Mn in bone. Thermal neutrons have a high cross section to interact with ^{55}Mn; the resulting 847 keV characteristic γ-rays can then be captured. By measuring those γ counts from the irradiated bone, MnBn concentration can be calculated. Based on simulation work, a deuterium-deuterium (DD) neutron generator system was selected, and optimal materials and thicknesses for neutron moderation, reflecting, and shielding were also determined in order to provide the highest yield of thermal neutrons. Hand bone has been chosen as the irradiation site to minimize the irradiation dose to human subjects. More recently, we have constructed a DD neutron generator with a flux up to 3×10^9 neutrons/sec. Hand phantoms doped with different Mn concentrations were irradiated using the optimized irradiation system. The Mn characteristic γ-rays were collected by a HPGe detector system with 100% relative efficiency and analyzed by a digital spectral processor. The detection limit was calculated to be about 1.5 μg Mn/g dry bone (ppm) with an irradiation dose of 50 mSv to the hand. The whole body effective dose was about 31 μSv. The current effort is devoted to reduce the detection limit to 0.75 ppm with a combination of four 100% HPGe detectors. Given the normal MnBn concentration of ~1 ppm in general population, this system appears to be useful in MnBn quantification in humans.
Supported in part by R21-OH010044 and RO1-ES008146

PS 1292 Induction of Heme Oxygenase-1 (HO-1) and Accumulation of Tellurium upon Exposure to Diphenyl Ditelluride and Tellurium Tetrachloride in HT-29 Human Colon Cells

P. Vij and D. Hardej. *Pharmaceutical Sciences, St. John's University, Queens, NY.*

Tellurium (Te) is a metalloid, with no known physiologic role in humans. Te containing compounds are being used in increasing quantities in industry, agriculture and organic synthesis in products such as optical blue ray discs, photographic materials and photoelectric cells. Increasing uses of such products suggests that human environmental exposure will increase in the future. The neurotoxicity of Te compounds has been documented however little has been reported regarding the gastrointestinal toxicity of this metalloid. Previous work in our lab has demonstrated the mechanism of cell death in HT-29 cells upon exposure to diphenyl ditelluride (DPDT) and tellurium tetrachloride ($TeCl_4$). The purpose of the present study was to evaluate the potential of tellurium compounds $TeCl_4$ and DPDT to induce oxidative stress by examining heme oxygenase-1 (HO-1) induction and metal accumulation in HT-29 human colon cancer cells. HO-1 is a cytoprotective enzyme activated by its substrate heme and to diverse stimuli. The induction of HO-1 is one of the most important events in the cellular response to pro-oxidative insults. Upon exposure to concentrations ranging from 62.5μM to 1000μM of $TeCl_4$ and DPDT in HT-29 human transformed colon cells, oxidative stress was confirmed by a significant increase in the HO-1 activity at the concentrations ranging from 250 μM to 1000 μM in HT-29 cells with DPDT and from 62.5 μM to 1000 μM with $TeCl_4$ treatment when compared to the control group. Intracellular tellurium levels were determined by Inductively Coupled Plasma Optical Emission Spectrometry (ICP-OES), and significant increases were observed at the concentrations ranging from 500 μM to 1000 μM after DPDT and 125 μM to 1000 μM after $TeCl_4$exposure. It is concluded that DPDT and $TeCl_4$ exposure increases the HO-1 activity along with the increase in the intracellular accumulation of the metalloid.

PS 1293 Translesion Synthesis Defends against Telomere Dysfunction Induced by Hexavalent Chromium

H. C. Pope-Varsalona, F. Liu and P. L. Opresko. *Environmental and Occupational Health, University of Pittsburgh, Pittsburgh, PA.*

Telomeres are repetitive nucleotide sequences that cap and protect chromosome ends. When telomeres become dysfunctional they contribute to a variety of pulmonary diseases. Our previous work established that DNA replication stress induced by the environmental pollutant hexavalent chromium Cr(VI) causes telomere loss and aberrations. Chronic inhalation of Cr(VI) leads to a variety of lung diseases, including fibrosis, and cancers. Cr(VI) forms a spectrum of DNA lesions that impede DNA replication and can cause collapse of the replication fork and chromosomal breakage. Telomeres are fragile DNA sites prone to breakage during replication stress. Cells have mechanisms for bypassing lesions that block replication forks called translesion synthesis (TLS). We hypothesize that Cr(VI)-induced DNA replication stress activates TLS DNA polymerase η (polη) that suppress Cr(VI)-induced mutagenesis and telomere dysfunction. Our research is investigating several endpoints of telomere dysfunction in human cells proficient and deficient in polη. We observe that cells deficient in polη are 53 fold more sensitive to low levels of Cr(VI) and show through flow cytometric analysis that polη deficient cells are delayed in S-phase of the cell cycle compared to isogenic controls. Using a combination of immunofluorescence and telomere fluorescence in situ hybridization (IF-teloFISH), quantification of replication stress at genomic and telomeric DNA show that Cr(VI) induces polη mobilization to stalled DNA replication sites at genomic and telomeric regions in human cells. Post Cr(VI) exposures, we identify telomeric aberrations by staining metaphase chromosomes with a fluorescent telomeric probe using teloFISH and observe a four-fold increase in aberrations in cells with dysfunctional polη. Our study demonstrates one mechanism by which Cr(VI) directly interacts with the genome, alters telomere integrity, and the cellular pathways that protect telomeres in the face of genotoxic replication stress.

PS 1294 Fish As Models for Investigating Metabolic Disruption Arising from Dietary Selenium Oversupplementation

D. Janz and J. Thomas. *Toxicology Centre, University of Saskatchewan, Saskatoon, SK, Canada.*

Selenium (Se) exhibits a narrow range between essentiality and toxicity in many animals. There is increasing concern that Se oversupplementation in humans can lead to symptoms of metabolic syndrome, including Type 2 diabetes. We have been using fish as comparative animal models to investigate mechanisms of metabolic disruption arising from excess dietary organoselenium. This work originated in field studies of Se-contaminated aquatic ecosystems, where five fish species exhibited consistent evidence of altered lipid and carbohydrate homeostasis. Similarly, in laboratory studies adult zebrafish fed diets augmented with seleno-L-methionine (1 [control, no supplementation], 3, 10 or 28 ug Se/g dry mass) for 90 days exhibited dose-dependent increases in whole body lipid (triacylglycerols) and carbohydrate (glycogen) stores. Despite greater energy stores, experiments in a swim tunnel respirometer showed that zebrafish fed the Se-augmented diets had a reduced swimming capacity, reduced aerobic scope, and a greater standard metabolic rate. To investigate potential mechanisms underlying these observations, mRNA expression of a variety of key proteins involved in lipid and carbohydrate regulation were determined using RT-PCR. Exposure to elevated dietary Se significantly down-regulated mRNA abundance of protein tyrosine phosphatase 1B (PTP 1B) in muscle, and beta-hydroxyacyl coenzyme A dehydrogenase (HOAD), sterol regulatory element binding protein 1 (SREBP 1) and methionine adenosyltransferase 1 alpha (MAT 1A) in liver of zebrafish. Additional studies in rainbow trout showed that chronic exposure to elevated dietary Se resulted in greater baseline plasma cortisol concentrations, but an attenuated cortisol response to acute stress challenges. Overall, these results have clear implications for the fitness of wild fish exposed to elevated dietary Se in contaminated aquatic ecosystems, and may provide insight into mechanisms of metabolic disruption in mammals, including humans, that receive dietary oversupplementation of organoselenium.

PS 1295 Effects of Uranyl Acetate on Etoposide-Induced DNA Damage and Repair in Human Bronchial Epithelial Cells (16HBE14o-)

M. Yellowhair[1] and R. Lantz[2]. [1]*Cancer Center, The University of Arizona, Tucson, AZ and* [2]*Cellular and Molecular Medicine, The University of Arizona, Tucson, AZ.*

It has been widely reported that metals can be genotoxic by several mechanisms including generation of reactive oxygen species and inhibition of DNA repair. There is an increased concern over environmental exposure to abandoned uranium mine tailings as well as occupational exposures to depleted uranium via military action. The aim of this study is to evaluate the ability of depleted uranium (DU) to inhibit double strand break DNA repair at low concentrations in human bronchial epithelial (16HBE14o-) cells. 16HBE14o- cells were co-exposed to 0.13 μM (30 ppb; current EPA standard in drinking water) of soluble depleted uranium as uranyl acetate (UA) in the presence of 0 – 25 μM of etoposide. UA cytotoxicity was assessed in vitro by the clonogenic survival assay. DNA damage response was assessed in vitro via flow cytometry to determine phosphorylation of the DNA repair proteins: ATM, SMC-1, and γ-H2AX. Replication protein A (RPA) activity was assessed by an ELISA assay and cell cycle arrest was assessed via flow cytometry. Findings from this work demonstrate that cells treated with UA did not induce phosphorylation of DNA repair proteins (pATM, pSMC-1, or pγ-H2AX) compared to etoposide treatments and untreated cells. Interestingly, the co-exposure of UA and etoposide reduced the amount of phosphorylated ATM and activated RPA after 48 and 60 hr, respectively. These results suggest that DU may inhibit double strand break DNA repair at low concentrations in the presence of a known DNA damaging agent. The inhibition of DNA repair by depleted uranium at environmentally relevant concentrations suggest a novel means by which uranium may exert its genotoxic effects. This work is supported by NIH Grants CA096281 (RCL), CCSG – CA 023074 (AZCC/ARL-Division of Biotechnology Cytometry Core Facility), CA09501, F31ES014971 (MY), U54CA143924, MGE@MSA (MY) and The Alfred P. Sloan Foundation (MY) for funding this project.

PS 1296 Gastric Reduction of Hexavalent Chromium in Fed and Fasted Human Stomach Samples

S. M. Hays[1], C. R. Kirman[1], M. Suh[2] and D. Proctor[2]. [1]*Summit Toxicology, Lyons, CO and* [2]*ToxStrategies, Mission Viejo, CA.*

The rate and capacity of gastric reduction of hexavalent chromium [Cr(VI)] are important determinants of dose delivery of Cr(VI) to the small intestines, which in turn is a determinant of potential cancer risk. Our previous experiments using fed rodent gastric contents and fasted human fluid found that the reduction of Cr(VI) exhibited a mixed second-order reaction with a pH dependent second-order rate constant. Potential uncertainties regarding dilution which may affect the concentrations of reducing agents and the second-order rate constant were noted. This study is an extension to our previous experiments. Stomach fluid samples were obtained from human volunteers in the fed and fasted (paired) states. Using speciated isotope dilution mass spectrometry, studies were conducted to ascertain the kinetics (rates and capacity) of the various gastric fluids to reduce Cr(VI), with emphasis on better characterization of conditions during a fed state and characterizing inter-individual variability. The effects of pH, dilution and redox potential were investigated. Alternative mathematical forms of the reduction model were considered. The human data confirm a significant pH dependence for the second-order rate constant which appears to be independent of dilution. Fasted human gastric fluid

has a lower pH (1.8±0.3) than pH in fed samples (2.7±0.7). In addition, fasted human gastric fluid has a lower capacity to reduce Cr(VI) per L stomach fluid (approximately half) as compared to fed gastric fluid. The results of these experiments are used to support human health risk assessment by modeling the extent of Cr(VI) escaping reduction in the stomach during fed and fasted states.

PS 1297 Temporal Changes in Rat Liver Gene Expression after Cadmium and Chromium Exposure

M. S. Madejczyk[1], C. E. Baer[4], W. E. Dennis[3], V. C. Minarchick[2], S. S. Leonard[2], D. A. Jackson[3], J. A. Lewis[3] and J. D. Stallings[3]. *[1]ORISE Postdoctoral Fellow at USACEHR, Fort Detrick, MD, [2]National Institute for Occupational Safety and Health, Morgantown, WV, [3]US Army Center for Environmental Health Research, Fort Detrick, MD and [4]Excet, Inc., Fort Detrick, MD.*

Our Nation's Guardians are at risk of exposure to a variety of environmental health hazards throughout their normal duty activities including deployments, training exercises, and homeland defense situations. Metals are widely used in large quantities in a number of industrial processes and are common environmental toxicants, which increases the possibility of our Soldiers being exposed at toxic levels. While metal toxicity has been widely studied, the exact mechanisms of toxicity remain unclear. In order to further elucidate these mechanisms and identify candidate biomarkers, rats were exposed via a single intraperitoneal injection to three concentrations of $CdCl_2$, $NiCl_2$ and $Na_2Cr_2O_7$, and livers were harvested 1, 3, or 7 days after exposure. Cd and Cr accumulated in the liver at 1 day post-exposure, while there was no accumulation of Ni. Cd levels remained elevated over the length of the experiment, while Cr levels declined. Differentially expressed genes were identified via microarray analysis. Both common and uniquely modulated transcripts and perturbed pathways were identified for the metal species. Enriched pathways and functions included hepatic injury, inflammation, cell cycle, tissue repair, and cancer. This work provides insight into the temporal effects and mechanistic pathways involved in acute metal intoxication, which may lead to the identification of candidate biomarkers.

This research was supported in part by an appointment to the Postgraduate Research Participation Program at the USACEHR administered by the ORISE through an interagency agreement between the US DOE and USAMRMC. Research was conducted in compliance with the Animal Welfare Act, and all other Federal requirements. The views expressed are those of the authors and do not constitute endorsement by the U.S. Army or NIOSH.

PS 1297a Toxicogenomic Study in Rat Thymus of F1 Generation Offspring following Maternal Exposure to Silver Ion

J. Yourick, X. Gao, V. Topping, T. Black, N. Olejnik, Z. Keltner, M. Scott and R. Sprando. *Division of Toxicology, Office of Applied Research and Safety Assessment, U.S. Food and Drug Administration, Laurel, MD.*

Silver-containing compounds or their mixtures are widely applied as antimicrobial agents onto food packaging materials, often in direct contact with the food. The extensive use of silver in the food industry raises concerns about its safety, toxicity and health risk. Data currently available revealed that in utero exposure to silver could adversely affect the developing immune system. However, further studies are needed to confirm that the previously observed adverse effects are due to silver ion alone, and to define the no observed effect level (NOEL). In the present study we used a toxicogenomic approach to study the effect of silver ion on the developing thymus at the transcriptional level using whole genome microarrays. Global gene expression changes in rat thymus of F1 generation pups at post natal day 26 following maternal exposure to silver acetate at 0, 0.4, 4.0, or 40.0 mg/kg in drinking water are reported here. Five female and 5 male pups were included in each dosing group. Gene expression profiling analyses identified only about a dozen differentially expressed genes (DEGs) in each dose group using a loose criterion of fold change (FC) > 1.5 and unadjusted $p < 0.05$, regardless whether the analysis was conducted within each gender group or with both gender groups combined. No dose-dependent effect was observed on the number of DEGs. In addition, none of these genes had a false discovery rate (FDR) < 0.05 after correction for multiple testing. These results indicate silver acetate up to 40.0 mg/kg did not affect gene expression in the developing thymus. Combined with the observation that thymus-to-body-weight ratios were not affected, and no histopathological abnormalities in thymus were identified in the pups, the current study using a toxicogenomic approach suggests that in utero exposure to silver ion up to 26.0 mg/kg (equivalent to 40.0 mg/kg silver acetate) did not have an adverse effect on the developing thymus.

PS 1297b Assessing Toxicity of FeMn Dust Particles from a South African Ferromanganese Smelter Works: *In Vitro* Studies on Primary Rat Astrocytes and BEAS-2B Cells

L. Koekemoer[1] and M. Gulumian[1, 2]. *[1]Toxicology and Biochemistry, National Institute for Occupational Health, Johannesburg, Gauteng, South Africa and [2]Haematology and Molecular Medicine, University of the Witwatersrand, Johannesburg, Gauteng, South Africa.*

Occupational exposure to manganese (Mn) may result in development of diseases associated with the lungs and brain. Even though evidence of Mn associated diseases exists, some studies have found no association between manganese levels in blood or urine and indicators of neurotoxic effects.
This study investigated the effects of ferromanganese (FeMn) dust, from a ferro-manganese smelter works, on primary rat astrocytes and human bronchial epithelial (BEAS-2B) cells. Particle size distribution, surface area and trace elemental composition were analyzed. Particle uptake was studied using dark field microscopy and viability determined using the xCELLigence RTCA system based on cell adherence. Nuclear translocation of Nrf2 and Nf-κB was studied using western blots and genotoxicity determined by the alkaline Comet assay. Min-U-Sil 5 was used as benchmark particles.
The presence of nano sized FeMn and its cellular uptake in both cell lines was confirmed. Treatment resulted in a dose-dependent decrease in viability of both cell lines for both particle types, with crystalline silica producing higher toxicity compared to FeMn.
Short term exposure to FeMn and silica led to an increase and long term exposure to a decrease in translocation of both the Nrf2 and Nf-κB transcription factors, in both cell types tested. This indicates that after longer periods of exposure, the antioxidant defences were unable to overcome the oxidative stress induced by these particles.
Results indicate that access of FeMn ultrafine particles to the brain may be possible in smelter workers, resulting in direct disturbances of cellular toxicity, viability and markers of oxidative stress in astrocytes. Lung epithelial cells come into contact with these particles first, thus resulting in similar disturbances in BEAS-2B cells. These results and further toxicity studies could help to establish more reliable biomarkers of Mn effect and exposure.

PS 1297c Interference Study of Conventional Assays, Caused by Gold Nanoparticles (AuNPs) Exhibiting Surface Plasmon Resonance (SPR)

M. Gulumian[1, 2], N. Sanabria[1] and C. Andraos[1, 2]. *[1]Toxicology, NIOH, Johannesburg, Gauteng, South Africa and [2]Haematology & Molecular Medicine, Wits, Johannesburg, Gauteng, South Africa.*

Plasmonic engineered NPs are popular in consumer- and medical-based industries due to their unique surface characteristics. Identifying the toxicity of NPs is critical given the increased exposure. The toxicity of NPs is often determined using conventional colorimetric and optical high-throughput toxicity systems that rely on absorbance, luminescence or fluorescence signals. However these systems are prone to interference by the NPs, which lead to erroneous results.
This study assessed citrate-capped AuNPs interference with:
1) Three cell viability systems (toxicity)
2) Three fluorescent dyes often used in high-throughput systems (geno-/toxicity)
3) The isolation, quantification and analysis of RNA (genotoxicity)
The AuNPs exhibited optical interference with the detection system and direct adsorption of assay components with two of the assays. In addition, the distinct SPR and large surface area of AuNPs lead to a quenching in fluorescence of all three fluorescent dyes. Total RNA, isolated from untreated BEAS-2B bronchial human cells, was spiked with AuNP. The resultant sample was quantified and a concentration-dependant quenching of the absorbance spectrum was observed. The RNA purity absorbance ratios were also altered. Differences were not observed using electrophoretic analyses of RNA integrity. However, treatment of BEAS-2B cells, with NPs under non-cytotoxic test conditions, showed slight RNA absorption interference between 190-220 nm. In addition, interference varied depending on the point of NP application and the use of RNA stabilising solutions.
Toxicity results should be interpreted with caution when using conventional systems. The best alternative would be the use of a system independent of dyes or optical devices such as those that implement impedance technology. The isolation, quantification, purity and integrity are critical points of analyses for RNA-based techniques. Hence, the observed quenching effect would cause quantification errors and obscured integrity validation for gene expression studies.

PS 1297d The Effects of Tellurium Compounds on the Viability of Rat Hippocampal Astrocytes Are Attenuated with Calcium Blocker

A. Forino and D. Hardej. *Pharmaceutical Sciences, St. John's University, Queens, NY.*

Tellurium (Te) is a metalloid belonging to group 6A of the periodic table along with Selenium (Se) and sulfur (S). Unlike S and Se, Te has not been found to have any physiologic role in mammals, although detectable levels of Te have been noted in humans through dietary and/or industrial exposures. Te compounds have been associated with both peripheral and central nervous system toxicity. Studies have suggested that nervous system disturbances with exposure to these compounds may be partially attributed to disruption of Calcium (Ca) homeostasis that results in destabilization of cytoskeletal proteins. The purpose of this study was to examine the relationship of Te exposure and effects on astrocyte viability and cytoskeleton and to determine if Ca plays a role in these changes. Rat hippocampal astrocytes were treated with 15.6, 31.2, 62.5, 125 and 250 μM of tellurium tetrachloride ($TeCl_4$) and diphenyl ditelliuride (DPDT) to assess changes in viability. Cytoskeletal preparations of treated and control cells were observed using scanning electron microscopy (SEM). Cells were subsequently treated with 125 μM concentrations of each of the compounds with and without the Ca blocker dantrolene for 24hrs to determine the effects of Ca on cell viability in cells treated with Te. Results indicate a significant reduction in cell viability at all Te doses when compared to untreated cells. Cells treated with 5 μM dantrolene and 125 μM $TeCl_4$ and DPDT showed significant increases in viability when compared to cells treated with Te alone. The cytoskeleton of Te treated cells observed using SEM demonstrated changes such as loss of crossbridging and condensation of cytoskeletal components when compared to untreated cells. It is concluded that Te decreases astrocyte viability and that the use of dantrolene significantly increases viability, suggesting that Ca plays a role in this process. Exposure to Te compounds results in cytoskeletal alterations when compared to non-exposed cells.

PS 1297e Investigating the Potential Carcinogenic Effects of Chronic Tungsten (VI) Oxide Exposure to Immortalize Human Lung Cells

F. Laulicht[1], L. Cartularo[1], S. Medici[2], M. F. Peana[2], M. A. Zoroddu[2] and M. Costa[1]. [1]*Environmental Medicine, NYU Langone Medical Center, Tuxedo, NY and* [2]*Department of Chemistry and Pharmacy, University of Sassari, Sassari, Sassari, Italy.*

Rationale: Tungsten oxide (WO3) is an occupational exposure hazard. The primary route of WO3 exposure is inhalation and WO3 is known as a pulmonary irritant. This work investigated exposure of WO3 to immortalized human bronchial epithelial cells (Beas-2B) to investigate cytotoxicity and carcinogenic potential.
Experimental procedures: Insoluble WO3 particles were sonicated to reduce aggregation and create suspensions of WO3 particles small enough for Beas-2B cells to engulf (<10 microns in diameter). Beas-2B cells were chronically exposed to varying doses (0.25, 0.5, 1.0, 5.0, 10 and 15 μg/cm2) of WO3 for 6 weeks. Proliferation rate was measured; soft agar cell migration testing and scratch test assays were performed.
Results: After 2 weeks, Beas-2B cells with the highest doses of WO3 started to proliferate just as quickly as the cells that had low doses of WO3. After 6 weeks of WO3 exposure, in the control transformation there was an average of 8 colonies per soft agar well. In the lower doses (0.25-1.0 μg/cm2) there was an average of 25 colonies per well. In the higher doses (5.0- 15.0 μg/cm2) colonies ranged from 30 to 75 per well. Scratch testing revealed that WO3 treated cells migrated significantly more quickly than control transformed cells.
Conclusions: Chronic treatment of Beas-2B cells with WO3 induced transformation in the cells. Inhaled WO3 may not only be a lung irritant, but also a potential pulmonary carcinogen at high doses.

PS 1297f Quercetin Inhibits Cr(VI)-Induced Lung Carcinogenesis by Targeting miR-21-Pdcd4 Signaling Pathway

P. Poyil[1, 2], D. Sasidharan Padmaja[1, 2], Y. Son[1, 2], J. Hitron[1, 2], Z. Zhang[1] and X. Shi[1, 2]. [1]*Graduate Centre for Toxicology, University of Kentucky, Lexington, KY and* [2]*Center for Research on Environmental Disease, University of Kentucky, Lexington, KY.*

Hexavalent chromium [Cr(VI)] is an important human carcinogen associated with pulmonary diseases and lung cancer. Cancer prevention using natural products has become an integral part of cancer control. Quercetin is one of the most abundant dietary flavonoids widely present in many fruits and vegetables, possesses potent antioxidant activity capable of protecting normal cells from various stimuli-induced oxidative stress and cell death. MicroRNA-21 (miR-21) is a key regulator of oncogenic processes. It is significantly elevated in the majority of human tumors and functionally linked to cellular proliferation, invasion and migration. Studies have shown that miR-21 exerts its oncogenic activity by targeting the tumor suppressor gene programmed cell death 4 (Pdcd4). The present study examined the effect of quercetin on the inhibition of Cr(VI) induced carcinogenesis and the role of miR-21-Pdcd4 signaling involved. Our results showed that quercetin decreased ROS generation induced by Cr(VI) exposure in Beas-2B cells. Chronic Cr(VI) exposure induced malignant cell transformation, increased miR-21 expression and caused inhibition of Pdcd4, which were significantly inhibited by the treatment of quercetin in a dose dependent manner. Stable knockdown of miR-21/ overexpression of pdcd4 in Beas-2B cells significantly reduced the Cr(VI) induced cell transformation. Furthermore, Quercetin inhibited the Cr(VI) induced E-cadherin reduction, and also beta-catenin/TCF-dependent transcription. Taken together, these results demonstrate that quercetin is able to protect Beas-2B cells from Cr(VI)-induced carcinogenesis by targeting MiR-21-Pdcd4 signaling.

PS 1297g Application of Lead Isotope Ratios to Lead Poisoning Investigations On-Farm

J. P. Buchweitz[1, 2], J. Zyskowski[3], L. Stensen[2] and A. Lehner[2]. [1]*Pathobiology and Diagnostic Investigation, Michigan State University, East Lansing, MI,* [2]*Toxicology Section, Michigan State University Diagnostic Center for Population and Animal Health, Lansing, MI and* [3]*Nutrition Section, Michigan State University Diagnostic Center for Population and Animal Health, Lansing, MI.*

Lead (Pb) is a common cause of heavy metal poisonings in cattle. Sources of Pb on-farm may include crankcase oil, machinery grease, batteries, plumbing, and paint chips. Consequently, consumption of, or exposure to, these sources may negatively impact animal health and, if present at subclinical concentrations, may be inadvertently introduced into the food supply by excretion in milk or distribution in beef cattle. Therefore, the scope of poisoning incidents must be clearly assessed and the source of intoxication mitigated to prevent future exposures. One valuable tool in the forensic assessment of lead source is Pb isotope analysis. We report on two cases in which the novel application of Pb isotope analysis by ICP-MS was extended to bovine blood and liver for comparison to environmental samples including paint chips and soil to elucidate lead source. Isotope ratios 208Pb/206Pb, 207Pb/206Pb, 207Pb/204Pb, and 206Pb/204Pb were calculated for blood samples across the entire herd in each case. Blood isotope profiles corresponded with exposure to paint chips obtained from sources unique to each herd. Although this resolved the poisoning incident for one farm, a subsequent poisoning event on the second farm prompted a more thorough investigation of the property. Pb quantitation and isotope profiling provided a direct link between an affected calf's liver and soil obtained from the farm's main barn but not from that of a secondary barn. These two cases highlight the use of isotope profiling as an advanced diagnostic technique for Pb source identification on-farm.

PS 1297h Chronic Arsenic Exposure *In Vitro* Causes Acquisition of Multiple Tumor Cell Characteristic in Human Pancreatic Epithelial Cells

W. Qu and M. P. Waalkes. *NTP, NIEHS, NIH, Research Triangle Park, NC.*

Arsenic is linked with human pancreatic diseases potentially including cancer. Emerging data indicates cancer stem cells (CSCs) may be critical to the carcinogenic process. Our prior work showed chronic cadmium exposure of a human pancreatic ductal epithelial (HPDE) cell line caused oncogenic transformation and formation of CSC-like cells. Thus, we studied if inorganic arsenic exposure could induce a similar tumor cell phenotype in HPDE cells and derivative non-adherent spheroids, which are enriched in stem cells (SCs or CSCs). HPDE cells were chronically exposed to sodium arsenite (2.5 μM) for up to 30 weeks and cancer cell characteristics were assessed including matrix metalloproteinase-9 (MMP-9) secretion, invasion, colony formation and expression of cancer relevant genes by RT-PCR or immunoblotting. Non-adherent spheroid formation was used to assess CSC-like production and tumor cell phenotype was assessed in such spheres. Chronic arsenic exposed (CAE) cells (30 weeks) showed morphological changes (loss of contact inhibition, atypical foci of cell mounding), increased MMP-9 secretion and colony formation, and marked over-expression of pancreatic cancer markers (*S100P, PSCA*), oncogenes (*C-myc, C-jun*), and the cell proliferation marker *Cyclin D1*, all typical for pancreatic cancer cells. CAE cells also became tolerant to arsenic (LC50 74.8 ± 1.9 μM) compared to control (18.1 μM ± 2.1 μM) which is common in chronic treatment. Compared to control, CAE cells produced 300% more non-adherent spheres, which contain an abundance of SCs or CSCs. CAE-derived spheres were more invasive, secreted more MMP-9, and over-expressed markers for pancreatic CSCs (CXCR4, CD133, CD44) and S100P. Single spheres from CAE cells rapidly produced aggressive, highly branched, poorly differentiated glandular-like

structures in Matrigel. Thus, chronic arsenic causes acquisition of multiple tumor cell characteristics in HPDE cells. These data support the plausibility of arsenic as a human pancreatic carcinogen.

PS 1297i Chronic Arsenic Exposure Induces Cancer Cell Characteristics in Human Peripheral Lung Epithelial Cells

R. J. Person, E. J. Tokar and M. P. Waalkes. *NTP, NIEHS, NIH, Research Triangle Park, NC.*

Inorganic arsenic is a human lung carcinogen. Here we study the ability of chronic inorganic arsenic exposure to induce a cancer phenotype in the immortalized, non-tumorigenic human lung epithelial cell line, HPL-1D. Signs of oncogenic transformation were assessed periodically during chronic sodium arsenite (2 μM) exposure, such as secreted matrix metalloproteinase-2 (MMP-2) activity, invasion, and expression of cancer-relevant genes at the transcript and protein levels. After 38 weeks of continuous arsenic exposure, secreted MMP-2 activity increased to 200% of control, a level typical of other cells lines that have acquired an arsenic-induced cancer phenotype. The invasive capacity of these chronic arsenic-treated lung epithelial (ATLE) cells was over 3-times control levels. Expression of lung cancer tumor suppressor genes SLC38A3 and TTF-1 at the protein level was markedly reduced in ATLE cells to 26% and 24% of control, respectively. Increases occurred in K-Ras oncogene (300 % of control) and both the ERK (274%) and p-ERK (152%) proteins in ATLE cells. Vimentin increased to 300% and E-Cadherin protein was reduced to 16% of control in ATLE cells indicative of epithelial-to-mesenchymal transition. Thus, ATLE cells appeared to have acquired multiple cancer cell characteristics, some of which are specific to lung. Additional evidence of an oncogenic phenotype in ATLE cells came from other molecular events linked to chronic arsenic exposure. ATLE cells showed reduced expression of the tumor suppressor genes *APC* (72% of control), *PTEN* (43%), and *CCND1* (76%) and the DNA damage response gene *ATM* (82%). Expression of the oncogene *AKT*. increased in ATLE cells to 242% of control. Chronic arsenic exposure increased expression of the major metallothioneins, MT-1A and MT-2A and stress response genes *HO-1* (690%) and *HIF-1*α (247%). Thus, it appears that arsenic can induce multiple cancer cell characteristics in human lung epithelial cells. This model can now be used to further assess mechanisms of arsenic-induced lung cancer.

PS 1297j Silencing KRAS Overexpression in Arsenic-Transformed Prostate Stem Cells Results in Signs of Malignant Phenotype Reversal

N. N. Ngalame, E. J. Tokar and M. P. Waalkes. *NTP, NIEHS, NIH, Research Triangle Park, NC.*

Inorganic arsenic is a human carcinogen that probably targets the prostate. Chronic arsenic exposure malignantly transforms the RWPE-1 human prostate epithelial line to CAsE-PE cells, and a derivative normal prostate stem cell (SC) line, WPE-stem to arsenic-cancer SCs (As-CSC). KRAS oncogene activation appears critical during this process, as CAsE-PE cells overexpress KRAS, and activation precedes transformation. As-CSCs also overexpress KRAS suggesting this is important in arsenic carcinogenesis in this key subpopulation. Thus, we hypothesize KRAS knockdown (KD) may reverse arsenic-induced malignant phenotype. RNA interference using shRNAmirs to obtain KRAS KD was used in As-CSCs. KRAS shRNAmir primarily expresses miRNA 30 transcript which targets KRAS to silence expression. As-CSCs were transduced with KRAS shRNA, or non-targeting control shRNA. Stable cell lines were generated by puromycin selection. Cells analyzed 2 weeks post transduction showed KRAS protein decreased to 5% of control in KD As-CSCs, confirming stable KD. KRAS KD decreased phosphorylated ERK by 60%, indicating inhibition of RAS/ERK signaling, a proliferation/survival pathway activated with arsenic transformation. Secreted metalloproteinase (MMP) activity increases in arsenic-induced malignant transformation, and by 4 weeks, KRAS KD decreased secreted MMP-9 (49%) and MMP-2 (39%) activity. Anchorage-independent growth (colony formation) is typical of cancer cells and correlated with cancer SCs. KRAS KD in As-CSCs decreased colony formation (40%) at 6 weeks after transduction. KRAS KD increased the cell cycle inhibitor proteins p16 (131%) and P21 (156%) and decreased the cell cycle activator *CCND1* transcript (26%), indicating reduced proliferation, consistent with a loss of rapid growth. KRAS KD increased (86%) protein levels of PTEN, a tumor suppressor gene inactivated in many cancers and in As-CSCs. Thus, KRAS silencing impacts arsenic-induced malignant phenotype at the level of CSCs, inducing loss of many typical cancer characteristics.

PS 1297k Differential DNA Methylation in Arsenic- or Cadmium-Transformed Malignant Prostate Epithelial Cells

K. E. Pelch, E. J. Tokar, B. Merrick and M. P. Waalkes. *NTP, NIEHS, NIH, Research Triangle Park, NC.*

Many inorganic carcinogens are weak mutagens, suggesting the epigenome is an important target. Previous work shows global DNA hypomethylation in human cells malignantly transformed by inorganic arsenic (iAs) and altered methylation patterns in iAs- or cadmium-transformed epithelial cells. In this work, the methylation status in the promoter region of six genes was assessed in the normal human prostate epithelial cell line (RWPE1) that was malignantly transformed by 10 μM cadmium for 11 weeks (CTPE) or 5 μM iAs for 31 weeks (CAsE-PE), at which time cells showed multiple markers of acquired cancer phenotype. Next generation sequencing of the transcriptome identified multiple misregulated genes. Of the most highly misregulated genes, 6 genes associated with stem cell function/dysfunction (*ALHD1A1, WNT4,* and *NES*), extracellular matrix (*HYAL1*), cell adhesion (*NTM*), or aggressive cancers (*S100P*) were chosen for in depth analysis of the DNA methylation profile. DNA was isolated, bisulfite converted, and combined bisulfite restriction analysis (COBRA) was used to identify differentially methylated CpG sites within 1000 bases of the transcription start site. Differential methylation was confirmed with bisulfite sequencing. All 6 genes showed differential methylation of at least one CpG site in transformants relative to control RWPE1 cells. Altered gene expression was inversely related to methylation status in 4 out of the 6 genes. Expression of *NES* (>15-fold) and *NTM* (>1000-fold) was decreased in the transformants compared to control. Both genes were hypermethylated near the transcription start site. Expression of *HYAL1* (>25-fold) and *S100P* (>40-fold) was increased in transformants relative to control and both genes were hypomethylated near the transcription start site. *ALDH1A1* and *WNT4* expression was increased in transformed cells versus control and both genes were hypermethylated relative to control. In conclusion, altered gene expression profiles observed in cadmium and iAs transformed cells may often result from altered DNA methylation status.

PS 1297l Arsenic Induces an Oncogenic Phenotype in Human Breast Epithelia through an Estrogen Receptor-Independent Pathway by Aromatase Activation

Y. Xu, E. J. Tokar and M. P. Waalkes. *NTP, NIEHS, NIH, RTP, NC.*

Inorganic arsenic has been linked to human breast cancer in some studies. Here, we tested the effects of inorganic arsenic exposure on the normal, estrogen receptor (ER)-negative breast epithelial cell line, MCF-10A. Cells were chronically exposed to sodium arsenite (500 nM) and markers of cancer phenotype and expression of genes relevant to breast cancer or stem cells (SCs) were examined. After 24 weeks of continuous arsenic exposure, increases in secreted metalloproteinase (MMP) activity, colony formation, invasion, and proliferation rate occurred, all typical cancer cell characteristics. The arsenic-transformed breast epithelial (ATBE) cells showed characteristics of a basal-like breast cancer, including ER-α, HER-2 and progesterone receptor negativity, and enhanced expression of breast cancer SC (CSC) markers, K5 and p63. Putative CD44+/CD24low/- breast SCs increased to 180% of control in ATBE cells as assessed by flow cytometry. In non-confluent culture, ATBE cells formed multilayer cell mounds, indicative of loss of contact inhibition, which showed high levels of K5 and p63 indicating the presence of CSCs. Epithelial-to-mesenchymal transition occurred starting from 8 weeks of arsenic exposure, as seen by cell morphology, increased *SNAIL1* and *VIMENTIN* expression and decreased *E-CADHERIN* expression. Aromatase, a key rate-limiting enzyme in estrogen synthesis, was overexpressed (mRNA, 540% of control; protein, 140% of control; week 8) starting early on in arsenic exposure. Immunofluorescence showed widely spread of aromatase overexpression in the ATBE cells. Levels of 17β-estradiol increased in ATBE cells and conditioned medium. The aromatase inhibitor, letrozole, abolished arsenic-induced 17β-estradiol increases, and over a 3-week period reversed arsenic-induced oncogenic phenotype. Thus, chronic arsenic exposure drives human breast epithelia into an oncogenic phenotype with an apparent overabundance of putative CSCs. Arsenic appears to transform breast epithelia through overexpression of aromatase, thereby activating oncogenic processes independent of ER.

PS 1298 Variable Cytotoxicity and Reactive Oxygen Species Generation in Pulmonary and Aortic Cells Exposed to Inorganic Arsenic and Monomethylarsonous Acid

R. Khalili, B. Welch, C. Pace, J. Kuzhippala and J. E. Angermann. *School of Community Health Sciences Environmental Physiology and Toxicology Laboratory, University of Nevada, Reno, Reno, NV.*

Chronic ingestion of arsenic produces myriad toxic effects including atherosclerosis and hypertension, but the cellular mechanisms by which vascular effects are produced remain unclear. The arsenic metabolite monomethylarsonous acid (MMAs) demonstrates elevated vascular toxicity relative to inorganic arsenic (iAs) and may therefore be linked to arsenic-induced vascular disease. The present study explores the role of iAs and MMAs on cytotoxicity, cellular morphology and ROS generation in two model vascular smooth muscle cell lines. Cytotoxic effects of iAs and MMAs on rat thoracic aorta smooth muscle cells (A7r5) and rat pulmonary arterial smooth muscle cells (rPASMC) in culture were examined for generation of malondialdehyde (MDA), hydrogen peroxide, and superoxide. Cytotoxicity, cell morphology, and mode of cell death were determined by cell counts, trypan blue exclusion, flow cytometry, MTT assay, and light microscopy. Cells treated with iAs or MMAs displayed cytotoxic effects and MMAs was significantly more toxic than iAs to both cell lines. After a 24 hour exposure, LC_{50}s in A7r5 were 11μM and 700nM when treated with iAs and MMAs, respectively. 10μM iAs and 500nM MMAs induced apoptosis in A7r5 and appeared to arrest cell growth in S phase. MMAs was significantly more toxic to rPASMC than iAs with an apparent 24h LC_{50} of 4.0μM relative to 27μM for iAs. No significant differences in MDA formation or superoxide production were observed following iAs or MMAs exposure in either line, although a significant increase in hydrogen peroxide was observed subsequent to iAs and MMAs exposure in both lines. These results suggest that the increased toxicity of MMAs may be in part due to increased hydrogen peroxide generation in A7r5 cells, but cytotoxicity is not solely attributable to oxidative stress when analyzed *in vitro*, suggesting that additional mechanisms are involved in arsenic-promoted vascular disease.

PS 1299 Differential Toxicity of Sodium Arsenite (AsIII) and Monomethylarsonous Acid (MMAIII) to Vascular Smooth Muscle and Endothelial Cells

B. Welch[1], R. Khalili[1], C. Martino[2] and J. E. Angermann[1]. [1]*School of Community Health Sciences Environmental Physiology and Toxicology Laboratory, University of Nevada, Reno, NV and* [2]*Department of Mechanical Engineering, University of Nevada, Reno, NV.*

Arsenic, a naturally occurring environmental contaminant, has been shown to create a redox state imbalance within numerous organs and tissues, resulting in increased steady-state concentrations of reactive oxygen species (ROS) such as superoxide anion, singlet oxygen, peroxyl/hydroxyl radicals, and hydrogen peroxide (H_2O_2). Although arsenic is primarily ingested in its inorganic form (sodium arsenite; iAsIII; iAs), the human metabolite monomethylarsonous acid (MMAIII; MMA) exhibits greater toxicity than tri- or pentavalent inorganic arsenic in the vasculature. In order to ascertain the potential for both iAs and MMA to enhance generation of ROS in vascular cell types, we examined the differential toxicity of iAs and MMA acid to rat aortic vascular smooth muscle (VSM; A7r5) cells and human umbilical vein endothelial cells (HUVECs), as well as the dynamics of arsenic-induced ROS production (as H_2O_2) in these model lines. The MTT assay was utilized to characterize iAs and MMA-induced changes in mitochondrial function, while H_2O_2 production following was quantified with the Amplex Red Assay. MMA was more highly toxic than iAs within both A7r5 cells and HUVECs, resulting in 80% reduction in mitochondrial viability (5μM, 24h exposure) relative to 20% reduction in mitochondrial viability following iAs exposure. Arsenic-induced H_2O_2 production was more substantial in A7r5 cells relative to HUVECs, with 2 hour iAs treatment causing a 10% increase and MMA a 60% increase over control. HUVECs showed a 20% increase in H_2O_2 production following 2h iAs treatment, whereas 2h MMA exposure did not cause a significant increase in H_2O_2 production. These results indicate that MMA is inherently more toxic than iAs to VSM and endothelial cells, and that H_2O_2 production is more prominent in VSM relative to endothelial cells, suggesting that mechanisms of cellular toxicity likely differ between these vascular cell types.

PS 1300 Arsenic-Induced Glycolysis during Malignant Transformation

F. Zhao, H. Li, C. Beeks, P. Severson, B. Futscher and W. T. Klimecki. *Pharmacology and Toxicology, University of Arizona, Tucson, AZ.*

Epidemiology studies have established a strong link between chronic arsenic(As) exposure and lung cancer. Currently, contribution of perturbed energy metabolism to carcinogenesis is an intensive area of research. In several human cell culture models (primary, immortal, malignant), we observed that non-cytotoxic exposure to As increased extracellular acidification rate(ECAR). Lactate accumulation caused by extracellular acidification, could be inhibited by 2-deoxy-D-glucose, a non-metabolized glucose analog. This established that As induces aerobic glycolysis(the Warburg effect), a metabolic shift frequently observed in the acquisition of malignancy. Our studies in Beas-2B(B2B), a non-malignant pulmonary epithelial cell line, found that the metabolic perturbation began early in the course of malignant transformation by As(8 wks). Correlated with the surge of glycolysis, we measured a 40% increase in mitochondria mass, suggesting that As may be damaging the mitochondria leading to biogenesis. Mitochondrial pyruvate dehydrogenase(PDH), an established target of As, controls the flow of pyruvate from glycolysis into the Krebs cycle. Intracellular metabolomics revealed 1.6-fold increase in pyruvate and 12-fold increase in lactate. Real-time ECAR established that glycolysis induction occurs within 20 minutes of As exposure, supporting a direct effect on PDH. Our evidence suggests that this metabolic shift is also sustained by HIF1A (hypoxia-inducible factor 1A). We found that As-exposed B2B accumulated HIF1A protein, and underwent transcriptional upregulation of HIF1A-target genes including pyruvate dehydrogenase kinase 2/3/4, inhibitor of PDH. Overexpression of HIF1A increases glycolysis 20% (vs. control), confirming that HIF1A can modulate glycolysis in B2B. Coincident with induction of glycolysis, we observed a decrease in E-cadherin expression, indicating loss of cell-cell adhesion and epithelial-mesenchymal transition, a hallmark of malignancy. Current efforts are aimed at dissecting the role that this metabolic disruption plays in malignancy in this model.

PS 1301 Arsenic Contaminated Drinking Water Deregulates Human Gene Expression Patterns in a Gender-Specific Manner in Bangladeshi Adults

A. B. Munoz[1], Y. Chervona[1], T. Kluz[1], M. Hall[2], M. Gamble[3] and M. Costa[1]. [1]*Environmental Medicine, New York University School of Medicine, Tuxedo, NY,* [2]*Department of Epidemiology, Mailman School of Public Health, Columbia University, New York City, NY and* [3]*Department of Environmental Health Sciences, Mailman School of Public Health, Columbia University, New York City, NY.*

Approximately 150 million people in at least 70 countries are exposed to arsenic via drinking water. Arsenic exposure is associated with skin, lung and bladder cancers, cardiovascular disease, kidney disease, and diabetes. Many questions remain regarding the mechanisms behind arsenic's pathogenesis including its potential role as an endocrine disruptor. Previous research in humans suggests that arsenic alters the abundance of post-translational histone modifications in a gender-specific manner. Twenty-nine study participants (55% male) from the FACT folate clinical trial in Bangladesh were selected with water arsenic exposure ranging between 50–500 ug/L As. RNA was extracted from peripheral blood mononuclear cells (PBMCs) and gene expression profiling was performed using Affymetrix 1.0 ST arrays. Differentially expressed genes were assessed between high and low groups for males and females separately and findings were validated using real-time PCR. Network analysis was performed using IPA (Ingenuity ® Systems, www.ingenuity.com). Among males, a total of 534 genes were differentially expressed ($p < 0.05$) in PBMCs from study participants with high arsenic exposure relative to those with low arsenic exposure. Females exhibited a total of 645 differentially expressed genes ($p < 0.05$). Only 42 genes overlapped between the two genders, with 28 out of 42 genes changing in opposite directions. Network analysis revealed both genders exhibited deregulation of the cardiovascular system through a distinct set of genes. Arsenic exposed adults exhibit gender-specific responses in gene expression. While responses are distinct, they exhibit similar features including cardiovascular deregulation.

PS 1302 Maladaptive Signaling from Arsenic Exposure Impairs Cardiac Bioenergetics and Enhances Autophagy

K. Beezhold, L. R. Klei, R. T. Cattley and A. Barchowsky. *EOH, University of Pittsburgh, Pittsburgh, PA.*

Environmental exposure to arsenic through drinking water causes cancers, as well as metabolic and cardiovascular diseases. Association of arsenic with cancer and many of its molecular mechanisms have been well studied, but much less is known of mechanisms for arsenic-promoted cardiac and vascular disorders. A low steady-

state level of cardiac autophagy is critical to maintaining heart homeostasis. While increased autophagy in response to stress such as ischemia or starvation is protective, excessive response to reperfusion after ischemia is detrimental. Stress-induced autophagy, such as in arsenic exposure, can be adaptive and prevent cell transformation. We hypothesized that arsenic exposure increases maladaptive signaling in cardiac tissue causing impaired bioenergetics and enhanced autophagy. DNA binding arrays identified several dysregulated transcription factor families in arsenic-exposed mouse hearts. Pro-autophagic FoxO transcription factors were increased up to 6-fold above control. Protein analysis by immunostaining and Western showed increased expression of both FoxO1 and 3a in the heart nuclei and DNA binding was confirmed by EMSA. Hearts from arsenic exposed (100 μg/L in drinking water for 2-5 wks) mice were analyzed for FoxO- associated signaling pathways. Upstream of FoxO3a activation, we observed increased in miR-143, a cardiac and autophagy associated miRNA that increases in FoxO3a protein expression. SRF, a transcription factor that drives miR-143 expression, was increased and ELK1, a MAPK family member that is a direct miR-143 target decreased. Downstream of FoxO3a we observed increased pyruvate dehydrogenase kinase 4 expression that may mediate starvation signaling indicative of impaired bioenergetics. These results suggest that arsenic increases cardiac autophagy by inducing autophagy regulating transcription factors (foxO) and by eliciting maladaptive starved signaling (ELK1 and PDK4). Supported by NIEHS F32 1F32 ES022134 01(KB) and NIEHS R01 ES013781(AB)

PS 1303 Global Assessment of Arsenic Pollution Using Sperm Whales (*Physeter macrocephalus*) As an Indicator Species

L. C. Savery[1, 2, 3], J. Wise[1], S. Wise[1, 2, 3], C. Falank[1, 2, 3], C. Gianios[1, 2, 3], W. D. Thompson[2, 3], C. Perkins[4], T. Zheng[5], C. Zhu[5] and J. P. Wise[1, 2, 3]. [1]*Wise Laboratory of Environmental & Genetic Toxicology, University of Southern Maine, Portland, ME,* [2]*Maine Center for Toxicology and Environmental Health, University of Southern Maine, Portland, ME,* [3]*Department of Applied Medical Sciences, University of Southern Maine, Portland, ME,* [4]*Center for Environmental Sciences and Engineering, University of Connecticut, Storrs, CT and* [5]*Yale School of Public Health, Yale University, New Haven, CT.*

Arsenic (As), a naturally occurring metalloid, is an oceanic pollutant of global concern due to its toxicity, ability to bioaccumulate and potential for increasing ocean levels to an unknown extent by anthropogenic activities. The sperm whale (*Physeter macrocephalus*) has a global distribution and high trophic level. The aim of this study was to establish a global and regional baseline of oceanic total As concentrations using free-ranging sperm whales as an indicator species. Skin biopsies (n = 342) were collected during the voyage of the *Odyssey* (2000-2005) from 17 regions considering gender and age in males. As was detectable in 99% of samples with a global mean of 1.9 ug/g ww ranging from 0.1 to 15.6 ug/g ww. Previous work in toothed whale skin found the mean As concentration to be 0.6 ug/g ww being 3 fold lower than these data. Global mean As concentrations were significantly different between females and males with males having a higher mean. Global mean As concentrations were significantly similar between age in males. As concentrations in two sloughed skin samples were similar to levels in skin biopsises from the same region indicating As is excreted by skin sloughing. Maldives, Seychelles and Sri Lanka had the highest regional means with 3.5, 2.5, and 2.4 ug/g ww, respectively. These data raise concern for As pollution in the Indian Ocean with levels reaching 13.8 ug/g ww. Literature suggests sources of As in this region are from naturally occurring sources and heavy use of As-containing pesticides and herbicides. More research is needed to determine the extent and sources for the elevated As concentrations in this region.

PS 1304 Evaluation of Arsenic (+3 Oxidation State) Methyltransferase Activity to Tellurite

M. Tokumoto, N. Kutsukake, E. Yamanishi, Y. Anan and Y. Ogra. *Laboratory of Chemical Toxicology and Environmental Health, Showa Pharmaceutical University, Machida, Tokyo, Japan.*

Inorganic arsenic is one of the distressing environmental contaminats, and many people suffer from its toxicity. Arsenite [As(III)] is metabolized with arsenic (+3 oxidation state) methyltransferase (As3MT), and the methylated metabolites are excreted into urine. It was reported that inorganic tellurium (Te) is simply methylated *in vivo*, and its ultimate methylated metabolite was excreted into urine. Although Te is also methylated as arsenic, the enzyme(s) being responsible for the Te methylation is still unclear. In this study we evaluated that As3MT metabolized inorganic Te and was involved in the reduction of Te toxicity. To obtain polyhistidine-tagged recombinant As3MT (rAs3MT), cDNA of human As3MT was inserted into pBAD, and rAs3MT was purified on a nickel ion-affinity column. The reaction mixture consisted of rAs3MT, S-adenosyl-L-methionine, glutathione and As(III) or tellurite [Te(IV)] in phosphate buffer and were incubated at 37°C for 4 h. The metabolites were determined by an HPLC coupled with an inductively coupled plasma-mass spectrometer. Although rAs3MT actually metabolized As(III) to dimethylated arsenicals, no methylated metabolites of Te(IV) with rAs3MT were detected under the reaction conditions. This result indicates that As3MT is a specific enzyme to metabolize As, and Te(IV) seems to be methylated by another methyltransferase and not As3MT. Next, siRNA targeting As3MT was introduced into human hepatoma cell line HepG2 cells to achieve the knockdown (KD) of As3MT. Then, the As3MT-KD cells and control siRNA-transfected cells were treated with As(III) or Te(IV) for 24 h. No apparent changes in the cell viability between As3MT-KD and control cells were observed when either As(III) or Te(IV) was exposed. As3MT did not protect the HepG2 cells from the cytotoxicities of As(III) and Te(IV). This can be explained by the suggestion that the cytotoxicities of some metabolic intermediates of As, such as trivalent methylated arsenicals, are equivalent to that of As(III), and Te(IV) is not metabolized with As3MT.

PS 1305 Ogg1 Genetic Background Determines the Genotoxic Potential of Environmentally Relevant Arsenic Exposures

A. Hernandez[1, 2], J. Bach[1], A. Sampayo-Reyes[3] and R. Marcos[1, 2]. [1]*Genetics and Microbiology, Autonomous University of Barcelona, Bellaterra, Barcelona, Spain,* [2]*CIBERESP, Barcelona, Spain and* [3]*Centro de Investigaciones Biomédicas del Noreste (CIBIN)-Instituto Mexicano del Seguro Social (IMSS), Monterrey, Nuevo León, Mexico.* Sponsor: A. Sampayo-Reyes.

Inorganic arsenic (i-As) is a well-established human carcinogen to which millions of people are exposed worldwide. It is generally accepted that the genotoxic effects of i-As after an acute exposure are partially linked to the i-As-induced production of reactive oxygen species; but it is necessary to better determine if chronic sub-toxic i-As doses are able to induce biologically significant levels of oxidative DNA damage (ODD). To fill in this gap we have tested the genotoxic and oxidative effects of environmentally relevant arsenic exposures using mouse embryonic fibroblast MEF mutant Ogg1 cells and their wild-type counterparts. Effects were examined by using the comet assay complemented with the use of FPG enzyme. Our findings indicate that MEF Ogg1-/- cells are more sensitive to arsenite-induced acute toxicicty, genotoxicity and ODD. Long-term exposure to sub-toxic doses of arsenite generates a detectable increase of ODD and genotoxic DNA damage only in MEF Ogg1 deficient cells. Altogether, the data presented here points out the relevance of ODD and Ogg1 genetic background on the genotoxic risk of i-As at environmentally plausible doses. The persistent accumulation of DNA 8-OH-dG lesions in Ogg1-/- cells during the complete course of the exposure suggests a relevant role in arsenic-associated carcinogenic risk in turn.

PS 1306 Arsenic, Obesity, and Inflammation Cytokines in Mexican Adolescents

M. Rubio-Andrade[1], G. G. Garcia-Vargas[1], S. J. Rothenberg[3], A. J. Steuerwald[4], P. J. Parsons[4], R. D. Zamoiski[2], V. M. Weaver[2], C. Resnick[2], E. Silbergeld[2], A. Navas-Acien[2] and E. Guallar[2]. [1]*Universidad Juarez Estado de Durango, Gómez Palacio, Durango, Mexico,* [2]*BSPH, Johns Hopkins University, Baltimore, MD,* [3]*Instituto Nacional de Salud Pública, Cuernavaca, Morelos, Mexico and* [4]*Wadsworth Center, NYSDOH, New York, NY.*

Evidence on the association of arsenic (As) exposures with obesity is considered as in-sufficient. Obesity is considered a disorder related to an inflammatory process, while arsenic also has an effect on the immune system. The aim of this cross-sectional study was to assess the association of arsenic exposure, obesity and inflammatory cytokines in adolescents exposed to arsenic via drinking water.
We studied 384 healthy adolescents 12-15 years of age, living in Torreon Coahuila, México. Participants with fish consumption in the previous week, or incomplete measurements were excluded. Total As concentrations in urine were measured using a inductively coupled plasma-mass spectrometer and expressed as μg/g creatinine. Adiposity was assessed using body mass index (BMI), sex- and age-standardized body mass index (zBMI), and bioimpedance segmental body composition (fat mass); cytokines were determined using ELISA method. The prevalence of obesity and overweight was 14.8% and 21.1% respectively. The median (IQR) of fat mass was 26.4% (19.9-32.75), which was significantly higher in female than males. The median (IQR) urinary As level was 36.2 (26.01, 46.8) μg/g creatinine. Only TNFa levels were higher in male adolescents. The median (IQR) of arsenic in urine in non obese subjects was 35.7 (27.4, 46.3) μg/g creatinine, and in adolescents with over-weight and obesity it was 36.6 (24.8, 47.5) μg/g creatinine. In a Spearman correlation analysis, arsenic exposure correlates with fat mass but not zBMI. IL 6 and TNFα correlates with zBMI and arsenic, and IL6 correlated with fat mass.
Our results showed a negative association of adiposity with arsenic exposure. Results of As and obesity association are in agreement with previous studies in human exposed to low levels of As in drinking water.

PS 1307 *In Utero* and Chronic Low-Dose As (III) Exacerbation of NAFLD and Alteration of Energy Metabolism

E. J. Ditzel[1], H. Nyugen[1], P. Parker[1] and T. D. Camenisch[1, 2, 3]. [1]*Pharmacology and Toxicology, University of Arizona, Tucson, AZ,* [2]*Steele Children's Research Center, Tucson, AZ and* [3]*Southwest Environmental Health Sciences Center, Tucson, AZ.*

Arsenic exposure is an ongoing health concern that has been increasingly linked to the development of cardiovascular disease and the metabolic syndrome. However, the role of low-dose As (III) exposure on the development of the metabolic syndrome remains controversial, and our study aims to explore mechanisms of As (III) toxicity on the development of the cardiometabolic syndrome. Male Swiss Webster mice were treated with 100ppb NaAsO2 in their water starting at embryonic day 5 (IU), after weaning (PN), or from embryonic day 5 onward (IU+). After weaning, all mice were fed a western diet. IU+ mice became overweight at week 5. The liver to body weight ratio in the IU and IU+ mice was elevated. Plasma HOMA-IR determined IU+ animals were insulin resistant. Liver H&E evaluation determined that all had microvesicular steatosis, but hepatocellular ballooning was most severe in the IU, PN, and IU+ mice. Liver evaluation with Masson's trichrome found fibrosis in the IU and IU+ livers. Oil-Red-O liver staining found steatosis in all groups with marginally higher lipid content in As (III) treated groups. Metabolomic analysis of plasma found changes in As (III) exposed animals that support an influence on energy metabolism: with effects evident in glycolysis, TCA cycle, and lipid metabolism. The histological, weight, and liver to body weight ratio findings are consistent with NAFLD (non-alcoholic fatty liver disease) suggesting that low-dose As (III) exposure, prenatal and chronic, predisposes mice to more severe NAFLD when on a western diet. Insulin resistance in IU+ animals suggests As (III) contribution to the development of the metabolic syndrome. The metabolomic findings are indicative of diverse changes in energy metabolism as a result of low-dose prenatal and/or chronic arsenic exposure. These data will be used to determine mechanisms behind metabolism alterations caused by As (III) so that therapeutic interventions can be developed.

PS 1308 Prenatal Arsenic Exposure and Proteomic Shifts in the Newborn

K. Bailey[1], J. E. Laine[2], J. E. Rager[1], E. M. Sebastian[1], A. F. Olshan[2], L. Smeester[1], Z. Drobna[3], M. Styblo[3, 1], M. Rubio-Andrade[4], G. G. Garcia-Vargas[4] and R. Fry[1]. [1]*Department of Environmental Sciences and Engineering, University of North Carolina, Chapel Hill, NC,* [2]*Department of Epidemiology, University of North Carolina, Chapel Hill, NC,* [3]*Department of Nutrition, University of North Carolina, Chapel Hill, NC and* [4]*Facultad de Medicina, Universidad Juárez del Estado de Durango, Gómez Palacio, Durango, Mexico.*

Prenatal exposure to inorganic arsenic (iAs) is associated with adverse health effects in infants, children, and adults, and yet the biological mechanisms that underlie these effects are understudied. In order to gain a better understanding of alterations in protein expression profiles associated with prenatal iAs exposure, we utilized samples from 50 mother-child pairs from a recently-established prospective pregnancy cohort in Gómez Palacio, Mexico. Concentrations of iAs in maternal drinking water (DW-iAs) ranged from below the limit of detection (LOD)-236 μg/L and the sum of iAs metabolites in maternal urine (total urinary arsenic; U-tAs) ranged from 6.19-319.7 μg/L. Using a high-throughput antibody array, we identified 111 cord blood proteins for which there was a significant association between protein expression in the newborn and maternal U-tAs. These proteins were enriched in functions including immune response and cellular growth/development. The newborns differed in the relationship between expression of these proteins and U-tAs in which this relationship was positive for "activator" newborns (n=30) and negative for "repressor" newborns (n=20). This activator/repressor status was associated with U-tAs and head circumference in newborn males. The molecular changes observed here may provide insight into the complex relationship between prenatal arsenic exposure, inter-individual differences in proteomic response to iAs, and susceptibility to adverse health outcomes.

PS 1309 Modification of Arsenic Metabolism by Sex Steroid Hormones in Hepatocytes (HepG2)

C. O. Puente-Valenzuela[1], E. Sierra-Campos[1], J. J. Duarte-Sustaita[1], L. M. Del Razo[2] and G. G. Garcia-Vargas[1]. [1]*Universidad Juarez del Estado de Durango, Gómez Palacio, Durango, Mexico and* [2]*Toxicología, CINVESTAV-IPN, Mexico, Distrito Federal, Mexico.*

Epidemiological studies suggest that women are more efficient to metabolize arsenic. In the present work was evaluated the effect of testosterone, progesterone and estradiol in the arsenic metabolism in the human hepatocytes cell line (HepG2). For the quantification of arsenic species cryo-trapping method (HG-CT-AAS) was used. LODs for the arsenic species were 0.7, 0.3 and 0.6 μM for iAs, MMA y DMA, respectively. HPLC-DAD was used for the quantification of GSH/GSSG ratio, a mobile phase containing 10 mM of Sodium Monobasic Phosphate in 2% of methanol was used in C18 column in reverse phase; the LODs for GSH and GSSG were of 1.0 μM for both. The cells were able to metabolize 0.2 μM of arsenite (Sodium Meta-Arsenite), generating the following profile of intracellular arsenic species: 36.8 % iAs, 21.2 % MMA and 42.0 % DMA, in 24 hr treatment, without decrease of cell viability (MTT Test). Sodium arsenite did not active the antioxidant system of GSH/GSSG, the ratio GSH/GSSG for the control cell (no arsenite added) was 3.17 and 2.83 when cells were treated with 0.2 μM sodium arsenite without statistic difference. For hormones assays a wide range of concentrations were used: for testosterone 100 – 1500 ng/dL, progesterone 750 – 12000 ng/dL, and estradiol 1.25 – 10.0 ng/dL. Finally, it was found that estradiol was able to change the profile of arsenical species, increasing the fraction of iAs at 37% and decreasing the DMA at 54% with respect to control cells, these changes were made at 5 pg/dL of estradiol. Based on the obtained results it can be concluded that estradiol modifies the metabolism of arsenic in the cell line HepG2.

PS 1310 Postnatal and *In Utero* Exposure to Methylated Arsenicals Enhances Atherosclerosis in the ApoE-/- Mouse Model

L. Negro Silva, M. Lemaire, C. A. Lemarié, S. Lehoux and K. K. Mann. *Lady Davis Institute for Medical Research, McGill, Montreal, QC, Canada.*

Epidemiologic data link arsenic exposure to an increased risk of cardiovascular diseases, such as atherosclerosis. Indeed, we have shown that 200 ppb sodium arsenite (NaAsO2) significantly enhances atherosclerotic plaque in apolipoprotein E (ApoE)-/- mice. However, different oxidation and methylation states of arsenic exist in the environment and are formed in vivo during biotransformation. However, the relative toxicity of these compounds is controversial. We hypothesized that methylated arsenicals would also promote atherosclerosis. We exposed male ApoE-/- mice to 200 ppb of NaAsO2, monomethylarsenate V (MMA V), monomethylarsenous III (MMA III), or dimethylarsenate V (DMA V) in the drinking water for 13 weeks. We compared arsenic-exposed animals with those on tap water and analysed plaque size in the aortic arch and aortic sinus. The en face staining of the aortic arch showed a greater lesion area in all arsenic-treated groups, where all, but the MMA V-exposed animals, were significantly increased from control. The plaque size in the aortic sinus was also increased. We have previously shown that NaAsO2 changed the composition of the plaque towards a more unstable phenotype. Using histochemistry, we observed less collagen and more lipids in plaque composition after MMA V and MMA III exposure, as reported for NaAsO2. Intriguingly, we have begun in utero exposures, where mice were exposed to 200 ppb DMA V from conception until weaning, and then kept on tap water for 13 weeks to compare with our postnatal exposures. Surprisingly, the in utero exposure to DMA V, which is considered less toxic, enhances atherosclerosis in ApoE-/- mice. Our data show that methylated-arsenicals also have the potential to increase atherosclerosis and alter plaque composition. These data suggest that methylation of arsenic may not protect against cardiovascular toxicity.

PS 1311 Reduction of Dimethylarsinic Acid in Rats and Rat Liver Cytosol—Role of Thioredoxin Reductase

B. F. Nemeti and Z. Gregus. *University of Pecs, Pecs, Hungary.*

Dimethylarsinic acid (DMAsV) is the main metabolite of inorganic arsenic in humans. Although its intrinsic toxicity is low, prolonged exposure can induce cancer. The toxicity of DMAsV (a pentavalent arsenical) mainly derives from its reduction to its trivalent form, dimethylarsinous acid (DMAsIII), which is much more cytotoxic due to its facile covalent reactivity with SH-groups. Rat liver cytosol, when supplemented with glutathione (GSH), catalyzes reduction of DMAsV to DMAsIII. On searching for enzymes that may carry out this toxification reaction, we observed that the specific thioredoxin reductase (TRR) inhibitor aurothioglucose and trivalent antimony inhibited the reduction of DMAsV by rat liver cytosol in concentration-dependent fashion, suggesting the possible role of TRR in this process. To test this hypothesis, we incubated DMAsV in the presence of GSH with liver cytosols from rats pretreated with an oleanolic acid derivative (CDDO), which increased cytosolic TRR activity markedly (+75%). We found that DMAsIII formation was 30% higher in the cytosol of CDDO-treated rats as compared to controls. However, when the incubations were supplemented with NADPH or the disulfide-reducing tris-carboxyethylphosphine, the difference disappeared. Furthermore, purified rat liver TRR neither reduced DMAsV nor did it augment cytosolic DMAsV reduction. The role of TRR in DMAsV reduction was also assessed in vivo in CDDO-treated rats. Rats are unique in that their hemoglobin avidly binds DMAsIII through a reactive cysteine residue, making the rat particularly suitable for following DMAsV reduction in vivo. Compared to controls,

however, the CDDO pretreatment did not alter the time course of the accumulation of DMAsIII in the blood of rats. In conclusion, the contribution of TRR to DMAsV reduction appears indirect. The activity of TRR may be indispensable for the reduction of DMAsV; however, at the quantity normally present in rat liver TRR does not limit the rate of DMAsV conversion to the highly toxic DMAsIII. Further research is warranted to identify the enzymes carrying out this important toxification step.

PS 1312 Dietary Methyl Donors Influence Arsenic Metabolism in Residents of Chihuahua, Mexico

M. Styblo[1], C. González-Horta[2], B. E. Sánchez Ramírez[2], L. Ballinas-Casarrubias[2], J. Hernández Ávila[3], R. Santos Luna[3], S. Román-Pérez[3], M. Ishida[2], D. Gutiérrez Torres[2], R. Hernández Cerón[4], D. Viniegra Morales[4], F. Baeza Terrazas[4], G. G. Garcia-Vargas[5], Z. Drobna[1], R. Fry[1], J. Buse[1], D. Loomis[6], L. M. Del Razo[7] and M. Mendez[1]. *[1]Nutrition, Univ North Carolina Chapel Hill, Chapel Hill, NC, [2]Universidad Autónoma de Chihuahua, Chihuahua, Mexico, [3]Instituto Nacional de Salud Pública, Cuernavaca, Mexico, [4]Colegio de Médicos Cirujanos y Homeópatas del Estado de Chihuahua, A.C., Chihuahua, Mexico, [5]Universidad Juárez del Estado de Durango, Gómez Palacio, Mexico, [6]IARC, Lyon, France and [7]Cinvestav-IPN, Mexico DF, Mexico.*

Inorganic arsenic (iAs) is a common drinking water contaminant known to increase risk of cancer and several non-cancerous diseases. iAs is metabolized via a pathway involving enzymatic methylation to methylarsenic (MAs) and dimethylarsenic (DMAs) prior to excretion. Higher proportions of urinary arsenic as iAs or MAs are thought to indicate an impairment in the capacity to methylate iAs and to increase health risks. Studies in Bangladesh suggesting dietary methyl donors, including folate and vitamin B12, may reduce iAs toxicity by enhancing DMAs production have yet to be confirmed in other populations. We explored associations between folate and vitamin B12 intakes and metabolites of iAs in urine of 771 adults in Chihuahua (Mexico) who were exposed to iAs in drinking water (<0.1-419.8 μg As/L). After adjusting for age and gender, adequate intakes of folate (>320 μg/day, 57% of the sample) were associated with higher %DMAs, a lower %iAs and higher MAs/iAs and DMAs/MAs ratios in urine, but only among subjects with high intakes of B12 (> the median of 1.85 μg/day). In contrast, among subjects with low B12 intakes, folate intake adequacy was associated with a reduction in %DMA and in the DMAs/MAs ratio, suggesting an impairment of the methylation capacity. Thus, B12 rather than folate intake may be the limiting factor in iAs metabolism in Mexican population.

PS 1313 Reduction of Dimethylarsenate to Dimethylarsenite by Rat Liver Cytosol: Further Characterization

Z. Gregus and B. F. Nemeti. *University of Pecs, Pecs, Hungary.*

Dimethylarsinic acid (DMAsV), the major urinary metabolite of inorganic arsenic, is weakly cytotoxic, however, its reduced form, dimethylarsinous acid (DMAsIII), is highly toxic. We have shown that rats and rat liver cytosol (RLC) reduce DMAsV in glutathione (GSH) dependent manner. GSH S-transferase omega 1 (GSTO1) can also reduce DMAsV, yet its role in DMAsV reduction in vivo or in cell extracts is uncertain. Our studies on reduction of DMAsV to DMAsIII in RLC yielded mixed findings, some compatible with involvement of GSTO1 in the cytosolic reduction of DMAsV, others not (Chem Res Toxicol 26: 432, 2013). Therefore, we carried out further investigations, using an improved GSTO1 assay and a DMAsV reduction assay, both in presence of GSH as a supporting substrate, to compare the features of these two enzymatic activities in RLC. Some of our findings indicate similar responsiveness, whereas others attest divergent characteristics: 1. Potent GSTO1 inhibitors (KT53, CMFDA) inhibited both GSTO1 activity and DMAsV reduction by RLC in the same concentration range. 2. Aurothioglucose and trivalent antimony weakly inhibited GSTO1 activity, but strongly inhibited DMAsV reduction by RLC. 3. The DMAsV reducing activity of some cytosols were low, but were normalized by NADPH. In contrast, the GSTO1 activity of all cytosols was similar and was not affected by NADPH addition. Further, a specific substrate of GSTO1 (4-nitrophenacyl-glutathione, 4NPG) inhibited DMAsV reduction, but this effect was alleviated with NADPH or the disulfide reducing TCEP, suggesting that GSSG, the byproduct of 4NPG reduction by GSTO1 and a known inhibitor of DMAsV reduction, may be involved. Additional studies revealed that the cytosolic DMAsV reducing activity is best supported by GSH, much less by cysteine, and not by other SH compounds tested. S-Alkyl-GSH compounds impaired DMAsV reducing activity in RLC, with their potency increasing with the length of alkyl chain. Thus, the GSH dependent DMAsV reducing enzyme in RLC has a GSH binding site. This feature may facilitate isolation of this hitherto unknown enzyme and its positive identification.

PS 1314 Chronic Exposure to Arsenic is Associated with an Elevated Cardiometabolic Risk in Chihuahua, Mexico

C. González-Horta[1], M. Mendez[2], B. E. Sánchez Ramírez[1], L. Ballinas-Casarrubias[1], M. Ishida[1], D. Gutiérrez Torres[1], R. Hernández Cerón[3], D. Viniegra Morales[3], F. Baeza Terrazas[3], G. G. Garcia-Vargas[4], Z. Drobna[2], R. Fry[2], J. Buse[2], D. Loomis[5], L. M. Del Razo[6] and M. Styblo[2]. *[1]Universidad Autónoma de Chihuahua, Chihuahua, Mexico, [2]University of North Carolina, Chapel Hill, NC, [3]Colegio de Médicos Cirujanos y Homeópatas del Estado de Chihuahua, A.C., Chihuahua, Mexico, [4]Universidad Juárez del Estado de Durango, Gómez Palacio, Mexico, [5]IARC, Lyon, France and [6]Cinvestav-IPN, Mexico DF, Mexico.*

Cardiometabolic (CM) risk is characterized by a group of factors that serve as indicators of an individual's overall risk for type-2 diabetes mellitus (DM) and cardiovascular disease (CVD). The traditional CM risk factors include dysglycemia, dyslipidemia, high blood pressure, inflammation, endothelial dysfunction, and obesity. Growing epidemiologic evidence suggests that exposure to some environmental chemicals, including inorganic arsenic (iAs), may increase risk of DM and CVD. The present cross-sectional study examined associations between iAs exposure and CM risk factors in a cohort of adult Chihuahua residents (n=933) who drank water containing 0.05 - 419.8 μg As/L. Results show that subjects in the highest exposure tertile (58.3 - 419.8 μg As/L) had higher levels of total cholesterol in plasma and were more likely to have dysglycemia (OR 1.60, 95%CI 1.09-2.32), hypertriglyceridemia (OR 1.53, 95%CI 1.07 - 2.20), and high blood pressure (OR 1.57, 95%CI 1.05 - 2.35) than subjects in the lowest exposure tertile (≤38.5 μg As/L). In addition, all these CM risk factors were positively associated with the ratio of dimethylarsenic (DMAs) to methylarsenic (MAs) and with %DMAs in urine. Thus, an increased capacity to convert iAs to DMAs may be a risk factor for CM disease in individuals exposed to iAs. Prospective studies are needed to examine causality of the association of CM risk with iAs exposure and to determine if iAs metabolism can modify this risk.

PS 1315 Inorganic Arsenite Suppresses Mast Cell Degranulation via a Pathway Target Upstream of Calcium Signaling

J. Shim[1], R. Kenndy[2], L. Weatherly[2], L. Hutchinson[1], J. Pelletier[1], B. Evans[1], H. Hashmi[1], K. Blais[1] and J. A. Gosse[1]. *[1]Molecular and Biomedical Sciences, University of Maine, Orono, ME and [2]Graduate School of Biomedical Science and Engineering, Orono, ME.*

Exposure to Arsenic (As) is a global concern and is linked to many diseases. Many millions of people worldwide are exposed to elevated levels of arsenic through drinking water, food, and other sources. Using a well-characterized mast cell model (RBL-2H3 cells), we previously demonstrated that inorganic Arsenic inhibits antigen-mediated mast cell degranulation. Found in the vast majority of human tissues, mast cells are critical players in numerous diseases, including allergy, asthma, infectious disease, cancer, and even many central nervous system disorders such as autism and anxiety. Mast cells secrete myriad effectors from cytoplasmic granules such as histamine and β-hexosaminidase. The present studies have been performed in order to investigate arsenic's molecular target in the degranulation pathway. We have found that Arsenic does not affect F-actin membrane ruffling of RBL-2H3 cells stimulated with antigen, suggesting that arsenic's target is not common to both the ruffling and degranulation pathways. We found that Arsenic dampens calcium influx, as measured by fluo-4 fluorescence. When stimulating degranulation while bypassing early signaling events, via the use of thapsigargin or calcium ionophore, we found no Arsenic effect on the degranulation response. Using an alternative, non-IgE-mediated mast cell stimulant, G-protein activator compound 48/80, we observed no Arsenic effect degranulation. Taken together with our earlier data showing an inhibition of IgE-mediated degranulation, this result suggests that arsenic's target in the degranulation pathway is upstream of calcium influx, protein kinase C, phospholipase D, and actin ruffling. Recently, we investigated arsenic's effect on phosphorylation using a sandwich ELISA and the data suggests that arsenic may be interfering with the phosphorylation of the early kinase Syk.

PS 1316 Arsenite-Induced ROS/RNS Generation Causes Zinc Loss and Inhibits the Activity of Poly(ADP-Ribose) Polymerase-1

X. Zhou[1], F. Wang[2], W. Liu[1], X. Sun[1], C. Chen[1], L. G. Hudson[1] and K. Liu[1]. *[1]College of Pharmacy, University of New Mexico, Albuquerque, NM and [2]Department of Nutrition and Food Hygiene, Fourth Military Medical University, Xi'an, Shaanxi, China.*

Arsenic enhances the genotoxicity of other carcinogenic agents such as ultraviolet radiation and benzo[a] pyrene. Recent reports suggest that inhibition of DNA repair is an important aspect of arsenic cocarcinogenesis, and DNA repair proteins

such as poly(ADP ribose) polymerase (PARP)-1 are direct molecular targets of arsenic. Although arsenic has been shown to generate reactive oxygen/nitrogen species (ROS/RNS), little is known about the role of arsenic-induced ROS/RNS in the mechanism underlying arsenic inhibition of DNA repair. We report herein that arsenite-generated ROS/RNS inhibits PARP-1 activity in cells. Cellular exposure to arsenite, as well as hydrogen peroxide and NONOate (nitric oxide donor), decreased PARP-1 zinc content, enzymatic activity, and PARP-1 DNA binding. Furthermore, the effects of arsenite on PARP-1 activity, DNA binding, and zinc content were partially reversed by the antioxidant ascorbic acid, catalase, and the NOS inhibitor, aminoguanidine. Most importantly, arsenite incubation with purified PARP-1 protein in vitro did not alter PARP-1 activity or DNA-binding ability, whereas hydrogen peroxide or NONOate retained PARP-1 inhibitory activity. These results strongly suggest that cellular generation of ROS/RNS plays an important role in arsenite inhibition of PARP-1 activity, leading to the loss of PARP-1 DNA-binding ability and enzymatic activity.

PS 1317 Protective Role of Vitamin E Succinate and Selenite in Arsenic-Intoxicated Hamster: Arsenic-Induced Oxidative Stress and Its Reversible Damage

A. Sampayo-Reyes[1], R. Dauder[2] and A. Hernandez[2]. [1]*Toxicology and Pharmacology, Centro de Investigaciones Biomedicas, Monterrey, Nuevo León, Nuevo León, Mexico and* [2]*Genetics, Universitat Autonomas de Barcelona, Barcelona, Bellaterra, Spain.*

We studied the effects of combined exposure to arsenic, selenite and vitamin E succinate. (i) oxidative stress and its correlation with glutathione and linked enzymes; (ii) alterations in the structural integrity of DNA with assay comet; and (iii) biochemical parameters. Efficacy of selenite and alpha-tocopherol succinate in reducing these changes was also determined. Hamsters were exposed to sodium arsenite, 100 ppm of arsenite via drinking water. Co-treatment with 8.5 mg/Kg/day of selenite or 6 mg/Kg/day of vit E was also carried out to assess whether those compounds exert any protective role, individually and in combination for twenty weeks. The samples of whole blood were collected at 24hrs and 20 week post-treatment and the assay was carried out to determine DNA damage as represented by comet tail-length and biochemical parameters assay. Arsenic species were measured in the urine by HPLC-ICP/MS. Exposure to arsenic altered the levels of oxidative stress enzymes. These changes were accompanied by increased reactive oxygen species (ROS) levels. Arsenic exposure led to a significant depletion of super oxide dismutase (SOD) activity with no effect on catalase and glutathione peroxidase (GPx) activities. The distribution of DNA migration revealed that the hamster exposed to arsenic showed more DNA damage than samples obtained from control. The results demonstrate a As toxic effect, and a noticeable protective effect of both vit E and selenite, coexposure had additional beneficial effects in restoring altered biochemical variables, maintaining pro-oxidant/antioxidant balance. Our experiments indicate the significant protective action of vitamin e succinate and sodium selenite on arsenic-induced toxicity in the hamster.

PS 1318 Prenatal Arsenic Exposure and the Epigenome: Altered microRNAs Associated with Innate and Adaptive Immune Signaling in Newborn Cord Blood

J. E. Rager[1], K. Bailey[1], L. Smeester[1], S. K. Miller[1], J. E. Laine[2], Z. Drobna[3], J. Currier[4], C. Douillet[3], A. F. Olshan[2], M. Rubio-Andrade[5], M. Styblo[1, 3], G. G. Garcia-Vargas[5] and R. Fry[1, 4]. [1]*Environmental Sciences and Engineering, University of North Carolina, Chapel Hill, NC,* [2]*Department of Epidemiology, University of North Carolina, Chapel Hill, NC,* [3]*Department of Nutrition, University of North Carolina, Chapel Hill, NC,* [4]*Curriculum in Toxicology, University of North Carolina, Chapel Hill, NC and* [5]*Facultad de Medicina, Universidad Juárez del Estado de Durango, Gómez Palacio, Durango, Mexico.*

The Biomarkers of Exposure to ARsenic (BEAR) pregnancy cohort in Gómez Palacio, Mexico was recently established to better understand the impacts of prenatal exposure to inorganic arsenic (iAs). In the present study, we examined a subset (n=40) of newborn cord blood samples for microRNA (miRNA) expression changes associated with in utero arsenic exposure. Levels of iAs in maternal drinking water (DW-iAs) ranged from below detectable values to 236 μg/L (mean=51.7 μg/L). Total urinary arsenic in maternal urine (U-tAs) was measured where tAs was defined as the sum of iAs and its monomethylated and dimethylated metabolites (MMAs and DMAs, respectively). Levels of U-tAs ranged from 6.2 to 319.7 μg/L (mean=64.5 μg/L). Genome-wide analysis revealed 19 miRNAs with increasing expression association with U-tAs. Transcriptional targets of the miRNAs were computationally predicted and subsequently assessed using transcriptional profiling. Pathway analysis demonstrated that the U-tAs-associated miRNAs are involved in signaling pathways related to known health outcomes of arsenic including cancer and diabetes mellitus. Immune response-related transcripts were identified with decreased expression levels associated with U-tAs, and predicted to be mediated by the arsenic-responsive miRNAs. Results of this study highlight miRNAs as novel responders to prenatal arsenic exposure that may contribute to arsenic-induced immunosuppression.

PS 1319 Arsenic Exposure Increases Monocytes Adhesion to the Vascular Endothelium, a Pro-Atherogenic Mechanism

M. Lemaire[1], R. M. Krohn[2], L. Negro Silva[3], C. A. Lemarié[4], M. Flores Molina[1], S. Lehoux[4], J. E. Smits[2] and K. K. Mann[1]. [1]*Oncology, McGill University, Montreal, QC, Canada,* [2]*Ecosystem and Public Health, University of Calgary, Calgary, AB, Canada,* [3]*Experimental Medicine, McGill University, Montreal, QC, Canada and* [4]*Medicine, McGill University, Montreal, QC, Canada.*

Arsenic exposure is linked epidemiologically to increased atherosclerosis, but the mechanisms by which arsenic enhances atherosclerosis are unknown. Monocytes, macrophages and platelets are key players in the early stage of an atherosclerotic lesion. Circulating monocytes and macrophages bind to the activated endothelium of vessels and migrate into the sub-endothelium where they become lipid-laden foam cells. This process can be facilitated by platelets, which favour monocyte recruitment to the lesion. Thus, we assessed the effects of arsenic exposure on platelet activation, platelet-monocyte aggregation and monocyte adhesion to endothelial cells. We observed no effect of arsenic on platelet activation or platelet-monocyte aggregation. Then, we assessed the monocyte adhesion to VCAM-1, an adhesion molecule normally found on activated endothelial cells. We found that 1) monocyte and macrophage adhesion to VCAM-1 is increased by arsenic; 2) the surface expression of the β1 integrin (CD29) that binds to VCAM-1 is increased on macrophages by arsenic; and 3) these effects can be inhibited by antioxidants. We extended these results using a co-cultured model of human endothelial and monocytic cells and an *ex vivo* organ culture system. We found that both cell types need to be exposed to arsenic to maximize monocyte adhesion in a dose-dependent manner, at concentrations as low as 10 ppb. Finally, we assessed the CD29 level on circulating monocytes in mice exposed to arsenic. Arsenic increased monocytic CD29 levels as compared to control animals, and addition of high selenium diet decreased CD29. Together, these data suggest that arsenic enhances atherosclerosis by increasing monocyte adhesion to endothelial cells, a process that is inhibited by antioxidants.

PS 1320 Synergistic Effect of Arsenic on Hexavalent Chromium Cytotoxicity and Genotoxicity in Human Lung Cells

J. Stewart, N. Nutter, J. P. Wise and H. Xie. *University of Southern Maine, Portland, ME.*

Hexavalent chromium (Cr(VI)) and inorganic arsenic are well known environmental and occupational hazards and are often found as mixed contaminants and wastes. Both of them are known human lung carcinogens. Despite that people are exposed to these metals simultaneously under most conditions, little is known about the potential co-exposure impact. Arsenic is known to inhibit DNA damage repair and our previous studies show that Cr(VI) induces DNA double strand breaks and neoplastic transformation in human lung cells. Thus, it is likely that co-exposure to Cr(VI) and arsenic could cause greater toxic effect. The objective of this study is to determine the ability of arsenic to increase Cr(VI) genotoxicity and carcinogenicity in human lung cells. We found that arsenic has a synergistic effect on Cr(VI) cytotoxicity. 0.5 uM arsenic alone induces 14 percent of relative cell death. Cr(VI)-induced cell death is increased from 32, 50 and 62 to 47, 65 and 80 percent of relative cell death, respectively after co-exposure to 0.5 uM arsenic and 0.1, 0.5 and 1 ug/cm2 lead chromate. Arsenic has a similar effect on soluble Cr(VI) compound, sodium chromate. Arsenic also causes an increase in Cr(VI)-induced chromosome aberration. 0.5 uM arsenic alone induces 9 metaphases with chromosome damage. When co-treated with 0.01, 0.05 and 0.1 ug/cm2 lead chromate, the number of metaphase with damage increased from 5, 6 and 19 to 16, 16 and 31, respectively. These data suggest that co-exposure to Cr(VI) and arsenic induces a synergistic toxic effect in human lung cells. Further work will include assessing the effect of arsenic on Cr(VI)-induced DNA double strand break and repair. This work is supported by NIEHS grants R15ES021587 (H.X.) and ES016893 (J.P.W.).

PS 1321 Tissue Distribution and Excretion of Arsenic and Selenium following Co-Administration of Diphenylarsinic Acid and Selenite in Rats

Y. Kobayashi and S. Hirano. *National Institute for Environmental Studies, Tsukuba, Japan.*

Diphenylarsinic acid (DPAA) is a chemical precursor as well as a degradation product of arsenic-containing chemical weapons such as diphenylarsine chloride. Toxicological findings on DPAA are limited as compared to inorganic arsenicals (iAs). Selenium (Se) is an essential element, and is known to interact with arsenic. We investigated metabolic interactions between Se and As in rats co-administered with DPAA and selenite in this study. Male Sprague-Dawley (SD) rats were injected intravenously with DPAA, selenite or co-administrated with As and Se, at a dose of 1.0 mg As or 1.0 mg Se/kg body weight, and urine and feces were collected separately for 24 h using metabolic cages . In a separate experiment SD rats were anesthetized with sodium pentobarbital, the bile duct was cannulated, and DPAA or/and selenite were administered intravenously at a dose of 1.0 mg As or 1.0 mg Se/kg body weight to study biliary excretion of Se and As. The bile fluid was collected on ice for 30 min up to 3 hr after the injection. The animals were sacrificed by withdrawing blood from the abdominal aorta under anesthesia at 24 or 3 h after the injection, and heparinized blood and tissue samples were collected. Selenite significantly reduced concentration of As in plasma 24 h after the administration. DPAA significantly reduced distribution of Se in kidney, and yet significantly increased excretion of Se into urine 24 h after the administration. On the other hands, selenite significantly reduced the biliary excretion of DPAA, and DPAA significantly increased the biliary excretion of selenium in 30 min after the administration and then significantly reduced the biliary excretion when DPAA and selenite were co-administered. DPAA significantly increased distribution of Se in whole blood, and significantly reduced distribution of Se in liver; however, distribution of As to blood and liver was not influenced by selenite 3 h after the administration. These results suggest that DPAA interacted with selenite, and changed distribution and excretion of these metalloids each other in rats.

PS 1322 Increased Expression of the Proto-Oncogene Anterior Gradient 2 in the MCF-10A Cell Line by Arsenite Exposure

J. Van Gieson, S. H. Garrett, D. A. Sens and S. Somji. *Pathology, University of North Dakota, Grand Forks, ND.*

Arsenite and cadmium are environmental carcinogens that have been implicated in various cancers. Previously, our laboratory has shown that arsenite and cadmium can cause malignant transformation of the immortal breast epithelial cell line MCF-10A. Microarray analysis of the transformed cells revealed an over-expression of the gene Anterior Gradient 2 (AGR2). These findings are significant since AGR2 is known to be overexpressed in estrogen receptor positive breast cancers. AGR2 is a pro-oncogeneic protein that is highly expressed in a variety of human cancers. It is known to play a role in promoting cellular transformation, tumor growth as well as metastasis. In this study, we validated the expression level of AGR2 in the parent MCF-10A cells as well as the arsenite and cadmium transformed MCF-10A cells using PCR and Western analysis. The data obtained indicated that the expression of AGR2 was significantly increased in the arsenite transformed cells compared to the cadmium transformed cells. We were also interested in determining if exposure to arsenite or cadmium could increase the expression of AGR2 in the parent MCF-10 cells. For this purpose MCF-10A cells were exposed to 4, 8 or 16 μM arsenite or 2, 4, or 6 μM cadmium for 48 hrs and the expression levels of AGR2 were determined. The data obtained showed that exposure to arsenite resulted in a significant increase in the expression of AGR2, whereas exposure to cadmium had no effect on the expression level of AGR2. These results suggest that arsenite has the potential to induce the pro-oncogenic protein AGR2, the expression of which may increase the metastatic potential of the cancer cells.

PS 1323 The Prebiotic Oligofructose Protects against Enhanced Liver Injury Caused by Arsenic in a Model of NASH

V. L. Massey, R. H. Schmidt, M. Tan, W. H. Watson and G. E. Arteel. *Pharmacology & Toxicology, University of Louisville, Louisville, KY.*

Arsenic, a ubiquitous drinking water contaminant, tops the ATSDR list of hazardous environmental chemicals and is a known hepatotoxin. This group showed that subhepatotoxic doses of arsenic sensitize the liver to experimental non-alcoholic fatty liver disease (NAFLD) caused by a high fat diet (HFD). It is now strongly suspected that an altered gut flora plays an important role in NALFD. Indeed, prebiotics (oligofructose; OFC), protect against experimental NAFLD, and correlate with repletion of commensal bacteria (e.g., *Bifidobacteria* spp.) in the GI tract. The purpose of the current study was to test the hypothesis that OFC protects against enhanced liver injury caused by arsenic in experimental NAFLD. Accordingly, male C57Bl6/J mice were fed low fat diet (LFD), HFD or HFD containing OFC during concomitant exposure to either tap or arsenic-containing water for 10 wks. Abundance of bacteria in cecal contents was determined by qPCR. Histological changes were determined by hematoxylin and eosin staining. Macrophage activation and fibrin deposition were determined by immunostaining. HFD caused fatty liver injury, as characterized by an increase in liver:body weight ratio, steatosis and transaminases. Arsenic synergistically enhanced HFD-induced liver damage, inflammation, and fibrin deposition. HFD and arsenic alone both altered content of cecal bacteria, and both decreased the abundance of Bifidobacterium spp; OFC supplementation protected against this effect. OFC supplementation also protected against the enhanced liver damage, inflammation, and fibrin accumulation caused by the combination of HFD and arsenic. These results indicate that enhanced HFD-induced liver damage caused by arsenic may be mediated, at least in part, by GI tract dysbiosis and that prebiotic supplementation may confer significant protective effects. Together, these data support our hypothesis that arsenic-mediated changes in the GI tract flora play an important factor in sensitizing the liver to injury.

PS 1324 Metabolomics Signature of Inorganic Arsenic-Associated Diabetes: Links to Amino Acid Metabolism

E. M. Sebastian[1], K. Bailey[1], C. González-Horta[2], B. E. Sánchez Ramírez[2], L. Ballinas-Casarrubias[2], M. Ishida[2], D. Gutiérrez Torres[2], R. Hernández Cerón[3], D. Viniegra Morales[2], F. Baeza Terrazas[3], L. M. Del Razo[4], G. G. Garcia-Vargas[5], R. Saunders[1], W. Jia[6], B. B. John[7], D. Loomis[8], Z. Drobna[1], M. Styblo[1] and R. Fry[1]. [1]*School of Public Health, University of North Carolina at Chapel Hill, Chapel Hill, NC,* [2]*Universidad Autónoma de Chihuahua, Chihuahua, Mexico,* [3]*Colegio de Médicos Cirujanos y Homeópatas del Estado de Chihuahua, Chihuahua, Mexico,* [4]*Centro de Investigación y de Estudios Avanzados del Instituto Politécnico Nacional, Chihuahua, Mexico,* [5]*Universidad Juárez del Estado de Durango, Gomez Palacio, Mexico,* [6]*University of Hawaii Cancer Center, Honolulu, HI,* [7]*School of Medicine, University of North Carolina at Chapel Hill, Chapel Hill, NC and* [8]*International Agency for Research of Cancer, Monographs Section, Lyon Cedex, France.*

The Chihuahua Cohort was established to study chronic disease associated with exposure to inorganic Arsenic (iAs) in drinking water, specifically diabetes mellitus (DM). The present study profiled the metabolomic shifts in a group of individuals selected from this cohort (91 diabetics and 86 non-diabetics) using both LC-MS and GC-MS platforms. Exposure to iAs was characterized by iAs levels in drinking water (DW-iAs) and by the sum of iAs metabolites in urine (U-tAs). Fasting plasma glucose (FPG) and 2-hour plasma glucose (2HBG) were recorded by a glucose tolerance test and were used to determine an individual's DM status. Levels of DW-iAs ranged from 0 to 419.7 μg/L, and U-tAs level ranged from 4.69 to 445.2 μg/L. Both urine and plasma metabolite levels were analyzed as they related to DM, iAs exposure or iAs-associated DM. Metabolites were identified that were specific to iAs exposure, as well as to DM. Notably, a metabolomic signature of 23 metabolites was identified that distinguishes iAs-associated DM. These metabolites reflect changes not only in glucose, but also in amino acid metabolism, providing additional evidence that iAs-associated DM may differ from the common type-2 DM.

PS 1325 Inorganic Arsenic Exposure and Bone Loss in Normal and Hypertensive Rats

C. Wu[1], B. Chen[1], H. Wu[1], C. Chiu[1], R. Yang[2], Y. Chen[3], C. Huang[4] and S. Liu[1]. [1]*Institute of Toxicology, College of Medicine, National Taiwan University, Taipei, Taiwan,* [2]*Department of Orthopedics, College of Medicine and Hospital, National Taiwan University, Taipei, Taiwan,* [3]*Department of Physiology and Graduate Institute of Basic Medical Science, College of Medicine, China Medical University, Taichung, Taiwan and* [4]*Graduate Institute of Chinese Medical Science, School of Chinese Medicine, College of Chinese Medicine, China Medical University, Taichung, Taiwan.*

Exposure to inorganic arsenic through drinking water is a major international public health issue. It can be absorbed via digestive tract or skin and then accumulated in the variant target oranges to disturb tissues functions. Previously epidemiological studies showed that arsenic exposure from drinking water could increase vascular disorders to elevate blood pressure or decrease bone mineralization. However, whether arsenic exposure from drinking water enhances the loss of bone mineralization during hypertension disease remains unclear. Here, we examined the changes of bone morphology and bone mineral density in normal (WKY) and spontaneously hypertensive rats (SHR) after exposure to inorganic arsenic from drinking water using micro-computed tomography (micro-CT) analysis. Rats were exposed with arsenic trioxide (As2O3) from drinking water for three months. The results showed that arsenic exposure obviously increased blood pressure in WKY

rats and significantly enhanced blood pressure in SHR rats in a dose dependent manner. The results of micro-CT-derived bone morphometry and density measurements showed that connectivity density, trabecular thickness, bone volume, trabecular bone number, trabecular separation, and bone mineral density were significantly changed in both WKY and SHR rats. However, no significant differences were observed in these bone parameters between SHR and WKY rats. Taken together, these results suggest that inorganic arsenic is capable of inducing bone loss in normal and hypertensive rats, but hypertension condition seems not to enhance the arsenic-induced bone loss.

PS 1326 *In Vivo* Mutagenicity Assay of Arsenite Using Gpt Delta Transgenic Mice

S. Takumi[1, 2], Y. Aoki[1], T. Sano[1], T. Suzuki[1], T. Nohmi[3] and K. Nohara[1]. *[1]National Institute for Environmental Studies, Tsukuba, Japan, [2]The Jikei University School of Medicine, Tokyo, Japan and [3]National Institute of Health Sciences, Tokyo, Japan.*

While arsenic has been classified as a Group 1 human carcinogen by the International Agency for Research on Cancer (IARC), the mutagenicity in animal model has not been fully characterized. The aim of this study was to assess the *in vivo* mutagenicity of arsenite in C57BL/6J gpt delta mice. Male gpt delta mice were given drinking water containing 85 ppm sodium arsenite for 3 weeks, and the hepatic genome was assayed for mutations 2 weeks later. The result of gpt mutation assays showed a significant increase in mutation frequency in the liver following arsenite exposure. Analysis of the mutation spectra revealed that 67% of mutations detected are G:C to A:T transitions and 6% are G:C to T:A transversions in the control group. In contrast, arsenite exposure resulted in a markedly higher rate of G:C to T:A transversions (46% of mutations detected). G:C to T:A transversions have been reported to be induced following formation of 8-hydroxy-2'-deoxyguanosine (8-OHdG), one of the major forms of oxidative DNA damage. We also detected a significant increase in 8-OHdG in the livers of the mice exposed to arsenite. These results demonstrate that arsenite induces G:C to T:A transversions through oxidative-stress-induced 8-OHdG formation *in vivo*. We also discuss the results of the DNA methylation analysis of gpt gene and the expression analysis of DNA repair genes.

PS 1327 N-Cadherin Up-Regulation in Arsenite and Cadmium-Transformed Urothelial Cells

E. Sandquist, X. Zhou, S. Somji, D. A. Sens and S. H. Garrett. *Pathology, University of North Dakota, Grand Forks, ND.*

The switch from E- to N-cadherin is a well-known indicator of the epithelial-to-mesenchymal transition occurring in bladder cancer. N-cadherin upregulation is correlated with tumor stage, increased recurrence, and decreased survival in patients. While the factors mediating the decrease in E-cadherin expression are well-established, little is known of the factors regulating the increase in N-cadherin expression. Environmental agents are the common cause of bladder cancer. Specifically, arsenite and cadmium are known carcinogens and implicated in the development of bladder cancer. Previous studies from our laboratory have shown that arsenite and cadmium can cause malignant transformation of normal immortalized bladder urothelial cells. These transformed cells can form tumors when injected sub-cutaneous or intraperitoneal into nude mice. The goal of the present study was to determine if there was a difference in expression levels of E- and N-cadherin in the transformed cell lines and the tumor heterotransplants. For this purpose real-time PCR was performed on RNA samples isolated from the transformed cell lines and the tumor heterotransplants. Western analysis was performed to determine the protein levels whereas immunohistochemical analysis was performed to determine the localization of the proteins within the tumor heterotransplants. The results obtained show that E-cadherin is expressed in the transformed cell lines as well the tumor heterotransplants. The expression of N-cadherin was very low in the parent UROtsa cells whereas the levels increased in the transformed cell lines. The expression level of N-cadherin decreased in the tumor heterotransplants compared to the cell lines. An interesting finding was the focal expression of N-cadherin in the intraperitoneal tumors suggesting that heavy metal exposure promotes the epithelial-to-mesenchymal phenotype and bladder cancer progression.

PS 1327a Effects of Inorganic Arsenic on Metabolism-Related Gene Expression in the Zebrafish—Relevance of Exposure Windows and Treatment Doses

S. Kalasekar, C. W. McCollum, M. Bondesson and J. Gustafsson. *University of Houston, Houston, TX.* Sponsor: D. Zalko.

Diabetes Mellitus is a metabolic disorder characterized by aberrant glucose homeostasis. The Centers for Disease Control and Prevention reported that, in 2011, 8.3% of the population of the United States suffered from this condition, with 90-95% of all patients being affected with Type 2 Diabetes (T2D). T2D is characterized by hyperglycemia, insulin resistance and aberrant pancreatic β-cell function. Many risk factors have been associated with T2D, such as age, obesity, family history, and genetic polymorphisms. More recently, it has been suggested that chemicals in the environment can contribute to the disease.
Arsenic is a widespread toxic chemical found in ground and drinking water, and has been correlated with diabetes risk in millions of people worldwide. Although some experimental studies suggest a link between arsenic exposure and diabetes, most of these studies investigate the effects of arsenic at high concentrations, and vary in the chosen exposure windows considerably.
Zebrafish are vertebrates very similar to humans genetically and physiologically. In our studies, we used the zebrafish as a model organism to take a closer look at arsenic as a potential diabetogen. Zebrafish embryos/larvae were exposed to arsenic at different developmental stages, and sacrificed for gene expression analyses. Treatment doses included very low, environmentally relevant concentrations, as well as higher concentrations. Our data shows that different doses and windows of arsenic exposure can affect the expression of genes related to carbohydrate metabolism in the zebrafish. Therefore, determining appropriate exposure windows and doses is critical for determining arsenic toxicity.

PS 1327b Effect of Three-Week Exposure of Manganese Chloride on Motor Activity and Metal Homeostasis in Rats

D. Saputra[2, 1], J. Chang[3], J. Kim[3] and K. Lee[1, 2]. *[1]Korea Institute of Toxicology, Jeongeup, Republic of Korea, [2]University of Science and Technology, Daejeon, Republic of Korea and [3]Pharmaceutical Sciences, Northeastern University, Boston, MA.*

Manganese neurotoxicity with Parkinson-like symptoms, called as manganism, has been observed in welders. Toxicity and transport of Mn can be modulated by body iron status. Conversely, manganese exposure can alter the body iron stores, leading to impaired iron homeostasis. In this study, investigation of manganese-associated motor activity, iron status, and metal brain deposition was performed by $MnCl_2$ aerosol exposure in SD rats. Rats (male, n=12) were exposed 4 hr/day for 3 weeks (13 exposures) to $MnCl_2$ (1.2 μm, 39 mg/m^3). Motor activity was assessed at the 2nd day after last exposure by rotarod test. Between exposure and control group, there was no significant difference in motor-related parameters. Brain, liver, and serum were collected. No body weight loss was observed. Liver and serum non-heme iron levels did not show any difference. Olfactory bulb, prefrontal cortex, and striatum were analyzed for Mn, Fe, Cu, and Zn levels. While other metal levels were not influenced, increased Mn levels were observed with significant differences compared to controls. There was a decreasing gradient from olfactory bulb to striatum of brain. This pattern is different to other intra-peritoneal injection or tracheal instillation. In latter case, Mn deposition showed higher level in striatum than in other parts of brain, probably due to blood-brain transport after pulmonary absorption to blood. Our study supports the idea that inhaled manganese transport occurs through olfactory pathway to the brain. The current study showed Mn deposition in the brain but did not show motor activity changes. It should be noted that other metal levels in the brain were not altered. Serum and liver non-heme iron showed no significant difference. Taken together, Mn exposure of 39 mg/m^3 does not alter motor activities, systemic iron status, and brain metal homeostasis in this experimental condition.

PS 1327c Fetal Arsenic Exposure As a Possible Contributor to Metabolic Syndrome Onset in Mice

P. Sanchez Soria, D. Broka, R. N. Hardwick, N. J. Cherrington and T. D. Camenisch. *College of Pharmacy,, Tucson, AZ.*

Exposure to environmental arsenic is a major concern in the United States and worldwide. Arsenicals have been associated with a number of diseases, including cardiovascular and metabolic diseases. Environmental exposures to toxicants throughout fetal development play a critical role as triggers of adult disease. This study aims at evaluating the contribution of fetal arsenic exposure to the onset of metabolic syndrome. Swiss Webster mice were exposed to either 100 ppb sodium arsenite or sodium chloride via the dam's drinking water from embryonic day

6 until birth. Mice were maintained on normal chow and water for 36 weeks. Weight and metabolic end-points were evaluated throughout the study. Blood plasma analysis demonstrated that in-utero (IU) arsenic-exposed mice exhibited a significant increase in blood glucose levels between weaning age and 4 months of age, remaining elevated after 8 months. On the other hand, glucose levels in control mice did not change over time. Similarly, IU arsenic-exposed mice showed a consistent elevation in total cholesterol, as well as LDL cholesterol at weaning age, 4 months and 8 months of age, when compared to control mice. Further analysis demonstrated the development of nonalcoholic fatty liver disease in IU arsenic-exposed mice, as evidenced by major morphological changes and an increase in steatosis concomitant with hepatocellular ballooning. Growth rates were not statistically different; however, IU arsenic-exposed mice showed a trend of heavier weights when compared to control mice. Taken together, these results suggest that IU arsenic exposure is a possible contributor to metabolic syndrome onset in mice.

PS 1327d Biological and Behavioral Modifiers of Urinary Arsenic Metabolic Profiles in a US Population

D. J. Thomas[1], E. E. Hudgens[2] and J. Rogers[3]. *[1]ISTD, NHEERL, U.S. EPA, Research Triangle Park, NC, [2]EHPD, NHEERL, U.S. EPA, Research Triangle Park, NC and [3]Westat, Rockville, MD.*

Relations between intensity of arsenic exposure from home tap water and levels of inorganic As (iAs) and its mono- (MAs) and di-methylated (DMAs) metabolites were examined in urine from 903 individuals ≥ 45 years of age who resided in Churchill County, Nevada, continuously for 5 or more years. Over a wide range of exposures (home tap water supplies contained <3 to 1200 μg of As per liter), concentrations of iAs, MAs, and DMAs strongly correlated with concentrations of As in home tap water. However, percentages of the summed iAs, MAs, and DMAs concentrations in urine accounted for by each species were unaffected by home tap water As concentration, suggesting that capacity for formation and excretion of methylated metabolites was not exceeded. Mean urinary iAs, MAs, and DMAs concentrations were significantly lower ($P<0.001$) in urine of women than in men; women had significantly lower iAs and MAs ($P<0.005$) and significantly higher DMAs percentages ($P<0.0001$) in urine than men. Age did not affect concentration of any arsenical in urine, although there were significant age-related trends for decreased iAs percentage ($P<0.0002$) and increased DMAs percentage ($P<0.01$). Body mass index (BMI) did not affect iAs, MAs, or DMAs levels in urine but BMI was significantly associated ($P<0.01$) with lower MAs percentage and increased DMAs percentage. Smoking status (assessed by urinary cotinine levels) was associated with significant trends for urinary iAs, MAs, or DMAs concentrations and for iAs, MAs, or DMAs percentages ($P<0.05$). These results indicate that among older Americans with a wide range of exposure to iAs from home tap water, both biological factors (gender, age, BMI) and behavioral factors (smoking) can affect profiles of arsenicals found in urine. These modifiers may contribute to interindividual and interpopulation variation in response to chronic exposure to As from water and other media. (This abstract does not reflect U.S. Environmental Protection Agency policy.)

PS 1327e Exposure Assessment to Arsenic by Total Arsenic and Speciation Analyses in Urine of Korean Adults

J. Park[1], H. Bae[1], D. Kang[1], D. Kim[1], B. Choi[1], K. Park[2], H. Lim[3], S. Eom[4], H. Kim[4], S. Oh[5] and H. Kwon[6]. *[1]College of Medicine, Chung-Ang University, Seoul, Republic of Korea, [2]Nano-Photonics Research Center, KIST, Seoul, Republic of Korea, [3]Neodin Medical Institute, Seoul, Republic of Korea, [4]College of Medicine, Chungbuk National University, Cheongju, Republic of Korea, [5]College of Human Ecology, Kyung Hee University, Seoul, Republic of Korea and [6]College of Medicine, Dankook University, Cheonan, Republic of Korea.*

Arsenic has been known a human carcinogen, which is widely distributed in the environment. This study was performed to evaluate the exposure level to arsenic in Korean adults. Diet intake and urine sample were obtained from 2,117 study subjects older than 19 years of age. Human exposure to the arsenic was assessed by using the concentrations of total arsenic and arsenic species such as As+5, As+3, MMA, DMA, arsenobetaine in urine. The estimation of diet intake was performed by using the data of individual food consumption from a 24 hrs recall study. Daily diet intake was estimated at 1,373.6 g. The geometric mean concentration of total arsenic in urine was 97.6 μg/L, which was determined by ICP-MS method. The speciation analysis of arsenic in urine was followed by using HPLC-ICP-MS method. Arsenobetaine was the most abundant species in urine. The geometric mean concentrations of arseinc species were 41.36 μg/L of arsenobetaine, 24.72 μg/L of DMA, 1.42 μg/L of MMA, 0.52 μg/L of As5+ and 1.42 μg/L of As3+. The significant relations were observed between fishes/shellfishes intakes and total arsenic and some species of arsenic such as arsenobetaine and DMA. And the consumption of seaweeds showed a positive relation with As3+ and DMA but not arsenobetaine. These findings suggest that the seafood might be a one of major source to the arsenic exposure in Korean adults.

PS 1327f The Roles of Sirt3/FOXO3a/MnSOD in Arsenic-Inhibited Insulin Stimulated Glucose Uptake in 3T3L1 Adipocytes and C2C12 Myotubes

D. Sasidharan Padmaja[1], P. Poyil[1, 2], X. Shi[1, 2] and Z. Zhang[1]. *[1]Graduate Center for Toxicology, University of Kentucky, Lexington, KY and [2]Center for Research on Environmental Disease, University of Kentucky, Lexington, KY.*

Chronic human exposure to inorganic arsenic (iAs) compounds, a potent environmental oxidative stress inducer, have been found to cause insulin independent type 2 diabetes mellitus (T2DM). The mechanisms underlying the diabetogenic effects of iAs is poorly understood. T2DM is characterized as insulin resistance in insulin-sensitive peripheral tissues, such as myotubes and mature adipocytes bearing an imbalance in the glucose homeostasis via inhibiting insulin-stimulated glucose uptake (ISGU). To investigate the role of oxidative stress in As-induced T2DM, both 3T3L1 adipocytes and C2C12 myotubes were chronically exposed to inorganic arsenic (iAsIII) for 8 weeks. The results show that iAs treatment significantly decreased ISGU. A decrease in the mitochondrial oxygen consumption rate (OCR), an increase in ROS production and a decrease in the mitochondrial membrane potential in iAs-treated 3T3L1 adipocytes and C2C12 myotubes were observed. Sirtuin3, a mitochondrial deacetylase was dramatically decreased along with its associated transcription factor of the forkhead family, Foxo3a upon iAs treatment. Further study finds that reduced Foxo3a activity by iAs exhibited a decreased binding affinity with the promoter binding site of manganese superoxide dismutase (MnSOD), an important mitochondrial antioxidant enzyme. Overexpression of Sirt3/MnSOD increased ISGU reduced by iAs, leading to amelioration of iAs-induced T2DM. Our results suggest that Sirt3/Foxo3a/MnSOD signaling plays a significant role in the inhibition of ISGU induced by chronic arsenic exposure.

PS 1328 Altered miRs Expression in hVM1 Cells Arsenic-Exposed during Differentiation

K. González-Palomo, C. Castillo, M. Jiménez-Capdeville and M. Salgado. *Facultad de Medicina-Departamento de Bioquimica, Universidad Autónoma de San Luis Potosi, San Luis Potosi, San Luis Potosi, Mexico.*

Although arsenic toxicity had been extensively studied and a number of its main effects identified, emerging reports point to new molecular targets and mechanisms of toxicity. Among them, epigenetic mechanisms seem to play a central role in the wide effects displayed by several xenobiotics, toxics and pollutants. Arsenic exposure alters DNA metyltransferase enzymes expression and activity, which is associated with whole-genome and gene specific methylation changes. In animal models, both hypometylation and hypermethylation of gene promoters associated with memory formation and learning have been demonstrated. Since there are controversial reports about arsenic-induced DNMT modifications, it is of interest to know whether arsenic influences other epigenetic players. Recently, microRNAs are considered among the main epigenetic factors through the post-transcriptional inhibition of several molecular targets and the regulation of physiological processes. This study was performed to know whether cell line of human neural stem cells derived from ventral mesencephalon (hVM1) exposed to arsenic during differentiation display alterations of miR-125b, 148a and 132 expression. Also, we wanted to know whether those changes would be associated with Nestin, CREB, BNDF and DNMT3b gene expression, using real time RT-PCR method. Statistically significant changes were observed in miR-125b and miR-148a expression level. Although hVM1 cells exposed to arsenic have a trend to down-regulation of miR-132, this effect was not statistically significant. Gene expression of the target proteins was significantly altered in exposed cultures. However, Nestin showed a negative correlation with miR-125b and that may have physiological interpretation. In conclusion, these results support that arsenic exposure induces changes of key microRNAs expression and therefore could affect neural differentiation in hVM1 cells.

PS 1329 Exposure to Manganese during Development Induces Lasting Motor and Cognitive Impairment in Rats

T. V. Peres[1, 3], H. Eyng[1], S. C. Lopes[2], D. Colle[1], F. M. Gonçalves[1], D. K. Rieger[1], A. Costa[1], M. W. Lopes[1], M. Farina[1], R. D. Prediger[2], M. Aschner[3] and R. B. Leal[1]. *[1]Departamento de Bioquímica, Universidade Federal de Santa Catarina, Florianópolis, SC, Brazil, [2]Departamento de Farmacologia, Universidade Federal de Santa Catarina, Florianópolis, SC, Brazil and [3]Department of Molecular Pharmacology, Albert Einstein College of Medicine, New York City, NY.*

Manganese (Mn) is an essential element, however exposure to high Mn levels may affect structures of the basal ganglia, leading to motor impairment similar to Parkinson's disease. The molecular mechanisms underlying Mn neurotoxicity, particularly in the developing central nervous system (CNS), need further investigation. Our goal was to investigate whether early-life exposure to Mn affects motor coordination and cognitive function in adulthood. Male Wistar rats were exposed to saline (control) or intraperitoneal MnCl2 (5, 10 or 20 mg/kg) injections from post-natal day (PND) 8 up to 12. Behavioral tests were performed on PND 60-63. Motor coordination was assessed in the rotarod. Object recognition task was used to evaluate short-term memory. Biochemical analysis of the striatum was performed on PND70. Rats exposed to 10 and 20 mg/kg Mn performed significantly worse on the rotarod apparatus compared to controls ($p<0.05$), establishing motor coordination impairment. Rats exposed to the highest Mn dose failed to recognize a familiar object when replaced by a novel object ($p<0.05$), attesting memory impairment. These effects were accompanied by decreased levels of non-protein thiols, e.g. glutathione ($p<0.05$), and increased levels of glial fibrillary acidic protein (GFAP) ($p<0.05$) in the striatum. This study documents that acute low-level exposure to Mn during critical neurodevelopmental period induces cognitive and motor dysfunctions that last into adulthood.
Supported by: CNPq, FAPESC, CAPES, FINEP. Travel support provided by CAPES Foundation – Ministry of Brazil

PS 1330 Chronic Developmental Exposure to Environmental Manganese (Mn) Reduces Rat Striatal and Cortical Dopaminergic Activity in Adulthood

S. M. Lasley[1], C. A. Fornal[1], S. Mandal[1], B. J. Strupp[2], S. A. Beaudin[3] and D. Smith[3]. *[1]U. Illinois Coll. Med., Peoria, IL, [2]Cornell U., Ithaca, NY and [3]U. California, Santa Cruz, CA.*

Compelling evidence exists that neurobehavioral function in children may be adversely affected by elevated Mn exposure. However, little is known of the neuronal mechanisms that may underlie the effects of early life exposure on neuromotor and cognitive deficits in adulthood. We assessed biogenic amine activity in striatum and prefrontal cortex of rats exposed chronically to Mn during early development or continuously to adulthood. Rat pups were orally exposed to 0, 25, or 50 mg Mn/kg/day from PN 1-21, or from PN 1 throughout life (N=8-12/group). In adulthood guide cannulae were implanted in striatum and cortex, and 3-5 days later microdialysis probes were inserted and perfused with a modified Ringer's solution. After allowing time for basal analyte concentrations to stabilize, perfusion was switched for 60 min to 120 mM K+ to depolarize the tissue, then perfusion was returned to the modified Ringer's. Collected fractions were analyzed by HPLC. At the time of microdialysis brain Mn values in the Early Life 25 and 50 groups were not different from controls (2.06 ug/g tissue), while Mn levels in the Lifelong 25 and 50 groups were increased by 11 and 23% over controls, respectively. Basal (pre-stimulus) extracellular levels of DOPAC were decreased 45 and 43% in the Early Life 50 and Lifelong 25 groups, respectively, compared to controls. Furthermore, extracellular dopamine (DA) was significantly diminished compared to Control values at 20 and 40 min after initiation of high K+ in the Early Life 25, Early Life 50, and Lifelong 25 groups with the latter being most affected. Reduced cortical DA responses were also found in both Lifelong groups. These findings are consistent with fine motor function deficits seen with these same treatments, which were most pronounced in the Lifelong 25 group (Beaudin et al., 2013). Collectively, these results define the negative impact of chronic exposure to environmentally relevant levels of Mn on CNS dopaminergic function. (Supported by ES018990)

PS 1331 Methylmercury Induces a Muscle-Specific Notch Target Gene and Disrupts Neuromuscular Development in the Embryo

M. D. Rand, G. Engel and A. Delwig. *Environmental Medicine, University of Rochester, Rochester, NY.*

Methylmercury (MeHg) is known to elicit neurological deficits in both motor and cognitive functions subsequent to prenatal exposure. The specificity of MeHg for neural targets that in turn compromise motor function is not completely understood. Studies in mammalian and insect cells have shown that MeHg induces expression of Notch pathway target genes, notably the Enhancer of split m-delta (E(spl)mδ) gene. Our earlier studies demonstrate that MeHg induction of E(spl)mδ occurs independent of the Notch receptor and thus may directly influence neural development. In this study we characterize E(spl)mδ expression in the Drosophila embryo under the influence of MeHg exposure. We show that MeHg specifically induces E(spl)mδ in vivo relative to other Notch target genes. MeHg-induced E(spl)mδ expression is not a by-product of a general stress response or a shift in developmental timing. MeHg also elicits phenotypes in the embryonic intersegmental and segmental motor nerves. However, genetic manipulations targeting expression of E(spl)mδ specifically to neurons does not elicit a motor nerve outgrowth phenotype. We now show that MeHg also evokes perturbations in embryonic muscle patterning. Furthermore, using a GFP reporter construct it is seen that E(spl)mδ expression localizes to specific subsets of the developing lateral and dorsal musculature that are innervated by the segmental and intersegmental motor nerves. Ectopic expression of E(spl)mδ in embryonic muscle has profound effects on muscle patterning and causes a segmental nerve phenotype similar to MeHg treatment. In contrast, targeting expression of the closely related Notch target gene Enhancer of split m-gamma (E(spl)mγ) to developing muscle shows no embryonic phenotype, whereas E(spl)mγ targeted to neurons is embryonic lethal. In summary these data highlight a novel mechanism whereby MeHg can engage the activity of a specific Notch pathway target gene to alter coordinated development of muscles and motor neurons.
(Funded by NIEHS R01 ES015550 and R03 ES021581 awarded to M.D.R.)

PS 1332 Genome-Wide Association Study of Methylmercury Tolerance and Susceptibility: Beneficial Effects of Caffeine

S. L. Montgomery, D. Vorojeikina and M. D. Rand. *Environmental Medicine, University of Rochester, Rochester, NY.*

Methylmercury (MeHg) is a persistent environmental toxin that humans are exposed to primarily through the consumption of fish and seafood. In a number of population studies the extent of MeHg toxicity varies among individuals despite similar levels of exposures, indicating that genetic differences play a role in MeHg tolerance and susceptibility. Furthermore, findings in a major epidemiological study in the Seychelles indicate diet and nutrition largely influences MeHg toxicity. Explicit dietary effects on MeHg toxicity can be seen with caffeine supplementation in a defined *Drosophila* developmental toxicity assay. To examine how genetic variation and dietary factors impact MeHg tolerance we employed a model organism with the *Drosophila* Genetic Reference Panel (DGRP) consisting of 192 genome-sequenced wild-caught inbred strains. We used the DGRP lines to perform a GWA study of MeHg tolerance on development (eclosion assay) in the presence and absence of caffeine. Genotype-phenotype association analyses for total eclosion on MeHg- and/or caffeine- containing medium were assessed on nearly 2.5 million SNPs using the DGRP webtool readily available to *Drosophila* investigators. We find that eclosion rates across 176 lines exhibits variance indicative of a quantitative trait for each treatment condition. Furthermore, caffeine alone, exhibits a slight overall toxic effect; however, for a majority of the DGRP lines, co-exposure with MeHg+caffeine rescues the observed MeHg-mediated toxicity. Preliminary analyses of the SNP association indicate between 50-150 genes significantly associated with the eclosion trait under MeHg or caffeine alone and MeHg+caffeine treatments. Several biological functions are revealed including nuclear functions such as transport and chromatin regulation. Validation of a number of these identified candidate genes is in progress. These results provide groundwork for future functional and translational experiments examining genes involved in MeHg toxicity.
(Funded in part by NIEHS R21ES019954)

PS 1333 Non-Linearity and Enhancement by Prenatal Stress of Developmental Methylmercury-Induced Neurochemical Changes

H. Weston, J. L. Allen, D. Weston, K. Conrad, S. Pelkowski, M. Sobolewski and D. A. Cory-Slechta. *Environmental Medicine, University of Rochester Medical School, Rochester, NY.*

Methylmercury (MeHg), through contamination of diet, and stress are co-occurring risk factors, share biological substrates, including the hypothalamic-pituitary-adrenal axis and brain mesocorticolimbic dopamine/glutamate systems, and can produce common adverse effects, including cognitive deficits. Collectively, these conditions suggest that MeHg effects could be enhanced by stress, particularly prenatal stress (PS) given the vulnerability of the fetus to MeHg. Rat dams were exposed to 0, 0.5 or 2.5 ppm MeHg chloride in drinking water from 2.5 weeks prior to breeding to weaning; a subset of each MeHg group also received restraint stress on gestational days 16-17. At 2 mos, corticosterone, total blood and brain Hg, and regional brain monoamine changes (frontal cortex, hippocampus,

nucleus accumbens, striatum, hypothalamus, olfactory bulb) were evaluated in one pup/gender/litter to preclude litter effects. Blood and brain Hg increased with increasing MeHg exposure; corticosterone levels were not influenced by MeHg or PS. Instances of non-linear monoamine concentration-effect curves with MeHg occurred in virtually every brain region, particularly in females, with alterations at 0.5 ppm, but not at 2.5 ppm. Further, multiple monoamine changes were seen only in the presence of MeHg + PS, particularly in striatum and frontal cortex in males, and hippocampus and nucleus accumbens in females. In females, MeHg+PS reduced hippocampal monoamines, and increased nucleus accumbens and olfactory bulb monoamines, whereas MeHg+PS decreased frontal cortex and striatum monoamines males. These results demonstrate that PS can enhance the neurotoxicity of MeHg. Consequently assessment of neurotoxic risk in the absence of PS may underestimate its hazardousness. These findings underscore the need to develop animal models more reflective of the multiplicity of risk factors in the human environment . Further, the non-linearity of MeHg effects raises concerns in relation to human health risk assessment. EPA RD 83457801

PS 1334 Preliminary Characterization of Neuroantibody (NAb) Associations with Hg and PCB in 7-Year-Old Faroese Children with Prenatal Exposure to Seafood Neurotoxicants

C. Osuna[1], P. Weihe[2], P. Grandjean[1, 3] and H. A. El-Fawal[4]. [1]*Harvard School of Public Health, Boston, MA,* [2]*Faroese Hospital System, Tórshavn, Faroe islands,* [3]*Institute of Public Health, University of Southern Denmark, Odense, Denmark and* [4]*Neurotoxicology Laboratory, Albany College of Pharmacy and Health Sciences, Albany, NY.*

Preclinical studies of neurotoxicity and human studies of neurodegeneration suggest that NAb may be useful biomarkers of insult. In a proof-of-concept study, archived sera from 38 children at the age of 7 (16 males; 22 female) were randomly selected from a birth cohort established in 1986-1987 as part of the Children's Health and the Environment in the Faroes. Maternal hair-Hg [MHg; geometric mean (IQR); 5.8 (2.6-10.9)μg/g], cord blood-Hg [CordHg;31.4(11-64)μg/L] and cord blood-PCB [CordPCB;2.0(1.3-2.9)μg/L], indicators of prenatal exposures, and blood-Hg [Hg7;1.3(5.5-22.8)μg/L] and serum-PCB [PCB7;1.6(0.97-2.9)μg/L] at the age of 7, current exposure indicators, were used. Titers of IgM and IgG against neurofilament (NF-L; NF-M; NF-H), cholineacetyltranferase (ChAT), GFAP, MBP, desmin (D) and actin (A) were measured. Positive associations (r=0.3-0.5; p<0.01) were observed for IgM titers against NF-L, NF-H, GFAP, MBP (and IgG), ChAT and A with Hg7. Higher titers of anti-NF-H and MBP, IgG, and anti-A and D, IgM, in girls were not significant (p=0.06-0.09). Stratification by MHg (< or >10 μg/g) or CordHg (< or >60 μg/L) indicated higher anti-NF-M and GFAP, IgM, while stratification by Hg7 (< or >10 μg/L) indicated higher anti-NF-L, NF-M, GFAP, MBP, ChAT and D, IgM, and anti-NF-M and GFAP, IgG (p<0.05) at higher exposure. Differences in anti-NF-M, GFAP, ChAT and D, IgM, and GFAP, IgG, occured at higher levels of PCB7(< or >10 μg/L). Multivariate regression indicated that Hg7 is the major determinant of NAb. After controlling for CordHg, CordPCB, and PCB7, 8 of 16 NAbs were significantly positively associated with Hg7. Taken together, this study suggests that NAb may be useful biomarkers of NS insult resulting from Hg exposure. This warrants further testing in a larger cohort with the incorporation of neurobehavioral assessment.

PS 1335 Ontogeny of Fc-Gamma Receptors in the Developing Rat Brain

P. Lein and M. Stamou. *Molecular Biosciences, School of Veterinary Medicine, UC Davis, Davis, CA.*

Immunoglobulin G (IgG) antibodies that cross-react with intracellular antigens in the developing brain have recently been identified in an experimental animal model of developmental mercury toxicity and in mothers at risk for having a child with autism. But whether these autoantibodies interfere with neuronal development remains controversial, in part because it is not clear how IgG would access an intracelullar neuronal target. Fcγ receptors (FcγR) bind the constant (Fc) region of immunoglobulin G (IgG), and mediate uptake of IgG and cellular responses triggered by IgG binding in immune cells. This raises the question of whether neurons in different brain regions also express functional FcγR. Investigation of FcγR expression by RT-PCR indicated that transcripts of FcγRI, FcγRIIa, FcγRIIb, FcγRIII and the neonatal FcRn are expressed in the cortex, hippocampus and cerebellum of naïve male and female rat pups on postnatal days (PND) 2 and 7, but at lower levels than in the liver and spleen. Transcript levels did not vary significantly as a function of sex or age, with the following exceptions: (i) FcγRIIa and FcγRIII were downregulated by PND7 in the spleen but not in brain or liver; (ii) FcRn was upregulated in the cerebellum but downregulated in the spleen at PND7 compared to PND2. To determine cell-specific expression, we also performed RT-PCR of these five FcγR isoforms in primary cultured cortical and hippocampal cells. All five transcripts were detected in both cell culture models at days *in vitro* ranging from 2 to 21. Immunocytochemical analysis indicates that FcγRI and FcγRII are predominantly expressed in neurons; whereas FcγRII FcγRIII and FcRn are predominantly expressed in astrocytes. We are currently designing assays to assess whether these receptors are functional in neurons. In summary, our data confirm that FcγR are expressed at the transcript and protein level in neurons and glial cells in different regions of the rat brain during neurodevelopment. This work supported by NIH grants R01 ES014901 and P42 ES04699.

PS 1336 Developmental Lead Exposure and the Exacerbation of Alzheimer's Pathology: An Immunological Analysis

A. vonderEmbse, D. Johnson, J. N. Franklin, Q. Hu and J. DeWitt. *Physiology and Toxicology, Brody School of Medicine, East Carolina University, Greenville, NC.*

Although Alzheimer's disease (AD) is typically a late-onset neurodegenerative disorder, there may be a period of susceptibility early in brain development which, if disrupted, may exacerbate the disease pathologies. We hypothesize that early exposure to a known neurotoxic and immunotoxic chemical, such as lead acetate, may alter microglia function and/or phenotype during this critical window of development, which then promotes amyloidosis or decreases microglia phagocytosis of amyloid-β, the protein associated with AD neuropathology. The exact mechanism by which microglia are involved with amyloid-β deposition or removal is currently contested in the scientific literature, although there is significant evidence for the colocalization of microglia and amyloid-β plaques. We investigated this "double-hit" model of the concurrent effects of environmental toxicant exposure and critical windows of development susceptibility through the use of a genetically predisposed triple transgenic mouse model (3XTgAD). Pups were orally gavaged with 100 parts per million of lead acetate and vehicle from postnatal day (PND) 5-15, a known postnatal period of vulnerability for microglia. At PND50, 90, and 180, hippocampus was isolated from brains of treated and control animals and stored for future analysis of microglia colocalization with amyloid-β. The remaining brain tissue was processed to measure microglial activity by flow cytometry. Activity of microglia from treated animals was increased relative to control animals. These initial data suggest that early-life exposure to an environmental agent, when given during a critical window of microglia maturation, changes microglial activity. We believe that these changes in activity alter the course of AD neuropathologies.

PS 1337 Chronic Lead Exposure during Early Development Alters Synaptogenesis and Synaptic Function through Inhibiting Wnt7a Activity

H. Wang, F. Hu and L. Xu. *School of Biotechnology and Food Engineering, Hefei University of Technology, Hefei, Anhui, China.* Sponsor: D. Fox.

Lead exposure has been implicated in the impairment of synaptic transmission and plasticity in the developing hippocampus. However, the mechanism remains unclear. Here we investigated whether chronic lead exposure during development affected hippocampal dendritic spine formation and synapse strength and if the Wnt signaling pathway was involved. Sprague–Dawley rats were exposed to lead only during lactation. The lead-exposed pups acquired lead via milk of dams whose drinking water contained 0.2% (1090 ppm) lead acetate from parturition to weaning, while the control dams remained on distilled water throughout the lactation period. Hippocampal lead accumulated significantly in lead-exposed rats (0.471 ± 0.11μg/g) compared with the controls (0.021 ± 0.002μg/g). Golgi-Cox staining method was used to examine the spine density of hippocampal CA1 pyramidal neurons in postnatal (PN) 14 and PN21 rats. Lead significantly down-regulated the spine density in both age groups. This was accompanied by a significant age-dependent decline of Wnt7a expression and stability of its downstream protein following chronic lead exposure. Furthermore, in cultured hippocampal neurons lead (0.1 and 1μM lead acetate) significantly decreased the spine density in a dose-dependent manner. Exogenous Wnt7a application restored the frequency of miniature excitatory postsynaptic currents (mEPSCs) in the Pb2+-treated cultures back to control levels. Additionally, the lead-induced decrease in the spine density was attenuated by Wnt7a, which also increased the stability of the downstream molecules in the Wnt signaling pathway. Our results suggest that lead negatively impacted spine growth and synaptic transmission of the developing hippocampus through alteration of the presynaptic Wnt7a signaling.(Supported by the National Key Basic Research Program of China (973 Program, No. 2012CB525003).)

PS 1338 Lead-Induced Alterations within the Excitatory GABAergic Pathway during Early Embryonic Zebrafish Development

S. Wirbisky, G. J. Weber, J. Lee, J. R. Cannon and J. L. Freeman. *Purdue University, West Lafayette, IN.*

Lead (Pb) is a non-essential toxic heavy metal; its use in industrial applications is widespread and has resulted in an increased risk of human environmental exposure. Multiple organs are targets of Pb toxicity; however, the central nervous system (CNS) is most sensitive during early development due to rapid cell proliferation and migration, axonal growth, and synaptogenesis. One of the primary components of CNS development is the GABAergic system. Gamma-aminobutyric acid (GABA) is the primary inhibitory neurotransmitter in the adult brain. However, during early development GABA functions as an excitatory neurotrophic factor which contributes to cell proliferation, neuronal differentiation and migration, and synaptogenesis. Studies report the effects of Pb on GABA in the mature brain, but little is known regarding the adverse effects of Pb exposure on the GABAergic system during embryonic development. To characterize the effects of developmental Pb exposure on the GABAergic system, zebrafish embryos were exposed to 10, 50, or 100 ppb (μg/L) Pb or a control treatment shortly after fertilization through 24, 48, 60, or 72 hours post fertilization (hpf). A dose-response was observed between Pb exposure and tissue uptake in zebrafish larvae. Genetic analysis showed that developmental Pb exposure caused either an increase or a decrease in mRNA expression of seven genes (gad2, gad1b, gabra1, gabbr1a, gat-1, gat-3, vgat) throughout the GABAergic pathway that was developmental time point and dose specific. GABA levels were analyzed and also revealed dose and time point specific alterations. These data provide evidence indicating that changes in gene expression throughout the GABAergic pathway do not cause similar immediate alterations in GABA levels and that the compensatory response of the GABAergic system is highly dependent upon dose and developmental time point. These data provide a framework for further analysis of the effects of Pb on the GABAergic system during the excitatory phase and transition to an inhibitory neurotransmitter during development.

PS 1339 Selective Loss of Parvalbumin-Positive GABAergic Interneurons by Pb2+: Examining Early-Life Pb2+ Exposure As a Risk Factor for Schizophrenia

K. Stansfield, K. Ruby and T. R. Guilarte. *Environmental Health Sciences, Columbia University, New York City, NY.*

Schizophrenia is a devastating neuropsychiatric disease that affects 1-2% of the worlds' population. Schizophrenia has a neurodevelopmental origin in which genetic and environmental risk factors come together to precipitate a schizophrenia phenotype later in life, typically in adolescence. One of the most replicated neuropathological findings in post-mortem brain tissue from schizophrenia subjects and in animal models of the disease is the loss of Parvalbumin-positive (PV+) GABAergic interneurons in the cerebral cortex (Lewis et al., 2005; Nature Reviews Neurosci, 6, 312) and hippocampus (Zhang et al., 2002; Schizophr research, 55(1-2):1-10). We hypothesized that if early life Pb2+ exposure is an environmental risk factor for schizophrenia (Guilarte et al., 2012; Neurotoxicology, 33(3):560-74), then it should recapitulate the loss of PV+ GABergic interneurons in these brain regions.

At postnatal day 50, or late adolescence, Pb2+-exposed animals exhibited a loss of PV+ interneurons in the dorsolateral prefrontal cortex, the CA1-CA3 regions of the pyramidal cell layer of the hippocampus, and in the caudal aspects of the striatum relative to controls. The loss of PV+ interneurons in these brain regions was confirmed by western blot of PV protein. Consistent with the GABAergic phenotype of PV+ interneurons, we also confirmed a loss of glutamic acid decarboxylase-67 protein (GAD67) by western blot.

Importantly, Pb2+ exposure did not alter the levels of calbindin and calretinin protein levels, suggesting that these GABAergic interneuron phenotypes are not affected. These findings implicate a cause and effect relationship between chronic early life Pb2+ exposure and a neuropathology that is hallmark of the schizophrenic brain. [Supported by NIEHS grant number ES006189 to TRG]

PS 1340 Cumulative Effects of Maternal Lead Exposure, Prenatal Stress, and Early Behavioral Adversity on Subsequent Learning and Short-Term Memory

D. A. Cory-Slechta[1], H. Weston[1], J. L. Allen[1], D. Weston[1], S. Pelkowski[1], K. Conrad[1], M. Sobolewski[1] and T. R. Guilarte[2]. [1]*Environmental Medicine, University of Rochester Medical School, Rochester, NY and* [2]*Environmental Health Sciences, Columbia University Mailman School of Public Health, New York City, NY.*

Children's early behavioral experience has profound and enduring impacts on subsequent life trajectory. This study sought to determine how lead (Pb) exposure and prenatal stress (PS) effects on learning and short-term memory were influenced by an early behavioral history of 'adversity' (exposure to forced restraint and forced swim; FRFS) vs. 'attainment' (food-rewarded fixed interval (FI) behavioral performance). Offspring of rats exposed to 0 or 50ppm Pb drinking water from 2 mos prior to conception through weaning ± PS (dam restraint, gestational days 16-17) were subsequently exposed to either FRFS or FI conditions. All were then tested on a repeated learning (RL) paradigm requiring learning of 2 response sequences (7 sessions) and then 3 response sequences (14 sessions) for food reward, followed by a novel object recognition (NOR) paradigm. Blood Pb levels averaged 20 ug/dl at 5-6 days of age and <3 ug/dl at 30 days. In initial tests, depending upon the particular sequence, early adversity significantly impaired learning of 2 lever sequences in both sexes, and of 3 response sequence learning for males relative to FI experience. In females, some effects were most pronounced in FRFS + Pb + PS females. Similarly, the greatest impairments in NOR memory occurred in FRFS + Pb+PS females who showed the lowest levels of novel object contact time. While clear individual differences within groups were seen, group median values for novel duration index showed a type of cumulative stressor decline across behavioral experience and Pb+PS conditions, such that highest median values were seen in the FI no Pb, no PS females, and lowest values in the FRFS 50ppm PS females. Collectively, these findings suggest that early life behavioral adversity can further exacerbate the effects of developmental Pb + PS, thus resulting in a cumulative detriment. ES006189 (T. Guilarte).

PS 1341 A Weight-of-Evidence Evaluation of the Association between Lead Exposure and Autism Spectrum Disorders

H. N. Lynch, M. Seeley and B. D. Beck. *Gradient, Cambridge, MA.*

It has been suggested that exposure to lead, a neurotoxin associated with cognitive and behavioral deficits, may be a risk factor for autism spectrum disorders (ASD), including autistic disorder, Asperger's syndrome, and pervasive developmental disorder - not otherwise specified. The etiology of ASD has been heavily researched over the last decade due to the dramatic rise in prevalence of ASD, which increased by almost 80% between 2002 and 2008. In 2008, approximately 1 in 88 children aged 8 years old had ASD. While some of this increase is the result of diagnostic advancement and awareness, these factors may not be entirely responsible for the rise. The heterogeneous nature of ASD and the varying severity of its symptoms, which are characterized by problems with communication and socialization and atypical behaviors and interests, suggest there are likely several potential causal pathways involving genetics in combination with other physiological and environmental risk factors. We conducted a systematic, objective, and transparent weight-of-evidence (WoE) analysis of the available epidemiologic literature to determine whether there is a reliable association between in utero or early childhood exposure to lead and the development or exacerbation of ASD. Our analysis indicated that epidemiologic studies that reported positive associations between lead and ASD have primarily assessed exposure based on lead levels in either hair or urine. In contrast, we determined that studies that assessed exposure in whole blood or teeth have found that lead levels were similar in individuals with and without ASD. Because lead biomarkers in teeth and blood are more reliable than those in hair or urine for estimating exposure, we conclude that greater weight should be given to teeth/blood studies, where no associations have been found. Ecological studies, while limited due to the lack of individual level exposure data, also have found no association between lead and ASD. Overall, we conclude that the WoE indicates that lead exposure is not associated with the development or severity of ASD.

PS 1342 Exposure to Concentrated Ambient Ultrafine Particulate Matter during Postnatal Brain Development and/or Adulthood Elicits Lateral Ventricle Dilation, Sustained Neuroinflammation, and Neurochemical Disruption Preferentially in Male Mice

J. L. Allen, S. Pelkowski, D. Weston, H. Weston, M. Sobolewski, D. Herr, B. Palmer, G. Oberdoerster and D. A. Cory-Slechta. *Environmental Medicine, University of Rochester Medical School, Rochester, NY.*

Links between autism, schizophrenia, and cognitive decline and exposure to ambient air pollution have been reported. Ultrafine (<100nm) particles are considered the most toxic of ambient particulates. To determine potential neurotoxicity of concentrated ambient ultrafine particles (CAPS) to developing brain, mice were exposed to CAPS during the first two weeks of life and/or in adulthood (PND60). Notably, CAPS produced lateral ventricle dilation only in male mice with either postnatal or adult exposure; ventriculomegaly has been shown to be characteristic of autism and schizophrenia. A lack of changes to the Aqueduct of Sylvius suggests a non-obstructive mechanism such as neuroinflammation. Additionally, CAPS caused glial disruption and an inflammatory response: microglial activation was seen in males, while both sexes showed a time-dependent astrocytic response. CAPS altered brain cytokines in a sex- and time point-dependent manner. Consistent with a neuroinflammatory response, females showed a transient increase in striatal IL-6 24 hours after postnatal exposure, but this had resolved by adulthood. Both sexes exhibited a protracted neuroinflammatory response to CAPS, with midbrain IL-1β in males and TNFα in females increased following postnatal only CAPS when brains were examined in young adulthood. CAPS also produced multiple changes in brain monoamine and amino acid neurotransmitters that were dependent on sex, timing of exposure, latency between exposure and sacrifice, and brain region. These included disruption of mesocorticolimbic monoamines and, in males, increased hippocampal glutamate, consistent with potential excitotoxicity. Thus, low level CAPS can produce neuropathology preferentially in males, with greater vulnerability during the postnatal period, that is consistent with features of profound neurodevelopmental disorders. ES019105

PS 1343 Gestation-Only Trichloroethylene Exposure Promotes Neural Oxidative Stress and Adverse Behavior in Association with Peripheral Immune Activation in Male Offspring

S. J. Blossom, G. Chandler and S. B. Melnyk. *Pediatrics, UAMS College of Medicine, Little Rock, AR.*

Mice exposed to trichloroethylene (TCE) postnatally from birth until 6 weeks of age demonstrated impaired glutathione redox homeostasis and increased biomarkers of oxidative stress in the brain and plasma. Here we confirm and extend these findings in mice exposed to TCE during gestation only. Similar to postnatal-only exposure, a targeted metabolomics analysis in gestation-only exposed mice revealed comprised glutathione redox disequilibrium and behavioral alterations characterized by increased locomotor and exploratory activity in male offspring at postnatal day (PND) 42. Accordingly, this TCE exposure induced a significant and dose-dependent increase in tyrosine oxidative end products including 3-nitrotyrosine in PND42 male offspring. 3-chlorotyrosine, an indicator of oxidative stress generated by immune activation, was also significantly elevated in the plasma of TCE exposed offspring. Because this result suggested that an immune component may be an important contributor to the neurotoxic effects observed in our model, peripheral CD4+ T cells, well-characterized targets of TCE immunotoxicity, were evaluated for a panel of inflammatory mediators. Gestational TCE exposure induced a dose-dependent increase in IFN-γ and IL-17 commensurate with a decrease in anti-inflammatory IL-10. These results point to the gestational phase as a critical window of TCE toxicity. Further study is needed to understand the relationship between peripheral immune dysregulation and neurotoxicity with developmental TCE exposure and whether or not epigenetic processes play a role.

PS 1344 The Effects of Bisphenol A on the Dopamine System in a Developing Rat Brain and a Rat Pituitary Cell Line

B. Nowicki[1], G. Robinson[2], M. Hamada[2] and D. Jones[2]. [1]*CHS, Midwestern University, Glendale, AZ and* [2]*AZCOM, Midwestern University, Glendale, AZ.*

Bisphenol-A (BPA) is an organic compound that has been increasingly used in the manufacturing of various consumer products. BPA is considered an environmental estrogen, which appears to disrupt the brain's dopaminergic system. In this study we utilized both in-vitro and whole animal models to examine the effects of BPA on the brain's dopamine (DA) system. GH3 cells, a rat pituitary cell line, were used to investigate the effects of BPA on cellular localization of the dopamine transporter (DAT) and DA-mediated cell signaling. Using western immunoblot analysis and measuring the ratio of membrane vs. cytosolic DAT protein it was shown that BPA altered normal DAT localization. Immunoblot and ELISA analysis was used to examine the effects on proteins (pERK and prolactin) involved in DA-mediated cell signaling. First, BPA increased pERK levels in a concentration-dependent manner as demonstrated with an ELISA kit. Moreover, this effect was attenuated when cells were pre-treated with a D2 receptor antagonist. Second, prolactin release is regulated, in part by DA; consequently, it may be affected by exposure to BPA. Immunoblot analysis of intracellular and extracellular prolactin levels indicated that BPA altered the normal release of prolactin in a DA D2 receptor-dependent manner. In addition to studies conducted in GH3 cells, an animal model (Sprague Dawley rats) was used to investigate the effects of developmental exposure to BPA on DA turnover. High performance liquid chromatography (HPLC) was used to measure the levels of DA and its metabolites. Using striatal tissue from rat pups developmentally exposed to BPA through maternal transfer, it was demonstrated that chronic exposure to BPA during the developmental period increased DA turnover. These results indicate that exposure to BPA appears to enhance DA neurotransmission and turnover which may play a role in cognitive deficits associated with the DA system.

PS 1345 Bisphenol A-Induced Neurotoxicity in the Developing Rat Pup and a Pituitary Cell Model

J. Olson[1], E. Faucheu[1], J. Trinh[2], M. Hamada[2] and D. Jones[2]. [1]*CHS, Midwestern University, Glendale, AZ and* [2]*AZCOM, Midwestern University, Glendale, AZ.* Sponsor: T. Monks.

Bisphenol A (BPA), is a an estrogenic compound used in the manufacturing of polycarbonate plastics and epoxy resins. BPA is toxic to multiple organ systems including the brain. Exposure to BPA during development has been shown to induce neuronal differentiation, decreased neuronal survival rate, and apoptotic celll death. The goal of this study was twofold; first, we examined the toxic effects of BPA on the developing rat brain and second, detailed mechanisms involved in toxicity and apoptotic cell death were examined in a rat pituitary cell line (GH3). A variety of markers for apoptosis in the striatum and pituitary of rat pups developmentally exposed to BPA through maternal transfer were examined. Results indicated signs of apoptotic cell death in tissue from 24 and 60 day old female rat pups that were exposed to BPA during development. BPA caused a significant decrease in the intracellular pool of glutathione suggesting that exposure increased the levels of reactive oxygen species (ROS). BPA increased the release of cytochrome c from the mitochondria. Caspase 3 activation increased following BPA exposure as indicated by increased levels of cleaved caspase 3. TUNEL staining showed evidence of apoptosis. GH3 cells were used to examine detailed mechanisms involved in BPA-induced apoptotic cascade including altered Ca^{2+} levels and mitochondrial permeability. Using a Ca^{2+} ionophore (Fura-3AM), it was demonstrated that BPA-treated cells had increased levels of intracellular Ca^{2+}. Concentration-dependent disruptions in mitochondrial membrane permeability were detected following treatment with BPA by staining the cells with rhodamine 123. These results indicate that developmental exposure to BPA appears to be neurotoxic in female rat pups by increasing cellular oxidative stress and triggering neuronal cell death. Interestingly, findings obtained from this study in female pups appear to contradict pervious findings in male pups, therefore suggesting that BPA-induced neurotoxicity may be different in females compared to males.

PS 1346 Abnormal Neuronal Migration and Behavior in Mice Exposed *In Utero* to Bisphenol A

W. Ling[1], T. Endo[1], W. Miyazaki[1], E. Kimura[1], K. Kubo[2], K. Nakajima[2], M. Kakeyama[1] and C. Tohyama[1]. [1]*Laboratory of Environmental Health Sciences, CDBIM, Graduate School of Medicine, The University of Tokyo, Tokyo, Japan and* [2]*Department of Anatomy, School of Medicine, Keio University, Tokyo, Japan.*

Developing brain is highly sensitive to environmental chemicals, and perturbation of the brain development can lead to cognitive impairment, as well as psychiatric and neurological disorders. Bisphenol A (BPA), a high volume chemical used for plastics, has been suspected to affect brain development, but its mechanisms of toxicity have been elusive. In this study we investigated whether and how the developing brain of mice born to dams exposed to low-dose of BPA was affected. Pregnant mice were exposed to BPA by implanting osmotic pump at a daily dose equivalent to 0, 40 (BPA-40), 400 (BPA-400) μg/kg from embryonic day 14.5 (E14.5) to E18.5. Neuronal migration, an essential process of cerebral cortical development, was analyzed on E18.5 by using an in utero electroporation technique. We found neuronal migration was significantly decreased in the BPA-40 group compared with the control group. Robo1, a neuronal guidance receptor gene, was significantly increased in the BPA-40 group, and TrkB, a gene that mediates neuronal differentiation and survival, was significantly increased in the BPA-400 group. In

addition, dopamine and its metabolites in the forebrain were significantly increased in BPA-400 group compared to BPA-40 group. Serotonin turnover, i.e., ratio of 5-HIAA to 5-HT, in the hindbrain was significantly decreased in BPA-400 group compared to the control group. Behavior of adult male mice born to BPA-exposed dams was examined using an automated apparatus, IntelliCage, under a group-housed condition (Endo et al., PLOS One, 2012). We found that the BPA-40 group significantly exhibited impulsive behavior compared to the control group. In conclusion, impulsive behavior observed in adulthood may have a fetal origin of perturbationin neuronal migration and related metabolic alterations in monoamine levels, both of which were induced by in utero exposure to BPA.

PS 1347 Enhanced Behavioral Toxicity Induced by Maternal Exposure to a Mixture of Low-Dose Endocrine Disrupting Chemicals

M. Sobolewski, K. Conrad, K. Martin, J. L. Allen, H. Weston, B. Lawrence and D. A. Cory-Slechta. *University of Rochester, Rochester, NY.*

Understanding the toxicity of low dose endocrine disrupting chemical (EDC) mixtures is critical, as research suggests that low dose early developmental EDC exposure can, through physiological reprogramming, alter the trajectory of adult disease onset. To assess how low dose developmental EDC exposure alters adult behavior, pregnant female mice were exposed to relatively low doses of four EDCs, Atrazine (ATR – 10mg/kg), Perfluorooctanoic acid (PFOA – 0.1 mg/kg), Bisphenol-A (BPA - 50μg/kg), 2,3,7,8-tetrachlorodibenzo-p-dioxin (TCDD – 0.25μg/kg) and their mixture (MIX), from gestational day 7 until weaning. Control litters were created at the same time. Adult offspring were tested for locomotor activity, food-rewarded fixed interval (FI) reinforcement schedule performance, and novel object recognition (NOR) performance. While behavioral deficits were observed in all 5 treatment groups, an enhanced effect was seen in male MIX offspring in increased FI response rates, suggesting an inability to inhibit responding. These were not seen in any other male treated group. In fact, ATR males exhibited significant reductions in FI rates, suggestive of reduced attention to task or impaired motivation. MIX females did not show enhanced FI alterations; but TCDD alone increased FI response rates. A robust decreased rate of exploration during initial exposure to the novel object paradigm occurred in all treatment groups in both sexes, particularly males. Deficits in short-term memory were observed in ATR, BPA and MIX male offspring; TCDD female offspring showed short-term memory deficits during NOR testing, spending significantly less time per each approach to the novel object. Deficits did not correspond to changes in locomotor activity in either sex. Taken together, behavioral deficits in learning/short term memory occurred after exposure to relatively low maternal doses of EDCs in mice. MIX treated males showed some evidence of enhanced effects highlighting the need for risk assessment of EDC mixtures. Supported by P30 ES001247.

PS 1347a Gestational Exposure to Inhaled Vapors of Ethanol and Gasoline-Ethanol Blends in Rats

P. J. Bushnell, T. E. Beasley, P. Evansky, S. A. Martin, V. C. Moser, K. L. McDaniel, J. Norwood, M. E. Gilbert, R. W. Luebke and J. M. Rogers. *NHEERL/ORD, US EPA, Research Triangle Park, NC.*

The US automotive fleet is powered primarily by gasoline-ethanol fuel blends containing up to 10% ethanol (E10). Uncertainties regarding the health risks associated with exposure to E10 prompted assessment of the effects of prenatal exposure to inhaled vapors of gasoline-ethanol blends containing greater amounts of ethanol. Pregnant Long-Evans rats were exposed to fuel vapors, 6.5 hr/day, on days 9–20 of gestation, and their offspring were assessed using a variety of tests for clinical, physical, immunological and neurodevelopmental effects. Results of tests of cognitive function are reported in other abstracts. This report compares effects of inhaled ethanol (E100) at concentrations of 0, 5000, 10000, or 21000 ppm with effects of vapors of gasoline lacking (E0) or containing 15% ethanol (E15) at concentrations of 0, 3,000, 6,000, or 9,000 ppm. Maximum concen¬trations were limited by the lower explosive limits of the vapors. None of the vapors caused overt maternal toxicity, changes in litter size or weight, or altered the weight gain of the pups. With E100, motor activity and a few measures of a functional observational battery (hindlimb grip strength, excitability) were altered, but not in a dose-related manner. No such changes were observed with E0 or E15. With one exception, no dose-related changes were observed for any agent on any clinical, developmental, or immunological endpoint. Urinary protein concentrations suggesting potential kidney dysfunction, measured in the offspring at 3 and 6 months of age, increased across dose and age after E15 exposure; increases not related to dose were seen after exposure to E0. However, the highest measured protein concentration (300 mg/dL) was lower than concentrations associated with kidney damage in this strain of rats (400 – 2500 mg/dL). Thus, even at these high concentrations, inhalation of these vapors does not appear to pose a serious public health hazard. This abstract does not represent EPA policy.

PS 1347b Prenatal Inhalation Exposure to Evaporative Condensates of Gasoline with 15% Ethanol and Evaluations of Sensory Function in Adult Rat Offspring

W. K. Boyes[1], L. L. Degn[1], D. Lyke[1], T. E. Beasley[1], P. Evansky[1], S. A. Martin[1], J. N. Ortenzio[1], L. N. Pantlin[2], P. J. Bushnell[1] and D. W. Herr[1]. *[1]USEPA, Research Triangle Park, NC and [2]Meredith College, Raleigh, NC.*

The introduction of ethanol-blended automotive fuels has raised concerns about potential health effects from inhalation exposure to the combination of ethanol and gasoline hydrocarbon vapors. Previously, we evaluated effects of prenatal inhalation exposure to 100% ethanol (E100) or to gasoline (E0) vapors on sensory function of the offspring as a component of a larger biofuels research program. This study evaluated effects of exposure to vapors from a blend of 15% ethanol /gasoline (E15) on the same set of outcome measures used previously. Pregnant Long-Evans rats were exposed to 0, 3K, 6K, or 9K ppm E15 vapors for 6.5 h/day over GD9 – GD20. Sensory evaluations of offspring (1 male pup/litter) began around PND106. Peripheral nerve function (compound action potentials, NCV), somatosensory (cortical and cerebellar evoked potentials), auditory (brainstem auditory evoked responses), and visual evoked responses were assessed. Visual function assessment included pattern elicited visual evoked potentials (VEP), VEP contrast sensitivity, dark-adapted (scotopic) and light-adapted (photopic) flash electroretinograms (ERG), and UV and green flicker ERGs. Although some minor statistical differences were observed for auditory and somatosensory responses, these changes were not systematically related to dose. All physiological responses showed changes related to stimulus intensity, and provided an estimate of detectable levels of change. Overall, the results identified no persistent dose-related functional impairments of the peripheral nerve, somatosensory, auditory, or visual systems resulting form gestational exposure to E15 vapors. Additional studies are in progress to evaluate the effects of exposure to the evaporative condensate vapors from a blend of 85% ethanol with gasoline (E85). This is an abstract of a proposed presentation and does not necessarily reflect EPA policy.

PS 1347c Effects of Ethanol-Gasoline Blended Fuels on Learning and Memory

T. E. Beasley[1], W. M. Oshiro[1], V. C. Moser[1], M. E. Gilbert[1], K. L. McDaniel[1], P. Evansky[2] and P. J. Bushnell[1]. *[1]TAD, US EPA, RTP, NC and [2]EPHD, US EPA, RTP, NC.*

The potential toxicity of ethanol-gasoline blended fuels to the developing nervous system is of concern. We previously reported an absence of effect on learning and memory as seen in a trace fear conditioning task and water maze task in offspring of dams exposed prenatally to the vapors of ethanol. However, a high number of anticipatory responses were noted in male offspring that completed a choice reaction time task (CRT). In order to further explore this apparent impairment of response inhibition, we evaluated effects of vapors from a blend of 15% ethanol /gasoline (E15) and 85% ethanol/gasoline using a Differential Reinforcement of Low-rate Response task (DRL). We also evaluated the effects of E15 and E85 on the trace fear conditioning task and water maze task. Pregnant Long-Evans rats were exposed to 0, 3000, 6000, or 9000 ppm E15 or E85 vapors for 6.5 h/day from GD9 to GD20. Male and female offspring (n=10/sex/group/vapor) were trained on the Morris water maze starting on postnatal day (PND) 76. Overall, acquisition of the task and working memory were not affected by E15 or E85. A second set of male and female offspring (n=16/sex/group/vapor) was assessed using a fear conditioning task. There were no differences among dose groups in either cue or context learning. Finally, a third group of male and female offspring (n=8/sex/group/vapor) was assessed using a DRL task. Overall, the results identified no significant dose-related impairments after exposure to E15 or E85, although there was a tendency for inhibitory control impairment in the 9000 E15 male offspring. These results suggest prenatal exposure to ethanol-gasoline blended fuels produce few if any effects on learning and memory. This abstract does not reflect EPA policy.

PS 1347d Deficits in Response Inhibition in Male Rats Prenatally Exposed to Vapor Condensates Made from Gasoline Containing Ethanol at 0% and 15%, but Not 85%

W. M. Oshiro[1], S. A. Martin[1], T. E. Beasley[1], P. Evansky[2] and P. J. Bushnell[1]. *[1]TAD/NHEERL/ORD, US EPA, RTP, NC and [2]EPHD/NHEERL/ORD, US EPA, RTP, NC.*

The impact of developmental exposure to inhaled ethanol-gasoline fuel blends is a potential public health concern. We previously reported that rats whose mothers inhaled ethanol (21,000 ppm) during pregnancy had increased levels of anticipatory responding on a choice reaction time (CRT) task. Thus, we used this task to investigate effects in the adult offspring of dams exposed to vapor condensates made from fuels blended with a range of ethanol concentrations, including gasoline alone (E0) and gasoline with 15% and 85% ethanol (E15 and E85, respectively). Each blend was investigated in separate cohorts. Within each cohort, dams were exposed for 6.5 h daily from gestational day 9 through 20 to concentrations of 0, 3,000, 6,000, or 9,000 ppm (n=8 per concentration). Male offspring were assessed during acquisition of both cued and uncued versions of the CRT and during asymptotic performance of the uncued task. During acquisition, increased anticipatory responding (elevated hold failures during a preparatory hold period) was observed in rats exposed to E0 (9,000 ppm) and E15 (6,000 and 9,000 ppm) indicating deficits in response inhibition. E15 offspring also had reduced accuracy (6,000 and 9,000 ppm) during acquisition of the cued CRT, suggesting additional deficits in processing visual information, and reduced decision times (6,000 ppm), indicating possible facilitation in this measure due to elevated hold failures. No effects were observed on any performance measure after exposure to E85, or, during asymptotic performances of the uncued CRT for any fuel blend. These data, combined with data from rats exposed to vapors of neat ethanol, indicate that prenatal exposure to ethanol and gasoline can cause deficits in response inhibition. However, 15% ethanol in gasoline appears to increase these effects, whereas 85% ethanol appears to diminish them. This abstract does not represent EPA policy.

PS 1347e Developmental Ethanol Exposure Alters Synaptic Plasticity in the Visual Cortex of C57/BL6 Mice: Implications for Fetal Alcohol Spectrum Disorders

E. L. Wong[1], G. O. Sipe[2], C. E. Lamantia[2] and A. K. Majewska[2]. *[1]Environmental Medicine, University of Rochester, Rochester, NY and [2]Neurobiology and Anatomy, University of Rochester, Rochester, NY.*

Ethanol consumption during pregnancy is the leading non-inherited cause of mental disability. However, little is known about how ethanol elicits mental disability and whether defects in synaptic plasticity play a crucial role. We targeted ethanol exposure to a period of intense synaptogenesis in early development during which neural networks are rapidly assembled. In mice this occurs early in postnatal life and corresponds to the third trimester in humans. On postnatal day 4 (P4), C57/BL6 pups housed with the dam alone from P0 were randomly assigned to separation control (SC), saline injected control (SIC), or EtOH injected (EI) groups. Daily from P4-P9, EtOH treated mice were subcutaneously injected with two doses of 1.8g/kg 20% EtOH two hours apart. 1.5 hours after the second dose, P4 pups achieved blood and brain alcohol concentrations of 372 ± 48 mg/dL and 300 ± 60 mg/dL respectively (high binge). We limited separation of the pups from the dam and littermates to ~10 minutes on dosing days for all three groups. No significant differences in weight among the three groups were observed through P21. During the critical period for ocular dominance plasticity (P28-P33), SC, SIC, and EI mice were either monocularly deprived for 4 days by suturing of the contralateral eye (deprived) or not sutured (non-deprived). Intrinsic optical signal imaging of the left visual cortex showed that non-deprived SC, SIC, and EI mice all had the normal contralateral eye bias. SC and SIC deprived mice demonstrated the expected shift from a contralateral to an ipsilateral eye bias, evidence of normal ocular dominance plasticity. However, EI mice remained contralaterally biased after 4 days of deprivation. We conclude that early life ethanol exposure can disrupt activity-dependent visual system plasticity later on in life.

PS 1347f Subcortical Band Heterotopia (SBH) in Rat Offspring following Maternal Hypothyroxinemia: Structural and Functional Characteristics

M. E. Gilbert[1], R. Ramos[2], D. McCloskey[3], J. Goodman[4] and A. F. Johnstone[1]. *[1]Toxicity Assessment Division, US EPA, Research Triangle Park, NC, [2]NY Institute Techology, Coll Osteopathic Med, Old Westbury, NY, [3]Psychology, CUNY, Staten Island, NY and [4]NY Institute Brain Res, Staten Island, NY.*

Thyroid hormones (TH) play crucial roles in brain maturation, neuronal migration, and neocortical lamination. Subcortical band heterotopia (SBH) represent a class of neuronal migration errors in humans that are often associated with childhood epilepsy. We have previously reported the presence of SBH in a rodent model of low level hypothyroidism induced by maternal exposure to propylthiouracil (PTU). Here we examined the dose-response characteristics of this developmental malformation, the connectivity of heterotopic neurons with other brain regions, and their functionality. Pregnant rats were exposed to varying concentrations of PTU through the drinking water (0, 1, 2, 3, 10ppm) from gestational day 6 to postnatal day 21, producing graded levels of TH insufficiency. Dose-dependent increases in the volume of the SBH present in the corpus callosum were documented, with clear presence at concentrations of PTU that resulted in only minor, not statistically reliable, reductions in maternal serum T4. SBH contain neurons, oligodendrocytes, astrocytes, and microglia. Both monoaminergic and cholinergic processes were prevalent in the SBH. Tracer studies revealed anatomical connectivity of SBH neurons to cortical neurons and synaptic functionality of these anatomical connections was verified by ex vivo field potential recordings. SBH persisted in adult offspring despite rapid return to euthyroid status at termination of exposure, and adult offspring displayed an increased sensitivity to seizures induced by the convulsant pentylenetrazol. A number of features of this model are attractive to the investigation of molecular mechanisms of cortical development, effectiveness of therapeutic intervention in hypothyroxenimia during pregnancy, and of the impact of very modest TH imbalance that accompanies exposure to environmental contaminants. (Does not reflect EPA policy)

PS 1347g Developmental Thyroid Hormone (TH) Disruption: In Search of Sensitive Bioindicators of Altered TH-Dependent Signaling in Brain

C. Wood, A. F. Johnstone and M. E. Gilbert. *Toxicity Assessment Division, US EPA, Research Triangle Park, NC.*

Thyroid hormones (TH) are essential for brain development, yet clear indicators of disruption at low levels of TH insufficiency not been identified. Brain TH is difficult to measure, but TH-responsive genes can serve as sensitive indicators of TH action in brain. Although a number of TH-responsive genes have been identified, limited data are available on genes responsive to levels of TH insufficiency typically induced by xenobiotics. This study identified TH-responsive genes in neonatal rat cortex in a low dose model of TH insufficiency based on propylthiouracil (PTU, 0 1 2 3 10 ppm in drinking water to dams GD6-PN21). A suite of genes were examined including genes previously shown to be responsive to TH deprivation or activated by T3 in vivo or in vitro, and genes implicated in brain development. PTU dose-dependently reduced serum T4 in dams and pups on postnatal day (PN) 4 to a maximum of ~30% of control, with more severe reductions seen in neonates on PN14 (T4 <10% of control at the highest dose). Expression of several genes was dose-dependently down-regulated by PTU (Mog, Parv, Hr, Bteb, NGF, Arc) while others critically involved in brain development or previously identified with severe hypothyroidism or T3 administration were not altered (BDNF, Reelin, CamkIV, Sox2, Pax6, Nurr1). Gene targets altered at the lowest dose of PTU (T4 of 85, 63, 54% of control in dams at weaning, PN4, PN14 pups) included Col11a2, Itih3,Gjb6, Agt, Erg1 and Parv. A number of genes in 'compensatory pathways' (Mct8, Oatpc, Dio2) remained unchanged. These data indicate that many genes previously implicated as "TH-responsive" may not be involved in brain dysfunction associated with moderate TH insufficiencies. They further suggest that compensatory 'protective' mechanisms may either be insufficiently activated or immature in the neonatal brain. The most sensitive gene targets identified here will be used to evaluate the fidelity of serum TH induced by environmental contaminants to predict disruption of TH action in brain. (Does not reflect EPA policy).

PS 1347h Embryonic Exposure to Dopamine D1 and D2 Antagonists Disrupts Swimming in Two Zebrafish Strains

A. N. Oliveri, J. M. Bailey and E. D. Levin. *Psychiatry, Duke University, Durham, NC.*

Background. Zebrafish like mammals have dopamine systems that are important for programming a variety of functions including motor behavior. Normal development of dopamine systems would likely depend on normal responsivity of dopamine D1 and D2 receptors during development. Objective. Embryonic zebrafish were used to assess the role of D1 and D2 receptor action on motor function. Methods. Zebrafish embryos from the AB and 5D strain were exposed to 0.5, 1.5 or 5 μM of a dopamine D1 antagonist, SCH23390 or a D2 antagonist, haloperidol dissolved in aquarium water, which served as the vehicle control. Exposure lasted from 5 hrs to 5 dpf. After exposure, fish were transferred to aquarium water with behavioral testing 24 hrs later. An automated system of data collection was used in which individual swim characteristics were calculated in real time under light (100% illumination) and dark (0% illumination) conditions controlled via a DanioVision observation chamber. Each trial commenced following a 10-min acclimation period in dark. Ten min intervals of light and dark conditions alternated twice each for a 50-min session. Swim data were analyzed by ANOVA with Dunnett's test for pair-wise comparisons. Results. Survival of embryos was unaffected by treatment or strain. There was a significant effect of strain during dark, with ABs traveling a greater distance than 5Ds. The highest dose of haloperidol (5 μM) nearly eliminated movement during both conditions for both strains. Significant decreases were seen with the intermediate haloperidol dose (1.5μM) and the highest dose of SCH 23390 (5 μM) during dark for both strains. Conclusion. Blockade of either D1 or D2 dopamine receptors during embryonic development caused lingering deficits in swimming behavior, suggesting toxicants that affect dopamine systems during development may have persisting behavioral consequences. Differences in baseline behavior between strains suggest strain may be an important variable when measuring early-life endpoints in Zebrafish. Research supported by Superfund Research Program ES010356, EPA Star grant 83554101

PS 1347i DOTC (Di-n-octyltin Dichloride) Affects Brain Development at Weaning and Young Adulthood in Perinatal-Exposed Rats As Demonstrated by Brain MRI and Genome-Wide Gene Expression

D. M. De Groot[1], R. Kayser[1], L. Linders[1], M. de Groot[1, 2], A. Wolterbeek[1], M. Radonjic[1], R. H. Stierum[1] and F. Kuper[1]. [1]*TNO, Zeist, Netherlands and* [2]*IRAS, Utrecht, Netherlands.*

Di-n-octyltin dichloride (DOTC) is known for its developmental and immunotoxic potency. Previously, we found effects of DOTC (30mg DOTC/kg body weight/day, via diet) on early development (increased birth weight) and on the developing immune system in a study according to the new guideline for an Extended One Generation Reproduction Toxicology study (OECD 433) (Tonk et al., 2011). No effects were found on the developing nervous system with conventional endpoints of behaviour and neuropathology. However/surprisingly, volumes of brain regions were significantly increased in the DOTC-exposed offspring at weaning (early adolescence). The effects on brain volumes did not persist into adulthood. Cerebrum and cerebellum appeared differently affected. Genome wide gene expression in brain tissue of the DOTC-exposed offspring was consistent with effects on immune-related pathways and developmental pathways, and confirmed the differences between cerebrum and cerebellum and between adolescent (PND 21) and young adult age (PND 60/70). Relevant genes in at least one of the DOTC conditions were Nrgrn, Shank 3, Igf1r, Cck, Apba2 (involved in neurodevelopment and function), and LOC679869, Foxp2, Itga11, Arhgap5, Cd47, Dlg1, Gas6, Cml5, Mef2c (involved in cell size, proliferation and organ development). The effects of DOTC on genes involved in (neuro)development may have led to the observed changes in brain volume and specific gravity at adolescent age. Similar effects on brain volume have been found in humans diagnosed for autism. Moreover, Shank3, foxp2, cck and apba2 are associated with autism in humans. Our results support the notion of a relationship between environmental exposure to chemicals and childhood diseases like autism.

PS 1347j Neuroantibodies (NAB) in African-American Children: Associations with Gender, Gluthathione-S-Transferase (GST) Pi Polymorphisms (SNP) and Heavy Metals

A. Cichewicz[1], E. E. Hudgens[2], J. E. Gallagher[2] and H. A. El-Fawal[1]. [1]*Neurotoxicology Laboratory, Albany College of Pharmacy and Health Sciences, Albany, NY and* [2]*Environmental Public Health Division, NHEERL, US EPA, Research Triangle Park, NC.*

Polymorphisms in GST are implicated in immune-mediated disease, heavy metal accumulation and neurodegeneration. Blood cell DNA/serum samples from 131 African-American children (9-12 years old, 71 males; 60 females) in the Mechanistic Indicators of Childhood Asthma (MICA) study were used to determine GSTPi SNPs [rs947895 (C>A), rs6591256 (A>G), rs1695 (A>G), rs1871042 (C>T) and rs17593068 (G>T)] by PCR for associations with NAb, IgM and IgG, against neurofilaments (NF-L, NF-M and NF-H), glial fibrillary acidic protein (GFAP) and myelin basic protein (MBP) and nail heavy metal levels (As, Cd, Cr, Cu, Fe, Hg, Mn, Pb, Se and Zn). Overall, non-parametric analysis indicated significant associations ($r=0.23$; $p<0.05$) between anti-NF-H and anti-MBP with As and Pb, while anti-GFAP was also associated with Pb levels. Heavy metal levels did not differ on stratification by gender. However, females had higher levels of anti-NF-L and anti-NF-H, IgM, and anti-NF-M, IgG ($p<0.05$). In females only, there were significant ($p<0.01$-0.05) positive associations of anti-NF-H, GFAP and MBP, IgG, with As, Cr, Fe, Mn, Pb and Se, and with Cd and Cu for anti-NF-H and GFAP. Genotype stratifications revealed significantly higher levels of As, Cd, Mn and Pb in children with the rs947895_AA and rs1871042_TT genotypes. Higher Mn and Pb levels were found in children with the rs1695_GG genotype. Stronger associations between NAb and several metals were observed in these genotypes with higher metal levels, These results suggest that NAb, may be useful for detection of nervous system involvement in environmentally and genomically vulnerable populations and that females may be at greater risk as established by the prevalence of autoimmunity in this gender. This abstract does not necessarily reflect U.S. EPA policy.

PS 1347k Human Stem Cell-Derived Neuron and Astrocyte Cocultures in a Developmental Neurotoxicity Screening Assay

A. Majumder[1, 2], X. Wu[2] and S. Stice[1, 2]. [1]*ArunA Biomedical Inc., Athens, GA and* [2]*University of Georgia, Athens, GA.*

There is a need for rapid, cost effective, in vitro methods to identify chemicals hazardous to human brain development. Various in vitro assays utilizing uniform neuronal lines are used in screening potential neurotoxins. However neural tissue in the human CNS has an abundance of astrocytes and astrocytes alter the neurotoxic potentials of multiple neurotoxins. Thus a representative assay should include both astrocytes and neurons. Also a direct comparison between rodent and human neurons demonstrated species specific differences in sensitivity to known neurotoxins, reinforcing the need to shift to human cells for increased species representation. Here we describe a scalable high content imaging (HCI) assay using human neurons with astrocytes and compare it to a human neuron only assay. Human neural progenitor cells (hNP1, ArunA Biomedical Inc) derived from pluripotent stem cells (hPSC) were differentiated independently to near pure neuronal and astrocytic populations. Neurons and astrocytes at desired stages of maturity were subsequently co-cultured on 96 well assay plates. The co-cultures and corresponding neuron only groups were treated with a range of doses of two neurotoxins, Bis-1 and Lead Acetate, and analyzed using an automated platform for changes in viability and neurite outgrowth, an endpoint relevant to neurodevelopment. Both compounds are known to affect neurite outgrowth in hPSC derived neurons (hN2, ArunA Biomedical Inc). While both co-culture and neuron only cultures had significantly reduced neurite outgrowth with treatment at higher doses, in presence of astrocytes the reduction of neurite parameters for each treatment was significantly lower than in its corresponding neuron only assay without effecting cell viability. This significant alteration in toxic response strongly suggests need for a multi-cellular assay as above for accurate predictions of neurotoxicity at the organismal level and addresses a major gap in current state of screening technology.

PS 1347l Aluminum Exposure from Developmental to Mature Brain: Long-Term Implications on Neurodegenerative Injury

Q. Niu and Q. Zhang. *School of Public Health, Shanxi Medical University, Taiyuan, Shanxi, China.*

The role of long term aluminum exposure on etiology of Alzheimer's disease has been a hot topic for many years. While the results remain to be contradictory, more and more reports in literature have provided the evidence of aluminum-induced neurodegeneration in human population as well as in mature or old animals. The research presented in this communication is focused on the neurodevelopmental

effects of aluminum exposure on females and offspring. The ICR female mice were exposed to nano-alumina for ten days before mating and the exposure continued to the birth of pups, with blank control and nanocarbon control groups. An exposure regimen by intranasal exposure at 10ul each time, 3 times per day was employed in this study. Neurobehavioral tests including physiological, reflex and sensory function test, endurance test, Morris water maze, location navigation, open field test were performed to detect the neurodevelopmental functions of the pups. The results showed that compared with blank controls, nearly all of the parameters in the functional tests in pups delivered by nano-alumina exposed mother mice were significantly lower than those in the pups delivered by blank mice ($p<0.05$). Our data suggest that maternal exposure to aluminum in pregnancy period induces the neurodevelopmental impairment, exemplified in cognitive deficits, which may progress toward the neurodegenerative injury when animals become matured.

PS 1348 Differential Toxico-Proteomics Study in CSF and CP of Manganese (Mn)-Exposed Rats and the PHB1's Role in Mn-Induced Cell Cycle Arrest

G. J. Li[1], Y. Dong[1], H. Jing[1], J. Liu[1], J. Ning[1], Y. Li[1], Z. Tan[1], Y. Liu[1], K. Wei[2], T. Zhang[2], C. Zhao[1] and L. Ma[1]. *[1]Beijing Municipal Centers for Disease Prevention and Control, Beijing Key Laboratory of Diagnostic and Traceability Technologies for Food Poisoning, Beijing, China and [2]Beijing Proteome Research Center, Beijing, China.*

Excessive Manganese (Mn) exposure may induce Parkinsonism; yet the mechanism has not been completely elucidated. Choroid plexus (CP), which constitutes blood-cerebrospinal fluid barrier (BCB), has been considered as a primary target in Mn-induced neurotoxicity. In our study, a total of 32 Mn-related differentially expressed proteins in CP were identified by 2D-PAGE combined with Nano-LC-MS/MS, and 123 Mn-related proteins in CSF by label-free nanoHPLC-Q-TOF -MS/MS in an Mn-toxicity rat model.We further verified the 6 selected Mn- related proteins (PHB1, VDAC, β-actin, STIP1, TTR, Vimentin) in a CP cell line Z310 in vitro, and in vivo. Besides, the cell cycle arrest effect of Mn on Z310 cells had been proved from our previous experiment. A so-called iron responsive element structure within the 3' untranslated region on prohibitin 1 (PHB1) mRNA is a newly found functioning element. We confirmed that upregulated PHB1 does play an essential regulatory role in Mn-induce Z310 cell cycle arrest, by WB, RT-PCR, Transfection and Flow cytometry followed by the establishment of PHB1 knockdowned Z310 cells. The involved signal transduction pathways deserve further investigation. (partly supported by NSFC Grant in China # 81373028, Capital Development Project 2011-1013-03, and Beijing Health Bureau Project-2011. Corressponding author: Guojun J. Li, guojunli88@yahoo.com).

PS 1349 Transport of α-Synuclein at the Blood-Cerebrospinal Fluid Barrier and Effects of Heavy Metal Toxicities: Potential Role in Parkinson's Disease Pathoetiology

C. A. Bates[1], X. Fu[1], D. Ysselstein[2], J. Rochet[2] and W. Zheng[1]. *[1]Health Sciences, Purdue University, West Lafayette, IN and [2]Medicinal Chemistry and Molecular Pharmacology, Purdue University, West Lafayette, IN.*

The blood-cerebrospinal fluid barrier (BCB) in the choroid plexus maintains the homeostasis of critical molecules in the brain by regulating their transport between the blood and cerebrospinal fluid (CSF). Little is understood about how the BCB regulates brain homeostasis of α-synuclein (a-Syn), a protein implicated in Parkinson's disease (PD) pathology. Previous findings in this lab show that the presence of manganese (Mn) or copper (Cu) in solution facilitates a-Syn aggregates in vitro and that exposure to toxic levels of Mn and Cu induces intracellular a-Syn aggregation in immortalized Z310 choroidal epithelial cells. The current studies were designed to test the hypotheses that concomitant exposure to both Mn and Cu accelerates the rate of a-Syn aggregation in solution and Mn toxicity may facilitate a-Syn transport across a monolayer of the modeled blood-CSF barrier. Our data revealed the combined exposure to Mn and Cu had a much slower rate of a-Syn aggregation in solution than did exposure to either metal individually ($p<0.05$). The Two-Chamber Transwell study demonstrated that while there was a significant decrease in intracellular a-Syn levels at 48 hr compared to 24 hr within each control or Mn treated group, the pretreatment with Mn had no significant effect on a-Syn transport across the primary rat choroidal epithelial monolayer at 24 or 48 hr. Overall, these findings suggest that Mn exposure increases a-Syn aggregation in the BCB; this increase, however, does not result in the increased efflux of a-Syn from the CSF to blood via the BCB. Mn or Cu alone participates in the process leading to a-Syn aggregation; their combined effect is not additive, but rather inhibitive. The exact role of Mn and Cu in a-Syn aggregation and the respective molecular interactions with a-Syn are currently under investigation.

PS 1350 The Environmental Neurotoxin Manganese Promotes Cell-to-Cell Transmission of α-Synuclein via Exosomes in Cell Culture and Animal Models of Parkinson's Disease

D. Harischandra, M. Neal, A. Kanthasamy, N. Panicker, H. Privitera, H. Jin, V. Anantharam and A. Kanthasamy. *Biomedical Sciences, Iowa State University, Ames, IA.*

The aggregation of α-Synuclein (αSyn) is considered a key pathophysiological feature of Parkinson's disease (PD). Recent studies suggest that prion-like cell-to-cell transfer of misfolded αSyn contributes to the spreading of αSyn pathology. However, the biological mechanisms underlying the propagation of the disease with respect to environmental neurotoxic chemical exposures are not well understood. Considering the role of the divalent metal manganese in PD-like neurological disorders, we characterized its effect on αSyn misfolding and protein aggregation. First, we established a MN9D dopaminergic cell line stably expressing wild-type human αSyn and treated it with non-toxic doses of manganese at various time points. Analysis of condition medium (CM) through Western blot showed that cells secreted αSyn into extracellular media following manganese exposure. Further characterization of CM through electron microscopy readily detected the membranous nano-sized vesicles with characteristic hallmarks of exosomes. Western blot and ELISA studies revealed that the exosomes do in fact contain αSyn. Furthermore, Nanosight particle analysis showed that manganese exposure can enhance the release of αSyn-containing exosomes. In functional studies, we demonstrated that exosomes released during manganese treatment can induce neuroinflammatory responses in primary microglial cultures and neurodegeneration in differentiated human dopaminergic cells (LUHMES) through the activation of caspase-3 signaling. Our preliminary studies showed for the first time that stereotaxic delivery of αSyn-containing exosomes isolated from manganese-treated MN9D αSyn-expressing cells into the striatum can initiate PD-like motor deficits in mice. Collectively, these results demonstrate that manganese exposure promotes αSyn secretion by forming exosomal vesicles, which subsequently evoke pro-inflammatory and neurodegenerative responses in both cell culture and animal models. (ES19267 ES10586 & NS65167)

PS 1351 Development of Organotypic Brain Slice Culture Model to Study Environmentally Linked Proteinopathies

N. Kondru, D. Harischandra, V. Anantharam, A. Kanthasamy and A. G. Kanthasamy. *Biomedical Sciences, Iowa State University, Ames, IA.*

A prion-like spreading of protein aggregates is emerging as a major pathophysiological mechanism of many neurodegenerative diseases commonly referred to as proteinopathies, which include PD, AD, HD and ALS. Environmental neurotoxicant exposure has been increasingly recognized in proteinopathies, but the lack of suitable model systems to study protein aggregation hinders our understanding of the propagation of these diseases. Organotypic brain slice cultures offer advantages over traditional cell culture methods as they resemble the intra-cerebral environment ex vivo. The goal of the present study is to establish an organotypic brain slice culture model for the investigation of the protein-misfolding mechanisms underlying environmentally linked proteinopathies. Among various brain slicing techniques, we found that the slices prepared from Compresstome brain slicer possess higher cell survival for a prolonged period. We further tested whether RML scrapie prion could infect the cerebellar organotypic slice cultures (COSCs). After 35 dpi with RML scrapie, brain homogenates successfully demonstrated scrapie prion infection in COSCs, as evidenced by limited proteolysis and Western blot analysis. The infection-induced gliosis in COSCs was also confirmed by immunostaining analysis of glial markers, Iba1 and GFAP. Next, we generated organotypic cortico-striatal slice cultures and tested the effect of the environmental neurotoxicants manganese and lead on protein aggregation. Western blot analysis revealed that exposure to both metals significantly induced hyperphosphorylated tau as well as activation of pro-apoptotic signaling as measured by proteolytic activation of PKCδ. Taken together, our results demonstrate that the organotypic brain slice culture is an excellent model for studying the effects of environmental factors on protein misfolding in various proteinopathies of the central nervous system. The brain slice culture model will also greatly minimize the animal use for studying neurodegenerative diseases (NIH ES 19276 and ES10586).

PS 1352 Manganese Exposure Downregulates Anti-Apoptotic STAT5b Signaling through an Sp1-Dependent Mechanism

D. Kim, A. Kanthasamy, H. Jin, V. Anantharam and A. G. Kanthasamy. *Biomedical Science Department, Iowa State University, Ames, IA.*

Chronic exposure to elevated level of Manganese (Mn) has been linked environmentally to Parkinson's disease-like neurological abnormalities. However, the precise mechanisms underlying Mn-induced neurotoxicity are still not well understood. In this study, we have identified that Mn exposure downregulates a key regulator of apoptotic cell signaling involving the signal transducer and activator of transcription (STATs). 300μM Mn exposure in N27 dopaminergic neuronal cells downregulated STAT5b expression both at the protein and mRNA levels, while STAT1 was unaffected, indicating an isoform-specific effect of Mn on STAT5b expression. To determine the functional consequence of STAT5b regulation during Mn neurotoxicity, we performed overexpression studies. Surprisingly, overexpressing STAT5b significantly protected against Mn-induced apoptotic cell death, suggesting the STAT5b plays a cell survival role in dopaminergic neuronal cells. STAT5b upregulation also increased anti-apoptotic Bcl2 expression. To further determine the molecular mechanisms underlying STAT5b downregulation during Mn neurotoxicity, we cloned the STAT5b promoter. Analysis of the 2.5-kb mouse STAT5b promoter region indicated that a proximal region near exon 1 contains the regulatory element in response to Mn exposure. Detailed mutational analyses of the potential transcription factor binding site revealed that a SP1 site located at between -210 and -194 may be required for the suppression of STAT5b in Mn-induced neurotoxicity. Finally, we extended our studies to an animal model of Mn-induced neurotoxicity. The results showed that oral administration of Mn (30 mg/kg bw) in C57 black mice for 30 days significantly reduced the expression of STAT5b in the substantia nigra compared to control mice. Taken together, these data suggest Mn exposure downregulates anti-apoptotic STAT5b signaling via an Sp1-dependent mechanism in dopaminergic neurons, which may significantly contribute to Mn neurotoxicity. (NIH grants ES10586 and ES19267).

PS 1353 Mutant Huntingtin Impairs Mn-Dependent p53 Activation in Human iPSC-Derived Neural Progenitors

A. Tidball[1], K. K. Kumar[1], M. Uhouse[1], R. Chamberlin[3], A. A. Aboud[1], J. X. Sun[1], T. V. Bichell[1], M. Odak[1], R. Carson[2], K. C. Ess[2], M. Neely[1], M. Aschner[4] and A. B. Bowman[1, 2]. [1]*Neurology, Vanderbilt University, Nashville, TN,* [2]*Pediatrics, Vanderbilt University, Nashville, TN,* [3]*Genetics Associates, Inc., Nashville, TN and* [4]*Molecular Pharmacology, Albert Einstein College of Medicine, Bronx, NY.*

Huntington's disease (HD) is a devastating neurodegenerative disease caused by the mutant Huntingtin protein. Expression of mutant Huntingtin is known to cause altered p53 signaling in cell and animal models as well as in patients. We tested the hypothesis that manganese (Mn) activates p53 signaling and that mutant Huntingtin protein would impinge on this cell stress pathway. We compared p53 activation in wild type (Q7) and mutant Huntingtin expressing (Q111) StHdh murine striatal cells and found that sub-lethal concentrations of Mn (25 μM) caused significant phosphorylation of p53(ser15) in both Q7 and Q111 cells as measured by immunoblotting. The mutant (Q111) cell line had a significantly diminished response. We then tested whether this phenotype is also seen in human cells. Human induced pluripotent stem cells (hiPSCs) from control and Huntington's disease human subjects were differentiated into neural progenitors expressing early striatal markers (e.g. FOXG1, ISLET1). These human neural progenitors showed the same diminished p53 response to Mn ; however, p53 activation after double-stranded DNA damage via neocarzinostatin resulted in greater p53 activation in HD iPS cells. Quantitative RT-PCR for p53-dependent transcripts (e.g. TIGAR, p21) confirmed manganese activation of the pathway and diminished responsiveness in HD cells. Under sub-lethal cell stress conditions, p53 activates pro-survival gene transcripts. Thus, diminished p53 responsiveness may reduce the ability of neurons to adapt to repeated cellular stress (e.g oxidative stress and nutrient deprivation). We are currently working to identify the kinase responsible for the Mn-dependent phosphorylation of p53 and mechanism by which Mn activates p53. NINDS: F31 NS077632 (AMT) NIEHS: ES016931 (ABB) and ES010563 (MA and ABB)

PS 1354 A High-Throughput Screen for Modulators of Neuronal Manganese Status

K. K. Kumar[1], A. A. Aboud[1], M. Odak[1], M. Uhouse[1], J. X. Sun[1], A. Tidball[1], M. Neely[1], M. Aschner[2] and A. B. Bowman[1]. [1]*Department of Neurology, Vanderbilt University School of Medicine, Nashville, TN and* [2]*Department of Molecular Pharmacology, Albert Einstein College of Medicine, Bronx, NY.*

There is strong evidence that both genetic and environmental factors play a critical role in the pathogenesis of many neurodegenerative diseases. Exposure to the heavy metal, manganese (Mn), shows a strong correlation with incidence of Parkinson's disease (PD). This study presents the results of a high-throughput screen (HTS) to identify novel modulators of neuronal Mn accumulation. Specifically, we screened multiple chemical libraries including: SPECTRUM, NIH Clinical Compounds, Chembridge/Chemdiv, and kinase inhibitors from Roche, GSK, and Enzo. Our goal was to identify agents with research utility in defining molecular mechanisms of neuronal Mn regulation and those with potential clinical efficacy in modifying Mn environmental risk in vivo.

We have successfully optimized the Cellular Fura-2 Manganese Extraction Assay (CFMEA) for HTS (Z-factor>0.5) in an immortalized murine striatal cell line (STHdhQ7/Q7). Subsequently, we conducted a screen of 40,000 small molecules. A subset of molecules was rescreened in duplicate given the known biological/medical relevance of the source libraries. These studies revealed 48 small molecule modifiers of Mn status that hit twice in both screens, and these molecules were selected for the generation of concentration response curves (CRCs). CRCs revealed dose-responsiveness for 28 of these small molecules, known to target cellular signaling pathways previously implicated in Mn toxicity, including p53 and AKT, as well as GSK3β, ALK, EGFR/ErbB2, ERK, and neurotransmitter trafficking proteins. Parallel studies have revealed induction of phosphorylated p53 and AKT at subtoxic physiological Mn exposures.

Future effort will characterize these HTS-identified modulators of Mn status for activity in human induced pluripotent stem cell (hiPSC)-derived nigral and striatal like neural progenitors.

Support: NIH/NIEHS RO1 ES010563 (MA and ABB) and RO1 ES016931 (ABB).

PS 1355 A Statistical Analysis of Z-Score Stringency in a High-Throughput Screen for Modulators of Neuronal Mn Status

M. Odak[1], K. K. Kumar[1], M. Aschner[2] and A. B. Bowman[1]. [1]*Neurology, Vanderbilt University Medical Center, Nashville, TN and* [2]*Molecular Pharmacology, Albert Einstein College of Medicine, Bronx, NY.*

Manganese (Mn) is an environmental risk factor for Parkinson's disease. We performed a high throughput screening (HTS) for small molecule modifiers (SMMs) of neuronal Mn status to improve understanding of Mn transport and handling in the central nervous system. Current practices in HTS analysis utilize a statistical z-score with an absolute value of 3.0 as a cut-off for potential hits. We evaluate the utility of this statistical cut-off in our novel Fura2-based fluorescent Mn assay by performing replicate HTS. We have evaluated the variability and general distribution of "true-positive" versus "false-positive" hits using MATLAB. We find that relaxing the z-score cut-off from 3.0 to 2.0 identified a substantial fraction of FDA-approved drugs that may have translational value that fell below the 3.0 z-score limit. The ultimate goal of this study is to identify an optimal z-score cutoff for our HTS Mn assay given the non-linear responses of this assay. A total of 3,391 compounds were tested in duplicate to find SMMs using a murine striatal cell line. This study revealed 48 compounds that hit on both days of testing. Concentration Response Curves (CRCs) were generated for these, and 29 compounds revealed a true dose-dependent effect on cellular Mn levels. 69% of these 29 compounds had a z-score above an absolute value of 3.0 on both days of testing and 31% of compounds had z-scores between 2.0 and 3.0 on at least one day of testing. Furthermore, there was only a marginal decrease in the True Positive Rate (TPR) from 43.2% to 42.9% and a marginal increase in the False Positive Rate (FPR) from 1.0% to 2.8% by relaxing the z-score cutoff to 2.0. Additional statistical characterization will seek to evaluate the efficacy of compounds identified with a relaxed z-score cutoff and their mechanisms influencing Mn accumulation in murine striatal cells to validate a relaxed z-score approach with Fura2-based HTS.

Supported by NIEHS R01 ES10563.

PS 1356 Wildtype Alpha-Synuclein-Mediated Protection against Mn Toxicity in PD-Associated *C. elegans* Mutants

S. Chakraborty[1], J. Bornhorst[4], S. Meyer[4], H. Lohren[4], T. Schwerdtle[4], A. B. Bowman[3] and M. Aschner[2]. [1]*Neuroscience Graduate Program, Vanderbilt University, Nashville, TN,* [2]*Pediatrics, Vanderbilt University, Nashville, TN,* [3]*Neurology, Vanderbilt University, Nashville, TN and* [4]*Institute of Food Chemistry, University of Münster, Münster, Germany.*

Environmental overexposure to the essential trace element manganese (Mn) can result in an irreversible condition known as manganism that shares similar neuropathology with Parkinson's disease (PD), with dopaminergic (DAergic) cell loss associated with motor and cognitive deficits. However, the mechanisms that mediate the pathophysiology of both disorders remain unclear. Many PD genes impart risk for autosomal recessive, early-onset PD, including *parkin/PARK2* and *dj-1/PARK7*. Another PD-associated gene is *SNCA*, encoding for the presynaptic protein α-synuclein. Using *Caenorhabditis elegans* (*C. elegans*), we hypothesized that a loss-of-function mutation in *parkin/pdr1* and *dj-1/djr1.1* would increase vulnerability to Mn toxicity and enhance DAergic neurodegeneration compared to wildtype (WT) worms, which may be altered by expression of WT human α-synuclein (α-Syn). Synchronous L1 worms from WT N2, *pdr-1(gk448)* and *djr1.1(tm918)* mutant strains were acutely exposed to $MnCl_2$ (0–10 mM) for 30 minutes. *pdr1* and *djr1.1* loss enhances intraworm Mn accumulation compared to WT ($p<0.001$) that is rescued in *djr1.1* mutants also expressing α-Syn ($p<0.001$). Interestingly, enhanced oxidative stress upon treatment in the deletion mutants ($p<0.001$) is also rescued in the presence of α-Syn. However, *pdr1* and *djr1.1* show differential degeneration profiles, with α-Syn unable to rescue DAergic cell loss in the *djr1.1* mutants. This was associated with increased *SNCA* mRNA and decreased *dat-1* mRNA levels in *djr1.1* mutants, compared to decreased *SNCA* mRNA and increased *dat-1* mRNA levels in *pdr1* mutants. Thus, we show (1) a novel, neuroprotective role for WT human α-Syn in the background of PD-associated genes against Mn toxicity that may be dependent on its expression level, and (2) support for the role of extracellular dopamine in exacerbating Mn neurotoxicity (Supported by NIEHS R01ES10563).

PS 1357 The Role of a Novel Genetic Factor (SLC30A10) in Manganese-Induced Toxicity in *C. elegans*

P. Chen[1], M. Neely[2], A. B. Bowman[2] and M. Aschner[1]. [1]*Molecular Pharmacology, Albert Einstein College of Medicine, Bronx, NY and* [2]*Neurology, Vanderbilt University Medical Center, Nashville, TN.*

Environmental or occupational exposure to manganese (Mn) causes a neuropathy resembling idiopathic Parkinson's disease (PD). Exposure to excessive Mn has been linked to mitochondrial dysfunction, oxidative stress, protein aggregation and disruption of iron homeostasis. However, the mechanisms that mediate these impairments remain largely unknown, partially due to limited knowledge about Mn transporters. Recently, newly identified mutant alleles in human *SLC30A10* have been found to cause Mn accumulation in the basal ganglia (Tuschl *et al.*, 2012). Patients with mutations in *SLC30A10* show symptoms of hepatic cirrhosis, dystonia, polycythemia and hypermanganesemia. Although clinical studies indicate the potential role of SLC30A10 in cellular efflux, the exact function has yet to be elucidated. Here, we present novel data on the role of SLC30A10 in *C. elegans*. A blast search found 5 potential SLC30A10 homologs in worms. Knock down of these genes resulted in no change (*cdf-2*) or an increase (*cdf-1, ttm-1* and *toc-1*) in survival after Mn exposure, indicating the worm homolog might function differently. Transgenic animals were generated expressing either WT or mutant SLC30A10 in different tissues of the worm. Somatic tissue expression of WT SLC30A10 increases survival rate after Mn exposure; whereas expression in DAergic neurons attenuates their Mn-induced neurodegeneration. In both tissues mutant SLC30A10 has no significant effect. To explore why mutant SLC30A10 loses its Mn-protection activity, we made transgenic animals expressing SLC30A10 fusion protein with a C-terminal green fluorescent protein (GFP) tag. We found that mutant SLC30A10 fails to localize to the cell surface, as the WT form does, and instead accumulated in the cytosol of both DAergic neurons and body wall muscle cells. All together, these results suggest that WT SLC30A10 protects cells from Mn induced toxicity and the mutant protein loses this activity, possibly due to its failure to localize to the cell surface (supported by NIEHS ES010563).

PS 1358 Factors Affecting Manganese Accumulations in Gill Mitochondria of *Crassostrea virginica*

A. Nuhar, T. Shoneye, E. J. Catapane and M. A. Carroll. *Biology, Medgar Evers College, Brooklyn, NY.*

Manganese (Mn) is a neurotoxin causing Manganism in people chronically exposed to elevated levels in their environment. Oxidative stress has been implicated as a factor underlying Mn toxicity and dopaminergic dysfunction. Mitochondria play a key role as both cause and target of oxidative stress damage. The mechanisms of damage caused by Mn is attributed to its capacity to produce toxic levels of free radicals and induce mitochondrial dysfunction, thus enhancing ROS production. Reports indicate Mn accumulates in mitochondria. Controversy exists as to the extent of Mn accumulation within mitochondria and whether this contributes to the cause of Manganism. We use the oyster, *Crassostrea virginica*, as a test animal to study Mn neurotoxicty. We found Mn disrupts the dopaminergic system and impairs mitochondrial respiration. We also found Mn accumulates within mitochondria of gill cells but the mechanism has not been well studied. Mn is believed to utilize mitochondrial Ca^{2+} uniporter and H^+ or Na^+/Ca^{2+} exchanger for movement in and out of mitochondria. We hypothesize Ca channel blockers will alter mitochondrial Mn accumulations. We homogenized and centrifuged gills to prepare mitochondria. Isolated mitochondria were treated with Ca channel blockers then Mn, pelleted and washed to remove non-accumulated Mn. Mitochondria were digested in HNO_3 in a Microwave Digester then analyzed for Mn in a Perkin Elmer AAnalyst 800 AA Spectrophotometer with a THGA Graphite Furnace. Mitochondria treated with Mn (1 - 5 mM for 5 min) exhibited accumulation up to 1000% compared to controls. The channels blockers, $LaCl_3$, diltiazem, verapamil and ruthenium red (0.25 - 2 mM) reduced accumulations. $LaCl_3$ was the most effective in the dose range tested, decreasing accumulations by 90%. The study shows isolated mitochondria accumulate Mn and the mechanism of influx and efflux can be affected by drugs that interact with the Ca uniporter and H or Na/Ca exchanger. This work was supported by grants 0516041171 of NYSDOE and 0622197 of the DUE Program of NSF.

PS 1359 The Toxic Effects of Manganese on Dopamine D2 Receptor Activation Is Not Due to Inactivation of the Phospholipase C Receptor Signal Transduction Component

K. Rogers, I. Beaubrun, M. A. Carroll and E. J. Catapane. *Biology, Medgar Evers College, Brooklyn, NY.*

Manganese (Mn), a neurotoxin causing Manganism, a Parkinsons-like disease disrupts dopaminergic neurotransmission. The mechanism is not fully resolved and reports postulate it to be more related to dopamine (DA) neuron dysfunction rather than degeneration. Lateral cilia of gill of *Crassostrea virginica* are controlled by serotonergic-dopaminergic innervations from their ganglia. DA causes cilio-inhibition, serotonin cilio-excitation. Our previous work showed post-synaptic DA receptors present in gill lateral cells are D2 type, that are G protein-coupled (Gαi/o) metabotrophic receptors. Gαi inhibits adenylyl cyclase and phospholipase C (PLC). We also showed Mn blocks cilio-inhibitory effects of DA by blocking DA post-synaptic receptor activity. The adenylyl cyclase component of the D2 receptor signal transduction pathway was not effected by Mn. We hypothesized the PLC component of the D2 pathway also would not be effected by Mn. To test this we measured cilia beating rates using stroboscopic microscopy. Applying serotonin (10^{-6} - 10^{-3}M) to gill increased cilia beating rates up to 25 beats/min. Applying DA (10^{-6} - 10^{-3}M) decreased rates to 0. Applying Mn (100 μM) prevented the cilio-inhibitory response. Adding m3M3FBS (10^{-6} - 10^{-3}M), a PLC activator, produced a dose dependent increase in beating. Adding U73122 (10^{-6} - 10^{-4}M), a PLC inhibitor, produced a dose dependent decrease in beating. Repeating these experiments in the presence of 100 μM of Mn had no effect on actions of either drug. The study further helps elucidate the neurotoxic mechanism of action of Mn by showing Mn disrupts DA actions at D2 post-synaptic receptors, but does not interfere at the level of adenylyl cyclase or PLC in the signal transduction pathway. This information is helpful to understand causes and potential therapeutic treatments of Manganism. This work was supported by grants NIGMS 2R25GM0600309, NYSDOE 0516041071 and NSF 0622197.

PS 1360 p-Aminosalicylic Acid Prevents the Loss of Immunofluorescence Emissions of Post-Synaptic Dopamine D2 Receptors Due to Manganese Treatment

Y. Chekayev, K. Loney-Walsh, M. A. Carroll and E. J. Catapane. *Biology, Medgar Evers College, Brooklyn, NY.*

Manganese (Mn) a neurotoxin causing Manganism, a Parkinsons-like disease, disrupts dopamine (DA) neurotransmission. The mechanism is not fully resolved and reports postulate it more related to dysfunction of DA D2 receptors than degeneration of DA neurons. Cilia of lateral gill cells of *Crassostrea virginica* are controlled by serotonergic-dopaminergic innervations. DA is cilio-inhibitory, serotonin cilio-excitatatory. We showed post-synaptic DA receptors in gill lateral cells are D2 type, Mn blocks cilio-inhibitory effects of DA, and DA toxicity is blocked by p-aminosalicylic acid (PAS). Questions exist whether Mn decreases the number of post-synaptic DA D2 receptors in brain. We used immunohistofluorescence to test if Mn decreases the number of DA D2 receptors in gill of *C. virginica* and if PAS prevented the decrease. Using 1° antibodies against D2 receptors and FITC-linked 2° antibodies, we quantified DA D2 receptors in gill. Animals were treated with 500 μM of Mn for up to 6 days. Controls were treated without Mn. Gills were excised, fixed, exposed to antibodies and paraffin embedded. Sections were viewed on a epilume fluorescence microscope with FITC filters, and a ProgRes C3 camera. Fluorescence was quantified using ImageJ software from NSF. Fluorescence in sections from animals treated up to 6 days with Mn (500 μM) showed progressive decrease in fluorescence of up to 36% of controls. Animals co-treated up with 500 μM of Mn and PAS did not show reduced fluorescence. The study shows negative correlation between fluorescence intensity of DA D2 receptors in Mn treated animals vs controls, and also shows PAS can negate the effect Mn treatments on D2 receptors. The question of whether the loss in fluorescence intensity is due to an actual decrease in D2 receptor number or if Mn is altering the protein conformation and ligand binding site of D2 receptors needs to be further explored. This work was supported by grants 2R25GM06003 of the Bridge Program of NIGMS, 0516041071 of NYSDOE and 0622197 of the DUE Program of NSF.

PS 1361 Altered Neurotransmitter Levels in Rats Exposed to Manganese: Relevance to Dopaminergic Dysfunction and Neurodegeneration

S. L. O'Neal, J. Lee, J. R. Cannon and W. Zheng. *Purdue University, West Lafayette, IN.*

Excessive exposure to Manganese (Mn) can cause neurologic symptoms similar to, but distinguishable from idiopathic Parkinson's disease (IPD). The question as to whether or not Mn exposure has direct effects on dopamine (DA) and other catecholamines thereby disrupting the nigrostriatal pathway is unanswered. This study was designed to test the hypothesis that subchronic Mn exposure alters neurochemistry. Adult male rats received IP injections of 6 and 15 mg Mn/kg (as MnCl2) as the low- and high-dose groups, respectively, or saline as the control, 5 days per week for 4 weeks. Animals were sacrificed 24 hr after the last injection, and striatum (STR), hippocampus (HP), and substantia nigra (SN) were dissected for quantification of neurotransmitters including: DA, 3,4-dihydroxyphenylacetic acid (DOPAC), homovanillic acid (HVA), 5-hydroxytryptamine (5-HT), 5-hydroxyindolacetic acid (5-HIAA), and γ-aminobutyric acid (GABA) by HPLC. Analysis revealed statistically significant differences in the neurotransmitter content of these three brain regions between control-, low-, and high-dose groups. The level of DA and its metabolites in STR were significantly higher in Mn-exposed animals than in controls ($p<0.05$); DA turnover in SN was also significantly higher in exposed animals than controls ($p<0.05$). Interestingly, GABA levels were significantly higher in HP in exposed animals than in controls. Analysis with atomic absorption spectrometry showed Mn exposure led to a significant accumulation of Mn and copper in the femur as well as other bone tissues. Neurotransmitter differences seen in the striatum may be of particular relevance because alterations could lead to heightened sensitivity to additional insults, particularly due to oxidative modifications of DA. This study provides evidence that dopaminergic neurotransmission is especially sensitive to Mn intoxication.

PS 1362 Half-Life of Manganese (Mn) in Murine Bone following Oral Exposure

W. Zheng, S. L. O'Neal, L. Hong and A. Jones. *School of Health Sciences, Purdue University, West Lafayette, IN.*

A short half-life of Mn in blood circulation, due mainly to the metal's unique property of intracellular distribution, renders it difficult to use blood Mn for risk assessment of Mn toxicity. Available data in literature indicate that bone is a major storage organ for Mn, accounting for 43% of total body Mn. However, the kinetic nature of Mn accumulation in bone, especially with regard to the half-life in bone, remained unknown. This study was designed to understand the time-dependence of Mn distribution in bone tissues with a specific focus on its elimination half-life (t1/2) after subchronic oral exposure. Adult male rats received 50 mg Mn/kg (as MnCl2) by oral gavage, 5 days per week for 0-6 weeks. Animals were sacrificed on 0, 2, 4 or 6 weeks for the uptake study, and on day 1, week 2, 4, 8, or 12 after the cessation of 6-week Mn oral exposure for the t1/2 study. The femur, tibia, humerus and parietal bones were collected at each time point for AAS analysis of Mn concentration in bone (MnBn). After 4-week exposure, MnBn began to show a significant increase in all bone samples analyzed. By the end of 6-week's treatment, there were about 2-3.2 fold increases of MnBn in all bones as compared to those day-0 samples. Bone samples were collected after the stop of 6-week Mn treatment for up to additional 12 weeks; a linear regression analysis of the terminal phase of MnBn-time courses was used to calculate the elimination rate constant (Ke), from which the half-lives were obtained (t1/2=0.693/Ke). The weight of bones did not differ between control and Mn-treated rats at the end of 18-week's experiment. The half-lives of Mn in rat femur, tibia, and humerus bone were calculated to be 77 (r=0.9780), 263 (r=0.9885), and 429 (r=0.9940) days, respectively. These data suggest that a 4-week Mn oral exposure can lead to a significant accumulation of Mn in bone tissues. Moreover, the weight bearing bones such as femur appear to have a shorter t1/2 than in non-weight bearing bones. Whether Mn in bone may serve as an internal source of exposure deserves further investigation. (NIH/NIEHS ES008146)

PS 1363 Olfactory Toxicity in Rats following Manganese Chloride Nasal Instillation

M. L. Foster[1], T. Francher[1], S. Traver[1], D. B. Rao[2], L. Lazarowski[1] and D. C. Dorman[1]. [1]*College of Veterinary Medicine, North Carolina State University, Raleigh, NC and* [2]*Integrated Laboratory Systems, Inc., Durham, NC.*

Occupational exposure to inhaled manganese (Mn) is associated with altered odor recognition (dysosmia); however, the dose response relationship between acute Mn exposure and dysosmia remains poorly understood. Following inhalation, Mn travels along the olfactory nerve from the olfactory epithelium (OE) to the olfactory bulb (OB). This pilot study evaluated two related hypotheses: (a) that intranasal Mn administration increases OE and OB Mn concentrations; and (b) intranasal Mn exposure impairs performance of previously trained rats on a go-no-go olfactory discrimination (OD) task. Male Sprague Dawley rats were trained to either lever press ("go") in response to a positive conditioned stimulus (CS+: vanillin) or to do nothing ("no go") when a negative conditioned stimulus (CS-: amyl acetate) was present. Following odor training, rats were randomly assigned to either a Mn (200 mM $MnCl_2$) or 0.9% saline treatment group (n = 4-5 rats/group). Intranasal administration of either saline or $MnCl_2$ was performed on isoflurane-anesthetized rats as 40 μL bilateral injections using PE10 tubing. Rats were retested 48 hours later using the vanillin/amyl acetate OD task, then euthanized by CO_2 inhalation, followed by collection of the OE and OB. Mn concentrations in tissue samples were analyzed by ICP-MS. An additional cohort of rats (n = 3-4/group) was instilled with the same amounts and euthanized 48 hours later for histopathology examination of the nasal tissue. Mn-exposed rats had increased Mn levels in both the OE and OB and decreased performance in the OD task when compared with control animals. Histopathological evaluation of the caudal nasal cavity showed moderate, acute to subacute suppurative inflammation of the OE and submucosa of the ethmoid turbinates and mild suppurative exudate in the nasal sinuses in animals dosed with $MnCl_2$. No changes were evident in the olfactory bulb. The nasal instillation and OD procedures developed in this study are useful methods to assess Mn-induced olfactory deficits.

PS 1364 Effects of Chronic Manganese Exposure on White Matter Tracts in the Nonhuman Primate Brain: A Diffusion Tensor Imaging Study

J. L. McGlothan[1], J. Hsu[2], S. Mori[2], J. S. Schneider[3] and T. R. Guilarte[1, 2]. [1]*Environmental Health Sciences, Columbia University Mailman School of Public Health, New York City, NY,* [2]*Radiology, Johns Hopkins School of Medicine, Baltimore, MD and* [3]*Pathology, Anatomy, and Cell Biology, Thomas Jefferson University, Philadelphia, PA.*

Exposure to excess levels of manganese (Mn) produces a neurological syndrome with psychiatric, cognitive, and motor abnormalities. Using magnetic resonance imaging (MRI), we have previously shown (Guilarte et al., 2006) that non-human primates exposed to Mn exhibit significant Mn accumulation in white matter (WM) where it is likely to produce toxic effects. Based on these findings, ongoing MRI studies included diffusion tensor imaging (DTI), a sensitive technique to evaluate WM tracts *in vivo*. A total of 7 adult male cynomolgus macaques (Control n=3 and Mn-exposed n=4) underwent DTI scans prior to and after 8 and 18 months

of Mn exposure (1.66-2.5 mg Mn/kg per injection, 2x per week). Eleven different WM tracts in the brain were evaluated for mean diffusivity (MD) and fractional anisotropy (FA). We found a significant increase in MD at 18 months in the external capsule of Mn animals (p=0.04), with no change of MD in any other WM tract or in controls. We also observed significant increases in FA in the genu (p=0.01) and splenium (p=0.04) of the corpus collosum in Mn monkeys at 18 months. A significant increase in FA observed in the posterior thalamic radiation of control monkeys at 8 (p=0.02) and 18 months (p=0.01) was not seen in the Mn animals. While these results are not consistent with a previous study in welders (Kim et al., 2011), increased FA has been noted in mental diseases such as schizophrenia and autism. FA is usually interpreted as a marker of white matter integrity and may be influenced by a multitude of factors including myelination, gliosis, edema, and inflammation. Since DTI is a fairly new technique and many factors may influence the interpretation of results, further studies are needed to understand the biological relevance of the changes observed in this study. [Supported by NIEHS Grant # ES010975]

PS 1365 Comparison of *In Vivo* Manganese Accumulation in Nonhuman Primate and Human Brains

C. Yeh[1, 2], J. L. McGlothan[3], E. J. Ward[1], S. Dharmadhikari[1, 2], S. Snyder[1], Z. Long[1, 2], J. S. Schneider[4], T. R. Guilarte[3] and U. Dydak[1, 2]. [1]*Health Sciences, Purdue Univ, W Lafayette, IN,* [2]*Radiology and Imaging Sciences, IUSM, Indianapolis, IN,* [3]*Env. Health Sciences, MSPH, Columbia Univ, New York, NY and* [4]*Pathology Anatomy and Cell Biology, Thomas Jefferson Univ, Philadelphia, PA.*

Recent studies have shown that while the primary target of manganese (Mn) deposition in the brain is the basal ganglia, cortical regions are also involved in Mn neurotoxicity. Here, we aimed to compare the in vivo accumulation of Mn in the cerebral cortex of non-human primates and occupationally exposed humans.
In a non-human primate study, 4 Mn-exposed and 3 control adult male cynomolgus monkeys underwent magnetic resonance imaging (MRI). A series of inversion recovery images were acquired at baseline and after 8 months of Mn/saline exposure (3.2-5 mg Mn/kg wk). In the human study, 3D T1 relaxation images were acquired from 8 career welders (avg airborne Mn 0.10 mg/m3) and 6 controls from a manufacturer in the U.S. T1 parametric maps were calculated after coregistration and normalization of the images to their respective brain atlas. The exposed groups were compared to the control groups pixel by pixel using a nonparametric Kruskal-Wallis test.
In both humans and monkeys, the T1 parametric maps show significantly higher Mn deposition in the basal ganglia, red nucleus and substantia nigra. Increased Mn was also found in the frontal, temporal and parietal lobe, especially in the insula, primary and supplementary motor cortex. However, significant Mn changes in the visuospatial pathway were only found in monkeys most likely due to the higher levels of Mn exposure than in the human subjects.
Our automatic pixel by pixel analysis on brain Mn concentration maps reveals significant Mn deposition in the cerebral cortex, including the motor regulating network which contributes to neural impulse generation, movement planning and execution, and may underlie the mechanism of Mn-induced neurological dysfunction. The comparison between human and monkeys provides in vivo evidence for similarities in Mn distribution across different species. (NIEHS ES010975, ES020529)

PS 1366 Manganese Neurotoxicity: *In Vivo* GABA Levels Correlate with Motor Deficits in US Welders

S. Dharmadhikari[1, 2], R. Ma[1, 2], Z. Long[1, 2], C. Yeh[1, 2], S. Snyder[1], E. Zauber[3], R. Garcia[4], M. Moriyasu[4], R. M. Bowler[5], J. B. Murdoch[6] and U. Dydak[1, 2]. [1]*School of Health Sciences, Purdue University, W Lafayette, IN,* [2]*Radiology and Imaging Sciences, Indiana Univ School of Medicine, Indianapolis, IN,* [3]*Neurology, Indiana Univ School of Medicine, Indianapolis, IN,* [4]*Alliant Intl Univ, San Francisco, CA,* [5]*San Francisco State Univ, San Francisco, CA and* [6]*Toshiba Medical Research Institute, Mayfield Village, OH.*

High manganese (Mn) exposure, as encountered in some occupational settings, has been associated with motor deficits. The primary sites for Mn deposition are the basal ganglia, which play an important role in movement via the interaction of glutamate (Glu) and γ-aminobutyric acid (GABA). We therefore measured in vivo GABA and Glu levels in Mn-exposed workers using magnetic resonance spectroscopy (MRS) and studied the relationship with fine motor skills.
Welders (n=13) and controls (n=11) were recruited from a US truck trailer manufacturer. Short-echo-time spectra were acquired from the frontal cortex and motor cortex to measure the sum of Glu and glutamine (Glx), and J-edited GABA spectra were acquired from thalamus and striatum. All subjects also underwent a neurological motor exam (UPDRS-III) and several fine motor tests.
Welders had significantly increased UPDRS-III scores and higher levels of thalamic GABA compared to controls. For all subjects increasing thalamic GABA levels correlated with increasing normalized scores of the parallel line test reflecting tremor level (r=0.437, p<0.05), and striatal GABA correlated with Finger Tapping, used to assess motor speed (r=-0.551, p<0.01). In the welders, significant inverse correlations were seen between frontal Glx levels and the grooved pegboard score (r=-0.803, p<0.01), and between motor cortex Glx levels and parallel line test scores (r=-0.651, p<0.05).
The significant correlations of thalamic GABA and frontal Glx levels with tremor level, as well as striatal GABA levels with motor skills, confirm the use of MRS to study neurotoxic effects of Mn on the direct and indirect pathways of the basal ganglia that lead to motor disturbances. (Supported by NIEHS R01 ES020529)

PS 1367 Increased Thalamic GABA in Chronic Manganese-Exposed Metal Workers and Manganism Patients

U. Dydak[1, 2], Y. Jiang[3], X. Li[4], L. Long[4], J. B. Murdoch[5], W. Zheng[1] and Z. Long[1, 2]. [1]*School of Health Sciences, Purdue Univ, West Lafayette, IN,* [2]*Dept. of Radiology and Imaging Sciences, IUSM, Indianapolis, IN,* [3]*Health Toxicology, Guangxi Medical University, Nanning, China,* [4]*Radiology, Guangxi Medical University, Nanning, China and* [5]*Toshiba Medical Research Institute, Mayfield Village, OH.*

Overexposure to manganese (Mn) has been reported to lead to parkinsonism symptoms. We hypothesize that hypokinetic symptoms associated with Mn overexposure correspond to elevated thalamic GABA levels leading to reduced glutamatergic projections to the cortex. Therefore we aimed to test whether Mn-exposed workers and manganism patients may have elevated thalamic GABA levels, as well as reduced cortical glutamate (Glu) levels.
A group of 20 Mn-exposed welders, 19 Mn-exposed smelters, 7 manganism patients and 37 controls were recruited from Guangxi Province, China. Each subject underwent magnetic resonance imaging and spectroscopy exams. Short-echo-time 1H spectra were acquired from the frontal cortex and thalamus to assess levels of Glu, the sum of Glu and its precursor glutamine (together denoted as Glx), and myo-inositol (mI, a glial marker). GABA-edited spectra were also acquired in the thalamus. Metabolites are expressed as ratios over creatine (Cr).
Over three years we consistently found significantly increased thalamic GABA/Cr in welders, smelters, and manganism patients compared to controls (p<0.01 for all comparisons). Smelters showed significantly decreased frontal Glu/Cr, thalamic Glu/Cr and thalamic Glx/Cr (p<0.05 for all comparisons). Moreover, welders had significantly increased frontal mI/Cr and both groups of workers had significantly decreased thalamic mI/Cr (p<0.05 for all comparison).
Overall our results suggest increased thalamic GABAergic inhibition in Mn-exposed workers and manganism patients, as well as decreased glutamatergic excitation and Glu-Gln cycling in the frontal cortex of smelters. These metabolic changes may aid in understanding the mechanism of Mn-caused motor and cognitive deficits. (Supported by NIH/NIEHS R21 ES017498, R01 ES020529 and NSF of China #81072320)

PS 1368 GABA Levels Correlate with Exposure Levels and Brain Deposition of Manganese in US Welders

R. Ma[1, 2], C. Yeh[1, 2], E. J. Ward[1], Z. Long[1, 2], J. B. Murdoch[3], S. Snyder[1], E. Zauber[4], F. Rosenthal[1] and U. Dydak[1, 2]. [1]*School of Health Sciences, Purdue Univ., W Lafayette, IN,* [2]*Radiology and Imaging Sciences, Indiana Univ. School of Medicine, Indianapolis, IN,* [3]*Toshiba Medical Research Institute, Mayfield Village, OH and* [4]*Neurology, Indiana Univ. School of Medicine, Indianapolis, IN.*

Excessive manganese (Mn) exposure has been associated with decline in cognitive and motor function. Our previous study in a cohort of highly Mn-exposed Chinese workers found significantly elevated thalamic γ-aminobutyric acid (GABA) levels. The current study explored the relationships among brain GABA levels measured in vivo by magnetic resonance spectroscopy (MRS), brain Mn deposition measured by MRI and individual Mn exposure levels in a typical US occupational setting.
Thirteen welders and eleven controls were recruited from a US truck trailer manufacturer. Subjects underwent personal air sampling and filled out a questionnaire of detailed work history for the estimation of individual exposure to respirable Mn. For each subject a series of 3D images were acquired on a 3T GE Signa MRI scanner and used to create high-resolution T1 relaxation maps, an inverse indicator of Mn deposition. GABA spectra were acquired from the thalamus with a TE68 MEGA-PRESS sequence and quantified using LCModel, a spectral fitting tool.
GABA levels were significantly higher in welders vs. controls [2.45±0.68 mM vs. 1.40±0.45 mM, p<0.001]. Increased thalamic GABA levels significantly correlated with (a) average exposure estimated for the previous three months before the MRI exam [R=0.649, p<0.05] and with (b) decreased T1 relaxation time in the substantia nigra, denoting increased Mn deposition [R=-0.589, p<0.05].

These results confirm the elevation of thalamic GABA levels in a typical US occupational setting. The significant correlations between increased GABA levels and recent exposure levels, as well as with brain Mn accumulation in the substantia nigra, suggest that GABA-edited MRS in conjunction with quantitative T1 relaxation MRI may serve as a biomarker of Mn exposure. (Supported by NIEHS R01 ES020529 and CDC/NIOSH T03 OH008615)

PS 1368a Potential Prevention Strategies to Reduce the Risk of Neurotoxicity Associated with Manganese-Containing Welding Fumes

K. Sriram, A. M. Jefferson, G. X. Lin, A. Afshari, S. Stone, W. McKinney, M. Jackson, M. J. Keane, B. T. Chen, D. G. Frazer and J. M. Antonini. *CDC-NIOSH, Morgantown, WV.*

Welding generates complex metal aerosols, inhalation of which is thought to cause Parkinson's disease (PD)-like neurotoxicity, due to the presence of manganese (Mn) in the welding electrodes. As neurological disorders are generally progressive in nature, with latency between insult and appearance of clinical symptoms, a logical approach for workplace safety and health is to prevent adverse exposures. For welding, this can be achieved by minimizing welding fume (WF) generation rate and/or suitably modifying existing welding practices to reduce toxic exposures. Here, we show that by specifically modulating welding voltage, keeping current and shielding gas constant, the fume composition and neurotoxicological properties of WF can be significantly altered. Rats were exposed by whole-body inhalation to filtered air or WF particulates generated by gas-metal arc-stainless steel welding (GMA-SS; 40 mg/m3; 3h/d x 10d) either at 25V (standard/low; LVSS) or at 30V (high; HVSS) voltage. Both conditions produced good weld quality and similar particulate morphology, although aerosols from HVSS welding comprised of a larger fraction of ultrafine particulates that are characteristically considered to be more toxic than their fine counterparts. Exposure to particulates from LVSS welding caused neuroinflammation (increased Ccl2, Tnfa, Nos2; 1.5 - 3.9 fold; $P<0.05$) and decreased PD-related proteins (Th, Park5, Park7; 18 - 47%; $P<0.05$) in the dopaminergic brain areas, striatum and midbrain. Paradoxically, exposure to particulates from HVSS welding did not elicit any dopaminergic neurotoxicity. We determined that the lack of neurotoxicity may be a consequence of the reduced solubility of manganese in HVSS fumes. Our findings show promise for modified welding practices as a potential prevention strategy for Mn-related neurotoxicity during welding; however, it warrants additional investigations to determine if such modifications can be suitably adapted at the workplace to avert or reduce neurological risks.

PS 1368b The Role of the Transient Receptor Potential Ankyrin 1 (TRPA1) Channel in Methylmercury (MeHg)-Induced Ca^{2+} Dysregulation

H. Hannon and W. D. Atchison. *Pharmacology/Toxicology, East Lansing, MI.*

MeHg biphasically elevates $[Ca^{2+}]_i$, with the first (P1) and second (P2) phases attributed to Ca^{2+} release from, in part, IP_3-sensitive intracellular stores and extracellular Ca^{2+} influx through Ca^{2+}-permeable ion channels, respectively. MeHg-induced $[Ca^{2+}]_i$ dysregulations have been correlated with reduced viability of susceptible neuronal populations *in vitro*. Because paresthesia is the preeminent sign of MeHg intoxication, and the size and number of neurons of the dorsal root ganglia (DRG) are reduced in poisoned individuals, molecular entities unique to DRG may heighten sensitivity to MeHg. Heterologous expression was used in this study to investigate the contribution of TRPA1, a Ca^{2+}-permeable ion channel highly expressed in DRG, in mediating Ca^{2+} dysregulation throughout acute MeHg exposure. HEK 293 cells were transfected with human TRPA1 72 hrs prior to single-cell microfluorimetry studies. Fura-2 AM, a ratiometric Ca^{2+} fluorophore, was used to measure relative changes in $[Ca^{2+}]_i$ in transfected cells throughout exposure to MeHg (1, 2 μM). Time-to-onset of P1 was hastened in TRPA1-HEK exposed to 1 μM MeHg, as compared to untransfected HEK (UT) (5.9±0.8 min and 11.1±0.5 min, respectively; mean ± SEM). This suggests that TRPA1 provides a more kinetically favorable route of entry for low [MeHg]. Expression of TRPA1 did not alter the time-to-onset of P2 between TRPA1-HEK (39.7±2.2 min) and UT (37.4±1.5 min) exposed to 1 μM MeHg. Similarly, TRPA1 expression had no effect on the times-to-onset of neither P1 nor P2 in TRPA1-HEK (4.4±0.7 and 26.1±2.7 min, respectively) and UT (5.1±0.2 and 24.3±0.9 min, respectively) exposed to 2 μM MeHg. These results suggest Ca^{2+} entry through TRPA1 does not significantly contribute to overall $[Ca^{2+}]_i$ dysregulation following MeHg exposure. This, combined with the fact that P1 is unaffected by TRPA1 expression at higher [MeHg], suggests that TRPA1 may be a sensitive target for time- and concentration-dependent block by MeHg. Supported by NIH grant R01ES03299.

PS 1369 Methylmercury Induces Apoptosis in Neuronal Cells through ROS-Mediated Endoplasmic Reticulum Stress-Regulated Signaling Pathway

Y. Chung[1], F. Tang[2], C. Su[3], T. Lu[4], C. Wu[5], K. Chen[7], D. Hung[8], Y. Chen[4], C. Yen[1] and C. Huang[6]. *[1]Department of Occupational Safety and Health, Chung Shan Medical University, Taichung, Taiwan, [2]Department of Occupational Medicine, Changhua Christian Hospital, Changhua, Taiwan, [3]Department of Otorhinolaryngology, Head and Neck Surgery, Changhua Christian Hospital, Changhua, Taiwan, [4]Department of Physiology and Graduate Institute of Basic Medical Science, China Medical University, Taichung, Taiwan, [5]Department of Public Health, China Medical University, Taichung, Taiwan, [6]School of Chinese Medicine, China Medical University, Taichung, Taiwan, [7]Department of Urology, China Medical University Hospital, Taichung, Taiwan and [8]Division of Toxicology, Trauma & Emergency Center, China Medical University Hospital, Taichung, Taiwan.*

Objectives: Methylmercury (MeHg) is a well-known environmental pollution. The human beings expose to methylmercury through ingestion, which can cause irreversible nervous system dysfunction and injuries. However, effects and possible mechanisms of MeHg-induced neurotoxicity remained unclear. In this study, we attempted to investigate the important roles of endoplasmic reticulum (ER) stress-regulated pathway in MeHg-induced neurotoxicity.
Results: MeHg significantly decreased cell viability in a dose-dependent manner (1-5 μM) and induced the increase in caspase-3 activity, annexin V-FITC binding, and the protein expressions of caspase cascades in Neuro-2a cells, indicating that MeHg could induce neuronal cell apoptosis. Moreover, exposure of Neuro-2a cells to MeHg could trigger ER-stress as indicated by several key markers (GRP-78, GRP-94, CHOP, and XBP-1) and upstream molecules (the phosphorylation of PERK, eIF2-α, and IRE-1), and caspase-12 cleavage. Pretreatment with antioxidant NAC and transfection with specific si-RNA (GRP-78, GRP-94, CHOP, and XBP-1, respectively) could effectively attenuate MeHg-induced cytotoxicity, apoptotic events and ER stress-related signals.
Conclusions: These results indicate that the ROS production triggered ER-stress signaling pathway involves in MeHg-induced neuronal cell apoptosis.

PS 1370 Effect of Methylmercury (MeHg) on RNA Expression of Voltage-Gated Calcium Channels (VGCCs) in Naïve and Differentiated F11 Cells

K. Z. Perez-Vale, H. Hannon and W. D. Atchison. *Pharmacol./Toxicol., Mich State Univ, E. Lansing, MI.*

MeHg is an environmental contaminant that elevates $[Ca^{2+}]_i$ in two kinetically-distinct phases. Phase one (P1) consists of Ca^{2+} release from intracellular storage organelles, whereas phase two (P2) results from an influx of Ca^{2+} through Ca^{2+}-permeable ion channels. MeHg-induced elevations in $[Ca^{2+}]_i$ have been correlated with increased cell death. This study surveyed VGCC RNA expression in MeHg-exposed F11 cells, an immortalized cell line derived from dorsal root ganglia. Changes in RNA expression of the pore-forming subunit of the L-, N-, P/Q-, R- and T-type VGCC isoforms (*cacna1c*, *1b*, *1a*, *1e*, and *1h*, respectively) following MeHg exposure was examined by polymerase chain reaction (PCR). F11 cells were cultured and differentiated (2 μM retinoic acid) for 24-72 hrs prior to 1 hr MeHg exposure (1, 2 and 5 μM). 24 hrs after MeHg exposure, RNA was isolated and converted to cDNA. PCR was performed on cDNAs and relative changes in RNA were determined by $2^{-\Delta\Delta Ct}$. Differentiation alone increases the RNA expression of *cacna1c* and *cacna1a* in F11 cells at 72 hours (2.55±0.05 and 2.51±0.05, respectively; mean fold-change ± SEM). Differentiated F11 cells also express low levels of RNA for *cacna1b* (1.01±0.04), *cacna1e* (0.45±0.04), and *cacna1h* (1.12±0.03); exposure to MeHg reduces RNA expression of these genes in a concentration-dependent manner, with 5 μM MeHg reducing *cacna1a*, *cacna1c*, and *cacna1h* RNA most markedly (0.45±0.06, 1.06±0.09, and 0.63±0.04, respectively). Downregulation of RNA expression was also dependent upon the differentiation time point; cells differentiated for longer periods displayed a greater reduction of *cacna1* expression universally. Changes in RNA expression may reflect a concomitant alteration in protein expression, thus these data may indicate distinct VGCC isoforms as critical contributors to Ca^{2+} influx in P2. Because RNA expression of *cacna1c* and *cacna1a* is most abundant following acute MeHg exposure, the L- and P/Q-type VGCCs may be significantly involved in cytotoxic mechanisms. Supported by NIH grant R01ES03299 and R25NS54467.

PS 1371 Methylmercury Attenuates A23187-Induced Increase in Dopamine Release of PC12 Cells

M. Khalid[1, 2], M. Rios[1, 3] and W. D. Atchison[1, 2, 3]. [1]*Department of Pharm/Tox, Michigan State University, East Lansing, MI,* [2]*Center for Integrative Toxicology, Michigan State University, East Lansing, MI and* [3]*CMIB, Michigan State University, East Lansing, MI.*

Methylmercury (MeHg) causes calcium (Ca)-dependent neurotoxicity, which includes increases in spontaneous release of neurotransmitters. Both intracellular Ca ($[Ca^{2+}]_i$) release and extracellular Ca entry contribute to this effect. Although an inextricable link between alterations in Ca homeostasis and MeHg-induced neurotoxicity has been demonstrated in the past, Ca's exact role is unclear. Previously, work in our lab has revealed a concentration- and time-dependent relationship between MeHg and extracellular dopamine (DA). In this study, we seek to manipulate $[Ca^{2+}]_i$ levels to further define Ca's relationship with MeHg and release of DA. A23187, a Ca^{2+} ionophore, which increases $[Ca^{2+}]_i$, was therefore used to elucidate the contribution of $[Ca^{2+}]_i$ on the quantity of DA released by rat pheochromocytoma (PC12) cells. Forty-eight hours before treatment, undifferentiated PC12 cells were seeded at a density of $7x10^5$ cells/mL in poly-D-lysine coated well plates. At time of experiment, cells were pre-treated with either vehicle or 1 μM A23187 for 30 min. Subsequently, treatment medium was replaced with either vehicle, 1 μM A23187, or a combination of 1 μM A23187 and 2 μM MeHg for an incubation period of 60 min. Following treatment, plates were centrifuged and treatment medium was collected for analysis by high performance liquid chromatography (HPLC) to quantify extracellular DA. Extracellular DA levels increased significantly following treatment with A23187, as compared to vehicle-treated controls. Although co-treatment with MeHg increased DA levels when compared with basal levels, it blunted the extent of increase caused by treatment with the ionophore alone. These data suggest that although MeHg is able to increase the level of DA released by PC12 cells, its effect is not directly correlated with the amount of Ca available in the intracellular space. Supported by a ViCTER supplement to NIH grant RO1ES03299 and T32ES007255.

PS 1372 Contribution of Cholinergic Receptors to Methylmercury-Induced Cytotoxicity in PC12 Cells

C. Colón[2], Y. Rodriguez[3], M. Rios[1] and W. D. Atchison[1]. [1]*Michigan State University, East Lansing, MI,* [2]*University of Puerto Rico, Cayey, Puerto Rico and* [3]*St. Mary's University, San Antonio, TX.*

Ca^{2+}-mediated cell death is a common response of neurons to methylmercury (MeHg) exposure. However, the pathways by which MeHg increases $[Ca^{2+}]_i$ and causes cell death appear to vary, and may reflect direct actions on receptors or release of neurotransmitters. Prior studies showed that cholinergic receptors (AChRs) are potential targets for MeHg-mediated Ca^{2+} dysregulation. However, the extent to which they respond to MeHg in the absence of ACh and their relative contributions to cytotoxicity are not known. We studied the role of AChRs in MeHg-induced cytotoxicity in rat PC12 cells, a model that expresses both muscarinic (mAChR) and nicotinic receptors (nAChR) but does not express glutamate receptors, an additional potential target for MeHg-induced elevation of $[Ca^{2+}]_i$. Nerve growth factor-differentiated PC12 cells were treated for 1h with 1, 2, or 5μM MeHg. Cytoxicity was examined using the Live Dead Assay® 1 or 24h after MeHg treatment concluded. Mecamylamine (MEC, 5μM) and atropine (10μM), nAChR and mAChR antagonists respectively, were used to determine the relative involvement of nAChRs and mAChRs to MeHg-induced cell death. Viability at 1 and 24h after MeHg was reduced in a concentration-, but not time-dependent manner. At 1h, MeHg-induced cytotoxicity ranged from 33% (1μM) to 57% (5μM) and at 24h from 35% (1μM) to 65% (5μM). Pretreatment with either MEC or atropine protected PC12 cells from MeHg-induced cell death at both time points, however protection was proportional to the [MeHg], i.e., protection against low [MeHg] (1 μM) was much more effective than that at 5μM MeHg. At 1μM MeHg protection ranged from 77-97% (3-23% cytotoxicity) at both 1 and 24h, whereas at 5μM MeHg protection was only in the range of 32-50%. Thus both mAChRs and nAChRs contribute to Ca^{2+}-induced cytotoxicity by MeHg. This occurs in the absence of a cholinergic agonist, suggesting direct actions of MeHg on AChRs. This project was supported by NIH grants: R25NS065777 and R25GM059429.

PS 1373 Methylmercury Exposure Inhibits NGF-Triggered TrkA Phosphorylation and Leads to Apoptotic Neuronal Cell Death in Differentiating PC12 Cells

M. Fujimura[1] and F. Usuki[2]. [1]*Basic Medical Sciences, National Institute for Minamata Disease, Minamata, Kumamoto, Japan and* [2]*Clinical Medicine, National Institute for Minamata Disease, Minamata, Kumamoto, Japan.* Sponsor: A. Naganuma.

Methylmercury (MeHg) is an environmental neurotoxicant which induces selective cell death in the nervous systems. In this study, we investigated the effect of MeHg on differentiating neurons using PC12 cells in the presence of nerve growth factor (NGF). NGF is known to enhance the vitality and cellular functions in neurons. The PC12 cells exhibited apoptosis 2 days after exposure to 100 nM MeHg in the presence of 50 ng/ml NGF. During the course of MeHg-induced apoptotic cell death, inhibition of neuronal cell differentiation preceded apoptosis. Time course study of immunocytochemistry and ELISA analyses for neurite specific protein namely, neurofilament triplet H protein (NF-H), demonstrated that MeHg inhibited the expression of NF-H protein before the induction of apoptosis. To further investigate the factors responsible for inhibition of neuronal cell differentiation and subsequent apoptotic cell death, we investigated the expression levels of neurotrophic factor receptors, tropomyosin receptor kinase (Trk) A, B, and C, which regulate neuronal cellular differentiation in neurons. Western blot analysis demonstrated that MeHg inhibited selectively the TrkA phosphorylation, whereas changes in the total TrkA, B, and C levels were not observed. Furthermore, we demonstrated that a GM1 ganglioside analog, which is known to enhance NGF-triggered TrkA phosphorylation, prevented the differentiating PC12 cells against MeHg-induced apoptotic cell death. These findings suggest that MeHg exposure inhibits NGF-triggered TrkA phosphorylation selectively and lead to apoptotic neuronal cell death in differentiating PC12 cells.

PS 1374 Inflammatory Response to Methlymercury or Manganese in Astrocytes and Microglia

N. L. Parmalee[1], Y. Yu[2], R. L. Davis[3] and M. Aschner[1]. [1]*Molecular Pharmacology, Albert Einstein College of Medicine, Bronx, NY,* [2]*Pediatrics, Vanderbilt University Medical Center, Nashville, TN and* [3]*Pharmacology and Physiology, Oklahoma State University Center for Health Sciences, Tulsa, OK.*

Exposure to metals, including methylmercury (MeHg) and manganese (Mn), has been shown to lead to selective neurotoxicity, causing cognitive and movement defects and neuronal cell loss. We report here the response in expression of the proinflammatory cytokine tumor necrosis factor-α (TNF-α) and chemotactic monocyte protein 1/chemokine C-C motif ligand 2 (MCP-1/CCL2) in both astrocytes and microglia following exposure to MeHg or Mn. Primary cultures of astrocytes and microglia from one day old neonatal rat brains were exposed to 50, 100, or 500 μM $MnCl_2$, or 1, 5, or 10 μM MeHg. Expression of TNF-α or MCP-1 was measured by ELISA and normalized against total protein as measured by bicinchonic acid assay. MeHg, but not Mn exposure induced expression of MCP-1 in both astrocytes and microglia in a concentration-dependent fashion. Mn exposure significantly reduced TNF-α expression in microglia. Microglia exposed to MeHg showed a concentration-dependent increase in TNF-α expression though the difference failed to reach statistical significance. Mn exposure had no effect on TNF-α levels in astrocytes, while exposure to Mn in microglia resulted in reduced levels of TNF-α. Astrocytes and microglia express proinflammatory cytokines and chemokines under disease or injury conditions, prompting changes in the blood brain barrier and infiltration of leukocytes, events that may lead to neuroprotection or to cell death. MCP-1 upregulation in both astrocytes and microglia suggest that exposure to MeHg induces a neuroinflammatory response. Astrocytes responded to MeHg with reduced TNF-α, the opposite of microglia, consistent with the idea that the two cell types respond differently based on differential uptake and sensitivity and thus may have differing roles in the etiologies associated with neurological disorders associated with MeHg or Mn exposures. Supported by NIH ES 007331 and ES 10563.

PS 1375 Comparative Effects of Methylmercury on Cerebellar and Cortical Astrocytes

R. J. Jaiman[1] and W. D. Atchison[1, 2]. [1]*Neuroscience Program, Michigan State University, East Lansing, MI and* [2]*Pharmacology & Toxicology, Michigan State University, East Lansing, MI.*

Although methylmercury (MeHg) primarily affects neurons, especially the granule cells in the cerebellum, astrocytes are also targets of the metal. MeHg-induced neurotoxicity in astrocytes has been studied extensively in the cortical layer. However, effects on cerebellar astrocytes are less studied, and regional differences can occur in

astrocytes between the two areas. The goal of this study was to compare the toxicity of MeHg on cerebellar and cortical astrocytes. Determining if MeHg differentially affects astrocytes from these two brain regions could help us understand cellular mechanisms underlying the preferential sensitivity of cerebellar granule cells to MeHg. Primary astrocyte cultures from the cerebellum and cortical forebrain layer were obtained from C57BL/6 male mice. At 14-15 DIV, cells were exposed for 3h to 0μM, 2μM, 5μM, 10μM, or 15μM MeHg. Cyotoxicity was measured 24h later using EthD-1 and Calcein AM. In parallel cell cultures, GFAP and the nuclear fluorogenic indicator DAPI were used to calculate the percentages of astrocytes in the cultures. The percentages in the cerebellar and cortical cell cultures were 58% and 62% respectively. The mean percentage of cell death in the cerebellum was: 0.5%, 26%, 52%, 88%, and 96% at 0, 2, 5, 10, or 15μM MeHg respectively. In the cortical layer it was: 1.3%, 50%, 81%, 88%, and 94% respectively. Cell viability of cortical astrocytes was significantly reduced at 2 -15 μM MeHg; in cerebellar astrocytes viability was reduced only at 5-15 μM. There was a significant difference at 2 μM and 5 μM of MeHg when cerebellar and cortical were compared. The LC50s of the cerebellum and cortical layers were 4.1 μM and 1.6 μM MeHg, respectively. Thus whereas cerebellar granule cells are more susceptible to MeHg, their attendant astrocytes are less sensitive to MeHg-induced cytotoxicity than are cortical astrocytes, and brain region-dependent differences in cytotoxicity of astrocytes occurs in response to MeHg. Supported by NIH grants R01ES03299, R25NS54467 and T32GM092715.

PS 1376 GABA$_A$ Receptors Are Not a Primary Contributor to Methylmercury-Induced Cell Death in Transiently Transfected HEK293 Cells

D. Wiwatratana[1], C. Colon Ortiz[2], N. Delvalle[2] and W. D. Atchison[1, 2]. [1]*College of Vet Med, Michigan State University, East Lansing, MI and* [2]*Pharm/ Tox, Michigan State University, East Lansing, MI.*

Altering of GABA type A receptors(GABA$_A$R)-mediated inhibitory function by MeHg contributes to cerebellar dysfunction. The effect is more pronounced in cerebellar granule cells (CGCs) than the neighboring Purkinje cells (PKCs). Differential effects of MeHg on these two types of neurons could relate to differential expression of GABA$_A$R subunits. CGCs express α_1 and α_6 subunits; PKCs express only α_1 subunits. The subunits confer markedly different properties to GABA$_A$Rs as they are preferentially co-expressed with different auxiliary subunits such as γ_{2s} and δ. The δ subunit is very important in CGC tonic inhibition. Its preferential disruption by MeHg could cause enhanced excitability in CGCs, and promote Ca-induced cell death. Two questions were tested: 1) does co-expression of differential auxiliary γ_{2s} and δ subunits with α_6 contribute to MeHg-induced cell death? 2) Will differential subunit combinations of α and β subunit-containing GABA$_A$Rs exacerbate MeHg-induced cell death? HEK293 cells were transiently transfected with combinations of GABA$_A$R subunits and exposed for 3 or 6h to 1, 2 or 5μM MeHg. Cell viability was assessed using a Live/Dead cytotoxicity assay. HEK293 cell death increased with increasing [MeHg] at both 3 and 6h exposure. No significant difference between these exposure exists. Acute mortality rate induced by MeHg is similar for GABA$_A$Rs having $\alpha_6\beta_2\gamma_{2s}$ and $\alpha_6\beta_2\delta$ compositions and did not increase over that of untransfected or GFP-transfected HEK cells. Comparisons of susceptibility to MeHg-induced cell death among differential GABA$_A$R subunit compositions also indicated no significant difference. HEK cells transfected with GABA$_A$R containing $\alpha_1\beta_2\gamma_{2S}$, $\alpha_1\beta_3\gamma_{2S}$, $\alpha_1\beta_2\delta$, $\alpha_1\beta_3\delta$, $\alpha_6\beta_2\gamma_{2s}$, $\alpha_6\beta_3\gamma_{2s}$, $\alpha_6\beta_2\delta$ and $\alpha_6\beta_3\delta$were no more susceptible to MeHg-induced cytotoxicity. While GABA$_A$Rs are very sensitive targets to MeHg, a simple direct action of MeHg on the receptor will not explain the heightened sensitivity of CGCs.

PS 1377 Effects of Methylmercury on *Caenorhabditis elegans* Calcium Ion Channel Mutant Strains

S. M. Spencley[1], K. R. Sherer[2], R. Hajela[1] and W. D. Atchison[1, 2]. [1]*Dept. Pharmacology/Toxicology, Michigan State University, East Lansing, MI and* [2]*College of Veterinary Medicine, Michigan State University, East Lansing, MI.*

Caenorhabditis elegans (C. elegans) strains KC136, CB55, DM612, JD21, MT6129, and DA995 were used to examine the percent viability for GOF or LOF L-, P/Q- or T-type voltage-gated Ca^{2+} channels (VGCCs) in the presence of methylmercury (MeHg) using a gel rite hanging drop medium. Exposure of L3 worms to 1.0-100 μM MeHg resulted in decreased viability with increasing [MeHg] for 24 and 48 h. We expected that GOF VGCC mutants would have decreased viability resulting from increased Ca^{2+} influx in the cell leading to excitotoxicity while LOF mutants would have increased viability after MeHg treatment; however, we observed the opposite effect. In general, LOF mutants for high-voltage activated VGCCs exhibited decreased viability when exposed to MeHg, while the null mutation for low-voltage activated VGCCs led to increased viability. GOF high-voltage activated VGCC mutants had increased viability. Two explanations for this result are either upregulation of other VGCC subtypes leading to increase Ca^{2+} influx or complete block of Ca^{2+} entry to the cell thus decreasing viability. A third possible explanation for these results is that mutants have decreased Ca^{2+} buffering capacity and physiologic Ca^{2+} levels lead to death. To further explore these possibilities, KC136 was pretreated with 0.25 or 0.5μM of the L-type VGCC antagonist nemadipine-A (NEM-A) before exposure to 1.0-100 μM MeHg. NEM-A can cross the *C. elegans* cuticle, unlike other antagonists such as verapamil. Pretreatment of KC136 with 0.25 μM NEM-A plus MeHg exposure had no significant effect. Pretreatment of KC136 worms with 0.5 μM NEM-A significantly decreased viability at lower [MeHg] over 24 h without any change at 48 h. However, the significant effect may be due to NEM-A alone rather than a compounded effect of NEM-A and MeHg exposure. Supported by NIH grant R01ES03299.

PS 1378 The Putative Multidrug Resistance Protein MRP-7 Inhibits Methylmercury-Associated Animal Toxicity and Dopaminergic Neurodegeneration in *Caenorhabditis elegans*

N. M. VanDuyn[1], W. Li[1], J. Trinidad[2] and R. M. Nass[1]. [1]*Pharmacology and Toxicology, Indiana University School of Medicine, Indianapolis, IN and* [2]*Chemistry, Indiana University, Bloomington, IN.*

Background: Recent epidemiological and vertebrate studies suggest that MeHg exposure may contribute to dopamine (DA) neuron vulnerability and the propensity to develop Parkinson's disease (PD). We have developed a novel *Caenorhabditis elegans* (*C. elegans*) model of MeHg toxicity and have shown that low, chronic exposure confers embryonic defects, developmental delays, and DA neuron degeneration. Aims/Objectives: In this study we asked what genes and molecular pathways are involved in MeHg-induced whole animal and DA neuron pathology. Methods: We utilized a reverse genetic screen, biochemical assays, immunofluorescence, transgenic *C. elegans*, RT-PCR, MS, Western analysis, and neuronal morphology analysis to characterize expression, localization and the role that SKN-1, MRP-7 and post-translational modifications play in MeHg-induced whole animal and DA neuronal death. Results: Over 17,000 genes were screened for whole animal sensitivity to MeHg, and 92 genes were identified (90% have strong human homologues) that affect whole animal and/or DA neuron pathology. Here we report detailed analysis of a putative plasma membrane transporter's role in MeHg-associated DA neuroprotection. Specifically we demonstrate that genetic knockdown of MRP-7 results in a 2-fold increase in Hg levels and a dramatic increase in stress response proteins associates with the endoplasmic reticulum, golgi apparatus, and mitochondria, as well as an increase in MeHg-associated animal death. Chronic exposure to low concentrations of MeHg induces MRP-7 gene expression, while exposures in MRP-7 genetic knockdown animals results in a loss of DA neuron integrity in without affecting whole animal viability. Conclusions: These studies show for the first time that a multidrug resistance protein is expressed in DA neurons, and its expression inhibits MeHg-associated DA neuron pathology. Support: NIEHS ES014459 and ES003299 to RN; and EPA STAR Graduate Fellowship to NVD.

PS 1379 NAD$^+$ Supplementation Attenuates Methylmercury Toxicity in *Caenorhabditis elegans*

S. W. Caito and M. Aschner. *Molecular Pharmacology, Albert Einstein College of Medicine, Bronx, NY.*

Methylmercury (MeHg) is a persistent pollutant with known neurotoxicity. MeHg causes oxidative stress and mitochondrial dysfunction *in vitro* and animal models. This can lead to altered cell metabolism and energetics. It has been reported that MeHg decreases cellular nicotinamide adenine dinucleotide (NAD^+), however the effects on NAD-dependent enzymes and cellular functions have not been characterized. *Caenorhaditis elegans* (*C. elegans*) is a powerful genetic model for the investigation of neurotoxicity of MeHg, as worms readily accumulate the metal, leading to decreased survival and dopaminergic neurodegeneration. Herein, we tested the hypothesis that NAD^+ supplementation could attenuate MeHg toxicity and dopaminergic (DAergic) neurodegeneration. Worms were treated with 1 mM NAD^+ prior to MeHg treatment and assessed for lethality. Treatment with increasing doses of MeHg decreased survival of *C. elegans* (LD_{50} = 20.24 μM), and NAD^+ pre-treatment significantly attenuated its toxicity (LD_{50} = 34.6 μM, $p < 0.001$). Furthermore, worms lacking *pnc-1*, the rate-limiting enzyme in NAD^+ synthesis, were highly sensitive to MeHg toxicity (LD_{50} = 3.598 μM, $p < 0.001$). As MeHg is implicated in DAergic neurodegeneration involved in Parkinson's disease, we determined whether DAergic-dependent behavior was altered by NAD^+depletion in response to MeHg treatment. Wildtype worms had significantly less DAergic behavior as measured by the basal slowing response ($p < 0.05$). The DAergic behavior was further decreased in *pnc-1* mutants treated with MeHg ($p < 0.05$), suggesting that DAergic-dependent behavior may be altered by NAD^+ levels. DAergic cell morphology was evaluated following NAD^+ supplementation in worms express-

ing MCherry under the dopamine transporter promoter. MeHg significantly altered neuron morphology, which was significantly improved by pretreatment with NAD^+. Overall our data suggests that MeHg toxicity and DAergic dysfunction are dependent on cellular NAD^+ levels, which may be due to alterations in cytoprotective NAD-dependent enzymes, such as sirtuins and PARPs.

PS 1380 Nuclear Factor Erythroid 2-Related Factor 2 (Nrf2) Is a Modulator of Methylmercury-Induced Neurotoxicity

M. Culbreth[1], E. B. Bisen-Hersh[2] and M. Aschner[1]. [1]*Molecular Pharmacology, Albert Einstein College of Medicine, Bronx, NY and* [2]*Anesthesiology, Vanderbilt University, Nashville, TN.*

Methylmercury (MeHg) is a neurotoxicant, which poses a continued health risk to the human population. Despite extensive research, its precise mechanism of action has not been fully elucidated. Furthermore, the genetic basis for MeHg susceptibility is not well defined. In order to explore genetic modulators of MeHg-induced neurotoxicity, we utilized the BXD recombinant inbred (RI) mouse cohort. This cohort consists of fully inbred strains, containing varied nuclear factor erythroid 2-related factor 2 (Nrf2) expression. Nrf2 is a well-established antioxidant gene that is activated in response to oxidative stress. We hypothesized that mice with high Nrf2 expression would be less vulnerable to MeHg-induced neurotoxicity versus those with low expression. Therefore, mice were selected that exhibited either high (BXD21, BXD31) or low (BXD28, BXD84) Nrf2 expression, and the role of Nrf2 in modulating MeHg-induced neurotoxicity was examined. Astrocyte cultures were prepared from post-natal day 1 (PND1) pups, and treated approximately 3 weeks post-isolation with 1, 5, or 10μM MeHg for 90 min. After exposure, cells were collected for western blot analysis. BXD21/31 mice had significantly higher baseline Nrf2 expression relative to BXD28/84 ($p<0.001$). Following MeHg exposure, BXD31 mice exhibited higher Nrf2 expression compared to BXD28 with an overall significant effect of strain ($p<0.001$), treatment ($p<0.001$) and interaction ($p<0.01$). In addition, BXD31 mice were less sensitive to the effects of MeHg based on MTT and LDH assays with an overall significant effect of strain, treatment, and interaction ($p<0.001$). These results provide evidence that Nrf2 expression plays a key role in modulating MeHg toxicity. The data also demonstrate the utility of the BXD RI mouse strains for understanding genetic susceptibility to MeHg. Future experiments will explore the impact Nrf2 expression has on measures of oxidative stress and redox status. (supported by NIEHS 1R01ES020852)

PS 1381 Disruption of Short-Term Synaptic Plasticity and Neuronal Repetitive Firing in Cerebellar Slices of Mice following Chronic Methylmercury Exposure

Y. Yuan, S. M. Ciotti, A. B. Bradford, D. Autio, R. Hajela and W. D. Atchison. *Pharmacology/Toxicology, Michigan State University, East Lansing, MI.*

The cerebellum is a primary target of methylmercury (MeHg) neurotoxicity. Following acute MeHg exposures in vitro, this effect involves presynaptic effects on transmitter release and elevation of [Ca2+]i. However, the extent to which the acute effects mirror chronic toxicity has not been reported. To study the chronic effects of MeHg on cerebellar synaptic function and neuronal excitability, we studied changes in short-term plasticity and neuronal firing in cerebellar slices of mice following exposure to 5 ppm MeHg in the drinking water for 6 (9 mos old) or 12 (15 mos old) mos. Paired-pulse evoked synaptic currents in Purkinje cells were recorded in sagittal slices using whole cell voltage-clamp recording mode by stimulating the white matter; single action potential (AP) or repetitive firing in Purkinje or granule cells were evoked by injecting short or long pulses respectively, of depolarizing currents using whole-cell current-clamp recording mode. Following 6 mos of MeHg exposure, no significant changes in paired-pulse responses or AP firing in Purkinje and granule cells were observed between control and MeHg-treated mice. However, after 12 mos of MeHg exposure, 36% and 64% of MeHg-treated mice showed paired-pulse depression (PPD) and facilitation (PPF), respectively. In contrast, 72% and 28% of control mice displayed PPD and PPF, respectively. This suggests that MeHg acts presynaptically to promote PPF because short-term plasticity is generally attributed to presynaptic alterations of transmitter release. Chronic (12 mo) MeHg exposure also significantly reduced the frequency of repetitive firing in granule but not Purkinje cells compared with those from control mice. Thus, 12 mo, but not 6 mo MeHg treatment shifts short-term plasticity in cerebellum from PPD to PPF. Cerebellar synaptic function was modified through direct actions on the nerve terminal. Cerebellar granule cells are more sensitive than are Purkinje cells to these effects. Supported by NIEHS/NIH grant ES0003299.

PS 1382 Chronic Methylmercury Disrupts Timing, Isradipine Prevents Disruption, and D-Amphetamine Partially Reverses It

D. A. Pope and C. Newland. *Auburn Univ, Auburn, AL.*

BACKGROUND. Nigralstriatal dopamine neurons have a unique, Cav1.3, L-type Ca++ channel that exhibits rhythmic oscillations in Ca++, conferring pacemaking activities. This may make them vulnerable to Parkinson's Disease (PD) or MeHg, since both are linked to disrupted intracellular Ca++ homeostasis. Isradipine (ISR), an L-type Ca++ blocker, prevents PD in model systems. Distorted timing is a behavioral correlate of PD. METHOD. Nine-month-old male BALB/c mice consumed 0 or 5 ppm of MeHg in drinking water and 0 or 2 ppm of dietary ISR and were trained to lever-press for milk. On most trials, milk followed a response on one lever under a Fixed Interval (FI) 8" or the other lever under a FI 32" schedule, but which lever produced milk was uncued and unpredictable. On "Omission" trials, no milk was delivered but responding was still monitored. Dependent variables included the time that subjects switched from the short to long FI and independence of responding on the two levers. RESULTS. On a trial, mice first responded on the FI 8" lever and then switched to the FI 32" lever. Mice exposed to MeHg without ISR switched sooner than all other groups. The timing of the two levers occurred independently for all groups except the MeHg-No ISR. For that group, this correlation was negative, an unusual finding also seen in PD. For the MeHg/no-ISR mice, low-dose d-amphetamine restored independence of time discrimination without affecting switch times; higher doses hastened switching, especially in the MeHg-No ISR group. Haloperidol delayed switch time for both ISR groups, and hastened it for groups with ISR. INTERPRETATION. Controls independently timed the two intervals and switch times lay close to the geometric mean of the two FIs. Timing was impaired for the MeHg-exposed mice in a manner similar to that reported with PD; switch times were sooner than the geometric mean. ISR prevented these disruptions, d-Amphetamine partially restored function to MeHg-exposed mice, and haloperidol interacted with ISR but not MeHg. [Supported by ES 003299].

PS 1383 Rotarod and Wheel-Running Reveal Age-Specific Effects of Methylmercury Toxicity and Neuroprotection by Nimodipine

C. Newland, A. N. Shen, D. A. Pope and C. W. Cummings. *Auburn Univ, Auburn, AL.*

BACKGROUND. MeHg toxicity has been linked to disrupted calcium homeostasis and Ca2+ accumulation in nerve terminals. Calcium channel blockers such as nimodipine (NIM) protect against MeHg's toxicity. Motor function tests like the rotarod and wheel-running have been used to detect early signs of MeHg neurotoxicty while overt neurological signs such as clasping reflex and ataxia come later. The goal of the current study was to examine age-related differences in the onset of MeHg toxicity, and the ability of dietary nimodipine to confer neuroprotection from chronic MeHg exposure. METHODS. Male BALB/c mice, ages 2.5 and 9 months (n=52 and n=62, respectively), were administered 0 ppm or 10ppm Hg as MeHg in drinking water and 0 ppm or 200ppm NIM in chow. Rotarod and wheel-running were evaluated approximately weekly and analyzed with 2 x 2 x 2 (Age X Water X Diet) between-group variables and exposure-duration as a repeated measure using linear mixed-effects. RESULTS. Older MeHg-exposed mice exhibited diminished rotarod performance before the younger MeHg-exposed mice did (exposure day 44 vs 86). Younger mice outperformed older mice overall. Wheel-running followed a similar pattern but with no age-related differences. Gross neurological signs such as clasping and hind-limb paralysis appeared later. Nimodipine delayed rotarod and wheel-running deficits in both age groups as evidenced by significant Age X MeHg X NIM X Exposure-day interactions. CONCLUSION. Chronic exposure to 10ppm MeHg alone decreased time spent on rotarod and distance run in an age-related manner. Chronic nimodipine delayed motor dysfunction in young and old animals but had no detectable effect of its own. Young mice out-performed older mice on rotarod. Rotarod and wheel-running revealed motoric deficits before the onset of MeHg-induced gross motor dysfunction. [Funded by NIH ES003299]

PS 1384 Brain Region-Dependent Effects of Methylmercury on Expression of Ligand and Voltage-Gated Calcium Channels in Rat

A. Colon-Rodriguez[1, 2, 3], R. Hajela[1] and W. D. Atchison[1, 2, 3]. [1]*Pharm/Tox, Mich State Univ, East Lansing, MI,* [2]*CMIB, Mich State Univ, East Lansing, MI and* [3]*CIT, Mich State Univ, East Lansing, MI.*

Methylmercury (MeHg) causes brain region-specific neurotoxicity and contributes preferentially to cell death in cerebellar granule cells (CGCs). MeHg disrupts synaptic transmission, resulting in alteration of Ca^{2+} homeostasis, manifesting as elevated $[Ca^{2+}]_i$, in both CGCs and motor neurons. Our aim was to compare the effects of low dose MeHg exposure on gene expression (measured via steady state mRNA levels) of subunits of voltage (VGCC) and ligand-gated ion channels, each of which could contribute to the MeHg-induced elevation of $[Ca^{2+}]_i$. Pore forming α_1 subunits of VGCCs (α_{1A}, α_{1B}, α_{1C} and α_{1E}); AMPA receptor (AMPAR) GluR1-4 and NMDA receptor (NMDAR) NR1, NR2A, and NR2C were compared between cerebellum (CB) and brainstem (BS). Identifying alterations in transcript levels following MeHg exposure can help identify targets in the pathways involved in differential susceptibility of these two regions. We hypothesized that effects would be more pronounced in the CB, due to the poor Ca^{2+} buffering capacity of CGCs. PND5 Sprague Dawley rats were dosed with 0.9% NaCl (control) or 1.5 mg/kg/day MeHg sc for 15 or 30 d; another group had a clearing period of 30 d. QPCR was performed on reverse transcript (cDNA) of RNA isolated from 10 mg of BS and CB. 15 d MeHg exposure decreased the levels of all VGCC subunits in the CB but not BS. At 30 d levels of all the VGCCs remained decreased in the CB, except for α_{1E}, which increased. In BS, 30 d exposure increased significantly VGCC levels; after 30 d of clearing all α_1 levels decreased except α_{1B} which increased. AMPAR GluR2 and GluR3 decreased in CB after 15 d exposure. After 30 d exposure and the clearing period only GluR3 increased. BS AMPAR levels increased after 15 d exposure, except GluR3. After 30 d exposure all AMPAR increased further, this increase persisted after the clearing period, except for GluR4. NMDAR levels increased in both the CB and BS after 30 d exposure. These observations demonstrate that MeHg affects gene transcription or stability of mRNA differentially for NMDAR, AMPAR, and VGCCs between themselves as well as in the CB and the BS. Decrease in VGCCs in the CB and increase in the BS, as well as the decrease of AMPARs in the CB and increase in the BS, support the idea that the CB is one of the most susceptible targets of MeHg toxicity, maybe due to its inability to compensate for MeHg effects on these key genes.

PS 1385 Postnatal Methylmercury Exposure Increases Rat Spinal Cord Expression of Glutamate Receptor mRNA

A. L. Perez-Medina[1], A. Colon-Rodriguez[1, 2, 3] and W. D. Atchison[1, 2, 3]. [1]*Pharmacology and Toxicology, Mich State Univ, East Lansing, MI,* [2]*Comparative Medicine and Integrative Biology program, Mich State Univ, East Lansing, MI and* [3]*Center for Integrative Toxicology, Mich State Univ, East Lansing, MI.*

In a mouse model of ALS methylmercury (MeHg) causes Ca^{2+}-dependent excitotoxicity in motor neurons. This effect involves increased sensitivity of Glutamate receptors (GluR), especially Ca^{2+}-permeable AMPA receptors (AMPARs). The objective of this study was to determine if motor neuron GluR expression was increased by a subacute MeHg treatment in a non-ALS animal model. If so, this might indicate that these targets are especially sensitive to MeHg, and in a susceptible genotype (such as the "ALS mouse model") lead to motor neuron toxicity. Quantitative real-time PCR (qPCR) was used to evaluate the NMDAR (NR1, NR2A, and NR2C) and AMPAR (GluR1, GluR2, GuR3, and GluR4) subunit mRNA expression. Sprague Dawley rats received 0.75, 1.5 mg/kg/day MeHg or 0.9% NaCl (control) sc. Treatment began at postnatal day 5 (PND5) and ended on PND20, and PND35. Another group of rats had an additional 30 days without treatment following the 30 days of MeHg exposure (PND65). RNA isolated from 10mg of lumbar and sacral spinal cord were submitted to reverse transcription PCR (RT-PCR). Resulting cDNA was used to perform qPCR. MeHg exposure led to alterations on the mRNA levels of the most abundant GLUR subunits in spinal motor neurons. At 15 days, 0.75 mg/kg/day MeHg increased the expression of all the GluR subunits studied. The effect was similar in the 1.5 mg/kg/day exposure group. At 30 days, 0.75 mg/kg/day MeHg exposure increased the expression of all the subunits. In the 1.5 mg/kg/day exposure group a similar but less pronounced increase occurred. The 60 day rats that had the 30 day "clearing" period also had an increase in expression after MeHg exposure, except the NR2A subunit whose expression was decreased in both treatment groups. In conclusion, subacute MeHg exposure causes enduring changes in expression of GluR subunits in rats. These can affect the ability of motor neurons to regulate $[Ca^{2+}]_i$. In genetically susceptible organisms, this could result in motor neuron death by excitotoxicity. (Supported by NIH grants R01ES03299 and R25NS065777)

PS 1386 Chronic Isradipine Treatment Alters Methylmercury-Induced Effects on Ion Channel Expression in Adult Mice

Z. Santana Rodriguez[1], A. Colon-Rodriguez[2, 3, 4] and W. D. Atchison[2, 3, 4]. [1]*Biology, Univ of Puerto Rico, Rio Piedras, San Juan, Puerto Rico,* [2]*Dept Pharm/Tox, Mich State Univ, East Lansing, MI,* [3]*CMIB, Mich State Univ, East Lansing, MI and* [4]*CIT, Mich State Univ, East Lansing, MI.*

Methylmercury (MeHg) alters synaptic transmission, and $[Ca^{2+}]_i$ homeostasis in motor neurons leading to excitotoxicity. $GABA_A$ receptor ($GABA_AR$) mediated synaptic inhibition, and block of voltage gated Ca^{2+} channels (VGCCs) play important roles in MeHg-induced alterations of $[Ca^{2+}]_i$ that lead to cell death. VGCC-mediated increases in $[Ca^{2+}]_i$ are decreased by VGCC antagonists, like isradipine (IS). The purpose of our study was to examine effects of chronic IS treatment on MeHg-induced changes in voltage- and ligand-gated ion channel mRNA expression levels. We hypothesize that IS will disrupt the changes in mRNA expression caused by MeHg alone. Three mo old Balb/c mice were exposed for 12 mo to 0 ppm (control), 5 ppm MeHg *ad lib* in drinking water, 3 ppm IS in food or combined treatment with MeHg and IS. RNA was isolated from 10 mg of brainstem (BS) tissue. QPCR was performed in reverse transcript of the isolated RNA of the $\alpha1$, $\beta1$, $\beta3$, $\gamma2$, and δ subunits of the $GABA_AR$ and the α_{1A}, α_{1B}, α_{1C} and α_{1E} subunits of VGCCs. MeHg had no effect on expression of $GABA_AR$ subunits. IS alone increased GABA $\beta3$ subunit expression. MeHg/IS increased the GABA δ subunit significantly compared to MeHg and IS alone. MeHg exposure had no effect on expression of the VGCCs α_1 subunits, however IS significantly upregulated the α_{1C} subunit compared to MeHg alone. MeHg/IS downregulated the α_{1B} and the α_{1E} subunits and upregulated the α_{1C} subunit significantly compared to MeHg alone. In conclusion, unaltered expression of VGCC and $GABA_AR$ subunits after chronic MeHg exposure could indicate that these ion channels are not primary targets of MeHg toxicity in the BS and also supports the idea that MeHg-induced alterations on $[Ca^{2+}]_i$ in motor neurons are mostly mediated by glutamate receptors. Increased expression of VGCCs and $GABA_ARs$ after IS and MeHg/IS exposure could reflect the BS ability to compensate for the block as a result of the VGCC antagonist and MeHg. (Supported by NIH grants R01ES03299 and R25NS065777).

PS 1387 Plasma Thiol Antioxidant Barrier As a Potential Biomarker for Methylmercury Intoxication

F. Usuki and M. Fujimura. *National Institute for Minamata Disease, Minamata, Japan.* Sponsor: A. Naganuma.

The critical role of oxidative stress in the pathogenesis of methylmercury (MeHg) cytotoxicity has been clarified in vitro and in vivo. It is important to identify a biomarker for MeHg intoxication. In this work, we examined the following 3 plasma oxidative stress markers: diacron reactive oxidant metabolites (d-ROM), thiol antioxidant barrier, and biological antioxidant potential (BAP), by using a free radical elective evaluator in MeHg-exposed rats. The results were compared to those obtained from rats administered with 0.2% (w/v) lead (Pb) acetate or 15 ppm cadmium (Cd) chloride in drinking water. Male Sprague-Dawley rats were administered with 20 ppm MeHg in drinking water. The changes in the 3 plasma oxidative stress markers, histopathology, body weight (BW), and clinical features were examined every week. BW significantly decreased from 2 weeks after MeHg exposure in MeHg-treated rats compared to the controls. MeHg-treated rats exhibited hind limb crossing at 3 weeks after MeHg exposure. Histopathological changes were observed in the cerebellum of rats exposed to MeHg for 4 weeks. Among the plasma oxidative stress markers, the level of thiol antioxidant barrier decreased at 2 weeks after MeHg exposure; however, no histopathological changes were observed at this stage. The d-ROM levels increased 3 weeks after MeHg exposure, whereas BAP levels did not change during 4 weeks of MeHg exposure. Although rats that were exposed to Pb for 4 weeks showed pathological changes in the hippocampus, no changes were observed in the plasma oxidative stress markers. Cd-treated rats also showed no changes in plasma oxidative stress markers. The high affinity of MeHg for the selenohydryl group, sulfhydryl group, or selenide may cause an early decrease in the level of plasma thiol antioxidant barrier. In contrast, oxidative stress in plasma may be delayed although Pb and Cd are known to induce oxidative stress in tissues. Our results suggest that thiol antioxidant barrier level in plasma is a potential biomarker for MeHg intoxication.

PS 1388 Arsenic Induces Reactive Oxygen Species-Caused Neuronal Cell Apoptosis through JNK/ERK-Mediated Mitochondria-Dependent and GRP 78/CHOP-Regulated Pathways

T. Lu[1], F. Tang[2], C. Su[3], C. Yen[4], C. Wu[5], K. Chen[6], Y. Chung[4], D. Hung[7], C. Huang[8] and Y. Chen[1]. *[1]Department of Physiology and Graduate Institute of Basic Medical Science, China Medical University, Taichung, Taiwan, [2]Department of Occupational Medicine, Changhua Christian Hospital, Changhua, Taiwan, [3]Department of Otorhinolaryngology, Head and Neck Surgery, Changhua Christian Hospital, Changhua, Taiwan, [4]Department of Occupational Safety and Health, Chung Shan Medical University, Taichung, Taiwan, [5]Department of Public Health, China Medical University, Taichung, Taiwan, [6]Department of Urology, China Medical University Hospital, Taichung, Taiwan, [7]Division of Toxicology, Trauma & Emergency Center, China Medical University Hospital, Taichung, Taiwan and [8]School of Chinese Medicine, China Medical University, Taichung, Taiwan.*

Recently, epidemiological studies have suggested a possible relationship between inorganic As (iAs) exposure and neurodegenerative disease development. However, the effects and underlying mechanisms of iAs-induced neuronal cell injuries are most unknown. The present study demonstrated that iAs significantly decreased cell viability and induced apoptosis in Neuro-2a cells. iAs also increased oxidative stress damage and induced several features of mitochondria-dependent apoptotic signals. Pretreatment with the antioxidant N-acetylcysteine (NAC) effectively reversed these iAs-induced responses. iAs also increased the phosphorylation of JNK and ERK1/2, but did not that p38-MAPK, in treated Neuro-2a cells. Additionally, exposure of Neuro-2a cells to iAs triggered endoplasmic reticulum (ER) stress identified through several key molecules (GRP 78, CHOP, XBP-1, and caspase-12), which was prevented by NAC. Transfection with GRP 78- and CHOP-specific si-RNA dramatically suppressed GRP 78 and CHOP expression, respectively, and attenuated the activations of caspase-12, -7, and -3 in iAs-exposed cells. Therefore, these results indicate that iAs induces ROS causing neuronal cell death via both JNK/ERK-mediated mitochondria-dependent and GRP 78/CHOP-triggered apoptosis pathways.

PS 1389 Identification of Novel Proteomic Biomarkers for Heavy-Metal-Induced Nephrotoxicity

Y. Shin[1], M. Akram[1], K. Kim[1], E. Kim[1], H. Kim[2] and O. Bae[1]. *[1]College of Pharmacy Institute of Pharmaceutical Science and Technology, Hanyang University, Ansan, Republic of Korea and [2]College of Pharmacy, Sungkyunkwan University, Suwon, Republic of Korea.*

Long-term exposure of low-dose heavy metals are well-established risk factors against human health. Among various organs, the kidney is one of the most sensitive targets of for heavy metal-associated toxicity. Development of novel biomarkers is essential to evaluate and predict nephrotoxicity following exposure to low-dose heavy metals. Here we tried to identify new biomarkers using proteomics approaches in kidney tissues isolated after heavy metal exposure. Male Sprague-Dawley rats received mercuric chloride (HgCl2) and cadmium chloride (CdCl2) by oral administration. Proteomic analysis with kidney samples revealed that expression of several proteins was elevated by Hg and Cd exposure, suggesting them as potential candidates for new biomarkers. We further measured the change of new biomarkers in renal tubular cells following heavy metals exposure. Interestingly, in normal rat kidney proximal tubular cells (NRK-52E), the change of expression level of these new candidates were well correlated to the extent of cytotoxicity induced by heavy metals. Notably, the increase of new biomarkers was observed in drug-exposed tubular cells, suggesting the potential use of these biomarkers. The change of the new biomarkers was comparable to that of traditional biomarkers for renal toxicity, such as Kim1, Lcn2, Spp1 and TIMP1. With this study, we identified new protein biomarkers as novel candidates for drug or heavy metal-induced renal toxicity. Superior correlation between cytotoxicity and the extent of these protein changes suggests that they can be useful biomarkers to evaluate or predict renal toxicity.

PS 1390 Expression of Copper (Cu) Transporting Genes in Subventricular Zone (SVZ) and Choroid Plexus (CP)

X. Fu, L. Hong, W. Jiang and W. Zheng. *School of Health Sciences, Purdue University, West Lafayette, IN.*

Our recent data using X-ray fluorescent microscopy suggests an age-related increase of Cu along the wall of brain ventricles called SVZ. Since the regulation of cellular Cu homeostasis involves a variety of Cu transporting proteins, chaperones and intracellular binding proteins, it becomes necessary to understand the expression of these Cu regulatory proteins and how they contribute to the high Cu concentration in SVZ. Anatomically, SVZ is in direct contact with cerebrospinal fluid (CSF) secreted by the CP where the blood-CSF barrier (BCB) is located. This study was designed to compare the gene expression of Cu regulatory proteins in SVZ and CP. SVZ and CP tissues were dissected from brains of 3-wk, 10-wk or 9-m old male Sprague-Dawley rats and SVZ tissues from 3-wk-old rats were used for the primary cultures of neural stem cells (NSCs) and choroidal epithelial cells (CECs). Target gene expression levels in tissues and cultured cells were analyzed using quantitative real-time RT-PCR and normalized with the internal reference gene Actb. Our data showed that the expression level of Cox17 was the highest in SVZ, followed by Ctr1 and Dmt1, while Ctr1 was expressed the most in CP followed by Cox17 and Dmt1, of all three ages. However, by comparison of gene expression, Cox17, Dmt1 and Ctr1 were about 2-, 4-, and 60-fold lower in SVZ than in the CP, respectively ($p<0.05$). Higher expression levels of Ctr1 and Dmt1 were observed in CP of 9-m old rats than 3- and 10-wk old animals ($p<0.05$). Atp7b had the lowest expression in both SVZ and CP of all animals. Furthermore, the expression level of Dmt1 was higher in NSCs than CECs ($p<0.01$), while CECs expressed more Atp7a and Atp7b than those in NSCs ($p<0.05$). These findings suggest the Cu regulatory gene expression pattern in SVZ is different from those in CP; furthermore the age appears to influence the expression of these Cu regulatory genes. (Supported in part by NIH/NIEHS ES-008146)

PS 1391 Effects of Copper in LPS-Treated Microglia

A. Rossi-George[1], C. Guo[2], E. Bini[1], Q. Chang[3], A. Kusnecov[3] and A. Gow[2]. *[1]Pharmacy Practice and Administration, Rutgers University, Piscataway, NJ, [2]Pharmacology and Toxicology, Rutgers University, Piscataway, NJ and [3]Psychology, Rutgers University, Piscataway, NJ.*

Microglia are resident immune cells of the nervous system. Resolution of a pathologic event is achieved through the release of a variety of products with nitric oxide (NO) being the most potent. Within neurodegenerative disease there is both persistent activation of microglia and accumulation of transition metals. We proposed that copper (Cu) would alter NO signaling by changing the redox environment of the cell. Previously we have shown in vitro that Cu(I), but not other transition metals, reduces NO output from microglial cells without altering iNOS production. In this study, we sought to determine the effects of Cu overload on behavior and on microglial activation. Starting at weaning, C3He wild type mice were exposed to 300mg/L of CuSO4 in drinking water for 4 months before undergoing behavioral testing. TXJ mice, which are unable to expel excess Cu, were also examined. Twenty-four hours after testing they were injected i.p. with LPS (0 or 25 mg/kg) and perfused 4 hours later. Results showed that in the cerebellum, wild type mice on the Cu diet had the highest copper content(5.39 ng/gr) which was statistically significantly different from that of the TXJ mice (4.181 ng/gr) which, in turn, was twice that of the control mice (2.181 ng/gr). Mice were measured for anxiety responses by open field test and motor control by rotarod. In the open field, Cu feeding increased anxiety in wild type mice, while these responses were unaltered inTXJ mice ($P <.0001$). These changes were not a result of loss of motor control as performance of Cu-treated mice was not different from that of controls on the rotarod. Notably, there was a significant gender bias to locomotor performance in response to Cu feeding.Cu levels in the cerebellum are correlated with behavioral measures and may be related to altered microglial activation as shown by IHC analysis following LPS accumulation.

PS 1392 The Neurotoxic Effects of Tributyltin on Male F1 Tokai High-Avoider (THA) Rats Evaluated by the Sidman Electric Shock Avoidance Test

M. Tsunoda[1], T. Hasegawa[1], T. Kido[2], M. Hosokawa[3], C. Sugaya[1], Y. Sugiura[1], H. Endo[4] and T. Watanabe[4]. *[1]Preventive Medicine, Kitasato University School of Medicine, Sagamihara, Kanagawa, Japan, [2]Public Health and Environmental Medicine, Jikei University School of Medicine, Tokyo, Japan, [3]Epidemiology and Environmental Health, Faculty of Medicine, Juntendo University, Tokyo, Japan and [4]Basic Clinical Science and Public Health, Tokai University School of Medicine, Isehara, Kanagawa, Japan.*

Wistar-derived Tokai High Avoider (THA) rats can achieve a stable learning ability in the Sidman electric shock avoidance test because of their innate high level of avoidance ability and small individual differences. Tributyltin (TBT) compounds have become known as common environmental pollutants. In our previous study, impaired learning ability was demonstrated in the THA rats exposed to TBT at 125 ppm in their food after weaning. In the present study, we evaluated the neurotoxic effects of TBT on male F1 THA rats by the Sidman electric shock avoidance test. The pregnant THA rats were exposed to TBT at 0 and 50 ppm in their food. The F1 rats were exposed to TBT via the placenta and their dams' milk, and the exposure was stopped 4 weeks after delivery (weaning time). From 6 weeks of age, the Sidman electric shock avoidance test sessions were performed for 60 min/day for 10 consecutive days. The rats could avoid electric shocks by pressing a lever.

Avoidance rates for shock exposures were calculated for the first and second halves (30 minutes each) of each session. There was no significant difference in mean body weight at 6 weeks of age between the TBT group and the control. A significantly lower mean value of the avoidance rates in the TBT group compared with that in the control was observed in the first 30 minutes of the sessions on day 1. The mean values of the avoidance rates in the first and second 30 minutes in the TBT group were lower than those in the control from days 2 to 8. These results indicate that the learning ability was impaired in the F1 THA rats exposed to TBT at 50 ppm in their dams' food.

PS 1392a Chronic Lead Exposure Reduces Presynaptic Vesicle Availability in Mossy Fiber-CA3 Synapses and Shaffer Collateral-CA1 Synapses in the Rat Hippocampus

S. Guariglia, J. L. McGlothan, K. H. Stansfield and T. R. Guilarte. *Columbia University, New York City, NY.*

Lead (Pb2+) exposure has been shown to impair presynaptic neurotransmitter release in both in vivo exposed animals and in cell culture models. The mechanism by which this impairment occurs has not been fully elucidated. However, our lab has previously shown that Pb2+ exposure during synaptogenesis inhibits vesicular release and reduces the number of fast-releasing sites in cultured hippocampal neurons (Neal et al., 2010). We hypothesized that the impairment of vesicular release and the reduction in the number of fast-releasing sites may be associated with reductions in the number of vesicles docked in the presynaptic active zone (PAZ). In the present study, we used transmission electron microscopy to examine presynaptic vesicle pools in Perforant Path-Dentate Gyrus, Mossy Fiber-CA3, and Shaffer Collateral-CA1 synapses to determine if in vivo Pb2+ exposure altered synaptic vesicle number. Vesicles within the presynaptic axon terminal were counted and the distance between the vesicle and the PAZ measured using LoClust (Nikonenko and Skibo, 2004). Vesicles were classified as docked if they contacted the PAZ; rapidly recycling if they were 200 nm or less from the PAZ; or resting if they were more than 200 nm from the PAZ. We found that Pb2+ exposure significantly reduced the number of docked vesicles in Mossy Fiber-CA3 and Shaffer Collateral-CA1 synapses and the number of vesicles in the rapidly recycling pool of Mossy Fiber-CA3 synapses. These data suggest that Pb2+ exposure interferes with presynaptic neurotransmitter release by reducing the number of vesicles available for release. These findings provide a novel mechanism by which Pb2+ exposure impairs vesicular release. Further, this study confirms our previous findings in hippocampal neurons in culture and corroborates current work in which in vivo Pb2+ exposure results in reduced vesicular release probability (Stanton et al., 2014, SOT Abstract). [Funded by NIEHS grants ES006189 and ES020465].

W 1393 Addressing Uncertainties of the Toxicology of Nanomaterials in Food and Food Contact Products

A. Santamaria. *Exponent, Houston, TX.*

Nanotechnology has the potential to revolutionize the food industry by improving the delivery of nutrients, providing brighter colors and enhanced flavors, increasing food longevity, imparting antibacterial or biosensor properties, and providing product traceability in food and food contact products. The food industry is incorporating nanoparticles such as nutrients, silver, titanium dioxide, amorphous silica, clay, and carbon nanotubes into a growing number of food and food contact products, so consumers are likely being exposed to a variety of nanoparticles through ingestion. At this point, there is little information available on the toxicokinetics (absorption, distribution, metabolism, and excretion) and/or toxicological effects of engineered nanoparticles following ingestion. In addition, few studies have been conducted to evaluate tissue localization of the nanoparticles and/or effects on gut flora (e.g., due to their antimicrobial properties). There is also a need to develop standard methods for evaluating the levels of nanoparticles in foods and/or the migration of nanomaterials from food packaging or products (e.g., cutting boards) into food items. Regulatory agencies such as the US FDA, USDA, US Environmental Protection Agency (EPA), and risk assessment agencies such as the EFSA may request that a company provide extraction and/or toxicological studies to address some of these uncertainties, particularly for novel nanomaterials that may be used in foods and as food contact substances. This SOT session aims to address what is known about the potential exposure levels for nanomaterials in foods and food contact products, toxicokinetics and/or toxicological effects following ingestion, and laboratory methods for measuring tissue localization or effects of nanoparticles on the gastrointestinal tract. An overview of what food and food additive companies may need to do to address current or future regulations and/or guidelines will be presented. The findings and recommendations from the collaborative research projects will also be discussed by the speakers of this workshop who have participated in those projects.

W 1394 Safety Considerations for the Use of Nanomaterials in Food and Food-Related Products: A US FDA Regulatory Perspective

S. Thurmond. *Center for Food Safety and Applied Nutrition, US FDA, Washington, DC.*

The US FDA has been developing nanomaterial-related industrial guidance that cover foods, food contact materials and food ingredient containing products over which the Agency has regulatory authority since the publication of its July 2007, report on nanotechnology. In addition, FDA is conducting research to gauge the utility of our currently recommended safety testing paradigms for assessing the potential for food-related nanomaterials to produce toxicity and/or carcinogenicity. Research is underway at the CFSAN and the National Center for Toxicological Research (NCTR) to evaluate the recommended standard battery of *in vitro* tests when used with nanoparticulates and nanoencapsulated products, and to identify possible replacement tests. Early results indicate that this standard safety assessment panel may need to be augmented with other *in vitro* tests, and that at least one or more of the current safety assessment assays may need to be replaced. *In vivo* studies are also being conducted by NCTR, in collaboration with CFSAN, to assess the potential for orally administered nanosilver to produce toxicity. These studies are also serving as a platform for the development of safety assessment methodologies for *in vivo* studies with nanomaterials. In addition, FDA is conducting research to assess whether nanomaterials are being incorporated into products over which it has little regulatory authority, such as dietary supplements. Analytical fieldwork conducted by the FDA Office of Regulatory Affairs indicates that certain marketed dietary supplements contain nanomaterials either as nanoparticulates or as nanoencapsulated products. While research on the safety assessment of orally available nanomaterials in food-related products is ongoing at FDA and elsewhere, this research is moving ahead at a relatively slow pace. This slow progress may be in part due to the lack of information on how nanomaterials interact with food matrices and, subsequently, with the alimentary tract.

W 1395 NanoRelease Food Additive Project—Developing Methods to Measure Characteristics Relevant to Nanomaterial Uptake from Food

R. Canady. *Center for Risk Science Innovation and Application, ILSI Research Foundation, Washington, DC.*

Nanoscience is providing valuable knowledge of particle toxicology; however, it is unclear how to use this knowledge to distinguish "engineered" particulate materials within a context of the particulate nature of traditional foods. When does a change in characteristics at nanoscale distinguish a particle from background particles? Should nanomaterials used at early stages in food processing be considered nanomaterials at ingestion if they have dissolved or bound to other food components? How do we know when the knowledge gained from pristine, extracted, dispersed nanomaterials in dose response evaluations applies to the transformed, aggregated, bound materials in food that reaches our mouths? The need for safe innovation coupled with a growing awareness of particulate toxicology for foods brought a diverse stakeholder group together in the NanoRelease project to the task of filling a basic methods gap in our ability to understand what is "nano" in the food we eat. Findings that lay a path toward addressing these questions will be presented from white papers prepared by the more than 70 experts of the project. The findings include a practical and neutral view of what may be nanoparticulate in food and what methods are needed to prioritize attention across the different types of particles of foods.

W 1396 Uptake and Distribution of Ingested Nanomaterials

S. M. Roberts. *University of Florida, Gainesville, FL.*

Engineered nanomaterials can be added directly to food to produce a beneficial effect in the consumer (e.g., increase the absorption of a nutrient) or a beneficial effect on the food itself (e.g., increased shelf life, enhanced flavor). Nanomaterials can also be introduced into food incidentally when used to improve food processing. The safety of nanomaterials in food depends in part on what happens when they enter the dynamic environment of the GI tract, and ultimately on the extent to which they are taken into the body and distributed. There are several challenges to assessing nanomaterial behavior and interactions in the GI tract. Some are common to studies of the potential toxicity of nanomaterials in general, including inconsistencies in the nanomaterials as manufactured, uncertainty as to how to express the nanomaterial dose or concentration, and difficulties in characterizing the nanomaterial, as well as in detecting and measuring them in biological systems. Other challenges are unique to the gastrointestinal tract, including an environmental that changes with respect to: pH, ionic strength, nature and composition of the sur-

rounding food matrix, anatomical absorptive surfaces, physical/chemical barriers to absorption (mucin layer), and microorganisms with which to interact as the nanomaterial transits the gut. The rate and location of dissolution or breakdown within the GI tract is likely to be an important factor in determining potential biological effects for some nanomaterials. Existing studies offer some insights into nanomaterial properties that can influence uptake from the GI tract and distribution in the body, but much work remains before the critical processes are well understood. In addition to the potential for systemic toxicity following uptake of nanomaterials (or dissolution or degradation products), local effects (e.g., cytotoxicity to cells lining the GI tract) and indirect effects (e.g., through effects on gut microflora or interference with absorption of nutrients) are also possible and merit consideration, at least for some nanomaterials.

W 1397 High-Throughput Testing Using a 3-Cell Gut Model for Hazard Identification of Nanomaterials in Food Products

C. M. Sayes. *Center for Aerosols & Nanomaterials Engineering, RTI International, Research Triangle Park, NC.*

The need to develop *in vitro* model systems for rapid and cost-effective screening of agricultural products is becoming increasingly necessary for the safety of food for human and animal consumption. This talk describes a 3-cell gut model developed for assessing the effects of nanomaterials and other man-made materials on bacterial biofilm and mammalian cells – the two types of cells found in the gut of humans and most animals. The system also probes the effects of a disrupted biofilm on normal epithelial cell function. Engineered nanoparticles are already being incorporated for innovative food packaging applications. Given the scenario of incorporating nanoparticles into food matrices, two distinct exposure populations and consequently two exposure routes can be easily identified: 1) Occupational exposures of industrial workers, by way of aerosolized nanoparticles, involved in the manufacturing of nano-enabled packaging materials. A reasonable exposure route for this scenario would be via inhalation and further digestion of the nanoparticles that remained in the pharyngeal cavity. 2) Consumer that ingest nano-enabled foods and possibly nanoparticles that may be released from food packaging. A common thread that links both the exposure populations and the two exposure routes is that the nanoparticles will eventually be "digested" and reach the small intestines of the gastrointestinal (GI) tract. In order to explore the physicochemical changes that nanoparticles go through during digestion and how these changes affect the digestive system and the commensal microbes that inhabit the human small intestine, we present a model that uses a gut co-culture model incorporating the Caco-2 cell line, HT-29 cells and a biofilm of commensal *Escherichia coli*. In this study, commonly used metal oxide and colloidal metal nanoparticles, some of which are known to have antimicrobial properties and have been used for nano-enabled packaging production are evaluated to study the physicochemical changes that such nanoparticles go through during digestion.

W 1398 Adverse Outcome Pathways: A Conceptual Framework for 21st Century Risk Assessment

J. Rowlands[1] and K. Crofton[2]. [1]*Toxicology and Environmental Research & Consulting, The Dow Chemical Company, Midland, MI and* [2]*National Center for Computational Toxicology, US Environmental Protection Agency, Research Triangle Park, NC.*

An Adverse Outcome Pathway (AOP) represents existing knowledge concerning the linkage between a molecular initiating event and an adverse outcome at the individual or population levels (Ankley, Bennett, et al. 2009). As such, it is a conceptual framework that describes known linkages between a chemical-induced initial molecular event that alters biochemical cellular processes that cascade via a series of key events observed as cellular, tissue, and anatomical changes, that ultimately culminates in an adverse outcome of relevance to human or ecological health. This workshop will provide a regulatory rationale for using AOPs, along with the types and amounts of data needed to construct an AOP. Further, the level of confidence in an AOP will be explored for usage in regulatory decision-making, whether priority setting for chemical toxicity testing or hazard prediction. The practical utility of AOPs for risk assessment of chemicals will be illustrated using three case study examples.

W 1399 Creations and Use of AOPs: Progress and Prospects

A. R. Boobis. *Centre for Pharmacology & Therapeutics, Imperial College London, London, United Kingdom.*

The AOP concept has its origins in ecotoxicology but is now receiving increasing attention for its applicability to human health effects. In this respect an AOP is essentially indistinguishable from a mode of action (MOA) for a toxic effect. Hence, the general principles of one should apply to the other. These include identification of necessary and measurable key events, the molecular initiating event comprising an early such event, the use of weight of evidence such as the modified Bradford Hill considerations proposed by WHO for evaluation of key events, the rigorous exclusion of alternative pathways, the biological linkage of key events to an adverse outcome and the systematic qualitative and quantitative comparison of key events in model systems with those in humans, as appropriate. In human health assessment, AOPs/MOAs were initially used in evaluating the relevance of a rodent carcinogenic response to humans where a qualitative conclusion was sought. With the extension of the approach to non-cancer endpoints, quantitative information obtained on intermediate events can be invaluable in dose-response assessment for human risk. There is a need to agree the core information necessary to establish a robust AOP, and for a central repository of such AOPs and the intermediate events involved. OECD with support of other organisations is currently preparing such a repository. Establishment of AOPs will be invaluable in the design of new evaluation methods. AOPs will provide a necessary bridge between such methods and systems approaches to risk assessment. There are still conceptual barriers to the AOP/MOA approach, with a failure to appreciate that primarily it is a means to organise information in a coherent, transparent manner, on the basis of explicit lines of evidence.

W 1400 Adverse Outcome Pathway (AOP) for Skin Sensitization

G. Patlewicz. *DuPont Haskell Global Centers for Health & Environmental Sciences, DuPont, Newark, DE.* Sponsor: J. Rowlands.

Skin sensitisation is a significant environmental and occupational health concern. As such, there exists an important need to accurately identify chemicals that have the potential to cause skin sensitisation. Assessment of skin sensitisation is still heavily reliant on the use of animals, in particular the local lymph node assay (LLNA) since no regulatory accepted alternative method exists. Despite the obvious complexity of the endpoint, quite a detailed mechanistic understanding both in terms of the underlying biological process and chemistry has been developed which has helped direct research into alternative (non-animal) approaches. Recently the OECD developed an Adverse Outcome Pathway (AOP) that describes in detail the key events underpinning skin sensitisation. Making the collective knowledge of the skin sensitisation process explicit in this way provides an invaluable roadmap to guide method development, evaluation and application. Indeed the OECD has also implemented this AOP into the OECD Toolbox, a tool for the development, evaluation and justification of chemical categories for read-across. This presentation will outline the AOP and illustrate its utility in developing Integrated Testing Strategies (ITS) and read-across by way of practical examples.

W 1401 Thyroid Hormone Adverse Outcome Pathway-Based Screening Assays for Thyroid-Disrupting Chemicals

K. Crofton. *National Center for Computational Toxicology, US EPA, Research Triangle Park, NC.*

Disruption of thyroid hormones (THs) adversely affects neurodevelopment in both rodent models and humans. Therefore it is critical to determine the potential thyroid-disrupting activity of thousands of environmentally-relevant chemicals. However, the complexity of thyroid hormone regulation necessitates screening assays for multiple molecular initiating events that are not currently associated with any screening assays. The amount of detail and linearity characterizing thyroid pathways between molecular initiating events and adverse outcomes varies substantially, both as a function of existing knowledge and application needs. Development of AOPs provides insight into the uncertainties in linking chemical use, exposure and outcome, thereby focusing research on critical data needs. Example applications include the impact of thyroid disruption on neurodevelopment where AOPs have led to more efficient predictive testing and reduced uncertainty in extrapolation of effects between rodents and humans. Well defined thyroid AOPs also provide the molecular targets and key events that foster focused development of high-throughput screening models. Lastly, AOPs provide a utilitarian framework for future efforts to build quantitative and qualitative models useful in understanding the degree of perturbation associated with adverse outcomes. *This abstract does not necessarily reflect US EPA policy.*

W 1402 Reproductive Adverse Outcome Pathways for Chemical Inhibitors of Steroid Synthesis in Fish

G. T. Ankley and D. L. Villeneuve. *Office of Research and Development, US EPA, Duluth, MN.* Sponsor: K. Crofton.

A key physiological process controlling reproductive success of oviparous vertebrates (fish, amphibian, reptiles, birds) involves production of the egg yolk protein precursor vitellogenin (VTG). VTG production is an estrogen receptor (ER)-mediated process that, in females, is controlled by the production of 17B-estradiol. As such, environmental contaminants (including several pesticides and pharmaceuticals) that affect steroid synthesis can impact reproduction in fish through their ability to inhibit VTG production. Given both physiological importance and sensitivity to chemical stressors, there has been a significant amount of effort expended on developing well-characterized adverse outcome pathways (AOPs) relating steroid synthesis and VTG production to reproductive impacts in individuals and populations of fish. This presentation will provide an overview of the research conducted to derive and evaluate these AOPs from a weight-of-evidence perspective, including characterization of molecular initiating and key events and documentation of linkages between these events. The talk also will discuss practical applications of the AOPs to different facets of both prospective and diagnostic ecological risk assessments.

W 1403 The Adverse Outcome Pathway for Hepatic Toxicity and Tumorigenesis in Rodents Initiated by Activation of the Aryl Hydrocarbon Receptor by Dioxin-Like Chemicals

J. Rowlands and R. Budinsky. *Toxicology and Environmental Research & Consulting, The Dow Chemical Company, Midland, MI.*

Despite extensive knowledge of the toxicology of dioxins, no AOP for rodent tumorigenicity has been formally documented using the Human Relevance Mode of Action framework that was developed by the International Programme on Chemical Safety (IPCS). An AOP for dioxin-like chemical-induced hepatotoxicity and tumor promotion has been developed. The AOP describes sustained activation of the aryl hydrocarbon receptor (AHR) that eventually promotes liver tumors in rodents through a number of Key Events (KEs) including inhibition of intrafocal apoptosis, increased cell proliferation of previously initiated foci, proliferation of oval cells and extensive hepatic toxicity that provides an ongoing regenerative stimulus. Data substantiating this AOP includes *in vivo* studies of liver toxicity, tumor promotion and carcinogenesis induced by 2,3,7,8-tetrachlorodibenzo-p-dioxin (dioxin) and dioxin-like chlorinated dibenzofurans. Where appropriate, substantiating data was considered from *in vitro* studies of normal primary rodent cells and immortalized and/or transformed rodent cells. This AOP can be used for regulatory decision making when prioritizing chemicals for further testing.

W 1404 Challenges Facing the Next Generation of Risk Assessment

R. Gentry[1] and B. J. Locey[2]. [1]*ENVIRON International Corporation, Monroe, LA and* [2]*ARCADIS, Ann Arbor, MI.*

Risk assessors continue to be faced with significant challenges due to the increase in technology and complexity of endpoints and datasets to be considered in understanding the potential for chemical exposure to result in adverse impacts on humans or the environment. This workshop will bring scientists from multiple disciplines together to discuss these challenges for both human and ecological risk assessment and the potential for innovative solutions. The goal of this workshop is to present the latest thinking on issues significant to the practice of risk assessment today in a forum that allows for expanded thinking and an exchange of ideas. New concepts and older concepts that are being revisited to address new challenges will be presented. Topics will include the critical need for interoperability of data and models for risk assessment, consideration of variability and uncertainty in risk assessment, weight-of-evidence approaches, challenges in dose-response modeling, and the current and future guidance from the National Research Council on risk assessment issues as we move forward in the 21st century. This workshop will be the second collaboration between members of the SOT Risk Assessment Specialty Section and the SETAC Human Health Risk Assessment Advisory Group and builds on the concepts presented in a workshop developed by these two specialty sections in 2012. The 2012 workshop was titled "Concepts Critical to the Next Generation of Human Health and Ecological Risk Assessment" and highlighted some of the challenges facing the next generation of risk assessors. The goal of that workshop was to provide information on new programs and approaches within regulatory agencies, as well as in the private sector, that rely on the integration of human, animal, or ecological data.

W 1405 Risk Assessment in the 21st Century: Interpreting New Guidance

T. E. McKone. *University of California Berkeley, Berkeley, CA.* Sponsor: R. Gentry.

Risk assessment has become a dominant tool for guiding public policy in protecting public health and the environment. In the last decades of the twentieth century, the National Research Council's Board on Environmental Studies and Toxicology (BEST) produced a number of reports guiding origins and development of the field of risk assessment—in particular the famous "Red Book". In the first decade of the twenty first century, BEST carried out three studies that resulted in reports that redefined and advanced the field of risk assessment as it enters the next century. These reports include "Toxicity Testing in the 21st Century: A Vision and a Strategy,' issued in 2007, "Science and Decisions: Advancing Risk Assessment," in 2009, and "Exposure Science in the 21st Century: A Vision and a Strategy," in 2012. In this presentation I will briefly review the key recommendations from these reports and consider the implications of these recommendations for the preparation and interpretation of risk assessment as tool for informing environmental health science.

W 1406 Dose-Response: Current Challenges and Opportunities for Improvement

N. B. Beck. *American Chemistry Council, Washington, DC.*

With the increase in the types of chemical-specific quantitative data available, dose response assessment is becoming a complicated task, requiring the consideration of more information than a single data set.. One of the most controversial areas in dose response modeling is related to understanding when the integration of the available data are sufficient to suggest an approach other than default, or linear modeling approach. This is a critical science policy decision and opinions are often different on what the appropriate answer should be. Nuances in EPA's 2005 Cancer Guidelines have led to different interpretations. Added to the complexity of a modeling approach are the challenges in addressing and accounting for the endogenous production of chemicals in the body. While novel approaches have been proposed, they are not yet universally accepted. Other challenges in dose-response include understanding whether effects are adaptive, compensatory or adverse and determining how to characterize toxicity that is due to less than lifetime exposures. Finally, the ultimate challenge may be developing consensus around an approach for addressing cumulative risks. This talk will use specific examples to discuss existing challenges, proposed solutions, and opportunities that may exist to more fully develop consensus within the risk assessment community.

W 1407 Weight of Evidence: Data Requirements and Approaches for Use in Regulatory Decision-Making

C. J. Borgert. *Applied Pharmacology and Toxicology, Inc., Gainesville, FL.*

Weight of Evidence (WoE) approaches are often used to critically examine, prioritize, and integrate information from different types of studies to reach general conclusions. In risk assessment, the questions posed in problem formulation determine the types of information sought and the ways the information is integrated and interpreted. Hypothesis-based (HB) approaches to problem formulation have been proposed and applied to a diverse array of risk assessment problems ranging from very narrow questions about whether particular chemicals pose specific hazards to broader questions regarding use of data in making regulatory decisions. Although proposed by different analysts, most HB-WoE approaches require: explicit hypotheses; a priori data collection and selection processes and methods of evaluating data quality, and; transparent descriptions of the decision algorithms or process that will be used to reach conclusions. This presentation will synthesize the key elements of HB-WoE approaches and illustrate a few diverse applications of the method, including in the evaluation of mode of action for carcinogen risk assessment, in evaluating data from the U.S. EPA's Endocrine Disruptor Screening Program, and in data quality evaluation for information used in regulatory decision-making.

W 1408 Challenges to Risk Assessment in the 21st Century: Characterizing Variability and Reducing Uncertainty in Risk Assessments

P. S. Price. *The Dow Chemical Company, Midland, MI.*

Uncertainty and variability have been important issues for risk assessment policy and practice since the beginning of chemical risk assessment in the 1950s. Dose response assessment is essentially a measure of variability in tolerance in humans

and there is an uncertainty factor assigned to address human variability. Exposure assessments have historically focused on defining a reasonable upper bound to the range of exposures that occurs because of variability in human behavior and spatial and temporal variation in the release, transport, and removal of chemicals in the environment. Risk assessment must make decisions under limited information since the mechanisms of action for toxicity and the key data on exposures may not be known. In addition many risk questions involve prediction of future exposures which cannot be measured. Arguably the entire field of risk assessment can be described as an attempt to make robust decisions under uncertainty. New tools in toxicology and exposure assessment promise to improve risk assessment by reducing uncertainty and by better characterizing the sources of variation. Advances in the field of toxicology promise to improve our understanding of the dose-response of key events that occur early in adverse outcome pathways. Such data can replace the current approach of evaluating every apical endpoint before setting a point of departure. Advances in modeling variation in adsorption, dispersion, metabolism, and excretion of chemicals are improving our ability to perform dose response modeling across human populations of varying ages. Advances in exposure information facilitated by improved monitoring and reporting technology promises to improve our understanding of how variation in human behavior affects exposures. Perhaps just as important, the rise of integrated information systems that facilitate sharing toxicity and exposure data and advances in behavior monitoring technology.

W 1409 Multiscale Modeling: Data Integration and Interoperability

A. M. Jarabek. *NCEA, US EPA, Research Triangle Park, NC.*

Risk assessment requires the analysis, translation, and integration of data from various disciplines (e.g., exposure and epidemiology), which often represent different levels of observation (e.g., individual versus population), in order to determine the potential for exposure and health effect(s) at multiple scales such as the subcellular, individual, population, or community levels. An appreciation of the need for collaboration across disciplinary silos spanning the continuum from source → exposure → dose → response → cost:benefit is advancing due to the call for sustainability characterizations and the recent decision by the World Health Organization (WHO) to include consideration of ecosystem services in the definition of human health. Additionally, advances in biotechnology and systems modeling are resulting in increasingly complex data repositories that require integration and management of large amounts of data to understand different adverse outcome pathways and to more accurately predict and diagnose factors contributing to disease. Interoperability, defined as the ability of two or more diverse systems or components to exchange information and use the information that has been exchanged in new applications, is thus necessary to support regulatory risk applications and tractable decision support. Considerations and challenges for interoperability in two domains, cultural (e.g., disciplinary assumptions, "narratives", practices, and defaults) and technical (e.g., hardware, software such as models, standards, and data management) are highlighted by a case study of vinyl chloride hepatotoxicity along with recommendations from on-going efforts that evolved from the 2012 SOT CCT meeting.
(The views expressed in this abstract are those of the author and do not necessarily represent the views or policies of the U.S. Environmental Protection Agency.)

W 1410 Contribution of Nonimmune Cells to Adverse Immune Responses: Implications for Toxicology

P. W. Karmaus[1] and B. L. Kaplan[2]. [1]*Immunology, St. Jude Children's Research Hospital, Memphis, TN and* [2]*Department of Basic Sciences, Mississippi State University, Mississippi State, MS.*

The potential for direct adverse effects of xenobiotics on the immune system is widely recognized. These intrinsic effects are often due to expression of target receptors for xenobiotics on immune cells or alteration of intracellular processes. However, novel evidence supports that cellular changes induced by xenobiotics in nonimmune cells can alter the competence of the immune system. Organs outside of the immune system are increasingly recognized for their ability to initiate and shape an immune response. These organs include, but are not limited to, the central nervous system, the mucosal areas such as the lung and the gut, the liver, and the cardiovascular system. The role of toxicants and their ability to modulate organ systems, thereby initiating or altering an immune response resulting in immunotoxicity, is poorly understood. Research highlighting how toxicant-induced changes in tissue physiology can result in pertubations of the immune system will be discussed. The focus of presentations will address the considerations for modeling and for assessing toxic responses and explore putative mechanisms.

W 1411 Cannabinoid-Induced Suppression of beta2AR+ B Cell Function

B. L. Kaplan. *Department of Basic Sciences, Mississippi State University, Mississippi State, MS.*

It is well established that immune cell function is regulated by various neurotransmitters. Early studies demonstrated that beta2 adrenergic receptor (AR) agonists such as norepinephrine and terbutaline could enhance antibody production. Cannabinoid compounds, including the psychotropic congener in marijuana, delta-9-tetrahydrocannabinol (THC), also regulate antibody production. Thus, the focus of these studies was to study the interaction between cannabinoid and adrenergic regulation of B cell function. Studies were performed to determine if beta2AR+ B cell function was affected by cannabinoid treatment. Following lipopolysaccharide (LPS) treatment in vitro, both beta2AR+ and beta2AR- B cells produce IgM, which was suppressed in a concentration-dependent manner by THC. THC also suppressed LPS-stimulated CD86 expression on beta2AR+ B cells. Together, these data demonstrate interactions between cannabinoid and adrenergic regulation of B cell function, and suggest that the immunotoxicity of cannabinoids might involve perturbation of adrenergic signaling. These data further suggest that mechanisms by which some xenobiotics produce immunotoxicity might involve mediators produced by non-immune cells.

W 1412 Amodiaquine-Induced Liver Injury: A New Animal Model of Immune-Mediated Toxicity

R. Li. *Bristol-Myers Squibb Company, New Brunswick, NJ.*

As in humans, amodiaquine causes a delayed onset of mild liver injury (2-3-fold ALT induction) in both rats and mice. Amodiaquine-induced liver injury was associated with anti-drug antibodies and is preventable by cyclosporine in rodents. Liver histology demonstrated activated Kupffer cells, microgranulomas and individual hepatocyte necrosis. Evidence for apoptosis-related mRNA changes (Caspase 1 etc.) in the liver and HMGB1 blood concentrations at 6 h and Day 7 implied that amodiaquine-induced apoptosis of immune and/or non-immune cells is an early event in the initiation of an immune response to mediate the development of liver injury. The release of "danger" signals from apoptotic cells into peripheral circulation might be predictive of potential immune activation and associated tissue damage. A better understanding of immunological responses to those danger signals might shed light on the mechanisms of drug-induced liver injury.

W 1413 Adverse Effects of Systemic Inflammation and Acute Phase Responses Induced by Toxicants

S. B. Pruett. *Department of Basic Sciences, Mississippi State University, Mississippi State, MS.*

Acute administration of ethanol adversely affects resistance to infection, but it is paradoxically associated with a late increase in pro-inflammatory mediators and acute phase proteins in animal models for sepsis. Further investigation has revealed that initial inhibition of pro-inflammatory responses occurs both locally and systemically, but when the ethanol has been cleared, pro-inflammatory and acute phase proteins are elevated in ethanol-treated animals compared to those treated with live bacteria or bacterial lipopolysaccharide. The initial inhibition of responses by ethanol seems to be mediated by direct inhibition of the earliest signaling events at toll-like receptors. Subsequent enhanced inflammation is due to increased bacterial load in animals treated with bacteria (due to poor early clearance), and this reflects poorer outcomes in sepsis in animal models and humans. Enhanced inflammation and acute phase responses 12-24 hr after ethanol can also be caused by increased gut permeability. As a consequence, first pass exposure of the liver to microbial products and subsequent systemic exposure to microbes are increased. The presence of the microbial components establish a net pro-inflammatory status. Overall, these results demonstrate the importance of the gut epithelial barrier as a target organ in regulating immune responses. This work was supported by a grant from the National Institute on Alcohol Abuse and Alcoholism (R01AA009505).

W 1414 The Role of Epithelial Cell-Derived Hypoxia Signaling in Establishing the Inflammatory Response to Allergens

J. J. LaPres. *Department of Biochemistry and Molecular Biology, Michigan State University, East Lansing, MI.*

Recently, our laboratory created an inducible, lung epithelia-specific hypoxia inducible factor 1α (HIF1α) knock out mouse, which has abnormal responses to inhaled cobalt and ovalbumin (OVA). For example, when the HIF1α-deficient mouse is exposed to cobalt it displays an asthma-like phenotype. In contrast, control mice display a Th1-mediated inflammation, similar to hard metal lung disease. Moreover, these HIF1α-deficient mice display an exacerbated response to the OVA challenge model of murine asthma. This suggests that loss of HIF1α in the lung epithelia biases the lung towards a Th2-mediated inflammation. Interestingly, to promote this change in innate immunity, recombination of HIF1α in the epithelial cells must be induced in the first two weeks of life. These results demonstrate that early childhood epithelial-derived HIF1α signaling is important in establishing the inflammatory response of the lung, presumably by regulating the transcription of key secreted immune factors. To identify these factors, a coculture system has been utilized to characterize the ability of epithelial-derived signaling (e.g., HIF1α specific and others) to influence immune cell function. These results highlight the need to assess early life events, such as premature birth and early viral exposure, which might permanently affect HIF1a signaling in the airway epithelium and thus alter the risk of toxicant exposure as adults. Finally, our future directions will focus on characterizing HIF1α-dependent secreted immune factors in the development of the lung's immunity using a combination of *in vitro* and *in vivo* models. The ultimate goal is to determine how epithelial-derived HIF1α-mediated signaling can impact immune cell populations and their function and link these changes to susceptibility to atopic diseases, such as asthma, later in life.

W 1415 Indirect Xenobiotic Immune Modulation: Risk Assessment

L. P. Myers. *US FDA, Silver Spring, MD.*

Xenobiotics can modulate the immune responses indirectly through various mechanisms. Occasionally, this indirect modulation can be difficult to assess or evaluate nonclinically. Limitations are commonly attributed to species specificity to targets that may not be expressed similarly between humans and nonclinical models. Even though the safety of these products may be difficult to assess, there are still paths forward for these pharmaceuticals. Following existing guidance (ICH M3 (R2) or ICH S6 in conjunction with ICH S8), immunomodulatory drugs can be evaluated for many immune alterations prior to human exposure. However, if the target (e.g., receptor or ligand) is species specific and does not allow for adequate safety assessment, then alternative models may be necessary to evaluate the safety of these products. In these cases, increased human monitoring and a more conservative approach may be suggested, depending on the pharmaceutical. Careful consideration of the drug product, PD effects in *in vitro* as well as *in vivo* models, as well as a case-by-case approach is the most common pathway for developing drugs that have unique immunomodulatory mechanisms. Thus, both standard nonclinical evaluations utilizing existing guidances as well as product specific assessments (a case by case approach) are used to evaluate the safety of immunomodulatory products during risk assessment of human pharmaceuticals.

W 1416 Developmental Toxicity from Chemical Mixtures: Research to Application in Susceptible Populations

D. J. Carlin[1] and M. Mumtaz[2]. [1]*NIEHS, Research Triangle Park, NC and* [2]*ATSDR, Atlanta, GA.*

The study of environmental chemical mixtures is highly complex and requires sophisticated approaches to determine which mixture component(s) contribute to health effects. Consideration of sensitive subpopulations such as pregnant mothers, the developing fetus, infants, and children, significantly increases the complexity due to chemicals exhibiting different effects depending on the timing of exposure. For example, it is well known that exposure to mixtures of inorganic metals (e.g., lead, cadmium, mercury, arsenic) and pesticides leads to neurological and other organ-specific health effects in adults, but the suite of health effects associated with these mixtures in the developing fetus and infant could differ from that of adults and is less understood. This workshop will focus on the health effects of chemical mixtures with particular attention to exposure to pregnant mothers, the developing fetus, and children, and will include discussion of toxicological studies, statistical and modeling approaches, and application to human health risk assessment in these susceptible populations. There is an impending need to understand interactions among components of mixture exposures in order to improve human health risk assessments in these susceptible populations.

W 1417 Chemical Mixtures, Developmental Windows, and Neurodevelopment

R. O. Wright. *Mount Sinai School of Medicine, New York, NY.*

Low level mixed exposures likely influence developmental trajectories and program later life health effects. Understanding mixed exposures requires prospective study designs to capture critical developmental windows of exposure and complex statistical approaches to assess whether combined exposures are synergistic in toxicity. In addition, mixtures studies often evaluate 2 or 3 way interactions, but methodologies are needed that can address higher order interactions. This presentation will include data on ongoing longitudinal studies of metal mixtures and childhood neurodevelopment conducted in 3 distinct birth cohorts. As an example, in a preliminary analysis of 350 children (final N =829 when study is complete) Bayley Scales of Infant Development in Bangladeshi children and metal exposure (As, Pb, Mn), we used adjusted multivariable Kernel Machine regression to assess the joint impact of these 3 metals. This type of model will test the best fit of the overall interaction data and allows for non-linear relationships between random variables. Splines will be used to present above results graphically, as multi-dimensional nonlinear interactions are difficult to present as simple beta coefficients. Lead and the middle tertiles of arsenic, and manganese exposure compared to the lowest tertiles were inversely associated with 24-month Bayley scores (β=-0.71, p=0.01; β=-2.13, p-val=0.01; β=-1.25, p-val=0.061, respectively). There was evidence of lead-arsenic interaction. Lead toxicity was increased among children in the third tertile of arsenic exposure, compared to children in thefirst tertile of arsenic (interaction β= -0.33, p-val=0.006). Further, nonparametric splines were used to explore non-linear effects of As and Mn, which were detected as an inverted-U relationship between manganese and the Bayley score at the second arsenic tertile (p-val=0.0003). Overall, these preliminary findings suggest that non-linear relationships exist within mixed exposures and statistical methodologies to detect such relationships should be employed.

W 1418 En Route to More Relevant Animal Models: Interactions of Chemical and Nonchemical Stressors in Developmental Neurotoxicology

D. A. Cory-Slechta. *University of Rochester School of Medicine, Rochester, NY.*

Understanding interactions of chemicals and/or nonchemical stressors is ultimately critical for understanding risks associated with chemical exposures. Such interactions may augment or even mitigate toxicity and are thus critical to risk assessment and public health. This talk will describe developmental neurotoxicity and behavioral/cognitive toxicity in animal models as well as in human studies in which interactions of chemical and or nonchemical stressors were examined, based on the fact that these were co-occurring risk factors in human populations and that they also shared biological substrates. These include animal models of neurotoxic metals (lead and methylmercury) combined with prenatal stress, and the translation of these efforts to assessment of the impacts of combined lead and stress in occupationally-exposed workers. In support of the need for more complex models, our animal studies demonstrate that neurotoxic effects of both Pb and of methylmercury, both behavioral and neurochemical changes, are enhanced by prenatal stress in a sex-dependent manner. Iron insufficiency represents another risk factor for cognitive development that co-occurs with elevated lead exposure across the world, and shares both biological substrates and profiles of adverse effects with lead. Our newly developed animal model demonstrates that brain and bone lead levels are elevated by iron insufficiency. Ongoing analyses of lead-iron insufficiency interactions from the Rochester cohort study of low level lead exposure in which both blood lead and iron status were measured at 6, 12, 18, 24, 36, 48 and 60 mos of age along with IQ and cognitive outcomes suggests enhanced IQ reductions with combined elevated blood lead and anemia plus iron deficiency.

W 1419 Toward the Rational Use of Exposure Information in Mixtures Toxicology

R. Tornero-Velez. *US EPA, Research Triangle Park, NC.* Sponsor: D. Carlin.

Of all the disciplines of toxicology, perhaps none is as dependent on exposure information as Mixtures Toxicology. Identifying real world mixtures and replicating them in the laboratory (or *in silico*) is critical to understanding their risks. Complex mixtures such as cigarette smoke, diesel exhaust, and disinfection byproducts may be replicated without difficulty because they are uniquely associated with reproducible processes such as combustion. On the other hand, chemical mixtures that arise from multiple sources are less tractable. Toxicologists often are faced with developing *ad hoc* rules for constructing test mixtures, or they simply test a few binary combinations. We examined monitoring data for pesticides in daycares (CCC) and homes (AHHS) and the evidence that points to patterns in how they

group. We applied approaches from the field of community ecology to test if these assemblages of "chemical species" are random or structured. Presence-absence matrices developed from CCC and AHHS datasets indicated structure comparable to the West Indian Finch matrix when species diversity metrics were applied; namely, the COMBO metric (number of unique combinations) and CHECKER metric (number of 2x2 checker matrices). This finding indicated that factors (e.g., social, economic, and technical) limit the spectrum of pyrethroid combinations observed in these datasets. Additional methods were used to identify frequently occurring k-way combinations from the CCC dataset. These approaches were used to inform pharmacokinetic studies and a cumulative probabilistic exposure-dose assessment.

W 1420 Application of a Weighted Quantile Sum Approach to Identifying Bad Actors in Mixtures of Environmental Chemicals: A Transgenerational Study of Reproductive Hazards

C. Gennings. *Virginia Commonwealth University Medical Center, Richmond, VA.*

Risk evaluation of environmental chemical exposures is impacted (i.e., inflated variance, confounding) by the complex correlation structure among components of chemical mixtures. We have developed a novel, empirical weighted quantile sum (WQS) method for identifying 'bad actors' in correlated data. Characterization of the method (reliability, validity) will be presented using simulated data. The approach will be demonstrated using fecundability as a measure of reproductive hazard in a transgenerational study of PCBs. We compared the results of WQS regression to those based on categorization of PCB compounds by (1) hypothesized biological activity previously proposed and widely applied, and (2) degree of ortho-substitution (mono, di, tri), in a study of the relation of maternal serum PCBs and daughter's time to pregnancy (TTP). The dominant functionality groups associated with longer TTP were the dioxin-like, anti-estrogenic group (average weight, 22%) and PCBs not previously classified by biological activity (54%). In contrast, the unclassified PCBs were not important in the association with shorter TTP, where the anti-estrogenic groups and the PB-inducers group played a more important role (60% and 23%, respectively). The highly chlorinated PCBs (average weight, 89%) were mostly associated with longer TTP; in contrast, the degree of chlorination was less discriminating for shorter TTP. Finally, PCB 56 was associated with the strongest relationship with TTP with a weight of 47%. WQS regression found some associations previously identified by two classification schemes, but also identified other bad actors. This empirical method can generate hypotheses about mixture effects and mechanisms and overcomes some of the limitations of standard regression techniques.

W 1421 A Risk Assessment and Regulatory Agency Perspective on Mixtures Affecting Susceptible Populations

M. L. Dourson. *Toxicology Excellence for Risk Assessment, Cincinnati, OH.*

In one sense, the study of mixtures to susceptible populations is easy. Since we are all exposed to mixtures of chemicals and nonchemical stressors, one needs to simply be observant. Unfortunately, the mixtures to which many of us are exposed (e.g., oxygen and arsenic) are not really of much interest to regulators. Of more interest are exposures to mixtures, especially to sensitive subgroups, about which toxic effects are known and for which we might be able to do something, such as the concentrations of methylmercury and PCBs in fish. This presentation will start with a brief explication of existing methods that allow risk scientists to gauge the safety of chemical mixtures, and then highlight comparative toxicokinetic and toxicodynamic data between adults and children, which can be used to improve the estimation of safety and risk to susceptible populations from chemical mixtures and nonchemical stressors. Our analysis of Seychelle and Faroe Islands cohorts revealed differing intakes of PCBs and methylmercury, and using benchmark doses (BMDs) analysis, revealed the presence in children or absence in adults of neurological effects. The impact of our findings on the development of a mixture Reference Dose (RfD) and nonchemical stressors in these populations will be discussed.

W 1422 Somatic Cell Therapy—Paradigms for Investigational New Drug (IND)-Enabling Programs, Scientific and Regulatory Considerations, and Clinical Translation

C. Lindamood[1], P. Au[2], L. E. Black[3], J. Hamilton[4], J. Cavagnaro[5], J. W. Ludlow[6] and C. Sachs[7]. *[1]CLIII Consulting, LLC, Hoboken, NJ, [2]Food and Drug Administration, Rockville, MD, [3]Charles River Laboratories, Inc., Reno, NV, [4]Athersys, Inc., Cleveland, OH, [5]Access BIO, Boyce, VA, [6]Zen Bio Inc., Research Triangle Park, NC and [7]Janssen Research and Development, LLC, Spring House, PA.*

There is significant interest in somatic cell therapies and their therapeutic potential to stimulate repair in diseased or injured tissue. Development of these therapies has been hindered by lack of knowledge of appropriate methods for assuring patient safety in clinical trials. Standard pharmacological and toxicological methods may not apply in safety evaluation of somatic cell therapies. Animal model selection, and safety concerns to be assessed, varies greatly depending upon clinical indication, source and type of cell therapy, and method of cell therapy delivery. The aim of this workshop is to provide insight into successful paradigms for IND-enabling studies supporting clinical evaluation of somatic cell therapies. Speakers with both regulatory and academic/industry development expertise in somatic cell therapy will provide presentations of program experience. The overall goal is to aid current investigators in the somatic cell therapy field, and to facilitate and expedite the development of somatic cell therapies in clinical medicine by sharing lessons learned from previous experiences.

W 1423 Developing Cell Therapy Products: US FDA Preclinical Regulatory Considerations

P. Au. *Office of Cellular, Tissue and Gene Therapies, Center for Biologics Evaluation and Research, US FDA, Rockville, MD.* Sponsor: C. Lindamood III.

The presentation intends to provide an overview of Center for Biologics Evaluation and Research (CBER)/ Food and Drug Administration (FDA) expectations for preclinical studies for cell therapy products. Because of the diversity and complex nature of these products, they preclude the application of traditional, standardized approaches for preclinical testing. The case-by-case review approach will be discussed and general preclinical study design considerations and potential pitfalls will be presented. The application of these recommendations will be illustrated by case examples.

W 1424 The Shaky Bridge: Animal Model Translation for Cell Therapies and Impact on Clinical Success

L. E. Black. *Charles River Laboratories, Reno, NV.*

Cell therapies are very diverse. One universal statement that can be made is that nonclinical toxicology programs (the backbone of risk assessment for clinical trials) are less established for cells compared to those conducted for drugs. This problem starts at the difficulty of characterizing the nature of the product itself, even in vitro. For instance, islet cells may control glucose levels in animal models of pancreatic failure, but the obvious test of their in vitro potency (response to glucose) may not work at all. With this being true, uncertainty applies to prospective risk assessment, where one would hope that vitro and in vivo effects translate to patients. The term hope is used because we seldom see an intact "bridge" of activity from in vitro to in vivo in cell therapy research programs. We often have to proceed on faith that 1) the cells manifested both their pharmacologic and their toxicologic potential in the animal, and 2) that this one species program is a sound basis for human risk assessment. This is a far cry from knowing that we injected a drug (like a hormone) into two species, measured the drug PK and receptor occupancy, and measured the products secreted by hormone after binding to its receptor, and then observed amelioration of disease. So the pharmacology "bridge" for cell therapies (intrinsic to their nature/complexity) is a shaky one. Looking to the future, what can we do to improve our animal models, cell pharmacology, and translation to risk assessment? A stronger bridge might enable trials in earlier stage patients, improving chances of regeneration, and gaining Proof of Concept to further design optimal therapy. Published examples of in vivo data will be discussed.

W 1425 Considerations in Dose Extrapolation of Stem Cell-Based Therapies: Optimizing First in Human Trial Design

J. Cavagnaro. *Access BIO, Boyce, VA.*

Initial clinical studies of stem-cell based therapies are conducted in subjects with disease rather than normal volunteers. As such the objective is not only to administer a safe but also an active dose. However, unlike small molecules or large molecule biological drugs, there is no standard algorithm for extrapolation of preclinical animal doses. The concept of exposure also differs. This presentation will discuss key design considerations in dose extrapolation based upon differences in cell type, delivery and disease indication.

W 1426 Intravenous Administration of Human Bone Marrow-Derived MultiStem® Cells after Ischemic Stroke: Preclinical Safety, Efficacy, and Mechanism of Action Studies to Support IND Submission and Clinical Trial Design

J. Hamilton. *Athersys, Inc., Cleveland, OH.* Sponsor: C. Lindamood III.

MultiStem® is an allogeneic adult bone marrow-derived cell therapy product that has received allowance from the FDA for testing in humans in the treatment of acute myocardial infarction, prophylaxis of graft-versus-host-disease in leukemia patients, inflammatory bowel disease, and ischemic stroke. It is the only cellular therapeutic currently being tested in acute ischemic stroke patients in the US. This presentation will describe the battery of preclinical safety, efficacy, and mechanism of action studies performed to support Investigation New Drug (IND) submission and clinical trial design for the ongoing Phase I/II trial. Preclinical safety studies that supported multiple IND submissions, or that were designed specifically to support use of MultiStem in ischemic stroke, will be highlighted. The presentation will also address some of the unique challenges posed by testing cellular therapies in preclinical animal models.

W 1427 Regeneration of Native-Like Neo-Urinary Tissue from Nonbladder Cell Sources—Development of the Neo-Urinary Conduit™

J. W. Ludlow. *Zen Bio Inc., Research Triangle Park, NC.* Sponsor: C. Lindamood III.

The possibility of creating a tissue engineered/regenerative medicine product facilitating urinary diversion without leveraging native gastrointestinal tissue as the raw material was the rationale underlying the development of the Neo-Urinary Conduit™ (NUC). The NUC is a cell/scaffold construct that upon attachment to native ureters mediates efflux of urine from the kidneys directly to the external surface of the body. Good Laboratory Practice (GLP) studies demonstrated that a synthetic, bio-polymeric scaffold composite seeded with autologous smooth muscle cells derived from adipose tissue is capable of creating a patent NUC comprised on native-like urinary tissue. The regenerated conduit was not associated with sequela commonly found with urinary diversions generated from intestinal tissue or with non-cell seeded synthetic scaffolds. This ability to create urologic structures de novo from synthetic scaffolds seeded with adipose-derived smooth muscle cells should facilitate the translation of urologic tissue engineering technologies into clinical practice. As a combination product, the NUC received allowance from the FDA in 2010 to begin a clinical trial in bladder cancer patients. The NUC is the first of an entirely novel category of neo-organs designed entirely by scientists to fulfill specific functional roles. In this case bypass of the bladder and direct efflux of urine from the body. Since this product contains a combination of cells and biomaterials, it does not fit the standard absorption, distribution, metabolism, and excretion (ADME) and toxicology paradigm of safety testing. The lesson learned here is that a substantial amount of additional information was needed to be provided to the Food and Drug Administration (FDA) in order to assess safety of this regenerative medicine product. This presentation will cover the in-process testing, acceptance criteria for release, assessment of fitness for use, and potency of the final product during the pre-clinical GLP studies designed to support submission of the Investigational New Drug (IND) application.

W 1428 Nonclinical Development of Human Umbilical Tissue-Derived Cells (hUTC) for Degenerative Retinal Diseases

C. Sachs. *Janssen Research and Development, LLC, Spring House, PA.*

A nonclinical development program using rats and pigs was successfully executed to support a First-in-Human (FIH) clinical trial for hUTC in Retinitis Pigmentosa. This program evaluated the safety and efficacy of hUTC, but also developed and characterized analogous cells from rats and minipigs to understand the immunology of cells in an allogeneic setting. In rats, the desired pharmacology was demonstrated in the Royal College of Surgeons model of degenerative retinal disease and ocular histopathology was used to evaluate potential effects of the disease state on the safety of hUTC. The rat was used to evaluate the tumorigenicity and biodistribution of hUTC following subretinal and systemic administration. However, anatomic constraints precluded the use of the clinical surgical procedure. A large animal species, the minipig, was used to evaluate the safety of the cells when administered by the surgical method of cell administration intended for patients. Based on anatomic considerations, cell doses were extrapolated across species based on retinal surface area. Taken together, results of these nonclinical studies supported the initiation of FIH clinical trials.

W 1429 The Promise of Translational Imaging in Nonclinical Safety Assessment

C. L. Chen[1], B. R. Berridge[5], J. Heyen[6], P. Hockings[4], A. G. Johnson[2], S. Liachenko[3] and M. G. Paule[3]. *[1]ILSI Health and Environmental Sciences Institute, Washington, DC, [2]Center for In Vivo Microscopy, Duke University, Durham, NC, [3]Division of Neurotoxicology, US FDA NCTR, Pine Bluff, AR, [4]Drug Safety and Metabolism, AstraZeneca, Mölndal, Sweden, [5]Safety Assessment, GlaxoSmithKline, Research Triangle Park, NC and [6]Pfizer, La Jolla, CA.*

This symposium is designed to explore how several clinical to preclinical translational imaging modalities can be efficiently and effectively integrated into contemporary drug development and chemical hazard assessment. Standard clinical imagers, such as Magnetic Resonance Imaging (MRI), Magnetic Resonance Spectroscopy (MRS), Echocardiography (Echo) and Positron Emission Tomography (PET) have demonstrated strong utility in the nonclinical setting by allowing for the ability to perform real-time, non-invasive, longitudinal animal studies that can provide morphological, functional, and molecular data. Additionally, these modalities greatly minimize the need for assumptions in data interpretation and reduce uncertainty during product development or risk assessment; therefore, the preclinical application of these imaging strategies and the integration of these capabilities into modern drug safety assessment and environmental hazard identification is a promising development with the potential to greatly impact the field. This workshop will provide an overview of the challenges facing clinical trials and opportunities for translational imaging to address these gaps. Imaging approaches that address major contributors to pharmaceutical attrition, including cardiovascular safety, drug-induced liver injury, and neurotoxicity, will be presented. Additionally, the panel discussion will explore the hurdles of validating the use of imaging modalities as a biomarker in the field and by regulators. Ultimately, this workshop aims to facilitate dialogue across disciplines for broader acceptance and implementation of translational imaging in improving preclinical safety assessment and basic toxicity studies.

W 1430 Translational Imaging Advances in Preclinical Assessment and Challenges for Regulatory Acceptance

B. R. Berridge. *Safety Assessment, GlaxoSmithKline, Research Triangle Park, NC.* Sponsor: S. Liachenko.

There is a potential disconnect between the very molecular approach we take to contemporary drug design and the very 'un-molecular' approach we take to assessing *in vivo* efficacy and safety. Nonclinical safety assessment of human pharmaceuticals typically involves a regimented series of studies that might lack a level of morphofunctional integration to be optimally instructive and translational. It may also lack the ability to understand the molecular relationship between drug and safety liabilities or use the data generated to leverage ever developing computational capabilities. Advances in *in vivo* imaging capabilities are providing an unprecedented opportunity to refine our traditional approaches and advance the translatability of our studies. Longitudinal studies that allow dynamic assessments of dynamic processes could be more instructive and require fewer animals. Molecular imaging capabilities are providing opportunities to visualize physiologic processes and their association with drug in living systems. Imaging can also make 'quantitative' what has traditionally been un- or semi-quantitative. This presentation will provide an overview of the advances in imaging technology and its application to animal models with quantitative endpoints that are also applicable to the clinical setting. We will put focus to integrated assessments of target organ morphology and function

to provide a more holistic understanding of drug effects and the ability to identify the most sensitive biomarker of that effect. Additionally, we will present challenges to applying novel approaches in very traditional paradigms and debate the risks and benefits of those approaches.

W 1431 *In Vivo* Imaging of Hepatobiliary Transporter Function

P. Hockings. *Drug Safety and Metabolism, AstraZeneca, Mölndal, Sweden.* Sponsor: S. Liachenko.

New response biomarkers that are sensitive and specific to detect early liver dysfunction prior to onset of irreversible liver damage are urgently needed. This presentation will describe a new *in vivo* imaging biomarker of hepatobiliary transporter function in the rat. A compartmental model was developed to characterize the pharmacokinetics of hepatic uptake and biliary excretion of the MRI contrast agent gadoxetate. Magnetic resonance imaging was used to continuously measure the concentration of gadoxetate in the liver and plasma for one hour after a bolus injection. The gadoxetate concentration in hepatocytes was estimated after correction for the gadoxetate concentration in plasma and the known volume fraction of extracellular space in the liver. An investigational hepatobiliary transporter inhibitor was shown to reduce both the rate of uptake of gadoxetate into the hepatocyte and the Michaelis–Menten constant characterizing its excretion into bile, whereas KM values for biliary efflux were increased. These effects were dose dependent and correlated with effects on plasma chemistry markers of liver dysfunction, in particular bilirubin and bile acids. The HESI liver imaging working group is evaluating the ability of this technique to quantitate *in vivo* hepatobiliary transporter function in a multi-site setting imaging using a known hepatobiliary transporter inhibitor. The potential to translate this to technique to evaluate risk in the clinic will also be discussed.

W 1432 Characterization of Drug-Induced Changes in the Cardiovascular System

J. Heyen. *Pfizer, La Jolla, CA.* Sponsor: M. Paule.

The expansion of cardiovascular (CV) imaging modalities from being utilized primarily in efficacy based approaches into safety studies has led to more robust analysis of drug induced CV changes. Advancements in Ultrasound (US) and Magnetic Resonance Imaging (MRI) coupled with adaption to scale for smaller species has enabled the adoption of these techniques into preclinical testing and facilitated their use in this arena. Conducting laboratories should have an understanding of data variability including intra and inter-observer errors and should have a robust training and qualification processes in place prior to data creation and study conduction. Likewise, opportunities and data for reverse translation investigations of drugs with identified clinical CV liability such as doxorubicin or trastuzumab are available and have been undertaken. Refinement of techniques and advancements in technology such as strain imaging and 3D small animal imaging will continue to increase the quality of preclinical CV imaging and will allow for thorough investigation of potential CV of novel drugs. This presentation will describe the efforts of a ILSI Health and Environmental Sciences Institute CV imaging working group has produced cross-site/company data around reproducibility and variability using a single compound. ANOVA analysis showed that for most of the parameters, there is no statistically significant site difference after adjusting for the baseline and vehicle effect. The median Intra-Class Correlation (ICC) for all parameters is only 12.7%, suggesting the variability of site effect is small compared to the overall variability. With proper training and equipment, this workgroup has demonstrated that it is possible to collect high quality on cardiac structure and function using these approaches in standard toxicology or stand alone preclinical studies. A description of how these techniques can inform clinical risk and influence prospective clinical trial design for compounds with identified preclinical signals will also be discussed.

W 1433 Magnetic Resonance Histology—Applications in Toxicology

A. Badea, A. G. Johnson, E. Calabrese, C. Liu and L. Xie. *Center for In Vivo Microscopy, Duke University, Durham, NC.* Sponsor: M. Paule.

Magnetic resonance imaging (MRI) has revolutionized clinical medicine. The same underlying technologies are now triggering a similar revolution in the basic sciences. Magnetic resonance histology (MRH) was first suggested in 1993. Through the use of very high magnetic fields, specialized rf coils, novel imaging strategies, and specialized active MR stains, we have increased the spatial resolution in MRH by more than five orders of magnitude over that which is common in clinical MRI. While a number of papers have demonstrated the utility of MRH in toxicology, it is still not part of the mainstream. This presentation will include a brief overview of the technology and three recent results demonstrating exciting options that MRH provides the toxicologist because of its unique characteristics. In the first study, a developmental atlas of the rat provides a diffusion tensor (DTI) atlas following myelination of the rat brain at nine time points between PND0 and PND80. Changes in the diffusion metrics closely follow the development of myelin and its compaction- areas usually only seen with more complex electron microscopy. A second study demonstrates the use of magnetic susceptibility imaging providing quantitative insight into renal fibrosis. The last study describes a comprehensive infrastructure for high throughput MRH and it's validation in a study of the effects of trimethyl tin. MRH is nondestructive, so tissues do not need to be physically sliced. Three-dimensional scanning allows viewing of whole specimens fully intact. Since the tissue is not dehydrated, morphologic measurements are considerably more accurate than with traditional techniques. Because the data can be acquired with isotropic spatial resolution, difficulties in obtaining homologous slices are virtually eliminated. A wide range of contrast mechanisms provides a rich set of biomarkers for tissue injury. Combining these attributes with sophisticated image registration algorithms allows us to produce atlases with quantitative biomarkers defining both severity and extent of injury in the entire organ.

W 1434 Preclinical Development of Neurotoxicity Biomarkers Using *In Vivo* MRI

S. Liachenko. *Division of Neurotoxicology, NCTR, US FDA, Pine Bluff, AR.*

Current approaches in the analysis of neuropathology in support of new drug submissions to the FDA (the use of several arbitrary histology slices) can sometimes result in false-negative findings due to significant undersampling. Non-invasive MRI can provide unique information about the three-dimensional structure and function of the whole brain *in vivo* with sufficient resolution and contrast to serve as a translatable neurotoxicity biomarker. Recently it has been shown in our lab that the value of the brain T_2 water relaxation as measured with MRI in rats is sensitive to the acute neurotoxicity caused by known neurotoxicants with the variety of mechanisms of action. T_2 relaxation provides the quantitative measure of the amount and extent of the changes in the brain tissue consistent with neurotoxicity. This presentation will describe the implementation of such imaging approach to develop a quantitative non-invasive biomarker of neurotoxicity by correlating the *in vivo* MRI T_2 maps to histopathology using the panel of known neurotoxicants at different doses and time points. For example, a single dose of kainic acid (10 mg/kg, intraperitoneal injection) led to the rapid development of T_2 lesion, detectable already at 2 hours post-injection (lesion volume = 10.8 ± 2.6 mm^3), which grew significantly at 48 hours post-injection (lesion volume = 86.2 ± 34.2 mm^3). This measure provided much earlier detection of the neurotoxicity than conventional histopathology score, which was 0 at 2 hours and 1.84 ± 0.49 at 48 hours post-injection (histopathology score range is from 0 [no damage] to 4 [maximum damage] and is assessed qualitatively). The use of such non-invasive MRI biomarkers may significantly increase the chance of the early preclinical detection of the small or transient neurotoxic changes and thus to optimize the costly process of drug discovery and development as well as enhance the safety of the final product.

W 1435 The Role of Toxicology in Undergraduate STEM Education Reform

R. S. Pollenz[1], J. Labov[3], M. M. Bourgeois[2], T. Dodd-Butera[6], B. W. Brooks[4] and T. L. Leavens[5]. [1]*Office for Undergraduate Research, University of South Florida, Tampa, FL,* [2]*Environmental and Occupational Health, University of South Florida, Tampa, FL,* [3]*National Academy of Sciences, National Research Council, Washington, DC,* [4]*Environmental Science, Baylor University, Waco, TX,* [5]*Pharmacokinetic Consultant, Cary, NC and* [6]*Nursing, California State University, San Bernardino, San Bernardino, CA.*

The attrition of undergraduates who enter STEM degree programs but do not earn a STEM undergraduate degree is an area of national concern. "Vision and Change in Undergraduate Biology Education," the 2011 report from AAAS/NSF, and "Engage to Excel," the 2012 report from the President's Council of Advisors on Science and Technology (PCAST), are two national calls to action on this issue and advocate for significant reform in the way undergraduate STEM education is delivered. A strategic goal of SOT is a commitment to education in toxicology and the recruitment of students and new members into the profession. Although the number of undergraduate toxicology degree programs is limited, toxicology is a STEM discipline and many SOT members currently engaged in teaching undergraduates incorporate toxicology into traditional STEM undergraduate degree programs such as biology, biomedical sciences, chemistry, public health, and nursing. The learning objectives of this interactive workshop are to, 1) provide context to the national call to action on undergraduate STEM education reform, 2) present four case studies of inquiry-based approaches in undergraduate STEM education that inspire

students about the multidisciplinary science of toxicology, and 3) engage attendees to develop an "action plan" that incorporates toxicology and inquiry into a current STEM undergraduate degree program. During the workshop attendees will have the opportunity to network with practitioners who can help inform their practice. This session should have widespread benefit to anyone engaged in teaching "toxicology" at any level of academia or industry who has an interest in innovations that help to engage trainees to "work the problem."

W 1436 The Changing National Landscape of STEM Education: Building Partnerships with Scientists and Educators

J. Labov. *National Academy of Sciences, National Research Council, Washington, DC.* Sponsor: R. Pollenz.

The improvement of STEM (science, technology, engineering, and mathematics) education has become a national priority at all levels of the education system. However, efforts to increase the numbers of students who enter and persist in STEM fields too often have been disjointed and have been undertaken without understanding the potential effects on other parts of the education system. This presentation will provide an overview of recent reports and their recommendations for improving STEM education, especially at the undergraduate level. It will explore the intersections between education and public policy and why college and university faculty should be aware of and involved with education policymaking. It also will describe how current efforts to improve STEM education in Grades K-12 will likely have major impacts on postsecondary education and how undergraduate education will influence K-12 education in the future.

W 1437 Case Study 1: Creating Research Experiences and Activities for Public Health Undergraduates through Teaching Enhancement (CREATTE)

M. M. Bourgeois. *Environmental and Occupational Health, University of South Florida, Tampa, FL.*

One of the challenges presented by a rapidly expanding undergraduate program like the B.S. in Public Health at USF is providing research opportunities for students. The Office for Undergraduate Research (OUR) developed the CREATTE (Creating Research Experience and Activities Through Teaching Enhancement) to address this need. Through the CREATTE initiative, faculty incorporated an authentic research experience within a structured course. The research experience tracks on the student's transcript and they also have the opportunity to present their work at the Undergraduate Research Colloquium. CREATTE funds cover sustainable supplies and 30 hours of effort from a graduate assistant. During Fall 2012, 12 students in Environmental Health Science were able to participate in a project involving K12 outreach. This area was chosen because it is a vital component of the public health mission to educate the community regarding scientific issues, particularly toxicology and risk assessment. Students were matched with local K-8 science classes based on curriculum needs. Students created age appropriate presentations and activities on public health topics for the Great American Teach In. Utilizing this preexisting infrastructure obviated the need for school board clearance. Feedback from the students and teachers allowed participants to develop templates for future students to emulate. A post survey of participating CREATE undergraduate researchers indicated a strong agreement that they developed enhanced research competencies, had a deeper understanding of the course material and would engage in addition research activities.

W 1438 Case Study 2: Integrating Toxicology into the Undergraduate Curriculum

T. Dodd-Butera. *Nursing, California State University, San Bernardino, San Bernardino, CA.*

Addressing the challenge of incorporating toxicology and environmental threats into undergraduate nursing education is critical for engaging future health professionals in the application of science for the benefit of society. Utilizing case study methodology as part of an overall educational program on environmental health for undergraduate nursing students, educational modules were developed addressing toxicokinetics, by utilizing a lecture format on a model of lead toxicity. Further, a clinical rotation for students at a poison control center demonstrated clinical toxicology approaches and poisoning prevention strategies for the benefit of public health. The blended learning approach addresses the focus of the STEM initiative on content delivery, and incorporates the "4 C's" noted by the National Education Association as essential tools for preparing 21st century students for a global society through appreciative inquiry. The integration of poisoning principles through critical thinking, communication, collaboration, and creativity, is also aligned with the commitment of the SOT to education and exposure to the interdisciplinary nature of toxicology. Attendance at a journal club was also part of the educational strategy, and covered topics such as environmental exposures, chemicals, drug overdoses, and unintentional poisonings. The culminating experience was a presentation at a poster session, addressing problem solving through evidence-based practice, and a collaborative approach to campus-community partnerships and service learning. Integration of toxicology into didactic and clinical experiences of undergraduate nursing students underscores the potential for innovative approaches in addressing STEM initiatives and SOT strategies for education across multiple scientific disciplines.

W 1439 Case Study 3: Integrating Toxicology into the Undergraduate Laboratory Curriculum

B. W. Brooks. *Environmental Science, Baylor University, Waco, TX.*

This session presents multiple strategies utilizing contemporary scientific laboratory techniques to integrate environmental research into laboratory courses. Such an approach enhances student's critical thinking skills and allows for application of toxicology practices. This session will also describe modules that allow laboratory approaches for defining contaminants of emerging concern.

W 1440 Case Study 4: Problem-Based Instruction of Pharmacokinetics

T. L. Leavens. *Pharmacokinetic Consultant, Cary, NC.*

The goal of STEM education is the development of competency and application of knowledge versus acquisition of knowledge. Therefore, courses that are structured based on the higher order objectives in Bloom's taxonomy of learning provide an ideal classroom environment, because they are focused on projects and case studies versus lectures. Some of the more recent techniques to achieve this learning environment are the flipped classroom and e-learning tools. The objective of this presentation is to demonstrate how to design a problem-based lecture for pharmacokinetics, a discipline in which problem-solving skills are critical. The presentation will focus on the absorption component of pharmacokinetics and demonstrate how to convert a lecture on the topic into a flipped class through the use of video clips, interactive case studies, and web-based applications.

S 1441 *In Vitro* Microphysiological Systems: Advancing Regulatory Science through Innovation

A. Bahinski[1] and S. C. Fitzpatrick[2]. [1]*Wyss Institute for Biologically Inspired Engineering at Harvard University, Boston, MA and* [2]*Center for Food Safety & Applied Nutrition, US Food and Drug Administration, College Park, MD.*

Development of safe and effective drugs is currently hampered by the poor predictive power of existing preclinical animal models that often lead to failure of drug compounds late in their development. Given the tremendous cost of drug development and the long timelines involved, major pharmaceutical companies and government funding agencies are now beginning to recognize a crucial need for new technologies that can quickly and reliably predict drug safety and efficacy in humans in preclinical studies. Advances in bioengineering, material sciences, microfabrication, and microfluidics technologies have enabled the development of microphysiological systems that mimic the functional units of an organ. These advances have made it possible to initiate the engineering of cellular microenvironments and/or functional units of lung, heart, blood vessels, muscles, bones, liver, nervous system (including eye), gut, and kidney. In general, these microphysiological systems, or human "organs-on-chips," use microscale engineering technologies combined with cultured living human cells to create microfluidic devices that recapitulate the physiological and mechanical microenvironment of whole living organs. The next challenge is to develop an integrated microsystem platform that can incorporate several different modular organs on a chip. These integrated microsystems would mirror the complex physiology and biology of the human body. An integrated microphysiological platform could further our understanding of disease etiology and fill the critical need for improved model systems to predict efficacy, safety, bioavailability, and toxicology outcomes for candidate compounds. This symposium will examine the building blocks needed to bring this new innovative technology into the regulatory arena, including the need for adequate stem cells, the development of representative organ systems, challenges to building a "human on a chip," and the pathway to qualification for regulatory use.

S 1442 The Importance of Partnerships for Innovation in Regulatory Science—The NCATS/US FDA/DARPA Partnership for Developing Microphysiological Systems

D. A. Tagle. *National Center for Advancing Translational Sciences (NCATS), NIH, Bethesda, MD.* Sponsor: A. Bahinski.

The goal of the new National Center for Advancing Translational Sciences (NCATS) is to catalyze the generation of innovative methods and technologies that will enhance the development, testing and implementation of diagnostics and therapeutics across a wide range of human diseases and conditions. By improving the process by which diagnostics and therapeutics are developed, NCATS strives to make translational science more efficient, less expensive and less risky. Partnerships between federal agencies and stakeholders are critical for innovation in regulatory science. The NCATS/FDA/ Defense Advanced Research Projects Agency (DARPA) partnership for the development of in vitro microphysiological systems is a groundbreaking example of the types of partnerships that are needed to bring innovative new technologies into the regulatory paradigm. NCATS, FDA and DARPA are collaborating to develop a chip to screen for safe and effective drugs which is far more swift and efficient than current methods. NCATS would help identify barriers to progress and provide science-based solutions to reduce costs and the time required to develop new drugs and diagnostics. FDA will help determine how this new technology can be utilized to assess drug safety, prior to approval for first-in-human studies. DARPA and NIH will facilitate collaborations between researchers and FDA to advance the goals of both programs. The two agencies, in coordination with FDA, solicited proposals from industry, government labs, academic institutions, and other research organizations on how best to develop the chip, bringing together the latest advances in engineering, biology, and toxicology to bear on this complex problem. Throughout the five year research plan, NCATS, FDA, and DARPA meet biannually with all the researchers.

S 1443 Good Cell Culture Practices and Their Application to iPSC for Neurotoxicity

T. Hartung. *Department of Environmental Health Sciences, Center for Alternatives to Animal Testing, Johns Hopkins Bloomberg School of Public Health, Baltimore, MD.*

In parallel with recent developments in bioengineering, advances in stem cell technology now make it possible to obtain tissues from humans with specific genotypes and/or disease phenotypes. Although these capabilities present unprecedented opportunities to create biomimetic devices with the potential to capture the dynamics of drug effects in the human body, challenges still remain in differentiating pluripotent cells to span the developmental spectrum. Increasing awareness of the problems of cell authenticity, differentiation, stability of karyotypes, insufficient documentation of experimental conditions etc. led to the development of Good Cell Culture Practice (GCCP) guidance (Coecke et al., 2005). This formed a basis for the current OECD guidance for Good Laboratory Practice for in vitro studies. The increasing use of embryonic stem cells prompted a workshop on how to adapt GCCP for this emerging field and is currently further adapted to induced pluripotent stem cells, which increasingly substitute for human embryonic stem cells. Such quality control is of critical importance for the organ-on-a-chip models currently fostered to ultimately allow a body-on-a-chip combination of several such organoids combined with microfluidics. Our ongoing development of a (developmental) neurotoxicity 3D model from iPSC within this program is used to illustrate the challenges and opportunities of GCCP.

S 1444 Successes and Challenges in Integrating Organ Chips: The Heart-Lung Micromachine

D. E. Ingber[1, 2, 3]. [1]*Wyss Institute for Biologically Inspired Engineering at Harvard University, Boston, MA,* [2]*Vascular Biology Program, Children's Hospital Boston and Harvard Medical School, Boston, MA and* [3]*School of Engineering and Applied Sciences, Harvard University, Cambridge, MA.* Sponsor: A. Bahinski.

Biomimetic 'organ-on-chip' microdevices composed of mechanically active microfluidic systems lined by living cells reconstitute organ-level structures and functions that can be utilized for *in vitro* safety and efficacy testing of drugs, nanotherapeutics and other medical products. Recent advances have made it possible to engineer biomimetic microsystems technologies that replicate the complex physiological functions and mechanical microenvironment of the breathing lung and beating heart. These technologies have been leveraged and combined to create an integrated 'Heart-Lung Micromachine'. We will demonstrate the ability of the lung and heart devices, both alone and in combination, to measure the toxic effects of aerosol-based drugs *in vitro*. Challenges encountered in developing aerosol delivery and integration will be discussed, as well as engineering principles used to overcome these issues. The device, which will utilize human cells, can potentially be multiplexed and automated to accelerate drug development, improve success of clinical trials and mitigate regulatory hurdles, while also significantly reducing medical product development costs.

S 1445 Challenges of Developing an Integrated "Human on a Chip" System

J. P. Wikswo. *Vanderbilt Institute for Integrative Biosystems Research and Education, Vanderbilt University, Nashville, TN.* Sponsor: A. Bahinski.

The sophistication and success of recently reported microfabricated organs-on-chips and human organ constructs have made it possible to design scaled and interconnected organ systems that may significantly augment the current drug development pipeline and lead to advances in systems biology. Physiologically realistic live microHuman (μHu) and milliHuman (mHu) systems operating for weeks to months present exciting and important engineering challenges such as determining the appropriate size for each organ to ensure appropriate relative organ functional activity, achieving appropriate cell density, providing the requisite universal perfusion media, sensing the breadth of physiological responses, and maintaining stable control of the entire system, while maintaining fluid scaling. Successful mHu and μHu systems for drug development and systems biology will require low-volume microdevices that support chemical signaling, microfabricated pumps, valves and microformulators, automated optical microscopy, electrochemical sensors for rapid metabolic assessment, ion mobility-mass spectrometry for real-time molecular analysis, advanced bioinformatics, and machine learning algorithms for automated model inference and integrated electronic control. These challenges will be discussed, as well as efforts developing functional prototype components being developed for successful system integration.

S 1446 Moving Innovation into Regulatory Reality

D. Jacobson Kram. *Center for Drug Evaluation and Research, US FDA, Silver Spring, MD.*

Validation of new toxicology tools would ensure that new innovative technologies become integrated into the regulatory review process quicker, but differing points of view exist on what these validation strategies would look like for in vitro toxicology tests. At FDA, "qualification" is a regulatory conclusion that, within a stated context of use, the results of an assessment with a drug development tool can be relied upon to have a specific interpretation and application in drug development and regulatory decisions. A new drug development tool such as an organ on a chip is qualified by regulatory authorities if there is appropriate data in support of its intended use. Once qualified, this tool can be used without the regulatory agency's need to reconsider and reaffirm its applicability. The US FDA's CDER Drug Development Tool Qualification Process involves a "fit-for-purpose"- based upon an evidentiary threshold approach that depends upon the intended context of use in drug development. The drug development tool qualification program is an objective, science-based approach for evaluating the relevance, quality, and reliability of a test based upon its intended use, for example as part of a screening program or as a definitive surrogate endpoint in a pivotal clinical trial. It serves as a model for the discussion of new validation approaches for the incorporation of innovative alternative test methods into a regulatory framework.

S 1447 Mechanisms of Metal-Induced Disruption of DNA Repair

H. Xie. *Wise Laboratory of Environmental and Genetic Toxicology, University of Southern Maine, Portland, ME.*

Metal compounds are found throughout the environment from natural sources and human activities. Industrial applications contribute significantly to human metal exposure. Some metals, including arsenic, cadmium, chromium, lead, and nickel have been classified as or considered to be human carcinogens. DNA molecules are continuously damaged by endogenous factors and environmental agents (e.g., UV, chemical toxicants, and biological toxins). Thus, the efficient repair of these lesions is crucial to maintaining DNA integrity. In recent years, mounting evidence has suggested that DNA repair processes are susceptible to carcinogenic metals. Chronic exposure to Cr(VI) was shown to inhibit the error-free DNA double-strand break repair pathway, homologous recombination. Cd(II) interferes with DNA mismatch repair by binding to specific sites on Msh2-Msh6 to block its DNA binding and ATPase activities. Ni(II) was found to compromise activity of xeroderma pigmentosum group A complementing protein (XPA) in nucleotide excision repair (NER) pathway by interfering with zinc finger structure of XPA. As(III), Co(II), Cd(II), Hg(II), and Pb(II) have been found to decrease the incision step or the polymerization step in NER system. Studies reported that low

concentrations of As(III) inhibit poly(ADP-ribose) polymerase (PARP)-1, leading to interference with DNA repair process triggered by UV radiation. It has been proposed that interference with DNA repair systems is one of the common modes of action for metal-induced carcinogenicity. It is of great interest and importance to understand the steps affected by metals in the repair pathway and the mechanism of the repair inhibition. The presentations in this symposium will highlight the latest findings on the molecular mechanisms of metal-induced inhibition of DNA repair.

S 1448 Impact of Cadmium and Copper on the Cellular Response to DNA Damage: Interference with Redox-Regulation

A. Hartwig, B. Fischer, C. Keil, S. Risnes and A. Semisch. *Karlsruhe Institute of Technology, Karlsruhe, Germany.* Sponsor: H. Xie.

The carcinogenicity of cadmium has been recognized for some decades, but the underlying molecular mechanisms are not completely understood. While direct DNA damage appears to be of minor importance, the interference with antioxidative defense systems as well as interactions with DNA repair processes, tumor suppressor functions, and signal transduction pathways have been described in diverse biological systems. Thus, cadmium has been shown to disturb nucleotide excision repair, base excision repair as well as mismatch repair, and the interference with cellular redox regulation by reaction with redox-sensitive protein domains or amino acids may provide one explanation for cadmium-induced carcinogenicity. Particularly sensitive targets appear to be proteins with zinc binding structures, present in DNA repair proteins such as XPA, PARP-1 as well as in the tumor suppressor protein p53. For example, cadmium inhibits poly(ADP-ribosyl)ation, and detailed investigations suggest a direct interaction with PARP-1, presumably by inactivation of thiol groups. Also, cadmium compounds provoke an unfolding of the "wild type" p53 conformation, leading to diminished expression of DNA repair proteins and via inhibition of apoptosis to a resistance towards DNA-damaging agents. Particularly the combination of these multiple mechanisms may give rise to a high degree of genomic instability in cadmium-adapted cells, relevant not only for tumor initiation, but also for later steps in tumor development. Nevertheless, the disturbance of cellular redox regulation may also occur in case of essential trace elements on conditions of cellular overload. One example is copper, where especially copper-based nanoparticles lead to high concentrations of copper ions in the cell nucleus and thus overcome homeostatic control. Consequences are elevated levels of oxidative DNA damage and pronounced inhibition of poly(ADP-ribosyl)ation.

S 1449 Inhibition of DNA Repair As a Mechanism of Arsenic Carcinogenesis

K. Liu, X. Zhou, K. L. Cooper, S. W. Burchiel and L. G. Hudson. *University of New Mexico, Albuquerque, NM.*

Inorganic arsenic is a complete carcinogen. In addition to the known direct carcinogenic actions of arsenic, there is substantial evidence that arsenic at low, non-carcinogenic levels amplifies the carcinogenic potential of other DNA-damaging agents such as benzo[a]pyrene and ultraviolet radiation (UVR). One hypothesis to account for arsenic co-carcinogenesis is inhibition of DNA repair proteins containing zinc finger DNA binding motifs. Research from our lab and others has demonstrated that low arsenite concentrations can enhance a variety of UVR-induced DNA damage, including 8-hydroxyl-2'-deoxyguanine (8-OHdG) formation, DNA strand break, cyclobutane pyrimidine dimers, and 6,4-photo product. Biochemical studies suggest that disruption of zinc finger DNA repair protein function represents an underlying mechanism for arsenic carcinogenicity. We find that specific zinc finger proteins with ≥ 3 cysteine residues are direct and sensitive molecular targets for arsenic, including xeroderma pigmentosum group A (XPA) and poly(ADP-ribose)polymerase (PARP)-1, which plays a critical role in nucleotide excision repair and base excision repair, respectively. Mass spectrometry analysis provides evidence that arsenite binds to the zinc finger moiety of PARP-1, preventing zinc binding, thus interrupting the function of PARP-1. We have shown that zinc reverses the inhibitory effects of arsenic on PARP-1 activity and arsenic augmentation of UV-induced DNA damage and mutagenesis. Furthermore, zinc prevents the effects of arsenic on UV-induced DNA damage in mouse skin in vivo, suggesting that supplemental zinc may offer a tractable approach to attenuate arsenic co-carcinogenesis in exposed human populations. Collectively our studies demonstrate that arsenite can interact with key DNA repair zinc finger proteins, resulting in modification of protein structure and function, leading to accumulation of DNA damage.

S 1450 Prolonged Exposure to Particulate Chromate Induces a Switch from Homologous Recombination Repair to Nonhomologous End Joining Repair in Human Lung Cells

J. P. Wise, Q. Qin, C. L. Browning, S. Wise, H. Xie and A. Holmes. *University of Southern Maine, Portland, ME.*

The interaction of genotoxic chemicals with DNA repair is a key consideration in understanding their overall toxic mechanism. This presentation describes an example of this interaction focusing on chromate. Particulate chromate is a known human carcinogen and genotoxic agent, but how it causes cancer is unknown. DNA double strand breaks (DSB) are a key factor in its carcinogenicity as particulate chromate-induced neoplastic transformation occurs in human lung cells with experimentally disrupted DSB repair, but not in human lung cells with robust intact DSB repair systems. Emerging data show that particulate chromate targets the homologous recombination repair pathway (HR) in human lung cells with unaltered repair pathways. For example, zinc chromate induces concentration-dependent increases in DSBs and chromosome aberrations. With longer exposure times, this damage remains elevated indicating that the damage continues to be produced. An evaluation of representative proteins of the major steps in HR repair signaling showed that the sensors of DSB repair (measured as gamma-H2A.X, 53BP1 and Mre11 foci) remain elevated in response to these breaks indicating they are unaffected by chromate. By contrast, the effector component of HR repair (measured as Rad51 response) is compromised by chromate. During the first 24 h of exposure, Rad51 response increases as expected, but from 48-120 h of exposure the response continually declines. The signal transduction response through ATM also increases during the first three days of exposure, but after 96 h of exposure, the ATM response dramatically falls off. Simultaneously, the expression of Ku80 and DNA-PKcs proteins increased as HR repair function decreases. Thus, particulate chromate induces a signaling switch from HR to NHEJ after prolonged exposures. The timing of this switch also correlates well with the onset of particulate chromate-induced genomic instability in human lung cells. This work was supported by NIEHS grant ES016893 (J.P.W.).

S 1451 Chemistry and Biology of Oxidatively-Induced Tandem Lesions of DNA

Y. Wang. *Department of Chemistry and Environmental Toxicology Graduate Program, University of California Riverside, Riverside, CA.* Sponsor: H. Xie.

Exposure to various toxic metals in the environment can lead to cellular production of reactive oxygen species (ROS), which can result in DNA damage. Although substantial repair studies have been conducted for the ROS-induced single-nucleobase lesions, not much is known about how oxidatively induced tandem DNA lesions are repaired in mammalian cells. Our LC-MS/MS/MS quantification results revealed that 8,5'-cyclo-2'-deoxyadenosine (cyclo-dA), 8,5'-cyclo-2'-deoxyguanosine (cyclo-dG) and the GT intrastrand crosslink are present at significantly lower levels in tissues of repair-competent animals than in Ercc1-deficient animals. Likewise, we found higher levels of these lesions in brain tissues of XPA-deficient patients than in repair-proficient individuals. Viewing that XPA and Ercc1 are required for nucleotide excision repair (NER), the above results support that these DNA lesions are substrates for NER *in vivo*. Additionally, we observed an age-dependent accumulation of these DNA lesions in mammalian tissues, suggesting that the accumulation of these DNA lesions may play an important role in aging-related pathological conditions. We also found, from the LC-MS/MS and plasmid-based *in vivo* transcription assay, that both cyclo-dA and cyclo-dG substantially blocked transcription in mammalian cells, and transcription bypass efficiency is much lower in NER-deficient mammalian cells than repair-proficient cells, suggesting again the compromised repair of these DNA lesions in XPA-deficient cells. Moreover, the LC-MS/MS method allowed for the identification and quantification of mutant transcripts produced from the transcriptional bypass of the cyclo-dA and cyclo-dG lesions. Together, our combined chemistry and biology approach led to important novel insights into the repair and biological consequences of the oxidatively induced tandem DNA lesions.

S 1452 Molecular Mechanisms Involved in Neuro/Glial Toxicity: From Oxidative Stress to Redox Signal Transduction

R. Franco. *School of Veterinary Medicine and Biomedical Sciences, University of Nebraska-Lincoln, Lincoln, NE.*

Oxidative stress, defined as the imbalance between the production of reactive oxygen (ROS) or nitrogen (RNS) species and the ability of cells to scavenge these reactive species and repair oxidative damage, has been largely reported to participate in environmental toxicity. Biomarkers of oxidative damage in proteins, lipids, and nucleic acids are inherent to neuronal toxicity associated with pesticides, metals,

and particulate matter. Electron-transfer processes called "redox signaling" play key messenger roles in biological systems. Initially, ROS/RNS formation was thought to lead to nonspecific cellular damage. However, recent *in vitro* and *in vivo* findings demonstrate that, in response to environmentally relevant doses toxicants, a specific set of redox signaling events play a major role activating specific signaling transduction cascades, regulating gene expression, enzyme activity, cellular metabolism, and cell fate outcome of neuronal and glial cells. In this session we will examine recent findings on the molecular mechanisms by which redox signaling regulates environmental neuro/glial toxicity. More specifically, the speakers will highlight the novel mechanisms by which mitochondrial redox homeostasis, iron-sulfur cluster oxidation, electrophile-adduct formation, thiols, transcription factor regulation, oxidative post-translational modifications, and oxidative DNA-damage regulate the toxicity of particulate matter, aldehydes, pesticides, and metals. This topic should be of great importance to biochemists, risk assessors, graduate students, postdoctoral trainees, and academics within distinct Specialty Sections.

S 1453 Mitochondrial Redox Mechanisms of Neurotoxicants Implicated in Parkinson's Disease

M. N. Patel. *School of Pharmacy and Pharmaceutical Sciences, University of Colorado, Aurora, CO.*

Environmental agents such as the redox cycling herbicide paraquat (PQ2+) that produce reactive oxygen species (ROS) have been linked to increased risk of Parkinson's disease (PD). Our research is focused on elucidating mitochondrial mechanisms by which environmental redox cycling agents produce ROS and the resultant redox signaling involved in dopaminergic degeneration associated with PD. Studies from our laboratory have shown that mitochondria via complex III play a novel role in PQ2+-mediated ROS production. Furthermore, at the molecular level, PQ2+-generated ROS can exert specific additive and/or synergistic neurotoxicity via specific redox signaling cascades including the inactivation of key mitochondrial enzymes such aconitase and thioredoxin reductase 2 (TrxR2). Both in vitro and in vivo studies suggest that post-translational inactivation of the iron-sulfur enzyme aconitase, by superoxide and consequent release of mitochondrial iron and hydrogen peroxide results in more potent oxidants e.g. hydroxyl radical that ultimately exert damage. We have recently shown that isolated brain mitochondria consume hydrogen peroxide in a substrate- and respiration-dependent manner predominantly via the thioredoxin / peroxiredoxin system and pharmacological inhibition of TrxR or lentiviral knock-down of TrxR2 sensitizes dopaminergic cells to sub-toxic concentrations of PQ2+. This talk will cover these novel mitochondrial redox mechanisms by which neurotoxicants mediate dopaminergic cell death.

S 1454 The Electrophile-Responsive Proteome As a Target for Environmental Neurotoxicants

R. LoPachin. *Montefiore Medical Center, New York City, NY.*

Many environmental toxicants are electrophiles that can form irreversible covalent adducts with nucleophilic amino acid residues. Discerning how these environmental chemicals interact with the electrophile-responsive proteome is a critical step in defining their respective mechanisms of neurotoxicity. A detailed understanding of acrylamide (ACR) chemistry led us to the identification of relevant protein targets and to the molecular mechanism by which this targeting causes neuronal cell death. The Hard and Soft, Acids and Bases (HSAB) theory evidenced that the αβ-unsaturated carbonyl structure of ACR is a soft electrophile that preferentially forms covalent bonds with soft nucleophiles. This was corroborated by proteomic and in chemico studies that identified the redox-sensitive targeted residues as nucleophilic sulfhydryl thiolates (-S-) located within cysteine-centered catalytic triads of enzyme active sites. The irreversible formation of thiolate adducts by ACR causes enzyme inhibition by disrupting nitric oxide (NO) signaling. ACR inhibits the function of presynaptic proteins involved in the synaptic cycle leading to loss of neurotransmission and subsequent retrograde nerve terminal degeneration. The electrophile vulnerability of nerve terminals is then, based on the slow turnover of resident proteins, the lack of Nrf2/Keap1 transcription-based defense mechanisms, and the dependency on NO signaling. ACR and other environmentally-derived type-2 alkenes might act synergistically with endogenous unsaturated aldehydes to mediate neuronal cell death and accelerate the progress of neurodegenerative diseases. ACR causes neurotoxicity by interacting with the electrophile-responsive proteome. These findings are broadly applicable since many environmental toxicants are electrophiles that can produce toxicity by reacting with nucleophilic residues on macromolecules. Proteome-environment interactions have significant implications for human health and risk assessment. (NIH grants ES03830-25 and ES07912-11)

S 1455 Redox Regulation of NF–κB p50 and M1 Polarization in Neurotoxic Microglia

M. L. Block. *Anatomy and Neurobiology, Virginia Commonwealth University, Richmond, VA.*

Microglia detect and respond to a diverse array of stimuli, including environmental toxicants, bacterial toxins, cytokines, neuronal damage, and disease proteins, where the activation state can be characterized as a pro-inflammatory (M1) or alternative (M2) response. M1 polarization is implicated in neurotoxic microglia activation, with both enhanced M1 activation and impaired resolution (M2 response). How ROS shift microglia to a neurotoxic phenotype is unknown. Here we identify the NF–κB p50 protein radical in neurotoxic microglia, demonstrating oxidative modification during M1 polarization. Nuclear extracts from microglia cultures treated with the peroxynitrite generator SIN–1 (1μM) and the ROS–generating pesticide paraquat (0.5μM) showed decreased NF-κB p50 DNA binding, confirming that microglial ROS impairs NF–κB p50 function. NF–κB p50 –/– mice were injected with LPS (5mg/kg IP) and cultures (NF–κB p50 –/– primary mixed-glia cells and siRNA NF–κB1knockdown in BV2 microglia) were treated with LPS (10ng/ml), which resulted in enhanced pro-inflammatory cytokine production and activated microglial morphology. Loss of NF–κB p50 function in microglia cultures impaired both M2 gene expression and the resolution of M1 genes. Mesencephalic neuron-glia cultures from NF–κB p50–/– mice treated with either LPS or paraquat showed enhanced DA neurotoxicity. Paraquat amplified the production of LPS–induced TNFα in microglial cultures only in the presence of functional NF-κB p50, emphasizing the importance of NF–κB p50 for priming. In vivo paraquat studies revealed that NF–κB p50–/– mice have enhanced activated microglial morphology and elevated motor behavior deficits in response to a single paraquat injection, supporting that the NF–κB p50–/– mice may already be primed. These data identify a critical redox signaling mechanism triggered by environmental toxicants that drive M1 polarization in microglia, where loss of NF–κB p50 function leads to elevated neuroinflammation, microglial activation, and DA neurotoxicity (Supported by the NIEHS R01ES016951).

S 1456 Redox Signaling and Methylmercury Toxicity

M. Aschner and M. Ni. *Department of Pediatrics, Vanderbilt University Medical Center, Nashville, TN.*

MeHg causes acute and chronic damage to multiple organs, most profoundly the central nervous system (CNS). We examined the effects of MeHg on microglial and astrocytic viability, reactive oxygen species (ROS) generation, glutathione (GSH) level, redox homeostasis, and NF-E2-related factor 2 (Nrf2) protein expression, the master switch of antioxidant responsiveness. Our data showed that MeHg (at relevant physiological concentrations of 1-5 microM) treatment caused a rapid (within 1 min) concentration- and time-dependent increase in microglial ROS generation, accompanied by a statistically significant decrease in the ratio of GSH and its oxidized form glutathione disulfide (GSSG) (GSH:GSSG ratio). MeHg increased the cytosolic Nrf2 protein level within 1 min of exposure, followed by its nuclear translocation after 10 min of treatment. Consistent with the nuclear translocation of Nrf2, quantitative real-time PCR revealed a concentration-dependent increase in the messenger RNA level of Ho-1, Nqo1, and xCT 30 min post MeHg exposure, whereas Nrf2 knockdown greatly reduced the upregulation of these genes. Furthermore, we observed increased microglial death upon Nrf2 knockdown by the small hairpin RNA approach. Additional studies established that microglia were more sensitive to MeHg than astrocytes, a finding consistent with their higher Hg uptake and lower basal GSH levels. Microglia also demonstrated higher ROS generation compared with astrocytes. Nrf2 and its downstream genes were upregulated in both cell types, but with different kinetics (much faster in microglia). In summary, microglia and astrocytes each exhibit distinct sensitivity to MeHg, resulting in their differential temporal adaptive responses. These unique sensitivities appear to be dependent on the cellular thiol status of the particular cell type. (Supported by R01ES07331 and R01ES020852).

S 1457 Repair of Mammalian Genome Damage Induced by Oxidative Stress and Their Linkage to Neurodegenerative Diseases

S. Mitra. *Radiation Oncology, The Methodist Hospital Research Institute, Houston, TX.* Sponsor: R. Franco.

Endogenous reactive oxygen species (ROS), respiration by–products, and ROS induced during toxic/inflammatory response generate multitude of mutagenic and toxic oxidized bases, and strand breaks in mammalian genomes whose repair via the base excision/single–strand break repair (BER/SSBR) pathway is essential for preserving genomic integrity. The lack of replicative repair in neural cell genome

could explain the linkage of some neurodegenerative diseases to deficiency in BER proteins. Dyshomeostasis of transition metals Fe/Cu as well as accumulation of genome damage have been implicated in Alzheimer's (AD) and Parkinson disease (PD). We postulate that Fe and Cu (at up to micromolar level) pose double jeopardy in that not only these metal ions could induce ROS and hence oxidized bases, but they also inhibit repair of such oxidized bases by inhibiting the BER–initiating DNA glycosyslases NEIL1/2, both in vitro and in human neuroblastoma (SH–SY5Y) cells at sub–micromolar concentration. Metal chelators and chemopreventive curcumin reverse NEILs' inhibition both in vitro and in cells, thus warranting exploration of their therapeutic potential. Oxidative stress has also been linked to many neurodegenerative diseases, associated with aggregation/misfolding of key proteins including RNA binding proteins (RNPs) such as TDP–43 and FUS/TLS. Aggregation of TDP–43 together with its nuclear clearance has been implicated in amyotrophic lateral sclerosis (ALS). While the etiologic role of RNPs in diseases including hnRNP–U, which we had earlier shown to enhance BER efficiency, is not completely understood, we observed direct role of TDP–43 in repair of endogenous and induced DNA double–strand breaks (DSBs) via non–homologous end joining. The observed increase in the level of strand breaks in postmortem ALS brain is consistent with our hypothesis that the loss of DNA strand break repair due to inactivation of specific RNPs including TDP–43 causes neural death and disease phenotypes. (Supported by USPHS grant R01 CA158910 (SM), Alzheimer's Association grant NIRG–12–242135 (MLH).

S 1458 The Role of the AhR in Stem Cell Development and Lineage Specification

D. H. Sherr[4], A. Puga[1], T. A. Gasiewicz[2], E. Papoutsakis[3] and G. Murphy[4]. *[1]University of Cincinnati, Cincinnati, OH, [2]University of Delaware, Newark, DE, [3]University of Rochester Medical Center, Rochester, NY and [4]Boston University, Boston, MA.*

For decades the aryl hydrocarbon receptor (AhR) has been studied for its mediation of the toxic and carcinogenic effects of ubiquitous environmental chemicals including dioxins, planar PCBs and PAHs. A subtext to this work has always been the nature of the "normal" physiological function of this evolutionarily conserved protein. In the last five years, several breakthrough studies have begun to reveal the significance of the AhR in normal biological processes. Similarly, technological advances developed in the last five years have allowed investigators, for the first time, to map out some of the most basic tenets of pluripotent and multipotent stem cell differentiation. The significance of this work cannot be over-stated since control of stem cell differentiation is a key to both organ generation/regeneration and cancer stem cell immortality. Here, we focus on the intersection of AhR and stem cell biology to highlight the importance of the AhR to the regulation of stem cell differentiation and to emphasize the potential for environmental AhR ligands to disrupt essential cell specification programs. We will discuss AhR control of: 1) pluripotent (embryonic stem cell and induced pluripotent stem cell) development into cardiomyocytes, erythroid lineage cells and megakaryocytes, 2) multipotent hematopoietic stem cell senescence and differentiation into lymphocytes, and 3) cancer stem cell development. In so doing, we will identify themes common to multiple developmental systems (e.g., common AhR signaling pathways, the role of the AhR in maintaining "stem-ness," and predicted outcomes after environmental chemical exposure). Symposium speakers will address the significant implications of their work for stem cell and AhR biology under normal physiological conditions and when impacted by exposure to environmental AhR ligands.

S 1459 The AhR Modulate Cardiomyogenesis in Embryonic Stem Cells

A. Puga. *Department of Environmental Health, University of Cincinnati, Cincinnati, OH.*

The aryl hydrocarbon receptor (AHR) is a critical mediator of gene-environment interactions that regulates the transcription of drug-metabolism genes and of genes involved in cell cycle regulation. Many AHR targets identified by genome-wide gene expression profiling, ChIP analyses and studies with orthologous genes in invertebrates have morphogenetic functions suggestive of an AHR regulatory function during embryonic development. To address this hypothesis, we studied the regulation of Ahr expression in mouse embryonic stem cells (ESC) and their differentiated progeny. In undifferentiated ESC, cooperative interactions between pluripotency factors OCT3/4, NANOG and SOX2 and Polycomb Group (PcG) proteins maintain AHR expression in a repressed state, while RNA polymerase II (RNAPII) bound at the Ahr transcription start site, drives synthesis of abortive transcripts. Ahr activation during differentiation follows from reversal of repressive chromatin marks, including release of pluripotency factors and PcG proteins from their binding sites, Sp factor transactivation, establishment of open chromatin marks and engagement of active RNAPII to drive full-length RNA transcripts. Formation of contractile cardiomyocytes during ESC differentiation was significantly inhibited by both AHR activation and repression. Analysis of temporal trajectories of global gene expression showed that activation of AHR signaling disrupts the concerted expression of genes that regulate multiple signaling pathways involved in cardiac and neural morphogenesis, including dozens of genes encoding homeobox transcription factors and Polycomb and Trithorax Group genes. The Ahr gene has a high degree of regulatory plasticity during embryonic development. Dynamic repression might be required to maintain pluripotency, but holding the gene poised for expression allows for a quick switch to activation as the need arises during differentiation. AHR activation by xenobiotics establishes a complex regulatory network that disrupts various aspects of embryonic development, including cardiomyocyte differentiation. Supported by NIEHS grants ES006273 and ES010807.

S 1460 The AhR Is a Key Factor in the Regulation of Hematopoietic Stem Cells and Their Protection from Premature Exhaustion, Stress, and Hematopoietic Disease

T. A. Gasiewicz[1], K. P. Singh[1], J. C. Bennett[1], F. Casado[2], J. Walrath[1] and S. Welle[1]. *[1]Department of Environmental Medicine, University of Rochester, Rochester, NY and [2]McMaster Stem Cell & Cancer Research Institute, Hamilton, ON, Canada.*

There has been much work to define a physiological role of the AHR in the immune system and possible relationships to human disease. Hematopoietic stem cells (HSCs) from global AHR-knock out (KO) mice are inherently hyperproliferative. These data, along with others, are consistent with a hypothesis that the AHR has an important role as a negative regulator of HSC proliferation. Functional and genomic analyses of HSCs from aging KO mice indicate that a lifetime of altered signaling pathways results in premature exhaustion, aging and a myeloproliferative disorder. Aging mice lacking AHR showed a decreased survival rate, splenomegaly, increased circulating white blood cells, hematopoietic cell accumulation in tissues, and anemia. There was also decreased self-renewal capacity of HSCs determined by competitive repopulation and serial transplantation. Some of the molecular changes observed in aging HSCS include altered content of ROS, p16Ink4a, and γ-H2A.X, and indicator of DNA damage. AHRKO mice develop multiple genomic changes (e.g. Srpk2, Rad50, mTOR, Creb1, Hes1, Pdp-1, Stra13) in HSCs at an early age that lead to the phenotypic changes characteristic of premature exhaustion. The most prominent gene changes were also associated with HSC hyperproliferation, leukemia, and accelerated aging. Pathway analyses also indicated an enrichment of genes associated with oxidative stress, acute myelogenous leukemia, aging and heat shock response, and the B-catenin/Wnt pathways. These data indicate that the AHR is a key cofactor in the regulation of HSCs and their protection from long-term stress, premature exhaustion, and age-related disease. Supported by NIEHS grants ES01247, ES07026, ES04862, and ES016606.

S 1461 A Role for the Aryl Hydrocarbon Receptor (AhR) on Platelet Function

E. Papoutsakis[1, 2], S. Lindsay[1, 3], J. Jiang[1] and D. Woulfe[2]. *[1]Department of Chemical & Biomolecular Engineering, University of Delaware, Newark, DE, [2]Department of Biological Sciences, University of Delaware, Newark, DE and [3]Nemours Center for Childhood Cancer Research, A.I. duPont Hospital for Children, Wilmington, DE.* Sponsor: A. Puga.

We recently1 identified AHR as a novel regulator of megakaryocytic polyploidization and differentiation. Although AHR-null mice exhibited roughly 15% fewer circulating platelets than WT mice, this was insuf-ficient to explain the bleeding phenotype we found in AHR-null mice. Instead, we hypothesized that platelets from AHR-null mice are functionally deficient. Indeed, we found that only 20% of AHR-null mu-rine platelets aggregated in response to 2 μg/mL collagen compared to 60% for WT platelets. Spreading assays confirmed that AHR-null platelets demonstrated nearly 40% less spreading in response to collagen-dependent signaling. Yet AHR-null platelets bound fibrinogen and spread in response to other platelet agonists including thrombin, ADP, and AYPGKF (a PAR4 agonist). AHR-null platelets expressed similar levels of CD41 and CD49b surface markers, but 15% less GPVI, one of the receptors involved in collagen signaling. We then investigated molecular mechanisms by which AHR could influence collagen signaling within platelets and found that AHR-null platelets have decreased Vav1 and Vav3 expression compared to WT platelets, leading to decreased PLCA2 tyrosine phosphorylation. In contrast, tyrosine phosphorylation of Syk, which lies upstream of Vav1 and Vav3 phosphorylation, remained unaltered and thrombin stimulation resulted in Rac1 activation of both WT and AHR-null platelets. These results show that the absence of AHR leads to downregulation of Vav1 and Vav3, which in turn leads to altered PLCA2 phosphorylation and reduced platelet activation specifically

in response to collagen, without impacting other platelet signaling pathways. This study advances our hypothesis2 that AHR influences multiple aspects of normal hematopoietic differentiation.

1. Lindsey S & Papoutsakis ET. Br J Haematol 152, 469-484 (2011).
2. Lindsey S & Papoutsakis ET. Stem Cell Rev 8, 1223-1235 (2012).

S 1462 The AhR Regulates the Production and Specification of Bipotential Hematopoietic Progenitor Cells

G. Murphy[1], B. Smith[1], S. Rozelle[1], A. Leung[1], J. Ubellacker[2], A. J. Parks[2], S. Nah[1], S. Monti[1] and D. H. Sherr[2]. [1]*Center for Regenerative Medicine (CReM), Section of Hematology and Oncology, Department of Medicine, Boston University School of Medicine, Boston, MA and* [2]*Environmental Health, Boston University School of Public Health, Boston, MA.*

Recent studies demonstrate that the AHR may regulate the hematopoietic and immune systems during development in a cell-specific manner. Our results indicate that AHR has a physiological and functional role in normal hematopoietic development, and that modulation of the receptor in bi-potential hematopoietic progenitors can direct cell fate. Using a novel, iPSC-based, chemically-defined, serum and feeder cell-free culture system, we demonstrate that a functional AHR is expressed in hematopoietic progenitor cells (HPs), and that remarkably, AHR activation of these HPs drives an unprecedented expansion of HPs, megakaryocyte (Mk)- and erythroid-lineage cells. Further AhR modulation directs cell fate, with chronic AhR agonism permissive to erythroid differentiation and acute antagonism favoring megakaryocyte specification. These results demonstrate a new platform for studying human red blood cell and Mk development that allows for exponentially greater production of RBCs and Mks in comparison to existing methodologies. This strategy relies on the first of its kind definition of the role of the AHR receptor in normal hematopoietic development using specialized ligands in hematopoietic progenitor cells. A useful outcome for this work will be the utilization of this in vitro platform for the clinically relevant production of blood products. An iPSC-based system, such as the one described here in which sufficient numbers of cells can be produced, should facilitate future clinical adaptation involving the transfusion of iPSC-derived red blood cells and platelets without problems related to immunogenicity, contamination, or supply. Supported by NLHBI U01 HL107443-01, an American Society of Hematology (ASH) Scholar Award, the National Blood Foundation (NBF), PO1 ES11624, P42 ES007381, and the Art beCAUSE Breast Cancer Foundation.

S 1463 The AhR Controls Breast Cancer Stem Cell Development and Function

D. H. Sherr[1], A. J. Parks[1], S. Monti[2], G. Murphy[2], O. Novikov[1], J. Ubellacker[1] and E. A. Stanford[1]. [1]*Environmental Health, Boston University School of Public Health, Boston, MA and* [2]*Department of Medicine, Boston University School of Medicine, Boston, MA.*

Tumor metastasis is the cause of death in nearly all breast cancer patients. Recent evidence suggests that metastasis is mediated, to a disproportionate extent, by chemo-resistant, long-lived breast cancer stem-like cells (BCSLC). BCSLC cells are defined by their expression of aldehyde dehydrogenase (ALDH), a set of genes associated with "stem-ness", the ability to self-renew, expression of properties consistent with epithelial-to-mesenchymal transition (e.g., metastatic potential), and resistance to chemotherapeutics. Studies from several laboratories, including three laboratories represented in this symposium, suggest that the AHR, a protein historically associated with tumorigenesis, is involved in the development and/or function of blood stem cells which share some properties with cancer stem cells. Therefore, we postulated that the AHR may play a role in either the development or function of BCSLC. Here, we present data demonstrating elevated levels of constitutively active AHR in BCSLC from aggressive human ER-, PR-, Her2- ("triple negative") and inflammatory breast cancers. The results indicate that AHR hyper-activation with exogenous ligands (FICZ, TCDD, DMBA) increases and AHR inhibition with pharmacological or molecular agents decreases expression of BCSLC characteristics including expression of ALDH1, several stem cell-associated genes including Notch1, Nanog, and Oct 4, chemo-resistance, and the ability to grow and produce progenitor cells in spheroid colonies. These results further implicate the role of environmental chemicals in breast cancer risk through induction of BCSLC characteristics and have significant implications for the potential to target the AhR for cancer therapy. Supported by PO1 ES11624, P42 ES007381, and the Art beCAUSE Breast Cancer Foundation.

S 1464 Three Dimensions of Nanomaterial Pulmonary Toxicity: Innate Immunity, TLRs, and Inflammasomes

J. M. Brown[1] and S. S. Nadadur[2]. [1]*Pharmaceutical Sciences, University of Colorado, Aurora, CO and* [2]*Division of Extramural Research, NIEHS, Research Triangle Park, NC.*

Nanotechnology is rapidly developing, resulting in the production of numerous engineered nanoparticles. These materials have many potential uses in engineering, electronics, and medicine owing to their unique size, strength, functionality and surface properties. However, these novel properties also contribute to their potential health risk. A major route of exposure for engineered nanomaterials occurs through inhalation, potentially leading to pulmonary toxicity. Immune activation and inflammation represents a common response observed across many pulmonary studies of nanoparticle inhalation in rodents. However, our mechanistic understanding by which the materials elicit immune activation is limited. Recent accumulating evidence supports the proposal that the initial pulmonary immune response to nanoparticle exposure is mediated via the innate immune system driving inflammation. Presentations in this session are aimed at elucidating the mechanisms of these innate immune responses to engineered nanomaterial exposure in the lung. This will include exploration of macrophage phenotypes, inflammasome activation, Toll-like receptors and, lastly, will explore the degradation of nanomaterials by immune cells and their defensive products. The outcome of this session is to gain state-of-the-art information on the mechanisms of the critical innate immune system response in the toxicology of nanoparticles and ultimately the development of safe nanotechnologies.

S 1465 Inflammasome Activation in Nanoparticle-Induced Lung Inflammation

A. Holian[1], R. F. Hamilton[1], N. Wu[2], D. W. Porter[3], S. Tsuruoka[4], S. Mitra[5] and T. A. Girtsman[1]. [1]*CEHS, University of Montana, Missoula, MT,* [2]*Mechanical & Aerospace Engineering, West Virginia University, Morgantown, WV,* [3]*CDC/NIOSH/HELD, Morgantown, WV,* [4]*Engineering, Shinshu University, Nagano, Japan and* [5]*Chemistry and Environmental Science, New Jersey Institute of Technology, Newark, NJ.*

The precise mechanisms responsible for engineered nanomaterial (ENM)-induced activity remain to be elucidated. Increasing evidence supports the notion that alveolar macrophages (AM) contribute to ENM-induced lung inflammation and pathology through the NLRP3 Inflammasome in a similar manner as has been implicated for a number of "danger" crystals in a process sometimes referred to as sterile inflammation. In order to characterize mechanisms involved in ENM inflammation studies have been conducted in vitro using THP-1 and NLRP3 KO cells and primary AM from mice and humans as well as in vivo studies using murine models. Two key steps regulate this process: 1) ENM-induced phagolysosomal membrane permeability (LMP) leading to the release of cathepsin B into the cytoplasm, which has been linked to NLRP3 Inflammasome assembly and Caspase-1 activation necessary for IL-1β to be cleaved from its pro-form, and 2) elimination of the NLRP3 Inflammasome complex by autophagy. The precise steps leading to LMP have not been defined, although generation of reactive oxygen species and/or some other property of ENM have been implicated. Acidification of lysosomes is necessary for LMP since imipramine and chloroquine can block NLRP3 Inflammasome activation and downstream inflammation. ENM length and surface characteristics of ENM are important factors in LMP. Increasing the aspect ratio and/or rigidity of ENM increases bioactivity, while carboxylation of ENM surfaces decreases bioactivity. Furthermore, while ENM induce autophagy, increasing autophagic flux can block IL-1β release from macrophages. Finally, comparing the outcomes from in vitro and in vivo studies suggest that IL-1β production from THP-1 cells can be used to predict in vivo outcomes and serve to prioritize in vivo studies.

S 1466 Lung and Pleural Innate Immune Responses to Engineered Nanomaterials

J. C. Bonner. *Biological Sciences, North Carolina State University, Raleigh, NC.*

The nanotechnology revolution offers enormous societal and economic benefits for innovation in the fields of engineering, electronics, and medicine. However, growing evidence indicates that some biopersistent engineered nanomaterials (ENMs), including carbon nanotubes (CNTs) and metal nanoparticles, have the potential to stimulate immune, inflammatory, or fibroproliferative responses in the lung and pleura. This presentation will focus on specific mechanisms through which CNTs or nickel nanoparticles modulate cellular signaling and innate immune responses of macrophages, fibroblasts, and mesothelial cells relevant to lung and pleural disease. One of the goals is to discuss new evidence from transgenic mouse models showing that these ENMs have the potential to shift allergic lung inflammation from a

Th2 response to a mixed Th1/Th2 or a Th17 immune response. These data have particular relevance in determining the immune effects of ENMs on susceptible individuals with pre-existing respiratory diseases such as asthma. The role of specific members of the STAT family of transcription factors will be highlighted as key regulators of ENM-modulated immune and allergic responses. Moreover, the role of alternative macrophage activation during allergy will be discussed in terms of modulating CNT-induced inflammasome activation and the lung fibroproliferative response. Another goal is to discuss novel mechanisms through which ENMs, particularly CNTs, stimulate macrophages and mesothelial cells to cause pleural immune and inflammatory responses that might lead to mesothelioma. Overall, it is anticipated that this presentation will shed light on adverse effects of ENMs on the innate immune system of rodents and this information could be used to predict disease outcomes for humans following occupational or environmental exposures.

S 1467 Influence of Carbon Nanoparticles on Toll-Like Receptor Activity and Pathogen Susceptibility

T. Sabo-Attwood[1], P. Sanpui[1], X. Zheng[1], J. Loeb[1], J. Lednicky[1], N. Afrooz[2] and N. B. Saleh[2]. [1]*University of Florida, Gainesville, FL and* [2]*University of South Carolina, Columbia, SC.*

The extraordinary physico-chemical properties that make nanomaterials promising for product enhancement applications may lead to adverse immune defense responses in humans. We have a particular interest in single-walled carbon nanotubes (SWNTs) and their ability to influence the behavior of infectious agents. Altering the normal response to pathogens can have critical consequences, particularly for agents such as influenza A viruses (IAV), that are notorious for causing pandemics. Recognition of foreign pathogens by toll-like receptors (TLRs) stimulates innate immunity as a primary defense mechanism to combat pathogens. To investigate the ability of SWNTs to modulate TLRs, we employed human cell lines that overexpress TLR2 or TLR3 which recognize microbial moieties of bacteria and viral RNA, respectively. Results from these studies show that SWNTs fail to activate the TLRs alone, however they repress the activity of zymosan, the natural receptor agonist for TLR2, while enhancing activity of the TLR3 agonist poly I:C. Furthermore, these observations are most significant for SWNTs with 6,5 chiral enrichment which form more stable and less dense clusters than other types of SWNTs. To determine if SWNTs influence virus infectivity and modulate TLR pathways in lung cells, we infected small airway epithelial cells with IAV H1N1 while co-exposing to SWNTs. In these studies SWNTs significantly enhanced IAV infectability as quantified by virus titers and immunohistochemistry. While we did not observe significant changes in TLR3 or 7 mRNA expression in these cells, but anticipate that SWNTs alter TLR activity. Studies are currently underway to address the precise role of TLRs in these observed effects both in vitro and in vivo. Overall results from these studies indicate that SWNTs have the potential to increase the susceptibility of lung cells to pathogenic infections and modulate TLR activity.

S 1468 Enzyme-Catalyzed Degradation of Carbon Nanotubes *In Vitro* and *In Vivo*

A. Star. *Department of Chemistry, University of Pittsburgh, Pittsburgh, PA.* Sponsor: J. Brown.

Because of the unique properties of carbon nanotubes (CNTs), such as small size, large surface area, high strength, and electrical conductivity, this nanomaterial has been used in high-performance composites, electronics, and medical therapeutics. Given the possible pro-inflammatory and toxic effects of CNTs, understanding of their interactions with living systems is important as applications employing this nanomaterial become mainstream. To this end, we studied degradation of CNTs with peroxidases including horseradish peroxidase (HRP), myeloperoxidase (MPO), and eosinophil peroxidase (EPO) as a function of their structure and surface functionalization. Initially, in-test-tube studies were conducted, where HRP, MPO, and EPO were incubated with hydrogen peroxide and halides. Characterization techniques demonstrated that the reactive intermediates generated via the peroxidase cycle and hypohalous acids (e.g., HOCl from MPO and HOBr from EPO) produced through the halogenation cycle degraded short-cut carboxylated single-walled CNTs. Encouraged by these initial results, cellular studies were implemented in which we demonstrated that short-cut carboxylated, IgG-coated single-walled CNTs could be phagocytosed and degraded by neutrophils, inflammatory cells containing high concentrations of MPO. Also, utilizing a cellular culture system consisting of highly purified murine eosinophils in which degranulation and exocytosis of murine EPO (mEPO) were triggered by cytochalasin B and a platelet-activating factor (PAF), significant degradation of carboxylated, single-walled CNTs was evidenced after 48 hours of treatment. Finally, *in vivo* studies demonstrated that the inflammatory response in MPO-knockout (k/o) mice was stronger than that in wild-type (w/t) C57B1/6 mice, and both CNT degradation and clearance from the lungs of MPO k/o animals were markedly less effective. Given the promising cell culture and *in vivo* degradation results obtained to date, we envision future applications, where carbon-based nano-containers will biodegrade via peroxidase-driven mechanism after they deliver their cargo to organ/cell targets.

W 1469 Improving the Safety of Dietary Supplements and Natural Health Products by Assessing Effects in Humans

J. C. Griffiths. *International, Council Responsible Nutrition, Washington, DC.*

The use of dietary supplements and other natural health products is widespread internationally. Despite large-scale use, the lack of premarket approval in some countries and a general lack of information on the safety of these products is a recognized problem. Animal studies and other translational methods can be used to assess the safety of dietary supplements, but direct premarket information on humans is seldom available. This necessitates the use of postmarket human surveillance data to evaluate the long-term safety of dietary supplements. Sources of such information range from poison control data, adverse event data reported to regulatory authorities, consumer AER complaints to the product manufacturer, and controlled trials in volunteers. The assessment of adverse events reported to regulatory authorities can be challenging due to under-reporting, although the reporting of serious adverse events and recordkeeping requirements for dietary supplement manufacturers became law in the US in 2007. Challenges in assessing adverse event reports are greater than for pharmaceutical drugs because of the complexity of dietary supplement products and the lack of standardized terminology. Other novel sources of information include poison control centers, which have been studied as potentially valuable sources of adverse reactions to dietary supplements. Although much less studied, controlled studies in humans have provided direct information that can be used to assess the safety of dietary supplements. This workshop brings together expertise ranging from clinicians to company-responsible care units to discuss, inform, and provide examples of how this information is finding use in regulatory environments, labeling, formulation/re-formulation decisions, and new directions in basic research.

W 1470 Introduction: The Use of Human Data in Assessing Dietary Supplement Safety

S. A. Jordan. *Marketed Health Products Directorate, Health Canada, Ottawa, ON, Canada.*

Human safety data on dietary supplements and natural health products can be intentionally obtained from appropriately planned and executed randomized, controlled, clinical trials and other controlled studies. Human safety data on these products can also be obtained from adverse reactions reported to regulatory authorities, as well as emergency room visits and poison centre calls. The use and interpretation of these data are associated with certain challenges; however, they serve as critical information in monitoring and improving the safety of dietary supplements and natural health products. Recognising that these products are used by a significant number of global consumers, human data is of paramount importance in furthering a better understanding of the safety of these ingredients and products.

W 1471 A Clinician's Perspective on Accurate Adverse Event Knowledge in the Emergency Setting

L. Nelson. *Department of Emergency Medicine, NYU Emergency Medicine Associates, New York City, NY.*

Dietary supplement use is widespread and generally safe, though efficacy for most is unproven. The use of such supplements in not typically spontaneously reported by the patient nor asked about by the clinician. This is due to several perceptions, some correct and others misguided, related to the risks and benefits of supplements. Many trained in modern medicine do not understand the degree to which dietary supplements are used by their patients, and often view their use with skepticism. Due to either real or anticipated cynicism, patients may withhold their use from their healthcare providers. Clinicians may not fully comprehend the potential pharmacologic activity of supplements and their potential to contribute to adverse drug reactions. On the other hand, patients may be misled by claims of efficacy or safety and may be overly committed to their clinical utility. An attempt to link an adverse event to a specific dietary supplement is complicated by a lack of adequate baseline data that is typically available for conventional pharmaceuticals, and a tendency to both overlook or overanalyze a relationship. This presentation will suggest how a clinician might better communicate with patients to help assess the likelihood of an adverse event to prevent and treat resulting illness.

W 1472 Natural Product Postmarket Surveillance: A Safety Net Designed to Detect Signals, Generate Hypotheses for Research, and Confirm Safety

R. Kingston. *SafetyCall International PLLC, University of Minnesota, Bloomington, MN.*

Dietary supplements and other consumer natural products typically contain ingredients with an inherently wide margin of safety. Despite this fact, various ingredients can be negatively affected by processing, solvent systems, unconventional or non-traditional use patterns, or combining with other ingredients in proprietary blends with similar safety caveats for individual ingredients or the finished product as a whole. Premarket clinical studies are not routinely required or performed on finished products so products consumed by the public may make their debut in large populations that essentially become the "test" market. In these circumstances, products may carry forward high expectations of safety, but often times the only method of safety confirmation and ongoing monitoring for toxicity issues is the postmarket system of safety surveillance (PMS). Robust PMS can help companies confirm safety expectations, identify emerging safety signals associated with the monitored product, and provide information vital to hypothesis generation leading to focused investigation conducted in more controlled clinical environments. In order for the process to work effectively and efficiently, PMS data must be mined for appropriate and actionable safety signals. This presentation focuses on natural product PMS systems and methods to evaluate and act on generated safety signals with real life market examples.

W 1473 Clinical Utility of Dietary Supplement Case Reports and Adverse Event Reports: A Pharmaceutical Scientist's Perspective

B. Gurley[2] and J. C. Griffiths[1]. [1]*International, Council Responsible Nutrition, Washington, DC and* [2]*College of Pharmacy, University of Arkansas for Medical Sciences, Little Rock, AR.*

Clinicians are oftentimes left scratching their heads when it comes to objectively evaluating the clinical utility of published case reports and/or adverse event reports regarding dietary supplements. Few clinical scientists conduct prospective research in the field and even fewer understand the pitfalls associated with dietary supplements. In short, understanding the medicine is often the easy part, making sense of the supplement and its safety and/or efficacy is the confusing aspect. This presentation will discuss some of the shortcomings associated with dietary supplement formulations (e.g., dissolution, bioavailability, adulteration, etc.) and how they either contribute to or detract from the clinical significance of a case report or adverse event report. Examples involving Ephedra, Kava kava, EGCG, and Ephedra-free supplements will be highlighted, including the results of controlled safety studies in humans.

W 1474 Systematic Analyses of Kava's Hepatotoxic Risk—What We Know and What We Do Not Know

C. Xing. *College of Pharmacy, University of Minnesota, Bloomington, MN.*

Kava had previously been used to treat anxiety in Europe. Reports of rare hepatotoxicity potentially linked to its use led to its removal from the European market. However, kava is experiencing global resurgence, particularly in the USA, as a dietary supplement with limited quality control. Since many factors may influence the composition of the final kava products, various hypotheses have been proposed for its hepatotoxic risk with no validation. This presentation will report our research progress in identifying the cause of kava's hepatotoxic risk using various model systems, and discuss our strategies that will validate such causes in humans with the ultimate goal to minimize such a risk. Studies are also ongoing to maximize kava's anxiolytic and other beneficial effects. The outcomes from these investigations are expected to help the successful reintroduction of safer forms of kava with substantial clinical benefit.

W 1475 Collection, Interpretation, and Utilization of Adverse Event Data within a Global Dietary Supplement Company

V. Frankos[2] and J. C. Griffiths[1]. [1]*International, Council Responsible Nutrition, Washington, DC and* [2]*Global Science, Safety & Compliance, Herbalife, Torrance, CA.*

This presentation will present how AER data is used from the perspective of a global dietary supplement manufacturer. Global AE collection helps dietary supplement companies monitor product safety and quality worldwide and make continuous improvements as necessary. AER-related quality issues can identify product QA/QC failures that necessitate changes in formulations or in rare cases lead to product recalls. Integrating post-market AER monitoring with product quality complaints ensures the most comprehensive investigative practices and allows sensitive signal detection. An increasing number of governments have mandatory collection and reporting requirements for AEs. Regulatory requirements are ever-changing. New regulations for reporting are being developed and enforced worldwide and regulatory authorities are now more frequently asking for adverse event information upon registration or re-registration of products. A robust AER system allows the development of Q&As that can be shared with health-care providers, distributors, or consumers. Systematic review of AE data provides a company's legal department necessary information regarding compensation requests/decisions. At times, AER-related complaints may identify ethics violations by sales and distribution personnel. These might include suggesting products might treat a disease or other off label claims. Finally, as is true for drugs, post market AER monitoring is the best way to accurately assess the long term safety of dietary supplement products and assure your customers that the products they are using are truly safe.

W 1476 Toxicogenomic Technologies Can Improve the Assessment of Xenobiotic-Induced Liver Injury and Inform Human Relevance

S. D. Hester[1] and V. S. Bhat[2]. [1]*ISTD/NHEERL/ORD, US EPA, Research Triangle Park, NC and* [2]*NSF International, Ann Arbor, MI.*

The liver has a central role in normal physiology and is a sentinel organ for sensing chemical exposure. As such, it is one of the most frequent target organs serving as the basis of environmental chemical regulation and clinical drug failures due to concerns for both cancer and noncancer effects. Toxicogenomics has evolved to enable toxicity testing and risk assessment paradigms to be more efficient and less reliant on long-term animal studies. There is also global interest in using 'omic tools to overcome obstacles encountered when interpreting liver injury seen in laboratory test systems. Factors contributing to species-selective hepatotoxicant responses among various mammalian species, particularly as mediated via xenobiotic receptors such as CAR, will be discussed. Case studies will highlight how 'omic technologies provide mechanistic data for hazard identification, dose-response, and quantitative risk assessment with a fraction of the resources compared to traditional assessments. Gene signatures relating molecular initiating events such as transcription factor activation to downstream key events such as cell proliferation have defined adverse outcome pathways and correlated to trans-activation profiles of human transcription factors. These efforts to anchor genomic biomarkers of liver injury to more traditional apical endpoints create precedence for the use of toxicogenomic approaches as the basis of chemical regulation. In drug safety research, genetically-diverse population-based pharmacogenetic approaches have informed idiosyncratic liver toxicity, yielded mechanistic insights, and predicted clinically-relevant drug-induced liver injury where classical safety assessment models failed. Systematic approaches, such as the US FDA's liver toxicity knowledge base (LTKB) that integrate pathways, genes, proteins, and drugs to characterize the risk of liver injury, will advance regulatory science, improve the new drug application review process, and refine targeted strategies for regulatory-oriented research.

W 1477 Interspecies Differences in Response to Hepatotoxicants

C. J. Omiecinski. *Center for Molecular Toxicology and Carcinogenesis, Pennsylvania State University, University Park, PA.*

In mammalian organisms, members of the nuclear and soluble receptor superfamilies contribute critically as xenobiotic sensors, serving as mediators of toxicological and physiological responses to chemical exposure. These xenoreceptors transcriptionally regulate a large network of genes encoding a functional web of responses that include the metabolism and transport of xenobiotics, regulation of lipid and energy homeostasis, and modulation of cell proliferation. Mouse models of receptor biology have been deployed widely to characterize these features. However, marked differences exist among mammalian species in their sensitivities and response to hepatotoxicants, responses that differ with respect to dose as well as qualitatively in gene expression signatures elicited from a given exposure paradigm. For example,

the constitutive androstane receptor (NR1I3) is necessary for the development of hepatocellular carcinoma in mice following promotion by non-genotoxic receptor activators such as the direct ligand, TCPOBOP, or indirect activators such as phenobarbital (PB). However, extensive epidemiological studies in human populations have ascertained no excess risk of liver cancers following chronic PB exposure. To allow biologically-based and scientifically defensible extrapolations of receptor function across mammalian species that accurately predict potential human toxicities, it is critical to delineate the molecular mechanisms underlying these differential responses. Surprisingly, results using chromatin immunoprecipitation and bioinformatics analyses have revealed extensive divergence among transcription factor binding sites between species. Species-selective splice variation in each receptor further defines inherent differences in species response. This presentation will focus on those features of xenobiotic receptors that contribute to the differences underlying species-selective response to hepatotoxicants.

W 1478 The Utility of Toxicogenomics in the Risk Assessment of Carcinogens: A Report on Two Health Canada Case Studies

C. L. Yauk[1], I. Moffat[2], N. Chepelev[1], A. Jackson[1], S. Labib[1], J. Bourdon[2], B. Kuo[1], J. Buick[1], F. Lemieux[2], A. Williams[1], S. Halappanavar[1], A. Malik[1], M. Luijten[3], J. Aubrecht[4], D. R. Hyduke[5], A. Fornace[6], C. Swartz[7], M. D. Waters[7], I. B. Lambert[8] and L. Recio[7]. *[1]Environmental Health Science and Research Bureau and Water, Health Canada, Ottawa, ON, Canada, [2]Water and Air Quality Bureau, Health Canada, Ottawa, ON, Canada, [3]National Institute for Public Health and the Environment, Bilthoven, Netherlands, [4]Drug Safety R&D, Pfizer, Groton, CT, [5]Biological Engineering Department, Utah State University, Logan, UT, [6]Biochemistry and Molecular and Cellular Biology, Georgetown University, Washington, DC, [7]Integrated Laboratory Systems, Research Triangle Park, NC and [8]Department of Biology, Carleton University, Ottawa, ON, Canada.*

Despite the numerous proposed applications of toxicogenomics in human health risk assessment, integrating standard genomics endpoints in chemical evaluations or using changes in pathway expression to identify points of departure is uncommon. We evaluated the utility of toxicogenomics data in the risk assessment of two well-established carcinogens, benzo(a)pyrene and furan, to demonstrate how genomics data may enhance or complement the current risk assessment process. Gene expression profiles and dose-response modeling were used to develop modes of action and establish pathway-based points of departure for these compounds. We found agreement between the derived points of departures and margins of exposure for apical and genomics endpoints for pathways indicative of key events in the genomics-proposed mode-of-action, as well as the most sensitive pathways. Our case studies demonstrate that toxicogenomics can be used to support and improve cancer risk assessment, assist in the prioritization and preliminary evaluation of potential chemical hazards, and enhance our knowledge of the mode of action of chemical carcinogens.

W 1479 Using Gene Signatures to Predict Molecular Initiating Events in Liver Adverse Outcome Pathways

C. Corton. *NHEERL/ORD, US EPA, Research Triangle Park, NC.*

Adverse outcomes such as liver cancer have been linked to molecular initiating events (MIE) and downstream key events to define adverse outcome pathways (AOP). Identification of gene sets (signatures) predictive of MIEs (i.e., transcription factor activation) were derived by comparing microarray profiles of chemically-treated wild-type or transcription factor (TF)-null mice. The signatures included those dependent on AhR, CAR, FXR, Nrf2, PPARalpha, and PXR, as well as TFs (glucocorticoid receptor and androgen receptor) regulated by hormones. Prediction tests of TF activation showed that balanced accuracies were ≥ 90%. The signatures were used to comprehensively assess TF activation or suppression in a mouse liver compendium of gene expression biosets (~1900) that included chemicals, genetic models and other conditions that can affect the outcome of hazard studies including diet and life stage. Many of the TFs were activated/suppressed by a large number of chemical and chemical-independent perturbations of the liver (CAR, PPARa, PXR, Nrf2), whereas AhR activation was primarily through chemical exposure. Pairs of TFs (i.e., CAR, PPARa, Nrf2 and PXR) were often co-activated by chemicals and gene knockouts. Predictions of TF behavior were used to link chemical exposure, MIEs and AOs in the mouse liver allowing a classification of chemicals by one or more AOPs. The information can be used in cumulative risk models that take into account chemical-independent effects on MIEs (This abstract does not represent US EPA policy.)

W 1480 Genetically Diverse Mouse Populations Facilitate Toxicogenetic Analysis of Drug-Induced Hepatotoxicity

A. H. Harrill[1, 3], M. Mosedale[1], H. Wu[2] and K. Adkins[2]. *[1]Institute for Drug Safety Sciences, The Hamner Institutes for Health Sciences, Research Triangle Park, NC, [2]Investigative Toxicology, DSRD, Pfizer, Groton, CT and [3]University of Arkansas for Medical Sciences, Little Rock, AR.*

Standard nonclinical models, including animals and average human hepatocytes, lack the genetic diversity necessary to model the breadth of toxicity responses observable across clinical populations. Thus, it is occasionally challenging to establish an animal model for a clinically relevant toxic reaction. Recent data indicate that mouse population-based models aid identification of genetically sensitive individuals that may then be used to study mechanisms of toxicity. Development of the macrolide antibiotic PF-04287881 was suspended following elevations in liver function tests observed in a Phase I clinical trial that were not predicted by standard nonclinical species. We demonstrated that a mouse diversity panel (MDP), comprised of genetically diverse inbred strains, could accurately predict the DILI potential of PF-04287881 to humans. Increases in liver biomarkers were associated with histopathological findings of single cell necrosis, hepatocellular hypertrophy and Kupffer cell vacuolation. Based on their unique injury profiles, four mouse strains were selected for transcriptomic analysis of PF-04287881 toxicity in the liver. The protein ubiquitination pathway was highly enriched among genes differentially expressed in strains exhibiting PF-04287881-induced hepatocellular necrosis. In contrast, expression changes associated with PF-04287881-induced phospholipidosis included genes involved in drug transport, phospholipid metabolism and lysosomal function. These findings demonstrate the potential for a mouse population-based approach to improve hazard identification in drug-safety testing as well as to yield mechanistic insights via toxicogenetic investigation.

W 1481 Overcoming Obstacles to Study Drug-Induced Liver Injury with Toxicogenomics towards a Regulatory Application

W. Tong. *Division of Systems Toxicology, NCTR, US FDA, Jefferson, AR.*

More than 25% of drugs on the market that ultimately fail and 40% that fail during clinical trials do so because of liver toxicity. As the leading cause of acute liver failure in the United States, drug-induced liver injury (DILI) has become a major concern in drug development and evaluation. The FDA's new initiative on advancing regulatory science has identified DILI as a key focus area in a concerted effort to broaden FDA's knowledge, create better evaluation tools, and identify safety biomarkers along the various stages of drug development. To enhance our understanding of liver toxicity, NCTR is developing a liver toxicity knowledge base (LTKB) to support research into relationships among DILI, pathways, genes and proteins, and drugs. The project uses a combination of data from the literature on selected drugs with specifically emphasis on toxicogenomics data to develop a systematic approach for defining the severity of risk of a drug for liver injury. These approaches have a potential to support the application review process and regulatory oriented research.

W 1482 Understanding Weight of Evidence: Exploring Different Approaches to Integrating Evidence from Diverse Data Streams

N. B. Beck[1] and J. E. Goodman[3, 2]. *[1]Regulatory and Technical Affairs, American Chemistry Council, Washington, DC, [2]Harvard School of Public Health, Boston, MA and [3]Gradient Corp, Boston, MA.*

While it can be straightforward to evaluate a single study, or a single evidence stream, evaluating an entire body of literature for hazard assessment or risk assessment, where one needs to integrate data that comes from multiple evidence streams (e.g., human data, toxicological data, and mechanistic information), can be more complicated. The integration of all this information is becoming increasingly complex and is particularly driven by the explosion in biological sciences and technologies that are dramatically reshaping both the volume and utility of mechanistic information. Mechanistic information, when coupled with classical endpoint-oriented toxicity data, offers a growing opportunity to more closely examine the toxicologic plausibility of observational associations obtained from epidemiologic studies. Different organizations have taken different approaches to the integration of evidence from diverse data streams, and no clear consensus approach currently exists. This workshop will explore and discuss some current approaches to integrating evidence from several organizations that develop assessments. This is timely and important, as in 2009 the National Academies (NAS) specifically called upon the US EPA to, among other things, improve the way in which evidence is synthesized within the Integrated Risk Information System (IRIS) assessments. The NAS panel acknowledged that there are existing approaches, currently used by

other government programs and elsewhere, for each of these steps and encouraged the US EPA to select from and adapt them. The session will describe, using specific examples, current frameworks that use different approaches to integrate epidemiologic, toxicological, mechanistic, and other data. In addition, seen through the lens of a state user, this perspective will describe what elements are necessary in order to apply and use an integrated evaluation. Time will be provided for a robust discussion and questions.

W 1483 Introduction: Setting the Stage

N. B. Beck. *Regulatory and Technical Affairs, American Chemistry Council, Washington, DC.*

A brief overview of the workshop goals will be provided. This includes discussion of the importance of understanding epidemiologic, toxicological and mechanistic information in order to appropriately incorporate and integrate the information into weight of evidence determinations and risk assessments to inform regulatory and non-regulatory decisions.

W 1484 Understanding Hypothesis-Based Weight of Evidence

L. R. Rhomberg. *Gradient, Boston, MA.*

Once a systematic approach to choosing and laying out evidence is accomplished, the challenge remains to integrate the information into a judgment about the degree of credence to be placed in the possibility of a causal effect in the target (human) population in view of the incomplete and often contradictory information at hand (including human, animal, and mechanistic information). This presentation proposes the Hypothesis-Based Weight-of-Evidence (HBWoE) approach to making, defending, and explaining the basis for such judgment. What makes data into "evidence" is that one proposes that causative forces of the agent underlying the study results may also apply to the target population – that is, bringing to bear study results as evidence entails a proposed generalization of the operation of causes, and one can then ask what other consequences of those proposed common causes should exist and whether they are in fact seen. Noting patterns of commonality and discordance, and attending to the further assumptions that are made to try to reconcile them with the hypothesized general causative properties helps to sort through and articulate the logic behind judgments about human risk potential. The key question is whether the proposed common causal effects (and proposed reasons for any apparent exceptions to their operation) make for a more plausible account of the whole array of available results than do alternative explanations, a view that implements the process that Bradford Hill envisioned for the use of his "considerations" for the evaluation of causality. The method will be illustrated using as examples the evaluation of whether formaldehyde is a cause of human leukemia and whether nasal tumors in a rat inhalation bioassay indicate tumor risk to humans.

W 1485 The US EPA Causality Framework for Assessment of Air Pollution-Related Effects

M. Ross. *Office of Research and Development, US EPA, Research Triangle Park, NC.* Sponsor: N. Beck.

The periodic review of U.S. National Ambient Air Quality Standards (NAAQS) for each of the six criteria air pollutants — ozone, particulate matter, carbon monoxide, nitrogen oxides, sulfur oxides and lead — starts with the synthesis and evaluation of the most policy-relevant science in Integrated Science Assessments (ISAs). EPA has developed an approach for formal characterization of the strength of the scientific evidence and drawing conclusions on causality for exposure-effect relationships. The framework establishes uniform language concerning causality and brings greater consistency and specificity to the ISAs. EPA drew on relevant approaches for similar scientific decision-making processes by EPA and other organizations. Findings from multiple lines of evidence — controlled human exposure, epidemiologic and toxicological studies — are evaluated and integrated to draw conclusions with regard to factors such as consistency, coherence and biological plausibility. The relative importance of different types of evidence varies by pollutant or assessment, as does the availability of different types of evidence for causality determination. The use of the framework is demonstrated with several examples of determinations for various health outcomes and pollutants, particularly drawing from the recently-completed ISA for Lead (Pb). Disclaimer: The views expressed are those of the authors and do not necessarily reflect the views or policies of the US EPA.

W 1486 The Office of Health Assessment and Translation Approach to Evidence Integration for Assessment of Noncancer Health Effects

A. A. Rooney, A. L. Boyles, M. S. Wolfe and K. Thayer. *Division of the National Toxicology Program, NIEHS, Research Triangle Park, NC.*

The NTP's Office of Health Assessment and Translation (OHAT) develops non-cancer hazard identification conclusions by integrating the evidence streams for human and non-human animal studies along with consideration of other relevant data (e.g., in vitro or mechanistic studies). Before combing the three evidence streams, confidence ratings are developed for a given outcome by considering the strengths and weaknesses of the collection of studies or body of evidence. Human and animal studies are evaluated separately using a framework based on the Grading of Recommendation Assessment, Development and Evaluation (GRADE) and Agency for Healthcare Research and Quality (AHRQ) approaches. Other relevant data are evaluated in parallel by assessing the support for biological plausibility provided by this evidence stream. A level of evidence for each health effect is developed that reflects both the overall confidence in the association between exposure to the substance and the outcome and the direction of the effect (i.e., toxicity or no toxicity). The hazard identification conclusions are developed based on the highest level of evidence for a health effect from each of the evidence streams in the final step of the evidence assessment process. First, the level of evidence for health effects conclusion based on human data is considered together with the level of evidence for health effects conclusion based on animal data to reach a hazard identification conclusion of: Known, Presumed, Suspected, Not Classifiable or Not Identified, to be a hazard to humans. Second, the conclusion is considered in context of other relevant data. The final hazard identification conclusion reflects the confidence in each evidence stream as well as the consistency in support (or potential opposition) between the three lines of evidence on the relationship between exposure to the substance and the health effect being examined.

W 1487 Modernizing Problem Formulation: Classical versus Mode-of-Action Approaches to Weight-of-Evidence Determinations

C. J. Borgert. *Applied Pharmacology and Toxicology, Gainesville, FL.*

In scientific investigations, the questions posed—i.e., the hypotheses tested—determine the measurements and conditions under which they are taken, the procedures used to record and analyze data, and the context in which results are interpreted. In risk assessment, the questions addressed are typically articulated in the problem formulation phase. Decades ago, regulatory agencies couched problem formulation according to the questions answerable by the science of the day. As regulatory requirements for risk assessment became codified, so too did the rudiments of problem formulation. Unfortunately, codifying problem formulation prevents risk assessment from evolving to keep pace with scientific advancements. Today, more specific questions can be addressed and answered more precisely with more advanced science, but this science is not being used effectively because typically, the risk assessment problem formulation step still poses antiquated questions. Problem formulation needs to be modernized so that modern science can better inform risk considerations. Using well-studied chemicals as examples, e.g., chloroform or cumene, three Weight of Evidence approaches - the classical IRIS Approach, the Human Relevance Framework Approach, and a Hypothesis-Based Mode of Action Approach - are applied, compared, and contrasted. The analysis illustrates why improving the problem formulation phase is critical to making risk assessment more scientifically accurate, more practical, and more relevant for protecting human health and the environment.

W 1488 The User Perspective—What Makes an Integrated Evaluation Useable and Most Useful?

L. Zeise. *Office of Environmental Health Hazard Assessment, California EPA, Oakland, CA.*

This talk will consider evidence integration from the perspective of a implementer and user. Regulatory guidance levels, hazard evaluations and risk assessments typically rely on general frameworks for integrating evidence, as reflected in the preamble the monographs of the International Agency for Research on Cancer, various US Environmental Protection Agency guidelines and similar guidance developed by states. The emerging approaches described in earlier talks in the session add more specificity to how individual studies and streams of evidence are weighed in reaching conclusions about hazard traits and levels of toxic activity. They differ in approach to data organization, framing questions for evaluation, search strategies, and study selection, as well as resource requirements for performing the evaluation. As these newer approaches are developing the nature and volume of the relevant scientific evidence available for evaluation continues to change. Elements of us-

ability and usefulness of the new approaches will be considered in the context of the types of problems environmental protection agencies are expected to address and the aims of transparency, understandability, scientific rigor and public health protection. Disclaimer: The views expressed are those of the author and do not necessarily reflect the views or policies of the Office of Environmental Health Hazard Assessment or the California Environmental Protection Agency.

W 1489 Discussion

J. E. Goodman[1, 2]. [1]*Gradient, Boston, MA and* [2]*Harvard School of Public Health, Boston, MA.*

A robust discussion and question-and-answer session will focus on the benefits of using a weight-of-evidence approach in general, and particular aspects of various approaches that differ.

PS 1490 AML Subtypes Reported in Cigarette Smokers: A Meta-Analysis

D. Pyatt[1, 3] and D. D. Alexander[2]. [1]*Summit Toxicology, Superior, CO,* [2]*Exponent, Boulder, CO and* [3]*School of Public Health, University of Colorado, Denver, CO.*

The relationship between cigarette smoking and an increased risk of AML has been well documented. While the overall risk is modest, the number of smokers is very large. As a result, cigarette smoking is currently considered the single most important cause of AML in the US. It is assumed that the leukemogenic activity of cigarette smoke is related to the benzene or benzene metabolite content. It is also well documented that AML is not a single disease, but comprised of several different subtypes (depending upon the classification system utilized). One is the M3 subtype (per the FAB) or acute promyelocytic leukemia (APL) that is distinctly different from other subtypes of AML in terms of its diagnostic criteria, treatment, cytogenetic abnormalities and prognosis. While many studies demonstrate the relationship between cigarette smoking and AML, there have only been six studies that have formally evaluated the risk between cigarette smoking and various subtypes of AML. All six of these studies reported elevations in most subtypes of AML but not APL or AML with t(15;17). Here we conducted a meta-analysis of this data set and determined that the overall risk for APL among smokers was statistically significantly suppressed [summary OR = 0.5, 95% CI 0.3-0.8], with good homogeneity between the studies. In contrast, the summary OR for the M2 subtype of AML was significantly elevated [OR = 2.03, 95% CI = 1.41-2.90]. These data indicate that cigarette smoking (or benzene exposure) is not likely a causative factor in the development of APL.

PS 1491 Evaluation of Pyridyloxobutyl DNA Adduct Formation in the A/J Mouse Model

A. Urban, P. Upadhyaya and L. A. Peterson. *University of Minnesota, Minneapolis, MN.*

Tobacco-specific nitrosamines represent an important class of carcinogens found in tobacco products. The tobacco-specific nitrosamine 4-(methylnitrosamino)-1-(3-pyridyl)-1-butanone (NNK) is a potent carcinogen in laboratory animals, and is a known human carcinogen. NNK is metabolically activated to generate both methyl and pyridyloxobutyl DNA adducts, which if not repaired could persist and lead to lung tumor formation. Methyl DNA adducts have been linked to the tumorigenic properties of NNK. However, the role of pyridyloxobutyl DNA adducts in tumor formation has not been elucidated. NNK generates four pyridyloxobutyl DNA adducts: O6-[4-3-(pyridyl)-4-oxobut-1-yl]deoxyguanosine (O6-pobdG), O2-[4-3-(pyridyl)-4-oxobuty-1-yl]deoxythymidine (O2-pobdT), 7 [4-3-(pyridyl)-4-oxobut-1-yl]-2'-deoxyguanosine (7-pobG), and O2-[4-3-(pyridyl)-4-oxobut-1-yl]-2'deoxycytosine (O2-pobdC). O6-pobdG is repaired by O6-alkylguanine-DNA alkyltransferase (AGT), and nucleotide excision repair may play a role in the repair of O2-pobdT. The possible repair pathways of the other pyridyloxobutyl DNA adducts are unknown. To determine the role of pyridyloxobutyl DNA adduct formation in the tumorigenic properties of NNK, DNA adduct levels and tumor yield were measured in the lungs of A/J mice in following treatment with the model pyridyloxobutylating agent 4-(acetoxymethyl-nitrosamino)-1-(3-pyridyl)-1-butanone (NNKOAc). The findings indicate that O2-pobdT accumulates in lung DNA. AGT depletion does not significantly affect O6-pobdG repair or tumor formation, suggesting that O6-pobdG is likely also repaired by pathways other than AGT. These results indicate that the formation and persistence of O2-pobdT may be important for tumorigenesis, and that multiple pathways are likely responsible for the repair of pyridyloxobutyl DNA adducts. [Supported by CA-115309 and CA-138338].

PS 1492 Modulation of IL-8 Signaling by AhR in Breast Tumor Microenvironment Involves miR-17

M. B. van Duursen, S. Nijmeijer, A. D. van den Brand, J. Villevoye and M. Van den Berg. *IRAS, Utrecht University, Utrecht, Netherlands.*

Tumor microenvironment, including the interaction between breast epithelial (tumor) cells and surrounding breast adipose fibroblasts (BAFs), is crucial for tumor development and progression. MicroRNAs (miRNA) have been suggested to play an important role in tumor microenvironment signaling. The aryl hydrocarbon receptor (AhR) has previously been shown to affect miRNA expression. We found AhR expression in cancer-associated breast fibroblasts to be higher than in healthy BAFs, which points to an endogenous role for the AhR in breast cancer pathogenesis. Therefore, we studied the effect of AhR activation on miRNA signaling in an in vitro breast tumor microenvironment. For that, we firstly determined expression of 84 abundantly expressed miRNAs in MCF-7 cells that were exposed to vehicle control (DMSO), non-toxic AhR agonist tranilast (100 μM) or TCDD (1 nM) using a miRNA PCR Array. Despite both being AHR agonists, changes in miRNA profiles upon exposure to TCDD and tranilast were apparently ligand-dependently altered. Notably, both TCDD and tranilast inhibited miR-17 expression, which has been shown to directly target the 3′ UTR of IL-8. Indeed, TCDD, and to a lesser extent tranilast, concentration-dependently increased IL-8 secretion by MCF-7 cells. Next, we determined IL-8 secretion and gene expression in MCF-7 cells co-cultured with BAFs, to mimic a more relevant tumor microenvironment. IL-8 secretion by mono-cultured BAFs was 54.7 pg/ml/48h and 9.3 pg/ml/48h by mono-cultured MCF-7 cells. Interestingly, IL-8 secretion in a BAF/MCF-7 co-culture was around 4-fold lower than in a mono-culture of BAFs, but similar to MCF-7 mono-cultured cells. Activation of AhR by tranilast resulted in a seemingly, yet not significantly, increase in IL-8 expression in BAF/MCF-7 culture. Considering the direct link between IL-8 and promotion of cancer (stem) cells in vitro and in vivo, these data warrant further studies on AhR-mediated modulation of miRNAs in the tumor microenvironment.

PS 1493 Decreased Expression of FRY, a Promoter of Epithelial Cell Differentiation, Is Associated with EMT and Clinical Progression of Breast and Prostate Cancer

H. Zarbl[1], N. Takizawa[2, 1], J. C. Graham[1], B. Estrella[1], X. Ren[3] and M. Fang[1]. [1]*Environmental and Occupational Health Sciences Institiute, Rutgers, The State University of New Jersey, Piscataway, NJ,* [2]*GeneAssess, Inc, North Brunswick, NJ and* [3]*Department of Social and Preventive Medicine, The State University of New York, Buffalo, NY.*

Rat strains vary in their susceptibility to mammary carcinogenesis following exposure to chemical carcinogens, hormones and ionizing radiation. Using quantitative trait locus mapping, we recently identified Fry, the mammalian ortholog of the furry gene in *Drosophila melanogaster*, as a carcinoma susceptibility gene. Fry orthologs in lower eukaryotes regulate epithelial cell differentiation and polarity. Accordingly, loss of FRY expression in human mammary epithelial and tumor cell lines reduced the expression of gene network associated with epithelial differentiation, morphology, polarity and adhesion. Ectopic expression of the wild-type FRY gene in human breast cancer cells restored a gene expression profile consistent with differentiation, suppression of epithelial-mesenchymal transition (EMT), and significantly diminished tumorigenicity *in vitro* and *in vivo*. To assess the role of FRY in human cancers, we used clinically annotated cancer cohorts available in the Oncomine 3.0 gene expression database. The results indicated that FRY was significantly decreased in, and associated with, progression in a broad spectrum of epithelial cell cancers. Analysis of human breast carcinomas tissue microarrays (TMAs) confirmed that decreasing nuclear accumulation of the FRY protein were correlated with negative hormone receptor status, cancer progression, poor clinical outcomes, and especially increased Elston tumor grade (undifferentiated tumor histopathology score). Analysis of TMAs comprised of human prostate tissue and cancers verified that decreased FRY was also associated with clinical progression and poor outcomes. Together, these findings suggest decreased nuclear accumulation of the FRY cancer susceptibility gene plays a critical role in the pathogenesis and progression of cancer in various tissues.

PS 1494 Carcinogenicity Testing of Eliglustat in the Mouse and Rat

R. Forster[1], R. Dagher[2], J. K. Marquis[2] and M. Watzinger[1]. [1]*CiToxLAB, Evreux, France and* [2]*Genzyme Corporation, Waltham, MA.*

Eliglustat is in development for oral treatment of the inherited metabolic disorder Gaucher disease type 1 (GD1). This lysosomal storage disease results from a deficiency of the catabolic enzyme acid-(β)-glucosidase leading to accumulation of glycolipid. The principal substrate of acid-(β)-glucosidase is glucosylceramide

(GL-1); eliglustat acts to reduce production of GL-1 by inhibition of glucosylceramide synthase. Since treatment of GD1 patients will require chronic treatment with Eliglustat, carcinogenicity studies are required. We have evaluated potential carcinogenicity in chronic (2-year) bioassays in the Swiss CD-1 mouse (by dietary administration) and Sprague-Dawley rat (by oral gavage). In the mouse study, treatment with eliglustat did not influence overall survival rates of treated mice at dose-levels up to 75 mg/kg/day. Reduced bodyweight gain at the high dose level indicated that the MTD had been achieved. At histopathology, no treatment related increases in tumour incidence were observed in any groups of eliglustat treated mice. Similarly, in the rat study there was no effect of eliglustat on the overall survival rates up to the high dose level (75 (males) or 50 mg/kg/day (females)). Reduced bodyweight gain at the high dose level indicated that the MTD had been achieved. At histopathology, no treatment related increases in tumour incidence were observed in any groups of eliglustat treated rats. The only neoplastic lesions that were noted were among those that occur spontaneously in these animal models. It was concluded that eliglustat is not carcinogenic after oral administration to mice or rats.

PS 1495 Characterization of a Hepatocyte Nuclear Factor 4 alpha Gene Signature in Chemical Carcinogen-Induced Hepatocellular Carcinoma

C. Walesky[1], S. Gunewardena[2, 3], B. Yoo[4], R. Li[1], G. Edwards[1] and U. Apte[1]. *[1]Pharmacology, Toxicology, and Therapeutics, University of Kansas Medical Center, Kansas City, KS, [2]Molecular and Integrative Physiology, University of Kansas Medical Center, Kansas City, KS, [3]Biostatistics, University of Kansas Medical Center, Kansas City, KS and [4]Kansas Intellectual and Developmental Disabilities Research Center, University of Kansas Medical Center, Kansas City, KS.*

HNF4α is known as the master regulator of hepatocyte differentiation. Previous studies from our laboratory have shown that HNF4α inhibits hepatocyte proliferation and is a potential tumor suppressor. We have shown that deletion of HNF4α resulted in an extensive promotion of DEN-induced hepatic tumors, which were highly proliferative and less differentiated. To further delineate the role of HNF4α in hepatic carcinogenesis, we performed RNA-seq analysis on DEN-induced HCCs obtained from HNF4α-null mice and WT mice along with normal liver tissue. Three separate DEN-induced tumors from WT and HNF4α-null mice were subjected to Illumina Hi-Seq-based RNA sequencing. A total of 2152 genes were differentially expressed in the HCC obtained from HNF4α-null mice. We performed a comparative genomics analysis using previously published ChIP-seq data to obtain a novel gene signature for tumors lacking HNF4α. This analysis revealed 322 genes, which were at least 2 fold differentially expressed and contained a putative HNF4a binding site within 10 kb of their respective transcriptional start site. We validated 20 of these genes that appear to be important in tumorigenesis using Real Time PCR. We further used this 20-gene signature to characterize HNF4α activity status in two unrelated liver tumor models, FXR-KO and Atg5-KO, which further validated our findings. Our data suggests that liver tumors that lack HNF4α tend to be highly aggressive and metastatic. We hypothesize that utilizing this HNF4α-gene signature will allow us to discover chemical carcinogens that inhibit HNF4α function without an observed decrease in HNF4α protein level and predict aggressiveness of HCCs.

PS 1496 HER2 Deregulates Critical Control Blocks to Promote Breast Cancer Metastasis

P. Gupta and S. K. Srivastava. *Biomedical Sciences, Texas Tech University, Amarillo, TX.*

The pre-clinical & clinical studies indicate that HER2 overexpression enhances metastatic properties of the cancer cells. The underlying mechanisms of enhanced metastatic potential of HER2 overexpressing cancer, remains largely unknown. Metastasis is a multi-step process, during which epithelial to mesenchymal transition (EMT) and anoikis (anchorage independent cell death) resistance occur as the two major logjams. EMT helps in achieving invasiveness and motility by cancer cells. Cancer cells attain resistance to anoikis to survive during their travel from primary site to secondary site of cancer. Our results show a novel role of HER2 in the acquisition of mesenchymal features and anoikis resistance. To delineate the mechanism of EMT modulation by HER2, we used MDA-MB-231 & MCF-7 cells with their syngeneic variants with stable HER2 overexpression (referred to as high HER2 or HH cells). The HH cells presented higher invasion and expression of mesenchymal markers like N-cadherin and ZEB-1, along with suppression of epithelial marker Cytokeratin-18.We also observed amplified expression of EMT regulators like SNAIL in HH cells. TGFβ is known to be a master regulator of EMT process. Interestingly, the HH cells manifested higher levels of TGFβ protein and mRNA, along with higher expression of SMADs. SMADs are classical downstream effector molecules for TGFβ. Taken together our results for the first time show a novel regulation of EMT by HER2 through TGFβ signaling. Furthermore, we observed a unique induction of HER2 expression in anoikis resistant cells. The silencing of HER2 resulted in reduced survival of anoikis resistant cells indicating its vital role for anoikis resistance. In addition, the stable overexpression of HER2 enhanced anoikis resistance significantly. These observations clearly suggest a two tier role of HER2 during the process of metastasis. Further mechanistic and pre-clinical in vivo studies are under progress. [Supported in part by R01 grants CA129038 (to S.K.S) awarded by the National Cancer Institute].

PS 1497 Expression of the Fry Mammary Carcinoma Susceptibility Gene during Mouse Embryological and Organ Development

B. Estrella[1, 2], L. M. Aleksunes[4, 1], M. Poulnas[4], M. Fang[1], K. R. Reuhl[1, 4, 3] and H. Zarbl[1, 3]. *[1]Environmental and Occupational Health Sciences Institiute, Robert Wood Johnson Medical School, Rutgers, The State University of New Jersey, Piscataway, NJ, [2]Joint Graduate Program in Toxicology, Rutgers, The State University of New Jersey, Piscataway, NJ, [3]Rutgers Cancer Institute of New Jersey, Rutgers, The State University of New Jersey, New Brunswick, NJ and [4]Department of Pharmacology and Toxicology, School of Pharmacy, Rutgers, The State University of New Jersey, Piscataway, NJ.*

Fry, the mammalian ortholog of the *Drosophila melanogaster* furry gene, encodes an evolutionarily-conserved protein involved in cellular differentiation, division, morphology, polarity, and adhesion through its interaction with the nuclear Dbf2-related (NDR) family of serine/threonine protein kinases. We identified Fry as a carcinoma susceptibility gene in differentially susceptible rat strains. Decreased nuclear expression of the FRY protein in breast cancer cell lines reduces the expression of gene network associated with epithelial differentiation. Ectopic expression of the wild-type Fry gene in human breast cancer cells restored a gene expression profile associated with differentiation, suppression of epithelial-mesenchymal transition (EMT). Cancer cells expressing wild-type Fry at physiological levels reacquired a non-transformed morphology *in vitro* and a non-tumorigenic *in vivo* phenotype in the nude mouse xenograft model. Despite Fry's role in differentiation and cancer, characterization of its expression during embryogenesis and development in mammals has yet to be examined. In this study, mouse embryo sections from days 11, 14, and 17 days post-coitum were examined by immunohistochemistry using our anti-Fry antibody to determine the expression and localization of Fry during embryogenesis. Results from this study showed intense nuclear staining and localization of Fry in ectodermal (brain), endodermal (lung), mesodermal (cardiac cells) derived tissues, and in the placenta at all three stages examined. These results suggest that Fry may participate in placentation as well as embryologic and fetal development.

PS 1498 Bile Acids Promote Diethylnitrosamine-Induced Hepatocellular Carcinoma via NF-κB-c-Jun Signaling Axis

L. Sun, G. Edwards, C. Walesky, P. Borude, B. Bhushan and U. Apte. *Pharmacology, Toxicology and Therapeutics, University of Kansas Medical Center, Kansas City, KS.*

Hepatocellular carcinoma (HCC) is the most common hepatic malignancy and the third leading cause of cancer related deaths. Previous studies have implicated bile acids in pathogenesis of HCC but the mechanisms are not known. We investigated the mechanisms of bile acids in promoting diethylnitrosamine (DEN)-induced HCC in mice. Male C57BL/6 mice were treated with DEN (15 μg/kg) at postnatal day 15 and were weaned on a normal rodent diet. At the age of 8 months these mice were fed either the normal rodent chow (control diet) or a diet containing 0.2% cholic acid (0.2% CA diet) for 2 months. Two other groups of mice without DEN treatment fed either control diet or 0.2% CA diet from 8 to 10 months of age served as controls. All mice were sacrificed at 10 months of age and evaluated for liver tumors. The data show that 0.2% CA treatment resulted in 3-fold increase in number and size of DEN-induced liver tumors. All tumors observed in DEN-treated mice were well-differentiated HCCs. Microarray analysis (Affymatrix Mouse 430_2.0 chip) combined with Ingenuity Pathway Analysis revealed that NF-κB and JNK signaling pathways were the main signaling pathways activated in the DEN-treated 0.2% CA-fed livers. Real Time PCR and Western blot analysis were used to confirm the microarray data. Livers of DEN-treated 0.2% CA-fed mice had significantly higher TNFα, IL-1β, MCP-1 mRNA, a significant increase in total and phosphorylated-p65 and phosphorylated IκBα (degradation form). Further analysis also revealed a substantial increase in JNK phosphorylation and c-JUN protein in DEN-treated 0.2% CA-fed livers. Additional analysis revealed that Wnt/β-catenin and Hippo Kinase signaling pathways, which are also involved in HCC pathogenesis, were activated in DEN-treated mice but were not different between DEN-treated control diet fed mice and DEN-treated 0.2% CA-diet fed

mice. Taken together, these data indicate that bile acid feeding results in promotion of DEN-induced HCCs via specific activation of NF-κB and JNK signaling pathways.

PS 1499 Repurposing the Antimalarial Amodiaquine for Autophagy-Directed Anti-Melanoma Intervention

S. Qiao, S. Tao, M. Rojo de la Vega, S. L. Park, A. A. Vonderfecht, S. L. Jacobs, D. D. Zhang and G. T. Wondrak. *Pharmacology and Toxicology, College of Pharmacy and Arizona Cancer Center, University of Arizona, Tucson, AZ.*

The autophagic-lysosomal pathway is a critical component of the cellular stress response. Cancer cells upregulate autophagic activity as a mechanistic adaptation to adverse conditions of the tumor microenvironment, and pharmacological inhibition of autophagic-lysosomal function has therefore emerged as a promising strategy for chemotherapeutic intervention. Here we demonstrate that autophagic-lysosomal blockade can be achieved in cultured A375 malignant melanoma cells using the clinical anti-malarial amodiaquine (AQ). Consistent with lysosomal expansion observed at the ultrastructural level, AQ-induced molecular changes were substantiated by accumulation of the lysosomal marker glycoprotein Lamp-1, the lipidated autophagosome marker LC3-II, and selective autophagy substrates (p62, alpha-synuclein). Monitoring autophagic flux by expression of a tandem fluorescent-labeled LC3 confirmed autophagic-lysosomal blockade associated with rapid inactivation of lysosomal cathepsins. 2D-Immunoblot-proteomics using an AQ-directed monoclonal antibody identified the eukaryotic translation initiation factor eIF4A as a specific protein target adducted by the electrophilic quinoneimine-metabolite of AQ. Array analysis revealed modulation of gene expression antagonizing heat shock response (HSPA8, HSPA1A, HSP90AA1) and cell cycle progression (CDKN1A, E2F1) confirmed by immunoblot detection (Hsp70, Hsp90, p21, E2F1). Consistent with these expression changes, AQ displayed anti-proliferative effects causing S-phase arrest at submicromolar concentrations targeting an array of malignant melanoma cell lines. AQ-treatment caused rapid induction of energy crisis and sensitized melanoma cells to starvation- and chemotherapeutics-induced cell death. Taken together, our data suggest feasibility of repurposing the clinical anti-malarial AQ for anti-melanoma intervention targeting autophagic-lysosomal function and proliferative control. [R01CA122484, R03CA167580, R21CA166926, ES007091, ES06694].

PS 1500 Epithelial-to-Mesenchymal Transition in Human BEAS and BZR Cells by Benzo(a)pyrene: Involvement of Aryl Hydrocarbon Receptor and Long Interspersed Nuclear Element-1

P. Bojang[1], H. Gao[2], M. T. Haeberle[3] and K. S. Ramos[1, 4]. [1]*Biochemistry and Molecular Biology, University of Louisville, Louisville, KY,* [2]*Center for Translational Research, University of Louisville, Louisville, KY,* [3]*Department of Medicine, University of Louisville, Louisville, KY and* [4]*Center for Environmental Genomics and Integrative Biology, University of Louisville, Louisville, KY.*

Benzo(a)pyrene (B(a)P), a ubiquitous environmental hydrocarbon, has been extensively linked to diseases of the lung including interstitial fibrosis and carcinogenesis. The present studies were conducted to evaluate molecular mechanisms of BaP pulmonary toxicity in human BEAS and BZR cells, non-transformed and transformed bronchial epithelial cells, respectively. Treatment with B(a)P was associated with Epithelial-to-Mesenchymal Transition (EMT), a response which was dependent upon the activation of Aryl Hydrocarbon Receptor (AhR) and Long Interspersed Nuclear Element-1 (L1). B(a)P inhibited expression of epithelial markers and increased the relative abundance of mesenchymal markers in both BEAS and BZR cells. Treatment with α-naphthoflavone (α-NF), a potent antagonist of AhR, attenuated the induction of mesenchymal markers. The EMT response involved induction of L1 at both the mRNA and protein levels. Inhibition of L1 expression through siRNA knockdown attenuated EMT suggesting that intact L1 expression is required for EMT. Together, these data indicate that EMT in human bronchial epithelial by BaP involves activation of AHR and L1.

PS 1501 Disruption of Circadian Rhythm Accelerates Lung Metastasis of Breast Cancer in C3(1)/SV40 T-Antigen (TAG) Transgenic Mice

M. Fang[1, 4], M. Palunas[2, 4], K. R. Reuhl[2, 4], P. Ohman-Strickland[3] and H. Zarbl[1, 4]. [1]*Robert Wood Johnson Medical School, Rutgers University, Piscataway, NJ,* [2]*School of Pharmacy, Rutgers University, Piscataway, NJ,* [3]*School of Public Health, Rutgers University, Piscataway, NJ and* [4]*Environmental & Occupational Health Sciences Institute, Rutgers University, Piscataway, NJ.*

Disruption of circadian rhythm promotes breast cancinogenesis, and is associated with cancer progression and decreased survival rate. To investigate the contribution of the circadian disruption to breast cancer metastasis, heterozygous female C3(1)/SV40 T-antigen (Tag) transgenic mice were maintained on chronic jet-lag protocol (~ 3 months) or regular light and dark cycles after weanling. Mammary tumor latency, incidence and multiplicity, as well as metastasis and inflammatory status of lung were evaluated by histopathology. Results showed that the mammary tumor appeared 16 days earlier and the average total tumor burden (volume and weight) was higher in the mice maintained on jet-lag compared to that in mice on regular light and dark cycles (control group). Lung micro-metastatic foci were also observed at least 13 days earlier, and lung metastasis multiplicity was significantly associated with group, with 288% more metastasis foci in jet-lag vs control group. No visible lung metastatic tumors were observed in heterozygous mice; however, the visible lung metastatic tumor rate, micro-metastatic foci multiplicity, and average foci size were increased in jet-lag vs control group in carriers. In addition, number of lung inflammation foci was significantly increased by circadian disruption, with 233% more inflammatory foci in jet-lag than control group during the early metastasis stage, suggesting that suppressed cellular immunity and overactive inflammatory responses contribute to the development of lung metastasis in this model. Taken together, our studies demonstrated that disruption of circadian rhythm caused by jet-lag accelerates the development and progression of both primary mammary tumor and lung metastasis. (Supported by NIEHS grants: U19ES011387, P30ES007033, and P30ES005022).

PS 1502 Ni+2-Induced Global De-Regulation of Gene Expression and Morphological/Neoplastic Transformation of C3H/10T1/2 Mouse Embryo Cells

J. R. Landolph[1, 2, 3], A. T. Pehl-DeSilva[2, 3], K. A. Akinwumi[1, 2], F. Tseng[1, 2], M. Trieu[1, 3] and S. Menon[1, 3]. [1]*Dept. Micro., Univ. South. Cal., L. A., CA,* [2]*Dept. Path., Univ. South. Cal., L. A., CA and* [3]*Cancer Center, Univ. South. Cal., L. A., CA.*

Nickel refining induced lung/nasal cancers in workers; Ni3S2/green NiO induced lung cancer in rats. Ni3S2/green/black NiOs induced morphological/neoplastic transformation in 10T1/2 mouse embryo cells. mRNA differential display showed differential expression (DE) of 150 genes between non-transformed (Tx)/2 MCA/4 NiO/NiS-Tx 10T1/2 cell lines. Ni/MCA-Tx cell lines contained a) ect-2 amplification/higher ect-2 mRNA/protein levels; b) higher levels of calnexin mRNA/protein; c) no DRIP80/β-centaurin-2 mRNAs. We hypothesized Ni+2 1) amplified ect-2, leading to higher levels of microtubules (MTs); 2) silenced β-2-centaurin-2, causing higher levels of microfilaments (MFs); and 3) silenced DRIP80, altering Ca+2 ion distributions, in Tx 10T1/2 cells. To test these hypotheses, we stained cells with fluor. phalloidin to decorate MFs, fluor. Ab to α-tubulin to decorate MTs, Fluo 3AM to stain Ca+2 ions, DAPI to decorate nuclei, and examined cells by confocal microscopy. In non-Tx 10T1/2 cells, MFs/MTs were distributed homogeneously. In NiS/green NiO-Tx cell lines, MFs/MTs were over-expressed, aggregated in areas, absent in others, changing shapes of Tx cells. In non-Tx cells, Ca+2 ions were found in a) State I, in low density cells, with a high nuclear concentration of Ca+2 ions; or b) State II, in high density cells, with more cytoplasmic Ca+2 ions. In 4 Ni/2 MCA-Tx cell lines, Ca+2 ions were in State II. We conclude Ni+2 ions a) mutated/amplified 6 target genes/silenced 9 target genes; b) amplified ect-2, causing higher levels of MTs/silenced β-centaurin-2, causing higher levels of MFs, changing cell shapes/gene expression in Tx cell lines; c) silenced DRIP80, altering Ca+2 ion distributions in Tx 10T1/2 cell lines. These Ni ion-induced events caused DE of 150 genes in Tx cell lines and induction/maintenance of Tx phenotypes. Supported by Grant ES03341/grants from M. S. Program in Micro. and Provost's Office at USC, to JRL.

PS 1503 Differential Modulation of p-4EBP1, p-ERK, and Cyclin D1 by Amuvatinib/Erlotinib Treatment in PTEN+ and PTEN- Prostate Cancer Cells

R. D. Canatsey[1], W. Cai[1], N. Mastrandrea[1], J. Gard[2], R. Nagle[2], T. J. Monks[1] and S. S. Lau[1]. [1]*Southwest Environmental Health Science Center, Dept. of Pharm/Tox, College of Pharmacy, University of Arizona, Tucson, AZ and* [2]*College of Medicine, University of Arizona, Tucson, AZ.*

Environmental exposure to carcinogens causes loss of tumor suppressor genes. Phosphatase and tensin homolog (PTEN) negatively regulates the AKT pathway, and the PTEN gene is mutated/deleted in ~70% of prostate cancer cases. Downstream of AKT, eukaryotic initiation factor 4E binding protein 1 (4EBP1) regulates cyclin D1 translationally. In contrast, ERK, a member of the mitogen activated protein kinase (MAPK) pathway, regulates cyclin D1 transcriptionally. Both the AKT and MAPK signaling pathways contribute to disease progression in prostate cancer. A PTEN-deficient human prostate cancer cell line, LNCaP, and a PTEN-positive human prostate cancer cell line, DU145, were used to examine the role of PTEN status in determining drug sensitivity to Amuvatinib, a receptor tyrosine kinase inhibitor, and Erlotinib, an epidermal growth factor inhibitor. 1D and 2D Western blot analysis revealed that combination drug treatment of LNCaP cells caused a decrease in 4EBP1 pSer65, pThr70 and pThr37/46, with a concomitant decrease in cyclin D1 protein. Such combination treatment, however, did not modulate pERK status. Moreover, single drug treatment with Amuvatinib, but not Erlotinib, decreased p-4EBP1 and cyclin D1 protein levels. In DU-145 cells, combination drug treatment had no effect on p-4EBP1 status, but decreased p-ERK and cyclin D1 protein levels. Additionally, single drug treatment with Erlotinib, but not Amuvatinib, caused a loss of p-ERK and cyclin D1. The data reveal the differential modulation of cyclin D1, and its upstream regulators, in the PTEN+ and PTEN- cell lines by Amuvatinib and Erlotinib. Such differential responses likely contribute to specific anti-tumor agent efficacy. An appreciation of factors that determine the cell-dependent modulation of cyclin D1 will assist in the selection of appropriate biomarkers to assist in directing patient-targeted therapy. (Ventana/Roche, P30 ES006694)

PS 1504 (-)-Epigallocatechin-3-Gallate Increases Cell Growth Inhibition Induced by Benzo[a]pyrene in Human Lung Epithelial Cells

M. Cromie, W. Zhu and W. Gao. *The Department of Environmental Toxicology, Texas Tech University, Lubbock, TX.*

Our recent study found that curcumin and vitamin E protected against the cellular and molecular damage in normal human lung epithelial cells (BEAS-2B) after exposure to the carcinogen, benzo[a]pyrene (BaP). Based on these findings, we further evaluated whether epigallocatechin-3-gallate (EGCG), an active compound isolated from green tea, exhibited similar properties. The cells were evaluated for changes in cell viability, cell cycle alterations, benzo[a]pyrene diol epoxidation (BPDE)-DNA adducts, mRNA expression levels of cytochrome P450 (CYPs), and expression of tumor suppressor and cell survival proteins. MTT assay found that BaP-inhibited cell growth/proliferation was enhanced with EGCG co-treatment. Flow cytometry analysis revealed that BaP caused significant G2/M phase arrest, and this increased G2/M arrest was more pronounced in cells co-treated with BaP and EGCG. HPLC analysis indicated that BPDE-DNA adducts were diminished significantly by EGCG treatment, with an 80% reduction. qRT-PCR analysis showed that CYP1A1 and CYP1B1 were dramatically increased after BaP exposure, but co-treatment with EGCG significantly reduced their expression. Additionally, western blot analysis demonstrated that co-treatment of BaP with EGCG enhanced p53 activation but caused a marked reduction in the activation of Akt, survivin, and NF-kB. Overall, EGCG augmented cell growth inhibition, decreased BPDE-DNA adducts, reduced CYP1A1 and 1B1 expression, and upregulated p53 activation, while decreasing Akt activation, and the expression of survivin and NF-kB in cells exposed to BaP. In conclusion, EGCG did not protect BaP-exposed cells through the same mechanisms as curcumin and vitamin E, although it could help impede the initial DNA damage caused by BaP.

PS 1505 Benzo(a)pyrene-Induced Colon Carcinogenesis in the Apc^{Min} Mouse Model

J. A. Mantey[1], P. V. Rekhadevi[2], D. L. Diggs[2], M. S. Niaz[2] and A. Ramesh[2]. [1]*Neuroscience & Pharmacology, Meharry Medical College, Nashville, TN and* [2]*Biochemistry & Cancer Biology, Meharry Medical College, Nashville, TN.*

Several epidemiological studies have reported a link between dietary exposure to polycyclic aromatic hydrocarbons (PAHs) and sporadic colon cancer. On average in the United States, colorectal cancers, which are predominantly due to sporadic, non-genetic causes, claim an estimated 60,000 lives/year. Therefore, we have employed the Apc^{Min} mouse model to study colon cancers induced by benzo(a) pyrene (BaP), a widely distributed prototypical PAH toxicant. Benzo(a)pyrene was administered to Apc^{Min} mouse mice in tricaprylin at doses of 25 and 50 μg/kg via oral gavage over a 60-day period. Blood, colon and liver were collected at the end of the exposure period. The tissues were evaluated for histopathology. The expression of BaP biotransformation enzymes (CYP1A1, CYP1B1 and GST) in the liver and colon were assayed. Tissue and plasma samples were analyzed by reverse phase-HPLC coupled with fluorescence detection for BaP metabolite concentrations. Additionally, DNA was isolated from the tissues. Oxidative damage to DNA was assessed using the Biovision DNA damage quantification kit. Benzo(a)pyrene-DNA adducts were resolved and quantified by the ^{32}P-postlabeling method. The metabolic fate of BaP was altered in a dose-dependent manner with the 50 μg/kg dose group registering an elevated expression of BaP biotransformation enzymes, greater concentration of BaP metabolites, abasic sites in DNA, BaP-DNA adducts and more adenomas compared to the 25 μg/kg dose group ($p < 0.05$). These findings establish that i) subchronic exposure causes sustained induction of BaP biotransformation enzymes and extensive metabolism of this toxicant; ii) the production of free radicals initiated DNA base pair damage, which in the absence of DNA repair, formed BaP-DNA adducts; and iii) a correlation between colon tumors and BaP-DNA adduct concentrations. Our studies provide concrete evidence that sustained dietary exposure to BaP contributes to the development of colon cancer.

PS 1506 Regulation of Gene Expression Profiles in Clear Cell Renal Cell Carcinoma by Cadmium Exposure

S. Brooks[1, 2] and W. Rathmell[1, 2]. [1]*UNC-CH, Chapel Hill, NC and* [2]*Lineberger Cancer Center, University of North Carolina at Chapel Hill, Chapel Hill, NC.*

Clear cell renal cell carcinoma (ccRCC), the predominant subtype of kidney cancer, displays variability in risk for developing metastatic disease, and tissue-based prognostic biomarkers are urgently needed. Recently, we used unsupervised bioinformatic strategies to demonstrate two subtypes of ccRCC, clear cell A (ccA) and clear cell B (ccB). The subtypes conveyed a prognostic value, with tumors displaying the ccA signature associated with better survival compared to ccB. We developed and validated a 34-gene subtype predictor to classify clear cell tumors as ccA and ccB using RNA-sequencing data from 380 ccRCC samples from The Cancer Genome Atlas (TCGA) and the NanoString platform with a cohort of 163 fixed archival samples collected at the University of North Carolina. This novel tool can be used to analyze risk for developing metastatic disease and as a baseline metric to elucidate specific effects of toxicants on renal tumor gene expression signatures that can provide insight into the molecular phenotype of ccRCC.
Heavy metals can induce nephrotoxicity altering gene expression in the kidney, and thus increasing the risk of developing RCC. In addition to transcript alterations, numerous studies have found that Cd exposure can result in epigenetic deregulation by changing DNA methylation levels. We have observed significant decreases in methylated sites associated with the 34 genes from the ccA/ccB algorithm among ccRCC tissue (n=17) compared to normal tissue (n=15) of smokers from TCGA. Smoking populations experience higher levels of cadmium exposure, as one cigarette may contain 1-2 ug cadmium. Interestingly, the majority of this cohort was either ccB subtype or had metastatic disease, suggesting a possible correlation between cadmium exposure and aggressive disease. Exploring both acute and chronic cadmium-induced global expression and epigenetic reprogramming can enhance our understanding of the genetic interactions that drive the biological responses to these exposures and their influence on prognostic signatures of RCC.

PS 1507 Overexpression of CRM1: A Characteristic Feature of the Transformed Phenotype in Lung Carcinogenesis

C. Lu[1], L. Chen[1], P. Keohavong[2] and W. Gao[1]. [1]*Texas Tech University, Lubbock, TX and* [2]*University of Pittsburgh, Pittsburgh, PA.*

Our initial studies using normal human lung epithelial cells, BEAS-2B, and a bitransgenic mouse model have suggested that chromosome maintenance region 1 (CRM1), a nuclear export receptor for various cancer-associated 'cargo' proteins (such as p53), played an important role in lung cancer development. The objectives of the present study were to investigate the CRM1 expression and/or its associated p53 alteration in the following four models: human lung tumor tissues, 4-(methylnitrosamino)-1-(3-pyridyl)-1-butanone (NNK, a tobacco specific carcinogen)-induced mouse lung adenocarcinoma, NNK-transformed lung epithelial cells (named as BEAS-2BNNK), and stably over-expression of CRM1 in BEAS-2B cells (named as BEAS-2BCRM1+). CRM1 was overexpressed in tumor tissues from both lung cancer patients and NNK-treated mice, and in BEAS-2BNNK cells. Cellular malignant transformation was observed in BEAS-2BNNK and BEAS-2BCRM1+ cells. Furthermore, increased p53 phosphorylation at Thr 55, which indicated p53 cytoplasmic localization and p53 degradation, was increased

in NNK-induced lung adenocarcinoma and BEAS-2BNNK cells. Moreover, the nuclear retention of p53 was significantly diminished in BEAS-2BCRM1+ cells compared to BEAS-2B cells. These data suggest that CRM1 plays a critical role in lung cancer progression and that such mechanisms may provide a novel target for developing lung cancer therapies.

PS 1508 GS-19, a Novel GSK Inhibitor Suppresses the Growth of Pancreatic Cancer Cells by Inhibiting EGFR/AKT/STAT-3 Signaling

A. Ranjan[1], A. Birkenfield[1], P. Gupta[1], J. Lu[2], D. H. Hua[2] and S. K. Srivastava[1]. [1]*Department of Biomedical Sciences & Cancer Biology Center, Texas Tech University Health Sciences Center, Amarillo, TX and* [2]*Department of Chemistry, Kansas State University, Manhattan, KS.*

The American Cancer Society estimates that over 43,000 new cases of pancreatic cancer are diagnosed each year in the United States, with a five-year survival rate below 6%. Conventional therapies are often of limited use because of the resistance development and cancer relapse. Therefore, identification of novel strategies to control and treat pancreatic cancer is of great importance. GS-19 is a novel compound designated as a GSK inhibitor and shown good activity in neural protective assay using MC65 cells. In this study, we determined the cytotoxic effects of GS-19 in pancreatic cancer cells. GS-19 treatment inhibited the growth of Panc-1 and BxPC-3 cells in a concentration-dependent manner. Both the cell lines treated with GS-19 exhibited G-1 cell cycle arrest as well as apoptosis. Western blot analysis of both BxPC-3 and Panc-1 cells treated with GS-19 inhibited the activation (phosphorylation) and expression of key survival signaling proteins such as EGFR, STAT3 and AKT. The apoptosis induced by GS-19 was associated with cleavage of caspase-3 and PARP. Taken together, our results suggest that GS-19 suppress pancreatic cancer cell growth by inhibiting EGFR/AKT/STAT-3 signaling. However, further mechanistic studies are in progress to establish the role of EGFR/AKT/STAT-3 signaling in pancreatic cancer cells and correlate it with G1 cell cycle arrest and apoptosis induced by GS-19. The studies in part were supported by R01 grant CA129038 awarded by NIH to S.K.S

PS 1509 Olive Oil As a Chemopreventive Agent against Benzo(a) pyrene-Induced Colon Cancer in Apc^{Min}Mouse

L. D. Banks[1], P. Amaoh[1], M. S. Niaz[1], M. K. Washington[2], S. E. Adunyah[1] and A. Ramesh[1]. [1]*Biochemistry & Cancer Biology, Meharry Medical College, Nashville, TN and* [2]*Pathology, Vanderbilt University Medical Center, Nashville, TN.*

Colorectal cancer (CRC) ranks third in terms of cancer-related mortalities, and sporadic colon cancers (representing 90% of the cases) are triggered by diet and exposure to environmental toxicants. In recent years, cancer prevention through dietary intervention gained significant attention. In the light of published reports that Mediterranean diet lessens the incidence of CRC, we investigated how olive oil, an essential ingredient of Mediterranean diet modulates the biotransformation of benzo(a)pyrene (BaP, a polycyclic aromatic hydrocarbon compound) and contributes to a reduction in colon tumors using an animal model. Our study model was the male Apc^{Min} mouse, which was validated in our lab for studying sporadic colon tumors induced by BaP. Mice were assigned to a control (vehicle only; n =7), or treatment group (BaP only, BaP + olive oil; n =7 per category). Treatment consisted of 50 and 100 μg BaP/kg body weight dissolved in tricaprylin (BaP-only group) or olive oil administered daily via oral gavage for sixty days. Post exposure, mice were sacrificed; colon and liver tissues were retrieved and evaluated for histopathology. Another set of tissues were used for studying the expression and activities of biotransformation enzymes (CYP1A1, CYP1B1, and GST) and analysis of BaP metabolites. A reduced incidence of adenomas in colons of mice that ingested BaP + olive oil compared to BaP only and control groups ($p < 0.05$) was seen. Additionally, there was a significant reduction in CYP but not GST protein expression in tissues in BaP + olive oil-treated mice compared to BaP only-treated mice. Lastly, BaP organic metabolite concentrations were reduced in plasma and tissues of BaP + olive oil group compared to BaP-treated groups, whereas BaP aqueous metabolite concentrations (especially the glucuronide and sulfate conjugates) showed an opposite trend. In summary, our studies suggest that olive oil exerts a chemopreventive effect against BaP-induced colon cancer.

PS 1510 Cannabidiol Inhibits Glioma Cell Proliferation and Downregulates Specificity Protein (Sp) Transcription Factors

S. Sreevalsan[1] and S. H. Safe[1, 2]. [1]*VTPP, Texas A & M University, College Station, TX and* [2]*Institute of Biosciences and Technology, Texas A&M Health Science Center, Houston, TX.*

Cannabidiol (CBD), a plant-derived cannabinoid has shown promise as an anti-cancer agent in treating glioblastoma multiforme (GBM), however the mechanism of action of CBD on GBM is not completely understood. Treatment of CCF-STTG1 cells with CBD for 24 hr significantly inhibited cell growth, downregulated pro-oncogenic factors including epidermal growth factor (EGFR), bcl-2 and survivin and induced PARP cleavage a marker for apoptosis. Research conducted in our laboratory has shown that these same responses and factors are regulated by specificity protein (Sp) transcription factors Sp1, Sp3 and Sp4 that are highly expressed in multiple cancer cells and tumors. Sp1, Sp3 and Sp4 are also highly expressed in CCF-STTG1 cells and knock-down of Sp1, Sp3 and Sp4 by RNA interference decreased expression of survivin, bcl-2 and EGFR suggesting that these oncoproteins are regulated by Sp transcription factors in CCF-SSTG1cells. Moreover concentrations of CBD (10-15 uM) that decreased EGFR, survivin, and bcl-2 expression also downregulated Sp1, Sp3 and Sp4 in CCF-STTG1 cells. Furthermore, treatment of CCF-STTG1 cells with 15 uM of CBD and co-treatment with 1 uM of AM 251 and AM630, cannabinoid receptor antagonists 1 and 2 respectively failed to reverse the effects of CBD on Sp proteins suggesting that CBD-dependent Sp downregulation is cannabinoid receptor-independent. These results demonstrate for the first time that the anticancer activity of CBD in gliomas may be due, in part, to downregulation of Sp transcription factors and Sp-dependent genes and the mechanism of action involved in Sp protein repression is currently being investigated.

PS 1511 Role of ROS in the Anticancer Activity of PEITC in Pancreatic Cancer

I. D. Jutooru, A. S. Guthrie, G. Chadalapaka and S. H. Safe. *Veterinary Physiology and Pharmacology,, College Station, TX.*

Phenethyl isothiocyanate (PEITC) is a natural compound found in cruciferous vegetables and has been shown to have anticancer activity in various cancers including pancreatic cancer. Previous studies have shown that PEITC induces reactive oxygen species (ROS) and selectively kills cancer cells. In this study, PEITC decreased cell proliferation, induced ROS and cleaved PARP which was further confirmed by Annexin V staining in Panc1, Panc28 and L3.6pL pancreatic cancer cell lines. PEITC decreased mitochondrial membrane potential (MMP) which was confirmed using JC-staining and transmission electron microscopy (TEM). PEITC also deceased Sp proteins Sp1, Sp3 and Sp4 and several Sp-regulated genes involved in cell survival (survivin, Bcl2), angiogenesis (VEGF, VEGFR1) and growth (cyclin D1, EGFR, cMet). Repression of Sp and Sp-dependent genes by PEITC was due to downregulation of microRNA-23a~27a and induction of zinc finger and BTB domain (ZBTB) containing 4, 10 and 34. These responses were reversed by antioxidants such as glutathione (GSH) indicating the mechanism of action of PEITC is through induction of oxidative stress. Thus, the anticancer activity of PEITC is due, in part, to activation of ROS, which in turn targets miR-23a~27a:ZBTB-Sp transcription factor axis. This results in decreased expression of Sp-regulated genes, growth inhibition, apoptosis and antiangiogenic responses. Studies have also shown that elevated levels of ROS can cause dynamic changes in surrounding chromatin including changes in nucleosome positioning, CpG island-containing promoters of genes such as ACTB, cMyc, SFRP5 and TIMP3 resulting in changes in histone marks, transcription and DNA methylation. Additionally, PEITC decreased cMyc as early as 3 hrs in panc1 and L3.6pL and these responses are currently being investigated.

PS 1512 Diindolylmethane (DIM) Analogs As a New Class of NR4A1 Antagonists

X. Li[1], S. Lee[2] and S. H. Safe[1, 2, 3]. [1]*College of Medicine, Texas A&M Health Science Center, College Station, TX,* [2]*Institute of Biosciences & Technology, Texas A&M Health Science Center, Houston, TX and* [3]*Veterinary Physiology and Pharmacology, Texas A&M University, College Station, TX.*

The nuclear receptor NR4A1 (TR3, Nur77) is highly expressed in solid tumors and result of knockdown by RNA interference (RNAi) indicates that NR4A1 exhibits pro-oncogenic activity. Transfection of RKO and SW480 colon cancer cells with oligonucleotides that target NR4A1 (siNR4A1) inhibited cell proliferation and induced apoptosis and this was accompanied by decreased expression of Bcl-2 and survivin. A series of 1,1-bis(3'-indolyl)-1-(p-substituted phenyl)methane analogs (C-DIMs) was screened for potential NR4A1 antagonist activity using luciferase

constructs contained multiple consensus NR4A1 response elements (NBRE-Luc and NurRE-Luc). Several C-DIM analogs including the p-bromophenyl (DIM-C-pPhBr), p-hydroxyphenyl (DIM-C-pPhOH), p-cyanophenyl (DIM-C-pPhCN) and p-carboxymethylphenyl (DIM-C-pPhCO_2Me) significantly decreased transactivation in cells transfected with NBRE-Luc and NurRE-Luc. The C-DIM compounds also decreased transactivation in RKO cells transfected with NBRE-Luc and FLAG-tagged wild type NR4A1 and mutants with C-terminal (ΔEF) and N-terminal (ΔAB) deletions indicating that both activation functions (AF1 and AF2) were inactivated by the C-DIM compounds. Treatment of RKO cells with DIM-C-pPhOH inhibited cell growth and induced apoptosis but did not decrease NR4A1 expression indicating that the C-DIM analogs represent a new class of NR4A1 antagonists.

PS 1513 Mechanistic Evaluation of the Chemopreventive Effects of Folic Acid and Tributyrin in a Rat Liver Carcinogenesis Model

A. de Conti[1], A. H. Guariento[2], K. S. Furtado[2], V. Tryndyak[1], F. A. Beland[1], I. Pogribny[1] and F. S. Moreno[2]. [1]*Division of Biochemical Toxicology, NCTR, Jefferson, AR and* [2]*Food and Experimental Nutrition, University of Sao Paulo, Sao Paulo, Sao Paulo, Brazil.*

The steady increase in the incidence and mortality of hepatocellular carcinoma (HCC) signifies a crucial need to understand better the pathogenesis of HCC to improve clinical management and prevention of the disease. The aim of this study was to investigate molecular mechanisms for the chemopreventive effects of folic acid and tributyrin alone or in combination on rat hepatocarcinogenesis. Male Wistar rats were subjected to a classic "resistant hepatocyte" model of liver carcinogenesis and treated with folic acid and tributyrin alone or in combination for 5 weeks during promotion phase of carcinogenesis. Treatment with folic acid and tributyrin alone or in combination substantially inhibited the development of preneoplastic hepatic lesions. Microarray analysis showed significant changes in gene expression. A total of 501, 655, and 940 of differentially expressed genes involved in cell cycle, p53-signaling, angiogenesis, and Wnt pathways was identified in the livers of rats treated with folic acid, tributyrin or folic acid and tributyrin. A detailed analysis of these differentially expressed genes revealed that treatments inhibited angiogenesis in the preneoplastic livers. This was evidenced by the fact that 30 out of 77 differentially expressed genes common to all three treatments are involved in the regulation of the angiogenesis signaling network. The inhibition of angiogenesis was confirmed by reduced levels of CD34 protein. In conclusion, the tumor-suppressing activity of folic acid and tributyrin is associated with inhibition of angiogenesis at early stages of rat liver carcinogenesis. Importantly, these data demonstrate that the combination of folic acid and tributyrin has stronger chemopreventive effect than each of the compounds alone.

PS 1514 Uptake, Internalization, and Quantification of LHRH-Tagged Gold Coated Superparamagnetic Iron Oxide Nanoparticles in Cancerous MCF-7 Cells

S. Khiste[1], S. Batra[2], S. Jeyaseelan[2], K. Challa[3], S. N. Murthy[1] and R. M. Uppu[1]. [1]*Environmental Toxicology PhD Program, Southern University and A&M College, Baton Rouge, LA,* [2]*Pathobiological Sciences, LSU School of Veterinary Medicine, Baton Rouge, LA and* [3]*Center for Advance Microstructure and Devices, Louisiana State University, Baton Rouge, LA.*

Magnetic nanomaterials have generated enormous interest in the recent past for various promising applications in biomedical research including drug delivery, magnetic resonance imaging, and cancer therapy. Previous studies from our laboratory have shown that gold coated superparamagnetic iron oxide nanoparticles (SPIONs@Au) linked to LHRH can selectively kill cancer cells expressing receptors for LHRH. In these studies, we used cysteamine to cross link SPIONs@Au to the carboxy terminal of LHRH. For the present study we synthesized SPIONs@Au linked to LHRH through the amino terminal using 12-mecaptododecanoic acid (MDDA) N-hydroxysuccinamide ester as the heterobifunctional agent. The resulting conjugates, SPIONs@Au-MDDA-LHRH were studied for their uptake and internalization by LHRH receptor over expressing MCF-7 cancer cells. When incubated SPIONs@Au-MDDA-LHRH (0.2 mg/mL) for 24 h, we found substantial uptake (180 pg/mL; measured by ICP) of the nanoparticles by MCF-7 cells. Transmission Electron Microscopy results show the evidence of clumps of SPIONs@Au-MDDA-LHRH indicating their uptake by endocytosis. The nanoparticulate clumps were found located inside the membranous compartment together with cell organelles like mitochondria and ended up in late endosomes (autophagosomes), confirming the endocytic pathway of uptake. Further studies are underway to examine the selective tumorocidal activities of SPIONs@Au-MDDA-LHRH under the influence of low strength magnetic field. These studies would pave way for designing nanomaterials with tumorocidal properties and better management of cancer patients [Support from NSF (HRD1043316), NIH (8P20GM103424), and LA BoR is acknowledged; corresponding author's email: rao_uppu@subr.edu].

PS 1514a The Effect on Endothelial Cell Proliferation of Oligosaccharides of Hyaluronan

J. Lichtenberg[1], B. M. Malle[2] and P. Koolwijk[3]. [1]*Toxicology, Novozymes A/S, Bagsvaerd, Denmark,* [2]*Biopharma Technical Services, Novozymes A/S, Bagsvaerd, Denmark and* [3]*Department of Physiology, VU University Medical Center, Amsterdam, Netherlands.* Sponsor: N. Berg.

The degredation products of hyaluronan (HA) are reported to stimulate endothelial-cell proliferation, migration, tube formation and promote neovascularization associated with angiogenesis whilst native high-molecular-weight HA is inhibitory to these processes (1,2). When degraded into oligosaccharides of 3 to 10 disaccharides units (o-HA) an angiogenic effect has previously been demonstrated on the chicken chorioallantoic membrane and in rat skin where the blood vessel numbers were found to increase (3). It is speculated if HA degraded into o-HA may represent a safety issue in the human body due to stimulation of endothelial cell proliferation. We have investigated the effects on endothelial cell proliferation of bacillus subtilis derived HA. We used oligosaccharides of 3-10 disaccharide units, 1.35 - 4.5 kDa and native HA of 2162 disaccharides units, 865 kDa. HUVEC (human umbelical vein endothelial cell) and MVEC (human foreskin microvascular endothelial cell) and different cell lines of MVEC were stimulated with o-HA at concentrations of 1, 10 and 25 μg/mL and with native HA at dose concentrations of 5 to 100 μg/mL.
Results:
We were unable to induce stimulation of endothelial cell proliferation by oligosaccharides. Treatment of endothelial cells by native HA did not inhibit endothelial cell proliferation or caused a decrease of tube formation in 3-D assay.
Conclusion:
Based on the current data the degradation of hyaluronan into oligosaccharides gives no cause for concern in terms of stimulation of endothelial cell proliferation, migration and potential neovascularization.
References:
1. Deed R. et al., Int. J. Cancer, 1997
2. Slevin M et al.Matrix Biology, 2007
3. Sattar et al., J. Invest. Dermatol, 1994.

PS 1514b Effects of *Adansonia digitata* Fruit Pulp Extract on Sodium Arsenite-Induced Toxicities in Rats

O. A. Odunola, A. M. Adegoke, M. A. Gbadegesin and O. P. Akinbobola. *Cancer Research and Molecular Biology Laboratories, Department of Biochemistry, University of Ibadan, Ibadan, Oyo State, Nigeria.*

Prolonged ingestion of arsenic contaminated water and the attendant toxic effects is of global concern. Anti-oxidants and anti-oxidant rich foods and herbal medicinal plants are being accessed for the management and prevention of arsenicosis. In this connection, we investigated the effect of the aqueous extract of the fruit pulp of *Adansonia digitata* L – Africa's upside-down tree (FPA) on sodium arsenite (SA) – induced clastogenicity and hepatotoxicity in rats. The negative control rats were exposed to distilled water only while the positive control group had 2.5 mg/kg body weight of SA. Test animals were pretreated with either 200 or 400 mg/kg body weight of FPA before challenge with SA. All treatments were done for fourteen days. Sodium arsenite significantly ($p<0.05$) increased the activities of serum gamma glutamyl transferase (γGT), alanine aminotransferase (ALT) and aspartate aminotransferace (AST), the number of micronucleated polychromatic erythrocytes (mPCEs) induced in the bone marrow, hepatic cells proliferation and lipid peroxidation as compared with the control. Pre-treatment with FPA significantly ($p<0.05$) reduced the activities of γGT, AST and ALT, the number of mPCEs induced, hepatic cells proliferation and lipid peroxidation. Limited histopatological examination of the liver showed that FPA reduced the severe portal congestion with periportal fibroplasia and cellular infiltration by mononuclear cells induced by SA. We therefore conclude that the aqueous extract of the fruit pulp of *Adansonia digitata* has the potential to remediate sodium arsenite induced toxicities probably through the radical scavenging anti-oxidant system.

PS 1515 Association of Serum Levels of the Organochlorine (OC) Compound DDE with Type 2 Diabetes (T2D) in Mississippi

E. C. Meek, J. A. Crow, L. Mangum, M. K. Ross, R. Wills and J. E. Chambers. *Center for Environmental Health Sciences, Mississippi State University, Mississippi State, MS.*

Recent studies have reported an association with higher OC levels in people with T2D compared to non-diabetics. OC compounds associated with greater prevalence of T2D include the legacy pesticides, such as DDT. Exposure to OC compounds is predicted to be higher in agricultural areas, such as the Mississippi Delta region, where OC pesticides were heavily used. Soil samples were analyzed for OC residues from 60 randomly selected sites in the Delta region and 60 sites in a non-Delta region. Serum samples were randomly collected from patients from both the Delta and non-Delta regions at the Veterans' Administration Hospital in Jackson, MS. Following IRB approved informed consent, male subjects who were either Caucasian (C) or African American (AA) and were at least 45 years of age were selected for participation. Serum samples and de-identified clinical and demographic data were collected from each subject. Serum and soil samples were analyzed by GC-MS for OC residues including DDE, the bioaccumulative metabolite of DDT, which was detected most often in both soils and people. 80% of the Delta soil samples had quantifiable levels of DDE compared to 23% of the non-Delta soil samples and were 10-fold higher. About half of the proposed 300 serum samples have been collected and analyzed. DDE levels were adjusted based on serum lipid levels and were about 1.2-fold higher in diabetics than non-diabetics, 1320 and 1160 ng/g lipid, respectively. Subjects from the Delta region had about 1.5-fold higher DDE levels than non-Delta subjects, 1560 and 1012 ng/g lipid, respectively. AA subjects had 2.6-fold higher DDE levels than C subjects, 1992 and 761 ng/g lipid, respectively. AA and C diabetics both had higher DDE levels than AA and C non-diabetics. These results suggest that higher environmental residue levels of OC compounds, such as DDE, may result in higher serum levels and may be important for developing a biomarker of T2D. (Supported by USEPA STAR RD-83479501-0).

PS 1516 Pb and Cd-Contaminated Soil May Cause Metal Accumulation and Epigenetic Alteration in Rat Tissues

Y. B. Yohannes[1], S. M. Nakayama[1], Y. Ikenaka[1], B. Oroszlany[1], N. Bortey-Sam[1], K. Muzandu[2], J. Yabe[2], T. Umemura[1] and M. Ishizuka[1]. *[1]Hokkaido Univ, Sapporo, Japan and [2]University of Zambia, Lusaka, Zambia.*

Metal pollution in African countries is serious problem. Metal and metallothionein (MT) levels in wild black rats (*Rattus rattus*) collected in mining area (Kabwe and Chingola) and control area (Lusaka) of Zambia were compared in order to assess effects of metal pollution on wild terrestrial animals. In addition, we exposed laboratory Wistar rat (*Rattus norvegicus*) to metal contaminated soil from Kabwe for 1 year in order to clarify biological and epigenetic effects of metals. In the laboratory soil exposure, male Wistar rats were divided to three groups by type of soil exposure; A) without soil exposed control, B) soil containing low metal levels (Pb: 75 mg/kg, Cd: 0.4 mg/kg) and C) soil containing high metal levels (Pb: 3757, Cd: 6). We analyzed metal and MT levels in various tissues of rats after 1 year exposure. Genome wide methylation status was determined in the liver, kidney and testis using LUMA (LUminometric methylation assay). Levels of DNA methyltransferase (Dnmt 1, Dnmt 3a and Dnmt 3b) mRNA expression in tissues were analyzed by quantitative real-time RT-PCR. In the field study, *R. rattus* in Kabwe accumulated significantly higher concentrations of Pb and Cd in various organs than rats from Lusaka. Higher MT-1/2 mRNA expression levels in *R. rattus* from Kabwe than those in rats from Lusaka were also observed. In the laboratory soil exposure, rats in the group C accumulated significantly high concentrations of Pb and Cd in liver, kidney, lung, brain and tibia compared to other groups. Significantly higher levels of MT-2 mRNA were expressed in the kidney of group C. Interestingly, Dnmt 3a/3b mRNA expressions and genome wide methylation status in testis were significantly higher in rats of group C, suggesting that Pb and Cd contaminated soil caused metal accumulation and epigenetic alteration in rat.

PS 1517 Improving Urine-Based Human Exposure Assessment of Short-Lived Chemicals Using Reverse Dosimetry and NHANES Physiological and Behavior Data: A Value-of-Information Approach for Bisphenol A

H. Shankaran[1, 3] and J. G. Teeguarden[1, 2]. *[1]Systems Toxicology and Exposure Science, Pacific Northwest National Laboratory, Richland, WA, [2]Department of Environmental and Molecular Toxicology, Oregon State University, Corvallis, OR and [3]Currently: Modeling and Simulation, AstraZenaca, Boston, MA.*

Assessment of human exposure to chemicals with short biological half-lives, for example, bisphenol A (BPA), from urine spot samples is subject to a unique set of uncertainties. The influence of these uncertainties on the distribution of human exposures derived from urine-spot samples is not known. We generated an NHANES-like synthetic set of urine spot sample BPA concentrations for a population of individuals using a physiologically based pharmacokinetic model, assumed distributions of exposures to BPA and physiological data (e.g. body weight, cardiac output) and behavioral data (e.g. fasting times, urine accumulation period, sampling time, distribution of meals) available in NHANES 2009-10. These data were used to reconstruct the distributions of human exposure to BPA using the conventional urine-flow method, and two PBPK model-based reverse dosimetry approaches. Replacing measured values with samples from distributions, the influence of each parameter on the accuracy of the reconstruction was assessed. The conventional urine-flow approach underestimated BPA exposure two fold at the mean. Where all parameters were known, the PBPK-model based approach accurately reproduced the exposure distribution. Fasting time had the greatest influence on the accuracy of the exposure reconstruction, followed by the urine accumulation period, and the distribution of BPA exposure over the course of the day. The tails of the distributions were affected most significantly, but mean values were typically within 10% of the actual values for the reverse dosimetry methods. Of the model-based reverse dosimetry approaches, the individual-based approach was more accurate than the Monte-Carlo sampling approach.

PS 1518 Cigarette Smoke-Induced Cytochrome P4501A1—Potential Biomarker of Endothelial Dysfunction

E. Fourie[1], J. Anderson[2], A. Warneke[4], K. Zehr[1], M. T. Walsh[1], M. Langsfeld[3] and M. K. Walker[1]. *[1]Pharmaceutical Sciences, University of New Mexico, Albuquerque, NM, [2]Pharmacy Practice and Administrative Sciences, University of New Mexico, Albuquerque, NM, [3]Surgery, University of New Mexico, Albuquerque, NM and [4]University of New Mexico Hospital, Albuquerque, NM.*

Endothelial dysfunction, the loss of endothelial-derived vasodilators, precedes the development of many cardiovascular diseases in smokers. Biomarkers of endothelial dysfunction are limited and none have been investigated specifically in the context of cigarette smoke (CS) exposure. We hypothesized that cytochrome P4501A1 (CYP1A1), an enzyme induced by CS in the vasculature, would represent a biomarker of endothelial dysfunction.

Methods. We exposed CYP1A1 wild type (WT) and knockout (KO) mice to mainstream CS for 2 hr/d 5 d/wk for 6 wks, and assessed endothelial-dependent vasodilation in pressurized mesenteric arterioles. Vessels were pre-constricted with phenylephrine and dose-dependent dilation to arachidonic acid (AA, 10^{-7}-$10^{-4.5}$ M) was assessed. We also recruited Hispanic, age- and sex-matched, healthy never (n=16) and current smokers (n=17), and measured flow-mediated dilation and CYP1A1 inducibility from serum using the CALUX assay.

Results. In mice, CS exposure significantly enhanced the dose-dependent vasodilatory response to AA in WT mice, but not in KO mice ($p<0.05$). In humans, we found that flow-mediated dilation was significantly impaired in cigarette smokers (never smoker, 12.5±1.5%; smoker, 5.8±1.4%; $p<0.05$), indicating endothelial dysfunction. While serum CYP1A1 inducibility was not detected in never smokers, it was detected in serum from 15 of 17 smokers. Further, we found that CYP1A1 inducibility tended to be positively correlated with flow-mediated dilation ($r=0.47$, $p<0.09$).

Conclusions. These data suggest CYP1A1 influences the vasodilation response following CS exposure and that serum CYP1A1 inducibility in cigarette smokers may be a biomarker of endothelial dysfunction.

Supported by University of New Mexico, Clinical Translational Science Center (HRRC 12-168), and Environmental Health Signature Program.

PS 1519 Rapid Determination of Mercapturic Acids from Acrylamide and Glycidamide in Human Urine

B. Wang, G. Zhao, S. Wang, J. Yu and F. Xie. *Zhengzhou Tobacco Research Institute, Zhengzhou, China.* Sponsor: R. Meng.

A sensitive and specific electrospray tandem mass spectrometry method using a column switching unit with trap column and analytical column was established to quantify the mercapturic acid (MAs) of acrylamide (AA) and glycidamide (GA) in human urine. Urine was spiked with deuterated internal standards and injected directly into LC–MS/MS. The Waters Symmetry ShieldTM RP18 and Waters Xbridge-C8 were used for trapping and hydrophilic MAs, respectively. With this method, the limits of quantitation for AAMA and GAMA in urine were 6ng/mL and 0.5ng/mL, respectively; the inter-day and intra-day precision of AAMA and GAMA ranged from 2.7% and 7.3%, and the recoveries ranged from 99.6% to 105.3%. The method was simple, sensitive and accurate. The developed method was also applied to analysis urines of smokers and nonsmokers, results showed that amount of AAMA, GAMA in smokers urine were much higher than that in nonsmokers, indicating that AAMA and GAMA may be effective biomarkers to estimate acrylamide exposure in smoking.

PS 1520 Oxidized Cardiolipins As a Biomarker of Mitochondrial Dysfunction Triggered by Pesticide, Rotenone

Y. Tyurina[1], A. Vikulina[1], V. Kapralova[1], D. Winnica[1], L. Sanders[2], T. Greenamyre[2], V. A. Tyurin[1] and V. E. Kagan[1]. [1]*EOH, University of Pittsburgh, Pittsburgh, PA and* [2]*Neurology, University of Pittsburgh, Pittsburgh, PA.*

Exposure to a commonly used pesticide, rotenone, has been associated with the development of Parkinson's disease. We demonstrated that treatment of human blood lymphocytes with rotenone resulted in decreased mitochondrial membrane potential, inhibition of mitochondrial respiratory complex I, induction of apoptosis and selective oxidation of mitochondrial phospholipid, cardiolipin (CL). Here, we used rat rotenone-infusion Parkinson disease model to assess possible accumulation of peroxidized phospholipids. Adult male Lewis rats (6 months old) were exposed to rotenone daily (3 mg/kg, I.P.) and sacrificed 1, 5 and 10-14 days thereafter. Substantia nigra was isolated and lipids were extracted. To enhance the sensitivity of LC-MS protocols for the detection of oxidation products, phospholipids were treated either with phospholipase A1 from Thermomyces lanuginosus (10 μl/μmol phospholipids) or phospholipase A2 form porcine pancreas (10U/μmol of phospholipids) to release fatty acids residues from sn-1 and sn-2 position, respectively. Using the combination of lipidomics and oxidative epitope-targeted enzymatic digestion of total phospholipids we found a decrease of polyunsaturated fatty acids (PUFA) esterified into phospholipids on day 1 and 5 after expose. In addition we were able to detect oxygenated species of PUFA that were represented by their hydroxy-derivatives. Moreover, a decrease of CL species containing PUFA and accumulation of its oxygenated molecular species was oserved. We conclude that CL oxygenation products may represent a new biomarker of rotenone-induced mitochondrial dysfunction associated with Parkinson disease. The study was approved by the Institutional Animal Care and Use Committee at the University of Pittsburgh in accordance with the guidelines published by the NIH. Supported by NIH ES020693, U19 AI068021, NIOSH OH008282.

PS 1521 N^6-Formyllysine As a Biomarker of Formaldehyde Exposure: Inhalation Studies in Rats Reveal Formation and Accumulation of N^6-Formyllysine Adducts in Nasal Epithelium

B. Edrissi[1], K. Taghizadeh[2], B. C. Moeller[3, 4], R. Yu[3], D. Kracko[4], M. Doyle-Eisele[4], J. A. Swenberg[3] and P. C. Dedon[1, 2]. [1]*Department of Biological Engineering, Massachusetts Institute of Technology, Cambridge, MA,* [2]*Center for Environmental Health Sciences, Massachusetts Institute of Technology, Cambridge, MA,* [3]*Department of Environmental Sciences and Engineering, University of North Carolina, Chapel Hill, NC and* [4]*Lovelace Respiratory Research Institute, Albuquerque, NM.*

There is increasing recognition that aberrant protein modifications play an important role in the pathophysiology of many human diseases. N^6-Formyllysine, a chemical homolog of the biologically important N^6-acetyllysine, has recently emerged as a widespread modification of proteins. With formaldehyde as the major source of N^6-formyllysine, we quantified endogenous and exogenous adducts in nasal epithelium of rats exposed by inhalation to 0.7, 2, 5.8, and 9.1 ppm [$^{13}C^2H_2$]-formaldehyde using liquid chromatography-coupled tandem mass spectrometry. Exogenous adducts were detected in nasal epithelium and not in lung, liver, or bone marrow, with concentration-dependent formation in total and fractionated (cytoplasmic, membrane, nuclear) proteins. Endogenous adducts dominated at all exposures, with a 6 hr 9.1 ppm exposure resulting in one-third of the total load of N^6-formyllysine being derived from exogenous sources. We have further examined N^6-formyllysine accumulation in several tissues from rats exposed by inhalation to 2 ppm [$^{13}C^2H_2$]-formaldehyde for 7, 14, 21, and 28 days (6hr/day) and determined loss of N^6-formyllysine over a 7 day post exposure period. Our results showed detection and accumulation of exogenous adducts in nasal epithelium and not in lung, liver, or bone marrow, with exogenous N^6-formyllysine levels showing a 2-fold increase over a 3-week exposure period. The post exposure studies indicateda $t_{1/2}$ of ~50 h for this adduct in total proteins. Formation and accumulation of N^6-formyllysin in proteins, including histones with important epigenetic regulatory roles, could be another mechanism contributing to formaldehyde toxicity and carcinogenicity.

PS 1522 Serial Measurements of BPA and BPS in Texas Mother-Infant Pairs from the 3rd Trimester of Pregnancy through the 4th Month of Lactation

A. J. Schecter[1], D. Cherry[2], C. Liao[3], S. Yun[3], K. Kannan[3], J. Moye[4], N. Thiex[5], W. C. Shropshire[1] and L. S. Birnbaum[6]. [1]*University of Texas School of Public Health, Dallas, TX,* [2]*University of Washington, Seattle, WA,* [3]*Wadsworth Laboratory, Albany, NY,* [4]*NICHD, NIH, Bethesda, MD,* [5]*South Dakota State University, Brookings, SD and* [6]*NCI, NIH, RTP, NC.*

Relatively little is known about in utero or early infancy exposure to Bisphenol A (BPA) and related bisphenols. Here we report on a formative prospective cohort study to monitor exposure to BPA and a BPA substitute, Bisphenol S (BPS), in mother-infant pairs in a rural Texas county. Participants were recruited from a pool of consented National Children's Study (NCS) mothers as well as volunteers from the same clinics as part of an NCS formative research project. The use of human subjects was approved by the IRB of the University of Texas Health Science Center at Houston and Battelle's IRB. Specimens were collected prospectively from the third trimester of pregnancy through the fourth month of lactation from 10 mother-infant pairs who completed the protocol. BPA and BPS were analyzed in 86 urine, 50 breast milk, and 7 plasma samples utilizing enzymatic hydrolysis followed by high performance liquid chromatography coupled with electrospray triple-quadrupole mass spectrometry. These data document measurement of BPA and BPS in each of these matrices: urine, plasma and milk. Maternal urine specimens here had higher geometric mean (GM) concentrations of BPA (2.04 ng/mL wet wt [ww]) and BPS (0.52 ng/mL ww) than infant urine BPA (1.85 ng/mL ww) and BPS (0.19 ng/mL ww). The breast milk GM concentration of BPA (0.52 ng/mL) was higher than the BPS concentration (0.07 ng/mL). BPA and BPS breast milk GM concentrations increased from one month (0.41 and 0.06 ng/mL respectively) to four months postpartum (0.64 and 0.14 ng/mL respectively). This study documents that a BPA substitute, BPS, is detectable in human urine, plasma and breast milk and suggests the importance of monitoring for potentially toxic chemical substitutes for BPA. This study was funded by NIH.

PS 1523 Measurement of Endogenous and Exogenous 1, N^2-Propano-Deoxyguanosine DNA Adducts by Liquid Chromatography—Tandem Mass Spectrometry

B. C. Moeller[1, 2], W. Bodnar[2], L. Collins[2] and J. A. Swenberg[2]. [1]*Lovelace Respiratory Research Institute, Albuquerque, NM and* [2]*Environmental Sciences and Engineering, University of North Carolina, Chapel Hill, NC.*

1,N^2-Propano-dG is a mutagenic DNA adduct formed by the reaction of 2'-deoxyguanosine (dG) with crotonaldehyde, a lipid peroxidation by-product. This lesion can also be formed by the reaction of two acetaldehyde (AA) molecules with dG to form an identical adduct. AA and crotonaldehyde are highly reactive chemicals that form a number of lesions on cellular macromolecules including DNA and proteins. AA is a ubiquitous environmental chemical with a variety of human exposures from industrial/occupational activities, consumer products, lifestyle choices (food/alcohol/cigarette consumption), and environmental sources. AA is also formed following the metabolism of vinyl acetate and ethanol. In addition, AA is endogenously produced as a by-product of cellular respiration and metabolism. Since both compounds are endogenously present and can have exogenous exposures, a sensitive 2-dimensional HPLC-tandem mass spectrometry method was developed to quantitate endogenously and exogenously formed 1,N^2-propano-dG adducts using [$^{13}C_2$]-stable isotope exposures. The method monitored the endogenous and exogenous (+2 and +4 m/z) adducts using selected reaction monitoring allowing for the differentiation between the potential causative agents for the formation of the lesion. The method was validated and had a limit of detection of 1 fmol on column. Reactions of AA and [$^{13}C_2$]-AA with an amino acid catalyst were used to confirm the ability to differentiate between labeled and unlabeled adducts with a 1:2:1 formation ratio between the different isotopic forms. Endogenous 1,N^2-Propano-dG was quantitated in non-exposed rodent lungs.

PS 1524 Relationship between Long-Term Exposure to Great Lakes Contaminants and Hematological Parameters in Great Lakes Anglers

F. D. Stephen[1], L. Georger[1], M. R. Bonner[3], P. J. Kostyniak[2, 3], J. R. Olson[2, 3], M. S. Bloom[4] and J. E. Vena[5]. *[1]Math & Natural Sciences, D'Youville College, Buffalo, NY, [2]Pharmacology & Toxicology, State University of New York at Buffalo, Buffalo, NY, [3]Social & Preventive Medicine, State University of New York at Buffalo, Buffalo, NY, [4]Environmental Health Sciences, State University of New York at Albany, Albany, NY and [5]Epidemiology and Biostatistics, University of Georgia, Athens, GA.*

The New York State Angler Cohort (NYSAC) was established to assess the association between past and current consumption of contaminated sport fish and wild life (duck and turtle) and both short-term and long-term health effects. Based upon reported consumption of Lake Ontario fish and wildlife and validated exposures to halogenated aromatic hydrocarbons (serum PCB153 and Mirex) a subgroup of the cohort was selected to participate in studies that would examine the effect that fish or fish/wildlife consumption has on different hematological and immune markers. Participants were divided into two groups; consumers with the highest serum mirex and PCB153 levels that also self reported consumption of Lake Ontario wildlife (n=27) and non-consumers who were matched to by age, sex and geographic area and reported having never consumed Lake Ontario wildlife (n=16). The objective of the current study was to analyze differences in hematological parameters in these groups including white blood count, red blood count, hemoglobin levels, hematocrit levels, platelet count and full leukocyte differential. In anglers with serum DDE levels (n=14) higher than that observed in non-consumers, our results showed positive correlations (albeit clinically insignificant) with increased red blood cell count (r=.632, p=.015), hemoglobin levels (r=.590, p=.027), hematocrit percentage (r=.589, p=.027) and decreased platelet counts (r=-.570, p=.033). From these data we concluded that long term consumption of fish and/or wildlife contaminated with persistent Great Lakes pollutants does not significantly alter hematological markers in humans. (Supported in part by ATSDR, Grant H75-ATH 298338)

PS 1525 Biomarkers of Acute Whole-Body Irradiation in the Göttingen Minipig

J. N. Smith, J. Lovaglio, J. Creim, R. K. Piper, E. Baker, K. Burnum-Johnson, P. Piehowski, R. D. Smith and K. D. Thrall. *Pacific Northwest National Laboratory (PNNL), Richland, WA.*

Current medical treatments for acute exposure to ionizing radiation are limited, and improved prophylactic and therapeutic methods are needed to protect and treat military personnel, first responders, and the general public from health hazards associated with ionizing radiation exposure. Efficacy trials of prospective therapeutics in humans are not feasible or ethical, and in such cases, the U.S. Federal Drug Administration (FDA) requires efficacy studies conducted in an appropriate, well-characterized animal model ("the Animal Rule" 21 CFR 314.600 for drugs). As part of that effort, we are characterizing biomarkers of acute whole-body irradiation in the Göttingen minipig. Minipigs were irradiated at historical 0 (sham), LD_{25}, LD_{50}, and LD_{75} dose levels using ^{60}Co as the radiation source. Blood was collected at regular intervals from 6 hr to 45 d post exposure. Biomarkers were quantified including blood cell differentials and chemistries; targeted biomarkers with enzyme-linked immunosorbent assay (ELISA) such as interlukin-6 (IL-6), C-reactive protein (CRP), and serum amyloid A (SAA); and global plasma protein kinetics with liquid chromatography coupled with ion mobility spectrometry and time of flight mass spectrometry (LC-IMS-TOF MS). Ongoing analyses demonstrate dose-dependent decreases in white blood cells and platelets (among other measures) and increases in biomarkers (including IL-6, CRP, and SAA) at or near the time of death. These biomarkers support the use of the Göttingen minipig as an animal model to evaluate medical countermeasures for acute radiation exposure. Work supported under Biomedical Advanced Research and Development Authority (BARDA) Contract No. HHSO1003300TI and PNNL Laboratory Directed Research.

PS 1526 Biomarkers of Aflatoxin Exposure in Bexar and Surrounding Counties: Enhanced Incidence in Humans following Severe Drought

S. Elmore[1], L. Tang[2], M. Rodriguez[3], M. F. Carden[3], H. G. Hayes[3], A. A. Romoser[1], J. Wang[2], B. H. Pollock[3] and T. D. Phillips[1]. *[1]Veterinary Integrative Biosciences, Texas A&M University, College Station, TX, [2]College of Public Health, University of Georgia, Athens, GA and [3]University of Texas Health Science Center-San Antonio, San Antonio, TX.*

Aflatoxins (AF) are produced as metabolites by the fungi *Aspergillus flavus* and *A. parasiticus* and frequently contaminate important commodities such as corn and peanuts. Drought and plant stress promote the growth of these fungi which can lead to the production of AFs. Aflatoxin B1 is the most prevalent and toxic of the AF congeners and is a known risk factor for development of hepatocellular carcinoma. The area between 40° N and S of the equator is now considered to be a "hotspot" for exposure, which includes parts of the Southern and Midwestern United States. With greater than 75% of the U.S. experiencing moderate to exceptional drought in 2012, and climate change that favors fungal growth, a wider distribution of *Aspergillus* and higher prevalence of AF contamination in staple foods such as corn is expected. In an ongoing clinical trial initiated in August 2012, a predominantly Hispanic study population in South Texas was screened for AF exposure through analysis of a short-term urinary AF biomarker, AFM1. AFM1 was detected in 22.05% (45/204) of study participant urines with an overall mean and range of 4.735±19.78 and ND-180.73 pg/mg creatinine, respectively. The levels and prevalence of AFM1 detected in 2012 were sustained throughout most of the sampling conducted in 2013, suggesting that the drought of 2012 played a key role in human AF exposures. Detection of urinary AFM1 was significantly associated with increased frequency of tortilla (p=0.0157) and peanut (p=0.0084) consumption, in addition to the amount of Mexican food (p=0.0006) and corn products (p=0.0208) ingested. Further work is warranted to correlate our findings with long-term serum biomarkers to reflect steady state exposures and associated impacts on health. This research was supported by NIH 1RO1MD005819-01.

PS 1527 Inflammatory Cytokine Profiles in the Plasma and Saliva of Chronic Smokers and Moist-Snuff Consumers

G. L. Prasad and B. A. Jones. *R & D, RJ Reynolds Tobacco Co, Winston-Salem, NC.*

Chronic cigarette smoking causes inflammation, as evidenced by higher White Blood Cell counts (WBCs) and other leukocyte subsets. While some reports indicate that generally healthy smokers (SMK) exhibit changes in the cytokines and other inflammatory mediators, additional work is needed in this area. Further, it has not been reported whether consumers of non-combustible tobacco, such as moist snuff, also experience increased inflammation. Recently, we observed that in contrast to SMK, the levels of WBCs and several major leukocyte subtypes in Moist Snuff Consumers (MSC) resemble more closely the Non-Tobacco Consumers (NTC). Here we present the levels of selected inflammatory cytokines from tobacco consumers from the same study.

Cytokine profiles of Human Inflammation MAP v1.0 panel (Myriad RBM) were generated from plasma and saliva samples collected from generally healthy adult male study subjects from SMK, MSC and NTC cohorts who fasted overnight from food and tobacco. Detailed bioinformatic analyses revealed that some cytokine levels are useful for differentiating the study cohorts. Among the most significant differences between SMK and NTC cohorts were Intracellular Adhesion Molecule 1 and Matrix Metalloproteinase-9 from plasma and Monocyte Chemotactic Protein-1 from saliva. The levels of these three cytokines, among others, were also significantly different between SMK and MSC cohorts. The differences between the two nonsmoking (MSC and NTC) cohorts, however, were fewer: levels of plasma ferritin, and salivary α1-Antitrypsin, α2 macroglobulin and fibrinogen differed between the MSC and NTC cohorts. Comparative analyses of the nonsmoking (MSC plus NTC) and smoking (SMK) cohorts revealed that additional cytokines such as interleukin-8 emerged as being highly significant ($p<0.01$). Overall, these findings show that SMK exhibited most differences in the inflammatory cytokine levels and suggest increased inflammation relative to MSC and NTC cohorts, with far fewer differences detected between MSC and NTC.

PS 1528 An Evaluation of Candidate Biomarkers of Biological Effect in Baseline Samples from Smokers, Never-Smokers, and Ex-Smokers

F. J. Lowe, L. E. Haswell, E. Papadopoulou, C. J. Shepperd and N. Newland. *Biosciences, British American Tobacco, Southampton, Hampshire, United Kingdom.* Sponsor: C. Meredith.

Biomarkers have been proposed as potential tools to assess the toxicity and disease risk of tobacco product use. Two key requirements of such biomarkers are that they are able to consistently distinguish between smokers and non-smokers, and that they are reversible upon smoking cessation. Candidate biomarkers were recently assessed for these requirements in a six month, clinical study based in Germany1. Biomarker levels from the baseline study time point were compared in 143 smokers, 61 never-smokers and 61 ex-smokers who were otherwise healthy and age/gender matched. Of the 27 candidate biomarkers assessed, the following were found to be significantly different between smokers and never-smokers; urinary 8-epi-PGF2α (Type III) and 11-dehydrothromboxane B2 ($P<0.001$), plasma MCP-1, neutrophil elastase, leukotriene B4, ascorbic acid, HDL and oxidised LDL cholesterol (all $P<0.001$), erythrocyte catalase activity and malondialdehyde (all $P<0.0001$), serum total anti-oxidant capacity ($P<0.0001$) and total white blood cell (WBC), neutrophil and monocyte count (all $P<0.0001$). Of these biomarkers urinary 8-epi-PGF2α (Type III), plasma MCP-1, neutrophil elastase, leukotriene B4, ascorbic acid, HDL and oxidised LDL cholesterol, erythrocyte catalase activity and serum total anti-oxidant capacity, total white blood cell (WBC), neutrophil and monocyte count were also found to be significantly different between current and ex-smokers ($P<0.05$), and hence indicate the potential for reversibility. These data indicate that 12 of 27 candidate biomarkers assessed in this study are potentially useful tools for the assessment of altered biological effects following a switch from a conventional combustible tobacco product, to a novel tobacco product with reduced machine-smoked toxicant yields or non-combustible nicotine delivery products, and in smoking cessation studies.

1.Shepperd C, Newland N, Eldridge A, Graff D, Meyer I. BMC Public Health. 2013; 13: 690. Registration No. ISRTCN81286286

PS 1529 Effects of Cadmium on Olfactory-Mediated Behaviors and Molecular Biomarkers in Coho Salmon

C. R. Williams and E. P. Gallagher. *Environmental and Occupational Health Sciences, University of Washington, Seattle, WA.*

The salmon olfactory system is sensitive to the toxic effects of metals. We analyzed olfactory-mediated alarm response behaviors, epithelial injury, and a suite of molecular biomarkers of olfactory function in juvenile coho salmon following acute exposures to cadmium (Cd). The molecular biomarkers analyzed included: four G-protein coupled receptors (GPCRs) representing the two major classes of odorant receptors (salmon olfactory receptor sorb and vomeronasal receptors svra, svrb, and gpr27); a marker of neurite outgrowth (nrn1); and markers of antioxidant responses to metals, including heme oxygenase 1 (hmox1) and peroxiredoxin 1 (prdx1). Coho received acute exposures to 3.7 ppb or 347 ppb Cd, and a subset of treated fish was then housed in clean water for 16 days before analysis. Coho exposed to 347 ppb Cd over 48 hrs exhibited a reduction in freeze responses as well as an extensive loss of olfaction accompanied by histological injury to the olfactory epithelium. This olfactory injury was accompanied by significant decreases in gene expression of the olfactory GPCRs and increased expression of hmox1. Persistent behavioral deficits, histological injury and altered expression of a subset of olfactory biomarkers were still evident in Cd-exposed coho following a 16-day depuration. Exposure to 3.7 ppb Cd also resulted in reduced freeze responses and histological changes to the olfactory epithelium within 48 hrs of Cd exposure, although the extent of olfactory injury was less severe than observed for fish in the high dose Cd group. Furthermore adverse behavioral effects were present in some coho receiving the low dose of Cd even following a 16-day depuration. In summary, acute exposures to environmental levels of Cd can cause persistent olfactory injury in coho salmon. Mechanism-based biomarkers of oxidative stress and olfactory structures can augment the evaluation of olfactory injury manifested at the physiological level. Supported by NIEHS P42 ES04696.

PS 1530 The Effect of Cigarette Smoke Exposure on the Proteomic Composition of Human Bronchial Epithelial Cell Airway Surface Liquid

G. J. Phillips[1], L. E. Haswell[1], C. Meredith[1], W. Fields[2], L. McIntosh[3], D. Chelsky[3], L. Cortes[3] and P. Croteau[3]. [1]*Bioassessment, British American Tobacco, Southampton, United Kingdom,* [2]*Bioassessment, R J Reynolds Co, Winston-Salem, NC and* [3]*Caprion Proteomics Inc, Montréal, QC, Canada.*

Human bronchial epithelial cells (HBEC) cultured in vitro secrete mucins and other proteins that mimic in vivo airway surface liquid (ASL). This study used proteomics to determine HBEC ASL composition and the effect of cigarette smoke exposure. A mass spectrometry multiple reaction monitoring (MRM) assay was also developed to quantify the ASL proteins that significantly changed after smoke exposure. HBECs were exposed to low dose or high dose cigarette smoke or air. ASL was collected, processed and analysed by reversed phase liquid chromatography-mass spectrometry and tandem mass spectrometry. ASL characterisation identified 487 proteins with high confidence, these included mucins and non-mucin proteins involved in cytoskeletal, signalling, proteolytic, calcium binding and immune system pathways. Smoke exposure resulted in significant differential protein expression with the greatest changes occurring 48 hours after low dose smoke exposure. The majority of differentially expressed proteins are related to inflammation and immune response, calcium binding and homeostasis, squamous cell differentiation and keratinocytes, protein metabolism, and oxidative stress. A MRM assay was developed for 154 proteins, of which 133 proteins were detected in ASL samples. Over 100 proteins were differentially expressed, with most proteins being up-regulated 48 hours after low dose smoke exposure. ASL analysis has been shown to be compatible with a proteomic approach. Many of the proteins identified have been previously detected in sputum, indicating HBEC ASL may be used to model smoke exposure in vitro. Construction of a smoke exposure specific MRM assay enables the quantitation of over 100 proteins in a single sample which may be used to further investigate the effects of smoke exposure in both in vitro ASL and in vivo sputum samples.

PS 1531 Metabolomic Analysis of the Effect of Occupational Exposure to Pyrethroid Pesticides

M. Ratelle[1], M. Bouchard[1] and C. Lin[2]. [1]*Department of Environmental Health and Occupational Health, University of Montréal, Montréal, QC, Canada and* [2]*Institute of Environmental Health, National Taiwan University, Taipei, Taiwan.*

Pyrethroids are one of the most commonly used insecticides in agriculture. They can cause neurotoxic, immune and endocrine effects. Perturbations of mechanistic pathways leading to such effects are however poorly understood. A recent approach in toxicology is to observe changes in endogenous metabolites to inform on mechanisms of toxicity. In an attempt to identify a possible spectrum of biomarkers of adverse effects of pyrethroids, a preliminary metabolomic analysis of urine samples of workers exposed to pyrethroids was conducted. Thirty agricultural workers from three different farms exposed to cypermethrin provided a complete first morning urine void before and after application or work in a treated-area (following the required re-entry delay). Metabolomic analyses of urine samples were conducted by 1H nuclear magnetic resonance (NMR) followed by orthogonal partial least squares discriminant analysis (OPLS-DA). Non-parametric Wilcoxon statistical analyses were conducted given the small sample size and the neither normal nor log-normal distribution of biomarkers. The results of OPLS-DA model show two different clusters between the pre-exposure and the post-exposure samples. Higher hippurate levels were found in post-exposure urine samples ($p<0.0001$), but lower excretion levels of betaine ($p=0.019$), guanidoacetate ($p=0.004$), lysine ($p<0.05$), alanine ($p=0.07$) and threonine ($p=008$). Hippurate is produced in presence of benzoic acid coming from exogenous or endogenous precursors and glycine. The main exogenous metabolite of pyrethroids is 3-phenoxy-benzoic acid, a possible substrate to hippurate. Hippurate is an uremic toxin, which interferes with normal physiological and metabolic processes; it is involved in the correction of metabolic acidosis, developing into one of the key consequences of kidney function reduction and acceleration of kidney disease progression. These metabolomic changes warrant further investigations of the possible mode of action of pyrethroids.

PS 1532 Development of Method for Detection of Aflatoxin B1-Lysine Adduct in Dried Blood Spot Samples

K. S. Xue, L. Tang, Y. Wang, M. Kang and J. Wang. *University of Georgia, Athens, GA.*

There is an increasing concern on aflatoxin (AF) associated growth and development inhibition among children. Previously, longer AF exposure was mainly previously assessed by analyses of serum AFB-lysine adduct. However, serum anal-

ysis involved withdrawal of blood with needle stick which limits the applicability to infants and young children. In this study we developed a method to detect AFB-Lysine adduct in dried blood spots (DBS) samples. Commercially available DBS cards were evaluated for accuracy to hold different quantity of whole blood. Different washing strategies were tested to effectively elute bound blood components, especially for total protein and albumin spotted on DBS card. The recovery is >95% with the optimized washing conditions. To further validate the method, F344 rats were dosed with a single dose of AFB1 of 0, 25, 75, 225, or 675 μg/kg bw or a repeated dose of AFB1 of 5, 10, 25, and 75 μg/kg bw for two weeks. Whole blood samples from dosed animals were collected via cardiopuncture before sacrifice and immediately processed to DBS cards (6 cards per animal) and stored at 4°C until analysis. The remaining blood was prepared for serum to serve as the control. The DBS cards containing AFB-lysine adducts were washed and extracted for recovering the total protein and albumin, which were measured and digested with pronase to release mono-AFB-lysine adduct. The digests were further concentrated and purified with the solid-phase extraction. The eluate was dried and reconstituted for analysis with HPLC-fluorescence detection using the same protocol for analysis of serum samples. The similar limit of detection of AFB-lysine adduct was achieved with the DBS cards, however, the recovery of the spiked levels of AFB-lysine adduct was lower (10-20%) in the whole blood DBS than the serum, which suggested that certain components in the whole blood may interfere with the recovery. Further study would aim to resolve the interference factors, in particular the hemoglobin components, in the colorimetric reading for protein quantification as well as the adduct enrichment process.

PS 1533 Toxic Effects of Low-Level Arsenic Exposure on Erythrocyte and Its Membrane Proteins in Male Rats

Q. Pei[1], J. Zhang[1], Y. Gao[1], F. Tian[1], N. Ma[2], C. Ma[1], Y. Miao[1] and X. Qin[3]. *[1]Shanxi Medical University, Taiyuan, Shanxi, China, [2]Suzuka University of Medical Science, Suzuka, Japan and [3]China Institute for Radiation Protection, Taiyuan, China.* Sponsor: P. Zhou.

Aim: The purpose of this study was to examine changes of the erythrocyte and RBC membrane proteins in male rats exposed to low-level arsenic through drinking water and to further explore the potential biomarkers of chronic arsenic poisoning.
Methods: 40 male Sprague-Dawley rats (body weight 140-160g) were randomly divided into 4 equal groups and repectively provided ad libitum access to drinking water containing sodium arsenite dissolved in tap water at arsenic levels of 0, 10, 60 and 360μg/L for 30 days. The RBC toxic effects were detected by different indicators and methods, including RBC parameters (Automated Hematology Analyzer), eryptosis rate (Flow Cytometry), erythrocyte morphology (Scanning Electron Microscopy). Erythrocyte membrane proteins were analyzed by sodium dedecyl sulfate-polyacrylamide gel electrophoresis (SDS-PAGE) and Immunofluorescence Assay (IFA).
Results: The results revealed that, compared with the control group, RBC parameters have not abnormal changes in exposure groups, but eryptosis rate increased significantly in 360μg/L arsenic exposure group. In the As treatment groups, and particularly in 360μg/L group, we observed more irregular-shaped erythrocytes and spheroechinocytes. Electrophoretic analysis showed decreased ankyrin expression and increased band 3 expression in 360μg/L dose group. Immunofluorescence confirmed that band 3 and CD35 increased and clustered to the RBC membrane in rats exposed to arsenic.
Conclusions: This study suggests that low levels of arsenic exposure can produce toxic effects on erythrocyte, resulting in increased eryptosis and abnormal RBC morphology, which may be related to erythrocyte membrane proteins abnormalities. Erythrocyte membrane proteins are more sensitive to low-level arsenic than RBC number and morphology. Erythrocyte membrane proteins may be the early biomarkers in patients of chronic arsenic poisoning.

PS 1534 Determination of Aflatoxin M1 in Breast Milk As a Biomarker of Maternal and Infant Exposure in Colombia

P. Sánchez[2] and G. Diaz[1]. *[1]Salud Animal - Facultad de Veterinaria, Universidad Nacional de Colombia, Bogota, Colombia and [2]Toxicología - Facultad de Medicina, Universidad Nacional de Colombia, Bogota, Colombia.*

Aflatoxins are secondary fungal metabolites that can contaminate human food supplies. Four aflatoxins are produced by fungi, being aflatoxin B1 (AFB1) the most common and toxic. AFB1 is considered to be the most potent naturally occurring liver carcinogen known to humans. Chronic exposure causes hepatocellular carcinoma with prevalence 16–32 times higher in developing countries compared to first-world countries. Aflatoxin M1 (AFM1) is a monohydroxylated metabolite from AFB1 that is secreted in milk and can be used as a biomarker of exposure to AFB1. Ingestion of contaminated food during pregnancy and lactation may expose the newborn to the deleterious effects of aflatoxins. For these reason, efforts made to measure toxins in breast milk are important to establish the contribution of these toxins to public health, especially to the health of the newborn.
The aim of the present study was to determine AFM1 levels in human breast milk using immunoaffinity column cleanup with high performance liquid chromatography and fluorescence detection. An in-house version of the ISO method used for cow's milk was performed. Breast milk samples were obtained from 50 nursery mothers chosen from those attending The Mercy Hospital Foundation located in Bogota, Colombia. Volunteers filled in a questionnaire giving their consent to analyse their samples and details of their socio-economical, demographical and clinical data. The intake of dietary sources of aflatoxins was assessed using a food frequency questionnaire.
A total of 45 of the samples tested positive for AFM1 (median 5.2 ng/L; range 0.9-18.5 ng/L). The present study demonstrates a high exposure of mothers and neonates to AFB1 and AFM1 in Colombia, and shows the need to regulate the presence of aflatoxins in human foods. Further research is needed to determine the presence of mycotoxins in foods and biological fluids as well as to device protection strategies in a country where mycotoxins in human foods are not regulated.

PS 1535 Association of Neuroantibodies (NAb), Lead (Pb), Vascular, and Inflammatory Biomarkers in Hemodialysis Patients (HD)

D. Mason[1] and H. A. El-Fawal[2]. *[1]ANephRx Core Laboratory, Albany College of Pharmacy and Health Sciences, Albany, NY and [2]Neurotoxicology Laboratory, Albany College of Pharmacy and Health Sciences, Albany, NY.*

Vascular disease, a complication of renal failure, contributes to neurodegeneration. Cognitive decline, with white matter involvement, and heavy metal accumulation have been reported in HD patients. This study investigated the association of BPb, intercellular- and vascular cell adhesion molecules (ICAM and VCAM), fibroblast growth factor-23 (FGF23) and Fetuin-A (FA) with NAb, IgG, against neurofilaments (NF-L, NF-M, NF-H), GFAP and myelin basic protein (MBP) in 229 HD patients. NAb against all proteins were significantly prevalent in HD, with anti-NF-H and anti-GFAP (90 and 80%, respectively) the most prevalent. All titers significantly correlated with each other ($r=0.4$-0.9; $p<0.0001$). Anti-NF-M, VCAM and FGF23 ($p<0.05$) correlated with BPb. ICAM, but not VCAM, directly ($p<0.001$) correlated with all NAb titers, while FA and FGF23 inversely correlated with NAb ($p<0.01$). Multivariable regression ($R^2=0.2$-0.4) indicated that the major determinants of anti-NF-M, NF-H, GFAP and MBP titers were BPb ($p<0.02$), FA ($p<0.0001$) and VCAM ($p<0.01$). ICAM was a significant ($p<0.001$) determinant for all, but GFAP. For anti-NF-L ($R^2=0.4$), the major determinants were FA ($p<0.0001$) and ICAM ($p<0.01$). The present study demonstrates a strong association between BPb in HD patients and biomarkers of nervous system insult, as well as the association with vascular markers. ICAM and VCAM biomarkers have been associated with neurodegenerative diseases and cognitive decline. FA is believed to be neuroprotective, its decline indicating risk as suggested in the literature. While FGF23 may pose a risk for cardiovascular disease, its activities mediated through klotho are believed to be protective. This is consistent with the inverse association with NAb. Taken together, this study demonstrates the utility of NAb as biomarkers and their strong association with factors that may contribute to neuropathology in HD patients.

PS 1536 Identification of Marker Components in the Volatile Organic Emissions of Fusarium Fungi

E. Savelieva[1], A. S. Radilov[1], A. I. Ukolov[1], T. Y. Gagkaeva[2], O. P. Gavrilova[2], N. S. Khlebnikova[1] and V. R. Rembovskiy[1]. *[1]Research Institute of Hygiene, Occupational Pathology and Human Ecology, Leningrad Region, Russian Federation and [2]All-Russia Research Institute of Plant Protection, St. Petersburg-Pushkin, Russian Federation.* Sponsor: K. Khamidulina.

The metabolomics of microorganisms, in particular, Fusarium micromycetes, places special focus on the quantitative and qualitative composition of their emitted volatile organic compounds (VOC), because the latter serve as markers in the identification and differentiation of toxin-producing fungi. The profile of VOCs emitted by microorganisms and, consequently, the set of markers indicative of the presence of certain microorganisms in the analyzed object depend on the experimental conditions. For reproducible metabolic profiles some standard experimental conditions should be developed and commonly accepted. To this end, more information on the metabolic profiles of microorganisms in various experimental conditions should be accumulated.

We performed a comparative study of the VOC profiles of *F. cerealis, F. culmorum, F. graminearum, F. langsethiae, F. poae*, and *F. sporotrichioides* strains at varied times of culturing in potato dextrose agar, using gas chromatography-mass spectrometry combined with solid-phase microextraction. The parameters subject to standardization in this technique are the type of microfiber and sampling temperature.
The experiments involved passive sampling VOCs on a carbon microfiber at 40°C from the equilibrium vapor over live toxin-producing fungi cultures grown in GC vials.
Evidence was obtained for close correlation between the quantity of trichodiene (marker of trochotecene toxins) emitted by Fusarium fungi and the quantity and composition of sesquiterpenes in the emissions. A series of marker VOCs emitted by Fusarium fungi in much higher concentrations than trichodiene were detected and structurally characterized. Research on their specificity is in progress.
The work was supported in part by the Russian Foundation for Basic Research (project no. 12-04-00927-a).

PS 1537 Smoking, Vitamin E Supplement Use, and Prostate Cancer Survival

K. Zu[1] and E. Giovannucci[2]. [1]*Gradient, Cambridge, MA and* [2]*Harvard School of Public Health, Boston, MA.* Sponsor: J. Goodman.

Smoking is associated with increased risks of prostate cancer incidence and mortality. The effect of Vitamin E in prostate cancer prevention has been hypothesized to be modified by smoking. Therefore, we examined the associations of prediagnostic smoking and vitamin E supplement use with survival, as well as with tumor biomarkers, among prostate cancer patients. For 6,025 men diagnosed with prostate cancer between 1986 and 2012 in the Health Professionals Follow-Up Study, we obtained information on smoking and other lifestyle factors through questionnaires and ascertained cancer-specific mortality from 1986 through June, 2013. We used Cox regression to estimate hazard ratios (HRs) and 95% confidence intervals (CIs), and employed tissue microarrays and immunohistochemistry to assess tumor biomarkers in a subset of men. Being a current smoker, or quitting smoking for less than a decade prior to cancer diagnosis (recent past smokers) was associated with poorer survival (HR=1.84, 95% CI: 1.27-2.68 and HR=1.36, 95% CI: 0.97-1.91, respectively), compared to never smokers. Men who had quit smoking for more than a decade (remote past smokers) at diagnosis had risks of cancer-specific mortality similar to those who never smoked (HR=1.05, 95% CI: 0.86-1.27). Among never or remote past smokers, vitamin E supplement use did not appear to change mortality risk (HR=1.03, 95% CI: 0.87-1.22). However, for current or recent past smokers, vitamin E supplement use reduced their mortality risk to a level similar to that of never smokers (HR=0.96, 95% CI: 0.63-1.49). Analyses of tissue biomarkers showed that vitamin E supplement use was associated with less angiogenesis and better differentiation in the tumor among current or recent past smokers. In conclusion, smoking at the time of prostate cancer diagnosis is associated with poorer survival. Taking vitamin E supplement reduces the elevated mortality risk among smokers to a level similar to those who never smoked. The protective effects of vitamin E among smokers may be mediated through inhibiting angiogenesis and promoting differentiation in prostate tumors.

PS 1538 Discovery and Validation of Serum Protein Biomarker Candidates for Early Detection of Hepatocellular Carcinoma (HCC)

G. M. Mustafa[1], J. R. Petersen[2], L. Cicalese[3], N. Snyder[4], L. Denner[5] and C. J. Elferink[1]. [1]*Pharmacology, University of Texas Medical Branch, Galveston, TX,* [2]*Pathology, University of Texas Medical Branch, Galveston, TX,* [3]*Surgery, University of Texas Medical Branch, Galveston, TX,* [4]*Hepatology, Kelsey Seybold Clinic, Houston, TX and* [5]*Internal Medicine, University of Texas Medical Branch, Galveston, TX.*

The projected rise in HCC is mainly due to HCV infection with onset of HCC coming several decades after initial infection. However, additional environmental risk factors including alcohol, tobacco and other dietary insults that induce liver injury increase the incidence of HCC. The poor survival due to late stage diagnosis makes successful intervention difficult. Due to the lack of suitable diagnostic tools with adequate sensitivity and specificity to detect HCC early, our efforts center on the discovery and validation of a panel of blood derived biomarkers for early HCC detection. Serum was obtained from individuals positive for HCV or clinically diagnosed with liver disease(pre-HCC) or HCC, prefractionated using aptamer-based technology, and further fractionated using 2D-Difference In Gel Electrophoresis. Pre-HCC and HCC profiles were compared and 24 spots in 2D-DIGE exhibiting a statistically significant ≥1.5X change between pre-HCC and HCC samples were identified by mass spectrometry. Of the 24 candidate,11 were decreased and 13 were increased in patients with diagnosed HCC relative to the HCV patients. Stable isotope O18/O16 labeling was used to verify the proteins identified by 2D-DIGE,and supported the development of selected reaction monitoring(SRM) assays. ApoA1 from the list was selected for SRM assay development as proof of concept in this biomarker discovery protocol using AQUA peptides, and was independently verified immunologically. Using MRM(multiple reaction monitoring) and dynamic MRM assays we are verifying the quantitative assay parameters for a panel of candidate biomarkers. The ability to rapidly quantify proteins in a highly multiplexed manner using MRM with internal standard peptides closes the gap between discovery and validation in the biomarker pipeline.

PS 1539 Assessment of Renal Injury from Vancomycin and Puromycin in Rats

H. Stock, H. H. Ng, N. Chini, D. Fairchild and J. C. Mirsalis. *Bioscience, SRI International, Menlo Park, CA.*

Traditional biomarkers of nephrotoxicity, blood urea nitrogen (BUN) and serum creatinine (sCRE), are relatively insensitive to acute renal damage, generally requiring a loss of up to two-thirds of kidney function to induce significant changes. We have evaluated a new generation of urinary renal biomarkers (LIPO-2, clusterin, osteopontin, TIM-1, Albumin) using MesoScale Discovery® (MSD) kits. Fifteen male rats were administered either vancomycin (70 or 300 mg/kg) or puromycin (10 or 40 mg/kg) via intraperitoneal (ip) dosing daily for 7 days. Male rats (5/timepoint) were sacrificed on Days 2, 8 and 21. Blood for clinical pathology as well as urine was collected on Days 2, 8, 13 and 21. Microscopic pathology revealed necrosis, inflammation, fibrosis, and regeneration in male rats treated with either 300 mg/kg or 40 mg/kg of vancomycin or puromycin. Vancomycin at 300 mg/kg produced elevations in sCRE (1.4- and 1.9-fold) and BUN (1.5- and 1.9-fold) on Days 2 and 8, respectively. Puromycin (40 mg/kg) produced elevations in sCRE (3.1-fold) on Day 13 and BUN (1.5- and 1.8-fold) on Days 8 and 13, respectively; however, of the traditional markers of kidney function, only BUN showed significant changes that were outside the levels of historical controls. In contrast, 300 mg/kg vancomycin produced elevations in urinary albumin (6.0-fold) on Day 8 only, while urinary clusterin (6.0- and 16.3-fold), LIPO-2 (2.7- and 2.1-fold), osteopontin (4.3- and 2.9-fold), and TIM-1 (40.3- and 24.5-fold) were elevated on Days 2 and 8, respectively. Puromycin (40 mg/kg) produced elevations in albumin (45.7-fold) on Day 2 only and clusterin (5.4- and 2.1-fold), LIPO-2 (4.5- and 1.5-fold), and TIM-1 (23- and 3.3-fold) were elevated on Days 13 and 21, respectively. No significant changes in renal histopathology or biomarkers were observed at lower doses of vancomycin or puromycin. These results indicate that the MSD kits provide excellent sensitivity for detection of renal toxicity in rats following treatment with either vancomycin or puromycin. Work supported by NIAID Contract N01-AI-70043.

PS 1540 Validation of an HbA1c Assay for Selection of Aged Cynomolgus Monkeys for Toxicology Studies

N. Doyle, F. Poitout, M. Zamfir and S. Y. Smith. *Charles River, Montreal, QC, Canada.* Sponsor: M. Vézina.

Diabetes occurs spontaneously in aged cynomolgus monkeys and its diagnosis or potential for development must be considered when using aged monkeys on long term toxicology studies. Standard clinical pathology parameters are shown to be inadequate in diagnosing diabetes. Serum glucose (GLU) levels in aged monkeys can vary significantly and GLU measurements are also insufficient to detect persistent hyperglycemia. Glycated hemoglobin (HbA1c) is formed by the non-enzymatic addition of GLU to Hgb. Its formation in blood is positively correlated with the magnitude and duration of hyperglycemia. HbA1c half-life is 2-3 months and its removal from the blood is dependent on the degradation of hemoglobin. Transient hyperglycemia does not significantly affect the concentrations of HbA1c. HbA1c is a recognized marker of long term hyperglycemic status. The HbA1c assay was validated using whole blood in EDTA collected from healthy and confirmed diabetic cynomolgus monkeys. The Roche Diagnostic HbA1c kit immunoturbidimetric assay (Tina-quant HbA1c®) was adapted to use with an automated chemistry analyzer (Modular Analytics, Hitachi®) to measure HbA1c in hemolyzed whole blood. The HbA1c limit of detection was 0.3-2.6 g/dL for hemoglobin values between 4-40 g/dL. Intra-assay and inter assay coefficients of variation were 0.1 and 8.4 % respectively. Linearity of dilution was acceptable down to dilutions of 15:100. Hemolyzed samples were stable for 24 hrs at room temperature, 3 days at 2-8°C, and 2 months at -20°C, and over 3 freeze/thaw cycles. Stability of whole blood in EDTA was 3 days at room temperature or at 2-8°C. Reference values for HbA1c obtained in healthy cynomolgus monkeys were: 0.3-0.4 g/dL, or 1.8-3.0% of total hemoglobin for glucose values below 112 mg/dL. Values obtained in diabetic monkeys were 0.6-0.7 g/dL for GLU values between 120-256 mg/dL. The addition of HbA1c measurements to the clinical chemistry health screen panel allows a better identification of aged animals at risk for diabetes and a better health monitoring of these animals during the study conduct.

PS 1541 Insulin-Stimulated Urinary Chromium Excretion Is Not a Biomarker for Chromium Nutritional Status

S. T. Love[1], K. R. Di Bona[2], S. Halder Sinha[1], D. McAdory[1], B. R. Skinner[1], J. F. Rasco[2] and J. B. Vincent[1]. [1]*Chemistry, The University of Alabama, Tuscaloosa, AL and* [2]*Biological Sciences, The University of Alabama, Tuscaloosa, AL.*

Recent studies have suggested that the status of chromium as an essential element should be reconsidered because the effects of chromium supplementation appear to be more pharmacological rather than nutritional. The pharmacological basis for chromium's effects may explain the inability of investigators to identify a biomarker for chromium status. One potential biomarker, urinary chromium excretion in response to a glucose or insulin challenge, has not been examined to date. Chromium is known to be mobilized in the body in response to insulin (or insulin release in response to a glucose challenge), resulting in an increase in urinary chromium excretion. In this study, the magnitude of increase in urinary chromium loss as a function of dietary chromium intake was evaluated as a potential biomarker for chromium. Zucker lean rats housed under carefully controlled metal-free conditions were fed a series of purified diets containing variable amounts of chromium (from 16 μg/kg diet to 2000 μg/kg) for 4 months. The 16 μg/kg diet contained less chromium than any diet examined to date. Urine samples were collected pre- and post-insulin and glucose challenges (0, 2 hours, 6 hours and 12 hours post injection). Urinary chromium levels were analyzed by the standard method of addition using graphite furnace atomic absorption. Rat blood iron levels were also measured to determine if the addition of chromium to the diet altered iron status. The study demonstrated that the chromium content of the diet had no affect on blood iron levels and also confirmed that insulin-stimulated urinary chromium excretion is not a useful biomarker for chromium nutritional status.

PS 1542 Sensitive Sites of Glycation of the Fibrinolytic System Protein Plasminogen: Implications for T2D Vascular Complications

O. R. Kinsky, A. M. Williams, T. L. Hargraves, G. Tsaprailis, T. J. Monks and S. S. Lau. *Southwest Environmental Health Sciences Center, Department of Pharm/Tox, College of Pharmacy, University of Arizona, Tucson, AZ.*

Reactive dicarbonyls, such as methylglyoxal (MG), are present in blood and react with arginines (R) of target proteins, leading to diabetic micro- and macrovascular complications. MG plasma concentrations reach 4.5 μM, which can triple as diabetic complications progress. Protein-MG adducts may drive retinopathy, neuropathy, and many other common diabetic complications. The irreversible modification of R residues by dicarbonyls causes a net loss of positive charge, most commonly via hydroimidazolone formation. Previous studies in our laboratory identified the fibrinolytic system protein plasminogen (Pg) as a sensitive target of MG adduction, with functional significance. Thus, molecular modeling indicated that modification of R561 at the cleavage site of Pg would impact enzymatic activation due to drastically altered energy of interaction. The current work has identified, via 2D gel and subsequent in-gel digestion, the most sensitive sites of R modification (R504, R530) by MG on the protein, both of which may have functional effects. Although R561 was found as an early target for modification, it was not amongst the first sites hit. The functional significance of Pg adduction by MG was further tested in vitro. Pg activation was significantly delayed via modification with 50 μM MG, as determined by cleavage of a chromogenic substrate (S-2251) by plasmin, the product of Pg activation. A preliminary group of ten human plasma samples were selected and analyzed via Orbitrap mass spectrometry to detect modifications. Two patients with a history of cardiovascular disease showed R modification on Pg, at R504 and R530. At the present time, Pg modification in human plasma samples are being examined in a cohort >150 samples. The findings indicate that MG-modification of Pg may disrupt the fibrinolytic cascade sufficient to represent an underlying mechanism of vascular complications in diabetics. (R24DK083948, ABRC, ES016652, T32ES007091, P30ES006694).

PS 1543 A Practical and Complementary Approach to De-Risk the Potential Nephrotoxic Liability of a Drug Candidate at an Early Stage of Development

F. Brouta[1], M. Cornet[1], S. H. Dhalluin[2] and B. O. Depelchin[1]. [1]*Non-Clinical Development, UCB Pharma, Braine l'Alleud, Belgium and* [2]*NPS Portfolio & Alliance Management, UCB Pharma, Anderlecht, Belgium.*

UCBx, a compound intended for potential use in cognitive disorders, was stopped in preclinical development because of kidney toxicity observed in a 4-week GLP rat toxicity study. Adverse histopathological findings in the kidney were characterized by dose-related tubular degeneration/necrosis along with tubular basophilia. Urine analysis performed using both Meso Scale Discovery (MSD) and Luminex platforms showed marked increases of two Drug Induced Kidney Injury (DIKI) biomarkers (clusterin and KIM-1) on the 3rd day of administration which correlated with histopathological renal lesions observed on Day 28.

In order to derisk the potential nephrotoxicity liability of UCBy, close backup molecule from the same chemical series, urine biomarker analyses were performed in a 4-day rat toxicity study using the MSD platform. In addition, kidney samples were collected at necropsy to perform toxicogenomics analysis. Data analysis showed no significant while modest changes in urinary DIKI biomarkers without distinguishing gene expression profiles or kidney histopathological findings.

These results enabled the compound to progress to a 4-week rat toxicity study. Investigations included the measurement of DIKI protein biomarkers using the MSD platform. Results confirmed the absence of kidney toxicity after repeated administration over 4 weeks and confirmed the predictive value of the renal biomarkers.

In conclusion, the paradigm of performing urinary DIKI biomarkers and toxicogenomics analyses as complementary approaches to histopathology at discovery phase of drug development allowed to quickly get an early assessment of the potential nephrotoxic liability, particularly when a cycle of validation has been performed with a lead molecule.

PS 1544 Investigation of Urine Renal Safety Biomarker Collection Methods and Reference Intervals in Healthy Volunteers

A. F. Baker, M. J. Topper, R. Mogg, M. Cisneroz, N. King, P. Steven, L. Delgado, S. Sultana, E. G. Walker, E. Dennis, J. Sauer, S. Adler and J. Mikl. *Critical Path Institute, Tucson, AZ.*

Due to the lack of sensitivity, and non-specific nature of, the standard of care renal safety biomarkers, including serum creatinine and blood urea nitrogen, there has been an on-going effort by industry and academia to identify improved biomarkers of renal function and injury. Previous studies have reported that biomarker instability in the urine may confound their utility. The purpose of this study was to investigate the impact of preservatives on biomarker stability in urine, as well as investigate impact of age and gender on urine biomarker reference intervals values in healthy volunteers. To compare the impact of preservation agents on biomarker stability we collected and stored urine samples from five healthy volunteers in three ways: 1) neat (without a preservative or buffer), 2) with a pH stabilizing buffer, or 3) with a protease inhibitor cocktail. Samples were analyzed for a panel of 16 urine biomarkers by Myriad Rules Based Medicine and/or by Pacific Biomarkers Inc. using a combination of multiplex luminex based assays (Myriad RBM), ELISA, enzymatic, or turbidometric assays. Values were normalized to urine creatinine concentrations. Our findings suggest that urine pH has a significant impact on the stability of several biomarkers including beta-2-microglobulin, interleukin-18, and glutathione-S-transferase-alpha. In order to calculate normal reference ranges two serial "neat" spot urine samples were collected three weeks apart from 81 volunteers ranging from age 20 to 70 years of age. A significant gender difference was observed in values for Cystatin C (CysC), Clusterin, kidney injury molecule-1 (KIM-1), N-acetyl-beta-D-glucosaminidase (NAG), and osteopontin (OPN). A significant difference in values was observed between groups aged 20 to 39 vs 40 to 70 years old for KIM-1 and NAG. Together, our results provide insights on sample collection and handling techniques, as well as intrinsic factors that influence normal reference values for urine renal biomarkers including gender and age.

PS 1545 Translational Biomarkers for Oxidative Stress Response: A Validation Study with Flutamide

M. Teppner[1, 2], B. Ernst[2] and A. Paehler[1]. [1]*Non Clinical Safety, Pharma Research and Early Development, pRED, F. Hoffmann-La Roche Ltd., Basel, Switzerland and* [2]*Institute of Molecular Pharmacy, University of Basel, Basel, Switzerland.* Sponsor: F. Boess.

Flutamide is a non-steroidal anti-androgen drug for the treatment of progressive prostate carcinoma. Bioactivation of flutamide as well as redox cycling of its nitrobenzene group is supposed to be involved in the genesis of idiosyncratic adverse drug reactions via cellular oxidative stress.

Here, we present on the quantification of biomarkers for flutamide toxicity from *in vitro* and *in vivo* studies. Rat and human hepatocytes were treated with 100 μM flutamide for 24 hours. Cellular ATP and LDH release were determined by biochemical means. Determination of oxidative stress was done by analysis of a panel of isoprostane biomarkers by HPLC-MS/MS. Flutamide was also administered per os to Fischer F344 rats (500 mg/kg). Circulating isoprostane levels and standard enzymes for liver damage were monitored in plasma.

In vitro, no significant change in energy status or membrane integrity was observed in hepatocytes. However, significantly increased concentrations for different isoprostanes were detected in rat and human hepatocytes: 15R-Prostaglandin D2 augmented by 4.6 resp. 6.5 fold, 5-iso Prostaglandin F2α-VI showed 6.2 resp.

7.8 fold higher levels upon flutamide treatment. Similar results were obtained in rats in vivo: None of the measured liver enzymes were increased upon flutamide treatment. Plasma levels of oxidative stress markers were considerably changed: 15R-Prostaglandin D2 was 12.5 fold higher in treated animals and substantial levels of 5-iso Prostaglandin F2α-VI were detected in treated animals, not in vehicle controls.
These results show that enhanced formation of isoprostanes in rat hepatocytes translates to the *in vivo* situation. Human cells exert a similar response upon flutamide treatment. The quantitation of oxidative stress biomarkers in human hepatocytes is suggested as mechanistic tool to early address a drug's susceptibility to cause hepatic injury especially in man especially when bioactivation is involved.

PS 1546 Qualification of Novel Urine Biomarkers of Nephrotoxicity in Rodents on MSD Platform

A. V. Lyubimov, A. Kuzmis, Y. Chen, A. Zakharov and A. Banerjee. *Pharmacology, Toxicology Research Laboratory, UIC, Chicago, IL.*

The kidney is a common target organ for drug-induced injury, which is routinely assessed during safety evaluations. A panel of novel kidney injury markers has been recently identified, allowing diagnosis of nephrotoxicity with sufficient sensitivity and specificity in comparison to the conventional markers (serum creatinine and blood urea nitrogen (BUN)). As a result, there is a need for efficient methods for quantification of these novel biomarkers in early kidney toxicity screening. The goal of this study was to perform an analysis of urinary biomarkers on rodent models of kidney injury with an ultimate aim to enable more informed preclinical monitoring of kidney function. Concentration of kidney injury biomarkers was determined in urine using standard multiplexed (rat panel) or single plex (mouse) assays based on the MesoScale Discovery (MSD) platform that were developed by us. Evaluated injury response biomarkers included: albumin, NGAL (Lipocalin-2), T cell-immunoglobulin-mucin (TIM-1), and osteopontin. TIM-1 and NGAL MSD rat panel did not detect mouse proteins. Assays for these two markers were developed and qualified at our laboratory. Kidney injury was induced by cisplatin (7 mg/kg, single i.p.) as well as gentamicin (100 mg/kg, 7 daily SQ injections) in two species, Sprague Dawley rats and C57Bl/6 mice. Normal ranges in rodent plasma were established and found to be above the LLOD for both species. Albumin, NGAL, and TIM-1 demonstrated high sensitivity in detection of kidney impairment. However, elevated NGAL and TIM-1levels were detected at earlier time points than that of albumin. Osteopontin was a good indicator of tubular injury in rats but not in mice. Further optimization of the MSD methods are being undertaken to provide more sensitive assays for multiplexed detection of excreted biomarkers of kidney injury. In addition, a sensitive creatinine LC-MS/MS method was developed and validated as the routinely used clinical chemistry analyzer method is below the limit of quantitation in mouse urine.

PS 1547 Validation of an Electrochemiluminescence Multiplexed Immunoassay for Mouse Inflammation: The V-PLEX™

M. J. Cameron[1], D. B. Gemani[1], J. Coash[2] and A. Aulbach[2]. [1]*Immunology, MPI Research, Mattawan, MI and* [2]*Clinical Pathology, MPI Research, Mattawan, MI.*

To support preclinical safety studies a new, commercially available mouse cytokine multiplex kit (IFN-gamma, IL-1 beta, IL-2, IL-4, IL-5, IL-6, KC/GRO, IL-10, IL-12p70 and TNF-alpha) from Meso Scale Discovery was validated under GLP (Good Laboratory Practice) conditions. V-PLEX products allow the end user flexibility to pick and choose analytes from a predefined menu. To demonstrate biological relevance and create positive controls, mice were dosed with LPS via intraperitoneal injection. Serum samples were collected at 30 minutes and 1, 4, 8, 12, 24, and 48 hours post-LPS administration. LPS treatment in the mouse caused significant up-regulation of IFN-gamma, IL-10, IL-12, IL-1beta, IL-5, IL-6, KC/GRO and TNF-alpha beginning by 1 to 4 hours post dose. The analytical validation consisted of 6 independent immunoassay runs. Quality Control Samples (QC's) were made by spiking calibrator into mouse serum. Inter assay precision and accuracy (ULOQ, QC high, QC mid, QC low, LLOQ), short and long term stability, bench top stability, freeze thaw stability, dilutional linearity, testing of incurred samples from an animal study, and parallelism were evaluated. The total error for individual calibrator points ranged from 0.8 to 38.43. The total error for the QC low, QC mid, QC high ranged from 10.3 to 30.7, 9.43 to 30.5 and 9.64 to 29.22 respectively. The calibrator spiked into matrix was found to be stable after 3 freeze and thaw cycles, at one week and one month of storage at -20 and -70 degrees. A consistent under recovery for IL-4 and IL-2 was noted. Dilutional linearity was found to be acceptable for all of the analytes with the exception of IL-4 and IL-2. When considering the validation data set as a whole, 8 of the 10 analytes performed well and are considered fit for use. The data set for IL-4 and IL-2 suggest that these assays should be used with caution. The V-PLEX product is a new multiplexing product offering greater end user flexibility and may become a valuable tool for mouse cytokine analysis.

PS 1548 A Modern Assessment of Clinical Pathology Biomarker Correlation between Nonclinical Species and Humans

A. Lynn, V. J. Kadambi and J. Senn. *Drug Safety Research and Evaluation, Takeda Pharmaceutical Company Limited, Boston, MA.*

Translatability of biomarkers from nonclinical species to humans is vital when predicting for toxicity and monitorable biomarkers in the clinic. To that end, we have used the database Pharmapendium to perform correlation analyses on commonly observed adverse alterations in standard clinical pathology endpoints used in nonclinical and clinical studies. Human data was compared with 3 commonly used nonclinical species: rat, dog, and primate. Analyses are limited to those drugs where clinical data only exists from the year 2000 to present. Our data show that there is no significant difference between either sensitivity or specificity values across species. The maximum difference observed was 8%, with the exception of circulating reticulocytes which showed increased specificity of 15% to 17% in primates as compared to dogs and rats, respectively. This finding gives credence to the statement that lesser animal models are as useful as higher animal models for predicting these clinical pathology changes in humans. Additionally, the standard nonclinical toxicology evaluation practice of using a rodent and non-rodent species (rat and dog or rat and monkey) slightly increased sensitivity by 2% to 17% while marginally reducing specificity by 0% to 8%. Interestingly, a further correlation analysis between species indicated that there was no significant overlap between clinical pathology changes in both rat and dog and rat and monkey. There were 7 to 76 drugs where both the rat and dog were tested and where the dog showed the change in the clinical pathology parameter of interest. In these cases, the rat showed a false negative rate up to 85%. There were 2 to 49 drugs where both the rat and primate were tested and where the primate showed the change in the clinical pathology parameter of interest. In these cases, the rat showed a false negative rate of up to 100%. These data give credence to the use of two animal species in order to safely choose biomarkers for monitoring in the clinic.

PS 1549 Simultaneous Determination of 15 Heterocyclic Aromatic Amines in Urines of Smoker and Nonsmoker Using HPLC-MS/MS

G. Zhao, Y. Fu, S. Wang, J. Yu, B. Wang and F. Xie. *Zhengzhou Tobacco Research Institute, Zhengzhou, China.* Sponsor: R. Meng.

A sensitive UHPLC-MS/MS method for the simultaneously determination of 15 heterocyclic aromatic amines (HAAs) was developed and applied to the analysis of human urines of smokers and nonsmokers. The limits of detection and quantitation of these HAAs approached 0.80-6.06 and 2.65-20.20pg/mL, respectively. The intra-day and inter-day precisions of all HAAs were ≤10%. For the high sensitivity and good precision, the method was successively applied to analysis urines of smokers and nonsmokers, 10 HAAs were detected, 9 HAAs were analyzed and compared between two groups. Analysis results showed that cigarette smoke could induce the increased exposure of AαC and DMIP. This was the first study that so many HAAs are detected simultaneously, and also the first comprehensive study of HAAs exposure induced by cigarette smoking.

PS 1549a Cross-Site Analytical Validation of the Cardiac Biomarker NT-proANP in Rat

H. M. Colton[4], P. Vinken[1], N. Goeminne[1], W. J. Reagan[2], W. Buck[3], J. Lai-Zhang[3], R. Liu[5] and M. Cisneroz[6]. [1]*Janssen R&D, Beerse, Belgium,* [2]*Pfizer Inc., Groton, CT,* [3]*AbbVie, North Chicago, IL,* [4]*GSK, Durham, NC,* [5]*Takeda, Cambridge, MA and* [6]*Critical Path Institute, Tucson, AZ.*

Natriuretic peptides have proven utility in human medicine and are candidate non-invasive translational cardiac safety biomarkers for drug development studies in rats. A working group within PSTC is qualifying NT-proANP as a circulating biomarker of drug-induced hemodynamic stress. Analytical validation of an ELISA specific for human but cross-reacting with rat NT-proANP (Biomedica / Alpco Diagnostics, Cat No 04-BI-20892) was conducted by 5 different laboratories. The following aspects were assessed: intra- and inter-assay precision, accuracy, dilutional linearity, limit of detection (LOD), upper and lower limit of quantification (ULOQ and LLOQ), sample freeze/thaw (F/T) stability and inter-laboratory reproducibility. The standard curve showed acceptable analytical performance in all laboratories, defined as CV ≤ 20% and accuracy ≤ 20%. Intra- and inter-assay

precision ranged from 3.9-14.3% and 8.7-34.5% respectively for serum spiked with calibrator and from 3.5- 15.5% and 8.9-32.8% respectively for serum spiked with heart lysate. Accuracy of calibrator spiked serum was between 76 and 112%, of serum spiked with lysate between 74 and 103% and of the kit QC between 90 and 116%. Recovery after sample dilution ranged from 85-121% with occasional evidence of greater variability in the lower concentration range. The average LOD was 0.036 nM. LLOQ was <0.63 nM and ULOQ was 10 nM. Recovery of samples undergoing up to 3 F/T cycles was between 83 and 118%. Overall inter-laboratory precision varied between 18 and 30%. In conclusion, analytical performance of the NT-proANP ELISA in rat serum samples met or exceeded the assay validation criteria.

PS 1549b Implications of Histopathology Methods in Biomarker Qualification

R. L. Rouse, M. Min, K. Shea, S. Stewart and T. Colatsky. *CDER, U. S. FDA, Silver Spring, MD.*

Identification of candidate biomarkers detecting very early tissue injury and attempts to qualify these novel biomarkers for regulatory consideration have placed a spotlight on the histological and histopathological methods used in evaluating candidate biomarkers. The number and locations of organ samplings, the impact of non-blinded evaluations, the methodology for inclusion or exclusion of spontaneous changes, and inherent differences in pathologists are sources of variation that could potentially impact biomarker assessment. Three FDA pathologists were recruited to participate in studies that were conducted through remote evaluation of digital images of hematoxylin and eosin stained slides of kidneys. Initial studies were created to maximize variability between pathologists by providing no specific directions or guidance, by providing no contextual information, and by allowing no collaboration or consultation between pathologists. Later studies were designed to minimize inter-pathologist variability. The same five image sets were used to generate quantitative estimates of proximal tubular tissue volume and epithelial cell counts in stereology software. Tissue sections serial to the H&E stained sections were immunohistochemically stained for the candidate biomarker and the biomarker was quantified through digital image analysis software. Log-linear modeling for variability was conducted using SAS PROC GENMOD and LogXact from Cytel, Inc. Receiver Operating Characteristic (ROC) analysis was used to assess biomarker performance. Results indicate that differences between pathologists are the largest source of variability in evaluations and that blinding does not generally make a significant difference. Pathologist variability can significantly influence biomarker performance assessment analyses but can be minimized by using techniques to increase pathologist consensus. Quantitative stereology and digital image analysis methods did not improve biomarker performance assessments when compared to typical semi-quantitative evaluations averaged across all pathologists.

PS 1549c Tobacco Smoke Is a Significant Source of 1, 3-Butadiene Exposure in the US Population: NHANES 2005–2006

U. Alwis, R. DeCastro and B. C. Blount. *Tobacco and Volatiles, Centers for Disease Control and Prevention (CDC), Atlanta, GA.* Sponsor: R. Wang.

1,3-Butadiene is a known human carcinogen that is used in polymer production, and is detected in gasoline vapor, automobile exhaust, and tobacco smoke. Urine samples collected as part of NHANES 2005-2006 were assayed for 1,3-butadiene exposure biomarkers [N-acetyl-S-(1-hydroxymethyl-2-propenyl)-L-cysteine (MHBMA1), N-acetyl-S-(2-hydroxy-3-butenyl)-L-cysteine (MHBMA2), N-acetyl-S-(4-hydroxy-2-butenyl)-L-cysteine (MHBMA3), and N-acetyl-S-(3,4-dihydroxybutyl)-L-cysteine (DHBMA)] using ultra high performance liquid chromatography coupled with electrospray ionization triple quad mass spectrometry (UPLC/ESI-MSMS). MHBMA3 was the most abundant among the monohydroxy metabolites. The limits of detection in urine for MHBMA3 and DHBMA were 0.6 and 5 ng/mL respectively. In sample-weighted statistical analysis of NHANES 2005-2006 data, the median MHBMA3 and DHBMA levels among smokers (n=600) were 334 and 28 μg/g creatinine, respectively, compared to 250 and 5 μg/g creatinine for non-smokers (n=2467). Linear regression analysis showed that serum cotinine among smokers is a positive predictor of 1,3-butadiene exposure as measured by urinary MHBMA3 (linear slope $p = 0.0002$) and DHBMA (borderline $p = 0.10$), consistent with tobacco smoke as a primary exposure source for 1,3-butadiene. The sample-weighted median metabolic molar ratio (DHBMA/ [DHBMA + MHBMA3]) was significantly lower among smokers (0.92; $p < 0.0001$) compared to non-smokers (0.98). Also, among smokers the sample-weighted median metabolic molar ratio was significantly higher among non-Hispanic Blacks (0.93; $p = 0.04$) and Mexican Americans (0.95; $p = 0.0001$) compared with non-Hispanic Whites (0.92). Among smokers, the sample-weighted Pearson correlations of serum cotinine with both MHBMA3 ($r = 0.61$, $p < 0.0001$) and DHBMA ($r = 0.19$, $p < 0.0001$) were statistically significant. This study provides the first nationally representative characterization of butadiene exposure as measured by urinary MHBMA3 and DHBMA, and underscores tobacco smoke as a major source of butadiene exposure.

PS 1549d Novel Rat Kidney Injury Biomarker Assays Using a Gyros Nanotechnology Platform

T. L. Wente, J. Mistry, C. Fry and Q. Xiao. *R&D, EMD Millipore, St. Charles, MO.* Sponsor: R. Wiese.

A leading cause of failure to any drug development program is toxicity in various organs such as the kidney. Traditional tests may not be specific enough for what is occurring and often cannot be detected until damage is irreversible. Many nephrotoxicity biomarkers may aid in the detection of damage to the kidneys and offer clues to specific kidney tissue injury in a more timely manner. We have developed rat KIM-1 and rat Clusterin GyroMark™ HT Biomarker assays as the first two toxicity biomarker assays in the Gyrolab™ xP Workstation platform. This automated compact disc-based nanotechnology uses microfluidic technology for sandwich ELISA immunoassay analysis using a biotinylated capture antibody and a fluorescence labeled detection antibody. This Gyros technology has features including small sample size (200 –1000 nL), high sensitivity, broad dynamic range, and short assay time (1 hour per assay). The KIM-1 assay has a dynamic range, sensitivity, spike recovery, dilution linearity, intra-, and inter-assay variations of 0.054-40 ng/mL, 0.04ng/mL, 94%, 110%, < 5% and < 10%, respectively for 1:2 diluted rat urine samples. The Clusterin assay has a dynamic range, sensitivity, spike recovery, dilution linearity, intra-, and inter-assay variations of 0.36-1500 ng/mL, 0.3ng/mL, 93%, 100%, < 10% and < 10% respectively for 1:10 diluted rat urine samples. Using these new GyroMark™ HT Biomarker assays, we evaluated rats treated with no, low, and high doses of gentamicin. Urine samples (n=36) were collected on day 0, 3, 7, and 14. A significant increase in these markers was observed at day 3, tapering off as animals recovered towards day 14. The KIM-1 and Clusterin assays were compared to a leading commercial ELISA platform and vancomycin treated rat urine samples (n=36) correlation was $r = 0.97$ and 0.87 respectively. The analytical and biological validation data demonstrate that our GyroMark™ HT toxicity biomarker assays, rat KIM-1 and rat Clusterin, are highly robust and reproducible, using a 1000 nL sample size and can be a useful tool in detecting kidney damage in rat urine samples for drug development and basic research.

PS 1549e Comparison of Two Commercial Immunoassays for Determination of Atrial Natriuretic Peptide in Sprague-Dawley Rat Serum

J. R. Turk, A. Farhad and M. Ameri. *CBSS, Amgen Inc., Thousand Oaks, CA.*

Atrial natriuretic peptide prohormone (proANP) is synthesized by the atrial myocytes. A stretch of the cardiomyocyte stimulates the release of proANP into the circulatory system. In circulation, proANP splits into a biologically active peptide known as α-ANP and an inactive N-terminal peptide (NT-proANP). NT-proANP has a long half-life and is less sensitive to the pulsatile secretions of ANP. Therefore, blood concentration of NT-proANP is used as a biomarker to evaluate cardiac health. Accurate determination of NT-proANP in preclinical animal models is important in safety and efficacy assessment of drug candidates. The objective of this study was to investigate two commercially available immunoassay kits for determination of NT-proANP in rat serum. Serum samples from 12 male and 12 female Sprague Dawley rats (10-14 weeks old) and plasma samples from a left anterior descending coronary artery-ligation (LADX) myocardial infarction study (n = 7) were used to evaluate a human specific ELISA kit with a colorimetric detection system from ALPCO (Salem, NH) and a rat-specific kit with an electrochemiluminescense detection system from Meso Scale Discovery (MSD, Gaithersburg, MD). The coefficient of variation (CV) was <16% using the ALPCO kit and <10% using the MSD kit. The spike-recovery using the ALPCO kit standard in pooled rat serum was 89 ± 9% and using the MSD kit standard in pooled rat serum was 110 ± 10%. No significant interference up to 4+ hemolysis was observed for either kit. Good correlation ($r = 0.92$) was observed between the two kits and NT-proANP was shown to be stable up to three freeze-thaw cycles in rat serum. Compared to the control rats, NT-proANP mean values were significantly higher ($p < 0.05$) in the LADX groups. In conclusion, both assays meet the feasibility acceptance criteria for determination of NT-proANP in rat serum. The ALPCO kit was fully validated for research and toxicology studies.

PS 1549f Multiplex Blood Biomarker Approach to Determine Drug-Induced Vascular Injury in Rat

D. Pepin, S. Harris, R. Maheshwari and W. Zheng. *EMD Millipore, St. Charles, MO.* Sponsor: P. Hewitt.

Vascular injury is a common finding during the pre-clinical safety study of drugs. A lack of understanding of mechanisms of drug-induced vascular injury (DIVI) in animals and the absence of qualified biomarkers have become significant barriers in the development of new therapeutic agents. Recently, a number of promising candidate biomarkers for DIVI have been nominated. However, any effort to further validate and evaluate these markers is impeded by the lack of qualified high-throughput assays.
Based on Luminex xMAP® technology, we developed three panels of multiplexed immunoassays to quantify 17 potential DIVI biomarkers in rat serum and plasma samples. These biomarker candidates included caveolin-1, CTGF, PAI-1, IL-6, MCP-1, CINC-1, TIMP-1, VEGF, TNF-alpha, adiponectin, sICAM-1, sE-selectin, von Willebrand Factor (vWF), alpha-2-macroglobulin (A2M), alpha-1-acid glycoprotein (AGP), fibrinogen and haptoglobin. Furthermore, fenoldopam induced rat DIVI models were used to validate the sensitivity and specificity of these assays.
To induce vascular injury, rats were treated with the vasodilator compound fenoldopam mesylate (FM). FM was administered by continuous intravenous infusion over 24 hours with a dose of 6 mg/kg/h. Subsequently to the infusion, serum and plasma samples were collected from each group of three rats on post-infusion day 1, 3, and 7. Sterile 0.9% saline was used in the vehicle control cohorts. MILLIPLEX® MAP Rat Vascular Injury Magnetic Bead Assays were used to measure 17 candidate protein biomarkers simultaneously from the rat serum and plasma samples. Fenoldopam treatment resulted in significant increase in blood biomarkers, consistent with its well described vasotoxic effect. Several biomarkers were found promising in this study, including A2M, sICAM-1, CTGF, vWF and TIMP-1. The simultaneous measurement of these proteins with multiplex technology offered a robust and convenient method to study these biomarkers. Taken together, our data demonstrate the feasibility of using the multiplex biomarker approach to detect the onset and progression of DIVI in pre-clinical drug safety studies.

PS 1549g Conjugate Formation of 1-Bromopropane with Glutathione *In Vitro*

C. Seo[1], Y. Um[1], H. Kim[2], M. Kang[1], H. Jeong[2] and T. Jeong[1]. [1]*College of Pharmacy, Yeungnam University, Gyeongsan, Republic of Korea and* [2]*College of Pharmacy, Chungnam National University, Daejeon, Republic of Korea.*

Glutathione (GSH) is a ubiquitous tripeptide in mammalian systems for playing critical roles, including defense against many electrophiles. 1-Bromopropane (1-BP) is widely used as a substitute for chlorofluorocarbons because of its lower ozone-depleting potency, high volatility and non-flammability. It has been known that 1-BP could produce GSH conjugates so that the homeostasis would be interrupted. In the present study, the formation of GSH conjugates of 1-BP was characterized in vitro by using mass spectrometry. Rat liver homogenates and cell cultures including MCF-7 and HepG2 cells were compared for their ability to form S-propyl GSH. In rat liver homogenates, S-propyl GSH was also produced concentration-dependently from 1 mM 1-BP. A time-course study indicated that Tmax for the formation of S-propyl conjugates would be 1 hr after the treatment with 1-BP. In addition, the production of S-propyl conjugates was associated with the decrease in the level of GSH in liver homogenates. In cell cultures, S-propyl GSH was only produced in MCF-7 cells, but not in HepG2 cells. In addition, the conjugates were mostly detected in the cultured media, indicating that conjugates are excreted from MCF-7 cells when produced. A time-course study indicated that Tmax for the excretion of S-propyl conjugates would be 8 hr after the treatment with 1-BP in MCF-7 cells. The present results indicated that S-propyl conjugates of 1-BP could be produced in vitro and that toxicologically 1-BP in MCF-7 cells might act differently from HepG2 cells. Supported by a grant from National Research Foundation of Korea (2010-0026220).

PS 1549h N-Terminal Pro-Natriuretic Peptides and Heart Rate As Cardiovascular Safety Biomarkers

S. K. Engle and D. E. Watson. *Toxicology, Eli Lilly and Company, Indianapolis, IN.*

Functional changes in the cardiovascular (CV) system, such as altered blood pressure, are not usually measured and frequently go undetected in conventional repeat-dose rodent safety studies during drug development. Likewise, in clinical drug development, functional changes in the CV system of humans can go undetected until late stage clinical trials. Sustained changes in blood pressure are important because even small changes in blood pressure have been suspected of producing undesirable CV effects such as cardiac hypertrophy and myocardial degeneration in animals, and Major Adverse Cardiovascular Effects (MACE) in patients. Natriuretic peptides (NP) are cardiac hormones which affect blood pressure and inhibit cardiac hypertrophy by promoting excretion of salt and water through the kidneys, relaxation of vascular smooth muscle, and direct effects on the heart. They have been shown to have utility as prognostic biomarkers of heart failure, cardiac hypertrophy, and left ventricular dysfunction in patients, and may be useful biomarkers in non-clinical species as well. We examined NTproANP and NTproBNP concentrations in plasma of rats administered sunitinib for four days, and nifedipine, fluprostenol, minoxidil, L-NAME, and L-thyroxine for fourteen days. Plasma NTproANP and NTproBNP concentrations were inversely related to blood pressure after administration of sunitinib, nifedipine, minoxidil, and fluprostenol. Administration of L-NAME caused hypertension and increased NTproBNP concentrations, and L-thyroxine caused systolic hypertension and increased heart weight with no change in either NP. Nifedipine and minoxidil caused increased heart weights which were correlated with NTproANP concentrations. Fluprostenol and L-NAME did not cause changes in heart weight, in spite of sustained changes in blood pressure and NTproANP and NTproBNP. Increased heart weights were best correlated with increased heart rates. These studies support further development of NPs as biomarkers of functional changes in the cardiovascular system of veterinary species.

PS 1550 Manganese Exposure Assessment—The Use of Toenails As a Biomarker of Exposure in US Welders

E. J. Ward[1], J. Bainter[1], S. Snyder[1], U. Dydak[1, 2] and F. Rosenthal[1]. [1]*Health Sciences, Purdue, West Lafayette, IN and* [2]*Radiology and Imaging Sciences, IUSM, Indianapolis, IN.*

Previous studies have shown that high exposure to manganese (Mn) in occupational settings may lead to neurological health effects. Currently, there is no established biomarker for Mn exposure. The objective of this study was to evaluate the hypothesis that toenail Mn concentration is reflective of an individual's Mn exposure from occupational and dietary sources in a population of welders.
Toenail clippings of all ten toes were collected from fifteen career welders and nineteen controls. The toenail samples were cleaned and sonicated in Triton X-100 surfactant, digested using microwave acid digestion and analyzed for Mn using Inductively Coupled Plasma Mass Spectrometry (ICP-MS) for Mn. Respirable Mn exposure was estimated using a model combining air samples, work histories, and modifying factors such as ventilation and use of personal protective equipment. Dietary Mn and Fe were estimated with a food questionnaire.
There was no significant difference between mean Mn concentration in right and left feet (4.89 vs. 4.27 ug/g, $p = 0.1856$). Toenail Mn levels were higher in welders than in controls (7.14 vs. 3.02 ug/g, $p = 0.0003$). Toenail Mn was significantly correlated with cumulative exposure to respirable Mn seven to twelve months prior to the toenail clipping date ($r2 = 0.31$, $p = 0.03$). When ratio of dietary intake of Mn to Fe, smoking, and age were included as covariates in the statistical model the correlation between respirable Mn exposure and toenail Mn improved (adjusted $r2 = 0.56$, $p = 0.003$). With two exceptions, toenail Mn was able to clearly distinguish exposed individuals from controls.
The significant correlation of toenail Mn with the cumulative Mn exposure seven to twelve months prior to the toenail being clipped is consistent with the average growth time of toenails. The results suggest that toenail Mn is a valid, reproducible, easy to acquire biomarker of Mn exposure, which is feasible to use in an industrial welder population. (Supported by NIEHS R01 ES020529 and CDC/NIOSH T03 OH008615)

PS 1551 Elevated Household Dust Mn Levels Are Associated with Children's Hair Mn in Communities Impacted by Ferroalloy Plants in Northern Italy

P. Bertrand[1], E. Lucas[1], F. Donna[2], M. Peli[2], R. Lucchini[2, 3] and D. Smith[1]. [1]*University of California, Santa Cruz, CA,* [2]*University of Brescia, Brescia, Italy and* [3]*Mount Sinai School of Medicine, New York, NY.*

Objectives: Determine the association between levels of manganese (Mn) and other metals in household dust samples with levels in exposure biomarkers (hair, blood, saliva, and fingernails) in Italian adolescents in communities with active and historic ferroalloy plant activity.
Rationale: Adolescents living in communities with ferroalloy plant activity exhibit deficits in olfactory and fine motor function. Household dust Mn concentrations have not previously been measured to assess contamination from ferroalloy plant emissions.

Approach: Indoor and outdoor household dust samples were collected in communities with an active ferroalloy plant (n=178), with historically active plants (n=166), and a control site (n=99), leached with 7.5N HNO3 and analyzed for Mn, Al, Fe, Cd, Cr, Cu, Pb, and Zn by ICP-AES.
Results: Household dust Mn levels were significantly different between all three study sites, with levels highest in the community with an active ferroalloy plant (median = 2060 ug/g, range 130 – 183,000) and lowest in the reference community (median = 320 ug/g, range 20 – 1050); dust Mn levels were ~3 to 7-fold higher in outdoor versus indoor samples across all three sites.
In homes of adolescents providing biomarker samples (n=98), there was a highly significant correlation (ρ=0.491, p<0.001) between dust Mn concentrations and household dust Mn loading levels, and a highly significant association between dust Mn concentrations and hair Mn levels (ρ=0.3254, p<0.0011, n=98). There was no association between dust Mn loading and hair Mn (ρ=0.1201, p=0.265), or between dust Mn concentrations and Mn levels in other biomarker tissues (-0.1104<ρ<0.1426, p>0.22).
Conclusion: Dust Mn levels provide an informative measure of environmental Mn contamination from ferroalloy plant emissions, and their association with a biomarker of Mn exposure suggests that dust may serve as an important Mn exposure pathway for adolescents.

PS 1552 Calibration and Improvements of a Portable XRF Technology to Quantify Lead in Bone *In Vivo*

A. J. Specht[1], M. Weisskopf[2] and L. H. Nie[1]. [1]*Health and Human Sciences, Purdue University, West Lafayette, IN and* [2]*Harvard School of Public Health, Harvard University, Boston, MA.*

Lead is a ubiquitous toxin, which has been shown to have adverse health effects on many systems in the body. Bone serves as a valuable biomarker for long-term lead exposure. We have developed a portable XRF device to measure lead in bone in vivo with recent advancements in device technology and calibration methods. The main goals in this study were to improve the sensitivity of the system, determine the best calibration method, and validate the system for in vivo measurement. We investigated four calibration methods, namely background subtraction, bone calibration, bone adjustment calibration, and traditional peak fitting. System calibration is very important, as with larger soft tissue thickness the detected lead x-ray signals can be low and difficult to quantify. The device was calibrated using phantoms of known lead concentrations for background subtraction and traditional peak fitting methods, bone of known lead concentrations for bone calibration method, and bone and phantom comparisons for bone adjustment method. Using these calibration methods we measured the bare cadaver bone and goat bone samples with Lucite used to replicate soft tissue, and cadaver bone with and without intact soft tissue. There was strong correlation between the K x-ray fluorescence (KXRF) and portable XRF bone lead results for bare cadaver and goat bones. There was also strong correlation between KXRF and portable XRF results for goat bone with Lucite, however, the results for cadaver bone with Lucite did not show the same correlation. As a further assessment of the device for in vivo situation, the cadaver bone with intact soft tissue was used, and the results of these experiments also showed a good correlation with previous KXRF data. Our results suggest that the portable XRF bone lead measurement has a detection limit of 3.4 ppm with 2 mm soft tissue thickness, that the best calibration method for use with in vivo data is the background subtraction method, and that the technology needs to be validated in a larger human population.

PS 1553 Health Monitoring of Residents Overexposed to Heavy Metals in Abandoned Metal Mine Areas

D. Kim, J. Ryu, S. Ahn and S. Yu. *Environmental Health Research, National Institute of Environmental Research, Inchon, Inchon, Republic of Korea.* Sponsor: J. Park.

Since 2008, the National Institute of Environmental Research (NIER) of Korea has conducted "The survey on Metal exposure and Health Effects of Residents in Abandoned Metal Mine Areas in Korea" for 38 abandoned metal mines in high soil pollution. Some metals in biological samples were higher than those of general population. However, we couldn't find out clear evidence of health effect.
For the high exposure residents, whose heavy metal levels in blood and urine of some residents exceeded the reference values, NIER established management guidelines to monitor and reduce the exposure level of heavy metals in blood and urine of residents in abandoned metal mine areas in 2009.
The main purpose of this study is to monitor and reduce heavy metal concentrations in blood and urine through continuous monitoring and communication with the residents and health check up in the abandoned metal mine areas.
The target population was 135 residents in 2011, who showed higher metal values in blood and urine than reference values, the analyses of metals in blood and urine with medical check-ups and survey of personal questionnaires were conducted. The reference values of heavy metals in this study were as follows: blood mercury is 15ug/L (HBM2); blood cadmium 5ug/L (WHO); urine cadmium 5ug/g-cr (HBM2); and urine arsenic 35ug/L (ACGIH BEI's). And the study results can be summarized as follows: the geometric mean of blood mercury concentration was 6.54ug/L; blood cadmium was 5.68ug/L; urine cadmium was 3.61ug/g-cr; and urine arsenic was 61.30ug/g-cr. The excess rate of blood mercury concentration was 16.3%(8 of 49 subjects); blood cadmium was 75.9%(22 of 29 subjects); urine cadmium was 33.9%(19 of 56 subjects); and urine arsenic was 75.0%(6 of 8 subjects). Based on the results, for the 44 subjects who showed decreased heavy metal levels lower than the reference values and no medical abnormalities, the follow-up study was completed.

PS 1554 Estimating Exposure to Metals in Smelter Material

M. Seeley[1], G. I. Greenberg[1], S. Thakali[2] and B. D. Beck[1]. [1]*Gradient, Cambridge, MA and* [2]*URS Corporation, Fort Washington, PA.*

Historically, discarded material from non-ferrous smelters, including oven bricks, broken pieces of retort, and residue from the inside of retorts (smelter material), have been used for construction and maintenance of road beds and bridges. In some cases, concentrations of arsenic (As), cadmium (Cd), lead (Pb), and zinc (Zn) can be elevated in this bulk material. If metals were transferred to hands and subsequently ingested, direct contact with these materials could represent a potential health risk. While there are multiple studies of transfer of soils to hands, data regarding transfer of metals from solid material to hands are limited. Therefore, we conducted a hand transfer study to simulate potential exposure under conditions expected to maximize transfer of the metals from smelter material to hands. Twenty six pieces of smelter material were collected alongside roads and bridges, wrapped, and shipped to a laboratory for handling by a study volunteer. Prior to handling the smelter material, the volunteer's hands were moistened, and the volunteer actively handled the material for 30 seconds by holding, turning, and transferring the material between his or her two hands. The volunteer's hands were then thoroughly rinsed, and the rinsate was evaluated for concentrations of As, Cd, Pb and Zn. Zinc was detected in 14 of the hand transfer samples and Pb and Cd were each detected in two; As was not detected in any of the samples. Our results showed that very little, if any, of the metals were transferred from the smelter material to hands, with no correlation between amount transferred to hands and concentration in the bulk material; there was some indication of a relationship between hand transfer and metal concentrations in the soil near the sample collection area. Based on this study, handling of smelter material does not represent a significant exposure source.

PS 1555 Research on Potential Exposure of Workers to Metals in Smelter Materials Used As Fill for Roads and Bridges

L. A. Beyer, M. Seeley, G. I. Greenberg and B. D. Beck. *Gradient, Cambridge, MA.*

In some areas of the United States, smelter material (brick, smelter residue, and retort) has been used for road construction. Workers may potentially be exposed to these materials when repairing roads and bridges. Our objectives were to measure the amount of metals workers might get on their hands as a result of contacting the smelter material used as fill, estimate intake by workers potentially contacting the materials, and assess risk.
We evaluated exposure to metals from direct contact with smelter material following a study procedure based on peer-reviewed methodology. According to a detailed protocol, volunteers handled the material in a manner simulating how workers would contact the material. The volunteer's hands were then rinsed, and the rinsate was analyzed for lead, zinc, arsenic, and cadmium. Zinc was detected most frequently and at the highest concentration, lead was detected in two samples, and cadmium was detected in two samples. Arsenic was not detected in any of the hand transfer samples. The maximum amount transferred to the hands for cadmium, lead, and zinc was 0.002 mg, 0.035 mg, and 0.98 mg, respectively.
Using these results, as well as site-specific information regarding potential worker contact with smelter materials and standard US EPA risk assessment methodology, we calculated exposure from dermal contact and inadvertent ingestion of material on hands. For handling smelter material, we calculated a hazard quotient (HQ) of 0.017 for cadmium (ingestion and dermal contact) and an HQ of 0.0015 for zinc (ingestion only, as there is no dermal absorption). The total hazard index was 0.02. For lead, we estimated the daily intake of 1.96 μg for a 70-kg man, which would have no detectable impact on blood lead levels. Because none of the metals are evaluated as carcinogens, direct handling of smelter material would not be associated

with an excess cancer risk. According to the calculations for workers, the potential health risks associated with handling smelter material were very low and did not exceed acceptable risk levels.

PS 1556 Arsenic Speciation in the Copper Tailings with the Effects of Magnetite Removal

L. Yunjia, H. Longbin and L. Zhao. *Sustainable Minerals Institute, University of Queensland, Brisbane, QLD, Australia.* Sponsor: H. Longbin.

Arsenic is considered as one of severe metalloid pollutants in the copper tailings, which may pose risks to the environment and human health. It is known that iron oxides are one of the most important adsorbents of minor elements due to their reactivity and large specific surface area, which can coprecipitate and adsorb arsenic. Magnetite (Fe3O4), counting for up to 30% of in copper tailings, may act as a sink mineral to prevent arsenic mobilization. However, the ore processing has recently changed to remove magnetite as a by-product for economic benefit, which reduce magnetite concentration from 20 – 30% to 5%. Thus may affect arsenic speciation and consequently mobilize arsenic in tailings. In this study, we compared the sequential leaching results from the old copper tailings (total arsenic concentration 330 mg/kg) with magnetite and new copper tailing without magnetite. There was 34% arsenic adsorbed with iron in old tailing, comparing to 7% arsenate in new tailings. Organic matter (biochar and mulch) were added in those tailings and two types of Australian native plants were planted in the pot experiment. The leachate was collected which may display the different adsorption effects of organic matter on arsenic due to the reduction of the arsenic adsorption caused by magnetite removal. The results will allow us to understand the changes of arsenic speciation under the effects of magnetite removal in copper tailings and show the effects of organic matter addition to the tailings. The results will be interpreted in terms of the influence of magnetite and organic matter, which will provide essential information for further phytoremediation practice.

PS 1557 Antioxidant Status and Levels of Some Essential Trace Elements and Heavy Metals in Individuals Occupationally Exposed to Municipal Solid Wastes

A. O. Odewabi[1] and M. Ekor[2]. [1]*Chemical Pathology and Immunology, Olabisi Onabnjo University Teaching Hospital, Sagamu, Nigeria and* [2]*Department of Pharmacology, School of Medical Sciences, University of Cape Coast, Cape Coast, Ghana.*

Objectives: Waste management workers (WMW) in Nigeria are at risk of work-related disorders. The aim of the present study was to determine blood concentration of some essential trace elements (Se, Zn, Cu, Mg, Mn, Fe), toxic metals (Pb, Cr, Hg,), and antioxidant/prooxidant markers [ferric reducing ability of plasma (FRAP), ceruloplasmin and thiobarbituric acid reactive substances (TBARS)] in municipal solid waste workers of Sagamu, South West Nigeria. Materials and Methods: A total of 75 subjects consisting of 30 WMW and 45 Non-WMW were recruited by purposive sampling. The element concentrations were measured by means of an atomic absorption spectrophotometer after wet-acid digestion. The validity and accuracy was checked by using certified reference materials. Ceruloplasmin TBARS and FRAP were determined using standard procedures. Results: WMW exhibited significantly higher lipid peroxidation, depletion of antioxidant and alterations of levels of trace element and heavy metals. Significant ($p < 0.001$) elevation of ceruloplasmin (Cp) was associated with significant ($p < 0.001$) increase in TBARS and significant decrease ($p < 0.001$) in FRAP when compared with control. Apart from significant ($p < 0.05$) decrease level of iron (Fe) and significant ($p < 0.001$) increases in lead (Pb) and copper (Cu) observed in WMW, other trace elements and heavy metals analyzed (manganese (Mn), magnesium (Mg), chromium (Cr), mercury (Hg), selenium (Se) and zinc (Zn)) did not change significantly ($p > 0.05$) when compared with the control. A negative correlation between Cp ($r = -0.182$; $p > 0.05$) and lead as well as a positive correlation between FRAP ($r = 0.277$; $p<0.05$), zinc ($r = 0.230$; $p<0.05$) and lead and between copper ($r = 0.541$; $p > 0.001$) and iron were observed in WMW. Conclusions: Exposure to MSW predisposes to oxidative stress and lead toxicity and Cp appears promising to monitor lead overload in Nigerian WMW.

PS 1558 Deriving Algorithms for Matrix-to-Matrix Relations and Reverse Dosimetry of Selenium from Pooled Biomonitoring Data

N. Noisel[1], M. Bouchard[1] and G. Carrier[1, 2]. [1]*Dept de Santé Environnementale et Santé au Travail, Université de Montreal, Montreal, QC, Canada and* [2]*Direction de la Santé Environnementale et de la Toxicologie, Institut National de Santé Publique du Québec (INSPQ), Montreal, QC, Canada.*

Biomonitoring is increasingly used to assess exposure to selenium (Se) in the population. However, there is little harmonization among protocols used in the different studies (varying biological matrices, differences in expression of results (concentrations versus amounts, units)). This makes inter-comparison of biomonitoring results across studies difficult. Hence, the aim of this study was to perform a systematic meta-analysis of the relationships between Se intakes and concentrations in different accessible biological matrices from an extended review of Se biomonitoring studies. Inclusion and exclusion criteria were used and led to select 75 published biomonitoring studies in humans. This represents 8628 individuals who provided biological samples aiming at documenting Se exposure and/or Se concentrations in two or more biological matrices. Mathematical algorithms that relate Se intakes to biological concentrations and establish matrix-to-matrix associations were derived from these pooled biomonitoring data. Logarithmic regressions showed good correlations between Se intakes and whole blood concentrations (R2 = 0.884), plasma concentrations (R2 = 0.863) and urinary excretion rates (R2 = 0.958). Blood and plasma concentrations were also strongly related (R2 = 0.874), as were whole blood concentrations and urinary excretion rates (R2 = 0.953). The log-regression coefficients allowed interpreting Se physiology. Se concentrations in plasma tend to plateau when daily intake exceed 150 μg/d, whereas Se in urine increases rapidly above this threshold. The application of the algorithms to other independent data sets confirmed that interpretation of results on the basis of Se in hair and toenail may be misleading if external contamination is not avoided. Finally, this approach based on pooled data has the advantage to cover a wide range of exposure and to provide results with a high level of confidence.

PS 1559 Semen Uranium Concentrations in Gulf War I Depleted Uranium-Exposed Veterans

K. S. Squibb[1, 2], D. Hoover[1, 2], S. E. Hines[1, 2], P. Gucer[1, 2], T. I. Todorov[3], J. Centeno[4], M. Oliver[1, 2], J. Gaitens[1, 2] and M. McDiarmid[1, 2]. [1]*Dept. of Veterans Affairs Medical Center, Baltimore, MD,* [2]*UM School of Medicine, Baltimore, MD,* [3]*Food and Drug Administration, College Park, MD and* [4]*Joint Pathology Center, Silver Spring, MD.*

The Department of Veterans Affairs' (VA) Depleted Uranium (DU) Follow-up Program provides health surveillance for Gulf War I and OIF Veterans who were in friendly-fire events involving DU munitions. Members of this cohort with retained embedded fragments continue to excrete high levels of urine uranium (uU) with a DU isotopic signature. The purpose of this study was to determine if 1) semen U levels are elevated in this cohort and 2) if they are correlated with U in other body compartments (urine, blood and plasma). Participants in the 2009 biennial surveillance visit provided blood, semen and 24-hour urine specimens. After collection, thirty-five (35) semen samples were incubated at 37o C for liquefaction; then transferred to acid-washed Teflon vials for sample preparation and U analysis by ICP-MS. Concentrations of U in semen ranged from <0.8-3,350 pg/g with a median of 4.2 pg/g. Associations were explored between U concentrations in semen, urine, blood and plasma using Spearman correlations. Semen U was positively correlated with other body compartment U concentrations for all participants: urine U (r=0.85), blood U (r=0.73), and plasma U (r=0.82) (p<0.000 for all correlations). Results indicate that U levels in semen reflect systemic concentrations, which have remained high for > 20 years in Veterans with DU embedded fragments. Data suggest that urine samples may be used to estimate semen U levels. Our previous work demonstrated no significant semen or sperm abnormalities when correlated with uU levels; thus, these data suggest that U is not a significant reproductive toxicant at low concentrations. Supported by the Department of Veterans Affairs and approved by the Baltimore VA Medical Center's Office of Research and Development and University of Maryland's School of Medicine Institutional Review Board.

PS 1560 On-Site Monitoring of Marcellus Drilling Operations

M. McCawley and T. L. Knuckles. *West Virginia University, Morgantown, WV.*

The West Virginia Natural Gas Horizontal Well Control Act of 2011 required determination of the effectiveness of a 625 foot set-back from the center of the pad of a horizontal well drilling site. An investigation was conducted at seven drilling sites to collect data on particulate matter (PM), volatile organic compounds

(VOCs), noise, radiation, and light levels. Measurements of air contaminants were taken during active drilling to characterize levels that might be found at 625 ft from the well pad center at unconventional gas drilling sites. While PM and VOC's were detected at the well sites, none were above National Ambient Air Quality standards (NAAQS) at the 625 ft setback limit. Activities at the well site however did not allow for a consensus comparison to the NAAQS values. Some benzene concentrations were found to be 85ppb, 10 fold higher than what the CDC calls the "the minimum risk level for no health effects" and sound levels could exceed 95 decibels. Since, not all of the studied contaminants emanate from the center of the pad, regulations could consider other reference points (such as roadways) from which to measure a setback distance but there does not appear to be a simple solution to specifying a single point to assure control. The activities follow the terrain of the site and the needs of the process. Activities associated with some possible sources of the studied contaminants can occur closer than 625 feet from a sensitive receptor. Studies have also shown that the meteorology (and topography) may be a more important factor than distance measured on a map for determining air contaminant concentration. While the levels of contaminants that were seen were not unexpected based on previous studies they did fluctuate over a wide range. Consideration needs to be given to increased quality control monitoring of the process using direct-reading monitors at sensitive locations near the well pad, connected wirelessly to the operations center at the pad which in turn can control output from all sources.

PS 1561 Potential for Exacerbation of Pediatric Asthma Due to Ultrafine Particle Exposure from Marcellus Shale Gas Drilling Operations

E. Eyoita[1], M. McCawley[1], S. Chatterjee[2], W. C. Mercer[2], W. W. Harris[2], T. L. Knuckles[1] and H. P. Gamble[2]. *[1]West Virginia University, Morgantown, WV and [2]Ohio County Health Department, Wheeling, WV.*

Marcellus Shale drilling operations utilize diesel engines which result in a release of ultrafine particles (UFPs; particles less than 0.1 μm) during combustion processes. Recent epidemiological studies have found a positive association between UFPs and pulmonary health effects in humans. Furthermore, UFPs are of increasing concern because studies show they exacerbate asthma symptoms, especially in children. In this paper, we describe sampling conducted in Ohio County, West Virginia using a new, battery-operated, portable differential mobility analyzer to measure the concentration and size distribution of UFPs to predict health effects that may occur in areas where the wells are located. This allowed not only total particle number concentration to be determined but also the lung dose to be estimated based on established lung deposition models. We measured concentrations that averaged as low as 4,000 to as high as 46,000 particles per cm3 in areas around drilling operations. These concentrations were generally found to be higher than the 8,000 particles/cm3 concentration associated with increased emergency room admissions for pediatric asthma. Moreover, these concentrations were consistent with ambient air particle counts of obtained near mountaintop mining operations, which have high levels of cardiovascular disease and cancer in the population. The concentrations of UFPs were similar between the two industrial sites. Collectively, these data suggest a substantial ultrafine particle exposure burden to the populace proximal to the mining and drilling operations, which may be driving some of the adverse respiratory and cardiovascular effects. Currently, the Environmental Protection Agency does not monitor ultrafine particle concentrations in these areas, nor are there proposed limits for exposure. Hence, a health monitoring plan needs to be put in place with local hospitals to assure protection of the health of the population.

PS 1562 Comparison of Airborne Exposures from Diesel and Biodiesel Emissions

R. J. Reed, R. Wagoner, E. Lutz and J. Burgess. *Community, Environment, and Policy, University of Arizona, Tucson, AZ.* Sponsor: C. Lantz.

Introduction: Biodiesel mixtures are being used in the mining industry as an alternative to diesel to meet emission standards set by the Mining Safety and Health Administration (MSHA). This study compares the airborne exposures of diesel and biodiesel-blend emissions in an underground mine.
Methods: Twenty-two non-smoking subjects were exposed to emissions from diesel fuel and, separately, a biodiesel-blend (75% biodiesel, 25% diesel) while operating a load-haul-dump (LHD) vehicle in an underground mine. Personal samples were collected for total diesel particulate matter (DPM), respirable DPM, respirable dust, formaldehyde, acetaldehyde, naphthalene, nitric oxide (NO), and nitrogen dioxide (NO2) and analyzed according to National Institute for Occupational Safety and Health (NIOSH) methods.
Results: The average sampling time was 203 ±18.7 minutes. Mean respirable DPM (309 ±134 and 207 ±111 ug/m3, p=0.006), acetaldehyde (0.044 ±0.04 and 0.029 ±0.01 ppm, p=0.021), and naphthalene (0.0013 ±0.0007 and 0.0006 ±0.0003 ppm, p=0.002) time-weighted average (TWA) exposure concentrations were greater for diesel fuel than the biodiesel-blend, while total DPM (539 ±209 and 753 ±243 ug/m3, p=0.014) and respirable dust (0.60 ±0.38 and 0.86 ±0.29 mg/m3, p=0.035) TWA concentrations were less for diesel compared to the biodiesel-blend. There was no observed difference in TWA concentrations for formaldehyde (0.136 ± 0.129 and 0.09 ±0.022, p=0.114), NO (10.9 ±4.2 and 12.0 ±4.8, p=0.259), or NO2 (1.33 ±0.66 and 1.26 ±0.61, p=0.949) between the diesel and biodiesel-blend.
Discussion: Our study demonstrates that use of biodiesel blends may reduce exposures to respirable DPM, acetaldehyde, and naphthalene.

PS 1563 Comparison of Acute Human Health Effects from Diesel and Biodiesel Emissions

V. Lee, A. Nielsen, E. Lutz and J. Burgess. *Community, Environment, and Policy, University of Arizona, Tucson, AZ.* Sponsor: C. Lantz.

Human and animal studies suggest that diesel exhaust (DE) not only impairs vascular and pulmonary function, but is a probable carcinogen. Within the mining industry, there has been a shift toward replacing diesel with a diesel/biodiesel mixture, despite what little is known about the acute health effects of biodiesel exhaust (BE) inhalation. Using a cross-over study design, 22 participants were exposed to DE and BE (the latter from a 25% diesel/75% biodiesel mixture) in an underground mine. Pre- and post-exposure flow mediated dilation (FMD) of the brachial artery, exhaled carbon monoxide (CO), exhaled nitric oxide (NO), and spirometry (forced expiratory volume in one second, FEV1) were evaluated. DE and BE exposure periods were separated by approximately 3 months for each participant. The changes in baseline and peak FMD readings pre- and post-exposure to diesel were not significantly different than those measured for biodiesel. There was a statistically significant increase in post-exposure exhaled CO measurements for both fuel types tested and in post-exposure exhaled NO measurements for DE only; however, these changes were not different between the two fuel types. There was a statistically significant decrease from the baseline FEV1 value of 4.22L to post-exposure values for both DE and BE exhaust (3.98L, p=0.0001; 4.13L, p=0.0461, respectively), as well as a difference between the two fuel types (p=0.022), with a greater decrease in FEV1 in participants exposed to DE. These findings indicate that inhalation of both DE and BE result in acute health effects. There were no differences in the changes in biomarkers between the two fuel types, except in the case of FEV1. Based on these limited data, switching from diesel to biodiesel resulted in only a small improvement in acute health effects.

PS 1564 Airborne Impacts of the Richmond, California, Chevron Refinery Fire: A Case Study Showing the Difficulty of Correlating Real-Time Data, Exposure Assessment, and Public Health Impacts

S. B. DuTeaux. *Office of Emergency Response, California Air Resources Board, Sacramento, CA.*

Shortly after 6:30 p.m. on August 6, 2012, hazardous materials responders and firefighters were called to a fire at the Chevron Refinery in Richmond, California. A shelter-in-place order was quickly issued for surrounding communities warning residents to stay inside and reduce exposure to the smoke. During the fire, Chevron personnel took 17 direct readings of air contaminants on the refinery property as well as 19 air grab samples downwind from the fire. All readings were either below the limit of detection and/or below the Reference Exposure Levels (RELs) established by the Office of Environmental Health Hazard Assessment (OEHHA) for sulfur compounds and hydrocarbons. Local environmental health and air quality agencies collected additional air grab samples in neighborhoods downwind from the fire. The samples were analyzed for toxic air contaminants with the results showing the presence of approximately 20 volatile chemicals. Concentrations were above typical background levels but below levels associated with adverse health effects. The exception was one sample that contained 7.41 μg/m3 acrolein, well above the OEHHA acute REL of 2.5 μg/m3. Concentrations of particulate matter from the smoke were below state and federal air quality standards, although marginally higher when compared to seasonally adjusted concentrations. With the exception of acrolein, no toxic air contaminants were detected at levels associated with adverse health effects and particulate matter levels were near normal. Even so, on the day of the fire over 360 patients were seen in area emergency departments and one adult and two children were hospitalized. In the ensuing weeks, over 15,000 individuals sought medical care mostly for minor nose, throat, or eye irritation or respiratory effects. This incident underscores the difficulty of conducting an exposure assessment for short-term releases as well as the challenge of aligning real-time concentration data with reported public health impacts.

PS 1565 Health Surveillance Study on Printed Electronics (PE) Workplace

J. Lee[1], E. Sohn[1], J. Ahn[2], K. Ahn[3], K. Kim[1], T. Lee[4], J. Shin[5], Y. Chung[1] and I. Yu[1]. *[1]Institute of Nanoproduct Safety Research, Hoseo University, Asan, Republic of Korea, [2]Myungji Safety and Hygiene Laboratory, Nonsan, Republic of Korea, [3]Department of Mechanical Engineering, Hanyang University, Ansan, Republic of Korea, [4]Korea Institute of Machinery and Materials, Daejeon, Republic of Korea and [5]Occupational Lung Diseases Institute, KCOMWEL, Ansan, Republic of Korea.*

PE using converging technologies, such as printing, fine mechanics, nanotechnology, electronics, and other new technologies raise additional health and safety concerns to those experienced in the traditional printing industry. We have conducted a health surveillance study in a PE workplace based on a walk-though survey and personal and area sampling, and collection of blood and urine samples. There was no indication of exposure to excess silver nanoparticles or carbon nanotubes. Exposure to organic solvents was lower than current occupational exposure limits in terms of TWA, yet there were some organic solvent exposure exceeding current OELs during short work duration. Lack of engineering controls, such as local exhaust ventilation, correct enclosure, and duct connection were found in the walk-through survey. Most workers showed normal range of blood biochemistry and hematology values except one worker who was advised to be checked by physician immediately. Some workers showed exceed levels of BEIs including carboxyhemoglobin (marker for methylene chloride exposure) and acetone (marker for isopropyl alcohol). The levels for hippuric acid and methyl hippuric were within normal ranges, indicating low exposure to toluene and xylene. Few office workers were exposed to low concentrations of methylene chloride, which was under investigation to find cause. Cleaning work, a major emission operation, was not conducted within a hood, and waste from the cleaning work was not properly disposed of. Therefore, the present health surveillance study on PE results suggested that the PE industry should take care of organic solvent exposure to protect workers from occupational safety and health risks. If PE process was in full scale with full shift in the clean room with recirculated air, it would be real health risk to PE workers.

PS 1566 Microcystin Extraction from Human Blood Serum: Pitfalls and Solutions

A. Heussner[1], D. R. Dietrich[1], S. Altaner[1], L. Kamp[2] and F. Rubio[2]. *[1]Human & Environmental Toxicology, University of Konstanz, Konstanz, Germany and [2]Abraxis LLC, Warminster, PA.*

Microcystins (MCs) contaminate water bodies due to cyanobacterial blooms all over the world leading to a public risk of intoxication by exposure to contaminated water, food (e.g. fish) or algal food supplements. In order to enable monitoring of human exposure, sensitive screening methods are needed. ELISA has been demonstrated as a robust routine tool for MC quantification in environmental samples. However, some problems regularly occur during sample preparation leading to MC loss and therefore underestimation of the true concentration. The aim of the current study was to assess the pitfalls of the MC-extraction method from complex media with more detail.

For this, MCs (MC-LR, MC-YR, MC-RR, MC-LA, MC-LW, MC-LF and defined MC mixtures; 1-1,000 μg/L) were spiked into human blood serum as a surrogate for very complex sample media and quantified using the commercially available Adda-ELISA (Abraxis, Warminster, PA, USA) after standard extraction (methanol extraction with subsequent SPE). To detect the potential influence of sample storage and preparation materials different types of material such as glass, standard polypropylene and surface-treated polypropylene were compared.

Loss of MC during preparation and storage is largely dependent on (i) the handling of the stored material, (ii) the 'surface' of the storage material and (iii) the hydrophobicity of the MCs.

PS 1567 Vegetable Uptake and Human Exposure Assessment from a Community Garden with Elevated ∑DDT

E. N. Liberda[1] and L. J. Tsuji[2]. *[1]School of Occupational and Public Health, Ryerson University, Toronto, ON, Canada and [2]Environment and Resource Studies/Health Studies, University of Waterloo, Waterloo, ON, Canada.*

Introduction

Two agroforestry gardens and an open garden were prepared to grow vegetables in a remote Canadian First Nation community. Soil was sampled at the beginning of the project, while, at the end of the season potatoes and beans were collected and matched to the previous soil plots. Contaminant analysis consisted of a suite of organochlorines including DDT/DDE/DDD (2,4-DDT, 4,4-DDT, 2,4-DDE, 4,4-DDE, 2,4-DDD, 4,4-DDD) and a suite of metals. Based on our ∑DDT findings, we performed an exposure assessment associated with ingestion of contaminated vegetables.

Methods

Soil samples were taken randomly in each of the three plots (Plot A and B were the agroforestry sites, while Plot C was the open site), and vegetable samples were later matched to the soil samples. Soil samples were taken to the depth of the rooting zone. All samples were sent directly to Queen's University, Analytical Services Unit, for organochlorine analysis via GC-MS and metal analysis via ICP-OES. Exposure assessment was based on the analytical results and standard Canadian food consumption data set by Health Canada.

Conclusion and Discussion

Exposure analyses associated with the ingestion of vegetables from Plot A, the elevated ∑DDT site, were orders of magnitude less than the regulatory guidelines (e.g., acceptable daily intake [ADI] or reference dose [RfD]). Soil levels of ∑DDT were found to exceed Canadian regulatory guidelines of 0.7 mg/kg for agricultural or residential/parkland use only in Plot A. Contaminated soil from Plot A was correlated with vegetable tissue concentrations. While human exposure to the contaminated vegetables through ingestion may not pose a health risk, the contaminated soil did exceed regulatory guidelines. Thus, produce from Plot A was not distributed to residents and use of the site was discontinued.

PS 1568 Population Variation in Biomonitoring Data for Persistent Analytes: An Examination of Multiple Population-Based Datasets

L. Aylward[1, 2] and J. Mueller[2]. *[1]Summit Toxicology, LLP, Falls Church, VA and [2]ENTOX, University of Queensland, Brisbane, QLD, Australia.*

National biomonitoring efforts designed to characterize the levels and distribution of pollutants in populations have typically relied upon a resource-intensive sampling strategy and analysis of hundreds or thousands of individual biological samples. In Australia, a series of studies relying on pooled serum samples, a less resource-intensive approach, has been employed to characterize central tendencies of concentrations of selected persistent analytes, but this approach does not provide estimates of typical upper bound concentrations. This analysis assesses the feasibility of an empirical approach to estimating population upper bound reference values based on the examination of population variation from available biomonitoring datasets from the US, Canada, Germany, and the Catalonian region of Spain, with the results tested against data from the Flemish population of Belgium. Arithmetic mean concentrations and the ratio of the 95th percentile to the mean (P95:mean) were assessed in each survey for defined age subgroups for three polychlorinated biphenyls (PCBs 138, 153, and 180), hexachlorobenzene (HCB), and p,p-dichlorodiphenyldichloroethylene (DDE). While arithmetic mean concentrations of each analyte varied widely across surveys, the P95:mean ratios were reasonably consistent across surveys for each analyte, with no clear variation across age groups. The results are consistent with generally lognormal distributions of analyte concentrations in the populations studied, with similar geometric standard deviations across surveys, even when the population means were significantly different. The central tendency estimate of P95:mean ratios was approximately 2.2 for the three PCBs and HCB and 3.0 for DDE, and the approach accurately predicted the 95th percentiles in the Flemish dataset. These results can be used in combination with the Australian pooled sampling results to estimate upper bound reference values for use in evaluating individual biomonitoring data for the included analytes.

PS 1569 Serum Steatohepatitis Biomarker and Proinflammatory Cytokine Elevation in Response to Polychlorinated Biphenyl Exposures in the Anniston Community Health Study (ACHS)

H. Clair[1], K. C. Falkner[1], R. A. Prough[2] and M. Cave[1, 3]. *[1]Department of Medicine/GI, University of Louisville, Louisville, KY, [2]Biochemistry, University of Louisville, Louisville, KY and [3]Robley Rex VAMC, Louisville, KY.*

Monsanto Corporation previously operated a PCB production facility in Anniston, Alabama, and high-level environmental polychlorinated biphenyl (PCB) contamination is present there. In order to study the health effects of PCBs, a residential adult cohort (Anniston Community Health Survey – ACHS) was previously assembled. Hypertension and diabetes were linked to PCB exposures in the ACHS. Nonalcoholic steatohepatitis (NASH) has previously been associated with PCB exposures in the National Health and Nutrition Examination Survey (NHANES). The objective of this study is to determine whether NASH biomarker and adipocytokine abnormalities are present in the ACHS cohort. Archived fasting serum samples were obtained from ACHS (n=625), an unexposed healthy control group (HC, negative controls, n=11), and unexposed subjects with biopsy-proven steatohepatitis related to obesity (NASH, positive controls, n=34). Cytokeratin 18

(CK18) M30 and M65 (hepatocellular apoptosis and necrosis biomarkers) and adipocytokines were measured. Group means were compared by ANOVA with significance set at $p<0.05$. CK18 M65 was increased in ACHS vs. HC, while CK18 M30 was decreased. Both CK18 M65 and M30 were decreased in ACHS vs. NASH. IL-6 and IL-8 were increased in ACHS vs. both HC and NASH. Of these, IL-8 was increased to the greatest extent in ACHS (52 fold vs. HC). TNFα was increased in ACHS vs. NASH. Compared to HC, adiponectin was decreased and leptin increased to similar degrees in both ACHS and NASH. Insulin was increased in NASH vs. both ACHS and HC. Steatohepatitis biomarkers were abnormal in ACHS. Some differences existed between ACHS and unexposed subjects with NASH apparently related to obesity. Liver injury in ACHS was characterized by necrosis with high-level elevation of IL-8. These data further implicate PCB exposures in steatohepatitis and systemic inflammation.

PS 1570 Quantification of Tissue Bisphenol A and Global Methylation Profiles in Kidney, Liver, and Placenta from 1st and 2nd Trimester Human Clinical Samples

M. S. Nahar[1], C. Liao[2], K. Kannan[2] and D. Dolinoy[1]. [1]*Environmental Health Science, University of Michigan, Ann Arbor, MI and* [2]*Wadsworth Center, New York State Department of Health, Albany, NY.*

The ubiquitous monomer, bisphenol A (BPA), is an endocrine active compound used in a variety of consumer products. BPA has been associated with adverse health outcomes ranging from reproductive dysfunction to chronic diseases. Studies suggest that BPA operates by altering DNA methylation or other epigenetic markers, especially during critical windows of development. Characterization of BPA levels and epigenetic profiles across multiple tissues are currently limited to animal models or not well defined. Herein, we report tissue concentrations of BPA and global DNA methylation levels in healthy 1st and 2nd trimester human kidney, liver, and placental specimens (matched N=12 per tissue) obtained from the University of Washington Laboratory of Developmental Biology. Total BPA concentrations, measured using liquid chromatography tandem mass spectrometry, significantly differed across matched specimens (p-value: 0.002) with geometric means at 0.81, 9.19, and 1.62 ng/g for kidney, liver, and placenta, respectively. When global methylation was quantified at long interspersed retrotransposons (LINE1) repetitive elements using pyrosequencing and at CCGG sites across the genome using the Luminometric Methylation Assay (LUMA), methylation significantly differed across kidney, liver, and placenta (p-values <0.001). Average LINE1 methylation was 77.9% in kidney, 79.5% in liver, and 58.3% in placenta, while average LUMA methylation was 76.9% in kidney, 66.4% in liver, and 59.1% in placenta. No significant association was observed between total BPA and global methylation in fetal kidney or liver. However, there was a 0.23% increase in LINE1 methylation with 1 ng/g increase in total BPA in placenta (p-value: 0.002). Results suggest that BPA concentrations and methylation profiles are tissue specific in early life, and characterizing these differences will be important for exposure and risk assessment.

PS 1571 Biochemical Parameters and Fluoride Levels in Serum and Urine of Livestock Animals Accidentally Exposed to Hydrofluoric Acid

H. Kang, Y. Park, D. Kim and B. So. *Veterinary Drugs and Biologics Division, Animal and Plant Quarantine Agency, Anyang, Republic of Korea.*

This study aimed to evaluate the exposure of hydrofluoric acid and health status in cattle and other livestock animals raised near hydrofluric acid accident place by determining the level of fluoride ion and biochemical parameters in urine and serum. Cattle (n=111), goats (n=25) and chickens (n=5) raised in the farm near accident place were selected. Urine or blood serum samples were taken from 10-20 % of cattle per farm considering population on 17 days later of accident. Concentrations of fluoride ion (F-) in the samples were analyzed by fluoride ion selective electrode method. The concentrations of creatinine, calcium ion and other biochemical parameters in serum and urine were determined using a biochemistry analyzer. The fluoride ion concentration in urine was normalized by divided by creatinine values of urine to normalize concentration of fluoride ion in urine. The mean concentration of fluoride ion in urine of cattle (expressed as F- mg/g creatinine) were 27.8 (100m), 24.4 (500m), 11.1 (800m), 16.3 (900m), 3.02 (1.2km), 9.16 (1.5 km) and 3.58 in control group. The mean levels of fluoride ion in serum of cattle (expressed as mg/L) were 0.23 (100m), 0.15 (500m), 0.23 (800m), 0.11 (900m), 0.07 (1.2km), 0.16 (1.5 km) and 0.10 in control group. The mean concentration of fluoride ion in serum of goat (expressed as mg/L) were 0.39 (100m), 0.31 (600m), 0.02 (900m), and 0.08 in control group. The mean levels of fluoride ion in serum of chicken (expressed as mg/L) were 0.35 (100m) and 0.02 (600m). The mean±SD concentration of calcium ion in serum of cattle exposed to hydrofluoric acid (mg/dL) were 9.72±0.41 (100m), 9.54±0.57 (500m), 8.31±0.44 (800m), 9.06±0.40 (900m), 8.36±0.89 (1.2km), 9.13±0.98 (1.5 km) and 10.48±1.43 in control group. This study showed that the level of fluoride in serum and urine of animals exposed to hydrofluoric acid were decreased depending on the distance from leakage site. However, concentration of fluoride ion in samples was below the reference level of fluoride toxicosis in cattle.

PS 1572 Comparison of the Kinetics of Various Biomarkers of Benzo[a]pyrene Exposure following Different Routes of Entry in Rats

M. Moreau[1] and M. Bouchard[1, 2]. [1]*Department of Environmental and Occupational Health, University of Montreal, Montreal, QC, Canada and* [2]*Chair in Toxicological Risk Assessment and Management, University of Montreal, Montreal, QC, Canada.*

Exposure to benzo(a)pyrene (BaP), a polycyclic aromatic hydrocarbon (PAH) classified as a known carcinogen in humans (IARC), is of great health concern for both workers and the general population. The project aimed at comparing the kinetics of key biomarkers of BaP exposure in rats following different routes of entry. Blood and excretion time courses of BaP and key biomarkers were assessed in rats exposed to a single intravenous, intratracheal, oral and cutaneous dose of 40μmol/kg BaP. BaP and several metabolites (3-and 7-OHBaP, 4,5-and 7,8-diol-BaP, tetrol, 1,6 -, 3,6- and 7,8-dione-BaP) were measured in blood, urine and feces collected at frequent intervals over 72 h post-treatment, using HPLC/fluorescence. Only 3-OHBaP was detectable in blood at all time points. In urine, total amounts of BaP metabolites excreted over the 0-72h period followed the order: 4,5-diolBaP≥3-OHBaP>7-OHBaP>7,8-diolBaP following intravenous injection and intratracheal instillation, 3-OHBaP>7-OHBaP>4,5-diolBaP>7,8-diolBaP after cutaneous application and 3-OHBaP>4,5-diolBaP≥7-OHBaP>7,8-diolBaP following oral administration. In feces, total amounts of BaP metabolites recovered over the same period were: 7-OHBaP≥3-OHBaP>>4,5-diolBaP>7,8-diolBaP following all administration routes. Diones were not detectable using the developed method. For all routes of administration, excretion of 4,5-diolBaP was almost complete over the 0-24 h period in contrast with 3- and 7-OHBaP. After intravenous injection, intratracheal instillation and oral treatment, peak excretion of 3- and 7-OHBaP was reached in the 0-24 h period but only after 48 h post-treatment following cutaneous application. This study confirms the interest of measuring multiple metabolites due to the route-to-route differences in relative excretion of the different biomarkers and in time courses of diolBaP versus OHBaP. Concentration ratio of the different metabolites may help indicate time and main route of exposure.

PS 1573 A Cellular Model to Evaluate Salivary Gland Uptake and Clearance of Pesticides: A Novel Non-Invasive Biomonitoring Strategy

C. Timchalk, J. N. Smith and T. J. Weber. *Systems Toxicology, Pacific Northwest National Laboratory, Richland, WA.*

The use of saliva as a biomonitoring matrix has potential to significantly advance quantitative dosimetry as an integral component within epidemiology studies. A major limitation for saliva biomonitoring has been an inability to identify which chemicals are readily cleared in saliva, at levels that can be detected analytically. To address this limitation, immortalized Par C10 cells (parotid gland origin) grown on a Transwell® insert (3 μm pore) were used to quantify the uptake and clearance of trichloropyridinol (TCPy) the metabolite of the insecticide chlorpyrifos. Cells seeded on Transwell inserts were maintained until 7-days post-confluence at which time they displayed expression of parotic acinar cell proteins and localization of tight junction proteins at points of cell-cell contact. For uptake/clearance studies a range of TCPy concentrations (0.2-10 μg/mL) were evaluated. TCPy was added to the basolateral chamber (lower chamber) and sampled from the apical chamber (upper chamber) longitudinally for 4 hours. In the absence of cells, TCPy rapidly diffused across the transwell; whereas, the transport rate was substantially reduced with cells, and apical concentrations of TCPy were proportional to dose. These in vitro results are consistent with in vivo pharmacokinetic model predictions where TCPy salivary gland clearance is described with a 1-compartment model and transfer from blood to saliva is via passive transcellular diffusion. These experiments have established the feasibility of utilizing an in vitro cell based uptake/clearance assay coupled with pharmacokinetic modeling as a novel chemical screening strategy to identify ideal chemical candidates for saliva biomonitoring. This approach will be further evaluated using a broader range of pesticides with varying physical and chemical properties. Once established, this approach can be exploited for biomonitoring without the need to conduct more challenging in vivo saliva clearance studies. Supported by CDC/NIOSH grant R01 OH008173.

PS 1574 Concentrations of Diacetyl and 2, 3-Pentanedione in Mainstream Cigarette Smoke: A Comparison to Workplace Exposures

J. S. Pierce[1], A. Abelmann[1], L. J. Spicer[1], R. Adams[1] and B. L. Finley[2]. [1]*Cardno ChemRisk, Chicago, IL and* [2]*Cardno ChemRisk, Brooklyn, NY.*

Diacetyl and 2,3-pentanedione inhalation have been suggested as causes of severe respiratory disease, including bronchiolitis obliterans, in food/flavoring manufacturing workers. Both compounds are present in many food items, tobacco, and other consumer products, but estimates of exposures associated with the use of these goods are scant.
A study was conducted to characterize exposures to diacetyl and 2,3-pentanedione associated with cigarette smoking. The yields (μg/cigarette) of diacetyl and 2,3-pentanedione in mainstream (MS) cigarette smoke were evaluated for six tobacco products (e.g., both full-flavor and light cigarettes of three different brands) under three smoking regimens (ISO, Massachusetts Department of Public Health, and Health Canada Intense) using a standard smoking machine.
The mean diacetyl concentrations in MS smoke ranged from 250-361 ppm for all tobacco products and smoking regimens, and the mean cumulative exposures associated with 1 pack-year ranged from 1.1-1.9 ppm-years. For 2,3-pentanedione, the mean concentrations in MS smoke ranged from 32.2-50.1 ppm, and the mean cumulative exposures associated with 1 pack-year ranged from 0.14-0.26 ppm-years.
We found that diacetyl and 2,3-pentanedione exposures from cigarette smoking far exceed occupational diacetyl exposures for most food/flavoring workers who smoke. This suggests that previous claims of a significant exposure-response relationship between diacetyl inhalation and respiratory disease in food/flavoring workers were confounded, because none of the investigations accounted for non-occupational diacetyl exposure, yet all of the cohorts evaluated had considerable smoking histories. Further, because smoking has not been shown to be a risk factor for bronchiolitis obliterans, our findings suggest that diacetyl and/or 2,3-pentanedione exposure is not a risk factor for this disease.

PS 1575 Headspace and Small-Chamber Studies of Airborne Diacetyl Concentrations Associated with Selected Food Flavoring Mixtures

P. K. Scott[1], A. Abelmann[2], H. Avens[3], S. Hoyt[4] and B. D. Kerger[5]. [1]*Cardno ChemRisk, Pittsburgh, PA,* [2]*Cardno ChemRisk, Chicago, IL,* [3]*Cardno ChemRisk, Boulder, CO,* [4]*Environmental Analytical Service, San Luis Obispo, CA and* [5]*Cardno ChemRisk, Aliso Viejo, CA.*

The accuracy and consistency of airborne diacetyl measurements can be significantly affected by a number of environmental and analytical factors that may increase variability of field measurements. Accordingly, airborne emissions modeling may augment field measurements in evaluating probable exposures to workers and others in a wide variety of settings where this common buttery food flavoring component may be found. We conducted a series of laboratory studies of emissions from pure diacetyl and spiked mixtures of selected vehicles used for adding flavorings to foods. The test materials included diacetyl (99% purity), 0.015 to 1.5% diacetyl in a water/propylene glycol mixture, deionized water, or soybean oil, and 3% diacetyl in a commercial steam distillate of milk fermentation known as 'butter starter distillate'. Diacetyl was quantified after direct injection via gas chromatography with flame ionization detection. Measured headspace concentrations were compared to estimated concentrations utilizing Raoult's law with and without UNIFAC activity coefficient corrections for each mixture. Headspace measurements averaged 60 to 90% higher than the ideal (Raoult's law) estimated values and the activity coefficient-adjusted estimates were 17 to 20% higher but within analytical error for the aqueous mixtures. At 1.5% diacetyl content, the magnitude of emissions from greatest to least was: steam distillate > water > water/propylene glycol > soybean oil. Furthermore, small chamber studies (ASTM D-5116) at 4 air changes per hour were compared to estimated values using a surface spill model; measured and modeled values were within 20% after incorporating the activity coefficient adjustments. We conclude that headspace (static) and small chamber (dynamic) measurements of airborne diacetyl are consistent with model-estimated concentrations after mixture-specific adjustment for activity coefficients.

PS 1576 Determination of Illicit Drug on the Hands of High-Volume Money Collectors Using LC- MS/MS

A. I. Hinds. *Toxicology, Colorado State University, Fort Collins, CO.*

Illicit drug use in the United States has been steadily increasing over the years. Contact transfer of illicit drugs from currency to the hands of individuals during the acts of drug trafficking has been seen in many countries worldwide. While this contamination of currency has been highly examined, the downstream transfer of illicit drug in occupational exposure has not been explored. This study examines whether high volume money collectors accumulate illicit drugs via contact transfer from the natural parameters of their occupation. Utilizing LC- MS/MS, ten hand samples from bank tellers were evaluated for content of cocaine, methamphetamine and oxycodone and other drugs. Samples were obtained from both hands of 5 individuals; four individuals work in a high volume money handling position. The fifth sample was a baseline comparison from an individual with no known background in this occupation. Cocaine was detected in ranges of 35ng- 450ng. Oxycodone and methamphetamine were detected in lower levels of 2ng- 7ng. The quantifiable presence of cocaine, oxycodone and methamphetamine illustrates the ability of crystal- and tablet-form drugs to affix in the fabric matrix of currency and transfer to skin via contact transfer under normal occupational parameters. These results further indicate that illicit drugs have the ability to transfer from currency to hands of high volume money collectors in detectable amounts. To our knowledge, this is the first research to demonstrate this occupational exposure and illustrates the need for more expansive investigation into this unique route of occupational exposure to illicit drug.

PS 1577 Development of a Targeted LC/MS Approach to Screen for 182 Pesticides in Urine Samples

A. Somers[1], T. Senn[2], D. Whittington[3], M. Vredevoogd[4], E. M. Vigoren[4], E. M. Faustman[4] and Y. Lin[4]. [1]*Life Sciences, Salish Kootenai College, Pablo, MT,* [2]*Pharmaceutics, University of Washington, Seattle, WA,* [3]*Medicinal Chemistry, University of Washington, Seattle, WA and* [4]*Environmental and Occupational Health Sciences, University of Washington, Seattle, WA.*

Pesticides are used all over the world and are found in many environments such as farmlands, agriculture facilities and residences. Many methods have been developed to detect specific pesticide residues in food and water. Exposure to high levels of pesticides can be harmful to agricultural workers and their families. Our goal on these studies was to develop a urinary screening method to determine whether individuals might be exposed to pesticides. We used mixtures of pesticide standards to develop a liquid chromatography tandem mass spectrometry method. A semi-quantitative curve was created by diluting the standard pesticide solutions. Urine samples were prepared by the addition of acetonitrile to precipitate proteins, and the supernatant was removed, evaporated and reconstituted for analysis. Standards and samples were analyzed using a Waters Xevo TQD UPLC-MS/MS. We monitored 182 pesticides using this method and screened 108 urine samples from adults and children. We found various pesticides present in the urine samples with the lower limits of detection ranging from 0.1 to 10 ng/mL. Examples include, but are not limited to, carbendazim, imidacloprid, isoxaben, methidathion, and quinalphos. Using this method, we can screen for pesticide exposure in urine samples from both adults and children. This screening technique will inform adaptive monitoring programs in which pesticides targeted are studied using specific and sensitive assays for more quantitative measurements of exposure.

PS 1578 NMR Analysis of the Antibiotic "Amoxicillin" in Urine

B. Huang and E. Champeil. *Sciences, John Jay College of Criminal Justice, New York City, NY.* Sponsor: S. Cheng.

The aminopenicillin, Amoxicillin, is used in many treatments against bacterial infections such as pneumonia, ulcers and urinary tract infections. However, when it is used incorrectly in combination with other drugs undesirable side effects can occur. Therefore, it is crucial to develop a method to accurately detect and quantify Amoxicillin in human biofluids. This research focuses on using 1H NMR spectroscopy for the analysis of Amoxicillin in urine samples. NMR spectroscopy is a powerful tool to analyze chemical structures. In addition, if a water suppression technique is used, direct analysis of aqueous based samples such as urine is possible without the need for separation and/or derivatisation steps. We present here initial results regarding the direct analysis of amoxicillin in urine using 1H NMR and a new water suppression technique PURGE (Presaturation Utilizing Relaxation Gradients and Echoes).We found that at small concentration, an extraction method of Amoxicillin from urine is necessary as some signals from the matrix interfere will those of Amoxicilin. We therefore also present a solid phase extraction method to isolate amoxicillin in urine samples at low concentrations before NMR analysis.

PS 1579 Silicone Wristbands As Personal Passive Samplers

K. Anderson[1], S. G. O'Connell[1] and L. Kincl[2]. [1]*Department of Environmental & Molecular Toxicology, Oregon State University, Corvallis, OR and* [2]*College of Public Health & Human Services, Oregon State University, Corvallis, OR.* Sponsor: G. Sower.

Active-sampling approaches are commonly used for personal monitoring, but are limited by energy usage and data that may not represent bioavailable concentrations. Current passive techniques are popular, but often involve extensive preparation, or are developed for only a small number of targeted compounds. In this work, we present a novel application for measuring environmental, bioavailable exposure with silicone wristbands as personal passive samplers. Laboratory methodology affecting pre-cleaning, infusion, and extraction were developed using commercially available silicone, and chromatographic background interference was reduced after solvent cleanup with good extraction efficiency (>96%). After finalizing laboratory methods, 49 compounds were sequestered during an ambient deployment which encompassed a diverse set of compounds including polycyclic aromatic hydrocarbons (PAHs), consumer products, personal care products, pesticides, phthalates, and other industrial compounds ranging in log Kow from -0.07 (caffeine) to 9.49 (tris(2-ethylhexyl) phosphate). In two hot asphalt occupational settings, silicone passive samplers sequestered 25 PAHs during 8- and 40-hour exposures, as well as 2 oxygenated-PAHs (benzofluorenone and fluorenone) suggesting sensitivity of the devices over a single work day or week ($p<0.05$, power = 0.85). Additionally, the amount of PAH sequestered differed between worksites ($p<0.05$, power = 0.99), suggesting evidence of spatial sensitivity and diverse applications.

PS 1580 Probabilistic Modeling of Baby Wipe Lotion Exposure

S. Dey[1], G. Carr[2] and S. Zhou[1]. [1]*Global Product Stewardship/Central Product Safety, The Procter & Gamble Company, Cincinnati, OH and* [2]*Quantitative Sciences, The Procter & Gamble Company, Cincinnati, OH.* Sponsor: S. Felter.

Reliable exposure data are essential in evaluating the safety of ingredients in any consumer product. Appropriate exposure assessment is particularly important for products targeted for children because children differ from adults in basic behavior patterns or product use pattern. The purpose of this study was to estimate the amount of lotion transferred from baby wipes to the babies' skin (mg/kg bw/day) using a probabilistic modeling approach. Three different variables, number of wipes used per day, body weight, and lotion transferred from baby wipes to baby skin, were combined to establish a distribution of lotion transfer values across the studied diaper wearing population. Habit and practice data on wipes usage from both the US and Germany were included. Gender, age, and weight were evaluated for their influence on the transfer. The data were analyzed using a probabilistic Monte Carlo simulation and a statistical population model of exposure was constructed to calculate total daily lotion transfer. The estimated 50th, 90th, and 95th percentiles of lotion transferred were predicted by the model against the child's age in months in relationship to the number of wipes used per day. Overall, the model indicates that exposure (mg/kg/day) declines in association with use of fewer wipes per day, as the child gets older. The average daily lotion transfer for a diapering period of 0-36 months ranged between 160 – 180 mg/kg/day (50th percentile) and 330 – 340 mg/kg/day (95th percentile) for US and Germany populations. This poster will provide a breakdown of age and gender specific value for lotion exposure. This model can be used for future assessments of exposure to baby wipe ingredient.

PS 1581 Air Pollution Exposure Model for Individuals (EMI) in Health Studies: Predicting Spatiotemporal Variability of Residential Air Exchange Rates

M. Breen[1], J. Burke[1], S. Batterman[2], A. Vette[1], G. Norris[1], C. Godwin[2], M. Landis[1], C. Croghan[1], B. Schultz[1] and M. Breen[3]. [1]*US Environmental Protection Agency, Research Triangle Park, NC,* [2]*University of Michigan, Ann Arbor, MI and* [3]*North Carolina State University, Raleigh, NC.*

In health studies, traffic-related air pollution is associated with adverse respiratory effects. Due to cost and participant burden of personal measurements, health studies often estimate exposures using local ambient air monitors. Since outdoor levels do not necessarily reflect personal exposures, we developed the Exposure Model for Individuals (EMI) in health studies. A critical aspect of EMI is estimation of the air exchange rate (AER) for individual homes where people spend most of their time. The AER, which is the airflow into and out of buildings, can substantially impact indoor air pollutant concentrations and resulting occupant exposures. Our goal was to evaluate and apply an AER model to predict residential AER for the Near-Road Exposures and Effects of Urban Air Pollutants Study (NEXUS), which is examining traffic-related air pollution exposures and respiratory effects in asthmatic children living near major roads in Detroit, Michigan. We developed an AER model to predict AER from building characteristics related to air leakage; local airport temperatures and wind speeds; and open windows. Cross validation was used with a subset of NEXUS homes (N=24) with daily AER measured on five consecutive days during fall 2010 and spring 2011. Individual predicted and measured AER closely matched with median absolute differences of 36% and 24% for the fall and spring, respectively. The model was then applied to predict hourly AER for all NEXUS homes (N=121) during the study (Sept. 2010 - Dec. 2012). The AER predictions show (1) substantial house-to-house (spatial) variations (0.1 - 2.0 h^{-1}) from building leakage differences; (2) slow oscillations from seasonal temperature changes; and (3) large transients from wind speed fluctuations. This study demonstrates the ability to predict spatiotemporal variability of residential AER in support of improving health study exposure assessments.

PS 1582 An Enterprise Integration Application for Chemical Information and Tools for Green Chemistry Initiatives

B. Ford[1, 3], A. Broughton[1, 3], N. Winje[1, 3], A. Sadovnikova[2, 3] and D. Johnson[1, 2, 3]. [1]*UC Berkeley, Berkeley, CA,* [2]*Univ Michigan, Ann Arbor, MI and* [3]*Elara Bioscience LLC, San Francisco, CA.*

As a collaborative effort between the Elarabio Internship programs in Molecular Toxicology at UC Berkeley and The Risk Science Center at the University of Michigan, an Open Access portal, ChemTIPSTER (Chemical Toxins In Products: a Safety, Toxicity, Environmental Resource) was created and linked to a cloud-based secure exchange, ToxPlatform, focused on the integration of services for multiple green chemistry initiatives. The goal was to provide consumers, industry stakeholders, environmental groups, and governmental agencies access to important information and tools to assess specific chemicals known or deemed to be of concern for human health and the environment while maintaining confidential business information (CBI) for product stakeholders. Additional research tools have also been incorporated into the portal that aid in the evaluation and creation of safer substitutes for hazardous ingredients in products. ToxPlatform provides enterprise level integration of a secure virtual data room with simple user access for publishing fully searchable documents with custom format types and owner defined sharing access. This secure transfer platform allows CBI to be maintained through business partners and departments, supply chains, and regulatory submissions. The initial content of both ToxPlatform and ChemTIPSTER focused on the Safer Consumer Products regulation of Cal EPA DTSC involved in ensuring that consumer products are safe and sustainable before they enter the marketplace. Specific projects associated through both systems included identification of chemicals within a product, connection of chemical structure to mechanisms of action related to associated hazard traits through chemical motifs, metabolites, and pathways, and the identification or design of safer alternatives. A case study with polymers used in garden hoses and chemical leakage of various phthalates and potential endocrine disruptors into water used for irrigation in organic gardening is highlighted.

PS 1583 Comparative Toxicity of Epicatechin vs. Borohydride-Reduced Nanosilver in Prokaryotic and Eukarytoic Models

K. Murphy[1], T. Collins[1], R. T. Posgai[1], B. Demmitt[1], S. M. Hussain[2], M. G. Nielsen[1], J. Robinson[1] and J. J. Rowe[1]. [1]*Department of Biology, Center for Tissue Regeneration and Engineering, University of Dayton, Dayton, OH and* [2]*Applied Biotechnology Branch, Human Effectiveness Directorate, Air Force Research Laboratory, Wright–Patterson Air Force Base, Dayton, OH.*

Nanosilver is increasingly finding use as an antibacterial agent in consumer goods and water purification in developing countries. Despite claims that it has no harmful effects on eukaryotes, toxicity tests in vitro and in vivo suggest otherwise. Powerful reductants used in traditional nanosilver synthesis may contribute to its toxicity. To test this hypothesis, we utilized epicatechin reduced AgNPs and compared their in vivo and in vitro toxicity to sodium borohydride reduced AgNPs. We also examined the antimicrobial activity of the two kinds of AgNPs using gram positive and gram negative microbial experimental systems. Both epicatechin (12nm) and sodium borohydride synthesized nanosilver (10nm) were effective antibacterial agents against Pseudomonas aeruginosa (Gram negative) and Staphylococcus aureus (Gram positive), however sodium borohydride reduced AgNPs were more effective. Conversely, only traditionally synthesized Ag NPs were toxic to eukaryotic organisms. HeLA cell culture experiments resulted in a LC50 of 113.56 ug/mL and Drosophila melanogaster ingestion experiments showed a LC50 of 26.14 ug/mL. Doses of epicatechin nanosilver up to 200ug/mL showed no toxicity in either eukaryotic model. Of great interest was the more sensitive effect of traditional AgNP on a whole organism compared to our in vitro system. Although the epicatechin

synthesized AgNPs had slightly less antibacterial activity than the borohydride synthesized AgNPs, we conclude that epicatechin synthesized nanosilver provides a safer alternative to traditional nanosilver in consumer and health applications.

PS 1584 Safety Assessment of Irganox 1076 Migration from Use in Food Contact Applications

A. P. Neal-Kluever and K. R. Hatwell. *Division of Food Contact Notifications, FDA, College Park, MD.*

This project is a post-market re-evaluation, initiated by the Office of Food Additive Safety (OFAS) to ensure that current exposures are accurately captured and the safety assessment considers all relevant toxicological information available since the time of premarket approval. The trigger for the postmarket evaluation of Irganox 1076 (stearyl 3,5-di-tert-butyl-4-hydroxyhydrocinnamate, CAS Reg. No. 2082-79-3) was an increase in submissions notifying for the food contact substance (FCS) in calendar year 2012. In order to assess the safety of Irganox 1076 from food contact applications, the US Food and Drug Administration (FDA) reviewed the available chemistry information on food contact applications, including the US regulatory status, uses, levels in food, and alternative approaches to calculate exposure. Upon completion of this in-depth market analysis, the cumulative dietary concentration (CDC) was determined to be 1.5 ppm (4.5 mg/p/d). A rigorous evaluation of the available toxicological information was performed, incorporating both the data submitted for the premarket notification and any new toxicology data published subsequently. A 2-year chronic rat feeding assay was selected as the critical study with a no-observed effect level (NOEL) of 64 mg/kg/d. This NOEL and the revised CDC provides a margin of exposure (MOE) of 850, which provides an adequate margin of safety (MOS) and remains protective of human health for the regulated uses.

PS 1585 Safety Assessment of R, S-Equol As a Dietary Supplement for Benign Prostatic Hyperplasia

E. D. Lephart. *PDBio, BYU, Provo, UT.* Sponsor: P. Damian.

Equol is a polyphenol, more specifically an isoflavonoid. Polyphenols are common micronutrients in the human diet and have been studies for their role in the prevention of cancer, cardiovascular, and age-related diseases. Several thousand molecules with a polyphenol structure exist in higher plants, and several hundred are found in edible plants. Equol was first discovered in the early 1980s in the urine of humans consuming soy foods (a key metabolite of daidzein). More recently, equol has been reported in fermented soybean foods at relatively high concentrations. Unlike other isoflavonoids (i.e., genistein or daidzein), equol has a chiral carbon; therefore it can occur as R- and S-isomers. R,S-Equol can be prepared by catalytic hydrogenation of daidzein to yield R/S-equol > 99 %. Equol is known for its anti-oxidant and anti-androgenic activities where both S- and R-equol specifically bind 5α-dihydrotestosterone (DHT) with high affinity, and thereby prevent it from binding the androgen receptor. Equol also binds to estrogen receptor beta & estrogen related receptor gamma that are beneficial for treating benign prostatic hyperplasia (BPH). The available toxicity data on R,S-equol and/or its isomers, combined with the widely disseminated knowledge concerning the normal human metabolism of daidzein to equol and the long history of consumption of equol from food provide a sufficient basis for assessment of the safety of R,S-Equol as a dietary supplement for BPH. Studies include absorption, distribution, metabolism & excretion (ADME)/toxicokinetic results, acute/subchronic toxicity, genotoxicity, reproductive & developmental toxicity findings. Also, clinical intervention results display safety, feasibility and efficacy of R,S-equol (6 mg twice/day) to treat middle-aged men with moderate to severe BPH symptoms. In conclusion, all data support the use of R,S-equol to be safe, well-tolerated and provide rapid beneficial therapy (within days to weeks) for BPH that can be used alone or in combination with current pharmaceuticals to improve prostate health.

PS 1586 Application of QSAR Models to Evaluate the Dermal Absorption of Cosmetic Ingredients

F. Liu[1], V. Tu[1], D. M. Frederick[1] and H. Frasch[2]. [1]*Revlon Research Center, Edison, NJ and* [2]*Health Effects Laboratory, NIOSH, Morgantown, WV.*

Systemic exposure to cosmetic ingredients is an important factor to take into account during human health safety evaluation of cosmetic products. The information on dermal absorption is critical in order to accurately evaluate the systemic exposure. In vitro methods have been widely applied to determine the dermal absorption of cosmetic ingredients. Also, QSAR models have been proposed and utilized to predict the dermal absorption of chemicals based on their chemical properties. To evaluate the performance of various QSAR models to predict the dermal absorption of cosmetic ingredients, an *in vitro* dermal absorption study was conducted using a porcine (pig) skin model. Diglycerin is a common humectant used in cosmetic products and was used as a model ingredient in the current study. The dermal absorption profile over a 24-hour exposure period was measured and the kinetic data were fitted to various diffusion models and a combined diffusion/binding model. The permeability coefficient (Kp) and lag time (τ) were estimated with these models. The Kp value was compared with those predicted from publically available QSARs models. The maximum flux values (Jmax) were calculated from the kp values. Based on the Jmax values, default % dose absorbed (Kroes et al., 2007) through the skin per 24 hours ranged from 40% to 80%. The dermal absorption determined from the actual data is generally in agreement with the QSAR model prediction. The current study supports the use of QSAR models to predict dermal absorption for safety assessment of cosmetic ingredients. We suggest that multiple prediction models for dermal absorption should be applied in the absence of experimental data and that the most conservative prediction should be used in systemic exposure assessment of cosmetic ingredients.

PS 1587 An Immature Human Reconstructed Epidermis Model to Assess Baby Personal Care Product Ranges

S. Catoire and H. Ficheux. *THOR Personal Care, Compiegne, France.*

The personal care market for children is rapidly expanding and increasingly requires a specific approach. Recent publications have re-evaluated the old notion that skin is fully matured at birth and have shown that baby skin differs in structure, function and composition from that of adults. In consequence, these qualitative and quantitative differences may facilitate the development of pathological conditions, such as topic dermatitis and irritant contact dermatitis. Therefore, the risk assessment of raw materials and finished products for baby cannot be extrapolated from human adult data but must be considered as a new approach with adapted models. In order to respect the morphology and properties of baby skin, especially the stratum corneum, an "immature" human reconstructed epidermis has been developed. It was used, at first, to assess skin irritation for a range of baby products. This new model is derived from a previously in-house developed human reconstructed epidermis model (VitroDerm).

During an internal validation, 67 infant formulations classified into 13 personal care product families (cleansing milk, shower gel, nappy cream, cleansing water, foam bath, liniment, wipes, protective stick, moisturising milk, sun cream, hydrastick, body cream, cold cream) were tested on both mature and immature epidermis. After 20h exposure on the mature model, none of the formulations reduced the percentage of cell viability to below 50% and were therefore classified as potentially non-irritant. However, 10 formulations decreased the cell viability to below 50% on immature epidermis, allowing the identification of potentially irritating formulations. A statistically significant difference (t test; $p<0.05$) was found when mature and immature models were compared as a whole. This difference became more relevant when stratified analysis was made between rinse off and leave on products. The improvement in the prediction of irritation with this new model allows a better risk assessment during the development of baby products and can be used as a tool to select the most appropriate ingredients during formulation.

PS 1588 Instant On-Site Glucose Measurements in Dogs

A. Makin, V. Golozoubova, J. Tovborg Jensen and J. Løgsted. *CiToxLAB, Lille Skensved, Denmark.*

In the pre-clinical studies where blood glucose levels are expected to be affected (e.g. tests of insulin and its analogues), instant on-site glucose measurement in small blood sample provides clear ethical and practical benefits. Methods for direct glucose measurements in whole blood are well established. However, the equipment is normally calibrated only for human use, and its suitability for glucose measurements in e.g. dog blood was therefore evaluated. We performed a study with the objective being to validate One Touch® UltraEasy® glucometer (the glucometer) for direct glucose measurements in dog blood as compared to standard laboratory measurement (Hitachi). Furthermore we evaluated the quality of blood samples collected from different sites (veins in the ear, foreleg or neck).

Samples measured using the glucometer were compared to samples analysed using the Hitachi. There was a linear relation between whole blood glucose measurements in a broad range of glucose levels ($R2=0.93$ for whole blood versus plasma or serum). Glucose levels corresponding to plasma glucose levels down to 3.4 mmol/L, can be measured successfully using the glucometer. Levels below that are outside the limit range, and would require plasma/serum glucose measurements.

Site of sample collection did not affect the results. However, ear sampling appeared to be more traumatic for the animals and is therefore not recommended for multiple sampling.

In conclusion, the glucometer can be used can be used successfully for monitoring of glucose status in dogs, resulting in less stress for the animals, faster delivery of results, and ecomical benefits.

PS 1589 Safety Assessment of Hazardous Chemicals in Art Materials

J. L. Doran, C. Tuinman, G. Goodfellow and J. Daniels. *Intrinsik Health Sciences, Inc., Mississauga, ON, Canada.*

The United States Consumer Product Safety Commission (CPSC) is responsible for protecting the public from unreasonable risks of injury or death associated with consumer products. As such, the Commission has enacted "The Labelling of Hazardous Art Materials Act" (LHAMA) as a regulation in order to protect users from the potential health hazards associated with exposures to chemicals present in art materials. Assessing the safety of art materials poses a significant challenge due to the range of age grades associated with the use of these products. Examples of chemical categories used in art materials that may be of concern include benzidine-based dyes, solvents, and heavy metal-containing pigments. The aim of this study was to evaluate the safety of substances flagged as potential chemical hazards when included as ingredients in art materials for various age grades and types of uses. Results of toxicological studies indicate that certain benzidine-based dyes, solvents, heavy metal-containing pigments, as well as controlled substances, are associated with toxicity concerns such as specific organ toxicity, neurotoxicity, reproductive toxicity, developmental toxicity, and carcinogenicity. Product formulation data, collected in a proprietary database over a three-year period, were analyzed in order to determine the levels and frequency of use of products containing these substances in various categories of art materials. Exposure considerations and scenarios designed to address chronic toxicity concerns from chemical exposures for children and adults as a result of intentional use and reasonably anticipated misuse of several different art materials were developed. Using the results of the toxicological studies and exposure scenarios developed by our group, we analyzed the margin of safety for the use of these chemicals of concern with respect to toxicity effects in art materials. The results of our studies suggest that chemicals of toxicological importance are currently in use at levels that indicate potential concerns for children and adults.

PS 1590 Broad Spectrum Safety of Meratrim: A Novel Weight-Management Ingredient

F. C. Lau[1], J. Lugo[1], Z. Saiyed[1], G. Trimurtulu[2], A. Krishnaraju[2] and K. Sengupta[2]. [1]*Research and Development, InterHealth Nutraceuticals Inc., Benicia, CA and* [2]*Research and Development, Laila Nutraceuticals, Vijayawada, India.*

Meratrim is a unique dietary ingredient consisting of extracts from *Sphaeranthus indicus* flower heads and *Garcinia mangostana* fruit rind. Clinical studies have demonstrated that Meratrim is effective and well-tolerated in weight management. The current research assesses the broad spectrum safety of Meratrim in a battery of animal and *in vitro* studies including acute oral, acute dermal, primary dermal irritation, primary eye irritation, mammalian erythrocyte micronucleus and chromosomal aberration tests, plus Ames' bacterial reverse mutation assay. A sub-chronic repeated-dose 90-day toxicity study was conducted to determine the no-observable-adverse-effect-level (NOAEL) of Meratrim.
The LD_{50} levels of Meratrim in Sprague-Dawley (SD) rats, as determined by the acute oral and acute dermal toxicity studies, were >5,000 and >2,000 mg/kg body weight, respectively. The primary skin and eye irritation tests classified Meratrim as non-irritating to the skin and mildly irritating to the eye. Genotoxicity studies showed that Meratrim is non-mutagenic. In the repeated-dose 90-day oral toxicity study, SD rats were orally gavaged with Meratrim at 0, 250, 500 or 1,000 mg/kg/day. Body weight, food and water consumption, selected organ weights, ocular health, hematology, blood chemistry and clinical chemistry were assessed. The animals were sacrificed at the end of supplementation (day 90) and histopathological examinations were conducted.
No morbidity, mortality, or significant adverse events were observed either during the course of the study or at 90 days. Based on these findings, the NOAEL of Meratrim is determined to be 1,000 mg/kg of body weight/day in male and female SD rats.
These results, combined with the tolerability of Meratrim in the human clinical trials, demonstrate the broad spectrum safety of Meratrim.

PS 1591 Application of Metabolomics in Short-Term *In Vivo* Rat Toxicity Studies

H. Kamp[1], E. Fabian[1], M. Herold[2], G. Krennrich[1], L. Ralf[2], W. Mellert[1], G. Montoya-Parra[1], E. Peter[2], T. Walk[2], V. Strauss[1] and B. van Ravenzwaay[1]. [1]*Toxicology, BASF SE, Ludwigshafen, Germany and* [2]*Metanomics GmbH, Berlin, Germany.*

In the past years it has been shown that metabolomics can serve as a powerful tool in toxdicological research. BASF's Experimental Toxicology and metanomics have developed the MetaMap®Tox database with rat plasma metabolome data for more than 500 reference compounds based on 28 day rat studies (OECD 407 design). Metabolome analysis in plasma was performed after 7, 14 and 28 days and relative levels of endogenous metabolites in treated rats versus controls were analyzed. These data are now routinely used to predict the systemic toxicity of new compounds at BASF. For many chemicals we have seen consistent changes of metabolites over all three time points. The purpose of the research reported here was to investigate for a number of compounds if these metabolite changes would also occur at earlier time points.
Therefore, groups of five female and male animals each were treated with four compounds for which time-consistent effects had been previously observed (Vinclozolin, Methimazole, MCPA, Cyclosporin A). Plasma samples were taken on day 3, 5, and 7, the metabolome analyzed and the results compared against the data already present in the data base. At day 7 there generally was a good concordance (> 80%) with the previous 28 day studies. The number of metabolites changed in the correct direction, and the strength of the change was reduced at day 5, but overall patterns were still identified. At day 3 metabolites changes diminished further. MCPA produced a clear pattern of metabolite changes at day 3 that was comparable to that of the 28 day study. Furthermore, a time-dependent increase in the strength of the metabolome changes was observed in this study. These results confirm the previously shown reproducibility and robustness of metabolome data and show a potential applicability of metabolomics also in shorter term toxicity studies.

PS 1592 A Novel 16 AirTEER Electrode System to Measure Transepithelial Electrical Resistance in Organotypic Cultures

S. Frentzel[1], M. Liley[2], S. Constant[3], M. Favre[2], A. Meister[2], S. Majeed[1], D. Kuehn[1], C. Mathis[1], A. Hayes[4] and J. Hoeng[1]. [1]*Research & Development, Philip Morris International, Neuchatel, Switzerland,* [2]*CSEM - Centre Suisse d'Electronique et de Microtechnique SA, Neuchatel, Switzerland,* [3]*Epithelix SàRL, Geneve, Switzerland and* [4]*Spherix Consulting, Rockville, MD.*

Understanding how substances or particles cross biological barriers is an essential element in toxicological and pharmacological studies. Changes in the integrity of such barriers can be assessed in relevant organotypic models by measuring the TransEpithelial Electrical Resistance (TEER). However it requires full immersion of the cells, making it impossible for model systems, growing at the air-liquid-interface (MucilAir, Epithelix) to be analyzed in a representative and realistic way. To circumvent this issue, we developed a new electrode (AirTEER) system, which allows electrical contact with the apical (air) side of the organotypic model via an aqueous drop that forms a conducting liquid bridge between the electrodes and the cells in the culture. Additional features implemented into AirTEER enable continuous, real-time measurements over longer period of time, which circumvent the need for repeated removal of the cultures from the incubator. The system also allows the simultaneous measurement of up to 16 culture wells at a time. Pilot experiments, applying known toxicants clearly demonstrated a loss in electrical resistance after exposure of MucilAir tissue samples to toxic vapors or single substances applied from the apical side. Additional experiments will be carried out to assess robustness of the system and confirmation of continuous TEER measurements over longer time periods will not harm MucilAir tissues. Taken together, the possibility of real-time measurements using AirTEER would greatly facilitate access to a range of data that are currently not available. Notably, it would allow detecting subtle alterations in membrane integrity of aerosol exposed cells in a realistic fashion and potentially indicate whether or not the observed toxicity is reversible over time.

PS 1593 The Use of Everted Rat Small Intestinal Sacs *In Vitro* to Estimate Relative Absorption Potential of a Series of Alpha Olefins

M. Penman[1], R. H. Powrie[2] and C. R. Elcombe[2]. [1]*Penman Consulting, Brussels, Belgium and* [2]*CXR Biosciences, Dundee, United Kingdom.*

Higher Olefins (HO) range from C6 to greater than C32 olefins with an alpha or internal double bond and with linear and/or branched carbon chains. In order to meet the extensive information requirement of REACH, data read across was used for more than 30 HOs. One of the hypotheses of a category approach for HOs

is that mammalian bioavailability would decrease as molecular weight increased. If this could be demonstrated experimentally, the case for read across would be strengthened, reducing the need for toxicity studies on all of the chemicals. The aim of this study was to determine and rank the absorption potential of a series of alpha-olefins using an in vitro everted rat small intestinal sac model. Everted rat intestinal sacs were prepared by everting a freshly excised proximal small intestine over a glass stirring rod. The everted intestines were filled with oxygenated Fed State Simulated Intestinal Fluid (FeSSIF, the serosal medium, Galia et al., Pharm. Res. 15, 698, [1998]) and divided into sacs (~ 2.5 cm) using sutures. Sacs were incubated (1 hr, 37°C) in flasks containing FeSSIF saturated with individual alpha-olefins. The serosal fluids were extracted with isooctane and analysed for olefin content using GC-FID. The absorption of 30 olefins with carbon chains of C6 to C27 was investigated. Marked inter-compound differences in absorption were observed, with the degree of absorption decreasing with increasing carbon number. C6 to C10 olefins were well absorbed, while those of C14 and above were either not absorbed or very poorly absorbed. Data such as these could be used to select representative compounds from a series to study further in vivo. This study was funded by the Higher Olefins and Polyalphaolefins Reach Consortium (HOPA), c/o Penman Consulting bvba, Brussels.

PS 1594 Evaluation of Nose-Only Inhalation Exposure to Aerosolized Benzyl Acetate in Sprague-Dawley Rats

J. Randazzo[2], D. T. Kirkpatrick[1], D. Vitale[1] and M. Singal[1]. [1]*Respiratory Science Program, RIFM, Inc., Woodcliff Lake, NJ and* [2]*Inhalation Toxicology, WIL Research, Ashland, OH.*

Benzyl acetate is a commonly used fragrance material that has been associated with skin sensitization. The study objective was to understand the effects of inhalation exposure in Sprague-Dawley (SD) rats when aerosolized benzyl acetate was administered by nose-only inhalation at 6.1, 61.4, and 614 mg/m^3 (equivalent to 1, 10, and 100 ppm), for 2 weeks (6 hours/day, 5 days/week) for a total of 10 exposures. Standard endpoints evaluated included: clinical observation; body and organ weights; hematology and serum chemistry evaluation; macroscopic/microscopic examination of selected organs; and bronchoalveolar lavage fluid (BALF) analysis for cellular markers of inflammation (i.e., clinical pathology parameters and cytology). As a positive control to validate the utility of various endpoint measures as indicators of pulmonary inflammation, a nose-only inhalation pilot was conducted with 25 mg/m^3 amorphous silica (0, 1, 2, 5 or 10 exposures). At all exposure levels, benzyl acetate was well tolerated. A nonadverse test substance-related increase in BALF lactate dehydrogenase was observed at the 614 mg/m^3 exposure concentration. Therefore, the no-observed-adverse-effect level (NOAEL) was considered to be 100 ppm (equivalent to 614 mg/m^3), the highest exposure concentration tested.

PS 1595 Development of *In Vitro* Screens for Chemical Disruptors of the Retinol Signaling Pathway

Y. Chen and D. H. Reese. *CFSAN/OARSA, U.S. FDA, Laurel, MD.*

Retinoic acid (RA), which regulates the expression of hundreds of protein coding and non-coding RNA genes, is essential for normal embryonic development and maintenance of cellular phenotype in adult animals. Intracellular levels of RA are controlled by the retinol signaling pathway (RSP) that regulates RA synthesis (from vitamin A; retinol) and its catabolism. Chemical disruption of the RSP can cause abnormally low or high cellular levels of RA resulting in abnormal embryonic development and adult disease. Our research focus is on the development and application of in vitro test systems for assessing the safety of chemicals in foods, food additives, dietary supplements, cosmetics and other consumer products. We are particularly interested in identifying chemicals that disrupt essential developmental signaling pathways such as the RSP. We recently described the development of a rapid, medium-throughput, gene-expression (RT-PCR) assay that uses the mouse P19 pluripotent stem cell to detect chemicals that disrupt the RSP. To provide enhanced throughput capability of our screen system, a new reporter assay was developed. A lentiviral vector was used to establish stable clones of the retinol-responsive C3H10T1/2 mouse multipotent stem cell that contain the Luc reporter gene under the control of the retinoic acid response element (RARE). Preliminary tests using this new RARE-Luc cell on several positive compounds demonstrate its ability to detect RSP disruptors. The assay can be optimized to be used in a Tox21 high-throughput screening platform. The RT-PCR-based assays will provide the flexibility of assessing the effect of chemicals using a broader range of endpoints. The advantages of these assays will be discussed. Assays for assessing chemical effects on other important developmental toxicity pathways can also be established using similar methods.

PS 1596 Evaluation of Nose-Only Inhalation Exposure to Aerosolized β-Ionone in Sprague-Dawley Rats

D. T. Kirkpatrick[2], J. Randazzo[2], D. Vitale[1] and M. Singal[1]. [1]*Respiratory Science Program, RIFM, Inc., Woodcliff Lake, NJ and* [2]*Inhalation Toxicology, WIL Research, Ashland, OH.*

β-Ionone is a commonly used fragrance material that has been associated with skin sensitization. The study objective was to understand the effects of inhalation exposure in Sprague-Dawley (SD) rats when aerosolized β-Ionone was administered by nose-only inhalation at 7.9, 79, and 790 mg/m^3 (equivalent to 1, 10, and 100 ppm) for 2 weeks (6 hours/day, 5 days/week) for a total of 10 exposures. Standard endpoints evaluated included: clinical observation; body and organ weights; hematology and serum chemistry evaluation; macroscopic/microscopic examination of selected organs; and bronchoalveolar lavage fluid (BALF) analysis for cellular markers of inflammation (i.e., clinical pathology parameters and cytology). As a positive control to validate the utility of various endpoint measures as indicators of pulmonary inflammation, a nose-only inhalation pilot was conducted with 25 mg/m^3 amorphous silica (0, 1, 2, 5 or 10 exposures). At all exposure levels, β-Ionone was well tolerated; however, adverse test substance-related effects were observed in the nasal cavity at the 790 mg/m^3 exposure concentration. Therefore, the no-observed-adverse-effect level (NOAEL) was considered to be 10 ppm (equivalent to 79 mg/m^3), the middle exposure concentration tested.

PS 1597 Evaluation of Nose-Only Inhalation Exposure to Aerosolized Phenyl Ethyl Alcohol in Sprague-Dawley Rats

D. Vitale[1], J. Randazzo[2], D. T. Kirkpatrick[2] and M. Singal[1]. [1]*Respiratory Science Program, RIFM, Inc., Woodcliff Lake, NJ and* [2]*Inhalation Toxicology, WIL Research, Ashland, OH.*

Phenyl ethyl alcohol is a commonly used fragrance material that has been associated with skin sensitization. The study objective was to understand the effects of inhalation exposure in Sprague-Dawley (SD) rats when aerosolized phenyl ethyl alcohol was administered by nose-only inhalation at 0.5, 5, and 50 mg/m^3 (equivalent to 0.1, 1, and 10 ppm), for 2 weeks (6 hours/day, 5 days/week) for a total of 10 exposures. Standard endpoints evaluated included: clinical observation; body and organ weights; hematology and serum chemistry evaluation; macroscopic/microscopic examination of selected organs; and bronchoalveolar lavage fluid (BALF) analysis for cellular markers of inflammation (i.e., clinical pathology parameters and cytology). As a positive control to validate the utility of various endpoint measures as indicators of pulmonary inflammation, a nose-only inhalation pilot was conducted with 25 mg/m^3 amorphous silica (0, 1, 2, 5 or 10 exposures). At all exposure levels, phenyl ethyl alcohol was well tolerated. However, test substance-related microscopic findings were noted in nasal levels II through VI in the 50 mg/m^3 group males, level VI in the 0.5 mg/m^3 group males, levels IV and V in all test substance-exposed female groups, and level VI in the 5 and 50 mg/m^3 group females, and exhibited increased incidence or severity of luminal secretions consistent with mucous. These nonadverse changes were more commonly observed and tended to be more severe in the caudal nasal sections (V and VI). In addition, test substance-related mononuclear infiltrates in the liver and histiocytic infiltrates in the lungs were noted in the 50 mg/m^3 group females, but were considered nonadverse. Therefore, the no-observed-adverse-effect level (NOAEL) was considered to be 10 ppm (equivalent to 50 mg/m^3), the highest exposure concentration tested.

PS 1598 Evaluation of Nose-Only Inhalation Exposure to Aerosolized Methyl Dihydro Jasmonate in Sprague-Dawley Rats

M. Singal[1], J. Randazzo[2], D. T. Kirkpatrick[2], F. G. Burleson[3] and D. Vitale[1]. [1]*Respiratory Science Program, RIFM, Inc., Woodcliff Lake, NJ,* [2]*Inhalation Toxicology, WIL Research, Ashland, OH and* [3]*Burleson Research Technologies, Morrisville, NC.*

Methyl dihydro jasmonate is a commonly used fragrance material that has been associated with skin sensitization. The study objective was to understand the effects of inhalation exposure in Sprague-Dawley (SD) rats when aerosolized methyl dihydro jasmonate was administered by nose-only inhalation at 0.93, 9.3, and 93 mg/m^3 (equivalent to 0.1, 1, and 10 ppm), for 2 weeks (6 hours/day, 5 days/week) for a total of 10 exposures. Standard endpoints evaluated included: clinical observation; body and organ weights; hematology and serum chemistry evaluation; macroscopic/microscopic examination of selected organs; and bronchoalveolar lavage fluid (BALF) analysis for cellular markers of inflammation (i.e., cytokines). As a positive control to validate the utility of cytokine measures as indicators of pulmonary inflammation, a nose-only inhalation pilot was conducted with 25 mg/m^3 amorphous silica (0, 1, 2, 5 or 10 exposures). At all exposure levels, methyl di-

hydro jasmonate was well tolerated with no test substance-related effects observed. Therefore, the no-observed-adverse-effect level (NOAEL) was considered to be 10 ppm (equivalent to 93 mg/m^3), the highest exposure concentration tested.

PS 1599 Evaluation of Nose-Only Inhalation Exposure to Aerosolized Hydroxycitronellal in Sprague-Dawley Rats

F. G. Burleson[3], M. Singal[1], J. Randazzo[2], D. T. Kirkpatrick[2] and D. Vitale[1]. *[1]Respiratory Science Program, RIFM, Inc., Woodcliff Lake, NJ, [2]Inhalation Toxicology, WIL Research, Ashland, OH and [3]Burleson Research Technologies, Morrisville, NC.*

Hydroxycitronellal is a commonly used fragrance material that has been associated with skin sensitization. The study objective was to understand the effects of inhalation exposure in Sprague-Dawley (SD) rats when aerosolized hydroxycitronellal was administered by nose-only inhalation at 0.70, 7.0, and 70 mg/m^3 (equivalent to 0.1, 1, and 10 ppm) for 2 weeks (6 hours/day, 5 days/week) for a total of 10 exposures. Standard endpoints evaluated included: clinical observation; body and organ weights; hematology and serum chemistry evaluation; macroscopic/microscopic examination of selected organs; and bronchoalveolar lavage fluid (BALF) analysis for cellular markers of inflammation (i.e., cytokines). As a positive control to validate the utility of cytokine measures as indicators of pulmonary inflammation, a nose-only inhalation pilot was conducted with 25 mg/m^3 amorphous silica (0, 1, 2, 5 or 10 exposures). At all exposure levels, hydroxycitronellal was well tolerated with test substance-related effects limited to non-adverse microscopic findings in the nasal cavity in the 70 mg/m^3 females. Therefore, the no-observed-adverse-effect level (NOAEL) was considered to be 10 ppm (equivalent to 70 mg/m^3), the highest exposure concentration tested.

PS 1600 Development of an Alternative Photosafety Assessment Approach for Cosmetic Ingredients Based on the Photochemical and Photo-Biochemical Properties

H. Nishida[1], M. Hirota[1], M. Kitagaki[1], S. Onoue[2], M. Kato[2], G. Suzuki[2], S. Yamada[2] and H. Kouzuki[1]. *[1]Shiseido Research Center, Shiseido Co. Ltd., Yokohama, Japan and [2]Department of Pharmacokinetics and Pharmacodynamics, School of Pharmaceutical Sciences, University of Shizuoka, Shizuoka, Japan.* Sponsor: T. Yoshida.

Development of non-animal safety evaluation methods for chemicals is necessary from the viewpoint of animal welfare and to meet the 7th Amendment of the European Cosmetics Directive. The purpose of the present study is to establish a photosafety assessment strategy for cosmetic ingredients using several in vitro assays. The strategy was based on photochemical and photo-biochemical properties of chemicals (51 chemicals including 34 phototoxins), which were investigated by UV/VIS spectral analysis, reactive oxygen species (ROS) assay and 3T3 neutral red uptake phototoxicity test (3T3 NRU PT). At first step, molar extinction coefficients (MEC) were calculated by UV/VIS spectral analysis to identify photochemical characters. Most phototoxins exhibited potent UV/VIS absorption with MEC of over 1000 L mol^{-1} cm^{-1} according to the positive criteria of ICH S10 draft guideline while false negative prediction occurred only on two cosmetic ingredients. The ROS assay was applied for further photochemical characterization to lessen the false negative results. The ROS assay did not provide any false negative predictions at least in this study, thus the ROS assay might be useful as photosafety assessment of cosmetic ingredients. In order to justify false positives from two assays, 3T3 NRU PT was conducted. Three chemicals that predicted as false positive in UV/VIS spectral analysis or ROS assay were evaluated as negative in 3T3 NRU PT. The tiered approach using these in vitro methods could be a promising non-animal test method for hazard identification of photoreactive chemicals.

PS 1601 Evaluation of the Subchronic Toxicity of Acetoxydihydrodicyclopentadiene

V. T. Politano and A. Api. *Research Institute for Fragrance Materials, Inc., Woodcliff Lake, NJ.*

The subchronic toxicity of acetoxydihydrodicyclopentadiene, a widely used fragrance ingredient, was investigated in an enhanced OECD 408 dietary 90-day toxicity study. Sprague-Dawley rats were fed dietary concentrations of 0, 200, 2000, 6000 and 20000 ppm acetoxydihydrodicyclopentadiene, equivalent of 0, 15.3, 154.9, 464.1 and 1504.6 mg/kg bw/day, respectively, for 90 consecutive days. In addition to the repeated dose endpoints, estrous cycling and sperm analyses were conducted. Statistically significant reductions in body weight gains were detected for males treated with 20000, 6000 or 2000 ppm and in females treated with 20000 ppm. Corresponding reductions in food consumption and efficiency were observed in the 20000 ppm group only. Males treated with 6000 and 20000 ppm showed statistically significant changes in clinical chemistry parameters. Increased kidney weights and reduced prostate and pituitary weights were recorded for all treated males. Males treated with 20000 ppm also had increased liver and adrenal weights. Females treated with 2000 and 6000 ppm had decreased liver weights. The treatment related histopathological findings were recorded only for males in kidneys (hyaline droplet nephropathy and renal tubular degeneration/regeneration), liver (hepatocellular hypertrophy and vacuolation), and adrenals (vacuolation of the zona fasciculata). No toxicologically significant effects were detected in females treated with 6000, 2000 or 200 ppm therefore the NOAEL for females was considered to be 6000 ppm. The kidney effects detected in males from all treatment groups were considered consistent with well documented changes related to alpha-2u-globulin accumulation and are peculiar to the male rat in response to treatment with some hydrocarbons. This effect is not indicative of a hazard to human health and, for the purposes of hazard evaluation the NOAEL for males should be regarded as 2000 ppm, or 154.9 mg/kg/day, based on alanine aminotransferase levels. Based on the current total systemic exposure from fragrance use of 0.0008 mg/kg/day, the margin of exposure is greater than 190000.

PS 1602 Optimization of a Primary Hepatocyte Assay for Prediction of Liver Carcinogenicity in Agrochemical Development

L. A. Murphy[1], L. Kan[1], M. J. LeBaron[1], D. R. Boverhof[1], J. Bailey[2], C. Terry[2], R. Billington[2] and R. J. Rasoulpour[1]. *[1]The Dow Chemical Company, Midland, MI and [2]Dow AgroSciences, Indianapolis, IN.*

Many chemicals, including agrochemical molecules, may induce rodent liver tumors through non-genotoxic mechanisms, and characterization of the mode-of-action (MoA) can have important implications for human health risk assessments. Prediction of this MoA early in molecule development may facilitate lead optimization of analogues and inform the subsequent integration of MoA endpoints into in vivo regulatory studies. Nuclear receptor (NR) activation (i.e.,aryl hydrocarbon receptor (AhR), constitutive androstane receptor (CAR), pregnane X receptor (PXR), and peroxisome proliferator-activated receptor alpha (PPARα)), can be an initial molecular event for in vivo non-genotoxic rodent liver tumorigenesis. Primary hepatocytes are a relevant system to predict in vivo hepatic NR activation and also have metabolic capacity. To optimize this assay, rat primary hepatocytes were exposed to prototypical NR activators 3-methylcholanthrene (AhR), phenobarbital (CAR), dexamethasone (PXR), or Wyeth-14643 (PPARα) followed by Cyp biomarker gene expression analyses to determine dynamic range and non-specific induction of Cyp responses, and establish criteria for positive NR activation responses. Halauxifen-methyl, a novel herbicide, was also analyzed in this assay to determine correlation of in vitro and in vivo gene expression responses. The in vitro Cyp responses for prototypical NR activators and halauxifen-methyl were consistent with in vivo Cyp induction. Although, variability in hepatocyte preparations can affect the dynamic range for Cyp induction, prototypical NR activators were run concurrently with each hepatocyte lot to define the inducibility of the system. A molecule was deemed positive for NR activation if Cyp gene expression responses were ≥40% of the prototypical NR activator response. This interpretation strategy was applied to assess NR activation potential of several new chemical entities and results indicate correlation between in vitro and in vivo gene expression responses.

PS 1603 Academic and Commercial Partnership: Identifying Sustainable Flame Retardants by Rapid *In Vivo* Screening

R. L. Tanguay. *Environmental and Molecular Toxicology, Oregon State Univ, Corvallis, OR.*

Fire prevention often requires the use of fire hardening strategies for combustible materials used in consumer products. Flexible polyurethane foams, widely used as cushioning and/or padding materials, are typical and fire hardening is often achieved with the addition of chemicals that interfere and resist combustion. It is well known that humans can be exposed to various compounds found in these products and there are mounting concerns that some of these chemicals may pose human health risks. Manufacturers are spending considerable effort to identify alternative high performing chemicals that are also inherently safer to use and need a robust and cost effective toxicity screening technique early in the product development process. A major complexity in assessing the potential hazard and risk posed by flame retardants is the diversity of chemical structures; and the chemical structure and toxicity relationships are not yet established for these compounds. We propose that a rapid multi-dimensional whole animal testing platforms can be a powerful tool to screen for, and identify chemicals with differential hazard potential. To test this hypothesis, we obtained 9 flame retardant chemicals from ICL Industrial Products for testing in our high throughput zebrafish testing facility. The identity of the compounds was blinded to the laboratory. We performed

our standard rapid throughput assessment of developmental and neurotoxicity in zebrafish. Broad concentration ranges, and all exposures were initiated at 6 hours post fertilization (hpf) and were continuous until 120 hpf. At 120 hpf, larvae were assessed for photo-induced locomotor activity and changes in a suite of 20 morphological endpoints. Five of the compounds displayed toxicity only at the highest test concentrations (64uM), one produced toxic effects at concentrations as low at 6.4 uM, and importantly, two of the compounds produced no adverse effects at any test concentration. These data indicate that it may be possible to proactively identify commercially important compounds with reduced hazard potential.

PS 1604 Development of Three-Dimensional Reconstructed Model for Human Skin Irritation and Corrosive Tests

C. Zhang[1], B. Chen[1], Z. Du[1], Z. Wang[2] and X. Zhang[1]. [1]*Forelandpharma Co Ltd, Beijing, Beijing, China and* [2]*Boston University, Boston, MA.* Sponsor: J. Wang.

In vitro models to study irritation, corrosivity and phototoxicity are important tools for research and development in the pharmaceuticals and cosmetic industries. Human skin is the best possible model for such in vitro studies. The commercially reconstructed human epidermis models are similar to the morphology, lipid composition and biomarkers of native human tissue and have been approved by European Centre for the Validation of Alternative Methods (ECVAM) for the validation of cosmetics. The models are available in many nations but not in China. Here, we describe the development of a constructed three-dimensional (3D) model using Chinese human skin cells, which consists of a "dermis" with fibroblasts embedded in rat type I collagen matrix and an "epidermis" comprised of differentiated keratinocytes. The main objectives of this study were to use our reconstructed 3D skin tissues for validation on in vitro tests for human skin irritation and corrosion, and for reliability and relevance to published references. For irritation study, the 3D skin tissues were exposed with cosmetics collected from both Western nations and China. MTT assay was performed for cell viability and ELISA was conducted for IL-1 release. For corrosive study, reference chemicals including severely corrosive, corrosive and non-corrosive compounds were used to validate whether our 3D skin model matched the criteria used by ECVAM. The results demonstrated our skin model could meet the criteria. Our data indicate that the reconstructed 3D Chinese skin model is a reproducible and sensitive tool to assess skin irritation and corrosion to cosmetics and chemicals.

PS 1605 Lauric Aldehyde: Ninety-Day Repeated-Dose Oral (Dietary) Toxicity in Rats

G. Ritacco, V. T. Politano and A. Api. *Research Institute for Fragrance Materials, Woodcliff Lake, NJ.*

Lauric aldehyde is a widely used as a fragrance material. This enhanced OECD 408 compliant study investigated the systemic toxicity of lauric aldehyde by dietary exposure. Ten rats /sex /dose were fed diets containing 0, 200, 2000, 6000 or 20,000 ppm lauric aldehyde for 90 days. Observations included clinical observations, outside cage observations, food consumption, body weights, functional observational battery, ophthalmoscopy, hematology, plasma chemistry, urinalysis, estrous cycling (weeks 6-7 and 12-13), sperm analyses, gross necropsy, and histopathology. There were no unscheduled deaths. No adverse effect in overall food consumption or food efficiency was detected. There were no toxicologically significant changes in clinical observations, functional battery tests, body weights, hematology, blood chemistry, or organ weights; no toxicologically significant abnormalities were detected at necropsy. There were no toxicologically significant effects on the concentration, motility or morphology of samples of epididymal sperm. There were no treatment related effects on the concentration of homogenization resistant epididymal or testicular spermatid counts. Males treated with 20,000 ppm lauric aldehyde showed a statistically significant increase in the number of abnormal sperm during morphological assessment, not associated with any other sperm related effects. Sperm morphological analyses were extended to the low and mid dose groups and sperm staging was conducted on all groups; no effects were observed. Therefore, it was considered not to be toxicologically relevant. There were no treatment related changes in any other parameters measured. Dietary administration of 200, 2000, 6000 and 20,000 ppm lauric aldehyde to rats did not result in any toxicologically significant effects. The No Observed Adverse Effect Level (NOAEL) was considered to be 20,000 ppm (equivalent to a mean achieved dose of 1410 mg/kg/d). With total systemic exposure of 0.0043 mg/kg/d, the margin of exposure for lauric aldehyde is >300,000, indicating a very low potential for toxicity.

PS 1606 Formulation, Analysis Method Development, and Validation for Dimethylaminoethanol Bitartrate in Gavage Dose Formulations

J. C. Blake[1], S. D. Cooper[1], M. C. Best[1], R. A. Fernando[1], V. G. Robinson[2] and S. Waidyanatha[2]. [1]*Analytical Chemistry and Pharmaceutics, RTI International, Research Triangle Park, NC and* [2]*Division of the National Toxicology Program, NIEHS, Research Triangle Park, NC.* Sponsor: K. Levine.

Dimethylaminoethanol (DMAE) and several of its salts are produced in quantities greater than 1,000 tons per year, thus are included in the category of High Production Volume Chemicals. DMAE and its salts are extensively used in waste water treatment, manufacture of polyurethane foams, water-based paints and surface coatings. Dimethylaminoethanol bitartrate (DMAE bitartrate) can be found in a number of dietary supplements, touted for its anti-aging effects in both skin and brain function.
The purposes of the current study were to formulate DMAE bitartrate in sterile water, and to develop and validate a formulation analysis method for DMAE bitartrate in sterile water as a gavage formulation for use in toxicology studies. The stability and the pH of the dose formulation were also evaluated. To achieve these objectives, a gas chromatographic method using flame ionization detection was developed for analysis of DMAE bitartrate in sterile water. The DMAE bitartrate was completely soluble in the vehicle up to 300 mg/mL. The method was successfully validated over the range 2.5 to 225 mg/mL and with a dilution verification to extend the range up to 300 mg/mL. The accuracy (relative error) was ≤ 9.4% and precision (percent relative standard deviation) was ≤ 2.8%. The limit of detection was determined to be 0.2 mg/mL and the limit of quantitation was 0.5 mg/mL. The range of pH of the formulations was between 3.4 and 3.6. The 10 mg/mL formulation demonstrated acceptable stability for 14 days showing recoveries of 93.7% and 94.8%, respectively. The composition of the DMAE bitartrate was also verified by the analysis of tartaric acid including the analyses after formulation storage. To date tartaric acid was found to be at a 1:1 molar ratio with DMAE through 21 days of storage.

PS 1607 Identification of Volatile Organic Compound Sources and Exposure Assessment of Upstream Oil and Gas Workers during Well Completion Activities

J. E. Snawder[1], M. J. Breitenstein[1], M. Alexander-Scott[1], E. J. Esswein[2], B. King[2] and M. Kiefer[2]. [1]*Applied Research & Technology, NIOSH, Cincinnati, OH and* [2]*Western States Office, NIOSH, Denver, CO.*

The National Institute of Occupational Safety and Health (NIOSH) is conducting research to assess chemical exposure risks to upstream oil and gas workers. Upstream oil and gas activities include site construction, drilling, well completions, extraction and well production services. Activities in each segment may present chemical hazards inherent to that activity. Well completion activities such as perforation and hydraulic fracturing, flowback, production testing and produced water management present the potential for exposures to volatile organic compounds (VOCs) including benzene, toluene, ethylbenzene, and xylenes (BTEX) and polyaromatic hydrocarbons (PAHs). Individual exposures were determined by sampling airborne VOCs in the personal breathing zone (PBZ), measurement of VOCs in exhaled breath and metabolites in urine. Identification of exposure sources and patterns of exposure were estimated through the use of photoionization detectors for VOCs, chemical specific colorimetric methods and infrared videography. VOCs including alkanes, alkenes, aromatic hydrocarbons and PAHs were detected in air samples. Real time measurement of VOCs including benzene, were highest near the headspace of tank hatches and worker exposures were reflective of time spent performing work near those sources. Mean level of benzene in PBZ samples was 0.156 ppm (0.497 mg/m3) and ranged from 0 – 0.59 ppm (0-1.88 mg/m3). Levels of BTEX in exhaled breath and urinary metabolites (BTEX and PAHs) were correlated to time spent near sources. In the case of the benzene metabolite, s-phenyl mercapturic acid the mean was 3.37 μg/g creatinine (range = 0–20 μg/g creatinine). Significant temporal variations in concentrations of VOCs (e.g., BTEX) were identified. The completions activity performed, proximity to the source, wind direction and weather conditions all effect the potential for short term and full-shift risks for exposure.

PS 1608 Probabilistic Hazard Assessment for Skin Sensitization Potency Using Machine-Learning to Design Integrated Testing Strategies

V. D. Rocha, T. Luechtefeld, A. Maertens, T. Hartung and A. Kleensang. *Environmental Health Science - CAAT, Johns Hopkins School of Public Health, Baltimore, MD.*

Skin sensitization is an important endpoint for risk assessment of new ingredients. The latest amendment of the EU Cosmetic Directive/Regulation and animal welfare call for implementation of animal-free alternatives for hazard assessment. Although *in vitro* testing has been successful for endpoints such as skin irritation, no single *in vitro* test can provide sufficient information about the potential hazard of ingredients. Several *in silico* and *in vitro* tests have been developed and validated considering the mechanism that trigger skin sensitization, and can be used as part of an Integrated Testing Strategies that ensure a reliable prediction. In this study, we combine heterogeneous input sources using a Random Forest and Bayesian Network to develop a probabilistic approach to hazard identification. These models were built on a combination of *in silico* and *in vitro* available data for 145 chemicals tested on two cell-based assays (KeratinoSens®, U-937), in chemico Direct Peptide Reactivity Assay, *in silico* data from Times, and skin penetration (Jaworska et al., 2013) to estimate skin sensitization potency as assessed by local lymph node assay. Furthermore, we develop and evaluate algorithms for the creation of conditional testing strategies from complex generative models. Our models are able to predict with an average balanced accuracies for four classes of skin sensitizers of approximately 61%, or 76% of accuracy when moderate and strong sensitizers had been treated as one class. At the moment we try to integrate additional data from chemicals and assays (e.g. Michael acceptor, h-CLAT, Lusens). Our results suggest that a generative machine learning model can be used to quantify the potency and probability of skin sensitization given *in vitro* and *in silico* data. These tools are a methodological opportunity for toxicologists consider to strengthen hazard decision-making based on incomplete pieces of information using a more precise approach compared to Weight-of-evidence methods.

PS 1609 Development of Noncancer Threshold of Toxicological Concern (TTC) Database to Support Alternative Assessment Methods for Cosmetics-Related Chemicals

K. Muldoon-Jacobs[1], A. R. Boobis[2], S. Barlow[3], S. P. Felter[4], H. M. Hollnagel[5], D. Keller[6], V. Vitcheva[1], K. Arvidson[1], A. P. Worth[7] and C. Yang[8]. *[1]US FDA CFSAN OFAS, College Park, MD, [2]Imperial College, London, United Kingdom, [3]Independent consultant, Brighton, United Kingdom, [4]Procter & Gamble, Cincinnati, OH, [5]Dow Europe GmbH, Horgen, Switzerland, [6]Henkel, Dusseldorf, Germany, [7]EC Joint Research Center, Ispra, Italy and [8]Altamira LLC, Columbus, OH.*

The Seventh Amendment of the European Cosmetics Directive requires replacement of animal studies in the assessment of cosmetic products and ingredients. The COSMOS consortium within SEURAT, a joint research cluster funded by the European Commission and Cosmetics Europe, has been engaged in development of computational methods and tools. A non-cancer repeat-dose toxicity database for cosmetics-related chemicals has been compiled to establish the COSMOS TTC database; this has been augmented with chemicals from the Munro dataset found in the Cosmetics Inventory. Lipid-soluble vitamins and essential amino acids were excluded from the database. The resulting TTC database contains information on over 550 chemicals, including their NOAELs and critical effects at the LOAELs. Over 20% of the toxicity data, selected from the lowest 10th percentile of NOAELs from each Cramer Class and studies showing large discrepancies across the data sources, were evaluated and documented transparently in two study review sessions. The chemical space of the new TTC database has been compared with that of other existing TTC databases, demonstrating its suitability of coverage for the assessment of cosmetic-related chemicals. Comparing the 5th percentile values of the distributions of NOAELs in the COSMOS TTC database with those from the Munro database showed that existing TTCs values are adequately protective. Strategies to apply this information to cosmetics-related chemicals will be described. The COSMOS TTC database will be made public and serve as a resource for alternative methods. *Authors thank COSMOS consortium. This abstract does not reflect the policy of US FDA, JRC, or EC.*

PS 1610 Evaluation of Four Alpha-Diketones for Toll-Like Receptor-4 (TLR-4) Activation in Human Embryonic Kidney Cells

K. Thuett[1], B. D. Kerger[2], D. J. Paustenbach[1] and B. L. Finley[1]. *[1]Cardno ChemRisk, San Francisco, CA and [2]Cardno ChemRisk, Aliso Viejo, CA.*

Animal studies of 2,3-butanedione (diacetyl) and 2,3-pentanedione inhalation have demonstrated severe inflammatory responses predominating in the upper airways of rats and mice, but no similar inflammatory responses were observed in humans. TLR-4 is an important pattern recognition receptor in the inflammosome cascade that triggers cytokine production and recruitment of immune cells to damaged or infected epithelial tissues. TLR-4 appears to play a role in chronic inflammatory conditions like Crohn's Disease, ulcerative colitis, and rheumatoid arthritis. Notably, some chemicals activate TLR-4 in rodents but not in humans. We utilized a human embryonic kidney cell assay (HEK293) to test for potential TLR-4 activation effects of 2,3-butandeione, 2,3-pentanedione, 2,3-hexanedione, and 2,3-heptanedione at test concentrations of 1, 10, 100, and 1,000 uM. The assay detects NF-kB induced expression of secreted alkaline phosphatase measured after 16 h incubation by a UV-VIS Spectrometer at 650 nm. *E. coli* K12 lipopolysaccharide (LPS) at 0.5 ng/ml served as a positive control and was added with each test compound to evaluate combined effects. None of the tested alpha-diketones were found to exhibit cytotoxicity, TLR-4 agonism, or combined effects with LPS at the highest test concentration of 1,000 uM. We conclude that human TLR-4 activation was not observed at relatively high concentrations of the tested alpha diketones. Investigation of rodent TLR-4 activity of these compounds might reveal a species difference in the inflammosome response compared to humans. It is also possible that metabolites or condensation products might be responsible for the severe inflammatory responses observed in the upper airways of rodents exposed to these compounds. Thus, further research is warranted.

PS 1611 High-Throughput Respirometric Assay Identifies Mitochondrial Toxicants in ToxCast Phase II

L. P. Wills[1], G. C. Beeson[1, 2], R. Schnellmann[2] and C. Beeson[1, 2]. *[1]MitoHealth Inc, Charleston, SC and [2]Drug Discovery and Biomedical Sciences, MUSC, Charleston, SC.*

The mitochondria are a common target of toxicity for drugs, industrial, and environmental chemicals because of their critical roles in aerobic metabolism and stress response. Previous high throughput screens (HTS) to identify mitochondrial toxicants use immortalized cell lines and focus on changes in membrane potential, which may not be sufficient to identify mitochondrial dysfunction. Primary cultures of renal proximal tubule cells (RPTC) are an excellent model because they derive their energy through aerobic metabolism, similar to that found *in vivo*, and have extensive transporters. We conducted a respirometric assay using RPTC and the Seahorse Bioscience Extracellular Flux Analyzer to screen 700 compounds (5 μM; 1 h) from the ToxCast Phase II library. Electron transport chain (ETC) inhibitors were defined as compounds that decreased respiration prior to a decrease in cell viability. Uncouplers were defined as compounds that caused > 15% increase in basal respiration. Of the assayed compounds, 397 (57%) were classified as ETC inhibitors, and 50 (7%) were uncouplers. A 480 compound subset was also examined in immortalized human renal cells (HK2) to determine differences in susceptibility to mitochondrial toxicity between primary and cultured cell lines. Of the assayed compounds, 282 (59%) were ETC inhibitors in RPTC, 219 (45%) inhibited the ETC in HK2, and 135 (28%) were common between both cellular models. Within the subset 17 (4%) were uncouplers in the RPTC, 74 (15%) uncoupled mitochondrial respiration in HK2, and only 3 (0.6%) were common between both cellular models. The observed differences between the RPTC and the cultured HK2 can be explained by the different metabolic profiles of the two models. This information will provide mechanisms and chemical-based criteria for assessing and predicting mitochondrial toxicity of new drugs, consumer products, and environmental agents. ToxCast Phase II was provided by the EPA. Funding was provided through grant 2R44-ES019378-02.

PS 1612 Electronic Cigarette Refill Fluids: Danger in a Bottle?

B. Davis, M. Dang, J. Kim and P. Talbot. *University of California Riverside, Riverside, CA.*

Electronic cigarettes (EC) are tobacco-free nicotine delivery devices that function by aerosolizing a solution composed of a humectant, flavoring and nicotine of varying concentrations. In this study, the nicotine concentration of 72 EC refill fluid (RF) products was quantified using high performance liquid chromatography (HPLC) and compared to manufacturer labeled concentrations to determine the accuracy of nicotine concentration labeling and the fidelity/consistency in

manufacturing of EC RFs. A subset of the 72 RFs were duplicate products, these were also evaluated by visual comparison of fluid coloration. A HPLC method was specifically created for the nicotine quantification of EC fluids. A Hewlett Packard Series 1100 HPLC with a Thermo Scientific Hypersil ODS C18, 200mm x 4.6mm, 5μm column was used with a flow rate of 0.8 mL/min and an injection volume of 5μL. An isocratic method was applied using a mobile phase of 76.9% water, 23% acetonitrile, and 0.1% triethylamine at a pH of 7.6. 50 of the 54 RFs labeled as containing nicotine had quantified nicotine concentrations that varied significantly from the manufacturer labels with a predominance of fluids (46 of 50) being in excess of labeled values. RFs labeled as zero nicotine were found to be nicotine free. Five products were unlabeled for nicotine concentration; three contained no nicotine, while the remaining two contained nicotine concentrations in excess of 100mg/mL. In duplicate comparisons of nicotine containing RFs, 16 of the 18 duplicates varied significantly in nicotine concentration from their mates. Of the 23 total duplicate pairs, 15 of 23 varied in coloration from their mates. Nicotine concentration labeling on EC refill products was often inaccurate, and some bottles that were not labeled had nicotine concentrations that would be lethal if inadvertently consumed by a child or adult. To ensure the reliability and safety of RFs, it is necessary to establish quality control guidelines for the manufacturing and labeling of RF products.

PS 1613 Cytotoxicity of Electronic Cigarette Refill Fluid Aerosols

R. Z. Behar, A. Razo and P. Talbot. *Cell Biology and Neuroscience, University of California, Riverside, Riverside, CA.*

Electronic cigarettes (EC) are nicotine delivery devices, often advertised for smoking cessation. The fluids used to refill these devices typically contain nicotine, a humectant, such as propylene glycol or vegetable glycerin, flavorings and contaminants. Few scientific studies have assessed possible health effects of EC aerosols on users, and it remains unclear whether they pose a health concern. Previously, 19 EC refill fluids from four companies were screened for cytotoxicity using human pulmonary fibroblasts (hPF) via the MTT assay. In this extension of the previous study, we produced aerosols from these fluids using the Vea EC from Johnson Creek and then tested them for cytotoxicity in the MTT assay on hPF, which model the adult lung. A comparison was made between the refill fluids applied to hPF and the aerosols produced from the fluids which were then used to treat the cells. Aerosols ranged in IC50 values (dose that inhibits survival by 50%) from 0.1054% to >1% (12 had low-cytotoxicity and 7 were moderately cytotoxic). For 68% of refill fluids (13 of 19), the corresponding aerosols had similar cytotoxicity. 11% of the fluids (2 of 19) were more cytotoxic than their aerosols. Finally, 21% of the products (4 of 19) were more potent as aerosols than as fluids. This latter observation is important as it shows that heating refill fluid can increase its cytotoxicity. The data further show that when screening for cytotoxicity of EC products, testing refill fluids on cells is not always representative of the effects of an aerosol on cell survival. Additionally, 2 of the 19 aerosols produced vapor effects at their high dose, and the dose range was then adjusted to eliminate vapor transfer into neighboring wells in the 96-well plate. This study is the first to compare the cytotoxicity of EC refill fluids and their aerosols on human cells. In addition, this study provides valuable insight into which of these EC refill products may be potentially harmful to users.

PS 1614 Apparent Lack of Cytotoxicity in Brands of e-Liquids Previously Reported As Being Cytotoxic

J. H. Lauterbach. *Lauterbach & Associates, LLC, Macon, GA.*

US sales of e-cigarettes (e-cigs) and e-liquids reportedly will exceed $1 billion in 2013. While there is much evidence to indicate that short-term use of e-cigarettes as a smoking cessation tool does not present undue health risks in healthy adults, little is known about health risks associated with long-term use of the product. To date there appears to have been only one report of *in vitro* toxicological assays that are commonly used to assess the toxicity of mainstream cigarette smoke being applied to the mainstream aerosol from e-cigs (Romagna *et al.*, 2013); but that research used puffing conditions now known to be inappropriate for e-cigs; and puffing of e-cigs is also known to give cytotoxic substances such as acrolein when dry puffs are taken (Farsalinos *et al.*, 2013). Thus, it makes sense to determine e-liquid cytotoxicity first. There has been one report (Bahl *et al.*, 2012) that described the use of the MTT *in vitro* assay with three different cell lines (hESC, mNSC, hPF) to estimate the cytotoxicity of e-liquids used to refill the reservoirs of e-cigs. While several e-liquids were reported to be cytotoxic, no cytotoxic compounds were identified in that report. For this research, four of the same brand-styles of flavors that were reported as cytotoxic by Bahl were obtained. An additional brand-style of e-liquid was obtained from another manufacturer. All five samples were assayed with the Neutral Red Uptake (NRU) cytotoxicity assays with CHO cells (assays were purchased from Labstat International ULC, Kitchener, ON, Canada), and a modification of Health Canada Method T-502 was used. There was no cytotoxicity at a concentration of 0.1%. In addition, each e-liquid was analyzed by GC-MS, and none of the compounds reported to cause e-liquid cytotoxicity such as allyl alcohol and diacetyl were found. However, one e-liquid was found to contain eugenol and cinnamaldehyde, compounds not usually used in cigarettes sold in the US.

PS 1615 VUSE Electronic Cigarette Aerosol Characterization

E. H. Theophilus[1], J. Rowe[1], S. Chouchane[2], K. Kilby[1], C. Rhoades[1], S. Alderman[1], W. Morgan[1] and R. J. Potts[1]. [1]*RJ Reynolds, Winston-Salem, NC and* [2]*Eurofins, Lancaster Labs, Winston-Salem, NC.*

Electronic cigarettes (e-cigs) are of high interest worldwide as alternatives to combustible cigarettes. R. J. Reynolds Vapor Company has introduced VUSE, an e-cig, in the US market in 2012. A main criticism of e-cigs from various groups is that there are not enough data on exposure to nicotine or other potential toxicants of interest. This poster presents mainstream aerosol chemistry data for different commercial VUSE products. Aerosol was collected using a 55/30/3 machine puffing regimen and either bell shaped or square wave puffing profiles. The test programs included evaluations of a subset of compounds currently listed on FDA's Harmful and Potentially Harmful Constituents list for combustible cigarettes. Individual constituent yields and chromatographic profiling data for different commercial VUSE products tested over different time intervals consistently indicated that: 1) compounds intentionally added to the formulation of the e-liquids (e.g., nicotine, glycerin) were measured in the aerosol, as expected; 2) toxicants of concern for combustible cigarettes were either below the limit of quantification or below the limit of detection in VUSE aerosols; and 3) VUSE aerosols were significantly less complex than mainstream smoke emitted from combustible cigarettes.

PS 1616 Safety Assessment of Potential Food Ingredients on Canine Primary Hepatocytes

L. W. Zhang[1], B. Jeffery[2], J. E. Riviere[1] and N. A. Monteiro-Riviere[1]. [1]*Department of Anatomy and Physiology, Kansas State University, Manhattan, KS and* [2]*Global Quality and Food Safety, MARS Inc., McLean, VA.*

Toxicity screening of pet food ingredients must first be conducted to assess their safety in dog food. Canine hepatocytes (CH) were isolated from the livers of dogs (n=3), euthanized for clinical reasons with owner consent, using a two-step collagenase perfusion method. CH were evaluated for viability with alamarBlue (aB) mitochondrial membrane potential (MMP) and reactive oxygen species (ROS) for 24h in some of the compounds. In addition, human and rat hepatocytes were used to compare to CH. Aflatoxin B1 (AB) and acetaminophen (APAP) were assessed to characterize and screen early toxic responses in CH and in pet food ingredients like clove leave oil (CLO) and eugenol (EUG). CH showed a decrease in viability with an LC_{50} of 3.38μg/ml and APAP with an LC_{50} of 3.11mg/ml, while the LD_{50} in human hepatocytes was 4.47μg/ml for AB and 3.45mg/ml for APAP, and rat LC_{50} of 5.36μg/ml for AB and 2.35mg/ml for APAP. MMP in CH showed a significant decrease by AB and APAP, and an increase in ROS especially with superoxide. In addition, CLO and EUG dosed at 1.5-fold dilution series ranging from 0.1% to 0.0029% in CH showed an increase in intracellular vacuoles when dosed at high concentrations greater than 0.0088%. CLO and EUG showed a decreased in viability from 0.030% at 24h with the same LC_{50} of 0.037%. In conclusion, CH were successfully isolated and well characterized for the assessment of toxicants and pet food ingredients, which is comparable to human and rat hepatocytes. The variable responses may be attributable to age and breed of dogs. (Supported by Mars Inc.)

PS 1616a Development of Formulation and Analysis Methods for Triphenyl Phosphate (TPP) in Rodent Feeds for Toxicology Studies

B. Collins[1], A. Mitchell[2], W. Vandaveer[2], V. Ault[2], N. Doll[2], S. Beckwith[2], N. Pearson[2], A. Mainey[2], K. Aillon[2], J. Algaier[2] and R. Harris[2]. [1]*National Toxicology Program (NTP) NIEHS, Research Triangle Park, NC and* [2]*MRIGlobal, Kansas City, MO.*

Aromatic phosphates (AP) are rapidly replacing brominated flame-retardants in commercial products. Most commercial APs are multi-component products containing ~20% TPP. Due to the lack of comprehensive toxicology data, TPP is under evaluation by the NTP. In support of planned toxicology studies, analytical methods were developed and validated for dose formulation characterization, including dose concentration, homogeneity, and stability of TPP in NIH-07 and NTP 2000 rodent meal feed. TPP-dosed feed (10 g) was extracted with 100 mL of acetonitrile (ACN):acetic acid (99:1; NIH-07) or 100 mL of ACN (NTP-2000)

and analyzed by HPLC/UV on an XTerra RP18, 5um column using a water:ACN gradient. This method, which was validated over a range of ~200 – ~5,000 ppm, was linear (r > 0.999), accurate (percent relative error < ±6.9%), and precise (relative standard deviation (% RSD) < 0.4%). TPP feed formulations were evaluated for factors influencing homogeneity, including TPP and feed particle size. Commercial TPP is supplied as 1-9 mm pellets, making formulation challenging. In this study, a ball-mill was used to grind TPP to a median diameter of ~420 μm to approximate feed particle diameter (median ~270 μm determined for 5 meal types). Homogeneity in NIH-07 and NTP 2000 was evaluated for two mixing procedures involving feed flour or an acetone/feed slurry. Both mixing procedures produced homogeneous formulations at 240 or 40,000 ppm (%RSD ≤ 5.0%), but the feed flour approach resulted in large TPP/feed agglomerates requiring extensive post-formulation particle size reduction. The 240-ppm TPP formulation was stable for 42 days in both diets, when stored at 4 or –20C, and for 7 days at ambient temperature when exposed to air and light in open feeders, but displayed an ~10% loss (NTP-2000) or an ~17% loss (NIH-07) after 24 hours when exposed to rodent urine/feces.

PS 1616b Using Cluster Approaches to Assess the Safety of Chemicals Used in Consumer Products

C. Baier-Anderson[1], C. Rudisill[2], L. Morlacci[2], M. Adams[1], B. Drake[1], J. Tunkel[2] and K. Mayo[1]. *[1]US EPA, Washington, DC and [2]SRC, Inc., North Syracuse, NY.*

There is a growing interest in the use of cluster-supported read across to obtain more efficient and accurate hazard assessments. While the practice of using structural analogs to evaluate data-poor chemicals is well established, the narrow-approach of "one analog to evaluate one chemical" can lead to inconsistent and inaccurate results, particularly when there is a need to assess a large number of chemicals. Assessing hazards in the context of small groups ("clusters") of structurally-related chemicals increases the overall confidence and the consistency of the hazard evaluation. The OECD and international regulatory authorities are increasingly looking to the use of clusters to maximize resources and animal welfare. This poster illustrates how the US EPA Design for the Environment Branch (DfE) is using chemical clusters to streamline hazard evaluation in a voluntary program that promotes the use of safer chemicals in consumer products.
Clusters can be assembled by professional judgment, but clustering software such as ChemACE, developed by US EPA to quickly create discrete clusters from user-defined chemical lists and with minimal refinement, can save time and effort during the initial grouping exercise. DfE uses ChemACE in the development of chemical clusters to evaluate chemicals against DfE's ecological, environmental fate, and human health criteria. Examples such as allyl esters, polycyclic musks and macrocyclic lactones, are used to illustrate how clusters are defined, used for read-across and provide assistance in decision-making. In addition to streamlining the evaluation process within DfE, this approach could be of further help for companies that are conducting hazard assessments under their own internal sustainability initiatives.

PS 1616c Toxicity of Tris(Chloropropyl)phosphate (TCPP) Dietary Exposure for 13 Weeks in Harlan Sprague-Dawley Rats and B6C3F1/N Mice

K. Ryan[1], A. R. Pandiri[3], D. Giri[5], K. Cimon[4], M. Buccellato[2], L. M. Fomby[2], M. Hejtmancik[2], D. Y. Vasconcelos[2], K. L. Witt[1], G. Travlos[1], D. Malarkey[1] and M. D. Stout[1]. *[1]DNTP, RTP, NC, [2]Battelle, Columbus, OH, [3]EPL, Inc, RTP, NC, [4]PC, RTP, NC and [5]PC, Houston, TX.*

TCPP is a high production volume flame retardant and plasticizer. It is recognized as a global contaminant but the hazard to humans remains unknown. The objective of this study was to evaluate the toxicity of TCPP in male and female mice and rats exposed via dosed feed for 13 weeks at 0, 1250 (mice only), 2500, 5000, 10000, 20000 and 40000 (rats only) ppm. In rats, perinatal exposure from gestation day 6 through postnatal day 21 (weaning) preceded the 13-week exposure. Exposure in mice began at 5-6 weeks of age. All rat dams exposed to 40000 ppm (gestation) and all male pups (first week post-weaning) from the 20000 ppm group either died or were humanely terminated due to overt toxicity. Body weights in all rats at weaning were 13-30% lower than controls, indicating an effect on weight gain. In mice, no treatment-related mortality or clinical signs of toxicity were observed. Terminal body weights were 12% (rats) and 29% (mice) lower than controls. Relative liver (rats, mice) and thymus (rats) weights were increased. Rats displayed increased serum cholesterol and decreases in hepatic enzymes; mice exhibited decreased blood leukocyte counts. In rats, microscopic changes included minimal to mild biliary hyperplasia and cortical hyperplasia in the thymus. In mice, hepatocellular hypertrophy and cytoplasmic alteration of male renal tubular epithelium were noted. In genotoxicity tests, TCPP did not induce mutagenicity in bacteria or chromosomal damage in peripheral blood of male or female rats, or female mice. Chromosomal damage in the form of micronucleated erythrocytes was seen in male mice. In summary, subchronic exposure to TCPP in feed resulted in reduced dam and pup survival (rats) and the liver, thymus and kidney were considered primary targets of toxicity. The NTP is currently evaluating the effects of TCPP on development, chronic toxicity, and carcinogenicity. This work was supported by the NIH.

PS 1616d Use of Chemical Safety Assessment and the TTC to Evaluate the Potential Toxicity of an Endoscopic Guidewire

N. S. Goud, M. Beauchane, J. Kapitan and E. E. Reverdy. *Corporate Toxicology and Biocompatibility, Boston Scientific Corporation, Natick, MA.*

An endoscopic, non-vascular guidewire (limited, less than 24-hour tissue contacting device) underwent a material and process change. To assess the potential impact of these changes to patient safety, the device was extracted with hexane or saline at 50 deg C and the resulting solutions were analyzed by various analytical test methods for extractable substances. GC-MS showed the presence of benzaldehyde, a commonly used food additive. The dose of benzaldehyde (10 μg) to which patients might be exposed from the use of guide wire was calculated to be about 70,000 times less than the published oral reference dose to man. Similarly, the total amount of 2-hydroxy-iso-butyrophenone present in the device (0.09 μg) was calculated to be 1000 times less than the proposed 90 μg/day dose limit for a Class III compound using the Threshold of Toxicological Concern (TTC) guidelines, implying a negligible genotoxicity or carcinogenic risk. The ICP-MS data showed the presence of several metallic elements such as zinc to which humans are exposed through various dietary sources. The estimated patient exposure to zinc from the use of the guidewire was calculated to be 285,714 times less than the prescribed daily upper intake level from US Food and Nutrition Board. Lastly, the device extract also showed the presence of tungsten (38 μg) which, based on the published NOAEL data, resulted in 138 times less than the tolerable exposure dose. The device extracts passed the required biocompatibility tests for safety evaluation. In summary, this study showed that chemical characterization of device extract is useful in determining potential toxicological risks, which may obviate the need for conducting further *in vivo* biocompatibility assays.

PS 1616e Diet Effects on Endpoints Relevant to Reproductive Toxicity Assessments in CD-1 Mice

K. Delclos[1], L. Camacho[1], S. Lewis[1], M. Vanlandingham[1], G. Olson[2], G. C. Gamboa Da Costa[1], K. Woodling[1], E. Sepehr[1], D. R. Doerge[1] and B. E. Juliar[1]. *[1]NCTR, Jefferson, AR and [2]Toxicologic Pathology Associates, Jefferson, AR.*

There are mixed reports on the reproductive effects of diet and dietary phytoestrogens on energy utilization, fat deposition, and reproductive parameters in CD-1 mice that could impact effects of hormonally active test agents. CD-1 weanlings were fed chow diets (NIH-41, Purina 5K96, Purina 5008/5001), purified AIN-93 (Growth and Maintenance), the AIN-93 formulation modified with ethanol-washed soy protein concentrate replacing casein (SPC), or SPC supplemented with isoflavones (SPC+ISF). NIH-41 served as the control diet and all diets were assayed for isoflavones and the estrogenic compounds zearalenone, coumestrol, and BPA. Serum was assayed for isoflavones. F_0 animals were mated. F_1 mice were evaluated for sexual development and subsets underwent uterotrophic assays and glucose challenge, as well as body composition analysis by dual-energy X-ray absorptiometry (DXA) at PND 21 and at termination (approximately PND 105). A subset of F_1 mice were mated to produce an F_2 generation terminated at PND 21. Body weights (BW) did not differ among diet groups in the F_0 generation and no differences in percent fat were indicated by DXA, although insulin levels were significantly lower (28-40%) and glucose elevated (14-19%) in F_0 males fed the AIN-93 and both SPC diets. In the F_1 and F_2 generations, BW in both sexes in the SPC and SPC+ISF groups was > 10% lower than the NIH-41 controls. Both sexes in both F_1 and F_2 generations fed the AIN-93 had an increased percent body fat (12-30%) at PND 21. The AIN-93 group had higher baseline glucose (F 17%, M 30%) but diet did not significantly affect responses to glucose or ethinyl estradiol (uterotrophic) challenges. Breeding performance did not differ among test groups in either generation, although there were testes effects (lower weight (22%), histology) in the AIN-93 group. All diets tested appeared suitable for reproductive assessments; isoflavone levels were not a major factor in the differences noted. (Support: NIEHS #AES12013/FDA #224-12-0003 IAG)

PS 1616f Chemical Characterization and Biocompatibility Investigation of One Drug-Combo Implant Devices for Neural Implication—Medtronic Antibiotics Impregnated Catheters

X. Deng, J. Bertrand and D. Amery. *Medtronic, Jacksonville, FL.*

Medtronic Antibiotics Impregnated Catheters (ARES) catheters are silicone elastomer catheters which are subsequently impregnated with proprietary antibiotics, which is the first drug-combo implant device in Medtronic Neurosurgery division. These catheters are permanently implanted ventricular and peritoneal catheters used as components of a shunt system in the treatment of hydrocephalus. The antibiotic impregnated ventricular and peritoneal catheters are line extensions of the currently offered standard Medtronic Neurosurgery catheters for use as components of a shunt system. To investigate the biological safety of the product for its usage as brain implant devices, series of chemical characterization and biocompatibility testing are undertaken. Drug elution study showed that the antibiotic is eluting at a rate and level that is not anticipated to cause significant patient adverse reactions. This product did not cause cytotoxicity in SK-N- MC neuronal cells after 48 hours exposure nor did it cause acute systemic toxicity in Swiss Albino mice. It did not induce skin irritation in rabbits or sensitization reactions in Guinea Pigs. More importantly, New Zealand White rabbits implanted with ARES did not demonstrate differences in measured parameters (clinical observation, clinical chemistry/hematology and histological pathology) that were considered to be attributable to ARES for a period of 13 weeks. As expected, ARES, which includes antibiotics, caused toxicity in some strains of the S. typhimurium tested in the bacteria reverse mutation assay. However, in the remaining bacteria strain, ARES did not induce any mutagenicity and it did not induce any genotoxic response in mouse lymphoma L5178Y cell lines. The base materials and impregnated antibiotics of the ARES catheters have been used in clinical settings for a long time without known genotoxic and carcinogenetic response, indicating low risk of genotoxicity and carcinogenecity for the ARES catheters.

PS 1616g *In Vitro* Assessment of Cardiotoxicity Hazard of Environmental Compounds Using Fast Fluorescence Imaging of Beating iPSC-Derived Cardiomyocytes

O. Sirenko[1], K. Ryan[2], F. Parham[2], M. Behl[2, 3], B. D. Anson[4], E. F. Cromwell[1] and R. R. Tice[2]. [1]*Research, Molecular Devices, Sunnyvale, CA,* [2]*National Toxicology Program, NIEHS/NIH, RTP, NC,* [3]*Kelly Government Solutions, RTP, NC and* [4]*Cellular Dynamics International, Madison, WI.*

A large number of environmental agents, with potential for human exposure, remain inadequately tested for toxicological effects. As an effort to develop and characterize in vitro model systems for toxicological screening, we used fast kinetic fluorescence imaging that monitored changes in intracellular Ca2+ using a calcium sensitive dye to screen a library of environmental chemicals and drugs for their ability to alter beating patterns in human iPSC-derived cardiomyocytes. These cardiomyocytes were exposed to a diverse set of 80 environmental chemicals. Compounds were screened for cardiotoxicity across a 7-point concentration at 30 min and 24 h of treatment. A number of physiological parameters of cardiomyocyte beating, such as beat rate, peak shape (amplitude, width, raise, decay, etc.) and regularity were collected using automated data analysis. Concentration-response profiles were evaluated using logistic modeling to derive a benchmark concentration (BMC) point-of-departure value, based on one standard deviation departure from the estimated baseline in vehicle treated cells. BMC values were used for cardiotoxicity classification and ranking. We found that number of environmental chemicals such as pesticides (permethrin, heptachlor, deltamethrin, dieldrine, carbaryl); flame retardants (isopropylated phenyl phosphate, 2- ethylhexyl diphenyl phosphate, 2,2'4,4-tetrabromodiphenyl ether); polycyclic aromatic hydrocarbons (acenaphthylene) and mitochondria toxins (rotenone) inhibited in vitro cardiomyocyte function. We applied the Toxicological Prioritization Index approach to integrate and display data across many collected parameters, to derive "cardiotoxicity" ranking of tested compounds. This approach can be utilized to prioritize suspected cardiotoxicants for in vivo hazard characterization and mechanistic follow-up studies.

PS 1617 Analysis of Four Hepatoxicants Using the xCELLigence Analytical System and HepaRG Cells

C. Jin[2], D. Steen[1], C. Chesne[1] and Y. A. Abassi[2]. [1]*Biopredic International, St. Gregoire, France and* [2]*ACEA Biosciences Inc, San Diego, CA.*

Hepatotoxicants act through different mechanisms and kinetics, and we reasoned that an analytical system allowing for convenient, kinetic monitoring of relevant effects combined with metabolically competent human hepatic cells, should facilitate recognition of the risk of hepatotoxicity. Our protocol involved culturing cryopreserved, differentiated HepaRG cells onto the xCELLigence 96-well cell culture plate, and after a four-day adaptation period, treating them with different concentrations of four compounds with known risk of hepatotoxicty-APAP, amiodarone, CsA, and troglitazone-and its eventual replacement the PPAR agonist rosaglitazone. The Cell Index (CI), an expression of the electrical impedance of adherent cells as measured on sensors in the culture plate wells by the xCELLigence Cell Analyzer, of treated cells was compared to the CI from HepaRG cells exposed to a 0.5% DMSO control at post-treatment time points 24, 48, 72, 96, and 168 hrs, during which time the medium was replenished every 48 hours. The CI was also assessed at 2, 5, 10, and 20 hours after treatment with eight APAP concentrations and control to determine if damage to the cells could be detected rapidly, since McGill et al reported significant glutathione depletion within three hours after exposing HepaRG to APAP.

With the exception of low concentrations, time and concentration-dependent effects were detected for all hepatotoxicants. 72 hours after treatment with 6uM of APAP and 50uM of amiodarone, the NCI of treated cells declined 70% and 83% respectively compared to the control cells. A marked CI decline in APAP treated cells vs control was detected within 10hrs. At 72+hrs. exposure to 200uM troglitazone demonstrated much stronger effect on the CI than 450uM of rosaglitazone.

We conclude that the combination of the HepaRG cells and xCELLigence system may sensitively detect risk of hepatotoxicity across a range of mechanisms.

PS 1618 Modeling of Inflammation-Mediated Liver Injury *In Vitro*

K. Balavenkatraman[1], B. Bertschi[1], M. Magnifico[2], A. Hauchard[1], S. Chibout[1], M. Uteng[1], J. Marlowe[2], P. J. Devine[2], F. Pognan[1] and A. Wolf[1]. [1]*Novartis Pharma AG, Basel, Switzerland and* [2]*Novartis Pharma AG, Cambridge, MA.*

Drug induced liver injury (DILI) is one of the leading causes for the discontinuation of drugs both in development and in post-marketing phase. Pre-existing liver inflammatory status might sometimes predispose patients to drug-induced hepatotoxicity.

A major contributor to liver inflammation is the resident macrophages, also referred to as Kupffer cells. However it is not feasible to profile all compounds during drug development in in vivo studies for their role in inflammation mediated liver injury in all preclinical species. An alternative is the use of in vitro approaches such as the co-culture of hepatocytes together with Kupffer cells or to treat hepatocytes with immunomediators such as TNFalpha to mimic inflammation mediated liver injury.

Mouse, rat, dog and human primary hepatocytes were cultured in a collagen-matrigel sandwich configuration and were primed with the immunomodulator TNFalpha. Two structurally related analogs – Trovafloxacin and Levofloxacin were used to validate this inflammatory model for liver injury. Cellular ATP (Adenosine Triphosphate) content and leakage of LDH (Lactate dehydrogenase) into the supernatant were measured.

Trovafloxacin, known to trigger hepatotoxicity in vivo, induced cytotoxicity in all tested species only in the presence of TNFalpha whereas Levofloxacin, which is innocuous in vivo, did not. A good correlation between the cellular ATP levels as well as the LDH released into the supernatant was observed. When hepatocytes were cultured without TNFalpha, both Trovafloxacin and Levofloxacin were devoid of any cytotoxicity.

This inflammatory-like model for drug-induced liver injury could be used to test compounds that are in development across various species.

PS 1619 Developing an Impedance-Based Cellular Assay with Human iPSC-Derived Cardiomyocytes to Quantify Modulators of Cardiac Contractility

C. W. Scott[1], X. Zhang[2], N. Abi Gerges[1], Y. A. Abassi[2] and M. Peters[1]. [1]*Drug Safety and Metabolism, AstraZeneca, Waltham, MA and* [2]*ACEA Biosciences, San Diego, CA.*

Cardiovascular toxicity is a prominent reason for late-stage failures in drug development, resulting in the demand for in vitro assays that can predict this liability in early drug discovery. Current in vitro cardiovascular safety testing primarily focuses on ion channel modulation and low throughput cardiomyocyte contractility measurements. The xCELLigence Real-Time Cell Analyser (RTCA) Cardio system utilizes label-free impedance technology to quantify beating properties of spontaneously beating cardiomyocytes in a medium throughout (96-well) mode. We tested both human induced pluripotent stem cell-derived cardiomyocytes (hIPS-CMs) and rat neonatal cardiomyocytes (rat-CMs) on the Cardio system. A set of 50 reference compounds were tested in concentration-response mode and the potency values for effects on beat rate and beat amplitude were determined. These compounds had previously been tested in vivo as well as in a low throughput in vitro optical-based contractility assay using electrically paced canine cardiomyo-

cytes (Toxicol Appl Pharmacol (2012) 260:162) and included negative and positive inotropes and no effect compounds. By comparing to the known in vivo contractility effects, hIPS-CM impedance had assay sensitivity, specificity and accuracy values of 90%, 74%, and 84%, respectively. These values compared favorably to the in vitro optical canine assay (83%, 84%, 82%) and were slightly better than impedance using rat-CMs (80%, 74%, 76%). The hIPS-CM and rat-CM impedance potency values spanned 5 orders of magnitude and correlated with values from the canine optical assay (r2=0.76 and 0.70, respectively). The Cardio system had >5X higher throughput than the optical assay. Thus, the hIPS-CM Cardio system assay can help detect the human cardiotoxic potential of novel therapeutics early in drug discovery and, if a hazard is identified, support the design-make-test-analyze cycle to mitigate this liability.

PS 1620 Assessment of Prolactin-Mediated Changes and Their Reversal in Molindone Treated Rats

S. Goel[1], S. Ganiger[2] and G. Krishna[1]. [1]*Supernus Pharmaceuticals, Inc., Rockville, MD and* [2]*Advinus Therapeutics Ltd., Bengaluru, India.*

Molindone, an antipsychotic, is known to modulate prolactin levels linked with reproductive changes in rodents. Such effects were further investigated in the current 6-month rat study with a reversal phase to better characterize changes for risk assessment. Wistar rats (12/sex/group) were dosed daily by gavage with molindone (males at 1, 3 and 10 mg/kg; females at 5, 20 and 60 mg/kg). Blood samples were analyzed for molindone and prolactin on Days 1, 180 and at a 2-month reversal period. Histopathology was performed on reproductive tissues. Results showed that plasma levels of molindone were more than dose proportional with Tmax between 0.25 to 1h postdose (PD). Prolactin levels peaked within 1h PD and were 284 and 335 ng/mL in males and 613 and 848 ng/mL in females, respectively, for Days 1 and 180. Prolactin levels remained elevated up to 2h PD in males and 8h in females. After 2-month recovery, prolactin levels reached basal levels, suggesting complete reversibility. Histopathologically, on Day 180, an increased vacuolation of mammary gland epithelium was noted in males at 3 and 10 mg/kg. In females, a diffuse glandular hyperplasia in mammary tissue was noted in all treated groups with minimal severity in 5 mg/kg, and minimal to mild severity in 20 and 60 mg/kg. At the end of recovery, histopathology changes in males were completely reversed; in females, they were completely reversed at 5 mg/kg, with signs of reversal at 20 and 60 mg/kg. Reversibility in prolactin and histopathology seen in this study validates the pharmacologically mediated effects of molindone and corroborate with the known role of prolactin in hormonal homeostasis and reproductive physiology. These changes are considered species-specific, similar to those seen with other antipsychotics in this class of drugs. It is concluded that the transient prolactin-mediated histopathology changes seen in this study are of negligible risk, if any, to humans, as such changes have not been reported in humans taking molindone as a therapeutic.

PS 1621 *In Vitro* Assessment of Intestinal Toxicity of Drugs Using an Electronic Impedance-Based Cell Monitoring System

C. Aruga, T. Fujita, T. Yamamoto and Y. Iwase. *Safety Research Laboratories, Mitsubishi Tanabe Pharma Corporation, Chiba, Japan.* Sponsor: J. Shinoduka.

Intestinal toxicity is a common problem in pharmaceutical development. In particular, the potential for diarrhea not caused by cytotoxicity is difficult to detect in rodent study because of the difference in the intestinal structures between rodent and human. As such, it is often first identified in dog or non-human primate study, or furthermore, in a clinical trial. Transepithelial electrical resistance (TEER) measurement has been used for the in vitro detection of diarrhea potential, especially due to barrier disruption, although its throughput was quite low. In this study, the usefulness of a real-time impedance-based cell monitoring system, xCELLigence (ACEA Biosciences, Inc.), which has a measurement principle similar to that of TEER, was evaluated as an effective assay system for detection of the potential for diarrhea in human.

HT29 cells, a human colon adenocarcinoma cell line, were seeded on 96-well E-plates, in which a sensor electrode array is incorporated in each well, and monitoring of cell impedance was initiated using xCELLigence. After 48 hrs incubation, the cells formed a confluent monolayer and the impedance became constant; then, cells were exposed to 19 compounds with or without diarrhea potential and cell impedance were monitored for 24 hrs.

As a result, remarkable reductions (>20% vs. vehicle control) of cell impedance were observed in the compounds that induced diarrhea due to barrier disruption: cytochalasin D, ethanol and okadaic acid. Slight reductions (15-20% vs. vehicle control) of cell impedance were observed in the compounds that induced secretory diarrhea, forskolin, sildenafil, IBMX and quinidine. On the other hand, no apparent change was observed in the compounds that induced diarrhea due to intestinal hypermotility, erythromycin and bethanecol, and in seven non-diarrhea-inducing compounds, except for loperamide. These results suggest the usefulness of the xCELLigence system as an effective assay to detect the potential for diarrhea in human.

PS 1622 A Comparison of Human Hepatocyte Systems and Conditions for Hepatotoxicity Screening

C. Storck, F. Wang, J. Kwagh, J. Megill and O. Flint. *Discovery Toxicology, Bristol-Myers Squibb, Princeton, NJ.*

Cultures of primary human hepatocytes (PHH), human induced pluripotent stem cell derived hepatocytes (hiPSCH; CDI, Madison, WI), and 5 immortalized THLE-5B (ATCC CRL 11113) human hepatocyte cell lines (one parental clone, Tc5, lacking CYP450 expression and 4 clones expressing either human CYP2C9, 2C19, 2D6 or 3A4 were compared for detection of hepatotoxicity (reduction of cellular ATP by 50% [IC50] at concentrations ≤ 50 μM). We used 40 hepatotoxic drugs (HD) labeled with a warning for serious (SHD, n = 20) or variable (VHD, n = 20) hepatotoxicity in human patients and 20 drugs not reported to be hepatotoxic (NHD). Cells were exposed to compounds at concentrations ≤ 200 μM for 4 days. In parental Tc5 cells, IC50 values of ≤ 50 μM were generated for 78% HD (31/40) and 15% of NHD (3/20). Metabolism by the Tc5 CYP expressing clones did not significantly increase the number of HD with IC50 values ≤ 50 μM but reduced the IC50 values for 5 SHD and 8 VHD and increased the IC50 values of 2/3 NHD to > 50 μM. In iPSCH and PHH, IC50 values ≤ 50 μM were respectively generated by 55% (22/40) and 53% (21/40) HD. PHH and hiPSCH generated the same number of false positives (5% [1/20]). These results support using the non-metabolizing Tc5 parent line to evaluate hepatotoxicity routinely, and use of the Tc5 clones subsequently to investigate the potential for toxification or detoxification. The iPSCH and PHH detect fewer HD and may be better reserved for compound specific mechanism studies. Finally, others have reported increases in the predictive value of hepatocyte cell systems co-treated with 1) DL-buthionine-(S-R)-sulfoximine to deplete glutathione, 2) a cytokine cocktail (TNFa, LPS, IL1a, IL6) to model immune stimulation under inflammatory conditions, or 3) galactose substituted medium to alter cell respiratory status. However, we found that these conditions did not improve the detection of HD in Tc5 cells after 4 days of culture.

PS 1623 A Chemical Derivative of Naturally Occurring Isothiocyanate, DJ4, Blocks Stress Fiber Formation

V. P. Kale, D. Desai, S. Amin, J. Hengst, S. Sung and J. Yun. *Pharmacology, Penn State College of Medicine, Hershey, PA.*

Isothiocyanates (ITC) are naturally occurring compounds found in many vegetables and are known for their antioxidant properties. We have developed a series of novel derivatives of ITC as a part of a cancer drug discovery program. Among the many derivatives tested, DJ4, dramatically altered the morphology of multiple cell types including cancer cells. Using confocal microscopy, detailed examination of the cytoskeletal structures of DJ4 treated cells revealed that DJ4 totally disrupted stress fiber formation without affecting microtubules. Given the known role of Rho family GTPases in cytoskeletal regulation, we hypothesized that DJ4 may exert its effects on stress fibers through modulation of signal pathways downstream of the Rho GTPases. Cellular mechanistic studies revealed that the DJ4-induced disruption of stress fibers was mediated by inhibition of Rho-associated kinases (ROCK) and myotonic dystrophy-related Cdc42-binding kinase (MRCK). In in vitro kinase activity studies, DJ4 inhibited phosphorylation of endogenous MYPT1 (myosin binding subunit of myosin phosphatase) which is a downstream substrate of ROCK and MRCK. Molecular docking of DJ4 onto the crystal structures of these kinases suggested that DJ4 binds at the ATP binding site of these kinases. In vitro biochemical studies using recombinant ROCK/MRCK and MYPT1 proteins confirmed that DJ4 potently inhibited ROCK1/2 and MRCKβ in an ATP competitive manner. Together these results demonstrated that DJ4-induced loss of stress fibers in the cells is at least, in part, mediated by direct inhibition of ROCK1, ROCK2 and MRCKβ. As stress fiber formation is involved in migration/invasion of cancer cells, these results further indicate the potential utility of DJ4 as a novel anti-metastatic agent.

PS 1624 Identification of Unknown Impurities in the Decorporation Agent 3, 4, 3-LI(1, 2-HOPO) Using UPLC Xevo-TOF MSMS Instrumentation

N. Panyala, M. Sturzbecher-Hoehne and R. J. Abergel. *Chemical Sciences Division, Glenn T. Seaborg Center, Lawrence Berkeley National Laboratory, Berkeley, CA.*

Identification of trace impurities in drugs and their structural elucidation is attaining much more interest due to their significant influence on drug activity.1-5 This structural information is very fundamental to know toxicity of trace impurities and their effect on drug activity especially at the preclinical stage.
The octadentate ligand 3,4,3-LI(1,2-HOPO), composed of four 1-hydroxy-pyridin-2-one (1,2-HOPO) units linked to a spermine scaffold through amide linkages, is undergoing preclinical development as an actinide decorporation agent6 that removes radioactive actinides from the body. In this study, 18 trace impurities were detected with the 3,4,3-LI(1,2-HOPO) ligand, using ultra-performance liquid chromatography coupled with photo-diode array UV detection and Electrospray Ionization-Quadrupole Time of Flight Mass spectrometry (UPLC-ESI TOFMS) via induced-in-source or collision induced mass fragmentation (Nozzle-Skimmer Fragmentation). Molecular ions were fragmented within the nozzle-skimmer region of the ESI mass spectrometer equipped with a TOF detector.
Of these 18 impurities, 8 are considered major impurities (detected over 0.1% threshold) and need to be characterized according to ICH guidelines. Structural elucidation of all 18 impurities was carried out via analysis of generated fragment ions using mass fragmenter, elemental composition softwares obtained from Waters Corporation (USA) and Molecular Fragment Calculator software. Proposed structures of impurities were further confirmed via isotopic modeling.

References

1. Narayanam M, et al. J Pharm Biomed Anal, 2013. S0731-7085(13): 00181-7.
2. Wu CS, et al. Rapid Commun Mass Spectrom, 2013. 27(9): 971-8.
3. Schmidt AH and Molnar I. J Pharm Biomed Anal, 2013. 78-79: 65-74.
4. Saini B and Bansal G. J Pharm Biomed Anal, 2013. 84C: 224-231.
5. Liu Y, Chen L, and Ji Y. J Pharm Biomed Anal, 2013. 81-82: 193-201.
6. Sturzbecher-Hoehne M, et al. Dalton Trans., 2011. 40(33): 8340-6.

PS 1625 Preclinical Assessment of Monocarboxylate Transporter 1 (MCT1) Inhibition on Retinal Function and Vision

E. A. Martin[1], A. E. Allen[2], R. J. Lucas[2], K. A. Greenwood[1] and W. S. Redfern[1]. [1]*Drug Safety and Metabolism, AstraZeneca, Alderley Park, Cheshire, United Kingdom and* [2]*Faculty of Life Sciences, University of Manchester, Manchester, United Kingdom.* Sponsor: R. Roberts.

Inhibition of monocarboxylate 1 (MCT1) is of interest to target highly glycolytic tumours. Inhibition of MCT1 leads to intracellular lactate accumulation, lactic acidosis and cell death. MCTs are expressed in many tissues including skeletal muscle, cardiac, testes, liver and eye. MCT1 is expressed abundantly in the retina. The high metabolic rate in the retina is supported mainly by glycolysis and the lactate produced is thought to fuel oxidative respiration in retinal cells such as photoreceptors. Hence, inhibition of MCT1 could lead to impaired retinal function. We have investigated the effect of AZD3965, an MCT1 inhibitor, preclinically in rats using OptoMotry (a visual acuity test) and electroretinography (ERG). For the OptoMotry test, albino rats were treated with AZD3965 for 7 days followed by 8 days recovery, and assessed pre-dose, on Days 1 and 4 of dosing and during the recovery phase. A dose related decrease in visual acuity was seen on Day 1 of dosing, which decreased further by Day 4. Slow, but complete recovery was seen after a week off dose. For the ERG, pigmented rats were treated with AZD3965 for 7 days followed by 7 days recovery. ERG measurements (scotopic and photopic) were taken pre-dose, on Day 1 and 7 of dosing and during the recovery phase. Rats were dark adapted prior to ERG, and anaesthetised during the procedure. AZD3965 had a dose-dependent effect on both scotopic and photopic ERGs within two hours of dosing. Interestingly, retinal function showed a significant recovery over the 7 days of repeated dosing, demonstrating partial restoration of function while being treated with compound. Further recovery was evident after cessation of dosing. These data show that MCT1 inhibition causes reversible visual and retinal functional disturbances in rats, and therefore a potential risk for patients. ERG offers a sensitive method for detecting retinal functional changes and is being used to monitor patients in the clinic.

PS 1626 Inhibition of MRP4- and BCRP-Mediated Transport by Tyrosine and Aurora Kinase Inhibitors

R. N. Hardwick[1], M. Snellings[2], B. C. Ferslew[2] and K. L. Brouwer[2]. [1]*Curriculum in Toxicology, University of North Carolina, Chapel Hill, NC and* [2]*Eshelman School of Pharmacy, University of North Carolina, Chapel Hill, NC.*

Tyrosine kinase (TKI) and aurora kinase (AKI) inhibitors are anti-cancer agents that target specific signaling pathways involved in aberrant cancer cell growth. TKI/AKIs interrupt these pathways by binding to the ATP-binding pocket of kinases to diminish their activity. Inhibition of ATP-binding cassette (ABC) efflux transporters can lead to intracellular accumulation of drugs, altered disposition, and toxicity. Some TKIs have been identified as inhibitors of ABC transporters commonly upregulated in malignant cells, including P-glycoprotein and breast cancer resistance protein (BCRP). However, the potential for TKIs/AKIs to inhibit other hepatic efflux transporters, namely multidrug resistance-associated proteins (MRPs), is largely unknown. The purpose of the current study was to compare the inhibitory potency of 20 TKIs and AKIs (0.1-100μM) against MRP4 and BCRP using inverted membrane vesicles. TKI/AKI inhibition of MRP4-mediated 3H-dehydroepiandrosterone sulfate (2μM;3.5min;n=3-6) uptake and BCRP-mediated 3H-estrone sulfate (1μM;1.5min;n=3-6) uptake was used to estimate a relative IC50. The ratio of the steady-state maximum total plasma concentration (Css) to the IC50 for each TKI/AKI was calculated to provide an estimate of the potential clinical relevance of inhibition for each transporter as determined by a Css/IC50 ratio ≥0.1. Inhibition of BCRP was prominent and included alisertib, barasertib, danusertib, enzastaurin, erlotinib, gefitinib, imatinib, lapatinib, neratinib, nilotinib, pazopanib, selumetinib, sorafenib, sunitinib, tozasertib, and vandetanib. TKI/AKIs exhibiting Css/IC50 ratios ≥0.1 for MRP4 included alisertib, danusertib, erlotinib, lapatinib, neratinib, nilotinib, pazopanib, sorafenib, tozasertib, and vandetanib. These findings may prove useful in the clinical interpretation of pharmacokinetic/pharmacodynamic outcomes in TKI/AKI combination treatment regimens. Current studies are underway to determine the TKI/AKI-mediated inhibition of MRP2 and MRP3.

PS 1627 Use of MALDI-Imaging As Part of an Integrated Approach to Predict the Nephrotoxic Potential of Polymyxin Derivatives

A. Gupta[1], R. Goodwin[2], N. Keirstead[2], A. Sathe[1], J. Harris[1], N. Johnson[2], A. Xue[2], C. Brown[2], D. Snow[2], F. McGrath[2], M. Pietras[2], L. Cheatham[2], P. I. Bentley[2], M. Blais[2], M. Wagoner[2], K. Thakur[1], T. Grebe[1], J. Swales[2], G. Kern[1], M. Hale[1] and J. Sasaki[2]. [1]*Infection Innovative Medicines Unit, AstraZeneca, Waltham, MA and* [2]*Drug Safety and Metabolism, AstraZeneca, Waltham, MA.*

Polymyxins, an older class of antibiotics, though are increasingly utilized as a last resort treatment for multi-drug resistant Gram negative infections, suffer from renal toxicity as a key dose-limiting liability. While in vitro cell-based screening systems and in vivo nonclinical toxicology models can provide useful insight, no single approach has been shown to accurately predict the nephrotoxic potential of these compounds. Our work investigated whether the renal effects of colistin and polymyxin B nonapeptide (PMBN) could be correlated to exposure differences observed in either in vitro models, or repeat dose in vivo rat toxicology studies. In rat in vivo studies, PMBN induced minimal nephrotoxicity, and was therefore expected to exhibit reduced renal exposure compared to colistin. Surprisingly, total kidney concentrations of colistin and PMBN differed by only 2-3 fold. MALDI imaging, a quantitative technique to measure compound concentration in specific tissue regions, was implemented to determine whether the cortical regions of the kidney (the site of renal injury) were subject to enhanced exposure in colistin-treated rats. The MALDI results indicate that colistin was concentrated in the cortical regions (medullary abundance was only ~10% of cortical abundance) of the kidney, whereas PMBN was distributed more evenly throughout cortical and medullary regions.
Additionally, when we compared the nephrotoxic potential and exposure differences of colistin and PMBN in various in vitro systems, the trends were similar to the in vivo data.
In summary, integrated assessment of in vivo tissue distribution and toxicology data, together with in vitro cytotoxicity and exposure measurements, can offer more accurate predictions of nephrotoxic liability.

PS 1628 A Real-Time *In Vitro* Safety Assessment Approach Utilizing a Simplified, Multiparametric Work Flow

A. L. Niles[1], M. Sobol[1], T. L. Riss[1], S. Einhorn[3], M. Zhou[2] and D. F. Lazar[1]. [1]*Promega, Madison, WI,* [2]*Promega Biosciences, San Luis Obispo, CA and* [3]*Cellular Dynamics International, Madison, WI.*

In vitro cytotoxicity is inextricably linked to a combination of compound dosage, exposure period, and intrinsic cell susceptibility. Current screening paradigms which utilize only endpoint measures in a defined cell type adequately address effects due to dosage, but often fail to define important toxicokinetic profiles or inherent mechanistic sensitivities. We investigated the use of a real-time cytotoxicity probe applied at the time of dosing with staurosporine, panobinostat, imantinib, terfenadine, colchicine, aflatoxin B1, bortezomib, camptothecin, valinomycin, nocodazole, methotrexate and ionomycin. Serial dilutions of these model compounds with the probe were delivered to iPS-derived, terminally differentiated hepatocytes and proliferating hepatoma and erthroid leukemia cell lines. Cytotoxicity data were collected at 4, 24, 48 and 72hr followed by a same-well multiplexed viability assay. The collated data revealed striking differences in toxicokinetics, potency and magnitude of response which positively correlated with known mechanism of action for the model compounds. The multiplexed viability data further served to either confirm observed cytotoxicity by inverse signal concordance, or suggest replicative perturbation in susceptible replicating cells. Furthermore, the use of cell types with differential capacity for phase I metabolism, allowed us to stratify cytotoxic risk based on mode-of-action of parent molecule toxicity and/or metabolic by-products owing to biotransformation. Lastly, the experimental approach taken was sufficiently predictive and informative to merit consideration for adoption as a new safety screening paradigm for new chemical entities.

PS 1629 Antimycobacterial Activity and Cytotoxicity of South African Rubiaceae Species, a Potential Source of Promising Antituberculous Remedies

A. O. Aro, L. J. McGaw and K. A. Eloff. *Paraclinical Sciences, University of Pretoria, Pretoria North, Gauteng, South Africa.*

Tuberculosis is an airborne contagious disease which has infected about one-third of the world's population with 1 in 10 latently infected individuals developing active disease in a lifetime. Although, the mortality rates of TB have reduced to about 1.7 million per annum, the incidence of new cases has increased due to the upsurge of HIV/AIDS. Toxicity associated with the presently available anti-TB drugs is a limitation to the treatment of TB leading to the failure of patient's compliance to the treatment. Medicinal plants are used in many part of southern Africa to treat TB-related symptoms including chest pain and coughing. In a preliminary screening process, plant species from the *Rubiaceae* family showed good activity against *Mycobacterium smegmatis*. Sixteen genera from the *Rubiaceae* family indigenous to South Africa were screened for their anti-TB activity against *M. smegmatis* and *M. aurum* using a two-fold serial microdilution assay while cytotoxicity was determined by MTT assay against C3A liver cells and Vero kidney cells. The selectivity index (SI) values were calculated. Six of the extracts showed good minimum inhibitory concentration (MIC) values ranging from 0.04-0.12 mg/ml. Thirteen extracts were relatively non-cytotoxic with LC50 values ranging from 0.1-0.7 mg/ml. *Oxyanthus speciosus* had the highest SI values (LC50/MIC) of 4.9 and 6.5 against *M. smegmatis* and *M. aurum* respectively (C3A cells) and 2.6 and 3.4 respectively (Vero cells). C3A cells were more sensitive to *Psychotria zombamontana* and *Pavetta lanceolata* than Vero cells, while *Psychotria capensis* was toxic to both C3A and Vero cell lines. In conclusion, *O. speciosus* may contain compounds which can act as leads for the development of new anti-TB drugs. Extracts containing several active compounds may also be promising remedies to act in conjunction with known anti-TB drugs to enhance their activity. Further work is continuing on isolation and identification of these compounds, and evaluation of fractions of the extracts for antimycobacterial activity.

PS 1630 Investigation of the Effects of Pyrrolamide Antibiotic Agents on Temperature in Rats

L. Wright[1], C. Sadler[1], J. Maynard[2], W. S. Redfern[1], J. McKay[1], H. Powell[1], J. Eakins[1] and S. Ricketts[2]. [1]*DSM, AstraZeneca, Macclesfield, United Kingdom and* [2]*PHC-Biomarker, AstraZeneca, Macclesfield, United Kingdom.* Sponsor: P. Duffy.

Administration of pyrrolamide antibiotic agents to rats was shown to be associated with reductions in core body temperature. We utilised a series of different techniques to gain an understanding of whether the changes in body temperature were related to effects on brown adipose tissue (BAT).

Core body temperature was assessed using digital rectal probes and transponders implanted subcutaneously into the interscapular region. Both methods demonstrated a decrease in core body temperature, which was variable between individual animals. Thermal imaging of the rats demonstrated a reduction in interscapular temperature suggesting decreased heat production, whilst there was no evidence of heat loss via the tail.

Metabolic rate (assessed using an oxymax open circuit calorimeter) demonstrated a slight decrease in group mean metabolic rate following administration of single doses of pyrrolamide compounds to rats when compared to controls; again with more marked effects seen in individual animals.

18F-Fluoro-Deoxyglucose Positron Emission Tomography (18F-FDG PET) imaging showed a significantly reduced 18F-FDG uptake in BAT compared with vehicle treated animals following administration of a single dose. However, inhibition of glucose metabolism was not specific to BAT, with significantly reduced 18F-FDG uptake observed in other tissues.

On repeat dosing in rats there was macrovesiculation/eosinophilia/coalescence seen in BAT by histology from Day 7 of dosing onwards. Enzyme histochemistry showed an increase in markers of oxidative phosphorylation (succinate dehydrogenase and cytochrome C oxidase) suggesting a change in mitochondrial function. The ultrastructure showed mitochondrial changes (increased condensation and/or number), and increased osmophilicity of lipid droplets inferring functional changes in mitochondria.

Current results support a conclusion of mitochondrial functional changes that in brown fat could have resulted in reduced thermogenesis.

PS 1631 Enhanced Sensitivity of Human and Animal Hepatocytes to Hepatotoxicants after a Prolonged Treatment Duration of 96 Hours

A. P. Li and U. Doshi. *In Vitro Toxicology, In Vitro ADMET Laboratories, Columbia, MD.*

In vitro hepatotoxicity evaluation in hepatocytes allows the selection of new chemical entities with reduced hepatotoxic liability for further development. Furthermore, multispecies evaluation in vitro aids the selection of the most appropriate animal for in vivo assessment of human hepatotoxic potential. We report here results with 12 model drugs with known animal in vivo and human clinical hepatotoxic potential: acetaminophen, aflatoxin B1, amiodarone, cyclophosphamide, troglitazone, rosiglitazone, ketoconazole, cerivastatin, fluvastatin,simvastatin, tacrine, and tamoxifen. Plateable cryopreserved hepatocytes from three human donors, Cynomolgus monkey, SD rat, CD-1 mouse and beagle dog were simultaneously evaluated in the same experiment for the assessment of potential species differences. The hepatocytes were plated in collagen-coated 384-well plates, with treatment initiated 4 hrs after plating for two treatment durations of 24 hrs and 96 hrs followed by quantification of cellular ATP contents. Increased cytotoxicity was observed for all hepatotoxicants at the prolonged treatment duration of 96 hrs. For several hepatotoxicants, the 96-hr treatment allowed clear distinction of species-differences which could not be observed with the 24-hr treatment. For instance, the hepatotoxic cerivastatin was highly cytotoxic (96-hr EC50 <3 uM) in human, monkey and dog hepatocytes, and substantially less cytotoxic in mouse and rat hepatocytes. Similarly, tacrine was cytotoxic after 96-hr treatment in human and monkey hepatocytes (EC50 of 19 to 41 uM) but non-cytotoxic to CD-1 mouse, SD-rat, and beagle dog hepatocytes. Neither cerivastatin nor tacrine was cytotoxic to human or animal hepatocytes up to the highest concentration evaluated of 100 uM at the shorter treatment time of 24-hrs. The results suggest that the prolonged 96-hr treatment of the hepatocytes significantly enhance the sensitivity of the cells to hepatotoxicants. Species-differences observed in vitro in this assay may aid the selection of the most appropriate animal model for in vivo safety evaluation.

PS 1632 A Novel 19-Substituted Benzoquinone Ansamycin Ameliorates A53T alpha-Synuclein-Induced Toxicity in a SH-SY5Y Cell Model of Parkinson's Disease through the Upregulation of Heat Shock Proteins and the Induction of Autophagy

D. Siegel[1], R. Xiong[1], R. Kitson[3], W. Zhou[2], C. J. Moody[3] and D. Ross[1]. [1]*Skaggs School of Pharmacy and Pharmaceutical Sciences, University of Colorado Anschutz Medical Campus, Aurora, CO,* [2]*School of Medicine, University of Colorado Anschutz Medical Campus, Aurora, CO and* [3]*School of Chemistry, University of Nottingham, Nottingham, United Kingdom.*

A major cause of neurodegenerative diseases including Parkinson's disease (PD) is the accumulation of misfolded protein aggregates that in turn leads to neurotoxicity. Targeting Hsp90 has been proposed as an attractive strategy to halt neurodegenerative diseases, and the benzoquinone ansamycin (BQA) Hsp90 inhib-

itors such as geldanamycin (GA) and 17-AAG have been found to protect against A53T α-synuclein induced toxicity in cell models of PD. However, current BQA inhibitors are relatively hepatotoxic in animal models, and a major mechanism of toxicity involves glutathione depletion as a result of arylation at the C19 position of the BQA. We have developed novel 19-substituted BQAs (19BQAs) as a means to prevent arylation and have validated that these compounds are unreactive at the 19-position using model thiols including glutathione. Our results show that 19BQAs exhibited little toxicity in SH-SY5Y cells relative to their parent quinones (GA, 17-AAG and 17-DMAG) using trypan blue, MTT and Annexin/PI apoptosis assays, while they retained the ability to induce heat shock proteins (HSPs) and autophagy as determined by increased levels of Hsp70, Hsp27 and LC3 II respectively. Transduction of mutant A53T human α-synuclein adenovirus in SH-SY5Y cells was further utilized to determine whether 19BQAs could ameliorate the neurotoxicity of mutant α-synuclein. 19-phenyl-GA, which caused potent induction of Hsp70, Hsp27, and LC3 II, significantly attenuated A53T α-synuclein-induced toxicity. These results indicate that 19BQAs may provide a means to modulate protein-handling systems in neural cells thereby ameliorating the aggregation and toxicity of proteins such as mutant A53T α-synuclein (supported by CA51210, ES018943 and Parkinsons UK).

PS 1633 High-Throughput *In Vitro* Toxicity Screening Using Autonomously Bioluminescent Human Cells in 2D and 3D Cultures

T. Xu[1, 2], J. D. Webb[1], A. Rogers[1, 2], D. Close[2], S. Ripp[1, 2] and G. S. Sayler[1, 2]. [1]*The University of Tennessee, Knoxville, TN and* [2]*490 BioTech Inc., Knoxville, TN.*

In vitro cell culture-based assays have increasingly become fast, high-throughput, and low cost alternatives to *in vivo* animal tests for tier I cytotoxicity screening of a large and still growing number of small molecule candidates in the drug development pipeline. Most of the current cell assays employ endpoint measurements that require cell destruction and/or substrate addition, thus limiting informational output to only intermittent single time point snapshots as well as requiring large numbers of samples be analyzed in parallel for basic toxicological kinetics studies. To overcome this disadvantage, we have demonstrated substrate-independent bioluminescent imaging in living human cells using a synthetically optimized bacterial bioluminescence (*lux*) reporter system. To evaluate its application for toxicity screening, *lux*-expressing autobioluminescent HEK293 cells were treated with the antibiotic Zeocin, whose toxicity was measured using the *lux*-based autobioluminescent assay, and the traditional MTT assay every 24 hours for 4 days. While the MTT assay required an individual set of samples for each time point, the substrate-free nature of the *lux*-system allowed for repetitive, near real-time monitoring of the same cell population over time. Exposure to 1000 μg Zeocin/ml yielded comparable toxicity profiles using both methods, reducing cellular activity to 11.9% and 13.9% compared to untreated cells after 2 days of exposure in the *lux* and MTT assay, respectively. The minimum concentration to induce 100% cell death ($p < 0.05$ compared to a medium control) within 4 days was determined to be 500 μg/ml in both assays. The ability to produce a measurable signal independently also facilitated the continuous monitoring of cell growth on a hyaluronan hydrogel 3D scaffold to more closely mimic *in vivo* conditions. Bioluminescence was detectable from untreated cells for at least 14 days in 3D culture. A rapid decrease in bioluminescence was similarly observed in 3D cultures within 1 day of Zeocin treatment.

PS 1634 Lack of Neuropathy after Long-Term Tedizolid Phosphate Administration in Rats

H. Hosako[1], A. Radovsky[1], D. Draganov[1], J. Vija[1] and K. Bartizal[2]. [1]*Toxicology, WIL Research, Ashland, OH and* [2]*Cubist Pharmaceuticals, San Diego, CA.*

A number of antibiotics, including linezolid (LZD), are associated with mitochondrial toxicity that can manifest as serious optic and/or peripheral neuropathy, primarily during long-term therapy. In a 6 month rat study, sciatic and optic nerve degeneration was observed with LZD exposures similar to those in humans. Tedizolid phosphate, a novel antibiotic prodrug given once/d for 6 days demonstrated noninferior efficacy to LZD twice/d for 10 days and may have less potential for mitochondrial toxicity. The neurotoxic potential of tedizolid phosphate in rats was examined in a robust 9 month study. Tedizolid phosphate in vehicle was administered orally to Long Evans rats (N = 366) once/d for 1, 3, 6, or 9 months at 7.5, 15, and 30 mg/kg (males) and 2.5, 5, and 10 mg/kg (females); dose levels were chosen to cover tedizolid exposures up to ≈ 10-fold of those in patients. Concurrent controls (N = 130) received vehicle only. The neurotoxic potential of tedizolid phosphate was thoroughly evaluated by a number of behavioral and neuropathological assessments. Toxicokinetics of the active moiety tedizolid were assessed throughout the study. There were no drug-related effects on survival, food consumption, functional observational battery assessments, locomotor activity, brain weight/measurements, ocular examinations, and macroscopic and microscopic neuropathological findings (including sciatic and optic nerves); of note, 9 month microscopic data are still being analyzed. Tedizolid exposure generally increased proportionally to dose, with little accumulation over time. Average and 9 month tedizolid steady-state exposures were ≈ 6-fold and 8-fold, respectively, of those in humans with standard 200 mg/d dose. This rigorous animal study showed no evidence of neurotoxic effects during long-term administration of tedizolid phosphate at systemic exposures considerably higher than achieved at the human therapeutic dose. These results suggest a reduced neurotoxicity risk with long-term tedizolid phosphate treatment relative to LZD.

PS 1635 Sequence Motifs Associated with Hepatotoxicity of Locked Nucleic Acid (LNA)-Modified Antisense Oligonucleotides

B. D. Hollingshead[1], A. D. Burdick[1], S. Sciabola[2], S. R. Mantena[1], R. Stanton[2], J. Warneke[1], M. Zeng[3], E. Martsen[3], A. Medvedev[3], S. S. Makarov[3], L. Reed[1], J. Davis[1] and L. O. Whiteley[1]. [1]*Drug Safety Research and Development, Pfizer, Cambridge, MA,* [2]*Oligonucleotide Therapeutic Unit, Pfizer, Cambridge, MA and* [3]*Attagene Inc, Morrisville, NC.*

Locked Nucleic Acids (LNAs) are third generation antisense oligonucleotide (ASO) modifications that improve target affinity, RNase H activation and stability. LNA modifications may increase the risk of hepatotoxicity compared to other types of ribose modifications. In vitro cytotoxicity screens have not been reliable predictors of hepatic toxicity in non-clinical testing; however, mice are considered to be a sensitive test species. To better understand the relationship between nucleotide sequence and hepatotoxicity, a structure-toxicity analysis was performed using two week tolerability studies in mice administered with LNA-modified ASOs at a dose of 25 mg/kg. ASOs targeting human Apolipoprotien C3 (Apoc3), CREB (cAMP Response Element Binding Protein) Regulated Transcription Coactivator 2 (Crtc2) or Glucocorticoid Receptor (GR, NR3C1) were classified based upon the presence or absence of hepatotoxicity in mice. From these data, a Random Forest classification model built from nucleotide sequence motif descriptors revealed two motifs (TCC and TGC) that were present only in hepatotoxic sequences. We found that motif containing sequences had higher propensity for binding hepatocellular macromolecules and increased P53 and NRF2 stress pathway activity. These results suggest in silico approaches can be utilized to establish structure toxicity relationships of LNA-modified ASOs and decrease the likelihood of hepatotoxicity in preclinical testing.

PS 1636 PARP Inhibitors and Centrosome Declustering: Bone Marrow Safety Implications

M. Crosby[1], R. Caccese[1], M. V. Nadella[1], K. Mikule[2] and J. Sasaki[1]. [1]*Drug Safety and Metabolism, AstraZeneca Pharmaceuticals, LP, Waltham, MA and* [2]*Oncology Innovative Medicines Unit, AstraZeneca, Waltham, MA.*

PARP inhibitors may selectively target cancer cells via centrosome declustering (CD). We explored the bone marrow (BM) safety profile of PARP inhibitors that induce CD and/or multipolar spindles (MPS) through *in vitro* and *in vivo* experiments. PARP inhibitors were synthesized and ranked according to CD and MPS-forming activities. Efficacy data suggested that this activity was PARP6-mediated. Although PARP6-dependent activity was considered to be cancer cell-specific, BM toxicity was observed in efficacy *in vivo* studies. To address the hypothesis that compounds inhibiting PARP1-3 could be responsible for the observed BM toxicity, we performed *in vitro* colony-forming cell (CFC) assays. We investigated 15 compounds with different MPS-inducing and PARP1 activities. The compounds' potencies in the CFC assays aligned with MPS-inducing activity, but not with PARP1 inhibition. To confirm the relationship between CD/MPS and BM toxicity *in vivo*, studies were conducted using enantiomers with differential MPS-inducing potencies (EC50s of 0.02 μM vs. inactive), but with similar PARP1 activities. The two compounds were dosed to give equivalent exposure over the course of 10 days (oral). Complete blood counts (CBCs) and BM flow cytometry revealed that BM toxicity occurred only in animals dosed with the enantiomer that caused MPS. Whereas there were peripheral, pancytopenic-suppressive changes with the active enantiomer, the inactive enantiomer showed no significant changes in CBCs. BM flow cytometry analyses showed significant reductions in lymphoid, myeloid, and erythroid cell populations, ranging from 70–100% over the course of the experiment with the active enantiomer. This was in contrast to the inactive enantiomer, which showed mild (10–20%) reductions in the same BM cell populations. The enantiomer experiment revealed that the proposed mechanism of PARP6-associated CD/MPS induction was independent of PARP1 and was directly associated with BM toxicity. Interestingly, this reflects a novel role for PARP6 in the BM.

PS 1637 Zebrafish-Based Screening to Prioritize Drug Development for Glioblastoma Therapy

L. Wehmas[1], J. A. Greenwood[2, 3], S. Liu[3], A. Punnoose[4] and R. L. Tanguay[1]. [1]*Environmental and Molecular Toxicology, Oregon State University, Corvallis, OR,* [2]*Environmental Health Sciences Center, Oregon State University, Corvallis, OR,* [3]*Biochemistry and Biophysics, Oregon State University, Corvallis, OR and* [4]*Physics, Boise State University, Boise, ID.*

Despite 30 years of extensive research on therapeutic development, the 5-year survival rate for patients diagnosed with glioblastoma remains less than 5%. The aggressive nature of glioblastoma often renders radiation and surgery ineffective. Thus, discovering new compounds that mitigate glioblastoma progression is vital to improving patient survival. We utilize an innovative orthotopic zebrafish xenograft model to assess drug efficacy at inhibiting human glioblastoma proliferation, invasion and angiogenesis within a 3-day time frame. Zinc oxide nanoparticles (ZnO-NPs) demonstrate preferential cytotoxicity to cancer cells in culture; therefore, we are interested in confirming whether this selective toxicity is conserved *in vivo*. Although ZnO-NPs prevented glioblastoma cell proliferation *in vitro*, preliminary experiments at exposure levels tolerable to the zebrafish revealed the ZnO-NPs significantly enhanced proliferation in the xenograft model. Knockdown of calpain 2 reduces glioblastoma invasion by ~90%; therefore, we are also interested in using our model to identify novel therapeutics that impede glioblastoma invasion through calpain 2 inhibition. *In vitro* testing of calpain 2 inhibitors identified two compounds that block glioblastoma invasion at low μM concentrations while causing minimal toxicity to the zebrafish making them ideal candidates for testing in the xenograft model. The results of screening putative anti-proliferative NPs and anti-invasive calpain 2 inhibitors will be compared to known chemotherapeutics LY294002, temozolomide and acivicin. Our approach holds promise for efficiently prioritizing novel glioblastoma therapeutics for future development. Research support: NSF 134468, NIEHS P30ES000210, ES016896 and T32ES07060.

PS 1638 Mutagenicity, Citotoxicity, and Genotoxicity Evaluation of Megazol Analogs

F. D. Mello[1], A. S. Carvalho[2], M. M. Bastos[2], N. Boechat[2], C. Aiub[3] and I. Felzenszwalb[1]. [1]*Department of Biophysics and Biometry, Rio de Janeiro State University, Rio de Janeiro, Rio de Janeiro, Brazil,* [2]*Institute of Pharmaceutical Technology, Oswaldo Cruz Institute, Rio de Janeiro, Rio de Janeiro, Brazil and* [3]*Department of Genetics and Molecular Biology, Federal University of the State of Rio de Janeiro, Rio de Janeiro, Rio de Janeiro, Brazil.* Sponsor: D. Oliveira.

Chagas disease is a protozoan zoonosis caused by *Trypanosoma cruzi* that has infected a large number of people. So far there is no effective drug for Chagas disease treatment. So, the Institute of Pharmaceutical Technology at Fiocruz has designed three nitro analogs of the nitroimidazole-thiadiazole megazol: PTAL 05-02 (5-(1-methyl-5-nitro-1H-2-imidazolyl)-1H-1,2,4-triazol-3-amine), PAMT 09 (2-amine-N-(1-methyl-4-nitro-1H-imidazole-5-yl)-5-(trifluoromethyl)-1H-1,2,4-triazole) and PTAL 04-09 (1-(1-methyl-4-nitro-1H-imidazole-5-yl)-1H-pirazole), whose toxicological properties were not evaluated. Then, this work investigates the mutagenic, cytotoxic and genotoxic activities of megazol and its nitro analogs. The *Salmonella* microsome assay was performed using the pre-incubation protocol with different strains of *Salmonella enterica* serovar Typhimurium (TA97, TA98, TA100, TA1535, TA102), and the Micronucleus assay was carried out with RAW264.7 macrophage rat cells. The assays were performed in accordance with OECD (1997 and 2010) standards. Megazol showed dose-dependent mutagenic and cytotoxic activity at very low concentration (0.05 μg/mL) for all *S. enterica* strains, with and without exogenous metabolic activation (S9 mix). PTAL 04-09 was the only analog to present mutagenic activity (TA100) at the higher concentration (50 μg/mL), with and without S9 mix. All of the nitro analogs presented cytotoxic activity to at least one strain (TA100 and/or TA1535), only with S9 mix. Moreover, all of them were capable of inducing micronucleus formation and showed cytotoxic effects (apoptosis and necrosis) at all concentrations (1.0 to 100 μg/mL). Our results showed that advances can be made in the development of new safe compounds to the Chagas' disease treatment.

PS 1639 Toxicological Safety Assessment of Novel 5, 6-Dihydropyridazine-1(4H)-Carbohydrazides: An Antitubercular Agents

R. Mishra[1, 2], A. A. Siddiqui[2], A. Husain[2], M. Rashid[2] and V. Srinivasan[3]. [1]*School of Pharmacy and Emerging Sciences, Baddi University of Emerging Sciences and Technology, Baddi, Himachal Pradesh, India,* [2]*Department of Pharmacy, Jamia Hamdard, New Delhi, India and* [3]*US Safety Evaluation, L'Oréal, Clark, NJ.*

Nowadays multidrug-resistan tuberculosis strain which is unaffected by the major anti-tuberculosis drugs currently on the market. That's why there is an urgency to develop new drugs and strategies to fight against tuberculosis or a tragedy may occur. A novel series of 5,6-dihydropyridazine-1(4H)-carbohydrazides and its analogs was synthesized and characterized spectroscopically. All the compounds were characterized and screened for in vitro anti-tuberculosis (anti-TB) activity against Mycobacterium tuberculosis H37Rv strains by using resazurin assay utilizing microtiter-plate method. These compounds also showed good antitubercular. Thus, the high level of activity shown by the compounds (7a, 7e) suggests that these compounds could serve as leads for development of novel synthetic compounds with enhanced anti-TB activity. After that, a toxicological safety assessment was conducted on 5,6-dihydropyridazine-1(4H)-carbohydrazides, to predict safety with oral consumption by rats. Two genotoxicity studies were conducted and no evidence of mutagenicity or genotoxicity was observed in the presence or absence of a rat liver S9 metabolic activation system at concentrations up to 5,000 μg of compound/plate in a chromosomal aberration assay. Studies conducted in Wistar rats included a 14-day acute oral toxicity study, and a 90-day repeated oral toxicity study. A 6-month repeated oral toxicity study was conducted in rats. In the 14-day study, the NOAEL was determined to be 5 g/kg bw. While a few statistically significant ($p<0.05$) findings were observed in the 90-day Wistar rat study, it was considered to be a sound basis for conducting a 6-month study. In the 6-month rat study, the no observed effect level was concluded as 1,000 mg/kg bw/d, the highest dose group tested. Finally, in a developmental toxicity study in rats no fetal abnormalities related to administration of the test article were observed.

PS 1639a Evaluation of Drug-Induced Cardiotoxicity in Zebrafish

R. Husain[1], G. Chimote[2], A. Damre[3], N. Pawar[2], J. Sreenivasan[2], S. Satapathy[3], V. Agarwal[2] and M. A. Mulla[1]. [1]*Toxicology, Piramal Enterprises Limited, Mumbai, Maharashtra, India,* [2]*Zebrafish & Nenotechnology, Piramal Enterprises Limited, Mumbai, Maharashtra, India and* [3]*Discovery DMPK, Piramal Enterprises Limited, Mumbai, Maharashtra, India.*

QT prolongation and the attendant risk of the malignant arrhythmia, torsades de pointes have led to the post marketing withdrawal of multiple medications from the market. Since drug-induced cardiotoxicity is difficult to predict, it has been major focus for regulatory scrutiny and is one of the most important areas of investigation in new drug development. Multiple new assays have been produced to the field in the last few years, highlighting not only to the importance of cardiotoxicity, but also the limited predictive utility of current techniques. Goal of present study was to establish correlation between Zebrafish cardiotoxicity and QT prolongation. QT prolonging and non-QT prolonging drugs (Amitryptaline, Amoxicillin, Bromocriptine, E-4031, Erythromycin, Haloperidol, Isoniazide, Linezolid, Methysergide, Pergolide, Quinidine, Rifampicin, Serotonin, Tamoxifen, Valproic Acid, Verapamil) were tested at different concentrations in Zebra fish cardiotoxicity assay. Three days post fertilization (dpf) zebrafish were incubated with drugs for 4 hours at 28°C. After incubation, parameters like heart rate, atrio-ventricular ratio, circulation defects, gross morphological defects, edema and thrombosis were recorded. Severe impairment of cardiac function after treatment with QT prolonging drugs resulted in the formation of pericardial edema, hemorrhage, bradycardia, as well as death. Results of Zebra fish cardio-toxicity were well correlated with hERG IC50 and effective therapeutic plasma concentration.

PS 1639b Identification of Compounds That Inhibit Dioxin Toxicity Using Cyp1a Reporter Zebrafish

S. Choi and K. Kim. *Chonnam National University Medical School, Gwangju, Republic of Korea.* Sponsor: H. Teraoka.

2,3,7,8-Tetrachlorodibenzo-*p*-dioxin (TCDD) is the unintentional byproduct of various industrial processes, is classified as human carcinogen and could disrupt reproductive, developmental and endocrine systems. Induction of cyp1a1 is used as an indicator of TCDD exposure. We sought to determine tissues that are vulnerable to TCDD toxicity using a transgenic zebrafish (*Danio rerio*) model. We inserted a nuclear enhanced green fluorescent protein gene (EGFP) into the start codon of a zebrafish cyp1a gene in a fosmid clone using DNA recombineering. The resulting recombineered fosmid was then used to generate cyp1a reporter zebrafish, embryos

of which were exposed to TCDD. Expression pattern of EGFP in the reporter zebrafish mirrored that of endogenous cyp1a mRNA. Using this transgenic cyp1a reporter zebrafish, we screened 6,400 small molecules for inhibitors of dioxin toxicity and identified several compounds that almost completely suppressed pericardial edema, a characteristic feature of dioxin toxicity in zebrafish embryos. We are currently testing efficacy of various derivatives of these compounds in the zebrafish embryos. Development of dioxin inhibitors will further understanding of dioxin toxicology and contribute to the treatment of dioxin intoxication.

PS 1639c Magnetic 3D Bio-Printing: A Novel High-Content Assay for Drug Toxicity Screening

H. Tseng[1], J. A. Gage[1], W. L. Haisler[2], S. K. Neeley[2], G. R. Souza[1] and T. C. Killian[3]. [1]*Nano3D Biosciences, Houston, TX,* [2]*Bioengineering, Rice University, Houston, TX and* [3]*Physics, Rice University, Houston, TX.* Sponsor: M. Wagoner.

A growing demand exists for the development of 3D cell culture models for drug screening that predict *in vivo* response more accurately than traditional 2D models. To meet this demand, we developed a real-time and dynamic 3D assay for drug screening based on magnetically bio-printed 3D cultures. This assay is based on the use of magnetic nanoparticles to rapidly assemble and print cells into 3D cellularized dots or rings that contract over time, and at rates that can vary with drug concentration.

Here, this assay was validated using 3T3 murine embryonic fibroblasts. 3T3s were first incubated overnight with the magnetic nanoparticle assembly and bio-printed the next day either into 3D dots or rings, and allowed to shrink over 5 hours. Contraction due to cell-cell interaction and migration was captured using a mobile device programmed to image whole plates of 3D cultures at specific timepoints, eliminating the need to image rings constantly under a microscope. This assay is label-free that allows for post-assay experimentation to explore mechanisms of action and yield more content per experiment.

This assay was validated as both a measure of drug response in 3D by comparing it to a 2D viability assay, as well as a high-content assay by fluorescent staining for viability and cytoskeletal organization, and compared to a 2D viability assay. With increasingly toxic drug concentrations, 3T3 dots and rings shrank at a slower rate, became less viable, and lost cytoskeletal organization. This assay was validated using retinoic acid, dexamethasone, doxorubicin, forskolin, fluorouracil, and norepinephrine, showing higher drug sensitivity compared to cells in 2D. Other cell types have been tested, including cancer cell lines, such as MCF-10A, and primary cell lines, like vascular smooth muscle cells.

PS 1640 Ocular Anatomical Features in Rabbits, Dogs, and Monkeys; a Comparison with Human Data

I. Atsumi, M. Kurata and H. Sakaki. *Toxicology, Senju Pharmaceutical Co., Kobe, Hyogo, Japan.*

In non-clinical studies for the development of ophthalmic products, laboratory animals such as rabbits, dogs, and cynomolgus monkeys are used frequently. The comparative researches for the ocular anatomy are essential for interpreting of data and extrapolating to human. However, the information has been scattered, and there is less comprehensive literatures easily to compare between the species. The purpose of this study is to provide direct and systematical comparison data of the ocular anatomical features from rabbits, dogs, and monkeys, and to compare with human data which were already established. The eyeballs from animals were all obtained from the purpose-breed animals ethically euthanized. After measuring the eyeball size (axial length, weight and volume), they are frozen. The frozen samples were dissected and measured for lens and vitreous size parameters during gradual throwing. As the result, the present study provided anatomical measurement values comprehensively for whole eyeball, lens, vitreous as well as body weight in each animal species. In comparison with human, the ratio were 0.39, 0.82 and 0.46-fold against human value (as 1) for eyeball weight, 1.71, 2.48 and 0.53-fold for lens weight, and 0.34, 0.73 and 0.55-fold for vitreous volume in rabbits, dogs, and monkeys respectively. Vitreous size was not directly depended on body weight of animals itself. This result enables us to set the dosage volume of drugs based on the size of animal eye. Furthermore, the ratio of dosage volume to eyeball size makes extrapolating to human more precise. In conclusion, this study provided a direct comparative data of ocular anatomical features in rabbits, dogs and monkeys and compared with human data. This would be useful for evaluating the non-clinical studies for ophthalmic products.

PS 1641 Retinal Toxicity Induced by a Novel Beta-Secretase Inhibitor in the Rodent

J. Werner[1], M. Fielden[1], J. A. Jamison[2], A. A. Coppi[1], D. Hickman[1], R. T. Dunn[1], E. Trueblood[1], C. Afshari[1] and R. Lightfoot-Dunn[1]. [1]*Amgen, Thousand Oaks, CA and* [2]*MPI Research, Mattawan, MI.*

Beta-secretase 1 (BACE1) represents an attractive target for the treatment of Alzheimer's disease; however, development of small molecule inhibitors has been challenging due to retinal toxicity in nonclinical studies. Retinal abnormalities have also been reported in a mouse knockout model, although such findings have not been replicated in other laboratories. In the course of compound development of a potent BACE1/2 inhibitor, we observed retinal degeneration characterized by loss of photoreceptors in the outer nuclear layer. To further investigate the retinal toxicity, a time-course investigational study was performed in the rat, which included retinal histomorphometry, fluorescence microscopy, electroretinography (ERG), and optical coherence tomography (OCT). Autofluorescent granules in the RPE were the earliest detectable change in the retina on day 4. Over the dosing period, the severity of AFG accumulation was dose- and time-dependent and associated with hypertrophy of the RPE. However, there were no test article-related changes noted in the neuro-retina and no changes observed by routine ophthalmoscopic examination after 28 days of dosing. Following 2 months of recovery, there was significant thinning of the retina at the highest dose, which was attributed to loss of photoreceptors in the outer nuclear layer. Electroretinography changes were observed as early as day 14, and before any detectable photoreceptor loss. There was also an increase in AFGs in alveolar macrophages of the lung. In separate studies, no retinal abnormalities were observed in BACE1 knockout rats or mice. In addition, an increase in AFG was observed in the RPE of BACE1 and BACE2 knockout mice treated with a BACE inhibitor for 14 days. Taken together, these results suggest that the retinal toxicity observed is an off-target effect that impairs phagolysosomal function in the RPE, which leads to photoreceptor dysfunction and retinal degeneration.

PS 1642 GSK2617971: *In Vitro* and *In Vivo* Characterization of a Mitochondrial Uncoupler

C. Hu[1], A. King[1], G. Brunori[2], A. Broom[2], J. Mangum[3], J. Armitage[2], R. Peterson[3], L. Day[4], L. King[1], S. Turner[1], D. J. Murphy[1], L. Schaller[5], J. Wilson[5], P. Turnbull[5], J. Lyon[2] and K. J. French[1]. [1]*Safety Assessment, GlaxoSmithKline, King of Prussia, PA,* [2]*Safety Assessment, GlaxoSmithKline, Ware, United Kingdom,* [3]*Safety Assessment, GlaxoSmithKline, RTP, NC,* [4]*Drug Metabolism and Pharmacokinetics, GlaxoSmithKline, King of Prussia, PA and* [5]*MM DPU, GlaxoSmithKline, RTP, NC.*

Adverse effects on mitochondria frequently underlie toxicities during drug development. Emerging technologies and increased mechanistic understanding have enabled more robust characterization of drug-induced effects on mitochondrial function both in vitro and in vivo. GSK2617971 ('971) is a pyrazole identified during development as a potent uncoupler of oxidative phosphorylation. In vitro, '971 caused rapid, dose-dependent increases (up to 200% versus vehicle) in mean oxygen consumption rate and mean extracellular acidification rate in C2C12 cells. In vivo, '971 demonstrated a steep dose-response tolerability profile with large individual variation, where only a 33% increase in mean plasma Cmax resulted in morbidity and death in rats given 100 mg/kg following a single dose versus rats given a well tolerated dose of 30 mg/kg/day for up to 7 days; however, in a separate study a single dose of 30 mg/kg induced hyperthermia (up to 5.1°C), a characteristic effect of uncoupling, and associated cardiovascular and respiratory response in 3 of 4 rats, among which one died of respiratory failure and cardiovascular collapse secondary to hyperthermia (> 42.5°C). At exposures below or equal to those that correlated with hyperthermia, functional effects (impaired mitochondrial calcium loading capacity, decreased mitochondrial membrane potential and decreased energy charge ratio) were observed in liver, skeletal muscle and kidney of rats given '971 versus vehicle and were consistent with minimal to moderate mitochondrial swelling as observed via electron microscopy. In conclusion, GSK2617971 is a potent uncoupler that exhibits functional and structural effects both in vitro and in vivo. The approaches utilized here are valuable for characterization of mito-toxicants during preclinical drug development.

PS 1643 The Mitosafe® Bioenergetic Balance Screen (BBS): An Innovative Cell-Based Profiler for Modulators of Mitochondrial Metabolism to Predict Hepatotoxicity

E. Cornille-Robert[1], P. Picamal[1], N. A. Compagnone[1], D. Hoet[2] and G. Labbe[2]. [1]*Predictive Toxicology Dept., ICDD, Meyreuil, France and* [2]*In Vitro Safety, Sanofi, Alfortville, France.* Sponsor: M. Doubovetzky.

Optimized methodologies are needed for predicting drug-induced hepatotoxicity, a frequent cause for drug withdrawal in clinical phases and post-marketing. Mitochondrial bioenergetics is impaired in drug-induced liver injuries. Thus the mitochondrial bioenergetic balance is a pertinent target to detect and eliminate potential hepatotoxic drugs at early pre-clinical stage. In this context, multiplexing is recognized to be more relevant than conventional end-point assays. The BBS measures, in the same non-permeabilized cells, oxygen consumption rate, lactate production rate, cellular ATP level and cell viability in an integrated multiplexed fashion.
We used the BBS in HepG2 cells with a set of 10 reference compounds, hepatotoxic, toxic to other organs, or well-tolerated, in dose-response to establish their bioenergetic profiles. Previous studies had shown that the BBS, used in a screening mode, testing compounds at a single dose, lacks specificity in recognizing hepatotoxic compounds. Using dose-response profiles increased the specificity of the BBS. Compounds toxic to other organs were not identified as hepato-toxicants. Moreover, we could generate an index of hepatotoxicity similar to that of LTKB's classification identifying compounds with severe, moderate and acceptable DILI concerns. The BBS classification index relied on the potential for activation of central metabolism to compensate mitochondrial bioenergetic liabilities, in drugs displaying lesser DILI concerns. Compared to the LTKB's classification the BBS had a sensitivity of 75% and a specificity of 100%. To validate our hypothesis, the analysis should be extended to a largest set of compounds and performed on metabolically competent cells. Overall our results suggest that the BBS bioenergetic profiling may be a useful outcome to assess hepatotoxicity potential in early preclinical drug development.

PS 1644 Mitochondrial Toxicity: Assessing *In Vitro-In Vivo* Correlative Risk in the Antiviral Human Rhinovirus Project (HRP)

M. S. Mondal[1], N. Keirstead[2], N. Johnson[2], L. Cheatham[2], H. Garside[3], M. Crosby[2], A. Chen[4], M. Rooney[4], P. Bhagunde[4], M. Cornebise[4], J. Wang[5], Q. Yu[4], M. Henteman[4], S. Butler[4], S. Brocklehurst[3] and J. Eakins[3]. [1]*Regulatory Safety, Drug Safety and Metabolism, Astrazeneca, Plc, Waltham, MA,* [2]*Drug Safety and Metabolism, Astrazeneca, Plc, Waltham, MA,* [3]*Drug Safety and Metabolism, Astrazeneca, Plc, Alderly Park, England, United Kingdom,* [4]*Infection iMed, Astrazeneca, Plc, Waltham, MA and* [5]*Pharmaceutical Development, Astrazeneca, Plc, Waltham, MA.*

Mammalian mitochondria possess a bacterial and viral ancestry [1]; as a consequence, antibacterial as well as some antiviral therapies could be prone to increased potential for mitochondrial toxicity. One such antiviral program, HRP identified a potential mitochondrial toxicity liability, during in-vitro screening using the glucose/galactose assay. AZN001, the original lead, had a Glu/Gal ratio of 8.5 that translated to IC50=15μM in the mitochondrial oxygen consumption assay. Although these in-vitro assays are considered predictive for mitochondrial toxicity, their actual translations in-vivo, including a quantitative in-vitro - in-vivo relationship and finding a molecular mechanism, are yet to be established. To address these points, AZN001 (top dose 750 mg/kg/d) has been tested in a 7-day rat study. Several parameters that can suggest mitochondrial dysfunction, including plasma lactate and transmission electron microscopy (TEM), were included in the study. As monitored by these in-vivo end points, a clear translation of in-vitro effects was observed. No clear guidance for a quantitative in-vitro and in-vivo relationship could be established. Additionally, an in depth in-vitro mechanistic study involving AZN001 and mitochondrial respiratory enzymes indicated potential inhibitions of mitochondrial complex I and/or complex V. In the light of these observations, the HRP team has implemented a suitable testing strategy for development of follow up lead candidates.
Reference(s)
1. Vafai, V.B. and Mootha, V. K. (2012) Mitochondrial disorders as windows into an ancient organelle Nature 491 (15), 374-383.

PS 1645 A Novel Assay for Detection of Drug-Induced Effects on Calcium-Dependent Platelet Activation

D. Petrucci, A. Murray and K. French. *GlaxoSmithKline, King of Prussia, PA.*

Platelets are central mediators of hemostasis at sites of injury, and as such, their regulation is tightly controlled. Platelet activation is initiated by various agonists, most of which require an elevation in cytosolic Ca^{2+} concentrations $[Ca^{2+}]_i$ for activity. Flow cytometry is a promising technique for the analysis of platelet phenotype and function. However, prior techniques for assessing drug-induced effects on platelet $[Ca^{2+}]_i$ did not enable pretreatment of *ex vivo* samples. To address this, an *ex vivo* human whole blood platelet activation assay was developed. Diluted whole blood platelets were loaded with the fluorescent Ca^{2+} indicator Fluo-3 AM to measure $[Ca^{2+}]_i$ alterations with $P2Y_1$ and/or $P2Y_{12}$ platelet receptor antagonists MRS2279 and 2MeSAMP, respectively. Activation with ADP caused a 4.4-fold increase in $[Ca^{2+}]_i$ over baseline. As expected, inhibition of the $P2Y_1$ receptor with MRS2279, caused a dose dependent decrease in $[Ca^{2+}]_i$ upon ADP activation (up to 74% inhibition at 300 μM). 2MeSAMP did not inhibit $[Ca^{2+}]_i$ at 100 μM. Inhibition of CD62P expression was consistent with $[Ca^{2+}]_i$ effects for MRS2279 (up to 60% at 300 μM), but not 2MeSAMP (up to 79% at 100 μM), indicating 2MeSAMP inhibits activation through a mechanism independent of the calcium pathway. A combination of both antagonists had a near complete inhibitory effect on calcium flux and activation demonstrated by decreased Fluo-3 AM fluorescence and CD62P expression. In conclusion, we have developed a novel flow cytometric assay that enables *ex vivo* manipulation of whole blood for evaluating potential drug-induced effects on $[Ca^{2+}]_i$. This assay can help investigate mechanisms of toxicity associated with platelet activation and alleviates the need to dose human subjects or animals. As a case study, we demonstrate disparate mechanisms of inhibition of platelet activation with known inhibitors of ADP-mediated signaling in platelets. Furthermore, the novel capability of *ex vivo* investigation of platelets is advantageous to guide future compound evaluations in preclinical safety studies.

PS 1646 Rapid Screening of Master Viral Stocks for Wild-Type Contamination

G. K. Massey[2], G. P. Gambill[2], A. D. Penman[1, 2] and K. K. Daniels[1]. [1]*Toxicology and Pathology Services, Southern Research Institute, Birmingham, AL and* [2]*Bioanalytical Sciences, Southern Research Institute, Birmingham, AL.*

Adenovirus 5 (Ad5) vectors are commonly used for vaccines and gene therapy. The E1A gene is required for viral replication. Some therapies take advantage of this property by inserting a therapeutic gene of interest in place of E1A. Since vector production requires the trans-complementation E1A, cell lines were generated to include the Ad5 sequence needed for replication. However, homologous recombination can occur during propagation, resulting in wild-type vector. These vectors are monitored for recombination to wild-type by their ability to infect cells lines without trans-complementation factors. Other gene therapy vectors take advantage of viral replication. For these vectors, a selective promoter replaces the E1A promoter so replication only occurs in cells of interest. These vectors are able to replicate, but only in the presence of cellular factors that activate the new promoter. If propagated in cell lines with wild-type sequence, homologous recombination can also occur, resulting in wild-type vector. Since both vectors are replication competent, there is difficulty distinguishing modified vector from wild-type Ad5. Therefore, a more specific test is needed to ensure vector stocks do not contain wild-type Ad5. Due to the specific and quantitative nature of real-time PCR, an assay for the wild-type promoter can be used to monitor for wild-type contamination of master viral stocks. Our method allows for the identification of 1-10 copies of wild-type Ad5 in the presence of 108 copies of modified vector. The method takes approximately 3-4 hours, allowing for same day results. Utilizing vectors from preclinical and/or clinical studies, we will present data demonstrating that using our method, 2 of the 4 vectors tested had appreciable levels of wild-type contamination. In conclusion, application of this method demonstrates the need to monitor vector quality throughout the production process and/or affirm vector specificity upon completion of production and prior to use in animal or human studies.

PS 1647 Understanding Mechanisms of Drug-Induced Liver Injury Using Primary Human Cell and Coculture Systems

F. Shah[1], E. Berg[2], M. A. Polokoff[2], J. Yang[2] and N. Greene[1]. [1]*Compound Safety Prediction Group, Pfizer Inc., Groton, CT and* [2]*BioSeek, a Division of DiscoveRx, South San Francisco, CA.*

Drug-induced liver injury (DILI) still remains a challenge to the pharmaceutical industries and regulatory authorities due to its idiosyncratic nature. Elucidating the mechanisms by which injury occurs in human hepatocytes and other liver cells is focus of attention. Here, we attempt to understand the mechanisms of DILI

using complex co-cultures of primary human cells (BioMAP systems). 10 discontinued Pfizer compounds and 25 known drugs (withdrawn from market or with black boxed-warnings) with clinical DILI and a small set of non-DILI compounds were retrieved from ToxCast Phase II dataset. These compounds were profiled in eight primary human cells (at multiple concentrations) including endothelial, epithelial, smooth muscle, fibroblasts and immune cells, stimulated with specific combination of inflammatory mediators, with activity in total of 87 protein read-outs. Compounds were classified based on their similarity in BioMAP profiles, which resulted in a number of unique clusters for DILI compounds. Some of these compounds exhibited overt cytotoxicity in multiple cell types, whereas others preferentially showed activity in one system (for e.g. fibroblasts). Also, a subset of them inhibits proliferation of multiple cell types. In contrast, the non-DILI compounds were weakly active or inactive. The discriminating read-outs between DILI and non-DILI set were identified using statistical computational approaches. Efforts are underway to understand the pathway-based mechanisms of DILI for a subset of compounds.

PS 1648 Assessment of Phencyclidine in the Evaluation of Physical Dependence in Rats Using the Nonprecipitated Withdrawal Test

P. Atterson, J. Toot, T. Pringle, M. Bennett and K. Landis. *WIL Research, Ashland, OH.*

Physical dependency assessments are conducted as part of the FDA and EMEA requirements pertaining to the medicinal product scheduling and investigation of dependence potential. Due to specific and often unique mechanisms of action for each drug class, it is necessary to evaluate and establish appropriate paradigms to assess physical dependency as part of a larger drug abuse liability (DAL) program. Therefore, the use of a validated and robust rodent model with appropriate non-precipitated withdrawal tests is necessary to adequately determine dependence potential. The objectives of this study were to establish standard withdrawal scores, changes in qualitative motor activity, and alterations in operant behavior assessments following chronic administration of the NMDA-R antagonist, phencyclidine (PCP). Phencyclidine was administered by subcutaneous injection to 8 groups of Wistar or Sprague Dawley adult male rats (n=6 rats/group) on an escalating dose regimen (up to 80 mg/kg/day) over the course of 21 to 28 days, followed by a 1 to 2 week withdrawal period. During the treatment and withdrawal phases, animals were monitored for body weight (BW), food consumption (FC), qualitative motor activity (MA), neurobehavioral/clinical observations (OBS), and operant scheduled behavior (OPB). During treatment, BW, FC, OBS, MA, and OPB were relatively consistent across PCP treatment groups, with characteristic increased motor activity and decreased motor coordination. Following the cessation of PCP dosing, OBS and initial MA were not significantly different across treatment groups, suggesting a lack of robust withdrawal behaviors. However, OPB assessments exhibited a significant decrease in OPB following the cessation of PCP dosing. These results demonstrate the importance of proper paradigm selection when designing specific DAL studies.

PS 1649 Investigation of the Method of Oral Mucosal Irritation Test by Oral Instillation in Rats

H. Kimoto, Y. Ito, S. Matsumoto and E. Hosoki. *Otsuka Pharmaceutical Co., Ltd., Tokushima, Japan.* Sponsor: W. Brock.

Evaluation for oral mucosal irritation is requested at the time of submission of new drug application when the clinical route of drug candidate intends to be intraoral administration. Generally, oral mucosal irritation tests have been conducted by applying test substances on the mucosa of cheek pouch in hamsters. In the present study, we conducted a cumulative oral mucosal irritation test in rats to evaluate the irritation potential of sodium dodecyl sulfate (SDS) according to the Cosmetic, Toiletry and Fragrance Association (CTFA) guidelines. Macroscopic and histopathological examination of oral mucosa was investigated. SDS was administered 4 times daily at 1-hr intervals for 4 or 10 days to rats under the different conditions as follows: instillation of 0.5%, 4% and 15% SDS (0.1 mL) into the oral cavity and application of 4% SDS (0.1 mL) with a paint brush to the labial mucosa and incisor gingiva of the mandibular oral vestibule. The irritation potential of SDS was evaluated on the basis of the daily mean total score (DMTS) and was classified as follows: Nonirritant (DMTS: 0), Mild irritant (DMTS: 0.5-1.0), Moderate irritant (DMTS: 1.1-2.0) and Severe irritant (DMTS: 2.1 and over). Macroscopic observations included sloughing on the incisor gingiva in the 4% SDS application and 15% SDS instillation groups. In addition, discoloration on the tongue was observed in the 15% SDS instillation group. The DMTS for 4% SDS application and 15% SDS instillation were 0.6 and 1.3, respectively. Therefore, SDS in each experiment was evaluated as "Mild irritant" and "Moderate irritant", respectively. By contrast, no oral mucosal irritation was observed in the 0.5% or 4% SDS instillation groups. In the histopathological examination, parakeratosis and thicking of the mucosal epithelium were observed on the labial mucosa in the 4% SDS application and 15% SDS instillation groups. It is suggested that this oral mucosal irritation test method by oral instillation in rats could be helpful to evaluate liquid drugs.

PS 1650 Comparative Subchronic Toxicity Studies in Rats of LY2963016 (LY), an Insulin Glargine Product, with USA-Sourced Lantus® (US–L) and EU-Sourced Lantus® (EU–L)

R. A. Byrd, J. L. Blackbourne, A. E. Schultze and J. L. Vahle. *Toxicology and Drug Disposition, Eli Lilly and Company, Indianapolis, IN.*

LY2963016 is an insulin glargine product, with an identical amino acid sequence to Lantus® insulin glargine. To support human clinical trials and in agreement with regulatory guidance for follow–on biologics, the toxicity of LY was characterized in rats alongside two reference insulin glargine products: US–L (Study 1) and EU–L (Study 2). Dosing was daily via subcutaneous injection for 4 wk. In Study 1, LY or US–L doses of 0, 0.3, 1.0, and 3.0/2.0 mg/kg were given. In Study 2, LY or EU–L doses of 0, 0.3, 1.0, and 2.0 mg/kg were given. The findings in Studies 1 and 2 were related to hypoglycemia or hyperinsulinemia at all LY and Lantus doses; the severity and duration of hypoglycemia was dose related. In Study 1, dosing was suspended at 3 mg/kg LY or US–L for 3 d due to multiple mortalities and associated severe hypoglycemia and then resumed at 2 mg/kg for the remainder of the study. Overall, the maximum tolerated dose (MTD) was exceeded in Studies 1 and 2 for LY, US–L and EU–L at ≥1.0 mg/kg based on hypoglycemia related mortalities. Hypoglycemia also occurred, but was tolerable with no associated mortality in the 0.3 mg/kg doses for LY, US–L and EU–L. Sciatic nerve degeneration, a common *sequelae* of sustained hypoglycemia, occurred at the high dose with LY, US–L and EU–L. At study termination, rebound hyperglycemia and pancreatic islet cell atrophy were observed at ≥1.0 mg/kg of LY, US–L or EU–L and was most likely due to down regulation of endogenous insulin synthesis secondary to hyperinsulinemia. Increased fat was observed in the skin, subcutis and injection sites at all doses of LY, US–L and EU–L consistent with lipogenic pharmacology typical of insulins. Based on the occurrence of intolerable hypoglycemia in rats at doses ≥1.0 mg/kg, the MTD and NOAEL (no–observed–adverse–effect level) was 0.3 mg/kg for LY, US–L and EU–L. Therefore, we conclude that the toxicity profiles of LY, US–L and EU–L are highly similar.

PS 1651 Glucocorticoid-Induced Bone Loss in Aged Rats Is Not Reversible

R. Samadfam, E. Lesage and S. Y. Smith. *Bone Research, Charles River, Montreal, QC, Canada.* Sponsor: M. Vézina.

The objective of this study was to investigate the effects of methylprednisolone (a glucocorticoid, 3 mg/kg/day) on bone when administered to aged rats (19 week old female Wistar Hannover) with an inactive growth plate, for 13 weeks followed by an 8-week recovery period. Effects on bone densitometry and bone geometry were evaluated (using pQCT) at baseline and Weeks 4, 13 and 19. In addition, body weight, food consumption, selected serum biochemistry and bone turnover markers were evaluated to add perspective on mechanisms underlying bone effects. Sharp decreases in body weights were noted one week following treatment compared to baseline with no further loss for the remainder of the treatment period. Steady weight gains for controls over the treatment period compared to a lack of gain (or loss during the first week) for treated animals, resulted in marked differences between treated and controls. Within 1 week of recovery, the body weights of the treated-animals were comparable to controls. Increases in food consumption were noted for treated versus controls that persisted during the recovery period. During the treatment period, decreases in bone formation marker (osteocalcin) were noted for treated animals compared to controls. However, at end of recovery, osteocalcin levels were slightly higher than controls. No effects were noted on bone resorption markers or serum phosphrous and calcium. At the proximal tibia metaphysis mean BMC (bone mineral content) and BMD (bone mineral density) were significantly lower than controls. At the diaphysis, significantly lower BMC was noted with lower bone diameter indices, indicating smaller bones. In general, effects on bone diameter and bone mass persisted during the recovery period, in spite of the slight increase in osteocalcin levels at the end of the recovery period. These data collectively indicate that treatment with methylprednisolone is associated with smaller and likely weaker bones. Furthermore, in aged rats these negative effects did not reverse following cessation of methylprednisolone treatment.

PS 1652 Rat-Specific MOA for Tumor Formation in Rats with the SGLT2 Inhibitor Canagliflozin

B. Feyen[1], E. Moesen[1], S. De Jonghe[1], P. Vinken[1], J. Ying Ma[2], M. D. Johnson[2], M. Srinivas[2], W. Coussement[1], Y. Van Bekkum[1] and L. Lammens[1]. [1]*Drug Safety Sciences, Janssen, Beerse, Belgium and* [2]*Drug Safety Sciences, Janssen, Raritan, NJ.*

Canagliflozin, a sodium glucose cotransporter 2 (SGLT2) inhibitor, caused renal tubular tumors (RTTs) and pheochromocytomas in a 24-month rat carcinogenicity study at the high dose.
Canagliflozin is also a low potency inhibitor of SGLT1 and causes carbohydrate (CHO) malabsorption at high doses in rats via inhibition of intestinal glucose transport leading to increased intestinal calcium absorption (secondary to acidification), hypercalciuria and hyperostosis. This carbohydrate malabsorption was believed to play a role in the induction of the renal and adrenal tumors.
A 6-month mechanistic study (with a 1 and 3 month interim evaluation) was performed in which rats were fed a glucose-free 40% fructose diet. The purpose of this study was to prevent carbohydrate malabsorption and its sequelae. Urinary calcium, development of hyperostosis, and serum 1,25-dihydroxyvitamin D and parathyroid hormone (PTH) were used to confirm the effectiveness of the intervention. In addition, cell proliferation was evaluated in kidneys and adrenal medulla by BrdU-immunohistochemistry and kidney injury was evaluated by KIM-1 immunohistochemistry, to evaluate the link between CHO malabsorption and kidney injury/cell proliferation (as proximal steps in tumorigenesis) in these target tissues.
Utilization of a glucose-free fructose diet prevented the effect on CHO malabsorption and its sequelae including hyperostosis and increased calcium absorption. Cell proliferation in the kidney and adrenal medulla was increased in rats administered canagliflozin (cana) fed a standard diet, and immunostaining was increased for the renal injury biomarker KIM-1. These effects were inhibited in cana-treated rats maintained on the glucose-free fructose diet indicating they are secondary to CHO malabsorption and are not direct effects of canagliflozin.
CHO malabsorption was absent in humans at clinical doses indicating that the tumor findings in rats are not clinically relevant.

PS 1653 Expanded Therapeutic Index of Antithrombin Silencing and Correction of APTT in a Hemophilia A Mouse Model

S. Barros, M. Carioto, J. Hettinger, Y. Jiang, J. Qin, H. Prabhala, A. Sehgal and A. Akinc. *Alnylam Pharmaceuticals, Cambridge, MA.*

ALN-AT3, a subcutaneously administered RNAi therapeutic targeting antithrombin (AT), is currently being developed for the treatment of hemophilia and rare bleeding disorders. It has previously been demonstrated that once weekly dosing of ALN-AT3 results in potent, dose-dependent and reversible silencing of plasma AT in multiple preclinical species. In the mouse, steady state ED50 knockdown was achieved following weekly doses of 0.5 mg/kg. This study evaluated the exaggerated pharmacology of ALN-AT3 when administered via weekly SC injections (x 7 wks) to wild-type (WT) vs. hemophilia A (HA) mice at 0, 10, 30, and 100 mg/kg (20-, 60- and 200-fold dose multiples of the mouse ED50). Test article-related effects were evaluated by clinical signs, BW, clinical pathology, organ weights, and histopathology of select tissues (eye, heart, kidney, liver, lung, spleen). The PD of ALN-AT3 was evaluated by plasma AT protein assay. Repeat dosing of ≥ 10 mg/kg ALN-AT3 to WT mice was not tolerated, as evidenced by early mortality, adverse clinical signs (ocular abnormalities, craniofacial swelling, lethargy), weight loss, clinical pathology changes (↓PLT, ↑NEU), ↑spleen weights, and microscopic findings in heart (thrombi) and eye (hemorrhage). Residual plasma AT protein in all animals was < 10% relative to control (> 90% on-target AT suppression). All findings were suggestive of thrombosis and DIC, consistent with the intended pro-coagulant effect of AT suppression. The findings in WT animals are also consistent with homozygous AT deficiency in humans, which is almost always lethal in utero. In contrast, ALN-AT3 was well tolerated in HA mice, with no adverse findings up to 100 mg/kg. In addition, HA mice exhibited significant reductions in APTT consistent with the therapeutic hypothesis of rebalancing the hemostatic system in the disease condition. Collectively, the data also suggest an expanded therapeutic index of AT suppression in the hemophilia disease condition.

PS 1654 Repeated-Dose Intramuscular (IM) Toxicity Study with Poly-α-L-Glutamic Acid (PLG) in New Zealand White Rabbits

L. Segal[1], E. Grosdidier[3], C. Sobry[3], G. Giordano[1], M. Damsten[1], R. Forster[3], K. Frazier[2] and E. Destexhe[1]. [1]*GlaxoSmithKline Vaccines, Wavre, Belgium,* [2]*GlaxoSmithKline Pharma, Upper Merrion, PA and* [3]*CiToxLAB, Evreux, France.*

The potential local and systemic toxic effects of five IM injections at 2 weeks intervals of the excipient PLG MW 2083 Da were studied in New Zealand White rabbits. PLG was administered at a dose of 6.25 mg/injection and compared with saline treatment. The PLG concentration, pH, osmolarity, sterility and endotoxin levels were verified at each day of injection. Rabbits were distributed in 3 subgroups (5/sex) sacrificed 1, 3 or 28 days post last dose (days 58, 60 or 85). Animals were observed for mortality/morbidity, clinical signs, and local injection site reactions. Body weight, food consumption, rectal temperature, and ophthalmology were evaluated prior to, during and after treatment. Hematology, coagulation, blood biochemistry and C-Reactive Protein (CRP) levels were evaluated prior to treatment and on days 2, 8, 53, 58, 64 and 85. After the treatment period all animals in each subgroup were sacrificed and examined macroscopically. Selected tissues were weighed and preserved. Microscopic examinations were performed on the kidneys only on day 58, and on all preserved tissues on day 60. No unscheduled deaths occurred during the study and no signs of systemic toxicity were observed. Animals treated with PLG had a higher incidence of reactions (mainly erythema) at injection sites relative to the controls, which persisted for up to 19 days. Since all local reactions were reversible, PLG was considered well tolerated locally. Mean body weight and food consumption were unaffected by PLG treatment. No remarkable effects on rectal temperature or ophthalmological findings were observed in the control or PLG groups. Hematology, coagulation parameters, blood biochemistry and CRP levels were unaffected by PLG exposure. IM administration of PLG did not induce any significant histopathological findings compared to saline, in particular, no kidney findings. The excipient PLG was considered to be well tolerated both locally and systemically following repeated IM injections in the rabbit.

PS 1655 Preclinical Safety Development of a New HSV-2 Prophylactic Candidate Vaccine to Support a First-in-Human Phase I Clinical Trial

D. Paul[1], V. Barban[2], A. Popineau[1] and S. J. Gould[1]. [1]*NonClinical Safety, Sanofi Pasteur, Marcy l'Etoile, France and* [2]*NonClinical Product Perfrmance, Sanofi Pasteur, Marcy l'Etoile, France.*

Herpes simplex type-1 (HSV-1) and type-2 (HSV-2) viruses belong to the herpesviridae family of viruses (members of the alphaherpesvirus subfamily), which can cause prevalent, lifelong genital, dermal and ocular infections resulting in a spectrum of clinical symptoms including cold sores, genital ulceration, corneal blindness and encephalitis.
HSV529, a viral vaccine candidate against HSV-2 wild type virus, is being developed to prevent HSV-2 genital infection. The vaccine is derived from a HSV-2 186 syn+-1 wild-type virus, where the UL5 and UL29 genes have been deleted, which are essential for viral replication.
To support a first-in-human study in healthy adults (18 to 40 years, ClinicalTrial.gov study code NCT01915212), a repeat dose toxicity and biodistribution studies were conducted in the guinea pig, which was selected as it is pathogenically sensitive to HSV-2 virus, closely mimics the human genital HSV-2 infection, and develops a positive humoral response to the vaccine.
The repeat dose study was conducted to assess the systemic toxicity and local tolerance and the biodistribution study was designed to evaluate the distribution, persistence, the ability to shed and to establish latency. In the repeat dose toxicity study, 4 intramuscular (IM) injections of a human dose (107 PFU/0.5 mL injection) induced a robust immune response. Effects were limited to reversible local reactogenicity and changes in the draining lymph nodes, related to immune stimulation. A transient minimal decrease in platelet count was also noted. The biodistribution study showed that following one IM injection at a human dose, no HSV529 was detected in any HSV-2 target organs and biofluids at the time points assessed. The study confirmed HSV529 was unable to distribute, propagate/replicate, shed or establish latency up to 45 days post injection. This data supported moving forward in a Phase 1 clinical trial with monitoring of local reactogenicity and platelet counts.

PS 1656 Mechanism of Platelet Reduction in Monkeys with BMS-986001, an HIV Nucleoside Reverse Transcriptase Inhibitor

M. Guha[1], M. S. Christin-Piche[2], S. Clark[1], R. Bunch[1], T. Sanderson[1] and M. Davies[1]. [1]*Drug Safety Evaluation, Bristol-Myers Squibb, Mount Vernon, IN and* [2]*Pre-Clinical Services, CRL, Montréal, QC, Canada.*

Overall, BMS-986001 has a consistent nonclinical toxicity profile, the primary target tissue being the erythroid series in bone marrow. However, in 6- and 9-month studies, 3 of 60 BMS-986001-treated monkeys (5%) developed severe platelet (PLAT) reductions accompanied by cutaneous petechiae only at the highest doses (200-300 mg/kg/d). In all 3 affected monkeys, the onset (Weeks 8-11) and magnitude (>50% reductions, and as low as 0.3% of pretest in individuals) of the PLAT reductions were generally similar and there was no overt bleeding. In the 6-month study, the 2 affected monkeys were euthanized (Week 14) and the 300 mg/kg/d dose was reduced to 200 mg/kg/d without further occurrences of low PLAT. The 1 affected monkey (200 mg/kg/d) in the 9-month study completed the dosing and PLATs recovered at the end of 1-month recovery period. Plasma BMS-986001 levels for these 3 monkeys were similar to other monkeys given the same dose; thus higher BMS-986001 exposure did not explain the PLAT reductions.
Drug-induced PLAT reduction can be caused by anti-drug antibodies (ADA). To determine if PLAT reductions were mediated by ADA, serum platelet-associated immunoglobulin (PAI) levels were measured using PLAT-coated 96-well ELISA and by FACS analyses. No circulating PAI was detected in serum of any affected monkey by ELISA. However, PLAT-bound PAI was detected in CD42+ PLATs (IgG-PE mean fluorescence intensity [MFI]: 27 - 109; control MFI: ≤7) correlating with the PLAT reduction in the 1 affected monkey, measured in the 9-month study. PLAT-bound PAI was not measured in the 2 euthanized monkeys from the 6-month study.
These results suggest that BMS-986001-induced PLAT reduction in monkeys may have been due to PLAT-bound ADA and only in the presence of BMS-986001. Despite moderate levels of PLAT-bound IgG (MFI: 26) in the 1 affected monkey in the 9-month study, PLAT counts recovered to pretest values at the end of drug-free recovery period.

PS 1657 NKTR-192, a Novel Polymer Conjugated Opioid Agonist, Demonstrates a Superior Preclinical Safety Profile to Traditional Opioids

C. Ji[1], X. Ge[1], E. G. Tonkin[1], M. K. Sievert[2] and T. D. Sweeney[1]. [1]*Toxicology, Nektar Therapeutics, San Francisco, CA and* [2]*Covance Laboratories, Madison, WI.*

NKTR-192 is a new chemical entity mu opioid agonist that uses Nektar's advanced polymer conjugate technology to achieve slow CNS uptake while maintaining adequate brain exposure with analgesia and is being developed for the treatment of moderate to severe acute pain. NKTR-192 produces full analgesic efficacy comparable to oxycodone in the mouse acetic acid writhing model. Orally administered NKTR-192 was evaluated in 28-day repeat dose toxicity studies with a 2-week recovery observation period at oral BID doses up to 180 mg/kg/day in rats and 30 mg/kg/day in dogs. Findings observed in both species are consistent with the pharmacology of a mu opioid agonist. Major dose-limiting toxicities with NKTR-192 included emesis in the dog, shallow respiration and hypoactivity in both dog and rat. Doses exceeding the MTD in dog (>20 mg/kg as a single dose) caused severe respiratory depression and sedation that required naloxone reversal. In rats given >150 mg/kg as a single dose, target organ toxicities (dilation and/or hemorrhage) were observed in the urinary bladder and kidney. These findings were completely reversed after a 2-week recovery period. Based on the 28-day repeat dose toxicity studies, NOAELs of 120 mg/kg/day (BID) and 30 mg/kg/day (BID) were established in rats and dogs, respectively. A dose of 120 mg/kg/day NKTR-192 in rats provides an adequate animal to human safety margin to support clinical development. Compared to a standard opioid (oxycodone), NKTR-192 demonstrates a clear separation of analgesia from CNS side effects with safety margins of 11-fold based on NOAEL and 45-fold for sedation, while oxycodone has narrower safety margins of 3-fold for toxicity and 24-fold for sedation.
In conclusion, NKTR-192 toxicology studies in rats and dogs support the safety of NKTR-192 for clinical development and appears to have a superior therapeutic index relative to traditional opioids.

PS 1658 Preclinical Safety Evaluation of MTL-005, a Novel Metalloporphyrin Radiosensitizer

J. Caldwell[1, 2] and C. Beattie[2]. [1]*University of Liverpool, Liverpool, United Kingdom and* [2]*MorEx Development Partners, London, United Kingdom.*

MTL-005 (copper meso-5,15-Bis[3-[(1,2-Dicarba-closo-dodecaboranyl)methoxy] phenyl]-meso-10,20-dinitroporphyrin) is under development as a radiosensitizer for use in head and neck cancer. In vivo it slows growth of murine squamous cell carcinomas and adenocarcinomas. Given i.p. to mice, it is cleared from the circulation and taken up by both normal tissues and tumors, with tumor concentrations up to 6 times higher than in muscle, skin, and brain. It concentrates in the liver and spleen and can be detected in both tumors and liver for at least 62 days post administration.
4 i.v. toxicology studies were carried out in rats and 2 in dogs. MTL-005 was dissolved in a mixture of dimethylacetamide, Solutol HS15 and PEG300 and diluted with 0.9% saline. Components of this vehicle are known to have toxic effects, especially in dogs. Rats were given 0, 20, 40 and 60 mg/kg (divided over 2 consecutive days)and dogs with 2 doses of 0, 1, 5 or 10 mg/kg given 14 days apart. Toxicities observed included body weight loss, reduced food consumption, dark discolouration of several organs, and reversible gastric epithelial hyperplasia (in rat at doses up to 30 mg/kg/day); and inflammatory changes at the infusion site, liver changes, and the death of 1 dog at 10 mg/kg. The vehicle may have contributed to the body weight, food consumption, and liver effects, as most of these signs were also observed in the vehicle controls. The MTD in rats was 40 mg/kg but a NOAEL could not be established due to the body weight losses observed both treated and control groups.
Dogs tolerated 1 or 5 mg/kg well but the vehicle contributed to the effects seen at 10 mg/kg. Liver histopathology findings and plasma chemistry changes associated with the vehicle were seen in all groups and liver histopathology findings persisted for 28 days. Injection site changes were reversible over 28 days. Again, a NOAEL could not be established.
These preclinical data were sufficient for regulatory approval of a Phase I clinical study of MTL-005 as an adjunct to radiotherapy in patients and this has now been initiated.

PS 1659 Certolizumab Pegol, a Humanized Antibody Fab Fragment, Pharmacokinetic Considerations in Juvenile Monkey

B. O. Depelchin[1], J. Tibbitts[4], I. Wakefield[2], T. Parton[4], L. King[4], S. Grote-Wessels[3] and P. Theil[1]. [1]*UCB, Braine-l' Alleud, Belgium,* [2]*NCSE Ltd, Shardlow, United Kingdom,* [3]*Covance, Munster, Germany and* [4]*UCB, Slough, United Kingdom.*

Certolizumab pegol, Cimzia (CZP), is a humanized antibody Fab fragment, with specificity for human tumor necrosis factor alpha, conjugated to polyethylene glycol (PEG). This drug is approved for adult indications in US, EU and Japan. Paediatric indications are under development.
Following recent recommendations from the health authorities (EMA, / CHMP/647258/2012) on pegylated proteins for paediatric uses, UCB initiated investigative activities in juvenile monkeys to address the expectations. First stage of the plan started with pharmacokinetic (PK) under single and chronic administrations in which total PEG plasma and CSF concentrations as well as urinary excretion of PEG related substances were evaluated using nuclear magnetic resonance (NMR). These data on PEG-moieties disposition complement the understanding of the vacuolation phenomenon observed with pegylated proteins including CZP. Single doses of 10, 20, or 50mg/kg CZP were given by SC route to 2 juvenile males and females. Weekly repeated doses of 10 or 50mg/kg were given SC over 12 weeks in juvenile male and female, followed by an 8 week observation period.
Steady states for both CZP and total PEG were observed after repeated dosing at 28 days post start, with single dose PK fully predictive of the multiple-dose PK. The multiple dose PK exhibited no change over time with an apparent terminal PK similar to those observed after single dose. The accumulation to steady state appeared kinetically similar for CZP and total PEG, achieving the concentration plateau at approximately 28 days. The concentration of PEG in CSF, either in the form of PEG or CZP, remained low, more than 1000 times lower than in plasma. The daily urinary PEG excretion rose to a steady state between 28 and 42 days.
Results after repeated CZP administration in juvenile monkey indicated PEG exposure was dose linear and that steady state plasma concentrations were reached at all doses, supporting a threshold concept for the formation of vacuolation.

PS 1660 Nonclinical Safety Assessment of Tofacitinib in the Juvenile Rat and Monkey

C. J. Bowman, M. Collinge, Z. Radi, T. T. Kawabata, W. M. Vogel and D. J. Ball. *Pfizer, Groton, CT.*

Tofacitinib (Xeljanz) is a novel oral inhibitor of intracellular Janus kinases (pan-JAK inhibitor) for the treatment of rheumatoid arthritis. JAK is critical for intracellular signal transduction of activated cytokine receptors, including those important for lymphocyte activation, proliferation and function. To support the use in pediatric patients as young as 2 years old with juvenile idiopathic arthritis, toxicity studies in juvenile rats and cynomolgus monkeys were conducted. Based on previous findings in adult animals, the immune, hematopoietic and reproductive systems were targeted for evaluation. A 39-week juvenile monkey study (with 26-week recovery) initiated in 14 month-old animals revealed decreased red blood cell parameters, lymphocyte and lymphocyte subset numbers, primary T-dependent antibody response and immune system organ weights during the dosing phase but partially to fully recovered by the end of the dose-free period. A one-month juvenile rat study with 2-month recovery was initiated in 3-week old rats to enable evaluation in animals roughly equivalent to the youngest patient age of 2 years old. In juvenile rats, expected effects on immune and hematology parameters were observed by the end of dosing but were no longer present at the end of the recovery period. Overall, the immune and hematopoietic effects observed in juvenile rats and monkeys were reversible and consistent with JAK inhibition and effects observed in adult animals. Lastly, effects on fertility were evaluated following tofacitinib oral administration in rats from weaning (3 weeks old) to sexual maturity. No effects on male or female reproduction were observed indicating no effect on development of reproductive system in juvenile animals. In summary, the results of these studies in rat and cynomolgus monkey demonstrate that in juvenile animals there were no novel toxicities, no permanent changes and no increased sensitivities relative to known effects of tofacitinib in adult animals thus supporting clinical trials in pediatrics.

PS 1661 Case Study: The Evolving Cardiac Risk Assessment for a Novel Anticancer Agent

R. J. Knight and C. Pollard. *Drug Safety and Metabolism, AstraZeneca, Alderley Park, Cheshire, United Kingdom.*

AZD7762 is a checkpoint kinase 1/2 inhibitor that was being developed as a first in class treatment for advanced solid tumours in combination with DNA-damaging agents. AZD7762 was well-tolerated in tumour-bearing mice, significantly enhancing the efficacious effects of chemotherapy or radiation. However, cardiovascular safety signals in preclinical studies led to a complicated and species-dependent cardiovascular risk profile. A profound, irreversible decrease in blood pressure and LVdp/dtmax was observed in the anesthetised dog. In a conscious dog telemetry model however, no effect on blood pressure was evident but there was a dose-dependent, transient, decrease in LVdP/dt max (up to 36% vs vehicle). There were no signs indicative of a similar haemodynamic change in the rat. However in toxicity studies, myocarditis and elevations in troponins and other biomarkers of myocardial injury were seen in a minority of rats (incidence approximately 1/6). No cardiac pathology was oberved in the dog at similar exposures. Investigative work suggested the myocarditis was an exacerbation of background pathology in the Wistar rat. The data indicated little or no safety margins to the predicted exposure levels required for efficacy in patients. Phase I clinical trials were conducted in 130 patients and included echocardiography, biomarkers of cardiac injury and stringent exclusion and stopping criteria. Cardiac adverse events were reported in 5 patients within the predicted biologically effective range, characterised by episodes of acute stress cardiomyopathy, decreased ejection fraction or elevations in troponin. Using extreme-values modelling of the clinical safety data, the overall risk/benefit profile for the intended indications was reviewed and further clinical development stopped.

This case study provides a useful example of how the emerging risk assessment was shaped by the complex preclinical cardiovascular profile, and the issues encountered in distinguishing a CV signal in patients with advanced cancer.

PS 1662 Infusion Administration of Lipid Emulsions in Preclinical Dog Studies—Practicality and Animal Welfare Consideration

S. Iqbal[1], H. van Wijk[1] and A. Castellernau[2]. [1]*Covance Laboratories Ltd, Harrogate, United Kingdom and* [2]*BBraun Melsungen AG, Melsungen, Germany.*
Sponsor: A. Jackson.

Parenteral nutrition (PN), treatment to prevent malnutrition, requires intravenous (IV) administration of lipid emulsions (LE): these qualify as IV drugs and are subject to all applicable safety regulations. LEs are typically formulated at fat concentrations of 10% or 20%, which optimally suit human energy requirements (i.e., metabolic rate of about 30kcal/kg/day equivalent to a fat dose of about 3g/kg/day). Preclinical testing of LEs requires consideration of the metabolic rate of the biological test system: this is 80-100kcal/kg/day for the dog, and 180kcal/kg/day for the rat (i.e., approximately 3- and 6-fold that of humans). Supplying these energy requirements with human-optimized LEs is challenging, due to the large volumes to be infused; for instance, supplying daily energy requirements to the rat and dog with a 10% LE results in infusion volumes 3- and 1.5-fold higher than the test system's total blood volume. Avoiding volume overload-related side effects required several steps, including delivery up to 24hrs and frequent monitoring of clinical signs (SC) and clinical pathology (CP) data. A dose escalation study was performed in dogs with an LE to assess the feasibility of administering volumes up to 68.81mL/kg. A cannula was implanted in the right jugular vein and connected to a subcutaneously implanted vascular access port (VAP) and accessed via needle. The other end of the infusion line was connected to a portable pump secured in a jacket. To acclimate animals to test article volumes, escalating amounts of saline were administered up to 1 week pretreatment. Animals were dosed on D1 at 27.52mL/kg over 24hrs and CS were reviewed every 4hrs. Daily bodyweight and food consumption was recorded and CP samples were collected 20hrs into infusion, allowing review of the CP data prior to dose escalation. In conclusion, animals tolerated infusion of large volumes of LE; however, precise monitoring and stepwise volume escalation were critical.

PS 1662a The Science behind Personal Care Products: A Hands-On Approach to Engaging K–12 Students

K. Sprugel[1] and R. Weeks[2]. [1]*Amgen Inc, Seattle, WA and* [2]*NWABR Volunteer, Seattle, WA.*

Making science relevant and hands-on is critical to engaging middle and high school students. Northwest Association for Biomedical Research (NWABR) has developed a four lesson curriculum, "Consumer Awareness: Personal Care Products Safety and Labeling" that investigates the science, labeling and safety testing behind personal care products. The lessons, which include a lotion-making lab, have been presented by teachers and toxicologists to diverse student audiences in classrooms and informal education workshops.

This four lesson curriculum reminds students that science is part of their everyday lives, especially if they are to be informed consumers. It makes science and toxicology relevant through the exploration of the science and safety testing behind personal care products. It emphasizes critical evaluation skills and a basic understanding of science and regulations. The curriculum guides students through the analysis of personal care products by incorporating multiple aspects of:

—Science: biology, chemistry, toxicology, math

—Research: drug development process, experimental design, evaluating sources of information

—Ethics: safety testing on animals and humans

—Social Responsibility: risk assessment and safety policies, consumer advocacy

The lessons and workshops can be tailored in length and depth to engage the target audiences in formal and informal learning environments. Training with the curriculum has been offered to over 270 teachers across the country. The kit loan program for teachers has reached over 11,400 students. Two hour workshops highlighting the lotion making lab and labeling have also been conducted with other groups such as Girl Scouts, after school programs and summer camps (~1000 students).

The curriculum addresses national Next Generation science education standards regarding the relationship of science, technology and society. It can also provide a context for introducing topics such as the process of drug development and careers in science.

The curriculum is freely available at https://www.nwabr.org/teacher-center/consumer-awareness#overview .

PS 1662b Strategy to Develop Expertise in Risk Assessment in Developing Countries

S. B. Barros[1], E. S. Nascimento[1], J. V. Camargo[2], E. M. Faustman[3], A. Hayes[4], L. Rosenheck[5] and G. D. Umbuzeiro[6]. [1]*USP, Sao Paulo, Brazil,* [2]*UNESP, Botucatu, Brazil,* [3]*U of Washington, Seattle, WA,* [4]*Harvard University, Boston, MA,* [5]*LR Risk Consulting Inc, Greensboro, NC and* [6]*UNICAMP, Limeira, Brazil.*

Although basic principles of toxicology are taught in undergraduate courses in Latin America (LA), chemical risk assessment (RA) is not a topic generally discussed even in graduate programs. To fill this gap, the Brazilian Society of Toxicology and IUTOX developed since 2008 a six days workshop, based on the IUTOX Risk Assessment Summer School concept, to respond to this need for well trained Risk Assessors and Managers (RAM) in both government and industry and to give current and future regulators an improved perspective on how toxicological

information should be used to make informed decisions that best protect human health and the environment. For the most part, participants prior to the workshop were not able to discriminate among strengths and weakness of the toxicological information or to select even the most relevant information for their RA. During the workshop, the RA process is stressed both in lectures and in the unique concept of participants' case reports. Lectures are limited with most of the time dedicated to small discussion groups working on individual case studies prepared by the participants in advance. These sessions focus on how to selected appropriate endpoints for the most realistic exposure scenario. After these discussions each student presents his/her RA in a plenary gathering that concludes with the best approach for the proposed problem. Because topics are selected in advance a broad array of examples allows participants to see the process unfold in many different scenarios. The distribution of participants, now over 106 scientists, among industry, governmental agencies and academics brings different approaches of the RA process from and back into these different sectors. Course evaluations clearly indicate: 1) improved understanding of the concepts of RA, 2) how to properly perform RAs, 3) importance of the course in training current and future RAM, and 4) the outstanding recognition of the course throughout LA.

PS 1662c National Library of Medicine Education-Related Resources in Toxicology, for 2014 and Beyond

P. J. Hakkinen, S. Publicker and J. E. Kelly. *National Library of Medicine, National Institutes of Health, Bethesda, MD.*

The U.S. National Library of Medicine (NLM) provides free resources for health and science professionals, educators and students, and the public. The Specialized Information Services Division (SIS) provides information resources and services in toxicology, environmental health, chemistry, and other topics. TOXNET (TOXicology Data NETwork) provides easy access to a large set of databases, including ones as diverse as the Hazardous Substance Data Bank (HSDB), Household Products Database (HPD), and the Comparative Toxicogenomics Database (CTD). A variety of training options to learn more about the TOXNET databases are available. Enviro-Health Links are guides to a variety of topics such as laboratory safety, nanotechnology and human health, tobacco, smoking, and health and climate change and health. SIS has several K-12 educational tools in environmental health: ToxMystery for elementary students, the Environmental Health Student Portal for middle school grades, and Tox Town for high school students. In addition, SIS had developed lessons plans and classroom activities for the resources as well as the K-12 Science and Health Education portal for access to free resources that introduce, reinforce, and supplement education programs with topics such as biology, careers, environmental health science/chemistry, forensics and medical technology, and genetics. Toxicology Tutors provide users of NLMs toxicology databases with a working knowledge of basic toxicology principles. ToxLearn, a joint effort between NLM and the Society of Toxicology from 2006-2013, will update and expand Toxicology Tutors. One module is available and others will follow as funding permits. SIS offers clinical toxicology-related training resources for first responders, first receivers, and others involved in responding to hazardous material (Hazmat) and other types of incidents. One way to stay up to date with SIS efforts is via Twitter (@NLM_SIS).

PS 1662d Completion of an SOT Web Portal for Submission and Accessing K–12 Outreach Activities

A. Slitt[1], D. R. Johnson[3] and T. K. Fick[2]. *[1]University of Rhode Island, Kingston, RI, [2]3M, Saint Paul, MN and [3]US Army, Clinton, MS.*

A K-12 outreach resource collection will soon be available for SOT members on the SOT website. Many SOT members are active in toxicology outreach, and many more would like to be but don't know where to start. This resource collection provides successful model activities that can be used in a range of circumstances (classrooms, career events, informal science education) classified by age level, topic, and with other attributes for ease of selection for those involved in K-12 education outreach. These examples are reviewed before acceptance and demonstrate what toxicologists do to increase our effectiveness as we interact with educators, parents, students, and communities.

The K-12 Sub-Committee strongly encourages members to contribute activities that they use in outreach. The SOT K-12 outreach web pages also include information about past Annual Meeting events and Regional Chapter outreach activities. This project comprises two major goals – first, creation of an efficient system to collect and categorize K-12 resources submitted by members and second, the creation of a searchable database on SOT's website with outreach resources that will be initially available to members, then at some point in the future available to the general public. Regional Chapter Contacts will assist with review and collection of website content.

The World Wide Web is a powerful tool that can educate and provide information to educators, parents, and students. We plan to utilize the web to make K-12 education outreach available to members and educators across the globe. This presentation is an opportunity to for the K-12 Sub-Committee to interact with SOT members who might have access to valuable teaching resources, which will benefit members and the public. We need your excitement and interest – submit your K-12 activities to the SOT web portal!

PS 1663 K–12 Education and Outreach: Inspiring Students Towards Careers in Science, Technology, Engineering, and Math (STEM)

V. S. Bhat[1], R. Donofrio[2], K. LeVanseler[2], A. Brackman[3], J. C. English[1], K. Cox[1], A. Gadoth[1] and A. D. Phelka[1]. *[1]Toxicology Services Dept., NSF International, Ann Arbor, MI, [2]Applied Research Center, NSF International, Ann Arbor, MI and [3]Chemistry Laboratory, NSF International, Ann Arbor, MI.*

Headquartered in Ann Arbor, Michigan since 1944, NSF International is an independent, not-for-profit organization dedicated not only to improving global human and environmental health, but also to fostering future stewards for this mission. Toxicologists, microbiologists, chemists, and engineers from NSF have led hands-on experiments to promote STEM education and mentor future leaders in public health and safety. Learning modules were developed to explore polymers by creating elephant toothpaste using dish soap, yeast and hydrogen peroxide. Other experiments emphasizing sustainable futures involved recycling, biodegradation, and home-made pH paper to learn about acid rain. Participating at local events such as the Maker Faire science festival in Detroit, Earth Day activities at the Science and Nature Center, workshops at the Hands-On Museum, and judging high school science fairs proves as rewarding for the mentors as the students. In conjunction with the American Red Cross and the Partnership for Food Safety Education, NSF International created the Scrub Club® (www.scrubclub.org), a fun website that teaches K-3rd grade children proper hand washing. The Centers for Disease Control and Prevention estimated that 164 million school days are lost each day due to illness. The site contains a webisode, interactive games, music and educational materials for teachers, parents, and kids. Materials are available for download in English, Spanish and French. NSF sponsored a Scrub Club® "Clean Hands" game for schools nationwide and toxicologists have visited local schools with stickers, magnets and tattoos. A growing number of local and regional school districts and public health departments also use this resource. NSF International's Applied Research Center is also a proud supporter of this year's SOT K-12 education outreach event for high school students and their mentors on Saturday March 22, 2014.

PS 1664 Evaluation of a Summer Undergraduate Fellowship in Toxicology and Environmental Health Sciences: Self-Assessment of Research Competencies

L. M. Aleksunes[1], E. Caswell[2], J. E. Gutierrez[2], L. E. Liang[2] and D. L. Laskin[1]. *[1]Pharmacology and Toxicology, Rutgers University, Piscataway, NJ and [2]Center for School and Community-Based Research and Education, Rutgers University, Piscataway, NJ.*

Rutgers University has developed a summer research fellowship program to promote pharmacology, toxicology and environmental health sciences as careers in biomedical research. The program consists of a 10-week basic science and translational research experience for undergraduates and was also designed to include weekly events including laboratory safety and responsible conduct of research training, a field trip to a pharmaceutical company, career development and research seminars and student presentations. To assess the improvement of participants in key areas, students completed an adapted version of the Undergraduate Research Student Self-Assessment survey from the University of Colorado at the beginning and the end of the 10-week fellowship. The response rates for the pre- and post-program surveys were 100% and 71%, respectively. The survey captured changes in three key areas: Application of Knowledge to Research (data analysis, problem solving), Scientific Abilities (daily independent and group activities), and Research Abilities (laboratory and presentation activities). A 7-point scale was used by participants to assess their level of confidence on 27 competencies. Significant improvement was observed in 15 of 27 competencies (55%). The greatest advancements were made in the ability of students to identify experimental limitations (31%), to determine the next step in a research project (26%) and to understand the connections between scientific disciplines (25%). A summer research program engages undergraduate students in full-time research experiences and provides unique opportunities to promote toxicology and environmental sciences as research areas for the next generation of scientists and enhances career development skills. Supported by ES020721, ES005022, and ASPET SURF.

PS 1665 A Model for a Residential High School Summer Research-Based Engagement Program to Inspire Students toward STEM Disciplines and Toxicology

Y. Franco[2], M. M. Bourgeois[3] and R. S. Pollenz[1]. [1]*Cell Biology, University of South Florida, Tampa, FL,* [2]*Secondary Education, University of South Florida, Tampa, FL and* [3]*Public Health, University of South Florida, Tampa, FL.*

Persistence of undergraduate students in STEM disciplines is an issue of national concern. This issue is particularly relevant to the field of toxicology because the number of BS-level toxicology programs is limited and undergraduates matriculation to graduate level toxicology programs is from other STEM disciplines. In addition, the ability to inspire undergraduate students toward the field of toxicology at institutions that do not offer a BS level toxicology degrees is typically through upper level toxicology-based elective courses that students who leave the STEM may never have a chance to take. Reports show that persistence can be increased if students participate in "high-engagement" STEM-based activities in high school and early in college. USF has developed summer residential STEM Academies that provides high school students an intensive 6-day program in several STEM disciplines. The Academy engages domestic and international students in inquiry, discovery, creativity and hands-on research. Faculty from key research centers and colleges, collaborate to emerge students in basic, clinical and translational research. Students are also exposed to the multitude of professional career options that interface with the STEM degree. Professional educators from local high schools and colleges build community within the cohort through individualized and group mentoring. To date 64 students have completed three different Academies and 100% of the participants have indicated that they are inspired toward a STEM degree program. In addition 100% of rising seniors who completed the program in 2012, enrolled in STEM undergraduate programs in Fall 2013. The presentation will outline i) the structure of the program, ii) the details for the engagement exercises, iii) the cost to implement, iv) assessment instruments and v) a model for a STEM Academy with focus on Environmental Health and Toxicology to be offered in summer 2014.

PS 1666 Creating Undergraduate Research Opportunities within Structured Courses through the CREATTE Initiative: Processes, Case Studies, and Outcomes

R. S. Pollenz. *Cell Biology, University of South Florida, Tampa, FL.*

Numerous reports show that early engagement of undergraduates in research activities improves academic performance, engagement in the discipline and the probability that the student will graduate within the discipline. Since there are national issues related to persistence in STEM disciplines, innovative methods to engage students in research activities are a focus on many curricular reform efforts. In addition, many large research universities face significant issues regarding the mentorship capacity to offer all students a research opportunity. To address these issues the Office for Undergraduate Research (OUR) developed the CREATTE program (Creating Research Experience and Activities Through Teaching Enhancement). CREATTE provides faculty teaching undergraduate courses modest funds to support a graduate student (2-3 hrs week) and sustainable supplies in support of research projects that are integrated into the course curriculum. During 2012-13, CREATTE program supported >700 students in research projects through this initiative. Courses in Public Health (Envir. Health Sci., Ecotoxicology), Integrative Biology (Epigenetics, Coastal Ecosystems), and Psychology (Statistics) all have relevance to students who may consider toxicology careers and graduate school. A post survey of participating CREATE undergraduate researchers indicated a strong agreement that they developed enhanced research competencies, had a deeper understanding of the course material and would engage in additional research activities. The presentation will outline i) the structure of the program, ii) case studies of research activities related to toxicology, iii) faculty time commitment, iv) and the assessment instruments used to validate the learning outcomes.

PS 1667 Escape from Toxic Island (Life Size!): A Toxicology Awareness Program Using Demonstrations and Hands-On Activities

D. Hardej[1, 2] and L. M. Hoffman[1, 2]. [1]*Pharmaceutical Sciences, St. John's University, Jamaica, NY and* [2]*MASOT, Bordentown, NJ.*

"Escape from Toxic Island (Life Size!)", is an educational program that was developed by the MASOT Education and Outreach Committee to teach basic toxicology concepts to middle school aged children. The program builds on the former program, "Escape from Toxic Island", by utilizing the participants as life–sized game pieces that are introduced to basic toxicology concepts and then move from station to station to view or participate in toxicology related tasks. An introduction, called the island tribunal, was first provided for the participants. This included basic concepts such as the dose-response, common terminology and introduction to Paracelsus. A demonstration of dose response followed the introduction. Participants proceeded to toxicology-related demonstrations or hands-on activities. The stations included, Lemons and Onions, a demonstration that linked exposure to mildly irritating substances to risk, Science Sleuth where participants learned about reading labels to determine hazards and classifying chemical agents, No Water Off a Duck's Back, that allowed participants to explore what happens to birds, humans and aquatic creatures when oil ends up in bodies of water, and Baggie Science, a station that investigated chemical changes. These resources were already available on SOT's website and were modified to fit the needs of the present program. A Poison Control Squad was added as a demonstration to bring awareness of the dangers of medicines that might mimic the look of popular candy and also the dangers of household chemicals that look like commonly ingested liquids, for example, pine cleaner and apple juice. For each activity, participants engaged in active dialog with the presenters so that assessment of the participant's prior knowledge of the topic could be made. Once the activities were completed, participants and presenters discussed their findings to verify the participants understanding of the topics.

PS 1668 Creating Research Opportunities in K–12 Outreach for Undergraduate Students

A. J. Abritis and M. M. Bourgeois. *EOH, USF COPH, Tampa, FL.*

K12 outreach is a vital component in our mission to educate the community about scientific issues, particularly toxicology and risk assessment. Using funds from the Office for Undergraduate Research at the University of South Florida, undergraduate students participate in an authentic research experience within a structured course. Each autumn, 15 – 20 undergraduate students develop short science lectures and age appropriate activities for traditionally underserved schools in the Tampa Bay area. These student offer these demonstrations as part of the Annual Great American Teach In (GATI), held during the celebration of American Education Week. They identify a relevant environmental or occupational health topic, conduct research and create presentations designed to convey their findings in age appropriate lecture and hands on activities. The experience is designed to meet three core criteria: i) Pose or work from defined research question, ii) Work individually or in groups to apply relevant methods of inquiry to produce original findings/products, iii) Present the findings/products to peer and professionals in formal (e.g. Undergraduate Research Colloquium or professional meetings) and informal (e.g. course setting) venues. Past projects have involved an exploration of dose, response and toxicity using familiar measurements and household substances, sustainable gardens and pesticide safety, environmental pollutants and water sanitation. The GATI project fosters community outreach at the K–12 level, introducing the importance of toxicology to a range of primary and secondary level students while allowing project undergraduates to learn the art of outreach, develop skills in critical thinking, and gain a pedagogical background on which to build an academic future, should they so choose.

PS 1669 Evaluation of Technical and Knowledge-Based Outcomes following Participation in a One-Week High School Research Program in Toxicology and Environmental Health Sciences

G. L. Guo[1, 2], J. E. Moscovitz[1, 3], A. Venosa[1, 3], L. M. Aleksunes[1, 2], A. Gow[1, 2] and D. L. Laskin[1, 2]. [1]*Pharmacology and Toxicology, Rutgers University, Piscataway, NJ,* [2]*Environmental and Occupational Health Sciences Institute, Rutgers University, Piscataway, NJ and* [3]*Joint Graduate Program in Toxicology, Rutgers University, Piscataway, NJ.*

As an applied science, students are often not exposed to the fields of toxicology and environmental health sciences until their undergraduate or graduate studies. The purpose of this summer program was to introduce rising sophomore, junior, and senior high school participants to the concepts of toxicology, provide hands-on laboratory training, and highlight various careers in toxicology and environmental sciences. Two groups of 23 students (n=46 total) participated in a non-residential, one-week summer program at Rutgers University that consisted of didactic (70%) and laboratory (30%) activities organized by toxicology graduate student and faculty instructors. Activities focused on dose-response relationships, experimental design, clinical toxicology, histology and pathology, epidemiology, and genetics. Pre- and post-student surveys aimed to assess student motivation to participate in the program, research and technical abilities, and basic toxicology knowledge. Students indicated that the greatest motivating factors to participate included an opportunity to explore their interest in science and gain hands-on laboratory experience. Self-assessment surveys revealed improved presentation skills (24%), labo-

ratory proficiency including DNA isolation (49%) and cell culture (31%) as well as assessment of patient clinical findings (32%). Using a true/false exam, student's knowledge of key toxicology concepts increased from the beginning (67% correct responses) to the end of the program (81% correct responses). The genetics, histology, and pathology labs received the highest ratings. A one-week summer laboratory and didactic program engages high school students in toxicology and environmental health sciences and improves laboratory and presentation skills as well as increases knowledge of key scientific concepts.

PS 1670 Using a Case Study Followed by a Lab Exercise to Examine Acetylcholinesterase Activity

M. J. Pomeroy-Black. *Biology, LaGrange College, LaGrange, GA.*

Allowing students to design and implement an experiment engages students far more than "cookbook labs". However, it can be difficult to create toxicology lab activities that require the students to do this. Using a case involving the paralysis of several dogs, students were drawn into the case prior to asking them to design and implement an experiment. Students were given background information about the dog's behavior and environment at which point they discussed possible causes of the paralysis, including demyelination and enzyme inhibition. They were presented with ambiguous data and ran lab tests to determine the cause of the paralysis in order that the dogs could be treated. Prior to running the tests students determined the appropriate controls, formulated a hypothesis and described the procedure for running the tests. Using a spectrophotometer and observing the intensity of fluorescence allowed the students to determine if the cause of the paralysis was acetylcholinesterase inhibition or demyelination. The instructor may ask students to present their research using an "integrated approach" to writing a research report.

PS 1671 A Toxicological Study Using Zebrafish (*Danio rerio*) As a Model

M. Reynolds-Walsh. *Washington College, Chestertown, MD.*

Only recently has it been adequately recognized that substances present in the environment can have adverse effects on developing organisms. Now, with environmental pollutants accumulating at an unprecedented rate, and with pharmaceuticals dominating western medicine, it is particularly important that we understand the effects of the substances to which we are exposed. Zebrafish (*Danio rerio*) has become a widely used model system for the study of vertebrate development. This system is particularly amenable for use in undergraduate laboratories because of the ease of collection and manipulation and the rapid rate of development. In this lab, students use zebrafish to examine the effects of nicotine, ethanol, and retinoic acid on normal development. Students first examine normal development and compare it to overall growth, dry weight, and behavior of zebrafish exposed to these chemicals. The students also collect data on LC50 and notochord length. The quantitative data is evaluated for statistically significant differences between treatments. Finally, students write a research proposal for an independent experiment in which they expose embryos to a toxicant of their choice, carry out the experiment, and present their findings. This lab introduces students to the use of animal models and incorporates experimental design and data analysis. More importantly, it introduces students to concepts and models in toxicology to increase their awareness and interest.

PS 1672 Incorporation of Evolution and Toxicology Enhances Conceptual Learning in Undergraduate Neuroscience Courses

S. K. Infante and C. P. Curran. *Biological Science, Northern Kentucky University, Highland Heights, KY.*

The field of neuroscience is inherently integrative and often requires understanding concepts from fields including molecular biology, toxicology, and evolution. Yet, few undergraduate courses focus on more than human neuroanatomy and physiology or rodent behavior. Therefore, we developed a transdisciplinary Advanced Neurobiology course from an evolutionary perspective, using toxicology principles to highlight gene-environment interactions and adaptations across major phyla. This lecture-lab course was also designed to align with the curricular objectives of the interdisciplinary Neuroscience minor. This presented the added challenge of creating an advanced course that serves students from different disciplines. Both lecture and lab highlighted evolutionary changes in the Animal Kingdom, beginning with sponges (Phylum Porifera) and moving through invertebrates (Phylum Cnidaria, Plathyhelminthes, Nematoda, Annelida, Arthropoda, and Mollusca) before focusing on vertebrates in Phylum Chordata. We incorporated historically relevant models in toxicology and neuroscience including *C. elegans, Drosophila, Aplysia*, zebrafish, and mice. For example, using *C. elegans,* students assessed chemotaxis and dose response to benzaldehyde. Students examined sex differences in alcohol preference using *Drosophila hydeii.* To accommodate different learning styles, we used various pedagogical tools to achieve each lab's learning objectives. We heavily emphasized problem-based and team-based learning in the laboratory setting and used similar tools in lecture. We also used various methods of assessment, including group activities, lab notebooks, presentations, and student peer reviews. Toxicological concepts (dose response, ADME, and duration of exposure) were emphasized when students designed and executed group experiments on the behavior of C57BL/6J mice treated with nicotine and caffeine. Overall, our course succeeded in providing undergraduate students with a well-rounded perspective of complex concepts in neuroscience and toxicology.

PS 1673 Sparking Toxicology Interest in High School Students

M. Lindsey[1, 2] and H. Ingram[2]. [1]*Southwest Environmental Health Sciences Center, University of Arizona, Tucson, AZ and* [2]*BIO5 Institute, University of Arizona, Tucson, AZ.*

SCOPE AND RATIONALE: "High school is where the pipeline begins," –Serrine S. Lau, PhD. The University of Arizona's (UA) KEYS High School Summer Research Internship has successfully hosted 188 high school students in toxicology and bioscience laboratories, who received academic credit for their internships.
DESCRIPTION: Highly achieving students, with interests in bioscience, bio-medical science, toxicology, environmental health and bioengineering, apply for this competitive 7-week program. Applicants submit a letter of interest, teacher recommendations, and transcripts. Accepted interns are interviewed to make compatible placements. In week 1, they develop hands-on laboratory research techniques, learn to read research papers, and hear about cutting-edge research. In weeks 2 through 7, they complete a research component for their lab. The program ends with a poster session, well attended by faculty members, graduate students, friends, and family members.
EVALUATION AND ASSESSMENT: Student work is assessed to gauge increased knowledge of research methodology, biotechnology skills, toxicology and environmental health. Assessors also measure self-confidence and communication skills. Faculty evaluations, intern formative evaluations, summative evaluations, and alumni surveys inform the development of KEYS. All 9 interns from the 2007 class have earned baccalaureate degrees and 8 are pursuing graduate, medical or pharmacy degrees. Interns have also been recognized in theses and dissertations.
CONCLUSIONS: High school students are capable of understanding and positively contributing to complex bioscience research such as toxicology. Real world science experiences, instruction, technical and science literacy, and supportive nurturing during and after the program are essential elements that promote student success. "It is an important program because it exposes the interns to all the aspects of the science community and career."–Georg Wondrak, PhD.

PS 1674 Implementation of an Academic Service Learning (AS-L) Project within an Undergraduate Course in Pharmacology

B. Billack. *St John's University, Jamaica, NY.*

Academic service learning (AS-L) is a type of active learning in which a student demonstrates knowledge and understanding through service to the community and reflection. The present report describes an activity in which AS-L was implemented as part of an undergraduate pharmacology course. The course is common to the curricula of the Doctor of Pharmacy, Physician Assistant and Toxicology programs at St. John's University. In the AS-L project, teams of up to 5 students were charged to develop a presentation concerning the nature of drugs or pharmaceuticals and their effects on the human body. Students could form their presentation around discussion topics such as drugs versus natural substances, the medical benefits of drugs, the possible toxicities of drugs both legal and illegal, or the mechanisms by which drugs enter or leave our bodies. The student teams then traveled to various service sites throughout the greater university community with the goal of community outreach through education. Included among the service sites was an "after school/weekend" program for teenagers in foster care, a "weekend" program for young students in middle school (grades 6-8), and a local food pantry with an adult cohort. Strengths and limitations of the AS-L project were noted. The major strength of the project, as indicated from student reflection papers, was that each student in the team became an active learner and the otherwise "passive learning" environment of the classroom became an active one at the service site. All students in the team presented and answered questions. A limitation of the activity is finding a suitable instrument for assessing student learning. Future ASL courses of this type are anticipated to include pre and post surveys. The details of this AS-L project have been submitted for publication in the Journal of Toxicological Education (www.JToxEd.org).

PS 1675 Community Engagement: Chromium Contamination and Human Exposure in Garfield, NJ

S. P. Doherty-Lyons[1], S. Bari[2], J. Leng[2], F. Gany[2] and J. T. Zelikoff[1]. [1]*New York University School of Medicine, Tuxedo, NY and* [2]*Memorial Sloan Kettering Cancer Center, New York City, NY.*

In September 2011, a southwest section of Garfield, NJ was designated an EPA superfund site, following a 1983 chromic acid (hexavalent chromium [CrVI]) spill from a partially-buried storage tank at a local electroplating plant. CrVI-contaminated water (and a resulting dust) was first found seeping into a local firehouse basement in Garfield in 1993, followed by 13 residential properties in 2000, and more recently in wells south of the Cr plume area and under the Passaic River to the neighboring town of Passaic. As part of the Community Outreach and Engagement Core of the NYU NIEHS Center of Excellence, residents of Garfield have begun participating in a community health survey as a way to express their concerns within the community. The demographics of the survey respondents demonstrated that 55% were female, 79% were white, 29% Hispanic, and a majority had finished high school. Thirty-two percent of the respondents said they were 'unsure' if they were exposed to chemicals or pollutants where they live, which suggests a limited awareness of chromium exposure in their community. When asked about environmental issues in their community, 67% and 71% of respondents were concerned about air and water quality, respectively. The top three health issues of concern were cancer (64%), asthma (48.5%) and respiratory illness (47%). While residents are still being recruited to participate in the community survey, healthy, non-smoking residents 18-65 yr-of-age who lived in Garfield for > 2 yr are being recruited to donate toenail clippings to identify potential total Cr exposure in residents within the last 18 months. If elevated Cr levels are detected in any of the toenail samples of residents, they will be asked to come back and provide a blood sample to determine whether there has been any recent Cr exposure (within the last 2 months). This community-based participatory research will help gauge the needs of the community and (hopefully) relieve the anxiety of the Garfield residents concerning Cr exposure (NYUNIEHS Ctr COEC ES017427).

PS 1676 Education to Action: Supporting Youth Leadership through Environmental Health Education

J. M. Gohlke[1], M. C. Bernhard[1], S. B. Tyson[2], K. Brown[2] and L. Antoine[1]. [1]*Environmental Health Sciences, University of Alabama at Birmingham (UAB), Birmingham, AL and* [2]*Friends of West End, Birmingham, AL.*

North Birmingham, AL has recently been the subject of environmental concerns due to heightened levels of arsenic and benzo(a)pyrene found in the soil and air. In Jan. 2012, areas surrounding several major industries were designated a Superfund emergency response area. Working with community partners, environmental health priorities were established. As a starting point and to address education needs in the community, we implemented an environmental health education program at Hudson K-8 school for children ages 8-15 and their families. We developed an inquiry-based curriculum and evaluation constructs in collaboration with community members and teachers at Hudson Elementary. The curriculum included hands-on, age appropriate programs with a focus on the environmental issues North Birmingham residents currently face. The ultimate goal of the program was to increase knowledge of how contamination is measured, how risks to health are determined, and demonstrate ways to identify and assess environmental health issues in your neighborhood. The program culminated in a final interactive demonstration of results led by the children, which was presented at a community-wide event in North Birmingham. Knowledge gained and risk perception was evaluated through pre and post- tests. In addition, community members also took a risk perception survey regarding the environmental issues in their community. They reported concern of chemicals in the community, concern that key decision-makers lack a good plan for addressing the needs of the community, and a willingness to become actively involved in projects to improve the social or environmental quality of their community. Outcomes of this initial program have resulted in the development of a plan to continue and potentially expand Education to Action to other area schools.

PS 1677 SOT Members Support K–12 Involvement and Outreach

C. L. McGinnis[1], A. L. Slitt[2] and N. W. Hurst[3]. [1]*Quinnipiac University, Hamden, CT,* [2]*University of Rhode Island, Kingston, RI and* [3]*Infinity Pharmaceuticals, Inc., Cambridge, MA.*

SOT has supported efforts related to K-12 outreach since the mid 1990's, however the level of involvement of SOT and Regional Chapter members in K-12 classrooms and informal education settings was unknown. The K-12 Regional Chapter Outreach Contacts proposed and developed a survey which was distributed to SOT and Regional Chapter members in September 2013. The goals of the survey were to: 1) assess the level of interest among SOT members in conducting outreach activities, 2) assess the level of member involvement in outreach activities, and 3) identify members who are currently involved or would like to participate in future outreach activities. Obtaining member input is critical in determining whether K-12 outreach aligns with the Society's strategic priorities of Building for the Future of Toxicology and Promoting the Recognition of Toxicology. Administered online, 475 SOT members responded, about 6% of the membership. Of these respondents, 31% are currently involved in outreach, 29% have been involved in the past but are not now, 33% are not involved but would like to be, and 7% are not interested in conducting K-12 outreach. Of the 272 who are involved, have been involved, or are interested in K-12 outreach, 60% had been or are involved with science fair projects and judging. The majority of survey respondents felt that SOT and the Regional Chapter should encourage and allocate resources for K-12 outreach. Support of the outreach activities through ideas and access to materials for classroom activities was ranked highly by the respondents. Outreach to high school students and teachers were ranked as the highest priorities for the Society's efforts. In conclusion, there is a strong level of interest in, support of, and engagement in K-12 outreach in a substantial subgroup of SOT members. Additionally, 286 members provided names which will allow us to segment the group by Regional Chapter and to contact these individuals to assist at the Regional Chapter and National levels.

PS 1678 Passive Sampling Devices Enable Capacity Building and Characterization of Bioavailable Pesticide Mixtures along the Niger, Senegal, and Bani Rivers of Africa

G. Sower[1], K. Anderson[1], D. Seck[2], K. A. Hobbie[1], A. Ndiaye Traore[2], M. McCartney[1], A. Ndaye[2], N. D. Forsberg[1] and T. A. Haigh[1]. [1]*Department of Environmental & Molecular Toxicology, Oregon State University, Corvallis, OR and* [2]*Centre Régional de Recherches en Ecotoxicologie et de Sécurité Environnementale, Dakar, Senegal.*

It is difficult to assess pollution in remote areas of less developed regions due to limited availability of energy, equipment, technology, trained personnel, and other key resources. Passive sampling devices (PSDs) are technologically simple analytical tools that sequester and concentrate bioavailable organic contaminants from the environment. Scientists from Oregon State University and the Centre Régional de Recherches en Ecotoxicologie et de Sécurité Environnementale (CERES) in Senegal developed a partnership to build capacity at CERES and to develop a pesticide monitoring project using PSDs. The partnership and dynamic process developed is applicable to equivalent capacity building programs. The project culminated in a field and laboratory study where paired PSD samples were simultaneously analyzed in African and US laboratories with quality control evaluation and traceability. The joint study included sampling from 63 sites across 6 western Africa countries, generating a 9,000 data point pesticide database with virtual access to all study participants.

PS 1679 The *Journal of Toxicological Education* (*JToxEd*)—A Milestone in Toxicology Education

J. P. Gray[1], B. Billack[2], M. G. Borland[3], S. M. Ford[2], M. A. Gallo[4], G. Hall[1], S. D. Ray[5], M. Reynolds-Walsh[6], A. L. Slitt[7], L. M. Williams[8] and S. M. Zamule[9]. [1]*Science, United States Coast Guard Academy, New London, CT,* [2]*Pharmaceutical Sciences, St. John's University, New York City, NY,* [3]*Chemistry & Biochemistry, Bloomsburg University, Bloomsburg, PA,* [4]*EOHSI, Rutgers University, Piscataway, NJ,* [5]*Pharmaceutical Sciences, Manchester University College of Pharmacy, Fort Wayne, IN,* [6]*Biology, Washington College, Chestertown, MD,* [7]*Biomedical & Pharmaceutical Sciences, University of Rhode Island, Kingston, RI,* [8]*Biology, Bates College, Lewiston, ME and* [9]*Biology, Nazareth College, Rochester, NY.*

The disciplines biology, chemistry, and biochemistry have been very successful in developing and publishing high quality, peer reviewed journals for decades targeting instructional design and educational strategies. Until now, the field of toxicology lacked a publication on toxicology education. The *Journal of Toxicological Education* (www.JToxEd.org) will fill this need, publishing peer-reviewed articles and peer-reviewed instructional materials for those interested in toxicology education. Accepted materials include but are not limited to lecture strategies, laboratory materials, pedagogy, recorded video or audio lectures, podcasts, and textbook and other book reviews. Materials targeted at any audience (post-graduate education to middle school and the general public) are accepted. The journal is open access and completely non-profit. There is no charge for publication in *JToxEd*, all submissions are posted online in the freely accessible Woods Hole Open Access Server (WHOAS) institutional repository of the Marine Biological Laboratory, and all articles are published under the Creative Commons license – authors retain full rights to their work, including the right to republish elsewhere. *JToxEd* is neither

affiliated with nor endorsed by the SOT, but fully supports the SOT educational mission and initiatives, and many of its editors serve or have served on educational committees of the SOT. *JToxEd* is actively seeking additional authors, reviewers, and editors.

PS 1680 A Unique Collaboration Producing Highly-Trained Toxicologic Pathologists: The MPI Research/Michigan State University Toxicologic Pathology Training Program

K. G. Nelson[1], S. D. Fitzgerald[2] and D. J. Patrick[1]. [1]*Pathology, MPI Research, Mattawan, MI and* [2]*Diagnostic Center for Population Animal Health, Michigan State University, East Lansing, MI.* Sponsor: C. Amuzie.

Well-trained toxicologic pathologists are a key component in the pharmaceutical, biomedical, chemical, and research toxicology fields, where interaction between toxicologists and pathologists familiar with toxicology is a vital aspect of compound and device development and research. Approximately 30% of entry-level pathologists are going into pharmaceutical, chemical, or contract research positions upon completion of their training programs. However, currently there are very few training programs that are oriented towards producing pathologists with extensive experience in laboratory animal pathology or toxicologic pathology. The MPI Research/Michigan State University Toxicologic Pathology training program was created in 2002 to address a shortage of these well-trained, boarded toxicologic pathologists. This unique residency consists of two years of a traditional anatomic veterinary pathology residency program at Michigan State University, followed by 12-15 months of focused toxicologic pathology training at MPI Research, a contract research organization that provides preclinical and early clinical research services. The program has included 10 anatomic pathology residents to date; of which seven have completed the program (two are currently in the program). The MPI/MSU combined residency program has produced residents that are well-prepared for the veterinary pathology board exam (100% pass rate) and produced well-trained and qualified toxicologic pathologists (86% employed in toxicologic pathology). The toxicologic pathologist employment environment has shifted since the program's inception, but a need for entry-level pathologists and researchers possessing focused knowledge and training in toxicologic pathology and the demands of the biopharmaceutical industry remains high. This program may serve as a model for developing other cooperative toxicologic pathology-focused training programs between industrial and academic interests.

PS 1680a Pedagogy and Policy: Teaching Effectiveness, Efficiency, and Equity

T. Dodd-Butera. *Nursing, CSU San Bernardino, College of Natural Sciences, San Bernardino, CA.*

Multiple conceptual frameworks exist for addressing health policy. Integrating a "3E" concept into class work can introduce principles of effectiveness, efficiency, and equity; and cultivate future policy makers in toxicology and public health. A logic model provides an illustration of an underlying conceptual framework and the logical connection within and between systems. Students in a course entitled, "Program Planning and Evaluation," constructed a logic model, using the example of policies addressing toxic exposures to the maternal-fetal environment. Incorporating tenets of public health and equity, the underlying assumption is that the "10 Essential Public Health Services" and "CDC Framework for Program Evaluation" provide the context for "3E" strategies to decrease toxic exposures before, during, and after pregnancy. Inputs involve cooperation of government and non-governmental organizations, development of community-campus partnerships, integration of research data and health education materials, and consideration of the importance of training current and future professionals of toxicology and public health. Proposed activities are assessed for effectiveness, cost and personnel efficiency, and determinants of health equity and social justice. Short and long-term outcomes are considered in relation to feasibility, propriety, and accuracy, in order to assess and evaluate programs and policies. Program and policy development in class work empowers students through education and experiential learning. Using a logic model provides an instructor with a reusable learning tool, which students can apply to other public health and toxicology issues for policy development in coursework and for future professional development.

PS 1681 Dioxin Exposure during Sexual Differentiation Causes Transgenerational Toxicity in Zebrafish

T. Baker[1, 2], R. E. Peterson[1, 2] and W. Heideman[1, 2]. [1]*Pharmacy School, University of Wisconsin-Madison, Madison, WI and* [2]*Molecular and Environmental Toxicology Center, University of Wisconsin-Madison, Madison, WI.*

Transient exposure of juvenile zebrafish to waterborne 2,3,7,8-tetrachlorodibenzo-p-dioxin (TCDD, 50 pg/ml) during gonad differentiation at 3 and 7 weeks post fertilization, respectively, causes changes in sex ratios, decreases in reproductive capacity, and increases in skeletal abnormalities of F0 generation adults. The goal of the present study was to determine if the adverse effects of TCDD exposure on the F0 generation would persist in the next two generations of TCDD lineage offspring (F1 and F2). It was found that changes in sex ratios, skeletal abnormalities, and reproductive capacity continued to be observed in the TCDD lineage F1 and F2 generations. While the F1 generation may have been exposed to TCDD as germ cells; the F2 generation was never exposed to TCDD. In the TCDD lineage F1 and F2 generations, the sex ratios showed both a significantly higher percentage of females and greater incidence of skeletal abnormalities with a scoliosis-like kink in the spinal column being most common. Decreased reproductive capacity also was observed in TCDD lineage F1 and F2 generations with both egg release and percentage of eggs fertilized significantly decreased compared to controls. Spawning of the TCDD lineage F2 generation males (never exposed to TCDD) with control females revealed that decreased egg release and egg fertilization was caused by the TCDD lineage F2 males. Thus, toxicity observed in three generations (F0, F1 and F2) of TCDD lineage zebrafish as well as in a TCDD lineage F2 male generation outcross, suggests that epigenetic transgenerational inheritance of TCDD toxicity occurs through the male germline. (Supported by UW Sea Grant, NIEHS, and NCATS)

PS 1682 Metabolomic Analysis of Embryonic Zebrafish Indicates Hyaluronic Acid As a Biomarker of Arsenic Exposure

Y. Nkrumah-Elie, J. Kirkwood, J. Stevens, E. Ho and R. L. Tanguay. *Environmental Health Sciences Center, Oregon State University, Corvallis, OR.*

Arsenic exposure has been associated with a myriad of human diseases including cardiovascular disease, cancers and neurological disorders; and developmental arsenic exposure may be relevant in the fetal onset of disease. The goal of this study was to use metabolomics to identify novel developmental targets of arsenic that may lead to adult onset diseases. To evaluate the impact of arsenic exposure in early development, dechorinated 5D zebrafish (*Danio rerio*) embryos were placed in control embryo media or embryo media containing 10 μM sodium arsenite at six hours post fertilization (hpf). Embryos were placed in the dark and allowed to develop uninterrupted in a 28 degree incubator. At 120 hpf, the embryos were prepared for metabolomics analysis. Briefly, 10 larvae were pooled in triplicate and metabolites were extracted using MeOH:RO water, 80:20, v:v, chilled to -80 degrees. Untargeted, unbiased metabolome profiles were developed using LC-MS/MS technology. ANOVA was utilized to compare resulting mass spectrometry features in the control and arsenic exposed zebrafish embryos. Arsenic exposure resulted in significantly altered features ($P<0.05$, 2-fold change) in the positive and negative ion modes, as modeled by principal component analysis and volcano plots. Preliminary analysis indicates that hyaluronic acid (HA) as one of the most significantly increased metabolites (4.57-fold change, $P=0.00094$) resulting from arsenic exposure. HA is a glycosaminoglycan produced by hyaluronan synthase 2 and is involved in cardiac valve development and migration of myocardial cells. HA has been shown to be overexpressed in arsenic induced liver dysfunction, is used as a biomarker of bladder cancer. Additionally, the HA receptor, CD44, is overexpressed in ovarian cancer. HA may be a biomarker of embryonic arsenic exposure and may help to elucidate the role of arsenic in the fetal onset of chronic diseases.

PS 1683 Multigenerational Effects of Benzo[a]pyrene Exposure on Survival and Developmental Deformities in Zebrafish Larvae

K. L. Willett, J. Corrales, C. Thornton and M. B. White. *Pharmacology and Environmental Toxicology, University of Mississippi, University, MS.*

Multigenerational impacts of polycyclic aromatic hydrocarbon (PAH) exposure are suggested in human cohort studies. To investigate mechanisms and developmental phenotypes associated with a dietary benzo[a]pyrene exposure, zebrafish were used. Only F0 adult zebrafish were fed 0, 10, 114, or 1012 μg BaP/g diet at a feed rate of 1% body weight twice/day (equivalent to 0, 0.21, 2.3 and 20 μg BaP/g fish) for 21 days. Three subsequent untreated generations of offspring (F1-F3) were assessed for mortality and time to hatch at 24, 32, 48, 56, 72, 80, and 96 hours post fertilization (hpf) and developmental deformities at 96 hpf. F1 mortality significantly increased in the higher BaP dose groups (2.3 and 20 BaP μg/g fish), but there

were no differences in the F2, F3, or F4 generations. Time to hatch in the higher doses significantly decreased in only the F1 and F4 generations. Multigenerational phenotypic impacts were caused in three generations (F1, F2, and F3) following the F0 exposure. Body morphology deformities (e.g. shape of body, tail and pectoral fins) were most extreme in the F1 generation although still present in the F2 generation. Craniofacial structures (e.g. length of brain regions and size of optic and otic vesicles), although not significantly affected in the F1 generation, emerged as significant deformities in the F2 generation and persisted through the F3 generation. Swim bladder impacts in the F1 generation corresponded to BaP treatment, but in the F3 generation fish in all treatments had affected swim bladders. Molecular analysis is now being used to elucidate mechanisms that are associated with the phenotypic deformities detected across generations. Supported by NIEHS R21ES019940.

PS 1684 Benzo(a)pyrene Exposure Induces Global Methylation, Dampens Met Expression, and Induces Negative Behavioral Responses in Offspring Mice

D. B. Hood[1, 3], Z. Li[1], M. Maguire[1], R. E. Rhoades[1], M. McCallister[1] and L. Rothblat[2]. [1]*Department of Neuroscience and Pharmacology, Center for Molecular and Behavioral Neuroscience, Meharry Medical College, Nashville, TN,* [2]*Department of Psychology, George Washington University, Washington, DC and* [3]*Division of Environmental Health Sciences, College of Public Health, Department of Neuroscience, College of Medicine, The Ohio State University, Columbus, OH.*

MET, encodes a pleiotropic receptor tyrosine kinase implicated in multiple cellular processes during development and is an autism risk gene. This study tested the hypothesis that in utero exposure to B(a)P aerosol during the critical period of neurogenesis negatively modulates postnatal Met expression, glutamatergic processes towards later-life behavioral phenotypes. On embryonic day 14-17, dams were exposed to B(a)P aerosol 100ug/m3 or carbon black only for 4 hours/day by nose-only inhalation. Birth indices and growth curves did not reveal any effects from exposure in offspring pups. Epigenetic assays revealed upregulation of global methylation in exposed Cprlox/lox offspring relative to controls. Developmental expression profiling for Met demonstrated negative modulation in B(a)P-exposed Metfx/fx/Emx1cre and Cprlox/lox offspring. in vivo microdialysis, spatial discrimination and executive learning, paradigms were used. Met offspring that were exposed in utero demonstrated a robust decrease in prefrontal cortical glutamate concentrations as compared to control Metfx/fx/Emx1cre offspring (PND100). Conversely, Cprlox/lox offspring that were exposed in utero demonstrated a robust increase in prefrontal cortical glutamate concentrations as compared to control Cprlox/lox offspring. In separate behavioral paradigms, Cprlox/lox offspring that were exposed in utero 100mg/m3 exhibited either significant impairments in 1) spatial discrimination or 2) contextual rule switching paradigms when required to respond in a context appropriate manner. These data provide insights into the potential mechanisms of Met action.

PS 1685 *In Vivo* Aryl Hydrocarbon Receptor-Mediated Developmental Toxicity Impairs the Adult Cardiovascular System

V. S. Carreira[1], Y. Fan[1], M. Jiang[2], S. Koch[2], M. Naticchioni[2], M. Smith[2], J. Rubinstein[2] and A. Puga[1]. [1]*Environmental Health, University of Cincinnati, Cincinnati, OH and* [2]*Internal Medicine, University of Cincinnati, Cincinnati, OH.*

Perturbations of developmental programs are key contributors to adult disease. Specifically, disruption of arylhydrocarbon receptor (AHR) homeostatic levels in vitro suggests that developmental exposure to the ubiquitous environmentally persistent organic pollutant (POP) 2,3,7,8-tetrachlorodibenzo-p-dioxin (TCDD) culminates in abnormalities of cardiomyocyte structure and function. TCDD is a prototypical AHR agonist, and the AHR pathway has been suggested to coordinate a complex regulatory network underlying attainment and maintenance of cardiovascular homeostasis during development. Nevertheless, the pathogenesis and phenotypes of TCDD developmental toxicity remains vague. The present work aims at understanding how an abnormal AHR homeostatic level during embryogenesis affects the adult cardiovascular system. C57BL/6J pregnant mice were oral-gavaged with TCDD (0.1 to 50 μg/Kg dosages) or vehicle control at key cardiogenesis time points. Embryos were harvested at representative time points or carried to term and adulthood. Naïve C57BL/6J Ahr-/- mice were also included for each time point. At all studied doses, embryos could be carried to term; however, all pups died within 24 hours post-partum at the three highest doses. Cardiac alterations consisted of sexually-dimorphic changes in molecular, functional, and structural endpoints, including altered compartment-specific transcriptome, cardiac morphometry, altered proliferation, as well as cardiac hypertrophy and failure protein markers, changes in baseline blood pressure, echocardiographic parameters, and cardiovascular challenge tolerance. Our findings underscore the developing heart as a target for developmental disruption by in-utero exposure to a POP and the role of this receptor in cardiovascular development and disease. Supported by NIH Grant 5R01ES06273.

PS 1686 The Effects of Endocrine Disruption on the Maturation of the Developing Human Fetal Prostate

C. M. Saffarini[1], E. V. McDonnell[1], A. Amin[2, 1], S. M. Huse[1], D. Spade[1], S. Kostadinov[3], S. J. Hall[1] and K. Boekelheide[1]. [1]*Pathology and Laboratory Medicine, Brown University, Providence, RI,* [2]*Pathology and Laboratory Medicine, Rhode Island Hospital, Providence, RI and* [3]*Pathology and Laboratory Medicine, Women and Infants Hospital, Providence, RI.*

The etiology of prostate cancer is unknown, although it has been suggested that early life exposures to various toxicants, such as estrogenic chemicals, may play an important role. Previous studies in animal models have demonstrated that early life exposures to estrogens are responsible for epithelial and stromal hyperplasia, inflammation, and prostatic intraepithelial neoplasia (PIN) lesions. We have developed a xenograft rodent model, using the renal subcapsular space as the implantation site, to characterize the growth and differentiation of human fetal prostate implants (gestational age 12-24 weeks) in athymic nude mice. This model evaluates the effects of both early and later-life exposures to either corn-oil (control) or 250 ug/kg/body weight of 17β-estradiol 3-benzoate post-transplant. Key characteristic prostatic markers responsible for epithelial and stromal maturation were assessed in both control and treated xenografts. The prostate markers, p63, Ki-67, Chromogranin A, prostate specific antigen, caldesmon, smooth muscle alpha actin, estrogen receptor-α and estrogen receptor-β were stained in 7, 30, 90, and 200 day xenografts. The endogenous rodent prostates exhibited atypical hyperplasia along with the presence of massive cellular debris after estrogen exposure, while the human prostates displayed basal cell hyperplasia as indicated by p63 staining. Utilizing a PCR array, a select panel of 40 prostate specific genes was chosen for analysis. Results from the PCR arrays revealed changes in genes responsible for mesenchymal development and ductal morphogenesis, as well as changes in the prostate cancer pathway. This study of human fetal prostate tissue will allow for future mechanistic studies investigating the origins of neoplastic prostatic disease, and the effects of estrogenic endocrine disrupting chemicals.

PS 1687 Application of a Novel Method for Identification of Murine Metastable Epialleles to Human Populations

C. Weinhouse, J. Kim, M. S. Nahar, K. E. Sant and D. Dolinoy. *Environmental Health Sciences, University of Michigan School of Public Health, Ann Arbor, MI.*

Metastable epialleles (MEs) represent genomic regions with highly variable, stochastically established epigenetic marks that respond to early life environmental exposures. We previously identified murine MEs using genome-wide expression arrays in liver, kidney, and brain tissues (N = 10 males; aged PND22) to filter for candidates with a high R-values, or ratios of inter-individual: inter-tissue variances in expression. DNA methylation at these loci is established early in development, when MEs are most vulnerable to disruptive reprogramming. Two murine candidate MEs identified via this novel method, *Dnajb1* (R = 1.67) and *Glcci1* (R = 1.61), were validated in A^{vy} mouse liver tissue. Percent liver methylation was variable in a promoter CpG island in *Dnajb1* (N = 11, 0-19%) and at two ERV class II repeats in *Glcci1* (Repeat 1, N = 10, 92-100%; Repeat 2, N = 9, 79-100%). Mean liver DNA methylation at *Glcci1* Repeat 1 was altered following in utero exposure to 50 mg bisphenol A (BPA)/kg diet (N = 91), as compared to controls (N = 79) ($p < 0.0001$), indicating environmental lability. Here, we demonstrate applicability of this microarray method in identifying human MEs (N = 10 males, N =10 females). Validation of the top two candidate MEs, *DDX3Y* (R-value = 14.1, N = 28) and *NUMA1* (R-value = 10.6, N = 47), in 1st and 2nd trimester human fetal liver, revealed large inter-individual variability in DNA methylation. Percent liver methylation at seven CpG sites at the *DDX3Y* locus ranged from 10%-32%, with site-specific variances of 6 to 57. Percent liver methylation at five CpG sites at the *NUMA1* locus ranged from 14%-43%, with site-specific variances of 20 to 98. These data represent preliminary validation of a novel expression microarray method for ME identification in humans, which was previously validated in mice. Identification of human MEs is an important step in focusing studies of population level epigenetic responses to toxicant exposures.

PS 1688 Perinatal Docosahexaenoic Acid Supplementation in Mice Suppresses Chronic Inflammatory Responses through Modulation of Notch Signaling

M. Ali, K. M. Heyob, M. S. Augustine, M. Velten and L. K. Rogers. *The Research Institute at Nationwide Children's Hospital, Columbus, OH.*

Backgound: Maternal inflammation contributes to premature delivery and premature infants routinely receive therapeutic oxygen. The long term pulmonary consequences of perinatal inflammation are unclear. We tested the hypothesis that a hostile perinatal environment induces chronic inflammation into adulthood causing increased oxidative stress and apoptosis. Furthermore, we hypothesize that these changes are modulated through activation on Notch-1 and Notch-2 signaling.
Methods. Pregnant C3H/HeN mice were injected with LPS or saline and placed on control or DHA supplemented diets on embryonic day 16. Once born, offspring were placed in room air (RA) or 85% O2 for 14 d then returned to RA for an additional 6 weeks. GSH and GSSG levels were measured in lung tissues using biochemical assays. 8-isoprostanes were measured by LC-MS/MS. Caspase 3, p53, and Bcl-2 were measured by western blot as markers of apoptosis. Notch-1 and -2 levels and downstream signaling cascade were assessed in lung tissues by western blot and immunohistochemistry.
Results: At 8 weeks of age, lower levels of GSSG and 8-isoprostanes were observed in the lungs of DHA supplemented mice. Decreases in caspase 3, p53 and Bcl-2 were observed in similar tissues. Total Notch-1 and -2 protein contents and nuclear localization were decreased in the lung tissues from DHA supplemented mice.
Conclusion: Perinatal inflammation causes long-term consequences which results in increases in oxidative stress and apoptosis into adulthood. These changes are likely to be modulated by alterations in Notch signaling. Maternal DHA supplementation prevented the long-term changes due to early inflammation and hyperoxia exposure indicating therapeutic potential for DHA for preterm infants

PS 1689 Gestational Nanomaterial Exposure: What Does the Future Hold?

T. R. Nurkiewicz[1], P. G. Stapleton[1], C. E. Nichols[2], J. Yi[1], V. C. Minarchick[1] and J. M. Hollander[2]. [1]*Phys. and Pharm., WVU, Morgantown, WV and* [2]*Exercise Phys., WVU, Morgantown, WV.*

As the potential for engineered nanomaterials (ENM) develops, so does the risk of inevitable exposure within non-occupational settings, including expecting mothers and their unborn young. This fetal programming after maternal ENM exposure may have effects lasting well into adulthood. Pregnant (GD 10) Sprague-Dawley rats were exposed to nano-titanium dioxide aerosols (count mode aerodynamic diameter of 144±8 nm, 11±0.3 mg/m3, 4 hrs/day) for an average of 5.5±0.5 days to evaluate the adult consequences of gestational ENM exposure. The calculated cumulative maternal deposition over the exposure time was 85±3 μg. This study focused on the microvascular health of the heart and uterus (<150 μm) of the surviving adult (8-10 weeks) female progeny using an isolated microvessel preparation. Coronary microvascular responsiveness is impaired after gestational ENM exposure, represented by an impaired endothelium-dependent dilation to mechanical (increased intraluminal flow, Flow, 5-30 μL/min), and metabolic stimuli (acetylcholine, ACh, 10-9-10-4 M), delayed smooth muscle relaxation (spermine-NONOate, 10-9-10-4 M), and a blunted α-adrenergic response of the smooth muscle (phenylephrine, 10-9-10-4 M). Uterine arteriolar endothelial reactivity was also significantly impaired overall. This dysfunction presented as abolished endothelium-dependent reactivity (ACh), impaired flow induced dilation (Flow), and reduced myogenic responsiveness (transmural pressure, 15-120 mm Hg). Mechanistically, we isolated and evaluated the mitochondria of the left ventricle and uterus, overall suggesting a reduction in respiratory control ratio within the left ventricle, indicating a mitochondrial defect. This could have the propensity to increase oxidative stress production, thereby affecting NO bioavailability. Collectively, gestational ENM exposure may lead to independent cardiovascular consequences for the exposed progeny. These impairments may increase cardiovascular disease susceptibility for future generations.
NIH-F32-ES023435 (PAS)
NIH-RO1-ES015022 (TRN)
NSF-1003907 (VCM)

PS 1690 Mono-2-Ethylhexyl Phthalate (MEHP) Exposure Modifies Embryonic Nutrition, One-Carbon Metabolism, and Epigenetic Programming in Organogenesis-Stage Mouse Conceptuses

K. E. Sant, J. L. Jilek, D. Dolinoy and C. Harris. *Environmental Health Sciences, University of Michigan, Ann Arbor, MI.*

Mono-2-ethylhexyl phthalate (MEHP) is a ubiquitous environmental and industrial plasticizer. MEHP stunts embryonic growth and delays closure of the neural tube (NTD). These defects can be prevented by supplementation of nutrients for one-carbon (C1) metabolism indicating a vital role for C1 activity in mechanisms of toxicity. These nutrients may alter DNA and histone methylation because they provide the methyl groups required for epigenetic modifications. Abnormal epigenetic programming during development has the potential to alter tissue patterning and disease susceptibility throughout the lifecourse. This study sought to determine whether MEHP alters embryonic nutrition and epigenetic programming during organogenesis. Gestational day (GD) 8 mouse conceptuses were explanted into whole embryo culture and exposed to low- (100 ug/ml) and high-doses (250 ug/ml) of MEHP for 24 h. Uptake of FITC-albumin was used to assess histiotrophic nutrition pathways (HNP), and MEHP significantly reduced HNP activity ($p<0.01$). Nutrient substrates of C1 pathways were measured using mass spectrometry. Vitamin B12 was reduced in low-dose samples ($p<0.001$) but remained unchanged at the high-dose. Choline and homocysteine also became reduced in the low-dose and unchanged in the high-dose. Betaine was reduced in both the low- and high-dose conceptuses ($p<0.01$). Folate also followed this trend but changes were not significant. Methionine, cysteine, and S-adenosylmethionine all increased with dose, but changes were not significant due to high intersample variability. Histone methylation at H3K4 and H3K27 loci was examined using a case-control design for MEHP treatment and NTDs. H3K4 was hypermethylated in embryos (EMB) that had NTDs ($p=0.015$). Treatment increased methylation at H3K27 in EMB ($p=0.074$). Overall, visceral yolk sacs were hypomethylated when compared to EMB ($p<0.01$). This work demonstrates the ability of MEHP to modify embryonic nutrition, C1 substrates, and epigenetics during organogenesis.

PS 1690a Ancestral Exposure to Methylmercury (MeHg) Induces Transgenerational Inheritance of Neurobehavioral Defects

T. A. Kalluvila[1], R. H. Klingler[2], M. A. Pickens[2] and M. J. Carvan[2, 1]. [1]*School of Public Health, University of Wisconsin-Milwaukee, Milwaukee, WI and* [2]*School of Freshwater Sciences, University of Wisconsin-Milwaukee, Milwaukee, WI.*

Exposure to low levels of MeHg during fetal development has been associated with neurodevelopmental and visual deficits in humans. According to the National Health and Nutrition Examination Survey (1999-2000), 15.7% of childbearing-aged women have the blood Hg concentration above the level that would cause developmental effects in the most sensitive children (5.95 ppb in cord blood). Prenatal exposure to MeHg affects neurodevelopment resulting in intellectual disabilities; as well as, sensory and motor dysfunctions. Zebrafish is a model organism for human biomedicine and has been used as a model for visual development due to similarity in physiological, morphological and genetic characteristics of vision with humans. In the current study, F1 generation zebrafish embryos (less than 4hrs post fertilization) were exposed to MeHg for 24hrs resulting in tissue residues of <0.1, <0.1, <0.1, 0.64, 6.94 and 25.62 ppb Hg by ICP-MS. Fish were raised to the F3 generation with no additional MeHg exposure. As F3 adults, the fish were analyzed for visual startle response, retinal electrophysiology and locomotor activity. Exposure of the grandparents to MeHg during development caused statistically-significant ($p<0.05$) reduction in visual startle responses, delayed response of potassium ion channels of the bipolar cells of retina and induced hyperactivity. Visual startle deficits were identified in 0%, 65%, 82%, 72%, 63% and 87% while hyperactivity was detected in 0%, 50%, 41%, 56%, 69% and 67% for each ancestral dose group, respectively. The proportions of fish that exhibit visual deficit or hyperactivity were dose dependent; the data suggests that the phenotypes are inherited independently. These are truly transgenerational phenotypes as the F3 generation was not directly exposed to MeHg neither as egg (F1) nor as germ cell (F2). If this is also seen in humans, our findings have significant implications for human health risk assessments and interventions.

PS 1690b *In Utero* Exposure to Diesel Exhaust Air Pollution Promotes Adverse Intrauterine Conditions, Resulting in Weight Gain, Altered Blood Pressure, and Increased Susceptibility to Heart Failure in Adult Mice

C. S. Weldy[1], Y. Liu[1], H. Liggitt[2] and M. T. Chin[1]. [1]*Medicine, Division of Cardiology, University of Washington, Seattle, WA and* [2]*Comparative Medicine, University of Washington, Seattle, WA.*

Exposure to PM2.5 during pregnancy promotes reduced birthweight, and the associated adverse intrauterine conditions may also promote adult risk of cardiovascular disease. Here, we investigated the potential for in utero exposure to diesel exhaust (DE) air pollution, a major source of urban PM2.5, to promote adverse intrauterine conditions and influence adult susceptibility to disease. We exposed pregnant female C57Bl/6J mice to DE (≈300 μg/m3 PM2.5, 6 hrs/day, 5 days/week) from embryonic day (E) 0.5 to 17.5. At E17.5 embryos were collected for gravimetric and pathological analysis. In addition, some dams exposed to DE were allowed to give birth to pups and raise offspring in filtered air (FA) conditions. At 10-weeks of age, body weight and blood pressure were measured. At 12-weeks of age, cardiac function was assessed by echocardiography. Susceptibility to pressure overload-induced heart failure was then determined after transverse aortic constriction surgery. We found that in utero exposure to DE increases embryo resorption, and promotes placental hemorrhage, focal necrosis, compaction of labyrinth vascular spaces, inflammatory cell infiltration and oxidative stress. In addition, we observed that in utero DE exposure increased body weight, but counterintuitively reduced blood pressure without any changes in baseline cardiac function in adult male mice. Importantly, we observed these mice to have increased susceptibility to pressure-overload induced heart failure, suggesting this in utero exposure to DE 'reprograms' the heart to a heightened susceptibility to failure. These observations provide important data to suggest that developmental exposure to air pollution may strongly influence adult susceptibility to cardiovascular disease.

PS 1691 Reproductive Parameters in a 90-Day Toxicity Study of Smart Herbal Purifier®—A Poly Herbal Supplement in Male Rats

Z. N. Igweze[1, 3], O. E. Orisakwe[2] and A. W. Obianime[3]. [1]*Pharmacology and Toxicology, Madonna University, Elele, Rivers State, Nigeria,* [2]*Toxicology Unit, Faculty of Pharmacy, University of Port-Harcourt, Port-Harcourt, Rivers State, Nigeria and* [3]*Department of Pharmacology, School of Basic Medical Sciences, University of Port-Harcourt, Port-Harcourt, Rivers State, Nigeria.*

Cases of reproductive failure after prolonged intake of herbal supplements have been reported in Nigeria. This study evaluates the testicular effects of Smart Herbal Purifier -a poly herbal supplement SHP in sexually albino rats. Subchronic toxicity of SHP was investigated in a 90 day repeated dose toxicity test in male Sprague – Dawley rats. The rats were divided into 30 per group received 0, 48, 240, and 480 mg/kg/day of SHP. Animals were sacrificed at 30, 60, and 90 days. Body weight and male reproductive parameters, weight of testes, testicular and epididymal sperm count, motility, morphology, debris and viability were recorded. Testosterone, leutinizing hormone, prolactin, follicular stimulation hormone and malondealdehyde were analysed. Histology of the testes was examined. A Mann–Whitney U-test was used in data analysis. Testicular sperm motility significantly decreased from 71.87±12.98% (control group) to 27.13±6.64% (480 mg/kg SHP) treated group. There was significant % increase in both testicular (19.10±5.78 in control group to 57.50±6.89 in 480 mg/kg SHP) and epididymal (14±0.00 in control group to 50.0±1.53 in 480 mg/kg SHP) sperm debris. SHP significantly ($p<0.05$) increased the FSH from 0.82±0.45 to 1.24±0.93 (Iμ/L) in the control and the 240mg/kg SHP treated groups respectively. Malonaldehyde was significantly ($p<0.05$) increased from 0.98±0.13 to 1.20±0.26 in the control and 480mg/kg SHP treated groups respectively. Histology of the testes of the treated group showed necrosis of the seminiferous tubules. SHP might be associated with some male reproductive toxicity concerns.

PS 1692 The Smokeless Tobacco Product, Gutkha, Alters Reproductive Parameters in Exposed Male Mice

K. Koenig[1], S. P. Doherty-Lyons[1], D. Willis[1], C. Hoffman[1], J. L. Blum[1], F. Gany[2] and J. T. Zelikoff[1]. [1]*Environmental Health Sciences, New York University, Tuxedo, NY and* [2]*Memorial Sloan-Kettering Cancer Center, New York City, NY.*

Smokeless tobacco (ST) has become more popular worldwide as cigarette smoking is increasingly restricted in public places. While studies regarding the health effects of cigarettes are numerous, there are limited data on the toxicological implications of ST. Gutkha, an ethnically-linked ST product, is a blend of powdered tobacco, areca nut, slaked lime, catechu, and spices, of which tobacco and areca nut are considered by IARC as Group I human carcinogens. The purpose of this comparative study is to elucidate the effects of gutkha on male reproductive parameters including sperm quality and DNA damage and hormone levels. Eight-week-old male mice, divided into four treatment groups, were treated daily for 3 wk (5 d/wk) via an oral mucosal route with 50 μl of water, nicotine, tobacco, or gutkha. Half the mice were sacrificed at 24 h post-exposure and the remainder were sacrificed after a 5-wk recovery period. Total sperm counts were dramatically decreased in the nicotine-, tobacco-, and gutkha-treated groups compared to controls at both post-exposure time points. While mice exposed to nicotine alone had significantly increased sperm abnormalities (compared to controls) at both time points, onset of total sperm abnormalities in the gutkha- and tobacco-treated mice was delayed, appearing only 5-wk after exposure. In all three treatment groups (compared to time-matched controls) sperm head abnormalities ranked highest at 5-wk post-exposure. Gutkha-exposed mice tended to have reduced serum testosterone levels. Findings here illustrate that exposure to gutkha adversely affects male reproductive parameters by altering sperm health and that, in addition to nicotine, other gutkha components are playing a role in disruption of sperm development. Results of this study imply a strong public health risk, particularly for male gutkha users of reproductive age. Supported by Memorial Sloan Kettering Cancer Center Pilot Program and NYU NIEHS Center Grant No. ES000260.

PS 1693 Reproductive Toxicity of *Terminalia arjuna* in Male Albino Rats

S. Chauhan[1] and S. Agrawal[2]. [1]*ICMR, New Delhi, India and* [2]*Bhilai Mahila Mahavidyalaya, Bhilai, Durg, India.*

Terminalia arjuna, a member of Family Combretaceae is used as a cardiotonic in Ayurvedic medicine. Oral administration of the alcoholic bark extract of the plant to different groups of albino rats at 150 and 600 mg per kg b wt for 12 and 24 days respectively caused reduction in the wet weight of testis, epididymis, vas deferens and accessory reproductive organs. Necrotic changes such as shrinkage of seminiferous tubules, formation of uni- and multinucleate giant cells and / or clumping of germ cells was seen in the testis. Deformation of the tubules in caput and cauda epididymis was observed along with exfoliation of germ cells in the lumen. The lumen of vas deferens was obliterated and lamina propria was infiltrated with channels. Biochemical studies revealed depleted testicular glycogen and increased phosphatase enzyme levels. The extract inhibited gain in weight of reproductive organs of immature castrated male rats administered testosterone propionate. Findings reveal toxicity of T.arjuna extract.

PS 1694 The Haemogram, Spermiogram and Histopathology of Testicles and Epididymis of Male Wistar Rat Treated with Aloe Vera Gel

M. O. Oyeyemi and O. S. Ajani. *Department of Veterinary Surgery and Reproduction, University of Ibadan, Ibadan, Oyo, Nigeria.* Sponsor: A. Oyagbemi.

This work was designed to investigate the possible toxicological effects of Aloe vera on the spemiogram and spermatozoa morphology in rats. This work is carried out using fifteen male Wistar rats, weighing between 0.15kg to 0.24kg and randomly assigned to three groups (A, B, C). Groups A and B were the experimental groups while Group C was the control group. The experimental groups A and B were treated with Aloe vera gel at 300mg/kg body weight and 200mg/kg body weight respectively for 10 days. The findings shows that the percentage motility of spermatozoa from groups A and B were 64.00±6.80 and 66.00±8.74 respectively which were significantly lower than group C value of 89±2.46% ($P<0.05$). The percentage liveability of the sperm cells of Groups A and B were 88.00± 3.74 and 85.00±4.48 respectively. These were significantly lower than the control value of 96.8±0.74. The sperm concentration of the experiment groups A and B (53.2±2.27 and 59.4±2.43 respectively) were also significantly lower than the control group 84.6±2.14 ($P<0.05$). The difference in the experimental values in this study are significant ($P<0.05$) lower than the control. This indicates that an increase in the administration of Aloe vera gel decreases the percentage liveability and motility of sperm cells which will affect fertility of male animals under study. In conclusion, the use of Aloe vera gel for more than 10 consecutive days has been found to have an adverse effect on the spermiogram and spermatozoa morphology of intact male rats at a dose of 300mg/kg body weight.

PS 1695 Manganese: A Potential Reprotoxicant?

D. McGough[1], L. Jardine[2] and M. Maher[3]. [1]*International Manganese Institute, Paris, France,* [2]*Charles River Edinburgh, Edinburgh, United Kingdom and* [3]*Intertek ASG, Manchester, United Kingdom.* Sponsor: W. Harvey.

In occupational settings there is a concern that high levels of exposure to manganese may occur and that this, in combination with continued low level exposure over long periods of time, may lead to some adverse health effects. Contradictory findings exist regarding reproductive performance following such exposures.
The aim of this study was to investigate if manganese is a reprotoxicant. Manganese chloride was selected as the most suitable form of manganese to assess reprotoxicity. Four groups of Sprague-Dawley rats, 20 per group (10 males and 10 females) were exposed to $MnCl_2$ via the inhalation exposure route (nose only) for 9 weeks at target concentrations of 0 (control air only) 5, 10 and 30 μg/L of Mn.
A slight intergroup difference in body weight gains and food consumption was seen in the low and mid doses but this was not positively attributed to $MnCl_2$ exposure. At the high dose level (30 μg/L) adverse clinical signs, including irregular respiration, were observed in 1 male and 2 females resulting in the premature sacrifice of these animals, and the cessation of exposure to the remaining animals in this group after approximately 3 weeks of treatment (early gestation).
At the end of the study, it was concluded that, under the conditions of this study, $MnCl_2$ exposure at target levels of 5 and 10 μg/L did not have an effect on mating performance; fertility or the duration of gestation and hence manganese was not considered to be a reprotoxicant at these exposure levels.

PS 1696 N-Acetylcysteine, but Not the Suspension of Treatment, Reverses the Effects of Arsenic Trioxide on the Mouse Male Reproductive System

R. F. Silva[1], L. R. Kiguti[3], C. S. Borges[2], P. V. Silva[2], G. Missassi[2], A. S. Pupo[3] and W. D. Kempinas[2]. [1]*State University of Campinas, Campinas, SP, Brazil,* [2]*Morphology, State University of São Paulo, Botucatu, SP, Brazil and* [3]*Pharmacology, State University of São Paulo, Botucatu, SP, Brazil.*

Arsenic trioxide (AT) has been shown effective in the treatment of acute leukemia. Due to its apoptosis-inducing activity, it can affect germ cells. The aim of this study was to evaluate the immediate effects of treatment with AT on reproductive system of Swiss male mice, after 50 days of suspension of the treatment and with the co-administration of the antioxidant N-acetylcysteine (NAC). For this, adult male Swiss mice were treated with distilled water (vehicle), 0.3 or 3.0 mg/Kg/day of AT (ACROS 1327-53-3), subcutaneously in 25 applications. At the end of treatment half of animals were killed to evaluate the effects on sperm parameters and the other half were kept without the drug for 50 days (spermatogenesis + sperm transit time) and then killed for assessment of possible reversibility of the effects. In another experiment, animals were treated with vehicle, 3.0 mg/Kg/day of AT, NAC and NAC + AT. The following material was obtained/determined at necropsy: vital and reproductive organs weights, sperm from the vas deferens for motility analysis and testis for determination of daily sperm production. The differences among groups were compared using ANOVA and Kruskall-Wallis, followed by Dunnett or Dunn's tests, respectively, with $p<0.05$. The animals treated with the higher dose of AT and killed right after the end of treatment showed reduction in seminal gland weight, number of motile sperm and daily sperm production, which remained altered after the suspension of treatment. However, when NAC was given in conjunction with AT these parameters were similar to the control group. The results show that AT was toxic for the mouse male, compromising sperm quality and quantity, and that these effects were persistent even after the suspension of the treatment. Furthermore, the administration of an antioxidant prevented the harmful effects of the drug on the male reproductive system.

PS 1697 Assessment of the Reproductive Toxicity of Inhalation Exposure to Ethyl Tertiary Butyl Ether in Male Mice with Normal, Low-Active, and Inactive ALDH2

R. Wang[1], Z. Weng[1, 2], K. Ohtani[1], M. Suda[1] and Y. Yanagiba[1]. [1]*Japan National Institute of Occupational Safety and Health, Kawasaki, Japan and* [2]*NCTR, Jefferson, AR.* Sponsor: N. Mei.

Ethyl Tertiary Butyl Ether (ETBE) has been used in recent years as a biofuel additive. Previous reports have shown that ETBE is low toxicity with the NOAEL at 500 ppm. However, ETBE is metabolized to acetaldehyde and other aldehydes, which are known with high toxicity. Aldehyde dehydrogenase2 (ALDH2) is the main enzyme to metabolize aldehydes, but approximately 40% East Asians are deficient in the enzyme activity. So far no data are available regarding ALDH2 polymorphisms related to the reproductive toxicity of ETBE. In this study, a series of experiments were performed in Aldh2 knockout (KO), heterogeneous (HT) and wild type (WT) C57BL/6 male mice exposed to ETBE and the data about general toxicity, testicular histopathology, sperm head numbers, sperm motility and sperm DNA damage were collected. The results showed that 13-week exposure to 500, 1750 and 5000 ppm ETBE significantly decreased sperm motility and increased levels of sperm DNA strand breaks and 8-hydroxy-deoxyguanosion in both WT and KO mice; the effects were found in 1750 and 5000 ppm groups of WT mice but in all three exposed groups of KO mice. In the 9-week experiment of exposure to lower concentrations of ETBE (50, 200 and 500 ppm), the remarkable effects of ETBE on sperm head numbers, sperm motility and sperm DNA damage were further observed in KO and HT mice exposed to 200 ppm ETBE, but not in WT mice. Our findings suggested that only exposure to high concentrations of ETBE might result in reproductive damages in mice with normal active ALDH2, while low active and inactive ALDH2 enzyme can significantly enhance ETBE-induced reproductive damage even at low concentrations of ETBE, mainly due to the accumulation of acetaldehyde as a primary metabolite of ETBE.

PS 1698 Comparison of Infant Background Data from Pre- and Postnatal Developmental Studies in Cynomolgus Monkeys of Mainland and Island Origins

N. Lalayeva[1], S. Oneda[1], N. Makori[1], R. E. Watson[1], S. Jacobson[1], S. M. Glaza[1], T. Beck[1] and K. Fukuzaki[2]. [1]*Safety Assessment, SNBL USA, Ltd., Everett, WA and* [2]*Corporate, Shin Nippon Biomedical Laboratories, Ltd, Tokyo, Japan.*

A retrospective analysis of infant cynomolgus monkey control data from enhanced pre- and post-natal developmental toxicology (ePPND) studies were evaluated from two different origins: Mainland (ML; Chinese and Cambodian) and Island (IL; Indonesian). Parameters assessed included mean gestation length, incidences of stillbirth/infant mortality, functional development, and common macroscopic and microscopic findings. Infant evaluations in ~40% of the studies were through three to six months, and ~20% were through the first year of age.
Mean gestation lengths in ML (n=135) and IL (n=66) animals were on the average 161 and 157 days, respectively. Incidences of stillbirths were comparable at 8.2% and 10.2% and infant mortality rates were 2.3% and 5.1%, respectively. There were no notable differences between the two origins in the functional development parameters. No major external or visceral malformations were observed in any of the infants. The most consistent minor skeletal findings/variations for ML and IL infants, respectively, included metaphyseal sclerosis (3/76 and 6/65) and stairstep to the cranial suture (0/76 and 3/65). Microscopic observations consistently recorded in ML and IL infants, respectively, included mononuclear cell infiltration in the kidney (13/65 and 13/67), lungs/bronchi (17/65 and 18/66), and liver (19/77 and 26/67); extramedullary hematopoiesis in the liver (20/77 and 29/67) and axillary lymph nodes [LN] (8/61 and 7/67); increased lymphocytes/lymphoid follicles in mandibular LN (10/61 and 18/41), mesenteric LN (14/61 and 18/67), and spleen (12/77 and 7/67); and vacuolization of the liver (8/77 and 11/67).
The incidences of macroscopic findings, including skeletal, were low in infants from both origins and were comparable with that of adult monkeys (Chamanza et al. 2010). These reference background data are a vital tool in the evaluation of ePPND preclinical studies in cynomolgus monkeys.

PS 1699 Nonhuman Primate DART Data Interpretation: Challenges Associated with Background Changes in Pregnant Cynomolgus Monkeys

S. Karanth, J. N. Tichenor, A. Wilcox, J. K. Meyer and G. J. Chellman. *Toxicology, Charles River Laboratories, Preclinical Services, Reno, NV.*

The use of nonhuman primates (NHPs) in nonclinical safety assessment, including developmental and reproductive toxicology (DART), has increased in recent years due to the growing number of biotechnology-derived drugs, many of which are pharmacologically active only in NHPs. Similar to humans, major physiological, anatomical, metabolic, and hormonal changes occur in cynomolgus monkeys during pregnancy. Pregnancy-related changes in hormone levels (including estradiol and progesterone), clinical pathology parameters, lymphocyte subpopulations, and bone biomarkers have been reported. Some of these changes may mimic the mode of action of the biopharmaceutical being tested and, therefore, pose challenges to interpreting the study data. In order to better understand the background changes during pregnancy in cynomolgus monkeys, we evaluated selected hormone, clinical pathology, and lymphocyte subpopulation data using our historical control database from Enhanced Prenatal and Postnatal Development (ePPND) studies. Our data indicate that serum cholesterol levels are significantly decreased during gestation in cynomolgus monkeys, which is in contrast to a reported increase in cholesterol in pregnant women. Similar to humans, glucose levels are moderately increased in cynomolgus monkeys during gestation. While serum estradiol levels show a gradual increase, peripheral B-lymphocyte levels are

significantly decreased during gestation in cynomolgus monkeys. Since lymphopoiesis of B-cells has been reported to be negatively affected by steroids, the decreased B-lymphocytes during pregnancy may be due to increased estradiol levels. Our data support the observation that there are species-specific differences in background levels of selected parameters during pregnancy. Some of the background changes in pregnant cynomolgus monkeys can be potentially similar to the mode of action of the drug being tested and/or different than observed in pregnant women, therefore posing unique challenges for interpreting DART data.

PS 1700 Telmisartan Attenuates the Somatic and Germ Cells Damage in Streptozotocin-Induced Diabetic Rat: Cellular and Molecular Mechanisms

S. Kushwaha and G. Jena. *Department of Pharmcaology and Toxicology, National Institute of Pharmaceutical Education and Research, Mohali, Punjab, India.*

Diabetes is a metabolic disorder that affects nearly every organ system. Telmisartan, an angiotensin type 1 receptor blocker, used in diabetes associated hypertension. Besides controlling blood pressure, telmisartan exhibits several other beneficial effects and provides new avenues in end-organ protection. Present study explored the possible protective mechanisms of telmisartan, in kidney and testes of diabetic rat. Male Sprague Dawley rats randomized into six groups: control, telmisartan control, diabetic control and diabetic group treated with telmisartan at the doses of 3, 6 and 12 mg/kg /day, per oral for 4 weeks. Animals were made diabetic by single dose of streptozotocin, i.p. (55 mg/kg). Results showed that telmisartan significantly protects kidney as observed from decreased DNA damage, cell death and reduced expression of nuclear factor kappa B (NF-κB), cyclooxygenase (COX-2) and connective tissue growth factor (CTGF). Telmisartan also attenuates testicular toxicity as observed by restored sperm counts, decreased sperm DNA damage and apoptotic cell death. Immunohistochemistry of 8-oxo-dG (8-oxo-7,8-dihydro-2'-deoxyguanosine) and 3-nitrotyrosine confirmed that telmisartan significantly reduced oxidative and nitrosative damage. Western blot analysis showed that telmisartan decreased the levels of NF-κB, interleukin 6 (IL-6), tumor necrosis factor alpha (TNF-α), phosphorylated extracellular signal-regulated kinase (p-ERK1/2), inducible nitric oxide synthase (iNOS), caspase-3 and increased peroxisome proliferator-activated receptor gamma (PPAR-γ) expression. Present results showed that telmisartan restored the status of the antioxidant enzymes, oxidative and nitrosative stress, reduced inflammation and cell death in kidney and testis of diabetic rat. Further, research is needed to validate the usefulness of angiotensin receptor blockers, telmisartan in diabetes associated end organ damage.

PS 1701 Expression and Localization of Xenobiotic Transporters in the Male Reproductive System

D. M. Klein[1], N. J. Cherrington[1] and S. H. Wright[2]. [1]*Pharmacology/Toxicology, University of Arizona, Tucson, AZ and* [2]*Physiology, University of Arizona, Tucson, AZ.*

The blood-testis barrier (BTB) prevents the entry of many compounds into the male genital tract (MGT) which is beneficial for the exclusion of reproductive toxicants, but may decrease drug efficacy for medications requiring entry to the MGT. Transporters expressed along this tract can influence the distribution of xenobiotics into the MGT by the uptake into the MGT, efflux back into the blood, or facilitating the accumulation of toxicants into specific MGT tissues. By determining the constitutive mRNA expression levels and subcellular localization of these transporters, their physiological function and effect on drug disposition may be better predicted. The aim of this study was to determine subcellular localization of MRP transporters in rodent, macaque, and human testis and to determine mRNA expression of 30 xenobiotic transporters in different sections of the MGT isolated from rats. Using immunohistochemistry, we determined that in all species, MRP1 is restricted to the basolateral membrane of Sertoli cells, MRP5 is located in Leydig cells, and MRP8 is located in round spermatids. MRP4 is expressed on the basolateral membrane of Sertoli cells in human and macaques, but on the apical membrane in rats. By using branched DNA signal amplification, we determined that the epididymis expressed at least moderate levels of 19 transporters, while the vas deferens expressed 15, seminal vesicles 23, and prostate 19. Knowledge of which transporters are expressed in each tissue may provide insight into how xenobiotics are able to bypass this distinct compartment thereby increasing efficacy of medications needing access to the MGT for full therapeutic effect.

PS 1702 Phthalate Metabolism and Kinetics in an *In Vitro* Model of Testes Development

S. Harris[1], S. Wegner[1], S. Hong[1,2] and E. M. Faustman[1,2]. [1]*Department of Environmental and Occupational Health Sciences, University of Washington, Seattle, WA and* [2]*Institute for Risk Analysis and Risk Communication, University of Washington, Seattle, WA.*

We developed an in vitro model of testes development (3D-TCS) using rat testicular cells overlaid with extracellular matrix, allowing for three dimensional growth and a physiologically stable culture system. One barrier preventing utilization of in vitro models in toxicity testing is the lack of metabolic systems which are present in vivo but not in vitro. Another challenge in interpretation of results from in vitro models is the lack of kinetic data for many compounds in in vitro systems. In the current study, we sought to perform a preliminary characterization of the inherent metabolic capabilities of the 3D-TCS as well as investigate the kinetic behavior of some common male reproductive toxicants (phthalates). 3D-TCS cells were cultured with three phthalate diesters (DEP, DBP and DEHP). Concentrations of phthalate parent compounds and monoester metabolites were then measured at 2, 8 and 24 hours post exposure in culture media and cell lysate via mass spectrometry. We used detected levels of monoester metabolites as an indication of phase I metabolism of phthalates diesters to monoesters via non-specific lipase activity. Monoester metabolites were detected in all phthalate treated cell media and cell lysate samples. Metabolite levels ranged from <0.01-16% of initial concentration of parent compound. Phthalate diesters partitioned between media and lysate in a manner dependent on each compound's logKow value. In addition, analysis of 3D-TCS microarray data indicated gene expression of several lipases as well as CYPP450's involved in steroid or lipid metabolism. These results provide evidence for the presence of significant CYPP450's, the metabolism of phthalate diesters in our testicular co-cultures and also provide important information about the kinetic behavior of phthalates in the 3D-TCS.

PS 1703 The Role of H19 Hypomethylation in Male Reproductive Toxicity Induced by Endocrine Disruptors p, p'-DDE

Y. Song. *Zhejiang Academy of Medical Sciences, Hangzhou, China.*

p,p'-Dichlorodiphenoxydichloroethylene (p,p'-DDE), the major metabolite of dichlorodiphe noxytrichloroethane (DDT), is a known persistent organic pollutant and male reproductive toxicant. However, the exact mechanism remains limited. Objective In the present study, we try to investigate the role of methylation of imprinted gene H19 in male reproductive toxicity induced by p,p'-DDE. Methods Timed-pregnant Sprague-Dawley rats were obtained from experimental animal center in Zhejiang Province. Young adult female rats were cohabited with male rats overnight, and onset of pregnancy was determined by the presence of a copulation plug after overnight mating (gestation day (GD) 0). From GD8 to GD15, the pregnant rats were dosed daily by gavage with com oil as vehicle control or 100 mg p.p'-DDE per kilogram of body weight. There were 6 dams in each group. The pregnant rats were allowed to deliver spontaneously. After parturition, the litter size was randomly reduced to 10 at birth to assure uniformity, and pups were kept with their respective dams until weaning on postnatal day (PND) 21, at which point litter mates of the same sex were housed up to 4 per cage till PND90. Results We found that transient exposure (daily gavage of 100 mg/kg body weight) of a gestating female rat to p,p'-DDE from gestation day 8 to 15 caused reduced sperm quality associated with Igf2-H19 ICR hypomethylation in the adult male F1 generation. Conclusion Reprogramming of imprinted gene may play critical roles in male reproductive toxicity induced by p,p'-DDE.

PS 1704 Developing a Screen for Analysis of Environmental Epigenetic Effects

J. A. Camacho and P. Allard. *Molecular Toxicology, UCLA, Los Angeles, CA.*

Many factors challenge the efficiency of assessing chemicals found in the environment. These include the vast number of compounds and toxicity endpoints to be tested as well as the vital need to replace rodents in order to quickly, economically and ethically assess chemical safety. Another important issue at hand is the long lasting effect, potentially spanning several generations, of chemicals in our environment and the lack of tools to comprehensively identify these. In order to address these issues, we propose the development of new technologies that can accurately determine the safety of chemicals for endpoints that are hard to study in vertebrate models.

Here, we establish the use of the genetic model system, the worm *Caenorhabditis elegans*, as a relevant model for epigenetic and reproductive toxicity assessment. We are taking advantage of *C. elegans* genetic tools to detect chemical disruption of the germline chromatin and in particular of evolutionary conserved epigenetic

marks. To this aim, we are making use of a worm strain where GFP is specifically epigenetically silenced in the germline. In order to validate the approach, the strain is exposed to inhibitors of histone modifications that have been well characterized in mammalian systems. These inhibitors should disrupt proper establishment and/or maintenance of epigenetic marks, and lead to desilencing of the transgene in the germline. Here, we report that exposure to the histone deacetylace inhibitor valproic acid causes a de-repression of the GFP transgene expression in germ cells indicating that continuous histone deacetylation is required for the epigenetic repression of the transgene in the germline. To our knowledge, this had not previously been shown in *C. elegans* or other species. These preliminary results offer us a reliable control to further test against environmental chemicals. Further work will examine the sum of pathways and enzymatic activities that lead to proper regulation of chromatin states in the germline. Together, we are designing a strategy that should offer a more comprehensive examination of the environmental effects of the epigenome.

PS 1705 Epigenetic Transgenerational Actions of Dibutyl Phthalate and Male Fertility

W. Wu, B. Yuan, J. Li, H. Gu, M. Chen, D. Wu, C. Lu, Y. Xia and X. Wang. *Nanjing Medical University, Nanjing, PR, China.*

Increased occurrence of reproductive disorders has raised concerns regarding the impact of endocrine-disrupting chemicals on reproductive health, especially when such exposure occurs during fetal life. A novel mechanism of posttranscriptional control mediated by microRNAs (miRNAs) has lately emerged as an important regulator of spermatogenesis. This study sought to investigate the epigenetic transgenerational effect of endocrine disrupting chemical dibutyl phthalate (DBP) on male fertility. Gestationg female rats were dosed with corn oil or DBP (5, 50, or 500 mg/kg/day, per os) during the period of gonadal sex determination (between embryonic days 8 and 15). We determined the expression levels of 760 mature miRNAs in F3 rat testes with or without prenatal DBP exposure using a miRNA microarray technique, verified by quantitative real-time PCR from F1 to F4. Dose-realted effects on male offspring included reduced sperm counts, sperm motility, and testicular and epididymal malformations. Of the screened miRNAs, 7 miRNAs were up-regulated and 152 miRNAs down-regulated (fold change > 2) in 5 mg/kg/day DBP treated group when compared with controls. There were 6 miRNAs up-regulated and 212 down-regulated in 500 mg/kg/day DBP treated group. The target genes of 15 aberrantly expressed miRNAs (fold change > 8) were involved in PI3K-Akt signaling pathway, Axon guidance, ErbB signaling pathway and Focal adhesion pathways. We found permanent alterations in expression levels of multiple miRNAs suggesting an epigenetic mechanism of action. We propose that the deleterious effects of DBP on the male reproductive system are mediated by aberrantly miRNA expression in the testes. Overall, these results suggest that DBP can alter miRNA expression in F3 testes, a potentially novel mode of DBP transgenerational effect.

PS 1706 Epigenetic Mechanisms of Cadmium-Induced Placental Insufficiency

M. L. Clive, P. Sysa Shah, N. Johnston, T. Hargest, D. Bedja and K. Gabrielson. *Environmental Health Sciences, Johns Hopkins Bloomberg School of Public Health, Baltimore, MD.*

Cadmium is an environmental toxicant primarily released from trash incineration and burning fossil fuels. Smoking is the most significant source of human cadmium exposure, followed by diet, air, and drinking water. Cadmium exposure during pregnancy has been identified as a cause of placental insufficiency (PI) and intrauterine growth restriction, but the mechanism is not fully understood. Cadmium can disrupt normal cell function by epigenetic mechanisms, including global DNA and promoter methylation changes and altered microRNA (miR) expression. Although observed in other tissues, such epigenetic effects have not been studied in the placenta. We hypothesized that cadmium induces PI by epigenetic mechanisms. Female C57BL/6 mice (~100 day old) were administered 20 ppm cadmium chloride in drinking water ad libitum 2 weeks before mating and throughout pregnancy. On gestational day 15.5, umbilical artery (UA) blood velocity was assessed via the Doppler pulse method, and then dams were euthanized. Fetal and placental tissues were weighed and evaluated by histopathology, TUNEL staining, Western blot, global DNA methylation analysis, and miR was quantified. Compared to controls, cadmium-exposed dams had significantly lower UA systolic velocity, increased placental cell death, smaller litter size, and increased fetal resorption rate. Cadmium-exposed placentas had altered expression of angiogenesis-related proteins, including increased VEGF receptor 2, and decreased eNOS and heat shock protein 90. Maternal hearts showed global hypomethylation with cadmium exposure. Placentas had significantly decreased expression of angiogenesis-related miR -126-5P. Cadmium exposure induced PI in this model. Cadmium altered the expression of angiogenesis related proteins and miRs in the placenta, and induced global hypomethylation in maternal hearts, providing evidence that cadmium induces PI via epigenetic mechanisms. Further investigations will seek to identify specific mechanisms.

PS 1707 Dynamic Expression of Imprinted Genes and Epigenetic Factors in an *In Vitro* Testicular Coculture

S. Wegner, S. Harris, S. E. Pacheco and E. M. Faustman. *Department of Environmental and Occupational Health Sciences, University of Washington, Seattle, WA.*

Male reproductive developmental processes are an important target of environmental contaminants. However, there are no validated *in vitro* models for screening the chemicals that remain untested for male reproductive toxicity. Perturbation of epigenetic factors during testis development is of particular concern given the importance of epigenetic regulation for spermatogenesis and the potential for epigenetic programming of germ cells to influence disease. Our lab has previously developed a 3D testis co-culture isolated from postnatal day 5 rats that corresponds to a key phase of male reproductive development *in vivo*. This co-culture can accurately distinguish between reproductively toxic and nontoxic phthalate esters, making it a promising model for toxicity testing. To characterize the developmental pathway dynamics and epigenetic transitions captured in our *in vitro* model, we evaluated global gene expression through time in culture. Primary rat testicular cells were co-cultured with a Matrigel overlay. Gene expression was measured using Affymetrix 1.0 ST arrays. Genes significantly changed over time were identified by univariate f-test (FDR< 0.1). Over the course of 72 hours in culture (corresponding to postnatal days 7-10 *in vivo*) expression of genes involved in spermatogenesis such as AR, Dazl, Dhh, Strbp, and Ace was significantly increased. A pathway analysis of gene expression in this 72 hour period reveals significant changes in GO terms related to DNA methylation and epigenetic regulation. This suggests dynamic epigenetic modulation of gene expression through time. In parallel we see significant changes in expression of a panel of genes known or predicted to be imprinted paternally (e.g. Cpa4, H19, Tmem88) or maternally (e.g. Spon2, Sox8, Fermt2). This baseline characterization indicates that our model provides a strong platform for evaluating the potential effects of environmental factors on imprinting and the epigenetic regulators of developmental processes. (FDA 1U01FD004242-01, and NIEHS T32 ES007032-35)

PS 1708 Age-Dependent Macrophage Infiltration into the Testis of Rats and Mice after Mono-(2-Ethylhexyl) Phthalate (MEHP) Exposure

C. Murphy, A. Stermer and J. H. Richburg. *Pharmacology & Toxicology, University of Texas at Austin, Austin, TX.*

The testis is an immune privileged organ, however infectious and non-infectious inflammation of the testis has been shown to cause infertility. Phthalates are chemical plasticizers that are known Sertoli cell toxicants. Here we characterize the infiltration of macrophages into the testis of immature (21d, 28d, and 35d) and mature aged Fisher rats (56d) at 12, 24, and 48 hours after a single dose (1 g/kg) of mono-(2-ethylhexyl) phthalate (MEHP). The testis of rats at 21 and 28d had a peak increase in the number of CD11b+ immunoreactive cells (neutrophil, macrophages, and dendritic cells) cells at 12h after MEHP treatment as quantified by flow cytometry. In 28d rats, CD11b+ cells remained significantly elevated at 48h while, in 21d rats it returned to control levels by 24h. The peak number of CD11b+ cells in 35d rats was delayed until 24h, remaining significantly elevated at 48h. In mature rats there was no increase in CD11b+ cells demonstrating differential responses of the testicular immune system at different developmental ages. Immunohistochemistry confirmed the increase of newly arrived macrophages (CD68+ cells). In all immature rats, monocyte chemoattractant protein-1 (MCP-1), the primary chemokine produced in the testis, was significantly increased at 12h after MEHP treatment. This was followed by peak germ cell apoptosis (85-95% of seminiferous tubules contained ≥4 TUNEL positive germ cells) at 24h post-treatment in immature rats. The timing of peak germ cell apoptosis was similar in mature rats, however they displayed a significantly lower incidence of MEHP-induced germ cell apoptosis (8% of seminiferous tubules contained ≥4 TUNEL positive cells). Taken together, these results suggest that MEHP-induced an increase in MCP-1, triggering migration of macrophages into the immature rat testis prior to the initiation of germ cell apoptosis. Thus, signifying a role of macrophages in exacerbating MEHP-induced germ cell apoptosis in an age-dependent manner.

PS 1709 Seminiferous Tubule Atrophy Occurs Regardless of X-Ray Exposure in the p53-Null Rat Testis

D. Spade, M. S. Dai, S. J. Hall and K. Boekelheide. *Pathology & Laboratory Medicine, Brown University, Providence, RI.*

DNA damage from x-radiation can lead to apoptosis through p53 signaling. In the mouse testis, germ cell death resulting from x-radiation is dependent on p53 signaling. We hypothesized that p53 was also essential for germ cell apoptosis in response to X-radiation in the rat testis. We exposed wild-type Sprague-Dawley and novel p53 knockout rats (SD- Tp53 tm1sage) (age 60 d), to 0, 0.5, or 5 Gy x-ray. Rats were euthanized at 3 h, 12 h, and 42 d after exposure. Body, testis, and epididymis weights were recorded. The terminal deoxynucleotidal transferase dUTP nick end labeling (TUNEL) assay, a measure of apoptosis, was performed in paraffin-embedded testes. Real-time RT-PCR for the death receptor gene Fas was performed. 13 d BrdU labeling was performed to characterize the spermatogonial stem cell population in unexposed knockout rats, and whole-mounted tubules were labeled for GFRA1, a marker of type A spermatogonia. X-radiation resulted in a significant increase in TUNEL labeling after 12 h in wild-type rats. However, frequent TUNEL positive cells, most often spermatocytes, were observed in p53-/- rats in all treatment groups. p53-/- rats displayed frequent, but variable, atrophy of seminiferous tubules and lower average testis weight. While Fas mRNA levels followed a similar trend to TUNEL frequencies, they did not differ significantly by treatment. GFRA1 staining showed similar populations of A spermatogonia in wild-type and p53-/- rats, and BrdU labeling in p53-/- testes gave an average 37% germ stem cell labeling index, indicating normal proliferative activity. Therefore, we conclude that the frequent TUNEL signal in p53-/- rats likely results from unresolved homologous recombination in spermatocytes during meiosis. Our data indicate that p53 plays a critical role in maintenance of spermatogenesis in the rat. While p53 is known to participate in resolution of DNA double-strand breaks in meiotic recombination, this represents a significant difference from data previously obtained in the mouse.

PS 1710 The Stage-Specific Apoptotic Response of the Rat Testis to Low-Dose 2, 5-Hexanedione and X-Irradiation Coexposure

N. Catlin, S. M. Huse and K. Boekelheide. *Brown University, Providence, RI.*

Testicular effects of chemical mixtures may differ from those of the individual chemical constituents. This study assesses the co-exposure effects of the model germ cell- and Sertoli cell-specific toxicants, X-irradiation (x-ray) and 2,5-hexanedione (HD), respectively. X-ray induces germ cell apoptosis and in high dose studies, HD has been shown to attenuate the x-ray induced germ cell apoptosis. Here, adult rats were exposed to different levels of x-ray (0.5Gy, 1Gy, 2Gy) or HD in the drinking water for 18 days (0.33%), alone or in combination. To assess cell type-specific attenuation of HD effects with x-ray co-exposure, we used laser capture microdissection (LCM) to examine a panel of apoptosis-related transcripts using PCR arrays. The apoptosis PCR arrays identified significant dose-dependent treatment effects on several genes, with down-regulation of DR5, Naip2, Sphk2, Casp7, Aven, Birc3 and upregulation of Fas. Both Casp7 and DR5 are key pro-apoptotic factors in the apoptosis pathway, and had the strongest down-regulation following 0.33% + 0.5Gy exposure, with maximum fold decreases of -6.37 and -4.17, respectively. The significant and simultaneous downregulation of pro- and anti-apoptotic transcripts is exacerbated, rather than ameliorated, by the addition of HD to the low dose of x-ray. These results indicate that the attenuation effect seen with the high dose co-exposure does not persist into the low dose range. However, the downregulation of anti- and pro-apoptotic transcripts as a result of 0.5Gy x-ray exposure may be an adaptive mechanism employed by the injured spermatogonia to evade apoptosis. These studies provide insight into cell-specific toxicant co-exposures and they illustrate that low dose and high dose responses can differ, and that the low dose response in not necessarily an extrapolation of the effects seen at high doses.

PS 1711 Surface Charged Iron Oxide Nanoparticles May Influence Reproductive and Developmental Toxicity in CD-1 Mice

K. R. Di Bona[1], Y. Xu[2], Y. Bao[2] and J. F. Rasco[1]. [1]*Department of Biological Sciences, The University of Alabama, Tuscaloosa, AL and* [2]*Department of Chemical and Biological Engineering, The University of Alabama, Tuscaloosa, AL.*

Iron oxide nanoparticles (NPs) are currently being investigated for many uses including biomedical imaging, soil/groundwater remediation, and drug delivery. The risk to pregnant women and the developing fetus is high, as the NPs have the potential to cross the placenta due their small size. Our lab has previously shown that pregnant CD-1 mice given a low (10 mg/kg body mass) intraperitoneal dose of NPs coated with either poly acrylic acid (PAA, negatively-charged) or polyethylenimine (PEI, positively-charged) for 8 consecutive days had significantly decreased maternal weight gain, increased fetal resorptions, and increased fetal liver iron concentrations compared to controls. These results raise concern about NP reproductive toxicity and how NP exposure might affect the developing fetus. In the current study, female CD-1 mice were given a low, medium, or high dose (10, 50, or 100 mg/kg body mass) of NPs during organogenesis (gestation day (GD) 8, 9, or 10) in order to observe if there is a dose related effect on reproduction and to examine if fetal bioaccumulation of NPs will result in decreased fecundity or malformations in the progeny. At low dosages, no adverse effects were observed. At the highest dosage, increased resorptions were observed for the PAA NPs given on GD 8 and the PEI NPs given on GD 10. The testes and uteri of the offspring were harvested and histologically examined for abnormalities. Increased uterine and decreased seminiferous tubule epithelial linings were observed in offspring of dams given the highest dosage of NPs; no changes in fecundity were observed in any group. While no negative reproductive effects were observed at the lower dosages, exposure to a high dosage of surface charged iron oxide NPs during pregnancy may result in increased fetal death and reproductive organ abnormalities in the offspring.

PS 1712 Long-Term Effects of Low-Dose Prenatal Exposure to Endocrine Disruptors on Male Reproduction and Development

S. Jones[1, 2], A. Boisvert[1, 3], T. Duong[1, 4], S. Francois[1, 4] and M. Culty[1, 2, 4]. [1]*Research Institute of the McGill University Health Center, McGill University, Montreal, QC, Canada,* [2]*Experimental Medicine, McGill University, Montreal, QC, Canada,* [3]*Medicine, McGill University, Montreal, QC, Canada and* [4]*Pharmacology & Therapeutics, McGill University, Montreal, QC, Canada.*

Environmental exposures to endocrine disruptors (EDs) are thought to contribute to idiopathic increases in male reproductive abnormalities. Although humans are exposed to a myriad of EDs from conception through adulthood, few studies have evaluated the effects of combined exposures, while animal studies often used doses exceeding environmental levels. We hypothesized that prenatal exposure to combined low dose of the phytoestrogen genistein and the plasticizer di-(2-ethylhexyl) phthalate (DEHP) might pose a greater risk to male reproduction than individual compounds.

Pregnant Sprague Dawley dams were gavaged from gestational day 14 to birth with either corn oil, genistein, DEHP or their mixture at 10 mg/kg/day, a dose at which either compound does not cause conspicuous long term effects. Adult serum testosterone levels were unchanged. However, histological analysis revealed increased interstitial fibrosis in testes of ED-exposed adult offspring, suggestive of premature aging. Quantification of elongated spermatids and quantitative PCR analysis (qPCR) of germ cell markers indicated adult germ cell alterations in ED-exposed rats.

Gene expression arrays identified 83 up-regulated and 171 down-regulated genes ($p<0.05$) in testicular RNA from ED-treated relative to control rats, including genes with explicit ties to male reproduction, such as FOXA3, PDGFRa and HSD3B1, suggesting disrupted testis development and function. These changes were further validated by qPCR.

These results show that prenatal exposure to a mixture of unrelated EDs at environmentally relevant doses permanently disrupt testicular gene expression profiles and histology in a manner different from individual compounds, highlighting a need for more realistic and comprehensive analysis of endocrine disrupting chemicals.

PS 1713 Perinatal Exposure to an Environmentally Relevant Mixture of Brominated Flame Retardants: Developmental and Metabolic Outcomes

E. W. Tung[1], A. Kawata[1], M. Rigden[1], P. L. Lefevre[2], R. G. Berger[2], A. C. Holloway[3], B. F. Hales[2] and M. Wade[1]. [1]*Hazard Identification Division, Health Canada, Ottawa, ON, Canada,* [2]*Pharmacology and Therapeutics, McGill University, Montreal, ON, Canada and* [3]*Obstetrics and Gynecology, McMaster University, Hamilton, ON, Canada.*

Polybrominated diphenyl ethers (PBDEs) and hexabromocyclododecane (HBCD) are brominated flame retardants (BFRs) that were used extensively as additives in commercial products. PBDE toxicity is primarily associated with endocrine disruption. Recent studies suggest that PBDEs induce insulin resistance in adult animals; however, the role that PBDEs may play in altering offspring susceptibility to metabolic syndrome has not been addressed. The purpose of this study was to examine the effects of perinatal exposure to an environmentally-relevant PBDE and HBCD mixture on postnatal development. Pregnant rats were exposed to the BFR mixture pre-conception through lactation by diet (0, 0.06, 20, 60 mg/kg). Developmental and pubertal markers were monitored. Oral glucose tolerance tests were performed at postnatal (PND) 90 and 180, with additional fasting blood samples collected (PND 21, 60, 150). Insulin-sensitive tissues were weighed at necropsies. BFR exposure did not alter early developmental markers (CRL, AGD, incisor eruption,

eye opening). Onset of puberty was accelerated in females (20 mg/kg); furthermore, males exhibited delayed onset of puberty (60 mg/kg). Body weight or food consumption has not differed among treatment groups to date. However, both male and female offspring had increased liver weights at PND 21 (20 and 60 mg/kg). Moreover, male fat pad weights were significantly decreased at PND 46 (20 mg/kg). PBDE exposure did not affect fasting glucose or insulin levels, and there was no evidence of impaired glucose tolerance (AUCglucose) or insulin resistance (AUCinsulin). In conclusion, perinatal BFR exposure alters reproductive development as indicated by accelerated onset of puberty in female offspring and delayed onset in males. Decreased fat pad weights in males at PND 46 indicate that BFR exposure may have metabolic effects.

PS 1713a Reproductive and Developmental Toxicology Assessment of Oral Dietary Calcium Formate in Yucatan Miniature Swine

T. Madsen[1], A. Stricker-Krongrad[1], D. W. Hobson[2], C. Selby[1], G. P. Georges[4], R. P. Hanzlik[3], D. Brocksmith[1], J. Liu[1] and G. Bouchard[1]. *[1]Sinclair Research Center, LLC, Columbia, MO, [2]LoneStar PharmTox, LLC, Bergheim, TX, [3]University of Kansas, Lawrence, KS and [4]Nephro-Tech 1, LLC, Shawnee, KS.*

Rational: Calcium Formate (CaF) is being considered as a dietary calcium supplement. Objective: Assess the reproductive/developmental toxicity of CaF using the miniature pig model when administered orally via food consumption. Experimental Procedures: Sixty (30 male and 30 female) sexually mature Yucatan miniature swine were gender paired for breeding and randomized into 3 gps of 10 pairs receiving untreated control, low dose (2.25% CaF), and high dose (4.5% CaF) in the daily diet. Standard reproductive and developmental variables were assessed, including clinical, gross, and microscopic pathology (parents and piglets).
Results:
Female fertility index/gp ranged from 80-100%; 170 offspring were recorded; viability was good. Length of gestation, birth wts and body wt change were comparable. Litter size was robust (range 5.4-7.1) for all groups.
CaF supplementation was associated with decreased (dec.) food intake in both parents in the high dose gp and with dec. weight gain in both parents during the premating phase of the study. These between gp differences persisted through the gestational phase for the females, but there was not a statistically significant increase (inc.) in the magnitude of these differences over time.
CaF supplementation was associated with inc. in serum calcium levels in both parents. Although statistically significant, the magnitudes of these differences were small, and well within the normal physiologic ranges.
There were no findings of toxicity in the offspring related to maternal exposure to dietary CaF.
Conclusion(s): Dec. food intake, dec. weight gain during premating phase, and inc. serum calcium were associated with oral dietary CaF administration. These findings were consistent with previous research, and/or represented expected responses to the administration of oral CaF supplementation.

PS 1713b Effect of Vincamine on the Reproductive System of Harlan Sprague-Dawley Rats and B6C3F1/N Mice

I. Surh[1], B. McIntyre[1], M. J. Hoenerhoff[2], D. M. Fallacara[4], D. Y. Vasconcelos[4], M. Vallant[3] and P. Chan[1]. *[1]Toxicology Branch, National Toxicology Program, National Institute of Environmental Health Sciences, Research Triangle Park, NC, [2]Cellular & Molecular Pathology Branch, NIEHS, RTP, NC, [3]Program Operations Branch, NIEHS, RTP, NC and [4]Battelle, Columbus, OH.*

Vincamine is an alkaloid extracted from the leaves of Vinca minor. The National Toxicology Program conducted short-term/pilot toxicity studies in Harlan Sprague Dawley rats and B6C3F1/N mice. Time-mated rats were dosed up to 1000 mg/kg from gestation day (GD) 6 through GD 21. All dams in the 1000 mg/kg groups were moribund on GD 7 and exhibited implants at necropsy. Dams dosed with ≥ 30 mg/kg did not produce pups, and the majority of undelivered dams had fetal resorptions when necropsied. Dams and pups in the 10 mg/kg dosage group did not exhibit any effects attributed to vincamine. Vincamine was subsequently administered up to 300mg/kg to time-mated female rats from GD 17 to GD 21 (after the period of major organogenesis), then postnatal day (PND) 1 through PND 20. Pups were administered vincamine from PND 12 to PND 20. Vincamine was well tolerated by the dams; all dams survived to study termination, and there were no treatment related effects on littering index, duration of gestation or maternal behavior. On PND1 and 4, vincamine administration was associated with lower pup body weights (100 and 300 mg/kg) and smaller litter size (300mg/kg). Mild testicular hypoplasia, and minimal ovarian hypoplasia were observed at dose levels ≥ 100 mg/kg at necropsy on ~ 21 days of age. In mice, vincamine was administered by gavage up to 1000 mg/kg for 14 days. Morbidity and mortality was observed at 500 (females) and 1000 (males and females) mg/kg. Consistent with the rat study, the testes were a target of vincamine exposure in male mice. A dose-dependent decrease was observed in testes and epididymides weights in the 500 and 1000-mg/kg groups. Testicular necrosis in the germinal epithelium of the seminiferous tubules was noted among males exposed to dose levels ≥ 250 mg/kg of vincamine. This work was supported by the NIH.

PS 1713c Dose Addition Predicts Effects of Phthalate Mixture on Male Reproductive Tract Development and Associated Fetal Testis Gene Expression in Rats

K. L. Howdeshell[1], C. V. Rider[1], J. R. Furr[2], V. S. Wilson[2] and L. E. Gray[2]. *[1]NTP/NIEHS, RTP, NC and [2]USEPA, RTP, NC.*

A challenge in cumulative risk assessment of phthalate esters is incomplete data on individual chemicals. The objective of the current study was to test whether dose addition (DA) and relative potency factor (RPF), which is a type of DA that relies upon a reference compound, would be better predictors than response addition (RA) of the effects of a 5 phthalate mixture on fetal testis gene expression (star, cyp11a, and insulin-like hormone 3) and hormone-sensitive male reproductive tract development when assumptions were made for missing individual phthalate data. We administered a dose range of the mixture (100, 80, 60, 40, 20, 10, 5 or 0% of top dose consisting of 300 mg/kg per chemical of benzyl butyl (BBP), di(n) butyl (DBP), diethyl hexyl phthalate (DEHP), di-isobutyl phthalate (DIBP) and 100 mg dipentyl phthalate (DPP)/kg)) via gavage to rat dams on GD8-18 (fetal gene expression study) or GD8-postnatal day 3 (in vivo study); we selected the ratio of the top dose so that each phthalate contributed equally to the reduction in fetal testosterone (T) production based on estimates of their potencies from previous studies. We compared observed mixture responses to model predictions of DA, RPF, and RA based on the logistic regression analysis of the individual phthalate data using DBP or DEHP as the reference phthalates. DA predicted the inhibition of fetal gene expression at GD18, decreases in neonatal anogenital distance and adult reproductive organ weights, and induction of juvenile areolae retention and adult reproductive malformations. RPF based on fetal T production was nearly as accurate as DA, while RA was never the best model. Similar results were obtained when the observed data of the mixture were force fit to the logistic regression parameters of the models. Therefore, dose addition was a good predictor of the mixture even in the face of incomplete data on the individual phthalates. This research was partially supported by an interagency grant by the NIH, NIEHS. This abstract does not necessarily reflect USEPA policy.

PS 1713d The Effects of Triclosan on the Male Reproductive System of the Rat

T. E. Stoker, G. W. Louis and D. Hallinger. *Endocrinology Branch, US EPA, Research Triangle Park, NC.*

Triclosan (TCS), a widely used antibacterial agent, has been shown to have endocrine disrupting activity in mammals. Although the majority of these studies report that TCS alters thyroid hormones, effects on the estrogenic and androgenic pathways have also been observed. These include reports indicating anti-androgenic activity of TCS in vitro and a decrease in serum testosterone (T) concentrations in vivo. In the first study, we further examined the effect of TCS on androgenic activity in the male rat using the Hershberger assay. Six-week old castrated male rats were gavaged for 10 consecutive days with 50 or 200 mg/kg of TCS or vehicle control (corn oil) to determine the presence of any potential androgenic effects. Other groups of rats were treated with testosterone proprionate (TP) (0.2 mg/kg, sq) alone or in combination with 50 or 200 mg/kg TCS to evaluate possible anti-androgenicity or TP potentiation by TCS. On day 10, the accessory sex tissues (glans penis, Cowper's glands, levator ani bulbo cavernosus muscle complex, seminal vesicles, and ventral prostate) were weighed. TCS alone did not alter the weight of any of the tissues. Also, TCS did not alter the weight of the tissues when given in combination with TP. As expected, TCS exposure (alone or in combination with TP) resulted in a dose-dependent decrease in serum thyroxine after a 10 day exposure to 50 and 200 mg/kg TCS. In a second in vitro study, we examined the effect of TCS on T production using the H295 cell line. Forskolin and prochloraz served as positive controls producing the expected increase and decrease in T production, respectively. TCS from 0.01 to 3.0 μM did not alter T. 10 μM 0f TCS induced 20% cytotoxicity. Thus, in the present study TCS did not have androgenic or anti-androgenic activity in the Hershberger assay and was without effect on steriodogenesis in the H295 cell line. Serum T4 was significantly decreased demonstrating that the doses selected were sufficient to cause a change in this hormone. This abstract does not necessarily reflect EPA policy.

PS 1713e Effect of Oral Bisphenol A (BPA) and Ethinyl Estradiol (EE2) on Genome-Wide Gene Expression in Prostates from 4-Day-Old Rats

L. Camacho, C. Chang, M. Basavarajappa, T. Han, J. C. Fuscoe, S. Lewis, M. Vanlandingham and K. Delclos. *NCTR, FDA, Jefferson, AR.*

Bisphenol A (BPA) is an industrial chemical used in the manufacture of polycarbonate and epoxy resins. The molecular pathways potentially modulated by doses of BPA below those needed to activate the estrogenic pathway remain poorly characterized. We assessed the effect of BPA on the gene expression in prostates from 4-day-old rats, an age when the internal levels of aglycone BPA are relatively high due to an immature metabolic system. NCTR Sprague-Dawley rats were dosed daily by oral gavage from gestation day 6 until delivery and their pups were directly dosed daily from the day after birth. Dose groups included naïve and vehicle controls, seven "low" BPA doses [2.5, 8, 25, 80, 260, 840, 2,700 μg/kg body weight (bw)/day], two high BPA doses (100,000, and 300,000 μg/kg bw/day), and two doses of the reference estrogen EE2 (0.5 and 5.0 μg/kg body weight (bw)/day). Genome-wide gene expression was assessed by DNA microarray in a subset of doses, and genes of interest were validated by quantitative real-time PCR using all study doses. Principal component analysis showed that samples segregate into three sub-groups: 1) vehicle and low BPA; 2) high BPA and low EE2; and 3) high EE2. The high EE2 dose modulated the largest number of genes, followed by the low EE2 dose. Genes commonly modulated by the high BPA and EE2, which included *Dclk3*, *Gnai2*, *Gzmc*, *Map4k5*, and *Pipc*, were modulated in the same direction by both chemicals. Modulation of genes in the "low" BPA dose range was inconsistently observed across all doses, with no dose-response pattern. These data suggest that BPA doses ≤ 2,700 μg/kg bw/day have limited effects in the gene expression in the rat prostate under our experimental conditions. This is consistent with the lack of "low" BPA effects observed in other endpoints, including prostate histopathology, examined in 90-day-old siblings from the same study. IAG FDA 224-12-0003/NIH ES12013.

PS 1713f Effects of Bisphenol A (BPA) on Transcription in Male and Female Rat Mammary Glands

M. Basavarajappa, C. Chang, T. Han, J. C. Fuscoe, K. Delclos and L. Camacho. *NCTR, FDA, Jefferson, AR.*

Bisphenol A (BPA) is a common component of epoxy resins and polycarbonate plastics, used in the manufacture of food and beverage containers and medical devices. Biomonitoring studies indicate there is nearly ubiquitous exposure to BPA. The molecular pathways potentially modulated by doses of BPA below the current no-observed-adverse-effect level [NOAEL; 5 mg BPA/kg body weight (bw)/day] remain poorly characterized. In the present study, we assessed the effects of BPA on the expression level of genes encoding estrogen receptors (ER; *Esr1* and *2*), ER-related receptors (*Esrra*, *b*, and *c*), G-protein-coupled ER (*Gper*), and DNA methyltransferases (*Dnmt 1*, *3a*, and *3b*) in the mammary gland of 4-day-old male and female rats by quantitative real-time RT-PCR. In addition, DNA microarray analysis of genome-wide gene expression was performed on the female mammary glands. Pregnant NCTR Sprague-Dawley rats were dosed daily by oral gavage with vehicle control, "low" BPA (2.5, 8, 25, 80, 260, 840, or 2,700 μg/kg bw/day), "high" BPA (100,000 or 300,000 μg/kg bw/day), or ethinyl estradiol (EE2; 0.5 or 5.0 μg/kg bw/day) from gestation day 6 until parturition, and the pups daily from the day after birth until postnatal day 4. A naïve (not dosed) control was also included. Neither BPA nor EE2 significantly affected the expression of the *Esr*, *Esrr*, or *Dnmt* genes in male and female mammary glands. Microarray data in female mammary gland indicate that several known estrogen-responsive genes were modulated by EE2, including *Akr1c13*, *Apln*, *Clock*, *Il4ra*, *Ramp3*, *Serpinb9*, *Spon1*, and *Trhr2*. Genes modulated by both BPA 300,000 and EE2 (one or both doses) included *Coro1c*, *Ctrc*, *Lgals4*, and *Ntng1*. In addition, several genes were modulated at doses below NOAEL, including *Fas* (BPA 2.5), *Ak7* (BPA 25), *Rab39* (BPA 260), and *Scn1a* (BPA 2,700). The expression changes below NOAEL were observed in single BPA doses and did not show any consistent dose response pattern. Future studies will explore further the effect of BPA in the genome-wide gene expression in the male rat mammary gland. IAG FDA 224-12-0003/NIH ES12013.

PS 1713g Aflatoxin B1 Interferes with Steroidogenic Machinery to Suppress Testosterone Secretion in Rats Leydig Cells

I. A. Adedara[1, 2], M. K. Nanjappa[1], E. O. Farombi[2] and B. T. Akingbemi[1]. [1]*Department of Anatomy, Physiology, and Pharmacology, Auburn University, Auburn, AL and* [2]*Drug Metabolism and Toxicology Research Laboratories, Department of Biochemistry, University of Ibadan, Ibadan, Oyo, Nigeria.*

Aflatoxin B1, the most potent of the naturally occurring mycotoxins, is a powerful carcinogen and has been implicated in testicular dysfunction in both animals and humans. We hypothesized that AFB1 might adversely impact Leydig cells which are the primary source of testosterone production essential for good quality semen production and reproductive success. Purified Leydig cells, isolated from testes of 35-day-old Long-Evans rats, were incubated with AFB1 singly or in combination with MAPK inhibitors. The data from radioimmunoassay and western blot analysis demonstrated that AFB1 significantly decreased both Leydig cells basal and LH-stimulated testosterone secretion. AFB1 significantly down-regulated steroidogenic acute regulatory protein (StAR), 3β hydroxysteroid dehydrogenase (3β-HSD), 17β-hydroxysteroid dehydrogenase enzyme (HSD17B3) but up-regulated cytochrome P450 side chain cleavage enzyme (CYP11A1) expression. AFB1-induced testosterone decrease was mediated by androgen receptor (AR) and insulin-like growth factor 1 receptor-beta (IGFR1B). AFB1 treatment increased ERK activation but decreased the activation of JNK and p38 MAPK. AFB1-induced decrease in testosterone secretion was attenuated by UO126 only. AFB1 did not affect luteinizing hormone receptor (LHR), estrogen receptor (ESR1), epidermal growth factor receptor (EGFR) and CYP17A1 expression. Taken together, AFB1 suppresses testosterone biosynthesis by interference with steroidogenic machinery in rat Leydig cells.
Keywords: Aflatoxin B1, Leydig cells, Testosterone, Rats.

PS 1713h Effect of Neonatal Exposure to Decabromodiphenyl Ether on Transcript Levels of Thyroid Hormone Receptor α and Androgen Receptor in Mouse Sertoli Cells

H. Miyaso[1, 3], N. Nakamura[2], Y. Matsuno[1, 3] and C. Mori[1, 3]. [1]*Center for Preventive Medical Science, Chiba University, Chiba, Japan,* [2]*Department of Pharmacology, Physiology and Toxicology, Food and Drug Administration, Jefferson, AR and* [3]*Department of Bioenvironmental Medicine, Graduate School of Medicine, Chiba University, Chiba, Japan.*

Decabrominated diphenyl ether (decaBDE) is one of flame retardants and is used in worldwide. Our previous study found postnatal exposure to decaBDE had adverse effect to male reproduction in mice. Mice were injected subcutaneously 0.025, 0.25, and 2.5 mg/kg decaBDE during postnatal day 1-5 and evaluated at 12 weeks of age. We identified that the transcript levels of thyroid hormone receptor α (Thra) decreased significantly in testes of 0.025 mg/kg decaBDE dose group, while no change of thyroid hormone (TH) levels was observed between control and all dose groups. In addition, our data showed that the transcript level of androgen receptor (Ar) in testes and the number of spermatozoa in epididymides also decreased significantly in 0.025 mg/kg decaBDE dose group. It has been reported that TH function is important for induction of Ar in Sertoli cells and that AR is necessary for production of spermatozoa, therefore it is suggested that decaBDE affect the transcript levels of Thra and Ar in Sertoli cells. To clarify this hypothesis, neonatal ICR male mice were injected with decaBDE by above described method and testes were collected at 12 weeks of age. Total RNA was extracted from isolated Sertoli cells and the transcript levels of Thra and Ar were evaluated by real-time RT PCR. Our data showed the decrease in transcript level of Thra in 0.025 mg/kg dose group compared to the control group. Moreover transcript level of Ar also decreased in 0.025 mg/kg dose groups. Our study suggests that postnatal exposure to decaBDE causes decreased transcript levels of Thra and Ar in Sertoli cells and results in decreased number of spermatozoa.

PS 1713i The microRNAs Pathway in Mechanism of Crude Oil-/Dispersant-Induced Reproductive Toxicity

X. Pan, Y. Zhang and J. R. Polli. *Biology, East Carolina University, Greenville, NC.*

Lines of evidence have demonstrated that dispersed oil affects reproduction, in a more potent manner than oil- and dispersant-alone exposures. However, the action mechanism of dispersed oil remains largely unknown. In this study, the model organism *Caenorhabditis elegans* (*C. elegans*) were employed to investigate impacts of crude oil/-dispersant exposures on sex cell development and underlying microRNA (miRNA)-mediated mechanisms. Worms were exposed to different diluted levels of crude oil-dispersant mixtures (20:1, v/v; at 500 ×, 2000 ×, and 5000 × dilutions) and same levels of oil-alone and dispersant-alone treatments. Histological results

show that the dispersed crude oil significantly increases the number of apoptotic cells and diploid sperms (immature) in treated worms' gonad when compared to controls at all exposure levels ($p < 0.05$). Genes involved in the apoptosis pathway were disregulated, which include ced-13, ced-3, ced-4, ced-9, cep-1, dpl-1, efl-1, efl-2, egl-1, egl-38, lin-35, pax-2, and sir-2.1. Given cep-1/p53 was activated at all dispersed oil treatments and the germ cell apoptosis was suppressed in the CEP-1 loss of function mutant, the increased apoptosis is likely CEP-1 dependent. A total of 231 microRNAs expressions were analyzed using quantitative real-time PCR; 59 miRNAs were up-regulated, while 82 were down-regulated. Heatmap clustering indicates that dispersed oil displayed a distinct miRNA expression profile compared to control, oil-alone, and dispersant-alone treatments. The gene targets and functions of miRNAs were analyzed using bioinformatics tools (TargetScan, miRanda, and KEGG). A variety of reproduction related pathways were found to be regulated by oil-dispersant affected miRNAs, including MAPK signaling pathway, Wnt signaling pathway, Hedgehog signaling pathway, and Oocyte maturation pathway, etc. This study provides mechanism understandings of crude oil/-dispersant induced reproductive toxicity.

PS 1713j High-Content Screen and Mechanistic Study of Environmental Reproductive Toxins in *C. elegans*

D. A. Parodi[1] and P. Allard[1, 2]. [1]*ISG, UCLA, Los Angeles, CA and* [2]*EHS, UCLA, Los Angeles, CA.*

Chemicals play an integral part of our everyday life despite their significant impact on human health and the environment. Global chemical production is doubling every 25 years, rapidly outpacing population growth, increasing both in volume and in the variety of the compounds released in the environment each year. Over the past several decades, the contribution of environmental exposures to the etiology of reproductive health effects of exposures has become an increasing cause for concern. However, there is tremendous difficulty in assessing safety of these chemicals due to their large number and also from the complexity of biological effects they elicit over a large range of doses. Here, I address these issues by using the genetic model system, the worm *Caenorhabditis elegans* in two ways. First, I aim to identify reprotoxic chemicals by screening chemicals for their ability to disrupt meiosis and induce aneuploidy in *C. elegans*. For this purpose, I developed a 384-well plate high-content microscopy assay that can accurately detect the induction of aneuploidy based on the emission of GFP fluorescence in aneuploid embryos (Allard et al, 2013). This assay will be used to screen ToxCast Phase I and II environmental chemical libraries and to identify a list of compounds with high aneugenicity. Second, a molecular and cellular mechanistic follow-up analysis of hits will be performed. Preliminary work indicates that worms exposed to 100uM Maneb, Feranimol or Diazinon show a significant induction in the number of germline apoptotic nuclei (2.7, 2.6 and 3.3-fold induction, respectively. $p<0.05$) and an increase in reduced nuclear density (2.8, 2.6 and 2.4-fold induction, respectively. $p<0.05$), suggesting that these compounds are potent reproductive toxicants causing germline maintenance disruption and acute germ cell death.
Together, these studies aim at developing unique methods to interrogate our chemical environment for its effect on germline maintenance and health.

PS 1713k Cross-Species Evaluation of Endocrine Disrupting Effects of Lead (Pb) on Maturation and Development

E. P. Hines, L. Vinikoor-Imler and M. G. Lassiter. *EMAG, NCEA, US EPA, Research Triangle Park, NC.*

In a cross-species evaluation conducted in support of the review of the US EPA National Ambient Air Quality Standards (NAAQS) for Lead (Pb), findings from epidemiologic, toxicological and ecological disciplines were used in a weight of evidence approach to evaluate reproductive and developmental effects of this metal, including endpoints associated with endocrine disruption. In the process of synthesizing information on reproductive effects of Pb for the 2013 Integrated Science Assessment for Lead (ISA), we noted that Pb is associated with maturational delays (e.g. puberty onset, developmental duration, life cycle length, metamorphosis) across a wide variety of organisms. A causal association between Pb exposure and developmental and reproductive endpoints for both human health and ecological receptors was reported. Moving beyond the synthesis conducted for the Pb ISA, we have reviewed the literature on changes in timing of developmental milestones associated with exposure to Pb. Evidence from multiple species points to an underlying common mode of action of Pb on the insulin-like growth factor signaling pathway; inhibin B was also affected in vertebrate models of Pb exposure. An interdisciplinary cross-species approach provided insights into endocrine disruption by Pb and a possible mode of action of this metal. Increased time to sexual maturation or delayed development may have consequences for reproduction and development across a broad range of species.

The views expressed in this poster are those of the authors and do not necessarily represent the views or policies of the U.S. Environmental Protection Agency.

PS 1713l Dual Role of microRNA-31 in 2, 3, 7, 8-Tetrachlorodibenzo-*p*-dioxin(TCDD)-Mediated Upregulation of CYP1A1 and FoxP3 in Activated T Cells

P. Mehrpouya, P. S. Nagarkatti and M. Nagarkatti. *Pathology, Microbiology and Immunology, University of South Carolina School of Medicine, Columbia, SC.*

TCDD, an environmental contaminant, is well known for inducing severe toxicity including immunosuppression. We examined the mechanisms by which TCDD affects T cell response to Staphylococcal enterotoxin B (SEB) and Pertussis Toxin (PTX). SEB, a superantigen, activates ~20% of T cells via Vβ8 T cell receptor and causes a robust release of pro-inflammatory cytokines. Pertussis Toxin promotes the generation of IL-17-producing CD4+ cells by inducing IL-6. We injected C57BL/6 mice with either SEB or PTX, and treated them with either vehicle or TCDD. Our studies showed that TCDD treatment of SEB-activated lymphocytes led to a decrease in Vβ8+ T cells. TCDD treatment of PTX-activated lymphocytes dampened Th17 cells while promoting FoxP3+ Tregs. TCDD also induced apoptosis in activated T cells, suppressed pro-inflammatory cytokines, IFN-γ, TNF-α and IL-6, and induced anti-inflammatory cytokine, IL-10. In order to determine the role of microRNA (miR) in TCDD-induced immune dysregulation, we performed high throughput miR analysis. In silico analysis demonstrated that miRs induced by TCDD regulated several pathways including induction of apoptosis, AhR signaling and Treg differentiation. Interestingly, miR-31 which was down regulated following TCDD treatment was found to be complementary to both the 3'-UTR of Foxp3 and CYP1A1 genes, which was validated by RT-PCR. Furthermore, miR-455 against ARNT target gene was also down-regulated in TCDD treated groups. In addition, miR-21 which targets the pro-apoptotic targets, Fas and FasL was down-regulated by TCDD, which correlated with the ability of TCDD to induce apoptosis. Together, our studies demonstrate that TCDD-mediated immune regulation may be mediated by altered expression of several microRNAs (Supported by NIH grants P01AT003961, P20 RR032684, R01AT006888, R01ES019313, R01MH094755 and VA Merit Award BX001357)

PS 1713m Relationship between Allergic Characteristics of Swine Husbandry Workers and Endotoxin Level in Swine Farm Dust

H. Kim[2], Y. Heo[1], K. Shin[1], J. Jo[1] and K. Roque[1]. [1]*Occupational Health, Catholic University of Daegu, Gyeongsan si, Republic of Korea and* [2]*Preventive Medicine, The Catholic University of Korea, Seoul, Republic of Korea.*

Animal husbandry workers could be exposed to various work hazards including toxic gases, chemicals, and endotoxin. Immunological evaluation on allergic hypersensitivity occurrence was undertaken for swine farm workers. Relationship between endotoxin level in dust collected from swine farms and immunological markers related with respiratory allergy was evaluated. Peripheral blood samples were collected from 10 workers at 10 swine farms in Korea. PBMCs were stimulated with PMA and ionomycin for 48 hours. The levels of cytokines at culture supernatants were determined using a ELISA kit. The concentration of particulate matter (PM10) in the indoor air of the swine farms was evaluated using a PVC membrane filter and mini volume air sampler, and endotoxin levels in the dust were measured by Limulus Amebocyte Lysate Kinetic QCL method. Levels of endotoxins in total dust were categorized into high (GM:109.35 EU/m^3) and low concentrations (GM:0.95 EU/m^3) for 5 swine farms, respectively. IL-4 levels were higher in the high endotoxin group than the low endotoxin group, while interferon-γ levels were lower in the high endotoxin group than the low endotoxin group. The ratio (IFNγ to IL-4) was lower in the high endotoxin group (1.15±0.60) than the low endotoxin group (3.09±2.38).The level of IL-13 was significantly higher in the high endotoxin group (1.12±0.37 ng/ml) than the low endotoxin group (0.37±0.04 ng/ml). Plasma IgE levels were five times higher in the swine farm workers than the seven control subjects not involved with animal husbandry at the same residential area as the swine farm workers. The house dust mite (*Dermatophagoides farinae, D. pteronyssinus*) and cockroach were the major respiratory allergens for swine farm workers.This study suggests that the immunological function of swine farm workers exposed to high level of endotoxin could be modulated toward allergic reactivities. [supported from Korean Rural Development Agency, PJ008678]

PS 1713n Glucose and Insulin Mediated Alteration in Metabolic Activity of U937 Cells

A. Engin, B. Karahalil and E. Coskun. *Department of Toxicology, Gazi University, Faculty of Pharmacy, Ankara, Turkey.*

By 2030, it is estimated that the number of people with diabetes will be more than 82 million in developing countries and more than 48 million in developed countries. In type 2 diabetes, insulin resistance and metabolic syndrome are associated with persistant hyperglysemia and chronic inflammation due to the macrophage activation by impaired glucose retention. Enhanced reactive oxygen production, increased modification in ligands and disruption in insulin signaling pathway are the main courses in the development of diabetic complications. The aim of our study is to evaluate the alteration in the metabolic activity of U937 human monocytic cell line by glucose and insulin. U937 cells were incubated with or without insulin (10 μU/ml – 60 μU/ml) and with various glucose concentrations (50 mg/dl – 500 mg/dl) that were determined due to the blood glucose levels of International diabetes classification. Metabolic activity of U937 cells were significantly increased in hypoglycemic conditions with 60 μU/ml insulin at 48 hours. However, higher glucose in combination with high insulin concentrations significantly decreased metabolic activity of the monocytic cells at 72 hours. These results indicate that chronic exposure to high glucose due to uncontrolled diabetes may alter the immune response realted to the changes in the metabolic activity of the immune system cells.
Acknowledgement: This study was supported by Gazi University, Scientific Research Projects Division, 02/2011-32.

PS 1713o Ascorbic Acid Improves Hyperoxia-Compromised Host Defense against *Pseudomonas aeruginosa* Infection in Mice

V. S. Patel[1], V. Sampat[1], M. Espey[3], H. Wang[2] and L. Mantell[1, 2]. [1]*Department of Pharmaceutical Sciences, St. John's University College of Pharmacy and Health Sciences, Jamaica, NY,* [2]*Centers for Inflammation and Immunology, The Feinstein Institute for Medical Research, North Shore-LIJ Health Science, Manhasset, NY and* [3]*National Institutes of Health, Bethesda, MD.*

Oxygen therapy using high concentrations of oxygen (hyperoxia) is associated with compromised host defense and greater susceptibility to bacterial infections, causing ventilator-associated pneumonia (VAP). Hyperoxia-induced excessive ROS production and accumulation of extracellular HMGB1 play critical roles in impairing macrophage's ability to phagocytose. Ascorbic acid (AA), an antioxidant, exhibits beneficial effects in various ROS-mediated diseases. The aim of this study was to determine whether AA could improve hyperoxia-compromised host defense and macrophage functions. C57BL/6 male mice were exposed to hyperoxia (≥99% O_2, 48 h) followed by intratracheal inoculation with *Pseudomonas aeruginosa*, and simultaneously treated with different concentrations of AA. RAW 264.7 cells (a macrophage like cell line) were also exposed to different concentrations of AA prior to 95% O_2 exposure, ROS levels, phagocytic activities and extracellular HMGB1 accumulation were analyzed. AA effectively improved bacterial clearance in lungs and airways of the mice. It significantly rescued the hyperoxia-compromised macrophage function of phagocytosis. Improved phagocytic activity was accompanied by reduced ROS levels as well as decreased accumulation of extracellular HMGB1. Our study demonstrates that AA, a cost-effective dietary supplement, could provide a rewarding aid in prevention and treatment of VAP.

PS 1713p Immunotoxicity of Sodium Methyldithiocarbamate: Potential Connections of Disparate Effects

W. Tan, B. Nanduri, X. Deng and S. B. Pruett. *Basic Sciences, Mississippi State University, Mississippi State, MS.*

Sodium methyldiothiocarbamate (SMD) is the third most abundantly used conventional pesticide in the U.S. We have previously reported mechanisms its immunotoxic effects, but we have not previously reported a comprehensive description of the effects of this compound on gene expression and host resistance in a mouse model. These effects are reported here, and they indicate that oral exposure to the compound and relatively high dosages (100-300 mg/kg) causes substantial decreases in innate immune and inflammatory responses to bacterial lipopolysaccharide (from *Escherichia coli*) or to viable bacteria. A series of SMD dosages most potently inhibited expression of genes related to interferon response and production pathways. These results suggested that the action of a strong interferon inducer might be inhibited to a greater extent than the action of a stimulus such as LPS or whole bacteria. Thus, polyinosinic-polycytidylic acid (poly I:C), the major ligand for TLR3 was investigated, and SMD was found to inhibit cytokine and chemokine induction by this compound at dosages as low as 10 mg/kg, which are substantially lower than required for inhibition of these responses by LPS or whole bacteria. Although, we have previously shown that SMD decreases survival in an *E. coli* model of sepsis, inhalation or dermal exposure are more likely routes for human exposure to SMD. We report here that inhalation of SMD or its major breakdown product (methylisothiocyanate) did not significantly decrease survival. However, survival was decreased by oral administration of SMD. The results indicate that survival in mice treated by inhalation was associated with rapid recovery of initial inhibition of decreased bacterial killing in phagocytic cells and decreased production of cytokines or chemokines. We now hypothesize that the effects of SMD on lethal outcome in sepsis on and TLR3 responses are related and that fully understanding this will also suggest reasons for differences in effects of dosage routes. This work was supported by a grant from NIEHS (R01ES01370803).

PS 1713q Immunotoxicity Profile following Exposure to Silt Deposit Dust Samples from Nellis Dunes Recreational Area, Clark County, Nevada

L. Murphy[1], W. B. David[2], R. M. Chow[2], M. Leetham-Spencer[1], M. Jensen[1], B. J. Buck[4], D. Goossens[4], Y. Teng[4], L. Gryder[3], S. Young[3], N. Walters[1], D. E. Keil[1], M. M. Peden-Adams[2] and J. C. Dewitt[5]. [1]*Microbiology, MSU, Bozeman, MT,* [2]*Harry Reid Center for Env. Studies, UNLV, Las Vegas, NV,* [3]*Anthropology, UNLV, Las Vegas, NV,* [4]*Geoscience, UNLV, Las Vegas, NV and* [5]*Pharmacology and Toxicology, ECU, Greenville, NC.*

The Nellis Dunes Recreation Area (NDRA) is a popular region for off-road vehicle driving that attracts over 300,000 commercial and personal riders each year. Trace metals that could potentially affect human health have been measured in soil and airborne dust samples. Map unit CBN7 is composed of aggregated silt deposits commonly found in badlands without rock or vegetative cover. Dust samples from CBN7 with a median grain size of 4.37μm were analyzed via inductively coupled plasma mass spectrometry (ICP-MS) and contained: 293.63 ppm Mn, 248.23 ppm Sr, 49.49 ppm Cr, 26.20 ppm Pb, and 23.51 ppm of As. B673CF1 female mice were exposed via oropharyngeal aspiration at doses of 0.01, 0.1, 1, 10, and 100 mg geological sample/kg/day at four intervals, each a week apart. No dose-responsive changes were observed in body or organ weights. Serum total bilirubin was dose-responsively increased beginning at 0.1 mg/kg/day. Serum creatinine levels were increased at 10 and 100 mg/kg/day whereas blood urea nitrogen was dose-responsively decreased beginning at 0.1 mg/kg/day. Blood neutrophil and lymphocyte numbers were increased at 10 and 100 mg/kg/day. Splenic CD8+ and CD4+/CD8+ T-cells were decreased; however, this was not clearly dose-responsive. No significant changes were detected in splenic B220 or thymic CD4/CD8. IgM antibody production was dose-responsively suppressed beginning at 0.1 mg/kg/day with an ED50 of 0.30 mg/kg/day. The LOAEL was 0.1 mg/kg/day whereas the NOAEL was 0.01 mg/kg/day as demonstrated by antigen-specific IgM production. Further studies will assess the potential health risks associated with recreation at this site.

PS 1713r Immunotoxicity Profile following Exposure to Geological Dust Samples Collected from Nellis Dunes Recreational Area Map Unit CBN2: Median Grain Size 4.5 μm

M. Leetham-Spencer[1], J. C. Dewitt[4], M. M. Peden-Adams[2], R. M. Chow[2], W. B. David[2], L. T. Murphy[1], M. Jensen[1], N. Walters[1], L. Gryder[3], B. J. Buck[5], D. Goossens[5], Y. Teng[5], S. Young[3] and D. E. Keil[1]. [1]*Microbiology, Montana State University, Bozeman, MT,* [2]*Harry Reid Center, University of Nevada, Las Vegas, NV,* [3]*Anthropology, University of Nevada, Las Vegas, NV,* [4]*Pharmacology and Toxicology, East Carolina University, Greenville, NC and* [5]*Geoscience, University of Nevada, Las Vegas, NV.*

Nellis Dunes Recreational Area (NDRA) is a highly popular ORV area near Las Vegas, NV. Soil and airborne dust in this area are rich in naturally occurring arsenic. This presentation focuses on data from CBN2, which is a yellow silt and clay unit mostly barren of vegetation. Dust samples with a median grain size of 4.5 μm were analyzed for total elemental composition via inductivity coupled plasma mass spectrometry. The following concentrations were found: As:136.82 ppm; Cr:38.74 ppm; Pb:22.71 ppm; Mn: 386.28 ppm; and Sr:424.89 ppm. B6C3F1 female mice were exposed to dust via oropharyngeal aspiration at doses of 0.01, 0.1, 1, 10, and 100 mg geological sample/kg body weight/day and a PBS control at four intervals, each seven days apart. After the exposure period, immunotoxicological assays were performed on secondary lymphoid tissues and blood was evaluated for clinical chemistry parameters and markers of oxidative stress. All comparisons were made to the control group. Across all doses, thymic CD4/CD8 subpopulations were decreased. Serum creatinine was dose responsively increased beginning at 1.0 mg/kg/day whereas blood urea nitrogen decreased at 10 and 100 mg/kg/day. Serum total bilirubin was increased at 100 mg/kg/day. No changes were seen in SOD, ROS, total glutathione, and total antioxidant capacity oxidative stress markers. Antigen specific IgM antibody production was dose responsively suppressed beginning at 0.1 mg/kg/day with an ED50 of 0.03 mg/kg/day. A LOAEL of 0.1 mg/kg/day and

a NOAEL of 0.01 mg/kg/day were determined from IgM antibody production. These, and additional data, will support an assessment of the potential health risk to people who recreate at the Nellis Dunes site.

PS 1713s Reducing Immunogenicity in a T Cell-Dependent Antibody Response (TDAR) in Cynomolgus Monkeys Leads to a Sensitive Assessment of Immunosuppression by Abatacept (CTLA4-Ig)

G. Bannish[2], M. S. Perpetua[1], A. J. Beavis[1], B. Fraszczyk[1], S. Harvey[1], T. Ziegelhofer[3], J. Doughty[1] and L. A. Coney[2]. *[1]Biomarkers, Bioanalysis, and Clinical Sciences, Huntingdon Life Sciences, East Millstone, NJ, [2]Biologics, Huntingdon Life Sciences, Huntingdon, Cambridgeshire, United Kingdom and [3]Cardiology/Infusion Technology, Huntingdon Life Sciences, East Millstone, NJ.*

The TDAR response is used to evaluate drug effects on the immune system, assessing antigen presentation and T and B lymphocyte function. Cynomolgus monkeys injected subcutaneously on 5 occasions over 15 days with 1 mg Keyhole Limpet Hemocyanin (KLH) in Incomplete Freund's Adjuvant (IFA) developed a robust IgM and IgG antibody response to KLH. Treatment of animals twice weekly with 8 mg/mL/kg Abatacept (CTLA4-Ig) by intravenous slow bolus injection did not diminish the antibody response. In a separate study, animals were injected with 100 ug KLH in the absence of adjuvant via intradermal injections. These animals developed a detectable IgM response with inverse titers of 25,000 ten days following primary immunization. IgG responses were detectable 14 days post primary injection with inverse titers of 12,000, and 7 days post secondary challenge with inverse titers of over 50,000. Treatment of a cohort of these animals with Abatacept led to an ablation of antibody responses. Antibody responses to KLH from animals were reduced but not ablated when treated with 1 mg/kg methotrexate via subcutaneous injection. Maximal mean IgM responses to KLH 10 days following primary immunization were reduced from 120,000 to 34,000. Maximal mean IgG responses to KLH were reduced from 1 x 10^6 to 0.66 x 10^6 with maximal responses delayed from 7 to 10 days post secondary KLH challenge. Combined, these data determine that excessive antigenic stimulation can overcome the immunosuppressive effects of Abatacept and define an alternate immunization strategy that is susceptible to immunosuppression. Utilizing an appropriate immunization strategy in TDAR assays and including biological immunosuppressant controls, this model is optimized for safety assessment of immunomodulatory biological drug products.

PS 1713t Sulforaphane Inhibits Vascular Inflammation in Mice and Prevents TNF-alpha-Induced Monocyte Adhesion to Primary Endothelial Cells through Interfering with the NF-κB Pathway

P. Nallasamy[1], H. Shah[1], E. Brooke[1], H. Zhu[2], Y. Li[2] and Z. Jia[1]. *[1]University of North Carolina at Greensboro, Greensboro, NC and [2]Campbell University School of Osteopathic Medicine, Buies Creek, NC.*

Tumor necrosis factor alpha (TNF-α) is a critical cytokine that plays important role in regulation of the toxic effects of a variety of chemicals and toxicants. Sulforaphane, a naturally-occurring isothiocyanate present in cruciferous vegetables, has received wide attention for its potential to improve vascular function in vitro. . However, its effect in vivo and the molecular mechanism of sulforaphane at physiological concentrations remain unclear. Here, we report that a sulforaphane concentration as low as 0.5 μM significantly inhibited TNF-α-induced adhesion of monocytes to human umbilical vein endothelial cells (HUVECs). Sulforaphane also significantly suppressed TNF-α-induced production of adhesion molecules. Furthermore, sulforaphane inhibited TNF-α-induced NF-κB transcriptional activity, IκBα degradation and subsequent NF-κB p65 nuclear translocation in endothelial cells, suggesting that sulforaphane can inhibit inflammation by suppressing NF-κB signaling. In an animal study, the physiologically-relevant dose of sulforaphane (300 ppm) in a mouse diet significantly abolished TNF-α-increased ex vivo monocyte adhesion and circulating adhesion molecules and chemokines in C57BL/6 mice. Histology showed that sulforaphane treatment significantly prevented the eruption of endothelial lining in the intima layer of the aorta and preserved elastin fibers' delicate organization as shown by Verhoeff-van Gieson staining. Immunohistochemistry studies showed that sulforaphane treatment also reduced VCAM-1 and monocytes-derived F4/80-positive macrophages in the aorta of TNF-α-treated mice. In conclusion, sulforaphane at physiological concentrations protects against TNF-α-induced vascular endothelial inflammation, in both in vitro and in vivo models. This anti-inflammatory effect of sulforaphane may be, at least in part, associated with interfering with the NF-κB pathway.

PS 1713u Pulmonary Toxicity and Global Gene Expression Changes in Response to Subchronic Inhalation Exposure to Crystalline Silica in Rats

P. Joseph, R. Sellamuthu, J. R. Roberts, S. Young, D. Richardson, W. McKinney, B. T. Chen, D. G. Frazer, J. Gu, M. L. Kashon and C. Umbright. *NIOSH, Morgantown, WV.*

Exposure to crystalline silica results in serious health effects, most notably, silicosis and cancer. An understanding of the mechanism(s) underlying the silica-induced pulmonary toxicity is critical for the intervention and/or prevention of adverse health effects. Rats were exposed by inhalation to silica at a concentration of 15 mg/m3, 6 hours/day, 5 days/week for 3, 6 or 12 weeks. Pulmonary toxicity and global gene expression changes were determined in the lungs of the control (air) and silica exposed rats at the end of each exposure period. Pulmonary toxicity, as evidenced by an increase in lactate dehydrogenase activity and accumulation of alveolar macrophages and infiltrating neutrophils in the bronchoalveolar lavage fluid, was seen in the rats depending on the silica exposure duration. The most severe histological changes, seen in the 12-week exposure group, consisted of chronic active inflammation, type II pneumocyte hyperplasia, and fibrosis. In addition, silica was visible in the lungs of the rats belonging to the 12-week exposure group. A significant increase in the number of neutrophils seen in the blood indicated silica-induced systemic inflammation in the rats. Microarray analysis of the global gene expression profiles of the lungs detected significant differential expression (FDR p <0.05 and fold change >1.5) of 38, 77 and 99 genes in the rats exposed to silica for 3-, 6- and 12-weeks, respectively, compared to the time-matched controls. Bioinformatics analysis of the differentially expressed genes identified significant enrichment of functions, networks and pathways related to inflammation, cancer, oxidative stress, fibrosis and tissue remodeling in the lungs of the silica exposed rats. Collectively, the results of our study provided insights into the molecular mechanisms underlying pulmonary toxicity following sub-chronic exposure to crystalline silica in rats.

PS 1714 Regulation of Covalent Modification of 2-Tert-Butyl-1, 4-Benzoquinone to Keap1 through Glutathione-Mediated *S*-Transarylation

Y. Abiko[1, 2] and Y. Kumagai[1]. *[1]Graduate School of Comprehensive Human Sciences, University of Tsukuba, Ibaraki, Japan and [2]Research Fellow of the Japan Society for the Promotion of Science, Tokyo, Japan.*

Butylated hydroxyanisole is a phenolic antioxidant and classified class-2B carcinogen. It is readily undergoes *O*-dealkylation to produce 2-*tert*-butyl-1,4-hydroquinone (TBHQ), which readily auto-oxidizes to the electrophlic metabolite 2-*tert*-butyl-1,4-benzoquinone (TBQ). TBQ causes activation of transcription factor Nrf2 copled to *S*-arylation of its negative regulator Keap1 through thiols with low p*Ka* values (Abiko Y et al., Toxicol Appl Pharmacol 255: 32-39, 2011). In a previous study, we found that glyceraldehyde-3-phosphate dehydrogenase (GAPDH) covalently modified with 1,2-naphthoquinone (1,2-NQ) undergoes *S*-transarylation by glutathione (GSH), resulting in a recovery of GAPDH activity through removal of the 1,2-NQ from modified GAPDH and a concomitant formation of a 1,2-NQH2-SG that readily oxidizes to 1,2-NQ-SG (Miura T et al., Chem Res Toxicol 24: 1836-1844, 2011). In the present study, we explored the possibility of GSH-dependent *S*-transarylation of Keap1-TBQ adduct. Pretreatment with L-buthionine-(*S,R*)-sulfoximine, a specific inhibitor for GSH synthesis, prior to TBQ exposure of HepG2 cells suggested that the Keap1-TBQ adduct appears to undergo GSH-mediated *S*-transarylation because the depletion of GSH in the cells affected Nrf2 activation and up-regulation of its downstream protein such as heme oxygenase-1 caused by TBQ. Supporting this, a cell-free study demonstrated that TBQ covalently bound to Keap1 with low p*Ka* thiols undergoes nucleophilic attack by GSH with a p*Ka* value of 9.12, thereby eventually eliminating Keap1 and forming GSH adducts of TB(H)Q such as TBHQ-SG, TBHQ-diSG, and TBQ-diSG as determined by LC-MS/MS analysis. These results suggest that cellular GSH plays a role in the reversible covalent modification of TBQ to Keap1 (Abiko Y and Kumagai Y., Chem Res Toxicol 26: 1080-1087, 2013).

PS 1715 An Imaging-Based RNAi Screen Identifies Novel Regulators of Nrf2 Activation

S. Hiemstra, B. Herpers, M. Niemeijer, S. Wink and B. van de Water. *Toxicology, LACDR, Leiden, Netherlands.*

Reactive oxygen species (ROS) are major inducers of cellular stress and cell death. The anti-oxidant response pathway is therefore a key mechanism in protecting cells against ROS-mediated toxicity. The transcription factor Nrf2 is a critical regulator of the antioxidant response pathway and fundamental in cytoprotection. The activity of Nrf2 is controlled through KEAP1-mediated ubiquitination and

subsequent proteasomal degradation. Moreover, various kinases can phosphorylate Nrf2 thereby affecting its stability. Accumulated Nrf2 translocates to the nucleus targeting the expression of multitude of anti-oxidant target genes, such as Srxn1. The entire signaling network that controls Nrf2 stability and functionality is so far unclear. To monitor the KEAP1/Nrf2/Srxn1 signaling pathway we apply live cell imaging and tagging these target genes with GFP using BAC recombineering. Using high throughput confocal imaging we can quantify the dynamics of Nrf2 activation and established the concentration time course dynamics of Nrf2 activation by, amongst others, iodoacetamide and CDDO-me. In order to provide full understanding of the upstream regulators of the Nrf2 pathway, we applied a siRNA knock-down based screen using the GFP-Srxn1 reporter as a downstream target of Nrf2. We screened all individual kinases, phosphatases, ubiquitinases and transcription factors for their involvement in Nrf2 activation. After knock-down, CDDO-me was used to activate Nrf2 followed by quantification of Srxn1-GFP expression. We observed ~50 target genes that enhance Srxn1-GFP expression and ~35 target genes that inhibit Srxn1-GFP expression after CDDO-me treatment, including both known and novel modulators. Pathway analysis was performed to identify the signaling networks that control Nrf2 activity. Individual hits were validated using alternative strategies to activate Nrf2 and there involvement in cytotoxicity was evaluated. This work contributes to more elaborate understanding of the signaling networks that control Nrf2 signaling in the context of xenobiotic-induced cytotoxicities.

PS 1716 Ambient Vapor Samples Activate the Nrf2-ARE Pathway but Not an Inflammatory Response in Human Bronchial Epithelial BEAS-2B Cells

Y. Shinkai[1, 2], S. Nakajima[2], A. Eiguren-Fernandez[3], E. Stefano[3], D. A. Schmitz[3], J. R. Froines[3], A. K. Cho[3] and Y. Kumagai[1, 2]. [1]*Faculty of Medicine, University of Tsukuba, Tsukuba, Ibaraki, Japan,* [2]*Graduate School of Life and Environmental Sciences, University of Tsukuba, Tsukuba, Ibaraki, Japan and* [3]*Southern California Particle Center, University of California Los Angeles, Los Angeles, CA.*

Ambient air pollutants have been reported to induce oxidative stress based inflammatory responses in humans and experimental animals. However, most of these reports describe the actions of the particulate phase of ambient and exhaust samples. We describe here results of studies investigating the actions of the vapor phase of ambient air samples collected in the midtown area of Los Angeles on human bronchial epithelial BEAS-2B cells using DNA microarray analysis. Among 26 genes whose expression increased fourfold or more, four genes were associated with detoxifying genes regulated by the transcription factor Nrf2. Consistent with these results, the vapor samples activate the Nrf2-ARE pathway, resulting in up-regulation of heme oxygenase-1 (HO-1), glutamate cysteine ligase modifier subunit, and cystine transporter (xCT) mRNA and proteins. No appreciable increases in pro-inflammatory genes were observed. These results suggest that ambient vapor samples activate the Nrf2-ARE pathway but not an inflammatory response. Also, treatment of the vapor samples with glutathione resulted in reduction in the Nrf2 activation and HO-1 induction, suggesting that electrophiles in vapor samples contribute to this Nrf2-dependent antioxidant or adaptive response.
[Reference] Shinkai Y et al., Environ Toxicol, 2013, in press

PS 1717 Proteomics Analysis to Identify Sensor Proteins with Covalent Modification Associated with 1, 4-Naphthoquinone-Induced Activation of Electrophilic Signal Transduction Pathways

R. Hirose[1], T. Miura[2], R. Sha[3], Y. Shinkai[1, 2], T. Tanaka-Kagawa[4] and Y. Kumagai[1, 2]. [1]*Environmental Biology Lab, Faculty of Medicine, University of Tsukuba, Tsukuba, Ibaraki, Japan,* [2]*Graduate School of Comprehensive Human Sciences, University of Tsukuba, Tsukuba, Ibaraki, Japan,* [3]*Leading Graduate School Doctoral Program, University of Tsukuba, Tsukuba, Ibaraki, Japan and* [4]*Division of Environmental Chemistry, National Institute of Health Sciences, Tokyo, Tokyo, Japan.*

While metabolic activation of naphthalene, yielding 1,2-naphthoquinone (1,2-NQ) and 1,4-NQ that can covalently bind to cellular proteins, has been recognized to be associated with its toxicity, the current consensus is that such electrophile-mediated covalent modification of sensor proteins with thiolate ions is also involved in activation of cellular signal transduction pathways for cellular protection against reactive materials. In the present study, we developed an immunochemical assay to detect cellular proteins adducted by 1,4-NQ. Dot blot analysis indicated that the antibody prepared against 1,4-NQ recognized the naphthalene moiety with the para-dicarbonyl group, rather than with the ortho-dicarbonyl group. Furthermore, little cross-reactivity of para-quinones with either a different number of aromatic rings (n = 1) or substituent groups was observed. With this specific antibody against 1,4-NQ, we identified nine target proteins of 1,4-NQ following exposure of human epithelial carcinoma cell line A431 to 1,4-NQ. Among them, heat shock protein 90 (HSP90) and HSP70 are of interest because covalent modification of these chaperones causes activation of heat shock factor-1, which plays a role in the cellular response against electrophiles such as 1,4-NQ. Thus, our method, which does not use radiolabeled compounds, would be applicable for exploring activation of electrophilic signal transduction pathways coupled to covalent modification of sensor proteins during exposure to naphthalene as well as 1,4-NQ.
[Reference] Hirose R et al., J Toxicol Sci, 2012, 891-898.

PS 1718 Role of Stress Response Proteins and Redox-Sensitive Transcription Factors in Chemically-Induced Liver Injury: Chemoprevention with Kolaviron and Curcumin

E. O. Farombi[1], S. Shrotriya[1, 2] and Y. Surh[1, 2]. [1]*Biochemistry, University of Ibadan, Ibadan, Oyo State, Nigeria and* [2]*Research Institute of Pharmaceutical Sciences, Seoul National University, Korea, Republic of Korea.*

Kolaviron, a bioflavonoid from the seeds of Garcinia kola and Curcumin, present in the rhizome of Curcuma longa have been reported to possess anti-inflammatory, antioxidant, anticarcinogenic and chemopreventive activities via multiple mechanisms. Biomarkers of hepatic oxidative injury, histological and immunohistochemical techniques were used to validate the biochemical mechanisms underlying the hepatoprotection of kolaviron and curcuimin. In addition, the protein expression levels of cyclooxygenase (COX-2) and inducible nitric oxide synthase (iNOS) and heme oxygenase activity (HO-1) and expression were evaluated by western blotting while DNA-binding activities of nuclear factor kappa B (NF-κB), NF-E2-related factor 2 (Nrf2) and activator protein-1(AP-1) were determined by Electrophoretic mobility shift assay. kolaviron reduced the Dimethyl nitrosamine (DMN)-induced markers of oxidative stress. Kolaviron inhibited the DMN-induced expression of COX-2 and iNOS. Immunohistochemical staining of rat liver verified the inhibitory effect of kolaviron on DMN-induced hepatic COX-2 expression. Furthermore, kolaviron abrogated DMN-induced binding activity of NF-κB as well as AP-1. Our data showed that curcumin increases HO-1 activity and HO-1 protein via activation of Nrf2 in rat liver. Also, Curcumin administration resulted in enhanced nuclear translocation and ARE-binding of Nrf2. Tetrahydrocurcumin lacking α- β unsaturated double bond elicits lower anti-inflammatory activity. Collectively, kolaviron inhibits COX-2 and iNOS expression through down regulation of NF-κB and AP-1 DNA binding activities while curcumin protects against DMN-induced hepatotoxicity through ARE-driven induction of HO-1 expression. Thus kolaviron and curcumin qualify as candidates for chemoprevention of hepatocarcinogenesis especially in regions where humans are exposed environmentally and through diet to liver toxic agents.

PS 1719 Ozone Induces Lung Epithelial Cell Inflammation through MAP Kinase Activation without NF-κB Activation

S. D. McCullough[1], K. E. Duncan[2], S. M. Swanton[1], L. A. Dailey[1], D. Diaz-Sanchez[1] and R. Devlin[1]. [1]*Clinical Research Branch, US Environmental Protection Agency, Chapel Hill, NC and* [2]*Center for Environmental Medicine, Asthma, and Lung Biology, University of North Carolina - Chapel Hill, Chapel Hill, NC.*

Ground-level ozone (O3), a ubiquitous air pollutant, is a strong oxidizing agent and potent inducer of airway inflammation via the induction of pro-inflammatory mediators such as IL-8, IL-6, and IL-1 alpha/beta. Previous attempts to characterize O3-mediated activation of these pro-inflammatory mediators have associated their up-regulation with activation of the canonical NF-κB pathway. However, these studies were conducted in transformed cell lines and thus may not accurately reflect what occurs in normal cells. With the increased availability of primary cells in recent years, we sought to test whether the previously established model of O3-dependent pro-inflammatory mediator expression applied to primary human bronchial epithelial cells (phBEC). Thus we characterized the O3-mediated activation of cellular signaling pathways in phBEC grown in air-liquid interface culture obtained from seven donors and in the bronchial epithelial cell line BEAS-2B. Despite observing activation of NF-κB signaling in the BEAS-2B cell line following O3 exposure, we were unable to detect its activation in phBEC following O3 exposure. Instead, we observed activation of the EGFR/MEK/ERK and MKK4/p38 pathways. Additionally, the inhibition of EGFR and p38 kinase activity during O3 exposure was sufficient to prevent the O3-mediated induction of pro-inflammatory mediators in phBEC. These novel findings indicate that the mechanism underlying the O3-induced expression of pro-inflammatory mediators in phBEC involves the activation of MAP kinases, not canonical NF-κB signaling. This discovery is an important step toward elucidating the molecular mechanisms associated with the adverse health effects of O3 exposure, predicting susceptible populations, and identifying strategies for therapeutic intervention.

PS 1720 Caloric Restriction Induces the Antioxidant Response in White Adipose Tissue

L. Armstrong and A. L. Slitt. *Biomedical and Pharmaceutical Sciences, University of Rhode Island, Narragansett, RI.*

Oxidative stress (OS) in adipose tissue (AT) causes metabolic dysfunction of fatty acid transport and dysregulation of AT expandability, which alters AT role in nutritional adaptation and glucose tolerance. Central obesity and insulin-resistance (IR) are important causative factors of metabolic syndrome directly related to AT and metabolic stress. Most notably, OS originating from obesity is considered to be a precipitating factor for obesity-induced IR in AT. In addition to nutritional excess, many chemicals of environmental concern can be deposited in AT and elicit adverse effects via inducing OS; the effects of these toxicants on AT dysfunction via OS is largely unknown. The objective of the study was to understand mechanisms by which caloric restriction (CR) bolsters the antioxidant response in AT to combat OS, and the physiological outcomes of this activation. ARE-hPAP, C57/BL6 (WT) and Nrf2KO mice were place on a restricted diet for approximately 6 weeks in order to determine if CR-induced Nrf2 activation of antioxidant pathway occurred. Nrf2 was induced 3-fold in ARE-hPAP and WT, resulting in an 88% and 84% loss in WAT mass respectively. The induction of Nrf2 was accompanied by a 3- and 2-fold increase in Nqo1 expression, and 4.5- and 3-fold increase in Sod1 expression, in respective cohorts. As growing scientific literature has implicated that obesity-related inflammation influences adipose Lpl activity, CR-induced antioxidant response in WAT may regulate triglyceride metabolism (TG). Lpl, a key enzyme essential for oxidation or storage of TGs in the blood and AT, was increased 2.4-fold in CR-WT mice, and a key regulator of its promoter, Pparγ, was induced 3.2-fold. The induced expression of both Lpl and Pparγ was abolished in CR-Nrf2KO mice, suggesting a role for Nrf2 in the regulation of TG metabolism in AT. Overall, the antioxidant response is induced in WAT via Nrf2 at the transcriptional level, and Nrf2 induction results in regulation of triglyceride metabolism, suggesting Nrf2 as a therapeutic drug target against OS-induced AT dysregulation.

PS 1721 Using In-Cell Proteomics to Assess the Effects of Mitochondrial Oxidative Phosphorylation Inhibitors on Cell Metabolism

H. Garside[1], R. A. Capaldi[2], X. Luo[2], A. P. Capaldi[3] and J. Eakins[1]. [1]*Drug Safety and Metabolism, AstraZeneca, Macclesfield, United Kingdom,* [2]*MetProf Inc, Tucson, AZ and* [3]*University of Arizona, Tucson, AZ.* Sponsor: P. Duffy.

HepG2 cells, like all cancer cells, generate energy from glucose by glycolysis, with little contribution from oxidative phosphorylation (OXPHOS). However, when glucose is replaced by galactose in the growth media, these cells use OXPHOS to generate energy by utilizing glutamine and asparagine in a process called anapleurosis. Comparison of cell viability in the different media is now used routinely to screen drugs for mitochondrial toxicity. Here using a novel In-Cell Proteomics method, we have expanded the evaluation of the effect of the classical inhibitors of OXPHOS: FCCP (uncoupler), oligomycin (ATP synthase inhibitor), myxathiazol (complex III inhibitor), and rotenone (Complex I inhibitor) on mitochondrial function and cell metabolism. Cells were incubated with compounds at 100uM in either glucose or galactose for 6, 24 or 72h prior to fixation. Protein levels were quantified using specific antibodies. All 4 compounds induced cell death by 6h in galactose based on cell appearance and reduction in MCl1 and PUMA levels. In parallel, there was dephosphorylation of both 4E-BP1 and the S6 ribosomal protein, indicating mTor involvement, and a strongly increased phosphorylation of eIF2α, consistent with a component of oxidative stress. In glucose there was no cell death at 6h with FCCP or oligomycin, but some apoptosis with rotenone and myxathiazol. Unlike galactose all 4 compounds induced a large increase in phosphorylation of both p38MAPK and c-Jun kinases in glucose along with increases in both fatty acid oxidation and synthesis along with ER stress based on the increased levels of ACADM, HADHB, ACC2 and CHOP1 respectively. Our results indicate considerable effect of OXPHOS inhibitors outside mitochondria, some but not all of which can be accounted for by loss of ATP production, indicating that other factors such as ROS and altered metabolic intermediates exiting this organelle provide retrograde signalling of mitochondrial stress to the rest of the cell.

PS 1722 The NF-kB Family Member RelB Controls microRNA miR-146a to Suppress Cigarette Smoke-Induced COX-2 Protein Expression in Lung Fibroblasts

C. J. Baglole, M. Zago, A. Rico de Souza, E. Hecht, S. Rousseau, Q. Hamid and D. H. Eidelman. *Medecine, McGill University, Montreal, QC, Canada.*

Rationale: Cigarette smoke (CS) is the leading cause of preventable death worldwide. Diseases due to cigarette smoke exposure, including chronic obstructive pulmonary disease (COPD), are associated with chronic inflammation typified by the heightened expression of cyclooxigenase-2 (COX-2). RelB is an NF-kB family member that suppresses the CS-induced COX-2 protein by an unknown mechanism. The ability of RelB to regulate COX-2 protein expression in response to cigarette smoke may be due to miR-146a, a miRNA which attenuates COX-2 expression in response to inflammatory stimuli. In this study we tested the hypothesis that RelB attenuation of cigarette smoke-induced COX-2 expression is due to regulation of miR-146a.
Methods: Relb+/+ and Relb-/- mouse lung fibroblasts were exposed to 2%-5% cigarette smoke extract (CSE) for 3, 6 or 8 hours. COX-2 protein and mRNA as well as miR-146a were analyzed by WB and/or qRT-PCR. Relb+/+ cells were transfected with Relb siRNA or a miR-146a inhibitor and then exposed to 2%-5% CSE for 8h. COX-2 protein and mRNA were then assessed by WB and qRT-PCR.
Results: CSE induced a significant increase in COX-2 protein expression in Relb-/- fibroblasts compared to Relb+/+ cells. Relb siRNA in Relb+/+ cells also increased COX-2 protein. Despite increased COX-2 protein in Relb-/- fibroblasts, there was a lack of Cox-2 mRNA, suggesting transcriptional induction of Cox-2 mRNA cannot account for the heightened protein expression. There was no difference in Cox-2 mRNA stability between Relb+/+ and Relb-/- cells. RelB regulated miR-146a in response to CSE and the inhibition of miR-146a potentiated CSE-induced COX-2 protein expression.
Conclusions: RelB prevents exaggerated COX-2 expression in response to CS by controlling miR-146a expression, an event which might be crucial in dampening smoke-induced damage. Thus, the RelB/miR-146a pathway may represent a new research direction with therapeutic potential for cigarette smoke-induced lung disease such as COPD.

PS 1723 Benzo[a]pyrene and β-Naphthoflavone Promote Nrf2 Nuclear Translocation in HepG2 Cells

E. C. Herrera-Cogco[1], L. Ramírez-Martínez[2], B. Munoz[1], A. Sánchez-Flores[3], F. Castorena[4], E. López-Bayghen[2] and A. Albores[1]. [1]*Toxicology, Cinvestav, Mexico, DF, Mexico,* [2]*Genetics and Molecular Biology, Cinvestav, Mexico, DF, Mexico,* [3]*Escuela Nacional de Ciencias Biológicas, IPN, Mexico, DF, Mexico and* [4]*Human Growth and Development Area, Tecnológico de Monterrey, Monterrey, NL, Mexico.*

Benzo[*a*]pyrene (BP), an ubiquitous environmental contaminant classified as a carcinogen, affects FTH1 transcription. FTH is the main intracellular iron storage protein that sequesters excess free iron to minimize generation of reactive oxygen species, therefore the gene is considered as antioxidant. On the other hand, Nrf2 is a transcription factor that regulates antioxidants gene expression through its Keap1 repressor. We compared the BP promotion of Nrf2 translocation to HepG2 cell's nucleus with that of β-naphthoflavone (β-NF), atypical synthetic Nrf2 inducer by Electrophoretic Mobility Shift Assays (EMSA). Either BP (5 μM) or β-NF (10 μM) promoted Nrf2 nuclear accumulation, however, Nrf2 was translocatedat 6 h after β-NF treatment whereas BP treatment did so 24 h afterwards. Docking analysis of β-NF or BP, and its metabolites, with Keap1 suggest that β-NF has higher association and lower dissociation capacities than BP. Even more, BP-diolepoxyde displayed the highest association and the lowest dissociation capacity with keap1, including the parent compound. These results suggest that BP metabolites (particularly BP-diolepoxide), but not the parent compound, are responsible for the Nrf2 translocation to the nucleus. The role Nrf2 nuclear accumulation and regulation on the FTH1 transcription remains to be investigated. (Supported by: Conacyt-SS162391, ICYTDF 51/2012, Proinnova 197755 and Conacyt scholarship 263803 to ECH-C).

PS 1724 Heat Shock Protein A6 Expression Is Increased by AP1 and Repressed by TNIP1

V. P. Ramirez[1], M. Stamatis[2], A. Shmukler[2] and B. J. Aneskievich[1]. [1]*Dept of Pharmaceutical Sciences, University of Connecticut, Storrs, CT and* [2]*PharmD Program, School of Pharmacy, University of Connecticut, Storrs, CT.*

Toxic insults or tissue trauma leads to the increased expression of heat shock proteins (HSP). A recently identified and thus least characterized member of the HSP70 family is HSPA6 (also known as HSP70B'). Like other HSPs, it protects cells from heat and chemical stress. However, its different affinity for protein sub-

strates distinguishes it from chaperone family members like HSPA1A (also known as HSP70). Compared to other HSPs, less is known about the transcriptional control of A6, a potentially important characteristic as A6 expression varies greatly amongst different cell types.
Using cultured HaCaT keratinocytes (KC), we observed constitutive and heat induced expression of A6. To identify transcription factors (TF) controlling its basal expression, the A6 3kb promoter was isolated and cloned into a luciferase reporter construct (LUC). Our results from transfected 5' promoter truncation constructs localized a positive regulatory region between -647 to -70bp. Internal promoter deletions within the -647bp LUC suggested a central fragment is crucial for the activation of the A6 promoter. Binding site specific mutants within this fragment determined AP1 plays a key role in A6 expression.
Our lab also observed reduced basal expression and halted stress inducibility of A6 due to overexpressed TNIP1, a protein involved in repressing the activation or activity of several TFs. Using a similar approach, we searched for TNIP1-regulated binding sites involved in A6 repression. Interestingly, the TNIP1-sensitive region (-647 to -70bp) lacks identified TNIP1 target TF binding sites. These results suggest that TNIP1 represses A6 through a novel TF target. Moreover, this work demonstrated A6 expression levels can be modulated to increase or decrease via activation of AP1 or TNIP1, respectively. Since HSPs protect cells from heat and chemicals and the skin is a barrier to such stressors, it is important to understand the mechanisms involved in HSP regulation in KCs.

PS 1725 Role of Cytokines in Regulation of Angiotensinogen in Human Hepatocytes

M. R. Karim, R. A. Ansari, M. A. Clark and S. A. Rizvi. *Pharmaceutical Sciences, Nova Southeastern University, Fort Lauderdale, FL.*

Increase in blood pressure and fibrotic transformation of liver is connected to the abuse of alcohol. Alcohol metabolism by the liver produces hepatic injury resulting in immune responses where the levels of cytokines, especially interleukin-1β (IL-1β), IL-6 and other cytokines are increased. IL-1β activates nuclear factor-kappaB (NF-κB) while IL-6 activates signal transducer and activator of transcription 3 (STAT3) transcription factor. In a cell based model, the effects of IL-1β (10ng/ml) and IL-6 (10 ng/ml) on angiotensinogen (AGT) secretion were studied by treating hepatocytes (HepG2 and Huh7) for 4hrs. and 12 hrs. In addition, NF-κB- mediated effects on secretion of AGT was studied by treating HepG2 and Huh7 with 50 nM phorbol 12-myristate 13-acetate (PMA) for 4hrs. and 12 hrs. It was observed that both PMA and IL-1β increased the secretion of AGT in HepG2 cells while such an effect was not pronounced in Huh7 cells. IL-6 treatment also increased the level of AGT secretion in HepG2 compared to Huh7 cells. It is concluded that human AGT which is a class II acute phase response protein can be modulated by NF-κB activation, and HepG2 hepatocytes are sensitive to NF-κB modulation whereas Huh7 hepatocytes are not.

PS 1726 Modification of Pattern Recognition Receptor Expression As a Potential Mechanism of GI Toxicity

G. Yanochko and B. Hirakawa. *Pfizer, Inc, San Diego, CA.*

Gastrointestinal toxicity is a common adverse effect of oncology drugs. Multiple mechanisms of toxicity are likely, particularly from kinase inhibitors, and include inhibition of proliferation, and changes in cell-cell adhesion, migration or differentiation. Epithelial cells of the gastrointestinal tract interact with the resident gut microflora via pattern recognition receptors (PRR), an interaction which helps maintain barrier integrity of the epithelial lining. Using IEC-6 cells as a model for the crypt cell population of the small intestine and IPEC-J2 cells as a model for the intestinal enterocyte population, we examined the gene expression of two PRRs, toll-like receptors (TLR) 2 and 4, after 48 or 72 hour in vitro exposure to the inflammatory cytokines (TNFα and IFNγ) or 5 kinase inhibitors.
IEC-6 cells had detectable levels of TLR4 expression but not TLR2 under standard growth conditions. IPEC-J2 cells expressed both TLR2 and TLR4 under standard growth conditions with approximately 1000 fold more TLR4 than IEC-6. 48 hour exposure of IEC-6 cells to 10 ng/mLTNFα or 10 ng/mL IFNγ did not induce TLR2 expression. TLR2 expression in IPEC-J2 cells was significantly decreased ~50% after 48 hour exposure to 10ng/mL TNFα but was not affected by IFNγ. Similarly, TNFα suppressed TLR4 expression in both IEC-6 and IPEC-J2. However, IFNγ increased TLR4 expression in IEC-6 but decreased TLR4 expression in IPEC-J2. Preliminary results suggest that kinase inhibitors cause similar changes in TLR gene expression in IEC-6 and IPEC-J2cells. After 72 hour in vitro exposure to 5 kinase inhibitors at concentrations that caused ~10% loss of viability, TLR2 and TLR4 were suppressed 50-60% in IPEC-J2 compared to vehicle-dosed cells. 4/5 kinase inhibitors affected TLR4 expression in IEC-6 cells with 20-70% suppression. These results suggest that modification of the interaction between gastrointestinal epithelium and microflora could be an additional mechanism of gastrointestinal toxicity.

PS 1727 MiRNAs Quantification and Evaluation of Suitable Housekeeping Genes in the Major Preclinical Species

A. Rogue, R. Forster, E. Floch and P. J. Nicholas. *CiToxLAB, Evreux, France.*

MicroRNAs (miRNAs) regulate nearly 60% of cellular protein expression and are the subject of intense research in both the therapeutic and diagnostic areas. Circulating miRNAs associated with proteins, exosomes and vesicles are proving to be highly sensitive and translatable biomarkers of drug-induced injury. With the advancing discovery of novel biomarkers, there is a growing need for sensitive and specific extraction and quantification methods. RT-qPCR has gained acceptance as a robust and reliable transcriptomic method to profile subtle changes in miRNA levels. For interpretation of results and to allow comparison between studies, the choice of a suitable reference miRNA to use as an internal control is a crucial factor. To date, there has been no systematic evaluation of RT-qPCR reference genes for the study of miRNAs expression in whole blood from pre-clinical species. In this study, the expression of two housekeeping miRNAs in whole blood, miR16 and miR103, selected from the literature, has been validated using two RT-qPCR kits: miRCURY LNA (Exiqon) and miScript (Qiagen). After comparison of the kits, the expression of these miRNAs was assessed in male and female animals from five pre-clinical species: rat, mouse, dog, mini-pig and primate. Differences were found between the two kits for the quantification of miRNA. The Qiagen kit was a robust method for analysis of miRNA with no inhibition from the matrix. The Exiqon kit was much more sensitive, with a quantification limit at 2 x 10-5 ng, but under comparable conditions it was more prone to PCR inhibition compared to the Qiagen kit miR-16 and miR-103 were quantified with highly similar Ct values ranging from 14.9-18.3 for miR-16 and 16.9-22.7 for miR-103 with rodents consistently expressing slightly lower levels than the other species. To investigate the suitability of each gene as a housekeeping gene, circulating miRNAs were collected from routine toxicology studies. These data demonstrate the suitability of miR-16 and miR-103 over the more commonly referenced U6 small nuclear RNA using the Exiqon kit.

PS 1728 Role of Hypoxiamimetics in Regulation of Angiotensinogen in Human Hepatocytes

R. A. Ansari, M. R. Karim, S. A. Rizvi and M. A. Clark. *Pharmaceutical Sciences, Nova Southeastern University, Fort Lauderdale, FL.*

Alcohol usage is linked to increased blood pressure and fibrotic transformation of the liver. Angiotensinogen (AGT), which produces angiotensin II (Ang II), an octapeptide, is involved in blood pressure regulation and fibrotic transformation of the liver after the death of hepatocytes. Ang II is produced from its precursor, AGT, by sequential action of renin followed by angiotensin converting enzyme (ACE). The levels of AGT are less than the Michaelis-Menten constant (Km) of renin. Therefore, an increase in blood AGT levels would result in a corresponding increase in Ang II levels that might play crucial role in blood pressure regulation and fibrogenic activity.
Alcohol metabolism by the liver produces oxidative stress that activates hypoxia inducible transcription factor-1alpha (HIF-1α). In addition, alcohol-mediated hepatic injury produces immune responses resulting into increased levels of interleukin-1β and other cytokines. IL-1β activates nuclear factor-kappa B (NF-κB) transcription factor. Since hepatocytes lose the ability to metabolize alcohol after several passages, in order to mimic the alcohol mediated HIF-1α activation, hypoxia mimetics were employed to investigate the effect of HIF-1α activation on AGT secretion. HepG2 and Huh7 hepatocytes were treated with deferoximine (60nM and 120 nM) and cobalt chloride (10μM and 20μM) for 4hrs. and 12hrs. and effects of treatments on AGT secretion were studied. It was observed that both the deferoximine and cobalt chloride increased the secretion of AGT. It is concluded that human AGT may possess hypoxia response element(s) which is responsible for the effects of hypoxia mimetics.

PS 1729 A Graph Theoretical Approach to Determine *In Vitro* Mode of Action

J. A. Vrana, H. N. Williams, A. A. Han and J. W. Boyd. *Chemistry, West Virginia University, Morgantown, WV.*

The prediction of xenobiotic exposure leading to long-term adverse reactions, such as off-target toxicity, cell death, and/or carcinogenesis, has been aggressively pursued in the toxicological and pharmaceutical communities. However, the development of computational models coupled with high-throughput screening assays capable of not only predicting a toxic outcome (e.g., cell death) but also the mode(s) of action contributing to this eventual fate have yet to fulfill these advantageous expectations. Previously, we have shown that 24 hour in vitro cell death can be forecasted at significantly early time-points by exploiting the rapid, endogenous pharmacodynamic response to xenobiotic exposure. This approach utilized protein phosphorylation responses of key proteins found in cellular death and survival pathways at time points relevant to critical signaling events to forecast the eventual cellular fate, irrespective of xenobiotic mode of action(s). However, the mode(s) of action contributing to the cell's predetermined fate remains elusive. To this end, we propose a graph theoretical approach to decode the early networked phosphoprotein response of select proteins following xenobiotic insult. In this proof-of-concept study, we monitored the phosphoprotein response of HepG2 cells exposed to TDZD-8 (GSK3 inhibitor) for a short amount of time (40 minutes) and a longer period of time (10 hours). Euclidean distances of these responses were used as weighted edges (protein-protein theoretical links) to compute the graph theoretical parameter, radiality, for each node (protein) measured. Radiality-based dose-response curves were then constructed to identify proteins related to alterations in network activity following TDZD-8 exposure. From this approach, the potential mode(s) of action at critical time points related to signaling events that are responsible for the cell's predetermined fate (i.e., cell death) may be elucidated, which will greatly impact xenobiotic high-throughput risk assessment in vitro as well as pharmaceutical adverse drug reaction analyses.

PS 1730 Regulation of Airway Mucin Gene Expression by *Aspergillus*

B. Lee, X. Zhou, L. Zhu and Y. Chen. *University of Arizona, Tucson, AZ.*

Environmental mold exposure causes or exacerbates respiratory disease and it is one of the most deleterious environmental hazards that could impact on our health. Aspergillus (ASP) is one of the most prevalent types of molds that are found indoors and outdoors. Bronchiectasis is the prominent symptom resulted from ASP exposure. Airway obstruction caused by mucus over-production and the damage to the tracheobronchial walls are the hallmarks of the bronchiectasis. Since epithelial injury and abnormal repair has been linked to mucus overproduction, we test the hypothesis that ASP damages airway epithelial cells to induce growth factor secretion and the activation EGFR pathway, which in turn elevates mucin expression and mucus production. In our study, ASP activated both Reactive Oxygen Species (ROS) generation and Calcium flux through a protease-dependent but PAR-independent pathway. ROS was critical for the induction of cell death, which Calcium flux was indispensable for mucin increase via a novel PKC-ERK pathway. Interestingly, this pathway was mostly EGFR-independent. Thus, delineating this novel mechanism will lead to the development of effective diagnostic and therapeutic reagents for the pulmonary diseases resulted from environmental mole exposure.

PS 1731 An Approach to Investigate Intracellular Protein Network Responses

A. A. Han[1], H. N. Williams[1], J. A. Vrana[1], N. Boggs[2] and J. W. Boyd[1]. [1]*Chemistry, West Virginia University, Morgantown, WV and* [2]*Applied Physics Laboratory, Johns Hopkins University, Laurel, MD.*

Modern toxicological evaluations have evolved to consider toxicity as a perturbation of biological pathways or networks. As such, toxicity testing approaches are shifting from common endpoint evaluations to pathway based approaches, where the degree of perturbation of select biological pathways is monitored. These new approaches are greatly increasing the data available to toxicologists, but methods of analyses to determine the inter-relationships between potentially affected pathways are needed to fully understand the consequences of exposure. An approach to construct dose-response curves that use graph theory to describe network perturbations amongst three disparate mitogen-activated protein kinase (MAPK) pathways is presented. Mitochondrial stress was induced in human hepatocytes (HepG2) by exposing the cells to increasing doses of the complex I inhibitor, deguelin. The relative phosphorylation responses of proteins involved in the regulation of the stress response were measured. Graph theory was applied to the phosphorylation data to obtain parameters describing the network perturbations at each individual dose tested. The graph theory results depicted the dynamic nature of the relationship between p38, JNK, and ERK1/2 under conditions of mitochondrial stress, and revealed shifts in the balance of these MAPK pathways at low doses. The inter-relationship, or crosstalk, amongst these 3 traditionally linear MAPK cascades was further probed by co-exposing cells to deguelin plus SB202190 (JNK and p38 inhibitor) or deguelin plus SB202474 (JNK inhibitor). The cells exposed to deguelin plus SB202474 resulted in significantly decreased viability, which could be visualized and attributed to the decrease of ERK1/2 network centrality. The approach presented here allows for the construction and visualization of dose-response curves that describe network perturbations induced by chemical stress, which provides an informative and sensitive means of assessing toxicological effects on biological systems.

PS 1732 The microRNA Pathway in Blast-Induced Neurotrauma

D. Dobbins, J. R. Polli, E. E. Connolly and X. Pan. *Biology, East Carolina University, Greenville, NC.*

A complex genetic response following traumatic brain injury (TBI) is associated with lingering neurologic and cognitive problems during neuroregeneration and mild TBI recovery. MiRNAs, a class of endogenous non-coding small RNAs, have been identified as a major gene regulator in most biological and metabolic processes. Aberrant expression of miRNAs is found in neurodegenerative diseases and other CNS disorders. Therefore, a dynamic miRNA network regulating TBI-induced gene expressions may represent the molecular signature of TBI pathophysiology. A mild brain injury rodent model was generated using an advanced blast simulator. As an acute response to 70 kPa over ambient pressure, the mRNA expressions of vitamin D receptor, progesterone receptor, and all selected inflammatory parameters were misregulated in blood and brain tissues. Our preliminary work has also histologically verified the mild brain injury and evaluated the memory and cognitive deficits using the Morris Water Maze. Compared to shams, intraventricular hemorrhages are common observations and blast-injured animals showed cognitive deficits and signs of depression behaviors. Twenty four miRNAs display aberrant expressions in blood of blast-injured animals collected seven days post-blast. miRNA markers target various neurological, inflammatory, and endocrinological pathways.

PS 1733 The Effect of Thiazolidinediones on Cell Metabolism

J. Eakins[1], R. A. Capaldi[2], X. Luo[2], A. P. Capaldi[3] and H. Garside[1]. [1]*Drug Safety and Metabolism, AstraZeneca, Macclesfield, United Kingdom,* [2]*MetProf Inc., Tucson, AZ and* [3]*University of Arizona, Tucson, AZ.* Sponsor: P. Duffy.

Several first generation thiazolidinediones used to treat diabetes have been either withdrawn (troglitazone) or have black box warnings (rosiglitazone and pioglitazone) due to toxicity. We have studied 4 thiazolidinediones: troglitazone, rosiglitazone, pioglitazone and WY14621 using a novel In-Cell Proteomics method that monitors the change in levels of, and altered post-translational modifications in, key proteins of metabolism. This method simultaneously shows the therapeutic effects of the drugs as well as adverse events likely due to toxicity. Treating HepG2 cells with 100uM of each for 6, 24 or 72h, all compounds have effects consistent with activation of PPARγ; they up-regulate both mitochondrial and peroxisomal lipid metabolizing enzymes. All but WY14621 also up-regulate levels of the enzymes of oxidative phosphorylation, Krebs cycle and pyruvate dehydrogenase consistent with PPARγ activators. Increased phosphorylation of S6 ribosomal protein (5-7 fold) over DMSO treated cells was observed, as would be expected given the enhanced protein synthesis. There were also increased levels of IREα, HSP60, SOD2 and catalase, but not SOD1, indicative of activation of the unfolded protein response and oxidative stress. Interestingly, troglitazone differs from the other compounds. In HepG2 cells this compound caused apoptosis with a strong reduction in the level of both MCl1 and PUMA, increases CHOP1 levels, indicative of strong oxidative stress, dephosphorylation of 4E-BP1, and up-regulation of beclin 1 at 6 but not 72h suggesting an attempted autophagy. Interestingly, when examined in cardiomyocytes, troglitazone shows all of the proposed therapeutic effects but does not induce apoptosis, and there is no increase in levels of Chop1, phospho-4E-BP1 or beclin 1, suggesting reduced cell stress compared to HepG2 cells. These results show the utility of a broad screen of metabolism by protein changes in identifying the different effects of compounds in a particular class and deciding between therapeutic versus toxic reactions.

PS 1734 High-Throughput Screening for Cellular Signaling Toxicity Provides Alternatives to Cytotoxicity Measures

C. L. Sherwood[1, 2, 3], M. McCorkel[2] and S. Boitano[1, 2, 4]. [1]*Arizona Respiratory Center, University of Arizona, Tucson, AZ,* [2]*BIO 5 Research Institute, University of Arizona, Tucson, AZ,* [3]*Southwest Environmental Health Sciences Center, University of Arizona, Tucson, AZ and* [4]*Physiology, University of Arizona, Tucson, AZ.*

Inhalation of toxicants such as tobacco smoke, air pollution and those from industrial processes (e.g. arsenic) can lead to respiratory dysfunction including Chronic Obstructed Pulmonary Disease (COPD). The respiratory epithelium provides the first line of defense against inhaled insults. The cells that comprise the airway epithelium coordinate innate immune defenses and initiate adaptive immune responses. Although it is well known that toxicant-induced COPD can result in part from dysfunctional airway epithelial cellular physiology, the mechanisms by which this occurs remain elusive. Traditional cellular toxicity assays represent an end point in toxicity analysis, however, diseases commonly progress with compromised cellular physiology in lieu of cell death. To better assess cell-compromising toxins, we have used the xCELLigence Real-Time Cell Analyzer (RTCA). RTCA is a high-throughput screening format (6x96-well plate) that uses impedance measurements to detect physiological changes in adherent cells. We monitored human bronchial epithelial cells for changes in response to paracrine signaling molecules critical to airway epithelial innate immunity (e.g., ATP). Responses in untreated cells were compared to responses in cells treated for 4 - 24 hrs with arsenic, nanoparticles, or tobacco product constituents. We found that these respiratory toxicants induced dose-dependent alterations of physiological responses. Importantly, this cell signaling toxicity was measured at doses much lower than required to observe cytotoxicity. Findings from the RTCA experiments were confirmed with more traditional cell signaling assays (e.g., digital imaging microscopy of Ca^{2+} signaling). In conclusion, the RTCA device offers a high-throughput approach to screening cells for toxin/toxicant-induced dysfunction independent of cell death and potentially important in toxin/toxicant-induced disease.

PS 1735 Forecasting Cell Death Dose-Response from Early Signal Transduction Responses *In Vitro*

J. W. Boyd, J. A. Vrana, H. N. Williams and A. A. Han. *Chemistry, West Virginia University, Morgantown, WV.*

The rapid pharmacodynamic response of cells to toxic xenobiotics is primarily coordinated by signal transduction networks, which follow a simple framework: the phosphorylation / dephosphorylation cycle mediated by kinases and phosphatases. However, the time course from initial pharmacodynamic response(s) to cell death following exposure can have a vast range. Viewing this time lag (between early signaling events and the ultimate cellular response) as an opportunity, we hypothesize that monitoring the phosphorylation of proteins related to cell death and survival pathways at key, early time-points may be used to forecast a cell's eventual fate, provided that we can measure and accurately interpret the protein responses. In this presentation, we focus on a three-phased approach to forecast cell death after exposure: 1) determine time-points relevant to important signaling events by exploiting the relationship between mitochondrial-driven energy metabolism and kinase response to estimate theoretical ATP production, 2) experimentally determine phosphorylation values for proteins related to cell death and/or survival pathways at these significant time-points, and 3) estimate the 24 hour plasma membrane degradation dose-response of cells to xenobiotic exposure from protein cluster analyses. To test this approach, we exposed HepG2 cells to two disparate treatments: a GSK3β inhibitor and a MEK inhibitor. After using our three-phased approach, we were able to accurately forecast the 24 hour HepG2 plasma membrane degradation dose-response from protein phosphorylation values as early as 20 minutes post-MEK inhibitor exposure and 40 minutes post- GSK3β exposure.

PS 1736 TC-PTP Inhibits UVB-Induced Keratinocyte Survival and Proliferation by Regulating Stat3 Signaling

J. W. Shin[1, 2], H. Lee[1, 2], L. D. Morales[2], T. J. Slaga[1] and D. J. Kim[1, 2]. [1]*Pharmacology, University of Texas Health Science Center at San Antonio, San Antonio, TX and* [2]*Edinburg Medical Research Division, University of Texas Health Science Center at San Antonio, Edinburg, TX.*

Ultraviolet B radiation (UVB) contributes to the development of skin cancer by creating DNA damage that can yield gene mutations which disrupt intracellular signaling mechanisms. One vital signaling mechanism is tyrosine phosphorylation signaling. We have previously shown that T-cell protein tyrosine phosphatase (TC-PTP) contributes to the rapid dephosphorylation /deactivation of Stat3 in response to UVB irradiation in keratinocytes. In the current work, we investigated the functional role of TC-PTP in keratinocyte survival and proliferation following UVB exposure. Knockdown of TC-PTP in mouse keratinocytes using siRNA significantly reduced apoptosis following UVB irradiation in comparison with control keratinocytes as evidenced by the decreased levels of activated caspase-3 and PARP cleavage. This reduction corresponded with an increased level of phososphorylated Stat3 in TC-PTP-deficient keratinocytes. Knockdown of TC-PTP in keratinocytes also significantly increased cell proliferation following UVB irradiation compared with control keratinocytes. Similar with these results, overexpression of TC-PTP in keratinocytes significantly increased apoptosis and decreased cell proliferation in response to UVB irradiation compared with control keratinocytes, which corresponded with a decreased level of phosphorylated Stat3. Treatment of TC-PTP-deficient keratinocytes with specific Stat3 inhibitor, STA21 significantly reduced cell viability, upon UVB exposure in comparison with untreated TC-PTP-deficient keratinocytes, which suggests that the effect of TC-PTP on cell viability is mediated by Stat3 dephosphorylation. Combined, our results indicated that TC-PTP plays an important role in the regulation of keratinocyte proliferation and survival after UVB exposure via modulation of Stat3 signaling. Furthermore, these results suggest that TC-PTP may be a novel potential target for the prevention of UVB-induced skin cancer.

PS 1736a Patterns of Gene Coregulation across Multiple Tissues Undergoing Toxicological Challenge

S. S. Auerbach[1], D. L. Svoboda[2], B. A. Merrick[1] and R. R. Tice[1]. [1]*National Toxicology Program, National Institute of Environmental Health Sciences, Research Triangle Park, NC and* [2]*Social and Scientific Systems, Inc, Durham, NC.*

Genes that are tightly co-regulated over toxicogenomic space represent gene networks that carry out specific adaptation and repair processes. Such networks reflect the emergent properties of the complex biological systems where they are manifest and therefore tend to be a more accurate reflection of the biological response than what is gleaned from generic gene set analysis. Here we present a data-driven approach to discover gene co-regulation modules manifest in rat liver, kidney, heart and thigh muscle following toxicological challenge. A number of modules were present at a biological process level across multiple tissues including cell cycle, proteasome function, complement/coagulation cascades, and cytoskeletal function. Other modules were more specific to one organ system, such as steroid metabolism (liver), fatty acid metabolism (liver) and oxidative metabolism (thigh muscle). Using transcription factor/microRNA enrichment we identified plausible driver of expression for each of the modules. Findings from this analysis suggested a substantial role for the regulatory factors Mir136 (fatty acid metabolism), Crem (steroid metabolism) and Nrf1/Pparg (proteasome function) in the response to toxicological challenge. Notably, variation in the co-regulation modules across tissues indicated alternative means of biological process activation (e.g., proteasome function appears to be predominantly effected by Nrf1 in the liver and Pparg in the muscle). Overall, the analysis provides a bottom-up deconvolution of toxicological perturbations that can be used in the development of data driven adverse outcome pathways which more accurately reflect the tissue specific signaling networks.

PS 1736b Regulation of Human CYP2C9 Expression by Electrophilic Stress Involves AP-1 Activation and DNA Looping

N. L. Makia[1], S. Surapureddi[1], R. A. Prough[2] and J. A. Goldstein[1]. [1]*Human Metabolism Group, Laboratory of Toxicology and Pharmacology, National Institute of Environmental Health Sciences (NIEHS), Research Triangle Park, NC and* [2]*Biochemistry and Molecular Biology, University of Louisville School of Medicine, Louisville, KY.*

CYP2C9 is an important enzyme that metabolizes therapeutic drugs, environmental chemicals and physiologically important endogenous compounds. CYP2C9 expression is induced by drugs such as rifampicin, St. John's Wort and phenytoin. Many drugs and foreign compounds are metabolized in the liver to electrophilic and reactive metabolites. The effects of these electrophilic metabolites on the regulation of CYP2C genes have not yet been investigated. Initial studies using primary human hepatocytes showed induction of both CYP2C9 and CYP2C19 genes by tert-butylhydroquinone (tBHQ). As a pro-oxidant, tBHQ regulates the expression of cytoprotective genes by activation of redox-sensing transcription factors, such as the nuclear factor E2-related factor 2 (Nrf2) and activator protein 1 (AP-1). The promoter region of CYP2C9 contains two putative AP-1 sites (TGAGTCA) at positions -2201 and -1930 which are also highly conserved in CYP2C19. Ectopic expression of Nrf2 had no effect on CYP2C9 luciferase activity, while the CYP2C9 promoter is activated by cFos and JunD. Using specific kinase inhibitors for MAPK, we showed that ERK and JNK are essential for tBHQ-induced expression of CYP2C9. EMSA assays demonstrate that cFos distinctly interacts with the distal site and JunD with the proximal AP-1 site. Chromosome conformation capture (3C) analyses confirmed the formation of a DNA loop in the CYP2C9 promoter allowing interaction between cFos at the distal site and JunD at the proximal site to

activate CYP2C9 transcription in response to electrophiles. These results indicate that oxidative stress generated by exposure to electrophilic xenobiotics and metabolites induces the expression of CYP2C9, thereby altering the metabolic clearance of therapeutic drugs and xenobiotics which are substrates of CYP2C9.

PS 1736c Dose-Specific Nicotine-Dependent Behaviors in *Caenorhabditis elegans*: Regulation of Nicotinic Acetylcholine Receptors

J. R. Polli and X. Pan. *Biology, East Carolina University, Cary, NC.*

Nicotine, the major psychoactive compound in tobacco, targets the nicotinic acetylcholine receptors (nAChRs) and leads to drug dependence. The nematode *Caenorhabditis elegans*' (*C. elegans*) genome encodes conserved and extensive nicotinic receptor subunits, representing an excellent system to investigate nicotine-induced cholinergic signaling in the context of drug addiction. However, the *in vivo* expression pattern of nAChR genes under chronic low-level nicotine exposure has not been systematically investigated in *C. elegans*. Here, we have reported the first *in vivo* expression of the 28 authentic nAChRs at the mRNA level following nicotine exposure in *C. elegans*. Chronic (24 hour) low-level (6.17-61.7 μM) nicotine exposure has been shown to change the expression of nicotinic receptors in a dose-specific manner. Worms exposed to 6.17 and 61.7 μM nicotine displayed nicotine-dependent behaviors. Quantitative real-time PCR results showed that five genes (lev-1, acr-6, acr-7, lev-8, and acr-14) were significantly up-regulated at 61.7 μM nicotine treatment, with worms showing significant withdrawal behaviors when the nicotine supply was discontinued. However, the 19.5 μM dosed worms did not exhibit the withdrawal behavior, which was accompanied by a general increase in nAChRs expressions. We have also predicted conserved microRNAs that may target these receptor genes using online algorithm tools. Quantitative real-time PCR results showed that several predicted miRNAs were co-expressed with their target nAChR genes, including let-7, miR-355, miR-70, and miR-71. This study provides useful information regarding the comprehensive *in vivo* expression pattern of the 28 "core" nAChRs and its relationship with addiction behaviors.

PS 1736d Nrf2 Protects Mitochondrial Degeneration by Oxidative Stress

J. G. Strom[1], B. Xu[1], J. A. Johnson[2] and Q. M. Chen[1]. [1]*Pharmacology, University of Arizona, Tucson, AZ and* [2]*School of Pharmacy, University of Wisconsin-Madison, Madison, WI.*

Oxidative stress plays an important role in cellular injury. Cells surviving oxidative stress often become enlarged with increased protein content. In the myocardium, enlargement of cardiomyocytes consequential to tissue injury contributes to mal-adaptive remodeling and subsequent development of heart failure. Here we address the role of mitochondria in cells surviving oxidative stress and becoming enlarged using primary cultured rat cardiomyocytes as an experimental model. These cells survive low to mild doses of H_2O_2, but develop hypertrophy. In control cells, mitochondria exist in elaborate and elongated networks. Within 24 hours after exposure to a mild dose of H_2O_2 (300 μM), the mitochondrial network was replaced by predominately individual, punctate mitochondria. Electron microscopy revealed H_2O_2-induced swelling of mitochondria with disorganized cristae and areas of condensation. Measurements of functional mitochondria showed a H_2O_2 dose-dependent (50 to 400 μM) decrease over a course of 5 days. At the protein and mRNA levels, H_2O_2 treatment resulted in a reduction of mitochondrial components, cytochrome c and cytochrome b. Nrf2 overexpression prevented H_2O_2 from inducing mitochondria morphological changes and the reduction of cytochrome c and cytochrome b. Although Nrf2 is known as a transcription factor regulating antioxidant and detoxification genes, Nrf2 overexpression did not reduce the level of protein oxidation as measured by carbonyl formation. We found that Nrf2 localizes to the outer mitochondrial membrane, suggesting a direct role in mitochondrial protection. Mitochondria prepared from the myocardium of Nrf2 knockout mice are more sensitive to permeability transition. Correlating with the protective effect of Nrf2 against mitochondrial decay, Nrf2 overexpression prevented H_2O_2 from inducing cardiomyocyte hypertrophy. These data suggest that mitochondrial decay due to oxidative stress contributes to cardiomyocyte hypertrophy and Nrf2 protects mitochondria from oxidant injury likely through direct interaction with mitochondria membrane.

PS 1736e RNA-Seq Analysis of the Functional Link between Vascular Disruption and Adverse Developmental Consequences

J. Franzosa[1], R. S. Settivari[2], R. Ellis-Hutchings[2], N. Kleinstreuer[3], K. Houck[1], E. W. Carney[2] and T. B. Knudsen[1]. [1]*NCCT, U.S. EPA, RTP, NC,* [2]*The Dow Chemical Company, Midland, MI and* [3]*ILS, Inc/NICEATM, NIEHS, RTP, NC.*

Vasculogensis and angiogenesis are complex processes necessary for normal development. High throughput-screening (HTS) efforts by the US EPA ToxCast program identified a diverse set of environmental chemicals that potentially disrupt biological targets associated with blood vessel formation and/or remodeling. To investigate embryonic responses to vascular disruption, gestation day 10 rat embryos were exposed *in vitro* to anti-angiogenic reference compounds 5HPP-33 (5, 15, 30 μM) or TNP-470 (0.25, 2.5, 25 μM) and vehicle controls. The major effects elicited after 48 h were embryo lethality (5HPP-33 ≥ 15μM) and dysmorphogenesis (TNP-470 ≥ 0.25 μM). RNA-Seq was conducted on RNA from embryos and yolk sacs (n= 8 embryos or 4 pools of 2 yolk sacs per concentration) at 4 h post-exposure, a time point selected to identify early transcriptional responses. Patterns of differentially expressed genes (DEGs) were tissue and concentration-dependent (apical vs transcriptional responses).Unsupervised hierarchical clustering of embryonic DEGs showed that transcriptional responses at the highest concentration of 5HPP-33 were similar to TNP-470 at any concentration. Pathway analysis revealed that the most significantly enriched pathway for exposures eliciting overt phenotypes, 5HPP-33 (30 μM) and TNP-470 (0.25, 2.5 and 25 μM) was the cellular p53 response pathway. Concentration-dependent effects were observed in embryonic DEGs directly related to known vasculogenesis targets (i.e. VCAM1, TNF, CASP8, HIF1A, AHR). These data demonstrate the importance of p53 signaling in developmental angiogenesis and support the hypothesis that conserved vascular disruption pathways can lead to developmental toxicity outcomes of with diverse phenotypes. The identification of altered vascular regulatory networks perturbed by developmental toxicants supports an adverse outcome pathway associated with disruption of the embryonic vasculature. *This abstract does not necessarily reflect US EPA policy.*

PS 1737 Developmental Neurotoxicity Assessment in a 3D Organotypic Neuronal Model Using a Metabolomics Approach

H. T. Hogberg, R. Bachinski, M. Bouhifd, G. Harris, A. Kleensang, S. Odwin-DaCosta, D. Pamies, L. Smirnova, L. Zhao and T. Hartung. *CAAT, Johns Hopkins University, Bloomberg School of Public Health, Baltimore, MD.*

The National Research Council report from 2007 "Toxicity Testing in the 21st Century: A vision and a strategy" (Tox-21c) has created an atmosphere of departure in the US. It suggests moving away from traditional animal testing to modern technologies based on pathways of toxicity. An area of toxicology where Tox-21c could have a significant impact is developmental neurotoxicity (DNT). There is concern that exposures to environmental chemicals contribute to the increasing incidence of neurodevelopmental disorders in children. However, due to lack of DNT studies only very few substances have been identified as developmental neurotoxicants. Moving towards a mechanistic science can help us identify the perturbed pathways that likely lead to these adverse effects.
A 3D rat primary organotypic neuronal model was exposed from day 7 up to 21 to suspected (developmental) neurotoxicants including pesticides, drugs and metals. Mass spectrometry based metabolomics measurements were performed and quantitative measurements of genes expressed in different cell types (neural precursor cells, neurons and glial cells). Mass spectrometry analysis showed differences in metabolite levels between control and treated cells in a concentration dependent manner. Signatures of changed features have been putatively identified and associated to perturbed pathways supported by gene expression data. For example metabolites involved in the biochemical pathway of the neuronal specific metabolite N-acetyl aspartate (NAA) (malate, aspartate, NAA and glutamate) were significantly decreased after exposure to lead chloride and maneb. In patients, the level of NAA has shown to be decreased in numerous neuropathological conditions such as brain injury, stroke and Alzheimers. It also indicates neuronal/axonal loss or compromised neuronal metabolism. Obtained data suggests that metabolomics could be a promising tool for developmental neurotoxicity assessment.
Funded by the FDA #U01FD004230

PS 1738 MiRNomics, Metabolomics, and 3D Neuronal Differentiation of LUHMES Progenitor Cells As an *In Vitro* Model for DNT Studies

L. Smirnova, G. Harris, J. Delp, H. T. Hogberg, D. Pamies, R. Bachinski and T. Hartung. *CAAT, Johns Hopkins Bloomberg School of Public Health, Baltimore, MD.*

This work aims to develop a human 3D brain model to identify changes in transcriptome, including microRNA expression (miRNomics), and metabolome after exposure to neurotoxicants. The LUHMES cell line differentiates rapidly and homogeneously into dopaminergic neurons (DNs) in traditional monolayer cultures. Knowing the fact that 3D culture conditions better mimic the in vivo response, we developed a 3D human neuronal model using LUHMES cells and constant gyratory shaking culture condition. The LUHMES cells have shown prolonged survival when cultured 3D compared to traditional monolayers. The differentiation in 3D aggregates was characterized by qRT-PCR, flow cytometry and immunocytochemistry. We observed increase of NeuN positive cells (mature neurons) and decrease Ki-67 positive cells (proliferating cells) in the course of differentiation by flow cytometry. During early stages of differentiation, 3D cultures did not contain any apoptotic cells. However, up to 30% of the cells within aggregates were apoptotic (Annexin V/caspase3 positive) at later time points (15-21 days) that could be reduced by decreasing the size of aggregates. We observed strong induction in gene expression of neuronal markers (β-III-Tubulin, DAT, synapsin 1, and TH) as well as neural-specific/enriched miRNAs (mir-124, mir-9, mir-128, mir-132, mir-133b, mir-137). To demonstrate the model's suitability for neurotoxicity testing, the aggregates were treated for 24 and 48 hours on day 6 and 12 of differentiation with dopaminergic neurotoxicants, MPP+ and rotenone. Perturbations in energy metabolism and stress response following mitochondrial complex 1 inhibition was characterized by LC-MS based metabolomics, transcriptomics, miRNA profiling and mitochondrial function assay. In conclusion, we have successfully developed a new 3D human model that can be used for (developmental) neurotoxicity testing.

PS 1739 Development of Calcium Responses and Electrical Activity in Differentiating Mouse Neural Progenitor Cells *In Vitro*

M. M. Dingemans, M. de Groot and R. H. Westerink. *Neurotoxicology Research Group; Institute for Risk Assessment Sciences; Faculty of Veterinary Medicine, Utrecht University, Utrecht, Netherlands.*

In vitro methods for developmental neurotoxicity (DNT) testing have the potential to reduce animal use and increase insight into mechanisms of chemical-induced alterations in the development of functional neuronal networks. Mouse neural progenitor cells (mNPCs) have proven valuable to detect DNT using biochemical and morphological techniques. However, their neurophysiological characteristics are still largely unknown.

We have therefore investigated calcium responses and electrical activity in primary mNPCs (using the Ca^{2+}-responsive dye Fura-2 and a multi-electrode array system, respectively) to explore their applicability for DNT testing with focus on neuronal function.

Immunocytochemistry reveals that mNPCs express neuronal, glial and progenitor markers at various differentiation durations. Stimulus-evoked changes in intracellular calcium concentration ($[Ca^{2+}]_i$) were investigated at 1, 7 and 14 days of differentiation. Increases in $[Ca^{2+}]_i$ are evoked by depolarization, acetylcholine, L-glutamic acid, dopamine, adenosine triphosphate and, to a lesser extent, by serotonin and gamma-aminobutyric acid. Notably, the percentage of responsive cells and response amplitudes indicate changes in the expression and functionality of related neurotransmitter receptors and calcium signaling pathways during *in vitro* differentiation. The development of functional intercellular signaling pathways is confirmed in mNPCs cultured on multi-electrode arrays, demonstrating that mNPCs develop spontaneous electrical activity within 1-2 weeks of differentiation. These data demonstrate that mNPCs develop functional neuronal characteristics *in vitro*, making it a promising model to study chemical-induced effects on the development of neuronal function.

This work is funded by the European Union [DENAMIC project; FP7-ENV-2011-282957] and The Netherlands Organization for Health Research and Development (ZonMw) [85300003].

PS 1740 Thyromimetic Effects of Araclor 1254 (AR) and Polybrominated Diether 100 (PBDE) on Angiogenesis (AG) Are Mediated via the αVβ3 Integrin Receptor

M. Alnamnakani[1, 2], S. A. Mousa[2] and H. A. El-Fawal[1]. [1]*Neurotoxicology Laboratory, Albany College of Pharmacy and Health Sciences, Albany, NY and* [2]*Pharmaceutical Research Institute, Albany College of Pharmacy and Health Sciences, Albany, NY.*

Neovascularization through AG is essential during neurogenesis. These events are affected by thyroid hormone (T3 and T4). While the mode of action of thyromimetic AR and PBDE remain equivocal, studies of AG have characterized the αvβ3 integrin receptor as a mediator of T3 and T4 activity and MAP kinase (MAPK) as an intracellular effector. The effects of AR and PBDE on AG, contributing to developmental neurotoxicity, were investigated at equivalent doses (0.01, 0.02, 0.05 and 0.10 μg/ml), compared to fibroblast growth factor (bFGF;1 μg/ml), T3 (6.5ng/ml) and vehicle controls (PBS) in the 10 day chick chorioallontoic membrane (CAM). Test concentrations on coverslips (total volume 20μl), were added to CAM and harvested after 3 days of incubation under conditions of O2/CO2 and humidity to quantify the perfusion area (A), total length (L) and number of branch points (B). Both AR and PBDE dose-dependently increased B at doses < 0.02 μg/ml and peaked at 0.05 μg/ml. Pro-AG responses to AR and PBDE were comparable to each other and to bFGF and T3 at the doses used (average 70%>PBS; $p<0.001$). However, vessels were thin and tortuous, with frequent evidence of micro-hemorrhaging. Compromised perfusion was supported by the lack of increases in A and L, despite the increase in B. T3/T4 receptor antagonist tetrac, a T4 derivative (2.5 μg/CAM), and XT-199 (2.5 μg/CAM), a αvβ3 receptor blocker, completely blocked the effects of both 0.05 μg/ml AR or PBDE. The MAPK blocker PD98059 (2.5 μg/CAM), used against 0.05 μg/ml AR, reversed its effects. Evidence of increased, but defective, AG with AR or PBDE suggests a toxicant-induced hypoxic response. These results demonstrate that AR and PBDE induce AG at low doses and identifies a pleiotropic target of these hormone-disrupting chemicals. Excessive vascularization with increased permeability and αvβ3 receptor dysfunction have been implicated in neurodegenerative diseases.

PS 1741 BDE-47 and BDE-49 Selectively Disrupt Axonal Outgrowth in Cultured Hippocampal Neurons

H. Chen, D. Yang and P. Lein. *University of California, Davis, Davis, CA.*

Polybrominated diphenyl ethers (PDBEs) are a class of brominated flame retardants that were widely used in textiles, polyurethane foams, and plastics. Higher body burdens of PDBEs in children have been associated with increased risk of cognitive deficits, including decreased attention and performance on intelligence tests. Despite this, the molecular and cellular mechanisms associated with PBDE developmental neurotoxicity are not clearly known. PBDEs share structural similarities to non-dioxin-like (NDL) polychlorinated biphenyls (PCBs). NDL PCBs interact with ryanodine receptors (RyRs), an intracellular calcium release channel, to promote dendritic arborization, which is a critical determinant of neuronal connectivity. PBDEs have similarly been shown to sensitize RyRs, suggesting that BDE congeners may also modulate neuronal connectivity. To test this hypothesis, we quantified axonal and dendritic outgrowth in primary dissociated hippocampal cultures after exposure to BDE-47, a highly abundant BDE congener with low RyR activity, or BDE-49, a less abundant congener with potent activity at the RyR. Both BDE-47 and BDE-49 significantly decreased axonal outgrowth and there were no significant differences between them with respect to the concentration-relationship to this effect. In contrast to NDL PCBs, neither congener altered dendritic outgrowth, as determined by morphometric assessment, nor synaptic connectivity, as quantified by ELISA for synaptophysin. These results suggest that both BDE-47 and BDE-49 can selectively disrupt axonal outgrowth, most likely via RyR-independent mechanisms. Supported by NIH grant R01 ES014901, P42 ES04699, T32 ES007059, and an unrestricted gift from the J.B. Johnson Foundation.

PS 1742 Assessing Genetic Susceptibility to Motor Function Deficits following Developmental Exposure to Polychlorinated Biphenyls

M. Stegman, C. P. Curran, S. K. Infante, M. Kromme, B. Hays, K. Taylor, H. Garber and A. Lang. *Biological Sciences, Northern Kentucky University, Highland Heights, KY.*

Polychlorinated biphenyls (PCBs) are ubiquitous industrial chemicals banned in the 1970s due to their wide-ranging toxicity. Children exposed in utero and lactationally have a higher risk of learning, memory and behavioral deficits. The goal of our research is to identify genes which affect susceptibility to these pollutants.

The enzyme CYP1A2 can sequester toxicants such as dioxins and coplanar PCBs The aryl hydrocarbon receptor (AHR) bind coplanar PCBs, initiating transcription of several genes including CYP1A2, a key detoxifying enzyme. Though it is also reportedly expressed in the cortex and cerebellum of the brain, its physiological function in the brain remains unknown. Previous work in our lab uncovered learning and memory deficits in *Cyp1a2(-/-)* knockout mice. Our current work compares *Ahr^{d}Cyp1a2(-/-)*, *Ahr^{b}Cyp1a2(-/-)*, and *Ahr^{b}Cyp1a2(+/+)* mice exposed during gestation and lactation to PCBs or the corn oil vehicle. Pregnant dams were treated from gestational day 0 (GD0) to postnatal day 25 (PND 25). We compared the three genotypes of mice using a battery of six tests: rotarod, gait analysis, sticker removal, pole climbing, balance beam, and grip strength. There was a significant main effect of treatment on all 5 days of testing ($P< 0.05$) and a significant gene x treatment interaction on Day 4 of testing ($P<0.05$) with PCB-treated *Ahr^{b}Cyp1a2(-/-)* mice showing the greatest impairments. There was a significant main effect of genotype and treatment in gait analysis with PCB-treated animals and *Ahr^{d}Cyp1a2(-/-)* mice having significantly longer stride lengths ($P<0.05$). There were no significant differences in the pole test. Both *Cyp1a2(-/-)* knockouts had significantly shorter latencies to traverse the beam ($P<0.001$). Further analysis will be required to determine if this indicates a difference in motor function or greater motivation to reach the safety of the darkened goal box.

PS 1743 Motor Dysfunction in Mice Varying at the AhR and Cyp1a2 Loci following Developmental PCB Exposure

C. P. Curran, S. K. Infante, M. Stegman, M. Kromme, A. Lang, K. Taylor, H. Garber and B. Hays. *Biological Sciences, Northern Kentucky University, Highland Heights, KY.*

Polychlorinated biphenyls (PCB) are persistent organic pollutants that bioaccumulate in the environment. Gestational and early developmental exposure to PCB can cause learning and memory deficits in children as well as behavioral problems. More recently, PCB exposure has been linked to an increased risk of Parkinson's disease. PCBs are found as mixtures of coplanar and noncoplanar congeners. Coplanar PCBs activate the aryl hydrocarbon receptor (AHR), which then leads to increased expression of cytochrome P450 CYP1A1 and CYP1A2. Maternal CYP1A2 can sequester PCBs in the liver, preventing their distribution to the fetus or through breast milk. Our previous work showed that genetic variation at the AhR and CYP1A2 loci alters susceptibility to PCB-induced neurotoxicity. Using a mouse model that models human variation in the AHR and CYP1A2 genes, we extended our previous work on learning and memory deficits to examine genetic susceptibility to PCB-induced motor dysfunction. Pregnant dams were treated with a PCB mixture by gavage on gestational day (GD) 10 and postnatal day (PND) 5. We began motor testing on offspring at PND 60. We found a significant main effect of treatment with PCB-treated animals having significantly shorter latencies to fall off the rotarod ($P<0.001$). We also found a significant effect of genotype with CYP1A2(-/-) mice showing significant impairment on rotarod compared with wild type mice ($P<0.001$). This suggests that CYP1A2 protein is essential to normal cerebellar function or development. There was a significant gene x treatment interaction in gait analysis with PCB-treated AhR^{d}CYP1A2(-/-) mice having longer stride lengths ($P<0.01$). Females showed significantly shorter latencies in the pole climb test and greater stride differentials. Together, these results suggest that the greatest effects of developmental PCB exposure are on cerebellar function rather than on nigrostriatal pathways.

PS 1744 Perinatal Exposure to PCBs Alters Amphetamine and Cocaine Behavioral Sensitization

M. M. Miller, J. N. Voeller, J. L. Nelms, A. E. Meyer and H. J. Sable. *Psychology, University of Memphis, Memphis, TN.*

PCBs alter brain dopamine (DA) function suggesting the reinforcing properties of psychostimulants may be modified by PCB exposure. Drug-induced psychomotor effects are assumed to share the same neural substrate mediating the reward circuit. We previously showed male rats perinatally exposed to an environmentally relevant PCB mixture exhibited enhanced locomotor activation following a single IP amphetamine (AMPH) injection (0.5 mg/kg) with attenuated behavioral sensitization following repeated administration of the same AMPH dose. This project determined if similar PCB exposure would alter the locomotor-activating effects of cocaine (COC). Dams were exposed to 0 (control), 3, or 6 mg/kg/day PCBs throughout gestation and lactation. Behavioral sensitization to COC was assessed in one adult male and female/litter. On PND 75, each rat was placed in a locomotor testing chamber and given 30 min to habituate. Next, an IP injection was administered followed by 60 min of activity testing. On day 1, the IP injection was saline while on days 2-7 and 14 it was 10.0 mg/kg COC. No PCB-related differences were observed following the first injection of COC. Behavioral sensitization in the 6 mg/kg/day PCB rats occurred after only the second COC injection which was earlier than in controls. Significant differences between these exposure groups were seen following the second (males) and third (females) injection of COC. All exposure groups exhibited similar COC behavioral sensitization by the fifth COC injection. Overall, an increase in locomotor activation (relative to controls) was observed after one injection of 0.5 mg/kg AMPH and two injections of 10.0 mg/kg COC. Repeated AMPH injections attenuated behavioral sensitization in PCB-exposed males relative to controls, but repeated COC injections did not. Thus, perinatal PCB-exposure can alter the locomotor activating effects and behavioral sensitization of psychostimulants – perhaps due to differences in DA function following PCB exposure. (Supported by NIEHS R00ES015428)

PS 1745 PFOS Induces Behavioral Alterations Compatible with ADHD in a Zebrafish Model of Developmental Neurotoxicity

S. Spulber[1], P. Kilian[1], S. Negri[2], M. Di Tuccio[2] and S. Ceccatelli[1]. [1]*Neuroscience, Karolinska Institutet, Stockholm, Sweden and* [2]*Environmental Research Center, Salvatore Maugeri Foundation, Pavia, Italy.*

Background: Perfluorooctane sulfonate (PFOS) is a widely spread environmental contaminant. It accumulates in the brain and has potential neurotoxic effects. The exposure to PFOS has been associated with higher impulsivity and increased ADHD prevalence.
Objectives: We investigated the effects of developmental exposure to PFOS in zebrafish larvae, focusing on the modulation of activity by the dopaminergic system.
Methods: We exposed zebrafish embryos to 0.1 or 1 mg/l PFOS and assessed swimming activity at 6 dpf. We analyzed the structure of spontaneous activity and the acoustic startle response. In addition, we investigated the effects of D-amfetamine on the alterations in spontaneous activity and startle response in zebrafish larvae.
Results: We found that zebrafish larvae exposed to 1 mg/L PFOS display a disorganized pattern of spontaneous activity consisting of less frequent, but more intense bouts of activity as compared with controls. In addition, the startle response is followed by persistent hyperactivity. D-amfetamine partly corrected the phenotype in zebrafish larvae exposed to 1 mg/L PFOS.
Conclusion: Developmental exposure to PFOS induces hyperactivity mediated by a dopaminergic deficit that can be corrected by D-amfetamine. Our data support the association of PFOS exposure with impulsivity and ADHD in children.

PS 1746 Early Embryonic 2, 3, 7, 8-Tetrachlorodibenzo-*p*-dioxin (TCDD) Exposure Disrupts Forebrain and Cerebral Vascular Development in Zebrafish

J. S. Plavicki, K. Miller, E. Christensen, R. E. Peterson and W. Heideman. *School of Pharmacy, University of Wisconsin at Madison, Madison, WI.*

TCDD is a persistent environmental contaminant that exerts toxicity by activating aryl hydrocarbon receptor (AHR) signaling. Using fluorescent-immunohistochemistry (F-IHC) and confocal microscopy, we examined TCDD-exposed and control zebrafish brains and found that TCDD exposure disrupts forebrain and cerebral vascular development. Within the forebrain, the olfactory bulbs (OB) and habenular nuclei were smaller and had reduced expression of activated leukocyte cell adhesion molecule, an axonal marker. F-IHC staining with a synaptic marker (synaptic vesicles) revealed disorganization within the OBs. We examined cerebral vasculature at 48, 72, 96, and 120 hours post fertilization (hpf) using a flk1:EGFP endothelial reporter line. To visualize vascular morphology, we collected a series of optical sections and generated brightest point projections using Olympus software. Cerebral vasculature malformations were identified in the fore-, mid- and hindbrains of TCDD-exposed embryos at all times examined. The presence of phenotypes at 48 hpf, prior to decreases in cardiac output, indicate that TCDD can impact vascular development independent of cardiac function. We also found that exposure to a sub-lethal level of TCDD (50 ppt) disrupts cerebral vasculature development. We blocked ahr translation using ahr2 and ahr1 morpholinos and observed fore- and midbrain vascular malformations. These phenotypes in zebrafish are consistent with AHR's role in mammalian vascular development. A common mechanism mediating TCDD-induced toxicity is downregulation of the transcription factor, sox9b. We are examining sox9b as a potential TCDD target in the developing nervous system and have found that loss of sox9b results in severe brain and vascular phenotypes. Thus, TCDD exposure disrupts brain and vascular development. Whether disrupted cerebrovascular development caused by fetal TCDD exposure in humans plays a role in neurodevelopmental disorders and cognitive impairment remains to be determined. (Supported by NIH ES012716).

PS 1747 Rapid Identification and Characterization of Neuromodulator Chemicals Using an Embryonic Zebrafish System

D. Reif[1], R. L. Tanguay[2], L. Truong[2] and D. Mandrell[2]. [1]*Bioinformatics Research Center, North Carolina State University, Raleigh, NC and* [2]*Department of Environmental and Molecular Toxicology, Oregon State University, Corvallis, OR.*

New strategies are needed to address the data gap between the bioactivity of chemicals in commerce and the environmental versus existing hazard information. This data gap is especially wide when considering toxicological endpoints that are difficult to measure using purely in vitro systems, such as abnormal behavior. We describe an embryonic zebrafish system where behavior can be both experimentally perturbed (6 doses of chemical and 1-second pulses of light) and measured (accompanying real-time, spontaneous movement) in a high-throughput fashion. This system is applied to characterize the behavioral response to 1060 ToxCast™ chemicals as hyperactive or suppressive to movement of 24 hours-post-fertilization (hpf) zebrafish embryos subjected to intermittent pulses of light. By dividing the experimental interval according to light pulses (Background = prior to first pulse; Excitatory = after first pulse; Refractory = after second pulse), we observe movement responses that can classify neuromodulator chemicals as eliciting light-independent movement alterations (102), light-dependent photomotor responses (231), or both (276). The chemicals can be further subdivided into a discrete number of prototype clusters based upon hypo- and/or hyperactivity patterns across light intervals. As an integrative measure of normal development, significant alterations in movement highlight neuroactive chemicals representing several modes of action. These early behavioral responses are predictive (relative risk $p < 0.05$) of 17 specific developmental abnormalities (including notochord defects) and mortality measured at 5 days-post-fertilization (dpf). Therefore, this system can provide for rapid characterization of chemical-elicited behavioral responses at an early developmental stage that are indicative of significant downstream hazard.

PS 1747a Predictions of Developmental Neurotoxicity Potential of TDCPP

V. C. Moser[1], P. M. Phillips[1], K. L. McDaniel[1], K. A. Jarema[1], K. B. Paul[2], J. M. Hedge[2], W. R. Mundy[2], T. J. Shafer[2] and S. Padilla[2]. [1]*TAD/NHEERL, US EPA, RTP, NC and* [2]*ISTD/NHEERL, US EPA, RTP, NC.*

Tris(1,3-dichloro-2-propyl)phosphate (TDCPP) is an organophosphate flame retardant with widespread usage and documented human exposures through food, inhalation, dust ingestion, and breast milk. Concern for neurodevelopmental effects in infants and children has been raised by findings of decreased neural proliferation in cell culture as well as abnormal development and altered thyroid hormones in larval zebrafish assays. We evaluated the potential for developmental neurotoxicity of TDCPP using in vitro and in vivo studies. With 1-hr exposure in vitro, decreased neuron firing rate was observed in micro-electrode arrays in rat cortical cell cultures at concentrations that did not impact cell viability. In larval zebrafish, acute exposure produced decreases in motor activity. Longer exposures (48 hr) in developing human hN2 cells produced <30% decrease in neurite outgrowth and cell viability only at high concentrations, and no changes were noted in rat cortical neurite outgrowth. Pregnant Long-Evans rats were orally dosed (0, 15, 50, or 150 mg/kg/d) from gestational day 10 to weaning, and offspring were evaluated on several physical and neurological parameters. Serum thyroid hormones were unaffected in offspring on postnatal day (PND) 6 or 22, and in dams post-weaning. Brain weight was unaltered in offspring at both ages, but liver weight was increased in high-dose dams. There were no differences in body weight or litter size at birth, but starting at PND6 the high-dose group showed a persistent impairment in weight gain. The ontogeny of righting reflex (PND 2-4) and of motor activity (PNDs 13, 17, 21) was not altered by treatment. Thus, acute exposures produced effects on larval zebrafish behavior and rat neuronal cell activity. Exposure during developmental processes in rat cortical cells and in rats during the preweaning period showed little to no evidence of specific developmental neurotoxicity. This is an abstract of a proposed presentation and does not reflect US EPA policy.

PS 1747b Impact of Perinatal TCDD Exposure on Neuroendocrine Stress Response System in Mice

S. L. Benner[1], T. Inoshita[1], Y. Ding[1], M. Kakeyama[1, 2] and C. Tohyama[1]. [1]*Grad School of Med., University of Tokyo, Bunkyo-Ku, Tokyo, Japan and* [2]*Grad. Sch. Biomed. Sci, Nagasaki University, Nagasaki, Nagasaki, Japan.*

Adversities during the perinatal period can disrupt the development of the neuroendocrine stress response system, which may influence the vulnerability to psychopathology later in life. The increasing trend of a prevalence of developmental and psychiatric disorders has been suspected of being induced at least partly by environmental chemical exposure during perinatal development. We have previously reported the lasting consequences of perinatal exposure to a low dose of 2,3,7,8-tetrachlorodibenzo-p-dioxin (TCDD) in cognitive, social, and emotional functions in mice. However, its effect on the development of the stress response system has not yet been defined. The current study thus aimed to examine whether an oral administration of 0, 0.6 or 3.0 μg TCDD/ kg on GD 12.5 in C57BL/6 mice induces a permanent impact on the stress response system of the male offspring. A series of stress challenges was conducted when they were adults (8-10 weeks), in order to characterize the hypothalamo-pituitary-adrenal (HPA) axis function. The TCDD-exposed offspring exhibited hypersensitivity of the HPA-axis as well as disruption in the central feedback regulation, and the endocrine phenotype was especially conspicuous in the higher dose, TCDD3.0 group. A significant reduction of corticotropin-releasing hormone (CRH) receptor gene expression was detected in the hippocampus of the TCDD3.0 adult mice, which was also confirmed in the TCDD3.0 neonatal hippocampus. Additionally, reductions in hippocampal ACTH receptor and glucocorticoid/mineralocorticoid receptor ratio were observed at the neonatal stage. The present results suggest that developmental programming of the stress response system is susceptible to a perinatal TCDD exposure, and that a reduced gene expression level of central feedback regulating molecules may underlie their exacerbated stress response.

PS 1747c Developmental Exposure to PCBs Differentially Alters Sensitivity to Audiogenic and Kindling-Induced Seizures in Rats

S. Bandara[1], S. L. Schantz[1] and M. E. Gilbert[2]. [1]*University of Illinois at Urbana-Champaign, Urbana, IL and* [2]*US EPA, Research Triangle Park, NC.*

Previously we reported an increased incidence of audiogenic seizures in offspring of rats exposed to an environmental mixture of polychlorinated biphenyls (PCBs). This study compares the proconvulsant properties of PCB exposure in audiogenic and electrical kindling seizure models. Adult male and female offspring exposed to the PCB mixture throughout gestation and lactation (0 or 6mg/kg/day) were subjected to an audiogenic seizure paradigm (100dB noise, 8 kHz, 2m) and behavioral seizure response (wild running, clonus) recorded. Male littermates were stimulated (1-s train of 60Hz pulses, 1ms pulsewidth, 50-200μA) through indwelling electrodes in the amygdala to establish a threshold for induction of an electrographic afterdischarge (AD). Thereafter, stimulation was delivered once daily at 200μA until a fully generalized seizure (Racine Scale) was evoked. Electrographic and behavioral seizure characteristics were recorded in response to each stimulation. Consistent with previous findings more PCB-exposed rats than controls exhibited clonic seizures (76% vs 22%) in response to noise. In contrast to an augmented audiogenic seizure response, PCBs delayed the development of electrical kindling (16.4 vs 11.6 ADs to 1st Stage 5 seizure). This delay occurred in the early stages as significantly more sessions were required to advance rats from focal (Stage 1-2) to generalized (Stage 3-5) seizures. Groups did not differ in AD thresholds. A trend towards longer cumulative AD duration to 1st generalized seizure was also evident in the PCB-exposed group. A dissociation of responsiveness based on seizure model indicates that while developmental PCB exposure has proconvulsive effects at the level of the auditory brainstem, the same exposure slowed the progression of behavioral manifestations from a focal seizure site in the forebrain. The latter may be reflective of impaired plasticity mechanisms previously reported in PCB-exposed animals. Does not reflect EPA policy; funded by ES15687.

PS 1747d Zebrafish Model of PCB Developmental Neurotoxicity

G. W. Miller and P. Lein. *Molecular Biosciences, University of California, Davis, Davis, CA.*

Despite being banned since the late 1970s, polychlorinated biphenyls (PCBs) remain persistent environmental toxicants that pose significant risk to the developing nervous system. We have demonstrated that some non-dioxin-like PCBs alter neuronal connectivity by promoting dendritic arborization in cultured hippocampal neurons via ryanodine receptor (RyR)-dependent mechanisms. Structure activity relationships (SAR) of RyR sensitization by PCBs has been established using mammalian cell culture. However, whether this SAR translates to in vivo developmental neurotoxicity of PCBs has yet to be tested. Low throughput and high costs make it challenging to perform extensive in vivo SAR studies in rodent models. To address this gap, we are evaluating the embryonic zebrafish as an in vivo model of PCB developmental neurotoxicity. As an initial assessment of the zebrafish model, we tested three PCB congeners that exhibit differing levels of RyR activity in mammalian cells: PCB 77 (negligible RyR activity), PCB 52 (moderate RyR activity), and PCB 95 (high RyR activity). Enzymatically dechorionated embryos were exposed to varying concentrations (0.1-1.7 uM) of these three congeners from 6 to 120 h post fertilization (hpf). Within each cohort of exposed embryos, a set of embryos were treated with vehicle (DMSO) and another set left untreated.

Embryos were observed at 24 and 120 hpf by stereomicroscope for mortality and gross malformations. At 24 hpf, no differences were observed between treatment groups. By 120 hpf, embryos treated with PCB 77 were not significantly different from vehicle controls or untreated embryos. In contrast, there were significant, concentration-related increases in gross malformations and mortality in embryos treated with either PCB 52 or PCB 95, with PCB 95 exhibiting significantly greater potency than PCB 52. These data correlate with the relative potencies of these PCB congeners on RyR activity, suggesting the feasibility of using embryonic zebrafish as a novel in vivo model to study the developmental effects of RyR-active PCBs. Supported by NIH (grant ES014901 and ES011269).

PS 1747e Sex-Dependent Effects of Lead and Prenatal Stress on Neonatal Stress Receptor and Adult Corticosterone Levels

S. Pelkowski[1], M. Sobolewski[1], H. Weston[1], S. Kidd[2], D. W. Anderson[2], J. S. Schneider[2] and D. A. Cory-Slechta[1]. *[1]Univ. of Rochester, Rochester, NY and [2]Thomas Jefferson Univ., Philadelphia, PA.*

Early life exposure to lead (Pb) and prenatal stress (PS) creates sex-specific alterations in CNS development, including the hypothalamic–pituitary–adrenal (HPA) axis, the major stress response system. The current study examined the potential sex specific effects of Pb ± PS on alterations in glucocorticoid (GR:NR3C1) and mineralocorticoid (MR:NR3C2) receptors in neonatal brain and in adult corticosterone levels. C57/Bl6 mouse dams received 0 or 100 ppm Pb water 2 mos prior to breeding through weaning. Half of these dams were exposed to restraint stress 3x/day for 30 min from GD 11-19, while the other half received no stress (NS). This yielded 4 treatment groups/sex: 0-NS, 0-PS, 100-NS and 100-PS. At PND 0 and PND 6, frontal cortex, hippocampus and cerebellum were collected, and the remaining brain used for receptor expression analysis. GR and MR levels were assessed in nuclear and cytosolic brain fractions. Both Pb and PS significantly reduced nuclear GR levels relative to 0-NS controls in females, whereas only PS (0-PS and 100-PS) significantly reduced nuclear MR levels. Males showed the opposite pattern, wherein Pb (100-NS and 100-PS) showed significantly elevated nuclear GR levels. At PND 60, sex-specific differences were also observed in corticosterone levels. Pb-treated males exhibited blunted baseline corticosterone levels, and PS-treated males exposed to acute handling stress displayed significantly elevated corticosterone responses. In contrast, no Pb ± PS-related changes in corticosterone occurred in females. These results show that early life exposure to Pb ± PS creates sex-specific alterations in stress physiology as found for both neonatal and adult neuroendocrine profiles. Altered corticosterone homeostasis has been associated with impaired cognitive function and neurological damage. Understanding the sex-specific response of the HPA axis to early developmental lead and stress exposure may increase our understanding of gender-specific neurobehavioral diseases. ES021534-01

PS 1748 Persistent Organic Pollutants and Different Types of Pesticides Can Interact during Brain Development to Exacerbate Behavioral and Cognitive Defects in Mice

H. Viberg, I. Lee, S. Buratovic, A. Fredriksson and P. Eriksson. *Environmental Toxicology, Uppsala University, Uppsala, Sweden.*

In the field of toxicology the tradition has been to investigate one substance/compound at the time without any thought of possible interactive effects concerning multiple exposures. Humans are continuously exposed to persistent organic pollutants, such as methylmercury (MeHg) and the perfluorinated compound perfluorohexane sulfonate (PFHxS), and different pesticides, such as the organophosphate chlorpyrifos and the organochlorine endosulfan. There is some information present about the developmental neurotoxicity of these individual compounds and we have recently seen that they, individually can induce behavioural disturbances such as deranged spontaneous behaviour and habituation, learning and memory defects and reduced cognitive functions, together with altered function of the cholinergic system, when the exposure occurs during a critical phase of neonatal brain development (PND 10). Therefore, in the present study we investigated how a combined exposure to MeHg and chlorpyrifos as well as a combined exposure to PFHxS and endosulfan could affect behaviour and cognitive function. Adult mice, neonatally exposed to 0.4 mg MeHg/kg bw and chlorpyrifos (5 or 10 mg/kg bw), showed a disturbed spontaneous behavior to a novel home environment and reduced habituation compared to the control animals and the individual exposures. The same was seen in adult mice neonatally exposed to PFHxS (6.1 or 9.2 mg/kg bw) and endosulfan (0.05 or 0.1 mg/kg bw). Interestingly, these effects seem to be of a synergistic nature, because effects were even seen for combinations of doses where the individual doses did not induce disturbances in spontaneous behavior to a novel home environment. These results indicate that the present methods of risk assessment can underestimate the potential risk with chemicals, since combinations of chemicals potentially can shift the dose-response curve.

PS 1749 Adult Dose-Response-Related Behavioral Effects of 4 Different Pesticides, after Neonatal Exposure

S. Hallgren, I. Lee, S. Buratovic, A. Fredriksson, P. Eriksson and H. Viberg. *Environmental Toxicology, Uppsala University, Uppsala, Sweden.*

There are several different types of pesticides globally used, all with their own characteristics and toxicological potency. In the present study we have exposed male mice neonatally to different doses of four different types of pesticides, carbaryl (carbamate) chlorpyrifos (organophosphate), cypermethrin (pyrethroid) and endosulfan (organochlorine), and tested them for spontaneous behavior in a novel home environment at adult age. The doses used were 0.5 – 20 mg carbaryl/kg bw, 0.1 – 5.0 mg chlorpyrifos/kg bw, 0.1 – 5.0 mg cypermethrin/kg bw and 0.05 – 20 mg endosulfan/kg bw. All four pesticides induced adult disturbances in the spontaneous behavior in a novel home environment, affecting cognitive function, at 2 months of age. Carbaryl induced a dose-response related effect on spontaneous behavior from 5 mg/kg bw and up, while chlorpyrifos only induced a weak effect with the highest dose tested (5 mg/kg bw). The pyrethroid cypermethrin induced dose-response related neurotoxicity from 0.5 mg/kg bw and up. The organochlorine endosulfan also induced dose-response related neurotoxicity from 0.1 mg/kg bw and up These disturbances also persisted when the animals were re-observed at 4 months of age, indicating that these effects are long-lasting or even irreversible. From this study we conclude that endosulfan seem to be the most potent, of these four compounds, to induce cognitive behavioral effects in the adult after neonatal exposure, while carbaryl has the lowest potency to induce these types of neurotoxic effects.

PS 1750 Developmental Exposure to Levels of Chlorpyrifos That Do Not Inhibit Brain Cholinesterase Induces Decreased Emotional Reactivity in Rodents

R. L. Carr, M. K. Ross and C. A. Nail. *Center for Environmental Health Sciences, Mississippi State University, Mississippi State, MS.*

Traditionally, chlorpyrifos (CPS) mediates its toxicity through inhibition of cholinesterase (ChE). However, in recent years, the toxicological effects of developmental CPS exposure have been attributed to an unknown non-cholinergic mechanism of action. We hypothesize that the endocannabinoid system may be an important target because of its vital role in nervous system development. We have previously reported that repeated exposure to 0.5 mg/kg CPS results in the inhibition of fatty acid amide hydrolase (FAAH), the enzyme that metabolizes the endocannabinoid anandamide (AEA), without measurable inhibition of ChE. This exposure resulted in the accumulation of AEA in the forebrain of juvenile rats. Current literature indicates that FAAH activity and AEA levels play an important role in the regulation of emotional reactivity. However, it is unclear if our observed changes in these parameters results in any changes in emotional reactivity. To determine this, 10 day old rat pups were exposed daily for 7 days to either corn oil or 0.5, 0.75, or 1.0 mg/kg CPS by oral gavage. On PND25, the rats were placed into a dark container in a novel open field and the latency to emerge from the container was measured. In this test, rats that stay in the dark for a long time are considered emotionally reactive. All CPS treated groups spent significantly less time in the dark prior to emerging as compared to control suggesting a decreased level of emotional reactivity induced by CPS exposure. Although not directly correlated, our data suggest that the alteration of endocannabinoid signaling during developmental exposure can lead to alteration of behavioral function.

PS 1751 Zebrafish Brain Development Is Altered by Early Exposure to the Organophosphate Chlorpyrifos

H. Richendrfer and R. Creton. *MCB, Brown University, Providence, RI.*

Pesticides are found ubiquitously in the environment because of their wide use in agriculture. While adults have enzymes that are able to break down pesticides, developing embryos lack the necessary enzymes for toxicant removal. Low doses of organophosphate pesticides during early embryonic development in animal models and humans have been documented to affect brain development and behavior. Because embryos are more vulnerable to pesticides, it is important to determine at which stages of development embryos are most affected by the exposure to organophosphate pesticides. Using zebrafish as a model system for pesticide exposure is advantageous because embryos can be exposed to organophosphates immediately after fertilization and large numbers of larvae can be used for high-throughput behavioral analysis and brain imaging. Using a high-throughput assay developed in our lab we have shown that low doses of a widely used organophosphate, chlorpyrifos (even in very low doses), affect discrete behaviors if administered during specific developmental time periods. Current studies in our lab utilize a transgenic line of zebrafish, Tg(elavl3:Kaede) for two-photon brain imaging. Embryos from this line

can be exposed to UV light during the first few days of development which 'marks' already present neurons a red fluorescence color, whereas newly born neurons will contain green fluorescence. Results of our current studies indicate that zebrafish treated with organophosphate pesticides show altered brain development compared to control zebrafish. The results of the present study suggest that the modified brain development seen in zebrafish may be indicative that chlorpyrifos is a contributing factor in neurodevelopmental disorders such as autism, ADHD, and anxiety. These results have the potential to affect dietary guidelines for pregnant women and children.

PS 1752 Modeling the Developmental Neurotoxicity of Chlorpyrifos in Human Neural Stem Cells: Role of Butyrylcholinesterase in Neuronal Differentiation

A. K. Tiethof[1, 2], R. P. Hart[3, 4], J. C. Moore[4, 5, 6] and J. Richardson[1, 2]. [1]*Environmental and Occupational Health Sciences Institute and Department of Environmental and Occupational Medicine, Robert Wood Johnson Medical School, Picataway, NJ,* [2]*Joint Program in Toxicology, Rutgers University, Piscataway, NJ,* [3]*Department of Cell Biology and Neuroscience, Rutgers University, Picataway, NJ,* [4]*The Human Genetics Institute of New Jersey, Picataway, NJ,* [5]*RUCDR Infinite Biologics, Piscataway, NJ and* [6]*Department of Genetics, Rutgers University, Piscataway, NJ.*

The organophosphorus pesticide chlorpyrifos (CPS) primarily exerts toxicity through inhibition of acetylcholinesterase (AChE). However, several studies hypothesized that additional targets of CPS may be responsible for its developmental neurotoxic effects. Butyrylcholinesterase (BChE) is the evolutionary counterpart to AChE. Both enzymes appear early in nervous system development prior to cholinergic synapse formation, with BChE expressed before AChE. Therefore, we hypothesized that BChE may be an important target of CPS during neuronal development. To model neuronal development in vitro, we used human neural stem cells (NSCs) derived from induced pluripotent stem cells (iPSC). After four days of Brain-derived neurotrophic factor (BDNF) induced neuronal differentiation of iPSC-derived NSCs, BChE activity increased 115%, while AChE activity was unchanged. BChE mRNA expression increased greater than two-fold, whereas AChE mRNA expression was not altered. Treatment of differentiating NSCs with chlorpyrifos (10 μm) continuously during differentiation caused the inhibition of AChE and BChE activity by 82% and 97%, respectively. However, CPS exposure had no effect on cell morphology, viability or the expression of the early neuronal differentiation marker HES5. To determine the role of BChE protein, shRNA was utilized to knock down expression of BChE. Preliminary results indicate a 74% decrease in HES5 after BChE knockdown, which suggests that BChE may play a role in the differentiation of NSCs independent of, or in addition to its enzymatic activity. Support provided by: R01ES015991 and P30ES005022.

PS 1753 Astrocytes Protect against Diazinon- and Diazoxon-Induced Inhibition of Neurite Outgrowth by Regulating Neuronal Glutathione

D. M. Pizzurro[1, 2], K. Dao[2] and L. G. Costa[2, 3]. [1]*Gradient, Cambridge, MA,* [2]*Department of Environmental and Occupational Health Sciences, University of Washington, Seattle, WA and* [3]*Department of Neuroscience, University of Parma, Parma, Italy.*

Evidence continues to emerge that demonstrates human exposure to various organophosphorus insecticides (OPs) is associated with neurobehavioral deficits in children. Focusing on the widely used OP diazinon (DZ) and its active oxygen metabolite, diazoxon (DZO), we explored their ability to impair neurite outgrowth in rat primary hippocampal neurons as a mechanism of developmental neurotoxicity. Both DZ and DZO (0.5-10 μM) significantly inhibited neurite outgrowth in hippocampal neurons at concentrations devoid of any cyototoxicity. These effects appeared to be mediated by oxidative stress, as they were prevented by antioxidants (melatonin, N-t-butyl-alpha-phenylnitrone, and glutathione ethyl ester). Inhibition of neurite outgrowth was observed at concentrations below those that inhibit the catalytic activity of acetylcholinesterase. Follow-up experiments in an indirect co-culture system demonstrated that the presence of astrocytes was able to protect against inhibition of neurite outgrowth by DZ and DZO. Astrocytes increased neuronal glutathione (GSH) in neurons to levels comparable to those of GSH ethyl ester. Astrocytes depleted of GSH by L-buthionine-(S,R)-sulfoximine (BSO) no longer conferred protection against DZ- and DZO-induced inhibition of neurite outgrowth. The findings indicate that DZ and DZO inhibit neurite outgrowth in hippocampal neurons by mechanisms involving oxidative stress, and these effects can be modulated by astrocytes and astrocyte-derived GSH. Oxidative stress from other chemical exposures, as well as genetic abnormalities that result in deficiencies in GSH synthesis and regulation, may render individuals more susceptible to these developmental neurotoxic effects of OPs.

PS 1754 Prenatal Dexamethasone, As Used in Preterm Labor, Exacerbates the Impact of Postnatal Chlorpyrifos Exposure on Serotonergic Pathways

F. Seidler, J. Card and T. A. Slotkin. *Pharmacology & Cancer Biology, Duke University Medical Center, Durham, NC.*

We examined the potential for prenatal dexamethasone treatment to create a subpopulation whose developing brain has been sensitized to the effects of subsequent postnatal chlorpyrifos exposure. Pregnant rats received a standard therapeutic dose (0.2 mg/kg) of dexamethasone on gestational days 17-19; pups were given subtoxic doses of chlorpyrifos on postnatal days 1-4, (1 mg/kg, <10% cholinesterase inhibition). We evaluated serotonin (5HT) synaptic function from postnatal day 30 to day 150, assessing the expression of 5HT receptors and the 5HT transporter in brain regions encompassing all the 5HT projections and cell bodies along with 5HT turnover (index of presynaptic impulse activity) in the cerebral cortex. These parameters are known targets for neurodevelopmental effects of dexamethasone and chlorpyrifos individually. In males, chlorpyrifos produced an overall elevation in the expression of 5HT synaptic proteins, with a progressive increase from adolescence to adulthood; this effect was lessened by prenatal dexamethasone treatment. The chlorpyrifos-induced upregulation was preceded by deficits in 5HT turnover, indicating that the receptor upregulation was an adaptive response to deficient presynaptic activity. Turnover deficiencies were exaggerated by dexamethasone treatment, thus worsening the functional impairment caused by chlorpyrifos. In females, chlorpyrifos-induced receptor changes were spared relative to those in males. Nevertheless, prenatal dexamethasone still exacerbated the 5HT turnover deficits and reduced 5HT receptor expression in females, demonstrating the same adverse interaction. Glucocorticoids are used in 10% of U.S. pregnancies, and are also elevated in maternal stress; consequently, our results indicate that this group represents a large subpopulation that may have heightened vulnerability to developmental neurotoxicants such as the organophosphates. (Support: NIH ES10356)

PS 1755 Ketamine Induces Neurotoxicity in the Developing Brain

J. Liu, X. Han and S. D. Soriano. *Anaesthesia, Harvard Medical School, Boston, MA.*

Ketamine, a non-competitive N-methyl-D-aspartate receptor (NMDA-R) antagonist, is commonly used to induce anesthesia and analgesia in infants and children undergoing surgery and painful procedures. However, little is known about how ketamine impact the developing nervous system, especially in infants and young children. In our previous studies, we found that ketamine activated aberrant cell cycle reentry and induced apoptosis by increasing expression of cyclin D1, cleaved-caspase-3 and Bim in vivo and in vitro. Ketamine also activated the AKT- GSK-3b (glycogen synthase kinase 3b) pathway in the developing rat brain. Based on these, we hypothesize how ketamine affects pathological neurodegeneration the developing rat brain.

Material and Methods: Sprague-Dawley postnatal day 7 (P7) rat pups were used for this study. Rats were given three doses of 5, 10 and 20 mg/kg body weight of ketamine (ket) and one control group. Each rat pup received 4 intraperitoneal doses of either saline, or ket at 90 minutes intervals over 6 h. After the 6 h treatment period, the animals were deeply anesthetized with pentobarbital (100 mg/kg, IP). Parts of the brain tissues were extracted and flash frozen in liquid nitrogen for western blotting analysis. The other parts were fixed in 4% paraformaldehyde for immunohistochemical assay. Apoptosis such as cleaved-caspase-3, TUNEL, and other protein expression such as Disrupted in schizophrenia-1 (DISC1) and early growth response-1 (EGR-1) were determined by immunofluorescent and western blotting assays.

Results and Conclusion: Ketamine could significant increase neuroapoptosis by increasing apoptosis and cleaved-caspase-3 expression in the rat brain tissues. Ket also significantly decreased the expression of DISC1 and EGR-1, indicating a reduction in developing neurite. These findings suggest that ketamine may induce neurodegeneration by regulating DISC1 pathway in the developing brain.

PS 1756 Using 2D and 3D Electron Microscopy Techniques to Study Mitochondrial Ultrastructure in the Developing Rat Brain after Ketamine Treatment

T. Eustaquio[1], A. Paredes[1], F. Liu[2], W. Slikker[3], M. G. Paule[2], P. C. Howard[1] and C. Wang[2]. [1]*Office of Scientific Coordination, USFDA-NCTR, Jefferson, AR,* [2]*Division of Neurotoxicity, USFDA-NCTR, Jefferson, AR and* [3]*Office of the Director, USFDA-NCTR, Jefferson, AR.*

Ketamine, an FDA-approved N-methyl-D-aspartate (NMDA) receptor antagonist, is commonly used for general pediatric anesthesia. Recent evidence has indicated that continuous exposure to ketamine induces extensive neuronal cell death in

the developing brains of experimental animals. It has been speculated that the underlying mechanism involves a compensatory upregulation of NMDA receptor subunits that amplifies intracellular calcium concentrations that are beyond the buffering capacity of the mitochondria. This results in loss of mitochondrial membrane potential and disruption of electron transport, eventually leading to elevated levels of reactive oxygen species and cell death. Little is known, however, about the overall changes in the mitochondrial ultrastructure that may accompany the distinct events in this cascade. The objective of this study is to utilize complementary methods of electron microscopy (EM) to study the mitochondrial ultrastructure in developing rat brains after ketamine treatment: classical transmission EM (TEM) to study single mitochondria in individual neuronal cells in 2D and serial block-face scanning EM (SBF-SEM) to study mitochondria-rich brain tissues in 3D. Postnatal day 7 rats were administered 6 injections of 20 mg/kg at 2-h intervals, a dose that was previously found to induce significant neurotoxicity in the frontal cortex. Severity grading of TEM micrographs showed a significant proportion of swollen mitochondria in the frontal cortex ($p = 0.02$), while 3D reconstructions of SBF-SEM data showed that mitochondrial volume was concurrently increased. Such alterations of mitochondrial ultrastructure are solid evidence indicating mitochondria play a critical role in ketamine-induced neuronal cell damage. This study demonstrates that quantitative 2D and 3D EM are valuable tools that can reveal how ultrastructure plays a critical role in understanding drug interactions.

PS 1757 Neonatal Low-Dose Coexposure to the Anaesthetic Agent Ketamine and Gamma-Radiation Causes Persistent Neurobehavioural Defects in Adult Mice

P. Eriksson[1], S. Buratovic[1], B. Stenerlöw[2], A. Fredriksson[1] and S. Sundell-Bergman[3]. *[1]Dept. Environmental Toxicology, Uppsala University, Uppsala, Sweden, [2]Dept. Radiology, Oncology and Radiation Science, Uppsala University, Uppsala, Sweden and [3]Dept. Soil and Environment, Swedish University, Uppsala, Sweden.*

Ionising radiation (IR) is widely used in the medical field for treating tumours, including tumours in the central nervous system, and for imaging techniques such as computed tomography (CT). There is a lack of knowledge and increasing concern about effects and consequences from low dose exposure during critical phases of brain development and the combination of IR and anaesthetic agents. In earlier studies we have seen that IR as well as the anaesthetic agent ketamine can induce persistent developmental neurotoxic effects. We have also recently reported that IR can interact with environmental agents, during a critical period of neonatal brain development, to exacerbated developmental toxic effect including reduced cognitive function in adults.
Neonatal NMRI male mice, 10 days of age, were exposed to a single s.c. dose of ketamine (7.5 mg/kg bw). One hour after the ketamine exposure the mice were irradiated with 137Cs gamma radiation (Rudbeck laboratory, Uppsala University). Mice were irradiated in plastic dishes with a surface dose-rate of around 0.2 Gy/min. The mice were irradiated at the doses of 0.05, 0.1 and 0.2 Gy, respectively, given at one occasion. The animals were subjected to spontaneous behaviour in a novel home environment at ages of 2- and 4-months. Neither the single dose of ketamine (7.5 mg/kg bw) nor the radiation dose of 0.05, 0.1 or 0.2 Gy affected the spontaneous behavior, but the co-exposure ketamine 7.5 mg/kg bw and to external gamma radiation 0.1 and 0.2 Gy caused developmental neurotoxic effects. The effects were also dose-response related. The study shows that co-exposure to IR and ketamine can interact and significantly enhance developmental neurotoxic effects, manifested as disrupted spontaneous behaviour in a novel home environment behaviour including reduced/lack of habituation which indicate reduced cognitive functions in the adults.

PS 1758 The Antirheumatic Drug, Leflunomide, Interferes with the Dopamine Synthesis Pathway

A. Planchart, L. St. Mary, K. Duke, M. Ihrie and C. J. Mattingly. *Biological Sciences, North Carolina State University, Raleigh, NC.*

Leflunomide belongs to a class of drugs known as disease-modifying antirheumatic drugs (DMARD), and is used to treat rheumatoid arthritis and systemic lupus erythematosus. Previous studies showed that Leflunomide, but not its metabolite A771726, activates the aryl hydrocarbon receptor (AHR) pathway presumably by binding to the receptor's ligand binding site, and increases transcription of CYP1A1. The AHR ligand, 2,3,7,8-tetrachlorodibenzo-p-dioxin (TCDD), causes severe craniofacial defects in model organisms, including zebrafish. The affected structures are derived from cranial neural crest cells (NCCs), which are multipotent cells originating at the interface of the neural ectoderm and underlying neural tube. NCCs migrate to distant regions of the embryo, and undergo differentiation to generate multiple cell types, including chondrocytes, neurons, and melanocytes. To determine if Leflunomide interferes with neural crest cell function, we exposed zebrafish embryos to 5 μM Leflunomide –half the concentration of previous studies examining its effect on AHR activation—and observed the absence of melanin synthesis. Melanin, or more specifically, eumelanin and pheomelanine, is derived from tyrosine in the same biochemical pathway that synthesizes the neurotransmitters dopamine, norepinephrine and epinephrine in dopaminergic neurons, which progressively degenerate in Parkinson's disease patients. We then used dat:gfp transgenic zebrafish, which express green fluorescent protein (GFP) under the control of the dopamine transporter promoter (dat), to examine the effect of Leflunomide exposure on dopaminergic neurons. We observed progressive loss of GFP in cells corresponding to dopaminergic neurons, which we confirmed by immunohistochemistry using antibodies to the rate-limiting enzyme, tyrosine hydroxylase. Our study demonstrates that Leflunomide may interfere with the normal function of dopaminergic neurons but further studies are required to determine susceptibility windows and risks in other species, including humans.

PS 1759 Cumulative Vaccination Alters Immune Responses in the Developing Brain

K. Streifel[1, 3], K. L. Jones[2], J. Van de Water[2, 3] and P. Lein[1, 3]. *[1]Department of Molecular Bioscience, University of California Davis, Davis, CA, [2]Department of Internal Medicine, University of California Davis, Davis, CA and [3]M.I.N.D. Institute, University of California Davis, Davis, CA.*

Peripheral immune activation triggered by infection during gestational and postnatal development has been linked to adverse neurodevelopmental outcomes. Vaccination also activates the peripheral immune system to generate an immune response that will protect against future pathogenic infections. While these vaccines have been individually tested for efficacy in protecting against pathogenic infection, there have been no studies investigating whether immune challenge through cumulative vaccination in early childhood alters neurodevelopment. To address this question, we used a rat model to assess whether treatment with the recommended childhood immunization schedule alters cytokine profiles and neuroinflammation. Because there is evidence that immune challenge can elicit altered immune responses in susceptible populations, we compared effects of immunization in rats with varying immune profiles: Lewis rats, which have a genetic predisposition to a Th1 pro-inflammatory response, and Brown Norway rats, which skew towards a Th2 allergy response. On postnatal day 10, rats were vaccinated according to the vaccination schedule typically administered humans at 2 months of age (RV, DTaP, Hib, PCV, and IPV). Controls received an equal volume of adjuvant and saline. Rats were euthanized 2 or 5 days post treatment. Quantification of cytokine levels using Luminex multiplex technology indicated that while there were no significant treatment effects on the peripheral response, there were treatment-related changes within the cortex, cerebellum and hippocampus in both sexes across both rat strains. Ongoing immunohistochemical studies are evaluating microglial and astroglial activation in these same brain regions. Whether these responses alter neurodevelopment has yet to be determined but is the focus of future studies.
Supported by Safe Minds and NIH (T32-MH073124).

PS 1760 Dysregulation of Autism-Associated Synaptic Proteins by Environmental Contaminants

G. Kaushik, J. C. Pfau, K. Aho and M. A. Thomas. *Biological Sciences, Idaho State University, Pocatello, ID.*

With the prevalence in U.S. as 1 in 50 children, a majority of cases of idiopathic autism in children likely result from unknown environmental triggers in genetically susceptible individuals. These triggers may include maternal exposure of a fetus to minute concentrations of pharmaceuticals and personal care products (PPCPs). Unmetabolized psychoactive pharmaceuticals reach drinking water through a variety of routes, including ineffectively processed sewage. Previous studies in our laboratory examined the extent to which gene sets associated with neuronal development were up- and down-regulated (enriched) in the brains of fathead minnows treated with PPCPs at environmental concentrations. Here, we tested two successive hypotheses 1) the enriched gene sets in fish brains were associated with Autism Spectrum Disorders (ASD) by analyzing the extent to which their protein products interacted with other proteins in a protein-protein interaction network, composed of known ASD-associated gene products and their interaction partners or degrees; 2) PPCPs would alter *in vitro* expression of ASD-associated synaptic proteins that had exceptional parameters within ASD-associated network. A network of 7212 proteins and 33,416 edges (connections) was generated and visualized by using the bioinformatics software package Cytoscape. We found that enriched gene sets from our previous study were more inter-connected than non-enriched sets in the network based on both degree and clustering coefficient. Within the significant gene sets, we listed key synaptic proteins that have been found to be associated with ASD in other studies. We differentiated human neuroblastoma cells for 2 weeks with 10μM retinoic acid (RA) and treated with environmentally relevant concentrations of fluoxetine, carbamazepine and venlafaxine, and analyzed expression of proteins

with flow cytometry. This study signifies that PPCPs alter the expression of key synaptic proteins that potentially contribute to neurological disorders like ASD by disrupting neuronal development.

PS 1761 Nicotine-Induced Insomnia in Larval and Juvenile Zebrafish

M. E. Wolter and K. R. Svoboda. *Joseph J. Zilber School of Public Health, University of Wisconsin-Milwaukee, Milwaukee, WI.*

At least 13% of pregnant mothers smoke while they are pregnant and the children of those mothers often sleep less than children born from mothers who do not smoke. In addition to these developmental consequences of smoking, adult smokers often report having problems associated with disrupted sleep. It is thought that these disruptions are related to nicotine which is a potent stimulant and a key ingredient found in cigarettes. The action(s) of nicotine are mediated by activation of neuronal nicotinic acetylcholine receptors (nAChRs) distributed throughout the nervous system. The pineal gland and the retina, two structures that are important for controlling the circadian rhythm (CR) express nAChRs in zebrafish. Thus, we hypothesized that an acute nicotine exposure would disrupt the CR and potentially create an "insomnia-like" phenotype in zebrafish. We evaluated the consequences of an acute, continuous nicotine exposure on the CR in one, two, and three week old zebrafish. One week old larvae exposed to 1μM nicotine had a disrupted CR. Two week old zebrafish exposed to 5μM nicotine had a disrupted CR, but a 1μM nicotine exposure had no effect on the CR. Interestingly, continuous exposure to both 1μM and 5μM nicotine disrupted the CR in 3 week old zebrafish. Along with the disruption in the CR, nicotine exposure consistently increased locomotor activity in the initial 6 hours of the CR. These results indicate that nicotine is capable of altering the "sleep state" of the zebrafish by creating an initial period of hyperactivity followed by a disruption in the circadian rhythm. When combined, we suggest that these phenotypes may be analogous to nicotine-induced insomnia in humans.

PS 1762 Coexposure to Gamma-Radiation and Nicotine during a Critical Period of Neonatal Brain Development Can Exacerbate Cognitive Defects in Adult Mice

S. Buratovic[1], B. Stenerlöw[2], S. Sundell-Bergman[3], A. Fredriksson[1] and P. Eriksson[1]. [1]*Dept. Environmental Toxicology, Uppsala University, Uppsala, Sweden,* [2]*Dept. Radiology, Oncology and Radiation Science, Uppsala University, Uppsala, Sweden and* [3]*Dept. Soil and Environment, Swedish University of Agricultural Sciences, Uppsala, Sweden.*

It is known that neonatal exposure to low doses of external γ-radiation as well as nicotine can affect cognitive functions in adult mice. The present study was carried out to investigate whether neonatal co-exposure to external γ-radiation and nicotine can exacerbate developmental neurotoxic effects, including altered susceptibility of the cholinergic system, in adult mice. Neonatal male NMRI mice were exposed to: 1) external γ-radiation (60Co, 0.2 Gy, dose-rate 0.07 Gy/min) on PND10, PND10 and 11 or PND10, 11 and 12, 2) 66 μg nicotine/kg bw s.c. twice daily on PND10, PND10 and 11 or PND10, 11 and 12, 3) 0.2 Gy and 66 μg nicotine /kg bw on PND10, PND10 and 11 or PND10, 11 and 12. Controls were exposed to saline and sham irradiated. At an adult age of 2 months animals were observed for spontaneous behaviour in a novel home environment and the variables locomotion, rearing and total activity were registered. Neurotoxic recordings regarding altered susceptibility of the cholinergic system, animals were injected with 80 μg nicotine/kg bw sc and observed for spontaneous behaviour. Animals exposed to 3 x 0.2 Gy as well as animals co-exposed to 3 x 0.2 Gy and 3 x 66 μg nicotine/kg bw showed a deranged spontaneous behaviour at 2 months of age. When challenged to nicotine (80 μg/kg bw) previously mentioned animals showed an increased susceptibility to nicotine at an adult age. All effects were significantly more pronounced in mice co-exposed to γ-radiation and nicotine. These results indicate that external γ-radiation and nicotine can interact to enhance behavioural defects at an adult age if the exposure occurs during a critical period of neonatal brain development. The increased susceptibility to nicotine and altered cognitive function suggests that the cholinergic system is a target system for this type of neurotoxic effects.

PS 1763 Integrating Kinetics and Dynamics for Domoic Acid: Lessons Learned from a Mouse Neurodevelopmental Study

J. Park[1, 3], M. Shiotani[1], S. Hong[1, 3], D. Wittington[2], T. B. Cole[1], W. C. Griffith[1, 3], T. M. Burbacher[1], L. G. Costa[1] and E. M. Faustman[1, 3]. [1]*Environmental and Occupational Health Sciences, University of Washington, Seattle, WA,* [2]*Medicinal Chemistry, University of Washington, Seattle, WA and* [3]*Institute for Risk Analysis and Risk Communication, University of Washington, Seattle, WA.*

Although human public health guidelines have been implemented to limit domoic acid (DA) ingestion from shellfish, consumption of DA contaminated seafood by pregnant women remains a concern as DA produced by harmful algal blooms of Pseudo Nitzschia could alter neurodevelopment of fetuses. To assess the effects of repeated, low-level DA exposures on early neurodevelopment, we conducted toxicokinetic and neurobehavioral studies on pregnant C57BL/6 mice and their offspring. Maternal non-symptomatic human-relevant doses of 0, 1, or 3 mg/kg of DA were administered orally in pregnant mice from gestational days (GD) 10 to 17. The toxicokinetics study showed significant DA accumulations in fetal brain and amniotic fluid over time. Maternal and fetal blood peaked at 1.2 and 3.4 hours after the last dose on GD17, respectively, suggesting that fetuses have delayed exposures to DA. Maternal and non-pregnant mice plasma clearance rates (95% CI) were 0.18 (0.16, 0.21) per hour, where up to 38% of DA in maternal blood was going into fetuses. The neurobehavioral tests revealed that offspring from DA exposed dams demonstrated significant dose and sex specific neurobehavioral effects in some of post weaning measurements, such as anxiety in elevated plus maze, walking patterns in CatWalk, home-cage behaviors, and memory in Morris water maze. Integration of kinetics and dynamics of DA were done by correlating areas under the curve and peak concentrations with neurobehavioral outcomes. Results from our studies add significant new information to the literature on kinetics and dynamics of DA with human-relevant exposure patterns, pathways, and levels. This work has been supported by the Pacific Northwest Center for Human Health and Ocean Studies (NIH: P50 ES012762 and NSF: OCE-0434087, OCE-0910624, and 1128883).

PS 1764 Neurohistopathology of Postnatal IP Dose of MK-801 in Juvenile Rats

R. M. Parker[1], D. C. Thake[2] and R. C. Switzer[3]. [1]*DART, Huntingdon Life Sciences, East Millstone, NJ,* [2]*MW ToxPath Sciences LLC, Chesterfield, MO and* [3]*NeuroScience Associates, Inc, Knoxville, TN.*

Characterization of low occurrence of isolated minimal or mild degeneration (DEG) and apoptosis (APO) in control brains is imperative to determine the difference between relationship of normal changes and the effects of a test article. The effects of MK-801 (a non-competitive NMDA antagonist with known neurotoxic properties) on the development of juvenile Sprague-Dawley rat brains were characterized. The MK-801 group received a single dose (3 mg/kg, IP) on PNDs 7, 8, 9, 11 13, 16, 23, 39, 69 or 111). The control article (distilled water, 5 mL/Kg, oral gavage) was dosed daily from PND 7 until the day prior to termination. Thirty or twenty rats per sex per time-point had brains perfused/harvested on PNDs 8, 9, 10 and 12, or on PNDs 14, 17, 24, 40, 71 and 113, respectively. The brains were embedded, coronally sectioned at 40μ (through the entire brain length), and stained with amino cupric silver (DEG changes) and caspase 9 stain (APO). Neurohistopathological evaluation of the entire brain for DEG and APO was performed.

APO and DEG was prevalent in numerous brain regions of younger control animals (primarily from PND 8 through PND 24). Therefore DEG and APO treatment effects are changes present in a given brain area, specific for each PND, that were greater in incidence or severity than control values. Increased DEG and APO were present in MK-801 animals at all time-points. Increased DEG and APO in MK-801 rats were present in a large number of brain sites in the earlier PNDs with severities ranging from minimal to marked while these changes at later PNDs were substantially diminished. Females generally had more brain sites involved than did males especially at the later PNDs. By PND 40, males typically had only 3 or 4 sites at which DEG was observed. APO that was present in MK-801 rats was generally distinct and unequivocal when compared with the control animals. Based on this data, isolated minimal or mild occurrences of DEG and APO should not be considered treatment related events in juvenile Sprague-Dawley rats.

PS 1764a Comparing the Neurotoxic Effects of Propofol and Ketamine in Rat Embryonic Neural Stem Cells

F. Liu[1], N. V. Sadovova[2], C. M. Fogle[1], T. A. Patterson[1], M. G. Paule[1], W. Slikker[1] and C. Wang[1]. [1]*National Center for Toxicological Research, Jefferson, AR and* [2]*Toxicologic Pathology Associates, Jefferson, AR.*

Propofol and ketamine are widely used in pediatric anesthesia and analgesia. To evaluate their developmental neurotoxicity and exmine underlying mechanisms, embryonic neural stem cells (NSCs) were used. NSCs were harvested from gestational day 14 rat fetuses and exposed on day 7 in culture to propofol at concentrations of 10, 50, 100, 300 and 600 μM, or ketamine at 1, 10, 100, and 500 μM ketamine in growth medium (GM) for 24 h or to 50 μM propofol or 10 μM ketamine in differentiation medium (DM). In GM propofol caused a dose-dependent reduction in NSC viability; while ketamine did not have this effect except at the very high concentration of 500 μM. At clinically-relevant concentrations in GM, propofol produced a dramatic increase in ROS generation and enhanced apoptosis as evidenced by an increase in Bax and in TUNEL-positive cells. Similar apoptotic effects were not observed at clinically-relevant dose of ketamine. No significant intracellular Ca2+ influx was detected when NSCs were stimulated with 50 μM NMDA in GM, suggesting there were no functional NMDA receptors expressed on NSCs in GM. In DM, most of the NSCs differentiated into neurons or glial cells. Differentiated neurons were identified using immuno staining with PSA-NCAM (a neuron-specific marker) and calcium influx stimulated with 50 μM NMDA suggested the existence of functional NMDA receptors. Propofol and ketamine significantly increased NSC ROS generation in DM. Propofol and ketamine caused neuronal damage but did not significantly affect glial cells. These observations suggest that ROS plays a key role in propofol and ketamine-induced neurotoxicity and that Ca2+ imaging and gene and protein arrays will be critical for defining associated mechanisms. In summary, an excitatory action of glutamate neurotransmission can be closely related to anesthetic-induced toxicity during development.

PS 1764b Understanding the Mechanism of Anesthetic-Induced Developmental Neurotoxicity Provides Pathways to Prevention

W. Slikker, F. Liu, N. V. Sadovova, S. Liu, X. Zhang, C. M. Fogle, T. A. Patterson, M. G. Paule and C. Wang. *NCTR/FDA, Jefferson, AR.*

Frequently used anesthetics have either NMDA-type glutamate receptor blocking or GABA receptor enhancing properties. To test the unifying hypothesis that exaggerated intracellular Ca2+ accumulation and mitochondrial dysfunction is a common pathway leading to neuroapoptosis following anesthesia, acetyl-L-carnitine (ALC), an anti-oxidant and mitochondrial protector, was used in a variety of in vivo and in vitro studies with and without concomitant exposure to ketamine or propofol. Embryonic neural stem cells were harvested from gestational day 14 rat fetuses and exposed on the 7th day in culture for 24 hrs to 1, 10, 100, and 500 μM ketamine in the growth medium, and/or in differentiation medium, or ketamine plus ALC (10 μM) for 24 hrs, followed by a 24-hr withdrawal period. Mitochondrial viability was not significantly affected, and no significant changes in calcium influx were detected on neural stem cells in growth medium (lack of functional NMDA receptor); whereas calcium influx was detected in neurons while in differentiation medium after stimulation with 50 μM NMDA. However, for those differentiated neurons, enhanced neuronal apoptosis was apparent as indicated by an increased number of TUNNEL-positive cells and a significantly decreased number of PSA (neuron-specific marker)-positive neurons. Additionally, co-administration of ALC effectively protected neurons (Ketamine plus 10 μM ALC for 24 hrs, followed by a 24-hr withdrawal period) from ketamine-induced neuronal damage. Like-wise, 24-hr exposure of neural stem cells to clinically-relevant concentrations of propofol (50 μM) resulted in apoptotic cell death that was attenuated by ALC. Together, these data support the hypothesis that oxidative stress and mitochondrial dysfunction is a common pathway to anesthetic-induced toxicity during develop and that decreasing oxidative stress provides a promising pathway to prevention of neurotoxicity.

PS 1764c Propofol Adverse Effects on Neural Stem Cell Differentiation and Viability

N. V. Sadovova[1], F. Liu[2], C. M. Fogle[2], M. G. Paule[2], W. Slikker[2] and C. Wang[2]. [1]*Toxicologic Pathology Associates, Jefferson, AR and* [2]*Neurotoxicology, NCTR/FDA, Jefferson, AR.*

Propofol is a commonly used short-acting general anesthesia drug. Propofol is a GABA receptor agonist and exerts its analgesic effect through GABA system. A growing body of data suggests that exposure to anesthetics during certain periods of brain development has long-term deleterious effects. To study the underlying mechanisms associated with propofol-induced neuronal toxicity and adverse effects, a neural stem cell model was utilized. Embryonic neural stem cells were harvested from gestational day 14 rat fetuses and maintained in growth medium for 7 days. On the 8th day cultures were exposed to 0 μM propofol (control) or 50 μM propofol (clinically relevant concentration) in differentiation medium for 48 h, followed by a 24 h withdrawal period. No significant effect on LDH release was observed from either control or propofol-exposed cultures. However, mitochondrial viability (MTT uptake) was significantly affected after propofol exposure. Propofol-induced damage was confirmed by an increased number of TUNEL-positive apoptotic cells. Propofol adverse effects on neural stem cells differentiation and viability were identified using PSA-NCAM a neuron-specific marker; a monoclonal antibody for oligodendrocyte (O4), and GFAP for astrocyte. Our data demonstrated that the number of PSA-NCAM positive neurons and O4 positive oligodendrocytes were remarkably reduced in propofol exposed cultures compared to control. However, no significant changes in astrocytes were detected (GFAP expression). These findings suggest that prolonged propofol exposure has significant adverse effects on neural stem cell differentiation, and produces enhanced neural cell damage including neurons and oligodendrocytes; propofol-induced neural cell damage is mainly apoptotic in nature.
Supported by NCTR/FDA (Experiment E-7417)

PS 1764d Evaluating Neural Progenitor Cell Expansion following Sevoflurane Exposure in Developing Rat Brain Using Micropositron Emission Tomography of [18F] Fluoro-L-Thymidine

S. Liu[1], M. G. Paule[1], X. Zhang[1], G. Newport[1], S. Apana[2], M. Berridge[2], W. Slikker[1] and C. Wang[1]. [1]*Neurotoxicology, National Center for Toxicological Research, Jefferson, AR and* [2]*3D Imaging, LLC, Little Rock, AR.*

Neural progenitor cell expansion is critical for normal brain development. During the brain growth spurt, exposures to general anesthetics which either block the N-methyl D-aspartate receptor (NMDAR) or enhance the γ-aminobutyric acid receptor type A ($GABA_AR$) can disturb the neuronal transduction. Few reports on the effects of anesthetic exposure on neural progenitor cell expansion *in vivo* had been published up to date. Here, minimally invasive micro positron emission tomography (microPET) coupled with 3' -deoxy-3' [^{18}F] fluoro-L-thymidine ([^{18}F] FLT) was utilized to detect the effects of sevoflurane exposure on neural progenitor cell proliferation. FLT, a thymidine analog, is taken up by cells and phosphorylated in the cytoplasm, leading to its intracellular trapping. The uptake and phosphorylation of FLT correlate highly with cellular proliferation. Intracellular retention of [^{18}F] FLT, thus, represents an observable in vivo marker of cell proliferation. Postnatal day (PND) 7 rats (n=10) were exposed to 2.5% sevoflurane mixed with O_2 for 9 hr. One wk post-exposure, the standard uptake values (SUVs) for [^{18}F]-FLT in the hippocampal formation were significantly attenuated in the sevoflurane-exposed rats in comparison with control ones (t test, $p < 0.05$), suggesting decreased uptake and retention (proliferation) in these regions. Two and four wk post-exposure SUVs for [^{18}F]-FLT were comparable in the sevo-exposed rats and control ones. Co-administration of 7-nitroindazole (7NI, 30 mg/kg, n=5), a selective inhibitor of neuronal nitric oxide synthase, moderately (around 15%) attenuated the sevo-induced decrease in [^{18}F]-FLT SUVs. These findings suggested that neural progenitor cell proliferation is significantly decreased following sevoflurane exposure in the developing rat brain.

PS 1764e Vigabatrin-Induced Effects on the CNS of Juvenile Rats: Further Characterization of Histological Findings

A. D. Rasmussen[1], K. M. Wegener[1], P. Mullins[2], E. Richmond[2] and N. Downes[2]. [1]*Regulatory Toxicology & Safety Assessment, H. Lundbeck A/S, Valby, Denmark and* [2]*Sequani Ltd, Ledbury, Herefordshire, United Kingdom.*

Vigabatrin is an oral antiepileptic drug (AED) marketed under the trade name Sabril as adjunct therapy for adults with refractory complex partial seizures and as a mono therapy for children aged 1 month to 2 years with infantile spasms. Vigabatrin causes irreversible inhibition of gamma-aminobutyric acid transaminase (GABA-T), the enzyme responsible for the catabolism of the inhibitory neurotransmitter gamma-aminobutyric acid (GABA), and oral treatment with this compound results in increased level of GABA in the cerebrospinal fluid and brain.
In the study presented here, administration of vigabatrin to juvenile rats during discrete periods of time (starting from day 4 of age) resulted in histopathological changes in the brain in terms of neuropil microvacuolation, as well as effects on myelination and on the oligodendrocytes. The variation in the location of the lesions appears to be consistent with the process of myelination previously reported in rats; in the youngest animals, myelination occurred mainly in the hind brain (medulla oblongata and pons) and there was no appreciable myelination in the

thalamus which showed minimal myelination on Day 7 and appreciable myelination by Day 10. It seems likely that the swollen oligodendrocytes seen after as the initial change in the thalamus represented an early stage in the development of the myelin lesion which was seen later as neuropil vacuolation.
The data presented here expand on previous knowledge on the histopathological findings reported in the developing nervous system of rats when exposed to Vigabatrin. A full account of the study data is pending publication during 2014.

R 1765 Hydraulic Fracturing: Are There Worker Health Issues?

D. Kaden[1], R. O. McClellan[4], J. E. Snawder[3], R. A. Nocco[2], M. Finn[1] and Z. Naufal[2]. [1]*ENVIRON International Corporation, Boston, MA,* [2]*Chevron, San Ramon, CA,* [3]*CDC-NIOSH, Williamstown, KY and* [4]*Consultant, Albuquerque, NM.*

Use of horizontal drilling and hydraulic fracturing in the US oil and gas (O&G) industry has expanded, with >500,000 workers in this industry in 2013. As with any industry, the workforce has the greatest potential for exposure to contaminants. Furthermore, due to the rapid expansion and need to work at multiple locations, many workers remain transient and work at different sites, often owned by different operators, which can lead to additional complexities when assessing exposures. O&G exploration using hydraulic fracturing has constantly evolved to increase efficiency in recovering oil and gas, which have market value, and further minimize any environmental and health hazards to workers and nearby residents. The highly sophisticated process holds potential hazards as high pressures are used transferring large volumes of water, sand (silica), and small quantities of specific chemicals from the surface to specific geologic structures. Extensive use is made of diesel-powered equipment. Current practices seek to recover and reuse injected fluids to minimize water consumption and the disposal of hazardous waste, including trace elements and naturally-occurring radioactive material. Toxicology and epidemiology have been used to guide improvements in technology (e.g., advanced diesel engines, fuels, and exhaust after-treatment to reduce diesel emissions of PM and NOx) and replace proppants/additives with more environmentally-friendly alternatives. Concern for occupational hazards, including minimizing exposure to noxious agents that may have immediate or long-term impact, is key to planning hydraulic fracturing operations.

IS 1766 Understanding the Implications of Breastfed Infant Exposures to POPs: How Can We Do Better?

G. M. Lehmann[1], D. G. Farrer[2], J. S. LaKind[3], M. Poulsen[4], H. A. El-Masri[1], E. D. McLanahan[1] and S. Haddad[5]. [1]*US EPA, Research Triangle Park, NC,* [2]*Oregon Health Authority, Portland, OR,* [3]*LaKind Associates, LLC, Catonsville, MD,* [4]*Oregon Department of Environmental Quality, Portland, OR and* [5]*Université de Montréal, Montréal, QC, Canada.*

Persistent organic pollutants (POPs), such as polychlorinated biphenyls (PCBs), may accumulate within a woman's adipose tissue over many years prior to pregnancy and may subsequently partition into human milk upon breastfeeding. As a result, infant POP intake from breastfeeding may be much greater than average daily maternal POP doses. The developmental period is critical because it sets the stage for lifelong health. Humans continue to develop postpartum, and effects of POP exposure during this period may persist into childhood, or even adulthood. Thus, it is important to be able to accurately assess early-life exposures to these chemicals. In many cases, current environmental exposure assessment methods do not account for differences between maternal and infant POP exposures. In order to fully consider the breastfeeding pathway when assessing risk from POP exposure, it is useful to have methods to estimate a breastfed infant dose based on an average daily maternal dose. In this session, PCBs will be considered as an example of POPs to which human mothers and their infants are commonly exposed. Models developed to estimate breast milk PCB concentrations based on lifetime maternal exposure will be presented, as will the potential application of these models for identifying health effects associated with PCB exposure during infancy. Furthermore, potential policy implications of addressing the difference between average daily maternal PCB dose and breastfeeding infant dose will be discussed. Although PCBs were chosen as an example to use for these discussions, lessons learned can be applied to many POPs, including emerging chemicals of concern. This session will be of interest to risk assessors and regulators who seek to include the breastfeeding exposure pathway in the consideration of risks to infants from POPs. [The views expressed here do not reflect the views or policies of the US EPA.]

EC 1767 Training and Continuing Education for the "Total Toxicologist": How Do We Optimize Training and Educational Opportunities for Different Job Sectors?

C. E. Sulentic[1] and D. A. Fox[2]. [1]*Wright State University, Dayton, OH and* [2]*University of Houston, Houston, TX.*

The training and continuing education of toxicologists is a priority for the SOT membership as demonstrated by the SOT Professional Needs Assessment Task Force (PNATF) and the Education Summit. But what defines a well-trained toxicologist or the "Total Toxicologist?" Does the definition vary depending on the employment sector? Do current graduate programs and continuing education programs provide the necessary and sufficient training for toxicologists? To initiate a discussion regarding these questions, SOT and the National Institute of Environmental Health Sciences sponsored the 2011 Toxicology Educational Summit, which brought participants from academia, industry, and government together to better define the necessary skill sets for the Total Toxicologist (*Tox Sci* 127:331, 2012). Conclusions from the Summit underscored a deficiency in critical thinking, communication skills, and practical application of laboratory data to drug development and risk assessment as well as a need for improved educational opportunities for mid-career toxicologists. Sustaining a career in the current and future global environment, with the ever-changing and rapid advances in technology, requires partnerships between academia, industry, and government to train and re-train the Total Toxicologist. The goal of this session is to offer multi-faceted perspectives on the skill sets (both hard and soft) required for a successful career as a Total Toxicologist and will include talks from early-, mid-, or late-career toxicologists currently employed in academia, industry (pharmaceutical and agricultural/chemical), or government. The session will also provide a brief summary of the results from the PNATF survey to offer a perspective from the SOT membership regarding their perceived training needs. This session should be of interest to students, postdocs, and early- and mid-career toxicologists and is consistent with SOT's goals to continue educational awareness and advancements for all toxicologists.

PS 1768 Pesticides-Induced Oxidative Damage: Possible *In Vitro* Protection by Antioxidants

K. A. Osman[1], A. K. Salama[2] and O. A. Omran[2]. [1]*Pesticide Chemistry & Technology Department, College of Agriculture, Alexandria, Egypt and* [2]*Medical Laboratories, Faculty of Science, Majmaah University, Majmaah, Saudi Arabia.*
Sponsor: K. Osman.

The in vitro the effect of selenium (Se) and a combination of vitamin E and vitamin C on some pesticides, viz atrazine, dimethoate, or endosulfan at three different levels of 10, 20, and 30 mM to induced biochemical alterations in rat erythrocytes and hepatocytes of rats was investigated by determining the levels of lipid peroxidation (nmoles MDA/mg protein), glutathione (μmole GSH/mg protein) and glutathione peroxidase (μmoles NADPH/min/mg protein). In comparison with the control, pesticides stimulated thiobarbituric acid reactive substances (TBARS) activity and glutathione peroxidase activity, enhanced the glutathione contents. Treatment with selenium and a combination of vitamin E and/or vitamin C potentially reduced the free radicals in erythrocytes or hepatocytes and ameliorated the oxidative stress induced by such pesticides. The results suggested that pesticides treatment increases in vitro lipid peroxidation, glutathione peroxidase level and glutathione content by increasing oxidative stress in erythrocytes and hepatocytes of rats and selenium and a combination of vitamin E and vitamin C can reduce this lipoperoxidative effect.

PS 1769 Effects of Aspirin on LPS-Induced Metabolic Stress in Mouse Macrophage and Human Hepatoma Cells

H. Raza, A. John and J. Shafarin. *Biochemistry, UAEU, Al Ain, United Arab Emirates.*

Nonsteroidal anti-inflammatory drugs (NSAIDs) have been reported to induce cytotoxicity in cancer and non-cancerous cells. Overdose of acetaminophen (APAP) has been known to cause liver injury in humans and experimental animals. Their precise molecular mechanisms, however, are not clearly understood. Our previous studies using HepG2 cells treated with aspirin and mouse macrophage J774.2 cells treated with APAP strongly suggest cell cycle arrest and induction of apoptosis associated with mitochondrial dysfunction and oxidative stress. Macrophages are known to play a critical role in toxicity as well as protection of target tissues against the toxicity induced by NSAIDs. In the present study, we have further demonstrated that macrophages are a more sensitive target for aspirin–induced toxicity than HepG2 cells in lipopolysaccharide (LPS)-treated – macrophage J774.2 and hepatoma HepG2 cells. A marked and differential alteration in oxidative stress, apoptosis, glutathione redox homeostasis and mitochondrial functions were ob-

served in these cells. Pre-treatment of the above cells with N-acetylcysteine, a known antioxidant, has also exhibited selective cytoprotective effects. Our results have suggested that altered glutathione (GSH)-redox metabolism, oxidative stress and mitochondrial function in macrophages and hepatoma cells play a critical role in LPS/NSAIDs-induced cytotoxicity. These results may help in better understanding the pharmacological, toxicological and chemopreventive properties of NSAIDs in cancer and non-cancerous cellular systems. (Supported by Sheikh Hamdan Medical Research Grant and Terry Fox Cancer Research Funds and a fund from CMHS Research Committee).

PS 1770 Brominated Diphenyl Ether-47 Induces Oxidative Stress and Inflammatory Pathways in Human Placental Cells *In Vitro*

H. Park and R. Loch-Caruso. *University of Michigan, Ann Arbor, MI.*

Polybrominated diphenyl ethers (PBDEs) are widely used flame retardant compounds. Brominated diphenyl ether (BDE)-47 is one of the most prevalent PBDE congeners found in human breast milk, serum and placenta. Exposure to BDE-47 has been linked to adverse pregnancy outcomes in humans including preterm birth, low birth weight and stillbirth. Although the underlying mechanisms of adverse birth outcomes are poorly understood, critical roles of oxidative stress and inflammation are implicated. The present study investigated BDE-47-induced oxidative stress and prostaglandin (PG) production in a human extravillous trophoblast cell line, HTR-8/SVneo. After 4, 12 or 24 h exposure of HTR-8 cells to BDE-47, intracellular glutathione (GSH) concentration, PGE2 release, and expression of 84 redox-regulated genes were assayed. Treatment of HTR-8 cells with 20 μM BDE-47 for 24 h resulted in differential expression of redox-sensitive genes compared to solvent control, as assayed with a commercial Oxidative Stress PCR Array. Treatment of HTR-8 cells with 5, 10, 15, and 20 μM BDE-47 for 24 h increased intracellular GSH levels compared to solvent control, consistent with increased mRNA expression of genes related to GSH synthesis. At 24 h, 20 μM BDE-47 induced significant increases in PGE2 release into the culture medium. The PGE2 increases were accompanied by significant 5.3, 4.4 and 4.7-fold increases in mRNA expression of the prostaglandin synthesis enzyme prostaglandin-endoperoxide synthase 2 at 4, 12 and 24 h, respectively. Furthermore, treatment with 15 and 20 μM BDE-47 significantly decreased mRNA expression of the prostaglandin catabolic enzyme hydroxyprostaglandin dehydrogenase. Because abnormal activation of oxidative stress and PG production can disrupt trophoblast functions that are necessary for placental development and successful pregnancy, further investigation is warranted of the impact of BDE-47 on trophoblast cellular responses.

PS 1771 Radical Acylation of L-Lysine-Containing Peptides and Soralbumin by Peroxynitrite-Treated Diacetyl and Methylglyoxal

E. J. Bechara[1, 2], R. Tokikawa[2], M. Machini[2], M. Uemi[1], N. A. Assunção[1] and A. A. Alves[1]. [1]*Ciências Exatas e da Terra, Universidade Federal de São Paulo, Diadema, São Paulo, Brazil and* [2]*Bioquimica, Universidade de São Paulo, São Paulo, São Paulo, Brazil.*

Highly reactive α-dicarbonyls such as diacetyl, methylglyoxal, 4,5-dioxovaleric acid, and 3-deoxyglucosone have been characterized as secondary catabolites that can aggregate proteins and form DNA nucleobase adducts in several human maladies. In vitro, diacetyl (DA) and methylglyoxal (MG) have also been shown to rapidly add up the peroxynitrite anion (k2 ~ 10exp4 to 10exp5 M-1s-1), a potent biological nucleophilic, oxidant and nitrating agent, followed by carbon chain cleavage to carboxylic acids from acetyl radical intermediate that can attach to amino acids added to the reaction mixtures. Here, using HPLC or CE coupled to ESI or MALDI-TOF/MS techniques, we show that the DA or MG/peroxynitrite systems are capable of acetylating the α- and ε-amino groups of terminal and/or inner L-Lys residues of synthetic KALA-OH, Ac-KALA-OH, K(Boc)ALA-OH, and Ac-A-E-F-K-F-A-L-NH2 as well as amino acid residues of bovine soralbumin in phosphate buffer pH 7.4. The pH profiles (6.2-8.2) of the reactions traced for the tetrapeptides are bell-shaped, peaking at approximately 7.5, therefore near the pKa values of both ONOOH and H2PO4- anion, which is in accordance with initiating phosphate-catalyzed nucleophilic addition of ONOO- anion to the α-dicarbonyl catabolite. CE or HPLC and MS analyses of reaction products confirmed αN- and εN-acetylation of Lys derivatives by DA as well as acetylation and formylation by MG. Moreover, the EPR MNP-CH3CO radical adduct signal was found to be quenched upon addition of L-His. These data raise the hypothesis of contributing radical acylation of proteins in epigenetic processes, where their enzymatic acetylation is a well-documented event, recently reported to be as critical to the cell cycle as phosphorylation. Also noteworthy is the observed formylation of L-Lys containing peptides by MG never reported to occur in proteins. Financial support: FAPESP, CNPq, INCT Redoxoma.

PS 1772 Mrp1 Protects against Doxorubicin-Induced Cardiotoxicity *In Vitro*

W. Zhang, D. Coy, J. Deng and M. Vore. *Graduate Center for Toxicology, University of Kentucky, Lexington, KY.*

Doxorubicin (DOX), an anthracycline used in cancer chemotherapy, is well known for its dose-limiting cardiotoxicity, due in part to DOX-induced oxidative stress. Here, we investigated the role of multidrug resistance-associated protein 1 (Mrp1), an ATP-binding cassette efflux transporter, in DOX induced cardiotoxicity. Cardiomyocytes (CM) and cardiac fibroblasts (CF) were isolated from C57BL/6J (WT) or Mrp1 knock out (KO) mice (1-3 days old), treated with saline (SAL) or DOX (0.5 – 3 μM) and examined 24 hrs later. DOX increased Mrp1 mRNA (~2 fold) and protein (~1.8 fold) expression similarly in both CM and CF. The MTS assay showed that CM from KO mice were more sensitive to DOX than WT, with an IC50 in KO of 0.94 μM (95% CI: 0.74 – 1.18) versus 1.60 μM (95% CI: 1.20 – 2.11) in WT. Furthermore, CM and CF from KO mice showed increased caspase 3 cleavage, PARP cleavage and γH2AX expression following DOX treatment, consistent with increased apoptosis and DNA damage in cells from KO mice. As an indicator of intracellular oxidative stress, the redox potential (*Eh*) of the GSH/GSSG pool was similar between WT and KO cells treated with either SAL or DOX. Despite this similarity, DOX treatment led to increased concentrations of GSH and GSSG in KO cells, but not WT cells. After DOX treatment, the KO CM had a 1.7 ± 0.3-fold higher GSH ($p < 0.05$) and a 1.8 ± 0.2-fold higher GSSG level ($p < 0.05$) than WT CM. Similar effects due to the loss of Mrp1 were observed in CF. Further studies showed that in KO cells, DOX led to increased expression of the rate-limiting GSH synthesis enzyme glutamate-cysteine ligase (GCL), including GCLc (catalytic subunit) and GCLm (regulatory subunit). Finally, expression of Nqo1, a downstream gene in the Nrf2 pathway, was significantly higher in both SAL and DOX-treated KO vs WT cells. These results suggest that despite comparable *Eh* for GSH/GSSG, cells from Mrp1 KO mice are under oxidative stress and show that Mrp1 protects against DOX induced cardiotoxicity in cultured CM and CF. (CA139844, AHA 13PRE17060037)

PS 1773 Disruption of Keap1/Nrf2-Antioxidant Response after Chronic Doxorubicin Exposure *In Vivo*

K. K. Nordgren and K. B. Wallace. *Biomedical Science, University of Minnesota Medical School, Duluth, MN.*

Doxorubicin (DOX), an anthracycline antineoplastic drug, is a widely used therapy for treating various human solid tumors and leukemias. Unfortunately, DOX therapy is limited by a cumulative, dose-dependent, and irreversible cardiomyopathy that occurs with repeated administration. A pivotal initiating event of DOX-induced cardiotoxicity is presumed to be the production of reactive oxygen species (ROS) and oxidation of lipids, DNA and proteins. We recently identified activation of the Keap1/Nrf2-antioxidant response system – a major cellular defense mechanism against oxidative stress – as an important response to acute DOX exposure *in vitro*. Specifically, increased autophagic degradation of the Keap1 regulator protein allowed increased abundance of transcription factor Nrf2 and downstream antioxidant gene activation. In the present study, we address the hypothesis that dysregulation of the Keap1/Nrf2-antioxidant pathway may contribute to the persistent DOX-induced cardiotoxicity after chronic exposure *in vivo*. Male, Sprague-Dawley rats received 6 weekly injections of 2 mg/kg (s.c.) DOX or saline followed by a 5 week drug-free period prior to analysis of cardiac tissue transcripts and proteins. At study completion, DOX treated rats had a mean body weight ~12% lower than saline treated rats, attributed to diminished growth rate. Cardiac tissue from animals exposed to DOX demonstrated a decrease in non-protein sulfhydryl groups, indicating a persistent increase in oxidative stress. Despite this, there was no activation of Nrf2-regulated genes, including *Nqo1*. Furthermore, protein concentration, but not gene expression, of Nrf2 was decreased by 19.4% ($p < 0.05$) with a corresponding increase of Keap1 protein content (65.7%, $p < 0.05$), suggesting overabundance of Keap1 results in increased degradation of Nrf2 transcription factor. These findings identify disruption of the Keap1/Nrf2 pathway as a potential contributing mechanism for persistent oxidative cardiotoxicity associated with chronic DOX administration. (Supported in-part by grants from the 3M Company and Whiteside Institute.)

PS 1774 Oxidative DNA Damage in Liver and Kidney of Weanling Rats due to Subchronic Coexistence of Aflatoxicosis and Protein Malnutrition

O. A. Rotimi[1, 3], O. Ademuyiwa[1], F. Oluwafemi[2] and E. A. Balogun[1]. [1]*Department of Biochemistry, Federal University of Agriculture, Abeokuta, Nigeria,* [2]*Microbiology, Federal University of Agriculture, Abeokuta, Nigeria and* [3]*Biological Sciences, Covenant University, Ota, Nigeria.*

The coexistence of aflatoxicosis and protein malnutrition in children is a major health burden in developing countries especially in sub-Saharan Africa. Hence, this study investigated the effects of the coexistence of Aflatoxin B1 (AFB1) poisoning and protein malnutrition on renal and hepatic antioxidant status and the integrity of genomic DNA in weanling rats. Eight groups of animals were used in this study; groups 1 and 2 were male and female animals fed normal protein diet (20% protein), groups 3 and 4 were male and female animals fed low protein diet (5%), groups 5 and 6 were male and female animals fed normal protein (20%) + 40ppb AFB1 and groups 7 and 8 were male and female animals fed low protein (5%) + 40ppb AFB1 respectively. At the end of eight weeks, rats were sacrificed after an overnight fast and liver and kidney were excised. Glutathione, glutathione transferase, superoxide dismutase, peroxidase, catalase and glucose-6-phosphate dehydrogenase were determined spectrophotometrically while genomic DNA fragmentation was determined by agarose gel electrophoresis after extraction of DNA from the tissues. Results showed that the coexistence significantly ($p<0.05$) decreased glutathione, glutathione transferase, and superoxide dismutase while it increased peroxidase in the kidney and liver. It significantly ($p<0.05$) increased catalase in the liver while a decrease was observed in the kidney. Furthermore, a decrease in glucose-6-phosphate dehydrogenase was observed in the liver while no significant ($p>0.05$) difference was observed in the kidney. Agarose gel electrophoresis showed DNA damage in the kidney of the rats while no difference in pattern was observed in the liver. Our results suggest that sub-chronic coexistence of AFB1 poisoning and protein malnutrition resulted in oxidative stress with a concomitant DNA damage in the kidney of weanling rats.

PS 1775 Boric Acid Activates PERK in DU-145 Prostate Cancer Cells

K. E. Yamada[1], S. Kobylewski[1] and C. D. Eckhert[2, 1]. [1]*Molecular Toxicology IDP, University of California, Los Angeles, Los Angeles, CA and* [2]*Environmental Health Sciences, University of California, Los Angeles, Los Angeles, CA.*

We have previously reported that physiological levels of boric acid (BA) (10 μM) activates the ATF4 branch of the unfolded protein response (UPR) in DU-145 prostate cancer cells. The ATF4 pathway is initiated by phosphorylation of eIF2α at Ser51 by GCN2, PERK, HRI, or PKR kinase. 10 μM BA treatment increases levels of ph-eIF2α/total eIF2α protein between 0.5-2 hours in DU-145 cells. We hypothesized that phosphorylation occurs through PERK, the kinase activated by ER stress. We used MEF WT cells and MEF PERK -/- cells to test if PERK is required for eIF2α phosphorylation upon BA treatment. MEF WT cells show an increase in ph-eIF2α/total eIF2α between 0.5-1 hours with 10 μM BA treatment. The increase in ph-eIF2α is not observed in 10 μM BA treated MEF Perk -/- cells over a 6 hour time course, indicating that PERK is required for BA induced phosphorylation of eIF2α. To further support the hypothesis that BA activates PERK, we tested for Nrf2 activation in DU-145 cells, another PERK dependent pathway. Nrf2 activation leads to translocation from the cytoplasm to the nucleus where it acts as a transcription factor for the antioxidant response element (ARE). We used immunofluorescence to show that 10 μM BA treatment resulted in Nrf2 translocation to the nucleus at 2 hours. In addition, we measured mRNA levels of three ARE genes (HMOX-1, NQO1, and GCLC) using real time PCR. 10 μM BA treatment results in an increase in mRNA levels of all three genes at 2 hours, following the temporal pattern observed in the immunofluorescence experiments. These results provide evidence that BA is an activator of PERK at physiological concentrations that can be achieved through diet.

PS 1776 DNA Fragmentation in Rats following Exposure to Delta 9-Tetra Hydrocannabinol

O. A. Dosumu[1], S. O. Rotimi[3], E. O. Abam[1, 4], O. Ademuyiwa[1], R. N. Ugbaja[1], O. B. Onunkwor[1], T. F. Akinhanmi[1, 2], O. O. Ogunrinola[1, 6], A. D. Wusu[1, 6], O. K. Afolabi[1, 5] and D. O. Babayemi[1]. [1]*Biochemistry, Federal University of Agriculture, Abeokuta, Ogun, Nigeria,* [2]*Chemistry, Federal University of Agriculture, Abeokuta, Ogun, Nigeria,* [3]*Biological Sciences, Covenant University, Ota, Ogun, Nigeria,* [4]*Biochemistry, Bell's University, Sango Ota, Ogun, Nigeria,* [5]*Biochemistry, Ladoke Akintola University of Technology, Ogbomosho, Oyo, Nigeria and* [6]*Biochemistry, Lagos State University, Ojoo, Lagos, Nigeria.*

Cannabis sativus preparations, having Delta 9-tetrahydrocannabinol (Delta 9-THC) as the major active compound, are used as illicit drugs and the use is often abused worldwide. Delta 9-THC is a potent inducer of cellular oxidative stress that could contribute significantly to cell injury and dysfunction. This study investigated the effect of repeated administration of Delta 9-THC on DNA damage in rat tissues. Delta 9-THC was administered orally in olive oil at 12.5mg/kg, 25mg/kg and 50mg/kg for 7 weeks to different groups of rats while control animals received the vehicle (Olive oil). Twenty four hours after the last administration, blood and other tissues (liver, kidney, brain, heart, testis and spleen) were removed from the animals and their DNA samples were extracted using the spin column technique. Oxidative DNA damage was assessed by agarose gel electrophoresis detection of DNA laddering. The DNA damages in the kidney, testis and spleen were observed at a dosage of 12.5mg/kg. In the liver and blood however, the DNA fragmentation was observed only in rats that received 25mg/kg and 50mg/kg. The integrity of DNA in the brain and heart was however preserved. The findings of this study demonstrate that exposure to Delta 9 –THC can result in DNA fragmentation in different tissues.

PS 1777 MALDI-Mass Spectrometry-Based Biochemical Microscopy of Cardiolipin Molecular Species in Brain Tissue

A. Amoscato[1], L. J. Sparvero[1], R. He[3], B. Pitt[1], H. Bayir[2, 1] and V. E. Kagan[1]. [1]*Environmental and Occupational Health, University of Pittsburgh, Pittsburgh, PA,* [2]*Critical Care Medicine, University of Pittsburgh, Pittsburgh, PA and* [3]*Pharmacy College, Jinan University, Guangzhou, China.*

Existing protocols associated with MALDI imaging mass spectrometry (MALDI-IMS) in the mapping of lipids on tissue sections fail to detect the mitochondria-unique phospholipid cardiolipin (CL), known to be essential for cell and mitochondrial physiology. We developed a new protocol enabling the "biochemical microscopy" of diversified individual molecular CL species. This has been achieved by the employment of: i) phospholipase C to reduce highly abundant phosphatidylcholine (PC) signals, ii) chemical crosslinking with 1-ethyl-3-[3-dimethylaminopropyl] carbodiimide hydrochloride (EDC) to block ion suppressive effects from carboxyl containing molecular species, iii) modified matrix application methods and ammonium acetate washes to enhance CL signal in negative ion mode. Using these treatments, we were able to visualize and map CL in rat brain tissue. We documented a spatial distribution for CL in the rat brain. The relative intensities of CL species m/z 1448 and 1450 were highest in the hippocampal area and decreased in intensity as one transitions from the hippocampus toward the white matter and cortex areas. Higher mass CL species displayed similar or increased intensities in the hippocampus and cortex areas. The developed protocol made possible MS/MS analysis of CL species in tissue sections resulting in the mapping of their fatty acyl fragments. The applicability of this newly developed MALDI imaging method to various CL species in the brain will provide insight into a variety of biologically important questions where brain functions are compromised.

PS 1778 Exposure to Zinc Induces Compartment Specific Redox Changes in Bronchial Epithelial Cells

P. Wages[1], R. Silbajoris[2], L. Brighton[3] and J. Samet[2, 1]. [1]*Curriculum in Toxicology, UNC, Chapel Hill, NC,* [2]*EPHD, NHEERL, EPA, Chapel Hill, NC and* [3]*CEMALB, UNC, Chapel Hill, NC.*

Zinc is a ubiquitous metallic component of ambient particulate matter (PM). Epidemiological and toxicological studies have specifically implicated zinc as a contributor to the health effects associated with PM inhalation. We have previously demonstrated that zinc can increase cytosolic hydrogen peroxide (H2O2)levels as well as increase the cytosolic glutathione redox potential (EGSH) by altering the ratio of reduced to oxidized glutathione. We recently provided evidence that the increased EGSH level is at least in part due to zinc-induced H2O2 production in the mitochondria. We therefore investigated the role of zinc exposure on the mitochondrial redox status by measuring the EGSH in mitochondria. Cultures of the human bronchial epithelial cell line BEAS 2B were transduced using lentiviral

vectors encoding the dynamic fluorescent sensors roGFP, which reports localized EGSH, or HyPer, which senses H2O2 levels. BEAS 2B cells were also transfected with a third fluorogenic probe, pHred, which measures the mitochondrial pH. Data from these sensors tracked in real time in cells undergoing exposure to 50 uM zinc/1 uM pyrithione using confocal live cell microscopy, showed that zinc induces mitochondrial increases in H2O2 and EGSH, while having no measurable effect on pH. Expression of cytosolic or mitochondrially targeted-catalase decreased the zinc-induced H2O2 levels as expected in each compartment but did not alter the mitochondrial increase in EGSH,. These data suggest that the zinc-induced cytosolic redox changes are caused by an increase in mitochondrial H2O2 production, but are distinct from the zinc-induced increase in mitochondrial EGSH as evident by the H2O2 independent increase in EGSH. This study further demonstrates the utility of using dynamic fluorogenic probes in evaluating xenobiotic-induced oxidative intracellular events in real time. THIS ABSTRACT OF A PROPOSED PRESENTATION DOES NOT NECESSARILY REFLECT EPA POLICY.

PS 1779 p97 Modulates Nrf2-KEAP1-Mediated Antioxidant Response

T. Wu, M. Kang, M. Long, S. Tao, E. Chapman and D. D. Zhang. *College of Pharmacy, University of Arizona, Tucson, AZ.*

The transcription factor Nrf2 has revealed as the master regulator of intracellular redox homeostasis. As an adaptive response to oxidative stress, Nrf2 activates transcription of a battery of genes encoding antioxidant protein, detoxification enzymes and xenobiotic transporters by binding to the cis-antioxidant response elements in the promoter region of these genes. Previous work by our lab and others demonstrated that Nrf2 is subject to poly-ubiquitin-mediated proteasomal degradation in a Keap1-dependent manner. Here we report a potential functional connection between protein quality control and Nrf2 activation. Genetic knockdown or pharmacological inhibition of p97, an AAA-ATPase governing critical steps in ubiquitin-dependent protein quality control and intracellular signaling pathways, resulted in an increase in Nrf2 protein level as well as increase Nrf2 target gene expression. We also demonstrated that p97 is in complex with Nrf2 and with Cul3-Keap1-Rbx1 E3 ligase complex using biochemical and proteomics analysis. Furthermore, indirect immunofluorescent staining reveals both inhibited p97 function and treatment with arsenite lead to increased autophagosome levels, implying the possible link between arsenic, p97, autophagy, Nrf2 upregulation and cellular toxicity. These findings not only suggest new regulatory mechanism of Nrf2-Keap1 pathway, but also offer a potential mechanism by which arsenic activates the Nrf2 pathway.

PS 1780 Microtubule-Associated Protein 1s (MAP1s) Is a Novel Component of the Noncanonical p62-Dependent Mechanism of Nrf2 Regulation

E. M. Rojo de la Vega Guinea, T. Wu, S. Tao, Y. Zheng and D. D. Zhang. *College of Pharmacy, University of Arizona, Tucson, AZ.*

Microtubule Associated Protein 1s (MAP1s) is a short and ubiquitously expressed member of the microtubule-associated protein (MAP) 1 family. Recent studies have identified a cytoprotective role for MAP1S as it enhances autophagy, which eliminates genome instability and protein aggregates, and protects against chemically-induced hepatocarcinogenesis. The interaction of MAP1s with several cellular components such as tubulin, actin, RASSF1A, LRPPCR and the autophagy protein LC3 has already been characterized. Here we identified that MAP1s and Keap1 are contained in the same protein complex through their interactions with p62, rather than through direct, ETGE motif-dependent MAP1s-Keap1 interaction. Moreover, MAP1s and Keap1 colocalized with p62 and LC3 in a punctate pattern that suggests that they all form part of an autophagic complex. Overexpression of MAP1s resulted in decreased protein levels of coexpressed Keap1, and treatment with the proteasome inhibitor MG132 resulted in a more dramatic decrease in Keap1 protein levels. On the other hand, treatment with diverse autophagy inhibitors prevented further Keap1 degradation. Additionally, Map1s knockdown resulted in increased protein levels of Keap1 and p62, with a concomitant decrease in Nrf2 signaling. In vivo, we saw that acute treatment of nude mice with the hepatic carcinogen diethylnitrosamine (DEN) resulted in MAP1s induction in liver. This induction of MAP1s also resulted in increased protein levels of p62, Nrf2, NQO1, and decreased protein levels of Keap1. Interaction between p62 and Keap1 was previously been shown to impede Nrf2 degradation, thereby favoring its stabilization and induction of downstream genes. Taken together, all these results suggest that Map1s is a novel component of the non-canonical pathway of Nrf2 activation mediated by p62.

PS 1781 Selenoprotein P Regulates PCB3 Metabolite-Induced Oxidative Stress and Toxicity in Human Keratinocytes

W. Xiao[1], Y. Zhu[1, 2], E. Sarsour[1], A. Kalen[1], N. Aykin-Burns[1, 3], D. R. Spitz[1] and P. Goswami[1]. [1]*Department of Radiation Oncology, The University of Iowa, Iowa City, IA,* [2]*Department of Radiation Oncology, Northwestern University, Chicago, IL and* [3]*Department of Pharmaceutical Sciences, University of Arkansas for Medical Sciences, Little Rock, AR.* Sponsor: L. Robertson.

Polychlorinated biphenyls (PCBs) and their metabolites are environmental pollutants that are believed to have adverse health effects presumably by inducing oxidative stress. To determine if 1-(4-Chlorophenyl)-benzo-2,5-quinone (4-ClBQ: metabolite of 4-monochlorobiphenyl, PCB3) induced oxidative stress is associated with changes in the expression of specific antioxidant genes, mRNA levels of 92 oxidative stress-response genes were analyzed using TaqMan® Array Human Antioxidant Mechanisms (Life technologies), and results were verified by performing quantitative RT-PCR assays. The expression of selenoprotein P (sepp1) was found to be significantly downregulated (8-10-fold) in 4-ClBQ treated HaCaT human skin keratinocytes, which correlated with a significant increase in MitoSOX oxidation. Overexpression of Mn-superoxide dismutase, catalase, or treatment with N-acetyl-L-cysteine suppressed 4-ClBQ-induced toxicity. Sodium selenite supplementation also suppressed 4-ClBQ-induced decrease in sepp1 expression, which was associated with a significant inhibition in cell death. Furthermore, HaCaT cells overexpressing sepp1 were resistant to 4-ClBQ induced oxidative stress and toxicity. These results demonstrate that SEPP1 represents a previously unrecognized regulator of PCB induced biological effects. These results support the speculation that selenoproteins can be an attractive countermeasure for PCB induced adverse biological effects.

PS 1782 17 alpha-Estradiol Down-Regulates Glutathione Synthesis in Serum-Deprived PC-12 Cells

I. Sørvik, K. E. Rakkestad, G. R. Øverby, K. B. Debernard, G. H. Mathisen and R. E. Paulsen. *Department of Pharmaceutical Biosciences, University of Oslo, School of Pharmacy, Oslo, Norway.* Sponsor: M. Løvik.

Estradiol is reported to have neuroprotective functions in the CNS. We have previously found that estradiol (10 μM) acted as an acute neuroprotector in cultured cerebellar neurons, but not as a long-term neuroprotector, since preconditioning reduced levels of glutathione, and hence decreased subsequent acute neuroprotection. Here, we demonstrate that 17α-estradiol (10 μM) enhanced serum deprivation-induced cell death in rat pheochromocytoma PC-12 cells whereas antioxidants C and E (vitamins C/E) in combination (2+10 μM) tended to protect. The present study further explored the mechanism behind the toxic effect of estradiol in serum deprived PC-12 cells and compared it with vitamins C/E. Serum deprivation-induced cell death was partly reduced by N-acetylcystein, a cysteine precursor with potential to restore glutathione levels. Serum deprivation reduced endogenous glutathione levels, while glutathione levels were further reduced with 17α-estradiol treatment, but not with vitamins C/E. In addition, 17α-estradiol down-regulated the promoter activity of the rate-limiting enzyme in glutathione production, glutamate-cysteine ligase (GCL), as well as c-Fos protein levels in serum deprived cells. The c-Fos transcription factor normally binds to the AP-1 response element in the GCL promoter resulting in increased production of glutathione e.g. as a response to oxidative stress. Over-expression of c-Fos partly restored the GCL promoter activity in serum deprived cells treated with 17α-estradiol. Nrf2, a transcription factor binding another response element in the GCL promoter was not affected by 17α-estradiol. In conclusion, our study presents evidence that 17α-estradiol has a long-term negative effect on the endogenous glutathione level through its ability to reduce c-Fos levels resulting in down-regulated glutathione synthesis during serum deprivation, and therefore 17α-estradiol does not rescue PC-12 cells from serum deprivation-induced cell death.

PS 1783 Pharmacological Inhibition of c-Jun N-Terminal Protein Kinase (JNK) Blocks Lipid Droplet Accumulation Caused by Malondialdehyde (MDA) and Intralipid in Rat Hepatocytes

A. R. Cardoso[2], E. L. Holmuhamedov[3], R. N. Deepe[1] and J. J. Lemasters[1]. [1]*Drug Discovery & Biomedical Sciences and Biochemistry & Molecular Biology, Medical University of South Carolina, Charleston, SC,* [2]*Biochemistry, University of São Paulo, São Paulo, Brazil and* [3]*Center for Integrative Research on Cardiovascular Aging, Aurora University, Milwaukee, WI.*

Mitochondrial dysfunction and reactive oxygen species (ROS) generation are implicated in non-alcoholic fatty liver disease (NAFLD). ROS lead to MDA formation from lipid peroxidation. Our aim was to elucidate whether MDA causes lipid droplet accumulation by activation of JNK. Primary rat hepatocytes were cultured

for 3 h and then incubated for 1 h with: 1) medium alone, 2) 25 μM MDA, 3) 0.2% Intralipid (emulsion of egg yolk and soybean triglycerides), 4) MDA plus intralipid, 5) 10 μM SP600125 (JNK inhibitor), and 6) MDA plus intralipid plus SP600125. Cells were then incubated with bodipy green, TMRM and propidium iodide (PI) to visualize neutral lipids, polarized mitochondria and non-viable cells, respectively, by confocal microscopy. After medium alone, hepatocytes displayed few lipid droplets. MDA alone did not increase lipid droplet accumulation but caused a decrease of mitochondrial membrane potential (ΔΨ) assessed by TMRM. Intralipid alone caused neither accumulation of lipid droplets nor a decrease of ΔΨ. However, MDA combined with Intralipid led to substantial increases of size and quantity of lipid droplets together with a decrease of ΔΨ. JNK inhibition with SP600125 blocked lipid accumulation and the decrease ΔΨ after MDA plus intralipid. No treatments induced PI staining. These results are consistent with our previous hypothesis that aldehydes like MDA inhibit mitochondrial voltage dependent anion channels (VDAC) with consequent inhibition of β-oxidation of fatty acids and mitochondrial ΔΨ formation (JBC 2012;287:7692-7700). However, steatosis only developed if a source of lipid was present. Interestingly, JNK inhibition abrogated steatosis induced by MDA plus Intralipid, suggesting that aldehyde-dependent VDAC closure occurs via a JNK-dependent pathway.

PS 1784 Development of a Novel Luminogenic Assay for H2O2 Detection

J. J. Cali, J. Schultz, S. Duellman, G. Vidugiris, H. Wang, W. Zhou and P. Meisenheimer. *Research, Promega Corporation, Madison, WI.* Sponsor: T. Riss.

H2O2 is a reactive oxygen species (ROS) that is convenient to measure because of a relatively long half-life and it is also useful as a general marker of oxidative stress. Common H2O2 reagents include fluorogenic probes that react directly with H2O2 or via catalysis by horseradish peroxidase (HRP). The direct probes are convenient for imaging ROS inductions, but tend to be non-selective among the various ROS and they deliver small assay windows in homogenous formats. While HRP-dependent probes are sensitive and selective, they are prone to high false hit rates in screens and perform poorly in cell based assays. To overcome these shortcomings we synthesize a cyanobenzothiazole derivative containing a borate ester and self-cleaving linker (2-ethynyl-6-((4-(4,4,5,5-tetramethyl-1,3,2-dioxaborolan-2-yl)benzyl)oxy)benzo[d]thiazole) to use as a luminogenic probe. The borate ester reacted directly and selectively with H2O2 to expose the linker and eliminate a free cyanobenzothiazole. The latter moiety reacts rapidly with D-cysteine to form luciferin, which in turn generates light with luciferase. Based on well-known characteristics of luciferase assays we expected low background, wide dynamic range, and low false hit rates. In a homogenous format cells were where exposed to test articles (e.g. ROS inducers) and probe, and then to a luciferase formulation containing D-cysteine. The luciferase produced light read on a luminometer in proportion to the H2O2 concentration of the sample. Prototypical ROS inductions were detected with high sensitivity and a wide dynamic range in a multiwell format. To test high throughput performance, we screened the 1280 compound LOPAC library against HepG2 cells. Cells in medium were compared to medium alone to select H2O2 modulators and to discriminate between cell-based and abiotic effects. LOPAC screens revealed a low false hit rate (0.5%) compared to an HRP based method (7.1%). These results indicate the assay obviates certain limitations of fluorescent methods and that it should prove effective for small scale and high throughput applications.

PS 1785 Nrf2 but Not NF-kB Is Activated by African Dust Organic Extract in BEAS-2B

R. I. Rodríguez and B. D. Jimenez-Velez. *Biochemistry and Center for Environmental and Toxicological Research, University of Puerto Rico Medical Sciences Campus, San Juan, Puerto Rico.*

Every year, African dust storms cross the Atlantic Ocean impacting the Caribbean region. Airborne particulate matter (PM) falls outs along its path. This matter contributes to the oxidative atmospheric potential of the environments and in organisms. The impact of this global phenomenon on the health of the Puerto Rican community continues to be evaluated. We previously reported the induction of IL-6 and IL-8 by African dust (ADE) in human bronchial epithelial cells (BEAS-2B). Here we expand our research to assess the activation of two trans factors 1) the nuclear erythroid 2-related factor 2 (Nrf2) and 2) the nuclear factor κB (NF-κB). The role of heavy metals and oxidant capacity were evaluated using deferoxamine mesylate (DF) and N-acetyl-L-cysteine (NAC), in cells treated with PM organic extracts (50μg/mL). Protein extracts were obtained using the Nuclear Extract Kit (Active Motif) according to the manufacturer and quantified by the Bradford assay. Activation of Nrf2 and NF-κB were determined by an ELISA base assay (Active Motif). Nuclear extracts including the activated transcription factors were added to a plate coated with the specific oligonucleotide containing a consensus-binding site for Nrf2 or NF-κB. Both ADE and Non-ADE extracts induce the activation of Nrf2 after 1 hr. This response is partly due to the oxidative capacity of ADE (not significant for Non-ADE) extract since it was significantly reduced by NAC. ADE and Non-ADE extracts triggered the activation of Nrf2 however; the magnitude of this activation was significantly increased for ADE. To our surprise we were unable to find any evidence for NF-κB activation after 1 or 4 hrs. This research demonstrates that African dust arriving Puerto Rico has an oxidative capacity capable of activating antioxidant defenses in lung cells. The activated molecules are good candidates for testing biomarkers of exposure to cellular stress during seasonal respiratory outcome. Support provided by MBRS-RISE Grant R25GMO61838.

PS 1786 Perfluorooctanoic Acid (PFOA) Causes Oxidative Stress in the Mouse Pancreas

L. M. Kamendulis, Q. Wu and B. A. Hocevar. *Environmental Health, Indiana University School of Public Health, Bloomington, IN.*

Perfluoroalkyl chemicals (PFCs) such as perfluorooctanoic acid (PFOA) are widely used in industrial and commercial applications and are environmentally and biologically persistent. In rodents, PFC exposure has been shown to lead to reduced body weight, liver hypertrophy, and decreased cholesterol levels. In addition, chronic exposure to PFCs induce liver, Leydig and pancreatic acinar cell tumors (PACTs) in rodents. Epidemiologic studies have also linked exposure to PFC compounds to adverse health effects in humans, several of which identified an association between PFC exposure and pancreatic disease. To address the effects of PFCs on the pancreas, we treated 8 wk old C57Bl/6 mice with vehicle or PFOA by gavage at doses of 0.5, 2.5 or 5.0 mg/kg BW/day for 7 days. In addition, a group of mice were treated with cerulein, which induces mild pancreatitis and produces an oxidative stress in the pancreas. Our results demonstrate that exposure to PFOA results in pancreatic toxicity, evidenced by increased serum levels of amylase and lipase in the PFOA treatment groups. PFOA accumulated in serum, liver and pancreas in a dose-responsive manner. Increased levels of the lipid peroxidation product F2α-isoprostane were observed in both the pancreas and liver (2.5-fold and 1.5 fold, respectively) indicating that PFOA induced oxidative stress in these tissues. In the pancreas and liver, F2α-isprostane levels were strongly correlated with PFOA content (r2 = 0.86, and 0.90, respectively). The mRNA expression of the cytosolic and mitochondrial forms of superoxide dismutase, (SOD1 and SOD2) was increased by ~2-fold in the pancreas of PFOA- treated mice, which was accompanied by an increase (24%) in the enzymatic activity of SOD. While the levels of GSH in the pancreas were not altered, the ratio of GSH:GSSG was significantly decreased by PFOA exposure. In contrast, PFOA increased GSH levels and the GSH:GSSG ratio in the liver. Collectively, these results support that PFOA exposure results in oxidative stress in the pancreas.

PS 1787 Investigating the Bioenergetic and Oxidative Impacts of Rapid Altitude Adjustment

M. K. Makley[1, 4], R. R. Chapleau[1, 4], A. G. Ntamack[2], R. A. James[2, 3], J. M. Gearhart[1, 4] and D. A. Mahle[4]. [1]*Henry M. Jackson Foundation, Wright Patterson AFB, OH,* [2]*NAMRU-D, Wright Patterson AFB, OH,* [3]*Camris International, Wright Patterson AFB, OH and* [4]*USAF 711HPW/RHDJ, Wright Patterson AFB, OH.*

Rapid ascent to high altitudes commonly results in a severe decrease in exercise performance and cognitive abilities. Many situations, in which rapid altitude changes are required, such as mountain rescues and flight, necessitate transport in aircraft or high-performance vehicles. Sprague-Dawley rats were elevated to three simulated altitudes for one hour (1,000, 10,000, or 20,000 feet) under constant oxygen levels. Liver, heart, and brain mitochondria were immediately isolated following exposure for evaluation of State 3, State 4, and uncoupler-stimulated respiration in a Seahorse XF Bioanalyzer. In addition to evaluating ATP production, spare capacity, and proton leak with the XF Bioanalyzer, measurements of the oxidative stress markers cytochrome c and thiobarbituric acid reactive substances (TBARS) were taken. Our results from heart tissue show that in addition to reduced oxygen delivery to organs, altitude affects the basic bioenergetics of the cell by reducing the oxidative capacity of the mitochondria. Although ATP production is maintained at a relatively constant level (0.25 pmoles/min), the mitochondrial membrane is weakened as indicated by an increase in proton leakage (42%). Furthermore, the levels of TBARS in the blood increase 28% with the raise in altitude to 20,000 feet, supporting our physiological observations. The decrease in spare respiratory capacity corresponding to a weakened membrane and the presence of oxidative stress markers suggests that additional stressors at altitude could have catastrophic outcomes. Future work will investigate the impact on mitochondrial function in unique brain regions as well as skeletal muscle effects.

PS 1788 Studying Nrf2-Mediated Oxidative Stress Response in Human Keratinocytes Exposed to Two Plant Polyphenols—Quercetin and Curcumin

P. Xue[1], B. Sun[1], J. Dong[1], Y. Adeleye[2], P. L. Carmichael[2], A. White[2], M. E. Andersen[1], R. A. Clewell[1] and J. Pi[1]. [1]*The Hamner Institute, Durham, NC and* [2]*SEAC, Unilever INC, Colworth Science Park, Bedfordshire, United Kingdom.*

Quercetin (QUE) and curcumin (CUR) are polyphenols found naturally in foods and used as additives in dietary supplements, spices and pigments. Both have anti- or pro-oxidant effects depending on dose and are of interest as possible nutriceuticals due to anticancer and antioxidant activities. Nuclear factor E2-related factor 2 (Nrf2) mediated transcriptional signaling through the antioxidant response element (ARE) is a major cellular defense mechanism against oxidative stress. To better understand the mechanism of action for QUE and CUR, we evaluated dose- and time-response of markers of oxidative stress (intracellular GSH/GSSG ratio, reactive oxygen species; ROS) and antioxidant response (Nrf1, Nrf2, IKKβ proteins, Nrf2-ARE reporter activation, Nrf2-dependent gene transcription) in immortalized human keratinocyte (HaCaT) cells. Glucose oxidase (GOX) and tert-butylhydroquinone (tBHQ) were positive controls. QUE and CUR increased cellular ROS within 1 hr at 10 and 20 μM. CUR, but not QUE, decreased intracellular GSH/GSSG at 18 hr. Activation of Nrf2 was rapid, with observed Nrf2-ARE-luc activity, nuclear accumulation of Nrf2, and Nrf2 target gene transcription (NADH quinone oxidoreductase 1; NQO1, heme oxygenase 1; HO1) occurring within 2 – 6 hr at doses similar to those causing ROS. Interestingly, CUR induced Nrf2-ARE-luc and HO1 expression were 4-10 fold higher than QUE, GOX or tBHQ. Only CUR showed a strong induction of Nrf1 and IKKβ proteins, and IL6 and TNFα mRNA, suggesting cross-talk with the Nrf1 and nuclear factor kappa-light-chain-enhancer of activated B cells (NFκB) pathways. Nrf1 binds the ARE and the NFκB inflammatory response pathway has cross-talk with Nrf2 signaling. Thus, while both QUE and CUR induce ROS and Nrf2-mediated antioxidant response, the stimulatory effect of CUR on ARE-mediated transcription appears to be amplified by the crosstalk with Nrf1 and NFκB pathways.

PS 1789 Ethacrynic Acid Enhances Oxygen Toxicity-Compromised Macrophage Functions by Inhibiting HMGB1 Release and NF-κB Activation

M. Wang[1], M. Muralidhar[1], R. A. Sitapara[1], S. Gorasiya[1], W. Wu[1] and L. Mantell[1, 2, 3]. [1]*Pharmaceutical Science, St John's University, Jaimaica, NY,* [2]*Center for Inflammation and Immunology, The Feinstein Institute for Medical Research, Manhasset, NY and* [3]*Center for Heart and Lung Research, The Feinstein Institute for Medical Research, Manhasset, NY.*

Prolonged exposure to hyperoxia can compromise macrophage functions, contributing to the development of ventilator-associated pneumonia (VAP). Accumulation of extracellular high mobility group box-1 (HMGB1) in airways of animals exposed to hyperoxia can cause macrophage dysfunction. Hence, inhibition of the release of nuclear HMGB1 into the extracellular milieu may help maintain macrophage functions under hyperoxic conditions. The present study investigates whether ethacrynic acid (EA), a diuretic, suppresses HMGB1 release from macrophages and modulates macrophage functions in hyperoxia. RAW 264.7 cells were treated with different concentrations of EA for 24 h in the presence of 95% O2. EA inhibited hyperoxia-induced HMGB1 release and improved hyperoxia-compromised macrophage phagocytic and migration functions. In addition, hyperoxia-induced NF- κB activation was inhibited in EA treated RAW 264.7 cells, suggesting EA inhibits HMGB1 release via modulating NF-κB. To further confirm the role of NF-κB in hyperoxia-induced HMGB1 release, BAY 11-7082, a selective inhibitor of NF-κB activation, was used. BAY 11-7082 significantly inhibited HMGB1 release, improved hyperoxia-compromised macrophage migration and phagocytic functions. These results suggest that EA enhances hyperoxia-compromised macrophage functions by inhibiting HMGB1 release from macrophage via reducing NF- κB activation. Therefore, NF-κB could be a potential target to improve hyperoxia-compromised macrophage functions.

PS 1790 Protection of HepG2 Cells from Acrolein Toxicity by CDDO-Im via Glutathione-Mediated Mechanism

H. Shah[1], C. Saunders[1], A. Speen[1], E. Brooke[1], P. Nallasamy[1], H. Zhu[2], Y. Li[2] and Z. Jia[1]. [1]*Department of Biology, University of North Carolina at Greensboro, Greensboro, NC and* [2]*Department of Pharmacology, Campbell University School of Osteopathic Medicine, Greensboro, NC.*

Acrolein is an environmental toxicant, mainly found in smoke released from incomplete combustion of organic matter. The compound is ubiquitously found in endogenous as well as exogenous environment. Several studies showed that exposure to acrolein can lead to liver damage. The mechanisms involved in acrolein-induced hepatocellular toxicity, however, are not completely understood. This study examines the toxic effects and cytotoxic mechanisms of acrolein on HepG2 cells. Acrolein at pathophysiological concentrations was shown to cause a concentration-dependent decrease in cell viability. Acrolein exposure was also found to cause apoptotic cell death and an increase in levels of protein carbonyl and TBARS (thiobarbituric reactive acid substances), markers of protein damage and lipid peroxidation, respectively, in HepG2 cells. Acrolein also rapidly depleted intracellular glutathione (GSH), phase II enzyme GSH-linked glutathione-S-transferases (GST) and aldose reductase (AR), three critical cellular defenses that detoxify reactive aldehydes. Results further showed that depletion of cellular GSH by acrolein preceded the loss of cell viability, which suggests that cellular GSH depletion may be an important event in acrolein-induced cytotoxicity. To further determine the role of cellular GSH in protecting against acrolein-mediated cytotoxicity, buthionine sulfoximine (BSO) was used to inhibit cellular GSH biosynthesis. It was observed that depletion of cellular GSH by BSO led to a marked potentiation of acrolein-mediated cytotoxicity in HepG2cells. Furthermore, induction of GSH levels by CDDO-Im, a triterpenoid compound, afforded protection against acrolein toxicity in a concentration-dependent manner via induction of GSH mechanism. This study may provide understanding on the molecular action of acrolein which may be important to develop novel strategies for the prevention of acrolein-mediated toxicity.

PS 1791 Methionine Sulfoxide Reductase A: A Novel Nrf2 Target Gene

B. Harder, S. Tao, W. Tian, G. T. Wondrak and D. D. Zhang. *Pharmacology and Toxicology, University of Arizona, Tucson, AZ.*

Methionine sulfoxide reductase A (MsrA) is an oxidoreductase repair enzyme responsible for catalyzing the stereospecific reduction of methionine-S-sulfoxide to methionine. Previous studies have shown that reactive oxygen species (ROS) can lead to the oxidation of methionine, thereby rendering proteins functionless. Reversal of this process by MsrA has been shown to restore protein function, and has been implicated in cellular senescence, the aging process, neurodegenerative diseases, and glucose homeostasis. The antioxidant response of MsrA is established, but the transcriptional regulation remains uncertain. Nrf2, a key regulator of the antioxidant response, is a transcription factor that is responsible for altering gene expression upon insult triggered by ROS. We predicted MSRA to be a novel target gene of Nrf2 based on 12 putative AREs contained within the promoter region. Preliminary data, through induction of Nrf2, identified that MsrA protein expression acts just as other well-established Nrf2 target genes. Subsequent knockdown of Nrf2 in HaCaT cells showed reduced protein level of MsrA. Taken together, our data indicate that MSRA is a novel target gene of Nrf2. The regulation of MsrA and its functional contribution to the Nrf2-mediated defensive response are currently under investigation.

PS 1792 Production of Reactive Oxygen Species by the Redox Cycling of 9, 10-Phenanthraquinone in Human Monocyte THP-1 Cells: Role of the Mitochondrial Electron Transport Chain

Z. Jia[1], H. Zhu[3], M. A. Trush[2] and Y. Li[3, 1]. [1]*Department of Biology, University of North Carolina at Greensboro, Greensboro, NC,* [2]*Bloomberg School of Public Health, Johns Hopkins University, Baltimore, MD and* [3]*Department of Pharmacology, Campbell University School of Osteopathic Medicine, Buies Creek, NC.*

Exposures to environmental pollution remains a major problem and poses continuing risks to human health. Airborne particulate matter (APM) contains large amounts of quinoid compounds and it has been shown that 9,10-phenanthraquinone alone compromises about 6% of the total organic extract of diesel exhaust particles. However, the potential involvement of 9,10-phenanthraquinone in APM-induced adverse effects remains unclear. In this study, we determined whether 9,10-phenanthraquinone could undergo redox cycling in human monocyte THP-1cells. Incubation of THP-1 cells with 9,10-phenanthraquinone at 0.1-1 μM resulted in a significant stimulation of potassium cyanide (KCN)-resistant oxygen consumption, indicating that 9,10-phenanthraquinone could undergo redox cycling in cells. Redox cycling of 9,10-phenanthraquinone in THP-1 cells led to production of reactive oxygen specides (ROS) as determined by luminol-derived chemiluminescence (CL). The 9,10-phenanthraquinone -induced luminol-derived CL in cells was inhibited by mitochondria inhibitor rotenone suggesting the involvement of the mitochondrial electron transport chain (METC) in mediating the redox cycling of 9,10-phenanthraquinone to produce ROS. In support of this process, incubation of 9,10-phenanthraquinone with mitochondria isolated from the THP-1 cells also stimulated ROS production. In summary, this study demonstrated that 9,10-phenanthraquinone produces ROS in THP-l cells and METC is a

critical site for PAH quinones to redox cycle for ROS generation. Over production of ROS in mitochondria may lead to preferential oxidative damage to mitochondrial enzyme complexes as well as mitochondrial DNA, a critical events in cardiovascular disorders, including atherogenesis, hypertension, myocardial infarction, and heart failure.

PS 1793 Approaches to Minimize Hyperoxia-Induced Impairment of Macrophage Phagocytic Function

W. Wu, L. K. Sharma and L. Mantell. *St. John's University, Jamaica, NY.*

Alveolar Macrophages (AM) play a significant role in maintaining homeostasis by clearing invading pathogens and scavenging dead cells. Prolonged exposure of animals to hyperoxia (supraphysiological concentrations of oxygen) can induce oxidative stress that impairs the alveolar macrophages' phagocytic function. This impairment has been attributed to the compromised host innate immunity and increased susceptibility to infections. Strategies aiming at improving hyperoxia-compromised phagocytic function might improve innate immunity in patients and reduce chances of serious infections. The objective of this study was to test whether altering the exposure pattern to hyperoxia can minimize the deleterious effects of hyperoxia on macrophages. We tested two exposure paradigms to address whether:1. the adverse effects of hyperoxia on macrophages are reversible. 2.Intermittent exposure to hyperoxia is less deleterious than continuous exposure in compromising phagocytic function. Here, we report that phagocytic function compromised by 24 hours of continuous hypreoxiacan was reversed upon subsequent exposure to room air for 24 or 48 hours. The extent of recovery is dependent upon the duration of both hyperoxic and normoxic exposure. Macrophages that were subjected to intermittent exposure to hyperoxia (2 hours break after 12 hours exposure) exhibited significantly higher phagocytic activity compared to those with continuous 24 hour exposure. Thus, either giving sufficient time to recover or using intermittent hyperoxia can significantly ameliorate the toxic effects of hyperoxia on macrophage function.

PS 1794 Identification of Novel Chemical Inhibitors of Nrf2-ARE Activity and Their Application in Sensitizing Human Acute Monocytic Leukemia Cells to Chemotherapy

H. Peng[2, 3], P. Xue[2, 4], Y. Hou[1, 2], H. Zhang[2, 4], B. Sun[2], J. Dong[2], T. Zhou[2], W. Qu[4], S. Peng[3], B. Nelson[2], R. A. Clewell[2], Q. Zhang[2], M. E. Andersen[2] and J. Pi[2, 1]. [1]*School of Public Health, China Medical University, Shenyang, Liaoning, China,* [2]*The Hamner Institutes for Health Sciences, RTP, NC,* [3]*Academy of Military Medical Sciences, Beijing, China and* [4]*Fudan University, Shanghai, China.*

Nuclear factor E2-related factor 2 (Nrf2) is a master regulator of the antioxidant response element (ARE)-dependent transcription and plays a pivotal role in chemical detoxification in both normal and tumor cells. In keeping with previous findings that Nrf2-ARE plays a critical role in chemotherapeutic resistance of cancer cells, stable knockdown of Nrf2 by lentiviral shRNA in human acute monocytic leukemia THP-1 cells resulted in sensitization to cytotoxicity induced by multiple chemotherapeutic agents, including arsenic trioxide (As2O3), etoposide and doxorubicin. We screened a panel of chemicals using a variety of human and mouse cell lines expressing an ARE-luciferase reporter, and found that a group of widely used anti-tubercular drugs, including ethionamide (ETH) and isoniazid (INH), displayed substantial inhibitory property against Nrf2-ARE activity. This inhibitory property was further validated by significant reduction in mRNA expression of multiple ARE-driven genes under basal and oxidative stress conditions. Suppression of Nrf2-ARE by ETH or INH significantly enhanced the sensitivity of THP-1 and several other cancer cells, such as human histiocyte lymphoma U937 cells, to As2O3-induced cytotoxicity as determined by cell viability assays, ATP production, cell cycle and apoptosis analysis. In THP-1 cells, the sensitization effect of ETH to As2O3-induced cytotoxicity is Nrf2 dependent, suggesting that Nrf2 is a potential target of the chemotherapeutics. To our knowledge, our study is the first to demonstrate that ETH and INH suppress Nrf2-ARE signaling and disrupt the transcriptional network of the antioxidant response, leading to sensitization of cancer cells to chemotherapeutic agents.

PS 1795 Radical-Containing Ultrafine Particulate Matter Suppresses Cardiomyocyte Nrf2-Signaling

G. Chuang and K. J. Varner. *Pharmacology, LSU Health Sciences Center, New Orleans, LA.*

Epidemiology studies have linked combustion-generated particulate matter to increased cardiac morbidity and mortality. To conduct prospective controlled-exposure studies, we synthesized a model particulate matter, DCB230, by chemisorption of 1,2-dichlorobenzene to 0.2 μm silica particles containing 5% Cu(II)O at 230°C. Electron paramagnetic resonance showed that DCB230 generates radicals in solution in a manner similar to particles collected by atmospheric sampling. We previously showed that DCB230 exposure produces cardiac inflammation and oxidative stress. Since cellular anti-oxidant status is critical in countering inflammation and oxidative stress, we hypothesized that DCB230 exposure exerts cardiotoxicity by adversely impacting the Nrf2 anti-oxidant response pathway. Temporally coinciding with cell death, 8 hour treatment with DCB230 (0-200 μg/mL) decreased total glutathione and Nrf2 protein level in HL-1 cardiomyocytes. Additionally, 100 μg/mL DCB230 treatment failed to induce transcription of canonical Nrf2-regulated genes Hmox1 and Nqo1. Because glutathione depletion leads to apoptosis, HL-1 cardiomyocytes were pre-treated with 5 mM n-acetylcysteine (NAC) to augment cytosolic glutathione levels, washed, and then treated with 100 μg/mL DCB230 for 2 hours in order to investigate whether glutathione depletion mediated cell death. Surprisingly, NAC pre-treatment failed to reverse the DCB230-induced decreases in pro-caspase 9, Nrf2, and mitochondrial membrane potential. These data indicate that DCB230 suppression of Nrf2 and subsequent induction of apoptosis in cardiomyocytes are not mediated by glutathione depletion. Instead, alternate Nrf2 mechanisms such as transcriptional regulation of mitochondrial bioenergetics and the anti-apoptotic protein Bcl-2 may be responsible. Importantly, these findings may explain in part the paradoxical observation of suppressed Nrf2 signaling in lungs of smokers and emphysema/COPD patients, despite their apparent high levels of oxidative stress and inflammation. Supported by NIH P42-ES013648, Sub-project 6661.

PS 1796 Transcriptomic Changes in a Murine Hyperoxic Lung Injury Model and Analysis of Sex-Specific Changes

K. Lingappan, W. Jiang, L. Wang, X. Couroucli and B. Moorthy. *Baylor College of Medicine, Houston, TX.*

Hyperoxia contributes to acute lung injury and inflammation in experimental animals, ARDS (acute respiratory distress syndrome) in adults and BPD (bronchopulmonary dysplasia) in preterm infants. Sex-specific differences in outcomes in these diseases are well-known. The mechanisms responsible for sex differences in the susceptibility towards hyperoxic lung injury (HLI) remain largely unknown. Our objective was to characterize sex-specific differences in the transcriptome and inflammatory markers in lung injury due to oxidative stress using microarray and luminex bead arrays. Male and female (8-10 wk) wild type (WT) (C57BL/6J) mice were exposed to hyperoxia (FiO2>0.95). Gene expression in lung tissue was studied using the Mouse Gene 1.0 ST Array (Affymetrix). A combination of fold change ≥ 1.4 and false discovery rate < 5% was used to define differentially expressed genes (DEGs). Overrepresentation of gene ontology terms representing biological processes among the DEGs were tested using a conditional hypergeometric test (p-value < 0.01). Signaling pathway impact analysis (SPIA) was also performed to measure actual perturbation in a given pathway under our experimental conditions. The suspension bead array revealed increases in mouse lung tissue homogenate levels of IL-6 (F>M) and VEGF (M>F) after hyperoxia. A total of 2209 (up-regulated (UR): 1385, down-regulated (DR): 824) and 2467 (UR: 1549, DR: 918) genes were differentially expressed following hyperoxia compared to room-air in females and males respectively. Comparison of DEG profiles identified 327 genes unique to females, 585 unique to males and 1882 common genes. DEGs involved in lung development, signaling pathways (NF-kappa B, MAP kinase) may explain the differences in sex-specific susceptibility to HLI. These findings provide novel insights into the mechanisms involved in HLI and suggest new pathways that need to be investigated as sex-specific biomarkers and possible therapeutic targets for HLI.

PS 1797 Altered Mitochondrial Bioenergetics in Response to Arsenic Exposure: New Outlook on Arsenic-Induced Toxicity

H. D. Chavan, K. Mickey and P. Krishnamurthy. *Pharmacology, Toxicology & Therapeutics, Kansas University Medical Center, Kansas City, KS.*

Arsenic is a human carcinogen that is ubiquitously present in the environment. Arsenic mediated toxicity is suggested to be due to the induction of reactive oxygen species. However, the origins of these radicals are not clearly understood. Here we show that arsenic exposure, at environmentally relevant concentrations, uncouples

oxygen consumption from ATP production in mammalian cells leading to increased electron leakage, decreased ATP production and reduced spare respiratory capacity. Analysis of the mitochondrial respiratory complex provides evidence implicating a dose dependent deregulation in respiratory complex activity in response to arsenic exposure, suggesting that mitochondrial dysfunction might contribute to arsenic mediated induction of reactive oxygen species. These data illustrate that mitochondria might be a primary target in arsenic-induced oxidative stress and understanding the mechanism by which arsenic deregulates mitochondrial respiratory complex activity and uncouples oxygen consumption from ATP production might provide an important cellular target in interventional remedy for arsenic-induced toxicity.

PS 1798 Keap1 Redox-Dependent Regulation of Doxorubicin-Induced Oxidative Stress Response in Cardiac Myoblasts

K. B. Wallace and K. K. Nordgren. *Biomedical Science, University of Minnesota Medical School, Duluth, MN.*

Doxorubicin (DOX) is a widely prescribed treatment for a broad scope of cancers, but clinical utility is limited by the cumulative, dose-dependent cardiomyopathy that occurs with repeated administration. DOX-induced cardiotoxicity is associated with the production of reactive oxygen species (ROS) and oxidation of lipids, DNA and proteins. A major cellular defense mechanism against such oxidative stress is activation of the Keap1/Nrf2-antioxidant response element (ARE) signaling pathway, which transcriptionally regulates expression of antioxidant genes such as *Nqo1* and *Gstp1*. In the present study, we address the hypothesis that an initial event associated with DOX-induced oxidative stress is activation of the Keap1/Nrf2-dependent expression of antioxidant genes and that this is regulated through drug-induced changes in redox status of the Keap1 protein. Incubation of H9c2 rat cardiac myoblasts with DOX resulted in a time- and dose-dependent decrease in non-protein sulfhydryl groups. Associated with this was a near 2-fold increase in Nrf2 protein content and enhanced transcription of several of the Nrf2-regulated down-stream genes, including *Gstp1*, *Ugt1a1*, and *Nqo1*; the expression of *Nfe2l2* (Nrf2) itself was unaltered. Furthermore, both the redox status and the total amount of Keap1 protein were significantly decreased by DOX, with the loss of Keap1 being due to both inhibited gene expression and increased autophagic, but not proteasomal, degradation. These findings identify the Keap1/Nrf2 pathway as a potentially important initial response to acute DOX-induced oxidative injury, with the primary regulatory events being the oxidation and autophagic degradation of the redox sensor Keap1 protein. (Supported in-part by grants from the 3M Company and Whiteside Institute.)

PS 1799 Retinoic Acid Receptor-Dependent Interactions Contribute to the Selective Cytoprotection Afforded by All-Trans-Retinoic Acid against Renal Injury

J. Sapiro, R. T. Miller, R. D. Canatsey, A. B. Romans, T. J. Monks and S. S. Lau. *SWEHSC, Pharmacology and Toxicology, University of Arizona, Tucson, AZ.*

Chemical-induced nephrotoxicity is a major cause of acute kidney injury. Pretreatment of LLC-PK_1 cells with all-*trans*-retinoic acid (ATRA, 25 μM, 24 hr) affords cytoprotection against chemical nephrotoxicants such as *p*-aminophenol (PAP, 150 μM, 3 hr), iodoacetamide (IDAM, 25 μM, 2 hr) and 2-(glutathion-*S*-yl)hydroquinone (MGHQ 300 μM, 2 hr) as assessed by the Neutral Red assay. In contrast, pretreatment of cells with ATRA provides no protection against cisplatin (25 μM, 24 hr) -induced apoptosis, suggesting that ATRA selectively protects against toxicants that induce necrosis and not apoptosis. The biological effects of retinoids are typically mediated through interaction with the nuclear retinoic acid receptors (RAR) and retinoid X receptors (RXR). While western blot analyses of nuclear lysate from LLC-PK_1 cells revealed the presence of both RAR and RXR, ATRA only induced the RAR isoforms. Since ATRA binds to the RAR/RXR heterodimer, we tested the hypothesis that other RAR agonists would provide protection against nephrotoxicants. Pretreatment of LLC-PK_1 cells with the pan-RAR agonist 4-[(E)-2-(5,6,7,8-tetrahydro-5,5,8,8-tetramethyl-2-naphthalenyl)-1-propenyl]-benzoic acid (TTNPB) (25 μM, 24 hr) protected against PAP (125 μM, 3 hr) and IDAM (20 μM, 2 hr) –induced nephrotoxicity. Pretreatment of LLC-PK_1 cells with the pan-RXR agonist, methoprene acid (25 μM, 24 hr), afforded minor protection against PAP (125 μM, 3 hr) but not IDAM (25 μM, 2 hr). The results are consistent with the view that ATRA-mediated cytoprotection involves interaction with the RAR receptor. During ATRA-mediated cytoprotection, the endoplasmic reticulum chaperone Grp78 was induced in a similar time-dependent manner to RAR. Thus, ATRA and/or analogs thereof, may serve as an effective therapeutic intervention prior to kidney transplantation, which causes ischemic-reperfusion renal injury (ES016578, ES006694, ES007091).

PS 1800 Administration of Sulindac, an NSAID, and Qurectin, an Antioxidant, in Combination Attenuates Bleomycin-Induced Lung Fibrosis in Wistar Rats

R. Verma[2], M. V. Patel[2], V. J. Piccirillo[1], P. Mehta[2], D. Gohel[2], T. Marvania[2] and S. Balakrishnan[3]. [1]*VJP Consulting, Inc., Ashburn, VA,* [2]*Department of Toxicology, Jai Research Foundation, Valvada, Gujarat, India and* [3]*Department of Zoology, The M.S. University of Baroda, Vadodara, Gujarat, India.*

Idiopathic pulmonary fibrosis is the most prevalent chronic lung disease. Inflammation and oxidative stress are considered major mechanisms that induce lung tissue inflammation and fibrosis. Studies have suggested that reactive oxygen species such as superoxide anion, hydrogen peroxide and hydroxyl radical are major mediators of lung inflammatory processes. The present study was conducted to evaluate the ameliorative effects of quercetin (a dietary flavonoid having strong antioxidant activity) alone and in combination with sulindac (non-steroidal anti-inflammatory drug) on lung injury induced by bleomycin. Following single intra-tracheal instillation bleomycin rats were treated by oral administration of either quercetin (100 mg/kg/day) or sulindac (20 mg/kg/day) for 20 days reduced the severity of bleomycin induced effects on relative lung weights, lung hydroxyproline contents and plasma TNF-α levels. However, subtle signs of toxicity persisted in the quercetin and sulindac treated groups. The combination of quercetin (50 mg/kg/day) and sulindac (10 mg/kg/day) was more effective in reducing bleomycin induced lung toxicity than the higher doses of each agent separately. Therefore, these results suggest that the concurrent administration of quercetin and sulindac in low doses are synergistic in protection of the lung from oxidative stress induced effects.

PS 1801 Dietary Flavonoid Quercetin Attenuates Bleomycin-Induced Pulmonary Fibrosis in Rats by Improving Lung Antioxidant Status

D. Gohel[2], V. J. Piccirillo[1], M. V. Patel[2], R. Verma[2], P. Mehta[2], T. Marvania[2] and S. Balakrishnan[3]. [1]*VJP Consulting, Inc., Ashburn, VA,* [2]*Deptartment of Toxicology, Jai Research Foundation, Valvada, Gujarat, India and* [3]*Department of Zoology, The M.S. University of Baroda, Vadodara, Gujarat, India.*

Lung fibrosis is a frequent side effect of the chemotherapeutic agent bleomycin. Reports suggest that reactive oxygen species may play a key role in the development of lung fibrosis from this agent. The present study examined the protective role, if any, of the dietary flavonoid, quercetin, against bleomycin induced lung fibrosis in rats. Animals were divided into a control group (0.5% carboxymethylcellulose orally for twenty days post sham intra-tracheal instillation of saline on day 0), a bleomycin group (6.5 U/kg body weight via single intra-tracheal instillation on day 0 followed by oral administration of 0.5% carboxymethylcellulose for twenty days) and a bleomycin plus quercetin group (single 6.5 U/kg intra-tracheal bleomycin instillation followed by oral administration of quercetin for twenty days). Our results show that bleomycin administration increased lipid peroxidation resulting in prolonged state of local tissue inflammation characterized by elevated levels of TNF-α even after twenty days of drug treatment. The prolonged oxidative stress resulted in excessive collagen deposition in the peribronchial and perialveolar regions of lung culminating in lung fibrosis. Twenty days of quercetin treatment following bleomycin administration stabilized tissue antioxidant capacity at normal levels with recovery from lung inflammatory changes. Trichrome stained lung tissue from the rats receiving repeated doses of this flavonoid revealed only basal levels of collagen deposition as confirmed by normal levels of hydroxyproline. The results of the present study strongly suggest that quercetin may be an effective protective agent against bleomycin induced pulmonary fibrosis.

PS 1802 Nrf2 Activation by the First-in-Class Direct Keap1-Nrf2 Interaction Inhibitor LH601A in Human Kidney Cells

G. Thorne[1], X. Wen[2], M. S. Joy[4], L. Hu[3] and L. M. Aleksunes[2, 5]. [1]*Dept of Pharmacy and Health Professions, Elizabeth City State University, Elizabeth City, NC,* [2]*Dept of Pharmacology and Toxicology, Rutgers University, Piscataway, NJ,* [3]*Dept of Medicinal Chemistry, Rutgers University, Piscataway, NJ,* [4]*Dept of Pharmaceutical Sciences, University of Colorado, Aurora, CO and* [5]*Environmental and Occupational Health Sciences Institute, Piscataway, NJ.*

Under basal conditions, the antioxidant transcription factor, Nuclear factor (erythroid-derived 2)-like 2 (Nrf2), is bound to the Keap1 (Kelch-like erythroid-cell-derived protein 1) protein and targeted for proteasomal degradation in the cytoplasm. In response to cellular injury or chemical treatment, Nrf2 activates the transcription of antioxidant, cell stress, metabolism and other protective genes and defends against kidney injury. LH601A is a first-in-class direct inhibitor of the Keap1-Nrf2 protein-protein interaction. We hypothesize that LH601A will activate Nrf2 signaling in human cultured kidney cells and protect against chemical-induced kidney

injury. For this purpose, human embryonic kidney 293 cells were treated with LH601A and the positive control indirect Nrf2 activator, sulforaphane (SFN). Nrf2 target genes and proteins (NADPH quinone oxidoreductase 1, Nqo1; heme oxygenase-1, Ho-1; and thioredoxin-1, TR1) were quantified by qPCR and western blot analysis. SFN and LH601A up-regulated Ho-1 mRNA (4- to 7-fold) and TR1 mRNA (2-fold) within 2 to 6 h which persisted through 16 h. SFN also increased Nqo1 mRNA by 2-fold at 6 h, however induction was not observed with LH601A until 16 h. In addition, SFN and LH601A elevated the Ho-1 protein expression by 3-fold at 16 h. Since Nrf2 activation can protect tissues from oxidative stress and injury, the direct inhibitor of the Keap1-Nrf2 interaction investigational drug LH601A may be used to activate the expression of protective genes and defend against kidney diseases. Supported by DK093903, DK080774, ES005022, ES020721, ES020522, and the SOT Intern Program.

PS 1803 A Novel Mitochondria-Targeted Antioxidant for Mitigation of Radiation

A. Banerjee, N. Sieracki, M. Bonini and A. V. Lyubimov. *Pharmacology, University of Illinois, Chicago, IL.*

Radiation-induced generation of excessive reactive oxygen or nitrogen species (ROS or RNS) leading to mitochondrial dysfunction, bone marrow damage, apoptosis and necrosis in the gastric mucosa is well understood. ROS/RNS removal by electron scavengers and antioxidants is a promising therapeutic strategy towards radiation exposure induced-damage. A series of novel antioxidants targeting the mitochondria were designed, synthesized, and structurally elucidated. The core scaffold contains a hydroxylamine moiety that protects the cell and mitochondria from oxidative damage by 2 synergizing mechanisms (enzymatic dismutation of superoxide radical and possible metal chelating). SMA-011 was selected from several novel compounds as the most promising for mitigation of γ-irradiation-induced death in C57Bl/6 mice. Preliminary studies showed that 1 mg/kg of SMA-011 provided as a single subcutaneous dose at 24 hr post irradiation (8.1 Gy) was well tolerated in mice. It was evident that after Day 12 post total body irradiation there was a drop in survival in the control group but not in the SMA-011-dosed group (90 % survival in SMA-011 group vs. 45% survival in the control group at Day 12) which was statistically significant on each day from Days 12 to 22 (45 % survival in SMA-011 group vs. 15 % in control by Day 30). In addition, SMA-011 when administered subcutaneously at 24 hr post irradiation also efficiently prevented loss of components of complexes I (NADPH dehydrogenase), III (cytochrome bc1 complex) and II (succinate dehydrogenase) in the heart and jejunum tissues collected at 48 and 120 hr. Furthermore, when a high dose of total body irradiation at 13 Gy was applied to C57BL/6 mice, SMA-011 showed good protection of the jejunum as well as prominent proliferative activity on Day 4 post irradiation observed through TUNEL and Ki-67 staining of the jejunum. Hence, the low toxicity, systemic availability and significantly increased survival rate indicates that SMA-011 has a good potential to serve as a radiation mitigating agent with possible alternate applications in other inflammatory diseases.

PS 1804 Fibrate Engagement of a Peroxisomal TSC Signaling Node Induces Autophagy via mTORC1 Repression

D. N. Tripathi[1], J. Zhang[1], J. Jing[1], A. Alexander[2], R. Dere[1] and C. L. Walker[1]. *[1]Center for Translational Cancer Research, IBT Texas A & M HSC, Houston, TX and [2]Department of System Biology, UT M D Anderson Cancer Center, Houston, TX.*

We have recently reported that the Tuberous Sclerosis Complex (TSC) signaling node (TSC1, TSC2, and Rheb) localizes to peroxisomal membranes, where it represses mTORC1 in response to ROS via a novel pathway involving ATM. In the present study, we sought to determine whether cells (rodent and human both) treated with clofibrate (PPAR activator), engage this signaling pathway, in response to ROS generated as a byproduct of increased peroxisomal β-oxidation of fatty acids, to restore peroxisomal homeostasis. In rat liver FAO cells, clofibrate activated PPARs resulting in increased transcription of peroxisomal proteins such as ACAA1 and EHHADH, and increasing ROS levels. Elevated ROS following clofibrate treatment lead to activation of ATM and its downstream effectors LKB1-AMPK-TSC2, which suppressed mTORC1 signaling as evidenced by decreased phosphorylation of S6K and S6. Interestingly, activation of this signaling pathway by clofibrate also occurred in MCF-7 (breast cancer) cells, which do not undergo peroxisome proliferation. Commensurate with suppression of mTORC1 in response to clofibrate, autophagy/pexophagy was induced in both rodent and human cells, as evidenced by an increase in the autophagosome marker LC3-II, decrease in the long-lived protein p62, increase in GFP-labeled puncta (autophagosomes) in cells stably expressing GFP-LC3, and detection of autophagosomes containing peroxisomes by electron microscopy. Together, these results provide compelling evidence that increased peroxisomal ROS induced by fibrates activate ATM, and the TSC signaling node resident at the peroxisome to suppress mTORC1 and induce autophagy/pexophagy, providing a mechanism by which cells can restore peroxisomal homeostasis in response to treatment with PPAR ligands.

PS 1804a Distinct Roles of Basal and Inducible Nrf2-Medicated Antioxidant Response against Cobalt Chloride-Induced Cytotoxicity in Human Keratinocytes

R. Zhao[1], L. Wang[1], M. Zhang[1], S. Jiang[1], J. Fu[2], J. Chen[1], B. Yang[3], X. Liang[3], D. Guan[1] and J. Pi[2]. *[1]School of Forensic Medicine, China Medical University, Shenyang, China, [2]School of Public Health, China Medical University, Shenyang, China and [3]China Medical University, Shenyang, China.*

Hypoxia is an important physipathological process that is involved in many cutaneous diseases and injuries. Nuclear factor E2-related factor 2 (Nrf2) is a master regulator of the antioxidant response element (ARE)-dependent transcription and plays a pivotal role in chemical detoxification in a variety of cells, including keratinocytes. This study was conducted to illustrate the role of Nrf2-medicated antioxidant response against chemical hypoxia-induced cell injury by cobalt chloride (CoCl2), in human keratinocytes. In HaCaT cells, acute CoCl2 exposure significantly increased the levels of intracellular reactive oxygen species (ROS) and the expression of Nrf2 and multiple ARE-regulated antioxidant genes in concentration- and time-dependent manners, showing that CoCl2 causes oxidative stress in the cells. Selective knockdown (KD) of Nrf2 by lentiviral shRNA dramatically reduced the basal and inducible expression of many antioxidant enzymes and sensitized the cells to acute cytotoxicity of CoCl2. In contrast, pretreatment of HaCaT cells with a well-known Nrf2 activator tert-butylhydroquinone protected the cells from CoCl2-induced cell injury in a Nrf2-dependent fashion. In addition, silencing of kelch-like ECH-associated protein 1 (Keap1), a Cul3-adapter protein that allows for Nrf2 to be ubiquinated and degraded by the proteasome complex, led to a dramatic resistance to CoCl2-induced cytotoxicity and apoptosis. Interestingly, knockdown of Keap1 markedly enhanced the basal activity of Nrf2, but reduced the induction of ARE-dependent genes by CoCl2, suggesting that basal activity of Nrf2 is more important than inducible expression of ARE-dependent genes in determining cellular sensitivity to the cytotoxicity of CoCl2. Taken together, our studies suggest that basal and inducible Nrf2-medicated antioxidant response may play distinct roles in human keratinocytes against CoCl2-induced cytotoxicity.

PS 1804b A Dilution Effect in the Malondialdehyde Measurement in Serum with High-Performance Liquid Chromatography-Tandem Mass Spectrometry

Q. Wu, L. M. Kamendulis and B. A. Hocevar. *Department of Environmental Health, Indiana University School of Public Health, Bloomington, IN.*

Oxidative stress is caused by an imbalance between free radicals and antioxidant defenses in the body, which is a prominent feature of many diseases. The overwhelming redox state can lead to damages to biomolecules including proteins, lipids, and DNA. Malondialdehyde (MDA) is one of the major secondary decomposition products of peroxidized polyunsaturated fatty acid and is one of most used biomarkers in oxidative stress studies. We developed and validated a sensitive method for the quantitation of MDA in mouse serum after derivatization with 2,4-dinitrophenyhydrazine (DNPH) by high-performance liquid chromatography with positive electrospray ionization coupled with tandem mass spectrometry (HPLC-ESI-MS/MS). In spite of the promising instrument measurement, a significant sample dilution effect in sample preparation was observed for the quantitative analysis of MDA for the same mouse serum. The measured MDA levels were 74.7, 20.6, and 3.4 μM for 5%, 40%, and 100% of serum samples, respectively. The possible reason for this phenomenon is a better hydrolysis of serum samples in a more diluted serum mixture, which released relatively more low-molecular mass aldehydes and competently derivatized with DNPH in the reaction. A decreased recovery of MDA was also demonstrated for the same serum spiked with acetone, formaldehyde, or 4-hydroxynonenal. Therefore, a cautionary note on sample dilution should be made before any conclusions are drawn for MDA measurements. And other more reliable biomarkers for oxidative stress such as 8-*iso*-PGF2α are also highly needed for oxidative stress studies.

PS 1804c Role of Cystine/Glutamate Transporter Slc7a11 in Bleomycin-Induced Lung Inflammation and Fibrosis in Mice

H. Cho, L. Miller-DeGraff and S. R. Kleeberger. *Laboratory of Respiratory Biology, NIEHS, NIH, Research Triangle Park, NC.*

Oxidative stress has been implicated in the pathogenesis of lung disorders including pulmonary fibrosis. Nrf2 has a protective role in these disorders via transcriptional induction of cytoprotective genes including thiol homeostasis enzymes. Glutathione is the most abundant cellular thiol and is essential in antioxidant defense. Solute carrier family 7 (cationic anionic amino acid transporter, y+ system), member 11 (Slc7a11, xCT) is an Nrf2 effector, and encodes a cystine/glutamate transporter that mediates entry of cystine into the cell coupling with efflux of glutamate to produce glutathione. We hypothesized that Slc7a11 is important to protection against pulmonary fibrosis. To test this hypothesis, bleomycin (0.5 U/Kg body weight) or vehicle was instilled in wild-type (WT) and mice with spontaneous mutation in Slc7a11 (C3H/HeSnJ-Slc7a11sut/J, Slc7a11-/-). Pulmonary injury responses were determined at 3, 7, 14, and 21 d after treatment. Bleomycin-induced influx of macrophages, neutrophils, eosinophils, monocytes, and lymphocytes in bronchoalveolar lavage fluids (BALF) were significantly higher in Slc7a11-/- mice than in WT mice (3-7 days). Pulmonary hemorrhage and appearance of uncommon inflammatory cells (e.g., atypical lymphocytes, basophils, megakaryocytes) in the BALF were enhanced in Slc7a11-/- than in WT after bleomycin. We found more lymphocytic nodules and diffused fibrotic lesions in Slc7a11-/- mice compared to WT mice 14-21 d post-bleomycin. Concurrently, gene expression and accumulation of lung collagen was significantly higher in Slc7a11-/- than in WT mice. Bleomycin also increased mRNA and protein levels of Slc7a11 in WT mice (3-21 days). Moreover, lung glutathione and its biosynthesis enzyme (glutamate-cysteine ligase) levels were increased post-bleomycin in WT mice while these changes were marginal in Slc7a11-/- mice. Results demonstrated that is Slc7a11 involved in protection against bleomycin-induced lung inflammation and fibrosis in the mouse.

PS 1805 Animal Behaviors Associated with Developmental Chlorpyrifos Exposure Are Inconsistent with Autism

A. Lavin Williams and J. M. DeSesso. *Exponent, Alexandria, VA.*

Animal models do not exactly replicate human psychiatric disorders; however, these models may be used to investigate whether the behaviors associated with certain exposures in animals parallel those observed in autism. According to the most current version of the Diagnostic and Statistical Manual of Mental Disorders (DSM-V), autism is diagnosed based on (1) persistent deficits in social communication and social interaction and (2) the presence of restricted, repetitive patterns of behavior, interests and activities. To address whether developmental chlorpyrifos (CYP) exposure was associated with autistic behaviors, a literature search was conducted to identify studies in rats and mice involving gestational or early postnatal exposure to CYP or CYP oxon (the active metabolite) and subsequent behavioral testing to assess social interactions and communication, stereotypic behaviors and other behaviors associated with novelty-seeking/anxiety. A total of 13 studies conducted in 6 different laboratories were identified. Analysis of these studies found that perinatal CYP exposure was generally associated with (1) no effect, increased social communications or conflicting findings in 6 of 7 studies; (2) no effect or increased social encounters in 4 of 4 studies; (3) no effect, reduced stereotypies or conflicting findings related to stereotypic behaviors in 9 of 9 studies; and (4) no effect or increased preference for novelty and reduced anxiety in novel environments in 5 of 7 studies. When a difference from control was observed, it was often in the opposite direction of what one would expect in autism. Based on these results, perinatal CYP exposure is not associated with the development of autism-like behaviors in rats and mice.

PS 1806 Toxicologic Assessment of Air Ion Exposures in Laboratory Animals

W. H. Bailey[2] and A. Lavin Williams[1]. [1]*Exponent, Alexandria, VA and* [2]*Exponent, Bowie, MD.*

Air ions are molecules of air that have become ionized—that is, they have either lost or gained an electrical charge. Air ions are natural phenomena generated by weather events, waterfalls, and geologic sources. Past speculation has suggested that exposure to positive air ions may be adverse to one's health, while exposure to negative air ions may be associated with beneficial health effects. The purpose of this research was to assess the potential health effects associated with exposure to air ions. A literature search was conducted to identify studies of laboratory animals exposed to positive or negative air ions. Topic areas of specific study included: behavior and brain activity; learning and memory; effects on serotonin and other neurotransmitters; tracheal function; respiratory infection; cardiovascular function; reproduction and growth; carcinogenesis; and other health outcomes. Many of these studies were found to be relatively old and also to suffer from various reporting and methodological deficiencies. The latter deficiencies include a failure to include sham exposures (i.e., controls were handled in a different manner than were treated animals) and to blind investigators as to the exposure status of the animals. Also, the vast majority of the studies on air ions (positive, negative or mixed ions) failed to control from the influence of potential confounding variables, including the presence of an electrical field and the production of noise, light, and ozone or other gaseous by-products. The most carefully controlled studies, however, consistently reported no effects of exposure on any of the health endpoints examined. In conclusion, based on the available literature, the data available from animal studies do not provide evidence of any adverse or beneficial effects of air ions exposure on health. This finding is consistent with comprehensive reviews and meta-analyses of human experimental studies of mood and behavior (Perez et al., 2013) and respiratory function, clinical pulmonary measures and asthmatic symptoms (Alexander et al., in press).

PS 1807 Assessment of Antiandrogenic Effects Observed following Exposure to Phthalates: An Evaluation of Concordance between Epidemiological, Animal, and Mechanistic Evidence

X. Arzuaga[1], A. Hotchkiss[1], T. Walker[1], C. J. Brinkerhoff[2, 1], K. Christensen[1] and G. S. Cooper[1]. [1]*ORD/NCEA, US EPA, Washington, DC and* [2]*Oak Ridge Institute for Science & Education, Oak Ridge, TN.*

Studies using various rat strains have consistently shown that phthalate exposure can interfere with normal development of the male reproductive system via inhibition of androgen synthesis and other hormones. In addition, epidemiological studies provide evidence of an association between gestational exposure to certain phthalates during pregnancy and anti-androgenic effects on the developing male reproductive system. However, studies using xenografts or ex vivo tissue cultures have reported that human fetal testis are unresponsive to phthalate-induced disruption in testosterone levels/production. These results question the validity of the rat model for assessment of potential human health effects. In order to address the utility of the rat model, a review and analysis of available evidence from epidemiological, animal, and ex-vivo studies on phthalate-induced effects in the developing male reproductive system and other androgen-regulated developmental outcomes was performed. While the ex vivo and xenograft data suggest that humans may be unresponsive to fetal phthalate exposure, experimental conditions including sample size, variability, and age of sampled human tissue should be taken into consideration in a weight of evidence evaluation. Overall, the evidence from epidemiological studies, animal bioassays, and mechanistic studies suggest that phthalate exposure can disrupt testicular androgen synthesis during early life stages. Based on these observed effects and given the uncertainties associated with the available xenograft and ex-vivo studies, rats are still considered a useful model for assessing phthalate-induced reproductive health effects in developing human males.
Disclaimer: The views expressed are those of the authors and do not necessarily represent the views or policies of the US EPA.

PS 1808 Evidence on the Carcinogenicity of Butyl Benzyl Phthalate (BBP) and Possible Mechanisms of Action

C. Hsieh, M. Sun, J. D. Budroe, M. S. Sandy and L. Zeise. *OEHHA, Cal/EPA, Sacramento, CA.*

BBP is a high-production chemical that is primarily used as a plasticizer in polyvinyl chloride products such as flooring materials. Its urinary monobenzyl phthalate metabolite is detected in biomonitoring studies indicating widespread human exposure. The chemical's carcinogenicity was reviewed to support a decision by a qualified panel of experts on whether or not it should be added to the Proposition 65 list of chemicals known to the state to cause cancer. OEHHA conducted a search of the scientific literature for information relevant to the carcinogenicity of BBP, up through October 4, 2013. 241 papers were identified, analyzed and summarized, as follows. BBP statistically significant increased the incidence of pancreatic acinar cell tumor, mononuclear cell leukemia, and adrenal medulla tumor in rats. In addition, rare tumors of the urinary bladder transitional epithelium were identified in treated female rats, accompanied by treatment-related increases in hyperplasia. While negative in Salmonella reverse mutation assays, BBP has tested positive in multiple other genotoxicity studies. In vitro findings include DNA base lesions in mouse bone cells, DNA single strand breaks in HepG2 cells and DNA-protein crosslinks (DPC) in rat liver cells. In vivo findings include DPC in mouse liver and sister chromatid exchanges and chromosomal aberrations in mouse bone marrow cells. Microarray and proteomic studies revealed BBP increased expression of several cancer pathway-related genes and proteins (e.g. VEGF, MYC and DEK). In human breast cells (HBC) in vitro and in rat breast cells in vivo, BBP increased markers of cell proliferation, angiogenesis, epithelial-mesenchymal transition, mi-

gration, and invasiveness. In addition, HBC treated with BBP formed tumors and increased angiogenesis in athymic nude mice. Accordingly, several possible non-exclusive mechanisms of carcinogenesis were identified, including genotoxicity, epigenetics, androgenic disruption, and peroxisome proliferator activated receptor-, aryl hydrocarbon receptor-, and estrogen receptor-mediated mechanisms.

PS 1809 Integrated Mechanistic Evidence on Noncancer, Portal-of-Entry Effects following Formaldehyde Inhalation

A. D. Kraft, B. S. Glenn, G. S. Cooper, B. F. Pachkowski, K. D. Salazar and J. M. Fritz. *US EPA, Washington, DC.*

Formaldehyde is a high production volume chemical with a multitude of industrial uses. Due to its high reactivity, the majority of inhaled formaldehyde is deposited in the upper respiratory tract. Formaldehyde exposure has been reported to cause a number of noncancer health effects, primarily at the portal-of-entry, including sensory irritation, impaired pulmonary function, asthma and immune effects, and respiratory tract pathology. This analysis attempts to cohesively and succinctly describe the mechanistic data related to these effects. Mode of action (MOA) data is typically described within a given health domain (e.g., supporting sensory irritation), and is most commonly used to inform biological relevance to humans. By evaluating the plausibility of the evidence, based on the chemical properties of formaldehyde and study design characteristics (e.g., route, duration, and levels of exposure), we identify and describe the potential mechanistic inter-dependencies across health effects. For example, stimulation of sensory nerve endings in the nasal mucosa can elicit an irritant sensation, but this stimulation may also initiate a release of tachykinins, eventually resulting in airway inflammation. Similarly, formaldehyde can initiate mucociliary changes that result in epithelial damage and cell proliferation, leading to lesions in the upper respiratory tract; however, thickened mucus and increased epithelial cell proliferation may also lead to pulmonary dysfunction. Detailing the plausibility of these mechanistic linkages and presenting this information schematically provides continuity and added clarity to MOA descriptions across health domains. This analysis allows for an effective evaluation of the potential biologic mechanisms that are most likely to be operative following formaldehyde exposure. Finally, this presentation facilitates a more integrated discussion of the potential relationship(s) between noncancer health effects and carcinogenicity. Disclaimer: The views expressed are those of the authors and they do not represent U.S. EPA policy or guidance.

PS 1810 Weight-of-Evidence Evaluation of Short-Term Ozone Exposure and Cardiovascular Effects

R. L. Prueitt[1], S. N. Sax[2], H. N. Lynch[2], J. C. Lemay[2], J. M. King[2] and J. E. Goodman[2]. [1]*Gradient, Seattle, WA and* [2]*Gradient, Cambridge, MA.*

There is a large body of research on the potential cardiovascular (CV) effects associated with ozone exposure, including epidemiology, toxicology, and controlled human exposure studies. US EPA is reviewing these data in its consideration of a revision to the ozone National Ambient Air Quality Standards (NAAQS). We conducted a weight-of-evidence (WoE) analysis to determine if there is an association between CV effects and short-term ozone exposure at levels below the current primary ozone NAAQS of 75 parts per billion (ppb). We utilized a novel WoE framework based on US EPA's NAAQS causality framework to critically evaluate and synthesize the relevant epidemiology, controlled human exposure, animal toxicology, and mechanistic data. We concluded that the epidemiology evidence of CV morbidity and mortality is inconsistent and lacks coherence across specific CV endpoints. Specifically, the lack of epidemiology evidence of morbidity effects is not coherent with reported mortality estimates. Toxicology studies, although somewhat more consistent, are of limited relevance because they are conducted at high exposure levels, well above the current NAAQS, and there is insufficient information on dose-response relationships. Furthermore, there is a lack of coherence between reported results from epidemiology studies (suggesting no effects) and results from animal studies (suggesting small effects at high exposure levels). Similarly, controlled human exposure studies report inconsistent effects after exposure to ozone levels above the current NAAQS. Studies that aim to identify potential mechanisms for CV effects of ozone by measuring various CV-related biomarkers also report inconsistent results with uncertain clinical significance, indicating that there is no clear biological mechanism for CV effects from ozone exposure. Overall, our WoE analysis does not support that CV effects are associated with short-term ozone exposure below the current NAAQS.

PS 1811 Do Asbestos-Induced Pleural Plaques Cause Lung Function Deficits?

L. E. Kerper[1], H. N. Lynch[1], L. C. Mohr[2] and J. E. Goodman[1]. [1]*Gradient, Cambridge, MA and* [2]*Medical University of South Carolina, Charleston, SC.*

While there is general agreement that pleural plaques are biomarkers of asbestos exposure, there is debate in the scientific community over whether pleural plaques cause lung function deficits. Many of the studies that addressed this issue were subject to certain limitations. In most studies, pleural plaques were diagnosed by radiography, which is less accurate than high resolution computed tomography (HRCT) and can lead to misdiagnoses. Some studies reported lung function changes in subjects that had lung abnormalities in addition to pleural plaques, so that the contribution of pleural plaques to deficits was unknown. To eliminate these sources of uncertainty, we conducted the first comprehensive analysis of the associations between pleural plaques and lung function based on epidemiology studies in which 1) pleural plaques were diagnosed by HRCT and 2) individuals were identified with pleural plaques and no other lung abnormalities. We identified and analyzed 16 relevant studies. We looked for patterns within and across studies and examined whether associations were reproducible. Only three of the 16 studies reported statistically significant associations between pleural plaques and some measure of lung function. Among these three studies, the lung function parameters were not consistent, suggesting that the associations were not likely causal. In addition, mean asbestos exposures in all three studies were higher in the subjects with pleural plaques than in the subjects without. This suggests that if the effects were not due to chance, the asbestos exposure itself, rather than pleural plaques, may have been responsible for observed lung function deficits. Taken as a whole, the direction of effect (i.e., lung function deficit vs. improvement) varied among studies, indicating the absence of even subtle effects and that the lack of effect noted in the majority of studies was not a result of low statistical power. We conclude that there is no reliable association between the presence of pleural plaques in asbestos-exposed populations and lung function deficits.

PS 1812 Firefighters' Inhalation Exposures and the Risk of Developing Multiple Myeloma

M. Peterson and P. A. Valberg. *Gradient, Seattle, WA.*

Firefighters encounter a complex mixture of chemicals under unique exposure conditions. The complexity in evaluating whether these exposures lead to occupational diseases has led 27 states to pass "presumptive causation" legislation, which assume all cancers that occur among firefighters are a result of on-the-job exposures. While such laws may be well intentioned, their scientific basis is dubious at best. Because a meta-analysis of firefighter data suggests these workers have a relative risk of 1.5 for multiple myeloma (MM), a cancer of cells in the hematopoietic system that can affect multiple sites in the body, including the bone, bone marrow, and kidney, we conducted a weight-of-evidence analysis to evaluate whether exposure to airborne chemicals typically identified in firefighting environments could be causally linked to increased risks. We examined a variety of factors in exposure, toxicological, and epidemiological studies, including study design, power, corroboration, relevance, and coherence within and among studies. Firefighters may inhale a variety of combustion products (including IARC Group 1 carcinogens) in both acute and more chronic scenarios (e.g., diesel exhaust). We found that for the well-studied IARC Group 1 chemicals, there was insufficient evidence that MM risk was increased with exposure. Many studies have sought to identify MM risk factors, but the results are inconsistent. Reviews and meta-analyses of MM among firefighters have reported modestly increased, but unstable, MM risks. Significant methodological issues cloud the interpretation of these meta-analyses. For example, only a few of the studies reported a statistically significant increase in MM in firefighter populations, and exposure information was often lacking. Because of a lack of concordance among the studies as to exposure and outcome, our evaluation found that airborne occupational exposures in firefighters are not causally associated with an increased risk of MM. Little is known about the etiology of MM, and job-related "presumptive causation" in the case of MM in firefighters is not supported by available scientific evidence.

PS 1813 Toxicological Review of Biocides Used in Hydraulic Fracturing

A. Pawlisz and A. L. LeBeau. *CRA, Dallas, TX.*

The use of hydraulic fracturing to extract gas and oil form shale formations has maintained its exponential growth in US and worldwide. Hydraulic fracturing consists of injecting water, friction reducers, proppants, disinfectants, surfactants, thickeners, scale inhibitors, corrosion inhibitors, and acids to promote flow of hydrocarbons otherwise bound in impermeable matrices. The rapid explosion of

volume and extent of fracking exploration has led to community, regulator, and health practitioner concerns over the potential health effects associated with exposure to fracking fluid constituents. Many of the disclosed ingredients are cited as harmless. However, there are certain chemical groups, such as antimicrobials, that have specific (by design) adverse biological activity. This presentation focuses on the identity and toxicity of fracking fluid constituents listed as having a disinfectant function. The methodology consisted of querying publicly-available databases used by the oil and gas industry to disclose chemical information. Data fields associated with chemical name, CAS number, additive concentration, and fracking fluid concentration were extracted for each disclosed biocide. Next, retrieved records were matched with toxicity data from open literature. The information on the stock as well as the formulated fluid concentrations, in concert with toxicity thresholds, was used to calculate Potential for Exposure Quotients (PEQs) under an accidental release scenario. Results for 2013 show that nearly 100 hydraulic fluid additives are categorized as a biocide and/or an antimicrobial agent. Some of the more commonly listed disinfectants are glutaraldehyde, naphthalene, ethoxylated nonylphenol, and tetrakis hydroxymethyl-phosphonium sulfate. Aldehydes were found to be the most common (N=1,678) toxic (lowest RfC of 8.0E-05 mg/m3) fluid ingredients with the highest PEQs (average fracking fluid concentration of 2.5%). For the purpose of this presentation, all findings are presented as summary tables for ease of reference and sharing of information.

PS 1814 Acute Effects of Acrolein in Human Volunteers during Controlled Exposure

A. Dwivedi, L. Ernstgård, L. Palmberg, J. C. Lorentzen and G. Johanson.
Institute of Environmental Medicine, Karolinska Institutet, Stockholm, Sweden.

Acrolein (ACR) is a reactive α, β-unsaturated aldehyde formed by burning wood, plastic, diesel fuel, paraffin wax, smoking and cooking. It is a common constituent of indoor air. There are limited toxicological data available, however, as ACR is highly irritating to the eyes and respiratory tract, irritation is considered to be the critical effect. The aim of the study was to determine thresholds for acute irritation and inflammation for ACR and thus improve the scientific basis for setting exposure limits. Nine healthy volunteers of each sex were exposed at six occasions for 2 h at rest to: clean air, clean air + ethyl acetate (EA), 0.05 ppm ACR, 0.05 ppm ACR + 15 ppm EA, 0.1 ppm ACR, and 0.1 ppm ACR + 15 ppm EA. The exposure conditions were carried out in a balanced order and were blinded to the volunteers. Symptoms related to irritation and central nervous system effects were rated on Visual Analogue Scales. EA was used to mask the potential influence of odor on the symptom ratings. The ratings of eye irritation increased during exposure to ACR in a dose dependent manner (median values 0 mm, 1.5 mm and 8 mm for control, 0.05 ppm and 0.1 ppm of ACR respectively, $p < 0.001$, Friedman test) with no influence by co-exposure to EA. No significant exposure related effects on pulmonary function or nasal swelling were found. Furthermore, no effects were seen on markers of inflammation and coagulation in blood (C-reactive protein, IL-6, serum amyloid A, fibrinogen factor VIII, von Willebrand factor and Clara cell protein) and induced sputum (cell count, differential cell count, IL-6 and IL-8). Blink frequency, recorded by electromyography, showed a dose-dependent increase ($p=0.049$) for exposure to ACR alone. However, this effect was not seen for combined exposure to ACR and EA. In conclusion, our study suggests that short-term exposure to 0.1 ppm ACR is mildly irritating to the eyes.

PS 1815 At the Intersection of Occupational Toxicology and Product Quality: Harmonization of Risk-Based Values in the Pharmaceutical Sector

P. Weideman[1], A. Maier[2], A. Willis[3], R. Sandhu[3] and S. Gomez[1]. [1]*Safety Assessment, Genentech, Inc., South San Francisco, CA,* [2]*Dept. of Environmental Health, University of Cincinnati College of Medicine, Cincinnati, OH and* [3]*Toxicology Excellence for Risk Assessment, Cincinnati, OH.*

Decisions based on health risk assessment are an integral part of pharmaceutical manufacturing. Occupational exposure limits (OELs) are a key tool for protection of workers. Acceptable daily exposures (ADEs) address residual carryover of active ingredients, as well as impurities. OELs and ADEs share a common risk method underpinning, i.e., the derivation of a point of departure (POD) and application of uncertainty factors. Despite similarities, regulatory drivers for OELs and ADEs differ reflecting their intended applications and that current guidelines are often unclear or inconsistent. The result is a confusing landscape of methods. We conducted a critical analysis of methods for risk values used in worker health vs. product quality. Recurring differences among these risk value communities include: 1) identifying effect levels (e.g., NOEL vs. NOAEL) as the POD, 2) calculating maximum daily doses and potential for dose accumulation, 3) addressing route-specific bioavailability, 4) considering severity of effects and data gaps, and 5) characterizing differences in toxicology among large and small molecule therapeutics and industrial chemicals. Despite these issues, commonality in data compilation and evaluation can be leveraged when applied in the context of a systematic data integration approach. Issue mapping was used to identify a path for effective use of data for risk value development and to improve translation of data for alternative risk value methods (e.g., OELs vs. ADEs). The result is improved consistency in risk values in the short-term with a longer-term opportunity to document best practices for risk-based assessments as applied in worker health and pharmaceutical product quality.

PS 1816 Cumulative Risks in Occupational Settings: A Checklist Tool to Support Decision Making

R. C. Lee[1], P. Nance[2], A. Lamba[3] and A. Maier[4]. [1]*Neptune and Company, Inc., Albuquerque, NM,* [2]*Toxicology Excellence for Risk Assessment, Cincinnati, OH,* [3]*US Environmental Protection Agency, Washington, DC and* [4]*University of Cincinnati, Cincinnati, OH.*

Cumulative risk assessments (CRAs) evaluate the likelihood of adverse health effects resulting from all routes of exposure to multiple stressors. Appreciable attention has focused on improving risk science methods in this area. For example, approaches have been published for addressing environmental exposures to mixtures of chemicals with a unifying mode of action or for assessing community level health impacts arising from diverse exposures. However, guidance for conducting CRAs for occupational scenarios is lacking. To address this gap, we conducted a critical analysis of current CRA frameworks to identify a set of techniques suitable for translation to occupational risk assessment. Consistent with elements of existing methods, we developed a refined CRA checklist tool with several features customized for consideration of the occupational environment. Key elements include: provisions for incorporating exposures by oral, inhalation and dermal routes (reflecting occupational plus non-occupational exposures); specific guidance for chemical stressors with a process for modifying the CRA based on presence of multiple stressors; and, a tiered risk system to select assessment needs and provide flexibility in applying any of several alternative validated models. The CRA checklist tool was also applied to published occupational exposure scenarios to identify areas in traditional occupational risk assessments that should be considered for more rigorous CRA. Overall, we found that the absence of a decision support tool yielded inconsistent consideration of CRA in occupational assessments. The evaluation also provided insights on data gaps that preclude conduction of high confidence CRAs for current occupational scenarios. Despite these gaps we demonstrated how a systematic decision tool can serve as a pragmatic solution for improving consistency in conducting occupational CRAs.

PS 1817 Improper Use of Haber's Law Results in Erroneous Fatality Estimation from Predictive Models

H. Salem[1, 2], J. Moser[2, 3] and D. R. Sommerville[1]. [1]*U.S. Army Edgewood Chemical Biological Center, Aberdeen Proving Ground, MD,* [2]*Chemical Security Analysis Center, Department of Homeland Security, Gunpowder (APG-EA), MD and* [3]*Battelle Memorial Institute, Columbus, OH.*

There are two common measures for inhalation exposure to a vapor/gas toxicant: the dosage (defined as the product of concentration and time [Ct]) and the toxic load (defined as $C^n t$, with n being the toxic load exponent). The historical and most-often used estimator is Ct (Haber's Law) which was developed in the early 1920s. However, it was soon determined that Ct was inadequate to account for changes in toxicity as a function of exposure duration. Thus, the toxic load was introduced (and subsequently popularized in the 1980s by ten Berge and his associates) as an empirical solution to the shortcomings of the Ct measure. The differences in lethality predictions between dosage and toxic load approaches were investigated via simulation for a target population of rats exposed to sarin. An n of 1.6 was used for the toxic load based on the rat study of Mioduszewski et al. (2002). The Haber (n = 1) and toxic load models were compared by modeling release of sarin from a fixed point over a spatially uniform population of rats in three different scenarios. In all three scenarios, the Haber model gave slight underestimates of fatalities until approximately 3-5 minutes following release, after which fatality estimates were at least 125% higher than those of the toxic load model. This demonstrates that unequal exposure over time within a population affects differences in fatality estimation between Haber and toxic load models. When n does not equal one, fatalities are erroneously estimated when using Haber's Law because time is unrealistically weighted against concentration. For chemicals with n greater than one, the Haber model can overestimate fatalities at low concentrations or long durations and underestimate fatalities at high concentrations or low durations. This relationship reverses for those chemicals with n less than one.

PS 1818 Impact of Nonconstant Concentration Exposure on Lethality of Inhaled Hydrogen Cyanide in the Rat: A Case Study for Assessing the Validity of Toxic Load Models

L. M. Sweeney[1], D. R. Sommerville[3], S. R. Channel[4], N. M. Gargas[2] and B. C. Sharits[2]. [1]*NAMRU Dayton, Henry M. Jackson Foundation, WPAFB, OH,* [2]*NAMRU Dayton, CAMRIS, WPAFB, OH,* [3]*Edgewood Chemical Biological Center, Aberdeen Proving Ground, MD and* [4]*Leidos, Linton, IN.*

The toxic load model (TLM) is an empirical approach in hazard assessment modeling for estimating the relationship between the inhalation toxicity of a chemical and the exposure duration. The toxic load (TL) is normally expressed as a function of vapor concentration (C) and duration (t), with TL equaling $C^n \times t$ being a typical form. Hypothetically, any combination of concentration and time that yields the same "toxic load" (cumulative exposure) will give a constant biological response. These formulas have been developed and tested using controlled, constant concentration animal studies, but the validity of applying these assumptions to time-varying concentration profiles has not been tested. Experiments were designed to test the validity of the TLM under conditions of non-constant acute exposure. Male Sprague-Dawley rats inhaled constant or pulsed concentrations of hydrogen cyanide (HCN) generated in a nose-only exposure system for 5, 15, or 30 minutes. The observed lethality of HCN for the 11 different C vs. t profiles was used to evaluate the ability of the TLM to adequately describe the lethality of HCN under the conditions of non-constant inhalation exposure. The TLM was found to be applicable under the tested conditions, with the exception of the median lethality of very brief, high concentration, discontinuous exposures.

PS 1819 A Framework for Risk Assessment for Less-Than-Chronic and Intermittent Exposures to Chemicals (Noncancer Endpoints)

L. T. Haber[1], B. Meek[2], A. Li-Muller[3], M. Yole[3], A. K. Mohapatra[3] and S. Petrovic[3]. [1]*Toxicology Excellence for Risk Assessment (TERA), Cincinnati, OH,* [2]*University of Ottawa, Ottawa, ON, Canada and* [3]*Health Canada, Ottawa, ON, Canada.*

Exposure to chemicals at contaminated sites, whether single, repeated or intermittent, may last for shorter periods of time than those upon which most guidance values are normally based. Because it is presently not feasible to conduct toxicity studies or develop Toxicity Reference Values (TRVs) specific to each scenario of interest, methods are needed to address this variety of scenarios, drawing as much as possible on existing guidance values. A working framework was developed to address non-cancer effects resulting from short-term and intermittent exposures to chemicals. The framework identifies key parameters relevant to the implications of duration and intermittency of exposure, and provides an integrated, tiered approach for applying increasing levels of toxicological understanding and expertise to exposure scenarios of interest, including consideration of both toxicokinetic (half-life) and toxicodynamic (persistence of effect) implications of intermittent exposures. It incorporates the use of TRVs based on exposure periods as similar as possible to the 'actual' exposure periods and the use of dose averaging under limited, specified conditions. Key data and information sources supporting consideration of less-than-chronic exposures are also documented, including: (1) references for a broad range of TRVs for less-than-chronic exposures from a variety of organizations, criteria for selection, and a description of their bases and applicability; (2) grouping of chemicals based on their half-lives and appropriate reference data sources, and (3) grouping of chemicals based on persistence of their effects. This framework will aid in improving the scientific basis for the evaluation of less-than-chronic and intermittent exposures in a variety of settings.
Disclaimer: The views expressed herein do not necessarily represent Health Canada policy.

PS 1820 Use of a Single-Pass, Nose-Only Exposure System to Simulate High Altitudes

R. A. James[1], D. A. Mahle[2], D. R. Mattie[3], P. R. Eden[4], W. R. Howard[5] and B. A. Wong[6]. [1]*Environmental Health Effects Research Directorate, Camris International, NAMRUD, Wright Patterson AFB, OH,* [2]*USAF 711 HPW/RHDJ, US Air Force, Wright Patterson AFB, OH,* [3]*USAF 711 HPW/RHDJ, US Air Force, Wright Patterson AFB, OH,* [4]*USAF 711 HPW/RHDJ, US Air Force, Wright Patterson AFB, OH,* [5]*Environmental Health Effects Research Directorate, US Navy, NAMRUD, Wright Patterson AFB, OH and* [6]*Environmental Health Effects Research Directorate, Henry M. Jackson Foundation, NAMRUD, Wright Patterson AFB, OH.*

The military has experienced a number of known or suspected hypoxia-related in-flight events in its pilots of high performance aircraft. Some contaminants, identified in breathing air supplied to pilots, are being investigated as a possible link to the hypoxia-related events. In order to evaluate possible hypoxia-related hypotheses in an animal model, a nose-only exposure system was adapted to expose rats to controlled levels of toluene under low pressure (high altitude) conditions. A 52-position nose-only exposure system (Lab Products, Seaford, DE) with closed animal containment tubes demonstrated the capability to hold an air supply at 5.0 L/min while adjusting exhaust flow to maintain an internal pressure to simulate altitudes of ambient, 10,000 or 20,000 feet above sea level. Toluene was mixed into the test atmosphere using either a gas cylinder containing a toluene-air mixture, or toluene vapor from a pressure vessel and maintained at 100 or 200 ppm in the test atmosphere. Oxygen was incorporated into the inlet stream at the higher altitude settings to maintain a partial pressure approximately equivalent to ambient. Special port valves were used to allow rat exposures to be staggered under simulated high altitude conditions for pharmacokinetic studies. An initial study was conducted in which adult male and female S-D rats were exposed to 200 ppm toluene for 1 hr using the single pass, nose only exposure system at simulated altitudes of 940 (ambient), 10,000 or 20,000 feet above sea level. The pharmacokinetics of toluene tissue uptake results are presented in a separate poster by Mahle et al. 2014.

PS 1821 Comparison of Liver Toxicity Potencies of Three Dinitrotoluene Compounds

Z. Yan[1] and J. Zhao[2]. [1]*ORISE, Cincinnati, OH and* [2]*National Center for Environmental Assessment, US EPA, Cincinnati, OH.*

Munitions compounds 2,4-dinitrotoluene (2,4-DNT) and 2,6-dinitrotoluene (2,6-DNT) are two of the six most common isomers of dinitrotoluene (DNT). Technical grade dinitrotoluene (tgDNT) is a mixture of the six DNT isomers and is comprised of 76% 2,4-DNT and 19% 2,6-DNT with the remaining 5% a combination of four other DNT isomers (2,3-, 2,5-, 3,4-, and 3,5-DNT). Toxicity studies and health assessments of 2,4-, 2,6-, and tgDNT have reported distinct liver effects. In order to compare liver toxicity potencies of these three DNTs, we reviewed available studies in dogs, rats, and mice and compared noncancer and cancer liver effects following oral subchronic- and chronic-duration exposure to 2,4-, 2,6- and tgDNT. Potential points of departure for liver effects were identified and used to compare their toxicity potencies. We then examined the potential mechanisms that could account for the differences in hepatotoxicity. Our results indicated that similar pathologic liver lesions were induced after chronic-duration exposure to the three DNTs and their progression can be summarized in four stages: liver degenerative effects and/or cell death, hyperplastic/regenerative effects, neoplastic nodules, and hepatocellular carcinoma. Based on available biotransformation, toxicogenomic and genotoxicity information, imbalanced detoxification due to covalent binding with proteins and DNA, production of reactive oxygen species, and inhibition of oxygen supply may all contribute to DNT-induced noncancer liver toxicity and carcinogenesis. While their potencies of noncancer liver toxicity are not significantly different, 2,6-DNT is the most potent liver carcinogen followed by tgDNT; 2,4-DNT is the least potent. The differences of liver cancer potencies are consistent with their potencies of DNT-induced hepatocyte genotoxicity. The views expressed in this abstract are those of the authors and do not necessarily reflect the views or policies of the U.S. Environmental Protection Agency.

PS 1822 Methylmercury Inhibition of Serum Paraoxonase 1 Activity and the Risk of Cardiovascular Disease

B. R. Sonawane[1], R. Nath[1], P. Lewandowski[2] and G. L. Ginsberg[3]. [1]*NCEA/ORD, US Envoronmental Protection Agency, Washington, DC,* [2]*School of Medicine, Deakin University, Geelong, VIC, Australia and* [3]*Connecticut Department of Public Health, Hartford, CT.*

Paraoxonase-1 (PON1) is an antioxidant enzyme present on high density lipoproteins and is known to be protective against atherosclerosis. PON1 has become a useful disease biomarker since low serum activity of this enzyme is associated with increased cardiovascular risk. PON1 also catalyzes the detoxification of organophosphates. Therefore, serum PON1 is essential for the prevention of two distinct adverse outcomes. The single sulfhydryl moiety on PON1 is believed to be the molecular target. Epidemiological and in vitro studies show that exposure to methyl mercury has been associated with a decline in PON1 activity. Based upon data from a native fish-eating population, methyl mercury exposure in the 0.1 to 0.3 μg/kg/day range is associated with substantial loss of serum PON1 activity. Using these data, we explored PON1 as a potential disease biomarker to estimate the cardiovascular risk from methyl mercury ingestion in the general population. The simulated shift in the population distribution of PON1 towards lower levels increases the percent of the population at risk for acute cardiovascular outcomes. This approach of evaluating mercury toxicity follows recommendations made in the National Academy of Sciences report "Science and Decisions" to explore the interaction between chemical toxicity and background disease. This example points out the emerging importance of disease biomarkers in chemical risk evaluation.

Disclaimer: The views expressed in this presentation are those of the authors and do not necessarily reflect the views and/or policies of the U.S. Environmental Protection Agency, Deakin University or the State of Connecticut.

PS 1823 Determination of the Relative Allergenicity of Food Products for Quantitative Hazard Assessment

A. Kruizinga, R. Klein Entink, M. Blom, G. Houben and J. van Bilsen. *TNO, Zeist, Netherlands.* Sponsor: R. Woutersen.

Currently, sustainable food production, including alternative protein sources, is receiving much attention and exploration of these sources is widely supported by international organizations. These alternative proteins sources should have the lowest allergy risk possible. Until now, accurate pre-marketing assessment of the allergenicity of new proteins is impossible. Moreover, existing guidance documents are restricted to qualitative assessment, have low predictive value and result often in an oversimplification in terms of hazard assessment. To overcome those limitations, we developed a two-dimensional scale for expressing allergenicity that allows a quantitative hazard characterisation of new proteins.
The two dimensions of the scale were defined as 1) the prevalence expressed as the percentage of the general population that has the allergy and 2) the potency of the protein expressed as the ED50 in mg-protein of the allergen (the dose that provokes objective allergic responses in 50% of the allergic persons). In terms of hazard characterization, severity of symptoms was not included, since this is a result of the nature of the exposure and the potency of the individual rather than an inherent and independent attribute of the allergen.
The scale was developed by ranking 11 allergenic products based on potency data from indivudal food challenges and 22 scientific papers on prevalence, selected after a critical review. The resulting 2-dimensional scale can be used to project a new protein on the scale and assess its potential hazard relative to the known allergens. In a next step, we aim to develop a model that predicts the position of a new protein on the scale using its physical, chemical and biological characteristics.

PS 1824 A 21st-Century Roadmap for Human Health Risk Assessment

A. R. Boobis[1], T. Pastoor[2], A. N. Bachman[3], S. M. Cohen[4], M. Dellarco[5], I. Dewhurst[6], J. Doe[7], N. G. Doerrer[8], M. Embry[8], A. Moretto[9], R. D. Phillips[3], J. Rowlands[10] and J. Y. Tanir[8]. *[1]Imperial College London, London, United Kingdom, [2]Syngenta Ltd., Greensboro, NC, [3]ExxonMobil Biomedical Sciences, Inc., Annandale, NJ, [4]University of Nebraska Medical Center, Omaha, NE, [5]National Institute of Child Health and Human Development, Bethesda, MD, [6]UK Chemicals Regulation Directorate, York, United Kingdom, [7]Parker Doe Partnership LLP, Cheshire, United Kingdom, [8]ILSI Health and Environmental Sciences Institute, Washington, DC, [9]University of Milan, Milan, Italy and [10]The Dow Chemical Company, Midland, MI.*

The ILSI Health and Environmental Sciences Institute (HESI) Risk Assessment in the 21st Century (RISK21) project was initiated to develop a scientific, transparent, and efficient approach to the evolving world of human health risk assessment. RISK21 developed a framework that reconsiders in the way chemical risk assessment information is obtained and used. It is a problem formulation-based, exposure driven, tiered data acquisition approach that allows an informed decision on human health safety to be made when sufficient evidence is available. This consistent approach maximizes the ability to inform decisions and optimize resource usage. Two case studies were developed to illustrate these principles. The first example identified testing needs for a new 'nth' in class pesticide to be used in mosquito netting, and illustrated how existing information from other pesticides in the same chemical class and knowledge of use patterns can inform data needs and decision making. The second example evaluated a large number of chemicals which might be present in drinking water, to prioritize which are of highest potential concern for human health risk assessment. Both case studies also identified key issues and possible approaches to address cumulative risk. The overall goal of these examples was not to make definitive risk assessment determinations but to establish the utility of the RISK21 framework in assessing the value of available information and making decisions about what, if any, additional information is needed to inform a decision.

PS 1825 Poor Pregnancy Outcome and Small for Gestational Age Associated with Blood Cadmium among Mothers in Malaysia

M. Jaafar[1], R. Sarimin[1], A. Ismail[1] and N. Ashikin[2]. *[1]Department of Community Health, National University of Malaysia, Cheras, Kuala Lumpur, Malaysia and [2]Toxicology and Pharmacology Unit, Institute of Medical Research, Kuala Lumpur, Kuala Lumpur, Malaysia.*

Cadmium is a known heavy metal that contaminate environment and causes health problems like Itai-itai disease. However, not many studies have been carried out to determine its pregnancy outcome. This cross-sectional study was conducted among pregnant mothers in the state of Selangor, Malaysia. The objectives were to determine blood cadmium concentrations and its impact on the pregnancy outcome.
A total of 280 third trimester pregnant mothers were involved in the study using a universal sampling method at selected health clinics from July to September 2007. A face to face interview using structured questionnaires was used. Pregnancy and delivery history were obtained from the antenatal record book. Blood samples were analysed for cadmium using GFAAS at IMR laboratory.
Mean of blood cadmium concentration was 1.47+0.44μg/l with minimum and maximum value of 0.12μg/l and 2.86μg/l, respectively. Mean age of respondents was 28.3+4.4 year-old. The factors that significantly associated with blood cadmium concentration were household income per month ($p<0.05$), spouse type of work ($p<0.05$), and current haemoglobin level ($p<0.05$). Using the multivariate analysis, haemoglobin level was significantly associated with blood cadmium (adjusted r2 = 0.152; $p<0.01$). Every incremental of 1g/dl of haemoglobin will reduce 0.13μg/l of blood cadmium level. The study also revealed an association between higher blood cadmium mothers with poor pregnancy outcomes ($p<0.01$) and small for gestational age (SGA) ($p<0.01$).
Even though the mean blood cadmium level in the study population was low compared to the reference value (10μg/dl), it showed that the environmental exposure to cadmium is real among pregnant mothers in this country. Proper education of public about the importance of avoiding exposure and emphasis on having an effective environmental management in maintaining a cadmium-free condition wherever possible are the ultimate aims of minimizing health impacts.

PS 1826 Lung Overload: Conclusions of an ECETOC Task Force

R. Kreiling[2], J. C. Carrillo[2], M. Kellert[2], W. Koch[2], N. Krueger[2], L. Levy[2], F. Linker[2], L. Ma-Hock[1], T. Petry[2], E. van Miert[2], D. Warheit[2], H. Vrijhof[2], H. Wiegand[2], B. van Ravenzwaay[1] and A. Poole[2]. *[1]Toxicology, BASF SE, Ludwigshafen/Rhein, Germany and [2]ECETOC, Brüssel, Belgium.*

Chronic exposures to high concentrations of poorly soluble, low toxicity particles (PSP) cause various toxicological effects in the lung. Lung overload is typified by impairment in alveolar macrophage (AM) mediated particle clearance and loss of AM mobility, suggesting a threshold mediated mode of action. The Task Force examined the current scientific understanding of the `lung overload` hypothesis and concludes:
1) inhalation exposure to high concentrations of PSP, irrespective of particle size, are eliciting comparable localized pulmonary toxicity via processes that are pro-inflammatory in nature, causing oxidative stress and an persistent pulmonary inflammatory response
2) the mechanisms of the described effects are clearly threshold related
3) adverse outcome pathway is largely common within all species and is applicable for nano and microscale particles
4) rats are the most sensitive species with regard to non-neoplastic and unique for neoplastic responses
5) epidemiological studies have not been able to detect an association between occupational exposures to PSP and an increased risk for lung cancer
6) differences of particle retention, distribution, clearance patterns and defense systems in the lungs of exposed rats vs. primates or humans, may account for both the greater sensitivity in rats and corresponding differences in pulmonary pathological responses to long-term particle exposures
7) differences in the biosolubility of deposited particles may accelerate or slow down the process of lung overload development
The derivation of health based Occupational Exposure Limits, a Derived No Effect Level, for PSP is justified. Because rats are more sensitive than humans and based on comparable biokinetics, an overall assessment factor of 1 for intra- and interspecies differences is sufficient. DNELs based on NOAELs/NOAECs from animal inhalation studies, adjusted for human equivalent concentrations by appropriate dosimetry modeling, is recommended.

PS 1827 A Decision Tree to Optimize Literature Identification for Pharmaceutical Risk Assessment

D. Lee[1], B. K. Gadagbui[1], J. F. Reichard[1], A. Willis[1], A. Maier[2] and R. Sandhu[1]. [1]*Toxicology Excellence for Risk Assessment (TERA), Cincinnati, OH and* [2]*University of Cincinnati, Cincinnati, OH.*

Risk assessment needs are complex for pharmaceuticals, including occupational health, patient safety, product quality and environmental impact. Assessments cover a range of substances including actives, intermediates, process reagents, excipients, degradants, contaminants and leachates. Optimizing literature identification ensures that key information is not missed and that time is not spent on unproductive database searches. Because of the diversity of scenarios and substances involved, a one-size-fits-all approach to literature identification is not efficient. We developed a decision tree for literature identification for pharmaceutical risk assessment. The decision tree starts with the identification of integrated scientific reviews or external risk assessments, followed by a binning strategy depending on the use or type of substance (e.g., active, food contact material, excipient, industrial chemical, endogenous substance). Criteria used for prioritization of search sites and databases within a bin included update frequency, level of peer review, completeness of data presentation, breadth of coverage for substances of interest, ease of data access, and level of regulatory recognition. If the literature does not identify sufficient high quality data, the focus shifts to a targeted determination of tools for addressing data gaps (e.g., in silico methods and the threshold of toxicological concern). This decision tree was tested on different types of substances and reduced the overall time spent in conducting the risk assessment. The difference between fee-based pharmaceutical literature resources was also compared to freely available resources using the decision tree, and the biggest impact of the paid resources appeared to be in the reduction in time needed to sort through data from multiple sources. The decision-tree approach is an important problem formulation tool ensuring that resources used are well aligned with the intended use of the risk assessment.

PS 1828 Use of Cluster Groups in Systematic Review of Literature

M. Cawley[1], M. Selgrade[1], C. F. Gibbons[2] and R. Jones[2]. [1]*ICF, International, Durham, NC and* [2]*NCEA, U.S. EPA, Washington, DC.*

Systematic review of the literature for risk assessment purposes can result in >10,000 references, which can be time and cost intensive to review in a traditional linear manner. Commercially available, visual analytics software enables clustering of similar references based on automated text analysis. References are clustered around key concepts that distinguish papers from the full set of results and can be prioritized for review by concept. We tested the efficacy of prioritizing references for review with this software using results from a comprehensive search of CrVI literature. Our initial search strategy resulted in approximately 9,000 references. We eliminated approximately 3,500 references electronically using additional key word searches and identified a batch of over 300 highly relevant 'seed' references. The remaining references along with seeds were clustered and about 1,600 references were found in clusters containing at least one seed reference. This group of references was prioritized for review and evaluated by multiple screeners. The remaining references underwent a traditional title and abstract review by a single subject matter expert. Ultimately, we found approximately 85% of the relevant animal and 70% of the relevant human hazard identification studies in the health effects cluster. Depending on the circumstances and size of clusters, references in clusters not identified as relevant can be handled in several ways: discard without review (not recommended), apply additional key word searches to prioritize further, or screen by a single (rather than multiple) reviewer. Based on our results, clustering references is an effective way to streamline review of large literature datasets as the bulk of the relevant literature was found within the health effects cluster. We conclude that clustering approaches have promise, but must be carefully tailored to individual needs. Additional comparisons of this type are warranted. The views expressed are those of the authors and do not necessarily represent the views or policies of the U.S. Environmental Protection Agency.

PS 1829 Evaluating Study Quality: A Comparison of the TOXR Tool and OHAT Approaches

R. Blain[1], A. S. Bale[2], A. L. Boyles[3], A. A. Rooney[3], D. Segal[2], C. Skuce[1] and M. Selgrade[1]. [1]*ICF International, Durham, NC,* [2]*EPA, Office of Research and Development, NCEA, Washington, DC and* [3]*NTP, National Institute of Environmental Health Sciences, Durham, NC.*

Standardization and documentation of criteria used to evaluate the quality of studies used in risk assessment is a recognized need in the environmental health sciences. The NTP Office of Health Assessment and Translation (OHAT) developed a method of evaluating animal and human studies for risk of bias based on criteria used in systematic reviews. The European Commission developed the ToxR tool to assess the reliability of toxicological data from in vitro and in vivo studies. Both methods are intended to evaluate studies in a systematic and transparent manner, but the approaches differ. The ToxR tool applies points based on a yes/no to a series of questions that leads to the assignment of Klimisch categories ranging from insufficient documentation to reliable without restrictions. The OHAT approach also has a series of questions with project-specific criteria for 4 possible ratings reflecting the potential for bias in the study, but no overall score is assigned. Seven reviewers independently used the OHAT method to evaluate 11 in vivo animal studies on thyroid effects previously evaluated using the ToxR tool. The purpose was to evaluate the OHAT tool for consistency among different reviewers and compare and contrast the strengths and weaknesses of the two tools. For both methods, we found that some questions were too vague, resulting in different interpretations. For the OHAT method, this could be due to our failure to tailor criteria ratings for this specific project as required. The ToxR Tool would also benefit from such tailoring. With both tools, high quality studies generally had the most similarity between the reviewers, while lower quality studies varied. Strengths and weaknesses were noted for both tools and opportunities for each to incorporate changes were suggested by the current comparison. This abstract does not reflect EPA policy.

PS 1830 Systematic Evaluation of Inhalation Studies for Exposure Quality: A Case Study with Formaldehyde

J. E. Whalan, A. M. Jarabek, J. J. Stanek, G. M. Woodall, P. G. Reinhart, A. Galizia, E. D. McLanahan, B. S. Glenn, A. Davis, A. D. Kraft, S. L. Makris and L. D. Burgoon. *National Center for Environmental Assessment, US EPA, Washington, DC.*

Misdosing can occur by any route of exposure, but it is a particular challenge for inhalation studies because of the inherent complexity of generating and characterizing consistent test atmospheres. There is an expectation that human and animal test subjects in a chamber study will be exposed under conditions that are carefully regulated, frequently measured, and clearly reported. Poor study design, human error, and problems with mechanical and electronic equipment can impair an inhalation exposure and undermine the validity of a study. A systematic approach to evaluating studies, when selecting inhalation studies for a chemical assessment, involves a toxicologist familiar with chamber operations evaluating each study for seven key elements of exposure quality: 1) test article characterization, 2) generation method, 3) analytical method, 4) analytical concentrations, 5) particle size characteristics, 6) chamber type, and 7) controls. Any deficiencies are recorded in a table and the study is ranked for its exposure quality and documentation. These rankings may determine whether a study is considered for hazard evaluation and/or dose-response analysis. The exposure quality evaluation of approximately 200 formaldehyde chamber studies is presented as an example. Nearly half of these studies are considered inadequate for hazard evaluation and/or dose-response analysis.
The views expressed are those of the authors, and do not necessarily represent the views or policies of the U.S. Environmental Protection Agency.

PS 1831 Development of a Database Tool to Track the Study Selection Process for Hazard Identification: Naphthalene Case Study

C. Keshava[2], K. Zaccaria[1], P. McClure[1], J. A. Stickney[1] and W. A. Chiu[2]. [1]*SRC, Inc., East Syracuse, NY and* [2]*National Center for Environmental Assessment, US EPA, Washington, DC.*

When developing a systematic review process for identifying relevant health effects literature for evaluation of chemical health hazards, transparency in the study selection process is imperative. Using naphthalene as a case study, a database tool was developed to organize and summarize the toxicological literature for this chemical and to communicate evaluation and selection of studies for hazard identification. The moderately-sized database for naphthalene consists of human case reports and epidemiology studies; chronic, subchronic, and acute animal toxicity studies; and mechanistic and genotoxicity studies. The database tool tracks study selection, evidence table and exposure-response array development, and quality-control review processes. Major features of the database tool are: 1) inclusion of all human and animal toxicity studies selected for full-text review from the systematic literature search, with brief study details and identification of all endpoints evaluated; 2) rationale for inclusion/exclusion of the study in evidence tables/exposure-response arrays; and 3) identification of endpoints with statistically significant findings. This case study of naphthalene demonstrates a database tool that organizes and tracks hazard identification activities, identifies potential data gaps, and reduces potential study-selection bias by transparently presenting pertinent information for all

potentially relevant studies. Additionally, this database tool effectively conveys the database's size and coverage of endpoints while communicating study-specific decisions in the hazard identification process.
Disclaimer: The views expressed in this abstract are those of the authors and do not necessarily reflect the views or policies of the U.S. Environmental Protection Agency.

PS 1831a Scientists' Attitudes toward Regulatory Risk Assessment

S. Lichter[3] and J. M. DeSesso[1, 2]. [1]*Exponent, Alexandria, VA,* [2]*Georgetown University, Washington, DC and* [3]*CMPA, George Mason University, Arlington, VA.*

Public debate over the scientific quality and accuracy of chemical risk assessments developed by federal programs is growing. This debate can be informed by accurate knowledge of expert opinion on these issues. Therefore, we conducted a survey on regulatory risk assessment (RRA) among scientists with knowledge and experience in this field. Members of Risk Assessment Specialty Section of SOT, Dose Response Section of the Society for Risk Analysis, and International Society for Regulatory Toxicology and Pharmacology were surveyed in February 2013 about problem formulation and analysis plans, the acquisition and evaluation of data, weight of evidence methodology, peer review, and the use of scientific risk evaluations in risk management decisions.
The 186 respondents largely agreed on proper procedures for conducting RRAs while disagreeing on whether these procedures are properly implemented in practice. Thus, 68% regard problem formulations and analysis plans as very important, but only 30 percent say they are usually conducted. Similarly, 69% find it very important for assessors to have access to raw data of critical studies, but 31% say it is usually made available. Over 90% emphasize the use of clear criteria for selecting and evaluating studies, but only 24% report that standardized protocols are usually implemented. Most (82%) believe the same evaluation criteria should be used for evaluating all studies regardless of their institutional origin. Eighty-nine percent believe weight of evidence methodology should be used but only 45% say WOE methods are usually applied, and 24% describe its use as consistent or transparent. Only 41% think risk management decisions are based on current knowledge of biology and toxicology. Finally, they believe risk managers give too much weight to politics, the media, and environmental groups, and too little weight to scientific factors and economic costs and benefits. These results suggest that numerous scientific concerns need to be addressed by federal officials in order to improve the use of risk assessments in the regulatory process.

PS 1831b US EPA's Framework for Human Health Risk Assessment to Inform Decision Making

J. W. Fitzpatrick[1], R. Schoeny[2], K. Gallagher[3] and E. V. Ohanian[3]. [1]*OSA, US EPA, Washington, DC,* [2]*ORD, US EPA, Washington, DC and* [3]*OW, US EPA, Washington, DC.*

The Framework for Human Health Risk Assessment to Inform Decision Making was developed by EPA's Risk Assessment Forum to be responsive to the decision making needs of the Agency. It addresses the recommendations presented in the National Research Council's (NRC's) Science and Decisions (2009) on the design of risk assessments, including planning, scoping, and problem formulation. The Agency's Risk Assessment Forum held broad based internal discussions prior to assembling a Technical Panel of senior risk assessors and risk managers from across the Agency to develop the Framework. Prior to releasing the final Framework, the Framework received extensive Agency review along with inter-agency and external peer reviews. In developing the final Framework the input from the review process along those received from the public were considered. In addition to the focus on planning, scoping and problem formulation, the Framework presents the concept of risk assessment that are "fit for purpose" and details that this is accomplished with an increased dialogue between risk assessors and risk managers to ensure that the risk assessment will inform the risk management options. The problem formulation phase described in the Framework emphases the development of a conceptual model that follows the source to outcome continuum for the risk assessment as a key input into the development of the analysis plan. . In accordance with longstanding agency policy, it also emphasizes the importance of scientific review and public, stakeholder and community involvement and links the reader to agency resources on these topics. This Framework will be instrumental in facilitating the implementation of existing and future EPA guidance for conducting human health risk assessments and in improving the utility of risk assessments that inform risk management decision-making processes. This presentation will discuss details of the Framework and associated implementation plans by the Agency.

PS 1831c When Does Exogenous Exposure to Endogenously Produced Chemicals and Essential Elements Become a Problem?

N. Birchfield, T. Berner, R. Nath, B. R. Sonawane, P. White, J. Ball, R. P. Subramaniam, C. J. Brinkerhoff, K. Hogan, J. Gift, B. Buckley, E. O. Owens, A. D. Kraft, B. S. Glenn, L. Flowers, J. Jinot and C. Scott. *Office of Research and Development, U.S. Environmental Protection Agency, Washington, DC.*

The U.S. Environmental Protection Agency's (EPA's) National Center for Environmental Assessment (NCEA) evaluates hazard and dose-response relationships for certain substances found in the environment in order to support EPA's risk assessment and risk management activities. Although chemical pollution is commonly considered to result from the release of anthropogenic contaminants to the environment, a number of these "contaminants" are produced either endogenously in healthy organisms or are required for normal metabolism. Some chemicals on EPA's chemical priority lists (e.g., HAPs, CCL, NAAQS), in addition to arising from human economic activities, are also produced endogenously in mammalian cells (e.g., methanol, formaldehyde, CO) or are essential elements (e.g., Zn, Mn, Cu). Chemicals that are endogenously produced or that are required for normal metabolism present unique challenges in evaluating hazards from their exogenous exposure. For instance, is there some level of change above normal internal concentrations that is needed to induce adverse effects? Are natural levels of endogenous chemicals harmless? How do exogenous exposures impact endogenous chemical levels? The purpose of this presentation is to articulate issues to consider in characterizing the toxicity of exogenous exposure to endogenous chemicals. To build more common understanding and consider issues specific to endogenous chemical health assessment, NCEA will be hosting a public workshop in 2014 on this evolving area of science. Disclaimer: The views expressed in this abstract are those of the authors and do not necessarily represent the views or policies of the EPA.

PS 1831d Environmental Epigenetics: Potential Application in Human Health Risk Assessment

S. P Kuppusamy[1], J. Phillip Kaiser[2] and S. C. Wesselkamper[2]. [1]*ORISE, ORD, NCEA, U.S. EPA, Cincinnati, OH and* [2]*ORD, NCEA, U.S. EPA, Cincinnati, OH.*

Although previous studies have shown a significant involvement of epigenetic dysregulation in human diseases, the applicability of epigenetic data in the current human health risk assessment paradigm is unclear. The goals of this study are to compare the relative sensitivities of epigenetic alterations (DNA methylation) with tumor incidence data and to explore the possibility of incorporating epigenetic data into the hazard identification step of human health assessments. DNA methylation alterations and tumor incidences in laboratory animal studies were analyzed from various toxicological databases for the following chemicals: di(2-ethylhexyl) phthalate, bromodichloromethane, dibromochloromethane, chloroform, hydrazine, trichloroethylene, benzidine, and trichloroacetic acid. All analyses involved conversion of animal doses to human equivalent doses. Benchmark dose values for tumor incidences were compared to no-observed-adverse-effect levels (NOAELs) for DNA methylation changes. In the absence of a NOAEL, a 10-fold uncertainty factor was applied to the lowest-observed-adverse-effect level (LOAEL) to approximate a NOAEL. This analysis revealed that DNA methylation is 1.2- to 25-fold more sensitive than the corresponding tumor incidence for all chemicals, except for trichloroacetic acid, where there is no difference in sensitivity. The predominant DNA methylation alteration was hypomethylation of either whole DNA or the promoter region of various oncogenes, and the exposure duration of epigenetic studies was shorter compared to a 2-year carcinogenicity study. This study shows that DNA methylation changes are more sensitive than tumor incidences and could potentially be considered as an alternative point of departure in human health assessments of suspected carcinogens. However, more research is needed to ascertain how epigenetic data can be applied in human health risk assessment. [The views expressed in this abstract are those of the authors and do not necessarily reflect the views or policies of the U.S. EPA]

PS 1831e New Concepts for Risk and Safety Assessment of Plant Food Supplements (PFS)

S. van den Berg and I. Rietjens. *Toxicology, Wageningen University, Wageningen, Netherlands.*

To adequately support the safe use of plant food supplements (PFS), uniform and well accepted procedures for risk and safety assessment are essential. While many consumers equal 'natural' with 'safe', PFS may contain compounds that are of concern for human health. A major bottle neck in the safety assessment of botanicals and botanical ingredients and thus also for PFS is the fact that some botanicals may

contain compounds that are both genotoxic and carcinogenic. Risk assessment of such compounds is complicated and an international scientific agreement on the best approach is currently lacking (EFSA, 2005). Therefore, new concepts were tested that could be of use for risk and safety assessment of PFS focusing on finding adequate ways to judge the risk or safety of PFS that may contain genotoxic carcinogens. This should ultimately give a better idea on when risk management actions would be needed, but also for which PFS there is no reason for concern even though they do contain limited amounts of genotoxic carcinogens. The new concepts tested include the margin of exposure (MOE) approach, a mode of action (MOA) based approach and a matrix effect approach. The MOE was found to be a valuable approach in risk and safety assessment of PFS that can be used to set priorities for risk management. Moreover, the integrated approach of in vitro and MOA based physiologically based kinetic (PBK) modeling was found to be a very useful addition to risk and safety assessment of PFS based on the MOE approach since it facilitates read-across and also provides a way to take matrix effects into account. Furthermore, the new concepts tested may prove a way forward to markedly reduce the number of experimental animals used for safety testing of PFS.
The research leading to these results has received funding from the European Community's Seventh Framework Programme (FP7/2007-2013) under grant agreement n° 245199. It has been carried out within the PlantLIBRA project (website: www.plantlibra.eu). This report does not necessarily reflect the Commission views or its future policy on this area.
EFSA, 2005. The EFSA Journal, 282, 1-31.

PS 1831f Probabilistic Environmental Hazard Assessments of ToxCast Phase I and II *In Vitro* Datasets

L. A. Kristofco[1], D. A. Dreier[1], E. S. Williams[1], J. Corrales[1], E. P. Gallagher[2], T. Kavanagh[2], A. Voutchkova[3], J. B. Zimmerman[4], P. Anastas[4] and B. W. Brooks[1]. *[1]Environmental Science, Baylor University, Waco, TX, [2]University of Washington, Seattle, WA, [3]George Washington University, Washington, DC and [4]Yale University, New Haven, CT.*

Little toxicology data exists for the majority of industrial chemicals. Our research group has examined approaches to utilize known toxicological data to predict thresholds of untested chemicals, and to select assays for assessing toxicity when multiple model systems exist. Here we employed chemical toxicity distributions (CTDs) to perform probabilistic hazard assessments (PHAs) using data from the U.S. EPA's ToxCast program. PHAs may predict toxicological potencies of similar chemicals, prioritize chemicals for additional toxicity testing, support read-across for regulatory purposes, and identify characteristics for sustainable molecular design. An initial PHA examined the comparative sensitivity of three in vitro assays for estrogenicity representing a diverse group of industrial chemicals and pesticides from ToxCast Phase I. CTDs were compared at 5th centiles for all compounds, common compounds, and organophosphates tested. When all available data were compared, a NCGC assay was most sensitive for estrogenicity as there was a 5% probability of detecting a compound that will elicit an estrogenic response at or below 0.089 mg/L. When only common compounds and organophosphates were considered, an Attagene assay was most sensitive assay with centiles of 0.13 mg/L and 1.8 mg/L, respectively. We then extended this PHA approach to examine additional data from ToxCast Phase II. A PHA of an oxidative stress assay demonstrated decreasing assay response with increasing assay duration, based on 0.58, 0.815, and 2.930 ug/L for 1hr, 24hrs and 72hrs, respectively. Conversely, a stress kinase assay did not display such a relationship with 5th centiles of 1.024, 0.655 and 1.122 ug/L for 1hr, 24hrs and 72hrs, respectively. Strengths and weaknesses of this approach continue to be explored.

PS 1831g Developing an Evidence-Based Rationale for Determining the Necessity of Repeat Inhalation Studies of Agrochemical Aerosols with Irritant Properties

P. Singh[1], P. M. Hinderliter[1], R. Chamanza[1], J. Wright[1], P. Whalley[1], A. Stevens[1], J. D. McDonald[2], P. J. Kuehl[2], M. Doyle-Eisele[2], C. Garner[2] and R. W. Lewis[1]. *[1]Syngenta, Greensboro, NC and [2]Lovelace Respiratory Research Institute, Albuquerque, NM.*

An evidence-based approach was used to determine whether repeat inhalation toxicity studies for two fungicide formulations, with varying potential to produce irritation, would provide new information of use in human health risk assessment. After considering the available acute inhalation and irritation toxicity data, a 2- or 4-week repeat exposure study was conducted with formulations of chlorothalonil and azoxystrobin, respectively, including histopathology of the respiratory tract. In addition, as part of the testing strategy for chlorothalonil, pharmacokinetic data from inhalation administration in rats was generated for route to route extrapolation of systemic availability. At the end of the repeat exposure studies, concentration-related squamous metaplasia was noted in the ventrolateral larynx and/or the nasal epithelium, consistent with changes commonly reported in rats following nose-only inhalation exposures to irritant chemicals. At minimal to mild grades of severity, these findings are non-adverse, and potentially reversible. Systemic absorption of chlorothalonil, following 6 hours of inhalation exposure to a concentration (0.004 mg/L) above those potentially relevant to maximum worker exposures, was not increased compared to oral absorption (14-23%), even with guideline sized particles (1-3 μm MMAD). The portal of entry toxicity of irritant aerosols generally limits the achievable exposure concentrations such that exposures typically cannot be high enough to produce expected systemic toxicity. Test guideline size particles have greater deposition and increased surface area than predominantly larger sized aerosols produced in the field, lowering the accuracy of human hazard prediction, especially for chemical irritants. These data support the use of an evidence-based approach in determining the need for repeat inhalation studies for the assessment of human health risk assessment from inhalation.

PS 1831h Comparison of Developmental and Neurotoxic Endpoints Observed in Experimental Animal Studies following Inhalation Exposure to n-Butanol and n-Butyl Acetate

J. Weaver[1], T. Blessinger[1], A. F. Sasso[1], S. L. Makris[1] and A. S. Bale[2]. *[1]National Center for Environmental Assessment, US-EPA, Washington, DC and [2]Drug and Chemical Evaluation Section, DEA, Washington, DC.*

Several studies have suggested that toxicity associated with n-butyl acetate may be informative of toxicity associated with n-butanol and vice versa. N-butyl acetate rapidly metabolizes to n-butanol; therefore, it is anticipated that the toxic effects observed following exposure to n-butyl acetate and n-butanol would be similar. A literature search was conducted to identify peer-reviewed studies that evaluated toxic health effects resulting from n-butanol or n-butyl acetate exposure. Most of these studies evaluated primarily neurotoxic and developmental toxicity endpoints. Toxicity endpoints from all of the studies were reviewed and toxicity effect levels were determined. To facilitate study comparisons, internal n-butanol blood levels were estimated by using a previously developed PBPK model (Teegarden et. al 2005). Studies investigating developmental effects of n-butyl acetate and n-butanol demonstrated similar dose related trends including decreased food consumption in dams and decreased fetal body weight. Endpoints consistent with neurotoxicity were not directly comparable between n-butanol (e.g., altered motor function) and n-butyl acetate (e.g., decreased absolute brain weight). In this case study, similar trends in toxicity were observed between n-butyl acetate and n-butanol in some developmental endpoints, suggesting that toxic effects identified following exposure to n-butyl acetate may be predictive of toxic effects observed as a result from exposure n-butanol.
The views expressed are those of the authors and do not necessarily reflect the views or policies of the U.S. EPA

PS 1831i Relative Oral Bioavailability of Benzo(a)pyrene from Soils at Environmentally-Relevant Concentrations

J. W. Munson[1], Y. W. Lowney[2], M. Ruby[3] and S. M. Roberts[1]. *[1]University of Florida, Gainsville, FL, [2]Exponent, Boulder, CO and [3]Integral Consulting, Louisville, CO.*

Several reports in the literature suggest that interactions between PAHs and soil diminish PAH bioavailability and thus reduce risk from incidental ingestion of PAH- contaminated soil. Various animal models and approaches have been used to estimate PAH bioavailability from soil. To facilitate PAH measurement, most of these studies were conducted using PAH concentrations that only occur at heavily contaminated sites. The objective of this study was to explore the influence of soil composition, PAH concentration, and source material type on PAH bioavailability using an approach capable of measuring uptake at low, environmentally-relevant PAH concentrations (down to 1 ppm or less). Contaminated soil samples were constructed using PAHs from three source materials (PAHs in solvent, soot, and fuel oil) to which 3H-benzo(a)pyrene (3H-BaP; total BaP concentrations of 1, 10, and 100 ppm) was added and weathered for eight weeks. Each soil was administered as a single dose to rats, and blood samples were taken over six days. Relative bioavailability (RBA) of the BaP from soil was estimated by comparing the area under the curve (AUC) for 3H concentration versus time in blood with the AUC observed from the same material dosed in a food matrix for comparison. Food was used for comparison because the cancer slope factor for BaP is derived from studies in rats in which the exposure medium is diet. The extent to which BaP RBA was diminished in soil versus food varied among the source materials. Differences were also observed among soils of different composition, suggesting that the nature of the soil as well as the source of PAH contamination can influence bioavailability. These data will be informative both in understanding soil-PAH interactions that affect bioavailability and form a basis for the development of in vitro approaches for PAH bioavailability estimation. Supported in part by a grant from SERDP.

PS 1831j *In Vitro* Toxicity Assessment of Dust Emissions from South African Gold Mine Dumps

C. Andraos[1, 2] and M. Gulumian[1, 2]. [1]*Toxicology, NIOH, Johannesburg, Gauteng, South Africa and* [2]*Haematology & Molecular Medicine, Wits, Johannesburg, Gauteng, South Africa.*

Background: Johannesburg (Jhb), South Africa, known as the golden city, is recognized for its large contribution to the gold mining industry. However, with this reputation comes the challenge of managing the mine waste produced. Currently there are over 380 mine dumps in and around Jhb, but despite efforts to contain the dust emitted from these dumps the exposure to surrounding communities is inevitable. This is due to the rapid expansion of communities moving closer to the dumps. Recently, residents have come forward with complaints including upper respiratory infections, bronchitis and asthma after moving to areas surrounding the dumps. Previous studies conducted in the US, Australia, Spain and UK have proven that dust from mine dumps could be a risk to communities through inhalation of ultrafine particulate matter (PM). Aim: The aim of this study was to determine whether communities in Jhb are also at risk by conducting a health risk assessment. Methods & Results: Exposure assessment showed that the daily concentrations of PM10 emitted from three mine dumps were well above the exposure limit of 180 μg/cm3 for the majority of the sampling period. Physicochemical analysis of dusts collected from the dumps showed the presence of nanoparticles (< 100 nm), known to lodge deep in the respiratory system and to reach internal organs via the bloodstream. High levels of transition metals known to generate free radicals were identified with elemental analysis. The dust also exhibited high surface activities with electron spin resonance spectroscopy, which might explain the dose-dependent toxicity observed with the BEAS-2B bronchial epithelial and U937 monocytic macrophage cell lines when using the xCELLigence impedance-based system. Time-dependent uptake of the particles into the cells was confirmed with the CytoViva Hyperspectral Imaging system. Conclusion: These results suggest a possible risk to surrounding communities. Current efforts are focused on the dose-response assessment and risk characterization to validate the current results.

PS 1831k Potential Mode of Action for Respiratory Effects following Exposure to Libby Amphibole Asbestos

M. R. Gwinn, A. M. Jarabek and B. R. Sonawane. *Office of Research & Development, US Environmental Protection Agency, Washington, DC.*

Evidence from different types of studies (in vitro assays, laboratory animal and occupational and epidemiological studies) and across multiple species point to fibrosis, lung cancer and mesothelioma as respiratory disease outcomes of interest after exposure to Libby Amphibole asbestos (LAA). We systematically reviewed and evaluated the published literature to identify potential mechanisms by which LAA may induce these effects, but a mode of action (MOA) specific to LAA cannot be established. Chronic inflammation, mutagenicity, cytotoxicity and regenerative proliferation can be hypothesized as relevant to an MOA for LAA carcinogenesis, but the temporal relationships and relative contribution of each mechanism remain to be elucidated. Further, the complexities of fiber toxicity make it difficult to distinguish different roles for these same mechanisms in the etiology of mesothelioma and fibrosis. Limitations of early study design and in presentation of the results also hinder insights on the role of specific fiber characteristics. Most experimental studies lack characterization of fiber size distribution, precluding dosimetry insights; while failure to provide results by cell type prevents an integrated understanding of tissue reactions. The route of exposure utilized for in vivo animal studies is particularly important; results obtained from non-physiologically relevant routes (i.e., intraperitoneal injection, gelatin implant) may not accurately reflect the dosimetry or response in occupational inhalation exposures. Although the limited mechanistic data infer biological effects similar to those of other mineral fibers following exposure to LAA, the existing literature is insufficient to establish a MOA for any of these disease outcomes in the respiratory tract.
DISCLAIMER: The views expressed are those of the authors and do not necessarily represent the views and/or policies of the Environmental Protection Agency.

PS 1831l Development of an Open-Source Integrated Test Strategy for Skin Sensitization Potency

J. Pirone[1], M. Smith[1], N. Kleinstreuer[2], T. A. Burns[2], J. Strickland[2], Y. Dancik[3], R. Morris[1], L. Rinckel[2], W. Casey[4] and J. Jaworska[3]. [1]*SSS, Inc., Durham, NC,* [2]*ILS, Inc., Research Triangle Park, NC,* [3]*P & G NV, Bever, Belgium and* [4]*DHHS/NIH, NIEHS/NTP/NICEATM, Research Triangle Park, NC.*

Regulatory authorities require testing to identify substances with the potential to cause allergic contact dermatitis so that appropriate labeling alerts users to the hazard and precautions necessary to minimize exposure. To reduce or eliminate animal use in testing, integrated test strategies (ITS) that combine in silico and in vitro test methods have been proposed. Scientists at the National Toxicology Program Interagency Center for the Evaluation of Alternative Toxicological Methods (NICEATM) and Procter and Gamble (P&G) are developing an open-source version of a previously published ITS for skin sensitization. The original ITS is based on a Bayesian network (BN ITS-2) using in silico and in vitro models that map to the OECD Adverse Outcome Pathway for skin sensitization. BN ITS-2 was developed using a commercial software package. To increase accessibility and algorithmic transparency, NICEATM and P&G developed open-source ITS-2 (OS ITS-2) with tools in R software for building and performing exact inference using a Bayesian network. R versions of widely used algorithms for supervised discretization and latent class learning were substituted for proprietary algorithms. The overall classification accuracies for the OS ITS-2 and the BN ITS-2 were the same, with three compounds misclassified by both methods. Two case studies of representative substances, chlorobenzene and 2-mercaptobenzothiazole, were evaluated using NICEATM's skin sensitization database, and value of information was assessed for the in vitro assays and in silico inputs. The OS ITS-2 provides availability, transparency, and represents a major step in allowing the ITS to be reproduced and tested, which is essential for use in a regulatory framework. The model is available on the NTP website (http://ntp.niehs.nih.gov/go/its).
This project was funded in whole or in part with Federal funds from the NIEHS, NIH under Contract Nos. N01-ES-35504 and GS-23F-9806H.

PS 1831m Prevalence of Molds in Residential Indoor and Outdoor Environments in Northern California and Its Implication in Health Risk Assessment

I. Arnould and S. Kim. *ToxiSan, Bangor, CA.*

Increasingly, airborne mold in home environments has been linked with asthma exacerbation and other respiratory diseases. The majority of these adverse health risk assessments due to mold exposure have been conducted with data from residential homes or buildings associated with dampness. While controlling indoor moisture and mold can help solve mold contamination problems and adverse health effects, very little attention is given to the mold prevalence and its health impacts in non-damp or "normal" indoor residential environments. In this study, we have performed visual inspection of residential homes in Northern California to assess whether mold or conditions indicating mold are present in the indoor air environments. We also collected air samples in order to: (1) capture and quantify a broad spectrum of fungal/mold spores present in the air, and (2) assess whether the levels suggest a fungal/mold problem in the indoor locations. Between 2006 and 2013, we collected and analyzed more than 900 samples (> 600 outdoor air samples; 300 indoor air samples). The results showed that: (1) molds are normally found in indoor air in particularly large numbers, 100 – 8,500 spores per cubic meter of indoor air (residential homes with no visual/known dampness); (2) the range of outdoor mold was 500 -38,000 spores per cubic meter, with four peaks in January, May, October, and November; (3) the four dominant airborne fungi were, yeast, *Cladosporium*, *Penicillium*, and *Aspergillus*; (4) individuals complaining about asthma and other respiratory effects were not well correlated with indoor environments with high spore counts. Our findings suggest that: (1) the ratio, not absolute spore counts, of indoor air spores to outdoor air spores in a given residence should be used as an accurate indicator of a mold problem in a residence, and (2) special emphasis should be given when conducting mold risk assessment with individuals who might be more susceptible to health problems from mold exposure (individuals with respiratory sensitivities and a compromised immune system).

PS 1832 Environmental Pesticides Induce Histones H3 and H4 Acetylation in Cell Culture Models of Parkinson's Disease: Interplay between Mitochondrial Dysfunction and Epigenetic Modifications in Parkinson's Disease

A. Charli, H. Jin, V. Anantharam, B. Natarajan, A. Kanthasamy and A. Kanthasamy. *Biomedical Sciences, Iowa State University, Ames, IA.*

Persistent exposure to environmental pesticides is implicated in the etiopathogenesis of Parkinson's disease (PD). Emerging epigenetic studies show that histone acetylation is one of the key modifications that can play a role in neurodegenerative processes. In this study, we examined the effects of commonly used pesticides that target mitochondrial complex-1, including rotenone, tebufenpyrad and pyridaben, on mitochondrial dysfunction and histone acetylation. Exposure of rat dopaminergic neuronal cells (N27 cells) to tebufenpyrad and pyridaben resulted in cytotoxic cell death in a dose-dependent manner. EC50 for tebufenpyrad and pyridaben was determined to be 3.985 and 3.776 μM, respectively. Furthermore, N27 cells exposed to tebufenpyrad and pyridaben showed a time-dependent increase in the levels of acetylated histones H3 and H4. The classic mitochondrial complex 1 inhibitor rotenone also induced histone H3 and H4 acetylation. Measurement

of ATP levels by luminescent assay showed that mitochondrial complex-1 inhibitors caused a significant reduction in ATP levels. Functional studies using the mitotracker green assay on N27 cells showed that exposure to complex 1 inhibitors caused significant damage in mitochondria. These results were also confirmed by fluorescence microscopy. Interestingly, pre-treatment with the HAT inhibitor anacardic acid (8.5uM) protected against tebufenpyrad and pyridaben–induced ATP reduction, H3 and H4 acetylation and cytotoxic cell death. Collectively, exposure to tebufenpyrad and pyridaben induced histone acetylation via mitochondrial dysfunction, which together may play a key role in dopaminergic neuronal degeneration (supported by NIH grant ES10586).

PS 1833 Comparison of *In Vitro* Cell Models for Assessment of Pesticide-Induced Dopaminergic Neurodegeneration

H. J. Heusinkveld and R. H. Westerink. *Neurotoxicology Research Group, Institute for Risk Assessment Sciences - University of Utrecht, Utrecht, Netherlands.*

Current biomedical and (neuro)toxicity research on (neuro)degenerative diseases relies strongly on animal models. For both ethical and technical reasons this use of laboratory animals is often undesirable. Current in vitro research largely relies on tumor derived- or immortalized cell lines. However, the suitability of cell lines for studying neurodegeneration is determined by their intrinsic properties.
We therefore characterized four different neuronal cell models (PC12, SH-SY5Y, MES23.5 and N27 cells) with respect to the presence of functional membrane ion channels and receptors. Furthermore, we assessed the effects of five known neurotoxic pesticides (rotenone, lindane, dieldrin, imazalil and dinoseb) on cytotoxicity, oxidative stress and parameters of intracellular calcium homeostasis using a combined aB/CFDA assay, a H2DCFDA assay and single cell fluorescent (Fura-2) calcium imaging, respectively.
Our results demonstrate considerable differences in intrinsic properties and pesticide-induced effects on cytotoxicity and oxidative stress, as well as on intracellular calcium homeostasis between the cell lines. The results thus indicate that care should be taken when interpreting (neuro)toxicity data as the chosen cell model may greatly influence the outcome.
This work was funded by the European Union-funded project ACROPOLIS (Grant Agreement KBBE-245163) and by the Faculty of Veterinary Medicine (Utrecht University).

PS 1834 Low Concentrations of Insecticides Induce Acute and Concentration-Dependent Effects on Calcium Homeostasis in PC12 Cells

M. Meijer and R. H. Westerink. *Neurotoxicology Research Group, Institute for Risk Assessment Sciences (IRAS), Utrecht, Netherlands.*

Insecticides are widely used and are well known neurotoxic chemicals. There are different classes of insecticides based on their reported primary mode of action. Since calcium plays a critical role in neuronal development, we tested whether selected organochlorines, organophosphates, neonicotinoids, carbamates and pyrethroids can disturb calcium homeostasis in PC12 cells.
Effects on basal calcium homeostasis were investigated using single cell fluorescence (Fura-2) microscopy. By depolarizing cells with high K^+-containing saline, effects on the depolarization-evoked increase in intracellular calcium ($[Ca^{2+}]_i$) through voltage-gated calcium channels (VGCCs) were also investigated.
The data demonstrate that endosulfan, chlorpyrifos and chlorpyrifos-oxon at 10 μM induce an acute but modest increase in basal $[Ca^{2+}]_i$. More importantly, most of the tested insecticides concentration-dependently inhibited the depolarization-evoked $[Ca^{2+}]_i$, with cypermethrin being the most potent compound with an IC_{20} of 0.009 μM. α-cypermethrin inhibited the depolarization-evoked $[Ca^{2+}]_i$ with 20% at 0.03 μM, chlorpyrifos at 0.08 μM, endosulfan at 0.1 μM, chlorpyrifos-oxon at 1 μM and parathion at 2.56 μM. Carbaryl, imidacloprid, paraoxon-ethyl and paraoxon-methyl did not inhibit the depolarization-evoked $[Ca^{2+}]_i$.
In conclusion, our data demonstrate that 1) insecticides concentration-dependently inhibit depolarization-evoked $[Ca^{2+}]_i$, and that 2) oxon metabolites are less potent compared to their parent compounds in inhibiting depolarization-evoked $[Ca^{2+}]_i$. This acute disturbance of calcium homeostasis may partly underlie insecticide-induced neurotoxicity.
This work was supported by the European Union [DENAMIC project; FP7-ENV-2011-282957] and the Faculty of Veterinary Medicine of Utrecht University.

PS 1835 Azole Fungicides Disturb Intracellular Ca^{2+} in an Additive Manner in Dopaminergic PC12 Cells

R. H. Westerink and H. J. Heusinkveld. *Neurotoxicology Research Group, Institute for Risk Assessment Sciences - Utrecht University, Utrecht, Netherlands.*

Humans are exposed to complex mixtures of pesticides and other compounds, mainly via food. Azole fungicides are broad spectrum antifungal compounds, widely used in agriculture as well as in human and veterinary medicine. The mechanism of antifungal action relies largely on inhibition of CYP51 inhibiting fungal cell growth and known adverse health effects of azole fungicides are thus linked to CYP inhibition. Additionally, azole fungicide-induced neurotoxicity has been reported, though the underlying mechanism(s) are largely unknown.
We therefore investigated the effects of a group of 6 azole fungicides (imazalil, flusilazole, fluconazole, tebuconazole, triadimefon and cyproconazole) on cell viability and on oxidative stress in dopaminergic PC12 cells using a combined alamar Blue/CFDA-AM and H_2DCFDA assay, respectively. As calcium plays a pivotal role in neuronal survival and functioning, effects of these 6 azole fungicides as well as binary and quaternary mixtures of azole fungicides on the intracellular calcium concentration ($[Ca^{2+}]_i$) were investigated using single-cell fluorescence microscopy in PC12 cells loaded with the calcium-sensitive fluorescent dye Fura-2.
Only modest changes in cell viability and ROS production were observed. However, 5 out of 6 azole fungicides induced an non-specific inhibition of voltage-gated calcium channels (VGCCs), though with varying potency. Experiments using binary IC_{20} and quaternary IC_{10} mixtures indicated that the inhibitory effects on VGCCs are additive.
The combined findings demonstrate modulation of intracellular Ca^{2+} via inhibition of VGCCs as a novel mode of action of azole fungicides. Furthermore, mixtures of azole fungicides display additivity, illustrating the need to take mixture effects into account in human risk assessment.
This work was funded by the European Union-funded project ACROPOLIS (Grant Agreement KBBE-245163) and by the Faculty of Veterinary Medicine (Utrecht University).

PS 1836 Atrazine Alters Neuronal Redox Status but Does Not Activate Nrf2

J. Roede[1, 3], D. I. Walker[2, 3] and J. M. Hansen[3]. [1]*Pharmaceutical Sciences, University of Colorado, Aurora, CO,* [2]*Civil and Environmental Engineering, Tufts University, Medford, MA and* [3]*Medicine, Emory University, Atlanta, GA.*

Atrazine (ATZ) is the second most commonly used herbicide in the United States and is widely applied to grain crops, such as corn, wheat, and sorghum. Because of its wide use, ATZ is the most commonly detected pesticide in ground water. ATZ can act as an endocrine disruptor as well as cause dopaminergic neuron death and behavioral phenotypes. The aim of this study was to characterize how subtoxic concentrations of ATZ and its metabolites alter neuronal redox status. SH-SY5Y neuroblastoma cells were treated with subtoxic concentrations of ATZ and its metabolites and alterations in cytoplasmic and mitochondrial peroxiredoxin (Prx) redox status as well as cellular GSH, GSSG and redox potentials (EhGSSG) were measured. Redox western blots showed that neither ATZ nor its metabolites, deethylatrazine (DEA), deisopropylatrazine (DIA), diaminochlorotriazine (DACT), altered cytoplasmic Prx1 redox status; however, acute exposure (4h) to DEA, DIA, or DACT resulted in slight oxidation of mitochondrial Prx3, but this effect normalized by 24h. Analysis of intracellular GSH, GSSG and EhGSSG showed that both ATZ and DIA significantly deplete GSH resulting in considerable oxidation of EhGSSG. Due to the ATZ-mediated decrease in intracellular GSH, we investigated if Nrf2 was activated by ATZ or its metabolites. Western blots of nuclear fractions showed a slight increase in Nrf2 nuclear translocation in DEA treated cells and a large increase following DACT treatment, but no increase in ATZ treated cells. Analysis of Nrf2-controlled genes (GCLC, NQO1, HO-1, Prx1) showed slight activation by DACT. GCLC expression was increased by ATZ, but it can be concluded that this mechanism may not be Nrf2-mediated. In conclusion, our results demonstrate that ATZ alters intracellular GSH redox status, but does not alter Prx redox or cause an increase in Nrf2 nuclear translocation or transcription.

PS 1837 Gestational and Lactational Drinking Water Exposure to Atrazine Causes Specific Behavioral Deficits and Selectively Alters Monoaminergic Systems in C57BL/6 Mouse Dams, Juvenile, and Adult Offspring

Z. Lin[1, 2], N. M. Filipov[1, 2] and C. A. Dodd[1, 3]. [1]*Physiology and Pharmacology, Univ. of Georgia, Athens, GA,* [2]*Interdisciplinary Toxicology Program, Univ. of Georgia, Athens, GA and* [3]*Biology, Fort Valley State University, Fort Valley, GA.*

Atrazine (ATR) is one of the most frequently detected pesticides in the U.S. water supply and limited evidence suggests that it may be a developmental neurotoxicant. The present study focused on behavioral and neurochemical (monoamine) alterations in C57BL/6 mouse offspring and dams exposed to low dose of ATR (3 mg/L) via the drinking water (DW) from gestational day 6 to postnatal day (PND) 23. Behavioral tests included open field, pole, grip strength, novel object recognition (NOR), forced swim (FS), and marble burying. Maternal and offspring (PND21, 35, and 70) body and brain weights were not affected by ATR. However, ATR exposure caused: (i) hyperactivity and decreased performance in the NOR in the dams; (ii) hyperactivity (males and females), increased immobile time in the FS (males), decreased performance in the pole test (females), and increased number of buried marbles (females) in the juvenile offspring (PND35); (iii) decreased performance in the NOR by females in the adult offspring (PND70). ATR exposure also increased striatal dopamine (DA) in the dam and juvenile offspring (males and females), but not in the adult offspring, and it decreased serotonin in the perirhinal cortex of female, but not male, adult offspring. These results suggest that perinatal exposure to environmentally-relevant DW levels of ATR targets the nigrostriatal DA pathway in the dam and offspring, alters motor and cognitive functions of the dam, induces a variety of sex-selective behavioral abnormalities involving motor and emotional functions in the juvenile offspring, and decreases cognitive function of female adult offspring, an effect that may be due to altered serotonin homeostasis in the perirhinal cortex.

PS 1838 *N*-Methyl-*D*-aspartate Receptor Activation May Contribute to Glufosinate Neurotoxicity

S. R. Lantz[1, 3], C. M. Mack[2], K. A. Wallace[2], E. F. Key[1], T. J. Shafer[2] and J. E. Casida[1]. [1]*Dept. of Nutritional Sciences and Toxicology, University of California, Berkeley, CA,* [2]*Integrated Systems Toxicology Division, NHEERL, ORD, U.S. Environmental Protection Agency, Research Triangle Park, NC and* [3]*Marquette Biological Station, U.S. Fish and Wildlife Service, Marquette, MI.*

Glufosinate (GLF) at high levels in mammals causes convulsions through a mechanism that is not completely understood. The structural similarity of GLF to glutamate (GLU) implicates the glutamatergic system as a target for GLF neurotoxicity. The current work examined GLF interaction with *N*-methyl-*D*-aspartate subtype GLU receptors (NMDAR) and GLT-1 transporters via [^{3}H]CGP39653 binding experiments and [^{3}H]GLU uptake assays, respectively. GLF effects on neuronal network activity were assessed using microelectrode array (MEA) recordings in primary cultures of cortical neurons. GLF and its primary metabolite *N*-Ac-GLF bind to the NMDAR; the IC_{50} value for GLF was 668 μM. Concentrations of GLF greater than 1 mM were needed to decrease GLU uptake through GLT-I. In MEA recordings from networks of rat primary cortical neurons, the concentration-responses for NMDA, GLF and *N*-Ac-GLF on network mean firing rates (MFR) were biphasic, increasing at lower concentrations and decreasing below control levels at higher concentrations. Stimulation of MFR occurred between 1-10 μM NMDA (320% control, max), 100-300 μM *N*-Ac-GLF (190% control, max) and 3-1000 μM GLF (320% control, max). The NMDAR antagonist MK801 attenuated both NMDA and GLF increases in MFR. The GLF concentration required to alter GLU transport through GLT-I is not likely to be attained in vivo, and therefore not relevant to the neurotoxic mode of action. However, toxicokinetic data from reports of intentional human poisonings indicate that GLF concentrations in the CNS after acute exposure could reach levels high enough to lead to effects mediated via NMDA receptors. Furthermore, the newly characterized action of *N*-Ac-GLF at the NMDA receptor suggests that both the parent compound and metabolite could contribute to neurotoxicity via this pathway. *This abstract does not reflect EPA Policy.*

PS 1839 Nrf2 Upregulation in Response to Paraquat Exposure in Rat Neuroblast Cells

L. Chen, A. Fowler, M. Narasimhan, L. Mahimainathan, D. Patel, M. Rathinam and G. I. Henderson. *Pharmacology and Neuroscience, TTUHSC, Lubbock, TX.*

The herbicide paraquat (1,1′-dimethyl-4,4′-bipyridinium dichloride, PQ) is widely used in agriculture. Numerous reports confirm that PQ is teratogenic yet the mechanisms underlying this remain incompletely defined. Our previous study showed that PQ elicited Nrf2 protein accumulation in the nucleus within 24hs with a significant dose-response effect ($p<0.05$), which suggested a potential neuroprotective role for Nrf2, a transcription factor which controls glutathione (GSH) homeostasis. To further evaluate the neuroprotective role of Nrf2 in response to PQ exposure, the following study addresses this in a rat neuroblast line. The results showed that after 24 hours of PQ exposure, GSH/GSSG ratios were decreased. However, while Nrf2 nuclear protein level increased, the luciferase assay showed that ARE-related activity was decreased. To address Nrf2 function, Nrf2 was silenced, resulting in enhanced PQ toxicity. Cells were further treated with PQ plus resveratrol (Res, 24h pretreatment) and results demonstrated that Res protects against PQ toxicity through Nrf2 alterations. PQ can inhibit neuroblast replication, and up-regulate Nrf2 expression along with its nuclear accumulation. However, the expected increase in luciferase activity does not occur. Silencing or up-regulation of Nrf2 showed that Nrf2 can play a cytoprotective role against PQ toxicity towards these neuroblasts, yet Nrf2 nuclear accumulation with luciferase activity decreasing might reflect a toxic effect of PQ on this system. In summary, PQ at physiologically relevant concentrations impaired viability and cellular redox potential of cells that are direct precursors of neurons in the developing brain. Cytoprotection and Nrf2/ARE responses in the presence of paraquat can be augmented by interventions that increase nuclear Nrf2, however the effectiveness of this may be reduced by a paraquat-related impairment of Nrf2/ARE interactions need further studies.

PS 1840 Paraquat and MPTP Induce Alterations in the Expression Profiles of microRNA in Neuro-2A Cells

H. Li, Q. Wang, N. Ren, Z. Wang and S. Wu. *Department of Occupational and Environmental Health, School of Public Health, Fujian Medical University, Fuzhou, Fujian, China.* Sponsor: Q. Zhang.

Recent evidence indicates that microRNAs (miRNAs) play a key role in neurodegenerative diseases. However, little is known about how these miRNAs contribute to dopaminergic neuronal damage by paraquat (PQ) and 1-methyl-4-phenyl-1,2,3,6-tetrahydropyridine (MPTP). Here we used microarray analysis to show that PQ and MPTP induce alteration of miRNA expression in a cell model of Parkinson's disease. The results reveal that treatment with 300 μM PQ caused miRNA deregulation in which 60 miRNAs were up-regulated and 228 miRNAs were down-regulated. Among the 288 miRNAs identified, the levels of six miRNAs (miR-297b-5p, miR-497-5p, miR-503-5p, miR-374-5p, miR-135b-5p, and miR-669e-3p) were changed more than 1.2-fold. Upon treatment with MPTP at 300 μM MPTP, a total of 576 mRNAs were deregulated; 506 miRNAs were up-regulated and 70 miRNAs down-regulated. Among the 576 miRNAs, miR-93-5p and miR-425-5p) had changes above 1.2-fold. These findings showed that both PQ and MPTP alter the miRNA expression, but each affects a different set of miRNA targets. Alterations in the expressions of miR-17-5p, miR-93-5p, miR-210-3p, miR-374-5p, miR-378-3p, miR-503-5p were verified by real-time quantitative reverse transcriptase polymerase chain reaction. Bioinformatics analysis indicated that aberrant expression of miR-17-5p potentially contributes to PQ-induced neurotoxicity. Taken together, our study demonstrates, for the first time, that characteristic changes in miRNA expression profiles occur after PQ and MPTP treatment, which suggests miRNA may be involved in the development of PQ and MPTP induced neurodegeneration as a molecular mechanism. This work was supported by the National Natural Science Foundation in China (Grant 81172715, 30800936), Fujian Province Funds for Distinguished Young Scientists (2012J06018) and Program for New Century Excellent Talents in Fujian Province University (NCETFJ, JA11103).

PS 1841 DDT and DDE Enhance the Toxicity of Amyloid Beta Peptides in *Drosophila*

L. DeRespiris[3], K. Carney[2], M. Konsolaki[2], K. R. Reuhl[3] and J. Richardson[1]. [1]*RWJMS, Piscataway, NJ,* [2]*Genetics, Rutgers University, Piscataway, NJ and* [3]*Pharmacology and Toxicology, Rutgers University, Piscataway, NJ.*

Environmental factors, such as pesticides are thought to play a significant role in the pathogenesis of diseases of the nervous system. DDT (dichlorodiphenyltrichloroethane) is a persistent synthetic organochlorine insecticide used to control ma-

laria and typhus. Although banned in the US, DDT is widely used today in Africa and there are still areas of contamination in the US. Recently, we found that serum levels of DDE, a metabolite of DDT, are associated with a diagnosis of Alzheimer's disease (Richardson et al., 2009) and that DDT changes the expression of amyloid precursor protein in cultured cells. To determine whether exposure to DDT or DDE affected these pathways in an intact organism, we utilized *Drosophila melanogaster* that express human Alzheimer's amyloid beta (Aβ) peptides and develop progressive neurodegenerative phenotypes and reduced lifespan. Initially, we tested the toxicity of DDT and DDE in wild type adult *Drosophila* and found that 100% of flies died by 5 days provided food containing 100μM DDT, whereas 50% of control flies lived to 30 days. Interestingly, DDE did not compromise viability at concentrations up to 1mM. In a developmental model, both pesticides caused developmental delays at concentrations as low as 10μM, a concentration that caused no lethality in adult flies. Based on these results, we treated Aβ-expressing *Drosophila* with 1μM DDT or DDE and measured changes in their lifespan. At 15 days of exposure, lifespan of DDT treated males was 12% lower compared to controls, whereas DDE-treated males had 18% lower viability. No changes in viability were observed in treated female flies. Our work suggests that sub-toxic levels of DDT and DDE may exacerbate the effects of Aβ in a *Drosophila* model of Alzheimer's and that these effects appear to be sex-specific. Supported by the SOT Intern Program and NIH grants P30ES005022 and R25ES020721.

PS 1842 Nanomolar Bifenthrin Alters Synchronous Ca^{2+} Oscillations and Cortical Neuron Development Independent of Sodium Channel Activity

Z. Cao[1], Y. Cui[1], H. M. Nguyen[2], D. P. Jenkins[2], H. Wulff[2] and I. N. Pessah[1]. [1]*Molecular Biosciences, School of Veterinary Medicine, UCDavis, Davis, CA and* [2]*Pharmacology, School of Medicine, UCDavis, Davis, CA.*

Bifenthrin is a relatively stable type I pyrethroid with broad agricultural and domestic uses that causes tremors and impairs motor activity in rodents. In this study we investigated the influence of nanomolar concentrations of bifenthrin on the synchronous Ca^{2+} oscillations (SCO) necessary for activity dependent dendritic development. Primary mouse cortical neurons were cultured 8-9 days *in vitro* (DIV) loaded with the Ca^{2+} indicator Fluo-4, and imaged using FLIPR Tetra. Acute exposure to bifenthrin rapidly increased the frequency of SCO 2.7-fold (EC_{50}=58nM) and decreased SCO amplitude by 36%. Changes in SCO properties were independent of modifications in voltage-gated sodium channels since 100nM bifenthrin had no effect on the whole-cell Na^+ current, nor influenced neuronal E_{rest} of cortical neurons. Moreover, the L-type Ca^{2+} channel blocker nifedipine failed to ameliorate bifenthrin-triggered SCO activity, and were not mediated by ryanodine receptor channel modification. By contrast, the mGluR 5 antagonist MPEP normalized the bifenthrin-triggered increase in SCO frequency without altering baseline SCO activity, indicating that bifenthrin amplifies mGluR 5 signaling independent of Na^+ channel modification. Competitive (AP-5) and noncompetitive (MK801) NMDAR antagonists partially decreased both basal and bifenthrin-triggered SCO frequency increase. Bifenthrin-modified SCO rapidly enhanced the phosphorylation of cAMP response element-binding protein (CREB). Sub-acute (48h) exposure to bifenthrin commencing 2 DIV enhanced neurite outgrowth and persistently increased SCO frequency and reduced SCO amplitude. Collectively these data identify a new mechanism by which bifenthrin potently alters Ca^{2+} dynamics and Ca^{2+}-dependent signaling in cortical neurons that have long term impacts on activity driven neuronal plasticity.

PS 1843 Protective Role of Melatonin against Alpha-Cypermethrin-Induced Oxidative Stress in Human Neuroblastoma Cell Line SH-SY5Y

A. Anadon, J. Del Pino Sans, M. A. Martínez, E. Ramos, I. Ares, V. Castellano, M. Martínez, M. R. Martínez-Larrañaga and A. Romero. *Departamento de Toxicologia y Farmacologia, Universidad Complutense de Madrid, Madrid, Spain.*

α-Cypermethrin, alpha-cyano pyrethroid insecticide, is a relatively potent neurotoxic associated with human health risks. In the present study the aims were, on one hand to investigate in an in vitro model the neuroprotective role of three well-known antioxidants, melatonin (MEL), Trolox and N-Acetylcysteine against α-cypermethrin induced neurotoxicity and on the other hand, to examine, by PCR array, the cell death pathway expression patterns in neuroblastoma cell line SH-SY5Y after pyrethroid exposure and the potential neuroprotective role of melatonin. Levels of both nitric oxide (NO) and lipid peroxides measured as malondialdehyde (MDA) were significantly increased after α-cypermethrin exposure, however selected antioxidants exerted different protective actions. Compared to other antioxidants, 1 μM MEL treatment showed the most effective protection against pyrethroid-induced lipid peroxidation and increased NO levels. We evaluated multiple cell death regulation genes after α-cypermethrin and α-cypermethrin plus MEL-treated cells, most of genes altered by the pyrethroid were partially or completely reverted by MEL treatment, among them, ATG16L1, BIRC3, FOXI1, IGF1, INS, IRGM, KCNIP1, MAG, RAB25, SCNA, S100A7A, SQSTM1, TNFRSF10A, TNFRSF11B and TNFRSF1A. These results suggest that oxidative stress is a key element in the neurotoxicity process induced by α-cypermethrin and a multitasking indolamine as MEL might be beneficial to prevent toxicity caused by α-cypermethrin or even other pyrethroids with similar action mechanism. This work was supported by projects Ref. BSCHGR58/08(UCM), Ref. No. S2009/AGR-1469(CAM) and Consolider-Ingenio 2010 No.CSD2007-063(MEC), Spain.

PS 1844 Pyrethroid Pesticides Directly Activate Microglia through Voltage-Gated Sodium Channels Leading to Increased TNF-alpha Release

J. Liu[1], M. M. Hossain[2] and J. Richardson[2]. [1]*Ernest Mario School of Pharmacy, Rutgers University, Piscataway, NJ and* [2]*Department of Environmental & Occupational Medicine, Rutgers Robert Wood Johnson Medical School, Piscataway, NJ.*

Microglia are considered to be the resident immune cells of the central nervous system and contribute significantly to ongoing neuroinflammation in a variety of neurodegenerative diseases. Recently, we identified that voltage-gated sodium channels (VGSC) are present on microglia cells and contribute to the release of the pro-inflammatory cytokine tumor necrosis factor alpha (TNFα) (Hossain and Richardson, 2013). Based on this finding and the fact that pyrethroid pesticides act on VGSC, we hypothesized that exposure of microglia to the pyrethroid pesticides, permethrin and deltamethrin, would activate microglia and increase release of TNFα. BV2 mouse microglial cells were seeded into a 96-well plate and treated with 0-100 μM deltamethrin or permethrin for 24 or 48 hrs and cell viability was assayed using Alamar blue. Cell viability decreased in a dose and time dependent manner for concentrations of deltamethrin and permethrin above 10 μM. Next, BV-2 cells were treated with vehicle, the VGSC blocker tetrodotoxin (TTX), or 0.5-5 μM deltamethrin or permethrin in the presence and absence of TTX for 24-48 hours. Media was removed and the concentration of TNFα was assayed using ELISA. TNFα release increased significantly in a dose and time-dependent manner for both deltamethrin and permethrin. TTX significantly reduced the pyrethroid-induced TNFα release, indicating that interaction with VGSC significantly contributed to release. From these data, we conclude that pyrethroid pesticides directly activate microglial cells through interaction with microglial VGSC. Because neuroinflammation plays a key role in many neurodegenerative diseases, these data provide an additional mechanism by which exposure to pyrethroids may contribute to neurodegeneration.

PS 1845 Repeated Pesticide Exposure Causes Hippocampal ER Stress, Neuroinflammation, and Cognitive Deficits in Mice

M. M. Hossain[1], E. DiCicco-Bloom[2] and J. Richardson[1]. [1]*Environmental and Occupational Medicine and Environmental and Occupational Health Sciences Institute, Rutgers-Robert Wood Johnson Medical School, Piscataway, NJ and* [2]*Neuroscience and Cell Biology, Rutgers-Robert Wood Johnson Medical School, Piscataway, NJ.*

Endoplasmic reticulum (ER) stress and neuroinflammation are implicated as significant contributors to neurodegeneration. Previously, we demonstrated that the widely used pyrethroid pesticide deltamethrin causes ER stress-mediated apoptosis in SK-N-AS neuroblastoma cells. However, whether this occurs in vivo remains unknown. Here, we investigated the effects of repeated deltamethrin exposure (3 mg/kg every 3 days for 60 days) on hippocampal ER stress, neuroinflammmation, and cognitive function in adult mice. Repeated exposure to low dose deltamethrin caused ER stress in the hippocampus, as indicated by increased CHOP (131%) and GRP78 (96%) levels. This was accompanied by increased levels of caspase-12 (110%) and activated caspase-3 (50%) in the hippocampus. Deltamethrin also induced microglial activation, as indicated by Iba-1 staining, and increased TNF-α mRNA expression (121%) and protein (465%) levels. To determine whether these effects lead to cognitive dysfunction, hippocampal-dependent learning and memory was evaluated with a spatial navigation task. Deltamethrin-treated animals exhibited profound deficits in the acquisition phase and in short-term and long-term memory. Additionally, deltamethrin exposure caused decreased BrdU-positive cells (36.54%) in the dentate gyrus (DG) of the hippocampus, suggesting impairment of hippocampal neurogenesis. Collectively, these results demonstrate that repeated deltamethrin exposure leads to ER stress, neuroinflammation, and apoptotic cell death in the hippocampus. Furthermore, impaired hippocampal neurogenesis may contribute to deficits in learning and memory by deltamethrin. Supported by NIH P30ES005022 and R01ES015991.

PS 1846 Effects of Permethrin on the Acoustic Startle Response in Adult Male Sprague-Dawley Rats

C. V. Vorhees[1], T. G. Osimitz[2], L. P. Sheets[3], D. Minnema[4], M. Brooks[5], D. W. Gammon[6] and M. T. Williams[1]. [1]*Child Neurology, Cincinnati Children's Research Foundation, Cincinnati, OH,* [2]*Science Strategies LLC, Charlottesville, VA,* [3]*Bayer CropScience, Research Triangle Park, NC,* [4]*Syngenta Crop Protection, Research Triangle Park, NC,* [5]*Ag-Chem Consulting LLC, Clifton, VA and* [6]*FMC Corp, Philadelphia, PA.*

Pyrethroids are synthetic insecticides derived from naturally-occurring pyrethrins. Type I pyrethroids induce tremor and Type II induce choreoathetosis and salivation. Both types act on voltage-gated sodium channels and some congeners have effects on calcium and chloride channels. At non-symptomatic doses, the acoustic startle response (ASR) is sensitive to the effects of these compounds. The ASR of adult male Sprague-Dawley rats was tested 2, 4, 6, and 8 h after oral administration of the Type I pyrethroid, permethrin, given once by gavage in 5 ml/kg corn oil at doses of 0, 60, 90, or 120 mg/kg. Response amplitude to a 120 dB mixed- frequency "white" noise stimulus was recorded for 100 ms after signal onset (Vmax in mV) using accelerometer-based force transducers (SR-LAB, San Diego Instruments). Test sessions consisted of a 5 min acclimation and 100 trials with an intertrial interval of 20 s. Rats were acclimated to the vivarium for 2 weeks, 2/cage. Rats were weighed, handled, and pre-tested to reduce stress. Pretest-1 consisted of ASR test with no treatment. Pretest-2 (24 h later) consisted of ASR test after 5 ml/kg corn oil gavage. Rats were assigned to groups matched for Pretest-2 ASR peak response amplitude. Data were analyzed by ANOVA (Dose x Time x Block; 10 trials/block; 1-between, 2-within design). Permethrin increased Vmax (Dose main effect: $p<0.001$) and interacted with time (Dose x Time: $p<0.001$), and block (Dose x Time x Block: $p<0.05$). The Dose x Time interaction showed no effects at 2 h, mid and high dose increases at 4 h, and increases at all doses at 6 h and 8 h. The low dose had less effect than mid and high doses but the latter two doses did not differ from one another. Future experiments will determine the effects of permethrin during development. (Supported by CAPHRA).

PS 1847 Acute Alterations in Thermoregulatory Response after Single-Compound and Joint Oral Exposure to Pyrethroid Insecticides in Infant Rats

C. S. Sosa Holt[1], U. Bardullas[2] and M. J. Wolansky[1, 3]. [1]*Quimica Biologica, Universidad de Buenos Aires (UBA), Buenos Aires, Argentina,* [2]*Departamento de Neurobiología Conductual y Cognitiva, Instituto de Neurobiologia, Universidad Nacional Autonoma de Mexico, Queretaro, Mexico and* [3]*IQUIBICEN (CONICET), UBA, Buenos Aires, Argentina.*

Most pyrethroid insecticides (PYRs) are classified as type-I or-II based on acute neurobehavioral effects in adult rodents. In rats, PYRs produce alterations in thermoregulatory response (TR): hyperthermia (type-I) or hypothermia (type-II).This dual classification distinguishes high-dose oral syndromes. However, recent evidence suggest that realistic exposures in humans are well below acute dose levels used to classify PYRs, and a greater commonality of clinical effects is observed at lower doses. In addition, while a greater vulnerability for pesticides has been recognized during early life, there is limited information on the age-related toxicity of PYRs. In this study, cypermethrin (CPM,type-II) and bifenthrin (BIF,type-I) dissolved in corn oil are evaluated in single-chemical and mixture assays using TR as an endpoint in Sprague Dawley rat pups (P20). Subcutaneous temperature was recorded by radiotelemetry before and after single-bolus oral dosing, at 30 min intervals during 5 h. Infants were slightly more sensitive than adults to both PYRs. Most important, BIF produced a biphasic response that had not been observed in a previous study in adults (Wolansky et al, 2007) with an initial mild increase followed by an evident decline in temperature at 2-4 h at doses above 12 mg/kg. A biphasic response was also observed after exposure to CPM, consistent with previous data in adults. When infants were administered a mixture of low-effective, equipotent doses of both PYRs, an apparent summation of the initial body heating effect was observed, and no hypothermic action was evident afterwards. The results are discussed in the context of the age-specific toxicodynamic and toxicokinetic factors determining qualitative divergence in toxic responses to pesticides during early development (UB and CSSH had equal contribution to this work)

PS 1848 Acute Exposure to a Glyphosate-Containing Herbicide Leads to Mitochondrial Dysfunction in *Caenorhabditis elegans*

C. E. Todt, R. Negga, S. K. Jadav, D. C. Bailey and V. A. Fitsanakis. *Biology, King College, Bristol, TN.*

Epidemiological studies indicate that pesticide usage positively correlates with neurodegenerative disorders, particularly Parkinson's disease. Further evidence suggests that exposure to glyphosate-containing pesticides, the most widely-used class of herbicides in the world, may lead to mitochondrial inhibition. This is in contrast to treatment with glyphosate by itself, which is relatively non-toxic, even to mitochondria. To further explore this potential relationship between Touchdown® (TD), a glyphosate-based herbicide, and mitochondrial inhibition, we acutely exposed second larval stage (L2) *Caenorhabditis elegans* (*C elegans*) to various concentrations (LC_{25}, LC_{50}, or LC_{75}) of TD as percent active ingredient (glyphosate). To determine whether mitochondrial function was compromised, assays were performed 24 hours post-acute TD exposure (30 min) to determine whether Complex II, Complex IV, or the proton gradient were adversely affected. Based on one-way ANOVA ($*p<0.05$), colorimetric data from Complex II and IV assays indicate that these complexes are not inhibited, but rather stimulated in a dose-dependent manner. Results relating to the integrity of the proton gradient indicate a statistically significant increase ($*p<0.05$) in tetramethylrhodamine ethyl ester (TMRE) accumulation, signifying not only an intact proton gradient, but perhaps uncoupling and an increase in proton concentration in the inner mitochondrial membrane space. These data suggest that acute exposure of *C elegans* to TD leads to mitochondrial dysfunction, which may contribute to neurodegeneration observed in previously published studies from this lab.

PS 1849 Chronic Exposure to TouchDown, a Glyphosate-Containing Herbicide, Leads to Mitochondrial Inhibition in *Caenorhabditis elegans*

D. C. Bailey, R. Negga, C. E. Todt, R. E. Barnett and V. A. Fitsanakis. *Biology, King College, Bristol, TN.*

Glyphosate-containing herbicides are some of the most widely-used pesticides in the world. Although glyphosate alone is relatively non-toxic, a growing body of evidence suggests that commercial formulations may lead to increases in oxidative stress and mitochondrial inhibition. Previous data from our lab demonstrated dopaminergic and GABAergic neurodegeneration in *Caenorhabditis elegans* (*C elegans*) when exposed to various concentrations of Touchdown® (TD). Since mitochondrial inhibition may lead to decreased neuronal viability, we sought to determine whether mitochondrial function was compromised. Therefore, we treated L2 worms with varying concentrations of TD followed by assays specific for mitochondrial complex activity. Initially we determined overall mitochondrial function using tetramethylrhodamine ethyl ester (TMRE) to measure the extent of proton gradient integrity. Results from TMRE assays indicated a dose-dependent decrease in dye accumulations in treated worms compared to control ($*p < 0.05$). Colorimetric data from Complex II studies suggested a dose-dependent relationship. At lower concentrations (LC_{25}, LC_{50}), Complex II activity was marginally inhibited. At the highest concentration (LC_{75}), however, Complex II activity was statistically significantly increased ($*p < 0.05$) compared to control worms. Complex IV studies suggested a slight increase in activity at all treatment concentrations compared to control, but this did not reach statistical significance. Therefore, it does not appear that Complex IV activity is inhibited by TD. Taken together, these data indicate that exposure of *C elegans* to TD leads to mitochondrial inhibition. Furthermore, since mitochondrial inhibition can lead to increased reactive oxygen species production, chronic exposure to TD could potentially result in neuronal degeneration, including that associated with Parkinson's disease.

PS 1850 Detection of Reactive Oxygen Species in *Caenorhabditis elegans* after Exposure to Glyphosate- or Mn/Zn Ethylene-*bis*-Dithiocarbamate-Containing Pesticides

A. D. Shelton, R. Negga, D. C. Bailey and V. A. Fitsanakis. *Biology, King College, Bristol, TN.*

The purpose of these studies was to determine if exposure of *Caenorhabditis elegans* (*C elegans*) to the glyphosate-containing herbicide, TouchDown(R) (TD), or the Mn/Zn ethylene-*bis*-dithiocarbamate-containing fungicide, Mancozeb (MZ), results in increased reactive oxygen species (ROS) production, specifically O^{2-} and H_2O_2. Initially double-stranded DNA was exposed to varying concentrations of TD or MZ for 6, 12, or 24 hours. DNA samples were then loaded on an agarose gel to determine if DNA nicking, due to putative ROS production, occurred. Results indicated a concentration-dependent increase in nicking in both TD and MZ treatments compared to control. To verify ROS production *in vivo*, *C elegans* were

exposed chronically (24 h) or acutely (30 min) to varying concentrations of TD or MZ, and assayed with dihydroethidium (DHE), for O^{2-}, or AmplexRed, for H_2O_2. DHE assays in either treatment paradigm (chronic or acute TD or MZ) indicated no statistically significant increase in O^{2-} at any concentration compared to control. Furthermore, chronic TD exposures followed by AmplexRed treatment showed no statistically significance difference compared to control. Conversely, worms treated acutely with TD showed a statistically significant (**p<0.01) increase in H_2O_2 in LC_{25} and LC_{50} groups compared to control. AmplexRed assays in worms following chronic MZ exposure indicated a statistically significant (***p<0.001) decrease in H_2O_2 in the LC_{25} group compared to control, but a dose-dependent upward trend in production of H_2O_2 with increasing concentration (LC_{25} vs LC_{50},***p<0.001; LC_{50} vs LC_{75},**p<0.01). AmplexRed results in acute MZ studies showed a statistically significant decrease in H_2O_2 in LC_{25} (***p<0.001) and LC_{50} (**p<0.01) treatment groups compared to control, but a statistically significant (***p<0.001) increase in this ROS in LC_{75} worms. Taken together, these data strongly support the hypothesis that both pesticides are capable of producing ROS, and that the ROS may be either H_2O_2 or hydroxyl radical.

PS 1851 Treatment of *Caenorhabditis elegans* with Either a Glyphosate-Containing Herbicide or Manzate Leads to Decreased ATP Levels

S. E. Orfield, R. H. Nichols, S. L. Burchfield and V. A. Fitsanakis. *Biology, King College, Bristol, TN.*

Epidemiological studies show a positive correlation between pesticide exposure and Parkinson's disease (PD) in humans. It is also known that patients with PD exhibit mitochondrial inhibition. Interestingly two widely-used agrochemicals, TouchDown® (TD), a glyphosate-containing herbicide, and Manzate (MZ), a Mn/Zn ethylene-*bis*-dithiocarbamate-based fungicide, are suspected of adversely affecting mitochondrial function. Furthermore, previous work in *Caenorhabditis elegans* (*C elegans*) from our lab has shown specific neurodegeneration in dopaminergic and GABAergic neuronal populations. To determine whether exposure to these pesticides could also result in potential mitochondrial dysfunction, we treated three groups of N2 (wild-type) strain *C elegans* with varying concentrations (LC_{25}, LC_{50}, LC_{75}) of the respective commercial-grade compounds as a percent active ingredient (glyphosate or Mn/Zn elthylene-*bis*-dithiocarbamate). Studies using chronic (24 h) or acute (30 min) exposure paradigms were conducted. Following the respective treatment, a luminescent probe was used to determine the relative amount of ATP in each group. Results indicated a statistically significant decrease (***p<0.001) in ATP production in the chronic LC_{75} TD treatment group compared to control. For acute treatment with TD, there was a statistically significant increase (***p<0.001) in ATP production in the LC_{25} group compared to all other groups, including control. When worms were treated with chronic MZ, there was an overall statistically significant decrease (***p<0.001) in ATP amount for each of the three treatment groups when compared to control. Finally, in worms from the acute MZ treatment studies, a strong trend suggested a decrease in ATP compared to control worms. Taken together, these data indicate a general reduction of ATP that could result from mitochondrial inhibition following exposure to these pesticides. Overall, these data suggest that chronic or acute exposure of *C elegans* to either TD or MZ could promote neurodegeneration via mitochondrial dysfunction.

PS 1852 Maneb (Manganous Ethylenebisdithiocarbamate) Alters Expression of Genes Involved in Oxidative Stress and Induces Stress Proteins in Rat Hippocampal Astrocytes

M. Akhtar and L. D. Trombetta. *Pharmaceutical Sciences, St. John's University, Queens, NY.*

Approximately 5.1 billion pounds of pesticides per year are used in the United States, of which 70 million pounds are fungicides. There is increasing evidence that pesticides are implicated in human health impairment. According to epidemiological and experimental studies, there is a strong association between pesticide use and neurodegenerative diseases. Maneb, a manganese containing ethylenebis[dithiocarbamate], is a broad-spectrum fungicide commonly used to control plant diseases on food and feed crops. Dithiocarbamates have been shown to produce reactive oxygen species (ROS), altering cellular antioxidant homeostasis that can lead to cellular stress. Astrocytes play a critical role in normal brain physiology and neuroprotection. In this study, Maneb's potential to alter the expression of genes involved in oxidative stress and antioxidant defenses and induction of stress proteins in rat hippocampal astrocytes was evaluated. Rat hippocampal astrocytes were exposed to 13.5 μM (LC_{50} concentration) of Maneb for 24 hours. Real-time PCR analysis indicated that Maneb exposure caused a 2-fold or greater change in the expression of stress responsive genes involved in ROS metabolism such as *Nqo1* and *Prdx1*, which were up-regulated, and *Txnrd2*, *Txnip*, *Gpx7*, *SOD3*, and *Dhcr24*, which were significantly down-regulated. In addition, Maneb exposure significantly modified the expression of several antioxidant genes including peroxidases *Ctsb*, *Ptgs1*, and *Ptgs2* that were up-regulated more than 2-fold, and *Prdx4* and *Nxn* antioxidant genes that were down-regulated upon Maneb exposure. Biochemical analyses following Maneb exposure revealed that there was a significant increase in the level of stress-inducible proteins, HO-1 and Hsp70. Maneb's ability to disrupt redox homeostasis and cause protein misfolding in rat hippocampal astrocytes suggests its potential to promote astrocytic dysfunction and neurotoxicity.

PS 1853 Manganese-Containing Dithiocarbamates-Induced Cell Death via Senescence Pathway

C. Ta and S. Cheng. *Sciences, John Jay College of Criminal Justice, New York City, NY.*

Cells are constantly exposed to various stresses. Cellular senescence is an irreversible cell cycle arrest for cells in response to DNA damage, oxidative stress, or oncogenic activation. Cell cycle progression is controlled by various cellular signaling pathways. The status of protein redox condition is the decisive key of regulation of these signaling pathways. One of the regulators associated with the protein redox status is NF-kappa B. It has been suggested that activation of NF-kappa B signaling has a causal role in promoting senescence. Study from Cheng's group has demonstrated that manganese-containing dithiocarbamate pesticides, maneb (MB) and mancozeb (MZ), at 50 uM activate NF-kappa B cascade, which is partially in response to its potentiated effect on 1-methyl-4-phenylpyridium (MPP+)-induced cell death in rat pheochromocytoma (PC12) cells. This study was designed to reveal the involvement of cellular senescence in MB- and MZ- induced cell death. The indicator of senescence is based on β-galactosidase activity at pH 6 (senescence-associated β-Gal; SA-β-Gal), which is only present in senescent cells, and not seen in pre-senescent, quiescent, or immoral cells. The results show an increase of SA-β-Gal activity in PC12 treated with MB and MZ (10 uM, 20 uM, and 50 uM) after 4 hours treatment and 24 hours recovery as compared to phosphate buffered saline (PBS) treated PC12 cells. The increase of SA-β-Gal was more perceptible in PC12 cells treated with low dose (10 uM) of MB and MZ as compared to the cells treated with higher doses (20 uM and 50 uM). This study demonstrates that non-toxic doses of MB and MZ (10 uM) can trigger cell cycle arrest in order for cells to compromise the cellular repair or commit cellular apoptosis.

PS 1854 Decreased Gene Expression of Acetylcholine Receptors and Acetylcholinesterase in the Honeybee due to Imidacloprid Exposure

C. C. Byrnes and J. A. Roling. *Biology Department, Bridgewater State University, Bridgewater, MA.*

Imidacloprid is a pesticide highly toxic to the honeybee's nervous system. It is a potential cause for Colony Collapse Disorder (CCD), when honeybees abandon their queen and hive to die. The honeybee hive numbers have dropped 40-50% in the last year alone. Honeybees are the most effective insect pollinators therefore it is critical to prevent any future decline. In order to understand how imidacloprid affects honeybee nervous systems, honeybees were exposed to a sugar solution containing 0 ug/L, 0.2 ug/L, 20 ug/L, or 2,000 ug/L imidacloprid for five days in glass jars. RNA was extracted, cDNA synthesized, and Quantitative PCR (QPCR) performed on 25 genes. Seven genes successfully amplified in QPCR. Gene expression was measured for acetylcholinesterase (Ache)-1 and acetylcholine receptor (AchR) α3, α4, and β2. These genes were selected because imidacloprid is believed to bind to the AchR, but is unrecognized by Ache. Gene expression was compared to the internal housekeeping genes 18s rRNA and actin. Ache-1 gene expression was statistically different at 20 ug/L, but not at 2,000 ug/L. The decreased gene expression of Ache-1 indicates there is less enzyme to break down acetylcholine. However, an excess of acetylcholine would cause over stimulation in nerves. Due to the excess of acetylcholine in the synapse at the nerve, the honeybee is believed to counteract the condition by reducing the number of acetylcholine receptors. This was verified in the AchR α3, α4, and β2 when exposed to 20 ug/L. Gene expression of the AchR subunits decreased to 5.3, 3.5 and 3.9%; respectively when compared to the control bees. Genes will be cloned and more nervous system genes including LCCH3 analyzed to further understand the mechanism of imidacloprid.

PS 1855 Differential Expression of MAP-2 (Microtubule Associated Protein-2) Gene Transcripts in the Central Nervous System of Hens Treated with DFP (Diisopropyl Phosphorofluoridate)

T. V. Damodaran[1, 2] and M. B. Abou-Donia[2]. [1]*Biology, North Carolina Central University, Durham, NC and* [2]*Pharmacology and Cancer Biology, Duke University Medical Center, Durham, NC.*

Organophosphorus-ester induced delayed neurotoxicity (OPIDN) is a neurodegenerative disorder characterized by ataxia progressing to paralysis with a concomitant central and peripheral, distal axonapathy. Diisopropylphosphorofluoridate (DFP) produces OPIDN in the chicken that results in mild ataxia in 7–14 days and severe paralysis as the disease progresses with a single dose. White leghorn layer hens were treated with DFP (1.7 mg/kg, sc) after prophylactic treatment with atropine (1 mg/kg, sc) in normal saline and serine (1 mg/kg, sc) in dimethyl sulfoxide, with appropriate controls. The hens were euthanized at different time points such as 1, 2, 5, 10 and 20 days, and the tissues from cerebrum, midbrain, cerebellum brainstem and spinal cord were quickly dissected and frozen. MAP-2 has been shown to be closely associated with CaM Kinase II and several other proteins of cytoskeleton. We used northern blots to investigate MAP-2 mRNA levels, while beta actin and 18S RNA were used as controls. The results indicate differential gene expression pattern for MAP-2 mRNA transcripts for both spatial and temporal aspects. Highly susceptible tissues like brainstem and spinal cord showed differential down-regulation at early time points followed by up regulated levels at later time points. Cerebellum, being a moderately susceptible tissue showed moderate levels of alterations in the gene expression of MAP-2 transcripts. Cerebrum, being resistant tissue also showed differential expression pattern. Differential levels of MAP-2 transcript levels in various regions may indicate differential levels of abnormal phosphorylation/dephosphorylation in the DFP-treated brain tissues during the OPIDN development. This new data further validates for our recent findings about the role of cell death and cell survival pathways acting via abnormal phosphorylation of cytoskeletal proteins in the initiation and progression of OPIDN.

PS 1856 Comparative Study on Short- and Long-Term Behavioral Consequences of Organophosphate Exposure: Relationship to AChE mRNA Expression

C. Lopez-Granero[1, 2], D. Cardona[2], N. L. Parmalee[1], E. Gimenez[2], R. Lozano[2], J. Barril[3], M. Aschner[1], F. Sanchez-Santed[2] and F. Cañadas[2]. [1]*Albert Einstein College of Medicine, New York, NY,* [2]*Universidad de Almeria, Almeria, Spain and* [3]*Universidad Miguel Hernandez, Elche, Spain.*

Organophosphates (OPs) affect behavior via the inhibition of acetylcholinesterase (AChE). While the cognitive short-term effects may be directly attributed to this inhibition, the mechanisms that underlie the long-term cognitive effects of OPs remain controversial. Accordingly, two experiments were designed to compare the effects of OPs on cognition and to ascertain whether long-term OPs effects, analogous to their short-term effects, are AChE-dependent. A single subcutaneous dose of 250 mg/kg chlorpyrifos (CPF), 1.5 mg/kg diisopropylphosphorofluoridate (DFP) or 15 mg/kg parathion (PTN) was administered to male Wistar rats. Spatial learning was evaluated 72 h or 23 weeks after exposure (experiment 1 and 2, respectively). Brain soluble and membrane-bound AChE activity, synaptic AChE-S mRNA, read-through AChE-R mRNA and brain acylpeptide hydrolase (APH) activity (as alternative non-cholinergic target) were analyzed once behavioral testing was completed (17 and 37 weeks after OPs exposure). CPF treatment ($p < 0.05$) caused both short- and long-term statistically significant effects on spatial learning, while PTN treatment ($p \leq 0.06$) led only to short-term effects. Long-term exposure to CPF and DFP significantly decreased AChE-S and AChE-R mRNA, while in the PTN group only AChE-S mRNA levels were decreased ($p < 0.05$). However, after long-term OP exposure, soluble and membrane-bound AChE activity was indistinguishable from controls ($p < 0.05$). Finally, no changes were noted in brain APH activity in response to OPs. This study demonstrates long term effects of OPs on AChE-S and AChE-R mRNA in the absence of changes in AChE soluble and membrane-bound activity. Thus changes in AChE mRNA expression suggest non-catalytic properties of the AChE enzyme. Supported by GV07/158, PSI2011-26237 from Spain. Travel support provided by NIEHS ES R01 07331.

PS 1857 Chlorpryifos Disrupts Social Behavior in Adult Zebrafish

J. M. Bailey, A. N. Oliveri and E. D. Levin. *Integrated Toxicology and Environmental Health Program, Duke University Medical Center, Durham, NC.*

Background. Organophosphate pesticides, including chlorpyrifos (CPF), are used worldwide in agricultural and household settings, leading to extensive human exposure. Experimental rodent studies and epidemiological reports show that that CPF exposure can disrupt several domains of cognitive function. The effects of this compound on social and emotional behavioral are, however, more poorly characterized. Objective. Here, we utilize the emerging zebrafish model to characterize the social-emotional effects of acute adult exposure to CPF. Methods. Male and female adult zebrafish were exposed for 24 hours to three concentrations of CPF (0.1 μm, 0.25 μm, 0.6 μm) via submersion. CPF was dissolved in DMSO and added to 3L glass tanks (sealed during exposure) containing 1L of zebrafish home-tank water. After exposure, all fish were transferred to un-dosed water. Exposure to water containing an equivalent concentration of DMSO alone under the same conditions served as the control. Behavioral testing commenced after 3 hours in un-dosed water. An automated system of data collection was used in which swim speed, pattern and trajectory where calculated in real time (Noldus® EthoVision software). Experimental conditions (image and location of shoal stimuli) were also controlled via EthoVision, creating a moderate-high throughput system for analyzing behavioral endpoints. Results. CPF exposure disrupted behavior at doses that did not cause overt toxicity and that did not reduce overall swimming behavior. In a dose dependent fashion, CPF attenuated the typical shoaling response observed in unexposed animals. Conclusion. These data show that zebrafish can be a useful model for understanding social or emotional effects of neurotoxicants. Moreover, we demonstrated deleterious effects on subtle domains of behavior that occurred despite the lack of overt toxicity or motoric impairment.
(Research supported by the Superfund Research Program ES010356)

PS 1858 Neurotoxic Effects of Repeated Exposure to Low-Dose Chlorpyrifos in Rats

Y. S. Lee[1], J. A. Lewis[2], D. A. Jackson[2] and J. D. Stallings[2]. [1]*ORISE/USACEHR, Frederick, MD and* [2]*US Army Center for Environmental Health Research, Frederick, MD.*

Acute exposure to high-dose organophosphate (OP) pesticides, such as chlorpyrifos (CPF), has been known to compromise neurobehavioral functions, including learning, memory and visuospatial reasoning. Recent studies suggest even a low-dose exposure to OP pesticides may pose significant health and environmental risks to military and civilians alike. We used a rat exposure model to elucidate effects and mechanisms of subacute low-dose CPF exposures. Rats exposed to 10 mg/kg CPF for 21 days displayed reduced body weight gain, increased movement following cued fear conditioning testing, and cholinesterase inhibition. Differential gene expression analysis by RNA-seq revealed increased mRNA expression of neuropeptide (*Npy, Cort*) or neuropeptide-binding (*Crhbp*) genes in the hippocampus of CPF-exposed animals. *Bdnf,* a known regulator of synaptic plasticity and neuronal functions, was also up-regulated in the response to CPF exposure. It was demonstrated by immunohistochemistry that more neuronal cells expressed NPY and CRHBP proteins in the hippocampus of rats exposed to CPF compared to unexposed animals. MicroRNA expression analysis by small RNA-seq suggested that the miR-132/miR-212 cluster may play a role in CPF-induced neurotoxicity. Pathway analysis identified potential downstream effects of low-dose CPF: increased risk of seizures and neurite outgrowth, synaptic depression, coordination, fertility and body size. Our study results indicate that a low-dose CPF exposure can alter mRNA and protein expression of key regulators of neurobehavioral functions, and that these gene expression changes may be linked to neurobehavioral toxicity of CPF.
This research was supported in part by an appointment to the Postgraduate Research Participation Program at the USACEHR administered by the ORISE through an IAA between the US DOE and USAMRMC. Research was conducted in compliance with the Animal Welfare Act, and all other Federal requirements. The views expressed are those of the authors and do not constitute endorsement by the US Army.

PS 1859 Chlorpyrifos Oxon Primes Microglia: Enhanced LPS-Induced TNFα Production

S. Brookins, S. Levesque, C. McGraw, T. Taetzsch and M. L. Block. *Anatomy and Neurobiology, Virginia Commonwealth University, Richmond, VA.*

Persian Gulf War veterans suffering from Gulf War Illness (GWI) experience a wide range of chronic and debilitating symptoms including cognitive dysfunction, depression, anxiety, muscle pain, migraine, and fatigue. Increasing evidence implicates microglia, the resident innate immune cells in the brain, and neuroinflammation in symptoms associated with GWI. Current hypotheses predict that "multiple hits" from environmental exposures, such as the organophosphate pesticide Chlorpyrifos (CPF), combined with low grade inflammation may initiate exaggerated and persistent central nervous system (CNS) pathology to drive GWI. CPF-oxon is an active CPF metabolite linked to deleterious CNS effects, but little is currently known of the physiological mechanisms underlying the CNS dysfunction. To begin to address how CPF may impact microglia, cultures were treated

with CPF oxon (1μM-1nM) and microglial activation was assessed. CPF oxon treatment in HAPI microglial cells resulted in elevated 30 minute superoxide and 3 hour H_2O_2 production, with no initiation of 6 hour TNFα nor 24 hour nitrite production. However, combined treatment with CPF oxon (0.5μM) and lipopolysaccharide (LPS)(5ng/mL) resulted in synergistically amplified TNFα production in both microglia and neuron-glia cultures. These findings support that CPF oxon may activate microglia to produce reactive oxygen species and prime microglia to be sensitive to additional pro-inflammatory stimuli.

PS 1860 *In Utero* Chlorpyrifos Exposure Leads to Behavioral Deficits and Alterations in Hippocampal GABAergic Synaptic Transmission

R. D. Burke, J. D. Pescrille, J. Mamczarz, E. F. Periera and E. X. Albuquerque. *Epidemiology and Public Health, Div. of Translational Toxicology, University of MD Baltimore, Baltimore, MD.*

Epidemiological studies have reported that children exposed in utero to organophosphorus pesticides, including chlorpyrifos (CPF), present higher incidence of cognitive deficits, attention deficit/hyperactivity disorder, and autism spectrum disorders than non-exposed children. We have reported earlier that guinea pigs born to dams exposed during the last ten days of pregnancy to CPF (25 mg/kg/day, sc), a dose that causes no overt signs of maternal toxicity, present significant cognitive deficits in the Morris water maze (MWM). Because spatial learning in the MWM is hippocampal dependent and increased GABAergic activity induces cognitive deficits, we hypothesized that cognitive deficits induced by prenatal exposure to CPF correlate with increased GABAergic transmission in the CA1 field of the hippocampus. To test this hypothesis, we used the whole-cell patch-clamp technique to record inhibitory and excitatory postsynaptic currents (IPSCs and EPSCs) from CA1 pyramidal neurons in hippocampal slices obtained from behaviorally tested adult male guinea pigs that had been prenatally exposed to CPF or vehicle during the last 10 days in utero. Spontaneous and miniature IPSC frequencies were higher in CPF-exposed guinea pigs. The increased GABAergic activity correlated with cognitive deficits presented by the CPF-exposed animals tested in the MWM. Spontaneous and miniature EPSCs were comparable between treatment groups. In addition, western blotting of hippocampal protein extracts revealed that CPF exposure had no significant effect on the levels of markers of specific interneuron populations, suggesting that an increase in the number of interneurons is unlikely to account for the increased GABAergic transmission. It is conceivable that prenatal exposure to CPF leads to long-lasting disruption of neurotransmitter systems, such as the nicotinic cholinergic system, known to play a key role in the modulation of hippocampal GABAergic transmission and cognitive functioning.

PS 1861 Prenatal Exposure to Chlorpyrifos Leads to MAPK Dysfunction and Epigenetic Modifications in the Brain

S. W. Todd[1, 2], W. R. Randall[1], E. F. Pereira[2], J. D. Pescrille[2], J. Mamczarz[2] and E. X. Albuquerque[2]. *[1]Toxicology, University of Maryland, Baltimore, Baltimore, MD and [2]Epidemiology and Public Health, University of Maryland, Baltimore, Baltimore, MD.*

Chlorpyrifos (CPF) is a commonly used organophosphorous pesticide that inhibits the enzyme acetylcholinesterase. Prenatal exposure to CPF has been correlated to late onset IQ loss, attention deficits, hyperactivity and autism spectrum disorders. These delayed effects following exposure are suggestive of intracellular signaling abnormalities likely related to genomic expression. To test these hypotheses we exposed guinea pigs prenatally to CPF and examined pups for mitogen activated protein kinase (MAPK) dysfunction as well as changes in histone modification. Pregnant guinea pigs were injected subcutaneously once daily with 25 mg/kg CPF or peanut oil for the last 10 days of pregnancy. On postnatal day 37-42, pups were evaluated for spatial memory retention using the Morris water maze (MWM). After testing, guinea pigs were euthanized and their brains were excised and processed. Processed brains were used in western blotting to identify intracellular proteins involved in activating histone kinases and acetyltransferases. The kinase p38 is a primary activator of mitogen- and stress-activated kinase (MSK), which is a principle histone H3 kinase. The expression of p38 kinase was significantly higher in whole-brain extracts of CPF treated pups. The MSK protein was shown to be significantly activated within the hippocampus of treated pups as well, while other MAPKs are still being analyzed. Levels of acetylated and phosphorylated histone 3, 2A and 2B were found to be altered in hippocampal and striatal brain regions. Additionally, we see sex specific deficiencies in escape latency and distance traveled in MWM, indicating an impaired working memory. Our findings suggest that low-level exposure to CPF during early development produces changes in MAPK signaling consistent with epigenetic modifications of histones. This can subsequently lead to long-term changes in gene expression and deficits in cognition.

PS 1862 Fipronil Disposition in the Brain and Changes in the Serotoninergic System

M. R. Martínez-Larrañaga, M. A. Martínez, I. Ares, R. Pita, M. Martínez, V. Castellano, A. Romero, E. Ramos and A. Anadon. *Departamento de Toxicologia y Farmacologia, Universidad Complutense de Madrid, Madrid, Spain.*

Fipronil is a pesticide with widespread utility in control of agricultural and domestic pests including many lepidopteran species, thrips, locusts, ants, cockroaches, fleas, and ticks. In insects, fipronil is recognized to act as a potent blocker of the GABA-regulated chloride channel in CNS. In vivo mammalian studies indicate that primary metabolic pathway for fipronil involves oxidative formation of the sulfone metabolite. This metabolite was reported to be more toxic to insects, mammals, fish and birds than parent compound itself. Because fipronil is used in home applications, recent concerns for potential adverse public health effects (vomiting, agitation and seizures) were raised. The goals of this study were to determine disposition of fipronil and its sulfone metabolite in brain and to assess the relevance of the kinetic results with changes on serotoninergic neurochemistry induced by fipronil. Two experiments were carried out: (1) Male Wistar rats treated with fipronil (single dose 10 mg/kg, per os) were killed at different times after treatment and brain samples were collected to determine fipronil and fipronil sulfone levels by HPLC-MS; (2) male Wistar rats treated with fipronil (10 mg/kg, per os, 5 days) and with corn oil (control animals) were killed 24h after dosing and brain regions isolated and content of 5-HT and 5-HIAA quantified by HPLC-ED. Results showed fipronil was distributed into CNS. Fipronil absorbed rapidly and eliminated slowly from the brain. The Cmax of fipronil and fipronil sulfone was 0.457 and 0.856 μg/g. Fipronil significantly ($P<0.001$) decreased 5-HT levels in hypothalamus (-22%), frontal cortex (-35%), hippocampus (-40%) and striatum (-45%) respect to controls. These results suggest a link between fipronil effect on serotoninergic system and its specific levels of brain concentration. Work supported by projects Refs. GR35/10-A UCM-BSCH, S2009/AGR-1469 (CAM) and Consolider-Ingenio 2010 No.CSD2007-00063 (MEC), Madrid, Spain.

PS 1863 Triclopyr: Subchronic Neurotoxicity Study in Fisher F344 Rats

M. Corvaro[1], M. Aggarwal[1], A. K. Andrus[2], R. M. Golden[2], R. Hukkanen[2], S. Marty[2] and D. L. Eisenbrandt[3]. *[1]Dow Agrosciences, Milton, United Kingdom, [2]Toxicology & Environmental Research and Consulting;, The Dow Chemical Company, Midland, MI and [3]Dow AgroSciences LLC, Indianapolis, IN.*

Triclopyr is a pyridine-based herbicide used mainly on non-crop areas to control broadleaf weeds and woody plants. A subchronic neurotoxicity study in rats was conducted.
Four groups of F344/DuCrl rats (10 animals/sex/group) were exposed to Triclopyr technical at levels of 0, 5, 25, or 200 mg/kg/day via the dietary route for 90 days. Neurotoxicity was evaluated using a functional observational battery (FOB), determinations of grip performance, rectal temperature, landing foot splay, and an automated test of motor activity (pre-exposure, weeks 2, 4, 8, and 13). General health condition (clinical observations, body weights, and food consumption) were evaluated weekly; ophthalmic examinations were given pre- and post-exposure. At the end of the study, 5 animals/sex/group were perfused for histopathologic evaluation of the central and peripheral nervous system (control and high-dose groups).
The no-observed-effect level (NOEL) for general toxicity was 25 mg/kg/day in both sexes based on: A) treatment-related decrease in body weight and food consumption of the high-dose group, beginning at the Week 2 and persisting throughout the study; B) increased urination of high-dose animals, observed at week 8 and Week 13 in FOBs. This finding was considered a secondary effect, as kidney effects (including: functional changes such as decreased urine specific gravity and glucose in the urine; proximal tubules impairment) were identified at 20 – 250 mg/kg/day in a previous 13-week dietary toxicity study using F344/DuCrl rats.
The NOEL for Triclopyr neurotoxicity was 200 mg/kg/day in both sexes as there were no effects on any parameter that would suggest a neurotoxic effect, including the examination performed both during in life and post mortem portion of the study. These results are consistent with previous toxicity studies, which showed no treatment-related neurotoxic effects across species.

PS 1863a Effects Produced by Single and Repeated Dosages of Fipronil on the EEG of Long-Evans Rats

D. Lyke, K. L. McDaniel, V. C. Moser and D. W. Herr. *TAD/NB, US EPA, Durham, NC.*

We have previously reported that various classes of pesticides have different effects on the non-stimulus driven EEG after acute treatment, including fipronil (25 or 50 mg/kg) (Lyke *et al.*, *Toxicologist*, 2010, 2011, 2012, 2013). In this study, we

compared the effects of single and repeated treatment with fipronil on the EEG. Fipronil is a member of the phenylpyrazole class of compounds that inhibits GABA receptors. Pilot studies indicated that 6 hours post dosing was the time of peak effect for neurological signs. Dosages for repeated treatments were chosen based on weight loss, regain, and neurological signs during pilot studies. Adult male Long-Evans rats were implanted with epidural screw electrodes. After about 1 week recovery, single exposure animals were dosed for 2 days with 1 ml/kg corn oil vehicle and then tested to allow acclimation to the procedures. On the third day, animals were dosed with corn oil, 5, or 10 mg/kg fipronil and tested 6 h later. Animals in the repeated dosing group were dosed for 14 consecutive days with corn oil, 5, or 10 mg/kg/day fipronil. Transient weight loss and occasional tremors were observed in the high dosage group, but these effects resolved after about 1 week. On days 12 and 13, animals had EEG recorded prior to dosing. On day 14, the rats were dosed 6 h prior to testing. Single treatment with these lower dosages did not significantly alter the EEG. However, repeated dosing with 5 or 10 mg/kg/day resulted in increases in the amplitude of the Delta (34 and 30% respectively) and Theta bands (41, 47%), and the area of the Theta band (30, 39%) compared to control. The area of the Gamma band was decreased at 5 (20%) and 10 mg/kg/day (22%) when recorded between the visual and frontal cortex, compared to control. The data confirm that fipronil alters CNS activity as measured by EEG. Additionally, dosages that were ineffective with a single treatment produced significant changes with repeated dosing. *This is an abstract of a proposed presentation and does not necessarily reflect EPA policy.*

PS 1863b Changes in Rat Serum Bionindicators after Single or Repeated Dosages of Fipronil

D. W. Herr[1], D. Lyke[1], R. McMahen[3], M. Strynar[3], J. M. Hedge[2], K. L. McDaniel[1] and V. C. Moser[1]. *[1]TAD/NB, US EPA, Durham, NC, [2]ISTD, US EPA, Durham, NC and [3]NERL, US EPA, Durham, NC.*

Acute exposure to different classes of pesticides produces different patterns of changes in serum bioindicators (Herr *et al.*, *Toxicologist*, 2013). We now examined profiles of bioindicators after 1 or 14 treatments with 0, 5, or 10 mg/kg/day fipronil (po). Adult male Long-Evans rats were evaluated for EEG changes (Lyke *et al.*, *Toxicologist*, 2014), and were sacrificed after testing (6 h). There were no changes in serum ALT, AST, LDH, or SDH. Serum T3 decreased after 1 or 14 treatments (10 mg/kg). Serum T4 decreased after 1 (10 mg/kg) or 14 treatments (5, 10 mg/kg/day). Serum samples were processed by Myriad RBM (RodentMAP® and Rat MetabolicMAP®). One exposure produced changes in 4 of 73 analytes, while 14 treatments altered 8 different analytes. Biocrates AbsoluteIDQ™ p180 analysis of plasma showed changes in metabolites, and repeated dosing produced more effects. Increased serum levels of the fipronil sulfone metabolite, and decreased levels of fipronil, were found with 14 treatments vs. 1 exposure. Data show that repeated treatment with fipronil results in different patterns of bioindicators compared to a single exposure, and may reflect changes in involvement of biological pathways. *This is an abstract of a presentation and does not necessarily reflect EPA policy.*

PS 1863c Chronic, but Not Acute, Treatment of *Caenorhabditis elegans* with TouchDown Leads to Increased Oxidative Stress

R. A. Donaldson, R. Negga and V. A. Fitsanakis. *Biology, King College, Bristol, TN.*

The purpose of this study was to determine if chronic (24 h) or acute (30 min) exposure of *Caenorhabditis elegans* (*C elegans*) to TouchDown™ (TD), a glyphosate-containing herbicide, resulted in increased oxidative stress. To verify if the glutathione pathway was activated following chronic TD treatment, CL2166 worms were treated with TD. This *C elegans* strain has glutathione-*S*-transferase (GST) tagged with green fluorescent protein (GFP) resulting in increased fluorescence when GST::GFP translation is up-regulated. This is generally interpreted as elevated oxidative stress. A concentration-dependent increase in fluorescence compared to control worms (***$p<0.001$) was observed. This was not the case for CL2166 worms treated acutely. To determine the specific reactive oxygen species that may contribute to increased GST::GFP transcription and translation, synchronized populations of wild-type (N2) *C elegans* were exposed chronically or acutely to varying concentrations (LC_{25}, LC_{50}, LC_{75}) of TD. Following incubation, worms were further exposed to dihydroethidium, (DHE) to detect O^{2-}, or hydroxyl radical and peroxynitrite sensor (HPF; Life Technologies). DHE assays detected no statistically significant increase in O^{2-} in any treatment paradigm at any concentration. Chronic TD exposure following treatment with HPF showed no statistically significant increases in fluorescence compared to control when HPF was added 24 h post treatment. A concentration-dependent trend towards increased HPF fluorescence was observed, however, when HPF was added immediately following TD incubation. Conversely, worms treated acutely with TD showed a strong trend towards decreased hydroxyl radical production compared to controls. Taken together, these data support the hypothesis that chronic, but not acute, exposure leads to increased GST::GFP transcription and translation that may be due, in part, to the production of hydroxyl or peroxynitrite radicals. Furthermore, it is likely that this increased oxidative stress could be the mechanism through which previously observed neurodegeneration in *C elegans* occurs.

PS 1864 Application of Proteomics to Identify Deregulated Proteins Associated with Idiosyncratic Liver Toxicity in a Rat Model of LPS/Diclofenac Co-administration

S. Ramm[1], B. Morissey[2], C. Rooney[2], S. Pennington[2] and A. Mally[1]. *[1]Department of Toxicology, University of Wuerzburg, Wuerzburg, Germany and [2]UCD Conway Institute, University College Dublin, Dublin, Ireland.* Sponsor: W. Dekant.

There is increasing experimental and clinical evidence to suggest that non-drug related risk factors such as an underlying disease, bacterial or viral infection, may contribute to idiosyncratic drug reactions (IDR). In our previous work we found that combined treatment of rats with therapeutic doses of diclofenac (Dcl), a model drug associated with drug idiosyncrasy in patients, and bacterial endotoxin (LPS) resulted in severe hepatotoxicity. In this study, we used an integrated discovery to targeted LC-MS proteomics approach combined with multiplex ELISA to identify liver and plasma proteins modulated by LPS/Dcl treatment, which may be mechanistically linked to or serve as potential safety alerts for IDRs.
In the absence of hepatotoxicity, LPS alone caused a marked increase in the concentration of various cytokines and other putative danger signals such as CINC-1 and HMGB1 in plasma as well as significant changes in 19/49 in liver proteins and 3/15 plasma proteins analyzed by LC-MS. The most prominent effect of Dcl alone was a significant rise in T-kininogen-1, an acute phase protein previously suggested as a sensitive marker for drug-induced liver injury, in both liver and plasma. This effect and LPS-mediated cytokine release were amplified in the combined LPS/Dcl treatment group. In addition, depletion of plasma fibrinogen β and γ, consistent with the suspected contribution of the hemostatic system and increased fibrin deposition to IDRs, was observed in the co-treatment group. In contrast, several proteins previously suggested as liver biomarkers such as clusterin did not correlate well with liver injury in this model.
Taken together, our analyses revealed proteomic changes associated with IDRs in a rat model of LPS/Dcl co-administration.

PS 1865 The Use of microRNAs to Explore the Mechanisms of Phenobarbital-Mediated Toxicity in the Rat

M. Osborne[1], R. Currie[2], J. Wright[2] and N. J. Gooderham[1]. *[1]Imperial College London, London, United Kingdom and [2]Syngenta, Bracknell, United Kingdom.*

Phenobarbital (PB) is a prototypical hepatic drug-metabolism inducer, and a model tumour promoter in the rat. Recent publications have suggested that alterations in microRNAs (miRNAs) can enhance our understanding of the mechanisms of PB-mediated toxicity. MiRNAs are small non-coding RNAs that suppress gene expression by inhibiting translation or stimulating transcript degradation of complementary mRNAs, with single mRNAs often targeted by multiple miRNAs. This study explored miRNA expression profiles in the liver from male Fischer rats which had been administered either a tumour promoting dose of PB (1000ppm) or a non-tumour promoting dose (50ppm) in the diet for 1, 3, 7, 14, 28 or 90 days. Previous work identified miR-182 was significantly increased compared to control after 90 days treatment using microarray profiling (Koufaris et al., (2012). Toxicolog Sci. 128(2): 532-43). With quantitativePCR assays we have demonstrated that miR-182 was significantly increased from 7 days onwards, compared to controls. In addition we showed that a predicted target of miR-182, glycine N-methyltransferase (Gnmt), and a validated target, forkhead box transcription factor O1 (FoxO1), were significantly down-regulated by 1000ppm PB compared to controls, and had a significant inverse correlation with miR-182 across the 90 days treatment period. FoxO1 is known to be an inducer of genes involved in cell cycle arrest and apoptosis, and Gnmt is known to indirectly regulate gene methylation and therefore gene expression. Decreases in these mRNA targets were dose concordant with the PB-induced phenotypic effects, transient hyperplasia at 3 days treatment (significantly decreased FoxO1 but unchanged miR-182), and global DNA hypermethylation at 14 days treatment (significantly decreased Gnmt and increased miR-182). These data lend support to the notion that miRNA expression profiles can be used to explore PB-mediated liver toxicity, offer insights into potential underlying mechanisms, and suggest the importance of temporal regulation.

PS 1866 Performance and Standardized Threshold of Traditional Serum Biomarkers for Diagnosis and Prediction of DILI in Rats

Y. Tonomura, Y. Kato, H. Hanafusa, Y. Morikawa, K. Matsuyama, T. Uehara, M. Ueno and M. Torii. *Drug Developmental Research Laboratories, Shionogi & Co., Ltd., Toyonaka, Osaka, Japan.* Sponsor: K. Nakamura.

Drug induced-liver injury (DILI) is one of the major safety concerns in drug development. Alanine and aspartate aminotransferase (ALT and AST) and functional biomarkers such as bilirubin have been widely used for monitoring of DILI. However, in preclinical, the diagnostic thresholds of these biomarkers have not been standardized among different testing facilities, and the predictive performance for future onset of hepatic lesions remains unclear. Here, we analyzed the data of large-scale toxicogenomics database, TG-GATEs, in which male Sprague-Dawley rats (N = 5253) were treated with 143 compounds with positive or negative hepatotoxicity for 3, 7, 14 and 28 days. Receiver operating characteristic (ROC) analysis was applied to assessment of the diagnostic or predictive performance of these traditional biomarkers. The threshold was expressed as percentage compared to the control mean for consistent evaluation among different testing facilities. Additionally, area under ROC curve (ROC-AUC) that means accuracy of biomarker was calculated. Regarding all hepatic lesions, the thresholds of AST and ALT were 111 to 116% and 113 to 123% compared to the control mean, respectively, with relatively high accuracy (ROC-AUC was 0.83 to 0.91 and 0.72 to 0.86, respectively). Furthermore, focusing on hepatic necrosis improved the ROC-AUCs of AST and ALT (0.82 to 0.98 and 0.84 to 0.91, respectively) with the following threshold; 116 to 130% and 115 to 126%, respectively. Additionally, the diagnostic performance of AST and ALT was almost equal to that of combinatorial usage by logistic regression model. However, we could not confirm the sufficient predictive performance of future hepatic lesion by these biomarkers. In conclusion, the results provide the information that enables consistent evaluation of these biomarkers by the standardized diagnostic threshold, and suggest that the performance of these biomarkers is limited to diagnostic case of hepatic lesion rather than the prediction.

PS 1867 Tissue Factor Decryption Contributes to Coagulation Triggered by Fas-Induced Hepatocyte Apoptosis

J. P. Luyendyk[1], A. K. Kopec[1], N. Joshi[2], H. Cline[1], C. E. Rockwell[2] and M. Lopez[1]. [1]*Pathobiology and Diagnostic Investigation, Michigan State University, East Lansing, MI and* [2]*Pharmacology/Toxicology, Michigan State University, East Lansing, MI.*

Liver parenchymal cell (i.e., hepatocyte) apoptosis is associated with activation of the blood coagulation cascade. Emerging evidence suggests that coagulation cascade activation may be a mechanistic biomarker of morbidity in patients with acute liver injury. Hepatocytes have been shown to express tissue factor (TF), the primary activator of blood coagulation, in an encrypted form that lacks procoagulant activity. We hypothesized that induction of hepatocyte apoptosis by the Fas death receptor pathway increases the procoagulant activity of hepatocyte TF. Jo2 antibody-induced coagulation cascade activation was significantly reduced in mice with hepatocyte specific TF deficiency. Treatment of primary mouse hepatocytes with Jo2 induced apoptosis as indicated by cleavage of caspase-3 and increased exposure of phosphatidylserine (PS) on the cell surface. Jo2 treatment increased TF-dependent coagulation factor Xa generation by hepatocytes and triggered the release of procoagulant TF-positive microparticles into the culture medium. Pretreatment with a caspase-3 inhibitor reduced Jo2-induced TF activity and microparticle procoagulant activity. The high affinity PS-binding protein lactadherin significantly reduced Xa generation by Jo2-treated hepatocytes and abolished microparticle procoagulant activity. The results indicate that the mechanism of Fas-dependent hepatocyte TF activation involves caspase-3 activation and PS exposure on the cell surface. This suggests that increased (hepatocellular) TF procoagulant activity could contribute to the prothrombotic state associated with hepatocyte apoptosis in chronic liver disease.

PS 1868 Toxicogenomic Analysis of Liver Samples from Rats Treated with a Spleen Tyrosine Kinase Inhibitor Reveals No Enrichment in Liver Injury Ontologies Despite Transaminase Elevations

B. D. Jeffy, K. Ghoreishi, R. Magpantay and M. Breider. *Exploratory Toxicology, Celgene Corporation, San Diego, CA.*

Treatment of rats with either a spleen tyrosine kinase (SYK) inhibitor CC0485118 or acetaminophen led to an increase in serum ALT and AST levels. However, liver histopathology changes (centrilobular hepatocellular necrosis) were evident only in the acetaminophen-treated animals To determine the mechanism of transaminase elevations induced by CC0485118 in the absence of liver injury, toxicogenomic analysis was conducted using liver RNA from the rats treated with either acetaminophen or CC0485118. Pathways analysis of toxicogenomic data from acetaminophen-treated rats showed enrichment in a variety of hepatotoxicity ontologies as well as regulation of genes in antioxidant response pathways, consistent with the known mechanism of acetaminophen-induced centrilobular necrosis. Conversely, gene expression analysis from livers of CC0485118 treated animals did not identify enrichment in any pathways related to liver injury but rather showed regulation of the SREBP1-ATF4 transcription factor pathway, cholesterol and fatty acid biosynthesis, and immune response pathways. In-depth analysis of the gene expression changes caused by treatment with CC0485118 suggested that induction of SREBP1 in turn led to a transcriptional increase in ALT2 gene expression. Taken together, data obtained from this study showed that although serum levels of ALT and AST were induced by both acetaminophen and CC0485118, lack of liver injury toxicogenomic markers and no morphological evidence of hepatocellular necrosis, suggests that liver enzyme elevation in CC0485118 in rats is not related to liver injury.

PS 1869 MiRNA-Seq Analysis of Livers of Rats Exposed to Phenobarbital

M. Flores Torres[1], J. Wright[2], R. Currie[2] and N. J. Gooderham[1]. [1]*Surgery and Cancer, Imperial College London, London, United Kingdom and* [2]*Syngenta, Jeallot's Hill International Research Centre, Bracknell, United Kingdom.*

MicroRNAs (miRNAs) are short, non-protein coding RNAs. They regulate gene expression by either inhibiting translation or promoting mRNA degradation, and are involved in diverse physiological and pathological events. Previous data from our group (Koufaris et. al. *Toxicolog Sci*:128, 532, 2012) showed that phenobarbital (PB, a CAR activator), induces dysregulation of the hepatic miRNAome in rat livers. The liver miRNAome associated with PB induced CAR activation was explored at different doses and time points using high-throughput sequencing of small RNAs (miRNA-seq), a powerful tool for discovery and profiling of miRNA expression, providing a deeper understanding of molecular toxicology. Male Han Wistar rats were dosed with PB (50 or 1000 ppm) for 28 days, and sacrificed after 1, 3, and 28 days. Total RNA was isolated from frozen livers and library constructs were generated (TrueSeq smallRNA kit, Illumina). miRanalyzer V0.3 and DESeq were used for bioinformatics and statistical analysis. qPCR was used to validate the expression of miRNA families and potential gene targets. Around 200 miRNAs were detected per sample; for 50 ppm, only day 28 had 2 differentially expressed miRNAs, PB 1000 ppm, showed 3, 16, and 4 miRNAs differentially expressed at days 1, 3, and 28. Histopathological evaluation showed hepatocellular centrilobular hypertrophy at 7 and 28 days, consistent with the known enzyme induction effects of PB. miR-21 was upregulated after 3 days, suggesting PB mediated dysregulation of epithelial mesenchymal transition (EMT). However, miR-30b was also induced after 3 days, and the miR-200 family was induced after 28 days, both of which would act to counter the EMT dysregulation. Consequently these findings suggest activation of a homeostatic response in EMT control in response to PB treatment, in order to preserve the epithelial nature of hepatocytes. This miRNA-seq approach enables a more detailed exploration of miRNAs and their response to hepatotoxicants, such as PB, helping elucidate underlying pathway perturbations.

PS 1870 Aroclor 1260 Exposure Causes Steatohepatitis and Activates Hepatic Receptors in an Animal Model of Diet-Induced Obesity

B. Wahlang[1], M. Song[1], L. Al-Eryani[1], H. Clair[1], J. Guardiola[1], K. C. Falkner[1], R. A. Prough[2], J. C. States[3] and M. Cave[1, 4]. [1]*Department of Medicine/GI, University of Louisville, Louisville, KY,* [2]*Biochemistry, University of Louisville, Louisville, KY,* [3]*Pharmacology & Toxicology, University of Louisville, Louisville, KY and* [4]*Medicine, Robley Rex VAMC, Louisville, KY.*

Polychlorinated biphenyls (PCBs) are persistent organic pollutants associated with nonalcoholic fatty liver disease (NAFLD). We demonstrated that PCB 153 worsened diet-induced obesity (DIO) and hepatic steatosis in mice fed high fat diet (HFD). We evaluated the effects of a PCB mixture, Aroclor 1260 (Ar), in a mouse model of DIO. Male C57Bl/6 mice were fed control diet (CD) or HFD. Ar (20 mg/kg or 200 mg/kg in corn oil) was administered by oral gavage. Serum, liver and fat samples were taken for immunohistochemistry, RT-PCR, lipid analysis and adipocytokine measurements. Ar(20mg/kg) was selected for further studies in PXR-/- and CAR-/- models. In mice fed HFD, Ar co-exposures were associated with increased lean mass (20 mg/kg) and decreased body fat mass (200 mg/kg). Mice fed HFD developed hepatic steatosis but this was not affected by Ar co-exposures. Ar worsened liver necro-inflammation in mice fed HFD. AST and ALT were increased in HFD+Ar(20 mg/kg); inflammatory foci and cellular necrosis were observed histologically in HFD+Ar animals. Expression of pro-inflammatory hepatic TLR4 target genes, including IL-6 and TNFα, were increased in HFD+Ar(20 mg/kg). Plasma IL-6 and tPAI-1 levels were increased in HFD+Ar(20 mg/kg). Hepatic gene expression of P450s including Cyp3a11 (Pregnane-Xenobiotic Receptor target) and Cyp2b10 (Constitutive Androstane Receptor target) was upregulated by Ar exposure in both CD and HFD-fed mice. Cyp1a2 (Aryl hydrocarbon Receptor target) was upregulated only in groups exposed to Ar(200 mg/kg). Aroclor 1260 worsened hepatic and systemic inflammation in the DIO model of NAFLD. These effects may be driven by dose and congener-dependent receptor activation. Environmental pollution may be a relevant "second hit" in the transformation of steatosis to steatohepatitis.

PS 1871 Secretome and Intracellular Metabolomics Analysis in HepG2 Cells after Exposure to Liver Toxicants

T. Ramirez[1], W. Mellert[1], A. Strigun[2], H. Kamp[1], T. Walk[2], L. Ralf[2] and B. van Ravenzwaay[1]. [1]*Toxicology, BASF SE, Ludwigshafen/Rhein, Germany and* [2]*metanomics, Berlin, Germany.*

The use of alternatives to animal testing has considerably increased in the last years, in addition to their major contribution to animal welfare, they open the possibility to better understand and explore the mechanisms underlying toxicity. New technologies, such as transcriptomics, proteomics and metabolomics provide the opportunity to obtain comprehensive information about the toxicological mode of action of compounds being in commerce and most importantly for compounds under development. The combination of in vitro systems coped to metabolomics not only enables the acquisition of quantitative information about the multi-parametric metabolic response of the cellular systems in normal and patho-physiological conditions, but also represents a major steps towards non-animal alternatives in toxicology. Herein, we report on our achievements on metabolomics coped to a liver in vitro model, 1) a highly stable method that can be reproducible along time, 2) the capacity to evaluate targeted metabolomics from cell secretome (>100 metabolites) and intracellular (>200 metabolites), 3) the identification of three liver toxicity modes of action; peroxisome proliferators, liver enzyme inductors and general liver toxicants. These data are the basis to broaden the use of metabolomics not only to identify other modes of action apart from liver toxicity, but also to use other in vitro models with the final aim to better elucidate the cellular changes/responses during toxicity

PS 1872 A Physiologically Relevant 3D Cell Culture Model for Hepatotoxic Studies

L. Price[4, 1], S. Ramaiahgari[1], M. den Braver[2], V. Terpstra[3], M. Coonen[5], D. Jennen[5], B. Herpers[4], J. N. Commandeur[2], J. H. van Delft[5] and B. van de Water[1]. [1]*Division of Toxicology, LACDR, Leiden, Netherlands,* [2]*Division of Molecular Toxicology, AIMS, Vrije University Amsterdam, Amsterdam, Netherlands,* [3]*Department of Pathology, Bronovo Hospital, The Hague, Netherlands,* [4]*OcellO, Leiden, Netherlands and* [5]*Department of Toxicogenomics, Maastricht University, Maastricht, Netherlands.*

In 2D culture, HepG2 cells have low expression of metabolic enzymes and drug transporters, which will compromise the validity of their use in safety assessment. Here we have developed a 3D cell culture model for the assessment of hepatoxicity. We cultured HepG2 cells in an extracellular matrix protein gel to establish 3D spheroid cultures resembling the in vivo architecture. There was a robust induction of morphological and functional differentiation, with a strong induction of metabolic enzymes and transporters, many of which are poorly expressed in monolayer cultures. Synthetic fluorescent bile acid analogue was used to determine biliary uptake and presence of bile canaliculi. HPLC analysis of testosterone metabolites revealed increased metabolic capacity. Microarray and QPCR analysis was performed to assess liver specific functions and Ingenuity pathway analysis (IPA) software was used to analyze gene expression data and study interaction of biological pathways. Comparative gene expression analysis of our 3D HepG2 cell culture model revealed its close resemblance to human liver gene expression at pathway level. Unlike primary hepatocytes in 2D culture, the metabolic competence of HepG2 in 3D could be retained for up to 4 weeks, making chronic exposures feasible. Toxicity assessment studies on this 3D model showed an increased sensitivity in identifying several hepatotoxic compounds. The assay is implemented in a 384 well format for low cost and increased throughput and represents a novel and more physiologically relevant method for assessing drug-induced liver toxicity.

PS 1873 Modified High-Content Imaging Micropatterned Hepatocyte Coculture Model for Predictive Toxicology

O. Trask[1], A. Moore[2], M. E. Andersen[1] and E. LeCluyse[1]. [1]*Institute for Chemical Safety Sciences, The Hamner Institutes for Health Sciences, Research Triangle Park, NC and* [2]*Hepregen Corporation, Medford, MA.*

Current in vitro hepatic models that have been used to identify drug- or chemical-induced hepatotoxicity, including HepG2, iPSC-derived, or primary hepatocytes, have intrinsic challenges, such as variable metabolic capacity, brief ex vivo life span in culture, and difficulties associated with measuring data reproducibly at the single cell level with standard automated microscopy HCS systems. In this study we utilized a micropatterned primary hepatocyte co-culture model as an enhanced approach to address the shortcomings of the current model systems for evaluation of in vitro hepatotoxicity using quantitative high content imaging. This co-culture model consists of primary hepatocytes that are micropatterned to form a discrete micro-architecture or "hepatocyte islands" surrounded by supporting fibroblasts resulting in extended life and metabolic function. Multiple HCS image capture and image analysis strategies were used to demonstrate methods to interrogate various 2D/3D morphometric parametric features such as size, shape, and intensity at the hepatocyte island or at the single cell level. Using this approach, subpopulations of both fibroblast stromal cells and hepatocytes were identified that exhibited modification in nuclear feature parameters, degradation of cell membrane, changes in mitochondria function, and mitochondria induced apoptosis using known positive control reference compounds (valinomycin and rotenone), negative control compounds (acetylcholine) and generating an 8-point concentration-response curve over 5 days in culture. Subpopulation analysis of the co-culture model showed compound-specific susceptibility in subpopulations of either stromal cells or hepatocytes. Our data clearly demonstrate that the micropatterned co-culture system is amendable for high content imaging and screening applications and provides a unique advantage over existing in vitro cell models for studying hepatotoxicity over prolonged periods of time.

PS 1874 Abnormal Immune Response to Antigen Challenge in Subjects with Alcoholic Cirrhosis: Baseline Data from the Zinc in Alcoholic Cirrhosis (ZAC) Trial

M. Mohammad[1], K. C. Falkner[1], S. Barve[1], Z. Zhou[2], C. McClain[1, 3] and M. Cave[1, 3]. [1]*Department of Medicine/GI, University of Louisville, Louisville, KY,* [2]*Nutrition, UNC-Greensboro, Greensboro, NC and* [3]*Robley Rex VAMC, Louisville, KY.*

Immune dysfunction contributes to liver disease progression and infection risk in alcoholic cirrhosis (AC). The purpose of the study is to better characterize liver injury biomarkers, adipokines, and immune function in subjects enrolled in a placebo-controlled, clinical trial of zinc sulfate for alcoholic cirrhosis (ZAC).
Baseline data of 17 consenting subjects with AC were compared to 8 non-drinking, healthy controls. Plasma adipokines and whole blood ex vivo lipopolysacharide-stimulated (LPS) and phytohemagglutinin-stimulated (PHA) cytokine production were measured by Luminex. Plasma cytokeratin 18 (CK18, M30 and M65) were measured by ELISA. Differences between the means (AC vs. controls) were evaluated by t-test using and statistical significance was set at $p<0.05$. The mean age (55.0±10.1 years) and BMI (26.2±3.9 kg/m2) in AC were similar to controls. Mean plasma CK18 M30 and M65 were increased in AC compared to controls ($p<0.05$). Mean insulin levels were increased in AC ($p<0.05$) while mean glucose levels were similar. There were non-significant trends towards higher adiponectin, leptin, PAI-1, and resistin in AC. Un-stimulated whole blood ex vivo production of IL-6, IL-8, IL-10, and TNF-α were increased in AC ($p<0.05$). Mean

LPS-stimulated cytokine production of IL-1β, IL-2, IL-4, IL-6, IL-10, IL-17a, TNF-α, MCP-1, and IFN-γ were not significantly different between groups. Mean PHA-stimulated cytokine production of IL-1β, IL-6, IL-10, and TNF-α were significantly decreased in AC ($p<0.05$). The 17 subjects had increased CK18, insulin resistance, and immune dysfunction. Un-stimulated IL-6, 8, 10 and TNF-α were increased in AC. LPS stimulation induced cytokine production to a similar degree in AC and controls indicating an absence of priming in AC. PHA stimulation failed to induce production of IL-1β, IL-6, IL-10, and TNF-α in AC, but not controls, suggesting abnormal T-cell function.

PS 1875 Combining Two High-Content Screening Approaches Measuring Phospholipidosis and Lysosomal Trapping with *In Silico* Modelling Approaches to Predict Phopholipidosis Occurrence in Humans

P. A. Walker, C. Bauch, S. Ellis, H. Woodhouse and C. Dilworth. *Cyprotex, Maccelsfield, United Kingdom.* Sponsor: C. Strock.

Phospholipidosis (PLD) is a lysosomal storage disorder characterised by excessive accumulation of intracellular phospholipids in tissues, such as the liver, kidney, brain and lung. It is well established that a large number of cationic amphiphilic drugs (CADs) have the potential to induce PLD. Phospholipids can accumulate in lysosomes, which are essential organelles in cellular biogenesis and when compromised could lead to cellular toxicity. Drug accumulation in lysosomes (lysosomotropism) is a direct mechanism known to result in PLD, however PLD can also occur indirectly by altering synthesis and processing of phospholipids. In this study fifty-six compounds (twenty-eight known to cause PLD in vivo, twenty-five not known to cause PLD in vivo and three compounds known to cause PLD specifically in the rat kidney.
In silico models based on physico-chemical properties can be used to predict in vivo PLD such as the Ploemen model (sensitivity 75%, specificity 86%, accuracy of 86%), here we show how the prediction of PLD in vivo can be improved by combining in silico models with two different high content screening (HCS) assays used to determine the accumulation of a PLD dye in vitro or the trapping of compounds within lysosomes (and exclusion of a lysosomal dye). We evaluated two cellular models HepG2 and H9c2 cells and show that HepG2 cells are more predictive than H9c2 cells with an accuracy of 91% and 80% respectively. On combining in silico and HCS in vitro approaches a sensitivity of 96%, specificity of 93% and an overall accuracy of 95% in predicting in vivo PLD was achieved.
These results demonstrate the applicability of in vitro and in silico approaches to understand the mechanism underlying PLD and the utility of these approaches as useful screening tools in the pharmaceutical industry for the selection of drug candidates with a low liability of PLD.

PS 1876 A Long-Term Perfused Immune-Liver Coculture System to Model Antituberculosis Efficacy and Drug-Induced Liver Injury

T. Gumbo[1], S. Shuford[2], S. Srivastava[1], C. Sherman[1], A. Dasgupta[3], D. Orr[2] and H. E. Crosswell[2]. [1]*Office of Global Health, University of Texas Southwestern, Dallas, TX,* [2]*KIYATEC, Greenville, SC and* [3]*Alternative Cellular Therapeutics, Marietta, GA.*

Pyrazinamide (PZA) is active in adult tuberculosis (TB) and can cause DILI. Meta-analysis of >13,000 patients on PZA suggest a non-dose dependent DILI mechanism. Novel 3D cultures approximate biology better than 2D. 3D perfusion systems may better mimic human pharmacokinetics (PK) and pharmacodynamics (PD) of drugs over time. To determine whether PZA DILI is dose dependent, we combined our hollow fiber system (HFS) TB model with a 3D perfused liver model to develop a dynamic PK/PD assessment of PZ activity. The 3DKUBE™(KIYATEC) HepG2 liver/fibroblast co-culture model (KIYATEC) was retrofitted into the HFS with Mycobacterium tuberculosis-infected THP-1 MPs and cultured for 28 days. The TB/ MP-Liver systems were exposed to 5 concentrations of PZA or controls [media (-); APAP (+)], with a 6 hour t1/2 to mimic pediatric PK. Viability, aspartate transaminase (AST), alanine transaminase (ALT) and lactate dehydrogenase (LDH), were measured weekly. HepG2 show a 4-fold increase in CYP3A4 expression of in perfused 3D co-culture as compared with 2D monolayer. PZA and APAP(t1/2) did not increase macrophage cell death. Drug accounted for 30% of the variance ($p=0.035$) of LFTS, driven by APAP versus negative control. The fold-change of AST, ALT, and LDH for negative controls versus APAP was 1.5±0.2 v. 2.1±0.3, 1.0±0.5 v. 3.0±1.4, and 0.3±0.1 v. 4.4±3.5, respectively. There was only weak PZA dose-response based on changes in LFTs, with an r2=0.21 (AST) and r2=0.32 (ALT), with decrease in AST and ALT changes as PZA dose increased. There was no convergence for LDH. There was no apparent increase in DILI with increase in PZA dose. Conclusion: Despite HepG2 limitations, a 3DKUBE HepG2 liver model exposed to human-like PKs in the HFS demonstrated increased LFTs with APAP, but no dose dependent DILI for PZA, similar to clinical findings. This system may be useful for identifying novel drugs with reduced toxicity in multi-drug TB.

PS 1877 Accelerated Cytotoxicity Mechanism Screening of Flutamide in Isolated Rat Hepatocytes

A. Maruf[1] and P. J. O'Brien[1, 2]. [1]*Pharmacology & Toxicology, University of Toronto, Toronto, ON, Canada and* [2]*Faculty of Pharmacy, University of Toronto, Toronto, ON, Canada.*

Flutamide (FLU) is a competitive antagonist of the androgen receptor which has been used in the treatment of metastatic prostatic cancer. FLU was reported to induce severe liver injury in some patients. The most common liver pathology was hepatic necrosis and cholestasis. The potential molecular cytotoxic mechanisms of FLU towards isolated male Sprague Dawley rat hepatocytes were investigated in this study using "Accelerated Cytotoxicity Mechanism Screening" (ACMS) techniques. A concentration-dependent increase in cytotoxicity, reactive oxygen species (ROS) formation and a decrease in % mitochondrial membrane potential was observed for FLU compared to control hepatocytes. We hypothesized that FLU produced hepatic necrosis through reactive metabolite(s) and ROS formation. Incubation of isolated hepatocytes for 2 hr with 75 μM flutamide induced an approximate 50% loss in hepatocyte viability (LC50, according to ACMS). A significant increase in FLU cytotoxicity and ROS formation was observed when glutathione (GSH) depleted hepatocytes were used and this toxicity was reversed by the addition of N-Acetyl-l-cysteine (a GSH precursor). Nontoxic concentrations of1-aminobenzotriazole (non-selective cytochorome P450 inhibitor), ketoconazole (a CYP3A inhibitor), α-napthoflavone (a CYP1A1/2 inhibitor) and menadione (an aldehyde oxidase inhibitor) significantly decreased FLU-induced cytotoxicity suggesting the involvement of cytochrome P450 and aldehyde oxidase catalyzed reactive metabolite(s) formation. Previous studies also found that rat and human microsomal cytochrome P450 oxidatively metabolized flutamide into electrophilic metabolite(s). TEMPOL (4-hydroxy-2,2,6,6-tetramethylpiperidin-1-oxyl), a known ROS scavenger and superoxide dismutase mimic, prevented hepatocyte death. DPPD (N,N'-diphenyl-1,4-phenylenediamine) also reversed toxicity caused by FLU. From the data that we obtained till date, it can be suggested that FLU caused reactive metabolite(s) and ROS formation leading to oxidative stress and mitochondrial injury.

PS 1878 A Novel Mouse Model for Phenytoin-Induced Liver Injury: Involvement of Immune-Related Factors and P450-Mediated Metabolism

E. Sasaki[1], K. Tsuneyama[2], T. Fukami[1], M. Nakajima[1] and T. Yokoi[1, 3]. [1]*Graduate School of Medical Science, Kanazawa University, Kanazawa, Ishikawa, Japan,* [2]*Graduate School of Medicine and Pharmaceutical Science for Research, University of Toyama, Toyama, Toyama, Japan and* [3]*Department of Drug Safety Sciences, Nagoya University Graduate School of Medicine, Nagoya, Aichi, Japan.*

Drug-induced liver injury is a major issue for drug development and clinical drug therapy; however, in most cases, it is difficult to predict or prevent these reactions due to a lack of proper animal models and unknown mechanisms of action. Phenytoin (DPH) is an anticonvulsant drug that is widely used for the treatment of epilepsy. Some patients who are administered DPH will suffer symptoms of drug-induced liver injury characterized by hepatic necrosis. However mechanism under the developing DPH-induced liver injury is largely unknown. In this study, we established a mouse model for DPH-induced liver injury and analyzed the mechanisms for hepatotoxicity in the presence of immune- or inflammation-related factors and metabolic activation. Female C57BL/6 mice were administered DPH for 5 days in combination with L-buthionine-S,R-sulfoximine (BSO) to deplete hepatic GSH contents. As a result, plasma alanine aminotransferase (ALT) levels were increased, hepatic lesions were observed during histological evaluations, hepatic glutathione levels were significantly reduced and oxidative stress marker levels were significantly increased. Inhibition of cytochrome P450-dependent oxidative metabolism significantly suppressed elevated plasma ALT levels and depleted hepatic glutathione levels. Among the innate immune factors, hepatic mRNA levels of NACHT, LRR, pyrin domains-containing protein 3, interleukin (IL)-1β, and damage-associated molecular patterns were significantly increased. In the adaptive immune response, Th17 cells-mediated inflammation was suggested. In conclusion, cytochrome P450-dependent metabolic activation followed by a stimulation of innate immune responses and IL-17-mediated inflammation are involved in DPH-induced liver injury.

PS 1879 An Environmental 2nd Hit: Effect of Vinyl Chloride Exposure on Liver Injury in Experimental Hepatotoxicity and in Humans

L. Anders[1], A. Douglas[1], J. Guardiola[1], V. L. Massey[1], I. Kirpich[2], M. Mohammad[2], K. C. Falkner[2], M. Cave[2, 3], C. McClain[2, 3] and J. Beier[1]. [1]*Pharmacology & Toxicology, University of Louisville, Louisville, KY,* [2]*Department of Medicine/GI, University of Louisville, Louisville, KY and* [3]*Robley Rex VAMC, Louisville, KY.*

Vinyl chloride (VC) is a ubiquitous environmental contaminant and ranks 4th on the ATSDR Hazardous Substances Priority List. We have previously reported increased hepatocellular necrosis in a highly exposed occupational cohort and in vitro models. The purpose of this study is to study hepatic injury in vivo and assess potential liver damage in a residential cohort of human subjects living adjacent to a VC chemical plant. C57Bl/6J mice received chloroethanol (ClEtOH), a major metabolite of VC, and lipopolysaccharide (LPS) 24 h after ClEtOH. Samples were harvested for determination of liver damage, inflammation and changes in carbohydrate and lipid metabolism. Apoptosis and necrosis biomarkers were measured in human serum. In mice, ClEtOH alone caused no detectable liver damage. LPS exposure caused oxidative stress, lipid accumulation and inflammation, which was exacerbated by ClEtOH preexposure. ClEtOH increased activation of recruited and resident monocytes as well as neutrophils and was coupled with an increase in transaminases over LPS alone, an increase in necroinflammatory foci and an increase in free fatty acids. The combination of ClEtOH and LPS decreased TUNEL-positive cells, suggesting a switch to necrotic cell death. Human subjects exposed to VC had elevated CK18 M65>M30 consistent with necrotic hepatocellular death, similar to the animal model. Taken together, ClEtOH sensitizes the liver to a "second hit." Chronic low-level environmental exposures increased hepatocellular necrosis in this cohort of residents. This serves as proof-of-concept that VC hepatotoxicity may be modified by endotoxemia, which commonly occurs in diet-induced obesity and NAFLD. These data implicate exposure to VC in the development of liver disease in susceptible populations.

PS 1880 Towards a Human 3D Biomimetic Liver Construct for the Investigation of Immune-Mediated Damage to Human "Sentinel" Biosensing Hepatocytes for Physiology and Predicting Toxicology

N. Senutovitch[1, 2], L. A. Vernetti[1, 2], A. Gough[1, 2], R. DeBiasio[1], T. Shun[1], A. Bakan[2, 1] and D. L. Taylor[1, 2]. [1]*Drug Discovery Institute, University of Pittsburgh, Pittsburgh, PA and* [2]*Computational and Systems Biology, University of Pittsburgh, Pittsburgh, PA.*

The early identification of drug induced human hepatotoxicity is essential to improve the safety of new drugs and to decrease the time and cost of development. To address this need, a 3D human liver sinusoidal unit and co-culture models were developed with endothelial cells to support human primary hepatocytes, stellate cells and immune responsive macrophages. Genetically encoded sub-sets of sentinel cell hepatocytes and stellate cells with fluorescence based biosensors provide live cell read-outs of key toxicity pathways such as ROS generation, mitochondrial function, apoptosis and immune-mediated cell damage. Sentinel cells include fresh and cryopreserved primary human hepatocytes, fetal hepatocytes, stem cell derived hepatocytes, HepG2 cells and LX-2 stellate cells. We have maintained and demonstrated: (a) response of the sentinel cells to hepatotoxic compounds up to 21 days in co-cultures of hepatocytes and endothelial cells; (b) testosterone metabolism in co-cultures for up to 21 days; (c) demonstrated hepatocytes with encoded biosensors will appropriately respond and then recover from sub-lethal concentrations of the oxidative stress and (d) show a gradual decrease in the intensity of mitochondrial function biosensor sentinel cells when monitored by daily high content screening in hepatocytes chronically treated with low concentrations of nefazodone. Finally, incorporation of human macrophages into a liver sinusoidal model showed LPS but not trovafloxacin induced release of TNF-alpha. In concordance with known immune-mediated liver toxicity, LPS and trovafloxacin but not LPS and levofloxacin or LPS and caffeine were shown to induce cytotoxicity in hepatocytes. Work is supported by NIH/NCATS grant 5UH2TR000503-02 and this is collaboration with the Martin Yarmush laboratory at the Center for Engineering in Medicine at Massachusetts General Hospital.

PS 1881 Dissecting Toxicity Mechanisms in Induced Pluripotent Stem Cell-Derived Hepatocytes and Hepatic Cell Lines

M. Liljevald[1], A. Sjögren[2], G. Brolén[3], J. Sagemark[1], X. Li[2], A. Jonebring[3], I. Cotgreave[1], B. Glinghammar[1] and T. B. Andersson[2]. [1]*Discovery Safety, AstraZeneca, Mölndal, Sweden,* [2]*DMPK RIA iMED, AstraZeneca, Mölndal, Sweden and* [3]*Discovery Sciences, RAD, AstraZeneca, Mölndal, Sweden.*

There is a huge interest in drug discovery research to use hepatocytes generated from human induced pluripotent stem cells (hiPSC) as an *in vitro* model to predict liver toxicity. However, little is known about the toxicity machinery in such cells. Therefore, we decided to shed light on this issue. We generated hiPSC by reprogramming human foreskin fibroblasts with modified mRNA (encoding OCT4, KLF4, SOX2, LIN28 and c-MYC), adopted them to grow as single cells in a monolayer and differentiated them into hepatocyte-like cells (hiPSC-Hep). The hiPSC-Hep expressed hepatic proteins and exhibited cytochrome P450 enzyme activity. Next, we compared the toxic response in hiPSC-hep, the hepatic cell lines HepaRG and Huh7, and cryopreserved primary human hepatocytes (cryo-hHep). Staurosporine decreased ATP levels in all cell types, but to a less extent in Huh7. Similarly, staurosporine activated caspases 3 and 7 in all cell types, but to a less extent in Huh7. Further, qRT-PCR analysis of a panel of genes important for apoptosis regulation and execution, followed by hierarchical clustering, showed that the cryo-hHep (three donors) were closer to each other than to any of the other cell types. A pathway enrichment analysis identified hiPSC-Hep as the cell type closest to cryo-hHep for several important apoptotic pathways. Next, the cells were treated with acetaminophen. The ATP response and activation of caspase 3 and 7 in the different cell types indicate that acetaminophen induced apoptosis in hiPSC-Hep, HepaRG and Huh7, but necrosis in cryo-hHep. Our study is an important contribution to the understanding of the toxicity machinery in hiPSC-Hep, which is crucial in order to evaluate their usefulness as an *in vitro* toxicity model.

PS 1882 Trovafloxacin Potentiates Lipopolysaccharide-Induced Tumor Necrosis Factor Release in RAW Cells in an ERK-Dependent Manner

K. L. Poulsen[1, 2], R. P. Albee[1], P. E. Ganey[1, 2] and R. A. Roth[1, 2]. [1]*Pharmacology and Toxicology, Michigan State University, East Lansing, MI and* [2]*Center for Integrative Toxicology, Michigan State University, East Lansing, MI.*

Trovafloxacin (TVX) is a fluoroquinolone antibiotic known to cause idiosyncratic drug-induced liver injury (IDILI) in humans. The mechanism underlying this toxicity remains unknown. An animal model of IDILI in mice revealed that TVX synergizes with inflammatory stress from bacterial lipopolysaccharide (LPS) to produce an hepatotoxic interaction that requires prolongation of the appearance of tumor necrosis factor-alpha (TNF) in the plasma. A model of TVX/LPS cotreatment was established in RAW 264.7 cells acting as a surrogate for TNF-releasing cells in vivo. Pretreating cells with TVX for two hours increased LPS-induced TNF protein release into culture medium in a concentration- and time-dependent manner. During the pretreatment period, TVX increased TNF mRNA, but this was less apparent after LPS addition, suggesting that the pivotal signaling events occurred during TVX pretreatment. TVX significantly increased TNF mRNA in part by increasing mRNA stability. ERK 1/2 (ERK) signaling can increase TNF mRNA transcription and stability, and this possibility was evaluated. Indeed, one hour of TVX exposure increased phosphorylation of ERK. An ERK-selective activation inhibitor, U0126, prevented ERK phosphorylation and abolished the TVX-mediated increase in TNF mRNA; however, it only decreased the early (<30 min) but not the later TVX-mediated increase in TNF mRNA stability. U0126 prevented the TVX-mediated increase in TNF protein release after LPS. These results demonstrated that TVX pretreatment of RAW cells increased TNF mRNA and enhanced LPS-induced TNF release in an ERK-dependent manner. (Supported by NIH grant R01 DK061315 and T32 ES007255.)

PS 1883 Early Identification of Clinically Relevant Drug Interactions with the Human Bile Salt Export Pump (BSEP; ABCB11)

P. Artursson[1], J. M. Pedersen[3, 1], P. Matsson[1], C. A. Bergström[1], J. Hoogstraate[2], A. Noren[1] and E. LeCluyse[3]. [1]*Uppsala University, Uppsala, Sweden,* [2]*Acturum Life Science AB, Sodertalje, Sweden and* [3]*The Hamner Institutes of Health Sciences, Research Triangle Park, NC.*

BSEP inhibition has been proposed as a contributor to drug induced liver injury (DILI). In this study we performed a detailed analysis of the role that BSEP inhibition plays in DILI and to what extent it can be used to predict DILI.
Inverted membrane vesicles and sandwich cultured human hepatocytes (SCHH) were used to determine the influence of drugs on BSEP-mediated taurocholate (TA) transport. The clinical impact of BSEP inhibition was evaluated by associ-

ating BSEP inhibition to the severity of drug induced liver injury DILI warnings in drug labels issued by the FDA. In addition, a structure activity model that correctly predicted 82 and 94% of inhibitors and non-inhibitors, respectively, was developed. A dataset of 250 compounds was screened for BSEP inhibition in membrane vesicles, and 86 BSEP inhibitors were identified. Structure-activity modeling identified BSEP inhibition to correlate strongly with compound lipophilicity, while positive molecular charge was associated with lack of inhibition. All approved drugs in the dataset (n=182) were categorized according to DILI warnings in drug labels issued by the FDA and a strong correlation between BSEP inhibition and DILI was identified. Among the approved drugs as many as 38 of the 61 (62%) identified BSEP inhibitors were associated with severe DILI and every second drug associated with severe DILI was a BSEP inhibitor. This is twice the levels observed for BSEP non-inhibitors. Results from SCHH show that BSEP inhibitors associated with severe DILI greatly reduced the canalicular efflux of TA, while BSEP inhibitors without the association to severe DILI did not.
BSEP inhibition in membrane vesicles was found to correlate to DILI severity, and altered disposition of TA in SCHH was shown to distinguish BSEP inhibitors associated with severe DILI from those with no or mild DILI.

PS 1884 Developmental Exposure to Bisphenol A (BPA) Induces Hepatic Lipid Accumulation Mediated through Nrf2 Activation

P. Shimpi[1], B. Rubin[2] and A. L. Slitt[1]. [1]*University of Rhode Island, Kingston, RI and* [2]*Sackler School of Graduate Biomedical Sciences, Tufts University, Boston, MA.*

BPA is a component present in some plastics, dental sealants, and thermal receipts. Urinary BPA levels have been positively associated with obesity in recent human studies. Rodent studies have also demonstrated that developmental BPA exposure can increase body weight and hepatic lipid accumulation. Recently, we described that Nrf2 pathway is associated with hepatic lipid accumulation via upregulation of lipid transport and synthesis gene expression. The mechanism of this BPA mediated lipogenic effect remains unknown, but is likely due to dysregulation of gene expression for lipid homeostasis. The present study examined whether developmental BPA exposure caused hepatic lipid accumulation through Nrf2-mediated upregulation of gene expression for lipid import and synthesis. Pregnant CD1 mice were administered 25 or 250μg BPA/kg/day via osmotic pump; after weaning on PND 20, the resulting daughters were exposed to BPA via drinking water until PND 35. BPA increased hepatic lipids in livers from PND35 and week 39 adult female offspring along with upregulation of genes for lipid uptake and synthesis, such as fatty acid synthase and acetyl CoA carboxylase. This was further associated with induction of transcriptional pathways that promote lipid import and synthesis, such as Peroxisome proliferator activated receptor-γ, and Sterol regulatory element binding protein 1c protein expression at PND32 and week 39. At week 39 mice, Nrf2 target genes Gclc and Nqo1 protein expression were increased with BPA exposure. BPA increased total acetylated Histone 3 K9 marks were increased in nuclear fractions from liver. Future studies will address the deeper mechanism by which BPA exposure causes dysregulation of lipid metabolism, by examining Nrf2 recruitment to the Ppar-γ and Srebp-1c promoters. Overall, our data illustrates that developmental BPA exposure causes increased hepatic lipids via increased expression of genes that control lipid import and synthesis, as well as decrease lipid export in liver.

PS 1885 Species Difference May Account for the Discrepancy in Predicting Drugs Causing Severe Drug-Induced Liver Injury (sDILI)

J. Zhang[1], U. Doshi[2], A. P. Li[2] and W. Tong[1]. [1]*Division of Bioinformatics and Biostatistics, FDA/NCTR, Jefferson, AR and* [2]*In Vitro ADMET Laboratories LLC, Columbia, MD.*

In a previous in vitro study with pooled human hepatocytes from U.S. population, elevation of ROS/ATP ratio has been identified as a potential biomarker to identify the drugs that cause sDILI such as acute liver failure (ALF). However, several drugs with ALF reported only in Sweden didn't cause the elevation, suggesting that genetic or environmental factors may play key roles in this regional discrepancy. Interestingly, these drugs were identified in high content assays with rat hepatocytes using DNA damage and steatosis as endpoints. To confirm this observation, these drugs were evaluated in rat hepatocytes with ROS/ATP ratio. Furthermore, human hepatocytes from 10 individual donors were evaluated in a subset of the drugs to investigate individual difference. Primary cultured hepatocytes from rats or human were treated with the drugs at eight concentrations and divided into two sets, one for the quantification of ROS, and the other for cellular ATP contents. ROS/ATP ratio was obtained for each concentration, and area under dose-response curve calculated. The results confirmed that most of these drugs indeed cause the elevation of ROS/ATP ratio in rat hepatocytes. In human hepatocytes, 8 Sweden drugs and 7 sDILI drugs were evaluated. The majority of findings from these 7 sDILI drugs tested on individual donors are consistent with the results from pooled samples. However, individual variances were observed on 8 Sweden drugs. As drug metabolism is susceptible to genetic and environmental factors, and interspecies differences exist in terms of catalytic activities, we hypothesize that drug metabolism differences between the Swedish and U. S. populations due to genetic variance may be responsible for the discrepancy in the manifestation of sDILI and indicate potential mechanisms involved in CYP-mediated metabolism. Differences in response between rat and human hepatocytes to these drugs further underscores the difficulty in the use of laboratory animals to prediction drug toxicity in human.

PS 1886 Trovafloxacin-Induced DNA Damage in HepG2 Cells Causes p21 Upregulation and Activation of ATR and Sensitizes Cells to TNF-Mediated Cytotoxicity Involving ERK

K. M. Beggs[1, 2], P. E. Ganey[1, 2] and R. A. Roth[1, 2]. [1]*Pharmacology and Toxicology, Michigan State University, East Lansing, MI and* [2]*Center for Integrative Toxicology, Michigan State University, East Lansing, MI.*

The fluoroquinolone antibiotic trovafloxacin (TVX) has caused idiosyncratic hepatotoxicity in humans, although the mechanism for this toxicity is unknown. In mice given TVX, liver injury occurred only upon coexposure to endogenously produced or exogenously administered tumor necrosis factor-alpha (TNF). Similarly, treatment of HepG2 human hepatoma cells with TVX and TNF resulted in cytotoxicity, whereas neither TVX nor TNF alone caused any cell death. TVX caused cell cycle arrest in HepG2 cells, and TVX/TNF-induced cytotoxicity was attenuated by NU6027, an inhibitor of the ataxia telangiectasia and Rad3-related (ATR) kinase. These results led to the hypothesis that TVX causes DNA damage and activates the DNA damage response pathway that contributes to cytotoxicity in the presence of TNF. In support of this hypothesis, TVX caused an increase in active ATR in the nuclei of cells. TVX treatment caused DNA damage in HepG2 cells at 24 hours, and this occurred earlier (12 hours) in cells treated with both TVX and TNF. None of the treatments caused a change in p53 expression; however, p21 mRNA transcripts were increased at 6 hours in TVX-treated groups, followed by increased protein at 12 and 24 hours. The DNA content of TVX-treated cells was also decreased at 24 and 48 hours. TVX treatment also resulted in activation of extracellular signal-regulated kinase (ERK), which was prevented by the ERK inhibitor U0126. Inhibition of ERK by U0126 did not alter the TVX-induced cell cycle arrest but did attenuate the cytotoxicity induced by TVX/TNF treatment. Taken together, these data suggest that DNA damage induced by TVX causes an increase in p21 expression, ATR activation and cell cycle arrest as well as activation of ERK, which plays a role in TVX/TNF-induced cytotoxicity of HepG2 cells. (Supported by NIH grant R01DK061315.)

PS 1887 Inhibition of Bile Salt Export by Marketed Drugs in Primary Hepatocytes from Human, Monkey, Dog, Rat, and Mouse

K. He[1], J. Zhang[2], L. Cai[1], M. Yang[1], S. Qin[1] and W. Tong[2]. [1]*Biotranex LLC, Monmouth Junction, NJ and* [2]*Division of Bioinformatics and Biostatistics, NCTR/FDA, Jefferson, AR.*

Cholestasis is one of the mechanisms of drug-induced liver injury (DILI). This study is to investigate the potential inhibition of bile salt export by drugs that are associated with cholestasis. The functional activity of bile salt export pump (BSEP) was determined in primary hepatocyte suspension with a sensitive LC-MS/MS method. Cryopreserved hepatocytes were incubated with bile acids in the presence or absence of the test articles. The fractions containing transported bile salts were separated by centrifugation and the concentrations of the bile salts were determined by LC-MS/MS. The BSEP activity was determined to be approximately 1.0, 3.0 (glycocholic acid), 2.7, 4.2, and 2.7 (taurocholic acid) nmole/million cells/hour for human, monkey, dog, rat, and mouse, respectively. Forty drugs were tested with human hepatocytes, including 7 drugs causing cholestatic injury, 12 vanishing bile duct syndrome (VBDS), 10 cholestatic hepatitis, 4 mixed injuries, 1 hepatocellular injury and 6 drugs with no DILI reported. The assay is sensitive and robust in identifying drugs causing cholestatic injury (6 out of 7) with potent inhibition of BSEP activity (IC50 < 10 μM in the order of potency, cyclosporine, ritonavir, saquinavir, troglitazone, atorvastatin, cerivastatin). None of the drugs causing VBDS and cholestatic hepatitis shows IC50 < 40uM except haloperidol, indicating that mechanisms other than BSEP inhibition may be involved in the development of these liver injuries. Drugs causing mixed injuries such as ketoconazole, pioglitazone and lovastatin are potent BSEP inhibitors (IC50 < 10 μM). Twenty four drugs were also tested in hepatocytes isolated from monkey, dog, rat and mouse, respectively. Species difference in potency was observed. In summary, a novel and

robust assay was developed using hepatocyte suspension from human and animal species to assess BSEP inhibition. Drugs causing cholestatic and mixed injury are highly associated with potent BSEP inhibition.

PS 1888 Role of Epithelial to Mesenchymal Transition in the Hepatic Fibrosis of OVE26 Type 1 Diabetic Mice

Q. Zhang[1, 2], X. Jiang[1], Y. Li[1], X. Miao[1], C. Zhang[1], L. Cai[1] and M. Cheng[2]. [1]*University of Louisville, Louisville, KY and* [2]*Guiyang Medical College, Guiyang, Guizhou, China.*

Diabetes is a global health issue. Diabetic liver injury is one of common complications in diabetic patients. Epithelial to mesenchymal transition (EMT) has been considered as an important mechanism in hepatic fibrosis. In the present study, therefore, we utilized OVE26 transgenic type 1 diabetes mouse model to investigate diabetic effect on EMT and its association with hepatic fibrosis. Serum glucose, aminotransferase and triglyceride levels of OVE26 and their wild-type (FVB) mice at 1, 3, 5 and 8 months old were measured. Hepatic pathology and fibrotic response were examined with HE, oil-red, and Sirius-red staining as well as Western blotting along with immunohistochemical staining for TGFβ1, CTGF, E-Cadherin, and αSMA protein expression. Compared to FVB mice, OVE26 mice exhibited significant increases in serum levels of glucose, aminotransferase and triglyceride. At ages of 5 and 8 months, OVE26 mice developed steatohepatitis in varying degrees, reflected by significant increases in oil-red staining, collagenous fiber hyperplasia, and Sirius-red staining, compared to age-matched FVB mice. The protein expression of TGFβ1, CTGF, αSMA, and fibronectin as index of EMT, detected by Western blotting and/or immunohistochemical staining, was significantly increased in 5- or 8-month old OVE26 mice compared to age-matched FVB mice. There was no significant difference between OVE26 and FVB for E-Cadherin expressions, examined with Western blotting. These results suggest that steatohepatitis is an early manifestation in the liver of diabetic mice, and developed into hepatic fibrosis at late stage, which may be related to the EMT.

PS 1889 FXR Regulates FoxO3 Activation in Ethanol-Induced Autophagy and Liver Injury

S. Manley[1], H. Ni[1], J. Williams[1], H. Yang[1], B. Kong[2], G. L. Guo[2] and W. Ding[1]. [1]*Pharmacology, Toxicology and Therapeutics, University of Kansas Medical Center, Kansas City, KS and* [2]*Pharmacology and Toxicology, Rutgers, Piscataway, NJ.* Sponsor: U. Apte.

Autophagy is a lysosomal degradation process and cellular protective mechanism. Alcoholic liver disease encompasses a wide spectrum of pathogenesis including steatosis, fibrosis, cirrhosis, and alcoholic steatohepatitis. Autophagy induction protects against alcohol-induced steatosis. We recently demonstrated that Farnesoid X Receptor deficient (FXR-/-) mice displayed impaired autophagy. We thus hypothesized that FXR-/- mice may have exacerbated liver injury after alcohol treatment. In the present study, we found that alcohol treated-FXR-/- mice had increased serum alanine aminotransferase (ALT) and hepatic triglyceride levels compared to wild type mice. Mechanistically, we found that ethanol treatment had decreased expression of various essential autophagy genes in FXR-/- mice than that of wild type mice. Interestingly, we further found that Forkhead box O3 (FoxO3), a transcriptional factor that regulates autophagy and many antioxidant gene expressions, is activated by ethanol to protect against ethanol-induced liver injury. Ethanol-induced FoxO3 activation was dramatically suppressed in the FXR-/- mice. These results suggest that FXR is a positive regulator for ethanol-induced FoxO3 activation and autophagy.

PS 1890 Global Proteomic Analysis of Acetaminophen Toxicity in 3D Human Liver Microtissues

C. Escher[2], R. Ossala[2], P. Gunness[1], M. Bober[2], F. Grimm[2], L. Reiter[2], Y. Butscheid[2] and S. Messner[1]. [1]*InSphero AG, Schlieren, ZH, Switzerland and* [2]*Biognosys, Schlieren, ZH, Switzerland.*

Early prediction of drug safety remains a challenge in preclinical phases of drug development. Global proteomic analysis may allow for a better understanding of the mode of action and mechanism of toxicity induced by drug treatment. In this study, a novel mass-spectrometric approach - Hyper Reaction Monitoring (HRM) – was used to quantify changes in protein expression in 3D human liver microtissues exposed to acetaminophen (APAP).
3D human liver microtissues were exposed to 8 concentrations of APAP (4 μM - 10'000 μM) over 72 hours. Microtissues were harvested and subjected to mass spectrometric analysis. For global proteome profiling the samples were measured, normalized and profiled using a previously generated library of over 1900 proteins. Treatment-dependent changes in protein expression were determined by performing pairwise t-test comparisons of each APAP concentration with untreated control.
Significant changes in the expression of 127 proteins were observed across all treatment conditions. Among these proteins, the expression of several phase I enzymes (CYPs 1A2, 2B6, 2C1, 2C8 and 2E1) were altered following drug treatment. Interestingly, exposure to a subtoxic (4 μM) concentration of APAP induced a 4 fold up-regulation of CYP1A2 protein expression, which supports the role of CYP1A2 in the bioactivation of APAP to its reactive metabolite in vivo. Cluster analysis revealed the up-regulation of membrane proteins, glycoproteins and fatty acid metabolism-related proteins. Down-regulated proteins included those involved in eicosanoid metabolism, suggesting interaction of APAP with its pharmacological target.
Taken all together, the results suggest that use of HRM for proteomic studies in 3D human liver microtissues is a powerful tool to detect early changes in the proteome and may allow for the better understanding of the mechanism of drug-induced toxicity and the identification of relevant early biomarkers of toxicity.

PS 1891 Integrated Proteomic and miRNA Transcriptional Analysis Reveals the Hepatotoxicity Mechanism of PFNA Exposure in Mice

J. Wang, Y. Shengmin, W. Zhang, H. Zhang and J. Dai. *Key Laboratory of Animal Ecology and Conservation Biology, Institute of Zoology, Chinese Academy of Sciences, Beijing, China.*

Perfluoroalkyl chemicals (PFASs) are a class of highly stable man-made compounds, and their toxicological impacts are currently of worldwide concern. Administration of perfluorononanoic acid (PFNA), a perfluorocarboxylic acid (PFCA) with a nine carbon backbone, resulted in dose-dependent hepatomegaly in mice (0, 0.2, 1 and 5 mg/kg body weight, once a day for 14 days) and an increase in hepatic triglycerides (TG) and total cholesterol (TCHO) in the median dose group, as well as serum transaminases in the high dose group. Using isobaric tags for relative and absolute quantitation (iTRAQ), we identified 125 hepatic proteins (60 up-regulated, 65 down-regulated) that exhibited statistically significant changes after PFNA treatment. Lipid metabolism process proteins were the most dominant in the up-regulated proteins. While down-regulated proteins were mainly involved in monosaccharide and amino acid metabolic processes. Three altered proteins by iTRAQ (Acsl1, Fbp1, and Glud1) were further confirmed by Western blot analysis. The mRNA analysis results further suggested that PFNA exposure not only resulted in a fatty acid oxidation effect, but also activated genes involved in fatty acid and cholesterol synthesis in the mouse liver. Additionally, three (two down-regulated, one up-regulated) and thirty (fourteen down-regulated, sixteen up-regulated) microRNAs (miRNAs) exhibited at least a two-fold alteration ($P < 0.05$) in the 1 and 5 mg/kg/d PFNA treatment groups, respectively, including hepatic disease related miRNAs, miR-34a and miR-200c. The repression effect of miR-34a on fucosyltransferase 8 (Fut8) and lactate dehydrogenase (Ldha) was confirmed by luciferase activity assay and western blot analysis. The results indicated that PFNA exerted a hepatic effect, at least partially, by miRNAs mediated post-translational protein repression.

PS 1892 Sertraline Induces Endoplasmic Reticulum Stress in Hepatic Cells

L. Guo[1], J. Xuan[1], L. Couch[1], A. Iyer[2] and S. Chen[1]. [1]*NCTR, Jefferson, AR and* [2]*University of Maryland, Baltimore, MD.*

Sertraline is generally used for the treatment of depression, and is also used for the treatment of panic, obsessive-compulsive, and post-traumatic stress disorders. Previously, we have demonstrated that sertraline caused hepatic cytotoxicity with mitochondrial dysfunction and apoptosis being the underlying mechanisms. In this study, we identified additional molecular mechanisms by microarray analysis and studies further by biochemical and molecular analyses. HepG2 cells were exposed to sertraline at various concentrations for 6 h and subjected to whole genome gene expression microarray analysis. Pathway analysis revealed that endoplasmic reticulum (ER) stress and MAPK signaling pathway are among the significantly affected biological changes. Following the results of microarray study, we validated the increased expression of ER stress makers by real-time PCR and Western blot. The expression of typical ER stress markers such as PERK, IRE1α, and CHOP were significantly increased. To better study ER stress-medicated drug-induced liver toxicity; we established in vitro systems monitoring ER stress response quantitatively and efficiently using Gaussia luciferase (Gluc) or secreted alkaline phosphatase (SEAP) as reporter. In these two reporter assays, sertraline showed inhibiting effect on the secretion of Gaussia or alkaline phosphatase. Moreover, we demonstrated that sertraline-induced apoptosis coupled to ER stress and the apoptotic effect

was attenuated by 4-phenylbutyrate, a potent ER stress inhibitor. In addition, we showed that MAP4K4-JNK signaling pathway participated in the process of sertraline-induced ER stress. In summary, for the first time, we defined that ER stress is a mechanism of sertraline-induced liver toxicity.

PS 1893 Sertraline, an Antidepressant, Induces Apoptosis in Hepatic Cells through the Mitogen-Activated Protein Kinase Pathway

S. Chen, J. Xuan, H. Lin, L. Couch, N. Mei, V. N. Dobrovolsky and L. Guo. *National Center for Toxicological Research, Jefferson, AR.*

Sertraline is generally used for the treatment of depression, and is also approved for the treatment of panic, obsessive-compulsive, and post-traumatic stress disorders. Previously, using rat primary hepatocytes and isolated mitochondria, we demonstrated that sertraline caused hepatic cytotoxicity and mitochondrial impairment. In the current study, we investigated and characterized molecular mechanisms of sertraline toxicity in human hepatoma HepG2 cells. Sertraline decreased cell viability and induced apoptosis in a dose- and time-dependent manner. Sertraline activated the intrinsic checkpoint protein caspase-9 and caused the release of cytochrome c from mitochondria to cytosol; this process was Bcl-2 family dependent because anti-apoptotic Bcl-2 family proteins were decreased. Pre-treatment of the HepG2 cells with caspase-3, caspase-8, and caspase-9 inhibitors significantly reduced the release of lactate dehydrogenase, indicating that sertraline-induced apoptosis is mediated by both intrinsic and extrinsic apoptotic pathways. Moreover, sertraline markedly increased the expression of TNF and the phosphorylation of JNK, ERK1/2, and p38. In sertraline-treated cells, the induction of apoptosis and cell death was shown to be the result of activation of JNK, but not ERK1/2 or p38 in the MAPK pathway. Furthermore, silencing MAP4K4, the upstream kinase of JNK, attenuated both apoptosis and cell death caused by sertraline. Taken together, our findings suggest that sertraline induced apoptosis in HepG2 cells via activation of the TNF-MAP4K4-JNK cascade signaling pathway.

PS 1894 High-Content Analysis of a High-Throughput Human *In Vitro* Metabolic Model

S. D. Cole[1, 2, 3], J. S. Madren-Whalley[1], A. P. Li[4] and H. Salem[1, 5]. [1]*US Army Edgewood Chemical Biological Center, Gunpowder, MD,* [2]*National Research Council, Washington, DC,* [3]*Defense Threat Reduction Agency, Fort Belvoir, VA,* [4]*In Vitro ADMET Laboratories, Inc., Columbia, MD and* [5]*Department of Homeland Security, Aberdeen Proving Ground, MD.*

Human xenobiotic metabolism and hepatotoxicity are important factors in toxicology studies conducted by the pharmaceutical industry and Department of Defense. Here we report an informative, high throughput in vitro method for studying the effects of human metabolism on the toxicity of compounds of interest. Using the integrated discrete multi-organ co-culture (IdMOC) system, we grew 3T3-L1 cells in monoculture and in the presence of primary human hepatocytes and, after toxicant exposure, conducted high content analysis. The fluorescence intensities of calcein-AM and ethidium homodimer-1, as well as nuclear area and cell density, were endpoints indicative of cytotoxicity caused by 4-aminophenol. We observed that the cytotoxicity of 4-aminophenol in 3T3-L1 cells cultured in the presence of hepatocytes was less than that observed for 3T3-L1 cells grown in monoculture, suggesting that metabolism of the parent compound imparted a protective effect on the 3T3-L1 cells. In this assay we were also able to observe the effects of the P450 enzyme inhibitor, 1-aminobenzotriazole, on the toxicity of 4-aminophenol and cyclophosphamide for 3T3-L1 cells grown in co-culture with hepatocytes. The use of IdMOC plates combined with high content analysis is therefore a multi-endpoint, high throughput capability for the measurement of human metabolism on xenobiotic toxicity in vitro.

PS 1895 Comparative Metabolism of Eight Model Pharmaceutical Compounds in Rat- and Human-Liver Microsomes, Suspension Hepatocytes, and Micropatterned Cocultures of Primary Hepatocytes

J. Enoru[1], W. DeMaio[1], A. Watanyar[1], K. Draper[1], A. Moore[2] and O. Ukairo[2]. [1]*Ricerca Biosciences, Concord, OH and* [2]*Hepregen Corporation, Medford, MA.*

In vitro metabolism evaluations for compounds in early development are typically conducted using liver microsomes and suspension hepatocytes. While these systems have been serving the drug development community, they have their limitations, with examples of "metabolite surprises" - where metabolites which were not predicted or observed *in vitro* or *in vivo* during pre-clinical studies, were observed in the clinic. Such surprises can have a significant impact on the timeline of a drug development program and has prompted investigations aimed at developing *in vitro* systems that can more accurately predict human *in vivo* metabolism.

In this study, the metabolite profile of eight model pharmaceutical compounds with various biotransformation reactions was investigated using a functionally stable model of primary hepatocytes [micropatterned co-cultures (MPCCs)] in parallel with the traditional liver microsomal and suspension hepatocyte systems. Incubations were performed for 0 and 60 min in liver microsomes; 0 and 2 hr in suspension hepatocytes; and 0, 4 hr, 2 days and 7 days in MPCCs. Metabolites were identified by LC/MS employing a narrow range of chromatographic conditions, representative of drug metabolism screening in an early development setting. Preliminary results show that MPCCs are more metabolically active than the traditional platforms, based on greater disappearance of test article and formation of metabolites. Formation of metabolites from non-P450 mediated reactions, especially UGTs, and secondary metabolites appear to be more predominant in MPCCs.

Results from this investigation support the usefulness of MPCCs for metabolite profiling studies with the potential of eliminating "metabolite surprises". MPCCs also provide the advantage that the cells maintain metabolic activity over an extended period in culture, which probably explains why secondary metabolites were more abundantly generated in this system.

PS 1896 Expression of Drug Processing Genes in Livers of Germ-Free Mice

F. Selwyn, J. Cui and C. D. Klaassen. *University of Kansas Medical Center, Kansas City, KS.*

Intestinal bacteria regulate many host functions, and may alter the expression of drug processing genes (DPGs) in the host. The purpose of this study was to characterize the expression of hepatic DPGs in mice lacking the normal complement of intestinal bacteria (germ-free mice) using RNAseq. Total RNA was isolated from the livers of adult male conventional (CV) and germ-free (GF) C57BL/6 mice (n=3 per group). The cDNA libraries were sequenced 50bp paired-end using an Illumina HiSeq2000 sequencer. Approximately 80-100 million reads were generated per sample and over 95% of the reads were mapped to the mouse mm10 genome (Tophat). The transcript abundance was estimated by Cufflinks, and differential expression was determined using Cuffdiff (FDR-BH<0.05). Ingenuity Pathway Analysis determined that drug-processing pathways rank among the top most differentially regulated networks in livers of GF mice. Cyp3a11, the cytochrome P450 enzyme (Cyp) that metabolizes more than 50% of drugs and is induced by PXR agonists, was decreased 87% in GF mice; Cyp2b10, the Cyp induced by CAR agonists was decreased 57% in GF mice; whereas Cyp4a14, a Cyp induced by PPARα agonists was increased 202%; and Cyp1a2, the Cyp induced by AhR agonists was increased 51%. The changes in mRNA of these Cyp genes do not appear to be due to mRNA changes in these receptors, because the mRNA of PXR was not altered, and the mRNA of CAR, PPARα and AhR were in fact increased. Not only were the Cyp mRNAs altered in the GF mice, but other DPGs, such as a number of glutathione transferases were down-regulated, whereas a number of sulfotransferases and uptake transporters and efflux transporters were up-regulated. In summary, this study suggests that intestinal bacteria regulate the mRNA expression of a large number of DPGs, and this may be responsible for some of the individual differences in drug responses.

PS 1897 Morphological Changes to Mitochondria in Response to Compounds with Different Modes of Action

A. Winkley, A. Davies, D. W. Brewster and S. Tekur. *DSE, Vertex, Cambridge, MA.*

Early identification of compounds that could be a cause of drug induced liver injury is a vital part of a risk avoidance strategy. Along with other factors, disruption of normal mitochondrial function has long been linked to hepatic damage. Mitochondrial function is often monitored by determination of ATP, or, in the more recent literature by direct measurement of the mitochondrial membrane potential (MMP). These studies are usually carried out with HepG2 cells which are an immortalized, transformed cell line that are difficult to image at the subcellular level due to the compact nature of the cytoplasm. The classical toxins rotenone, oligomycin, bendamustine, BAM7, wortmannin, antimycin, anisomycin and amiodarone were used to investigate the utility of using mitochondrial morphology in WS1 fibroblasts as a potential screening endpoint for toxicity assessment. MMP was measured up to 6 hours and compared to changes in mitochondrial morphology. WS1 fibroblasts are a primary human cell line that forms a flat monolayer in culture making them relevant to human risk assessment and amenable to high content imaging. Results from this study demonstrate that mitochondrial networks can be readily visualized in WS1 cells and quantified with appropriate stains and that changes in mitochondrial morphology, such as fragmentation due to a toxic

insult can be detected. Using morphology we are able to differentiate between compounds more readily than typical MMP staining; this was very evident with rotenone, oligomycin and antimycin that had comparable effect on MMP but very different effects on mitochondrial morphology. In addition we also found underlying morphology changes with compounds not thought of as classical mitotoxins such as anisomycin, showing the added benefit of a more phenotype based risk assessment tool. This first experiment has shown the great potential for using mitochondrial morphology as a screen, further studies are planned to follow up with a more diverse set of compounds, incorporating further mitochondrial endpoints for added context.

PS 1898 *In Vivo* Extrapolation of *In Vitro* Drug-Induced Hepatocyte Accumulation of Triglycerides to Predict Steatosis in Rodents and Humans

P. Patel, M. Atari, H. Woodhouse, P. A. Walker and S. Thomas. *Cyprotex, Maccelsfield, United Kingdom.* Sponsor: C. Strock.

Drug-induced liver injury (DILI) is one of the main causes of late-stage attrition in the development of drugs. Hepatic steatosis (fatty accumulation of the liver) can lead to DILI. Although it is considered to be a relatively mild side-effect of drugs, it may indicate more serious underlying causes, such as inhibition of mitochondrial respiration.
Here we report an in vitro in vivo extrapolation (IVIVE) of an in vitro steatosis assay to in vivo triglyceride accumulation in the rat on exposure to model steatotic compounds. The dose-response of triglyceride accumulation to compound exposure was measured in HepG2 cells using high content screening (HCS). The IVIVE is based around a mathematical model of hepatocyte triglyceride (TG) production and very low density lipoprotein (VLDL) production and export. TG accumulation data obtained by HCS was converted to quantitative fluxes to TG, and the effects of drugs on this flux were modelled as kinetic effects on CO2, TG and VLDL production. In this way, direct (modulation of TG and/or VLDL fluxes) and indirect (inhibition of mitochondrial pyruvate oxidation) causes of steatosis can be explored. Casting the effects as kinetic parameters in this way enables the effects of exposure to be directly and quantitatively simulated.
The prediction of steatosis in vivo was performed by using known plasma concentrations of drugs to drive the simulated response of intrahepatic TG accumulation. Good agreement was observed between predicted and observed accumulation in vivo for model drugs. Exercising the model enables examination of the expected effects of drugs on mitochondrial respiration as well TG/VLDL metabolism.
Using the steatosis model with PBPK modelling to predict drug concentrations, the in vivo steatosis dose response could be predicted directly from in vitro data, and also used to aid optimization of dosing regimes to minimise steatosis whilst maintaining efficacy.

PS 1899 Using *In Silico* Modeling to Understand the Role of BSO in GSH Metabolism

S. Das, R. Kumar, A. Khanna, S. Louha, K. Rajendran, B. Thota, D. Raman, D. Srivastava, N. Rajeswara, N. Mandyam, S. Raghavan and K. Subramanian. *Strand Life Sciences, Bangalore, India.*

It is believed that one of the key roles played by BSO is to inhibit the transport of cysteine, an essential amino acid across the hepatocyte cell membrane. Since cysteine is a rate-limiting substrate for GSH synthesis by gamma-GCS, BSO could lower cellular GSH by substrate inhibition. One of the facts that support this hypothesis is that lowered GSH levels are observed in presence of upregulated gamma-GCS. To test the validity of this hypothesis and other competing ones, we treated HepG2 cells with BSO for a period of 24 hours and assayed GSH, ATP, ROS and gamma-GCS levels at various time points. To understand the impact of cysteine availability for GSH synthesis, we also performed the same experiments by culturing the cells in excess cysteine containing media.
BSO induces an increase in ROS generation and hence depletion of cellular ATP and GSH. Addition of excess cysteine in the culture media recovered the ATP levels and reduced ROS levels. However the addition of excess cysteine did not recover the GSH, although the gamma-GCS activity remained up regulated. To understand what could be contributing to this behaviour, we fed the experimental observations into our in silico model of liver metabolism (Virtual Liver) and performed simulations to mimic the experimental conditions and to test various hypotheses for the action of BSO and cysteine in the liver. Our analysis indicates that the direct inhibitory effect of BSO on gamma-GCS activity has a greater impact than reduced cysteine availability in lowering cellular GSH levels. ATP and ROS recovery in the presence of additional cysteine is via a GSH independent route.

PS 1899a Validation of a 3-Dimensional Liver Microtissue Model for Long-Term Hepatotoxicity Studies

S. Messner[3], T. Moeller[1] and B. Larson[2]. [1]*BioreclamationIVT, Halethorpe, MD,* [2]*BioTek, Winooski, VT and* [3]*InSphero, Schlieren, Switzerland.*

In vitro animal models have revealed multiple mechanisms of action (MOA) of diclofenac-related hepatotoxicity, including oxidative stress and mitochondrial permeability transition (MPT), and CYP-related metabolic activation and the formation of reactive metabolites. The combined hepatotoxic effect of these MOAs usually occurs within weeks of therapy commencement, emphasizing the need to incorporate in vitro safety testing periods similar to clinical exposure. However, primary hepatocytes cultured in a two-dimensional (2D) manner have been shown to undergo rapid loss of differentiated function and metabolic capacity and have less complex inter-cellular and cell-matrix interactions compared to in vivo.
Here we demonstrate a 3D cell culture model in which hepatocytes dispensed into a hanging drop re-aggregate into a functional liver microtissue. Assessment of hepatocellular function and toxicity were measured by luminescent and image-based markers for CYP3A4 activity, ATP content, membrane integrity, mitochondrial superoxide production and MPT formation. CYP3A4 was found to be 100X greater in microtissues than in 2D. CYP activity and cell viability after 14 days of culture in 3D remained at 100% of day 1 levels, while 2D culture values dropped below 50%. Oxidative stress and MPT pore opening were observed after 3 and 7 day diclofenac incubations, respectively, confirming similar MOA using 3D cell culture. However, the time to reach a diclofenac cytotoxicity EC50 of 300 μM as measured by membrane integrity was 3 days with microtissues in contrast to 2 hours using 2D cell culture, as previously shown by other researchers. The potential of 3D cell models to better mimic clinical exposure timelines may lead to better correlation when performing long-term cytotoxicity studies while maintaining the benefits of specific in vitro assays to determine MOAs.

PS 1899b Detection of Human Hepatic Toxicity in Chimeric Mice with Humanized Liver by Human ALT1 ELISA System

C. Tateno[1, 2], H. Iwanari[3], T. Shimada[1], T. Kimura[4], C. Yamasaki[1], M. Kakuni[1] and Y. Ishida[1, 2]. [1]*PhoenixBio Co., Ltd., Higashihiroshima, Japan,* [2]*Liver Research Project Center, Hiroshima University, Hiroshima, Japan,* [3]*Quantitative Biology and Medicine, RCAST, Tokyo University, Tokyo, Japan and* [4]*Institute of Immunology Co., Ltd., Tokyo, Japan.* Sponsor: M. Hayashi.

To predict human (h-) hepatic toxicity a suitable animal model is needed because some medicines or chemical entities confirmed to be safe in experimental animals are toxic to the h-liver. We developed chimeric mice with h-hepatocytes (PXB-mice®), which have been used for Drug Metabolism and Pharmacokinetics (DMPK) studies and hepatitis B or C virus (HBV or HCV)-infection studies, to predict h-metabolism and chemical efficacy for HBV or HCV. Since >70% of the PXB-mice livers are repopulated with h-hepatocytes as well as <30% mouse (m-) hepatocytes, whether m- or h-hepatocytes are the cause of a chemical-induced increase in ALT activity cannot be distinguished. ALT1 and ALT2 are isotypes of ALT; the former is a cytoplasmic protein and the latter is a mitochondrial protein with indistinguishable enzyme activity. Therefore, to identify h-specific hepatotoxicity, we produced h-ALT1-specific antibodies not crossed with m-ALT1, m-ALT2, or h-ALT2 by immunization with recombinant h-ALT1 protein synthesized by Baculovirus. Using 2 types of h-ALT1 antibodies we developed a h-ALT1 sandwich ELISA system, and detected h-ALT1 protein in PXB-mouse plasma. PXB- and SCID mice were administered aflatoxin B1 (AFB-1) or CCl4 orally for 7 days, and the ALT activities and h-ALT1 concentrations in plasma were measured periodically. ALT activity was found to be higher in the AFB-1-treated PXB-mice than the AFB-1-treated SCID mice, and the kinetics of ALT activity was similar to h-ALT1 protein levels in the PXB-mice. Conversely, ALT activity was higher in the CCl4-treated SCID mice than the CCl4-treated PXB-mice, and the kinetics of ALT activity was different from h-ALT1 levels in the PXB-mice. Therefore, AFB-1 and CCl4 are more toxic for h-hepatocytes and m-hepatocytes, respectively. In conclusion, using the h-ALT1 ELISA system, h-specific hepatic toxicity was detected quantitatively in the PXB-mice.

PS 1899c Development of High-Throughput AlphaLISA Immunoassays to Quantify ALT and AST Levels in Human Primary Hepatocytes Culture Supernatant

E. Doudement, H. Uppal, D. L. Misner and D. M. Dambach. *Safety Assessment, Genentech Inc, S. San Francisco, CA.*

Alanine aminotransferase (ALT) and Aspartate aminotransferase (AST) levels in blood are routinely used as a marker for liver function and elevations in these enzyme levels are associated with liver injury. Since compound attrition in pre-

clinical and clinical development is commonly due to drug-induced liver injury, compounds are screened for hepatotoxicity using in vivo and in vitro approaches. Currently, existing methods to quantify AST and ALT in hepatocyte culture supernatant require high volumes, thereby reducing throughput capacity and often showing high variability. Herein we describe development of high throughput assays using AlphaLISA technology to measure AST and ALT in cell culture supernatant. Human primary hepatocytes were treated with Amitriptyline, a known hepatotoxicant that increases AST and ALT, at 1mM for 2h as a positive control and non-treated hepatocytes served as a negative control. The assay development steps included robustness of positive control for hepatotoxicity, identification of 2 specific antibodies for ALT and AST, optimization of antibody/bead concentrations, buffers, and incubation time. Specificity and matrix tolerance of the assay were also tested. Optimized ALT and AST AlphaLISA in vitro assays are high throughput (384 well plate), requiring 5 µl of sample, demonstrated to work on both culture supernatant and cell lysate, detected enzymes levels (and not their activity) and did not require washes like conventional ELISA. Availability of such assays enables in vitro hepatotoxicity studies to be done in 384 well plates and to be monitored over time in long term studies by collecting culture supernatant at various time points.

PS 1899d MicroRNA miR122 Induction by Bile Salt Export Pump (BSEP) Inhibiting DILI Drugs in Primary Cultured Human Hepatocytes

Q. Yang, U. Doshi and A. P. Li. *In Vitro ADMET Laboratories, Advanced Pharmaceutical Sciences, Columbia, MD.*

MicroRNA miR122 is a promising novel plasma biomarker for early detection of liver damage, as changes in plasma level would occur before the elevation of alanine aminotransferase and aspartate aminotransferase activities. As of this writing, little is known about the regulation of miR122 expression in hepatocytes. In our laboratory, we embarked upon the evaluation of miR122 expression in hepatocytes treated with various drugs known to be associated with drug induced liver injuries (DILI). Hepatocytes from three donors were treated for 8 hrs with ten drugs with known clinical hepatotoxicity: the hepatotoxic disulfiram, ketoconazole, troglitazone, nefazodone, valproic acid, zomepirac, ifosfamide, tamoxifen, and the relatively less toxic ibuprofen and rosiglitazone. RT-PCR was used for the quantification of miR122. Dose-dependent and significant induction of miR122 was observed in hepatocytes from all three donors at the highest concentration evaluated of 250 uM for disulfiram (42 to 130 fold), troglitazole (15 to 225 fold), and nefazodone (10 to 26 fold). It is interesting to note that all three drugs are associated with DILI and are known to be potent BSEP inhibitors. The induction of miR122 by BSEP inhibiting DILI drugs suggesting a possible mechanistic link between bile salt accumulation and miR122 expression. Further research is being performed in our laboratory with additional DILI drugs and BSEP inhibitors to verify this apparent correlation which may aid mechanistic understand of DILI. The results also suggest that quantification of miR122 induction in cultured hepatocytes may be an useful in vitro screening assay for identification of drug candidates with DILI potential during drug development.

PS 1899e "Inside-Out" Membrane Vesicles: An *In Vitro* Model to Study Transporter-Mediated Drug Interactions Which Can Lead to Liver Toxicity

A. Gao[1], N. Li[2], S. Parikh[2], J. Bourgea[2] and C. J. Patten[2]. [1]*Corning Life Sciences, Kennebunk, ME and* [2]*R&D, Corning Life Sciences, Bedford, MA.* Sponsor: C. Crespi.

Multidrug resistance proteins (MRPs), in particular MRP2, and the bile salt export pump (BSEP), are the two major ABC efflux transporters which contribute to drug induced liver toxicity. MRP2 is essential for hepatobiliary elimination of many drugs, drug conjugates and endogenous compounds, such as bilirubin glucuronides. MRP2 dysfunction caused by inherited MRP2 deficiency or drug mediated inhibition results in hyperbilirubinemia. BSEP is the rate-limiting step of bile salt transport across hepatocyte membranes. Disruption of BSEP in hepatocytes leads to accumulation of cytotoxic bile salts in the liver, resulting in liver toxicity, e.g., cholestasis. In light of the evidence showing the importance of MRP2 and BSEP in drug induced liver toxicity, the International Transporter Consortium (ITC) recommends evaluating the potential interaction of NMEs (new molecular entities) with MRP2 and BSEP. This study focused on the use of "inside-out" membrane vesicles, which are prepared from insect cells (Sf9) infected with baculovirus expressing human MRP2 or BSEP cDNA, to access drug interactions for these transporters in vitro. The data demonstrate that in the presence of ATP, MRP2 vesicles showed significant uptake (~10-fold) for leukotriene C4 (LTC4) and estradiol-17β-glucuronide, known MRP2 substrates, compared to control samples (vesicles assayed with the non-hydrolyzable ATP analog AMP). Taurocholate, a BSEP probe substrate, showed more than 20-fold uptake activity in BSEP vesicle, compared to the control. MRP2 mediated uptake of the probe substrate LTC4 was significantly inhibited by known MRP2 modulators, e.g. MK571, benzbromarone, terfenadine and indomethacin. BSEP mediated taurocholate uptake was shown to be inhibited by known BSEP inhibitors, e.g. cyclosporine A, glibenclamide and troglitazone, etc. The data indicates that "inside-out" membrane vesicles are a quick and useful tool to screen MRP2 and BSEP inhibitors which can potentially cause liver toxicity in vivo.

PS 1900 Connexin 32 Maintains Stemness of Hematopoiesis

Y. Hirabayashi[1], B. Yoon[2], I. Tsuboi[3], J. Kanno[1], J. E. Trosko[4] and T. Inoue[3]. [1]*Div. of Cell. & Molecul. Tox., Nat'l Inst. of Health Sciences, Tokyo, Japan,* [2]*Lab. of Histology & Molecul. Pathogenesis, School of Vet. Med., Kangwon Nat'l Univ., Chuncheon, Republic of Korea,* [3]*Nihon Univ. School of Med., Tokyo, Japan and* [4]*Michigan State Univ., East Lansing, MI.*

We previously reported on the role of connexin (Cx) 32 during steady-state hematopoiesis and its potential protective role against leukemogenesis. Here, we examined the hematopoietic progenitor cell (HPC) kinetics by evaluating the percentage of cycling HPCs by continuous bromodeoxyuridine (BrdUrd) incorporation in vivo for up to 3 months, followed by ultraviolet-A exposure to eliminate BrdUrd incorporating cells. As a result, the percentage of the entire cycling fraction of primitive HPCs without Cx32 apparently increased continuously although that with Cx32 was maintained at a certain level from 8 weeks until 18 months of age. This is consistent with the observations of a larger number of HPCs and a smaller number of hematopoietic stem cells (HSCs) in aged Cx32-KO mice than in wild-type mice, which are in contrast to young mice with/without Cx32.
Then, we examined the bone-marrow reconstitution capability of HSCs from Cx32-KO mice by serial transplantation of cells in the lineage-negative, c-kit-positive, and Sca1-positive (LKS) fraction from wild-type and Cx32-KO mice with freshly isolated bone marrow cells to prevent an acute radiation injury. Although both groups showed reconstituted hematopoiesis without any significant differences in various hematopoietic parameters in the primary, and secondary recipients, clear differences in the parameters in the LKS fraction solely from the secondary recipients were observed. Namely, four out of seven recipients in the wild-type group showed over 0.5% donor cells (average percentage and standard deviation for 4 mice, 25.1±27.9%), whereas none of the five recipients in the Cx32-KO group showed more than 0.5% donor cells. These findings in this study taken together with the previous findings imply that Cx32 plays an essential role in maintaining self-renewal proliferation of HSCs to prevent their exhaustion and in suppress neoplastic changes.

PS 1901 A Novel CXCR4 Antagonist SDF-1βP2G Enhances Ischemic Angiogenesis via Endothelial Progenitor Cell Mobilization, Infiltration, and Incorporation

X. Yan[1, 2], L. Cai[1, 2] and Y. Tan[1, 2]. [1]*Kosair Children's Hospital Research Institute, Department of Pediatrics, University of Louisville, Louisville, KY and* [2]*Chinese-American Research Institute for Diabetic Complications, Wenzhou Medical College, Wenzhou, Zhejiang, China.*

Stromal cell derived factor 1 (SDF-1) and C-X-C chemokine receptor type 4 (CXCR4) axis plays a critical role in angiogenesis. However, the multi-functional characteristics of native SDF-1 limit its potential application. We developed a novel CXCR4 antagonist namely, SDF-1βP2G (P2G), which was derived from human native SDF-1β to block CXCR4 and promote mobilization of endothelial progenitor cells (EPCs) necessary for vascular injury recovery and angiogenesis. P2G exerted antagonistic effects against CXCR4 by promoting CXCR4 internalization and competitively inhibiting downstream signaling in vitro, and does- and time-dependently mobilization of EPCs (CD31+/c-Kit+) from bone marrow into blood in vivo. Moreover, intravenous administration of P2G significantly stimulated ischemic angiogenesis, blood reperfusion and skeletal muscle regeneration in an acute hindlimb ischemia model. Mechanistic study showed that P2G significantly stimulated EPCs mobilization in the peripheral blood and promoted their infiltration into ischemic skeletal muscle tissues and incorporation into the newly formed blood vessel. In addition, P2G enhanced the activation and/or expression of angiogenesis and progenitor cell chemotaxis-related factors including Akt, ERK, mTOR, MMP-9, SDF-1/CXCR4 and VEGF. Furthermore, neutralization of VEGF with its specific antibody abolished P2G-induced blood reperfusion and angiogenesis. More importantly, no obvious inflammatory and apoptotic effects were observed in multiple organs after P2G administration. These data suggest that the novel antagonist of CXCR4, P2G, can be successfully utilized to stimulate ischemic angiogenesis and muscle regeneration through mobilization of EPCs in a VEGF dependent manner. Our work has demonstrated for the first time that P2G is a non-toxic, specific CXCR4 antagonist with a great potential for clinical application for ischemic vascular diseases.

PS 1902 Evaluation of Cell Health *In Vitro* Using Video Bioinformatics

S. C. Lin, B. Davis, H. Yip and P. Talbot. *Cell Biology and Neuroscience, University of California, Riverside, CA.*

The efficiency of in vitro toxicological assays can be increased by evaluating changes in cellular behavior and morphological characteristics during treatment. CL-Quant, a video bioinformatics (VBI) analysis tool, includes various modules for analyzing biological endpoints, and users can also introduce new protocols. Here, three cell health quantification modules were used: (1) growth, (2) migration, and (3) reactive oxygen species (ROS) production. Time-lapse videos of cigarette smoke exposed cells were collected using a Nikon BioStation. To evaluate pluripotent stem cells, colony area (pixels) was measured at each time point. For single cell proliferation of neural and NTera stem cells, confluency (pixels) was measured in each frame to obtain growth rate. Smoke exposure inhibited growth of all cell types when compared to the control. Colony migration was studied by extracting information on: migration rate, displacement (distance between the starting and ending points), and total distance travelled. Average distance travelled by treated colonies was less than the control. The gap closure assay was used to measure single cell migration, and neural stem cell migration was more sensitive to smoke exposure than NTera cells. To verify the accuracy of the automated VBI tool, a set of images from each experiment was analyzed for ground truth (ImageJ software). CL-Quant and ImageJ analyses produced similar results for all assays. We also examined levels of ROS, which often increase when cells are stressed and can lead to severe cell damage, and cell death. To quantify ROS production, cells were pre-loaded with MitoSox, a mitochondrial ROS (superoxide) indicator, then treated with chemicals and imaged at 2 to 3 minute intervals. A CL-Quant protocol was created to measure and to graph intensity, an indicator of ROS production over time. Smoke treated cells showed increased ROS production. Our studies demonstrate that CL-Quant can be used to evaluate biological parameters associated with cell health, and these parameters can be applied to toxicological studies.

PS 1903 Delayed Electrophysiologic and Proarrhythmic Effects of Kinase Inhibitors Assessed in Human Induced Pluripotent Stem Cell-Derived Cardiomyocytes (hiPSC CM)

H. Shi[1], M. Huang[1], D. Xing[1], J. Zhu[1], G. Lewen[2], S. P. Adams[1] and P. C. Levesque[1]. [1]*Discovery Toxicology, Bristol-Myers Squibb, Princeton, NJ and* [2]*Research Informatics and Automation, Bristol-Myers Squibb, Princeton, NJ.*

Some kinase inhibitors prolong QT interval and cause ventricular arrhythmia in patients due to direct (acute) and indirect (delayed) inhibition of multiple cardiac ion channels including hERG and Na channels. Standard cell-based assays are only able to detect the direct or acute ion channel effects and do not predict proarrhythmic potential, particularly when limited to assessment of individual recombinant channels expressed in cell lines. The coupling of high-resolution multi-electrode array (MEA) technology with hiPSC CM allows detailed and spatial analysis of acute and delayed effects on field potential duration (FPD, QT surrogate) and conduction velocity (CV), as well as proarrhythmic signals (PAS). Kinase inhibitors (nilotinib and BMS-A), and the direct hERG blocker (dofetilide), were evaluated in hiPSC CM using MEA. Dofetilide increased FPDs and elicited PAS within 20 minutes at 3 and 10 nM; the effects were sustained over 24 hours. The PAS were associated with 5 patterns of increasing severity: alternans, aberrant repolarizations, afterdepolarizations, intermittent polymorphic tachycardia, and fibrillation. For kinase inhibitors, consistent with the direct inhibition of hERG and Na channels in patch-clamp assays, within 30 minutes nilotinib at ≥ 1 μM and BMS-A at ≥ 3 μM elicited PAS, increased FPDs and decreased CVs. With 24 hour treatment, these effects worsened for both compounds. Within 30 minutes, 0.1 and 0.3 μM nilotinib and 1 μM BMS-A did not significantly affect FPDs and CV, and PAS were also not detected; effects, however, were observed after 2 hours exposure. The dose- and time-dependent effects of kinase inhibitors on FPD, CV and PAS predict proarrhythmic potential of the agents. The hiPSC MEA assay enables preclinical evaluation of both acute (direct channel) and delayed electrophysiologic effects and proarrhythmic potential (possibly related to kinase inhibition).

PS 1904 Aluminum Maltolate Interferes with Gene Expression of Epigenetic Modifying Enzymes in Mouse Embryonic Stem Cells

A. Aliberti and F. A. Barile. *Pharmaceutical Sciences, St. John's University College of Pharmacy, Queens, NY.*

The fetal basis of adult disease hypothesis postulates that prenatal exposure to environmental factors such as metals increases susceptibility to adulthood diseases via epigenetic mechanisms. For example, exposure to aluminum (Al) has been implicated in dialysis encephalopathy syndrome and Alzheimer's disease. Thus, using mouse embryonic stem (mES) cells as a model of early embryogenesis, we studied if Al could induce alterations in gene expression patterns of epigenetic modifying enzymes, such as those involved in DNA methylation and histone maintenance. In initial experiments, stem cells treated with aluminum chloride ($AlCl_3$; 150-2500 μM for 24-hrs) showed a statistically significant increase in cell viability as compared to control except at the highest concentration. Since Al readily forms complexes in the environment, aluminum maltolate (AlMal) was subsequently used to assess toxicity. Exposure to AlMal (150-750 μM) caused a significant, dose dependent decrease in cell viability (IC_{50}: 530 μM). As a control, maltol alone (450-2250 μM) did not significantly decrease cell viability except at the highest concentration. Combinations of $AlCl_3$ and Mal also decreased cell viability at 600:1800 and 750:2250 μM combinations. As with previous gene expression experiments performed with $CdCl_2$ (SOT abstract #1197, 2013), AlMal (150 μM and 300 μM for 24-hrs) also caused a two-fold or greater increase in Aurkc (phosphorylase necessary for proliferation in the pre-implantation blastocyst), as well as to Ciita (class II transactivator). Exposure to 300 μM AlMal resulted in at least a two-fold down-regulation of Dnmt3a and Dnmt3b (DNA methyltransferases), Ehmt2 (lysine methyltransferase), Hdac11 (histone deacetylase), and Prmt3 (arginine methyltransferase), all of which regulate embryogenesis. Consequently, AlMal appears to interfere with expression of genes for epigenetic modifying enzymes essential for embryonic development.

PS 1905 Lineage Stage Specific Modulation of Rat Hepatic Stem/Progenitor Cell Growth by Activation of the Aryl Hydrocarbon Receptor (AhR)

J. A. Harrill[1], B. Parks[1], E. Wauthier[2], J. Rowlands[3], L. M. Reid[2] and R. S. Thomas[1]. [1]*The Hamner Institutes for Health Sciences, Research Triangle Park, NC,* [2]*Program in Molecular Biology and Biotechnology, Department of Cell Biology and Physiology, University of North Carolina, Chapel Hill, NC and* [3]*The Dow Chemical Company, Midland, MI.*

A novel culture system was established for rat hepatic stem cells (rHpSCs) and their descendants, hepatoblasts (rHBs), and accompanying mesenchymal precursor support cells (angioblasts and precursors of endothelia and stellate cells). This was achieved using a combination of long-chain hyaluronan plating substratum and Kubota's Medium (KM), a serum-free medium designed for endodermal stem/progenitors. Supplementation of KM with leukemia inhibitory factor (LIF) increased the growth of desmin+ mesenchymal cell precursors accompanied by a selective increase in the growth of rHBs. This model was used to examine lineage stage-specific effects of structurally diverse AHR agonists on rHpSC and rHB growth. Automated high content image analysis and bipartite fluorescent surface area density (FSAD) gating methods demonstrated that the growth of rHpSCs was stimulated by AHR agonists 2,3,7,8-tetrachlorodibenzo-p-dioxin, 6-formylindolo[3,2-b]carbazole and 3-3'-diindolylmethane. These effects occurred at concentrations which produced persistent activation of AHR as assessed by Cyp1a1 induction. TCDD stimulation of rHpSC growth was concurrent with a marked loss rHBs resulting in selective expansion of rHpSCs. The findings provide mechanistic insight into a potential lineage stage-specific mode-of-action for promoting TCDD-induced rat liver tumorigenesis.

PS 1906 Aflatoxin B1 Effects on Differenciation, Proliferation, and Cell Death on Human Adult Hepatic Stem/Progenitor Cells

W. Hassen[1], S. Gerbal-Chaloin[2], I. Iankova[2], C. Duret[2], P. Briolitti[2], J. Ramos[3] and M. Daujat-Chanvanieu[2]. [1]*Department of Cellular Physiology and Toxicology, Institute of Biotechnology, Monastir, Tunisia,* [2]*Hepatic Differentiation of Stem Cells and Biotherapy of Liver Diseases, Normal and Malignant Stem Cells, Inserm U1040, Research Institute of Biotherapy, University of Montpellier, Montpellier, France and* [3]*University Hospital of St Eloi, CHU St Eloi, Montpellier, Montpellier, France.* Sponsor: A. Lopez de Cerain.

AFB1 (AFB1) is a mycotoxin naturally occurring in common food and pointed out as a major risk factor for Hepatocellular carcinoma (HCC). Recent data suggest that HCC may derivate from endogenous liver stem/progenitor cells undergoing blocked ontogeny rather than dedifferentiation of adult hepatocytes. We have previously isolated a population from the human liver suspected to represent progenitor cells since they express typical progenitor markers, exhibit a marked proliferative potential, differentiate into hepatocyte-like cells that express an intermediate hepato-biliary phenotype when cultured under appropriate conditions, and are able to engraft and differentiate in vivo after transplantation in mice liver in a regenerative context.
The present study addresses the effect of AFB1 on the behavior of these human hepatic progenitor cells as possible initiator of cell transformation leading to HCC. To this end, we investigate different toxicological endpoints in response to AFB1

treatment, including Cytotoxicity, DNA Damage and Repair, Oxidative Stress, Cell Death Patterns in addition to Cell Proliferation versus Differentiation. The major finding of our work is that AFB1 induces in a time and concentrations dependent manner a striking inhibition of differentiation as evidenced by reduced albumin, HNF4 α, α-Antitrypsin expression and enhances cell proliferation. In addition, AFB1 induced DNA damage, activate DNA repair pathway and induces oxidative damage and apoptotic cell death. Altogether, our data suggest that AFB1 is likely to initiate tumor transformation from hepatic adult Stem/Progenitor cells, the resident progenitor population of the adult human liver.

PS 1907 Low Levels of Aryl Hydrocarbon Receptor Expression in Mouse Embryonic Stem Cells Deregulate Pluripotency Balance

C. Ko, Y. Fan, Q. Wang and A. Puga. *Environmental Health, University of Cincinnati, Cincinnati, OH.*

Embryonic stem cells (ESC) are highly proliferative and display an unusual cell cycle distribution, lacking G1 and G2 checkpoints due to the continuous activity of cyclin dependent kinases and retinoblastoma (RB) protein. A shortened G1 phase combined with S-phase accumulation contributes to high proliferative rates, closely related to ESC's self-renewal and pluripotency, under the control of pluripotency factors. Discontinuous expression of these factors creates heterogeneous responses to differentiation stimuli within the population of ES cells. The aryl hydrocarbon receptor (AHR) acts as a mediator of xenobiotic toxicity as well as a cell cycle modulator through interactions with RB and regulation of proteins involved in the G2/M transition. Our recent data revealed that in murine ESC, pluripotency factors and polycomb group proteins repress Ahr expression; this result, along with the pausing of RNA polymerase II on the Ahr proximal promoter and the increase of Ahr expression upon differentiation, suggest that AHR may play a regulatory role during early embryogenesis. To investigate whether low levels of Ahr expression had a functional role in ESC physiology, we analyzed the cell cycle distribution of Ahr+/+ and Ahr-/- ES cells. Cultures of both cells grew at similar proliferation rates, but Ahr-/- ESC accumulated in S phase with reduced G1 and G2/M phases compared to Ahr+/+ ESC. To further characterize AHR-expressing ESC, we sorted AHR-expressing (AHR+) and not-expressing (AHR-) cells from cultures of Ahr+/+ ES cells and followed their fate in culture. After two days in culture, we observed the appearance of AHR- in AHR+ cultures and vice versa; Immunofluorescence analyses indicated that AHR-positive ESC expressed lower levels of pluripotency factors OCT4 and NANOG, suggesting that AHR expression in ESC may disrupt the homeostatic regulation of the undifferentiated, pluripotent state and may contribute to altered responses to differentiation stimuli. Supported by NIH Grant 5R01ES06273.

PS 1908 Predictive Assays for Cardiotoxicity Using Embryonic Stem Cell-Derived Cytiva™ Cardiomyocytes (hESC-CM)

K. F. Marcoe, J. Chesnut-Speelman, T. Arnold, S. Wang, J. Kushleika, Y. Zhao and U. Warrior. *Toxicology Cellular Services, Eurofins Cerep-Panlabs, Redmond, WA.*

Cardiovascular toxicity is a major cause of failed drug development and withdrawals. Predictive toxicology screening assays enabling early identification and deselection of compounds that have potential to cause either functional (changes in contractility) or structural (morphological damage or loss of viability) cardiotoxicity are required. Multiplexed high content screening (HCS) with automated fluorescence microscopy and image-based technology was used to develop cellular assays that detect key mechanisms relevant to drug- induced cardiotoxicity. The following parameters were evaluated: cell count (nuclear dyes); calcium mobilization (Fluo-4 AM); mitochondrial membrane potential (TMRM); membrane permeability (TOTO-3); B-type natriuretic peptide (BNP) peri-nuclear protein expression (anti-BNP); alpha-actinin protein disruption (anti-alpha-actinin, sarcomeric); and troponin I protein integrity (anti-troponin I). Studies were undertaken in hESC-CM at 24 and 72 h. Twelve compounds including 8 clinically approved structural cardiotoxins, 3 functional cardiotoxins and 1 non-cardiotoxin were evaluated. IC50 values demonstrated high concordance with published values. More adverse effects were observed at 72 h with 4 of the structural cardiotoxins (mitoxantrone, sunitinib, sorafenib and amiodarone) significantly modulating all assay parameters. Mitochondrial membrane potential (MMP) was the most sensitive and specific indicator of structural cardiotoxicity. Cmax values demonstrated correlation with MMP ($r = 0.91$) and BNP expression ($r = 0.92$) indicating toxicity detection at in vivo therapeutic levels. We developed assays to evaluate functional cardiotoxicity potential using the multi-electrode array platform (MEA) by measuring beat period, spike amplitude and field potential duration. This study demonstrates the utility of HCS and MEA assays using hESC-derived cardiomyocytes to facilitate cardiotoxicity hazard identification and provide insight into the intricate mechanisms implicated in cardiotoxicity.

PS 1909 Early Activation of Aryl Hydrocarbon Receptor Alters the Expression of Homeobox Transcription Factors That Control Cardiomyocyte Differentiation

Q. Wang, J. Chen, C. Ko, Y. Fan, Y. Xia, M. Medvedovic and A. Puga. *University of Cincinnati, Cincinnati, OH.*

The aryl hydrocarbon receptor (AHR) is a critical mediator of gene-environment interactions. The prototypical ligand for the receptor is the environmental pollutant TCDD. Genome-wide gene expression profiling suggests that disruption of AHR homeostatic levels during embryonic stem cell (ESC) differentiation alters the expression of homeobox transcription factors (HTFs) that control cardiomyocyte (CM) differentiation. To further characterize how AHR regulates the expression of HTFs during CM differentiation, we isolated Ahr+/+, Ahr+/- and Ahr-/- ESC from C57BL6 mice. TCDD treatment significantly inhibited the formation of contractile CM nodes during Ahr+/+ and Ahr+/- ESC differentiation while Ahr-/- ESC were resistant to TCDD-induced cardiotoxicity. The most critical time window of TCDD toxicity for Ahr+/+ and Ahr+/- ESC CM differentiation was during the early differentiation time, between day 0 and day 3. Global expression analysis of differentiating cells from day 1 to day 4 showed that activation of AHR disrupts the concerted expression of genes involved in cardiac differentiation, while the onset of HTFs involved in CM differentiation was delayed in Ahr-/- cells. We used plasmids with a reporter of eGFP under the control of promoters of the master cardiac regulator Nkx2-5 or the pacemarker Shox2 to analyze interactions between these homeobox genes in transfected mouse hepatoma cells treated with TCDD or not. TCDD treatment significantly down-regulated Nkx2-5 promoter-driven while up-regulated Shox2 promoter-driven eGFP expression. These data suggest that AHR activation by TCDD induces the repression of genes involved in cardiac differentiation through the inhibition of NKX2-5-regulated genes and that loss of AHR delays CM differentiation. AHR function appears to be the coordination of a complex regulatory network responsible for attainment and maintenance of cardiovascular homeostasis. Supported by NIEHS 5R01 ES006273.

PS 1910 *In Vitro* Multiparameter Assessment of Cardiotoxicity in Human Induced Pluripotent Stem Cell (iPSC)-Derived Cardiomyocytes

M. L. Wolfe[1], B. D. Anson[2] and H. Ma[1]. [1]*Cellular and Molecular Biology, MPI Research, Mattawan, MI and* [2]*Cellular Dynamics International, Madison, WI.*
Sponsor: T. Rogers.

Cardiotoxicity is one of the leading causes of drugs failing during clinical trials and being withdrawn from the market. Implementation of an in vitro cell-based predictive assay early in the drug discovery process would help improve early compound attrition and develop safer drug candidates. We tested compound-treated human induced pluripotent stem cell (iPSC)-derived cardiomyocytes (iCell® Cardiomyocytes) using the Thermo Scientific ToxInsight® IVT platform to determine the cardiotoxicity risk of a compound through the measurement of multiple toxicity biomarkers in individual cells. The compounds we investigated are known cardiotoxic compounds (Doxazosin, Rosiglitazone and Nilotinib) and non-cardiotoxic compound (Aspirin). Each compound was tested at six concentrations in triplicate. The use of multiple dyes allows for high sensitivity and specificity for predicting cardiotoxicity by simultaneously detecting six multiplexed cellular targets and properties associated with cell loss, cellular redox stress, apoptosis and mitochondrial stress. Furthermore, the extracellular supernatants can be analyzed for a biomarker of hypertrophy, brain natriuretic peptide (BNP), for a seventh cardiotoxicity parameter. The cardiotoxicity profile generated by the multiparametric data for the test compounds may help determine the mechanism of toxicity between classes of therapeutic reagents.

PS 1911 Evaluation of a 3D Stem Cell Model of Intestinal Epithelium to Predict and Model Enterotoxicity

M. Wagoner[1], M. V. Nadella[1], R. Caccese[1], K. Adams[1], J. Sasaki[1] and Y. P. Dragan[2]. [1]*Safety Assessment, AstraZeneca Pharmaceuticals, Waltham, MA and* [2]*E.I. du Pont de Nemours and Company, Wilmington, DE.*

Cancer therapies are often dose-limited by their toxicity in rapidly proliferating, non-neoplastic tissues. The intestinal epithelium is the most rapidly dividing tissue in adult mammals, turning over every 5-7 days, and thus requiring continual

proliferation, differentiation and stem cell self-renewal. Unintended perturbation of any one of these processes by pharmaceuticals can cause enterotoxicity. To date, scaleable in vitro systems for the prediction and modeling of enterotoxicity have been limited to immortalized cell lines, which recapitulate only a fraction of the cell types and processes unintentionally perterbed by enterotoxins. Here, we describe an in vitro model that captures critical aspects of enterotoxicity including proliferation, differentiation and stem cell self-renewal. This murine 3D crypt-villus organoid, termed a MiniGut or intestinal enteroid, is sensitive to a multitude of mechanisms of enterotoxicity caused by both marketed pharmaceuticals as well as pharmaceutical compounds in development. The data presented in this work indicates that in addition to detecting the enterotoxicicity inherent in chemotherapies such as 5-fluorouracil and irinotecan, the intestinal enteroid model is able to distinguish between toxic and non-toxic drug candidates in a medium throughput fashion. Furthermore, our results indicate that intestinal stem cells and their progeny are maintained in their native niches in the MiniGuts, enabling perturbations in stem cell self-renewal and differentiation observed in vivo to be modeled in vitro. MiniGut intestinal enteroids recapitulate the complex interplay of 5 different epithelial cell types, including the critical stem cell compartment, and will serve as a valuable in vitro screen for drug-induced enterotoxicity in ways that were previously only possible in vivo.

PS 1912 Characterization of a Brain Microphysiological System for Studying Gene/Environment Interactions

D. Pamies[1], G. Makri[3], J. P. Bressler[2], K. M. Christian[3], G. Harris[1], C. O'Driscoll[2], L. Smirnova[1], P. Marina[2], R. Bachinski[1], T. Hartung[1] and H. T. Hogberg[1]. [1]*CAAT, Johns Hopkins, Bloomberg School of Public Health, Baltimore, MD,* [2]*Kennedy Krieger Institute, Johns Hopkins Bloomberg School of Public Health, Baltimore, MD and* [3]*Institute for Cell Engineering, Johns Hopkins School of Medicine, Baltimore, MD.*

There is a concern that chemical exposure might contribute to neurological disorders. However, the neurotoxic potential of many chemicals remains unknown, as current *in vivo* (developmental) neurotoxicity tests are expensive, time consuming and with doubtful relevance for humans. Moreover, the difficulty of studying interactions between human genetics and environmental factors leads to lack of knowledge about the events that induce neurological diseases. Microphysiological systems (MPS), promise to generate more complex *in vitro* human models that better simulate the organ's biology and function. The recent discovery of induced pluripotent stem cells (iPSC) gives a range of possibilities allowing cellular studies of individuals with different genetic backgrounds (e.g. human disease models). Application of iPSCs from different donors in MPS gives the opportunity to better understand disease and can be a novel tool in different fields, such as drug development, toxicology and medicine. In order to generate a brain-on-a-chip, in the last year, we have established a 3D model consisting of aggregating cultures of iPSC-derived neural cells based on our experience with 3D rat primary aggregating brain cell cultures. Characterization of the model has been obtained. mRNA and microARN levels have been studied as well as size, apoptosis and cell type populations. Human 3D aggregates stain positively for different neuronal markers after 4 and 8 weeks of differentiation. In addition, qPCR analyses show higher expression of various neuronal differentiation markers in 3D cultures compared to 2D culture, showing a faster maturation in the 3D system. Here we present the applications of this emerging technology and identify possible future directions of our developed 3D brain MPS. Funded by NIH (#1U18TR000547)

PS 1913 The Potential Therapeutic Role of Secreted Antiviral Entry Inhibitory (SAVE) Peptides Expressed by Transduced Mesenchymal Stem Cells (MSCs)

N. Lee[1, 3], E. Walker[1], L. Egerer[2], D. Laer[2], B. Bunnell[1, 3] and S. Braun[1, 3]. [1]*Regenerative Medicine, Tulane National Primate Center, New Orleans, LA,* [2]*Division of Virology, Innsbruck Medical University, Innsbruck, Austria and* [3]*Biomedical Sciences, Tulane University, New Orleans, LA.*

The population of people living with human immunodeficiency virus (HIV) has remained relatively stable due to antiretroviral therapy. However, still the pace of new infections continues at far too high a level. We have shown that expression of the membrane-associated and secreted C46 peptides, members of the new fusion inhibitor class of antiretroviral drugs, efficiently block infection of new cells by interfering with the function of HIV-1 gp41. To evaluate the potential therapeutic role of the Secreted Anti-Viral Entry inhibitory (SAVE) peptide in transduced mesenchymal stem cells (MSCs), we measured the inhibition of HIV infection in vitro with C46-transduced MSCs. First, we transduced human and rhesus MSC with retroviral and lentiviral vectors (LV) expressing GFP (LZRS-GFP: MLV and HRST-GFP: LV), membrane-bound C46 (M218: MLV), or the secreted C46 (T-60: MLV and T-42: LV). Fluorescent microscopy and flow cytometry demonstrated that up to 69% of LV-transduced MSCs and 293T control cells expressed GFP. Molecular analysis of MLV ψ packaging element revealed that up to 25.5% of the human MSCs, rhesus MSCs, and 293T cells were transduced with the T-60 and M218 vectors. C46 was detectable in SAVE-transduced MSCs by western blot using 2F5 antibody. We sequentially conducted the single round infection assay to measure the inhibition of viral infection in vitro with conditioned medium from the SAVE-transduced MSCs. The data showed that conditioned medium from C46 and SAVE transduced rhesus bone marrow derived-MSC blocked the infection of the HIV vectors by from 60-75%. In order to test whether transduction and the insertion of the trans-gene affect the differentiation of MSCs potency, we have conducted osteogenic, adipogenic, and chondrogenic differentiation assay on SAVE-transduced rhesus bone marrow derived MSCs.

PS 1914 Foetal-Derived Human Neural Stem/Progenitor Cells (h-NPCs): Safety Profile in the Mouse following Single Intracerebroventricular (ICV) Administration

G. Di Gallo[1], E. Riccardi[1], C. I. Bernardi[1], E. Brambilla[2], F. Ruffini[2] and G. Martino[2]. [1]*Preclinical Development, Accelera S.r.l., Nerviano - Milano, Italy and* [2]*Division of Neuroscience, San Raffaele Hospital - Experimental Neurology Institute, Milano, Italy.* Sponsor: M. Brughera.

Foetal derived human neural stem/progenitor cell (h-NPCs) transplants have potential as therapeutic candidates to treat a vast number of disorders of the central nervous system (CNS). The biological activity of these stem cells has been analyzed extensively in vitro and in vivo, (1, 2) supporting neuroprotective strategies and clinical translation in human therapy for the major components of the CNS (i.e. brain, spinal cord and eye).
To investigate any potential adverse effect of stem cell therapy, h-NPCs were given as a single intracerebroventricular (IVC) administration to CD-1 mice treated daily with cyclosporin to better simulate the possible clinical use in humans, and the animals were carefully observed for a period of 90 days thereafter.
No mortality related to the biological effect of h-NPCs occurred, and no significant signs of toxicity were recorded either in clinical signs, body weights, food intake, clinical pathology, and at gross and histological examinations.
From the results obtained it was concluded that h-NPCs given as single ICV administration to CD-1 mice do not exert any local or systemic toxicity even following a relatively extended period of observation, supporting their safe application in clinical testing.
1. Ann Tsukamoto, Nobuko Uchida, Alexandra Capela, Thorsten Gorba and Stephen Huhn. Stem Cell Research & Therapy 2013, 4:102
2. Stefano Pluchino et al. Annals of Neurology 2009, 66:343

PS 1915 High-Throughput Developmental Toxicology Screening Platform Using Human iPSC-Based Transcriptional Analysis

R. Abujarour, B. Valamehr, M. Robinson and P. Flynn. *Fate Therapeutics, San Diego, CA.* Sponsor: R. Totah.

One of the most promising alternative in vitro developmental toxicity assays is the Embryonic Stem Cell Test (EST) which is based on the ability of mouse embryonic stem cells (ESCs) to differentiate into beating cardiomyoctes as determined by morphological assessment. However, the EST is low throughput, lacks quantitative molecular endpoints, requires inter-species extrapolation and does not inform about a toxicant's mode of action. Unlike mouse ESCs, human ESCs and human induced pluripotent stem cells (hiPSCs) are difficult to culture as single cells and thus are not compatible with high throughput manipulations. We have previously developed a single-cell handling and hiPSC culture system based on novel small molecules, enabling scaled culture and multi-well assay development. In the present study we demonstrate a novel and potentially powerful developmental toxicity screening platform using single cell hiPSCs as an in vitro model for embryonic development, and transcriptional analysis to track changes in conserved developmental signaling pathways as predictors of developmental toxicity. Feeder-free and single cell-seeded hiPSCs were exposed in 96-well plate to three definitive teratogens (methyl mercury, thalidomide and valproic acid) and DMSO (solvent) in 6 concentrations for 48hr. Gene expression analysis of developmentally-regulated genes (developmental signaling pathways, pluripotency and lineage specifications) was performed by high-content RT-PCR using microfluidic chips capable of performing 2,304 unique PCR reactions (48 samples and 48 gene targets). All the three teratogens inhibited pluripotency genes and activated differentiation genes to variable degrees. Further, effects on developmental signaling pathways were mapped, revealing unique toxicant-specific signatures on teratogen exposure. We believe this study demonstrates the potential for hiPSC-based teratogen characterization and enables the further identification of toxicology signatures for prospective toxicology screening.

PS 1916 Arsenic-Induced Aberrant Gene Regulation of Human Adipose-Derived Mesenchymal Stem Cells

J. J. Shearer and M. L. Figueiredo. *UTMB, Galveston, TX.*

Inorganic arsenic is a worldwide contaminant commonly found in drinking water. Although the EPA has classified it as a human carcinogen the mechanistic details are still being elucidated. Current data suggests cancer associated with arsenic exposure is the result of genome instability and subsequent aberrant gene transcription rather than direct mutagenicity. Epidemiological studies have suggested a correlation between arsenic exposure and the incidence of prostate cancer. Malignant transformation by chronic arsenic exposure already has been shown in prostate-derived epithelial stem cells. We want to build on these findings by looking at another potential target of arsenic as the trigger of prostate cancer, periprostatic adipose tissue. The thickness of periprostatic adipose tissue has been correlated to the severity of prostate cancer and has been shown to be a rich source of human adipose-derived mesenchymal stem/stromal cells (hASC). Our hypothesis is that arsenic may be able to transform hASC in the periprostatic adipose tissue in order to promote prostate tumor progression. hASC have been isolated from prostate tumors in humans and data suggests they are derived from the periprostatic adipose tissue. Therefore, the goal of this project is to begin to deduce the malignant effects arsenic has on hASC, starting with examining dysregulation in gene expression. After chronic exposure of hASC to an environmentally relevant level of arsenic (sodium arsenite 1 μM), a 14.5 fold increase in interleukin-6 expression was detected by qPCR analysis after 6 weeks. In addition, genes associated with chromatin remodeling (HDAC1), cellular invasiveness (MMP-9) and cancer stem cells (NOTCH1) are becoming differentially expressed as we continue the course of arsenic exposure (9 weeks). These results suggest a reprogramming of hASC gene transcription induced by arsenic that may have the potential to alter the microenvironment surrounding the prostate, likely increasing cancer susceptibility (Supported by T32ES007254).

PS 1917 A Biomarker-Based Developmental Toxicity Screen Using Human Induced Pluripotent Stem Cells for Compound Prioritization

L. A. Egnash, J. A. Palmer, A. Smith, K. R. Conard, P. R. West, R. E. Burrier, E. Donley and F. R. Kirchner. *Stemina Biomarker Discovery, Inc., Madison, WI.* Sponsor: L. Recio.

Assessing potential developmental toxicity of new chemicals is resource intensive, time consuming, and requires large numbers of laboratory animals. Availability of more predictive developmental toxicity screens based on human cells will reduce costs, increase pharmaceutical and chemical safety, and reduce the risk of false-negatives due to inter-species differences. Our previous work has established that an hES cell culture based system can be used to predict human teratogenicity as an effective compound screening tool. The present work extends this idea to human iPS cells derived from the genetic manipulation of human somatic cells. iPS cells are phenotypically and genetically similar to hES cells (i.e. morphology, proliferation, gene expression) and are being used by many researchers to overcome the moral, ethical and political controversies surrounding hES cells. The current studies compare the metabolic similarities between human iPS and hES cells in response to compound exposure. Using both targeted and untargeted metabolomics approaches, we tested 31 compounds with known teratogenicity in human iPS cells and compared the results to those obtained using hES cells. For targeted metabolomics experiments, iPS cells were exposed to 9 concentrations of each compound. Spent media was collected and analyzed by high resolution LC/MS to determine the relative abundance of the biomarkers present in the system. For untargeted metabolomics experiments, cells were exposed to 3 concentrations of each compound and spent media was analyzed using a UPLC-ESI-QTOF mass spectrometry method that measured a broad range of small molecules. Using the biomarkers and assay parameters identified using hES cells, the iPS cell-based biomarker assay identified known developmental toxicants with 81% accuracy (75% sensitivity, 87% specificity). Establishing a developmental toxicity assay using iPS cells harnesses the predictive power of the hES cells without the ethical controversy, thus enabling validation for regulatory purposes.

PS 1918 Investigation of Mitochondrial Toxicity in Stem Cell-Derived Cardiomyocytes

S. Schwengberg[1, 2], R. Kettenhofen[2], J. Hynes[3], C. Carey[3], E. Clarke[4] and H. Bohlen[2]. [1]*Cells at Work Consulting & Services, Dueren, Germany,* [2]*Axiogenesis AG, Cologne, Germany,* [3]*Luxcel Biosciences, Inc., Cork, Ireland and* [4]*ReachBio LLC, Seattle, WA.*

Mitochondrial dysfunction has been implicated in the etiology of drug-induced cardiotoxicity, one of the most common causes for drug withdrawal. Screening for compounds with such liabilities has been difficult due to the lack of relevant cell models and assay technologies. Stemcell-derived cardiomyocytes provide a homogenous, reproducible and physiologically relevant cardiomyocyte cell system. Apart from the use in cardiac electrophysiology, these cells allow a detailed assessment of cell metabolism and mitochondrial function when combined with suitable assay technology, e.g. probes for the assessment of cellular O2 consumption.
We have examined the feasibility of such an approach by using mouse or human stemcell-derived cardiomyocytes cultured in 96 well plates. Rotenone, FCCP, and Antimycin were used as model compounds, and their effect on O2 consumption was continuously measured post treatment using the MitoXpress® Xtra probe (Luxcel Biosciences). FCCP (↑), Rotenone (↓), and Antimycin (↓) revealed typical O2 consumption profiles illustrating a capacity to specifically detect perturbed OXPHOS immediately post-treatment. Additionally, the influence of culture media containing glucose (4.5 g/L) or galactose (1.8 g/L) on susceptibility of mouse cardiomyocytes to mitochondrial toxicants have been assessed. Using the xCELLigence (ACEA Biosciences Inc.), we could demonsrate that although the onset of the effect of doxorubicin and FCCP was faster in cardiomyocytes cultured in glucose media, the overall effect of both compounds after 48h of treatement in both media was similar. Only the ETC I inhibitor Rotenone showed an increased effect both on onset and severity if cells were cultured in galactose.
Our results demonsrate the combination of cell and assay systems to be capable of delineation of mitochondrial inhibition and uncoupling from non-specific cytotoxicity as well as the detection of redox cyclers, a particularly important mechanism in drug-induced cardiotoxicity.

PS 1919 Monitoring of Calcium Transients of Human Cardiomyocytes Derived from Induced Pluripotent Stem Cells As a Predictive Tool for High-Throughput Assessment of Cardiac Toxicity

R. Kettenhofen[1], A. Duenbostell[1], T. Niedereichholz[2], J. D'Angelo[2], H. Horai[2], S. Schwengberg[1, 3], H. Bohlen[1] and T. Licher[4]. [1]*Axiogenesis AG, Cologne, Germany,* [2]*Hamamatsu Photonics K.K., Hamamatsu City, Japan,* [3]*Cells at Work Consulting & Services, Dueren, Germany and* [4]*Sanofi-Aventis Deutschland GmbH, Frankfurt, Germany.* Sponsor: E. Clarke.

Early assessment of cardiotoxic potentials is desired to avoid costly failures of drug candidates in the late phases of the drug development process. Since screening for hERG channel modulation is not sufficient to assess a comprehensive view on potential adverse effects on the heart, there is a need for a predictive cardiotoxicity assay suitable for high throughput screening (HTS). Directed differentiation and a transgenic approach allow for a specific selection of pure, human induced pluripotent stem cell-derived cardiomyocytes (hiPSCM). The hiPSCM reveal spontaneous contraction and typical physiological properties compared to their primary counterparts and can be generated in the quality, stability and amounts required in HTS. We have used the FLIPR Calcium 5 Assays Kit together with the Hamamatsu FDSS μCell and the FLIPR to monitor and analyze the effect of more than 35 standard compounds on the parameter of cytosolic free calcium ([Ca2+]i) transients from hiPSCM in a 384 well format. Each compound was tested in a full dose response with at least 3 replicates for each concentration. The compounds tested comprise known modulators of cardiac sodium, calcium, potassium (including several hERG blockers), and hyperpolarization-activated ion channels as well as GPCRs, connexins, and ion exchangers and pumps. Typical modulations of [Ca2+]i transients in terms of frequency, duration, peak amplitude, slope (rise and decay), and rhythmicity were analyzed and correlated to the known mode of action of the compounds. The results from our study reveal that modulation of [Ca2+]i transients is predictive for a broad range of cardiotoxic compounds. Based on these results, the described assay system is a cost effective, predictive in vitro system to assess cardiac liabilities at an early state of the drug development process.

PS 1920 An *Ex Vivo* Platform to Evaluate the Differential Effects of Potential Therapies on Leukemia Progenitors (CFU-L) vs. Normal Bone Marrow (NBM) Progenitors (CFU-GM)

E. Clarke, B. Kyriss and A. Mergaert. *ReachBio LLC, Seattle, WA.*

Acute myeloid leukemia (AML) is a malignant disease characterized by rapid growth of myeloid cells in the marrow. This year, 14,500 new cases will be diagnosed in the US, claiming the lives of approximately 10,000. Nearly 40 years have passed since the development and implementation of cytarabine (Ara-C) and daunorubicin (DNR) combination therapy as a standard of care. Yet the genetically heterogeneous characteristics of AML demands the development of novel treatment strategies. In support of this end, the colony forming cell (CFC) assay provides an ex vivo platform in which novel compounds can be tested for efficacy alone or together with current combination therapies. Using the CFC assay we evaluated the toxicity of the AML drugs DNR, Ara-C and clofarabine on AML cancer "stem cells" and NBM CFU-GMs. NBM (n=4) and AML marrow (n=3) were cultured in semisolid methylcellulose-based media (ColonyGel) at 37°C, 5% CO2. Test compounds were added over a broad concentration range in triplicate and CFU-GM and CFU-L were enumerated microscopically after 14 days. Mean IC50 values for DNR, Ara-C, and clofarabine for CFU-GM and CFU-L were 11.5, 15.8 and 29.3 μM and 5.45, 2.9 and 2.2 μM, respectively. These data confirm greater (i.e. selective) killing of CFU-L vs NBM CFU-GM for all individual compounds. We extended this study to evaluate multi-combination therapies using calculated IC25 values for DNR and Ara-C on CFU-L (3 and 2 μM, respectively) and assessed this drug duo together with clofarabine. The combination of DNR and Ara-C at their IC25 concentrations inhibited CFU-L by approximately 50% in all AML marrows and inhibited NBM CFU-GM by 20%. When clofarabine, at its IC25 (1.5 μM) was added to DNR and Ara-C, an increased inhibition of CFU-L (70%, n=2) was observed while NBM CFU-GM inhibition was only increased to 24%. Thus, CFC assays provide a platform to evaluate novel targeted therapies with the current standard of care drug combinations, and can ascertain their selective effect on leukemic vs normal progenitors.

PS 1921 Cryopreserved Hepatocytes and Stem Cell-Derived Hepatocyted As Microphysiological 3D Liver Models in LiverChip

C. Rowe[1], E. Large[1], T. Cornforth[1], A. Robinson[1], A. Marguerie[2], L. Wray[2], M. Yeo[2], E. Sceats[1] and D. Hughes[1]. [1]*Zyoxel Ltd, Oxford, United Kingdom and* [2]*Definigen Ltd, Cambridge, United Kingdom.* Sponsor: S. Tannenbaum.

Liver functions rapidly decline in vitro when hepatocytes are cultured as monolayers. Human primary cell use is also hindered by unpredictable supply and quality of fresh cells. Cryopreservation techniques have partially circumvented the supply problem although cells quickly deteriorate. Similarly, methods to differentiate hepatocyte-like cells from induced pluripotent stem cells (iPSCs) can derive cells with liver disease phenotypes, such as Alpha 1 antitrypsin (A1AT) deficiency, although the cells may not be reaching the fullest possible maturity. We investigate the LiverChip in vitro 3D platform to model liver physiology through improved maintenance of primary liver cells with greater longevity and to further mature hepatocytes derived from iPSC cells to model pathophysiology. In LiverChip, cryopreserved primary human hepatocytes formed 3D tissues with metabolic activity, albumin production and urea output for at least 3 weeks. Through a DARPA funded project a liver microphysiological system based on the co-culture of primary human hepatocytes and kupffer cells was developed. Co-cultures displayed physiological responses to lipopolysaccharide exposure, including down-regulation of CYP3A, and secretion of pro-inflammatory cytokines IL-6 and TNF-alpha. Human iPSC-derived hepatocyte-like cells displayed enhanced hepatic function in LiverChip, compared with 2D monolayers. Analysis of secreted alpha fetoprotein, albumin, A1AT and fibrinogen demonstrated that LiverChip supports iPSC-derived cells with more advanced maturity than 2D culture. In conclusion, LiverChip is a perfused culture system supporting functional primary human liver cells to model hepatic tissue. LiverChip also has utility in further maturing iPSC-derived hepatocyte-like cells to recapitulate the physiology and pathophysiology of liver cells in health and disease.

PS 1922 LiverChip 3D Liver Platform Distinguishes between Known Hepatotoxic Drugs and Closely Related Structural Analogues

I. Taylor, C. Rowe, E. Large, T. Cornforth, A. Robinson, E. Sceats and D. Hughes. *Zyoxel Ltd, Oxford, United Kingdom.* Sponsor: S. Tannenbaum.

Primary human hepatocytes have many applications in drug discovery with plated or suspension cells used in assays for developing and testing candidate drugs. However, the attrition rate of drug candidates in late clinical phases, post-marketing drug withdrawal, and need for black box safety warnings due to hepatotoxicity demonstrate that many hepatotoxic drugs are not effectively screened out. There is great interest in 3D culture systems that re-form liver-like tissues from isolated human cells, and support liver physiology, to improve the predictivity of hepatotoxicity studies. LiverChip is a perfused culture system in which isolated liver cells re-form liver-like tissue structures in sinusoid-like channels in a porous scaffold. Tissues maintain measurable liver functions, including drug metabolism, with clearance of probe drugs correlating well with known hepatic clearance in man. Here we investigate LiverChip as a tool to distinguish between known hepatotoxic drugs and closely-related non-toxic structural analogues using multiples of human maximum plasma levels (Cmax). Human liver tissues were pre-formed in LiverChip for 3 days and then exposed to 0, 1, 3, 10, 30 and 100x Cmax concentrations of drugs for a further 6 days. Hepatocyte perturbations were assessed by measured disturbances in phenotypic liver markers, reduced mitochondrial activity and overt cytotoxicity was measured by leakage of intracellular enzymes. LiverChip experiments could identify known hepatotoxins with different mechanisms. Drugs that elicit hepatotoxicity in man through the formation of reactive metabolites (e.g. Clozapine), mitochondrial dysfunction (e.g. Tolcapone) or biliary transporter inhibition (e.g. Bosentan) could be distinguished from their non-toxic structural analogues. In conclusion, LiverChip is an effective tool for discovery toxicology with utility during selection of analogous lead compounds to identify safer new drugs with the lowest risk hepatotoxic potential.

PS 1922a Tobacco Smoke Effects on an Endothelial Cell Model Derived from Inducible Pluripotent Stem Cells

D. Gerhold[1], D. Kuo[1], G. Chen[2], G. Chen[2], J. Braisted[1], J. Zhu[2] and M. Boehm[2]. [1]*Toxicology, NIH/NCATS National Center for Advancing Translational Sciences, Rockville, MD and* [2]*NHLBI, NIH, Bethesda, MD.* Sponsor: M. Xia.

Tobacco smoke causes 3-fold more deaths from heart attack, stroke, and vascular disease, than from cancers. Endothelial cell responses to tobacco were studied to elucidate vascular disease/toxicity mechanisms. Human inducible Pluripotent Stem cells (iPSC) were differentiated to form an Endothelial Cell model (iECs). These iECs (98%) express the endothelial cell marker proteins: CD31 and VE-Cadherin. iECs or primary cultured human endothelial cells were cultured from: aorta (AECs), human coronary artery (CAECs), or umbilical vascular endothelial cells (HUVEC); and treated with tobacco smoke extract or vehicle. Viability was measured using an [ATP] assay and gene expression profiles were determined using qPCR and whole-genome mRNA sequencing (RNAseq). The majority of gene expression responses to tobacco by primary endothelial cells were recapitulated by iECs. Each cell line also yielded unique gene responses to tobacco according to RNAseq analysis. This work has revealed transcriptional responses of endothelial cells to tobacco that predispose humans to: vascular clotting, oxidative damage, hypertension, arterial calcification, and cytotoxicity. Further work will identify tobacco smoke components that trigger each event, and will identify biomarkers for these adverse events.

PS 1922b Neural Stem Cell Susceptibility to Japanese Diesel Exhaust Particulate Matter

C. Hegg, C. Jia and L. Koch. *Pharmacology and Toxicology, Michigan State University, East Lansing, MI.*

Environmental air pollutants negatively affect cognitive brain functions such as learning and memory and cause progressive neurodegeneration through unknown mechanisms. Although these deficits are associated with changes in neurogenesis (stem cell proliferation, differentiation and survival), few studies have examined the consequences of environmental air pollutants on neurogenesis. We examined the effects of 28 day daily intranasal exposure to particles isolated from Japanese diesel exhaust (DEPs, 1 mg/kg) or the organic extract of the DEPs (extracts) in C57Bl/6 male mice (6 weeks old; n=6/group). Behavior and proliferation in the dentate gyrus and subventricular zone of the lateral ventricles, areas of continuous neurogenesis affected by Alzheimer's disease, were examined. Exposure to DEPs or extracts did not alter weight gain compared to vehicle control (0.05% DMSO; $p>0.05$). There was no anxiolytic effect of DEPs or extracts as measured using the elevated plus maze behavior test at exposure day 9 and 27 ($p>0.05$ v. vehicle). These results indicate there was no overt toxicity associated with the treatments in this study. Proliferation, assessed by BrdU incorporation, was quantified in 8 planes through the dentate gyrus. A significant decrease in BrdU incorporation was observed in the DEP treatment group only ($p<0.05$ v. vehicle). BrdU incorporation in the subventricular zone region was such that counting individual cells was not possible. However, analysis of immunoreactivity using fluorescence intensity measurements indicated there was a trend for decreased BrdU incorporation in the subventricular zone of DEP-exposed mice compared to vehicle. Collectively,

this study demonstrates that chronic exposure via nasal aspiration of an ultrafine particulate, but not the organic component, decreases the ability of stem cells to proliferate in two brain regions that undergo neurogenesis. These data suggest that there are interrelationships between air pollution, neuronal stem cells and neurodegenerative diseases.

PS 1922c Clostridial Toxins Cause Synaptic Inhibition in Networked Populations of Stem Cell-Derived Neurons

P. McNutt, P. H. Beske, K. S. Hubbard, M. E. Lyman and K. M. Tuznik. *USAMRICD, Aberdeen Proving Ground-Edgewood Area, MD.*

Following internalization into presynaptic termini, the two families of clostridial neurotoxins (CNTs) botulinum neurotoxin (BoNT) and tetanus neurotoxin (TeNT) cleave proteins associated with synaptic vesicle release, preventing the exocytosis of neurotransmitters. To date, no cell-based model used in CNT research has been shown to form functioning synapses, limiting the ability to conduct target discovery or therapeutic screening. Stem-cell derived neurons have recently been proposed as a next-generation cell-based platform for neurotoxicity research. Whole-cell patch clamp electrophysiology indicates that ESNs develop mature electrical responses and form a complex, synaptically coupled network with an excitatory:inhibitory balance by 18 days in vitro (DIV). Hypothesizing that synaptically coupled ESNs may undergo synaptic inhibition in the presence of BoNT/A, we evaluated the effects of intoxication on functional measurements of synaptic activity at DIV 24. Treatment of ESNs with 0.01 mouse lethal units of BoNT serotype A (BoNT/A) resulted in the significant loss of synaptic function, as determined by significant reductions in synaptically driven excitatory potentials and miniature excitatory post-synaptic currents (mEPSCs). Notably, inhibition of miniature inhibitory post-synaptic currents (mIPSCs) was a leading indicator of intoxication, being >80% inhibited within 30 min, whereas significant decrements in mEPSC activity were not apparent until 60 min. Long-term patch clamp assays indicated that addition of BoNT/A perturbed the excitatory/inhibitory balance within minutes, producing an epileptiform network response that progressively increased through 40 min. These data suggest that electrophysiological characterization of trans-synaptic activity may comprise a novel, rapid screen for the presence of functional toxin in forensic, pharmaceutical, environmental and/or food samples, as well as provide a physiologically relevant in vitro model for drug screening and mechanistic research

PS 1922d Characterization of Functionally Networked, Central Nervous System Neurons Derived from Stem Cells As an *In Vitro* Platform for Neurotoxin Research

M. E. Lyman, P. McNutt, K. S. Hubbard, P. H. Beske and K. M. Tuznik. *USAMRICD, Aberdeen Proving Ground-Edgewood Area, MD.*

Recently, there has been a strong emphasis on developing an in vitro model for botulinum neurotoxin (BoNT) research that combines the biological relevance of primary neurons with the scalability, reproducibility, and genetic tractability of continuous cell lines. However, no cell-based platform recapitulates the sensitivity of primary neurons to BoNTs, suggesting that neurogenic cell lines do not accurately model the mechanisms of toxin internalization and activity. Here, we present a novel system to efficiently derive high yield, high purity neurons (ESNs) from murine embryonic stem cells (ESCs) for neurotoxin research. This approach produces terminally differentiated and synaptically coupled populations of networked glutamatergic (90%) and GABAergic (10%) neurons within three weeks. RNA sequencing was used to correlate cellular gene expression with the functional onset of network activity during differentiation and neuronal maturation. Bioinformatic analysis revealed a dynamic transcriptional profile, culminating with a population containing mature, VGLUT2+ glutamatergic and GABAergic neurons. Neuronal maturation was confirmed using immunocytochemistry, which revealed the appropriate compartmentalization of neurotypic proteins in concordance with a decrease in markers of pluripotency. Electrophysiologic characterization confirmed maturation-dependent intrinsic neuronal properties, the development of a synaptically coupled neural network exhibiting miniature excitatory and inhibitory post-synaptic currents and an emergent excitatory:inhibitory balance. We have shown that ESNs are sensitive to a wide array of neuromodulatory toxins, including botulinum neurotoxins, tetanus toxin and glutamate, among others. The ability to produce a networked neuronal population that exhibits the appropriate pathophysiological response to intoxication by neurotropic toxins confirms the suitability of derived neuron networks for basic research and drug discovery.

PS 1922e Transcriptomic Effects of Curcumin and Piperine in Breast Stem Cells

J. Colacino[1], S. P. McDermott[2], M. A. Sartor[3], M. Kakarala[4], M. S. Wicha[2] and L. S. Rozek[1]. [1]*Environmental Health Sciences, University of Michigan School of Public Health, Ann Arbor, MI,* [2]*Comprehensive Cancer Center, University of Michigan, Ann Arbor, MI,* [3]*Computational Medicine and Bioinformatics, University of Michigan, Ann Arbor, MI and* [4]*Van Andel Research Institute, Grand Rapids, MI.*

Curcumin and piperine have been shown to have cancer preventive activity in preclinical models. We have previously shown these compounds limit stem cell self renewal. Normal and breast cancer stem cells exist in two states, with each cell type having unique properties. The objective of this study is to identify the mechanisms of action of curcumin and piperine in breast stem cells, using cell type specific RNA sequencing (RNA-seq) on breast cancer cell lines and normal breast cells. Breast cancer cell lines SUM149, T47D, and MCF7 were cultured as mammospheres and treated with curcumin (2.5μM - 15μM) and piperine (5μM and 10μM) individually and in combination. Normal breast cells isolated from reductive mammoplasty patients (n=13) were treated as mammospheres with 5μM curcumin and 5μM piperine. We used fluorescence activated cell sorting to isolate ALDH+ and ALDH-/CD44+/CD24- stem cell fractions of SUM149, treating with 5μM curcumin and 5μM piperine for 24hrs. RNA-seq libraries were prepared with the NuGen Encore Complete kit and sequenced on an Illumina HiSeq 2500. In cell lines, curcumin and piperine inhibited mammosphere formation in a dose-dependent manner. In primary breast cells, curcumin, piperine, and the combination inhibited mammosphere formation 28% (p=0.0004), 24% (p=0.01), and 42% (p=0.0002) respectively. In both stem cell fractions, curcumin induced differential expression of similar genes, including AREG, EPGN, BAMBI, ALDH3B2, and CYP1B1. Pathway analyses showed that curcumin induced expression changes related to cholesterol and steroid biosynthesis and oxidoreductase activity. Ongoing experiments will quantify the transcriptomic effects of these compounds in normal breast stem cells. These findings point to novel regulation of stem cell self renewal and provide biomarkers of efficacy for future cancer prevention trials.

PS 1922f Development of a Human Adipose Stem Cell Model for Chemical Obesogen Screening

C. Deisenroth and B. Foley. *The Hamner Institutes for Health Sciences, Research Triangle Park, NC.*

The relationship governing environmental influence on an individual's genetic predisposition toward obesity is a complex one. A largely unexplored avenue is the notion of obesogens; environmental endocrine disrupting chemicals (EDC) that may alter the propensity towards obesity, particularly during prenatal and early life exposure. In an effort to establish a human-based high-throughput platform for obesogen screening, human adipose stem cells (ASC) were selected as a biologically relevant model. Differentiation of multipotent ASC through a committed progenitor stage to terminal adipocytes requires a chemical cocktail capable of coordinated perturbation of multiple signaling pathways. Initial assessment demonstrated that omission of any single chemical component in the cocktail significantly decreased or inhibited ASC differentiation potential. In order to define a cocktail that would prime ASC for commitment to the adipocyte lineage and facilitate dose-response assessments to novel chemical obesogens, thiazolidinedione, dexamethasone, and phosphodiesterase inhibitor were screened in combination across a five-point dose-response to determine relative rates of differentiation. A quantitative fluorescence-based readout of neutral lipid accumulation was used as a phenotypic endpoint to define the priming cocktail suitable for screening. Peak relative lipid accumulation exhibited a 5-fold change increase over primed controls (Z'=0.47), demonstrating a suitable dynamic range for the assay. In addition, characterization of key adipogenesis biomarkers was assessed at the transcript and protein level to characterize the differentiation capacity of the priming cocktail. Subsequent exposure of primed ASC to reference compound tributyltin, the hallmark obesogen, demonstrated dose-dependent modulation of adipose stem cell fate. Development of a high-throughput human adult stem cell based platform is useful for unbiased screening of novel EDC's capable of modulating adipogenesis.

PS 1923 Cytoprotective Effects of the Antioxidants Tempol and WR-1065 in Human Lymphoblastoid Cells Exposed to Zidovudine (AZT)

M. O. On'Gele[1], H. Braun[1], K. Divi[1], M. C. Poirier[1], J. B. Mitchell[2] and O. Olivero[1]. [1]*Carcinogen-DNA Interactions, National Cancer Institute, Bethesda, MD and* [2]*Tumor Biology Section, National Cancer Institute, Bethesda, MD.*

Antiretroviral Nucleoside Reverse Transcriptase Inhibitors (NRTIs) are used in drug combinations to treat Human Immunodeficiency Virus-1 (HIV-1) infection. AZT is an NRTI that becomes incorporated into DNA, acts as a DNA replication chain terminator, induces aneuploidy and mutations in mice and humans, and is tumorigenic in mice. The Cytokinesis Block Micronucleus (CBMN or Cytome) assay is a comprehensive system used to measure DNA damage occurring as a result of genotoxic insult. Molt-3, human lymphoblastoid cells exposed to AZT for 52 hours, were arrested with Cytochalasin B (Cyt B) for the last 28 hours, and the binucleated cells, which by definition completed one cell division, were scored for: micronuclei (MN); chromosome bridges (NPBs); nuclear buds (NBs); Apoptotic/Necrotic (A/N) cells and Nuclear Division Index (NDI). We hypothesized that the antioxidants Tempol and WR-1065 would protect against AZT-induced genotoxicity. Molt-3 cells were seeded into 24-well plates and exposed to 10 μM AZT, 10 μM AZT plus 5 μM WR-1065, or 10 μM AZT plus 200 μM Tempol. Cyt B was added for the last 24 hours to arrest cell growth. The NDI was similar for all groups, indicating that the different treatments did not alter cell viability. Molt-3 cells exposed to AZT and examined by Cytome assay had significant increases in MN, NBPs, NBs, and A/N, compared to unexposed controls. Cells treated with either Tempol or WR-1065 had significantly-reduced AZT-induced MN. In addition, WR-1065, but not Tempol, reduced the levels of A/N. In the presence of AZT, Tempol significantly reduced levels of NBs, while WR-1065 reduced the levels of NPBs. Overall, the Cytome assay provided a useful indicator of AZT-induced genotoxicity, and demonstrated that the antioxidants Tempol and WR-1065 each protect against different AZT-induced genotoxic end points. The data implies different mechanisms of protection for the two antioxidants.

PS 1924 Prolonged Exposure to Particulate Chromate Inhibits Homologous Recombination Repair Proteins

C. L. Browning[1, 2], H. Xie[1, 2], Q. Qin[1], J. Masson[3] and J. P. Wise[1, 2]. [1]*Wise Laboratory of Environmental and Genetic Toxicology, Maine Center for Toxicology and Environmental Health, University of Southern Maine, Portland, ME,* [2]*Graduate School of Biomedical Sciences and Engineering, University of Maine, Orono, ME and* [3]*Genome Stability Laboratory, Laval University Cancer Research Center, Quebec City, QC, Canada.*

Particulate hexavalent chromium (Cr(VI)) is a known human lung carcinogen that produces several forms of DNA damage, including DNA double strand breaks (DSBs). The homologous recombination (HR) repair pathway is utilized by cells to repair DSBs in an error-free manner during late S-G2 and mitosis. Our previous studies show that prolonged Cr(VI) exposure induces persistent DSBs levels and that defective repair of these DSBs allows for neoplastic transformation of human lung cells. However, few studies have investigated the effect of particulate Cr(VI) exposure on HR repair proteins. In this study, we analyzed the effect of particulate Cr(VI) exposure on key HR proteins: one of the DSB sensors, MRE11, the signal transducer, ATM, a key repair effector, RAD51, and the RAD51 transporter, RAD51C. We exposed human lung fibroblasts to zinc chromate for 24-120 hours. After exposure, the response of these proteins was measured by western blotting or a nuclear foci formation assay. Our data shows an increase in nuclear MRE11 foci formation, phosphorylated ATM protein expression, RAD51 protein expression and nuclear foci formation and RAD51C nuclear foci formation after 24 h Cr(VI) exposure, suggesting that HR repair is activated. However, prolonged Cr(VI) exposure inhibits phosphorylated ATM protein expression, RAD51 protein expression and nuclear foci formation and RAD51C nuclear foci formation. These results suggest that prolonged Cr(VI) exposure inhibits HR repair signaling through the regulation of RAD51. Ongoing work is investigating the effect of prolonged Cr(VI) exposure on RAD51C protein expression, RAD51/RAD51C co-localization and RAD51 transport kinetics. This work was supported by NIEHS grant ES016893 (J.P.W).

PS 1925 Targeted Ubiquitination and Degradation of Human DNA Ligase I by the CUL4-DDB1 Ubiquitin Ligase Complex

Z. Peng and A. Tomkinson. *Internal Medicine, Univ of New Mexico, Albuquerque, NM.*

Human DNA ligase I (hLIGI) is required for efficient DNA replication, recombination and repair. Here, we report a mechanism that controls the programmed degradation of hLIGI via targeted ubiquitination. In this study, a proteomic approach was used to screen interacting proteins of hLIGI in 293T cells. Mass spectrometry analysis reveals several proteins in the hLIGI immunocomplex including cullin4A (CUL4A) and damage-specific DNA binding protein 1 (DDB1). We confirmed that CUL4A and DDB1 as hLIGI-associated proteins by immunoprecipitation, which suggests that DDB1 acts as an adapter to link LIGI to CUL4 to form the E3 ubiquitin ligase complex. Furthermore, the level of hLIGI was reduced in confluent MCF10A cells and under stress conditions; while treatment with the proteasome inhibitor, MG132 prevented this reduction. We also found that hLIGI ubiquitination ultimately led to its degradation via the proteasome pathway, at least in part initiated by the Cul4-DDB1 complex. Mutations or inhibitors that blocked the modification at any step in this pathway would suppress hLIGI degradation. These findings may represent a newly identified regulatory mechanism used by cells to ensure the normal DNA replication and is essential for the maintenance of genome stability.

PS 1926 Activation of ATM-Dependent Genotoxic Signaling in Human Lung Cells by Formaldehyde

S. Ortega Atienza, J. Morse and A. Zhitkovich. *Pathology and Molecular Medicine, Brown University, Providence, RI.*

Formaldehyde (FA) is a carcinogenic aldehyde that produces DNA-protein crosslinks as the main form of DNA damage. Human exposure to exogenous FA primarily occurs via inhalation and is found in many occupational settings and among tobacco smokers. In this work, we examined whether the alkylating agent FA was capable of engaging ATM kinase that is traditionally associated with the stress signaling elicited by DNA double-stranded breaks (DSB). We found that FA provoked a rapid activation of the ATM pathway in normal and transformed human lung cells. In response to FA, ATM underwent activating Ser1981 autophosphorylation and phosphorylated two major proteins in its signaling network, CHK2 kinase and chromatin-associated KAP1. However, unlike DSB, FA-activated ATM did not target the transcription factor p53. Inhibition of RNA polymerase II had no effect on ATM activity, arguing against the possibility that ATM was triggered by collision of transcription complexes with bulky DNA-protein crosslinks. Activation of ATM was absent in nondividing cells and found exclusively in S-phase in cycling cell populations. The presence of DSB-sensing MRN complex was not required for FA-induced ATM responses, pointing to a noncanonical mechanism of activation. Inhibition of ATM kinase activity resulted in elevated levels of chromosomal breaks in normal human lung cells, indicating a protective role of ATM-induced signaling in suppressing gross genetic abnormalities by carcinogenic FA.

PS 1927 p53 Regulation of the GADD45a Gene Is Restricted to Genotoxin Exposure As a Consequence of a Requirement for p53/WT1 Interaction in the Promoter

R. Walmsley[1, 2] and D. Johnson[3]. [1]*Faculty of Life Sciences, University of Manchester, Manchester, United Kingdom,* [2]*Gentronix Ltd, Manchester, United Kingdom and* [3]*Animal Molecular Biology, Harper Adams University, Newport, United Kingdom.*
Sponsor: S. Dertinger.

Rationale: p53 is required for genotoxin and non-genotoxin induced apoptosis. However expression of the p53 target GADD45a, exploited in the GreenScreen HC genotoxicity assay, is very specifically induced by genotoxins. This study was conceived to explain the conundrum. The GADD45a p53 response element is in intron 3, however the GADD45a promoter has a WT1 response element binding site and other studies have demonstrated that WT1 and p53 proteins can interact. Furthermore, WT1 binding is supressed by Myc in the absence of DNA damage. The purpose of this study was therefore to test the hypothesis that GADD45a specificity is a consequence of WT1 mediation of p53 regulation.
Experimental approach: site directed mutagenesis was used to disrupt either or both of the p53RE and WT1RE in GADD45a-GFP reporter plasmids, and these were transfected into p53 competent TK6 cells and closely related p53 mutant WI-L2-NS cells. These new cell lines were then challenged with the following mechanistically diverse genotoxins: methyl methanesulphonate, cisplatin and mitomycin C, hydroxyurea, aphidicolin, 5′fluorouracil and benomyl. GFP expression data was collected using the standard GreenScreen assay protocols.

Results: GFP synthesis induced by all compounds in TK6 cells carrying the unmodified reporter. GFP synthesis was reduced in p53 mutant and wild type cells carrying modified reporter plasmids. The reduction was greatest in cells carrying the mutated p53 RE.
Conclusions: These experiments demonstrate that both WT1 and p53 response elements are involved in GADD45a regulation. This allows the conclusion that the induction of GADD45a requires p53, but specificity to genotoxins is a consequence WT1 controlled access to the promoter, which in turn is regulated by Myc.

PS 1928 Oxidative DNA Damage/Repair Induces Inflammatory Gene Expression in the Airways by 8-Oxoguanine DNA Glycosylase-Mediated Cell Signaling

L. Aguilera-Aguirre[1], A. Bacsi[1], T. G. Wood[2], A. R. Brasier[2, 3, 4], B. T. Ameredes[2, 3, 4], X. Ba[1] and I. Boldogh[1, 2]. *[1]Microbiology and Immunology, University of Texas Medical Branch, Galveston, TX, [2]Sealy Center for Molecular Medicine, University of Texas Medical Branch, Galveston, TX, [3]Institute for Translational Sciences, University of Texas Medical Branch, Galveston, TX and [4]Internal Medicine, University of Texas Medical Branch, Galveston, TX.*

Environmental pollutants cause oxidative stress in the airways and increase the levels of 8-oxoguanine (8-oxoG) in the DNA of lung epithelium due to guanine's lowest redox potential among DNA bases. 8-oxoguanine DNA glycosylase-1 (OGG1) excises and releases 8-oxoG during DNA base-excision repair (BER). Accumulation of 8-oxoG in the DNA has been linked to various inflammatory diseases including asthma. However, little is known about the role of OGG1-BER in pathogenesis of airway diseases. We observed activation of small GTPases upon OGG1-BER, or addition of 8-oxoG base to OGG1 proficient cells or mouse lungs in vivo. Therefore, we proposed that OGG1-BER and consequent activation of small GTPases mediate signaling for pro-inflammatory gene expression. To test our hypothesis, we challenged BALB/cJ mice intranasally with OGG1-BER product 8-oxoG, and used next-generation RNA-Sequencing technology to investigate the whole-genome gene expression in the lungs. The most overrepresented pathway was inflammation-related signaling. The majority of upregulated pro-inflammatory genes (≥ 3-fold expression) were NF-κB-dependent. We confirmed the expression levels of selected genes by qRT-PCR. In line with these observations, challenged mice with 8-oxoG or glucose oxidase (to induce OGG1-BER) showed significant induction of airway inflammation as determined by the number of neutrophils in bronchoalveolar lavage fluid compared to control ($p < 0.0001$). We conclude that OGG1-BER-triggered inflammatory gene expression in the lungs is a novel mechanism through which environmental pro-oxidant pollutants can induce airway inflammatory diseases.
Supported by: NIEHS T32ES007254, NCATS 1UL1TR000071 and NIEHS RO1 ES18948

PS 1929 Interpreting *In Vitro* Micronucleus Positive Results: Simple Biomarker Matrix Discriminates Clastogens, Aneugens, and Irrelevant Positive Agents

S. Bryce[1], J. Bemis[1], S. Dertinger[1], J. Mereness[1], M. Schuler[2], R. Spellman[2], J. Moss[2] and D. Dickinson[2]. *[1]Litron Laboratories, Rochester, NY and [2]Pfizer, Groton, CT.*

The specificity of *in vitro* mammalian cell genotoxicity assays is considered relatively low, as they yield a high incidence of positive results that are not expected to have *in vivo* relevance. We set out to develop a rapid, effective follow-up testing strategy that predicts whether apparent *in vitro* micronucleus (MN)-inducing effects are due to a clastogenic, aneugenic, or secondary irrelevant mode(s) of action. Priority was given to biomarkers that could be multiplexed onto flow cytometric acquisition of MN frequencies, or could be accomplished in parallel using a homogeneous-type assay. A training set of 30 chemicals comprised of clastogens, aneugens, and misleading positives was studied in human TK6 cells over a range of closely spaced concentrations in a continuous exposure design. In addition to MN frequency, the following endpoints were investigated: cleaved PARP-positive chromatin, cleaved caspase 3-positive chromatin, EMA positive chromatin, polyploid nuclei, phospho-histone H3-positive cells, TMRE negative cells, cellular ATP levels, cell cycle perturbation, and shift in γ-H2AX fluorescence relative to solvent control. Logistic regression identified endpoints that effectively predicted chemicals' a priori classification. Cross validation indicated that a promising base model includes γ-H2AX shift and change in phospho-histone H3-positive events (25/30 correct calls). Improvements were realized when one or two additional endpoints were included (26 - 30/30 correct calls). These models were further evaluated with a test set of 10 chemicals, and by evaluating 3 chemicals at a collaborating laboratory. The resulting data support the hypothesis that a matrix of high throughput-compatible biomarkers can effectively delineate two important modes of genotoxic action, as well as identify cytotoxicity that can lead to irrelevant positive results.

PS 1930 Error-Prone Double-Strand Break Repair Plays a Predominant Role in Oxidative Stress-Induced Mutagenesis

V. Sharma[1], L. Collins[1], W. Sun[2], J. A. Swenberg[1] and J. Nakamura[1]. *[1]Department of Environmental Sciences and Engineering, UNC, Chapel Hill, NC and [2]Department of Genetics, UNC, Chapel Hill, NC.*

Endogenous and exogenous oxidative DNA damage has been implicated in degenerative diseases and carcinogenicity. To counter this oxidative DNA damage, mammalian cells possess error-free DNA-repair systems. In contrast, a few DNA repair pathways in cells do not possess high fidelity and result in mutations. Little is known about the comparative contribution of each error-free and error-prone DNA repair protein/pathway in the oxidative stress induced DNA damage response (DDR) and mutations. Therefore, in the present study, using H2O2 as a model compound, we sought to understand the mechanisms of DDR and mutations caused by low level of oxidative stress and identify DNA repair pathways that may affect oxidative stress induced susceptibility to mutagenesis. DDR analyses were performed in different repair protein deficient DT40 cells. Rev1, Rad54, Rad51c, XRCC2, Fen1, Ku70 and Lig IV deficient cells showed comparatively more hypersensitivity to H2O2. All Ku70, DNA PKcs and Lig IV (NHEJ proteins) deficient cells tested in our study revealed a drastic decrease in mutation frequency despite the presence of equivalent levels of 8-oxodG as in the wild type DT40 cells. These data indicate a ROS induced mutagenic pathway in vertebrate cells proceeds via DNA double strand breaks (DSBs) and error-prone NHEJ repair. Current data combined with our previous reports of abasic site clusters in intact human cultured cells suggest that endogenous and exogenous oxidative stress may cause clustered DNA damage which may lead to DSBs with complex DNA ends and repairing such DSB with NHEJ may result in mutations even in the absence of DNA replication. It has been reported that NHEJ-deficient mice show early aging and less spontaneous tumor formation. Therefore, we are currently hypothesizing that mutations induced by oxidative stress through error-prone DSB repair pathway may be involved in etiology of wide variety of human diseases.

PS 1931 A New Mode of Action for the Cytolethal Distending Toxin

B. Salles, E. Bezine, Y. Fedor, J. Vignard, E. Boutet-Roubinet and G. Mirey. *Toxalim, INRA, Toulouse, France.*

The Cytolethal Distending Toxin (CDT) is a virulence factor produced by many pathogenic bacteria like Escherichia coli, Helicobacter hepaticus, Haemophilus ducreyi etc. The CDT production allows bacteria to persistently colonize the body, evade the immune system, induce inflammation and trigger genetic instability. In addition, it has been shown that CDT induces DNA double-stranded breaks (DSB), leading to cell cycle arrest and to cytotoxicity, associated with a characteristic cellular distension.
In order to characterize the type of DNA damage induced by CDT, we studied the cell sensitivity to different CDT doses, with the cell cycle as read-out. Thanks to comet assay and immunofluorescence, we have shown that at doses 1000 times lower than those used previously in the literature, CDT induces multiple single-strand breaks. When cells are going through S phase, a replicative stress is induced and DNA damage degenerate into DSB. Indeed, with a PCNA marker, we observed an S-phase slowing down and an increase of the number of cells in late S-phase. Moreover, these CDT-induced DNA damage cause the activation of the pathway involving the RPA, ATR and CHK1 proteins, characteristic of a replicative stress. Finally, we have shown that the activation of the ATM pathway, due to DSB induction, happens later after the CDT treatment. Therefore, the importance of the S-phase passage for the CDT cytotoxicity suggests that proliferating cells are more sensitive to CDT than quiescent cells.
Our work underlines the complex mechanism of CDT action. It will help in the characterization of CDT-expressing bacteria and may open new therapeutic approaches, for example by targeting the mechanisms of associated genotoxicity.

PS 1932 Investigating Mechanisms of Mitochondrial DNA Damage-Mediated Developmental Arrest

E. Turner[1], L. Donoghue[1], C. Hopkins[2], T. Brock[2] and J. N. Meyer[1]. [1]*Nicholas School of the Environment, Duke University, Durham, NC and* [2]*Knudra Diagnostics, Salt Lake City, UT.*

Persistent mitochondrial DNA (mtDNA) damage in response to ultraviolet C radiation (UVC) results in developmental delay or arrest in *Caenorhabditis elegans* (Bess et al., 2012 *Nucleic Acids Res* 40:7916). We are testing several hypotheses on the mechanism of this delay, including the role of oxidative stress and insulin signaling, using deletion mutants and stress-inducible fluorescent reporter strains. Age-synchronized wild-type and mutant nematodes were plated on agar in the absence of food and exposed to 7.5 J/m2 UVC 0, 24 and 48 h after plating. Nematodes were then transferred to plates with food and growth was measured with a COPAS Biosort using extinction, or optical density, as a proxy for size 24, 48, and 72 h after transfer. Fluorescence in reporter strains was also measured. We identified developmental delays and a 50% reduction in the size of UVC –treated *sod-2* mutants and developmental delays in *sod-3* mutants relative to wild-type nematodes after UVC treatment (SOD-2 and SOD-3 are mitochondrial superoxide dismutases). These data support the hypothesis that UVC-induced damage causes mitochondrial oxidative stress. Our data also show significant delay in *daf-16* (mu86); *glp-1* (e2141) and *daf-16* (mgDf47); *glp-1* (e2141) mutants relative to wild-type nematodes, but not *daf-16* (mu86) without the deletion in *glp-1* (DAF-16 functions in insulin signaling and stress resistance and GLP-1 is required for germline proliferation; absence results in adults composed only of somatic cells). This suggests that insulin signaling promotes development in the context of persistent mtDNA damage, but only in the absence of germ cells. Finally we observed induction of hsp-16.2 and hsp-60 in biosensors of heat-shock proteins localized in the cytosol and mitochondria respectively, in response to UVC radiation, suggesting damage to both mitochondrial and cytosolic proteins.

PS 1933 Impact of p53 Functionality in *In Vitro* Mammalian Cell Toxicity Testing

R. Smith, J. Whitwell and J. Clements. *Covance Laboratories, Harrogate, United Kingdom.* Sponsor: J. Bhalli.

The number of *in vitro* mammalian cell positives that do not correlate with follow-up *in vivo* genotoxicity and carcinogenicity testing is of concern (1). p53 competent cells of human origin may provide more predictive data for assessment of human hazard and risk and less misleading *in vitro* positives compared to traditionally used rodent cell lines lacking wild-type p53 function (2). It remains unclear whether cell species origin or p53 status impacts their ability to accurately predict genotoxicity in the *in vitro* mammalian cell tests.
Cells lacking wild-type p53 may underestimate cytotoxicity with the analysis of inappropriately high concentrations for genotoxicity compared to a p53 functional cell line. Three closely related human lymphoblastoid cell lines that differ in p53 status were tested; TK6 express wild-type p53, NH32 are p53 null, WTK1 overexpress mutant p53, similar to commonly used rodent cells. Ethyl methanesulfonate (EMS), etoposide and paclitaxel (taxol) were tested according to regulatory guidelines and cytotoxicity determined using relative populating doubling. Apoptosis was also determined using caspase-3/7 activity.
NH32 were sensitive to the cytotoxic effects of EMS compared to TK6 and WTK1. In contrast NH32 underestimated cytotoxicity with etoposide compared to TK6 and WTK1. A similar cytotoxic response was observed in all three cell lines with taxol; however, cytotoxicity was observed at lower concentrations in TK6. The apoptotic response to each compound in WTK1 was significantly reduced compared to TK6, which demonstrate increases in apoptosis typical of a p53 functional cell line. NH32 demonstrated similar levels of apoptosis to WTK1 following etoposide and taxol treatments but was more similar to TK6 in the response to EMS.
The results showed that p53 deficient cell lines do not consistently underestimate cytotoxicity and the cytotoxic response is drug specific. Other factors associated with loss of p53 function or species origin may be more relevant to the reported high number of *in vitro* positives.

1. Kirkland, et al (2005) Mut Res, 584, 1-256
2. Fowler, et al (2012) Mut Res, 742, 11-25

PS 1934 Evaluation of DNA Repair Center Kinetics after Treatment with Chemicals Causing Linear and Nonlinear Dose-Response Curves for Micronuclei

B. Sun[1], O. Trask[1], S. Ross[1], P. L. Carmichael[2], Y. Adeleye[2], M. E. Andersen[1] and R. A. Clewell[1]. [1]*The Hamner Institute, Durham, NC and* [2]*SEAC, Unilever INC, Colworth Science Park, Bedfordshire, United Kingdom.*

We evaluated the broad dose-response for micronuclei (MN; permanent chromosomal damage) in human p53-competent fibrosarcoma HT1080 cells for 8 prototype genotoxic chemicals with different modes of action. Neocarzinostatin (NCS; γ-irradiation mimic), methyl methanesulfonate, ethyl nitrosourea (MMS, ENU; alkylating agents), H_2O_2 (oxidative damage), quercetin and curcumin (QUE, CUR; oxidative polyphenols), exhibited threshold-like dose-response curves, while curves for etoposide (ETP; topo II inhibitor) and mitomycin C (MMC; DNA crosslinker) were more linear. To determine if DNA repair processes could help explain the observed dose-response behavior for MN, we used 2D/3D microscopy imaging to measure the dose response and time course for DNA repair center (DRC) formation. DRCs are aggregation sites of repair proteins into cytological foci that form at sites of double stand breaks (DSBs) and replication stress. Observation of formation and dissolution of DRCs allows evaluation of DNA repair dynamics. We developed a high content assay to quantitate DRCs by visualizing and counting nuclear foci that contained two essential components of DRCs - p53BP1 and p-H2AX. Dose-response and time course measurements were performed with two representative chemicals that either showed linear (ETP) or non-linear (NCS) MN induction. ETP induced DRCs were not significantly resolved even at low-concentrations (0.02 μM). NCS showed a very different DRC kinetics. At low doses (5 ng/mL NCS), DRCs were formed quickly and were resolved between 3 and 7 hr. At higher doses of NCS, however, the number of DRCs remained high out to 24 hr. These results indicate that cells appear to more efficiently repair DSBs induced by NCS than ETP at low doses, and this differential repair efficiency may explain the distinct shape of dose response curves for the two chemicals.

PS 1935 The Bystander DNA Double-Strand Breaks Induced by Alpha-Particles and the Protective Effect by Vanillin Derivative VND3207

P. Zhou[1, 2], H. Guan[1], C. Fan[1, 2], Y. Wang[1], X. Liu[1] and B. Huang[2]. [1]*Radiation Toxicology and Oncology, Beijing Institute of Radiation Medicine, Beijing, China and* [2]*Institute for Environmental Medicine and Radiation Hygiene, The University of South China, Hengyang, Hunan Province, China.*

Radiation-induced bystander effect is defined as the biological effects induced in cells that are not directly targeted by a charged particle and, but are received the signals from these irradiated proximity cells. In order to investigate the bystander DNA double-strand breaks (DSB) and its protection measure, we have firstly estabolished a new bystander experimental model of co-culture human fibroblast cells. The red fluorescence fusion protein of HsBrk1-RFP was used to mark the cytoplasm in one cell line to distinguish the irradiated target cells (HFS-RFP) and the non-irradiated bystander cells (no mark HFS) in the co-culture cellular model. Cells were irradiated with α-particle, and the DNA double-strand break and repair kinetics were analyzed by the immunostaining observation of γH2AX foci. Whether 0.1 Gy or 0.2 Gy α-particle irradiation, the same time-kinetics of γH2AX foci production and abatement were observed in both irradiated HFS-RFP cells and the bystander non-irradiated HFS cells, in which the highest level of γH2AX foci was detected at 1 h post-irradiation, then diminished. There is no significant difference between the yields of DSB in the bystander cells proximity to 0.1 Gy or 0.2 Gy irradiated cells. VND3207 is a novol vanillin derivative, and was found to has a radioprotection effect through its capabilities as a powerful antioxidant, in minimizing DNA damage via provoking DNA-PKcs activity. It can also protects the mice from the radiation induced carcinogenesis. Here we further unvealed that VND3207 can protect the bystander cells from the DNA double-strand breaks induced by damage signals from the proximity irradiated cells. Conclusion: A new bystander effect research model was established through the co-culture cells model. The vanillin derivative 3207 effectively protects the cells from the bystander DNA double-strand breaks.

PS 1936 UV-Induced DNA Damage and Repair Regulation at Ends of Chromosomes

D. Parikh and P. L. Opresko. *University of Pittsburgh, Pittsburgh, PA.*

Ultra-violet (UV) irradiation is the most ubiquitous environmental inducer of skin cancer and melanomas. Telomeres are DNA-shelterin protein complexes at ends of chromosomes, characterized by presence of unique TTAGGG repeats. The thymine repeats (TT) on G-rich strands of telomeric DNA are hotspots for the

formation of cyclobutane pyrimidine dimers (CPD) and 6-4 photoproducts (6-4 PP) induced by UV light exposure. Recent reports suggest that telomeres are either deficient in photoproduct removal or are repaired slower than the bulk genome. DNA photoproducts can cause mutations and block DNA replication, unless they are repaired by nucleotide excision repair (NER) pathway system. We report here a novel, independent assay that we have established to measure the persistence or repair of photoproducts in telomeric DNA compared to the bulk genome, using specific antibodies against CPDs and 6-4PPs following exposure of cells to UVC. We observed that CPDs decreased in genomic DNA after 12-24 hours but persisted in telomeric DNA. Southern blot assays using radio-labeled oligonucleotides that bind to telomeric DNA confirmed enrichment of telomeres in purified fractions. To investigate possible mechanisms for this repair inhibition, we tested directly effect of shelterin protein TRF2 on NER protein XPF-ERCC1 via enzyme activity assays. We discovered that nuclease cleavage activity of purified XPF-ERCC1 on a stem-loop DNA substrate was completely abolished by TRF2. Our results provide the first direct biochemical evidence towards quantifying critical UV damage at telomeres and elucidating NER pathway regulation by shelterin.

PS 1937 Effects of Cadmium and 17α-Ethinylestradiol on Benzo(a) pyrene Adduct Formation

K. E. Germ, S. Tang and G. D. Mayer. *Environmental Toxicology, Texas Tech University, Lubbock, TX.*

Xenoestrogens have been increasingly associated with various adverse health conditions, including cancer. It is known that both cadmium and 17α-ethinylestradiol are ubiquitous environmental contaminants, and that low-dose exposures can illicit mechanistic effects in vivo. Nucleotide excision repair is the DNA repair mechanism responsible for the removal of bulky DNA adducts, which, if gone un-repaired, may lead to DNA mutations. Cadmium and 17α-ethinylestradiol are known to enhance hormonal responses *in vivo* and *in vitro*, and have roles in the advancement of hepatocellular carcinoma. Additionally, they are known to down-regulate multiple DNA repair mechanisms, including the nucleotide excision repair pathway. We pre-exposed human hepatocellular carcinoma (HepG2) cells to various concentrations of 17α-ethinylestradiol, a synthetic estrogen, and cadmium, to see if such pre-exposure to these compounds had any effect on bulky DNA adduct repair when the same cells were subsequently exposed to the pro-carcinogen, benzo(a)pyrene. Cells were exposed to two different concentrations of benzo(a)pyrene for varying amounts of time up to 48 hours. We then quantified benzo(a)pyrene diol-epoxide adducts at each of 6 time-points using high performance liquid chromatography with fluorescence detection. Our data indicate that with 17α-ethinylestradiol pre-exposure, efficient adduct repair was delayed, as adducts continued to be detected up to 48 hours of exposure. Also, after cadmium pre-exposure, adduct formation increased over time throughout the 48 hour timepoint. Results demonstrate that in HepG2 cells, both 17α-ethinylestradiol and cadmium exposures affect the prevalence and repair rate of benzo(a)pyrene-DNA adducts.

PS 1938 Integration of Genomic Biomarkers in Cancer Risk Assessment for Xenobiotics with Positive Findings in Chromosome Damage Assays

H. Li[2], D. R. Hyduke[4], C. L. Yauk[3], J. Aubrecht[1] and A. Fornace[2]. [1]*Dept of Drug Safety Evaluation, Pfizer Inc, Groton, CT,* [2]*Georgetown University, Washington, DC,* [3]*Health Canada, Ottawa, ON, Canada and* [4]*Utah State University, Logan, UT.*

Despite scientific progress in understanding cancer mode of action, experimental approaches for assessing oncogenic risk for chemicals relies mainly on traditional methods. The currently used *in vitro* genotoxicity testing battery does not offer sufficient mechanistic information for assessing oncogenic risk to humans. Recent advances in molecular biology and bioinformatics have enabled interrogating cellular responses to chemical exposure at the genomic level. This approach has revealed molecular pathways and networks that are mechanistically involved in chemical carcinogenesis. We have focused on application of a transcriptomic biomarker approach in the p53-wt human cell line TK6 to facilitate oncogenic risk assessment by assessing genotoxicity and other mechanisms for drug candidates and environmental chemicals. We have constructed a reference database containing gene expression profiles of 27 model agents with a broad range of toxic mechanisms. A genotoxic-signature biomarker comprising of 65 genes, TGx27.65, has been identified from the reference database by using the nearest shrunken centroids (NSC) algorithm. TGx-27.65 discriminates genotoxic from non-genotoxic agents with 100% accuracy after 10-fold cross validation. In a subsequent biomarker validation study, 42 chemicals were selected to test TGx-27.65 's performance on genotoxicity identification. All chemicals with direct DNA-damaging mechanisms were classified as "genotoxic" by transcriptomics assay with TGx-27.65. Interestingly all except one out of eleven chemicals with false positive results in *in vitro* chromosome aberrant assay were not classified as "genotoxic" using TGx-27.65. We have examined the inter-laboratory reproducibility of this biomarker and tested the application of TGx-27.65 in assessing chemicals that need metabolic activation. Advanced bioinformatic analysis further identified gene markers that significantly correlate with various toxic mechanisms.

PS 1939 Developmental Exposure to Ultraviolet C Radiation Results in Altered Energy Production Later in Life in *Caenorhabditis elegans*

J. Rooney, R. K. Bodhicharla, A. S. Bess, M. C. Leung, I. T. Ryde, A. Luz and J. N. Meyer. *Nicholas School of the Environment, Duke University, Durham, NC.*

Mitochondrial genomes encode for 13 proteins that are essential components of the electron transport chain (ETC) and are normally present at between 1000 and 100,000 copies per cell. However, this number is greatly reduced during specific developmental stages, representing a potential critical window for mitochondrial genotoxicant exposure. Mitochondrial DNA (mtDNA) is more susceptible than nuclear DNA (nucDNA) to damage by many environmental pollutants, for reasons including absence of Nucleotide Excision Repair (NER). NER is a highly functionally conserved DNA repair pathway that removes bulky, helix distorting lesions such as those caused by ultraviolet C (UVC) radiation and many environmental toxicants, including benzo[a]pyrene (BaP). In the current experiment we tested the hypothesis that UVC induced mtDNA damage during larval development would alter energy production throughout the life of the nematode. We exposed first larval stage *C. elegans* to a serial UVC dose that results in the accumulation of mtDNA damage while allowing for repair of nuclear DNA damage, and measured ATP levels, mtDNA and nucDNA copy numbers, oxygen consumption and expression of mitochondrial genes throughout the life of the worms. ATP levels were measured as luminescence using the firefly luciferase expressing PE255 glp-4(bn2) strain (provided by Cristina Lagido, University of Aberdeen). mtDNA copy number and gene expression were measured via real time PCR. ATP levels were significantly lower, and the mtDNA to nucDNA copy number ratio was slightly, but significantly reduced in response to UVC. Oxygen consumption was also reduced at 8 and 12 days post UVC. Interestingly, there was no decrease observed in mtDNA or nucDNA encoded mitochondrial transcripts. These results indicate that mtDNA damage during development can alter energy production throughout the life of the nematode, and highlights the potential for a critical window of exposure.

PS 1940 Investigating Genetic Susceptibility to Mitochondrial Toxicity

A. Luz and J. N. Meyer. *Nicholas School of the Environment, Duke University, Durham, NC.*

Genetic variation within the human populous causes a range of sensitivities to various toxicants, including some that target the mitochondria. For example, the antibiotic gentamycin, which targets the bacterial ribosome, can also cause hearing loss. Adverse effects can be worsened in certain individuals carrying a point mutation that renders the mitochondrial 12S rRNA, which is evolutionarily related to the bacterial rRNA, more bacteria-like. In addition to pharmaceuticals, many environmental pollutants are also known mitotoxicants; however, whether these toxicants pose an increased risk to individuals suffering from mitochondrial disease is unknown. Using a UVC exposure protocol that allows for the accumulation of mitochondrial (mtDNA), but not nuclear DNA damage, we found that *C. elegans* carrying a deletion in the *fzo-1* gene are extremely sensitive to UVC-induced mtDNA damage. *fzo-1* and its human orthologs *MFN1* and *MFN2* play a major role in mitochondrial dynamics (outer membrane fusion), and the *fzo-1* deletion results in highly fragmented mitochondria. The removal of UVC-induced mtDNA damage is *fzo-1*-dependent in *C. elegans*, and mutations in *MFN2* cause Charcot-Marie-Tooth neuropathy type 2A in humans. Utilizing the *fzo-1* mutant we are screening environmental mitotoxicants for exacerbation of growth inhibition, because larval development is dependent on mitochondrial function. Initial screens have demonstrated that chronic, low doses of rotenone (0.25 μM), and paraquat (150 μM) significantly delay the growth of *fzo-1* mutants, compared to wild-type worms. To further test the role of mitochondrial dysfunction in larval developmental delay, we will analyze mitochondrial fitness by measuring oxygen consumption with a Seahorse XFe24, ATP production with an *fzo-1* strain expressing an ATP-luciferase transgene, and mtDNA damage and copy number with a QPCR assay. This research aims to help fill a knowledge gap that leaves an already susceptible population of individuals at an even higher risk to certain environmental exposures. Funded by NIEHS 1R01-ES017540-01A2 and Duke University Graduate Fellowship.

PS 1941 Investigations of Dose-Response for Key Events in the Mode of Action (MOA) for Propylene Oxide (PO)-Induced Mutagenicity in TK6 Cells

L. H. Pottenger[1], M. R. Schisler[1], F. Zhang[1], N. Visconti[1], Z. Ji[1], D. Delker[2], L. G. McFadden[1], M. J. Bartels[1], B. Gollapudi[3] and M. J. LeBaron[1]. [1]*The Dow Chemical Company, Midland, MI,* [2]*University of Utah, Salt Lake City, UT and* [3]*Exponent, Midland, MI.*

PO, a reactive chemical, induces nasal tumors in rodents upon chronic high-dose inhalation exposures. It is mutagenic *in vitro* and weakly clastogenic *in vivo*. To investigate thresholds for PO-induced mutagenicity, dose-responses for several hypothesized key event biomarkers were assessed in TK6 cells. Triplicate cultures were treated with 0.5 to 50 μg PO/ml, and evaluated for: mutant frequency (HPRT MF), micronucleus (MN), Comet, GSH-PO conjugate, N7-hydroxypropylguanine (N7-HPG) adducts, and 2 homeostasis/oxidative stress markers (cytosol 8-OH-GTP, 8-OH-dG). Data were analyzed for point-of-departure (POD) metrics: No-Genotoxic-Effect-Levels (NOGELs), bilinear threshold dose (Td), and benchmark dose (BMD). Exposure biomarkers: N7-HPG adducts, not detected in controls, increased linearly with PO dose; GSH-PO increased over control levels at ≥5 μg/ml PO. Oxidative biomarkers 8-OH-dG and 8-OH-GTP were affected; all treated groups had decreased 8-OH-GTP and increased 8-OH-dG adducts vs controls. Biomarkers of genotoxic effects, HPRT MF and MN, with Comet, had NOGELs of 25, 25, and 10 μg/ml, respectively. Bilinear Td and BMD analyses of MF data gave a Td of 5.72 and a good fit for BMD10 (4.99) and BMR (9.51). Neither MN nor Comet data had a good fit for BMD. DNA from 57 pooled mutant clones (0, 5, 50 μg PO/ml) underwent NexGen sequencing to determine mutational spectra (MS) spanning the full-length 45kb human HPRT1 gene. The MS showed a difference in transversions in the top dose group vs. controls, where A:T→T:A mutations predominated; low dose MS (MF not increased) did not have a similar change. Integration of such dose-response data for biomarkers of hypothesized key events, along with the determination of MS data, support the determination of *in vitro* NOGELs, or thresholds, for certain key events including genotoxic effects, and provide key perspective on the threshold MOA of PO. Sponsored by the Cefic PO & PG SG.

PS 1942 Depleted Uranium Induces DNA Damage and Alteration of DNA Repair Proteins in Human Lung Epithelial Cells

H. Xie, V. Sekeroglu, Z. Sekeroglu, C. Falank, A. Holmes and J. P. Wise. *University of Southern Maine, Portland, ME.*

Depleted uranium (DU) is commonly used in military applications and is also used in civilian industry and thus exposure of soldiers and others is frequent and widespread. DU is considered a probable human carcinogen, affecting the bronchial cells of the lung, however, how DU causes lung cancer is uncertain. In this study, we use the human bronchial epithelial cell line (BEP2D) to investigate the genotoxicity effect of DU and the underlying mechanisms. We found that DU weakly causes chromosome damage after a 24 h exposure but induces time-dependent increase in chromosome damage after 48 h and 72 h exposure. DU also induces DNA double strand breaks measured by comet assay. Doses of 0.25, 2.5 and 25 ug/cm2 uranium trioxide increases comet tail length of 0, 2 and 7, respectively after a 24 h exposure. Both 48 h and 72 h DU treatment induces a similar increase in tail length. We next investigated whether DU affects DNA double strand break repair pathway. We found that 24 h DU treatment does not affect the DNA damage sensor step measured as Mre11 expression but 48 h and 72 h exposure of 25 ug/cm2 uranium trioxide inhibits Mre11 expression. DU treatment increases phosphorylated ATM but inhibits Rad51 expression. Our study demonstrates that DU induces genotoxicity and may interfere with DNA repair in human bronchial epithelial cells. This work was supported by ARO grants # W911NF-04-1-0240 and W911NF-08-0333 (J.P.W.).

PS 1943 Antimutagenic Effect of *Curcuma longa* L. and Photoactivated Cow Urine Using Salmonella Reverse Mutation Assay

R. M. Nagane[1], N. N. Patel[1], K. E. Tendulkar[1], N. U. Dhumal[1], K. D. Vashi[1] and V. J. Piccirillo[2]. [1]*Toxicology, Jai Research Foundation, Vapi, Gujrat, India and* [2]*VJP Consulting, Inc., Ashburn, VA.*

Bacterial short-term assays are useful tools to evaluate antimutagenesis due to their simplicity and flexibility.to design experiments that allow clarification of antimutagenesis mechanisms. This study was undertaken to assess the antimutagenic potential of aqueous extract of *Curcuma longa* L. and photo-activated cow urine against well known direct acting mutagens [9-Aminoacridine hydrochloride hydrate (9-AA), 2-Nitrofluorene (2-NF), sodium azide (SA) and Mitomycin-C (MMC)] in Salmonella reverse mutation assay using the pre-incubation method with five histidine deficient (his-) mutant tester strains (TA1537, TA1535, TA98, TA100 and TA102). The extract of *Curcuma longa* and photoactivated cow urine were selected because of their s strong antioxidant properties. Aqueous extract was prepared from *Curcuma longa* L. as per published procedures in EMEA/HMPC/456848/2008 while photo-activated cow urine was obtained from Gurukul, Gujarat. The results of extract of *Curcuma longa* and photo-activated cow urine, showed a dose-dependent antimutagenic response in the Salmonella reverse mutagenicity assay in the absence of S9. Extract of *Curcuma longa* inhibited revertants by about; 26-43% induced by 9-AA in TA1537, 22-39% induced by SA in TA1535, 33–81% induced by 2-NF in TA98, 30-95% induced by SA in TA100 and 18-62% induced by MMC in strain TA102 at different concentrations. Photo-activated cow urine inhibited revertants by about; 10-18% induced by 9-AA in TA1537, 13-54% induced by SA in TA1535, 9-55% induced by 2-NF in TA98, 16-86% induced by SA in TA100 and 20-60% induced by in MMC in TA102 at different concentrations. Concurrent negative controls (distilled water, aqueous extract of *Curcuma longa* and photo-activated cow urine) showed revertants within normal historical range. These data suggest that aqueous extract of *Curcuma longa* L. and photo-activated cow urine have promising antimutagenic properties against direct acting mutagens.

PS 1943a Comparison of Genotoxic Effects of Major Diesel Exhaust Components in Human Alveolar Basal Epithelial Cells (A549)

P. Rossner[1], J. Stolcpartova[1], J. Schmuczerova[1], A. Milcova[1], E. Hruba[2], M. Machala[2] and J. Topinka[1]. [1]*Institute of Experimental Medicine, Prague, Czech Republic and* [2]*Veterinary Research Institute, Brno, Czech Republic.*

Internal combustion engines (ICE), including diesel engines, power most of the motorized road vehicles. ICE are a major source of air pollution in metropolitan areas. Among other compounds they emit polycyclic aromatic hydrocarbons (PAHs) and their nitro-derivatives. Genotoxicity of benzo[a]pyrene (B[a]P), a model PAH, and PAH nitro-derivatives (1-nitropyrene (1-NP) and 3-nitrobenzantrone (3-NBA)), was studied in a model cell line A549. The cells were treated for 4 and 24 hours with different concentrations of tested compounds (B[a]P: 0.1 and 1 μM; 1-NP: 1 and 10 μM; 3-NBA: 0.5 and 5 μM) and several endpoints, including bulky DNA adducts and oxidative stress markers (lipid peroxidation, protein and DNA oxidation) were analyzed. All tested compounds increased bulky DNA adduct levels after both the 4-h and 24-h treatment, although the effect of 1-NP was relatively weak. A 24-h treatment resulted mostly in higher DNA adduct levels than the 4-h treatment with the exception of 3-NBA. 1-NP induced protein oxidation after both the 4-h and 24-h treatment. Interestingly, lipid peroxidation measured as levels of 15-F2t-isoprostane decreased after the B[a]P treatment, but was elevated after incubation of the cells with 1-NP and 3-NBA. 8-Oxo-7,8-dihydro-2'-deoxyguanosine (8-oxodG), a marker of oxidative DNA damage, was not affected by either compound and/or treatment period. Our data highlight differences in genotoxic mechanisms of PAHs and their nitro-derivatives, particularly for oxidative stress markers. Supported by the Czech Science Foundation (13-01438S) and by EU LIFE+ Program (LIFE-ENV-CZ-651).

PS 1943b Nitroxide TEMPO: A Genotoxic and Oxidative Stress Inducer in Cultured Cells

X. Guo, R. A. Mittelstaedt, L. Guo, J. G. Shaddock, R. H. Heflich, M. M. Moore and N. Mei. *NCTR, Jefferson, AR.*

Low molecular weight nitroxide, 2,2,6,6-Tetram ethylpiperidine-1-oxyl (TEMPO), is a stable free radical which has been widely used throughout chemistry and biochemistry as process intermediates. Due to its antioxidant abilities and protective properties in various pathological situations, some studies have proposed them as potential therapeutic agents for medical applications. Thus, the potential risks of TEMPO need to be addressed. In this study, we investigated the cytotoxicity and mutagenicity of TEMPO using the mouse lymphoma assay (MLA) and in vitro micronucleus assay (MN). In the absence of metabolic activation (S9), 3mM TEMPO produced significant cytotoxicity and marginal mutagenicity in the MLA; whereas in the presence of S9, treatment of mouse lymphoma cells with 1–2mM TEMPO resulted in dose-dependent decreases of the relative total growth and increases in mutant frequency. In the MN assay, treatment of TK6 human lymphoblastoid cells with 0.9–2.3mM TEMPO increased the frequency of both micronuclei (a marker for clastogenicity) and hypodiploid nuclei (a marker of aneugenicity) in a dose-dependent manner, with the responses being greater in the presence of S9. Within the dose range tested, TEMPO also induced increased generation of reactive oxygen species and decreased glutathione levels in mouse lymphoma cells. In addition, the loss of heterozygosity (LOH) analysis showed that the majority of TEMPO-induced mutants, both in the presence and absence of S9, produced

high levels of LOH at the Tk locus only, indicating allele loss of ≤34Mbp. These results indicate that TEMPO is mutagenic in the MLA and induces micronuclei and hypodiploid nuclei in TK6 cells. Oxidative stress may account for part of the genotoxicity induced by TEMPO in both cell lines.

PS 1943c 454 Next-Generation Sequencing Reveals a Catalogue of SNPs and Novel Genetic Anomalies in the Transcriptome of TK6 Cells

J. Revollo, D. Petibone, S. M. Morris, B. Green and B. Ning. *Division of Genetic and Molecular Toxicology, National Center for Toxicological Research, Jefferson, AR.* Sponsor: S. Chigurupati.

TK6 cells are a human lymphoblastoid cell line originally derived from a patient suffering from spherocytosis that were subsequently mutagenized with the intercalating agent ICR-191 to create a heterozygous thymidine kinase locus (TK+/-). Since TK6 cells are heterozygous for the TK gene but wild-type for the p53 gene, they are routinely used to assess the mutagenicity of chemicals by using loss of heterozygosity of the remaining wild-type TK allele as a reporter. Despite their common use and importance in genetic toxicology, little is known about other genetic abnormalities these cells possess and how these may affect their response to genotoxicants. To determine if TK6 cells carry DNA sequence changes that may affect their response to DNA damaging agents, we used 454 Next Generation Sequencing to characterize the TK6 transcriptome. We detected 2572 genetic variations arising from nuclear DNA and 46 from mitochondrial DNA, from a total of 7471 detected genes. Among the anomalies mapping to nuclear DNA, 1089 are known SNPs, while 1483 are novel. Among the anomalies mapping to mitochondrial DNA, 36 are known SNPs, while 10 are novel. Importantly, we detected several anomalies that could affect the genotoxic profile of these cells, such as a frame-shift mutation in the heavy subunit of ferritin (FTH), and clinically-relevant SNPs at the xenobiotic metabolizing enzyme NADPH quinine oxidoreductase 1 (NQO1) and the thiopurine drugs metabolizing enzyme thiopurine S-methyltransferase (TPMT) loci, among many others. Our data provides a preliminary catalogue of the altered DNA sequences present in the transcriptome of TK6 cells.

PS 1943d MGMT Promoter/Enhancer Haplotypes Alter Transcription Factors Binding

M. Xu, I. Nekhayeva, C. E. Cross, J. Speidel and S. Abdel-Rahman. *UTMB, Galveston, TX.*

The *MGMT* gene encodes the direct reversal DNA repair protein O6-methylguanine-DNA methyltransferase, which preferentially removes adducts resulting from exposure to alkylating agents from the O6 position of guanine. Recently, we sequenced 104 DNA samples from healthy individuals and identified several single nucleotide polymorphisms (SNPs) in the *MGMT* promoter/enhancer (P/E) region. We found that, due to linkage disequilibrium, these SNPs form defined haplotypes. To determine the functional significance of these haplotypes, we transfected luciferase-reporter constructs representing the different haplotypes into glioblastoma cells and determined their effect on *MGMT* promoter activity. The results showed that *MGMT* P/E haplotypes, rather than individual SNPs, differentially regulate *MGMT* transcription. However, the mechanism(s) by which these haplotypes affect *MGMT* transcription remains elusive. Using in-silico analysis, we found that several of the SNPs in our population are within or in close proximity to putative transcription factor (TF) binding sites including AP-1, NF-1, Ap-2α, GCF and c-Myc. We therefore hypothesized that *MGMT* P/E haplotypes affect TF binding leading to alteration in *MGMT* transcription. To test our hypothesis we conducted a TF binding profile for different *MGMT* haplotypes using the Promoter Binding TF Profiling Plate Array assay (Signosis, Inc.), which allowed us to evaluate binding of 48 TFs to the *MGMT* P/E. We found a significant difference in TF binding depending on the *MGMT* P/E haplotype evaluated, indicating that the haplotypes do alter TF binding. These data provide a mechanistic explanation to our findings demonstrating that *MGMT* P/E haplotypes influence promoter activity and could explain the well-documented interindividual sensitivity to environmental and therapeutic alkylating agents (Supported by T32-07454; P30 ES006676 and JSME bridging grants).

PS 1943e Exploring *In Vivo* Genotoxicity Thresholds through an Integrated Evaluation of 5-FU

S. C. Gehen[1], D. Geter[2], K. Pant[3], J. Mehta[1], R. Billington[1] and B. Gollapudi[2,4]. [1]*Dow AgroSciences, Indianapolis, IN,* [2]*The Dow Chemical Company, Midland, MI,* [3]*BioReliance, Rockville, MD and* [4]*Exponent, Inc, Midland, MI.*

5-fluorouracil (5-FU) was discovered at trace levels during residue assessments of an investigational agricultural product. To characterize potential health risk associated with this residue, focused hazard and exposure assessments were conducted. While 5-FU has genotoxic potential under some conditions, information relevant to dietary exposure was lacking. To assess the potential genotoxic hazard of 5-FU under relevant exposure conditions, F344/DuCrl rats received a dose of 6 mg/kg/day 5-FU by diet for 14 days. Dose-level selection was based on a dietary exposure estimation of 0.0005 mg/kg/day and a 10,000-fold margin of exposure. Multiple guideline genotoxicity end-points were integrated in a single study using the same group of animals. Specifically, the end-points evaluated were unscheduled DNA synthesis [UDS] in hepatocytes, primary DNA damage [Comet assay] in stomach and duodenum cells and formation of micronucleated polychromatic erythrocytes [MNT] in bone marrow. Sensitivity of the system was confirmed by positive control animals which received single gavage doses of either dimethylnitrosamine (35 mg/kg) or cyclophosphamide monohydrate (40 mg/kg/day) and ethyl methanesulfonate (200 mg/kg/day) prior to study termination. All responses were compared to untreated animals. The study results showed 5-FU did not induce a significant increase in the mean number of net nuclear grain counts in hepatocytes isolated from treated animals in the UDS assay, there was no primary DNA damage as measured by the Comet assay, and there was no significant increase in the number of micronuclei in the polychromatic erythrocytes in bone marrow of the treated rats. Under the conditions of this study, it is concluded that 5-FU is non-genotoxic when administered in the diet to rats at levels 10,000-fold higher than predicted human exposure. This study demonstrates the utility of an integrated testing approach for genotoxic potential as well as exposure-based dose-level selection to characterize human risk.

PS 1943f Timecourse of Altered Hepatic Nucleotide Excision Repair Activity following Treatment of Mice with the Tobacco-Specific Carcinogen 4-(Methylnitrosamino)-1-(3-Pyridyl)-1-Butanone

C. M. Harris and T. E. Massey. *Pharmacology and Toxicology Graduate Program, Department of Biomedical and Molecular Sciences, Queens University, Kingston, ON, Canada.*

4-(Methylnitrosamino)-1-(3-pyridyl)-1-butanone (NNK) is a genotoxic carcinogen found in tobacco and tobacco smoke. This carcinogen forms apurinic sites as well as methyl and pyridyloxobutyl (POB) adducts on DNA, which can lead to mutations and neoplasms if the DNA damage persists. The objective of this study is to assess the impact of NNK on repair of NNK-derived POB DNA adducts by the nucleotide excision repair (NER) pathway, and to determine the mechanism by which NNK alters NER. Using an in vitro NER activity assay, we examined the effect of a tumorigenic dose of NNK (10μmol in 0.1mL saline) on repair of a POB damaged plasmid by nuclear extracts from livers of NNK- or saline-treated A/J mice (n=4), at 2, 4, 12, 24 and 72h post-injection. NNK treatment caused a trend towards increased repair activity at 4h (p=0.38) and 72h (p=0.36), and at 24 h, a time-point associated with maximal DNA damage, the increase (48%) was statistically significant (p=0.03). In contrast, at 12h post injection, we observed a significant decrease (84%) in repair activity (p=0.04). NNK treatment did not significantly affect levels of the key NER proteins XPA and p53, although at 24h a trend towards increased p53 occurred (p=0.28). Overall, NNK appears to have time-dependent effects on NER activity of mouse liver. At a time point of maximal DNA damage, an increase in repair activity would help to decrease the likelihood of DNA damage persistence and fixation of mutations. The decrease in repair observed at 12h may be related to diurnal variation in mouse NER activity. Results to date do not support a role for XPA or p53 in the effects of NNK on repair of POB adducts. Supported by CIHR grant No. MOP-89698.

PS 1943g Non-B-DNA-Induced Mutagenesis in Eukaryotes

J. McKinney and K. Vasquez. *Pharmacology & Toxicology, University of Texas at Austin, Austin, TX.* Sponsor: R. Finch.

DNA can adopt alternative structures that do not conform to the Watson-Crick B DNA helix (i.e. non-B DNA structures), including H-DNA and Z-DNA. Sequences that can adopt non-B DNA structures are very abundant in human genomes, and we and others have shown that non-B DNA can cause genomic instability. However, the mechanisms involved are not well characterized. Importantly,

H-DNA and Z-DNA-forming sequences co-localize with chromosomal breakage hotspots, such as those found in cancer-related chromosomal translocations, implicating non-B DNA in cancer etiology. Non-B structures cause distortions in the double helix, and therefore, may be recognized as DNA "damage" by repair proteins. Preliminary data from our lab have shown that nucleotide excision repair (NER) and mismatch repair (MMR) proteins are involved in H-DNA-induced mutagenesis in yeast and mammalian cells. Based on these results it is plausible that repair proteins from multiple pathways participate in error-generating repair of non-B DNA structures, resulting in genomic instability. Thus, we hypothesize that NER and MMR proteins are involved in Z-DNA-induced mutagenesis in eukaryotes. The long-term goal of this project is to determine the mechanism(s) involved in non-B-DNA-induced genetic instability. We have developed a genetic instability reporter system using a yeast artificial chromosome (YAC) containing naturally occurring non-B DNA-forming sequences capable of forming Z-DNA found at a translocation breakpoint in human cancer. We screened a yeast gene knock-out library using the YAC reporter system to identify proteins that play a role in DNA structure-induced genetic instability. Thus far we have determined that several NER and other repair proteins are involved in Z-DNA-induced mutagenesis in yeast. We will continue to screen MMR proteins. Future experiments will confirm these results in human cells, and further characterize the roles of proteins identified in the yeast screen using biochemical and cell-based assays.

PS 1943h Reduction of Genotoxicity from External and Endogenous Sources with Yel002

M. J. Davoren and R. H. Schiestl. *Environmental Health Science, UCLA, Los Angeles, CA.*

Genotoxicity, is a persistent, yet often sinister health threat. A large amount of damage resulting from exposure to massive amounts ionizing radiation, for example, can cause death by killing the radiation sensitive dividing cells of our bone marrow and gut lining. However, oftentimes the effects of lesser doses are often not observed until the development of delayed diseases, such as cancers, a long period after the initial genotoxic insult.

Ataxia Telangiectasia, or AT, is a severe progressive and terminal disease. By lacking a critical DNA repair enzyme, sufferers of AT essentially accumulate genotoxic damage in their cells at a greatly increased rate, succumbing to cancers at the median age of 22.

The development of a drug capable of mitigating the damage caused by multiple sources of genotoxicity via the upregulation of DNA repair mechanisms is of critical importance for the rescue of both healthy people exposed to genotoxic events such as radiation exposure and those individuals with endogenous DNA repair disorders, such as AT sufferers. Through a high-throughput, yeast based screen, the Schiestl Lab at UCLA has identified a number of compounds capable of reducing both radiation associated death and mutation rates. When the compounds were later tested in mice, one compound, designated Yel002, stood out as particularly effective, capable of cutting the death radiation of C3H mice irradiated at the LD100 level of 8 Gy down to 25%.

Given the sustained effectiveness of Yel002 as a radiation damage mitigator, it was decided to investigate whether it could protect against other sources of DNA damage, such as the endogenous repair disorder AT. Two strains of ATM deficient mice were injected once weekly with 75 mg/kg Yel002 in saline solution. Over a 97 week experimental period, we were able to observe an increase in life expectancy from 42 to 52 weeks with these weekly doses (generally caused by a delay in the development of terminal lymphoma) In addition, we hope to further increase the effectiveness of Yel002 with a new, more bioavailable formulation, currently showing promise in radioprotection experiments.

PS 1943i Somatic and Germ Cell Mutant Analysis in the Big Blue® Transgenic Mouse Mutation Assay with N-Ethyl-N-nitrosourea (ENU)

R. R. Young[1], H. Dinesdurage[1], D. Bruning[1], M. McKeon[1], T. Vidmar[2] and M. Aardema[3, 1]. [1]*Toxicology, BioReliance, Rockville, MD,* [2]*BioSTAT Consultants, Inc, Portage, MI and* [3]*Marilyn Aardema Consulting, LLC, Fairfield, OH.*

The new OECD Technical Guideline 488 (2011, revised 2013) for transgenic rodent mutation (TRM) assays has led to renewed interest in the Big Blue® assay to follow-up positive genotoxicity or carcinogenicity results. To requalify the assay in our laboratory to OECD standards, the frequency of *cII* mutants in somatic tissue (liver and bone marrow) and germ cell (testis and cauda) were assessed in ENU-exposed male C57BL/6 homozygous Big Blue® mice. Mice were treated with vehicle control (VC) for 28 days (pH 6 aqueous buffer, N=16) or ENU on days 1-3, (74 mg/kg day 1, 40 mg/kg day 2 and 3, N=30). Half the animals were necropsied on study day 31 or day 77. Low sperm DNA yields at day 31 and significantly reduced ($p<0.05$) testes weight (days 31 and 77) and cauda weight (day 77) in ENU-treated mice were consistent with reported effects of ENU exposure. At Day 31, statistically significant increases in mutant frequencies were observed in liver (6X increase; 189 ± 50 x 10^{-6} for ENU vs 33 ± 5 x 10^{-6} for VC); bone marrow (15X increase; 711 ± 207 x 10^{-6} for ENU vs 48 ± 18 x 10^{-6} for VC); and testis (6X increase 148 ± 49 x 10^{-6} for ENU vs 23 ± 7 x 10^{-6} for VC). At day 31 significant increase in mutant frequency was not observed in caudal sperm (1.4X increase, 39 ± 23 x 10^{-6} for ENU vs 28 ± 11 x 10^{-6} for VC) which is consistent with germ cell toxicity at this time point. At Day 77, significant increases in mutant frequencies were observed in liver (7X; 310 ± 94 x 10^{-6} for ENU vs 43 ± 11 x 10^{-6} for VC); and bone marrow (17X increase; 543 ± 177 x 10^{-6} for ENU vs. 32 ± 18 x 10^{-6} for VC). Day 77 caudal sperm and testis are under evaluation. Excellent homogeneity and reproducibility was obtained in *cII* mutant frequencies in our laboratory. The GLP Big Blue C57BL/6 *cII* mutation assay at BioReliance is experimentally and statistically robust, conforms to past experience, literature expectations and regulatory guidelines, and is a useful tool for assessment of mutations *in vivo*.

PS 1943j Integration of *Pig-a* and Micronucleus Endpoints into the Big Blue® Transgenic Mouse Mutation Assay: Results for Benzo(a)pyrene (BaP) and N-Ethyl-N-nitrosourea (ENU)

L. F. Stankowski[1], M. Aardema[2], R. Kulkarni[1], T. E. Lawlor[1], M. McKeon[1], Y. Xu[1], D. Torous[3], S. Dertinger[3] and R. R. Young[1]. [1]*BioReliance, Rockville, MD,* [2]*Marilyn Aardema Consulting, LLC, Fairfield, OH and* [3]*Litron Laboratories, Rochester, NY.*

Integration of multiple endpoints into *in vivo* genotoxicity assays provides a broad assessment of genotoxic potential while reducing the use of animals. We examined the induction of micronuclei and the *Pig-a* mutant phenotype in reticulocytes and mature red blood cells (mnRET and RET^{CD24-}, and mnNCE and RBC^{CD24-}, respectively) in the peripheral blood of male Lambda LIZ/*lacI* C57BL/6 homozygous (Big Blue®) transgenic mice. Animals were treated with vehicle (olive oil) or BaP (50 mg/kg/day) on Days 1-28, or ENU (40 mg/kg/day) on Days 1-3. Peripheral blood was collected ~3 hours before animals were sacrificed on Day 31 (as per OECD Test Guideline 488), for tissue collection for determination of *cII* mutant frequencies, the Big Blue® transgenic endpoint. Micronucleus and *Pig-a* mutant frequencies were determined by flow cytometry using MicroFlow® and MutaFlow® kits (after immunomagnetic enrichment), respectively (Litron Laboratories). BaP induced statistically significant increases in mnRET, mnNCE, RET^{CD24-} and RBC^{CD24-} (1.54-, 2.09-, 616- and 100-fold, respectively; all $p< 0.001$). ENU induced statistically significant increases in mnNCE, RET^{CD24-} and RBC^{CD24-} (1.39-, 1050- and 207-fold, respectively; all $p< 0.001$), but not mnRET (as expected due to the short term dosing regimen and turnover of mnRET into mnNCE in mice). The sensitivity and power of the high throughput *Pig-a* method is demonstrated by its detection of relatively small net increases in mutant frequencies (the 100-fold increase in RBC^{CD24-} observed for BaP represented an increase of ~14 x 10^{-6} over a vehicle control value of 0.14 x 10^{-6}). Analysis of *cII* mutant frequencies in somatic and germ cell tissues is ongoing. This study demonstrates the ability to integrate multiple endpoints into the Big Blue® Transgenic Mouse Mutation Assay for a comprehensive assessment of genotoxicity.

PS 1944 Comparative Cytotoxicity of Nanosilver in HepG2 and Caco2 Cells

S. C. Sahu, J. Zheng, J. Ihrie, J. Yourick and R. Sprando. *Toxicology, US Food and Drug Administration, Laurel, MD.*

Increasing human exposure to nanosilver in consumer products is of concern. We evaluated two widely used human cell culture models, HepG2 and Caco2 cells, for screening cytotoxicity of food- and cosmetic-related nanosilver. We characterized nanosilver by DLS, TEM and ICP-MS analysis. Average size of nanosilver determined by our TEM analysis was 20.4 nm and showed no agglomeration. Concentration of nanosilver determined by our ICP-MS analysis was 0.962 mg/ml. Our ICP-MS and TEM analysis suggested uptake of 20 nm silver by both cell types. Cytotoxicity of 20 nm silver was determined in HepG2 and Caco2 cells at concentrations 0.1, 1.0, 10.0 and 20.0 μg/ml. A significant concentration-dependent cytotoxicity of nanosilver was observed in HepG2 cells in concentration range 1 to 20 μg/ml and at a higher concentration range 10 to 20 μg/ml in Caco2 cells compared to control. When both cell types were exposed to nanosilver there was a significant concentration-dependent decrease in dsDNA content indicating increased DNA damage in concentration range 1 to 20 μg/ml. No oxidative stress was noted in either cell type tested at concentration range used. Nanosilver treatment induced a significant concentration-dependent decrease in mitochondria membrane potential in both cell types indicating increased mitochondria injury in concentration range 1 to 20 μg/ml for HepG2 cells and at a higher concentration range 10 to 20 μg/ml for Caco2 cells. These results indicated that HepG2 cells were more sensitive to nanosilver than Caco2 cells. It is believed that oxidative

stress leads to cytotoxicity of nanoparticles in general.. However, we did not detect nanosilver-induced oxidative stress in either of cell types in concentration range used. Our results suggested that oxidative stress did not contribute to observed cytotoxicity of nanosilver. A different mechanism of nanosilver cytotoxicity initiated by mitochondria injury is suggested. In summary, our results indicated that widely used in vitro models, HepG2 and Caco2 cells, are excellent models for screening cytotoxicity of nanomaterials.

PS 1945 Induction of Autophagy at Noncytotoxic Concentrations of Silver Nanoparticles in HepG2 Cells

A. Mishra, Q. Zhang, G. Kumar, B. Casey and P. L. Goering. *CDRH, USFDA, Silver Spring, MD.*

Silver nanoparticles (AgNP) are increasingly used in medical and consumer products to exploit their antimicrobial properties, but health risks associated with exposure have not been fully evaluated. Further studies are needed to more fully understand the bioactivity of AgNP and identify biomarkers of toxicity. Autophagy is a part of the lysosomal-mediated pathway that functions to sequester and remove unnecessary and misfolded cytoplasmic proteins. Recent studies have shown that nanoparticles of varying chemistries and size can activate the autophagic-lysosomal pathway leading to cytotoxicity. The goal of this study was to: 1) evaluate AgNP cytotoxicity in cultured human HepG2 cells, 2) evaluate autophagy and apoptotic responses induced by AgNP, and 3) determine if LC3B protein, a pro-autophagic marker, can serve as a molecular biomarker to predict AgNP-induced cytotoxicity. HepG2 cells were studied since liver is a primary organ for systemic nanoparticle accumulation. AgNP (10, 50 and 100 nm) were characterized for size and shape using TEM and DLS. Cells were incubated with AgNP (0.1, 0.5, 1, 5, 10, or 50 μg/ml) for 12 and 24 hr. Cytotoxicity was assessed by trypan blue exclusion and XTT assays. Apoptosis (Annexin V) was assessed by flow cytometry. Confocal and fluorescence microscopy were used to detect lysosomal activity (Lysotracker DND), autophagy (Cyto-ID green), and LC3B. Cytotoxicity was observed only after 24 hr post-exposure at the highest concentrations of AgNP (10 and 50 μg/ml) but not at lower concentrations (less than 5 μg/ml). Apoptosis was detected only after 24 hr post-exposure at 10 and 50 μg/ml. No significant apoptosis was detected at 12 hr post-exposure at all the concentrations. In contrast, autophagic vacuoles and increased expression of LC3B were observed at 12 and 24 hr post-exposure at non-cytotoxic concentrations (less than 5 μg/ml). In conclusion, the data demonstrated that 1) autophagy was induced at non-cytotoxic AgNP concentrations, and 2) LC3B may serve as a sensitive biomarker to detect early toxicity in AgNP-exposed cells.

PS 1946 Flow Cytometry-Based Evaluation of Silver Nanoparticle Cytotoxicity: Role of Serum Concentration in Media

G. Kumar[1], W. Wei[2], H. Degheidy[1], B. Casey[1] and P. L. Goering[1]. *[1]CDRH, FDA, Silver Spring, MD and [2]University of Maryland, College Park, MD.*

Nanoparticles (NPs) when exposed to clinically relevant media, e.g., serum or blood, are immediately coated with proteins and lipids. The adsorbed biomolecules can significantly alter the physiochemical properties (size, charge, shape, surface functionalities) of NPs and hence, highly influence NP tissue disposition, cell uptake, and biological responses. NPs, due to their nanoscale properties, also interfere with colorimetric in vitro cytotoxicity assays such as MTT or LDH. However, assays that do not use spectrophotometric detection, such as flow cytometry (FC) based assays, are less likely to be influenced by NP interference. The aim of this study was to 1) compare the cytotoxicity of silver nanoparticles (AgNPs) pre-mixed with cell culture media (with varying FBS concentration) in L-929 fibroblasts compared to direct addition (no pre-mixing) of AgNPs to the cells, and 2) evaluate the use FC-based assays to assess cytotoxicity of AgNPs. To assess the effects of premixing on cytotoxicity, AgNPs (10 nm diameter) were added to cells either following pre-mixing with cell culture media (supplemented with 0.1, 1, or 5% FBS) for 24 hr or directly added without pre-mixing. After 24 hr exposure to the cells, cytotoxicity was assessed by MTT and FC based assays. The degree of cell necrosis and apoptosis was assessed using 7-AAD and Annexin V dyes, respectively. MTT data showed that AgNPs added directly to cells produced a particle concentration (μg/ml)-dependent decrease in viability, i.e., AgNPs pre-mixed with cell culture media supplemented with 0.1% FBS were more toxic as compared to premixing of AgNPs with media supplemented with 5% FBS. FC data showed that the degree of necrosis and apoptosis of cells when exposed to AgNPs was dependent on the concentration of both AgNPs and FBS in cell culture media used for premixing. The data showed that AgNPs premixed for 24 h with cell culture media were less cytotoxic as compared to no premixing. The results indicate that NP sample preparation methods influence biological testing outcomes.

PS 1947 Size- and Surface Coating-Dependent Uptake and Cellular Responses of Iron Oxide Nanoparticles in Human Mammary Healthy and Breast Cancer Epithelial Cells

Q. Zhang[1], S. Rajan[1], K. M. Tyner[2], B. Casey[1], C. Dugard[3], Y. Jones[3], A. Paredes[3], C. Clingman[2], P. C. Howard[3] and P. L. Goering[1]. *[1]CDRH, FDA, Silver Spring, MD, [2]CDER, FDA, Silver Spring, MD and [3]NCTR, FDA, Jefferson, AR.*

Superparamagnetic iron oxide nanoparticles (SPIONs) have received great attention due to their promising use as magnetic resonance imaging (MRI) contrast agents. In this study, we evaluated the cellular uptake and biological responses in vitro of ultrasmall SPIONs used for MRI breast cancer imaging. We compared the cellular responses between primary breast epithelia isolated from healthy and breast cancer donors after exposure to different sizes and surface coatings of USPIONs (10 nm and 30 nm bare, 10 nm and 30 nm PEG-coated). The particles were characterized using transmission electron microscopy (TEM), dynamic light scattering and gel electrophoresis. Cellular interactions with USPIONs were assessed by confocal microscopy and TEM imaging analysis. Cellular uptake of USPIONs was quantified using inductively coupled plasma mass spectrometry. Cell viability was measured by MTT and neutral red uptake assays. T2* weighted MRI scans were performed to demonstrate the potential for image contrast enhancement using a 4.7T MRI scanner. Results showed cell association/internalization of USPIONs was size- and surface coating-dependent; higher cellular uptake of 10 nm and 30 nm bare particles was observed in both cell types compared with PEG-coated particles. Cell uptake for 10 nm and 30 nm bare particles was higher in tumor cells from 2 of 3 tested donors compared to healthy cells from 3 donors. Cytotoxicity was minimal except at high concentrations of 200 and 400 ug/ml for all tested particles. Significantly enhanced MRI contrast was observed following exposure to 10 and 30 nm bare particles compared to PEG-coated particles in both cell types. These data indicate that cell responses following exposure to USPIONs are dependent on particle properties. The results provide useful information to better evaluate the safety and efficacy of USPIONs used as MRI contrast agents for breast cancer imaging.

PS 1948 Influence of Single-Walled Carbon Nanotubes with Different Physico-Chemical Properties on the Cellular Responses in Alveolar Epithelial Cells and Macrophages

K. Fujita[1, 2], S. Endoh[2], J. Maru[2], H. Kato[1, 2], N. Shinohara[1, 2], M. Horie[3] and M. Fukuda[2]. *[1]National Institute of Advanced Industrial Science and Technology (AIST), Tsukuba, Japan, [2]Technology Research Association for Single Wall Carbon Nanotubes (TASC), Tsukuba, Japan and [3]University of Occupational and Environmental Health, Kitakyushu, Japan.*

Impurity-free single-walled carbon nanotubes (SWCNTs)—relatively small bundles and a short linear shape (CNT-1), large bundles and a long linear shape (CNT-2), and commercial SWCNTs with residual metals (CNT-3) as a reference sample did not cause a significant inhibition of cell proliferation, induction of apoptosis, or arrest of cell cycle progression in A549 human alveolar epithelial cells. However, CNT-2–treated cells significantly increased the level of intracellular reactive oxygen species (ROS), in a dose-dependent manner, and the levels of these ROS were higher than those of CNT-1–treated cells or CNT-3–treated cells. On the other hand, treatment of NR8383 rat alveolar macrophage cells with CNT-1, CNT-2, and CNT-3 resulted in slight inhibition of cell proliferation. The levels of IL-1b, MIP-1a, MCP-1 and intracellular ROS generation in CNT-2–treated cells were significantly higher than that in CNT-1–treated cells. CNT-1, CNT-2, and CNT-3 were phagocytosed in vacuoles. Expression of many genes involved in the inflammatory response, their response to oxidative stress, and the expression of extracellular matrix metalloproteinases (MMPs) were markedly upregulated in cells exposed to CNT-2 or CNT-3. These results suggest that the size and length of the bundles of SWCNTs dispersed in cell culture medium, even in the same bulk SWCNTs, are critical parameters of the cellular processes and elicit stress-related cellular responses in alveolar macrophages. We propose a model in which MMPs or inflammatory cytokines derived from alveolar macrophages activated by phagocytosis of SWCNTs induce degradation of the extracellular matrix, and consequently, may cause pulmonary inflammation in alveolar epithelial cells as an indirect effect. This research was funded by NEDO, Japan (P10024).

PS 1949 Comparative Biocompatibility of Nano-Anticancer Drugs

S. Lee[1], J. Son[1], D. Khang[2] and S. Kim[1]. [1]*Phamacology, Kyungpook National Univ, Daegu, Republic of Korea and* [2]*School of Materials Science and Engineering and Center for NBECS, Gyeongsang National University, Jinju, Republic of Korea.*

The drug delivery system (DDS) has become increasingly attractive in cancer therapy since it can improve drug efficacy and reduce side effects of drugs on normal tissues. Formulating small molecule drugs into nanoparticles (NPs), such as liposomal or carbon nanotube (CNT), allows for a significant reduction of adverse effects while maintaining antitumor efficacy. However, biosafety and biocompatibility of nano-anticancer drug are not much scrutinized in terms of toxicological aspect. In this study, we demonstrated comparative toxicity of pegylated liposomal doxorubicin (Doxil) and doxorubicin (Dox)-linked CNT (Dox-CNT) in various cell lines. We used four types of cell lines such as Raw 264.7, HepG2, AML-2, and SK-MES-1 as target organ cells. We found that Dox-CNT induced greater cytotoxicity than Doxil in four types of cells. Specifically, Dox-CNT enhanced cytotoxicity through cellular uptake and production of reactive oxygen species in Raw 264.7 and HepG2 cells. Dox-CNT caused apoptosis and necrosis through CNT-induced ROS production at concentration of cell viability 75% in all the cells. However, Doxil increased apoptosis through Dox-induced changes of mitochondria potential in Raw 264.7 and SK-MES-1 cells. Both of Dox-CNT and Doxil has no significant effect on expression of pro-inflammatory cytokines in all the cells. Our results suggest the importance of biocompatibility during the design of new nano-anticancer drugs.

PS 1950 Protein Carbonylation As a Marker of Oxidative Stress Induced by Nanoparticles: Analysis of 16 Inorganic Nanoparticles

M. D. Driessen[1], R. Ossig[2], J. Schnekenburger[2], A. Vennemann[3], M. Wiemann[3], A. Luch[1] and A. Haase[1]. [1]*German Federal Institute for Risk Assessment, Berlin, Germany,* [2]*Biomedical Technology Center, University of Münster, Münster, Germany and* [3]*IBE R&d gGmbH, Münster, Germany.*

The BMBF-funded project "nanoGEM" follows a systematic approach to understand hazards associated with different types of nanoparticles (NP). Oxidative stress is considered to be a major paradigm to explain NP toxicity. Here we focused on protein carbonylation as a consequence of oxidative stress for a set of 16 different nanoparticles, used as either plane ("pristine") materials or with different surface coatings. In parallel several in vitro and in vivo toxicity endpoints have been analyzed.
We used NP of 10nm (ZrO2), 15nm (SiO2) and 50nm or 200nm (Ag), furnished either with acidic, basic or polymeric functionalities and TiO2, ZnO, BaSO4 and AlOOH as references. Characterization followed the nanospecific REACH guidance R7.1. In a screening approach we studied time- and dose-dependent carbonylation of all 16 NP in NRK-52E cells via 1D immunoblots. Data were correlated with cytotoxicity (WST-8, LDH assay) and ROS formation (DCFDA assay). Furthermore we applied a 2D proteomics approach combined with MALDI-MS/MS to identify the modified proteins. Finally for several NP we analyzed lung tissues after in vivo instillation in mice.
Eight out of 16 NP induced protein carbonylation in NRK-52E cells. Observed protein carbonylation correlated well with overall toxicity. The 2D approach revealed a complex and distinct pattern of carbonyls. Modified proteins were identified as proteins of cytoskeleton, HSP or proteins of major cellular pathways (i.e. glycolysis). We also observed carbonyl modifications in the lung tissue homogenates of rats intratracheally instilled with the same NP.
Taken together, analysis of protein carbonylation appears useful to describe toxic effects of NP and to better understand underlying molecular mechanisms.

PS 1951 ERK Pathway Is Activated in Bare-FeNPs-Induced Autophagy

E. Park[1], M. Cho[3], H. Umh[2], Y. Kim[2], S. Kim[1] and J. Kim[1]. [1]*Department of Molecular Science and Technology, Ajou University, Suwon, Gyeonggi-Do, Republic of Korea,* [2]*Department of Chemical Engineering, Kwangwoon University, Seoul, Republic of Korea and* [3]*College of Veterinary Medicine, Seoul University, Seoul, Republic of Korea.*

Iron oxide nanoparticles (FeNPs) are known to be one of the most biocompatible and safe nanoparticles. However, their long-term persistence remains a problem, and macrophages play as an important mediator in continuous stimulation of the immune system due to biopersistence of nanoparticles. In the present study, we identified the mechanisms underlying the uptake and toxicity of bare-FeNPs using RAW264.7 cells, a mouse peritoneal macrophage cell line. The bare-FeNPs penetrated the cell membrane through electrostatic interactions together with the general phagocytic pathway. At 24 h after exposure, they distributed freely in the cytosol or within autophagosome-like vacuoles. Bare-FeNPs induced decrease in the cell viability along with the cell cycle arrest in G1 phase. In addition, they increased the generation of ROS and the secretion of NO and TNF alpha as well as the expression of SOD-1 and -2 proteins, which are an anti-oxidant. While, the mitochondrial calcium level, the intensity of labeled mitochondria, and ATP production decreased. The levels of autophagy-related proteins such as p62, beclin1, ATG5, and LC3B increased in a dose-dependent manner together with the levels of ATF 3, p-EGFR and p-ERK proteins. However, the level of p-JNK protein clearly decreased. TEM images also showed that damaged organelle exist within autophagosome-like vacuoles with bare-FeNPs. On the basis of these results, we suggest that bare-FeNPs induce autophagy by initiating oxidative stress in RAW264.7 cells. Furthermore, ERK, but not JNK, pathway is activated in bare-FeNPs-induced autophagy.

PS 1952 Hidden Hazards of Nanoparticles: Crosstalk between Toxicogenomics, DNA Damage, and Cell Death

Q. Saquib[1], A. A. Al-Khedhairy[1], M. A. Siddiqui[1], J. A. Siddiqui[1], M. Faisal[2], S. Dwivedi[1], S. T. Khan[1] and J. Musarrat[3]. [1]*Department of Zoology, College of Science, King Saud University, Riyadh, Saudi Arabia,* [2]*Department of Botany, King Saud University, Riyadh, Saudi Arabia and* [3]*Department of Agricultural Microbiology, Aligarh Muslim University, Aligarh, India.*

The rationale of this study is to provide first evidence on the crosstalk between toxicogenomic changes, DNA damage and cell death induced by NiO and ZnFe2O4-NPs in HepG2 and WISH cells. Ultrastructure analysis revealed NPs translocation in cell cytoplasm and induction of DNA damage. MTT and NRU assays showed cytotoxicity of 20.6%, 64.48% in HepG2 and 18.4%, 50.73% in WISH cells. Flow cytometric analysis exhibited high ROS and nitric oxide generation along with 1.2-fold fluorescence enhancement in mitochondrial membrane potential ($\Delta\Psi$m) in NiO-NPs treated HepG2 and 0.9-fold decline in ZnFe2O4-NPs treated WISH cells. Ca2+ influx and esterase activity in HepG2 cells exhibited 474.6% and 128% greater values after NiO-NPs exposure. Cell cycle analysis of HepG2 and WISH cells exhibited 30.5% and 15.2% of apoptotic cells upon NiO and ZnFe2O4-NPs treatment. qPCR analysis of p53, caspases 3 and 9 genes showed 2.0, 1.2 and 1.1-fold upregulation in HepG2 cells. WISH cells also exhibited 5.3, 1.6, and 14.9-fold upregulation of p53, caspases 3 and bax genes. The RT2 Profiler™ PCR array data of 84 genes responsible for oxidative stress and human toxicity elucidated up-regulation of mRNA transcripts of GDF15, DDIT3, CXCL10, NOS2 and HSPA6 in range of 2.0 to 4.6-folds. Also, ZnFe2O4-NPs treated WISH cells elucidated differential up-regulation IL-1b, NFKB1, NOS2 and CCL21 genes in range of 1.5 to 3.7-folds. Furthermore, immunofluorescence analysis of NiO-NPs treated HepG2 cells exhibited translational activation of p53, bax, bcl2, cyto c, PARP and MAPK proteins. In conclusion, the significant ROS production, reduction in $\Delta\Psi$m, DNA damage, and activation of genes linked to inflammation, oxidative stress, proliferation, DNA damage and repair could serve as predictive toxicity and stress markers for toxicological assessment of NPs induced cellular and genetic damage in exposed human population.

PS 1953 Lung Tissue Culture Model for Assessment of Cytotoxicity and Inflammation Induced by Inhalable Carbon Black Nanoparticles

A. Braun[1, 4], O. Danov[1, 4], J. Kopf[1], M. Stroebele[2], T. Hansen[1], H. Fehrenbach[3] and K. Sewald[1, 4]. [1]*Fraunhofer Institute for Toxicology and Experimental Medicine, Hannover, Germany,* [2]*Karlsruhe Institute of Technology, Karlsruhe, Germany,* [3]*Airway Research Center North, Member of the German Center for Lung Research, Borstel, Germany and* [4]*Biomedical Research in Endstage and Obstructive Lung Disease Hannover (BREATH), Member of the German Centre for Lung Research (DZL), Hannover, Germany.* Sponsor: C. Dasenbrock.

Carbon black nanoparticles (CBNP) are produced in several megatons per year and are used in the industry mainly in tires, inks and for stabilization of elastomers. CBNP have a large surface area to volume ratio and can be covered with polycyclic aromatic hydrocarbon (PAH). CBNP were evaluated as possible cancerogenetic. However, it is remain unclear whether the effects are caused by PAH known to be cancerogenic or by CBNP itself. This study focused on evaluation of one CBNP without PAH (Printex® 90), two CBNP with only one PAH (Printex® 90 Benzo[a]pyrene and Printex® 90 9-Nitroanthracene) as well as one covered with different PAH (acetylene soot). Precision cut lung slices (PCLS) were used as acute exposure model.
PCLS (murine, rat and human) were exposed to different concentrations of Printex® 90, acetylene soot, Printex® 90 Benzo[a]pyrene and Printex® 90 Nitroanthracene for 24 h. The size distribution of stable particle suspension in DMEM medium was determined by dynamic light scattering. Viability of PCLS

was assessed by LIVE/DEAD® staining and determination of metabolic activity using the WST-1 assay. Pro-inflammatory immune responses were assessed in tissue lysate and quantified using ELISA (e.g. IL-1α, IL-1β, TNF-α, CXCL-8). Printex® 90 nanoparticles were nearly non toxic in PCLS of all three species at concentrations between 0.7 and 66 μg/mL. Compared to these results Benzo[a]pyrene and 9-Nitroanthracene coating showed a toxic effect at 50 μg/mL. Acetylene soot showed 1.5-fold increase in metabolic activity compared to medium control after 24 h exposure. A 40 % decrease to medium control in release of pro-inflammatory cytokines were observed at the concentration of 66 μg/mL for all CBNP.

PS 1954 Long-Term Exposures to Low Doses of Cobalt Nanoparticles Induce Cell-Transformation Enhanced by Oxidative Damage

R. Marcos[1, 2], B. Annangi[1], J. Bach[1], G. Vales[1], L. Rubio[1] and A. Hernandez[1, 2]. [1]*Universitat Autonoma de Barcelona, Cerdanyola del Valles, Spain and* [2]*CIBERESP, Barcelona, Spain.* Sponsor: A. Sampayo.

A weak aspect of the in vitro studies devoted to get information on the toxic, genotoxic and carcinogenic properties of nanomaterials is that they are usually conducted under acute-exposure and high-dose conditions. This makes difficult the extrapolation to human beings. To overcome this point we have evaluated the cell transforming ability of cobalt nanoparticles (CoNPs) after long-term exposures (12 weeks) to sub-toxic doses (0.05 and 0.1 μg/mL). To get further information on whether CoNPs-induced oxidative DNA damage is relevant for CoNPs carcinogenesis, the cell lines selected for the study were the wild-type mouse embryonic fibroblast (MEF) and its isogenic Ogg1 knockout partner, unable to properly eliminate the 8-OH-dG lesions from DNA. Our initial short-term exposure experiments demonstrate that low doses of CoNPs are able to induce ROS and that MEF Ogg1-/- cells are more sensitive to CoNPs-induced acute toxicity and oxidative DNA damage. On the other hand, long-term exposures of MEF cells to sub-toxic doses of CoNPs were able to induce cell transformation, as indicated by the observed morphological cell changes, significant increases in the secretion of metalloproteinases (MMPs), and anchorage-independent cell growth ability, among other cancer-like phenotypic hallmarks. Interestingly, such changes were significantly dependent on the cell line used, the Ogg1-/- cells being particularly sensitive. Altogether, the data presented here confirms the potential carcinogenic risk of CoNPs at environmentally plausible doses and points out the relevance of ROS and Ogg1 genetic background on CoNPs-associated effects.

PS 1955 *In Vitro* 3D Collagen-Based Hydrogel Model to Evaluate Cytotoxicity of Silver Nanoparticles

N. Bhatt[1, 2], G. Kumar[1], J. Stegemann[2], H. Degheidy[1] and P. L. Goering[1]. [1]*CDRH, FDA, Silver Spring, MD and* [2]*Dept Biomed Engineering, University of Michigan, Ann Arbor, MI.*

Nanomaterials are finding increasing uses in the medical device industry in applications such as medical implants, scaffolds and antimicrobial surface coatings. Currently, nanoparticle (NP) toxicity is typically studied in either 2D cell monolayer in vitro models or in vivo animal models; both models have inherent advantages and disadvantages. Studies using 2D models are easy and fast; however, they do not represent the complexity of native tissue. In contrast, in vivo experiments offer the full complexity of tissues, but have high cost and pose difficulty in tracking NP tissue distribution. Alternative 3D collagen matrix-based models offer several advantages to traditional models: in vitro cellular responses can be studied in a physiologically-relevant microenvironment and longer term in vitro exposures are possible. An advantage of 3D models for nanoparticle toxicity testing is that a uniform cell exposure is attained as the limitations of diffusion (smaller NPs) and sedimentation (larger NPs) of particles during exposure are mitigated. The goal of this study was to evaluate the feasibility of using a 3D tissue culture model to assess the cytotoxicity of silver nanoparticles (AgNPs). L-929 fibroblast cells were pre-mixed with type-1 collagen, crosslinked at 37oC to form 3D hydrogels, and allowed to adhere to the collagen matrix for 24 h. After 24h exposure to 10, 100, or 200 nm AgNPs at different concentrations (1, 25, and 50 μg/ml), cells were harvested from hydrogels via collagenase digestion. Harvested cells were exposed to 7-AAD dye and cell viability was measured using flow cytometry. Cytotoxicity was dependent on both dose and size of AgNPs. Cells treated with 10nm AgNPs at 50 μg/ml exhibited a 93% decrease in viability. However, less than 3% decreases in cell viability were observed after exposure to 100nm and 200nm AgNPs. The data showed that a fabricated 3D in vitro cell culture model can be used to evaluate the cytotoxicity of NPs and can bridge the gap between 2D cell culture and animal models.

PS 1956 Nanosilver-Induced Apoptosis in Cell Lines Depends on the Presence of p53

R. Foldbjerg and H. N. Autrup. *Environmental and Occupational Medicine, Aarhus University, Aarhus, Denmark.*

Silver nanoparticles (Ag NPs) are widely used in consumer products and great efforts are made to elucidate the toxicological mechanisms. Activation of apoptosis after exposure to Ag NPs was investigated in 3 cell lines (CaCo-2, A549, and A549-p53-/-). The Ag NPs (16 nm) were previously characterized (Foldbjerg et al, Toxicol. Sci., 2013). Ag NPs reduced the cellular viability (measured by the MTT assay) by 80% in CaCo-2 cells and 35% in A549 cells at the highest NP concentration (30 μg/mL). Using the annexin V/PI assay, cell death was mainly detected as apoptosis in A549 cells and necrosis in CaCo-2 cells. Thus, cell death induced by Ag NPs may occur by different mechanisms in A549 and CaCo-2 cells. One of the major apoptosis pathways is via the activation of caspases. In A549 cells, a significant increase in caspase-3/7 and -9 activity was observed upon Ag NP exposure. In contrast, the caspase activity in Ag NP-treated CaCo-2 cells was unchanged compared to vehicle controls. CaCo-2 cells lack functional p53 and further studies in A549-p53-/- cells verified that p53 is necessary for caspase-3/7 activation upon Ag NP exposure. Increased caspase activity could, however, be induced by the mdm-2 inhibitor, Nutlin-3, demonstrating that the caspase machinery is fully functioning in CaCo-2 and A549-p53-/- cells. These results indicate that Ag NPs induce caspase-dependent apoptosis in A549 cells and caspase-independent necrosis in CaCo-2 cells. The classical route of caspase-9 activation includes loss of mitochondrial membrane potential (MMP). To confirm this route, the MMP of A549 cells exposed to Ag NPs was measured by JC-1 staining. Interestingly, Ag NPs did not affect the fraction of cells with low MMP suggesting activation of caspase-9 by a mitochondria-independent route. This route may involve calcium fluxes since Ag NP exposure induced a dose-dependent increase of cytosolic [Ca2+] in both A549 and CaCo-2 cells as determined by Fluo-4 fluorescence. We therefore speculate that Ag NPs may induce ER stress leading to calcium release and subsequent caspase activation in cells with wild type p53.

PS 1957 Silver Nanoparticle-Induced Apoptosis, Genotoxicity, and Oxidative Stress in CHO Cells

P. J. John[1], K. K. Awasthi[1], A. Awasthi[1], N. Kumar[2] and P. Roy[2]. [1]*Zoology, University of Rajasthan, Jaipur, Rajasthan, India and* [2]*Biotechnology, Indian Institute of Technology, Roorkee, Uttarakhand, India.* Sponsor: S. Rana.

Silver has been used for decades owing to its health benefits as an antimicrobial and antifungal substance. Due to the novel properties of silver, silver nanoparticles are used in electronics, biosensing, photographic processing, medical applications and in many common household products, thus increasing their concentration in the environment and concern about the evaluation of its toxicity. For the present study, the Chinese Hamster Ovary (CHO) cells were exposed to various dose concentrations of silver nanoparticles i.e. 25, 50 and 100 μg/ml in invitro and were compared with that of the control. Cellular morphology, mitochondrial function (MTT assay), mitochondrial membrane potential, anti-oxidant enzymes assay (CAT, SOD, GPx, GST, GR activities as well as total Glutathione level) and comet assay were performed to assess the toxicity. Ag NPs caused decreased mitochondrial membrane potential and comparable CAT, SOD, GPx, GST, GR activities. Comet tail length, tail moment and percent DNA in tail were also found to be increased in dose dependent manner. In summary, the results suggest that Ag NPs at low concentration cause cytotoxicity, oxidative stress induced apoptosis and damage to DNA and other cellular components.

PS 1958 Influence of Capping Agents on Cellular Uptake of Silver Nanoparticles and the Resultant Toxicity

F. Zhang, B. Lau and E. D. Bruce. *Ecological, Earth and Environmental Sciences, Baylor University, Waco, TX.*

Nanomaterials, especially silver nanoparticles (AgNPs) have been applied to numerous commercial products. Accordingly, there are raising concerns that exposure to these nanoparticles may cause potential adverse effects on humans as well as the environment. Humans are exposed to AgNPs mainly via inhalation and ingestion, and the potential toxicity has been attributed to nanoparticle-cell interactions, such as the adsorption and internalization of nanoparticles, however, little is known about the mechanisms of these interactions and the factors influencing them. This experiment was carried out to quantitatively and mechanistically investigate the role of capping agents of AgNPs on cellular uptake by cells in the epithelial lining of the human lung and colon. In vitro studies of human bronchoalveolar carcinoma derived cells (A549) and colon adenocarcinoma (Caco-2) are used to quantify the uptake kinetics and the extent of internalized AgNPs and to investigate the uptake

mechanism among different capping agents. AgNPs cytotoxicity is evaluated by lactate dehydrogenase (LDH) release and cell viability, which is also compared to the toxicity caused by Ag+ treatments. We observed Ag+ significantly reduced cell viability and triggered LDH release, however, no such changes were observed from AgNPs-treated cells. In addition, cellular inflammatory response and DNA damage will also be assessed and presented as part of AgNP toxicity mechanism investigation. Results of this study can be applied to facilitate the risk assessment process, limiting the hazards associated with occupational/consumer exposure to silver nanoparticles.

PS 1959 Partial Reduction of Silver Nanoparticle-Dependent Cytotoxicity and Stress Activation following Magnetic Field Exposure

N. J. Braun[1], K. K. Comfort[2] and S. M. Hussain[3]. [1]*Department of Biomedical Engineering, Purdue University, West Lafayette, IN,* [2]*Chemical and Materials Engineering, University of Dayton, Dayton, OH and* [3]*Molecular Bioeffects Branch, Human Effectiveness Directorate, Air Force Research Laboratory, Wright Patterson AFB, OH.*

Silver nanoparticles (AgNPs) have become incorporated into a number of consumer, industrial, and medical applications, owing to its tremendous, innate plasmonic and antimicrobial properties. However, AgNPs also induce a strong cytotoxic response, brought on by an excess of cellular stress and DNA damage, which has severely limited the inclusion of AgNPs in nano-based biological applications, such as drug delivery and bio-imaging techniques. Previous investigations into magnetic field (MF) exposure have determined the potential of MFs to reduce the stress response in cellular systems; however the ability of a MF to protect cells from AgNPs has yet to be explored. This study sought to identify if concurrent exposure to 10 nm AgNPs and a 30 mT static MF could reduce the cytotoxic and stress responses in a murine neural stem cell line (NE-4C). This study identified that the presence of a MF provided a layer of protection from negative AgNP effects, with a 15% increase in viability noted up to a threshold concentration of 10 μg/mL. This partial recovery of AgNP dependent cytotoxicity was found to correlate with increased ki67 expression and a substantial decrease in the NE-4C stress response, including reactive oxygen species production and NFκB and c-Jun expression. As neurological models are highly susceptible to stress, this study identified MF stimulation as a potential mechanism to counteract detrimental AgNP effects in neural cells; thereby demonstrating that a joint AgNP and MF system may be advantageous to progress neurological nano-based applications.

PS 1960 Ionic Dissolution of Silver Nanoparticles Is the Root Cause behind the Differential Disruption of EGF Signal Transduction

K. K. Comfort[1], E. Maurer[2] and S. M. Hussain[2]. [1]*Chemical and Materials Engineering, University of Dayton, Dayton, OH and* [2]*Molecular Bioeffects Branch, Human Effectiveness Directorate, Air Force Research Laboratory, Wright Patterson AFB, OH.*

In recent years, the field of nanotoxicology has begun exploring the ability of low, relevant dosages of nanomaterials to impact normal cellular functionality, such as signal transduction. Previously, we identified that silver nanoparticles (AgNPs) reduced epidermal growth factor (EGF) dependent signaling. It has also been elucidated that the generation of silver ions is the origin behind the well-established cytotoxic response of AgNPs in a cellular system. However, it has yet to be explored whether the ionic dissolution or the interaction between the particles and the cell surface receptors is the driving force behind AgNP dependent signaling alterations. As such, the goal of this study were to determine if the disruption of EGF signaling transduction was a result of the ionic dissolution or the AgNPs themselves, in a human keratinocyte cell model. Following separation of the AgNPs from the generated ions through tangential flow filtration, it was discovered that the kinetic dissolution was the principle cause for observed modifications to the EGF signaling network, as evaluated through Akt and Erk phosphorylation. The silver ions alone produced a 20% loss of signaling activation, whereas treatment with the particles alone induced no modifications. To explore if this phenomena was sustained or transient, EGF signaling activation was re-evaluated 72 hours after the removal of the AgNPs. Modulation of the cellular response to EGF stimulation still existed, however, after this extended time frame an augmentation in signaling was found; indicating the HaCaTs were in recovery mode. In conclusion, this study demonstrated that at low dosages of AgNPs, the disruption to cellular functionality is driven by the rate of ionic dissolution and is sustained for several days post AgNP removal; further illuminating the long term potential for damage following exposure.

PS 1961 Design and Validation of Nanomaterial Aerosol Exposure Techniques for *In Vitro* Toxicology

C. Grabinski[1, 2], M. Sankaran[2] and S. M. Hussain[1]. [1]*Molecular Bioeffects Branch, Air Force Research Laboratory, Wright Patterson AFB, OH and* [2]*Department of Chemical Engineering, Case Western Reserve University, Cleveland, OH.*

Traditional in vitro toxicology studies are often conducted by dispersing nanomaterials (NMs) in biological media for administration to cells in a static condition, which does not depict realistic inhalation exposure. The objective of this study was to validate a previously designed system to mimic inhalation exposure by delivering well-characterized NM aerosols to cells grown at the air-liquid interface. Silver NMs were exposed either as dispersion in biological media or as an aerosol generated from powder. The aerosolized NMs were characterized in real-time for size distribution and concentration simultaneously to being introduced into the nanoaerosol exposure chamber and deposited onto cells using electrostatic deposition. A human type II pneumocyte and alveolar macrophage co-culture was grown in the chamber and exposed to either the dispersion or aerosol. Post-exposure, the viability was assessed using the Alamar Blue assay, the cell morphology was evaluated using fluorescence microscopy and NM uptake was imaged using electron microscopy. Results showed that the NMs exhibited unique agglomeration patterns and dosimetry when exposed at the air-liquid interface as a dispersion versus aerosol. This led to differences in the cellular response and NM uptake. This study demonstrates a promising step forward in the development of a standardized realistic exposure method for assessing NM toxicity to lung cell models in vitro.

PS 1962 Strain-Dependent Responses to Quantum Dots in Mouse Hepatocytes

T. Ward[1], R. S. McMahan[3], C. White[1], J. Shang[2], X. Hu[2], X. Gao[2], D. L. Eaton[1], T. Kavanagh[1], W. C. Parks[3] and W. A. Altemeier[3]. [1]*Department of Environmental and Occupational Health Sciences, University of Washington, Seattle, WA,* [2]*Department of Bioengineering, University of Washington, Seattle, WA and* [3]*Department of Medicine, University of Washington, Seattle, WA.*

Quantum dots (Qdots), a new class of fluorescent nanoparticles, have unique properties that have enabled new opportunities in many areas including optoelectronics, photovoltaics, drug delivery, and biomedical imaging. Despite widespread industrial use and promise for commercial and diagnostic applications, the toxicity of many Qdots remains largely unknown. Many nanoparticles are known to be pro-inflammatory, especially when taken up by tissue macrophages that can elaborate pro-inflammatory cytokines and chemokines. Several in vivo studies have shown that injection of Qdots into rats or mice results in rapid clearance from the blood, with most of them ending up in the liver, spleen, and lymph nodes. In this study, we aim to determine how hepatocytes respond to Qdots, and whether toxic and immunomodulatory effects of Qdots are strain-dependent. We used an in vitro model of exposure to primary hepatocytes cultures from C57BL/6J and A/J strains of inbred mice to determine strain-dependent phenotypes related to exposure to tri-n-octylphosphine oxide, poly (maleic anhydride-alt-1-tetradecene) (TOPO-PMAT) coated CdSe/ZnS Qdots. We cultured primary hepatocytes from C57BL/6J and A/J mice and treated them with various doses of Qdots for 4 hours. We found that Qdot uptake in primary hepatocytes was dose-dependent and significantly higher in hepatocytes from A/J mice than those from C57BL/6J mice. We also measured pro-inflammatory cytokines by qPCR, and found that Qdots induced strain-dependent expression of Il-6 and Cxcl1 mRNA in primary hepatocytes, with cells from A/J mice demonstrating more sensitivity than C57BL/6J cells. Collectively, these data suggest that genetic background plays a significant role in Qdot uptake and inflammation. The A/J strain is more susceptible to Qdot-induced inflammation than C57BL/6J, consistent with in vivo data.

PS 1963 Quantifying the Impact of Ag Nanoparticle Structure and Dissolution in Cell Culture Media on Cell Exposure and Biological Impact

P. Munusamy[1], S. Chen[2], B. Leo[2], C. Liu[1], J. N. Smith[1], B. D. Thrall[1] and D. R. Baer[1]. [1]*Pacific Northwest National Laboratory, Richland, WA and* [2]*Imperial College, London, United Kingdom.*

In vitro studies using bone marrow derived macrophages and RAW 264.7 cells show that 24 hr exposure to 20 nm Ag particles causes cytotoxicity at concentrations ≥ 10 μg/ml. Understanding the actual dose of nanoparticles and Ag ions to the cell requires knowledge of nanoparticle agglomeration, deposition, dissolution, and transformation in cell culture media. We have examined particle dissolution at suspension concentrations from 1 μg/ml to 50 μg/ml and changes of particles for two 20 nm nanoparticles synthesized in different ways. One set of particles was prepared with a 7-8 nm Au core that helped produce particles of uniform

size. Ag coatings were made up of several Ag crystallites that nucleated on the Au producing many highly defective interfaces. In contrast, pure Ag particles were less uniform in shape but had a more ordered 'single' crystal structure with slip plane or grain-boundary defects. Dissolution was studied in RPMI+FBS culture medium by measuring the appearance of Ag in the supernatant as a function of time up to 24 hours. High resolution (HR)-TEM and STEM images after solution exposure showed that the pure Ag particles maintained structural integrity compared to Ag/Au particles where Ag layer had a non-uniform dissolution sometimes exposing the Au core. Dissolution was increased for 20 nm Ag/Au particles in comparison to pure Ag. An equation relating the kinetics of dissolution, the surface area of particles and an effective solubility constant was used to examine dissolution behaviors. For solution concentrations ≥ 10 μg/ml, dissolution parameters within each particle type are consistent regardless of particle concentration. The effective solubility constant for 20nm particles with the Au was higher than that observed for pure Ag particles. At solution concentrations < 10 μg/ml, solution kinetics and rates appear to be less than would be expected from the behaviors at higher concentrations. Reasons for this difference are under study.

PS 1964 Does Microfluidic Dispersion Influence the Toxicity of Geometric TiO2 Nanomaterials?

T. B. Tilly[1, 2], L. L. Kerr[2], L. K. Braydich-Stolle[1], J. J. Schlager[1] and S. M. Hussain[1]. [1]*Molecular Bioeffects, AFRL, Dayton, OH and* [2]*Chemical, Paper, and Biomedical Engineering, Miami University, Oxford, OH.*

Tunable chemical and physical properties of engineered nanomaterials are achievable by changing their geometry and morphology. Titanium dioxide (TiO2) based nanofilaments—nanotubes, nanowires, nanorods—have gained interest in sensing, electrical, and environmental fields due to their superior performance over TiO2 nanoparticles. Their application in the medical field for drug delivery, implant coating, and bioimaging is just now being realized, however their biocompatibility is not fully understood. Thus, safety assessment of geometric TiO2 nanomaterials is critical for protecting workers, patients, and bystanders as these technologies become widely implemented. The tendency of TiO2 based nanofilaments to aggregate and agglomerate make toxicity results controversial because of the challenge in differentiating whether the observed toxicity was caused by the nanofilaments or aggregates. TiO2 nanofilaments aggregate and are difficult to disperse homogeneously in solution by conventional methods, like sonication and voxtexing. In this study, a microfluidic device was utilized to produce the stable, homogeneous dosing solutions necessary for in vitro toxicity evaluation by eliminating any toxicity caused by aggregated TiO2 nanofilaments. The quality of the dispersion provided by this method allows for toxicity results to be directly correlated to the TiO2 nanostructure itself. The biocompatibility of four TiO2 nanogeometries—nanotubes, nanowires, nanorods, and nanoparticles—were assessed in nasal epithelial cells (RPMI 2650). All TiO2 based nanomaterials dispersed by the microfluidic method were biocompatible in RPMI 2650 cells at the concentrations tested. Whereas 100 μg/ml concentrations of nanowires and nanotubes dispersed by sonication reduced viability up to 27%, indicating that in vitro toxicity results may be controlled by the dispersion of dosing solutions.

PS 1965 Low-Level Exposure to Silver Nanoparticles-Induced Hypertrophy, Multinucleation, and Senescence in Lung Epithelial Cells

D. Ellis[2, 1], C. E. Sulentic[1] and S. M. Hussain[2]. [1]*Department of Pharmacology & Toxicology, Wright State University, Dayton, OH and* [2]*Molecular Bioeffects Branch, Bioeffects Division, Air Force Research Laboratory, Wright Patterson AFB, OH.*

Nanotechnology is a rapidly expanding discipline focused on manipulating materials at the nanometer scale. Considerable research has focused on the antibacterial properties of silver nanoparticles (AgNPs), resulting in several commercial products. The bactericidal activity of AgNPs stems from shedding of silver ions and their binding critical biomolecules. The toxic activity in mammalian cells is proposed to derive from oxidative stress caused by the particles and the ions release. In addition, AgNPs may reside in biosystems, producing long-term stress directly or through slow dissolution to ions. As a result, AgNP exposure raises concern over environmental and human health effects. Long-term stress and oxidative damage can induce cellular senescence, or permanent growth arrest. This project tested the potential for AgNPs to induce senescence in A549, epithelial cells during extended exposure at a sub-lethal concentration. Cells were exposed to AgNPs for 1 to 4 days at 10 μg/mL, a level that did not cause overt toxicity by MTS assay but caused oxidative stress measured using a Dichlorofluorescein probe. After 3 to 20 days of recovery, induction of senescence was assessed by observing cell morphology, measuring proliferation, and testing for senescence-associated β-galactosidase (SA-β-Gal) activity. AgNPs caused an increase in the number of hypertrophic cells and cells with SA-β-Gal activity, indicating senescence was induced. Proliferation was relatively unaffected suggesting that many A549 cells were able to subvert full growth arrest; however most hypertrophic cells were multinucleate implying that they could not complete cytokinesis. Taken together, these results indicate that AgNPs induced a senescence-like phenotype in A549 cells despite their resistance to growth arrest.

PS 1966 Evaluation of Tungstate Nanoparticle Cytotoxicity

K. M. Dunnick[1, 2], M. A. Badding[1], D. Schwegler-Berry[1], N. R. Fix[1], S. Wong[1, 2] and S. S. Leonard[3, 4]. [1]*NIOSH, Morgantown, WV,* [2]*West Virginia University, Morgantown, WV,* [3]*State University of New York at Stony Brook, Stony Brook, NY and* [4]*Brookhaven National Laboratory, Upton, NY.*

Alkaline-earth metal tungstate AWO_4 (A= Ca, Ba, Sr) nanoparticles are currently being used in a variety of applications, including use as components of medical equipment, optical fibers, and scintillator detectors. This versatility may lead to increases in manufacturing within the next 10 years and may subsequently result in more cases of occupational exposure. Therefore, it is important to assess the effects of tungstate nanoparticles on cellular systems. RAW 264.7 macrophage cells were used to assess tungstate nanoparticle toxicity and changes in reactivity based on shape (sphere vs. wire), size, and chemistry. Enhanced dark field microscopy and scanning electron microscopy were used to evaluate nanoparticle-cell association over multiple time points up to 7 hours. To assess uptake, transmission electron microscopy was implemented. Both wires and spheres showed cell surface interactions; however, only spheres were engulfed. To assess intracellular reactive oxygen species (ROS) production, a DCFH assay was performed. Results showed that nanowire-exposed cells had significantly increased levels of ROS over a 7 hour time-course, while nanosphere-treated cells did not. This may be a result of association versus engulfment. Based on ROS production and cell-particle interactions, overall cellular cytotoxicity was measured. A caspase activation assay was used to assess apoptosis, and an MTT assay was employed to determine cell viability. Minimal caspase activity was measured after 24 hours with both spheres and wires. Wire-cell interactions resulted in cell death after 24 hours and sphere treated cells had minimal changes in viability. This data shows that tungstate nanoparticles are not explicitly toxic; however, wires appear to be more reactive than spheres, and have an initial, but manageable toxic effect on cells.

PS 1967 *In Vitro* Cytotoxicity Assay of TiO_2 Nanoparticles in Pulmonary Epithelial and Macrophage-Like Cells

K. Iwasawa[1], T. Aoyama[1], K. Harano[1], N. Shinohara[2], G. Zhang[2], M. Gamo[2] and Y. Sakai[1]. [1]*Institute of Industrial Science, the University of Tokyo, Tokyo, Japan and* [2]*RISS, National Institute of Advanced Industrial Science and Technology, Tsukuba, Japan.* Sponsor: H. Kojima.

Recent advances in nanotechnology have increased the development and production of many new nanomaterials, and this raises concerns about possible human health risk. To establish alveolar cell-based assay systems, human epithelial and macrophage-like cell lines (A549 and THP-1) were used.

First, we investigated the A549 cell viability after exposure to the nanoparticles (Φ21 nm TiO_2) at various initial densities. When the cells are cultured at a low density, the drastic decrease of viability (50%) was observed. In contrast, when the cells are cultured at a high density to form cell monolayer, the viability decreased only slightly. In addition, in cocultues of A549 monolayer and THP-1, there were no viability changes, presumably because particles are firstly phagocytized by THP-1 or macrophages. These results show that we have to carefully choose the culture conditions according to the objectives such as screening with high sensitivities or physiological relevancy.

Second, nanoparticles permeation was investigated using A549 and THP-1 cell-based alveolar model formed on semi-permeable membranes and relevant numerical simulation describing dynamic equilibrium among the apical side, alveolar cells, macrophages and basolateral sides. With biological kinetic parameters obtained in the cell-based assay, the numerical model largely described the concentration changes in the assay system. By changing some parameters such as scale of the model to overcome the limitations of existing culture models, it was indicated that the combination use of *in vitro* cell-based tissue models and numerical simulations made us possible to predict the permeation of particles through the alveolar tissue.

PS 1968 Differential Mode of Nano-Bio Interaction by Graphene Nanomaterials

N. Chatterjee, H. Eom and J. Choi. *University of Seoul, Seoul, Republic of Korea.*

The wide applications of Graphene nanomaterials and its derivatives have emphasized the need for further mechanistic insight to predict the consequences of environmental health and safety impacts of its exposures. However, little information is available on their toxicity and bio-compatibility. In this current study, we report the impact of differential functionalization of graphene in the interaction with HepG2 cells. We performed a comprehensive study on the toxicity of graphene oxide (GO) and reduced graphene oxide (rGO) on human hepatoma cells (HepG2) and two different kind of GO- few layer graphene (FLGO) and single layer graphene (SLGO), three kind of graphene nanoplatelets (GNP), pristine GNP, GNP-NH2, GNP-COOH on human bronchial epithelial (Beas2B) cells. We used the standard toxicity endpoints such as, cell viability, uptake, apoptosis, ROS formation, DNA damage etc. Furthermore, we also carried out the details of physio-chemical properties of graphene nanomaterials by using Raman spectroscopy, AFM, TEM and XPS etc. The results showed that the differential modes of nano-bio interaction of graphene nanomaterials are influenced by its chemical modification, layer number and functionalization which in turn would direct its further biomedical application. In summary, our results present a paradigm for analyzing surface functionality-activity relationship of graphene naomaterials with tissue specific evaluation could eventually be utilized for more efficient and innocuous applications, specifically in biomedical field.

PS 1969 Amorphous Silica Nanoparticle-Mediated Hepatotoxicity: A System Toxicology Approach

H. Eom, N. Chatterjee and J. Choi. *University of Seoul, Seoul, Republic of Korea.*

The wide applications of synthetically manufactured amorphous silica nanoparticles (aSiNP) range from daily life uses such as paints, varnishes, glue, desiccants, plastics, toothpaste, pharmaceuticals, cosmetics, food packaging and as food additives etc, and extended to diagnostic and biomedical fields such as bioimaging, drug and gene delivery, cancer therapy etc. However, the toxic potentiality and bio-compatibility of aSiNP remains to be elucidated. The present study aims to investigate the molecular mechanisms and pathways involved in aSiNP mediated toxicity with systems toxicology approach. The standard toxicity endpoints such as, cytotoxicity, DNA damage, ROS formation, significant modulations of antioxidant as well as DNA repair genes expressions were evident in aSiNP exposed HepG2 cells. Furthermore, the global gene expression changes and subsequent pathway analysis revealed that steroid, lipid and cholesterol biosynthesis pathways are mainly triggered due to aSiNP exposure at 100 mg/L for 24 h. In addition, aSiNP exposures also affect glutathione metabolism as well as xenobiotic and drug metabolism pathways in HepG2 cells. The observed changes in cellular oxidative stress and lipid/cholesterol biosynthesis pathway can be considered as the potential mechanism of aSiNP mediated hepatotoxicity. Our findings could eventually help in designing of future applications of aSiNP, specifically in drug delivery system and other biomedical purposes.

PS 1970 Cerium Oxide Nanoparticles Air Exposure: A Comparison Study Using a Human 3D Airway Model and A549 and Beas-2B Cell Lines

I. M. Kooter[1], Y. Staal[2], M. Grollers-Mulderij[1], M. Steenhof[1], E. Duistermaat[2], F. A. van Acker[2], E. Schoen[1], E. van Someren[1] and F. Kuper[1]. *[1]TNO, Utrecht, Netherlands and [2]TNO Triskelion BV, Zeist, Utrecht, Netherlands.* Sponsor: R. Wouters.

Human 3D airway models are fully differentiated and functional models of the respiratory epithelium and therefore may be positioned in safety evaluation of nanoparticles entering the airways. They are cultured at an air liquid interface (ALI), allowing relevant exposure via air. To investigate the respiratory effects of nanoparticles, we performed air exposures of nano-CeO_2 and micro-CeO_2 using MucilAir human 3D bronchial model and compared these to Beas-2B and A549 cell lines.
MucilAirTM and A549 or BEAS-2B cell lines were exposed at ALI conditions in Vitrocell exposure modules to 0, 50, 224, 1000 mg/m^3 CeO_2 for 1 hour. After a 24 hours post-incubation period, cells were analyzed for oxidative stress, inflammation, cytotoxicity, genotoxicity and RNA expression.
Comparison of cell models showed that MucilAir cells are less affected by the air stream compared to the A549 or BEAS-2B cells (based on IL-8 and LDH). MucilAir cells showed a slight HO-1 response for both nano-CeO_2 and micro-CeO_2 exposure, where cell lines did not. In contrast Beas-2B cell line showed an inflammatory response (IL-8) upon nano-CeO_2 exposure where MucilAir does not. Both A549 and Beas-2B cell lines showed a dose response in the Comet assay upon nano-CeO_2 exposure in contrast to MucilAir. These differences between MucilAir and the cell lines are confirmed by the gene expression analyses.
Comparison of the nano-CeO_2 and micro-CeO_2 exposures showed that prominent effects were found for nano-CeO_2 exposure only. Nano-CeO_2 exposure resulted in an increase in IL-8 for the Beas-2B cell line where micro-CeO_2 exposure does not. A dose response on genotoxicity is observed for both the nano-CeO_2 exposed cell lines only.
Summarizing, our results show that the MucilAir human 3D airway model is more resistant to air stream and nano-CeO_2 compared to the cell lines. We conclude that the use of human 3D airway models might predict a more realistic response where cell lines might overestimate the effect of nanoparticles.

PS 1971 Zinc Oxide Nanoparticles Induce Cytotoxicity in Human Endothelial Colony-Forming Cells

Y. Suzuki[1], S. Tada-Oikawa[1], G. Ichihara[2], K. Izuoka[1] and S. Ichihara[1]. *[1]Mie University, Tsu, Japan and [2]Nagoya University Graduate School of Medicine, Nagoya, Japan.*

Background: Metal oxide nanoparticles have been widely used in industry, cosmetics, as well as biomedicine. However, cardiovascular effect of exposure to metal oxide nanoparticles remains elusive. It is known that the endothelial progenitor cells (EPCs) contribute to postnatal endothelial repair and regeneration. Although recent studies indicated that, in humans and mice, the number of EPCs is decreased by exposure to PM2.5, the effect of metal oxide nanoparticle on EPCs remains unclear at the cellular level. The present study investigated the cytotoxicity, apoptosis and the tube formation induced by nano-sized zinc oxide (ZnO) particles using human endothelial colony forming cells (ECFCs), that participate in postnatal vasculogenesis.
Method: ECFCs were exposed to nano-sized and macro-sized ZnO for 24 hours. Cellular viability was determined by the MTS assay, which measures the reduction of {3-(4,5-dimethylthiazol-2-yl)-5-(3-carboxymethoxyphenyl)-2-(4-sulfophenyl)-2H-tetrazolium} (MTS) to formazan in viable cells. Apoptotic cells were counted by flow cytometry using Annexin V-FITC to stain apoptotic cells. For capillary-like tube formation assay, ECFCs were placed in 24-well plates pre-coated with solidified Matrigel Matrix and cultured for 24 hours. Capillary-like tubular structures were photographed, and the number of incorporated ECFCs in tubules was determined.
Results and Discussion: The 24-hour exposure to nano- and macro-sized ZnO reduced the cellular viability in a dose-dependent manner and increased apoptotic cells in ECFCs. The functional capacity for tube formation of ECFCs on Matrix gel was reduced in the cells exposed to nano- and macro-sized ZnO particles compared with the control cells. The study indicates that exposure to nano- and macro-sized ZnO particles may attenuate function of vasculogenesis in ECFCs.

PS 1972 Biological Evaluation of Ultrananocrystalline and Nanocrystalline Diamond Coatings

S. Skoog[1, 2], G. Kumar[2], J. Zheng[2], A. Sumant[3], P. L. Goering[2] and R. Narayan[1]. *[1]Joint Dept. of Biomedical Eng., UNC & NCSU, Raleigh, NC, [2]CDRH, US FDA, Silver Spring, MD and [3]Center for Nanoscale Materials, Argonne National Laboratory, Argonne, IL.*

Biomaterials with nanoscale surface features have been increasingly investigated for medical device applications in an effort to achieve desired tissue-material interactions. Ultrananocrystalline diamond (UNCD) and nanocrystalline diamond (NCD) thin films are distinguished by their grain size with UNCD having 2-5 nm grain size and NCD with grain sizes of 10 nm and above (up to 500 nm). Both UNCD and NCD exhibit material properties similar to those of natural diamond, including mechanical robustness, chemical inertness, biocompatibility, and excellent tribological properties, which make them ideal implant coating materials. Recently, UNCD and NCD have been investigated as coatings for orthopedic, dental, ophthalmic, and cardiovascular device applications. The aim of this study was to evaluate the in vitro biocompatibility of UNCD and NCD coatings and to determine if surface roughness and grain size affect cellular response. Thin films of UNCD and NCD with varying levels of surface roughness (grain sizes 5-350 nm) were deposited on silicon substrates using microwave plasma chemical vapor deposition (MPCVD). Scanning electron micrographs and atomic force micrographs revealed uniform films with different scales of surface roughness; Raman spectroscopy confirmed the presence of carbon bonding typical of diamond thin films. Cell attachment, morphology, viability, and proliferation responses of human bone marrow stromal stem cells to UNCD and NCD surfaces were evaluated. In vitro cell viability and proliferation data showed that UNCD or NCD films have no major adverse cytotoxic effects. No significant differences in cell viability or cell proliferation were noted among diamond films (UNCD or NCD) of different

nanoscale roughness. Our in vitro data shows that UNCD and NCD coatings have superior in vitro biocompatibility profiles irrespective of their roughness and grain size making them desirable for use in implantable medical devices.

PS 1973 Preparation, Characterization and Antimicrobial Activity of Eu3+-Doped Hydroxyapatite Nanopowders

J. F. Delgado-Jimenez[1, 2], R. Agustin-Serrano[2], E. Reyes-Cervantes[2], J. L. Varela[2], R. Gonzalez-Rodriguez[4], J. A. Quenel[1], T. D. Palacios-Hernandez[1, 3] and E. Rubio-Rosas[2]. *[1]DCQB, Universidad de las Americas Puebla, San Andres Cholula, Puebla, Mexico, [2]CUVyTT, Benemerita Universidad Autonoma de Puebla, Puebla, Puebla, Mexico, [3]CB, Universidad Popular Autonoma del Estado de Puebla, Puebla, Puebla, Mexico and [4]Texas Christian University, Fort Worth, TX.*

Hydroxyapatite [(HAp) - Ca10(PO4)6(OH)2] is a bioceramic which corresponds 65% of human hard tissue. This material has received intense research due its biocompatibility, osteoconductivity, bioactivity, non-toxicity and non-immunogenicity. Herein we propound the lanthanide introduction of Eu3+ ions into HAp as a functional mimic of Ca2+ ions for biological imaging. Luminescent HAp nanorods were prepared by means of a microwave-assisted hydrothermal method. In a typical process and without further purifications, (NH4)2HPO4 were dissolved in 25 ml of tridistilled water to form solution A. CaCl2 and Eu(NO3)3*H2O were dissolved in 25 ml of tridistilled water to obtain Solution B. Subsequently Solution A was poured into solution B. After a basic pH adjustment the suspended white precipitate was irradiated with microwaves within Teflon vessels. The nanopowders were characterized by XRD, SEM, TEM, AFM, SAED, TGA/DSC, UV-Vis, FTIR and EDX to determine cristallinity, morphology, thermal stability and optical properties. In general terms, the synthetic biomaterial was doped with 1, 2.5 and 5% of total weight. XRD patterns ratified high crystalline HAp with hexagonal structure. In addition Europium Oxides were absent demonstrating Eu3+ introduction in the lattice. Microscopy techniques revealed nanorods in the range of 14-25 nm. Eu3+ impurities presence also was confirmed by elemental analysis. Finally, Eu3+ modified nanoparticles were evaluated upon *Staphylococus aureus* and *Escherichia coli* as biological *in vitro* models through antibiogram technique. The test was design using several concentrations of the product (10, 1, 0.1 and 0.01 mg/ml). The materials obtained didn't show toxicity evidences, opening the possibility of being used for potential medical applications.

PS 1973a Silver Nanoparticles and Ionic Silver Have Opposite Effects on Spontaneous Activity and Pharmacological Responses in Neuronal Networks *In Vitro*

J. D. Strickland[1], J. Crooks[2], D. Hall[2], K. Dreher[2] and T. J. Shafer[2]. *[1]NCSU, Raleigh, NC and [2]NHEERL, ORD, U.S. Environmental Protection Agency, Research Triangle Park, NC.*

Silver nanoparticles (Ag NP) are used in a wide range of consumer and medical products because of their antimicrobial properties. In vivo studies have demonstrated that Ag NPs translocate to distal organs, including the brain, following inhalation and ingestion. Thus, it is essential to examine neuronal function as part of assessing potential human health impacts of Ag NPs. The present study examined effects of $AgNO_3$, 3 citrate coated and 3 PVP coated Ag NPs (10, 50, and 75 nm) on network function in primary cultures of cortical neurons using microelectrode array recordings. Non-cytotoxic concentrations of Ag NPs and $AgNO_3$ (0.078-0.63 and 0.08-1.7 μg/ml, respectively) were determined after a 48 hr exposure using Cell Titer Blue and Neutral Red assays. Between days 12-19 in vitro, baseline activity (1 hr) was recorded prior to exposure to Ag NPs. Changes in number of total spikes (TS) and number of active electrodes (AE), relative to controls, were assessed 1, 24 and 48 hr after exposure to FBS pre-coated Ag NP suspensions or $AgNO_3$. After 48 hr, the response to a challenge with the $GABA_A$ antagonist, bicuculline (BIC; 25 μM), was assessed. Citrate coated 10 nm Ag NP caused statistically significant concentration-related increases in AEs at 24 hr. After BIC treatment, PVP coated 75 nm Ag NP caused statistically significant increases in AE (0.6 μg/ml) and TS (0.3 μg/ml). $AgNO_3$ had opposite effects on TS and AEs, causing statistically significant decreases in AEs (0.9 and 1.7 μg/ml), negative concentration-related trends in AEs at 24 and 48 hr, and a significant concentration-related decrease in TS following BIC challenge. These results indicate that Ag NP size and coating affect their ability to disrupt either spontaneous or $GABA_A$ receptor mediated neuronal activity in vitro. In addition, the direction of the effect on neuronal activity for Ag NP was opposite that of $AgNO_3$, indicating ionic silver does not mediate these effects. (This abstract does not reflect Agency Policy.)

PS 1973b *In Vitro* Cytotoxicity and Phagocytosis of Silver Nanomaterials in Murine Macrophages

T. D. Green[1], A. Badawy[2], T. Tolaymat[3] and D. J. Thomas[1]. *[1]ISTD, NHEERL, ORD, EPA, RTP, NC, [2]Civil & Environ. Engin., University of Cincinnati, Cincinnati, OH and [3]LPRCD, NRMRL, ORD, EPA, Cincinnati, OH.*

Manufactured silver nanomaterials (AgNPs) are used as antimicrobials in many consumer products. Although increased use of AgNPs increases risk of exposure through inhalation or ingestion, there are few data on human health risks associated with exposure to these materials. Here, we evaluated the toxicity of AgNPs in the murine macrophage J774A.1 cell line. Macrophages play a key role in the inflammatory response by phagocytosis of pathogens, debris, and foreign particles. Phagocytosis of AgNPs by macrophages could expose these cells to Ag and alter their cell structure and function. We used two *in vitro* cytotoxicity assays, lactate dehydrogenase (LDH) release and the reduction of 3-(4,5-dimethylthiazol-2-yl)-2,5-diphenyltetrazolium bromide (MTT), to compare cytotoxic effects of ionic Ag (Ag nitrate), polyvinylpyrrolidone PVP coated-AgNPs (MHD =13 nm), hydrogen reduced H_2-AgNPs (14 nm), and citrate AgNPs (12 nm). Cells were exposed to ionic Ag (1-216 ppm), PVP-coated AgNPs (34-8640 ppm), H_2-AgNPs or citrate-AgNPs (135-4320 ppm), either in media alone or in media supplemented with 1% fetal bovine serum (FBS), for 1, 4, or 24 hr before assessment of cellular status. The net phagocytosis of these cells was determined using a phagocytosis assay following (1 or 4 hr) exposures to ionic Ag and AgNPs at lower concentrations. LDH leakage increased after exposure to ionic Ag and AgNPs indicating that all compounds produced damage to cell membranes. Each AgNP diminished MTT reduction capacity of J774A.1 cells with a 50% reduction in activity with exposure to low parts per million concentrations of Ag. Compared with AgNPs, ionic Ag was a more potent cytotoxicant. It also appears that there is both a time and concentration dependent reduction in phagocytosis following exposure. These results indicate that higher concentrations of AgNPs can affect cell viability, the integrity of cell membranes, metabolic competency of cells, and the functional ability to phagocytize. (This abstract does not reflect U.S. EPA policy.)

PS 1973c Mechanistic Study of Silver Nanoparticle-Induced DNA Damage in L5178Y Mouse Lymphoma Cells

H. Lin[1], W. S. Lam[1], X. Guo[1], S. L. Dial[1], J. Yan[1], T. Chen[1], T. Ingle[1], A. Paredes[1], Y. Jones[1], P. C. Howard[1], M. M. Moore[2] and N. Mei[1]. *[1]NCTR/FDA, Jefferson, AR and [2]ENVIRON International Corporation, Little Rock, AR.*

Silver nanoparticles (AgNPs) are increasingly used in diverse applications because of their unique size and characteristics. Numerous studies have shown that exposure to AgNPs can induce the cytotoxic and genotoxic effects on mammalian cells both in vivo and in vitro assays, implying that AgNPs may increase the risk of adverse health effects. In our study, PVP- and citrate- coated 50 nm AgNPs in Fischer's medium (F5p) were shown to be stable at 37 °C using NanoSight and TEM analysis. DNA damage caused by 50 nm AgNPs was evaluated in vitro using hOGG1 and Endonuclease III-modified Comet assays. The L5178Y/Tk+/—3.7.2C mouse lymphoma cells were treated for 4 hours with different concentrations (10, 20, 35 and 50 μg/ml) of 50 nm AgNPs coating with PVP or citrate. The results indicated that the percentage of DNA in the tail (% tail DNA) was increased in L5178Y cells treated with 20, 35, and 50 μg/ml AgNPs (both PVP- and citrate-coated) compared to negative controls, but that % tail DNA was not altered significantly by 10 μg/ml AgNPs. Moreover, the western blotting demonstrated that the expression of γ-H2AX and OGG1/2 were dramatically increased in cells treated with both PVP- and citrate-coated AgNPs at concentrations of 20 μg/ml and greater. Furthermore, a pathway-specific mouse oxidative stress was also utilized to explore the potential role of oxidative stress in AgNP- induced DNA damage response. The PCR array analysis indicated that the expression of genes associated with oxidative stress was significantly altered by the AgNP treatment. Taken together, these results suggest that treatment with 50 nm AgNPs induce DNA damage in L5178Y cells, and possibly their ability to produce oxidative stress may contribute to DNA damage.

PS 1973d An Evaluation of the Potential Phototoxicity of CeO2 Nanoparticles in Retinal Pigment Epithelial Cells *In Vitro*

L. N. Pantlin[2], J. N. Ortenzio[1], V. Holub[1], L. L. Degn[1], R. Zucker[1] and W. K. Boyes[1]. *[1]USEPA, Research Triangle Park, NC and [2]Psychology, Meredith College, Raleigh, NC.*

Cerium dioxide (CeO2) engineered nanoparticles (NP) are used as fuel-borne catalysts in off-road diesel engines, which can lead to exhaust emissions of respirable CeO2 NP. Other metal oxides may act as photo-catalysts which generate free radicals upon exposure to UV radiation or visible light. This study tested the hypothesis that CeO2 NP would cause a dose-dependent phototoxic reaction in human-de-

rived retinal pigment epithelial cells (ARPE-19) after UV exposure. CeO2 NP samples (Alfa Aesar, 36-99nm; NanoAmor, 6-60nm) were suspended in cell culture media with 10% fetal bovine serum (FBS) at concentrations: 0, 3, 10, 20, 30, 55, 100 or 20υg/ml TiO2 NP (Degussa P25; positive control) and administered to ARPE-19 cells grown in 24-well plates. Plates were either exposed to UV radiation (90min) or kept in the dark. After 24hrs, cell viability was determined with a calcein-AM/propidium iodide stain. Exposure to higher concentrations of CeO2 NP and exposure to UV light (290-400nm) reduced cell viability in CeO2 NP compared to dark plates. When a 2.5% CuSO4 solution filter restricted light exposure to the UVA (320-400nm) range, there was no difference in viability between UVA exposed cells and dark controls. The results showed significant effects of irradiation ($F(2,165) = 3.87$, $p = 0.02$) and between the cerium samples ($F(2,165) = 1.91$, $p < .0001$). CeO2 NanoAmor participated in phototoxic reactions with UVB, but not UVA wavelengths. Both CeO2 NP samples were less potent phototoxicants than TiO2 NP. Dark-field microscopy and flow cytometry light scatter confirmed CeO2 NP uptake into ARPE-19 cells in a dose-dependent manner. At concentrations higher than 3 υg/ml CeO2 NP formed visible intracellular agglomerates, which were spatially arranged around the nucleus and presumed to be associated with the endoplasmic reticulum and mitochondria. In summary, NanoAmor showed a more phototoxic response to UV irradiation (290-320nm) than Alpha Aesar, but was less phototoxic than TiO2. This does not reflect EPA policy.

PS 1973e Comparing Bioactivity Profiles of Diverse Nanomaterials Based on High-Throughput Screening (HTS) in ToxCast™

A. Wang[1], J. Franzosa[1], I. Shah[1], D. L. Filer[1], N. Kleinstreuer[2], S. Marinakos[3] and K. Houck[1]. *[1]US EPA, Durham, NC, [2]ILS, Durham, NC and [3]Duke Univ, Durham, NC.*

Most of the over 2800 nanomaterials (NMs) in commerce lack hazard data. Efficient NM testing requires suitable toxicity tests for prioritization of NMs to be tested. The EPA's ToxCast program is evaluating HTS assays to prioritize NMs for targeted testing. Au, Ag, CeO2, Cu(O2), TiO2, SiO2, and ZnO nanoparticles, their ion and micro counterparts, carbon nanotubes (CNTs), asbestos, and pesticides containing nano-Cu(O) - total 62 samples - were screened at 6 -10 concentrations each. A total of 262 bioactivity/toxicity endpoints in cells and zebrafish embryos were measured. Cellular stress and immune response pathways were primarily affected. NM's core chemical composition was more important than size for bioactivity. NMs had similar profiles as their ion counterparts, suggesting ion shedding was a key factor in mechanism of action. Ag, Cu, and Zn (nano, ion) were more cytotoxic and active in more assays than others. While 3 asbestos samples had similar immune response profiles, 6 CNTs had profiles distinctive from asbestos. Potential bioactivity targets that were not directly measured were suggested by reference profiles similar to our data, e.g. similar profiles of a microtubule stabilizer interfering with mitosis and our nano-TiO2. Dividing endpoints into cytotoxicity and various functional categories, we developed a ToxPi-based ranking approach for in vitro bioactivity. Samples active in more categories at lower concentrations were ranked higher than samples active in fewer categories and/or at higher concentrations. Ag, Cu, and Zn samples were ranked as high in vitro bioactivity; asbestos, Au, CeO2, some CNTs, and some TiO2 samples were ranked as low. Recognizing our assays using submerged cells may be poor models for inhalation effects, this ranking may be more appropriate for oral effects. We demonstrated that HTS assays can identify affected cellular pathways, predict targets, and may be useful for ranking NMs for specific purposes. This abstract does not necessarily reflect EPA policy.

PS 1973f Silver Nanoparticles Induce Antiproliferative Effects on Airway Smooth Muscle Cells: Role of Nitric Oxide and Muscarinic Receptor Signaling Pathway

C. Gonzalez[1, 2], M. A. Ramirez-Lee[1], H. Rosas-Hernandez[1, 2], S. Salazar-Garcia[1], J. M. Hernandez[1], R. Espinosa-Tanguma[1], F. J. Gonzalez[1] and S. F. Ali[2]. *[1]Laboratorio de Fisiologia Celular, Universidad Autonoma de San Luis Potosi, San Luis Potosi, SLP, Mexico and [2]Division of Neurotoxicology, NCTR, Jefferson, AR.*

Silver nanoparticles (AgNPs) are used to manufacture materials with new properties and functions. However, little is known about their toxic or beneficial effects on human health, especially in the respiratory system, where its smooth muscles (ASM) regulates the airway contractility by different mediators, such as acetylcholine (ACh) and nitric oxide (NO). The aim of this study was to evaluate the effects of AgNPs on ASM cells. Exposure to AgNPs induced ACh-independent expression of the inducible nitric oxide synthase (iNOS) at 100μg/mL, associated with excessive production of NO. AgNPs induced the muscarinic receptor activation, since its blockage with atropine and blockage of its downstream signaling pathway inhibited the NO production. AgNPs at 10 and 100μg/mL induced ACh-independent prolonged cytotoxicity and decreased cellular proliferation mediated by the muscarinic receptor-iNOS pathway. However, the concentration of 100μg/mL of AgNPs induced muscarinic receptor-independent apoptosis, suggesting the activation of multiple pathways. These data indicate that AgNPs induce prolonged cytotoxic and anti-proliferative effects on ASM cells, suggesting an activation of the muscarinic receptor-iNOS pathway. Further investigation is required to understand the full mechanisms of action of AgNPs on ASM under specific biological conditions.

PS 1973g Laser 3D Printing with Nanoscale Resolution: Improving Biocompatibility and Mitigating Toxicity from Photoinitiators

P. E. Petrochenko[1, 2], R. Narayan[2], P. L. Goering[1] and A. Ovsianikov[3]. *[1]CDRH, USFDA, Silver Spring, MD, [2]Joint Dept Biomed Engr, UNC-CH, Chapel Hill, NC and [3]Inst Materials Sci Technol, TU Wien, Vienna, Austria.*

Recent developments in laser-assisted 3D printing using two-photon polymerization (2PP) allow for previously unattainable submicron resolution and show promise for creating 3D cell scaffolds for regenerative medicine and tissue engineering applications. A significant barrier to using 2PP for biological applications exists due to the toxicity of photoinitiators required for polymerization. The goals of this study were to 1) demonstrate two approaches for creating nanotextured, porous 3D scaffolds using 2PP, and 2) develop a model system to evaluate in vitro cell responses, such as cell growth, protein adsorption, and toxicity, to nanoscale variations on material surfaces or to residual chemicals used in scaffold fabrication. The first approach involves printing a 3D scaffold from a urethane diacrylate-based elastomer, removing residual toxic substances and seeding cells. The second approach, involves trapping cells directly in a methacrylamide-modified gelatin matrix. Results from the first method indicate that stable scaffolds with porosities of over 60% can be custom printed to fit standard 96-well plates. Human bone marrow stromal cells grown on 3D scaffolds exhibited increased growth and proliferation compared to smooth 2D scaffold controls. Scaffolds adsorbed larger amounts of proteins due to a greater surface area and allowed cells to attach in multiple planes and infiltrate the porous scaffolds. Results from the second approach indicated some dead MG63 osteosarcoma cells and L929 fibroblasts in encapsulated regions. In order to mitigate photoinitiator toxicity, 3 antioxidants -Trolox (water-soluble vitamin E), vitamin C, and glutathione – were used. Preliminary results demonstrated decreased cytotoxicity. The data indicate that 2PP is a promising technique for fabricating custom 3D scaffolds, including the potential for cell encapsulation.

PS 1973h *In Vitro* Penetration of Polyethylene Glycol- and Citrate-Coated Silver Nanoparticles into Human Skin

V. Topping[1, 2], K. Belgrave[1, 2], Z. Keltner[1], R. Sprando[1], J. Yourick[1] and M. E. Kraeling[1]. *[1]Office of Applied Research and Safety Assessment, US FDA, Laurel, MD and [2]ORISE, US DOE, Oakridge, TN.*

Silver nanoparticles (AgNP) are used as an antimicrobial in a variety of cosmetic products. There are concerns about the potential safety associated with human skin exposure. This study was conducted to investigate the in vitro penetration of neutrally charged polyethylene glycol (PEG) and negatively charged citrate (CIT) coated 20 nm AgNPs into excised human skin. AgNPs were first characterized to confirm the size, shape, charge, agglomeration state and stability of the particles. Circular punches of dermatomed human cadaver skin from two donors were placed into flow-through diffusion cells, and 0.01% and 0.001% aqueous solutions of PEG and CIT coated AgNPs were applied once to the surface of the skin in duplicate. These concentrations were chosen as they were relevant to current commercially available cosmetics. After 24 hours, the skin samples were washed with a 1% soap solution and distilled water, removed from the diffusion cells, and tape-stripped twice to remove unabsorbed surface AgNPs. Each skin disc was prepared for analysis by taking half for inductively coupled plasma mass spectrometry (ICP-MS) analysis and the other half for Transmission Electron Microscopy (TEM). Preliminary ICP-MS analysis revealed an increase in silver content (ng silver/g of skin) of PEG and CIT samples at both concentrations when compared to untreated control skin. There was a 20-fold and 9-fold increase in silver content of the 0.01% PEG and CIT AgNP samples compared to the 0.001% treatments, respectively. TEM images of skin samples coincided with ICP-MS results, with 20 nm CIT and PEG coated AgNPs localized in the stratum corneum and upper epidermis. Higher concentrations of AgNP solutions corresponded with increased skin silver content. This study indicates that human skin silver content increased after an application of neutrally and negatively charged aqueous AgNPs for 24 hours, and these particles may penetrate into the upper epidermis.

PS 1973i *In Vitro* Penetration of Anionic Dendrimer Nanoparticles into Pig and Human Skin

K. Belgrave[1], V. Topping[1], X. Gao[1], K. Schlick[2], E. Simanek[2], S. Man[3], A. K. Patri[3], R. Sprando[1], J. Yourick[1] and M. Kraeling[1]. [1]*Office of Applied Research and Safety Assessment, USFDA, Laurel, MD,* [2]*Department of Chemistry, Texas Christian University, Fort Worth, TX and* [3]*Nanotechnology Characterization Laboratory, Leidos Biomedical Research, Inc., Frederick National Laboratory for Cancer Research, Frederick, MD.*

Dendrimers are highly branched stable polymeric nanoparticles with terminal functional groups capable of binding other molecules which could be used to increase delivery of chemicals to skin. The surface charge of the dendrimers may affect skin absorption of bound cosmetic ingredients. We previously evaluated the skin penetration of amine-terminated polyamidoamine (PAMAM) dendrimer nanoparticles. Alexa Fluor 568 (~1 equivalent per dendrimer) was conjugated to terminal amines on the dendrimers via amide bonds for confocal imaging. In this study, we examined the skin penetration of generation 3, generation 4, generation 5 and generation 6 PAMAM dendrimers further conjugated with succinic anhydride (negative surface charge). Free unconjugated fluorophore was removed by ultrafiltration followed by gel filtration, and characterized. Dendrimers were applied (0.2% concentration) in aqueous solutions or cosmetic emulsion formulation onto viable pig or human cadaver skin assembled in diffusion cells. After a 24 hour exposure, the extent of skin penetration was determined by laser scanning confocal microscopy. Most fluorescence from the applied dendrimers appeared in the stratum corneum (SC) or in hair follicles of both pig and human skin. Fluorescence appeared in the upper regions of the epidermis of pig skin with the small generation dendrimers using both the low (12.8 μl) and high (40 μl) volume solution applications. With the emulsion, most of the generations of various dendrimer species remained in the SC or penetrated pig skin through hair follicles. In human skin, small generation dendrimers penetrated skin with the low and high volume solutions and emulsion application. Dendrimers of all generations applied in emulsion mostly remained in the SC of human skin.

PS 1973j *In Vitro* Penetration of Neutral Dendrimer Nanoparticles into Pig and Human Skin

M. Kraeling[1], K. Belgrave[1], V. Topping[1], X. Gao[1], K. Schlick[2], E. Simanek[2], S. Man[3], A. K. Patri[3], R. Sprando[1] and J. Yourick[1]. [1]*Office of Applied Research and Safety Assessment, USFDA, Laurel, MD,* [2]*Department of Chemistry, Texas Christian University, Fort Worth, TX and* [3]*Nanotechnology Characterization Laboratory, Leidos Biomedical Research, Inc., Frederick National Laboratory for Cancer Research, Frederick, MD.*

Dendrimers are highly branched stable polymeric nanoparticles that may be synthesized to specific nano-sizes, shapes, and surface chemistry. We examined the effect of polyamidoamine (PAMAM) dendrimer size and surface functionalization on skin penetration. PAMAM dendrimer nanoparticles were conjugated with Alexa Fluor 568 (~1 equivalent per dendrimer) via amide bonds for confocal imaging. Generation 3, generation 4, generation 5 and generation 6 PAMAM dendrimers were further conjugated with glycidol to impart no charge (neutral). Free unconjugated fluorophore was removed by ultrafiltration followed by gel filtration, and characterized. Glycidol dendrimers were applied (0.2% concentration) in aqueous solutions or cosmetic emulsion formulation onto viable pig or human cadaver skin assembled in diffusion cells. After a 24 hour exposure the extent of skin penetration was determined by laser scanning confocal microscopy. Most fluorescence from the applied glycidol dendrimers appeared in the stratum corneum (SC) and in hair follicles of both pig and human skin. In pig skin, fluorescence appeared in the upper regions of the epidermis for all generation dendrimers using the high volume (40 μl) solution applications. Penetration was less apparent using the lower volume (12.8 μl) solution applications, with most of the dendrimers remaining in the SC. Some smaller generation dendrimers penetrated into the upper epidermis. With the dendrimer emulsion vehicle application, there was marginal epidermal penetration for the small generation dendrimers. In human skin, epidermal penetration was not as extensive with the high and low volume solution and emulsion applications as compared to pig skin. Dendrimers applied in emulsion mostly remained in the SC of human skin.

PS 1974 An Improved Dispersion Method (Taquann Method) of Multiwall Carbon Nanotube for a Whole-Body Inhalation Exposure System

J. Kanno, Y. Taquahashi, Y. Ogawa, A. Takagi, M. Tsuji and K. Morita. *Division of Cellular and Molecular Toxicology, National Institute of Health Sciences, Tokyo, Japan.*

Inhalation is a major route of nanomaterial exposure for humans. To test its toxicity, the whole body inhalation exposure experiment is essential. Multi-wall carbon nanotube such as Mitsui MWNT-7 is a mixture of single fibers of various length and width, their agglomerates and aggregates. And yet, human exposure would result in alveolar lesions by single fibers; the aggregate/agglomerate will sediment fast in the ambient air and will be filtered out effectively by the upper respiratory tract. In contrast, bulk MWNT-7 applied to experimental animal by intratracheal spraying or pharyngeal aspiration often show bronchitis/bronchiolitis with granuloma evoked predominantly by the aggregate/agglomerate. Here, we report a new whole body inhalation exposure system based on an idea of liquid-phase filtering/dispersion and critical point drying to effectively remove the aggregate/agglomerates and disperse MWNT-7 into dry single fibers without dispersant and changes in fiber length and width distribution ("Taquann Method", J Tox. Sci. 38:619-628, 2013). The MWNT-7 was suspended in Tert-butyl alcohol, freeze-and-thawed, filtered by a vibrating 25 micrometer mesh Metallic Sieve, snap-frozen by liquid nitrogen, and vacuum-sublimated in order to avoid re-aggregation of the single fibers by surface tension. An aerosol generation system ("Direct injection system") was developed for Taquann-dispersed MWNT-7 (T-CNT). T-CNT was loaded in a newly designed cylindrical cartridge case and injected into the chamber by compressed air. Aerosol in the chamber consisted predominantly of well-dispersed single fibers showing length and width distribution similar to those of the original sample, and these single fibers were found in the alveolar spaces of mice exposed. This system is relatively inexpensive and optimal for testing inhalation toxicity of nanomaterial samples in well-dispersed, dispersant-free aerosol with minimum mechanical fragmentation. (Supported by the Health and Labour Sciences Research Grant, MHLW, Japan)

PS 1975 Effects of Prenatal Inhalation Exposure to Copper Nanoparticles (Cu NPs) on Dams and Offspring in Mouse Model

A. Adamcakova-Dodd[1], L. S. Powers[2], K. N. Gibson-Corley[3], M. F. Monick[2], V. Grassian[4] and P. S. Thorne[1]. [1]*Occupational and Environmental Health, Univ of Iowa, Iowa City, IA,* [2]*Internal Medicine, UI, Iowa City, IA,* [3]*Pathology, UI, Iowa City, IA and* [4]*Chemistry, UI, Iowa City, IA.*

Increasing number of individuals may be exposed to nanomaterials during pregnancy. Our aim was to determine if prenatal inhalation exposure to Cu NPs has an effect on dams and offspring and if their Th1/Th2 cytokine profiles were influenced. Physicochemical characteristics of Cu NPs were evaluated. Pregnant and non-pregnant mice (C57Bl/6J) were exposed to Cu NPs in the whole-body exposure chamber for 4 hrs/day on gestation day (GD) 3-19 (3.5 mg/m3). Animals were euthanized either immediately post exposure (on GD 19) or 7 wks later. Bronchoalveolar lavage (BAL) fluid was analyzed for total and differential cell counts and cytokines. Cu content was determined in lungs and blood of dams, placentas and blood of pups. Dam's lungs and placentas were evaluated for histopathological changes. Gene expressions of Th1/Th2 profiles were analyzed in lungs and spleens of pups. Survival rate of pups at 7 wks of age was lower if they were exposed to Cu NPs during gestation, compared to controls (76% vs. 83%). The average litter size, male/female ratio, birth weight as well as body size at birth were not different between Cu NP-exposed and control mice. Both pregnant and non-pregnant mice exposed to Cu NPs had significant pulmonary inflammation with increased number of neutrophils in the BAL fluid/mouse (1,637 and 1,985 x 103, respectively) compared to pregnant and non-pregnant controls (0.431 and 0.415 x 103, respectively). Perivascular lymphoplamacytic cuffing was found in the lungs of exposed mice and was more pronounced in the non-pregnant group. Similarly, levels of following cytokines (IL-12(p40), G-CSF, GM-CSF, KC, MCP-1, MIP-1α, MIP-1β, RANTES and TNF-α) in BAL fluid were significantly higher in non-pregnant than pregnant exposed mice. Cells counts and levels of Th1/Th2 cytokines measured in BAL fluid of pups were not different in Cu NP-exposed mice and controls. Supported by NIEHS/NIH P30 ES005605.

PS 1976 Health Surveillance Study on MWCNT Manufacturing Workers

J. Lee[2], S. Park[2], J. Lee[1], J. Shin[2], Y. Lee[2], J. Baek[2], J. Hwang[2], K. Ahn[3], J. Park[4] and I. Yu[1]. *[1]Institute of Nanoproduct Safety Research, Hoseo University, Asan, Republic of Korea, [2]Occupational Lung Diseases Institute, Ansan, Republic of Korea, [3]Department of Mechanical Engineering, Hanyang University, Ansan, Republic of Korea and [4]College of Medicine, Chung-Ang University, Ansan, Republic of Korea.*

Although many in vivo and in vitro toxicology studies on multi-walled carbon nanotubes (MWCNTs) indicate that exposure to MWCNTs may induce potential human health effect, actual health effect of MWCNTs among exposed workers have not been known. The levels of exposure and internal doses of MWCNT are becoming more and more important for estimating the health effects resulting from exposure to MWCNTs, yet information on biomonitoring and exposure is very difficult to obtain from MWCNT manufacturing workers. We have conducted a health surveillance study in a workplace which manufactures MWCNTs, including the assessment of personal and area exposure levels to MWCNTs, a walk-through evaluation of the manufacturing process, and the collection of blood and exhaled breath condensates from the exposed workers. Additionally, a lung function test was conducted to the MWCNT manufacturing workers and office workers. The workers were exposed to 112-229 μg/m^3 total suspended particulates 6.2-9.3 μg/m^3 elemental carbon near the range recommend exposure level suggested by NIOSH. The workers exhibited normal range of hematology and blood biochemistry values and normal range of lung function parameters. On analysis of EBC, malondialdehyde (MDA), 4-hydroxy-2-hexenal, and n-Hexanal levels in the exposed workers showed a significant increase when comparing with the office workers. The MDA level was significantly correlated with blood molybdenum (Mo) concentration, suggesting usefulness of MDA in EBC and Mo as biomarkers of MWCNT exposure.

PS 1977 The Effects of Pharyngeal Aspiration-Exposure to Zinc Oxide Nanoparticles on Pulmonary Fibrosis Induced by Bleomycin in Mice

W. Wu[1], G. Ichihara[1], S. Tada-Oikawa[2], Y. Suzuki[2], J. Chang[1], N. Hashimoto[3], Y. Hasegawa[3], D. W. Porter[4], V. Castranova[4], C. Gabazza[5], E. Gabazza[5] and S. Ichihara[2]. *[1]Occupational and Environmental Health, Nagoya University Graduate School of Medicine, Nagoya, Japan, [2]Mie University Graduate School of Regional Innovation, Tsu, Japan, [3]Respiratory Medicine, Nagoya University Graduate School of Medicine, Nagoya, Japan, [4]National Institute for Occupational Safety and Health, Morgantown, WV and [5]Mie University Graduate School of Medicine, Tsu, Japan.*

The present study investigated underlying mechanism of pulmonary fibrosis caused by exposure to ZnO nanoparticles, in a mouse model of pulmonary fibrosis induced by bleomycin (BLM). The mouse model was completed by constant subcutaneous infusion of 100 mg/kg bleomycin sulphate using osmotic mini-pumps. Female C57BL/6Jcl mice were divided into BLM and non-BLM groups. In each group, two doses (10, 30 μg/mouse) of ZnO nanoparticles with primary diameter of 20 nm were delivered into the lungs through pharyngeal aspiration. Bronchoalveolar lavage fluid (BALF) and the lungs were collected 10 days after administration under deep anesthesia. Exposure to ZnO nanoparticles dose-dependently increased the lungs weight. Histopathologically, slight and severe thickness was observed within interalveolar septum in low and high dose groups, respectively, which was accompanied by dose-dependent increase in total cells, macrophages, lymphocytes and neutrophils in BALF. The increase in total protein in BALF at high dose indicated increased permeability of air-blood barrier. IL-1 beta and MCP-1 in BALF were significantly higher in all BLM groups as opposed to the low levels in non-BLM groups, indicating lasting inflammation after exposure in BLM groups. Moreover, in BLM groups, ZnO nanoparticles led to dose-dependent increase in IL-1 beta and MCP-1, suggesting higher susceptibility to ZnO nanoparticles in this mouse model. This study suggested severer inflammation was caused by ZnO nanoparticles in the BLM mouse model of pulmonary fibrosis at the early stage.

PS 1978 Effects of Nanoparticle Pre-Exposure Dispersion Status on Bioactivity in the Mouse Lung

T. M. Sager[1, 2], M. Wolfarth[2], V. Castranova[2] and A. Holian[1]. *[1]University of Montana, CEHS, Missoula, MT and [2]NIOSH, Morgantown, WV.*

From a toxicology perspective, nanoparticles possess two features that promote their toxicity. The first involves physical-chemical characteristics, including particle surface area. The second is the ability of the nanoparticle to traverse cell membranes. These two characteristics are influenced by placing nanoparticles in liquid medium prior to animal exposure. Nanoparticles tend to agglomerate in suspension, making it difficult to accurately deliver them for in vivo or in vitro experiments. Thus, we hypothesize that the nanoparticle dispersion status will correlate with the in vivo bioactivity/toxicity of the particle. The proposed questions of this study are of great importance to the nanotechnology/toxicology community, namely the highly debated question of whether nanoparticle dispersion status (pre-exposure) is of importance. To test our hypothesis, nano-sized nickel oxide was suspended in four different dispersion media (PBS, dispersion medium (DM), Survanta, or Pluronics). At each respective dose, well-dispersed and poorly dispersed (suspensions were sonicated utilizing a Branson Sonifer 450, 25W continuous output, 20 min or 5 min, respectively) suspensions were created. Mice (male, C57BL/6J, 7 weeks old) were given 0-80 μg/mouse of nano-sized nickel oxide in the different states of dispersion via pharyngeal aspiration. At 1 & 7 days post-exposure, mice underwent whole lung lavage (WLL) to assess pulmonary inflammation and injury as a function of dispersion status, dose, and time. Results show that pre-exposure dispersion status correlates with particle bioactivity. In fact, the particle/media combination that produced the smallest hydrodynamic particle size (nano-NiO2 suspended in DM & sonicated for 20 min. = 7.5 nm) produced a greater increase in PMNs, LDH activity, as well as albumin levels in WLL fluid than the other nano-nickel/suspension media combinations. These results indicate that a greater degree of pre-exposure dispersion increases particle bioactivity/toxicity in the lung. This work was supported by NIH grant F32 ES021341.

PS 1979 Effects of Multiwalled Carbon Nanotube Solubility on Inflammation and Lung Function

D. Botelho[1], A. Porter[2], F. Chung[3], T. Tetley[3], J. Zhang[4] and A. Gow[1]. *[1]Toxicology, Rutgers University, Piscataway, NJ, [2]Materials, Imperial College, London, United Kingdom, [3]National Heart & Lung Institute, Imperial College, London, United Kingdom and [4]Nicholas School of the Environment & Duke Global Health Institute, Duke University, Durham, NC.*

Multi-walled carbon nanotubes (MWCNTs) have high ξ potential, are relatively insoluble in aqueous solvents, and interact with hydrophobic materials. These properties are altered by functionalization. Due to complexity of MWCNTs it is important to study organ level effects. To study effects of MWCNTs on the lung we use a suspension method involving native surfactant. This method is effective at keeping MWCNTs in suspension despite functionalization. We hypothesized that increasing solubility of MWCNTs in the aqueous environment would shift the organ level response to inflammation from interaction with the lung lining fluid. C57Bl6J mice were intratracheally instilled with MWCNTs (30-50nm OD, 0.5-2μm length) at 1.5μg/g body weight. 2 types of MWCNT were examined—functionalized by carboxylation or acid-purified. 1 day post instillation, the functionalized MWCNT treated mice showed neutrophilia (147.1 ± 105.67 v 2.5 ± 0.92 x10^3) and increased cell count (196.5 ± 113.02 v 57.0 ± 8.25 x10^3) vs control. Purified MWCNT mice did not display significant inflammation (18.5 ± 15.62 v 2.5 ± 0.92 x10^3 neutrophils; 63.0 ± 15.09 v 57.0 ± 8.25 x10^3 total cells). Lung function was not affected by functionalized MWCNTs but purified MWCNTs increased lung stiffness, consistent with surfactant disruption. 3 days post instillation, neutrophilia resolved in functionalized MWCNT treated mice, but protein concentration increased vs control (0.2 ± 0.03 v 0.1 ± 0.02 μg/μl total protein). Purified MWCNT mice do not show increased tissue stiffness. Both MWCNT treated groups demonstrated significant decrease in collectin content. These data are consistent with functionalization "revealing" the MWCNTs to inflammatory system and reducing effect on lung function. Supported by NIH Grants 5U19ES019536-02 & 5T32ES007148

PS 1980 Pre-Exposure to Nontoxic Levels of Magnetite Nanoparticles Sensitizes Mice to Pulmonary Infection by *Streptococcus pneumoniae*

J. G. Pounds[1], J. N. Smith[1], J. Klein[1], H. D. Jolley[1], V. K. Kodali[1], K. Rosso[1], B. D. Thrall[1], C. F. Frevert[2], S. J. Skerrett[2] and J. G. Teeguarden[1]. *[1]Systems Toxicology, Pacific Northwest National Laboratory, Richland, WA and [2]Medicine, University of Washington, Seattle, WA.*

Two major forms of iron oxide are preferred for medical applications due to their perceived biocompatibility. Pretreatment of cultured macrophages with non-cytotoxic doses of superparamagnetic iron oxide (SPIO) reprogramed ~500 genes in response to subsequent challenge by endotoxin, suppressing activation of both pro- and anti-inflammatory pathways and diminished bacterial phagocytosis (Kodali et al. 2013). Herein we characterize and confirm the potential impaired clearance of bacteria by mice pretreated with SPIO. We administered 0 or 1.0 μg SPIO/gbw to C57BL/6 by oropharyngeal aspiration (OPA) and evaluated the pro-inflammatory response by measuring cytokines in BALF collected 1-28 d post-dosing. No statistical changes in cytokine levels were observed at 1-28 d post-dosing confirming that

SPIO is not strongly pro-inflammatory. The bioavailability of aspirated SPIO (by ICP-MS) was <0.1% and was cleared from the lung with a half-time of 7-8 days indicating that the lung retained a significant amount of SPIO at the time of bacterial instillation (24 hr post-dosing). Finally, mice were administered 0, 5, 30, or 100 μg SPIO by OPA 24 hr prior to intra-nasal instillation of 50k colony forming units (CFU) of S. pneumoniae. The SPIO doses were selected to represent the mouse equivalents of human occupational exposure for 1, 5, and 20 d at the Permissible Exposure Limit. The low pyrogenic/inflammatory potential of these exposures was confirmed by the absence of changes in surface body temperature. However, mice pretreated with 30 or 100 μg SPIO exhibited a 3.6- and 7.0-fold increase, respectively, in CFU recovered from the lung, indicating mice exposed to SPIO had reduced lung clearance of S. pneumoniae. These studies suggest that the direct toxicity of SPIO may be less important than those effects elicited by SPIO interaction with other stressors. Supported by NIEHS NCNHIR Consortium ES019544

PS 1981 A Comparative *In Vivo* Screening of Nine Classes of Multiwalled Carbon Nanotubes for Acute Lung Toxicity in Mice

M. Cartwright[1], S. Schmuck[1], C. White[1], C. Corredor[2], D. Botta[1], D. K. Scoville[1], C. Chisholm[1], J. Posner[2, 3], T. Gordon[4] and T. Kavanagh[1]. *[1]Environmental and Occupational Health Sciences, University of Washington, Seattle, WA, [2]Chemical Engineering, University of Washington, Seattle, WA, [3]Mechanical Engineering, University of Washington, Seattle, WA and [4]Environmental Medicine, New York University, Tuxedo, NY.*

Multi-walled carbon nanotubes (MWCNTs) present potential health risks during their manufacture and handling in the electronics and medical industries. To improve understanding of MWCNT behavior following inhalation, we are investigating how aggregative characteristics, aspect ratio, surface carboxylation, and purity from trace metals affect MWCNT pulmonary toxicity in vivo. To characterize aggregative behavior, we used dynamic light scattering to assess the hydrodynamic radii and zeta potentials of nine classes of MWCNTs in dispersion medium (DM). In order to assess pulmonary toxicity, we exposed eight-week-old male A/J mice via oropharyngeal aspiration to DM vehicle or a single MWCNT class at 40 μg/mouse, and sacrificed the mice after 24 hours. Treatment with unpurified and carboxylated MWCNTs was associated with lung inflammation as indicated by flow cytometric and cytospin analyses of neutrophil influx into bronchoalveolar lavage fluid (BALF). Across all MWCNT classes, we found no evidence of alveolar/capillary barrier dysfunction or frank cellular damage as indicated by BALF supernatant total protein or lactate dehydrogenase activity. Similarly, no evidence of severe oxidative stress was detected in lung tissue as indicated by total glutathione levels. Our results indicate that high-dose exposure to unpurified and carboxylated MWCNTs causes acute lung inflammation but not frank cellular toxicity in the short term. This work was supported by NIH Grants U19ES019545 and P30ES007033, and NSF grants CBET-0932885 and DGE-0718124.

PS 1982 Inhalation of Nanosized Titanium Dioxide Alters Cardiovascular Autonomic Function

T. L. Knuckles, J. Yi and T. R. Nurkiewicz. *Center for Cardiovascular and Respiratory Sciences, West Virginia University, Morgantown, WV.*

Nanotechnology is a rapidly growing field with the potential to influence all aspects of modern life. However, the cardiovascular toxicity of nanomaterials is not well understood. We have previously demonstrated a disruption in normal microvascular function following nanomaterial exposure via alterations in autonomic control. Presently, using a telemetry and a baroreflex function model, we show changes in autonomic control following inhalation exposure to nanosized titanium dioxide (nano-TiO_2) for 4 hours for 2 days at 6 mg/m^3. Telemeterized rats were acclimatized and exposed to sham (day 0), then nano-TiO_2 or sham on 2 consecutive days (days 1, and 2). Renal sympathetic nerve activity (rSNA), mean arterial pressure (MAP) and heart rate (HR) were continuously monitored. 24 h after the last exposure, baroreflex sensitivity was measured with phenylephrine (PE; 1-8 μg/kg) or sodium nitroprusside (SNP; 5-20 μg/kg). MAP increased during nano-TiO_2 relative to day 0 and sham (max ΔMAP sham -8.1±4.3 mm Hg, nano-TiO_2 3.0±2.1 mm Hg). The nano-TiO_2-induced MAP increases were largely driven by diastolic blood pressure (DBP) increases (day 1: sham DBP 98±3.5 mm Hg, nano-TiO_2 110±2.3 mm Hg), suggesting an enhanced peripheral resistance. Overnight, rSNA and HR were significantly elevated following exposure, suggesting an augmentation in the normal sympathetic nerve diurnal pattern (max; ΔHR sham 3±5 BPM, nano-TiO_2 14±1 BPM: ΔSNA sham -2.2±0.9 μV, nano-TiO_2 0.84±0.6). PE infusion enhanced and prolonged the depression in HR following nano-TiO_2 exposure compared to sham (max ΔHR - sham 13±1 BPM, nano-TiO_2 -15±1), suggesting increased parasympathetic signaling, which could be mitigated with hexamethonium or atropine. Nano-TiO_2 exposure significantly enhanced MAP depression by SNP (max ΔMAP -34±1.5 mm Hg sham, -41±1.3 mm Hg nano-TiO_2), though the mechanism unclear. Considered together, engineered nanomaterial exposure may alter cardiovascular function through autonomic signaling that is not obvious under resting conditions. (Funding NIH ES015022, TRN)

PS 1983 Endothelial Cells As Biosensors to Assess the Vascular Inflammatory Potential of Serum following Nanomaterial Exposure

M. Aragon[1], M. Dunlap[1], J. R. Roberts[2], A. Erdely[2] and M. Campen[1]. *[1]University of New Mexico, Albuquerque, NM and [2]NIOSH, Morgantown, WV.*

Assessing mechanisms underlying the adverse vascular health effects of systemic inflammation induced by inhaled toxins presents a substantial research challenge. We have developed an ex vivo model that allows for a realistic exposure method to better elucidate the mechanisms involved in a living system. This approach applies serum from exposed animals to cultured primary endothelial cells, as this is the component in direct contact with the vascular endothelium. Here, we apply this assay paradigm to assess the impact of pulmonary exposures to multi-walled carbon nanotubes (MWCNT) or graphene. Mice were exposed to varying doses (4, 10 or 40 μg) of MWCNT, various types of graphene, or carbon black via pharyngeal aspiration, and serum was collected at 4 and 24 h post-exposure. Serum collected from 19 d inhalation exposures to 0.5 or 5.0 mg/m3 MWCNT was also assayed for endothelial activation. Serum from exposed mice induced an up-regulation of endothelial cell surface VCAM and ICAM expression, along with elevations in mRNA at the 4 h time point. Multiple sizes of graphene were tested; the smallest sizes (<2 μm x <2 μm x 1-2 nm and 5 μm x 5 μm x 7 nm) induced up-regulation of surface VCAM, but were overall less potent than carbon black, used as a control particle. Furthermore, we assessed nitric oxide (NO) generation by endothelial cells using electron paramagnetic resonance (EPR) methods, and found that NO was decreased via treatment with serum from MWCNT-exposed mice following stimulation with 2 mM ATP. Microarray analysis of endothelial cell response to serum from the inhalation and instillation exposures revealed a common set of response elements. In conclusion, pulmonary exposure to carbon-based nanomaterials alters circulating factors which promote endothelial cell activation and decreased NO bioavailability.

PS 1984 Surface Amination Enhances the Toxicity of Silica-Coated Silver Nanoparticles

J. A. Bonventre[1], B. Harper[1] and S. L. Harper[1, 2]. *[1]Environmental & Molecular Tox, Oregon State University, Corvallis, OR and [2]Chem., Biol. & Env. Eng, Oregon State University, Corvallis, OR.*

Surface charge can greatly influence the toxicity and bioavailability of engineered nanoparticles (NPs). Positively charged NPs generally elicit greater toxicity than comparable negative or neutrally charged particles. The effect of amination on NP toxicity was investigated in embryonic zebrafish, a model vertebrate. Embryos were exposed to 0.5-100ppm suspensions of 80nm silica (Si) or 70nm silver with 20nm Si-coating (AgSi), or aminated NPs of like size and composition. Surface amination significantly increased the toxicity of the NPs. Si NPs did not induce mortality or morbidity at the tested concentrations, whereas aminated Si induced 58% mortality at 100ppm. Both AgSi NPs were significantly more toxic to embryos than Si NPs. AgSi NPs significantly delayed development at 24 hours post fertilization in 25 (50%), 50 (64%) and 100 (75%) ppm treatments, and caused significant mortality beginning at 10ppm. In comparison, aminated AgSi NPs delayed development significantly as low as 1 ppm and induced significant mortality at 5ppm, with 100% mortality above 50ppm. Both AgSi NPs induced significant sublethal effects, including craniofacial and fin malformations, edemas, and body curvatures. When similar silica coated Ag NPs with varied surface amination levels (0.5x, 1x, and 2x) were tested at the same concentrations, the AgSi-1x was significantly more toxic than the 0.5 or 2x AgSi NPs, inducing mortality at 100 (95%) ppm. In contrast, AgSi-2x only induced 38% mortality at 100 ppm, and AgSi-0.5x NPs did not cause toxicity at any concentration tested. Increased amination was observed to alter the stability of the aminated NP dispersions in the exposure media, with the 2x NPs being the least stable in suspension. Our results suggest that increasing surface amination only leads to increased toxicity when bioavailability is held constant, highlighting the importance of understanding NP stability and bioavailability during exposure.

PS 1985 Establishment of an Inexpensive, *In Vivo* Screening Tool for Nanomaterial Safety Using the Adult Zebrafish

N. Elrod[1], J. Brady[1, 2], L. K. Braydich-Stolle[3], S. M. Hussain[3] and J. Speshock[1]. [1]*Biology, Tarleton State University, Stephenville, TX,* [2]*Texas A&M AgriLife Research Institute, Stephenville, TX and* [3]*Air Force Research Laboratories, Wright-Patterson Air Force Base, OH.*

Current toxicological assessment of the safety of nanomaterials is lagging well behind the synthesis and consumer use. This is largely due to the lack of a quality inexpensive model for toxicological assessment. Cell cultures are inexpensive and can provide some indications on biological properties, but they do not convey a complete account for cell-to-cell communication. Mammalian models can allow for a greater understanding of toxicology and biodistribution. However, adequate mouse studies can be cost prohibitive. This study examines the potential for an inexpensive alternative *in vivo* model using the adult zebrafish, *Danio rerio*, for assessment of nanomaterial immunotoxicology. Zebrafish have many homologous proteins shared with humans and other mammals and can be bred and maintained for very little cost. Having been completely sequenced, many biomarkers for stress, toxicity and inflammation have been identified in the zebrafish. This preliminary assessment has determined the extent of biodistribution, inflammation, and toxicity using 10 nm silver nanospheres and it has been determined that the nanomaterials do not cause mortality or significant morbidity after a one-time intradermal exposure at 10 or 50 μg/mL and can distribute throughout the fish as evidenced by differential effects on various target organs. Quantitative PCR, ICP-MS, and transmission electron microscopy where used to measure the biodistribution and inflammatory responses of the silver nanoparticles. All target organs had measurable amounts of silver nanoparticle detected and a mild inflammatory response at 24-hours post-inoculation was observed. The establishment of the adult zebrafish *in vivo* model for immunotoxicology could allow for an inexpensive comparative analysis of a wide array of nanomaterial sizes, shapes, and compositions for determination of their safety and distribution.

PS 1986 Genetic Influence of Pulmonary Response to Silver Nanoparticles Exposure and Candidate Gene Identifications

M. Hernandez, K. Galdanes, L. Chen and T. Gordon. *Environmental Health Science, NYU, Tuxedo, NY.*

Within the last few decades, the use of nano-materials and products for multi-application uses has seen exponential growth, while information on the toxicity of these nano-materials is still largely unknown. This study evaluated the variation of response in numerous murine strains to examine genetic susceptibility to silver nanoparticles (AgNPs). Previously, 8 strains of inbred mice were acutely exposed via oropharyngeal aspiration to a dose of 0.25μg/g body weight of 20nm silver citrate, with observed polymorphonuclear neutrophil (PMN) responses between 1.4-60% (DBA/2J<C57BL/6J< AKR/J< 129SI/SvJ< A/J< FVB/NJ< C3H/HeJ< Balb/cJ). Increased protein levels occurred most predominantly and significantly in the three most PMN-sensitive strains (FVB/NJ, C3H/HeJ, BALB/cJ) and was decreased in the three lowest PMN-responsive strains (DBA/2J, C57BL/6J, AKR/J). Cytokine analysis revealed significant differences in VEGF and MDC in FVBN/J mice and RANTES in C3H/HeJ. Currently, in collaboration with the University of Washington, a total of 30 strains have been combined to assess genetic susceptibility via pulmonary inflammation and injury endpoints (%PMN, protein, lactate dehydrogenase release, cytokine analysis) as well as haplotype association mapping for identifying candidate genes, responsible for the influence of genetics on the pulmonary response to AgNPs. Based upon previous and current findings on inter-strain response variation, these mouse models, representative of a genetically varied population, displayed a susceptibility pattern among strains. Ultimately, these findings further support the link between genetic background and the elusiveness of the link between sensitivity mechanisms and innate inter-species responses to AgNPs.

PS 1987 Effects of Nanosilver and Silver Nitrate Exposure on Ionic Regulation and Nanoparticle Size Characterization Using Field-Flow Fractionation in Fathead Minnows

A. D. Hawkins[1], C. Thornton[1], A. Bednar[2], A. J. Kennedy[2], J. A. Steevens[2], J. Cizdiel[1] and K. L. Willett[1]. [1]*University of Mississippi, Oxford, MS and* [2]*ERDC, Vicksburg, MS.*

Silver nitrate (AgNO3) and silver nanoparticles (AgNPs) damage and alter the fish gills after acute exposure. Ionic regulation in fish gills can be perturbed by AgNO3 exposure primarily due to the inhibition of Na,K-ATPase. One proposed mechanism of silver nanoparticle toxicity is from the release of silver ions; however, AgNPs can accumulate and have unique toxic effects on different biological targets. In order to understand the relationship between silver exposure and ionic regulation, fathead minnows were exposed for 96 hr to 20 nm PVP- or citrate-coated silver nanoparticles (PVP-AgNPs; citrate-AgNPs) or AgNO3 at two nominal concentrations (20 and 200 μg/L) or (2 and 6 μg/L), respectively. FHM gills were paraffin embedded, sectioned and immunohistochemistry was performed for the presence of Na,K-ATPase. Also, Na,K-ATPase activity was measured in fish gills and GI tract in order to further understand the effects of the Ag-NPs on ionic exchange. The distribution of silver was quantitated following acid digestion and ICP-MS analysis. No detectable silver accumulation occurred in the brain. Exposure to 6 μg/L AgNO3 produced the highest silver bioaccumulation in the skin, liver, and gill, while exposure to 200 μg/L citrate-AgNPs produced the highest bioaccumulation in the GI tract. AgNP size was measured in GI tract and gill tissue after exposure using field-flow fractionation (FFF) interfaced to ICP-MS. AgNPs detected in GI tissue displayed heteroaggregation with particle sizes ranging from 20-70 nm, while AgNPs in gill tissue were less aggregated with particle sizes from 20-40 nm. FFF data indicated that AgNPs were still in particle form after uptake which may be related to their differential tissue accumulation and toxicity compared to ionic silver. This research is supported by US Army ERDC grant: W912HZ-09-C-0033.

PS 1988 Unique Particle Effects in Fathead Minnow Gill Gene Expression and Uptake following Exposure to Nanosilver and Silver Nitrate

N. G. Reyero Vinas[1, 2], A. D. Hawkins[3], C. Thornton[3], A. J. Kennedy[2], J. A. Steevens[2], K. Bu[4], J. Cizdiel[4] and K. L. Willett[3]. [1]*Mississippi State University, Vicksburg, MS,* [2]*ERDC, US Army, Vicksburg, MS,* [3]*ETRP, University of Mississippi, University, MS and* [4]*Chemistry, University of Mississippi, University, MS.*

Silver exposure is toxic to fish due to disturbances of normal gill function. A proposed toxicity mechanism of silver nanoparticles (AgNPs) is derived from the release of silver ions, similar to silver nitrate (AgNO3). However, AgNPs can have unique toxic effects. To determine if differences between AgNO3 and AgNP toxicities exist, fathead minnows (FHM) were exposed to 20 nm PVP- or citrate-coated silver nanoparticles (PVP-AgNPs; citrate-AgNPs) at the nominal concentration of 200 μg/L or AgNO3 at nominal 6 μg/L for 96 hr (n=5). Gills were dissected and microarray analysis was performed on the gills. Hierarchal clustering of FHM gene expression results revealed that all the control, AgNO3, and PVP-AgNP exposed fish clustered by treatment. In citrate-AgNP exposed fish, 67% clustered uniquely together but 33% clustered with the AgNO3 exposed fish. There were 115 differentially expressed genes shared among all Ag treatments compared to controls. However, there were 481, 406, and 715 differentially expressed genes unique to AgNO3, PVP-AgNP, and citrate-AgNP, respectively. In addition, ToxList and IPA analysis indicated several common toxic endpoints such as oxidative stress and cell death consistent with silver toxicity; however, this analysis also indicated some unique pathways between nanosilver and AgNO3. Silver bioaccumulation was quantitated in the skin matrix, liver, GI and brain. Highest accumulation of silver following AgNO3 treatment was observed in skin and liver (84 and 1,500 ng/g, respectively). The highest accumulation of silver following AgNP treatments was observed in the GI tract (24,000 and 19,000 ng/g for PVP-AgNP and citrate-AgNP, respectively). These results indicate that there was differential silver accumulation and gill gene expression depending on exposure to AgNO3 or AgNPs. Supported by ERDC grant: W912HZ-09-C-0033.

PS 1989 Investigating the Influence of Oral Exposure to Silver Nanoparticles on Intestinal Microbiota in Nonhuman Primates

G. K. Hinkley[1], T. M. Ngo[2], M. Ukhanova[2], J. W. Munson[1], V. Mai[2] and S. M. Roberts[1]. [1]*Physiological Sciences, University of Florida CEHT, Gainesville, FL and* [2]*Emerging Pathogens Institute, University of Florida, Gainesville, FL.*

Silver nanoparticles (AgNPs) are used for their antimicrobial activity in a wide range of applications and consumer products. Some of the uses of AgNPs, such as in food packaging, likely result in ingestion. In addition to the possibility of direct toxicity from ingested AgNPs, toxicity could also occur indirectly through disruption of normal gastrointestinal microbiota. In this study, male non-human primates (*Macaca fascicularis*) (n=5) were given 20 nm AgNPs in 10mL of Gatorade (62.5 μg/mL) once daily for 8 days. AgNPs were characterized with respect to primary particle size and agglomeration state both as received and in the Gatorade dosing vehicle. Feces were collected on the day before the first dose and the day after the last dose, as well as 1 week after treatment stopped. On a separate occasion, the same animals received a control treatment (Gatorade only) and feces were collected on the same schedule. High throughput 16S rRNA sequencing was used to determine if AgNP treatment had an influence on the overall microbiota diversity and prevalence of specific operational taxonomical units (OTUs). When

investigating overall diversity at the phylum level no significant differences were observed. However, when analyzing specific OTUs at the 98% similarity level, we observed more than 30 in which the number of sequences increased upon nanoparticle exposure but only three in which sequence numbers decreased. In contrast, the number of OTUs with significant increases/decreases was similar for the vehicle-control treatment. This observation suggests that AgNPs select for, rather than against particular gut bacteria. These results demonstrate that AgNPs affected gut microbiota under the conditions of the study. Prediction of potential corresponding health impacts will require additional analysis of the data.

PS 1990 Histopathological Analysis of Malignant Tumors Induced by Intraperitoneal Injection of Carbon Nanotubes

S. Rittinghausen[1], B. Bellmann[1], A. Hackbarth[1], H. Ernst[1], U. Heinrich[1], A. Leonhardt[2] and D. Schaudien[1]. [1]*Fraunhofer Institute for Toxicology and Experimental Medicine, Hannover, Germany and* [2]*Leibniz Institute for Solid State and Materials Research, Dresden, Germany.* Sponsor: C. Dasenbrock.

Biological effects of tailor-made multi-walled carbon nanotubes (MWCNTs) were investigated in vivo in a 2-year carcinogenicity study in a project funded by the German Federal Ministry of Education and Research (contract no. 03X0109A).
Five male Wistar rats per group (total of 500 rats) were treated once by an intraperitoneal (i.p.) injection of a low (1x109 WHO fibers) and high (5x109 WHO fibers) dose each of MWCNTs (MWCNT 1, 2, 3 and 3a) suspended in artificial lung medium, also used as negative control. Amosite asbestos (0.1x109 WHO fibers) served as positive control. It is well known that only fibrous but not granular dusts can cause tumors in rats after i.p. application. Moribund rats were sacrificed and necropsy comprising all organs was performed. A histopathological classification of tumors and in addition, immunohistochemistry was conducted to compare the induced tumors with mesotheliomas occurring in humans.
The treatments induced mesotheliomas in all dose groups, whereas incidence and time to tumor were different between the groups. Rats treated with MWCNTs 3 (L= 8.57 μm; D: 0.085 μm) and 3a (L= 9.3 μm; D= 0.062 μm) were killed moribund between 8 and 12 months after treatment and exhibited high tumor incidences in the low and high dose groups. The survival time of rats treated with MWCNTs 2 (L= 10.24 μm; D= 0.04 μm) was even longer but resulted also in high tumor incidences in both dose groups in relation to the positive control. For MWCNTs 1 (L= 7.9 μm; D= 0.037 μm) the survival time for the low dose was similar to the amosite asbestos (L= 13.95 μm; D= 0.39 μm) positive control. Overall, tumor incidences were lower than for MWCNTs 2, 3 and 3a.
Most tumors were histologically and immunohistochemically classified as malignant mesotheliomas comparable to those in humans, revealing a predominantly superficial growth on the serosal surface of the peritoneum especially the diaphragm.

PS 1991 Safety Evaluation of Fullerene Nanoparticle and Fullerene Whisker *In Vivo* Experiment

I. Yoko, G. Hasegawa and M. Nakao. *Kurume University, Kurume, Japan.*

[Purpose] We previously reported that fullerene whisker (FNW) with an average length of about 6 micrometer and an average diameter of about 660 nanometer seemed to be a safe nano-product similar to C60s in vitro (SOT annual meeting, 2010). Its unique properties make itself as a material for promising carbon device. This study was conducted to study its chronic effects compared with those of fullerene particles (C60) in vivo experiment. [Methods] FNWs (J Mater Res 17:83-88, 2002, 99.9% pure C60) and C60 (99.95% pure) were tested with the dose levels of 0.001, 0.01, 0.1, 1.0 microgram/mouse. ICR male and female mice were instilled trachealy under anesthesia with suspended test materials. The survival time, tumorigenesis and the gene expression profiles on the lung using whole mouse genome oligo DNA microarray kit (41174 probs) were studied. [Results] 1. Mice were observed maximum for 512 days after the treatment with various concentration of the material. In Kaplan-Meier analysis there is a significant difference among the FNW, C60 and Control groups in both male and female. The FNW group showed shorter half-life than those of the C60 and Control groups. 2. On macroscopic findings of the lung at autopsy, lung tumor were observed only in the FNW group (2/19 male, 2/16 female) dose-independently. 3. Number of gene-up-regulation or down-regulation was small in FNW- and C60- treated mice. However, Wt1 and Klrb1b genes were up-regulated and Klra 17 gene was down-regulated in the FNW-treated mice. Other many tumorigenic genes did not change clearly in the FNW-treated mice. [Conclusion] Down-regulation of Klra17 gene and up-regulation of Klrb1b gene may reveal that NK activity was reduced in the mice treated with FNW. These results suggest that FNW cannot be concluded to be as safe as the particles C60 in vivo. It will require more detail in vivo for safety evaluation of FNW.

PS 1992 Repeated-Dose Toxicity Testing of 9 Nanoparticles with Different Surface Functionalizations

W. Wohlleben[3, 1], R. Büsen[1], H. Kamp[1], V. Strauss[1], M. Dammann[1], S. K. Treumann[1], S. Gröters[1], K. Wiench[2], B. van Ravenzwaay[1] and R. Landsiedel[1]. [1]*Experimental Toxicology and Ecology, BASF SE, Ludwigshafen/Rhein, Germany,* [2]*Product Safety, BASF SE, Ludwigshafen/Rhein, Germany and* [3]*Polymer Physics, BASF SE, Ludwigshafen/Rhein, Germany.*

Oral uptake of nano-materials from food or cosmetics by consumers is likely to occur at low doses over long periods of time. To date, only few reports on in vivo effects of nano-materials upon subacute or subchronic oral exposure are available. The majority of these investigations address the effects of silver nanoparticles and none of these reports any non-transient toxicologically relevant effects.
Here, we present the results of two subacute oral toxicity studies in Wistar rats employing nine nano-materials with different surface functionalizations. The primary particle size was 10 nm (ZrO2), 15 nm (SiO2), 30 nm (BaSO4, OECD NM220) and 50 nm or 200 nm (Ag). The particles were coated with acid-, amino-, PEG-, acrylic- and electro-steric-functionalities.
The nano-materials were applied as suspensions via oral gavage at limit dose for 28-days. The studies were performed according to the OECD test guideline (TG) 407 including clinical observations, clinical pathology and (histo-)pathology. In addition to the basic haematological and clinical chemistry parameters, the acute phase proteins haptoglobin and alpha-2-macroglobulin as well as the protein troponin I were determined. Furthermore, mass spectrometry-based metabolite profiling was performed in serum samples making use of the MetaMap®Tox database to determine and assess metabolite patterns.
Test substance-related adverse effects were not observed with any of the nine nano-materials. Although tested at limit dose, no changes during clinical examinations, clinical pathology or pathology parameters were observed. The determination of acute phase proteins as well as troponin I did not reveal treatment-related effects. Furthermore, there were no matches with specific toxicity patterns in the MetaMap®Tox.

PS 1993 Comparative Biochemical and Histopathological Evaluation of PEG-Coated and Noncoated Gold Nanoparticles in Sprague-Dawley Rats

A. Patlolla[1], C. Collier[2] and P. B. Tchounwou[3]. [1]*Biology/Environmental Science, Jackson State University, Jackson, MS,* [2]*Environmental Science, Jackson State University, Jackson, MS and* [3]*Jackson State University, Jackson, MS.*

Nanoparticles (NPs) offer a great possibility for biomedical application, not only to deliver pharmaceutics, but also to be used as novel diagnostic and therapeutic approaches. Currently, there are no data available regarding to what extent the degree of the toxicity and the accumulation of gold nanoparticles (GNPs) are present in in vivo administration. The aim of this study was to assess the effects, after oral administration, of poly-ethylene-glycol (PEG) coated and non-coated GNPs on various hepatotoxicity markers such as alanine (ALT), aspartate aminotransferases, alkaline phosphatase, induction of reactive oxygen species and histopathological analysis in the mouse model. Sprague -Dawley rats were exposed to four different concentrations of PEG-coated and non-coated GNPs (12.5, 25, 50 and 100 μg/kg BW) and a control. Samples were collected 24 hours after the last treatment following standard protocols. Exposure to PEG-coated and non-coated GNPs enhanced the activities of serum amino-transferases (ALT/AST), alkaline phosphatases (ALP) and concentration of lipid hydro peroxide compared to control. Histopathology of exposed liver showed a statistically significant effect in the morphological alterations of the tissue compared to controls. However, PEG-coated GNPs demonstrated enhanced hepatotoxic effect than non-coated GNPs. The cellular findings reported here do suggest that both GNPs has the potential to induce hepatotoxicity in Sprague-Dawley rats through activation of the mechanisms of oxidative stress, which is of sufficient significance to warrant in vivo animal exposure studies. However, more studies to clarify the role of encapsulation in the in vivo toxicity of GNPs, are required and parallel comparison is preferred.

PS 1994 The Effects of Metal Oxide Nanoparticles on Angiogenesis in Transgenic Zebrafish

J. Chang[1, 2], G. Ichihara[1], Y. Shimada[3], S. Tada-Oikawa[2], Y. Suzuki[2], R. Sehsah[1], M. Kato[1], T. Tanaka[3] and S. Ichihara[2]. [1]*Occupational and Environmental Health, Nagoya University Graduate School of Medicine, Nagoya, Aichi, Japan,* [2]*Mie University Graduate School of Regional Innovation Studies, Tsu, Japan and* [3]*Molecular and Cellular Pharmacology, Pharmacogenomics and Pharmacoinformatics, Mie University Graduate School of Medicine, Tsu, Japan.*

The present study investigated the effects of exposure to metal oxide nanoparticles on the angiogenesis using transgenic (TG) zebrafish. The study also examined the potential mechanisms that may be involved in those effects using human umbilical vein endothelial cells (HUVECs). TG (nacre/fli1:EGFP) zebrafish were exposed to nano-sized titanium dioxide (TiO2), silica dioxide (SiO2), and copper oxide (CuO) particles at the concentrations of 0.01, 1 and 100 μg/ml from 1 dpf (day-post-fertilization) to 5 dpf. Angiogenesis were evaluated morphologically at the end of the exposure.
Exposure to CuO particles reduced the number of subintestinal vessels running transversely in TG zebrafish. In zebrafish exposed to CuO particles, the expression of vascular endothelial growth factor (VEGF) and VEGF receptor was down-regulated in the endothelial cells separated by Fluorescence Activated Cell Sorter (FACS). Moreover, HUVECs exposed to CuO particles showed reduction of the cell viability and increase in the apoptotic index in a dose-dependent manner. The study suggested that nano-sized CuO particles inhibit the angiogenesis due to reduction of VEGF expression and induction of apoptosis.

PS 1995 The Effect of Silica Nanoparticles on Endocytosis and Reproduction in *Caenohabditis elegans*

H. Eom, N. Chatterjee and J. Choi. *School of Environmental Engineering and Graduate School of Energy and Environmental System Engineering, University of Seoul, Seoul, Republic of Korea.*

Silica nanoparticles (SiNPs) are one of the popular nanomaterials used in industrial manufacturing, synthesis, engineering and medicine. Recently some toxicity and related mechanisms of silica nanoparticles have been reported, but it also remains thorough research. In this study, the toxic mechanism of SiNPs was investigated in the nematode, *Caenohabditis elegans* by using survival, reproduction test, microarray and pathway analysis. Physicochemical characterization of SiNPs was performed using dynamic light scattering (DLS) and zeta potential. No mortality was found for 24h exposure SiNPs however, reproduction was significantly decreased at the same concentrations. To gain a potential mechanism of toxicity, microarray followed by pathway analysis was conducted on *C. elegans* exposed to 10 mg/L SiNPs (decreased 20 % reproduction). Microarray results indicated that genes involved in reproduction were down-regulated in *C. elegans*. Pathway analyses result suggests endocytosis pathway being involved as a mechanism of uptake. Involvement of endocytosis pathway in SiNPs was assessed using specific inhibitors (Methyl-β-cyclodextrin, chlorpromazine, and LY294002 for caveolin-, clathrin-, and pinocytosis-mediated endocytosis, respectively). The inhibitor assay indicated an internalization process by clathrin-madiated endocytosis is involved in SiNPs. In addition, to confirm the effect of reproductive toxicity through endocytosis, reproduction test was conducted using endocytosis defective mutants, such as chc-1, cav-1, cup-2 and rme-8. Overall results suggest that SiNPs may affect reproductive toxicity via endocytosis pathway in *C. elegans*.
Key word: silica nanoparticle, reproduction, endocytosis, *C. elegans*, microarray, pathway analysis

PS 1996 *In Vivo* Invasion of Chorioallantoic Membrane by Lung Adenocarcinoma Cells Exposed to Titanium Dioxide Nanoparticles

A. Déciga-Alcaraz[1], E. I. Medina-Reyes[1], V. Freyre-Fonseca[1, 2], N. L. Delgado-Buenrostro[1], J. O. Flores Flores[3] and Y. I. Chirino[1]. [1]*Facultad de Estudios Superiores-Iztacala, National University of Mexico, Estado de Mexico, Mexico,* [2]*Escuela Nacional de Ciencias Biológicas, Instituto Politécnico Nacional, Distrito Federal, Mexico and* [3]*Centro de Ciencias Aplicadas y Desarrollo Tecnológico, National University of Mexico, Distrito Federal, Mexico.*

Background. Titanium dioxide nanoparticles (TiO2 NPs) is one of the most produced nanomaterial around the world and it has been classified by the International Agency for Research in Cancer as a possibly carcinogenic to human (Group 2B) in occupational settings. TiO2 NPs exposure induces several cellular alterations; however, cell invasion has less investigated.
Aim. We hypothesized that human tumor cells can acquire a more invasive phenotype after TiO2 NPs exposure. To test this hypothesis, lung adenocarcinoma A549 cells were exposed to nanospheres of TiO2 NPs (1, 5 and 10 μg/cm2) and nanobelts of TiO2 NPs to 10 μg/cm2 for 7 days. Then, 30 000 cells were mixed with collagen type I and placed on top of chicken chorioallantoic membrane (CAM) of leghorn white chicken eggs, which were previously incubated during 11 days at 37°C and 80% humidity. After 5 days, CAM was harvested and sectioned (6 μm) to perform hematoxillin and eosin (H&E) staining and immunohistochemistry (IHC) of cytokeratin 8, Gli1 and Ki67 in order to localize the human tumor cells in the CAM.
Results. Transmission electronic microscopy of TiO2 NPs nanospheres and nanobelts showed agglomerates of 588 nm and 454 nm respectively, in cell culture media plus 10% serum fetal bovine with zeta potential of -21 mV and -27 mV, respectively. H&E and IHC showed that the A549 cells treated with both shapes of TiO2 NPs had higher capacity to invade, detected by cytokeratin 8, and to proliferate detected by Gli1 and Ki67 in the CAM.
Conclusion. A549 cells treated with TiO2 NPs were more invasive and had higher capacity to proliferate in comparison with untreated cells in the CAM.

PS 1997 Secondary Mechanisms Drive Silica Nanomaterial Genotoxicity As Shown by the OGG1 Comet Assay and Genomic Analysis

A. Sullivan[1], T. Downs[1], Y. Shan[1], R. Adams[1], M. Crosby[2] and S. Pfuhler[1]. [1]*Mason Business Center, The Procter & Gamble Company, Mason, OH and* [2]*AstraZeneca Pharmaceuticals, Waltham, MA.* Sponsor: C. Ryan.

The safety profile and potential mode(s) of action (MoA) by which nanomaterials (NMs) may induce genotoxicity are not fully understood. Using amorphous silica (15nm Levasil® 200) at 50mg/kg, we examined a range of biomarkers after a single i.v. injection to male Wistar rats. Two studies were conducted; the first examined a wide range of time points; 4, 8, and 24h and second study investigated further early responses at 1, 2 and 4h. The second study also included an additional positive control, the model oxidant KBrO3. No significant increases in direct DNA damage were detected in the liver using the alkaline comet assay at any of the time points examined (2, 4, 8, and 24h). However, in the second study there was a small, but significant, increase in oxidative DNA damage at the 4h time point measured by the OGG1 modification of the comet assay in animals treated with the silica NM, while the positive control showed a strong increase in oxidized bases in the liver and the kidney (a target organ of KBrO3). Liver tissue was also analyzed for the transcriptional expression of genes by microarray analysis. Genes involved in responding to oxidative stress (Ho-1), inflammation (Ccl2), DNA damage (p53) and immune challenges (NfKB1(p105/p50)) were all upregulated in animals treated with silica NMs beginning at the earliest time points measured, 1 and 2h. These responses peak at 4h (Ho-1) or 8h (Ccl2, NfKB1, p53). In contrast, the KBrO3 treatment did not trigger an increase in Ccl2 while the other genes were increased in a highly significant manner. These data are supported by the patterns evident in heat maps representing genes involved in regulation of the pathways mentioned above. These results are in line with our previous data linking moderate DNA damage caused by silica NM with a tissue damaged mediated inflammatory response (Downs et al, Mutat Res, 745 (2012) 38-50), while our model oxidant KBrO3 showed strong DNA oxidative damage.

PS 1998 Generation of Titanium Dioxide Nanoparticle Aerosols for Biodisposition Kinetic Assessment

I. Pujalté, D. Dieme, S. Haddad and M. Bouchard. *Universite de Montréal, Montréal, QC, Canada.*

The intensive use of titanium dioxide nanoparticles (TiO2 NPs) in industrial products makes it one of the most produced NPs worldwide. Risk assessment studies are necessary, but limited data are available on NP disposition after inhalation. This study focused on the generation of TiO2 NP aerosols and their disposition kinetics in rats.
Adult male Sprague-Dawley rats were exposed acutely by inhalation «head-nose only » to 15 mg/m3 of commercial anatase TiO2 NPs (~20 nm) during 6 h. Blood was withdrawn at 0, 2, 4, 6, 24 and 48 h post-dosing (n = 6 rats per time point) and rats were sacrificed at 0, 1 and 2 days after onset of exposure (n=6 rats per group). Aerosols were generated with a collision 6-jet nebulizer and granulometry and concentrations were determined in real time using SMPS, CPS and Dusttrak. Ti levels were quantified by ICP-MS in blood, tissues (lungs, liver, kidneys, spleen), and excreta (urine, feces). Physiological parameters were also monitored.
Stable concentrations of poorly-agglomerated TiO2 NP aerosols were generated, with a mean aerodynamic diameter of 72 nm. Highest Ti concentrations were found in lungs at 24 and 48 h (on average 167 and 194 μg Ti/g), suggesting a persistence of NPs at the site-of-entry (0.08 μg/g pre-exposure). An increase in blood

Ti concentrations was quickly observed in the first 24 h post-dosing; after 24 h, Ti was non-detectable in blood. No significant increases in kidney concentrations of Ti were observed post-dosing. Significant increases in Ti concentrations were observed in liver and spleen 24 h post-dosing compared to pre-exposure levels, but not at 48 h (mean of 107 and 75 ng/g liver 24 and 48 h post-dosing versus 45 ng/g pre-exposure; corresponding values in spleen of 53, 76 and 29 ng/g). Significantly higher Ti concentrations were also found in feces post-dosing (on average 139 and 80 μg/g at 24 and 48 h versus 31 μg/g pre-exposure). No change in organs or body weights was observed through time. Further works are in progress to generate different aerosol exposure conditions.

PS 1999 Impact of Liposome-Induced Complement Activation on Tumor Growth and Angiogenesis

B. Rowland, M. Sabnani, R. Rajan, M. Markiewski and I. La-Beck. *Texas Tech University Health Science Center, Abilene, TX.* Sponsor: A. Elder.

Rationale: Acute infusion reactions in response to Doxil® (pegylated liposomal doxorubicin; PLD) are mediated by anaphylatoxins (C5a) generated from liposome-induced complement (C)-activation. Since C5a was reported to promote tumor growth through recruitment of myeloid derived suppressor cells (MDSCs), we postulate that liposome induced C-activation can promote tumor proliferation and lead to treatment resistance. Thus, we conducted studies to determine impact of this carrier on tumor progression.
Methodology: C57BL/6 mice bearing syngeneic TC-1 flank tumors were treated with a single dose (n= 10) or 4 weekly doses (n = 9) of non-drug loaded liposome (LIPO; identical to PLD carrier) or vehicle. Tumor volume was monitored and at endpoint tumors were processed for single cell suspension, tissue lysate, and frozen section. Cells were stained for MDSCs (CD11b+Gr1+) and analyzed by flow cytometry. C-activation (C3b/iC3b/C3c) was quantified in lysate via indirect ELISA. Tumor sections were stained for vasculature (CD31) and microvessel density in whole sections was quantified using digital pathology and image analysis algorithms.
Results: Tumor volumes were 2-fold larger in LIPO treated mice than in controls, 653 ± 144 and 218 ± 58 mm3, respectively ($p<0.05$). Tumors in LIPO treated mice had higher microvessel density than controls, 20.8 ± 0.1 and 15.0 ± 0.1 vessels/mm2, respectively ($p<0.01$). In LIPO versus control groups, there was increased C-activation (8.8% and 3.9% of positive reference, respectively) and MDSC infiltration (2.6% and 0.5%, respectively) in tumors.
Conclusions: Contrary to the prevailing paradigm that they are inert drug carriers, our data showed that liposome induced C-activation can promote tumor growth and angiogenesis through increased tumor recruitment of MDSCs. Ongoing studies will clarify this mechanism of resistance and develop strategies for mitigating unwanted immune effects to enhance antitumor efficacy. These results will have major implications for the future development of anticancer liposomes.

PS 2000 The Comparative Effects of Nanoporous and Colloidal Silica Nanoparticles in Atopic Dermatitis

S. Kim. *Pharmacology, Kyungpook National University Medical School, Daegu, Republic of Korea.*

Nanoparticles (NPs) are incorporated into a variety of skin care products. Recently, NPs have been identified as causative agents affecting skin barrier penetration and immunologic responses. Thus, understanding epidermal and dermal penetration, as well as possible toxicity of NPs is important to skin inflammatory diseases. The aim of our study was defining the effects of pore structural conditions of silica NPs in atopic dermatitis (AD) condition. Both nanoporous (NPS) and colloidal (Col) silica NPs (100 and 500 μg/ear) were topically applied to female BALB/c mice during 3 weeks. Topical application of NPs during 3 weeks elicited aggravation of AD symptoms. In both histology and FACS analysis, NPS NPs showed significant increase of ear and epidermal thickness, infiltration of immune cells (eosinophils, mast cells) and proliferation of immune cell than Col NPs. NPS NPs led to significant increase in serum immunoglobulin (total IgE, DFE specific IgE and IgG2a) and histamine. NPS NPs induced higher expression of Th1, Th2 and Th17 cytokines. Interestingly, NPS-induced AD symptoms were significantly reduced by oil treatment. To define the underlying mechanisms of action, human keratinocytes (HaCaT) model was used. NPS NPs induced higher expression of pro-inflammatory cytokines and chemokines by the up-regulation of nuclear factor-κB in HaCaT cells. The results indicate that in vivo exposure to NPS NPs caused more damage to skin inflammation than that of Col NPs through the hydroscopic property. These results suggest the importance of verification of biocompatibility of NPs in dermal exposure.

PS 2001 5-Day Repeated Inhalation Toxicity of Graphene Nanopowder

J. Shin[1], J. Kim[2], J. Baek[1], J. Hwang[1], J. Lee[1], T. Kim[2], E. Kim[2] and I. Yu[2]. *[1]Occupational Lung Diseases Institute, KCOMWEL, Ansan, Gyeonggi, Republic of Korea and [2]Institute of Nano Products Safety Research, Hoseo University, Asan, Chungnam, Republic of Korea.*

Graphene has increased attraction recently in many applications such as a display screens, solar cells, electric circuits, as well as medical and industrial processes due to their unique electronic and chemical properties. However, relatively little is known about the hazard assessment and human health of graphene. We evaluated the acute pulmonary toxic effect of graphene via nose-only inhalation exposure for 5 consecutive days (6h/day). Male SD rats were divided into 3 groups (5 rats in each groups), the fresh air control (0 mg/m3), low (0.68 ± 0.14 mg/m3), and high (3.86 ± 0.94 mg/m3) concentration group, respectively. We measured lactate dehydrogenase (LDH) and microalbumin (mALB) levels in bronchoalveolar lavage (BAL) fluid on day 1, 3, and 28 after 5 days exposure of graphene. To evaluate the biopersistence of graphene, we observed the deposition of graphene in alveolar macrophages via high resolution illuminator (CytoViva, USA). There was no statistical significant difference in mean concentrations of LDH and mALB of exposed groups compared to control group on all post-exposure groups (1, 3, and 28 days). The deposition of graphene in alveolar macrophages was observed in all post exposure groups. In this study, there was no acute pulmonary toxic effect of graphene in BAL fluid; however, it is necessary to evaluate the physico-chemical characterization and sub-acute or -chronic inhalation toxicity of graphene

PS 2002 Acute Effects of Multiple-Dose Metallofullerene Exposures in Mice after Intraperitoneal Exposure

V. Wallace[1], J. Hinckley[1], B. S. Jortner[1], M. Ehrich[1] and Z. Zhou[2]. *[1]Virginia-Maryland Regional College of Veterinary Medicine, Blacksburg, VA and [2]Luna NanoWorks, Danville, VA.*

Gadolinium metallofullerene (Gd3N@C80) is a fullerene compound, a nanoparticle that contains carbon atoms oriented in a hollow sphere formation with gadolinium encapsulated within the cage. Gd3N@C80 has been proposed as a MRI contrast agent in medical imaging techniques, and also suggested for use for prevention of organophosphate poisoning. Although current published in vitro and in vivo studies utilizing single-dose Gd3N@C80 have not revealed toxic responses, studies examining multiple dose effects of these compounds have not been performed. This study investigates the acute effect of multiple doses of Gd3N@C80 derivatives on mice (male, CD-1 strain). The treatment group received three 8 mg/kg doses intraperitoneally (IP; n=12) and control mice received a saline solution IP (n=6). Dosing was done at 0, 4, and 7 hours, with behavioral observations made throughout the day. Mice were sacrificed at either 10 or 24 hours post-exposure, at which times samples were collected for clinical pathology analysis (hematology, serum biochemistry, urinalysis), and the major organs for histology. No abnormalities were detected in any study parameters, indicating that our multiple doses of Gd3N@C80 did not elicit acute toxicity in mice. Funded by NIH T350D011887 as part of the Summer Veterinary Student Research Program.

PS 2003 BrdU Screening—a Short-Time Test for Reliable Prediction of Carcinogenicity for MWCNT

A. Hackbarth[1], D. Schaudien[1], B. Bellmann[1], H. Ernst[1], A. Leonhardt[2], U. Heinrich[1] and S. Rittinghausen[1]. *[1]Fraunhofer Institute for Toxicology and Experimental Medicine, Hannover, Germany and [2]Leibniz Institute for Solid State and Materials Research, Dresden, Germany.* Sponsor: C. Dasenbrock.

Since the discovery of the excellent features of MWCNT, there has been an increase in potential applications, despite the fact that they have been discussed to have a toxic potential depending on their length and fiber-like shape. For this reason, potential adverse biological effects of MWCNT have been investigated in vivo (rat) in a project funded by the German BMBF (contract No. 03X0109A). Tailor-made MWCNT with different lengths and diameters were produced, suspended in artificial lung medium and injected intraperitoneally in rats in two dose groups (low: 1x109 WHO fibers; high: 5x109 WHO fibers) in a BrdU screening test (MWCNT 1, 2, 3) and a carcinogenicity study (MWCNT 1, 2, 3, 3a). Long amosite asbestos (0.1x109 WHO fibers) served as positive control, ground MWCNT and Printex 90 (5 mg/rat) as negative control. Suspension and length/diameter distribution were measured in SEM.

Proliferation of cells in the diaphragmatic peritoneum was investigated as a short-time screening test 3 and 6 months after i.p. injection of fibers in rats, using the BrdU method and measurement of peritoneal thickness. Furthermore, animal mortality and tumor development were monitored over two years in a carcinogenicity study.
There was a time-independent significant increase in cell proliferation after injection of MWCNT 1(high) (L=7.9 μm; D=0.037 μm), MWCNT 2(low/high) (L=10.24 μm; D=0.04 μm), and MWCNT 3(low/high) (L=8.57 μm; D=0.085 μm), like after exposure to long amosite asbestos (L=13.95 μm; D=0.39 μm) as positive control. MWCNT 2(high) and 3(low/high) induced significant dose-dependent thickening of the peritoneum after i.p. injection, independently of time.
In the carcinogenicity study, MWCNT 2, 3 and 3a (L=9.3 μm; D=0.062 μm) showed a higher mesothelioma incidence than MWCNT 1.
In conclusion, some MWCNT (MWCNT 2, 3) mediate enhanced proliferation of peritoneal cells in the diaphragm in rats, which may result in mesothelioma development.

PS 2004 Silver Nanoparticles, Injected Intravenously, Accumulate in the Spleen of Mice and Cause Major Changes in Immune Cell Profiles

D. Willis[1], P. L. Goering[2], T. H. Umbreit[2], H. Degheidy[2], Q. Zhang[2], J. Zheng[2], B. Casey[2], L. Graham[2], L. Chen[2], M. Betz[2] and J. T. Zelikoff[1]. *[1]Environmental Medicine, NYU School of Medicine, Tuxedo, NY and [2]Center for Devices and Radiological Health, FDA, Silver Spring, MD.*

Silver nanomaterials are increasingly being used as antimicrobial agents in medical devices, yet their effects on immunocompetence are unclear. This study investigated modulation of immune cell profiles and cell activation in the spleen by iv exposure of adult male mice to silver nanoparticles (AgNP), as well as particle distribution in the liver, kidneys, and spleen. Mice, injected each day for 2 days with a total of 66 or 300 μg of either 20 or 110 nm AgNP (or sodium citrate vehicle), were sacrificed 1 d later and splenic cells examined by flow cytometry. Analysis revealed that injection of 66 μg of 20 nm AgNP increased Th2 cells and decreased effector memory cells, while exposure to the same dose of larger-sized AgNP had no effect on percentages of CD3+,CD4+, Th1, Th2, Th17 cells, CD4/CD8 ratio or total memory/naïve/central memory/effector memory cells compared to controls. At 300 μg, 20 nm AgNP significantly decreased the number of naïve CD4+ cells and CD3+CD4- cells, while increasing total/activated central memory cells, total/activated effector memory cells, total memory cells, and natural killer cells; exposure to the same dose of 110 nm AgNP increased activated CD11c+ cells (macrophages). ICP-MS analysis demonstrated that the highest concentrations of silver were in the spleen following the 300 μg AgNP exposure, with an average concentration reaching a peak of 151 and 41.5 μg/g following exposure to 20- and 110 nm-sized AgNP, respectively. Relative weight of the spleen was increased significantly following 20 nm AgNP exposure. These data indicate that systemic exposure to AgNP accumulates in the spleen, adversely affects spleen weight and modulates the systemic immune response, accumulates in the spleen, and adversely affects spleen weight in a dose-dependent manner with smaller size particles leading to more marked effects. Supported by NSF/FDA Scholar-in-Residence at FDA program - #1237451.

PS 2004a Thirty-Day Whole-Body Inhalation Toxicity and Tissue Burden Study of Multiwalled Carbon Nanotubes in Harlan Sprague-Dawley Rats and B6C3F1 Mice

B. C. Sayers[1], M. D. Stout[1], M. F. Cesta[1], N. A. Moore[2], G. L. Baker[2], K. M. Patton[2], B. K. Hayden[2], J. A. Dill[2] and N. J. Walker[1]. *[1]Division of the National Toxicology Program, National Institute of Environmental Health Sciences, Research Triangle Park, NC and [2]Battelle Toxicology Northwest, Richland, WA.*

Multiwalled carbon nanotubes (MWCNTs) are a diverse class of high aspect ratio nanoscale materials that vary in size (length, diameter) and composition (surface functional groups, metal catalyst residue). The similarity of MWCNTs to harmful high aspect ratio fibers has generated concern for toxicological potential of MWCNTs. This study was designed to evaluate the toxicity of MWCNTs (length x diameter: 2.6 um x15 nm, purity: 99%, nickel content: 0.52%) in Harlan Sprague Dawley rats and B6C3F1/N mice exposed via whole body inhalation. Male and female rats and mice (35/sex/group) were exposed to 0, 0.1, 0.3, 1, 3, or 10 mg/m3 MWCNTs for 5 days/week (6 hours/day). The day after the last exposure, core group animals (10/sex) received complete necropsy and histopathological examinations. Blood and lungs were collected from animals in the tissue burden groups (25/sex) on postexposure day 0 (10/sex), 14, 42 and 126 (5/sex) and analyzed for nickel as a surrogate for MWCNT. Dose-dependent increases (incidence and/or severity) in chronic lung inflammation and pulmonary associated lymph node hyperplasia were observed in both species and sexes. Significantly increased lung weights were observed in female rats exposed to 10 mg/m3 and both male and female mice exposed to ≥ 3 mg/m3 ($p \leq 0.01$). Clearance rates of MWCNT from the lung were similar in both sexes and species and decreased markedly in animals exposed to ≥ 3 mg/m3 (T1/2 ≈ 5-21 mo) compared to the 0.1, 0.3 and 1 mg/m3 dose groups (T1/2 ≈ 2-3 mo). The long clearance half lives, large lung burdens and lung lesions in animals exposed to MWCNT ≥ 3 mg/m3 suggest that lung overload occurred. The data from this study will be used to design a chronic whole-body inhalation toxicity study of MWCNTs. This work was supported by the NIH, National Institute of Environmental Health Sciences.

PS 2004b Cerium Oxide Nanoparticles Induced Lung Fibrosis Involving Epithelial-Mesenchymal Transition (EMT)

J. Y. Ma, B. D. Dolash, M. Barger, D. Schwegler-Berry, R. R. Mercer and V. Castranova. *PPRB/HELD, NIOSH, Morgantown, WV.*

Recently cerium compounds have been used as diesel fuel additives to increase fuel combustion efficiency and decrease diesel soot emissions. However, detection of cerium oxide nanoparticles (CeO_2) in the diesel exhaust by emission tests are a caused of health concern. Our previous studies have shown that exposure of rats to CeO_2 induces sustained pulmonary inflammation and mediator production, and lung fibrosis. The current objective is to evaluate the effects of CeO_2 on functional change of alveolar type II cells (ATII) leading to EMT. Male Sprague Dawley rats were exposed to CeO_2 (3.5 mg/kg) by a single intratracheal instillation and sacrificed at various times post exposure. ATII were isolated from lung tissues at 28 days post exposure and purified by panning. Alveolar macrophages (AM) were isolated by bronchoalveolar lavage (BAL). The first BAL fluid (BALF) and AM-conditioned medium obtained after a 24 h incubation time were saved for further analysis. Lung fibrosis was evident by increased hydroxyproline content and enhanced Sirius Red staining for collagen in lungs at 28 days after CeO_2 exposure. Scanning electron micrographs indicate CeO_2-induced ATII hypertrophy. Confocal microscopic analysis demonstrated that exposure to CeO_2 increased the presence of stress actin, expressed as α-smooth muscle actin (α-SMA) in ATII at 28 days post exposure and caused CeO_2-induced EMT. CeO_2 exposure significantly increased the fibrogenic cytokine,TGF-β1, in AM-conditioned media, and increased matrix metalloproteinases and soluble collagen in BALF, at 3 and 28 days post exposure, respectively. In vitro exposure of ATII or a rat type II cell line (RLE-6TN) to TGF-β1 significantly increased α-SMA expression and altered morphology. In addition, exposure of type II cells to BALF significantly increased α-SMA expression, suggesting CeO_2 exposure induced mediators in the BALF significantly modified cell function. These results demonstrate that CeO_2-induced EMT of ATII may play important role in lung fibrosis. These findings suggest potential health effects of CeO_2 exposure.

PS 2004c Cytotoxicity and Genotoxicity Assessment of Silver Nanoparticles in Mouse

T. Chen[1], Y. Li[1], J. A. Bhalli[2], W. Ding[1], J. Yan[1], M. G. Pearce[1], C. K. Cunningham[3], Y. Jones[3], W. A. Monroe[3], T. Zhou[4] and P. C. Howard[3]. *[1]Division of Genetic and Molecular Toxicology, FDA/National Center for Toxicological Research, Jefferson, AR, [2]Covance Laboratories Inc, Indianapolis, IN, [3]Nanotechnology Core Facility, FDA/National Center for Toxicological Research, Jefferson, AR and [4]Center for Veterinary Medicine, FDA, Rockville, MD.*

Silver nanoparticles (AgNPs) are among the most commercially used nanomaterials and their toxicity and genotoxicity are controversial. Although many in vitro studies have been conducted to evaluate the genotoxicity of AgNPs, in vivo genotoxicity studies on the nanomaterials are limited. Given the unique physicochemical properties and complex pharmacokinetics behavior of nanoparticles (NPs), in vivo genotoxicity assessment of AgNPs is badly needed. In this study, the clastogenicity and mutagenicity of AgNPs with different sizes and coatings were evaluated using mouse micronucleus (MN) assay, Pig-a assay and Comet assay. Five 7-week-old male B6C3F1 mice per group were treated with 5 nm polyvinylpyrrolidone (PVP)-coated AgNPs at a single dose of 0.5, 1.0, 2.5, 5.0, 10.0 or 20.0 mg/kg body weight (bw) via intravenous injection for both the MN and Pig-a assays; or with 15–100nm PVP- or 10–80nm silicon-coated AgNPs at a single or 3-day repeated dose of 25.0 mg/kg bw for the MN assay and Comet assay in mouse liver. Inductively coupled plasma mass spectrometry (ICP-MS) and transmission electron microscopy (TEM) analyses indicated that AgNPs reached the testing tissues (bone marrow for the MN and Pig-a assays and liver for the Comet assay). Although there was a reduction of reticulocytes in the PVP-coated AgNPs-treated animals, indicating cytotoxicity of the AgNPs, none of the treatments resulted in a significant increase of either mutant frequencies in the Pig-a gene or the percent of micronucleated reticulocyte over the concurrent controls. However, both the PVP-

and silicon-coated AgNPs induced oxidative DNA damage in mouse liver. These results demonstrate that the AgNPs can reach mouse bone marrow and liver, and generate cytotoxicity to the reticulocytes and oxidative DNA damage to the liver.

PS 2004d One Year Pulmonary Outcomes After Exposure to Carbonaceous Nano-Engineered Materials and Asbestos

A. A. Shvedova[1], N. Yanamala[1], E. K. Kisin[1], A. R. Murray[1], A. Hubbs[1], P. Keohavong[2], L. P. Sycheva[3], V. E. Kagan[2] and V. Castranova[1]. *[1]HELD/PPRB, CDC/NIOSH, Morgantown, WV, [2]University of Pittsburgh, Pittsburgh, PA and [3]Sysin Research Institute of Human Ecology and Environmental Health, Moscow, Russian Federation.*

Single-walled carbon nanotubes (SWCNT) and carbon nanofibers (CNF) are carbonaceous nanoparticles sharing fibrous morphology with a well-known, naturally occurring, toxic fiber, asbestos. Both short- and long-term outcomes of pulmonary exposure to asbestos, ranging from inflammation and fibrosis to mesothelioma and lung cancer, are well described. To date, no data are available describing long-term adverse effects of pulmonary exposure to SWCNT or CNF. Thus, a direct comparison of chronic effects of SWCNT, CNF and asbestos is of significant importance. Here, we assessed inflammatory, fibrogenic and genotoxic effects of SWCNT, CNF, and asbestos in C57BL/6J mice one year after a single pulmonary exposure by pharyngeal aspiration and inhalation. We provide evidence that up to one year after exposure, SWCNT, CNF and asbestos persist in the lung and regional lymphatics. All three particles induced chronic bronchopneumonia and lymphadenitis, accompanied by pulmonary fibrosis. While CNF and asbestos were found to promote the greatest degree of inflammation, followed by SWCNT, the latter was the most fibrogenic of all three types. SWCNT induced cytogenetic alterations including micronuclei and nuclear protrusions in vivo. Notably, SWCNT and CNF, but not asbestos, increased the incidence of K-ras oncogene mutations in lungs. No lung tumor incidence occurred after 1 year post exposure in any group. Inhalation exposure to SWCNT showed significantly greater inflammatory, fibrotic and genotoxic effects than bolus pharyngeal aspiration thus indicating that bolus exposure does not over-predict pulmonary response and appears useful for hazard determination. Overall, our data suggest that long-term pulmonary toxicity of particles with high aspect ratios - SWCNT, CNF and asbestos – is defined not only by their fibrous morphology but also by the chemical composition, specific surface area and type of exposure.

PS 2004e Effect of Prenatal Exposure to Carbon Black Nanoparticle on Gene Expression in the Spleen of Offspring Mouse

M. Umezawa[1, 2], S. Okamoto[1], R. Shimizu[1] and K. Takeda[1, 2]. *[1]Department of Hygienic Chemistry, Faculty of Pharmaceutical Sciences, Tokyo University of Science, Noda, Chiba, Japan and [2]The Center for Environmental Health Science for the Next Generation, Research Institute for Science and Technology, Tokyo University of Science, Noda, Chiba, Japan.* Sponsor: K. Nohara.

Objective: We recently found that exposure of pregnant mouse to carbon black nanoparticle (CB-NP) decreased T cells in the spleen of offspring during the neonatal period. The aim of the present study was to examine the effect of prenatal exposure to CB-NP on gene expression in the spleen of offspring in a mouse model.
Methods: CB-NP (PRINTEX90 from Degussa; primary particle size: 14 nm; surface area 300 m^2/g) was suspended at 5 mg/mL in water, sonicated for 30 min, and then filtrated through a 450-nm filter immediately before administration. The peak size of the aerodynamic diameter distribution of CB-NP in the suspension was 68 nm. Pregnant ICR mice were treated with the CB-NP suspension (95 μg/kg/time) by intranasal instillation on gestational days 5 and 9. Spleen was collected from male and female offspring mice at 5 days post-partum. All animals were treated and handled in accordance with national guidelines for the care and use of laboratory animals. Gene expression in the tissues was examined by cDNA microarray using a SurePrint G3 Mouse Gene Expression 8×60K microarray (Agilent). Gene Ontology, canonical pathway and transcription factor related to the genes dysregulated by prenatal CB-NP treatment were bioinformatically extracted.
Results: The genes differentially expressed by prenatal CB-NP treatment in the spleen of both male and female offspring were enriched in a transcription factor GATA1, which are closely associated with erythrocyte development. The genes annotated to GATA1 were upregulated and included Cxcr5, Hes1, Irs1, Dnase1l3, Nf1a, and Nf1b. Interestingly, previous studies indicated that Hes1 inhibits the function of GATA1 and the development of erythroid and megakaryocytic cells.
Conclusion: The effect of prenatal exposure to CB-NP through the airway on the spleen was associated with upregulation of genes related to GATA1 in neonatal mouse.

PS 2004f Quantum Dot-Induced Changes in Pulmonary Function Are Mouse Strain Dependent

D. K. Scoville[1], D. An[2], C. Carosino[1], C. White[1], M. Cartwright[1], S. Schmuck[1], X. Gao[3], W. C. Parks[2], W. A. Altemeier[2] and T. Kavanagh[1]. *[1]Environmental and Occupational Health Sciences, University of Washington, Seattle, WA, [2]Medicine, University of Washington, Seattle, WA and [3]Bioengineering, University of Washington, Seattle, WA.*

Quantum dots (QDs) are photostabile fluorescent nanoparticles commonly composed of a cadmium selenide (CdSe) core, a zinc sulfide (ZnS) shell, and coatings specific to a variety of uses in electronics and biomedical research. QDs can cause inflammation and toxicity in the respiratory tract when inhaled, instilled, or aspirated. In this study we investigated whether pulmonary aspiration of 12 nm diameter tri-n-octylphosphine oxide, poly(maleic anhydride-alt-1-tetradecene) coated CdSe/ZnS QDs (TOPO-PMAT QDs) causes functional changes in mouse lung mechanics in a mouse strain dependent fashion. C57BL/6J and A/J mice were dosed with 6 μg Cd equivalents/ kg body weight of a 10 nM TOPO-PMAT QD solution or an equal volume of saline vehicle via oropharyngeal aspiration. At 24 hours, mice were anesthetized, intubated via tracheotomy, and connected to a flexiVent instrument. Lung mechanics were measured repeatedly during a progressive nebulized methacholine challenge (0-50 mg/ml). There were statistically significant increases in total lung resistance, tissue damping, and lung elastance with methacholine challenge after TOPO-PMAT QD treatment in A/J but not C57BL/6J mice. There were also statistically significant increases in baseline airway resistance and lung compliance in A/J compared to C57BL/6J mice. Thus, TOPO-PMAT CdSe/ZnS QDs negatively affected pulmonary function in a mouse strain-dependent manner. It is important that genetic susceptibility be considered in risk assessment strategies for QDs and other engineered nanomaterials. Supported by NIH Grants U19ES019545, P30ES007033, and R01HL086883.

PS 2004g The Mitochondrial Effects of a Chronic Exposure to a Low-Dose of Silver Nanoparticles Are Rescued by an Antioxidant

C. M. Palmeira[1, 2], J. S. Teodoro[1, 2], R. Silva[2], A. T. Varela[1, 2], F. V. Duarte[1, 2] and A. P. Rolo[1, 3]. *[1]Center for Neurosciences and Cell Biology, University of Coimbra, Coimbra, Portugal, [2]Department of Life Sciences, University of Coimbra, Coimbra, Portugal and [3]Department of Biology, University of Aveiro, Aveiro, Portugal.*

Manufactured silver nanoparticles (AgNPs) are a ubiquitous presence in daily life, for they are used in numerous applications, from ultrasensitive molecular sensing and diagnostic imaging, agents for photodynamic therapy, burn and wound dressing, to dental-bonding agents and sunscreens, cosmetics and fuel cells, tires, optics, clothing and electronics. The same properties that make AgNPs so useful could also prove harmful when interacting with humans and the environment. Most of the works so far have unveiled a strong induction of oxidative stress as main mechanism of toxicity. However, these studies are mainly focused on short-term exposure and, consequently, higher doses. As such, we aimed to understand how long-term exposure to a relative low-dose of AgNPs could affect various biological systems, with a particular focus on mitochondrial bioenergetics and if these effects could be reverted by a simultaneous treatment with a known antioxidant, N-acetylcysteine (NAC). Other objectives were to understand if there is a preferential target organ in the body and if the size of the AgNPs was a determinant factor in the registered alterations.
In accordance with European and national animal use guidelines, 10-week old male Sprague-Dawley rats were intraperitoneally (i.p.) injected with 200 μg/Kg (w/w) of either 10 nm or 75 nm AgNPs, with and without a 30min previous NAC 100 mg/Kg i.p. injection. We uncovered a NAC-reversible, non-size dependent negative effect of AgNPs in various functions (membrane potential, oxygen consumption, ATP generation, amongst others) of isolated liver, kidney and, to a lesser extent, heart mitochondria. Our data demonstrates that even a low-end dose exposure to AgNPs has a pernicious effect in the long term, which begs for further assessment of the indiscriminate use and exposure to AgNPs.

PS 2004h Nanoceria *In Vivo* Biotransformation Is Associated with Loss of Its Pro-Oxidant Brain Effects

U. Graham[5], S. S. Hardas[2], R. Yokel[1], P. Wu[3], E. Grulke[3], M. T. Tseng[4] and D. Butterfield[2]. *[1]Pharm Sci, U KY, Lexington, KY, [2]Chemistry, U KY, Lexington, KY, [3]Chemical & Materials Engineering, U KY, Lexington, KY, [4]Anatomical Sciences & Neurobiology, U Louisville, Louisville, KY and [5]CAER, U KY, Lexington, KY.*

Background: Nanoceria has many commercial uses and is being developed as an antioxidant therapeutic. It persists in the rat for 90 days with little quantitative reduction, primarily in the liver, where it produces granuloma. It produces pro-ox-

idant effects in the brain up to 30 days after administration. Objectives: Determine nanoceria's physicochemical characteristics in the liver and effects on brain oxidative stress for 90 days after administration. Methods: A citrate-stabilized cubic 30 nm ceria (85 mg/kg) was iv infused once to rats, terminated 1 h to 90 days later. Controls received vehicle. Multiple oxidative stress endpoints were determined in the brain. Nanoceria in the liver was examined using HR-TEM, electron energy loss spectroscopy (EELS), energy-dispersive X-ray spectroscopy (EDS), and selected area electron diffraction (SAED). Results: Following similar administration of a 5 nm ceria, oxidative stress was seen in the brain up to 30 days after 30 nm ceria, including elevated protein carbonyl, catalase, and heat shock protein 70 levels and decreased GSH/GSSG. Ninety days after its administration oxidative stress endpoints were at control levels. HR-TEM of the liver revealed nanoceria particles were highly fragmented and rounded along their edges and the appearance of clouds containing copious of 1 to 3 nm ceria (verified by EELS, EDS, and SAED) near the nanoceria agglomerates. EELS showed the 1 to 3 nm ceria had a reduced valence (Ce3+) state, indicating in vivo processing shifted nanoceria to a form having higher free radical scavenging activity. The temporal association between nanoceria biotransformation in the liver and reversal of nanoceria-induced oxidative stress in the brain suggests a cause and effect relationship. Conclusion: Nanoceria's long term fate and effects warrant further study to better understand its adverse and beneficial nature. Support: US EPA STAR Grant RD-833772.

PS 2005 Cannabinoid Receptor Function on Bone Marrow-Derived Dendritic Cells

J. Suarez-Martinez[1, 2], R. Crawford[1] and N. E. Kaminski[1, 3]. [1]*Center for Int Tox, Michigan State University, E. Lansing, MI,* [2]*Comp Med and Int Biol, Michigan State University, E. Lansing, MI and* [3]*Pharm and Tox, Michigan State University, E. Lansing, MI.*

Dendritic cells (DCs) are professional antigen presenting cells indispensible in linking the innate and adaptive immune response. DCs comprise a heterogeneous population of cells. Each distinct subset has its unique set of surface markers and different abilities to respond to environmental stimuli and process antigen. Cannabis is the most frequently consumed illicit drugs in the world. Mammals express at least two types of cannabinoid (CB) receptors, Cannabinoid receptor 1 (CB_1) and Cannabinoid receptor 2 (CB_2). Previous studies in our lab have shown that the antiviral response (HIV and influenza) in $CB_1^{-/-}CB_2^{-/-}$ (KO) mice was markedly increased compared to WT due to a deregulation of IL-17 producing T cells primarily attributable to DC. The role of the CB receptors on DC development, function and susceptibility to exogenous cannabinoid compounds such Δ^9-tetrahydrocannabinol (Δ^9-THC) has not been characterized. The objective of the present study was to determine CB receptor function in the development and maturation of DC subsets from mouse bone marrow. Bone marrow was extracted from femurs and tibias of WT (C57bl6) and KO mice and stained for DC markers. Our results indicate that the percent of DC populations, determined by CD11c expression, composes 4% of freshly isolated bone marrow cells in WT mice and 10% in KO mice. We also found that WT bone marrow has a higher percent of MHCI+ and CD86+ cells. On the other hand, KO mice demonstrated a slightly higher percent MHCII+ cells. Looking at specific subpopulations within CD11c+ cells we found that plasmacytoid DCs had a higher percent in WT meanwhile CD8α DCs and monocyte DCs composed a higher percent in the KO mice in comparison to WT. Interestingly, CD8α and monocyte DC surface expression of maturation markers MHCII and CD86 were below that of the WT mice. Our findings suggest a possible role of CB receptors in DC maturation and subset development. (This work was supported by DA007908)

PS 2006 Cannabinoid Regulation of Peripheral Sympathetic Neuronal Activity: Possible Role in Cannabinoid-Mediated Immunosuppression

T. J. Simkins[3, 4], D. Fried[2], J. J. Galligan[2, 3], J. L. Goudreau[2, 3, 4], K. J. Lookingland[2, 3, 4] and B. L. Kaplan[1]. [1]*Department of Basic Sciences, Center for Environmental Health Sciences, Mississippi State University, Mississippi State, MS,* [2]*Department of Pharmacology and Toxicology, Michigan State University, East Lansing, MI,* [3]*Neuroscience Program, Michigan State University, East Lansing, MI and* [4]*Center for Integrative Toxicology, Michigan State University, East Lansing, MI.*

Cannabinoids are compounds derived from *Cannabis sativa* that exhibit immunosuppressive effects. Cannabinoids are also known to inhibit neurotransmitter (NT) release in the central nervous system. Therefore, it was hypothesized that inhibition of NT release might contribute to cannabinoid immunosuppressive mechanisms. NTs are implicated in immune homeostasis; for example, norepinephrine (NE) modulates antibody production. However, it is not known to what extent cannabinoids interact with NTs to cause immunosuppression. *In vivo*, NE innervation of the spleen capsule is known to cause spleen contraction during times of hypoxia as well as in response to an immune challenge. Therefore, we utilized NE-induced splenic contraction as a tool to probe the role of cannabinoids in regulating spleen capsule sympathetic neuronal activity in wild-type and cannabinoid receptor dual knockout (CB1/CB2 KO) mice. It was discovered that NE-induced spleen capsule contraction was significantly attenuated in CB1/CB2 KO mice. However, this effect was not observed in response to electrical stimulation of spleen capsule sympathetic axon terminals, suggesting a potential role for non-adrenergic signaling in contraction. Additionally, spleens from CB1/CB2 KO mice have decreased spleen capsule thickness that iss not due to decreased smooth muscle content. Overall, these studies suggest that the mechanism by which cannabinoids regulate splenic sympathetic activity *in vivo* could involve interaction with one or more NTs. The results from these studies could identify neuronal mediators involved in the immunosuppressive effects of cannabinoids.

PS 2007 Modulation of HIVGP120 Antigen-Specific Immune Responses by Δ9-Tetrahydrocannabinol *In Vivo*

W. Chen[1, 3], R. Crawford[3], B. L. Kaplan[2, 3], K. Smith[3] and N. E. Kaminski[2, 3]. [1]*Microbiology and Molecular Genetics, Michigan State University, East Lansing, MI,* [2]*Pharmacology and Toxicology, Michigan State University, East Lansing, MI and* [3]*Center for Integrative Toxicology, Michigan State University, East Lansing, MI.*

Approximately 25% of HIV patients use marijuana for its putative therapeutic benefit; however, it is unknown how cannabinoids affect the immune status of immunocompromised HIV patients. Previously, a surrogate *in vitro* mouse model was established to investigate the effects of cannabinoids on the early stages of the anti-HIV response. Specifically, $CD8^+$ T cell proliferation and gp120-specific IFNγ production were induced, which were suppressed or enhanced by Δ^9-tetrahydrocannabinol (THC), the predominant psychoactive compound in marijuana, depending on the magnitude of cellular activation. To determine whether THC has similar effects *in vivo*, a mouse model to stimulate the HIV_{gp120}-specific immune response has also been established. Vector plasmid VRC2000 or gp120-expressing plasmid VRCgp120 was injected intramuscularly into mice. The gp120-specific IFNγ response was detected, when splenocytes were restimulated with gp120-derived peptide 81, which was identified as being immunodominant among 211 tested peptides comprising gp120. In addition, both T cell and non-T cell populations were activated in response to VRC_{gp120} stimulation, as evidenced by increased expression levels of surface activation markers (e.g., CD69, CD80, major histocompatibility complex II). Furthermore, both the gp120-specific IFNγ response and the magnitude of cellular activation were enhanced in cannabinoid receptor (CB) 1 and 2 knockout mice compared to wild type mice. THC further increased the above-mentioned response in wild type mice, but showed minimal to no enhanced effect in knockout. Overall, our findings suggest that THC modulates HIV antigen-specific immune responses *in vivo* in a CB1/CB2-dependent manner. (Supported by NIH DA07908)

PS 2008 Δ9 Tetrahydrocannabinol (THC) Expands and Activates Highly Immunosuppressive MDSCs via S100A8 Secretion

J. M. Sido, P. S. Nagarkatti and M. Nagarkatti. *Pathology, Immunology & Microbiology, University of South Carolina School of Medicine, Columbia, SC.*

Marijuana is a widely used drug of abuse. With the recent legalization of marijuana for recreational purpose, in two states, as well as medicinal purpose, in 21 states, understanding the impact of cannabinoids is now paramount. We focused on the mechanism by which Δ9 tetrahydrocannabinol (THC), the psychoactive ingredient found in the *Cannabis sativa* plant, causes immunosuppression. Earlier studies from our lab have demonstrated that THC induces myeloid derived suppressor cells (MDSCs) resulting in immune suppression. However, the precise mechanism of THC-mediated MDSC induction and activation is not fully understood. In this study, we determined the mechanism by which THC induces the generation and activation of a highly immunoregulatory MDSC population. We found that THC-induced MDSCs (THC-MDSCs) had significantly increased levels of suppressive function, secretion of signal transducer and activator of transcription (Stat) 3 activating cytokines, and S100A8 protein compared to naive bone marrow resident MDSCs (BM-MDSCs). THC-induced granulocytic and monocytic MDSC subsets were more suppressive than BM-MDSC subsets. Additionally, arginase1 (Arg1), a known immunoregulatory molecule, was elevated in THC-MDSCs compared to BM-MDSCs. Increased levels of IL-6 and IL-10 in THC-MDSCs correlated with elevated Stat3 activation. S100A8 is a protein which has been shown in tumor models to drive MDSC accumulation and activation, but its role in THC-mediated MDSC induction is not known. Phosphorylated Stat3 has been shown to bind the promoter region of S100A8 and increase transcription. Use of the S100A8 depletion antibody (8H150 at 20 mg/mouse) led to a 1.8 fold decrease in the accumulation of THC-MDSCs and impacted their suppressive function. Together, these data suggest a key role for S100A8 in THC-induced expansion

and activation of highly suppressive MDSCs. (Supported in part by NIH grants P01AT003961, R01-AT006888, -ES019313, -MH094755, P20RR032684 and VA Merit Award BX001357)

PS 2009 The Role of Chemical Sensitizer's Reactivity in the Generation of Reactive Species and the Activation of the Nrf2 Pathway in THP-1 Cells

S. Karaki[1], M. Pallardy[1], C. Migdal[1], M. Azoury[1], E. Gimenez-Arnaud[2], J. Lepoittevin[2] and S. Kerdine-Römer[1]. *[1]UniverSud, INSERM UMR 996, Faculté de Pharmacie, Châtenay-Malabry, France and [2]Université de Strasbourg, CNRS UMR 7177, Laboratoire de Dermatochimie, Strasbourg, France.*

Allergic contact dermatitis is generally induced by electrophilic chemicals which trigger reactive species (RS) production and provoke an electrophilic stress leading to the accumulation of the transcription factor nuclear related factor 2 (Nrf2) in dendritic cells and cell lines such as THP-1.
We investigated if a correlation exists between the reactivity of chemical sensitizers toward amino-acids and the generation of RS [reactive oxygen species (ROS) and reactive nitrogen species (RNS)], and to determine if this chemical stress induced by chemicals sensitizers participated to the accumulation of the Nrf2 protein.
This work was conducted in THP-1 cells. Production of RS was measured using the H2DCFDA probe and flow cytometry. Nrf2 accumulation was detected by western blotting.
Chemicals sensitizers-induced RS seemed to be correlated with Nrf2 protein fold induction. Our data revealed that chemicals reacting with both lysine and cysteine showed the highest potency for inducing RS compared to cysteine-only reactive chemicals or lysine-only reactive chemicals. As a model sensitizers, 2,4-dinitrochlorobenzene (DNCB) and cinnamaldehyde (CIN) induced RS production and Nrf2 accumulation. However, Nrf2 expression was inhibited only in the presence of the thiol antioxidant N-acetyl-L-cysteine (NAC), but not with a phenyl-alpha-tert-butyl-nitrone (PBN; a non-thiol antioxydant) or with the anti-oxidant vitamin E. These results suggested that thiol groups are playing a key role in DNCB- and CIN induced Nrf2 accumulation and that cellular stress provoked by RS may play a secondary role in Nrf2 activation.
Cysteine/lysine and cysteine-reactive chemicals were correlated to the RS generation. RS production by chemical sensitizers was associated with Nrf2 protein accumulation. However Nrf2 accumulation seemed to be independent from RS production.
Karaki S. & Migdal C. contributed equally to this work.

PS 2010 Protein Kinase CK2 and JNK Control Nrf2/Keap1 Activation in Response to Skin Contact Sensitizers in THP1 Cells

M. de Bourayne[1], Z. El Ali[1], O. Filhol Cochet[2], C. Cochet[2], M. Pallardy[1] and S. Kerdine-Römer[1]. *[1]INSERM URM-996, Univ Paris Sud, Châtenay-Malabry, France and [2]INSERM U1036, iRTSV, CEA, Grenoble, France.*

Dendritic cells (DC) exposure to skin contact sensitizers such as dinitrochlorobenzene (DNCB) or cinnamaldehyde (CinA) induces an up-regulation of phenotypic markers and cytokines secretion that are regulated by mitogen-activated protein kinases (MAPKs). Chemical sensitizers generate a chemical stress that is perceived by DCs as a danger signal leading to DC maturation. Nrf2/Keap1 pathway is central to detect cellular stress. In absence of electrophile or oxidative stress, Keap1 associates with Nrf2 and targets Nrf2 for proteasomal degradation. Under chemical stress, Keap1 conformation is modified, Nrf2 is released and translocates to the nucleus, acting as a transcription factor binding on antioxidant response element (ARE) in target genes promoters, such as heme oxygenase ho-1, or nadph quinone oxidoreductase nqo-1.
Since sensitizers activate both MAPKs and Nrf2 in DC, we address the question whether Nrf2 accumulation by contact sensitizers depends on MAPKs pathway, or other kinases like the protein kinase CK2.
THP1 cell line is in validation for the detection of chemicals sensitizing potential, and is used as "DC-like" model. THP1 cells were stimulated by DNCB and CinA, and use of a recombinant phosphatase highlighted that Nrf2 exists as a phosphorylated form. Moreover, pretreatment of THP1 cells with CK2 and JNK inhibitors abolished Nrf2 accumulation in response to chemical sensitizers, indicating the importance of CK2 and JNK in Nrf2/Keap1 pathway activation. Using a biotin ARE probes approach, we found both phosphorylated c-jun, the main effector of JNK, and Nrf2 bound on ARE in response to CinA and DNCB.
We are currently investigating, the importance of CK2 and JNK in DC maturation and activation in response to sensitizers.

PS 2011 Nrf2 Controls Dendritic Cells Survival in Response to Contact Sensitizers through bcl-2 and Antioxidant Genes Expression

Z. El Ali[1], C. Deloménie[2], M. Pallardy[1] and S. Kerdine-Römer[1]. *[1]INSERM URM-996, Univ. Paris Sud, Châtenay-Malabry, France and [2]IFR141-IPSIT, Univ. Paris Sud, Châtenay-Malabry, France.*

Dendritic cells (DC) are professional antigen presenting cells playing a major role in the induction of primary immune response. Contact sensitizers, such as dinitrochlorobenzene (DNCB) or cinnamaldehyde (CinA) are known to induce reactive oxygen species (ROS) production.
The Nrf2/Keap1 pathway is central for detoxification. In the absence of a chemical stress, Keap1 associates with Nrf2 and leading to its degradation. In the presence of an electrophilic compound, Keap1's conformation is modified leading to Nrf2 translocation to the nucleus and transcription of its target genes. We have demonstrated that contact sensitizers like DNCB or CinA induce Nrf2 accumulation in human DC.
To elucidate the role of Nrf2 in DC survival, nrf2 WT or KO bone marrow-derived DC (BMDC) were treated with DNCB or CinA for 24h. Results showed (1) an increase of apoptotic cells and (2) a decrease in living cells in absence of Nrf2. An increase of caspase 3/7 activity, a rapid loss of mitochondrial membrane potential ($\Delta\Psi m$) and a higher ROS production were observed in nrf2-/- DC compared to nrf2+/+ DC in response to DNCB or CinA. Our results also showed that DNCB and CinA induced the expression of the anti-apoptotic gene, bcl-2, in a Nrf2-dependent manner.
To further investigate the cytoprotective role of Nrf2 against chemical sensitizers, qPCR array of 43 genes was performed. Our results reveal that Nrf2 can upregulate catalase (cat), heme oxygenase (hmox-1), nadph quinone oxydoreducatase (nqo-1), glutathione peroxidase 1 (gpx1), glutathione reductase (gsr) and gutathion-S-transferase (gsta4, gstm1).
These results suggest that Nrf2 plays a role in cell survival and protects DC from contact sensitizers via the transcriptional activation of anti-apoptotic and antioxidant genes.

PS 2012 Nrf2 Has Differential Effects on the Early Events of Murine T Cell Activation

A. E. Turley[1, 3], J. W. Zagorski[2] and C. E. Rockwell[1, 3, 2]. *[1]Pharmacology and Toxicology, Michigan State University, East Lansing, MI, [2]Cellular and Molecular Biology, Michigan State University, East Lansing, MI and [3]Center for Integrative Toxicology, Michigan State University, East Lansing, MI.*

Nuclear factor erythroid 2-related factor 2 (Nrf2) is a widely expressed transcription factor activated by cell stress, including reactive oxygen species and electrophilic stimuli. Nrf2 regulates a battery of detoxification, antioxidant, and metabolizing enzymes necessary for a cell to respond to stressors. Nrf2 is activated by many different compounds, including environmental contaminants such as arsenic, and synthetic food preservatives such as tBHQ (tert-butylhydroquinone). There is increasing evidence that Nrf2 modulates a number of different immune responses. Nrf2 null mice develop a lupus-like autoimmune disease, and show increased susceptibility to sepsis and inflammatory injury. More recently, our laboratory has shown that Nrf2 inhibits some of the early events of human T cell activation. The purpose of the present studies was to characterize the role of Nrf2 in early events of T cell activation. The Nrf2 activator, tBHQ, inhibited production of IFNg and IL-2 by murine splenocytes activated with anti-CD3/anti-CD28. Unexpectedly, other events of early T cell activation, such as induction of CD25 and CD69, were not affected by tBHQ. To characterize this further, we investigated the effect of Nrf2 on CD25/CD69 induction at multiple time-points using a number of different T cell activators, including anti-CD3/anti-CD28, concanavalin A and PMA/ionomycin. Regardless of time-point or activator, there was consistently no effect on CD25/CD69 expression. Overall, these studies demonstrate Nrf2 has differential effects on early events of T cell activation in murine splenic T cells. (This work is supported by NIH grant ES018885).

PS 2013 Inhibition of IL-2 Production by the Nrf2 Activator, tBHQ, Correlates with Inhibition of NFκB Activation in Activated Jurkat T Cells

J. W. Zagorski[1, 3], A. E. Turley[1, 2], H. E. Dover[1, 2], K. R. VanDenBerg[1, 2], J. R. Compton[1, 2] and C. E. Rockwell[1, 2, 3]. [1]*Pharmacology and Toxicology, Michigan State University, East Lansing, MI,* [2]*Center of Integrated Toxicology, Michigan State University, East Lansing, MI and* [3]*Cellular and Molecular Biology, Michigan State University, East Lansing, MI.*

The transcription factor, nuclear factor erythroid 2-related factor 2 (Nrf2), is activated upon cellular stresses, such as the presence of reactive xenobiotics and/or oxidative stress. After activation, Nrf2 accumulates in the nucleus and induces the transcription of its target genes, including HMOX and NQO1. Numerous studies have shown that Nrf2 plays a role in inflammatory diseases, including autoimmunity. Recently, we have shown that activation of Nrf2 in CD4+ murine T cells skews differentiation toward that of a TH2 phenotype. Although shown to be immunomodulatory in mice, the role of Nrf2 in human immune cells is largely uncharacterized. Therefore, the purpose of the present studies was to determine the effects of the Nrf2 activator, tBHQ, upon the early events following human CD4+ T cell activation. Treatment of human Jurkat T cells with tBHQ markedly inhibited the production of IL-2 and moderately inhibited the expression of CD25, the high-affinity IL-2 receptor. The inhibition of IL-2 by tBHQ correlated with a decrease in the transcriptional activity of NFκB, a key transcription factor in the regulation of the IL-2 promoter. Collectively, our studies demonstrate that the Nrf2 activator, tBHQ, markedly inhibits IL-2 production in activated Jurkat T cells, which is likely due to inhibition of NFκB activation. (This work is funded by NIH grants ES018885 and GM092715).

PS 2014 Maintenance of Long-Term Self-Renewal in Hematopoietic Stem Cells by Aryl Hydrocarbon Receptor-Dependent Regulation of Reactive Oxygen Species during Fetal Development

E. Tate[1], Y. Chen[2], D. Wang[2] and M. D. Laiosa[1]. [1]*Zilber School of Public Health, UW-Milwaukee, Milwaukee, WI and* [2]*Blood Research Institute, Milwaukee, WI.*

Determining the mechanism by which in utero activation of the Aryl hydrocarbon receptor (AHR) in hematopoietic stem cells (HSC) impairs the process of self-renewal will provide insight into a spectrum of blood disorders ranging from stem cell exhaustion to leukemia. The AHR is a ligand-activated transcription factor and studies in AHR deficient mice have elucidated a role for the AHR in hematopoietic stem cell quiescence. The mechanism by which cells remain in this low proliferative state is unknown. Alterations in reactive oxygen species (ROS) have been shown to adversely impact HSC self-renewal possibly due to DNA damage. Furthermore, the ligand-activated AHR has been implicated as a modulator of cellular respiration. With this knowledge, we hypothesized that the AHR is a negative regulator of aerobic respiration in HSC, such that ligand-activation disrupts this regulation, leading to increased ROS in anaerobic cells adversely impacting long-term self-renewal. To test the hypothesis, we exposed pregnant C57Bl/6 mice to 3ug/kg of the AHR agonist 2,3,7,8 Tetrachlorodibenzo-p-dioxin (TCDD) and analyzed ROS in HSC from fetuses ranging in age from gestational day (GD) 7.5 to GD 14.5. We used fetuses because of the developmental age dependent transitions that occur in HSC respiratory activity. We found that on GD 7.5 and 11.5, there was a 50% increase in ROS production in HSC (defined as Lin-Sca+cKIT+CD150+), followed by a 30% decrease in the HSCs on GD 14.5. Furthermore, in a competitive irradiation/reconstitution assay testing long-term self-renewal function, HSC from control fetal livers out competed HSC exposed to TCDD in utero by nearly three to one after three serial bone marrow transplants. These data suggest that the AHR plays an important role in maintaining metabolic homeostasis in HSC, and that ligand activation increases oxidative stress, adversely impacting long-term self-renewal. This research was supported by NIEHS under award number R00 ES016585.

PS 2015 Impaired by TCDD of Human Hematopoietic Stem Cells to B Cell Lineage Commitment

J. Li[1, 3], A. Phadnis-Moghe[1, 3], R. Crawford[2, 3] and N. E. Kaminski[1, 2, 3]. [1]*Genetics Program, Michigan State University, East Lansing, MI,* [2]*Department of Pharmacology and Toxicology, Michigan State University, East Lansing, MI and* [3]*Center for Integrative Toxicology, Michigan State University, East Lansing, MI.*

2,3,7,8-Tetrachlorodibenzo-p-dioxin (TCDD) is a potent immunomodulator which effects a wide range of immune components and immune responses. In vitro studies have shown that human mature B cells are vulnerable to suppression by TCDD. However, the effect of TCDD on the human B cell developmental process has not previously been investigated. To address this question, an in vitro culture system was established to recapitulate human B cell development. Specifically, hematopoietic stem cells (HSC) are co-culturing with irradiated human primary bone marrow stromal cells. In three weeks of culture, we observed a downregulation of HSC marker CD34 as cells underwent development, as well as an upregulation of IL-7R, which indicated lymphoid lineage restriction. More importantly, generation of lineage-committed B cells was observed by the co-expression of B220 and CD19 in approximately 20% of the cell population. These data illustrated establishment of an in vitro model system of human B cell development from HSC. The objective of the present study was to employ this model system to investigate the effect of TCDD on B cell development. HSC were treated with TCDD (1, 10 and 30nM) and/or vehicle (0.02% DMSO). Comparing to the vehicle control, TCDD reduced cell number in a concentration-dependent manner. Apoptosis analysis using Annexin V and 7-AAD suggested the decrease of cell number was not due to cytotoxicity of TCDD. Likewise, TCDD decreased CD34 and IL-7R expression and ultimately the number of B220+CD19+ lineage-committed B cells that were generated from HSC. Together, these data for the first time suggested that TCDD altered early human B cell development. Research is supported in part by NIH ES002520 and NIH P42 004911.

PS 2016 TCDD-Aryl Hydrocarbon Receptor (AhR) Pathway-Mediated Suppression of Human B Cell Activation Involves BCL-6 in Human Primary B cells

A. Phadnis-Moghe[1, 2], R. Crawford[2, 3] and N. E. Kaminski[2, 3]. [1]*Genetics Program, Michigan State University, East Lansing, MI,* [2]*Center for Integrative Toxicology, Michigan State University, East Lansing, MI and* [3]*Dept. Of Pharmacology and Toxicology, Michigan State University, East Lansing, MI.*

Activation of B cells via CD40 receptor ligation concomitantly with signaling through cytokine receptors IL-2, IL-6 and IL-10, drives B cell proliferation and differentiation. Impaired human B cell activation hampers B cell progress towards differentiation. Environmental contaminants such as TCDD are known to markedly affect B cell activation and differentiation. Hence, the objective of the present study was to investigate the mechanism underlying suppression of human B cell activation by TCDD. BCL-6 was identified as a likely candidate owing to its role as a transcriptional repressor of B cell activation and differentiation. In the presence of TCDD, BCL-6 protein levels were elevated in human B cells. Concomitant with this TCDD-mediated increase in BCL-6 a decrease in B cell activation was evident through the attenuation of surface CD80 and CD69. In addition, it was observed that BCL-6 could repress CD80 in presence of TCDD by binding to the enhancer region of CD80. To further ascertain the role of BCL-6 in the suppression of B cell activation, the small molecule inhibitor of BCL-6 repression, 79-6, was utilized. Treatment of activated B cells with TCDD in combination with 79-6 reversed the suppression of CD80 levels and partially reversed the suppression of CD69 levels thereby providing evidence for a role by BCL-6 in regulation of B cell activation. Further, involvement of the AHR signaling pathway in BCL-6 regulation and in B cell activation was demonstrated using the AHR low affinity ligand, monochlorinated dibenzo-p-dioxin (MCDD), which had no effect on BCL-6 protein levels or on B cell activation. Collectively, these results suggest that suppression of human B cell activation, especially of CD80 occurs, in part, due to deregulation of BCL-6 by the TCDD-AHR pathway. Supported in part by NIH R01 ES002520 and P42 ES004911.

PS 2017 Developmental Activation of the AhR Enhances the CD4+ T Cell Response in the Influenza Virus-Infected Lung

L. Boule[1], B. Winans[2] and B. Lawrence[1, 2]. [1]*Microbiology and Immunology, University of Rochester Medical Center, Rochester, NY and* [2]*Environmental Medicine, University of Rochester Medical Center, Rochester, NY.*

Recent discoveries suggest that developmental exposure to certain pollutants increases the severity of respiratory infections later in life, but the mechanism by which this occurs is unknown. The aryl hydrocarbon receptor (AhR) is a ligand-regulated transcription factor that binds a broad variety of anthropogenic and naturally derived chemicals. It is expressed by immune cells, and upon activation can alter the function of the immune system. Using a mouse model, developmental exposure to the potent AhR ligand 2,3,7,8-tetrachlorodibenzo-p-dioxin (TCDD) alters the immune response to the common respiratory pathogen influenza A virus. Developmentally exposed offspring have a poorer $CD8^+$ T cell response to infection; yet, have more bronchopulmonary inflammation and an elevated number of immune cells in their lungs. We report here that, in contrast to $CD8^+$ T cells, the percentage of activated, virus-specific $CD4^+$ T cells doubles in the lungs of offspring of TCDD-treated dams. To understand if the increase in $CD4^+$ T cells in the lung is due to $CD4^+$ T cell intrinsic or extrinsic influences of developmental exposure to TCDD, we performed reciprocal adoptive transfers of naïve $CD4^+$ T

cells. We determined that the enhanced CD4+ T cell response to influenza virus infection is due to indirect effects of developmental exposure on these cells. This is the first report demonstrating that AhR activation during development alters the pulmonary CD4+ T cell response to influenza virus infection, an effect which may lead to more bronchopulmonary inflammation, contributing to increased severity of respiratory infections.

PS 2018 Suppression by 2, 3, 7, 8-Tetrachlorodibenzo-*p*-Dioxin (TCDD) of IL-2 Plus IL-21-Induced B Cell Activation

B. Avalos[1], A. Phadnis-Moghe[2, 3] and N. E. Kaminski[3, 4]. [1]*Biology, Univ. of Puerto Rico, San Juan, Puerto Rico,* [2]*Genetics, Michigan State University, East Lansing, MI,* [3]*Center for Integrative Toxicology, Michigan State University, East Lansing, MI and* [4]*Pharmacology and Toxicology, Michigan State University, East Lansing, MI.*

2,3,7,8-Tetrachlorodibenzo-*p*-dioxin (TCDD) is the most toxic compound among the group of halogenated aromatic hydrocarbons found in our environment. TCDD is known to adversely affect the adaptive immune system. Studies using rodents have shown that TCDD affects the differentiation of B cells into antibody-secreting cells. Recent work using human primary B cells has shown that B cell activation is suppressed significantly by TCDD, thereby, subsequently affecting the process of B cell differentiation. Specifically, B cells activated with CD40 ligand (CD40L) and cytokines IL-2, IL-6 and IL-10 show suppression of B cell activation markers CD80, CD86, and CD69. IL-21 is a cytokine known to enhance the proliferation of B cells, playing a vital role in their differentiation. Hence, the goal of this study was to understand the effects of TCDD on CD40L and IL-2 plus IL-21-induced human B cell activation. Flow cytometry was used to measure levels of B cell activation markers in primary human B cells activated with CD40L and cytokines in presence of TCDD. Furthermore, changes in mRNA levels of Src-homology phosphatase-1 (SHP-1), a gene known to be altered in B cell activation, were also investigated. Our results show that TCDD-treatment led to a decrease in the percent and mean fluorescence intensity of B cell activation markers CD80, CD86 and CD69 from three individual human donors. Additionally, the mRNA levels of the gene SHP-1 were increased in presence of TCDD as expected. Overall, our results show that TCDD suppresses the CD40L and IL-2 plus IL-21-induced B cell activation, which occurs independent of the cytokine-stimulation used and may involve increased SHP-1 expression. (Supported by NIH R01ES002520)

PS 2019 Evaluation of Aryl Hydrocarbon Receptor (AhR) Polymorphism G1661A on TCDD-Mediated Biological Activity in the Human B Cell

N. Kovalova[1], R. Crawford[2] and N. E. Kaminski[2]. [1]*Pharmacology and Toxicology, Michigan State University, East Lansing, MI and* [2]*Center for Integrative Toxicology, Michigan State University, East Lansing, MI.*

2,3,7,8-tetraclorodibenzo-p-dioxin (TCDD)-mediated suppression of antibody responses is dependent on the AHR, a ligand activated transcription factor belonging to the basic helix-loop-helix/PAS family. Prior studies have demonstrated that TCDD directly targets B cells to suppress antibody responses. We have also shown that human B cells exhibit similar sensitivity to TCDD-mediated suppression of the IgM response as "responsive" mouse strains, with one important exception; of the donors we have assayed, approximately 1 in 6 are refractory to suppression of the IgM response by TCDD. AHR sequencing of human "responders" and "non-responders" revealed that a number of non-responders express a G1661A AHR SNP. Therefore, we hypothesized that loss of sensitivity to TCDD-induced suppression of the IgM response is due to a G1661A polymorphism within the AHR. To test this hypothesis, the AHR null SKW 6.4 human B cell line was transduced to establish SKW-AHR+ and SKW-ΔAHR cell lines that stably express the wild type (WT) or G1661A polymorphic form of the human AHR, respectively. SKW-AHR+ and SKW-ΔAHR cells express similar levels of AHR mRNA, as determined by qRT-PCR. TCDD-induced Cyp1B1 mRNA expression levels was markedly lower in SKW-ΔAHR than in AHR+ cells, suggesting decreased transactivation potency of the G1661A AHR, compared to WT. To establish the effects of G1661A polymorphism on TCDD-induced IgM response, LPS-activated SKW cell lines were treated with increasing concentrations of TCDD and assayed for secreted IgM. IgM quantification by ELISA demonstrated comparable suppression of secreted IgM by TCDD in SKW-AHR+ and SKW-ΔAHR. Moreover, the slope of the concentration-response curves for TCDD-mediated IgM suppression for SKW-AHR+ and SKW-ΔAHR cells were similar. We conclude that the G1661A human AHR SNP alone did not attenuate TCDD-induced IgM suppression but did alter sensitivity to induction of CYP1B1. (Supported by NIH P42 ES004911 and NIH R01ES002520.)

PS 2020 Immunologic Comparison between Wild Type and Aryl Hydrocarbon Receptor (AhR$^{-/-}$) Null Rats Treated with a TCDD Dosing Regimen That Causes Hepatic Inflammation

R. Crawford[1], S. D'Ingillo[1], A. Phadnis-Moghe[1], W. Chen[1], J. Suarez-Martinez[1], J. Li[1], N. Kovalova[1], B. L. Kaplan[1], J. A. Harrill[2], R. S. Thomas[2] and N. E. Kaminski[1]. [1]*Center for Integrative Toxicology, Michigan State University, East Lansing, MI and* [2]*The Hamner Institutes for Health Sciences, Research Triangle Park, NC.*

TCDD treatment has been demonstrated to induce rat liver tumors. Recently, a mode-of-action was proposed that involves TCDD-mediated, AhR–dependent hepatic inflammation as a key event in the promotion of rat liver tumors by TCDD. To investigate the above mode-of-action, AhR$^{-/-}$ Sprague Dawley rats were established, and their immune system comprehensively characterized. The objective of the present study was to compare the immune status of AhR$^{-/-}$ rats and age matched wild type controls after administration of TCDD (0, 3, 22, 100, 300, or 1000 ng/kg/day) by oral gavage 5 days/week for 4 weeks; a dosing regimen that induces hepatic inflammation. The immunologic evaluation included enumeration and quantification of resting and activated (LPS, PWM or anti-rat CD3/28) splenic leukocyte populations. Comprehensive phenotyping of splenic leukocytes for B cells, T cell subtypes, monocyte-derived lineages, neutrophils and NK cells was conducted. TCDD produced a dose-dependent decrease in the percentage of NK and NKT cells in WT rats, with no effect on the AhR$^{-/-}$ rats at any of the TCDD doses. In contrast, AhR$^{-/-}$ rats had a higher percentage of NK and NKT cells compared to WT rats. LPS-activated WT but not AhR$^{-/-}$ splenocytes showed a marked decrease in proliferation at the two highest doses. TCDD treatment had no effect on PWM or anti-rat CD3/28 activated splenocytes from either WT or AhR$^{-/-}$ rats. Differentiation to a high IgM producer with LPS was significantly suppressed by TCDD treatment in WT at 300 and 1000 ng/kg/day but not in splenocytes from AhR$^{-/-}$ rats. In addition, the percentage of high IgM producers was significantly higher in the AhR$^{-/-}$ compared to WT. These studies suggest that the AhR plays a role in the maintenance of immune homeostasis and/or regulation. Funded by Dow Chemical Company.

PS 2021 TCDD-Induced Activation of the Human IgH hs1, 2 Enhancer Is Not Altered by Mutation of Transcription Factor Binding Sites within the Polymorphic Region

A. Snyder, S. Ochs, B. Johnson and C. E. Sulentic. *Pharmacology and Toxicology, Wright State University, Dayton, OH.*

The environmental contaminant 2,3,7,8-tetrachlorodibenzo-ρ-dioxin (TCDD) is a suppressor of immunoglobulin (Ig) expression in various animal models. This effect appears to be mediated through the aryl hydrocarbon receptor (AhR). When activated by ligand, the AhR binds to dioxin response elements (DRE) leading to altered transcriptional activity. Our previous results identified DRE sites and TCDD-induced binding of the AhR to these sites within a transcriptional regulatory region (3'IghRR) that controls Ig heavy chain expression. The 3'IghRR consists of four enhancer regions (hs3A; hs1,2; hs3B, hs4) and is sensitive to TCDD-induced inhibition, which correlates with TCDD-induced inhibition of Ig expression. In humans, the hs1,2 enhancer (hu-hs1,2) is polymorphic and has been associated with certain autoimmune diseases. We have identified TCDD-induced activation of the hu-hs1,2 enhancer and a decrease in enhancer activity with deletion of the polymorphic region. The objective of the current study was to utilize mutational analysis and luciferase reporter constructs to evaluate the contribution of each transcription factor binding site within the polymorphic region to hu-hs1,2 activity and modulation by TCDD. TCDD induced a similar fold-induction in hu-hs1,2 reporter activity regardless of which transcription factor was mutated; whereas these mutations lead to an increase in basal hs1,2 activity. Evaluation of the binding sites 5' of the polymorphic region demonstrated an increase in hs1,2 activity when the Oct site was mutated and a marked decrease in activity when the AP-1/ETS site was mutated. However, these mutations had little effect on TCDD-induced activation. These results suggest a complex interaction of proteins binding within the hu-hs1,2 enhancer and a consistent increase in hs1,2 activity by TCDD. A better understanding regarding the role of the hu-hs1,2 enhancer and how TCDD modulates its activity may lead to insights into the etiology of autoimmune disorders associated with the hs1,2 polymorphism.

PS 2022 Elucidating the Role of the Polymorphic Human hs1, 2 Enhancer in the Effects of TCDD

A. K. Freiwan, B. Johnson and C. E. Sulentic. *Wright State University, Dayton, OH.*

2,3,7,8-Tetrachlorodibenzo-p-dioxin (TCDD) is a potent environmental toxin known to inhibit immunoglobulin (Ig) gene expression in various animal studies. We have identified the mouse 3'Ig heavy chain regulatory region (3'IghRR) as a sensitive transcriptional target of TCDD, which may mediate the inhibitory effect of TCDD on Ig expression. Interestingly, the human hs1,2 enhancer is polymorphic and has been associated with a number of autoimmune diseases. Suggesting a species difference, TCDD inhibited mouse hs1,2 enhancer activation and activated basal human hs1,2 (hs-hs1,2) enhancer activity. The objective of this study was to determine the effect of stimulation and TCDD on hu-hs1,2 enhancer activity using a human B-cell line (CL-01) and luciferase reporter constructs regulated by each of the human hs1,2 alleles. Our results verity that TCDD alone activates each of the hu-hs1,2 alleles. Surprisingly, B-cell stimulation through TLR 7 and 8 by R848 inhibited basal activity of the hu-hs1,2 alleles and TCDD co-treatment reversed this inhibition. In contrast, R848 induced Ig secretion and activated a 3x NF-κB luciferase reporter, therefore confirming functional signaling through the TLRs and activation of the CL-01 B-cell line. R848 also induced class switch recombination from IgM to IgG. Furthermore, TCDD inhibited both IgM and IgG secretion in cells stimulated with R848. These results suggest that the hu-hs1,2 enhancer may be a negative regulator of 3'IghRR activity and Ig expression. Alternatively, the hs1,2 enhancer may function differently when studied in isolation as compared to its function in the intact 3'IghRR. Future studies will evaluate the effect of TCDD in the absence or presence of stimulation on the activity of the entire human 3'IghRR and its other enhancers, hs3 and hs4. Elucidating the role of the polymorphic hs1,2 enhancer in 3'IghRR activity and the effect of TCDD on the enhancers of the 3'IghRR may provide insights into the etiology of autoimmune diseases associated with the hs1,2 polymorphism. (Supported by NIEHS R01ES014676)

PS 2023 Benzo(a)pyrene Exposure Suppresses FcγRII (CD32)-IgG Antibody Complex Binding by Disruption of Lipid Raft Membrane Integrity

R. S. Clark[1], D. B. Hood[2], M. Maguire[1] and A. Ramesh[3]. [1]*Neuroscience and Pharmacology, Meharry Medical College, Nashville, TN,* [2]*Division of Environmental Health Sciences, College of Public Health and Department of Neuroscience, College of Medicine, Ohio State University, Columbus, OH and* [3]*Biochemistry and Cancer Biology, Meharry Medical College, Nashville, TN.*

The fundamental requirement in activation of macrophage effector functions is the binding of immunoglobulins to Fc receptors. The FcγRIIa (CD32) immunoreceptors have been reported to either constitutively reside in or associate with detergent resistant membranes (DRMs) upon binding to IgG, the most abundant Ab class in circulation. Previous research suggests that exposure to benzo(a)pyrene, B(a)P, an environmental toxicant, suppresses macrophage effector functions but the mechanism remains undefined. The purpose of this study was to elucidate the mechanism of B(a)P-induced suppression by examining the effects of B(a)P exposure on CD32-lipid raft interactions in the regulation of IgG binding to CD32. B(a)P exposure altered lipid raft integrity by depleting membrane cholesterol at over a 50% depletion rate (577.8 ± 204.6, $p < 0.001$). The exposures also lead to a 30% (216.2 ±, 142.7 $p < 0.05$) reduction in affinity or an exclusion of CD32 from lipid rafts. The 50% diminution in membrane cholesterol as well as the 30% exclusion of CD32 from lipid rafts caused significant suppression of CD32-mediated IgG binding by 60% (486.2 ± 166.7, $p < 0.001$) which suggests that intact lipid rafts are required for IgG complex binding to CD32. Future studies are directed at establishing whether B(a)P-induced suppression increases macrophage susceptibility to microbial infection.

PS 2024 Wear Particles Derived from Metal Hip Implants Generates Multinucleated Giant Cells in a 3-Dimensional Peripheral Tissue-Equivalent Model

D. K. Dutta[1], P. A. Potnis[1], K. Rhodes[2] and S. C. Wood[1]. [1]*CDRH/ OSEL/ DB, FDA, Silver Spring, MD and* [2]*University of Maryland, College Park, MD.* Sponsor: P. Goering.

Multinucleate giant cells (MGCs) are created by the fusion of 5 to 15 monocytes or macrophages. MGCs can be generated by hip implants at the site where the metal surface of the device is in close contact with tissue. MGCs play a critical role in the inflammatory processes associated with adverse events like aseptic loosening of the prosthetic joints and bone degeneration as observed in some patients. Upon interaction with metal wear particles, endothelial cells can upregulate bioactive molecules and pro-inflammatory cytokines that can enhance a localized immune response. However, the role of endothelial cells in the generation of MGCs has not been completely investigated. We first developed a three-dimensional peripheral tissue-equivalent model (PTE) consisting of collagen gel, with a monolayer of endothelial cells on gel surface and human peripheral blood mononuclear cells (PBMCs) on top, which mimics peripheral tissue under normal physiological conditions. The cultures were incubated for 14 days with Cobalt chromium alloy (CoCr ASTM F75, 1-5 microns) wear particles, PBMC were allowed to transit the endothelium and harvested cells were analyzed for MGC generation using propidium iodide (PI) by flow cytometry. Increase in forward scatter (cell size) and in the PI uptake (DNA intercalating dye) was used as a measure of MGCs. Our results show that endothelial cells induce generation of MGCs 4 fold higher in 3-dimentional PTE system as compared to traditional 2-dimensional culture plates. Furthermore, we also checked whether increase in particle to cell ratio affects MGC generation. We found that increase in dose of particle to cell ratio decreases MGC generation compared to control, indicating that cells underwent apoptosis or necrosis with higher particle concentration. In sum, we have established a robust and relevant model to follow MGCs formation using flow cytometry. We observed a consistent generation of metal wear particle-induced MGCs which herald MoM hip failure.

PS 2025 Dermal Exposure to Triclosan Induces Changes in Expression of Innate and Adaptive Immune Genes in a Mouse Model

S. Anderson, N. B. Marshall, C. M. Long, K. L. Anderson, E. Lukomska and B. J. Meade. *NIOSH, Morgantown, WV.*

Triclosan has had widespread use in the general population as an antimicrobial agent and is commonly found in consumer products such as soaps, deodorants, toothpastes, shaving creams, mouth washes, and cleaning supplies. Triclosan has recently attracted the attention of the scientific community, regulatory agencies and the general public because of its high production volume, widespread applications and reports of endocrine-disrupting effects. A positive association between urinary levels of triclosan and diagnosis of allergies, hay fever, and sensitization to aeroallergens and foods has been identified. While not generally considered to be a sensitizing chemical, work by our group has recently shown that dermal exposure to triclosan at concentrations similar to those in consumer products augmented the allergic response to a known allergen in a mouse asthma model. However, the specific mechanism of this augmentation has yet to be elucidated. These studies were conducted to investigate the mechanism responsible for the augmented allergic response following dermal triclosan exposure. BALB/c mice were exposed dermally on the ears to concentrations of triclosan ranging from 0.75-3% (0.375-1.5mg/mouse/day) for up to 9 consecutive days. Expression of immune genes in the ears and lymph nodes of mice following exposure was analyzed using quantitative polymerase chain reaction. Robust thymic stromal lymphopoietin (TSLP), IL-1 beta, TNF-alpha increases and modest CCL22 & IL-22 dose responsive increases in gene expression were observed in the ears. In the lymph node draining the exposure site, dose responsive increases in CCL22 & IL-4 and decreases in T-bet, IFN-gamma, TNF-alpha & IL-1beta gene expression were observed. A decrease in expression of RORgammat was observed in both the ear and lymph nodes following exposure to 3% triclosan. These results suggest that triclosan may augment allergic responses by modulating both innate and adaptive genes.

PS 2026 The α7 Nicotinic Acetylcholine Receptor Agonist GTS-21 Improves Bacterial Clearance in Mice by Restoring Hyperoxia-Compromised Macrophage Function

R. A. Sitapara[1], L. K. Sharma[1], V. S. Patel[1], C. R. Ashby[1], S. Gorasiya[1], M. Zur[1] and L. Mantell[1, 2]. [1]*Department of Pharmaceutical Sciences, St. John's University, Queens, NY and* [2]*The Feinstein Institute for Medical Research, North Shore-LIJ Health System, Manhasset, NY.*

Mechanical ventilation with supraphysiological concentrations of oxygen (hyperoxia) is routinely used to treat patients with respiratory distress. However, prolonged exposure to hyperoxia compromises macrophages' ability to phagocytose and clear bacteria. Previously, we have shown that hyperoxia induced the release of nuclear protein, high mobility group box-1 (HMGB1), into both the airways of hyperoxia-exposed mice and the extracellular milieu of cultured macrophages. Extracellular HMGB1 can impair macrophage phagocytosis and increase mortality of mice infected with *Pseudomonas aeruginosa* (PA). GTS-21, an α7nAChR agonist, can inhibit endotoxin-induced HMGB1 release. The aim of this study was to determine whether GTS-21 can inhibit hyperoxia-induced HMGB1 release into the extracellular milieu, enhance macrophage function, and improve bacterial clearance in mice under hyperoxic conditions. GTS-21 (0.04, 0.4, and 4 mg/kg)

was systemically administered to mice that were exposed to hyperoxia (≥99% O_2) and subsequently challenged with PA. We found that 4 mg/kg of GTS-21 significantly increased bacterial clearance, decreased acute lung injury and accumulation of airway HMGB1. To investigate the cellular mechanism of these observations, RAW 264.7 cells, a macrophage-like cell line, were incubated with different concentrations of GTS-21 prior to exposure to 95% O_2. We found that GTS-21, at 5, 25, and 50 μM, inhibited HMGB1 release and significantly enhanced macrophage phagocytic activity. Together these results indicate that GTS-21 is effective in inhibiting hyperoxia-induced HMGB1 release, enhancing macrophage function, and improving bacterial clearance under hyperoxic conditions. Therefore, the α7nAChR represents a possible pharmacological target to improve the clinical outcome of patients on ventilators by augmenting host defense against bacterial infections.

PS 2027 Regulation of Epithelial B Cell Activating Factor by Ribosomal Insults

K. Do[1], D. Kim[2] and Y. Moon[1]. [1]*Deaprtment of Microbiology and Immunology, Pusan National University School of Medicine and Immunoregulatory Therapeutics Group in Brain Busan 21 Project, Yangsan, Republic of Korea and* [2]*National Institute of Animal Science, RDA, Suwon, Republic of Korea.*

Although the activation of B cells in the gastrointestinal tract is of great importance in the context of immunity to pathogens and mucosal inflammatory diseases, little is known about the mechanisms responsible for the local activation of B cells in the subepithelial area of the intestine. Epithelium-derived BAFF is the major modulator of B cell development and Ig class switching. The present study was performed to address the molecular mechanism of BAFF expression in gut epithelial cells in the presence of proinflammatory stimuli. Inflammation-induced BAFF expression in mucosal epithelial cells might be responsible for diverse mucosa-associated diseases linked to intestinal inflammation and autoimmunity. Although BAFF was marginally expressed in unstimulated epithelial cells, BAFF mRNA was significantly upregulated by proinflammatory IFN-γ. Furthermore, IFN-γ triggered JAK/STAT1 signals via the cytokine receptor, which contributed to epithelial BAFF upregulation. In terms of signaling intervention, ribosomal insult attenuated IFN-γ-activated JAK/STAT signal transduction and subsequent BAFF induction in gut epithelial cells. Ribosomal insults led to the superinduction of SOCS3 by enhancing its mRNA stability via HuR RNA-binding protein. Upregulated SOCS3 then contributed to the blocking of the JAK/STAT-linked signal, which mediated BAFF suppression by ribosomal stress. All of these findings show that ribosomal stress-induced SOCS3 plays a novel regulatory role in epithelial BAFF production, suggesting that epithelial ribosomal dysfunction in association with SOCS3 may be a promising therapeutic point in BAFF-associated human mucosal diseases. (This work was carried out with the support of "Cooperative Research Program for Agriculture Science & Technology Development (Project No. PJ008405032012)" Rural Development Administration, Republic of Korea).

PS 2028 NKG2D-RAE-1 Mediates the Interaction between Intestinal Epithelial Cells and Intraepithelial Lymphocytes in Food Allergy

R. Pieters[1], L. Kruijsen[1], C. Giannakou[1], L. Boon[2], J. Smit[1] and M. Bol-Schoenmakers[1]. [1]*Institute for Risk Assessment Sciences, Immunotoxicology, and Immunology Division, Utrecht University, Utrecht, Netherlands and* [2]*Bioceros Inc, Utrecht, Netherlands.*

Responses to ingested food proteins in the gut usually result in oral tolerance. Failure in oral tolerance induction may cause allergic sensitization, but the mechanism behind this is not yet fully understood. Previously, we found that allergic sensitization in a mouse peanut allergy model to peanut (PE) plus cholera toxin (CT) resulted in decreased numbers of gut intraepithelial lymphocytes (IEL, including gammadelta T cells) and that specific triggering of gammadelta T cells increased the allergic response. We therefore hypothesize that food allergies may be critically regulated by IEL responding to intestinal epithelial stress. Since clearance of stressed cells involves ligation of Natural Killer Group 2 Member D (NKG2D) on IEL and NK cells, we aimed to investigate the involvement of NKG2D on IEL during allergic sensitization.
Sensitization of C57BL/6 mice via intragastric treatment with PE plus CT resulted in increased NKG2D expression on IEL. Furthermore, duodenum and ileum showed increased mRNA levels for the NKG2D ligand RAE-1, and for the Th2-skewing cytokine IL-33. In addition, when mice were treated with anti-NKG2D blocking antibody during intragastric sensitization, levels of PE-specific IgG1 and IgE were significantly enhanced.
The present results point towards involvement of epithelial cell perturbations and subsequent NKG2D-RAE-1-mediated response by IEL in allergic sensitization. Together, these data demonstrate the potential involvement of intestinal stress, e.g. by luminal contents such as food constituents, pharmaceuticals or microbial components, in allergic sensitization.

PS 2029 Oxycyte®, a Perfluorocarbon (PFC) Emulsion, and Its Effects on Immunocompetence

S. Anderson[1], V. J. Johnson[2], G. Burleson[2] and T. Bradshaw[1]. [1]*Oxygen Biotherapeutics Inc, Morrisville, NC and* [2]*Burleson Research Technologies, Inc., Morrisville, NC.*

Oxycyte, a 60% w/v perfluoro(t-butylcyclohexane) intravenous emulsion, is being developed for the treatment of traumatic brain injury (TBI). PFC emulsions are cleared from circulation via the mononuclear phagocyte system (MPS), namely macrophages, monocytes, and neutrophils. Thus there is concern that PFCs may have a negative impact on immunocompetence. We evaluated Oxycyte's effect on viral and bacterial clearance in host resistance models and on *ex vivo* macrophage function. BALB/c mice received saline, Oxycyte (3, 6, or 12 mL/kg) or an immunomodulatory control followed an hour later by infection with influenza virus (~4 x 10^4 PFU), *Streptococcus pneumoniae* (~1 x 10^7 CFU/mouse) or *Listeria monocytogenes* (~1 x 10^3 CFU/mouse). Influenza viral titers and influenza-specific IgM and IgG were assessed in lung homogenates. Lung or spleen and liver homogenates were assessed for *S. pneumonia* and *L. monocytogenes* titers, respectively. *Ex vivo* macrophage phagocytosis was assessed 7 days following Oxycyte treatment. Oxycyte caused a slight stimulation of the T-dependent antibody response (TDAR) to influenza (increased antibody). The rate and efficiency of viral clearance was no different for the Oxycyte treatment groups than the controls with influenza viral load reduced by ~4 logs by Day 6 and completely cleared by Day 8. Saline and all Oxycyte treatment groups achieved ~5 log reduction in *S. pneumoniae* within 24 hours of infection. Treatment of mice with Oxycyte resulted in 80-100% mortality by Day 4 following *L. monocytogenes* infection. Oxycyte dose-dependently increased *ex vivo* splenic macrophage phagocytosis 7 days after *in vivo* administration. Overall, these studies demonstrate that treatment of mice with Oxycyte did not impact the efficient clearance of either Influenza virus or *S. pneumoniae* at any dose level. However, Oxycyte decreased the ability of mice to defend against systemic *L. monocytogenes* infection.

PS 2030 Leptin Mediated CD57 Expression on CD8+ve Cytotoxic T Cells Are Crucial for Toxicity-Induced Nonalcoholic Steatohepatitis

R. K. Seth[1], S. Das[1], A. Kumar[2], A. Chanda[1], M. B. Kadiiska[2], G. Michelotti[3], J. E. Manautou[4], A. Diehl[3] and S. Chatterjee[1]. [1]*Environmental Health Sciences, University of South Carolina, Columbia, SC,* [2]*Free Radical Metabolism Group, Institute of Environmental Health Sciences, Research Triangle Park, NC,* [3]*Division of Gastroenterology, Duke University, Durham, NC and* [4]*Pharmaceutical Sciences, University of Connecticut, Storrs, CT.*

Environmental toxins induce a novel CYP2E1/leptin signaling axis in liver. This in turn activates a poorly characterized innate immune response that contributes to nonalcoholic steatohepatitis (NASH) progression. To identify the relevant subsets of T-lymphocytes in CYP2E1-dependent, environment-linked NASH, we utilized a model of diet induced obese (DIO) mice that are chronically exposed to bromodichloromethane (BDCM). Mice deficient in CYP2E1, leptin (ob/ob mice), or both T and B cells (Pfp/Rag2 double knockout (KO) mice) were used to delineate the role of each of these factors in metabolic oxidative stress-induced T cell activation. Results revealed that elevated levels of lipid peroxidation, tyrosyl radical formation, mitochondrial tyrosine nitration and hepatic leptin as a consequence of metabolic oxidative stress caused increased levels of hepatic CD57, a marker of peripheral blood lymphocytes including NKT cells. CD8+CD57+ cytotoxic T cells but not CD4+CD57+ cells were significantly decreased in mice lacking CYP2E1 and leptin. There was a significant increase in the levels of T cell cytokines IL-2, IL-1β, IFN-γ in BDCM exposed DIO mice but not in mice that lacked CYP2E1, leptin or T and B cells. Apoptosis as evidenced by TUNEL assay and levels of cleaved caspase-3 was significantly lower in leptin and Pfp/Rag2 KO mice and highly correlated with protection from NASH. The results described above suggest that higher levels of oxidative stress-induced leptin mediated CD8+CD57+ T cells play an important role in the development of NASH. It also provides a novel insight of immune dysregulation and may be a key biomarker in NASH.

PS 2031 Automated High Content Imaging of NF-κB Signaling Modulation in Drug-Induced Liver Injury (DILI)

S. Huppelschoten, B. Herpers, L. Fredriksson, S. Wink, K. Yan and B. van de Water. *LACDR, Toxicology, Leiden University, Leiden, Zuid-Holland, Netherlands.*

Drug-Induced Liver Injury (DILI) is the most important reason to withdraw initially approved drugs from the market, to stop the development of novel drugs during the clinical test phase and for failure of FDA approval. Currently, the very heterogenic group of chemicals inducing idiosyncratic DILI cannot be predicted in vitro, in vivo or even in clinical trials. This illustrates the necessity of a better understanding of underlying mechanisms. DILI parent compounds or metabolites induce cellular stress, which can ultimately lead to cell death. Drug exposure combined with pro-inflammatory cytokine stimulation does synergistically increase apoptosis, which indicates that cytokine signalling plays an important role in the development of idiosyncratic DILI. The major pro-inflammatory cytokines in the liver activate NF-κB, a transcription factor regulating immune reactions, cell growth and death. To gather more insight in the activation of NF-κB and its importance in DILI, we have generated HepG2 Bacterial Artificial Chromosome (BAC) GFP-based reporter cell lines of the most important players in the NF-κB signalling cascade. We established and carefully characterized GFP-BAC cell lines of IκBα, RelA and Icam1 and determined the effect of DILI-inducing compounds on pro-inflammatory cytokine signalling by live confocal microscopy. The time-resolved dynamics of the expression and/or localization of these genes was determined at a single cell level at different cytokine and DILI compound concentrations. A large panel of DILI compounds affected the kinetics of IκBα degradation, RelA nuclear translocation and Icam1 expression induced by either TNFα or IL1β. For various compounds this was directly associated with enhanced cytotoxicity of combined DILI/cytokine exposure. We propose that our novel high content imaging approach would be an effective means to pin-point DILI hazard for novel drug candidates.

PS 2032 Effect of 1-Bromopropane on Expression of IL-4 and IL-5 and Secretion of β-Hexosaminidase by Calcium Influx in RBL-2H3 Cells

H. Han[1], H. Kim[1], K. Lee[2], T. Jeong[3] and H. Jeong[1]. *[1]Pharmacy, Chungnam National University, Daejeon, Republic of Korea, [2]College of Pharmacy, Chonnam National University, Gwangju, Republic of Korea and [3]College of Pharmacy, Yeungnam University, Gyeongsan, Republic of Korea.*

1-Bromopropane (1-BP) is an alternative to ozone-depleting chlorofluorocarbons that has a variety of potential applications as a degreasing agent for metals and electronics, coating agent and as a solvent vehicle for spray adhesives in the workplace. Although 1-BP has been recently reported to generate neurotoxicity, reproductive toxicity, hepatotoxicity, and immunotoxicity in rodents and human, there is little information about the effect of 1-BP on the mast cell degranulation and allergic responses. This study investigated the effect of 1-BP on degranulation and inflammatory mediator production in RBL-2H3 cells. 1-BP significantly increased release of beta-hexosaminidase and histamine in mast cells. 1-BP also increased the production and mRNA expression of pro-inflammatory cytokines such as IL-4 and IL-5. In addition, 1-BP increased IL-4 promoter and NF-AT-driven luciferase activity. Furthermore, 1-BP increased phosphorylation of Ca2+/calmodulin-dependent kinase (CaMKIIalpha), PKCdelta, Akt and MAP kinase. 1-BP increased influx of extracellular Ca2+ in RBL-2H3 cells. 1-BP induced release of beta-hexosaminidase and inhibited by treatment with a p38 inhibitor (SB203580), an ERK inhibitor (PD98059), a JNK inhibitor (SP600125), and a Calcium inhibitor (W7). These results demonstrated that 1-BP enhances mast cell-derived allergic inflammatory reactions by inducing beta-hexosaminidase and histamine release and pro-inflammatory cytokine expression via extracellular calcium influx.

PS 2033 Renal Dendritic Cells Attenuate Cisplatin Neprotoxicity Independent of Neutrophil Regulation

R. K. Tadagavadi, G. Guofeng, W. Wang and W. Reeves. *Department of Medicine, Pennsylvania State University College of Medicine, Hershey, PA.*

Cancer chemotherapy can produce sterile inflammation with associated tissue injury and organ dysfunction. Cisplatin is a very effective chemotherapeutic agent used against a wide range of solid tumors. Major adverse effects of cisplatin therapy are immunotoxicity and acute kidney injury. Neutrophils are reported to infiltrate and exacerbate injury in a wide range of sterile inflammatory models of tissue injury. Here, we studied the kinetics of neutrophil infiltration into kidneys and their role in cisplatin-mediated kidney injury. Mice treated with cisplatin showed a marked decrease in total blood leukocytes but a 5-fold elevation in neutrophils at 72 hrs after cisplatin treatment. In kidneys, cisplatin treatment caused a 2 fold increase in total kidney leukocytes as early as 24 hrs after cisplatin treatment. Renal infiltration of myeloid cells in cisplatin treated mice was prominent; monocytes and neutrophils were elevated by 10 fold as compared to saline treated mice. We depleted neutrophils using a neutrophil-specific antibody (clone 1A8) to examine the functional relevance of infiltrating neutrophils in cisplatin nephrotoxicity. This antibody resulted in greater than 90% depletion of neutrophils. Of note, depletion of neutrophils had no impact on the extent of cisplatin-induced kidney injury or renal dysfunction as compared to non-depleted mice. Earlier, we reported that dendritic cell depletion in CD11c-DTR mice causes exacerbation of kidney injury and a dramatic increase in renal neutrophils as early as 24 hrs after cisplatin treatment. Thus, we also examined the role of neutrophils in dendritic cell depleted mice treated with cisplatin. Dendritic cell depletion resulted in worse renal dysfunction in spite of neutrophil depletion, suggesting that dendritic cell mediated protection occurs independent of its effects on neutrophils. These data demonstrate that cisplatin nephrotoxicity is independent of neutrophil-mediated inflammation and dendritic cells protect kidneys via neutrophil-independent mechanisms.

PS 2034 Entecavir: Chemokine Receptor 2 (CCR2)-Mediated Chemotaxis As a Mode of Action for Mouse-Specific Pulmonary Macrophage Accumulation

G. L. Gong[1], J. Pang[2], Q. Zhao[2], E. Janovitz[1] and L. D. Lehman-McKeeman[1]. *[1]Discovery Toxicology, Bristol-Myers Squibb, Princeton, NJ and [2]Disc Biology Immunology, Bristol-Myers Squibb, Princeton, NJ.*

Entecavir (ETV; Baraclude®) is a marketed guanosine nucleoside analog that inhibits hepatitis B viral replication. In preclinical studies, ETV caused lung toxicity in mice but not in rats, dogs or monkeys. Microscopically, lungs from ETV-treated mice (10 mg/kg; 1 mo) showed alveolar septal thickening and accumulation of macrophages, and bronchoalveolar lavage analysis revealed a 3-fold increase in alveolar macrophages, with no effects on other inflammatory cells. CCR2 null mice were resistant to ETV-induced macrophage accumulation suggesting a role for this receptor in the ensuing pulmonary toxicity. To further evaluate the role of CCR2 in macrophage accumulation, ETV was evaluated for chemotactic activity in mouse and human monocytic cell lines. Although weaker than monocyte chemotactic protein-1 (MCP1; optimum concentration <10 nM), ETV was a chemotaxin in mouse WEHI 274.1 cells with maximum chemotaxis observed 75 nM. In contrast, ETV was not chemotactic in human THP-1 cells at concentrations up to 6 μM. ETV also exhibited chemotactic activity in mouse peripheral blood mononuclear cells (PBMCs) with an optimal concentration of 222 nM, but showed no activity in PBMCs from CCR2 null mice. To further test species differences in chemotaxis, the effect of ETV in PBMCs from rats and humans was studied. ETV showed weak chemotaxis for PBMCs isolated from Sprague-Dawley rats, with optimal chemotactic activity at 2 μM. In contrast, no chemotactic activity was observed in human PBMCs at ≤ 6 μM. These results indicate that ETV-induced pulmonary macrophage accumulation and lung toxicity is dependent on CCR2-mediated monocyte chemotaxis. As the chemotactic activity was specific for mice, lung toxicity was not predicted as a potential liability of ETV therapy.

PS 2035 Differential Infiltration of Macrophages into the Testis after Mono (2-Ethylhexyl) Phthalate Exposure in F344 Rats and C57B6/J Mice

A. Stermer, C. Murphy and J. H. Richburg. *Pharmacology and Toxicology, University of Texas at Austin, Austin, TX.*

Different strains and species of animals are used for both toxicological studies and basic research. Often general similarities in toxicity between animals exist, but sensitivities and specific mechanisms of toxicity can vary. Phthalates, ubiquitously used plasticizers, are known Sertoli cell toxicants. Mono (2-ethylhexyl) phthalate (MEHP) induced testicular injury has been studied in rats and mice, where inflammatory signaling has been shown to mediate germ cell apoptosis in the common MEHP mechanism. Yet, rats have been shown to have 30 fold lower LOAEL than mice. To further define this difference we analyzed germ cell apoptosis and immune infiltration into the testis of F344 rats and C57B6/J mice. MEHP (1g/kg, gavage) or equivalent volume vehicle was given to 28-day (d) rats and mice. Testes were collected 12, 24, and 48 hours (h) after exposure. Single cell suspensions were isolated from the interstitum of one testis, reacted with anti-CD11b (monocytes, macrophages, neutrophils) and quantified through flow cytometry. Germ cell apoptosis was measured by TUNEL. Rats showed peak number of CD11b+ cells 12h after exposure compared to controls. Over time (24 and 48h) the number of cells after exposure remitted, but remained significantly higher than controls. The CD11b+ cells were identified as newly arrived macrophages through CD68 immunohistochemistry. Mice showed a higher control number of CD11b+ cells compared to rats, but no differences between treatments existed. Peak apoptosis, at 24h in both species, was greater in rats than in mice (98% and 23% TUNEL pos-

itive tubules, respectively). Immunofluorescence showed localization of monocyte chemoattractant protein-1 (MCP-1) in the peritubular myoid cells in the rat, but none in the mouse. Rat expression of MCP-1 was significantly increased 12h after MEHP treatment, as determined by ELISA. These findings show that macrophage infiltration precedes and correlates with increased apoptosis, suggesting species dependent exacerbation of germ cell apoptosis after MEHP exposure.

PS 2036 Methylenediphenyl Diisocyanate Binds Membrane and Intracellular Proteins of Intact THP-1 Cells

M. Mhike[1, 2], J. M. Hettick[2], B. F. Law[2], T. A. Bledsoe[2], I. Chipinda[2], A. R. Lemons[2], B. J. Green[2], A. P. Nayak[2], R. Simoyi[1], D. Beezhold[2] and P. D. Siegel[2]. *[1]Chemistry, Portland State University, Portland, OR and [2]Allergy and Clinical Immunology Division, Centers for Disease Control, Morgantown, WV.*

Diisocyanates (dNCO) are used in the production of polyurethane products and can cause occupational asthma. Although dNCO asthma displays the same pathological hallmarks as other allergic asthmas, dNCO-specific IgE can only be detected within a small subset of dNCO asthmatics. Because of this low prevalence, we propose that methylenediphenyl diisocyanate (MDI) may adduct to cell membrane and intracellular proteins, contributing to the development of non-IgE asthma. In this study, human monocytic leukemia (THP-1) cells were exposed to varying concentrations of MDI. After exposure, cells were processed into soluble and membrane fractions, dialyzed, and analyzed for extent of MDI protein binding, following acid hydrolysis, by quantification of the MDI hydrolysis product, methylenedianiline (MDA). Proteins were electrophoresed on sodium dodecyl sulfate polyacrylamide gels and protein bands were excised, hydrolyzed and analyzed for MDA. Proteins from the bands were identified using proteomic mass spectrometry. Protein bound MDI was detected in a dose-dependent manner and quantified from the membrane and soluble fractions of MDI exposed THP-1 cells. Eleven bands from the soluble fraction and 2 bands from the membrane fraction were identified as containing MDI bound proteins. The extent of MDI intracellular protein binding was not affected by cytochalasin D, a chemical which binds actin filaments and inhibits active uptake into cells. Proteins identified in the soluble fraction were all of intracellular origin suggesting that reactive MDI can cross the cell membrane and subsequently haptenate intracellular proteins. The results of the present study support the potential involvement of dNCO haptenated membrane and intracellular proteins in development of asthma.

PS 2037 Biodistribution of Reolysin® (Pelareorep) in Sprague-Dawley Rats to Support the Use of This Orphan Virus As an Investigational Drug for Cancer Treatment

A. Parenteau[2], R. Chakrabarty[1], H. Tran[1], A. Hagerman[1], S. Serl[1], B. Thompson[1], M. Coffey[1], R. Tavcar[2], I. Boulay[2], M. Bigras[2] and R. Forster[3]. *[1]Oncolytics Biotech Inc., Calgary, AB, Canada, [2]CiToxLAB North America, Laval, QC, Canada and [3]CiToxLAB France, Evreux, France.*

Reolysin® (pelareorep) is a clinical formulation of the human Reovirus Type 3 Dearing strain. The clinical safety and efficacy of Reolysin® as an oncolytic therapy in humans is being tested on an assortment of cancer indications as a mono and/or combination therapy. Reovirus has many inherent characteristics that make it a potential candidate for virotherapy, including: the rapid and natural spread through the haematogenous route, the ability to overcome immunological barriers thereby reaching tumor sites, and being replication-competent. The purpose of this study was to elucidate the bio-distribution pattern of Reolysin® in healthy Sprague-Dawley rats. Following a single 15-minute intravenous infusion (at dose levels of 6.5E+07, 6.5E+08 and 6.5E+09 viral particles/animal, based on an average body weight of 225 grams) via the tail vein in Sprague-Dawley rats, the levels of virus genome were determined in 16 organs/tissues by RT-qPCR (Reverse Transcriptase-Quantitative Polymerase Chain Reaction) over a 336 hr follow-up period. Maximal reovirus RNA levels were observed in the spleen, indicating its involvement in viral uptake and clearance, followed by heart, ovaries, tail (infusion site), liver and lungs. All the organs/tissues demonstrated unquantifiable levels of reovirus genome at the end of the follow-up period, suggesting substantial to complete viral clearance. Several studies in the last decade have described the use of reovirus for treating ovarian cancers. An increase of reovirus genome in ovaries at 24 hr post infection was noted. The results will aid in the design of additional exploratory clinical trials for Reolysin®.

PS 2038 Multi-Endpoint Assessment of Bone Marrow Toxicity in Sprague-Dawley Rats

J. Piccotti, K. Ghoreishi, L. Alvarado, R. Magpantay, S. Couto and M. Breider. *Exploratory Toxicology, Celgene Corporation, San Diego, CA.*

Bone marrow toxicity is often an unwanted side effect of kinase inhibitors. We previously demonstrated bone marrow hypocellularity in rats dosed with CC0485118, a small molecule kinase inhibitor of spleen tyrosine kinase (Syk) and Janus kinase-2 (Jak-2). The current study was conducted to further characterize the bone marrow toxicity caused by CC0485118 using a recently developed bone marrow flow cytometry assay. In this study, male Sprague-Dawley rats received once daily oral (gavage) doses of CC0485118 at 25, 50 and 200 mg/kg for 7 consecutive days. CD71+ cells and CD11b/c+ cells were measured by flow cytometry in femurs of vehicle- and test article-treated rats approximately 24 hours after the last dose to assess compound effects on the erythroid and myeloid lineages, respectively. Bone marrow toxicity also was assessed by measuring peripheral blood reticulocyte counts and by histopathologic examination of the sternum. Treatment of rats with CC0485118 at 200 mg/kg resulted in a moderate reduction in total nucleated cells (TNC) in the bone marrow, compared to vehicle control rats. This finding was confirmed by moderate to marked bone marrow hypocellularity observed microscopically and was consistent with a moderate drop in reticulocytes. The relative percentages of CD11b/c+ myeloid cells were mildly increased in rats dosed at 200 mg/kg. However, a mild to moderate reduction in the absolute numbers of both CD71+ erythroid cells and CD11b/c+ myeloid cells were observed in these animals, resulting in no change in the myeloid to erythroid ratios (M:E) compared to controls. Thus, the flow cytometry data demonstrated toxicity to both the erythroid and myeloid lineages by CC0485118. The results of this study demonstrated that measuring CD71+ and CD11b/c+ cells in rat bone marrow can be used to complement histopathologic examination by assessing compound effects on the myeloid and erythroid lineages. Future studies will further test the sensitivity and predictability of this assay by using compounds that differentially target myeloid or erythroid cells.

PS 2039 Cysteine Microenvironment Determines Nitrosylation Status: Lessons from Proteome Analysis of NOS2 and GSNOR Knockout Mice

C. B. Massa[1], P. T. Doulias[2], H. Ischiropoulos[2] and A. Gow[1]. *[1]Toxicology, Rutgers, Piscataway, NJ and [2]Pediatrics, University of Pennsylvania, Philadelphia, PA.*

S-nitrosylation of cysteine residues to form a nitrosothiol (SNO) is a key mechanism in regulating the pathophysiological response to NO production. The subset of cysteine residues that form SNO upon NO exposure is small presumably determined by the chemistry of nitrosylation. We propose that loss of inducible nitric oxide synthase (NOS2) will reduce the number of SNO proteins, while loss of the SNO degrading enzyme S-nitrosoglutathione reductase (GSNOR) will produce additional SNO proteins through transnitrosation. SNO proteins were isolated from lungs of wild-type C57Bl6/J, GSNOR-/- and NOS2-/- mice (3/genotype) using mercury-resin capture. Lungs were perfused and stored at -80 C before homogenization in HEPES (pH 7.4) with DTPA and protease inhibitors in amber glass vials. Detection and validation of SNO sites was performed using the mass spectrometry approach of Doulias et. al. Briefly, free thiols were blocked by alkylation, then samples underwent UV photolysis to cleave the S-N bond of SNO. Denitrosylated thiols were captured by incubation on organo-mercury resin and trypsin digested on-column. Bound peptides were eluted with performic acid, and sequenced using tandem LC/MS/MS and SEQUEST protein identification. In WT lung 297 SNO sites were detected. As predicted, NOS2 loss reduced the SNO protein number to 88, with all SNOs observed in the WT mouse. In the GSNOR-/- mouse 89 SNO residues were identified, with 47 not seen in WT mice. Distributions of SNO hydropathy estimates from adjacent amino acids were compared between genotype by Kruskal-Wallis. While loss of NOS2 did not alter the hydropathy distribution vs. WT mice, GSNOR-/- has selective loss of hydrophobic SNOs. Primary sequences were analyzed to assess how local amino acid composition impacts SNO formation. GSNOR loss altered abundance of specific residues and residue classes (charged, polar and hydrophobic) relative to WT mouse, supporting a role for thiol microenvironment in determining selectivity.

PS 2040 Assessment of Sensitization Potential of Textile Dyes Using a Nonradioactive Local Lymph Node Assay and an *In Vitro* Loose-Fit Coculture-Based Sensitization Assay

V. Ahuja[1], A. Sonnenburg[2], S. Sharma[1] and R. Stahlmann[2]. [1]*Drug Safety Assessment, Novel Drug Discovery & Development, Lupin Ltd. (Research Park), Pune, India and* [2]*Institute of Clinical Pharmacology and Toxicology, Charité-Universitätsmedizin Berlin, Berlin, Germany.*

Contact dermatitis is one of the most common skin diseases, with a great socio-economic impact. Disperse dyes, which are suitable for dyeing synthetic fibers, are responsible for the great majority of allergic contact dermatitis cases to textile dyes. The aim of the present study was to study the sensitization potential of textile dyes using a non-radioactive biphasic murine local lymph node assay (LLNA) and an *in vitro* Loose-fit Co-culture based Sensitization assay (LCSA). In biphasic LLNA, female BALB/c mice were shaved over a surface of approximately 2 cm square on back and treated with various concentrations of textile dyes. The 'sensitization' treatment included application of 50 µl of test substance on the back daily on days 1-3 followed by 'challenge' treatment on days 15-17 with application of 25 µl of test substance on the dorsum of both ears. End-points on day 19 following deep carbon-di-oxide anesthesia included thickness and weight of an ear biopsy, lymph node weight, lymph node cell count and the proportion of various lymphocyte subpopulations. The LCSA involved single layer of human non-differentiating keratinocytes and of allogenic floating monocytes which are cocultured in serum-free medium in the presence of a cytokine cocktail. The coculture develops into a system consisting of activated keratinocytes and dendritic cell-related cells. The half-maximal increase in CD86 expression on the dendritic cell-like cells (EC50 values) was used to compare the sensitizing potential of tested substances. The results showed the usefulness of the modified biphasic LLNA to study sensitization potential of textile dyes. The results from LCSA correlated well with data derived from the modified version of LLNA and human data. The LCSA represented a suitable test system to simultaneously analyze irritative and sensitizing properties of chemicals altogether.

PS 2040a Influence of Nickel Rich $PM_{2.5}$ Exposure on MAPKs and NF-κB Signaling and Inflammatory Cytokines

B. A. Narayanan[1], J. Blum[1], D. Tian[1], N. K. Narayanan[1], J. T. Zelikoff[1], J. Niu[2], Q. Qu[1], M. Costa[1] and L. Chen[1]. [1]*Environmental Medicine, NYU School of Medicine, New York City, NY and* [2]*Public Health, Lanzhou University, Gansu, Gansu, China.*

Fine ambient particulate matter ($PM_{2.5}$) exposure is associated with adverse health effects due to, in part, its oxidative stress and proinflammatory potentials. However, the impact of specific major components of airborne PM on human health and the mechanisms involved remain unclear. Previously, we showed that $PM_{2.5}$ induces oxidative stress and inflammation in residents of two Chinese cities, Jinchang (JC) and Zhangye (ZH). $PM_{2.5}$ concentrations in these cities were comparable except for the level of nickel (Ni) which was found to be >82fold higher in JC than in ZH. In this study, we tested the hypothesis that Ni-rich $PM_{2.5}$ induces an inflammatory response by triggering the MAP kinase pathways and thus enhance pro-inflammatory cytokine production. For these studies either male FVBN mice were exposed 3x/wk for 3 wks to $PM_{2.5}$ from either Chinese city, or female B6C3F1 mice were exposed to concentrated $PM_{2.5}$ from Sterling Forest, Tuxedo, NY (SF) between conception and gestational day 16. Tissue samples (liver, lung and heart) from PM-exposed mice or filtered air (FA) control mice were collected. Western blot analyses revealed changes in pAkt (serine 478), and p38 MAP kinase (>3-fold each, increase) in the heart, liver and in the lungs in response to Ni rich PM2.5 compared to FA. Although no significant changes in expression of NF-κBp65 or NF-κBp52 was noted in heart and liver, an increase in NF-κBp65 (>4fold) was evident in lung. Elevated levels of cytokines IL-6 and IL-1β (>2fold and >5fold, respectively) were evident in serum samples of both Ni-rich PM and SF PM. Taken together, these findings suggest that inflammation, pulmonary and liver toxicity induced by Ni-rich $PM_{2.5}$exposure may occur through differential signaling pathways involving growth factor regulated (ERK1/2) or oxidative stress (p38) MAP kinase pathways. MAPKs and NF-κB could have synergistic roles in IL-6 and IL-1β induction that could promote transcription of critical genes involved in the inflammatory process.

PS 2040b Potential Immunotoxicity of a Polyfluoroalkyl Substance Replacement of Perfluorooctanoic Acid

J. DeWitt[1], B. R. Rushing[1], Q. Hu[1] and M. Strynar[2]. [1]*Pharmacology and Toxicology, East Carolina Univ, Greenville, NC and* [2]*Human Exposure & Atmospheric Sciences Division, MDAB, US EPA, RTP, NC.*

Perfluorooctanoic acid (PFOA) is a perfluoroalkyl substance (PFAS) that has been used as a surfactant in the production of myriad industrial and consumer products. However, its presence in the environment and and demonstrated multisystem toxicity in several animal models led to a voluntary phase-out by several US manufacturers. A potential replacement for PFOA is undecafluoro-2-methyl-3-oxahexanoic acid (U2M3). Exposure to PFOA and related PFASs suppresses T cell-dependent antibody responses (TDAR) in mice without observable impacts on T or B cell numbers. This study evaluated TDAR in mice exposed to U2M3. Doses were based on publicly available information indicating a NOAEL of 10 mg/kg/d for evidence of regenerative anemia. Adult male and female C57BL/6 mice were gavaged with 0, 1, 10, or 100 mg/kg/d of U2M3 per BW for 28d. After 24d, mice were immunized with a T cell-dependent antigen. On day 29, animals were euthanized and sera were evaluated for IgM TDAR. U2M3 exposure did not alter BW or lymphoid organ weights; liver weights were increased in males and females at 10 (~40%) and 100 (~140%) mg/kg U2M3 relative to controls. Mean IgM serum titers of males dosed with 100 mg/kg were statistically suppressed by 10% relative to controls; female responses did not vary statistically from controls. Splenic CD45R B cell numbers were suppressed in males exposed to 100 (10%) mg/kg, but no other changes in numbers of splenic lymphocytes were observed for males or females at any dose. Serum concentrations for 100 mg/kg after 28d of exposure were 21595 ng/mL for males and 7132 ng/mL for females, which may partially explain the lack of TDAR suppression in females. However the relevance of the TDAR response and serum concentrations to organisms environmentally-exposed is unknown as environmental concentrations of this potentially emerging compound also are unknown. This abstract does not represent EPA policy.

PS 2040c Ah Receptor Activation Alters the Phenotype and Function of Pulmonary Innate Lymphocytes

D. M. Shepherd[1], B. P. Seaver[1, 2] and C. A. Beamer[1, 2]. [1]*Biomedical & Pharmaceutical Sciences, University of Montana, Missoula, MT and* [2]*Center for Environmental Health Sciences, University of Montana, Missoula, MT.*

The lung is a unique immunological site because it is constantly exposed to potentially harmful pathogens, including airborne particulate and microorganisms. The aryl hydrocarbon receptor (AhR), a ligand-activated transcription factor, acts as a regulator of mucosal barrier function and may influence immune responsiveness through changes in gene expression, cell-cell adhesion, and cytokine expression in the lung. Innate lymphoid cells (ILCs) play important roles in innate immune responses to infection and allergens, repair after tissue damage, and lymphoid tissue formation and homeostasis. Although the AhR has emerged as a critical regulator of ILCs and inflammation in the gastrointestinal tract; its role as a regulator of ILCs and inflammation in the respiratory tract remains largely undefined.

In this study, we tested the hypothesis that activation of AhR signaling pathways alters the phenotype and function of respiratory ILCs. CD45+CD90.2hiLineage- ILCs were expanded in the lungs of naïve Rag1-/- mice using rmIL-33 and isolated using a combination of anti-CD90.2 magnetic beads and flow cytometry. Purified ILCs were re-stimulated in culture with 50ng/ml rmIL-33 in the presence or absence of the prototypic AhR ligand TCDD, as well as the natural AhR ligands, indole 3-carbinol (I3C) and (1'H-indole-3'-carbonyl)-thiazole-4-carboxylic acid methyl ester (ITE) for 7 days. Concomitant exposure to AhR ligands altered the phenotype and activation of lung ILCs in a dose dependent manner as measured by changes in the expression of cell surface markers (Sca-1, ICOS, CD44, and CD39) and production of cytokines (IL-5 and IL-22). Collectively, our data suggest that AhR activation may modulate respiratory immunity via changes in the phenotype and function of ILCs.

This work is supported by NIEHS/NIGMS grant R01-ES013784 (DMS), NIEHS grant R15-ES020993 (CAB), and NIGMS grant P30GM103338. The contents are solely the responsibility of the authors and do not necessarily represent the official view of NIH.

PS 2041 Failure of Reversal of Oxidative Damage in Renal Tissues of Lead Acetate-Treated Rats

A. S. Akinrinde[1], T. O. Omobowale[2], A. A. Oyagbemi[1], A. B. Saba[1], B. S. Ogunpolu[2] and O. T. Daramola[2]. [1]*Dept of Vet. Physiology, Biochemistry and Pharmacology, University of Ibadan, Nigeria, Ibadan, Oyo, Nigeria and* [2]*Veterinary Medicine, University of Ibadan, Nigeria, Ibadan, Oyo, Nigeria.*

Removal of lead from the environment of man or otherwise, the movement of man from lead-contaminated areas has been employed as a means of abatement of the toxic effects of lead. Whether toxic effects in already-exposed individuals subside after lead withdrawal remains unanswered. In order to understand the reversibility of nephrotoxicity induced by lead acetate, male Wistar rats were orally exposed to 0.25, 0.5 and 1.0mg/ml of lead acetate for 6 weeks. One-half of the rats were sacrificed at 6 weeks while the other half remained for an additional 6 weeks after withdrawal of lead. There were significant ($p<0.05$) increases in Glutathione S-transferase (GST), Catalase (CAT), Superoxide dismutase (SOD), Hydrogen peroxide (H2O2) generated and Malondialdehyde (MDA) in a dose-dependent manner, with concomitant reduction in glutathione (GSH) content and Glutathione peroxidase (GPx) activity. The pattern of alterations in most of the oxidative stress and antioxidant parameters remained similar in rats from the withdrawal period, although CAT and SOD activities reduced, in contrast to their elevation during the exposure period. Serum creatinine levels were significantly ($p<0.05$) elevated in both exposure and withdrawal experiments. The weights of kidney tissues were, however, not significantly altered throughout the study period. The results suggest that lead acetate-induced nephrotoxicity indicated by induction of oxidative stress and disruption of antioxidant parameters were not reversed even after removal of lead for the time course of the study in male rats.

PS 2042 Disposition and Toxicity of Mercury in Aging Rats

C. Bridges, L. Joshee and R. K. Zalups. *Mercer University, Macon, GA.*

Progressive loss of functioning nephrons, secondary to age-related glomerular disease, can impair the ability of the kidneys to effectively clear metabolic wastes and toxicants from blood. Additionally, as renal mass is diminished, cellular hypertrophy occurs in the remaining nephrons that remain (primarily along the proximal tubule). Consequently, we hypothesize that the remaining functioning nephrons are at an increased risk of being intoxicated by nephrotoxic compounds, such as the acute nephrotoxicant, inorganic mercury (Hg^{2+}). The purpose of the present study was to characterize the renal pathological effects of aging on the renal disposition and toxicity of Hg^{2+} using young adult and two-year old rats. Paired groups of animals were injected (i.v.) with either a 0.5 μmol/kg non-toxic or a 2.5 μmol/kg nephrotoxic dose of mercuric chloride. Significant differences were detected between corresponding groups of young and aged rats. Plasma creatinine, blood urea nitrogen and renal biomarkers were greater in both groups of aged rats than in corresponding young adult rats. Histologically, evidence of glomerular sclerosis, tubular atrophy, interstitial inflammation and fibrosis were significant pathological features in kidneys of aged animals. In addition, proximal tubular necrosis, especially along the straight segments in the inner cortex and outer stripe of the outer medulla was a prominent feature in the renal sections from both aged and young rats treated with the nephrotoxic dose of Hg^{2+}. Our findings indicate that aging has a profound effect of the renal disposition of administered Hg^{2+} and reduces renal overall function more significantly in aged rats than young rats.

PS 2043 Profiling of Human, Canine, and Rat Urine Samples Using Bio-Plex Pro RBM Kidney Toxicity Assays

W. Tan[1], H. Schnaars[2], K. Marshall[2], H. Akey[2], L. Stephen[2], A. Baugher[1], D. Jethwaney[1] and C. Linnevers[1]. [1]*Bio-Rad Inc, Hercules, CA and* [2]*Myriad RBM Inc, Saranac Lake, NY.* Sponsor: E. Dominic.

Acute kidney injury (AKI) is a serious medical condition caused by a variety of bodily insults, including trauma from an accident, ICU acute renal failure, or exposure to nephrotoxic agents. From a pharmaceutical industry standpoint, drug-induced toxicity is a serious issue, sidelining 30% of therapeutics overall, from preclinical lead compounds to marketed drugs (Bonventre et al. 2010). Early detection of AKI along with proper treatment regimens is critical in the prevention of further loss of kidney function. The current clinical criterion for the diagnosis of AKI relies on traditional tests (glomerular filtration rate and blood urea nitrogen) that employ late biomarkers that are detectable days or weeks after kidney damage has occurred. Researchers are looking for biomarkers that are sensitive, specific, and early indicators of AKI. Further, level monitoring should be cost effective and permit rapid reporting of results (Slocum et al. 2012). In collaboration with Myriad RBM, the Predictive Safety Testing Constortium (PSTC), and the European Medicines Agency (EMEA), we have developed seven panels of magnetic bead-based assays using the Luminex xMAP technology. These assays employ a standard sandwich enzyme immunoassay method using a 96-well plate format. Assay performance was evaluated according to standard verification and validation parameters, including assay sensitivity, precision, accuracy, working ranges, specificity and linearity of dilutions. The assays demonstrated excellent precision, sensitivity and broad working assay range. We observed robust performance in human, canine and rat urine samples across a range of physiological conditions, from normal to diseased and drug-treated. The multiplex immunoassays enable rapid and combinatorial evaluation of multiple proteins. This permits researchers to detect key proteins that maybe upregulated within hours of kidney damage, providing valuable information throughout the drug development process, from lead optimization to preclinical and clinical protocol decision making.

PS 2044 Protection against Type 2 Diabetes-Induced Nephropathy by Multiple Exposures to Low-Dose Radiation Was Associated with Improvement of Dyslipidemia and Insulin Resistance and Suppression of Renal Inflammation and Oxidative Stress

C. Zhang[1, 2, 3], M. Shao[1, 2], L. Cai[1, 2, 3] and X. Lu[2]. [1]*Chinese-American Research Institute for Diabetic Complications, Wenzhou Medical University, Wenzhou, China,* [2]*Ruian Center of Chinese-American Research Institute for Diabetic Complications, the Third Affiliated Hospital of the Wenzhou Medical University, Wenzhou, China and* [3]*KCHRI & Department of Pediatrics, University of Louisville, Louisville, KY.*

The aims of the present study were to investigate whether LDR can prevent type 2 diabetes-induced renal damage and to explore the possible mechanism. Mice were fed with a high-fat diet for 12 weeks, followed by a single injection of streptozotocin to develop a type 2 diabetic mouse model. Then, these mice were exposed to LDR at different doses (25, 50, and 75 mGy) for 4 or 8 more weeks with HFD treatment. The kidney weight, renal function, blood glucose level, and insulin resistance were examined. The pathological changes were measured by hematoxylin and eosin, periodic acid Schiff, and Masson's trichrome staining. Systematic and renal lipid profiles were detected by ELISA. Renal inflammation, oxidative stress, and fibrosis were assessed by real-time PCR, western blot assays, and immunohistochemical staining. HFD/STZ-induced type 2 diabetic mice exhibited severe pathological changes in the kidney and renal dysfunction. Exposure of the mice to LDR for 4 weeks, especially at 50 and 75 mGy, prevented most of the abnormalities. The beneficial effects became weaker after LDR treatment for 8 weeks. LDR also attenuated serum lipid levels and subsequent lipotoxicity characterized by insulin resistance, inflammation, and oxidative stress in the diabetic kidneys. Finally, the LDR-induced anti-oxidative effect was due to upregulation of renal nuclear factor E2-related factor-2 expression and function. These results suggest that LDR prevented type 2 diabetes-induced kidney injury. The protective mechanisms may be mainly attributed to the prevention of dyslipidemia and the subsequent lipotoxicity-induced insulin resistance, inflammation, and oxidative stress.

PS 2045 Attenuation of Hyperlipidemia- and Diabetes-Induced Early-Stage Apoptosis and Late-Stage Renal Dysfunction via Administration of Fibroblast Growth Factor 21 Is Associated with Suppression of Renal Inflammation

X. Lu[1], C. Zhang[1, 2, 3], X. Li[2] and L. Cai[1, 2, 3]. [1]*Ruian Center of Chinese-American Research Institute for Diabetic Complications, The Third Affiliated Hospital of the Wenzhou Medical University, Ruian, Zhejiang, China,* [2]*Chinese-American Research Institute for Diabetic Complications, Wenzhou Medical University, Wenzhou, China and* [3]*KCHRI & Department of Pediatrics, University of Louisville, Louisville, KY.*

Lipotoxicity is a key feature of the pathogenesis of diabetic kidney disease, and is attributed to excessive lipid accumulation (hyperlipidemia). Increasing evidence suggests that fibroblast growth factor (FGF)21 has a crucial role in lipid metabolism under diabetic conditions. The present study investigated whether FGF21 can prevent hyperlipidemia- or diabetes-induced renal damage, and if so, the possible mechanism. Mice were injected with free fatty acids (FFAs, 10 mg/10 g body weight) or streptozotocin (150 mg/kg) to establish a lipotoxic model or type 1 diabetic model, respectively. Simultaneously the mice were treated with FGF21 (100 μg/kg) for 10 or 80 days. The kidney weight-to-tibia length ratio and renal function were assessed. Systematic and renal lipid levels were detected by ELISA and Oil Red O staining. Renal apoptosis was examined by TUNEL assay. Inflammation, oxidative stress, and fibrosis were assessed by Western blot. Acute FFA administration and chronic diabetes were associated with lower kidney-to-tibia length ratio, higher lipid levels, severe renal apoptosis and renal dysfunction. Obvious inflammation, oxidative stress and fibrosis also observed in the kidney of both mice models. Deletion of the fgf21 gene further enhanced the above patho-

logical changes, which were significantly prevented by administration of exogenous FGF21. These results suggest that FFA administration and diabetes induced renal damage, which was further enhanced in FGF21 knock-out mice. Administration of FGF21 significantly prevented both FFA- and diabetes-induced renal damage partially by decreasing renal lipid accumulation and suppressing inflammation, oxidative stress, and fibrosis.

PS 2046 ALDH16A1 Interacting with HPRT1 in the Purine Salvage Pathway

M. M. Sandoval, V. Vasiliou, Y. Chen, B. C. Jackson and R. Johnson. *Pharmaceutical Sciences, University of Colorado, Aurora, CO.*

Purpose: Gout, a common form of inflammatory arthritis, is strongly associated with elevated uric acid concentrations in the blood (hyperuricemia). A recent study identified a rare single nucleotide polymorphism in the aldehyde dehydrogenase 16A1 (ALDH16A1) gene, ALDH16A1*2, shows a strong association with hyperuricemia and gout (Stefansson, 2011). ALDH16A1 is a novel and unique member of the ALDH superfamily in relation to its protein structure and has been identified as a binding partner of multiple proteins. Hypoxanthine-phosphoribosyltransferase (HPRT1) is a potentially important binding target for ALDH16A1 in the context of gout pathophysiology because it plays a key role in the purine salvage pathway and reduced/absence of its activity are known to cause hyperuricemia and gout. The purpose of this study is to determine if ALDH16A1 plays a role in hyperuricemia and gout by modulating HPRT1 in the purine salvage pathway.
Methods: Molecular modeling was performed to determine if ALDH16A1 is catalytically inactive and the binding ability with HPRT1.
Transfection and immunoprecipitation were performed to assess the ex vivo interaction between ALDH16A1 and HPRT1.
Uric acid generation in transfected cells overexpressing ALDH16A1 was determined to assess the possible role of ALDH16A1 in the purine salvage pathway.
Results: Molecular modeling predicts human ALDH16A1 protein would lack catalytic activity due to the absence of the catalytically important cysteine residue (Cys-302) as well as a loss of substrate binding and cofactor binding (NAD+) pockets. Molecular modeling as well as ex vivo interaction studies implies that ALDH16A1, but not ALDH16A1*2, may interact with HPRT1. The decrease in uric acid generation in ALDH16A1 overexpressing cell lines implies a possible role of ALDH16A1 in the purine metabolism pathway.
Conclusion: These results lead to the intriguing possibility that association between ALDH16A1 and HPRT1 may be required for optimal HPRT1 activity; disruption of this interaction may contribute to the hyperuricemia seen in ALDH16A1*2 carriers.

PS 2047 The Possible Role of Fluoride on Aggravation of Tubulointerstitial Fibrosis Caused by Unilateral Ureteral Obstruction through TGF-β1

T. Kido[1, 2], M. Tsunoda[2], C. Sugaya[2] and H. Yanagisawa[1]. [1]*Public Health and Environmental Medicine, The Jikei University School of Medicine, Tokyo, Japan and* [2]*Preventive Medicine, Kitasato University School of Medicine, Sagamihara, Kanagawa, Japan.*

Fluoride (F) is an environmental pollutant. The contamination of ground water by F has been reported in China, India, Iran, and Argentina. Since F is filtered by the kidney, humans or experimental animals with renal insufficiency may be affected by F more seriously. We used the tubulointerstitial fibrosis model of rats induced by unilateral ureteral obstruction (UUO). We examined whether or not F deteriorates tubulointerstitial fibrosis in rats with UUO. In this study, the pathological changes and the expression of TGF-β1 mRNA in the renal cortex of rats were examined. Left ureter was ligated and sham-operation was done in 7-week-old male rats weighing 240-260g. F was administered to rats with UUO at 0, 75 and 150 ppm and sham-operated rats at 0 and 150 ppm in drinking water for 2 weeks. The kidneys obtained were immediately harvested, decapsulated and carefully dissected into the cortex on ice. Real-time PCR was performed for the analysis of TGF-β1 mRNA. The cortex was also pathologically examined by Masson-trichrome stain. Body weight of rats with UUO exposed to 150 ppm of F was significantly lower than that of rats with UUO exposed to 0 and 75 ppm of F. The average of water intake in rats with UUO exposed to 75 and 150 ppm of F was significantly lower than that in rats with UUO that were not exposed to F. Masson-trichrome stain revealed the deterioration of tubulointerstitial fibrosis in the renal cortex of rats with UUO exposed to 150 ppm of F. The expression of TGF-β1 mRNA was increased in rats with UUO exposed to 150ppm of F than in those exposed to 0 and 75ppm of F. These observations suggest that F develops tubulointerstitial fibrosis in rats with UUO via increased action of TGF-β1.

PS 2048 Effects of Cadmium (Cd) on the Localization of Cystatin C and Megalin in Rat Kidney

W. C. Prozialeck, A. Van Dreel, J. Edwards, P. C. Lamar, C. Ackerman, I. Stock and A. Papaeliou. *Dept of Pharmacology, Midwestern University, Downers Grove, IL.*

Cadmium (Cd) is a nephrotoxic environmental pollutant for which there is a need for improved biomarkers of toxicity. Cystatin C is a low molecular weight protein (13.3 kilodaltons) that is being investigated as a potential biomarker of the early stages of Cd-induced kidney injury. During recent studies in this area, we found that the general patterns of cystatin C localization in the proximal tubule seemed to correspond to, but not exactly mimic, those of the proximal tubule transport protein megalin and that Cd seemed to alter the localization of both proteins. In the studies described here, we have developed a procedure for the dual immunofluorescence labeling of cystatin C and megalin in single sections of rat kidney. Cryosections were incubated overnight in primary antibodies-rat antimegalin (abcam;as7699) and goat anticystain C (abcam; ab117642)-followed by incubation in the respective secondary antibodies, a TRITC conjugated chicken anti rabbit IgG (abcam; ab6826) and an Alexafluor 488 conjugated donkey anti goat IgG (abcam; ab150129), and then processed for confocal microscopic imaging. In control samples, both cystatin C and megalin exhibited speckled patterns of labeling in an area just beneath the brush border of the proximal tubule epithelial cells. By contrast tissue samples from animals that had been treated with Cd (0.6 mg subcutaneously, 5 days per week for 6, 9 or 12 weeks) showed diffuse labeling of both molecules along the apical cell surface, with retraction and deterioration of the apical brush border. These changes coincided with an increase in the urinary excretion of cystatin C. These results provide further evidence that Cd increases the urinary excretion of cystatin C and they suggest that this effect may result from disruption of the megalin-mediated transport in the proximal tubule.

PS 2049 Zn-Excess Intake Increases Systemic Blood Pressure and Deteriorates Renal Function through Superoxide Radical-Induced Oxidative Stress

H. Yanagisawa and T. Kido. *Department of Public Health and Environmental Medicine, The Jikei University School of Medicine, Tokyo, Japan.* Sponsor: M. Tsunoda.

In recent years, foods and tablets with addition of the essential trace element, zinc (Zn), have been sold for the maintenance of good health and for health promotion. However, Zn toxicity due to zinc-excess intake has not been fully established. Using rats fed 22 g/day of a control diet containing 0.005% (1.1 mgZn/day) Zn or two Zn-excess diets containing 0.05% (11 mgZn/day) or 0.2% (44 mgZn/day) Zn for 4 weeks, we examined whether or not Zn-excess intake affected systemic blood pressure (BP) and renal function. An increase in Zn intake elevated systolic BP, diastolic BP and mean arterial pressure (MAP), and reduced renal blood flow (RBF) and inulin clearance in a dose-dependent manner. This decline in inulin clearance may be the result of a fall in RBF. Administration of the nitric oxide (NO) synthase inhibitor, L-NAME, markedly increased MAP and significantly decreased RBF in the three groups of rats. Inversely, administration of the exogenous superoxide radical scavenger, tempol, significantly decreased MAP and substantially increased RBF in the three groups of rats. Resultantly, tempol dramatically restored MAP and RBF levels in rats fed two Zn-excess diets to levels comparable to those observed in rats fed a control diet. These observations suggest that both an elevation in systemic BP and a reduction in RBF seen in the two Zn-excess diet groups result from a decrease in the action of the vasodilator, NO through the formation of peroxynitrite based upon the non-enzymatic reaction of NO and increased superoxide radical. Indeed, the activity of the endogenous superoxide radical scavenger, Cu/Zn-superoxide dismutase, was significantly reduced in the vessel wall of rats fed two Zn-excess diets vs. a control diet. Thus, Zn-excess intake increases systemic BP and deteriorates renal function through the oxidative stress caused by superoxide radical. In addition, the lowest observed adverse effect level (LOAEL) of Zn appears to be approximately 11 mg/day.

PS 2050 Epigenetic Changes in p21 Expression in Renal Cells after Exposure to Bromate

N. E. Scholpa, X. Zhang and B. S. Cummings. *Pharmaceutical and Biomedical Sciences, University of Georgia, Athens, GA.*

This study tested the hypothesis that bromate (KBrO3)-induced renal cell death is mediated by epigenetic mechanisms. Global DNA methylation, as assessed by 5-methylcytosine staining, was not changed in normal rat kidney cells treated with acute cytotoxic doses of KBrO3 (100 and 200 ppm), as compared to controls. However, KBrO3 treatment did increase p38, p53 and histone 2AX (H2AX)

phosphorylation, and p21 expression. Treatment of cells with inhibitors of DNA methyltransferase (5-azacytidine or 5-Aza) and histone deacetylase (trichostatin A or TSA) in addition to KBrO3 increased cytotoxicity, compared to cells exposed to KBrO3 alone. 5-Aza and TSA co-treatment did not alter p38 or p53 phosphorylation, but slightly decreased H2AX phosphorylation, and significantly decreased p21 expression. We also assessed epigenetic changes in cells treated under sub-chronic conditions with environmentally relevant concentrations of KBrO3. Under these conditions (0-10 ppm KBrO3 for 28 days), we detected no increases in cell death or DNA damage. In contrast, slight alterations were detected in the phosphorylation of H2AX, p38 and p53. Sub-chronic low dose KBrO3 treatment also induced a biphasic response in p21 expression, with lower concentrations increasing expression, but higher concentrations decreasing expression. Methylation specific PCR demonstrated that sub-chronic KBrO3 treatment decreased the methylation of cytosine bases in the p21 gene, as compared to controls. Decreases in cytosine methylation correlated to alterations in p21 protein expression. Collectively, these data show the novel finding that KBrO3-induced renal cell death is altered by inhibitors of epigenetic modifying enzymes and that KBrO3 itself induces epigenetic changes in the p21 gene.

PS 2051 Effects of Proguanil Hydrochloride on Selected Hematological, Liver, and Kidney Function Indices in Rats

J. O. Adebayo, M. A. Adekunle, Z. A. Ajao, F. O. Audu, R. A. Adeyemo and E. A. Balogun. *Biochemistry, University of Ilorin, Ilorin, Kwara, Nigeria.*

Proguanil is a prophylactic antimalarial drug often used in combination with other drugs, such as atovaquone. However, the toxicity of this compound has not been fully elucidated. In this study, effects of sub-chronic administration of proguanil on selected haematological, liver and kidney function indices were investigated. Forty rats were randomly divided into four groups (i.e. A, B, C and D). Rats in group A (control) were orally administered distilled water while rats in groups B, C and D were orally administered 2.86, 5.71 and 11.43 mg/kg body weight of proguanil hydrochloride respectively for 28 days. The rats were then sacrificed and the full blood count with selected liver and kidney function indices were determined. The results revealed that the drug, at all doses, caused no significant alteration (P>0.05) to platelet count, total white blood cell count, percentage neutrophils, percentage lymphocytes and serum urea, uric acid and creatinine concentrations compared to controls. Moreover, the drug at all doses did not significantly alter (P>0.05) γ-glutamyl transferase activity compared to control. However, the haemoglobin concentration, red blood cell count, mean corpuscular volume, mean corpuscular haemoglobin concentration, mean corpuscular haemoglobin, packed cell volume and serum albumin concentration were significantly reduced at the highest dose of the drug administered compared to controls. The results suggest that proguanil may cause haemolysis and inhibit albumin synthesis in the liver at higher doses; thus, its abuse should be avoided.

PS 2052 Proteomic Biomarkers for Early Detection of Acute Kidney Injury (AKI) in Rats

H. Kim[1], T. Kim[1], E. Lee[2], E. Park[2], B. Jung[1], M. Shin[1] and B. M. Lee[1]. *[1]School of Pharmacy, Sungkyunkwan University, Suwon, Republic of Korea and [2]College of Pharmacy, Pusan National University, Suwon, Republic of Korea.*

Traditional urinary biomarkers for the diagnosis of acute kidney injury (AKI) are insensitive and nonspecific. Our studies were carried out to evaluate whether aldo-keto reductase subfamily (Akr7a1) and selenium-binding protein-1 (SBP-1) are present in acute renal failure and might serve as a urinary marker of AKI. Previously, these proteins were newly identified by proteomic analysis in the kidney of rats treated with mercury chloride (5 mg/kg). In this study, cisplatin, gentamycin, cyclosporin A, and mercury chloride were administered to rats for 1, 3, and 5 days. We compared expression levels of matrix metalloproteinase-9 (MMP-9), N-acetyl-beta-D-glucosaminidase (NAG), and kidney injury molecule-1 (KIM-1) as biomarkers for the detection of AKI. Blood and urine samples were analyzed to detect conventional biomarkers for AKI. Blood urea nitrogen (BUN) and serum creatinine (sCr) levels were slightly increased in the neprotoxicants-treated groups when compared to control group. In contrast, urinary Kim-1, MMP-9, and NAG levels were significantly increased. The mRNA expressions of Akr7a1 and GSTP1 dose-dependently increased in the kidney, whereas SBP-1 mRNA levels were significantly decreased. In histopathological examination, proximal tubular damage was observed only in the high dose of nephrotoxicants. These results suggest that Akr7a1 and SBP-1 might be used as early biomarkers for the detection of AKI.

PS 2053 Deficiency in Mdr1/MDR1 Increases Paraquat Accumulation and Toxicity in Mice and Human Renal Proximal Tubule Cells

X. Wen[1], C. J. Gibson[1], I. Yang[2], B. Buckley[2], J. Richardson[2, 3], M. J. Goedken[4] and L. M. Aleksunes[1, 2]. *[1]Pharmacology and Toxicology, Rutgers Univ, Piscataway, NJ, [2]Environmental and Occupational Health Sciences Institute, Rutgers Univ, Piscataway, NJ, [3]Environmental & Occupational Medicine, Rutgers Univ, Piscataway, NJ and [4]Pathology, Merck Research Laboratories, Kenilworth, NJ.*

Paraquat is a highly toxic herbicide that targets the lungs and kidneys following acute exposures. Prior studies demonstrated that the organic cation transporter 2 and multidrug and toxin extrusion 1 protein contribute to the urinary excretion of paraquat in the kidneys. The purpose of this project was to determine whether the multidrug resistance protein 1 (MDR1/Mdr1, Abcb1) also participates in the efflux of paraquat from the kidneys and protects against renal injury. Paraquat transport and toxicity were quantified in human renal proximal tubule epithelial cells (RPTEC) that endogenously express MDR1. Inhibition of MDR1 function by PSC833 or siRNA increased the cellular accumulation of paraquat in RPTEC cells by ~50%. Reduced efflux was accompanied by enhanced cytotoxicity of paraquat (50% decrease in the LC50 value) in PSC833-treated cells. To determine the role of Mdr1 in vivo, renal paraquat accumulation and subsequent nephrotoxicity were assessed in wild-type and Mdr1a/1b-null mice administered paraquat (10 or 30 mg/kg, i.p.). The kidneys of Mdr1a/1b-null mice had a 750% higher paraquat concentration compared to wild-type mice at 4 h. This was accompanied by significantly greater mRNA induction of kidney injury-responsive genes Kim-1 and Nqo1 in paraquat-treated Mdr1a/1b-null mice. Histopathological analysis confirmed the enhanced paraquat toxicity, as more extensive tubular degeneration was observed in Mdr1a/1b null mice compared to wild-type mice. In conclusion, Mdr1/MDR1 contributes to the elimination of paraquat from the kidneys and protects against toxicity (Supported by DK093903, ES020522, ES005022, ES007148).

PS 2054 Bisphenol A Induces Inflammatory Response and Cytokine Release in Renal Mesangial Cells

B. Chen[1], C. Wu[1], S. Liu[1], C. Chiang[2], C. Huang[3] and Y. Chen[4]. *[1]Institute of Toxicology, College of Medicine, National Taiwan University, Taipei, Taiwan, [2]Department of Integrated Diagnostics & Therapeutics, College of Medicine and Hospital, National Taiwan University, Taipei, Taiwan, [3]Graduate Institute of Chinese Medical Science, School of Chinese Medicine, China Medical University, Taichung, Taiwan and [4]Department of Physiology and Graduate Institute of Basic Medical Science, China Medical University, Taichung, Taiwan.*

Bisphenol A (BPA) is a common ingredient of plastic products, which wildly exists in daily life. In addition to reproductive toxicity, renal toxicity has also been implicated during BPA exposure. BPA exposure has been demonstrated to be associated with low-grade albuminuria in adults. Mesangial cells play an important role in renal glomerular filtration rate. However, the detailed action and mechanism of BPA-induced renal toxicity are still unclear. Here, we investigated the effect and possible mechanism of BPA on glomerular mesangial cells. In this study, mouse mesangial cell (MMC) were treated with 0~100 μM BPA. Cell viability was not affected by 25 and 50 μM BPA after 24 h treatment, but cell viability was decreased to 90% under treatment with 100 μM BPA. BPA 100 μM did not increase the cell apoptosis by PI-Annexin V staining. BPA treatment also did not change the caspase-3 and PARP cleavages in MMC. In renal cells, cyclooxygenase (COX)-2/prostaglandin (PG) E2 and interlukin-1β release were the inflammatory markers. After BPA treatment, COX-2 protein expression and PGE2 secretion and nuclear factor κ-B (NFκB)-p65 phosphorylation in MMC were increased in a dose dependent manner. The interleukin-1β levels were also increased in MMC culture medium after BPA treatment. BPA could also activate the AMP-activated protein kinase (AMPK), which plays an inflammation regulator. Taken together, these results indicate that BPA at non-cytotoxic concentrations is capable of increasing the expression/secretion of COX-2/PGE2 and cytokines in MMC, and imply that BPA may cause inflammatory response in renal glomeruli and influence the renal function.

PS 2055 Cell-Based Approach to Predict Kidney Toxicity

M. Adler[1, 2], E. M. Gottwald[1, 2], A. K. Ajay[1, 2], X. Lu[3], M. Hafner[2], A. Subramanian[3], P. Sorger[2] and V. S. Vaidya[1, 2]. *[1]Brigham and Women's Hospital, Boston, MA, [2]Harvard Medical School, Boston, MA and [3]Broad Institute of MIT and Harvard, Cambridge, MA.*

Kidney toxicity due to drugs and environmental contaminants accounts for significant patient mortality and morbidity. Current approaches to conduct safety and risk assessment of compounds rely predominately on animal studies and ex-

trapolation of the dose effects to humans although the typical response of animal models and humans can differ greatly. The objective of this study was to develop a cell-based high-throughput assay to identify potential nephrotoxic compounds using primary human proximal tubular epithelial cells (HPTEC). We show that HPTECs grown in a monolayer possess structural (e.g. expression of zonula occludens-1, cytokeratin 18) and functional characteristics (transport and glutathione activity) that are more representative of human kidney than immortalized kidney cell lines. To identify a biomarker of kidney toxicity *in vitro*, we treated HPTECs with known nephrotoxicants (cyclosporin A, cisplatin, tacrolimus, gentamicin, tobramycin, aristolochic acid, cadmium chloride, ochratoxin A, doxorubicin) as well as a non-toxicant (carboplatin) in at least 6 concentrations for 3, 6, 12 and 24 h. We measured 1,000 selected transcripts, which are a reduced representation of the genome and from which the remainder of the transcriptome can be computationally inferred. Heme oxygenase-1 (HO-1) was identified as one of the most differentially expressed genes after incubation with kidney toxicants, confirming *in vivo* reports of its significant increase in mice, rats and humans during kidney injury. Increases in the HO-1 mRNA (RT-PCR) and protein (ELISA) levels correlated well with morphological changes in the cells. We then developed and optimized a homogenous time-resolved fluorescence (HTRF) assay that allows high-throughput measurement of HO-1. Alterations in the HO-1 levels measured by HTRF correlated with ELISA (r2=0.97). We demonstrate an alternative approach to prescreen a large number of compounds for kidney toxicity, thus reducing and replacing the use of animals in preclinical toxicity studies.

PS 2056 Cyclosporin A-Induced Apoptosis in Renal Proximal Tubular Epithelial Cells Is Associated with Trb3 Induction

D. Germano, M. Uteng, S. Chibout, F. Pognan and A. Wolf. *Discovery & Investigative Safety, Novartis Pharma AG, Basel, Switzerland.*

Cyclosporine (CsA) is currently the primary immunosuppressant for the prevention of allograft rejection in solid organ transplantation. However, chronic treatment with CsA results into nephrotoxicity. Tubular cell apoptosis contributes to the pathogenesis of renal injury, but the molecular mechanisms are poorly understood. CsA is known to provoke endoplasmic reticulum (ER) stress, but the role of mediators involved in the processes leading to apoptosis remains elusive.
In this study the immortalized human renal proximal tubular epithelial cell line (RPTEC/TERT1) was used. Occurrence of reactive oxygen species (ROS), depolarization of mitochondrial membrane potential ($\Delta\Psi$m), apoptosis by caspase 3/7 activation and necrosis were measured with the use of specific fluorescent dyes by high content imaging (HCI) microscopy technology. Exposure of RPTEC/TERT1 to CsA for 48 hours resulted into dose-dependent ROS production, increased apoptosis and necrosis. The expression of ER stress-related genes CHOP, ATF4 and Trb3 together with pro-apoptotic genes was markedly increased. Silencing of Trb3 with specific siRNA resulted into decreased dissipation of mitochondrial membrane potential and protected significantly from CsA-induced apoptosis and necrosis. In addition, Trb3 silencing promoted the activation of the AKT-dependent pro-survival pathway following CsA exposure.
Thus, our data suggests that Trb3 has a crucial role during ER stress-induced apoptosis upon treatment with CsA, and therefore serve as a potential target for nephroprotective treatments.

PS 2057 MiR-27b Regulates Podocyte Function by Targeting Adenosine Receptor

Z. Li, B. L. Homer, S. O'Neil and R. Nassirpour. *Pfizer, Andover, MA.*

MicroRNAs (miRNAs) have been shown to be crucial not only in kidney development and normal renal function but also in various kidney diseases. In this study, we investigated the potential role of miRNAs as key regulators of podocyte injury. We first characterized the miRNA expression patterns in glomeruli as well as in primary podocyte cultures isolated from three different mammalian species: mouse, rat, and non-human primate (NHP). Profiling miRNA expressions led to the identification of a list of highly-conserved glomerulus-enriched and podocyte enriched miRNAs. We then examined if podocyte injury induced by application of a nephrotoxicant, puromycin aminonucleoside (PAN), alters the expression pattern of miRNAs *in vitro*. As reported previously, PAN not only induced apoptosis but also significantly down-regulated several podocyte enriched miRNAs, including miR-27b. By manipulating the expression level of this miRNA, we found that overexpression of miR-27b *in vitro* enhanced PAN-induced apoptosis in podocytes while its inhibition promoted survival. Target identification analysis identified Adora2b as a potential target for miR-27b. In fact, ectopic expression of miR-27b suppressed both Adora2b mRNA and protein expression in primary podocyte cultures. Not surprisingly, inhibition of miR-27b increased the transcript and protein expression levels of Adora2B. Dual luciferase binding assays further confirmed Adora2b as a direct target of miR-27b. We then investigated whether Adora2B modulation by miR-27b is regulating PAN induced podocyte injury by examining the impact of direct alteration of Adora2b expression on cell phenotype *in vitro*. Knockdown of Adora2b remarkably suppressed cell proliferation and induced apoptosis, similar to the phenotypes we had observed with miR-27b over expression. Additionally, stimulating the adenosine signaling by an Adora2b ligand reduced PAN induced apoptosis in primary podocyte cultures. Taken together, our data strongly suggest that miR-27b plays a pivotal role in regulating PAN induced podocyte injury by directly targeting Adora2b

PS 2058 Inhibitors of Ceramide Synthesis Protect Mice from Cisplatin-Induced Acute Kidney Injury

T. Dupre, A. R. Mather and L. J. Siskind. *Pharmacology and Toxicology, University of Louisville, Louisville, KY.*

Acute kidney injury (AKI) resulting from cisplatin administration remains to be an obstacle in chemotherapeutic treatments. Cisplatin-induced AKI involves apoptotic and necrotic cell death of the proximal tubules (PT), pathways known to be regulated by the sphingolipid ceramide. PT cells grown in culture elevate ceramides when treated with apoptotic or necrotic doses of ceramide as a result of the activation of ceramide synthase (CerS) and acid sphingomyelinase (aSMase), respectively. Thus, we hypothesize that inhibitors of ceramide synthesis will protect mice from cisplatin-induced nephrotoxicity. To test this hypothesis, we used cisplatin-induced (25 mg/Kg) AKI in C57BL/6 mice. At twenty-four hours C16, C20, and C24:1-ceramides were increased in the kidney cortex of cisplatin treated mice, concomitant with elevated CerS and aSMase activities. Mice pretreated for 3 days with the de novo synthesis inhibitor myriocin and the aSMase inhibitor amitriptyline were protected from cisplatin-induced AKI. At 72 h post cisplatin injection, serum creatinine and BUN levels were measured, showing a significant decrease in mice pretreated with ceramide inhibitors as compared to the levels observed in vehicle control mice. In conclusion these data indicate that inhibitors of aSMase and de novo ceramide synthesis protect mice from cisplatin-induced nephrotoxicity. As amitriptyline is already FDA approved for use in humans and myriocin is well tolerated in multiple mammalian models, these data these data show high potential for translational use for the prevention of AKI during chemotherapy treatment. This work was supported by R01 DK093462 (to L.J.S.).

PS 2059 Methyl Isobutyl Ketone (MIBK) Induces an Exposure-Related Increase in Measures of α2u-Globulin (α2u) Nephropathy in Male but Not Female F344 Rats

S. Borghoff[1], G. C. Hard[2], T. S. Poet[3], J. Davis[4], S. M. Green[5], B. J. Hughes[6], T. Mensing[7] and S. S. Sarang[8]. [1]*ToxStrategies, Inc, Cary, NC,* [2]*Private Consultant, Tairua, New Zealand,* [3]*Summit Toxicology, Richland, WA,* [4]*ILS, Inc, Morrisville, NC,* [5]*Eastman Chemical, Kingsport, TN,* [6]*Dow Chemical, Midland, MI,* [7]*Sasol Solvents, Moers, Germany and* [8]*Shell International, Houston, TX.*

Chronic exposure to MIBK caused an increased incidence of renal tubule adenomas and occurrence of renal tubule carcinomas in male, but not female rats. A number of chemicals have been shown to cause male rat renal tumors through the α2u nephropathy-mediated mode of action (MOA). The objective of this study was to evaluate the ability of MIBK to induce measures of α2u nephropathy in male and female F344 rats following exposure to the same inhalation concentrations used in the cancer bioassay (0, 450, 900, or 1800 ppm). Rats were exposed 6 hours/day for 1 or 4 weeks and kidneys excised approximately 18 hours post exposure to evaluate hyaline droplet accumulation (HDA), α2u staining of hyaline droplets, renal cell proliferation, and to quantitate renal α2u concentration at both 1 and 4 weeks. There was an exposure-related increase in all measures of α2u nephropathy in the male, but not female rat kidneys. The hyaline droplets present in the male rat kidney stained positively for α2u. The changes in HDA and α2u concentration were comparable to d-limonene, an acknowledged inducer of α2u nephropathy. In a separate in vitro investigation using a two-compartment vial equilibration model to assess the interaction between MIBK and α2u, the dissociation constant (Kd) was estimated to be 1.27×10^{-5}M. This Kd is within the range similar to other chemicals known to bind to α2u and cause nephropathy. Together, the exposure-related increase in measures of α2u nephropathy, sustained increase in renal cell proliferation along with an indication of reversible binding of MIBK to α2u, support the inclusion of MIBK in the category of chemicals exerting renal effects through a protein droplet α2u nephropathy-mediated MOA.

PS 2060 Ameliorative Effects of Metformin on Aristolochic Acid-Induced Renal Toxicity in Mice Due to Its Ability to Control Methylglyoxal and N^{ε}-(Carboxymethyl)Lysine Accumulation

T. Huang[1], Y. Li[1], S. Chen[1], Y. Lee[2], L. Tien[2] and J. Lee[1]. [1]*School of Pharmacy, Taipei Midecal University, Taipei, Taiwan and* [2]*School of Medicine, Fu-Jen Catholic University, New Taipei City, Taiwan.*

Aristolochic acid (AA)-induced renal lesions are related to increased renal levels of methylglyoxal (MGO) and N^{ε}-(carboxymethyl)lysine (CML) which is an advanced glycation end product (AGE). Metformin is a generally accepted drug for the treatment of type 2 diabetes mellitus, and is considered as an MGO scavenger and AGE inhibitor. This study investigated the renal MGO and CML scavenging ability of metformin, and its effect on renal function in C57BL/6 mice with AA-induced renal lesions. Mice were treated with metformin orally (12 or 24 mg/kg BW/day) for 15 days, and injected intraperitoneally with AA (5 mg/kg BW/day) for 8 days since day 8. Following injection of AA into mice for 8 days, decreased renal function was observed according to biochemical indexes and histopathological test results. Administration of metformin ameliorated the renal lesions, especially at a dose of 12 mg/kg BW. The concentration of renal MGO in AA-injected, untreated mice (without metformin) was approximately 6-fold higher than that in the control mice (37.33 ± 9.78 vs. 5.89 ± 2.64 μg/mg of protein, $p < 0.01$, respectively). CML was also observed in the renal tubules of AA-injected, untreated mice by immunohistochemistry. Administration of metformin at the two tested doses reduced renal MGO levels to 9.81 ± 5.04 μg/mg of protein in the 12 mg/kg BW-treated mice and 17.79 ± 7.88 μg/mg of protein in the 24 mg/kg BW-treated mice, and attenuated the accumulation of CML in the kidney. In this study, we found that metformin decreased renal MGO and CML levels, and improved renal function in AA-injected mice, which confirmed that metformin may be a suitable therapy for AA nephropathy due to its ability to control MGO and CML accumulation.

PS 2061 Altered Expression of Renal Drug Transporters in Multiple Rodent Models of Nonalcoholic Steatohepatitis

M. Canet, R. N. Hardwick, A. D. Lake, A. L. Dzierlenga, J. Clarke and N. J. Cherrington. *Pharmacology and Toxicology, University of Arizona, Tucson, AZ.*

Nonalcoholic fatty liver disease (NAFLD) is the most common form of chronic liver disease in Western society. NAFLD represents several stages of liver damage ranging from simple steatosis to the more advanced nonalcoholic steatohepatitis (NASH). Current experimental models of NASH include diet-induced models such as the methionine and choline deficient (MCD) diet as well as genetically obese models such as the leptin-deficient, ob/ob mice. Previous investigations have demonstrated alterations in the expression and activity of multiple hepatic drug transporters in human NASH, but little information is currently known regarding extra-hepatic regulation of drug transporters in NASH. The purpose of the current study was to characterize and investigate the regulation of renal drug transporters across multiple experimental rodent models of NASH. Both rat and mouse NASH models were utilized in this investigation and include; the MCD diet, atherogenic diet, ob/ob and db/db mice, and fa/fa rats. Histologic and pathological evaluations confirmed that the MCD and atherogenic rats as well as the ob/ob and db/db mice all developed NASH. In contrast, the fa/fa rats did not develop NASH however, despite a lack of liver damage; renal histology suggests that the fa/fa rats develop significant renal injury in comparison to the NASH-confirmed models. Investigation into the kidney mRNA expression of drug transporters showed that among the rodent models, the animals with confirmed NASH such as the rat MCD diet model and the ob/ob and db/db mice developed more, total alterations in mRNA and protein expression. In general, the majority of drug efflux transporters are induced by NASH whereas uptake transporters are both induced and repressed at the mRNA and protein level. These results suggest that NASH alters the expression and possibly function of renal drug transporters, which would disrupt drug elimination mechanisms in the kidney.

PS 2062 Resveratrol Reduces Doxorubicin Cytotoxicity in Human Kidney (HK-2) Cells

L. K. Vu[2], G. O. Rankin[1], H. Hedrick[1], J. G. Ball[1] and M. Valentovic[1]. [1]*Pharmacology, Physiology and Toxicology, Marshall University School of Medicine, Huntington, WV and* [2]*University of Charleston, Charleston, WV.*

Doxorubicin (DOX), or Adriamycin, is a cancer chemotherapeutic agent used in treatment of breast, ovarian, small cell lung cancer, acute and chronic lymphoid leukemia. DOX is both cardiotoxic and nephrotoxic. Resveratrol (RES) is a phytochemical found in grapes, berries, and nuts. RES possesses antioxidant and anticancer properties. This study tested the hypothesis that RES will reduce DOX cytotoxicity in human noncancerous renal proximal tubular epithelial cells (HK-2) and RES will attenuate DOX mediated oxidative stress. HK-2 cells were grown for 48 h. Cells were next pre-incubated for 1 h with 0 (DMSO), 5, or 7.5 uM RES followed by a 24 or 48 h co-incubation with 0, 1, or 2 uM DOX. Cell viability was assessed using an MTT assay. Results showed that DOX decreased cell viability in a concentration dependent manner and RES increased cell viability in cells exposed to DOX. Protein carbonyls, an indicator of oxidative stress and detected by Oxyblot Western analysis, were increased by DOX and reduced by RES. Additionally, RES decreased protein carbonyls in cells exposed only to RES. ADP/ATP assay determined RES preservation of cellular ATP following DOX exposure. RES reduced DOX cytotoxicity in HK2 cells at DOX concentrations that are clinically relevant. (Supported by NIH Grant 5P20RR016477 to the West Virginia IDeA Network for Biomedical Research Excellence).

PS 2063 Inhibition of TGF-β1-Induced Renal Epithelial Mesenchymal Transition by Chrysin

R. Nagavally and S. M. Ford. *Toxicology Program, St. John's University, Jamaica, NY.*

Epithelial mesenchymal transition (EMT) has been suggested as mechanism in the development of fibrosis, such as occurs in the response to certain toxicants. It is a process in which a polarized epithelial cell is converted into a motile mesenchymal cell. Mesenchymal-specific proteins required for movement, invasion and fibrosis are acquired as the epithelial cell proteins necessary for the function of epithelial tissue are lost. In the current study, we tested the effect of a flavonoid in a cell-culture model of EMT. To induce EMT, we use transforming growth factor-β1 (TGF-β1) which is a cytokine activated in most cases of fibrotic injury. Chrysin, a flavonoid extracted mainly from passion flowers, was examined for its ability to inhibit EMT induced by TGF-β1 in the LLC-PK_1 cell line. Cells were treated with TGF-β1 alone or TGF-β1 + chrysin. Effects on the mesenchymal markers collagen, α-smooth muscle actin, and vimentin were evaluated as indicators of EMT. The amount of collagen in the cells was determined by the Sirius red assay. Collagen content was significantly increased from 93 ± 8 μg collagen/ mg total protein in the control group to 127 ± 8 μg collagen/ mg total protein in the TGF-β1 treated group. In the group treated with both TGF-β1 + chrysin, collagen was significantly reduced to 104 ± 6 μg collagen/ mg total protein. The expression of α-smooth muscle actin and vimentin was determined by immunocytochemistry. Mouse primary antibodies were tagged using an anti-mouse IgG conjugated with FITC. The specimens were evaluated by widefield microscopy at 20X magnification. Treatment with TGF-β1 increased the expression of mesenchymal markers, whereas in the presence of TGF-β1 + chrysin the expression of both α-smooth muscle actin and vimentin resembled the untreated controls. These results demonstrate that chrysin can inhibit TGF-β1-induced EMT in LLC-PK_1 cells.

PS 2064 Exploration of the Role of Renal Biotransformation in 3, 4, 5-Trichloroaniline Nephrotoxicity *In Vitro*

C. Racine, D. Anestis and G. O. Rankin. *Pharmacology, Physiology & Toxicology, Marshall University, Huntington, WV.*

Chlorinated anilines are common intermediates in the production of agricultural products. Exposure to chlorinated anilines occurs through industrial, agricultural and environmental settings. One chlorinated aniline of interest in our laboratory is 3,4,5-trichloroaniline (3,4,5-TCA). Previous studies have shown that 3,4,5-TCA can induce nephrotoxicity in vitro. The purpose of this study was to explore the role of renal biotransformation enzyme systems on 3,4,5-TCA nephrotoxicity using an in vitro model. The current study utilized isolated renal cortical cells (IRCC) from male Fischer 344 rats. IRCC (3 ml: 4.0 X 106 cells/ml) were treated with 0.5 mM 3,4,5-TCA or DMSO (vehicle) control for 120 minutes. Cytotoxicity was determined using lactate dehydrogenase (LDH) release assays. In some experiments, cells were pretreated with either an antioxidant [ascorbate (2.0 mM), glutathione (1.0 mM), N-acetyl-L-cysteine (2.0 mM) or α-tocopherol (1.0 mM)], a flavin monooxygenase (FMO) inhibitor [methimazole (1.0 mM), or N-octylamine (1.0)], a cytochrome P450 (CYP) inhibitor [metyrapone (1.0 mM) or piperonyl butoxide (PIBX; 1.0 mM)], or a cyclooxygenase inhibitor [indomethacin (1.0 mM)]. 3,4,5-TCA nephrotoxicity was not significantly attenuated by pretreatment with methimazole or N-octylamine, suggesting that FMO mediated oxidation does not play a significant bioactivating role in 3,4,5-TCA nephrotoxicity. Pretreatment with indomethacin, a cyclooxygenase inhibitor, significantly attenuated toxicity. The CYP inhibitor PiBx also significantly attenuated 3,4,5-TCA toxicity, while metyrapone pretreatment provided no significant attenuation of toxicity. All antioxidant pretreatments significantly attenuated 3,4,5-TCA nephrotoxicity. These results suggest that free radicals and oxidative stress may play a role

in 3,4,5-TCA nephrotoxicity in vitro, and that these oxidative species arise from biotransformation by cyclooxygenase activity or via CYP isozymes inhibited by PiBx but not metyrapone.

PS 2065 Renal Epithelial Hyperplasia Caused by Urinary Crystals of a Novel GKA and Its Metabolites after Acute Dosing in Sprague-Dawley Rats

E. Tien[4], J. R. Turk[4], N. Everds[4], Q. Ye[1], M. Nguyen[4], P. Cao[3], J. Schroeder[4], R. Kelly[2], L. Jin[1] and C. Afshari[4]. *[1]Pharmacokinetics and Drug Metabolism, Amgen, Inc., South San Francisco, CA, [2]Pharmaceutics, Amgen, Inc., South San Francisco, CA, [3]Molecular Structure and Characterization, Amgen, Inc., South San Francisco, CA and [4]Comparative Biology and Safety Sciences, Amgen, Inc., Thousand Oaks, CA.*

Renal toxicity caused by crystal formation in the urine is well-established for some drugs, industrial chemicals, food additives, and naturally occurring toxins but toxicity typically requires long term dosing to cause measurable changes in urinary system morphology and/or function. Compound A, a novel glucokinase activator (GKA), caused crystal formation in the urine with accumulation in the collecting ducts accompanied by renal transitional epithelial hyperplasia with neutrophil infiltration after only 4 consecutive daily doses in female Sprague Dawley rats. A second study dosing Compound A at 600mg/kg/day for 1, 2 or 4 consecutive days was performed to explore the unusually rapid progression of the hyperplasia and identify the crystals. Findings after a single dose included crystals in urine and kidneys and clinical pathology changes indicating inflammation and decreased renal function. Additional findings after 2 doses included renal transitional epithelial hyperplasia with neutrophil infiltration. No changes were observed in urinary bladder epithelium. Crystals in the kidneys were identified as Compound A and two major metabolites by MALDI mass spec imaging. Urinary system findings observed with Compound A have not been seen with other internally tested GKAs of similar structure nor GKAs reported in the literature, suggesting that it is unrelated to the biology of glucokinase activation. The renal toxicity caused by Compound A highlights possible rapid onset of such effects and acute toxicity studies could benefit from additional endpoints to more clearly define the nature of such findings if the potential exists for renal toxicity to occur.

PS 2066 Are Succinate and Diglycolic Acid Taken Up into Human Kidney Proximal Tubule Cells by the Same Sodium Dicarboxylate Transporters?

C. N. Robinson, G. M. Landry, C. Dunning and K. McMartin. *Pharmacology, Toxicology & Neuroscience, LSU Health Sciences Center, Shreveport, LA.*

Diglycolic acid (DGA) is now considered to be the primary toxic metabolite of diethylene glycol (DEG), leading to the acute kidney injury from DEG overdose. DGA is a four-carbon dicarboxylic acid, with structural similarity to the TCA cycle intermediate, succinate. We hypothesize that DGA and succinate are taken up by the same sodium dicarboxylate transporter (NaDC) located in the proximal tubule cells of the kidney. This study compared the intracellular uptake of DGA and succinate, via apical (NaDC-1) and basolateral (NaDC-3) transporters. Human kidney proximal tubule cells were cultured until confluent, then subcultured onto membrane inserts in 24 well plates, that allow for distinct apical and basolateral uptake. Using 14C-substrates, uptake was measured at increasing time points and concentrations for both succinate and DGA, along with measurements of sodium dependence of the NaDC transporters. Cellular uptake of succinate from both the apical and basolateral membrane demonstrated sodium dependence, suggesting mediation via NaDCs, with somewhat higher uptake by the apical NaDC-1. Uptake of DGA was not sodium dependent from the apical direction and was not saturable, suggesting a transporter-independent mechanism. Basolateral uptake of DGA was sodium-dependent and was saturable with a Km of about 16 mmol/L. The magnitude of DGA uptake at non-toxic concentrations was greater from the basolateral side than the apical. These results suggest that DGA and succinate transport have differing characteristics in human kidney cells.

PS 2067 Transporter Function and Response to Nephrotoxicants in a p16-Modified Human Renal Proximal Tubule Epithelial Cell Line

T. Steiner, N. Venkatraman, Y. Xiao, J. Blasberg, M. Bourner and D. C. Thompson. *Sigma-Aldrich, St. Louis, MO.*

Kidney toxicity is a continuing concern during drug development. Although primary human kidney cells are available and a handful of immortalized kidney cell lines currently exist, there is a need for improved assay systems. We modified human primary renal proximal tubule epithelial cells by knocking out p16, a cyclin dependent kinase inhibitor, thereby enabling extended cell proliferation. The resulting cell line was characterized for the presence of proximal tubule cell markers as well as several functional properties, including transporter activity and response to known human nephrotoxicants. Two uptake (OAT1, OCT1) and two efflux (MDR1, MRP2) renal transporters were studied. Transporter assays were carried out on poly-D-lysine coated 24-well plates at a seeding density of 0.5 million cells/well for 10 (uptake) or 30 min (efflux). Concentration-dependent uptake of the OCT1 substrate tetraethylammonium (TEA) and the OAT1 substrate p-aminohippuric acid (PAH) were observed. Verapamil and probenecid inhibited TEA and PAH uptake by 33 and 66%, respectively. For the efflux transporters, MRP2-mediated efflux of carboxydichlorofluorescein (CDCF) was inhibited using MK571, leading to a 3.25-fold increase in intracellular CDCF. Similarly, MDR1-mediated efflux of calcein was inhibited with cyclosporine A, leading to a 7-fold increase in intracellular calcein. The cell line was also tested for sensitivity to several nephrotoxicants. Concentration-dependent cytotoxicity (48 hr, MTT assay, IC50) was observed with each of the test compounds, including gentamicin (3 mM), cisplatin (20 μM), tacrolimus (75 μM), potassium dichromate (25 μM) and diglycolic acid (7.5 μM), the proposed nephrotoxic metabolite of diethylene glycol. The presence of functional uptake and efflux transporters coupled with toxicant sensitivity suggest that the cell line may be useful for drug-transporter interactions and the early detection of renal toxicants.

PS 2067a Development and Characterization of a Novel Cell-Based Model to Study MATE1- and MATE2K-Mediated Drug Uptake and Interactions

C. J. Patten, J. Wang, K. Cooper, J. Bourgea, A. Gao and N. Li. *Corning Life Sciences, Bedford, MA.* Sponsor: C. Crespi.

Transporter involved drug-drug interactions (DDIs) in the kidney can prolong the drug elimination half-life, leading to accumulation of victim drugs in the body, consequently causing pharmacological problems or renal toxicity. Multidrug and toxin extrusion transporters (MATEs), e.g. MATE1 and MATE2K, localized on the apical membrane of proximal tubule cells are major transporters which mediate the excretion of important medications into the urine. Several studies have demonstrated that apical efflux by MATEs is one of the sites of DDI in the kidney. Therefore, the International Transporter Consortium (ITC) recommends studying the potential interaction of new molecular entities (NMEs) with MATE1 and 2K. A new "Thaw and Go" cell-based transporter model has been developed to evaluate MATE1 and MATE2K-based interactions, which enables early in vitro evaluation of potential MATEs involvement in drug induced renal toxicity. In the presence of oppositely directed H+-gradient or ammonium chloride-induced intracellular acidification, the transport activity of various cations, such as tetraethylammonium (TEA), metformin and 1-methyl-4-phenylpyridinium (MPP) were significantly stimulated in hMATE1 and hMATE2K expressing cells for more than 10 fold compared to the control cells expressing the empty vector. The concentration dependent uptake of TEA and metformin in hMATE1 and hMATE2K demonstrated "simple" Michaelis-Menten kinetics with Km value of 260uM and 355uM in MATE1, and 755uM and 1.2mM in MATE2K respectively. The inhibitory parameters of known drug inhibitors for MATEs verapamil, quinidine, cimetidine and ritonavir were also determined using this model, which are comparable to literature reports. The study demonstrates the model is a compliant and useful in vitro tool to screen MATE1 and MATE2K involved drug interaction and/or drug induced renal toxicity in early stages of drug development.

S 2068 Exploring the Interface between Air Pollution and Metabolic Syndrome: The Bittersweet Dilemma

U. P. Kodavanti[1] and J. G. Wagner[2]. *[1]EPHD, NHEERL, US EPA, Research Triangle Park, NC and [2]Cardiorespiratory Toxicology, Michigan State University, East Lansing, MI.*

The metabolic syndrome (MetS) affects approximately 32% of the US population and is expected to grow to 34% by 2020. The conventional risk factors, such as diet and sedentary lifestyle, do not fully explain this rising epidemic. Multiple lines

of epidemiological evidence show associations of high ambient air pollution with the incidence of metabolic disease, such as diabetes, and risk factors that comprise the metabolic syndrome. Coincident with uncontrolled air pollution in developing countries are improved lifestyle (less physical activity) and calorie-rich diets. These imply that there is likely an interaction between diet, metabolic processes, and injuries induced by inhaled pollutants. While new research on the contribution of air pollution to cardiometabolic derangements is emerging, the mechanisms by which airborne materials can affect multiple cardiovascular and metabolic pathways are unknown. The goal of this session is to present new data from both animal and human studies to shed light on the interaction of air pollutant exposure with both the incidence and exacerbation of diabetes, obesity, and cardiovascular disease. Some key issues to be addressed by presentations in this session include: What behavioral, dietary, and environmental factors contribute to the development of MetS and, subsequently, to type 2 diabetes and cardiovascular disease? How do obesity and other metabolic abnormalities interact to promote cardiovascular disease? How do air pollutants alter cardiometabolic outcomes during controlled versus natural exposures in humans? How does diet-induced metabolic syndrome alter cardiovascular responses to single and multipollutant exposures? How does obesity predispose for exaggerated airway responses to pollutants? Lastly, how do air pollutants alter stress pathways and energy expenditure? Together, the presentations begin to answer these critical questions and provide some seminal examples of the toxic interface between diet, metabolic homeostasis, and air pollutant exposure.

S 2069 The Role of Overweight and Obesity in the Diabetes and Cardiorenal Syndrome

J. R. Sowers. *Department of Internal Medicine, Diabetes and Cardiovascular Center, University of Missouri, Columbia, MO.* Sponsor: U. Kodavanti.

The presence of a group of interactive maladaptive factors including hypertension, insulin resistance, metabolic dyslipidemia, obesity, microalbuminuria, and/or reduced renal function constitutes the cardiorenal metabolic syndrome (CRMS). Overweight, obesity, diabetes and chronic kidney diseases (CKD) have grown to pandemic proportions in industrialized countries during the past decade. The fact that these interactive factors promote heart and renal disease has been documented in large population-based studies. Obesity seems to be the driving force behind the development of heart disease, diabetes and CKD and therefore the CRMS. The relationship between overweight/obesity, insulin resistance and kidney disease begins in early childhood and appears to be related to overconsumption of high-fructose corn syrup and insufficient physical activity. Today, 13 million children are obese, and over 70% of these children are likely to become obese adults. Indeed, approximately 30% of male and 34% of female adults in the United States are obese. This lifestyle-related epidemic will be a major societal medical and economic problem that will accentuate the current epidemic of CRMS in the United States and other industrialized and emerging industrialized countries. This presentation will review the potential mechanisms by which obesity and other metabolic abnormalities interact to promote diabetes and cardiovascular disease. Some of the potential mechanisms might explain the role of air pollutants in exacerbating cardiometabolic disease.

S 2070 The Effects of Air Pollution Exposures on Aspects of the Metabolic Syndrome in Humans

R. Brook. *Division of Cardiovascular Medicine, University of Michigan, Ann Arbor, MI.* Sponsor: U. Kodavanti.

Particulate matter (PM) air pollution is associated with an increased risk of cardiovascular (CV) events over periods of both short and long-term exposures. While PM is capable of promoting CV morbidity by a variety of mechanisms, an important pathway may be via the potentiation of facets of the metabolic syndrome (MetS) including hypertension and insulin resistance. We have undertaken a series of human studies in the US and China that evaluated the acute and sub-acute effects of PM exposures upon several aspects of the MetS in humans. First, we performed a series of randomized double-blinded cross-over studies of acute exposures to rural coarse concentrated ambient PM (CAP). Systolic (0.32 ± 0.74 mm Hg, p=0.021) and diastolic (0.27 ± 0.77 mm Hg, p=0.05) blood pressure (BP) linearly increased during the inhalation of coarse CAP [76.2 ± 51.5 μg/m-3] compared to filtered. Heart rate was higher and the ratio of low-to-high frequency heart rate variability increased together with circulating endothelial progenitor cells during CAP exposures. Second, the homeostasis model assessment of insulin resistance (HOMA-IR) was measured in 25 healthy adults living in rural Michigan were transported to an urban location for 5 consecutive days of daily 4-5-hour-long ambient air pollution exposures. A 10 μg/m−3 increase in sub-acute fine PM exposures was associated with increased HOMA-IR (+0.7, p=0.023) and reduced heart rate variability (standard deviation of normal-to-normal intervals). Lastly, we evaluated the association between personal exposure to combustion-related BC [median=4.1 μg/m−3] with ambulatory BP and autonomic function in Beijing, China. An interquartile range increase in BC during the previous 10 hours was associated with an increase in systolic BP of 2.20 mmHg and diastolic BP of 1.55 mmHg. This series of experiments demonstrates that exposures to fine and coarse PM, as well as BC, are capable of increasing BP and impairing metabolic insulin sensitivity in humans. PM air pollution may be an important environmental factor contributing to global epidemic of the MetS.

S 2071 Cardiometabolic Interactions of Diet and Air Pollution: Field Studies with Multipollutant Atmospheres

J. G. Wagner. *Cardiorespiratory Toxicology, Michigan State University, East Lansing, MI.*

Metabolic conditions such diabetes, insulin resistance and metabolic syndrome (MetS) might predispose an individual to adverse cardiovascular responses to air pollutant exposures. While health complications from exposure to various airborne pollutants have been modeled in rodents with hypertension and various cardiac diseases, comparable studies in animal models of metabolic disorders have not been conducted. This presentation will briefly survey the use of relevant animal models that study cardiovascular and metabolic outcomes, and will then focus on new results from a series of studies that use the high fructose-fed (HFr) rat model of diet-induced CMS. HFr- rats were exposed to ozone, fine particulate matter (PM2.5) or their combination, to test the hypotheses that 1) adverse cardiovascular effects of air pollution would be exacerbated by the MetS and 2) coexposure to multipollutants would induce greater toxicological responses than to single pollutants. Prior to exposures, HFr rats had dyslipidemia, hepatic lipidosis, and elevated blood pressure (BP) and heart rate (HR), but had depressed heart rate variability (HRV). Reductions in BP and HR by air pollutant exposures were exacerbated and prolonged in HFr rats. Interestingly, insulin resistance and lipid derangements were less severe in HFr rats after exposures. Results using this novel model of CMS will contribute to the development of prevention and intervention strategies to protect this susceptible population from the adverse cardiovascular effects of multipollutant atmospheres.

S 2072 Augmented Pulmonary Responses to Acute Ozone Exposure in Obese Mice: Roles of TNFR2, IL-13, and IL-17A

S. A. Shore. *Department of Environmental Health, Harvard School of Public Health, Boston, MA.* Sponsor: U. Kodavanti.

Acute ozone exposure results in more inflammation, greater changes in pulmonary mechanics, and greater airway hyperresponsiveness (AHR) in obese than lean mice. These obesity-related differences in ozone responses are observed both in genetically obese mice and in mice with diet induced obesity. Because obese mice have increased circulating TNFα, and because TNFα has been shown to play a role in responses to acute ozone in lean mice, we examined the role of TNFα in the augmented responses to acute ozone exposure of obese mice. Lean wildtype (WT) and TNFR2 deficient (TNFR2-/-) mice, and obese Cpefat and TNFR2 deficient Cpefat mice (Cpefat/TNFR2-/-) were exposed to ozone (2 ppm for 3 h) or air. Ozone-induced increases in pulmonary mechanics, airway responsiveness, and cellular inflammation were greater in Cpefat than WT mice. In lean mice, TNFR2 deficiency ablated ozone-induced AHR, without affecting pulmonary inflammation, whereas in obese mice, TNFR2 deficiency augmented ozone-induced AHR but reduced inflammatory cell recruitment. Interestingly, ozone caused pulmonary expression of IL-13 in Cpefat but not WT mice. In Cpefat mice, anti-IL-13 attenuated ozone-induced increases in pulmonary mechanics and inflammation, but not AHR. There was no effect of anti-IL-13 in WT mice. Ozone also caused greater IL-17A expression in lungs of obese versus lean mice, and anti-IL-17A treatment attenuated ozone induced AHR and inflammation in obese but not lean mice. CD4+ cells were the source of both the IL-13 and the IL-17A induced by ozone in obese mice. These results indicate that pulmonary responses to ozone are not just greater, but qualitatively different in obese versus lean mice. In particular, in obese mice, ozone induces activation of CD4+ T cells, causing release of IL-13 and IL-17A that exacerbate the pulmonary effects of ozone, in part via synergism with TNFα. The majority of the population of the US is either obese or overweight. Our results emphasize the need for improved understanding of the effects of ozone in this population.

S 2073 Emerging Evidence of Ozone's Metabolic Effects and Potential Mechanisms

U. P. Kodavanti. *EPHD, NHEERL, US EPA, Research Triangle Park, NC.*

Recent evidence suggests that air pollutant exposure impacts key metabolic processes and is linked to metabolic syndrome. Because ozone (O3) does not translocate systemically, neuronal pathways and/or systemic mediators released from lung injury are proposed to account for the metabolic impairment. Our studies provide evidence that short-term O3 exposure induces reversible metabolic alterations, including glucose intolerance and increases in blood leptin, glucose, fatty acids, and amino acids in rodent models. These metabolic alterations are reflected in transcriptional changes in the liver, consistent with increased catabolism (i.e., increased energy expenditure and reduced lipid synthesis). Liver metabolic processes are likely coordinated with changes in adipose and muscle metabolism. Because these O3-induced systemic changes are accompanied by large increases in circulating catecholamine (i.e., stress response), derangement of neurohormonally-mediated metabolic processes likely play a key role. Experiments using adrenalectomized rats confirm the role of circulating adrenal hormones for the induction of the acute metabolic response after acute O3 exposure. Collectively, data show that short-term air pollution exposure results in increased energy expenditure. Conversely, the hypothermic and bradycardia responses noted in rodents exposed to air pollutants suggest reduced energy demand. Currently systems approaches such as transcriptomics, proteomics, and metabolomics are being used to determine how these acute metabolic responses induced by O3 might relate to adaptation, and when elicited chronically, may result in disease (e.g., obesity, insulin resistance, and/or type 2 diabetes). (This abstract does not reflect USEPA policy).

W 2074 Advances in the Application of Imaging Technologies to Developmental Toxicology

S. L. Makris[5], V. Sutherland[1], C. W. Lo[2], M. G. Paule[3] and L. D. Wise[4]. *[1]Reproductive Toxicology, Bristol-Myers Squibb Company, New Brunswick, NJ, [2]Department of Developmental Biology, University of Pittsburgh, Pittsburgh, PA, [3]Division of Neurotoxicology, NCTR, US FDA, Jefferson, AR, [4]Developmental & Reproductive Toxicology, Merck Research Laboratories, West Point, PA and [5]National Center for Environmental Assessment, US EPA, Washington, DC.*

The multiple imaging modalities utilized in developmental science have allowed for the ability to visualize everything from gene activation in a zebrafish embryo to developmental stages in a growing conceptus to malformations in scores of rodent fetuses in a high-throughput manner. This workshop is designed to showcase the advantages of the various imaging systems utilized in developmental studies and their benefits to basic researchers, preclinical experimenters, and clinicians alike. Presentations include examples of the diverse imaging tools (confocal episcopic fluorescence, 2-photon microscopy, ultrasound, micro-MRI, PET, and micro-CT) currently being utilized for developmental (including neurodevelopmental) toxicology studies and how these techniques are being applied to help understand the normal versus a diseased state. The potential for expanded application of developmental imaging data in a regulatory context for pharmaceuticals and environmental chemicals is widely recognized. However, there are challenges in implementing this conceptual shift in the methods traditionally used for hazard characterization and in applying the results in decision-making. Technical and methodological standards need to be developed; validation studies will be necessary to demonstrate the sensitivity, specificity, and reliability of the methods to support utilizing them in a regulatory context; and laboratories will need to weigh the cost of implementing an imaging protocol against the potential gains in technical efficiency and increased study sensitivity.

W 2075 Lightsheet Microscopy for Rapid High-Resolution of Fluorescent Reporters and Fusion Proteins in Developing Zebrafish

K. J. Clark. *Biochemistry and Molecular Biology Department, Mayo Clinic, Rochester, MN.* Sponsor: V. Sutherland.

To date, 3- and 4-dimensional imaging modalities have had limited utility in assessment for purposes of drug development. New microscopy techniques are rapidly improving our means to visualize dysmorphogenesis and biological function in developing zebrafish. Our laboratory is producing a number of BioBanner transgenic fish lines that will produce a short half-life green fluorescent protein in response to cell signaling. One of our BioBanner fish lines, contains glucocorticoid response elements that are bound by activated glucocorticoid receptor to produce GFP in response to glucocorticoids like cortisol or fluticasone. The Lightsheet microscope uses cylindrical lenses to create laser sheets that illuminate a single z-plane at a perpendicular to the collection objective(s). This narrow plane of excitation reduces sample phototoxicity and allows capture of an entire z-plane at once, which greatly speeds collection of 3- and 4- dimensional imaging. Rapid imaging of entire zebrafish larvae at single time-points or over extended periods of time provides insight into biological responses throughout development. This presentation will provide an overview of the basic principles of Lightsheet microscopy, describe our glucocorticoid-responsive BioBanner fish, and provide sample Lightsheet images obtained from these fish.

W 2076 High-Throughput Phenotyping Pipeline Using Multiple Imaging Modalities for the Diagnosis of Structural Birth Defects in Fetal/Newborn Mice

C. W. Lo[1], X. Liu[1], A. Kim[1], Y. Chen[1], Y. Li[1], N. Klena[1], L. Leatherbury[2], R. Francis[1] and K. Tobita[1]. *[1]Department of Developmental Biology, University of Pittsburgh, Pittsburgh, PA and [2]Children's National Medical Center, Washington, DC.* Sponsor: V. Sutherland.

We conducted a large-scale forward genetic screen in mice with chemical mutagenesis to elucidate the genetic etiology of structural birth defects. For this study, we developed a sophisticated mouse phenotyping pipeline entailing the combined use of noninvasive in utero fetal ultrasound imaging of pregnant dams, with follow up analysis of the abnormal fetuses and neonates using a combination of micro-CT, micro-MRI and histopathology examination by confocal episcopic fluorescence image capture (EFIC). Confocal EFIC imaging is a histological imaging technique ideally suited for the analysis of complex anatomy associated with structural birth defects, as it allows any standard paraffin embedded sample to be imaged using native tissue autofluorescence, generating high resolution registered 2D image stack of the specimen suitable for seamless digital resectioning in any orientation and also rapid 3D rendering. Using this combined approach, we have screened over 70,000 fetal mice encompassing 4X genome coverage, and have recovered over 2,000 mutants exhibiting a wide spectrum of birth defects, including eye/craniofacial/brain malformations, limb and other skeletal anomalies, neural tube closure defects, congenital heart disease, and visceral organ defects such as multiple organ cysts, polycystic kidney disease, biliary atresia, intestinal malrotation/obstruction, kidney agenesis, hydronephrosis, hydroureter and bladder obstructions, thymus aplasia, and other visceral organ anomalies. Using whole mouse exome sequencing analysis, we have recovered the disease causing mutations in over 100 of the mutant mouse lines recovered from the screen. Together, these studies show the efficacy of our phenotyping pipeline for the diagnosis of birth defects in fetal/neonatal mice. Supported by NIH grant HL098180

W 2077 PET/CT Approaches to Imaging Aspects of Neurotoxicity in the Developing Animal

M. G. Paule. *Division of Neurotoxicology, NCTR, US FDA, Jefferson, AR.*

This presentation will address the use of PET coupled with CT technology to monitor aspects of general anesthetic-induced neurotoxicity in both rodents and nonhuman primates. General anesthetics are capable of causing increases in apoptotic brain cell death in animal models when exposures occur during the brain growth spurt. This abnormal cell death has been associated with subsequent cognitive deficits in both rodents and nonhuman primates. Naturally, there is concern over the use of these agents in the pediatric setting. Specific PET markers of apoptosis (radiolabeled Annexin V and DFNSH) have been used to follow the onset, time course and severity of this exposure-related phenomenon in rodents, but, as of yet, similar markers capable of crossing the primate blood-brain barrier have not been identified. Under the presumption that apoptotic phenomena likely activate glial cells in the CNS, a marker of glial cell activation (FEPPA) is being used as a surrogate marker for cell damage/death. FEPPA targets the Transporter Protein (TSPO)/Peripheral Benzodiazepine Receptor (PBR) which is located on the mitochondrial membrane and is overexpressed in activated glial cells. Early data indicate that FEPPA does in fact access the nonhuman primate brain and, in animals exposed to general anesthetics, exhibits increased retention times suggesting increased glial activation, presumably in response to brain cell damage.

W 2078 Recent Applications of Micro-CT Imaging in Preclinical Developmental Toxicology

C. Winkelmann. *Imaging Department, Merck Research Laboratories, West Point, PA.* Sponsor: V. Sutherland.

Micro-computed tomography (micro CT) for the evaluation of fetal skeletal morphology has become a routine GLP procedure in this laboratory. The presentation will provide an overview of basic principles of micro-CT including acquisition,

reconstruction, visualization, segmentation, and registration. Examples of analyses using segmentation and registration of skeletal elements and visceral organs, which required contrast staining, will be presented. It will be evident that these latter techniques offer the potential for automated analysis of morphology. The use of micro-CT in other laboratories to assess development will be briefly reviewed. Conduct of positive control studies and studies with new drug candidates show that micro-CT evaluation of the fetal skeleton is equal to conventional evaluations after alizarin red staining. Relative to alizarin red evaluations, micro CT evaluations have not changed the NOEL and/or LOEL of a study. The incidences of a few minor skeletal abnormalities are either increased (e.g., incomplete ossification of sternebra 5 in rats and of metacarpal 1 in rabbits) or decreased (e.g., trace supernumerary ribs in rats) across all groups including controls by micro-CT compared to alizarin red evaluation. These differences are mainly due to the slightly lower resolution of the current scanner; however, a different scanner with higher resolution is under evaluation. Results of a study that scanned postnatal rat pups to assess skeletal changes in the same animals over time will be discussed. Such procedures will be useful in performing longitudinal studies. The ready availability of electronic images provided ample material for development of a web-based atlas. Discussion will conclude with our current efforts directed toward automated segmentation and analysis of all fetal rabbit skeletal elements in order to flag potentially abnormal fetuses for manual micro-CT evaluation.

W 2079 Imaging Data for Scientific Decision-Making in a Regulatory Context

S. L. Makris. *ORD, NCEA, US EPA, Washington, DC.*

Imaging technologies that facilitate high resolution evaluation of the developing fetus and/or neonatal individual have been utilized with outstanding success in developmental research and clinical practice for many years. Innovative application of current technologies has historically been used to resolve complex scientific issues. In the research and clinical communities, there is a high degree of confidence in the derived information. Yet, there are likely to be many challenges that arise in bridging the gap between these widely accepted applications and regulatory decision-making for pharmaceuticals and environmental chemicals. This presentation will address the ways in which imaging technologies have been utilized in a regulatory context to date, and how they might be utilized in the future, particularly in the field of developmental toxicology. The pathway to achieve this goal remains under discussion. There are recognized benefits of implementing an organized and collaborative effort to address the collection, interpretation, and application of developmental toxicology imaging data. Establishing technical standards for imaging hardware and software, as well as methodological best practices for technological processes and procedures, would be useful in standardizing imaging within and across laboratories. Validation of developmental imaging technologies would need to include a demonstration of such inter- and intra- laboratory consistency in the detection of morphological alterations during development, the ability to detect effects from known developmental toxicants (positive reference chemicals), and evidence that imaging techniques provide, at the very least, a similar level of sensitivity and specificity as conventional developmental toxicity testing methods. Additionally, issues of increased efficiency, and cost vs. benefit would need to be explored. In spite of the many challenges, there is widespread consensus on the potential usefulness of imaging data for the characterization of developmental hazard.

W 2080 Beyond hERG: Novel Cardiovascular De-Risking Strategies and Their Regulatory Acceptance

J. Davis and T. Brabham. *Pfizer, Andover, MA.*

Whether drug development is prosecuting small molecule or biologic programs, cardiovascular safety is still one of the leading causes of compound attrition. The rationale for attrition has gone far beyond the traditional drug-induced long QT syndrome associated with inhibition of the human Ether-a-go-go Related Gene (hERG). Pharmaceutical companies have built-in greater controls for eliminating that hurdle by using sensitive high-throughput *in vitro* screens around this and other important cardiac ion channels that have significantly reduced arrythmogenic risks. Despite these advances, adverse effects on the cardiovascular system remain a multifactorial risk, difficult to discern, especially during early drug discovery stages. Recent comprehensive preclinical attrition data has demonstrated that hemodynamic alterations, vasculitis, and left ventricular cardiac hypertrophy are increasing in incidence in short- and long-term animal studies. Unlike the well-established mechanistic link between hERG and QT prolongation, these unique pathologies either lack suitable investigative tools and models, or have a lack of confidence in the underlying mechanisms preclinically. This challenge is compounded by the advancement of molecules that act as novel targets for which limited safety data are available. However, in the past couple of years promising advances have been made in *in vitro* and *ex vivo* assay development, which have the potential to impact industry cardiovascular safety de-risking standards much as hERG screening did. Investigators are exploring more integrative tactics, by effectively employing predictive *ex vivo* tissues baths as well as stem cell-derived human cardiomyocytes to rank-order and/or advance suitable drug candidates. While developing innovative tools is important, it's also clear, as the diversity of pharmaceutical drug products evolve into a more challenging target space (i.e., kinase inhibition), these inherent risks need to be evaluated on par with regulatory expectations.

W 2081 Study of Cardiovascular Safety of Small Molecules and Biologics: The State of Science, Challenges, and Gaps

A. S. Bass[1] and F. Sannajust[2]. *[1]Discovery Sciences Support, Merck & Co., Boston, MA and [2]Safety and Exploratory Pharmacology, Merck & Co., West Point, PA.*

The search for innovative approaches allowing early prediction of cardiovascular toxicity of small molecules or biologics is urgently needed. Despite significant efforts to identify new methodologies and assays that accurately predict the risk of cardiovascular toxicity, everyone recognizes that validation of these test systems is only evident from the number of new molecules safely brought to the marketplace. The story of the hERG channel assay and the impact that it has had on removing from development those molecules that pose a risk of proarrhythmia exemplifies both the science and strategy that goes into validation of an assay. Possessing data which describing a molecule's profile on other established mechanisms of cardiovascular toxicity, e.g., effects on receptors, ion channels, transporters, kinases and intracellular organelles (e.g., mitochondria), sets up a "theoretical" concern, a hypothesis, amendable to further testing. In the case of these simple biologic targets and those associated with more complex cardiovascular toxicities, quantitative translation and predicting adverse events remain to be established. Translational biomarkers, testing in viable organs or tissues harvested from patients and study of pluripotent stem cells offer hope of resolving some of the challenges of translational biology. However, considered as steps in the lead optimization phase, *in vitro* assays do not fully represent the integrated physiology of animals or patients. Furthermore, there are adverse cardiovascular events for which the underlying pathophysiology is not well understood. These latter cases are emblematic of challenges faced by the scientific community. For those investigators, a "line of sight" to de-risking the potential for cardiovascular toxicity of a promising new drug begins in early discovery and continues through to the post-marketing phase.

W 2082 Regulatory Expectations for Submission of Novel *In Vitro* Assays Addressing Cardiovascular Risk

T. Papoian. *US FDA, Silver Spring, MD.* Sponsor: J. Davis.

The potential for bio-pharmaceuticals to possess unintended clinical effects on the cardiovascular system during the drug development process is an important regulatory concern. Although in vitro and in vivo preclinical models have been designed to effectively screen bio-pharmaceuticals for specific cardiovascular liabilities, such as QT interval prolongation and other proarrhythmic effects, failure to prevent cardiovascular risk in humans continues to occur, particularly with compounds that do not specifically interfere with cardiac ion channels. Examples for improvement in screening for potential cardiotoxicity would be development of more human-specific models, such as human induced pluripotent stem cell-derived (iPSC) cardiomyocytes. Although this and other in vitro models are gaining acceptance among bio-pharmaceutical companies for initial screening of candidate compounds for further development, the predictivity, reliability and regulatory acceptance of submitted data generated from such newer in vitro models requires proper validation and qualification, so that appropriate decisions regarding human risk assessment during subsequent clinical testing can be made with an acceptable degree of confidence. Regulatory agencies, such as the FDA, clearly have been supportive of such efforts to develop better predictive in vitro models that can improve drug safety for subsequent testing and therapeutic use in humans. Some of the regulatory expectations for submission of novel in vitro assays to address non-proarrhythmic cardiovascular risk will be discussed.

W 2083 Translation of Models for Assessment of Hemodynamic Endpoints

J. Heyen[1], M. Hemkens[1], W. Hu[3], C. Northcott[4], L. Warren[5], A. Bassyouni[1], S. Jenkinson[1], J. Steidl[4], T. Brabham[4] and J. Davis[2]. *[1]Global Safety Pharmacology, Pfizer, San Diego, CA, [2]Investigative Toxicology, Pfizer, Cambridge, MA, [3]Investigative Toxicology, Pfizer, San Diego, CA, [4]Global Safety Pharmacology, Pfizer, Groton, CT and [5]Compound Safety Prediction, Pfizer, Groton, CT.*

Hemodynamic effects of non-cardiovascular compounds continue to be a challenge in drug development. Early compound selection employing a robust cardiovascular ex vivo/in vivo screening funnel can lead to improved decision making and project efficiencies. To this end, understanding of the cross model and cross-species translation can significantly inform decision making and compound advancement. The translational relationship between in vitro and in vivo such as the isolated rat aorta and conscious rat telemetry is explored and defined for select chemical series and mechanisms. These assays have optimized detection/differentiation of compounds with potential hypotensive risk associated with a mechanistic structure-activity-relationship (SAR). Key relationships in this strategy included the establishment of in vitro concentrations relevant to observed in vivo effects. Several case studies will be shared demonstrating key impacts and decision making criteria. Additionally, the understanding cross species in vivo translation and effects can strengthen decision making and improve the ability to achieve the ultimate goal of predicting human outcomes.

W 2084 Development of Tools for Early Assessment of Cardiac Hypertrophy Risk during Drug Development: Leveraging Cell Models and Gene Expression Analysis

T. K. Baker and G. H. Searfoss. *Investigative Toxicology, Eli Lilly and Company, Indianapolis, IN.* Sponsor: J. Stevens.

Cardiac hypertrophy is initiated and maintained by a wide array of endocrine, paracrine, and autocrine growth factors in response to increased work load, injury, or defects in contractile performance. Cardiac hypertrophy is clearly double-edged, where under exercise or pregnancy it is beneficial and referred to as physiologic, but under sustained hypertension or aortic stenosis cardiac hypertrophy is pathologic. Both types of hypertrophy are characterized by an increase in cardiomyocyte size, but only pathological hypertrophy is associated with increased apoptosis and fibrosis as well as functional changes such as altered cellular Ca2+ homeostasis, ion channel remodeling, reduced contractile force and relaxation velocity. While initially an adaptive response that attempts to maintain cardiac output, sustained cardiac hypertrophy induced by pathological stimuli is a leading predictor for the development of heart failure. Drug-induced cardiac hypertrophy often manifests in the later stages of preclinical safety testing. In response to this late stage risk, an early safety assessment screening paradigm has been developed using iPS derived human cardiomyocytes, which are phenotypically and functionally more reflective of cardiac myocytes in vivo. Upon treatment with molecules associated with the induction of cardiac hypertrophy we have characterized these cells using endpoints that represent the hallmarks of cardiac myocyte hypertrophy including; cytoskeleton remodeling, induction of the fetal reversion gene expression program, and secretion of natriuretic peptides. In addition, new approaches that leverage high content imaging and computational systems biology have been applied to the model, which allow for a more thorough characterization and deeper understanding of drivers of cardiac myocyte hypertrophy.

W 2085 Applications of Stem Cell-Derived Cardiomyocytes—From Basic Research to Arrhythmia Prediction to Potential Regulatory Implications

K. L. Kolaja. *Cellular Dynamics International, Montclair, NJ.*

Within the basic science community, *in vitro* models and approaches that improve the early understanding of compound's beneficial or deleterious effects as well as accurately reflect diseased tissues are sorely needed. Breakthroughs that enable research to make faster, more accurate, human relevant decisions would be embraced by regulatory agencies as well as companies who make products (be it chemical, food, drugs, etc). Recent advancements in the ability to manufacture stem cell-derived tissues has enabled drug discovery scientists to create relevant models for pharmacology and toxicology investigations using pluripotent stem cells of human origin. Specifically to benefit drug-induced cardiotoxicity, stem cell-derived cardiomyocytes have been made in high quality, purity, and quantity and confirmation of their expression, function, and response to cardioactive molecules has occurred. Across a set of nearly 80 compounds, stem cell-derived cardiomyocytes were shown to respond in a clinically meaningful manner to drugs that induce arrythmia. This approach is being adopted by pharmaceutical companies as a means to better assess drug-induced arrhythmia at early stages of drug development and is in the early stages of consideration by regulatory agencies as a surrogate for extensive clinical data. In addition, mechanistic studies in stem cell-derived cardiomyocytes have been conducted to investigate potential kinases that mediate sunitib-induced cardiotoxicity. While the utility of stem cell-derived cardiomyocytes as a model for cardiotoxicity has not been broadly studied, a real opportunity exists to evaluate effects in a human cell system that is stably beating and maturing *in vitro*. A higher level of opportunity exists since stem cell-derived cardiomyocytes are being made from a genetically diverse set of individuals which will allow interrogation of the relationship of genetics and drug-induced cardiotoxicity in an *in vitro* manner.

W 2086 Cardiovascular Risk Assessment for Biopharmaceuticals

H. M. Vargas. *Safety & Exploratory Pharmacology, Amgen, Inc, Thousand Oaks, CA.* Sponsor: J. Davis.

Biopharmaceutical (BP) drugs are innovative medicines that have revolutionized the treatment of human disease, and offer the opportunity to develop new therapeutics with high specificity for their human target, long half-life and target coverage, and low risk for "off-target" pharmacology. While BP attrition due to safety concerns is generally considered to be low, especially for risks like QTc prolongation, these novel therapeutics may have functional cardiovascular effects that require evaluation during nonclinical drug development. The cardiovascular evaluation of BP products requires a science-based, case-by-case approach, as each biological modality will have unique pharmacological characteristics that influence the testing strategy. The integration of safety pharmacology endpoints into general (repeat-dose) toxicity studies is a rational paradigm for assessing potential changes in the cardiovascular system, but requires thoughtful planning. In some cases, dedicated and optimally-designed nonclinical cardiovascular safety studies may be needed to assess a functional risk triggered by target-pharmacology concerns. For example, implant telemetry studies may be needed to detect small changes in arterial blood pressure after acute and chronic exposure. This presentation will cover some examples of cardiovascular strategies used to evaluate novel biopharmaceuticals.

W 2087 Communication and Engagement with the Public about Toxicology in a World That Misunderstands Science and Scientists: How Do You Make Your Message Relevant and "Sticky"?

B. L. Kaplan[1] and S. J. Hermansky[2]. *[1]Center for Environmental Health Sciences, Department of Basic Sciences, Mississippi State University, Mississippi State, MS and [2]Research and Quality Innovation, ConAgra Foods, Omaha, NE.*

Dissemination of scientific results drives innovation and productivity in all fields, including toxicology. It is critical to effectively communicate findings to colleagues, peers and trainees in written and oral forms and most of us are comfortable in this arena. However, it is more difficult to communicate results and translate risk to the lay public that listens to messages through an emotional lens—especially in the world of social media that defines "experts" based upon frequency and volume of communication rather than demonstrated expertise. Certainly, the public faces a barrage of environmental health issues associated with alleged hazards due to contamination of food, water, air and soils. To make appropriate decisions, the public, media and legislators need information in a readily understandable format presented in a way that resonates with them. In general, communicating and engaging with the lay public is not addressed as part of graduate training, and, therefore, even accomplished toxicologists who are effective scientific communicators find themselves underprepared. Communication directed "at" lay audiences, even that which uses appropriate terminology, is often ignored and does not "stick" with the target audience. Moreover, it is now clear that effective public communication must exceed simple dissemination of results; all stakeholders, including affected communities and populations, should be engaged by toxicologists in bidirectional discussions that facilitate learning by both scientists and the public on an emotional and transparent level. Four actors from four different vantage points will present on the role scientists should play in communication and engagement with the public about toxicology. A discussion panel will follow.

W 2088 To Speak or Not to Speak.That Is the Question.And the Challenge

M. P. Holsapple. *Battelle, Columbus, OH.*

Practically every member of the SOT has been given an opportunity to speak about their research in a scientific setting –highlight their hypothesis, describe methods, present results, make interpretations, defend their conclusions. Because the above is centered on THEIR work, it is generally a comfortable experience, and there is no question that these presentations highlight the values and impacts of the science of toxicology. Far fewer members of the SOT are called upon to provide a non-scientific perspective on what it means to be a toxicologist, or on why the science of toxicology should be viewed by the public as value-added. The focus of this presentation will be on the challenges inherent in serving as a spokesperson for science and our Society. The first question is – Should the SOT enlist its members to occasionally communicate on behalf of science, toxicology and the Society? The short answer is 'yes' based on past practices - there are examples of how the SOT has reached out to its members for this type of communication. The second question is - What are the challenges inherent in communicating on these subjects? One of the strengths of the SOT is the diversity of its membership, and any message offered needs to leverage that diversity. Even though toxicology is one of the most integrated sciences currently being practiced, and there is an increasingly greater emphasis on the need for multi-disciplinary research teams, toxicology continues to struggle with an 'identity crisis' that is common across the sciences today. Societal perceptions are changing and must be anticipated. The impacts of "chemophobia", and the perception that all toxicologists do is 'tell us that everything is harmful' can impact our effectiveness and credibility. There are also examples of the "good guy/bad guy" syndrome, as in "bad guys" are in industry or government, and "good guys" are in academia. Ultimately, we must recognize that in spite of the challenges, the failure to speak about the value of the SOT, and of the science that exists at its core, could marginalize our discipline, and indeed all of science, in the eyes of the public.

W 2089 The New Universe of "Knowledge"

S. J. Hermansky. *Research and Quality Innovation, ConAgra Foods, Omaha, NE.*

Information availability, whether accurate or not, is rapidly evolving and continues to change how we perceive and interact with the world in which we live. The definition of "expert" is no longer based on education and training but on the frequency and passion of communication. How this new universe of knowledge affects our world cannot be ignored when a single person has the power to initiate movements that rapidly and completely demonize finely textured ground beef ("pink slime") or cause major companies to reformulate products to eliminate a specific ingredient. As scientists, we must adapt our communication style to this new world or be drowned out or, worse, become irrelevant. This is no easy task as we work to protect integrity and credibility for ourselves and our employers. Accomplishing real and persistent change in our approach to communication requires a commitment of time and resources and an effort to understand the emotional drivers in this new universe of "knowledge." Not only does our ability to influence our stakeholders and public behavior depend on it, the very role of science in society depends on it.

W 2090 Values, Trust, and Science

C. Arnot. *Center for Food Integrity, Gladstone, MO.* Sponsor: S. Hermansky.

All organizations operate through social license or the privilege of operating with minimal formalized restrictions (regulation or legislation). A social license is granted when you operate in a way consistent with the ethics, values and expectations of your stakeholders (customers, employees, community, regulators, legislators, the media). Once lost, either by reducing or eliminating public trust, social license is replaced by various levels of control designed to compel performance consistent with expectations. Operating with a social license is flexible and low cost while operating with a high degree of social control increases costs and reduces flexibility. A radical example of lost social license is Arthur Anderson and Enron. After the collapse of Enron, the accounting profession lost its social license. Freedom enjoyed by scientists is in jeopardy as stakeholders raise questions about the trustworthiness of today's science-based industries. Our research, focused on the food industry, demonstrated that three primary elements drive trust: competence, confidence, and influential others. Competence is about skills and technical ability. Historically, we as scientists have focused our communication on this believing stakeholders will make logical data based decisions. However, with today's social media, competence no longer ensures public trust. Thus, consumers focus on other aspects of communication including confidence: the perception that the communicator has shared values and ethics and a belief they will do the right thing. Similarly, consumers turn to other sources of information or their "influential others" (family and friends). Our research also demonstrated that confidence, or shared values, is much more important than competence for consumers. This research should be relevant to today's crisis of science communication. New ways of engaging communicating are required if we want to build trust and maintain social license. A major driver of trust in today's world is a non-negotiable focus on transparency. To succeed, we need to demonstrate our commitment to practices that are ethically grounded, scientifically verified and economically viable.

W 2092 Databases Facilitating Systems Biology Approaches to Toxicology

S. M. Bello[1] and M. Shimoyama[2]. [1]*Mouse Genome Informatics, The Jackson Laboratory, Bar Harbor, ME and* [2]*Rat Genome Database, Medical College of Wisconsin, Milwaukee, WI.*

The application of systems biology approaches to toxicology promises discovery of new molecular and genetic connections, the ability to draw novel inferences about mechanisms and modes of actions, and the ability to build better predictive models. However, a systems biology approach first requires identifying appropriate data from a vast array of possible data types and resources. By using multiple high-quality databases, researchers can pull together the required gene, pathway, chemical relationship, and other information needed to build their predictive model. To best use these resources, one first needs to know what resources exist, what the strengths and limitations of the resources are, and how to efficiently retrieve data from them. This session will provide an introduction to several types of resources, including model organism (Mouse Genome Informatics, Rat Genome Database), pathway (Reactome), and toxicology (Comparative Toxicogenomics Database, EPA Dashboard) databases. The goal of this session is to familiarize participants with the power and limitations of publicly available databases that may be used to build and refine models of biological systems that can be applied to toxicology research. Talks will present content overviews for each database and demonstrate data retrieval and analysis capabilities. Speakers also will be available for interactive demonstration sessions during the meeting (see the US EPA booth for dates and times).

W 2093 Mouse Genome Informatics: Using Data Integration to Facilitate Discovery of Relationships Among Genes

S. M. Bello, M. Ringwald, J. E. Richardson, J. A. Kadin, C. J. Bult, J. A. Blake and J. T. Eppig. *Mouse Genome Informatics, The Jackson Laboratory, Bar Harbor, ME.*

The Mouse Genome Informatics Database (MGI, www.informatics.jax.org) is the free international resource for the genetics, genomics, and biology of the laboratory mouse. MGI integrates biological data about the laboratory mouse, including mutant phenotypes, human disease associations, developmental gene expression, gene functions, and tumor biology, from a variety of different sources. MGI uses multiple ontologies and vocabularies including the Gene Ontology (GO), Mammalian Phenotype Ontology (MP), and Mouse Anatomical Dictionary, to annotate data from direct submissions, high throughput projects, and published literature. Data integration and use of ontologies allows users to identify and retrieve annotated data sets with varying levels of specificity. For example, using the recently created MouseMine resource at MGI (www.mousemine.org) a user can generate a list of genes associated with iron ion homeostasis, binding and/or transport, refine this list to only those genes with mutations resulting in neurological or behavioral defects then export the final list in a variety of formats. Or a user can exploit specific MGI query forms to identify genes known to be expressed in the developing autonomic nervous system, then export this list to the batch query tool to retrieve all phenotypes associated with mutations in these genes. This talk will describe some of the ways data are brought in and integrated into MGI, how ontologies can be used to facilitate identification of specific data sets, and how MGI tools may be used for bulk data entry and retrieval. An emphasis will be placed on data types that may be useful in building mechanistic or predictive models for use in toxicology.
The Mouse Genome Database (MGD) at MGI is supported by NIH/NHGRI grant HG000330. MouseMine is supported by NIH/NHGRI grant HG004834.

W 2094 Chemical Connections at the Rat Genome Database

M. Shimoyama. *Rat Genome Database, Medical College of Wisconsin, Milwaukee, WI.* Sponsor: S. Bello.

The Rat Genome Database (RGD) is the premier site for genetic, genomic, physiological and phenotype data for the laboratory rat. RGD provides an integrated research platform for investigators through the integration of multiple datasets and software tools. To meet the needs of the many investigators who use rat in toxi-

cology and pharmacology studies, RGD provides comprehensive data on chemical-gene and drug-gene interactions with specific chemical pathways visualized on its Genome Browser. RGD also has an extensive set of molecular pathways with interactive diagrams including pharmakcokinetic and pharmacodynamics pathways and pathways affected by the presence of toxins and chemicals. RGD also provides comprehensive phenotype measurement data for various strains through its PhenoMiner tool with many records for measurements in which chemicals have been used as stressors, induction agents or phenotype modifiers. The Gene Annotator tool allows users to analyze functional similarities and differences in gene sets and identifies and visualizes subsets of genes associated with particular chemicals and diseases, chemicals and pathways or chemicals and biological processes. Such sophisticated software tools and query systems help users navigate the data to identify new connections and make RGD truly a research platform.

W 2095 The Reactome Knowledgebase: Using Open-Source Data Analysis Tools to Reveal Biological Pathways in Toxicological Data Sets

M. E. Gillespie. *St. John's University, Queens, NY.*

Identify the relevant toxicological pathway from molecular participants is a daunting task. Whether the researcher is taking a detailed look at a small number of proteins or sifting through a large data set identify the functional biological pathway is a critical step. Reactome is an open-source, open access, manually curated and peer-reviewed pathway database. Pathway annotations are authored by expert biologists, in collaboration with Reactome editorial staff and cross-referenced to many bioinformatic databases. Pathway and Expression Analysis tools analyze user supplied data sets permitting ID mapping, pathway assignment and over-representation analysis. The rich detail of the Reactome data set combined with the analysis tools available, provide the toxicologist with an accessible method of identifying biological pathways

W 2096 The Comparative Toxicogenomics Database (CTD): Facilitating Mechanistic Understanding of Chemical Effects

C. J. Mattingly. *Biology, North Carolina State University, Raleigh, NC.*

The Comparative Toxicogenomics Database (CTD; http://ctdbase.org) is a publicly available resource that informs hypothesis development about mechanisms of chemical actions and the impact of environmental exposures on human health. CTD contains manually curated data describing chemical-gene interactions and chemical-disease and gene-disease relationships. Curated data are integrated with external data sets (e.g., Gene Ontology and pathway data) and tools that allow users to navigate and analyze biological relationships relevant to environmental health. This presentation will describe CTD functionality and highlight several new analysis and data visualization features. It will also include information about emerging projects, including the modifications to chemical representations, text-mining workflows for identifying chemical-gene-disease data, novel pathway development tools, and exposure data curation.

W 2097 Interactive Web Application (Chemical Safety for Sustainability Dashboard) for Computational Toxicology Data Exploration

M. T. Martin. *US EPA, Research Triangle Park, NC.*

The USEPA has developed a web-based interface (Dashboard) to synthesize data from the ToxCast and ExpoCast project in the federated Aggregated Computational Toxicology Resource (ACToR) database into customized information displays. The Chemical Safety for Sustainability (CSS) Dashboard is built upon a flexible infrastructure, allowing multiple views of ACToR data organized to support user-specific needs. The users select sets of chemicals and data to focus on for data exploration and analysis. The data are organized into data classes to present all relevant information for a given pre-defined grouping of data such as hazard and exposure or in vivo and in vitro data. The CSS Dashboard provides data class views relevant to the data types and will continuously expand the viewing options. Within the Data Explorer mode, the user can view summarized information for the various data classes across all selected chemicals. In contrast, the Chemical Explorer mode permits viewing of the highly detailed data including concentration response plots and curve-fitting parameters across hundreds of high-throughput screening assays and chemicals. Chemical-specific scores that consider all information in each data class is presented in a dynamic summary table with a default score (e.g., average AC50 across assays within the in vitro hazard data class). Users can adjust default score criteria or apply expert knowledge to modify particular scores, with all decisions saved for sharing or later consideration. The scores are carried over into the Prioritization Mode where the chemicals are ranked in a weight-of-evidence scheme including an implementation of the Toxicological Prioritization Index (ToxPi). The ToxCast Dashboard will serve as the primary portal for ToxCast and Expocast data and model release and public user-interaction. This abstract does not necessarily reflect U.S. EPA policy.

W 2098 Genomics in Toxics Regulation and Litigation in the Era of Whole Genome Sequencing

A. R. Schatz[2] and G. E. Marchant[1]. [1]*College of Law, Arizona State University, Tempe, AZ and* [2]*Global Safety & Environment, Merck & Co, Whitehouse Station, NJ.*

Genomic and other 'omic data are increasingly being used in both toxic tort litigation and environmental standard-setting. For example, defendants are beginning to request genetic testing of toxic tort plaintiffs to demonstrate alternative causation, while plaintiffs are using genomic biomarkers in appropriate cases to buttress their proof of specific causation. On the regulatory side, the US Environmental Protection Agency is increasingly using genetic susceptibility data to identify susceptible subgroups in setting ambient air quality standards, while using toxicogenomic data to evaluate and characterize the toxicology of pesticides and chemicals. These initial applications of genomic data are setting the precedents and creating the pathways for much broader use of genomic data in both the toxic tort litigation and environmental regulation contexts as we rapidly move into the era of whole genome sequencing. This year, tens of thousands of people will have their genome sequenced. That number is expected to rapidly climb to the millions and perhaps even hundreds of millions over the next few years. This session will discuss current applications of genomic data, and how whole genome sequencing will greatly increase the availability and use of genomic data, in both the litigation and regulatory domains. It will also discuss the complex ethical, legal, and social issues the increased use of genomic data will present in these contexts, including informed consent, disclosure and access issues, the "right not to know," privacy and confidentiality issues, and the rights and responsibilities of those that produce and are harmed by toxic substances with differential genetic susceptibility.

W 2099 Incorporating Genomic Data into the Risk-Analysis Paradigm

H. J. Clewell. *The Hamner Institutes For Health Sciences, Research Triangle Park, NC.*

Genomic data are increasingly being used to assess and manage potential health risks from drugs and environmental chemicals. Gene array data can provide information on the mode of action for toxicity of a compound and, when coupled with Benchmark Dose modeling, can be used to determine acceptable exposures and evaluate population variability. In addition, whole-genome or whole-exome sequencing can help to identify individuals with known genetic susceptibility factors for a particular adverse health outcome. This presentation will discuss how genomic data are now, and are likely to be in the future, incorporated into risk assessment and risk management, and some of the scientific challenges and policy/ethical issues that this category of data present.

W 2100 Regulatory Applications and Implications of Whole Genome Sequencing

M. A. Rothstein. *Institute for Bioethics, Health Policy and Law, University of Louisville School of Medicine, Louisville, KY.* Sponsor: G. Marchant.

This presentation will review the various applications and implications of WGS data for regulation of toxic chemicals, including how to regulate for individuals with genetically-variable sensitivities; setting uncertainty factors based on genetic susceptibility data, relationships between genetic susceptibilities and ethnic background, whether genetically at-risk individuals be able to accept increase risk in the workplace, and the appropriate role for warnings, labels, and self-help with respect to genetic susceptibilities.

W 2101 Genome Sequence Data and Toxic Torts

A. J. Harris. *ENVIRON, Little Rock, AR.*

Validated biomarkers of exposure, effect and susceptibility obtained from toxicogenomics studies are potentially very powerful tools to establish or negate causation in toxic tort. For example, increased "chromosomal abnormalities" in plaintiffs might be used to establish that exposure to DNA damaging agents has occurred, but cannot be used for establishing general causation due to lack of chemical specificity. On the other hand, genetic polymorphisms that affect DNA repair may impair an individual's response to genotoxic agents, (i.e. more susceptible to exposure) or indicate that an individual carrying that biomarker will have an increased "baseline" of chromosomal abnormalities, altering the biomarker dose-response curve in establishing or negating causation criteria and suggesting an alternate cause of elevated genotoxic biomarkers. The use of biomarkers in toxic tort is increasing; however, in many cases, the biomarkers in question have not been sufficiently validated to demonstrate that reported changes in gene expression patterns or changes in circulating cytokines/proteins levels are indeed causally related to overexposure to a specific chemical or class of chemicals. Proper validation of a defensible biomarker developed from toxicogenomics data includes reproducibility by one or more independent scientific investigators, demonstration of dose-response and specificity, development of a blind test set as confirmation of the methodology, data transparency, and the absence of non-specific or confounding responses. This presentation will discuss the potential use of WGS sequence data in toxic tort litigation, beginning with current uses and applications of genomic data in toxic tort litigation. It will then evaluate the implications of much greater availability and use of genetic data as WGS becomes more prevalent, and some of the issues this will create for the litigation system and the individual participants.

W 2102 Next Generation Sequencing and Genetic Liability

G. E. Marchant. *College of Law, Arizona State University, Tempe, AZ.*

This presentation will address some of the broader liability issues created by the rapid development of next generation sequencing (NGS). Building on the previous presentation, it will give some previous examples of genetic data being used in toxic tort cases, and demonstrate how NGS data is likely to greatly expand the use of genomic data in toxic tort cases. It will also describe other liability contexts, such as medical malpractice liability for health care providers and testing laboratories, that are also likely to expand in the NGS era, again building on existing cases and case law. Finally, the presentation will raise some of the broader ethical issues raised by the use of genetic data in tort litigation, including informed consent, data reporting and disclosure, the "right not to know," and privacy.

W 2103 Is Manganese-Induced Parkinsonism Mediated via Dopamine Neuron Degeneration or Dysfunction?

W. Zheng[1] and T. R. Guilarte[2]. [1]*School of Health Sciences, Purdue University, West Lafayette, IN and* [2]*Environmental Health Science, Columbia University, New York City, NY.*

Degeneration of dopamine (DA)-containing neurons in Substantia Nigra Pars Compacta (SNpc) is responsible for clinical manifestation of idiopathic Parkinson's disease (IPD). Manganese (Mn) intoxication is known to cause a clinical syndrome that partially overlaps with those typically seen in IPD. Cumulative data from clinical observations, animal experiments, and imaging approaches have come to the point of inciting a discussion on whether the neurotoxicity mediated by Mn on the DAergic system is one of dysfunction, degeneration, or both. This workshop brings together internationally recognized experts in the field with their diverse experimental observations on Mn-DA research to address this issue. The session starts with a brief introduction of the nigrostriatal pathway in movement disorders, followed by a description of the topic in question. The first speaker presents neuropathological features of human brains collected from autopsy workers chronically exposed to Mn. The second speaker shows clinical data from subjects exposed to the eliciting drug and discusses the integrity of DA terminals. The third speaker discusses the observations from nonhuman primate studies suggesting that Mn-induced movement abnormalities are associated with an impaired DAergic function. The fourth speaker reports the data from a rat model on Mn accumulation in SNpc and neurochemical changes in brain by synchrotron X-ray fluorescent and neurochemical/pathological analyses. The last speaker demonstrates the temporal relationship of injury vis-à-vis the affected neurotransmitter systems in a *C. elegans* model. The topic on DA dysfunction, degeneration, and related entwining processes will further the current understanding of the contribution of dysfunction vs. degeneration in environmental etiology of neuronal diseases. The session will be of interest to a broader audience and, in particular, to those engaged in toxicological research related to Mn toxicity, IPD and neurodegenerative diseases, neuroscience, neurotoxicology, and systems biology.

W 2104 Pre- and Post-Synaptic Dopaminergic Dysfunction in Mn-Exposed Workers

B. A. Racette[1] and G. Nelson[2]. [1]*Neurology, Washington University School of Medicine, St. Louis, MO and* [2]*Division of Epidemiology and Biostatistics, University of the Witwatersrand, Johannesburg, South Africa.* Sponsor: W. Zheng.

The role of the dopaminergic system in the clinical syndrome associated with Mn has been controversial. PET imaging with [18F]fluorodopa (FDOPA) is a noninvasive measure of nigrostriatal dopaminergic neuron integrity. Ultimately, neuropathologic examination of brains of exposed workers is the most definitive approach to identify causative pathways. To assess the pre- and post-synaptic dopamine system in humans with occupational Mn exposure, we conducted molecular neuroimaging with FDOPA PET in 40 Mn-exposed welders and neuropathologic assessment of the corpus striatum in eight Mn miners and compared both to matched controls. None of these workers had a diagnosis of a Mn-related clinical syndrome. For the PET studies, basal ganglia volumes of interest were identified for each subject and the uptake of FDOPA, Ki, was generated for each region. For the pathologic assessment, we compared mean cell density of neurons, astrocytes, and microglia in the caudate, putamen, and globus pallidus interna and externa in Mn miners with non-Mn miners. In the FDOPA PET study, repeated measures general linear model (GLM) analysis demonstrated a strong interaction between diagnostic group and region. The regional pattern of uptake in welders was most affected in the caudate > anterior putamen > posterior putamen. Histopathology of Mn miner brains revealed a trend towards lower mean neuron and astrocyte density compared to non-Mn-miners in the caudate nucleus and putamen. There was higher mean microglia density in Mn miners than non-Mn- miners in the globus pallidus interna and externa. The ratio of astrocytes to microglia in each brain region was lower in Mn miners as compared to non-Mn miners. The FDOPA PET studies in Mn-exposed welders indicate dysfunction in the presymptomatic nigrostriatal dopamine system. The neuropathology studies in Mn miners suggest that chronic, low-level Mn exposure may be associated with selective toxicity to astrocytes and neurons and microglial response in the corpus striatum.

W 2105 Manganese-Induced Parkinsonism in Methcathinone Abusers

K. Sikk[1], S. Haldre[2], S. Aquilonius[3] and P. Taba[2]. [1]*Department of Neurology, North Estonia Central Hospital, Tallinn, Estonia,* [2]*Department of Neurology and Neurosurgery, University of Tartu, Tartu, Estonia and* [3]*Department of Neuroscience, Neurology, Uppsala University, Uppsala, Sweden.* Sponsor: W. Zheng.

Methcathinone abuse is a new cause of manganism. This psycho-stimulant is prepared from pseudoephedrine using potassium permanganate as an oxidant. The final mixture contains high concentrations of manganese (Mn). Methcathinone abuse is an important cause of parkinsonism among young Estonian patients. We describe the clinical, biological, neuroimaging characteristics and follow-up results in a large cohort of intravenous methcathinone users. The most prevalent symptoms are symmetrical bradykinesia, dystonias, early postural, gait and speech impairment; rest tremor is rarely present and rigidity is mild. The syndrome is irreversible after cessation of exposure and there is a trend of worsening. Plasma Mn concentrations in active uses are significantly higher than those in former users; so are the hair Mn levels. By MRI T1-weighted images, all active users show a symmetric hyper-intensity in globus pallidus, substantia nigra, periaquaductal grey matter and cerebral pedunculi, less in putamen, caudate nucleus, dentate nucleus and white matter. FDG PET in former users shows decreased brain metabolism mainly in the central part of the brain, including the basal ganglia, thalami, and the surrounding white matter. Whether these changes are mainly Mn induced, as the clinical syndrome, or correspond to the effect of long-term methcathinone abuse cannot be concluded. DAT SPECT results indicate that the presynaptic neurons in the nigrostriatal pathway are intact in former methcathinone abusers. Further, the data show no decrease in the level of postsynaptic D2 receptors in striatum. Evidence from our neuroimaging studies support the hypothesis that accumulation of Mn in the brain is not associated with the degeneration of dopaminergic neurons as in PD, instead the dopaminergic system could be dysfunctional.

W 2106 Nigrostriatal Dopamine System Dysfunction in Manganese-Exposed Nonhuman Primates

T. R. Guilarte. *Environmental Health Sciences, Columbia University Mailman School of Public Health, New York City, NY.*

It has long been recognized that chronic manganese (Mn) exposure in humans produces a neurological syndrome comprising psychiatric, cognitive and movement abnormalities that resemble some aspects of idiopathic Parkinson's disease (PD). However, examination of the literature also indicates significant differences between Mn-induced parkinsonism and PD. For example, Mn-induced parkinsonism does not seem to be responsive to l-dopa therapy, an effective treatment for PD. Our laboratory has been examining the effect of chronic exposure to moderate levels of Mn in non-human primates in order to assess the effects on the nigrostriatal dopaminergic system using Positron Emission Tomography (PET) as well as other neuropathological endpoints. Our results indicate that the most affected parameter of the dopaminergic synapse is the ability to release dopamine. No significant changes were measured in dopamine transporter levels indicating that dopamine terminals do not degenerate as a result of Mn exposure. A small but significant decrease was also measured in the level of D2-dopamine receptors in the striatum. These findings indicate that chronic exposure to moderate levels of Mn does not result in the degeneration of dopamine neurons but it results in dopamine neuron dysfunction since they cannot release dopamine. More recent evidence indicates that a similar decrease in dopamine release measured by PET is present in dopamine terminals innervating the frontal cortex. In general, dopamine neuron dysfunction may be a common mechanism to explain cognitive and motor function deficits associated with Mn neurotoxicity. [Supported by NIEHS grant number ES010975]

W 2107 Accumulation of Manganese in Substantia Nigra and Alterations in Brain Neurochemistry following Subchronic Manganese Exposure in Rats

W. Zheng[1], Y. Pushkar[2] and J. R. Cannon[1]. [1]*School of Health Sciences, Purdue University, West Lafayette, IN and* [2]*Physics, Purdue University, West Lafayette, IN.*

Numerous studies on manganese (Mn)-induced parkinsonism indicate an interaction between Mn and dopaminergic neurotransmission. However, the lack of distinct T1 signal by MRI in substantia nigra (SN) in Mn-exposed human brain, along with other study results, has led to the assumption that Mn toxicity may take place in brain regions other than the dopamine (DA) neuron-enriched SN. To better characterize Mn toxicity, we developed a high spatial resolution synchrotron X-ray fluorescence imaging technique (XRF) as a new quantitative tool to study Mn distribution following in vivo Mn exposure. Sprague-Dawley rats received daily ip. injections of 6 mg Mn/kg, as MnCl2, 5 days/wk for 4 wks. Brains were processed for imaging analysis and tyrosine hydroxylase (TH) immunohistochemistry for DA neurons. Our XRF data confirmed previous observations by atomic absorption spectrophotometry that subchronic Mn exposure resulted in a significant accumulation of Mn in globus pallidus (GP), thalamus, cortex and choroid plexus ($p<0.05$). Moreover, we found that Mn accumulated to a great extent in pars compacta of the SN (~5 fold increase in Mn levels in SNpc after exposure), whereas the increase of Mn levels in cortex, GP, thalamus and cortex was 1.8, 3.8, and 3.9 fold, respectively. Confocal images of TH-stained SN area revealed a diminished TH immunoreactivity in Mn-treated rats. Preliminary quantification of neurotransmitters (dopamine, serotonin, norepinephrine, and GABA) by HPLC showed that Mn elicited detectable changes in the levels of multiple neurotransmitter systems in several brain regions likely including SN. These observations present a linkage between Mn exposure and neuronal toxicity, which may render the nigrostriatal DA system more susceptible to degeneration. The single cell imaging of Mn from rat brain tissues and neuropathological examination are currently in progress and the results may provide direct evidence of Mn interaction with DA neurons. (Supported by NIEHS RO1-ES008164; R00-ES019879)

W 2108 Manganese (Mn) Interaction with Dopaminergic Neurons: Evidence from *C. elegans*

M. Aschner, C. Au and A. Benedetto. *Department of Pediatrics, Vanderbilt University Medical Center, Nashville, TN.*

Parkinson's disease (PD)-mimicking drugs and pesticides, and more recently PD-associated gene mutations, have been studied in cell cultures and mammalian models to decipher the molecular basis of PD. Thus far, a dozen of genes have been identified that are responsible for inherited PD. However they only account for about 8% of cases, most of the cases likely involving environmental contributions. Environmental manganese (Mn) exposure represents an established risk factor for PD, and both PD and Mn-intoxicated patients display a characteristic extrapyramidal syndrome primarily involving dopaminergic (DAergic) neurodegeneration with shared common molecular mechanisms. To better understand the specificity of DAergic neurodegeneration, we studied Mn toxicity in *Caenorhabditis elegans* (*C. elegans*). Combining genetics and biochemical assays, we established that extracellular, and not intracellular, dopamine (DA) is responsible for Mn-induced DAergic neurodegeneration and that this process (1) requires functional DA-reuptake transporter (DAT-1) and (2) is associated with oxidative stress and lifespan reduction. Overexpression of the anti-oxidant transcription factor, SKN-1, affords protection against Mn toxicity. We identified three new divalent metal transporter (DMT1)-like genes in *C. elegans*: smf-1, smf-2 and smf-3. In the worm, deletion of smf-1 or smf-3 led to an increased Mn tolerance, while loss of smf-2 led to increased Mn sensitivity. Translational GFP-fusions revealed that SMF-1 and SMF-3 strongly localize to partially overlapping apical regions of the gut epithelium, suggesting a differential role for SMF-1 and SMF-3 in Mn nutritional intake. Conversely, SMF-2 was detected in the marginal pharyngeal epithelium, possibly involved in metal-sensing. Analysis of metal content upon Mn exposure in smf mutants revealed that SMF-3 is required for normal Mn uptake, while smf-1 was dispensable. Combined, these studies establish the utility of *C. elegans* in identifying Mn transporters and deciphering mechanisms of Mn-induced neurodegeneration (Supported by R01ES07331 and R01ES020852).

W 2109 Science-Based Preclinical Safety Assessment: Decision-Making to Enhance Regulatory Success

R. Roberts[1] and M. Hinrichs[2]. [1]*AstraZeneca, Macclesfield, United Kingdom and* [2]*MedImmune, Gaithersburg, MD.*

Diversity is increasing in the biological targets, pharmacological strategies, and types of chemistry being investigated in first-time-in-human (FTIH) studies; similarly, there is growing information, guidance, and experience to protect volunteer/patient safety. In response, regulatory toxicology strategies have diversified and evolved from those practiced only a decade ago, reflecting advances in science and technology and the experiences of individuals and organizations. In this context, this workshop will consider the key question: Are these 'diversities' complementary and working expeditiously to bring important new (and safer) medicines to patients? In order to address this, speakers will cover the four key areas of small molecules, traditional biologics, innovative biologics, and nucleotide constructs. The presentations will include specific discussion of the science and technology in each area, will consider strategic and tactical issues such as study design, species selection, target organ toxicity profiles, and regulatory guidance relevant to safety assessment. Building on this, each talk will be illustrated with case studies that address the question. This will be followed by a regulatory perspective covering issues and challenges associated with novel pharmacologic targets and new molecular chemistries balancing innovation with the need to ensure volunteer/patient safety. Overall, the presentations will provide clear information illustrated by examples on the different strategies employed for the different types of chemistries with an emphasis on relevance and outcome. The session will be of broad interest to academic, industry, regulatory, and consultant toxicologists who wish to be updated in this critical and evolving area.

W 2110 Regulatory Toxicology Testing for Small Molecules: Strategies and Outcome Analysis

R. Roberts, S. Horner, D. Lees, D. Ryan, R. Callander and S. Robinson. *AstraZeneca, Macclesfield, United Kingdom.*

Preclinical toxicology studies of up to 1 month duration are frequently used to support single or multiple dosing for a similar duration in Phase I clinical trials (ICH Guideline M3(R2), 2009), although for oncology Phase I trials in advanced cancer, dosing can continue beyond the duration of toxicology cover according to the patient's response (ICH Guideline S9; 2009). An analysis of target organ toxicities in these studies for 77 AstraZeneca candidate drugs (CDs) revealed a pattern of target organ toxicities that was largely similar across most therapeutic areas although the oncology/infection therapeutic area differed with a larger range of organs affected. For the 75 CDs for which both rodent and non-rodent studies were conducted, new target organs were identified in non-rodents for 43 of the CDs and the changes seen only in non-rodents included organ systems of high relevance for human risk assessment such as the liver, male reproductive tissues and CNS. Overall, these data on small molecule target organ toxicities provide new insights into drug toxicity profiles in preclinical species and additionally confirm the value of using non-rodents as a second species in toxicity testing to support human safety. As such, these approaches have been successful in supporting robust decisions around risk assessment for traditional pharmacological targets and small molecule chemistries, but how have these regulatory strategies fared when applied to more challenging targets and more sophisticated chemistries? In addition, what recent innovations have been developed in the field of small molecule toxicology? One interesting trend is the in-

clusion of safety pharmacology endpoints into general toxicology studies; these can provide useful data and are resource efficient. A further notable trend is a shared aim across the Pharma industry of reducing attrition in the GLP toxicology phase of candidate drug testing. Our data have shown that failures in this phase can be significantly reduced by extending the dose range finding studies and also by front loading the non-rodent telemetry.

W 2111 Risk Assessment of "Traditional" Biologics

L. Andrews. *Sanofi, Waltham, MA.*

This presentation will address the issues and challenges presented in preclinical risk assessment of pharmacological targets and molecular constructs produced by recombinant technologies such as hormones and cytokines where multiple pre-clinical test species may be inappropriate. As the activity of the biologic therapeutic is frequently species specific, the selection of appropriate animal models or surrogates is crucial to generating useful data. Some animal test systems have been refined to alleviate the inter-species issues, and alternative in vitro strategies have also been identified which could significantly reduce or eliminate testing. However the cost benefit of approaching the development of a "non-traditional" biologic either through the use of a surrogate or the use of an animal model still raises many questions. The focus of this presentation is to discuss and disseminate the problems and potential solutions associated with the development and safety testing of biological-based products. Considerations will be given to the use of transgenic animals, homologous molecules and in vitro systems that may be more predictive of safety and translatability than traditional speices/tests. In addition, review of the recent regulatory guidelines including S6 addendum, S9 and other relevant guidances will be highlighted as to their impact on the development of large molecules. Specific examples will be given to illustrate the utility of many of these alternative strategies. Case examples will include the use of a transgenic animal for a development program (including DART), the use of a surrogate antibody and the potential challenges of relevance and translatability and a unique development program using an animal model of diseaese and the predictivity of this model to the clinic

W 2112 Risk Assessment of Humanized Monoclonal Antibodies, Antibody-Drug Conjugates, and Novel Antibody Constructs

M. Hinrichs, L. A. Iciek, K. P. McKeever and P. C. Ryan. *MedImmune, Gaithersburg, MD.*

Rapid advances in the field of protein engineering have led to the development of novel biologic drug platforms such as targeted nanoparticles, antibody drug conjugates (ADC), bispecific antibodies, and Fc mutated monoclonal antibodies. These emerging drugs continue to present new regulatory safety assessment challenges despite decades of practical experience with more traditional biologic agents. While the basic principles outlined in the recent addendum to ICH S6(R1) Preclinical Safety Evaluation of Biotechnology-Derived Pharmaceuticals can be applied to regulatory safety testing of novel biologics, the unique characteristics of each platform necessitates a science-based case-by-case approach often involving the use of safety testing methods that have not yet been standardized. This presentation will cover the scientific aspects of safety study design and species selection for two types of novel biologic platforms, bispecifics and ADCs. Case examples will be presented to highlight the strategic thinking and individualized approach required when evaluating the safety of new biologic technologies. The presentation will conclude with a discussion of the clinical relevance and current limitations of nonclinical testing strategies to focus on areas that could be improved in the future.

W 2113 Safety Assessment of Oligonucleotide Constructs

S. Henry. *Preclinical Development, Isis Pharmaceuticals, Inc., Carlsbad, CA.*

This presentation will address the strategy, issues and challenges presented in risk assessment of oligonucleotide constructs such as antisense inhibitors and microRNAs. The basic principles of safety testing generally apply to oligonucleotide based therapeutics, but there are unique considerations related to targeting RNA expression in terms of general tolerability and exaggerated pharmacologic assessments. These considerations with regards to the site of action, interspecies cross-reactivity, and nonspecific effects influence the choice of animal models and the design of toxicology studies. Existing guidance's for traditional drugs or biotherapeutics do not perfectly apply to oligonucleotides, but sufficient experience has been gained over the years to outline strategies and several points to consider documents have been written or are in preparation. Among the unique aspects are that oligonucleotides are intended to engage intracellular targets (i.e., RNA) so tissue uptake is important. Assessment of effects related to both the chemical platform and the intended pharmacology are emphasized more than other drug platforms. Most unique for this class of chemical is the consideration of differences in genetic sequence between animal models that must be considered. The interspecies difference in sequence homology often limit the activity of the human drug in animal models, but the ability to rationally design species-active inhibitors makes the use of surrogate inhibitors relatively straight forward. This talk will focus on strategies to deal with the challenges to ultimately provide meaningful safety assessment for new drugs that translate to patients. An example of a safety/pharmacodynamics relationship for an antisense inhibitor of Factor XI that incorporates mouse, monkey and human data will be presented.

W 2114 Regulatory Authority Experience with Diverse Molecular Chemistries and Preclinical Safety Assessments Supporting First Time in Humans

D. Jacobson Kram. *US FDA, Silver Spring, MD.*

Novel pharmacologic targets and new molecular chemistries raise challenging regulatory issues. A balance must be struck between supporting innovation in drug discovery while insuring volunteer/patient safety. For healthy volunteers there is no risk/benefit paradigm and the bar for safety is high. The lack of historical information on clinical toxicities for novel pharmacologic targets argues for conservatism in selecting a safe start dose and dose escalation scheme. FDA's guidance "Estimating the Maximum Safe Starting Dose in Initial Clinical Trials for Therapeutics in Adult Healthy Volunteers" discusses situations where the start doses based on animal toxicology NOAELs should be lowered; one of the listed reasons is "novel therapeutic target." For biologic drugs in this category a MABEL (minimal anticipated biological effect level) approach has been proposed. The need for such an approach was largely triggered by the cytokine release syndrome seen after the first dose in the Tegenero 1412 phase 1 study. This paradigm may have to be altered when the patient population has a serious and life threatening indication such as cancer. In these instances, patients should not be repeatedly exposed to drug doses that are not expected to have pharmacological effects. Other approaches could include microdose testing when investigating pharmacokinetics and bioavailability and the use of surrogate molecules when the drug only binds to the human target. In general, selection of the start dose for first in man studies with novel pharmacologic targets and/or new molecular chemistries should err on the side of safety i.e. lower start doses, slower dose escalation, protracted timing between dosing of participants and careful monitoring.

HH 2115 A History of the 3Rs in Toxicity Testing: From Russell and Burch to 21st Century Toxicology

M. L. Stephens[1] and N. Mak[2]. *[1]CAAT, Johns Hopkins University, Baltimore, MD and [2]Alternatives Research and Development Foundation, Jenkintown, PA.*

The 3Rs—replace, reduce, and refine—have become the internationally established framework guiding the development of alternatives to animal experimentation in toxicology. Yet this framework languished for two decades after it was first proposed in 1959 by British scientists William Russell and Rex Burch. Then, as the animal experimentation controversy intensified in the 1980s, the concept of alternatives became politically charged, with some arguing that *in vivo* experiments could be replaced readily and others arguing that they were irreplaceable. A generation or so later, following the 2007 publication of a US National Research Council (NRC) report *Toxicity Testing in the 21st Century, a Vision and Strategy*, prominent scientists began predicting the near elimination of animal use in toxicity testing through the development of "21st-Century Toxicology." How have we gotten from Russell and Burch to the beginnings of 21st-Century Toxicology? In this session, we will present results from comprehensive citation and literature searches that track the influence of Russell and Burch's 3Rs framework and the prevalence of 3Rs-related research in toxicology over time. We will also draw on timelines of various 3Rs activities, including the founding of 3Rs organizations, centers, journals and websites, funding sources, the organization of workshops and conferences, the enactment of animal welfare/alternatives laws, and other milestones, to inform our historical analysis. We will present a historical narrative framed around four phases of activity: incubation (1959–1979), increasing acceptance and spread (1980–early 1990s), maturation (early 1990s–2007), and paradigm shift (2007–present). The impact of more than 50 years of 3Rs activity will be measured in part by focusing on the validation and regulatory acceptance status of alternative methods and trends in animal-use statistics, concluding with a discussion of remaining challenges to the development, validation, regulatory acceptance, and implementation of 3Rs methods.

IS 2116 Leadership In Science: Skills and Styles

B. Mahadevan[1], P. Rao[2], L. S. Birnbaum[3], H. I. Swanson[4], M. Aardema[5] and L. Burns Naas[6]. [1]*Regulatory Affairs, Abbott Nutrition, Abbott Laboratories, Columbus, OH,* [2]*Global Regulatory Affairs & Safety Sciences, Bristol Myers Squibb, Princeton, NJ,* [3]*NIEHS, RTP, NC,* [4]*Molecular and Biomedical Pharmacology, University of Kentucky, Lexington, KY,* [5]*Marilyn Aardema Consulting LLC, Scientific Advisor, BioReliance, Rockville, MD and* [6]*Drug Safety Evaluation, Gilead Sciences Inc, Foster City, CA.*

In the 21st century, more than any other time in history, science is a team sport and requires cross-disciplinary/cross-functional interaction to meet the objectives and gain results. These interactions across multiple disciplines often require careful management and skillful leadership. Often times we fall prey to the belief that "a leader is always born". However, all of us "lead" in everyday life subconsciously or rather unconsciously. A question that begs to be asked is, "Why should anyone be led by me?" The answer can be elusive and requires the recognition that not all leaders are born. Good leaders can be developed. This, of course, leads to question, "How?" That again has to be addressed directly in terms of tangible competencies and behaviors. Is this due to the perception that the scientific ladder and management ladder are parallel, and one cannot support the other? The 21st century demands that each of us "own" our careers as well as the contributions towards society in a variety of ways. The time has arrived to spur the enthusiasm to "lead" in all fronts—the classroom to the boardroom and beyond. This informational session will include presentations by key leaders from academia, industry, government, and consulting. The speakers will introduce the concept of leadership as it relates to the current and emerging work environment, followed by a testimonial of core skills and styles required to be an effective leader. The testimonials will be individual but will provide set of tangible core qualities that are key to succeed and lead—at all levels. The session is designed for presentation and includes time for questions and discussion.

IS 2117 Recent Challenges Beyond the Usual Toxicological and Public Health Challenges in Africa

A. M. Kadry[1], S. Myers[2], E. Afriyie-Gyawu[3], S. Soliman[4] and M. T. Ahmed[5]. [1]*Office of Research and Development, National Center for Environmental Assessment, US EPA, Washington, DC,* [2]*Department of Pharmacology and Toxicology, University of Louisville, Louisville, KY,* [3]*College of Health and Human Sciences, Georgia Southern University, Statesboro, GA,* [4]*Pesticide Chemistry and Toxicology, Alexandria University, Alexandria, Egypt and* [5]*Pesticide Chemistry and Toxicology, Suez Canal University, Ismalia, Egypt.*

Africa has shown strong levels of economic growth over the last ten years, with African countries among the fastest movers on the United Nations Development Program's (UNDP) Human Development Index. However, there are still a large number of toxicological problems and environmental challenges that face the continent. While considerable work has been done to recognize the hazards of air pollution and minimize its extent in many of the world's cities, the major metropolitan areas of several African cities still suffer from excessive air pollution. Air pollution can come from a variety of sources, including vehicle exhaust, uncontrolled industrial production, resource extraction, as well as various industrial emissions. Disposal of scrap tires is also a serious challenge facing several African countries. The unregulated widespread practice of using scraps of tires as a source of energy in several African countries may raise concerns for food, public health, and environmental safety. Tires are a very rich source of energy; however, tires are made of a complex mixture of ingredients that release toxic chemicals upon burning. The appropriate storage, labeling, and the judicial use of pesticides also pose a challenge. There are large numbers of pesticide stockpiles scattered over the continent, often stored haphazardly. In many African countries, empty pesticide containers are used to store fuel, food, and water. There are 50,000 metric tons of obsolete and banned pesticides still in use in many African countries. This informational session should enhance our understanding of the opportunities for increased global research initiatives focusing on solving the new emerging toxicological challenges facing Africa.

PS 2118 Comparison of the Rabbit, Diabetic Miniature Swine and Nonhuman Primate to Evaluate the Clinical Biopotency of Insulin Products

S. Renna[1], A. Stricker-Krongrad[1], L. Brown[1, 2], E. C. Blair[1], T. Madsen[1], B. C. Hanks[1, 2], J. Liu[1] and G. Bouchard[1, 2]. [1]*Sinclair Research Center, LLC, Auxvasse, MO and* [2]*Sinclair BioResources, LLC, Auxvasse, MO.*

The potency of human insulin has classically been evaluated following the U.S. Pharmacopeia (USP) guideline for comparison to an international standard (IS) of activity (IU). However, since insulin analogues are intentionally different and cannot be standardized against IS, there is a need for a bioassay to assess clinical specific activity (U). To this extent, we compared the biopotency (U) of different insulin products in rabbits, in type 1 diabetic miniature swine and in normal non-human primates, and used human and pork insulin as reference standards. New Zealand White rabbits were fasted and injected subcutaneously (s.c.) at a dose level of 0.5 U/kg. Yucatan miniature swine (*Sus scrofa*) were made diabetic by intravenous administration of alloxan and insulin products were injected s.c. at dose level of 0.1 U/kg in overnight fasted animals (no feed or insulin for 18 h). Normal insulin suppression tests (nIST) were conducted in fasted male cynomolgus primates (*Macaca fascicularis*) receiving a bolus intravenous (i.v.) infusion of glucose (ivGTT; 0.25 g/kg) and treated with somatostatin. Insulin products were given at dose level of 0.05 U/kg. Glucose levels were recorded using handheld glucometer devices. The blood glucose kinetic (BGPK) and the blood glucose area under the curve (BGAUC) were used to assess biopotency in the rabbit and in the diabetic miniature swine. The slope of the blood glucose clearance (kG) was used to assess biopotency during the nIST. Our data indicate that the biopotency of insulin products can be assessed using BGAUC and kG, but that only the type 1 diabetic miniature swine can discriminate between differences in biopotency for all aspects of BGPK. Conclusions: The BGPK for short-acting human and pork insulin were similar in the rabbit assay but their respective BGAUCs were different (ratio of 1.2). Accordingly pork insulin was more potent during nIST in the non-human primate (slope of -0.012 vs. -0.010; pork and human, respectively).

PS 2119 Evaluation of Phototoxicity of Intravitreal Injected Porphyrin in Albino Rabbit

T. Aya, K. Watanabe, S. Tsukamoto, Y. Oshita, T. Mochizuki, Y. Yao, K. Hosoi and K. Kawazu. *Santen Pharamceutical Co., LTD., Ikoma-shi, Nara, Japan.*

For ophthalmic medications, phototoxicity is one of the toxicities which would be a concern during drug development. Although there are several in vitro phototoxicity assays, no in vivo studies have been established to assess ocular phototoxicity. The purpose of this study was to develop appropriate study conditions to evaluate ocular phototoxicity for intravitreal injective solutions by using Porphyrin [4,4',4'',4'''-(Porphine-5,10,15,20-tetrayl) tetrakis (benzenesulfonic acid) tetrasodium salt hydrate] in albino rabbits.

The Porphyrin has absorbing spectrum in a visible light range, was administered bilaterally to rabbit eyes at 0 to 0.2 mg/eye (20 μL/eye) by single intravitreal injection. Just after dosing, one of the eyes from each animal was irradiated with a solar simulator (SOL-500, Hönle) for 2 hours under anesthesia. The eyes were kept open by lid retractors and saline was instilled periodically in order to prevent corneal drying during irradiation. The irradiation intensity was approximately 20 J/m2 as UV-A at the cornea. Ocular phototoxicity was evaluated by ophthalmological examinations at 1 to 8 days after the irradiation. The animals were euthanized after the irradiation and their eyes were examined histopathologically.

In the ophthalmological examinations, vitreous hemorrhages and vitreous opacity, etc. were found in 0.06 and 0.2 mg/eye groups. In the histopathological examinations, hyperplasia of lens epithelium, focal degeneration and thinning of retina, vacuolation and necrosis of nerve fiber etc. were observed. These findings were confirmed only in the porphyrin-dosed and light-irradiated eyes. The findings were considered to be phototoxicity caused by porphyrin.

In our conclusion, in vivo ocular phototoxicities were detected in this study. Further investigation is needed to extrapolate the results on human subjects. This is the first step for the establishment of in vivo phototoxicity model for intravitreal injective solutions.

PS 2120 Development of a Novel Model of Latent Oncogenic Herpesvirus Reactivation for Immunotoxicologic Evaluations

R. Mikkelsen[1], J. Aligo[2], M. R. Walker[2], D. Weinstock[2], F. G. Burleson[1] and G. Burleson[1]. [1]*Burleson Research Technologies, Inc., Morrisville, NC and* [2]*Biologics Toxicology, Janssen Pharmaceuticals, Inc., Spring House, PA.*

In immunotoxicology testing, major objectives include determining the test article's effect on susceptibility to infectious or neoplastic disease, and ability to induce hypersensitivity and autoimmunity. Immunotoxicity caused by a pharmaceutical or chemical compound may be reflected in an impaired clearance of an infectious agent, increased sensitivity to opportunistic infections, reduced efficacy of immunization, or reactivation of latent infections. Host resistance models provide the only means to directly assess compound toxicity to the total immune response, since pathogen clearance by the host requires complex interactions between innate and adaptive immunity.

Development of a murine gammaherpesvirus 68 (MHV-68) infection model was performed to facilitate identification of pharmaceutical agents that cause reactivation of latent viral infections, such as Epstein Barr Virus (EBV) in humans. Both MHV-68 and EBV are B-lymphotropic, establish latency after acute lytic infection, and are associated with the development of lymphomas.
The model was developed using cyclosporine A as a positive immunomodulatory control. Cyclosporine A blocks calcineurin activity, which prevents activation of cytokine genes in T cells, leading to decreased T cell growth and activity. Cytotoxic T lymphocytes are critical for control of latent MHV-68 infection in the spleen. C57BL/6 mice were infected with 50,000 PFU MHV-68 and treated with 50 mg/kg cyclosporine A by the intraperitoneal route. Primary infection and viral reactivation in the spleen were measured by plaque assay for cell-free infectious virus, and qRT-PCR for latent and lytic mRNA viral transcripts. Infected splenocytes were quantified by infectious center assay. MHV-68 was detected in spleens of C57BL/6 mice treated with cyclosporine A 31 days following primary infection.

PS 2121 Efficacy and Pharmacokinetics of Brincidofovir for Treatment of Lethal Rabbitpox Virus (RPXV) Infection in NZW Rabbits; A Model of Human Smallpox

I. M. Grossi[1], S. Foster[1], K. Van Sickle[1], L. Keilholz[1], M. Rose[1], T. Brundage[1], J. Long[2], R. Krile[2] and L. C. Trost[1]. [1]*Pharm/Tox, Chimerix, Inc., Durham, NC and* [2]*Tox, Battelle Biomedical Research Center, Columbus, OH.*

Brincidofovir [BCV (CMX001)] inhibits viral replication and is active against all 5 families of dsDNA viruses causing human disease. Chimerix is developing BCV for multiple indications leading with prevention of CMV in transplant patients. Jointly, BCV is being developed for treatment of smallpox under the "Animal Rule". This randomized, blinded, placebo-controlled study determined the efficacy of BCV for prevention of mortality caused by intradermal infection with a lethal inoculum of RPXV strain Utrecht.
Infected rabbits were randomized to treatment at the first observation of secondary lesions. Treatment regimens consisted of 3 oral doses spaced at 48 hours beginning at randomization. Doses of 5/5/5, 20/5/5 and 20/20/20 mg/kg BCV were evaluated. Compared to placebo, a statistically significant, dose dependent increase in survival was observed at the 20/5/5 and 20/20/20 mg/kg doses; demonstrating that BCV is effective for treatment of lethal poxvirus infection when administered after appearance of clinical signs of disease, specifically appearance of secondary lesions remote from the inoculation site.
An independent cohort of rabbits was added to study the PK of the 20/5/5 mg/kg regimen of BCV, when dose was initiated Day 4 post-infection. The concentration of cidofovir-diphosphate (CDV-PP), the active antiviral, was assessed in peripheral blood mononuclear cells (PBMCs) to support scaling to a human dose for treatment of smallpox. Rabbit PBMC CDV-PP exposure was less than or equal to that in humans given doses currently under evaluation in clinical studies for other dsDNA viruses. These data support the feasibility of scaling doses of BCV that are effective in a lethal animal model of smallpox to a human dose that is under evaluation in a Phase 3 clinical study for prevention of CMV. This work was supported by the Biomedical Advanced Research and Development Authority (BARDA) under contract HHSO100201100013C.

PS 2122 Effect of Prandial Status on Plasma Bile Acids Composition in Dogs

I. L. Csanaky[1], P. Shipkova[2], D. Robertson[2], M. Reily[2], A. J. Lickteig[1], M. Pratt-Hyatt[1], C. D. Klaassen[1] and L. D. Lehman-McKeeman[2]. [1]*University of Kansas Medical Center, Kansas City, KS and* [2]*Bristol-Myers Squibb Co, Princeton, NJ.*

Bile acids (BAs) play a central role in liver function, but they are known to be toxic to the liver. It is assumed that changes in composition and/or concentrations of a specific BA in plasma may be pathognomonic for specific liver diseases. This study aimed to determine the physiological composition and changes of plasma BAs in beagle dogs in fasted and fed states. Plasma samples were collected at 9 am, 2 pm (2 hrs after feeding), 4 pm and the next day at 9 am from male (M) and female (F) dogs. The plasma BAs were quantified with UPLC-MS/MS. The total BA concentration in plasma of F dogs was about double that of M dogs at all time points. At 9 am (fasted) the majority of BAs were taurine (T)-conjugated BAs (M:70%, F:84%), a smaller proportion were unconjugated BAs (M:29%, F:13%), with a minimal proportion of glycine-conjugated BAs (M:1.4%, F:3.4%). The most prominent BAs in canine plasma were: TCA>TDCA≥TMCA>TCDCA~TUDCA~TLCA. The concentration of plasma BAs increased after feeding, reaching peaks nearly 10-fold higher 4 hours after feeding than the fasted state, and the BA concentrations returned to basal levels by the next morning. The proportion of T-conjugated BAs increased to ~96% after feeding and returned to the basal proportion by the next morning. The inter-individual variation of BAs was 3 to 10 fold at each time point. In summary, (1) the majority of plasma BAs in dogs was taurine conjugates, (2) feeding increased plasma BAs by about an order of magnitude, due primarily to increased taurine-conjugated BAs, (3) basal concentrations of BAs were higher in F than M dogs, (4) and there were large inter-individual differences in plasma BAs. These findings demonstrate that physiological BA concentrations in plasma of dogs are influenced markedly by prandial status, and slightly by gender. These physiological variations may complicate the interpretation of plasma BA concentrations in pathological conditions.

PS 2123 Assessment of DNA Copy Number Alterations in Fibrosis-Associated Mouse Liver Tumors

G. Silva[1], G. Chappell[1], T. Uehara[1], I. Pogribny[2] and I. Rusyn[1]. [1]*Environmental Sciences and Engineering, University of North Carolina, Chapel Hill, NC and* [2]*National Center for Toxicological Research, US Food and Drug Administration, Jefferson, AR.*

Hepatocellular carcinoma (HCC) is a prevalent human cancer with rising incidence worldwide. Human HCC is typically associated with chronic liver inflammation and cirrhosis. To better understand the pathogenesis of liver cancer, we studied molecular mechanisms of liver cancer development using a human-relevant mouse model of fibrosis-associated hepatocarcinogenesis. We observed more than double the incidence of liver tumors in B6C3F1 male mice treated with the N-nitrosodiethylamine (DEN; single ip injection of 1mg/kg at 14 days of age) and carbon tetrachloride (CCl4; 0.2ml/kg, 2/week ip starting at 8 weeks of age for 14 weeks), as compared to mice treated with DEN or CCl4. The increased incidence of liver tumors in this model was associated with epigenetic events indicative of genomic instability. Thus, we hypothesized that DNA copy number alterations, a prominent feature of genomic instability, are prevalent in the liver tissues of mice with fibrosis-associated HCC. We evaluated gains and losses of genomic DNA in both tumor and surrounding fibrotic liver by array comparative genomic hybridization. Recurrent copy number alterations were identified by defining altered segments of DNA and calculating their frequency. We found considerable variation in the frequency of alterations between the tumors and the matched non-tumor tissues. Several regions of gain or loss observed in the tumors were also detected in non-tumor tissues, but at a lower frequency. This indicates that genomic instability increases with disease progression, and demonstrates genomic changes in pre-neoplastic tissues. Collectively, these data show that genomic instability plays a role in fibrosis-associated HCC in the mouse. This copy number data can also be used to identify genes that play a functional role in cancer development. Importantly, DNA copy number data is an endpoint used by The Cancer Genome Atlas project, and can be used to explore the human relevance of our model of HCC.

PS 2124 Expression of Cysteine-Rich Secretory Protein LCCL Domain Containing 2 [CRISPLD2] Is Associated with Bile Duct Hyperplasia and Pericellular Fibrosis in Nonalcoholic Steatohepatitis

C. Saravanan[1], C. Spence[2], J. Trevaskis[2], X. Wang[2], J. Galarneau[1], W. Chutkow[2] and K. Mansfield[1]. [1]*Discovery and Investigative Pathology, Novartis Institutes for Biomedical Research, Cambridge, MA and* [2]*Cardiovascular and Metabolism, Novartis Institutes for Biomedical Research, Cambridge, MA.* Sponsor: V. Sasseville.

Nonalcoholic steatohepatitis (NASH) is a fibro-inflammatory liver disease associated with metabolic syndrome in human that can progress to cirrhosis and hepatocellular carcinoma by unknown mechanisms. Histologically, NASH is characterized by hepatocellular steatosis, lobular inflammation, bile duct hyperplasia (BDH), and pericellular fibrosis. Studies in the past have shown that degree or stage of fibrosis positively correlates with the extent of BDH. However, the interactions among the diverse hepatocellular populations in this unique pattern of fibrogenesis are poorly understood. Previously, our group developed a mouse model of NASH, wherein the histopathologic features were similar to that of the human disease. The goal of the present study was to characterize the molecular mechanisms of BDH and its role in fibrogenesis during progression of NASH. We performed gene expression microarray analysis of RNA from liver tissue of ob/ob (leptin-deficient) mice fed either high-fat [ob/ob HFD] or chow diet [ob/ob LFD] for 16 weeks. Of particular interest the gene encoding CRISPLD2, a secretory protein reported to be critical for epithelial morphogenesis during lung and kidney development, is among the top differentially up-regulated genes in ob/ob HFD mouse liver. A combined in situ hybridization, histochemistry, immunohistochemistry and image analysis suggested that CRISPLD2 was expressed in hepatic stellate cells that accompany the BDH and fibrous tracts. These data suggest that CRISPLD2 may play a role in the development of BDH, and hence fibrogenesis, during the progres-

sion of NASH. Further characterization of the role of CRISPLD2 may help us to understand the complex interplay among the diverse cell types in the progression of pericellular fibrosis.

PS 2125 Repetitive Exposures to Low Dose X-Rays Radiation Attenuates Testicular Apoptotic Cell Death in Type 2 Diabetic Rats via Akt-Mediated Nrf2 Activation

Y. Zhao[1], X. Chen[1], J. Dai[2], Y. Tan[2], L. Cai[2, 1] and W. Li[1]. *[1]Cancer Center, First Hospital, Jilin University, Changchun, Jilin, China and [2]KCHRI at Department of Pediatrics, University of Louisville, Louisville, KY.*

Infertility is a common complication in diabetic men due to the loss of germ cells. Our previous study had demonstrated that repetitive exposures to low dose X-rays radiation (LDR) can attenuate type 1 diabetes-induced testicular apoptotic cell death. To define whether repetitive exposures to LDR can also attenuate type 2 diabetes (T2DM)-induced testicular apoptotic cell death, T2DM rats were established by high fat diet feeding, followed by a small dose of streptozotocin. After diabetes onset, diabetic and age-matched control rats were treated with or without LDR at 25 mGy for 4 weeks every other day. Western blotting assay revealed that testicular apoptosis was significantly increased in T2DM rats by detecting AIF, along with increased oxidative and nitrosative damage, by detecting 3-NT and 4-HNE, and increased ER stress, by detecting CHOP and caspase 12. All these effects were attenuated by repetitive exposures to LDR. Mechanistic studies showed that Akt-mediated GSK-3β was down-regulated, but Akt negative regulators PTP1B and TRB3 were up-regulated in T2DM group. T2DM-induced the above testicular Akt related changes were partially prevented by repetitive exposures to LDR. Expression of Nrf2 and its downstream gene NQO-1 was up-regulated in T2DM group, and further up-regulated by exposures to LDR. Nrf2-related downstream anti-oxidants, such as SOD activity and catalase content were decreased in T2DM group by quantification assays, and these effects were attenuated by exposures to LDR. Therefore, the attenuation of T2DM-induced testicular apoptotic cell death by repetitive exposures to LDR is likely mediated by up-regulation of Akt/Nrf2-mediated anti-oxidative pathway.

PS 2126 Hematopoeitic Characteristics of the Macaque following a Single Dose OF Irradiation

R. Love[1], N. Makori[1], S. M. Glaza[1], T. Beck[1] and K. Fukuzaki[2]. *[1]Safety Assessment, SNBL USA, Everett, WA and [2]Corporate, Shin Nippon Biomedical Laboratories, Ltd., Tokyo, Japan.*

In continuing efforts to develop well defined animal models for the acute radiation syndrome under the FDA Animal Rule (21CR314, subpart 1), whole body irradiation (TBI) was applied to six cynomolgus macaques at a total dose of 7.55 Gy using a LINAC source. Various parameters were monitored for 59 days including hematology (24 time points), body weights, body temperature, food consumption, cageside and detailed clinical observations. A well defined veterinary medical treatment regimen and supportive care measures were provided for the irradiated animals. Necropsy was performed on day 59 and organs and tissues were evaluated macro and microscopically.
Results: 50% of the animals were euthanized by day 37. As expected following accurate TBI, decreases in neutrophil and platelet parameters were seen following irradiation on day 1. Study endpoints, in addition to survival, included the cell nadirs, the day of and duration of neutropenia (ANC <500μL, ANC <100μL) and thrombocytopenia (PLT <20,000μL), and time to recovery to an ANC >1,000μL and PLT >20,000μL. Lethal doses of TBI administered reduced the circulating ANC to <500μL by day 8 for all irradiated animals and to <100μL between day 10 and day 12. The average nadir at 7.55 Gy was 18μL. The ANC of survivors recovered to ≥100 μL by day 22 and one non-survivor recovered to this level on day 28. Only surviving animals attained recovery to ANC ≥500 μL (between day 22 and day 25). The first day the PLT count decreased to <10,000μL ranged from day 12 to day 14. The PLT count continued to decrease and the duration of thrombocytopenia (PLT <20,000 μL) ranged from day 12 to day 25 for surviving (and the one non-survivor) animals, with the exception of one survivor (SSAN 10) that showed decreased counts sporadically until scheduled necropsy on day 59. The animals required a range of 10 to 20 days to recover to PLT counts ≥20,000μL, with the exception of one animal discussed above (SSAN 10) who showed continued sporadic decreases. The results of this study support an LD50/59 of 7.55 Gy.

PS 2127 Dry Eye Symptoms in a Mouse Model of Mucin Deficiency

X. Zhou and Y. Chen. *University of Arizona, Tucson, AZ.*

Millions of Americans suffer from dry eye. The symptoms include: ocular surface discomfort, often described as feelings of dryness, burning, a sandy/gritty sensation, itchiness, visual fatigue, sensitivity to light, and blurred vision. The environmental (e.g. smoke, dust, low humidity, light etc.) and occupational (e.g. CO, CS2) stressors can induce or exacerbates dry eye by reducing ocular mucous cells and mucin production. In one of the dominant dry eye diseases- Sjögren syndrome, the patients have markedly reduced conjunctival goblet cells and the goblet cell-specific mucin-MUC5AC. However, there is no experimental evidence causally linking the mucin deficiency and the pathogenesis of dry eye. In the present study, a Muc5ac knockout (KO) mouse model was created so that one major ocular mucin-Muc5ac is deleted. The mice was subject to various physiological measurements as compared to its wide-type (WT) control. Interestingly, the mean tear break up time (TBUT) values were significantly lower and corneal fluorescein staining scores were significantly higher in KO mice as compared to WT. But the tear volume was not changed. Despite the lack of Muc5ac expression in the conjunctiva of KO mice, Muc5b expression was significantly increased in these mice. Corneal opacification, varying in location and severity, was found in a few KO mice but not in WT mice. The present results suggest a significant difference in the quality, but not the quantity, of tear fluid in the KO mice compared to WT mice. Therefore, we, for the first time, demonstrate that the lack of a major ocular mucin-Muc5ac causes dry eye.

PS 2128 Toxic Milk Leads to the "Mask" Phenotype in Hephaestin Knockout Mice

K. E. Page[1], E. Lachenauer[1], J. Luong[1], C. Han[1], H. Irimagawa[1], Y. He[1], D. W. Killilea[2], D. M. Frazer[3], G. J. Anderson[3], B. K. Fuqua[3] and C. Vulpe[1]. *[1]Nutritional Science and Toxicology, University of California, Berkeley, Berkeley, CA, [2]Children's Hospital Oakland Research Institute, Oakland, CA and [3]QIMR Berghofer Medical Research Institute, Brisbane, QLD, Australia.*

Iron is an essential element that is required for many cellular functions. Multiple symptoms of iron deficiency have been reported in humans, including anemia, hair loss, stunted growth, and reduced oxygen transport. Mammalian iron intake is mediated in two different ways, across the placenta during fetal growth, and through the intestine during postnatal growth and development. We previously identified hephaestin (Hp), a copper-iron ferroxidase, which plays a key role in intestinal iron transport. Hephaestin oxidizes iron and works in conjunction with ferroportin to facilitate iron export from enterocytes and its efficient binding to plasma transferrin. Null mutations in the Hp gene cause an accumulation of intracellular iron, specifically in the intestine. During analysis of the Hp null mice, we discovered that neonates born to Hp knockout (Hp KO) dams developed truncal hair loss (the "mask" hair loss phenotype) that resolved after weaning. The same phenotype was also observed in pups born to mothers with intestine-specific knockout of Hp (even WT (floxed) pups born to these mothers), suggesting that lack of maternal Hp in the intestine alone is responsible for the mask phenotype. In order to determine the stage (ante and/or post natal) at which lack of maternal Hp leads to pup hair loss, we performed cross-fostering studies. Wild-type pups fed by Hp KO dams presented with the "mask" phenotype, whereas, all pups fed by the WT dams had normal hair growth. Histology of the affected skin of pups fed by Hp KO dams showed disorientation and keratinization of the follicles, follicular infundibular plugging and some tortuosity to the hair canals. Our findings suggest the involvement of a "toxic milk" phenotype involving low iron levels in the milk causing this phenotype.

PS 2129 Alterations of Contractile Gene Expression (Mypt1, CPI-17, and Myosin Kinase) in RUPP, L-NAME, and Adriamycin Rodent Models of Preeclampsia

J. Toot[1] and J. Reho[2]. *[1]WIL Research, Ashland, OH and [2]Department of Medicine, Division of Cardiology, University of Maryland, Baltimore, MD.*

Preeclampsia (PE) is a pregnancy disorder that is characterized by a variety of complications, including high systemic blood pressure and deficits in renal hemodynamics. These PE related changes result in the characteristic reduction in placental perfusion pressure and compromised vascular function. In particular, this altered vascular reactivity is potentially due to a complex mechanism involving endothelial dysfunction and changes in vascular smooth muscle (VSM) contractile properties. The VSM of the microvasculature (i.e., meseneteric arteries) is distinct both phenotypically and functionally from that of the large conduit arteries, with many of the the associated hemodynamic factors responsible for these differences still remaining undefined. Therefore, the objective of this study was to investigate and characterize the expression of several key contractile genes (Mypt1, CPI-17, and Myosin

Kinase) in various rodent models of PE (i.e., RUPP, L-NAME, and Adriamycin). Of particular interest is myosin phosphatase (MP), which acts as a central mediator of vascular function and can be used as a model to determine the VSM phenotype. Alternative splicing of exon 24 (E24) of the MP targeting subunit (Mypt1) generates isoforms that determines the VSM response to NO/cGMP mediated vasorelaxation. Fast contracting (E24+) isoforms are predominant in mesenteric artery VSM while slow contracting (E24-) isoforms are expressed in large artery VSM. Control and SHAM operated pregnant rats expressed the E24+ isoform of Mypt1 in mesenteric arteries. Hypertension during pregnancy resulted in a moderate shift in Mypt1 isoforms in L-NAME and RUPP mesenteric arteries, while Adriamycin treatment lead to a significant shifting of the Mypt1 from the E24+ to E24- isoform ($p<0.05$) in mesenteric arteries. These data indicate a potential compensatory mechanism of the VSM involved in the pathology associated with PE.

PS 2129a Variability in Neurotoxicity: Who Is Susceptible and Why

G. Alam[1], D. B. Miller[2], J. P. O'Callaghan[2], L. Lu[3], R. W. Williams[3] and B. C. Jones[1]. [1]*Biobehavioral Health, The Pennsylvania State University, University Park, PA,* [2]*CDC-NIOSH, Morgantown, WV and* [3]*University of Tennessee Health Sciences Center, Memphis, TN.*

There is increasing interest in differential susceptibility among humans to toxicants, as well as a growing appreciation that multiple gene variants, exposure history, and complex gene-environment interactions (GXE) are critical determinants of disease and risk. For example, individuals who carry a mutation in the glutathione S-transferase gene have far higher risk for developing Parkinson's disease when exposed to paraquat (PQ) (Goldman et al. Mov Disord 27:1652,2012). More refined animal models, in particular genetic reference families of mice, now make it practical to replicate, extend, and mechanistically validate findings from epidemiological and genetic studies of humans. In fact, Liang and colleagues validated the findings of Goldman in glutathione deficient mice (Toxicol Sci 134:366,2013). These families, including the BXD and the Collaborative Cross, provide tight experimental control, but incorporate a very high level of genetic diversity. They are ideal for mechanistic studies of GXE and can now be reliably exploited to define single gene polymorphisms, important biochemical, and molecular mechanisms of toxicity. To illustrate, we studied the neurotoxicity of PQ and MPTP in BXD recombinant inbred mouse strains. Toxicity of PQ is highly variable among these strains and covaries with PQ-related disruption of iron regulation in the midbrain. We also studied effects of MPTP on striatal dopaminergic neurotoxicity among 10 BXD lines and found that 12.5 mg/kg MPTP s.c. caused a variation of 20 – 90% in neurotoxicity as determined by reductions in dopamine and its metabolites, tyrosine hydroxylase protein and elevations in GFAP, an astrocyte marker of neurotoxicity. Furthermore, the variation in dopaminergic neurotoxicity among strains was not due to altered metabolism of MPTP to MPP+, the proximal neurotoxicant. Genetic reference panels can provide valuable information on potential genetic differences in susceptibility and GXE.

PS 2129b Nuclear Receptor Small Heterodimer Partner (SHP) Modulates Circadian Clock Control of ER Stress Signaling in Alcoholic Liver Disease (ALD)

L. Wang, H. Tsuchiya and Y. Zhang. *University of Utah, Salt Lake City, UT.*
Sponsor: G. Guo.

[Purpose] In the past decade, our research has focused on elucidating the molecular mechanisms by which SHP (Nr0b2) regulates liver and metabolic diseases. Highlights of our findings include revealing the role of SHP in fatty liver, liver cancer, and microRNA regulation. In this study, we use SHP-/- mice and the an alcohol binge model to investigate how the liver circadian clock regulates ER stress and fatty liver.
[Methods] The NIAAA binge model was established using 8 weeks old, male C57BL/6 (WT) and SHP-/- mice (Nat Protoc 2013; 8:627–637). The mice were acclimatized to a control liquid diet for 5 days, then fed with 5% Lieber-DeCarli diet or pair-fed for 10 days. On day 11, mice were gavaged with maltose (control) or alcohol solutions at zeitgeber time (ZT) 3 (9 am) and sacrificed at ZT12, 18, 0, and 6. Serum and liver were collected. GC/MS and RNA-sequencing (RNA-seq) were used to identify clock regulated metabolites and genes, respectively. Transient transfection, luciferase reporter assay, ChIP assay, gel-shift assay, Co-IP, Western blots, adenovirus overexpression, siRNA knockdown, and qPCR were used to elucidate the molecular mechanisms.
[Results] Metabolomics revealed a global alteration by alcohol in the oscillation of intermediate metabolites in pathways of glucose, lipid, and amino acid metabolism in SHP-/- mice. Liver SREBP-1c protein cleavage and TG content exhibited a rhythmic pattern of changes. The rhythmicity of core clock genes (Clock, Bmal1, Npas2) and nuclear receptors (Rorα, Rorγ, Rev-erbα) was disturbed by alcohol. Hepatic lipid metabolic genes and ER stress markers exhibited strong oscillations, which were perturbed by alcohol binge. We identified Chop as a circadian clock controlled gene that involves the Rorα/Rorγ/Rev-erbα/SHP regulatory cascade.
[Conclusions] We provide a unique model for future investigation of the role of environmental chemical exposures in the development of metabolic diseases.
[Grant Support] NIH DK080440 and AHA GIA (L.W.).

PS 2129c Mammary Gland Tumor Promotion by IGF1 and an Insulin Analogue in the p53+/R270HWAPCre Mouse Model

B. ter Braak[1], K. Siezen[3], B. van de Water[1] and J. van der Laan[1, 2, 3]. [1]*Toxicology, LACDR, Leiden University, Leiden, Zuid-Holland, Netherlands,* [2]*National Institute of Public Health and the Environment, Bilthoven, Netherlands and* [3]*Medicines Evaluation Board, Utrecht, Netherlands.*

Insulin analogues are chemically modified molecules with improved pharmacokinetic parameters compared to regular human insulin. Although these compounds have been tested for carcinogenic side-effects with the standard two-year in vivo assays in rodents, there are some concerns raised by several epidemiological studies in which an association is suggested between the use of some insulin analogues and the cancer incidence in these diabetic patients.
In this study the new p53R270H/+WAPCre mouse model, which will develop spontaneous human relevant mammary gland specific tumors, was used. We frequently injected this model with insulin NPH, insulin glargine, insulin X10 (AspB10) or IGF1. We hypothesized that injections with possible carcinogenic compounds would increase the number of tumors that are formed, decrease the latency time for tumor development, lead to different types or more aggressive tumors. We found that both X10 and IGF1 significantly decreased the latency time for tumor development (for glargine a slight, non-significant effect was observed). A Western blot analysis was done on all primary mammary gland tumors (n=170) to investigate the IR/IGF1R/HER2/ESR/p-Ekt/p-Akt/ and Catherin status. Hierarchical clustering of this data revealed that X10 and IGF1 induced tumors showed a distinct protein-expression profile that was characterized by high p-Erk levels, suggesting an important role of MAPK signalling cascade in tumor progression/initiation in insulin analogue induced tumors.
These results also indicate that the use of a tissue specific cancer model, like the p53R270H/+WAPCre mouse model, can be used to discriminate between mitogenic and non-mitogenic compounds.

PS 2129d Characteristics of IgG Deposit and Neurodevelopmental Protein Expression in Brain of BTBR T+tf/J Mouse Fetus

Y. Heo[1], S. Hwang[1], C. Kim[1], H. Kim[2], K. Shin[1] and J. Jo[1]. [1]*Occupational Health, Catholic University of Daegu, Gyeongsan si, Republic of Korea and* [2]*Preventive Medicine, The Catholic University of Korea, Seoul, Republic of Korea.*

Autism is a brain developmental disorder with social interaction defects, communication faults, and repetitive behaviors. The cause of autism is not clearly defined. Since the presence of autoantibodies against brain antigen was reported in autistic children and their mothers, autoimmunity is considered being involved in pathogenesis of autism. BTBR T+tf/J (BTBR) mouse was recently reported as a animal model for investigation of autism because of its similarity in behavioral abnormalities with human autistic subjects. Neuro-inflammation could mediate generation of autoantibodies to brain antigen resulting in altered brain development. To evaluate the presence of brain autoantibodies and expression status of proteins related with brain development at fetal stage, fetus of BTBR mice were obtained at day 18 of prenatal period. FVB mice were used as a control strain because of its positive social behaviors. Thirty one and twenty seven fetus were obtained from three pregnant BTBR and FVB dams, respectively. Deposit of IgG isotype in fetal brain was evaluated using brain homogenates by ELISA. Expression of glial fibrillary acidic protein (GFAP), brain-derived neurotrophic factor (BDNF), nerve growth factor (NGF), and myelin basic protein (MBP) was examined using the fetal brain homogenates. Level of brain IgG2a, IgG2b, and IgG3 deposit was significantly higher in BTBR fetus than FVB fetus, but no difference was found for IgG1 between the two strains. Expression of GFAP, NGF, and MBP was significantly lower in BTBR fetus than FVB fetus, but level of BDNF was not different between the two strains. Overall, this study suggest that pre-natal alteration in expression of various proteins related with brain development could lead to occurrence of autism. In addition, accumulation of autoantibody against brain antigen at fetal stage could result in pathogenesis to brain development. [supported by National Research Foundation of Korea 2010-0022169]

PS 2130 Lifetime Carcinogenicity Studies in the CD-1 Mouse: Historical Data for Survival and Neoplasms

J. Le Bigot, C. Thirion-Delalande, B. Palate and R. Forster. *CiToxLAB, Evreux, France.*

The availability of historical data for survival and tumor incidences can be useful in the overall interpretation of lifetime carcinogenicity bioassays. Survival data and incidences of neoplastic lesions were compiled for CD-1 mice from the same supplier used as control animals in nine carcinogenicity studies of 104 weeks. All studies, terminated between 2005 and 2011, were performed in our facility, with standardized environment, housing, feeding, necropsy, tissue sampling and trimming procedures, application of common diagnostic criteria and peer review. The mean survival rate of male and female mice was similar (respectively 45% and 43% at terminal sacrifice). The most common causes of unscheduled death or moribundity in males during the course of the studies were, by decreasing order, tumors (mostly from hemolymphoreticular system, lung or liver), atrial thrombosis, amyloidosis, skin lesion, various inflammatory processes or nephropathy. In females, the most common causes were tumors from the hemolymphoreticular system or from another origin (mainly lung or uterus), amyloidosis, skin lesion or nephropathy. In males, the most common neoplasms originated from lungs (adenoma and carcinoma; >25%), liver (adenoma and carcinoma; >25%) and lymphoreticular system (10% malignant lymphoma) while females had mostly malignant lymphoma (>25%). The other common tumors seen with an incidence above 1% were found in various organs, i.e. Harderian gland, uterus, ovaries, adrenal gland, pituitary gland, mammary gland, testis and kidney or testis, in addition to systemic tumors (mainly histiocytic sarcoma and hemangiosarcoma). The incidences of the principal tumors were compared to published data. There were no marked differences with the exception of the slightly higher incidence of malignant lymphoma in the males and females from our facility. These data were also compared study per study, revealing no major differences. This suggested that major tumor types were stable during this 6-year period with no evidence of strain drift.

PS 2131 Historical Control Data Generated in a 2-Year Life Span Study in Wistar Rats (Crl:Wi(Han)) Demonstrate a Reliable Model for Carcinogenicity Studies

M. Kunze[1], P. Allingham[1], A. Leoni[1], A. Albrecht[1], W. Riedel[1], S. Gähler[2], G. Pohlmeyer-Esch[3], K. Weber[2] and J. F. Hardisty[4]. *[1]BSL BIOSERVICE Scientific Laboratories GmbH, Planegg, Germany, [2]AnaPath GmbH, Oberbruchsiten, Germany, [3]KALEIDIS, Saint-Louis, France and [4]EPL Inc., Durham, NC.*

The aim of this study was to obtain historical background data in Wistar rats collected over a period of 2 years as an essential prerequisite of carcinogenicity studies with this rat strain.
Specific pathogen free Crl:Wi(Han) Wistar rats obtained from Charles River, Germany were maintained untreated and provided ad libitum rodent diet. A 104-week study was conducted with 50 males and 50 females to investigate the survival, body weight development, health condition, clinical pathology and incidences of non-neoplastic and neoplastic lesions.
At study completion a high survival rate of 86 % in males and 74 % in females was observed. Body weights developed as expected, but reached extremely low mean values (<500g in male and <300g in female animals). Clinical findings and clinical pathology results were within the expected range. When compared to other rat strains, a low number of spontaneous lesions were observed at necropsy.
The general tumor profile was within the range of expected lesions (pituitary adenoma, mammary tumors, hepatocellular, thyroid and adrenal gland neoplasms, Leydig cell tumors). In contrast, the Wistar specific thymoma, but also skin and ovarian neoplasms were of very low incidence. Rare tumors included cases of hibernoma, two nasal cavity tumors (adenoma, hemangiosarcoma), and parotid gland adenoma. Amongst pre-neoplastic and nonneoplastic lesions, there was a low incidence of foci of hepatocellular alteration, especially for basophilic cell foci, a common finding in Wistar rats. The severity degrees of other findings were significantly lower than noted in other rat strains.
These results show that this Wistar rat strain maintained on Altromin 1324 diet at BSL offers a reliable model for the evaluation of carcinogenic potential of compounds especially in studies that are designed to exceed the standard duration of 2 years.

PS 2132 A One-Year Feeding Study for WistarHannover GPT Delta Transgenic Rat

H. Takagi[1], Y. Nozaki[1], A. Kawada[1], M. Yamada[2], K. Masumura[2] and T. Nohmi[3]. *[1]Biotechnical Center, JAPAN SLC, Inc., Hamamatsu, Japan, [2]Division of Genetics and Mutagenesis, National Institute of Health Sciences, Tokyo, Japan and [3]Biological Safety Research Center, National Institute of Health Sciences, Tokyo, Japan.* Sponsor: A. Nishikawa.

Transgenic rodent gene mutation assays, recently adopted as OECD test guideline TG488, are useful methods to evaluate in vivo mutagenicity of chemicals in a target organ. The multiple copies of genetically neutral transgenes that contain reporter genes for mutation analysis are integrated in the chromosome of the transgenic rodents. However, biological identities between the transgenic and non-transgenic animals are not well demonstrated. To evaluate the characteristics of WistarHannover gpt delta transgenic (Tg) rat in general toxicity study, we investigated the clinical and pathological features of the gpt delta transgenic and non-transgenic WistarHnnover rats in one-year feeding study. The six week-old Slc:WistarHannover/Rcc-Tg(gpt delta) and Slc:WistarHannover/Rcc (60 animals/sex/strain) were employed for this assessment. Twenty animals in each sex were subjected to necropsy at 13, 26 and 52 weeks after starting, then, clinical and pathological assessments were conducted. In Slc:WistarHannover/Rcc-Tg(gpt delta), the values of several parameters in hematology, clinical biochemistry and organ weights were different from those in Slc:WistarHannover/Rcc with statistical significance. These alterations, however, were within the range of historical control data of in housed Slc:WistarHannover/Rcc, and thus were considered to be incidental. In histopathology, spontaneous lesions in WistarHannover such as fibrosis in the heart, microgranuloma in the liver and so on were observed in both strains. These results suggested that there were no remarkable differences which indicate phenotypic modulation in Tg rats, and supported the conclusion that Slc:WistarHannover/Rcc-Tg(gpt delta) has similar characteristics to WistarHannover.

PS 2133 Carcinogenic Monitoring Data on RasH2 Mice to Guarantee a Long-Term Biologic Stability

K. Urano[1], K. Machida[1], T. Mizushima[1], C. Nishime[1], E. Nishinaka[2], R. Inoue[1], M. Yasuda[1] and H. Tsutsumi[1]. *[1]Central Institute for Experimental Animals, Kawasaki, Japan and [2]JAC, LTD., Tokyo, Japan.*

Laboratory mice, which are used for the regulatory purposes such as carcinogenicity tests, are required long-term biological stability during the mass production and over successive generations. CByB6F1-Tg(HRAS)2Jic (rasH2) mice have been known for having a high susceptibility to human carcinogens and mainly used for the short-term carcinogenicity test for pharmaceuticals. In order to guarantee the biological equivalence and stability of the phenotype, mainly the carcinogenicity susceptibility of rasH2 mice produced by two major breeding facilities of this strain in the world, Taconic (Germantown, NY, USA) and CLEA Japan (Fuji, Shizuoka, Japan), we have periodically compared the carcinogenic response of these mice to the standard positive control compound N-methyl-N- nitrosourea (MNU). Thirty male and 30 female rasH2 mice were obtained from Taconic and CLEA Japan and were divided into two groups for each sex. Vehicle or 75 mg/kg MNU were intraperitoneally injected once at 7 weeks of age and the treated mice were observed for 26 weeks. Body weight gain and survival rate were similar between the mice from these two breeding facilities. No significant difference was observed in the incidence of major MNU-induced tumors in rasH2 mice such as forestomach papilloma and carcinoma, malignant lymphoma, skin papilloma and lung adenoma between the mice from Taconic and CLEA Japan. The data was also comparable to the background data of the last 2 decades such as the ILSI/HESI International Act data (Usui *et al.*, 2001) and the first large-scale monitoring data in 2006 (Machida *et al.*, 2008). This result suggests that carcinogenicity susceptibility of rasH2 mice have been maintained since their establishment and their biological quality has also been guaranteed for the regulatory purposes.

PS 2134 Ranges of Commonly Evaluated Clinical Chemistry, Hematology, and Coagulation Parameters from Clinically Healthy Cynomolgus Monkeys of Asian Origin

L. Lanning[1], K. Taylor[2] and J. Hewitt[2]. *[1]Office of Regulatory Affairs, NIH/NIAID/DMID, Bethesda, MD and [2]Office of Biodefense, Research Resources, and Translational Research, NIH/NIAID/DMID, Bethesda, MD.*

Cynomolgus macaques (*Macaca fascicularis*), also known as crab-eating macaques, are important species in the product development of both drugs and biologics. Historically, studies conducted in cynomolgus macaques were primarily for the determination of the safety of products. With the issuance of the FDA's final rule, 'New Drug and Biological Drug Products; Evidence Needed to Demonstrate

Effectiveness of New Drugs When Human Efficacy Studies Are Not Ethical or Feasible'(21 CFR 314.600 for drugs; 21 CFR 601 Subpart H for biological products), nonhuman primates, including cynomolgus macaques, have also become essential animal models to address product efficacy.
A comprehensive set of well-documented reference values for hematology, clinical chemistry and coagulation parameters can assist in interpreting clinical pathology data from cynomolgus macaques. These values provide data essential for the characterization of the cynomolgus macaque, as is required of an animal model in support of product development under the 'Animal Rule'. In addition, reference ranges assist in evaluating the overall health status of each animal as well as serving as a baseline for evaluation/interpretation of any changes that occur due to disease and/or toxicity.
The values summarized and presented in this poster are intended to provide veterinary clinicians, researchers and toxicologists with reference ranges for hematology, clinical chemistry and coagulation parameters commonly evaluated in toxicology and/or efficacy studies. Analyses were performed using samples collected from clinically normal, healthy, naïve, young adult, cynomolgus macaques of Asian origin. Methods of collection, sample handling and analysis are described. Samples were collected and analyzed as part of multiple studies across multiple sites sponsored by the National Institute of Allergy and Infectious Disease (NIAID).

PS 2135 Comparison of Historical Control Parameters Derived from Subchronic Studies Conducted in CD®IGS Rats Fed 5002 or 5CR4 Certified Diets

M. A. Morse[1], B. Jacob[2] and A. M. Sargeant[2]. [1]*Toxicology, Charles River Laboratories, Spencerville, OH and* [2]*Pathology, Charles River Laboratories, Spencerville, OH.*

LabDiet certified rodent 5002 and 5CR4 diets are two diets used in GLP toxicology studies. One of the major differences between the two diets is the protein content (5002: 20% protein; 5CR4: 14% protein). To assess possible differences in the effects of these diets on toxicologic endpoints, historical control parameters from 28-day and 90-day studies conducted within the last 5 years in male and female CD®IGS rats (Crl: CD(SD)) were compared for each diet. Among the parameters evaluated were body weights, food consumption, hematology parameters, coagulation parameters, clinical chemistry parameters, organ weights, and histopathology findings in selected tissues. There were no notable differences in body weights, body weight gain, or food consumption in rats fed 5CR4 diet when compared to rats fed 5002 diet. Higher levels of triglycerides and cholesterol were among the few differences in clinical pathology parameters observed in male and female rats fed 5CR4 diet when compared to rats fed 5002 diet, which may be related to a slightly higher fat content in the 5CR4 diet. Kidney weights were approximately 10% greater in male rats and female rats fed 5002 diet when compared to rats fed 5CR4 diet, but there were no microscopic correlates for this apparent organ weight difference. Other organ weights were more comparable between groups of rats fed each diet. There were no notable differences in histopathology findings in the liver, lung, or kidneys in rats fed 5002 diet or 5CR4 diet. Overall, there were very few differences in historical control parameters detected in rats fed 5CR4 diet in comparison to 5002 diet, and the two diets are quite comparable when used in subchronic studies in CD®IGS rats.

PS 2136 Comparison of Rodent Euthanasia Using Carbon Dioxide (CO2) by Pre-Filled, Slow-Filled, and Rapid-Filled Methods in Mice

J. K. Herman[1], J. Seeman[2], B. Joachim[1], T. Richer[4], M. Logan[3] and L. W. Dochterman[3]. [1]*Toxicology, Covance Laboratories, Madison, WI,* [2]*Lab Animal Medicine, Covance Laboratories, Madison, WI,* [3]*Pathology, Covance Laboratories, Madison, WI and* [4]*Toxicology Operations, Covance Laboratories, Madison, WI.*

The AVMA Guidelines for the Euthanasia of Animals (2013) states that pre-filled CO2 chambers are unacceptable and a slow-fill method with a rate of approximately 10% to 30% per minute is optimal due to lower potential for pain or distress. To evaluate the proposed procedure, three methods of CO2 delivery for euthanasia were compared in mice: fully charged chamber (Group 1, n=5; 100% CO2), rapid fill (Group 2, n=8; 80% CO2 per minute) and slow fill (Group 3, n=8; 30% CO2 per minute). Blood was collected via cardiac puncture for analysis, necropsy was performed and histological changes were assessed. Mean onset of tachypnea was 11, 15 and 20 seconds while mean time to respiratory cessation was 35, 56 and 141 seconds for Groups 1, 2 or 3, respectively. Ataxia, tachypnea, open-mouth breathing, and recumbency occurred in all groups but onset was more rapid in Group 1 while overall durations were longest in Group 3. Mean pH of the mixed venous samples were 7.10, 7.05 and 6.88 for Groups 1, 2 and 3, respectively, although the partial pressure of oxygen and hemoglobin oxygen saturation were consistent across groups. Additionally, Group 3 animals had macroscopic observations of dark red discoloration of all lung lobes correlating microscopically to lung congestion and hemorrhage. In conclusion, based on shorter time to respiratory cessation, milder clinical pathology changes and lack of microscopic changes, the fully charged chamber is considered to be more humane than using a slow fill technique. However, given the recent guideline changes, we propose utilizing the rapid-fill method for the euthanasia of rodents via CO2 as this method appeared more humane compared to the slow-fill method. Given the variability in the blood pH, toxicokinetic evaluation may also be affected based on variability in plasma protein binding when using the slow filled method.

PS 2137 Effects of Blood Collection via Catheter on Hematology and Coagulation Parameters in Rats

A. M. Brooks, A. N. Alexander, L. Hudgens and R. Hall. *Toxicology, Covance Laboratories Inc., Madison, WI.*

The purpose of this study was to determine the optimum blood collection method in rats treated with Alteplase (Activase®), an on-the-market anticoagulant, and compare clinical pathology data after various collection methods. Five groups of male rats (5/group in 3 treated groups, 3/group in 2 control groups) were catheterized via femoral vein for intravenous (IV) dosing. Animals in 3 of those groups (1 control and 2 treated) were also catheterized in the jugular vein; this second catheter was connected to an injection port and used for blood collections.
Alteplase (20 mg/kg, 1 mg/mL) was administered IV to treated groups over approximately 1 hour. Control groups received sterile saline at the same dose volume and duration. Blood for hematology and coagulation were collected approximately 10 minutes after the end of infusion. Samples were collected directly from the jugular vein (JB) or via catheter with (CBH) or without (CB) heparin lock.
Alteplase administration produced pharmacologically expected mildly prolonged PT (30% higher), moderately prolonged APTT (49% higher), and moderately lower fibrinogen concentration (58% lower) for JB animals (compared to JB controls). However, coagulation data from samples collected via catheter showed significant artifact compared to data from JB samples, even in untreated animals. Virtually no APTT data could be obtained from CBH or CB animals; the few samples that did produce data showed abnormally extended times (67.9-80.3 seconds vs. 17.1 18.1 seconds for JB controls). Plasma samples also showed slight hemolysis for animals bled by CB (2/5 samples) or CBH (2/3 control and 3/5 Alteplase samples) techniques. Hemolysis was not present in plasma samples from control or treated JB animals, and APTT was measurable in all of these plasma samples. Between control groups, CBH collection resulted in lower platelet counts than did JB collection (28% lower).
In conclusion, direct venous blood collection is preferred when assessing coagulation and hematology endpoints in rats; collection via catheter should be avoided in this model.

PS 2138 Characterization of Background Routine and Specialization Ocular Endpoints Used in Juvenile NHP Toxicology Studies

K. Tenneson, S. Wise and M. Vézina. *Ocular and Neuroscience, Charles River, Montreal, QC, Canada.*

In recent years there has been an increased emphasis on non-clinical testing of pharmaceutical and biopharmaceutical products for the pediatric population. With larger numbers of new chemical entities undergoing toxicology testing, ocular changes may also be detected. Ophthalmologic examinations are a common endpoint on toxicology studies and can detect unanticipated ocular effects; however, other parameters may also provide relevant information. As the non-human primate (NHP) is often the most appropriate species for the testing on biologics, we characterized the full battery of standard and specialized ocular endpoints in juvenile non-human primates (18 to 23 months; n=4 animals) to determine whether they exhibited significantly different profiles than observed in older animals. No abnormal findings were observed during examinations, which consisted of a biomicroscopic (slit lamp) examination for evaluation of the adnexa and anterior portion of the eyes, funduscopic (direct and indirect ophthalmoscopy) examination to evaluate the ocular fundus. Effects on intraocular pressure (IOP) can occur in response to a test article or to ocular inflammation. In young animals, mean IOP values were 15 ± 4 mmHg; approximately 14% lower than background ranges in older animals (2 to 5 years; n=172 eyes). Mean corneal thickness measured using a hand-held pachymeter (451 ± 25 μm) or specular microscope (457 ± 15 μm) were slightly higher than those measured in older populations (422 ± 21 μm; n=12 eyes). Corneal endothelial cell density was overall higher in juvenile animals (mean =3519 cells/mm^2 vs. 2936 cells/mm^2), however, fewer of these consisted of the typical hexagonal shape compared to older animals (61% vs 71%). In conclusion, background ocular characteristics are generally similar between juvenile and older

animals, however, there are some differences which should be taken into consideration when evaluating the results in toxicology studies to facilitate the recognition of test article-related changes.

PS 2139 Data Comparison of the Respiratory Parameters during the Acclimatization Phase of Rat Snout-Only and Whole-Body Plethysmography Studies

S. Moore, R. Armstrong and S. Jordan. *Huntingdon Life Sciences, Huntingdon, United Kingdom.* Sponsor: D. Mitchell.

Prior to the exposure phase of a snout-only plethysmography (SOP) or whole-body plethysmography (WBP) study, the animals are trained to the restraint procedure over a period of days. The aim is to minimise any stress-related elevations in respiratory minute volume (RMV) values, which may mask potential effects of the administered test material. Measurements of tidal volume (TV), respiration rate (RR) and RMV were conducted over a number of consecutive days. For SOP, the animals were held in restraining tubes and for WBP they had freedom of movement in a small chamber. Mean data (n=8) for the SOP study gave elevated RMV values of up to 637mL/min on Day 1 after 10mins, which decreased to 229mL/min by 30mins and 200mL/min by 60mins. For Day 3 to 5, the RMV had decreased to between 405 and 420mL/min after 10mins, 185 and 198mL/min by 30mins and 189 and 203mL/min by 60mins. The values from the period 30 to 60mins are similar to published data (1). These changes in RMV were due to increases in the RR (up to 399 breaths per minute (bpm) as only a marginal effect on TV was observed. Mean RMV data (116 to 138mL/min) for the WBP study gave little change with acclimatisation number and duration. Comparing the two approaches, RR values were initially considerably higher for SOP (up to 399bpm) but after 30mins were similar (123bpm for SOP and 124bpm for WBP). There was also a marked difference in mean TV values, 1.75mL/min for SOP and 1.06mL/min for WBP. In conclusion, the method of restraint has a marked effect on RR, TV and RMV and additional study design considerations needs to be given prior to conducting SOP studies.

(1) Alexander DJ et al, (2008). Association of Inhalation Toxicologists (AIT) working party recommendation for standard delivered dose calculation and expression in non-clinical aerosol inhalation toxicology studies with pharmaceuticals. *Inhalation Toxicology*, 20, 1179-1189.

PS 2140 Comparison of 4DCT-Derived Ventilation Maps to Deposition Patterns of Inhaled Particulates in Healthy and Diseased Rat Lungs

R. E. Jacob[1], W. J. Lamm[2], D. R. Einstein[1, 3], M. Kueger[2], R. W. Glenny[2] and R. A. Corley[1]. [1]*Pacific Northwest National Laboratory, Richland, WA,* [2]*Pulmonary and Critical Care Medicine, University of Washington, Seattle, WA and* [3]*Mechanical Engineering, University of Washington, Seattle, WA.*

Changes in lung mechanics due to disease can strongly impact airflow dynamics and ventilation patterns. We have demonstrated that non-invasive, *in vivo* 4DCT imaging (3D imaging at multiple time points in the breathing cycle) can be used to map heterogeneities in ventilation patterns of rats under healthy and disease conditions. To validate such maps we exposed rats to fluorescent microspheres (FMS) by inhalation and examined 3D particle deposition patterns using cryomicrotome imaging. In these studies, eleven male Sprague-Dawley rats (231±7g) were given an intratracheal dose of either 10 U/kg elastase in 0.2 mL saline or 0.2 mL saline only to a single lobe. Four weeks after dosing, rats were surgically intubated, mechanically ventilated with a tidal volume of ~2.0 mL, and imaged at 100 ms temporal resolution over the full breathing cycle by 4DCT. Immediately following imaging, rats were transferred to another ventilator with the same tidal volume and exposed to an aerosol of ~1 micron FMS for 5 minutes. After the exposure, the lungs were removed, filled with an embedding medium, and frozen for cryomicrotome sectioning. The cryomicrotome captured images of inhaled particle deposition throughout the entire lung, where the fluorescent signal intensity indicates ventilation. Comparisons between 4DCT ventilation maps and FMS deposition patterns showed strong correlations ($r=0.75$, $p<0.0005$) in ventilation patterns, where gross ventilation defects due to the disease were observed. By comparison, control rats showed few, if any, ventilation anomalies. We conclude that ventilation maps derived from non-invasive 4DCT imaging can be useful for predicting aerosol deposition in inhalation studies, evaluating lung disease and disease progression, and assessing treatment efficacy.

PS 2141 Development of an Impedance-Based Model For Assessment of Cardiopulmonary Function in Rabbits

M. Horsmon[1], N. M. Vincelli[2] and R. Kristovich[1]. [1]*US Army Edgewood Chemical Biological Center, Gunpowder, MD and* [2]*Leidos, Gunpowder, MD.* Sponsor: S. Hulet.

Improving the quality of physiologic data collected from research animals in toxicology studies is paramount. This is most easily accomplished by collecting as much data as possible from a single animal, thereby reducing animal use and error associated with satellite groups. The present study investigates the feasibility of applying a large animal implantable telemetry device capable of providing data on animal activity, core body temperature, blood pressure (BP), electrocardiogram (ECG), and impedance-based respiratory parameters in the rabbit. Six New Zealand white rabbits were implanted with a modified TL11M3-D70-PCTR device from data sciences international. The first task was to develop an optimal implantation technique that yields calibrated tidal volume (Vt) measurements that are within 10% of those obtained simultaneously from a pnemotachograph (PNT), low noise ECG, and stable BP. The second task was to challenge with a known respiratory stimulant (doxapram HCl, 5.0mg/kg I.V.) to assess linearity of the calibration across a range of Vt. Of the three electrode placements attempted, only one resulted in calibrations consistently under 10% error. Optimal electrode placement results in calibrated Vt measurements within 1.7% (±1.6%) of those obtained from a PNT during normal tidal breathing, 6.0% (±3.6%) following doxapram HCl injection and 7.3% (±4.4%) following saline injection. Vt range for normal tidal breathing and saline injection was 9-15mL, and following doxapram injection was 25-30mL. Similar error ranges were associated with derived flow parameters. Increases in mean BP of 25.0mmHg (±6.82mmHg) and decreases in heart rate of 56.3bpm (±6.82bpm) were associated with doxapram injection only. No departure from normal body temperature was observed in any group. The development of this model offers a solution to monitoring cardiopulmonary function the rabbit.

PS 2142 Comparison of Cardiovascular Parameters Recorded via Radio-Telemetry in Göttingen and Chinese Bama Minipigs

S. Mason, L. Qu, R. Wu, S. McPherson and Q. He. *WuXi AppTec, Suzhou, China.*

Introduction: Minipigs are routinely used for regulatory toxicity testing, including assessment of cardiovascular effects of a drug via telemetry. In the USA and Europe, the Göttingen minipig is often selected for such studies, while in China, the Bama minipig is usually the species of choice. The objective of this study was to compare the hemodynamic and electrocardiographic parameters of the Göttingen and Chinese Bama minipigs, using the standard telemetry methodology.

Method: Six Bama minipigs were surgically implanted with radiotelemetry transmitters (DSI TL11M2-D70-PCT). Systemic blood pressure, modified Lead II ECG intervals, and heart rate were recorded continuously for repeated intervals of approximately 24 hours using the DSI Ponemah software (version 5.00). The control cardiovascular data for Göttingen minipigs were obtained from literature (Markert et al, 2008).

Results and discussion: The mean systolic and diastolic pressures for Bama pigs were 134 and 95 mmHg, respectively, compared with the published values of 122 and 86 mmHg for Göttingen animals. Baseline heart rates were slightly higher for the Bama pigs (88 bpm) compared with the Göttingen pigs (71 bpm). Associated with the difference in heart rate, there were some small differences in quantitative ECG parameters, most notably for the QRS duration (39 ms for Bama and 56 ms for Göttingen) and QT-interval (295 ms for Bama and 320 ms for Göttingen). Much of the difference in heart rate and derived ECG intervals may be attributable to variations in housing and husbandry practice. In particular, the timing of feeding relative to data collection is an important factor as postprandial increases of 8-10% in heart rate have been demonstrated in minipigs. In summary, the cardiovascular parameters collected from telemetry-instrumented Bama minipigs were broadly similar to those reported from Göttingen animals, and this strain of animal is considered suitable for assessment of effects of new drugs on the cardiovascular system.

PS 2143 Comparative Sensitivities of the Rat, Dog, and Monkey Larynx and Tracheal Bifurcation in Inhalation Toxicity Studies

A. M. Pilling[2], V. Mowat[1] and D. J. Alexander[3]. [1]*Pathology, HLS, Huntingdon, United Kingdom,* [2]*Toxpath Consultancy Ltd, Stradbroke, Suffolk, United Kingdom and* [3]*DA Nonclinical Safety Ltd, Godmanchester, Cambs, United Kingdom.* Sponsor: D. Mitchell.

Introduction
In this review, a comparative assessment of the larynx and carina from rat, dog and cynomolgus monkey is undertaken, to compare sensitivities and to assess their relevance for man. In inhalation toxicity studies, the authors have observed that drug induced lesions are frequently reported in the larynx and tracheal bifurcation (carina) in the rat, but less so in the dog or primate. This review is based on observations made by the authors over several years, and on data from inhalation studies compiled at one site.
Histopathological sections of the upper respiratory tract tissues, including the larynx and carina, were prepared and evaluated according to the protocols in use at the different sites, in accordance with best practice guidelines. Data from several inhalation studies run at one site on different rodent and nonrodent species were collated and tabulated. They indicated that some test articles which induce lesions in the upper respiratory tract in rodents, notably in the larynx, do not cause histopathological changes in the dog or primate, supporting the authors' observations.
The rat larynx is far more sensitive than the dog and monkey in its response to inhaled xenobiotics, due to the relatively thin epithelial lining, in association with increased mucosal deposition of aerosol particles. The carinal ridge at the tracheal bifurcation is also a well-defined point of impaction for inhaled particles, and is more frequently injured in rodents than in dogs and primates, due to its relatively thin epithelium and airflow dynamics.
Conclusion
Personal observations and available data indicate that drug induced lesions are more frequently reported in the larynx and tracheal bifurcation (carina) in the rat than in the dog or primate, bringing into question the relevance of these rodent findings for humans.
These observations suggest the human larynx is closer to the beagle dog and cynomolgus monkey in its response to inhaled xenobiotics.

PS 2144 Species-Related Differential Sensitivity for Assessing Hemodynamics and Respiratory Function Using Combined Telemetry-Plethysmography Model

E. Hayes, S. Rompion, S. Goineau, P. Guillaume and G. Froget. *Porsolt, Le Genest Saint Isle, France.*

Simultaneous monitoring of cardiovascular and respiratory parameters in conscious non-restrained animals could be useful in safety evaluation. However, the choice of the animal species may be crucial.
We investigated the sensitivity of the 3 commonly used rodent species to the effects of clonidine (1 mg/kg, i.p.), verapamil (30 mg/kg, p.o.) and theophylline (100 mg/kg or 50 mg/kg in mice, p.o.) on cardio-respiratory function using combined telemetry and plethysmography. Telemetered rats, guinea-pigs and mice were placed into plethysmography chambers to simultaneously assess hemodynamics (Heart Rate, HR; Mean Arterial Blood Pressure, MAP) and respiratory function (Minute Volume, MV).
Clonidine decreased HR in rats (-38%, $p<0.001$) and mice (-31%, $p<0.01$) but not in guinea-pigs. Clonidine also increased MAP (+35%, $p<0.01$) and tended to reduce MV (-22%, NS) in rat only. In rats and mice, verapamil decreased MAP (-27% and -25%, $p<0.01$) and increased HR (+16% and +12%, $p<0.05$). Hemodynamic parameters were not modified in guinea-pigs. Verapamil had no effect on ventilation in the 3 species. Theophylline increased HR in rats, mice and guinea-pigs (+59%, +39% and +32%, $p<0.001$) but had no effect on MAP. Theophylline exhibited respiratory stimulant properties in rats (MV, +68%, $p<0.05$) and mice (MV, +203%, $p<0.01$) but not in guinea-pigs.
These findings suggest that, in contrast to cardiac risk assessment with regards to evaluation of QT interval prolongation, both rats and mice are more sensitive than guinea-pigs in the combined telemetry-plethysmography model for assessing hemodynamics and respiratory function in early safety pharmacology studies.

PS 2145 Effect on Dosimetry of Altered Respiratory Minute Volume During Inhalation Exposure

X. Li, S. Oag, P. McDonald and P. Smith. *Inhalation Toxicology, Charles River Edinburgh, Edinburgh, United Kingdom.* Sponsor: W. Harvey.

For most rodent inhalation studies, the achieved dose is estimated based on the calculated respiratory minute volume (RMV) according to animal body weight using one of the commonly accepted algorithms, like Guyton, McMahon, Bide or AIT formula. However, such estimates will not be accurate if the inhaled material has a local irritating effect on the respiratory system, with consequent effects on the respiratory pattern and RMV. Under such circumstances, the inhalation dose may be miscalculated by use of standard algorithms. The current study was designed to investigate the effect of a known respiratory irritating agent (Code: SA) on the RMV of rats. SA was aerosolised and administrated to the rat via the nose-only inhalation route for 10 min at three different aerosol concentrations using a flow past system. Animal RMV was assessed using a head out plethysmography system before, during and after inhalation exposure. Our investigations revealed that the RMV values decreased significantly during inhalation exposure to SA compared with the values obtained before inhalation exposure in the same animals. The reduction was mainly due to decreased tidal volume and was largely concentration-dependent. At the high concentration, the measured RMV value was less than 50% of the RMV value estimated according to the McMahon formula. The investigation justifies our approach of using the measured RMV value rather than calculated RMV (based on animal body weight) for a better estimate of achieved doses during inhalation exposure to test items which may have an irritant effect on the respiratory system.

PS 2146 Implantation of Left Ventricular Pressure Telemetry with Solid Tip ECG in the Cynomolgous Macaque: Surgical and Anaesthetic Considerations

K. Read. *Veterinary Services, Huntingdon Life Sciences, Alconbury, United Kingdom.* Sponsor: D. Mitchell.

Objectives: Implantation of a D70-PCTP transmitter allows measurement of cardiovascular parameters for safety pharmacology and toxicology studies. Historically, we have implanted ECG electrodes subcutaneously over the thorax in the primate, resulting in a variable signal with a large noise:signal ratio. The solid-tip negative ECG electrode configuration aims to eliminate muscle noise and movement artefact from the ECG waveform.
Method: A balanced anaesthetic technique is used and multimodal analgesia is provided. The dual pressure catheters are surgically implanted into the apex of the left ventricle via a midline laparotomy and incision in the diaphragm, and into the abdominal aorta via the left femoral artery. The device body is anchored in the abdominal cavity to measure core body temperature. The positive ECG electrode is positioned on the diaphragm close to the apex of the heart, and the negative ECG electrode advanced into the superior vena cava via the right internal jugular vein. The final position of the negative ECG electrode is ascertained at surgery by monitoring ECG morphology.
Results: The solid-tip ECG configuration ensures the procedure for implantation is reproducible and simplified compared to subcutaneous placement. Waveforms from these implants are considered good, and all animals recovered well without complications. Our peri-operative protocol provides stable anaesthesia and suitable analgesia for this procedure. To date none of our macaques implanted with this device have required surgical repair.
Conclusions: The solid-tip ECG D70-PCTP device provides improvements in ECG waveform quality in the primate, and also animal welfare due to decreased surgical/anaesthesia time and fewer surgical repairs.
References: Data Sciences International (2011) Solid Tip Lead Surgical Manual. Available at: www.datasci.com

PS 2147 Onset of Sexual Maturity in Female Göttingen Minipigs

B. Peter[1], E. de Rijk[1], H. Lorentsen[2], A. Zeltner[2] and H. Emmen[1]. [1]*Toxicology, WIL Research, Den Bosch, Netherlands and* [2]*Ellegaard Göttingen Minipigs A/S, Dalmose, Denmark.*

In drug development minipigs may be used as a non-rodent alternative to dogs or non-human primates. For general toxicity studies, the animals should be sexually mature at start of the study. Based on breeding experience, female Göttingen minipigs are considered to reach sexual maturity at 4-5 months of age. To investigate this further, a study with young sows at 3-4 months of age (housed in the same room as adult boars) was performed. Twice weekly, they were observed for signs of heat (vulva redness/swelling, mounting) and blood samples were taken for progesterone analysis. In addition, body weights were recorded every 2 weeks. After the completion of 1-2 cycles of progesterone release, females were sacrificed. To check

whether the female minipigs were actually sexually mature, the reproductive organs (ovaries, uterus, pituitary gland) were weighted and histopathologic examination of reproductive-related organs (ovaries, uterus and cervix, vagina, mammary gland and pituitary) was performed.
Before reaching sexual maturity, very low concentrations of progesterone (< 1 ng/mL) and/or signs of heat were detected sporadically. The first cycle of progesterone release, indicative of a functional corpus luteum, was noted in 7/13 sows at 3.7-4.2 months (8.4-12 kg) and for another 6/13 sows at 6.1-6.5 months (12.1-16 kg) of age. The estimated cycle length was 17-22 days. Signs for heat were not always noted around expected ovulation. Histopathological examination of the reproductive organs confirmed that all 13 sows were sexually mature.
In conclusion, the age range when female Göttingen minipigs reach sexual maturity (3.7-6.5 months) is much longer than anticipated. Hence, care should be taken when designing toxicity studies with young sows and interpreting data hereof. Progesterone analysis proved to be a reliable method to detect sexual maturity during in-life.

PS 2148 Ovarian Cycle Features in Socially Housed Cynomolgus Monkeys (*Macaca fascicularis*)

A. Mitchell[1], C. M. Luetjens[2], S. M. Henwood[1] and G. F. Weinbauer[2]. [1]*Covance Laboratories, Madison, WI and* [2]*Covance Laboratories GmbH, Muenster, Germany.*

Social housing of macaques is a standard and common requirement of up-to-date primate husbandry. Unlike in male animals, social housing can have profound effects on ovarian cyclicity and potentially on female fertility. Among these effects are interruptions or irregularities of the ovarian cycles. However, these cycle disturbances vanish as animals are socially housed over prolonged periods of time. Since this laboratory has long-lasting experience in ovarian cycle monitoring/social housing, a retrospective analysis of cycle patterns was undertaken. Beyond that, a comparison of menstrual cycle data was conducted for two locations (US vs. Europe) with highly comparable husbandry approaches/vaginal swabbing collection and criteria. Daily vaginal swab data were available from 5447 ovarian cycles of Asian origin animals. Animals were housed socially for a period of at least 3 months. The swabs were rated from no to heavy menstruation. Menstrual cycle length was categorized (C1, C2, and C3) depending on the cycle length difference between consecutive cycles with C1 being a regular cycle, C2 a prolonged cycle and C3 a comparatively irregular cycle. Cycle durations below 20 days and over 50 days were excluded from analysis. Interestingly, more than 85% of animals were in the C1 category, indicating a stable and regular cycle during prolonged social housing with only 3 - 8% of animals each being either in category C2 or C3. A direct comparison between the two sites (4755 vs. 692 cycles) confirmed a similar distribution of C1, C2, and C3 categories for each site with differences below 5% within each category. In conclusion, social housing – in the longer term – has beneficial effects on ovarian cycle regularity and stability, at least in the cynomolgus monkey model. Also, ovarian cycle data are similar between different locations. Hence, social housing is recommended for mature/fertile animals even though this might impose prolonged baseline periods in order to stabilize ovarian functions.

PS 2149 Development of a Novel Duodenal Catherization Model in the Minipig Using an Implant Modified from the Clinic

R. Rose and K. Read. *Veterinary Services, Huntingdon Life Sciences, Alconbury, United Kingdom.* Sponsor: D. Mitchell.

Objective: A minipig duodenal catheterization model was developed to investigate local irritancy of a test compound. Direct duodenal dosing is clinically required for certain medications. As this study was concerned with local irritancy, it was essential to limit variables and use the same implants that would be used clinically. To make the minipig model directly comparable to the clinical trials, the surgical implant selected was specifically modified from a PEG tube and intestinal line used in human medicine (Freka®).
Method: Cadaver trials were undertaken in three minipigs to determine the optimum implant dimensions, and to perfect the surgical technique looking at both standard and minimally invasive approaches. A preliminary trial in three minipigs revealed the tendency for the intestinal catheter to be drawn back into the stomach, possibly due to the retention of a matt of fibrous material when the animals are bedded on straw. Two alternative methods were developed, one altering the position of the PEG tube in the stomach and the other avoiding use of the PEG tube and placing the intestinal catheter directly into the duodenum, via modification with a retention bead and Dacron mesh. Post-operative orthoganol view radiographs were taken on the pilot study to ensure the correct location of the catheter in all animals during the dosing period.
Results and conclusion: The pilot work proved the direct duodenal placement method was a successful and robust model allowing progression to the dose range finding and main studies. The surgical approach and fixation technique of the intestinal catheter will be explained visually. The presentation will also detail feeding considerations, anaesthesia, analgesia and post-operative catheter maintenance regimes.
Rita Rose BSc, MA, VetMB, MSc(WAH), MRCVS

PS 2150 Comparison of Cynomolgus and Marmoset Monkeys for Preclinical Testing of Biopharmaceuticals

W. Frings and B. Niggemann. *Covance Laboratories GmbH, Muenster, Germany.*

Biopharmaceuticals, unlike chemically synthesized compounds, frequently exhibit species-specific activity. For many biopharmaceuticals, e.g. monoclonal antibodies, nonhuman primates frequently constitute the only or the most relevant species. The most commonly used species is the cynomolgus monkey (*M. fascicularis*), an Old World monkey. New World monkeys, e.g. the marmoset monkey (*Callithrix jacchus*) are also being used occasionally. Within the primate pedigree Old World monkeys are more closely related to humans compared to New World monkeys. In many instances, safety assessment of biopharmaceuticals requires evaluation of the immune system. In this work, relevant differences between cynomolgus and marmoset monkeys are compared. Functional immunotoxicology tests are easier to be performed in cynomolgus monkeys due to better functionality of human assays or blood volume limitations in marmosets. On the other hand some leukocyte CD markers better resemble the human distribution in marmosets. Development of anti-drug antibodies (ADA) is often a critical limitation for the evaluation or maximum duration of preclinical studies with biopharmaceuticals. Based upon the phylogenetic distance a higher risk of ADA development in marmosets can be assumed. However, data from approx. 200 animals/species exposed to human antibodies reveal 6 % of cynomolgus and only 2 % of marmosets developed detectable ADA responses impacting toxicokinetics. In conclusion, whilst cynomolgus monkeys are the preferred non-human primate model, marmosets provide a relevant alternative in certain instances.

PS 2151 Hepatic Microsomal UDP-Glucuronosyltransferase (UGT) Activities in Microminipig

E. Higashi[1], A. Ando[1], S. Iwano[1], N. Murayama[2], H. Yamazaki[2] and Y. Miyamoto[1]. [1]*Toxicology and Pharmacokinetics Laboratories, Toray Industries, Inc., Kanagawa, Japan and* [2]*Laboratory of Drug Metabolism and Pharmacokinetics, Showa Pharmaceutical University, Tokyo, Japan.*

Microminipig, a small minipig (< 10 kg body weight in adult) is developed as a novel experimental animal for nonclinical pharmacology/toxicology studies in Fuji Micra Inc. (Shizuoka, Japan). To understand the results of nonclinical studies, we need to comprehend species differences in drug metabolism between human and microminipig. It has been reported that there is some overlap in microminipig and human cytochrome P450 substrate specificity, with high P450 2D-madiated activity in liver microsomes. Glucuronidation catalyzed by UDP-glucuronosyltransferase (UGT) is a predominant phase II biotransformation reaction in the metabolism. The purpose of the present study is to identify the characteristics of hepatic UGT activity of microminipig by a comparison with those of human and other experimental animals.
In vitro UGT activities in liver microsomes from microminipig, human, mouse, rat, dog, monkey and minipig were investigated. Glucuronides of estradiol, imipramine, serotonin, propofol and 3'-Azido-3'-deoxythymidine (AZT), a selective substrate of human UGT1A1, 1A4, 1A6, 1A9 and 2B7, respectively, were measured by LC/MS/MS.
Estradiol glucuronidation activity of microminipig was higher than that of human and other animals. Imipramine-*N*-glucuronidation, a distinctive conjugation by human UGT1A4, was catalyzed by microminipig liver microsomes, but not by dog liver microsomes. Serotonin and propofol glucuronidation activities in microminipig were similar to those in human. Low AZT glucuronidation activity in microminipig was observed as similar to that in rodents or dog. UGT activities in microminipig were similar to those in minipig. It is suggested that microminipig is useful for nonclinical studies as one of non-rodent species on UGT activity.

PS 2151a Quantity of Plasma Not a Constraint to Measure Clinical Chemistry Analytes

S. Jana, V. Goyal, S. Pandey, A. Gothi, S. Kakade and R. Nirogi. *Discovery Toxicology, Suven Life Science Ltd, Hyderabad, Andhra Pradesh, India.*

Clinical chemistry is an essential analytic tool in many areas of research, drug assessment and development. In research involving mice or other small animals, limited amount of blood that can be collected pose a challenge and limit the prac-

tical utility of clinical chemistry analyses on serum or plasma. To overcome this problem, multiple cohort of animal are being used for different activities at different time leading to extra animals and additional resources, and limit the suitability of interpretation of results which are derived from different animals. The aim of this study was to prove the hypothesis that diluted plasma can be used in toxicity studies involving mice to determine various clinical chemistry parameters from the same animal without compromising the quality of data. Blood samples were collected from the mice; two aliquots were prepared, one used for dilution and other one kept undiluted. First aliquot was diluted 2, 3, 5 and 10-fold with water for injection. Analysis was carried out using automated clinical chemistry analyzer. Results were compared with the results from non diluted plasma of same mice. Most of the clinical chemistry parameters were well within the range of undiluted samples except electrolytes. For electrolytes, we tried dilution with different diluent like reagent grade water type I, Cal A (Randox), plasma, normal saline and water for injection albeit without any success. Nevertheless, when specimen dilution will permit essential testing on small, valuable or fewer animals, all specimen dilutions should be performed identically throughout the study.

PS 2151b Determining the Effect of Storage Conditions on Different Coagulation Parameters

S. Pandey, V. Goyal, A. Gothi, S. Jana, S. Kakade and R. Nirogi. *Discovery Toxicology, Suven Life Science Ltd, Hyderabad, Andhra Pradesh, India.*

Coagulation parameters viz. prothrombin time (PT), activated partial thromboplastin time (APTT) and fibrinogen are usually included in clinical and preclinical safety studies of xenobiotics. The analysis is generally performed along with the terminal sacrifice where lots of activities are scheduled. Thus there are likely chances of delay in analysis particularly when blood for coagulation is collected via abdominal vena cava. In this experiment we tried to find out the variation that is caused by delay in analysis as well as variation due to storage conditions. Animals were bled under proper anesthesia and plasma was separated immediately. Aliquots of plasma were prepared and stored for 6, 24 and 48 hours at room temperature, refrigerated and freezing conditions. Stability of analytes in blood was also evaluated at refrigerated condition for 6 h. All parameters from all storage conditions including fresh plasma were analyzed using semi automated coagulometer. PT was found to be consistent at all three storage conditions up to 6 hours. APTT was also consistent at room and refrigeration temperature up to 6 hours but not at freezing temperature. Fibrinogen was found to be the most stable parameter that showed consistency in results even up to 48 hours. All three coagulation parameters were stable in blood kept refrigerated through 6 hours. In conclusion, plasma for PT and APTT can be stored and analyzed without any significant changes up to 6 hours from the time of blood collection if stored either at room or refrigerator temperature while fibrinogen level testing can be extended up to 48 h after collection.

PS 2151c Basal and Short-Term Food Denial Stress-Induced Plasma Cortisol in Four Lineages of Miniswine

A. Stricker-Krongrad[2], N. Patel[1], N. Yumibe[1], D. Yurek[1], N. Huang[1], S. Renna[2], D. White[2], L. Brown[2], J. Liu[2] and G. Bouchard[2]. [1]*Eli Lilly & Company, Indianapolis, IN and* [2]*Sinclair Research, Auxvasse, MO.*

Rationale: To compare basal and stress response plasma cortisol levels.
Experimental Procedures: Four lineages of miniswine (MS) were evaluated for cortisol levels. Included were Hanford, Yucatan, Sinclair S-1 and Gottingen strains. Animals were age and weight-matched, non-diabetic, castrated juvenile males (4.2-5.1 mos age) weighing 11-14 kg. Sixteen animals were studied (N = four for each lineage group). Standard manipulations for blood sampling by VAP were used. Baseline cortisol levels were measured over seven sampling points and averaged. A short-term stressor was applied (food denial or the presentation of a feed bin into animal room without offering feed for ~30 min). The animals were then fed and cortisol samples taken at ~30 min post initial food exposure.
Results: Sinclair lineage baseline plasma cortisol levels were the lowest of the four lineages prior to the stress event. Average cortisol levels: Sinclair < Yucatan ~ Hanford ~ Gottingen. The cortisol levels post-stress were elevated for all lineages. The Yucatan and Gottingen were hyper-responders while the Hanford was a moderate responder, and the Sinclair a low to non-responder. All animals except one Sinclair showed an increase in cortisol. The post-stress cortisol for Yucatan increased an average of 129%, Gottingen 125%, Hanford 71%, and Sinclair 14%. The response difference between baseline and post stressor cortisol levels in Sinclair was significantly smaller than responses in Yucatan and Gottingen (Tukey-Kramer HSD, $p<0.05$).
Conclusions: The Sinclair lineage had the lowest average basal cortisol level. The stressor increased cortisol from a range of 14% to 129% (means) across the four lineages. All lineages responded to the stressor as reflected by increased plasma cortisol but the Sinclair increase was very modest. The Sinclair lineage was essentially a non-responder to the short-term stressor (food denial).

PS 2151d Successful Social Housing of Mature Male Cynomolgus Macaques in Mixed Sex Rooms

D. M. Abney[1], K. Harding[2], J. Toscano[1], L. Poor[1], E. Moreau[3], H. Moomaw[1], D. Reim[1] and C. Winnicker[4]. [1]*Charles River Laboratories, Reno, NV,* [2]*Charles River Laboratories, Houston, TX,* [3]*Charles River Laboratories, Senneville, QC, Canada and* [4]*Charles River Laboratories, Wilmington, MA.* Sponsor: R. Kaiser.

At Charles River Laboratories (CRL), we are committed to ensuring all our animals have the highest level of care and welfare. To this end, our social housing program includes placing all animals in pairs or groups. We have a rate of almost 100% success social housing juvenile and sub-adult animals as well as adult females. Social housing of sexually mature males can be a challenge. Some publications suggest that it is not advisable to attempt adult male introductions in mixed sex rooms of rhesus macaques (*Macaca mulatta*). However separating animals into single sex rooms introduces a potential scientific confound as well as operational inefficiencies, and to our knowledge this data has not been published for cynomolgus macaques (*Macaca fascicularis*). Data was collected from two CRL sites which are actively social housing mature males. For the purposes of data collection, sexually mature males were defined as 5 years of age and 5kg or greater. As is common in toxicology research, all animals had a narrowly defined weight range. A pair/group was considered 'successful' if they had maintained compatibility for a minimum of two weeks. All social housing attempts were made in rooms with females present and visible to the males. A total of 21 rooms were analyzed, and 81% of the rooms surveyed had success in pairing the majority of males in the room. Fifteen rooms had a success rate of 75% - 100% (median 92%) with over 280 male animals being socially housed. This data shows that mature males can be successfully socially housed in rooms with females. The ability to compatibly socially house mature males in mix sex rooms does not compromise welfare and allows for greater flexibility of vivarium space usage.

PS 2152 Surgical and Nonsurgical Options for Dosing of Centrally Administered Compounds and CSF Sampling in Toxicity Studies Using Cynomolgus Monkeys

C. Rose, S. H. Korte, F. Runge and B. Niggemann. *Covance Laboratories GmbH, Muenster, Germany.* Sponsor: G. Weinbauer.

In preclinical toxicology, the cynomolgus monkey represents the predominant non-human primate species. In terms of drug delivery, crossing the blood-brain barrier is often an important need in pharmaceutical development. This work gives an overview about available techniques and our experience. Opt.A: Under sedation, in juv. (11 months and 0.8 kg) to mature (≥ 5 kg) animals, lumbar spinal needle injection was feasible at 3 times within 24 hrs (n=+1000) for dosing (1-3mL) or CSF sampling (1-3mL). Opt.B: Animals of the same age range underwent intrathecal administration (0.02 mL/kg/hour) with a surgically implanted lumbar port system (n=+480) for a duration of 13 wks, with 50% port patency for CSF. Opt.C: Dual port surgery with implantation (n=3) of a cisterna magna and lumbar port allowed multiple CSF samplings with chair-restrained and non sedated animals, while dosing continuously through the lumbar port. The cisterna magna port showed a 100% port patency for 4 wks, hence required precaution when handling the animals to avoid catheter blocking or relocation. Opt.D: So far 9 months patency was achieved for an implanted intraventricular port (n=1) to allow a more robust and practicable CSF withdrawal (daily: 8 times, each 0.3mL). For the proper location of the lateral ventricle, a template atlas of the macaque brain for digital imaging and quantitative neuroanatomy was used. Non-stereotactic surgeries were conducted using SoloPort™ MID LOVOL; 3 Fr polyurethane catheter; round tip; 60cm, 2 movable beads (Solomon Scientific, USA) as also performed in clinical settings. Post surgery the animal received an antibiotic and flunixin as analgesic for 5 days. A wash out period, was scheduled prior to start of first dosing. In conclusion, all described techniques were successfully conducted with juvenile and mature group housed cynomolgus monkeys in accordance with European requirements. It is now possible to perform the full regime of clinical settings in this species for withdrawal of CSF, as well as for administration of centrally active drugs

PS 2153 Selection of Ocular Histology Tissue Sections Based on Ophthalmic Examination Findings

M. C. Collins. *Preclinical Services, Charles River Laboratories, Reno, NV.*

Standard procedures for collection and sectioning of eyes may not be sufficient when ocular findings are noted during ophthalmic examinations. Routine histologic sections of the eye are collected cutting by a section parallel to the ciliary artery to include cornea, iris, lens, retina, macula, optic disc, and optic nerve. While this process provides a tissue section that includes the most important ocular structures, this section may be insufficient if ocular findings have been noted in regions that are not centrally-located or if the test article targets the eye. Data from ophthalmic exams can be used to determine the best location to collect histologic sections of the eye.

Cynomolgus monkeys with pre-existing ophthalmic findings such as lens opacity, optic disc pallor, and retinal changes were selected for evaluation. An ophthalmic examination via slit lamp biomicroscopy and indirect ophthalmoscopy was conducted. Detailed information regarding the location of the ocular finding was recorded. For lens and fundus findings, a photograph was collected at the time of ophthalmic examination. At necropsy, the globes were collected separately. A standard histologic section and additional sections were collected based on location information from the ophthalmic data.

The routine section rarely included affected regions of the eye. Only in cases of optic disc findings was there a good likelihood of seeing the affected region on the routine slide. Non-central retina findings and lens findings were less often visible in routine sections. Using detailed descriptions from ophthalmic examination and photographs, the likelihood of collection a tissue section that included the region of ophthalmic findings was improved.

The routine section only provides the opportunity to evaluate ophthalmic findings if they are present in the region that is sectioned. For non-central findings, data from ophthalmic exams (including photographs) can be used to hone in on a tissue section more likely to include the affected region.

PS 2154 Dermal Administration in Toxicity Studies Using the Cynomolgus Monkey

S. H. Korte and B. Niggemann. *Covance Laboratories GmbH, Muenster, Germany.* Sponsor: G. Weinbauer.

The cynomolgus monkey represents an important primate model for preclinical safety evaluation, and in rare cases drugs must be administered topically (epicutaneous administration). The current work describes the conduct and practicability of long duration administration (4-8 hours) of a gel-like test item (0.5 mL/kg/dose) over a period of 4 weeks. Following calculation of the required body surface area, the application site was shaved (e.g. 15 times 10 cm), so that the area was clearly separated from the remaining coat. Vehicle or appropriate concentration of the formulated test article was uniformly applied with a plastic card in equal thickness to the shaved area at the animals back, covered with a soft cloth and fixed with tape. In addition, a thin elastic tape was rolled around the animal's body for additional fixation. A jacket was used for further protection of the dosing site. The animals underwent a 3 day jacket training to ensure comfort when wearing the jacket and to reduce the risk of manipulation by cage partners. At the end of the exposure period and after the skin assessment all application sites were cleaned with water for injection and additionally back and hands/feet were washed with an anti-allergic olive-based soap. Hereby, possible contamination should be further reduced. Great care was given to ensure protection of the dosing area to avoid accidental exposure or cross contamination with other group housed monkeys. All animals were examined for signs of erythema, eschar formation and oedema at the dosing site(s) according to a modified Draize scheme (Draize, 1944). At necropsy, skin samples were taken from (a) application site (back), (b) non-dosed area (lower back, adjacent to application site), and (c) non-dosed area (abdomen), for comparison. In conclusion, the described technique was successfully conducted with group housed cynomolgus monkeys. However, some incidences of cross contamination did occur. Future work therefore shall evaluate the practicability of a thin body coat partly also covering legs and arms.

PS 2155 Comparative Analysis of Cynomolgus Monkeys Behaviour by 24 Hour Time-Lapse Video Monitoring in Toxicity Studies

C. M. Luetjens. *Covance Laboratories GmbH, Muenster, Germany.* Sponsor: G. Weinbauer.

The cynomolgus monkey represents the predominant non-human primate species when it comes to preclinical safety evaluation of new medical products but rarely rely on behavioural aspects of undisturbed animals. Therefore, a video monitoring study was conducted with 12 animals divided in three animals per group. Repeated monitoring in a longitudinal study on three different occasions was performed in an interval of six weeks. The grouped animals were acquainted to each other and to the European style cages which are equipped with separating steel bar boxes. A video system monitored the animals for 24 hours in a light/dark regime of 12/12h adapted biweekly in a dark phase to red-light, with weak light emission. The videos were captured with software to monitor three animals on a single data file. To keep the total analysis time manageable all analyzed videos were only observed for six hours in total, always in the same daily time frames for all observed animals: Four hours at day light and two hours during the night. A qualitative behavioural scoring was utilized by timing the actions of the individual monkeys, divided into the following five different categories: 1) moving slowly, 2) sitting or lying calmly, 3) sitting on the water tap at the back, 4) wandering or climbing, and 5) the total number of behavioural changes. The observations demonstrated a high intra- and inter-variation of behavioural actions. The total number of behavioural changes was similar for the simultaneously monitored animals compared to the animals repeatedly monitored: 57.3 ± 18.0 compared to 53.3 ± 15.1 changes, respectively. The longest observed category (over 2 hours) was the mean time of sitting or lying calmly (which is mainly during the night) followed by sitting on the water nipple for almost two hours. In conclusion, this study demonstrated the feasibility of video recording of undisturbed cynomolgus monkeys over 24 hours. The results of this study will help detection and comparison of clinically relevant or adverse treatment effects normally not seen by short cage side observations.

PS 2156 Investigation of a Suitable Method for Monkey Semen Collection

G. Lei, S. McPherson, W. Hongping, C. Barker, S. Mason and Q. He. *WuXi AppTec, Suzhou, China.*

The cynomolgus monkey (*Macaca facicularis*) is routinely used in preclinical toxicity testing. For certain drug indications it is important to have sexually mature animals on the studies. For males the presence of sperm in the ejaculate is one of the criteria for determination of sexual maturity. The intent of this study was to evaluate a reliable and repeatable method of semen collection. A total of 36 male cynomolgus monkeys, approximately 5 years of age or older and weighing 4.4 to 6.9 kg, were individually housed in stainless steel cages elevated off the floor, in HEPA-filtered rooms with a 12-hour light cycle. Semen was collected using a modified penile electroejaculation method (Mattison, et al., 2011). Semen collection was attempted in normal restraint chairs using minimal restraint. A gauze strip moistened in 0.9% saline was wrapped around the penis. Two electrodes from the stimulator were attached to the gauze. The stimulator settings were 10 to 30 pulses per second, and 1 to 3-ms duration. The voltage was varied from 0 to 50 V. The lowest voltage was initially used and then gradually increased as required. The head of the penis was held inside an appropriate volume tube opening to catch the entire ejaculate, which was immediately transported to the laboratory for sperm count. The semen weight was also recorded. If no ejaculation occurred the animal was allowed to rest for at least 1 min and the stimulation was repeated. If no ejaculation occurred within 10 min, the animal was returned to his cage. Semen collection was attempted from the animal again with a minimum of 24-hour of rest between collection attempts. The success rate for semen collection was 86% at the first attempt and 100% within 2 days. The ejaculate parameters results obtained (weight 0.02 to 1.9 g and sperm count 2.7 x 107 to 5.8 x 108) were comparable to the literature (Niehoff, et al. 2010). The results demonstrated that this semen collection method may be used during the conduct of preclinical toxicity testing and the results can support the determination of the sexual maturity of the male non human primate.

PS 2157 Collection of Semen Samples from Rabbits in Drug Disposition Studies

J. D. Stuhler[1], J. Relph[1], M. Jensson[1], T. Eckhoff[1], F. Thalacker[1] and V. Tedesco[2]. [1]*Metabolism, Covance Laboratories, Madison, WI and* [2]*Novartis Pharmaceuticals Corporation, East Hanover, NJ.* Sponsor: V. Dinkel.

The rabbit semen collection model is a useful tool for the investigation of drug distribution into semen. Rabbits are relatively low cost, easy to manipulate in this application, and provide adequate sample volumes for analysis. This study describes a relatively simple and convenient method for collecting semen from rabbits for quantification of drug levels in drug disposition studies. The method used in this study is a modification of the procedures reported by Naughton et al. (2003) and Bredderman et al. (1964).

In two studies with separate groups of rabbits (acclimated to laboratory conditions for 1 to 3 weeks before study initiation), 10 of 11 rabbits on test produced semen samples over an 8-day sample collection period. Postdose sample weights ranged

from 0.111 to 0.541 grams (mean 0.320 ± 0.148 grams) in the first study, and from 0.220 to 1.54 grams (mean 0.483 ± 0.324 grams) in the second study. All sample weights met the minimum sample size criterion for analysis.
Difficulties were generally minor and included one animal for which no postdose samples were produced, and 5 samples (from a total of 56 collected samples) that were noted as being pink (n=2) or yellow (n=3) in color, possibly indicating blood or urine contamination.
Serial blood samples for pharmacokinetic analysis were collected from the same animals used for semen collections.
This project demonstrates that semen samples can be reliably collected from rabbits over an extended period of time in drug disposition studies. A lengthy acclimation or training period was not required to achieve the study objectives. Semen sample weights were variable, but in all cases were sufficient to meet the analytical requirements of the study.

PS 2158 Hepatic Portal Vein Catheterization in the Dog

H. Murphy and K. Read. *Veterinary Services, Huntingdon Life Sciences, Alconbury, United Kingdom.* Sponsor: D. Mitchell.

Objectives: Catheterisation of the hepatic portal vein in the dog has been described for infusion, withdrawal, and measurement of portal pressure. Historically a number of techniques have been described, with no major refinements to the procedure in recent literature. A study required investigation of the extent of first-pass metabolism of test article when delivered orally.
Methods: Four beagle dogs were implanted with a modified polyurethane catheter (tapering from 6F to 4F at the tip with a suture bead 100mm from tip). The catheter was advanced into the hepatic portal vein from either the caudal pancreatico-duodenal vein, or the cranial mesenteric vein. The catheter was connected to a subcutaneous vascular access port tunnelled to an accessible site over the thorax. Peri-operative analgesia, anaesthesia and antibiosis were provided. Patency was maintained by regular flushing with heparinised saline, and the catheter locked with heparinised saline between access points.
Results: Literature regarding this procedure describes difficulties with patency, in particular thrombophlebitis and clot formation over the catheter tip. However, the implants in this study remained patent for the post-operative period and the dogs were used successfully on study, with the collection of all required portal vein samples. Blood flow through the catheter was positional in one animal.
Correct catheter placement was confirmed on necropsy, and examination of the catheter tip indicated no macroscopic clot formation.
Conclusions: Catheterisation of the hepatic portal vein using this technique appears to provide reliable portal blood sampling over 6 weeks. With further implantations, refinements can be made to the peri-operative protocol and the flushing regime.
References:
Rendall M (1965) New technique for portal catheterisation in dogs. Gut. Pages 613-614
Denton AE, Gershoff SN, Elvenjem CA (1953) A new method for cannulating the portal vein of dogs. Journal of Biological Chemistry. 204 pages 731-736

PS 2159 Advances in Intranasal Delivery for Two Commonly Used Preclinical Test Systems

M. C. Freke[1], J. Douville[1], D. O. Clarke[2], A. Everly[2] and A. Viau[1]. [1]*Inhalation Toxicology, Charles River, Montreal, QC, Canada and* [2]*Nonclinical Safety Assessment, Eli Lilly and Company, Indianapolis, IN.*

As appropriate, the regimens and routes of administration for the nonclinical testing of novel chemical entities should mimic the intended regimens and routes of administration used in clinical trials. Intranasal drug delivery to animal species commonly used in nonclinical testing presents its own unique challenges.
The purpose of this investigation was to assess the tolerability of repeated intranasal dose delivery in two commonly used species, the rat and dog, at total daily dose volumes that would be necessary to achieve the intended targeted doses in proposed toxicity studies. Acclimation to the intranasal dosing techniques and necessary handling was performed over 2 -3 days using a calibrated micropipette set to deliver 40 µL saline for rats or a commercially available nasal spray pump set to deliver 150 µL saline per actuation for dogs. On each dosing day, rats were dosed during 8 discrete sessions with a maximal accumulated volume of 160 µL/nostril/session, whereas dogs were dosed during 16 discrete sessions with a total volume of 600 µL/nostril/session. Tolerability was assessed by noting the incidence of struggling, saline reflux and/or number of partial doses given.
It was concluded that the total volume and number of dosing sessions selected were well tolerated by each species; however, the time between sessions was critical to the success of the dose administration technique. Dogs tolerated 30 minutes between dosing sessions, whereas 1 hour between sessions was preferable to allow rats to relax suitably before the next session. The results demonstrate that multiple intranasal dosing sessions to achieve high total daily intranasal dose volumes can be tolerated by rats and dogs, two commonly used test species, provided there is a suitable interval between sessions.

PS 2160 Packed Cell Reinjection As a Technique for Serial Blood Sampling in Rats

P. S. Coder, S. M. Davis, R. Moehle, A. Obrecht and D. G. Stump. *WIL Research, Ashland, OH.*

For laboratory animal species, the total amount of blood withdrawn depends upon the weight of the animal and the time between successive collections. Withdrawal of too much blood, without intravenous fluid replacement can result in hypovolemic shock. Withdrawal of smaller volumes at intervals too frequent to allow for blood cell replacement can result in anemia. In general, for rats, it is recommended to collect no more than 3 samples, at a volume less than 20% of the total blood volume over a 24-hour period. This approach necessitates combining data across animals for the purposes of toxicokinetic/pharmacokinetic analyses. In order to allow serial blood sampling from adult rodents, WIL Research has recently established the technique of packed cell reinjections. While this method has been used in academia, to the best of our knowledge, it has not been used previously in regulatory toxicology. Adult female rats were surgically implanted with femoral vein catheters with SAI Quick Connect harnesses with injection caps and jacket adaptors. Catheter patency was maintained by use of a heparinized saline lock. Blood samples were collected at 6 timepoints over two 24-hour periods in one week. Between collection and reinjection, catheters were flushed with saline and a heparin lock was maintained. Samples were centrifuged, plasma was removed and the cell pellet was resuspended in sterile saline to make a cell suspension, which was reinjected back into the animal. Catheters were flushed with saline and a heparin lock was reapplied. Subsequently, catheter patency was monitored on a twice-weekly basis for 4 weeks to facilitate inclusion of additional sampling intervals. Thirteen (13) of 15 females survived the packed cell reinjection procedures, with patent catheters. Over the course of 4 weeks, gradual reduction in percentage of patent catheters was noted, with >50% patent at termination. These newly established procedures allow us to collect up to 12 serial samples (0.4-0.5 mL/sample) during a one week period.

PS 2161 Blood Capillary Microsampling in Suckling Rats—Reduction in and/or Elimination of the Need for Satellite Pups

N. S. Powles-Glover[1], S. Clubb[2], L. Jardine[2] and J. Stewart[1]. [1]*AstraZeneca, Macclesfield, United Kingdom and* [2]*Charles River, Edinburgh, United Kingdom.* Sponsor: W. Harvey.

Toxicology studies in suckling rats often include satellite animals (3/sex/timepoint) for toxicokinetic (TK) purposes where blood is collected (typically >200µL) as a terminal procedure. Blood microsampling using a tail vein, capillary tube method has been used for TK profiling of satellite pups in an oral gavage repeat dose toxicology study where 5x32µL blood samples were collected from Postnatal day (PND) 14 pups (weighing ca 34g) and again at end of study on PND35. There were no clinical observations in the sampled pups and their weight gain matched that of unsampled control pups. Use of microsampling at PND14 and PND35 reduced the number of satellite pups from 60 to only 6 pups.
Numbers of animals could be reduced even further if (limited) TK sampling could be done in main study pups. However there is concern that this might affect critical toxicological endpoints. An experiment was performed to emulate studies that finish at the end of the suckling period. 3 x 32µL blood samples were taken from 10 pups/sex within a 24 hour period at PND19 (ca 40-43g) and the following were measured at termination on PND20: clinical pathology, spleen and liver weights plus histopathology. There was an equal sized unsampled concurrent control group. There were no in-life observations or histopathological differences but there was a slight (non statistically significant) increase in splenic weight. In the terminal blood samples, females showed a slight but statistically significant decrease in red blood cell count (to 0.94x of control) plus slight (non significant) decreases in haemoglobin and haematocrit. The males showed a slight (non significant) increase in reticulocyte counts (to 1.05x of control). However, all values were within the concurrent control range. It was concluded that the nature and severity of the effects of microsampling 96µL blood in a PND19 suckling rat does not preclude the microsampling of main test pups provided care is taken to match blood loss in the control and judgement is used in the interpretation of findings.

PS 2162 Quantified Electroencephalography (qEEG) in Safety Pharmacology

G. Froget, E. Esneault, G. Peyon, D. Babin and V. Castagné. *Porsolt, Le Genest Saint Isle, France.*

Quantified Electroencephalography (qEEG) is a highly relevant translational technique able to measure the global effects of drugs on brain electrical activity. The aim of this study was to investigate the effects of 4 drugs with well-known side-effects, scopolamine, clozapine, ketamine and amphetamine on EEG in the conscious rat. Fourteen telemetered rats were implanted with two surface electrodes over the fronto-parietal cortex. After post-surgical recovery, animals were administered with vehicle or a drug and EEG was recorded over 60 minutes, starting 15 or 30 minutes after systemic injection. The differences of the spectral power between vehicle and the different treatments were assessed for each frequency band.
Scopolamine (0.5 mg/kg) clearly increased theta and alpha frequencies over 60 minutes with similar effects on delta frequencies from 0 to10 minutes. A significant increase of alpha and beta frequencies was observed with clozapine (2 mg/kg). Ketamine (30 mg/kg) globally increased total spectral power with marked effects on delta, beta and gamma frequencies. Amphetamine (4 mg/kg) tended to increase alpha frequencies but significantly decreased beta to gamma frequencies.
The increase of slow waves (delta to theta) potentially relates to the amnesic effects reported for scopolamine. Hyperactivity induced by amphetamine or ketamine potentially relates to the increase of theta to beta frequencies. An increase of intermediate frequencies is characteristic of a sedative-like effect, as observed with clozapine on beta frequencies. These results suggest that qEEG is a sensitive and reliable translational tool to predict potential adverse effects induced by new compounds on the central nervous system.

PS 2163 Serotonin Reduction Impairs Executive Function and Induces Submissive-Like Behavior in Mice: A Validation Study of a New Cognitive Test for Chemical Risk Assessment

T. Endo[1], S. Benner[1], W. Ling[1], N. Endo[1], E. Kimura[1], C. Tohyama[1] and M. Kakeyama[1, 2]. [1]*Laboratory of Environmental Health Sciences, Center for Disease Biology and Integrative Medicine, Graduate School of Medicine, the University of Tokyo, Tokyo, Japan and* [2]*Department of Neurobiology and Behavior, Graduate School of Biomedical Sciences, Nagasaki University, Nagasaki, Japan.*

Environmental chemical exposure has been suspected to be responsible for a recent increase in the incidence of pervasive developmental disorders. To study the possible causal relationship, we recently developed a new behavioral test method, using an apparatus named IntelliCage, which can analyze the executive function and social behavior in group-housed mice in a highly reproducible manner (Endo et al., Behav. Brain Res., 2011; PLOS ONE, 2012). In the present study, we have validated the reliability of this method by applying it to an assessment of chemically-induced serotonin reduction model mice as a widely accepted model of executive function and social behavioral impairments. C57BL/6J male mice were administered 4-chloro-DL-phenylalanine (PCPA), a tryptophan hydroxylase inhibitor, at a daily dose of 0 or 25 mg/kg for 4 weeks using osmotic mini-pump. Throughout this period, the two groups of mice were housed together in an IntelliCage and subjected to the behavioral flexibility test that consists of acquisition of place learning and its serial reversals. As a result, the PCPA group was found to perform less efficient in reversal learning than the control group. The PCPA group was also found to have submissive-like behavior under a competitive condition throughout the test. These results were essentially consistent with previous studies showing that serotonin reduction induces behavioral inflexibility and social behavioral abnormalities in monkeys and humans. In conclusion, the present behavioral test was validated as a reliable method for assessing abnormality in higher brain function in group-housed mice, and could be a useful method to evaluate neurotoxicity of various chemicals.

PS 2163a A Simple Method of Cerebrospinal Fluid Collection from Conscious Beagle Dogs and Its Application As a Surrogate for the Assessment of CNS Exposures

V. Goyal, S. Pagrut, S. Pandey, S. Jana, A. Gothi, S. Kakade, G. Bhyrapuneni and R. Nirogi. *Discovery Toxicology, Suven Life Science Ltd, Hyderabad, Andhra Pradesh, India.*

Many central nervous system (CNS) drug discovery programs require the successful collection of cerebrospinal fluid (CSF) for assessing CNS penetration and distribution of new chemical entities. Evidence from preclinical and clinical studies suggests that drug concentration in CSF appears to be reasonably accurate in predicting unbound drug concentration in the brain. Therefore, CSF can be used as a useful surrogate for in vivo assessment of CNS exposure and provides an important basis for the selection of drug candidates for entry into development. For repeated collection of CSF from dog, either dog has to be surgically cannulated or anesthetized several times which may interfere the pharmacokinetic (PK) property of the drug of interest. The objective of the present investigation was to develop a systematic approach to simplify the technique for collecting CSF from cisterna magna of the conscious Beagle dogs. Dog is placed either in lateral recumbency with the head flexed ventrally to 90 degree or alternatively in standing position comfortably and bent the neck at 90 degree to the table with the help of an assistant. Neck should be flexed so that space of insertion can be visible. A 20 - 24 gauge needle is inserted into depression just behind the pointed occipital protuberance; direction of needle should be first slight transverse then obliquely into cistern magna. A slight popping sensation is observed when needle in subarachnoid space. CSF will come out with pressure inside the space as well as by gravity into collection tube. Multiple sampling can be done by this method using same animals to determine PK parameters. The same animal can be used again after appropriate wash out period. In our laboratory, we have used this technique several times to determine the drug CSF concentrations successfully. This method can be used for CSF PK without use of anesthesia or any surgical intervention.

PS 2163b Phosgene-Induced Lung Injury in the Conscious Pig

S. Graham[1], A. J. Smith[1], R. L. Perrott[1], B. J. Jugg[1] and A. M. Sciuto[2]. [1]*Dstl, Salisbury, United Kingdom and* [2]*USAMRICD, Aberdeen Proving Ground, MD.*

Currently no medical countermeasures exist for phosgene poisoning and treatment is supportive in an intensive care setting. Small animal models have been used to screen candidate therapies, however, extrapolation of therapeutic benefit to man requires verification in a larger animal model e.g. the pig. There is therefore a requirement to test the efficacy of treatments against a consistent, well characterised injury.
Animals were surgically implanted with a telemetry transmitter and exteriorised catheters to enable venous and arterial blood samples to be taken. After recovering from surgery (1 week) and baseline measurements (1 week), animals were exposed to either air or phosgene under anaesthesia, then recovered and monitored, fully conscious for 24 h.
Air exposed and phosgene exposed (Mean inhaled dose ± S.E.M., 0.793 ± 0.03 mg/kg) animals were successfully recovered and monitored to 24 h post-exposure. The phosgene exposed animals had a moderate/severe lung injury at 24 h compared to the air exposed animals.
Phosgene produced an increase in the amount of protein in the terminal bronchoalveolar lavage (BAL) fluid of the phosgene exposed animals (Mean ± S.E.M., 0.82 ± 0.3 mg/ml). The lung wet weight to body weight ratio (LWW:BW) and lung wet weight to dry weight ratio (LWW:DW) are measures of extravascular lung water and indicate the degree of alveolar permeability. There was an increase in the LWW:BW ration in the phosgene exposed animals when compared to the air exposed animals (Mean ± S.E.M., 16.16 ± 1.81 versus 8.01 ± 0.13). There was also an increase in the LWW:DW ration in all the lung lobes sampled in the phosgene exposed animals compared to the air exposed animals. Phosgene increased the number of neutrophils recruited to the lungs compared to the air exposed animals. The feasibility and reproducibility of the dose of phosgene producing a severe, but non-lethal lung injury at 24 h in which to test therapeutic candidates has been demonstrated.
© Dstl Crown Copyright 2014. Published with the permission of the Defence Science and Technology Laboratory on behalf of the Controller of HMSO.

PS 2163c LCt50 Determination of Sarin and Soman in Conscious Guinea Pigs (GP) Using a Nose-Only Vapor Inhalation Model

W. Holmes, D. Paradiso, J. Koenig, R. B. Lee, J. H. McDonough and D. Anderson. *USAMRICD, Aberdeen Proving Ground, MD.* Sponsor: J. Grahm.

Sarin and soman are organophosphorus compounds that pose both a military and a civilian threat. Because of the volatility of these agents, inhalation is likely the primary route of exposure. The toxicology of these inhaled agents has been under-investigated to date. This study was conducted to evaluate the dose-relationship curve and establish the lethal concentration of 50% of the exposed population (LCt50) for both sarin and soman in unanesthetized GP using a newly developed nose-only vapor exposure system. GP were placed in a double compartment Plexiglas chamber separated by rubber neck and rubber nose seals which was then mounted to a 12-port nose-only inhalation tower. Respiratory parameters were monitored with a pneumotach and transducer during the exposure. GP were exposed to sarin or soman vapor via a Brooks vapor-generating system for 20 min in the concentration range of 13.1 to 21.8, and 13.7 to 24.5 mg/m3, respectively. LCt50 estimates (± 95% confidence intervals [CIs]) were determined using a stage-wise adaptive dose design analysis. The LCt50 for sarin was calculated to be 14.3 mg/m3 (CI:14.0-

14.6) and 18.4 mg/m3 (CI:16.7-20.2) for soman. Acetylcholinesterase (AChE) activity was measured in whole blood (WB) and from red blood cells (RBC) immediately following death. AChE activity was greatly depressed in both RBC and WB with maximal levels of activity being 15.5% and 10.5% of baseline, respectively, and means of 8.39% and 5.35% of baseline, respectively. This model provides a precise, accurate and realistic nerve agent vapor inhalation exposure system that can be used to test potential therapeutic compounds against these volatile nerve agents. The views expressed in this poster are those of the author(s) and do not reflect the official policy of the DoA, DOD, or the U.S. Government. The experimental protocol was approved by the USAMRICD IACUC and all procedures were conducted in accordance with the principles stated in the Guide for the Care and Use of Laboratory Animals and the Animal Welfare Act of 1966 (P.L. 89-544), as amended.

PS 2164 The Endogenous Arylhydrocarbon Receptor Ligand 6-Formylindolo[3, 2-b]Carbazole (FICZ) Is a Phototoxic UVA-Sensitizer in Epidermal Keratinocytes and Reconstructed Human Skin

R. Justiniano, S. L. Park, S. Qiao, C. M. Cabello and G. T. Wondrak. *Pharmacology and Toxicology, College of Pharmacy and Arizona Cancer Center, University of Arizona, Tucson, AZ.*

6-Formylindolo[3,2-*b*]carbazole (FICZ) is a physiological high affinity ligand for the mammalian aryl hydrocarbon receptor (AhR) regulating expression of AhR target genes including cytochrome P450 1A1 (*CYP1A1*). Cutaneous formation of FICZ occurs through ultraviolet (UV)-driven photo-oxidation of its precursor L-tryptophan, and FICZ is thought to potentiate the UVB-induced stress response in human skin through AhR activation. Here we demonstrate for the first time that FICZ displays nanomolar activity as a phototoxic UVA-sensitizer targeting human skin cells through photodynamic induction of oxidative and proteotoxic stress. In human HaCaT keratinocytes, induction of apoptosis was observed in response to the combined action of solar simulated UVA (3.3 J/cm2) and FICZ (10 nM), but did not occur upon exposure to UVA or FICZ only. FICZ-phototoxicity was also observed in an epidermal tissue reconstruct (EpidermTM) exposed to FICZ and UVA, as evident from sunburn cell formation and proteolytic activation of caspase 3. Gene expression array analysis revealed that FICZ caused upregulation of *CYP1A1* independent of UVA exposure. In contrast, induction of cellular heat shock (*HSPA6*, *HSPA1A*), ER stress (*DDIT3*), and oxidative stress (*TXNRD1*, *HMOX1*, *AKR1C2*, *SPINK1*) response gene expression was observed only upon combined exposure to UVA and FICZ, further substantiated by immunoblot detection (p-eIF2α, p-p38, HO-1). FICZ photosensitization was associated with induction of pronounced intracellular photooxidative stress that could be antagonized by singlet oxygen quenchers (sodium azide, DABCO). Taken together, our data demonstrate that the endogenous AhR ligand FICZ displays pronounced photodynamic activity in epidermal keratinocytes and reconstructed human skin, representing a novel mechanism of UVA phototoxicity that may be operative in human skin. Supported by grants from NIH [R01CA122484, R03CA167580, R21CA166926, ES007091, ES06694].

PS 2165 Linalool and Limonene in Fragranced Products: Stability and Quantification of Potentially Sensitizing Hydroperoxides

G. Adamson[3], S. Kern[1], H. Dkhil[2] and A. Natsch[1]. [1]*Givaudan Schweiz AG, Duebendorf, Switzerland,* [2]*Givaudan France SA, Argenteuil, France and* [3]*Givaudan US, East Hanover, NJ.*

Upon exposure to air, linalool and limonene can form sensitizing hydroperoxides. Positive patch tests to the hydroperoxides in dermatitis patients were reported. Due to a lack of analytical evidence it is unclear under which conditions, and from which sources, the public might be exposed to sufficient quantities of these oxidized products for induction of skin sensitization to occur. We developed analytical methods using mass spectrometry in combination with gas chromatography (GC-MS) and liquid chromatography (LC-MS) for the oxidation products. We performed stability studies to follow the fate of linalool and limonene in fine fragrances and antiperspirants, since these product types lead to highest consumer exposure to these ingredients. We found a high stability of linalool and limonene in the products investigated. We detected very low levels (around 0.07%) of linalool hydroperoxide in linalool obtained from natural sources. This level remained constant upon storage. Low levels of linalool hydroperoxide were detected in a commercial fragrance but degraded at elevated temperature to non-sensitizing secondary oxidation products. Aged fine fragrances retrieved from consumers contained a median of 2430 μg/g of linalool and 7 μg/g of linalool hydroperoxide. Corrected for matrix effects, concentrations are twofold higher. In antiperspirants, we detected no oxidation products. A novel method for limonene hydroperoxide detection is presented, but limonene hydroperoxide levels stay below limit of detection of this method (< 50 μg/g) in tested products. In conclusion, low levels of linalool and limonene hydroperoxide in fragranced products may originate from raw materials, but we found no evidence for hydroperoxide formation during storage of representative perfume-containing consumer products. The typical concentrations found in the fragrance samples are around three orders of magnitude below the experimental concentration inducing skin sensitization in animal tests.

PS 2166 Vetiveryl Acetate Evaluated for Potential Phototoxicity Utilizing a Human Epidermal Model and Patch Testing

J. F. Lalko and A. Api. *Research Institute for Fragrance Materials Inc., Woodcliff Lake, NJ.*

Vetiveryl acetate is utilized as a fragrance ingredient in a variety of consumer and personal care products, being appreciated for it woody note in perfumery. The UV spectrum for this material demonstrates absorption in the region of 290 – 700nm, and therefore has the potential to be photoactivated. In order to determine the potential for phototoxic effects, a phototoxicity test in a three dimensional human epidermal model (EST1000) was conducted. This assay is based upon a comparison of the cytotoxic effects of the test material following exposure to a non-toxic dose of UV light. Cytotoxicity is expressed as a reduction in the mitochondrial conversion of MTT [(3-4,5-dimethyl thiazole 2-yl) 2,5-diphenyl-tetrazoliumbromide] to formazan. A material is considered to have a phototoxic potential if one or more concentrations +UVA (60 min with 6 J/cm^2) results in a decrease in relative cell viability of ≥ 30%, when compared to the identical concentration –UVA. Vetiveryl acetate was tested at five concentrations ranging from 0.1 to 10% (v/v) in 1:3 Ethanol:Diethyl phthalate (EtOH:DEP). In the EST1000 model, no phototoxicity was observed to vetiveryl acetate over the range of concentrations tested. Additionally, historical studies conducted in animal models indicate a lack of phototoxicity up to 100%. A confirmatory phototoxicity patch test was conducted in a group of human volunteers with a concentration series of 2.5%, 7.5% and 25%. These concentrations of vetiveryl acetate were confirmed as having no phototoxic effects in humans following the phototoxicity patch test.

PS 2167 *In Vivo* Phototoxicity Evaluation in Hairless Mice followed by 8-Methoxypsoralen, Lomefloxacin, and Ofloxacin

Y. Takahashi, S. Utsunomiya, T. Yamada, Y. Yamashita, N. Koyashiki, A. Arima, H. Sameshima and R. Nagata. *Shin Nippon Biomedical Laboratories, Ltd. (SNBL), Kagoshima, Japan.*

Purpose: The ICH S10 draft consensus guideline "Phototoxicity Evaluations of Pharmaceuticals" is in the Step 3 consultation period in Sept 2013. However, this draft guideline does not currently specify species/strain selection or test procedures for *in vivo* phototoxicity studies. Therefore, in order to select a suitable positive control compound and animal strain, we examined *in vivo* phototoxicity in 2 strains of hairless mice after administration of 3 known phototoxicants, 8-methoxypsoralen (8-MOP), lomefloxacin HCl (LMFX), and ofloxacin (OFLX).
Method: Seven-week-old HR-1 and SKH1-E hairless mice (Hoshino Laboratory Animals, Inc., Japan, and Charles River, NC, respectively) were orally given 8-MOP (10 and 20 mg/kg), LMFX (50 and 100 mg/kg), and OFLX (300 and 1000 mg/kg), and irradiated with ultraviolet A at 20 J/cm ^{2} (λ=352 nm) from a Dermaray M-DMR-50 (Toko Electric Co., Ltd., Japan) apparatus 30 min later. The expression of phototoxicity was evaluated in each strain with the following items: auricle thickness, skin reactions at the auricle and on the back with the Draize method at 0.5, 24, 48 and 72 hr after irradiation, and ophthalmology and histopathologic changes in the auricular and back skins, eyeballs, and optic nerves (HE staining) at 72 hr.
Result: Male HR-1 mice given 8-MOP showed very slight erythema and edema at the auricle and back at 24 hr and an increased edema score (3; moderate) at 72 hr, auricle thickening and eyelid edema. Histopathology revealed inflammation, degeneration and necrosis in the skin and eyelids. These reactions were also observed, but to a lesser extent, after other phototoxicant treatments (order of severity: 8-MOP > LMFX > OFLX). No marked sex or strain (HR-1 vs. SKH1-E) differences were noted.
Discussion: We judged that both investigated strains were appropriate, and 8-MOP was the most appropriate positive compound, for phototoxicity tests in hairless mice.

PS 2168 Development of an Alternative Method for Assessment of Skin Sensitization Using the *In Vitro* IL-18 Reconstructed Human Epidermis (RHE) Model

S. M. Furst[1], H. Lineberry[1], H. Aloor[1], J. Therrien[1] and E. Roggen[2]. [1]*Safety Assessment, Stiefel a GSK company, Research Triangle Park, NC and* [2]*3Rs Management and Consulting ApS, Lyngby, Denmark.*

Several efforts are underway, in line with the 3Rs philosophy, to develop and validate in vitro testing methods for sensitization, as alternatives to the traditional in vivo models. The first living cells of the skin to encounter sensitizing chemicals are mainly keratinocytes. Of the cytokines produced by keratinocytes, IL-18 plays a key role in skin sensitization induction. The use of keratinocytes and skin cultures provides a valuable, simplified in vitro model to evaluate the sensitization potential of topically applied compounds. An IL-18 assay has been developed detecting changes in IL-18 levels upon exposure to chemicals using human keratinocyte cell lines (www.sens-it-iv.eu). More recently, a model using RHE was found to have advantages of decreased variability, better representation of human exposure and the ability to test water insoluble/unstable compounds as well as final product/formulations. The IL-18 RHE protocol was adapted using EpiDermTM and three known contact sensitizers (resorcinol, weak; cinnamaldehyde, moderate; 2,4-dinitrochlorobenzene, strong). Chemical dilutions were made and applied topically to the RHEs for 24 hours. Cell viability (MTT) and IL-18 levels (ELISA) were used as measures of sensitization. Criteria were established as an IL-18 Stimulation Index (SI) value >1.6x with a cell viability between 5%-50% for at least one concentration. Results indicated the test was simple to perform with slight modifications for the type of cultures used. Reproducible results were obtained for the moderate and strong sensitizers with varying results for the weak sensitizer, resorcinol. The variability in results may stem from differences in stratum corneum barriers between types of RHE cultures. In conclusion, IL-18 production by RHE represents a promising and easily adaptable model for the screening of chemicals for sensitization potential and reducing the use of animals for testing.

PS 2169 TRPA1 Inhibitors Counteract Inflammation and Edema in a Mouse Model of CS Tear Gas Agent-Induced Cutaneous Injury

S. Achanta[1], S. Balakrishna[1], N. Chintagari[1, 2], B. F. Bessac[1, 3], A. Sui[1] and S. E. Jordt[1]. [1]*Pharmacology, Yale University, New Haven, CT,* [2]*US Food and Drug Administration, Bethesda, MD and* [3]*Texas A & M Health Science Center, Kingsville, TX.*

The deployment of the tear gas agent, CS (2-Chlorobenzalmalononitrile), for riot control has significantly increased in recent years. CS induces severe pain, blepharospasm, lachrymation, and airway obstruction. CS is strongly electrophilic, causing tissue injury associated with inflammation and edema.
We recently identified the sensory neuronal ion channel, Transient Receptor Potential Ankyrin 1 (TRPA1), as a key target for CS to induce acute irritation and pain, and as a mediator of neurogenic inflammation. Here, we used mice to examine the effects of TRPA1 gene deletion and pharmacological TRPA1 inhibitors on CS induced cutaneous injury.
Cutaneous injury was induced by application of 10 μl CS agent (200 mM in DMSO) to each side of the right ears of 8 week old C57BL6 male mice, or male Trpa1-/- mice (n≥5 per group). The left ears were treated with vehicle only. TRPA1 inhibitors, HC-030031 or A-967079, were administered i.p. to WT mice at 200 or 100 mg/kg, respectively, 30 minutes and again 4 hr post CS exposure. Plasma extravasation was monitored 6 hr post exposure by in vivo infrared fluorescent imaging using contrast agent injected IV 2 hr post exposure. Edema formation was monitored by measurements of ear thickness and ear biopsy weights, and cytokine inflammatory markers (MMP-9, IL-1β, KC/CXCL1, and MIP-2/CXCL2) were quantified by ELISA in skin sample protein extracts.
CS induced strong plasma extravasation, tissue swelling, and dramatic increases in inflammatory cytokine levels in the mouse ear skin. These injury parameters were strongly reduced in Trpa-/- mice. Treatment of WT mice with TRPA1 inhibitors recapitulated the effects observed in TRPA1-deficient mice, including diminished plasma extravasation, swelling, and cytokine levels.
These findings identify TRPA1 is a crucial mediator of CS-induced tissue injury, with TRPA1 inhibitors as effective countermeasures reducing key injury parameters when administered post exposure.

PS 2170 Differential Induction of DUOX Isoforms by Arsenite and Vanadate: A Novel Role for Reactive Oxygen?

T. Hill[1, 2] and R. H. Rice[1]. [1]*Environmental Toxicology, University of California at Davis, Davis, CA and* [2]*School of Nursing, University of Northern Colorado, Greeley, CO.*

Dual oxygenase (DUOX) 1 and 2 are membrane bound proteins of the NOX superfamily that have been linked to specific inflammatory or cellular repair functions. Our previous work has demonstrated selective induction/switching of DUOX isoforms by the cytokines IFN-γ and IL-4 in cultured human keratinocytes and bronchial epithelium. Similarities between the biochemistry of keratinocyte differentiation and DUOX regulation suggest DUOX perturbation could be a source of epidermal barrier defects that enhance toxicant penetration. Arsenic toxicity is characterized by ROS generation and is reported to involve NOX activity. Water pollutants from mining activity that contain metal ions such as vanadate also generate ROS at high concentration. We examined the effects of these known water contaminants on DUOX induction using an established exposure model for heavy metals in spontaneously immortalized human keratinocyte (SIK) cultures and real time QPCR. We find that most metal/metalloid compounds suppress the cytokine induction of both DUOX isoforms. However, arsenite exposure causes incomplete suppression of DUOX2, while vanadate amplifies DUOX2 induction by IFN-γ beyond its normal efficacy. DUOX2 inductions by IFN-γ, as well as its amplification by vanadate, are completely suppressed in the presence of 30 mM dimethylthiourea, a known ROS scavenger. Similarly, glutathione depletion using 0.5 μM buthionine sulfoxime replicated the increased efficacy of DUOX2 induction by IFN-γ seen with vanadate. These findings suggest a novel role for ROS in DUOX2 gene induction and provide additional insight into arsenic toxicity as well as the mechanistic contribution of DUOX biology to differentiating epithelium. Future studies on the role of DUOX in keratinocytes may provide a novel mechanistic approach to assess the effects of environmental and industrial toxicants on healthy skin and wound healing.

PS 2171 Involvement of Reactive Oxygen Species (ROS) and Gene Expression Profile in Response to p-Phenylenediamine and Components of Permanent Hair Dyes in Human Keratinocytes (HaCaT) Cells and Human Skin Explants

T. Zanoni[1], A. Bast[1, 2], G. Hageman[1, 2], S. S. Maria-Engler[1] and D. P. de Oliveira[1]. [1]*Environmental Toxicology, University of Sao Paulo-USP, Ribeirao Preto, Brazil and* [2]*Toxicology, University of Maastricht, Maastricht, Netherlands.*

Para-phenylenediamine (PPD) is an aromatic amine present in about 70% of all hair dyes worldwide. PPD is primarily used as a dye intermediate after reaction with H2O2 (oxidizing agent) and Resorcinol(R) (coupler). It penetrates the hair shaft permanently modifying the hair colour. Sensitization to PPD is known to cause of allergic contact dermatitis. However, the molecular mechanism of PPD-induced skin toxicity remains unclear. We investigated the induction of Reactive Oxygen Species (ROS) and the involvement of gene expression of certain genes that appear to be involved in toxicity of PPD. We tested the ROS induction potential of PPD in presence and absence of the coupler Resorcinol and oxidizing agent H2O2 in monolayer using immortalized keratinocytes (HaCaT) that are the first contact point after dermal exposure, as well as human skin explants. For HacaT cells in monolayer, the dose of 100μg/mL, increased the intracellular levels of ROS after 1 hour of incubation. After 24 hours of incubation the dose of 20 μg/mL was able to increase the levels of 8-oxo-dG and malonaldehyde (MDA) was formed. Besides, we observed that the addition of H2O2 decreased the intracellular levels of ROS and the levels of 8-oxodG, while the levels of MDA were not decreased by the addition of H2O2. Using the human skin explants, we demonstrate that the exposure to PPD, PPD-H2O2-R and PPD-R on commercial concentration, upregulates the expression of genes involved in inflammatory responses, responses to oxidative stress and metabolism of xenobiotics by cytochrome P450 on human epidermis. Our results indicate that oxidative stress is involved on the mechanism of PPD-epidermis toxicity in monolayer and in skin explants. This study helps to elucidate the toxic effects in response to PPD and components of hair dyes on human skin.

PS 2172 Dermal Absorption *In Vitro* and Its Influencing Parameters

K. Guth, E. Fabian, S. Wölk, B. van Ravenzwaay and R. Landsiedel. *Toxicology, BASF SE, Ludwigshafen/Rhein, Germany.*

Skin absorption is an in vitro method described in OECD guideline 428 and the technical guidance GD 28. Since study design dependent parameters can be varied, we performed systematic parameter variations under defined experimental conditions to understand their potential influence.

We investigated dermal absorption with skin preparations of rats, pigs and humans in Franz like diffusion cells. Experiments were performed to address the following parameters: ex vivo skin preparations (gender, age, localization, preparation), reconstructed skin models, storage and freezing-cycles, static versus flow through, concentration of test compounds, donor vehicle and receptor fluids. We used different model compounds, e.g. testosterone, caffeine which were analyzed by liquid scintillation counting, HPLC or photometry. Absorbed dose (%), permeation rates and permeability constants (Kp) were calculated.
Variations in skin preparation and testing in static or in flow-through systems had no remarkable influence on Kp. Main impacts on Kp were observed for ex vivo vs. reconstructed skin preparations, thickness of SC, test-substance concentration, donor vehicle and receptor fluid: In our experiments the barrier function of reconstructed skin was inappropriate for absorption testing. Since the test substance, its concentration and donor vehicle are reflected by the applied formulated product these parameters have to parallel the real exposure scenario and will intentionally predetermine the study results. The influential effect of the receptor fluid was related to the solubility of the test substance in the chosen solvents. This relation was obvious e.g. for the lipophilic compound testosterone where a higher Kp and absorbed dose was observed for ethanol:water (1:1 / v:v) in comparison to 5% aqueous BSA.
Taken together, the results of the current investigations can be taken into account for the establishment of a standardized experimental set up for dermal absorption studies in vitro, whereby the identified mayor influential parameters should be carefully addressed

PS 2173 Evaluation of Age, Storage, and Skin Preparation Technique on Dermal Absorption in Rat Skin

S. Chaudhuri, A. T. McCoy, F. Zhang, S. C. Hansen, L. K. Sosinski and M. J. Bartels. *Toxicology, The Dow Chemical Company, Midland, MI.*

Dermal uptake is a common route of exposure for chemicals and can have a substantial impact on exposure and risk assessments. Accurate in vitro dermal penetration data from rat skin is critical for triple pack studies where these data are used in conjunction with in vitro human and in vivo rat results to correctly extrapolate to human in vivo absorption levels. The present study evaluated the quantitative impact of age, storage and skin preparation technique on dermal absorption of three test chemicals (benzoic acid, caffeine and testosterone) in rat skins. Juvenile (4-5 wk old) rat skin was compared to mature adult rat skin (12-15 wk old). The data indicated that flux and absorption were consistently increased by approximately two-fold in juvenile rats compared to adult rats with all 3 test materials. Storage of rat skins at -80°C did not significantly affect flux or absorption values, compared to fresh skin samples, however, there was an overall 33% decrease in the number of viable skins when frozen, compared to fresh skins. The extent of hair clipping for preparation of the skin samples is also critical in dermal absorption experiments. Data indicated that extensive clipping (7-8 passes), to remove most of the epidermal hair, resulted in 2-3fold higher flux rates, with 87% of skin samples failing integrity tests. In contrast integrity was maintained in 100% of the skin samples that were subject to moderate clipping (2-3 passes). Flux and absorption were increased approximately 2-3 fold in skin samples subject to more extensive clipping compared to those treated more moderately with all the 3 test materials. Collectively, the data suggest that age of rats and clipping technique substantially affect the rate of dermal absorption during in vitro dermal experiments, while prolonged storage may lead to material wastage due to loss of integrity in skin samples. As a result, appropriate experimental design is critical for an accurate assessment of this major exposure route.

PS 2174 The Effect of Coformulants on Dermal Uptake—A Raman Study

T. Patel[1], D. Salazar[3], G. Bell[3], J. Wright[3], B. Parr-Dobranzski[3], A. Ghaemmaghami[2], P. Williams[1], C. J. Roberts[1] and F. R. Rose[1]. [1]*School of Pharmacy, University of Nottingham, Nottingham, United Kingdom,* [2]*School of Life Sciences, University of Nottingham, Nottingham, United Kingdom and* [3]*Syngenta Ltd, Jealott's Hill International Research Centre, Berkshire, United Kingdom.*
Sponsor: P. Botham.

The Organisation for Economic Co-operation and Development (OECD) guidelines on the conduct of *in vitro* dermal absorption investigations have attempted to standardise global practises. However, the methods used to evaluate epidermal accumulation such as 'tape stripping' have yet to be formalised and can give rise to large sources of variability. Thus, there is a strong need to develop alternative methods to investigate compound localisation within skin samples. Confocal Raman spectroscopy (CRS) is a radiolabel free, rapid, optical, non-invasive method which allows compounds to be identified within dermal tissue. In this study, CRS was used to determine testosterone localisation within *ex vivo* 300 μm dermatomed pig skin samples treated with the compound in solutions ((1:1) *v/v*) containing either; Emulsogen EL360, propylene glycol, or Tween 20. A LabRAM HR (Horiba Scientific) imaging spectrometer was employed for the analysis of the treated skin samples (n=6), using an IR laser at 785 nm coupled with a Synapse CCD detector. Spectra were obtained from the surface of the skin to a maximum depth of 150 μm at 0, 1, 2, 3, 4, 5, 6 and 24 hour time points to mimic real-time exposure. CRS spectra for the pig skins demonstrated good reproducibility with some spectral differences noticed. Spectral intensity decreased with increasing depth, as expected. Emulsogen EL360, Tween 20 and propylene glycol all appeared to influence the absorption of 30.0 mg/mL testosterone through the skin. The spectra obtained also suggested that the stratum corneum was the main barrier to testosterone absorption. These findings show that the CRS method has the potential to determine epidermal compound accumulation, which will help to inform the likely systemic bioavailability of residues within skin, providing an alternative tool for standardised dermal risk assessment.

PS 2175 Skin Absorption of Performance Amines Used in Metalworking Fluids

L. Roux, J. Brooks, J. Yeatts and R. E. Baynes. *NCSU, Raleigh, NC.*

Every year, ten million workers are exposed to metalworking fluids (MWFs) which may be toxic, especially to the respiratory system and the skin. There are four types of MWFs: neat oils and three water-based MWFs (soluble oil, semi-synthetic and synthetic) which are diluted with water and whose composition varies according to the mineral oils ratio. MWFs also contain various additives such as biocides and corrosion inhibitors. The absorption of six amines used as corrosion inhibitors and biocides in MWF was determined in porcine-skin flow-through diffusion cell experiments with three radiolabeled ethanolamines (mono-, di- and tri-ethanolamine, MEA, DEA and TEA respectively) and a mixture of three GC-amenable amines (dibutylethanolamine, dicyclohexylamine and diphenylamine). The test compounds were dosed in four vehicles (water and three generic water-based MWF formulations) and analyzed using a scintillation counter or a gas chromatography/mass spectrometer. The six compounds were significantly ($p<0.05$) more absorbed in water (e.g. 1.15±0.29 %dose (DEA in Water)) compared to other formulations (e.g. 0.13±0.01 %dose (DEA in semi-synthetic MWF)) and absorption was greatest for dibutylethanolamine in all the formulations. Generic soluble oil formulation tended to increase the permeability and the absorption of MEA, DEA and TEA. Permeability coefficients were significantly higher ($p<0.05$) with TEA relative to the other test compounds (e.g. 4.22E-04±5.3E-05 cm/h (TEA in synthetic MWF) VS 1.23E-04±1.0E-05 cm/h (MEA in synthetic MWF)), except for MEA in generic soluble oil formulation. Future research will confirm these findings with *in vivo* studies in pigs and dermatotoxicity studies will be conducted to compare the relative safety of these compounds in MWF. With this data, the MWF industry would be able to alter their MWF formulation to protect the metalworkers' health.

PS 2176 *In Vitro* Human Skin Permeation: Example of CMI/MI and Tolylfluanid, Two Irritant, and Sensitizer Biocides

A. Berthet[1], P. Spring[2], N. Charriere[1], D. Vernez[1] and N. B. Hopf[1]. [1]*Institute for Work and Health, Lausanne, Switzerland and* [2]*Dermatology, Centre Hospitalier Universitaire Vaudois, Lausanne, Switzerland.*

Biocides are recognized as skin irritants or sensitizers. Known for its antibacterial effects, the mixture methylchloroisothiazolinone (MCI) and methylisothiazolinone (MI) is considered an irritant and may cause contact allergy even after a single exposure. Tolylfluanid, an anti-fouling biocide for paints, is also a known irritant and sensitizer in addition to being classified as a "probable human carcinogen" by the US EPA. Dermal risk estimates are based on dermal permeation rates; however, few human skin permeation studies are available for these biocides. The goals of this study were to: i) measure permeation rates of these three biocides separately and in various commercial products, and ii) quantitatively assess their irritant effects to skin using dermatopathological methods. All experiments were performed using newly harvested human skin obtained from plastic surgery. The dermatomed skin was mounted onto a flow-through diffusion cell system and different concentrations of aqueous standards or commercial products were applied; MCI/MI (75:25, 150:50, 375:125, 750:250 ppm) and MI alone (500 ppm). Exposure lasted for 6 to 24 hours. MI permeates faster than MCI (<1h and 4 to 5 h, respectively), possibly due to retention of MCI in the skin. No tolylfluanid (50, 100, 500 ppm) was found in the receptor liquid, however the metabolite, 4-dimethylaminosulfotoluidid (DMST), was measured 2 to 3 h after the tolylfluanid application. The histopathological results showed a dose-response with focal spongiotic change in epidermis following 6h exposure to 750/250 ppm CMI/MI solution and 24h exposure to 375/125 ppm. No focal spongiotic change was observed after exposure to MI or tolylfluanid. Overall, our results show that human skin permeations are different from study results using animal skin.

PS 2177 The *In Vitro* SkinEthic RHE Skin Corrosion As a Reference Test Method in the Acute Testing Strategy

V. Leblanc[1], C. Tornier[2], M. Grandidier[1], C. Robert[2], N. Seyler[2], J. Cotovio[1] and N. Alépée[1]. *[1]L'Oréal, Aulnay sous Bois, France and [2]L'Oréal, Gerland, France.* Sponsor: D. Bury.

Skin irritation and skin corrosion refer to localized toxic effects resulting from a topical exposure of the skin to a substance. The Globally Harmonized System of Classification and Labeling of Chemicals (GHS) define skin irritation as "the production of reversible damage» and skin corrosion as "irreversible damage" to the skin following the application of a substance. A number of validated, non-animal methods to determine skin corrosion and irritation are available. As such, the SkinEthic Reconstructed Human Epidermis (RHE) test method has been adopted within the context of OECD TG 431 (skin corrosion) and OECD TG 439 (skin irritation).
Updated approaches to the use of tiered and integrated testing strategies for predicting skin corrosion/irritation potential without the use of animals are discussed in the present study. Illustration is provided by combining both SkinEthic RHE skin corrosion and irritation test methods for evaluating the stepwise testing strategy (Top down and Bottom-Up approaches).
All 50 reference chemicals listed in either OECD TG431 or 439 were evaluated in both skin irritation and corrosion SkinEthic RHE validated methods.
Amongst the 22 known in vivo corrosive chemicals, 95% were correctly predicted as corrosives. Therefore those 21 chemicals were also defined as irritants. The substances were well classified by using the top-down approach which consists of conducting primarily skin corrosion test method.
Considering the non irritant chemicals, 100% (10/10) of the correctly classified in vitro irritants were also identified as non corrosives. Thus, when applying the bottom-up approach, the GHS classification of those substances was accurately defined by performing the skin irritation evaluation.
In conclusion, the results suggest that testing strategy is not a strict sequence and that stepwise procedure, weight of evidence and testing should be considered as acceptable approaches to structure relevant information of the substance used for hazard assessment.

PS 2178 *In Vitro* Skin Corrosion and Irritation Assessment of Ingredients Using EpiSkin Model: Top-Down and Bottom-Up Approaches

M. Grandidier, J. Cotovio and N. Alépée. *L'Oréal, Aulnay sous Bois, France.* Sponsor: D. Bury.

The OECD adopted a tiered approach for dermal testing described in the revised TG 404. Data from structurally related chemicals (e.g. pH extremes), human data and experience (weight of evidence) are sometimes sufficient for classifying the skin irritation/corrosion potential of chemicals. If this information is not sufficient, validated in vitro methods can then be used e.g. in vitro EpiSkin methods accepted in both OECD TG 431 (skin corrosion) and TG439 (skin irritation).
The aim of the study is to present the Top-Down and Bottom-Up approaches to the use of tiered in vitro testing strategies for predicting skin corrosion/irritation potential without the use of animals.
For such purpose, 98 chemicals (partially from EURL-ECVAM validation studies and OECD TG431 & TG439) were evaluated in both skin corrosion and irritation EpiSkin methods.
Amongst the 35 in vivo non irritants, 85% might be correctly classified in vitro as irritants (I). Therefore those 35 chemicals were also defined as non corrosives (NC). Thus, when applying the bottom-up approach the GHS classification of those substances was accurately defined by performing the skin irritation evaluation.
Considering the 40 known in vivo corrosives (C), all chemicals were correctly predicted as C and also identified as I. The substances are well classified by using the top-down approach which consists of conducting primarily skin corrosion test method.
Amongst the 23 in vivo I but NC chemicals, 20 out of 23 were correctly classified as I. The 3 others were therefore not classified as C (true false negatives). By applying the top-down approach, 6/20 irritants might be misclassified as C (false positives C) whereas they were well classified as irritants only using the bottom-up approach. The bottom-up approach is more accurate for those chemicals.
The use of existing data and a tiered in vitro approach should be sufficient and consider in the context of the revision of OECD TG404. This comprehensive evaluation should also facilitate regulatory acceptance decision on the methods, and it proposed uses.

PS 2179 The Usefulness of the Validated SkinEthic RHE Method to Identify Skin Corrosive UN GHS Subcategories

C. Tornier[1], C. Robert[1], J. Cotovio[2] and N. Alépée[2]. *[1]L'Oréal, Gerland, France and [2]L'Oréal, Aulnay sous Bois, France.* Sponsor: D. Bury.

The SkinEthic Reconstructed Human Epidermis (RHE) test method has been adopted within the context of OECD TG 431 for distinguishing corrosives and non-corrosives. The EU CLP classification system requires subcategorising of corrosive chemicals into the three UN GHS subcategories 1A, 1B and 1C. Since the SkinEthic RHE method was originally validated to discriminate corrosives from non-corrosives, the present study was undertaken to investigate its usefulness to discriminate skin corrosive UN GHS subcategories.
In total 84 substances were tested in three independent runs and two prediction models (PM) were assessed, representing a pre-defined validated prediction model (PM-A) and an alternative one defined post-hoc (PM-B). The results obtained with both PM were reproducible, as shown by the > 92.9% concordance of classification between runs for discriminating corrosives versus non-corrosives, and the > 85% concordance for discriminating the GHS subcategories versus non-corrosives. Moreover results confirmed a high sensitivity of the SkinEthic™ RHE method to predict corrosives (94.9%) and good specificity (> 73.7%) independent of the PM applied.
Regarding the identification of UN GHS corrosive subcategories, when considering the 30 reference chemicals as recommended in the recently revised OECD TG 431 (2013), PM-A and PM-B achieved 78.9% and 83.3% accuracy respectively for the identification of GHS subcategories and non-corrosives. They correctly predicted 90% of GHS subcategory 1A and 80% of GHS non-corrosive substances independent of the PM used.
In conclusion, the SkinEthic RHE test method is highly reproducible and sensitive for discriminating corrosive from non-corrosive substances. Furthermore it allows reliable identification of skin corrosive GHS subcategory 1B-and-1C substances using the PM-A and PM-B, and of GHS subcategories 1A using the PM-B. Due to its high sensitivity, the test method provides high safety standards for skin corrosion testing.

PS 2180 Chronic Solar Simulated UVR Exposure Alters Histone Modifications at Photoaging Gene Promoters in Human Dermal Fibroblasts

L. Passantino[1], M. Matsui[2] and M. Costa[1]. *[1]Nelson Institute of Environmental Medicine, New York University, New York City, NY and [2]Estee Lauder Companies, Inc., Melville, NY.*

UVR exposure from sunlight is a major contributing factor to the photoaging of skin. Photoaging of the dermal matrix is characterized by reduced collagen and elastin synthesis, wrinkle formation, and elevated matrix metalloproteinase (MMP) activity. The epigenetic profiles of aged cells are different from those of young cells. It is therefore possible that UVR could induce epigenetic changes, and this could mediate the photoaging process in skin. In this study, chronic solar simulated UVR (ssUVR)-induced alterations to histone 3 tails, DNA methylation, and gene expression were characterized in cultured primary neonatal human dermal fibroblasts. The cells were irradiated with 12 J/cm^2 ssUVR once per day every 3 to 4 days over a 2 week period. The cells were then cultured for an additional week without irradiation, and were collected at the end of this recovery period. Affymetrix GeneChips were used to compare the gene expression profiles of irradiated and sham irradiated cells. Chronic ssUVR significantly altered 2,678 genes (p-value ≤ 0.05, fold-change cut-off = 1.1), including genes relevant to photoaging and epigenetic modulation. Histone modifications and DNA methylation were studied by chromatin immunoprecipitation and pyrosequencing of sodium bisulfite-converted DNA, respectively. MMP1, MMP 2, MMP3, and dermatopontin were up regulated by chronic ssUVR, and H3K9 dimethyl was reduced in these gene promoters. H3K27 trimethyl was decreased in the MMP1 and MMP2 promoters. H3K9 acetylation was increased at the promoters of MMP1 and MMP3. Lysyl oxidase homolog 3 (LOXL3) and leprecan-like 1 gene expression was down regulated by chronic ssUVR, and decreased H3K4 trimethyl was observed in these gene promoters. Increased H3K9 dimethyl and H3K27 trimethyl were observed in the LOXL3 promoter. Differential DNA promoter methylation was not found in these genes. These findings indicate a role for epigenetics in the photoaging process.

PS 2181 Timecourse of Recovery following UV-Induced Damage Using a Full-Thickness Human Skin Equivalent

M. A. Bachelor, P. J. Hayden, M. Klausner, G. Stolper, J. Oldach and M. Li. *MatTek Corporation, Ashland, MA.*

Solar ultraviolet (UV) radiation is known to have deleterious effects on human skin. The UVB (280-320 nm) and UVA (320-400 nm) spectrum of solar radiation have been shown to affect keratinocytes, the major cellular constituent of the epidermis, by causing direct DNA damage and/or indirect DNA damage and cytotoxicity through the formation of reactive oxygen species. In the present study, a commercially available human skin equivalent (HSE) (EpiDerm-FT™) and excised human skin was exposed to solar-simulated light to gain insight into the temporal UV-induced response of human epidermal tissue. In vitro HSEs were irradiated with a single UVR dose approximately equivalent to either 6 or 9.5 minimal erythemal doses (MEDs) for an individual of EPA skin phototype 2. Cutaneous damage and recovery were then monitored for a period of seven days. Histological analysis showed a dose dependent formation of apoptotic sunburn cells in epidermal KCs at 24 hrs post-irradiation. By day 3 post-irradiation, a thinning of the viable epidermal cell layers was evident with maximum epidermal degeneration observed at day 4. Resumption of epidermal proliferation and differentiation was evident in both 6 and 9.5 MED tissues by days 5-7, leading to regeneration of viable epidermal layers. Excised human skin tissues irradiated with the same UV doses displayed responses very similar to those observed in the in vitro HSEs. DNA damage indicated by cyclopyrimidine dimer (CPD) formation was assessed by immunohistochemistry. CPD positive basal KCs decreased steadily in number each day, and were almost completely undetectable seven days post-irradiation. CPD formation could be completely blocked through topical application of OTC sunscreens. Finally, elevated levels of IL-8 and MMP-1 were induced following UV-irradiation demonstrating an early inflammatory response followed by an extended period of matrix remodeling activity. These results demonstrate that HSEs are useful for UV-induced photocarcinogenesis studies and evaluation of sunscreens.

PS 2182 Effect of Exposure Area on Nerve Agent Absorption through Skin *In Vitro*

C. Dalton, S. Graham and J. Jenner. *Biomedical Sciences, Dstl, Salisbury, United Kingdom.*

Static diffusion cells are used to determine the penetration of chemicals through skin *in vitro*. These chemicals may be constituent parts of topically applied pharmaceutical formulations, being evaluated for hazard assessment purposes or for medical countermeasure development. Static diffusion cells traditionally have a limited surface area defined by the edge of the donor chamber over which a penetrant may spread during a diffusion cell study. Should the penetrant spread rapidly to this containment limit the penetration rate can be determined. Where chemicals are applied within vehicles, creams and ointments and are applied over the entire skin surface area within the diffusion cell, spread to the containment limit occurs at study commencement. However, for the hazard assessment of small droplets of toxic chemicals, such as organophosphate nerve agents, limiting skin surface spread *in vitro* could lead to underestimation of percutaneous penetration and hence underestimation of systemic toxicity *in vivo*. This study considered the dependency of the percutaneous penetration of the nerve agents ^{14}C-VX and ^{14}C-GD on skin surface spread on pig and guinea pig skin. Two types of static diffusion cell were used with areas of 2.54 cm^2 and 14 cm^2 available for diffusion. For both VX and GD lateral diffusion (either on the skin surface or within the superficial layers) was measured by autoradiography. Chemical spread to the edge of the 2.54 cm^2 cell but not the 14 cm^2 cell. Amounts of nerve agent penetrating in the 2.54 cm^2 cell were less than in the 14 cm^2 cell, but penetration rates expressed per unit area were similar. The results support the conclusion that the smaller diffusion cell artificially limited the skin surface spread of both ^{14}C-VX and ^{14}C-GD resulting in less chemical penetrating at the same rate. This study has shown that it is important account for surface area spread when reporting nerve agent absorption through skin.
© Crown copyright 2013. Published with the permission of the Defence Science and Technology Laboratory on behalf of the Controller of HMSO.

PS 2182a *In Vitro* Dermal Permeation of Nicotine from Surrogate E-Cigarette Liquids

H. Frasch and A. M. Barbero. *National Institute for Occupational Safety and Health, Morgantown, WV.* Sponsor: S. Anderson.

Rationale and Scope: Nicotine (NIC) in propylene glycol (PG) plus flavorings form the main delivery components of electronic cigarettes (e-cigarettes). Some flavoring constituents, e.g. limonene, are known to enhance dermal penetration. Workers mix these liquids and fill e-cigarette cartridges in the manufacturing process, creating the potential for dermal exposure. No information currently exists on the dermal absorption of nicotine from propylene glycol vehicle. Therefore, *in vitro* human epidermal permeation of NIC from 24 mg/mL ("high strength") solutions in PG and from neat NIC were measured. Preliminary studies from 24 mg/mL NIC in PG with the addition of 5% (w/w) limonene were also undertaken. Procedures: Both steady-state fluxes (Jss, μg/cm^2/h) and lag times (τ, h) were determined from infinite dose exposures of 8 h (neat NIC, 9 samples from 3 donors) or 26 h (NIC + PG, 9 samples from 3 donors; NIC + PG + limonene, 3 samples from 1 donor) using static diffusion cells. NIC was quantified by HPLC. Results: Jss from NIC + PG was 4.0 ± 2.3 (mean ± SD). Addition of 5% limonene substantially enhanced flux to 84 ± 23. Jss from neat NIC was 175 ± 57. Measured τ's were: NIC + PG: 10.1 ± 3.3; NIC + PG + limonene: 5.2 ± 2.6; neat NIC: 1.9 ± 0.7. Application of a risk assessment paradigm predicts, for an 8 h exposure to the volar surface of fingertips (73 cm^2) followed by washing, the following average total NIC uptakes (mg): NIC + PG: 7.3; NIC + PG + limonene: 110; neat NIC: 152. Because the typical NIC intake from a smoked cigarette ≈ 1 mg, these numbers may also be thought of as "cigarette equivalents" consumed over an 8 h work shift. Conclusions: These data suggest the potential for substantial systemic nicotine uptake from occupational exposures in the manufacture of e-cigarettes. The addition of flavorings may significantly enhance systemic uptake.

PS 2182b Using Mode of Action in Predicting Skin Toxicity

V. Veljovic, D. Mitic Potkrajac, B. Rakic and G. Apic. *Cambridge Cell Networks Ltd, Novi Sad, Serbia.*

The aim of this study was to develop and test different skin toxicity Modes of Action (MOA). MOA describes the key events and processes starting with interaction of an agent with the cell leading to different biological response. MOA can be looked at as a representation of existing knowledge concerning the linkage(s) between initial chemical binding, defined as the molecular initiating event (MIE), intermediate events on cell, tissue and organ level and biological outcome. MOA can be used to identify key events for which non-animal tests can be developed, thereby facilitating mechanism-based, predictive toxicological assessments with low uncertainty and high human relevance.
We focused on 5 well studied skin toxicants and based on the present knowledge, created their biological network. In addition we created a computational model of biological pathways describing cellular processes activated by these compounds by manually annotating and processing molecular information from the literature from the public domain (PubMed articles and FDA reports) and made the data computable. Moreover, we created bioinformatics analysis tools for assessing chemical structure similarity, allowing us to group the compounds based on their chemical structure in addition to their MOA.
We tested this database for other known skin toxicants that are not covered by the database. Based on their structure similarity to other skin toxicant and/or know biological interaction partners we were able to predict skin toxicity of these compounds and suggest possible MOA.

PS 2182c Identification of Putative Skin Sensitizers Using QSAR Models Enriched by *In Vitro* Data

A. Tropsha[1], V. Alves[2], E. Muratov[1], D. Fourches[1], J. Strickland[3], N. Kleinstreuer[3] and C. Andrade[2]. [1]*UNC-Chapel Hill, Chapel Hill, NC,* [2]*Federal University of Goiás, Goiânia, GO, Brazil and* [3]*ILS, Inc., Research Triangle Park, NC.*

Repetitive exposure to a chemical agent can induce an immune reaction in susceptible individuals leading to skin sensitization. We have developed computational models capable of accurately assessing the skin sensitization potential of environmental chemicals. To this end, we have (i) compiled, curated, and integrated the largest publicly-available database of skin-sensitizing chemicals; (ii) used this data to generate and validate QSAR models for skin sensitization; and (iii) employed these models to identify putative sensitizers among chemicals in the Scorecard and Tox21 databases. A random forest method was employed for QSAR modeling of compounds characterized by SiRMS and Dragon descriptors, and the OECD-compliant model validation workflow was followed. The overall classification accuracies of QSAR models discriminating sensitizers from non-sensitizers were 68-88% when evaluated on several external validation sets. When compared to the OECD QSAR toolbox skin sensitization module, our models afforded significantly higher Positive and Negative Predictive Rates. When applied to chemicals within the applicability domains, the models could reliably identify positive and negative sensitizers with 94% and 71% certainty, respectively. Statistically significant descriptors from high-accuracy models yielded SAR rules that could guide structural optimization of chemicals of interest. Using these models, we have identified putative skin sensitizers in the ScoreCard and Tox21 databases as primary hits for

further experimental testing. The addition of ToxCast in vitro assays as biological descriptors for hybrid QSAR modeling improved the quality of resulting models and enabled deeper interpretation of these models in terms of underling MOAs.

PS 2183 Phosphoramide Mustard-Induced DNA Adduct Formation and DNA Damage Repair Response Induction in Rat Ovarian Granulosa Cells

S. Ganesan and A. Keating. *Animal Science, Iowa State University, Ames, IA.*

Cyclophosphamide (CPA) is used to treat cancer in children and women. Phosphoramide mustard (PM), the ovotoxic metabolite of CPA, destroys rapidly dividing cells by forming NOR-G-OH, NOR-G and G-NOR-G adducts with DNA, which can ultimately lead to DNA damage. DNA repair processes are constantly active and cell death can occur when normal repair processes fail. Previous studies have shown that PM induces DNA damage in rat ovaries. This study was designed to investigate PM-induced DNA adduct formation and induction of the DNA repair response using rat spontaneously immortalized granulosa cells (SIGC). Cells were treated with vehicle control (1% DMSO) or PM (3 or 6 μM) for 24 or 48hrs. Cell viability was reduced ($P < 0.05$) after 48 hrs in cells treated with 3 or 6 μM PM. The NOR-G-OH DNA adduct was detected by treatment with 6 μM PM after 24 hrs (8*105 relative abundance) compared to control (1.3*105). The G-NOR-G DNA adduct was formed after 48 hrs by both 3 (4.5*105) and 6 μM PM (4.5*105) compared to control (2*105) treatments. Phosphorylated H2AX (γH2AX), a marker of DNA double stranded break occurrence, was increased by exposure to 6 μM PM after 24 hrs. After 24h of PM exposure, 3 μM PM decreased mRNA expression of the DNA repair genes Atm (0.6-fold ± 0.09), Parp1 (0.7- fold ± 0.01), Brca1 (0.5-fold ± 0.07), Rad51 (0.6-fold ± 0.04) Xrcc6 (0.7-fold ± 0.06) and Prkdc (0.6-fold ± 0.07) while, in contrast, mRNA levels of Atm (1.2-fold ± 0.5), Parp1 (1.16-fold ± 0.4), Brca1 (1-fold ± 0.3), Rad51 (2.3-fold ± 0.7), Xrcc6 (1-fold ± 0.3) and Prkdc (1.1-fold ± 0.1) were increased ($P < 0.05$) by 6 μM PM compared to control. After 48hrs, both PM concentrations increased ($P < 0.05$) Atm (3 μM: 2.1-fold ± 0.6; 6 μM: 1.3-fold ± 0.3) and Parp1 (3 μM: 4-fold ± 0.8; 6 μM: 1.2-fold ± 0.4) mRNA levels relative to control treated cells. These data support that PM induces DNA adduct formation in ovarian granulosa cells causing DNA damage and eliciting the ovarian DNA repair response in a dose- and time-dependent manner (Supported by ES016818 to AFK).

PS 2184 *In Utero* BPA Exposure May Cause Transgenerational Reproductive Effects in Mice

A. Ziv-Gal, W. Wang, C. Zhou and J. A. Flaws. *Comparative Biosciences, University of Illinois at Urbana-Champaign, Urbana, IL.*

Bisphenol A (BPA) is an endocrine disrupting chemical that is widely used in the manufacture of epoxy resins and polycarbonate plastics. Some studies suggest that in utero BPA exposure affects ovarian development and function in the F1 generation of mice; however, the reproductive effects on consecutive generations are unknown. In this study, pregnant dams (FVB mice; F0) were orally dosed with vehicle control, BPA (0.5, 20, and 50 μg/kg/day), or diethylstilbestrol (DES; 0.05 μg/kg/day; positive control) daily from gestation day 11 until birth. Female F1 pups were allowed to reach sexual maturity and then were mated with proven male breeders to produce a F2 generation. Sexually mature females from the F2 generation were placed into two breeding studies, which were initiated at the ages of three and six months. At the end of each breeding study several reproductive outcomes in F2 females were assessed. Those include, litter size, average pup weight, male/female pups ratio, and percentage of dead pups in each treatment group on postnatal day 0. The results indicate that 20 μg/kg/day BPA exposure significantly increased the percentage of dead pups as F2 dams aged from three to six months. The percentage of dead pups was 1.9±1.2% at three months compared to 29.5±8% at six months (n=9-11 breeding pairs; p=0.02). Further, 0.5 and 50 μg/kg/day BPA resulted in a trend of an increased percentage of dead pups as dams aged from three to six months. Additionally, 0.5 μg/kg/day BPA exposure significantly increased average pup weight compared to control (control: 1.4±0.03g versus BPA 0.5: 1.6±0.03g, n=7-12 breeding pairs; p=0.01) at six months. DES had a similar effect on average pup weight (control: 1.4±0.03g versus DES: 1.7±0.1g, n=7-12 breeding pairs; p=0.03) at six months. Collectively, these data suggest that exposure of F0 pregnant dams to BPA affected the viability and the weight of the pups born to F2 dams. Additionally, these effects were more severe as the dams age. Supported by: NIH P01ES022848 (JAF) and NIH R0183459301 (JAF).

PS 2185 Genistein Exposure Inhibits Growth and Alters Steroidogenesis in Adult Mouse Antral Follicles

J. Peretz and J. A. Flaws. *Comparative Biosciences, University of Illinois at Urbana-Champaign, Urbana, IL.*

Genistein is an isoflavone phytoestrogen found naturally in a variety of plant structures, including soybeans, lentils, sunflower seeds, and chickpeas. However, the majority of human genistein exposure originates from soy-based dietary products such as soy milk and soy protein. Phytoestrogens have the potential to mimic, enhance, or impair the components of the estradiol biosynthesis pathway, which could alter follicle growth. Though some studies have inconsistently indicated that genistein affects granulosa cell proliferation and hormone production, no studies have examined the effects of genistein exposure on intact antral follicles. This study tested the hypothesis that genistein (6.0 and 36μM) inhibits follicle growth and steroidogenesis in mouse antral follicles. To test this hypothesis, antral follicles were isolated from adult, cycling mice and cultured with either vehicle control (dimethylsulfoxide; DMSO) or genistein (6.0 and 36μM) in supplemented α-minimum essential media for 96 hours (h). Every 24h, individual follicle diameters were measured and, after culture, media were collected and subjected to enzyme-linked immunosorbent assays for measurements of progesterone, androstenedione, testosterone, and estradiol levels. The results indicate that genistein (36μM) significantly inhibited follicle growth beginning at 72h compared to control (DMSO: 114.1 ± 0.81; genistein 36μM: 98.8 ± 3.44; percent change, n=3, $p \leq 0.05$). Additionally, genistein (6.0 and 36 μM) significantly inhibited estradiol and androstenedione levels at 96h compared to control (for estradiol, DMSO: 6764 ± 571pg/mL; genistein 6.0μM: 1376 ± 485pg/mL; genistein 36μM: 1048 ± 216pg/mL; n=3, $p \leq 0.05$). Conversely, genistein (36μM) significantly increased progesterone levels at 96h compared to control (DMSO: 24.1 ± 5.6ng/mL; genistein 36μM: 104.7 ± 26.6ng/mL; n=3, $p \leq 0.05$). Further, genistein had no effect on testosterone synthesis. Collectively, these data indicate that genistein is toxic to antral follicles, impairing follicle growth and altering steroidogenesis.
Support: NIH R01ES019178.

PS 2186 Di(2-ethylhexyl) Phthalate May Accelerate Early Ovarian Folliculogenesis by Increasing pAKT Levels in the Ovary

P. R. Hannon and J. A. Flaws. *Department of Comparative Biosciences, University of Illinois, Urbana, IL.*

Di(2-ethylhexyl) phthalate (DEHP) is a plasticizer in consumer, medical, and building products. Humans are exposed to DEHP daily via ingestion, inhalation, and dermal contact, representing a public health concern. Little is known about the effects of DEHP on normal ovarian function. Our lab has shown that 10 and 30 day exposure to DEHP accelerates primordial follicle recruitment to the primary stage of development in mice. Immature follicles at this stage rely on proper regulation of the phosphatidylinositol 3-kinase (PI3K) signaling pathway for primordial follicle survival, quiescence, and activation of folliculogenesis. We have reported that DEHP exposure for 30 days dysregulates the mRNA expression of key factors in the PI3K pathway; however, the effects at 10 days and the level of the key regulator of PI3K signaling, pAKT, in response to DEHP treatment are unknown. Thus, we tested the hypothesis that 10 day DEHP treatment increases the level of pAKT in the ovary to promote accelerated early folliculogenesis. To test this hypothesis, CD-1 mice (post-natal day 39) were orally dosed with corn oil (vehicle control) or DEHP (20μg/kg/day-750mg/kg/day) daily for 10 days. The ovaries were subjected to immunohistochemistry, and the percentage of positive staining for pAKT was calculated and compared across treatment groups (n=3/group). DEHP significantly increased pAKT in the whole ovary at all doses compared to controls (vehicle: 1.7±0.2; 20μg/kg: 5.3±0.9; 200μg/kg: 6.7±2.0; 20mg/kg: 7.8±3.4; 750mg/kg: 7.6±1.6%). DEHP also significantly increased pAKT in primordial follicles at all doses compared to controls (vehicle: 2.8±0.5; 20μg/kg: 10.4±2.6; 200μg/kg: 8.8±2.3; 20mg/kg: 7.2±0.7; 750mg/kg: 8.3±1.4%). Furthermore, DEHP significantly increased pAKT in primary follicles at the 20μg/kg-20mg/kg doses compared to controls (vehicle: 12.9±0.6; 20μg/kg: 28.9±2.4; 200μg/kg: 17.8±0.7; 20mg/kg: 24.4±3.0%). These data provide mechanistic evidence that DEHP may induce acceleration of early folliculogenesis by increasing pAKT levels in the ovary. Supported by R01ES019178.

PS 2187 Phosphoramide Mustard-Induced Changes in Glucose Metabolism in the Neonatal Rat Ovary

J. A. Madden and A. Keating. *Animal Science, Iowa State University, Ames, IA.*

Phosphoramide mustard (PM) is an ovotoxic metabolite of the anti-neoplastic drug cyclophosphamide. PM targets all follicle types ultimately leading to ovarian failure and infertility. Although recognized as an ovotoxicant, the ovarian response

to PM is largely unknown, thus this study investigated whether PM might impact ovarian energy production by evaluating potential changes in glucose metabolism gene expression. Postnatal day 4 (PND4) F344 rat ovaries were cultured in media and treated on alternate days with vehicle control (DMSO; CT) or PM (60 μM). Following 2 or 4 days (d) of culture, RNA was isolated and a drug metabolism RT^2 *Profiler* PCR array was performed. Relative to CT treated ovaries there was no impact of PM exposure on mRNA levels of glucose metabolism genes investigated after 2d. However, following 4d of PM exposure, mRNA levels of three glycolytic genes decreased ($P < 0.05$): glucose-6-phosphate isomerase (*Gpi*; 29% decrease), hexokinase-2 (*Hk2*; 57% decrease) and lactate dehydrogenase A (*Ldha*; 39% decrease). *Hk2* and *Gpi* are the first two enzymes of glycolysis, while *Ldha* catalyzes the final step. The mRNA level of aryl hydrocarbon receptor nuclear translocator (*Arnt/Hif1b*), a transcription factor regulating glycolytic gene expression, was also decreased ($P < 0.05$; 25% decrease) at 4d and unchanged at 2d, compared to CT. These results suggest that glycolysis may be decreased or slowed by PM, reducing the ovarian capacity to convert glucose to pyruvate, which could potentially be involved in PM-induced ovotoxicity. (Supported by ES016818 to AFK).

PS 2188 A Short Low-Dose Exposure to Di-n-Butyl Phthalate (DBP) Disrupts 17Beta-Estradiol Production in CD-1 Female Mice

A. Acuff and Z. R. Craig. *School of Animal and Comparative Biomedical Sciences, University of Arizona, Tucson, AZ.*

Di-n-butyl phthalate (DBP) is present in consumer products such as plastics, cosmetics, insecticides and oral medications. We have shown previously that DBP disrupts 17β-estradiol (E_2) production by mouse ovarian antral follicles treated in vitro. To date, no studies have evaluated the effects of DBP on these parameters following short in vivo exposures with low doses of DBP. Thus, the purpose of this study was to determine whether a 10-day oral exposure to DBP at low doses would alter E_2 production in female mice. We based our low doses on the Tolerable Daily Intake (TDI; 0.01 mg/kg/day) and the Oral Reference Dose (RfD; 0.1 mg/kg/day) for DBP. A 1000 mg/kg/day dose was included to mimic previous in vivo high dose studies with DBP. Young CD-1 mice (35 days old, n=8/group) were dosed orally with tocopherol-stripped corn oil (vehicle), 0.01 mg/kg/day (TDI), 0.1 mg/kg/day (RfD), and 1000 mg/kg/day (HIGH) for 10 days. Body weights were recorded throughout the study and animals were euthanized within one hour of their last dose. Uteri, kidneys, adrenals, spleen, and liver were excised and weighed to assess toxicity to these tissues. Blood samples were collected to measure circulating levels of E_2. No differences in body weight and weight gain were observed between control and DBP-treated mice. DBP dosing did not affect uterine, kidney, adrenal, and spleen weight, but, animals dosed with the TDI had significantly decreased liver weights. Compared to vehicle-treated controls, mice treated with the TDI showed a trend ($p=0.06$) for decreased circulating E_2, while mice treated with the RfD and the high dose had significantly lower circulating E_2 than controls ($p \leq 0.05$; OIL: 8.85 ± 0.56 pg/mL, TDI: 6.67 ± 0.80 pg/mL; RfD: 6.58 ± 0.49 pg/mL; HIGH: 5.05 ± 0.90 pg/mL). Our findings of decreased circulating E_2 in DBP-treated mice suggest that this phthalate disrupts steroidogenesis in female mice at low doses with relevance to human exposure. Supported by NIH grants K99/R00ES021467 (ZRC).

PS 2189 Temporal Impact of Obesity on Expression of Genes Encoding Enzymes Involved in Ovarian Xenobiotic Biotransformation

J. Nteeba and A. Keating. *Department of Animal Science, Iowa State University, Ames, IA.*

Obesity is associated with type 2 diabetes, compromised reproductive health and birth defects in offspring. Obesity is also allied with elevated blood glucose and insulin levels, altering insulin's action on various organs including the ovary. In extra-ovarian tissues, insulin regulates xenobiotic biotransformation enzymes, potentially through phosphatidylinositol 3-kinase (PI3K) signaling. Xenobiotic chemicals can target the ovary and destroy the primordial follicles as well as other follicle types, leading to premature ovarian failure, infertility and other health impairments. Despite strong association between obesity and elevated plasma insulin, whether obesity influences ovarian xenobiotic biotransformation remains poorly understood. This study therefore, investigated the temporal effect of obesity on ovarian expression of genes encoding cytochrome P450 isoform 2E1 (*Cyp2e1*) and microsomal epoxide hydrolase (*Ephx1*). 4 weeks old female wild type normal non-agouti (a/a; designated lean; n = 20) and agouti lethal yellow (KK.Cg-Ay/J; designated obese; n = 20) mice were utilized. Glucose tolerance testing followed by euthanasia and ovary collection was performed at 6, 12, 18 or 24 weeks (n = 5 per group) of age. Total RNA was isolated and cDNA (1:25) were amplified using primers specific for mouse *Cyp2e1* and *Ephx1*. Relative mRNA expression of each gene was normalized using *Gapdh* as a housekeeping gene. Statistical analysis was performed using the T-test function of GraphPad Prism 5.5 software with a statistical significance level set at $P < 0.05$. Obesity had a differential effect on ovarian *Cyp2e1* and *Ephx1* expression over time. Relative to their lean counterparts, in a time-dependent manner, ovaries from obese mice displayed decreased ($P < 0.05$) *Cyp2e1* on one hand and increased ($P < 0.05$) *Ephx1* mRNA levels, supporting that *Cyp2e1* and *Ephx1* may have some common transcriptional regulator. These results indicate that obese females may have increased susceptibility to ovotoxicant-induced reproductive health impairments.
This work was supported by ES016818 to AFK.

PS 2190 Examining Triclosan-Induced Potentiation of the Estrogen Uterotrophic Effect

G. W. Louis[1, 2], D. Hallinger[1] and T. E. Stoker[1]. [1]*Endocrine Toxicology Branch, US Environmental Protection Agency, Research Triangle Park, NC and* [2]*Oak Ridge Institute for Science and Education, Oak Ridge, TN.*

Triclosan (TCS), a widely used antibacterial, has been shown to be an endocrine disruptor. We reported previously that TCS potentiated the estrogenic effect of ethinyl estradiol (EE) on uterine growth in rats orally administered 3 μg/kg EE and TCS (2 to 18 mg/kg) in the uterotrophic assay, whereas TCS alone had no effect. We further characterized this potentiation by evaluating the effect of co-exposure with lower doses of EE (0.125 to 2 μg/kg) that are comparable to the concentrations in hormone replacement therapies. We found that TCS correspondingly potentiated the uterotrophic effect (both in uterine weight and epithelial cell height), but at significantly lower doses of EE (LOEL = 0.25 μg/kg). In the current study, we evaluated the effects of TCS with a xenoestrogen in the uterotrophic assay to determine whether the effect is specific to only co-administration with EE. Female rats were exposed to 100 and 200 mg/kg of nonylphenol (NP), a pesticide with ER agonist activity, in addition to an EE-treated positive control group. NP induced a significant increase in uterine weight, but to a lesser extent than the EE-induced response. Animals co-treated with TCS and NP also had a significant increase in uterine weight compared to vehicle controls, but this difference was not significantly different from NP alone. To examine the cellular mechanism by which TCS potentiated the EE uterotrophic effect, we conducted an *in vitro* estrogen receptor (ER) transactivation assay, which revealed that TCS alone does not activate the ER. Cotreatment of TCS with estradiol did not alter the maximal response suggesting that TCS does not antagonize nor potentiate the ER. These results provide evidence that the potentiation of the estrogenic response by TCS is not at the level of the ER. Further studies are needed to evaluate the role of TCS in altering estrogen metabolism. *This work does not necessarily reflect EPA policy.*

PS 2191 Propylparaben Has No Estrogenic Activity When Administered for 3 Months in Juvenile Rats

L. Sivaraman[1], L. Pouliot[2], Y. Zhao[1], G. Liu[1], H. Shen[1], B. Wang[1], C. Parrula[1], T. Brodie[1], M. J. Graziano[1] and M. E. McNerney[1]. [1]*Bristol-Myers Squibb Co., New Brunswick, NJ and* [2]*Charles River Laboratories Preclinical Services, Montreal, QC, Canada.*

BACKGROUND: Parabens, esters of p-hydroxybenzoic acid, are used as antimicrobial preservatives in pharmaceuticals. There has been considerable controversy regarding the potential of parabens for estrogen-mimetic activity, and widespread concern regarding their use in pediatric medicinal formulations. The scientific literature contains conflicting results from several studies. We designed and conducted a comprehensive study to determine the potential of propylparaben (PB) to elicit estrogen-mimetic effects. OBJECTIVES: 1). Determine the potential estrogen-mimetic effects of PB in juvenile rats; 2). determine the systemic exposures to PB and metabolites; and 3). evaluate the reversibility of any observed changes. METHODS: PB was administered by oral gavage once daily to groups of Crl:CD(SD) rats at doses of 0 (vehicle), 10, 100, or 1000 mg/kg from Postnatal Days (PNDs) 4 through 90. Evaluations included clinical observations, body weight, food consumption (after weaning on PND 21), evidence of sexual maturation (vaginal opening and preputial separation), clinical pathology, anatomic pathology of male and female reproductive tracts, and toxicokinetic profiles on PND 7, 21 and 83. Recovery phase evaluations additionally included estrus cyclicity, mating (PND 91) and fertility assessments. Evaluations of the offspring included viability, birth weight, litter size, clinical observations, and examinations of pups for evidence of dysmorphology. RESULTS: PB was well tolerated by neonatal, juvenile, and adult rats when administered from PND 4-90 at doses ≤1000 mg/kg/day. There were no effects of PB on sexual maturation or reproductive function in male or female rats, nor changes in organ weights or microscopic pathology of reproductive tissues suggestive of estrogen mimetic effects of PB or its metabolites. Exposures to PB and metabolites were confirmed in toxicokinetic evaluations. CONCLUSION: Propylparaben is not an estrogen-mimetic in juvenile rats.

PS 2192 Combined Repeated-Dose Toxicity Studies with the Reproduction/Developmental Toxicity Screening Tests for Perfluorotetradecanoic Acid and Perfluorohexadecanoic Acid in Rats

A. Hirose[1], S. Fujii[2], T. Suzuki[3], H. Kato[1], T. Kawamura[1], M. Matsumoto[1], M. Takahashi[1], M. Hirata-Koizumi[1], T. Nishimura[4], M. Ema[5] and A. Ono[1]. *[1]Division of Risk Assessment, National Institute of Health Sciences, Tokyo, Japan, [2]Safety Research Institute for Chemical Compounds Co., Ltd., Sapporo, Japan, [3]Tokyo Metropolitan Institute of Public Health, Tokyo, Japan, [4]Teikyo Heisei University, Tokyo, Japan and [5]National Institute of Advanced Industrial Science and Technology, Tsukuba, Japan.*

Perfluoroalkyl carboxylic acids (PFCAs) are environmental pollutants which are of concern due to their possible effects on human health. Although many toxicological researches have been performed, there is little information about the toxicity of PFCAs with a carbon chain length C11 and above. In order to obtain initial toxicological information for such long-chain PFCAs, combined repeated dose toxicity studies with the reproduction/developmental toxicity screening tests were conducted in the Japanese safety examination of existing chemicals and safety programmes. Presented here are the results for perfluorotetradecanoic acid (PFTeDA, C14) and perfluorohexadecanoic acid (PFHxDA, C16) concluded recently. Male and female rats were administered by gavage with PFTeDA at 1, 3 or 10 mg/kg/day or with PFHxDA at 4, 20 or 100 mg/kg/day, and each female was mated with a male in the same dose group after 14-day administration. Males were dosed for a total of 42 days and females were dosed throughout the gestation period until day 5 after parturition. PFTeDA and PFHxDA mainly affected the liver, causing hypertrophy of hepatocytes and fatty change, at middle and high doses. PFTeDA also induced follicular cell hypertrophy in the thyroids at middle and high doses. The only observed reproductive/developmental effect was an inhibition of postnatal body weight gain of pups at a maternal toxic dose of PFTeDA. The NOAELs for the repeated dose and reproductive/developmental toxicity were concluded to be 1 and 3 mg/kg/day for PFTeDA and 4 and 100 mg/kg/day for PFHxDA, respectively.

PS 2193 Inhalation Exposure of Pregnant Mice to Concentrated Airborne Particulate Matter Leads to Adverse Obstetric Outcomes Associated with Particular Exposure "Windows"

J. L. Blum, L. Chen and J. T. Zelikoff. *Environmental Medicine, New York University School of Medicine, Tuxedo, NY.*

Epidemiologic studies suggest a strong causal link between exposure to airborne particulate matter (PM) during pregnancy and preterm birth (PTB) and low birth weight (LBW). However, these studies are often in disagreement regarding which particular time points are most sensitive or whether such effects are cumulative. Previously, we showed that inhalation exposure of timed-pregnant mice to concentrated $PM_{2.5}$ (CAPs) collected from Tuxedo, NY, throughout pregnancy (6 hr/d from gestational day (GD) 0 through GD16) at a concentration of ~160 μg/m^3 resulted in PTB and LBW. Using the same exposure paradigm, mice were assigned to one of four exposure windows (Win) corresponding to specific events during development (Win 1–GD0-5; Win 2-GD6-14; Win 3-GD14-17; and, Win 4 GD0-16). Mean daily CAPs concentration for each exposure window was 178, 193, 171, and 173 μg/m^3 for windows 1-4, respectively. CAPs exposure induced PTB ranging from 0.4d for Win 2 to 0.6d in Win 4 compared to time-matched controls corresponding to ~1 wk preterm in humans. Exposure to CAPs resulted in LBW with pups from Win 1, 2, and 4 being ~10% lighter than FA exposed litters. Placental weight on GD17 was decreased by ~8% by CAPs exposure, but only for those mice prenatally exposed later in pregnancy (Win 3). These experimental data provide feasibility for the epidemiological association between PM exposure and PTB/LBW and show for the first time that there are particularly sensitive gestational windows for PM exposure that are clearly related to adverse obstetric outcomes. Alterations in fetal development and growth can have lifelong effects such as increased rates of learning and behavioral difficulties, along with later life susceptibilities to disease (e.g., type 2 diabetes). These data demonstrate the public health risk associated with PM exposure and effects specific to a particular gestational window of vulnerability. Supported by March of Dimes and the NYU NIEHS Center Grant ES000260.

PS 2194 *In Utero* Exposure of F-344 Rats to Low Levels of Dietary Zeranol Induces Transgenerational Effects on Sexual Development and Susceptibility to Chemically-Induced Mammary Carcinogenesis

C. Lewis[1], J. T. Barrett[1, 2], P. Vakil[2], M. A. Gallo[1, 2] and H. Zarbl[1, 2]. *[1]GSBS, RWJMS-Rutgers University, Piscataway, NJ and [2]EOHSI, Rutgers University, Piscataway, NJ.*

Zeranol (Zer) is a potent semi-synthetic derivative of zearalenone, a myco-estrogen produced by Fusarium that contaminate grain. After its growth promoting effects on livestock were noted in the early 1970's, Zer was developed as a substitute for diethylstilbestrol (DES) to enhance desirable qualities of meat. Zer is widely used in the North and South America but banned in much of Europe and Asia. Zer is detected in the finished product, is extremely stable at cooking temperatures and has a long half-life in humans. Accidental and occupational exposures to Zer have been associated with precocious puberty. Our recent studies in prepubescent girls indicate that human exposure is primarily via the consumption of beef and corn, and urinary levels of unconjugated Zer was associated with altered onset of puberty, height and weight (Bandera et al., 2011). Our studies in rats indicated that exposure to Zer (between PND-9 to term) at doses within the human ADI (1.25μg/kg/day) via the maternal diet, resulted in precocious puberty in females F1 progeny, defined by a 3 day decrease in age at vaginal opening. F1 male progeny showed feminization as assessed by decreased ano-genital distance and decreased sperm count. F1 females treated with a single carcinogenic dose of N-Nitroso-N-methylurea (NMU) showed decreased latency and increased incidence of mammary tumors. Similar effects on puberty and carcinogenesis were also observed in the F2 progeny, but only if both the dam and the sire were exposed to Zer *in utero*. Preliminary studies of the F3 progeny demonstrated a trend towards decreased litter sizes, notably a significant decrease in fecundity, number of male offspring and a 3 day delay in vaginal opening. Together these studies suggest that *in utero* exposure to the Zer produces transgenerational effects on sexual development and susceptibility to chemical-induced carcinogenesis.
Supported by a Grant from The New Jersey Commission on Cancer Research.

PS 2195 Transfer of Triclocarban through Gestation and Lactation

H. Enright[1], V. Lao[1], M. Sarachine Falso[2], B. A. Buchholz[2], K. Kulp[1] and M. A. Malfatti[1]. *[1]Biosciences and Biotechnology Division, Lawrence Livermore National Laboratory, Livermore, CA and [2]Center for Accelerator Mass Spectrometry, Lawrence Livermore National Laboratory, Livermore, CA.*

It has been demonstrated that a variety of chemicals are not removed after wastewater treatment, which results in their release back into the water supply and environment. These chemicals may act as endocrine disrupting compounds (EDC), which can affect the function of the endocrine system and adversely affect progeny and/or (sub)-populations. To date, studies evaluating the effects of EDC during periods of development are lacking, including quantitative measures of accumulation after exposure. We are measuring the transfer and accumulation of the EDC, triclocarban (TCC), from mother to offspring both in utero and through lactation using accelerator mass spectrometry (AMS). The high sensitivity of AMS allows for assessment of environmentally relevant concentrations of TCC (pM-nM).
^{14}C-labeled TCC was administered to pregnant female mice through their drinking water (100nM) during gestation and lactation using custom made water bottles. In utero, detectable quantities of TCC were found in fetal (~0.1%ID) and placental tissue (<0.02%ID). An increase in accumulation of TCC was observed through lactation (~6 pmol TCC/gram) compared to the gestation only exposure group (~2 pmol TCC/gram). Taken together, these data indicate that TCC is transferred from mother to offspring through two routes: across the placental barrier and through lactation. While low levels of TCC transfer were observed in mice, these findings suggest that if TCC is similarly transferred in humans, there may be implications after exposure on human health. Further studies are needed to identify whether low levels of TCC accumulation can interfere with reproduction and development and if these effects are dose dependent.
This work performed under the auspices of the U.S. Department of Energy by Lawrence Livermore National Laboratory under Contract DE-AC52-07NA27344. LLNL-ABS-644431

PS 2196 Plasma Microsampling of the Female Mouse and Fetus for Pharmacokinetic Profiling of Monoclonal Antibodies

E. Marsden[1], S. Haertle[2], L. Reynaud[1] and S. Baudet[1]. [1]*WIL Research Europe-Lyon, St Germain-Nuelles, France and* [2]*MorphoSys AG, Planegg, Germany.*

Microsampling-coupled bioanalytical techniques are becoming powerful tools for use in pre-clinical studies, particularly with rodents, where optimizing blood use is paramount to try and avoid or reduce the need for satellite animals.
In a series of intravenous (bolus) single and repeat dose pharmacokinetic investigations in the mouse with IgG antibodies, serial blood microsamples (30 µL each) were taken from the non-anesthetized adult female using K2-EDTA Microvette tubes via the saphenous vein and single microsamples from the gestation day 15, 16.5 or 18 fetus by cardiac puncture using insulin syringes. The fetal samples were pooled by litter (approximately 30 µL) into K2-EDTA microtubes. Adult and fetal plasma (approximately 10 µL each) was obtained by centrifugation. Amniotic fluid was also sampled using insulin syringes. All samples were stored frozen in cryotubes (between -15 and -25 °C) until analysis.
For quantifying the test item in the plasma and amniotic fluid, highly selective and sensitive ligand-binding assays were developed using Electro-Chemo-Luminescence (ECL) detection. Based on the characteristics of the test item and its target antigen, assay plates were either coated indirectly using biotin labeled recombinant antigen captured via streptavidin, or directly using idiotypic anti-drug antibodies. Only 2 µL of the plasma or 4 µL of amniotic fluid were diluted in assay buffer to analyze each sample in duplicate within the assay plate. The bound test item was detected by ECL-labeled secondary detection antibodies (e.g. anti Fc or Fab antibodies). Bioanalysis of IgG antibodies was feasible with microsamples using the described assay setup and provided a precise, accurate and specific quantification of the test item with low limits of quantification between 10-100 ng/mL back calculated for undiluted plasma/amniotic fluid samples.
We conclude that microsampling-coupled bioanalytical techniques provide ethical, scientific and financial advantages with respect to conventional pharmacokinetic methods for biologicals.

PS 2196a Mammary Gland Histopathology of the Harlan Sprague-Dawley Rat: A Model for Mammary Tumor Susceptibility Studies following Perinatal Endocrine Disrupting Compound Exposures

J. P. Stanko and S. E. Fenton. *National Toxicology Program Laboratory, NTP/NIEHS, Research Triangle Park, NC.*

The Harlan Sprague Dawley rat (Hsd:SD) is one of the current rat models used in National Toxicology Program (NTP) studies. The present study was conducted to understand various physiological and reproductive parameters of untreated Hsd:SD female rats and also to report the incidence and tumor types following 7,12 dimethylbenz-α-anthracene (DMBA)-induced mammary carcinogenesis in these rats. Pregnant female Hsd:SD rats (n=22) were obtained from Harlan Laboratories Inc. (Indianapolis, IN). Puberty was assessed in female offspring by recording the day of vaginal opening (VO). Necropsy was conducted on a subset of female offspring (n = 10 dams represented) on postnatal day (PND) 45 and mammary glands were collected for whole mount preparation and developmental assessment. The remaining female offspring received 30 mg DMBA/kg BW in 5ml sesame oil/kg BW by oral gavage on PND45. Necropsy of all females was conducted at week 24 post-DMBA administration. The mean gestation period of dams that delivered viable litters was 22.7 ± 0.1 d (n=17) with a mean litter size of 11.3 ± 0.8 pups and a mean pup weight of 9.9 ± 0.2 g. The mean age at VO was 37.7 ± 0.5 d (n=12 litters) and the mean BW at VO was 118.1 ± 2.2 g. At necropsy 24 weeks post-DMBA administration, 71% (66/93) of the females exhibited at least one tumor with a mean multiplicity of 2.2 ± 0.2 tumors/rat. A total of 153 neoplasms were observed, comprised primarily of adenocarcinomas (80/153) and fibroadenomas (64/153). An interesting observation was the presence of adenocarcinomas arising within a fibroadenoma (7/153), described as a focally adenocarcinomatous change within a well-defined primary fibroadenoma. While these lesions are rare, the overall tumor incidence and multiplicity of DMBA-treated Hsd:SD rats falls within ranges reported for other rat strains used under various test guidelines. These data should be considered when determining the DMBA dose and age of administration in future studies.

PS 2196b Early-Life Mammary Effects in Male and Female Rats following Low-Dose Maternal and Drinking Water Exposure to a VOC Mixture

A. J. Filgo[1, 2], E. Quist[1, 3] and S. E. Fenton[1]. [1]*NTP Labs, DNTP, NIEHS, NIH, DHHS, Research Triangle Park, NC,* [2]*Curriculum in Toxicology, University of North Carolina, Chapel Hill, NC and* [3]*Comparative Biomedical Sciences, College of Veterinary Medicine, NC State University, Raleigh, NC.*

Volatile organic compounds (VOCs) such as benzene, trichloroethylene, trans-1,2, dichloroethylene, tetrachloroethylene, and vinyl chloride are common industrial pollutants used in a number of cleaning agents and solvents. Ingestion and inhalation are the most common routes of reported environmental or occupational exposures. In the U.S., spikes in birth defects, infant mortality, reproductive cancers and leukemia have occurred in areas where high levels of VOCs were detected in drinking water supplies. We tested the effects of water-borne VOCs on mammary development in rats following prenatal and early life exposures. Timed-pregnant Harlan Sprague Dawley rats (n=12 dams/dose group) and their offspring were given access to water containing mixtures of these 5 VOCs at 5 or 10 times the concentrations measured in contaminated U.S. well water. Dams and pups were exposed from gestation day (GD) 10 until sacrifice. Litter sizes were equalized after birth. Mammary glands were collected for whole mount and immunohistochemistry assessment on PND 23 and 48 of both males and females. The whole mounts were scored on a scale of 1-4, where 1 is least developed and 4 is most developed. At PND 23, males treated with 5X and 10X VOCs had higher developmental scores than controls, which reached significance at 10X VOCs. Neither treated group of PND23 females was significantly different from control. However, at PND 48 both treated groups of both males and females had significantly higher developmental scores than the control groups. There was no apparent effect of the contaminated water on estrogen and progesterone receptor levels in the immunostained sections. These data suggest that the VOCs mixture accelerates mammary development in both male and female rats, with the effect most evident post-puberty.

PS 2196c Altered Mammary Development As a Result of *In Utero* Exposure to a High and Low Dose of Inorganic Arsenic (iAs) in the CD-1 Mouse

D. K. Robinson[1, 2], S. E. Fenton[2], K. Rodriguez[3] and H. Yao[3]. [1]*Toxicology, University of North Carolina at Chapel Hill, Cary, NC,* [2]*NTP Laboratory, NIEHS, RTP, NC and* [3]*Laboratory of Reproductive and Developmental Toxicology, NIEHS, RTP, NC.*

Mammary morphogenesis begins during early embryonic development, but exponential growth and differentiation doesn't occur until the onset of puberty. Early life exposure to environmental contaminants may result in altered mammary gland developmental timing during puberty and lactation, and increased susceptibility to breast cancer. Arsenic (iAs) exposure via contaminated drinking water is a global threat that has resulted in endocrine disruption and various cancers. The effect of arsenic on mammary gland development of female CD-1 mice was evaluated following their exposure from gestational days (GD) 10-18 (dams given 0 [control], 10 ppb or 42.5 ppm sodium arsenite in drinking water). Mammary whole mounts and tissue sections from contralateral glands were collected from 3 wk, 4 wk, 6 mo and 1 yr old female offspring. The effects of developmental iAs exposure were evident at all ages examined. At 3 wk of age iAs caused different effects at high and low doses. The 10ppb group exhibited a delayed phenotype 1.8±0.11 and 1.8±0.19 (4th and 5th glands respectively) in comparison to control (2.1±0.26 and 2.25±0.38). However, 42.5 ppm offspring presented with accelerated growth, (2.9± 0.19 and 3.4±0.19). By 6 mo both 10 ppb and 42.5 ppm (2.7±0.4 and 3.4±0.29, respectively) exhibited significantly advanced growth compared to control (1.9±0.37). Histological evaluations in the 10 ppb group at 6 mo of age demonstrated disorganized luminal epithelium, with papillary structures forming within ducts, surrounded by excess amounts of collagen. The 42.5 ppm dose group exhibited a varied morphology; sparse ductal structures, with small lumens and dense epithelium. The severity of these findings increased with age. These finding may implicate early iAs as a potential toxicant that can alter proper mammary gland development thus increasing the susceptibility of the gland to form cancer.

PS 2196d Prenatal PFOA Exposure Mediates Effects in the Murine Mammary Gland through Endocrine Disruption

M. B. Macon[1, 2] and S. E. Fenton[2]. [1]*Curriculum in Toxicology, UNC-CH, Chapel Hill, NC and* [2]*NTP Laboratory, NIEHS, NIH, RTP, NC.*

Our laboratory has shown that low-dose prenatal perfluorooctanoic acid (PFOA) exposure delays mammary gland development in CD-1 mice. Through a systems biology approach, we characterized PFOA effects in the mammary tissues through

analysis of whole mounts, microarrays, qPCR, Western blots, histology, immunohistochemistry, and serum PFOA and steroid hormone analysis. Developmental scoring of mammary whole mounts indicated PFOA-induced mammary delays persisted into adulthood. These morphological alterations were characterized as increased collagen density, active terminal end buds and reduced side branching; changes were observed even though serum PFOA concentrations had reached control levels. Ppar, Wnt, and Esr1 (Erα) were identified as candidate gene pathways by microarray analysis; RNA post-transcriptional modification and lipid metabolism were top molecular functions. Updated array analysis predicted Pparα and γ, dihydrotestosterone and beta-estradiol to be upstream regulators of PFOA altered genes with Pparα and γ predicted to be inhibited and dihydrotestosterone and beta-estradiol predicted to be activated. qPCR validated changes in Ppar targeted and steroid related genes. Western blot analysis of selected genes revealed increased protein expression of Pparγ and Erα in whole cell lysates at PND 7 with non-significant increases in Pparα and Pparβ/δ; Erα protein expression was reduced by PND 21. Results from blots coincided with IHC stained sections for Erα that was reduced at PND 21 and 56. No change was observed in serum estradiol or progesterone, however testosterone levels were reduced at PND 21 and DHEA levels were reduced at PND 56. Changes in hormone levels over time were different in PFOA-treated animals compared to controls for estradiol, testosterone, and DHEA, suggesting that PFOA has an overarching effect on sex steroid hormone synthesis. Collectively, these data show prenatal PFOA exposure disrupts the endocrine system to have localized effects on the maturation of the mammary gland at serum levels that overlap with human exposures.

PS 2196e Mode of Action and Human Relevance Assessment of Male CD-1 Mouse Renal Adenocarcioma Associated with Lifetime Exposure to Empagliflozin

J. A. Phillips[1], M. E. Taub[1], N. Ishiguro[2], S. VanTongeren[1], B. Knight[1], E. C. Ludwig-Schwellinger[3], J. Yuan[1], J. D. Smith[1], H. Yu[1], P. A. Escobar[1], W. T. Loging[1] and W. W. Ku[1]. *[1]Boehringer Ingelheim Pharmaceuticals, Inc., Ridgefield, CT, [2]Kobe Pharma Research Institute, Kobe, Japan and [3]Boehringer Ingelheim Pharmaceuticals, GmbH, Biberach, Germany.*

In the 2-year carcinogenicity study with empagliflozin (dose levels of 100, 300 and 1000 mg/kg/day) in CD-1 mice, an increased incidence of renal tubular adenomas and carcinomas was identified in the male high dose (1000 mg/kg/day) group. Renal tumors were preceded by non-neoplastic degenerative/regenerative tubular changes and were not observed in female mice, and rats or humans of either gender. A nongenotoxic tumorigenic mode of action comprised of five key events is presented through analysis of all available data. The mode of action initially involves predisposed background renal pathology in male mice exacerbated by pharmacologic activity of SGLT2 inhibition, and additional compound-related renal metabolic stress imposed by a male mouse kidney-specific cytotoxic aldehyde oxidative metabolite product. The convergence of these initial key events during chronic treatment promotes conversion to constitutive cellular proliferation (tumors and renal cysts) in male mice, which is likely driven by depletion of oxidative stress handling reserve. The described mode of action requires that all five key events are operative to present a carcinogenicity risk in the CD-1 mouse. Not all key events are present in the context of female mice, rats or humans or present for other osmotic diuretics or other SGLT2 inhibitors. The overall weight of evidence supports a nongenotoxic mode of renal tumorigenesis specific to the male mouse that is not relevant to humans of either gender. This is additionally supported by a predominant oxidative pathway of empagliflozin metabolism in the mouse, compared to a predominant conjugative pathway (O-glucuronidation) in humans.

PS 2196f General Toxicology and Carcinogenicity Assessment of Empagliflozin, an SGLT2 Inhibitor for the Treatment of Type 2 Diabetes Mellitus

M. Bogdanffy, R. F. Stachlewitz, S. VanTongeren, B. Knight, W. W. Ku, S. G. Emeigh Hart and K. T. Blanchard. *Nonclinical Drug Safety, Boehringer Ingelheim Pharmaceuticals, Inc., Ridgefield, CT.*

Empagliflozin selectively inhibits sodium glucose co-transporter SGLT2 thereby reducing renal reabsorption of glucose as a therapeutic modality for type 2 diabetes mellitus. In pivotal toxicity studies in CD-1 mice, Wistar (Han) rat, and Beagle dogs, most toxicity was consistent with secondary pharmacology related to urinary glucose loss and electrolyte imbalances including decreased body weight and body fat, increased food consumption, diarrhea, dehydration, decreased serum glucose and increases in other serum parameters reflective of increased protein metabolism and gluconeogenesis, urinary changes such as polyuria, and glucosuria. At high multiples of the therapeutic exposure, microscopic changes were observed in kidney and some soft and vascular tissues, and included tubular karyomegaly, single cell necrosis, cystic hyperplasia and hypertrophy (mouse), renal mineralization (rat), and tubular nephropathy and interstitial nephritis (dog). Empagliflozin is non-genotoxic in a standard battery of gene mutation and chromosomal damage assays. In rat and mouse carcinogenicity studies, empagliflozin induced no tumors in females. Benign hemangiomas of the mesenteric lymph node and Leydig cell tumors were observed in male rats, both of which are common to the SGLT2 class, strain of rat, or may be of secondary relationship to treatment. Renal tumors were observed in male mice at 1000 mg/kg/day, an exposure approximately 45- and 113-fold above the therapeutic doses of 25 and 10 mg, respectively. As described in related abstracts, the mode of action for these tumors is dependent on the natural predisposition of the male mouse to renal pathology and a metabolic pathway not reflective of humans. The male mouse renal tumors are considered not relevant to humans. Evaluations of photoabsorption spectrum and distribution of 14C-labelled empagliflozin to eye and skin coupled with the results of general toxicology studies revealed no potential for phototoxicity.

PS 2196g A Predominant Oxidative Renal Metabolite of Empagliflozin in Male Mice Is Cytotoxic in Mouse Renal Tubular Cells but Not Genotoxic

J. D. Smith, Z. Huang, H. Maw, R. Nardi, P. Foppiano, L. Her, W. Loging, P. A. Escobar, J. A. Phillips, H. Yu, M. E. Taub and W. W. Ku. *Boehringer Ingelheim Pharmaceuticals Inc., Ridgefield, CT.*

In a mouse 2 year carcinogenicity study with the SGLT2 inhibitor empagliflozin (dose levels of 100, 300 and 1000 mg/kg/day), an increased incidence of renal tubular adenomas and carcinomas was identified only in the male high dose group. Renal tumors were preceded by a number of renal degenerative/regenerative findings in only male high dose mice. Empagliflozin is not genotoxic, which supports a nongenotoxic mode of action. Cross species *in vitro* metabolism studies identified a male mouse predominant oxidative renal metabolite (M466/2) that spontaneously degrades under physiological conditions to a phenol metabolite (M380/1) and reactive 4-OH crotonaldehyde (4-OH CTA). *In vitro* toxicity studies were conducted to evaluate the cytotoxic and genotoxic potential of empagliflozin and synthesized M466/2. M466/2 was tested in both the bacterial reverse mutation (Ames) and *in vitro* mammalian (CHO) cell micronucleus assays to evaluate genotoxic potential. A primary mouse renal tubular epithelial (mRTE) cell model was used to assess the cytotoxic potential of empagliflozin and M466/2, showing that M466/2-derived *in vitro* 4-OH CTA exposure is cytotoxic to mRTE cells but is not genotoxic. Bioanalysis of M466/2 in *in vitro* incubation test media demonstrated exposures comprising >75% of M380/1, implying a stoichiometric release of reactive 4-OH CTA. In contrast, empagliflozin is not cytotoxic or mitogenic in mRTE cells. Broad panel *in vitro* pharmacology profiling revealed no off-target activities for empagliflozin suggestive of alternative modes of action. In conclusion, a male mouse predominant renal metabolite M466/2 is associated with the male mouse specificity in renal injury and tumor response. These *in vitro* data showed that M466/2-derived 4-OH CTA exposure is cytotoxic to renal tubule cells and can contribute to additional compound related renal metabolic stress and further chronic low level renal injury that support a nongenotoxic mode of tumor pathogenesis.

PS 2196h Pathogenesis of Renal Injury in the Male CD-1 Mouse Associated with Exposure to Empagliflozin

B. Knight, S. Emeigh Hart, J. A. Phillips, S. Koegler, J. Hall and W. W. Ku. *Boehringer Ingelheim Inc., Ridgefield, CT.*

An increased incidence of renal tubular adenomas and carcinomas was identified in the 2-year CD-1 mouse carcinogenicity study with empagliflozin (SGLT2 inhibitor) in high dose (1000 mg/kg/day) male mice. A 13-week mouse renal pathogenesis study was conducted with empagliflozin to evaluate dose-dependency and temporal onset of non-neoplastic degenerative/regenerative tubular changes which precede neoplasia. Male and female CD-1 mice were given daily oral doses of 0, 100, 300, or 1000 mg/kg, (corresponding carcinogenicity study dose levels) for 1, 2, 4, 8 or 13 weeks. The maximum expected pharmacology with secondary osmotic diuresis was observed by Week 1 at > 100 mg/kg/day in both genders. Histopathologic kidney changes were first detected after 4 weeks of dosing in the male 1000 mg/kg/day dose group, with progressive increases in the incidence and/or number of findings in this dose group so that they were more readily detected during Weeks 8 and 13. Changes detected starting on Week 4 consisted of minimal single cell necrosis and minimal increases in mitotic figures. These changes persisted at an increased incidence at weeks 8 and 13, and were accompanied by minimal to mild karyomegaly, minimal proximal convoluted tubular epithelial cell hyperplasia and a corresponding increase in Ki-67 positive nuclei in epithelial cells of the proximal convoluted tubules. There were no corresponding changes in serum chemistry or urinalysis parameters indicative of any physiologically meaningful effect on renal function and thus these findings were not considered to be

adverse. Similar changes were not identified in lower dose groups in males nor were they present in females of any dose group. Overall, the study results support early compound-related degenerative/regenerative changes only in high dose male CD-1 mice as a key contributing feature to a nongenotoxic mode of renal tumor pathogenesis.

PS 2196i RNA-Seq Reveals Molecular Changes in Renal Injury Associated with Exposure to Empagliflozin in the Male CD-1 Mouse

J. Yuan[1], P. Pande[1], J. Hill[2], Y. Wang[2], D. Hall[3], J. Mikl[3] and W. W. Ku[1]. *[1]Nonclinical Drug Safety, Boehringer Ingelheim Pharmaceuticals, Inc., Ridgefield, CT, [2]Scientific Knowledge Discovery, Boehringer Ingelheim Pharmaceuticals, Inc., Ridgefield, CT and [3]Biometrics and Data Management, Boehringer Ingelheim Pharmaceuticals, Inc., Ridgefield, CT.*

In the CD-1 mouse 2-yr carcinogenicity study with empagliflozin, an increased incidence of renal tubular adenomas/carcinomas was observed in the high dose (1000 mg/kg/day) male group. To gain better understanding of the molecular changes in mouse kidney to support a tumorigenic mode of action, we have utilized RNA-seq to evaluate gene expression changes in mice dosed with empagliflozin at 1000 mg/kg/day in a 13-week renal pathogenesis study. Enriched renal cortex was collected at 1, 2, 4, 8 and 13 weeks, and the whole transcriptome in kidney was profiled. The transcriptome was compared between vehicle and empagliflozin treated male and female mice. Data showed male mouse-specific changes in kidney over 13 weeks of dosing. Consistent with the expected pharmacologic activity of SGLT2 inhibition and compound related renal metabolic stress, early treatment-related male-specific expression changes were noted in osmolarity regulation, drug metabolism and transport at Weeks 1 and 2, followed by changes in immunity and complement system genes at Week 4. Treatment-related changes in genes and pathways related to p53 regulated cell proliferation, oxidative stress and renal injury were observed in high dose males at Week 8 and the number of genes with significant expression change dramatically increased at Week 13. The later expression changes were consistent with the increased appearance of degenerative/regenerative renal tubular changes only in high dose male. In contrast to males, observed expression changes were less apparent in female mice. Consistent with a nongenotoxic tumorigenic mode of action, no expression changes in DNA damage/repair pathways were identified. Overall, observed molecular changes in the male mouse complement the renal pathological changes in supporting a nongenotoxic tumorigenic mode of pathogenesis for empagliflozin.

PS 2196j Nonclinical Safety Assessment of Exendin (9-39) in Juvenile Rats and Dogs

K. E. Elsass[2], N. Bordelon[2], M. Lynch[2], M. Hawk[2], T. Arndt[2], P. Hong[2], K. Knostman[2], D. DeLeon[3] and P. S. Terse[1]. *[1]National Center for Advancing Translational Sciences, Bethesda, MD, [2]Battelle, Columbus, OH and [3]The Children's Hospital of Philadelphia, Philadelphia, PA.*

Exendin (9-39) is being developed for the treatment of congenital hyperinsulinism, the most common cause of persistent hypoglycemia in children. Toxicology studies were conducted in Sprague Dawley rats (7±1 days of age) and beagle dogs (13 days of age) to support its clinical evaluation. In 14-day non-GLP studies, TID subcutaneous (SC) doses of 15, 50, and 150 mg/kg/dose were administered to rats and 5, 15, and 40 mg/kg/dose were administered to dogs. Based on the lack of toxicologically significant findings, TID doses for GLP 28-day studies were increased to 20, 80, and 300 mg/kg/dose for rats and 10, 30, and 100 mg/kg/dose for dogs. Toxicological endpoints evaluated included: clinical observations, body weight, food consumption, clinical pathology, CNS assessment (rats), electrocardiography (dogs), toxicokinetics, and histopathology. The only Exendin (9-39)-related observations noted were increased serum glucose in female rats, decreased serum triglycerides in male rats, and increased urine volume in male dogs. In the cardiovascular safety pharmacology study, beagle dogs (7 to 8 months old) were administered a single SC dose of vehicle or 5, 20, or 80 mg/kg Exendin (9-39) in a 4 x 4 Latin-square design. No toxicologically significant findings were observed. A dose proportional increase in Exendin plasma exposure was observed; combined average AUClast on Day 28 in male and female rats at the 300 mg/kg/dose was 249,000 ng.h/mL and at the 100 mg/kg/dose in dogs was 340,500 ng.h/mL. In conclusion, based on the available data, no observed adverse effect levels were 300 mg/kg/dose in rats and at 100 mg/kg/dose in dogs using TID subcutaneous dosing schedule.
(Supported by NCI-SAIC Contract No. HHSN261200800001E, NICHD and NINDS under BrIDGs Program).

PS 2196k ETI-204 Nonclinical Safety Assessment of CNS Findings from Inhalational Anthrax Animal Studies

B. Yamamoto[1], M. T. Butt[2], N. Serbina[1], H. Tang[1] and A. Shadiack[1]. *[1]Elusys Therapeutics, Pine Brook, NJ and [2]Tox Path Specialists, Frederick, MD.*

Inhalational anthrax (IA) can result in progressive hemorrhagic meningoencephalitis and death. Antibodies against *Bacillus anthracis (Ba)* toxin components (antitoxins) are strategies to treat IA. ETI-204 is a monoclonal antibody against the protective antigen component of *Ba* toxins currently in development for IA disease treatment. No *Ba* antitoxin-related changes are typically observed in the CNS of IA study survivors (monkeys, rabbits), however, in IA infected non-survivors, *Ba* antitoxins have been associated with extravascular bacteria and higher incidence of acute inflammatory reactions in leptomeninges compared to controls that tend to die with no CNS changes or with just intravascular bacteria. Because of a putative *Ba* antitoxin CNS effect, ETI-204 CNS safety was assessed.
Cynomolgus monkeys or NZW rabbits were aerosol exposed with ~200 LD_{50} of *Ba* spores and dosed with ETI-204 (1-32 mg/kg, IV) and the brains from 78 monkeys and 86 rabbits were examined microscopically. Brains of 15 non-*Ba*-exposed rabbits dosed with ETI-204 (16-32 mg/kg/dose x4, IV) were also examined.
There were no ETI-204-related changes in IA study survivors or in ETI-204 exposed, non-infected rabbits, indicating no direct ETI-204 CNS effect. In IA infected monkeys and rabbits, there was a higher incidence of meningitis and extravascular bacteria in ETI-204-treated non-survivors (all doses) compared to controls that tended to die with no CNS changes or had just intravascular bacteria.
CNS findings in ETI-204-treated non-survivors were consistent with IA and an immune response to extravascular bacteria. One hypothesis is in non-survivors, *Ba* antitoxins do not reach the brain in sufficient quantities or in time to prevent bacterial extravasation, inflammatory reactions, and death, or the *Ba* infection is too severe to save the host with *Ba* antitoxin treatment alone. ETI-204 has not been shown to be toxic to the CNS, and ETI-204 IA survival benefit appears to outweigh any potential CNS risk.
Federally supported by ASPR/BARDA under Contract No. HHSO100201000026C.

PS 2196l Nonclinical Assessment of NRX-1074, an Orally Bioavailable NMDAR Partial Agonist

G. W. Wolfe[1], M. M. Vegarra[1], C. S. Godin[1], D. Houck[2] and J. Gidda[2]. *[1]Smithers Avanza, Gaithersburg, MD and [2]Naurex, Inc, Evanston, IL.*

NRX-1074, a partial agonist of the NMDAR receptor, is an orally bioavailable molecule that is being developed for major depressive disorders. Studies have shown promising ketamine-like efficacy signatures without apparent safety issues. As part of an IND, studies were conducted included *in vitro* genotoxicity, blood compatibility, safety pharmacology, and repeat-dose studies. NRX-1074 did not result in genotoxicity or hemolysis. No adverse effects were noted on the respiratory or central nervous systems in rats at 700 mg/kg, PO and in the cardiovascular system in dogs at 70 mg/kg, IV and 300 mg/kg, PO. In the Repeat-Dose Studies, animals were dosed daily for 28 days via oral gavage at 0, 30, 200 or 600 mg/kg/day (rats) or 0, 30, 70, 200 mg/kg/day (dogs) or daily for four weeks by IV injection at doses of 100 (200) mg/kg/day (rats) or 70 mg/kg/day (dogs). Parameters evaluated in both studies included mortality, physical examinations, cageside observations, body weight, food consumption, ophthalmology, clinical pathology, gross pathology, absolute/relative organ weights, histopathology, ECGs (dogs only) and toxicokinetics. In the oral gavage studies up to 600 mg/kg/day (rats) and 200 mg/kg/day (dogs) and in the intravenous studies up to 100 mg/kg/day (rats) and 70 mg/kg/day (dogs), no treatment-related effects were noted during the dosing or recovery period. IV administration of NRX-1074 at 200 mg/kg resulted in mortality in rats. The no-observed-effect level (NOEL) for NRX-1074 when administered orally for at least 28 days to rats and dogs was 600 and 200 mg/kg/day for the oral route, respectively, and 100 and 70 mg/kg/day, respectively for the intravenous route. The oral HED's were 97 and 108 mg/kg in rats and dogs, respectively and intravenous HED's were 16 and 38 mg/kg in rats and dogs, respectively, suggesting the rat as the most sensitive species.

PS 2196m Comparative Prolactin Study in Mouse and Rat Using CNS Drugs: Molindone, Haloperidol and Reserpine

S. Ganiger[1], H. Krishnappa[1], S. Sulaiman[1], S. Goel[2] and G. Krishna[2]. *[1]Safety Assessment, Advinus Therapeutics Ltd, Bangalore, Karnataka, India and [2]Supernus Pharmaceuticals, Inc, Rockville, MD.*

Typical antipsychotics have high affinity for dopamine D2 receptors and known to increase blood prolactin in both rodents and humans. Two independent studies were conducted to investigate and compare the prolactin and its reversal to basal

levels over a 24h postdose (PD) in Wistar rats and 32h PD in Swiss albino mice. Groups of rats and mice were treated with single doses of molindone (5 and 60 mg/kg; oral), haloperidol (20 and 100 mg/kg; oral), or reserpine (10 and 50 mg/kg; subcutaneous). These drugs were selected based on their potential to increase prolactin. Blood samples were drawn over 6 time points and prolactin levels were measured using validated ELISA method. Molindone resulted in peak prolactin levels at 0.25h PD and returned to baseline by 24h in both species. In general, haloperidol and reserpine showed treatment related increase in prolactin, though at a slower rate compared to molindone in rats and mice. The prolactin levels reached basal levels in male rats and mice by the last sampling time studied. However, in females the prolactin was decreased but remained elevated by last sampling time compared to controls. This study demonstrates, rodents experience prolactin surges that are physiologically required for reproductive effects of test-drugs. The changes in prolactin correlated with plasma drug levels and were higher in females than in males for all three drugs. Rapid reversal of prolactin in molindone treated animals compared to haloperidol and reserpine correlates to its short half-life. These data are considered to be of significant value in comparative human risk assessment of test drugs.

PS 2196n Assessment of Prolactin-Mediated Changes and Their Reversal in Molindone-Treated rasH2 Mice

G. Krishna[1], S. Ganiger[2] and S. Goel[1]. [1]*Supernus Pharmaceuticals, Inc., Rockville, MD and* [2]*Advinus Therapeutics Ltd., Bengaluru, India.*

Molindone, an antipsychotic, is known to modulate prolactin levels linked with reproductive changes in rodents. Such effects were further investigated in 6-month mouse study with a reversal phase to better characterize risk assessment. Groups of rasH2 mice were dosed daily by gavage with molindone at 5, 15 and 50 mg/kg. Blood samples were analyzed for molindone on Day 180 and prolactin on Days 1, 180 and at a 2-month reversal period. Histopathology was performed on reproductive tissues. Results showed that plasma levels of molindone were more than dose proportional with Tmax at 0.25h postdose (PD). Prolactin levels peaked within 0.5h PD and were 255 and 272ng/mL in males and 1313 and 2454ng/mL in females, respectively, for Days 1 and 180. Prolactin levels remained elevated up to 1h PD in males and 3h in females but returned to basal levels by 24h PD. Further, after 2-month recovery, prolactin levels were at basal levels, suggesting complete reversibility. Histopathologically, on Day 180, changes in ovaries included retention of eosinophilic corpora lutea and interstitial atrophy of diffuse nature in all of the treated groups. Atrophy of uterus and vagina were observed in these groups. At the end of recovery, these changes were completely reversed at 5 and 15 mg/kg, with signs of reversal at 50 mg/kg. In males, there was no histopathology changes noted. Reversibility of prolactin levels and histopathology seen in this study confirms the pharmacologically mediated effects of molindone and corroborate with the known role of prolactin in hormonal homeostasis and reproductive physiology. These changes are considered rodent-specific, similar to those seen with other antipsychotics in this class of drugs. It is concluded that the transient prolactin-mediated changes seen in this mouse study are of negligible risk, if any, to humans, because such changes have not been reported in humans taking molindone as a therapeutic.

PS 2196o The Role of Receptor Occupancy Analysis during Preclinical Development of Biologics

S. Kirk, K. Troth, A. Head and W. Beck. *Covance Laboratories Ltd, Harrogate, United Kingdom.*

Pre-clinical safety assessment of biopharmaceuticals provides many challenges, including the potential for the production of anti-drug antibodies (ADA) when a human (or humanised) protein is administered to an animal system. ADA production may lead to loss of exposure and activity of the biotech product resulting in limited toxicology information. In this study, we highlight the critical role of reliable receptor occupancy (RO) data in confirming exposure to a biotech derived protein (Bio-A) specific for receptors on a sub-set of lymphocytes, during a 26 week regulatory study in the mouse.
Prior to starting the 26 week study an RO method was validated to determine the proportion of bound and free target receptors on lymphocytes in the presence / absence of Bio-A. Both evaluations established good reproducibility (CV <27%) whilst requiring minimal quantities of blood. At Week 13 of the 26 week mouse study, ADA production and a drop in systemic levels of Bio-A suggested loss of exposure, especially in the low dose group. RO analysis on a sub-set of animals indicated that the majority of low dose mice had reduced levels of bound Bio-A and high levels of free receptors. However, in the remaining mice, Bio-A was still bound to the surface of lymphocytes. Based on the possibility that exposure still persisted in some animals it was decided that additional blood be taken from the toxicology animals at necropsy to evaluate the level of free receptors in each. This additional analysis was possible in the mouse as the RO validation had established a method where this could be evaluated in blood samples of 50µL. Evaluation of free receptors in the low dose group, contradicted the ADA and TK data, suggesting that the majority of mice were still exposed and rendering these animals valid for assessment of toxicity over the 26 week period.
In conclusion, establishment of a robust method to measure RO provided vital information regarding exposure levels that allowed a proportion of the low dose animals to be used to for histopathology evaluation, when the TK and ADA data suggested otherwise.

PS 2196p De-Risking Potential Infection Risk with Anti-CSF-1

K. S. Rajapaksa, W. Lin, E. Suto, Z. Huang, J. Eastham-Anderson, P. Katavolos, C. D. Austin, D. M. Danilenko, J. DeVoss, W. Lee, F. Martin and A. A. Zarrin. *Genentech, South San Francisco, CA.*

Colony-stimulating factor-1 (CSF-1) promotes differentiation, proliferation and migration of monocytes/macrophages, which are involved in innate and adaptive immunity. Macrophages are implicated in variety of inflammatory diseases; therefore, anti-CSF-1 therapeutic antibodies can be beneficial in several indications such as rheumatoid arthritis (RA). A safety concern when targeting this pathway is increased infection risk due to the role of monocytes/macrophages in immunity; therefore, 2 mouse studies were conducted to evaluate the anti-CSF-1 safety profile and infection risk.
The overall safety profile of anti-CSF-1 was evaluated in an 84d repeat dose study, where administration of anti-CSF-1 (twice weekly; i.p.; 200ug/mouse) resulted in decreased macrophages in spleen, lung, kidney and liver. There was a minimal to mild increase in ALT, AST and CK, consistent with the role of liver macrophages in clearing serum enzymes. No anti-CSF-1-related anatomic pathology findings were observed. Collectively, these findings are consistent with pharmacology of anti-CSF-1.
Infection risk with anti-CSF-1 was interrogated by evaluating the response to *Listeria monocytogenes* challenge in a head-to-head comparison to a TNFa inhibitor (TNFRII-IgG), the biologics standard of care for RA. A mouse *Listeria* infectious challenge model was chosen because the primary response to *Listeria* is driven by macrophages and RA patients treated with TNFa inhibitors are at an increased risk of infections with *Listeria*. While anti-CSF-1 treatment (twice weekly; i.p.; 200ug/mouse; up to 42d) did result in increased mortality compared to isotype antibody-treated controls, the onset and rate of mortality was significantly later and lower than that observed with TNFRII-IgG (twice weekly; i.p.; 150ug/mouse; up to 14d). These data suggest that anti-CSF-1 maybe associated with less risk of infection compared to TNFa inhibitors.

PS 2196q A Method Validation for the Screening and Confirmation of Neutralizing Antibodies (NAb) against PEG-IL-29 in HCV Human Sera Using a Cell-Based Assay with a Bioluminescent Detection Platform

J. Hantash. *Biotechnology Services, Tandem Labs Inc., West Trenton, NJ.* Sponsor: Z. Radi.

A cell based assay for the determination of PEG-IL-29 neutralizing antibody in human HCV positive sera was developed and validated in support of bioequivalence studies. The assay utilized a cell line that was engineered to over-express the IL-29 receptor containing a Luciferase reporter construct with ISRE and STAT binding elements directly upstream of a luciferase reporter gene.
Positive Quality Control and test HCV positive serum samples containing Anti-PEG-IL-29 antibodies (antibody/PEG-IL-29) mix was added to an overnight seeded cell culture plate and incubated. ONE-Glo solution was added and the signal was measured. Samples were determined to be "positive" or "negative" for neutralizing activity based on a comparison of the mean response of the positive control to the mean response of the negative control. Samples are considered positive if the % Neutralization value is greater than or equal to the assay cut point.
25 HCV positive Human Sera lots were tested to determine the neutralization cut point of the assay, which was found to be ≥26%. For quality control samples tested at two concentrations (1000 and 500 ng/mL), precision (%CV) ranged from 0.1 to 25.7% and 0.0 to 23.7%; respectively. The assay sensitivity was 250 ng/mL with a drug tolerance ≥2ng/mL. For selectivity, 10 out of the 10 HCV positive Human Sera lots tested showed neutralization (%) <26%. Positive control samples showed bench top stability for 20 hours (neutralization ranged from 34 to 38%) and freeze thaw stability for up to 8 cycles (neutralization ranged from 44 to 65%). Long term stability at -80°C was proven for up to 182 days (neutralization ranged from 30 to 57%). The validated Nab cell based assay in HCV positive Human Sera successfully met all standard assay-validation parameters and was suitable for use in bioequivalence studies.

PS 2196r Assessing Safety and Efficacy of Anti-CD20 Biologics in Human Immune System Mice

K. E. Howard, X. Li, J. Austin and C. Gonzalez. *CDER/OTS/OCP/DARS, US FDA, Silver Spring, MD.* Sponsor: J. Weaver.

Testing of biological drug products for safety and efficacy in animal models has been difficult to assess because common models such as rodents, canines and non-human primates do not necessarily share common biological receptors with humans. A new animal model, the human immune system mouse, has recently emerged in widespread use for infectious disease pathogenesis and vaccine testing research. We utilize human immune system mice that have human thymus and liver implanted underneath the kidney capsule and are engrafted with human hematopoietic stem cells. To test the ability of this model assess the efficacy and safety of biological drug products in vivo, we tested the anti-CD20 product rituximab.
Mice were pretreated with anti-histamines and anti-inflammatory products, as recommended per package label. A single treatment was administered at three different doses; 2 mg/kg (low), 8 mg/kg (middle), and 15 mg/kg (high). The drug was diluted in saline to concentrations of 0.2 – 0.75 mg/ml prior to i.v. administration to reduce the likelihood of immediate hypersensitivity reaction. Samples for flow cytometric assessment and serum were taken immediately prior to administration and then at 1, 2, 5, 8, 11, 16, and 21 days post-treatment. Mice were euthanized at days 8, 11, 16 and 21 post-administration to determine the completeness and durability of B-cell depletion in blood, spleen and bone marrow. Results showed that human immune system mice experienced full B-cell depletion in a dose-dependent manner, with the low dose group substantially reconstituted at day 8 and the high dose group still depleted at day 21 post-administration. Adverse effects observed included off-target depletion of T-cells that was donor dependent, which has also been shown to occur in some human patients. These results demonstrate that human immune system mice can respond biologically in a dose-dependent manner to anti-CD20 drug products and recapitulate the pharmacodynamics and adverse events observed in humans.

PS 2196s Recombinant H7N9-Avian Influenza Vaccine: A 57-Day Repeat-Dose Intramuscular Toxicity Study with and without Saponin-Based Adjuvant Matrix M in the New Zealand White Rabbit

M. M. Vegarra[1], C. S. Godin[1] and D. Flyer[2]. [1]*Smithers Avanza, Gaithersburg, MD and* [2]*Novavax, Inc, Rockville, MD.*

A recombinant virus-like particle (VLP) vaccine against avian influenza A (H7N9) is being developed to protect people from a pandemic threat. The purpose of the study was to evaluate the potential toxicity of the H7N9 avian Influenza VLP Vaccine when administered by IM injection on Study Days 1, 15, and 29 to New Zealand White rabbits, with or without the addition of the saponin-based adjuvant Matrix M. Matrix M was also evaluated without the influenza antigen. This study also investigated the reversibility of any treatment-related toxicity during a 28-day no-treatment recovery period. Fifty rabbits/sex were randomly assigned to 5 groups (10 animals/sex). The animals were treated via IM injection on SD 1, 15, 29, and subjected to a full gross necropsy on SD 31 (terminal) or 57 (recovery). Evaluations included mortality, physical examinations, cage-side, and Draize observations, body weights, body weight changes, food consumption, body temperatures, ocular examination, clinical pathology (clinical chemistry, hematology, coagulation, and C Reactive Protein [CRP]), gross pathology, absolute and relative organ weights, histopathology, and immunology analysis. Treatment with H7N9 VLP Vaccine had no effect on mortality, physical examinations, cage-side observations, body weights, body weight changes, food consumption, ocular findings or organ weights in either sex. The body temperatures were similar to the control group on SD 29 and 30 at 6 and 24 hours after the third dose, respectively. There were no clinical pathology effects attributable to the test articles. CRP values showed high variability and were sporadically increased at the sample points two days after injections. The increase was transient, levels returned toward baseline, and there were no significant differences in placebo and actively-treated groups at recovery. Histopathology findings were non-adverse intended pharmacologic effects of immune stimulation. Seroconversion was observed in 100% of animals which received the vaccine.

PS 2196t Characterization of Ototoxic Synergism between Kanamycin and Amitriptyline in Guinea Pigs

M. M. Abernathy, R. Tapp, D. Gauvin and T. Baird. *Neurobehavioral Sciences, MPI Research, Mattawan, MI.* Sponsor: J. Heward.

Amitriptyline has been demonstrated an efficacious therapy for preventing noise induced hearing loss in preclinical models. It has been shown that aminoglycoside antibiotics engage similar mechanisms of auditory hair cell damage as those involved in noise-induced lesions. A study was conducted to assess the efficacy of amitriptyline in protecting auditory hair cells from kanamycin-induced damage. Male guinea pigs (n=46) were intraperitoneally administered sterile water, or either of two doses (5 or 15 mg/kg) of amitriptyline. One hour post-dose, saline or kanamycin was administered (400 mg, s.c.). This dosing regimen was conducted once a day for 9 days. Auditory brainstem response (ABR) evaluations were conducted pre-test and Day 9, in the left ear of each animal at 32 kHz. After the final ABR collection, the left temporal bone was collected, auditory hair cell hair cell analysis conducted, and cytocochleograms created for those animals in which hearing deficits were observed. The results of the ABR evaluations showed that 400 mg/kg kanamycin produced an average threshold increase of 20 dB. Surprisingly, the 15 mg/kg dose of amitriptyline caused moderate increases in the auditory threshold in 25% of the animals. When the 15 mg/kg dose of amitriptyline was administered in combination with 400 mg/kg kanamycin, the auditory insult was exacerbated, inducing an average threshold increase of 70 dB. The 5 mg/kg dose of amitriptyline did not afford any protection when administered with kanamycin, as auditory thresholds were similarly increased by an average of 20 dB. The cytocochleogram data confirmed that the kanamycin lesions, including amitriptyline co-administration, were a direct result of cytotoxicity. The cytocochleograms from the affected amitriptyline treated animals revealed no significant hair cell loss, which may indicate pathology within the auditory nerves. This study revealed the first instance of amitriptyline-induced ototoxicity in guinea pigs, and advises that amitriptyline may not be a suitable preventative therapy for kanamycin-induced hearing loss.

PS 2196u Sildenafil-Induced Changes in Auditory Brainstem Response in Mice

Y. Kuroiwa[1], T. Ogawa[1], Y. Nakayama[1], K. Maeda[1], Y. Tuda[2], A. Nakamura[1], T. Enami[1], S. Okazaki[1] and H. Kuse[2]. [1]*BoZo Research Center Inc., Gotemba, Shizuoka, Japan and* [2]*BoZo Research Center Inc., Kannami, Shizuoka, Japan.* Sponsor: W. Ruddock.

Auditory brainstem response (ABR) recording in animals is a useful method to investigate ototoxicity of chemicals. Several animals, including rabbits, guinea pigs and rats, are used to investigate ototoxicity. The phosphodiesterase 5 inhibitor sildenafil was reported to induce sudden hearing loss in humans. We used mice in this study to induce hearing loss by small amounts of chemicals and investigated the ototoxicity of sildenafil by ABR recording. B6C3F1 male and female mice were administered 20 mg/kg/day of sildenafil for 2 weeks and then 40 mg/kg/day for an additional 2 weeks. ABR was recorded from 6 male and 6 female mice under isoflurane anesthesia every week during the administration period. Acoustic clicks were delivered through an inner-type earphone, 1000 responses to repetitive stimuli at a rate of 20 Hz were averaged and analyzed for 10 msec. The stimulus intensity was delivered between 20 and 90 dB sound pressure level (SPL). After 7 days of sildenafil administration, a slight increase in amplitude of wave I or II was observed sporadically. This slight change was considered to be a precursory phenomenon of subsequent hearing changes. Then, after 21 days of sildenafil administration (7 days after increasing to 40 mg/kg), the ABR threshold shift rose up to 60 dB SPL and decreased in amplitude, suggesting hearing dysfunction by sildenafil treatment. After 28 days of sildenafil administration, the ABR threshold returned to a normal level; however, the amplitude of waves I and II with 90 dB SPL was rather increased abnormally and the wave pattern was deformed. At this dose level, we could not reveal the effects of sildenafil on the latency of ABR or histopathological changes in the cochlea. These results suggest that sildenafil affects auditory function in mice. Further dose-finding trials would be required.

PS 2196v When a Convulsion Is Not a Seizure: Behavior and EEG Studies with SCH A in the Beagle Dog

M. Kallman[1], M. Sgro[1], C. Markgraf[2] and L. Ballering[2]. [1]*Covance Laboratories, Greenfield, IN and* [2]*Merck Research Laboratories, Lafayette, NJ.*

Dose escalation studies in the beagle dog with SCH A, a CNS-targeted compound, elicited convulsions in a male and a female dog at doses of 600 mg and 1000 mg, respectively.
To evaluate brain activity preceding and accompanying convulsions and to correlate findings with plasma concentrations, a follow up study was conducted in EEG telemeterized beagle dogs. Male Beagle dogs (n=4) were implanted with DSI 3-biopotential leads monitoring EEG from right and left cortices and EMG. In a dose-escalation design, dogs were administered single oral doses of 300, 600, 1000 and 2000 mg/kg SCH A. EEG was recorded for 12 h and behavior was observed for approximately 10 hours following each dose. Following 1 day wash-out, the same dose was administered again for toxicokinetic analysis. Blood samples were taken at 1, 2, 4, 8 and 24 h post-dose.

Administration of SCH A produced increased salivation and emesis at doses equal to or greater than 300 mg/kg and mild to severe tremor at doses equal to or greater than 600 mg/kg. Tremor occurred 30-60 minutes post-dose and increased in magnitude with increasing dose. Two animals appeared to be more sensitive to these effects, showing more severe findings and findings at lower doses than the other two animals. EEG analysis showed no evidence of seizure-related waveforms in any animal. TK analysis showed that mean AUC values increased with increasing dose, and mean Cmax values increased from 300-1000 mg/kg, with no further increase at 2000 mg/kg. Individual inter-animal variability made difficult the determination of a PK-PD relationship. It did not appear that there was a strong correlation between plasma concentration and clinical signs following oral administration of SCH A. Oral administration of SCH A was not accompanied by adverse changes in brain activity, as assessed by EEG.

PS 2196w The Effect of Anesthetic on QT Interval Measurements in Guinea Pigs

L. A. Neves, H. Wang, J. Huang, P. B. Senese and M. R. Gralinski. *CorDynamics, Inc., Chicago, IL.*

Anesthetized guinea pig is a widely used model for early screening of drug-candidate effects on cardiovascular function. This species is gaining traction for use in conscious screening telemetry studies. For unconscious work, the majority of published studies use sodium pentobarbital (NaP) as the anesthetic of choice. However, NaP is an antagonist of the inward rectifying cardiac potassium channel IKs. Since the IKs is a component of the guinea pig cardiac repolarization sequence, this species can be exquisitely sensitive to IKs blockade. In this study we investigated the baseline vulnerability of the anesthetized guinea pig for safety pharmacology screening of drugs with potential to prolong the QT interval. Male guinea pigs (400-550g) were anesthetized with ketamine/xylazine (87/5 mg/kg, KET) or NaP (15-30 mg/kg) and surgically instrumented with a Millar catheter to measure arterial pressure. Electrocardiograms were recorded and PR interval, QRS duration, QT/QTc interval and arrhythmogenesis were monitored. Monitored parameters were compared with measurements obtained previously in conscious guinea pigs (CON). NaP anesthetized guinea pigs exhibited baseline QTcB intervals (342±3 ms, $p<0.05$) that were significantly increased compared to CON cohort (256±6 ms). QTcB intervals in the KET group (307±7 ms, $p<0.05$) were also increased as compared to CON group, but the changes were significantly less robust. Lower HR was observed in the KET group (215±9 bpm, $p<0.05$) as compared to CON (258±13 bpm) and NaP (250±6 bpm) groups. QRS duration was increased in the KET (45±0.8 ms) and NaP (44±0.3 ms) groups as compared to CON guinea pigs (29±1.3 bpm, $p<0.05$). No change in mean arterial pressure was observed between the groups. In summary, the choice of anesthetic appears to influence the QT interval in anesthetized guinea pigs compared to conscious animals. It is possible that anesthetics with additional inherent IKs blockade may overly sensitize the animal to agents that prolong the electrocardiographic QT interval. Consideration should be taken when selecting anesthetics for this model.

PS 2196x IG-001 Suppressed Hypersensitivity Reactions versus Taxol® in Beagle Dogs

O. J. D'Cruz, J. Hsu and V. Trieu. *Sorrento Therapeutics, Irvine, CA.*

Study Purpose: Hypersensitivity reactions (HRs) are known adverse effects of Taxol® chemotherapy. Taxol® is formulated in Cremophor EL (Cr-EL) which triggers HRs requiring premedication. Abraxane®, a Cr-EL-free albumin-bound formulation (nab-Pac), has low incidence of HRs. IG-001 is a novel Cr-EL-free, non-biologic nanoparticle formulation being developed as an alternative to nab-Pac. We report the suppressed HRs for IG-001 vs Taxol® in beagle dogs as the most sensitive species.
Methods: Sixty-five beagle dogs (33 M and 32 F) were evaluated in 3 GLP studies. In a dose-escalation study, 9 dogs received a 30 min intravenous (iv) infusion of IG-001 (1.1-4.5 mg/kg) or Taxol®) (0.1-1.1 mg/kg). In the single (n = 24) or repeated 5-cycle (n = 32) dosing studies, dogs received IG-001 (1.5-4.5 mg/kg for 3 hr) or Taxol®) (0.1-2.5 mg/kg for 30 min), the latter group with antihistamine premedication. Measurements included clinical observations, body weight, food consumption, hematology, blood chemistry, and histopathology.
Results: Minimal clinical signs were noted at IG-001 doses of 1.1 or 2.2 mg/kg, but 4.5 mg/kg was associated with moribundity. Taxol® produced HRs at 0.1 mg/kg and above, necessitating premedication and shortening of infusion time from 3 hr to 30 min. The MTD was >2.2 mg/kg for IG-001 and 0.2 mg/kg for Taxol®. HRs to IG-001 was limited to only 2 of 32 (6.25%) dogs from the dose-escalation study. The HRs occurred after 3 or 4 doses within 3 or 5 weeks. No HR was noted with the IG-001 vehicle or those treated with IG-001 in the single- and repeated-dose studies. Excluding the severe HRs observed in the Taxol® group, body weight, food consumption, clinical signs, and hematology responses were comparable between IG-001 and Taxol®.
Conclusions: Taxol® infusion in the canine model resulted in severe HRs requiring antihistamine premedication and a reduction in infusion time. IG-001 was better-tolerated without premedication at substantially higher doses and with a low potential to produce HRs. IG-001 could potentially be a safe and effective alternative to nab-Pac.

PS 2196y Repeat-Dose Rabbit Vaginal Tolerance/Toxicity Study of Diindolylmethane Cream for Topical Treatment of Cervical Intraepithelial Neoplasia

T. L. Horn[1], M. Muzzio[1], C. J. Detrisac[2], M. A. Zeligs[3], D. L. Boring[4] and D. L. McCormick[1]. *[1]IIT Research Institute, Chicago, IL, [2]Pathology Associates, Chicago, IL, [3]BioResponse Nutrients, LLC, Boulder, CO and [4]National Cancer Institute, Bethesda, MD.*

Cervical Intraepithelial Neoplasia (CIN) is a premalignant condition characterized by dysplastic changes in the cervix. Because it can be identified by screening and may progress to invasive malignancy, CIN is an attractive target for cancer prevention. Indole-3-carbinol and its condensation product, diindolylmethane (DIM), have chemopreventive activity in several carcinogenesis models. As a result of its superior stability, DIM is being evaluated in clinical trials for cancer prevention in several sites, including the cervix. A preclinical study was performed to characterize the local and systemic effects of intravaginal administration of DIM (DIM Vaginal Cream, BioResponse LLC, Boulder, CO [BR-DIM-VC]). Groups of 5 NZW rabbits received intravaginal instillation of the maximum feasible volume (1.0 ml) of BR-DIM-VC (0% [placebo], 2%, 4%, or 6%) on alternate days for two weeks. Exposure to BR-DIM-VC induced no mortality and had no effect on body weight. The results of clinical and physical observations, clinical chemistry, hematology, and coagulation assays were comparable in all groups. Vaginal pH was unchanged by exposure to BR-DIM-VC. Vaginal irritation scoring demonstrated dose-related vaginal edema and erythema in rabbits treated with BR-DIM-VC. At 2%, 4/5 rabbits were normal; 1 rabbit demonstrated very slight edema (no erythema). At 4%, 2/5 rabbits were normal; 3 rabbits demonstrated very slight edema with barely perceptible erythema. At 6%, 1/5 rabbits was normal, 2 rabbits demonstrated very slight edema with very slight erythema, and 2 rabbits demonstrated slight edema with well-defined erythema. No vaginal edema or erythema was seen in placebo-treated rabbits. Repeat-dose intravaginal administration of BR-DIM-VC on alternate days for two weeks induced no systemic toxicity in rabbits. BR-DIM-VC did induce very slight to slight vaginal irritation in a dose-related fashion. (HHSN261201200025I)

PS 2196z A Retrospective Analysis of the Effect of Housing Conditions on Body Weight, Food Consumption and Survival in Rat Carcinogenic Rat Studies

D. Zhao[1], C. N. Papagiannis[2], D. W. Poage[2], R. L. Yeager[1], D. R. Davila[1], J. Hiner[2] and L. Shu[3]. *[1]Preclinical Safety, AbbVie Inc, North Chicago, IL, [2]MPI Research, Mattwan, MI and [3]Statistics, AbbVie Inc, North Chicago, IL.*

Rodent toxicology studies have historically been performed in wire-bottom cages. However, both the National Research Council (NRC) and Association for the Assessment and Accreditation of Laboratory Animal Care (AALAC) International, recommend housing rats in solid-bottom cages with bedding to prevent development of foot lesions and/or stress responses. A retrospective analysis of Sprague-Dawley rat carcinogenicity study data (n=25 control groups) compared the effects of individual vs. pair housing and wire-bottom vs. solid-bottom caging on body weight, food consumption and survival. Survival was analyzed by the Cox proportional hazards model; body weight was analyzed by the Gompertz non-linear mixed model and food consumption was analyzed by the mixed effects ANOVA Model. For rats housed individually in solid-bottom cages, average body weights were higher compared to rats housed individually in wire-bottom cages. The body weight differences become significant around Week 25 in males and Week 45 in females, and continued until the end of study. At Week 104, the average difference in males was about 50 g or 5% and in females was about 55 g or 11%. The differences in average body weight did not correspond with a significant difference in average food consumption or in survival rates. For pair-housed rats in solid-bottom cages, average food consumption was lower (~7% in males; ~8% in females) than rats housed individually. This difference in average food consumption corresponded with a slightly lower average body weight (Week 104, ~3% in males; ~9% in females) and a marginal improvement in survival (in females only, Week 104, ~15%). In conclusion, this analysis demonstrates that housing conditions (individual vs. paired and wire-bottom vs. solid-bottom) may affect body weight, food consumption, and survival on two-year rat carcinogenicity studies.

PS 2196aa Global Cross-Company Data-Sharing on the Use of Recovery Animals for Human Safety Assessment

F. Sewell and K. Chapman. *National Centre for the Replacement, Refinement & Reduction of Animals in Research (NC3Rs), London, United Kingdom.* Sponsor: L. Burns Naas.

An international expert group which includes 32 organisations (pharmaceutical and biotechnology companies, contract research organisations and regulatory bodies) has shared data on the use of recovery animals in the assessment of pharmaceutical safety for early development. The group has used this data as an evidence-base to make recommendations on the inclusion of recovery animals in toxicology studies to best assess human safety, while reducing animal use. The initiative is led by the NC3Rs in collaboration with the Medicines and Healthcare products Regulatory Agency (MHRA).
Recovery animals are used in pharmaceutical development to provide information on the potential for a toxic effect observed in animals to translate into long term human risk. They are included on toxicology studies to assess whether effects observed during dosing persist or reverse once treatment ends. It is a regulatory requirement to assess recovery at some point during drug development.
The group devised a questionnaire to collect information on the use of recovery animals in general regulatory toxicology studies to support first-in-human clinical studies. Questions focused on study design (e.g. species, recovery duration and the number of animals used), the rationale behind inclusion or exclusion (case-specific vs. default inclusion), and the impact this had on internal and regulatory decisions. Data on 137 compounds (53 biologicals and 78 small molecules) from 259 studies was provided by 22 companies and showed that there was wide variation in where, when and why recovery animals were included. We found that recovery animals were included on all studies for 85% biologicals and 65% small molecules. Recovery animals were included on more than one dose group for 70% biologicals and 25% small molecules. The number of recovery animals used per compound ranged from 0 to over 100. An analysis of individual study and programme design shows that there are opportunities to reduce the use of recovery animals in certain circumstances which would not impact drug development.

PS 2196bb Comparison of the Expression of ALP Isoenzymes in Serum among Five Animal Species Used in Toxicity Studies

K. Goto[1], Y. Nishihara[1], J. Kobayashi[1], A. Okamuro[2], H. Mizuguchi[2], T. Narita[2], R. Haneda[2] and K. Hatayama[1]. [1]*BoZo Research Center Inc., Gotemba, Shizuoka, Japan and* [2]*Bozo Research Center Inc., Kannami, Shizuoka, Japan.* Sponsor: W. Ruddock.

Alkaline phosphatase (ALP, EC 3.1.3.1.) in serum is measured frequently in toxicity studies. ALPs exist widely in the whole body and are highly expressed in the liver, bone, small intestines, kidney and placenta in humans. ALP in serum is the sum of that transferred into the blood stream from organs and tissues. ALP isoenzymes in serum are important items for the evaluation of organ toxicity, but they have not yet been well-examined in experimental animals. In this study, a human serum ALP isoenzyme analysis kit (AlkPhor System, Jokoh Co., Ltd., Tokyo, Japan) for polyacrylamide gel disk electrophoresis was applied to mice, rats, guinea pigs, rabbits and dogs, and the expression of ALP isoenzymes in serum was compared among them. As a result, bone ALP was commonly observed in all animal species examined and it decreased with age. Liver ALP was also common in all animal species. It had less activity in untreated animals, but it remarkably increased in the cholestasis model. Intestinal ALP and high molecular weight intestinal ALP were detected only in rats and decreased by fasting. Intestinal-type ALP was specific to guinea pigs and hardly observed in untreated animals. High molecular weight ALP was specific to rabbits and was low in untreated animals. Atypical ALP was specific to dogs and was identified as bone-type ALP corresponding to the human variant bone ALP isoenzyme. Corticosteroid-induced ALP was also specific to dogs, increased with age, and showed individual differences. As stated above, a total of eight ALP isoenzymes were identified in serum among five animal species. Bone and liver ALPs were common to 5 animal species while the others were found in specific animal species with characteristic nature. The present results strongly suggest that analysis of ALP isoenzymes in serum of animal species used in toxicity studies is important to evaluate toxicities.

PS 2197 Aryl Hydrocarbon Receptor Activation Impairs Insulin Signaling through Degrading IRS-1

C. Wang[1], C. Xu[1], S. Krager[2], C. Jaeger[1], K. Bottum[2] and S. Tischkau[1]. [1]*Pharmacology, SIU School of Medicine, Springfield, IL and* [2]*Internal Medicine, SIU School of Medicine, Springfield, IL.*

Epidemiological studies have shown that exposure to persistent organic pollutants (POPs) is associated with increased risk of type 2 diabetes. Most of POPs function through activation of the aryl hydrocarbon receptor (AhR), and our previous studies have shown that AhR knockout (AhRKO) mice exhibits enhanced insulin sensitivity. In this study, we explored the effects and mechanisms of AhR agonists on the insulin signaling pathway using wild-type (WT) and AhRKO mice, as well as hepatoma cells, Hepa-1c1c7 (c7). In c7 cells, AhR agonists 2,3,7,8-Tetrachlorodibenzo-p-dioxin (TCDD) and beta naphthoflavone (BNF) decreased insulin receptor substrate 1 (IRS-1) protein expression and inhibited AKT phosphorylation, but did not change IRS-1 mRNA, TNF-α or phospho-JNK levels. AhR knockdown with specific siRNA partially reversed the BNF or TCDD-mediated IRS-1 protein decrease. Furthermore, the proteasome inhibitor, MG132, partially restored AhR agonist-mediated IRS-1protein degradation. In addition, AhR activation by its agonists compromised the insulin signaling pathway and caused hyperglycemia in WT mice, but not in AhRKO mice. Taken together, these data indicate that AhR activation induced IRS-1 ubiquitin-dependent degradation leading to insulin resistance and hyperglycemia. Our findings provide an insight into the mechanisms underlying environmental contaminants-induced diabetes and identify AhR signaling as a novel therapeutic target.

PS 2198 Exposure to p, p'-Dichlorodiphenyldichloroethylene (DDE) Promotes Fasting Hyperglycemia in Male C57BL/6 Mice

G. E. Howell[1], J. Kilic[2], E. C. Meek[1] and J. E. Chambers[1]. [1]*Center for Environmental Health Sciences, Mississippi State University College of Veterinary Medicine, Mississippi State, MS and* [2]*Biological Sciences, Mississippi College, Clinton, MS.*

It is estimated that approximately 8.3% of the U.S. population have either diagnosed or undiagnosed diabetes mellitus. Out of these cases of diabetes mellitus, approximately 90-95% of these cases are type 2 diabetes mellitus (T2D). Although the exact cause of T2D remains an enigma, predisposing factors include age, weight, poor diet, and a sedentary lifestyle. Until recently the association between exposure to environmental contaminants and the occurrence of diabetes had been unexplored. However, based on epidemiological studies, we now know that elevated serum concentrations of persistent organic pollutants, especially organochlorine pesticides or their metabolites, are positively associated with increased prevalence of T2D and insulin resistance. Our current line of investigation is to determine if this association is causative or coincidental. In the present study, male C57BL/6 mice were exposed to DDE (2.0 mg/kg) or vehicle (corn oil; 1 ml/kg) for five days then fasting blood glucose, glucose tolerance, and insulin challenge tests were performed following a seven day resting period. Exposure to DDE significantly elevated fasting blood glucose levels compared to vehicle. Intraperitoneal glucose tolerance tests and phosphorylation of a key insulin signalling intermediate, Akt, in the liver and skeletal muscle following intraperitoneal insulin administration were comparable between vehicle and DDE treated animals. In summary, exposure to DDE does produce fasting hyperglycemia. However, this fasting hyperglycemia does not appear to be mediated by insulin resistance based on our glucose tolerance and insulin challenge testing. Thus, the current study reveals that exposure to DDE does alter systemic glucose metabolism and may be a contributing factor to the development of hyperglycemia associated with diabetes. (Supported by NIH grant# 7R15ES019742-03)

PS 2199 PCB126 Alters Adipogenesis and Induces Metabolic Disruption in a Human Adipocyte Model

G. S. Gadupudi[1, 3], F. Gourronc[2], A. J. Klingelhutz[2] and L. W. Robertson[1, 3]. [1]*Graduate Program in Human Toxicology, University of Iowa, Iowa City, IA,* [2]*Microbiology, University of Iowa, Iowa City, IA and* [3]*Occupational & Environmental Health, University of Iowa, Iowa City, IA.*

Polychlorinated biphenyls (PCBs) are persistent, organic, lipophilic pollutants that bio-accumulate, mainly in white adipose tissue. Adipocyte tissue plays key roles in energy/metabolic homeostasis and disruption of its function leads to disease. Epidemiological studies indicate that exposure to PCBs is associated with obesity, diabetes, hypertension, hepatic steatosis and dyslipidemia. PCB126 (3,3′,4,4′,5-pentachlorobiphenyl), a potent aryl hydrocarbon receptor (AhR) agonist, causes wasting disorder, dyslipidemia, and hepatic steatosis in animal models and insulin resistance and glucose intolerance in "in-vitro" animal cells. However,

the mechanism causing these effects and their relevance to human disease is not well understood. In this study, we have used unique immortal human preadipocytes that can be differentiated into adipocytes to evaluate the effects of PCBs on adipocyte biology. Exposure of the preadipocytes to PCB126 at concentrations of 0.1 - 10 μM caused a dose-dependent decrease in subsequent differentiation to adipocytes. Reduced differentiation was marked by significant decreases in accumulation of lipids, mRNA expression of adipocyte differentiation markers (PPARγ2, CEBPα, aP2 and adiponectin; $P < 0.05$) and genes in the insulin signaling pathway (IRS-1 and GLUT4). Strikingly, the decrease in adipocyte differentiation was more profound in preadipocytes exposed to PCB126 before differentiation compared to exposure during differentiation, the latter being the treatment regimen used in previously reported studies. These results indicate that PCB126 may maintain pre-adipocytes in an undifferentiated state, possibly leading to expansion and metabolic disruption that can initiate metabolic syndrome. These interesting observations warrant further research in order to understand the mechanism by which PCB126 causes inhibition of adipocyte differentiation and the roles of adipose tissue in PCB126 induced toxicity.

PS 2200 TCDD Treatment Enhances Hepatic Stellate Cell Activation during Experimental Liver Fibrosis

C. L. Lamb, W. A. Harvey and K. A. Mitchell. *Biological Sciences, Boise State University, Boise, ID.*

2,3,7,8-Tetrachlorodibenzo-*p*-dioxin (TCDD) and related chemicals are widespread environmental pollutants that elicit toxicity through the aryl hydrocarbon receptor. It was recently shown that exposure to TCDD enhances gross markers of liver damage during experimental liver fibrosis. Liver fibrosis is a wound healing response characterized by the deposition of excessive or abnormal extracellular matrix by myofibroblasts, namely hepatic stellate cells (HSCs). Previous studies in our laboratory revealed that TCDD treatment enhances activation of a human HSC line *in vitro*. The goal of the present study was to determine if TCDD increases HSC activation *in vivo* using two mouse models of liver fibrosis: bile duct ligation (BDL) and carbon tetrachloride (CCl_4) administration. For the BDL model system, C57Bl/6 mice were treated with TCDD (20 ug/kg) or peanut oil (vehicle) one day prior to surgery and euthanized 3 and 7 days later. For the CCl_4 model system, CCl_4 (5 ul/g) was administered twice a week for 6 weeks, and TCDD (20 ug/kg) or vehicle was given during the last 2 weeks. In BDL mice, TCDD treatment elicited a 3- to 6-fold increase in plasma alanine aminotransferase levels and caused marked expansion of periportal bile ducts. Immunofluorescence staining revealed that TCDD treatment increased expression of the HSC activation marker, alpha-smooth muscle actin (αSMA), in areas surrounding the bile ducts, which coincided with a three-fold increase in αSMA transcript levels in the whole liver. In the CCl_4 model, a 50% increase in liver-body weight ratio was observed in TCDD-treated mice compared to mice that received CCl_4 alone. TCDD treatment also elicited a 5-fold increase in hepatic αSMA transcript levels and enhanced collagen deposition, as revealed by increased Sirius red staining. These results indicate that TCDD treatment enhances HSC activation *in vivo*, which may contribute to the exacerbation of liver damage observed in TCDD-treated mice during experimental liver fibrosis.

PS 2201 Congener- and Species-Specific Differences in Relative Effect Potencies of Dioxin-Like Compounds between *In Vitro*-Exposed Human Peripheral Blood Lymphocytes and Mouse Splenic Cells

K. van Ede, K. Gaisch, M. Van den Berg and M. B. van Duursen. *Toxicology, IRAS, Utrecht University, Utrecht, Netherlands.*

Human risk assessment for dioxin-like compounds is typically based on the concentration measured in blood serum multiplied by their assigned toxic equivalency factor (TEF). Consequently, the actual value of the TEF is very important for accurate human risk assessment. In this study we investigated the effect potencies of 3 polychlorinated dibenzo-p-dioxins (PCDDs), 6 polychlorinated dibenzofurans (PCDFs) and 10 polychlorinated biphenyls (PCBs) relative to the reference congener 2,3,7,8-tetrachloro-dibenzo-p-dioxin (TCDD) in in vitro exposed primary human peripheral blood lymphocytes (PBLs) and mouse splenic cells. REPs were determined based on cytochrome P450 (CYP) *1A1*, *1B1* and the aryl hydrocarbon receptor repressor (*AhRR*) gene expression as well as CYP1A1 activity in human PBLs and *Cyp1a1* gene expression in mouse splenic cells. Results show that estimated median human REPs (n = 4-6 donors) for 1,2,3,4,6,7,8-heptachlorodibenzo-p-dioxin (1234678-HpCDD), 2,3,4,7,8,-pentachlorodibenzofuran (4-PeCDF), 1,2,3,4,7,8-hexachlorodibenzofuran (123478-HxCDF) and 1,2,3,4,7,8,9-heptachlorodibenzofuran (1234789-HpCDF) were with 0.1, 1.1, 1 and 0.09 respectively, significantly higher compared to those estimated for mouse with REPs of 0.05, 0.45, 0.09, 0.04, respectively. Opposite to these results, for 3,3',4,4',5-pentachlorobiphenyl (PCB 126), the estimated median human REP of 0.001 was 30-fold lower compared to the mouse REP of 0.03. Furthermore, human REPs for 1234678-HpCDD, 4-PeCDF, 123478-HxCDF, 1234789-HpCDF and PCB 126 were all outside the half log uncertainty range that is taken into account in the WHO-assigned TEFs, which are predominantly based on rodent studies. Together, these data show congener- and species-specific differences in REPs for some but not all dioxin-like congeners tested. Taking these congener- and species-specific REPs into account might improve human risk assessment.

PS 2202 Measurement of Protein Adducts Formed by Quinoid Metabolites of Polychlorinated Biphenyls (PCBs)

M. Li[1], L. W. Robertson[1, 2], P. A. Kapke[3] and G. Ludewig[1, 2]. [1]*Interdisciplinary Graduate Program in Human Toxicology, The University of Iowa, Iowa City, IA,* [2]*Department of Occupational and Environmental Health, The University of Iowa, Iowa City, IA and* [3]*Hybridoma Facility, Iowa State University, Ames, IA.*

Recently unexpected high levels of indoor PCB air concentrations were found in a large number of public elementary school classrooms. Most of the airborne PCBs are lower chlorinated congeners, from mono- to tetra-chlorinated PCBs. Lower chlorinated biphenyls can be metabolized to dihydroxy metabolites and further oxidized to quinoid metabolites both *in vitro* and *in vivo*. Quinoid metabolites of PCBs may form adducts at nucleophilic sites of proteins. Using radioactively labeled PCB3, we previously had observed hemoglobin adducts *in vivo* and covalently bound adducts with nuclear protein in livers. Our current objective is to establish the methodologies to quantitatively measure the adducts formed by PCB3 quinones, and to determine the distribution of protein adducts and the target proteins in cells treated with PCB3 and metabolites. Monoclonal antibodies against PCB3 quinone protein adducts may be employed to screen tissues for such adducts and to isolate adducted proteins. Two types of immunogens of PCB3 quinones were synthesized. PCB3 quinones were linked with keyhole limpet hemocyanin (KLH) or N418 through N -succinimidyl 3-(2-pyridyldithio)-propionate (SPDP). These antigens were injected repeatedly into mice. Four hybridoma lines with strong antibody production were chosen for further analysis of antibody specificity. In addition a method is being developed to quantify protein adduction by detaching bound quinone molecules from the proteins, isolating and quantifying them. To establish this method, PCB3-para-quinone was incubated with bovine serum albumin (BSA). Protein adducts were hydrolyzed under mild acidic conditions and extracted with hexane. Quinoid PCB residues in the extracts were determined by HPLC and confirmed by mass spectrometry. In future experiments GC/MS or LC/MS will be used to increase detection limits. (Supported by NIEHS Superfund Program P42 ES013661)

PS 2203 The Effects of Polycyclic Aromatic Hydrocarbons on Cellular Proliferation and Viability in Clone-9 Rat Liver Cells

S. J. Gray and E. D. Bruce. *Environmental Science, Baylor University, Waco, TX.*

Polycyclic aromatic hydrocarbons (PAHs) have been labeled contaminants of concern due to their carcinogenic potential, insufficient toxicological data, ubiquity, and inconsistencies in the composition of environmental mixtures. These factors interfere with understanding the toxic potential of this class of compounds, particularly in mixtures. Characterizing the non-carcinogenic toxicity of PAH compounds will contribute to toxicity assessments, understanding mixture interactions, and the management of human health risks. The objective of this study was to observe cellular responses from PAH concentrations. Clone-9 rat liver cells were grown in culture and tested to observe acute toxicity. In paired trials, cells were exposed to 15 parent and methylated PAHs for a period of 24 hours, with concentrations ranging from 0.25-20 parts per million (ppm). At 100% confluence, Janus green B staining was performed to observe cellular viability and proliferation. Many of the tested compounds displayed minimal toxicity, with no observed inhibition of proliferation or viability except at the highest concentration. Benzo[a]pyrene (BaP) displayed slight toxicity, with a decline in proliferation only at 20 ppm. There was no observed response from benzo[e]pyrene, benzo[k]fluoranthene, chrysene and phenanthrene. 3,6-dimethylphenanthrene, 7,12-dimethylbenz[a]anthracene and 9,10-dimethylanthracene displayed severe toxicity, impairing both proliferation and viability in a dose-responsive manner. The results for the parent compounds concur with available literature, which acknowledge carcinogenesis as the primary health concern rather than non-carcinogenic toxicity at environmentally-relevant concentrations. However, our findings suggest that methylated PAHs can be much more toxic than the parent compounds. Further research will compare these results to trials using binary PAH mixtures for the purpose of characterizing mixture effects.

PS 2204 Biotranformation of BDE-100 to Potentially Toxic Metabolites: Predominant Role of Human CYP2B6

M. S. Gross[1], D. M. Butryn[1], B. P. McGarrigle[2], D. S. Aga[1] and J. R. Olson[2]. [1]*Chemistry, University at Buffalo, Buffalo, NY and* [2]*Pharmacology and Toxicology, University at Buffalo, Buffalo, NY.*

Polybrominated diphenyl ethers (PBDEs) are additive flame-retardants used in numerous consumer products, resulting in their presence as widespread environmental contaminants. Recent studies have suggested that hydroxylated metabolites of PBDEs accumulate in human serum at levels similar to or greater than their parent PBDEs. Furthermore, it has been suggested that bioactivation through oxidative metabolism may add to the neurotoxic potential of PBDEs, however, insufficient data exists on the metabolism of PBDEs in humans. The purpose of this study was to characterize the in vitro metabolism of 2,2',4,4',6-pentabromodiphenyl ether (BDE-100), one of the most abundant PBDEs found in humans, by recombinant human cytochrome P450s (CYPs) and pooled human liver microsomes (HLMs). Recombinant CYPs (1A1, 1A2, 2A6, 3A4, 2B6, 2C8, 2C9, 2C19, 2D6, and 2E1) were individually incubated with 20 μM BDE-100 to monitor CYP-specific metabolism. For kinetic studies, recombinant CYP2B6 and HLMs were incubated with BDE-100 (0-60 μM). Analysis was completed by gas chromatography-mass spectrometry after derivatizing the hydroxylated-BDE metabolites (OH-BDEs) to their methylated derivatives using (trimethylsilyl) diazomethane. CYP2B6 was found to be the predominant CYP responsible for the formation of five mono-OH-BDE and two di-OH-BDE metabolites observed for BDE-100. One metabolite was identified as 6′-OH-BDE-100 through use of an authenticated standard. Utilizing fragmentation characteristics of methoxylated-BDEs (MeO-BDEs), it is hypothesized that two meta-OH-BDEs and one para-OH-BDE are among the remaining OH-BDE metabolites. Kinetic studies of BDE-100 metabolism by CYP2B6 and HLMs found Km values ranging from 3.7-5.9 μM and 4.7-5.6 μM, respectively, suggesting a high affinity towards the formation of OH-BDEs. Our results will ultimately better inform future studies investigating the potential of PBDEs and their metabolites to produce neurotoxic and other health effects. (NIEHS grant #ES021554)

PS 2205 Enantioselective Disposition of 2, 2', 3, 5', 6-Hexachlorobiphenyl (PCB 95) and Its Metabolites in Mouse Dams Dosed during Pregnancy

I. Kania-Korwel[1], C. Barnhart[2], K. M. Truong[2], P. Lein[2] and H. Lehmler[1]. [1]*Department of Occupational and Environmental Health, Univ of Iowa, Iowa City, IA and* [2]*School of Veterinary Medicine, University of California, Davis, CA.*

Racemic PCB 95 has been implicated as a developmental neurotoxicant. Although studies in adult female mice show a dose-dependent enantiomeric enrichment of PCB 95 and its hydroxylated metabolites (OH-PCBs), the effect of pregnancy on the enantioselective disposition of PCB 95 in laboratory animals has not been investigated. This is an important question since pregnancy-related changes in cytochrome P450 and enantioselective transfer of PCBs and OH-PCBs to the fetus and neonate could potentially modulate enantiomeric enrichment of PCB 95 and its metabolites. This study investigates dose-dependent differences in the enantioselective disposition of PCB 95 and OH-PCBs in female C57Bl/6 mice (8.5 weeks old) fed daily with racemic PCB95 (0.1, 1 or 6 mg/kg) or vehicle (peanut oil) in peanut butter, starting two weeks before mating and continuing throughout gestation and lactation. The levels and enantiomeric enrichment of PCB 95 and OH-PCBs were determined in adipose, blood, brain and liver. There was an increase in PCB 95 and OH-PCB levels with increasing dose in all tissues. Adipose had the highest level of the parent compound; blood had higher OH-PCBs levels than liver, and no metabolites were detected in brain or adipose. PCB 95 displayed clear enantiomeric enrichment in all tissues, with enantiomeric fractions (EF) ranging from 0.26 ± 0.01 (adipose) to 0.11 ± 0.02 (liver). These EF values are comparable to observed previously in PCB 95-treated adult mice. Our findings suggest that pregnancy-related changes in P450 enzyme levels and transfer to the offspring do not significantly change the enantiomeric enrichment of PCB 95 in adult female mice. Future studies are needed to better understand the toxicological implications of the enantiomeric enrichment of PCB 95 and its metabolites in mice and, ultimately, PCB exposed humans. [Supported by NIH grants, ES014901, ES017425 and ES007059]

PS 2206 Decreased Hepatocyte Nuclear Factor 4 alpha Activity As a Mechanism of Hepatomegaly Induced by PFOA and PFOS

S. McGreal[1], A. McCarthy[1], C. Walesky[1], M. Manley[1], C. S. Lau[2], B. Hagenbuch[1] and U. Apte[1]. [1]*Department of Pharmacology, Toxicology and Therapeutics, University of Kansas Medical Center, Kansas City, KS and* [2]*National Health and Environmental Effects Research Laboratory, U.S. Environmental Protection Agency, Research Triangle Park, NC.*

Perfluorooctanoate (PFOA) and Perfluoroctanesulfonate (PFOS) are synthetic perfluorinated carboxylic acids and are persistent organic pollutants with significant reproductive, hormonal and hepatic effects. PFOA and PFOS induce hepatomegaly in rodents, mechanisms of which are not completely clear. Recent in vitro studies indicate that PFOA and PFOS can bind and inhibit HNF4α activity in hepatic cell lines. Previous studies in our laboratory have shown that inhibition of HNF4α results in hepatomegaly. Based on these data, we investigated whether loss of HNF4α function is involved in hepatomegaly induced by PFOA and PFOS. Male CD1 mice treated with PFOA (3 mg/kg) and PFOS (10 mg/kg) once a day for seven days by oral gavage exhibited significant increase in liver to body weight ratio along with increased PCNA positive cells in the liver. PFOA and PFOS treatment decreased in HNF4α protein levels in the liver without affecting its mRNA levels. Western blot analysis showed increase in Cyclin D1 protein levels upon PFOA and PFOS treatment. Further, Real Time PCR analysis of several known and novel HNF4α target genes revealed that PFOA and PFOS exposure resulted in a significant increase in the expression of pro-mitogenic genes normally down regulated by HNF4α including cdkn3, egr1, cyp2c37, ccnd1, akr1b7, myc, and ugt2b17. Consistent with these observations, human hepatocyte treated for 48 hours with 100 μM PFOS showed an increase in mRNA of Ccnd1, Osgin1, Cdkn3, Ces3, genes that are negative targets of HNF4α and a decrease in Apoa2, Apob, F12, genes which are positive targets of HNF4α. Taken together, these data indicate that PFOA and PFOS-induced decrease HNF4α protein and activity, may be involved in hepatomegaly induced by these chemicals.

PS 2207 Low-Dose Perfluorooctanesulfonic Acid (PFOS) Induces Hepatic Lipid Accumulation and Dampens Caloric Restriction-Induced Lipid Loss in Mice

D. Salter, J. Xu, W. Wei, L. Armstrong and A. L. Slitt. *Biomedical and Pharmaceutical Sciences, University of Rhode Island, Kingston, RI.*

A combination of caloric restriction (CR), dietary modification, and exercise is the recommended therapy to reverse nonalcoholic fatty liver disease. The ability to mount an effective response to caloric restriction required to effectively shift hepatic metabolism to fatty acid oxidation depends upon induction of Sirtuins, AMP-activated kinase, and Peroxisome proliferator-activated receptor-γ coactivator 1 α (PGC-1α). PFOS, a fluorosurfactant previously used as a stain repellent and anti-stick material, is persistent in the environment and considered an "emerging contaminant" by the EPA. PFOS (1-10 mg PFOS/kg/day) induced hepatic lipid accumulation associated with altered lipid metabolism gene and protein expression in mice. We hypothesized that PFOS interferes with the beneficial effects of CR on hepatic lipid utilization and glucose homeostasis. Adult male C57BL/6 mice were fed ad libitum or 25% reduced calorie diet concomitant with 100 μg PFOS/kg/day for 6 weeks. PFOS significantly increased percent body weight after 4 weeks of administration, but did not significantly alter CR-induced percent weight loss over 6 weeks. Further studies indicated that PFOS (50 nm, 1, 5, 10, and 50 uM) increased adipogenesis in 3T3-L1 cells through induction CEBPs and PPARγ. PFOS also increased hepatic triglyceride accumulation and lipid loss after CR was lower in PFOS treated mice but not associated with significant changes in lipogenic gene mRNA expression. We also evaluated PFOS effects on glucose tolerance and found that it interfered with CR-induced improvement of glucose tolerance. This was further associated with suppression of hepatic Glut-2 and IRS-1 mRNA expression and PFOS stimulation of glucose production in isolated hepatocytes. Overall, a relatively low sub-chronic administration of PFOS had disruptive effects for lipid and glucose homeostasis under ad libitum and CR conditions.

PS 2208 Bile Salt Transporters Are Involved in the Disposition of Perfluoroalkyl Sulfonates in Rats and Humans

W. Zhao[1], J. Zitzow[2], D. J. Ehresman[2], S. Chang[2], J. L. Butenhoff[2] and B. Hagenbuch[1]. [1]*Pharmacology, Toxicology and Therapeutics, The University of Kansas Medical Center, Kansas City, KS and* [2]*Medical Department, 3M Center, St. Paul, MN.*

Perfluoroalkyl sulfonates (PFSAs) are persistent environmental contaminants present in human serum. Pharmacokinetic studies in animal models suggest that the long half-lives of certain PFSAs such as perfluorohexanesulfonate (PFHxS) and

perfluorooctanesulfonate (PFOS) are in part, due to strong hepatic accumulation and slow renal elimination. Studies in rats have indicated that PFOS undergoes enterohepatic circulation and in humans, cholestyramine treatment appeared to enhance its fecal excretion. Given that the sodium dependent bile acid uptake transporter Na^+/taurocholate cotransporting polypeptide (NTCP) expressed at the basolateral membrane of hepatocytes, the apical sodium dependent bile acid transporter (ASBT) mainly expressed at the apical membrane of enterocytes and the bile salt efflux pump (BSEP) expressed at the apical membrane of hepatocytes are essential for the enterohepatic circulation of bile acids, we tested whether PFSAs are substrates of these transporters in rats and humans. We used CHO Flp-In cells stably expressing human NTCP and HEK293 cells transiently expressing rat NTCP, as well as rat and human ASBT to measure the uptake of perfluorobutanesulfonate (PFBS), PFHxS, and PFOS in the presence or absence of sodium. In addition, Sf9 vesicles expressing human BSEP were used to test whether PFBS, PFHxS or PFOS would inhibit taurocholate transport by human BSEP. The results demonstrate that both rat and human NTCP can transport PFBS, PFHxS and PFOS. However, human ASBT only transports PFOS while rat ASBT transports none of the PFSAs. Transport of taurocholate by human BSEP was inhibited by both PFHxS and PFOS. We further characterized transport by performing time and concentration dependent uptake studies. In conclusion, these results suggest that the long half-live and the hepatic accumulation of PFOS in humans are, at least in part, due to transport by NTCP, ASBT and BSEP.

PS 2209 Evaluation of 6-Week Dietary Exposure to 100 ppm Perfluorooctane Sulfonate (PFOS) and Normal Choline or High Choline in Sprague-Dawley Rats

B. D. Bagley, S. Chang, D. J. Ehresman and J. L. Butenhoff. *3M Company, St. Paul, MN.*

Perfluorooctane sulfonate (PFOS) is a bioaccumulative and environmentally persistent chemical that has been detected in the serum of occupationally exposed workers as well as the general population. In toxicology studies, PFOS administration (at doses several orders of magnitude greater than the general population exposure) has produced hepatocellular hypertrophy, hepatocellular vacuolation, increased liver triglycerides, and decreased serum cholesterol. Many of these observations are similar to those reported in choline deficient animal models used to investigate non-alcoholic hepatic steatosis. Choline is a nutrient used as the primary positively charged ion for cell membrane formation and very low density lipoprotein packaging. PFOS creates an ion complex with choline in solution and in ex vivo liver which may constitute a choline sink leading to a choline deficient phenotype. The central hypothesis is that at high doses PFOS makes an ion complex with choline in the liver and produces a choline deficient phenotype in the treated animals which may be exacerbated by increased lipid β-oxidation. To investigate this hypothesis, Sprague Dawley rats (6/sex/group) received diets containing normal choline, high choline, 100 ppm PFOS with normal choline or 100 ppm PFOS with high choline for 6 weeks. The total consumed PFOS dose achieved approximately 200 mg/kg which approximates the acute oral LD50 in rats (i.e., 251 mg/kg). As such, mortality, seizure, and sensitivity to light and touch were noted in PFOS-exposed animals. Hepatocellular vacuolation and microscopic evidence of peroxisome proliferation were noted in PFOS-exposed animals. The hepatic vacuoles were a result of lipid accumulation based on Oil Red O staining. Choline supplementation showed a trend towards decreased hepatic lipid concentration in PFOS-treated male rats. Additional studies are needed to further investigate this potential relationship between PFOS and choline.

PS 2210 Perfluoroalkyl Acids in River and Sea Water of Japan

N. Saito[1], N. Shimizu[2] and S. Tsuda[1]. *[1]Iwate Institute of Environmental Health Sciences, Morioka, Japan and [2]LSCA, Application Centre, Agilent Technologies Japan Ltd, Tokyo, Japan.*

Environmental waters such as river water (RW) and sea water (SW) are expected to be the major exposure sources of Perfluoroalkyl acids (PFAA) to humans via tap water and food fish. At the 2013 Annual Meeting of SOT, we reported that perfluorohexanoate released from the source to the river is rapidly contaminating surrounding SW and gradually contaminating tap water in the nearby areas. In the present study, we analyzed using LC-MS/MS the vast range of PFAA (from C4 to C16 carboxylates; and CS4, CS6, CS8 and CS10 sulphonates) sampled from RW in Japan (98 locations) and SW around Japan (31 locations) in 2010 and 2011, respectively. In the RW, C8, C9, C6 and CS8 showed high average concentrations of 3.22, 1.38, 1.37 and 1.10 ng/L, respectively. In the SW, the concentrations of C6, C8, C9, and CS8 were also high and were 0.35, 0.92, 0.50 and 0.27ng/L, respectively. In the RW, Pearson's correlation coefficients (r) showed highly significant correlations between each of C8, C9, C6 and CS8. The r values for couples of C8, C9 and CS8 were very high, and C9 vs C8, C9 vs CS8 and C8 vs CS8 were 0.846, 0.843 and 0.792, respectively. The r of C6 vs C8 was 0.742. The r values for C6 vs CS8 and C9 were 0.616 and 0.600, respectively. In the SW, the correlations between each of four PFAA reflected those of the RW: they were high and highly significant.The high concentrations of C8, C9 and CS8 with high correlation coefficients may explain their long usage for the similar purpose and their persistence. As a substitute for C8, C6 is recently introduced and manufactured in the same factory once produced C8. The high r value for C6 vs C8 may reflect the release of C6 and C8 from the same source. Unlike CS8 and C8, C9 or C6 is not officially regulated. The bioaccumulation of PFAA with longer carbon chain is generally greater than the shorter one. The effect of C9 on peroxisome proliferator-activated receptor alpha is strongest among known PFAA. Thus, observation should be necessary on this persistent chemicals, as well as newly contaminating C6.

PS 2211 Mortality Experience of APFO Production Workers

B. Alexander[1], K. Raleigh[1], G. Ramachandran[1], T. Church[1], L. Scott[1], S. Mongin[1], P. Logan[2], S. Morey[3] and G. Olsen[2]. *[1]University of Minnesota, Minneapolis, MN, [2]3M Company, St. Paul, MN and [3]More Consulting, Inc, St. Paul, MN.*

Background: The ammonium salt of perfluorooctanoic acid (APFO) is used in fluoropolymer production. APFO dissociates in biologic media to perfluorooctanoate (PFOA); a chemical that has an environmental presence with uncertain human health effects. We evaluated the mortality experience of employees of an APFO manufacturing plant. Methods: This cohort mortality study followed 9,027 employees including 4,668 from a site that produced APFO from 1947-2000 and 4,359 from a non-APFO facility in the same geographic area. Yearly APFO exposure was estimated using a job and task-based APFO exposure matrix developed from industrial hygiene monitoring data, expert judgment, and production information. APFO production workers were categorized into quartiles of cumulative exposure with those from a non-APFO plant as a non-exposed reference population. Standardized mortality ratios (SMR) and 95 percent confidence intervals (95% CI) were estimated using state referent mortality data from 1960-2008. Standardized rate ratios (SRR) and 95% CI were estimated for the exposed population and each APFO exposure quartile in comparison to the non-exposed worker population. Study was approved by Univ of MN IRB. Results: We observed 2,954 deaths (SMR = 0.93 (95% CI=0.89-0.96)). Cancers of a prioi interest (Obs total, Obs exposed, [SRR (95% CI)]) included liver (15, 8, [1.5 (0.5-4.2)]), pancreatic (48, 18, [0.8 (0.4-1.5)]), kidney (24, 6, [0.4: (0.1-0.9)]), bladder (16, 8, [1.3 (0.5-3.6)]), and prostate (72, 23 [0.6 (0.4-1.0)]). There was little evidence of an exposure response association comparing exposure quartiles to the referent population. The SRR for pancreatic cancer in the highest exposure category was elevated, but imprecise [obs= 6, SRR=2.2 (95% CI=0.6-7.7)]. The SRR for heart disease was 0.81 (95% CI=0.70-0.94), with a SRR of 1.2 (95% CI=0.6-2.2) in the highest exposure category. Conclusion: In this study, occupational exposure to APFO was not associated with a greater risk of death from all causes or specific causes of death.

PS 2212 iTRAQ Protein Profile Analysis of Mouse Testis after Perfluorooctanoate (PFOA) Exposure

H. Zhang[1], L. Yin[1], L. Bin[2], Y. Shengmin[1] and J. Dai[1]. *[1]Institute of zoology, Beijing, China and [2]Anhui University, Hefei, China.*

Perfluorooctanoic acid (PFOA) is a stable man-made compound with many industrial and commercial uses. Concern has been raised that it may induce hepatotoxicity, immunotoxicity, developmental effects and some other toxicological effects. However, the testicular toxicity of PFOA and its underlying mechanism is not well known. In this study, male mice were exposed to 0, 0.08, 0.31, 1.25, 5 and 20 mg/kg/day of PFOA for 28 days. Absolute testis weight was diminished at the highest dose, as well as testosterone and progesterone levels in serum and testis were all inhibited at doses of 1.25,5 and 20 mg/kg/day. In addition, the seminiferous tubules were damaged in a different degree after PFOA exposure. After iTRAQ labeling combined with two-dimensional liquid chromatography and tandem mass spectrometry (2DLC–MS/MS) analysis, 93 differentially expressed proteins between the control and the 5 mg/kg/d PFOA treated mice were successfully identified. These proteins were mainly involved in cell proliferation, lipid metabolism, steroid metabolism and spermatogenesis, nucleic acid metabolism, stress response and apoptosis, and others. In addition, serum and testis cholesterol were all reduced after PFOA exposure, and the mRNA and protein expressed levels of genes involving in cholesterol transport and testosterone synthesis were all inhibited by PFOA. Thus, we speculated that the decrease of serum cholesterol might play an important role in testicular toxicity of PFOA.

PS 2213 Effects of Perfluorooctanoate (PFOA) and Perfluorooctanesulfonate (PFOS) on Cholesterol Efflux in Macrophage-Derived Foam Cells

J. Vanden Heuvel[1, 2], J. A. Garban[1] and J. T. Thompson[1]. [1]*Veterinary and Biomedical Sciences, Penn State University, University Park, PA and* [2]*Indigo Biosciences, Inc., State College, PA.*

Cholesterol metabolism and efflux from peripheral cells, such as macrophages and foam cells, is a critical part of reverse cholesterol transport (RCT), a metabolic process that has implications for atherosclerosis and cardiovascular diseases. There have been several conflicting studies that suggest environmental and occupational exposure to Perfluorooctanoate (PFOA) and Perfluorooctanesulfonate (PFOS) affects RCT and cholesterol metabolism. However, the data from animal studies and from examination of potential mechanisms of action raise questions as to whether there is a direct causality of PFOA and PFOS exposure and hypercholesterolemia. In these studies we have directly examined effects of PFOA and PFOS on cholesterol efflux and in genes involved in this process. PFOA and PFOS are agonists for nuclear receptors that increase cholesterol efflux, such as the peroxisome proliferator-activated receptors (PPARs). Importantly, in THP-1 differentiated into macrophage-derived foam cells, PFOA and PFOS increased cholesterol efflux to either HDL or apoA. Comprehensive gene expression analysis by microarray is being pursued to determine the key genes being regulated by these perfluorinated compounds in foam cells that impact RCT. These studies will also assist in the identification of genes that are sensitive to PFOA and PFOS exposure that can be utilized in biomonitoring studies. Taken together, these studies suggest that PFOA and PFOS exposure affects cholesterol efflux, but not in a manner consistent with a negative health impact.

PS 2213a Tetrabromobisphenol A versus Bisphenol A: Excitation-Contraction Coupling Impairment through Divergent Mechanisms

R. Zhang and I. N. Pessah. *Department of Molecular Biosciences, School of Veterinary Medicine, University of California, Davis, Davis, CA.*

Bisphenol A (BPA) and its brominated derivative tetrabromobisphenol A (TBBPA) are high production volume chemicals utilized in the manufacture of various consumer products. While these chemicals share the same chemical backbone, the halogenation on TBBPA may produce activity on a distinct set of molecular targets versus BPA. The targets we investigated are those involved with skeletal muscle excitation-contraction (EC) coupling and relaxation, namely 1) the dihydropyridine receptor (DHPR), 2) the type 1 ryanodine receptor (RyR1), and 3) the sarcoplasmic/endoplasmic reticulum Ca^{2+} ATPase (SERCA). TBBPA indeed had concentration-dependent interactions with these targets: 1) it inhibited specific [^{3}H]PN200 binding to DHPR with an IC_{50} of ~0.4 μM; 2) it elicited an increase in specific [^{3}H]ryanodine binding to RyR1, achieving >1500% of vehicle control at 30 μM, and induced rapid efflux of Ca^{2+} from actively loaded microsomes; 3) it inhibited the biochemical activity of SERCA with an IC_{50} of ~13.3 μM. In contrast, BPA had no influence on specific [^{3}H]PN200 binding, SERCA activity, and Ca^{2+} efflux. However, surprisingly, both TBBPA and BPA impaired EC coupling in primary skeletal myotubes. In field stimulated myotubes loaded with the Ca^{2+} indicator fluo-4, 10 μM TBBPA rapidly diminished evoked Ca^{2+} transient amplitudes, achieving complete transient abrogation within 15 min of exposure, and increased baseline intracellular Ca^{2+} levels. BPA did not modify baseline Ca^{2+} levels, and while BPA also diminished Ca^{2+} transient amplitudes, complete abrogation was not achieved. These results indicate that while TBBPA is able to potently modify Ca^{2+} dynamics in myotubes via interactions with DHPR, RyR1 and SERCA (which are indeed detrimental to muscular function), such interactions are not necessary for impairing skeletal EC coupling. The mechanism(s) by which BPA impairs skeletal EC coupling warrant further investigation. Sponsored by NIH P42 ES04699, P01 11269, U.S. EPA R833292, R829388, T32 HL 86350, and T32 ES 7059.

PS 2213b An Evaluation of Gestational Exposure to Perfluorooctanoic Acid (PFOA): Effects on Body Composition and Physiological Factors

D. L. Diggs, J. Norwood, C. Wood, M. Lin, J. M. Rogers, C. S. Lau and B. D. Abbott. *ORD, NHEERL, TAD, DTB, US EPA, Durham, NC.*

Exposure to environmental pollutants can be a factor for induction of metabolic disorders. This study examined if exposure to PFOA during development could alter body composition and other physiological outcomes. Study 1: Pregnant CD-1 mice were gavaged with PFOA at 0, 0.001, 0.01, 0.1, or 0.3 mg/kg body weight (bw) from gestation day (GD) 1 – 17. At weaning, pups were fed a high fat (HFD) or control (CD) diet. Body composition, blood pressure (bp), and gene expression in tissues of offspring were examined. Male- BW increased in 0 mg PFOA+HFD vs 0 mg PFOA+CD and 0.01 mg PFOA+HFD vs 0.01 mg PFOA+CD. In HFD, bw decreased in 0.3 vs 0 mg PFOA. There were no effects on percent of body fat. At postnatal day (PND) 90, diastolic bp was decreased in 0.1 and 0.3 mg PFOA+HFD vs 0 mg PFOA+HFD and increased in 0.3 mg PFOA+HFD vs 0.3 mg PFOA+CD. The bp effects of 0.1 mg PFOA+HFD persisted to PND 180. Female- At 0 and 0.001 mg PFOA+HFD had increased weight gain vs CD. The %fat increased in 0.001 vs 0 mg PFOA+HFD. At PND 180, diastolic bp decreased in 0.01 and 0.3 mg PFOA+CD vs 0 mg PFOA+CD. Differential gene regulation was produced by HFD and PFOA in white fat and liver at 52 weeks of age. At 0.001 mg PFOA+HFD vs 0.001 mg PFOA+CD, 3 genes in white fat and liver were under-expressed while 14 genes in white fat and 19 in liver were over expressed. At 0.01 mg PFOA+HFD vs 0.01 mg PFOA+CD, 3 genes in white fat and 4 genes in liver were under-expressed while 14 genes in white fat and 15 in liver were over-expressed. Study 2: Pregnant mice were fed NIH-31 (low phytoestrogen) diet and dosed with PFOA at 0, 0.01, 0.1, or 1 mg/kg from GD 1 – 17. Pups remained on the NIH-31 diet. There were no age- or dose-related differences in bw or %body fat in either sex. In summary, exposure to PFOA and HFD produced sex-dependent changes in bw, body composition, and bp response in mouse offspring exposed to the chemical during perinatal development. This abstract does not necessarily reflect USEPA policy.

PS 2214 Cardiovascular Effects of Lead, Inorganic Mercury, and Methylmercury: Potential Risk to Humans

T. Wildemann[1, 2], S. D. Siciliano[1, 2] and L. P. Weber[1, 3]. [1]*Toxicology Graduate Program, University of Saskatchewan, Saskatoon, SK, Canada,* [2]*Soil Science, University of Saskatchewan, Saskatoon, SK, Canada and* [3]*Veterinary Biomedical Sciences, University of Saskatchewan, Saskatoon, SK, Canada.*

Humans are exposed to lead, inorganic Hg and methylmercury in the environment. The European Food Safety Authority (EFSA) estimated average human exposures of 0.68 μg Pb/kg-bw/d, 0.08 μg Hg(II)/kg-bw/d and 0.039 μg MeHg/kg-bw/d. Epidemiological studies show an association between exposure to Pb or Hg and hypertension. The study objective was to explore cardiovascular effects of sub-chronic Pb or Hg exposure in rats to determine NOAELs for human health risk assessments.

Male rats (n = 3-6) were exposed for 4 weeks to lead acetate (Pb; 4 – 45000 μg/kg-bw/d), mercury chloride (Hg(II); 7 – 4000 μg/kg-bw/d) or mono-methylmercury chloride (MeHg; 4 – 1607 μg/kg-bw/d) in the drinking water. Echocardiography, carotid artery ultrasound and intra-arterial blood pressure were performed after 4 weeks.

Dose-response curves for most cardiovascular effects were U-shaped. Blood pressure was significantly increased for Pb ≥ 2000 μg/kg-bw/d (~20 mmHg systolic) as well as for MeHg ≥ 7 μg/kg-bw/d (~40 mmHg systolic and diastolic), while Hg(II) had no effect on blood pressure. MeHg ≥ 7 μg/kg-bw/d also increased pulse pressure and heart rate, while Pb and inHg had no effect. Pb ≤ 57 μg/kg-bw/d decreased blood pressure and increased carotid diameter (vasodilation) with compensatory increase in stroke volume. In contrast, Hg(II) ≤ 29 μg/kg-bw/d reduced carotid diameter (vasoconstriction) with compensatory decrease in stroke volume, while MeHg showed no effect.

Cardiovascular responses to Pb, Hg(II) and MeHg were U-shaped, but both Pb and MeHg increased blood pressure at higher doses. Based on the increased blood pressure response, NOAELs (safety factor of 100) for humans were estimated as 0.57 μg Pb/kg-bw/d, 0.29 μg Hg(II)/kg-bw/d and 0.04 μg MeHg/kg-bw/d. Thus, risk of cardiovascular disease might be increased by Pb in the general European population and by MeHg for high fish consumers.

PS 2215 Stainless Steel Leaches Nickel and Chromium into Foods during Cooking

K. A. Hobbie, K. L. Kamerud and K. Anderson. *Department of Environmental & Molecular Toxicology, Oregon State University, Corvallis, OR.* Sponsor: G. Sower.

Toxicological studies show that oral doses of nickel and chromium can cause cutaneous adverse reactions such as dermatitis. Additional dietary sources, such as leaching from stainless steel cookware during food preparation, are not well characterized. This study examined stainless steel grades, cooking time, repetitive cooking cycles, and multiple types of tomato sauces for their effects on nickel and chromium leaching. While a dose of only 67 μg of nickel was associated with cutaneous reactions in 40 percent of nickel sensitive participants. We found depending on cooking conditions 88 to 1,000 ug Ni per serving of tomato sauce cooking in stainless steel. Like nickel, we found chromium leached from stainless steel into tomato sauce, from 86 to 900 ug Cr in a single serving of tomato sauce. All tomato sauce samples that were cooked in the presence of stainless steel using typical cooking

procedures showed significantly elevated Ni and Cr concentrations. In addition to other natural dietary sources, stainless steel cookware can significantly contribute to overall nickel and chromium consumption.

PS 2216 Oxidative Stress and Heavy Metal Toxicity in Work Place Exposure to Heavy Metals in Nigeria

O. M. Akinosun and O. S. Adeleye. *Chemical Pathology, University of Ibadan, Nigeria, Ibadan, Oyo, Nigeria.*

Heavy metals contamination of the environment is of major concern because of their toxicity and threat to human life and the environment. Studies have shown that the air in the work environment usually contains a number of chemicals, which when inhaled and absorbed by the body, pose a potential risk for workers' health.Though, most metals are essential for proper functioning of the human biological system, humans are not adapted to dealing with them at concentrations higher than the reference values.
Presence of elevated concentrations of heavy metals can result in induction of oxidative stress via production of reactive oxygen species or reduction of antioxidant defences, disruption of calcium homeostasis, induction of DNA damage, interaction with sulfhydryl groups, disturbances in the heme biosynthetic pathway, and some are known human carcinogens.
Accumulating evidence also indicates that work place exposure leading to generation of free radicals, accompanied by inadequate antioxidants in the body leading to oxidative stress is on the increase. This study assesses work place exposure to heavy metals in thirty-seven metal workers and thirty-six age and sex matched office workers serving as controls. Ten (10) mls of venous blood was collected from each subject into lithium-heparin bottle and this was used to determine Total Plasma Peroxides (TPP) by the FOX2 method while Cadmium (Cd), lead (Pb), zinc (Zn), Manganese (Mn), Ferritin were determined by atomic absorption spectrophotometer. There was significant increase at $p<0.05$ in Lead (0.0159 ± 0.0029) μg/L and Mn (31.92 ± 7.79) μg/dL in the exposed group than the controls and significant positive correlation between TPP and Pb. Significant decrease $p<0.05$ in Ferritin (96.38 ± 8.22) μg/L in the exposed was also observed. Occupationally exposed workers are prone to heavy metal toxicity with increased free radical generation which may lead to increased chronic disease manifestations and even cancers. Increase intake of antioxidant supplements may be beneficial as well as using safety/protective apparels.

PS 2217 Gene Expression Profiling in Saudi Individuals Exposed to Environmental Heavy Metals

I. M. Attafi[1], S. A. Albakheet[3], K. S. Famulski[2] and H. M. Korashy[3]. [1]*Poison Control Center, Jazan Health Affairs, Jazan, Saudi Arabia,* [2]*Alberta Transplant Applied Genomics Centre, University of Alberta, Edmonton, AB, Canada and* [3]*Pharmacology and Toxicology, King Saud University, Riyadh, Saudi Arabia.*

The aim of this study was to evaluate the effects of long-term exposure to environmental heavy metals on the gene expression profile of individuals live near to mining areas at Mahd Ad-Dahab region, Saudi Arabia. For this purpose, microarray analysis was conducted in an attempt to evaluate the alteration of gene expression profile of gene-regulated diseases and to identify potential biomarkers that may be involved in the response to heavy metals toxicity. Sixty healthy volunteers were divided to two groups; exposed group consisted of 40 male residents in the heavy metal-polluted area, whereas the control group consisted of 20 male residents in a non-polluted area (Riyadh). Our results showed that the plasma levels of Pb, Cd, and Hg were found to be significantly high in the heavy metal-exposed group. Total RNA was isolated from whole blood using PAXgene Blood RNA tubes and reversed transcribed and hybridized to the gene array using the Affymetrix U219 GeneChip. Microarray analysis identified 425 genes are differentially expressed in heavy metal-exposed groups. The alteration of many genes of interest revealed by microarray analysis suggests that these genes play a role in heavy metal-induced toxicity. Some of these genes were confirmed by RT-PCR analysis. The commonly significant differentially expressed genes in the heavy metal-exposed groups were analyzed for network, functional, canonical pathways, and upstream regulators using the Ingenuity Pathway Analysis (IPA) software. Renal and urological diseases, developmental disorders, and hematological diseases were the most significant diseases that are associated with heavy metal-exposed groups. The following genes participate in renal disease induction (such as SNRPG, UQCRB and AIF1) could be used as early biomarkers for renal toxicity. IPA also indicated that MYC might be the major upstream regulator of gene dataset.

PS 2218 Are Metals in Rolling Tobacco Less Risky Than Cigarettes?

M. C. Rubio-Armendáriz[1], C. Silva[1], D. González-Weller[1], Á. J. Gutiérrez[1], G. Luis-González[1], A. Hardisson[1] and A. Anadon[2]. [1]*Toxicología, Universidad de La Laguna, La Laguna, S/C de Tenerife, Islas Canaria, Spain and* [2]*Toxicología y Farmacología, Universidad Complutense, Madrid, Madrid, Spain.* Sponsor: A. Anadón.

Smoking is a major public health problem and an important source of exposure to toxic elements, including metals. The presence of metals in tobacco depends mainly on where the tobacco was grown and the production process.

Objectives: a) to quantify the concentrations of metals (Al, B, Ba, Ca, Cd, Co, Cr, Cu, Fe, K, Li, Mg, Mn, Mo, Na, Ni, Pb, Si, V, Zn) in 23 brands of rolling tobacco and to compare them with the concentrations previously found in cigarettes, b) to compare metals levels across different brands and producers, and with/without additives.
Materials and Methods: 34 samples from 23 different brands of rolling tobacco sold on the island of Tenerife (Spain) were analyzed by Inductively Coupled Plasma-Optical Emission Spectrometry (ICP-OES).
Results: Mean concentrations of metals in rolling tobacco were (mg/kg): Al (207.97); B (9.20); Ba (31.91); Ca (9189.74); Co (0.23); Cr (0.62); Cu (8.65); Fe (167.23); K (9767.13); Li (14.66); Mg (2257.74); Mn (56.29); Mo (0.09); Na (458.99); Ni (0.75); Si (644.28); V (0.29); Zn (17.45). Mean levels in rolling tobacco with/without additives were (mg/Kg): Al (223.3/181.7); B (8.499/9.735); Ba (28.97/2.150); Ca (8297/9873); Co (0.196/0.182); Cr (0.703/0.259); Cu (8.619/9.524); Fe (164.5/141.8); K (7567/10206); Li (19.05/13.69); Mg (1945/2449); Mn (42.54/53.71); Mo (0.075/0.117); Na (497.3/497.1); Ni (0.776/0.638); Si (649.7/629.5); V (0.358/0.343); Zn (12.92/20.12). Average Cd levels (mg/Kg) were 0.396 (range 0.129–1.035); levels with/without additives were 0.208/0.484. Average Pb levels (mg/Kg) were 0.327 (range 0.131–0.759); levels with/without additives were 0.339/0.326.
Conclusions: The levels of Al, Co, Cr, Mn, Ni, Cd and Pb in rolling tobacco are roughly half of those previously detected in tobacco cigarettes (mg/Kg: Al (428); Co (0.56); Cr (1.442); Mn (112.026); Ni (2.238); Cd (0.810); and Pb (0.602)). The use of additives in the production of rolling tobacco does not affect the levels of metals significantly.

PS 2219 Evaluation of Electric Arc Furnace-Processed Steel Slag for Dermal Corrosion, Irritation, and Sensitization

M. Suh[1], J. J. Yzenas[2] and D. Proctor[1]. [1]*ToxStrategies, Mission Viejo, CA and* [2]*Edw. C. Levy Company, Valparaiso, IN.*

Electric arc furnace (EAF) steel slag is alkaline (pH of ~11-12) and contains metals that are known dermal sensitizers, most notably chromium and nickel. As such, EAF slag has potential to cause dermal irritation and sensitization at sufficient dose, but no published study has characterized the potential for dermal effects associated with EAF slag. To assess dermal irritation, corrosion, and sensitizing potential of EAF slag, in vitro and in vivo dermal toxicity assays were conducted following Organisation for Economic Co-operation and Development (OECD) guidelines. In vitro dermal corrosion and irritation testing (OECD 431 and 439) of EAF slag was conducted using human epiderm model. In vivo dermal toxicity and delayed contact sensitization testing (OECD 404 and 406) were conducted in rabbits and guinea pigs. Chemical properties of EAF slag were also characterized. Calcium, iron, silicon and magnesium oxides were the major constituents of EAF slag, each contributing more than 10% of the slag composition. Other elements measured in the EAF slag at higher concentrations were manganese, aluminum and chromium, but nickel was measured at relatively low concentrations. Barium and chromium were the only constituents detected in the TCLP extraction leachate, and they were measured concentrations of 0.798 and 0.250 mg/l, respectively. EAF slag was not corrosive and not irritating in any in vitro and in vivo dermal toxicity tests. The results of the delayed contact dermal sensitization test indicate that EAF slag is not a dermal sensitizer. These findings are supported by the observation that metals in EAF slag occur as oxides of low solubility with leachates that are well below TCLP limits. Metals in slag are tightly fused to the physical matrix limiting the mobility of metal constituents that may be of concern for dermal effects. Based on these results and in accordance to the OECD guidelines, EAF slag is not considered a dermal sensitizer, corrosive or irritant.

PS 2220 MicroRNA Expression Profiles and ICP-MS Hair Analysis of Individuals Living Down-Wind of an Active, Open-Pit Copper and Molybdenum Mine in an Urban Superfund Site

H. Dysinger, K. Hailer, D. Hobbs and M. Calhoun. *Chemistry, Montana Tech of the University of Montana, Butte, MT.*

Butte, Montana, a town of approximately 35,000 residents, is a part of the largest superfund site in the United States. One of the unique aspects of Butte's history is that surface mining and smelting activities occurred, and continue today, in close proximity to Butte's historically dense urban population. This has resulted in homes and neighborhoods in Butte with high concentrations of a variety of toxic metals (and metalloids) including arsenic, lead, copper, zinc, mercury and cadmium. Therefore it is likely that people living near areas of active mining, or the numerous areas of uncovered smelter wastes, may have been chronically exposed through air, water or soil to this suite of potential toxins. In this study, volunteers were recruited based upon mapping and demographic data to determine if potential chronic exposure to these metal mixtures could lead to changes in miRNA expression patterns. Human hair and nasal cell samples were collected from individuals of various ages, living within close proximity to current surface mining as well as near historic mine tailings (n=16). Control samples were collected from individuals living in Bozeman, MT (n=8,) a town without historical or current mining practices. Elemental analysis was performed on the hair samples by ICP-MS and several metals were found to be elevated in the Butte population, including copper and molybdenum. Preliminary miRNA data show a number of up-regulated micro RNAs that are putative oncomirs (mir-93-5p, mir-106b-5p). There is also a down-regulation in the Butte population of miRNAs known to participate in regulation of inflammatory responses (miR-146b-5p and miR-146a-5p). These preliminary data illustrate the need for additional study and data collection of samples from individuals living downwind of an active open-pit copper mine.

PS 2221 Initial Characterization of Metal Exposures in Community Residents Living Adjacent to the Black Leaf Pesticide Manufacturing Complex

I. Kirpich[1], M. Mohammad[1], K. C. Falkner[1], G. E. Arteel[2], R. Barnett[1], J. C. States[2], R. A. Prough[3] and M. Cave[1, 4]. *[1]Department of Medicine/GI, University of Louisville, Louisville, KY, [2]Pharmacology & Toxicology, University of Louisville, Louisville, KY, [3]Biochemistry, University of Louisville, Louisville, KY and [4]Robley Rex VAMC, Louisville, KY.*

Black Leaf is an abandoned industrial site in Louisville, KY with exceptionally high-level soil contamination by organochlorine pesticides (OCP) – exceeding the Residential Screening Level (RSL) by up to 18,000-fold. However, the site is also contaminated to a lesser degree with arsenic, lead, and polycyclic aromatic hydrocarbons. Black leaf is surrounded by the Park Hill Neighborhood, and in 2013 EPA began remediating residential yards with soil contamination. The aim of this study was to determine if adult Park Hill residents living adjacent to Black Leaf had elevated levels of arsenic and lead; and to determine if levels correlated with soil mapping data and pro-inflammatory cytokine elevation. Blood lead and creatinine-adjusted random urine arsenic levels were determined by inductively coupled Plasma/Mass (ICP/MS). Serum pro-inflammatory cytokines were measured by Luminex analysis. The mean age of voluntary participants (n=53) was 52.4±16.0 years with 18.6±19.4 years of residence near Black Leaf. Participants were predominantly female (66.0%) and African American (79.2%). Two participants living adjacent to an on-site arsenic "hotspot" had very high urine arsenic levels (175 and 60 mcg/g creat). These residents also had marked elevation in serum IL-8 levels (137 and 116 pg/ml). Mean blood lead levels were 3.4±1.1 mcg/dL (adult reference range <10 mcg/dL). Two adult study participants living near an on-site "hot-spot" had exceptionally high levels of arsenic and IL-8. These findings are remarkable because soil levels of arsenic were much lower than OCPs when compared by respective RSLs. These positive findings suggest that further characterization of OCP levels, their biologic effects, and the potential response to soil remediation should be performed in Park Hill residents living near the Black Leaf Chemical Site.

PS 2222 Influence of Light/Dark Condition on Bioaccumulation and Toxic Severity of Heavy Metals in Mice

N. Miura and K. Ohtani. *National Institute of Occupational Safety and Health (JNIOSH), Kawasaki, Japan.*

We recently reported that cadmium (Cd)-induced mortality was markedly different by injection timing meaning light/dark cycle affect the severity of Cd-induced toxicity. In this study, we report further evidences for the diurnal variation of toxicities induced by heavy metals such as chromium and nickel in mice. Male C57BL/6J mice adapted for 14 days with assigned to 6 groups of 5 animals were administrated intraperitoneally (i.p.) with potassium dichromate (50 mg/kg) or nickel sulfate (60 mg/kg) at different hours in the day (10:00, 14:00, 18:00, 22:00, 2:00 and 6:00 h), describing as zeitgeber time (ZT); ZT2, ZT6, ZT10, ZT14, ZT18 and ZT22. The mortality was observed until 14 days after the injection. As a result, mice were more sensitive to Ni during light phase (ZT2 to ZT6) while more resistant during dark phase as same as the result of Cd. In case of Cr, however, mice were more sensitive at late-light to mid-dark phase (ZT10 to ZT18). Therefore, 1) mice had clear diurnal variation to metal-induced toxicity, and 2) the daily fluctuation of metal sensitivity differed depending on metal compounds, probably depending on the valence of metal ion. We further investigated that Cd accumulation in the liver was significantly rose at light-phase exposure compared to dark-phase exposure. Our results clearly indicate that light/dark condition affects on severity of metal-induced toxicity and metal bioaccumulation.

PS 2223 Safety Evaluation of Tibetan Medicine Zuotai in Mice

L. Wei, C. Li, Y. Du, D. Wang, X. Chen and H. Yang. *Pharmacology and Safety Evaluation Key Laboratory of Tibetan Medicine in Qinghai Province, Northwest Institute of Plateau Biology, Chinese Academy of Sciences, Xining, China, Xining, Qinghai, China.* Sponsor: X. Huang.

Zuotai (gTso thal) is one of the most famous and important drugs in traditional Tibetan medicine, which is composed of mercuric sulfide, sulfur, ashes of eight metals and eight minerals, and other adjuvants. The objective of the present study is to assess the safety of Zuotai in mice. KM mice were used to evaluate the safety of Zuotai through acute toxicity test, sub-acute toxicity test and long-term accumulative toxicity experiment. The result of acute toxicity test in mice shows that there no appears dead or obviously poisoning phenomenon, although the dose is up to 80 g/kg/day. The sub-acute toxicity test in mice for 30 day found that Zuotai can reduce significantly CREA (Creatinine), ALT (Alanine Aminotransferase) and AST (Aspertate Aminotransferase) levels in serums under low dose (13.34 mg/kg/day) and medium dose (53.36 mg/kg/day), and increase markedly the levels of CREA, ALT, AST, MDA (Malondialdehyde) in serums under high dose (2 000 mg/kg/day). Long-term accumulative toxicity experiment in mice showed that the mercury in KM mouse kidney began to increase significantly under clinical equivalent dose (6.67 mg/kg/day) in 2.5th months, then reduced gradually to normal levels after discontinuation. However, the amounts of mercury in liver, spleen and brain had no significant change. Although the ratio of AST/ALT appeared lower significantly at 4.5th months, the levels of CREA, ALT, AST, TBIL (Total Bilirubin) and BUN (Blood Urea Nitrogen) in serums had no distinctive difference at same time. In additional, the histological structures of the kidney, liver and spleen of mice were changed slightly at the 4.5th month and gradually recovered to normal after 1.5 month of withdrawal. And, the body weights of treated group mice had no difference comparing with control group. The present research suggests that the toxicity of Zuotai is tiny. However, Zuotai may result in mercury accumulation in kidney or other organs under high dose and long-term medication.

PS 2224 Development and Validation of a Method to Measure a Suite of Organotin Compounds in Serum from Danish Women of Child Bearing Age

V. G. Robinson[2], K. Thayer[2], K. Levine[1], R. A. Fernando[1] and S. Waidyanatha[2]. *[1]RTI International, Research Triangle Park, NC and [2]Division of the National Toxicology Program, National Institute of Environmental Health Sciences, Research Triangle Park, NC.*

Organotin compounds have had many industrial uses, including use as plasticizers and antifouling agents in marine paints. These compounds are known to be environmentally persistent, which can lead to human exposure, most commonly through consumption of contaminated fish. The aim of this study was to develop and validate a method to measure butyltin, dibutyltin, tributyltin, phenyltin, diphenyltin, and triphenyltin, with validation ranges for all six tin species spanning approximately 0.30 to 12.7 ng/mL. Serum samples from Danish women of childbearing age were diluted 1:5 with an eluent containing 0.5% triethyl amine, 0.075% tropolone, 5.5 % acetic acid, and 65% methanol in deionized water and centrifuged prior to analysis by an ion-pair reverse-phase ultra-performance liquid chromatography coupled to sector field inductively coupled plasma mass spectrometry (IPRP-UPLC-ICP-SFMS). Using this method, a complete separation was achieved for all tin species in a single chromatographic run within three minutes. The experimentally determined limit of quantitation (ELOQ) for each compound was approximately 0.30 ng/mL, while the limit of detection (LOD) for each compound was approximately 0.05 ng/mL in serum. The method was validated for accuracy (%relative error within ±15% for non-ELOQ standards), precision (%relative standard deviation ≤15% for non-ELOQ standards), linearity (correlation coefficients > 0.99), and specificity. This method will be applied to measure organotin compounds in serum samples collected from women of childbearing age.

PS 2225 Evaluation of the Design, Performance, and Metal Emissions of Electronic Cigarettes

M. T. Williams[1, 2], A. Villarreal[2], K. Bozhilov[3] and P. Talbot[2]. [1]*Environmental Toxicology, University of California, Riverside, Riverside, CA,* [2]*Cell Biology and Neuroscience, University of California, Riverside, Riverside, CA and* [3]*Central Facility for Advanced Microscopy, University of California, Riverside, Riverside, CA.*

Electronic cigarettes (EC) are novel nicotine delivery devices. Based on our earlier data, we hypothesized that new models of EC will vary in their performance characteristics and have heavy metals in their aerosol. We investigated this hypothesis using 10 brands of cartomizer EC and three approaches that included dissections, performance, and elemental analysis of EC aerosols. All 10 brands had the same basic design components, which consisted of wires, solder joints, air-tubes, a mouthpiece, fluid, and fibers. Four brands had been used prior to packaging, while six were in pristine condition. The flow rate required for aerosol production ranged from 4–21 mL/s. During "smoke out", flow rate was constant for 5 brands, but had to be increased periodically to produce aerosol in 5 brands. Within brands, pressure drop was relatively stable, but varied between brands (12-330 mm H2O). Aerosol density oscillated during "smoke out" for all 10 brands. The elemental composition of EC aerosol and smoke from conventional cigarettes was compared using inductively coupled plasma optical emission spectroscopy. Of 62 elements screened, 21 were present in EC aerosols. Eight (Al, B, Ba, Na, Pb, Si, Sr, Zi) were, in general, less abundant in EC aerosol than in conventional cigarette smoke. In contrast 12 (Ag, Ca, Cr, Cu, Fe, Mg, Mn, Ni, Se, Sn, Ti, Zn) were more abundant in EC aerosol than in smoke. One major selling brand had about 3.4 times as much silicon as the conventional brands and a different leading brand of EC had about 500 times as much tin in its aerosol than the conventional cigarette smoke. In summary, the cartomizers, while similar in design, varied in performance. All 10 cartomizers had metals in their aerosol. The health effects of metal exposure from EC are not yet know.

PS 2226 Oxidized LDL As a Marker of Cardiovascular Disease Risk in a Navajo Population Exposed to Heavy Metal Mining Contaminants

M. E. Harmon[1], C. Miller[2], M. Campen[1], C. Shuey[3], M. Cajero[2], S. Lucas[1], B. Pacheco[2], S. Ramone[3], T. Nez[3] and J. L. Lewis[2]. [1]*College of Pharmacy, University of New Mexico, Albuquerque, NM,* [2]*Community Environmental Health Program, University of New Mexico, Albuquerque, NM and* [3]*Southwest Research and Information Center, Albuquerque, NM.*

Numerous abandoned mines within the Navajo Nation contribute uranium, arsenic and other heavy metals to the soil and groundwater. Environmental exposure to heavy metal contaminants may promote or exacerbate cardiovascular disease (CVD). Evidence is emerging that pre-existing metabolic disease may increase an individual's susceptibility to vascular toxicity of heavy metal contaminants. To assess the potential impact of these contaminants on the cardiovascular health of exposed individuals, we examined traditional (IL-6, CRP) and novel (oxLDL) plasma biomarkers in a large community of the Navajo Nation. Samples and data were obtained in partnership with the DiNEH project through a culturally appropriate community-based participatory approach. Biomarker data were linked to geospatial and well water data on contamination sites using traditional linear regression and Bayesian models. Estimated annual intake of arsenic is a significant predictor of oxLDL. To examine a possible mechanism for this finding, and because copper, another metal, is known to directly oxidize LDL, we investigated if arsenic and uranium could also directly oxidize LDL. Human LDL was incubated with varying concentrations of sodium arsenite and/or uranyl acetate for up to 5 hours. Oxidation of LDL was determined by ELISA, to assess protein-specific modification, and lipid oxidation was assessed by TBARS assay. We found that arsenic oxidizes LDL at all concentrations tested. Uranyl acetate does not seem to oxidize LDL at low concentrations, and uranyl acetate appears to reduce the oxidizability of sodium arsenite when both are present. In summary, oxLDL seems to trend with arsenic in drinking water. Arsenic appears to directly oxidize LDL, which could be a potential mechanism to explain chronic CVD health outcomes.

PS 2227 Biomonitoring Trace Metals in Seminal Plasma and Urine and Their Relationships with Male Reproductive Endpoints

K. Kantaria and A. Jeng. *School of Community and Environmental Health, Old Dominion University, Norfolk, VA.*

The objective of the study was to examine any association between exposure to trace metals and parameters of semen quality in human male subjects. Metals (lead, Pb, copper, Cu, cadmium, Cd, zinc, Zn, and selenium, Se) in the seminal plasma and urine of the human male subjects (n =196) were analyzed by flame atomic absorption spectrometry, electrothermal atomic absorption spectrometry or atomic absorption spectrometry. Multinomial logistic regression analysis was conducted to assess the correlation between metal concentrations and semen quality parameters, where those parameters were dichotomized in categories less than or greater than the World Health Organization reference levels (concentration > 20 x 106/ml, motility ≥ 40%, and vitality ≥ 58%). Pearson's Product Moment Correlation Coefficient was used to assess overall correlations between metal concentrations and sperm quality parameters. Metals in most urine samples (> 98.5%) were detectable. Metals in seminal plasma were detectable except Pb and As, with 79 % and 51% of all the samples, respectively, below the detection limits. Metal concentrations in seminal plasma and urine did not correlate with each other. Concentrations of all of the metals in seminal plasma and urine were not significantly different between those in dichotomized categories. However, Cd and As in urine, adjusted for creatinine levels, were negatively correlated with vitality and morphology by means of % of amorphous heads, while Zn was positively correlated with sperm concentrations. Cd and As in urine may affect sperm vitality and morphology. However, lack of correlation between metals in seminal plasma and urine suggested future studies are needed to determine a suitable biological matrix for assessing reproductive capacity endpoints.

PS 2228 Toxic Metal Levels in Children Residing in a Smelting Craft Village in Vietnam: A Pilot Biomonitoring Study

S. K. Miller[1], A. P. Sanders[1], V. Nguyen[2], J. B. Kotch[3] and R. Fry[1, 4]. [1]*Environmental Health Sciences and Engineering, Gillings School of Global Public Health, University of North Carolina, Chapel Hill, NC,* [2]*Department of Maternal and Child Health, Gillings School of Global Public Health, University of North Carolina, Chapel Hill, NC,* [3]*Department of Surgery, School of Medicine, University of North Carolina, Chapel Hill, NC and* [4]*Curriculum in Toxicology, School of Medicine, University of North Carolina, Chapel Hill, NC.*

In Vietnam, pollution caused by small-scale domestic smelting of automobile batteries into lead ingot is a growing concern. The smelting craft village of Nghia Lo, Vietnam, has attracted the attention of health and environmental experts due to its extremely high lead levels in water, soil, dust, and foods. Despite the threat of toxic metal exposure, biomonitoring among susceptible populations, such as children, has not been previously conducted. In this pilot study, twenty children from Nghia Lo ages 18 months to four years were selected for capillary whole blood and toenail biomonitoring. Blood lead levels and toenail levels of arsenic, cadmium, chromium, lead, manganese, and mercury were measured. All 20 children had detectable levels of blood lead and every child had levels that exceeded the CDC guideline level of 5 μg/dL. Eighty percent of tested subjects had blood lead levels higher than 10 μg/dL. Five children (25%) had lead levels greater than 45 μg/dL, the level of recommended medical intervention. Average toenail lead, manganese, and mercury levels were 157, 7.41, and 2.63 μg/g, respectively, well above levels previously reported in children. Significant correlations were found between toenail metal levels including chromium and manganese and lead and cadmium ($r>0.65$, $p<0.001$). Linear regression showed that closer residential distance to a smelter was associated with increased blood lead levels ($p<0.05$). The results suggest an urgent need to control toxic metal exposure sources related to domestic smelting and seek treatment for children residing in these villages with the highest blood lead levels.

PS 2229 Assessment of Heavy Metal Residues in Food Crops Irrigated by Municipal Wastewater

M. M. Shereif. *Chemistry, King Saud University, Riyadh, Riyadh, Saudi Arabia.*
Sponsor: A. Kadry.

The heavy metal residues of Fe, Zn, Cu, Ni and Mn were assessed in three food crops, barley *Hordeum Vulgar* (grain crop); broad beans *Visia faba* (legume) and rape seed *Brassica nupus* (oil crop) irrigated with municipal wastewater. Results showed that Mn and Ni were significantly higher at all crops irrigated by municipal wastewater. However, the effect of municipal wastewater irrigation was insignificant on Zn and Cu residues when compared to groundwater irrigation. The residues of Fe and Mn in straw of all wastewater irrigated crops were significantly higher than in grain and seeds. However, there were no significant differences between the residues of the heavy metals Cu, Zn and Ni in all crops irrigated by municipal wastewater or groundwater. The study approved the need of proper regulations for disposal, recycling and application of municipal wastewater to agricultural lands.

PS 2230 Novel Oral Detoxification of Mercury, Cadmium, and Lead with Thiol-Modified Mesoporous Silica

T. Sangvanich[2], D. Castro[1, 2], W. Ngamcherdtrakul[2], J. Morry[2], W. Yantasee[1, 2] and G. Fryxell[3]. [1]*PDX Pharmaceuticals, Portland, OR,* [2]*Biomedical Engineering, Oregon Health and Science University, Portland, OR and* [3]*Pacific Northwest National Laboratory, Richland, WA.*

Thiol modified mesoporous silica (SH-SAMMS) was developed as an oral drug for the prevention and treatment of heavy metal poisoning. SH-SAMMS was first evaluated for the removal of methyl mercury (MeHg(I)), inorganic mercury (Hg(II), lead (Pb(II)), and cadmium (Cd(II)) in terms of binding capacity and rate in synthetic matrices mimicking conditions of gastric and intestinal fluids. SH-SAMMS was found to be superior to SAMMS with carboxylic and phosphonic acid based ligands as well as other commercially available chelating sorbents. Furthermore, SH-SAMMS could effectively remove soluble mercury from digested fish without significantly affecting the levels of most essential minerals found in fish. SH-SAMMS retained Hg(II) and MeHg(I) tightly inside the nano-size pores, preventing micron-size bacteria from converting the mercury species to more mobile forms. Rats fed with diet containing MeHg(I), Cd(II), and Pb(II) and SH-SAMMS for two weeks had blood Hg levels that were significantly lower than rats fed with the metal rich diet containing metals only. Upon cessation of the metal rich diet, continued administration of SH-SAMMS for two weeks facilitated the clearance of Hg faster and greater than those not fed with SH-SAMMS. Rats receiving SH-SAMMS were also protected from body weight loss associated with the metal poisoning. Retention of Hg and Cd in major organs was lowest in rats fed with SH-SAMMS throughout the entire study of 4 weeks. For Pb, while its retention in most tissues of rats was negligible (with the exception of bone), the reduction of blood Pb by SH-SAMMS was significant. SH-SAMMS did not change the levels of essential elements including zinc, sodium, phosphorus, potassium, calcium, and iron in blood and all tissues compared to the control. Only small reduction in blood Cu was observed due to SH-SAMMS, but not more than that of rats receiving metal rich diet alone.

PS 2231 Vulnerability of Frontal Cortex to Chronic Manganese Exposure in Welders

Z. Long[1, 2], C. Yeh[1, 2], X. Li[3], S. Snyder[1], E. Zauber[4], Y. Jiang[3] and U. Dydak[1, 2]. [1]*School of Health Sciences, Purdue Univ., West Lafayette, IN,* [2]*Dept. of Radiology and Imaging Sciences, Indiana Univ. School of Medicine, West Lafayette, IN,* [3]*Guangxi Medical Univ., Nanning, China and* [4]*Dept. of Neurology, Indiana Univ. School of Medicine, Indianapolis, IN.*

Historically the basal ganglia were thought to be the main target of manganese (Mn) neurotoxicity. Recent evidences shows significant effects of Mn exposure on the frontal cortex. The aim of this study is to test the vulnerability of the frontal cortex in Mn-exposed welders.

29 welders (14 from China and 15 from the U.S.) and 33 age- and gender-matched controls (23 from China, 10 from the U.S.) were recruited. Each subject underwent the same magnetic resonance imaging and spectroscopy exams. MR spectra were acquired from the frontal cortex, thalamus, motor cortex and striatum in the U.S. cohort, while from the frontal cortex, thalamus, hippocampus and posterior cingulated cortex (PCC) in the Chinese cohort. Brain metabolites were quantified including myo-inositol (mI), glutamate (Glu), creatine (Cr). A series of high resolution inversion recovery images and multi-echo gradient echo images were acquired to calculate T1 and T2* values, which quantitatively measure brain Mn and Fe levels, respectively. Metabolic changes, T1 and T2* values of the same brain regions were compared between welders and controls within each cohort.

Both welder groups showed significantly reduced T1 values in many brain regions including the frontal cortex, and significantly reduced T2* values only in the frontal cortex. Chinese welders showed significant changes in Glu, Cr and macromolecules in the frontal cortex, mI in the thalamus and PCC, no changes in the hippocampus, while U.S. welders also showed more changes in the frontal cortex, without any changes in the other regions.

Overall, the frontal cortex of both welder groups showed more metabolic changes and Fe deposition assessed by reduced T2* values, indicating the frontal cortex may be particularly vulnerable to Mn exposure in welding fumes (Supported by NIH/NIEHS #R01 ES020529, National Science Foundation of China Grant #81072320)

PS 2232 Measuring Community Lead (PB) Toxicity: Filling the Prevention Gap to Advance from Reactive to Proactive Medicine

H. W. Mielke[1], C. R. Gonzales[2], E. T. Powell[2] and P. W. Mielke[3]. [1]*Pharmacology, Tulane University School of Medicine, New Orleans, LA,* [2]*Lead Lab, Inc., New Orleans, LA and* [3]*Colorado State University, Fort Collins, CO.*

A child's blood Pb assay is often the first realization that exposure to environmental Pb has occurred. A critical gap is an investigative protocol that preempts harmful childhood Pb exposure. Mapping soil Pb and blood Pb evokes a novel approach. New Orleans was split into high (≥100 mg/kg) and low (<100 mg/kg) soil Pb census tracts (CT). Four soil sample locations, busy streets, residential streets, house sides, and open spaces (away from streets and houses), represent each CT. Soil and blood Pb concentrations within the high and low Pb census tracts were analyzed by multi-response permutation procedures (MRPP) and p-Values were <10E-16. Pre-Katrina children's blood Pb ≥ 5 μg/dL in high and low Pb CTs were 58.5% and 24.8%, respectively. Post-Katrina children's blood Pb ≥ 5 μg/dL in high and low Pb CTs decreased to 29.6% and 7.5%, respectively. In high Pb CTs, median soil Pb for busy streets, residential streets, house sides, and open space sample locations were 367, 313, 1228, and 103 mg/kg, respectively; in the low Pb CTs median soil Pb for busy streets, residential streets, house sides, and open spaces were 64, 46, 32, and 28 mg/kg, respectively. The best predictor of children's blood Pb is residential street-side samples systematically collected throughout residential New Orleans. Soils in high Pb CTs lack a margin of safety. Low Pb CTs were safer by factors ranging from 3 to 38 depending on soil sample location. Patterns of lead from decades of Pb deposition were not worsened by post-Katrina renovations. Contrarily major improvements are materializing in selected communities. Low Pb soils are available at the city outskirts to remedy Pb contamination. All large cities probably present similar characteristics as New Orleans. Soil Pb maps are a diagnostic tool that assist with comprehending and promoting proactive childhood Pb exposure prevention at the community scale.

Funding support by U.S. HUD (Grant # LALTT0002-11) to Tulane University.

PS 2233 Correlation of Blood Cr (III) and Adverse Health Effects: Application of PBPK Modeling to Determine Nontoxic Blood Concentrations

A. Monnot, W. V. Christian, D. J. Paustenbach and B. L. Finley. *ChemRisk, San Francisco, CA.*

Chromium (Cr) (III) is a trace metal essential to human health and exposure typically occurs via the diet on a daily basis. Some groups of individuals, such as those consuming Cr(III) supplements or patients with Cr-containing implants, may have elevated blood Cr(III) concentrations. Although blood Cr(III) concentrations are thought to be an accurate metric of exposure, little is known about the relationship between these concentrations and possible adverse health risks. This study evaluated the various effects reported in animal and human epidemiological studies of Cr(III) exposure in an attempt to correlate them with blood Cr(III) concentrations. The target endpoints identified in this analysis included the hematological, hepatic, and renal systems. Animal and human physiological based pharmacokinetic (PBPK) models were used to estimate steady state blood Cr(III) concentrations from a variety of dosing regimens. Our results suggest that blood Cr(III) concentrations as high as 480–580 μg/L are not associated with any responses. For each of the three health endpoints considered in this analysis (hematological, hepatic, and renal) no adverse effects were observed below 3,700 μg/L. Some hematological responses were observed at 3,700 μg/L, and adverse effects clearly occurred at 7,500 μg/L. These findings can be used to assess potential health risks to individuals with elevated blood Cr(III) concentrations.

PS 2234 The Effect of Seasonal Variation on the Concentration of Metals in Water, Fish, Aquatic Plant, and Soil Sediment in El-Fayoum, Egypt

K. A. Abdou[1], A. A. Sharkawy[2], M. M. Mahmod[1] and E. O. Hamed[3]. [1]*Department of Toxicology and Forensic Medicine, Faculty of Veterinary Medicine, Beni Suef University, Beni Suef, Beni Suef, Egypt,* [2]*Department of Toxicology and Forensic Medicine, Faculty of Veterinary Medicine, Assiut University, Assiut, Assiut, Egypt and* [3]*Biochemistry Department, Animal Health Institute, Animal Health Institute, El-Fayoum, El-Fayoum, Egypt.* Sponsor: A. Kadry.

The effect of Seasonal variation on the concentration of seven metals: cadmium (Cd), lead (Pb), iron (Fe), manganese (Mn), zinc (Zn) and copper (Cu) was evaluated in water, two species of most consumed fishes (*Tilapia nilotica* & *Claries lazera*), an aquatic plant (*Ceratophillyum demersum* L), and soil sediments in Wadi Al Raiyan lakes, El-Fayoum, Egypt. Samples were collected in summer and winter 2010-2011. Metals concentrations were measured by Atomic Absorption

Spectroscopy. The studied metals were detected in all the examined samples. Zn had the highest concentration among the metals detected in water. Pb, Cd, Zn, Fe, Cu, Mn concentrations were below the Egyptian permissible limit. Cu, Pb and Cd concentrations in water samples during summer season is much higher than their concentrations in water during winter season, while the Zn and Fe concentrations in water samples during winter season is much higher than there concentrations in water during summer season. Mn concentration in water samples were the same during winter and summer seasons. Iron concentration in *Ceratophyllum demersum* L. was above the Egyptian permissible limit. In addition, Cd, Zn, Cu and Pb concentrations in plant samples during summer season were higher than the concentrations in winter season. Fe concentration in plant samples during winter season was higher than the concentrations in summer season. The investigated metal concentrations in the soil sediment and tissues of *Tilapia nilotica* and *Claries lazera* fish samples were above the Egyptian permissible limits. The significance of these findings is discussed.

PS 2234a Comparison of Lead Exposure in Different Production Plants

J. Valachova, O. Osina, T. Vasicko and L. Musak. *Jessenius Faculty of Medicine, Comenius University, Martin, Slovakia.*

Goal of this work was to determine lead (Pb) concentrations in blood of exposed humans by atomic absorption spectroscopy and inductively coupled plasma-mass spectrometry. The authors examined the heparinized blood of 4 cohorts.
The first cohort was 17 Slovak workers, the average age 40.18 ± 13.31 (x ± RSD) years, who tested the functionality of conveyor belts intended for the transport of bulk material with a content of Pb. Workers did not use any personal protective equipment (respirators). There were found high levels of Pb in blood. The average value of Pb concentration after 2-5 months was 364.1 ± 144.2 μg.1-1. Increased values of Pb in blood over the biological limit (>400 μg.1-1) were indicated in 6 workers.
The second cohort were 282 glass factory employees with the average age 37.52 ± 7.86 years and the average blood concentration of Pb was 333.4 ± 169.7 μg.l-1. The employees have been producing glass from liquid lead glass batch at different working positions more than one year. The increased concentrations (over 400 μg.l-1) were found in 101 cases that was more than 35.82%. The highest values (more than 700 μg.l-1) were found in five glass blowers. This was higher than a binding biological value which must not be exceeded.
The next cohort was from the new metallurgical plant with Pb risk but with the modern technology. The group of 18 employees with the average age 47.67 ± 11.23 years and the average blood concentration 137.8 ± 76.7 μg.l-1. Modern and clean production resulted to the safe levels of Pb in blood.
As a control cohort was used the group of similar size and similar age structure with other than lead metal exposure.
All workers with values more than 400 μg.l-1 were invited on our clinic for mobilization treatment. We found important to monitor the exposed group regularly. We recommend to establish a regular medical control of exposure level.

PS 2234b Manganese Accumulates in Leaves of Radishes Grown in Manganese-Supplemented Soils

S. Clarke-Lambert, M. Stapleton, K. Ruddock and D. Skeete. *Biology, Medgar Evers College, Brooklyn, NY.* Sponsor: E. Catapane.

Manganese (Mn) is a naturally occurring element, essential in trace amounts for living organisms, but is potentially toxic in high concentrations. Certain occupations including mining, welding and steel manufacturing can expose workers to chronically high levels of airborne Mn, leading to a clinical condition known as Manganism, which has Parkinson like symptoms. Recent studies report excess dietary Mn can impair immune and reproductive functions in birds. Previously we showed Mn is present in some commercially available fertilizers. We hypothesize plants grown in soils high in Mn or supplemented with fertilizers containing Mn will accumulate Mn in leaves and fruits. To test this we grew radishes in soils supplemented with fertilizers containing Mn, as well as in soil without added Mn. Samples (0.5 g) of each of the fertilizers as well as radish leaves were digested with HNO3 in a CEM Discovery Microwave Digester. Digested samples were analyzed for Mn levels using electrothermal vaporization with deuterium lamp background correction in a Perkin Elmer AA800 Atomic Absorption spectrophotometer with a THGA graphite furnace. We found that leaves from plants grown in soils supplemented with Mn accumulated Mn up to about 104 μg/gm tissue. The control leaves contained 25.28 μg/gm of Mn, which was significantly less than all the experimental groups. On the other hand, the soil that contained fertilizer had a significantly higher concentration of Mn than the plant tissue. The highest concentration of Mn recorded in the soil with Mn supplement fertilizer was 1709 μg/gm, while the lowest concentration was 1280 μg/gm. The study shows that plants will accumulate Mn from the soil and that use of fertilizers with high concentrations of Mn will increase the accumulations, possible creating a situation where animals and people ingesting the fruits and vegetables might be subjected to elevated Mn levels. This work was supported by grants 0516041071 of NYSDOE and 0622197 of the DUE Program of NSF.

PS 2234c Environmental Uranium Exposure and Immune Function among Navajo Community Members—DiNEH Study

J. Ong[1], E. Erdei[1], R. L. Rubin[2], C. Miller[1], B. Pacheco[1], M. Cajero[1], C. Shuey[3, 1] and J. L. Lewis[1]. [1]*College of Pharmacy-Community and Environmental Health, University of New Mexico, Albuquerque, NM,* [2]*University of New Mexico Health Sciences Center, School of Medicine, University of New Mexico, Albuquerque, NM and* [3]*Southwest Research and Information Center (SRIC), Albuquerque, NM.*

Navajo commmunites have long been concerned that environmental uranium (EU), a consequence of extensive uranium (U) mining on Navajo lands, contributes to poor health outcomes among tribe members. EU exposures may contribute to disease through contaminated water consumption, dust inhalation and radiation exposure. Based on our past and ongoing work with another tribe, which shows immune response alterations due to metal exposures, our research team began immune function studies on a subset of Navajo participants in the Diné Network for Environmental Health (DiNEH) study (n=268). We aimed to study potential causes of autoimmune disease (AD) as a follow-up to information generated from the total DiNEH sample (N=1,304). Statistical modeling and geospatial data of abandoned U wastes and participants' homes indicate an association between EU exposures and self-reported AD. To investigate immune system responses, we determined lymphocyte subpopulations and measured serum cytokines using flow cytometry. Whole blood samples were used to identify T cells(CD3+), T helpers (CD4+), T cytotoxic (CD8+), B cells (CD19+), natural killer (NK) cells, and HLA-DR+ activated immune cells. Pro- and anti-inflammatory cytokines, as well as antinuclear and specific autoantibodies, were measured in serum using enzyme-linked immunosorbent assays (ELISA). Regression modeling indicates that DiNEH participants who reported increased EU exposure had increased proportion of activated T cells and decreased proportion of B cells and other antigen-presenting cells. Such cellular changes can lead to lower production of protective antibodies against invading pathogens. Alterations in cytokine production indicated an inflammatory response. These findings indicate altered immune response among the participants related to EU exposure.

PS 2234d Pilot Study of Environmental Monitoring of Konya Region near Abandoned Mercury Mine in Turkey

B. Karahalil[1], M. Ulukaya[1] and O. Alp[2]. [1]*Toxicology Department, Gazi University Faculty of Pharmacy, Ankara, Turkey and* [2]*Analytical Chemistry, Gazi University Faculty of Pharmacy, Ankara, Turkey.*

Hundreds of pollutants are discharged into the environment every day. Of these, heavy metals are regarded as serious pollutants of the aquatic environment because of their environmental persistence and tendency to be concentrated in aquatic organisms.Abandoned mines are an important global concern and continue to pose potential threats to human health including environmental damage/s. There is not any specific regulation for mining wastes in Turkey and this situation puts the mining wastes into the dangerous category. Therefore, this study focuses on the environmental effects of the abandoned mercury mines. To demonstrate environmental mercury contamination, fish samples were collected from two different regions which were contaminated and uncontaminated region. As a biomarker of environmental exposure the levels of Hg in fish samples were measured by Cold Vapor-Atomic Absorption Spectrometry (CVAAS). In fish samples, the levels of Hg were 0.504 ± 0.475 (mg/kg) (Mean ± SD) in Group 1 and 0.04 ± 0.054 (mg/kg) (Mean ± SD) in Group 2. Our data suggested that although mercury mine was closed long time ago, mining waste is still a problem and continues to contaminate the environment.

PS 2234e Comparative Study of US EPA's Building Assessment and Survey Evaluation Database

R. DeHate[1], B. Skelly[1], G. T. Johnson[2] and R. D. Harbison[2]. [1]*GEI Consultants, Inc, Valrico, FL and* [2]*College of Public Health, University of South Florida, Tampa, FL.*

In 2001 the United States Environmental Protection Agency (EPA) published the results of an indoor air quality study conducted at randomly selected public and commercial office buildings across the U.S. The Building Assessment and Survey

Evaluation (BASE) database has been used extensively for comparative background values for indoor air in commercial buildings for risk assessments and soil vapor intrusion assessments. EPA's BASE study sampled 100 buildings with a total of 298 sample sets. For this comparative study we collected indoor air samples from 137 sites and compared these data to the background values found in the BASE study. We collected a total of 794 indoor air sample sets that were analyzed for volatile organic compounds using EPA Method TO-14A and TO-15. The BASE study used a combination of two sample collection methods: 6 liter SUMMA canisters and multi-sorbent tubes. This study utilized only SUMMA canisters and all samples were sent to an approved laboratory for analysis. The BASE method reporting limits ranged from 0.2 to 7.0 μg/m3. Our data set was then compared to the minimum, maximum, means and the 25th, 50th, 75th, 90th, 95th and 99th percentile values in the BASE data set. Our results show that although similar to the background dataset there were enough differences to conclude that the "background" dataset is limited and should be expanded to include additional data. This additional data is readily available through State programs that have been collecting indoor air samples through a variety of programs including soil vapor intrusion assessments. This expanded dataset would be more reflective of actual background; allowing further evaluation of the data sets for more accurate risk assessment of the human population that it is being applied to.

PS 2234f Videographic Methodology for Quantification of Dermal Contact with Water During Recreational Beach Use

C. B. Roberts, L. Stuchal and S. M. Roberts. *University of Florida, Gainesville, FL.*

When ocean water contaminants threaten the shoreline, risk to public health from contaminant exposure during recreational beach use must be evaluated and managed. This risk depends in large part upon the extent of contact with water by beach users, including both skin surface area exposed and duration of contact. Currently, there are almost no data of this type available. The objective of this project is to determine the extent of water contact by the public during recreational beach use and how contact is influenced by weather and water conditions. Permanently mounted, high resolution video cameras are used to capture subject behavior on a public beach in Florida following an IRB approved protocol. Because the study involves passive observation of individuals in public, consent of subjects is not required. Video files are evaluated by an analyst post- hoc (i.e., not in real time). Potential subjects are restricted to those who spend their entire time on the beach within the field of view of the cameras so that the full extent of water contact during the day can be measured. Subjects are classified by gender and approximate age (adult, child, toddler) based upon appearance and are assigned a subject number. From the group of potential subjects identified for each study day, a subset is randomly selected for quantitative analysis. For each subject, the approximate extent and time of immersion are determined in time steps from the video files. The skin surface area exposed is assumed based upon age/gender classification and median body weight and surface area data from NHANES. An exposure time and average skin surface area in contact with water for the day is calculated for each subject. Ambient air and water temperatures are also recorded and will be used in a later phase of the study to develop a predictive model of water exposure on the beach as a function of weather conditions. Information derived from this study will be of value in risk assessment for estimating exposure to water borne contaminants on public beaches.

PS 2234g Plasma Hydroxylated Polybrominated Diphenyl Ethers (HO-PBDEs) in Californian Women of High Risk for Birthing an Autistic Child

Y. Lin[1], I. Hertz-Picciotto[2], D. Tancredi[2], I. N. Pessah[1] and B. Puschner[1]. *[1]VM: Molecular Biosciences, University of California, Davis, Davis, CA and [2]Public Health Sciences, University of California, Davis, Davis, CA.*

Exposure to the polybrominated diphenyl ethers flame retardants (PBDEs) causes concern for carcinogenicity, neurotoxicity, reproductive toxicity, and thyroid toxicity. Hydroxylated PBDE metabolites (HO-PBDEs) are of increasing toxicological interest because of their greater biological activity compared to parent compounds. Little is known about the extent and patterns of HO-PBDEs during pregnancy, especially in populations susceptible to heritable neurodevelopmental disorders. We measured plasma HO-PBDE levels using LC/MS-MS in Californian women enrolled in MARBLES (Markers of Autism Risk in Babies-Learning Early Signs), who are at high risk for birthing an autistic child. Twelve HO-PBDEs were measured in plasma from 79 women collected during each trimester and at delivery (194 samples total). HO-PBDEs were extracted by solid phase extraction and derivatized by dansyl chloride to enhance the detection sensitivity of LC/MS-MS. Compared to other studies, women enrolled in MARBLES had significantly higher mean concentrations of 4'-HO-BDE17 (1.02 ng/g lipid versus not detected), 2'-HO-BDE28 (0.2 ng/g lipid versus not detected), 3-HO-BDE47 (1.59 versus 0.1 ng/g lipid) and 6-HO-BDE47 (0.92 versus 0.3 ng/g lipid). Plasma HO-PBDEs increased with each calendar year between 2006 and 2009. Specifically, samples collected in 2006 and 2007 had significantly lower levels ($p < 0.05$) of 2'-HO-monobromodiphenyl ether (0.006 and 0.034 ng/ml), 2'-HO-2,4-dibromodiphenyl ether (0.161 and 0.171 ng/ml) and 3'-HO-2,4-dibromodiphenyl ether (0.107 and 0.200 ng/ml) compared to 2009 (0.054, 0.243 and 0.315 ng/ml, respectively). Due to the increase of total plasma lipids during gestation, HO-PBDEs expressed on ng/g lipid basis decreased with gestational stage. The determination of plasma HO-PBDE levels in MARBLES mothers suggests a substantial exposure to PBDEs. Further studies are needed to correlate maternal PBDE and HO-PBDEs exposures with neurodevelopmental toxicity.

PS 2234h Exposure Monitoring for Natural and Anthropogenic Polybrominated Diphenyl Ethers (PBDE) and Derivatives in Puget Sound, Washington, Area Volunteers

I. Schultz[1] and L. Kuo[2]. *[1]Marine Sciences, Pacific NW National Lab, Sequim, WA and [2]Pacific NW National Lab, Sequim, WA.*

Synthetic polybrominated diphenyl ethers (PBDEs) have been widely used as flame retardants in many consumer products including electronic devices. The most important routes of human exposure appear to be from contaminated food and contact with dust found in households and workplaces. Structurally related derivatives of PBDEs are the hydroxylated (OH-PBDEs) and methoxylated forms (MeO-PBDEs). Experimental evidence suggests the OH-PBDEs pose greater health risks than other forms of PBDEs. Certain OH-PBDEs and MeO-PBDEs are also marine natural products and it is unclear although likely, that marine fish and shellfish, which bioaccumulate these compounds serve as a vector for human exposures. In this study, we are measuring approximately 120 different PBDE, OH-PBDEs and MeO-PBDEs in household/workplace dust and blood plasma samples provided by human volunteers living in the Puget Sound region of Washington State and working in either the commercial fishing or recycling industries. The commercial fishing occupation is largely an outdoor activity that promotes above average seafood consumption while electronic recycling may expose workers to dust with higher than average levels of PBDEs. Thus, comparison of PBDE levels in samples associated with these occupations may provide insight on the relative importance of dust vs. food as a source of PBDEs. Initial results suggest the pattern of PBDE distribution in volunteers that consume low amounts of seafood are more comparable relative to those from volunteers consuming higher than average amounts of seafood. For example, no MeO-PBDEs were detected in volunteers consuming low amounts of seafood. Also, comparison of results from volunteers of white-European, African-American and Hispanic ethnicity suggested ethnicity was not an important variable in determining PBDE congener content of plasma relative to occupation and other lifestyle attributes. Supported by NIOSH Grant 1R21OH010259-01A1.

PS 2234i High-Throughput Modeling of Indoor Exposures to Chemicals

C. I. Nicolas[1, 3], M. R. Goldsmith[2], B. K. Ahir[1, 3], T. B. Knudsen[1], J. Rabinowitz[1], W. Setzer[1], K. Mansouri[1, 3] and J. F. Wambaugh[1]. *[1]NCCT, U.S. EPA, RTP, NC, [2]NERL, U.S. EPA, RTP, NC and [3]ORISE, Oak Ridge, TN.*

Risk due to chemical exposure is a function of chemical hazard and exposure. Proximate sources of exposure due to the presence of a chemical in consumer products are identified as key drivers of exposure and are not well quantified. The ExpoCast project is developing a model that forecasts indoor exposure to chemical additives in textiles. Flame retardant chemicals are found in flooring, upholstery, and articles of clothing. Depending on their physicochemical properties, they may bio-accumulate in the indoor environment at higher magnitudes than in the outdoor environment, which is correlated with high indoor exposure rates. Halogenated flame retardants, such as polybrominated diphenyl ethers, are semi-volatile organic compounds (SVOCs) that are potentially harmful to humans. In this study, ExpoCast predicted emissions of 74 chemicals found in 32 flooring materials for which gas phase concentrations were measured by Wilke et al. (2004).[1] Flooring materials include a range of natural and synthetic floor coverings, installations, and adhesives. Emissions calculations principally depend on the gas-phase concentration of the SVOC in the material as well as the surface area of that source.[2] A linear regression yielded R^2 and p values of approximately 0.3 and 2.0E-12, respectively, with logP and vapor pressure being the most significant predictors for gas-phase concentration followed by their presence in adhesives and resilient flooring. These results potentially allow for the forecasting of gas-phase concentrations of chemicals for which their analytical data in flooring materials are lacking. Data generated from high throughput exposure methods are then combined with high-throughput screening data from the ToxCast project in order to scientifically assess risk in a time and cost effective manner. As a result, comprehensive risk assessment of indoor use chemicals may be achieved. This abstract does not necessarily reflect EPA policy.

1. Wilke et al. Indoor Air 2004, 14, 98-107
2. Little et al. Environ. Sci. Technol. 2012, 46, 11171-11178

PS 2234j Consumer Exposure to Bisphenol A from Plastic Bottles Depends on Degree of Usage

F. Bidabadi and M. A. Yakubu. *Environmental & Interdisciplinary Sciences, Texas Southern University, Houston, TX.*

Bisphenol A (BPA) is an organic compound with a weak estrogenic property, the health effects of BPA remain inconclusive but It is agreed that it has low acute toxicity. Because of the ubiquitous presence of BPA in our daily lives, there is concern about its ability to leach from products into consumables creating adverse health effects. Such scenarios led "BPA free" products. We have characterized the presence of BPA in various plastic products: baby bottles, water and food containers; investigated the effects of temperature, and degree of use on BPA leachates. Various plastic baby bottles, water/sports bottles, and food containers were filled with water, boiled to 90, 95, or 100oc for 36, 48, 60 times/hours, sample collected along with 0.5gm from different plastics were extracted and analyzed along with standard using HPLC-Uv-Vis at 225-310 nm; with a mobile phase (acetonitrile: water (70:30 v/v)) and mass confirmed with MALDI-TOF for BPA and metabolites. HPLC: BPA elutes with a mean retention time (RT) of 7.35 +/- 0.05 min and quantification showed differential leaching of BPA from different plastic containers depending on the temperature and extent of use. Microwaving water in plastic containers showed temperature and time-dependent concentration of BPA leachates. Analysis of different containers showed presence of BPA in all samples except from Ziploc Smart Snap. MALDI-TOF analysis of sample extracts confirmed presence of BPA and other derivatives. Most of the plastic containers tested leached BPA from baby bottle, water bottles and food containers even those labeled "BPA free" except Gumdrop baby bottle and Ziploc Smart Snap. Concern remains of how free and safe are plastic containers labeled "BPA free"? Though, BPA has low estrogenic activity and not considered a major threat to human health, but manufacturers of consumer products need to live up to their product standard and avoid the guessing game. However, more research is required to identify conditions that lead to BPA leach from products and the long term toxic effects of BPA.

PS 2234k Direct Determination of BPA, BPA Glucuronide, BPA Sulfate, and BPS in Human Urine

R. Gerona[1], A. J. Schecter[2], M. Friesen[1], D. Cherry[3], N. Thiex[4], W. C. Shropshire[2] and J. Moye[5]. *[1]U California, San Francisco, CA, [2]U Texas School of Public Health, Dallas, TX, [3]U Washington, Seattle, WA, [4]South Dakota State University, Brookings, SD and [5]NICHD, NIH, Bethesda, MD.*

Bisphenol A (BPA) is a high production volume chemical widely used in the production of polycarbonate plastics and epoxy resins found in commercial products to which nearly 100% of humans are exposed. With increasing public objections to the use of BPA, manufacturing companies have resorted to replacing BPA with alternatives like BPS. However, BPS has a similar structure to BPA and is expected to be endocrine disrupting like BPA. BPA has been associated with a variety of adverse health effects in laboratory animals and humans.
We used a novel liquid chromatography- tandem mass spectrometry (LC-MS/MS) method in a pilot study to directly measure BPA and its metabolites, BPA glucuronide and BPA sulfate, in 15 urine samples of 1st trimester pregnant women enrolled in a rural Texas US National Children's Study. Unlike most urine studies, we were able to speciate between BPA glucuronide and BPA sulfate, and eliminate the need for enzymatic hydrolysis in measuring BPA metabolites. The observed geometric means for BPA in free, glucuronide, and sulfate forms are 0.06, 7.20 and 0.22ng/mL (0.04, 4.57, and 0.14 ug/g Cr) respectively. The observed geometric mean for total BPA is 0.84 ng/mL (5.02 ug/ gCr). This level is higher than all reported urine BPA measurements and may have resulted from improved accuracy and analyte recovery using our direct method.
We also developed an LC-MS/MS method for measuring BPS (LOD= 0.01ng/mL). The observed geometric means for free, conjugated and total BPS in our cohort are 0.01, 0.13 and 0.13 ng/mL (0.01, 0.08 and 0.08 ug/g Cr) respectively. These results imply that although BPS is detected in our cohort, BPA remains to be more pervasive among this group of pregnant women from rural Texas. However, since we have a limited number of subjects in this pilot study, this requires follow-up in larger cohorts.

PS 2234l Application of Physiologically-Based Pharmacokinetic Modeling of Bisphenol A to Estimation of Daily Intake Amounts by Age and Gender

D. Jeong[1], S. Kim[1], H. Moon[2], J. Park[3], K. Kim[1], K. Choi[1] and S. Kim[1]. *[1]Environmental Health, Seoul National University, Seoul, Republic of Korea, [2]Marine Sciences and Convergent Technology, Hanyang University, Ansan, Republic of Korea and [3]Environmental Health Sciences, Soonchunhyang University, Asan, Republic of Korea.*

Bisphenol A (BPA), easily found in many consumer products, has been measured in biological media among general population in many countries due to concerns of endocrine disturbance. Recently, Korean government completed the first phase of nation-wide human biomonitoring survey for 6311 adults representing general Korean population (2009-2011), and published two other reports of biomonitoring including younger subjects (n = 253) and a birth cohort (n = 235). The objectives of the presenting study are to predict the levels of exposure to BPA using physiologically-based pharmacokinetic (PBPK) modeling and to make assess the risk of BPA in Korean population by age and gender. We adapted a published PBPK model of monkeys exposed to BPA (Fisher et al, 2011) by using typical human physiological parameters and validated the kinetic parameters by fitting the model to published measurement of human PK profiles. For reverse-dosimetry, we constructed exposure conversion relationship (ECR) chart of urinary levels of BPA and average daily intake amount at various levels of exposure with assumption of continuous exposure to BPA for 24 hr. Model uncertainty was addressed by 1,000 iterations of Markov Chain Monte-Carlo simulation for selected parameters after sensitivity analysis by body weight. According the ECR chart estimated daily intakes (EDI) were: 0.030 (95% CI: 0.021 – 0.043) μg/kg/d for adolescents (age 13-18), 0.010 (0.007 – 0.014) μg/kg/d for male adults (19+ yr), 0.009 (0.006 – 0.013) μg/kg/d for female adults, 0.040 (0.029 – 0.056) μg/kg/d for pregnant women at delivery. While the estimated HQ ranged 0.0002 to 0.0008 based on tolerable daily intake (50 μg/kg/d), sensitive population (adolescents and pregnant women) seemed exposed relatively more. Considering that reference value should be more conservative for the susceptible, the actual risk might be underestimated.

PS 2234m High-Throughput Exposure Estimation Using NHANES Data

C. L. Strope[1], B. A. Wetmore[3], W. Setzer[1], J. Rabinowitz[1], R. Pearce[1], K. Dionisio[2] and J. F. Wambaugh[1]. *[1]National Center for Computational Toxicology, Environmental Protection Agency, Durham, NC, [2]National Exposure Research Laboratory, Environmental Protection Agency, Durham, NC and [3]The Hamner Institutes for Health Sciences, Durham, NC.*

In the ExpoCast project, high throughput (HT) exposure models enable rapid screening of large numbers of chemicals for exposure potential. Evaluation of these models requires empirical exposure data and due to the paucity of human metabolism/exposure data such evaluations include large uncertainty. Wambaugh et al. (2013; ES&T) used CDC National Health and Nutrition Examination Survey (NHANES) as a data source for urinary biomarkers of human chemical exposure and developed an exposure prediction model that had large uncertainties. To reduce the uncertainties, we developed a one-compartment pharmacokinetic (PK) model for relating both serum and urine biomarkers to probable chemical exposures. The PK model was parameterized with metabolic clearance and volume of distribution data compiled from literature sources. This expanded the chemical space explored beyond the urine evaluation chemicals by incorporating serum and blood biomarker concentrations to include environmentally persistent chemicals such as perfluorinated and polychlorinated biphenyl chemicals. Exposures were inferred probabilistically, using Markov Chain Monte Carlo (MCMC) to estimate the distribution of parent chemical exposures consistent with the biomarker data. By incorporating up to 50 additional metabolites from the NHANES data, we reduced the uncertainty in the parent chemical exposure inferences. The incorporation of a more diverse set of metabolites and corresponding reduction in uncertainty in ExpoCast predictions will play a key role in the confident application of exposure models in prioritization and risk assessment contexts. This abstract does not necessarily reflect EPA policy.

PS 2234n Inferring Population Exposure from Biomonitoring Data on Urinary Concentrations

W. Setzer, J. Rabinowitz and J. F. Wambaugh. *National Center for Computational Toxicology, US EPA, Research Triangle Park, NC.*

Biomonitoring studies such as the National Health and Nutrition Examination Survey (NHANES) are valuable to exposure assessment both as sources of data to evaluate exposure models and as training sets to develop heuristics for rapid-expo-

sure-assessment tools. However, linking individual measurements of urine concentrations of a metabolite back to an individual's exposure rate is generally difficult, because: urine concentrations need to be converted to excretion rates; parent chemical exposures are inferred from multiple, sometimes overlapping metabolites measured in urine; and the same observation may be due to a less-recent, large exposure or a more-recent, smaller exposure. While individual measures are problematic, we demonstrate approaches to solutions for the above problems for population distributions of exposure. We calibrate models for gender-, ethnicity-, age-, and bodyweight-dependent predictors of creatinine production rate for the US population, based on the 2009-2010 NHANES sample. We use Bayesian methods to infer parental exposure given measurements on metabolites, allowing for the fact that multiple parents may result in the same metabolite. Results of simulations with stochastic exposure scenarios demonstrated that simple models assuming steady-state exposure give approximately the correct population median, but that the population variance of exposure depends on the exposure variance, the frequency of exposure events, and aspects of pharmacokinetics, and is thus is more problematic. However, the population variance can be bounded, and even uncertain knowledge of pharmacokinetic properties can help improve exposure estimates. This abstract does not necessarily reflect EPA policy.

PS 2234o Urinary Arsenic Metabolism Profiles of Workers in a Copper Mining and Smelting Plant

S. Xi, Q. Sun, S. Liu and G. Sun. *Department of Environmental and Occupational Health, School of Public Health, China Medical University, Shenyang, China.*
Sponsor: J. Pi.

Introduction: Inorganic arsenic (iAs) exposure is potential occupational hazard in copper mining and smelting. After absorption, As undergoes successive reductions and methylations metabolism. As excretion profile was related with environmental arsenic levels, individual arsenicosis risk, sex, age, nutritional status and body weight. The current investigation was carried out to evaluate As exposure and the urine metabolite profiles of workers with different jobs in a copper mining and processing plant in China. Methods: A total of 170 male workers in 5 different departments (administrative employees (Group 1), copper ore miners (Group 2), copper ore grinding and milling (Group 3), electrolytic procession (Group 4) and copper smelters (Group 5)) of a copper mining and processing plant were randomly recruited. Subject age, job history, alcohol and smoking habit, dietary habits, et al. were collected. Blood pressure, height and weight were measured and body mass index (BMI) was calculated. Spot urine samples were collected and determined for iAs, MMA, DMA, and trimethylated arsenic (TMA) by atomic absorption spectrophotometer with an arsenic speciation pretreatment system. Results: The highest urinary levels of iAs, MMA and DMA were found in the Group 5. There was a statistically higher excretion of urinary As in the Group 4 and 5 compared to Group 1, 2 and 3 ($p < 0.05$). In Group 4 and 5, 77.8% and 93.3% of workers had total urinary As values higher than 50μg/g Cr, and significantly higher than that of Group1, 2 and 3. There was a statistically higher excretion of urinary DMA in the workers of BMI>25 and intake seafood in recent 3 days. The odds of subjects with urine As exceeded 50μg/g Cr were positively and significantly associated with different production type (OR=1.907; CI=1.387-2.621; p=0.000) and BMI (OR=1.504; CI=1.009-2.242; p=0.045). Conclusion: The workers in copper production plant presented significantly elevated levels of iAs, MMA, DMA and TAs, especially for smelters and workers of electrolytic process.

PS 2234p Urinary Arsenic Concentration As a Biomarker of Exposure to Arsenic in Drinking Water

L. Schwarcz, B. Malczewska-Toth and H. Krapfl. *New Mexico Department of Health, Santa Fe, NM.*

In New Mexico (NM), arsenic in groundwater has been measured as high as 600 μg/L. Arsenic in drinking water is a potential public health concern in areas of NM where concentrations in groundwater exceed the Environmental Protection Agency maximum contaminant level of 10 μg/L. Approximately 90% of NM's drinking water supply comes from groundwater. A biomarker of arsenic exposure could estimate the contribution of arsenic from drinking water. The analysis evaluated how well urinary arsenic concentration is associated with arsenic concentration in drinking water among NM biomonitoring project participants.
Data were utilized from three NM Department of Health projects conducted from 2004 through 2012, which included volunteer participants residing in 76 communities. For this analysis, only adults who provided samples of their drinking water, a spot urine sample and completed an exposure assessment survey were included (N=1009). Total arsenic concentrations from drinking water and urine samples were analyzed. Sample collections and analytical methods applied were similar among the biomonitoring projects, therefore, it was concluded that the results could be pooled for analysis. A multiple regression model was developed to evaluate the effect of drinking water arsenic concentration on urinary arsenic level, with adjustment for variables such as age, sex, dietary supplement use, tobacco use, fish/seafood consumption, and daily water consumption.
After adjusting for relevant covariates, for each 1 μg/L increase of total arsenic in drinking water, there was a 2.7% increase in creatinine-corrected total urinary arsenic concentration.
Urinary arsenic concentration can serve as a biomarker of exposure to arsenic in drinking water; however, other factors also contribute to urinary arsenic levels. Education about the importance of arsenic testing and methods of reducing arsenic in drinking water, especially for those on private wells, can positively affect health behavior of communities at risk for excessive exposure to arsenic.

PS 2234q A Comprehensive Evaluation of Inorganic Arsenic in Food and Considerations for Dietary Intake Analyses

A. Lewis, H. N. Lynch, G. I. Greenberg and M. C. Pollock. *Gradient, Cambridge, MA.*

Arsenic (As) can exist in the environment in several different forms, and each form has unique chemical characteristics that influence its toxicity. Within the last decade or so, the increased focus on speciated As (both the inorganic and organic forms) and its potential toxicity has resulted in a large body of literature on speciated As in different food types. We evaluated the state of knowledge of As speciation in food and calculated the average levels of several species of As measured in food. Because inorganic arsenic (inAs) is considered the most toxicologically important form of As, we focused our analysis on papers presenting information on total inAs and speciated inAs (inAs3+ or inAs5+). Other As species (e.g., monomethylarsonic acid [MMA], dimethylarsinic acid [DMA]) were also evaluated when presented with inAs information. Publications were drawn from the peer-reviewed literature and reports by authoritative health agencies. We compiled a large database of measurements, including over 6,000 unique inAs data points. Our analysis demonstrated that inAs in foods can vary widely by type and even by sample, with mean inAs concentrations ranging from undetectable (in milk) to 8,100 μg/kg (in seaweed/algae). After seaweed, the highest mean inAs concentrations were found in rice-based products such as flour and bran, followed by rice and rice cereals. We also found a high percentage of non-measurable As in many food types. We believe this is one of the first analyses to combine data from the available literature on speciated arsenic to calculate summary statistics for a variety of food types. The applicability of our analysis is limited, however, by uncertainties introduced by unclear study methodology and inconsistencies in the available data. Calculations of dietary intake of As must consider study quality, the treatment of undetectable concentrations of As species, and the consumption patterns of the population of interest.

PS 2234r Organic Chemical Exposure and Dose from Paper Products: A New Suite of Integrated Predictive Models

M. Posson, K. T. Bogen, M. Glomski and P. Sheehan. *Health Sciences, Exponent, Inc., Oakland, CA.*

A suite of models was developed to estimate consumer exposures to organic chemicals in paper packaging. These models estimate chemical dose to consumers for different paper-product categories using corresponding representative NHANES 2003–2008 food-consumption data and migration-related physico-chemical parameters compiled for >120 chemicals (e.g., molecular weight, temperature-specific vapor pressure, water solubility, and log octanol-water partition coefficient). Data from a review of more than 80 studies on chemical migration from paper into food products and food simulants were extracted into a database used to fit physico-chemical regression (PCR) models that predict the extent of chemical migration over time using three different paper characteristics (basis weight, presence of paper coating, and contact area), under seven different conditions of storage and handling. The models developed address exposure by ingestion, wet-dermal contact, and dry dermal contact. The approach developed to assess chemical exposures from paper products was illustrated using three examples of dry fatty foods under heated, room, and frozen temperatures represented by French fries, cakes, and frozen lasagna, respectively. Each example was investigated for a total (n) of 97 to 116 chemicals with a broad range of chemical properties. Simplified PCR models, involving two or three parameters, were determined to accurately predict each corresponding set of chemical-specific doses via the ingestion pathway: 0.999 (French fries, n = 116), 0.988 (cakes, n = 113), and 0.927 (frozen lasagna, n = 97). Dry dermal dose fractions were found to be negligible, except for in the case of French fries (average ~12%). The wet dermal contact model is applicable only to paper products that become wetted during use (e.g., paper towels). The suite of models can be used to screen consumer exposures to organic chemicals in paper packaging under a variety of conditions and is effective for product stewardship assessments and compliance with consumer-based laws or regulations.

PS 2234s Exploring Exposure Pathways with Chemical/Product Categorical (CPCat) Data

K. Dionisio[1], A. Frame[1], M. Goldsmith[1], J. F. Wambaugh[1], A. Liddell[1], T. Cathey[2], D. Smith[1], J. Vail[1] and R. Judson[1]. [1]*US EPA, RTP, NC and* [2]*Lockheed Martin, Durham, NC.*

We are exposed to thousands of chemicals over our lifetimes. A major challenge to risk assessors is to understand how and when chemical exposures occur, and which "exposure pathways" contribute the most. An informatics-driven approach to assigning "product-use" categories to product "ingredients" will help prioritize which chemicals will be given more scrutiny for a target population (life-stage, gender, ethnicity), identifying (a) human activities that result in increased chemical exposure while (b) reducing the dimensionality of hazard assessment to a tangible subset for risk characterization. How chemicals are used is directly related to their potential exposure routes, and in the sense of near-field source apportionment, to the identification of chemical-specific use-to-receptor exposure pathways. We have developed the Chemical/Products Categories Database (CPCat) to explore these pathways. CPCat is a relational database comprised of chemical "use category" information, including both consumer- and industrial-process based uses for chemicals, using mined and curated data from 14 major sources from multiple countries, including data from regulatory bodies, manufacturers and retailers. CPCat contains information on 42K unique chemicals mapped to a set of >700 use categories. We provide an example of how CPCat can be used to link life-stage to use-pattern to products and their ingredients for children's exposure. CPCat can be used to identify chemicals that children would potentially be exposed to, and the major activity/source of such exposures; a database query of the "child" or "baby" keywords results in the identification of 1,300 chemicals, of which the majority are associated with the "child toy" CPCat category. This information can then be used to rank plausible exposures of chemicals which may be investigated for potential biological activity. The entire database and a set of tools will be made publicly available. *The views expressed in this abstract are those of the authors and do not reflect the views or policies of the U.S. EPA.*

PS 2234t Naturally-Occurring Airborne Diacetyl Concentrations Resulting from Roasting and Grinding Coffee Beans in an Industrial Setting

S. Gaffney, C. J. Ronk, B. L. Finley, J. L. Henshaw, J. S. Pierce, L. McCarthy, J. Lotter and A. Abelmann. *Cardno ChemRisk, San Francisco, CA.*

Diacetyl is added to many food products to impart a buttery flavor. There is ongoing debate as to whether occupational exposures to diacetyl are associated with an increased risk for certain respiratory diseases, particularly bronchiolitis obliterans (BO). While some believe that the weight of evidence points to a causative relationship, others have noted contradictory evidence, including that diacetyl also occurs naturally in many foods (e.g., wine and dairy products) and other consumables (e.g., tobacco). Studies have shown that diacetyl emissions from these products can exceed exposures in food and flavoring manufacturing settings, and yet they have not been associated with an increased risk of BO. Coffee is another potential source of diacetyl exposure. During roasting, naturally occurring amino acids and sugars in coffee beans undergo a Maillard reaction to create diacetyl. However, there are no published data on diacetyl emissions associated with processing coffee beans. We measured airborne concentrations of naturally-occurring diacetyl at a facility that roasts and grinds coffee beans with no added flavoring agents. A total of 36 task-based stationary air samples were collected at breathing zone height over the course of three 60-lb roasting batches that lasted 37-41 min each, and three 15-lb grinding batches lasting 8-11 min each; all samples were analyzed using OSHA 1012 method. Diacetyl concentrations ranged from undetectable to 3.6 ppb in the immediate work area of a roasting operator, and from undetectable to 3.9 ppb 7-15 ft from the roaster during roasting operations. During grinding, diacetyl concentrations ranged from 110-390 ppb in the immediate work area of a grinding operator, and from 18-36 ppb approximately 6 ft from the grinder. Our findings suggest that naturally occurring diacetyl is released from processing coffee at concentrations that may exceed proposed occupational exposure limits. These results may be useful for evaluating whether or not diacetyl exposure increases the risk of BO.

PS 2234u Serum Ferritin, Calcium, Albumin and Ascorbic Acid Levels in Smokers in Calabar, Nigeria

E. R. Egbe[1], Y. D. Obisesan[1] and S. T. Maleghemi[2]. [1]*Medical Laboratory Science, University of Calabar, Calabar, Cross River, Nigeria and* [2]*Community Medicine, University of Calabar, Calabar, Cross River, Nigeria.* Sponsor: J. Anetor.

Rationale and scope of the study: Exposure to tobacco smoke is injurious to health, this study aims at comparatively assessing the toxic effect of cigarette smoking on the biochemical substances that promotes healthy living. One hundred and eighty subjects voluntarily enrolled for this study after obtaining informed consent and ethical clearance. Subjects were between 24 - 65 years of age, subdivided into active (60) and passive (60) smokers and non smokers(60).
Method: Enzyme linked immunosorbent assay technique was used for the estimation of serum ferritin while calcium, albumin and ascorbic acid were analyzed colourimetically. Result: Serum Calcium, albumin and ascorbic acid levels were significantly lower($P<0.05$) in active and passive smokers than non smokers while ferritin was significantly elevated ($P<0.05$) in the smokers than non smokers. Correlation analysis supports prolonged exposure to cigarette smoke with increased ferritin levels. Conclusion: Elevated ferritin in smokers is consequent on alveolar macrophage stimulation while depleted biomolecules is a product of toxic cotinine metabolites.

PS 2234v Estimated HPHC Intakes from SNUS Consumption: Comparison with Dietary Intakes

P. Begemann[1], O. Mudasiru[1], C. Ward[1], M. Curvall[2] and L. Rutqvist[2]. [1]*Health Sciences, ENVIRON International Corporation, Arlington, VA and* [2]*Swedish Match, Stockholm, Sweden.*

More than 8000 different components have been identified in tobacco and tobacco smoke. In 2012, the FDA released a list of close to 100 "Harmful or Potentially Harmful Constituents (HPHCs)" in tobacco products and tobacco smoke that it determined have the potential to cause direct or indirect harm. The objective of the present study was to compare estimated daily intakes of relevant HPHCs from consumption of snus, a traditional Swedish moist snuff, to intakes from the diet.
Average and worst case scenarios were based on analyses of 35 HPHCs and additional PAHs and volatile nitrosamines in 8 Swedish Match (SM) snus products, extraction data (where available), and data on snus consumption. The worst case calculations used the highest HPHC concentration from SM Brand Testing and upper bound daily snus consumption. For the comparison to dietary intakes, average population-based intakes from public health agencies, guidelines, or concentrations in common foods were used. HPHC concentrations below the laboratory limits of detection (LOD) were taken into account as $LOD/\sqrt{2}$.
The analysis showed that snus use results in HPHC intakes either lower or generally similar to those from food. For example, intakes of all analyzed PAHs, acetaldehyde, most metals, acrylamide, and aflatoxins were, even under worst case conditions and assuming 100% extraction, below the average or within the range of estimated dietary intakes. Using similar methods and the latest published concentrations in cigarette main stream smoke, tobacco-specific nitrosamine intakes were found to be similar for average snus use and smoking.
This comparison between intakes of HPHCs is not intended to directly address health risks of the particular components, and potential local effects were not considered. Limitations of the approach include assumptions regarding extraction and uptake of HPHCs from snus and food; however assumptions were conservative and therefore the estimated exposures from snus consumption for most current users would not likely be higher than calculated in this analysis.

PS 2234w Dermal Absorption of Benzo[a]pyrene: Assessment of Flux from Aged Soil and Application to Risk Assessment of Contaminated Sites

J. Kissel[1], A. Bunge[2], Y. W. Lowney[3] and M. Ruby[4]. [1]*University of Washington, Seattle, WA,* [2]*Colorado School of Mines, Golden, CO,* [3]*Exponent, Boulder, CO and* [4]*Integral Consulting, Louisville, CO.*

Soil cleanup standards are based in part on predicted human exposure to soil contaminants. Chemicals in soil may be transferred to the skin surface upon dermal contact, and from there, systemically absorbed. Because dermal absorption from soil is generally not rapid, characterization of the rate of uptake is important in predicting absorbed dose. For PAHs, USEPA currently recommends that risk assessments assume the dermal absorption of PAHs from soils to be 13% of the total applied dose. However, fractional absorption is not independent of load. Dermal absorption is best described in terms of gradient-driven flux. In order to update existing knowledge regarding potential for dermal absorption of PAHs from contaminated soil, we conducted experiments with four soils of varying organic carbon and

black carbon content. Aging of radiolabelled benzo(a)pyrene (BaP) on the soils was conducted for eight weekly cycles in which soils were wetted and dried. Eight- and 24-hr absorption experiments were then conducted in vitro using heat-separated human cadaver epidermis to assess the flux of BaP from each soil and to investigate the effect of soil characteristics and BaP concentrations on flux. Experiments were also conducted with BaP delivered in solvent to permit comparison to absorption from a soil matrix. Uptake (as assessed by radiolabel recovered from swabbed skin) of solvent-deposited BaP was more rapid than penetration to receptor fluid, reflecting lag time in skin. Uptake and penetration from aged soils at nominal initial concentrations of 3 and 10 ppm BaP were correspondingly lower, reflecting reduced thermodynamic activity in soil. This research is particularly relevant in light of EPA's draft toxicity profile for BaP, which introduces a Dermal Cancer Slope Factor for use in risk assessment of BaP exposures, including exposures from soil.

PS 2234x Hematoxicity and Genotoxicity in Children Exposed to Benzene in a Petrochemical Area in México

P. Nadia[1], R. Diana[2], H. Alejandra[1], E. D. Israel[2] and M. Brenda[1]. [1]*Instituto de Ciencias de la Salud, Universidad Autónoma del Estado de Hidalgo, Pachuca, Hidalgo, Mexico and* [2]*Universidad de Guanajuato, Guanajuato, Mexico.* Sponsor: M. Gonsebatt.

Background Children living in Tula, Hidalgo, México, are exposed to pollutants from petrochemical and chemical industries located in the area. The Secretaría de Medio Ambiente y Recursos Naturales (SEMARNAT) reports emissions to environment of some toxic compounds. Benzene emission has been reported to the enviroment and it is well known that is an hematotoxic and genotoxic compound.
Objective The aim of this study was to evaluate the genotoxicity and hematological effects in children environmentally exposed to benzene.
Methods Samples of urine, blood and buccal epithelium were obtained from 26 children (6-8 years old). Exposure to benzene was assessed by determination of an urine metabolite: trans, trans-muconic acid (t,t-MA). Micronucleous frecuency (MNf) was evaluated in buccal epithelial cells and hematological parameters were determined.
Results: Expossure assessment indicates that the 35% of children have levels above de Biological Exposure Index (500 μg/gCreatinine). The mean of the t,t-MA urinary levels was 460.7 μg/gCreatinine; this value is above of levels reported in previous studies in children from Italy, Thailand and México. In the hematological status assessment, 100% of children have some hematic parameter abnormal. The 78% have hemoglobin levels above normal values for the age group; 42% has altered leukocytes (10% lymphopenia, 19% granulocytes alterations, 22% monocytes). The preliminary results (n = 8) the mean of MNf was 12.7/1000; this value is three times higher than those reported in other studies in children. No statistic significant correlation between benzene exposure and hematological parameters was found.

PS 2234y Refined Exposure Assessment for Three Active Ingredients of Humidifier Disinfectants

J. Lee[1], J. Kwon[2] and C. Kim[1]. [1]*Institute of Environmental Protection and Safety, NeoEnBiz Co., Bucheon, Republic of Korea and* [2]*Division of Environmental Science and Ecological Engineering, Seoul, Republic of Korea.* Sponsor: J. Choi.

Exposure assessment for three major active ingredients used for humidifier disinfectants, polyhexamethylene guanidine (PHMG), oligo(2-(2-ethoxy)ethoxyethyl guanidinium chloride (PGH), and 5-chloro-2-methylisothiazol-3(2H)-one/2-methylisothiazol-3(2H)-one (CMIT/MIT) mixture, were conducted in a bedroom using an air sampler for a refined risk assessment. The experimental site was selected to reflect consumer exposure conditions. Aerosols formed by a humidifier were sampled during 8 h at 7.5 L min-1. Absorbed PHMG and PGH by the sampler were quantified using a spectrophotometric method and an HPLC-UV detection was used for CMIT/MIT. Three exposure scenarios were assumed for adding humidifier disinfectants to the humidifier water at 1, 2, and 10 times the volume recommended by the product suppliers and the humidifier was on at its maximum rate of producing aerosols in order to consider reasonable worst-cases. Sampled mass of PHMG and PGH ranged 200~2800 μg and 140~1900 μg, respectively, under different exposure conditions, whereas absorbed mass of CMIT/MIT was barely detected at the detection limit of 0.11/0.29 mg/L only at 10 times the recommended level. The resulting risk quotients for PHMG and PGH ranged 1400~20000 and 1000~13000, indicating that health risks could be significant. For CMIT/MIT mixture, risk quotients were much smaller than estimated by assuming that they are conservative in the indoor environment probably due to oxidative reactions. Refined exposure assessment presented here may provide a useful tool for assessing risks posed by active ingredients in spray-type biocidal products.

PS 2234z Evaluation of Asbestos Exposure Associated with Research Laboratories

G. T. Johnson[1], E. Garcia[1], D. Newfang[1], J. Coyle[1], C. Blake[2] and R. D. Harbison[1]. [1]*College of Public Health, University of South Florida, Tampa, FL and* [2]*Bureau Veritas North America, Kennesaw, GA.*

Asbestos containing materials have been used for decades in research laboratory products and include transite, tong asbestos sleeves, gloves, gauze pads, and other materials. These materials typically contain chrysotile asbestos with concentrations raging up to 80%. The objective of this study was to evaluate asbestos exposure from selected products with simulated laboratory use. An environmental chamber was used to simulate laboratory application of the products. Bulk samples of various products were tested before and after use. Industrial hygiene personal and area air samples were collected during all testing following NIOSH 7400/7402 methodologies. Phase contrast microscopy (PCM) and transmission electron microscopy (TEM) were used for sample analyses. Collection of personal and area air samples varied between 4 and 6 hours. Analysis of personal air samples using PCM, showed airborne fiber concentrations as high as 0.058 f/ml during use of tongs fitted with asbestos sleeves. Further analysis using TEM showed the highest asbestos level of 0.0036 f/ml. Manipulation of transite board resulted in personal TWA asbestos levels as high as 0.02 f/ml. Analysis of area air samples during heating of gauze pads using PCM showed airborne fibers concentrations ranging from less than 0.007 to 0.009 f/ml. When analyzed using TEM, asbestos levels ranged from 0.001 to 0.002 f/ml. Personal samples were in similar ranges. Some asbestos was lost from gauze pads during use. Asbestos–containing gauze pads produce de minimis air levels of asbestos when heated. Testing of various asbestos containing materials used in research laboratories indicate low potential for asbestos fiber exposures.

PS 2234aa Managing the Risk of Occupational Allergy in the Enzyme Detergent Industry

D. Basketter[1], F. H. Kruszewski[2], S. Mathieu[3], D. Kirchner[4], A. S. Panepinto[4], M. Fieldsend[5], V. Siegert[6], F. Barnes[7], R. Bookstaff[4], M. Simonsen[8] and B. Concoby[9]. [1]*DABMEB Consultancy Ltd., Sharnbrook, United Kingdom,* [2]*American Cleaning Institute, Washington, DC,* [3]*A.I.S.E., Brussels, Belgium,* [4]*Procter & Gamble Company, Cincinnati, OH,* [5]*Unilever, Sharnbrook, United Kingdom,* [6]*Henkel AG & Company, Duesseldorf, Germany,* [7]*Robert McBride Ltd., Manchester, United Kingdom,* [8]*Novozymes A/S, Bagsvaerd, Denmark and* [9]*DuPont Company, Palo Alto, CA.*

Enzyme proteins have long been recognized to have a potential to cause occupational allergy. Consequently, enzyme detergent manufacturers have chosen to implement a number of control measures to ensure that the hazard does not translate into health effects in the workforce. A determination has been provided on how risk management guidelines for the industry, as developed by the American Cleaning Institute and the International Association for Soaps, Detergents and Maintenance Products, were actually implemented in practice and the resulting experience of workplace exposures and health impacts. Both medical surveillance and air monitoring practices associated with the implementation of industry guidelines at over 100 manufacturing facilities over a five year period were evaluated with respect to the prevalence of allergic antibody and occupational respiratory allergy. In the five years of experience reviewed herein, results from air monitoring and health surveillance show success in both areas at a level of greater than 99%. The data show that by using the approaches described for the limitation of exposure, for good occupational hygiene, and for active health monitoring, the respiratory allergenic hazard associated with enzyme proteins can be successfully managed to ensure the safety of the workforce.

PS 2235 Asbestos Content of Heavy Equipment Brake-Wear Debris and Associated Airborne Exposures during Brake Work

M. Grespin[1], E. Donovan[1], R. Ward[1], A. Madl[2] and B. L. Finley[3]. [1]*Cardno ChemRisk, San Francisco, CA,* [2]*Cardno ChemRisk, Aliso Viejo, CA and* [3]*Cardno ChemRisk, Brooklyn, NY.*

Asbestos-containing brake linings were commonly used in heavy construction equipment until the 1980s. However, asbestos exposures and potential health risks associated with brake repair on heavy equipment have not been comprehensively evaluated. The present study determined whether individuals working with heavy equipment brake components, or bystanders to such work, were exposed to chrysotile asbestos above exposure limits dependent upon chrysotile content of equipment brake wear debris (BWD) and type of machinery. Publicly available published and unpublished studies examining BWD asbestos content in various heavy equipment were identified. Variables potentially contributing to BWD and airborne asbestos concentrations included common brake job practices, infrequent

manipulative activities, cleaning methods, and brake component dimensionality. Tasks included combinations of changing brakes, inspection of brake pads, glazing brakes with sandpaper, and cleaning with solvent or compressed air. The degree to which airborne asbestos concentrations correlated to BWD composition and physical characteristics, the type of heavy machinery, and the brake work activities was determined. Most, but not all, BWD samples contained less than one percent chrysotile by weight. For air samples, phase contrast microscopy results for personal, bystander or area samples did not exceed 0.622 total f/cc based on short-term, task-based sampling. 8-hr time weighted average concentrations did not exceed 0.045 asbestos f/cc after adjusting for asbestos content using transmission electron microscopy. These results are consistent with those observed for smaller vehicles, including automobiles. This suggests that individuals working with these materials would not have been exposed to asbestos above contemporaneous or current exposure limits, regardless of BWD chrysotile content. It is unlikely that the dimension of brake components influences the degree to which mechanics working with such products were historically exposed to asbestos.

PS 2236 Determination of Air Conc. and Exposure to Spores from Microbe-Based Cleaning Products: Influence of Human Activity and Vacuuming

N. W. Berg[1], J. Sedivy[2], R. Testman[3], K. Acedo[3] and T. G. Osimitz[4]. *[1]Novozymes A/S, Bagsvaerd, Denmark, [2]Novozymes Biologicals, Inc., Salem, VA, [3]Golden Pacific Laboratories, Fresno, CA and [4]Science Strategies, LLC, Charlottesville, VA.*

Microbe-based carpet cleaning products contain non-pathogenic, highly specialized microbes that produce appropriate enzymes in the presence of soils ceasing production when the stains or soils have been removed. These products are used in homes and institutions and potential for human exposure from residues in the air and on treated surfaces exists. The purpose of this study was to determine the air conc. of viable bacterial spores after use of two microbe-based carpet cleaning products based on a blend of *Bacillus* spores: a whole room consumer-use product and machine applicator & a spot treatment product using a trigger sprayer. The influence of choreographed human activities on airborne spore levels was investigated. Studies were conducted in a simulated residential exposure room carpeted with plush nylon carpet and equipped with impingers to collect airborne spores.
Airborne spore levels were elevated after application of either product but quickly returned to values similar to the 95th percentile or less of field measurements of airborne spores in indoor settings. Vacuuming and passage of time continued to cause a decrease in airborne levels. The trigger sprayer for spot application produced levels of airborne spores slightly above the provisional threshold limit (TLV) of 1x104 CFU/m3, established for airborne microbes in occupational settings. The spores are, however, mainly carried in non-inhalable water-based particles. So although airborne spore counts in the spot application exceeded the TLV, trigger sprayer products typically produce non-inspirable particles that, despite their presence, actually pose minimal potential for pulmonary exposure.
Based on the data from these exposure studies, and a critical evaluation of the published literature, it is concluded that carpet cleaning products containing a mix of *Bacillus* spores can be regarded as safe for the users.

PS 2237 A Continuing Legacy of Chlordane and Dieldrin?—A Case Example of Pesticides in Well Water in Stamford, Connecticut

S. M. Rusnak[1] and A. Fountain[2]. *[1]CT Dept. of Public Health, Hartford, CT and [2]Stamford Department of Health, Stamford, CT.*

The Connecticut Department of Public Health (CT DPH), the Connecticut Department of Energy and Environmental Protection (CT DEEP), and the city of Stamford have been involved over the past four years with a number of contaminated private wells in Stamford. Banned pesticides, dieldrin and chlordane, were discovered in several private wells at levels exceeding Connecticut's state drinking water guidelines. The source of the contamination was originally thought to be a nearby landfill, but it is now believed to be from either home pesticide treatment for termites or agricultural use several decades ago. The well contamination issue was originally thought to be limited to a small area of Stamford, but now it is known to be more widespread. To better understand the scope of the pesticide contamination in Stamford, the Stamford Health Department launched a small random sampling program and a subsidized city testing program. There are almost 2000 wells that have been tested to date where approximately 15% of wells tested have either dieldrin and/or chlordane present with 6% exceeding state drinking water guidelines. The maximum concentrations of chlordane and diedrin in wells are 7.4 and 1.3 parts per billion (ppb), respectively, and 25 and 43 times the state drinking water guidelines. Using these maximum levels for chlordane and dieldrin, the lifetime cancer risk from drinking the contaminated water is up to 5 excess cancer cases out of a population of 10,000. The city of Stamford, with assistance from CT DEEP and CTDPH, took a proactive approach and placed many of these homes on whole house filters and later to municipal water. CT DEEP, CTDPH, and the city of Stamford have taken a number of actions to deal with the private well contamination and inform the community. The pesticide contamination in Stamford raises broader questions about the past practice of treating home foundations for termite control using chlordane and dieldrin and the nature and scope of potential impacts to groundwater quality in Connecticut and possibly other states.

PS 2238 Surface Water Risk Assessment of Pesticides in Ethiopia

B. M. Teklu[1], P. I. Adriaanse[2], M. M. Terhorst[2], J. W. Deneer[2] and P. J. van den Brink[1, 2]. *[1]Aquatic Ecology and Water Management, Wageningen University, Wageningen, Netherlands and [2]Altera, Wageningen University and Research centre, Wageningen, Netherlands.* Sponsor: A. Patrick.

Scenarios for future use in the pesticide registration procedure in Ethiopia have been devised for 3 separate Ethiopian locations, which are considered to be protective for 99% of Ethiopia. The scenarios estimate concentrations in surface water resulting from agricultural use of pesticides for a small stream and for 2 types of small ponds (Adriaanse et al., 2013). Preliminary results from scenario calculations will be presented.
On the basis of volume of use, application rate in Ethiopia and acute human toxicity the 7 pesticides considered to be of most risk to humans were selected, assuming exposure as a result of the consumption of surface water. Estimates of exposure concentrations in surface water were established using modelling software also applied in the EU registration procedure (PRZM and TOXSWA). Calculations generated the 99-percentile maximum concentration for use in human risk assessment and the 90-percentile maximum concentration for use in ecotoxicological risk assessment. Input variables included physicochemical properties, and data such as crop calendars, irrigation information, meteorological information and detailed application data which were specifically tailored to the Ethiopian situation.
The results indicate that for all the pesticides investigated the acute human risk resulting from the consumption of surface water is low to negligible, whereas agricultural use of Chlorothalonil and Endosulfan may result in medium to high risk to aquatic species.
Key words: Risk assessment, pesticides, models simulation, aquatic ecosystem, Ethiopia

PS 2239 Human Health Risk Assessment of Metals in Fish in Ghana

D. Doke and J. M. Gohlke. *Environmental Health Sciences, Univ of Alabama at Birmingham (UAB), Birmingham, AL.*

Fish advisories have been established by many nations to protect the public from potentially harmful health effects linked to eating contaminated fish. Advisories are based on estimations of cancer and non-cancer health risks associated with concentrations of contaminating chemicals found in fish, and the average levels of consumption of fish in the population. Fish is an important source of nutrition in Ghana; however, little is known about potential health effects associated with eating fish in Ghana. The overall aim was to estimate the extent of contamination of the fishery resource so as to inform guidelines on fish consumption. We gathered information on levels of metals in fish in Ghana from scientific publications identified using the PubMed database. We estimated human health risk by calculating a hazard quotient based on the reported levels of mercury in fish and compared risk across different fish species and water bodies in Ghana. Mercury was the only metal in which there was sufficient data to estimate human health risk from eating fish caught in Ghana. The mean for all the recorded values for mercury concentrations in fish was 0.10 mg/kg wet weight. This concentration is associated with a hazard quotient of greater than 1, meaning that adverse health effects are possible. Generally, lower concentrations of mercury were found in fish from the lakes sampled while higher concentrations were detected in fish from rivers, particularly in gold mining areas of Ghana. Our results indicate mercury found in fish may be causing health effects, such as impaired neurological development. It is important for the government and relevant agencies in Ghana to consider a mechanism to effectively monitor pollution, issue fish consumption advisories when warranted, and determine and remediate the source of contamination, which likely includes mercury emissions from artisanal mining based on the heightened levels found in fish from rivers in the gold-mining region.

PS 2240 Exposure Assessment of Children Ingesting Pb in Lipstick and Its Comparison to Regulatory Values

M. Lippi, M. Abramson, W. V. Christian and A. Monnot. *ChemRisk, San Francisco, CA.*

The lead (Pb) content consumer products has become an increasing concern over the past several years. In 2007, the Campaign for Safe Cosmetics published the test results of 33 lipstick samples and found that 61% contained lead, with a maximum Pb concentration of 0.65 ppm. In 2010 the US FDA tested 400 lipstick samples and found a median Pb concentration of 0.9 ppm and a maximum Pb concentration of 7.19 ppm. To assess the safety of these lipsticks in instances where children might intentionally or incidentally ingest lipstick products, we used the US EPA's Integrated Exposure Uptake Biokinetic (IEUBK) Model for Lead in Children to determine the blood Pb concentrations of children (aged 0-7) ingesting varying amounts of lipstick of different Pb concentrations. Modeled blood Pb concentrations were then compared to the estimated blood Pb concentration for the US Consumer Product Safety Commission's (CPSC) guideline of 15 ug Pb/day (orally) and to the Centers for Disease Control (CDC) and US EPA actionable blood Pb levels (BLL) of 5 ug/dL and 10 ug/dL, respectively. The maximum estimated geometric mean blood Pb level resulting from the ingestion of the CPSC guideline was 3.8 ug/dL, assuming inclusion of background sources in the guidance value. The amount of the highest concentrated lipstick (7.19 ppm) required to yield a blood Pb concentration in the range generated by the CPSC guidance value and the US EPA BLL (3.8 – 10 ug/dL) was 0.25 – 4.94 g lipstick/day; this is equivalent to ingestion of around 1/50th to 2/5th of a 3.0 oz tube of lipstick/week, assuming concomitant background exposure. The amount of lipstick with the FDA median concentration of 0.9 ppm that would need to be ingested to reach this blood Pb concentration range was 2.0 – 39.4 g lipstick/day, or around 1/5th to three 3.0 oz tubes of lipstick/week. Our results suggest that the safety of these products and cosmetics should be assessed not only by the presence and amounts of hazardous contents, but also through an assessment of estimated exposures and comparison to health based standards.

PS 2241 Improving Emergency Preparedness: Reviewing Respiratory Irritants of Hazardous Chemicals to Enhance the Chemical Mixture Methodology

H. Dixon[1, 4], C. Nix[2, 4], J. Yao[4], H. Fournier[3, 4], S. Folkens[3, 4], C. Glantz[4] and X. Yu[4]. [1]*University of Puget Sound, Tacoma, WA,* [2]*University of Ashland, Ashland, OH,* [3]*Wittenberg University, Springfield, OH and* [4]*Pacific Northwest National Laboratory, Richland, WA.*

The U.S. Department of Energy and other public and private sector entities programs use the Chemical Mixture Methodology (CMM) for emergency response planning for facilities that have the potential for an airborne release of hazardous chemicals. The CMM calculates hazard indices (HIs) for each chemical in a mixture based on two components: the estimated concentration of the chemical at a given receptor location and the known health-based concentration limit for exposure to the chemical. If the combined HI for a chemical mixture exceeds unity, it indicates that the health effects from the release could inhibit an individual's ability to perform protective actions. Health code numbers (HCNs) identifying specific toxic effects (e.g., brain, liver) are then used to provide a more detailed and accurate evaluation of the potential health effects from exposure to an airborne chemical mixture. The current CMM's method combines moderate and severe respiratory irritants in one HCN and it does not consider mild effects. The CMM research team hypothesized that by separating respiratory irritants effects into severe, moderate, and mild HCNs and applying appropriate weighting factors, the CMM would provide a more accurate assessment of health effects for chemical mixtures that include respiratory irritants. During a summer internship for undergraduate students, the two lead authors reviewed over 1,000 chemicals in the CMM data set that are classified as respiratory irritants and reassessed HCNs based on data from 11 technical references. The interns then conducted a preliminary evaluation of the benefit of the revised approach using 127 test cases (one-third of the CMM testing database). Results show that the new HCNs reduced HI values in 44% of the test cases, with differences of ≥5% occurring in about 89% of all the test cases. This confirms that the revised respiratory irritants enhance the CMM.

PS 2242 Health Effects of Mercury in Flared Natural Gas

S. Yu[1], L. Hall[1], S. Karania[2], H. Wong[2] and M. Keinath[2]. [1]*ENVIRON International Corporation, Emeryville, CA and* [2]*ENVIRON International Corporation, San Francisco, CA.*

Mercury is a naturally-occurring volatile contaminant of natural gas; concentrations range from <0.01 to 2000 μg/m3 worldwide depending on the geologic deposit. Hydraulic fracturing has revolutionized the scale of natural gas extraction, with certain shale deposits supporting thousands of active wells. At production platforms, large volumes of natural gas are flared (burned) to remove unwanted gas; in the process mercury may be released to ambient air. Mercury is a well-recognized toxin that can affect the nervous, immune, and other systems.

We used a range of published natural gas mercury levels, well completion flared gas volumes, and a screening level dispersion model (SCREEN3) to model mercury concentrations in ambient air near a model gas well. We speciated total mercury emissions into elemental and mercuric forms and considered soil deposition and mercury methylation. Potential health effects from inhalation, ingestion, and dermal exposure to different mercury species were evaluated by applying USEPA exposure parameters and standard toxicity reference levels.

Our results indicate that maximum annual average airborne concentrations of mercury occur approximately 1000 meters from the well. Based on modeled concentrations, mercury emitted from flaring during the completion phase of a single well does not pose chronic health concerns (hazard index [HI] <1). There are many uncertainties inherent in this screening-level assessment, including modeling emissions from a single well, inclusion of only a single category of flare source, the mercury concentration of natural gas, the use of a screening air dispersion model, and mercury speciation and deposition. While preliminary, given the complexity of active high-density natural gas well fields with diverse mercury content, a refined risk assessment should be performed to ensure that health risk impacts are appropriately characterized.

PS 2243 TCE, Vapor Intrusion, and Risk Management: A Case Study

J. M. LaVelle. *CDM Smith, Green Valley, AZ.*

New toxicological information has prompted USEPA to consider acute *in utero* toxicity at low levels of TCE in the air. Further, data reported from studies of vapor intrusion suggest both high variability in indoor levels, and little correlation with parameters such as temperature and pressure differentials, shallow soil vapor concentrations, precipitation, and soil characteristics. If acute effects from inhalation of TCE do occur, they may occur on few days per year, and these days cannot be reliably predicted. This dilemma presents challenges when assessing risks from acute exposure to TCE in air. Key questions include: how often will extreme concentrations occur?; what extremes might be expected?; how likely are these extremes to occur during the window for heart development?; what data are needed to support risk assessment that addresses these issues?; how should the results of the analysis be interpreted? These issues were considered where one unit of a building is used as a church. The unit is adjacent to a source of TCE contamination and overlies a "plume" of TCE vapors. Indoor air concentrations in this unit have varied somewhat over time, but have often been within an order of magnitude of the lowest air concentration of TCE being considered as a threshold for teratogenic effects (2 $\mu g/m^3$). A one-dimensional stochastic analysis, using data from residential situations to estimate frequency and magnitude of TCE excursions, occupancy information appropriate for church use, a target of indoor air concentration of 2 $\mu g/m^3$, and a window early in pregnancy for developmental effects on the heart, suggest low probability of pregnant women being present at times when TCE concentrations could be toxic. A "worst case" might suggest a few percent of days in a year; a "best" case might suggest a few percent of days over two or three years. Unless understanding of vapor intrusion improves substantially, risk managers may have to decide where along a continuum of days per unit time where risks become acceptable. The situation appears similar to that of lead, where an acceptable target is based on achieving target blood lead levels in percentage of children.

PS 2244 Risk Assessment of Biogas Trace Constituents

K. Kloc, A. G. Salmon, R. H. Lam, D. Siegel and M. Marty. *Office of Environmental Health Hazard Assessment, California Environmental Protection Agency, Oakland, CA.*

California law required OEHHA, working with the California Air Resources Board (CARB), to develop a human health risk assessment for residential and occupational exposure to toxic constituents present in biogas, a source of fuel methane and alternative to natural gas. Our study focused on the three most likely biogas sources for California in coming years: municipal landfills, municipal wastewater treatment plants, and dairy farm wastes. More than 300 trace constituents have been identi-

fied in raw biogas from these sources, including numerous straight and branched alkanes, alkenes, aldehydes, esters, alkyl benzenes, thiols, sulfides, organometals, organosilicon compounds, and many regulated toxic volatile organics. We collated risk-estimating criteria (i.e., toxicity values) for the biogas constituents from databases published by OEHHA, the U.S. EPA, and two other federal agencies. In some cases, we grouped chemicals whose toxicological properties were judged to be similar, and developed a single toxicity value for each group. Approximately 50 constituents lacked either individual or group risk criteria and could thus not be quantitatively assessed (e.g. several benzene derivatives and alkyl sulfides). We obtained air concentration estimates from CARB and evaluated cancer and non-cancer risks using standard assessment methods developed by OEHHA. Twelve biogas constituents were determined to be of health concern to consumers or workers based upon screening thresholds for carcinogens (1 or 30-per-million additional risk, respectively) and non-carcinogens (a hazard quotient > 0.01 or 0.3, respectively). The constituents were: Alkyl Thiols, Antimony, Arsenic, Copper, p-Dichlorobenzene, Ethylbenzene, Hydrogen Sulfide, Lead, Methacrolein, n-Nitroso-di-n-Propylamine, Toluene, and Vinyl Chloride. As a result of the assessment, biomethane producers will be required to test for these chemicals to ensure that they are adequately removed from raw biogas during processing. OEHHA will update the risk assessment as new information becomes available.

PS 2245 A Global Harmonized Risk Assessment for Volatile Cyclic Siloxanes (D4 and D5)

R. Gentry[1], C. Van Landingham[1], T. Greene[1], T. Guerrero[2] and K. P. Plotzke[3]. *[1]ENVIRON International Corporation, Monroe, LA, [2]Silicones Environmental, Health and Safety Center, Washington, DC and [3]Dow Corning Corporation, Midland, MI.*

Octamethylcyclotetrasiloxane (D4) and Decamethylcyclopentasiloxane (D5), two low molecular weight cyclic siloxanes, are used globally as intermediates in the production of several widely-used industrial and consumer products. Their global use requires consideration of consumer use information and risk assessment requirements from various sources and authoritative bodies. A global "harmonized" risk assessment was conducted to meet requirements e for substance-specific risk assessments conducted by regulatory agencies such as the US EPA's Integrated Risk Information System (IRIS) and Health Canada, various independent scientific committees of the European Commission, as well as provide guidance for chemical safety assessments under the REACH Regulation in Europe, and other relevant authoritative bodies. This risk assessment incorporates global exposure information combined with a Monte Carlo analyses to determine the most significant routes of exposure, utilization of a multi-species, multi-route physiologically-based pharmacokinetic (PBPK) model to estimate internal dose metrics, benchmark modeling to determine a point of departure (POD), and a Margin of Safety (MOS) evaluation to compare the estimates of intake with the POD. Because of the unusual pharmacokinetic behaviors of D4 and D5including high lipophilicity, high volatility with low blood-to air-partition coefficients, and extensive metabolic clearance that regulate tissue dose after exposure, the use of a PBPK model was essential to provide a comparison of a dose metric that reflects these processes. The characterization of the potential for adverse effects after exposure to D4 and D5 using a MOS approach based on an internal dose metric removes the subjective application of uncertainty factors that may be applied across various regulatory agencies and allows examination of the differences between internal dose metrics associated with exposure and those associated with adverse effects.

PS 2246 Proposed Methodology for Risk Assessment of Groundwater High in Nitrates for Distillation Processes

L. A. Haighton, H. Fikree, J. W. Card and V. Lee-Brotherton. *Cantox Health Sciences International, Mississauga, ON, Canada.*

Groundwater in agricultural regions often exceeds the nitrate Maximum Contaminant Level (MCL) of 10 mg/L as nitrogen (~45 mg/L as NO_3) and reducing NO_3 below the MCL can be costly. The MCL is based on a link to infant methemoglobinemia from studies circa 1950. While later research questions this relationship, the MCL is the legal limit. A risk assessment was completed to support the safety of groundwater NO_3 levels above the MCL for use in distillation of plant oils for dietary supplement uses by children (age ≥3) and adults. The method considers the acceptable daily intake (ADI) for NO_3 (mg/kg/d), body weight of consumer (BW, kg), fraction of total daily exposure from supplement use [allocation factor (AF), %], the daily supplement dose (g/d), volume of water (mL) needed to produce 1 g of oil [distillate ratio (DR), mL/g], and partitioning to the oil phase [partitioning factor (PF), %]. Values used in this assessment: ADI=3.7 mg/kg/d (as NO_3) from JECFA (since supplement is not for infants); BW=10 kg; AF=assumed 20%; Dose=4 g/d; DR=30 mL/g; PF=100% (worst case) or 0.0041% (reasonable case based on log K_{ow} of -4.39). The NO_3 concentration in groundwater resulting in an exposure equal to 20% of the ADI from consumption of the supplement and assuming a worst case scenario of all NO_3 from water ending up in the oil (PF=100%) was calculated to be 62 mg/L based on the following equation: $Conc_{water}$ (mg/L)=[ADI (mg/kg/d) x BW (kg) x AF (%) x 1000 mL/L]÷[(Dose (g/d) x DR (mL/g) x PF (%)]. However, as NO_3 is a highly water soluble compound, the realistic PF value of 0.0041% (based on the log K_{ow} of NO_3) should be used in estimating the amount of NO_3 that would partition to the oil. Using this PF value, the groundwater concentration of NO_3 that would equal 20% of the ADI from use of the supplement is 1,504,065 mg NO3/L. This concentration could never be reached in groundwater. Thus, as essentially zero NO_3 in groundwater would likely partition to the oil, otherwise potable groundwater containing NO_3 levels above the MCL may still be safe for oil distillation.

PS 2247 Risk from Exposure to Triorthocresyl Phosphate (TOCP) in Aircraft Cabins and Flight Decks

C. Y. Chan, L. J. Swenson, J. Hobden, N. A. Moore and B. J. Kelman. *Veritox, Inc., Redmond, WA.*

There has been and continues to be concern in the airline industry about pilot and flight attendant exposure to TOCP, a well-known neurotoxin. Oil used in jet engines may contain 1-3% tricresyl phosphate of which 0.1- 1% is TOCP. The workplace 8 hour time weighted average OSHA Permissible Exposure Limit (PEL), NIOSH Recommended Exposure Limit (REL), and ACGIH Threshold Limit Value for TOCP are all 0.1 mg/cubic meter. Investigations of in-plane air contamination by aircraft turbine engine oil via engine bleed air supply systems have reported no levels of TOCP above limits of detection (LOD, 0.000009-0.001059 mg/cubic meter) in the cockpits or cabins of sampled aircraft. Since there is no inhalation toxicity factor for TOCP, we performed a risk assessment comparing the acceptable daily intake based on an oral exposure with exposure at the LOD and PEL. Our assessment indicates that pilots and flight attendants are not exposed to sufficient TOCP to cause any adverse health effects. Our assessment is consistent with recent publications reporting that there are no detectable biomarkers of exposure to TOCP in flight crews.

PS 2248 Exposure to Vitamin A (Retinol and Retinyl Esters) from Cosmetics Increases the Proportion of the Population That Exceeds the Upper Intake Level

R. B. Hetland[1], B. Granum[1], J. E. Paulsen[1], V. Thrane[1], J. L. Lyche[1], C. Lutzow-Holm[2], T. O. Fotland[1], I. L. Lillegaard[1] and I. Steffensen[1]. *[1]Norwegian Scientific Committee for Food Safety, Oslo, Norway and [2]External Expert, Oslo, Norway.*

Vitamin A, a group of compounds including retinol (ROL) and retinyl esters, is required in numerous physiological functions. ROL and retinyl esters are widely used in cosmetics such as anti-wrinkle creams and moisturisers due to their positive effects in the skin.

The Norwegian Scientific Committee for Food Safety (VKM, 2012) performed a risk assessment of ROL and retinyl esters in cosmetics based on the tolerable upper intake level (UL) of 3000 μg ROL equivalents (RE)/day (SCF, 2002) and the lower guidance level (GL) of 1500 μg RE/day for individuals at risk of osteoporosis and bone fracture (EFSA, 2008).

Oral intake of vitamin A was estimated based on national food consumption surveys. Systemic exposure dose from cosmetics (with 0.05 and 0.3% RE) was estimated based on The Scientific Committee for Consumer Safety's Notes of Guidance for the Testing of Cosmetic Ingredients (2010) and a study by Yourick et al. (2008).

Intake of vitamin A is high in parts of the Norwegian population; the most important source is diet. Use of food supplements contributes significantly and increases the proportion of the population exceeding the UL. The contribution from cosmetics to the total intake of ROL and retinyl esters is most prominent for 13-year-olds (23% of UL) and adults (29% of UL).

Excess exposure to vitamin A is of concern for individuals at risk of osteoporosis and bone fracture (e.g. post-menopausal women). About 10% of adult women in Norway exceed the GL of 1500 μg RE/day by intake from food and food supplements alone. The additional contribution of retinol and retinyl esters from cosmetics increases this proportion to ca. 75% which means a significant increase in number of individuals at risk of osteoporosis and bone fracture.

Acknowledgement. The assessment was performed by the VKM Panel on Food Additives, Flavourings, Processing Aids, Materials in Contact with Food and Cosmetics.

PS 2249 Assessment of Potential Health Risks on the Basis of the Character and Degree of Chemical Pollution of the Environment

M. I. Kombarova, A. S. Radilov and V. R. Rembovskiy. *Research Institute of Hygiene, Occupational Pathology and Human Ecology, Leningrad Region, Russian Federation.* Sponsor: K. Khamidulina.

Health risks to the population living in the protective action zone of the Maradykovsky Chemical Weapons Storage and Destruction Facility (CWSDF), Kirov Region, Russia, were assessed. The risk assessment process included four steps (hazard identification, dose–response evaluation, exposure assessment, and risk characterization) and involved ranking possible carcinogenic and non-carcinogenic hazards from exposure to pollutants emitted by the CWSDF, preliminary ranking potential carcinogens on the basis of the total annual emission and the weighting coefficient of carcinogenic activity, and emission dispersion modeling.
Ranking the atmospheric pollutants of the CWSDF allowed identification of priority pollutants to be monitored, which included 1–13 non-carcinogens (sulfur dioxide, fuel-oil ash from power stations, nitrogen dioxide, PM 10, C12-C19 alkanes, nitrogen oxide, sodium sulfate, potassium sulfate, sodium carbonate, sodium diphosphate, manganese and its compounds, and carbon monoxide); specific pollutants: RVX, 2-(diethylamino)ethyl isobutyl sulfide (DS), isobutyl methylphosphonic acid (IMPA), and monoethanolamine; and carcinogens: soot, benz[a] pyrene, and gasoline.
The respiratory system, central nervous system, vision organs, and digestive tract were found to be the target organs for chronic inhalation exposure to the priority pollutants.
The potential health risks were calculated using the average annual concentrations of the priority pollutants in the CWSDF emissions in the chosen reference points.
The noncarcinogenic risks for specific priority pollutants were as follows: IMPA 0.00001–0.00086; DS 6.3E-008–2.2E-005; RVX 9.9E-007–2.4E-005. The carcinogenic risks varied in the ranges 1.54E-08–7.14E-07 for benz[a]pyrene and 5.93E-10–6.57E-09 for carbon (soot). The chronic non-carcinogenic and carcinogenic risk parameters were at acceptable levels for all reference points.
The work was supported in part by the International Science and Technology Center (project. no. 3697).

PS 2250 *In Vitro* Bioactivity in ToxCast Assays for Fruit and Vegetable Extracts

B. A. Wetmore[1], E. Berg[2], M. A. Polokoff[2], R. S. Thomas[3] and M. E. Andersen[1]. [1]*The Hamner Institutes for Health Sciences, Research Triangle Park, NC,* [2]*BioSeek, a Division of DiscoveRx, Inc., South San Francisco, CA and* [3]*National Center for Computational Toxicology, USEPA, Research Triangle Park, NC.*

The ToxCast and Tox21 programs have generated *in vitro* screening data for over 1000 chemicals to aid in hazard identification and setting chemical testing priorities. These data, together with high-throughput pharmacokinetic data, are used to infer possible toxic responses and external concentrations required to elicit these effects. There is only limited experience in evaluating dose-response for natural products in these assays. In this study, juices were extracted from 30 organically grown fruits and vegetables. These juices were screened in concentration-response format across multiple cell types using the BioMap platform to assess similarities of pathway responses of the extracts with those of database compounds. Bioactivities noted with unpeeled potato juice were immunomodulatory and tissue remodeling activities across endothelial, peripheral blood mononuclear and fibroblast cells. This pattern of response was similar to quercetin, a plant-derived flavonoid. Broccoli juice initiated anti-proliferative effects on endothelial, fibroblast and smooth muscle cells with significant similarity to mitomycin C (374 ng/mL; Pearson, r=0.806) and the fungicide mancozeb (40 uM; Pearson, r=0.776). To relate *in vitro* concentrations to administered dose, the filtered juice yield per g item was used with the plasma volume of a 70kg adult to approximate % juice present in systemic circulation after eating. This value was used as a surrogate for target tissue concentration. The activity described for broccoli was elicited at 0.5%, the amount of juice anticipated in the circulation following consumption of 2 cups of broccoli. Importantly, the bioactivities noted do not necessarily lead to adverse effects. These data provide context for assessing the in vivo relevance of *in vitro* concentration-response and bioactivity data generated in ToxCast and similar screening programs. *This abstract does not necessarily reflect EPA policy.*

PS 2250a Merging ExpoCast™ with ToxCast™: Incorporating High-Throughput Exposure Predictions with Dosimetry-Adjusted *In Vitro* Bioactivity to Inform Toxicity Testing Strategies

M. B. Black[1], J. F. Wambaugh[2], M. Sochaski[2], R. Judson[2], S. S. Ferguson[3], K. Houck[2], H. J. Clewell[2], M. E. Andersen[1], R. Thomas[2] and B. A. Wetmore[1]. [1]*The Hamner Institutes for Health Sciences, Research Triangle Park, NC,* [2]*National Center for Computational Toxicology, USEPA, Research Triangle Park, NC and* [3]*Life Technologies, Durham, NC.*

Our previous work incorporating dosimetry and exposure with high-throughput screening (HTS) enhanced the utility of HTS data by translating *in vitro* bioactivity concentrations to external exposures required to achieve these levels internally. These oral equivalents were compared against exposure estimates to provide a margin of exposure (MOE). ToxCast Phase I chemicals are primarily food use pesticides for which regulatory estimates are available. As ToxCast efforts transition to chemicals lacking exposure information, exposure prediction tools become increasingly important. In this study, *in vitro* hepatic clearance and plasma protein binding were measured to estimate dosimetry-adjusted oral equivalents for Phase II chemicals. Chemical exposures were predicted from HT far-field mass balance models coupled with a predictor for near-field human exposure. Joint regression on all factors provided a calibrated consensus exposure prediction and a measure of variance conveying the uncertainty of the predictions. These values were compared against the calculated oral equivalents to assess the potential that actual exposures might elicit bioactivity. Exposure predictions across the lower and upper 95th confidence interval typically spanned eight orders of magnitude. Comparison of the minimum oral equivalent to the upper bound exposure prediction indicated that 49 and 95 of the 178 chemicals had MOEs < 1 and < 100, respectively. Application of these HT tools provides a first order approximation of MOEs to aid in prioritization of testing. Efforts are underway to reduce the uncertainty in the exposure predictions and increase the utility of this approach. *This abstract does not necessarily reflect EPA policy.*

PS 2250b Development of Reverse Toxicokinetic Models to Correlate *In Vitro* and *In Vivo* Estrogen Receptor Activity

X. Chang[1], N. Kleinstreuer[1], P. Ceger[1], J. T. Hamm[1], B. Jones[1], L. Rinckel[1] and W. Casey[2]. [1]*ILS, Inc., Research Triangle Park, NC and* [2]*DHHS/NIH, NIEHS/NTP/NICEATM, Research Triangle Park, NC.*

Through the U.S. Tox21 high-throughput screening (HTS) program, efforts are underway to use quantitative high throughput in vitro assays to assess chemical effects across multiple cellular pathways, including the estrogen receptor (ER) pathway. HTS assays provide an efficient way of identifying potential biological targets for chemicals. However, the nominal in vitro assay concentrations may not accurately reflect the potential in vivo effects of these chemicals due to the differences in bioavailability and clearance. A set of pharmacokinetic models was developed to correlate in vitro concentrations with potential in vivo effects for Tox21 chemicals with potential to interact with the ER. These models estimate the daily oral doses in laboratory animals and humans for Tox21 ER active chemicals that would result in a steady-state in vivo blood concentration equivalent to the in vitro AC50 (concentration at 50% maximum activity) values identified using HTS assays that specifically target the ER pathway. These models were built using published experimental data and quantitative structure–activity relationship predictions for hepatic metabolic clearance and unbound plasma protein fraction for tested chemicals. The models were also adapted to incorporate infant physiology to include this most vulnerable human population. Using daily oral doses estimated from the model, Tox21 ER active chemicals were ranked, with chemicals having the lowest effective dose in these models being considered the most likely to interact with the ER in vivo, either as agonists or antagonists. The estimated oral dose for a subset of chemicals was also compared to the in vivo dose range reported to elicit ER-related effects.
This project was funded in whole or in part with Federal funds from the NIEHS, NIH under Contract No. N01-ES-35504.

PS 2250c Estimation of Methylmercury Intake Doses in the South Korea Population Using a PBPK Model

S. Lee[1], Y. Tan[2], J. Sobus[2], M. Phillips[3] and S. Kim[1]. [1]*School of Public Health, Seoul National University, Seoul, Republic of Korea,* [2]*NERL, US EPA, RTP, NC and* [3]*NERL, US EPA, Duluth, MN.*

Recently, South Korea has measured total mercury (Hg) in blood as part of Korean National Environmental Health Survey (koNEHS) in 6311 subjects representing Korean general population. About 25 % of the biomarker measurements were above the German HBM1 (biomonitoring guidance value) of 5 μg Hg/L; and

about 1% was above the HBM2 of 15 μg Hg/L. Among the various mercury-containing compounds, methylmercury (MeHg) is the most toxic because of its ability to be readily absorbed and to accumulate in the body. It has been linked to developmental deficits in children and increased risk of cardiovascular disease in adults. US EPA has set a guidance value for MeHg exposure, but it is reported as a daily intake dose, requiring an exposure reconstruction step in order to compare the measured biomarker concentrations with average intake. Thus, the current study used these biomarker data to further investigate the potential of this population being exposed to MeHg at or above the U.S. Reference Dose (RfD) of 0.1 μg MeHg/kg/day. First, total blood Hg concentrations were converted to MeHg using a randomly selected MeHg/Hg ratio from a previously reported distribution measured among South Korean. Next, these estimated blood MeHg concentrations were used to reconstruct MeHg intake amounts using a published physiologically based pharmacokinetic (PBPK) model for MeHg. Monte Carlo analysis was conducted to account for variability in physiology and pharmacokinetics in estimating the distribution of MeHg intake. The resulting mean amount was 2.88 μg/day, which is comparable to the estimate from the South Korean environmental monitoring report in 2011 based on MeHg residues in fish (2.8 μg/day). The estimated mean dose was 0.045 μg/kg/day, which was approximately half of the RfD; and above 10% of the estimated doses were higher than the RfD. Additional analysis will be conducted to examine what variables are associated with those biomarker measurements that are higher than the other guidance values.

PS 2250d Protecting Astronaut Health at First Entry into Vehicles Visiting the International Space Station: Insights from Whole-Module Offgas Testing

V. E. Meyers[1], T. F. Limero[2], V. DeVera[2], P. F. Cheng[2], J. J. Hand[2], J. B. Trowbridge[2] and J. T. James[1]. *[1]NASA JSC, Houston, TX and [2]Wyle Integrated Science and Engineering, Houston, TX.*

NASA has accumulated considerable experience in offgas testing of whole modules prior to their docking with the International Space Station (ISS). Since 1998, the Space Toxicology Office has performed offgas testing of the Lab module, both MPLM modules, US Airlock, Node 1, Node 2, Node 3, ATV1, HTV1, and three commercial vehicles. The goal of these tests is twofold: first, to protect the crew from adverse health effects of accumulated volatile pollutants when they first enter the module on orbit, and secondly, to determine the additional pollutant load that the ISS air revitalization systems must handle. In order to predict the amount of accumulated pollutants, the module is sealed for at least 1/5th the worst-case time interval that could occur between the last clean air purge and final hatch closure on the ground and the crew's first entry on orbit. This time can range from a few days to a few months. Typically, triplicate samples are taken at pre-planned times throughout the test. Samples are then analyzed by gas chromatography and mass spectrometry, and the rate of accumulation of pollutants is then extrapolated over time. The analytical values are indexed against 7-day spacecraft maximum allowable concentrations (SMACs) to provide a prediction of the total toxicity value (T-value) at the time of first entry. This T-value and the toxicological effects of specific pollutants that contribute most to the overall toxicity are then used to guide first entry operations. Finally, results are compared to first entry samples collected on orbit to determine the predictive ability of the ground-based offgas test.

PS 2250e Public Health Concerns Surrounding Fine Particulate Matter Generated from Hydraulic Fracturing

A. LeBeau and A. Pawlisz. *CRA, Dallas, TX.*

To evaluate the potential impact of fine particulates on public health in communities relatively close to hydraulic fracturing (i.e., fracking) activities, a preliminary evaluation of available particulate matter (PM2.5) data from three air monitoring stations in the Dallas, TX area was conducted. Annual air quality monitoring data for 2013 was obtained from the Texas Commission of Environmental Quality (TCEQ) web site. Air quality monitoring stations in Texas Region 4 sampled and monitored ambient air and meteorological conditions to generate the hourly averages that were used for this data analysis. The monitoring stations selected for this evaluation were: C56 at Denton Airport South; C52 near Midlothian, TX; and C1044 near Italy, TX. The stations were selected due to the fact that they recorded PM2.5 and wind direction data that were needed to evaluate any potential impacts from fracking activities. These locations were also identified due to their relative distance from the potential influence of the Dallas/Fort Worth metro area. Geometric means of annual PM2.5 concentrations were determined for each location, for both PM2.5 appearing to originate from heavy fracking activity and for PM2.5 appearing to originate from a direction relatively free of fracking activity. Wind direction was used to estimate the origin of the PM2.5. At all three locations, the annual PM2.5 concentration from the direction of fracking was significantly elevated in comparison to the PM2.5 concentration facing away from the heaviest fracking activity in the area (i.e., C56: Toward Fracking (TF) PM2.5=7.6 μg/m3 vs. Away from Fracking (AF) PM2.5=6.2 μg/m3, p=<0.001; C52: TF PM2.5=9.0 μg/m3 vs. AF PM2.5=5.8 μg/m3, p<0.001; C1044: TF PM2.5=7.6 μg/m3 vs. AF PM2.5=6.3 μg/m3, p<0.001). No direction-specific concentrations were above the primary EPA annual PM2.5 air quality standard of 12 μg/m3. These preliminary data indicate that mean PM2.5 levels from the direction of fracking are significantly higher than those from the direction that is relatively free of nearby fracking activities; however, the levels are not above the annual EPA standard.

PS 2250f Cancer Risk of PAHs in Particulate Matter from Biofuel Combustion

D. A. Sarigiannis, S. P. Karakitsios, D. Zikopoulos, S. Nikolaki and M. Kermenidou. *Chemical Engineering, Aristotle University of Thessaloniki, Thessaloniki, Greece.*

The risk of cancer attributable to PAH exposure has been assessed, in the light of increased use of biomass for space heating associated to the financial crisis over the last couple of winters. Ambient air PMx was sampled in several urban sites, and analysed chemically for PAHs and levoglucosan, used here as the most specific tracer of biomass combustion. Internal exposure to PAHs was estimated taking into account the deposition of the respective PM fractions across the human respiratory tract (HRT). Deposition at different regions of the HRT was carried out using the Multiple-Path Particle Dosimetry (MPPD) model. MPPD calculates the deposition and clearance of mono- and poly-disperse aerosols in the respiratory tract of rats and human adults and children (deposition only) for particles ranging from ultrafine (0.01 microns) to coarse (20 microns) sizes. Potential cancer risk due to exposure to the mixture of PAHs in urban ambient air was calculated according to the toxicity equivalence factor (TEF) approach using as basis the benzo(a)pyrene (B[a]P) cancer potency. The BaP-TEQ (Toxicity Equivalent Quotient) (carcinogenic equivalent, in ng/m3) was calculated by multiplying the concentrations of each compound in the PAH mixture with the respective TEF for cancer potency relative to BaP. To estimate cancer risk the TEQ of the respective fraction of particulate matter deposited across HRT daily, was multiplied to a dose-response function, derived by the B[a]P Inhalation Unit Risk (the latter is equal to 0.88E-6 (ng/m3)-1). Significant variation in risk was observed among different age groups, much larger than variation due to geospatial attributes. The risk for children is four times higher than for adults. Only limited difference was found between traffic and urban background sites in the winter (mean cancer risk for both is close to 10-6). The carcinogenic potency of PM emitted from biofuel combustion (main PM source of the urban background pollution) was slightly higher compared to the potency of traffic-originated PM when using conventional fuel types.

PS 2250g Data Source Summary Documents (DSSDs) Derived for Updated Drinking Water Standards and Health Advisories (DWSHA) Tables

D. J. Stewart[1, 2], C. Bast[2], C. S. Wood[2] and S. S. Kueberuwa[3]. *[1]University of Tennessee, Knoxville, TN, [2]Oak Ridge National Laboratory, Oak Ridge, TN and [3]U.S. Environmental Protection Agency, Washington, DC.*

The DWSHA tables, sponsored by the U.S. Environmental Protection Agency's (EPA's) Office of Water (OW), summarize the drinking water regulations and Health Advisory (HA) values as well as the reference dose (RfD) and cancer risk values for drinking water contaminants. The tables provide Maximum Contaminant Level Goals (MCLGs), Maximum Contaminant Levels (MCLs), and HAs. HAs in the tables are guidance values based on non-cancer health effects for different durations of exposure (one-day, ten-day, and lifetime) or a specific probability of cancer (10-4 – 10-6 cancer risks).

HAs are recommendations for unregulated drinking water contaminants to protect public health as needed. Based on EPA policy, all DWSHA Tables published after 2012 will calculate lifetime HAs for all contaminants with RfDs, regardless of their carcinogenicity status. This will allow risk assessment managers to compare the noncancer and cancer values and determine which level provides a more meaningful scenario-specific risk reduction.

A systematic review of the DWSHA table was initiated in 2012 to ensure that the benchmark values are consistent with the most current EPA assessments and all contaminants with RfDs have lifetime HAs. A total of 75 RfD and oral slope factor updates were identified that needed to be confirmed. The associated DWEL, Lifetime HA, or Cancer Risk values are being recalculated accordingly. Additionally, 29 contaminants without lifetime HAs will be reviewed. These changes are summarized in Data Source Summary Documents (DSSDs), along with principal study information and uses and occurrence, and hyperlinked to the DWSHA Tables. Quality assurance/control is an ongoing process to review

completed DSSDs and updated DWSHA tables. The 2014 DWSHA tables will provide hyperlinks to 33 DSSDs. Every fall, the DWSHA tables will be verified and updated, and new DSSDs will be hyperlinked, as applicable.

PS 2250h Toluene and Dibutyl Phthalate in Nail Lacquers: A Proposition 65 Exposure Assessment

J. Keenan, L. Kopelovich and N. Jacobs. *Cardno ChemRisk, San Francisco, CA.*

Toluene and Dibutyl Phthalate (DBP) can be found in many consumer products, including nail lacquers. In 2012, the California Environmental Protection Agency (Cal EPA) evaluated 25 nail products and found that 64% of lacquer polishes contained toluene and 28% contained DBP. Concentrations of toluene and DBP ranged from 42 to 190,000 ppm and 14,000 to 88,000 ppm, respectively. Exposure to these chemicals is regulated by the California Safe Drinking Water and Toxic Enforcement Act of 1986 (commonly referred to as Prop 65). The purpose of this study was to estimate consumer exposure to toluene and DBP from nail lacquers via dermal and inhalation exposure routes. Using the results collected by the Cal EPA, a Prop 65 exposure assessment was performed based on minimum, median, and maximum toluene and DBP concentrations in nail lacquer. Inhalation exposure was estimated using standard conservative exposure assessment equations, and dermal exposure was calculated using SkinPerm Quantitative Structural Activity Relationship methodology. The Maximum Allowable Dose Level (MADL) of toluene is 7000 μg/day and assumes that 50% of the inhaled toluene is absorbed. To compare the total absorbed toluene concentration from nail polish application to the MADL, we combined the estimated dermal exposure with 50% of the calculated inhalation exposure. Our estimated absorbed toluene dose for a consumer ranged from 39.5 to 1.8 x 10^5 μg/day. Overall, most concentrations of toluene reported by the Cal EPA resulted in exposures that fell below the Proposition 65 MADL; however, higher toluene concentrations resulted in exposure values that exceeded the MADL. Given the negligible volatilization rate of DBP, only dermal exposure was evaluated. Consumer DBP exposure ranged from 3.4 x 10^3 to 4.2 x 10^5 μg/day. All estimated DBP exposures were above the MADL of 8.7 μg/day.

PS 2250i A Tiered Safety Assessment Approach for Evaluating Chemicals in Consumer Products and Applications for Asthma Risk Management

M. J. Vincent[1], A. Maier[2], M. Jayjcok[3], B. Gadagbui[1], A. Parker[1] and S. Ross[1]. [1]*Toxicology Excellence for Risk Assessment, Cincinnati, OH,* [2]*University of Cincinnati, Cincinnati, OH and* [3]*Jayjock & Associates, Langhorne, PA.*

Asthma is a complex syndrome with potentially severe consequences. The number of affected individuals is growing, although the reason for the increase is uncertain. Substantial evidence that exposure to some chemicals is linked to asthmatic responses increases the need for effective management of potential chemical exposures . A safety assessment approach tailored to the screening of asthma risks from consumer product ingredients was developed for use as a risk management tool. Several key features of the approach advance the use and integration of assessment resources often used for asthma investigations. First, a quantitative health benchmark for asthma or related endpoints (irritation and sensitization) is provided that extends the assessment beyond qualitative hazard classification methods. Second, a parallel structure includes methods for dose-response assessment of asthma endpoints and for scenario specific exposure estimation. The two parallel tracks are integrated in a risk characterization step. Third, a tiered assessment structure is provided to accommodate different amounts of data for both dose-response assessment (i.e., use of existing benchmarks, hazard banding, or the threshold of toxicological concern) and exposure estimation (i.e., use of empirical data, model estimates, or exposure categories). Tools building from traditional methods and resources have been adapted to address specific issues pertinent to asthma toxicology (e.g., mode-of-action and dose-response features) and the nature of consumer cleaning product use scenarios (e.g. product use patterns and exposure durations). A case study for acetic acid, as used in various sentinel products and residential cleaning scenarios, was developed to refine and verify relationships among tiered approaches within the safety assessment methodology with the goal that each lower data tier in the approach provides a similar or greater margin of safety for a given scenario.

PS 2250j Automatic Topic Classification for Environmental Human Health Assessment

K. L. Painter[1], S. J. Dutton[2], E. O. Owens[2] and L. D. Burgoon[2]. [1]*Oak Ridge Institute for Science and Education/Environmental Protection Agency, Research Triangle Park, NC and* [2]*Environmental Protection Agency, Research Triangle Park, NC.*

In environmental risk assessment, information about potential health risks of chemicals released into the environment is compiled and distilled for use in informing public policy. The U.S. Environmental Protection Agency (EPA) produces Integrated Science Assessments (ISA) that provide a review of literature on air pollutants, including ozone and nitrogen oxides (NOx). The review process currently requires much human labor to sort through the thousands of potentially-relevant documents published each year, a problem this study seeks to alleviate by using automated topic classification methods. For this study, abstracts and titles of scientific documents about ozone and NOx were labeled by subject matter experts in four domains relevant to ISAs: toxicology, atmospheric science, epidemiology, and exposure science. In addition, documents not relevant to the four domains were included to simulate the background articles that we want to filter out of consideration. The labeled documents were used to train models using a Naive Bayes Multinomial classifier, via the Weka data mining platform. For the NOx documents, recall (% of all documents in a class that are classified correctly) for scientific domains ranged between 76% and 92%, with precision (% of classified documents that are in the desired class) between 38% and 75%. For ozone documents, recall ranged from 85% to 89%, with precision between 67% and 97%. Finally, to demonstrate that models can be generalized to accurately predict topics for documents on new chemicals, models trained on NOx documents were used to classify ozone documents (recall: 77-81%, precision: 65-84%), and vice versa (recall: 68-83%, precision 67-81%). The views expressed in this abstract are those of the authors and do not necessarily represent the views of policies of the EPA.

PS 2250k Use of Text-Mining and Machine Learning to Prioritize the Results of a Complex Literature Search

B. Howard[1], R. Shah[1, 4], V. Walker[2], S. Holmgren[3] and K. Thayer[2]. [1]*Sciome LLC, RTP, NC,* [2]*OHAT, National Toxicology Program, NIEHS, RTP, NC,* [3]*Office of Scientific Information Management, NIEHS, RTP, NC and* [4]*SSS, Durham, NC.*

As part of the effort to conduct various meta-analysis studies, literature reviews and technical reports, toxicologists routinely conduct complex searches of the scientific literature. These searches can yield thousands or tens of thousands of candidate documents. Human curation of this large literature set is resource intensive. To that end, we have developed and implemented, in collaboration with NIEHS, tools and procedures that can assist researchers in prioritizing, filtering and organizing these large literature search results. To demonstrate the effectiveness of this approach, we tested our software using a set of 48,638 articles identified by researchers as potentially relevant in a review of the transgenerational inheritance of health effects. Given only the title and abstract information available from PubMed, human curators applied complex inclusion and exclusion criteria to identify the relevant subset from these candidates. This time-consuming baseline approach identified 765 relevant "included" documents, 47,873 "excluded" documents. Compared to the manual process, the system we have developed makes this baseline approach more efficient by (1) Prioritizing the results such that relevant documents are more likely to appear near the top of the ranked results list, and (2) Organizing/clustering search results according to major themes and topics in a manner that makes it more manageable to navigate the resulting literature. For example, using a randomly selected "seed" consisting of only 50 included and 50 excluded documents, our system ranked the remaining unlabeled documents such that 56% and 93% of the included documents occurred in the top 10th and 50th percentiles, respectively. Furthermore, the system conveniently organizes the document set for interactive browsing using MeSH terms and other user-defined categories. Together, these facilities will allow researchers to identify relevant literature more efficiently, and to spend more time on the analysis and interpretation of the resulting documents.

PS 2250l HAWC (Health Assessment Workspace Collaborative): A Modular Web-Based Interface to Facilitate Development of Human Health Assessments of Chemicals

A. J. Shapiro and I. Rusyn. *Env. Sci. and Engin., Univ. North Carolina at Chapel Hill, Chapel Hill, NC.*

Regulatory agencies conduct assessments of the potential for chemicals to pose a threat to human health. Such assessments typically consist of a critical review of available studies to identify adverse health effects to characterize exposure-response relationships. In addition to the systematic review of pertinent studies and the

analyses of available data, opportunities for public input and multiple levels of scientific review are also critical steps to engage stakeholders who may be affected. The overall framework for how assessments are performed and what information should be evaluated is well established, yet the format and the process for how assessments are conducted remain to be a notable and persistent challenge. In this project, we aimed at addressing these challenges by creating a modular, web-based content-management system to synthesize multiple data sources into overall human health assessments of chemicals. We created an online tool, HAWC (Health Assessment Workspace Collaborative, https://hawcproject.org/) which integrates and documents the overall workflow from literature search and review, to data extraction, evidence synthesis through visualization tools, dose-response analysis, uncertainty characterization, and customized reports. Crucial benefits of such a system include improved integrity of the data and analysis results, greater transparency, standardization of data presentation, and increased consistency. By utilizing a web-based workspace, assessment team members can collaborate on the same project rather than share files and track edits. Utilizing HAWC as a web-based portal for reviewers and stakeholders, all interested parties have dynamic access to completed and ongoing assessments. Overall, this project creates a clear summary of the results of the assessment, and a source for primary data and/or tabulated study summaries and visual aids that constitute the scientific justification for its conclusions.

PS 2251 Toxic Effects of Secondhand Smoke-Revealing Mechanism by Systems Biology Approach

D. Mitic Potkrajac[1], B. Rakic[1], A. Price[1], G. Apic[1] and R. B. Russell[2].
[1]Cambridge Cell Networks Ltd, Cambridge, United Kingdom and [2]Cell Networks, University of Heidelberg, Heidelberg, Germany.

The aim of this study was to investigate mechanism that enables tobacco smoke components to induce cardiovascular system toxicity. Secondhand smoke (or ETC) contains around 90 known toxic compounds emitted from tobacco combustion. We focused on 8 compounds labeled as harmful and potentially harmful constituents (HPHCs) by FDA and present mainly in the side-stream smoke with side-stream to mainstream smoke ratio of two. We created a computational model of biological pathways describing cellular processes activated by these compounds by manually annotating and processing molecular information from the literature from the public domain (PubMed articles and FDA reports) and made the data computable. We generated a comprehensive database of known side effects and protein targets of these 8 compounds. By applying bioinformatics analysis tools to this data we have identified several adverse effects regarding heart diseases, reproductive and developmental toxicity. For each of these adverse effects we generated the hypothesis of mechanism of action that is supported by current knowledge.

PS 2252 Profiling Environmental Chemicals That Induce the Antioxidant Response Pathway Using Cell-Based Assays and Cheminformatics Tools

M. T. Kim[1, 2], A. Sedykh[3], J. Zhang[1, 2], R. Huang[4], M. Xia[4] and H. Zhu[1, 2]. *[1]Chemistry, Rutgers, The State University of New Jersey, Camden, NJ, [2]Center for Computational and Integrative Biology, Rutgers, The State University of New Jersey, Camden, NJ, [3]Multicase Inc., Beachwood, OH and [4]NIH National Center for Advancing Translational Sciences, Department of Health and Human Services, Rockville, MD.*

Oxidative stress causes cell damage which can lead to a variety of neurodegenerative diseases. Exogenous compounds that induce oxidative stress cause cell damage which triggers the transcription of antioxidative genes located in the antioxidant response element (ARE) signaling pathway. This process is essential for alleviating cell injury, but the mechanisms that lead to cytotoxicity and further animal toxicity are still unclear. Previously, a cell-based ARE beta-lactamase reporter gene assay was used to screen 1,408 compounds in the National Toxicology Program (NTP) library in a Quantitative High Throughput Screening (qHTS) format. Then, compounds that induced the ARE pathway were identified. In this study, we first used various Quantitative Structure-Activity Relationship (QSAR) approaches to develop predictive ARE models. The resulting models were used to virtually screen other compounds of interest (e.g. Tox21 chemical library). Next, we used our in-house automatic profiling tools to gather and analyze available animal toxicity data for each of the compounds in both the NTP-1408 and the extended chemical library. The in vitro and in vivo relationship established by this step could be used to develop predictive models for complicated animal toxicity endpoints (e.g. those of neurotoxicity). The final alternative computational toxicity predictors could be used to prioritize potentially toxic compounds that cause oxidative stress and induce the ARE pathway.

PS 2253 Improving the Development of Adverse Outcome Pathways: Lessons Learned from the AhR Rodent Liver Tumor and AhR Avian Teratogenicity/Embryolethality AOPs

R. A. Becker[1], T. Simon[2], G. Patlewicz[3], S. W. Kennedy[4], A. Farhat[4] and R. Budinsky[5]. *[1]American Chemistry Council, Washington, DC, [2]Ted Simon LLC, Winston, GA, [3]Dupont Haskell Global Centers, Newark, DE, [4]Environment Canada, Ottawa, ON, Canada and [5]The Dow Chemical Company, Midland, MI.*

An adverse outcome pathway (AOP) represents the sequence & causal linkages between initial molecular events, key events and an adverse outcome. As part of the OECD AOP Programme, we separately developed an Aryl Hydrocarbon Receptor (AHR) AOP for rat liver tumor promotion (RLTP) & an AHR AOP for avian deformities/lethality & then collaborated to enter these in the AOP Wiki (beta). Differing levels of polymorphism-dependent AHR activation provides strong evidence identifying AHR activation during critical periods of avian development as the molecular initiating event (MIE) for avian teratogenicity/embryolethality. While AHR binding is the initial molecular event, there is strong evidence that sustained AHR activation for a significant portion of the lifespan is the MIE causally related to RLTP. In developing & adapting these for the AOP Wiki, we arrived at a recommendations applicable to other AOPs; these are 1) recognizing that while receptor binding & acute changes in gene transcription may be the IME, they do not always predict the MIE & the Wiki should be revised accordingly; 2) expanding the AOP Wiki structure beyond key events to include a) associative events (biomarkers that are not themselves necessary for the adverse outcome but are reliable indicators for key events) & b) modulating factors (e.g., aspects of homeostasis or other factors that may alter the occurrence &/or dose-response of the MIE or subsequent key events); 3) the need for a robust & transparent framework to document scientific confidence for use of the AOP & assays that measure responses related to each specific key event for predictive toxicology; & 4) the need to discuss explicitly application of the AOP for each different regulatory purpose: priority setting; chemical categorization; integrated approaches to testing & assessment (IATA); and screening level hazard/risk assessment.

PS 2254 Data Mining Approach to Formulate Alerting Chemotypes for Liver Steatosis/Steatohepatitis/Fibrosis

A. S. Mostrag-Szlichtyng[1], V. Vitcheva[4], M. D. Nelms[2], P. Alov[4], I. Tsakovska[4], S. J. Enoch[2], A. P. Worth[3], M. T. Cronin[2] and C. Yang[1]. *[1]Altamira LLC, Columbus, OH, [2]Liverpool John Moores University, Liverpool, United Kingdom, [3]European Commission - Joint Research Centre, Institute for Health & Consumer Protection, Ispra, Italy and [4]Bulgarian Academy of Science, Institute of Biophysics and Biomedical Engineering, Sofia, Bulgaria.*

COSMOS oRepeatToxDB, oral repeat-dose toxicity database, is designed with an ontology describing toxicological effects at each dose level using controlled vocabulary, thus enabling mechanistic data mining. Observations are also coupled to organism-level sites and more specific effects at lower levels are formulated within hierarchical framework: organs/systems→segments/tissues→cells/organelles. The majority of biological/chemical processes occur at the cell/organelle level, and so interactions between chemicals and proteins/genes are investigated in order to associate chemical structures with phenotypic effects resulting from related toxicity mechanisms. Furthermore, common structural fragments are extracted and refined into mechanistic chemotypes representing underlying molecular initiating events. We present a data mining case for liver steatosis, steatohepatitis and fibrosis. Over 20% of cosmetics-related chemicals in this database were associated with lipid deposition, fatty changes, cytoplasmic vacuolization, cellular infiltration and inflammation in various hepatocytes, ultimately leading to fibrosis. Combined phenotypic effects and morphological changes at various sites were mapped onto chemical compounds. Applying the ToxPrint chemotypes to these compounds, the set of alerting chemotypes for liver steatosis/steatohepatitis/fibrosis was identified. They include alcohols, diols, glycol ethers, aminophenols, tertiary amines, aromatic amines, polychlorinated short alkanes, halogenated amines, and Michael acceptors. Identification of these alerting chemotypes can be considered as the initial step in developing the categories used in safety/risk assessment. This approach also provides a way to investigate molecular pathways relevant to toxicological mechanisms. Supported by EU FP7 COSMOS Project.

PS 2255 Novel Expert Reports for Drug-Induced Kidney Injury (DIKI)

G. Apic[1], A. Stelkic[1], D. Mitic Potkrajac[1], V. Veljovic[1] and R. B. Russell[2]. [1]*Cambridge Cell Networks Ltd, Cambridge, United Kingdom and* [2]*Cell Networks, University of Heidelberg, Heidelberg, Germany.*

Nephrotoxicity and functional impairment in the kidney caused by drugs, have increased in recent years and become one of the major stumbling blocks in new drug candidates' safety. Currently, there are predominantly pre-clinical animal tests and in vitro models for assessing drug induced kidney injury (DIKI). The aim of this study is to develop, accelerate and ratify a unique computational model as a strategy in predicting drug induced organ injury, including DIKI. We manually annotated publicly available data (more than 10 000 articles) and proprietary company datasets (several thousand gene expression observations) related to nephrotoxicity, to build a complex molecular network of genes, proteins and chemicals within the knowledge base. We focused on known DIKI associated drugs, together with their metabolites, signaling molecules, nuclear hormone receptors and all known affected proteins for each relation within the knowledge base, with the ultimate goal in predicting possible kidney injury of a drug. We tested our system with the current standards of renal function, as blood urea nitrogen and serum creatinine, which were confirmed as proof of the concept for the DIKI. In addition, our model also confirmed recently discovered beta-2-microglobulin as molecule that could be used for detecting kidney injury.

PS 2256 Identification of Adverse Outcome Pathways for the Nephrotoxicity of Nucleoside and Nucleotide Antiviral Drugs

W. C. Drewe[1], A. Cayley[1], R. Benz[2], N. L. Kruhlak[2] and B. Surfraz[1]. [1]*Lhasa Limited, Leeds, West Yorkshire, United Kingdom and* [2]*Center for Drug Evaluation and Research, Food and Drug Administration, Silver Spring, MD.*

Adverse outcome pathways (AOPs) describe the mechanistic link between a molecular initiating event (MIE) and an adverse toxicity outcome (AO). Anti-viral drugs, a class of compounds categorized as one of the most toxic in the FDA CDER urinary tract toxicity dataset, were investigated to identify the mechanisms leading to renal toxicity.

The FDA CDER urinary tract toxicity dataset is based on the post-marketing adverse events of 1609 chemicals. Dataset clustering based on 70% sub-structure similarity provided five clusters covering purine and pyrimidine nucleosides, their corresponding phosphonate nucleotide analogues, and other structurally related compounds. These classes were then investigated for the mechanistic pathways which lead to nephrotoxicity and the preparation of structural alerts for toxicity prediction.

Four structural toxicity alerts were successfully implemented. These were based on publicly available *in vivo* reports of nephrotoxic events in man and other mammals, and data from relevant mechanistic *in vitro* assays. The collated data was also used to generate plausible mechanisms to describe the nephrotoxicity of anti-viral drugs in man and other mammals.

We report the construction of AOPs to describe the mechanisms of the *in vivo* nephrotoxicity of anti-viral drugs. Structurally related nucleoside and nucleotide drugs lead to histologically and biochemically proven structural and functional alterations of both proximal tubular and glomerular cells. Proximal tubulopathies such as Fanconi syndrome and acute tubular necrosis, and glomerulopathies such as minimal change nephropathy and focal segmental glomerulosclerosis have been reported. Mitochondrial toxicity has been implicated in these highly metabolically active renal cells as one potential MIE, which is likely to be related to the clinical mode of action of these compounds *in vivo*. Furthermore, these compounds can act as potent inhibitors of mitochondrial polymerase gamma, which leads to mitochondrial toxicity.

PS 2257 Using Adverse Outcome Pathways to Identify Existing Knowledge for Mechanisms of Teratogenicity Resulting from Endocrine Disruption

M. L. Patel[1], A. Cayley[1], W. C. Drewe[1], R. Benz[2], N. L. Kruhlak[2] and B. Surfraz[1]. [1]*Lhasa Limited, Leeds, United Kingdom and* [2]*Center for Drug Evaluation and Research, Food and Drug Administration, Silver Spring, MD.*

Adverse Outcome Pathways (AOPs) can be used to describe how exogenous chemicals may perturb a complex biological system. The endocrine system is involved in many regulatory processes including the development and function of the reproductive system. We investigated how disruption of steroidal hormone homeostasis within these systems may lead to teratogenicity.

We analysed rodent fetal dysmorphogenesis data (2141 chemicals) within the FDA CDER reproductive toxicity non-proprietary dataset. These data were investigated to identify pathways leading to teratogenic outcomes. Androgen receptor binding, estrogen receptor binding, 5alpha-reductase inhibition and aromatase inhibition were amongst the identified modes of action. Further literature work was undertaken to identify plausible supporting data, pathways and mechanisms.

It was found that disruption of these pathways by xenobiotics and the subsequent mis-regulation of hormones can lead to teratogenic effects in developing sex organs and cause specific syndromes of defects in offspring. In rodent studies the most sensitive period of treatment is late organogenesis. Compounds may interact with various parts of these pathways rather than just at one point. Different receptor binding sites have a high degree of similarity and substrates may act as both agonists and antagonists depending on the conditions present. The sex which is predominantly affected can depend on the target and the type of binding. 5alpha-reductase inhibitors predominantly affect male offspring whereas the effects of estrogen receptor antagonism can predominantly be seen in female offspring. Investigations for compounds inhibiting the aromatase enzyme highlight data and knowledge gaps in the literature.

We report the construction of AOPs for *in vivo* teratogenicity, where the molecular initiating events are receptor based. The AOP framework helps to view how subtle differences in perturbation of the pathways can affect the final outcome.

PS 2258 Arsenic and Pancreatic Cancer: A Computational Systems Toxicology Analysis of Risk

R. Coronel, C. Han, K. Kan, P. Nguyen and D. Johnson. *Nutri Sci & Toxicology, UC Berkeley, Berkeley, CA.*

Pancreatic cancer (PaCa) affects more than 40,000 people in the United States and is currently the 4th leading cause of cancer death. Its etiology has been linked to genetics, diet, smoking, and environmental factors such as pesticides and dyes. In 2007, a pancreatic cancer cluster was discovered in Oroville, California, where Koppers Co., Inc., a wood treatment facility, released copper chromated arsenic into the city's drinking water. A recent spatial modeling study done in Florida concluded that living within 1 mile of a known arsenic-contaminated well significantly increases the risk for PaCa. In this study, we sought to further investigate this association by using a computational systems toxicology approach to explore the influence of arsenic on the activity of candidate genes involved in PaCa. Arsenic, arsenite, arsenate, arsenicals, and arsenic acids were identified as the primary forms of arsenic in drinking water that are potentially associated with PaCa progression. We utilized the Comparative Toxicogenomics Database (CTD), KEGG, GeneCards, PubChem, T3DB, ToxNet, and Pathway Commons to generate an integrated PaCa/As pathway demonstrating the carcinogenic effects of these forms of As on target genes. Computational analysis highlighted As associated manipulation of the TNF ligand family, suggesting a relationship between As exposure and tumorigenesis. COX-2, HIF-1α and VEGF pathway mediation of angiogenesis alternatively constitute potential As associated tumor vascularization and supplementation for cancer growth. Furthermore, upregulation of CTNNB1 as a result of As toxicity also contributes to cell adhesion via the Wnt signaling pathway. Downregulation of genes implicated in NOTCH1 activation in tumor suppression were also expressed in As exposed cells. As upregulates NFE2L2 resulting in resistance against oxidative stress in cancerous cells. BCL2L1 upregulation prevents apoptosis, thus allowing tumor survival. These combinative effects of As toxicity associated with PaCa provide additional evidence for environmental concerns for As contamination in water and risk for PaCa.

PS 2259 Breast Cancer-Relevant Biological Pathways in the US EPA ToxCast and US NTP Tox21 Hazard Screening Programs

R. Rudel and J. M. Ackerman. *Silent Spring Institute, Newton, MA.*

Breast cancer is the most common cause of death of middle-aged American women and few preventable risk factors have been identified. Identifying breast carcinogens could lead to risk reduction, but this has not been a focus of toxicological research. High throughput screening initiatives such as Tox21 and ToxCast hold great promise for filling in data gaps on chemical hazards. We investigated the coverage of current ToxCast and Tox21 assays with respect to breast cancer-relevant pathways such as endocrine and cancer hallmark endpoints identified previously by an expert panel, comparing the two to identify gaps. We systematically searched ToxCast and Tox21 assay descriptions for keywords reflecting endocrine, cancer hallmark, and related pathways. We also searched for assays conducted in breast cells or with proteins isolated from breast cells. We verified our results with members of the ToxCast team.

ToxCast and Tox21 contain several assays intended to evaluate chemicals' effects on endocrine signaling pathways and cancer hallmark pathways, both categories of pathways believed to be important in breast cancer etiology. However, other im-

portant pathways and endpoints, including Her2, ER-β, and expression of breast cancer-relevant genes, are less well represented, whether because they were not prioritized, or because of difficulties in developing suitable high throughput assays. ToxCast and Tox21 currently include assays measuring ER, PR, AR, and aromatase activity, as well as cell growth kinetics, cell cycle perturbations, steroidogenesis, and apoptosis, in breast cells or proteins isolated from breast cells. Measurement of gene expression, growth signals, metabolism, and other endpoints in breast cells might provide additional important information about breast cancer risk. This disease-focused approach can be extended to other health effects, such as neurotoxicity or asthma, in order to suggest additional assays for high throughput screening projects.

PS 2260 High-Content Screening of Rodent Mammary Gland Carcinogens in Two Breast Cell Lines

J. M. Ackerman[2], C. Vulpe[1], A. Tagmount[1] and R. Rudel[2]. [1]*University of California, Berkeley, CA and* [2]*Silent Spring Institute, Newton, MA.*

Breast cancer is the most common cause of death of middle-aged American women and few preventable risk factors have been identified. Identifying breast carcinogens could lead to risk reduction, but this has not been a focus of toxicological research. High throughput testing methods, such as those being developed in US EPA ToxCast and NTP Tox21 programs, have the potential to identify carcinogens more quickly and cheaply than traditional rodent bioassays; the predictive power of these methods is still being evaluated. We used high content screening to measure the responses of two human mammary epithelial cell types, MCF7 (derived from a tumor) and MCF10A (derived from normal cells), to 24 and 72 hour exposures to a set of 111 chemicals relevant to breast cancer. Endpoints included measurements of DNA damage repair (P53, pH2AX), mitochondrial health, and cytoskeletal integrity (tubulin), among others, but no endocrine-related pathways. Because few human breast carcinogens have been identified, we tested 74 rodent mammary carcinogens (MCs), 19 "non-carcinogens" that did not induce any tumors in NTP bioassays, and 18 chemicals that disrupt mammary gland development in rodents. Comparing the two time points, assays run with 72 hours of exposure were more sensitive than those measured after 24 hours of exposure in either cell line, with more chemicals showing activity and more of the active chemicals showing activity at lower doses. Comparing the two cell lines, most assays were more sensitive in MCF10A than in MCF7 after 24 hours, and more sensitive in MCF7 than in MCF10A after 72 hours. Chemicals previously demonstrated to be genotoxic without metabolic activation in the Ames assay did not show more activity than Ames-negative chemicals in the two assays reflecting DNA damage repair (p53 and pH2AX). Additional research is required to relate high content screening endpoints to standard toxicity tests such as genotoxicity batteries and Ames, and to understand the importance of cell line and exposure conditions.

PS 2261 Re-Evaluation and Expansion of the US FDA/CDER Rodent Carcinogenicity Database for Structure-Based Analysis

D. Guo, B. L. Minnier, L. Stavitskaya and N. L. Kruhlak. *FDA, Silver Spring, MD.* Sponsor: R. Rouse.

A high-quality database of well-characterized toxicities linked to chemical structures is crucial to the development of structure-activity relationships. In order to have available the most accurate experimental data possible for structure-activity relationship development and read-across purposes, we re-analyzed the results of laboratory testing of the 1683 chemicals in the FDA/CDER rodent carcinogenicity database using contemporary standards, with a focus on extracting additional data fields and employing a more structured format for data archiving than in previous efforts. Test protocols were re-evaluated by OECD TE 451 and ICH S1B standards, including the selection of test animals, dosage, dosing duration and study duration, clinical examinations and histopathology evaluations. For pharmaceuticals, statistical significance in pair-wise comparison to concurrent controls (Fisher's Exact Test or an equivalent statistical analysis) was defined for rare tumors as $p \leq 0.025$ and common tumors as $p \leq 0.005$. For other chemicals, significance was defined for rare tumors as $p \leq 0.05$ and common tumors as $p \leq 0.01$. A numerical activity scale algorithm was designed to consistently quantify and stratify the results of the rodent carcinogenicity studies to enable more sophisticated computer analyses of structure-based trends. Among all reviewed chemicals, 190 are rodent carcinogens which cause tumors in male and female rats and mice, 364 are non-carcinogens. 98 out of the 190 carcinogens target the same organs across species and gender. The number of chemicals that are tumorigenic to male rats, female rats, male mice and female mice is 519, 482, 447, and 459, respectively. The most common tumor sites are the liver and lung. All organ-specific carcinogenicity data, supporting citations, and their respective chemical structures will be made available to the FDA/CDER community as a structurally searchable data repository, facilitating complex structure- and text-based queries, and supporting the development of quantitative structure-activity relationships.

PS 2262 Establishing Best Practice for the Application of a Novel Statistical-Based Model to Evaluate Potential Mutagenic Impurities under ICH M7

C. Barber[1], T. Hanser[1], N. L. Kruhlak[2] and L. Stavitskaya[2]. [1]*Research, Lhasa Limited, Leeds, United Kingdom and* [2]*US Food and Drug Administration, Silver Spring, MD.* Sponsor: C. Marchant.

Under the emerging International Conference on Harmonisation (ICH) M7 guideline, a safety assessment of a pharmaceutical impurity may, in some instances, be performed using *in silico*-based methods without the need for *in vitro* testing. Such assessments should consist of a statistical-based method (QSAR) and an expert rule-based method (SAR), both of which should be consistent with OECD guidelines for the regulatory use of (Q)SARs. These models need to be appropriately applied to ensure accurate and trustworthy predictions are generated. Furthermore, model predictions should be transparent and scientifically explicable to support the expert assessment recommended under the guideline.

In this work, we present best practice for the application of a new statistical-based QSAR software, Sarah Nexus, for the assessment of the genotoxic potential of pharmaceutical impurities. Sarah Nexus utilizes a novel machine-learning approach based upon self-organizing hierarchical networks, and was used to construct a statistical model based upon *Salmonella* mutagenicity data. The methodology allows for the tuning of model performance to balance sensitivity against specificity, as well as overall accuracy against coverage. To establish best practice, optimal model application settings were assessed using two independently-derived external validation sets containing 513 (19% positive) and 809 (42% positive) compounds. The same optimal settings of 10% sensitivity (defines the relative impact of positive signals) and 10% equivocal (the threshold under which the signal is not strong enough for the model to make a call) were identified for both cases, resulting in balanced accuracy of 74 and 77%, sensitivity of 64 and 68%, and specificity of 86 and 85%, respectively, for the two validation sets. While coverage is reduced to 81 and 86% under these conditions, this is considered an acceptable trade-off in favor of overall improved accuracy and, in particular, improved sensitivity.

PS 2263 Genotoxic Risk Assessment of Impurities in Drug Substances

S. Raimondo, L. Marocchio, Z. Cimarosti and L. Costa. *Safety Assessment, Aptuit, Verona, Italy.* Sponsor: C. Powell.

CPMP/SWP/5199/02 (2006) guidelines for Europe and FDA draft guidance (2008) for US are the current main reference documents for dealing with genotoxic and carcinogenic impurities in drug substances. An international effort for addressing different approaches and sometimes inconsistencies or gaps in the multiple guidances or papers published from different international bodies (ICH, EMA, PhRMA, FDA) is ongoing by the International Harmonization Conference (ICH), which M7 guideline is currently in step 2.

In this poster focus is given to the genotoxic impurity issue, describing the internal (Aptuit) Genotoxic Risk Assessment (GRA) process and presenting an overview of the results obtained from GRAs performed in the past three years. A perspective and process change once M7 guidance is released is also presented/discussed. GRA is an integrated, multidisciplinary process, involving essentially chemists, analysts and toxicologists, with the aim to evaluate the potential presence of genotoxic (DNA reactive, mutagenic) impurities in drug substance. The chemical route is first evaluated for potentially mutagenic compounds as defined by the "Genotoxic Impurities of High Concern" list of functional groups. Intermediates, reagents, major by-products (including reaction of reagents with solvents) and degradants are considered. Chemical structure rising concern are submitted to Derek Nexus (Lhasa Limited) for identification of structural features alerting for mutagenicity and carcinogenicity; those with confirmed alerting structure are submitted to the Ames test. Genotoxins should be removed or controlled at TTC (Threshold of Toxicological Concern) level. The group has evaluated in the past three years 20 synthetic routes (133 chemical stages), for an overall amount of approx 800 chemical structures assessed, of which 97 structures were recommended to DEREK screen. For most of these structures a control strategy was developed and only 59 were actually submitted to the analysis in silico. From these, 16 were confirmed to have mutagenicity and/or carcinogenicity concern. Ames test resulted positive for 3 structures.

PS 2264 Can Public Data Improve Mutagenicity Predictions for Proprietary Compounds?

R. V. Williams, C. Barber and C. Marchant. *Lhasa Limited, Leeds, United Kingdom.*

It has long been axiomatic that predictive toxicology models built on data available in the public domain can encounter problems when attempting to predict proprietary data, e.g. from a drug development program. Conversely, model performance against public data is often used to support the selection of models for specific applications and such analyses are often published. One outcome of some recent model development work has been to produce metrics that can be used to experimentally test the axiom and assess the validity of basing conclusions on public data. A large data set, based primarily on public data, was used to identify improvements to an expert knowledge base for (Ames test) mutagenicity. These improvements were implemented as new or modified structural alerts, and were incorporated into successive knowledge base iterations. The performance of each iterative build was evaluated against a large public data set (Benchmark) and a proprietary data set (Vitic Intermediates).
Our analysis showed that the addition (or modification) of structural alerts consistently improved the detection of mutagens within the Benchmark data set. However, this improvement was not mirrored against the Vitic Intermediates data set.
It can be concluded that performance against public data should be weighted accordingly when considering the use of models within a given chemical space. This experimentally supports the original axiom, at least in part, and suggests that building a model comprising only of public datasets (however large) may not be sufficient to allow accurate predictions within proprietary chemical space. However, further analyses would be required to verify the robustness of this conclusion (e.g. other pharmaceutical data sets) and also to read-across these results into other domains (e.g. agrochemicals or personal care products). Future work will focus on this, as data become available.

PS 2265 An Improved Workflow to Perform *In Silico* Mutagenicity Assessment of Impurities As Per ICH M7 Guideline

S. Chakravarti and R. D. Saiakhov. *MultiCASE Inc, Beachwood, OH.* Sponsor: G. Klopman.

Purpose: Use of *in silico* tools is one of the central points of ICH M7 guideline. However computational assessment of DNA reactive impurities in real life is still challenging. Purpose of this study is to develop and apply an effective workflow using a QSAR statistical system and a quantitative read across modeling methodology to obtain reliable genotoxicity assessments adhering to the ICH M7 recommendations. The novel multi-tier methodology provides the detailed information of toxicity alerts and reduces false positives, false negatives while increasing the test coverage. This *in silico* approach can be successfully used for assessment of mutagenicity of new drug candidates, impurities and metabolites.
Method and Data: CASE Ultra is a QSAR statistics based computer program that automatically extracts structure-activity knowledge from chemical databases and applies the knowledge for predicting activity in test chemicals. Several models, developed by MultiCASE Inc alone and within Research Cooperation Agreement with Center for Drug Evaluation and Research of FDA were utilized, as well as a read across modeling technique for quantitative prediction of toxicity that uses the neighborhood profiles of chemicals. A multi-tier approach in combining several models and read across engine for bacterial mutagenicity evaluation resulted in significant improvements in the sensitivity, specificity and coverage. The details of the methodology and results of prediction for a large external test set are presented.
Results of the Study: The improvements in the predictive performance as a result of the effective workflow is demonstrated for various scenarios of *in silico* mutagenic impurity assessments, using an external validation set and real life case studies as examples.

PS 2266 Development of an *In Silico* Profiler for Mitochondrial Toxicity

M. D. Nelms[1], M. T. Cronin[1], A. N. Richarz[1], C. Yang[2] and S. J. Enoch[1].
[1]*School of Pharmacy and Chemistry, Liverpool John Moores University, Liverpool, United Kingdom and* [2]*Altamira LLC, Columbus, OH.*

Disruption of normal mitochondrial functioning can result in cell death and is implicated within a variety of diseases. There are a number of mechanisms by which normal functioning can be impaired these include, but are not limited to, uncoupling of oxidative phosphorylation, inhibition of the electron transport chain and membrane permeability induction. Mitochondrial toxicity has been identified as a source of chronic toxicity in a number of drugs leading to their withdrawal from the market. Thus, the ability to identify chemicals potentially capable of this type of toxicity would be of benefit in the risk assessment process. Despite this, few in silico methods have been developed capable of making such predictions. Therefore, the purpose of this study was to develop an in silico profiler consisting of a series of structural alerts related to the mechanisms involved in mitochondrial toxicity. Data for 288 compounds identified as being either toxic or non-toxic to mitochondria were extracted from the literature. Structural similarity was undertaken to group the data, producing fourteen categories, from which nine structural alerts were identified, covering nine chemical classes and five mechanisms of mitochondrial toxicity. The nine chemical classes covered include lidocaine derivatives, thiazolidinediones, anthracyclines and cholic acid derivatives. The identified mechanisms were uncoupling of oxidative phosphorylation, inhibition of the electron transport chain, induction of membrane permeability transition, alternative electron acceptance and initiation of the death receptor pathway. These structural alerts were supported by mechanistic information from the literature allowing the chemistry of the Molecular Initiating Event to be defined. In addition, a new structure knowledge representation method, chemotype, is also used to extract mechanistic alerts from the dataset. The alerting chemotypes can also be deployed in KNIME node or on ChemoTyper (free software from FDA). Supported by the EU FP7 COSMOS Project.

PS 2267 Computational Identification of Active Phytochemicals and Potential Mechanisms for the Alleviation of Bleomycin-Induced Pulmonary Fibrosis

N. Chan, E. Perez, S. Li and D. E. Johnson. *Nutritional Sciences & Toxicology, UC Berkeley, Berkeley, CA.*

Bleomycin (BLM), a chemotherapy drug used in the treatment of Hodgkin's Lymphoma can induce pulmonary fibrosis. This deleterious side effect has been treated in integrative medicine with Hu-qi-yin, a Traditional Chinese Medicine (TCM) recipe. Additionally, the dietary supplement α-lipoic acid has been suggested as a possible treatment based on efficacy in a BLM-induced pulmonary mouse model. In this computational research, we identified potentially active phytochemicals in Hu-qi-yin and sought to verify the potential role of α-lipoic acid in inhibiting or alleviating pulmonary fibrosis. The TCM Database@Taiwan was used to identify 686 phytochemicals in the TCM recipe. Several other web-based resources were used to investigate, integrate, and screen disease genes, chemical-gene interactions, and protein binding interactions; the most important being the Comparative Toxicogenomics Database (CTD) and the Search Tool for Interactions of Chemicals (STITCH). Three genes most highly associated with the pulmonary fibrosis pathway using an inference score were transforming growth factor β1 (TGF β1), tumor necrosis factor (TNF) and chemokine ligand 2 (CCL2). Of the 686 phytochemicals, 54 had direct interactions with one or more BLM-induced genes, while 11 chemicals had indirect interactions. Although some chemical compounds were found to increase the expression of one or more of the genes, the majority of compounds displayed inhibitory effects against TNF, CCL2 or TGF β1. The study of α-lipoic acid suggested an inhibitory effect to TGF β1. This study supports a molecular explanation for the potential therapeutic effects observed with Hu-qi-yin and α-lipoic acid. Furthermore, the results suggest that isolated phytochemicals from Hu-qi-yin may possibly work in concert with α-lipoic acid to alleviate BLM- induced pulmonary fibrosis.

PS 2268 EDCs DataBank: 3D-Structure Database of Endocrine Disrupting Chemicals

D. Montes-Grajales and J. Olivero-Verbel. *Environmental and Computational Chemistry Group, University of Cartagena, Cartagena, Colombia.*

Endocrine disrupting chemicals (EDCs) are a diverse group of compounds that affect the endocrine system and have been epidemiologically associated with adverse health effects. However, major protein targets or toxicity mechanisms for many of these compounds are unknown. The aim of this work was to develop EDCs DataBank, the first database of EDCs with three-dimensional structures available for virtual screening. This database was built on MySQL using the EU list of potential endocrine disruptors and TEDXList. It contains three-dimensional structures available on PubChem, as well as a wide variety of information, including sources and biological information from different databases and text mining tools such as PubMed, Fable, ToxCast and LigerCat, making it useful for almost any kind of research regarding EDCs. The web platform was developed using HTML, CSS and PHP languages, which let the use of dynamic contents in a graphic environment and the creation of interactive histograms and scatter plots by the user, as tools that may help the analysis of the information available for each selected compound. Currently, EDCs DataBank has 602 molecules, including flavonoids, pesticides, industrial products, and other low molecular weight xenobiotics. This database is fully searchable and the 3D-structures of the molecules can be downloaded in

several formats, all together or separately. This database could be employed for application in docking studies, high-throughput virtual screening and protein interaction analysis, among others. EDCs DataBank will be available at http://edcs.unicartagena.edu.co. D. Montes is sponsored by Colciencias, 567-2012.

PS 2269 Computational Prediction of Off-Target Selectivity of Small Molecules Based on Ligand Set Similarity Using SEAware: Similarity Ensemble Approach Software

M. Fielden[1], M. Keiser[2], E. Gregori-Puigjané[2], J. Houze[1], W. Zhong[1] and C. Fotsch[1]. [1]*Amgen, Thousand Oaks, CA and* [2]*Seachange Pharmaceuticals, San Francisco, CA.*

In silico prediction of off-target pharmacology and adverse effects for small molecule drugs has been hampered by small and/or poorly representative training sets, and subsequently low predictivity. Here we present the results of an evaluation of the Similarity Ensemble Approach (SEA) to large scale prediction of off-target pharmacology. SEA calculates whether a molecule will bind to a target based on the chemical features it shares with known ligands, using a statistical model to control for random similarity. An independent test of over 200 proprietary compounds was evaluated for off-target interactions in comparison to actual ligand binding or enzyme inhibition data across approximately 150 targets. Using a training set based on publically available data (ChEMBL14), the prediction accuracy was poor and close to random (AUC of 0.53), however a second independent test set of over 850 well known drugs and chemicals had improved prediction accuracy (AUC of 0.79). As a result it was hypothesized that good prediction accuracy could be obtained if the training and test set compounds were structurally similar. To that end, we generated a training set based on a large comprehensive collection of internal drug-target interaction data and subsequently evaluated the algorithm using a 3-fold cross-validation approach. Using various affinity thresholds and compound fingerprinting methods, we consistently achieved high global prediction accuracy (AUC > 0.9). Sensitivity and specificity for individual off-targets could be optimized with altered thresholds to limit the number of false positives and still achieve a useful level of sensitivity. These results highlight the possibility of providing advanced knowledge of hundreds of off-targets based on structural information alone. It is anticipated such methods will be useful to guide selectivity screening strategies during lead optimization and provide novel insights to off-target toxicities not otherwise known.

PS 2270 Molecular Dynamic Simulation Studies of Bisphenol A and Its Analogs with Estrogen Related Receptor-Gamma and Human Androgen Receptor

R. M. Uppu[1, 2]. [1]*Dept of Biology, Chemistry and Environmental Toxicology, Southern University and A & M College, Baton Rouge, LA and* [2]*Biological Sciences, Louisiana State University, Baton Rouge, LA.*

Bisphenol A (BPA) and several of its analogs are high volume chemicals used mainly in the manufacturing of polycarbonate plastics. It has long been recognized that BPA and its analogs behave as xenoestrogens, and can cause reproductive disorders. We have recently determined the free energies of binding of BPA and its chlorinated and nitrated products to the estrogen-related receptor-gamma (ERRγ) and compared the binding energies observed with the natural ligand, estradiol. These studies hold promise for characterizing binding pockets and changes in free energy of binding for biologically-relevant bisphenols and their environmentally-generated derivatives. The present study focuses on extending the molecular docking calculations/simulations to various BPA analogs based on binding to not only ERRγ but also to human androgen receptor (hAR) by performing Free Energy Perturbation (FEP) using NAMD software. The absolute binding free energies of the ligand complexes are computed by running annihilations forward and backward with explicit solvent. Restraining potentials were removed during the simulations to observe changes in conformational and translational energies of the ligand and receptor upon binding. The whole system was minimized and equilibrated before running the said annihilations to remove steric hindrance(s) between atoms. The net binding free energies of BPA and its analogs thus calculated are analyzed and compared with those of experimental values which revealed strong binding affinity of compounds towards the receptors when compared to the natural ligand. The results from this study are promising as they can be used to characterize binding pockets and changes in free energy of binding of BPA and helps in identifying the most significant molecular targets for xenoestrogens in general and BPA in particular [Support from NSF (HRD1043316) and the US DoEd (PO31B040030) is acknowledged; corresponding author's email: rao_uppu@subr.edu].

PS 2271 Amoxillin- and Pefloxacin-Induced Ionoregulatory Disruptions in Rat Tissues

S. O. Rotimi[1, 4], D. Ojo[2], E. A. Balogun[1], O. Talabi[3] and O. Ademuyiwa[1]. [1]*Department of Biochemistry, Federal University of Agriculture, Abeokuta, Abeokuta, Ogun, Nigeria,* [2]*Department of Microbiology, Federal University of Agriculture, Abeokuta, Abeokuta, Ogun, Nigeria,* [3]*Health Centre, Federal University of Agriculture, Abeokuta, Abeokuta, Ogun, Nigeria and* [4]*Department of Biological Sciences, Covenant University, Ota, Ogun, Nigeria.*

Antibiotics are among the commonly prescribed and abused drugs in medicine. Their use is often associated with a variety of side/toxic effects. In order to investigate whether amoxillin and pefloxacin perturb electrolyte homeostasis, rats were treated with therapeutic doses of each antibiotic for 5 and 10 days respectively. Twenty four hours and 5 days after antibiotic withdrawal, blood and other tissues (liver, kidney, brain, heart and spleen) were removed from the animals analysed for their electrolyte contents and activities of Na+-K+- and Ca2+-Mg2+-ATPases. Molecular docking of the antibiotics against rat's alpha-3 subunit of Na+-K+-ATPase (NCBI accession number: gil6978547) and Ca2+-ATPase (NCBI accession number: gil16758008) was also performed. After 5 days of pefloxacin administration, the activity of Ca2+-Mg2+-ATPase in erythrocyte ghost, liver, kidney, brain and heart dropped to 75%, 71%, 91%, 92% and 42% of the control respectively. Na+-K+-ATPase activity was reduced to 48% and 59% of the control in the kidney and brain respectively. There was however a reversal in the activities of renal and cardiac Na+-K+-ATPase as well as splenic and cardiac Ca2+-Mg2+-ATPase 5 days after the withdrawal of amoxicillin treatment. These culminated in hyponatremia, hypokalemia, hypocalcemia and hypomagnesemia. By day 15 however, there was a resolution of the ionoregulatory disruption. In silico docking revealed that three hydrogen bonds are formed between amoxillin and Glu818, Tyr1012, Arg930 and Arg827 of Na+-K+-ATPase. Pefloxacin however forms only one hydrogen bond with Arg930 of the enzyme. Only Glu875 and Pro828 of Ca2+-ATPase form hydrogen bond with amoxillin and pefloxacin respectively. The findings of this study further revels the pattern and mechanisms of ionoregulatory disruptions by these antibiotics.

PS 2272 Enhanced Alternatives Analysis: Automated Evaluation of Chemical Hazard Attributes to Identify Preferred Substitutes

P. J. Beattie, J. P. Rinkevich and J. Orchard-Hays. *SciVera, LLC, Charlottesville, VA.*

Many companies, especially downstream users of chemicals, are moving toward improved chemicals management by establishing programs to better understand the chemicals in their products. In addition to collecting specific chemical ingredient information, companies are tasked with identifying chemicals of concern and prioritizing where to take action. One aspect of this process is to utilize Restricted Substance/Authoritative Lists (RSLs). A more robust approach focuses on understanding the underlying hazard data in the scientific literature to identify critical endpoints.

Benefits of an enhanced process for evaluating chemicals in products beyond basic RSL review includes predicting which chemicals are likely to be added to RSLs in the future and reducing cost of chemical substitution via proactive efforts.

Our research made use of the SciVera Lens attributes-based chemical hazard assessment database and several accompanying automated analytical tools to identify the gap between chemicals on key RSLs and chemicals with reported high hazard (based on GHS criteria). The results are based on analysis of the set of over 135,000 chemicals in the SciVera Lens and European Chemical Agency (ECHA) databases and a group of over 40 common RSLs.

The analysis focused on the Developmental-Reproductive (D-R) endpoint due to the fact that several RSLs identify this endpoint as the rationale for listing. The results indicate that more than 30 percent of chemicals with reported scientific data for high D-R hazards were not on any RSL and greater than 50 percent when assessed against specific D-R lists.

This analysis confirms that a hazard attributes-based assessment, when combined with the efficiency and consistency of automated techniques, provides for a more robust and predictive approach for alternatives assessment, allowing users to identify chemicals of potential concern prior to inclusion on an RSL, thereby reducing the potential for regrettable substitutions.

PS 2273 *In Silico* Workflow for Assessing Skin Irritation, Penetration, and Sensitization Potentials Using Chemotype-Based Models and Alerts

J. Rathman[2, 3], J. Schwöbel[1], T. Magdziarz[1], A. S. Mostrag-Szlichtyng[2], A. Tarkhov[1], L. Terfloth[1] and C. Yang[2, 3]. [1]*Molecular Networks GmbH, Erlangen, Germany,* [2]*Altamira LLC, Columbus, OH and* [3]*Chemical and Biomolecular Engineering, The Ohio State University, Columbus, OH.*

We present an *in silico* workflow for evaluating chemical toxicity instigated upon dermal contact. The first step identifies compounds that will not be absorbed and removes these from further consideration. Compounds that are absorbed and cause skin irritation are identified next, while absorbed non-irritating compounds are passed on to the next module for evaluation of skin sensitization potential. Probable metabolites are added to the workflow along with the parent molecules. Skin sensitization potential is predicted by modeling mouse local lymph node assay (LLNA) data, with values ranging from non-sensitizing to weak, moderate, strong or extreme. Covalent modification of proteins by sensitizers by well-known reaction mechanisms represents the molecular initiating event for the induction. ToxPrint chemotypes, structural fragments encoded with physicochemical properties and electronic system information, are used to categorize chemicals into MIE classes. Skin metabolic rules, coded in chemotypes, were also used to predict bioavailability and reactivity. Results from multinomial ordinal classification QSAR models for each MIE class are combined using a rigorous weight-of-evidence approach that explicitly quantifies the uncertainty associated with each prediction. Our approach has been externally validated using skin irritation and sensitization results from literature studies. The workflow effectively separates irritants from non-irritants. Approximately 70% of sensitizers are predicted in the correct category and better than 90% are predicted within one category or their reported experimental value. Further, all sensitizers are associated with chemotype alerts, illustrating the power of this approach in overcoming limitations of classical structural alerts. The workflow comprehensively addresses chemical toxicity via dermal contacts.

PS 2273a Computational Molecular Modeling for the Assessment of Nanoparticle Toxicity: Interactions with Biomolecules

N. Yanamala[1], V. E. Kagan[2] and A. A. Shvedova[1, 3]. [1]*HELD/PPRB, CDC/NIOSH, Morgantown, WV,* [2]*Department of Environmental and Occupational Health, University of Pittsburgh, Pittsburgh, PA and* [3]*Department Physiology and Pharmacology, West Virginia University, Morgantown, WV.*

Over the past two decades, nanotechnology has emerged as a key player in various disciplines of science and technology. A detailed understanding of the molecular details of interactions between nanoparticles (NP) and biomolecules is crucial for obtaining adequate information on mechanisms of action of nanomaterials and their possible toxicological outcomes. There has been a recent surge in the application of in silico based methods and approaches to address interactions of NPs with biomolecules providing insights into their mechanisms. To do this, we used structure-based computational modeling as a tool to predict the molecular interactions between carbonaceous NPs and cellular proteins and lipids. We demonstrated that specific interactions of NPs with proteins/lipids resulted in a coating on its surface, ultimately masking their inherent properties, thus leading to modified distribution in cells, recognition and uptake by cells. We also provide evidence that interactions of basic/positively charged amino acids of the enzymes (e.g. peroxidases) with the carboxyl moieties on carbon nanotubes and graphene – positioning them in close proximity to the catalytic site of the enzyme – are essential for the effective catalysis and safe degradation of these materials in vivo. Structure based computational modeling is a useful and effective approach that could facilitate the design and development of safe engineered nanomaterials.

PS 2273b Benchmarking Assessment of Open Source and Newly Released *Salmonella* Mutagenicity (Q)SAR Models for Potential Use under ICH M7

L. Stavitskaya, B. L. Minnier and N. L. Kruhlak. *Food and Drug Administration, Silver Spring, MD.* Sponsor: R. Rouse.

The current draft of the International Conference on Harmonisation (ICH) M7 guideline describes the use of (quantitative) structure-activity relationship ((Q) SAR) models during drug safety evaluation. The guideline, however, does not specify the use of any particular model, but instead recommends that the models meet the general definition of statistical or rule-based methodologies, and allow the identification of structural alerts. In this study, we evaluated the performance of Toxtree, a freely-available, open source SAR model and two newly-released, commercial (Q)SAR programs, Sarah Nexus and Leadscope Expert Alert System, as potential candidates for qualifying pharmaceutical impurities. To effectively assess the performance of Toxtree, an in-house Salmonella mutagenicity database of 3979 compounds (43% positive) and a highly-curated version of the Hansen dataset of 3734 compounds (58% positive) were used. Performance statistics for the two datasets ranged from 79% to 85% sensitivity and 83% to 73% negative predictivity, respectively. The performance of the statistical-based system, Sarah Nexus, was assessed using the in-house Salmonella dataset after removal of compounds that overlapped with the training set. The resulting dataset comprised 809 chemicals (42% positive), and yielded sensitivity and negative predictivity of 68% and 79%, respectively. The rule-based Leadscope Expert Alert System was evaluated using the curated Hansen dataset of 3734 chemicals (58% positive) and yielded performance of 85% sensitivity and 78% negative predictivity. These performance statistics compare favorably with those of the three most widely-used commercial model systems tested with the same data sets, indicating their suitability for the qualification of pharmaceutical impurities under ICH M7.

PS 2273c Pragmatic Issues in Applying Multiple *In Silico* Systems for Drug Safety Assessment

R. Benz[1], K. P. Cross[2] and G. J. Myatt[2]. [1]*OmnyCorp, Rockville, MD and* [2]*Leadscope, Inc., Columbus, OH.*

The current draft of the International Conference on Harmonisation (ICH) M7 guidelines on the "Assessment and control of DNA reactive (mutagenic) impurities in pharmaceuticals to limit potential carcinogenic risk" outlines the use of two complementary in silico methodologies to qualify impurities as not mutagenic, alongside an expert review. One system should be an expert alert-based system with the other a statistical-based methodology. The practical use of multiple systems presents a number of challenges and this poster enumerates and quantifies the performance implications of three important issues. Firstly, it discusses how mechanistically plausible alerts with limited supporting data (termed "indeterminant alerts") should be used and interpreted as part of an overall M7 assessment. Secondly, it discusses the importance of applicability domains when using alert-based systems. Finally, it reviews methodologies for combining the results from different in silico systems, along with available experimental data. A highly-curated version of the Hansen dataset of 3734 compounds with Salmonella data was used to evaluate the performance of the combined systems. By using a series of consensus rules combining both predictions and experimental data, the resulting sensitivity increased in a range from 9.1% - 12.1% and negative predictivity increased by 10.6% - 15.6% over using individual systems alone.

PS 2273d Metabolism Simulation and Toxicity Prediction in the Evaluation of Food Ingredient/Contaminant Safety

L. Terfloth[1], K. Arvidson[2], K. Muldoon-Jacobs[2], P. Volarath[2], A. Tarkhov[1], T. Magdziarz[1], J. Rathman[3, 4], D. Hristozov[4] and C. Yang[1, 4]. [1]*Molecular Networks GmbH, Erlangen, Germany,* [2]*Center for Food Safety and Applied Nutrition, Office of Food Additive Safety, U.S. Food and Drug Administration, College Park, MD,* [3]*Chemical and Biomolecular Engineering, The Ohio State University, Columbus, OH and* [4]*Altamira LLC, Columbus, OH.*

During the safety assessment of food additives and their impurities, metabolic knowledge becomes critical when *in vivo* data are unavailable for the specific compound. Inclusion of metabolism information into the *in silico* workflow is therefore a pre-requisite for the US FDA's Chemical Evaluation and Risk Estimation System (CERES). The chemical space of food additives was profiled using public ToxPrint and metabolic (human liver and S9-fraction) chemotypes. Chemotypes are structural fragments encoded with physicochemical properties, and are considered as alerts when associated with a specific endpoint. The metabolic potential was predicted by applying a diverse set of over 100 phase I as well as more than 20 phase II conjugation reactions of human liver metabolic chemotypes. As an example, the effect of S9 metabolic chemotypes on Ames mutagenicity was analysed against the food additives. Although nearly 20% of the compounds were perceived as genotoxic carcinogens by chemotype alerts, only 4% of such compounds were actually predicted to be mutagenic under CERES mechanistic QSAR paradigm. Nearly 50% of the food additives predicted to be mutagenic were matched with chemotype alerts for genotoxic carcinogens. When repeating the analysis after removing the compounds that may be detoxified by S9, the reliability of the genotoxic alerts is increased almost 3 times. This study demonstrates the value of the use of metabolic rules in conjunction with known chemotype alerts to reduce the false positive rate of structural rules. Implementation of the metabolic rulebase in CERES is also presented. The research was funded by EU FP7 and Cosmetics Europe. (Grant n° 266835).

PS 2273e Comparison of Pattern Recognition Methods for Toxicogenomics Time Series

D. M. Hendrickx, D. Jennen, J. J. Briedé, R. Cavill, T. M. de Kok and J. Kleinjans. *Toxicogenomics, Maastricht University, Maastricht, Netherlands.* Sponsor: H. van Loveren.

Establishing relationships between gene expression and phenotypic endpoints is important to discover mechanisms of action of a toxic compound. In this study, pattern recognition methods for the identification of genes whose expression time-courses are associated with phenotypic endpoints are compared.
Pattern recognition methods have been shown to be very effective in answering many biological questions, because biological entities belonging to the same cluster are assumed to be functionally related (1,2). To compare pattern recognition methods for identification of gene-phenotypic endpoint relationships from time-courses, four representative methods were chosen: k-means clustering (1), short time series expression miner (STEM)(3), linear mixed model (LMM) mixtures (4) and dynamic time warping (DTW4omics)(5). The four methods were applied on two published data sets on a human liver carcinoma cell line (HepG2): the response to benzo(a)pyrene (6) and menadione (7). Both data sets consist of time-series of both gene expression and phenotypic endpoints.
Lists of genes associated with an endpoint were identified and the overlap among the four methods determined. Gene Ontology (GO) and pathway analysis were applied on the gene lists.
Gene, pathway and GO lists show low overlap among the methods and each method provides biologically relevant information (large overlap with the literature). Additionally, relationships not occurring in the literature represent new hypotheses. Testing these hypotheses experimentally can lead to the discovery of new mechanisms of action for a toxic compound.

1. Liao TW Pattern Recognition 38, 1857-1874 (2005).
2. Bar-Joseph Z Bioinformatics 20(16), 2493-2503 (2004).
3. Ernst J & Bar-Joseph Z BMC Bioinformatics 7:191 (2006).
4. Celeux G et al. Statistical Modelling 5, 243-267 (2005).
5. Cavill R et al. PLoS One 8(8):e71823 (2013).
6. van Delft JH et al. Toxicol Sci 117, 381-392 (2010).
7. Deferme L et al. Toxicology 306, 24-34 (2013).

PS 2273f Constructing a Cleft Palate Adverse Outcome Pathway through HTS Data and Literature Mining Integration

N. C. Baker[1], N. S. Sipes[2], M. Hutson[3] and T. B. Knudsen[2]. [1]*Lockheed Martin, Research Triangle Park, NC,* [2]*NCCT, US Environmental Protection Agency, Research Triangle Park, NC and* [3]*Departments of Physics and Biological Sciences, Vanderbilt University, Nashville, TN.*

Interpreting EPA's ToxCast in vitro assay data in the context of Adverse Outcome Pathway (AOP) development is a significant challenge. While chemical activation in these assays may shed light on the molecular initiating event, the downstream effect of these activities at higher levels of biological organization (e.g., cellular, tissue, organ) leading to a potential toxicity endpoint can be difficult to identify. In this study we have used MeSH term annotations extracted from the biomedical literature to explore the relationship between the ToxCast assays significantly associated with cleft palate/cleft lip (CP/CL) toxicants and their possible downstream cellular, tissue, and organ level phenotypes. Approximately 60 ToxCast chemicals were identified as CP/CL toxicants either through the in vivo toxicity reference database, ToxRefDB, or literature reports. There were 29 ToxCast assays significantly ($p <= 0.05$) associated with these chemicals from univariate analyses. These 29 assays were associated with 18 unique genes and proteins. The MeSH terms for each of these genes and proteins were used to search a literature database of over 10 million articles to find the cellular, tissue, and organ MeSH annotation terms co-occurring with the genes and proteins. The co-occurrences counts calculated for the 66,275 resulting articles produced interesting significant connections. The ToxCast target leukocyte elastase, for instance, is highly co-annotated with the terms Cell Adhesion, Extracellular Matrix, and Connective Tissue, suggesting it should be examined for a possible role in extracellular matrix regulation during palate development. While cleft palate is used as an example, this robust literature mining technique has the potential to provide insight into AOP development for a broad range of toxicity endpoints. This abstract does not necessarily reflect US EPA policy.

PS 2273g Warning from Fold Change: Prediction of Potential Toxicity Based on Drug-Induced Genomic Expression Change

K. Wang[1, 2] and J. C. Fuscoe[1]. [1]*National Center for Toxicological Research, Food and Drug Administration, Jefferson, AR and* [2]*Bio-X Institutes, Shanghai Jiao Tong University, Shanghai, China.*

Background
Even though many techniques (from chemical structure analysis to animal/human clinical trial) are used to detect safety risks in drug development, some drugs with unanticipated severe toxicity still enter the market, leading to urgent demand for new methods of drug safety evaluation. Here we applied transcriptomic data from multiple types of cultured human cells in the Broad Institute Connectivity Map database to the systematic prediction of severe adverse reactions, i.e., myocardial infarction and liver injury.
Methods
We found that drugs with common risks generally lead to similar patterns of in vitro expression change. Based on the guilt-by-association principle, we selected a series of well-known drugs with safety risks as benchmarks and then established computational models to (1) 'score' the risk of different drugs according to their expression similarity to the benchmarks; and (2) highlight the key genes associated with, or responsible for, drug toxicity.
Results
It was found that, after scoring the myocardial risks of ~1,300 drugs, 43% of the drugs with FDA black box warnings were ranked in the 2% of top-scoring drugs. In addition, the high-scoring drugs were found to disturb specific genes related to the cardiovascular system, suggesting important clues to underappreciated toxicological mechanisms. A similar benchmarking and scoring strategy with drugs associated with liver injury also showed unique expression patterns and identified 8 additional suspicious drugs for further examination.
Conclusions
These results collectively suggest that with appropriate data analysis methods, drug-induced genomic expression changes in in vitro culture systems, such as the CMAP project, are a valuable source of information for drug safety evaluation and systems toxicology research. Specifically, we show that severe myocardial risks can be effectively addressed by transcriptomic data analysis.

PS 2273h Development of QSAR Models for Prediction of Hepatotoxicity Using Post-Market Data from US FDA's AERS Database

N. L. Kruhlak[1], L. Stavitskaya[1], K. P. Cross[2] and X. Zhu[1]. [1]*CDER/OTS/OCP/DARS, US Food and Drug Administration, Silver Spring, MD and* [2]*Leadscope Inc., Columbus, OH.* Sponsor: R. Rouse.

Drug-induced liver injury (DILI) is one of the most common drug-induced adverse events (AEs) leading to life-threatening conditions such as acute liver failure. It is also the second most common cause for post-market withdrawals or warnings. Efforts to develop new predictive methods to assess the likelihood of a drug being a hepatotoxicant have been challenging due to the complexity and idiosyncrasy of clinical manifestations of DILI. The FDA adverse event reporting system (FAERS) contains post-market data that depict the morbidity of AEs. In previous work, a set of 2029 unique and modelable drug entities with 13,689 drug-AE combinations was extracted from the AERS database using 38 hepatotoxicity-related query preferred terms, to serve as a basis of a quantitative structure-activity relationship (QSAR) training set. In the current study, additional filtering was performed to remove low confidence negative data and the resulting dataset of 1314 compounds, where the percentage of actives in the set was 50%, was used to build QSAR models with Leadscope's Predictive Data Miner software. Cross-validated QSAR performance for the prediction of DILI yielded concordance of 70%, with sensitivity and positive predictivity of 73 and 69%, respectively. These results represent an increase in sensitivity of 21% over earlier QSAR models for DILI based on post-market data. An assessment of domain of applicability using a large dataset of drug product structures (n=5081) yielded coverage of 85% when the model was applied without excluding structures predicted with 0.4 to 0.6 probability. An additional analysis of the QSAR training set using a set of human hepatotoxicity alerts from the Derek Nexus knowledgebase yielded predictions with specificity and positive predictivity of 74% and 64%, respectively. These two complementary approaches show utility when used in combination for the prediction of DILI for early screening of pharmaceutical candidates for hepatotoxic potential, as well as to support regulatory safety decision making.

PS 2273i A Database of *In Vivo* Estrogenic Activity for EDSP21 Reference Chemicals

P. Ceger[1], N. Kleinstreuer[1], X. Chang[1], B. Jones[1], J. T. Hamm[1], L. Rinckel[1], D. Rotroff[2] and W. Casey[3]. [1]*ILS, Inc., Research Triangle Park, NC,* [2]*NC State University, Raleigh, NC and* [3]*DHHS/NIH, NIEHS/NTP/NICEATM, Research Triangle Park, NC.*

Currently mandated testing for potential estrogenic activity will involve thousands of chemicals, cost millions of dollars, and take decades to complete using current validated tests. High throughput screening and computational toxicology tools may streamline this process by the quick and cost-effective identification of endocrine active chemicals (EACs). Access to a comprehensive database of high-quality in vivo EAC toxicology data is critical for the validation of in silico models and in vitro assays. The database can be used to prioritize chemicals for screening. Validation of HTS assays using the database will enable replacement of current validated in vitro screening assays with validated HTS assays. The results of these tests will better inform and target in vivo screening assays. To create such a database, we reviewed the current scientific literature, identified high-quality in vivo endocrine disruption testing data, and compiled the data into a single database. Initial review focused on the estrogenic effects of 52 reference chemicals selected by the EPA and NTP. Studies including data for these 52 chemicals on a number of different estrogenic endpoints (i.e., uterotrophic, pubertal, multigenerational, etc.) were identified. Data from the studies were extracted and compiled using a standardized ontology. An R script was developed to evaluate the quality of the data according to modified Klimisch criteria in an efficient and standardized manner. Data that were classified as reliable were added to the database, which is available on the NTP website (http://ntp.niehs.nih.gov/go/40658). This database constitutes a critical resource for validating in vitro and in silico models of estrogenic activity.
This project was funded in whole or in part with Federal funds from the NIEHS, NIH under Contract No. N01-ES-35504.

PS 2273j Using Weighted Entropy to Rank Chemicals in Tox21 Phase II BG1 ER-Luc Estrogen Receptor Assays

K. Shockley. *Biostatistics Branch, National Institute of Environmental Health Sciences, Research Triangle Park, NC.* Sponsor: R. Tice.

Quantitative high throughput screening (qHTS) assays from Phase II of the Tox21 collaboration provide concentration-response profiles for thousands of chemicals. It is necessary to be able to rank chemicals using data generated from such large scale screening experiments in order to efficiently prioritize environmental agents for possible endocrine disruption effects. Rankings are typically based on parameter estimates derived from fits to a pre-specified model, such as the logistic Hill Equation model. In particular, chemicals are often ranked using AC_{50} parameter estimates from the Hill Equation model, where an AC_{50} value represents the concentration exhibiting 50% of maximal induction along a sigmoidal curve. However, rankings based on this metric can be unreliable due to large errors associated with the parameter estimates when response data does not adequately fit the assumed model structure. Here, we describe an alternative approach for ranking chemicals in qHTS experiments based on weighted entropy scores (*WES*). *WES* provides a measure of average activity level that can be calculated from the observed response values and the underlying assay detection limits. We use *WES* to rank chemicals based on 15-point concentration-response data obtained from Tox21 Phase II BG1 ER-Luc estrogen receptor agonist and antagonist assays. A total of 276 substances in agonist mode, and 134 chemicals in antagonist mode, produced consistently high *WES* scores across in all three experimental runs (WES ≥ 2 bits). Only 38 compounds in agonist mode, and 32 compounds in antagonist mode, were ranked in the top 1,000 compounds by *WES* and AC_{50}. No significant correlation was observed when comparing ranks based on *WES* and AC_{50} for the 11,776 tested substances in agonist mode or antagonist mode.

PS 2273k FDALabel Database: Enabling Insights from Drug Labeling to Accelerate Advancement of Translational and Regulatory Sciences in Drug Safety

H. Fang[1], S. C. Harris[2], Z. Liu[2], J. Xu[2], Q. Shi[3], P. C. Howard[1] and W. Tong[2]. [1]*Office of Scientific Coordination, NCTR/FDA, Jefferson, AR,* [2]*Division of Bioinformatics and Biostatistics, NCTR/FDA, Jefferson, AR and* [3]*Division of Systems Biology, NCTR/FDA, Jefferson, AR.*

FDA drug labels represent the consensus and combined experience of regulators, drug sponsors and manufacturers, and scientific experts with information about product indications, target populations, and adverse drug reactions (ADRs). The amount of information captured in drug labels has grown rapidly, and the total number has likewise increased with around 400 to 500 new or updated drug labels being added weekly from the SPL (Structured Product Labeling) group in the FDA. This rapid pace of change, along with the breadth and depth of information contained in drug labels, highlights the need for a powerful search tool. FDALabel (http://www.fda.gov/ScienceResearch/BioinformaticsTools/ucm289739.htm) is a freely available, web-based, comprehensive drug label database with powerful full-text query capabilities. The database contains the full set of approximately 50,000 FDA-approved drug labels downloaded weekly from the National Library of Medicine's DailyMed archive (http://dailymed.nlm.nih.gov/). The simple search options in FDALabel include full-text search as well as searches within only the product or generic name. The advanced search options allow querying text based on any combination of specific sections, dosage forms, document types, market categories, market date and other information. We have selected study cases in this poster, including a pharmacogenomics biomarker study and also an ADR study which utilizes MedDRA standard terminologies. FDALabel provides researchers, regulators, drug developers, and physicians an effective and efficient means of accessing the rich amount of information contained in FDA drug labels. It also opens the possibility for novel uses of drug labels in supporting the FDA's goals of advancing translational and regulatory sciences, e.g., by identifying trends in ADRs or by identifying ADRs that are associated with increased risks to public health.

PS 2273l ToxCast Assay Annotation: An Application of BioAssay Ontology to Produce an Assay Metadata Reference with Extensions to the Assay Target Annotations

J. Phuong[1, 2], L. Truong[1], K. Houck[1], R. Judson[1] and M. T. Martin[1]. [1]*National Center for Computational Toxicology, Office of Research and Development, US EPA, Research Triangle Park, NC and* [2]*Dept of Environmental Science and Engineering, Univ of North Carolina at Chapel Hill, Chapel Hill, NC.*

High-throughput screening (HTS) and high-content screening (HCS) assays have changed the pace of chemical data collection for gene-protein, cellular, whole-embryo, and pathway-based responses. However, without the necessary assay metadata, it becomes a challenge to communicate what kind of data an assay reports. Integrative semantic resources such as the BioAssay Ontology (BAO) were developed to facilitate the annotation of assay parameters. We have used BAO with expansions to its vocabulary to produce the ToxCast Assay Annotation, a metadata resource to aid in the communication and use of EPA's ToxCast HTS and HCS assays. The ToxCast Assay Annotation describes 941 analyzed readouts (assay endpoints), which have complete ToxCast Phase I and II chemical set testing data (about 1000 chemicals). The annotation includes over 40 descriptor-classes (e.g., assay design type, detection technology type, and key assay reagent), which have been organized to aid in communication and analysis. In addition to BAO, various ontology sources such as the GPCR ontology and NCI thesaurus were incorporated for an abstract view of the target annotations. Where applicable, the conceptual difference between the technological target (e.g., mRNA, chemical, or protein) and the intended target (e.g., transcription factor activity, enzyme activity, or signaling pathway activity, respectively) are separately annotated. This annotation allows for a clear and concise reference for interpreting the ToxCast data, allows for identification of comparable ToxCast assay endpoints, and offers the potential to link with other HTS data repositories. This abstract does not necessarily reflect Agency policy.

PS 2273m Predictive Toxicology Tools Application in Contaminated Sites Health Risk Assessment and Remediation

A. K. Mohapatra[1] and B. Hardy[2]. [1]*Environmental Health Program, Health Canada (Praries Region Alberta), Calgary, AB, Canada and* [2]*Douglas Connect GmbH, Zeiningen, Switzerland.*

Health Canada (HC) has developed a tool that lists remediation technologies and a decision matrix for evaluating chemical exposure issues. We reviewed current practices involved in the design and intended use of the tool, evaluating the use of various toxicology data resources and predictive tools in providing value to risk management decision making, including the use of human health risk characterization data and tools in remedial alternatives and option analyses. We evaluated Petroleum Hydrocarbons, PAHs (e.g., Benzo[a]pyrene, Naphthalene), Chlorinated Hydrocarbons (e.g., Tetrachloroethylene and by-products) and Perfluorinated chemicals (e.g., Perfluorooctane Sulfonate). The research included consideration of the physical and chemical properties of the contaminants, reactivity, fate and transport, and the spatial and temporal exposure analysis including analysis of multiple sources of in silico, in vitro, and in vivo data and consensus models under a Weight of Evidence framework. The methodology was applied to case studies by selecting specific remedial technologies (e.g., bioremediation and chemical based remediation) and prioritizing site-specific contaminants and used to support risk-based predictions and recommendations for management of the contaminated sites. We were able to integrate relevant background knowledge, new data and predictive

models on those test chemicals from publicly available toxicology databases and resources including OpenTox, ToxBank, Comparative Toxicogenomics Database, TG-GATES, SEURAT, PubChem, and Tox21 databases for risk assessment and management decision-making supported by the remediation tool for contaminated sites and identified data gaps and limitations in applications. Disclaimer: "This poster abstract is based on a report to be finalized under contract to HC, Contaminated Sites Division; however, the abstract, the report and the poster does not necessarily reflect the opinion of HC nor is it HC guidance."

PS 2273n Web Application Supporting Chemical Safety Decisions

S. Watford[1, 2], J. Edwards[3], R. Judson[1], M. Linnenbrink[1], J. Kancherla[1] and M. T. Martin[1]. *[1]USEPA/ORD/NCCT, Research Triangle Park, NC, [2]University of North Carolina, Chapel Hill, NC and [3]ICF International, Durham, NC.*

The Tox21 and ToxCast chemical testing programs have generated millions of datapoints for thousands of chemicals. To allow for easier public access to this data, the USEPA has developed the Interactive Chemical Safety for Sustainability (iCSS) Application. iCSS is a web-based dashboard that synthesizes multiple sources of data into customized information displays. iCSS is built using both Zend Framework 2 and Sencha's Ext JS. Both frameworks provide a separate MVC architecture that allows separation of backend support and frontend displays. Data are grouped into three data classes: Hazard, Exposure, and Persistence/Bioaccumulation Potential. The users select (sub)sets of chemicals and types of data to focus on for the prioritization process. While not all chemicals will have complete information across all data classes, each class reports available data including relevant high-throughput assay results, regulatory information, and in vivo toxicity data. Custom widgets display each type of information according to its nature (e.g. dose-response plots or tables for assay data and summary tables for exposure information). Chemical-specific scores that consider all information in each data class are presented in a dynamic summary table that highlights areas deserving additional attention. Users can adjust global score criteria or apply expert knowledge to modify particular scores, with all decisions saved for sharing or later consideration. The scores are carried over into a prioritization process where the chemicals are ranked in a weight-of-evidence scheme to identify candidates for focused assessment. The aggregation of relevant data and use of web applications to generate custom displays streamlines the toxicity assessment process and allows users to zoom from larger chemical subsets down to finely focused chemical-wise views. The iCSS will serve as a portal for ToxCast data access for risk managers and the public. This abstract does not necessarily reflect U.S. EPA policy.

PS 2273o Pharmacokinetic Triage for Environmental Chemicals

J. F. Wambaugh[1], C. Strope[1], C. Nicolas[1], R. Judson[1], M. Goldsmith[1], H. A. El-Masri[1], B. A. Wetmore[2], J. P. Sluka[3], A. Tropsha[4], S. Bosgra[5], I. Shah[1], R. S. Thomas[1] and W. Setzer[1]. *[1]US EPA, RTP, NC, [2]The Hamner Institutes for Health Sciences, RTP, NC, [3]Indiana University, Bloomington, IN, [4]University of North Carolina, Chapel Hill, NC and [5]Utrecht University, Utrecht, Netherlands.*

Pharmacokinetic (PK) models aid in determining whether chemical exposures produce potentially hazardous tissue concentrations. For bioactivity identified *in vitro* (*e.g.* ToxCast™) – hazardous or not – PK models can forecast exposure thresholds, below which no significant bioactivity is expected. Successful methods have been developed for pharmaceutical compounds to determine PK from limited *in vitro* measurements and chemical structure-derived property predictions. These high throughput (HT) PK methods provide a more rapid and less resource–intensive alternative to traditional PK model development. Unfortunately, predictions from HTPK approaches have demonstrated mixed success for environmental chemicals when compared to predictions made by PK models developed with extensive *in vivo* data. Here we tested assumptions of previous HTPK approaches using a simple physiologically-based PK (PBPK) model and *in vitro* data for 232 chemicals in human and 39 chemicals in rat. We then analyzed the discrepancy between the predictions of HTPK and *in vivo* literature PK data for 44, mostly pharmaceutical, chemicals to characterize those properties that correlate with poor predictive ability (*e.g., in vitro* HTPK data, physico-chemical descriptors, chemical structure, and predicted transporter affinities). We propose a framework for PK triage in stages: First, *in vitro* measurements and *in silico* predictions determine whether the simplest HTPK approaches are likely to be sufficient. Second, identify and collect any additional, targeted *in vitro* data that is needed. Third, identify those chemicals most likely to require traditional, *in vivo* PK methods. This methodology allows prioritization of PK resources and characterizes the confidence in HTPK model predictions for potentially thousands of environmental chemicals that currently have no PK data. *This abstract does not necessarily reflect EPA policy.*

PS 2273p Estimation of Octanol/Water Partition Coefficient and Aqueous Solubility of Environmental Chemicals Using Molecular Fingerprints and Machine Learning Methods

Q. Zang, K. Mansouri and R. Judson. *National Center for Computational Toxicology, US EPA, Research Triangle Park, NC.*

Octanol/water partition coefficient (logP) and aqueous solubility (logS) are two important parameters in pharmacology and toxicology studies, and experimental measurements are usually time-consuming and expensive. In the present research, novel methods are presented for the estimation of both logP and logS of environmentally interesting chemicals solely based upon simple binary molecular fingerprints on a single data set which consists of 993 training samples and 251 test samples. A group of quantitative structure-property relationship (QSPR) models were developed using four approaches with different complexity: multiple linear regression (MLR), random forest (RF) regression, partial least squares regression (PLSR), and support vector regression (SVR). Genetic algorithms (GA) and RF method were employed to select the most information-rich subset of descriptors for obtaining reliable and robust regression models with high prediction performance. It was found that MLR, PLSR and SVM exhibited satisfactory predictive results with low prediction errors and substantially outperformed RF. MLR coupled with GA for descriptor selection was clearly superior to all other approaches and achieved correlation coefficients of 0.936 and 0.927 between the calculated and experimental data on the validation set for logP and logS, respectively. The inclusion of logP and molecular weights (MW) as two descriptors into logS models significantly improved the prediction accuracy, especially for RF modeling. The present study demonstrates that molecular fingerprints are very useful descriptors, GA is a very efficient feature selection tool and the selected descriptors can effectively model the two properties, and simple methods such as MLR give better results than more complicated methods. These models can be used for rapidly and accurately predicting logP and logS of environmental chemicals. This abstract does not necessarily reflect U.S. EPA policy.

PS 2273q Screening Environmental Chemicals in Metabolically Competent Human-Derived Hepatocytes

J. Jack[1, 2], J. Franzosa[1], P. G. Kothiya[1], J. Bonzo[3], P. Hurban[4], S. Siferd[4], S. Ferguson[5], J. Liu[1], S. D. Hester[1], A. Lake[1], K. Houck[1] and J. F. Wambaugh[1]. *[1]US EPA, Research Triangle Park, NC, [2]North Carolina State University, Raleigh, NC, [3]Life Technologies, Frederick, MD, [4]Expression Analysis, Research Triangle Park, NC and [5]NTP, NIEHS, Research Triangle Park, NC.*

ToxCast™ is the U.S. EPA's screening program comprising hundreds of relatively inexpensive and high-throughput assays to compare thousands of chemicals to reference toxicants and evaluate potential bioactivity. A new suite of assays aimed at investigating gene specific perturbations elicited by environmental chemical exposure in metabolically-competent, human-derived HepaRG cell line was designed and optimized. Briefly, cells were treated with individual chemicals in an eight-point concentration-response format in duplicate for 48 hours in a 96-well plate format. Total RNA was collected for gene expression profiling via real-time quantitative polymerase chain reaction (qRT-PCR). We evaluated the expression of a diverse set of 93 genes representative of various biological processes and disease states including: cell proliferation, survival, and death; nuclear receptor (NR) mediated metabolism and transport; oxidative stress; steatosis and fibrosis. Many of the genes are known to be transcriptionally regulated by key NRs, including CAR, PXR, PPARa, and HNF4a. Additionally, we evaluated reference plates with dilutions from high concentrations (*e.g.* 1 mM) of known toxicants phenobarbitol (PB), alfatoxin B1, omeprazole (OMP), fenofibric acid, and chenodeoxycholic acid (CDCA). These results demonstrated that the HepaRG cells elicited classically reported expression responses indicative of CAR/PXR, AhR, and FXR activation upon exposure to PB, OMP and CDCA, respectively. Evaluating thousands of chemicals in this assay provides unique insight into endogenous gene signaling networks intrinsic to key hepatocellular processes and disease states in humans. *This abstract does not necessarily reflect U.S. federal government policy.*

PS 2273r Prioritization of the Tox21 10k Library for Xenobiotic Metabolism and Toxicity Studies Using *In Silico* Metabolism Models

S. Ferguson[1], N. Kleinstreuer[2], M. Lawless[3] and R. R. Tice[1]. *[1]DHHS/NIH, NIEHS/DNTP, Research Triangle Park, NC, [2]ILS, Inc., Research Triangle Park, NC and [3]Simulations Plus, Lancaster, CA.*

One of the challenges within the U.S. Tox21 high throughput screening program is the lack of in vitro approaches incorporating xenobiotic metabolism. To help address this issue, in silico methods (ADMET-Predictor) have been employed to

identify and prioritize chemicals likely to undergo xenobiotic metabolism transformations (human) for studies in assays using metabolically-competent cells (e.g., primary hepatocytes, HepaRG). Three general criteria were used for prioritization: 1) chemicals predicted as substrates for human metabolism enzymes, 2) chemicals predicted to undergo extensive metabolism, and 3) chemicals predicted to generate metabolites with structural alerts for toxicity endpoints. Over the 18 xenobiotic metabolism enzymes (P450s and UGTs) predicted, true positive prediction rates of 87.7% (CYP1A2), 90.4% (CYP2C9), 76.6% (CYP2C19), 93.2% (CYP2D6), and 93.5% (CYP3A4) were observed for established substrates of 5 major xenobiotic metabolism pathways (quantitative models). Applying ADMET Predictor to 8,193 unique chemicals in the 10K library, 47,320 hits were predicted. Intrinsic clearance predictions were generated for each chemical and these data were combined using the ToxPi application to rank chemicals based on extent of metabolism weighted to relative expression levels in human liver. Using MedChem Studio, 168,805 unique metabolites were predicted. These structures were analyzed in various toxicity prediction models (e.g., estrogenic/androgenic activity, mutagenicity) to rank molecules based on anticipated toxicity. Rankings (Tox Risk) revealed various structures including 49 with nitroso groups (e.g. N-Nitrosopiperazine) out of the top 100 (96 predicted metabolites). 2,152 unique molecules made up the high risk mutagenicity ranking list with 15 out of 61 PAHs (i.e. benzo(a)pyrene) in the 10k library. These criteria were combined (e.g., CLINT, anticipated toxicities) to generate a prioritized list of chemicals for near term studies in metabolically-competent systems.

PS 2273s *In Vitro* Screening of 1877 Industrial and Consumer Chemicals, Pesticides, and Pharmaceuticals in up to 782 Assays: ToxCast Phase I and II

R. Judson[1], K. Houck[1], M. T. Martin[1], A. M. Richard[1], T. B. Knudsen[1], N. S. Sipes[1], I. Shah[1], S. B. Little[1], J. F. Wambaugh[1], M. Linnenbrink[1], J. Franzosa[1], J. Phuong[1], P. G. Kothiya[1], K. W. McLaurin[1], D. L. Filer[1], M. C. Leung[1], C. Strope[1], L. Truong[1], R. Thomas[1], D. Smith[1], D. Reif[2], D. Rotroff[2], N. Kleinstreuer[4], M. Xia[3] and R. Huang[3]. *[1]US EPA, Research Triangle Park, NC, [2]North Carolina State University, Raleigh, NC, [3]NIH, NCATS, Rockville, MD and [4]NICETM, Durham, NC.*

The U.S. EPA and Tox21 partners screened 1,877 chemicals, including pesticides; food, cosmetics and personal care ingredients; pharmaceuticals; and industrial chemicals. Testing used 782 in vitro assays across 7 technologies and biological formats (cell-free, cell lines and primary cells, multiple tissues). Assays were run in concentration-response (~0.01 to ~100 μM) with replicates and controls. We report several key findings. First, in 91% of the genes assayed for which we have reference chemicals (defined as a chemical with a known molecular target, 75 out of 313 genes total), a reference chemical is in the top quartile of potency. Second, 41% of chemicals show a "burst" of non-specific activity related to cell stress / cytotoxicity. On average, once ~5% of assays are activated by a chemical, there is a linear increase in the number of cytotoxicity/cell-stress-related hits relative to hits in other assays (R2=0.84). This indicates a potential for non-specific assay activity. In a set of 40 chemicals with both ToxCast and in vitro pharmacokinetic data, the burst concentration corresponds roughly to concentrations predicted to be seen in vivo at the maximum tolerated dose (MTD) in rat 2 year chronic cancer studies (78% of MTDs were in the burst region). Cholinesterase inhibitors were a prominent exception, with MTDs all below the burst range, since the MTD is driven by cholinesterase activity rather than systemic effects. Finally, chemicals were ranked by relative potency and target specificity to provide a quantitative metric to prioritize chemicals for further study. About ~1% of chemical-gene combinations show potent and specific activity (~3 hits per chemical on average). This abstract does not necessarily reflect Agency policy.

PS 2273t Using ToxCast Nuclear Receptor Activity to Predict Liver Toxicity

J. Liu[1, 2], R. Judson[1], M. T. Martin[1] and I. Shah[1]. *[1]National Center for Computational Toxicology (NCCT), US EPA, Durham, NC and [2]University of Arkansas at Little Rock/University of Arkansas for Medical Sciences, Little Rock, AR.*

Nuclear receptors (NR) are molecular initiating events in pathways to rodent liver cancer. 260 out of 309 ToxCast Phase I chemicals induced liver lesions in rat according to guideline testing studies from ToxRefDB. We used supervised machine learning to systematically investigate the accuracy of 621 ToxCast Phase I high-throughput screening (HTS) assays for classifying 260 chemicals into 10 types of adverse chronic hepatic histopathological outcomes. Predictive models using a variety of classification algorithms (LDA, Naïve Bayes, SVM) yielded a cross-validation balanced accuracy of 68.7% (±8.9%) for proliferative effects; 58% (±2.3%) for chronic hyperplasia and 63.2% (±3.8%) for hypertrophy. Univariate analysis of 621 HTS assays based on statistical correlation with corresponding in vivo endpoints revealed distinct associations between NR assays and liver endpoints categories. Next, all 91 NR assays out of 621 HTS assays were selected, including: retinoic X receptor-like (RXRα/β); peroxisome proliferator-activated receptor-like (PPARα/γ/δ); constitutive androstane receptor (CAR; NR1I3); pregnane X receptor(PXR; NR1I2); liver X receptor (LXR; FXR; NR1H); steroid receptor-like (SR; ERα/β; ERRα/β; AR); aryl hydrocarbon receptor (AhR); retinoic acid receptor (RARα/β/γ; NR1B); RAR-related orphan receptor (RORα/β/γ; NR1F); thyroid hormone receptor (THRα/β); vitamin D receptor (VDR; NR1I1). Using these 91 NR assays for supervised machine learning produced in classification accuracy to 73.1% (± 9.0%) for proliferative effects, 60.1% (±2.5%) for chronic hyperplasia and 65.2% (±4.2%) for hypertrophy. This work documents the accuracy of using nuclear receptor activity for predicting non-genotoxic rodent hepatocarcinogens, and, more broadly, it highlights the relevance of using molecular initiating events for prioritizing environmental chemicals.
This abstract does not represent EPA policy.

PS 2273u *In Silico* Study of ToxCast GPCR Assays by Quantitative Structure-Activity Relationships (QSARs) Modeling

K. Mansouri, N. S. Sipes and R. Judson. *EPA, Research Triangle Park, NC.*

Several thousand chemicals were tested in 700 toxicity-related in-vitro HTS bioassays through the EPA's ToxCast and Tox21 projects. This chemical set only covers a portion of the chemical space of interest for environmental exposure, leading to a need to fill data gaps with alternative methods. A cost effective and reliable approach to fulfill this task is to build Quantitative Structure-Activity Relationships (QSARs). In this work, a subset of 1800 ToxCast chemicals was used to build QSAR models for multiple ToxCast assays to predict activity of chemicals in a larger environmental database of ~30K structures. The initial molecular targets for this project were a set of 18 G-Protein Coupled Receptor (GPCR) assays. These assays are part of the aminergic category which was among the most active within the biochemical assays. The QSAR predictions were based on two levels; the first was a classification into active/non-active chemicals; then regression models were built to predict the AC50 potency values of the bioassays for the active chemicals. Different software packages were used to calculate constitutional, topological and fingerprinted molecular descriptors based on two-dimensional structures. Then several classification and regression model-fitting methods including PLS-DA, SVM, MLR, PLS and kNN were tested. The overall approach also included variable selection techniques such as Genetic Algorithms that were applied in order to select the most predictive molecular descriptors for each assay. The models were evaluated using n-fold cross-validation and forward validation on a held-out subset of the initial data. Finally, the applicability domains of the models were defined. Using PLS-DA for the human histamine H1 GPCR assay, a classification accuracy of 94% was reached with a non-error rate of 89% in fitting and 80% with 5-fold cross-validation with only 2 latent variables. This work shows the promise of using in vitro data to develop structure-based models for use in predicting target activity across the diverse space of environmental chemicals. This abstract does not necessarily reflect U.S. EPA policy.

PS 2273v Predicting Toxic and Therapeutic Mechanisms of the ToxCast Chemical Library by Phenotypic Screening

K. Houck[1], N. Kleinstreuer[2], J. Yang[3], E. Berg[3], T. B. Knudsen[1], A. M. Richard[1], M. T. Martin[1], D. Reif[4], R. Judson[1] and M. A. Polokoff[3]. *[1]National Center for Computational Toxicology, US EPA, Research Triangle Park, NC, [2]ILS/NICEATM, NIEHS, RTP, NC, [3]BioSeek/DiscoveRx, S. San Francisco, CA and [4]NCSU, Raleigh, NC.*

Addressing safety aspects of drugs and environmental chemicals relies extensively on animal testing. However the quantity of chemicals needing assessment and challenges of species extrapolation require development of alternative approaches. Using 8 primary human cell systems (BioMAP), we screened in concentration-response format 776 chemicals from the ToxCast Phase II library (http://epa.gov/ncct/toxcast/chemicals.html) for perturbation of physiologically important pathways. Cell systems consisted of combinations of endothelial, peripheral blood mononuclear, bronchial epithelial and coronary artery smooth muscle cells; fibroblasts and keratinocytes. Chemical-response signatures from 87 endpoints covering molecular functions relevant to toxic and therapeutic pathways were generated. Assessment of profiling data by unsupervised clustering using Self Organizing Maps and supervised analysis using Support Vector Machine algorithms grouped chemical/concentration by potential mechanism class providing insight into polypharmacology and potential off-target effects of drugs. Clusters contained diverse mechanistic activity including kinase, TNFα, phosphodiesterase and Hsp90 inhibitors; Ah, estrogen and glucocorticoid receptor modulators; disruptors of mitochondrial and tubulin function; histamine antagonists; and statins. Novel associations identified included induction of tissue factor in endothelial cells by ER antagonists, AhR

agonists and mTOR inhibitors, all chemical classes with susceptibility to venous thrombosis. Further, structure-based analysis demonstrated associations between chemical categories and mechanism class predictions. Our results yielded an extensive list of potential toxicological targets and biological pathways that we are incorporating into a chemical prioritization strategy for chemicals of concern to the Agency. This work does not necessarily reflect official Agency policy.

PS 2273w Predictive Models for Mechanism-of-Action Classification of Chemicals Using Phenotypic Data

E. Berg, J. Yang and M. A. Polokoff. *BioSeek LLC, South San Francisco, CA.*

Introduction. There is increasing interest in applying in vitro methods to characterize the potential toxicity of drugs and chemicals. Methods that would allow automatic classification of in vitro activity profiles into mechanism classes could be helpful in prioritizing novel agents. Methods. We have developed primary human cell-based assay panels in which chemical effects on the expression of protein biomarkers are measured. Eighty-eight selective, well-characterized tool compounds representing 28 distinct mechanism classes relevant to key biological and toxicity mechanisms were profiled in a standardized panel of 8 assay systems that had been previously used for testing >1000 chemicals and materials for the Environmental Protection Agency's ToxCast program (Houck, 2009). The resulting dataset of 83 endpoint measurements was then used to build predictive models for each of the 28 mechanism classes using machine learning. A support vector machine (SVM) approach gave the best performance, and so was applied to build a series of two-class SVM models for each mechanism class. Results. These models were then applied to evaluate several libraries and collections of bioactive materials including diversity and kinase focused libraries, biologics and natural products. Compounds from all collections types were highly active in phenotypic assays (hit rates of 7-60% at 1-5 μM). Analysis of a kinase-focused library and a set of environmental bio-actives revealed 48-57% of actives could be classified into one of the 28 tested mechanism classes. The most common mechanisms were mitochondrial inhibitors (14-27%) and microtubule inhibitors (4-10%). Proteasome inhibitors and cAMP elevators were more frequent in the environmental bioactive collection. Conclusions. These results suggest that compounds with potentially undesirable mechanisms are surprisingly common in most compound collections including libraries used for high throughput screening. This method may be useful for library characterization, determining compound mechanisms of action, and chemical prioritization.

PS 2273x Read-Across Driven by Molecular Initiating Events: Comparison of *In Silico* Profiling with Experimental Results for Reactivity

A. N. Richarz[1], T. W. Schultz[2], C. Yang[3], M. T. Cronin[1] and S. J. Enoch[1]. [1]*School of Pharmacy and Chemistry, Liverpool John Moores University, Liverpool, United Kingdom,* [2]*College of Veterinary Medicine, The University of Tennessee, Knoxville, TN and* [3]*Altamira LLC, Columbus, OH.*

Grouping or category formation allows the filling of data gaps by read-across to predict toxicity. Ideally it should be based on mechanistic similarities. Adverse Outcome Pathways (AOPs) link the chemistry of the Molecular Initiating Event (MIE) to effects and thus provide a mechanistic framework for the category formation. Covalent binding to biological proteins is an important MIE for toxicological endpoints including skin and respiratory sensitization, liver toxicity and elevated acute toxicity. A profiler (a collection of 108 structural alerts based on organic reaction mechanisms) has been developed to group compounds according to their protein binding capability. However, the alerting potential has not been evaluated in terms of the applicability domain and ability to create robust categories. Therefore, the ability of the alerts to profile 27 sulfur-containing industrial chemicals from a range of chemical classes (mercaptans, sulfides, disulfides, sulfoxides, sulfones, sulfonates, sulfates; saturated and unsaturated) was investigated. To achieve this aim, *in silico* predictions were compared with experimental results. Compounds were considered to be protein binders when reactive towards glutathione *in chemico* and demonstrating excess toxicity in the *Tetrahymena pyriformis* assay. The prediction of protein binding for thiols, disulfides, saturated sulfonates and sulfates (via S_N2 reaction), unsaturated sulfoxides, sulfones and sulfonates (via Michael addition) was verified experimentally with distinct excess toxicity for Michael addition. The *in silico* profiler was able to predict reactivity and differentiate reaction mechanisms related to reaction potency; this was associated with the degree of saturation of the compounds. The knowledge from this analysis was coded into a new set of chemotypes to better group compounds to perform read-across.
Supported by the EU FP7 COSMOS Project and ECHA.

PS 2273y ToxBank Integrated Data Analysis of SEURAT-1 Reference Compounds

B. Hardy[1], G. J. Myatt[2], P. Kohonen[3] and R. C. Grafström[3]. [1]*Douglas Connect GmbH, Zeiningen, Switzerland,* [2]*Leadscope, Columbus, OH and* [3]*Karolinska Institute, Stockholm, Sweden.*

The SEURAT-1 (Safety Evaluation Ultimately Replacing Animal Testing-1) research cluster is comprised of seven EU FP7 Health projects and is co-financed by Cosmetics Europe. The SEURAT-1 strategy is to adopt a mode-of-action framework to describe repeated dose toxicity to derive predictions of in vivo toxicity responses. ToxBank is the cross-cluster infrastructure project which provides a web-accessible shared repository of research data and protocols. Experiments generate dose response data over multiple timepoints using different omics platforms including transcriptomics, proteomics, metabolomics, and epigenetics over different cell lines and a common set of reference compounds (details available at wiki.toxbank.net). Data is also generated from functional assays and bioreactors and supplemented with in silico approaches. This complex and heterogeneous data is consolidated and harmonized through the ToxBank data warehouse in order to perform an integrated data analysis. We describe for 14 reference compounds the meta-analysis of multiple types of time-dependent dose response omics and functional data combined with in vitro and in vivo background knowledge including consideration of modeling variations in biokinetic responses. Open TG-GATEs human in vitro liver data of the reference compounds includes reactive compounds (e.g., acetaminophen, CCl4), mitochondrial disruptors (e.g., Rotenone), promiscuous binders (e.g., valproic acid, amiadarone), nuclear hormone receptor ligands (e.g., tamoxifen, WY14643), selective binders (e.g. fluoxetine) and cardiotoxins (e.g., Doxorubicin, Nifedipine). Adverse events of interest that are represented include cytotoxicity, fibrosis, steatosis, cholestasis and phospholipidosis. Overall we obtained 31,717 differential expression results with 14 compounds from the 45 comparisons, with Doxorubicin providing over 5000 results. Pathway enrichment analysis of Doxorubicin identified a number of key pathways including mismatch repair after 24 hours treatment and TNF-signaling at high doses after 24 hours.

PS 2273z Protein-Fragment Complementation Assays Detect and Describe Nuclear Receptor Activity across the ToxCast Chemical Library

D. L. Filer[1], R. Judson[1], D. Rotroff[1], D. Reif[2], A. M. Richard[1], K. Houck[1] and M. T. Martin[1]. [1]*US EPA NCCT, Research Triangle Park, NC and* [2]*Genetics, NCSU, Raleigh, NC.*

The USEPA ToxCast program has tested thousands of environmental chemicals in hundreds of assays to inform toxicity models and prioritization for further toxicity testing. Previously ToxCast only included assays measuring transcriptional surrogates for nuclear receptor (NR) activation. Protein-fragment complementation assays (PCA) directly quantify NR activation by measuring protein:protein interactions driven by ligand activation through receptor hetero- or homodimerization or coactivator recruitment. Using PCA we tested 1820 chemicals at six doses (0.3 - 100μM) and two times points to measure activity changes in estrogen receptors alpha (ERα) and beta (ERβ), androgen receptor (AR), peroxisome proliferator-activated receptor gamma (PPARγ), and retinoic acid receptor alpha (RXRα). Of the tested chemicals, 536 (~29%) showed activity in at least one assay. We demonstrated these assays enable the quantification of chemical-receptor interactions spanning full agonist to partial agonist to full antagonist response with known reference chemicals. We obtained this information with a single gain-of-signal readout, removing confounding cytotoxicity issues common to loss-of-signal antagonist assays. We distinguished ER antagonist reference compounds by their potency (AC50 < 1μM) and high efficacy (above 200% of 17β-estradiol controls). The homogenous detection technology and readouts also enabled combining assay results to interpret and compare across receptors. Out of 71 chemicals active in all six ER assays, we identified 9 chemicals (including mifepristone, genistein, and daidzein) as ERβ potency-selective ligands. Incorporation of these data into multiple-technology consensus models for prediction of hormone receptor activity will contribute to EPA's endocrine disruptor screening program (EDSP21). This abstract does not necessarily reflect Agency policy.

PS 2273aa ToxCast Workflow: Big Data Processing and Analysis of High-Throughput Screening Assays for Environmental Chemicals

P. G. Kothiya[1], D. Reif[2], R. Judson[1], D. L. Filer[1], A. M. Richard[1] and M. T. Martin[1]. [1]*National Center for Computational Toxicology, Environmental Protection Agency, RTP, NC and* [2]*Department of Genetics, North Carolina State University, Raleigh, NC.*

US EPA's ToxCast program is generating data in high-throughput screening (HTS) and high-content screening (HCS) assays for thousands of environmental chemicals, for use in developing predictive toxicity models. Currently the ToxCast screening program includes over 1800 unique chemicals and over 700 bioassays. Data collection from multiple assay vendors and collaborators in diverse formats, data standardization, and normalization, coupled with the needs for data transparency and consistency have posed major technical and scientific challenges to the program. We developed the ToxCast data workflow to allow for consistent cross-technology analysis and data reporting. The ToxCast workflow consists of 8 levels: "Data Processing/Normalization" (levels 1-4) and "Curve- fitting/ Hit-calling" (levels 5-8). The first half of the pipeline includes data preparation, mapping, batch effect correction, normalization and transformation to standard file-format. The curve-fitting and hit-calling process consists of cytotoxicity-point and outlier detection/masking, concentration activity estimates using dose-response modeling, and identifying & filtering confounded activity calls based on other assays. To increase curve-fitting and hit-calling accuracy, the ToxCast workflow incorporates a data-scan feature in the early stage of processing to identify noise and response variation. Moreover, the ToxCast workflow standardizes the analysis of highly-heterogeneous chemical assay data sets by accepting heterogeneous data formats, allowing for rapid processing with a convenient interface enabling easier access and interpretation of data at all levels for repeatable and transparent analyses. The finalized results have been uploaded into the ToxCast Dashboard for data integration and analysis, as well as to serve as the primary portal for publication and data release. This work does not necessarily reflect Agency policy.

PS 2273bb A Data Analysis Pipeline for Tox21 Quantitative High-Throughput Screening Assays and Its Application to Toxicity Profiling of Flame Retardants

J. Hsieh[1], A. Sedykh[2], M. Behl[1], R. Huang[3], M. Xia[3] and R. R. Tice[1]. [1]*DNTP/ NIEHS, Durham, NC,* [2]*MultiCASE Inc., Cleveland, OH and* [3]*NCATS, Rockville, MD.*

Tox21, a federal inter-agency collaboration involving NIEHS/NTP, EPA, FDA, and NCATS, is currently screening a 10K (~8,300 unique) compound library against toxicity pathways using a quantitative high throughput screening (qHTS) approach. Goals of Tox21 include in vitro activity profiling, prioritization for in vivo toxicity testing, and in vivo toxicity prediction. However, directly using qHTS data for in vitro activity profiling is challenging due to presence of non-reproducible artifacts (e.g., noise and technical artifacts at either well or plate level) and compound-dependent assay interference. Moreover, profiling of low-reproducible weak signals, which may serve as early indicators for toxicity, is also challenging. To account for these issues, we first implement a signal processing protocol to clean up signals. Second, we stratify and normalize signals based on a modified logistic function to give less weight to weak signals. Third, we flag the compounds whose reproducible signal could be artificial due to assay interference by incorporating counter-screens data such as auto-fluorescence and cytotoxicity. The pipeline has been applied to 32 readouts covering 20 pathways of interest. We find that after applying the signal processing protocol, signal reproducibility greatly improves (by up to 0.4, Pearson's r). Also, after flagging the signals caused by assay interference, the actual number of active compounds noticeably drops (by as much as 7%). We demonstrate the in vitro activity profiling results using 49 brominated or organophosphate flame retardants. Many of the known chemical-target interactions are captured and novel interactions are prioritized based on their activity strength. We conclude that the pipeline is useful for signal profiling and in vitro activity profiling (especially weak, which tend to be less reproducible), which then can be used for predictive human disease model building and compound prioritization, respectively.

PS 2273cc Alternative Methods for Toxicity Testing for Human Health Risk Assessment

D. Petersen, J. C. Lambert, S. C. Wesselkamper and J. Zhao. *EPA, Cincinnati, OH.*

Techniques used in toxicity testing for the 21st century, hold the promise of reducing the time, expense and numbers of animals required for evaluating potential hazards to human health. However, translation of data from non-traditional toxicology studies and alternative platforms for the purposes of human health risk assessment continues to be an area of concern. For example, toxicogenomic (including metabolomics, proteomics, and transcriptomics) endpoints evaluated from in vivo study designs often correlate closely with apical/phenotypical endpoints both quantitatively and qualitatively. However, correlations between apical/phenotypical endpoints and ex vivo, in vitro, and in silico approaches are less intuitive. Yet, all of these approaches have been tested and validated to various extents. We present case studies comparing the application of QSAR, read-across, and transcriptomic approaches to traditional methods in establishing points of departure for human health risk assessment.
The views expressed in this abstract, are those of the author[s] and do not necessarily represent the views or policies of the U.S. Environmental Protection Agency.

S 2274 Clinical Evaluation of Emerging Biomarkers of Drug-Induced Liver Injury

J. Aubrecht[1], S. J. Schomaker[1], A. H. Harrill[2], H. Jaeschke[3] and J. H. van Delft[4]. [1]*Dept of Drug Safety Evaluation, Pfizer Inc., Groton, CT,* [2]*Hamner-UNC Institute for Drug Safety Sciences, The Hamner Institutes for Health Sciences, Research Triangle Park, NC,* [3]*Dept. of Pharmacology, Toxicology & Therapeutics, University of Kansas Medical Center, Kansas City, KS and* [4]*Department of Toxicogenomics, Maastricht University, Maastricht, Netherlands.*

Drug-induced liver injury (DILI) remains the primary cause of drug failures during clinical development and post-marketing. It is estimated that up to 40% of potentially hepatotoxic compounds in humans go undetected in preclinical studies that utilize conventional biomarkers. Serum alanine aminotransferase (ALT) activity is a widely used clinical biomarker to assess the risk of liver injury during drug development and approvals by regulatory agencies. Since ALT increases may be transient, thus less clinically relevant, the development of alternative biomarker strategies capable of differentiating transient ALT increases from those that progress to severe DILI is essential. Several biomarkers identified by evidence from peer-reviewed literature and datasets at various institutions are being evaluated as potential DILI biomarkers by individual scientists and international research consortia such as Innovative Medicines Initiative and Critical Path Institute's Predictive Safety Testing Consortium. In this symposium we will discuss gaps and opportunities for clinical evaluation of DILI biomarkers and their application in DILI biomarkers strategies. Special attention will be given to the evaluation of protein- and miRNA-based biomarkers for detection of DILI in the clinic including their potential to facilitate the understanding of underlying toxic mechanisms. Furthermore, we will introduce the application of NextGen Sequencing in DILI biomarker research in human subjects.

S 2275 Clinical Evaluation of Emerging Biomarkers of Drug-Induced Liver Injury: Gaps and Opportunities

J. Aubrecht. *Dept of Drug Safety Evaluation, Pfizer Inc., Groton, CT.*

Drug-induced liver injury is a serious complication in drug therapy that is a primary cause of drug failure during clinical development. Commonly used biomarkers, particularly the serum transaminases (ALT, AST) and bilirubin (TBil) serve as useful indicators of hepatocellular of cholestatic liver injury. Because ALT is a very sensitive biomarkers of DILI, the differentiation of ALT increases that spontaneously resolve from the ones that signal serious liver injury is very difficult. On the other hand, increases of TBil levels that are considered a hallmark of severe DILI occur only after significant damage has already occurred. Therefore the development of new biomarker strategies capable of assessing the risk of clinically relevant liver injury in early stages is essential. Because prospective clinical studies evaluating performance of biomarkers of DILI are ethically not feasible, biomarker research of DILI in human subjects requires new approaches. Here we will focus on current status, gaps and opportunities in the development and evaluation of new clinical DILI biomarker strategies including the utilization of samples from subjects with variety of liver impairments via retrospective study design as well as validation and qualification process including the impact of international collaborative efforts.

S 2276 Evaluation of Emerging Biomarkers of DILI in Human Populations

S. J. Schomaker. *Department of Drug Safety Evaluation, Pfizer Inc., Groton, CT.*

Hepatotoxicity remains a major challenge in drug development. Although alanine aminotransferase (ALT) remains the gold standard biomarker of liver injury, alternative biomarker strategies to better predict the potential for severe drug-induced liver injury (DILI) are essential. Here, we evaluated the utility of glutamate dehydrogenase (GLDH), purine nucleoside phosphorylase (PNP), malate dehydrogenase (MDH), and paraxonase 1 (PON1) as indicators of liver injury in cohorts of human subjects, including healthy subjects across age and gender, subjects with a variety of liver impairments, and several cases of acetaminophen poisoning. GLDH and MDH had a strong correlation with elevated ALT levels and possessed a high predictive power for liver injury, as determined by ROC analysis. In contrast, PON1 and PNP did not detect liver injury in our study. Finally, evaluation of patients with acetaminophen-induced liver injury provided evidence that both GLDH and MDH might have utility as biomarkers of DILI in humans. This study is the first to evaluate GLDH, MDH, PON1, and PNP in a large number of human subjects and, and it provides an impetus for prospective clinical studies to fully evaluate the diagnostic value of GLDH and MDH for detection of liver injury.

S 2277 Mechanistic Biomarkers of Mitochondrial Dysfunction during Drug-Induced Liver Injury in Humans

H. Jaeschke. *Dept. of Pharmacology, Toxicology & Therapeutics, University of Kansas Medical Center, Kansas City, KS.*

Extensive progress has been made during the last decade in the understanding of mechanisms of drug-induced liver injury (DILI), especially acetaminophen (APAP) hepatotoxicity, in experimental animals. Binding of reactive metabolites to cellular, in particular mitochondrial proteins, mitochondrial dysfunction and oxidant stress, MAP kinase activation, nuclear DNA fragmentation and mitophagy are critical events. Mitochondria clearly emerged as the converging point of various signaling pathways leading to cell death. Despite the progress in animals, the understanding of DILI mechanisms in humans is limited. The presentation will focus on a mechanistic serum biomarker approach to study mechanisms of cell injury, especially mitochondrial dysfunction, in human APAP overdose patients and in mice. Biomarkers that are being used in patients after validation in experimental animals (APAP, furosemide toxicity), include the mitochondrial matrix enzyme GLDH, mitochondrial DNA, nuclear DNA fragments (generated by endonuclease G from mitochondria), and various acylcarnitines. These studies have demonstrated the successful use and some caveats of mechanistic biomarkers in humans suggesting that mitochondrial damage and nuclear DNA fragmentation are critical components of liver injury mechanisms in patients. In addition, the use of these biomarkers as predictors for acute liver failure will be discussed.

S 2278 Novel Liver Biomarkers Provide Insight into Benign Drug-Induced ALT Elevations in the Clinic

A. H. Harrill. *University of Arkansas for Medical Sciences, Little Rock, AR.*

Aminotransferase elevations can be an important indicator of overt liver injury in the clinic; however, there are several drugs in clinical use that cause benign alanine aminotransferase (ALT) elevations yet have no injury risk. Novel biomarkers are currently in development to more accurately discern acute drug-induced liver injury potential and we hypothesized that these newer biomarkers would not be elevated in the context of benign drug-induced ALT elevations. To test this hypothesis, ALT, glutamate dehydrogenase (GLDH), sorbitol dehydrogenase (SDH), high mobility group box 1 protein (HMGB1), cytokeratin 18, and miRNA(miR)-122 were assessed in the serum of healthy volunteers enrolled in two separate clinical studies of heparin or cholestyramine administration. Elevations in all of the novel biomarkers were found to be coincident with ALT in both clinical studies. We conclude that the novel biomarkers may have less utility to be predictive of overt hepatotoxicity that previously assumed. Yet, it is clear that the pattern of biomarker elevations provide important insights into the mechanisms underlying the low-level liver injury that occurs following exposure to heparin (i.e. necrosis with secondary activation of an innate immune response) and cholestyramine (i.e. necroapoptosis).

S 2279 Application of NextGen Sequencing for Discovery of Novel miR-Based Candidate Biomarkers of DILI in Human Subjects

J. H. van Delft. *Department of Toxicogenomics, Maastricht University, Maastricht, Netherlands.* Sponsor: J. Aubrecht.

MicroRNAs are stable and reliably detectable in blood. Recently, levels of circulating microRNAs such as miR122 and miR192 have been shown to respond to treatment with hepatotoxicants. Since microRNAs are either organ speciffic and/or associated with molecular pathways, microRNA-based biomarkers provide exciting opportunities. Deep sequencing technologies for microRNAs (smallRNA-seq) provide the most unbiased assessment of the many microRNA variants that can exist. In this study, we have compared profiles of circulating microRNA in human subjects with accidental acetaminophene (APAP) overdose with matched controlled subjects. We have identified over 30 microRNA species with time dependent response to APAP overdose. The set included known microRNAs such as miR122 and miR192 as well as novel, so far unknown, microRNAs whose levels drastically increased upon the hepatotoxic exposure. We have confirmed the identified microRNAs by independent RT-PCR methods, and evaluated their levels in other subjects with liver impairments.

S 2280 Does Evolution Matter in Toxicity Testing? Rethinking Cross-Species Extrapolation in Hazard Characterization

M. C. Leung and T. B. Knudsen. *National Center for Computational Toxicology, US EPA, Research Triangle Park, NC.*

Training in evolutionary thinking can help biomedical researchers, clinicians, and toxicologists ask useful questions that they might not otherwise pose. Emerging high-throughput technologies, predictive toxicology, and bioinformatics, as well as alternative toxicity models such as bacteria, yeast, *C. elegans*, zebrafish, and stem cells, provide new information across the phylogenetic tree at a molecular scale to support human health risk assessments. These novel approaches also create an opportunity to consider what role evolution plays in toxicity testing, particularly in cross-species toxicity extrapolation of pollutants and manufactured chemicals. This symposium aims to generate discussion on evolution and three specific aspects of toxicity testing: (1) how can the phylogeny of species-xenobiotics interaction influence the design and interpretation of high-throughput screens with microbes and alternative animal models; (2) how can the molecular evolution of naturally-occurring toxins and species interaction in the natural world inform the hazard characterization of pollutants and manufactured chemicals; and (3) how can comparative physiology in both vertebrates and invertebrates influence the development of adverse outcome pathways for human health risk assessments.

S 2281 Evolutionary Approaches in Cross-Species Toxicity Extrapolation: A Naturalist's Perspective

R. DeSalle and M. E. Siddall. *Division of Invertebrate Zoology, American Museum of Natural History, New York City, NY.* Sponsor: M. Leung.

A basic tenet of evolutionary biology is that species adapt to changes in its environment, including chemical exposures, over extended time and multiple generations. The mechanism of natural selection allows their progeny to eventually survive and reproduce in the changed environment (i.e. evolutionary fitness). While the choice of test animal species in laboratory toxicity testing is often based on the conservation of biology with humans, a better understanding in molecular evolution and comparative toxicology of naturally-occurring toxins can also inform the hazard characterization of pollutants and manufactured chemicals. This presentation will introduce the principal concepts of evolutionary biology that are applicable in toxicological sciences, including site directed mutagenesis, phylogenetic inference, purifying selection, and plant-herbivore coevolution. Specific examples of living poisonous and venomous species will be given, including toxicological cocktails (e.g. venoms or suites of alkaloids acting in concert) as well as proteinaceous toxins (e.g. enzymes or physiological pathway inhibitors). Their relevance to hazard characterization of environmental toxicants will be discussed.

S 2282 A High-Throughput DNA Damage Platform and Engineered Mice for Fluorescence Detection of Mutations Together Provide Insights into Ancient Strategies of DNA Repair

B. P. Engelward, J. Ge, D. K. Wood, D. M. Weingeist and O. Kiraly. *Department of Biological Engineering, Massachusetts Institute of Technology, Cambridge, MA.*

Both the evolution of species and the clonal selection of cells into tumors require a balance between genomic stability and diversification. DNA repair is essential for preserving DNA sequence information, and many DNA repair processes have been conserved across species. During evolution from microbes to mammals, key repair activities were not only conserved, but they were also leveraged to address selective pressures specific to mammals, such as antibody diversification. The role of base excision repair (BER) in these contexts will be presented. To learn more about BER in humans, we recently developed a novel high-throughput DNA repair platforms for assessing DNA repair capacity in eukaryotic cells. The "CometChip" leverages photolithography to enable hundreds of samples to be assessed for their DNA damage levels in parallel, enabling studies of inter-individual variation in DNA repair. Here we show that BER is highly variable in cells from ethnically diverse individuals. In addition to BER, we are also very interested in repair that is facilitated by homologous recombination (HR). Ironically, the BER pathway, while critical for removing damaged bases, also creates single strand breaks as repair intermediates. HR is required to tolerate the presence of these DNA repair intermediates. Here we describe the development of novel fluorescence based animal models in which rare cells that have undergone HR can be detected within intact tissues. A fundamental discovery resulting from this model is that BER in mammals puts pressure on HR under normal physiological conditions, raising the possibility that one DNA repair pathway creates selective pressure for another.

S 2283 Molecular Evolution of Transcription Factors in Zebrafish and Killifish: Implications for Biomedical and Environmental Toxicology

A. R. Timme-Laragy[1, 2] and M. E. Hahn[2]. [1]*School of Public Health and Health Sciences, University of Massachusetts, Amherst, MA and* [2]*Department of Biology, Woods Hole Oceanographic Institution, Woods Hole, MA.*

Small fish models such as the zebrafish are commonly used in toxicity and pharmaceutical testing, particularly to screen for early life stage effects, as well as in mechanistic studies. It is important to consider the evolutionary relationship between these fish models and humans, as fish have undergone at least one genome duplication event, and for many mammalian transcription factors fish often have duplicate copies (co-orthologs). Here, we will present the comparative evolutionary relationship of two families of genes encoding toxicologically relevant transcription factors—the aryl hydrocarbon receptor (Ahr) and nfe2-related (Nrf) gene families—and their associated signaling pathways. We will compare the Ahr and Nrf genes in two small fish models, the killifish (Fundulus heteroclitus) and zebrafish (Danio rerio), with those in humans and rodents, focusing on multiple fish Ahr (Ahr1a, Ahr1b, Ahr2a, Ahr2b) and Nrf2 (Nrf2a, Nrf2b) genes. We will discuss the implications of transcription factor multiplicity for biomedical and environmental toxicology, including both the challenges and the opportunities provided by differences in gene number and function among fish and mammals. [NIH grants F32ES017585, R01ES016366, and R01ES006272]

S 2284 The Comparative Toxicogenomics Database (CTD): Leveraging Species Diversity to Understand Mechanisms of Toxicity

C. J. Mattingly. *Department of Biology, North Carolina State University, Raleigh, NC.*

Extrapolation of animal and in vitro toxicology studies to humans remains a major challenge to improving understanding about the mechanisms of chemical actions and predicting exposure risks. The Comparative Toxicogenomics Database (CTD; http://ctdbase.org) is a publicly available resource that aims to advance understanding about environmental effects on human health and the underlying molecular mechanisms. It provides manually curated data describing chemical-gene-disease interactions from diverse species (vertebrates and invertebrates) and experimental systems (in vitro and in vivo) with external data sets and computational tools to enable user-driven cross-species environmental health studies. Comparisons of data across species and experimental systems are critical for determining the degree to which molecular and phenotypic responses are conserved. The degree of conservation is often indicative of fundamental biological mechanisms and pathways, and helps to inform mechanistic hypotheses and identify appropriate experimental models for specific research questions. This presentation will discuss the comparative data content in CTD, provide examples of cross-species analysis capabilities for mechanistic studies and describe future curation and integration initiatives that will further expand the comparative analysis capacity of CTD.

S 2285 A Conceptual Framework for Cross-Species Extrapolation to Support Chemical Risk Assessment

G. T. Ankley. *Office of Research and Development, US EPA, Duluth, MN.* Sponsor: M. Leung.

A challenge for both human health and ecological toxicologists is the transparent application of mechanistic (e.g., molecular, biochemical, histological) data to risk assessments. The adverse outcome pathway (AOP) is a conceptual framework designed to meet this need. Specifically, AOPs portray causal and predictive linkages between molecular-initiating events (MIEs) and adverse outcomes of regulatory significance in individuals or populations. Collecting, analyzing and communicating toxicological data through the use of AOPs enhances aspects of risk assessments related to extrapolation of chemical effects across biological levels of organization, chemical structures, and species. For the latter, consideration of taxonomic conservation of pathways, especially in terms of MIEs, provides a robust basis for cross-species extrapolation. This presentation will provide an overview of the AOP concept, review the roles of various national and international workgroups focused on the development and application of AOPs, and present examples of utility of the concept in different risk assessment/regulatory scenarios focused on cross-species extrapolation. This abstract does not reflect official EPA policy.

S 2286 Neurobehavioral Impacts of Early-Life Manganese Exposure: Linking Human and Animal Model Studies

D. Smith[1], R. Lucchini[2, 4], R. O. Wright[2], E. Haynes[3], M. Arora[2] and S. A. Beaudin[1]. [1]*Microbiology and Environmental Toxicology, University of California Santa Cruz, Santa Cruz, CA,* [2]*Department of Preventive Medicine, Icahn School of Medicine at Mount Sinai, New York City, NY,* [3]*Department of Environmental Health, University of Cincinnati, Cincinnati, OH and* [4]*Occupational Health, University of Brescia, Brescia, Italy.*

This symposium will highlight advances in our understanding of the complex causal relationships between early-life environmental manganese (Mn) exposure and lasting neurobehavioral impairment, gained through the coordinated integration of epidemiological and animal model studies. Behavior and cognitive function are among the most important public health outcomes, since the potential loss of neurological functioning early in life due to toxic exposures may result in diminished academic and economic productivity that can persist over the life span. Motor abnormalities are likewise relevant in relation to neurodegenerative disorders, leading to Parkinsonian disturbances in the aged. Multidisciplinary investigations that synthesize advances in developmental testing, animal toxicology, exposure assessment, statistical modeling, and epidemiology are necessary to gain insights into the impacts of early-life Mn exposure—impacts that have direct implications for public health. This symposium will address this research need through presentation of coordinated human and animal research that focuses on comparable neurophenotypes across species and age ranges, and that incorporates novel exposure-assessment tools, such as Mn levels in shed deciduous teeth, to assess the impacts of early-life and lifelong Mn exposure over distinct developmental windows/life stages.

S 2287 Animal-Human Correlates of Early-Life Mn Exposure and Executive Functioning

R. O. Wright. *Department of Preventive Medicine, Icahn School of Medicine at Mount Sinai, New York City, NY.* Sponsor: D. Smith.

This presentation will highlight a critical issue in the neurotoxicology of manganese (Mn) - the translation of animal results to humans. Because human randomized trials of Mn exposure cannot be conducted for Mn or any potentially neurotoxic agent, translation of animal study neurotoxicology research to humans must involve epidemiologic observational studies. Animal/human studies planned in tandem could also better elucidate mechanisms of action in the CNS. Human and animal studies seldom measure the same functional domains or address exposures at the same life stages, at least not in a coordinated fashion. Although there are several caveats when extrapolating results from animals to humans, one caveat, the use of different neurophenotypes, can be overcome given the development of computerized tests of animal/human behavior, such as the virtual radial arm maze (VRAM), the delayed spatial alternation and temporal response differentiation test

(a fixed interval response), and the continuous performance test (CPT), among others. In preliminary analysis of Italian children performing the Virtual Radial Arm Maze Increased hair Mn was not associated with latency (2.8 sec 95%CI -1.3-6.7) but was associated with increased total distance traveled (0.6 95%CI 0.0-1.3) and increased working memory count ratio (1.48, 95% 1.09-2.01), suggesting worse performance overall on this task in Mn-exposed children. In the delayed spatial alternation task performed in a Mexico cohort of 2 year olds, blood Mn was inversely associated with total number of errors performed correctly (-0.84, 95% CI -1.5, -0.15). Potential links to animal studies with similar designs will be discussed.

S 2288 Neurodevelopmental Effects of Ambient Exposure to Manganese in Appalachian Children Residing near a Ferromanganese Refinery

E. Haynes. *Department of Environmental Health, University of Cincinnati, Cincinnati, OH.* Sponsor: D. Smith.

Airborne manganese (Mn) exposure can result in neurotoxicity in workers and adults exposed to high levels of Mn, yet there is limited data on its effects on children. Marietta, Ohio has the longest operating ferromanganese refinery in the United States. The goals of the research were to characterize environmental exposures to Mn and determine the effect of chronic exposure on neurobehavior in children. A total of 408 children ages 7-9 years were enrolled in the Marietta Community Actively Researching Exposure Study (CARES). Internal dose measures were determined for lead, Mn, and secondhand tobacco smoke exposure. Children with hair Mn concentrations greater 610 ng/g, had a 3 point mean decrease in full scale IQ compared to children with hair Mn in the low and middle tertiles. In backward elimination regression modeling, ln hair Mn was also statistically and inversely associated with full scale IQ (β = -1.88; $p<0.008$) after adjusting for parent IQ, parent education, and gender. Additionally, ln blood Mn was also significantly associated with internalizing problems ($p<0.03$), but not ln hair Mn. Increases in hair and blood Mn and a decrease in time-weighted distance from the refinery were also significantly associated with poor postural instability. Presentation of these results will include discussion on SHS, an alternative source of Mn, and will be integrated similar epidemiological studies in Mexico and Italy, as well as the animal model studies presented in this symposium.

S 2289 Manganese Exposure across Different Life Stages Produces Comparable Deficits in Neuromotor Function and Olfactory Discrimination

R. Lucchini[1, 2]. [1]*Department of Preventive Medicine, Icahn School of Medicine at Mount Sinai, New York, NY and* [2]*Occupational Medicine, University of Brescia, Brescia, Italy.*

Results from our cross-sectional epidemiological study on environmental metal exposure in children and elderly living in the vicinity of previous and currently active ferroalloy plant emissions in northern Italy will be presented, and integrated with other epidemiological studies in Mexico and Ohio, as well as the coordinated animal model studies presented in this symposium. Our studies in Italy have comprehensively assessed Mn exposure over the lifespan, as well as olfactory function (using the Sniffin' Sticks test for odor identification) and motor function (using coordination tasks for fine movements and hand dexterity) in both adolescents and elderly age groups. Results show that adolescents and elderly exhibited similar impairment patterns of odor identification and motor coordination. Regression models showed negative associations of odor identification, motor coordination and hand dexterity with surface soil Mn concentrations among both adolescents and elderly. Elderly showed negative associations of odor identification and motor coordination with Mn in airborne particulate matter and in surface soil. Notably, the fine motor deficits have been reproduced in the coordinated animal model studies, discussed below. These data suggest that the common dopaminergic regulation of olfactory and motor functions is likely to represent the critical site of Mn toxic action.

S 2290 Validation of Novel Exposure Biomarkers in Manganese-Exposed Rats and in a Cohort of Children at Risk of Environmental Manganese Exposure

M. Arora. *Department of Preventive Medicine, Icahn School of Medicine at Mount Sinai, New York City, NY.* Sponsor: D. Smith.

This presentation will integrate assessment and validation of novel Mn exposure biomarkers across the animal model and epidemiological studies presented in this symposium. Transfer of manganese (Mn) across the placenta is tightly regulated and maternal blood levels do not accurately reflect fetal exposure and furthermore, because of complex kinetics, blood Mn in children may not precisely measure postnatal exposure. Consequently, measuring Mn exposure during the prenatal and early childhood periods remains a major challenge in studies exploring health outcomes of early life Mn exposure. To address this, we undertook detailed studies on rats exposed to controlled doses of Mn for different durations including early life exposure (low and high doses) and lifelong exposure (low and high doses). Results show that tooth-Mn levels accurately reflect both short- and long-term exposure and are also predictive of levels in other tissues including bone and brain. To validate this in humans, we undertook a prospective study comparing Mn levels in environmental and biological matrices with tooth-Mn levels measured using a laser ablation method that allowed us to develop a temporal map of Mn exposure over the prenatal and early postnatal periods. Results confirm that the tooth-Mn biomarker can be used to reliably reconstruct perinatal Mn exposure.

S 2291 Fine Neuromotor Deficits following Early and Lifelong Manganese Exposure, and the Efficacy of Oral Methylphenidate Treatment to Alleviate Motor Function Deficits

D. Smith. *Microbiology and Environmental Toxicology, University of California Santa Cruz, Santa Cruz, CA.*

Results from the epidemiological studies presented above indicate that environmental manganese (Mn) exposure produces lasting deficits in fine motor function in children and the elderly. To address this and establish exposure causality, we used a rodent model and the Montoya staircase and Ladder Rung Walking tests to determine whether developmental Mn exposure produces long-lasting deficits in sensorimotor performance in adulthood. Long-Evans male neonate rats were exposed daily to oral Mn from postnatal day 1-21 (early life only), or from PND 1 - throughout life. Results revealed that early life Mn exposure alone caused long-lasting impairments in fine motor control of reaching skills at the higher, but not lower Mn dose, lifelong Mn exposure led to widespread impairment in reaching and grasping/retrieval performance in adult rats, with the lower Mn dose group showing the greatest impairment, and lifelong Mn exposure produced similar (higher Mn group) or more severe (lower Mn group) impairments compared to their early life-only Mn exposed counterparts. Results of the Ladder Walking test, and the efficacy of oral methylphenidate treatment to alleviate lasting deficits will also be presented. These results substantiate the emerging clinical evidence in children reported above showing associations between environmental Mn exposure and deficits in fine sensorimotor function.

S 2292 Attentional Deficits in Early-Life and Lifelong Manganese-Exposed Rats and Their Reversal with Oral Methylphenidate Treatment

S. A. Beaudin. *Microbiology and Environmental Toxicology, University of California Santa Cruz, Santa Cruz, CA.*

As suggested by results from the epidemiological studies presented above and elsewhere, overexposure to manganese (Mn) in early life is associated with attention deficit with hyperactivity disorder in children, but the specific nature and causal relationship of these attentional deficits have yet to be demonstrated. To address this, we determined whether early life Mn exposed rats exhibited persistent deficits in visual attentional processes and impulsive behavior in adulthood, and if lifelong Mn exposure caused similar or more severe attention deficits than early life exposure alone. The Mn-exposed groups showed normal visual attention performance in vigilance tasks. However, the Mn-exposed groups displayed deficits in attentional accuracy when required to attend selectively to visual cues in the presence of olfactory distracters. Notably, impulse control was not measurably impaired in the Mn groups. The results substantiate the emerging epidemiological evidence and show that developmental Mn exposure can cause selective attentional deficits across a range of doses and exposure durations, including lasting susceptibility to greater distractibility in adulthood. The efficacy of oral methylphenidate to ameliorate the attention deficits will also be presented – these latter results will inform the mechanistic basis for these deficits as well as the potential efficacy of MPH for treating Mn-related attentional deficits in children.

W 2293 Are Biofuels More or Less Toxic than Conventional Fuels and What Are the Implications for Human Exposure and Risk?

A. M. van Erp[1] and M. C. Madden[2]. [1]*Health Effects Institute, Boston, MA and* [2]*US EPA, Research Triangle Park, NC.*

During the past decade, the use of biofuels such as biodiesel and bioethanol has been steadily increasing as a viable alternative to the use of petroleum-based fuels. Although there are clear advantages in terms of energy security and climate change, there are several unknowns about the long-term effects of the use of biofuels on the environment and on human health. Because there are many different biofuels and biofuel blends that originate from different feedstocks, evaluating their effects on the environment and human health over their entire lifecycle becomes rather complex. Although there may be reductions in emissions of certain compounds, there may also be unintended consequences. For example, adding bioethanol to gasoline reduces emissions of benzene and other hydrocarbons, but increases the levels of toxic aldehydes in the engine exhaust, and also leads to increased evaporative emissions. While first-generation biofuels such as ethanol derived from corn are now widespread, next-generation fuels such as those produced by microorganisms are under development. The workshop will start with an overview of the types of biofuels that are currently available and recent results of comparative emissions-testing programs in the US. We will then present the latest results from several research programs to evaluate the emissions and comparative toxicity of biofuels, including *in vitro* testing for genotoxicity, *in vivo* evaluation of pulmonary and cardiovascular effects, and the toxicity of fatty acid methyl esters (FAME) that are found in biodiesel. In addition to new results regarding emissions testing, the workshop will discuss different approaches and harmonization of toxicity testing *in vitro* and *in vivo*. Finally, we will conclude with approaches to assess human exposure and health impacts. [This may not represent official US EPA policy.]

W 2294 Biofuel Usage, Composition, and Engine Emissions

K. Hoekman. *Desert Research Institute, Reno, NV.* Sponsor: A. van Erp.

This presentation will provide an overview of biofuels in the United States, with a focus on biodiesel and other biodistillate fuels. In recent years, the volume of biofuels has increased steadily due to a variety of legal and regulatory drivers for the promotion of biofuels. These drivers and their influence on current and predicted future volumes of different kinds of biofuels will be presented. Currently, there are many different biodistillate fuels in use or under development but it is difficult to predict what their effect will be in terms of future market shares. This presentation will provide an overview of the main kinds of biofuels, including the major categories of biodistillates, explaining their terminology, feedstocks, manufacturing processes, compositions, and properties.

Fuel composition is inevitably linked to vehicle emissions and their potential air quality and public health impacts. Emissions standards for diesel engines and vehicles have become much more stringent over time. Compliance with these standards has been achieved by a combination of engine and fuel modifications, and utilization of emissions control systems. The incremental emissions impacts of biodiesel compared to conventional diesel fuel have been investigated extensively. There is widespread agreement that in most situations, biodiesel blends provide modest reductions in emissions of carbon monoxide (CO), total hydrocarbons (HC), and fine particulate matter (PM), but slight increases (or no change) in emissions of nitrogen oxides (NOx). The effects of other biodistillate fuels upon these so-called "criteria emissions" have not been studied as thoroughly, but are probably similar to the effects of biodiesel.

Emissions of non-criteria pollutants including mobile source air toxic (MSAT) emissions are also of concern, especially in terms of the use of bioethanol and the formation of aldehydes. However, much less information is available regarding the impacts of biodiesel, and other biodistillates, on MSAT emissions. This area will be discussed, other open issues will be identified, and recommendations for additional work will be presented.

W 2295 *In Vitro* Toxicological Evaluations of Emissions from Heavy-Duty Vehicles Using Biofuel Blends

N. Kado and C. F. Vogel. *Environmental Toxicology and Center for Health and the Environment, University of California Davis, Davis, CA.*

The evaluation of the potential health effects from exposure to emissions from motor vehicles presents numerous challenges because these emissions are complex mixtures chemically, vary with fuel and engine type, and the emissions may be altered due to evolving control strategies and technologies. One approach toward evaluating these complex particle and vapor-phase mixtures is to use screening tools, such as directed chemical analyses and in vitro biological analyses. An example of this approach is the detailed emissions study of biodiesel, renewable diesel, and ultra-low sulfur diesel fuels, which was conducted as part of a multi-investigator and multi-institutional study on regulated emissions as well as unregulated toxic emissions. Samples from heavy-duty trucks following standard test cycles on a chassis dynamometer were evaluated chemically and in a screening effort using in vitro assays. These assays included mutagenicity tests and expressions of inflammatory and oxidative stress markers in human macrophage cells and lung epithelial cells. The trend for many of the tests/species compared to ultra-low sulfur diesel fuel was lower with increasing biofuel blends, but with some tests/species, results were higher with certain biofuel blends. This presentation and discussion will provide a brief overview of some of the in vitro evaluations with focus on heavy-duty vehicle tests. (The abstract and opinions are of the authors and do not represent policy of the California Air Resources Board or the University of California)

W 2296 Comparative Toxicity and Mutagenicity of Biodiesel Exhaust

I. Gilmour[1], D. Demarini[2], N. K. Fukagawa[3], U. P. Kodavanti[1], A. K. Farraj[1], M. S. Hazari[1] and S. H. Gavett[1]. [1]*EPHD, US EPA, Durham, NC,* [2]*ISTD, US EPA, Durham, NC and* [3]*University of Vermont, Burlington, VT.*

Biodiesel (BD) is commercially made from the transesterification of plant and animal derived oils, and the composition of biodiesel exhaust (BE) depends on the type of fuel, the blend ratio and the engine and operating conditions. While numerous studies have characterized the health effects associated with petroleum diesel (PD) emissions following controlled animal and human exposures, information on pure and blended BD emissions are far more limited. We developed a test program to compare the mutagenicity and toxicity of 100% (B100) or a 20% mix (B20) of soy-based BD exhaust to emissions from conventional PD (B0). Exhaust was generated by a 0.32 L Yanmar engine driving a 3.8 kW Pramac generator with a constant load of 3 kW and diluted to target concentrations of 0, 50, 150, or 500 μg/m3 as determined by TEOM. Average NO (ppm) at the 500 μg/m3 level were 15.2 (B100), 12.7 (B20) and 14.8 (B0). Rats and mice were exposed independently for 4 hours per day for up to 6 weeks depending on the experimental protocol and model system. In general, B0 had the greatest pro-inflammatory effects in normal mice while both B0 and B100 potentiated plaque formation in ApO E mice. The B0 and B100 also caused changes in heart rate variability and systemic inflammatory responses in hypertensive rats. Organic extracts of B0 were the most mutagenic while the B20 was intermediate and the B100 was low. Overall, BD did not seem to be any more toxic than PD and in many cases had less effect. (This abstract does not represent U.S. EPA policy.)

W 2297 Approaches to Comparative Biofuels Toxicity Testing and Recent Results from Europe

M. Gerlofs-Nijland. *National Institute for Public Health and the Environment, Bilthoven, Netherlands.*

On a regular basis new combustion or after treatment technology is brought on the market to meet the new stricter standards or to reduce the costs to meet the current regulations. The use of new (bio)fuels and fuel additives is also increasing to reduce the emission of CO2 and to be less dependent on natural petroleum. The current type approvals are mostly not sufficient to examine the effects for man and the environment. This implies that when harmfulness is examined for a specific biofuel, opposite outcomes could be reached by different institutes due to diverse measurement set up and risk assessment. This presentation will discuss the difficulties in testing toxicity of emissions associated with combustion of biofuels, given the large number of permutations of possible fuel and engine combinations. With regard to measuring/limiting air pollution exposure and its health impact caused by automotive emissions, and more specifically biofuel combustion, there are no common testing guidelines and standards on which to base policy. Clearly, it would be preferable to come to agreement on a harmonized approach for in vitro and in vivo testing, so that new fuels that come to market can be assessed relatively quickly and in standardized way. One of the main questions is what biological pathways and health outcomes should be covered in such "screening" evaluations. So far, mutagenicity and genotoxicity have been a major focus but other end points should be considered as well, given the increasing evidence of cardiovascular and other health effects associated with inhalation of combustion products. In addition, a standardized approach is needed for the generation of combustion aerosols and exposure conditions to really support comparative hazard screening. Examples of recent results from Europe including human exposure studies will be shown as illustrations.

W 2298 Human Health Impact Assessment of Biofuels

M. Egyed, N. Edmonds, N. Charman, S. Lamy and M. Rouleau. *Health Canada, Ottawa, ON, Canada.* Sponsor: A. van Erp.

Transportation fuel use represents a key source of air pollutant exposure, particularly in urban areas where mobile source emissions and large populations overlap. Changes in fuel composition can substantially alter the complex mixture of combustion emissions. The increased use of biofuel blends over the past decade and development of policies to promote their uptake necessitate detailed evaluation of the associated health implications. Health Canada (HC) has developed a risk assessment framework to evaluate health impacts of non-conventional fuels and applied it to biofuels. The approach used is: 1) comparative (basecase vs. new fuel) in order to estimate the incremental health risks/benefits of biofuels; and 2) comprehensive, with a focus on principal pathways of risk. The recent HC biodiesel (BD) assessment includes a review of the relative toxicity of BD emissions compared to diesel emissions, and modeling of the impact of the use of BD blends (5% or 20% by volume in ultra low sulphur diesel) in on-road heavy duty vehicles on Canadian air emissions, air quality and resulting health impacts. Incremental health impacts are estimated based on concentration-response functions linking ambient air pollutants with increased risk of premature mortality, hospital admissions, emergency room visits and respiratory outcomes. It is estimated that BD blend use in Canada would reduce emissions of particulate matter, carbon monoxide, volatile organic compounds and polycyclic aromatic hydrocarbons, and increase emissions of nitrogen oxides. These effects are expected to attenuate by 2020 due to the incorporation of new technology vehicles in the fleet. Changes in air pollutant levels due to BD use are expected to be small (<1%), and the associated health impacts minimal. The health effects literature on the comparative toxicity of BD emissions was limited for most endpoints. It was concluded that compared to diesel exhaust, BD exhaust is unlikely to elicit greater respiratory toxicity and may be less mutagenic. Biofuel research to address risk assessment needs and a comparison with the US approach will be reviewed.

W 2299 Role of Circulating Factors in Mediating Systemic Toxicity of Inhaled Substances

L. Chen[1] and M. Campen[2]. [1]*Environmental Medicine, New York University School of Medicine, Tuxedo Park, NY and* [2]*Pharmaceutical Sciences, University of New Mexico, Albuquerque, NM.*

Air pollution has been long known to cause chronic and acute systemic health effects, including cardiovascular and possibly neurodegenerative diseases, but the pathway by which inhaled substances drive effects beyond the lung is unclear. The lung provides an effective barrier against most gaseous and particulate components of air pollution, and those that are taken up systemically are often in remarkably low concentrations. Moreover, several studies fail to see the same effects at relevant concentrations when particulates are delivered by gavage, intravenously, or in cell culture studies, implying that there is a lung-specific reaction that occurs to drive the systemic effects. Recent studies have revealed that inhalation exposures to a variety of pollutants can lead to the generation of circulating bioactive factors that drive endothelial cell activation and may also be responsible for neuroinflammation. Circulatory changes include generation of adducted proteins, altered metabolites and lipids, and altered function of lipoproteins. The identity of the causal component(s) in the circulation remains unclear, but ongoing lipidomic and metabolomic research is providing important insights. This workshop will highlight a number of advances in this area related to exposures to particulate matter, metals, ozone, combustion mixtures, and nanomaterials.

W 2300 Influence of $PM_{2.5}$ Exposure on the Receptor for Advanced Glycation End Products: Insight into an Emerging Risk for Diabetes

J. M. Vaughan[1], B. Narayanan[1], A. Schmidt[2] and L. Chen[1]. [1]*Environmental Medicine, New York University, New York City, NY and* [2]*Medicine, New York University, New York City, NY.*

Diabetics are a particularly vulnerable population to the adverse cardiopulmonary effects of particulate air pollution (PM)- this is often attributed to enhanced inflammation and endothelial dysfunction. Recent reports have implicated activated receptors for advanced glycation end-products (RAGE) as an integral factor in the inflammatory processes in cardiovascular dysfunction and diabetes; nonetheless, it is unclear whether ambient air pollutants (PM) alone/or in combination with other endogenous factors may contribute to the activation of RAGE. In this study, we have determined that sRAGE was significantly (P=0.0358) higher in serum samples of residents in Jingchang (538.7±37.5 ng/ml) than that measured in Zhangye (452.6±29.1ng/ml). This change was due to higher levels of Ni, Cu, As, and Se in PM2.5 in Jinchang than that in Zhangye. We also found a dose dependent increase in cell proliferation and small increases in sRAGE activity when human vascular endothelial cells exposed to ambient PM. Immunofluorescence detection showed an elevated number of cells positive for membranous RAGE expression; accompanied with a two-fold increase in mRNA for RAGE and NF-κB. Furthermore, results also showed a >2 fold increase of ATF4 and NF-κB in cells treated with PM+BSA. We also measured the expression of other non-glycated ligands (S100, HMGB1). Using siRNA to silence RAGE in human endothelial cells and RAGE knock out mice, we have confirmed the plausible interaction between PM and RAGE and verified that RAGE is a potential inflammatory mediator of inhaled ambient PM.

W 2301 Carbon-Based Engineered Nanomaterial Exposure Alters Circulating Factors that Induce Endothelial Activation and Impairment of Nitric Oxide Synthesis

A. Erdely[1] and M. Aragon[2]. [1]*CDC-NIOSH, Morgantown, WV and* [2]*University of New Mexico, Albuquerque, NM.*

Carbon-based engineered nanomaterials (ENM), including carbon nanotubes (CNT), graphene, and fullerenes, have profound utility in medicine, electronics, and composites. While the surface is just being scratched on the diverse applications, a growing workforce is subject to exposure by inhalation. *In vivo* studies identify pulmonary cytotoxicity, inflammation, and fibrosis as a result of carbon-based ENM exposure. In addition to the pulmonary response, effects related to cardiovascular dysfunction included vascular inflammation and oxidative stress, endothelial dysfunction, and increased atherosclerotic plaque formation. The mechanisms linking the initial pulmonary exposure to resultant cardiovascular dysfunction are under investigation. Given the apparent toxicity of certain ENM and the vast number of ENM including various permutations of each, controlled toxicology studies in humans are not practical. Therefore, a translational *in vitro* screening assay was developed for rodents to assess the potential cardiovascular toxicity of ENM. Specifically, this particular study explored the ability of circulating factors after pulmonary exposure to affect mechanisms related to vascular dysfunction. Serum collected from mice exposed to carbon black, multi-walled CNT, or varying types of graphene were incubated with murine primary endothelial cells. The serum from exposed mice increased endothelial cell surface expression of VCAM-1 and ICAM-1 as early as 4 hr post-exposure when compared to respective shams. In addition, the serum from exposed mice reduced ATP-stimulated endothelial cell nitric oxide production by 25%. These results complement end point cardiovascular effects and showed the presence of circulating factors contributing to vascular dysfunction following carbon-based ENM exposure. Furthermore, the methodological design allows for interpretation of systemic effects in an unbiased approach while providing a platform for comparative studies of differing ENM in a translational context.

W 2302 Endothelial Cell Pattern Recognition Receptors, CD36 and LOX-1, Contribute to Responses to Pollution-Induced Circulating Factors

M. Campen. *Pharmaceutical Sciences, University of New Mexico, Albuquerque, NM.*

Our laboratory initially discovered that the serum from health human volunteers contains a bioactive component following controlled exposures to diesel or nitrogen dioxide that can activate inflammatory endothelial cell responses. While we have eliminated the possibility that common cytokines are the driving factor(s) in this response, the identity of the biochemical ligands that drive such responses remains unknown. However, we have considered the possibility that multligand pattern recognition receptors (PRRs), as mediators of response to extracellular damage, could play a specific role in endothelial cell responses to pollution induced circulating factors. Two specific receptors have been investigated: cluster of differentiation 36 (CD36) and the lechtin-like oxidized low density lipoprotein receptor-1 (LOX-1). These observations help explain systemic vascular inflammatory effects of diverse inhaled pollutants such as ozone and PM, along with complex mixtures from combustion sources. Ongoing translational work enables cumulative response patterns in controlled settings to improve assessment of relative toxicity of individual components and mixtures of pollutants.

W 2303 Ambient PM and Diesel Exhaust Alter Functionality of HDL

J. Araujo. *School of Medicine, University of California Los Angeles, Los Angeles, CA.* Sponsor: M. Campen.

We and others have shown that exposure to concentrated ambient particles and motor vehicle emissions induce lipid peroxidation in the lungs, circulating blood and systemic tissues such as the liver and the aorta. It is unclear however, whether effects induced in the lungs are required for the induction of systemic vascular effects. It is possible that circulating factors such as plasma lipoproteins could be altered and serve as mediators of the systemic toxicity of inhaled substances. This presentation will focus on our studies designed to evaluate the functional changes induced by air pollutants on plasma HDL lipoproteins, their relationship to lipid peroxidation in the lungs, circulating blood and systemic tissues and the activation of endogenous peroxidation pathways.

W 2304 Systemic Effects of Inhalation Exposure Mediated by 'Omic Perturbation in Serum

A. K. Ottens. *Neurosciences, Virginia Commonwealth University, Richmond, VA.* Sponsor: M. Campen.

Recent studies suggest that inhalation exposure to ozone generates circulating factors in blood that can result in systemic health consequences, including activation of microglia and inflammatory responses in the brain; however, the nature and complexity of these products have remained a mystery. As ozone rapidly reacts in the lung surfactant, the generation of pulmonary-derived modified lipids, proteins, or small molecules may be a plausible outcome that leads to systemic effects. Through recent development of a label-free quantitative data-independent Omic platform, analysis of serum factors reveals a diverse and dose-dependent molecular perturbation with broad biochemical implications. Specific effects observed in coronary vascular and nervous systems will be discussed related to the compositional alterations in the serum.

W 2305 The Use of Dogs and Minipigs As an Alternative to the Nonhuman Primate in Nonclinical Safety Assessment of Biopharmaceuticals

J. A. Wisler[2] and J. Bluemel[1]. [1]*MedImmune, Gaithersburg, MD and* [2]*Amgen, Thousand Oaks, CA.*

Appropriate species selection is paramount for the nonclinical safety evaluation of biopharmaceuticals. Regulatory guidance requires the use of a pharmacological responder species, in particular for biopharmaceuticals. Most often the nonhuman primate (NHP) is considered as the only pharmacologically relevant species, and especially the cynomologus monkey is frequently used for nonclinical safety studies. In recent years, ethical concerns, increased public scrutiny, and issues of availability and transportation of NHPs have put considerable pressure on researchers worldwide to improve study designs and to intensify the search for alternative species. Besides recent activities to improve study designs to reduce the number of animals used, there is a sense of urgency to intensify the search for alternative species and consider nontraditional approaches beyond the use of "standard" toxicology species. Species like the dog and minipig are meanwhile widely used in toxicity studies for chemical-derived pharmaceuticals but rarely considered for nonclinical safety evaluation of biopharmaceuticals. The limited availability of scientific background data, e.g., pharmacogenomic or physiology comparisons, and limited regulatory experiences are considered as major obstacles for a wider use of dogs and minipigs for biopharmaceutical safety testing. A better understanding of factors like sequence homology, target/ligand expression, downstream signaling, effector functions, and antibody kinetics, as well as the availability of tools like species-specific background databases, *in vitro* assays, or reagents, would greatly facilitate the use of dogs and minipigs. Increased use of dogs and minipigs for nonclinical safety assessment of biopharmaceuticals would in turn increase the regulatory confidence and experience. The objective of this workshop is to review and discuss recent progression and challenges in the scientific characterization of dogs and minipigs and discuss their utility and limitations for regulatory safety testing of biopharmaceuticals.

W 2306 The Immune System and Immune Function Testing in the Dog and Minipig

H. N. Lebrec. *Toxicology Sciences, Amgen Inc., Thousand Oaks, CA.*

Reactivity with canine and minipig targets and to some extent the level of immunogenicity of human/humanized proteins in these species may be limitations to their use with regards to safety assessment of biopharmaceuticals. However, tools are available or can be developed to address immunology-related questions. The availability of appropriate knowledge and analytical tools regarding the immune system may be critical for proper nonclinical safety assessment of biopharmaceuticals in the dog and in the minipig from the following standpoints: demonstration of species relevance (on target specific binding, pharmacodynamics); conduct of immunotoxicology assessments (including immunophenotyping of subpopulations of lymphocytes and functional assessments [e.g., T cell-dependent antibody response [TDAR], cytotoxic T cell activity, NK function); assessment of immunogenicity and documentation of immunogenicity-related toxicity. This presentation will provide a comparison of the human, dog, and minipig immune system (overall structural and functional organization, ontogeny, innate immunity, humoral and cell-mediated immunity). It will then provide an overview of the tools available to document and characterize immunotoxicity in the dog and minipig (with a focus on TDAR and immunophenotyping), as well as existing gaps. It will then discuss available methods for documentation of anti-drug antibodies, circulating or tissue immune complexes.

W 2307 The Dog and Minipig As Pharmacology Models to Evaluate Biopharmaceuticals

N. Dybdal. *Safety Assessment Pathology, Genentech, South San Francisco, CA.*

Whether being considered for use in general toxicology or pharmacology studies, the many features of the dog and minipig which make them attractive for consideration as a non-rodent toxicology species must never overshadow the need to first determine if their use is appropriate and justified biologically. First the species specificity of the biopharmaceutical must be characterized and relevance in dog and/or minipig must be established (e.g. is the protein appropriately cross-reactive with the target – receptor/ligand). The biological pathway of concern needs to be characterized and comparative activity and control of the pathway understood (e.g. downstream signaling, effector function). Although the potential immunogenicity of the biopharmaceutical may present a challenge, duration of dosing, dose or schedule can often be managed to help avoid this issue. Immunogenicity of foreign proteins reflects a challenge to the feasibility of conducting studies in dogs and minipigs and should not be confused with an opportunity for use of these species as predictive models of immunogenicity in humans. This presentation will provide case examples of the use of dogs and minipigs as pharmacology models. In these examples the obstacles remaining will be balanced against the opportunities and growing feasibility of fully realizing the benefits of conducting pharmacology studies of biopharmaceuticals in these species.

W 2308 Animal Model Genomic Data Aids Species Selection in Pharmaceutical Discovery and Development

J. J. Vamathevan. *Computational Biology, GlaxoSmithKline, Stevenage, United Kingdom.* Sponsor: J. Wisler.

Improving drug attrition remains a challenge in pharmaceutical discovery and development. A major cause of early attrition is the demonstration of safety signals which can negate any therapeutic index previously established. Safety attrition needs to be put in context of clinical translation (i.e. human relevance) and is negatively impacted by differences between animal models and human. In order to minimize such an impact, an earlier assessment of pharmacological target homology across animal model species will enhance understanding of the context of animal safety signals and aid species selection during later regulatory toxicology studies.
This talk will cover the genomes of the scrofa Göttingen minipig and the *Canis familiaris* beagle. Comparative analysis of these genomes with other key model organisms, namely mouse, rat, cynomolgus macaque, rhesus macaque, two related breeds (*S. scrofa* Duroc and *C. familiaris* boxer) and human reveal considerable variation in gene content. Key genes in toxicology and metabolism studies, such as the UGT2 family, CYP2D6, and SLCO1A2, displayed unique duplication patterns. The use of simple phylogenetic tools allow for the comparisons of known human drug targets prior to starting safety studies. Example studies of such drug targets have revealed surprising variation such as species-specific positive selection, duplication and pseudogenized targets. These data will facilitate the more effective use of animals in biomedical research as well as enhance the understanding of the context of animal safety signals and aid species selection during later regulatory toxicology studies.

W 2309 Regulatory Acceptance of Nontraditional Animal Models for Safety Assessment: EU Perspective

J. van der Laan. *Section on Pharmacology, Toxicology and Biotechnology (FTBB), Medicines Evaluation Board, Utrecht, Netherlands.* Sponsor: J. Bluemel.

Animal welfare is enshrined in the Treaty of the EU. The revision of the Directive on animal protection in the EU was discussed intensely under the framework of the European Commission, because the use of animals, particularly the nonhuman primate (NHP), for testing purposes is a sensitive issue in Europe. The European Community funded a Specific Support Action (SSA) to evaluate the potential impact of toxicity testing in minipig as an alternative approach in regulatory toxicity testing, with the aim of contributing to replacement, refinement and reduction of animal testing. This SSA was named the RETHINK project. The use of NHP and minipig as animal models have been discussed in different forums and this presentation focuses on the minipig as an alternative and draws extensively on RETHINK. The EU launched the Directive 2010/63 indicating that the use of NHP in biomedical research is of the greatest concern to the general public. It is recognized that the use of live animals continues to be necessary to protect human health, but the use of NHP should be restricted to potentially life-threatening conditions in humans or in relation to cases of debilitating conditions. An important application of NHP is in the area of biotechnology-derived proteins. ICH S6(R1) guidance recommends the use of a relevant species, i.e., a species that does respond to the pharmacological action of the product. Because of the high specificity of biopharmaceuticals there is an important restriction in the choice of species. In most cases the cynomolgus monkey is the default species being chosen. Based on the EU-legal restrictions mentioned above the minipig might be considered as an important 'alternate' species. There are several opportunities and challenges in using minipig as the nonrodent species of choice.
- Application of minipigs in the testing strategy of dermally-applied products
- Limitations in reproductive and developmental toxicity testing of biopharmaceuticals
- Cardiovascular functioning in minipigs as a model for humans.

These topics will be discussed using case reports.

W 2310 Regulatory Acceptance of Nontraditional Animal Models for Safety Assessment: US Perspective

A. Jacobs. *US FDA, Silver Spring, MD.*

Although the International Conference on Harmonization Guideline ICH M3(R2) indicates the use of nonrodents for some studies of pharmaceutical products, the specific nonrodent species is not specified. Dogs are used most frequently. However, there may be reasons that dogs may not be the best model for a particular drug. Minipigs are being used increasingly for evaluation of both toxicity, especially for dermally applied drugs, and for various efficacy models. Hamsters may be used for the evaluation of intraoral drugs and for carcinogenicity studies. When nontraditional species are used, there may be less historical information available and unique issues of their care, and differences in physiology and anatomy and susceptibility to infection need to be understood. Use of nontraditional animal species can be proposed by a drug sponsor to a reviewing division with supporting data and reasons for using a particular species.

RI 2311 When the Dust Settles: Exposure Assessment and Health Effects from Dust Exposures in the Arid Southwest

R. Lantz. *Dept of Cellular and Molecular Medicine, University of Arizona, Tucson, AZ.*

In the arid southwestern United States, respirable dust levels in the atmosphere can be problematic due to the low humidity and strong winds. Over the last several years, these conditions have led to increased incidence of high dust exposures, especially in densely populated regions. Based on climate change models, these conditions are expected to worsen, with the southwestern US projected to be among the regions that will be most affected by these changes. This issue can be particularly acute just downwind from sources such as roads or legacy mine tailing sites, where dusts can contain high levels of respirable particulate matter that may also contain metals, including arsenic, copper, chromium, and cadmium, and legacy waste from hundreds of abandoned uranium mines in the region. Dusts and pollutants generated by other sources can also contribute to decrement in air quality and increased risk of adverse health outcomes. Airborne pollutants have long been implicated as potential etiological agents in the development of asthma and other diseases. In addition, exposure to airborne particulates exacerbates the pulmonary responses in already sensitized individuals. Further complicating these responses is the fact that ingestion of high levels of arsenic in drinking water is occurring simultaneously in the southwestern US. This session will focus on these important regional issues. Talks will present data on exposure assessment and characterization of dusts from roads and legacy mines. Potential adverse health outcomes from these exposures will be presented. The impact of these exposures on native populations will also be discussed. Data from both population and laboratory-based research will provide excellent examples and information related to the effects of exposure to dusts and metal-containing dusts. This will be of interest to those involved in metal toxicology, pulmonary toxicology, developmental toxicology, public health, risk assessment, and regulatory management.

RI 2312 Influence of Collection Region and Site Type on the Composition of Paved Road Dust: It's Not Just Dirt!!!

J. D. McDonald. *Lovelace Respiratory Research Institute, Albuquerque, NM.*

Exposures to particulate matter (PM) re-suspended by traffic from paved roads are ubiquitous, but little is known about the variability in composition of paved road dust (PRD). This knowledge gap hinders estimates of exposure to PM components near roadways. Respirable fractions of PRD collected from multiple U.S. regions and site types were analyzed to explore chemical composition and variability. Fifty samples were collected from streets, traffic arterials, street canyons, freeways, and industrial sites in six urban regions in the southwestern, Southern California, northeastern, and southeastern U.S. regions and five rural sites. Samples were sieved, aerosolized, and size-classified into fine (PM2.5) and coarse (PM10-2.5) fractions. Analyses included metals and other elements, organic and elemental carbon, inorganic ions, endotoxin and glucan. Crustal elements, organic carbon, and reactive metals comprised the PRD mass with smaller fractions of elemental carbon and inorganic ions. Proportions of many inorganic components were strongly correlated between particle sizes, but fine and coarse organic carbon poorly correlated. Composition varied both among and within regions and site types, with evidence that chemical signatures varied more systematically by region than by site type. Local sources strongly influenced some samples. Samples from large urban areas had greater contents of reactive metals, but these comprised less than 0.2% of the mass. Near-feedlot samples had high levels of endotoxin. The results provide insight into the variability of PRD composition, differences between re-suspended PRD and regional airborne PM, and improved source signatures for estimates of exposure to different PM components near roadways. An initial assessment of the inhalation toxicology of resuspended dust from Phoenix was assessed in mice. ApoE mice were exposed by inhalation for 60 days and evaluated for lung inflammation and cardiovascular response. Road dust overall showed less toxicity than similar exposed groups that were treated to vehicle exhaust.

RI 2313 Multimedia Exposure to Metals near a Mine Tailings Site

M. Loh. *Community, Environment and Policy, University of Arizona, Tucson, AZ.* Sponsor: R. Lantz.

An important pathway of exposure to mine tailings waste involves dust, especially in arid climates. Dust can be both inhaled and ingested. The latter route is particularly important with respect to children, who exhibit behaviors that predispose them to ingesting more dust per unit body weight than adults. Inhalation cannot be ignored, as this route of exposure for metals has not been well explored. Inhalation of metals such as arsenic may contribute to whole body dose as well as cause localized pulmonary effects. This study reports the results of exposure assessment of residents living near a legacy mine tailing site where they may have higher exposures to certain metals. The aim is to investigate whether there is a relationship between living near a former mine and smelter site in Arizona and exposure to metals, particularly arsenic (As) and lead (Pb), via soil, dust, and water. Metals were measured in residential soil, dust, water, urine and toenail samples from 31 children in 18 households up to 5 miles from a former mine and smelter site. Soil from the house perimeter and dust from vacuum bags were collected, sieved to <63 μm before nitric acid digestion and analysis via ICP-MS. Water and urine were analyzed without digestion, while toenails were washed, digested and analyzed. Blood lead was tested by an independent, certified laboratory. The majority of water Pb concentrations and blood Pb were below the limit of quantification. Total urinary As was above the NHANES 2009 geometric mean for ages 6-11 years with about 16% of the children above the 90th percentile, indicating a possible local source of exposure. Children do not appear to be highly exposed to lead from the tailing/smelter site. This may be due to the bioavailability of the metals, parameters that must be considered when determining exposure and biological effects. Further work will examine the spatial gradient between the site and environmental and biomarker levels, as well as other potential predictors of biomarker levels.

RI 2314 Effects of *In Utero* and Early Postnatal Exposures to Metal-Containing Dusts

R. Lantz. *Dept of Cellular and Molecular Medicine, University of Arizona, Tucson, AZ.*

In the arid Southwest of the United States, dusts, especially downwind of legacy mine tailings and smelters, can contain high levels of metals, including arsenic. The levels of arsenic in these dusts can be an order of magnitude above ambient levels. In addition, because of high levels of arsenic in drinking water, simultaneous exposure to arsenic from water and from airborne particulate dust occurs. Exposure to airborne toxicants, that are downwind of toxic sources, can cause adverse health effects. Exposure of pregnant female mice to air pollutants has been shown to alter lung function and to enhance sensitization and airway reactivity in offspring. *In utero* and/or postnatal exposure to cigarette smoke, ambient urban air particles or metals leads to increased airway reactivity, decreased surface to volume ratios in the lung and altered lung function in the offspring. In this study, we examined the effects of inhalation of arsenic compounds during sensitive developmental time periods. Mice were exposed by inhalation to dusts containing various forms of arsenic that can be found in mine tailings or downwind of smelters, either during *in utero* development, after birth or both. Pulmonary function, structure and inflammation were analyzed to determine the effects of these exposures on the developing lung. The effect of combined inhalation and ingestion was also analyzed. Alterations in lung resistance, elastance and airway reactivity were seen. These changes correlated with alterations that occurred in the connective tissue around airways. The responses depended on the form of arsenic that was inhaled as well as the developmental time when the exposures occurred. Children living in an arid region of Mexico who would be expected to be exposed both through ingestion and inhalation of arsenic showed decrements in lung function. These data indicate that inhalation of dusts containing arsenic during sensitive developmental times may result in altered pulmonary function and structure later in life.

RI 2315 Metals, the West, and Translational Science

J. L. Lewis. *Community Environmental Health Program, University of New Mexico, Albuquerque, NM.*

The western US has been heavily mined for a range of heavy metals, leaving the majority of the 500,000 abandoned mines in the US behind. Among these abandoned mines are also more than 10,400 abandoned uranium mine waste sites scattered throughout the west, with more than 1100 located on the Navajo Nation. Arsenic, both naturally occurring and as a co-contaminant in mine waste, also complicates exposures through its presence in unregulated water sources relied on by up to 30% of the populations in some of these regions. Evaluating the impact of these mixed-metal exposures in Western communities is further complicated by the fact that the sites often impact rural and tribal communities that have not been adequately represented in the research base from which toxicity has been evaluated. Evaluating the health impacts of the unique mixtures in the waste within the context of existing lifestyle and risk factors presents unique challenges, and an opportunity for developing novel approaches that integrate disciplines including population science, toxicology, and clinical care with physical sciences and novel statistical approaches to understand the complex interactions. We have been able to build on a diversity of strengths to develop an integrated transdisciplinary response to these issues and to begin not only characterizing the problems, but identifying interventions, informing clinical care, and informing policy to reduce the impact on our communities. In Navajo communities, we have found that while exposures in communities during the active phase of mining increased the risk for kidney disease, chronic lower dose exposures to legacy waste increase the likelihood of hypertension, autoimmune disease and immune dysfunction in adults. We are currently investigating the relationship between these exposures to mixed metals in legacy waste, reproduction, and development in Navajo children. These community-based approaches also represent efforts to integrate Western science with Native learning models and underscore the importance and impact of translational science in meeting the needs of improving community health.

PL 2316 Metabolic Pathways Related to Inflammation Are Disrupted by Arsenic in the Livers of Mice Fed a Western Diet

W. H. Watson[1], X. Shi[2], X. Wei[2], I. Koo[2], R. H. Schmidt[3], X. Yin[2], S. Kim[2], A. Vaughn[1], C. McClain[1, 4], G. E. Arteel[3] and X. Zhang[2]. *[1]Department of Medicine/GI, University of Louisville, Louisville, KY, [2]Chemistry, University of Louisville, Louisville, KY, [3]Pharmacology & Toxicology, University of Louisville, Louisville, KY and [4]Robley Rex VAMC, Louisville, KY.*

Arsenic is a widely-distributed environmental component that is associated with a variety of cancer and non-cancer adverse health effects. Additional lifestyle factors, such as diet, contribute to the manifestation of disease. Recently, arsenic was found to increase inflammation and liver injury in a dietary model of fatty liver disease. The purpose of the present study was to investigate potential mechanisms of this diet-environment interaction via a high throughput metabolomics approach. GC×GC-TOF MS was used to identify metabolites that were significantly increased or decreased in the livers of mice fed a Western diet (a diet high in fat and cholesterol) and co-exposed to arsenic-contaminated drinking water. The results showed that there are distinct hepatic metabolomic profiles associated with eating a high fat diet, drinking arsenic-contaminated water, and the combination of the two. The high fat diet significantly altered nine metabolites, and the addition of arsenic resulted in further changes to three of these metabolites as well as introducing changes in six additional metabolites. The profiles of altered metabolites were consistent with perturbations in the metabolism of glutathione, short-chain fatty acids and medium-chain fatty acids. Of particular interest was the apparent block in the synthesis of glycine when arsenic was combined with a high fat diet. Glycine can inhibit inflammatory signaling by hepatic Kupffer cells in other model systems, and the decrease in glycine levels seen in our model may account for the observed increase in inflammatory cytokines and markers of Kupffer cell activation. These results point to potentially novel mechanisms by which arsenic can promote the progression of fatty liver disease.

PL 2317 Organic Species of Arsenic Have Adverse Effects on *Pseudomonas aeruginosa*-Induced Immune Response

E. Notch, R. Barnaby, B. Coutermarsh, V. Taylor, B. Jackson and B. Stanton. *Geisel School of Medicine at Dartmouth, Hanover, NH.*

Arsenic is the number one environmental contaminant of concern with regard to human health. Epidemiological studies have linked arsenic exposure with lung disease, including bacterial infections, and chronic obstructive pulmonary disease, which are associated with *Pseudomonas aeruginosa* (*Pa*) infection. Animal models have also shown that arsenic alters the immune response. Little is known about effects of low doses relevant to US population exposure or the contributions of organic arsenic to altered immune response. This study examined impacts of inorganic sodium arsenite (iAs^{III}) and two major metabolites, monomethylarsonous acid (MMA^{III}) and dimethylarsenic acid (DMA^{V}), on *Pa* induced cytokine secretion by primary human bronchial epithelial cells (HBEC). Exposure of HBEC to iAs (10ppb) did not alter *Pa* induced cytokine secretion. In contrast, 5ppb DMA significantly decreased IL-8, IL-6, CXCL1 and CXCL2 secretion after *Pa* stimulation compared to cells exposed to *Pa* alone. Exposure to 5ppb MMA increased *Pa* induced IL-8, and CXCL2 secretion. These alterations in HBEC proinflammatory cytokine secretion can impact macrophage recruitment or amplification of chemotactic stimulus through reduced macrophage cytokine secretion. Differentiated THP-1 cells (macrophages), were exposed to purified CXCL1 and CXCL2 at concentrations based on HBEC secretion. Lower concentrations of CXCL1 and CXCL2, equivalent to those released by HBEC exposed to DMA and *Pa*, reduced THP-1 IL-8 and IL-1β secretion. Higher concentrations of CXCL1 and CXCL2, equivalent to those released by HBEC exposed to MMA and *Pa*, significantly increased THP-1 IL-1β secretion. This suggests that MMA will enhance inflammatory response potentially leading to lung damage and DMA will suppress inflammatory response resulting in increased pathogen burden. These results demonstrate that exposure to low levels of organic arsenic, that may occur from ingestion of rice and rice based products, have untoward effects on the respiratory immune response to *Pa* infection.

PL 2318 Arsenic Exposure and Cell-Mediated Immunity in Preschool Children in Rural Bangladesh

S. Ahmed[1, 2], Y. Wagatsuma[3], M. Kippler[1], R. Raqib[2] and M. E. Vahter[1]. [1]*Institute of Environmental Medicine (IMM), Karolinska Institutet, Stockholm, Sweden,* [2]*International Centre for Diarrheal Disease Research, Bangladesh, Dhaka, Bangladesh and* [3]*University of Tsukuba, Tsukuba, Japan.*

Prenatal arsenic exposure is associated with reduced infant's thymic size and function and increased morbidity, indicating arsenic-related impaired immune maturation. In this follow-up study, we evaluated the persistence of arsenic-related impaired immunity by measuring the delayed type hypersensitivity response (DTH) in pre-school aged children, in relation to prenatal and concurrent arsenic exposure. Children born in a longitudinal mother-child cohort in rural Bangladesh were studied at 4.5 years (n=577). Exposure to arsenic was assessed by the concentrations of arsenic metabolites in maternal urine (U-As) collected in gestational week 8 (GW8), as well as in children's concurrent urine. U-As was measured by HPLC online with ICP-MS. Children were given an intradermal injection of purified protein derivative (PPD), and the diameter (mm) of induration was measured after 48 hours. Plasma levels of 27 cytokines were analyzed by multiplex cytokine assay. Concurrent, but not prenatal, arsenic exposure was associated with increased risk of not responding to PPD (induration <5mm) injection. The odds ratio (OR) of not responding to PPD was 1.91, (95% confidence interval (CI): 1.18, 3.07) in children in the highest quartile of U-As (125-1228 μg/L) compared with lowest quartile (12-34 μg/L). The associations were stronger in underweight children and those in families with low socioeconomic status. Concurrent arsenic exposure was inversely associated with Th1 cytokines (IL-2 and TNF-α) (regression coefficient (95% CI): -0.38 (-0.69, -0.06); and -1.17 (-2.38, 0.05), respectively) and, thus, Th1/Th2 ratios (IL-2/IL-4 and IL-2/IL-10). In subsequent stratified analyses, these associations were more evident in underweight children and those in families with low socioeconomic status. In conclusion, arsenic exposure appeared to impair cell-mediated immunity in children by reducing the DTH, presumably linked to reduced Th1 cytokines.

PL 2319 Inhibition of Arsenic-Induced Unfolded Protein Response Prevents Endothelial Activation and Inhibits Atherosclerosis in APO E-Knockout Mice

S. Srivastava, S. D. Sithu, N. S. Wickramasinghe, E. Vladykovskaya, P. Haberzettl, A. Agarwal, M. Winner, R. E. Hamid-Berair and S. E. D'Souza. *University of Louisville, Louisville, KY.*

Epidemiological and animal studies suggest that exposure to arsenic exacerbates atherosclerosis. However, the mechanisms by which arsenic exerts its atherogenic effects are not known. We observed that exposure of endothelial cells to sodium arsenite for 4 days increased the expression of pro-inflammatory chemokine IL-8 by 5-fold and molecular chaperones of protein folding - GRP78 and HERP by 2-fold. Moreover, acute exposure of sodium arsenite (2-6 hours) to endothelial cells increased the surface expression of adhesion molecules ICAM-1, VCAM-1 and E-Selectin by 1.2-1.5-fold; leukocyte adhesion by 1.3-2.5-fold; leukocyte trans-endothelial migration by 2.5-4.0-fold; and expression of pro-inflammatory cytokines and chemokines by 27-150-fold. Acute exposure of endothelial cells to sodium arsenite also activated the IRE-1 and ATF-6 arms of unfolded protein response (UPR) and increased the expression of molecular chaperones. Knockdown of IRE-1 by siRNA and adenoviral transfection with ATF-6 prevented sodium arsenite-induced endothelial activation. Similarly, phenyl butyric acid (PBA), a chemical chaperone of protein folding, prevented sodium arsenite-induced endothelial activation. Moreover, feeding PBA to apoE-null mice for 16 weeks inhibited sodium arsenite-induced UPR in atherosclerotic lesions; expression of adhesion molecules on endothelial cells lining the atherosclerotic lesions; lesional and systemic inflammation and prevented the arsenic-induced exacerbation of lesion formation in the aortic valve. Together, these data suggest that arsenic causes endothelial activation and exacerbation of atherosclerosis by triggering UPR and chemical chaperones of protein folding could prevent arsenic-induced exacerbation of atherogenesis and inflammation.

PL 2320 Arsenite Exposure-Induced Lymphocytes G0/G1 Arrest Is Attributable to p130 Accumulation via p16 Increase

K. Okamura[1, 2] and K. Nohara[1, 2]. [1]*Center for Environmental Health Sciences, National Institute for Environmental Studies, Tsukuba, Japan and* [2]*Grad. Sch. of Life &Environ. Sci., University of Tsukuba, Tsukuba, Japan.*

Arsenite exposure induces immunosuppression, but the mechanism is not precisely elucidated. Previously, we clarified that exposure of mouse B lymphoma cell line A20 to arsenite induces G0/G1 arrest by increasing the amount of p130, a member of the retinoblastoma (RB) family, without changing the mRNA level. In this study, we sought the mechanism how p130 was increased by arsenite exposure. Since p130 has been reported to be undergone degradation following phosphorylation and subsequent ubiquitination and proteasome degradation, we focused on whether this pathway functions in A20 cells. Treatment of A20 cells with MG-132, a proteasome inhibitor, increased the amount of p130, which clarified that the pathway functions in A20 cells at steady state, and it was also expected that arsenite exposure increases p130 by inhibiting proteasome degradation. In consistent with the notion, the ubiquitination level of p130 in the arsenite treated cells was lower than MG-132 treated cells, and arsenite exposure was shown to increase hypo-phosphorylated p130. These results suggested that arsenite exposure inhibits proteasome-degradation of p130 by suppressing phosphorylation and following ubiquitination. Previous studies indicated that phosphorylation of RB proteins were regulated by cyclin dependent kinase inhibitors (CDKI), notably p21 and p16. The results of the present study showed that arsenite exposure increased mRNA levels of both *p16* and *p21*, but only *p16* siRNA suppressed the p130 increase by arsenite.p16 is reported to inhibit phosphorylation of RB proteins by interacting with cyclin-dependent kinase 4 (cdk4) and competitively inhibiting its activity on RB proteins. We also demonstrated that arsenite exposure increased the complex of p16 and cdk4. In conclusion, the results of the present study suggest that arsenite exposure increases p130 by inhibiting its phosphorylation and following ubiquitin-proteasome degradation via induction of p16.

PL 2321 Obesity and Lung Inflammation after Asbestos Exposure

T. A. Brown and A. Holian. *Center for Environmental Health Sciences, University of Montana, Missoula, MT.*

Rational: Asbestos exposure can lead to physiological consequences including chronic inflammation, asbestosis, pleural plaques, and mesothelioma. However, individual responses to particles differ, including asbestos. Obesity is one factor associated with differences in severity of asbestos-related disease. Furthermore, body mass index has been correlated with some diseases (viz., pleural plaques and pleural thickening) in the case of Libby asbestos exposure. Asbestos exposure leads to activation of the NLRP3 inflammasome, a pro-inflammatory protein complex that leads to the release of IL-1β, a phenomenon also seen in obesity. Using a murine model of diet-induced obesity we determined if obesity lead to a greater inflammatory response, including increased inflammasome activation, after asbestos exposure and if chronic exposure leads to more severe lung pathology, i.e., tissue fibrosis.
Methods: C57Bl/6 mice were put on a high fat diet for 12 weeks until they were 25% heavier than mice on the control diet. Alveolar macrophages were collected and exposed to asbestos for 24 hr to determine the level of inflammasome activation via IL-1β release. Mice were also exposed to asbestos for 24 hr in vivo and cytokine production and inflammation in the lavage fluid was determined. Finally, mice were examined after 8 weeks of asbestos exposure and the level of tissue fibrosis was determined.
Results: Alveolar macrophages isolated from obese mice showed increased inflammasome activation compared to normal diet mice after asbestos exposure. Additionally, obese mice had greater levels of inflammatory cytokines and granulocyte influx in the lungs after a 24 hr asbestos exposure. After long-term exposure to asbestos obese mice showed trends towards greater levels of fibrosis in the lungs.
Conclusion: Diet induced obesity caused greater levels of inflammation after asbestos exposure in the lungs due, at least in part, to excess inflammasome activation. This increased level of inflammation lead to a trend for greater levels of tissue fibrosis after long-term exposure.

PL 2322 The Characteristics of Activated Lymphocytes in Silicosis Differing in Th17 Phenotype from Systemic Scleroderma

Y. Nishimura[1], S. Lee[1], N. Kumagai-Takei[1], H. Matsuzaki[1], H. Hayashi[2], W. Fujimoto[2], Y. Morita[3], M. Kusaka[4] and T. Otsuki[1]. [1]*Hygiene, Kawasaki Medical School, Kurashiki, Japan,* [2]*Dermatology, Kawasaki Medical School, Kurashiki, Japan,* [3]*Rheumatology, Kawasaki Medical School, Kurashiki, Japan and* [4]*Kusaka Hospital, Bizen, Japan.*

Inhalation of silica causes lung pneumoconiosis, silicosis, the patients with which occasionally suffer from autoimmune diseases including systemic scleroderma (SSc). We hypothesized an immunological effect of silica exposure, and examined immunologically patients with silicosis and SSc using flow cytometry, realtime PCR and multiplex technology. Both the patients with silicosis and SSc showed increases in CTLA-4, CXCR3 and IL-1R1 on CD4+ T cells and CD25, FasL, CXCR3 and HLA-DR on CD8+ T cells. Additionally, silicosis showed increases in CD45RO on CD8+ T cells and FasL on NK cells, but SSc did not. Foxp3 mRNA level was high in CD4+ T cells of silicosis as well as SSc, but IL-1R1 mRNA was high only in SSc. Silicosis showed high TNF-α mRNA in stimulated CD4+ T cells,

whereas SSc showed high IL-17A mRNA. Both stimulated CD8+ T cells of silicosis and SSc showed high mRNA levels of granzyme B, IFN-γ and FasL. IP-10, MCP-1 and TNF-α levels in plasma were high in silicosis as well as SSc. These results indicate that silicosis and SSc patients have several similar characteristics of increases in regulatory T cells, activated CD4+ and CD8+ T cells and inflammatory chemokine and cytokine, and that Th17 function increases in CD4+ T cells of SSc patients. The similarities between silicosis and SSc suggest a potentially immune-activating effect of exposure to silica, leading to autoimmune diseases. The difference in characteristics observed in both the diseases might contribute to understanding pathogenesis of autoimmune diseases following exposure to silica.

PL 2323 Transient Receptor Potential Cation Channel A1 (TRPA1) Mediates Decrements in Cardiac Mechanical Function and Dysrhythmia Caused by a Single Air Pollution Exposure in Mice

N. Kurhanewicz[1], R. McIntosh-Kastrinsky[1], A. Ledbetter[2], L. Walsh[2], A. K. Farraj[2] and M. S. Hazari[2]. *[1]University of North Carolina, Chapel Hill, NC and [2]Environmental Public Health Division, USEPA, Research Triangle Park, NC.*

Time-series studies indicate that the risk of cardiac events and arrhythmia increase significantly in the hours to days directly following exposure to air pollution. Previous studies have demonstrated that pharmacological inhibition of transient receptor potential cation A1 (TRPA1) attenuates diesel exhaust-induced cardiac arrhythmia. In this study, we sought to further confirm the role of TRPA1 in acute cardiovascular dysfunction due to air pollution exposure by utilizing a TRPA1 knockout mouse model. We hypothesized that acrolein and ozone (O3), both potent TRPA1 agonists, would cause decrements in cardiac function and electrical disturbances via TRPA1 mediated mechanisms. Conscious, unrestrained C57BL/6 (wt) and TRPA1 knockout (ko) mice were exposed to 3ppm acrolein for 3 hours, or 0.3ppm O3 for 4 hours; separate groups were exposed to filtered air (FA). Electrocardiogram (ECG) was recorded continuously before, during and after exposure. 24 hours post-exposure, cardiac function was assessed using a Langendorff cardiac perfusion preparation. Acrolein exposed wt mice demonstrated a significant decrease in HR during exposure as well as an increased incidence of arrhythmia compared with FA controls. Acrolein also produced a significant increase in ventricular relaxation, whereas exposure to O3 produced a significant decrease in contractility and relaxation in wt mice. No effects were seen in acrolein or O3 exposed ko mice. These data indicate that TRPA1 mediates, at least in part, the development of acute cardiac function decrements and dysrhythmia following exposure to either of these two relatively ubiquitous pollutants. While both acrolein and O3 are TRPA1 agonists, they appear to cause divergent cardiac responses, which suggest the underlying mechanisms are more complex than mere sensory activation.(This abstract does not reflect EPA policy)

PL 2324 Inhalation Exposures to Ozone Induce Insulin Resistance and Pulmonary Pathology in Type II Diabetes-Prone Mice

K. Allen, R. Lewandowski, J. G. Wagner and J. R. Harkema. *Great Lakes Air Center for Integrated Environmental Research, Michigan State University, East Lansing, MI.*

Introduction: Epidemiological studies suggest that diabetics may be more susceptible to the adverse health effects of air pollution. Mice chronically exposed to particulate air pollutants induce insulin resistance (IR), an early indicator of type II diabetes (T2D). In the present study we tested the hypothesis that episodic inhalation exposures to a common gaseous air pollutant, ozone (O3), will induce early onset of IR in mice genetically prone to develop T2D.
Methods: Male C57BL/6, KK, and KKAy mice were exposed to 0 ppm (filtered air; FA) or 0.5 ppm O3, 4h/day, for 13 weekdays. Two hours after the last exposure, mice were subjected to insulin tolerance tests (ITT) and then sacrificed 24 hours postexposure. Mice received a single intraperitoneal injection of insulin and blood glucose levels were measured at 0, 10, 20, 30, 60, 90, 120 and 130 minutes after injection. Bronchoalveolar lavage fluid (BALF) was analyzed for inflammatory cells, and lungs were processed for light microscopy.
Results: Normoglycemic, C57BL/6 mice exposed to FA or O3 had normal ITT. In these mice, O3 caused modest increases in the number of BALF inflammatory cells and minimal to mild pulmonary pathology. In contrast, O3 induced greater increases in BALF inflammatory cells in the hyperglycemic KK mice, along with more severe pulmonary pathology. Marked IR was present in O3-, but not FA-, exposed KK mice. Both FA- and O3-exposed, hyperglycemic KKAy mice developed IR. KKAy mice exposed to O3 had the greatest numbers of BALF inflammatory cells and the most severe pulmonary pathology of all the mice on study.
Conclusions: Episodic O3 exposures caused an early onset of IR in mice genetically prone to T2D. These hyperglycemic animals had greater O3-induced lung injury and inflammation compared to normoglycemic, insulin responsive mice. These results suggest that people at risk for T2D may be more susceptible to respiratory and metabolic health effects caused by elevated concentrations of ambient O3. Funded by USEPA RD83479701.

PL 2325 Ozone-Induced Impairment of Systemic Metabolic Processes: Influence of Prior Ozone Exposure and Metformin Pretreatment on Aged Wistar Kyoto (WKY) Rats

V. L. Bass[1], D. Andrews[2], J. Richards[2], M. Schladweiler[2], A. Ledbetter[2], D. B. Miller[1] and U. P. Kodavanti[2]. *[1]UNC, Chapel Hill, NC and [2]NHEERL, US EPA, Research Triangle Park, NC.*

Ozone (O_3) exposure is associated with adverse cardiopulmonary health effects in humans and thought to produce metabolic impairment, such as insulin resistance. Recently, we showed that acute O_3 exposure caused glucose intolerance and increased serum leptin and epinephrine in aged Brown Norway rats. We hypothesized that 1) subchronic pre-exposure to O_3 at a young age would predispose rats to exacerbated metabolic effects of subsequent O_3 exposure later in life and 2) metabolic effects of O_3 would be diminished in aged rats pretreated with metformin to improve glucose uptake in tissue. WKY rats were exposed to O_3 at 0 or 0.5 ppm 6h/dx2days/week x 13 weeks starting at 3 months of age. To study the effects of pre-exposure, the same rats were re-exposed to 0 or 1ppm ozone acutely for 6h at 14 months of age. To examine if treatment to improve glucose uptake would reduce the effects O_3, another group of 18 month old WKY rats were treated with the anti-diabetic drug metformin in drinking water (3g/L) for 2 weeks prior to a 6h/day x 2 day acute exposure to 0 or 1ppm ozone. Glucose tolerance tests, serum, and Broncheoaveolar lavage fluid (BALF) analyses were done immediately after exposure in both studies. Marked age-related impairment of glucose tolerance was observed. Additionally, O_3 exposure caused further impairment of glucose tolerance. O_3 exposure resulted in acute lung injury/inflammation and increases in serum levels of leptin, insulin, cholesterol and triglycerides in aged WKY rats. Pre-exposure to O_3 had no significant impact on any of these parameters. Treatment with metformin did not reduce O_3-induced lung injury or glucose intolerance, but decreased serum leptin and insulin in all rats. Our results suggest that pre-exposure to O_3 does not impact response to re-exposure at an older age. We believe that the metabolic effects of O_3 are not mediated by impaired cellular glucose regulation. (Does not reflect US EPA policy).

PL 2326 Serum Metabolomic Profiling and Liver Transcriptomic Analysis Provides Mechanistic Evidence of Ozone (O3)-Induced Systemic Metabolic Impairment

D. B. Miller[1], E. D. Karoly[2], W. Ward[3], D. Andrews[3], V. L. Bass[3], M. Schladweiler[3], A. Ledbetter[3] and U. P. Kodavanti[3]. *[1]University of North Carolina-Chapel Hill, Chapel Hill, NC, [2]METABOLON INC., Durham, NC and [3]NHEERL, U.S. EPA, RTP, NC.*

Recently, air pollution has been linked to insulin resistance and obesity but the mechanisms remain to be elucidated. We have recently shown that acute O3 exposure induces glucose intolerance, hyperglycemia and increases in leptin and epinephrine in rats. Here, we hypothesized that the metabolic effects of O3 are associated with global changes in liver fatty acid and amino acid metabolism and that global metabolomic and transcriptomic approaches will provide insight into the mechanisms by which O3 might contribute to increased insulin resistance and/or obesity. Male Wistar Kyoto (WKY) rats were exposed to air or 1 ppm O3, 6 hrs/day for 1 or 2 days and liver gene expression and serum metabolomic analysis were performed immediately after. Metabolomic analysis identified O3 effects on numerous small metabolite biomarkers. O3 increased blood glucose, long chain free fatty acids, cholesterol and decreased 1,5-anhydroglucitol (AG); biomarkers of insulin resistance. Metabolites of glycolysis were increased, however; intermediates of the TCA cycle and bile acids were decreased in the serum by O3. Branched chain amino acids were increased, suggesting muscle amino acid catabolism. Of particular interest, metabolites that are associated with gut microbiome (e.g. phenylacetylglycine) were also markedly affected by O3. Liver gene expression profile after O3 exposure correlated with the serum metabolite changes. For example, elevated serum fatty acids coincided with decreased expression of lipid biosynthetic genes, suggesting that the liver might have initiated homeostatic control for metabolic changes. In conclusion, our metabolomic and genomic analyses show that O3 induces acute systemic alterations reflective of changes in glucose, lipid, and amino acid metabolism which upon chronic exposure might contribute to insulin resistance and obesity. (Does not reflect EPA Policy).

PL 2327 Ccr2 Regulates Inflammatory Cell Accumulation in the Lung and Tissue Injury following Ozone Exposure

A. M. Groves, M. Francis, M. Mandal, H. Choi, J. D. Laskin and D. L. Laskin. *Rutgers University, Piscataway, NJ.*

Ccr2 is a chemokine receptor that mediates the migration of macrophages (MP) to sites of injury. In these studies we analyzed the role of Ccr2 in ozone-induced inflammatory cell trafficking to the lung. Treatment of C57Bl/6 mice with ozone (0.8 ppm, 3 h) resulted in increased bronchoalveolar lavage (BAL) protein after 24-48 h, indicative of alveolar epithelial injury. This was associated with a time-related increase in CD11b+ inflammatory cells in the lung. The majority of these cells expressed CD11c and F4/80 indicating that they are mature lung MP. Ly6C is expressed at high levels on proinflammatory MP. CD11b+F4/80+Ly6Chi proinflammatory MP increased in the lung after ozone, peaking at 24-48 h. CD11b+F4/80+Ly6Clo antiinflammatory MP also increased in the lung, peaking 48-72 h after ozone. Loss of Ccr2 resulted in a decrease in ozone-induced accumulation of CD11b+ cells in the lung. This was correlated with decreases in CD11b+F4/80+Ly6Chi and CD11b+F4/80+Ly6Clo MP subpopulations. Whereas decreases in proinflammatory Ly6Chi MP persisted for at least 72 h post ozone, decreases in antiinflammatory Ly6Clo MP were transient, and by 72 h were near control levels. CD1b+F4/80+Ly6g+Ly6c+ myeloid-derived suppressor cells (MDSC), which display antiinflammatory activity and are known to migrate to sites of injury, were increased in the lung 48 h after ozone. Loss of Ccr2 resulted in a persistent increase in MDSC. Changes in lung MP and MDSC were linked to reduced toxicity of ozone, measured by BAL protein levels. The effects of loss of Ccr2 on splenic monocytes, which function as an extramedullary source of inflammatory cells were also analyzed. Ozone caused a decrease in Cd11b+F4/80-Ly6Chi proinflammatory monocytes in the spleen; this response was attenuated in Ccr2-/- mice 24-72 h after ozone. These results demonstrate a key role of Ccr2 in ozone-induced inflammatory cell emigration into the lung and toxicity. Moreover, it appears that the effects of Ccr2 are predominantly on proinflammatory MP. NIH ES004738, CA132624, AR055073, ES007148, ES005022.

PL 2328 Development of Eosinophilic Rhinitis and Nasal Tissue Remodelling in Mice Episodically Exposed to Ozone

C. Ong, K. Allen, C. Brandenberger, D. Jackson-Humbles, L. Bramble, R. Lewandowski, J. G. Wagner and J. R. Harkema. *Great Lakes Air Center for Integrated Environmental Research, Michigan State University, East Lansing, MI.*

Introduction: Ozone (O3) is an oxidant air pollutant in photochemical smog. While nasal epithelial injury and remodelling have been reported in laboratory animals repeatedly exposed to O3, associated granulocytic rhinitis and pro-inflammatory cytokine expression have not been fully characterized. We investigated the temporal changes in granulocyte influx, cytokine gene expression, and epithelial remodelling in the nasal mucosa of mice episodically exposed to O3.
Methods: Male mice were exposed to 0 or 0.5 ppm O3 for 1, 2, 4, 9, or 24 weekdays (4h/day). Airway mucosa from nasal turbinates and lateral wall were analyzed for cytokine and epithelial gene expression. Nasal tissues were prepared for light microscopy and morphometry. Immunohistochemistry was used to identify neutrophils, eosinophils, and chitinase-like proteins (Ym1/Ym2). Epithelial mucosubstances were histochemically detected.
Results: 1-day-O3 exposure induced a neutrophilic influx with few eosinophils and concurrent epithelial necrosis. These responses were associated with overexpression of KC, MIP-2, IL-1β, IFNγ, IL-5, IL-6 and eotaxin genes. After repeated O3 exposures, neutrophils waned and eosinophils increased, along with epithelial regeneration and remodelling. 9-day-O3 mice had marked eosinophilic rhinitis with few neutrophils, mucous cell metaplasia and increased epithelial Ym1/Ym2 proteins. Concurrently there was overexpression of Gob5, Muc5AC, IL4, IL5, eotaxin and Ym2 genes. 24-day-O3 mice developed marked eosinophilic rhinitis, epithelial hyperplasia, mucous cell metaplasia, hyalinosis, and increased Ym1/Ym2 expression.
Conclusion: Repeated, episodic O3 exposures in mice induce Th2 cytokine overexpression, eosinophilic rhinitis, epithelial remodelling, and increased epithelial chitinase-like proteins. These results suggest an etiologic role of ambient ozone in the development of nonallergic eosinophilic rhinitis. Funded by USEPA RD83479701.

PL 2329 Acute Fine Ambient Particulate and Ozone Coexposures in Durham, North Carolina: Influence of Season on Particle Chemistry and Cardiovascular Responses in Rats

A. K. Farraj, L. Walsh, N. Coates, F. Malik, D. Winsett, K. Kovalcik, J. McGee, M. A. Higuchi and M. S. Hazari. *US Environmental Protection Agency, Research Triangle Park, NC.*

Evidence from epidemiological and controlled human exposure studies points to synergistic effects of co-exposure to ambient particulate matter (PM) and gases including ozone (O3). Although evidence for synergism is growing, seasonal variability in PM composition adds considerable complexity to the elucidation of mechanistic underpinnings that drive these responses. The purpose of this study was to assess the impacts of season on PM chemistry and cardiovascular responses resulting from exposure to an air pollution mixture. We conducted summer (August, 2011) and winter (February, 2012) co-exposures to concentrated ambient particulates (CAPs) and O3 in Durham, NC. Rats monitored for heart rate and electrocardiogram (ECG) were exposed once for 4 hrs by whole-body inhalation to fine CAPs (target concentration: 150 ug/m3) using a Harvard Fine Particle Concentrator with/without 0.2 parts per million O3 or filtered air. Sensitivity to arrhythmia was measured in a separate cohort as the threshold dose of aconitine required to elicit cardiac arrhythmia. PM elemental composition and carbon fractions were analyzed by high resolution inductively coupled plasma–mass spectrometry and thermo-optical pyrolytic vaporization, respectively. CAPs concentration and median particle size during the summer were 172 ug/m3 and 325 nm, respectively. Because of lower ambient PM during the winter exposure, the CAPs concentration was below target, averaging 85 ug/m3 with a particle size of 155 nm. Rats exposed to summer CAPs or O3 alone developed ventricular premature beats and tachycardia at significantly lower doses of aconitine than air controls. CAPs and ozone co-exposures did not augment this response. There was no effect of exposure on arrhythmia sensitivity during the winter. PM chemistry and rat ECG and heart rate variability are currently being analyzed (This abstract does not reflect EPA policy).

PL 2330 Does Obesity Increase Susceptibility to Ozone? Respiratory, Behavioral, and Metabolic Assessments in Brown Norway Rats

C. J. Gordon[1], A. F. Johnstone[1], P. Phillips[1], U. P. Kodavanti[2] and K. A. Jarema[1]. [1]*Toxicity Assessment Division, US EPA, Research Triangle Park, NC and* [2]*Environmental Public Health Division, US EPA, Research Triangle Park, NC.*

There may be a link between obesity and susceptibility to the respiratory, cardiovascular, and other health effects of air pollutants. Furthermore, it has been proposed that some air pollutants are obesogenic and may contribute to obesity. In view of the epidemic growth of obesity and type II diabetes, it is imperative to develop animal models to study the links between obesity, metabolic syndrome, and exposure to air pollutants. Male, 3 month-old rats were fed control, high fat (60% of calories), or high fructose (60% of calories) diets. Percent body fat was monitored every 2 wk using a Bruker L90 minispec. Rats were then exposed to filtered air (FA) or 0.8 ppm ozone (O3) for 6 hr, 1 d/wk for 4 wk. Food consumption was assessed following O3 exposure. After 4 months, both diets led to increases in %body fat (3% for high fat; 1.5% for high fructose) and impaired glucose tolerance. Body weight was similar for the high fat and control rats, but lower for high fructose rats. O3 led to impaired respiratory responses measured in Buxco chambers. Enhanced Pause (penH) assessed 1 d post-exposure rose significantly but diet had no effect. Body fat was reduced by 2% after 3 weeks of O3 in all diet groups. Exposure to FA also led to significant reductions in body fat and net fat loss was greatest in the control group. Motor activity measured 1 d after O3 was significantly reduced in the control diet group but not high fat or high fructose groups. Food intake of high fat group increased significantly following O3. Housing rats for 6 hr in the Hinner exposure chambers appears to have led to a stress-induced decrease in body fat, a response accentuated by O3. Increasing %body fat by treatment with high fat/high fructose diets failed to alter respiratory susceptibility to O3. The increase in food consumption of high fat animals may indicate an obesogen-like effect of O3. This is an abstract of a proposed presentation and does not reflect US EPA policy.

Notes

Notes

Author Index

The numerals following the author's names refer to the abstract numbers. The asterisk after the abstract number indicates the author is the first presenter.

A

Aardema, M 1943i, 1943j, 2116
Abadin, H G 223f, 410
Abam, E O 1249, 1264, 1266, 1273*, 1776
Abassi, Y A 1617, 1619
Abatan, O M 793
Abbas, I K 963
Abbott, B D 2213b
Abbott, D 348
Abdel-Naim, A B 1110a
Abdel-Rahman, S 978d, 1110a, 1943d
Abdel-Rasoul, G 689
Abdelaziz, A 1180
Abdo, N 165*
Abdou, K A 2234*
Abe, F R 789*
Abe, T 432
Abelmann, A 1574, 1575, 2234t
Abergel, R J 894, 1624
Abernathy, M M 2196t*
Abi Gerges, N 1619
Abiko, Y 1714*
Abler, L L 905, 1087s
Abney, D M 2151d*
Abolaji, A O 173n*
Abongwa, M 1145*
Abou-Donia, M B 1855
Aboud, A A 1353, 1354
Aboyewa, O A 788
Abplanalp, W T 1121*
Abraham, L 231, 628
Abramson, M 2240
Abritis, A J 1668*
Abujarour, R 1915*
Abukharmah, J 383
Acali, S 1055
Acedo, K 2236
Acevedo, F 1229*
Achanta, S 2169*
Achanzar, W E 109
Ackerman, C 1252, 2048
Ackerman, J M 2259, 2260*
Acosta Amado, R 408a, 1019
Acuff, A 2188*
Adachi, R 988
Adair, K R 312f
Adamcakova-Dodd, A 515, 896, 1975*
Adams, K 1911
Adams, L 96e*
Adams, L L 239
Adams, M 1616b
Adams, R 146, 614*, 1574, 1997
Adams, S P 1903
Adamson, G 2165*
Adebayo, J O 499, 2051*
Adebayo, S A 785*
Adebiyi, O E 793*
Adedapo, A A 809*
Adedara, I A 1713g*
Adeduntan, S D 1073
Adegboyega, A M 813b*
Adegoke, A M 1514b
Adekunle, M A 2051
Adeleye, O S 2216
Adeleye, Y 162, 1788, 1934
Ademuyiwa, O 321, 1249, 1264, 1266*, 1273, 1774, 1776, 2271
Adeogun, A A 650
Adeogun, A O 462, 1073*, 1074
Adeoye, B O 809
Ader, A G 649a
Adeshina, F 624, 625, 626
Adeyemi, O O 663
Adeyemo, O K 669c*
Adeyemo, R A 2051
Adhikari, B 1171
Adkins, A L 581a
Adkins, K 125, 543, 1480
Adler, M 2055*
Adler, S 380, 1544
Adriaanse, P I 2238
Adunyah, S E 1109, 1509
Afaq, F 552e
Afolabi, O K 1249, 1264, 1266, 1273, 1776
Afolayan, G O 804*
Afriyie-Gyawu, E 2117
Afrooz, N 594, 1467
Afshari, A 1229a, 1368a
Afshari, C 98, 1641, 2065
Aga, D S 2204
Agarwal, A 2319
Agarwal, C 553, 554, 555
Agarwal, N 654
Agarwal, R 554*, 555
Agarwal, V 1639a
Agbaje, E O 804
Aggarwal, M 64, 1863
Aggerbeck, M 1011, 1158
Agim, Z S 378h, 923*
Agrawal, S 1693
Aguilar Alonso, P 1244
Aguilera-Aguirre, L 921, 1928*
Agusa, T 516, 519, 1259*
Agustin-Serrano, R 1973
Ahir, B 418a
Ahir, B K 1087p*, 2234i
Ahlberg, E 1126
Ahmad, B 813c
Ahmad, T 541*
Ahmed, M T 2117
Ahmed, S 1036, 2318*
Ahn, J 1565
Ahn, K 593, 1565, 1976
Ahn, S 1553
Aho, K 1760
Ahuja, V 2040*
Ai, D 674
Ai, Y 942a
Aiba, T 978b*
Aillon, K 877, 1616a
Ainscough, J 992
Aiub, C 1638
Ajani, O S 1694
Ajao, Z A 2051
Ajay, A K 2055
Ajibade, T O 803*
Akahori, Y 1087c
Akerstrom, M 74
Akey, H 2043
Akhtar, M 1852*
Akiba, E 591
Akinbobola, O P 1514b
Akinc, A 1653
Akindahunsi, A A 1198
Akingbemi, B T 1713g
Akinhanmi, T F 1776
Akinloye, D I 808*
Akinosun, O M 2216*
Akinrinde, A S 481, 1267, 1270, 2041*
Akinwumi, K A 788*, 1502
Akram, M 1123, 1389
Al Juboori, A 336
Al-Eryani, L 676, 1159*, 1870
Al-Khedhairy, A A 1952
Al-Refai, A M 175
Al-Shabanah, O A 504
Alabdouli, K 336
Aladdin, M M 394*
Alam, G 2129a*
Alaniz, R 1130
Albakheet, S A 2217
Albassam, M 104
Albee, R P 1197, 1882
Albers, P 332
Albertini, R J 467b
Albores, A 595, 1723
Albrecht, A 2131
Albrecht, P P 260
Albrekt, A 1062g
Albuquerque, E X 1860, 1861
Aldelemy, M L 504
Alderman, S 1615
Aldossari, A 826*
Aldous, K 265
Alegria-Torres, J 144
Alejandra, H 2234x
Aleksunes, L M 48*, 191, 562, 1162, 1497, 1664*, 1669, 1802, 2053
Aleman, J 574
Alépée, N 402, 1027, 1029, 2177, 2178, 2179
Alexander, A 1804
Alexander, A N 469, 953, 2137
Alexander, B 2211*
Alexander, C 1103
Alexander, D D 227, 777, 1490
Alexander, D J 2143
Alexander-Scott, M 1607
Algaier, J 877, 1616a
Alharthy, K M 208*
Ali, L 1180
Ali, M 1688*
Ali, S F 173m*, 353, 378i, 603b, 942e, 1973f
Ali, Z 978e
Aliberti, A 1904*
Aligo, J 2120
Allais, L 185*
Allard, P 151, 172, 1704, 1713j
Allen, A E 1625
Allen, J L 1333, 1340, 1342*, 1347
Allen, K 1008, 2324*, 2328
Allen, P 324
Allingham, P 2131
Allison, P 497
Almazrou, D 1200f*
Alnamnakani, M 1740*
Aloor, H 2168
Alov, P 2254
Alp, O 2234d
Alsahwi, N 122f
Alsop, D H 534, 1013*
Altaner, S 1566
Altemeier, W A 1962, 2004f
Altmann, H M 1087s
Aluru, N 965
Alvarado, A 603i
Alvarado, L 2038
Alves, A A 1771
Alves, J 675
Alves, V 2182c
Alwis, U 1549c*
Alyea, R 160*
Alzualde, A 148*
Amacher, D E 619
Amaoh, P 1509
Amaraneni, M 897*
Amberg, A 220*
Ambolet-Camoit, A 1011
Ambrosio, M 27, 632
Ameredes, B T 921, 1235, 1928
Ameri, M 1200b, 1549e
Amery, D 1616f
Amin, A 1686
Amin, S 1138, 1139, 1623
Amlund, H 782
Ammar, D A 555
Amoo, L B 862
Amos-Kroohs, R M 1087m*
Amoscato, A 1002, 1777*
An, D 894, 2004f
An, Y 418e
Anadon, A 1843*, 1862, 2218
Anan, Y 1304
Anand, S 685, 689b, 897
Anandhan, A 926
Anantharam, P V 362*
Anantharam, V 362, 927, 936, 937, 1285, 1350, 1351, 1352, 1832
Anastas, P 1831f
Anders, L 1879*
Andersen, M E 69, 76, 89, 94, 160, 162, 438, 439*, 695*, 1140, 1788, 1794, 1873, 1934, 2250, 2250a
Anderson, A A 954b
Anderson, D 570, 577, 2163c
Anderson, D S 828*
Anderson, D W 954h, 1747e
Anderson, G J 2128
Anderson, J 1518
Anderson, K 1280, 1579*, 1678, 2215
Anderson, K L 141, 142, 841c, 2025
Anderson, M E 388, 1042
Anderson, O S 964
Anderson, S 841c, 887, 2025*, 2029*
Anderson, S E 141, 142, 1229a
Anderson, T 669d
Andersson, M 941
Andersson, T B 1881
Ando, A 2151
Andón, F T 586
Andrade, C 2182c
Andraos, C 1297c, 1831j*
Andres, D K 570*
Andrews, D 1205, 2325, 2326
Andrews, L 267, 2111*
Andrews-Cleavenger, D 98
Andrus, A K 1863
Aneskievich, B J 1724
Anestis, D 2064
Anetor, G O 862
Anetor, J I 862*
Ang, C 669d
Angalakurthi, S 574
Angelini, D J 173a
Anger, W K 81, 689
Angermann, J E 1298, 1299
Angermeier, E 539a
Ankisetty, S 652
Ankley, G T 440d, 440e, 1402*, 2285*
Annangi, B 1954
Ansari, G A 384
Ansari, R A 1725, 1728*
Anson, B D 32*, 1616g, 1910
Antczak, P 173p, 418d
Antoine, D 105
Antoine, L 1676
Antonini, J M 20, 1229a*, 1242a, 1368a
Antonsen, B L 655
Anttila, M 343e
Aoki, Y 1326
Aoyama, T 1967
Apana, S 1764d
Api, A 420, 1601, 1605, 2166
Apic, G 2182b, 2251, 2255*
Appell, A 570
Apte, U 1173, 1495, 1498, 2206
Aquilonius, S 2105
Aquino, K 424*
Aragon, M 1983*, 2301
Arai, Y 822
Araki, T 954
Aranda-Rodriguez, R 1012
Aranibar, N 853
Araujo, J 19*, 2303*
Arbildua, J 1280
Arbuckle, T E 96h
Arcaroli, J 1095
Arce-Nazario, J 666
Archer, F E 383
Ares, I 1843, 1862
Arif, A 813c
Arima, A 2167
Armento, A 173k, 1040
Armitage, J 1642
Armstrong, L 1720*, 2207
Armstrong, R 2139
Arndt, T 2196j
Arnold, J 857
Arnold, L L 255
Arnold, T 1908
Arnot, C 2090*
Arnould, I 1831m*
Aro, A O 1629*
Aronstam, R S 603c
Arora, M 2286, 2290*
Arowojolu, A 862
Arrington, J E 406*, 408
Arteel, G E 1323, 2221, 2316
Arthur, J 108, 111
Arturo, G T 848a
Artursson, P 79, 901, 1883*
Aruga, C 1621*
Arvidson, K 27, 30*, 1609, 2273d
Arzuaga, X 1807*
Asaoka, Y 450
Asare, B 1072
Ascah, A 471
Aschner, M 38*, 566, 1329, 1353, 1354, 1355, 1356, 1357, 1374, 1379, 1380, 1456*, 1856, 2108*
Aseffa, B 514
Asgharian, B 66, 67, 774*
Ashby, C R 2026
Ashikaga, T 1029

Author Index (Continued)

The numerals following the author's names refer to the abstract numbers. The asterisk after the abstract number indicates the author is the first presenter.

Ashikin, N ... 1825
Ashkenazi, A ... 269
Ashley-Koch, A E ... 343b
Ashoor, R ... 97
Ashwini, S ... 834
Ashwood, P ... 698
Asomugha, A L ... 1200c
Asomugha, R N ... 1200c*
Assaf, N ... 60
Assunção, N A ... 1771
Ataku, H ... 988
Atanasova, N ... 1087m
Atari, M ... 1898
Atchison, W D ... 1256, 1368b, 1370, 1371, 1372, 1375, 1376, 1377, 1381, 1384, 1385, 1386
Athar, M ... 552e
Atnikov, K ... 581
Atosuo, J ... 343e
Atsumi, I ... 1640*
Attafi, I M ... 2217*
Atterson, P ... 503, 1648*
Au, C ... 2108
Au, P ... 1422, 1423*
Aubrecht, J ... 13, 1478, 1938, 2274*, 2275*
Audu, F O ... 2051
Auerbach, S S ... 122, 958, 1736a*
Augustine, A ... 343d*
Augustine, K ... 222
Augustine, M S ... 1688
Aulbach, A ... 1547
Ault, V ... 1616a
Aumsuwan, P ... 978e*
Austin, C D ... 2196p
Austin, C P ... 173b
Austin, J ... 2196r
Authier, S ... 274, 275, 344, 471
Autio, D ... 1381
Autrup, H N ... 1956
Avalos, B ... 2018*
Avalos, J ... 1020
Avens, H ... 1575
Avlasevich, S ... 452
Awasthi, A ... 1957
Awasthi, K K ... 1957
Awodele, O ... 804
Ay, M ... 936*, 937
Aya, T ... 2119*
Ayehunie, S ... 173k, 1035, 1040*, 1053
Ayers, S D ... 1135
Aykin-Burns, N ... 1781
Aylward, L ... 1065, 1568*
Ayoola, S O ... 651*
Ayotte, P ... 1255
Azab, S S ... 1110a
Azevedo, R ... 552a
Azimian, S ... 308
Azoury, M ... 123*, 987, 2009

B

Ba, X ... 1928
Baba, N ... 1259
Babayemi, D O ... 1249, 1264, 1776
Babica, P ... 1103
Babick, F ... 332
Babin, D ... 2162
Babin, M C ... 558, 564, 567
Babu, S ... 841e*
Bach, J ... 1305, 1954
Bachelor, M A ... 1038, 2181*
Bachinski, R ... 1737, 1738, 1912
Bachman, A N ... 1824
Bachour El Azziz, P ... 1192, 1193
Bacsi, A ... 1928
Bacus, S ... 1112
Badawy, A ... 1973b
Badding, M A ... 1208*, 1966
Badea, A ... 1433*
Badger, T M ... 254
Badisa, V ... 1264c
Bae, H ... 1327e
Bae, O ... 1122, 1123, 1389
Bae, S ... 1229b
Baek, J ... 1976, 2001
Baer, C E ... 1297
Baer, D R ... 814, 1963
Baeza Terrazas, F ... 1312, 1314, 1324
Bagchi, D ... 339
Bagchi, M ... 339*
Baghdasarian, A ... 542
Bagley, B D ... 2209*
Baglole, C J ... 906, 1722*
Bahinski, A ... 1441*
Bahl, V ... 1056*
Bai, Y ... 493
Baier-Anderson, C ... 1616b*
Bailey, D ... 901c
Bailey, D C ... 1848, 1849*, 1850
Bailey, J ... 1602
Bailey, J M ... 1347h, 1857*
Bailey, K ... 229, 1308*, 1318, 1324
Bailey, L A ... 611*
Bailey, W H ... 1806*
Bain, L J ... 176
Bainter, J ... 1550
Bainy, A ... 1147
Baird, C ... 624, 626
Baird, T ... 2196t
Baird, W M ... 539d, 876a
Bajt, M ... 1196
Bak, S ... 653
Bakan, A ... 1880
Baker, A F ... 1544*
Baker, E ... 1525
Baker, G L ... 5*, 2004a
Baker, N C ... 96e, 418a, 1087p, 2273f*
Baker, S ... 1039
Baker, T ... 1031, 1681*
Baker, T K ... 434, 2084*
Balaguer, P ... 149
Balakrishna, S ... 2169
Balakrishnan, S ... 399, 1800, 1801
Balandaram, G ... 246*, 1155
Balavenkatraman, K ... 873, 1618*
Balbuena, P ... 160, 240*
Baldrick, P ... 288
Baldwin, W S ... 522*
Bale, A S ... 349*, 1829, 1831h
Ball, D J ... 1660
Ball, G L ... 607
Ball, J ... 1831c
Ball, J G ... 1186, 2062
Ball, N N ... 885
Ballering, L ... 2196v
Ballinas-Casarrubias, L ... 1312, 1314, 1324
Balogun, E A ... 499*, 808, 1249, 1264, 1266, 1273, 1774, 2051, 2271
Balyan, R ... 893*
Banda, M ... 265a*
Bandara, S ... 1747c*
Banerjee, A ... 1546, 1803*
Banerjee, B D ... 551*
Banerjee, N ... 1110b*
Banks, L D ... 1509*
Banks, P ... 307
Bannish, G ... 404, 1713s*
Bante, H ... 727*
Bantseev, V ... 273
Bao, Y ... 1711
Barban, V ... 1655
Barbellion, S ... 220
Barber, C ... 2262*, 2264
Barbero, A M ... 2182a
Barchowsky, A ... 1302
Bard, J ... 526
Bardullas, U ... 1847
Barger, M ... 2004b
Bari, S ... 1675
Barile, F A ... 368, 960, 1904
Barker, C ... 2156
Barker, D ... 869, 970
Barker, M ... 338
Barks, A K ... 964
Barletta, M ... 498
Barlow, S ... 1609
Barnaby, R ... 2317
Barnes, E ... 183, 184*
Barnes, F ... 2234aa
Barnett, G W ... 922a
Barnett, R ... 2221
Barnett, R E ... 1849
Barnett Bucherl, S ... 613
Barnhart, C ... 351*, 2205
Barnhill, L ... 942b
Baron, R ... 581k
Barouki, R ... 870, 1011, 1158
Barr, D B ... 868
Barrass, N C ... 272
Barregard, L ... 74
Barres, J ... 815
Barrett, G ... 632
Barrett, J T ... 2194
Barril, J ... 1856
Barros, S ... 1653*
Barros, S B ... 1662b*
Barroso, J ... 1027*, 1029
Barrow, W ... 883
Bartels, M J ... 61, 64, 82*, 688, 885, 1099, 1941, 2173
Bartizal, K ... 1634
Bartlett, M ... 683
Barton, H A ... 6, 80*
Barve, P ... 869
Barve, S ... 869, 970, 1182, 1874
Basavarajappa, M ... 1713e, 1713f*
Basketter, D ... 2234aa*
Basnakian, A G ... 312b*
Bass, A S ... 2081*
Bass, V L ... 1232, 2325*, 2326
Bassett, L ... 152
Bassyouni, A ... 2083
Bast, A ... 335, 2171
Bast, C ... 625*, 2250g
Bastiaensen, N ... 1063
Bastos, M M ... 1638
Basu, N ... 41*
Basu, P ... 334*
Batchelder, E ... 182, 377
Batchelor, T P ... 392
Bates, A ... 1018b
Bates, C A ... 1349*
Bates, M ... 140*, 318
Batke, M ... 631
Batra, S ... 1514
Bats, A ... 1158
Battelli, L A ... 23
Batterman, S ... 1581
Bauch, C ... 1875
Baudet, S ... 2196
Bauer, A K ... 1103
Bauer, D ... 761*
Bauer, R A ... 390
Bauer, R N ... 874
Baugher, A ... 2043
Baumgart, B ... 850
Baun, A ... 836
Bauter, M R ... 327*
Bayir, H ... 1777
Baynes, R E ... 2175
Beach, A ... 306
Beach, T ... 552f
Beall, H D ... 298
Beamer, C A ... 2040c
Beasley, T E ... 1347a, 1347b, 1347c*, 1347d
Beattie, C ... 1658
Beattie, P J ... 2272*
Beaubrun, I ... 1359
Beauchane, M ... 1616d
Beauchane, M P ... 948, 949, 951
Beaudin, S A ... 1330, 2286, 2292*
Beavis, A J ... 404*, 1713s
Becak, D P ... 484
Bechara, E J ... 1771*
Becher, R ... 134
Beck, B D ... 251, 611, 1341, 1554, 1555
Beck, N B ... 9*, 1406*, 1482*, 1483*
Beck, T ... 197, 1698, 2126
Beck, W ... 2196o
Becker, R A ... 637, 1065, 2253*
Beckwith, S ... 1616a
Bedja, D ... 1706
Bednar, A ... 1987
Beeks, C ... 1300
Beeson, C ... 108, 1611
Beeson, G C ... 1611
Beeton, C ... 901c
Beevers, C ... 454, 456*
Beezhold, D ... 142, 2036
Beezhold, K ... 1302*
Begemann, P ... 2234v*
Beger, R D ... 99
Beggs, K M ... 1886*
Begley, T J ... 526
Behar, R Z ... 645, 1613*
Behl, M ... 378c, 1616g, 2273bb
Behle-Wagner, C ... 1032
Behr, J ... 365
Behringer, S ... 581h
Behrsing, H ... 173l*
Behrsing, T ... 616*
Beier, J ... 1879
Beilstein, P ... 333
Beker, A ... 154
Beland, F A ... 257, 265b, 632g, 956, 957, 1087b, 1513
Belcher, L A ... 328
Belgrave, K ... 173g, 1973h, 1973i*, 1973j
Beliveau, M ... 581
Bell, G ... 2174
Bellmann, B ... 1990, 2003
Bello, S M ... 2092*, 2093*
Bellwon, P ... 164*
Belmonte, J ... 85
Beltran, M ... 1090
Bemis, J ... 452, 1235*, 1929
Benahmed, M ... 1078
Bench, G ... 1110e
Bendjama, K ... 112*
Benedetto, A ... 2108
Benelli, C ... 1011
Benignus, V ... 632c
Benner, S ... 2163
Benner, S L ... 1747b*
Bennett, J C ... 1460
Bennett, M ... 1648
Bennett, M B ... 1015
Bentley, E ... 273
Bentley, P I ... 1627
Benton, B J ... 570
Benz, R ... 2256, 2257, 2273c*
Berezowski, K ... 1024*
Berg, E ... 1647, 2250, 2273v, 2273w*
Berg, M ... 504c*, 1229g
Berg, N W ... 2236*
Berger, R G ... 1713
Bergström, C A ... 1883
Bergström, U ... 941
Berhane, K ... 1242i
Berkbigler, J ... 1000*
Berlin, K ... 883
Bernal, A ... 233
Bernal-Barragan, H ... 315
Bernard, L ... 149
Bernardes, M ... 552a
Bernardes, M F ... 312, 458, 677*
Bernardi, C I ... 1914
Bernardini, G ... 835
Berner, T ... 1831c
Bernhard, M C ... 235*, 1676
Bernier, L ... 345, 861
Bernstein, A I ... 371
Bernstein, D M ... 1215*
Berridge, B R ... 1429, 1430*
Berridge, M ... 1764d
Bers, D M ... 1116
Bertelsen, L O ... 1018d
Berthet, A ... 2176*
Bertinetti-Lapatki, C ... 104*
Bertrand, J ... 1616f
Bertrand, P ... 1551*
Bertschi, B ... 1618
Beske, P H ... 1922c, 1922d
Bess, A S ... 1939
Bessac, B F ... 2169
Bessems, J ... 96c
Best, D S ... 1018a
Best, M C ... 1606
Bestman, J ... 223a
Beswick, E ... 143
Betz, M ... 2004
Beyer, B ... 220
Beyer, L A ... 1555*
Beygui, R ... 1116

The numerals following the author's names refer to the abstract numbers. The asterisk after the abstract number indicates the author is the first presenter.

Bezine, E ... 1931
Bhagunde, P ... 1644
Bhalli, J A ... 453*, 2004c
Bhaskaran, V ... 1177
Bhat, S A ... 813c
Bhat, V S ... 606, 608, 1476, 1663*
Bhatia, S ... 420*
Bhatnagar, A ... 15*, 1121, 1239
Bhatt, N ... 1955*
Bhattacharya, K ... 586*
Bhattacharya, S ... 94*, 438, 439, 1140
Bhattacharyya, M ... 1264a*
Bhattacharyya, S ... 99
Bhavaraju, L ... 1234*
Bhopale, K K ... 384
Bhusari, S ... 955*
Bhushan, B ... 1173*, 1498
Bhuyan, P ... 359*
Bhyrapuneni, G ... 2163a
Bialecki, R A ... 346
Bichell, T V ... 1353
Bichteler, A ... 628, 781
Bidabadi, F ... 2234j*
Bienstock, R ... 31
Bigras, M ... 2037
Bihaqi, S W ... 939
Bilgesu, S ... 603d
Billack, B ... 572, 576, 580, 1674*, 1679
Biller, M ... 699
Billington, R ... 64, 1602, 1943e
Bills, A J ... 475
Bin, L ... 2212
Bing, N ... 1128
Bingman, T S ... 467d
Bini, E ... 1391
Binkowski, B ... 167
Birch, E M ... 603e, 603f, 1242g
Birchfield, N ... 1831c*
Bircsak, K M ... 191*, 562
Birkenfield, A ... 1508
Birnbaum, L S ... 901b, 922d, 1522, 2116
Bisen-Hersh, E B ... 1380
Bisesi, J ... 594
Bishop, J ... 938
Bishop, M E ... 467a
Bisson, W ... 1139
Biswas, R ... 588
Bittner, G D ... 161
Blaauboer, B J ... 1041, 1048*, 1075
Black, K ... 846
Black, L E ... 1422, 1424*
Black, M B ... 2250a*
Black, T ... 1297a
Blackbourne, J L ... 1650
Blackman, B ... 1061, 1129a
Blain, R ... 1829*
Blair, E C ... 2118
Blais, K ... 382, 1315
Blais, M ... 1627
Blake, C ... 2234z
Blake, D J ... 1216*
Blake, J A ... 2093
Blake, J C ... 1606*
Blakemore, W ... 341, 342, 343*, 343f, 845
Blanc, E ... 1011
Blanchard, K T ... 2196f
Blanchet, D ... 170
Bland, S D ... 673
Blasberg, J ... 2067
Blaszkewicz, M ... 545
Bledsoe, T A ... 2036
Blessinger, T ... 96i, 1831h
Blickenstaff, N ... 876c*
Block, M L ... 928, 1455*, 1859
Blom, M ... 1823
Blomeke, B M ... 982
Blomet, J ... 985
Bloom, L ... 1128
Bloom, M S ... 1524
Blossom, S J ... 137, 966, 1343*
Blount, B C ... 1549c
Bloxham, P ... 467d
Bluemel, J ... 2305
Blum, J ... 2040a
Blum, J L ... 75, 1692, 2193*
Blumberg, B ... 739*
Blythe, L L ... 336
Bober, M ... 1890
Boberg, J ... 1018d
Bobst, S M ... 719, 721*
Bodar, C ... 658
Bodhicharla, R K ... 1939
Bodin, J ... 134*
Bodnar, W ... 978, 1107, 1110g, 1152, 1523
Boechat, N ... 1638
Boehm, M ... 1922a
Boekelheide, K ... 168, 1686, 1709, 1710
Bogdanffy, M ... 2196f*
Bogen, K T ... 243*, 604, 605, 2234r
Boggs, N ... 1731
Bohlen, H ... 1918, 1919
Boisvert, A ... 1712
Boitano, S ... 1734
Bojang, P ... 1500*
Bol-Schoenmakers, M ... 1041, 2028
Boldogh, I ... 921, 1928
Boley, S E ... 901c
Bolger, M ... 440j
Bollman, M A ... 1006a
Bolt, A M ... 1283*
Bolton, D ... 271
Bolton, J L ... 790, 796
Bolts, S ... 500
Bombick, B ... 95
Bommegowda, S ... 689a
Bondesson, M ... 149, 150, 1327a
Bonini, M ... 1803
Bonk, T ... 1018e
Bonnel, D ... 901e*
Bonner, J C ... 582, 583, 584, 603g, 1466*
Bonner, M R ... 689, 1524
Bono, C ... 397
Bonvallot, N ... 1009
Bonventre, J A ... 838, 1984*
Bonzo, J ... 2273q
Boobis, A R ... 1399*, 1609, 1824*
Booc, F T ... 208
Bookstaff, R ... 2234aa
Boon, L ... 2028
Bordelon, N ... 2196j
Borders, J ... 312f
Borgert, C J ... 1407*, 1487*
Borges, C S ... 1696
Borghoff, S ... 622, 623, 2059*
Boring, D L ... 2196y
Borland, M G ... 260*, 1679
Bornhorst, J ... 1356
Borrebaeck, C A ... 1062g
Borrelli, K M ... 268
Borsay Horowitz, D ... 1087h
Bortey-Sam, N ... 843, 1516
Bortner, C D ... 1087r
Bortoli, S ... 1011
Borude, P ... 1173, 1498
Bose, R ... 40
Bosgra, S ... 430, 2273o
Boskovic, G ... 909
Boss, G R ... 581d
Bostrom, M A ... 958
Bot, C ... 1118*
Botelho, D ... 1979*
Botta, D ... 1981
Bottum, K ... 1153, 2197
Bouchard, G ... 886, 1713a, 2118, 2151c
Bouchard, J ... 888
Bouchard, M ... 83, 839, 1531, 1558, 1572, 1998
Boudreau, M D ... 841b
Bouhifd, M ... 1737
Boulay, I ... 2037
Boule, L ... 2017*
Bourdon, J ... 1478
Bourgea, J ... 1899e, 2067a
Bourgeois, J ... 1087n*
Bourgeois, M M ... 122i*, 299, 1435, 1437*, 1665, 1668
Bourne, C ... 883
Bourner, M ... 2067
Bousquet, R W ... 1229d
Boutet-Roubinet, E ... 1931
Bovee, T ... 1067
Boverhof, D R ... 398, 399, 408a, 1019, 1602
Bowen, E ... 1039*
Bower, D ... 459
Bowers, E C ... 396*
Bowler, R M ... 1366
Bowman, A B ... 1353, 1354, 1355, 1356, 1357
Bowman, C J ... 278*, 1660*
Bowyer, J F ... 934
Boyce, R ... 698
Boyd, J W ... 1729, 1731, 1735*
Boyd, K N ... 1021*
Boyd, R ... 841a*
Boyd, W A ... 173d, 173o*
Boyer, C S ... 1126
Boyer, J A ... 1136
Boyes, W K 96b, 632c, 1062f, 1347b*, 1973d
Boykin, E H ... 145a, 980, 1204, 1205
Boyle, S ... 312f
Boyles, A L ... 1486, 1829
Boysen, K ... 669d
Bozhilov, K ... 2225
Bølling, A K ... 134
Brabham, T ... 1128*, 2080, 2083
Brackman, A ... 1663
Bradfield, C A ... 1087u
Bradford, A B ... 1381
Bradley, J ... 378*
Bradshaw, T ... 887, 2029
Brady, J ... 1985
Braisted, J ... 1922a
Braithwaite, E ... 1264b*
Brambila, E ... 1244*
Brambilla, E ... 1914
Bramble, L ... 140, 2328
Branam, A ... 905
Brandenberger, C ... 140, 2328
Brands, R ... 1048
Brandt, C R ... 744*
Brannick, K ... 1071
Brant, A ... 343
Brasier, A R ... 1928
Bratz, M ... 167
Braue, C R ... 581c, 581e
Braun, A ... 1051, 1057, 1953*
Braun, H ... 1923
Braun, N J ... 1959*
Braun, S ... 1913
Bravo, J ... 901f
Braydich-Stolle, L K ... 8, 832, 1964, 1985
Breech, K ... 126
Breen, M ... 1581*
Brees, D ... 873
Breider, M ... 1200, 1868, 2038
Breitenstein, M J ... 1607
Brenda, M ... 2234x
Brennan, A ... 103
Brennan, R J ... 2
Breslin, W ... 278
Bressler, J P ... 1912
Brewer, P ... 408
Brewster, D W ... 500, 1897
Breyfogle, B ... 1038*
Bridges, C ... 2042*
Briede, J ... 1104
Briedé, J J ... 2273e
Briffaux, J ... 185
Briggs, K ... 426
Brighton, L ... 1778
Brignolo, L ... 124
Brinkerhoff, C J ... 891*, 1807, 1831c
Briolitti, P ... 1906
Briones, J ... 514
Brismar, K ... 550
Brittain, M K ... 567*
Brittebo, E B ... 941
Broadfoot, B ... 966
Brocato, J A ... 1207*
Brochu, P ... 93
Brock, T ... 1932
Brock, T O ... 1280
Brock, W J ... 725*, 726*
Brocklehurst, S ... 1644
Brocksmith, D ... 1713a
Brockway, B ... 477
Brockway, M ... 477*
Brodbeck, C ... 1050
Broderick Pritty, M ... 876b*
Brodie, T ... 2191
Brodsky, B ... 566
Broka, D ... 497, 1327c
Brolén, G ... 1881
Bronstein, J ... 942b
Brook, R ... 2070*
Brooke, E ... 1713t, 1790
Brookins, S ... 928, 1859*
Brooks, A M ... 2137*
Brooks, B W ... 649b, 1435, 1439*, 1831f
Brooks, J ... 2175
Brooks, M ... 378e, 1846
Brooks, S ... 1506*
Broom, A ... 1642
Brorby, G ... 231, 781
Broschk, S ... 173
Broughton, A ... 1582
Brouta, F ... 1543*
Brouwer, K L ... 1626
Brouwers, T ... 1280
Brower, J ... 1222, 1242e*
Brown, A M ... 478
Brown, C ... 1627
Brown, J ... 1186
Brown, J M ... 485, 596, 821, 826, 1464*
Brown, J S ... 72
Brown, K ... 1676
Brown, L ... 886, 2118, 2151c
Brown, R ... 429
Brown, T A ... 696*, 2321*
Brown, T L ... 361
Browning, C L ... 1450, 1924*
Bruce, E D ... 1958, 2203
Bruckner, J V ... 683*, 684, 685, 897
Bruening-Wright, A ... 478
Brundage, T ... 2121
Bruning, D ... 1943i
Brüning, T ... 1007
Brunnemann, K D ... 171
Brunori, G ... 1642
Bruun, D ... 124, 360*, 557, 579
Bryce, S ... 452, 1929*
Brzak, K A ... 688, 1099
Bu, K ... 1988
Buccellato, M ... 1616c
Bucek, A ... 394
Buchanan, L V ... 851
Buchholz, B A ... 2195
Buchweitz, J P ... 1297g*
Buck, B J ... 1713q, 1713r
Buck, W ... 1549a
Buckley, B ... 846, 1831c, 2053
Buckpitt, A R ... 1219
Budinsky, R ... 467b, 1132*, 1403, 2253
Budroe, J D ... 1808
Budzynski, E ... 273
Buentello, A ... 316
Buettner, A ... 1203
Bugarski, A D ... 1242g, 1242h
Bugel, S M ... 181, 211*
Bui, J ... 686
Bui, L ... 1158
Bui, Q ... 328
Buick, J ... 1478
Buist, H E ... 430
Bult, C J ... 2093
Bumcrot, D A ... 942a
Bunce, R A ... 883
Bunch, R ... 854, 1656
Bunge, A ... 2234w
Bunnell, B ... 1913
Buratovic, S ... 1748, 1749, 1757, 1762*
Burbacher, T M ... 1763
Burchfield, S L ... 1851
Burchiel, S W ... 143, 513, 1449
Burdick, A D ... 1635
Burdock, G A ... 343g
Burgess, J ... 1562, 1563
Burgher, F ... 985
Burgoon, L D ... 1830, 2250j
Burke, J ... 1581
Burke, M ... 958
Burke, R D ... 1860*
Burleson, F G ... 400, 407, 1598, 1599*, 2120

Author Index (Continued)

The numerals following the author's names refer to the abstract numbers. The asterisk after the abstract number indicates the author is the first presenter.

Burleson, G 400*, 407, 2029, 2120
Burn, B R 487*
Burnett, J 901f
Burns, T A 1831l
Burns Naas, L 2116
Burnum-Johnson, K 1525
Burpee, B 382
Burrier, R E 1917
Burt, D 380
Bus, J 9
Buschmann, J 599*
Buse, J 1312, 1314
Büsen, R 597, 634*, 1992
Buser, M C 223f, 223g, 235a*
Bushel, P R 101
Bushman, W 1006
Bushnell, P 1062f
Bushnell, P J 96b, 632c, 1347a*, 1347b, 1347c, 1347d
Bussiere, J L 269, 898
Butenhoff, J L 352, 1135, 2208, 2209
Butler, S 1644
Butryn, D M 2204
Butscheid, Y 1890
Butt, M T 942a, 2196k
Butterfield, D 2004h
Butz, J 863
Buxton, S 1145
Byrd, R A 1650*
Byrnes, C C 1854*
Bystrek, M V 312f

C

Caballero-Gallardo, K 147, 667*
Cabanski, M 415*
Cabello, C M 308, 2164
Caccese, R 1636, 1911
Cachau, R E 603i
Cai, B 182, 377*
Cai, J 480, 911
Cai, L 295, 480, 482, 483, 493, 1094, 1887, 1888, 1901, 2044, 2045, 2125
Cai, W 916*, 1503
Caiment, F 101
Caito, S W 1379*
Cajero, M 2226, 2234c
Calabrese, E 1433
Caldwell, J 1658*
Caldwell, R 899
Calhoun, M 2220
Cali, J J 527, 1784*
Callander, R 284, 2110
Callard, I P 1087k
Calley, J 101
Callis, C 1028
Calufetti, S 1028*
Calvano, J 109*
Camacho, J A 1704*
Camacho, L 122c, 1616e, 1713e*, 1713f
Camacho, O 443
Camargo, J V 1662b
Camenisch, T D 496, 497*, 1307, 1327c
Cameron, C 857
Cameron, D 1020
Cameron, G 307
Cameron, M J 342, 845, 1547*
Cammack, J N 1*
Campbell, A 837
Campbell, J 69*
Campen, M 16*, 1242e, 1983, 2226, 2299, 2302*
Campion, C 1163b*
Campleman, S 231
Campos, A d 784*
Cañadas, F 1856
Canady, R 1395*
Canas, J 669d
Canatsey, R D 1503*, 1799
Caner, Y 66
Canerdy, T D 673
Canet, M 2061*
Cannon, J R 378h, 923, 933, 1 338, 1361, 2107
Cantrill, C 689b
Cao, H 440b
Cao, P 2065
Cao, W 1002
Cao, X 1062b*
Cao, Z 114, 360, 1842*
Capaldi, A P 1721, 1733
Capaldi, R A 1721, 1733
Cappellini, D 1280
Capshaw, Z 233
Carakostas, M 337
Carathers, M R 1025
Card, J 1754
Card, J W 621*, 2246
Carden, M F 317, 1526
Cardona, D 1856
Cardoso, A R 1783*
Carette, D 681
Carey, C 1918
Carioto, M 1653
Carlander, U 86*, 815
Carleer, J 11
Carlin, D J 53*, 1416*
Carll, A P 1242b*
Carlson, P 913
Carlsson, L 1126
Carmichael, C 103
Carmichael, P L 162, 1117, 1788, 1934
Carney, E W 146, 408a, 1019*, 1736e
Carney, J 327
Carney, K 1841
Carosino, C 603*, 2004f
Carr, G 1580
Carr, R L 1750*
Carrao, A 1020*
Carratt, S 848c
Carreira, V S 1271, 1685*
Carrier, G 1558
Carrillo, J C 1826
Carroll, M A 1358, 1359, 1360
Carroll Turpin, M A 501*
Carsillo, M 102
Carson, R 1353
Carter, D 292*
Carter, W T 581g*
Cartier, C 133
Cartularo, L 1245*, 1297e
Cartus, A T 523*
Cartwright, M 1981*, 2004f
Caruso, J 136
Caruthers, N 136
Carvalho, A S 1638
Carvalho, C M 39*
Carvan, M J 804, 1690a
Casado, F 1460
Cascio, W 492, 876d
Case, M 876d
Casey, B 1945, 1946, 1947, 2004
Casey, W 161*, 173b, 173h, 440h, 1062c, 1831l, 2250b, 2273i
Casida, J E 1838
Casillas, R P 559, 563, 565, 575
Casinghino, S 397
Cassee, F R 591
Castagné, V 2162
Castellano, V 1843, 1862
Castellernau, A 1662
Castellon, B T 841d
Castillo, C 1328
Castorena, F 1723
Castranova, V . 23, 585, 587, 590, 591, 603d, 830, 1977, 1978, 2004b, 2004d
Castro, A 467
Castro, D 915*, 2230
Caswell, E 1664
Catapane, E J 1358, 1359, 1360
Cathey, T 2234s
Catlin, N 1710*
Catoire, S 1587*
Cattley, R T 1302
Caudill, J 1022
Cavagnaro, J 1422, 1425*
Cavanaugh, J 312c
Cave, M 676*, 970, 1159, 1188, 1569, 1870, 1874, 1879, 2221
Caverly Rae, J 328
Cavieres, M 1087q*
Cavill, R 2273e
Cawley, M 1828*
Cawthon, D R 504c
Cayley, A 2256, 2257
Cearfoss, J M 1018
Ceccatelli, S 40*, 1745
Cederbaum, A 1200d
Ceger, P 173b, 173h, 2250b, 2273i*
Celander, M 1147
Celver, J 550
Centeno, J 1559
Cepa, S 1200b
Cepeda, C 858
Cera, C 526
Cerignoli, F 1119
Cerreta, J M 831
Cervelli, J A 563, 565
Cerven, D R 1025
Cesta, M F 2004a
Chadalapaka, G 1105*, 1106, 1143, 1511
Chakrabarty, R 2037
Chakraborty, S 1356*
Chakravarti, S 440i, 440k, 2265*
Challa, K 1514
Challis, K 1087d
Chamanza, R 1831g
Chamberlain, M 1134*
Chamberlin, R 1353
Chambers, H W 540, 556, 568
Chambers, J E 540, 556, 568*, 678, 679, 1515, 2198
Champeil, E 1578
Chan, C Y 2247*
Chan, K M 904
Chan, L 153, 223b, 1255
Chan, M P 638*
Chan, N 2267*
Chan, P 1713b
Chan, S 223a*
Chan, T 327
Chanda, A 2030
Chandler, C 254
Chandler, G 966, 1343
Chandler, J D 1001*
Chandler, K J 440c
Chandra, D 173o
Chandrasekaran, A 62
Chandy, K 901c
Chaney, S 352
Chang, C 418e, 552c, 833, 1713e, 1713f
Chang, H 575
Chang, J .. 312a, 1087, 1242c*, 1286*, 1327b, 1977, 1994*
Chang, J S 122*
Chang, Q 1391
Chang, R 437*
Chang, S 290*, 352, 1135, 2208, 2209
Chang, X 1149, 2250b*, 2273i
Chang, Y 177, 300*, 575*
Channel, S R 1818
Chao, M 177, 300, 312a, 1242c
Chao, S 670
Chapkin, R 1130
Chapleau, R R 440g, 1787
Chapman, E 1779
Chapman, K 2196aa
Chapman, V 971*
Chappell, G 978*, 2123
Chappelle, A H 236
Charbonneau, M 829
Charles, K 1018b
Charli, A 1832*
Charman, N 2298
Charoensuk, V 159*
Charriere, N 2176
Chatterjee, N 1968*, 1969, 1995
Chatterjee, S 736*, 1187, 1561, 2030
Chaudhary, S C 552e
Chaudhry, A R 909
Chaudhuri, S 2173*
Chauhan, S 1693*
Chavan, H D 1797*
Chavez-Munguia, B 595
Chavira-Ramirez, R 530
Chawsheen, H 1102
Cheatham, L 1627, 1644
Chekayev, Y 1360*
Chellman, G J 11, 1699
Chelsky, D 1530
Chen, A 1644
Chen, B 1325, 1604, 2054*
Chen, B T 10, 23, 603d, 841c, 1229a, 1242a, 1368a, 1713u
Chen, C 243, 685*, 1316
Chen, C L 1429*
Chen, D 954f, 1087t
Chen, G 1922a, 1922a
Chen, H 475, 509*, 884, 1741*
Chen, J 425, 550, 598, 1157, 1804a, 1909
Chen, K 296, 1369, 1388
Chen, L ... 245, 674*, 794, 823, 824, 825, 828, 1207, 1242, 1282, 1507, 1839*, 1986, 2004, 2040a, 2193, 2299*, 2300
Chen, M 89, 585, 603k, 830, 1705
Chen, P 509, 884, 1357*
Chen, Q M 1736d
Chen, R 819
Chen, S ... 790, 796, 1089, 1195, 1892, 1893*, 1963, 2060
Chen, T 114, 265d, 1282, 1973c, 2004c*
Chen, W 1182*, 2007*, 2020
Chen, X 173c*, 603k, 2125, 2223
Chen, Y 151*, 177, 223c, 296*, 300, 346, 357, 467b, 904*, 1077, 1095, 1325, 1369, 1388, 1546, 1595*, 1730, 2014, 2046, 2054, 2076, 2127
Chen, Z 263
Cheng, G 1250
Cheng, M 1888
Cheng, P F 2250d
Cheng, S 786*, 1853
Cheng, T 1242d*
Cheng, W 440d, 440e*
Cheng, X 910
Cheng, Y 223b*, 1106*
Chepelev, N 1478
Cherney, B 954a
Cherrington, N J 547, 735, 1183, 1327c, 1701, 2061
Cherry, D 1522, 2234k
Cherry, W 338
Chervona, Y 1301
Chesne, C 1150, 1617
Chesnut-Speelman, J 1908
Cheu, M 269
Cheung, F 408
Chevallier, A 1158
Chhimwal, R 398, 399
Chiang, C 2054
Chiang, H 511*
Chiang, Y 369
Chibout, S 873, 1618, 2056
Chigurupati, S 934*
Chihara, K 201
Child, J 641
Child, M 1053
Chillrud, S 825
Chilton, J 1058
Chimote, G 1639a
Chin, M T 1690b
Chini, N 1539
Chintagari, N 2169
Chipinda, I 2036
Chirino, Y I 1996
Chirmule, N 898
Chisholm, C 1981
Chitrakar, R 1229e*
Chittiboyina, S 548*
Chiu, C 1325
Chiu, W A 630, 1831
Chivers, S 278
Cho, A K 1716
Cho, H 1804c*
Cho, K H 194
Cho, M 290, 1951
Cho, S 641
Choi, B 942d, 1327e
Choi, C 1166, 1167
Choi, H 395, 993*, 1005, 2327
Choi, J 506, 787, 795, 797a, 799*, 801, 802, 999*, 1968, 1969, 1995
Choi, K 1087e, 1087g, 1223, 1233, 2234l
Choi, S 1023, 1243, 1639b*
Choi, T A 894*
Choi, Y 353, 790, 1125*, 1190

The numerals following the author's names refer to the abstract numbers. The asterisk after the abstract number indicates the author is the first presenter.

Cholanians, A B 924*
Choo, E 954g
Choongo, K 843
Chorley, B 1154
Chotibut, T 501, 935*
Chou, C 509, 574, 884*, 1242d
Chouchane, S 1615
Choudhury, E A 640*
Chow, C 503
Chow, R M 1713q, 1713r
Christensen, E 1746
Christensen, K 96i, 1807
Christian, B 740*
Christian, K M 1912
Christian, W V 954d*, 2233, 2240
Christin, E 681
Christin-Piche, M S 121, 1656
Chu, A 436*
Chu, C 535
Chuang, G 1795*
Chuang, Y 177, 300
Chuaqui, C 1126
Chukwuka, A V 1074
Chun, Y 293*, 1023
Chung, F 1979
Chung, J 1122
Chung, M 1242c
Chung, Y .. 21, 296, 357, 799, 800*, 801, 802, 1369*, 1388, 1565
Church, R J 106*
Church, T 2211
Churchill, G A 279
Chutkow, W 2124
Chuva de Sousa Lopes, S M 163
Ciarlo, M 649b
Cicalese, L 1538
Cichewicz, A 1347j*
Cichocki, J 1201, 1218, 1219*
Cimarosti, Z 2263
Cimon, K 1616c
Ciotti, S M 1256, 1381
Cisneros, B 595
Cisneroz, M 1544, 1549a
Cizdiel, J 1987, 1988
Clair, H 676, 1159, 1569*, 1870
Clark, A J 885, 1099
Clark, D L 118*
Clark, E S 318*
Clark, J M 378e
Clark, K J 2075*
Clark, M A 1725, 1728
Clark, R D 440j
Clark, R S 2023*
Clark, S 850, 1157, 1656
Clarke, D O 2159
Clarke, E 270, 1918, 1920*
Clarke, J 547*, 669d, 1183, 2061
Clarke-Lambert, S 2234b*
Claude, N D 987
Claville, M O 525, 841e
Clemens, G R 847
Clements, J 753, 756*, 1933
Clements, P J 427
Clendaniel, A N 838*
Clewell, A 329
Clewell, H J 60*, 69, 75, 76, 89, 91, 92, 96c, 240, 266, 438, 689b, 2099*, 2250a
Clewell, R A 160, 162*, 240, 1140, 1788, 1794, 1934
Cline, H 1191, 1867
Clingman, C 1947
Clippinger, A J 1037*
Clive, M L 1706*
Close, D 1633
Clougherty, J E 1242b
Cloutier, Y 829
Clubb, S 2161
Coash, J 1547
Coates, N 2329
Coats, J R 671*
Cobb, G 669d
Cobb, J 877
Coccini, T 835*
Cochet, C 2010
Cochrane, L 343
Coder, P S 2160*
Coffey, M 2037
Cohen, J 814, 817*
Cohen, S 157
Cohen, S M 255, 265c, 1824
Cohen, Y 816
Colacino, J 1922e*
Colagiovanni, D B 1100*
Colatsky, T 1549b
Colbry, D 440
Cole, B 1061, 1129a
Cole, J A 1163b
Cole, S D 173a, 1894*
Cole, S H 986
Cole, T B 686, 1763
Coleman, J D 248
Colle, D 1329
Colleluori, D M 943
Colli-Dula, R C 914*
Collier, C 1993
Collinge, M 1660
Collins, B 877, 1616a*
Collins, L 1110g, 1523, 1930
Collins, M A 236
Collins, M C 2153*
Collins, R 476
Collins, T 1583
Collis, L 1128
Colón, C 1372*
Colón, F 875
Colon Ortiz, C 1376
Colon-Rodriguez, A 1384*, 1385, 1386
Colton, H M 1549a*
Coman, G 876c
Comfort, K K 8, 1959, 1960*
Commandeur, J N 1872
Comotto, J 301*
Compagnone, N A 1643
Composto, G M 563, 565
Compton, J R 2013
Conard, K R 1917
Concoby, B 2234aa
Coney, L A 1713s
Cong, B 367
Cong, M 167
Conklin, D J 14*, 17*, 1121, 1235, 1239
Connolly, E E 1732
Connor, A 278
Connor, M P 505
Connors, K 649b
Conolly, R B 438, 440d*, 440e
Conrad, K 1333, 1340, 1347
Conrad-Vlasak, D 950
Constant, S 860, 1592
Conway, M 1129e
Cooke, G 338
Cool, D R 361
Coonen, M 1872
Cooney, C 966
Cooper, B T 1015
Cooper, G S 1807, 1809
Cooper, K 2067a
Cooper, K L 1449
Cooper, N 1121
Cooper, S D 1606
Cope, R 1087w, 1087x*
Copeland, L B 145a, 1006a, 1205
Copelnd, C 145a
Copeman, C 861
Coppi, A A 1641
Corbett, N E 1083
Corcoran, G B 719*
Cordero Badillo, Z I 968*
Cordier, A 873
Coriano, C 1069*
Corley, R A 773*, 882, 2140
Cornebise, M 1644
Cornet, M 1543
Cornforth, T 1921, 1922
Cornille-Robert, E 1643*
Coronel, R 2258*
Corrales, J 208, 1683, 1831f
Corredor, C 1981
Correll, J 1141
Corsini, E 984*
Cortes, L 1530
Corton, C 690*, 692*, 1154, 1479*
Corvaro, M 1019, 1863*
Cory-Slechta, D A 954h, 1333, 1340*, 1342, 1347, 1418*, 1747e
Coskun, E 1713n
Cosmanescu, A 85
Costa, A 1329
Costa, L 2263
Costa, L G 1753, 1763
Costa, M 969, 1207, 1245, 1282, 1297e, 1301, 2040a, 2180
Costin, G 173k, 1028
Côté, J 83*
Cotgreave, I 1881
Cotovio, J 170, 402, 2177, 2178, 2179
Cottom, J 452
Couch, L 1195, 1892, 1893
Coulter, S J 922d
Coumoul, X D 1158*
Couroucli, X 538*, 539, 1796
Coussement, W 348, 1652
Coutermarsh, B 2317
Couto, S 2038
Couttet, P 873
Covington, T R 87
Cowden, J 776
Cox, B 223h
Cox, J 757
Cox, K 607*, 1663
Coy, D 1772
Coyle, J 299*, 2234z
Crago, J P 205*
Craig, A M 336
Craig, E 649*
Craig, Z R 2188
Cravero, A 665
Crawford, R 2005, 2007, 2015, 2016, 2019, 2020*
Crawley, J N 557
Creighton, M 668
Creim, J 1525
Creton, R 1751
Creutzenberg, O H 599, 600*, 601
Cridge, B 791
Crofton, K 1066, 1398, 1401*
Croghan, C 1581
Cromie, M 1504*
Cromwell, E F 1616g
Cronin, M T 26*, 27, 28, 29*, 30, 31, 431, 632, 2254, 2266, 2273x
Crooks, J 440c, 841d, 1973a
Crosby, L M 1018b*
Crosby, M 1636*, 1644, 1997
Cross, C E 978d*, 1943d
Cross, K P 459, 2273c, 2273h
Cross, M 1120
Crosswell, H E 1876
Croteau, P 1530
Croutch, C R 877*
Crow, J A 1515
Crowell, S 70, 71
Crump, K S 781*
Cruz-Torres, I 1256*
Cruze, C 878
Csanaky, I L 2122*
Cucullo, L 354
Cuddapah, S 967
Cuellar-Kingston, N 337
Cuevas, E 173m, 378i, 603b, 942e*
Cui, J 49, 917*, 1896
Cui, Y 659, 1842
Culbreth, M 173i, 1380*
Culty, M 1712
Cummings, B S 683, 684, 685, 897, 2050
Cummings, C W 1383
Cummings, K J 1208
Cumpston, A 1229a
Cumpston, J 603d, 1229a
Cunningham, C K 2004c
Cupi, D 836*
Curran, C P 1672, 1742, 1743*
Currie, R 238*, 1090, 1865, 1869
Currier, J 1318
Currow, B 277
Curtin, M 527*
Curvall, M 2234v
Cutting, E 665
Cutuli, F 173l
Czich, A 220

D

D'Amico, L J 891
D'Angelo, J 1919
D'Cruz, O J 2196x*
D'Ingillo, S 2020
D'Souza, S E 2319
D'Agostino, J 533
Dadhania, V P 1164*, 1165
Dadson, O A 689
Dagher, R 1494
Dahlén, S 586
Dahm, M 22*
Dahms, J K 945
Dai, J 265e*, 976*, 1891, 2125, 2212
Dai, M S 1709
Dail, M 540*, 678
Dailey, L A 396, 1231, 1719
DaileySterling, F 1243
Dakoulas, E W 467e
Dalal, V R 398, 399*
Dalrymple, A 443*
Dalton, C 2182*
Dambach, D M 1899c
Dammann, M 1992
Damodaran, T V 1855*
Damre, A 1639a
Damsten, M 1654
Dancik, Y 1831l
Dandekar, D 689a
Dang, M 1612
Dang, Z 658*
Daniels, J 1589
Daniels, K K 1646
Daniels, M 980, 1204, 1205
Danilenko, D M 954g, 2196p
Dankovic, D A 632f*
Dann, S 1129
Danov, O 1953
Dao, K 1753
Dao, T 581e*
Dao, T L 581c
Daramola, O T 481, 1267, 1270, 2041
Darbonne, W 269
Darney, S P 418a
Darrah, P 271
Das, J K 1062i*
Das, M 778
Das, N 977
Das, S 88, 1059, 1187*, 1899*, 2030
Das, S R 212
Dasenbrock, C 1226*
Dasgupta, A 1876
Dasgupta, U B 977
Dasmahapatra, A K 214*, 978e
Daston, G 4, 146
Datko-Williams, L 1018c*
Datta-Chaudhuri, T B 173a
Dauder, R 1317
Daujat-Chanvanieu, M 1906
Däumling, C 642
Dave, N 1087l
Davenport, L L 827*, 1087m
David, R 256, 912*, 1110
David, S 185
David, W B 1713q, 1713r
Davidson, M 166
Davies, A 1897
Davies, M 849*, 850, 851, 852, 854, 1656
Davila, D R 2196z
Davis, A 1830
Davis, A L 308*
Davis, A P 411*, 423
Davis, B 1612*, 1902
Davis, C 130, 131
Davis, J 324, 878, 1635, 2059, 2080*, 2083
Davis, K J 467a
Davis, M A 173l, 1062d
Davis, R L 1374
Davis, S M 2160
Davis-Bruno, K 11
Davoren, M J 1943h*

Author Index (Continued)

The numerals following the author's names refer to the abstract numbers. The asterisk after the abstract number indicates the author is the first presenter.

Dawkins, J ... 485
Day, B J ... 359, 577, 1001
Day, L ... 1642
Day, T A ... 671
De Abrew, K N ... 146
de Bourayne, M ... 2010*
de Conti, A ... 957, 1513*
de Groot, M ... 356*, 1347i, 1739
De Groot, D M ... 1347i*
De Jesus, S ... 574
De Jonghe, S ... 1080, 1652
de Kok, T M ... 2273e
De la Rosa, J ... 667
De La Rosa, V ... 418d
De Luna -Lopez, C ... 313
de Oliveira, D P ... 2171
De Prins, S ... 223h*
de Rijk, E ... 2147
De Smedt, A ... 1027
De Waal, E J ... 348
De Wever, B ... 1027
de Zafra, C ... 269*
Dean, C G ... 661
DeAngelo, A B ... 1018a
Deans, R ... 12
Dearfield, K L ... 47*
Dearing, D ... 539a
Dearman, R J ... 971, 989, 990, 991*, 992
Debernard, K B ... 1782
DeBiasio, R ... 1880
DeCastro, R ... 1549c
Déciga-Alcaraz, A ... 1996*
Dedon, P C ... 1521
Deeb, T Z ... 552g
Deepe, R N ... 1783
Deering-Rice, C ... 1238*, 1241
Deferme, L ... 1104*
DeGeorge, G L ... 1025, 1033, 1034, 1035*
Degheidy, H ... 122b, 1946, 1955, 2004
Degitz, S ... 1087d
Degn, L L ... 96b, 1347b, 1973d
Degonkar, R ... 417
DeGroot, D E ... 1146
Deguchi, J ... 201, 1046
Deguchi, Y ... 472
DeHate, R ... 2234e*
Deisenroth, C ... 1922f*
Dekant, W ... 164
Dekker, C L ... 391
Del Pino Sans, J ... 174*, 1843
Del Razo, L M ... 144, 1309, 1312, 1314, 1324
Delarue-Cochin, S ... 987
Delbeke, K ... 1280
Delclos, K ... 1616e*, 1713e, 1713f
DeLeo, P ... 649b
DeLeon, D ... 2196j
Delgado, L ... 1544
Delgado-Buenrostro, N L ... 1996
Delgado-Jimenez, J F ... 1973*
Delker, D ... 1941
Dell, L ... 778
Dellarco, M ... 1824
Delluc, S ... 987
Deloménie, C ... 2011
DeLoughery, Z ... 1268
Delp, J ... 1738
Delvalle, N ... 1376
Delwig, A ... 1331
Demady, D ... 743*
DeMaio, W ... 285, 1895
Demarini, D ... 2296
Demchuk, E ... 410*, 433
Demmitt, B ... 1583
Demokritou, P ... 814, 817, 830
Den Besten, P K ... 173o
den Braver, M ... 1872
Deneer, J W ... 2238
Deng, J ... 1772
Deng, X ... 1616f*, 1713p
Denison, M ... 902, 907, 1146*
Denker, J A ... 478
Denner, L ... 1538
Dennis, E ... 1544
Dennis, W E ... 1265, 1297
Denslow, N D ... 669c, 914
Denton, R R ... 222
Denvir, J ... 909
Depelchin, B O ... 1543, 1659*
Dere, R ... 1804
DeRespiris, L ... 1841*
Derk, R ... 585, 830
Derrick, J ... 989
Dertinger, S ... 3, 452*, 1929, 1943j
DeRusha, C E ... 954b
Derzi, M ... 276*
Desai, D ... 1139, 1623
Desai, V ... 100*
Desai, V G ... 122d, 978a
DeSantis Rodrigues, A ... 578*
Deschl, U ... 171
Descotes, J ... 401*
DeSesso, J M ... 1805, 1831a
DeSimone, M C ... 261*
Destexhe, E ... 1654
Detrisac, C J ... 2196y
Detroyer, A ... 435
DeVera, C ... 1018b
DeVera, V ... 2250d
Devine, C ... 583
Devine, P J ... 1618
Devlin, R ... 1231, 1719
DeVoney, D ... 239
DeVoss, J ... 2196p
Dewailly, E ... 1255
Dewhurst, I ... 1824
Dewitt, J C ... 1713q, 1713r
DeWitt, J ... 699, 1336, 2040b*
DeWoskin, R ... 72*, 1087p
Dey, R D ... 392
Dey, S ... 1580*
Dhakal, K ... 515*
Dhalluin, S H ... 714*, 1543
Dhar, D ... 555
Dharmadhikari, S ... 1365, 1366*
Dhawan, P ... 866
Dholakiya, S L ... 368*
Dhumal, N U ... 1943
Dhungana, S ... 539e
Di Bona, K R ... 1541, 1711*
Di Gallo, G ... 1914*
Di Giulio, R ... 223e*
Di Tuccio, M ... 1745
Diagne, G ... 286
Dial, S L ... 319, 1973c
Diala, E I ... 862
Diallo, O N ... 121
Diamante, G ... 489*
Diamond, G L ... 72
Diana, R ... 2234x
Diaz, D ... 954g
Diaz, E ... 1242b
Diaz, G ... 1534
Diaz-Sanchez, D ... 396, 876d, 1242i, 1719
DiCicco-Bloom, E ... 178, 1845
Dickinson, A M ... 1036
Dickinson, D ... 1929
Dickman, K ... 508
Diehl, A ... 2030
Diehl, L ... 504a*
Dieme, D ... 839*, 1998
Dietert, R R ... 44*
Dietrich, D R ... 365*, 900, 1087c, 1566
Dietz, B M ... 790*, 796
Diggs, D L ... 1505, 2213b*
Dill, J A ... 2004a
Dillon, C ... 877
Dillon, D ... 443
Dillon, L M ... 851
DiLorenzo, A ... 1243*
Dilworth, C ... 1875
Dimitrov, S ... 435
Dimitrova, N ... 435
Dinesdurage, H ... 1943i
Ding, H ... 1129c
Ding, W ... 467a*, 1889, 2004c
Ding, X ... 508, 528, 531, 532*, 533
Ding, Y ... 1747b
Dingee, C ... 943
Dingemans, M M ... 1739*
Dinu, C A ... 589
Dionisio, K ... 2234m, 2234s*
Director-Myska, A E ... 923
Dissen, E K ... 223i, 632i*
Ditzel, E J ... 1307*
Divakaran, K ... 192*
Divi, K ... 1923
Divi, R L ... 705, 848
Dix, D J ... 173b, 418b
Dixit, R ... 7
Dixon, D ... 1110f
Dixon, H ... 2241*
Dixon, J ... 183
Dixon, M J ... 183
Dkhil, H ... 2165
Do, K ... 2027*
Do, M ... 507*, 797b
Doan, C J ... 318
Dobbins, D ... 1732*
Dobrovolsky, V N ... 453, 1893
Dochterman, L W ... 2136
Dodd, C A ... 996, 1837
Dodd, D E ... 1217*
Dodd-Butera, T ... 876b, 1435, 1438*, 1680a*
Dodge, D G ... 251*
Dodmane, P R ... 255*
Doe, J ... 1824
Doepker, C L ... 337
Doerge, D R ... 96f, 96g, 957, 1616e
Doerrer, N G ... 1824
Doherty, K ... 1112*
Doherty-Lyons, S P ... 1675*, 1692
Doke, D ... 1263, 2239*
Dolan, L ... 343g*
Dolash, B D ... 2004b
Dolinoy, D ... 964, 1570, 1687, 1690
Doll, N ... 1616a
Domashevskiy, A ... 786
Dominguez, M ... 603i
Domoradzki, J ... 901d*
Donald, C ... 301
Donaldson, R A ... 1863c*
Donde, H ... 869*
Donepudi, R ... 994
Dong, C ... 590
Dong, H ... 790
Dong, J ... 266, 1788, 1794
Dong, W ... 208
Dong, Y ... 351, 1348
Donley, E ... 1917
Donna, F ... 1551
Donnell, J ... 1058
Donner, E M ... 328, 467d
Donofrio, R ... 1663
Donoghue, L ... 1932
Donovan, E ... 2235
Dons, E ... 223h
Doran, J L ... 1589*
Dorko, K ... 1181
Dorman, D C ... 626, 1363
Dorr, T ... 1089
Dorsey, R M ... 173a
Dorta, D J ... 312, 457, 458, 677
dos Santos, G ... 270*
Doshi, U ... 529*, 1631, 1885, 1899d
Dossin, E ... 1054
Dostal, M ... 706, 844
Dosumu, O A ... 1249, 1266, 1273, 1776*
Dosunmu, A N ... 788
Doudement, E ... 1899c*
Doughty, J ... 1713s
Douglas, A ... 1879
Douglas, C ... 469
Douglas, D ... 581
Douillet, C ... 1318
Doulias, P T ... 2039
Douoguih, M ... 271
Dourson, M L ... 632j, 1087w*, 1087x, 1421*
Douville, J ... 345*, 2159
Dover, H E ... 2013
Downes, N ... 1764e
Downs, T ... 1997
Doyle, N ... 1540*
Doyle-Eisele, M ... 1107, 1222*, 1229f, 1236, 1242e, 1521, 1831g
Dragan, Y P ... 1911
Draganov, D ... 1634
Drake, B ... 1616b
Draper, K ... 285, 878, 1895
Dreher, K ... 764*, 1973a
Dreier, D A ... 1831f
Drewe, W C ... 2256*, 2257
Drey, H ... 469
Driessen, M D ... 1950*
Drobna, Z 229, 1308, 1312, 1314, 1318, 1324
Droege, W ... 1087i
Druwe, I L ... 35*
Du, K ... 1172*, 1253
Du, Y ... 2223
Du, Z ... 1604
Duan, J ... 171, 467a
Duan, X ... 312d
Duarte, F V ... 2004g
Duarte-Sustaita, J J ... 1309
Dubnicka, T ... 343d
Dubois, J ... 1018c
Ducheneaux, C ... 135
Duclos, M ... 401
Duellman, S ... 1784
Duenbostell, A ... 1919
Duerr, J ... 942c
Duffy, P ... 847*
Dugard, C ... 1947
Dugas, T R ... 501
Duguay, F ... 471*
Duistermaat, E ... 1970
Duke, A ... 574
Duke, K ... 1758
Dumais, A ... 1225*
Dumont, C ... 121*
Duncan, K E ... 1231, 1719
Dungar, B ... 1082
Dunlap, M ... 1983
Dunlevy, J R ... 244*
Dunn, A R ... 371
Dunn, K ... 877
Dunn, R T ... 1157, 1641
Dunnick, J K ... 922d
Dunnick, K M ... 1966*
Dunning, C ... 2066
Duong, T ... 1712
Dupre, T ... 2058*
Durand, P H ... 681
Duret, C ... 1906
Durham, P ... 641
Duringer, J M ... 336*
DuTeaux, S B ... 1564*
Dutta, D K ... 289, 2024*
Dutton, N ... 234*
Dutton, S J ... 2250j
Dvonch, T ... 1240
Dwivedi, A ... 1814*
Dwivedi, S ... 1952
Dybdal, N ... 269, 2307*
Dydak, U ... 1365, 1366, 1367*, 1368, 1550, 2231
Dye, J A ... 980, 1204
Dymacek, J ... 590
Dysinger, H ... 2220*
Dzierlenga, A L ... 1183*, 2061

E

Eagle, E ... 815
Eakins, J ... 1630, 1644, 1721, 1733*
Earhart, J J ... 297*
Eastham-Anderson, J ... 2196p
Eaton, D L ... 1962
Eaton, L ... 990*
Ebert, R ... 631
Eckhert, C D ... 1775
Eckhoff, T ... 2157
Eckstrum, K ... 1071*
Edelman, P ... 951
Eden, P R ... 895, 1820
Edmonds, N ... 2298
Edoff, K ... 40
Edrissi, B ... 1521*
Edwards, G ... 1173, 1495, 1498
Edwards, J ... 186, 1252*, 2048, 2273n
Edwards, J A ... 333*
Edwards, L ... 670
Edwards, P ... 848c*, 1218
Eftim, S ... 9

The numerals following the author's names refer to the abstract numbers. The asterisk after the abstract number indicates the author is the first presenter.

Egbe, E R ... 2234u*
Egerer, L ... 1913
Egnash, L A ... 1917*
Egner, P ... 526
Egyed, M ... 2298*
Ehresman, D J ... 352, 1135*, 2208, 2209
Ehrich, M ... 2002
Eid, A ... 939*
Eidelman, D H ... 906, 1722
Eiguren-Fernandez, A ... 1716
Einhorn, S ... 1045, 1628
Einstein, D R ... 2140
Einstein, F ... 994
Eisenbrandt, D L ... 1863
Ekker, M ... 153
Eklund, C R ... 632b, 632c
Ekor, M ... 1557
El Ali, Z ... 2010, 2011*
El Sayed, K A ... 798
El-Fawal, H A 938*, 1334, 1347j, 1535, 1740
El-Masri, H A ... 96b, 96e, 1766, 2273o
El-Nezami, H ... 1008
El-Saied, E M ... 1179
El-Sayed, R ... 586
El-Tawil, O S ... 1179*, 1179*
Elcock, L ... 689a
Elcombe, C R ... 1134, 1593
Eldridge, S ... 1062d
Elferink, C J ... 292, 1538
Elford, P ... 888
Elgamal, M ... 1180
Eliasen, L ... 134
Elkhouly, A ... 336
Ellingwood, A ... 118
Elliott, D M ... 385*
Ellis, D ... 1965*
Ellis, S ... 1875
Ellis-Hutchings, R ... 1736e
Ellison, C A ... 81
Ellithi, M ... 1180*
Elmore, S ... 343j, 1232, 1526*
Elnagar, K ... 938
Eloff, K A ... 785, 1629
Eloi Atkintunde, M ... 698*
Elrod, N ... 1985*
Elsass, K E ... 2196j*
Ema, M ... 2192
Embry, M ... 1824
Emeigh Hart, S ... 2196h
Emeigh Hart, S G ... 2196f
Emm, E J ... 581i
Emmen, H ... 2147
Emond, C ... 815
Enami, T ... 2196u
Endo, H ... 1392
Endo, M ... 587, 591
Endo, N ... 2163
Endo, T ... 1346, 2163*
Endoh, S ... 592, 1948
Endres, J R ... 329
Engel, G ... 1331
Engelward, B P ... 2282*
Engin, A ... 1713n*
Engle, S K ... 101, 1549h*
Englert, N ... 954e*
English, J C ... 607, 608*, 1663
Enoch, S J ... 2254, 2266, 2273x
Enoru, J ... 285, 1895*
Enright, H ... 2195*
Ensley, S ... 362
Enters, K ... 640
Entezari, M ... 940*
Eom, H ... 1968, 1969*, 1995*
Eom, I ... 1229b
Eom, S ... 353, 1260, 1327e
Eppig, J T ... 2093
Epstein, P ... 480
Erdei, E ... 135*, 2234c
Erdely, A ... 20*, 22, 486, 603d, 1983, 2301*
Erickson, S ... 137*, 966
Eriksson, P ... 1748, 1749, 1757*, 1762
Ernst, B ... 1545
Ernst, H ... 600, 1215, 1990, 2003
Ernstgård, L ... 1224*, 1814
Erraguntla, N K ... 610*, 780
Ersson, L ... 941*
Erstenyuk, A ... 265b
Erwin, K ... 223e
Escher, C ... 1890*
Escher, S ... 631*
Escobar, P A ... 2196e, 2196g
Escudero-Lourdes, C ... 144*, 957
Eskenazi, B ... 707
Eskin, E ... 1281
Esneault, E ... 2162
Espejel, M ... 343a
Espey, M ... 1713o
Espinosa-Tanguma, R ... 1973f
Espinoza, C F ... 603i
Espiritu, D ... 497
Esposito, E R ... 312f*
Ess, K C ... 1353
Essex, A ... 182*, 377
Esswein, E J ... 1607
Estrella, B ... 1493, 1497*
Eugster, E ... 379
Eustaquio, T ... 1756*
Evangelista, E ... 1129f
Evangelista, H ... 784
Evans, B ... 382, 1315
Evans, J ... 182, 377
Evans, K ... 467f
Evans, M B ... 235
Evansky, P 96b, 1062f, 1347a, 1347b, 1347c, 1347d
Everds, N ... 1157, 2065
Everly, A ... 2159
Ewart, S ... 968
Eyng, H ... 1329
Eyoita, E ... 1561*

F

Fabbri, M ... 732*
Fabian, E ... 120, 1591, 2172
Fadeel, B ... 586
Fader, K A ... 903*
Fagbohun, O A ... 1073, 1074
Fahlman, R ... 542
Fahmi, T ... 312b
Fairbrother, W G ... 550
Fairchild, D ... 1539
Fairweather, D ... 394
Faisal, M ... 1952
Fajardo, A M ... 1144
Falank, C ... 1303, 1942
Falciani, F ... 173p, 418d
Falkenstein, M ... 363
Falkner, K C ... 676, 1159, 1188, 1569, 1870, 1874, 1879, 2221
Fallacara, D M ... 1713b
Famulski, K S ... 2217
Fan, C ... 1935
Fan, J ... 909
Fan, L ... 369
Fan, X ... 536
Fan, Y ... 1271, 1685, 1907, 1909
Fan, Z ... 858
Fang, G ... 1110c
Fang, H ... 1087a, 2273k*
Fang, J ... 257, 1087b*
Fang, L ... 954f
Fang, M ... 1493, 1497, 1501*
Fant, M ... 1087n
Farahat, F ... 81, 689
Farahat, T ... 689
Faranda, A ... 467d
Farcas, M ... 1242g*
Farhad, A ... 1549e
Farhat, A ... 2253
Farina, M ... 1329
Farman, C ... 273
Farmen, M ... 101
Farombi, E O ... 173n, 1713g, 1718*
Farooq, A ... 813c
Farraj, A K ... 492, 2296, 2323, 2329*
Farrer, D G ... 1766
Fasullo, M ... 524, 526*
Fatkhutdinova, L M ... 603e*, 603f
Faucheu, E ... 1345
Faulk, C ... 964*
Faulkner, D ... 418d, 524
Faustman, E M ... 1577, 1662b, 1702, 1707, 1763
Favre, M ... 1592
Fay, K ... 669e*
Feaver, R ... 1061
Fedak, K ... 233*
Fedan, J S ... 1242a
Fedor, Y ... 1931
Fegert, I ... 1087v
Feher, D ... 995
Fehrenbach, H ... 1953
Feinleib, M ... 223i, 632i
Feldpausch, A ... 778
Fell, L ... 612
Fellows, M ... 757
Felter, S P ... 1609
Felty, Q H ... 1062i
Felzenszwalb, I ... 466, 784, 1638
Fendorf, S ... 1087l
Feng, S ... 182, 377
Feng, W ... 351, 480, 1188, 1189, 1194
Fennell, T ... 75, 484, 485, 539e*
Fensterheim, R J ... 467b
Fenton, S E ... 1087r, 2196a, 2196b, 2196c, 2196d
Fenu, L ... 79
Ferency, G ... 406, 408
Ferguson, H ... 331, 341, 342, 343, 343d, 811, 845
Ferguson, S ... 2273q, 2273r*
Ferguson, S S ... 2250a
Fernandes, A S ... 466
Fernández Tamayo, N ... 1244
Fernandez-Salguero, P ... 1158
Fernando, H ... 384*
Fernando, R A ... 198*, 1606, 2224
Ferraz, E A ... 466*
Ferreira, D W ... 172*
Ferro, A ... 131
Ferslew, B C ... 1626
Feyen, B ... 1652*
Ficheux, H ... 1587
Fick, T K ... 1662d
Fiebelkorn, S A ... 70, 237*
Field, L ... 1129b
Fielden, M ... 1157, 1641, 2269*
Fields, V ... 935
Fields, W ... 95*, 1530
Fieldsend, M ... 2234aa
Figueiredo, M L ... 1916
Figueroa, M ... 875
Fikree, H ... 621, 2246
Filbert, V ... 326
Filer, D L ... 173j, 1066, 1973e, 2273s, 2273z*, 2273aa
Filgo, A J ... 1087r, 2196b*
Filhol Cochet, O ... 2010
Filipczak, P ... 581k*
Filipov, N M ... 996, 1837
Fils-Aime, S ... 1264c
Finch, G ... 276
Finkelstein, J N ... 552f
Finkelstein, Y ... 566
Finley, B L ... 77, 225, 232*, 603j, 614, 954d, 1227, 1228, 1574, 1610, 2233, 2234t, 2235
Finn, M ... 1765
Finn, P ... 267
Fioravanzo, E ... 27, 28*, 29
Fisch, A ... 552c
Fischer, B ... 1448
Fischer, M ... 1226
Fischer, S ... 104
Fisher, C D ... 101, 102*, 122e
Fisher, J ... 90, 96f, 173c, 440f
Fisher, J W ... 96g*
Fisher, M ... 96h
Fisher, R ... 859
Fisher, S J ... 179
Fite, T ... 312b
Fitsanakis, V A ... 1848, 1849, 1850, 1851, 1863c
Fitzgerald, L M ... 622, 623
Fitzgerald, S D ... 1680
Fitzmaurice, A G ... 942b
Fitzpatrick, J W ... 1831b*
Fitzpatrick, S C ... 1441
Fitzsimmons, P N ... 669e
Fix, N R ... 488, 1966
Flannery, B ... 557*
Flaws, J A ... 1071, 2184, 2185, 2186
Fleischer, J ... 618, 620*
Flick, M J ... 1191
Flint, O ... 855, 856, 857*, 1622
Floch, E ... 1727
Flor, S ... 1068*
Flores, H ... 269
Flores, L ... 603i
Flores Flores, J O ... 1996
Flores Molina, M ... 1283, 1319
Flores Torres, M ... 1869*
Florian, L ... 560
Flowers, L ... 1831c
Flyer, D ... 2196s
Flynn, P ... 1915
Flynn, T J ... 169*, 1043
Fofaria, N M ... 354, 1098*
Fogle, C M ... 1764a, 1764b, 1764c
Foldbjerg, R ... 1956*
Foley, B ... 1922f
Foley, M ... 468, 474, 475
Folkens, S ... 2241
Follansbee, M H ... 72
Foltz, D ... 1031
Folz, R ... 1239
Fomby, L M ... 1616c
Foos, B P ... 892
Foppiano, P ... 2196g
Ford, B ... 1582*
Ford, J ... 96b
Ford, M ... 350
Ford, R ... 420
Ford, R D ... 122a
Ford, S M ... 1679, 2063
Foreman, J E ... 636*
Forgacs, A L ... 173j, 343c*
Forino, A ... 1297d*
Fornace, A ... 1155, 1156*, 1478, 1938
Fornal, C A ... 1330
Fornara, A ... 586
Forreryd, A ... 1062g
Forsberg, E M ... 268
Forsberg, N D ... 1678
Forster, J ... 1181
Forster, R ... 274, 275, 344, 401, 471, 888, 1225, 1494*, 1654, 1727, 2037, 2130
Fort, D J ... 202
Fort, M ... 406
Fostel, J ... 173b
Foster, M L ... 1363*
Foster, S ... 2121
Fotland, T O ... 2248
Fotsch, C ... 2269
Fountain, A ... 2237
Fourches, D ... 2182c
Fourie, E ... 1518*
Fournier, H ... 2241
Fournier, K ... 1009*
Fowler, A ... 1839
Fowler, D A ... 90
Fowler, K ... 95
Fowler, S ... 157
Fox, D A ... 312e, 352*, 1767
Frady, S L ... 223d
Frame, A ... 2234s
Francher, T ... 1363
Francis, M ... 395*, 2327
Francis, R ... 2076
Francis Stuart, S D ... 1246*
Franco, R ... 926, 1452*
Franco, Y ... 1665*
Francois, S ... 1712
Frandsen, H ... 1018d
Franklin, J N ... 699*, 1336
Franklin, P ... 197
Franklin, S ... 327
Frankos, V ... 1475*
Franks, D G ... 209
Fransson, M N ... 74*
Frantz, B ... 341, 342, 343, 343d, 811, 845
Frantz, S W ... 901c
Franz, B ... 166*
Franzen, A ... 71

Author Index (Continued)

The numerals following the author's names refer to the abstract numbers. The asterisk after the abstract number indicates the author is the first presenter.

Franzosa, J 1736e*, 1973e, 2273q, 2273s
Frasch, H 1586, 2182a*
Fraschini, M 901f
Fraszczyk, B 1713s
Fraunfelder, F W 745*
Frawley, R P 145b*
Frazer, D G 23, 603d, 1229a, 1368a, 1713u
Frazer, D M 2128
Frazier, K 1654
Fredenburgh, L 581k
Frederick, D M 1586
Fredriksson, A 1748, 1749, 1757, 1762
Fredriksson, L 1047, 1168, 2031
Freed, T A 198
Freedman, J H 173d, 173o, 1245, 1264b
Freeman, E 647*
Freeman, J J 265
Freeman, J L 203, 204, 221*, 1277, 1338
Freiwan, A K 2022*
Freke, M C 2159*
French, J E 1110f
French, K 1645
French, K J 1642
Frentzel, S 413, 415, 860, 1055, 1592*
Frericks, M 1078
Freshwater, L L 476
Frevert, C F 602, 1980
Freyberger, A 1087c
Freyre-Fonseca, V 1996
Fried, D 2006
Friedman, M A 914
Friesen, M 2234k
Frings, W 2150*
Frisbee, J 872
Fritsche, E 746, 752*
Fritz, H A 1227, 1228*
Fritz, J M 239*, 1809
Froget, G 2144, 2162*
Froines, J R 1716
Fronczek, F R 525
Fruin, S 1242i
Fry, C 1549d
Fry, R 229, 1308, 1312, 1314, 1318, 1324, 2228
Fryxell, G 2230
Fu, A 96g
Fu, J 440b, 1804a
Fu, P 1094
Fu, X 85, 1349, 1390*
Fu, Y 1549
Fuentes, J 1087n
Fueta, Y 180*
Fujibuchi, W 978b
Fujii, S 653, 2192
Fujimoto, W 128, 2322
Fujimura, M 1373*, 1387
Fujisawa, N 200*
Fujita, H 1087
Fujita, K 592, 1948*
Fujita, T 1621
Fujiwara, R 190*
Fujiwara, Y 1247, 1248
Fukagawa, N K 2296
Fukami, T 537, 975, 1878
Fukuda, M 1948
Fukumuro, M 447, 467c
Fukushima, T 1174*
Fukutomi, Y 988
Fukuzaki, K 197, 1698, 2126
Fulford, D 326
Fuller, B 343d
Funabashi, H 201, 1046
Fuqua, B K 2128
Furlong, C E 116, 686
Furniss, M 1062d
Furr, J R 1713c
Furst, S M 2168*
Furtado, K S 1513
Fuscoe, J C 100, 122d, 956, 978a, 1713e, 1713f, 2273g
Fussell, K 1078*
Futscher, B 1300

G

Gabazza, C 1977
Gabazza, E 1977
Gabos, S 1024
Gabrielson, K 1706
Gabrilovich, D 1002
Gadagbui, B 2250i
Gadagbui, B K 632j*, 1827
Gadhia, S R 960*
Gadoth, A 606*, 1663
Gadupudi, G S 2199*
Gaffney, S 2234t*
Gaffney, S H 1227, 1228
Gage, J A 1639c
Gagkaeva, T Y 1536
Gähler, S 2131
Gaikwad, S S 464
Gaisch, K 2201
Gaitens, J 1559
Gajewski, P D 363*
Galarneau, J 2124
Galbiati, V 984
Galdanes, K 823, 824, 825, 1986
Gales, S 272
Galizia, A 1830
Gallacher, M 102, 122e
Gallagher, A 778
Gallagher, E P 340, 1529, 1831f
Gallagher, J E 1347j
Gallagher, K 1831b
Galli, C L 984
Galligan, J J 2006
Gallo, M A 1679, 2194
Gallucci, R 979
Gambill, G P 1646
Gamble, H P 1561
Gamble, M 1301
Gamboa da Costa, G 122c, 632g*
Gamboa Da Costa, G C 1616e
Gammon, D W 62, 378e, 683, 685, 689b, 897, 1846
Gamo, M 1967
Gandolfi, A J 143
Ganerup, N 7
Ganesan, S 2183*
Ganey, P E 1197, 1199, 1882, 1886
Ganiger, S 1620, 2196m*, 2196n
Gany, F 1675, 1692
Gao, A 1899e*, 2067a
Gao, H 1500
Gao, W 1504, 1507
Gao, X 173g*, 603, 1297a, 1962, 1973i, 1973j, 2004f
Gao, Y 114, 265d, 1533
Garantziotis, S 583, 603g, 603h
Garban, J A 2213
Garber, H 1742, 1743
Garbow, J 579
Garcia, E 2234z
Garcia, H D 632d*
Garcia, R 1366
Garcia-Cantillo, A 667
Garcia-Montes de Oca, F G 530*
Garcia-Vargas, G G .. 229, 1306, 1308, 1309, 1312, 1314, 1318, 1324
Gard, J 1503
Gardella, K 1110c*
Gardner, D R 805
Gardner, S T 656
Gargas, N M 1818
Garibaldi, P 324
Garlick, R 577
Garner, C 1831g
Garner, L 223e
Garofolo, F 294*, 879, 880, 881
Garrett, S H 244, 1251, 1274, 1322, 1327
Garrett, T L 361
Garry, M R 227, 777*
Garside, H 1644, 1721*, 1733
Gash, D M 942a
Gasiewicz, T A 259, 1458, 1460*
Gassner, G 514
Gaston, J 670*
Gatlin, D 316
Gato, W E 122a, 309*, 922a, 922b
Gatti, D M 279*
Gaukler, S 283*
Gaultier, E 133
Gauthier, L 1128
Gautier, J 380
Gauvin, D 2196t
Gavett, S H 56*, 1205, 1217, 2296
Gavin, T 1170
Gavrilova, O P 1536
Gaytan, B 418d, 524*
Gbadegesin, M A 813b, 1514b
Ge, J 2282
Ge, X 1657
Ge, Y 1101
Gearhart, J M 87, 96, 96f, 440g, 556, 573, 1787
Gebhart, A 609
Geboy, N 1018b
Gee, S J 876
Geertz, M 415
Gehen, S C 63, 408a, 1019, 1943e*
Geiger, D 597
Gelineau-van Waes, J B 343b
Gemani, D B 1547
Gennings, C 1420*
Genter, M 725, 729*, 827
Gentry, R 70, 71, 1404*, 2245*
George, M H 1018a
George, N 440f
Georger, L 1524
Georges, G P 1713a
Geraci, C 8
Gerbal-Chaloin, S 1906
Gerberick, G 982, 992
Gerde, P 1229
Gerecke, D R 563, 565, 575, 578
Gergel, L E 268
Gerger, C J 491
Gerhardt, G A 942a
Gerhold, D 1922a*
Gerlach, C V 212*
Gerlofs-Nijland, M 2297*
Germ, K E 1937*
Germano, D 2056*
Germolec, D R 145b
Gerona, R 2234k*
Gershwin, M 902
Geter, D 1943e
Gettmann, K 616
Ghaemmaghami, A 2174
Ghaisas, S 937
Ghanem, C I 366*
Ghare, S 970*
Ghilardi, N 954g
Ghoreishi, K 1200*, 1868, 2038
Ghose, R 387
Ghosh, A 80
Ghosh, C 1, 122b
Gianios, C 1303
Giannakou, C 2028
Gibbons, A T 848
Gibbons, C F 1828
Gibbs, S 581j
Gibbs-Flournoy, E 1204*
Gibson, C J 2053
Gibson-Corley, K N 1975
Gidda, J 2196l
Gift, J 1831c
Gigliotti, A 1236
Gilbert, J 378, 1115
Gilbert, K 137, 966*
Gilbert, M E 1347a, 1347c, 1347f*, 1347g, 1747c
Gilbert, S G 649d*
Gilger, B 742*
Gill, M W 851*
Gill, P S 99
Gill, R 136
Gill, S S 338*
Gillespie, M E 2095*
Gillet, M 133
Gilmour, I 980, 1204, 1205, 1232, 2296*
Gimenez, E 1856
Gimenez-Arnaud, E 123, 2009
Ginsberg, G L 892, 1822
Giordano, G 1654
Giovannucci, E 1537
Girer, N 1137*
Giri, D 1616c
Girtsman, T A 1465
Giusto, K 572
Glantz, C 2241
Glaza, S M 1698, 2126
Glazier, J A 85
Glenn, B S 239, 1809, 1830, 1831c
Glenny, R W 2140
Glick, A 126
Glinghammar, B 1881
Glista-Baker, E 874*
Glomski, M 2234r
Glorennec, P 1009
Glover, K P 263*
Glynn, M 225, 614, 1227, 1228
Go, R 1087g*
Go, Y 868, 1254*
Goad, P T 504c
Gobejishvili, L 869, 970
Godard-Codding, C 669d
Gödecke, T 790
Godin, C S 271*, 277, 2196l, 2196s
Godleski, J J 1242b
Godoy, R 153
Godwin, C 1581
Godwin, H 833
Goebel, C 982*, 1031
Goedken, M J 2053
Goel, S 1620*, 2196m, 2196n
Goeminne, N 1549a
Goerdetier, D 1055
Goering, P L .. 1945, 1946, 1947, 1955, 1972, 1973g, 2004
Gogal, R M 188, 1284*
Gohel, D 347, 403, 405, 1800, 1801*
Gohlke, J M 235, 1263, 1676*, 2239
Goineau, S 2144
Goksøyr, A 1147
Goldberg, A 305, 306*
Golden, R M 1863
Golden, T 389*
Goldhaber, S 609*
Goldman, J M 1018a
Goldring, C 716*
Goldsmith, M 2234s, 2273o
Goldsmith, M R 2234i
Goldsmith, R B 173d*
Goldstein, J A 954e, 1736b
Goldstone, J V 1147
Golka, K 363, 545*
Gollapudi, B 3*, 467b, 1941, 1943e
Golozoubova, V 1588
Golub, M 848b*
Gomes, J 1200g*
Gomez, A 906
Gomez, S 1815
Gonçalves, F M 1329
Gong, G L 2034*
Gong, Z 1101
Gonzales, C R 2232
Gonzalez, C 378i, 942e, 1973f*, 2196r
Gonzalez, C P 931*
Gonzalez, F 245, 246, 247, 260, 1155, 1163
Gonzalez, F J 1973f
González, S K 595
Gonzalez Suarez, I 1054, 1055*
Gonzalez-Barranco, P 315
González-Horta, C . 797c, 1312, 1314*, 1324
González-Palomo, K 1328*
Gonzalez-Rodriguez, R 1973
González-Weller, D 2218
Goodale, B C 181
Gooderham, N J . 256, 912, 1110, 1865, 1869
Goodfellow, G 1589
Goodman, J 1347f
Goodman, J E 9, 1482, 1489*, 1810, 1811
Goodman, M 9
Goodwin, B 467g*, 1063
Goodwin, N C 279
Goodwin, R 1627
Goodyear, S 915
Goossens, D 1713q, 1713r
Gora, L 1199
Gorasiya, S 1789, 2026

The numerals following the author's names refer to the abstract numbers. The asterisk after the abstract number indicates the author is the first presenter.

Gordon, C J 2330*
Gordon, M K 312a, 575, 578, 581f, 1242c
Gordon, O 958
Gordon, T 823, 824, 825, 828, 1210, 1981, 1986
Gornati, R 835
Gosse, J A 382, 1315
Goswami, D G 554, 555*
Goswami, P 1781
Gothi, A 2151a, 2151b, 2163a
Goto, K 2196bb*
Goto, S 1046*
Gottwald, E M 2055
Goud, N S 1616d*
Goudarzi, M 1155
Goudreau, J L 2006
Gough, A 1880
Gould, S J 1655
Gourronc, F 2199
Govindraj, M 998
Gow, A 389, 858, 998, 1391, 1669, 1979, 2039
Gow, J 998
Gowda, K 1138
Gowda, S 383
Goyak, K 265
Goyal, V 2151a, 2151b, 2163a*
Grabinski, C 8, 1961*
Grace, C 282
Grafström, R C 2273y
Graham, J C 1493
Graham, L 2004
Graham, S 2163b*, 2182
Graham, U 2004h*
Gralinski, M R 2196w
Grandidier, M 2177, 2178*
Grandjean, P 1334
Granum, B 782*, 2248
Grascha, P 985
Grassetti, A 1132
Grassian, V 1975
Gray, J P 1083, 1679*
Gray, K 703
Gray, L E 1713c
Gray, S J 2203*
Gray, W G 792
Graza, S 197
Graziano, M J 849, 850, 851, 852, 854, 1089, 2191
Grebe, T 1627
Green, A 324, 1110g
Green, A L 973*
Green, B 552c, 1943c
Green, B J 2036
Green, B T 805
Green, C E 581d
Green, L 1100
Green, M 419
Green, R 238, 327, 343g, 1090
Green, S 1268
Green, S M 2059
Green, T D 1973b*
Greenamyre, T 1520
Greenberg, G I 1554, 1555, 2234q
Greene, N 1647
Greene, T 2245
Greenhaw, J 99
Greenwood, J A 1637
Greenwood, K A 1625
Greggs, B 649b
Gregori-Puigjané, E 2269
Gregory, J 586
Gregory, P A 918
Gregory, S G 343b
Gregus, Z 1311, 1313*
Grespin, M 2235*
Griffioen, J 1204
Griffith, W C 1763
Griffiths, J C 1469*, 1473, 1475
Griggs, A M 923
Grimaldi, M 149
Grimm, F 1890
Grizzle, T B 887*
Grogg, M 832*
Grollers-Mulderij, M 1970
Grondin, C J 423*
Grondin, R 942a*
Groom, S 344, 1225
Groothuis, G M 1062h*
Grosdidier, E 1654
Grosh, J 474
Gross, A D 671
Gross, M S 2204*
Gross, S A 233
Grossi, I M 2121*
Grote-Wessels, S 1659
Groten, J P 1154*
Gröters, S 597, 1078, 1220, 1221, 1992
Groth, E 649d
Groves, A M 552f, 2327*
Gruenig, F 186
Grulke, E 2004h
Grummt, T 451, 467h
Grund, E 417
Grundén, S 1030
Grunwald, W 361
Gryder, L 1713q, 1713r
Gu, C 1206
Gu, H 1705
Gu, J 508, 1713u
Gu, Q 378i, 603b*, 942e
Gu, S 915
Gu, T 550
Gu, X 1184*
Guallar, E 1306
Guan, D 1804a
Guan, H 1935
Guardiola, J 1870, 1879
Guariento, A H 1513
Guariglia, S 1392a*
Gucer, P 1559
Guedj, E 415, 860
Guerra, F A 317
Guerrero, A 406, 1157
Guerrero, T 2245
Guerrero-Castilla, A 667
Guerrette, Z 618*
Guertz, M 860
Guguen-Guillouzo, C 1192*
Guha, M 1656*
GuhaMazumder, D N 977
Guilarte, T R . 1288, 1289, 1339, 1340, 1364, 1365, 1392a, 2103, 2106*
Guillaume, P 2144
Guillette, L 1279
Guillouzo, A 1192, 1193*
Guillouzo, C 1150, 1193
Gukasyan, H 97
Gullick, D 683
Gulumian, M 1297b, 1297c*, 1831j
Gumbo, T 1876*
Gunawan, R 646
Gunewardena, S 49, 1495
Gunness, P 1047*, 1890
Guo, C 998*, 1391
Guo, D 2261*
Guo, G L 973, 1162, 1669*, 1889
Guo, J 1117
Guo, L . 173l, 319, 1062d*, 1195, 1892*, 1893, 1943b
Guo, N L 590
Guo, T 387, 662
Guo, T L 145b
Guo, X 319, 1943b*, 1973c
Guofeng, G 2033
Gupta, A 1627*
Gupta, P 1496*, 1508
Gupta, R C 673*
Gupta, S 551
Guralnik, M 572
Gurevich, I 1176
Gurley, B 1473*
Gustafsson, J 149, 150, 1327a
Guth, K 2172*
Guthrie, A S 1511
Gutierrez, A 877
Gutierrez, J C 188
Gutierrez, J E 1664
Gutiérrez, J 2218
Gutiérrez Torres, D 1312, 1314, 1324
Gutjahr-Gobell, R 1087h
Gutkin, D W 1242g
Gutting, B 581b*
Guy, P 1054
Guy, R H 632
Guyton, K Z 630
Guzylack, L 133*
Gwavava, P 791*
Gwinn, M R 1831k*
Gwinn, W M 1229d*

H

Haag, V 401
Haarmann-Stemmann, T 902
Haas, R 469
Haase, A 1950
Haber, L T 63, 68, 467b, 1819*
Haberzettl, P 1121, 1239*, 2319
Habibovic, A 390
Hack, C 87*, 96, 440f
Hack, E 895
Hackbarth, A 1990, 2003*
Hackenberg, M 265d
Hackett, E 848b
Haddad, S 632e*, 839, 1012, 1766, 1998
Hadiya, K 405
Hadrup, N 1018d, 1175
Haeberle, M T 1500
Haedo, R 1118
Haenen, G 335
Haertle, S 2196
Hafeez, M 807
Hafez, M M 504
Hafner, M 2055
Hageman, G 2171
Hagenbuch, B 900, 2206, 2208
Hagerman, A 2037
Haggard, D E 181*
Hahn, M E 209*, 1147, 2283
Hahn, R A 575, 578, 581f
Hahn, W R 1025
Hai, C 1212
Haigh, T A 1678
Haighton, L A 621, 632h, 2246*
Hailer, K 2220
Haines, C 1134
Haisler, W L 1639c
Hajela, R 1377, 1381, 1384
Hajirahimkhan, A 790
Hakkinen, P J 1662c*
Halappanavar, S 1478
Halayko, A J 921
Hald, K 424
Halder Sinha, S 1541
Haldre, S 2105
Hale, M 1627
Hales, B F 1713
Hales, D B 309
Hall, D 378a*, 378b, 1973a, 2196i
Hall, G 1679
Hall, J 2196h
Hall, L 561, 2242
Hall, M 1301
Hall, M L 995
Hall, P A 847
Hall, R 2137
Hall, S 1087d
Hall, S J 1686, 1709
Hallberg, L M 921, 1235
Hallgren, S 1749*
Hallinger, D 1713d, 2190
Halpert, J R 539a
Hamada, M 1344, 1345
Hamadeh, H 98
Hamed, E O 2234
Hamernik, K L 1087c
Hamid, Q 906, 1722
Hamid-Berair, R E 2319
Hamilton, J 1422, 1426*
Hamilton, R 352
Hamilton, R F 1465
Hamilton, T 581a
Hamlin, D M 119*
Hamlin, R 477
Hamm, J T 440h*, 1149, 2250b, 2273i
Hammerman, K 103
Hammock, B D 876
Hamre, J 173l
Han, A A 1729, 1731*, 1735
Han, C 2128, 2258
Han, H 2032*
Han, S 549
Han, T .. 100, 122d, 956, 978a*, 1713e, 1713f
Han, X 263, 467d, 1755
Hanafusa, H 1866
Hand, J J 2250d
Haneda, R 2196bb
Haney, J T 610, 780*
Hanig, J P 378f
Hanke, N 475
Hanks, B C 886*, 2118
Hanlon, P 811
Hannon, H 1368b*, 1370
Hannon, P R 2186*
Hansen, D K 173c
Hansen, E 154
Hansen, J M 194, 1836
Hansen, S C 2173
Hansen, T 512*, 600, 1953
Hanser, T 2262
Hantash, J 2196q*
Hanzlik, R P 1045, 1713a
Hao, R 1141
Happo, M 1206
Harano, K 1967
Harbison, R D 299, 419, 1087n, 2234e, 2234z
Hard, G C 2059
Hardas, S S 2004h
Hardej, D 680, 1278, 1292, 1297d, 1667*
Harder, B 1791*
Hardiman, G 654
Harding, K 2151d
Hardisson, A 2218
Hardisty, J F 2131
Hardwick, R N 547, 1327c, 1626*, 2061
Hardy, B 431, 2273m, 2273y*
Hardy, J 282
Hardy, K D 552b*
Hardy, P A 942a
Hargest, T 1706
Hargraves, T L 1542
Hargreaves, A 748*
Hargreaves, V 95
Harischandra, D 1350*, 1351
Harkema, J R . 5, 140, 440, 771*, 1240, 2324, 2328
Harmon, M E 2226*
Harney, J 864*
Harper, B 816*, 838, 1984
Harper, S L 816, 838, 1984
Harper, T 292, 513*, 539d
Harrer, H 314
Harrill, A H 106, 543, 813d, 1480*, 2274, 2278*
Harrill, J 504c
Harrill, J A 1132, 1905*, 2020
Harris, A J 2101*
Harris, C 194, 1690
Harris, C M 1943f*
Harris, G 1737, 1738, 1912
Harris, J 1627
Harris, K 792, 1109*
Harris, M A 779, 1290
Harris, P 1062a
Harris, R 877, 1616a
Harris, S 1549f, 1702*, 1707
Harris, S C 2273k
Harris, W W 1561
Harrison, B S 596
Harrison, P 642
Harrison, R 1204
Harrouk, W A 173c
Hart, D 1030
Hart, J A 352
Hart, R P 1752
Hartnett, J 167
Hartog, M A 531*, 532
Hartung, T 1443*, 1608, 1737, 1738, 1912
Hartwig, A 1448*
Harvest, G 550
Harvey, S 404, 1713s
Harvey, W A 2200
Harvilchuck, J A 567

Author Index (Continued)

The numerals following the author's names refer to the abstract numbers. The asterisk after the abstract number indicates the author is the first presenter.

Harvison, P J ... 1200f
Hasan, M ... 942
Hasegawa, G ... 1991
Hasegawa, R ... 432
Hasegawa, T ... 1392
Hasegawa, Y ... 1977
Haselman, J T ... 1087d
Hashiguchi, K ... 472
Hashimoto, K ... 110*
Hashimoto, N ... 1977
Hashmi, H ... 382, 1315
Hass, U ... 1018d
Hassen, W ... 1906*
Hassoun, E ... 1018*
Haswell, L E ... 1528, 1530
Hatayama, K ... 2196bb
Hatayama, T ... 128
Hatef, E ... 223i
Hathcock, J N ... 343h
Hattan, D ... 632g
Hattori, C ... 446*
Hatwell, K R ... 1584
Hatzakis, E ... 1141
Hauchard, A ... 1618
Hausherr, V ... 378d*
Havics, A ... 613
Hawk, M ... 581h*, 2196j
Hawkins, A ... 355
Hawkins, A D ... 1987*, 1988
Hawkins, B ... 627
Haws, L C ... 622, 623*, 779, 1290
Hayashi, A ... 978b
Hayashi, H ... 128, 961, 2322
Hayashi, M ... 432, 447, 467c
Hayashi, S ... 324
Hayden, B K ... 2004a
Hayden, P J ... 1035, 1038, 1040, 1053*, 2181
Hayes, A ... 413, 415, 860, 1054, 1055, 1087i, 1203, 1592, 1662b
Hayes, E ... 2144*
Hayes, H G ... 317, 1526
Haynes, E ... 2286, 2288*
Hays, B ... 1742, 1743
Hays, M ... 980
Hays, S M ... 779, 1065, 1296*
Hazari, M S ... 492*, 2296, 2323, 2329
He, C ... 662
He, G ... 1146
He, J ... 189
He, K ... 1887*
He, Q ... 287, 473, 2142, 2156
He, R ... 1777
He, Y ... 1281, 2128
Head, A ... 2196o
Heart, E A ... 1083*
Hebert, L ... 215
Hebert, V Y ... 501
Hecht, E ... 906, 1722
Heck, D E ... 559, 562, 563*, 565
Hecker, M ... 173
Hedge, J M ... 1747a, 1863b
Hedrick, E ... 1131*
Hedrick, H ... 1186, 2062
Heflich, R H ... 3, 453, 1062b, 1943b
Hegde, V L ... 922*, 962
Hegg, C ... 1922b*
Heideman, W ... 490, 504b, 1681, 1746
Heindel, J J ... 703*
Heindel, N ... 561
Heinonen, T ... 1062a, 1087o*
Heinrich, U ... 1990, 2003
Hejtmancik, M ... 1616c
Helliwell, S B ... 873
Helmcke, K J ... 38
Helmer, M ... 365
Hemkens, M ... 864, 1128, 2083
Henderson, G I ... 1839
Henderson, K A ... 581h
Henderson, R ... 1280*
Henderson, W M ... 1087f
Hendricks, C ... 267
Hendrickx, D M ... 2273e*
Hendriksen, P ... 408b*
Hendry-Hofer, T ... 577
Hendy, O ... 689
Hengst, J ... 1623
Hengstler, J G ... 363, 545
Hennan, J K ... 851
Hennen, J ... 982
Hennig, B ... 1124
Hennings, L ... 254
Henningsen, G M ... 624
Henriques, T A ... 899*
Henriquez, A R ... 1230*
Henry, S ... 1171, 2113*
Henshaw, J L ... 2234t
Henteman, M ... 1644
Hentges, K ... 184, 195
Henwood, S M ... 186*, 2148
Heo, Y ... 1229b*, 1713m, 2129d*
Heppenheimer, A ... 1062*
Her, L ... 2196g
Herbert, R A ... 813a, 1110f
Herman, D ... 1242f
Herman, E ... 100
Herman, J K ... 953, 2136*
Hermansky, S J ... 2087, 2089*
Hernandez, A ... 1305*, 1317, 1954
Hernandez, C ... 1235
Hernandez, J M ... 1973f
Hernandez, L ... 603i
Hernandez, L L ... 1087s
Hernandez, M ... 1986*
Hernández, L G ... 343a
Hernández Ávila, J ... 1312
Hernández Cerón, R ... 1312, 1314, 1324
Herold, M ... 120, 1591
Herpers, B ... 1168, 1715, 1872, 2031
Herr, D ... 1342
Herr, D W ... 378a, 1347b, 1863a, 1863b*
Herrera-Cogco, E C ... 1723*
Herring, A H ... 229
Herrmann, J ... 859
Herry, L ... 870
Herting, G ... 1280
Hertz-Picciotto, I ... 698, 2234g
Hess, A ... 1057
Hester, S D ... 65, 1062f, 1476*, 2273q
Hesterberg, T ... 504c, 1229g*
Hetland, R B ... 1084, 2248*
Hettick, J M ... 2036
Hettinger, J ... 1653
Heusinkveld, H J ... 1833*, 1835
Heussner, A ... 1566*
Hew, K M ... 391
Hewitt, J ... 2134
Heydens, W F ... 330
Heyen, J ... 1128, 1429, 1432*, 2083*
Heyob, K M ... 1688
Hibatallah, J ... 1027
Hibbard, N ... 166
Hibi, D ... 442
Hickman, D ... 1641
Hiemstra, S ... 173f, 1715*
Hien, T ... 1125
Higashi, E ... 2151*
Higgins, M ... 1200b
Higley, E ... 173
Higuchi, M A ... 5, 10, 1062f, 2329
Hilberer, A ... 1020
Hill, J ... 544, 2196i
Hill, K ... 689a
Hill, T ... 2170*
Hillenweck, A ... 149
Hinckley, J ... 2002
Hinderliter, P M ... 684, 1831g
Hinds, A I ... 1576*
Hiner, J ... 2196z
Hines, E P ... 1713k*
Hines, R N ... 53, 189, 192
Hines, S E ... 1559
Hinkley, G K ... 1989*
Hinrichs, M ... 2109, 2112*
Hinton, D E ... 841
Hirabayashi, Y ... 1900*
Hirakawa, B ... 1726
Hirano, S ... 822, 1321
Hirata-Koizumi, M ... 460, 2192
Hirayama, T ... 472
Hirose, A ... 199, 432, 460, 2192*
Hirose, R ... 1717*
Hirota, M ... 1600
Hirvonen, M ... 983, 1206
Hitron, J ... 1297f
Hixon, G ... 231, 628*, 781, 1280
Ho, B C ... 1151*
Ho, E ... 1682
Ho, I ... 369
Hoban, D ... 328
Hobbie, K A ... 1678, 2215*
Hobbs, C A ... 324*
Hobbs, D ... 2220
Hobden, J ... 2247
Hobson, B A ... 579*
Hobson, D W ... 1713a
Hocevar, B A ... 548, 1786, 1804b
Hock, M B ... 898
Hockings, P ... 1429, 1431*
Hoekman, K ... 2294*
Hoenerhoff, M ... 955
Hoenerhoff, M J ... 1713b
Hoeng, J ... 413, 415, 860, 1054, 1055, 1203, 1592
Hoet, D ... 1643
Hoffman, A D ... 669e
Hoffman, C ... 355, 1692
Hoffman, G ... 280
Hoffman, L M ... 680*, 1667
Hoffmann, A ... 902
Hoffmann, S ... 954b
Hofman-Hüther, H ... 327
Hofsteen, P J ... 490, 1129d*
Hogan, K ... 1831c
Hogberg, H T ... 1737*, 1738, 1912
Hogrefe, C ... 848b
Hokey, D A ... 271
Holbrook, M ... 468
Holden, P ... 833
Holian, A ... 140, 588, 1465*, 1978, 2321
Holladay, S D ... 188*, 1284
Holland, N ... 702*, 707*
Holland, N A ... 484*, 485
Hollander, J M ... 486, 1689
Hollert, H ... 173
Hollingshead, B ... 1128
Hollingshead, B D ... 1635*
Hollnagel, H M ... 1609
Holloway, A C ... 1713
Holman, N S ... 388
Holmes, A ... 1272, 1276*, 1450, 1942
Holmes, T ... 1202*
Holmes, W ... 570, 577, 2163c*
Holmgren, S ... 2250k
Holmquist, A ... 1251
Holmuhamedov, E L ... 1783
Holsapple, M P ... 2088*
Holub, V ... 1973d
Homer, B L ... 2057
Hong, H ... 955, 1087a*
Hong, L ... 1362, 1390
Hong, M ... 293
Hong, P ... 2196j
Hong, S ... 1702, 1763
Hongping, W ... 2156
Honma, M ... 460
Hood, A ... 949, 951*
Hood, D B ... 1684*, 2023
Hood, L ... 418c
Hoofnagle, A N ... 116
Hoogstraate, J ... 901, 1883
Hoover, D ... 1559
Hoover, J ... 669d
Hope, E ... 945, 946*
Hopf, N B ... 2176
Hopkins, C ... 1932
Horai, H ... 1919
Horie, M ... 1948
Horn, K ... 850*, 853, 854
Horn, T L ... 2196y*
Horne, B ... 581j
Horne, C ... 649b
Horner, M J ... 898
Horner, S ... 284, 2110
Hornung, M W ... 1087d*
Horsmon, M ... 2141*
Horvath, C ... 267*
Hosako, H ... 1634*
Hosoi, K ... 2119
Hosokawa, M ... 1392
Hosoki, E ... 1649
Hossain, M M ... 1844, 1845*
Hotchkiss, A ... 1807
Hotchkiss, J A ... 82, 688*, 770*
Hotchkiss, M G ... 1087f
Hou, F S ... 603c
Hou, M ... 1117
Hou, Y ... 1794
Houben, G ... 1823
Houck, D ... 2196l
Houck, K ... 173b, 223d, 343c, 378b, 418b, 1149, 1736e, 1973e, 2250a, 2273l, 2273q, 2273s, 2273v*, 2273z
Houdeau, E ... 133
Houle, C ... 125
Houston, J B ... 689b
Houthoff, E ... 1030
Houtman, R ... 1063*, 1150, 1154
Houze, J ... 2269
Howard, B ... 2250k*
Howard, K E ... 2196r*
Howard, P C 598, 1756, 1947, 1973c, 2004c, 2273k
Howard, W R ... 895, 1820
Howdeshell, K L ... 1713c*
Howell, B A ... 412
Howell, G E ... 679, 2198*
Hoyt, S ... 1575
Hristova, M ... 390
Hristozov, D ... 30, 431*, 2273d
Hruba, E ... 1943a
Hsaio, J ... 1171
Hsia, F K ... 948*
Hsieh, C ... 1808*
Hsieh, E J ... 116
Hsieh, H ... 827
Hsieh, J ... 173b, 173h, 343c, 1149, 2273bb*
Hsieh, W ... 89
Hsu, C ... 1149*
Hsu, J ... 1364, 2196x
Hsu-Kim, H ... 841
Hu, B ... 674
Hu, C ... 1642*
Hu, F ... 1337
Hu, H ... 408*, 687
Hu, J ... 533*
Hu, L ... 346*, 794, 1802
Hu, Q ... 699, 1336, 2040b
Hu, R ... 98
Hu, W ... 97, 1128, 2083
Hu, X ... 896*, 1962
Hua, D H ... 1508
Hua, M ... 645*
Huang, B ... 1578*, 1935
Huang, C 296, 357*, 1325, 1369, 1388, 2054
Huang, D ... 159
Huang, D Y ... 1024
Huang, H ... 939
Huang, J ... 577, 1001, 1087, 2196w
Huang, L ... 947, 954f, 1151
Huang, M ... 856, 1903
Huang, N ... 2151c
Huang, R ... 173b*, 173h, 444, 467g, 1149, 2252, 2273s, 2273bb
Huang, S ... 860
Huang, S S ... 153*
Huang, T ... 496*, 2060*
Huang, W ... 48, 50*, 97
Huang, X ... 813*
Huang, Y ... 603c*, 943
Huang, Z ... 1003, 2196g, 2196p
Hubbard, F ... 877
Hubbard, K S ... 1922c, 1922d
Hubbard, T D ... 1139*
Hubbs, A ... 2004d
Hubbs, A F ... 23
Hudgens, E E ... 1327d, 1347j
Hudgens, L ... 953*, 2137
Hudson, A ... 125, 397*
Hudson, L G ... 143, 1316, 1449
Hudson, S L ... 1263*
Huen, K ... 707
Hugentobler, M ... 333
Hughes, B J ... 885, 2059
Hughes, D ... 1921, 1922

The numerals following the author's names refer to the abstract numbers. The asterisk after the abstract number indicates the author is the first presenter.

Hughes, J M ... 1136, 1138
Hughes, M F ... 603a*
Hughes, V S ... 119
Hui, J Y ... 202*
Hui, S T ... 1281
Hukkanen, R ... 1132, 1863
Hulderman, T ... 603d
Hulla, J E ... 649c*
Hulsizer, S ... 360
Hummer, J ... 1242g
Humpf, H ... 314
Humphreys, W G ... 855
Hunault, C C ... 96c
Hüner, H ... 173
Hung, D ... 1369, 1388
Hung, G ... 1171
Hunter, D D ... 392
Hunter, D L ... 173i
Hunter, E S ... 769*
Hunter, S ... 440c, 1018a
Huppelschoten, S ... 2031*
Hurban, P ... 2273q
Hurst, N W ... 1677
Hurt, R ... 668
Husain, A ... 1639
Husain, R ... 1639a*
Huse, S M ... 1686, 1710
Hussain, N ... 940
Hussain, S ... 583, 603g*, 603h
Hussain, S M ... 8*, 832, 1583, 1959, 1960, 1961, 1964, 1965, 1985
Hussin, H F ... 798
Hutchinson, L ... 382, 1315
Hutson, M ... 418a, 2273f
Hutson, P ... 1006
Huttunen, K ... 983
Hutzler, C ... 1067
Hwang, G ... 1253*, 1257
Hwang, J ... 441*, 593, 1976, 2001
Hwang, M ... 1260
Hwang, S ... 2129d
Hwang, Y ... 1166, 1167
Hyduke, D R ... 1478, 1938
Hynes, J ... 1918
Hyvärinen, A ... 983

I

Iadonato, S P ... 901c
Iankova, I ... 1906
Iatropoulos, M J ... 171
Ibor, O R ... 1074*
Ichihara, G ... 502, 1087, 1971, 1977, 1994
Ichihara, S ... 502*, 1087, 1971, 1977, 1994
Ichimura, R ... 1070, 1160, 1161
Iciek, L A ... 2112
Ickstadt, K ... 545
Idowu, A A ... 651
Igweze, Z N ... 1691*
Ihrie, J ... 1944
Ihrie, M ... 1758
Iida, M ... 653*
Ijeh, I I ... 1200c
Iji, O T ... 650*
Ikarashi, Y ... 199
Ikemoto, T ... 1259
Ikenaka, Y ... 517, 521*, 843, 1516
Imai, D M ... 124
Imaida, K ... 1091, 1092, 1093, 1213
Imam, M S ... 841b*
Imam, S Z ... 378i, 942e
Imaoka, M ... 494
Imerman, P ... 362
Imhoff-White, F ... 791
Inada, H ... 201
Inceoglu, B ... 360
Infante, S K ... 1672*, 1742, 1743
Infante-Ramírez, R ... 797c
Ing, B R ... 689b
Ingber, D E ... 1444*
Ingber, S Z ... 223g*
Ingelman-Sundberg, M ... 1047
Ingham, P ... 157
Ingle, T ... 598, 1973c
Ingram, H ... 1673
Inhof, C J ... 612
Inoshita, T ... 1747b
Inoue, K ... 1070, 1160*, 1161
Inoue, R ... 2133
Inoue, T ... 1093, 1900
Inselman, A ... 173c
Int Panis, L ... 223h
Inturi, S ... 553, 554
Iqbal, S ... 901f, 1662*
Iregren, A ... 1224
Irimagawa, H ... 1281*, 2128
Irwin, J J ... 410
Irwin, W A ... 312e*
Isales, G ... 152, 155, 156
Ischiropoulos, H ... 2039
Ishida, K ... 898*
Ishida, M ... 1312, 1314, 1324
Ishida, Y ... 1899b
Ishiguro, N ... 2196e
Ishihara, Y ... 669a, 669b
Ishii, Y ... 442
Ishizuka, M ... 517, 521, 843, 1516
Ismail, A ... 1825
Ismail, A A ... 689
Israel, E D ... 2234x
Ito, K ... 110
Ito, T ... 241
Ito, Y ... 1649
Itoh, S ... 446
Itoh, T ... 190
Ivanov, N ... 413
Ivask, A ... 833
Iwamura, A ... 537
Iwanari, H ... 1899b
Iwano, S ... 2151
Iwasawa, K ... 1967*
Iwase, Y ... 455, 1621
Iwata, H ... 516, 517, 519, 653, 1259
Iyer, A ... 1195, 1892
Izuoka, K ... 1971

J

Jaafar, M ... 1825*
Jablonski, R ... 325
Jack, J ... 2273q*
Jack, L ... 391
Jackson, A ... 1478
Jackson, A R ... 922
Jackson, B ... 665, 2317
Jackson, B C ... 552*, 1095, 2046
Jackson, D A ... 1297, 1858
Jackson, G ... 1053
Jackson, J ... 627
Jackson, M ... 612*, 1229a, 1368a
Jackson-Humbles, D ... 2328
Jacob, B ... 2135
Jacob, C C ... 632g
Jacob, R E ... 2140*
Jacobs, A ... 759, 2310*
Jacobs, M ... 1087c
Jacobs, N ... 2250h
Jacobs, S L ... 1499
Jacobson, S ... 1698
Jacobson Kram, D ... 1446*, 2114*
Jadav, S K ... 1848
Jadhav, S ... 347*, 403
Jaeger, C ... 1153, 2197
Jaeger, T ... 1242b
Jaeschke, H ... 708, 713*, 867, 1172, 1178, 1181, 1196*, 2274, 2277*
Jaetae Seo, F ... 841e
Jäger, M ... 173
Jahangardi, R ... 520
Jaillet, L ... 888
Jaiman, R J ... 1375*
Jain, A K ... 553, 554
Jaiswal, A K ... 1083
Jaiswal, S ... 398, 399
Jalava, P I ... 1206*
James, A ... 895
James, J T ... 632d, 2250d
James, L P ... 99
James, R A ... 1787, 1820*
Jamieson, J ... 1128
Jamison, J A ... 1641
Jan, Y ... 559*
Jana, S ... 2151a*, 2151b, 2163a
Jang, H ... 539a
Jang, S ... 871
Jankovich, A ... 310
Janovitz, E ... 850, 1089, 2034
Janz, D ... 1294*
Jarabek, A M 775*, 1217, 1409*, 1830, 1831k
Jardine, L ... 1695, 2161
Jarema, K A ... 173i, 1747a, 2330
Jaskot, R ... 1204
Jaspers, I ... 874, 1242i
Javdan, M ... 940
Javier, C L ... 848a
Jaworska, J ... 1831l
Jay, J W ... 922a*
Jayaraman, A ... 1130
Jayaraman, S ... 1087h
Jayasundara, N ... 223e
Jayjcok, M ... 2250i
Jayyosi, Z ... 1113
Je, I ... 999
Jefferson, A M ... 1368a
Jeffery, B ... 320, 1616
Jeffrey, A M ... 171, 467a
Jeffy, B D ... 202, 1200, 1868*
Jeliazkova, N ... 431
Jena, G ... 465*, 1097, 1700
Jeng, A ... 1077*, 2227
Jenkins, D P ... 1842
Jenkins, S V ... 598
Jenkinson, S ... 2083
Jennen, D ... 1872, 2273e
Jenner, J ... 2182
Jensen, K F ... 173i
Jensen, M ... 1713q, 1713r
Jensson, M ... 2157
Jeon, R ... 871
Jeong, D ... 2234l*
Jeong, H ... 506, 507, 787, 795, 797a, 797b, 799, 800, 801, 802*, 1166, 1167, 1549g, 2032
Jeong, T ... 440l, 890*, 1200e, 1200i, 1549g, 2032
Jessop, F ... 588*
Jestoi, M ... 343e
Jethwaney, D ... 2043
Jett, D ... 558, 564, 567
Jetten, M ... 1062h
Jetter, J ... 1204
Jeyaseelan, S ... 1514
Ji, C ... 1657*
Ji, F ... 659
Ji, X ... 603k
Ji, Z ... 1941
Jia, C ... 1922b
Jia, K ... 532
Jia, W ... 1324
Jia, Z ... 1229e, 1713t, 1790, 1792*
Jiang, H ... 1102
Jiang, J ... 1003, 1461
Jiang, M ... 1685
Jiang, S ... 122a, 1804a
Jiang, W ... 535, 538, 539, 1390, 1796
Jiang, X ... 295, 493, 1888
Jiang, Y ... 813, 1367, 1653, 2231
Jianshe, W ... 976
Jiko, H ... 1116
Jilek, J L ... 194*, 1690
Jiménez-Capdeville, M ... 1328
Jimenez-Velez, B D ... 875, 981, 1785
Jin, C ... 954f*, 1617*
Jin, H . 927, 936, 937, 1285, 1350, 1352, 1832
Jin, L ... 2065
Jin, M ... 999
Jin, S ... 787*, 797a, 799, 800, 801
Jin, U ... 1130*, 1131
Jindo, T ... 494
Jing, H ... 1348
Jing, J ... 1804
Jinot, J ... 1831c
Jirau, H ... 875*
Jo, E ... 1229b
Jo, J ... 1713m, 2129d
Joachim, B ... 2136
Joca, L ... 776
Johanson, G ... 74, 86, 642*, 643, 815, 1224, 1814
Johansson, H ... 1062g
Johansson, M ... 643*
Johari, S ... 660
John, A ... 1769
John, B B ... 1324
John, J ... 418b
John, P J ... 1957*
John, T N ... 352
John-Baptiste, A ... 97
Johns, D ... 1018c
Johnson, A ... 938
Johnson, A G ... 1429, 1433
Johnson, B ... 2021, 2022
Johnson, B P ... 1087u*
Johnson, C ... 1232
Johnson, D 424, 436, 437, 1230, 1336, 1582, 1927, 2258
Johnson, D E ... 2267
Johnson, D L ... 778
Johnson, D R ... 669d*, 841a, 1662d
Johnson, G T ... 299, 419, 1087n, 2234e, 2234z*
Johnson, J ... 1151
Johnson, J A ... 1736d
Johnson, M D ... 1080, 1652
Johnson, N ... 1627, 1644
Johnson, R ... 2046
Johnson, V J ... 43*, 407*, 2029
Johnson, W D ... 889
Johnson-Restrepo, B ... 667
Johnston, C J ... 552f*
Johnston, N ... 1706
Johnstone, A F ... 1347f, 1347g, 2330
Jokinen, M P ... 1110f
Jokiniemi, J ... 1206
Jolley, H D ... 602, 814, 1980
Jolliet, O ... 815
Jolly, P ... 343j
Jonaitis, T ... 632h*
Jonebring, A ... 1881
Jones, A ... 1362
Jones, B ... 2250b, 2273i
Jones, B A ... 1527
Jones, B C ... 2129a
Jones, C P ... 841d
Jones, D ... 1344, 1345
Jones, D P ... 115, 418, 421, 422, 868*, 1254
Jones, I W ... 1018e
Jones, K L ... 1759
Jones, L A ... 193
Jones, R ... 776, 1828
Jones, S ... 1712*
Jones, S Z ... 874
Jones, Y ... 1947, 1973c, 2004c
Jonsson, M ... 343e
Jonsson, P ... 150
Jordan, E ... 1058
Jordan, S ... 2139
Jordan, S A ... 1470*
Jordt, S E ... 2169
Jortner, B S ... 2002
Jose, C C ... 967*
Joseph, D ... 987
Joseph, L B ... 563, 565*
Joseph, P ... 1713u*
Joshee, L ... 2042
Joshi, A ... 292
Joshi, K P ... 498*
Joshi, N ... 1191*, 1867
Joshi-Barve, S ... 869, 970, 1182
Joubert, P ... 1229e
Joy, M S ... 1802
Juarez, Z N ... 603i
Juberg, D R ... 61, 82, 688
Judson, R ... 173b, 223d, 1062f, 1066, 1087p, 2234s, 2250a, 2273l, 2273n, 2273o, 2273p, 2273s*, 2273t, 2273u, 2273v, 2273z, 2273aa
Jugg, B J ... 2163b
Juliar, B E ... 1616e
Jung, B ... 942, 2052
Jung, D ... 665*
Juran, S A ... 1224
Justiniano, R ... 2164*
Jutooru, I D ... 1105, 1106, 1511*

Author Index (Continued)

The numerals following the author's names refer to the abstract numbers. The asterisk after the abstract number indicates the author is the first presenter.

K

Kabadi, P K ... 603l*
Kabakoff, B ... 269
Kabalo, A N ... 843
Kabayama, K ... 954
Kabiersch, G ... 323
Kacew, S ... 1087w, 1087x
Kadambi, V J ... 7, 102, 122e, 1548
Kaden, D ... 70, 71, 1765*
Kadiiska, M B ... 1006b*, 2030
Kadin, J A ... 2093
Kado, N ... 2295*
Kadota, T ... 113*
Kadry, A M ... 2117*
Käfferlein, H U ... 1007
Kagami, Y ... 653
Kagan, V E .. 603e, 603f, 1002, 1003*, 1242g, 1520, 1777, 2004d, 2273a
Kahn, E ... 902
Kakade, S ... 2151a, 2151b, 2163a
Kakarala, M ... 1922e
Kakeyama, M ... 1346, 1747b, 2163
Kakuni, M ... 1899b
Kalasekar, S ... 1327a*
Kalbasi, A ... 122f*
Kale, V ... 797*
Kale, V P ... 1623*
Kalen, A ... 1781
Kallman, M ... 2196v*
Kalluvila, T A ... 1690a*
Kamal, A ... 1240
Kamdem, J P ... 173n
Kamendulis, L M ... 548, 1786*, 1804b
Kamerud, K L ... 2215
Kaminski, N E 438, 730*, 2005, 2007, 2015, 2016, 2018, 2019, 2020
Kammerer, A ... 510
Kamp, H ... 120, 1591*, 1871, 1992
Kamp, L ... 1566
Kan, K ... 2258
Kan, L ... 1019, 1602
Kan, R K ... 581c*, 581e
Kanbara, C ... 519
Kancherla, J ... 892, 2273n
Kandarova, H ... 762*
Kane, A ... 603l, 668
Kang, B ... 246
Kang, D ... 1125, 1327e
Kang, H ... 1044, 1571*
Kang, K ... 1125
Kang, M ... 226*, 317, 810, 890, 942, 1532, 1549g, 1779
Kang, S ... 1122
Kang, W ... 890
Kania-Korwel, I ... 2205*
Kanie, S ... 1091, 1092, 1213
Kanki, M ... 961
Kannan, K ... 1522, 1570
Kanno, J ... 1900, 1974*
Kansy, M ... 79*
Kant, R ... 555
Kantaria, K ... 2227*
Kanthasamy, A ... 362, 927, 927, 936, 936, 937, 937, 1285, 1285, 1350, 1350, 1351, 1352, 1832, 1832
Kanthasamy, A G ... 362, 1351, 1352
Kanungo, J ... 173m, 378i, 942e
Kaphalia, B S ... 384
Kapitan, J ... 1616d
Kapke, P A ... 2202
Kaplan, A ... 637
Kaplan, B L ... 1410, 1411*, 2006, 2007, 2020, 2087*
Kappen, C ... 187*
Kapralova, V ... 1520
Karabekian, Z ... 1129c
Karahalil, B ... 1713n, 2234d*
Karaki, S ... 123, 2009*
Karakitsios, S P ... 2250f
Karalius, B J ... 268
Karania, S ... 2242
Karanth, S ... 1699*
Karbowski, C M ... 98*
Karchner, S I ... 209, 965, 1147
Karim, M R ... 1725*, 1728
Karlsson, O ... 941
Karmaus, P W ... 1410*
Karmaus, W ... 997
Karner, T ... 900
Karoly, E D ... 2326
Kasaian, M ... 103, 1128
Kasamoto, S ... 447
Kashon, M L ... 23, 1713u
Kaski, S W ... 581c
Kasurinen, S ... 1206
Katavolos, P ... 954g, 2196p
Katche, C G ... 1072*
Katewa, A ... 954g
Kato, H ... 592, 1948, 2192
Kato, K ... 455
Kato, M ... 1087, 1600, 1994
Kato, Y ... 1866
Kaur, N ... 157
Kaushik, G ... 1760*
Kauss, M A ... 1060*
Kavanagh, M ... 338
Kavanagh, T ... 546, 603, 1831f, 1962, 1981, 2004f
Kavlock, R ... 173b
Kavlock, R J ... 418b
Kawabata, T T ... 125, 986, 1660
Kawada, A ... 2132
Kawamoto, T ... 107
Kawamura, S ... 265c
Kawamura, T ... 2192
Kawamura, Y ... 196*
Kawata, A ... 1713
Kawazu, K ... 2119
Kaweeteerawat, C ... 833*
Kayser, R ... 1347i
Ke, S ... 911
Keane, M J ... 1242h, 1368a
Kearney, K ... 503*
Kearns, A K ... 298*
Keating, A ... 2183, 2187, 2189
Keaton, M ... 250
Keebaugh, A J ... 1242f*
Keenan, J ... 2250h*
Keene, A M ... 76, 122b
Kegler, D ... 635
Kehe, K ... 463*
Keightley, A ... 121
Keil, A M ... 1200f
Keil, C ... 1448
Keil, D E ... 1713q, 1713r
Keil, K P ... 905, 1087s*
Keilholz, L ... 2121
Keinath, M ... 2242
Keirstead, N ... 104, 1627, 1644
Keiser, M ... 2269
Keler, T ... 268
Keller, D ... 27, 1037, 1609
Keller, J ... 1220*
Kellert, M ... 1826
Kelly, A ... 132*
Kelly, A D ... 1283
Kelly, J E ... 1662c
Kelly, K ... 122c
Kelly, K A ... 372*, 373, 374, 700*
Kelly, R ... 2065
Kelm, J M ... 1047
Kelman, B J ... 2247
Keltner, Z ... 1297a, 1973h
Kemler, R ... 163
Kemp, J M ... 979*
Kempinas, W D ... 379, 1696
Kenndy, R ... 1315
Kennedy, A J ... 1987, 1988
Kennedy, L H ... 505*
Kennedy, R ... 382
Kennedy, R T ... 719, 724*
Kennedy, S W ... 2253
Kenneke, J F ... 96e
Kent, S T ... 235
Kentala, D ... 901c
Kenyon, E ... 632b*, 632c
Keohavong, P ... 1507, 2004d
Kerdine-Römer, S ... 123, 2009, 2010, 2011
Kerger, B D ... 77, 225*, 1575, 1610
Kermenidou, M ... 2250f
Kern, G ... 1627
Kern, P ... 1029
Kern, S ... 2165
Kerns, S ... 877
Kerper, L E ... 611, 1811*
Kerr, L L ... 1964
Kerr, R P ... 1284
Kerzic, P ... 228*
Keshava, C ... 1831*
Keteles, K ... 72
Kettenhofen, R ... 1918, 1919*
Key, E F ... 1838
Keyser, B ... 570
Khalid, M ... 1371*
Khalifa, A E ... 1110a
Khalil, N M ... 433
Khalili, R ... 1298*, 1299
Khaliullin, T ... 603e, 603f*
Khan, I A ... 214, 978e
Khan, M ... 138, 139
Khan, S I ... 978e
Khan, S R ... 542*
Khan, S T ... 1952
Khanal, T ... 506*
Khang, D ... 1949
Khanna, A ... 88, 1059*, 1899
Khetani, S ... 1042
Khetani, S R ... 33*
Khiste, S ... 1514*
Khlebnikova, N S ... 1536
Khoder, M ... 1207
Khosa, R ... 812
Khuc, T ... 467g, 1063
Ki, S ... 1200e, 1200i
Kidd, S ... 954h, 1747e
Kido, T ... 1392, 2047*, 2049
Kiefer, M ... 1607
Kierski, M ... 647
Kiguti, L R ... 1696
Kijima, A ... 442
Kilby, K ... 1615
Kilford, P ... 901f
Kilian, P ... 1745
Kilic, J ... 2198
Killgore, J ... 669d
Killian, T C ... 1639c
Killilea, D W ... 1281, 2128
Kim, A ... 837, 2076
Kim, A H ... 866
Kim, C ... 2129d, 2234y
Kim, C H ... 933
Kim, C S ... 1018f*
Kim, D ... 230, 386, 549*, 942d*, 1110d*, 1327e, 1352*, 1553*, 1571, 2027
Kim, D J ... 1736
Kim, E ... 519, 653, 1123, 1389, 2001
Kim, G ... 890
Kim, H ... 353, 506, 507, 787, 795*, 797a, 799, 801, 871, 876, 890, 942, 1110b, 1166, 1167, 1200e, 1223, 1233, 1260, 1327e, 1389, 1549g, 1713m*, 2032, 2052*, 2129d
Kim, J . 117, 440l, 549, 593*, 660, 708*, 710*, 1286, 1327b, 1612, 1687, 1951, 2001
Kim, K ... 117*, 482, 482, 1122*, 1123*, 1125, 1389, 1565, 1639b, 2234l
Kim, M ... 490, 1257*
Kim, M T ... 2252*
Kim, P ... 1223, 1233
Kim, R ... 581e
Kim, S ... 117, 117, 440l, 999, 1087e*, 1200e*, 1831m, 1949, 1951, 2000*, 2234l, 2234l, 2250c, 2316
Kim, T ... 593, 660, 871, 2001, 2052
Kim, Y 353*, 482, 593, 980*, 1229b, 1260, 1951
Kimbell, J ... 67
Kimber, I ... 971, 989, 990, 991, 992*
Kimber, M J ... 671
Kimbrough, C ... 479
Kimmel, T A ... 613*, 649a
Kimoto, E ... 80
Kimoto, H ... 1649*
Kimura, E ... 1346, 2163
Kimura, T ... 1899b
Kimura, Y ... 988
Kincl, L ... 1579
Kindrat, I ... 265b*
Kindt, E ... 97
King, A ... 1642
King, B ... 1607
King, B L ... 411
King, C ... 1204, 1232
King, D H ... 1087r, 1110f
King, J M ... 1810
King, L ... 1642, 1659
King, N ... 1200b, 1544
Kingston, R ... 1472*
Kinniburgh, D W ... 159, 1024
Kinsky, O R ... 1542*
Kinter, L B ... 759*
Kipen, H ... 858
Kippler, M ... 2318
Kiraly, O ... 2282
Kirby, P ... 101, 102, 122e
Kirchner, D ... 2234aa
Kirchner, F R ... 1917
Kirk, S ... 2196o*
Kirkpatrick, D T ... 67, 1594, 1596*, 1597, 1598, 1599
Kirkwood, J ... 1682
Kirman, C R ... 617, 779*, 1065, 1296
Kirpich, I ... 1879, 2221*
Kishi, R ... 89
Kishi, S ... 1091, 1092, 1093, 1213
Kisin, E ... 1242g
Kisin, E K ... 603e, 1242h*, 2004d
Kissel, J ... 2234w*
Kissling, G ... 1087r
Kitagaki, M ... 1600
Kitamura, S ... 1086
Kitazawa, T ... 539c
Kitchin, K T ... 841d*
Kitson, R ... 1632
Kiyosawa, N ... 494
Klaassen, C D 49, 547, 917, 1185, 1896, 2122
Klapacz, J ... 1099*
Klausner, M ... 1038, 1040, 2181
Kleeberger, S R ... 1804c
Kleensang, A ... 1608, 1737
Klei, L R ... 1302
Klein, C ... 355
Klein, D M ... 1701*
Klein, J ... 1980
Klein, T ... 408
Klein Entink, R ... 1823
Kleindienst, T E ... 10
Kleinjans, J ... 1062h, 1104, 2273e
Kleinman, M T ... 353, 1242f
Kleinoeder, T ... 431
Kleinstreuer, N ... 4, 440h, 1062a, 1062c*, 1087o, 1736e, 1831l, 1973e, 2182c, 2250b, 2273i, 2273r, 2273s, 2273v
Klena, N ... 2076
Klimchak, N A ... 304
Klimecki, W T ... 1300
Klinefelter, G ... 1018a
Klingelhutz, A J ... 2199
Klinger, A R ... 244
Klingler, R H ... 1690a
Kloc, K ... 2244*
Kluz, T ... 969, 1207, 1245, 1301
Knaak, J B ... 81
Knapp, B ... 901c
Knapp, D M ... 104
Knebel, J ... 512, 601*, 1050
Knecht, A ... 207*
Knight, B ... 2196e, 2196f, 2196h*
Knight, R J ... 1661*
Knill, A ... 277
Knipping, E ... 1222, 1229f
Knostman, K ... 581h, 2196j
Knuckles, T L ... 1560, 1561, 1982*
Knudsen, G A ... 901b*, 922d
Knudsen, T B ... 4*, 418a, 418b, 1062a, 1087o, 1087p, 1736e, 2234i, 2273f, 2273s, 2273v, 2280
Knutson, S ... 652
Ko, C ... 1907*, 1909
Ko, H ... 763*
Kobayashi, J ... 2196bb
Kobayashi, N ... 199*
Kobayashi, S ... 591
Kobayashi, Y ... 1321*
Kobets, T ... 265b, 957*, 978
Kobilinsky, L ... 786

Koblis, K ... 647
Kobs, C ... 581j
Kobylewski, S ... 1775
Koch, L ... 1922b
Koch, S ... 1685
Koch, W ... 1226, 1826
Koci, J ... 320*
Kock, M ... 356
Kodali, V K ... 602*, 814, 1980
Kodama, Y ... 1160, 1161
Kodavanti, P S ... 378g
Kodavanti, U P 1230, 1232, 2068*, 2073*, 2296, 2325, 2326, 2330
Koegler, S ... 2196h
Koekemoer, L ... 1297b*
Koenig, E ... 101, 102, 122e
Koenig, J ... 581e, 2163c
Koenig, K ... 1692*
Koga, T ... 472, 1155*
Kogel, U ... 1054*
Kohonen, P ... 2273y
Koibuchi, N ... 1087
Koivisto, P ... 343e
Kokkonen, u ... 343e
Kolaja, K L ... 12, 2085*
Kolesar, J ... 1069
Kolker, A ... 1018b
Kolle, S ... 634, 1057
Koller, L D ... 626
Kollessery, G J ... 161
Kolodzieyski, L ... 286
Koltick, D ... 1287, 1291
Komatsu, H ... 113
Komatsu, T ... 539c
Kombarova, M I ... 2249*
Kondo, Y ... 241
Kondraganti, S R ... 535*
Kondru, N ... 1351*
Kong, B ... 1162, 1889
Kong, M ... 1235
Kong, X ... 1087n
Kongsbak, K G ... 1018d, 1175*
Konsolaki, M ... 1841
Koo, E ... 277
Koo, I ... 2316
Koolwijk, P ... 1514a
Kooter, I M ... 1970*
Kopec, A K ... 1191, 1867
Kopelovich, L ... 2250h
Kopf, J ... 1953
Kopf, P G ... 1082*
Koponen, H ... 1206
Koppen, G ... 223h
Korashy, H M ... 2217
Korbas, M ... 218
Kormendy, Z ... 382
Korolev, A ... 429
Korrapati, M ... 111*
Korte, J ... 1087d
Korte, S H ... 2152, 2154*
Kosharskyy, B ... 1170
Kosian, P ... 1087d
Kosior, K ... 223
Kostadinov, S ... 1686
Kostadinova-Angelova, R M ... 413, 415
Kostrub, C ... 286
Kostyniak, P J ... 1524
Kosyk, O ... 978, 1152
Kotch, J B ... 2228
Kothiya, P G ... 2273q, 2273s, 2273aa*
Koturbash, I ... 972
Kouzuki, H ... 1600
Kovacs, K ... 574
Kovalcik, K ... 2329
Kovalova, N ... 2019*, 2020
Kovochich, M ... 603j
Kovoor, A ... 550
Kowalski, J ... 223
Koyama, K ... 591
Koyashiki, N ... 2167
Koyner, J ... 105
Koziel, J ... 362
Kracko, D ... 1107, 1202, 1229f*, 1521
Kraeling, M ... 1973i, 1973j*
Kraeling, M E ... 1973h
Kraft, A D ... 239, 1809*, 1830, 1831c
Krager, S ... 1153, 2197
Krakowiak, P ... 698
Kramer, J W ... 478
Kramer, L R ... 246
Kramer, N ... 1048
Krantz, D ... 929, 930
Krantz, T ... 980, 1204, 1232
Krapfl, H ... 2234p
Krasnow, R ... 391
Krausz, K ... 1163
Krcha, M ... 1028
Kreckler, L ... 474*
Kreider, M ... 954d
Kreiling, R ... 1826*
Kremer, J J ... 475*
Krennrich, G ... 120, 1591
Kreps, M ... 137
Kretser, A ... 1017
Kreutzer, R ... 873
Krewski, D ... 1200g
Krieger, S M ... 688
Krile, R ... 2121
Krishan, M ... 1017*
Krishna, G ... 1620, 2196m, 2196n*
Krishna, S ... 996*
Krishnamurthy, P ... 1797
Krishnan, K ... 96a*
Krishnan, P ... 249*
Krishnappa, H ... 2196m
Krishnaraju, A ... 1590
Kristofco, L A ... 1831f*
Kristovich, R ... 2141
Kroese, E ... 430*
Krohn, R M ... 1319
Kroll, K J ... 669c
Krolski, M ... 683
Kromidas, L ... 420
Kromme, M ... 1742, 1743
Krueger, N ... 1826
Kruhlak, N L ... 2256, 2257, 2261, 2262, 2273b, 2273h*
Kruijsen, L ... 2028
Kruizinga, A ... 1823*
Krul, C ... 635*
Krupp, E ... 220
Kruse, S E ... 340
Kruszewski, F H ... 2234aa
Krzyzewski, S ... 1042
Ku, W W .. 544, 2196e, 2196f, 2196g, 2196h, 2196i
Kuan, N ... 1090
Kubaszky, R ... 275*
Kubik, L ... 350*
Kubo, K ... 1346
Kubota, A ... 517, 519, 1147
Kubota, R ... 199
Kueberuwa, S S ... 2250g
Kueger, M ... 2140
Kuehl, P J ... 883*, 1202, 1831g
Kuehn, D ... 413, 415, 860, 1592
Kugler, J ... 163*
Kühne, R ... 631
Kulkarni, R ... 467e*, 1943j
Kulp, K ... 1110e, 2195
Kumagai, Y ... 1258, 1714, 1716, 1717
Kumagai-Takei, N ... 127, 128, 129, 2322
Kumar, A ... 2030
Kumar, B ... 871*
Kumar, D ... 553, 554, 555
Kumar, G ... 1945, 1946*, 1955, 1972
Kumar, K K ... 1353, 1354*, 1355
Kumar, N ... 1957
Kumar, P ... 339
Kumar, R ... 88*, 522, 1059, 1899
Kume, T ... 537
Kumer, S ... 1181
Kumsher, D ... 1265
Kung, M H ... 265*, 636
Kunito, T ... 1259
Kuniyasu, H ... 322
Kuno, T ... 1093
Kunze, M ... 2131*
Kuo, B ... 1478
Kuo, D ... 1922a
Kuo, E ... 965*
Kuo, L ... 2234h
Kupcho, K R ... 291
Kuper, F ... 134, 1347i, 1970
Kupsco, A J ... 213*
Kurata, M ... 1640
Kurhanewicz, N ... 2323*
Kurita, H ... 908*, 978b
Kuroda, K ... 442*
Kuroiwa, Y ... 2196u*
Kuroki, H ... 1086
Kusaka, M ... 128, 2322
Kuse, H ... 2196u
Kushida, M ... 265c
Kushleika, J ... 1908
Kushwaha, S ... 1700*
Kusnecov, A ... 1391
Kutsukake, N ... 1304
Küttler, K ... 1220
Kuuspalo, K ... 1206
Kuzhippala, J ... 1298
Kuzmis, A ... 1546
Kwagh, J ... 855, 856*, 857, 1622
Kwan, M ... 1255
Kwekel, J C ... 100, 122d*, 978a
Kwon, H ... 230*, 1260, 1327e
Kwon, J ... 1223*, 1233, 2234y
Kwon, M ... 1044
Kwon, O ... 440l*, 942, 1200e
Kwon, Y ... 293
Kyriss, B ... 1920

L

La Merrill, M ... 682
La-Beck, I ... 1999
Labash, C ... 452
Labbe, G ... 1643
Labib, S ... 1478
Labov, J ... 1435, 1436*
LaBranche, T ... 1128
Lacey, C J ... 561
Lachenauer, E ... 2128
Lad, S ... 1005
Laer, D ... 1913
Laffan, S B ... 11
Laflamme, M ... 1129c
Lahoti, T S ... 260, 1136*, 1138
Lai, Y ... 262*, 901
Lai-Zhang, J ... 1549a
Laine, J E ... 229*, 1308, 1318
Laiosa, M D ... 2014
Laird, B D ... 1255*
Lake, A ... 2273q
Lake, A D ... 65*, 547, 2061
Lake, B G ... 60, 265c, 689b*
LaKind, J S ... 1766
Lalayeva, N ... 197, 1698*
Lalko, J F ... 2166*
Lam, R H ... 2244
Lam, W S ... 1973c
Lamantia, C E ... 1347e
Lamar, P C ... 2048
Lamb, C L ... 2200*
Lamb, M ... 1126
Lamba, A ... 1816
Lambert, E ... 633
Lambert, I B ... 1478
Lambert, J C ... 2273cc
Lambert, P ... 122h
Lame, M ... 1127
Lamime, S ... 539a
Lamm, S H ... 223i*, 632i
Lamm, W J ... 2140
Lammens, L ... 1080, 1652
Lamore, S D ... 1111, 1126*
Lamoureux, D ... 1242b
Lampo, A ... 348
Lamy, S ... 2298
Lan, Y ... 431
Lancaster, J ... 492
Landauer, M R ... 552d*
Landis, K ... 1648
Landis, M ... 1581
Landis, R W ... 350
Landolph, J R ... 1502*
Landreman, A ... 167*
Landry, G M ... 2066
Landry, T ... 1040
Landsiedel, R ... 173, 597, 634, 1057, 1220, 1221, 1992, 2172
Lang, A ... 1742, 1743
Lang, C ... 96h
Langley, M R ... 936, 937*
Langohr, I ... 140
Langsfeld, M ... 1518
Lanham, K A ... 504b*
Lanning, L ... 2134*
Lantz, R ... 1295, 2311*, 2314*
Lantz, S ... 353
Lantz, S R ... 1838*
Lantz-McPeak, S ... 173m, 378i, 603b, 942e
Lao, V ... 2195
Laporta, J ... 1087s
LaPres, J J ... 1214, 1414*
Lardie, T S ... 467b, 885
Large, E ... 1921, 1922
Larkin, A J ... 876a*
Larocque, N ... 179
Larson, A ... 951
Larson, B ... 307, 1899a
Larson, J L ... 244
Larson, T ... 54*
Lash, L H ... 310*
Lasher, M A ... 673
Laskin, D L ... 383, 389, 395, 559, 561, 562, 563, 565, 571, 1005, 1664, 1669, 2327
Laskin, J D ... 395, 559, 561, 562, 563, 565, 571, 1005, 1275, 2327
Lasley, S M ... 1330*
Lassiter, M G ... 1713k
Latendresse, J R ... 1062b, 1164, 1165
Lati, E ... 985
Latinwo, L ... 1264c
Lau, B ... 1958
Lau, C S ... 2206, 2213b
Lau, F C ... 1590*
Lau, S S 311, 370, 916, 924, 1503, 1542, 1799
Lauan, M ... 516*
Laudet, V ... 149
Lauenstein, L ... 1057
Lauer, F T ... 143*, 513
Laulicht, F ... 1245, 1297e*
Laumbach, R ... 858
Lauterbach, J H ... 1614*
Lauterstein, D E ... 355*
Lavado, R ... 652, 654
LaVelle, J M ... 2243*
Lavergne, S N ... 132
Lavin Williams, A ... 1805*, 1806
Law, B F ... 2036
Lawana, V J ... 927*
Lawless, M ... 440j*, 2273r
Lawlor, T E ... 1943j
Lawrence, B ... 1347, 2017
Lawrence, J ... 1200b, 1242b
Laws, S C ... 1087c, 1087f*, 1087h
Lawson, M ... 1132
Lawton, M ... 112
Lay, J M ... 411
Layko, D ... 1132
Lazar, D F ... 291, 1628
Lazarowski, L ... 1363
Le, J N ... 376*
Le Bigot, J ... 2130*
Le Guevel, R ... 1192
Le Sommer, C ... 160
Leach, K ... 1129
Leach, M W ... 276
Leal, R B ... 1329
Leatherbury, L ... 2076
Leavens, T L ... 1435, 1440*
LeBaron, M J ... 3, 753, 755*, 972, 1602, 1941
LeBeau, A ... 2250e*
LeBeau, A L ... 1813
Leblanc, A ... 1011*
Leblanc, V ... 2177*
Lebrec, H N ... 2306*
LeCluyse, E ... 388, 1042, 1045, 1140, 1873, 1883
LeCureux, L ... 1177*
Ledbetter, A ... 1232, 2323, 2325, 2326
Lednicky, J ... 1467
Lee, B 1125, 1166, 1167*, 1190, 1229b, 1730*

Author Index (Continued)

The numerals following the author's names refer to the abstract numbers. The asterisk after the abstract number indicates the author is the first presenter.

Lee, B M ... 2052
Lee, C ... 733*
Lee, D ... 1200i, 1827*
Lee, D U ... 954g*
Lee, E ... 2052
Lee, H ... 593, 603c, 1736
Lee, I ... 175*, 1748, 1749
Lee, J 593, 593, 660, 776*, 933*, 1125, 1166*, 1167, 1247, 1248*, 1257, 1277*, 1338, 1361, 1565*, 1976*, 1976*, 2001, 2060, 2234y*
Lee, K ... 290, 646, 802, 848c, 1125, 1130, 1190*, 1211, 1229b, 1286, 1327b, 2032
Lee, M ... 418e*, 1023, 1122, 1125
Lee, N ... 1913*
Lee, R ... 509
Lee, R B ... 581i, 2163c
Lee, R C ... 1816*
Lee, S ... 127, 128*, 129, 440l, 871, 876, 1125, 1130, 1131, 1143, 1200e, 1200i, 1200i, 1512, 1949*, 2250c*, 2322
Lee, S A ... 574
Lee, T ... 100, 1200i, 1565
Lee, V ... 1563*
Lee, W ... 871, 2196p
Lee, W M ... 867
Lee, Y ... 369, 801*, 871, 1976, 2060
Lee, Y S ... 1858*
Lee-Brotherton, V ... 2246
Lees, D ... 284, 2110
Leet, J K ... 152*
Leetham-Spencer, M ... 1713q, 1713r*
Lefebvre, D ... 96h*
Lefevre, A C ... 655
Lefevre, P L ... 1713
LeFew, W ... 378b, 440c*
Lehman, R ... 665
Lehman-McKeeman, L D .. 1177, 2034, 2122
Lehmann, D M ... 145a*
Lehmann, G M ... 1766*
Lehmler, H ... 510, 515, 1068, 2205
Lehner, A ... 1297g
Lehoux, S ... 1310, 1319
Lei, G ... 2156*
Leifer, K ... 586
Lein, P ... 124, 351, 360, 557, 579, 697, 1335*, 1741, 1747d, 1759, 2205
Lemaire, B ... 1147
Lemaire, M ... 1310, 1319*
Lemarié, C A ... 1310, 1319
Lemasters, J J ... 708, 709*, 1783
Lemay, J C ... 1810
Leme, D M ... 451*, 467h
Lemieux, F ... 1478
Lemire, M ... 1255
Lemke, S L ... 330
Lemons, A R ... 2036
Lemus, R ... 612
Lena, C ... 870
Lencina, C ... 133
Leng, J ... 1675
Lennon-Hopkins, K ... 411
Leo, B ... 1963
Leon Carrion, S ... 193
Leòn Chàvez, B ... 1244
Leonard, H D ... 1229a
Leonard, S S ... 488, 1208, 1297, 1966
Leonhardt, A ... 1990, 2003
Leoni, A ... 2131
Lephart, E D ... 1585*
Lepoittevin, J ... 123, 2009
Leppänen, H ... 983
Lepsy, C ... 122f
Leptak, C ... 13
Leroux-Petersen, D ... 879*
Leroy, F ... 170
Lesage, E ... 1651
Leung, A ... 1462
Leung, M C ... 418a*, 1087p, 1939, 2273s, 2280*
Leung, P ... 902
Leuschner, J A ... 581c, 581e
LeVanseler, K ... 1663
Leverette, R ... 1015*
Levesque, P C ... 851, 856, 1903
Levesque, S ... 928, 1859
Levin, E D ... 1347h, 1857
Levine, K ... 2224
Levoe, S N ... 124*
Levy, D D ... 467a
Levy, L ... 1826
Lewandowski, P ... 1822
Lewandowski, R ... 2324, 2328
Lewandowski, T A ... 613
Lewen, G ... 1903
Lewin, G ... 599
Lewis, A ... 639, 2234q*
Lewis, C ... 2194*
Lewis, E M ... 11, 898
Lewis, J A ... 1265, 1297, 1858
Lewis, J L ... 135, 2226, 2234c, 2315*
Lewis, R W ... 1831g
Lewis, S ... 100, 1616e, 1713e
Lezama Pacheco, J ... 1087l
Li, A A ... 59*
Li, A P ... 529, 1631*, 1885, 1894, 1899d
Li, B ... 312d*
Li, C ... 122b, 552e, 2223
Li, D ... 815*
Li, F ... 1163
Li, G J ... 1348*
Li, H ... 586, 954f, 1156, 1300, 1840*, 1938*
Li, J ... 101, 223i, 865*, 943, 1117, 1250, 1705, 2015*, 2020
Li, K L ... 954a*
Li, L ... 528*, 532, 533
Li, M ... 659, 2181, 2202*
Li, N ... 1899e, 2067a
Li, R ... 80, 1412*, 1495
Li, S ... 418*, 922c*, 942b, 2267
Li, W ... 855*, 932*, 942c, 1212*, 1250, 1378, 2125
Li, X ... 393*, 913, 1121, 1200h, 1367, 1512*, 1881, 2045, 2145*, 2196r, 2231
Li, Y ... 367*, 483, 483, 533, 1229e, 1348, 1713t, 1790, 1792, 1888, 2004c, 2060, 2076
Li, Z ... 114, 265d, 1684, 2057*
Li-Muller, A ... 1819
Liachenko, S ... 378f*, 1429, 1434*
Liang, J ... 461
Liang, L ... 359, 925
Liang, L E ... 1664
Liang, X ... 1804a
Liang, Y ... 868, 1254
Liang, Y W ... 538
Liao, C ... 1522, 1570
Liao, H ... 21
Libalova, H ... 706, 844*
Liberda, E N ... 1567*
Librizzi, J ... 343d
Licari, P ... 327
Liccione, J ... 312e
Licher, T ... 1919
Lichtenberg, J ... 1514a*
Lichter, S ... 1831a*
Lickfeldt, D W ... 688
Lickteig, A J ... 547, 2122
Liddell, A ... 2234s
Liebsch, M ... 1057
Liggitt, H ... 1690b
Lightfoot-Dunn, R ... 1641
Liley, M ... 1592
Lilius, E ... 343e
Liljevald, M ... 1881*
Lille-Langøy, R ... 1147
Lillegaard, I L ... 782, 2248
Lim, H ... 1327e
Lim, J ... 1260*
Lim, K ... 1023*, 1122
Lim, Y ... 549
Lima, A ... 552a*
Lima, F ... 805
Limaye, P ... 689a
Limero, T F ... 2250d
Lin, C ... 177, 1531
Lin, G X ... 1368a
Lin, H ... 103*, 122f, 319, 1062b, 1893, 1973c*
Lin, M ... 21, 436, 2213b
Lin, S C ... 1902*
Lin, W ... 2196p
Lin, Y ... 191, 892, 959, 1577, 2234g*
Lin, Z ... 1837*
Linak, W ... 1232
Lindamood, C ... 1422*
Lindberg, C ... 152
Linders, L ... 1347i
Lindsay, S ... 1461
Lindsey, M ... 1673*
Lindstedt, M ... 1062g
Lineberry, H ... 2168
Ling, W ... 1346*, 2163
Lingappan, K ... 539, 1796*
Linker, F ... 1826
Linnenbrink, M ... 2273n, 2273s
Linnevers, C ... 2043
Liong, M ... 603j*
Liou, S ... 21*
Lippi, M ... 2240*
Lipscomb, J C ... 6, 632b
Liqing, H ... 1206
Litoff, E J ... 522
Littke, M H ... 602
Little, S B ... 2273s
Liu, A ... 852, 855
Liu, C ... 1433, 1963
Liu, D ... 312d
Liu, F ... 367, 1212, 1242i, 1293, 1586*, 1756, 1764a*, 1764b, 1764c
Liu, G ... 2191
Liu, H ... 393, 674
Liu, J ... 65, 176*, 367, 886, 1185, 1348, 1713a, 1755*, 1844*, 2118, 2151c, 2273q, 2273t*
Liu, K ... 143, 1316, 1449*
Liu, R ... 816, 1549a
Liu, S ... 296, 357, 508*, 1325, 1637, 1764b, 1764d*, 2054, 2234o
Liu, T ... 511
Liu, W ... 1316
Liu, X ... 687, 1935, 2076
Liu, Y 169, 550, 705, 848*, 886, 1043*, 1144, 1188, 1189*, 1194, 1291*, 1348, 1690b
Liu, Z ... 62*, 2273k
Lizarraga, L E ... 370*
Lo, C W ... 2074, 2076*
Loader, J ... 577
Loccisano, A ... 70, 89
Locey, B J ... 1404
Loch-Caruso, R ... 1770
Loeb, J ... 1467
Logan, D ... 877
Logan, M ... 2136
Logan, P ... 2211
Loging, W ... 2196g
Loging, W T ... 2196e
Loguinov, A ... 173p
Loh, M ... 2313*
Lohr, K ... 371
Löhr, C V ... 539d
Lohren, H ... 1356
Loisel-Joubert, S ... 173e, 440a
Loizou, G D ... 440f
Lombardi, T ... 223
Lommen, A ... 1062h
London, B ... 525*
Loney-Walsh, K ... 1360
Long, C M ... 141, 142*, 2025
Long, J ... 2121
Long, L ... 1367
Long, M ... 1779
Long, Z ... 1365, 1366, 1367, 1368, 2231*
Long-Roldán, K L ... 1256
Longbin, H ... 1556
Longnecker, M P ... 89, 91, 92
Lookingland, K J ... 2006
Loomba, D ... 436
Loomen, J ... 1002
Loomis, D ... 1312, 1314, 1324
LoPachin, R ... 1170*, 1454*
Lopert, P ... 925*
Lopes, M W ... 1329
Lopes, S C ... 1329
Lopez, M ... 1867
López-Bayghen, E ... 1723
Lopez-Gonzalez, M L ... 530
Lopez-Granero, C ... 1856*
López-Marure, R ... 595
Lorber, M ... 96i
Lorello, L G ... 276
Lorentsen, H ... 2147
Lorentzen, J C ... 1814
Lotersztajn, S ... 1158
Lotter, J ... 2234t
Louha, S ... 88, 1059, 1899
Louis, G W ... 1713d, 2190*
Loukotková, L ... 632g
Lovaglio, J ... 1525
Love, R ... 2126*
Love, S T ... 1541*
Lovik, M S ... 134
Lowe, F J ... 1528*
Lowe, J ... 632j
Lowney, Y W ... 1831i, 2234w
Lowry, D T ... 23
Lozano, R ... 1856
Løgsted, J ... 1588
Lu, C ... 687*, 1507*, 1705
Lu, H ... 49
Lu, J ... 1045*, 1508
Lu, L ... 2129a
Lu, T ... 296, 357, 1369, 1388*
Lu, X ... 2044, 2045*, 2055
Lu, Y ... 1200d*
Lu, Z ... 461*
Luanpitpong, S ... 830
Lucak, J ... 883
Lucas, E ... 1551
Lucas, R J ... 1625
Lucas, S ... 2226
Lucchini, R ... 1551, 2286, 2289*
Luch, A ... 163, 1067, 1950
Luckett-Chastain, L R ... 979
Lucot, J B ... 361
Luczak, M W ... 1268, 1269*
Ludewig, G ... 1068, 2202
Ludlow, J W ... 1422, 1427*
Ludwig-Schwellinger, E C ... 2196e
Luebke, R W ... 1347a
Luechtefeld, T ... 1608
Luerman, G C ... 478*
Luetjens, C M ... 2148, 2155*
Lugo, J ... 1590
Lugokenskia, T H ... 173n
Luijten, M ... 1478
Luis-González, G ... 2218
Luithardt, H ... 378, 1115
Lukomska, E ... 141, 142, 2025
Lulla, A ... 580*, 942b*
Lum, B ... 269
Lumen, A ... 96g, 440f*
Lumley, L A ... 581i
Lumpkin, M H ... 71*
Luna, M ... 886
Lund, A K ... 18*, 1222
Lundell, B ... 943*
Lundqvist, J ... 1081*
Lunt, S Y ... 414
Luo, G ... 954e
Luo, J ... 936, 1285*
Luo, M ... 92
Luo, X ... 1721, 1733
Luo, Y ... 1200a
Luong, J ... 2128
Lupton, S ... 334
Lusis, A J ... 1281
Lust, R M ... 484
Lute, J ... 850
Lutz, E ... 1562, 1563
Lutzow-Holm, C ... 2248
Luyendyk, J P ... 1191, 1197, 1867*
Luz, A ... 1939, 1940*
Ly, H J ... 316
Lyche, J L ... 2248
Lyke, D ... 1347b, 1863a*, 1863b
Lyman, M E ... 581a, 1922c, 1922d*
Lyn-Cook, L E ... 467a
Lynch, B S ... 343i*
Lynch, H N ... 1341*, 1810, 1811, 2234q
Lynch, K ... 380
Lynch, M ... 2196j
Lynn, A ... 1548*
Lyon, J ... 1642
Lyubimov, A V ... 1546*, 1803

The numerals following the author's names refer to the abstract numbers. The asterisk after the abstract number indicates the author is the first presenter.

M

Ma, C ... 1533
Ma, D ... 527
Ma, H ... 138*, 1910
Ma, J ... 436
Ma, J Y ... 830, 2004b*
Ma, L ... 855, 1094, 1348
Ma, N ... 1533
Ma, R ... 1366, 1368*
Ma-Hock, L ... 597*, 1057, 1220, 1221, 1826
Maarschalkerweerd, T ... 154
MacAdam, D ... 995
MacCoss, M J ... 116
MacGregor, J T ... 452
Machala, M ... 1943a
Machida, K ... 2133
Machini, M ... 1771
Mack, C M ... 378a, 1838
Mackay, W J ... 326*
MacKenzie, D ... 143, 1144
MacKenzie, P I ... 918
MacKenzie, S ... 328*
Mackey, A ... 1129a
Mackey, S ... 391
MacMillan, D ... 96b
Macon, M B ... 2196d*
MacPhail, R C ... 173i, 378g
Madanayake, T ... 919*
Madden, J A ... 2187*
Madden, M ... 1018c
Madden, M C ... 876d, 1234, 2293
Madden, S ... 901e
Maddox, J R ... 343b
Madeen, E ... 539d, 882*
Madejczyk, M S ... 1297*
Mader, R ... 901f*
Madl, A ... 603j, 2235
Madren-Whalley, J S ... 1894
Madrid, O ... 1087q
Madsen, T ... 1713a*, 2118
Maecker, H T ... 391
Maeda, A ... 450*
Maeda, J ... 1160, 1161*
Maeda, K ... 2196u
Maeda, M ... 127, 129
Maeda, N ... 110
Maertens, A ... 1608
Mafirakureva, N ... 1062h
Magdy, D ... 1180
Magdziarz, T ... 2273, 2273d
Magee, B ... 615*
Maghni, K ... 829
Maginnis, G ... 633
Magnifico, M ... 1618
Magpantay, R ... 1200, 1868, 2038
Maguire, M ... 1684, 2023
Mahadevan, B ... 331*, 2116*
Mahajan, P R ... 994*
Mahalingaiah, P S ... 1096*
Maher, J ... 1200b
Maher, M ... 1695
Maheshwari, R ... 122g, 441, 1549f
Mahimainathan, L ... 1839
Mahle, D A ... 87, 96, 895*, 1787, 1820
Mahmod, M M ... 2234
Mahoney, K M ... 688
Mai, V ... 1989
Maibach, H I ... 876c, 985
Maier, A ... 63*, 613, 1815, 1816, 1827, 2250i
Maier, M ... 332*
Maier, M S ... 1064*
Maillere, B ... 987
Mainelis, G ... 846
Mainey, A ... 1616a
Maisonet, M ... 89
Maisonneuve, J L ... 121
Maiuri, A ... 1199*
Majeed, S ... 413, 415, 1592
Majewska, A K ... 1347e
Majkova, Z ... 876*
Majumder, A ... 1347k*
Majumder, M ... 977*
Mak, N ... 2115
Mak, T ... 1156
Makarov, S S ... 1635
Makia, N L ... 1736b*
Makin, A ... 1588*
Makley, M K ... 573, 1787*
Makori, N ... 197, 407, 1698, 2126
Makri, G ... 1912
Makris, S L ... 1830, 1831h, 2074*, 2079*
Malarkey, D ... 955, 1616c
Malaviya, R ... 561*, 571
Malczewska-Toth, B ... 2234p
Maldonado, A ... 652*
Maldonado-Rojas, W ... 783*
Maleghemi, S T ... 2234u
Malek, D E ... 954c
Malenke, J R ... 539a
Malfatti, M A ... 882, 1110e, 2195
Malik, A ... 1478
Malik, D S ... 1110*
Malik, F ... 2329
Malik, I ... 383
Mallampalli, R ... 1003
Malle, B M ... 1514a
Mallela, R K ... 967
Mally, A ... 1864
Mamczarz, J ... 1860, 1861
Man, S ... 1973i, 1973j
Manautou, J E .. 366, 1169, 1176, 1184, 1201, 2030
Mandal, M ... 389, 395, 1005*, 2327
Mandal, S ... 1330
Mandeville, P ... 144
Mandrell, D ... 1747
Mandyam, N ... 88, 1059, 1899
Mangelsdorf, I ... 631
Mangipudy, R ... 109
Mangum, J ... 1642
Mangum, L ... 679*, 1515
Manibusan, M K ... 1087c
Manjanatha, M G ... 319, 467a, 467b*
Manka, D ... 1061, 1129a
Manke, A ... 589*
Mankus, C ... 1053
Manley, M ... 2206
Manley, S ... 1889*
Mann, D A ... 1045
Mann, K K ... 1283, 1310, 1319
Manno, R ... 1132
Mannozzi, J T ... 326
Mansfield, K ... 2124
Mansour, A ... 1207
Mansouri, K ... 2234i, 2273p, 2273u*
Mantell, L ... 1713o, 1789, 1793, 2026
Mantena, S R ... 1635
Mantey, J A ... 1505*
Manwaring, J ... 1031*
Manzo, L ... 835
Mao, Z ... 603k
Marc, P ... 427*
Marceau, G ... 286*
Marchand, A ... 1012*
Marchant, C ... 2264
Marchant, G E ... 719, 722*, 2098, 2102*
Marchitti, S A ... 96e
Marcinek, D J ... 340
Marcoe, K F ... 1908*
Marcos, R ... 1305, 1954*
Marcotte, E ... 121
Marcus, M ... 89
Marczynski, B ... 1007
Marescotti, D ... 1055
Marguerie, A ... 1921
Maria-Engler, S S ... 2171
Marier, J F ... 581
Marina, P ... 1912
Marinakos, S ... 1973e
Marinovich, M ... 984
Markell, L K ... 263, 467d*
Markgraf, C ... 2196v
Markham, D A ... 885
Markiewski, M ... 1999
Marlot, P ... 165
Marlowe, J ... 1618
Marocchio, L ... 2263
Marone, P ... 327
Maronpot, R R ... 324
Marquis, J K ... 1494
Marroquin-Cardona, A G ... 315
Marsden, E ... 2196*
Marsh, H C ... 268
Marsh, K ... 899
Marshall, B ... 470
Marshall, K ... 2043
Marshall, N B ... 141*, 142, 1229a, 2025
Marshburn, J D ... 603g
Marsillach Lopez, J ... 116*
Marsters, J ... 883
Martin, C ... 1057
Martin, C A ... 929, 930*
Martin, E A ... 1625*
Martin, F ... 413, 415, 2196p
Martin, G ... 681
Martin, K ... 1347
Martin, M T ... 31, 173b, 173e, 173j*, 378b, 418b, 440a, 1066, 1087p, 2097*, 2273l, 2273n, 2273s, 2273t, 2273v, 2273z, 2273aa
Martin, P L ... 278
Martin, R J ... 1145
Martin, S A ... 96b*, 1347a, 1347b, 1347d
Martín-Pardillos, A ... 495
Martínez, M ... 1843, 1862
Martínez, M A ... 1843, 1862
Martínez-Larrañaga, M R ... 1843, 1862*
Martinez-Leija, M E ... 840, 978c*
Martino, C ... 1299
Martino, G ... 1914
Martino, J ... 1272*
Martinozzi Teissier, S ... 170, 1029
Martsen, E ... 1635
Marty, M ... 2244
Marty, S ... 82, 1863
Maru, J ... 592, 1948
Maruf, A ... 1877*
Maruyama, T ... 978b
Marvania, T ... 1800, 1801
Maryoung, L A ... 654*
Mason, D ... 938, 1535*
Mason, M ... 1276
Mason, S ... 287, 473, 2142*, 2156
Massa, C B ... 2039*
Massey, G K ... 1646*
Massey, T E ... 1943f
Massey, V L ... 1323*, 1879
Masson, J ... 1924
Mastrandrea, N ... 916, 1503
Masumori, S ... 447, 460, 467c
Masumura, K ... 442, 2132
Masuno, K ... 1174
Masure, E ... 219*
Mata, J E ... 462
Matevia, M ... 1036*
Mathavan, S ... 157
Mather, A R ... 2058
Mathias, R ... 877
Mathieu, L ... 985*
Mathieu, S ... 2234aa
Mathis, C ... 413, 415, 860*, 1054, 1055, 1592
Mathisen, G H ... 1782
Mathur, S X ... 101
Matsson, P ... 79, 1883
Matsui, M ... 2180
Matsumoto, H ... 591
Matsumoto, K ... 196
Matsumoto, M ... 460, 2192
Matsumoto, S ... 1649
Matsumura, F ... 107
Matsuno, Y ... 1713h
Matsushima, S ... 1174
Matsushita, D ... 472
Matsushita, K ... 442
Matsuyama, K ... 1174, 1866
Matsuzaki, H ... 127, 128, 129*, 2322
Matta, J L ... 467
Mattes, W B ... 728*, 813d
Matthews, C ... 581j
Matthews, J B ... 906
Mattick, J S ... 731*
Mattie, D R ... 440f, 624, 1010*, 1820
Mattingly, C J ... 210*, 411, 423, 1758, 2096*, 2284*
Mattis, N D ... 922b*
Mattison, D R ... 96f
Matulka, R A ... 327
Matute, J ... 343b
Matz, C J ... 68
Maurer, E ... 1960
Maurer, T S ... 80
Mav, D ... 955
Maw, H ... 2196g
Mawn, M P ... 467d
Maxwell, G ... 1029
Mayer, A M ... 995
Mayer, G D ... 1937
Maynard, J ... 1630
Mayo, K ... 1616b
Mayo-Perez, A ... 299
Mazur, C ... 96e
Mazzei, J ... 784
McAdory, D ... 1541
McArthur, A G ... 209
McArthur, V ... 1284
McAughey, J ... 66
McCabe, M J ... 136
McCallister, M ... 1684
McCarthy, A ... 30, 2206
McCarthy, L ... 2234t
McCartney, M ... 1678
McCarver, D ... 189*, 192
McCawley, M ... 1560*, 1561
McClain, C ... 869, 970, 1182, 1188, 1189, 1194, 1874, 1879, 2316
McClanahan, M ... 625
McClellan, R O ... 1765
McCloskey, D ... 1347f
McClure, L A ... 235
McClure, P ... 1014*, 1831
McCluskey, J D ... 419
McCollum, C W ... 149*, 1327a
McConnell, E R ... 778
McConnell, R ... 1242i
McCorkel, M ... 1734
McCormick, D L ... 889, 2196y
McCormick, J ... 1229e
McCormick, R ... 1234
McCoy, A T ... 64, 2173
McCue, C E ... 1083
McCullough, S D ... 396, 1231, 1719*
McDaniel, C ... 540
McDaniel, K L . 1347a, 1347c, 1747a, 1863a, 1863b
McDermott, S P ... 1922e
McDiarmid, M ... 1559
McDonald, A ... 1018a
McDonald, J D 10, 581k, 1202, 1222, 1229f, 1236*, 1242e, 1831g, 2312*
McDonald, P ... 2145
McDonnell, E V ... 1686
McDonough, J H ... 552g, 2163c
McDonough, P ... 182, 377
McDougall, R ... 81, 89
McDuffie, J E ... 106, 380*
McElroy, C ... 577*
McElroy, M ... 901e
McFadden, L G ... 64, 1941
McGarrigle, B P ... 2204
McGaw, L J ... 1629
McGee, J ... 980, 1205, 1232, 2329
McGee, M A ... 1205*
McGee, S ... 309
McGee, S P ... 997
McGill, M R 867*, 1172, 1178, 1181, 1196
McGillicudy, S ... 382
McGinnis, C ... 157*
McGinnis, C L ... 223*, 1677*
McGinnis, P M ... 625
McGlothan, J L ... 1288, 1289, 1364*, 1365, 1392a
McGough, D ... 1695*
McGrath, F ... 1627
McGrath, P ... 303*
McGraw, C ... 928, 1859
McGreal, S ... 2206*
McIntosh, L ... 1530
McIntosh, M ... 122h
McIntosh-Kastrinsky, R ... 2323
McIntyre, B ... 145b, 1713b
McKay, J ... 1630
McKee, J M ... 1062f
McKeever, K P ... 2112

Author Index (Continued)

The numerals following the author's names refer to the abstract numbers. The asterisk after the abstract number indicates the author is the first presenter.

McKeon, M ... 1943i, 1943j
McKim, J M ... 166, 170, 343f*, 845, 1037
McKim, K L ... 265a
McKinney, J ... 1943g*
McKinney, W ... 603d, 1229a, 1368a, 1713u
McKinney, W J ... 5
McKone, T E ... 1405*
McLanahan, E D ... 96b, 1766, 1830
McLaurin, K W ... 440a*, 2273s
McLellan, C J ... 606, 607, 608
McLoughlin, C E ... 486, 696, 841c*, 1242a
McMahan, R S ... 1962
McMahen, R ... 1863b
McMartin, K ... 2066
McMaster, M ... 179
McMullen, P D ... 94, 160, 162, 1140*
McNally, K ... 440f
McNamee, P ... 1027
McNerney, M ... 1110e*
McNerney, M E ... 2191
McNutt, P ... 581a, 1922c*, 1922d
McPherson, S ... 287*, 473, 2142, 2156
McQuaid, S ... 327
McQueen, C A ... 735*
McQuistan, T ... 882
McShan, W M ... 979
McVay, M ... 1042
Meade, B J ... 141, 142, 2025
Meade, M L ... 573*
Means, J C ... 309, 922a, 922b
Medeiros, R ... 552a
Medici, S ... 1297e
Medina-Reyes, E I ... 1996
Medvedev, A ... 1635
Medvedovic, M ... 425, 1909
Meech, R ... 918
Meek, B ... 6, 1819
Meek, E C ... 556, 568, 1515*, 2198
Megaraj, V ... 528
Meger, M ... 1018e
Meghazzi, M ... 344
Megill, J ... 1622
Mehendale, H M ... 1164, 1165*
Mehrpouya, P ... 1713l*
Mehta, J ... 1943e
Mehta, P ... 347, 403*, 1800, 1801
Mehta, R D ... 445
Mehta, V ... 905, 1087s
Mei, C ... 508
Mei, N ... 319*, 1893, 1943b, 1973c
Meighan, T G ... 1229a
Meijer, M ... 1834*
Meireles, G ... 664
Meisenheimer, P ... 527, 1784
Meister, A ... 1592
Mekenyan, O ... 435
Melchers, D ... 1150, 1154
Melching-Kollmuss, S ... 1078
Mellert, W ... 120, 634, 1591, 1871
Mello, F d ... 1638*
Melnyk, S B ... 1343
Menard, A L ... 581*
Ménard, S ... 133
Mencalha, A ... 466
Mendell, J T ... 734*
Mendez, A M ... 840*
Mendez, M ... 1312, 1314
Mendez, M A ... 603i
Mendoza, R ... 1218
Mendrick, D L ... 13, 99, 813d
Meng, Q ... 1275
Mengel, M ... 863
Menke, A ... 154
Menon, S ... 1502
Mensing, T ... 2059
Mercado, F ... 603i
Mercer, K E ... 254*
Mercer, R R ... 2004b
Mercer, W C ... 1561
Mercola, M ... 767*
Meredith, C ... 71, 237, 443, 1530
Mereness, J ... 452, 1929
Mergaert, A ... 1920
Merrell, M D ... 520*
Merrick, B ... 1297k
Merrick, B A ... 122, 958*, 1736a
Merrill, E A ... 440g*
Merrill, G F ... 546
Merrill, S J ... 429
Mesens, N ... 154
Messersmith, W ... 1095
Messner, S ... 1047, 1890, 1899a*
Metryka, O ... 990
Metushi, I G ... 1045
Meulenbelt, J ... 96c
Mewes, K ... 1027
Meyer, A ... 669, 675*
Meyer, A E ... 1744
Meyer, J K ... 1699
Meyer, J N ... 223e, 841, 931, 1932, 1939, 1940
Meyer, M ... 874
Meyer, S ... 1356
Meyer, S A ... 798*
Meyers, V E ... 2250d*
Meyo, J ... 223c
Mhike, M ... 2036*
Miao, X ... 1888
Miao, Y ... 1533
Michaut, V ... 170
Michelotti, G ... 2030
Michikawa, T ... 242
Mickey, K ... 1797
Miedema, A ... 343d
Mielke, H W ... 2232*
Mielke, J ... 343d
Mielke, P W ... 2232
Mierke, D R ... 132
Migdal, C ... 123, 2009
Mihalchik, A ... 587*
Mikaelian, I ... 104
Mikaelian, R ... 274*
Mikkelsen, R ... 400, 407, 2120*
Mikl, J ... 1544, 2196i
Mikule, K ... 1636
Milanez, S ... 626*
Milcova, A ... 706, 1943a
Millan, A ... 495
Millar, M ... 1090
Miller, A ... 58*
Miller, A L ... 581f*
Miller, C ... 135, 2226, 2234c
Miller, D B .. 372, 373, 374*, 581i, 700, 1232, 2129a, 2325, 2326*
Miller, E ... 574
Miller, G W ... 371*, 868, 1747d*
Miller, K ... 1746
Miller, K E ... 467e
Miller, L D ... 842
Miller, M M ... 1744*
Miller, M S ... 381*, 842
Miller, R ... 1236
Miller, R T ... 1799
Miller, S ... 431
Miller, S K ... 1318, 2228*
Miller, S M ... 552g
Miller Holt, J C ... 1018e*
Miller-DeGraff, L ... 1804c
Millet, M ... 1027
Mills, E M ... 250
Mills, L J ... 1087f, 1087h*
Min, E ... 577, 1001
Min, M ... 1549b
Minami, K ... 961
Minarchick, V C ... 488*, 872, 1297, 1689
Miner, W ... 476*
Minnema, D ... 378e, 684, 1846
Minnier, B L ... 2261, 2273b
Minsavage, G D ... 636
Mir, M R ... 813c
Miranda, M C ... 603i
Mire-Sluis, A ... 954a
Mirey, G ... 1931
Mirowsky, J E ... 1231*
Mirsalis, J C ... 1539
Mishin, V ... 562, 1275
Mishra, A ... 1945*
Mishra, M ... 1102*
Mishra, R ... 1639*
Mishra, V ... 923
Misner, D L ... 375, 866, 1060, 1899c
Misra, M ... 1015
Missassi, G ... 1696
Mistry, J ... 405, 1549d
Mistry, P ... 1039
Mitchard, T ... 847
Mitchell, A ... 1616a, 2148*
Mitchell, J B ... 1923
Mitchell, K A ... 2200
Mitchell, N J ... 343j
Mitchell, V K ... 1241*
Mitic Potkrajac, D ... 2182b, 2251*, 2255
Mitkus, R J ... 78
Mitra, S ... 1457*, 1465
Mitsumori, K ... 961
Mittelstaedt, R A ... 467b, 1943b
Miura, N ... 2222*
Miura, T ... 1717
Miyakawa, K ... 1197*
Miyamoto, M ... 477
Miyamoto, N ... 1114
Miyamoto, Y ... 450, 2151
Miyani, V ... 603a
Miyashita, C ... 89
Miyaso, H ... 1713h*
Miyayama, T ... 822*
Miyazaki, W ... 1346
Miyazawa, M ... 1062e*
Mizuguchi, H ... 2196bb
Mizuhashi, F ... 467c
Mizukawa, H ... 517*, 519
Mizushima, T ... 2133
Mochizuki, T ... 2119
Moehle, R ... 2160
Moeller, B C ... 883, 1107, 1242e, 1521, 1523*
Moeller, N ... 120
Moeller, T ... 307*, 1899a
Moesen, E ... 1652
Moffat, G J ... 278, 898
Moffat, I ... 1478
Mogg, R ... 1544
Moggs, J ... 971
Moghe, A ... 970
Mohammad, M ... 1874*, 1879, 2221
Mohammed, J ... 126
Mohammed, M ... 383*
Mohamud, W W ... 550
Mohapatra, A K ... 1819, 2273m*
Mohr, L C ... 1811
Moilanen, L H ... 945, 946
Moisan, E ... 121
Moland, C ... 100, 122d, 978a
Molitor, B ... 343d
Mondal, M S ... 1644*
Mongin, S ... 2211
Monick, M F ... 1975
Monks, T J ... 311, 370, 916, 924, 1503, 1542, 1799
Monnot, A ... 2233*, 2240
Monroe, W A ... 2004c
Monteiro-Riviere, N A ... 320, 632, 818, 819, 820*, 1616
Montes-Grajales, D ... 305, 306, 2268*
Montgomery, B ... 957
Montgomery, S L ... 1332*
Monti, S ... 1462, 1463
Monticello, T M ... 7*
Montoya-Parra, G ... 120*, 1591
Moody, C J ... 1632
Moomaw, H ... 2151d
Moon, H ... 2234l
Moon, Y ... 386, 993, 2027
Moore, A ... 1873, 1895
Moore, C ... 364*
Moore, J C ... 1752
Moore, J E ... 842
Moore, M M ... 319, 467b, 753*, 754*, 1943b, 1973c
Moore, N A ... 2004a, 2247
Moore, R W ... 905
Moore, S ... 2139*
Moors, M ... 40
Moorthy, B ... 535, 538, 539*, 1796
Morales, L ... 467
Morales, L D ... 1736
Morales-Rivera, J A ... 894
Morales-Soto, W ... 666*
Morano, M I ... 1151
Moreau, E ... 2151d
Moreau, M ... 1572*
Moreira, J ... 669, 675
Morelli, J ... 1113
Moreno, F S ... 1513
Moreno Lopez Malo, T ... 1244
Moretto, A ... 1824
Morey, S ... 2211
Morgan, D L ... 1110f*, 1229d
Morgan, E T ... 520
Morgan, J ... 656
Morgan, M ... 1087j
Morgan, R ... 1200b*
Morgan, S ... 7
Morgan, W ... 1615
Mori, C ... 1713h
Mori, S ... 1364
Morikawa, T ... 1160, 1161
Morikawa, Y ... 961, 1866
Morin-Kensicki, E ... 250
Morishita, M ... 815, 1240
Morisseau, C ... 876
Morissey, B ... 1864
Morita, K ... 1974
Morita, Y ... 2322
Moritz, W ... 1047
Moriyasu, M ... 1366
Morlacci, L ... 1616b
Morre, J ... 513
Morris, G ... 909
Morris, J B ... 770, 772*, 1201, 1218, 1219
Morris, R ... 1831l
Morris, S ... 96f, 299
Morris, S M ... 1943c
Morrison, J ... 1232
Morrison, L ... 283
Morry, J ... 915, 2230
Morse, J ... 1268, 1926
Morse, M A ... 2135*
Moscovitz, J E ... 1162*, 1669
Mosedale, M ... 543*, 1480
Moser, J ... 325*, 1817
Moser, V C ... 1347a, 1347c, 1747a*, 1863a, 1863b
Moses, M ... 13
Moses, M A ... 252, 259*
Mosher, S ... 223d*
Moss, J ... 1929
Moss, S J ... 552g
Mostrag-Szlichtyng, A S ... 2254*, 2273
Motomura, Y ... 954
Moudgal, C ... 173k*
Mounho-Zamora, B ... 269
Mousa, S A ... 1740
Mowat, V ... 2143
Moye, J ... 1522, 2234k
Moyer, B ... 1163a*
Mu, Y ... 122b*
Mubarokah, S N ... 918*
Mudasiru, O ... 2234v
Mueller, J ... 1568
Muenyi, C S ... 193*
Muldoon-Jacobs, K ... 27, 1609*, 2273d
Mulla, M A ... 1639a
Muller, R E ... 1242i*
Müller, L ... 874
Müller, S ... 463
Mulliner, D ... 220
Mullins, P ... 1764e
Mummery, C L ... 163
Mumtaz, M ... 96d, 1416
Mumy, K L ... 1010
Mun, G ... 1020
Mundy, W ... 35, 378c
Mundy, W R ... 1747a
Munir, P ... 165
Munley, M T ... 842
Munoz, A B ... 1301*
Munoz, B ... 1723
Munoz-Elias, E J ... 901c
Munson, J W ... 1831i*, 1989
Munusamy, P ... 814, 1963*
Murai, H ... 241
Muralidhar, M ... 1789
Muralidhara, S ... 684, 685, 897

Muratov, E ... 2182c
Murayama, N ... 1150, 2151
Murbach, T ... 329*
Murdoch, J B ... 1366, 1367, 1368
Murenzi, E ... 378e
Muriana, A ... 148
Muro, I ... 1110c
Murphy, C ... 1708*, 2035
Murphy, C G ... 411
Murphy, D J ... 1642
Murphy, G ... 1458, 1462*, 1463
Murphy, H ... 2158*
Murphy, K ... 1583*
Murphy, L ... 1713q*
Murphy, L A ... 64, 972, 1602*
Murphy, L T ... 1713r
Murr, A S ... 1018a
Murray, A ... 1645
Murray, A R ... 2004d
Murray, H ... 223f
Murray, I A ... 1133*, 1136, 1137, 1138
Murry, C ... 1129d
Murthy, S N ... 1514
Musak, L ... 2234a
Musarrat, J ... 1952
Muse, W T ... 581i
Muskhelishvili, L ... 1062b
Mussio, J ... 1062d
Mustafa, G M ... 1538*
Mustafin, I ... 603e
Mutka, S ... 1100
Mutlu, E ... 1110g*
Muto, S ... 455*
Mutsuga, M ... 450
Muwanika, R ... 226
Muzandu, K ... 843, 1516
Muzzio, M ... 889*, 2196y
Mweene, A ... 843
Myatt, G J ... 459*, 2273c, 2273y
Myers, L P ... 1415*
Myers, M B ... 265a
Myers, S ... 2117
Myhre, A ... 467d

N

Na, H ... 416*
Naciff, J M ... 146*
Nadadur, S S ... 1464
Nadeau, K ... 391
Nadella, M V ... 1636, 1911
Nadia, P ... 2234x*
Nagahori, H ... 265c
Nagai, M ... 447
Nagane, R M ... 464, 1943*
Naganuma, A ... 1253, 1257
Nagarkatti, M ... 385, 569, 922, 962, 963, 1004, 1713l, 2008
Nagarkatti, P S ... 385, 569, 922, 962, 963, 1004, 1713l, 2008
Nagata, M ... 446, 1174
Nagata, R ... 197, 472, 954, 2167
Nagavally, R ... 2063*
Nagle, R ... 1503
Nah, S ... 1462
Nahar, M S ... 1570*, 1687
Naik, P ... 354*
Nail, C A ... 1750
Nair, P ... 906
Nair, V ... 258*
Naito, H ... 1087
Nakajima, K ... 1346
Nakajima, M ... 537, 975, 1878
Nakajima, S ... 1716
Nakamaura, R ... 988
Nakamura, A ... 2196u
Nakamura, H ... 653
Nakamura, J ... 1930
Nakamura, M ... 1150
Nakamura, N ... 1713h
Nakamura, R ... 988
Nakano, Y ... 1091*, 1092, 1093, 1213
Nakao, M ... 669a*, 669b, 1991
Nakatsu, S ... 517
Nakayama, S M ... 843*, 1516
Nakayama, Y ... 2196u
Nallasamy, P ... 1229e, 1713t*, 1790
Nam, D ... 117
Nam, S ... 942
Nam, W ... 1200i
Nance, P ... 1816
Nanduri, B ... 1713p
Nanjappa, M K ... 1713g
Naoumov, N ... 873
Narain, N ... 417
Narasimhan, M ... 1839
Naravaneni, R ... 445*
Narayan, R ... 1972, 1973g
Narayanan, B ... 1242, 2300
Narayanan, B A ... 2040a*
Narayanan, N K ... 2040a
Narayanan, P ... 118, 406
Nardelli, L ... 402
Nardi, R ... 2196g
Narita, T ... 2196bb
Narotsky, M G ... 1018a
Nascimento, E S ... 1662b
Nascimento, T K ... 173n
Nash, D ... 1232
Nass, R M ... 932, 942c*, 1378
Nassirpour, R ... 2057
Natale, N R ... 298
Natalia, G ... 669c
Natarajan, B ... 1832
Nath, R ... 1822, 1831c
Nathanail, A ... 343e
Naticchioni, M ... 1685
Natsch, A ... 408a, 2165
Natsume, M ... 447
Naufal, Z ... 1765
Nault, R ... 414, 440*, 903
Naumann, B D ... 649a
Navarrete, E ... 1116*
Navarrette, P ... 188
Navarro-Yepes, J ... 926*
Navas-Acien, A ... 1306
Nawrot, T ... 223h
Nayak, A P ... 2036
Ndaye, A ... 1678
Ndiaye Traore, A ... 1678
Neagu, D ... 431
Neal, B ... 689a*
Neal, M ... 1285, 1350
Neal-Kluever, A P ... 1584*
Nedelcheva, D ... 435
Neeley, S K ... 1639c
Neely, M ... 1353, 1354, 1357
Neft, R ... 454*
Negga, R ... 1848, 1849, 1850, 1863c
Negri, S ... 1745
Negro Silva, L ... 1310*, 1319
Neier, K ... 232, 1227*, 1228
Nekhayeva, I ... 1943d
Nelen, V ... 223h
Nelms, J L ... 1744
Nelms, L ... 125
Nelms, M D ... 2254, 2266*
Nelson, A ... 286
Nelson, B ... 1794
Nelson, D ... 850
Nelson, G ... 2104
Nelson, J ... 469
Nelson, K ... 1028
Nelson, K G ... 341, 342, 845, 1680*
Nelson, L ... 1471*
Nelson, M R ... 581a
Nelson, N ... 1183
Nemec, M ... 1110b
Nemeti, B F ... 1311*, 1313
Nett, T ... 122h, 1080
Neuhaus, V ... 1051*
Neves, L A ... 2196w*
Newfang, D ... 2234z
Newhouse, L ... 414
Newland, C ... 1382, 1383*
Newland, N ... 1528
Newport, G ... 1764d
Nez, T ... 2226
Ng, C ... 276
Ng, H ... 1087a
Ng, H H ... 1539
Ng, K ... 130, 131
Ng, S P ... 1052*
Ngalame, N N ... 1297j*
Ngamcherdtrakul, W ... 915, 2230
Ngo, H ... 1084
Ngo, T M ... 1989
Nguyen, A H ... 898
Nguyen, H M ... 1842
Nguyen, J ... 1252
Nguyen, M ... 2065
Nguyen, P ... 848, 2258
Nguyen, T ... 1
Nguyen, T A ... 302*
Nguyen, V ... 2228
Nhim, C ... 987
Ni, H ... 1889
Ni, M ... 1456
Niaz, M S ... 1109, 1505, 1509
Nicholas, P J ... 1727
Nichols, A C ... 656*
Nichols, C E ... 486*, 1689
Nichols, D P ... 1001
Nichols, J W ... 669e
Nichols, R ... 1141
Nichols, R H ... 1851
Nicholson, S ... 572
Nicoara, O ... 105*
Nicolas, C ... 2273o
Nicolas, C I ... 2234i*
Nie, H L ... 1291
Nie, L H ... 1287*, 1552
Niedereichholz, T ... 1919
Niedzwiecki, A ... 1088
Niehof, M ... 512
Niehoff, M ... 468*
Nielsen, A ... 1563
Nielsen, M G ... 1583
Niemeijer, M ... 1715
Niessen, K V ... 560
Nigg, E ... 1272
Niggemann, B ... 468, 2150, 2152, 2154
Niino, N ... 494
Nijmeijer, S ... 1492
Nikam, K R ... 464
Nikolaki, S ... 2250f
Nikolic, D ... 790
Niles, A L ... 1628*
Ning, B ... 552c*, 1943c
Ning, J ... 1348
Ninomiya, F ... 1091, 1092, 1093*, 1213
Nioi, P ... 98, 1157
Nirogi, R ... 2151a, 2151b, 2163a
Nisanian, M ... 1284
Nishi, K ... 954*
Nishida, H ... 1600*
Nishihara, K ... 444*
Nishihara, Y ... 2196bb
Nishijima, K ... 988
Nishijou, T ... 1062e
Nishikawa, A ... 442
Nishimaki-Mogami, T ... 988
Nishime, C ... 2133
Nishimura, T ... 2192
Nishimura, Y ... 127, 128, 129, 2322*
Nishinaka, E ... 2133
Nishio, N ... 1046
Niu, J ... 2040a
Niu, Q ... 1347l*
Niu, W ... 425
Nix, C ... 2241
Nixon, M ... 324
Nkrumah-Elie, Y ... 1682*
Nkurunziza, P M ... 226
Nkwata, A ... 226
Noah, T ... 874
Noçairi, H ... 170
Nocco, R A ... 1765
Nocka, K ... 1128
Noel, A ... 829*
Nogueira, L ... 572
Noh, K ... 890
Noh, M ... 1123
Nohara, K ... 241*, 242, 1326, 2320
Nohmi, T ... 442, 1326, 2132
Noisel, N ... 1558*
Nolen, G ... 173c
Nomiyama, K ... 517, 519
Nomura, N ... 1046
Nong, A ... 93*, 96h, 1012
Nong Wang, X ... 1036
Nony, P A ... 1229g
Nordgren, K K ... 1773*, 1798
Noren, A ... 901, 1883
Nörenberg, A ... 449*
Norman, K ... 1020, 1021
Norris, G ... 1581
Northcott, C ... 2083
Norton, C ... 641, 1235
Norwood, J ... 1347a, 2213b
Notch, E ... 2317*
Note, R R ... 170*, 435
Novikov, O ... 264, 1463
Nowicki, B ... 1344*
Nowinski, S M ... 250
Nozaki, Y ... 2132
Ntamack, A G ... 1787
Ntapisha, J ... 843
Nteeba, J ... 2189*
Nuhar, A ... 1358*
Nukada, Y ... 1062e
Numano, T ... 199
Nunez, V ... 929*
Nungester, W ... 504a
Nurkiewicz, T R ... 488, 872, 1689*, 1982
Nurmela, J ... 1206
Nutter, N ... 1320
Nyagode, B A ... 520
Nycz, C ... 944*
Nygaard, U C ... 134, 391*
Nyska, A ... 1132
Nyugen, H ... 1307

O

O'Brien, B ... 978
O'Brien, E ... 390*
O'Brien, M H ... 1087k*
O'Brien, P J ... 1877
O'Brien, T ... 1022
O'Callaghan, J P . 372, 373*, 374, 700, 2129a
O'Connell, J R ... 552c
O'Connell, S G ... 1579
O'Driscoll, C ... 1912
O'Hara, M ... 282*
O'Keefe, M ... 334
O'Leary, M ... 135
O'Loughlin, K ... 581d*
O'Neal, S L ... 1361*, 1362
O'Neil, S ... 2057
O'Toole, T ... 1121
Oag, S ... 2145
Obejero-Paz, C A ... 478
Oberdoerster, G ... 1342
Öberg, M ... 643
Obianime, A W ... 1691
Obiorah, M ... 178*
Obisesan, Y D ... 2234u
Obrecht, A ... 2160
Obringer, C ... 1031
Ochs, S ... 2021
Oda, S ... 975*
Odak, M ... 1353, 1354, 1355*
Odewabi, A O ... 1557*
Odewumi, C ... 1264c*
Odnevall Wallinder, I ... 1280
Odukoya, O O ... 1249, 1264, 1266, 1273
Odunola, O A ... 788, 813b, 1514b*
Odwin-DaCosta, S ... 1737
Oelgeschlaeger, M ... 163
Oesterling Owens, E ... 1018c
Oestreich, J ... 1118
Ofelia, P A ... 848a
Ogawa, K ... 442
Ogawa, T ... 2196u
Ogawa, Y ... 1160, 1161, 1974
Ognibene, T ... 882
Ogra, Y ... 1304
Ogunlana, O E ... 1198
Ogunpolu, B S ... 481, 1267, 1270, 2041
Ogunrinola, O O .. 1249*, 1264, 1266, 1273, 1776
Oguntade, B ... 321
Oh, H ... 1200i
Oh, S ... 787, 797b*, 1190, 1327e
Ohanian, E V ... 1831b

Author Index (Continued)

The numerals following the author's names refer to the abstract numbers. The asterisk after the abstract number indicates the author is the first presenter.

Ohlsson Andersson, Å 1076, 1081
Ohman-Strickland, P 858, 1501
Ohno, Y 961
Ohsako, S 978b
Ohta, S 1086
Ohtani, K 1697, 2222
Ojima, A 1114
Ojo, D 2271
Okafor, P N 1200c
Okamatsu, G 539c
Okamoto, S 2004e
Okamura, K 241, 2320*
Okamuro, A 2196bb
Okazaki, S 2196u
Okazaki, T 954
Okeyo, G 1118
Okonkwo, N 514*
Okuda, Y 265c*
Ola, E 260
Ola-Davies, O E 462*, 1073
Olagunju, J A 1198
Olanrewaju, A I 321
Olatunji, O A 788
Olawuwo, O S 462
Olayemi, F O 803, 806*
Oldach, J 1053, 2181
Olden, K 959*
Oldenburg, S 819
Oldham, M 5
Olejnik, N 1297a
Olguin, S 1144*
Olie, J 96c*
Olin, J 173i, 1062a
Oliveira, D P 451, 457, 458, 467h, 664*, 789
Oliveira, G A 467h*
Oliver, L D 954d
Oliver, M 1559
Oliver, V 122h
Olivera, D 570
Oliveri, A N 1347h*, 1857
Olivero, O 705, 1923
Olivero-Verbel, J 147, 305, 306, 667, 783, 2268
Oller, A R 1280
Ollerstam, A 1229c
Olsen, G 1135, 2211
Olsen, J 408
Olshan, A F 229, 1308, 1318
Olson, G 632g, 841b, 1616e
Olson, J 1345*
Olson, J R 81, 689*, 1101, 1524, 2204
Olson, K 1200b
Olszyk, D 1006a
Olubanke, O O 1198*
Oluwafemi, F 1774
Olvera, J 574
Omiecinski, C J 1477*
Omobowale, T O 481*, 1267, 1270, 2041
Omoluabi, O 387
Omoruyi, I M 323*
Omotainse, S O 808
Omotosho, I O 1209*
Omran, O A 1768
Omura, K 961*
On'Gele, M O 1923*
Oneda, S 197*, 1698
Ong, C 2328*
Ong, J 135, 2234c*
Onishchenko, N 40
Ono, A 460*, 961, 2192
Onoue, S 760*, 1600
Onunkwor, O B 1249, 1266, 1273, 1776
Onwordi, C T 321*
Ooi, J 500
Ooms, T G 889
Opperhuizen, A 335
Opresko, P L 1293, 1936
Orchard-Hays, J 2272
Ordoñez, P 443
Orem, W 1018b
Orfield, S E 1851*
Orisakwe, O E 1200c, 1691
Orlicky, D 553, 554, 1095
Oroszlany, B 843, 1516
Orr, D 1876
Orr, M 1254
Orr Gandy, K 1004*
Ortega, S A 269
Ortega Atienza, S 1926*
Ortenzio, J N 1347b, 1973d
Ortiz-Martinez, R 313*
Ortiz-Martínez, M G 981*
Ortiz-Sanchez, C M 467*
Osborne, C 577
Osborne, M 1865*
Osgood, R S 1103*
Oshida, K 450
Oshiro, W M 96b, 1347c, 1347d*
Oshita, Y 2119
Osifeso, O O 788
Osimitz, T G . 60, 378e, 684, 685, 689b, 897, 1087i*, 1846, 2236
Osina, O 2234a
Osinski, M 475
Oskarsson, A 1076*, 1081
Osman, K A 1768*
Ossala, R 1890
Ossig, R 1950
Osterbauer, C 995*
Ostrander, G 652
Osuna, C 1334*
Otieno, M 106
Otsuki, T 127*, 128, 129, 2322
Ottens, A K 2304*
Ouédraogo, G 170, 173e, 440a
Ovesen, J L 1271
Ovsianikov, A 1973g
Owens, E O 1831c, 2250j
Owolabi, O B 788
Oyagbemi, A A 481, 809, 1267*, 1270, 2041
Oyeyemi, M O 1694*
Øverby, G R 1782

P

P Kuppusamy, S 1831d*
Pabon, L 1129d
Pacanowski, M A 552c
Pace, C 1298
Pacheco, B 135, 2226, 2234c
Pacheco, S E 1707
Pachkowski, B F 1809
Padilla, S 173i*, 223d, 440h, 1062a, 1747a
Paehler, A 1545
Page, K E 1281, 2128*
Pagrut, S 2163a
Painter, K L 2250j*
Paisley, B M 434*
Pajaro-Castro, N 147*
Pakbin, P 837, 1242f
Palacios-Hernandez, T D 603i, 1973
Palaniyandi, S 1255
Palate, B 2130
Palekar, A 1062a
Palestino, G 840
Pallardy, M 123, 987*, 2009, 2010, 2011
Palm, J 901
Palmberg, L 1814
Palmeira, C M 2004g*
Palmer, B 1342
Palmer, J A 1917
Palpant, N 1129d
Palunas, M 1501
Pamies, D 1737, 1738, 1912*
Pan, L 674
Pan, X 409*, 1713i*, 1732, 1736c
Pande, P 544*, 2196i
Pandey, S 2151a, 2151b*, 2163a
Pandiri, A R 955, 1616c
Pandya, J D 378g*
Pandya, M 347, 403
Panepinto, A S 2234aa
Pang, J 954g, 2034
Pani, J 1018e
Panicker, N 1350
Pannirselvam, M 500*
Pant, K 1943e
Panter, K E 805
Pantlin, L N 1347b, 1973d*
Panyala, N 1624*
Panzica-Kelly, J 222
Papadopoulou, E 1528
Papaeliou, A 2048
Papagiannis, C N 2196z
Papapostolou, V 1242b
Papoian, T 2082*
Papoutsakis, E 1458, 1461*
Paquette, D 274, 275
Paradiso, D 570, 577, 2163c
Parchment, R 1062d
Paredes, A 841b, 1756, 1947, 1973c
Parenteau, A 2037*
Parham, F 1616g
Parikh, D 1936*
Parikh, S 1899e
Park, B 797a*, 799, 802
Park, E 1951*, 2052
Park, H 549, 1770*
Park, J 933, 942d, 1260, 1327e*, 1763*, 1976, 2234l
Park, K 1327e
Park, N 293
Park, S 386*, 539b*, 1166, 1167, 1976
Park, S L 871, 1499, 2164
Park, S S 686
Park, W 942
Park, Y 1044, 1571
Parker, A 63, 2250i
Parker, P 1307
Parker, R M 1764*
Parkins, R 1199
Parks, A J 264, 1462, 1463
Parks, B 1281, 1905
Parks, W C 1962, 2004f
Parmalee, N L 1374*, 1856
Parmentier, C 164
Parod, R J 617*
Parodi, D A 1713j*
Parr-Dobranzski, B 2174
Parrill-Baker, A 505
Parrula, C 2191
Parsons, B L 265a
Parsons, G 583
Parsons, P J 1306
Parsons, P P 238
Parton, T 1659
Partridge, C R 72
Passantino, L 2180*
Pastoor, T 1824
Pastor, M 428*
Patel, D 1839
Patel, M 576
Patel, M L 2257*
Patel, M N 359, 925, 1453*
Patel, M V 347, 398*, 399, 403, 405, 1800, 1801
Patel, N 398, 399, 2151c
Patel, N N 464*, 1943
Patel, P 1898*
Patel, S 256*
Patel, T 2174*
Patel, V S 1713o*, 2026
Patil, M 970
Patlewicz, G 1400*, 2253
Patlolla, A 1993*
Patlolla, B 1116
Patri, A K 1973i, 1973j
Patrick, D J 1680
Patshin, E S 828
Patten, C J 1899e, 2067a*
Patterson, A 1133, 1141
Patterson, T A 1764a, 1764b
Pattnaik, N 1243
Patton, K M 581j, 2004a
Paul, D 1655*
Paul, K B 1066*, 1747a
Paula, E S 467h
Paule, M G 96f, 173m, 378f, 378i, 603b, 934, 942e, 1429, 1756, 1764a, 1764b, 1764c, 1764d, 2074, 2077*
Pauli, G F 790, 796
Paulsen, J E 2248
Paulsen, R E 1782
Pauluhn, J 10*, 25*, 1212
Paustenbach, D J 77, 225, 603j, 1610, 2233
Pavilonis, B 672*
Pavuk, M 234
Pawar, N 1639a
Pawlisz, A 1813*, 2250e
Peana, M F 1297e
Pearce, M G 467a, 2004c
Pearce, R 2234m
Pearson, J N 359
Pearson, N 1616a
Pearson, N J 888*
Pechacek, N 1022*
Peck, M 1203
Peden, D B 1242i
Peden-Adams, M M 1713q, 1713r
Pedersen, J M 901*, 1883
Pedersen, M 1018d
Peeples, C 76*
Peffer, R C 238
Pegram, R A 632b
Pehl-DeSilva, A T 1502
Pei, Q 1533*
Pei, X 922c
Peijnenburg, A 408b, 1062h
Peitsch, M 413, 415, 860, 1054, 1055, 1203
Pelch, K E 958, 1297k*
Peli, M 1551
Pelkowski, S 1333, 1340, 1342, 1747e*
Pellerin, M 343
Pelletier, J 382, 1315
Peltonen, K 343e*
Pendse, S 94, 162, 1140
Peng, H 1117, 1794*
Peng, L 49
Peng, S 1117*, 1794
Peng, S J 871
Peng, Z 1925*
Penman, A D 1646
Penman, M 1593*
Pennell, K D 115, 868
Pennington, K L 255
Pennington, M W 901c
Pennington, S 1864
Pepin, D 1549f*
Perdew, G H .. 1133, 1136, 1137, 1138*, 1139, 1141
Perdu, E 149
Pereira, E F 1861
Pereira, L C 312, 457, 458*, 677
Peres, T V 1329*
Peretz, J 2185*
Perez, E 2267
Perez, V 227*, 777
Perez-Martinez, A S 144
Perez-Medina, A L 1385*
Perez-Vale, K Z 1370*
Periera, E F 1860
Perkins, C 1303
Perkins, R 1087a
Permenter, M 1265*
Perpetua, M S 404, 1713s
Perrard, M 681*
Perrott, R L 2163b
Perry, C S 622, 623
Person, R J 1297i*
Pery, A R 28, 29
Pescrille, J D 1860, 1861
Pessah, I N 351, 360, 682, 698, 1842, 2213a, 2234g
Pestka, J J 140, 318, 409
Peter, B 2147*
Peter, E 120, 1591
Peters, J M 245, 246, 247, 249, 260, 1155, 1156
Peters, M 1111*, 1126, 1619
Petersen, D 649c, 2273cc*
Petersen, J R 1538
Petersen, S 174
Peterson, J D 1200h*
Peterson, K E 964
Peterson, L A 1491
Peterson, M 1812*
Peterson, R 1642
Peterson, R E 490, 504b, 905, 1681, 1746
Peterson, S M 203, 1277
Petibone, D 1943c
Petrash, J 555
Petren, S 168
Petrick, J S 330*
Petriello, M C 1124*
Petrikovics, I 574*

The numerals following the author's names refer to the abstract numbers. The asterisk after the abstract number indicates the author is the first presenter.

Petrochenko, P E ... 1973g*
Petrovic, S ... 1819
Petrucci, D ... 1645*
Petry, T ... 1826
Pettit, A ... 858*
Pettit, S D ... 764, 765*
Peyon, G ... 2162
Peyret, T ... 96a
Pfannenbecker, U ... 1027
Pfau, E ... 632j
Pfau, J C ... 55*, 130, 131*, 1760
Pfister, J A ... 805
Pfuhler, S ... 753, 758*, 1997
Phadke, D P ... 122, 958
Phadnis-Moghe, A ... 2015, 2016*, 2018, 2020
Phalen, R F ... 5
Phan, A M ... 370
Phat, S ... 417
Phatak, M ... 425
Phelka, A D ... 606, 1663
Philbert, M A ... 350
Phillip, O S ... 792*
Phillip Kaiser, J ... 1831d
Phillips, B ... 1203
Phillips, E ... 324
Phillips, G J ... 1530*
Phillips, J A ... 380, 2196e*, 2196g, 2196h
Phillips, J I ... 1215
Phillips, K ... 1089
Phillips, M ... 2250c
Phillips, M B ... 96i*
Phillips, P ... 2330
Phillips, P M ... 1747a
Phillips, R D ... 1824
Phillips, T D ... 316, 317, 343j, 1526
Phonethespwath, S ... 452
Phuong, J ... 2273l*, 2273s
Pi, J ... 439, 1788, 1794, 1804a
Piaia, A ... 427
Picamal, P ... 1643
Piccirillo, V J ... 347, 398, 399, 403, 405, 464, 1800, 1801, 1943
Piccotti, J ... 1200, 2038*
Pickens, M A ... 1690a
Picon-Rubio, F ... 315
Pidathala, A ... 247
Piehl, M ... 1025*, 1035
Piehowski, P ... 1525
Pierce, J S 232, 614, 1227, 1228, 1574*, 2234t
Pierre, S ... 1158
Piersma, A H ... 1079
Pieters, R ... 216, 635, 1041, 2028*
Pietras, M ... 1627
Pike, A F ... 1048
Pilling, A M ... 2143*
Pinette, J ... 215*
Pinkerton, K E ... 828
Pino, M A ... 576*
Pinto, C L ... 149, 150*
Piper, J ... 467b
Piper, R K ... 1525
Piroird, C ... 402*
Pirone, J ... 173d, 1831l*
Pirow, R ... 1057
Pita, R ... 1862
Pitt, B ... 1777
Pizzurro, D M ... 1753*
Planchart, A ... 210, 1758*
Plant, T M ... 379
Platoff, G ... 558, 564, 567
Platzack, B ... 346
Plautz, J R ... 632
Plavicki, J S ... 490, 504b, 1746*
Pleil, J ... 876d
Plöttner, S ... 1007*
Plotzke, K P ... 901d, 2245
Plummer, S ... 1090*
Plunkett, L M ... 637*
Po, I ... 578
Poage, D W ... 811*, 2196z
Poet, T S ... 61, 82, 2059
Pognan, F ... 426, 427, 873*, 1618, 2056
Pogribny, I ... 2, 265b, 956, 957, 978, 1513, 2123
Pohjanvirta, R ... 323
Pohl, H ... 223f, 1014
Pohl, J ... 194
Pohlenz, C ... 316
Pohlmann, G ... 600
Pohlmeyer-Esch, G ... 2131
Pointis, G ... 681
Pointon, A ... 1120
Poirier, M C ... 702, 705*, 848, 1923
Poitout, F ... 1540
Polakoff, B M ... 59
Poland, B ... 646*
Politano, V T ... 1601*, 1605
Pollard, C ... 1661
Pollard, K M ... 135
Pollenz, R S ... 1435*, 1665, 1666*
Polli, J R ... 1713i, 1732, 1736c*
Pollock, B H ... 317, 1526
Pollock, M C ... 2234q
Polokoff, M A ... 1647, 2250, 2273v, 2273w
Polzer, F ... 365
Pombo, M ... 1127*
Pomeroy-Black, M J ... 1670*
Ponnusamy, L ... 1096
Poole, A ... 236*, 1826
Pooler, C E ... 467d
Poor, L ... 2151d
Pope, D A ... 1382*, 1383
Pope-Varsalona, H C ... 1293*
Popineau, A ... 1655
Popovech, M A ... 823*, 824, 825
Popovici, A ... 683
Porter, A ... 1979
Porter, D W ... 23, 587, 591, 1465, 1977
Posgai, R T ... 1583
Poshiya, M ... 405
Posnack, N ... 1129c*
Posner, J ... 1981
Posson, M ... 2234r*
Potdar, S ... 312c*
Poth, A H ... 173, 1032*, 1062
Potnis, P A ... 289*, 2024
Pottenger, L H ... 1941*
Potter, D ... 1200b
Potts, R J ... 71, 1615
Potts, W ... 283
Pouliot, L ... 2191
Pouliot, M ... 274, 275, 471
Poulnas, M ... 1497
Poulsen, K L ... 1882*
Poulsen, M ... 1766
Poulton, E ... 1113*
Pounds, J G ... 602, 1980*
Povinelli, R J ... 429
Powell, E T ... 2232
Powell, H ... 1630
Powell, W H ... 1142
Powers, J E ... 505
Powers, L S ... 1975
Powles-Glover, N S ... 2161*
Powrie, R H ... 1593
Poyil, P ... 1297f*, 1327f
Poynter, M E ... 390
Prabhala, H ... 1653
Pradeep, P ... 429*
Prajapati, B ... 398, 399
Prajapati, M V ... 831*
Pramanik, K C ... 247*
Prasad, G L ... 1527*
Prater, M R ... 188
Pratt, L F ... 1033*, 1035
Pratt-Hyatt, M ... 2122
Prediger, R D ... 1329
Prefontaine, A ... 861*
Pregenzer, J ... 343f
Price, A ... 2251
Price, A K ... 746*, 747*, 751
Price, H ... 1110f, 1229d
Price, J ... 1119
Price, L ... 1872*
Price, O ... 66*, 67
Price, P S ... 61*, 82, 1408*
Price, R J ... 689b
Priestley, P J ... 470*
Primerano, D ... 909
Prince, L ... 218*
Pringle, R ... 556*, 568
Pringle, T ... 1648
Pritzlaff, A M ... 260
Privitera, H ... 1350
Proal, A ... 46*
Proctor, D .. 231*, 779, 781, 1290, 1296, 2219
Proctor, M ... 524
Prokopczyk, B ... 248
Proost, J ... 1062h
Proper, S P ... 1214
Proscura, E ... 566
Proudlock, R ... 467f*
Prough, R A ... 676, 1159, 1569, 1736b, 1870, 2221
Prozialeck, W C ... 2048*
Prueitt, R L ... 1810*
Pruett, S B ... 679, 1413*, 1713p
Prussia, A ... 433*
Pryor, A W ... 1061
Przygoda, R T ... 954c*
Psurny, E ... 581j
Publicker, S ... 1662c
Puchalski, J ... 408
Puente-Valenzuela, C O ... 1309*
Puga, A . 908, 1271, 1458, 1459*, 1685, 1907, 1909
Pugh Bishop, S ... 169, 1043
Pujalté, I ... 839, 1998*
Pulliam, S R ... 1109
Punnoose, A ... 1637
Pupo, A S ... 1696
Puppala, D ... 1129*
Purmal, A ... 503
Puschner, B ... 364, 2234g
Pushkar, Y ... 2107
Putt, D A ... 310
Pyatt, D ... 228, 1490*
Pyram, B ... 215

Q

Qi, L ... 895
Qi, Q ... 367
Qian, G ... 317
Qian, H ... 101
Qian, Y ... 587, 590
Qiao, J ... 272
Qiao, S ... 308, 1499*, 2164
Qin, J ... 1653
Qin, Q ... 272, 1450, 1924
Qin, S ... 418c, 1115, 1887
Qin, T ... 265d*
Qin, X ... 1533
Qing, T ... 1195
Qu, L ... 473*, 2142
Qu, Q ... 969, 1185*, 2040a
Qu, W ... 1229d, 1297h*, 1794
Qualls, C W ... 1061
Quell, S J ... 145a
Quenel, J A ... 1973
Quezada-Tristan, T ... 313
Quintanilla-Vega, B ... 926
Quist, E ... 1087r*, 2196b

R

Raaijmakers, J ... 635
Rabinowitz, J ... 2234i, 2234m, 2234n
Racette, B A ... 2104*
Racheed, S ... 574
Racine, C ... 2064*
Racine Miousse, I ... 972
Radhakrishnan, J ... 797
Radi, Z ... 1660
Radilov, A S ... 1536, 2249
Radonjic, M ... 1347i
Radovsky, A ... 1634
Raetzman, L ... 1071
Raftery, T ... 152, 155*, 156
Rager, J E ... 1308, 1318*
Raghavan, M ... 1148
Raghavan, S ... 88, 1059, 1899
Rahn, J J ... 223a
Raigneau, M ... 880*
Raimondo, S ... 2263*
Rajan, R ... 1999
Rajan, S ... 1947
Rajapaksa, K S ... 2196p*
Rajendran, K ... 88, 1059, 1899
Rajeswara, N ... 88, 1059, 1899
Rajnarayanan, R V ... 1072
Rakic, B ... 2182b, 2251
Rakkestad, K E ... 1782
Raleigh, K ... 2211
Ralf, L ... 120, 1591, 1871
Ralston, N V ... 37*, 42*
Ramachandran, G ... 2211
Ramagopal, M ... 846
Ramaiah, S K ... 103, 122f
Ramaiahgari, S ... 1872
Raman, D ... 88, 1059, 1899
Ramesh, A ... 1109, 1505, 1509, 2023
Ramirez, F M ... 311*
Ramirez, T ... 173, 634, 1871*
Ramirez, V P ... 1724*
Ramirez-Lee, M A ... 1973f
Ramírez-Martínez, L ... 1723
Ramm, S ... 1864*
Ramoju, S ... 1200g
Ramone, S ... 2226
Ramos, E ... 1843, 1862
Ramos, J ... 1906
Ramos, K S ... 1500
Ramos, R ... 1347f
Ramos, R F ... 796
Ramu, J ... 378f
Rana, J R ... 464
Rancourt, R C ... 554
Rand, M D ... 218, 1331*, 1332
Randall, C M ... 173a*
Randall, M J ... 390
Randall, W R ... 1861
Randazzo, J ... 67, 1594*, 1596, 1597, 1598, 1599
Randell, S ... 603h
Ranjan, A ... 1508*
Rankin, G O ... 541, 2062, 2064
Rao, D B ... 1363
Rao, P ... 2116
Rao, R ... 569*, 922
Rappold, A ... 876d
Raqib, R ... 2318
Rasco, J F ... 1541, 1711
Rasdall, J A ... 122a*
Rashid, M ... 1639
Rasmussen, A D ... 1764e*
Rasmussen, E ... 122a
Rasmussen, K ... 469*, 953
Rasmussen, T P ... 1176
Rasoulpour, R J ... 64, 972, 1602
Ratelle, M ... 1531*
Rath, M ... 1088
Rathinam, M ... 1839
Rathman, J ... 27, 31, 2273*, 2273d
Rathmell, W ... 261, 1506
Ratjani, K ... 989*
Rattray, M ... 183
Ravagli, C ... 427
Ravelo, D ... 185
Ravenscroft, S ... 1120*
Ravindran, A ... 126*
Rawlinson, P ... 1039
Ray, R ... 570
Ray, S D ... 297, 1679
Raza, H ... 1769*
Razo, A ... 1613
Razzaq, R ... 813c
Read, K ... 2146*, 2149, 2158
Reagan, W J ... 1549a
Rebeca Yasmin, P R ... 848a*
Recio, L ... 240, 324, 1110g, 1478
Redfern, W S ... 1625, 1630
Reed, D R ... 946
Reed, L ... 1635
Reed, M S ... 194
Reed, R J ... 1562*
Reeder, A ... 1143*
Reese, D H ... 1595
Reeves, W ... 2033
Regalia, D ... 504a
Rehman, M U ... 813c*
Reho, J ... 2129
Reibling, K ... 1128
Reichard, J F ... 425*, 1827
Reid, D ... 550

Author Index (Continued)

The numerals following the author's names refer to the abstract numbers. The asterisk after the abstract number indicates the author is the first presenter.

Reid, L M ... 1905
Reif, D 173b, 210, 223d, 1062f, 1747*, 2273s, 2273v, 2273z, 2273aa
Reif, D M ... 418b
Reigan, P ... 552
Reilly, C A ... 1238, 1241
Reilly, T P ... 1089
Reily, M ... 853, 2122
Reim, D ... 2151d
Reimschuessel, R ... 632g
Reineke, H ... 1129d
Reinhart, P G ... 1830
Reisfeld, B ... 84, 137
Reisinger, K ... 1029
Reiter, L ... 1890
Rekhadevi, P V ... 1505
Relph, J ... 2157
Rembovskiy, V R ... 1536, 2249
Remmer, H A ... 350
Ren, H ... 841d
Ren, J ... 272, 346
Ren, N ... 1840
Ren, X ... 1101*, 1493
Renaud, H J ... 49
Renna, S ... 2118*, 2151c
Renshaw, E ... 850
Resnick, C ... 1306
Retamal Marin, R ... 332
Retter, M ... 118
Rettie, A E ... 552b
Reuhl, K R ... 1497, 1501, 1841
Reuter, S ... 1129b
Reverdy, E E ... 948, 949*, 951, 1616d
Revollo, J ... 1943c*
Revskoy, S ... 158*
Reyero Vinas, N G ... 1988*
Reyes-Cervantes, E ... 1973
Reymick, J ... 934
Reyna, M ... 424
Reynaud, L ... 2196
Reynolds, J E ... 945*
Reynolds, S H ... 23
Reynolds-Walsh, M ... 301, 1671*, 1679
Reznik, S E ... 572, 580, 994
Rho, G ... 871
Rhoades, C ... 1615
Rhoades, R E ... 1684
Rhodes, K ... 2024
Rhomberg, L R ... 1484*
Riccardi, E ... 1914
Rice, A ... 603g, 603h
Rice, E ... 382
Rice, J R ... 173o
Rice, M ... 355
Rice, R ... 1026
Rice, R H ... 2170
Richard, A M ... 31*, 418b, 2273s, 2273v, 2273z, 2273aa
Richards, I ... 122i
Richards, J ... 1204, 1205, 1230, 1232, 2325
Richards-Waugh, L ... 541
Richardson, C J ... 1087l*
Richardson, D ... 1713u
Richardson, J ... 48, 51*, 973, 1752, 1841, 1844, 1845, 2053
Richardson, J E ... 2093
Richarz, A N ... 27, 431, 2266, 2273x*
Richburg, J H ... 1708, 2035
Richendrfer, H ... 1751*
Richer, T ... 2136
Richmond, E ... 1764e
Richter, P ... 1062b
Richter, R J ... 116, 686
Rick, D ... 64
Rick, D L ... 688
Ricke, E ... 252*
Ricke, W A ... 252, 259
Ricketts, S ... 1630
Rico de Souza, A ... 1722
Rider, C V ... 813a*, 1713c
Ridge, L ... 184
Riedel, W ... 2131
Rieger, D K ... 1329
Rietjens, I ... 1831e
Rigden, M ... 1713
Riley, R T ... 314, 343b*
Rinckel, L ... 173h*, 1831l, 2250b, 2273i
Ringeissen, S ... 435*
Ringwald, M ... 2093
Rinkevich, J P ... 2272
Rios, M ... 1371, 1372
Rioux, J ... 577
Ripp, S ... 1633
Ripp, S L ... 276
Risnes, S ... 1448
Riss, T L ... 291*, 1628
Risvanis, J ... 277*
Ritacco, G ... 1605*
Ritchie, G ... 581h
Ritchie, R ... 1087l
Ritter, D ... 1050*
Rittinghausen, S ... 1990*, 2003
Riu, A ... 149, 150
Rivera, P ... 1243
Rivera-Soto, R ... 1214*
Riviere, J E ... 320, 818*, 819, 1616
Rizvi, S A ... 1725, 1728
Rizvi, S M ... 1148
Robers, M ... 167
Robert, C ... 2177, 2179
Roberts, A ... 343i, 669d
Roberts, C B ... 2234f*
Roberts, C J ... 2174
Roberts, D ... 420
Roberts, J R .. 486, 841c, 1242a, 1713u, 1983
Roberts, K C ... 1217
Roberts, L J ... 232
Roberts, R ... 284*, 990, 2109*, 2110*
Roberts, S M ... 1396*, 1831i, 1989, 2234f
Robertson, A P ... 1145
Robertson, D ... 853*, 2122
Robertson, L W ... 515, 2199, 2202
Robillard, T ... 345
Robinson, A ... 1921, 1922
Robinson, C N ... 2066*
Robinson, D K ... 2196c*
Robinson, G ... 1344
Robinson, J ... 1583
Robinson, J F ... 179*
Robinson, M ... 1915
Robinson, P J ... 87, 96, 440g
Robinson, S ... 284, 2110
Robinson, V G ... 198, 1606, 2224*
Robson, S C ... 122f
Rocha, J B ... 173n
Rocha, V d ... 1608*
Roche, B ... 581h
Rochet, J ... 378h, 923, 1349
Rockwell, C E ... 145, 1867, 2012, 2013
Rodd, A L ... 668*
Rodeheaver, D P ... 1026
Rodrigues, L ... 417
Rodrigues Hoffmann, A ... 316
Rodriguez, J ... 954b
Rodriguez, K ... 2196c
Rodriguez, M ... 1526
Rodriguez, Y ... 1372
Rodríguez, G ... 875
Rodríguez, P ... 875
Rodríguez, R I ... 1785*
Rodríguez Salazar, T ... 343a
Rodríguez-Yáñez, Y ... 595*
Rodriquez, P ... 1280
Rodwell, D E ... 617
Roede, J ... 418, 1836*
Roederer, M ... 271
Roelen, B A ... 1075
Roelofs, M ... 1079*
Rogers, A ... 1633
Rogers, J ... 1327d
Rogers, J M ... 1347a, 2213b
Rogers, K ... 1359*
Rogers, L K ... 1688
Rogers, R A ... 1215
Roggen, E ... 2168
Roggen, E L ... 1062g*
Rogissart, A ... 220
Rogue, A ... 888, 1727*
Rohlman, D ... 81, 689
Rohr, A C ... 1222, 1229f, 1240
Rohrer, P ... 1169*, 1176
Rojanasakul, Y ... 585, 589, 830
Rojas, I ... 1163a
Rojo de la Vega, M ... 1499
Rojo de la Vega Guinea, E M ... 1780*
Roling, J A ... 661, 1854
Rolls, B A ... 921*
Rolo, A P ... 2004g
Román-Pérez, S ... 1312
Romans, A B ... 1799
Romero, A ... 1843, 1862
Romero, E G ... 1238, 1241
Romoser, A A ... 316, 317, 343j, 1526
Rompion, S ... 2144
Rondelli, C M ... 978d
Ronis, M J ... 254
Ronk, C J ... 225, 2234t
Roome, N ... 220
Roomi, M ... 1088*
Rooney, A A ... 1486*, 1829
Rooney, C ... 1864
Rooney, J ... 1939*
Rooney, M ... 1644
Roosen, W F ... 348*
Roper, C ... 632
Roque, K ... 1713m
Rosaldo, J J ... 922b
Rosas-Hernandez, H ... 378i*, 603b, 942e, 1973f
Rosato, K ... 219
Rose, C ... 2152*
Rose, F R ... 2174
Rose, K ... 388*, 1042
Rose, M ... 2121
Rose, R ... 2149*
Roseman, J ... 877
Rosen, M B ... 440c
Rosenfeld, C ... 343d
Rosengren, R J ... 791
Rosenheck, L ... 1662b
Rosenspire, A J ... 136*
Rosenstein, M C ... 411
Rosenthal, F ... 1368, 1550
Rosenthal, G J ... 1100
Rosini-Marthaler, L T ... 109
Ross, D ... 358, 1632
Ross, J ... 378b, 825
Ross, M ... 1485*
Ross, M K ... 679, 1515, 1750
Ross, S ... 160, 240, 1934, 2250i
Rossi, F ... 835
Rossi-George, A ... 1391*
Rossner, P ... 706, 1943a*
Rossnerova, A ... 706
Rosso, K ... 1980
Roszell, L E ... 627
Rotella, D P ... 259
Roth, A B ... 104
Roth, R A ... 1197, 1199, 1882, 1886
Rothblat, L ... 1684
Rothe, H ... 632, 982, 1031
Rothenberg, S J ... 1306
Rothrock, G ... 641
Rothstein, M A ... 2100*
Rotimi, O A ... 1774*
Rotimi, S O ... 1776, 2271*
Rotroff, D ... 173b, 2273i, 2273s, 2273z
Rouleau, M ... 2298
Rouse, R L ... 1549b*
Rousseau, S ... 1722
Roux, L ... 2175*
Rowe, C ... 1921*, 1922
Rowe, J ... 1615
Rowe, J J ... 1583
Rowland, A M ... 919
Rowland, B ... 1999*
Rowland, D ... 579
Rowland, J ... 65
Rowlands, J . 1132, 1398*, 1403*, 1824, 1905
Rowley, S D ... 359
Roy, D ... 1087j*
Roy, P ... 1957
Roy, S ... 1278*
Royland, J E ... 378g
Rozek, L S ... 1922e
Rozelle, S ... 1462
Rua, D ... 632
Ruark, C D ... 96*, 96f
Rubin, B ... 1884
Rubin, R L ... 135, 2234c
Rubinstein, J ... 1685
Rubio, F ... 1566
Rubio, L ... 1954
Rubio-Armendáriz, M C ... 2218*
Rubio-Andrade, M .. 229, 1306*, 1308, 1318
Rubio-Rosas, E ... 1973
Ruby, K ... 1339
Ruby, M ... 1831i, 2234w
Ruddock, K ... 2234b
Rudel, R ... 524, 2259*, 2260
Ruden, M ... 1264c
Rudisill, C ... 1616b
Rudraiah, S ... 366, 1176*
Ruff, J ... 283
Ruffini, F ... 1914
Rugen, P J ... 1030*
Ruiz, P ... 96d*
Rumbeiha, W K ... 362
Rundell, J ... 467f
Rundhaug, J E ... 250
Runge, F ... 2152
Runyon, S ... 391
Ruppert, G W ... 901c
Rushing, B ... 699
Rushing, B R ... 2040b
Rushmore, T H ... 1200f
Rushton, E ... 467b
Rusnak, S M ... 2237*
Russel, F ... 1062h
Russell, R B ... 2251, 2255
Rusyn, I ... 165, 630, 978, 1152, 2123, 2250l
Rutqvist, L ... 2234v
Ruus, A ... 782
Ruusunen, J ... 1206
Ryan, A M ... 427
Ryan, D ... 2110
Ryan, E ... 1025
Ryan, G A ... 203*
Ryan, K ... 1616c*, 1616g
Ryan, P C ... 2112
Rychlik, K ... 343j*
Ryde, I T ... 931, 1939
Rydnert, F ... 1062g
Ryu, J ... 1553
Ryu, S ... 117

S

Saba, A B ... 481, 1267, 1270*, 2041
Sabbisetti, V ... 122g
Sabelli, R ... 881*
Sabet, S ... 541
Sable, H J ... 1744
Sabnani, M ... 1999
Sabo-Attwood, T ... 594, 997, 1467*
Sabolsky, E M ... 488
Sabourin, C L ... 581h, 581j
Sabourin, P ... 581h, 581j*
Sachs, C ... 1422, 1428*
Sacks, J ... 776
Sadekar, N ... 1261*
Sadik, A M ... 901b
Sadler, C ... 1630
Sadovnikova, A ... 1582
Sadovova, N V ... 1764a, 1764b, 1764c*
Sadowski, R N ... 132
Saengtienchai, A ... 521
SaénzPardo-Reyes, E ... 797c
Safe, S H ... 258, 305, 306, 1105, 1106, 1130, 1131, 1143, 1510, 1511, 1512
Saffarini, C M ... 1686*
Saffour, K ... 64
Saforo, D J ... 304
Sagemark, J ... 1126, 1881
Sager, T M ... 486, 1978*
Saghir, S A ... 901a*
Sahneh, F D ... 818
Sahu, S C ... 1944*
Saiakhov, R D ... 440i, 440k*, 2265
Saito, K ... 1062e
Saito, N ... 591, 2210*
Saito, T ... 978b
Saiyed, Z ... 1590
Sakaguchi, H ... 1029, 1062e

The numerals following the author's names refer to the abstract numbers. The asterisk after the abstract number indicates the author is the first presenter.

Sakai, K ... 1262
Sakai, S ... 988*
Sakai, Y ... 1967
Sakaki, H ... 1640
Sakamoto, M ... 1262
Sakamura, S ... 173b
Saks, M J ... 719, 720*
Sakuratani, Y ... 432
Salahpour, A ... 371
Salama, A K ... 1768
Salama, M M ... 1180
Salawu, O A ... 807*
Salazar, D ... 2174
Salazar, K D ... 1809
Salazar-Garcia, S ... 1973f
Salbaum, J ... 187
Saldívar, L V ... 343a*
Saleh, N B ... 594, 1467
Saleh, S M ... 1179
Salem, H ... 173a, 1817*, 1894
Salgado, M ... 840, 974, 978c, 1328
Salib, M ... 539a
Salisbury, T B ... 909*
Salles, B ... 1931*
Sallsten, G ... 74
Salmen, R ... 486
Salminen, W F ... 99, 813d
Salmon, A G ... 2244
Salter, D ... 2207*
Salvador-Silva, M ... 947*
Salvatore, M F ... 935
Samadfam, R ... 1651*
Samala, R ... 893
Sameshima, H ... 472, 954, 2167
Samet, J ... 1778
Sampat, V ... 1713o
Sampayo-Reyes, A ... 1305, 1317*
Sanabria, N ... 1297c
Sánchez, B N ... 964
Sánchez, P ... 1534*
Sánchez Ramírez, B E ... 797c*, 1312, 1314, 1324
Sanchez Soria, P ... 497, 1327c*
Sánchez-Flores, A ... 1723
Sanchez-Martin, F J ... 1271*
Sanchez-Rueda, E G ... 603i*
Sanchez-Santed, F ... 1856
Sanders, A P ... 2228
Sanders, J M ... 901b, 922d*
Sanders, L ... 1520
Sanders, M ... 500
Sanderson, J ... 306
Sanderson, T . 305*, 849, 850, 851, 852, 854, 857, 1656
Sandhu, R ... 1815, 1827
Sandoval, M M ... 2046*
Sandquist, E ... 1327*
Sandy, M S ... 1808
Sangaraju, D ... 978
Sangtian, S ... 603g, 603h
Sangvanich, T ... 915, 2230*
Sankar Ganesh, P ... 834
Sankaran, M ... 1961
Sannajust, F ... 2081
Sano, T ... 122e, 242, 1326
Sanpui, P ... 1467
Sanquer, S ... 870*
Sant, K E ... 194, 1687, 1690*
Santamaria, A ... 1393*
Santana, L ... 1129f
Santana Rodriguez, Z ... 1386*
Santos, R R ... 1075
Santos Luna, R ... 1312
Sanz, F ... 427, 428
Saoo, K ... 1091, 1092
Sapiro, J ... 1799*
Saputra, D ... 1211, 1286, 1327b*
Saquib, Q ... 1952*
Saraceni-Richards, C ... 411
Sarachine Falso, M ... 2195
Sarang, S S ... 2059
Sarangarajan, R ... 417
Saravanan, C ... 2124*
Sargeant, A M ... 2135
Sargent, L M ... 23*
Sarigiannis, D A ... 2250f*
Sarimin, R ... 1825
Sarkanen, R ... 1062a, 1087o
Sarkar, K ... 1110c
Sarkar, S ... 378f, 603b, 934
Sarma, A ... 417
Sarsour, E ... 1781
Sartor, M A ... 1922e
Sarvazyan, N ... 1129c
Sasaki, E ... 537, 1878*
Sasaki, J ... 1111, 1627, 1636, 1911
Sasaki, K ... 988
Sasidharan, A ... 819*
Sasidharan Padmaja, D ... 1297f, 1327f*
Sasik, R ... 654
Sasso, A F ... 73*, 1831h
Sastre, M ... 467
Satapathy, S ... 1639a
Sathe, A ... 1627
Sato, K ... 196
Sato, R ... 1242b
Sato, S ... 978b
Satoh, M ... 1247*, 1248
Sauer, J ... 1544
Saul, J ... 468
Saunders, C ... 1790
Saunders, E L ... 823, 824, 825*
Saunders, R ... 1324
Savary, C ... 164
Savelieva, E ... 1536*
Savery, L C ... 1303*
Sawada, K ... 1114
Sawyer, A Y ... 944, 954b
Sax, S N ... 1810
Sayama, A ... 494
Sayed-Ahmed, M ... 504*
Sayers, B C ... 2004a*
Sayes, C M ... 641*, 1397*
Sayler, G S ... 1633
Sayre, P ... 24*
Sbarra, A N ... 581c
Scanlan, L D ... 173p*
Sceats, E ... 1921, 1922
Schaller, L ... 1642
Schantz, S L ... 1747c
Schatz, A R ... 649a, 2098*
Schaudien, D ... 600, 1990, 2003
Schauer, W ... 1100
Schaupp, C M ... 546*
Schecter, A J ... 1522*, 2234k
Schenk, L ... 643, 648*
Schepky, A G ... 1029*
Schick, S ... 1056
Schiestl, R H ... 1943h
Schindler, A ... 841
Schisler, M R ... 972*, 1941
Schladweiler, M ... 1230, 1232, 2325, 2326
Schlage, W K ... 415
Schlager, J ... 440g
Schlager, J J ... 573, 1964
Schlatter, H ... 982
Schlenk, D ... 205, 213, 489, 652, 654
Schlezinger, J J ... 1085
Schlick, K ... 1973i, 1973j
Schlink, S ... 886
Schlosser, P M ... 73
Schlotman, K ... 204*
Schmeits, P C ... 408b
Schmidt, A ... 1242, 2300
Schmidt, F ... 220
Schmidt, R H ... 1323, 2316
Schmidt, T ... 164
Schmitt, T ... 1181
Schmitz, D A ... 1716
Schmuck, S ... 1981, 2004f
Schmuczerova, J ... 706, 1943a
Schmued, L ... 378f, 934
Schnaars, H ... 2043
Schneider, A J ... 905*
Schneider, J ... 474, 954h*
Schneider, J S ... 1364, 1365, 1747e
Schneider, S S ... 634, 1078, 1087v*
Schneider, X ... 1057
Schnekenburger, J ... 1950
Schnelle, A ... 1186*
Schnellmann, R ... 108, 111, 708, 712*, 1611
Schöbel, N ... 378d
Schoen, E ... 1970
Schoen, K ... 1067
Schoeny, R ... 1831b
Schoeters, G ... 223h
Scholpa, N E ... 2050*
Schomaker, S J ... 2274, 2276*
Schones, D E ... 967
Schönlau, C ... 173
Schoof, R ... 778*
Schrenk, D ... 523
Schrickx, J ... 1041
Schroeder, A ... 440e
Schroeder, J ... 1157, 2065
Schroeder, L ... 282
Schroeter, J D ... 67*
Schubauer-Berigan, M ... 22
Schuchardt, S ... 600
Schuetz, C ... 273
Schuetz, J ... 1163
Schug, T ... 703
Schuh, J C ... 740, 741*
Schuler, F ... 104
Schuler, M ... 1929
Schultz, B ... 1581
Schultz, I ... 2234h*
Schultz, J ... 1784
Schultz, T W ... 420, 2273x
Schultze, A E ... 1650
Schumacher, J ... 289
Schüürmann, G ... 631
Schwab, C ... 31
Schwarcz, L ... 2234p*
Schwegler-Berry, D ... 841c, 1208, 1229a, 1242a, 1242g, 1966, 2004b
Schwengberg, S ... 1918*, 1919
Schwerdtle, T ... 1356
Schwöbel, J ... 2273
Sciabola, S ... 1635
Sciaky, D ... 411
Scinicariello, F ... 223f*, 223g, 235a
Sciullo, E ... 616
Sciuto, A M ... 2163b
Scoglio, C ... 818
Scornet, N ... 987
Scott, C ... 1831c
Scott, C W ... 1111, 1126, 1619*
Scott, L ... 2211
Scott, M ... 1297a
Scott, M A ... 1197
Scott, M P ... 689b
Scott, N ... 441
Scott, P K ... 1575*
Scott, W ... 97
Scoville, D K ... 1981, 2004f*
Scribner, K C ... 504c, 1229g
Scribner Doering, K ... 286
Seabra, V M ... 552a
Seagrave, J ... 1229f, 1236
Searfoss, G H ... 2084
Seaver, B P ... 2040c
Sebastian, A ... 378g
Sebastian, E M ... 1308, 1324*
Seck, D ... 1678
Seder, R ... 271
Sedivy, J ... 2236
Sedykh, A ... 440i*, 440k, 2252, 2273bb
Seeger, T ... 560
Seeley, J ... 226
Seeley, M ... 1341, 1554*, 1555
Seeman, J ... 2136
Seemann, D ... 899
Segal, D ... 1829
Segal, L ... 1654*
Sehgal, A ... 1653
Sehr, A ... 451, 467h
Sehsah, R ... 1994
Seidler, F ... 1754*
Seifert, A W ... 418a
Seinen, W ... 1048
Sekeroglu, V ... 1942
Sekeroglu, Z ... 1942
Sekino, Y ... 180
Selby, C ... 1713a
Selgrade, M ... 1828, 1829
Selinski, S ... 545
Sell, S ... 508
Sellamuthu, R ... 1713u
Selwyn, F ... 917, 1896*
Seman, N ... 550
Semisch, A ... 1448
Senese, P B ... 2196w
Sengupta, K ... 1590
Senn, J ... 102, 1548
Senn, T ... 1577
Sens, D A ... 244, 1251, 1274, 1322, 1327
Sensenhauser, C ... 1200b
Senutovitch, N ... 1880*
Seo, C ... 890, 1549g*
Seo, J ... 942*
Sepehr, E ... 1616e
Sepulveda, M M ... 203, 221
Serbina, N ... 2196k
Serl, S ... 2037
Serve, K ... 130*
Seth, R K ... 1187, 2030*
Sethi, P ... 684*
Setser, J ... 633*
Settivari, R S ... 146, 408a*, 1019, 1736e
Setzer, W ... 418b, 632a, 2234i, 2234m, 2234n*, 2273o
Severson, P ... 1300
Sewald, K ... 1051, 1057*, 1953
Sewell, F ... 2196aa*
Sexton, K G ... 978
Seyler, N ... 2177
Sgro, M ... 2196v
Sha, R ... 1717
Shaddock, J G ... 1943b
Shadiack, A ... 2196k
Shafarin, J ... 1769
Shafer, T J ... 35, 378a, 378b, 378c*, 1747a, 1838, 1973a
Shah, E J ... 361*
Shah, F ... 1647*
Shah, H ... 1229e, 1713t, 1790*
Shah, I ... 418b*, 690, 694*, 1973e, 2273o, 2273s, 2273t
Shah, K ... 347, 403
Shah, M Y ... 813c
Shah, P ... 122e, 387*
Shah, R ... 122, 955, 958, 2250k
Shah, S ... 603d
Shah, S V ... 312b
Shai, J L ... 785
Shaiba, L A ... 701*
Shalat, S L ... 846*
Shamy, M ... 1207
Shan, Y ... 146, 1997
Shang, J ... 603, 1962
Shang, P ... 393
Shankaran, H ... 814, 1517*
Shannahan, J ... 821*, 826
Shao, J ... 687
Shao, K ... 629*
Shao, M ... 2044
Shapiro, A J ... 630, 2250l*
Shapiro, D ... 1238, 1241
Sharanek, A ... 1192, 1193
Sharits, B C ... 1818
Sharkawy, A A ... 2234
Sharma, L K ... 1793, 2026
Sharma, M ... 550*
Sharma, N ... 254
Sharma, S ... 445, 857, 2040
Sharma, T ... 551
Sharma, V ... 1930*
Shaw, P K ... 298
Shaw, S ... 1229f
Shea, D ... 165
Shea, K ... 1549b
Shealy, D ... 561
Shearer, J J ... 1916*
Sheashaa, H ... 1180
Sheehan, D ... 173k
Sheehan, P ... 605*, 2234r
Sheets, L P ... 378e, 1846
Shell, S ... 1112
Shelton, A D ... 1850*
Shelton, M ... 878*
Shelton, S D ... 467b
Shen, A N ... 1383
Shen, C ... 550
Shen, H ... 920*, 2191

Author Index (Continued)

The numerals following the author's names refer to the abstract numbers. The asterisk after the abstract number indicates the author is the first presenter.

Shen, J ... 420, 561
Shen, L ... 1171
Shen, Y ... 511
Sheng, L ... 533, 662
Shengmin, Y ... 976, 1891, 2212
Shepard, K ... 324
Shepherd, D L ... 486
Shepherd, D M ... 2040c*
Shepperd, C J ... 1528
Shereif, M M ... 2229*
Sherer, K R ... 1377
Sheridan, J ... 906
Sherman, C ... 1876
Sherman, J H ... 330
Sherr, D H ... 264, 1458*, 1462, 1463*
Sherratt, P J ... 202
Sherwood, C L ... 1734*
Sherwood, D ... 841
Shi, H ... 36*, 856, 1903*
Shi, L ... 265d, 552c, 1195
Shi, Q ... 99, 813d, 1200a*, 2273k
Shi, W ... 367
Shi, X ... 1297f, 1327f, 2316
Shi, X C ... 1242h
Shibata, N ... 1150
Shibuya, A ... 190
Shiga, A ... 467c
Shih, T A ... 581e
Shim, E ... 848
Shim, I ... 1223, 1233*
Shim, J ... 382, 1315*
Shima, Y ... 653
Shimada, T ... 1899b
Shimada, Y ... 1994
Shimizu, M ... 518*, 1150
Shimizu, N ... 2210
Shimizu, R ... 1086*, 2004e
Shimizu, Y ... 669a, 669b
Shimomoto, T ... 322*
Shimoyama, M ... 2092, 2094*
Shimpi, P ... 1884*
Shin, J ... 593, 1565, 1976, 2001*
Shin, J W ... 1736*
Shin, K ... 1713m, 2129d
Shin, M ... 2052
Shin, S ... 293
Shin, Y ... 1123, 1389*
Shinde, M ... 405
Shines, C ... 1229d
Shinjo, K ... 241
Shinkai, Y ... 1716*, 1717
Shinn, W ... 581d
Shinohara, N ... 592*, 1948, 1967
Shiotani, M ... 1763
Shipkova, P ... 853, 2122
Shipkowski, K A ... 582*, 583, 584
Shishido, S N ... 302
Shiyanov, P ... 87, 895
Shmukler, A ... 1724
Shockley, K ... 173b, 173h, 2273j*
Shoda, L ... 412*
Shohatee, A ... 657*
Shoieb, A M ... 276
Shoneye, T ... 1358
Shoots, J ... 1142*
Shore, S A ... 2072*
Showker, J L ... 343b
Shropshire, W C ... 1522, 2234k
Shrotriya, S ... 1718
Shu, L ... 2196z
Shubitowski, D ... 968
Shuey, C ... 2226, 2234c
Shuford, S ... 1876
Shukla, A ... 57*
Shuldiner, A R ... 552c
Shull, J ... 1069
Shumway, L J ... 581c
Shun, T ... 1880
Shurin, M ... 1242g
Shvedova, A A ... 603e, 603f, 1242g, 1242h, 2004d*, 2273a
Siciliano, S D ... 2214
Sidaway, J ... 1120
Siddall, M E ... 2281*
Siddeek, B ... 1078
Siddens, L K ... 513
Siddiqui, A A ... 1639
Siddiqui, J A ... 1952
Siddiqui, M A ... 1952
Sido, J M ... 2008*
Siegel, D ... 358, 1632*, 2244
Siegel, P D ... 142, 2036
Siegert, V ... 2234aa
Sielken, R L ... 780
Sieracki, N ... 1803
Sierra-Campos, E ... 1309
Sierra-Santoyo, A ... 530
Sievers, C ... 1069
Sievert, M K ... 1657
Siezen, K ... 2129c
Siferd, S ... 2273q
Sifre, M I ... 1087r
Signoretto, E ... 835
Sikk, K ... 2105*
Silayeva, L ... 552g
Silbajoris, R ... 1778
Silbergeld, E ... 45*, 1306
Siler, S Q ... 412
Silinski, M A ... 198
Sills, R ... 955
Silva, C ... 2218
Silva, G ... 2123*
Silva, P V ... 1696
Silva, R ... 828, 2004g
Silva, R F ... 1696*
Silverman, J L ... 557
Sim, J ... 440l, 1200e, 1200i*
Simanek, E ... 1973i, 1973j
Simeonov, A ... 173b
Simic, D ... 850, 854
Simion, F ... 1020
Simkins, T J ... 2006*
Simmendinger, P ... 1221
Simmers, M ... 1061*, 1129a
Simmons, J ... 1018a*
Simmons, S O ... 1066
Simon, B R ... 253*
Simon, T ... 96d, 719, 723*, 2253
Simonich, M T ... 181
Simonsen, M ... 2234aa
Simoyi, R ... 2036
Simpson, P ... 189
Singal, M .. 67, 1594, 1596, 1597, 1598*, 1599
Singer, T ... 104
Singh, K P ... 1096, 1460
Singh, N ... 927
Singh, N P ... 922, 963*
Singh, P ... 1831g*
Singh, S ... 1095*
Singh, U ... 922, 963
Singhal, A ... 604*, 605
Singhal, R ... 1197
Singleton, S T ... 81*, 689
Sinko, P J ... 561, 563
Sioson, C ... 954g
Sioutas, C ... 837, 1242f
Sipe, G O ... 1347e
Sipes, N S . 418a, 1087p, 2273f, 2273s, 2273u
Sippula, O ... 1206
Siraki, A G ... 542
Sircar, C ... 265
Sirenko, O ... 1616g*
Siskind, L J ... 2058
Siso, S ... 579
Sitapara, R A ... 1789, 2026*
Sithu, S D ... 2319
Sitzmann, B ... 877
Siva Prasad, B ... 834*
Sivagas, S ... 425
Sivaraman, L ... 278, 2191*
Sizemore, D ... 271
Sjögren, A ... 1881
Sjögren, B ... 1224
Skeete, D ... 2234b
Skelly, B ... 2234e
Skerrett, S J ... 602, 1980
Skibba, M ... 295*
Skinner, B R ... 1541
Skoog, S ... 1972*
Skov, K ... 1018d, 1175
Skuce, C ... 1829
Slade, D ... 877
Slaga, T J ... 1736
Slattery, M ... 652
Slauter, R ... 343d, 901c
Sleiman, M ... 1056
Slikker, W . 96f, 1756, 1764a, 1764b*, 1764c, 1764d
Slitt, A ... 1662d*
Slitt, A L ... 48, 52*, 738*, 1677, 1679, 1720, 1884, 2207
Sloan, M E ... 235
Slob, W ... 632a*
Slotkin, T A ... 1754
Sluka, J P ... 85*, 2273o
Slusser, A ... 244, 1251*
Sly, E A ... 1021
Smart, R C ... 1108
Smeester, L ... 229, 1308, 1318
Smela, E ... 173a
Smirnova, L ... 1737, 1738*, 1912
Smit, J ... 2028
Smith, A ... 1917
Smith, A J ... 2163b
Smith, A T ... 101*, 102
Smith, B ... 1462
Smith, C ... 552g*
Smith, C V ... 410
Smith, D ... 1087l, 1330, 1551, 2234s, 2273s, 2286*, 2291*
Smith, G J ... 1201*, 1219
Smith, H W ... 119
Smith, J D ... 2196e, 2196g*
Smith, J N ... 814, 1525*, 1573, 1963, 1980
Smith, K ... 2007
Smith, K J ... 1133
Smith, L C ... 997*
Smith, L J ... 1276
Smith, M ... 173o, 1685, 1831l
Smith, M J ... 145b
Smith, M T ... 920
Smith, P ... 1141, 2145
Smith, Q R ... 893
Smith, R ... 577, 756, 1933*
Smith, R D ... 1525
Smith, R J ... 632f
Smith, R W ... 248*
Smith, S ... 343d
Smith, S Y ... 281, 1540, 1651
Smits, J E ... 1319
Snawder, J E ... 1607*, 1765
Snel, C ... 154
Snellings, M ... 1626
Snelten, C ... 796
Snider, T H ... 558*, 564, 573
Snoke, D ... 219
Snow, D ... 1627
Snow, S J ... 1232*
Snyder, A ... 2021*
Snyder, C A ... 375*
Snyder, N ... 1538
Snyder, R ... 539e
Snyder, R J ... 596, 603g, 603h*
Snyder, S ... 1365, 1366, 1368, 1550, 2231
So, B ... 1044, 1571
Soares, B ... 1288*
Sobh, M ... 1180
Sobol, M ... 1628
Sobolewski, M ... 954h, 1333, 1340, 1342, 1347*, 1747e
Sobry, C ... 1654
Sobus, J ... 96i, 2250c
Sochaski, M ... 2250a
Sofidiya, M O ... 809
Sohn, E ... 660*, 1565
Sohn, W ... 898
Sokolowski, K B ... 178
Solak, K ... 1075*
Solar, D ... 122f
Soldatow, V ... 1152
Soliman, S ... 2117
Solmonson, A ... 250*
Somers, A ... 1577*
Somji, S ... 244, 1251, 1274, 1322, 1327
Sommers, C H ... 326
Sommerville, D R ... 1817, 1818
Son, J ... 1949
Son, Y ... 1275*, 1297f
Sonawane, B R ... 892, 959, 1822*, 1831c, 1831k
Sonee, M ... 106, 380
Song, C ... 1211
Song, J ... 1211*
Song, M ... 440l, 1200e, 1870
Song, N ... 593
Song, Y ... 1089, 1703*
Songonuga, A ... 788
Sonnenburg, A ... 2040
Soonpaa, M ... 1129b
Sorger, P ... 2055
Soriano, J ... 603i
Soriano, S D ... 1755
Sorribas, V ... 495*
Sosa, C ... 495
Sosa Holt, C S ... 1847*
Soshilov, A ... 907*, 1146
Sosinski, L K ... 2173
Soucy, N V ... 950*
Sousa, H ... 552a
Southgate, J ... 1039
Souza, A O ... 312, 457*, 458
Souza, G R ... 1639c
Sower, G ... 1678*
Sowers, J R ... 2069*
Sowers, M J ... 848
Sørvik, I ... 1782*
Spade, D ... 1686, 1709*
Sparavalo, O ... 572*
Sparvero, L J ... 1777
Spatafora, C ... 1076
Specht, A J ... 1552*
Speen, A ... 1229e, 1790
Speidel, J ... 1943d
Spellman, R ... 1929
Spence, C ... 2124
Spencer, R M ... 418a, 1087p
Spencley, S M ... 1377*
Speshock, J ... 1985
Spicer, L J ... 1574
Spiess, P ... 390
Spirkl, H ... 220
Spitz, D R ... 1781
Sprando, R 173g, 632g, 1297a, 1944, 1973h, 1973i, 1973j
Spratt, M ... 1053
Spring, P ... 2176
Sprugel, K ... 1662a*
Spulber, S ... 1745*
Squibb, K S ... 1559*
Sram, R J ... 706*, 844
Sreenivasan, J ... 1639a
Sreevalsan, S ... 1510*
Sridharan, G ... 1130
Srinivas, M ... 1080, 1652
Srinivasan, V ... 1639
Sriram, K ... 1368a*
Srivastava, D ... 88, 1059, 1899
Srivastava, R K ... 552e*
Srivastava, S ... 1876, 2319*
Srivastava, S K ... 1098, 1496, 1508
St. Mary, L ... 1758
Staal, Y ... 1970
Stabler, L ... 1284
Stachlewitz, R F ... 2196f
Stackley, K D ... 223a
Staflin, K ... 375
Stahl, M ... 942b
Stahlmann, R ... 2040
Staley, J J ... 885
Stallings, J D ... 1265, 1297, 1858
Stallons, L J ... 108*, 111
Stamatis, M ... 1724
Stamou, M ... 697*, 1335
Stanek, J J ... 1830
Stanek, L W ... 1018c
Stanford, E A ... 264*, 1463
Stanko, J P ... 2196a*
Stankowski, L F ... 1943j*
Stanley, U K ... 1198
Stansfield, K ... 1288, 1289, 1339*
Stansfield, K H ... 1392a
Stanton, B ... 665, 2317
Stanton, P K ... 1289*
Stanton, R ... 1635
Stapleton, H ... 173p

The numerals following the author's names refer to the abstract numbers. The asterisk after the abstract number indicates the author is the first presenter.

Stapleton, M ... 2234b
Stapleton, P G ... 488, 872*, 1689
Star, A ... 586, 1468*
Starch, B A ... 280
Starkey, C B ... 655*
Starobin, J ... 492
Starr, T B ... 1107
Staska, L ... 23
States, J C ... 304*, 1159, 1870, 2221
Staub, D ... 468
Stauber, J ... 901e
Stavanja, M S ... 467b, 640
Staveley, J ... 647
Stavitskaya, L ... 2261, 2262, 2273b*, 2273h
Stebbings, R ... 1036
Steele, C ... 326
Steen, D ... 1617
Steenhof, M ... 1970
Steevens, J A ... 841a, 1987, 1988
Stefano, E ... 1716
Steffensen, I ... 782, 1084*, 2248
Steffy, D A ... 656
Stegeman, J J ... 1147*
Stegemann, J ... 1955
Steger-Hartmann, T ... 426*, 427
Stegman, M ... 1742*, 1743
Steidl, J ... 2083
Steiner, K ... 900*
Steiner, T ... 2067*
Steinfath, M ... 1057
Steinritz, D ... 463
Stelkic, A ... 2255
Stemmer, P M ... 136
Stenerlöw, B ... 1757, 1762
Stensen, L ... 1297g
Stephen, F D ... 1524*
Stephen, L ... 2043
Stephens, M L ... 2115*
Stermer, A ... 1708, 2035*
Stern, M ... 870
Sterner, T R ... 1010
Steuerwald, A J ... 1306
Steven, P ... 1544
Stevens, A ... 1831g
Stevens, E ... 1087u
Stevens, J ... 1682
Stevens, R C ... 686
Stevens, T ... 876d*
Stevens, Z ... 1040
Stewart, D J ... 2250g*
Stewart, J ... 1320*, 2161
Stewart, S ... 1549b
Stice, S ... 1058, 1347k
Stickney, J A ... 1831
Stierum, R H ... 430, 1347i
Stine, B ... 899
Stine, C ... 632g
Stintz, M ... 332
Stirdivant, S ... 1242e
Stock, H ... 1539*
Stock, I ... 2048
Stocking, K ... 1200b
Stoker, T E ... 1713d*, 2190
Stokes, A ... 479*
Stolcpartova, J ... 1943a
Stolper, G ... 2181
Stolte, M ... 220, 427
Stolz, D ... 1003
Stone, S ... 1368a
Stoner, M ... 161
Storck, C ... 855, 856, 857, 1622*
Storrs, P ... 938
Stout, K ... 371
Stout, M D ... 813a, 1616c, 2004a
Stoute, M ... 1225
Strader, L F ... 1018a
Strauss, V ... 120, 1078, 1220, 1591, 1992
Strazdas, L ... 173k
Streifel, K ... 1759*
Stricker-Krongrad, A ... 886, 1713a, 2118, 2151c*
Strickland, J ... 1831l, 2182c
Strickland, J A ... 1062c
Strickland, J D ... 1973a*
Strigun, A ... 1871
Strock, C ... 378, 1115*
Stroebele, M ... 1953
Strom, J G ... 1736d*
Strope, C ... 2273o, 2273s
Strope, C L ... 2234m*
Struck, M C ... 273
Strupp, B J ... 1330
Strynar, M ... 1863b, 2040b
Stuchal, L ... 2234f
Stueckle, T A ... 585*, 589, 830
Stuhler, J D ... 2157*
Stump, D G ... 2160
Sturzbecher-Hoehne, M ... 1624
Stybayeva, G ... 1129c
Styblo, M ... 229, 1308, 1312*, 1314, 1318, 1324
Su, C ... 296, 357, 1369, 1388
Su, Z ... 265d, 552c
Suarez, J S ... 1018a
Suarez-Martinez, J ... 2005*, 2020
Subramaniam, R P ... 239, 1831c
Subramanian, A ... 2055
Subramanian, K ... 88, 1059, 1899
Suda, M ... 1697
Suemizu, H ... 1150
Sugaya, C ... 1392, 2047
Sugaya, T ... 113
Sugihara, K ... 1086
Sugita-Konishi, Y ... 442
Sugiura, Y ... 1392
Suh, M ... 231, 779, 781, 1290, 1296, 2219*
Sui, A ... 2169
Sulaiman, S ... 2196m
Sulentic, C E ... 1767*, 1965, 2021, 2022
Sullivan, A ... 1997*
Sullivan, B P ... 1197
Sullivan, J T ... 7
Sullivan, P G ... 378g
Sultana, S ... 1544
Sumant, A ... 1972
Sumner, S C ... 484, 485
Sun, B ... 162, 240, 1140, 1788, 1794, 1934*
Sun, G ... 312d, 2234o
Sun, H ... 969*, 1207, 1245
Sun, J X ... 1353, 1354
Sun, L ... 1498*
Sun, M ... 1808
Sun, Q ... 2234o
Sun, R ... 1005
Sun, W ... 1930
Sun, X ... 217, 266*, 1316
Sundell-Bergman, S ... 1757, 1762
Sundius, L ... 1229c
Sung, S ... 1623
Sung, T ... 1167
Sunil, V ... 561
Sunmonu, T O ... 808
Suñol, C ... 749*
Surapureddi, S ... 954e, 1736b
Surfraz, B ... 2256, 2257
Surh, I ... 1713b*
Surh, Y ... 1718
Sushynski, C ... 901d
Sussman, R ... 649a*
Sutherland, V ... 2074
Suto, E ... 2196p
Sutter, C H ... 193, 505, 1163b
Sutter, T R ... 193, 505, 1163b
Suzuki, D ... 1160
Suzuki, G ... 1600
Suzuki, K ... 447, 516
Suzuki, S ... 686*
Suzuki, T ... 241, 242*, 1326, 2192
Suzuki, Y ... 113, 502, 1971*, 1977, 1994
Svedberg, E ... 901
Svoboda, D L ... 1736a
Svoboda, K K ... 578
Svoboda, K R ... 1761
Swackhamer, B J ... 948
Swales, J ... 1627
Swan, G E ... 391
Swanson, H I ... 2116
Swanson, T ... 1128
Swanton, S M ... 1719
Swaroop, A ... 339
Swartz, C ... 324, 1478
Swat, M ... 85
Sweeney, L M ... 68, 1010, 1818*
Sweeney, T D ... 1657
Swenberg, J A . 262, 1107, 1110g, 1521, 1523, 1930
Swenson, L J ... 2247
Swezey, R ... 581d
Switzer, R C ... 1764
Sycheva, L P ... 2004d
Symington, S B ... 378e*
Sysa Shah, P ... 1706
Szabo, N J ... 327

T

Ta, C ... 1853*
Taba, P ... 2105
Tablin, F ... 1127
Tachovsky, J A ... 231
Tada-Oikawa, S ... 502, 1971, 1977, 1994
Tadagavadi, R K ... 2033*
Taetzsch, T ... 928*, 1859
Taggart, R ... 841
Taghizadeh, K ... 1521
Taghreed Farahat, T ... 81
Tagle, D A ... 1442*
Tagmount, A ... 2260
Taguchi, K ... 113
Tailhardat, M ... 1027, 1029
Taimi, M ... 1040
Takada, S ... 201
Takagi, A ... 1974
Takagi, H ... 2132*
Takahashi, K ... 450
Takahashi, M ... 1070, 1160, 2192
Takahashi, T ... 1257
Takahashi, Y ... 2167*
Takasaki, W ... 110, 446, 494
Takasu, S ... 442
Takasuna, K ... 110
Takeda, K ... 2004e
Takeda, S ... 444
Takenouchi, O ... 1062e
Takeuchi, H ... 265c
Takeuchi, K ... 591
Takeyoshi, M ... 1087c
Takigiku, R ... 878
Takizawa, N ... 1493
Takumi, S ... 242, 1326*
Tal, T L ... 96e, 1062a*
Talabi, O ... 2271
Talamás-Rohana, P ... 797c
Talamo, F ... 415, 860
Talbert, D ... 1112
Talbot, P 645, 1056, 1612, 1613, 1902, 2225
Talcott, S ... 1110b
Talele, T ... 576
Talikka, M ... 413*
Talkington, B ... 590*
Tallkvist, J ... 1081
Tam, H W ... 1108*
Tambe, M A ... 378h
Tan, M ... 1323
Tan, W ... 1713p*, 2043*
Tan, Y ... 96i, 480, 482, 483*, 1901, 2125, 2250c
Tan, Z ... 1348
Tanabe, S ... 517, 519, 1259
Tanaka, J ... 447*
Tanaka, R ... 467c*
Tanaka, S ... 467c
Tanaka, T ... 1994
Tanaka-Kagawa, T ... 1717
Tancredi, D ... 2234g
Tang, F ... 1369, 1388
Tang, H ... 2196k
Tang, K ... 202, 1200
Tang, L ... 217, 226, 317*, 810, 1526, 1532
Tang, S ... 1937
Tanguay, R L ... 181, 207, 211, 212, 1603*, 1637, 1682, 1747
Taniguchi, T ... 1114*
Tanir, J Y ... 1824
Tansey, M G ... 520
Tao, S ... 1499, 1779, 1780, 1791
Tapp, R ... 2196t
Taquahashi, Y ... 1974
Tarcha, E J ... 901c*
Tardif, R ... 829
Tarkhov, A ... 31, 2273, 2273d
Tarnow, P ... 1067*
Tartaro, K R ... 125
Tassinari, M ... 173c
Tasso, M J ... 312*, 457, 458, 677
Tate, E ... 2014*
Tateno, C ... 1899b*
Tatu, C ... 1018b
Tatum-Gibbs, K R ... 1062f*
Taub, M E ... 2196e, 2196g
Täubel, M ... 983
Taurin, S ... 791
Tavcar, R ... 344*, 1225, 2037
Taylor, A ... 582, 583*, 584
Taylor, D L ... 1880
Taylor, G ... 1229d
Taylor, I ... 1922*
Taylor, K ... 1742, 1743, 2134
Taylor, M ... 76
Taylor, V ... 2317
Tchao, R ... 1200f
Tchounwou, P B ... 1993
Tedesco, V ... 2157
Teeguarden, J G ... 602, 814*, 1517, 1980
Tegenge, M ... 78*
Teklu, B M ... 2238*
Tekur, S ... 1897
Temming, R ... 1079
Templier, M ... 1027
Tendulkar, K E ... 1943
Teng, C T ... 1063
Teng, Q ... 173p
Teng, Y ... 1713q, 1713r
Tenin, G ... 184
Tennant, A ... 173i
Tenneson, K ... 2138*
Teodoro, J S ... 2004g
Teppner, M ... 1545*
ter Braak, B ... 2129c*
Teraoka, H ... 539c*
Terashita, N ... 472
Terfloth, L ... 27, 28, 29, 2273, 2273d*
Terhorst, M M ... 2238
Terpstra, V ... 1872
Terranova, R ... 971
Terry, C ... 64*, 1602
Terse, P S ... 467e, 2196j
Terskikh, A ... 4
Teshima, R ... 988
Testman, R ... 2236
Tetley, T ... 1979
Teunis, M ... 635
Tewari-Singh, N ... 553*, 554, 555
Tewolde, T S ... 790
Texiera-Clerc, F ... 1158
Thackaberry, E A ... 273*
Thai, S ... 841d
Thakali, S ... 1554
Thake, D C ... 1764
Thakur, K ... 1627
Thakur, V S ... 538
Thalacker, F ... 2157
Tham, K Y ... 916
Thapa, D ... 486
Tharmann, J ... 163
Thayer, K ... 1486, 2224, 2250k
Thébaud, S ... 286
Theberge, A B ... 252
Theil, P ... 1659
Theis, L ... 1032
Theophilus, E H ... 1615*
Therrien, J ... 2168
Thibault, S ... 97
Thiermann, H ... 463, 560*
Thierry-Mieg, D ... 552c
Thierry-Mieg, J ... 552c
Thiex, N ... 1522, 2234k
Thirion-Delalande, C ... 2130
Thomas, D ... 814
Thomas, D J ... 1327d*, 1973b
Thomas, E R ... 206*
Thomas, F K ... 198
Thomas, J ... 1294
Thomas, L J ... 268*

Author Index (Continued)

The numerals following the author's names refer to the abstract numbers. The asterisk after the abstract number indicates the author is the first presenter.

Thomas, M A ... 1760
Thomas, N ... 768*
Thomas, R ... 2250a, 2273s
Thomas, R F ... 1232
Thomas, R S ... 146, 1132, 1905, 2020, 2250, 2273o
Thomas, S ... 1898
Thomas, T ... 1116
Thompson, B ... 2037
Thompson, C M ... 622, 623, 628, 779, 1290*
Thompson, D ... 552, 1095
Thompson, D C ... 2067
Thompson, E ... 582, 583, 584*
Thompson, J T ... 248, 2213
Thompson, K ... 2
Thompson, K E ... 11*
Thompson, L C ... 485, 596*
Thompson, R ... 632j
Thompson, T A ... 1144
Thompson, W D ... 1303
Thomson, J ... 715*
Thorne, D ... 443
Thorne, G ... 1802*
Thorne, P S ... 515, 896, 1975
Thornton, C ... 208, 1683, 1987, 1988
Thorpe, R ... 989
Thorsheim, H R ... 893
Thorsrud, B A ... 331, 341, 342, 343, 845*
Thota, B ... 88, 1059, 1899
Thrall, B D ... 602, 814, 1963, 1980
Thrall, K D ... 1525
Thrane, V ... 2248
Threadgill, D W ... 261
Thuett, K ... 1610*
Thurman, D ... 272
Thurmond, S ... 1394*
Thurston, G D ... 1210
Tian, D ... 2040a
Tian, F ... 1533
Tian, W ... 1791
Tian, Y ... 911
Tibbitts, J ... 1659
Tice, R R ... 122, 173b, 173h, 444, 467g, 958, 1063, 1616g, 1736a, 2273r, 2273bb
Tichenor, J N ... 1699
Tidball, A ... 1353*, 1354
Tien, E ... 2065*
Tien, L ... 369*, 2060
Tierney, K ... 654
Tiesman, J P ... 146
Tiethof, A K ... 1752*
Tijani, A Y ... 807
Tijerina, P B ... 824*
Tillmann, T ... 600
Tilly, T B ... 1964*
Tilton, S C ... 2*, 602
Timchalk, C ... 1573*
Timme-Laragy, A R ... 209, 2283*
Tirkkonen, J ... 983*
Tirmenstein, M ... 109, 1089*
Tirrell, S ... 102
Tischkau, S ... 1153, 2197
Titorenko, V ... 306
Tluczkiewicz, I ... 631
Tobita, K ... 2076
Todd, S W ... 1861*
Todorov, T I ... 1559
Todt, C E ... 1848*, 1849
Tohamy, A F ... 1179
Tohyama, C ... 200, 978b, 1346, 1747b, 2163
Toimela, T ... 1062a, 1087o
Tokar, E J ... 12*, 958, 1297i, 1297j, 1297k, 1297l
Tokikawa, R ... 1771
Tokumoto, M ... 1247, 1248, 1304*
Tolaymat, T ... 1973b
Tolba, M F ... 978d, 1110a*
Tolbert, P ... 868
Tolliver, L M ... 603c
Tomar, S ... 922
Tomblin, J K ... 909
Tomkinson, A ... 1925
Tomlinson, C ... 1163a
Ton, T ... 955
Toneva, M ... 286
Tong, F ... 671
Tong, S ... 177
Tong, W ... 173b, 418e, 552c, 1087a, 1481*, 1885, 1887, 2273k
Tong, Z ... 1200
Tonkin, E G ... 1657
Tonomura, Y ... 1866*
Toole, C ... 173j
Toot, J ... 1648, 2129*
Topinka, J ... 706, 844, 1943a
Topiwala, K ... 312b
Topper, M J ... 1544
Topping, V ... 173g, 1297a, 1973h*, 1973i, 1973j
Torii, M ... 1174, 1866
Tornero-Velez, R ... 1419*
Tornesi, M ... 278
Tornier, C ... 2177, 2179*
Torous, D ... 1943j
Torous, D K ... 452
Torres, G B ... 343a
Torres, O ... 343b
Torres-Saavedra, P ... 479
Toscano, J ... 2151d
Toselli, P ... 1250
Totah, R ... 1129f*
Totpal, K ... 269
Tovborg Jensen, J ... 1588
Towery, K L ... 1191
Toyama, T ... 1258
Tralau, T ... 1067
Tran, D ... 505
Tran, H ... 2037
Tran, K I ... 837*
Tran, T ... 507
Tran, V ... 422*, 868
Tranchemontagne, Z ... 382
Trask, O ... 1873*, 1934
Trausch, I ... 952*
Traver, S ... 1363
Travlos, G ... 1087r, 1110f, 1616c
Tremblay, C M ... 93
Tremblay, J ... 286
Trent, J O ... 304
Tretyakova, N ... 978
Treumann, S K ... 1992
Trevaskis, J ... 2124
Trickler, W ... 353
Trieu, M ... 1502
Trieu, V ... 2196x
Trimurtulu, G ... 1590
Tringali, C ... 1076
Trinh, J ... 1345
Trinidad, J ... 932, 942c, 1378
Tripathi, D N ... 1804*
Trivedi, P P ... 1097*
Troese, M ... 1033, 1034*, 1035
Trombetta, L D ... 572, 580, 657, 680, 1261, 1852
Troncy, E ... 274, 275, 471
Tropsha, A ... 2182c*, 2273o
Trosko, J E ... 1900
Trost, C ... 273
Trost, L C ... 2121
Troth, K ... 2196o
Trouba, K J ... 852*, 853
Troutman, J ... 982
Trowbridge, J B ... 2250d
Truchon, G ... 829
Truchot, N ... 185
Trueblood, E ... 1157*, 1641
Truisi, G ... 164
Truong, K M ... 682*, 2205
Truong, L ... 31, 173e*, 181, 207, 440a, 1747, 2273l, 2273s
Trush, M A ... 1792
Trusk, P B ... 1112
Tryndyak, V ... 956*, 957, 1513
Tsakovska, I ... 27, 28, 29, 2254
Tsaprailis, G ... 1542
Tschudi-Monnet, F ... 751*
Tseng, C ... 177*, 300, 312a, 1242c
Tseng, F ... 1502
Tseng, H ... 1639c*
Tseng, M T ... 2004h
Tsou, T ... 511
Tsuboi, I ... 1900
Tsuchiya, H ... 2129b
Tsuchiyama, H ... 450
Tsuda, S ... 2210
Tsuji, J S ... 227, 243, 632d, 777
Tsuji, L J ... 1567
Tsuji, M ... 107*, 1974
Tsukamoto, S ... 2119
Tsuneyama, K ... 1878
Tsunoda, M ... 1392*, 2047
Tsuruoka, S ... 587, 591*, 1465
Tsutsumi, H ... 2133
Tu, S ... 794
Tu, V ... 1586
Tuckfield, C ... 1284
Tuda, Y ... 2196u
Tugendreich, S ... 603d
Tuinman, C ... 1589
Tumu, H ... 572
Tung, E W ... 1713*
Tunkel, J ... 1616b
Turk, J R ... 98, 1061, 1549e*, 2065
Turley, A E ... 2012*, 2013
Turnbull, P ... 1642
Turner, E ... 1932*
Turner, P ... 1008
Turner, S ... 1642
Turteltaub, K W ... 882, 923, 1110e
Tuznik, K M ... 581a*, 1922c, 1922d
Tvermoes, B E ... 77
Twaddle, N C ... 96f
Tyburski, J B ... 1156
Tyner, K M ... 1947
Tyson, S B ... 1676
Tyurin, V A ... 1002*, 1003, 1520
Tyurina, Y ... 1003, 1520*

U

Ubellacker, J ... 1462, 1463
Uchida, M ... 653
Uchino, K ... 592
Udasin, R G ... 562*
Udawatte, D J ... 913*
Ueda, M ... 467c
Uehara, T ... 961, 1866, 2123
Uemi, M ... 1771
Ueno, M ... 1174, 1866
Ueno, S ... 180
Uesugi, M ... 1114
Uetrecht, J ... 1045
Ugbaja, R N ... 1776
Uhouse, M ... 1353, 1354
Ujawane, D ... 405*
Ukairo, O ... 1042*, 1895
Ukhanova, M ... 1989
Ukolov, A I ... 1536
Ulukaya, M ... 2234d
Um, Y ... 890, 1549g
Umbreit, T H ... 2004
Umbright, C ... 1713u
Umbuzeiro, G d ... 1662b
Umemura, T ... 442, 843, 1516
Umezawa, M ... 2004e*
Umh, H ... 1951
Unice, K ... 77*
Uno, F ... 447
Uno, Y ... 455
Upadhyaya, P ... 1491
Upham, B L ... 1103
Uppal, H ... 866*, 1060, 1899c
Uppal, K ... 418, 421*, 422, 868
Uppu, R M ... 525, 841e, 1514, 2270*
Uramaru, N ... 1086
Urano, K ... 2133*
Urban, A ... 1227, 1228, 1491*
Urban, J D ... 337*
Urushidani, T ... 961
Ushijima, T ... 242
Uski, O ... 1206
Usui, Y ... 591
Usuki, F ... 1373, 1387*
Uteng, M ... 873, 1618, 2056
Utoh, M ... 1150
Utsunomiya, S ... 2167
Uyeminami, D ... 828

V

Vaessen, S ... 1041
Vahle, J L ... 1650
Vahter, M E ... 2318
Vaidya, V S ... 13*, 105, 2055
Vail, J ... 2234s
Vakil, P ... 2194
Valachova, J ... 2234a*
Valamehr, B ... 1915
Valberg, P A ... 1812
Valderas, M ... 883
Valdez-Flores, C ... 780
Valdivia, A G ... 313
Valdivia, P A ... 35, 378b*
Valentine, R ... 467b
Valentovic, M ... 1186, 2062
Vales, G ... 1954
Vallant, M ... 1713b
Valley, M P ... 291
Valverde, R ... 206
Vamathevan, J J ... 2308*
van Acker, F A ... 1970
Van Assche, F ... 1280
Van Bekkum, Y ... 348, 1652
Van Beneden, R J ... 913
van Beuningen, R ... 1063, 1150*, 1154
van Bilsen, J ... 1823
van Breemen, R B ... 790
van de Ligt, J ... 337
Van de Mieroop, E ... 223h
van de Water, B ... 173f, 1168*, 1715, 1872, 2031, 2129c
Van de Water, J ... 698, 1759
van Delft, J H ... 1872, 2274, 2279*
van den Berg, S ... 1831e*
Van den Berg, M ... 1075, 1079, 1492, 2201
van den Brand, A D ... 1492
van den Brink, P J ... 2238
van der Laan, J ... 2129c, 2309*
Van der Valk, J ... 635
van der Vliet, A ... 390
van der Weijden, V ... 154
Van Dreel, A ... 2048
van Duursen, M B ... 1075, 1079, 1492*, 2201
van Ede, K ... 2201*
van Erp, A M ... 2293*
Van Gieson, J ... 1322*
Van Goethem, F ... 154
Van Landingham, C ... 70*, 778, 901d, 2245
van Lipzig, M M ... 430
Van Loveren, H ... 408b
van Miert, E ... 1826
Van Poppel, M ... 223h
van Ravenzwaay, B ... 120, 173*, 597, 634, 1078, 1087v, 1220, 1221, 1591, 1826, 1871, 1992, 2172
Van Rompay, A R ... 1037
Van Sickle, K ... 2121
van Someren, E ... 430, 1970
van Thriel, C ... 378d, 750*
Van Vleet, T R ... 850, 853, 854*
van Wijk, H ... 288*, 1662
Van Winkle, L S 532, 828, 848c, 1218*, 1219
Vandaveer, W ... 1616a
Vandebriel, R ... 635
Vanden Heuvel, J ... 248, 1135, 2213*
VanDenBerg, K R ... 145*, 2013
VanDuyn, N ... 942c
VanDuyn, N M ... 932, 1378*
Vanetti, I ... 835
Vanié, P J ... 1255
Vanlandingham, M ... 1616e, 1713e
Vantangoli, M M ... 168*
VanTongeren, S ... 2196e, 2196f
Varela, A ... 281*
Varela, A T ... 2004g
Varela, J L ... 1973
Varela Silva, J A ... 974*
Vargas, H M ... 766*, 2086*
Varner, K J ... 487, 1795
Varonka, M ... 1018b
Varsally, W ... 418d
Vasan, S K ... 550
Vasconcelos, D Y ... 1616c, 1713b

The numerals following the author's names refer to the abstract numbers. The asterisk after the abstract number indicates the author is the first presenter.

Vashi, K D ... 1943
Vasicko, T ... 2234a
Vasiliou, V ... 552, 1095, 2046
Vasquez, K ... 1943g
Vasquez, K O ... 1200h
Vaughan, J M ... 823, 1242*, 2300*
Vaughn, A ... 2316
Vayas, K ... 561
Vega, R ... 1119
Vegarra, M M ... 2196l, 2196s*
Veljkovic, E ... 1203*
Veljovic, V ... 2182b*, 2255
Velmurugan, K ... 1103
Velten, M ... 1688
Vena, J E ... 1524
Venhorst, J ... 430
Venkatraman, N ... 2067
Vennemann, A ... 1950
Venosa, A ... 561, 571*, 1669
Veress, L ... 577
Veríssimo, G F ... 669*, 675
Verma, A ... 551
Verma, N ... 812*
Verma, R ... 1800*, 1801
Verma, S ... 1145
Vermeulen, N ... 1062h
Verner, M ... 89*, 632e
Vernetti, L A ... 1880
Vernez, D ... 2176
Veronesi, B ... 820
Verougstraete, V ... 1280
Verwei, M ... 632, 1041
Vetrano, A M ... 383
Vette, A ... 1581
Vezina, C M ... 905, 1087s
Vézina, M ... 2138
Viau, A ... 2159
Viberg, H ... 175, 1748*, 1749
Vicario-Rodriguez, L ... 183
Vickers, A ... 859*
Vidanapathirana, A K ... 485
Vidmar, T ... 476, 1943i
Vidugiris, G ... 1784
Vignand, P ... 185
Vignard, J ... 1931
Vigoren, E M ... 1577
Vij, P ... 1292*
Vija, J ... 1634
Vijay, V ... 100, 122d, 978a
Vikulina, A ... 1520
Vilcassim, M ... 1210*
Villalobos, A R ... 1246
Villalobos, J A ... 894
Villarreal, A ... 2225
Villarreal-Guerra, J M ... 315*
Villeneuve, D L ... 4, 440d, 440e, 1402
Villevoye, J ... 1492
Vincelli, N M ... 2141
Vincent, J B ... 1541
Vincent, M J ... 2250i*
Vinci, T ... 581h
Vinggaard, A ... 1018d*, 1175
Viniegra Morales, D ... 1312, 1314, 1324
Vinikoor-Imler, L ... 1713k
Vinken, P ... 1080*, 1549a, 1652
Virdi, P ... 853
Visconti, N ... 408a, 1941
Vishnudas, V ... 417
Vispute, S ... 910*
Vitale, D .. 67, 1594, 1596, 1597*, 1598, 1599
Vitale, L A ... 268
Vitcheva, V ... 27, 1609, 2254
Vito, S ... 360
Vitsky, A ... 97
Vladykovskaya, E ... 2319
Vock, E H ... 171
Voeller, J N ... 1744
Voels, B ... 1274*
Vogel, C F ... 107, 902*, 2295
Vogel, M ... 1128
Vogel, P ... 1163
Vogel, S ... 1057
Vogel, W M ... 1660
Vogels, J T ... 430
Voit, E ... 868
Volarath, P ... 2273d
Vollmer, G ... 173
Volz, D ... 152, 155, 156*, 212
vonderEmbse, A ... 1336*
Vonderfecht, A A ... 1499
VonTungeln, L ... 632g
Vore, M ... 1772
Vorhees, C V ... 827, 1087m, 1846*
Vorojeikina, D ... 1332
Voss, K A ... 314*, 343b
Voutchkova, A ... 1831f
Vrana, J A ... 1729*, 1731, 1735
Vredenburg, G ... 1062h
Vredevoogd, M ... 1577
Vrijhof, H ... 1826
Vrolijk, M ... 335*
Vu, L K ... 2062*
Vu, Y ... 686
Vuillaume, G ... 1054, 1203
Vulimiri, S V ... 239, 892*
Vulpe, C 173p, 418d*, 524, 1281, 2128, 2260
Vydynathan, A ... 1170
Vynckier, A ... 348

W

Waalkes, M P 12, 958, 1110f, 1229d, 1297h, 1297i, 1297j, 1297k, 1297l
Wachholder, R ... 271
Waczuk, E P ... 173n
Wade, M ... 616, 1713
Wadhwa, M ... 989
Wagatsuma, Y ... 2318
Wages, P ... 1778*
Wagner, J G . 815, 1240*, 2068, 2071*, 2324, 2328
Wagner, S ... 415
Wagoner, M ... 1627, 1911*
Wagoner, R ... 1562
Wahlang, B ... 676, 1159, 1870*
Wahlin, M ... 552b
Wahlström, E ... 1229c
Waidyanatha, S ... 198, 877, 1606, 2224
Wakatsuki, T ... 1129e*
Wakefield, I ... 1659
Walb, M C ... 842
Walesky, C ... 1173, 1495*, 1498, 2206
Walk, T ... 120, 1591, 1871
Walker, C L ... 1804
Walker, D ... 443
Walker, D I ... 115*, 422, 868, 1836
Walker, E ... 1913
Walker, E G ... 1544
Walker, L ... 95, 1026
Walker, L A ... 978e
Walker, M K ... 1518
Walker, M R ... 2120
Walker, N J ... 2004a
Walker, P A ... 1875*, 1898
Walker, T ... 1807
Walker, V ... 2250k
Wall, H G ... 1217
Wallace, J ... 326
Wallace, K A ... 35, 378c, 841d, 1838
Wallace, K B ... 1773, 1798*
Wallace, V ... 2002*
Walmsley, R ... 1927*
Walrath, J ... 1460
Walsh, L ... 2323, 2329
Walsh, M T ... 1518
Walters, N ... 1713q, 1713r
Wambaugh, J F ... 96e, 223d, 2234i, 2234m, 2234n, 2234s, 2250a, 2273o*, 2273q, 2273s
Wamhoff, B R ... 1061, 1129a*
Wan, J ... 500
Wan, L ... 1008*
Wang, A ... 1973e*
Wang, B ... 618, 619*, 620, 850, 852, 1519*, 1549, 2191
Wang, C ... 1153, 1194, 1194, 1756, 1764a, 1764b, 1764c, 1764d, 2197*
Wang, D ... 2014, 2223
Wang, F ... 857, 1316, 1622
Wang, G ... 138, 139*, 911*
Wang, H ... 157, 527, 550, 603, 842*, 1337*, 1713o, 1784, 2196w
Wang, J ... 97*, 139, 217, 226, 312a*, 317, 367, 687, 810, 852, 1242c, 1242d, 1526, 1532, 1644, 1891*, 2067a
Wang, J D ... 575
Wang, K ... 2, 265d, 418c*, 978a, 2273g*
Wang, L 535, 538, 539, 585, 589, 830*, 1796, 1804a, 2129b*
Wang, M ... 461, 1789*
Wang, Q ... 191, 1206, 1840, 1907, 1909*
Wang, R ... 598, 1697*
Wang, S ... 796*, 1519, 1549, 1908
Wang, W ... 1071, 2033, 2184
Wang, X ... 146, 157, 603k, 662, 958, 1087t, 1705, 2124
Wang, Y . 265a, 532, 662*, 810*, 1194, 1451*, 1532, 1935, 2196i
Wang, Z ... 1604, 1840
Wappel, R ... 1112
Ward, A ... 678*
Ward, C ... 2234v
Ward, E J ... 1365, 1368, 1550*
Ward, J B ... 1235
Ward, M D ... 1006a*
Ward, R ... 2235
Ward, T ... 1962*
Ward, W ... 2326
Warheit, D ... 1826
Warheit, D B ... 8, 1052
Warmke, T ... 441
Warneke, A ... 1518
Warneke, J ... 1635
Warner, W A ... 851
Warren, L ... 2083
Warrior, U ... 1908
Washington, M K ... 1109, 1509
Watanabe, G ... 1070
Watanabe, K ... 110, 2119
Watanabe, M ... 442
Watanabe, T ... 1392
Watanyar, A ... 285*, 1895
Waters, M D ... 1478
Watford, S ... 2273n*
Watkins, P B ... 34*, 106, 412, 1045
Watkins, S ... 1003
Watrud, L ... 1006a
Watson, D E ... 101, 102, 1549h
Watson, P ... 1229g
Watson, R E ... 197, 1698
Watson, S ... 539e
Watson, W H ... 1323, 2316*
Watt, J ... 1085*
Watzinger, M ... 1494
Wauthier, E ... 1905
Weatherly, L ... 382*, 1315
Weaver, E ... 1064
Weaver, J ... 1831h*
Weaver, J L ... 122b
Weaver, M J ... 298
Weaver, R ... 987
Weaver, V M ... 1306
Webb, J D ... 1633
Webb, P ... 1135
Weber, E ... 122h*, 1018e
Weber, G J ... 203, 204, 221, 1338
Weber, K ... 2131
Weber, L P ... 491*, 2214
Weber, T J ... 1573
Webster, L ... 1200b
Webster, T ... 1016*, 1085
Weeks, R ... 1662a
Wegener, K M ... 1764e
Wegner, S ... 1702, 1707*
Wehmas, L ... 1637*
Wei, C ... 509
Wei, K ... 1348
Wei, L ... 2223*
Wei, Q ... 1102
Wei, W ... 1946, 2207
Wei, X ... 2316
Wei, Y ... 224*, 528
Weideman, P ... 1815*
Weigand, R ... 1090
Weihe, P ... 1334
Weinbauer, G F ... 2148
Weinberger, B ... 383
Weiner, M L ... 341*, 342, 343, 845
Weingeist, D M ... 2282
Weinhouse, C ... 1687*
Weinstein, J ... 1232
Weinstock, D ... 2120
Weisel, C ... 672
Weiser, T ... 157
Weisskopf, M ... 1552
Welch, B ... 1298, 1299*
Welch, K ... 805*
Weld, M ... 338
Weldy, C S ... 1690b*
Welge, P ... 1007
Welle, S ... 1460
Welsh, C ... 90
Welsh, W ... 1275
Wen, X ... 1802, 2053*
Wendt, A ... 134
Weng, Z ... 552e, 813d*, 1200a, 1697
Wente, T L ... 1549d*
Werner, C ... 1087v
Werner, J ... 1641*
Werts, S ... 1183
Wesselkamper, S C ... 1831d, 2273cc
West, K ... 966
West, N ... 469, 953
West, P R ... 1917
Westerholm, E ... 648
Westerhout, J ... 1041
Westerink, R H ... 356, 1739, 1833, 1834, 1835*
Weston, D ... 1333, 1340, 1342
Weston, H 1333*, 1340, 1342, 1347, 1747e
Westphal, T ... 1018b
Wetmore, B A 146, 2234m, 2250*, 2250a, 2273o
Whalan, J E ... 1830*
Whalen, C C ... 226
Whalley, C E ... 581i
Whalley, P ... 1831g
Whelan, M P ... 691*
Whitaker, R M ... 111
White, A ... 359, 1788
White, C . 546, 553, 554, 577, 603, 683, 684, 685, 897, 1962, 1981, 2004f
White, D ... 2151c
White, G A ... 467a
White, J ... 419*
White, K L ... 145b
White, M ... 622, 623
White, M B ... 1683
White, P ... 753, 757*, 1831c
White, R ... 850, 854
White, R D ... 952
White, S ... 429
Whiteley, L O ... 1635
Whitley, E ... 362
Whittaker, M H ... 618, 619, 620
Whittaker, R ... 1119*
Whittemore, S L ... 215, 219
Whitten, D A ... 409
Whittington, D ... 1577
Whitwell, J ... 756, 1933
Whritenour, J ... 125, 397, 986
Wicha, M S ... 1922e
Wickliffe, J K ... 253, 1235
Wickramasinghe, N S ... 2319
Wiegand, H ... 1826
Wiegers, T C ... 411
Wiemann, M ... 1950
Wiench, K ... 1220, 1221*, 1992
Wiese, R ... 441
Wignall, J ... 630*
Wijeyesakere, S J ... 1148*
Wikoff, D ... 622*, 623
Wikswo, J P ... 1445*
Wilcox, A ... 1699
Wild, D J ... 693*
Wild, S L ... 898
Wildemann, T ... 2214*
Wilderman, R ... 539a*
Wildwater, M ... 216*
Wilga, P C ... 343f, 1037, 1151
Wilhelm, C ... 558, 564*
Wilkerson, C G ... 409
Wilkie, A ... 1018c
Wilkins, D E ... 118
Wilkinson, J ... 167
Will, Y ... 714

Author Index (Continued)

The numerals following the author's names refer to the abstract numbers. The asterisk after the abstract number indicates the author is the first presenter.

Willett, C ... 1036
Willett, K L ... 208, 1683*, 1987, 1988
Williams, A ... 1478
Williams, A M ... 1542
Williams, C D ... 1172, 1178*, 1196
Williams, C R ... 1529*
Williams, D ... 122c*
Williams, D E ... 513, 539d, 876a, 882
Williams, E ... 649b*
Williams, E S ... 1831f
Williams, F M ... 632*
Williams, G M ... 171*, 467a
Williams, H N ... 1729, 1731, 1735
Williams, J ... 1889
Williams, J P ... 552f
Williams, K ... 1191
Williams, K D ... 280*
Williams, L ... 223c*
Williams, L M ... 1679
Williams, M T ... 827, 1087m, 1846, 2225*
Williams, P ... 995, 2174
Williams, R V ... 2264*
Williams, R W ... 2129a
Williams, S ... 1284
Williams, W ... 145a
Willinger, L ... 312f
Willis, A ... 68*, 1815, 1827
Willis, D ... 1692, 2004*
Willis, R ... 1232
Wills, L P ... 1611*
Wills, R ... 540, 1515
Willson, G A ... 1217
Wilrich, P ... 1280
Wilson, C ... 863*
Wilson, D ... 1019
Wilson, J ... 1642
Wilson, J Y ... 534*, 1013
Wilson, M J ... 253
Wilson, V S ... 1066, 1087c*, 1713c
Wilt, N ... 173k, 1020, 1028
Wimalasena, R ... 878
Winans, B ... 2017
Windt, H ... 1226
Wingard, C J ... 484, 485*, 596
Winje, N ... 1582
Wink, S ... 173f*, 1168, 1715, 2031
Winkel, D ... 627*
Winkelmann, C ... 2078*
Winkley, A ... 1897*
Winner, M ... 2319
Winnica, D ... 1520
Winnicker, C ... 2151d
Winsett, D ... 2329
Winslow, J ... 842
Winters, J ... 240, 324
Wirbisky, S ... 204, 221, 1338*
Wirnitzer, U ... 288
Wise, C ... 448*, 1279
Wise, J ... 378h*, 448, 1303
Wise, J P . 448, 1272, 1276, 1279, 1279, 1303, 1320, 1450*, 1924, 1942
Wise, K ... 1065*
Wise, L D ... 2074
Wise, L M ... 132
Wise, S 448, 1276, 1279*, 1303, 1450, 2138
Wisialowski, T ... 1128
Wisler, J A ... 2305*
Witt, K L ... 173b, 444, 467g, 1616c
Witters, H ... 1037
Wittington, D ... 1763
Witzmann, F A ... 821
Wiwatratana, D ... 1376*
Wohlleben, W ... 597, 1992*
Woitkowiak, C ... 173
Wolansky, M J ... 1847
Wolenski, F ... 122e*
Wolf, A ... 873, 1618, 2056
Wolf, C J ... 418a
Wolf, J ... 1290
Wolf, M F ... 954b*
Wolfarth, M ... 1978
Wolfe, G W ... 2196l*
Wolfe, M L ... 1910*
Wolfe, M S ... 1486
Wolfinger, D ... 173k
Wölk, S ... 2172
Wolter, M E ... 1761*
Wolterbeek, A ... 154*, 1347i
Wolters, J ... 1104
Wolton, K ... 195*
Woltosz, W ... 440j
Won, S ... 787
Wondrak, G T ... 308, 1499, 1791, 2164
Wong, A ... 161
Wong, A W ... 343h*
Wong, B A ... 895, 1010, 1820
Wong, C ... 369
Wong, E L ... 1347e*
Wong, G ... 942c
Wong, H ... 2242
Wong, L ... 1006*
Wong, S ... 1966
Woo, H ... 1122
Wood, C ... 1347g*, 2213b
Wood, C E ... 65, 1232
Wood, C S ... 624*, 2250g
Wood, D K ... 2282
Wood, S C ... 289, 2024
Wood, T G ... 1928
Woodall, G M ... 632c*, 1830
Woodhouse, H ... 1875, 1898
Woodling, K ... 1616e
Woodruff, T J ... 630
Woods, C G ... 1140
Woodward, C E ... 661*
Woodward, R A ... 705, 848
Wooldridge, M ... 815
Woolhiser, M R ... 398, 399
Worek, F ... 560
Worley, R R ... 90*
Wormser, U ... 566*
Wortelboer, H ... 1041*
Worth, A P ... 27, 28, 29, 1609, 2254
Woulfe, D ... 1461
Woutersen, R A ... 635
Wray, L ... 1921
Wright, C ... 1110c
Wright, F A ... 165, 630
Wright, G M ... 958
Wright, J ... 183*, 184, 195, 238, 1039, 1090, 1831g, 1865, 1869, 2174
Wright, L ... 1630*
Wright, L K ... 581i*
Wright, M S ... 1186
Wright, P F ... 663
Wright, R O ... 704*, 1417*, 2286, 2287*
Wright, S H ... 1701
Wrzesinski, C ... 419
Wu, B ... 659
Wu, C ... 296, 357, 1325*, 1369, 1388, 2054
Wu, D ... 1087t*, 1705
Wu, H . 60, 89, 91*, 92, 125*, 543, 1325, 1480
Wu, J ... 511, 717*
Wu, K C ... 417*
Wu, L ... 1102
Wu, N ... 1465
Wu, P ... 2004h
Wu, Q ... 1786, 1804b*
Wu, R ... 2142
Wu, S ... 1840
Wu, T ... 1779*, 1780
Wu, W .. 21, 1242i, 1705*, 1789, 1793*, 1977*
Wu, X ... 510*, 1058*, 1347k
Wu, Y ... 257*, 884, 1087b
Wu, Z ... 392*, 1282
Wulff, H ... 1842
Wurpel, J ... 498
Wusu, A D ... 321, 1249, 1264*, 1266, 1273, 1776
Wyllie, S ... 122e
Wynne, R ... 254

X

Xi, S ... 2234o*
Xia, M ... 173b, 173h, 444, 467g, 1149, 2252, 2273s, 2273bb
Xia, Q ... 1094*
Xia, X R ... 1237*
Xia, Y ... 603k*, 1705, 1909
Xiang, Y ... 413, 415, 860, 1054
Xiao, Q ... 1549d
Xiao, W ... 1781*
Xiao, Y ... 2067
Xie, F ... 393, 533, 536, 1519, 1549
Xie, H .. 922c, 1272, 1279, 1320, 1447*, 1450, 1924, 1942*
Xie, J ... 393
Xie, L ... 159, 1433
Xie, W ... 737*
Xie, Y ... 1181*
Xin, Y ... 493*
Xing, C ... 1474*
Xing, D ... 1903
Xiong, K ... 1103
Xiong, R ... 358*, 1632
Xu, B ... 603k, 967, 1736d
Xu, C ... 1153*, 2197
Xu, J ... 2207, 2273k
Xu, K ... 1087t
Xu, L ... 1337
Xu, M ... 978d, 1943d*
Xu, T ... 1633*
Xu, W ... 1069
Xu, Y ... 1297l*, 1711, 1943j
Xuan, J ... 1195*, 1892, 1893
Xue, A ... 1627
Xue, K S ... 317, 810, 1532*
Xue, P ... 1788*, 1794

Y

Yabe, J ... 843, 1516
Yabe, T ... 201
Yafawi, R L ... 97
Yajima, K ... 1150
Yakubu, M A ... 2234j
Yamada, H ... 961
Yamada, J ... 432
Yamada, K ... 455
Yamada, K E ... 1775*
Yamada, M ... 2132
Yamada, S ... 1600
Yamada, T ... 201, 265c, 432*, 1046, 2167
Yamaguchi, M ... 1086
Yamakawa, K ... 1091, 1092*, 1093, 1213
Yamamoto, B ... 2196k*
Yamamoto, M ... 1262*
Yamamoto, S ... 128
Yamamoto, T ... 472, 1621
Yamamura, E ... 455
Yaman, H ... 581f
Yamanishi, E ... 1304
Yamasaki, C ... 1899b
Yamashita, A ... 201*
Yamashita, S ... 242
Yamashita, T ... 196, 432
Yamashita, Y ... 2167
Yamauchi, K ... 669b*
Yamauchi, T ... 196
Yamazaki, H ... 518, 1150, 2151
Yamazoe, Y ... 432
Yamoto, T ... 110
Yan, J ... 265d, 1973c, 2004c
Yan, K ... 2031
Yan, X ... 482, 483, 1901*
Yan, Y ... 1242d
Yan, Z ... 1821*
Yanagiba, Y ... 1697
Yanagisawa, H ... 2047, 2049*
Yanamala, N ... 1242g, 2004d, 2273a*
Yang, B ... 1804a
Yang, C ... 26, 27*, 28, 29, 30, 31, 431, 632, 1609, 2254, 2266, 2273, 2273d, 2273x
Yang, C S ... 794
Yang, C Z ... 161
Yang, D ... 1741
Yang, E ... 911
Yang, H ... 1166, 1167, 1229b, 1889, 2223
Yang, I ... 2053
Yang, J ... 1647, 2273v, 2273w
Yang, M ... 416, 539b, 1887
Yang, Q ... 1899d*
Yang, R ... 1325
Yang, X ... 96f*, 96g, 99*, 813d, 841*, 922, 962*, 963
Yang, Y ... 177
Yang, Z ... 217*
Yanochko, G ... 864, 1726*
Yantasee, W ... 915, 2230
Yao, H ... 2196c
Yao, J ... 2241
Yao, P ... 245*
Yao, Y ... 1282*, 2119
Yaren, H ... 581f
Yasuda, M ... 2133
Yasugi, S ... 1259
Yasuhara, T ... 669a
Yauk, C L ... 1478*, 1938
Ye, D ... 293
Ye, Q ... 2065
Ye, X ... 379*
Yeager, R ... 899
Yeager, R L ... 2196z
Yeatts, J ... 2175
Yee, N ... 197
Yeh, A ... 340*
Yeh, C ... 1365*, 1366, 1368, 2231
Yellowhair, M ... 1295*
Yemitan, O K ... 663*
Yen, C ... 296, 357, 1369, 1388
Yeo, M ... 1921
Yerges, L M ... 552c
Yeung, D T ... 558, 564, 567
Yi, H ... 1044*
Yi, J ... 872, 1689, 1982
Yi, O ... 230
Yi, S ... 539b
Yin, L ... 2212
Yin, X ... 480, 2316
Yin, Z ... 644*
Ying Ma, J ... 1652
Yingling, B M ... 1242a*
Yip, H ... 1902
Yohannes, Y B ... 843, 1516*
Yokel, R ... 2004h
Yoko, I ... 1991*
Yokohira, M ... 1091, 1092, 1093, 1213*
Yokoi, T ... 537*, 975, 1878
Yokouchi, Y ... 494*
Yole, M ... 1819
Yoo, B ... 49, 1495
Yoo, C ... 1087j
Yoo, H ... 1152*
Yoo, J ... 519*
Yoon, B ... 1900
Yoon, M ... 60, 75, 76, 89, 91, 92*, 266, 689b
Yoon, Y ... 708, 711*, 1125
Yoshida, E ... 1258*
Yoshida, M ... 1070*, 1160, 1161
Yoshikawa, T ... 472*
Yoshinari, K ... 432
Yoshioka, W ... 200
You, D ... 794*
You, H ... 539d*
You, M ... 511
Young, B ... 1018c
Young, J F ... 96f
Young, R K ... 1246
Young, R R ... 1943i*, 1943j
Young, S ... 1713q, 1713r, 1713u
Younis, H S ... 1171*
Yourick, J . 173g, 1297a*, 1944, 1973h, 1973i, 1973j
Yousefi, P D ... 707
Yozzo, K ... 152, 155, 156
Ysselstein, D ... 1349
Yu, D ... 552c
Yu, H ... 272*, 346, 2196e, 2196g
Yu, I ... 593, 660, 1565, 1976, 2001
Yu, J ... 1519, 1549
Yu, L ... 114*, 265d
Yu, Q ... 1644
Yu, R ... 1107*, 1521
Yu, S ... 1553, 2242*
Yu, T ... 422
Yu, X ... 2241
Yu, Y ... 1166, 1167, 1374
Yu, Z ... 965
Yuan, B ... 1705
Yuan, H ... 1117
Yuan, J ... 544, 2196e, 2196i*
Yuan, Y ... 1381*
Yucesoy, B ... 43
Yue, M S ... 490*
Yumibe, N ... 2151c

Yun, J 1623
Yun, K 440l
Yun, S 1522
Yunjia, L 1556*
Yunokawa, H 978b
Yurek, D 2151c
Yzenas, J J 2219

Z

Zaas, S 1235
Zaccaria, K 1831
Zacharewski, T R 414*, 440, 903
Zago, M 906*, 1722
Zagorski, J W 2012, 2013*
Zailani, H I 499
Zakharov, A 1546
Zalko, D 149
Zalups, R K 2042
Zalyalov, R 603f
Zamfir, M 1540
Zamoiski, R D 1306
Zamora, M 424
Zamule, S M 1679
Zang, Q 2273p*
Zanoni, T 2171*
Zarbl, H 973, 1493*, 1497, 1501, 2194
Zaroogian, G 1087h
Zarrin, A A 2196p
Zauber, E 1366, 1368, 2231
Zawia, N 939
Zebedeo, C N 130, 131
Zehr, K 1518
Zeidler-Erdely, P C 603d*, 1229a
Zeigler, B 342*, 845
Zeise, L 1488*, 1808
Zeligs, M A 2196y
Zelikoff, J T 75, 355, 1282, 1675, 1692, 2004, 2040a, 2193
Zelko, I 1239
Zeltner, A 2147
Zeng, M 1635
Zhan, L 973, 1129b*
Zhang, A 440b*
Zhang, C 222*, 295, 483, 1604*, 1888, 2044*, 2045
Zhang, D D 1499, 1779, 1780, 1791
Zhang, F 885*, 1026*, 1099, 1941, 1958*, 2173
Zhang, G 1967
Zhang, H 874, 997, 1101, 1229c*, 1794, 1891, 2212*
Zhang, J 418e, 639*, 962, 963, 1182, 1533, 1804, 1885*, 1887, 1979, 2252
Zhang, L 659*, 920, 1087*, 1141*, 1170
Zhang, L W 820, 1616*
Zhang, M 1189, 1194*, 1804a
Zhang, Q 438*, 439, 536*, 1347l, 1794, 1888*, 1945, 1947*, 2004
Zhang, R 2213a*
Zhang, T 1117, 1348
Zhang, W 976, 1087t, 1772*, 1891
Zhang, X 1604, 1619, 1764b, 1764d, 2050, 2316
Zhang, X L 1289
Zhang, Y 598*, 603b, 1163*, 1713i, 2129b
Zhang, Z 122b, 265e, 482*, 942a, 964, 1297f, 1327f
Zhao, B 922c
Zhao, C 1188*, 1189, 1348
Zhao, D 2196z*
Zhao, F 1300*
Zhao, G 1519, 1549*
Zhao, J 444, 649, 1146, 1149, 1821, 2273cc
Zhao, L 1556, 1737
Zhao, Q 2034
Zhao, Q J 6*
Zhao, R 1804a*
Zhao, W 855, 2208*
Zhao, X 590
Zhao, Y 75*, 266, 1250*, 1908, 2125*, 2191
Zhao, Z 157
Zhdanov, D D 312b
Zheng, J 1944, 1972, 2004
Zheng, M 813, 1250
Zheng, T 1276, 1303
Zheng, W 122g*, 346, 1291, 1349, 1361, 1362*, 1367, 1390, 1549f, 2103*, 2107*
Zheng, X 594*, 1467
Zheng, Y 482, 1780
Zhitkovich, A 1268*, 1269, 1926
Zhong, F 273
Zhong, M 1282
Zhong, W 2269
Zhong, X 48, 49*
Zhou, C 2184
Zhou, H 813, 874, 1185
Zhou, M 1628
Zhou, P 581f, 813d, 1935*
Zhou, S 480*, 482, 483, 1580
Zhou, T 1794, 2004c
Zhou, W 1632, 1784
Zhou, X 244, 533, 842, 1316*, 1327, 1449, 1730, 2127*
Zhou, Y 418c
Zhou, Z 1874, 2002
Zhu, B 245, 247
Zhu, C 1303
Zhu, H 1229e, 1713t, 1790, 1792, 2252
Zhu, J 224, 1903, 1922a
Zhu, L 1730
Zhu, S 1108
Zhu, W 1504
Zhu, X 986*, 2273h
Zhu, Y 536, 855, 1781
Ziegelhofer, T 1713s
Ziemann, C 601
Zierau, O 173
Zikopoulos, D 2250f
Zimmerman, J B 1831f
Zimmermann, L 900
Zimprich, C A 167, 291
Zink, D 718*
Zitzow, J 2208
Ziv-Gal, A 2184*
Zmirou-Navier, D 1009
Zollinger, T 971
Zong, C 1087
Zoroddu, M A 1297e
Zu, K 1537*
Zucker, R 1973d
Zur, M 2026
Zurlinden, T 84*, 137
Zwickl, C M 434
Zychowski, K 316*
Zyskowski, J 1297g

Notes

Abstract Keyword Index

The numerals following each keyword refer to the relevant abstract number(s).

'Omics ... 173p
'Omics Technology ... 120, 1591
(Developmental) Neurotoxicity .. 750, 1329
(Non)genotoxicity ... 1104
[18F]FLT ... 1764d
1-Bromopropane ... 1549g, 2032
1, 1-Diphenyl-2-Picrilhydrazyl (DPPH) ... 793
1, 3-Butadiene ... 978, 1549c
1, 4-Dioxane ... 446
1, 4-Naphthoquinone ... 1717
13-Week Dietary Study ... 343g
17α-Estradiol ... 1782
1H NMR ... 1578
2-Aminoanthracene (2AA) ... 922a, 922b
2-Arachidonylglycerol ... 440g
2-Ethylhexyl p-methoxycinnamate ... 145b
2, 3-Pentanedione ... 632f
2, 3, 7, 8-Tetrachlorodibenzo-*p*-dioxin (TCDD) ... 903, 1163b, 1681
2, 5-Dichlorophenol ... 224
21-Day Pups ... 897
2DE and MALDI-TOF/TOF ... 516
3-D *In Vitro* Models ... 603l
3-Dimensional ... 1876
3-Methylcholanthrene ... 535
3D ... 1872
3D Airway ... 1970
3D Baby Skin Model ... 1587
3D Bio-Printing ... 1639c
3D Cell Culture ... 307, 912
3D Cell Culture Models ... 1955
3D Cells ... 758
3D Cellular Microarray ... 539b
3D Culture ... 291
3D Culture System ... 1921, 1922
3D Culture Systems ... 413
3D Human Skin Model ... 1604
3D *In Vitro* Culture ... 168, 1899a
3D Printing ... 1973g
3D Skin Model ... 1034
3D Tissue Constructs ... 1037
3D-Human Dermal Equivalents ... 762
3R ... 634
3Rs ... 901f, 2115
3Rs Committment ... 759
4-Aminopyridine ... 625
4-Methyl-2, 4-bis(4-hydroxyphenyl) pent-1-ene (MBP) ... 357
4-Methylimidazole ... 539e
4-Vinylcyclohexene ... 173n
4EBP1 ... 1503
5-Day Repeated ... 2001
5-Fluorouracil ... 1943e
50 Hz ELF-EMF Exposure ... 356
5002 Diet ... 2135
6-Formylindolo[3, 2-b] Carbazole (FICZ) ... 2164
9, 10-Phenanthraquinone ... 1792
A-431 Skin Cell ... 576
a-Synuclein ... 1349
A/J Mice ... 1091
A53T α-Synuclein ... 1632
AB-RAGE ... 942e
Abandoned Mine ... 1553, 2234d
ABC Transporters ... 366, 901
Abcb11 ... 1163
ABCC4 Gene ... 1184
ABCG2 ... 1081
ABR ... 2196u
Absorption ... 77, 1593, 2174, 2175
Abuse ... 498
Academic Service Learning ... 1674
Accelerator Mass Spectrometry ... 2195
Acceptance ... 634
Acephate 97 DF ... 399
Acetaldehyde ... 467b, 1110g, 1523
Acetaminophen 84, 99, 366, 417, 418c, 713, 867, 1044, 1178, 1179, 1181, 1186, 1201, 1890
Acetaminophen Hepatotoxicity ... 1172, 1197
Acetaminophen Toxicity ... 1173
Acetaminophen-Induced Hepatotoxicity ... 1005
Acetylcholine ... 1854
Acetylcholinesterase ... 581e, 1670, 1856
Acidic Fibroblast Growth Factor ... 295
Aconitum brachypodum Diels ... 813
Acoustic Startle ... 1846
Acrolein ... 17, 390, 1121, 1182, 1229e, 1790
Acrylamide ... 914, 1454, 1519
Actinide Chelating Agent ... 894
Active Transport ... 440i
Acute & Subacute ... 812
Acute and Subchronic Toxicity Studies 807
Acute Behavioral Neurotoxicity ... 632c
Acute Exposure ... 63
Acute Inhalation Exposure ... 632c, 1818
Acute Kidney Injury ... 108, 2052
Acute Lung Injury ... 531, 581k, 596
Acute OP Intoxication ... 579
Acute Oral Toxicity ... 435
Acute Phase Response ... 1230
Acute Toxicity ... 170, 610, 813
Ad5 ... 1646
Adam8 ... 122a
Adansonia digitata ... 1514b
Adaptive Stress Response ... 173f
Additivity ... 1018c
Adenovirus ... 1646
ADHD ... 51, 230, 1745
Adherens Junction ... 1242c
Adipogenesis, Nuclear Receptors, Lipogenesis ... 2199
Adipose Tissue ... 1720
Adipose-Derived Stem Cell ... 1044
ADME ... 49, 1396
ADMET ... 440i, 1183
ADP ... 1645
Adverse Drug Reaction ... 547, 745
Adverse Events ... 1469, 1470, 1471, 1472, 1473, 1475
Adverse Immune Reactions ... 1036
Adverse Outcome Pathway ... 29, 239, 418d, 432, 690, 749, 776, 1399, 1400, 1401, 1402, 1403, 2285
Adverse Outcome Pathways ... 691, 746, 1398, 2256, 2257
Adverse Reactions ... 124
Aerosol . 828, 1229, 1594, 1596, 1597, 1598, 1599, 1961, 2225
Aerosol Delivery ... 271
Aerosols ... 1222
Afficacy ... 552c
Aflatoxin ... 316, 1526, 1774
Aflatoxin B1 ... 122, 526, 1713g, 1906
Aflatoxin Exposure ... 317, 1532
Aflatoxin M1 ... 313, 1534
Aflatoxin-Albumin Adduct ... 1532
Aflatoxins ... 226, 315
Africa ... 843, 2117
African Dust ... 981, 1785
AGE ... 322, 942d
Aged Rats ... 1651
Agent Orange ... 581g
Aggregations ... 598
Aging ... 122d, 318, 350, 942, 2042
Aging and Environmental Health ... 2325
Agrochemicals ... 1019
Ah Receptor . 1133, 1137, 1139, 1141, 1142, 1146
AhR ... 215, 223c, 292, 504b, 507, 737, 902, 906, 907, 978c, 1133, 1136, 1137, 1138, 1139, 1141, 1163a, 1492, 1685, 2014, 2016, 2020, 2253
AhR and Liver Fibrosis ... 2200
AhR Knockout Mice ... 1087u
AhR Ligands ... 1130
AhR Polymorphisms ... 2019
AIDS ... 1923
Air Ions ... 1806
Air Modeling ... 1575
Air Monitoring ... 2236
Air Pollution ... 14, 15, 16, 17, 18, 19, 844, 876a, 1206, 1242b, 1242e, 1275, 1342, 1690b, 1810, 2068, 2071, 2300
Air Pollution Exposure Model ... 1581
Air Pressure ... 87
Air Toxics ... 231
Air-Liquid Interface ... 173a, 1961
Air-Liquid Interface Culture ... 1062b
Airborne Chemicals ... 1062f
Airborne Concentrations ... 1564
Airborne Particulate Matter ... 2070
Aircraft ... 2247
Aircraft Lubricant ... 2247
Airway ... 848c
Airway Inflammation ... 801, 1719, 1928
Airway Pathology ... 771
Airway Sensory Irritants ... 2323
Airways Hyperresponsiveness ... 392
Alchornea cordifolia ... 803
Alcohol ... 214, 875, 1188, 1347e
Alcohol-Induced Liver Disease ... 1156
Alcoholic Fatty Liver Disease ... 2129b
Alcoholic Liver Disease ... 1155, 1189
Alcoholic Pancreatitis ... 384
Aldehyde ... 1783
Aldehyde Acrolein ... 954f
Aldehyde Dehydrogenase ... 552
ALDH16A1 ... 2046
ALDH1B1 ... 1095
ALDH1L1 ... 373, 374
ALDH2 Knockout Mice ... 1697
Aldose Reductase ... 1790
Aldosterone ... 1082
Algal ... 327
Alisporivir ... 873
Alkaline Phosphatase ... 1048
Alkaline Phosphatase (ALP) ... 2196bb
Alkenylbenzene ... 523
All-Trans Retinoic Acid ... 1799
Allelochemical ... 652
Allergen ... 1823
Allergen Sensitization ... 390
Allergic Contact Dermatitis ... 1034, 1831l
Allergic Inflammation ... 582
Allergy ... 141, 337, 988, 1006a, 1713m
Allopurinol ... 1178
Allosteric Modulation ... 440b
Aloe vera ... 1694
Alpha-Cypermethrin ... 1843
Alpha-Synuclein ... 929
Alpha-Tocopherol ... 78
AlphaLISA ... 1899c
ALT ... 1899c
ALT1 ... 1899b
Alternative ... 944, 1030, 2273s
Alternative Flame Retardant ... 1616a
Alternative Flame Retardants ... 1603
Alternative Fuels ... 1010, 2244
Alternative *In Vitro* Method ... 943
Alternative Methods 120, 635, 1062c, 1591, 1704, 2055, 2273cc
Alternative Methods to Animal Experiments ... 164, 1062h
Alternative Model ... 1057
Alternative Model Organism ... 173o
Alternative Models ... 173c, 1041, 1747a
Alternative Screening Technology ... 1713j
Alternative Test Methods ... 1398
Alternative Testing ... 764, 765, 766, 767, 768, 769, 1973e
Alternative to Animal Experiments ... 430
Alternative to Animal Methods ... 1608
Alternatives ... 1582
Alternatives Assessment ... 2272
Alternatives to Animal Model ... 354
Alternatives to Animal Testing ... 1021
Altitude ... 895, 1820
Aluminum ... 782, 1347l, 1904
Alzheimer's Disease . 939, 942d, 1277, 1841
Ambient Air ... 837
Ambient Particles ... 1242d
Ambient Traffic Related Particulate Matter ... 1242i
Ambient Vapor Sample ... 1716
Ambystoma ... 1142
American Board of Toxicology ... 649c
Ames ... 467f
Ames Assay ... 467d
Ames Salmonella/Microsomal Assay ... 1242h
Ames Test ... 462, 2263
Amines ... 1030, 1222, 1229f, 2175
Amino Acid Metabolism ... 343d
Aminoglycoside Antibiotics ... 2196t
Amorphous Silica ... 599, 601
Amorphous Silica Nanoparticles (aSiNP) ... 1969
Amoxicillin ... 1578
Amoxillin ... 2271
Amphibian ... 1142
Amphibian Model ... 1087d
AMPK ... 1166, 1167, 1194
Amyloid Beta ... 942d, 1841
Analytical Methods ... 946
Anaphase Promoting Complex ... 304
Anaphylaxis Model ... 401
Anatomy ... 1640
Androgen Receptor Binding ... 173
Androgens ... 1087s
Andrographis paniculata ... 809, 813b
Anesthetics ... 1764b
Anesthetized Guinea Pig ... 2196w
Aneugens ... 464
Angelica sinensis ... 790
Angiogenesis ... 1087o, 1513, 1514a, 1740, 1901
Angiotensinogen ... 1725, 1728
Animal Alternatives ... 1023, 1031
Animal Model ... 508, 1203, 1878, 2120, 2141
Animal Models ... 406, 1713a, 2121, 2151c, 2160, 2196a
Animal Models of Human Disease ... 935
Animal Sham Dosing ... 2139
Animal Welfare ... 2196z
Annexin ... 1200h
Annexin A1 ... 1164
Annotation ... 421
Anoikis ... 1496
Anoikis Resistance ... 1098
Antagonist ... 1131
Anterior Keratectomy ... 859
Anthelmintics ... 1145
Anthranilic Diamide ... 682
Anthraquinone ... 604, 605
Anthrax ... 581b, 2196k
Anti-BPDE-DNA-Adducts ... 1007
Anti-Inflammation ... 809
Antiandrogen ... 530
Antiandrogenic ... 1079
Antiapoptotic Proteins ... 312c
Antibiotic Resistance ... 1284
Antibiotics ... 1630, 1634
Antibody ... 989
Antibody Response ... 1713s
Antibody-Mediated ... 269
Anticancer Agent ... 797c
Anticancer Drug ... 1637
Antigen-Specific Response ... 2007
Antihistamine ... 581c
Antimicrobial Activity ... 603i
Antimutagenicity ... 1943
Antinuclear Antibodies ... 131
Antioxidant ... 793, 1218, 1219, 2216
Antioxidant Defense System ... 1267

Antioxidant Response 1720
Antioxidant Responsive Element (ARE) 1775
Antioxidants 808, 809, 1696, 1923
Antiplatelet Antibody 1656
Antiproliferative Effects 1973f
Antisense 2113
Antisense Oligonucleotide 1171
Antithrombin 1653
Antitoxin 2196k
Antitubercular Activity 1639
Antitumor Activity 298
Antiviral Drugs 2256
Antral Follicle 2185
AOP 96e, 747, 748, 750, 751, 752, 2253
AOPs 4
APAP 1176, 1180
Apc Min Mouse 1505, 1509
APFO 2211
Apolipoprotein 678
Apoptosis 188, 290, 293, 296, 297, 302, 303, 309, 312a, 797b, 797c, 978d, 1369, 1867, 1881, 1893, 1945, 1956, 1971, 2030, 2125
Apoptosis; Reactive Oxygen Species 1388
Apoptosis/Cell Death 312, 385
Apoptosis/Cell Survival 1108, 1243
Appalachia 1018b
Aquaculture 316
Aquatic 669d, 1987
Aquatic Nanotoxicology 660, 668
ARE Assay 2252
Aristolochic Acid 265d, 2060
ARNT 1110c
Aroclor 1870
Aromatase 1087h
Aromatase (CYP19) 1075
Aromatase Knockdown 208
Arrhythmia 477, 492, 1114, 1119, 2085, 2323
Arrhythmias 498
Arsenic 144, 145, 176, 223i, 229, 241, 242, 243, 312d, 497, 632i, 776, 777, 913, 958, 1297h, 1297i, 1297j, 1297k, 1297l, 1298, 1299, 1300, 1301, 1302, 1303, 1305, 1307, 1308, 1310, 1314, 1315, 1316, 1317, 1318, 1319, 1320, 1321, 1323, 1324, 1327c, 1327d, 1328, 1449, 1556, 1682, 1797, 1916, 2226, 2234p, 2234q, 2258, 2316, 2317, 2318, 2319
Arsenic Biotransformation 1309
Arsenic Exposure 1306, 1327a, 1533
Arsenic Metabolism 1312
Arsenic Speciation 1327e
Arsenic Trioxide 1696
Arsenic; Neurotoxicity 1388
Arsenicals 496
Arsenite 143, 240, 244, 1304, 1322, 1326, 1327, 2320
Artemisia annua L. Extract 1166
Aryl Hydrocarbon Receptor 212, 264, 502, 908, 909, 922c, 1087g, 1127, 1132, 1133, 1136, 1137, 1138, 1139, 1141, 1144, 1153, 1500, 1742, 1743, 1905, 1907, 1909, 2017, 2040c, 2197
Aryl Hydrocarbon Receptor (AhR) . 200, 1458, 1459, 1460, 1461, 1462, 1463, 2164
Aryl Hydrogen Receptor 2283
Arylesterase 540, 1273
As3MT 1304
Asbestos 53, 54, 55, 56, 57, 58, 127, 129, 130, 131, 1811, 1831k, 2234z, 2235
Ascorbic Acid 1713o, 2234u
Aspergillus 1730
Aspirin 1769
Assay 376
Assay Interference 1297c
Assay Validation 291
Assessment 1018e, 1580
AST 1200, 1899c
Asthma 390, 392, 582, 643, 921, 968, 1201, 1561, 2250i
Asthma Bronchiale 844
Astrocyte Neuron 1347k
Astrocytes 1261, 1278, 1297b, 1297d, 1380
Astrogliosis 372, 373, 374
Ataxia 1943h
Atherosclerosis 1310, 1319, 2319
Atomic Absorption Spectroscopy 343a
Atopic Dermatitis 799, 2000
ATP-Binding Cassette Transporters 1626
Atrazine 203, 204, 206, 221, 655, 1836, 1837
Atropine 558
Atropisomers 2205
Attention Deficits 2292
Audiogenic Seizures 1747c
Auditory 2196u
Auditory Safety 2196t
Autism 180, 1684, 1805, 2129d, 2234g
Autism Spectrum Disorder 1341
Autoantibodies 234, 1347j
Autoantibody 2129d
Autoimmune 46, 55, 1335, 2234c, 2322
Autoimmune Disease 103, 134
Autoimmune Diseases 122f, 128
Autoimmunity 136, 138, 139, 140
Automated Analysis 2272
Autonomic Function 1982
Autonomous Bioluminescence 1633
Autophagy 312a, 588, 710, 926, 1097, 1123, 1190, 1499, 1798, 1804, 1889, 1945, 1951
Autosomal Gene Mutation 453
AVMA 2136
AVPV 174
Azole Fungicides 1835
B Cell 136, 1411, 2019
B Cell Activation 2018
B Cell Lineage Commitment 2015
B-catenin 254, 905
B[a]P 208, 974
BAC-TRAP 373, 374
Bacillus anthracis 883
Background 287, 2234e
Background Data 1698, 2126, 2132
Bacteria 1931
BAFF 2027
Baikal Seal 519
Bakuchiol 437
Bama Pig 2142
Barrier Disruption 1621
Basal Insulin 1650
Base Excision Repair 1457, 2282
Bayesian 479
BBDR 61
BBDR-HPT Axis Model 440f
BBS 1643
BCL-6 248
BCOP 1020, 1021, 1022
BCRP 191
BDE 47 457
BDE-153 458
BDE100 2204
Bead-Based Immunoassay 441
Beas2B Cells 1968
Behavior 557, 848b, 1347h, 1748, 1749, 1805, 1806, 1837, 1857, 2155
Behavioral Experience 1340
Behavioral Sensitization 1744
Behavioral Testing 173i
Behavioral Toxicity 1347
Belomycin 1977
Benchmark Dose 617, 629, 1264a, 1478
Benchmark Dose Modeling 618, 622, 623, 630
Benchmark Doses 1009
Benzene 228, 235, 237, 1560, 2234x
Benzo(a)pyrene 71, 615, 616, 1077, 1109, 1500, 1505, 1509, 1723
Benzo[a]pyrene 491, 1271, 1572, 1683
Benzopyrene 2023
Benzyl Acetate 1594
Beryllium 781
Beta-Alanine 811
Beta-Ionone 1596
Beta-Secretase 1641
Bifenthrin 62, 1842
Bifurcation 438
Big Blue Transgenic Mouse 1943i
Bile Acid 1200b, 2122
Bile Acids 1498
Bile Duct Hyperplasia 2124
Bile Salt Export Pump (BSEP/ABCB11) 1883, 1887
Biliary Excretion 901, 1883
Binary PAH Mixtures 223e, 1007
Binding 684
Binding Assay 1087c
Bioaccessibility 1255, 1280
Bioaccumulation 663, 669d, 669e
Bioactivation 253, 552b, 1042
Bioanalysis 294, 878, 879, 880, 881
Bioanalytical Method Validation 877
Bioassay 1090
Bioavailability 28, 1556, 1831i
Biochemical 1993
Biochemistry 514
Biocide 1813, 2176
Biocompatibility 947, 951, 1616f
Biocompatibility Testing 899, 950
Biocorona 818
Biodegradation 586
Biodiesel 2294, 2296, 2298
Biodiesel Biofuel Blends 2295
Biodiesel Exhaust 1234, 1562
Biodiesel Inhalation Exposure 1563
Biodiesel/Diesel Exhaust 1242g
Biodiesel/Diesel Exhaust Particulate Matter 1242h
Biodisposition Kinetics 839
Biodistribution 888, 896, 901e, 2037
Biodistribution Kinetics 1998
Bioenergetics 312e, 378g
Biofuel 1347b, 1347c, 1347d, 2250f, 2294, 2297, 2298
Biofuels 1006a, 1347a, 2293
Biogas 2244
Biogenesis 712
Bioindicator 651, 1863b
Bioinformatics 418, 423, 425, 2097, 2250j, 2273y
Bioinformatics Tools 2092, 2093, 2094, 2095, 2096
Biokinetic Model 77
Biokinetics 1220
Biological Activity 1973
Biological Agents 2236
Biological Matrices 1558
Biological Modeling 94, 96e, 96i, 137, 440d, 440e, 2250f
Biological Models 2092
Biological Pathways 1062g, 2095
Biologicals 2196
Biologics 267, 419, 2111, 2196r
Biomaker 286
BioMap 1647
Biomarker 13, 99, 100, 101, 106, 114, 117, 122a, 122b, 122c, 122e, 122g, 272, 372, 380, 417, 722, 1387, 1389, 1515, 1521, 1525, 1536, 1538, 1539, 1549d, 1549e, 1549f, 1550, 1644, 2043, 2196bb, 2278
Biomarker of Arsenic Toxicity 1682
Biomarker Qualification 1434, 1549b
Biomarkers 84, 97, 102, 105, 107, 111, 119, 216, 343j, 867, 1006b, 1023, 1297, 1334, 1524, 1528, 1529, 1531, 1543, 1546, 1549c, 1929, 2052, 2226, 2255, 2274, 2275, 2276, 2277, 2279, 2286, 2290
Biomarkers and Biomonitoring 81, 662, 1558
Biomarkers for Exposure 116
Biomarkers of Arsenic Toxicity 977
Biomarkers of Exposure 83, 1526
Biomonitoring 96h, 116, 778, 1065, 1552, 1568, 1570, 1573, 2234l, 2234n, 2234p
Biomonitoring Data 2250c
Biopharmaceutical 269
Biopharmaceuticals 989, 2086, 2150, 2196o, 2305
Biopotency 886, 2118
Biosimilar 276
Biotherapeutics 294
Biotransformation 509, 512, 539a, 652, 2004h, 2234h
Biotransformation/Cytochrome P450 520
Biphenyl 1099
Birth Defects 424
Bisphenol A 539b, 621, 1071, 1344, 1346, 1517, 1570, 1713e, 1713f, 1884, 2054, 2184, 2213a, 2234k, 2234l, 2270
Bisphenol A (BPA) .. 52, 96h, 134, 357, 945, 946, 1129c, 1345
Bisphenol S 151, 2234k
Bisphenols 1064
Biz-2 792
Bizzy Nut 792
Black Carbon 223h, 1210
Bladder Cancer 244
Bladder Cancer Risk 545
Bleomycin 1211, 1800, 1801, 2267
Blood 598, 848a, 2234a
Blood Lead Level 230, 632d
Blood Lead Levels 778
Blood Mercury 1260
Blood Pressure 223f, 2049
Blood Profiles 806
Blood Sampling 2160
Blood Vessel 485
Blood Volume Reduction 861
Blood-Brain Barrier 18, 354, 378i, 942e
Blood-Testis Barrier 1701
BMAA 941
BMDL 604
BMP 163
BMP2-Inducible Kinase 222
BMS-986094 ..... 849, 850, 851, 852, 853, 854, 855, 856, 857
Body Composition 281, 2213b
Bone 1085, 1325, 1362, 1651
Bone Homeostasis 1283
Bone Loss 802
Bone Marrow Micronucleus Test 462
Bone Marrow Safety 1636
Bone Marrow Toxicity 866, 2038
Bone Marrow Transplantation 1900
Boric Acid 1775
Botanicals 790
Botulism 581
Bovine 1297g
BPA 1522, 2234j, 2268
BPS 1522
Brain 40, 366, 824, 1087n, 1342, 1347g, 1391
Brain Aging 378g
Brain Development 1346
Brain Disposition 1862
Brain Imaging, Transcriptomics 1347i
Brain Metastases 893
Brain Microvessel Endothelial Cells 353
Brain Slice Culture 1351
Brake Dust Inhalation 1215
Breast Cancer 264, 265a, 436, 915, 978e, 1096, 1297l, 1463, 1493, 1496, 1501, 1922e, 2129c, 2259, 2260
Breast Milk 1534
Breastfeeding 632e

Brominated Fire Retardants 1087x
Brominated Flame Retardant 457, 901b, 922d
Brominated Flame Retardants 1087w
Bromodichloromethane 736, 1187, 2030
Bromopropane 1087
Bronchial Epithelial Cells 603h, 860
Bronchiectasis 1730
Bronchiolitis Obliterans 2234t
BSEP 1200b, 1899d
Budding Yeast 524, 526
Building Air Exchange Rate 1581
Bulky DNA Adducts 1943a
Butachlor 50% EW 398
Butanol 349
Butter Flavoring 1575, 1610
Butyl Benzyl Phthalate 1808
Butyrylcholinesterase 1752
Bystander Effect 1935
C-C Chemokine Receptor 2 (CCR2) 1005
C-DIMs 1131, 1143
c-Jun-N-Terminal Kinase 1172, 1181
C. elegans 38, 172, 173o, 364, 932, 1378, 1736c, 1848, 1849, 1863c, 1995
C. violaceum 499
C57BL/6 Mice 1747b
Ca2+ Imaging 1833
Ca2+ Oscillations 1842
Caco-2 with CES-2 266
Caco2 680
Cadiotoxicity 1129e
Cadmium 74, 244, 301, 904, 960, 1062b, 1200d, 1245, 1246, 1247, 1248, 1249, 1250, 1251, 1252, 1253, 1254, 1264a, 1264b, 1264c, 1269, 1274, 1297k, 1322, 1327, 1448, 1506, 1706, 1825, 1937, 2048, 2222
Cadmium Oxide Nanoparticles 75
Caenorhabditis elegans 151, 931, 1377
Caffeic Acid Phenethyl Ester 797a, 1110a
Caffeine 343i
Calcineurin Activity 870
Calcium 382, 1371
Calcium Channel Blockers 570
Calcium Channels 1377
Calcium Dysregulation 1368b, 1372
Calcium Homeostasis 1256, 1834
Calcium Mobilization 1645
Callahan Mine Superfund Site 665
Caloric Restriction 738, 2207
Calorie Restriction 1720
Calreticulin 1148
Camels 336
CamKII 306
CAMVA 1020, 1022
Cancer 225, 252, 732, 734, 783, 1274, 1297k, 1300, 1322, 1327, 1491, 1499
Cancer Dose-Repsonse 243
Cancer Mode of Action 239, 1831k
Cancer Prevention 249
Cancer Progression 1493
Cancer Risk Assessment 261, 619
Cancer Stem Cell 265e
Cancer Stem Cells 264, 1463, 1920
Cancer Therapy 259, 466, 1514
Canine 404
Canine Kidney 320
Cannabinoid Receptor 214
Cannabinoid Receptors 2005
Cannabinoids 922, 1510, 2006
Capecitabine 893
CAR 1134
CAR/PXR 265c, 1135, 1151
Carbamazepine 1174
Carbendazim 681, 689a
Carbohydrate Malabsorption 1652
Carbohydrate Metabolism 1011, 1327a
Carbohydrazides 1639
Carbon 1240
Carbon Black 668
Carbon Black Nanoparticles 1953, 2004e
Carbon Capture 1229f
Carbon Monoxide 921
Carbon Nanomaterials 1468, 2301
Carbon Nanotube 20, 21, 25, 592, 603e, 1974, 1983
Carbon Nanotubes 22, 23, 584, 595, 603f, 1467, 1468, 1949, 1981
Carbon Tetrachloride 412
Carbon-Based Nanomaterials 24, 603l
Carbonyl Sulfide 362
Carboxylesterase 51
Carboxylesterases 189
Carcinogen 2194
Carcinogenesis 255, 265d, 265e, 961, 972, 1088, 1090, 1103, 1105, 1110g, 1290, 1297e, 1447, 1449, 1495, 1508, 1808, 1831d, 2131
Carcinogenesis Testing in Zebrafish 511
Carcinogenic Pathways 240
Carcinogenic Polycyclic Aromatic Hydrocarbons 706
Carcinogenicity ... 23, 265, 780, 1990, 2133, 2261
Carcinogenicity Study 2196z
Carcinogenicity Testing 1494
Cardiac 215, 1302, 1661, 2084
Cardiac Biomarker 1549a
Cardiac Cell Therapy 871
Cardiac Contractility 1619
Cardiac EMT 496
Cardiac Fibrosis 502
Cardiac Functionality 1060
Cardiac Insulin Resistance 483
Cardiac Lipotoxicity 482
Cardiac Toxicity 486, 717, 1129c
Cardiac Troponin 500
Cardiogenesis 184
Cardiolipin 1003, 1520, 1777
Cardiometabolic Risk 1314
Cardiomyocyte 478, 764, 765, 766, 767, 768, 769, 1129b
Cardiomyocyte Differentiation 163, 1909
Cardiomyocytes 36, 1126, 2085
Cardiomyogenesis 1459
Cardiomyopathy 480, 493
Cardiopulmonary 2141
Cardiopulmonary Toxicology 1242
Cardiorespiratory 491
Cardiotoxicity 32, 36, 100, 110, 481, 494, 504, 1062d, 1111, 1113, 1115, 1117, 1120, 1129, 1129f, 1616g, 1639a, 1772, 1903, 1908, 1910, 1918, 1919, 2082
Cardiotoxicity Mechanisms 1112
Cardiovascular 14, 16, 17, 152, 156, 468, 469, 473, 474, 475, 479, 488, 492, 504c, 581h, 1128, 1235, 1240, 1249, 1549e, 1549h, 1787, 1795, 2069, 2080, 2081, 2142, 2214, 2301, 2329
Cardiovascular and Blood Pressure Data 504a
Cardiovascular and Respiratory Safety Assessment 503, 1432
Cardiovascular Development 1087u
Cardiovascular Disease 15, 499, 1528, 1685, 1822, 2213
Cardiovascular Drug Safety 851, 2196w
Cardiovascular Effects 876d, 1810
Cardiovascular Function 1982
Cardiovascular Safety 477, 2086
Cardiovascular Safety Pharm Study 503
Cardiovascular Toxicity 500
Cardiovascular Toxicology 487, 546
Career 2116
Carnosine 811
Carrageenan 341, 342, 343, 343f
CASE Ultra 440k
Category Formation 435, 2273x
Catheterized 2137
Causation 233, 719, 721, 724
Caveolin-1 1124
ccA/ccB 1506
CCR2 2034
ccRCC 1506
CD 405
CD24 Knockout 453
CD25 2012
CD32 2023
CD36 737
CD4 966
CD4 Cells 141
CDISC-SEND 427
Cdx2 918
Cell 376
Cell Culture 603b, 1617
Cell Cycle 301, 603c, 906, 913, 1900
Cell Cycle Arrest 2320
Cell Cycle Regulation 587
Cell Death 312f, 603c, 1735
Cell Death Pathways 1784
Cell Death/Apoptosis 304, 1345
Cell Differentiation 176
Cell Impedance 1621
Cell Proliferation 195, 257
Cell Signaling 1734, 2050
Cell State 418b
Cell Toxicity 1831j, 2203
Cell Transformation 830
Cell Type 393
Cell Viability 291, 527
Cell-Based 2196q
Cell-Based Assay 1151
Cell-Based Screening 167, 920
Cell-Mediated Immunity 2318
Cellular Toxicity 1055
Cellular Uptake 1958
Centrosome 1272
CeO2 Nanoparticles 815, 841d, 1973d
Ceramide 2058
Cerebrospinal Fluid (CSF) 2163a
Cerium Oxide 2004b
Cerium Oxide Nanoparticles 1232
Ceriumoxide 1970
CFD-PBPK 772, 773
CFD-PBPK Model 69
CFU-GM 798, 1920
Chagas Disease 1638
Challenges 2117
Characteristics 1395
Characterization 641
Checkpoint Kinase 1661
Chelation 2230
Chemical Allergen 984
Chemical Allergy 971, 985
Chemical Database 30
Chemical Databases 421
Chemical Dispersants 448
Chemical Domain 30
Chemical Mixture Methodology 2241
Chemical Prioritization 647
Chemical Reactivity 2273, 2273d
Chemical Release 644
Chemical Respiratory Allergy 991
Chemical Risk Assessment 30, 160
Chemical Safety 2273n
Chemical Sensitizer 2009
Chemical Stress 123
Chemical Threat 360
Chemical Warfare Agent 626
Chemical Warfare Nerve Agent 2182
Chemical Weapons 567, 2249
Chemical-Disease Interactions 421
Chemicals of Concern 1582
Chemicals Used in Household Products 1223
Cheminformatics 433
Chemoprevention 794, 813c, 1513, 1718
Chemoprotection 985
Chemotaxis 2034
Chemotherapy 308, 2187, 2196x
Chemotherapy-Induced Toxicity 173l
Chemotypes 31, 2254
Chicken Liver 171
Child Development 704
Childhood Allergy 107
Childhood Obesity 235a
Children 96g, 223h, 843, 846, 848a, 1417, 1551, 1580, 1589, 1766, 2228, 2232, 2234x, 2287, 2288, 2289
Children Exposure 632e
Children's Health 703
Chiral Enrichment 594
Chiral PCBs 510
Chlordane 2237
Chlorination 661
Chlorine 626, 627
Chloroacetates 1018
Chloroanilines 2064
Chloromethyl/Methyl-Isothiazolinone (CMIT/MIT) 2234y
Chlorpromazine 1192
Chlorpyrifos 61, 81, 82, 654, 670, 687, 688, 689, 1750, 1752, 1805, 1857, 1858, 1860, 1861
Chlorpyrifos (CPF) 1859
Chlorpyrifos Oxon 688
Cholestasis 1192, 1193, 1887
Cholesterogenesis 1266
Cholesterol 1207, 1264
Cholesterol Transport 2213
Choline 2209
Cholinergic Receptors 1372
Cholinesterase Inhibition 688
Cholorogenic Acid 1110b
Chorioallantoic Membrane 1996
Choroid Plexus 1246, 1390
Choroid Plexus (CP) 1348
Chromatin Immunoprecipitation 973
Chromatin Structure 954f
Chromium . 73, 780, 954d, 969, 1269, 1271, 1272, 1290, 1293, 1296, 1320, 1675, 2222, 2233
Chromium (VI) 265e, 1924
Chromium Biomarker 1541
Chromolaena odorata 1200c
Chromosomal Aberration 650
Chromosome Aberration 461
Chronic Beryllium Disease 781
Chronic Exposure 1382
Chronic Inflammation 996
Chronic Obstructive Airways Disease 1209
Chronic Obstructive Pulmonary Disease 997
Chronic Toxicity 284
Chrysin 2063
Chrysotile 1215
Chrysotile Asbestos 1229g
Cichlids 1073
Cigarette 1490
Cigarette Smoke 255, 354, 393, 415, 443, 531, 874, 1216, 1504, 1518
Cigarette Smoke Exposure 413
Cigarette Smoke Exposure *In Vitro* 1054
Cigarette Smoke Particles 66
Cimzia 1659
Circadian Clock 2129b
Circadian Rhythm 1501, 1761, 2222
Circulating Biomarker 122f
Circulating microRNA 102
Circulating microRNAs 109
Circulating miRNAs 122f, 976
Circulatory Changes 2299
Cisplatin 312b, 2058
Clastogenicity 813b

Clastogens ... 464
Cleaning Products ... 649b
Clearance ... 592
Cleft Palate ... 183, 2273f
Clinical ... 2, 2278
Clinical Chemistry ... 2151a
Clinical Medicine ... 1471
Clinical Pathology ... 287, 1548, 2134, 2137
Clinical Toxicology ... 876b
Clinical Trial ... 88
Clofibrate ... 1804
Clostridial Neurotoxins ... 1922c
Cluster ... 1616b
Cnestis ferruginea ... 806
CNS Effects ... 1224
CNS Safety ... 2196k
CNTs ... 591
CO2 ... 2136
Coagulation ... 1867
Coagulation Parameters ... 2151b
Coal ... 667
Cobalt ... 77, 954d, 1214, 1268, 1269, 1276
Cobalt Chromium ... 603j
Cobalt Nanoparticles ... 1954
Cobalt, Metal ... 1414
Cobinamide ... 581d
Cocaine ... 1288
CoCl2 ... 1804a
CoCr-Alloy Particles ... 289
Cocrystals ... 525
Coculture ... 590, 1967
Cocultures ... 1042
Coffee ... 2234t
Cognitive Deficits ... 1845
Cohort Study ... 243
Colitis-Associated Colon Carcinogenesis ... 1097
Collagen ... 1006
Collagen-Induced Arthritis ... 999
Colloidal Silica ... 2000
Colombia ... 667
Colon ... 1109, 1505, 1509
Colon Cancer ... 1095, 1110b, 1512
Colon Carcinoma ... 322
Colorant ... 948, 949
Colorectal Cancer ... 256
Column Switching Technique ... 1519
Combination ... 1, 447
Combined Exposures ... 1416, 1748
Comet Assay ... 443, 467c, 789, 1957
Communication ... 2087, 2088, 2089, 2090
Community Ecology ... 1419
Community Education ... 876b
Community Engagement ... 1675
Community-Engaged ... 1676
Comparative Metabolism ... 1895
Comparative Toxicity ... 632f
Comparative Toxicogenomics Database ... 2096
Comparative Toxicology ... 2281
Complement ... 743
Complex Mixtures ... 1271
Comprehensive Measurement ... 455
Computational ... 440, 581b, 2234i
Computational Approaches ... 694
Computational Biology ... 2255
Computational Model ... 2182b
Computational Modeling ... 552, 1087p
Computational Modelling ... 79
Computational Models ... 770, 771, 772, 775
Computational Predictions ... 2273a
Computational Toxicology ... 26, 220, 429, 433, 440c, 1066, 1140, 2097, 2273c, 2273m, 2273n, 2273v, 2273z, 2273cc
Conazole Fungicides ... 1079
Concentrated Ambient Fine Particulate Matter ... 1239
Concentration Addition ... 1016
Concentration Response ... 2273j
Concentration-Response ... 614
Confocal Microscopy ... 1025
Confocal Raman Spectroscopy ... 2174
Congener and Species-Specific REPs ... 2201
Congenital Hyperinsulinism ... 2196j
Connexin 43 ... 575
Consequence Assessment ... 325
Consequence Modeling ... 325
Constitutive Androstane Receptor (CAR) ... 50, 1160, 1161
Construction Materials ... 642
Consumer Products ... 1589, 2234s, 2250i
Contact Allergy ... 982
Contact Dermatitis ... 876c, 979, 2040
Contact Hypersensitivity ... 126, 986
Contact Sensitizer ... 123
Content-Management System ... 2250l
Continuing Education ... 1767
Contractility ... 1120
Conventional Toxicity Assays ... 1297c
Convulsion ... 2196v
Convulsions ... 552g
Cookstove ... 1204
COPD ... 1203
Copper ... 1391, 1448, 2220
Copper Mining and Smelting ... 2234o
Copper Nanoparticles ... 1975
Copy Number Variation ... 2123
Coregulator Recruitment ... 1150
Coregulators ... 1063, 1154
Corneal Damage ... 578, 581f
Corneal Endothelial Cells ... 581a
Corneal Wound Repair ... 859
Corticoids ... 1212
Cosmetic ... 1029
Cosmetic Ingredients ... 27, 1586, 1600
Cosmetics ... 632, 632h, 782, 1604, 2240, 2248
Cosmetics Regulation ... 648
Countermeasure ... 581d
Courtroom ... 719, 720
Covalent Modification ... 1717
COX-2 ... 679
Coxsackievirus ... 394
cPLA2 ... 200
CPT I ... 504
Cramer ... 420
Criteria Air Pollutants ... 1018c
CRM1 ... 1507
Crocidolite ... 1215
Crontonaldehyde ... 1523
Crop Protection Formulations ... 408a
Cross-Reactivity ... 145a
Cross-Species Dosimetry ... 69
Cross-Species Extrapolation ... 2280, 2284, 2285
Crude Oil ... 979
Crude Oil/Dispersant ... 1713i
Cryopreserved Hepatocytes ... 1631
Crystal ... 2065
Crystalline Silica ... 140, 1713u
CSAF ... 61
CSF ... 2152
CSF Sampling ... 344
CSF-1 ... 2196p
CSF1-R ... 1200
CT Radiation ... 842
CT Scanning ... 901c
Cu Nanoparticles ... 833
Cu Transporting Genes ... 1390
Cumulative Risk ... 692
Cumulative Risk Assessment ... 231, 1816
Cumulus-Oocyte Complex ... 1075
Curcuma longa L. ... 1943
Curcumin ... 794, 940, 1922e
Cutaneous Wound Repair ... 575
Cyanide ... 581d, 581j
Cyanide Antidote ... 574
Cyanobacteria ... 995
Cyanuric Acid ... 632g, 890
Cyclin ... 916
Cyclin D1 ... 1503
CyclinD2 ... 1129b
Cyclooxygenase ... 1234
Cyclosporin ... 1193
Cyclosporin A ... 2056
Cynomolgus ... 186, 468
Cynomolgus Macaque ... 118
Cynomolgus Macaques ... 125
Cynomolgus Monkey ... 197, 407, 472, 954, 1061, 2126, 2152, 2154, 2155, 2156
Cynomolgus Monkeys ... 344, 1656
CYP Enzymes ... 505
CYP Expression ... 1110
CYP Inhibition ... 505
CYP1A1 ... 904
CYP1A1/1B1 Activities ... 1007
CYP1A1/2, CYP3A4 ... 1043
CYP1B1 ... 293, 505, 506
CYP2A5 ... 1200d
CYP2B ... 522, 1200i
CYP2B6 ... 527, 541, 2204
CYP2J2 ... 1129f
CYP2S1 ... 919
CYP450 ... 1087f
Cypermethrin ... 1531
CYPs ... 517
Cystatin C ... 2048
Cyto/Genotoxicity ... 1279
Cytochrome C ... 1278
Cytochrome P450 .. 512, 514, 516, 524, 530, 531, 534, 536, 552b, 652, 954e, 1151, 1218
Cytochrome P450 (CYP) ... 539d, 1736b
Cytochrome P450 1A1 (CYP1A1) ... 1518
Cytochrome P450 2A13 ... 511
Cytochrome P450 2B ... 539a
Cytochrome P450 Reductase ... 508, 510
Cytochrome P4501A1 ... 535, 539
Cytokine ... 484, 1547
Cytokine Analysis ... 270
Cytokine Profiles ... 1759
Cytokine Signaling ... 2031
Cytokine Storm ... 270
Cytokines ... 991, 994, 1199, 1208, 1264c, 1713p, 1725, 2317
Cytoprotection ... 1170
Cytoskelton Molecules ... 127
Cytotoxic ... 649a
Cytotoxicity ... 312, 449, 677, 784, 785, 947, 954c, 1199, 1276, 1376, 1614, 1628, 1629, 1933, 1944, 1957, 1959, 1973b, 1978, 2004c
Cytotoxicity Profiling ... 307
Cytotoxicity Screening ... 1633
Danio rerio ... 1681
Daphnia magna ... 173p
Daphnia pulex ... 1263
DART ... 1698, 1699
Data Analysis ... 378a, 2273y, 2273aa
Data Integration ... 423, 425, 1409, 2273l, 2273m, 2273y
Data Sharing ... 644
Database ... 432, 892, 1087a, 2261, 2273k
Daycare ... 1419
DcR3 ... 128
DDE ... 1515, 2198
DDI ... 440i
DDT ... 1567
Death Protein sPLA2 ... 1165
Decabromodiphenyl Ether ... 1713h
Dechlorane Plus ... 659
Decision Making ... 1824
Decorporation Agent ... 1624
Degradation ... 1925
Degranulation ... 1315, 2032
DEHP ... 96i, 177, 300, 2186
Delayed Effect ... 1070
Delta 9-Tetrahydrocannabinol ... 1776
Delta-9-Tetrahydrocannabinol ... 569, 2007
Deltamethrin ... 689b, 1845
Deltamethrin, Cis-Permethrin, Transpermethrin ... 897
Dendrimers ... 1973i, 1973j
Dendritic Arborization ... 351
Dendritic Cell ... 122b
Dendritic Cells ... 126, 1002, 2005, 2011
Dental Material ... 945, 946
Deoxynivalenol ... 318
Depleted Uranium ... 1295, 1559, 1942
Depression ... 996
Dermal Absorption ... 1586, 2172, 2173
Dermal Administration ... 2154
Dermal Exposure ... 632, 648, 2234f
Dermal Risk Assessment ... 762
Dermal Toxicity ... 2219
Dermatotoxicity ... 572
Detergents ... 2234aa
Detoxification ... 539a
Development ... 195, 205, 209, 1071, 1129d, 1712, 1860, 2074, 2075
Development Neurotoxicity ... 201
Developmental ... 636, 1343, 1736e, 2079
Developmental and Reproductive Toxicity ... 201, 220
Developmental and Reproductive Toxicology ... 2196a
Developmental Biology ... 216
Developmental Cardiotoxicity ... 207
Developmental Delay ... 1713k
Developmental Immunotoxicity ... 1660, 2017
Developmental Immunotoxicology ... 1336
Developmental Neurotoxicity ... 155, 175, 207, 1344, 1345, 1738, 1739, 1747a, 1748, 1749, 1753, 1764, 1764b, 1837, 2077
Developmental Neurotoxicology ... 1336, 1347e, 1347i, 1747e
Developmental Origins of Adult Disease ... 48, 52, 1087u
Developmental Origins of Health and Disease ... 1687
Developmental PAH Toxicity ... 223e
Developmental Regulation ... 1497
Developmental Stress ... 1087m
Developmental Toxic Effects ... 217
Developmental Toxicity ... 35, 89, 173m, 207, 223b, 223d, 617, 1087o, 1087r, 1087v, 1087w, 1915
Developmental Toxicology ... 75, 199, 489, 1595, 2078
Developmental Toxicology Assay ... 1917
Dexamethasone ... 910
DFP ... 579, 1855
DHA ... 1688
Di-n-Butyl Phthalate ... 198
Di(2-ethylhexyl)phthalate ... 1129c
Diabetes 188, 295, 339, 711, 879, 880, 1083, 1252, 1324, 1515, 1540, 1542, 1700, 2198, 2324
Diacetyl ... 232, 614, 632f, 1574, 1575, 1610, 2234t
Diarrhea ... 1621
Diastolic Pressure ... 2213b
Dibenzo[def, p]Chrysene ... 513, 539d
Dibutyl Phthalate ... 1705
Dichlorophenols ... 223g
Dichloropropene ... 63
Diclofenac ... 859
Dieldrin ... 2237
Diesel ... 1236
Diesel and Silica ... 1242a
Diesel Emission Particles ... 1922b
Diesel Emissions ... 504c
Diesel Exhaust 492, 504c, 1232, 1233, 1235
Diesel Exhaust Particle ... 68
Diesel Exhaust Particles ... 312a, 353, 1242c
Diesel Inhalation Exposure ... 876d, 1563
Diet ... 1163a, 1616e
Diet-Induced Obesity ... 1870, 2071
Dietary ... 1567
Dietary Carcinogens ... 256

The numerals following each keyword refer to the relevant abstract number(s).

Dietary Exposure 2234q
Dietary Supplements 343d, 343h, 1469, 1470, 1471, 1472, 1473, 1474, 1475
Diethanolamine 619
Diethylene Glycol 2066
Differential Display 1502
Differential Toxicity 1583
Differentiation 603h
Differentiation/Proliferation 1906
Diffusion Tensor Imaging (DTI) 1364
Diindolylmethane 305, 1512, 2196y
Diisobutyl Carbinol 885
Diisobutyl Ketone 885
DILI 34, 418e, 1481, 1876, 1899d, 2278
DILI Prediction System 1643
Dilution 2151a
Dimethylarsenic 1311, 1313
Dinitrotoluene 1821
Dioxin 334, 907, 1158, 1639b, 2021
Dioxin Responsive Element 922c
Dioxin-Like Compounds 2201
Dioxins 96d
Diphenyl Ditelluride 1297d
Discovery Safety Assessment 1636
Disease 638
Disease and Susceptibility 956
Disinfection By-Products 1018a
Dispersant 668
Dispersants 669c
Dispersion Method 1974
Disposition 901d, 2157
Disposition/Pharmacokinetics 883, 901b
Dissolution 1963
Distribution 154
Dithiocarbamates 1853
Diversity Outbred 279
Division 1549f
DMAE Bitartrate 1606
DMSO Induction 1043
DNA 1491
DNA Adduct 455, 467a, 1094, 1523
DNA Adducts 1110g
DNA Damage 162, 171, 319, 324, 467c, 1449, 1457, 1938, 1973c, 2183, 2282
DNA Damage and Repair . 444, 1448, 1928, 1935
DNA Double-Strand Break 442, 467g, 1942
DNA Double-Strand Break Repair 1450
DNA Double-Strand Breaks 1450, 1931
DNA Fragmentation 1776
DNA Ligase I 1925
DNA Methylation .. 242, 955, 963, 966, 968, 969, 978a
DNA Methyltransferases 965
DNA Repair . 1295, 1447, 1451, 1930, 1934, 1943f
DNA Synthesis 1129b
DNA-Reactive Carcinogens 171
DNase I 312b
DNEL 612, 643
DNEL Derivation 1826
DNT 1737
DNT Test 1058
Dog 539c, 2122, 2158, 2305, 2306, 2307, 2308
DOHAD 964
Domoic Acid 1763
Dopamine 371, 924, 1288, 1330, 1371, 1379, 2103, 2105, 2108
Dopamine Release 2106
Dopamine Transporter 942c
Dopaminergic 1758, 2107
Dopaminergic Neurotoxicity 935, 1344, 1347h
Dorsal Root Ganglion 173l
Dose Addition 1713c
Dose Extrapolation 96g
Dose Formulation 1606
Dose Response 1934
Dose-Response 630, 632a, 632i, 1404, 1406
Dose-Response Assessment 606, 1831c
Dose-Response Modeling 628
Dosimetry 95, 440h, 817, 1227
Dosimetry Modeling 67
Doxil 1949
Doxorubicin . 1117, 1772, 1773, 1798, 2062
Doxycycline 509
Draize Eye Test 1027
Dried Blood Spots 1532
Drinking Water 173o, 661, 1314, 2250g
Drivers of Irritation 1027
Drosophila 218, 1332
Drosophila melanogaster 1062f
Drug 335, 1149
Drug Abuse Liability 1648
Drug Cardiotoxicity 109, 1112
Drug Combo Device 1616f
Drug Development 525, 2196l, 2196v
Drug Hypersensitivity 986
Drug Interaction 518
Drug Metabolism 157, 549, 552, 883, 917
Drug Metabolizing Enzymes 387
Drug Permeation 1040
Drug Processing Genes 1896
Drug Safety 267, 552c, 1481, 1514a, 1544, 2273k
Drug Safety Assessment 1432, 2196l, 2196o, 2273h
Drug Toxicity 2196l
Drug Transporters 80
Drug-Allergy 987
Drug-Drug Interactions 440j, 2067a
Drug-Drug Interactivity 1899e
Drug-Induced Hepatotoxicity 529, 1899b
Drug-Induced Kidney Injury 2255
Drug-Induced Liver Injury . 412, 537, 1168, 1199, 1618, 1647, 1866, 1878, 1883, 1898, 2031, 2273g
Drug-Induced Liver Injury (DILI) 1868, 1887, 2274, 2275, 2276, 2277, 2279
Drug-Induced Nephrotoxicity 105
Drug-Induced Vascular Injury 112, 1549f
Drugs 875
Dry Eye 2127
dsRNA 330
Duodenal 2149
DUOX 2170
Dust 2311, 2312, 2313, 2314, 2315
DXA 281
Dynamics 711
Dyslipidemia 678
E-Cigarette 1614, 1615
E-Liquid 1614
E-Screen, A-Screen 1068
e15 ..... 1347b
Early Life Stages 608
Early Menarche 92
Earthworm 659, 834
Ebselen (EB-1) 580
ECG 477, 2146
ECG and QT Prolongation 472
Echinacea 798
Ecological Risk Assessment 662
Ecotoxicity 834
Ecotoxicological Assays 664
Ecotoxicology 655, 656
Ecotoxicology in Nematodes 662
Education 1435, 1436, 1437, 1438, 1439, 1440, 1662c, 1665, 1668, 1671, 1672, 1674, 1680, 1680a
Education and Career Development ... 1767
Education and Outreach .. 1663, 1667, 1677
Education Outreach 1662a
EEG 274, 275, 1863a, 2196v
EETs 1129f
Effects 1200c
Effects of Storage 2151b
Efficacy 564, 2121
EGCG 259, 1504
EGFR Signaling 1163b
EHMC 145b
Electric Arc Furnace 2219
Electrocardiogram 498
Electrocardiography 1242f
Electroencephalography (EEG) 2162
Electrolyte 2271
Electron Microscopy 1756
Electronic Cigarette 1015, 1615
Electronic Cigarettes 645, 1202, 1612, 1613, 2182a, 2225
Electrophile 1714, 1716
Electrophiles 1454
Electrophilic Stress 1736b
Electrophysiology 180, 1060, 1145
Electroretinogram 1641
Eleiyele Lake 1073
Elemental Analysis 1281
Elemental Imaging 1287
Eliglustat 1494
ELISA 863, 878
Embryo Development 440l
Embryo-Fetal Development 282
Embryonic Nutrition 1690
Embryonic Stem Cell 1909
Embryonic Stem Cell Differentiation 173g
Embryonic Stem Cell Test 173c
Embryonic Stem Cells 179, 1904, 1907
Embryonic Zebrafish 1747d
Emergency Response 1564
Emergency Risk Assessment 96c
Emission 642
Empagliflozin . 2196e, 2196f, 2196g, 2196h, 2196i
Emphysema 1250
EMT 247, 1496, 1888
Emulsion 78
Enantia chlorantha 793
Endocannabinoid 1750
Endocrine 211, 440e
Endocrine Activity 1087a
Endocrine Disrupting Chemicals 1072, 1087g
Endocrine Disrupting Compound 2195
Endocrine Disrupting Compounds 323
Endocrine Disruption 489, 1066, 1074, 2196d, 2250b, 2257, 2273i
Endocrine Disruptor 132, 223, 922d, 1018d, 1065, 1712
Endocrine Disruptor Screening 160, 161
Endocrine Disruptors 133, 173, 179, 551, 681, 1067, 1078, 1082, 1347, 2196c
Endocrine Screening 1087c
Endocrine Toxicology 1087j
Endocrine-Disrupting Toxicity 168
Endocytosis 841
EndoG 312b
Endogenous 1831c
Endogenous Adducts 1107
Endoplasmic Reticulum 1253
Endothelial Cells 1229e
Endothelial Dysfunction 595, 1121, 1125, 1518
Endothelial Progenitor Cells 1123
Endothelial Progenitor Cells (EPCs) ... 1901
Endothelial Spheroid 1062i
Endothelium 1922a
Endotoxin 1713m
Endotoxins 981
Energy 1018b
Energy Drinks 343i
Energy Homeostasis 1087k
Engine Emissions 1562, 1943a
Engineered Nanomaterials . 828, 872, 1689, 1973d, 1982
Engineered Tissue 1129e
Enolate 1170
eNOS 497, 787, 797a
Entecavir 2034
Enteric Bacteria 1284
Enterotoxicity 1911
Entropy 2273j
Environment 1351
Environmental Agents 1616g
Environmental Chemical 1149
Environmental Chemicals 1087o
Environmental Contaminants 424
Environmental Disease 730
Environmental Epigenetics 978
Environmental Estrogen 252
Environmental Exposure Limits 1264a
Environmental Exposures 48, 379, 669
Environmental Factors 638
Environmental Health Sciences 1669
Environmental Pollutants 107, 703, 921
Environmental Pollution 650
Environmental Risk Assessment 658, 2250g
Environmental Risk Factors 43, 44, 45
Environmental Toxicology 132
Enzymatic Biomarker 651
Enzyme 892
Enzyme Linked Immunosorbent Assay (ELISA) 669
Enzymes 2234aa
Eosinophils 118, 2328
EP Receptors 174
Epicardium 184, 490
Epicatechin 1583
Epidemiological Study 21
Epidemiology 9, 54, 89, 225, 227, 1341, 2070
Epiderm 943
Epigallocatechin Gallate 813d
Epigenetic 954g, 964, 969, 1707
Epigenetic Changes 974
Epigenetic Programming 1690
Epigenetic Toxicology 1840
Epigenetics 50, 187, 355, 702, 908, 954e, 954h, 956, 957, 958, 959, 960, 961, 963, 965, 967, 970, 971, 972, 973, 975, 978a, 978b, 978c, 978e, 1282, 1516, 1687, 1704, 1706, 1831d, 1832, 1861, 1904, 2008, 2050, 2180
Epigenome 968
Epigenomics 704, 707
Epithelial Barrier 1726
Epithelial-to-Mesenchymal Transition 1500
Epithelial-to-Mesenchymal Transition (EMT) 2004b, 2063
Epithelium 848c
Equol 1585
ER Stress 869, 1168, 1195, 1845, 1892
Erionite 130
ERK Pathway 1092, 1951
ERK/JNK 1736b
Erythrocyte 1267
Erythrocyte Membrane Proteins 1533
Essential Elements 609
Essential Oil 2166
Essential Oils 312f, 467
Estradiol 1077, 2188
Estrogen 173h, 1090, 2190
Estrogen Activity 1064
Estrogen Agonists 1831f
Estrogen Chemical Carcinogenesis 796
Estrogen Receptor 173b, 211, 1087c
Estrogen Receptor (ER) 1072
Estrogen Receptor Alpha 1110a
Estrogen Receptors 1069
Estrogen-Related Receptor 2270
Estrogenic Activity 161, 1067
Estrogens 1087a
Estrous Cycle 467c, 1070
Ethanol 194, 254, 912, 1200d, 1200e, 1413, 2294
Ethanol Hepatotoxicity 299, 1889

Ethics ... 2102
Ethinylestradiol ... 1087t, 1937
Ethionamide ... 1794
Ethyl Tertiary Butyl Ether ... 1697
Ethylenebisdithiocarbamate ... 680
Etofenprox ... 673
Eukaryotic Initiation Factor ... 786
Europium ... 1973
Euthanasia ... 2136
Evidence ... 720
Evidence Integration ... 1482, 1483, 1484, 1485, 1486, 1487, 1489
Evolution ... 2280, 2281
Ex Vivo ... 443, 603, 1051
Ex Vivo Imaging ... 2078
Excipient ... 1654
Executive Function ... 2163
Exogenous Adducts ... 1107
Experimental Autoimmune Encephalomyelitis (EAE) ... 942
Experimental Design ... 629
ExpoCast ... 2234m, 2234n, 2250a
Exposome ... 115, 422, 868, 1684
Exposure ... 82, 88, 411, 423, 1517, 1552, 1567, 1571, 1574, 1580, 1830, 2234i, 2234z, 2235, 2293
Exposure Assessment ... 20, 22, 603f, 1554, 1562, 1564, 1565, 1976, 2234p
Exposure Biomarkers ... 1572
Exposure Guidelines ... 627
Exposure Inference ... 2234m
Exposure Levels ... 1210
Exposure Modeling ... 1062h
Exposure Pathways ... 72
Exposure Reconstruction ... 2250c
Exposure Sources ... 2234s
Exposure Study ... 1814
Extracellular Signal-Regulated Kinases 1/2 ... 257
Extractables and Leachables ... 954a
Extracts ... 603i, 949, 951
Eye and Skin Corrosion and Irritation ... 1028
Eye Irritation ... 1019
Eye Stinging ... 1025
FACS ... 405
Factfinder ... 720
FAS ... 258
Fasting ... 865
Fat Accumulation ... 1194
Fatty Acid Ethyl Esters ... 384
Fatty Acids ... 190, 522
Fatty Liver ... 522, 2209
FcRn ... 278
FcγR ... 1335
FDA Drug Label ... 2273k
Fecundability ... 1420
Feed Formulation ... 1616a
Fellowship ... 1664
Fenhexamid ... 1087g
Ferritin ... 2234u
Ferritine ... 1723
Ferromanganese ... 1297b
Fertility ... 2148
Fertilizer ... 2234b
Fetal and Maternal Exposure Ratio ... 898
Fetal Brain Development ... 177
Fetal Origins of Disease ... 702, 707, 1690b
Fetal Programming ... 1689
FGF21 ... 910, 1189
Fiber ... 53
Fibrates ... 1160
Fibrin(ogen) ... 1191
Fibrinolysis ... 595
Fibroblast Growth Factor 21 ... 1188, 2045
Fibroblasts ... 1722
Fibrosis 552f, 603g, 1006, 1158, 1191, 1977, 2124
Fibrosis Biomarkers ... 603e
FICZ ... 1146
Fipronil ... 1862, 1863a, 1863b
Firefighter ... 1812
First-in-Human ... 2196aa
Fish ... 343a, 651, 669d, 669e, 1087h, 2234
Flame Retardant ... 173p, 622, 623, 1616a
Flame Retardants ... 212, 378c, 1713, 2234h
Flavinoid ... 1110e
Flavonoids ... 312
Flavoring Agents ... 67
Flow Cytometry 118, 404, 453, 1929, 1946, 2038
Flt3L ... 268
Fluorescently Labeled ... 838
Fluoride ... 495, 2047
Fluoro-Jade ... 603b
Fluoxetine ... 848b
Flutamide ... 1545, 1877
FMO3 ... 518, 1176
FOB ... 346
Folate ... 548, 1312
Folliculogenesis ... 2186
Food ... 331, 1017, 1395
Food Additive ... 324, 1394
Food Allergy ... 2028
Food and Pharmacology ... 635
Food Contact Materials ... 1584, 2234r
Food Contamination ... 325
Food Drinks ... 321
Food Flavorings ... 232
Food Ingredient ... 329
Food Ingredients ... 320, 1616
Food Juices ... 321
Food Processed Chemical ... 338
Food Safety ... 47, 326, 328, 333, 334, 338, 339, 343c, 343e, 1018d, 1526, 2234r
Food Safety/Nutrition ... 343d, 343h, 1713a
Foreign Body Granuloma ... 124
Formaldehyde ... 239, 262, 920, 1107, 1110f, 1521, 1809, 1830, 1926
Formulation ... 574
Fosb ... 242
Foxq1a ... 210
FQPA ... 59
Fra-1 ... 1264b
Fracking ... 1560, 1561, 2250e
Fracturing ... 1765
Fragrance ... 1605
Fragrance Ingredient ... 1601
Framework ... 1819, 1824, 1831b
Fresh Water Fish ... 650
Fresno, California ... 424
Frontal Cortex ... 2231
Fruit Pulp Extract ... 1514b
FRY Protein ... 1497
Fuels ... 2293
Fullerene ... 1991
Fullerene *In Vivo* ... 2002
Fumonisin ... 343b, 343j
Fumonisin B_1 ... 314
Fumonisins ... 315
Function ... 378b, 378c
Functional Profiling ... 418d
Functional Proteomics ... 1063, 1154
Fundulus heteroclitus ... 665
Fungi ... 1536
Furan ... 957
Furosemide ... 525, 1185, 1196
Fusarium ... 343b
FXR ... 1149, 1162, 1889
GABA ... 557, 1338, 1366, 1367, 1368, 1764e
GABAa Receptor ... 1376
GADD45a ... 1927
Ganoderma lucidum ... 1242c
Gap Junction ... 302
Gasoline ... 96b
Gasoline Vapor ... 1347a
Gastrointestinal Model ... 332, 779
GDL 1 Cells ... 467b
Gender ... 122i, 1301
Gender Difference ... 544, 1172
Gene Expression ... 173n, 187, 309, 414, 416, 603d, 706, 823, 844, 922a, 922b, 1207, 1301, 1384, 1713f, 1713u, 1938, 1988, 2273e, 2273q
Gene Expression Analysis .. 842, 1245, 1265
Gene Induction ... 527
Gene Microarray ... 942
Gene Mutation ... 447
Gene Regulation ... 911, 975
Gene Regulation/Signal Transduction ... 1106
Gene Signatures ... 1479
Gene Therapy ... 744
Gene-Environment ... 411
Gene-Environment Interactions ... 1743
General Anesthetics ... 2077
Generalized Additive Models ... 231
Genetic ... 41
Genetic Diversity ... 1480
Genetic Instability ... 1943g
Genetic Polymorphisms ... 552a
Genetic Risk Factor ... 543
Genetic Sequencing ... 2098, 2101
Genetic Susceptibility ... 1493, 1986, 2004f
Genetic Toxicology ... 3, 459, 753, 756
Genetic Variation ... 1281
Genetics Reference Panel ... 1062f
Genistein ... 333, 552d, 2185
Genome Profiling ... 526
Genome-Wide Association Study ... 1332
Genomic ... 722
Genomic Database ... 2093, 2094
Genomic Sequencing ... 2102
Genomics ... 122d, 702, 841d, 2099, 2308
Genotoxic Impurities ... 2263, 2265
Genotoxicity ... 23, 300, 319, 326, 441, 442, 449, 452, 457, 458, 460, 466, 467, 467e, 467f, 467g, 664, 1110, 1235, 1276, 1320, 1639, 1808, 1926, 1934, 1938, 1942, 1943e, 1943h, 1952, 1997, 2004c, 2004d, 2260
Genotoxicity Risk Assessment ... 454
Genotoxicology ... 1638
Genotoxin ... 1931
Geographic Clusters ... 2258
Germ Cell Toxicity ... 1693
Germ Cells ... 1700
Germ-Free ... 1896
Germline Disruption ... 1713j
Gestational Diabetes Mellitus ... 191
Gestational Exposure ... 2196b
Ghana ... 2239
GHS ... 639, 1022
GI Toxicity ... 1803
Giant Cells ... 2024
Ginkgo biloba Extract ... 1161
Ginkgo biloba ... 319, 955
GIS ... 666
Glia ... 1374, 1456
Glial-Neuronal Interactions ... 1753
Glioblastoma ... 1637
Glioma Cells ... 1510
Global Phosphoproteome ... 440l
Glomerulus ... 106
Gloxylase ... 203
Glucocorticoid ... 1651
Glucocorticoid Stress Response ... 1747e
Glucocorticoids ... 1754
Glucose ... 1713n
Glucose Metabolism ... 2187, 2325
Glucose Restriction ... 865
Glucose Tolerance ... 2330
Glucose-6-Phosphatase, Catalytic Subunit (G6PC) ... 922a
Glufosinate ... 1838
Glutamate Cysteine Ligase ... 1782
Glutamate Signaling ... 378d
Glutaredoxin ... 559
Glutathione ... 537, 1204, 1313, 1836, 1878
Glutathione-S-Transferase ... 1347j
Glyoxals ... 1771
Glyphosate ... 1848, 1849, 1850, 1851, 1863c
Gold Nanoparticles ... 598, 840
Gold Nanoparticles (Au NPs) ... 841e
Gold Nanorods ... 603k
Gonadectomy ... 1093
Göttingen Minipig ... 1525
Göttingen Minipigs ... 2147
Gout ... 2046
gp130 ... 596
GPCR ... 2273u
Gpt Delta Mouse ... 1326
Gpt Delta Rat ... 2132
Graph Theory ... 1731
Graphene ... 593, 1983, 2001
Graphene Nanomaterials ... 1968
Graphene Oxide ... 593
Green Tea Polyphenol ... 810
GRHL3 ... 1187
Groundwater ... 223i, 2246
Group House ... 346
GSH Conjugate ... 1094, 1549g
GSK3B ... 365, 916
GSNO Reductase ... 998
Guidance ... 1405
Guinea Pig ... 401
Gulf War Illness ... 1859
Gut Microbiota ... 1989
Gut Microflora ... 1726
Gutkha ... 1692
Gyrolab ... 119
h-ARS ... 2126
h-CLAT ... 1062e
H-FABP ... 504
H295R ... 1076
Haber's Law ... 1817
HaCaT ... 1804a
Hair Dyes ... 982
Hair Loss ... 2128
Hairless Mice ... 2167
Half-Life ... 469, 1362
Halogenated Phenolic Compound ... 1086
Hamsters ... 2310
Hand Bone ... 1291
Haploid ... 920
Haptenation ... 2036
Harmful Algae Blooms ... 364
Harmful and Potentially Harmful Constituents ... 2234v
Hazard Assessment ... 639, 649b, 1829, 2297
Hazard Characterisation ... 991, 1823
Hazard Identification ... 1831, 1831c
Hazardous Chemicals ... 96c
HbA1c ... 1540
HCN ... 1818
HDAC Inhibitors ... 973
HDL Cholesterol ... 2303
HDPE Reference Control ... 952
Health Code Numbers ... 2241
Health Disparities ... 959
Health Hazards ... 21
Health Monitoring ... 1553
Health Policy ... 1680a
Health Risk ... 2250d
Health Surveillance ... 1565, 1976
Heart ... 499, 504b
Heart Development ... 188
Heart Failure ... 1690b
Heart Rate Variability ... 1242b
Heart Weight ... 479
Heat ... 235
Heat Shock Protein ... 308, 1717, 1724
Heat Shock Proteins ... 1632
Heavy Metal ... 153
Heavy Metals ... 1389, 1555, 2216, 2217
Heavy Metals Residues ... 2229
Heavy-Duty Diesel Vehicle Emissions ... 2295

KEYWORD INDEX

Hematopoiesis 228, 1460, 1462, 2014
Hematopoietic 954g
Hematopoietic Stem Cells 687, 1900
Hematotoxicity 803, 2234x
Hemodialysis 938, 1535
Hemodynamic 473
Hemodynamics 2083
Hemophilia 1653
hepa-1 Cells 535
HepaRG 2273q
Hepatic 1177, 1200c
Hepatic Biochemical Parameters 1198
Hepatic Fibrosis 1888
Hepatic Gene Expression 1175
Hepatic Glutathione 1165
Hepatic Lipidosis 1157
Hepatic Metabolism 1087f
Hepatic Portal Vein 2158
Hepatic Protein Expression 192
Hepatic Steatosis 1153
Hepatic Stellate Cells and Liver Fibrosis 2200
Hepatic Stem Cell 1905
Hepatic Toxicity 1171
Hepatocarcinogen 450
Hepatocarcinogenesis 265b, 1100, 1104, 1513
Hepatocellular Carcinoma 246, 733, 955, 1538, 1937, 2123
Hepatocellular Tumors 265c
Hepatocyte 1192, 1200a, 1880
Hepatocyte Accumulation 1898
Hepatocyte Nuclear Factor 4 alpha 1495, 2206
Hepatocytes 307, 449, 669e, 1042, 1193, 1873, 1899a, 1921
Hepatomegaly 2206
Hepatoprotection 137
Hepatosteatosis 1200e
Hepatotoxicity 34, 94, 117, 269, 418b, 543, 713, 716, 803, 976, 1044, 1045, 1046, 1047, 1169, 1170, 1174, 1176, 1179, 1185, 1195, 1196, 1200, 1270, 1431, 1473, 1474, 1477, 1617, 1622, 1635, 1872, 1891, 1892, 1899a, 1922, 2273h, 2274, 2275, 2276, 2277, 2279
Hepatoxicity 32, 33, 388
Hepatoxicology 1412
HepG2 ..... 299, 458, 677, 1200f
HepG2 Cells 467h, 1245, 1769, 1944, 1968, 1969
Hephaestin 2128
Herbal Formulation 1590
Herbal Supplement 798, 1691
Herbicides 1863
Herpesvirus 1655, 2120
Hershberger 1713d
hESC-CM 1908
Heterocyclic Amines 923
Heterocyclic Aromatic Amines 1549
Heteroprotection 1164
Hexachlorophene 378f
Hexavalent 780
Hexavalent Chromium 610, 779, 1279, 1297f
Hexavalent Chromium (Cr (VI)) 1110d
HGPRT Locus 461
High Density Lipoprotein 19
High Glucose 1123
High School 1665, 1673
High School Education 1662a, 1669
High Throughput 440
High-Content 1639c
High-Content Analysis 1894
High-Content Imaging 173f, 1055, 1058, 1715, 1873, 1910
High-Content Screening 152, 155, 156, 418b, 1347k, 2260
High-Fat Diet 1153, 1166, 2330
High-Fructose Diet 2330
High-Performance Metabolic Profiling 115
High-Resolution Metabolomics 868
High-Throughput 173h, 1639c, 2273o, 2273z
High-Throughput Screen 534, 1355
High-Throughput Screening 467g, 1066, 1734, 1747, 1919, 2250b, 2259, 2273aa, 2273t, 2282
High-Volume Horizontal Hydraulic Fracturing 1282
Hip Implant 603j, 954d
Hippocampus 178, 1289, 1392a
hiPSC-Hepatocytes 1881
Histaminergic Reaction 288
Histology 942a
Histone Acetylation 1101
Histone Deacetylase 52
Histone Methylation 962
Histone Modification 50, 927
Histone Modifications 954f, 967
Histones 954h
Histopathological 1993
Histopathology 440
Histopathology Methods 1549b
Historical Data 2130
HIV 1913
HIV Drugs 869
HIV Transmission 705
HIV-Antiretrovirals 848
HIVgp120 2007
HMGB1 ..... 588, 940, 1789, 2026
HNF4A 918
HO-1 1292
HO-PBDEs 2234g
Homologous Proteins 2111
Homologous Recombination Repair 1924
Honeybee 1854
Hops 796
Hormone 252, 649a, 2268
Host-Microbe Interaction 45
House Dust 1551
Household Cleaner 813a
Housekeeping Genes 1727
Housing 633
HPLC 675
HPRT1 2046
Hras 265a
HSP 1724
Hsp90 Inhibitors 1632
HT-29 1292
Hu-hs1, 2 Enhancer 2022
Huh7 Cells 1043
Human 810, 1327d, 2172, 2273w
Human Adipose-Derived Mesenchymal Stem Cells 1916
Human Androgen Receptor 2270
Human B Cells 2016, 2018
Human Dendritic Cell 1062g
Human Development 731
Human Embryonic Stem Cells 2082
Human Epidermal Keratinocytes 820
Human Exposure 226, 2234s
Human Exposure Level 1031
Human Exposures 2217
Human Fibroblast-Like Synoviocytes 999
Human Health 730
Human Health Assessment 630, 2250l
Human Health Benchmarks 609
Human Health Effects 20
Human Health Risk Assessment 47, 770, 1555, 1809, 1815
Human Hematopoietic Stem Cell 2015
Human HepaRG Cell Line 1011
Human Hepatocyte Correlation 285
Human Hepatocytes 529, 1631
Human iPSC 1881
Human Kidney 74
Human Kidney Proximal Tubule Cells 2067
Human Neural Stem Cell (NSC) 290
Human Neurotoxicity Screening 1347k
Human Peripheral Blood Lymphocytes 2201
Human Placenta 191
Human Population 317
Human Prostate 1686
Human Relevance 236
Human Renal Proximal Tubule Cells 718
Human Risk Assessment 773, 774, 775
Human Safety Assessment 2196aa
Human Safety Data 1469, 1470
Human Serum 1566
Human Serum Albumin 440b
Human Skin 2176
Human Skin Equivalents 1032
Human Skin Explants 2171
Human Skin Sensitization 1036
Human Stem Cell 35
Human Stem Cell-Derived Cardiomyocyte 717, 1903
Human Stem Cells 32, 34, 36, 1622
Human Trophoblast 1770
Human-Induced Pluripotent Stem Cells 717, 718, 1112, 1915, 1922a
Humanized Mouse 1899b
Humanized Mouse Model 2129c, 2196r
Humidifier Disinfectants 2234y
Huntington's Disease 1353
Hyaluronan 1514a
Hybrid QSAR 429
Hydraulic Fracturing 1813, 2242
Hydrocarbon 1347b
Hydrofluoric Acid 1571
Hydrogen Sulfide 1258
Hydrolyzed Wheat Protein 988
Hydroperoxides 2165
Hydroquinone 460, 607
Hydroxyapatite 1973
Hydroxycitronellal 1599
Hydroxyl Radical 1275
Hydroxyproline 1800
Hyperkeratosis 193
Hyperlipidemia 2045
Hyperoxia 539, 1713o, 1789, 1793, 1796, 2026
Hyperoxic Lung Injury 538
Hyperplasia 255, 2065
Hypersalinity 654
Hypersensitivity 145a, 145b, 984, 1033, 1035, 2025, 2196x
Hyperspectral Dark Field Microscopy 821
Hypertension 1242b, 1325
Hypertrophy 2084
Hypoglycemia 2196j
Hypospadias 418a
Hypothalamic Pituitary Gonadal Axis 440e
Hypothalamic-Pituitary-Testicular Axis 1080
Hypothyroxenemia 1347f
Hypoxia 1728
Hypoxia Inducible Factors 1214
Ibandronate Sodium 437
ICH Guidelines 2265
ICH M7 ..... 2262, 2264, 2273c
ICP-OES 2218
Identification 1536
Idiopathic Autism 1760
Idiopathic Pulmonary Fibrosis 997, 1800
Idiosyncratic 1882
Idiosyncratic Drug-Induced Liver Injury 1864, 1886
Idiosyncratic Hepatotoxicity 529, 552b, 1886
IgE Allergy 2234aa
IGFR 258
IL-17 121
IL-18 1034
IL-1b 583
IL-2 2013
IL33 1128
Illicit Drug 1576
Imaging 2074, 2075, 2079
Imaging Mass Spectrometry 1777
IMI-eTOX 427
Imidacloprid 1854
Immune 1880, 2004, 2306
Immune Development 44, 342, 845
Immune Dysfunction 970, 1874
Immune Parameters 845
Immune Privilege 741
Immune Response 135, 342
Immune Suppression 922
Immune System 133, 696, 697, 698, 699, 700, 701, 841c
Immune-Mediated Drug Hypersensitivity Reactions 125
Immunoglobulin 2021
Immunologic Comparison 2020
Immunology 1466
Immunomodulation 2040c
Immunophenotyping 404, 408
Immunosuppressant 405
Immunosuppression . 140, 962, 1713s, 2006
Immunotoxicity 43, 143, 197, 401, 403, 408b, 1008, 1610, 2025, 2029, 2033, 2040b, 2318
Immunotoxicity Testing 986
Immunotoxicology 391, 397, 406, 740, 741, 742, 743, 744, 745, 1205, 1410, 1411, 1412, 1413, 1414, 1415, 1713l, 1713q, 1713r, 1985
Impairment 723
Impedance 1118, 1126, 1617
Imprinted Gene 1703
Impurities 1827
Impurity 277
In Silico 85, 1059, 2262, 2265
In Silico Methods of Prediction 693
In Silico Prediction 459, 1875, 2269
In Silico Profiler 2266
In Silico Tools 429
In Silico Toxicology 426, 428
In Utero 2184
In Vitro 146, 173f, 408a, 757, 817, 944, 1019, 1037, 1039, 1047, 1059, 1062d, 1231, 1530, 1549g, 1587, 1707, 1872, 1948, 1967, 2173, 2203, 2273r, 2273s
In Vitro Aerosol Exposure 1015, 1050, 1052
In Vitro Airway Model 1053
In Vitro Alternative 162
In Vitro Alternative Method 168, 1033, 1915
In Vitro Alternative to Animal Testing 160, 163, 512, 954b, 1024, 1029, 1050, 1052
In Vitro Alternatives 1280
In Vitro and Alternative Methods 2273v
In Vitro and *In Vivo* 1636
In Vitro Assay 397, 1633
In Vitro Assays 408b, 1028
In Vitro Carcinogenicity 1062
In Vitro Characterization 1833
In Vitro Culture Models 755
In Vitro CYP Induction Assay 285
In Vitro Cytotoxicity 1877, 1972
In Vitro Genotoxicity 1927
In Vitro Hazard Identification 753, 754, 758
In Vitro Hepatic Models 1873
In Vitro Hepatotoxicity 1622
In Vitro HTS 2250
In Vitro In Vivo Efficacy 574
In Vitro Inhalation Toxicity 1052
In Vitro Liver Model 716, 1309
In Vitro Lung Model 1613
In Vitro Metabolism 539e
In Vitro Methods 2273w
In Vitro Methods 64
In Vitro MicroFlow® Kit 451
In Vitro Micronucleus 464

In Vitro Micronucleus Assay 756
In Vitro Model 1046, 1397
In Vitro Models 830
In Vitro Neurotoxicity 1833, 1834, 1835, 1843
In Vitro Neurotoxicology 356
In Vitro Phototoxicity Testing 759, 762
In Vitro Positives 1933
In Vitro Prediction 1031
In Vitro Safety Testing 173k
In Vitro Screening 167, 2297
In Vitro Skin Absorption 2182, 2182a
In Vitro Skin Irritation 943
In Vitro Skin Sensitization 1029, 1062g
In Vitro Skin Sensitization Test 2168
In Vitro Systems 714
In Vitro Testing 755
In Vitro to *In Vivo* Extrapolation .. 690, 694, 695, 2250b
In Vitro Toxicity Assay 1631
In Vitro Toxicity Profiling 2273bb
In Vitro Toxicity Testing 467d
In Vitro Toxicology 1035, 1894, 1955
In Vitro-In Vivo Translation 1644
In Vitro, *In Silico* 1899
In Vivo 1985, 2004, 2080
In Vivo Comet Assay 454, 467A
In Vivo Gene Mutation 1943I
In Vivo Genotoxicity 600, 601
In Vivo Glucose Measurement 1588
In Vivo Imaging 1200H, 2140
In Vivo Metabolism 314, 510, 539E
In Vivo Micronucleus 1943J
In Vivo Mutagenesis 456
In Vivo Studies 894, 1978, 2273I
In Vivo Testing 303
IND-Enabling Toxicology 268
India 977
Indium Particles 1229d
Indoor Air 2234e
Indoor Air Quality 642
Indoor Exposure 1581
Indoor Mold 983
Induced Pluripotent Stem Cell 715, 1354
Induced Pluripotent Stem Cell-Derived Hepatocytes 1045
Industrial Hygiene 1816
Infant 197
Infant Formula 331, 341
Infants 1698, 1847
Infection 1713o
Infection Risk 2196p
Infectious Diseases 226
Inflammasome 57, 603g
Inflammation 122i, 132, 144, 223h, 359, 388, 393, 396, 785, 902, 992, 1001, 1005, 1006b, 1040, 1046, 1048, 1110b, 1136, 1138, 1206, 1216, 1224, 1237, 1242g, 1410, 1688, 1708, 1770, 1814, 2004d, 2321, 2327
Inflammation Bowel Disease 536, 933
Inflammatory 2054
Inflammatory Cytokine 1527
Inflammatory Cytokines 270, 1306
Inflammatory Effects 520
Inflammatory Response 2035
Influenza 874
Influenza Virus 1467, 2017
Informatics 876a
Infusion 185, 469, 953, 2149
Infusion Models 2137
Infusion Pump 953
Inhalant 1787
Inhalants and Cardiopulmonary 1232
Inhalation . 5, 10, 56, 66, 70, 597, 603d, 610, 631, 895, 896, 1202, 1205, 1225, 1227, 1229a, 1229b, 1229c, 1229f, 1233, 1236, 1286, 1594, 1596, 1597, 1598, 1599, 1695, 1820, 1830, 1831g, 1961, 1970, 2001, 2143, 2145, 2159, 2163c, 2193, 2296, 2303
Inhalation Dose 1817
Inhalation Dosimetry 67, 68, 770, 771, 772, 773, 774, 775, 1018f, 2250f
Inhalation Exposure 1217, 1347a, 2299
Inhalation Exposures 2139
Inhalation Nanotoxicology 600, 601, 2004a, 2004f
Inhalation Study 1220
Inhalation Toxicity 62, 593, 1057, 1221, 1229g, 1242d, 1975
Inhalation Toxicology 131, 1053, 1242
Inhalation, Disposition 515
Inhaled Dusts 1208
Inhaled Particles 2140, 2301
Inhibitor 1639b
Injury 561, 1218
Innate and Acquired Immunity 742
Innate Immunity 46, 407
Innate Lymphoid Cells 2040c
Inorganic Arsenic 1325, 1327f
Inorganic Arsenic (iAs) 2196c
Inorganic Mercury 1264
Insect 147
Insecticide 671
Insecticides 1014, 1834
Insulin 886, 1713n, 2118
Insulin Analogues 2129c
Insulin Glargine 1650
Insulin Resistance 482, 1239, 2324
Insulin Signaling 1932
Insulin Signaling Pathway 2197
Intake Assessment 2234v
Integrated Test Strategy 1831l
Integrated Testing Strategy 1608
Integrating Evidence 1488
Integrative Approach 170
IntelliCage 2163
Interaction 1321
Interactions 343i, 1012
Interferon 1713p
Interleukin-1 ..... 990, 992
Interleukin-6 256
Intermittent Exposure 1819
International Conference on Harmonisation (ICH) 2273b
Internships 1673
Interoperability 431, 1409
Intestinal Absorption 79
Intestinal Barrier 1041, 1413
Intestinal Epithelium 2028
Intestinal Hydrolysis 266
Intestinal Organoid 1911
Intestine 536, 917, 2027
Intradermal Injection 2196s
Intraepithelial Lymphocytes 2028
Intrahepatic Cholestasis of Pregnancy 1163
Intranasal Drug Delivery 2159
Intraocular Drug 273
Intraocular Lens 273
Intrathecal Administration 345
Intrathecal Dosing 344
Intratracheal Dosing 1225
Intratracheal Instillation 592, 1979
Intravaginal 2196y
Intravenous 280
Intravenous Infusion 288, 1662
Intraventricular 2152
Intronic Exonization 1184
Invasion 1996
Iodide Uptake 1087b
Iodotyrosine Deiodinase 1086
Ion Channels 1385
Ion Dissolution 1960
Ionizing Radiation 1757, 1762
IOP 2138
iPS Cardiomyocytes 1114, 1910
iPS Cells 1353
iPSC 375, 871, 1113, 1462, 1616g, 2084
iPSC-Derived Cardiomyocytes 1062d
Irganox 1076 1584
IRIS 73
Iron 1281, 1286, 2128
Iron Deficiency 1087m, 1263
Iron Metabolism 265b
Iron Oxide Nanoparticles 1711, 1947, 1951, 1980
Iron Sucrose 888
Iron Supplement in Pregnancy 862
Irritation 1038, 1224, 1587, 1814
IRS-1 2197
Ischemia-Reperfusion 108, 484
Ischemia/Reperfusion Injury 487
ISO 10993 950
Isoenzymes 2196bb
Isoflavone 1585
Isolated Perfused Rat Lung 1226
Isolated Rat Hepatocytes 1877
Isoniazid 542, 1045, 1794
Isoprostane 1545
Isoproterenol 110
Isothiocyanate 1623
Isotopes 1297g
Isotopic Lead 848a
iTRAQ 2212
ITS 2177, 2178
IV Infusion 345
IVIVE 632b, 901, 1087d, 2273o
Jacket 471
Jacketed External Telemetry 504a
Jacketed External Telemetry (JET) 472
Japanese Rice Fish 214
Jatropha 669a, 669b
Jejunum 903
Jet Fuels 1010
JET-BP 470, 474
JNK 1783
JNK/ERK/ER Stress 296
Jurkat T Cells 2013
Juvenile 185, 345, 2138, 2161
Juvenile Bone 847
Juvenile Immunotoxicity 1660
Juvenile Nonclinical Toxicology Study 1660, 2191
Juvenile Sensitivity 60
Juvenile Toxicology 2196j
Juvenile Toxicology Study 341, 343, 847
K–12 Education . 1662c, 1662d, 1676, 1677
K–12 Education Outreach 1662a, 1662d, 1663, 1677
K–12 Outreach 1668
Kaempferol 1087e
Kahweol 795, 797b
Karyorrhexis 347
Kava Kava 1474
KCC2 ..... 552g
Keap1 ..... 1714, 1779, 1780
Keap1, Nrf2 ..... 1773, 1798
Keratinocyte 1724, 1736
Keratinocytes 2168
Ketamine 1755, 1756, 1757, 1764a
Kidney 111, 122c, 286, 297, 508, 544, 1248, 1251, 1539, 1549d, 2042, 2050, 2051, 2055, 2056, 2061, 2062, 2063, 2065, 2067a
Kidney Biomarker 113
Kidney Injury 2196h
Kidney Toxicity 2043
Kinase Inhibitor 866, 1903
Kinase Inhibitors 1126, 1626
Kinases 1129, 2010
Kindling 1747c
Kinetic Modeling 25
Kinetically-Derived Maximum Dose 901a
Kinetics 154
Kisspeptin 205
Knockout Mice 1479
Knockout Rat 1132, 1134, 1157
Knowledge Base 691
Kola Acuminate 792
KRAS Mutation 1092
L-FABP 113
Label-Free 1619
Laboratory 2234z
Laboratory Study 1671
Lactobacillus rhamnosus GG Culture Supernatant 1194
Lactonase 540
Lactoperoxidase 586
Langerhans 990
Larynx 2143
Late Organogenesis Embryo Culture 1087q
Latent Reactivation 2120
Lauric Aldehyde 1605
LC-MS 294
LC-MS/MS 674, 1576, 2234k
LC-QTOF/MS 1000
LC/MS 1577
LC/MS/MS 455
LCt50 ..... 2163c
Leachates 2234j
Lead 223f, 663, 964, 1273, 1277, 1288, 1289, 1297g, 1338, 1339, 1340, 1341, 1392a, 1552, 1713k, 2232, 2234a, 2240
Lead (Pb) 939, 954h
Lead (Pb2+) 1337
Lead Acetate 481, 1267, 1270, 2041
Lead Exposure 778
Lead Poisoning 843
Lead Tissue Concentrations 72
Lead-Induced Dyslipidemia 1266
Leader 2116
Learning 655
Learning and Memory 827
Leelamine 1200i
Leflunomide 1758
Legal 2098
Leptin 506
Lessons from Genetic Toxicology 754
Leukemia 237, 1110f, 1490
Leukemia Therapy 1920
Leukocytes 1087r, 2033
Leydig Cell Tumor 1080
Leydig Cells 1713g
LHRH-SPIONs 1514
Libby Amphibole Asbestos Fibers 1217, 1831k
Ligand Promiscuity 1146
Ligand Specificity 907
Limb Defects 1087q
Limb Development/Birth Defects 1087p
Lipid 1190, 1662
Lipid Droplets 1002
Lipid Metabolism 150
Lipid Oxidation 15
Lipid Peroxidation 14, 16, 18, 19, 1198, 1790, 2030
Lipid Rafts 2023
Lipidomic 1264
Lipidomics 384
Lipogenesis 1167
Lipopolysaccharide 995
Liposome 1999
Literature Mining 2250k, 2273f, 2273i
Literature Review 1828, 2250k
Literature Search 1827
Litigation 721
Liver 85, 122a, 246, 388, 710, 735, 813d, 910, 957, 961, 978a, 1047, 1048, 1100, 1158, 1162, 1169, 1186, 1200b, 1200f, 1297, 1476, 1495, 1616, 1797, 1821, 1867, 1874, 1880, 1884, 1890, 1896, 1922, 2051, 2124, 2207, 2208
Liver Cancer 1498
Liver Carcinogenesis 65, 1602
Liver Development 189
Liver Fibrosis 2123
Liver Hypertrophy/Carcinogenesis 1160, 1161
Liver Inflammation 1618, 2316

KEYWORD INDEX

Liver Injury 292, 1164, 1165, 1178, 1412, 1718, 1879
Liver Injury Biomarker 1866
Liver Lipid Metabolism 735
Liver Micronucleus 450
Liver Micronucleus Assays 446
Liver Microsomes 2151
Liver Regeneration 1173
Liver Steatosis/Steatohepatitis/ Fibrosis 2254
Liver Toxicity . 169, 309, 1152, 1200g, 1865, 1871, 1899e
Liver X Receptor 150
Livestock Animal 1571
LLNA 440k
LNA 1635
Locomotor Activity 996
Lolitrem B 336
Long Noncoding RNAs 1105
Long-Term Culture 1051
Long-Term Post-Exposure 2004d
Low-Dose 1078
LPS 1769
LRRK2 933
Lung 561, 583, 831, 1213, 1229b, 1229c, 1242a, 1466, 1530, 1796, 2163b, 2321
Lung Burden, Translocation 2004a
Lung Cancer 223i, 236, 247, 312f, 632i, 1250, 1504, 1507
Lung Carcinogenesis 1092, 1093
Lung Deposition Modeling 66
Lung Development 848c
Lung Epithelial Cells 585, 1003, 1414
Lung Fibrosis 589, 1217, 1801
Lung Function 1811, 1979
Lung Inflammation 1981, 2072
Lung Injury 173a, 389, 539
Lung Overload 1826
Lung Tissue Slices 980
Lung Toxicity 980, 1229d
Lung Tumorigenesis 1091
LY2963016 1650
Lymph Node 971
Lymphocyte 954g
Lymphocyte Subsets 400
Lymphocytes 2320
Lysosomal Trapping 1875
MABEL 2114
Macaque 2146
Machine Learning 440k
Macrophage 389, 552f, 1319, 1882
Macrophage Function 397
Macrophage Phenotype 998
Macrophages 826, 1229d, 1793, 1973b, 2327
Magnetic Field 1959
Magnetite 1980
Major Histocompatibility Complex Alleles 125
MALDI 1627
Male Fertility 1079
Male Genital Tract 1701
Male Germ Cells 603k
Male Reproduction 1709, 1712
Male Reproductive Development 1707, 1713c
Male Reproductive Parameters 1691
Male Reproductive Toxicity 689a, 1692, 1693, 1703, 1710
Male Reproductive Toxicology 2227
Male Reproductive Tract 418a
Males 186
Malignant Transformation 1101
Malondialdehyde 1804b
Mammals 521
Mammary 1081
Mammary Carcinogenesis 2196a
Mammary Gland 1713f, 2196b, 2196c
Mammary Gland Development 2196d
Mancozeb 657
Maneb 680, 1852
Manganese 862, 1087l, 1286, 1291, 1329, 1330, 1349, 1350, 1352, 1353, 1355, 1357, 1358, 1359, 1360, 1361, 1362, 1366, 1374, 1550, 1551, 1695, 2103, 2104, 2107, 2108, 2234b, 2286, 2287, 2288, 2289, 2290, 2291, 2292
Manganese (Mn) 1364, 1365, 2106
Manganese Exposure 1327b, 1367, 1368, 2231
Manganese Neurotoxicity 1348, 1354, 1356, 1363, 1368a
Manganism .. 1285, 1358, 1359, 1360, 2105, 2234b
Manzate 1850, 1851
MAP Kinases 387
MAP Kinases Pathways 1719
MAP1s 1780
MAPK Kinases 312c
MAPK Pathway 1893
MAPK Signaling 1731
Margin of Exposure 604, 605
Marine Mammal 1259
Markers of Inflammation 983
Masa 315
Mass Spectrometry 343j, 422, 573, 1451, 1804b
Mast Cell 382, 1315
Maternal Plasma 2234g
Maternal Toxicity 1087v
Maternal-Fetal Environment 1680a
Math 581b
Mathematical Modeling 440c
Matrix Metalloproteinase-9 1088
Maturation 684, 2005
Maturity 2148
Maximum Tolerated Dose 901a
MCF-7 1096
MCF-7 Cell Assay 161
MCMC 96a
MDA-MB-231 791
MDMA 370
Mdr1/MDR1 2053
MDSC 922, 2008
MDSCs 1999
MEA 478
Mechanism 37, 349, 708, 1445
Mechanism-Based 170
Mechanism-Based Toxicity Screen 173d
Mechanisms 412, 555, 671, 1196, 1441, 1442, 1443, 1444, 1446
Mechanisms of Toxicity 1410
Mechanistic 1899
Mechanistic Evidence 1809
Mechanistic Model 1729
Mechanistic Modeling 435
Mechlorethamine 572
Mechlorethamine (HN2) 580
MED25 ..... 954e
Medical Countermeasures 2121
Medical Device 948, 950, 952, 954c
Medical Devices 954a, 954b, 1616d
Medicinal Plant 1629
Medicinal Plants 785, 804
Megalin 2048
MEHP 300
Melamine 632g, 890
Melanoma 260
Melatonin 148, 1097, 1843
Memory 363
Menidia beryllina 669c
Menstrual Cycles 2148
Mercapturic Acid 1519
Mercuric Sulfide 2223
Mercury 37, 38, 39, 40, 41, 42, 135, 136, 649d, 1255, 1259, 1261, 2042, 2234d, 2242
Mercury Toxicity 2230
Mesenchymal Tumors 225
Meso Scale Discovery 1547
Mesoporous Silica Nanoparticle 2230
Mesoporous Silica Nanoparticles 915
Mesothelioma 53, 57, 584, 1213, 1229g
Meta-Analysis 1490
Metabolic 1327c
Metabolic Modification 1721, 1733
Metabolic Profile 2234o
Metabolic Syndrome 872, 1294, 1307, 2068, 2069, 2070, 2073, 2326
Metabolism 48, 517, 519, 539b, 757, 810, 855, 882, 885, 896, 1300, 1327d, 1702, 1713, 1894, 2273d, 2273r
Metabolism, Differentiation, Insulin Resistance 2199
Metabolites 852
Metabolome 120, 1591
Metabolomic 414
Metabolomic Profiling 1175
Metabolomics 110, 117, 169, 250, 418, 603k, 853, 1000, 1156, 1242e, 1254, 1307, 1324, 1531, 1682, 1737, 1738, 1917, 2316
Metabolomics *In Vitro* 1871
Metagenomics 46
Metal 612, 1280, 1447
Metal Alloy 2215
Metal Binding Protein 1259
Metal Exposure 1675, 2215
Metal Homeostasis 1327b
Metal Mine 1553
Metal Mixtures 2220
Metal Oxide 1994
Metal Oxides 1966
Metal Pollution 1516
Metal Toxicology 1287
Metal-on-Metal Hips 289
Metallic 832
Metallic Allergen 122b
Metallofullerene 2002
Metalloporphyrin 1658
Metallothionein .. 480, 483, 822, 1244, 1274
Metals 229, 301, 603a, 611, 656, 1265, 1284, 1297, 1297h, 1297i, 1297j, 1318, 1327c, 1378, 1529, 1713q, 1713r, 2214, 2215, 2218, 2225, 2228, 2234, 2311, 2312, 2313, 2314, 2315
Metastable Epiallele 1687
Metastasis 1501
Metformin 507, 1183
Methadone 369, 541
Methamphetamine 369
Methamphetamine-Neurotoxicity 378i
Methcathinone 2105
Methionine; Methionyl Peptides 841e
Method Refinement 1588
Method Validation 1606
Methotrexate 552a
Methyl Dihydro Jasmonate 1598
Methyl Honokiol 482
Methyl Isobutyl Ketone 2059
Methylation 958, 965, 1310, 1570
Methylene Diphenyl Diisocyanate 236, 2036
Methyleugenol 523
Methylglyoxal 1542, 2060
Methylmercury 218, 750, 1256, 1257, 1262, 1263, 1331, 1332, 1333, 1368b, 1370, 1372, 1373, 1374, 1376, 1377, 1379, 1380, 1381, 1382, 1383, 1384, 1385, 1386, 1387, 1456, 1690a, 1822, 2239
Methylmercury (MeHg) 178, 290, 1258, 1371, 1375, 2250c
Methylmercury Neurotoxicity .. 1369, 1375
Methylphenidate 96f
MGMT Polymorphism 1943d
MGMT Promoter Haplotype 1943d
MHC Class I 1148
MIC-1 993
Mice 1804c
Micro-CT 2076, 2078
Micro-Environment 33
Microarray 1713e, 1796, 1995
Microarray Gene Expression 146, 903, 2217
Microarrays 1948
Microbiome 43, 44, 45, 47, 1130, 1323
Microcystin 364, 365, 900
Microcystins 1566
Microelectrode Array 1973a
Microelectrode Arrays 378a, 1116
Microfluidic 1964
Microglia 928, 940, 995, 1391, 1455, 1859
Microgravity 632d
Microminipig 2151
Micronization 1229
Micronucleated Polychromatic Erythrocytes 788
Micronuclei 452, 1110
Micronucleus 445, 467h, 1929
Micronucleus Test 447
Micronutrients 1088
microPET 1764d
Microphysiological System 1912
microRNA 99, 100, 101, 103, 142, 204, 418c, 569, 732, 963, 978d, 1004, 1121, 1302, 1318, 1492, 1705, 1713l, 1738, 1840, 1891
microRNA Reprogramming 734
microRNAs 97, 733, 978c, 1713i, 1865, 1869
Microsampling 2161, 2196
Microscopy 463
Microsomes 1895
Microvascular Health 1689
Microvascular Physiology 872
Microwave Popcorn 232
Midbrain Drug Delivery 942a
Migration 182
Milk 313
Mineral Oil 1067
Mini Excitatory Postsynaptic Current (mEPSC) 1337
Miniature Swine 2118
Mining 1018b
Minipig . 470, 2149, 2305, 2306, 2307, 2308, 2309
Minipigs 504a, 2310
Miniswine 886
miR-21-Pdcd4 Signaling 1297f
miR122 ..... 1899d
miRNA 98, 104, 106, 122c, 122d, 265d, 1727, 2057
miRNA Expression 2220
miRNA Sequencing 1869
miRNAs 906, 1722, 1732
Misoprostol 1087q
Mitochondria 108, 111, 115, 223a, 250, 306, 310, 312e, 486, 708, 710, 711, 712, 713, 813d, 823, 867, 1003, 1195, 1200a, 1358, 1453, 1611, 1630, 1642, 1643, 1736d, 1756, 1797, 1832, 1897, 2004g
Mitochondria Toxicity 848
Mitochondria-Mediated Apoptosis 298
Mitochondrial Biogenesis 797
Mitochondrial Disease 1940
Mitochondrial DNA Damage 857, 1932, 1939
Mitochondrial Dysfunction 340, 937, 1721, 1733, 1848, 1939
Mitochondrial Electron Transport Chain 1792
Mitochondrial Inhibition 1849, 1851
Mitochondrial Toxic Oxidative Stress 862
Mitochondrial Toxicity 873, 1644, 1918, 1939, 1940, 2266
Mitogne-Activated Protein Kinases 1388
MitoPark 936
Mitophagy 709
Mitotic Arrest 304
Mixture 1009, 1012, 1078
Mixture Toxicology 1011
Mixtures 96b, 253, 1008, 1014, 1016, 1017, 1018, 1018a, 1018c, 1018d, 1033, 1222, 1347, 1416, 1417, 1418, 1419, 1420, 1421, 1710, 1847, 2228
MK-801 348

The numerals following each keyword refer to the relevant abstract number(s).

MLL ... 687
MMP-9 ... 795
MN Assay ... 1943b
Mn SOD ... 1186
MoA ... 1099, 2182b
Mode of Action ... 64, 238, 605, 607, 1602, 1941
Model ... 440g
Model Uncertainty ... 632a
Modeling ... 882
Models ... 816
Models Simulation ... 2238
Modes of Action ... 1871
Modified Ames ... 265
Mold Risk Assessment ... 1831m
Molds in Residential Environments ... 1831m
Molecular Biology ... 1386
Molecular Dynamics ... 440b
Molecular Epidemiology ... 233
Molecular Evolution ... 2283
Molecular Imaging ... 901e
Molecular Initiating Event ... 2273x
Molecular Profiling ... 988
Molecular Structure and Dynamics ... 2273a
Molindone ... 1620, 2196m, 2196n
Moniliformin ... 343e
Monitoring ... 2133
Monkey ... 272, 346
Monkeys ... 1540
Mono(2-Ethylhexyl) Phthalate ... 383
Monoclonal Antibodies ... 278
Monoclonal Antibody ... 899, 2202
Monoclonal Antibody Clearance ... 898
Monocyte Adhesion ... 1229e
Monocytes ... 395
Monocytes/Macrophages ... 2196p
Monomethylarsonous Acid ... 143, 1101
Monoterpene ... 813a
Monte Carlo ... 2243
Monte Carlo Simulation ... 91
Montmorillonite ... 316
Morinda morindoides ... 808
Morphine ... 368
Morphine Dependence ... 367
Morpholino Antisense Oligos ... 222
Morphological and Neoplastic Cell Transformation ... 585
Morphology ... 1897
Mortality Rates ... 638
Mothers and Infants ... 1522
Motor ... 1366
Motor Activity ... 1327b
Motor Deficit ... 1365
Motor Function ... 2291
Mouse ... 450, 581j, 1914, 2130
Mouse Diversity Panel ... 543
Mouse Ear Vesicant Model (MEVM) ... 580
Mouse Embryonic Stem Cells ... 368, 960
Mouse Hepatocytes ... 1962
Mouse Liver Tumors ... 1099
Mouse Lymphoma Assay ... 1943b
Mouse Models ... 978, 2093
Mouse Mutagenesis ... 2076
Mouse Prostate Development ... 905, 1087s
MPPD Modeling ... 774
MRI ... 378f, 579, 1367, 2231
MRI T1 Relaxation Time ... 1365
MRL ... 1560
mRNA Expression ... 1370
MRP ... 218, 562
Mrp1 ... 1772
MSC ... 1085
MSD ... 1546
MsrA ... 1791
MTF-1 ... 1264b
mTOR ... 258, 919
MTT ... 789
MTT Assay ... 1056
Mucin ... 1730, 2127
Mucosal Exposome ... 993
Multielectrode Array ... 375, 1739
Multigenerational ... 241
Multiple Myeloma ... 1812
Multiple Sclerosis ... 1004
Multiple-Dose Safety ... 2002
Multiplex ... 122g
Multiplex Assay ... 441
Multiplex Assays ... 2043
Multiplexing ... 1547
Multiscale Models ... 428
Multiwall Carbon Nanotube ... 199
Multiwall Carbon Nanotubes ... 485, 585
Multiwalled Carbon Nanotubes 587, 603g, 603h, 2004a
Municipal Wastewater ... 2229
Muscle Coordination ... 805
Mustard ... 581h
Mustard Toxicity ... 576
Mutagenesis ... 1943g
Mutagenic Activity ... 1242h
Mutagenicity ... 240, 784, 1638, 2262, 2264, 2296
Mutagenicity and Markers of Inflammation ... 2295
Mutagenicity, Genotoxicity ... 446
MutaMouse ... 456
Mutation ... 241, 1326, 1943c
Mutation Assay ... 324
MWCNT ... 588, 590, 1976, 1990, 2003
Mycotoxin ... 343e
Mycotoxins ... 217
Myelodysplastic Syndrome ... 228
Myh10 ... 184
Myocardial Toxicity ... 2273g
Myocarditis ... 394
Myocardium ... 490
N-(Carboxymethyl)Lysine ... 2060
N-Acetyltransferase 2 ... 545
n-Butanol ... 1831h
n-Butyl Acetate ... 1831h
N-ethyl-N-nitrosourea ... 445
N-Methyl-D-Aspartate (NMDA) Receptor ... 1838
N-Methylpyrrolidine ... 280
N-Nitrosomorpholine (NMOR) ... 608
N6-Formyllysine ... 1521
Nab ... 2196q
NAC ... 1264c
nAChRs ... 1736c
NAD ... 1379
NAD(P)H: Quinone Oxidoreductase 1 (NQO1) ... 358, 1083
NADPH Oxidases ... 289
NAFLD ... 956, 1159
Nano Aerosol Inhalation ... 829
Nano Risk Assessment ... 1953
Nano TiO2 ... 834
Nano-Anticancer Drug ... 1949
Nano-bio Interactions ... 2273a
Nanocapsules ... 603i
Nanoceria ... 2004h
Nanocomposite ... 641
Nanocrystalline Cellulose ... 838
Nanocrystalline Diamond ... 1972
Nanomaterial ... 603d, 814, 816, 1395, 1983, 1991, 1994
Nanomaterials ... 486, 597, 832, 841a, 1221, 1397, 1465, 1954, 1992
Nanometals ... 830
Nanoparticle ... 818, 820, 824, 831, 841, 1347l, 1795, 1963, 1973a, 2004b
Nanoparticle Array ... 602
Nanoparticle Inhalation ... 1053
Nanoparticle Physicochemical Composition ... 819
Nanoparticle Protein Corona ... 819
Nanoparticle Toxicity ... 1711
Nanoparticles ... 86, 603a, 603c, 822, 836, 839, 888, 1393, 1396, 1947, 1971, 1973i, 1973j, 1980, 1998
Nanoporous Silica ... 2000
Nanoscale Particles ... 841b
Nanoscale Surface Coatings ... 1972
Nanosilver ... 484, 841c, 1944, 1956, 1973b, 1973h, 1986, 1987, 1988
Nanosilver Particles ... 660
Nanosilver Wires ... 660
Nanostructured Material ... 332
Nanotechnology ... 1394, 1466, 2196x
Nanotexture ... 1973g
Nanotoxcity ... 832
Nanotoxicity ... 603b, 835, 1952
Nanotoxicity *In Vitro* ... 1946
Nanotoxicology . 8, 488, 582, 590, 599, 602, 603, 817, 829, 833, 838, 841d, 1464, 1468, 1514, 1962, 1966, 1973e, 1978, 1986
Nanotube ... 1964
Nanotubes ... 583, 596
Naphthalene ... 69, 532, 533, 1219, 1831
NASH ... 1183, 1323, 2061
Natriuretic Peptide ... 1549a, 1549e
Natriuretic Peptides ... 1549h
Natural ... 2234h
Natural Killer Cell Activity ... 407
Natural Product ... 813c
Natural Products ... 329, 385, 670, 783, 797, 2250
Natural Toxin ... 159
Navajo ... 2234c
Near-Infrared Fluorescence ... 1200h
Neighborhood Environment ... 959
Nek2 ... 1272
Nelumbo nucifera Leaf Extract (NNE) ... 296
Neonatal Exposure ... 842, 1070
Neonatal Hyperbilirubinemia ... 190
Neonatal Manganese Exposure ... 1087m
Neoplastic Transformation ... 1502
Nephropathy ... 2044, 2059
Nephrotoxicants ... 2067
Nephrotoxicity ... 114, 122g, 380, 495, 632g, 1389, 1543, 1549d, 1799, 2033, 2041, 2053, 2058, 2064, 2066, 2256
Nephrotoxicity Prediction ... 1627
Nerve Agent ... 359, 556, 558, 581c, 581i
Nerve Agent Antidote ... 568
Nerve Agents ... 560
Network ... 418d
Network Analysis ... 1054
Network Motif ... 438
Neural ... 376, 1616f
Neural Crest Precursors ... 182
Neural Differentiation ... 1328
Neural Progenitor Cell Niche ... 752
Neural Stem Cell Differentiation ... 1764c
Neural Stem Cells . 1056, 1752, 1764a, 1914
Neurite Outgrowth ... 378d, 1058, 1842
Neuroantibodies ... 701, 938, 1334, 1535
Neuroapoptosis ... 1764
Neurobehavior ... 181
Neurobehavioral ... 581h, 777, 1763
Neurobehavioral Defects ... 1690a
Neurobehavioral Effects ... 227
Neurobiology ... 1672
Neuroblast ... 1839
Neurochemistry ... 1333
Neurodegeneration ... 378h, 927, 930, 931, 1357, 1378, 1452, 1764, 2108
Neurodegenerative Diseases ... 935
Neurodevelopment 210, 223a, 1347g, 1418, 1751
Neurodevelopmental ... 1335, 1347f
Neurodevelopmental Toxicity ... 2205
Neuroendocrine Stress Response System ... 1747b
Neurogenesis ... 178, 1922b
Neuroimmunotoxicology ... 1336, 1411
Neuroinflammation ... 361, 440g, 566, 751, 1759, 1844, 2304
Neurological Effects ... 611
Neuromodulation ... 1747
Neuromuscular ... 1331
Neuron ... 35, 377
Neuronal Degeneration ... 347
Neuronal Excitability ... 1381
Neuronal Function ... 1739
Neuronal Networks ... 1922d
Neuronal Protein ... 2129d
Neuropathology ... 1087n, 2104
Neuroprotection ... 700, 934, 1383
Neurotoxicant ... 1758
Neurotoxicity ... 147, 175, 347, 349, 357, 363, 370, 375, 378, 378b, 378c, 378e, 378f, 378g, 567, 659, 683, 746, 748, 749, 751, 945, 1087, 1262, 1297b, 1334, 1347l, 1350, 1360, 1392, 1454, 1529, 1634, 1740, 1741, 1755, 1757, 1762, 1764c, 1832, 1838, 1861, 1863, 1863a, 1863b, 1973a, 2286, 2287, 2288, 2289, 2290, 2291, 2292
Neurotoxicity Assessment ... 348
Neurotoxicity Screening ... 173i, 378a
Neurotoxicology ... 352, 355, 362, 696, 697, 698, 699, 700, 701, 723, 932, 1339, 1359, 1373, 1386, 1433, 1434, 1746, 1747e, 1852, 1858, 1912, 1922d
Neurotoxin ... 941
Neurotransmitter ... 1289, 1361
Neurotrauma ... 1732
Neutron Activation Analysis ... 1291
Neutron Technology ... 1287
Neutropenia ... 279
Neutrophils ... 383
New Concepts ... 1831e
New Drug Development ... 1625
New York City Subway ... 1210
Newborns ... 706
Next-Generation Sequencing ... 1943c
NF-B ... 928, 1455, 1722, 1789
NF-E2-Related Factor 2 (Nrf2) ... 572, 1124, 1736d
NF-kappaB ... 902, 1498
NFkappaB ... 1110c
NHANES ... 96d, 223g, 235a, 2234n
NHEJ ... 1930
NHEK ... 1163b
NHP ... 1699
Nickel ... 967, 1268, 1502, 2040a
Nicotine ... 173m, 1612, 1736c, 1761, 1762, 2182a
Nicotinic Acetylcholine Receptors ... 805, 1145
Nicotinic Receptor ... 560
Nimodipine ... 1383
Nitrated Fatty Acids ... 383
Nitrates ... 2246
Nitric Oxide ... 488, 497, 858, 998, 1973f, 2039
Nitrogen Dioxide ... 1231
Nitrogen Mustard .. 553, 554, 555, 561, 562, 565, 571, 575
Nitrosamines ... 1089
Nitrosative Stress ... 139
Nitrosothiol ... 2039
NLRP3 Inflammasome ... 1465
NMDA-Glutamate Receptor ... 749
NNK ... 1093, 1507, 1943f
Nnt ... 925
NOD2 ... 386
Non-B-DNA ... 1943g
Non-BPA ... 1064
Non-Coplanar PCBs ... 1147
Non-Genomic Pathway ... 1127
Non-Hodgkin's Lymphoma ... 251
Non-PRASA ... 666
Nonalcoholic Fatty Liver Disease ... 676, 735
Nonalcoholic Steatohepatitis ... 547, 800, 1187, 1569
Nonanimal Methods ... 1062c
Nonchemical Stressors ... 1418
Nonclinical Juvenile and Pediatric ... 845, 1659

The numerals following each keyword refer to the relevant abstract number(s).

Nonclinical Safety Assessment 268, 282
Nonclinical Toxicology 113, 276
Noncoding RNA 1106
Noncoding RNAs 730
Nongenotoxic Carcinogenesis 2196h
Nonhuman Primate 474, 889
Nonhuman Primate (NHP) 2309
Nonhuman Primates 2134, 2150
Noninvasive 471, 1573
Nonmotor Symptoms 937
Nonparametric Method 629
Nonparametric Splines 1417
NOS-2 ..... 581k
Notch 1331, 1688
Novel Biologics 2112
Novel Drug Targets 1105
NR4A1 ..... 1131, 1143
Nrf 223c
Nrf2 ..... 145, 312d, 493, 1169, 1185, 1380, 1715, 1716, 1723, 1779, 1785, 1788, 1791, 1794, 1802, 1804a, 1836, 1839, 2012, 2013
Nrf2 Activation 209, 2010, 2011
Nrf2 Pathway 2009
NRT1 705
NRTI 1656
NSRL 619, 620
Nuclear Factor E2-Related Factor-2 2044
Nuclear Receptor 1512, 2273t, 2273z
Nuclear Receptor and ER Stress 2129b
Nuclear Receptors 739
Nucleoside 849, 850, 851, 852, 853, 854, 855, 856, 857
Nucleoside Analogs 1923
Nucleotide Excision Repair 1943f
Nutrient Deprivation 709
Nutrition 327, 339, 1662
o-Phenylphenol (OPP) 606
Oatp 900
OATP1B1 ..... 440j
OATP1B3 159
Obesity 149, 223g, 1163a, 1252, 1306, 2068, 2069, 2072, 2189, 2321
Obesogen 679, 739, 1084, 1922f
Objectivity 724
Obstructive Sleep Apnea 480
Occupational 235, 612, 1607, 1816
Occupational Exposure 22, 1208, 1242a, 1557, 1576, 1966, 2234a
Occupational Exposure Level 611
Occupational Exposure Limit 613, 1010
Occupational Health 613
Occupational Risk 1815
Occupational Risk Assessment 781
Ochratoxin A 442
Octamethylcyclotetrasiloxane 901d
Ocular 947, 2138
Ocular Delivery 273
Ocular Histology 2153
Ocular Injuries 555
Ocular Irritancy 1024
Ocular Irritation 1020, 1021, 1025
Ocular Safety 1640
Ocular Safety Assessment 740
Ocular Toxicity 1641
Ocular Toxicology 581a, 740, 741, 742, 743, 744, 745, 2153
OECD 2179
OECD Guideline 407 1992
OECD Guideline 428 2172
OECD Test Guidelines 691
OECD TG 488 ..... 1943i
Off-Targets 220
Offgassing 2250d
OGG1 1928
Ogg1 Knockout Cells 1305
Ogun River 1074
Oil 343g
Oil and Gas 1607
Oil Pollution 669c
Oil Spill 448
Olefins 1593
Oleic 327
Olfaction 654
Olfactory Toxicity 1363
Oligodendrocyte 1764e
Oligonucleotide 1635
Oligonucleotide Constructs 2113
Oligoquat M 461
Olive Leaves 1179
Olney 348
Omega-3 Fatty Acids 340
Oncology 277
Oncomutations 265a
One-Carbon Metabolism 1690
Ontogeny 49, 192, 892
Ontology 427, 2273l
Ontology Data Mining 2254
OP Pesticides 1858
Operant Behavior 1363
Ophthalmic 2153
Ophthalmology 2119
OPIDN 1855
Opioid Receptors 368
Opioids 1657
Optical Coherence Tomography 954
Optineurin 378h
Oral Exposure 599, 1989, 2234r
Oral Mucosal Irritation 1649
Oral Toxicity 581j
Organ Toxicity 1180
Organ Weight 1229c
Organ-on-Chip 1441, 1442, 1443, 1444, 1445, 1446
Organ/Tissue Toxicity 158
Organic Pigments 1221
Organochlorine 678
Organochlorine Pesticide 2221
Organochlorine Pesticides 551
Organogenesis 194
Organohalogen Compounds 517
Organophosphate 556, 564, 568, 1750, 1751, 2163c
Organophosphate Pesticides 686, 689, 1754
Organophosphates 116, 748, 1856
Organophosphorus Insecticides 1753
Organotin DOTC 1347i
Organotins 739, 2224
Organotypic 1038, 1592, 2181
Organotypic Model 860
Organotypic Tissue Models 415
Organs Specific Genotoxicity 451
Orphan Virus 2037
Osteoblast 173c
Osteoblast Differentiation 1283
Osteoporosis 437, 632d
Ototoxicity 2196t, 2196u
Outreach 1676
Ovary 2183, 2186, 2187, 2188, 2189
OVE26 1888
Oxazolidinones 1634
Oxidation 1006b
Oxidative 1785
Oxidative Damage 1954
Oxidative DNA Damage . 467a, 1305, 1451, 1774
Oxidative Environmental Pollutants 1778
Oxidative Injury 310
Oxidative Potential 1275
Oxidative Stress 122i, 209, 292, 297, 312c, 481, 538, 559, 565, 577, 657, 752, 808, 833, 927, 1001, 1018, 1104, 1182, 1200g, 1270, 1343, 1387, 1452, 1453, 1455, 1457, 1545, 1557, 1736d, 1768, 1770, 1781, 1784, 1786, 1788, 1799, 1804b, 1831f, 1850, 1930, 1932, 1943a, 1950, 1973c, 2004h, 2041, 2252
Oxidative Stress and Apoptosis 213
Oxidative Stress and Inflammation 813c, 1997
Oxidative Stress-Antioxidant Imbalance 173n
Oxidized LDL 2226
Oxime 556, 564
Oxycyte 887, 2029
Oxygenation 518
Oxytocin 122h
Ozone 394, 396, 1230, 1231, 1810, 2302, 2324, 2325, 2326, 2327, 2328, 2329
Ozone Exposure 1719, 2072, 2073
Ozone Inhalation Exposure 876d
p-Phenylenediamine 2171
p, p'-DDE 679, 1703
P.R.I.T.* 1050
p38-MAPK 302
P450 ..... 528, 532, 533, 539c, 549
P450s 1742
p53 ..... 1248, 1268, 1709, 1927, 1933, 1956
p62 1780
p97 1779
PAH 215, 219, 615, 667, 882, 1103
PAH-DNA Adducts 513
PAHs 616, 1831i, 2234w
Paired Housing 2196z
Palate Development 183
PAMP 166
PAN-Induced Injury 2057
Pancreas 98, 134, 1786
Pancreatic Cancer 248, 548, 1106, 1508, 1511, 2258
Pancreatic Toxicity 97
Pancreatitis 873
PAR-4 1197
Parabens 266
Paracetamol 272
Paradichlorobenzene 224
Parameter Variation 632b
Paraoxonase 1249, 1273
Paraoxonase 1 ..... 686, 1822
Paraoxonase 1 (PON1) 568, 707
Paraquat 1839, 1840, 2053
Parent/Metabolite Drugs and GWAS 165
PARG 311
Parition Coefficients 897
Parkinson's Disease 153, 371, 378h, 923, 924, 925, 926, 928, 929, 930, 931, 932, 933, 934, 937, 942a, 942b, 942c, 1285, 1350, 1354, 1355, 1356, 1368a, 1453, 1520, 2103
Parkinsonism 2106
PARP 311
PARP-1 1316
PARP-1 Inhibitor 576
Particle Deposition 1018f
Particles 1282
Particokinetics 814
Particulate Chromate 1450
Particulate Matter 1207, 1241, 1831j, 2040a, 2193, 2250e, 2300, 2303, 2329
Particulate Matter Air Pollution 487, 1018f
Particulate Matter Dust 1243, 1713r
Particulate Matteral 1238
Particulates 951
Partition Coefficient 96, 2273p
Passive and Active Transport 79
Passive Sampling 1579, 1678
Passive Sampling Device 1579
Patch Testing 876c
Pathology 1990
Pathophysiology 312e
Pathway 411, 1129
Pathway Analysis 1254
Pathway and Network Analysis 1731
Pathways 4
Pattern Recognition 2273e
Pattern Recognition Receptors 2302
PBDE 92, 93, 1200g
PBDEs 340, 1741, 2204
PBPK 60, 73, 82, 84, 85, 87, 90, 96a, 96d, 96e, 96f, 96h, 617, 632b, 632c, 2234l
PBPK and Biological Modeling 76
PBPK Model 72, 86, 91, 93, 96b, 815
PBPK Modeling 70, 71, 75, 80, 96g, 2245
PBPK/PD Modeling 81
PC12 Cells 356
PCB 515, 519, 1569, 1740
PCB Sulfate Monoester 1068
PCB126 ..... 1062i
PCBs 1087j, 1524, 1747c
PCBs, POPs, Toxicity, Glucose Intolerance 2199
PCR 1646
Pedagogy 1674, 1679
Pediatric 11
Pediatrics 2077
Peer Review 1831a
Pefloxacin 2271
PEG-IL-29 ..... 2196q
Pegylated Proteins 1659
PEGylation 1657
PEITC 1511
Pentachloroanisole (PCA) 223b
Pentachlorophenol (PCP) 223b
Peptide Microarray 1063, 1150, 1154
Peptides 566
Percutaneous 2234w
Percutaneous Absorption 1973h
Perennial Ryegrass 336
Perfluorinated Compounds 2213
Perfluoroalkyls 1135
Perfluorocarbon 887, 2029
Perfluorocarboxylic Acids 2192
Perfluorochemicals 352
Perfluorononanoic Acid 976, 1175
Perfluorooactanoic Acid 2213b
Perfluorooctanesulfonate 1084
Perfluorooctanesulfonic Acid 738
Perfluorooctanoic Acid 1084, 2211, 2212
Perfluorooctanoic Acid (PFOA) 91
Perinatal Exposure .. 133, 703, 1347e, 1713b
Perinatal TCDD Exposure 1747b
Peripheral Neuropathy 173l
Permeability 353
Permethrin 689b, 1846
Permitted Daily Exposure 621
Peroxiredoxin 1 1102
Peroxisome Proliferator-Activated Receptor Alpha 1152
Peroxynitrite 1771
Persistent and Bioaccumulating Toxic Pollutant 632e
Persistent Organic Pollutant 2198
Persistent Organic Pollutants (POPs) 93, 901b, 1766
Personal Care 173k
Pesticide 558, 669, 670, 675, 930, 1841, 1855, 1860, 2237
Pesticide Mixtures 165
Pesticide Residue 672
Pesticide Residues 674
Pesticides 59, 65, 175, 567, 676, 677, 846, 929, 1524, 1573, 1577, 1749, 1768, 1831g, 1835, 1852, 1863c, 2238
PET 2104
Petroleum 265
PFAA 2210
PFAS 2040b
PFHxA 2210
PFNA 1891, 2210
PFOA 90, 1786, 2040b, 2196d, 2211
PFOA/PFOS 2206
PFOS 1745, 2207, 2209
PFSAs 2208
Phage Display 876
Phagocytosis 602, 1793
Phamacokinetics 164
Pharmaceutical Intermediates 1028
Pharmaceutical with Endocrine Disrupting Property 658
Pharmaceuticals 283, 1013, 1827, 2310

Pharmacodynamics 901c, 1729, 1735
Pharmacogenetics 546
Pharmacogenomic 1480
Pharmacogenomics 552c
Pharmacokinatics 880
Pharmacokinetic 70, 818, 881, 2163a
Pharmacokinetic Modeling 2234m
Pharmacokinetic Models 1876
Pharmacokinetic Variability 92
Pharmacokinetics 62, 71, 78, 122h, 276, 878, 879, 884, 887, 889, 891, 894, 901c, 901d, 1296, 1440
Pharmacology 2307
Pharmacophore 1069
Phase II Conjugation Reaction 521
Phencyclidine 1648
Phenobarbital 265c, 1200i, 1865, 1869
Phenolic 791
Phenolic Dye 789
Phenotype Prediction 545
Phenyl Ethyl Alcohol 1597
Phenylethylamines 169
Phenylpropanoid 523
PhIP 923, 1110e
Phorbol Ester 669a
Phorbol Esters 669b
Phosgene 570, 581k, 1212, 2163b
Phosphatase 1736
Phospholipidosis 1266, 1875
Photo-Activated Cow Urine 1943
Photoaging 2180
Photodamage 709
Photosafety 760, 761, 763, 1600
Photosensitivity 761
Phototoxicity 759, 760, 761, 763, 1973d, 2119, 2166, 2167
Phthalate 198, 2188, 2250h
Phthalate Mixture 1713c
Phthalates 1702, 1708, 1807
Phylogenetics 2281
Physiologically Based Pharmacokinetic Modeling 89, 96
Physiologically Based Pharmacokinetic Models 891
Phytochemicals 436, 2267
Phytoestrogen 1075, 1087e
Phytoestrogens 211, 1069, 1616e
Pig 2163b
Pig-a 452, 1943j
Pig-a Mutation 445
Piglet Model 331
Pigmentation 219
Pioglitazone 1198
Pipeline 1673
Piperonyl Butoxide 673
PIRC Rat 1109
Pituitary 1071
PK 96i
PKD1 936
PKPD Modeling 581
Plac1 ..... 1087n
Placenta 978d, 994, 1497
Placental Barrier 1110e
Placental Exposure 705
Placental Insufficiency 1706
Placental Transfer 278
Plagiarism 725, 726, 727, 728, 729
Plant Food Supplements 1831e
Plant Toxins 805
Plasma 2151a
Plasma Microsampling 901f
Plasminogen 1542
Plasmonic Nanoparticles 1297c
Plastics 2234j, 2268
Platelet Activation 1127
Platelets 1191, 1461, 1645
Platinum 145a
Platycodon grandiflorum 799, 800, 801, 802
Pleural Fibrosis 130
Pleural Plaques 1811
Pluripotency 1907
Pluripotent Stem Cells 1917
PM2.5 ..... 1237, 1240, 2250e
Poison Prevention 876b
Pokeweed Antiviral Protein 786
Policy 640, 649d
Pollen 1006a
Poly (ADP-Ribose) Polymerase (PARP) 299
Poly-α-L Glutamic Acid 1654
Poly(ADP-Ribose)Polymerase-1 138
Polybrominated Diphenyl Ether 181
Polybrominated Diphenyl Ethers 1082
Polybrominated Diphenyl Ethers (PBDEs) 179, 410
Polychlorinated Biphenyls . 351, 1068, 1742, 1743, 1744, 1781, 2202, 2205
Polychlorinated Biphenyls (PCBs) 234, 1124, 1747d
Polycyclic Aromatic Hydrocarbon 1684
Polycyclic Aromatic Hydrocarbons 235a, 2203
Polycyclic Aromatic Hydrocarbons (PAHs) 539d
Polyhexamethyleneguanidine Phosphate 1211
Polyhexmethylene Biguanidine (PHMG) 2234y
Polymorphism 549, 1347j
Polymorphisms 41, 541
Polyphenols 1788
PON1 SNPs 540
Poorly Soluble Particles with Low Toxicity 1826
POPs 1568, 1678
Population Health 2249
Population-Based *In Vitro* Testing 165
Population-Based PBPK Modeling 440f
Porcine Model 871
Poria cocos 1167
Portal-of-Entry 1831g
Postmarket Surveillance 1472
Postnatal Development 1713
Posttranslational 439
Potassium Heptaoxodichromate VI 788
Potency 1821
PPAR 249
PPAR Beta/Delta 246, 248
PPAR-Alpha 1140
PPAR-Beta 245, 247, 1155
PPAR-Gamma 149, 1085
PPARs 260
PPARα−/− 1156
pQCT 281
Prandial Status 2122
Precision-Cut Lung Slices 1051, 1057, 1953
Preclinical Database 426
Preclinical Safety 1658
Preclinical Safety Evaluation 2109
Preclinical Toxicology 284, 2159
Prediction 418e
Prediction Model 1032
Prediction Models 693, 1735
Predictive Methods 2273w
Predictive Model 2272
Predictive Models 173e, 459
Predictive Toxicity 440a, 1062a
Predictive Toxicology . 1087p, 1113, 2273m, 2280
Preeclampsia 2129
Pregestational 1087t
Pregnancy 229, 485, 1162, 2129
Pregnancy Outcome 1825
Pregnane X Receptor (PXR) 1147, 1157
Pregnant Mouse 898
Prenatal 1347c, 1347d
Prenatal Benzo[a]pyrene 538
Prenatal Exposure 1308, 1975, 2004e
Prenatal Stress 1333, 1340
Preservatives 321
Preterm Birth 994, 2193
Preterm Labor 1754
Prevalence of Molds 1831m
Primary Hepatocyte 1602
Primary Human Cells 2273v
Primary Human Hepatocytes 1181
Primary Podocyte 2057
Primate 633
Printed Electronics 1565
Proarrhythmia 1116
Probabilistic Risk Assessment 440f, 1831f
Problem Formulation 1831a
Processed Food 323
Prochloraz 1081
Prodrug 893
Prodrugs 794
Product Safety 640
Product Safety Assessment 328
Products 1
Profenofos 689
Progesterone 2147
Proguanil 2051
Proinflammatory 1171
Prokineticin 2 1285
Prolactin 378i, 1620, 2196m, 2196n
Proliferation 1039
Promethazine 581c
Promotion 1103
Prophylactic Vaccines 2196s
Propofol 1764a, 1764c
Proposition 65 ..... 620, 632h
Proprietary Data 2264
Propylene Oxide 1941
Propylparaben 2191
Prostacylin 1234
Prostate 1713e
Prostate Cancer .. 249, 259, 305, 310, 1110a, 1503, 1537, 1686, 1916
Prostate Development 1686
Prostatic Inflammation 1006
Protea cynaroides 791
Proteasomal Inhibition 358
Proteasome 926
Protein 1823
Protein Acylation 1771
Protein Adducts 2202
Protein Carbonyls 1950
Protein Corona 821
Protein Folding 1148
Protein Immunogenicity 989
Protein Kinase RNA-Like ER Kinase (PERK) 1775
Protein Kinases 908
Protein Malnutrition 1774
Protein Oxidation 350
Proteinopathies 1351
Proteom 1890
Proteomics 114, 409, 516, 1265, 1308, 1530, 1538, 1721, 1733, 1950, 2052, 2304
Proteosomal Degradation 992
Proteotoxicity 308, 1499
Prototypic Modified Risk Tobacco Product 1055, 1203
Provisional Advisory Levels 624, 625
Proximal Tubular Cells 2056
PSD95 377
Pseudomonas 2317
Psychoactive 723
Psychoactive Pharmaceuticals 1760
Psychostimulants 1744
PTE 2024
Pterostilbene 889
Pubertal Onset 1087t
Puberty 379, 1713k, 2194
Public Database 431
Public Health 1437
Publication 1679
Pulmonary 841c, 1204, 1205
Pulmonary and Cardiovascular Function 1563
Pulmonary Arterial Hypertension 501
Pulmonary Effects 1220
Pulmonary Exposure 815
Pulmonary Fibrosis 901e, 1211, 1804c, 2267
Pulmonary Inflammation 825
Pulmonary Injury 571
Pulmonary Toxicity 395, 603l, 1223, 1242g, 1713u
PXR 911
Pyrethroid 51, 1844
Pyrethroid Insecticides 189, 1846
Pyrethroids 60, 83, 378e, 683, 684, 685, 689b, 846, 1847
Pyrrolizidine Alkaloid 1094
Q-VD-OPh 361
QA/QC 1475
qHTS 173b, 757, 2273bb, 2273j
QSAR 96a, 433, 1616b, 2182c, 2273c, 2273h, 2273r, 2273u
QSAR Modeling 2252
QSAR Models 440j, 1586
QSPR 2273p
QT 1114
QT Interval 2196w
Qualification 277, 380
Quantitation 683
Quantitative Adverse Outcome Pathways 440d
Quantitative Analysis 408
Quantitative Bioanalysis 881
Quantitative High-Throughput Screening 444, 755
Quantitative Proteomics 542, 573
Quantitative Structure Activity Relationship 2273b
Quantum Dot Nanoparticles 2004f
Quantum Dots 603, 1962
Quercetin 797, 936, 1297f, 1801
Quinones 358
Rabbit 196, 847, 2141, 2157
Rad51 1924
Radiant Catalytic Ionization 326
Radiation 552d, 552f, 1525, 1803
Radiation Mitigator 1943h
Radiation Protection 865, 1935
Radioimmunoassay 122h
Radiosensitizer 1658
RAGE 322
Range in Noncancer Risk 632j
Ras Sindoor 1261
RasH2 2133
Rat 56, 343g, 811, 1129a, 1533, 1549h, 1601, 1649, 2064, 2145
Rat Blood 400
Rat Kidney Cells 1627
Rat miRNA Body Atlas 101
Rat Model 860, 2094
Rats 685, 1713g, 2038
RBL-2H3 2032
RccHan Wistar 914
REACH 636, 648
Reactive Blue 15 664
Reactive Metabolite 537
Reactive Oxygen Species 359, 1784, 1792, 1993, 2171
Reactive Oxygen Species (ROS) 587, 589, 837
Reactive Oxygen/Nitrogen Species 1803
Reactive Species 123, 2009
Reactive Sulfur Species 1258
Reactive Textile Dyes 451
Read-Across 29, 1593
Real-Time 1628
Real-Time Cell Analyzer 159
Receptor 1134
Receptor Occupancy 2196o
Receptors 1159, 1242, 1477

Reconstituted Human Corneal Epithelium Model ... 1026
Reconstructed Human Epidermis Model ... 2168
Reconstructed Vaginal Tissue Model ... 173k
Recovery ... 1566
Recovery Animals ... 2196aa
Recovery Groups ... 284
Red Blood Cells ... 1768
Red Ginseng ... 1200e
Red Seabream ... 653
Redox Biology ... 1102, 1795, 2039
Redox Cycling ... 1083
Redox Environment ... 194
Redox Potential ... 591
Redox Signaling ... 1452, 1778
Redox Status ... 1456
Reduction ... 1296, 1311, 1313
Reference Clustering ... 1828
Reference Concentration ... 632j
Reference Dose ... 777
Refill Fluid ... 1612
Refinement ... 1226
Regional Divergence ... 1885
Regorafenib ... 1200a
Regulation ... 2100
Regulatory ... 2082
Regulatory Acceptance ... 635
Regulatory and Safety Evaluation ... 1441, 1442, 1443, 1444, 1445, 1446
Regulatory Considerations ... 465
Regulatory Guidelines ... 456, 2250g
Regulatory Risk Assessment ... 631
Regulatory Safety Evaluation ... 2109, 2114
Regulatory Science ... 2110
Regulatory Testing ... 2112
Regulatory Toxicity Testing ... 2309
Regulatory Toxicology ... 185, 639, 1415
Reinstated Behavioral Sensitization ... 369
Release ... 641
Remediation ... 467d
Renal ... 1543
Renal Biomarkers ... 1544
Renal Cell Carcinogenesis ... 253, 261
Renal Dysfunction ... 2045
Renal Function ... 2049
Renal Proximal Tubule Cells ... 320
Renal Toxicity ... 649, 718, 1546
Renal Transport ... 2066
Renal Transporters ... 2067
Renal Tumor ... 2196e
Renal Tumors ... 2196f, 2196g, 2196i
Reovirus ... 2037
Repair ... 1936
Repeat Dose ... 26
Repeated-Dose Toxicity ... 164, 432, 1605, 2192
Repeated-Dose Toxicity Study ... 1601
Repeated-Dose Toxicology Studies ... 1992
Replication Stress ... 1293
Reporter Assays ... 167
Reporter Cell Lines ... 285, 2031
Reproduction ... 1713i
Reproduction and Development ... 1087x
Reproductive ... 1699, 2079
Reproductive Adverse Outcome ... 1087j
Reproductive Health ... 1807
Reproductive Organs ... 1620, 2196n
Reproductive System ... 1713b
Reproductive Tissue ... 790
Reproductive Toxicity ... 151, 637, 841, 1696, 1697, 1702, 1704, 1713a, 1713j
Reproductive Toxicology . 1616e, 2191, 2196
Reproductive/Developmental Toxicity ... 216, 1711, 2192
Reprotoxicity ... 1695, 2161
Research Fraud ... 725, 726, 727, 728, 729
Reserpine ... 2196m
Resources ... 1662d
Respiratory ... 1201
Respiratory Disease ... 1243
Respiratory Distress Syndrome ... 1163
Respiratory Function ... 1806
Respiratory Irritants ... 2241
Respiratory Safety Assessment ... 2236
Respiratory Toxicology ... 396, 1734
Respiratory Tract ... 828
Respiratory Tract Dosimetry ... 1228
Respiratory, Lung ... 577
Respirtory Rate ... 2139
Response Inhibition ... 1347d
Resveratrol ... 1076, 2062
Retina ... 352, 863
Retinal Function ... 1625
Retinal Pigment Epithelium ... 954
Retinal Toxicity ... 1625
Retinol Signaling ... 1595
Reverse Dosimetry ... 1517, 2250a, 2273o
RGS9 ... 550
Rhabdomyosarcoma ... 1143
Rhesus ... 848b
Rheumatoid Arthritis ... 552a
Rhinitis ... 2328
Rho Kinase ... 1623
Rhus trilobata ... 797c
Ribosomal Insults ... 386, 2027
Ribotoxic Stress Response ... 409
Ricin ... 581h, 624
Ring-DIMs ... 306
Risk ... 335, 1393, 2234e
Risk and Safety Assessment ... 434, 954a
Risk Assessment ... 6, 24, 25, 59, 63, 65, 68, 86, 227, 237, 338, 406, 420, 425, 440d, 465, 606, 607, 608, 609, 613, 614, 616, 622, 623, 626, 628, 632a, 637, 640, 643, 649b, 649d, 782, 1014, 1017, 1062h, 1290, 1398, 1404, 1405, 1406, 1407, 1408, 1409, 1415, 1421, 1476, 1478, 1482, 1483, 1484, 1485, 1486, 1487, 1488, 1489, 1616d, 1661, 1662b, 1713q, 1766, 1813, 1819, 1824, 1829, 1831, 1831b, 1831d, 1831e, 1831h, 1831j, 1897, 2055, 2099, 2113, 2117, 2214, 2229, 2234f, 2238, 2244, 2245, 2248, 2249, 2250i, 2250j, 2273, 2273d, 2273cc, 2285, 2298
Risk Assessment and Regulations ... 1815
Risk Assessment Methods ... 1008
Risk Assessment Tool ... 2232
Risk Characterization ... 647
Risk Framework ... 24
Risk Management ... 1831b
RMV ... 2145
RNA ... 330, 731
RNA Sequencing ... 909
RNA-Seq ... 49, 122, 181, 183, 263, 911, 917, 1736e, 2196i
RNAi Therapeutic ... 1653
Rodent ... 861, 2143, 2144, 2162, 2261
Rodents ... 288
Rolling Tobacco ... 2218
ROS ... 591, 1059, 1096, 1298, 1299, 1511, 1804, 2170
ROS Assay ... 1600
ROS;ER Stress ... 1369
ROS/ATP Ratio ... 1885
ROS/RNS ... 1316
Rotenone ... 1520
RT-qPCR ... 1727
RTCA Technology ... 1024
Ryanodine Receptor ... 351, 682, 1741, 1747d
S-Adenosylmethionine ... 939
S-Methoprene ... 673
S-Nitrosoglutathione ... 1100
S-Transarylation ... 1714
Safe Starting Dose ... 2114
Safer Consumer Products ... 1582
Safety ... 119, 475, 1119, 1128, 1628
Safety and Toxicology ... 1590
Safety Assessment ... 328, 329, 333, 381, 621, 972, 1036, 1061, 1062, 1129a, 1429, 1430, 1584, 1585, 1589, 1603, 1616, 1616b, 2173, 2179
Safety Assessment: Nonpharmaceuticals ... 1616d
Safety Assessments ... 343h
Safety Evaluation ... 2223
Safety Pharmacology ... 473, 476, 503, 1118, 2081, 2086
Safety Prediction ... 430
Salmonella Mutagenicity ... 2273b
Salubrinal ... 305
Salvia plebeia ... 999
Sampling Methods ... 983
Sandalwood ... 467
Sanionia uncinata ... 784
Saponins ... 799, 800, 801, 802
Sarin ... 361, 573, 581e, 581ji
Scavenger Receptors ... 826
Schizophrenia ... 1339
Science-Based Decision Making ... 2109
Scientific Ethics ... 725, 726, 727, 728, 729
Scientific Literacy ... 1668
Scratch ... 182
Screening ... 173j, 378b, 467f, 1908
Screening-Level Risk Assessment ... 647
SD Rat ... 287
Seafood Safety ... 2239
Seahorse Bioscience Extracellular Flux Analyzer ... 1611
SEAP ... 343f
Sebaceous Glands ... 563
Second Species ... 636
Secondary Pharmacology ... 2269
Secondhand Smoke ... 392, 2251
Seizure ... 275
Seizures ... 360
Selected Reaction Monitoring ... 418c
Selenium ... 39, 42, 213, 1255, 1262, 1278, 1321, 1558
Selenium Toxicity ... 1294
Selenoprotein P ... 1781
Semen ... 1559, 2157
Semi-Generic PBTK Model ... 96c
Semi-Natural Enclosures ... 283
Semi-Volatile Organics ... 1242f
Senescence ... 1853, 1965
Sensitivity ... 121
Sensitization ... 142, 2040
Sensitizers ... 2010, 2011
Sepsis ... 1713p
Serious Eye Damage/Eye Irritation ... 1027
Serotonin ... 501, 2163
Serotoninergic System ... 1862
Sertraline ... 1893
Serum ... 2304
Serum Deprivation ... 1782
Serum Gamma Glutamyl Transferase ... 223f
SES ... 230
Sesamin ... 787
Sex ... 318
Sex Differences ... 1219
Sex Hormones ... 1309
Sex-Specific ... 501
Sexual Development ... 379
Sexual Maturity ... 2147, 2156
SGA ... 1825
SGLT2 ... 2196e, 2196f, 2196g
SGLT2 Inhibitor ... 1652
Sh-SY5Y ... 365
SHE Cell Transformation Assay ... 1062
Short-Term Assays ... 2182c
Short-Term Synaptic Plasticity ... 1381
Sidman Electric Shock Avoidance Test ... 1392
Signal Transduction ... 912, 984, 1251, 1960, 2040a
Signaling Mechanisms ... 1729
Signaling Pathways ... 695
Silibinin ... 553
Silica Nanoparticle ... 1995
Silica Nanoparticles ... 600, 1984, 1997
Silicosis ... 128, 2322
Siloxanes ... 2245
Silver ... 814, 822, 823, 824, 841a, 841b, 1963, 1985
Silver Acetate ... 841b
Silver Ion ... 1297a
Silver Nanoparticle ... 1945, 1959, 1960
Silver Nanoparticles ... 819, 825, 826, 827, 1583, 1946, 1955, 1957, 1958, 1965, 1973c, 1973f, 1984, 1989, 2004, 2004c, 2004g
Silver Nanotoxicology ... 821
Simulation Modeling ... 646
Single Domain Antibody ... 876
Single-Walled Carbon Nanotubes .. 586, 594, 1948
siRNA ... 330, 840, 915
siRNA Screen ... 1715
Sirt3/FOXO3a/MnSOD ... 1327f
Skeletal Muscle ... 2213a
Skeleton ... 1087l
Skin . 463, 553, 554, 603a, 1030, 1303, 1973h, 2154, 2166, 2170, 2174, 2175
Skin Cancer ... 1108
Skin Corrosion ... 2177, 2178, 2179
Skin Explant ... 985
Skin Inflammation ... 979
Skin Injury ... 563, 565, 2169
Skin Irritation ... 944, 1604, 2177, 2178
Skin Metabolism ... 28
Skin Penetration ... 1973i, 1973j
Skin Permeability ... 28
Skin Permeation ... 2176
Skin Sensitization ... 402, 408a, 982, 990, 1032, 1035, 1037, 1062c, 1062e, 1608, 1831l, 2165, 2182c, 2273
Skin Toxicity ... 2182b
SLC30A10 ... 1357
Slc7a11 ... 1804c
Sleep ... 274
Sleep-Wake ... 148
Sloughing ... 1038
Small Fish Model ... 2283
Small Intestine ... 1040
Smartphone ... 876a
Smelter ... 1554
Smoke ... 95
Smokeless Tobacco ... 2234v
Smoker and Nonsmoker ... 1549
Smokers ... 2234u
Smoking ... 645, 1528, 1537, 1574
Smoothing Splines ... 628
SNP ... 548
SNPs ... 1238, 1260
Social ... 633
Social Housing ... 186, 2151d
Sodium Arsenite ... 788, 813b, 1514b
Sodium Channels ... 378e
Soil ... 669a, 841a, 1831i, 2234w
Solar Radiation ... 2119
Solatenol ... 238
Soluble Epoxide Hydrolase ... 876
Solvent ... 147
Soman ... 552g
Somatic Cell Therapy ... 1422, 1423, 1424, 1425, 1426, 1427, 1428
Sonic Hedgehog ... 176
SOT Code of Ethics ... 581g
Southwest ... 2311, 2312, 2313, 2314, 2315
Soy ... 323
Sp1 ... 1352
Spacecraft ... 2250d
Spatial Learning ... 1856
Speciation ... 2234q
Speciation Analysis ... 2224
Species Comparison ... 1640
Species Difference ... 500, 1885
Species Diversity ... 521
Species Extrapolation ... 96f
Species-Specificity ... 2035
Specificity Protein Transcription Factors ... 1510
Sperm Collection ... 2156
Sperm Parameters ... 1692

Sperm Whale ... 448, 1303
Spermiogram ... 1694
Spheroid ... 1120
Sphinganine 1-Phosphate ... 343b
Spinal Cord ... 1385
Spirometry ... 1209
Spleen ... 395, 2004e
Spleen Monocyte ... 571
Spondias mombin ... 462
Sprague-Dawley Rat ... 1773
Sprague-Dawley Rats ... 1225
Spray Dryer ... 1229
SRBCs ... 403
SSRIs ... 1013
Stable Primary Hepatocytes ... 1895
Standard of Knowledge ... 649c
Standard Operating Procedure ... 422
Standards ... 724
Staphylococcal Enterotoxin B ... 385
Staphylococcal Enterotoxin B (SEB) ... 569
StAR ... 172
STAT3 ... 372, 466, 1098
STAT5 ... 1352
Statin ... 1122
Statins ... 547
Statistical Approaches ... 1420
Statistics ... 476
Steatosis ... 736, 737, 738, 1783, 1884, 1898
Steel Slag ... 2219
STEM ... 1435, 1436, 1438, 1439, 1665, 1666
Stem Bark Extract ... 807
Stem Cell ... 764, 765, 1119, 1129e, 1619, 1764d, 1922e
Stem Cell Differentiation ... 440c
Stem Cell Models ... 1902
Stem Cell-Derived Cardiomyocytes ... 856, 1918, 1919
Stem Cell-Derived Neuron ... 1922d
Stem Cell-Derived Neurons ... 1922c
Stem Cells ... 12, 33, 40, 714, 766, 767, 768, 769, 1116, 1129d, 1297j, 1297l, 1328, 1458, 1459, 1460, 1461, 1764b, 1911, 1912, 1913, 1921, 1922f, 2080, 2081, 2085
Stem Cells and Toxicity Testing ... 714, 716, 1422, 1423, 1424, 1425, 1426, 1427, 1428, 1902
Stem Cells Drug Discovery ... 1118
STEM Education ... 1663
Stem/Progenitor Liver Cell ... 1906
Steroid ... 649a
Steroidogenesis ... 173j, 1076, 2185
Steroids ... 997
Steviol Glycoside ... 337
Store-Operated Calcium Channels ... 311
Store-Operated Calcium Entry ... 570
Strain Difference ... 1174
Strain Differences ... 825
Stress ... 1087v, 1253
Stress Fiber ... 1623
Stress Response ... 439
Striatum ... 1329, 1330
Stromal Cell-Derived Factor 1 (SDF-1) ... 1901
Structural Alert ... 2263
Structural Alerts ... 29, 2266, 2273x
Structural Birth Defects ... 2076
Structural Elucidation of Drug Impurities ... 1624
Structure-Toxicity Relationship ... 434
Study Quality ... 1829
Styrene ... 514
Subchronic Toxicity ... 1087i, 1242d
Substantia Nigra ... 367, 2107
Substructure Identification ... 434
Subventricular Zone ... 1390
Sulfate, Urinary Marker ... 515
Sulfide ... 362
Sulfiredoxin ... 1102
Sulforaphane ... 493, 874, 1713t
Sulfur Mustard ... 463, 559, 562, 563, 577, 581a
Sunscreen ... 877, 2181
Superfund Site ... 1087k
Superoxide ... 1117
Superparamagnetic Iron Oxide Nanoparticles ... 1947
Supplement ... 335
Supplements ... 2246
Surface ... 597
Surface Amination ... 1984
Surface Area ... 952
Surface-Active Agents ... 1226
Surfactant ... 1979
Surgery ... 1244, 2158
Survival ... 2131
Susceptibility ... 776, 1416, 2071, 2100
Susceptible ... 1421
SWCNTs ... 589
Swine Husbandry ... 1713m
Swiss Albino Mice ... 403
Synapse ... 377, 1337, 1392a, 1922c
Synaptic Proteins ... 1760
Synthetic Amorphous Silica ... 332
Synuclein ... 924
Syringe Weights ... 953
System Biology ... 2092
Systematic Review ... 1828, 2250l
Systemic Inflammation ... 1527
Systemic Toxicity ... 173e, 554, 2299
Systems Approach to Biomarker Discovery ... 187
Systems Biology ... 417, 695, 1736a, 2073, 2251
Systems Biology and Toxicology ... 410, 413, 415, 2259
Systems Modeling ... 88, 1899
Systems Toxicology ... 418a, 690, 1969
Syzygium guineense ... 807
T Cell ... 127, 145, 1004, 2012
T Cell Responses ... 391
T. arjuna Toxicity ... 1693
T1 ... 1368
T2DM ... 1327f
Tamoxifen ... 1087f, 1087h
Target Organ Toxicities ... 2110
Target Organ Toxicity ... 157
Tauroursodeoxycholic Acid (TUDCA) ... 934
Taxol ... 436
TB Therapy ... 542
TBBPA ... 922d
tBHQ ... 312d
TBI ... 1732
TCDD ... 174, 193, 200, 223c, 414, 490, 504b, 581g, 653, 904, 905, 922c, 1685, 1746, 2014, 2015, 2016, 2018, 2019, 2020
TCDD and Liver Fibrosis ... 2200
TCE ... 632j
TCE Acute Toxicity ... 2243
TCPP ... 1616c
TDAR ... 1713s
TDCPP ... 1747a
TDI ... 142
Tear Gas ... 2169
TEER ... 1592
TEF ... 1016
Telemetry ... 274, 275, 468, 471, 475, 476, 2142, 2144, 2146, 2162
Tellurite ... 1304
Tellurium ... 1292
Tellurium Tetrachloride ... 1297d
Telmisartan ... 80, 1700
Telomerase ... 298
Telomere ... 1936
Telomere Length ... 144
Temperature ... 1630
TEMPO ... 1943b
Teratogenesis ... 804
Teratogenicity ... 2257
Terpenes ... 671
Test Battery ... 1062e
Testicular ... 295
Testicular Cancer ... 245
Testicular Toxicity ... 681, 2035, 2212
Testing Strategy ... 658
Testis ... 1708, 2125
Testis Histopathology ... 1709
Testosterone ... 1009, 1091, 1807
Tetrabromobisphenol A ... 1087i, 1087w, 1087x, 2213a
Tetrachloroethylene ... 251
Tetracycline ... 509, 884
Tetramethylenedisulfotetramine ... 557
TETS ... 360
Texas ... 317
Text Mining ... 2250j, 2250k
Textile ... 876c
Textile Dye ... 467h
Textile Dyes ... 2040
TGF ... 267
TGF-beta2 ... 496
Th17 ... 2322
Thalidomide ... 173g, 196, 202, 1150
THC ... 962, 2008
Therapeutics ... 260
Therapy ... 560
Thiazolidinedione ... 1200f
Thioacetamide ... 454
Thiocyanate ... 1001
Thioethers ... 841e
Thioredoxin/Peroxiredoxin ... 925
Thioredoxine Reductase ... 1311
Thirdhand Smoke ... 1056
THP-1 Cells ... 837, 2036
Threshold ... 438, 1943e
Threshold Dose-Response ... 1941
Threshold of Toxicological Concern (TTC) ... 26, 27, 420, 632, 949, 1609
Thresholds of Toxicological Concern (TTC) ... 419
Thrombin ... 1197
Thrombocytopenia ... 866
Thrombosis ... 954b
Thymus ... 408, 1297a
Thyroid ... 234, 1087d, 1087i
Thyroid Hormone ... 1087, 1347f, 1347g, 1713d
Thyroid Hormone Metabolism ... 1086
Thyroid Receptors ... 1135
Thyroid Tumor ... 238
Tibetan Medicine ... 2223
Tight Junction ... 942e, 1062b
Tight Junctions ... 193
Tilapia guineensis ... 663
Time Series ... 2273e
Timing ... 1382
TiO_2 ... 1967
TISMO ... 1213
Tissue Injury ... 102, 122e, 708
Titanium Dioxide ... 620, 632h, 820, 839, 1964, 1998
Titanium Dioxide Nanoparticles ... 829, 1996
TK Modeling ... 74
TK-PK ... 2160
TLR-4 ... 1180
TLR4 ... 166, 343f
TLRs ... 387
TNF ... 1168
TNF-Alpha ... 520, 974, 1618
TNF-α ... 1713t
Tobacco ... 355, 674, 1015, 1018e, 1922a
Tobacco Products ... 646, 1527, 1613
Tobacco Smoke ... 1549c
Tobacco Smoking ... 391, 416
Tobacco-Control Policy ... 646
Tobacco-Specific Nitrosamines ... 511
Tocopherylquinone ... 1144
Toenails ... 1550
Toll-Like Receptor ... 166, 594, 1237
Toll-Like Receptors ... 981, 1467
Toluene ... 87, 895, 1820, 2250h
Tonnage ... 644
Topography ... 645
Tort ... 719, 721, 722
Tort Liability ... 2102
Total Arsenic ... 1327e
Tox21 .. 31, 173d, 173h, 444, 753, 754, 1595, 1737, 2273bb
Tox21 10K ... 173b
ToxCast ... 31, 173j, 223d, 343c, 418e, 440h, 1611, 1647, 1747, 1973e, 2250, 2250a, 2273aa, 2273f, 2273l, 2273q, 2273s, 2273u
ToxCast Chemical ... 524
ToxCast Hepatic Outcomes ... 694
ToxCastDB ... 2273t
Toxic Effects ... 2251
Toxic Industrial Chemicals ... 627
Toxic Load Model ... 1817, 1818
Toxic Torts ... 2101
Toxicant-Associated Steatohepatitis ... 1569
Toxicity ... 37, 38, 39, 42, 615, 712, 849, 850, 854, 1087l, 1206, 1209, 1233, 1616c, 1655, 1657, 1694, 1958, 2234d
Toxicity Biomarkers ... 109
Toxicity Data ... 426
Toxicity Pathways ... 1868
Toxicity Prediction ... 428, 430, 693, 2269
Toxicity Study ... 812
Toxicity Testing ... 439
Toxicity Testing in the 21st Century ... 162
Toxico-Proteomics ... 1348
Toxicogenetic ... 1480
Toxicogenetics ... 279, 2129a
Toxicogenomics ... 122, 1214, 1297a, 1476, 1478, 1479, 1481, 1736a, 1952, 2096, 2098, 2101, 2284
Toxicogenomics and Mode of Action ... 408b, 692
Toxicogenomics, Hepatotoxicity, Liver ... 692, 1868
Toxicokinetic Model ... 83
Toxicokinetic Study ... 877
Toxicokinetics ... 64, 343, 685, 890, 899, 901a, 901f, 1260, 1572, 1763
Toxicologic Pathology ... 1680
Toxicological Database ... 27
Toxicological Profile ... 410
Toxicology ... 1393, 1394, 1396, 1397, 1669, 1787, 1914, 2074, 2183
Toxicology Education ... 1662c, 1670, 1679
Toxicology Endpoints ... 861
Toxicology in *C. elegans* ... 1356
Toxicology Testing ... 2110
Toxicology Training ... 1767
Toxoplasma gondii Infection ... 363
ToxRefDB ... 440a
Trace Elements ... 343a
Trace Metals ... 1557, 2227
Traffic-Related Air Pollution ... 858
TRAIL ... 293
Training ... 1680
Transcript ... 1177
Transcript Profile ... 146
Transcription ... 173d, 1725, 1728
Transcription Factor Binding ... 1943d
Transcription Factors ... 1718
Transcription Initiation ... 1184
Transcriptome ... 544, 653, 1943c
Transcriptome Change ... 2273g
Transcriptomics ... 418, 914, 1054, 1061
Transcriptomics/Gene Expressing ... 173g
Transfection ... 840
Transgenerational ... 221, 1681, 2184
Transgenerational Effect ... 1705
Transgenerational Inheritance ... 1690a
Transgenic Animals ... 2111
Transgenic Mouse ... 460
Transgenic Mouse Mutation Assay ... 1943j

KEYWORD INDEX

Translation ... 409, 2083
Translational ... 2, 7
Translational Biomarker ... 103, 112
Translational Imaging ... 1429, 1430, 1431, 1432, 1433, 1434
Translational Science ... 1422, 1423, 1424, 1425, 1426, 1427, 1428
Translational Toxicology ... 870, 1548
Translesion Synthesis ... 1293
Transplacental Exposure ... 848
Transplantation ... 870
Transport ... 1349, 2208
Transporter ... 1177, 1899e
Transporters ... 2067a
Trauma ... 875
Treatment ... 1212
Treg ... 129
Tri-Ortho-Cresyl Phosphate ... 378d
Tribbles 3 ... 483
Tributyltin ... 223, 1392
Trichloroethene ... 138, 139
Trichloroethylene ... 137, 261, 966, 1152, 1343
Triclocarban ... 2195
Triclopyr ... 1863
Triclosan .. 141, 257, 382, 661, 1087b, 1087e, 1713d, 2025, 2190
Triglicerides ... 1002
Trihalomethanes, Haloacetic Acids ... 1018a
Triorthocresyl Phosphate ... 2247
Tris(Chloropropyl)phosphate ... 1616c
Trivalent Chromium ... 1541
Trovafloxacin ... 1882, 1886
TRP Channels ... 1368b
TRPA1 ... 1238, 1241, 2169, 2323
Tryptophan Metabolites ... 1130
TSPO ... 172
TT21C ... 1140
TTC ... 948
TTC Concept ... 631
Tube Formation ... 1971
Tuberculosis ... 271, 1629
Tubulointerstitial Fibrosis ... 2047
Tumor ... 2130
Tumor Immunity ... 129
Tumor Metastasis ... 1098
Tumor Microenvironment ... 732, 1492
Tumor Necrosis Factor ... 909
Tumor Promoter ... 254
Tumor Promotion ... 263
Tumor Suppressor ... 584
Tumorigenesis ... 245, 250
Tumors ... 1089
Tungsten ... 1283, 1297e
Tungsten Oxide ... 831
Turtle ... 206
Two Photon Polymerization ... 1973g
Type 2 Diabetes ... 858, 2044, 2125, 2300
Tyrosine Kinase Inhibitors ... 1626
U937 Cell Line ... 1713n
Ubiquitination ... 1925
UGT ... 975, 2151
UGT1A1 ... 190
UGT1A8 Gene Regulation ... 918
UGT2B15 ... 192
Ultrafine ... 1561
Ultrafine CAPs ... 1242f
Ultraviolet Radiation ... 126
Umu Test ... 836
Uncertainty ... 440a, 1408
Uncoupler ... 1642
Undergraduate ... 1435, 1436, 1437, 1438, 1439, 1440, 1672
Undergraduate Education ... 1666, 1670
Undergraduate Research ... 1664, 1666
Unfolded Protein Response 213, 552e, 2319
Unilateral Ureteral Obstruction ... 2047
UPLC TOFMS ... 1624
UPLC-MS/MS ... 198
Upper Respiratory Tract ... 1228
Uranium ... 2234c
Uranyl Acetate ... 1295
Uric Acid ... 1125, 1190
Urinary Arsenic ... 2234o
Urinary Bladder ... 1089
Urinary Bladder Cancer ... 551
Urinary Cotinine ... 416
Urinary microRNA ... 105, 122e
Urinary System Toxicity ... 813a
Urine ... 675, 1327e, 1539, 1577, 1578
Urine Uranium ... 1559
Urines ... 1549
Uro-Epithelium ... 1039
Usnic Acid ... 494
Uterotrophic ... 2190
UV ... 263, 2181
UV DNA Damage ... 1936
UV Light ... 836
UV Radiation ... 783
UVA ... 2164
UVB ... 1108, 1736
UVR ... 2180
V-akt Murine Thymoma Viral Oncogene Homolog 1 ... 922b
Vaccine ... 121, 581, 1654, 1655
Vaccine Constituents ... 419
Vaccine Safety ... 271
Vaccine Safety Assessment ... 2196s
Vaginal Irritation ... 2196y
Validation ... 402, 634, 1549a, 2224
Vapor ... 1018e
Vapor Intrusion ... 2243
Vapor Uptake ... 1228
Vapors ... 1227
Variability ... 96, 1408
Variation Analysis ... 779
Vascular ... 1535, 2302
Vascular Calcification ... 495
Vascular Inflammation ... 1713t
Vascular Injury ... 1129a
Vascular Insulin Resistance ... 1125
Vascular Remodeling ... 1122
Vascular Smooth Muscle .. 1122, 1298, 1299
Vascular Toxicity ... 1062a
Vasculature ... 1239, 1746
Vasculitis ... 104
Vasculogenesis ... 1736e
Vegetable ... 884
VEGFR3 ... 1062i
Vehicle ... 280
Vehicle Side Effects ... 124
Vehicular Exhaust ... 1242e
Ventilation ... 2140
Ventral Tegmental Area ... 367
Ventriculomegaly ... 1342
Vero Cell ... 813
Vesicant Injury ... 578, 581f
Vesicants ... 552e
Veterinary ... 539c
VGCC ... 1256
Video Bioinformatics ... 1902
Video Monitoring ... 2155
Videography ... 2234f
Vigabatrin ... 1764e
Vincamine ... 1713b
Vinclozolin ... 530
Vinyl Acetate ... 467b
Vinyl Chloride ... 1879
Virtual Tissue ... 94
Vitamin A ... 2248
Vitamin B12 ... 1312
Vitamin D ... 938
Vitamin E ... 1144, 1537
Vitamin E Succinate ... 1317
Vitellogenin ... 206, 1073, 1074
VITROCELL VC10 ... 95
VMAT2 ... 370, 371
VOCs ... 1012, 1087r, 2196b
Volatile Organic Compounds ... 1607
Voltage-Gated Calcium Channels ... 1370
Voltage-Gated Ion Channels ... 1384
VPA ... 180
VUSE ... 1615
Waist Circumference ... 224
War Threat ... 552e
Water ... 2234
Water Solubility ... 2273p
Weak Genotoxins ... 465
Wear Debris ... 603j
Wear Particles ... 2024
Web Application ... 2097, 2273n
Weight Management ... 1590
Weight of Evidence 1404, 1407, 1482, 1483, 1484, 1485, 1486, 1487, 1488, 1489, 1831a
Welding ... 1229a
Welding Fumes ... 1368a
Whisker ... 1991
White Cheese ... 313
White Matter ... 1364
Whole Genome DNA Methylation ... 977
Whole Genome Sequencing ... 2100
Whole-Body ... 581i
Whole-Body Inhalation ... 1974
Whole-Body Plethysmography ... 2144
Whole-Mount *In Situ* Hybridization ... 196
Wild Black Rat ... 1516
Wild Mice ... 283
Wild Yam ... 978e
Wildfire Particulate Matter ... 980
Wildlife ... 1279
Wistar Hannover ... 2132
Wistar Rat ... 2131
Withdrawal ... 1648
Wnt Signaling ... 1095
Wnt/Beta-Catenin Signaling ... 1173
Women ... 2116
Worker Exposure ... 1555
Workers ... 603e
Working Group ... 58
Working Memory ... 1347c
Workplace ... 603f
Wound Healing ... 578, 864
xCELLigence ... 478
Xenobiotic Biotransformation ... 546, 2189
Xenobiotic Transport ... 900, 1701
Xenobiotic Transporters ... 2061
Xenobiotics ... 1477
Xenoestrogens ... 1072
Yeast-Based Assay ... 173
Zanthoxylum armatum ... 812
Zearalenone ... 217
Zebrafish ... 148, 149, 150, 152, 153, 154, 155, 156, 157, 158, 173i, 173m, 201, 202, 203, 204, 205, 210, 212, 221, 222, 223, 223a, 223d, 303, 440h, 440l, 491, 534, 581e, 657, 804, 816, 942b, 1013, 1062a, 1087k, 1129d, 1147, 1277, 1294, 1327a, 1338, 1347h, 1603, 1639a, 1639b, 1671, 1745, 1751, 1761, 1857, 1994, 2075
Zebrafish Development ... 208, 1683
Zebrafish Embryonic Heart ... 223e
Zebrafish Xenograft Model ... 1637
Zeranol ... 2194
Zilpaterol ... 863
Zinc ... 1229a, 1244, 1246, 1778, 2049
Zinc Oxide ... 1229b, 1977
Ziram ... 942b
α-Hexylcinnamaldehyde ... 398, 399
α2u-Globulin ... 2059
α7nAChR ... 2026

Notes

The Official Journal of the Society of Toxicology

Toxicological Sciences

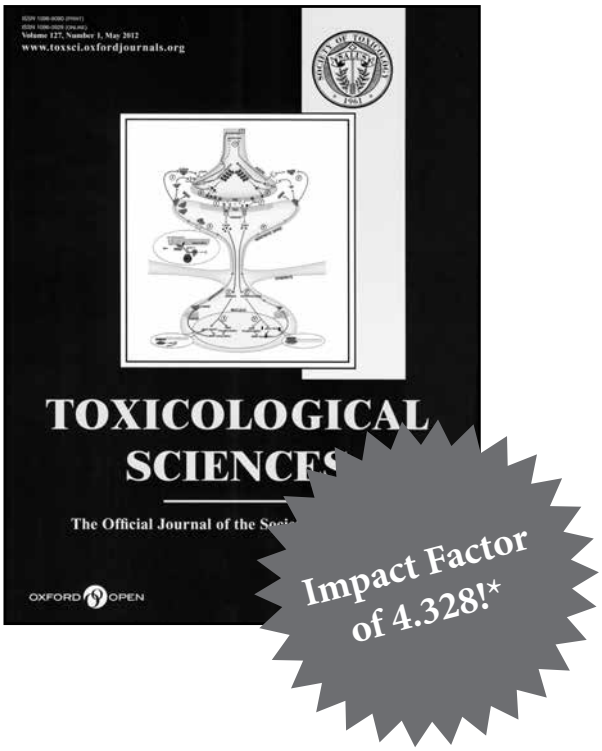

- *A top original research journal in Toxicology*
- *Ranked 8 out of 85 in this category*
- *Advance Access—quick online publication, weeks ahead of print*
- *Optional open access for authors*

VISIT OUR BOOTH AT TOXEXPO 2014

OR VISIT US ONLINE AT

www.toxsci.oxfordjournals.org

* 2012 Journal Citation Reports (Thomson Reuters, 2013)

OXFORD OPEN

OXFORD UNIVERSITY PRESS

53rd Annual Meeting and ToxExpo™

March 23-27, 2014

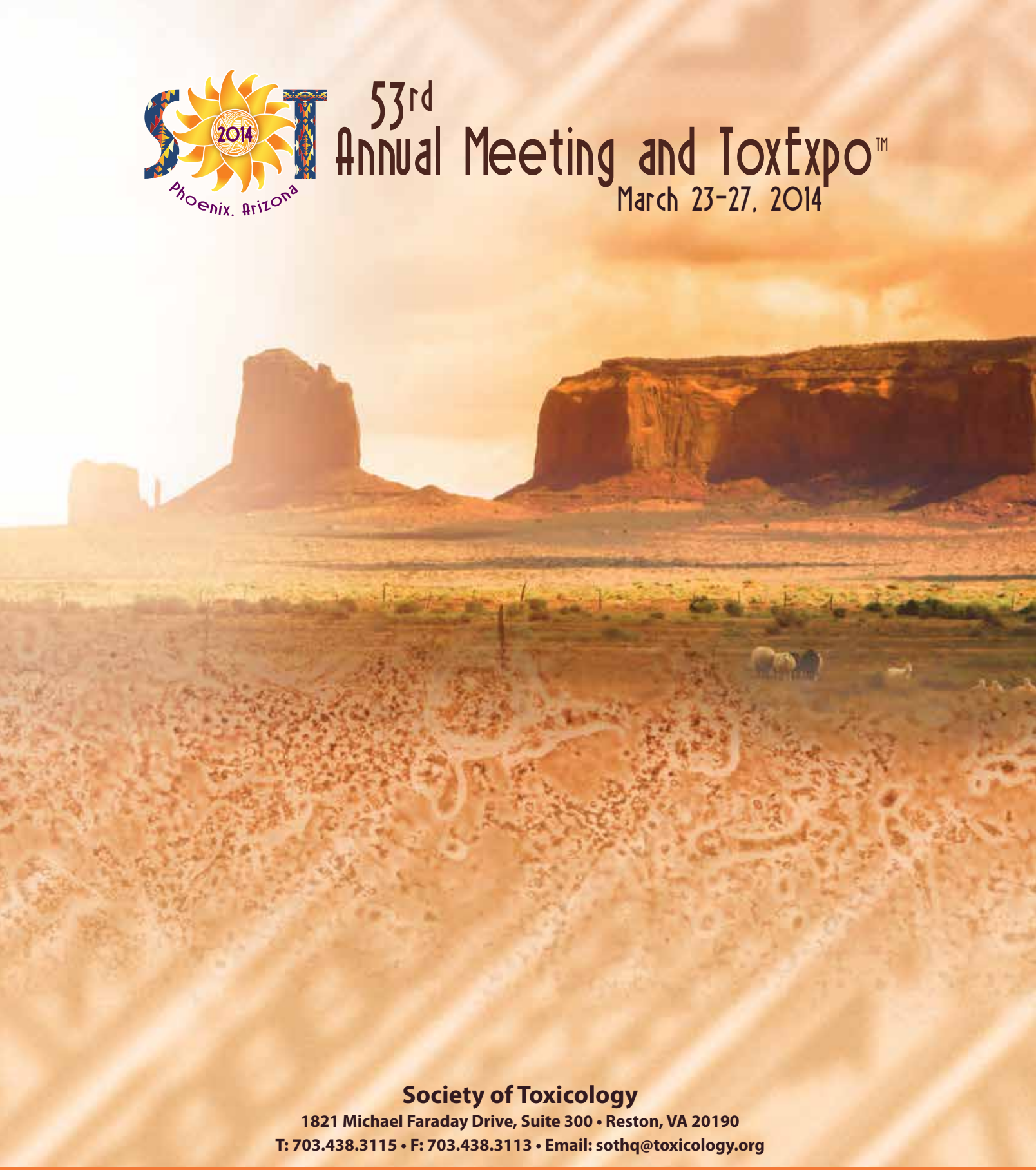

Society of Toxicology

1821 Michael Faraday Drive, Suite 300 • Reston, VA 20190

T: 703.438.3115 • F: 703.438.3113 • Email: sothq@toxicology.org

www.toxicology.org

FSC

© Mixed Sources

Product group from well-managed forests, controlled sources and recycled wood or fiber

www.fsc.org Cert no. XXX-XXX-XXXX

© 1996 Forest Stewardship Council

We are proud to print this publication entirely on Forest Stewardship Council certified paper. FSC certification ensures that the paper in this publication contains fiber from well-managed and responsibly harvested forests that meet strict environmental, social, and economic standards.